

1001

Nestin-positive Cells Become Osterix-expressing Osteoblast Precursors in the Perichondrium during Early Endochondral Bone Development. Noriaki Ono^{*1}, Wanida Ono², Paul Frenette³, Henry Kronenberg².¹Massachusetts General Hospital & Harvard Medical School, USA, ²Massachusetts General Hospital, USA, ³Ruth L. & David S. Gottesman Institute for Stem Cell & Regenerative Medicine, USA

Nestin-positive cells that support hematopoietic stem cells are putative mesenchymal stem cells in adult bone marrow. The relationship of these cells to osteoblast precursors in fetal life is unknown. Previous studies have shown that, during early endochondral bone development, osterix-expressing osteoblast precursors in the perichondrium translocate to the marrow space in a pericyte-like manner. To determine the possible involvement of nestin-positive cells in this process, we studied triple-mutant mice carrying a green fluorescent protein under the nestin promoter (Nes+ or Nes-GFP) and an inducible cre recombinase under the osterix promoter (Ox-CreER) that activates a Rosa26 tomato reporter upon tamoxifen injection. At embryonic day 10.5 (E10.5), Nes+ cells were distributed throughout the limb bud in a reticular manner, and most of these cells coexpressed the endothelial marker, CD31. When the distinct growth cartilage started to elongate at E12.5, Nes+ cells were found in the innermost portions of the perichondrium (PC), but not within the cartilage itself. At E13.5, Ox+ cells began to appear in the PC adjacent to the incipient hypertrophic cartilage (HC). In this part of the PC, most of the Nes+ cells were also positive for either Ox or CD31. We thereafter chased the descendants of these Ox+ cells (Ox-E13.5 cells) by a pulse-chase protocol. Ox-E13.5 cells translocated into the future marrow space, proliferated and differentiated into osteoblasts of the spongiosa. After E15.5, Nes+ cells were found in the innermost portions of the PC and the primary spongiosa, while Ox+ cells were found in the PC adjacent to the HC and in trabecular/cortical bone. Many Ox-E13.5 cells also expressed Nes-GFP in the primary spongiosa and contributed extensively to bone formation after 3 days of chase at E16.5. However, Ox-E13.5 cells did not express Nes-GFP in the perichondrium at E16.5. Furthermore, when chased further for 7 days until the time of birth (P0), Ox-E13.5 cells seldom expressed Nes-GFP in the primary spongiosa, and no Nes+ Ox-E13.5 cells were found in the perichondrium. Interestingly, Ox-E13.5 cells disappeared almost completely by postnatal day 21, with only a few osteocytes and bone lining cells remaining in the diaphysis. These findings indicate that Nes+ cells are heterogeneous in the embryonic perichondrium, and that a subset of Nes+ cells becomes Ox+ cells during bone development. Ox-expressing cells do not indefinitely renew themselves.

Disclosures: Noriaki Ono, None.

1002

c-Cbl Silencing in Mesenchymal Cells Promotes Osteoblast Differentiation by Decreasing STAT5-Runx2 Interaction. François-Xavier Dieudonné^{*1}, Nicolas Sèvre¹, Jing-Jie Weng², Yeu Su², Pierre J. Marie¹. ¹Inserm UMR-606 & University Paris Diderot, France, ²Institute of Biopharmaceutical Sciences, National Yang-Ming University, Taiwan

Ubiquitin ligase-dependent degradation of proteins is an important process governing bone cell proliferation, differentiation and apoptosis. The E3 ubiquitin ligase c-Cbl is responsible for the downregulation of multiple proteins including receptor tyrosine kinases (RTKs). We previously showed that selective inhibition of c-Cbl interaction with RTKs results in increased mesenchymal cell differentiation into osteoblasts. In this study, we investigated whether overall silencing c-Cbl in mesenchymal cells might promote osteoblast differentiation, and we determined the mechanisms involved in this effect. Using two shRNA targeting distinct c-Cbl domains that interact with either RTK or ubiquitin, we found that c-Cbl silencing increased cell proliferation in murine C2C12 and C3H10T1/2 multipotent mesenchymal cells, and human clonal multipotent bone marrow-derived F/Stro-1A+ stromal cells. Additionally, c-Cbl silencing increased alkaline phosphatase (ALP) staining and activity and promoted the expression of osteoblast markers (Runx2, ALP, type I collagen) in these mesenchymal cell lines. This positive effect on osteoblast differentiation translated into increased matrix mineralization *in vitro*, showing that overall c-Cbl silencing increases osteogenic differentiation in murine and human mesenchymal cells. Analysis of the molecular mechanisms revealed that c-Cbl silencing increased the expression of platelet-derived growth factor receptor alpha and insulin like growth factor receptor, suggesting that these receptors may mediate part of the effect of c-Cbl silencing on osteoblast differentiation. We performed immunoprecipitation (IP) analyses with the goal of identifying other target proteins that may mediate the effect of c-Cbl in mesenchymal cells. IP analyses revealed that c-Cbl physically interacts with STAT5, and that STAT5 interacts with Runx2 in mesenchymal cells. Silencing c-Cbl using shRNA increased STAT5 protein level which resulted from decreased c-Cbl-mediated ubiquitination of STAT5. Pharmacological inhibition of STAT5 activity abrogated the positive effect of c-Cbl shRNA on osteoblast gene expression and *in vitro* osteogenesis. The data reveal that overall inhibition c-Cbl promotes the osteogenic differentiation program in murine and human mesenchymal cells, and indicate that this effect involves decreased c-Cbl-mediated STAT5 ubiquitination resulting in increased STAT5-Runx2 interaction. This uncovers a novel mechanism by which c-Cbl controls the osteogenic capacity of mesenchymal cells.

Disclosures: François-Xavier Dieudonné, None.

1003

Fate Mapping with Osterix Cre Mice Reveals the Origin and Contribution of Bone Marrow Mesenchymal Stem Cells. Peter Mave^{*}, Yaling Liu, Sara Strecker, Liping Wang, Mark Kronenberg, David Rowe. University of Connecticut Health Center, USA

The developmental origin of adult bone marrow mesenchymal stem cells and their *in vivo* differentiation into more mature cell types has remained speculative. Here we carry out fate mapping studies utilizing Osterix-EGFPcre and Osterix-CreERT mice by intercrossing these lines with a floxed-stop tdTomato Cre reporter line (Ai9). Bone marrow stromal cultures derived from Osterix-EGFPcre;Ai9 mice result in the fluorescent marking of an adherent, mesenchymal population that is present at the earliest stages of culture and retains BMSC-like multipotent properties. Assessment of Ai9 Cre reporter expression in the bone marrow identifies several connective tissue related cell types in addition to cells of the osteoblast lineage, including reticular, vascular smooth muscle, adipocytic, and perineurial cells. Interestingly, adipose tissue and smooth muscle lined blood vessels lying outside the bone do not retain Cre reporter expression, suggesting a distinct origin and novel compartmentalization within the bone marrow. Temporal activation of Osterix-CreERT at E14.5 substantiates our constitutive Osterix-EGFPcre fate mapping studies and provides evidence that the embryonic perichondrium is a multipotent progenitor cell population that gives rise to much more than the osteoblast lineage and is the likely source of adult BMSCs. Furthermore, transplantation of adult BMSCs derived from Osterix-EGFP;Ai9 day 5 stromal cultures into a long bone defect resulted in the differentiation of Ai9 marked BMSCs into many of the same cell types defined by our fate mapping studies, including reticular cells, marrow adipocytes, and osteoblasts. Collectively, our studies indicate that BMSCs originate from an osterix-expressing perichondrial precursor cell population and they contribute to an array of connective tissue related cell types present within the bone marrow.

Disclosures: Peter Mave, None.

1004

Nocturnin, a Marrow Stromal Cell Deadenylase, Regulates Lineage Allocation Through Changes in Mitochondrial Bioenergetics. Anyonya Guntur^{*1}, Phuong Le¹, Sheila Bornstein², Sutada Lotinun³, Roland Baron⁴, Carla Green⁵, Clifford Rosen². ¹Maine medical center research institute, USA, ²Maine Medical Center, USA, ³Harvard School of Dental Medicine, USA, ⁴Harvard School of Medicine & of Dental Medicine, USA, ⁵Department of Neuroscience, University of Texas Southwestern Medical Center, USA

Nocturnin (*Noc*), a circadian deadenylase regulated by PPARG, is highly expressed in bone marrow stromal cells (MSCs). *Noc*-/- mice are lean, resistant to high fat diet induced obesity and have high bone mass. Rosiglitazone (Rosi) an agent that activates PPARG, markedly enhances the expression of *Noc*, causes significant trabecular bone loss and increases marrow adipogenesis in mice. Thus we hypothesized that *Noc* is important in regulating stromal cell fate either towards the adipogenic or osteogenic lineage in response to Rosi. To test this further, we treated 12 wk *Noc*-/- mice and their age- and gender matched WT controls(+/+) with 20 mg/kg/day Rosi for 8 wks. Unlike +/+ mice, Rosi treated *Noc*-/- mice had a two fold increase in trabecular BV/TV and a nearly 2 fold rise in BFR/TV (p<0.05) despite no change in total osteoblast number. We next studied the amino acid sequence of NOC and identified a mitochondrial target sequence in the N-terminus with a very high probability (0.98%) of localization to the mitochondria. Utilizing an epitope tagged NOC expression plasmid, we showed that NOC co-localizes with a resident mitochondrial protein, suggesting a potentially novel role for this deadenylase, either directly or indirectly by regulating mitochondrial metabolism. To study if *Noc* determines cell fate by influencing cellular bioenergetics and function, we tested the metabolic profile of MC3T3E1 cells over expressing *Noc* and compared them to GFP control cells. Previously, we showed that over-expression of *Noc* in pre-osteoblastic cells inhibited osteogenesis and conversely in 3T3L1 cells enhanced adipogenesis, two distinct cell types with different energy needs. To define the role of mitochondrial bioenergetics in cell fate, we utilized the XF24 extracellular flux analyzer and studied the oxygen consumption rate (OCR) and extracellular acidification rate (ECAR) of MC3T3E1 cells in response to mitochondrial stress during a pre differentiation state. *Noc* over expressing cells had lower basal OCR as well as reduced ECAR (i.e. a measure of glycolysis) compared to GFP expressing control cells. Taken together these data suggest that *Noc*, by targeting the mitochondria, affects bioenergetics thereby regulating cellular work and lineage allocation. Importantly, we hypothesize that the intracellular machinery controlling glucose and oxygen uptake in the mitochondria is a powerful influence on ultimate MSC fate.

NIH Grant AR45433

Disclosures: Anyonya Guntur, None.

1005

Osteoblastic Differentiation of Bone Marrow Stromal Cells is Sexually Dimorphic. Stefano Zanotti^{*}, Ernesto Canalis. St. Francis Hospital & Medical Center, USA

Skeletal integrity is preserved by the coordinated activity of osteoblasts and osteoclasts, and a decline in the number and function of osteoblasts may reduce bone mass. Osteoblastogenesis, the commitment of bone marrow stromal cell precursors to the osteoblastic lineage, determines osteoblast number. Although sex determines bone mass in humans and rodents, the mechanisms involved are understood poorly. Therefore, we tested whether primary bone marrow stromal cells harvested from male or female littermate mice, either from a tropism for Friend leukemia virus-B (FVB) or C57BL/6 genetic background, display a different potential for osteoblastic differentiation. Cells from FVB and C57BL/6 female mice exhibited suppressed formation of mineralized nodules when compared to cells from male littermates. Accordingly, alkaline phosphatase activity, and alkaline phosphatase and osteocalcin transcript levels, were reduced by 80% in cells from female mice in relation to cells from males, indicating that osteoblastogenesis *in vitro* is sexually dimorphic. These findings acquire further relevance in the study of osteoblastogenesis in genetically modified mouse models, which often display a sexually dimorphic skeletal phenotype. This was tested in a model of conditional inactivation of hairy and enhancer of split (*Hes1*), a Notch target which is a determinant of osteoblastogenesis. Conditional inactivation of *Hes1* in osteoblasts increased bone mass by enhancing bone formation exclusively in male mice, and *Hes1* inactivation in bone marrow stromal cells had a sexually dimorphic effect on osteoblastogenesis. *Hes1* null cells from male mice exhibited enhanced formation of mineralized nodules and alkaline phosphatase activity, whereas in *Hes1* null cells from females both parameters of osteoblastogenesis were suppressed. In conclusion, bone marrow stromal cells from female mice exhibit reduced potential for osteoblastic differentiation than cells from males, a difference that is accentuated in the context of *Hes1* inactivation. Therefore, cells from donors of different sexes should retain their individual identity for the study of osteoblastogenesis.

Disclosures: Stefano Zanotti, None.

1006

Wnt7b Promotes Bone Formation in vivo. Jianquan Chen^{*1}, Xiaolin Tu², Kyusang Joeng¹, Liang Ma¹, Fanxin Long³. ¹Washington University, USA, ²Indiana University School of Medicine, USA, ³Washington University School of Medicine, USA

Wnt signaling has emerged as an important mechanism for regulating both embryonic skeleton development and postnatal bone formation. However, the endogenous Wnt ligands involved in these processes and their specific downstream mechanisms are not well understood. We have previously shown that Wnt7b is expressed in the osteogenic perichondrium during embryonic limb development, and mouse embryos lacking Wnt7b in osteoprogenitor cells exhibit a delay in ossification. To investigate further the role of Wnt7b in both embryonic and postnatal bone formation, we generated a knockin mouse line (termed as R26-Wnt7b) by targeting Wnt7b cDNA into the ubiquitously active Rosa26 locus so that Wnt7b can be overexpressed in a Cre-dependent manner. Constitutive activation of Wnt7b expression with either Sp7-Cre or 2.3Col1-Cre led to a generalized increase in bone mass, a phenotype that began in the late-stage embryo and intensified in postnatal life. The increase of bone mass was caused by a combination of increased osteoblast number and enhanced osteoblast activity, without an overall change in bone resorption activity. To test whether Wnt7b can stimulate bone formation specifically in the postnatal animal, we generated a BAC transgenic mouse line (referred as Runx2-rtTA) by inserting the cDNA for reverse tetracycline transactivator (rtTA) into the Runx2 locus so that the expression of rtTA is driven by the Runx2 regulatory elements. Induction of Wnt7b expression by doxycycline in 1-month-old mice with the genotype of Runx2-rtTA; TetO-Cre; R26-Wnt7b stimulated bone formation, without overtly affecting bone resorption. In summary, these findings identify Wnt7b as a potent bone anabolic signal that can function both in the embryo and in the postnatal skeleton.

Disclosures: Jianquan Chen, None.

1007

PTH Signaling in Osteoblasts Necessary for Vascular Invasion of Cartilage. Tao Qiu^{*1}, Janet Crane², Chunyi Wen³, Lingling Xian¹, William Lu⁴, Xu Cao². ¹Johns Hopkins University School of Medicine, USA, ²Johns Hopkins University, USA, ³Li Ka Shing Faculty of Medicine, University of Hong Kong, Hong Kong, ⁴The University of Hong Kong, Hong Kong

Longitudinal growth of postnatal bone requires precise control on growth plate cartilage from chondrocytes through autocrine, paracrine, and endocrine hormone signaling. However, it is not clear how the cartilage is regulated by the endocrine signals. Parathyroid hormone (PTH) regulates both bone remodeling and cartilage development. To examine its effect on the longitudinal growth of bone, knockout mice were generated with deletion of the PTH receptor (PTH1R) in mature osteoblasts using the osteocalcin-promoter (*OC-cre:PTH1R^{fl/fl}*) where PTH signaling is well

documented to occur. The mice exhibited postnatal growth retardation with profound defects in growth plate cartilage, ascribable predominantly to a reduction in hypertrophic differentiation of chondrocytes, expansion of pre-hypertrophic zone, and decreased bone formation at trabecular bone and metaphyseal periosteum, resulting in premature closure of the growth plates and shortened long bones. This cartilage phenotype is distinct to those seen in the mice with the chondrocyte-specific deletion of PTH1R, in which the chondrocyte differentiation is accelerated. Therefore, PTH signaling in osteoblasts may signal to chondrocyte hypertrophy as loss of this signaling pathway impairs chondrocyte differentiation in growth plate cartilage.

Mechanistic analysis revealed that endochondrial angiogenesis and vascular invasion of cartilage were impaired in *OC-cre:PTH1R^{fl/fl}* mice, suggesting that the disrupted supply of blood vessels attenuated the chondrocyte hypertrophy. To test whether the loss of the vasculature was sufficient to restrain chondrocyte differentiation and rule out the effect of mosaic-expression of osteocalcin-Cre in cartilage, we studied a mouse model with deficiency of PECAM-1, a primary constituent of vascular endothelial cell-cell junctions, reasoning that the disruption of the vasculature alone would then mimic the effect of *OC-cre:PTH1R^{fl/fl}* mice on chondrocytes. Indeed, PECAM-1 knockout mice exhibit a similar bone phenotype to that seen in *OC-cre:PTH1R^{fl/fl}* mice. Importantly, PECAM-1 knockout mice showed a dramatic decrease in the number of hypertrophic chondrocytes, as demonstrated by significantly decreased expression of ColX. These studies identify PTH as an external organizer of cartilaginous growth plate in longitudinal growth of bone and reveal a previously unrecognized function for bone and osteoblasts in maintaining chondrocyte hypertrophy in postnatal life.

Disclosures: Tao Qiu, None.

1008

Parathyroid Hormone-related Peptide (PTHrP) Inhibits Chondrocyte Hypertrophy by Promoting Nuclear Translocation of Histone Deacetylase (HDAC) 4. Shigeki Nishimori^{*1}, Forest Lai¹, Elena Kozhemyakina², Eric Olson³, Andrew Lassar², Henry Kronenberg¹. ¹Massachusetts General Hospital, USA, ²Department of Biological Chemistry & Molecular Pharmacology, Harvard Medical School, USA, ³UT Southwestern Medical Center At Dallas Department of Molecular Biology, USA

Both PTHrP and HDAC4 delay chondrocyte hypertrophy but the molecular mechanisms of these processes have not been clarified. Lassar's group used primary chick chondrocytes and a chondrogenic cell line to show that PTHrP uses HDAC4 nuclear translocation to accomplish this delay in differentiation (MCB 2009). Here we report *in vivo* genetic and molecular evidence that supports this hypothesis.

Three genetic tests support the hypothesis that PTHrP and HDAC4 work in a common pathway: (1) The HDAC4 knockout (KO) mouse shows a phenotype similar to that of the PTHrP KO mouse; (2) Even though PTHrP heterozygotes (HET) and HDAC4 HET have normal growth plates at birth, the PTHrP and HDAC4 double HET mouse exhibits accelerated chondrocyte hypertrophy; and (3) The effects of transgenic (Tg) expression of PTHrP driven by the collagen 2 (Col2) promoter to suppress chondrocyte hypertrophy (Col2-PTHrP-Tg; Wier et al, PNAS 1996) is blocked by knocking out the HDAC4 gene (HDAC4-KO; Col2-PTHrP-Tg).

Class IIa HDACs (HDAC4, 5, 7, 9) have large N-terminal extension with conserved binding sites for the chaperon protein 14-3-3 and the transcription factor myocyte enhancer factor 2 (MEF2). Class IIa HDACs shuttle between nucleus and cytoplasm through regulated phosphorylation and dephosphorylation at the 14-3-3 binding sites. Lassar's group used their *in vitro* model to show that PTHrP signaling leads to dephosphorylation of HDAC4 phospho-S246, through activation of protein phosphatase 2A. Freed of binding to cytoplasmic 14-3-3 proteins, HDAC4 then translocates to the nucleus and represses the action of MEF2C, the master transcriptional regulator of chondrocyte hypertrophy.

To assess HDAC4 nuclear translocation downstream of PTHrP signaling *in vivo*, we examined HDAC4 cellular localization by immunohistochemistry using confocal fluorescent microscopy. Nuclei of the proliferating chondrocytes in the newborn Col2-PTHrP-Tg mouse show intense and dense HDAC4 signals. In contrast, in the newborn PTHrP KO mouse, HDAC4 signals are sparse in the nuclei, but high in the cytoplasm. We also assessed phosphorylation of S246 of HDAC4 in both mice using an HDAC4 phospho-S246 specific antibody. HDAC4 phospho-S246 was detected in the PTHrP KO mouse but not in the Col2-PTHrP-Tg mouse by immunohistochemistry and Western blot. These results are consistent with the idea that PTHrP inhibits chondrocyte hypertrophy by inducing HDAC4 dephosphorylation and subsequent HDAC4 nuclear translocation.

Disclosures: Shigeki Nishimori, None.

1009

Nmp4/CIZ Closes The Parathyroid Hormone Anabolic Window By Suppressing The Osteoprogenitor Pool. Paul Childress*¹, Yongzheng He², Mark Hood, Jr.³, Marta Alvarez¹, Melissa Kacena¹, Michael Hanlon⁴, Bryce McKee³, Feng-Chun Yang⁵, Joseph Bidwell¹. ¹Indiana University School of Medicine, USA, ²Department of Pediatrics, Indiana University School of Medicine, USA, ³Department of Anatomy & Cell Biology, Indiana University School of Medicine, USA, ⁴Iowa State University College of Veterinary Medicine, USA, ⁵Indiana University, USA

Parathyroid hormone (PTH) anabolic potency or its anabolic window for treating osteoporosis is intrinsically limited by unknown mechanisms. We have previously reported that disabling the transcription factor *Nmp4/CIZ* in mice expands this anabolic window while modestly elevating bone resorption. This previous study showed that wild type (WT) and *Nmp4*-knockout (KO) mice exhibited equivalent PTH-induced increases in bone after 2wks of treatment but by 7wks the null mice showed significantly more new bone. Interestingly, at 3wks of treatment serum osteocalcin, a marker for bone formation and osteoblast number peaked in WT mice but continued to increase in the null mice. To determine if this is when bone formation diverges between the genotypes and to investigate its cellular basis here we treated 10-wk-old null and WT animals with human PTH (1-34) [30 µg/kg/day] or vehicle for 3wks. At the end of treatment femoral trabecular architecture was evaluated using microCT analysis and bone marrow (BM) and peripheral blood (PBL) phenotypic cell profiles were assessed with clonogenic assays, flow cytometry, and hematology profile analyses. To analyze the data we employed a two-way ANOVA using genotype and treatment as the independent variables. If a genotype x treatment interaction was indicated, the data were analyzed by a Tukey HSD post hoc test to determine significant differences between the experimental groups. Statistical significance was set at $p < 0.01$. Hormone-treated *Nmp4*-KO mice gained over 2-fold more femoral trabecular bone (BV/TV) than did WT animals during the 3wk treatment period. There was no difference between genotypes in BM cellularity or the profiles of several blood elements. However, there was a 4-fold increase in *Nmp4*-KO CFU-F-ALK PHOS+ colonies (osteoprogenitors), a 1.6-fold increase in KO CFU-GM colonies (osteoclast progenitors), and a 2-fold increase in null BM CD8+ T-cells (which support osteoprogenitor differentiation). PTH had no effect on the size of any cell population. We propose that the extended and augmented anabolic activity in the *Nmp4*-KO mice first appears at 3wks of treatment and derives from an expanded osteoprogenitor pool, bolstered by the increase in BM CD8+T cells, thus sustaining bone formation after the WT osteoprogenitors are depleted. Additionally, this enhanced KO bone formation activity eclipses the elevated null osteoclastogenesis from the modestly enlarged CFU-GM pool.

Disclosures: Paul Childress, None.

1010

G-protein Stimulatory Subunit Alpha and q/11 Family Together Maintain Stem-like Chondrocytes in the Quiescent Stage. Andrei Chagin*¹, Tatsuya Kobayashi², Jun Guo², Takao Hirai³, Karuna Vuppapalati⁴, Min Chen⁵, Stefan Offermanns⁶, Susan Mackem⁵, Lee Weinstein⁷, Henry Kronenberg². ¹Karolinska Institutet, Sweden, ²Massachusetts General Hospital, USA, ³Kyoto Prefectural University of Medicine, Japan, ⁴Karolinska Institute, Sweden, ⁵National Institutes of Health, USA, ⁶Max-Planck-Institute for Heart & Lung Research, Germany, ⁷National Institute of Diabetes & Digestive & Kidney Diseases, USA

Parathyroid hormone (PTH)-related protein (PTHrP), regulated by Indian hedgehog and acting through the PTH/PTHrP receptor (PPR), is crucial for normal cartilage development. Recently we have shown that ablation of the PPR in postnatal chondrocytes leads to disappearance of the epiphyseal growth plate. We have also observed ectopic apoptosis in the resting zone of the growth plate where stem-like chondrocytes are located. To explore the mechanism whereby PPR signaling controls the fate of these resting zone chondrocytes, we have examined in vivo the roles of the G proteins activated by the PPR in chondrocytes in preventing disappearance of the growth plate.

First, we generated mice with tamoxifen-inducible and cartilage-specific ablation of the heterotrimeric G-protein stimulatory subunit alpha (G_{α}). We found that inactivation of G_{α} in postnatal chondrocytes causes dramatically impaired bone growth associated with accelerated chondrocyte hypertrophy and growth plate disorganization. In contrast to mice lacking the PPR in cartilage, a disorganized remnant of growth cartilage persists in mice lacking G_{α} in cartilage. Slowly proliferating, stem-like chondrocytes were labeled with BrdU followed by a "chase" period; the recruitment of these chondrocytes into the proliferative pool was accelerated upon G_{α} ablation. In contrast, these cells underwent apoptosis upon ablation of the PPR. These contrasting fates of stem-like chondrocytes might contribute to remnant formation when only G_{α} is ablated in the growth plate. Matings to generate mice with defects in signaling by other G-proteins activated by the PPR showed that G_{α} synergizes with the Gq/11 family of heterotrimeric G-proteins in causing malformation of the growth plate, that inactivation of both pathways leads to apoptosis of stem-like chondrocytes and disappearance of the growth plate, and that neither G12/13 nor XLas do not contribute to the PPR phenotype. We conclude that G_{α} is the major mediator of the anti-differentiation

action of the PPR on postnatal chondrocytes, while activation of both G_{α} and Gq/11 signaling is required to maintain stem-like chondrocytes in the quiescent phase.

Disclosures: Andrei Chagin, None.

1011

Hes1 is a Notch Target Gene that can Regulate Mesenchymal Progenitor Cell Proliferation and Differentiation during Skeletal Development. Timothy Rutkowski*¹, Anat Kohn¹, Anthony Mirando², Ryoichiro Kageyama³, Matthew Hilton². ¹University of Rochester, USA, ²University of Rochester Medical Center, USA, ³Kyoto University, Japan

We previously demonstrated that RBPjk-dependent Notch signaling suppresses mesenchymal progenitor cell (MPC) differentiation and induces proliferation during skeletogenesis. Several *Hes/Hey* factors are direct targets of RBPjk-dependent Notch signaling and critical Notch pathway components in progenitor cells. We also showed that knockdown of *Hes1* in MPCs resulted in accelerated differentiation during *in vitro* chondrogenesis, suggesting the importance of HES1 in this process. To determine whether HES1 is sufficient and/or required for MPC proliferation and differentiation during skeletal development in vivo, or whether HES1 is the sole regulator of the Notch-mediated suppression of MPC differentiation, we analyzed HES1 gain-of-function (GOF) (*Prx1Cre; Rosa-Hes1^{fl/fl}*), HES1 loss-of-function (LOF) (*Prx1Cre; Hes1^{fl/fl}*), and HES1 deficient Notch GOF (*Prx1Cre; Rosa-NICD1^{fl/+}; Hes1^{fl/fl}*) mice. Embryos were analyzed at E11.5, E12.5, E14.5, and E18.5 via whole-mount skeletal staining, ISH, and IHC of limb sections, and real-time RT-PCR of RNA isolated from limb-buds. Analyses demonstrated that HES1 GOF mutants exhibited reduced size of condensations and delayed chondrocyte gene expression via real-time RT-PCR and ISH. Proliferation analyses also indicated that HES1 GOF mutants had elevated MPC proliferation. These data demonstrate that sustained HES1 signaling is sufficient to induce MPC proliferation and delay differentiation but cannot block MPC differentiation and arrest chondrogenesis identical to sustained NOTCH1 signaling (*Prx1Cre; Rosa-NICD1^{fl/+}*). Interestingly, HES1 LOF embryos were analyzed using similar methods to determine whether MPC differentiation was accelerated as previously observed in RBPjk LOF mutants, although no striking chondrogenic changes were observed. Similar to other HES1 LOF models, we observed elevated *Hes5* gene expression in limb-bud MPCs following removal of *Hes1*, suggesting compensation from other *Hes* genes. Lastly, to determine whether *Hes1* is the sole Notch target required during Notch-mediated suppression of MPC differentiation, we analyzed HES1 deficient Notch GOF mice. Analyses demonstrated that sustained NOTCH1 signaling continued to suppress MPC differentiation in the absence of *Hes1*. Collectively, these data indicate that HES1 signaling is sufficient to delay MPC differentiation and induce proliferation, although additional HES/HEY factors or other Notch targets may be important in Notch-mediated regulation of MPCs during skeletogenesis.

Disclosures: Timothy Rutkowski, None.

1012

Postnatal Growth Plate Integrity and Function Require Ext1 Expression and Heparan Sulfate Production. Federica Sgariglia*¹, Eiki Kovama¹, Julianne Huegel², Maurizio Pacifici², Motomi Enomoto-Iwamoto¹. ¹Children's Hospital of Philadelphia, USA, ²Thomas Jefferson University, USA

The growth plate is the key engine for skeletal development during embryogenesis and continues to function in skeletal growth until the end of puberty when skeletal maturity is reached. The prenatal and postnatal integrity and function of the growth plate are regulated by a complex array of local and systemic factors. Many of these factors, including hedgehog proteins and bone morphogenetic proteins, interact with heparan sulfate that in turn influences their distribution, availability and signaling activity. To determine whether the growth plate requires heparan sulfate continuously, we conditionally inactivated Ext1, the major Golgi-associated enzyme for HS synthesis, in cartilage at postnatal stages by mating *Ext1* floxed mice with *Col2-CreER* mice. Given that Cre effectiveness is usually not complete, we compared mice with the genotypes *Ext1^{fl/fl}; Col2CreER* and *Ext1^{fl/-}; Col2CreER*, expecting the latter to display more effective ablation. Mice and appropriate controls were injected with tamoxifen at postnatal day 5 (P5) and examined at various time points over the following 8 weeks. Limb and axial skeletal specimens were analyzed by soft x-ray, µCT, histology and gene expression. Anatomically, the mutant mice displayed growth retardation, scoliosis and limb deformities, especially bowing of the forearm, by 2 to 4 weeks post injection. Histologically, the mutant growth plates in long bones and ribs were disorganized. A major and consistent feature was a lateral expansion of the growth plates such that the extra cartilaginous tissue draped and surrounded the underlying trabecular bone. The organization of the ectopic cartilaginous tissue resembled that of a growth plate but oriented perpendicularly to the main growth plate axis, with small immature chondrocytes facing the adjacent periosteum and hypertrophic chondrocytes facing native growth plate and bone. Analyses of gene expression and protein signaling patterns indicated significant changes in growth plate regulatory circuits. Some of the injected *Ext1^{fl/-}; Col2CreER* mice died prematurely, possibly reflecting complete Ext1 ablation. The data indicate that heparan sulfate is in fact required for postnatal growth plate function and progression of normal skeletal growth. The aberrant ectopic cartilage in mutants is reminiscent of that forming in patients with

Hereditary Multiple Exostoses, a pediatric pathology caused by *Ext1* mutations, providing further clues as to the pathogenesis of exostosis formation.

Disclosures: *Federica Sgariglia, None.*

1013

Sclerostin Antibody Improves Bone Mass and Mechanical Properties in *Brtl/+* Model of Osteogenesis Imperfecta When Administered During Growth. Benjamin Sinder^{*1}, Logan White¹, Michael Ominsky², Michelle Caird¹, Joan Marini³, Kenneth Kozloff⁴. ¹University of Michigan, USA, ²Amgen Inc., USA, ³National Institute of Child Health & Human Development, USA, ⁴University of Michigan Department of Orthopaedic Surgery, USA

Osteogenesis imperfecta (OI) is a genetic collagen disorder characterized by brittle bones and presents most severely in children. Anti-resorptive bisphosphonates have their major effect on trabecular bone and have been used with mixed success to treat pediatric OI during growth. Enhanced cortical bone would be valuable for OI amelioration, however no anabolic therapy has demonstrated consistent effectiveness. Sclerostin is a negative regulator of the Wnt pathway, and a neutralizing sclerostin antibody (Scl-Ab) has demonstrated potential anabolic efficacy in other models of bone fragility. Previously, we have shown that Scl-Ab stimulates new bone formation in osteoblasts harboring a type I collagen mutation¹ and improves bone mass and mechanical properties in an adult mouse model of OI². No studies to date have investigated Scl-Ab in the rapidly growing OI skeleton. Therefore the purpose of this study was to evaluate Scl-Ab during growth in the *Brtl/+* mouse model of dominant OI with G349C substitution on one *coll1a1* allele. Three week old male WT and *Brtl/+* were treated with Scl-Ab or Vehicle twice per week, for five weeks, at 25mg/kg. All changes are $p < 0.05$ unless otherwise noted, $n = 7-8$ /group. Body weight was not affected by Scl-Ab. MicroCT of the distal metaphyseal femur revealed that in WT, Scl-Ab increased Tb.BMD (66%) and BV/TV (56%) by increasing both Tb.Th (31%) and Tb.N (18%). In *Brtl/+*, Scl-Ab treatment increased Tb.Th (12%) with a trend towards increased Tb.BMD (30%, $p = 0.10$). However, neither BV/TV ($p = 0.26$) nor Tb.N ($p = 0.54$) were significantly altered, suggesting a reduced response to Scl-Ab in *Brtl/+* femoral trabecular bone. At femoral mid-diaphysis, microCT analysis showed Scl-Ab significantly increased cortical thickness (WT 23%; *Brtl/+* 24%), cross sectional area (WT 28%; *Brtl/+* 27%), and the medial-lateral moment of inertia (WT 41%; *Brtl/+* 35%) by similar amounts in both genotypes. Functionally, Scl-Ab increased femoral diaphyseal Ultimate Force (WT 66%; *Brtl/+* 47%) and Stiffness (WT 49%; *Brtl/+* 67%) as measured by four-point bending. Post yield displacement was not affected by Scl-Ab in *Brtl/+*, suggesting that treatment did not change material brittleness. In summary, Scl-Ab increased bone mass and improved whole bone mechanical properties in young *Brtl/+* mice. These initial data support that Scl-Ab may be beneficial for the treatment of OI patients by reducing fracture risk.

References: 1) Sinder et al ORS 2011; 2) Sinder et al ASBMR 2011

| | WT Veh | WT Scl-Ab | Brtl Veh | Brtl Scl-Ab |
|---------------------------------|----------------|-----------------|----------------|-----------------|
| Trab. μCT | | | | |
| BV/TV (%) | 19.8 \pm 3.2 | 31.0 \pm 6.7* | 15.9 \pm 3.2 | 18.8 \pm 4.2 |
| Tb.Th (μ m) | 39.2 \pm 1.3 | 51.4 \pm 7.1* | 37.8 \pm 4.1 | 42.5 \pm 4.0* |
| Tb.N (#/mm) | 5.06 \pm .76 | 5.99 \pm .49* | 4.20 \pm .79 | 4.39 \pm 0.73 |
| Tb.BMD(mg/cc) | 258 \pm 28 | 430 \pm 80* | 213 \pm 38 | 278 \pm 53 |
| Cort. μCT | | | | |
| CSA (mm ²) | 0.91 \pm .08 | 1.16 \pm .22* | 0.71 \pm .11 | 0.90 \pm .07* |
| Cort. Th. (mm) | 0.20 \pm .01 | 0.24 \pm .03* | 0.16 \pm .02 | 0.20 \pm .01* |
| M/L MOI (mm ⁴) | 0.17 \pm .03 | 0.24 \pm .09* | 0.12 \pm .02 | 0.16 \pm .02* |
| 4pt Bending | | | | |
| Ult. Load (N) | 27 \pm 2 | 45 \pm 11* | 17 \pm 4 | 25 \pm 5* |
| Stiffness(N/mm) | 194 \pm 25 | 291 \pm 53* | 128 \pm 32 | 214 \pm 34* |
| PYD (mm) | 0.15 \pm .06 | 0.37 \pm .21* | 0.06 \pm .06 | 0.07 \pm .04 |

Data is mean \pm S.D. * $p < 0.05$ effect of Scl-Ab within genotype.

Table: MicroCT and mechanical four-point bending data.

Disclosures: *Benjamin Sinder, None.*

1014

Treatment with Sclerostin Antibody Improves Bone Mass and Whole Bone Strength in the *Crtap-/-* Model of Recessive Osteogenesis Imperfecta. Ingo Grafe^{*1}, Tao Yang², Erica Homan², Elda Munivez², Caressa Lietman², Brian Dawson², Gautam Sule², Terry Bertin², Franklin Asuncion³, Hua Zhu Ke³, Michael Ominsky³, Brendan Lee⁴. ¹Department of Molecular & Human Genetics, Baylor College of Medicine, USA, ²Baylor College of Medicine, USA, ³Amgen Inc., USA, ⁴Baylor College of Medicine & Howard Hughes Medical Institute, USA

Standard treatment for patients with Osteogenesis Imperfecta (OI) is limited to antiresorptive bisphosphonates, which do not completely correct the bone fragility and seem to be less effective in adults. Sclerostin antibody (Scl-Ab) has been shown to have beneficial osteoanabolic effects in models of osteoporosis and forms of OI resulting from mutations in the genes encoding type I collagen. However, Scl-Ab treatment has not been studied in models of OI caused by defects in posttranslational collagen modifications, where the pathomechanism may differ. Cartilage associated protein (CRTAP) plays a role in posttranslational type I collagen modification and its loss of function results in recessive OI in a mouse model and in patients. In this study we investigate the effects of Scl-Ab treatment in *Crtap-/-* mice.

Six week old female *Crtap-/-* mice were treated with Sclerostin antibody (Scl-Ab) for 6 weeks (25 mg/kg, s.c. injection, twice per week), PBS treated *Crtap-/-* and wildtype (WT) mice served as controls. After treatment, spines and femurs were analyzed by microCT, biomechanical properties were assessed by 3-point bending of femurs.

Compared to PBS treated *Crtap-/-* mice, microCT analysis of vertebral body L4 showed significant increases in bone volume (BV/TV, +104%), trabecular number (Tb.N, +45%), trabecular thickness (Tb.Th, +41%) and BMD (+10%) in Scl-Ab treated *Crtap-/-* mice. Compared to WT mice, Scl-Ab fully reversed the reduction in Tb.Th and BMD in *Crtap-/-* mice, while BV/TV and Tb.N remained reduced. Femurs of Scl-Ab treated *Crtap-/-* mice demonstrated significant increases in cortical thickness (+37%), CSMI (+41%) and BMD (+23%) compared to PBS treated *Crtap-/-* mice and were no longer lower than in WT mice. Biomechanical testing of the femur midshaft showed that *Crtap-/-* mice had significantly reduced whole bone strength parameters, and Scl-Ab significantly increased maximum load (+41%) and stiffness (+48%) to WT levels. At the material level, *Crtap-/-* mice had reduced post-yield displacement and toughness, reflecting the increased tissue brittleness expected with OI. Scl-Ab did not significantly affect these material properties.

Scl-Ab treatment improves bone mass and microarchitecture in *Crtap-/-* mice, resulting in increased whole femoral bone strength without an effect on material properties. The findings of this study suggest that Scl-Ab treatment may have beneficial effect in the treatment of patients with recessive OI.

Disclosures: *Ingo Grafe, None.*

1015

***Pbx1* Is a Likely Candidate Gene for the Development of Fibro-osseous Lesions in Mice.** Cheryl Ackert-Bicknell^{*1}, Annerose Berndt², Clinton Cario², Beth Sundberg¹, John Sundberg¹. ¹The Jackson Laboratory, USA, ²University of Pittsburgh School of Medicine, USA

Fibro-osseous lesions are benign changes wherein normal bone is replaced with fibrovascular stroma. In humans, these lesions are found primarily in the jaw and tubular bones. They are more common in African American women, suggesting both a hormonal and a genetic etiology. In mice, there is also a higher incidence in females, however, these lesions occur primarily in the sternbrae, long bones, and vertebrae. In this study, we first determined the frequency and severity of fibro-osseous bone lesions in 12 and 20 month old female mice from 28 inbred strains. We then used these data to perform genome wide association (GWA) mapping to identify genetic loci associated with the development and severity of these lesions. Specifically, bones (calvaria, shoulder and elbow with associated long bones, hip and knee with associated long bones, ribs, and vertebrae from the thoracic, lumbar, and coccygeal regions) were examined histologically for the presence of fibro-osseous lesions. At 12 months of age, these lesions were rare; occurring in 3% of the 370 mice examined. At 20 months of age, these lesions affected 20% of the 280 mice examined, and were observed in 15 of the 28 strains. GWA scans for data collected from the 20 month old mice were performed using the efficient mixed-model association (EMMAX) algorithm using a 4 million SNP panel. Genetic loci associated with lesion development were mapped to Chromosome (Chr) 1 at 170.2 Mb, Chr 5 at 138.8 Mb, and Chr 15 at 68.7 Mb. The loci on Chrs 1 and 15 were also associated with lesion severity. *Pbx1*, is located at the peak for the locus on Chr 1. *Pbx1* binds to many transcription factors, is involved in organ development and is a suppressor of osteoblastogenesis. Furthermore, this gene is an oncogene and studies have shown that *Pbx1* guides Estrogen receptor alpha (*Esr1*) to target genes in aggressive breast cancer. In summary, we have shown that the mouse is an ideal model for the study of the pathological progression and genetic etiology of bone fibro-osseous lesions. Given the known functions of the *Pbx1* gene and the results of our genetic mapping study, we suggest that polymorphisms in *Pbx1* are associated with the development of this condition.

Disclosures: *Cheryl Ackert-Bicknell, None.*

1016

The Glucocerebrosidase (Gaucher Disease) Gene Functions in Immune Regulation and Skeletal Homeostasis. Pramod Mistry¹, Tony Yuen^{*2}, Ling-Ling Zhu², Jun Liu¹, Stephanie Halene¹, Mei Yang¹, Jameel Iqbal², Ruhua Yang¹, Wajahat Mehal³, Wei-Lien Chuang³, Dhanpat Jain¹, Jianhua Li⁴, Harry Blair⁵, Li Sun², Mone Zaidi⁶. ¹Yale School of Medicine, USA, ²Mount Sinai School of Medicine, USA, ³Genzyme Corporation, USA, ⁴Toussaint School of Medicine, USA, ⁵University of Pittsburgh, USA, ⁶Mount Sinai Medical Center, USA

The heterogeneous clinical presentation of patients with Gaucher Disease (GD1) cannot simply be explained by the lysosomal accumulation in macrophages of lipid substrates of the mutated enzyme glucocerebrosidase (GBA1). This macrophage-centric view also does not endorse emerging aspects of the disease, such as malignancies, gammopathies, autoimmune diathesis, Parkinson's disease, and osteoporosis, all of which are resistant to macrophage-directed enzyme replacement therapy. To understand the pathophysiology of the multi-system involvement in GD1, and to unravel new functions of the GBA1 gene in normal physiology, we conditionally deleted the gene using an Mx1 promoter in the hematopoietic and mesenchymal cell lineages in mice, *hitherto* termed GD1 mice. We fully recapitulated the visceral manifestations of human GD1. GD1 mice were also severely osteoporotic, with a marked reduction in bone formation rates *in vivo* and osteoblastogenesis *ex vivo*. Cytokine measurements, microarray analysis, and flow cytometry revealed widespread dysfunction of unexpected immune cell populations. Notably, the thymus exhibited the earliest and most striking alterations reminiscent of impaired T-cell maturation, aberrant B-cell recruitment, and enhanced antigen presentation. In contrast to the profound defects in the thymus, there were only limited cellular defects in peripheral lymphoid organs, namely the spleen, lymph nodes and bone marrow; these changes were restricted to mice with severe disease. The cellular changes were accompanied by elevated Th1 and Th2 cytokines that tracked with disease severity. Furthermore, as disease severity correlated with accumulating GBA1 substrates, namely glucosylceramide (GL1) and glucosylsphingosine (Lyso-GL1), we studied the effects of each lipid on the proliferation of bone marrow hematopoietic stem cell precursors (HSCs). The proliferation of multipotent precursors (MPP), short-term HSCs, and long-term HSCs was inhibited significantly by both GL1 and Lyso-GL1 *in vitro*. This suggests a direct role for lipid substrates in causing the extensive immune dysfunction in GD1. The results not only demonstrate that *GBA1* has a role in immune regulation, but also provide the first direct evidence for the involvement of cell lineages other than mononuclear phagocytes, most notably, T-cells, B-cells, dendritic cells, and osteoblasts, in the pathophysiology of GD1. Important therapeutic implications may eventually follow from these studies.

Disclosures: Tony Yuen, None.

1017

A Mouse Model of Cushing's Syndrome due to a Corticotrophin Releasing Hormone (*Crh*) Promoter Mutation develops Steroid Induced Osteoporosis. Liz Bentley^{*1}, Christopher Esapa², M. Andrew Nesbit², Rosie A Head², Holly Evans³, Darren Lath³, Tertius A Hough¹, Christine Podrini⁴, William Fraser⁵, Martin D Fray¹, Peter Croucher⁶, Matthew Brown⁷, Steve D. M. Brown¹, Roger D. Cox¹, Rajesh Thakker⁸. ¹MRC Harwell, United Kingdom, ²University of Oxford, United Kingdom, ³University of Sheffield, United Kingdom, ⁴Wellcome Trust Sanger Institute, United Kingdom, ⁵University of East Anglia, United Kingdom, ⁶Garvan Institute of Medical Research, Australia, ⁷Diamantina Institute of Cancer, Immunology & Metabolic Medicine, Australia, ⁸Nuffield Department of Clinical Medicine, University of Oxford, United Kingdom

Glucocorticoid-induced osteoporosis (GIOP) is a common condition for which effective and satisfactory treatments are not available. The availability of a mouse model for GIOP would facilitate investigations and *in vivo* assessment of treatments. In the course of our phenotype-driven screens of mouse mutants induced by the chemical mutagen N-ethyl-N-nitrosourea (ENU), we observed a mutant mouse with obesity, hyperglycaemia and low bone mineral density, features that are consistent with Cushing's syndrome. This phenotype was inherited as an autosomal dominant trait and the disease locus was mapped to chromosome 3 and to a 6.2Mbp interval that contained the gene encoding corticotrophin releasing hormone (*Crh*). DNA sequence analysis of the *Crh* gene did not identify any coding region mutations, in affected mice, but instead a T to C transition at -120bp, within the *Crh* promoter, was identified. Luciferase reporter assays demonstrated that this T to C transition resulted in a >2 fold increase in transcription activity in Neuro2a cells ($p < 0.001$). *In vivo* assessment of *Crh*^{120/+} mice revealed them to have, when compared to wild-type (*Crh*^{+/+} mice), elevated plasma concentrations of corticosterone (mean \pm SEM: *Crh*^{120/+} = 721.8 \pm 88.8 ng/ml; *Crh*^{+/+} = 414.3 \pm 59.5 ng/ml, $p = 0.01$), glucose (*Crh*^{120/+} = 24.12 \pm 4.23 mmol/L; *Crh*^{+/+} = 11.43 \pm 1.11 mmol/L, $p = 0.01$) and insulin (*Crh*^{120/+} = 3.99 \pm 0.55 ng/ml; *Crh*^{+/+} = 1.01 \pm 0.09 ng/ml, $p < 0.0001$). An analysis of cortico-endosteal bone structure using dynamic histomorphometric studies revealed that both male and female *Crh*^{120/+} mice, when compared to *Crh*^{+/+} mice, had reductions in mineralising surface area (males: *Crh*^{120/+} = 14.6 \pm 2.8; *Crh*^{+/+} = 56.8 \pm 3.4, females: *Crh*^{120/+} = 30 \pm 2.9; *Crh*^{+/+} = 63.8 \pm 5.4, $p < 0.01$),

mineral apposition rate (males: *Crh*^{120/+} = 1.2 \pm 0.2; *Crh*^{+/+} = 1.7 \pm 0.2, females: *Crh*^{120/+} = 1.4 \pm 0.2; *Crh*^{+/+} = 2.2 \pm 0.2, $p < 0.05$) and bone formation rate (males: *Crh*^{120/+} = 0.4 \pm 0.04; *Crh*^{+/+} = 1.1 \pm 0.1, females: *Crh*^{120/+} = 0.5 \pm 0.1; *Crh*^{+/+} = 1.6 \pm 0.1, $p < 0.01$). Further analysis of osteoblasts and adipocytes in bone, using static histomorphometry, showed a reduction in osteoblast number ($p < 0.05$) and the percentage of cortico-endosteal bone covered by osteoblasts ($p < 0.05$) in both male and female *Crh*^{120/+} mice which was accompanied by an increase in adipocytes in the bone marrow ($p < 0.01$). Thus, our studies have established a mouse model for Cushing's syndrome that develops osteoporosis.

Disclosures: Liz Bentley, None.

1018

A Key Pathological Role for the Wnt/b-catenin Signaling Pathway in Hypophosphatemic Rickets/Osteomalacia. Shuxian Lin^{*1}, Yong Jiang², Zhaowen Zong², Min Liu³, Ying Liu², Baozhi Yuan⁴, Marc Drezner⁴, Hua Zhu Ke³, J.Q. Feng². ¹Baylor College of Dentistry, USA, ²Baylor College of Dentistry, Texas A&M, USA, ³Amgen Inc., USA, ⁴University of Wisconsin, USA

Deletion or mutation of *Dmp1* or *PheX* leads to a hypophosphatemic rickets/osteomalacic disorder, in which increased FGF23 plays a key pathological role, although neither DMP1 nor PheX directly regulates FGF23 homeostasis. In this study, we initially showed that immunohistochemical evaluation of osteoblast/osteocytes from *Dmp1* knockout mice reveals elevated b-catenin expression levels. Subsequently, we crossed 3.2 kb-Col1^{ER} and Cre/ Catnb^{+/lox(ex)3} mice to generate offspring with constitutively activated b-catenin at postnatal day 3. Unexpectedly, these mice manifested a rickets phenotype, resembling that in *Dmp1* KO and *Hyp* mice, which included greatly expanded growth plates, short limbs and tail, malformed epiphysis, and defected metaphyses. To determine whether blocking Wnt/b-cat signaling will rescue the phenotype in *Dmp1* knockout mice, we crossed *Dmp1* knockout and 2.3 *Col1-Dkk1* transgenic mice, generating offspring that overexpressed DKK1 (a potent inhibitor of Wnt/b-catenin signaling pathway) in osteoblasts. By 3-weeks, the targeted expression of DKK1 and consequent blockade of Wnt/b-catenin signaling significantly improved the following elements of the rickets/osteomalacic phenotype: 1) FGF23, PTH, and Pi levels; 2) skeleton length (long bone and vertebrae); 3) growth plate thickness; 4) epiphysis and metaphysis phenotype; 5) cell proliferation (BrdU); 6) molecular bone markers (FGF23, b-catenin, Col I, BSP, OPN, OSX, E11 and SOST), and 7) bone mineralization and formation rates. By 8 weeks, the *Dmp1* knockout phenotype was further improved. Taken together, we demonstrate for the first time that an abnormal high level of Wnt/b-catenin expression in *Dmp1* knockout mice is a key pathologically local factor responsible for defects in osteoblast maturation into osteocytes and high FGF23 expression, leading to hypophosphatemic rickets. This study has clinical relevance, as a high Pi diet alone fails to fully restore the osteomalacic status in patients, and normalizing the Wnt/b-catenin signaling may benefit these patients. (This research was supported by DE018486).

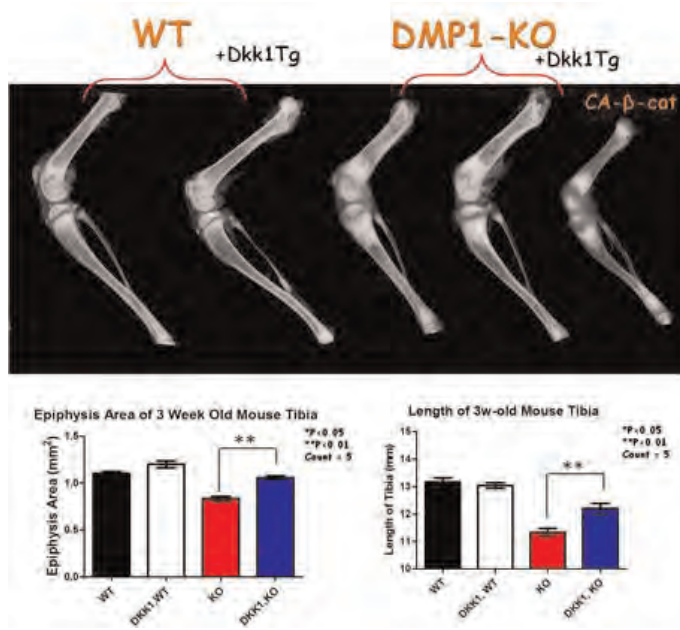


Fig 1. Longbone Morphology

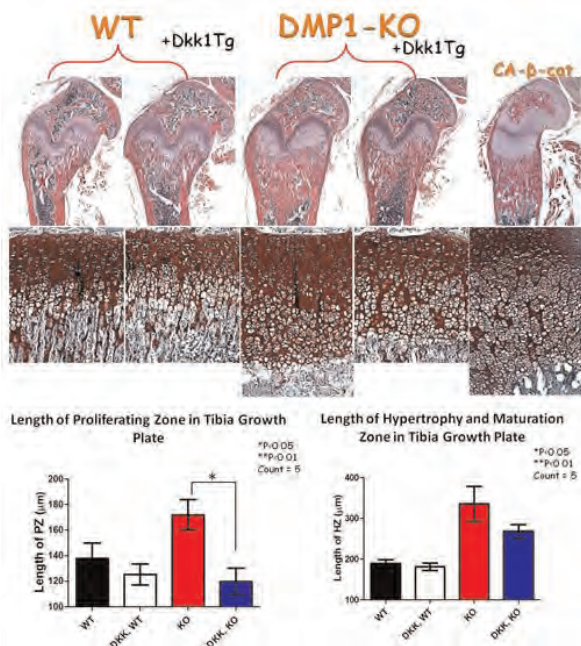


Fig 2. Epiphysis, Metaphysis and Growth Plate Phenotype

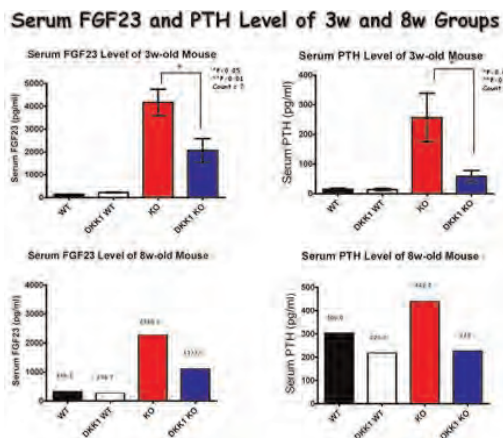


Fig 3. Serum FGF23 and PTH Level of 3w and 8w Groups

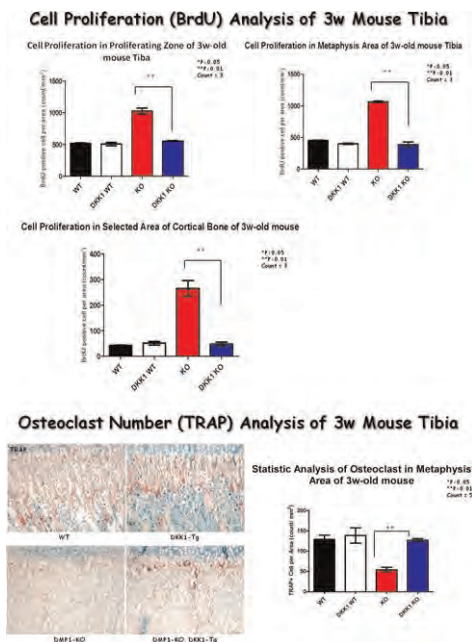


Fig 4. Cell Proliferation (BrdU) and Osteoclast Number (TRAP) Analysis of 3w Mouse Tibia

Beta-catenin, OSX, E11 Staining of 3w Mouse Longbone

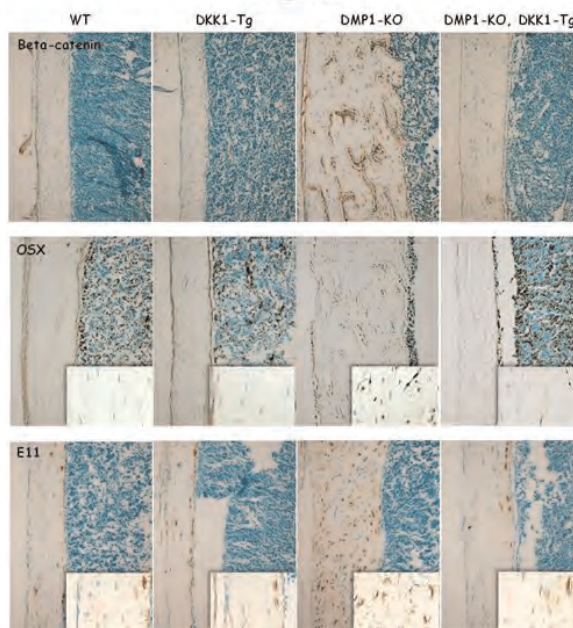


Fig 5. Beta-catenin, OSX, E11 Staining of 3w Mouse Longbone

Disclosures: Shuxian Lin, None.

This study received funding from: NIH

1019

Lack of Value of Serum Sex Steroid Measures in the Prediction of Osteoporosis and Fracture Risk in Community-dwelling, Ambulatory Older Men. Eric Orwoll¹, Jodi Lapidus¹, Ying Wang¹, Carrie Nielson¹, Andrew Hoffman², Howard Fink³, Gail Laughlin⁴, Sundeep Khosla⁵, Oregon Health & Science University, USA, ²Stanford University, USA, ³GRECC, Minneapolis VA Medical Center, USA, ⁴University of California, San Diego, USA, ⁵College of Medicine, Mayo Clinic, USA

Serum estradiol (E), sex hormone binding globulin (SHBG) and testosterone (T) have all been associated with BMD and fracture risk in populations of older men. Measures of T are commonly used in clinical evaluations of osteoporosis in men, but the value of these measures for risk assessment in individuals has not been formally assessed.

In the MrOS Study, 1563 community-dwelling, ambulatory men >65 yrs had baseline assays of E and T by mass spec, and SHBG by RIA. We assessed baseline BMD and subsequent BMD change by DXA, and ascertained incident fractures over 10 yrs. The value of T, E and SHBG levels for predicting the rate of BMD change was assessed via fit statistics from linear regression models. The ability of T, E and SHBG to predict BMD status (T score <-2.5 vs >-2.5) and fracture risk was assessed via logistic regression models. We initially considered models that were unadjusted, thus simulating the clinical situation, but also considered models with age and BMI adjustments. Finally, we examined clinical thresholds of E, T and SHBG to assess predictive utility. For each model we computed the area under the receiver operating characteristic curve (AUROC) to evaluate discriminative ability, and used net reclassification improvement (NRI) and integrated discrimination improvement (IDI) to assess improvement in risk prediction over a baseline model containing age, BMI and BMD.

Results: T, E and SHBG provided virtually no benefit for the prediction of BMD status, BMD loss or fracture risk. For instance, the AUROCs for hip fracture prediction using continuous T, E or SHBG alone were between 0.54-0.59 whereas the AUROC using baseline age+BMI+ BMD was 0.82. Moreover, when added to age+BMI+BMD, measures of sex steroids and SHBG (examined as continuous variables) did not improve the predictive value for any endpoint (p values for NRI and IDI insignificant for all). When conventional cutpoints for low sex steroids were examined there was no improvement. Results were unchanged when bioavailable T and E were examined. When only men with low BMD (T score -1.0 to -2.5) were analyzed the results were essentially the same.

Summary: In individual older men there appears to be low predictive value for sex steroid and SHBG measurements in assessing BMD status, rate of BMD change or fracture risk. There is little indication for including T, E or SHBG measures for estimating the risk of developing osteoporosis or fracture in community-dwelling older men.

Disclosures: Eric Orwoll, None.

1020

Serum DKK-1 Levels and the Risk of in Relation to the Occurrence of Osteoporosis-related Fractures : The CEOR Study. Mohammed-Salleh Ardawi¹, Abdulraheem Rouzi², Sharifa Al-Sibiani³, Nawal Al-Senani⁴.
¹Center of Excellence for Osteoporosis Research & Faculty of Medicine, Saudi Arabia, ²Center of Excellence for Osteoporosis Research & Department of Obstetrics & Gynecology, Faculty of Medicine & KAU Hospital, King Abdulaziz University, Saudi Arabia, ³Center of Excellence for Osteoporosis Research, & Department of Obstetrics & Gynecology, Faculty of Medicine & KAU Hospital, King Abdulaziz University, Saudi Arabia, ⁴Center of Excellence for Osteoporosis Research & Department of Obstetrics & Gynecology, Faculty of Medicine, & KAU Hospital, King Abdulaziz University, Saudi Arabia

Background: Dickkopf-1 (DKK-1) is involved in the regulation of bone formation through the inhibition of the Wnt/ β -catenin signaling pathway. DKK-1 over-expression in osteoblasts results in osteopenia and inhibits fracture repair, whereas DKK-1 activation in osteoblasts contributes to the pathogenesis of glucocorticoid- and/or estrogen deficiency-mediated osteoporosis. We therefore hypothesized that postmenopausal women with increased circulating DKK-1 levels have a greater risk for osteoporosis-related fractures (ORFs).

Subjects and Methods: We examined the association between circulating DKK-1 [measured by ELISA method, (Biomedica Gruppe, Biomedica Medizinprodukte GmbH & Co KG, Austria)] levels and the risk of ORFs in 707 postmenopausal women, 50 years of age or older in a population-based study with a mean follow-up period of 5.2 ± 1.3 years. Multivariate Cox proportional-hazards regression models were used for analysis of the risk of fracture with adjustment for age, body-mass index and other potential risk factors that may be associated with the risk of fracture or with higher circulating levels of serum DKK-1.

Results: High serum DKK-1 levels were associated with an increased risk of ORFs (Table 1). Following adjustment for age and other confounders, the relative risk of ORFs for each increment of 1 SD in DKK-1 level was about 2-fold among postmenopausal women. [RR = 1.98 (95% CI: 0.98-4.20)]. Further, women in the highest quartile of DKK-1 levels had an increase in the risk of ORFs so that the risk was 3.4-fold for DKK-1. The risk of ORFs that was attributable to DKK-1 levels (in the highest quartile) was estimated at 31.7%. The association between DKK-1 levels and the risk of fracture seems to be independent of bone mineral density and other confounding risk factors for fracture.

Conclusions: Higher serum DKK-1 levels are associated with a greater risk of ORFs independent of several other risk factors among postmenopausal women. Serum DKK-1 measurement holds promise as a risk factor for ORFs in postmenopausal women.

Table 1: Increased levels of serum DKK-1 and the risk of ORFs in postmenopausal women.

| | Relative risk (95% CI) for 1 SD increase | | Relative risk (95% CI) for levels < highest quartile | |
|----------------------|--|------------------|--|------------------|
| | Unadjusted | Adjusted | Unadjusted | Adjusted |
| Serum DKK-1 (pmol/L) | 1.86 (0.87-3.79) | 1.96 (0.97-4.12) | 3.36 (1.61-7.05) | 3.38 (1.49-7.89) |

All relative risk values were adjusted for age, BMI, BMD, hand grip strength, physical activity-score, dietary calcium intake, hand grip strength and BMD. Q1, Q2, Q3, Q4 quartiles for serum DKK-1 (pmol/L) were: Q1 = <81.9; Q2 = 81.9-105.2; Q3 = 105.3-133.2; Q4 = >133.2, respectively.

Table.1

Disclosures: Mohammed-Salleh Ardawi, None.

1021

Association between Hypovitaminosis D, Secondary Hyperparathyroidism, Bone Loss and Hip Fractures in the Prospective Population-based OPRA Study of Elderly Women. David Buchebner¹, Fiona McGuigan², Karl Obrant³, Paul Gerdhem⁴, Kristina Akesson⁵.
¹Halmstad Hospital, Sweden, ²University of Lund, Malmö, Skane University Hospital, Malmö, Sweden, ³University Hospital, Sweden, ⁴Karolinska Institutet, Sweden, ⁵Skane University Hospital, Malmö, Sweden

Background: Deficiency in vitamin D can cause secondary hyperparathyroidism, high bone turnover, bone loss and mineralization defects and is suggested to play a role in the development of osteoporosis and fragility fractures. In this study we investigated long term assessment of serum vitamin D and PTH to determine if hypovitaminosis D and elevated PTH lead to higher bone loss and increased hip fracture incidence in elderly women.

Methods: Study participants were Swedish women from the population based Malmö OPRA cohort. 1044 women, all 75y old, attended at baseline (BL), 715 attended at 5y. Bone mineral density (BMD) was assessed using a Lunar DPX-L DXA scanner. Serum 25-hydroxy vitamin D (25OHD) was available for 987 (BL), and 640 (5y) women, classified as: >75 nmol/l; 50-75 nmol/l; <50 nmol/l. Serum PTH

measurements were available for 999 (BL), and 694 (5y) women, classified as: normal (<6.8pmol/l) or high (>6.8pmol/l). Fracture data was ascertained from X-rays at the Dept. Radiology, Skane University Hospital, Malmö for mean follow-up of 9.0 years (range 7.4-10.9).

Results: Bone loss at 5 years was higher at the hip in women who, at both BL and 5y, had the lowest 25OHD (<50 nmol/l) compared to the other 2 groups (≥ 50 nmol/l): FN (16.7% v 6.9% v 7.8%); Troch (16.5% v 7.7% v 7%) and TH (10.7% v 6.2% v 6.5%) (p<0.). Similarly for PTH, there was higher loss in the high compared to the normal PTH group: FN (11.6% v 7.5%); Troch (9.8% v 7%); TH (8.7% v 6.3%). Women with low 25OHD (<50 nmol/l) and high PTH lost significantly more bone, with the highest loss at the trochanter.

The proportion of women who had 25OHD <50nmol/l at baseline was 4%, increasing to 17% at 5y. Of those who were low at baseline, 17% sustained at least one hip fracture during follow-up compared to 11% who had a hip fracture and had >50 nmol/l values (p=ns). Of the women who were low at 5y, 16% sustained at least one hip fracture during follow-up compared to 7% who had a hip fracture and values >50 nmol/l (p<0.05). S-PTH was not associated with more fracture, irrespective of 25OHD.

Conclusions: In this population sample of elderly women, vitamin D and PTH played a role in long term bone loss. Vitamin D status was associated with increased hip fracture incidence, whereas we could not confirm the hypothesis of elevated PTH increasing the risk of hip-fractures.

Disclosures: David Buchebner, None.

1022

Bone Turnover Marker Balance and Turnover: Association with Fracture Risk in the OPUS Study. Fatma Gossiel¹, Richard Jacques², Judith Finigan³, David Reid⁴, Christian Roux⁵, Dieter Felsenberg⁶, Claus-C Glueer⁷, Richard Eastell³.
¹The University of Sheffield, United Kingdom, ²School of Health & Related Research, University of Sheffield, United Kingdom, ³University of Sheffield, United Kingdom, ⁴University of Aberdeen, United Kingdom, ⁵Hospital Cochin, France, ⁶Charité - Campus Benjamin Franklin, Germany, ⁷Christian Albrechts Universitaet zu Kiel, Germany

Postmenopausal osteoporosis is characterised by an increase in bone turnover and an imbalance between bone resorption and bone formation. An approach has been described 'The Bone Marker Plot' that allows calculation of the rate of bone turnover and balance between bone formation and bone resorption from measurement of bone turnover markers. The aim of this study was to apply this approach to the prediction of fractures in older women. We studied 745 older women (55 to 80 years) and 213 younger women (20 to 39 years) from the Osteoporosis and Ultrasound Study (OPUS). We included women with bone turnover marker measurements who had no disease known to affect bone turnover, no anti-resorptive treatments close to baseline or during the study, and, if in the older group, were postmenopausal. We measured serum procollagen type I N-propeptide (PINP) and C-telopeptide of type I collagen (CTX) by automated immunoassay analyser (iSYS, IDS) on the samples taken at baseline. We calculated the multiple of the median for bone formation (PINP) and bone resorption (CTX) and the rate of bone turnover was calculated as the square root of the sums of the squared multiples of medians and the balance was calculated from the ratio of the formation multiple of median to the resorption multiple of median. The data were log transformed. We collected information about non-vertebral fractures by questionnaire and vertebral fractures by spinal radiographs after an interval of 6 years. There were 115 women with incident fractures over 6 years (23 vertebral, 92 non-vertebral). The older women had higher rates of bone turnover and more negative balance than the younger women (Mahalanobis distance 0.83, p<0.001). The women with vertebral fractures had more negative balance than those without fractures (odds ratio 0.61, 95% CI 0.40 to 0.93, p=0.020) but not significantly different turnover. The women with non-vertebral fractures had more negative balance than those without fractures (odds ratio 0.65, 95% CI 0.45 to 0.94, p=0.021) but not significantly different turnover. This suggests that balance rather than turnover may be an important determinant of fracture risk in older women.

Disclosures: Fatma Gossiel, None.

This study received funding from: IDS

1023

Can Functional Muscle Testing Improve Fracture Risk Assessment in an Ageing Female Population. Nicola Crabtree¹, Natalie Bebbington², Katie Stant³, Helen Duff³, Jim Parle³, Neil Gittoes⁴.
¹Birmingham Children's Hospital, United Kingdom, ²Queen Elizabeth Hospital Birmingham, United Kingdom, ³University of Birmingham, United Kingdom, ⁴Queen Elizabeth Hospital, Edgbaston, United Kingdom

Osteoporotic fracture risk increases with age and decreasing bone density. Additionally, ageing causes muscle mass to decline and the risk of falling to increase. However, falls risk is currently not included in the frequently used fracture risk calculator (FRAXTM). The aim of this study was to investigate the relationship between bone strength, muscle function and previous fracture in a sub group of the SCOOP study cohort.

The SCOOP study is a RCT which aims to demonstrate whether community-based screening for osteoporosis reduces the incidence of fractures and is cost effective in older women. It is a 7-year prospective study which has recruited 12,495 women between 70 and 85 years. As part of the study DXA scanning was offered to women considered to be at high risk of fracture estimated from clinical risk factors. At our centre, 1692 subjects were recruited of whom 390 attended for DXA scanning. Of these, 290 had muscle function assessed using the chair rising test (CRT) on the Leonardo™ ground force reaction plate. Hip strength index (HSI) was estimated using the advanced hip analysis tools on the GE Lunar iDXA™.

A significant decrease with age was observed for femoral neck BMD, yet HSI remained constant (1.42[0.37]). A significant decrease was noted in muscle power ($p < 0.0001$) and this correlated with a small but significant increase in chair rise time ($p = 0.015$). Women with $HSI \leq 1$ were significantly slower (3.0 vs. 2.4s per chair rise, $p = 0.005$) and had less muscle power (4.4 vs. 5.8 Watts/kg, $p < 0.0001$) than those with $HSI > 1$. Previous fracture incidence was greatest (73.9%) in those women where $FSI \leq 1$ and $CRT > 2.5$ secs and lowest (34.6%) in those where $FSI > 1$ and $CRT \leq 2.5$ secs, suggesting that those with the lowest bone strength and highest risk of falling had the greatest risk of fracture.

Identifying those persons who have both reduced bone strength and reduced muscle strength may better predict future fracture in an ageing female cohort and timed chair rises may prove to be a simple but useful addition to FRAX™ when considering future fracture risk.

Disclosures: Nicola Crabtree, None.

1024

Osteoporosis Screening in Women 50-64 years-old: Comparison of U.S. Preventive Services Task Force 2011 Screening Strategy and Two Traditional Screening Strategies in Women's Health Initiative participants. Carolyn Crandall¹, Joseph Larson², Meghan Donaldson³, Andrea LaCroix², Jane Cauley⁴, Jean Wactawski-Wende⁵, Margery L.S. Gass⁶, John Robbins⁷, Nelson Watts⁸, Kristine Ensrud⁹. ¹University of California, Los Angeles, USA, ²Fred Hutchinson Cancer Research Center, USA, ³University of British Columbia/Vancouver Coastal Health Research Institute, Canada, ⁴University of Pittsburgh Graduate School of Public Health, USA, ⁵University at Buffalo, USA, ⁶The North American Menopause Society, USA, ⁷University of California, Davis Medical Center, USA, ⁸Mercy Health Osteoporosis & Bone Health Services, USA, ⁹Minneapolis VA Medical Center / University of Minnesota, USA

Purpose. For women age 50-64, the U.S. Preventive Services Task Force (USPSTF) recommends bone mineral density (BMD) testing if the 10-year major fracture risk is $\geq 9.3\%$ using Fracture Risk Assessment Tool (FRAX without BMD). The impact of this strategy compared with others (the Simple Calculated Osteoporosis Risk Estimation [SCORE] and the Osteoporosis Self-Assessment Tool [OST]) on the number of younger postmenopausal women identified for BMD testing and proportion of those with osteoporosis correctly identified are uncertain. In addition, it is uncertain how the USPSTF strategy compares with other strategies to discriminate between those with and without osteoporosis.

Methods. We examined baseline questionnaire and BMD data from participants aged 50-64 years at the 3 clinical sites of the WHI that measured BMD (dual energy-x-ray absorptiometry). We included data from all participants aged 50-64 years who were not using bisphosphonates, raloxifene, calcitonin, or parathyroid hormone ($N = 5165$). We assessed the proportion of women who would be recommended for BMD screening using the USPSTF approach, OST (OST score < 2) and SCORE (score > 7) strategies. We calculated the percentage of women in specific T-score categories (T-score > -1 , $-1 \leq T\text{-score} < 2.5$, and T-score ≤ -2.5) who would be recommended for BMD testing and assessed the sensitivity, specificity, and area under the receiver operating curve (AUC) to discriminate those with and without osteoporosis as defined by T-score ≤ -2.5 .

Results. The proportions of women who would be selected for BMD testing were: 15.2% for the USPSTF (FRAX), 31.5% for SCORE, and 36.0% for OST strategies. Under the USPSTF (FRAX) strategy, only 34.1% of women with T-score ≤ -2.5 would be recommended for BMD testing, compared with 74.0% with SCORE and 79.8% with OST. The sensitivity, specificity, and AUC for identifying T-score ≤ -2.5 were 34.1%, 85.8%, and 0.60 for the USPSTF (FRAX), 74.0%, 70.8%, and 0.72 for SCORE, and 79.8%, 66.3%, and 0.73 for OST screening strategies. Stratifying for baseline hormone therapy use did not substantially alter these results.

Conclusions. Among women aged 50-64, the proportion with T-scores ≤ -2.5 identified was 1/3rd using USPSTF strategy, 3/4 using SCORE strategy, and 4/5 using OST strategy. The USPSTF strategy was modestly better than chance alone and inferior to conventional SCORE and OST strategies in discriminating between women with and without osteoporosis.

| | | Sensitivity, specificity, and AUC for identifying low BMD or osteoporosis | | | | | |
|--------------|----------------------------------|---|------------------|------------------|-------------------------|------------------|------------------|
| | | T-score ≤ -2.5 | | | -1 $>$ T-score > -2.5 | | |
| HT Use | | Sens (95% CI) | Spec (95% CI) | AUC % | Sens (95% CI) | Spec (95% CI) | AUC % |
| HT Users | USPSTF (FRAX risk $\geq 9.3\%$) | 38.1 (29.5-46.7) | 84.8(83.5-86.1) | 0.61 (0.57-0.66) | 18.9 (16.8-20.9) | 88.1 (86.4-89.7) | 0.53 (0.52-0.55) |
| | SCORE (> 7) | 73.0 (65.2-80.9) | 71.9 (70.3-73.5) | 0.72 (0.68-0.76) | 39.4 (36.8-42.0) | 82.2 (80.3-84.2) | 0.61 (0.59-0.62) |
| | OST (< 2) | 81.0 (74.0-87.9) | 63.0 (61.3-64.8) | 0.72 (0.68-0.76) | 51.7 (49.0-54.3) | 76.5 (74.4-78.6) | 0.64 (0.62-0.66) |
| Non-HT Users | USPSTF (FRAX risk $\geq 9.3\%$) | 30.3 (22.4-38.2) | 87.3 (85.9-88.8) | 0.59 (0.55-0.63) | 15.7 (13.5-17.9) | 90.4 (88.6-92.3) | 0.53 (0.52-0.55) |
| | SCORE (> 7) | 75.0 (67.5-82.5) | 69.1 (67.1-71.1) | 0.72 (0.68-0.76) | 46.0 (42.9-49.1) | 84.6 (82.3-86.8) | 0.65 (0.63-0.67) |
| | OST (< 2) | 78.8 (71.7-85.9) | 70.9 (68.9-72.8) | 0.75 (0.71-0.78) | 45.1 (42.1-48.2) | 87.2 (85.1-89.2) | 0.66 (0.64-0.68) |

Sensitivity, Specificity, and AUC of the 3 strategies

Disclosures: Carolyn Crandall, None.

1025

Inhibition of Sclerostin With AMG 785 in Postmenopausal Women With Low Bone Mineral Density: Phase 2 Trial Results. Michael R. McClung¹, Andreas Grauer², Steven Boonen³, Jacques P. Brown⁴, Adolfo Diez-Perez⁵, Bente Langdahl⁶, Jean-Yves Reginster⁷, Jose R. Zanchetta⁸, Leonid Katz², Judy Maddox², Yu-Ching Yang², Cesar Libanati², Henry G. Bone⁹. ¹Oregon Osteoporosis Center, USA, ²Amgen Inc., USA, ³Leuven University, Belgium, ⁴Laval University & CHUQ Research Centre, Canada, ⁵Autonomous University of Spain, Spain, ⁶Aarhus University Hospital, Denmark, ⁷University of Liège, Belgium, ⁸Instituto de Investigaciones Metabólicas, Argentina, ⁹Michigan Bone & Mineral Clinic, USA

Purpose: In preclinical studies, administration of antibodies that neutralize sclerostin result in increased bone mass and strength. We report the primary and key secondary endpoints of a phase 2 trial, evaluating the efficacy and safety of the human sclerostin antibody AMG 785/CDP7851 in postmenopausal women with low bone mineral density (BMD).

Methods: This international, randomized, placebo-controlled, phase 2 study enrolled postmenopausal women aged 55 to 85 years with a lumbar spine, total hip, or femoral neck T-score ≤ -2.0 and ≥ -3.5 . During the first 12 months, women were randomized to one of 5 regimens of subcutaneous AMG 785 (70 mg QM, 140 mg QM, 210 mg QM, 140 mg Q3M, 210 mg Q3M) or placebo, and one of 2 open-label active comparators: 70 mg weekly oral alendronate (ALN) or 20 μ g daily subcutaneous teriparatide (TPTD). The primary endpoint was percentage change from baseline in lumbar spine BMD at month 12 (AMG 785 compared with placebo).

Results: The women enrolled in the study ($N=419$) had a mean age of 67 years, and mean lumbar spine, total hip, and femoral neck T-scores of -2.3 , -1.5 , and -1.9 , respectively. All AMG 785 doses significantly increased BMD compared with placebo at each of the 3 sites at month 12 ($p < 0.005$). The largest gains were observed with AMG 785 210 mg QM which resulted in rapid increases in BMD reaching 11.3% at the lumbar spine and 4.1% at the total hip (Figure). These increases were significantly greater than those achieved with ALN and TPTD ($p < 0.0001$). All doses of AMG 785 increased serum PINP and reduced serum CTX from baseline by week 1. Bone turnover marker changes with ALN and TPTD showed expected profiles (ie, decreases in both markers with ALN, and increases in both markers with TPTD). In general, adverse events were balanced between the placebo and total AMG 785 groups with the exception of generally mild injection site reactions (4% placebo; 12% AMG 785).

Conclusion: AMG 785 led to rapid and marked increases in lumbar spine and hip BMD which were superior to those observed with ALN and TPTD. These gains are a testimony to the mechanism of action evidenced by a simultaneous stimulation of bone formation and decrease in bone resorption. AMG 785 was generally well tolerated. These data support the continued clinical investigation of AMG 785 as a potential therapeutic agent for the treatment of women with postmenopausal osteoporosis.

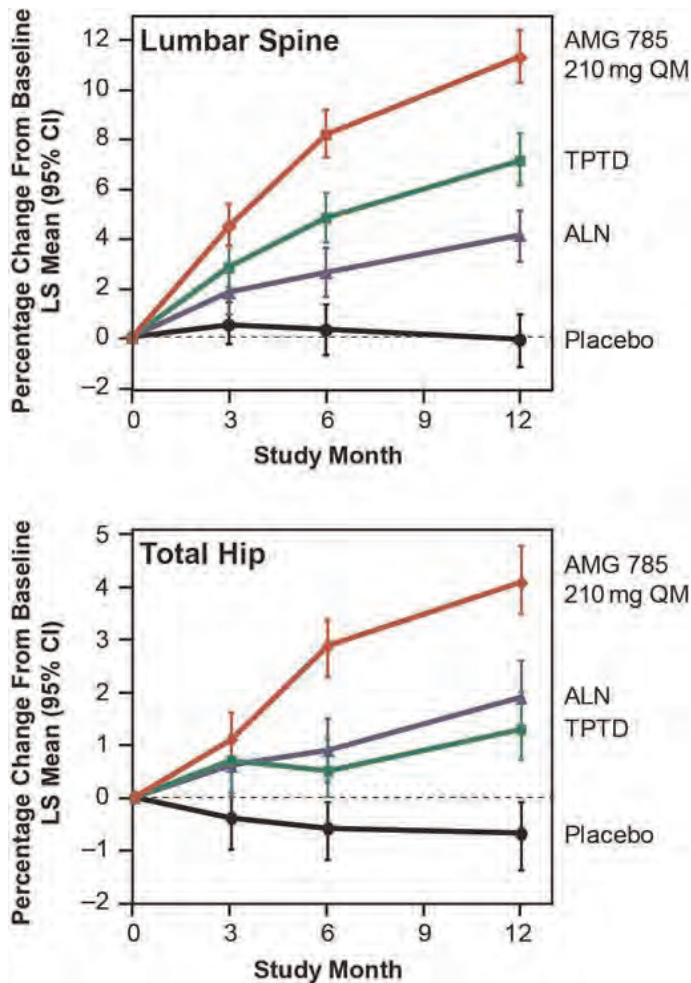


Figure
 Disclosures: Michael R. McClung, Amgen, Lilly, Merck, Novartis, 2; Amgen, Lilly, Novartis, Warner-Chilcott, 1; Amgen, Merck, 6
 This study received funding from: Amgen Inc. and UCB Pharma

1026

Blosozumab, a Humanized Monoclonal Antibody against Sclerostin, Demonstrated Anabolic Effects on Bone in Postmenopausal Women. Juliet McCole¹, Theresa Womack², Leijun Hu², Cheng Cai Tang³, Alan Chiang². ¹Eli Lilly & Company, Erl Wood, United Kingdom, ²Eli Lilly & Company, USA, ³Eli Lilly & Company, Singapore

Objective: Two clinical studies were conducted to assess the safety, tolerability, pharmacokinetics (PK), pharmacodynamics (PD), and potential immunogenicity of single and multiple escalating doses (IV and SC) of blosozumab in postmenopausal women, including prior/current alendronate users.

Research Design and Methods: These phase 1 studies were subject- and investigator-blind, placebo-controlled, randomized studies evaluating escalating doses of blosozumab: single IV doses up to 750 mg, single SC dose of 150mg, multiple IV doses up to 750mg every 2 weeks (Q2W) and multiple SC doses up to 270mg Q2W. Up to 8 subjects were randomized to each dose in the single dose study and up to 12 subjects to each dose in the multiple dose study. Safety parameters, including adverse events, and pharmacodynamic effects, including bone mineral density (BMD) and immunogenicity, were assessed for up to 12 weeks after the final dose of blosozumab.

Results: Blosozumab was well tolerated with no safety concerns identified following single or multiple administrations up to 750mg. Clinically and statistically significant bone biomarker responses were observed in sclerostin, procollagen-1 N-terminal peptide (PINP), bone specific alkaline phosphatase (BSAP), osteocalcin (OC), and carboxyterminal cross-linking telopeptide of collagen type 1 (CTx). A clinically and statistically significant anabolic response on bone was demonstrated through BMD following single and multiple (up to 5) administrations of blosozumab. There was up to a 3.41% (1.35,5.47) and up to a 7.71% (5.74, 9.67) [least-squares mean (90% confidence interval)] change from baseline in lumbar spine BMD at Day 85 following a single or multiple administration of blosozumab, respectively. The effects generally showed dose-related effects over the dose range tested and prior alendronate use did not appear to have a major impact. Antibodies to blosozumab were detected

but there was no pattern with regards to dose or route of administration and no suggestion of a neutralizing effect in terms of PK or PD parameters.

Conclusions: Blosozumab was well tolerated and exhibited anabolic effects on bone in these studies. These data support further investigation of blosozumab as a potential anabolic therapy for osteoporosis.

Disclosures: Juliet McCole, Eli Lilly and Company, 3
 This study received funding from: Eli Lilly and Company

1027

Effects of Odanacatib on BMD and Overall Safety in the Treatment of Osteoporosis in Postmenopausal Women Previously Treated with Alendronate. Tobias De Villiers¹, Sydney Bonnick², Alberto Odio³, Santiago Palacios⁴, Roland Chapurlat⁵, Boyd Scott⁶, Celine Le Bailly De Tillegem⁷, Carolyn DaSilva⁸, Albert Leung⁹, Deborah Gurner¹⁰. ¹Mediclinic Panorama, South Africa, ²Clinical Research Center of North Texas, USA, ³Alta California Medical Group, USA, ⁴Instituto Palacios, Salud y Medicina de la Mujer C/Antonio Acuña, Spain, ⁵E. Herriot Hospital, France, ⁶Merck & Co., Inc., USA, ⁷Merck Sharp & Dohme Corp., USA, ⁸Merck, USA, ⁹Merck Research Laboratories, USA, ¹⁰MSD, USA

Odanacatib (ODN) is a potent, orally-active cathepsin K inhibitor being developed for the treatment of postmenopausal osteoporosis. This study evaluated the effects of ODN 50mg once weekly (OW) on BMD and biochemical markers of bone turnover in patients previously treated with alendronate (ALN) (dosed daily or weekly) for ≥3years as well as the safety and tolerability of ODN. This study was not designed nor had the power to evaluate the effect of ODN on fractures.

This was a randomized, double-blind, placebo-controlled, 24-month study. The primary endpoint was % change from baseline at Month 24 of femoral neck (FN) BMD. 243 postmenopausal women ≥60 years of age with low BMD T-score (T-score range ≤-2.5 but >-3.5) at the total hip, FN or trochanter but no history of hip fracture and who had been treated with ALN for ≥3years were randomized in a 1:1 ratio to receive ODN 50mg OW or placebo OW for 24 months. All patients received vitamin D₃ 5600 IU/wk and calcium supplementation (to 1200 mg/day). BMD was assessed by DXA at baseline, 6, 12 and 24 months. Biochemical markers of bone turnover (s-CTX, u-NTx, s-BSAP and s-PINP) were measured at baseline and 3, 6, 12, 18 and 24 months.

In the placebo group, BMD at the FN and trochanter were not significantly different from baseline levels for the first 12 months, but declined significantly from baseline by Month 24 (-0.94% and -1.35%, respectively). Total hip BMD declined in a linear manner from baseline to month 24 (-1.87% at 24 months). At the lumbar spine (LS), BMD was not significantly different from baseline for the entire 24 months of the study. In the ODN group, BMD changes from baseline at 24 months were significant vs placebo at all 3 hip sites and the LS. The changes from baseline were 1.73%, 1.83%, 0.83% and 2.28%, respectively, for the FN, trochanter, total hip and LS. ODN 50mg OW significantly decreased the biomarker of bone resorption, u-NTx/Cr, and significantly increased biomarkers of bone formation, s-PINP and s-BSAP, compared to placebo. The increase observed for the bone resorption marker s-CTX with ODN treatment was unexpected. AEs were comparable between the 2 treatment arms. The overall safety profile appeared similar between ODN 50mg OW and placebo.

In this study ODN provided incremental BMD gains in osteoporotic women following ALN treatment. Biomarker results suggest that ODN decreases bone resorption while preserving bone formation.

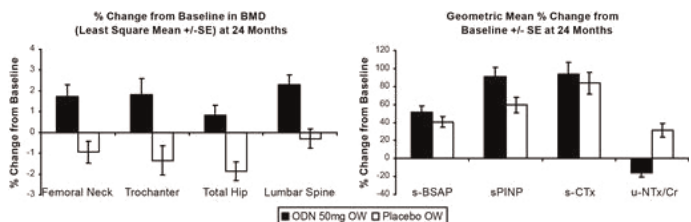
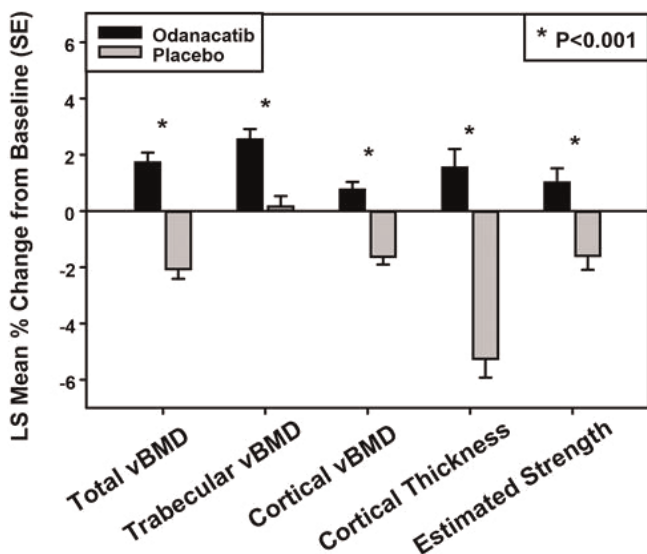


Fig 1
 Disclosures: Tobias De Villiers, Merck Sharp & Dohme Corp., 1; Merck Sharp & Dohme Corp., 9
 This study received funding from: Merck Sharp & Dohme Corp.

Effects of Odanacatib on the Distal Radius and Tibia in Postmenopausal Women: Improvements in cortical geometry and estimated bone strength. Anne De Papp¹, Angela Cheung², Sharmila Majumdar³, Kim Brixen⁴, Roland Chapurlat⁵, Bernie Dardzinski¹, Antonio Cabal¹, Nadia Verbruggen⁶, Shabana Ather⁷, Elizabeth Rosenberg¹. ¹Merck & Co., Inc., USA, ²University Health Network, Canada, ³University of California, San Francisco, USA, ⁴Institute for Clinical Research, Denmark, ⁵E. Herriot Hospital, France, ⁶Merck Sharpe & Dohme, Belgium, ⁷Merck & Co, Inc., USA

The cathepsin K inhibitor odanacatib (ODN), a novel antiresorptive that preserves bone formation, is currently in phase 3 development for postmenopausal osteoporosis. In a phase 2 study, 5 years of ODN 50 mg once weekly progressively increased areal BMD at the lumbar spine and total hip (11.9 % and 8.5% from baseline, respectively). ODN reduced bone resorption markers while preserving bone formation markers. In an OVX primate model, ODN has been shown to increase cortical thickness and periosteal bone formation at the central femur and femoral neck. In order to determine the effect of ODN on cortical geometry and to estimate bone strength, we conducted a randomized, double-blind placebo-controlled trial, using high resolution quantitative computerized tomography (HR-pQCT) of the distal radius and distal tibia. A total of 214 postmenopausal women, of mean age 64.0 ± 6.8 years and baseline lumbar spine T-score -1.81 ± 0.83, were randomized to oral ODN 50 mg or PBO weekly for 2 years. Lumbar spine areal BMD % change from baseline at 1 year (primary endpoint) was statistically significantly greater for ODN than PBO (3.49% treatment difference, p<0.001). After 2 years, there were significantly greater improvements with ODN than PBO in total, trabecular, and cortical volumetric BMD; cortical thickness; and estimated strength (failure load) of the distal radius using HR-pQCT-based finite element analysis (exploratory endpoints, FIGURE). At the radius, odanacatib attenuated the increase in cortical porosity that was seen in the placebo group (treatment difference in least squares mean % change from baseline -7.68, p=0.066). At the distal tibia, changes in volumetric BMD and cortical thickness were similar to changes at the radius. Safety and tolerability were similar between treatment groups. In conclusion, odanacatib increased cortical and trabecular density and improved cortical thickness of the distal radius and distal tibia, and improved the estimated bone strength in the distal radius compared to placebo.

Figure. Distal Radius HR-pQCT Endpoints in Postmenopausal Women at Month 24



NOTE: HR-pQCT endpoints were exploratory and there was no adjustment for multiplicity.
vBMD=volumetric bone mineral density

Fig

Disclosures: Angela Cheung, Merck Sharp and Dohme, 3
This study received funding from: Merck Sharp and Dohme

Bone Material Strength in Bisphosphonate-related Atypical Femoral Fractures Measured by 'in vivo' Microindentation. Robert Guerri Fernandez^{*1}, Jose Manuel Quesada Gomez², Xavier Nogues³, Leonardo Mellibovsky⁴, Lluís Puig⁵, Guv Yoskovitz⁶, Natalia Garcia Giralt⁵, Elisa Torres del Pliego⁷, Paul Hansma⁸, Adolfo Diez-Perez⁹. ¹Fundacio IMIM, Spain, ²Quesper R&D, Spain, ³Institut Municipal D'Investigació Mèdica, Spain, ⁴Hospital del Mar. IMIM. URFOA., Spain, ⁵Hospital del Mar. IMIM. URFOA, Spain, ⁶IMIM, Spain, ⁷Hospital del Mar. IMIM.URFOA, Spain, ⁸University of California, Santa Barbara, USA, ⁹Parc De Salut Mar, Spain

Atypical femoral fractures (AFFx) associated with long-term bisphosphonates (LTB) treatment are a growing safety concern. Their aetiology is not known but a deep alteration in bone material strength is likely given their clinical characteristics. In an AFFx series, we analyzed the strength of bone material by microindentation.

Patients and methods

Four groups of patients were included: 6 AFFx, 38 typical osteoporotic fractures, 6 LTB and 20 controls without fracture. A general laboratory work-up, bone densitometry by dual-energy X-ray absorptiometry, and bone microindentation testing at the tibia was done in all patients. Total indentation distance (Total ID), Indentation distance increase (IDI) and Creep indentation distance (Creep ID) were measured (microns). Age-adjusted ANCOVA analysis was used for comparisons between groups.

Results: Control individuals were significantly younger than the fracture groups. Bisphosphonate exposure was on average 5.5 years (range 5-12) for the AFFx group and 5.4 years (range 5-8) for the LTB group. Total ID (microns) was 36 (±6) for controls, 38(±4) for LTB, 46(±4) for AFFx and 47 (±13) for typical femoral fractures (mean ± SD), and IDI values were 13 (±2), 16 (±6), 19 (±3) and 18 (±5), respectively.

After adjusting by age, statistically significant differences were seen between controls and typical (P<0.001) and atypical fractures (P=0.03) for Total ID as well as for IDI (P<0.001 and P<0.05 respectively). There were no differences in Creep ID between groups.

Conclusions: Our data suggest that patients with AFFx have a deep deterioration in bone material strength at a tissue level not seen in LTB-treated cases. Since patients on bisphosphonates at risk of AFFx are not detected by bone mineral density tests, this finding strongly suggests an underlying bone condition in this subset of patients.

Disclosures: Robert Guerri Fernandez, None.

Quantitative Bone Histomorphometry in Patients with Bisphosphonate-Associated Atypical Subtrochanteric Femur Fractures Before and after 12 months of Teriparatide. Paul Miller^{*1}, Ed McCarthy². ¹Colorado Center for Bone Research, USA, ²John Hopkins Medical School, USA

Purpose: Atypical subtrochanteric femur fractures (ASFF) have been associated with long-term bisphosphonate (BP) administration. The mechanism whereby BP's may be linked to the greater risk of ASFF is unknown, but may be associated with a reduction in bone remodeling. Recombinant human 1-34 parathyroid hormone (rh-1-34 PTH) increases bone remodeling. It is unknown what effect administration of rh 1-34 PTH may have on remodeling in these patients. We report the results of paired bone biopsies done before and 12 months after treatment with rh 1-34 PTH in 15 patients with bisphosphonate associated ASFF.

Methods: Fifteen post-menopausal women on long-term alendronate who presented with ASFF underwent double tetracycline labeled transiliac bone biopsies between 6 weeks to 7 months following their ASFF. All patients already had intramedullary rods placed. The patients then received teriparatide (rh 1-34 PTH), 20ug/day for 12 months at which time a second biopsy was obtained from the opposite iliac crest. Quantitative histomorphometric analysis was performed and parameters were compared to published normative reference standards as well as to each patient's baseline biopsy.

Results: The baseline mineral apposition rate (MAR) in the group averaged 0.278 um/day (normal: 0.66-0.83 um/day) and was zero in 7 patients. After teriparatide administration the average MAR increased to 0.647 um/day. All 7 patients who had immeasurable MAR at baseline increased their MAR following teriparatide (average: 0.673 um/day). Likewise the bone formation rate (BFR) at baseline averaged 1.692 %/yr (normal: 8.6-21.8 %/yr) and was also zero in the same 7 patients that had immeasurable MAR. Following teriparatide the BFR increased in all patients, including the 7 with immeasurable MAR to an average of 4.03 %/yr.

Conclusions: Bone remodeling in patients with bisphosphonate associated ASFF is, on average, lower than published normal reference values but increase after discontinuation of bisphosphonates and 12 months of teriparatide administration. The baseline biopsies were heterogeneous in their quantitative parameters, though 7/15 patients had immeasurable MAR and BFR. The observations in this uncontrolled analysis do not confirm any pathophysiological link between bisphosphonate exposure and the development of ASFF but do suggest that (along with BP discontinuation) teriparatide may increase MAR and BFR in these patients who present with these ASFF. It remains unknown if teriparatide would prevent early fractures from progressing.

Disclosures: Paul Miller, None.

1031

Mechanoregulation of Cortical and Trabecular Bone Adaptation Measured by Examining Dynamic Bone Morphometry and the Mechanical Environment. Annette Birkhold^{*1}, Hajar Razi¹, Richard Weinkamer², Georg Duda¹, Sara Checa¹, Bettina Willie¹. ¹Julius Wolff Institute, Charité Universitätsmedizin Berlin, Germany, ²Max Planck Institute of Colloids & Interfaces, Germany

Bone can adapt to mechanical stimuli to attain its structure. However, the exact mechanisms of adaptation remain unclear. We hypothesize that both trabecular and cortical bone adapt to a similar amount to changes in the global loading by reduced resorption and increased formation.

We performed in vivo loading on the left tibia of ten female adult (26wk old) C57Bl/6 mice (right limb as internal control). In vivo microCT was performed at day 0, 5, 10, and 15. Images were registered with an algorithm overlaying data of the same limb at different time points. Resulting volumes were separated into trabecular and cortical bone. Constant, formed and resorbed bone volumes (BV), as well as corresponding parameters normalized to the total bone volume (BV/TBV), formation and resorption surface areas (SA) and normalized parameters (SA/TSA), bone formation (BFR) and resorption rates (BRR), mineral apposition (MAR) and resorption rates (MRR) were determined and validated with histomorphometry data. The local mechanical strains were determined with finite element method using a submodelling technique. Regional elasticity was in accord with the average BMD of the fibula, distal and proximal tibia. FEMs were validated with strain gauge data.

Mechanical loading significantly increased surface area of trabecular bone formation, but not MAR. The effect of loading on formed surface area was more prominent in cortical than in trabecular bone (cortical 6.6, trabecular 2.0 fold increase). Resorption area was reduced in cortical and trabecular bone (cortical 1.9, trabecular 1.5 fold decrease), but MRR was not altered. Higher strain levels were predicted in the cortical region (tensile 533-1627 microstrain, compressive 378-3012 microstrain) than in the trabecular region (tensile 393-707 microstrain, compressive 388-1442 microstrain).

Bone adapts to the loading by an increased formation and a reduced resorption, but in cortical bone the increase in bone apposition was much greater (figure). These data suggest adaptation is likely caused by a higher amount of osteoblast being recruited (or lining cells turning into osteoblasts), rather than by increasing the velocity of bone formation. The relationship between increased area of formation in cortical bone and higher tissue strain indicates that a threshold for increasing the number of osteoblasts may exist. Further investigations will determine local differences in the mechano-responsiveness of cortical and trabecular bone, as well as age related alterations.

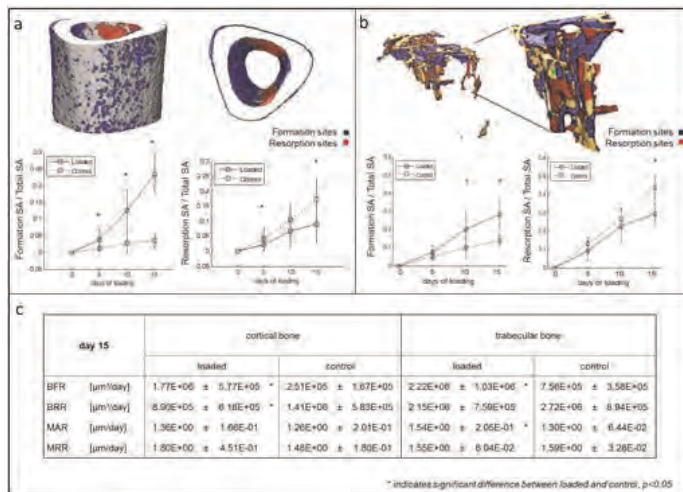


Fig: Areas of formation and resorption a: Cortical b: Trabecular c: Formation and resorption rates

Disclosures: Annette Birkhold, None.

1032

Force Induced Cytoskeletal Reorganization in MSC Requires mTORC2 Signaling at Focal Adhesions. Buer Sen^{*1}, Zhihui Xie², Natasha Case³, William Thompson⁴, Maya Styner³, Janet Rubin³. ¹University of North Carolina At Chapel Hill, USA, ²University of North Carolina, USA, ³University of North Carolina, Chapel Hill, School of Medicine, USA, ⁴University of Delaware, USA

The ability of cells to sense and transduce mechanical input involves focal adhesions (FA), which transmit outside-in information via integrins to signaling molecules co-localized within the FA. We published that mTORC2 (the rapamycin-insensitive rictor-associated mTOR) is a novel target of mechanical force: mTORC2

activates Akt, which through GSK3β inhibition leads to increased β-catenin and inhibition of adipogenesis of mesenchymal stem cells (MSC). Interestingly, mTORC2 has been shown to have a role in generating baseline cytoskeletal structure. As we have previously shown that MSC respond to mechanical input by generating more cytoskeletal structure, i.e., increased FAs connected by F-actin stress fibers, we wished to ascertain if mechanically activated mTORC2 was involved in this cytoskeletal reorganization. To activate mTORC2 signaling we applied cyclical strain (100 cycles x 2% strain) to marrow derived MSCs. RNA silencing of rictor (partner of mTOR) prevented strain, but not insulin, induced Akt serine 473 phosphorylation, confirming the role of mTORC2 signaling in Akt activation by strain. We next immunoprecipitated with vinculin to capture FA associated proteins: acute strain application induced both rictor and Akt association with FAs. Immunofluorescence staining for vinculin and rictor confirmed that mechanical loading induced rictor co-localization at FAs. Inhibition of mTOR activity blocked strain induced association of rictor/Akt with vinculin. The initial recruitment of mTORC2 to vinculin was shown to rely on tension development from disordered actomyosin as inhibition of myosin II kinase eliminated mechanical Akt activation and prevented the association of rictor/Akt with FAs. mTORC2 was next shown to be critical for the cytoskeletal reorganization induced by strain; FA assembly and their interconnection by radial stress fibers was completely prevented by both rictor silencing and by inhibition of mTOR. We further ascertained that the mTORC2 effector, Akt, was required for FA assembly, as inhibition of Akt activity phenocopied mTORC2's role in cytoskeletal reorganization. Our data shows that mechanically-induced rictor/Akt association with FA-vinculin is critical for strain-induced radial stress fiber association at the focal adhesion complex. As such, strain activation of mTORC2 prevents adipogenesis of MSC both through initiating β-catenin signaling and by increasing focal adhesion assembly.

Disclosures: Buer Sen, None.

1033

Cumulative Effects of Strontium Ranelate and Free-fall Impact Exercise in a Female Ovariectomized Rat Model. Priscilla C. Aveline^{*1}, Jérôme Touvier¹, Eric Lespessailles¹, Claude-Laurent Benhamou¹, Gael Y. Rochefort². ¹EA4708 I3MTO, Orléans Hospital, France, ²EA4708 I3MTO, Orléans Hospital, France, France

Physical exercise is known to exert beneficial effects on bone status. Strontium Ranelate (SrRan) was shown to have anti-osteoporotic properties in clinical studies and animal models. The combination SrRan + physical exercise has not yet been tested. We have mounted a study testing impact activity (EXE), or SrRan, or both in female rats either ovariectomized (OVX) or not (SHAM).

We have studied 8 groups of 12 female Wistar rats, 5 weeks old at baseline: SHAM (Sh), SHAM/SrRan (ShSr), SHAM/EXE (ShE), SHAM/EXE/SrRan (ShESr), OVX (O), OVX/SrRan (OSr), OVX/EXE (OE) and OVX/EXE/SrRan (OESr). Animals in the EXE groups were subjected to 10 impacts per day from 45 cm high, 5 days a week during 8 weeks. SrRan group animals were treated orally with 625 mg/kg of SrRan in 0.5 % carboxymethylcellulose (vehicle) per day during 8 weeks. Bone mineral density (BMD) and content (BMC) (whole body and left femur) were measured by DXA (Hologic Discovery) at weeks 0, 4 and 8. Morphological properties of trabecular and cortical bone from femur, tibia and L2 to L4 vertebrae were analyzed by µCT (Skyscan, 1072). A technique of image analysis assessing bone cortical geometry was settled. Osteocyte apoptosis was studied by cleaved caspase-3 immunostaining and expressed as a percent of total cells.

MicroCT analysis (femur, tibia and L2-L4 vertebrae) showed a deleterious effect of OVX, and a beneficial effect of SrRan and of EXE on BV/TV, Tb.N, Tb.Th, Tb.Pf, Tb.Sp and SMI. A significant additive effect of SrRan and EXE on these parameters was found. Cortical thickness was increased in SrRan groups; Ct.Po and Po.N were improved at femur and tibia levels in the SrRan groups, and significantly more in the EXE + SrRan groups.

OVX groups had a significantly higher osteocyte apoptosis versus SHAM animals. EXE did not significantly reduce osteocyte apoptosis in SHAM and OVX groups while SrRan significantly reduced osteocyte apoptosis in all groups. There was no significantly cumulative effect of EXE and SrRan on this parameter.

These data suggest that physical activity and SrRan may have a cumulative effect both on trabecular bone mass and microarchitecture as well as on cortical geometry and porosity. SrRan significantly reduced osteocyte apoptosis in cortical bone without significant cumulative effect with EXE. These data constitute the first description of an additive effect of SrRan plus EXE on bone status, and of a beneficial effect of SrRan on osteocyte apoptosis.

Exercise during recovery from HU proved beneficial to most densitometric and biomechanical properties of bone as measured at the end of recovery and after a subsequent period of disuse (2nd HU). Cancellous bone strength exhibits the most dramatic increases with exercise during recovery and is well preserved after the 2nd HU. Thus, incorporating resistance exercise during recovery from disuse not only provides benefits during reloading but also for subsequent unloading even with cessation of exercise.

Disclosures: Yasaman Shirazi-Fard, None.

1035

Site- and Compartment-specific Effects of Microgravity on the Skeleton in Mice Flown on the STS-135 Shuttle Mission. Rachel Ellman^{*1}, Virginia Ferguson², Eric Livingston³, Michael Lemus³, Leann Louis¹, Jordan Spatz⁴, Kelly Warmington⁵, Hong Lin Tan⁵, Dave Hill⁵, Marina Stolina⁵, Denise Dwyer⁵, Sutada Lotinun⁶, Roland Baron⁷, Chris Paszty⁸, Louis Stodieck², Mary Boussein¹, Ted Bateman⁹. ¹Beth Israel Deaconess Medical Center, USA, ²University of Colorado, USA, ³University of North Carolina, Chapel Hill, USA, ⁴Harvard-MIT Division of Health Sciences & Technology (HST), USA, ⁵Amgen Inc., USA, ⁶Harvard School of Dental Medicine, USA, ⁷Harvard School of Medicine & of Dental Medicine, USA, ⁸Amgen, Inc., USA, ⁹University of North Carolina, USA

Astronauts have high rates of bone loss following exposure to microgravity. Yet, the mechanisms that contribute to this profound bone loss are incompletely understood. Animal models are commonly used to study interactions between reduced loading and bone loss, but there are few data describing bone responses to microgravity in mice. Thus, the aim of this study was to assess site-specific changes in bone and muscle in mice exposed to microgravity via a 13 day flight on the space shuttle Atlantis. Female C57Bl/6N mice (9 wks old) were assigned to flight (FL, n=15) or ground-controls (GR, n=14) according to total body (TB) BMD and body mass. Mice were acclimated to cages and food for 2 weeks prior to start of the study. Outcomes included: in vivo BMD (total body, spine, leg and arm), ex vivo normalized muscle mass, and microarchitecture (tibia, femur, humerus), as well as serum markers of bone metabolism at end of study. Results: While both groups lost body weight (-8 and -6% in GR and FL), total lean/fat mass ratio did not differ between groups. There was significant muscle atrophy in hindlimbs (-3 to -18% in GR vs. FL, p < 0.05), but not in the forelimbs, where biceps mass was 18% higher in FL vs. GR (p < 0.05). Bone changes followed similar pattern as muscle, with greater effects in the hindlimb than forelimb. TB and leg BMD increased in GR, but acquisition was diminished with spaceflight (TBMD: 6.6% vs. 2.2% in GR vs. FL; Leg BMD: 9.0 vs. 1.3% in GR vs. FL, p < 0.01 for both), whereas arm BMD did not differ between groups. Tb.BV/TV was approx. 35% lower in FL vs. GR at the proximal tibia and distal femur (p < 0.01), but was only 22% lower in FL vs. GR at the proximal humerus (p < 0.05). Tb.Th was lower in FL than GR (-14 to -22%, p < 0.05), but Tb.N was unaffected. Cortical BA/TA was 4-8% lower in FL vs. GR at mid-tibia and femur, but was unchanged at the humerus. Serum measures were consistent with both lower bone formation (decr. osteocalcin and PINP) and higher bone resorption (decr. OPG, incr CTX1) in FL vs. GR. Serum sclerostin levels did not differ between groups at study end. In summary, short exposure to microgravity (13 days) induced significant deterioration of bone that was more pronounced in the hindlimb than forelimb, consistent with changes in muscle mass. Increased use of the forelimbs in the cages with wire floors and walls may have provided some protection from effects of microgravity in the forelimb.

Disclosures: Rachel Ellman, None. This study received funding from: Amgen Inc.

1036

Connexin 43 Deficiency Protects Against Skeletal Changes Associated with Mechanical Unloading. Shane Lloyd^{*1}, Gregory Lewis², Yue Zhang¹, Emmanuel Paul², Henry Donahue¹. ¹The Pennsylvania State University College of Medicine, USA, ²Penn State College of Medicine, USA

Gap junctions (GJs) are small protein channels that allow for direct cell-to-cell communication. Connexin 43 (Cx43) is the predominant GJ in bone and has been shown to have an integral role in the skeletal response to mechanical loading both in vitro and in vivo. However, little work has focused on the role of Cx43 in the response to unloading. Practical unloading scenarios include extended bed rest due to neurological injury, reduced physical activity associated with aging, or the microgravity environment.

We utilized skeletally mature mice with an osteoblast and osteocyte specific, osteocalcin-driven deficiency of Cx43 (cKO) or their wild-type (WT) littermates. Mice were subjected to three weeks of normal loading conditions (Control) or unloading via hindlimb suspension (Suspended) (4 groups, n=10-15/group). Mice were subjected to baseline and endpoint MicroCT scans. Dual-label quantitative dynamic histomorphometry was conducted.

At baseline, cKO mice demonstrated a cortical osteopenic phenotype, with reduced cortical thickness and bone mineral density and increased porosity. There was no trabecular phenotype. Loss of trabecular bone following three weeks of unloading was significantly attenuated in cKO mice (Figure 1AB). In cKO, there was reduced loss of trabecular BV/TV (-53% vs. -67%, p < 0.01), trabecular thickness (-21% vs.

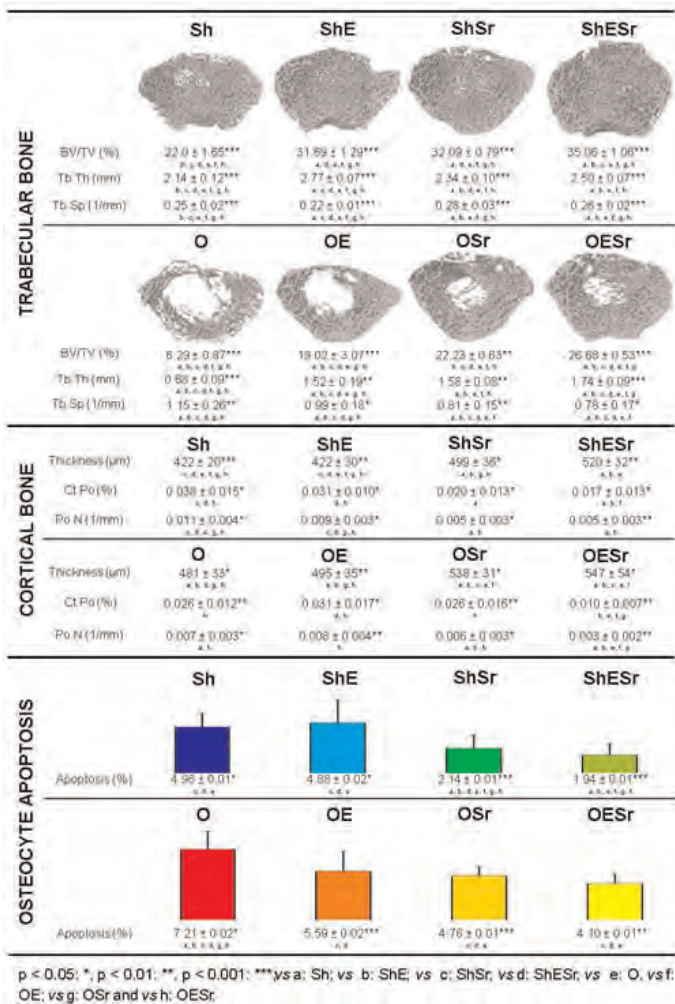


Figure 1 (Aveline et al.)

Disclosures: Priscilla C. Aveline, SERVIER, 6 This study received funding from: Servier

1034

Exercise during Recovery between Two Bouts of Disuse Mitigates Bone Loss on Second Exposure. Yasaman Shirazi-Fard^{*}, Estela Gonzalez, Joshua Davis, Ramon Boudreaux, Derrick Morgan, Kevin Shimkus, Susan Bloomfield, Harry Hogan. Texas A&M University, USA

The bone response to repeat exposures of disuse remains a concern for astronaut health and for clinical patients experiencing periods of bed rest or non-weightbearing. Previously, we reported that, regardless of age, bone loss during a subsequent period of disuse is milder than the initial exposure. This experiment assessed effects of resistance exercise during recovery between two bouts of disuse in distal femur metaphysis (DFM) and femur diaphysis (FD) bone. We hypothesized that exercise would not only enhance recovery but would also mitigate impact of the 2nd disuse.

Adult male Sprague-Dawley rats (6mo.) were assigned to age-matched cage controls (CC) and hindlimb unloaded (HU) groups by body weight and total (integral) vBMD. HU animals were exposed to 28d of hindlimb suspension (1HU), followed by 56d of recovery (1HU+R), and then a 2nd HU exposure (2HU). HU animals also performed squat jumping resistance exercise during recovery for 7 weeks (3d/wk) with exercise intensity increasing weekly. Groups (n=15) were euthanized at baseline, the end of the exercise protocol (1HU+EX, CC9), and after the 2nd HU (2HU+EX, CC10). Excised femora were scanned by pQCT at DFM and FD and tested to failure by 3-pt bending at FD and reduced platen compression at DFM.

DFM total BMC and vBMD for 1HU+EX recovered more completely (+23.1%, +14.3%) compared to 1HU+R (+3.6%, +3.9%). During the 2nd HU, tot BMC in 2HU+EX increased (+2.9%) while 2HU decreased (-1.9%). Tot vBMD decreased during the 2nd HU in both 2HU+EX (-2.0%) and 2HU (-6.9%). FD cortical BMC and vBMD recovered more in 1HU+EX (+10.7%, +2.4%) than 1HU+R (+7.4%, +0.16%). Cortical vBMD in 2HU+EX increased 3.8% vs. a decrease of 1.8% in 2HU. Exercise did not improve FD ultimate strength during recovery or during the 2nd HU. DFM ultimate stress from RPC testing increased +217% for 1HU+EX compared to 114% for 1HU+R and was significantly higher in 2HU+EX compared to 2HU by 342% or CC10 by 183%.

-35%, $p < 0.001$), and connectivity density (-50% vs. -64%, $p < 0.05$). There was no difference in loss of cortical bone between genotypes. Bone formation was dramatically suppressed during unloading of WT mice at both the endocortical (-100% Ec.BFR, -70% Ec.MS/BS) and periosteal surfaces (-60% Ps.BFR, -38 Ps.BFR ($p < 0.05$ for all)). This was not observed in cKO mice, where bone formation and mineralizing surface were maintained at control levels (Figure 2).

Taken together, these results indicate that defective Cx43 expression and/or gap junctional intercellular communication desensitizes bone to the effects of mechanical unloading, and that this may be due to an inability of mechanosensing osteocytes to effectively communicate the unloading state to osteoblasts to suppress bone formation. Combined with published reports from our laboratory demonstrating that Cx43 cKO mice have increased sensitivity to mechanical loading, these findings suggest that Cx43 may be a potential therapeutic target for investigation as a countermeasure to unloading and age-related bone loss.

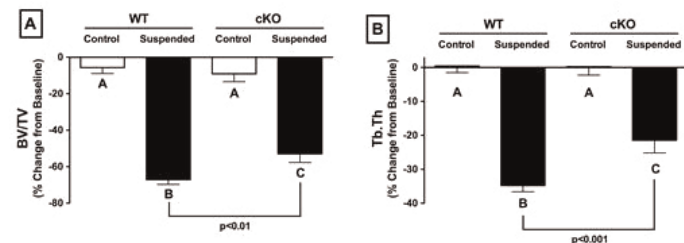


Figure 1. Attenuated loss of trabecular bone volume fraction and trabecular thickness.

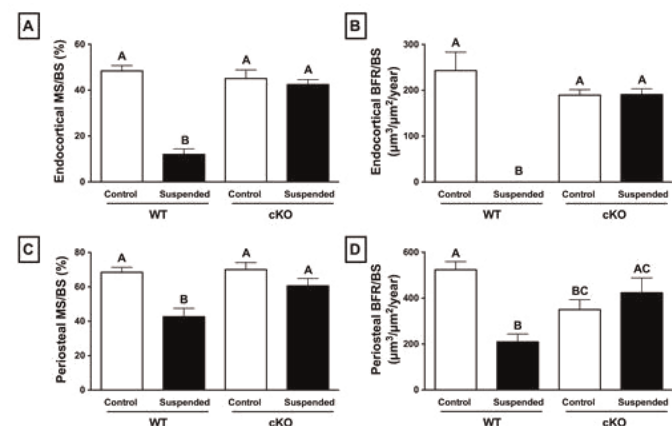


Figure 2. Preservation of mineralizing surface and bone formation rate.

Disclosures: Shane Lloyd, None.

1037

Osteocytes in the Homeostasis of Remote Organs. Mari Sato^{1*}, Noboru Asada¹, Kentaro Minagawa¹, Yuko Kawano¹, Hiroki Kawano¹, Kanako Wakahashi¹, Akiko Sada¹, Kyoji Ikeda², Toshimitsu Matsui¹, Yoshio Katayama¹. ¹Hematology, Dept. Med., Kobe Univ., Japan, ²National Center for Geriatrics & Gerontology, Japan

Reduced mechanical stress to bone in bedridden patients and astronauts leads to osteoporosis and immune suppression, and osteocytes are known as mechanosensory cells in bone. Here we show amazing functions of osteocytes to regulate an immune organ, thymus, and a metabolic organ, liver, both remote from bone. We utilized transgenic (TG) mice in which inducible and selective ablation of osteocytes is achieved *in vivo* through targeted expression of diphtheria toxin (DT) receptor. A single injection of DT in TG mice at 15 weeks of age generates osteocyte-less (OL) mice. Three weeks after DT injection, OL mice displayed severe lymphopenia and thymic atrophy (90% reduction in cellularity, $n=8$, $p < 0.0001$), but these phenotypes were restored as osteocytes were replenished 3 months after DT injection. B cell precursors in the bone marrow (BM) were also drastically decreased (pre-B cells by 89%, $n=3$, $p < 0.05$; pro B cells by 79%, $n=3$, $p < 0.01$), however, common lymphoid progenitors were only minimally affected (34%, $n=10$, $p < 0.01$). Hematopoietic stem cell activity, as assessed by competitive repopulation, and colony-forming myeloid precursors were not impaired. Analysis of B-lymphoid long-term BM cultures revealed that OL BM failed to produce B cells because of depletion of lymphoid-supporting CD45-VCAM-1+ stromal cells. Moreover, immunohistochemical analysis of the thymus showed that K8+ cortical thymic stromal cells were greatly reduced and their mesh network became sparse. Neither *in vivo* supply of T cell progenitors nor humoral factors by sharing the circulation with a normal partner in parabiosis rescued the thymic atrophy in OL mice. These results suggest that thymic atrophy in the absence of osteocytes was due to impaired thymic microenvironment. Since they also suggest that osteocytes control thymic stroma via a non-humoral signal, we speculated the involvement of the nervous system. To test this, we ablated osteocytes following destruction of ventromedial hypothalamic nucleus (VMH) or arcuate nucleus (ARC)

which controls food intake as well as bone mass. Although thymic atrophy was not restored, VMH or ARC destruction in OL mice unexpectedly caused massive fatty liver, which implies that some signal from osteocytes may normally suppresses fat accumulation in the liver caused by excessive food intake. Collectively, these results uncover surprising functions of osteocytes in the homeostasis of multiple remote organs.

Disclosures: Mari Sato, None.

1038

PTH/PTHrP Receptor Signaling in Osteocytes Regulates Anabolic and Catabolic Bone Responses to PTH by Modulating Bone Remodeling via Sclerostin and RANKL Expression. Vaibhav Saini^{1*}, Keertik Fulzele², Kevin Barry³, Dean Marengi³, Sutada Lotinun⁴, Roland Baron⁵, Paola Pajevic Divieti⁶. ¹MGH, Harvard Medical School, USA, ²Massachusetts General Hospital; Harvard Medical School, USA, ³MGH, USA, ⁴Harvard School of Dental Medicine, USA, ⁵Harvard School of Medicine & of Dental Medicine, USA, ⁶MGH- Harvard Medical School, USA

PTH is the only available anabolic agent to treat osteoporosis. Osteocytes may partially mediate the anabolic effects of PTH by suppressing Sclerostin, a Wnt signaling inhibitor. To investigate the role of PPR signaling in osteocytes, we generated mice lacking PPR in osteocytes (OcyPPRKO). Littermates carrying the floxed PPR alleles were used as controls. qPCR showed significantly decreased PPR transcripts in the osteocyte-enriched long bones of OcyPPRKO compared with control, demonstrating successful PPR ablation. Next, the role of PPR signaling in osteocytes in anabolic and catabolic bone responses was evaluated. For anabolic regimen, 8-week-old females were injected with 80µg/kg/day hPTH(1-34) for 4 weeks whereas for catabolic treatment, 13-week-old males were infused for 2 weeks with 100µg/kg/day. MicroCT analysis of femurs showed significantly higher cortical thickness ($p < 0.05$, $N > 4$) and bone area ($p < 0.05$, $N > 4$) in control animals treated with intermittent PTH as compared with vehicle whereas, as expected, continuous PTH induced a significant decrease in bone volume ($p < 0.05$, $N = 6$) and trabecular number ($p < 0.05$, $N = 6$) and increase in trabecular spacing ($p < 0.05$, $N = 6$) in control mice. In contrast, these parameters remained unchanged in OcyPPRKO mice treated with intermittent or continuous PTH. Histomorphometric analysis of anabolic or catabolic response to PTH in OcyPPRKO showed significantly reduced osteoblast numbers ($p < 0.05$, $N > 4$), and reduced, though not significant, osteoclast numbers were observed in OcyPPRKO than control. TRAP staining showed a lack of multinucleated TRAP+ osteoclasts in OcyPPRKO trabecular and cortical bone as compared with control. Immunohistochemistry of tibiae showed increased Sclerostin and decreased RANKL expression in osteocytes of OcyPPRKO than control. Lastly, to determine osteoclastogenic potency, osteoclast precursors from wild type spleens were co-cultured with osteocyte-enriched long bones from OcyPPRKO and control. Upon PTH treatment, a significantly reduced number of multinucleated osteoclasts were detected in OcyPPRKO co-culture compared to control ($p < 0.05$, $N = 3$). Osteoprotegerin treatment completely abrogated osteoclast formation in both groups, indicating that PPR signaling in osteocytes regulates osteoclastogenesis via a RANKL-mediated pathway. In summary PPR on osteocytes regulates RANKL expression, which in turn regulates osteoclast formation, and thus bone remodeling.

Disclosures: Vaibhav Saini, None.

This study received funding from: NIH

1039

Inhibition of Wnt1 Class Induced Lrp6 Signaling Normalizes Bone Mass in *Sost*; *Lrp5* Double Knockout Mice. Ming-Kang Chang^{1*}, David Jenkins², Ina Kramer¹, Seth Ettenberg², Marcel Merdes¹, Christine Henninger¹, Feng Cong², Michaela Kneissel¹. ¹Novartis Institutes for Biomedical Research, Switzerland, ²Novartis Institutes for BioMedical Research, USA

Sclerostin, encoded for by *Sost*, is an osteocyte secreted negative regulator of bone formation. Sclerostin is thought to exert its action by binding to the Wnt co-receptor Lrp5 and possibly Lrp6 thus blocking Wnt/beta-catenin signaling in cells of the osteoblastic lineage. We have shown previously that *Sost*; *Lrp5* double knockout (dKO) mice present with reduced bone overgrowth compared to *Sost* single knockout (KO) mice. To test whether the remaining bone overgrowth could be abolished by blockage of Lrp6 mediated Wnt signaling, we utilized three Lrp6 targeting antibodies that recognize different epitopes on Lrp6 and have distinct modes of action as previously described (1). First we injected 12-week-old *Sost* KO and control females ($n=5-8$ /group) for one month either with antibody A - blocking Wnt1 class mediated signaling, but potentiating Wnt3a class mediated signaling, or antibody B - displaying the reverse pattern, or antibody C - blocking both types of signaling, or vehicle. Computed tomography analysis revealed that blocking Wnt1 class mediated signaling reduced the abnormal bone gain in *Sost* KO mice and to a lesser extent also reduced growth related bone gain in control mice. This effect was irrespective of enhancement (antibody A) or blockage (antibody C) of Wnt3a class mediated signaling. Reversely and consistently, promotion of Wnt1 class mediated signaling in the absence of Wnt3a class mediated signaling (antibody B) further enhanced the abnormal bone gain of *Sost* KO mice and induced bone gain also in control mice. These data indicate that sclerostin mediates its action *in vivo* in part by interfering with signaling induced upon

Wnt1 class ligands binding to Lrp6, but not by Wnt3a class ligands. Hence, we next administered antibody A for one month to 12-week-old *Sost;Lrp5* dKO females in addition to *Sost* KO and control mice (n=8-10/group). The antibody reduced as expected again abnormal bone gain in *Sost* KO mice, while impacting bone density also in wildtype mice, though to a smaller extent. Importantly, the partial bone overgrowth still present in *Sost;Lrp5* dKO was completely abolished upon antibody treatment. Together, we conclude that sclerostin indeed exerts its action *in vivo* by targeting both Lrp5 and Lrp6 to block Wnt/ β -catenin signaling. Moreover the data suggest that Wnt1 type ligand mediated signaling has a dominant role in adult bone mass regulation over Wnt3a type ligand mediated signaling.

1 Ettenberg et al. PNAS 107(35)

Disclosures: Ming-Kang Chang, Novartis, 3
This study received funding from: Novartis

1040

Expression of Notch in Osteocytes Prevents Disuse Osteoporosis. Ernesto Canalis*¹, Kristen Parker², Jian Feng³, Stefano Zanotti¹. ¹St. Francis Hospital & Medical Center, USA, ²Saint Francis Hospital & Medical Center, USA, ³Texas A&M Health Science Center, USA

Notch are transmembrane receptors that play a role in cell fate decisions, and regulate skeletal development and osteoblast differentiation. In osteoblasts, Notch inhibits cell differentiation and function, and causes osteopenia. However, in osteocytes the function of Notch is unknown. Since osteocytes are mechanosensing cells, we first determined whether Notch is responsive to mechanical signals in these cells. Fluid flow shear stress (2-16 dynes/cm²/2h) induced the expression of the Notch target genes hairy enhancer of split (Hes)1 and Hes related with YRPW motif (Hey)1 and 2 in MLOY4 osteocytes, confirming activation of Notch signaling by mechanical stress. To establish the function of Notch in osteocytes, *Rosa^{Notch}* mice, where the Notch intracellular domain (NICD) is expressed under the control of the *Rosa* promoter following the excision of an intervening *loxP*-flanked STOP cassette, were crossed with transgenics expressing Cre under the control of the *Dentin matrix protein 1* (*Dmp1*) promoter. *Dmp1-Cre;Rosa^{Notch}* mice exhibited a marked increase in cancellous bone volume, and suppressed bone resorption due to the induction of osteoprotegerin without an inhibition of receptor activator of nuclear factor κ B ligand (RANK-L). Since the unloading of the skeleton is characterized by decreased bone formation and increased resorption leading to bone loss, we postulated that Notch expression in mechanosensing osteocytes may preserve bone mass during unloading. To test this hypothesis, the quadriceps and triceps surae muscles of *Dmp1-Cre;Rosa^{Notch}* and control mice were paralyzed with botulinum toxin A and sacrificed after 3 weeks. Microarchitectural analysis revealed a decrease in trabecular bone volume/tissue volume from (means \pm SEM; n, 5-6) $5.6 \pm 0.4\%$ in control limbs to $1.6 \pm 0.2\%$ in botulinum paralyzed limbs of control mice. In contrast, the bone volume of *Dmp1-Cre;Rosa^{Notch}* mice was increased to $15.7 \pm 2.6\%$ in control limbs and did not change in paralyzed limbs, where it was $15.7 \pm 2.7\%$. Histomorphometry revealed that osteoclast surface was increased in paralyzed limbs of control mice, but not of *Dmp1-Cre;Rosa^{Notch}*. The results indicate that Notch is activated in osteocytes by mechanical stress and can prevent bone loss in an experimental model of disuse osteoporosis, and as a consequence protect the skeleton during unloading. Modulation of Notch in osteocytes may serve as a therapeutic approach in disuse osteoporosis.

Disclosures: Ernesto Canalis, None.

1041

RANKL Produced by Osteocytes Contributes to the Bone Loss Induced by Hyperparathyroidism. Jinhu Xiong*, Melda Onal, Stavros Manolagas, Charles O'Brien. Central Arkansas VA Healthcare System, Univ of Arkansas for Medical Sciences, USA

Parathyroid hormone (PTH) regulates calcium homeostasis in part by stimulating the rate of bone remodeling; and it stimulates bone resorption in part by stimulating production of RANKL. Recently, osteocytes were shown to be a major source of RANKL for osteoclastogenesis in remodeling bone under normal conditions or for the loss of bone induced by unloading. However, it remains unclear whether osteocytes supply the RANKL responsible for the increase bone resorption during hyperparathyroidism. To address this question, mice lacking the RANKL gene specifically in osteocytes were placed on a calcium deficient diet which induces secondary hyperparathyroidism. Mice lacking RANKL in osteocytes, hereafter referred to as conditional knockout (KO) mice, were generated by crossing mice harboring a RANKL conditional allele with DMP1-Cre transgenic mice, which express the Cre recombinase in osteocytes. Five-month-old conditional KO mice and their control littermates were fed a calcium-deficient diet or a control diet for 4 weeks. Dietary calcium deficiency induced an increase in circulating PTH in both control and conditional KO mice; however, the increase in PTH was significantly greater in the conditional KO mice. As expected, dietary calcium deficiency induced bone loss in control mice as measured by DEXA. This bone loss was significantly attenuated in mice lacking RANKL in osteocytes. Micro-CT analysis revealed that there was a decrease in femoral cortical thickness and an increase in cortical porosity in control mice fed the calcium deficient diet compared with mice fed the normal diet, but both of these changes were completely abrogated in the conditional KO mice. Consistent with these findings, dietary calcium deficiency induced a significant increase in

RANKL expression in the bones of control mice but not in conditional KO mice. Moreover, osteoclast-specific gene expression was significantly elevated in the bone of control mice fed the calcium-deficient diet but this did not occur in the conditional KO mice, suggesting that dietary calcium deficiency induced a significant increase of bone resorption in control mice but not in the conditional KO mice. Taken together, these results demonstrate that RANKL produced by osteocytes is essential for the increase in bone resorption and the bone loss caused by hyperparathyroidism, thereby demonstrating that osteocytes are an important target cell for hormonal control of mineral homeostasis.

Disclosures: Jinhu Xiong, None.

1042

Direct Regulation of the RANKL Gene by PTH in Osteocytes Is Required to Stimulate Bone Resorption in the Adult Skeleton. Abdullah Ben-Awadh*, Naomie Olivos, Nicoletta Bivi, Matthew Allen, Lilian Plotkin, Xiaolin Tu, Teresita Bellido. Indiana University School of Medicine, USA

PTH increases osteoclasts by upregulating RANKL in osteoblastic cells, but the precise differentiation stage of the PTH target cell remains undefined. Recent findings demonstrate that PTH regulates gene expression in osteocytes and that these cells are an important source of RANKL. We therefore investigated whether direct regulation of the RANKL gene by PTH in osteocytes is required to stimulate bone resorption. To address this question, we examined resorption and RANKL expression in transgenic mice in which PTH receptor signaling is activated only in osteocytes (DMP1-caPTHRI) crossed with mice lacking the distal control region regulated by PTH in the RANKL gene (DCR^{-/-}). Longitudinal analysis of circulating CTX in male mice showed elevated resorption in growing mice of all genotypes that progressively decreased to plateau at 3-5 month of age. Resorption was significantly higher (~100%) in DMP1-caPTHRI mice and non-significantly lower (15-30%) in DCR^{-/-} mice, versus wild type littermates (wt) across all ages. CTX in compound DMP1-caPTHRI;DCR^{-/-} mice was similar to DMP1-caPTHRI mice at 1 and 2 months of age, but deletion of the DCR gradually corrected the increased resorption exhibited by DMP1-caPTHRI mice. By 3 months of age, CTX in compound mice was significantly lower compared to DMP1-caPTHRI mice (50% higher than wt), and by 5 months, it was undistinguishable from wt mice. Micro-CT analysis revealed lower material density in the distal femur of DMP1-caPTHRI mice, indicative of high remodeling, and this effect was partially corrected in compound mice. Consistent with previous results, the increased resorption exhibited by DMP1-caPTHRI mice was accompanied by elevated RANKL mRNA in bone at 1 and 5 months of age. RANKL closely matched resorption in DMP1-caPTHRI;DCR^{-/-} compound mice. Thus, RANKL levels were similar to DMP1-caPTHRI mice at 1 month and reduced to wt levels at 5 month of age. The same pattern of expression was observed for M-CSF, a survival factor for osteoclast progenitors and mature osteoclasts previously shown to be upregulated by RANKL *in vitro*. We conclude that resorption induced by PTH receptor signaling requires direct regulation of the RANKL gene in osteocytes. Moreover, whereas DCR-independent mechanisms operate in the growing skeleton, DCR-dependent, cAMP/PKA/CREB-activated mechanisms mediate resorption induced by PTH receptor signaling in the adult skeleton.

Disclosures: Abdullah Ben-Awadh, None.

1043

Gna13 as a Novel Negative Regulator of Osteoclast Differentiation and Activation Inhibits RANKL/AKT/NFATc1 Signaling. Mengrui Wu*¹, Wei Chen², Yi-Ping Li². ¹The University of Alabama at Birmingham, USA, ²University of Alabama at Birmingham, USA

Osteoclasts are the principle bone-resorbing cells, with its activity delicately modulated to maintain bone homeostasis. Osteoclast aberration results in diseases like osteoporosis and rheumatoid arthritis. Positive regulation of osteoclast by RANKL-axis signaling has been extensively studied during past decades, while negative regulation remains unclear. To explore the potential negative regulators of osteoclast differentiation and activation, we used microarray assay, RNAi knockdown and *in vitro* function analysis approaches, and identified Gna13 as the candidate molecule. To confirm the *in vitro* results, we generated mice specifically lacking Gna13 in the monocyte and osteoclast (CKO) by crossing Gna13^{fl/fl} mice with Lyz2-cre mice and Cathepsin K-Cre mice. The femur from a 2-month old CKO and wildtype (WT) mice were analyzed by X-ray, μ -CT, and histology (n \geq 4 per group). CKO mice demonstrated severe osteoporosis phenotype. TRAP staining of the femur sections showed that the osteoclast number in the CKO mice was increased two folds compared to those found in the WT mice. To study the bone resorption difference, CKO RANKL induced bone marrow cells were cultured on bone slides. CKO cells displayed increased osteoclast formation, larger cell size, larger actin ring on bone slides, and increased Cathepsin K secretion, compared with those of the WT cells. Bone resorption pit assay and medium CTX-I Elisa showed that bone resorption by CKO osteoclasts was increased (3-fold, p \leq 0.05) when compared with that of the WT osteoclasts. To study the regulatory mechanism of Gna13, the activity of BTK, ERK, p-38, JNK and AKT in response to RANKL was examined in the CKO and WT osteoclasts. AKT phosphorylation was largely increased in both pre-osteoclasts and osteoclasts in the absence of Gna13. Both mRNA and protein levels of NFATc1 were increased in CKO osteoclasts (2.5-fold, p \leq 0.05). Meanwhile, much more NFATc1 was observed in the nuclei of CKO osteoclasts. Interestingly, Src (upstream of PI3K/

AKT) inhibitor, pp2, rescued the CKO osteoclast aberration, indicating that Src may be involved in the Gna13 regulation pathway. In conclusion, our study demonstrated that Gna13, as a novel regulator of bone resorption, negatively regulates osteoclast differentiation and activation by inhibiting RANKL/AKT/NFATc1 signaling. Our results indicate that Gna13 may serve as a novel therapeutic approach for osteoporosis and other Osteoclast aberration related diseases.

Disclosures: Mengrui Wu, None.

1044

VPS35 Haploinsufficiency Results in an Osteoporotic Pathology Due to an Impaired RANK Trafficking and Increased RANKL-induced Hyper-resorptive Osteoclast Formation. Wen-Cheng Xiong^{*1}, Wen-Fang Xia², Fulei Tang², Xu Feng³, Lin Mei². ¹Medical College of Georgia, USA, ²Georgia Health Sciences University, USA, ³University of Alabama at Birmingham, USA

Bone remodeling, a dynamic process coordinated by osteoblastic bone formation and osteoclastic bone resorption, is essential for maintenance of healthy bone mass and normal bone structure. It is regulated by multiple factors, including PTH (parathyroid hormone) or PTHrP (PTH related peptide), Wnt, and RANKL (receptor activator of nuclear factor- κ B ligand). Retromer, a complex consisting of a VPS35-VPS29-VPS26 trimer and a sortin nexin (SNX) dimer, mediates selective endosome-to-Golgi retrieval of numerous membrane receptors, including wtless (a "receptor" for Wnt secretion) and PTH1R (type I receptor for PTH/PTHrP). Whereas these retromer cargos are important modulators of bone remodeling, retromer's function in this event remains largely unknown. Here we provide evidence for VPS35, a major component of retromer, in regulating osteoclastogenesis and bone remodeling. Hemizygous deletion of Vps35 in mouse led to osteoporotic-like phenotype, including decreased trabecular and cortical bone volumes, reduced trabecular thickness and density, and enlarged bone marrow cavity in long bones. These deficits appeared to be largely due to the increase of hyper-resorptive osteoclastogenesis in the mutant mice. Further mechanistic studies demonstrate that VPS35 is highly expressed in osteoclasts and its progenitor cells, in addition to osteoblasts. VPS35 expression in osteoclastic progenitor cells (e.g., macrophages) is necessary for RANKL induced retrograde trafficking of RANK and RANK inactivation. Loss of VPS35 function in macrophages results in an enhanced RANKL sensitivity and sustained RANKL-driven signaling. These results thus reveal an unrecognized function of VPS35/retromer in controlling RANK receptor trafficking and signaling in time and space and demonstrate an important role for VPS35/retromer in preventing hyper-resorptive osteoclast formation and osteoporotic pathology.

Disclosures: Wen-Cheng Xiong, None.

1045

The SH3BP2 Cherubism Mutation Promotes TNF Induction of Osteoclastogenesis Independent of RANKL. Tomoyuki Mukai^{*1}, Shu Ishida², Teruhito Yoshitaka³, Yasuyoshi Ueki⁴. ¹University of Missouri - Kansas City, USA, ²University Missouri-Kansas City School of Dentistry, USA, ³University Missouri-Kansas City School of Dentistry, USA, ⁴University of Missouri-Kansas City School of Dentistry, USA

TNF is an inflammatory cytokine known to play a key role in osteoclastogenesis. The precise mechanisms for TNF-induced osteoclast differentiation are not fully understood. While TNF has been reported to directly induce osteoclast differentiation, this is controversial as RANKL has been proposed to be responsible for all osteoclast formation. Gain-of-function mutations in SH3BP2, an adapter protein, are responsible for the craniofacial disorder, cherubism. In the mouse model of cherubism, elevated levels of systemic TNF and RANKL-induced osteoclastogenesis were observed compared to wild type. Since depletion of TNF in homozygous cherubism mice (KI/KI) corrects bone loss to control levels, we hypothesized that SH3BP2 plays a role in TNF direct induction of osteoclastogenesis. To test this hypothesis, primary bone marrow macrophages (BMMs) isolated from wild-type and SH3BP2 heterozygous mutant cherubism mice (KI/+) were cultured with M-CSF (25ng/ml) and TNF (100ng/ml) in the absence of RANKL for 4 days. We discovered that KI/+ BMMs form greater numbers of TRAP-positive multinucleated cells compared to wild-type BMMs (1143 \pm 58 vs 42 \pm 20 cells/well) and these TNF-induced osteoclasts resorb mineralized matrix. OPG-Fc failed to inhibit osteoclastogenesis, suggesting that TNF induces osteoclastogenesis independently of RANKL in KI/+ BMMs. Both type I and II TNF receptors (TNFRs) were required, as neutralizing antibodies against either receptor suppressed TNF-induced osteoclastogenesis. Specific inhibitors for Syk and Src also suppressed the osteoclastogenesis. Next we cultured NFATc1-deficient KI/+ BMMs with TNF and found that the NFATc1-deficient cells failed to differentiate into osteoclasts. Finally, to confirm the *in vivo* effect of the SH3BP2 mutation on TNF-induced osteoclastogenesis, recombinant TNF (1.5mg/mouse) was subcutaneously injected onto calvarial bones for 5 days in KI/+ mice, which unlike KI/KI mice, do not develop elevated systemic TNF. Histomorphometric analysis showed that osteoclast numbers per bone perimeter and eroded surface per bone surface are increased in TNF-treated KI/+ mice compared to TNF-treated wild-type mice (17.6 \pm 11.2 vs 6.5 \pm 4.6, 21.6 \pm 12.0 vs 9.2 \pm 9.4 %, respectively). In conclusion, the gain-of-function mutation in SH3BP2 enhanced TNF-induced osteoclastogenesis by mechanisms dependent on Syk, Src, and

NFATc1, and independent of RANKL. These data suggest that SH3BP2 is a novel regulator of inflammatory osteoclastogenesis.

Disclosures: Tomoyuki Mukai, None.

1046

Canonical and Non-Canonical BMP signaling Pathways Regulate Osteoclastogenesis. Aaron Broege^{*}, Lan Pham, Ann Emery, Melissa Stemig, Michael O'Connor, Anna Petrvk, Eric Jensen, Kim Mansky, Raj Gopalakrishnan. University of Minnesota, USA

We have previously shown that BMP2 acts directly on osteoclastic cells to enhance their differentiation. In the current study we further tested the requirement of BMP signaling for osteoclastogenesis by (a) characterizing the skeletal phenotype of mice carrying targeted deletion of *BMPRII* in osteoclasts using *LysM-Cre (BMPRII;LysM-Cre)* and (b) investigating the role of canonical and non-canonical BMP pathways during osteoclast differentiation. μ CT analysis of *BMPRII;LysM-Cre* showed increased trabecular bone volume fraction at 3 and 6 months compared to WT. Osteoclasts from *BMPRII;LysM-Cre* bone marrow monocyte (BMM) cultures were smaller than controls, and showed reduced expression of key genes involved in osteoclastogenesis including NFATc1, cathepsin K, OC-STAMP and Acp5. Investigation of the status of BMP signaling showed that phospho-Smad1/5/8 (P-SMAD1/5/8) levels were similar in osteoclasts from knockouts and WT controls. On the other hand, phospho-p38 (P-p38) levels were reduced in knockout osteoclasts compared to WT controls. These results suggest that reduced osteoclastogenesis and increased bone phenotypes in *BMPRII;LysM-Cre* are due to a reduced signaling through non-canonical BMP pathways. To further understand the mechanism of BMPs' regulation of osteoclastogenesis, we investigated both canonical and non-canonical BMP pathways at various time points in BMM cultures. In control cultures stimulated with RANKL, we detected P-p38 on day 1 and day 2 with a gradual decrease to undetectable levels at later time points, while P-SMAD 1/5/8 was not detected until osteoclasts began to fuse (day 3) and remained at detectable levels through day 5. Exposure of WT BMMs to Noggin on day 1 of the differentiation was sufficient to completely block osteoclast differentiation, indicating an early requirement for BMP signaling. At these early timepoints, treatment with exogenous BMP2 increased P-p38, whereas at late times P-SMAD1/5/8 was stimulated. Treatment with dorsomorphin or LDN193189, which preferentially inhibit the canonical pathway, inhibited osteoclast formation only when present on day 3 and later, suggesting that canonical BMP signaling is required for osteoclast fusion. Together, these results show that BMPs are required for osteoclastogenesis *in vivo* and that BMPs regulate osteoclast formation through distinct pathways at different phases of the differentiation process.

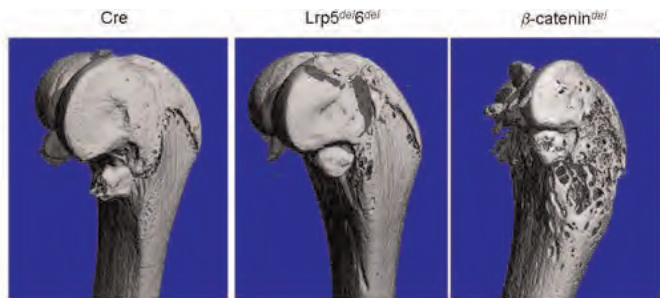
Disclosures: Aaron Broege, None.

1047

Deletion of Wnt Receptors Lrp5 and Lrp6 or β -catenin in Late Osteoclast Precursors Differentially Suppress Osteoclast Differentiation and Bone Metabolism. Ming Ruan¹, Larry Pederson¹, Christine Hachfeld¹, Michael Thomson², Y.S. Prakash³, Alan Howe⁴, Bart Williams⁵, Rachel Davey⁶, Sundeep Khosla⁷, Jennifer Westendorf⁸, Merry Jo Oursler^{*8}. ¹Endocrine Research Unit, Mayo Clinic, USA, ²Anesthesiology, Mayo Clinic, USA, ³Anesthesiology & Physiology, Mayo Clinic, USA, ⁴Department of Pharmacology, University of Vermont College of Medicine, USA, ⁵Van Andel Research Institute, USA, ⁶University of Melbourne, Australia, ⁷College of Medicine, Mayo Clinic, USA, ⁸Mayo Clinic, USA

The positive effects of canonical Wnt signaling on osteoblasts and bone formation are well known and have produced promising new anabolic therapies. However, little consideration has been given to other possible Wnt responding cells in the bone environment. It was recently shown that β -catenin suppression in osteoclasts causes osteopenia and increases osteoclast differentiation. Because β -catenin is involved in many Wnt-independent cellular processes this suggests but does not confirm a direct role for Wnts in osteoclast differentiation. In this study, we examined the bone microarchitecture of mice lacking the Wnt receptors, Lrp5 and Lrp6 (*Lrp5/6^{del}* mice) or β -catenin (β -cat^{del} mice) in cathepsin K-positive osteoclast precursors using *Cre/Lox* approaches. Trabecular bone density was reduced and osteoclast numbers were elevated in both models. One striking difference was the presence of large areas of cortical bone loss at the metaphyses of the β -cat^{del} bones, but not the *Lrp5/6^{del}* bones (see figure below). Histomorphometric analyses revealed a high turnover phenotype including increased bone formation in the β -cat^{del} bones, whereas the *Lrp5/6^{del}* bones exhibited a more muted phenotype and no increased bone formation compared to the β -cat^{del} bones. Deletion of either Lrp5 and Lrp6, or β -catenin increased osteoclast differentiation *in vitro* whereas Wnt3a suppressed differentiation in wildtype marrow cultures *in vitro*. Investigation of the mechanisms revealed that Wnt3a suppresses osteoclast differentiation by inducing the phosphorylation and inactivation of the crucial transcription factor NFATc1. Wnt3a also suppressed RANKL and M-CSF induced NFATc1 nuclear accumulation. Wnt3a rapidly activated Ca²⁺ influx through L type channels and activation of the AC/cAMP/PKA pathway in wildtype and β -cat^{del} precursors, but not in the *Lrp5/6^{del}* cells. Gene expression studies revealed that *Lrp5/6^{del}* precursors express high levels of the Wnt signaling inhibitors Dkk1,

Dkk2, and Sost compared to either control or β -cat^{del} precursors. Wnt3a also suppressed expression of these genes in wildtype osteoclast precursors. These data indicate that both canonical and non-canonical Wnt signaling suppress osteoclast differentiation whereas noncanonical signaling enhances coupling between bone resorption and bone formation.



Disclosures: Merry Jo Oursler, None.

1048

The Calcium-activated Potassium Channel SK4 (KCNN4/ IKCa1/KCa3.1) Modulates Bone Homeostasis via Osteoclasts. Heeseog Kang^{*}, Xiaojing Xu¹, Qing Zhang¹, Michael Kim¹, Jodi Carlson Scholz¹, Aruna Behera², Donald Souza², Jie Zheng², James E Melvin³, Gerald Nabozny², Jun Li², Agnès Vignery¹. ¹Yale University, USA, ²Boehringer Ingelheim, USA, ³University of Rochester, USA

The formation of multinucleate osteoclasts requires the fusion of macrophages, which is an essential step for efficient resorption of bone as fusion failure leads to accumulation of brittle bone such as in osteopetrosis. Since macrophage fusion is a rare event, our hypothesis has been that the fusion machinery is transiently induced at the onset of fusion. To identify the molecular players of the macrophage fusion machinery, we previously subjected fusing macrophages from rat lungs and human monocytes to genome-wide oligonucleotide microarray analysis. We discovered the induced expression of the calcium-activated potassium channel SK4 (KCNN4/IKCa1/KCa3.1). The role of SK4 is to set the cell membrane potential at negative values so as to aid in the electrochemical transport of other ions such as Cl⁻ and Ca⁺⁺. By mediating the efflux of K⁺, SK4 helps maintain the cell membrane potential to allow sustained Ca⁺⁺ influx into cells. We observed that the SK4 inhibitors TRAM-34 and ICAGEN-17043 inhibit the fusion of human monocyte- and mouse bone marrow-derived macrophages in a dose-dependent manner. Using mice null in SK4, we found that SK4-deficient bone marrow-derived macrophages show a delay in fusion that is RANKL dose-, and time-dependent. To ask whether calcium plays a role in signaling downstream of SK4, we subjected fusing bone marrow macrophages to real time PCR, western blot analysis and immunofluorescence. We observed a decrease in NFAT2 protein expression and translocation to the nucleus in SK4 null osteoclasts. Using fura-2 to image intracellular calcium, osteoclasts deficient in SK4 demonstrated a decrease in the amplitude of calcium oscillations. SK4-null macrophages also showed a decrease in Akt (ser473) phosphorylation in response to activation by RANKL, and by LPS. We then compared the bones from SK4 null mice, male and female, to wild types. Mice deficient in SK4 had a high bone density (pQCT, microCT) when compared with wild type littermates, which was associated with a decrease in osteoclast number (histomorphometry). Finally, we observed that SK4 null mice were partially protected from LPS-induced calvarial bone resorption, and from inflammation in response to antibody-induced arthritis. Together, our data strongly suggest that the calcium-activated K channel SK4 plays a central role in the formation and activation of osteoclasts and participates in the physiological and inflammation-induced regulation of bone mass.

Disclosures: Heeseog Kang, None.

This study received funding from: *Boehringer Ingelheim Pharmaceutical, Inc.*

1049

The Role of Osteal Macrophages in Anabolic Actions of PTH in Bone. Sun Wook Cho^{*}, Fabiana Soki², Amy Koh³, Matt Eber³, Pavam Entezam³, Laurie McCauley². ¹Seoul National University Hospital, South Korea, ²University of Michigan School of dentistry, USA, ³University of Michigan, USA

Bone marrow contains a population of resident macrophages termed osteomacs, which play a role in bone modeling, repair and hematopoietic stem cell niche maintenance. The purpose of this study was to determine the role of osteomacs in anabolic actions of PTH in bone. The macrophage fas-induced apoptosis (MAFIA) mouse model was utilized where the c-fms promoter activated by the synthetic dimerizer (AP20187) leads to Fas-mediated apoptosis of myeloid cells. AP20187 (AP) (10mg/kg) or vehicle was administered for 3d for initial macrophage depletion then every third day (1mg/kg) for 6wks to 16-22wk MAFIA mice, and intermittent PTH (50 mg/kg/d) was administered daily starting 4d after the initial AP dose until

ethanasia. AP-treated mice had ~80% depletion of macrophages (c-fms⁺F4/80⁺CD11b⁺Gr1⁺ or CD68⁺ via flow cytometric analysis) compared to vehicle treated mice. In bone, both trabecular and cortical bone volume and thickness were significantly reduced in AP-treated versus vehicle treated mice. PTH increased trabecular bone volume, number and thickness in vehicle-treated mice which was significantly attenuated in AP-treated mice. Consistently, PTH increased serum PINP and TRAP5b in vehicle but not AP-treated mice. To further investigate the function of late differentiated macrophages in PTH anabolism, clodronate-liposomes which induce apoptosis of phagocytic macrophages were utilized. Sixteen week old male wild-type C57Bl6 mice were treated with clodronate or PBS-loaded liposomes for 6 weeks, and intermittent PTH or vehicle control was administered from d4 until euthanasia resulting in 4 treatment groups. F4/80⁺CD11b⁺Gr1⁺ cells were significantly reduced (~50%) but CD68⁺ cells were increased (~15%) in the clodronate liposome groups. Increased trabecular bone volume and trabecular numbers were found in clodronate liposome-treated mice vs. PBS liposome mice. Intermittent PTH treatment to clodronate-treated mice resulted in prominent increases in trabecular bone mass, surpassing the PTH anabolic action observed in vehicle-treated mice. Taken together, depletion of c-fms⁺ myeloid-lineage cells resulted in osteopenic phenotypes with reduced effects of PTH anabolic actions in bone, whereas depletion of late-differentiated macrophages resulted in increased bone mass and anabolic PTH actions. These data suggest anabolic actions of PTH are associated with specific macrophage populations in bone.

Disclosures: Sun Wook Cho, None.

1050

Impaired Anabolic Action of PTH on Bone Formation in Fgf2 Knockout Mice is mediated by Attenuated Wnt Signaling. Yurong Fei^{*}, Liping Xiao², Marja Marie Hurley³. ¹New York University College of Dentistry, USA, ²University of Connecticut Health Center, USA, ³University of Connecticut Health Center School of Medicine, USA

Parathyroid hormone (PTH) is currently the only anabolic agent for treatment of osteoporosis in the U.S. However, the detailed mechanisms of its action are not fully defined. We previously showed that the anabolic bone effects of PTH require fibroblast growth factor 2 (FGF2). PTH treatment increases serum FGF2 in osteoporotic patients and PTH induces FGF2 and FGF receptor mRNA expression in osteoblasts. However, the anabolic effect of PTH on bone is impaired in *Fgf2*^{-/-} mice. Intermittent FGF2 treatment promotes osteoblast differentiation and bone formation *in vitro* and *in vivo*. However, bone formation is significantly reduced in *Fgf2*^{-/-} mice. PTH anabolic response also requires Wnt signaling and we recently reported that FGF2 modulates Wnt signaling in osteoblasts. We hypothesize that the impaired bone response to PTH in *Fgf2*^{-/-} mice is partially due to attenuated Wnt signaling. Three month-old *Fgf2*^{+/+} and *Fgf2*^{-/-} littermate male mice were treated with human rPTH (1-34) 20µg/kg body weight for 8 hours (n=3). Total RNA was extracted from tibia and protein was from femur. The data presented are pooled from two independent experiments. Ligand Wnt10b has been demonstrated to promote bone formation. We observed that PTH treatment markedly increased expression of Wnt10b mRNA and protein in *Fgf2*^{+/+} mice but not in *Fgf2*^{-/-} mice. Wnt antagonist SOST mRNA expression was significantly higher in *Fgf2*^{-/-} group, which may contribute to reduced bone formation. However, PTH treatment decreased SOST expression in *Fgf2*^{-/-} mice significantly. DKK2 is critical for osteoblast mineralization. PTH treatment significantly increased DKK2 mRNA in *Fgf2*^{+/+} mice but reduced DKK2 expression significantly in *Fgf2*^{-/-} mice. For Wnt receptor, we observed that PTH treatment significantly increased Lrp6 expression in *Fgf2*^{+/+} but not in *Fgf2*^{-/-} mice. β -catenin, an essential factor in Wnt signaling, is a positive regulator of bone formation. PTH treatment increased β -catenin mRNA expression significantly in *Fgf2*^{+/+} but not in *Fgf2*^{-/-} mice. Therefore, PTH treatment increased Wnt signaling in *Fgf2*^{+/+} mice, which is important for bone formation. However, attenuated Wnt signaling was observed in *Fgf2*^{-/-} mice, which may contribute to the impaired bone response of PTH. These data suggest that the impaired bone anabolic response to PTH in *Fgf2*^{-/-} mice is partially mediated by attenuated Wnt signaling.

Disclosures: Yurong Fei, None.

1051

The Sclerostin-Independent Bone Anabolic Activity of Intermittent PTH Treatment is Mediated by T Cell Produced Wnt10b. Jau-Yi Li^{*}, Jonathan Adams², Ming-Kang Chang³, M. Neale Weitzmann², Michaela Kneissel³, Roberto Pacifici². ¹Emory University, USA, ²Emory University School of Medicine, USA, ³Novartis Institutes for Biomedical Research, Switzerland

Blunted production of the Wnt inhibitor sclerostin (Scl) accounts for part of the bone anabolic activity of intermittent PTH (iPTH) treatment. However Scl-independent mechanisms of action of iPTH remain to be determined. iPTH promotes bone anabolism by increasing T cell production of the Wnt ligand Wnt10b. We thus investigated the contribution of T cell produced Wnt10b to the Scl-independent effects of iPTH. To avoid the confounding effect of the altered basal bone mass of Scl null mice have, we used an anti Scl mAb to neutralize Scl *in vivo*. 6 wk old WT mice, T cell deficient TCRb^{-/-} mice, TCRb^{-/-} mice previously reconstituted with WT T cells, and TCRb^{-/-} mice reconstituted with Wnt10b^{-/-} T cells were injected for 4 weeks with iPTH alone (hPTH1-34 at 80 µg/kg/day SC), Scl-ab alone (50 mg/kg once weekly IV),

or iPTH + Scl-Ab. PTH, vehicle and an isotype matched irrelevant Ab (Irr.Ig) were used as controls. Spine mCT measurements in WT mice revealed that bone volume (BV/TV) was increased 23.6 % by iPTH alone, 59.3 % by Scl-Ab alone, and 77.5 % by treatment with iPTH plus Scl-Ab. Combined treatment was more efficacious than Scl-Ab alone ($\Delta = 18.2\%$, $p < 0.05$), confirming that part of the anabolic activity of iPTH is Scl-independent. Identical results were obtained in TCRb^{-/-} mice reconstituted with WT T cells. By contrast, iPTH did not increase BV/TV nor potentiated the effect of Scl-Ab in TCRb^{-/-} mice and TCRb^{-/-} mice with Wnt10bKO T cells. Scl Ab alone had equal activity in all groups of mice. These findings indicate that T cell production of Wnt10 accounts for the Scl-independent anabolic effects of iPTH. iPTH alone increased serum levels of the bone formation marker PINP, and potentiated the increase in PINP induced by Scl Ab in T cell replete mice. By contrast, iPTH had no effects on serum bone formation markers in TCRb^{-/-} mice and TCRb^{-/-} mice with Wnt10bKO T cells. Moreover, iPTH and iPTH + Scl Ab increased ex vivo osteoblast (OB) differentiation and life span in T cell replete mice, but not in mice lacking T cells or T cell production of Wnt10b. By contrast, in vivo Scl-Ab treatment alone had no effects on OBs ex vivo, thus suggesting that iPTH regulates some aspects of OB differentiation and life span through a Wnt10b-dependent, Scl-independent mechanism. In summary, we show here that the Scl-independent activity of iPTH is completely accounted for by T cell produced Wnt10b.

Disclosures: Jau-Yi Li, None.

1052

PTH Induces Differentiation of Mesenchymal Stem Cells by Enhancing BMP Signaling. Bing Yu^{*1}, Xiaoli Zhao², Chaozhe Yang³, Janet Crane⁴, William Lu⁵, Mei Wan⁶, Xu Cao⁴. ¹Johns Hopkins School of Medicine, USA, ²The University of Hongkong, Hong Kong, ³The University of Alabama at Birmingham, USA, ⁴Johns Hopkins University, USA, ⁵The University of Hong Kong, Hong Kong, ⁶Johns Hopkins University School of Medicine, USA

Parathyroid hormone (PTH) stimulates bone remodeling and induces differentiation of bone marrow mesenchymal stem cells (MSCs) by orchestrating activities of local factors such as bone morphogenetic proteins (BMPs). The activity and specificity of different BMP ligands are controlled by various extracellular antagonists that prevent the binding of BMPs to their receptors. Low-density lipoprotein receptor-related protein 6 (LRP6) has been shown to interact with the extracellular signaling pathways of both PTH and BMP by forming a complex with PTH1R or sharing common antagonists with BMPs. Here we show that PTH induces the differentiation of MSCs into osteoblastic lineage through enhancement of BMP signaling by modifying the extracellular antagonist network assembled by LRP6. We found that single PTH injection increased the level of phosphorylated Smad1 (p-Smad1) in osteoblastic-like cells on the bone surface of 8-wk old mice, and the p-Smad1+ MSCs were elevated from 12.1% to 81.2% at 30 min after PTH injection. Importantly, PTH increased Smad1 phosphorylation and MSCs differentiation, antagonizing inhibitory effect of noggin, an BMP extracellular antagonist. Further, PTH enhanced pSmad1 was abolished in PTH1R^{-/-} OC59 cells, indicating that this effect is PTH1R-dependent. The results suggest that PTH enhances BMP signaling through regulation of extracellular antagonists.

We then examined whether PTH-induced PTH1R endocytosis plays a role in its effect on enhancing BMP signaling in MSCs. PTH-elevated phosphorylation of Smad1 was inhibited by blocking PTH1R endocytosis with β -arrestin knockdown or endocytosis inhibitor treatment. We also found that PTH enhances the phosphorylation of Smad1 through stimulating the endocytosis of the LRP6/PTH1R complex. Deletion of LRP6 with Ade-Cre in *lrp6* flox/flox MSCs elevated Smad1 phosphorylation to the level seen with PTH treatment in the presence of LRP6. However, in the LRP6-deficient cells, PTH did not further enhance the phosphorylation of Smad1, indicating that the PTH effect is LRP6-dependent. In addition, PTH stimulated 125I-BMP2 cell surface binding in a dose- and time-dependent manner by inducing the internalization of LRP6/PTH1R complex. Taken together, our results suggest that PTH enhances BMP signaling by inducing the endocytosis of LRP6-organized extracellular network of BMP antagonists and subsequent enhanced binding of BMPs to their receptors, leading to enhanced osteoblast differentiation of MSCs.

Disclosures: Bing Yu, None.

1053

The p27 Pathway Modulates The Regulation of Skeletal Growth and Osteoblastic Bone Formation by Parathyroid Hormone-Related Peptide. Jing Zhang^{*1}, Min Zhu², David Goltzman³, Andrew Karaplis³, Dengshun Miao⁴. ¹Nanjing Medical University, China, ²Nanjing Medical University, China, ³McGill University, Canada, ⁴Nanjing Medical University, Peoples Republic of China

We previously demonstrated that parathyroid hormone-related peptide (PTHrP) 1-84 knockin (*Pthrp* KI) mice, in which the nuclear localization sequence and the C-terminal region of PTHrP are deleted, displayed skeletal growth retardation and defective osteoblastic bone formation, however, the mechanism is unclear. Microarray analyses of differential gene expression profiles were performed in long bone extracts from *Pthrp* KI mice and their WT littermates. Results revealed that the expression

levels of p27, p57 and p53 were up-regulated 8.3, 6.5 and 5.4 fold, respectively, whereas the expression levels of cyclin E, cyclin D1, CDK2, Runx2, Osterix and ALP were down-regulated 5.4, 5.4, 5.3, 5.1, 5.8 and 5.2 fold, respectively, in *Pthrp* KI mice relative to WT littermates. To determine whether the cell cycle inhibitor p27^{Kip1} was involved in the regulation by PTHrP of skeletal growth and development *in vivo*, we generated compound mutant mice which are homozygous for both p27 deletion and the *Pthrp* KI mutation (*p27^{-/-}Pthrp* KI), and compared *p27^{-/-}Pthrp* KI mice with *p27^{-/-}Pthrp* KI, and WT littermates. Phenotypes were analyzed by histopathological, immunohistochemical, cellular and molecular approaches. Deletion of p27^{Kip1} in *Pthrp* KI mice resulted in a longer lifespan, increased body weight and improvement in skeletal growth, although *Pthrp* KI mice were not normalized. At 2 weeks of age, skeletal growth parameters, including length of long bones, size of epiphyses and PCNA positive chondrocytes, BMD and BMC, trabecular bone volume, osteoblast numbers, and ALP, type I collagen and osteocalcin positive bone areas were increased in *p27^{-/-}* mice, and reduced in both *Pthrp* KI and *p27^{-/-}Pthrp* KI mice compared to WT mice; however these parameters were increased in *p27^{-/-}Pthrp* KI mice compared to *Pthrp* KI mice. As well, the mRNA expression levels of Runx2, ALP, and type I collagen and protein expression levels of osteocalcin and PTHR, IGF1 and Bmi-1, and the numbers of total CFU-f and ALP positive CFU-f generated from bone marrow cell cultures, were similarly increased in *p27^{-/-}Pthrp* KI mice compared to *Pthrp* KI mice. Our results demonstrate that deletion of p27^{Kip1} in *Pthrp* KI mice can partially rescue defects in skeletal growth and osteoblastic bone formation by enhancing endochondral bone formation and osteogenesis. These studies therefore indicate that the p27 pathway may function downstream in the action of PTHrP to regulate skeletal growth and development.

Disclosures: Jing Zhang, None.

1054

Bone Loss in Lactating Mice Requires RANKL Signaling. Laleh Ardeshirpour^{*1}, Pamela Dann², Cristina Dumitru², Marina Stolina³, Paul Kostenuik³, John Wysolmerski⁴. ¹Yale University, USA, ²Yale School of Medicine, USA, ³Amgen Inc., USA, ⁴Yale University School of Medicine, USA

Lactation is associated with rapid bone loss suggesting that the maternal skeleton is an important source of calcium for milk production. Previous studies have suggested that bone resorption during lactation is mediated by increased RANKL signaling. To test this concept, we treated 15-week-old, lactating CD-1 mice with saline or recombinant OPG (OPG-Fc; 10mg/kg) every 4th day for the first 12 days post-partum. As expected, OPG-Fc effectively reduced TRACP 5b, osteocalcin and type I procollagen levels. OPG-Fc also completely eliminated bone loss during lactation. In controls, serial DEXA scans revealed a decline in BMD of 20% \pm 0.9 at the spine, 13% \pm 1.4 at the femur and 13% \pm 0.8 for the total body. In contrast, OPG-Fc treatment led to increases in BMD of 10% \pm 1.9 at the spine, 3% \pm 2.4 at the femur and 5% \pm 1.7 for the total body. Similarly, in OPG-Fc-treated mice, micro-CT revealed higher trabecular BV/TV, thickness, number and density, and increased cortical thickness and decreased porosity. Histomorphometry confirmed the higher bone volumes, trabecular thickness and trabecular numbers in OPG-Fc-treated lactating animals compared to controls. Consistent with the turnover markers, OPG-Fc significantly lowered osteoblast numbers and surfaces as well as bone formation rates. However, in contrast to the TRACP 5b data, there were many osteoclasts still present in the OPG-Fc treated bone. These cells appeared larger than normal and were often near but not on bone surfaces. Finally, despite the complete abrogation of bone loss, OPG-Fc-treated mice exhibited no obvious impairment of lactation. Circulating calcium levels were within the normal range although circulating PTH levels were slightly elevated. There was no increase in the levels of circulating 1,25(OH)₂ Vit D in OPG-Fc-treated mice. OPG-Fc also had no effect on litter size or pup growth, demonstrating normal milk production. In contrast, preliminary studies show that the combination of a low calcium (0.01%) diet and OPG-Fc results in a 60% maternal mortality. In conclusion, osteoclastic bone resorption but not osteoclast survival depends on RANKL signaling during lactation. In addition, in the presence of adequate dietary calcium, skeletal calcium mobilization is not essential for normal lactation. Inhibiting RANKL signaling will allow us to better understand the normal interplay between skeletal and dietary sources of calcium during milk production.

Disclosures: Laleh Ardeshirpour, None.

1055

The Risk of Hip Fracture after Initiating Antihypertensive Drugs in the Elderly. Debra Butt^{*1}, Muhammad Mamdani², Peter Austin³, Karen Tu³, Tara Gomes³, Richard Glazier³. ¹University of Toronto, Canada, ²Li Ka Shing Knowledge Institute, St. Michael's Hospital, Canada, ³Institute for Clinical Evaluative Sciences, Canada

Evidence indicates that initiating antihypertensive drugs in the elderly has been associated with an immediate increased risk of falls. However, it is unknown if initiation of antihypertensive drugs (thiazide diuretics, angiotensin II converting-enzyme inhibitors, angiotensin II receptor blockers, calcium channel blockers or beta-adrenergic blockers) is associated with an immediate increased risk of hip fractures. Our study examined the association between the initiation of monotherapy with any

of the five antihypertensive drug classes commonly used for the treatment of hypertension in the elderly and immediate increased risk of hip fracture.

A population-based, self-controlled case series design using healthcare administrative databases was conducted to identify patients initiating an antihypertensive drug from the over 1.6 million elderly residents in Ontario, Canada. A cohort of newly treated hypertensive elderly patients was linked to the occurrence of hip fractures from April 1, 2000 to March 31, 2009 to create exposed cases. The risk period was the first 45 days following antihypertensive therapy initiation with control periods before and after treatment in a 450-day observation period. The outcome measure was the first occurrence for a proximal femoral fracture during the risk period. The analysis determined the relative incidence (incidence rate ratio, IRR), defined as the hip fracture rate in the risk period compared to control periods.

Of the 301 591 newly treated hypertensive community-dwelling elderly, 1 463 hip fractures were identified during the observation period. Hypertensive elderly initiated on an antihypertensive drug had a 43% increased risk of having a hip fracture during the first 45 days following treatment initiation relative to the control periods, IRR 1.43 (95% confidence interval, CI 1.19 to 1.72). The IRR estimates were generally consistent amongst the five different classes of antihypertensive drugs, but only the angiotensin II converting-enzyme inhibitors (IRR 1.53, 95% CI 1.12 to 2.10) and beta-adrenergic blockers (IRR 1.58, 95% CI 1.01 to 2.48) demonstrated statistical significance.

Antihypertensive drugs were associated with an immediate increased hip fracture risk during the initiation of treatment in hypertensive community-dwelling elderly. Precautions should be undertaken to minimize the risk of hip fractures when initiating antihypertensive drugs in the elderly.

Disclosures: Debra Butt, None.

1056

Risk of Hip Fracture Associated with Non-Benzodiazepine Hypnotics in Subgroups of Nursing Home Residents. Sarah Berry^{*1}, Yoojin Lee², Shubing Cai², Vincent Mor², David Dore². ¹Hebrew SeniorLife/Beth Israel Deaconess Medical Center, USA, ²Warren Alpert Medical School of Brown, USA

Purpose: It is important to identify subgroups of nursing home residents that are particularly vulnerable to injurious falls when using hypnotic drugs. We conducted a case-crossover study to estimate the association between non-benzodiazepine hypnotic drugs and risk of hip fracture among a nationwide sample of long-stay nursing home residents, overall and stratified by functional characteristics.

Methods: Participants included 26,618 long stay U.S. nursing home residents aged ≥ 50 years with a hip fracture (7/1/2007-12/31/2008) from a sample of over one million patients in fee-for-service Medicare Parts A & D. Hip fractures were defined using ICD-9 primary diagnostic and procedural codes. Dispensings of non-benzodiazepine hypnotic drugs (zolpidem, eszopiclone, zaleplon) were ascertained using Medicare Part D claims. Stratifying characteristics were ascertained using the Minimum Data Set. The odds ratios of hip fracture were estimated using conditional logistic regression models by comparing the prevalence of non-benzodiazepine hypnotic dispensings during the 0-15 days before the hip fracture (hazard period) with the prevalence of dispensings during the 30-45 and 60-75 days before the hip fracture (control periods). Analyses were stratified by cognition, bladder function, and ability to transfer.

Results: Among participants, 1,737 were dispensed a non-benzodiazepine hypnotic before the hip fracture, and 599 participants with exposure-discordant pairs were included in analyses. Mean age was 82 yrs (± 10 yrs), and 78% were female. The risk of hip fracture was elevated during the 0-15 days following dispensing of a non-benzodiazepine hypnotic (OR 1.49; 95% CI 1.26, 1.76). The association between non-benzodiazepine hypnotics and hip fracture was somewhat greater in residents with moderate or severe cognitive impairment, intermittent urinary incontinence, and among residents that were independent or severely impaired with transfers (Table 1); however, these differences remain consistent with chance.

Conclusions: In nursing home residents, risk of hip fracture was elevated following dispensing of a non-benzodiazepine hypnotic. There were no clear differences in risk by cognition, bladder function, and ability to transfer. Caution should be used when prescribing a non-benzodiazepine hypnotic to nursing home residents.

| Resident characteristic | Categories | Odds ratio | 95% confidence intervals |
|-------------------------|--|------------|--------------------------|
| Cognition | Intact or mild impairment | 1.39 | 1.13, 1.71 |
| | Moderate or severe impairment | 1.69 | 1.27, 2.26 |
| Bladder function | Always continent or always incontinent | 1.42 | 1.26, 1.75 |
| | Intermittently incontinent | 1.62 | 1.21, 2.15 |
| Ability to transfer | Independent | 1.63 | 1.13, 2.37 |
| | Mild impairment | 1.34 | 1.05, 1.71 |
| | Moderate or severe impairment | 1.62 | 1.21, 2.18 |

Table 1

Disclosures: Sarah Berry, None.

1057

Implications of Expanding Indications for Initiation of Drug Treatment to Prevent Fracture in Older Men. Kristine Ensrud^{*1}, Kathy Wilt Peters², Brent Taylor³, Margaret Gourlay⁴, Meghan Donaldson², William Leslie⁵, Terri Blackwell⁶, Howard Fink⁷, Eric Orwoll⁸, John Schousboe⁹. ¹Minneapolis VA Medical Center / University of Minnesota, USA, ²San Francisco Coordinating Center, USA, ³University of Minnesota, USA, ⁴University of North Carolina, USA, ⁵University of Manitoba, Canada, ⁶CPMC RESEARCH INSTITUTE, USA, ⁷GRECC, Minneapolis VA Medical Center, USA, ⁸Oregon Health & Science University, USA, ⁹Park Nicollet Clinic/University of Minnesota, USA

Incremental effects of broadening the definition of osteoporosis (OP) and use of FRAX treatment thresholds on the proportion of older men identified as appropriate for initiation of drug treatment are uncertain. The extent to which observed-to-predicted fracture probability ratios differ across groups of untreated men identified using distinct criteria is also unknown. To address these questions, we sequentially applied the WHO OP definition, NOF OP definition, and FRAX treatment thresholds to 5882 men ≥65 years not taking bisphosphonates at the MrOS baseline exam. We then calculated observed 10-year probabilities for confirmed incident hip and major osteoporotic fracture events over time using cumulative incidence estimation, accounting for the competing risk of mortality. Predicted probabilities of hip and major osteoporotic fracture were calculated using FRAX with femoral neck BMD. Among the 5882 men, 130 (2.2%) were identified with OP using the WHO definition and an additional 422 were identified with OP using the NOF definition (total OP prevalence 9.4%). Applying FRAX treatment thresholds, 936 additional men were identified as eligible for treatment (i.e. high fracture risk) raising the total prevalence of men meeting indications for drug treatment to 25.3%. Observed fracture probabilities incrementally decreased across groups identified using different criteria (p<0.001), with highest probabilities among men identified with OP by the WHO definition (Table). Ratios of observed-to-predicted fracture probabilities were markedly greater than 1.0 among men with OP, especially those identified by WHO criteria, but were close to 1.0 among men without OP, including those at both high and low fracture risk. In conclusion, choice of definition of OP and use of FRAX treatment thresholds have major impacts on the proportion of men identified as warranting drug therapy to prevent fracture. Observed 10-year probabilities of hip and major osteoporotic fracture are highest among men identified with OP by the WHO definition, a group for which FRAX models with BMD underestimate actual risk. In the context of these findings and evidence suggesting lack of benefit of drug treatment in reducing nonvertebral fracture risk in the absence of OP, randomized trials are needed to evaluate efficacy of treatment in older men identified using criteria other than BMD-defined osteoporosis prior to expanding indications for initiation of drug treatment to prevent fracture.

| | Osteoporosis by WHO ¹ criteria (n=130) | Osteoporosis by NOF (but not WHO) ² criteria (n=422) | No Osteoporosis by WHO or NOF criteria High Fracture Risk ³ (n=936) | No Osteoporosis by WHO or NOF criteria Low Fracture Risk ³ (n=4394) | p-trend |
|--|---|---|--|--|---------|
| Hip Fracture | | | | | |
| Observed 10-year probability, (95% CI) | 20.6 (14.0, 28.1) | 6.8 (4.6, 9.5) | 6.4 (5.0, 8.1) | 1.5 (1.1, 1.9) | <0.001 |
| Predicted 10-year probability, mean (95% CI) | 9.5 (8.2, 10.7) | 4.3 (3.9, 4.7) | 5.8 (5.6, 6.1) | 1.2 (1.1, 1.2) | <0.001 |
| Major Osteoporotic Fracture | | | | | |
| Observed 10-year probability, (95% CI) | 30.0 (22.3, 38.1) | 17.5 (14.0, 21.3) | 12.0 (10.0, 14.1) | 4.8 (4.2, 5.4) | <0.001 |
| Predicted 10-year probability, mean (95% CI) | 17.4 (16.0, 18.8) | 10.8 (10.3, 11.3) | 12.5 (12.2, 12.7) | 5.9 (5.9, 6.0) | <0.001 |

*Observed probabilities calculated using cumulative incidence estimation accounting for competing risk of mortality; Predicted probabilities calculated using FRAX models with femoral neck BMD (version 3.3)
¹WHO definition of osteoporosis based on use of female specific T score of -2.5 or below at femoral neck
²NOF definition of osteoporosis based on use of male specific T score of -2.5 or below at femoral neck, total hip, or lumbar spine
³High fracture risk as defined by FRAX (with BMD) 10-year probabilities of hip fracture ≥3% or major osteoporotic fracture ≥20%; Low fracture risk as defined by FRAX (with BMD) 10-year probabilities of hip fracture <3% and major osteoporotic fracture <20%

Table

Disclosures: Kristine Ensrud, None.

1058

Association of Stressful Life Events with Accelerated Bone Loss in Older Men: the Osteoporotic Fractures in Men (MrOS) Study. Howard Fink^{*1}, Michael Kuskowski¹, Jane Cauley², Brent Taylor³, John Schousboe⁴, Peggy Cawthon⁵, Kristine Ensrud⁶. ¹GRECC, Minneapolis VA Medical Center, USA, ²University of Pittsburgh Graduate School of Public Health, USA, ³University of Minnesota, USA, ⁴Park Nicollet Clinic/University of Minnesota, USA, ⁵California Pacific Medical Center Research Institute, USA, ⁶Minneapolis VA Medical Center / University of Minnesota, USA

According to the allostatic load hypothesis, stressful life events (LE) may lead to various adverse health outcomes. In prior prospective analyses, we found that LE were independently associated with an increased risk of falls and that an age-adjusted association of LE with an increased risk of clinical fractures was in part due to lower BMD among those with LE. The current analyses explore whether LE are associated with higher rates of bone loss.

We used data from MrOS, a longitudinal cohort study in community-dwelling men aged ≥65 yrs. Total hip (TH) BMD was collected at baseline (V1) and at a second clinic visit (V2), approximately 4.6 years later. Information on several types of LE (e.g. wife/partner serious illness, loss of/separation from other close relative or friend) during the past 12 months was collected in a mailed interim questionnaire (IQ)

mid-way between V1 and V2 and in another questionnaire at V2. We used age and multivariate (MV) linear regression to model the association of LE with annualized percent TH BMD loss between V1 and V2, and logistic regression to model the risk of accelerated TH BMD loss (>1 SD more loss than the mean annualized percent change, i.e. loss exceeding -1.24%/yr) between V1 and V2.

Of 5229 men with V2 data, 76% reported >1 type of LE at either IQ or V2, including 24% with 2 types of LE and 21% with 3 or more types of LE. Among 4388 men with TH BMD measurement at both V1 and V2, mean annualized TH BMD loss was -0.36% (SD 0.88) and 13.9% of men were defined as having accelerated TH BMD loss. After age-adjustment, any LE (vs. none) was not associated with a higher rate of TH BMD loss ($p=0.10$), but the number of types of LE was associated with a higher rate of TH BMD loss ($p<0.001$). Odds of accelerated TH BMD loss were higher among men with any type of LE (age-adjusted OR for any event vs. none, 1.4 [95% CI, 1.1-1.7]), and increased in a graded fashion, corresponding with an increased number of types of LE (vs. none) (Table). Associations were attenuated but remained significant after MV adjustment, including for percent weight change between V1 and V2 and mood symptoms.

In this older male cohort, stressful life events were associated with a dose-related, but modest increase in odds of concurrent accelerated TH bone loss independent of other explanatory factors. Future studies are needed to confirm these findings and to investigate the mechanism that may underlie this association.

Table: Stressful life events (LE) and odds of accelerated V1 to V2 TH BMD loss, OR (95% CI)

| Model | Any type of LE | Sum of types of LE | 1 type of LE | 2 types of LE | 3+ types of LE |
|---------------------------|----------------|--------------------|----------------|----------------|----------------|
| Age only | 1.4 (1.1-1.7) | 1.2 (1.1-1.3) | 1.2 (0.95-1.6) | 1.3 (1.01-1.7) | 1.7 (1.3-2.2) |
| Base MV model* | 1.3 (1.00-1.6) | 1.1 (1.03-1.2) | 1.1 (0.9-1.5) | 1.3 (0.97-1.7) | 1.4 (1.1-1.9) |
| MV* + wt change | 1.2 (0.96-1.5) | 1.1 (1.01-1.2) | 1.1 (0.9-1.5) | 1.2 (0.9-1.6) | 1.3 (1.00-1.8) |
| MV* + wt change + mood sx | 1.2 (0.96-1.5) | 1.1 (1.01-1.2) | 1.1 (0.8-1.5) | 1.2 (0.9-1.6) | 1.3 (1.00-1.8) |

*Base MV model adjusted for the following V1 measures: age, weight, education, history of fracture before age 50 yrs, diabetes, stroke, MI, Parkinson's disease, low mood symptoms, self-reported health status, IADL impairment, gait speed, and chair stand completion time.

Table

Disclosures: Howard Fink, None.

1059

Lower Fracture Risk in Older Men with Higher Sclerostin Concentration – A Prospective Analysis from the MINOS Study. Pawel Szulc^{*1}, Cindy Betholon², Olivier Borel³, Roland Chapurlat⁴. ¹INSERM UMR 1033, University of Lyon, Hopital E. Herriot, Pavillon F, France, ²INSERM UMR 1033, France, ³Inserm, France, ⁴E. Herriot Hospital, France

Sclerostin is a glycoprotein synthesized by osteocytes and it inhibits bone formation. Its relationship with fracture in older men has been rarely explored so far. We measured serum concentration of sclerostin (Quidel-TECOMEDICAL, San Diego, CA) in 711 men aged 50 and older. Bone mineral density (BMD) was measured at the lumbar spine, hip and distal forearm (HOLOGIC 1000W). Serum sclerostin increased with age ($r=0.30$, $p<0.001$). After adjustment for age, weight, height, current smoking, bioavailable estradiol and parathyroid hormone, BMD of all the skeletal sites correlated positively with serum sclerostin ($r=0.25$ to 0.30 , $p<0.001$) and increased by 0.27 to 0.51 SD /SD increase in sclerostin. In similar multivariable models, serum concentrations of osteocalcin, bone alkaline phosphatase, N-terminal propeptide of type I procollagen and C-terminal telopeptide of type I collagen (CTX-I) as well as urinary excretion of total and free deoxypyridinoline and CTX-I correlated negatively with serum sclerostin ($r=-0.09$ to -0.24 , $p<0.05$ to 0.001) and decreased by 0.10 to 0.25 SD per SD increase in sclerostin.

During 10 years of follow-up, 76 men sustained at least one fragility fracture. The distribution of fracture incidence per quintiles of sclerostin was as follows: 12.9% (lowest quintile), 15.2%, 13.1%, 6.7%, 5.3% (highest quintile) ($p<0.005$). We compared fracture risk in the two highest quintiles combined vs three lower quintiles combined using logistic regression adjusted for age, BMI, age and BMI interaction, BMD, bone width (for femoral neck and distal radius), prevalent fracture, prevalent falls, and severe abdominal aortic calcification. Men with higher sclerostin concentration had lower risk of fragility fracture (e.g., after adjustment for hipBMD, OR= 0.53, 95%CI: 0.29, 0.97; $p<0.05$). Similar results were obtained in the models adjusted for BMD and width of tubular bones (e.g., femoral neck, OR= 0.49, 95%CI: 0.27, 0.89; $p<0.05$). When the analysis was limited to 47 men who sustained major fragility fractures (vertebra, hip, femur, tibia, pelvis, proximal humerus, multiple ribs), the results were similar (e.g., lumbar spine: OR= 0.44, 95%CI: 0.19, 0.99, $p<0.05$).

In conclusion, in older men, higher serum levels of sclerostin are associated with lower risk of fracture, higher BMD and lower levels of biochemical bone turnover markers.

Disclosures: Pawel Szulc, None.

1060

Bone Mineral Density and Mortality in Two Large Prospective Population-based Cohort Studies: Strongest Relation with Death due to Chronic Lung Disease. Natalia Campos-Obando^{*1}, Martha Castano-Betancourt², Ling Oei³, Oscar Franco⁴, Albert Hofman⁵, Bruno H. Ch. Stricker⁶, Fernando Rivadeneira⁷, Andre G. Uitterlinden⁸, M. Carola Zillikens². ¹Department of Internal Medicine, Erasmus University Medical Center, Netherlands, ²Department of Internal Medicine, Department of Epidemiology, Erasmus University Medical Center, Netherlands, ³Department of Internal Medicine, Erasmus University Medical Center, Netherlands, ⁴Cardiovascular Epidemiology Group, Erasmus University Medical Center, Netherlands, ⁵Department of Epidemiology, Erasmus University Medical Center, Netherlands, ⁶Department of Epidemiology, Department of Internal Medicine, Erasmus University Medical Center, Netherlands, ⁷Department of Epidemiology, Department of Internal Medicine, Erasmus University Medical Center, Netherlands, ⁸Department of Epidemiology, Department of Internal Medicine, Erasmus University Medical Center, Netherlands

Osteoporosis has been associated in some studies with cardiovascular disease (CVD) and all-cause and CVD mortality. Using two cohorts from the Rotterdam Study (RS-I and -II) we assessed the relation between femoral neck bone mineral density (FN BMD) and all-cause and cause-specific mortality divided into 7 groups based on ICD-10 codes: CVD, Cancer, Trauma, Infectious diseases, Dementia, Lung Diseases, and other causes. In 5,779 elderly participants from RS-I and 2,055 from RS-II BMD was measured at baseline and survival analyses were done using Cox proportional hazards models, adjusted for age, BMI and smoking, followed by meta-analysis. Hazard Ratios (HR; [95%CI]) are expressed for each standard deviation (SD) decrease in BMD. After mean follow-up of 14.5 (RS-I) and 9.0 (RS-II) years there were 2,832 and 220 deaths, respectively. An inverse relationship was found between BMD and all-cause mortality in males only: HR for RS-I: 1.09 [1.03-1.16] $P=0.004$; for RS-II: 1.30 [1.08-1.57] $P=0.005$; joint meta-analysis: 1.11 [1.05-1.17] $P=0.0003$. Adjustment for incident fractures did not essentially change these results. The strongest relation between BMD and cause-specific mortality was an inverse relation with mortality due to lung diseases (chronic obstructive pulmonary diseases (COPD)). This result was consistent in both cohorts and across genders (meta-analysis HR 1.90 [1.51-2.39], $P=4\times 10^{-8}$) and persisted after adjusting for steroid use and excluding prevalent COPD. There was an inverse association of BMD with trauma-related mortality in females only (HR: 1.71 [1.17-2.50], $P=0.006$). Also in females, there was a borderline significant trend for increased cancer-related mortality with increasing BMD. In both genders a decreased BMD was associated with increased dementia-related mortality only when prevalent cases were also included (meta-analysis HR: 1.23 [1.04-1.47], $P=0.018$). In RS-I but not in RS-II, there was a significant inverse relation between BMD and other causes of mortality in both genders (unattended-, unspecified- and sudden-death (HR 1.19 [1.08-1.31], $P=0.0003$)). We did not find a relation between BMD and mortality due to CVD or infections in either sex. In conclusion, FN BMD was inversely associated with all-cause mortality in elderly males but not females and strongly related to COPD mortality in both genders within two prospective population-based studies. No association was found between BMD and CVD mortality in either males or females.

Disclosures: Natalia Campos-Obando, None.

1061

Sclerostin Inhibition Improves Bone Mass, Bone Strength, and Bone Defect Regeneration in Rats with Type 2 Diabetes Mellitus. Christine Hamann^{*1}, Martina Rauner², Yvonne Hoehna³, Ricardo Bernhardt⁴, Jan Mettelsiefen³, Claudia Goettsch⁵, Klaus-Peter Guenther³, Franklin Asuncion⁶, Michael Ominsky⁶, Lorenz Hofbauer³. ¹Dresden Technical University Medical Center, Germany, ²Medical Faculty of the TU Dresden, Germany, ³Dresden University Medical Center, Germany, ⁴Technische Universität Dresden, Germany, ⁵Brigham & Women's Hospital Cardiovascular Division, USA, ⁶Amgen Inc., USA

Type 2 diabetes mellitus results in increased risk of fracture and delays in healing after a fracture has occurred. Better therapies are needed to prevent fractures and improve healing in these diabetic patients. ZDF fa/fa rats are an established model of type 2 diabetes mellitus and exhibit low bone mass and delayed bone defect healing. We tested whether antibodies against sclerostin (Scl-AbVI), an inhibitor of Wnt signaling, reverse the skeletal deficits of diabetic ZDF rats.

Gap defects of 3 mm were created at the femur of 11-week old diabetic ZDF fa/fa and non-diabetic ZDF +/- rats and stabilized by an internal plate. Saline or 25 mg/kg Scl-Ab was administered s.c. twice weekly for 12 weeks in diabetic and non-diabetic rats ($n=10$ /group). Bone mineral density (BMD), bone mass and strength were assessed using pQCT, μ CT, and biomechanical testing. Dynamic bone histomorphometry was used to assess bone formation, and the filling of the femur gap defect was analyzed by μ CT.

Diabetic rats displayed lower spinal and femoral bone mass compared to non-diabetic rats, and Scl-Ab treatment markedly enhanced bone mass of the femur and

the spine of diabetic rats. Scl-Ab also reversed the deficit in bone strength in the diabetic rats, with 65% and 89% increases in maximum load at the femoral shaft and neck, respectively. ZDF fa/fa rats had a 23% decrease in the material properties ultimate strength and modulus compared to +/+ rats, suggesting that bone quality was impaired by diabetes in this model. Scl-Ab modestly improved these parameters in diabetic rats, though its primary effect on whole bone strength was due to increased bone mass. The lower bone mass in diabetic rats was associated with a 65% decrease in vertebral bone formation rate, which Scl-Ab was able to increase by 6-fold, consistent with an anabolic effect. While non-diabetic rats filled 57% of the femoral defect, diabetic rats filled only 21%. Scl-Ab treatment significantly increased defect regeneration in both groups by 47% and 74%, respectively.

Sclerostin inhibition reverses the adverse effects of type 2 diabetes mellitus on bone mass and strength, and improves bone defect regeneration in rats.

Disclosures: Christine Hamann, None.

1062

Blosozumab, a Humanized Monoclonal Antibody, and A Chimeric Rodent Monoclonal Antibody Against Sclerostin Robustly Increase Bone Formation Activity in Intact Monkeys and Ovariectomized Rats. Yanfei Ma¹, Todd Page¹, Qianqiang Zeng¹, Mary D Adrian¹, David Halladay¹, Xuhao Yang¹, Masahiko Sato², Henry Bryant¹, Venkatesh Krishnan¹, David Waters¹, Rohn Millican¹, Jude Onyia¹, Stuart Kuhstoss¹. ¹Eli Lilly & Company, USA, ²Lilly Research Labs, USA

Loss-of-function mutations in the sclerostin gene result in a high bone mass phenotype in humans and knock-out mice. We examined the skeletal effects of a humanized anti-sclerostin antibody (blosozumab) in monkeys and a separate mouse/rat chimeric monoclonal anti-sclerostin antibody (sclerostin Ab) in rats. Rats were ovariectomized (OVX) at 6 months of age and permitted to lose bone for 1 month to establish osteopenia before initiation of treatment. A chimeric antibody was administered at doses up to 14 mg/kg once weekly (q7) or up to 28 mg/kg once every 2 weeks (q14) subcutaneously for 8 weeks (n=7/group). Compared to OVX IgG controls, bone mineral density (BMD) was increased with sclerostin Ab treatments in lumbar vertebrae (LV), and mid femur (MF) or distal femur at 14mg/kg q7 and at the 14 and 28 mg/kg q14 doses. Biomechanical load-to-failure analyses showed that LV, MF and femoral neck sites were strengthened to a similar extent with normalized time exposure between the q7 and q14 dosing regimens. Bone parameters increased in a dose dependent manner and compared favorably to PTH 1-38 (10µg/kg daily). Bone histomorphometry confirmed that sclerostin Ab increased trabecular area and thickness to sham- ovariectomy (Sham) levels in the proximal tibia metaphyses. Cortical area and thickness above Sham levels were observed in high dose groups in the mid shaft. The mineralizing surface and bone formation rate were higher in sclerostin Ab treated rats than those of IgG controls on trabecular, endocortical and periosteal surfaces. In the cynomolgus monkeys, blosozumab was administered up to 100 mg/kg weekly by intravenous injection to 3 year old males and females (n=4-6/dose/sex) for 9 months. The bone formation biomarker procollagen-1 N-terminal peptide (PINP) was increased at all dose levels and peaked at day 85. QCT analyses showed higher cortical bone mineral content (BMC), cortical area, thickness in tibial shaft, and trabecular BMC and BMD at the tibial metaphysis compared to vehicle controls in both genders at study termination. These results confirm the bone anabolic profile of sclerostin inhibition with selective monoclonal antibodies. The robustly enhanced bone microstructure and strength suggest therapeutic potential for blosozumab.

Disclosures: Yanfei Ma, Eli Lilly Company,
This study received funding from: Eli Lilly Company

1063

Sclerostin Antibody Treatment Improves Bone Mass, Microarchitecture and Mechanical Properties in Mice Exposed to Microgravity: Results from the STS-135 Shuttle Mission. Mary Bouxsein¹, Ted Bateman², Andrea Hanson³, Travis Pruitt⁴, Eric Livingston⁵, Michael Lemur⁵, Leeann Louis⁶, Rachel Ellman¹, Jordan Spatz⁷, Kelly Warmington⁸, Hong Lin Tan⁸, Dave Hill⁸, Denise Dwyer⁸, Alicia Ortega⁹, Schweta Maurya¹⁰, Marina Stolina¹¹, Sutada Lotunun¹², Roland Baron¹³, Chris Paszty¹⁴, Virginia Ferguson⁹. ¹Beth Israel Deaconess Medical Center, USA, ²University of North Carolina, USA, ³University of Washington, USA, ⁴Clemson University, USA, ⁵University of North Carolina, USA, ⁶Center for Advanced Orthopedic Studies, Beth Israel Deaconess Medical Center, USA, ⁷Harvard-MIT Division of Health Sciences & Technology (HST), USA, ⁸Amgen Inc, USA, ⁹University of Colorado, USA, ¹⁰University of Colorado, USA, ¹¹Amgen Inc., USA, ¹²Harvard School of Dental Medicine, USA, ¹³Harvard School of Medicine & of Dental Medicine, USA, ¹⁴Amgen, Inc., USA

Despite rigorous nutritional and exercise countermeasures, astronauts lose bone mass at 10 times the rate of postmenopausal women. Sclerostin is a potent inhibitor of bone formation and expression levels of *SOST*, the gene producing sclerostin, increase

with unloading and may mediate disuse-induced bone loss. We tested the ability of a sclerostin antibody (SclAb) to improve bone mass, microarchitecture and strength in mice exposed to 13 days of microgravity on the space shuttle Atlantis (STS-135). Female C57Bl/6N mice (n=14-15/gr, 9 wks old) were assigned to flight vehicle (FL-VEH), flight SclAb (FL-SclAb), ground vehicle (GR-VEH), or ground SclAb (GR-SclAb), and injected with SclAb (100 mg/kg, SC, Amgen) or vehicle 1 day prior to launch. Ground-controls housed identically as the flight mice. Results: Spaceflight negatively influenced BMD, microarchitecture and strength. SclAb treatment markedly improved BMD, bone microarchitecture and mechanical properties in both GR and FL mice at multiple skeletal sites, such that bone properties in FL-SclAb were equal to or greater than GR-VEH (Table). Specifically, microgravity inhibited gains in total body BMD seen in these young mice (p<0.05 vs FL); whereas SclAb led to greater increases in total body BMD in both environments (p<0.01 vs VEH). Tibial and femoral Tb.BV/TV by µCT were 35% lower in FL-VEH than GR-VEH, and 2-3 fold higher in Scl-Ab treated mice, regardless of loading. Midshaft Ct.Th was 5-9% lower in FL-VEH vs GR-VEH, and increased by SclAb treatment, such that values in FL-SclAb were similar to ground controls. Three-point bending of the femoral diaphysis showed decreased stiffness (-16%, p<0.05) and failure load (-11%, p<0.05) in FL-V vs GR-V, while SclAb preserved these properties in FL-SclAb mice at GR-VEH levels. Bone formation, assessed by quantitative histomorphometry, was significantly reduced by spaceflight, and was 3-fold higher in SclAb treated mice. Consistent with this, serum PINP and osteocalcin were lower, and CTX1 higher in FL-VEH vs GR-VEH, while serum osteocalcin and PINP were significantly higher in SclAb-treated mice regardless of loading condition. In conclusion, a single injection of SclAb not only inhibits bone loss in mice exposed to microgravity, but improves bone mass and microarchitecture to levels similar to ground controls, demonstrating that the anabolic effect of sclerostin inhibition occurs even in the absence of normal mechanical loading.

| | GR-VEH | GR-SclAb | FL-VEH | FL-SclAb |
|---------------------------|-------------|---------------|-------------------------|--------------|
| Total body BMD (% change) | 6.6 ± 3.2 | 20.5 ± 2.2* | 2.2 ± 2.2 ^Δ | 14.0 ± 2.2* |
| Leg BMD (% change) | 9.0 ± 4.4 | 25.3 ± 6.2* | 1.3 ± 2.5 ^Δ | 18.0 ± 1.8* |
| Prox Tibia Tb.BV/TV (%) | 10.7 ± 2.5 | 19.4 ± 3.5* | 6.7 ± 1.1 ^Δ | 15.5 ± 2.1* |
| Distal Femur Tb.BV/TV | 9.1 ± 1.3 | 17.1 ± 3.0* | 5.8 ± 1.0 ^Δ | 11.7 ± 2.5* |
| Tibia Ct.Thickness (µm) | 192 ± 9 | 219 ± 7* | 183 ± 6 ^Δ | 200 ± 9* |
| Femur Ct.Thickness (µm) | 161 ± 6 | 190 ± 9* | 147 ± 7 ^Δ | 172 ± 11* |
| Femur Stiffness (N/mm) | 93.6 ± 11.5 | 104.8 ± 14.7* | 78.2 ± 9.4 ^Δ | 98.7 ± 10.9* |
| Femur Failure Load (N) | 13.9 ± 1.4 | 16.7 ± 2.0* | 12.4 ± 1.2 ^Δ | 15.3 ± 1.6* |

^Δ p < 0.05 vs GR-Veh, * p < 0.05 vs Veh-treated within same loading group

Table

Disclosures: Mary Bouxsein, Amgen Inc, 6
This study received funding from: Amgen Inc

1064

Increased Bone Mass and Bone Strength by Sclerostin Antibody Is Maintained by a RANKL Inhibitor in Ovariectomized Rats with Established Osteopenia. Xiaodong Li¹, Kelly S. Warmington², Qing-Tian Niu², Frank J. Asuncion², Denise Dwyer², Mario Grisanti², Chun-Ya Han², Paul J. Kostenuik², Marina Stolina², Michael S. Ominsky², Hua Zhu Ke². ¹Amgen, Inc., USA, ²Amgen Inc., USA

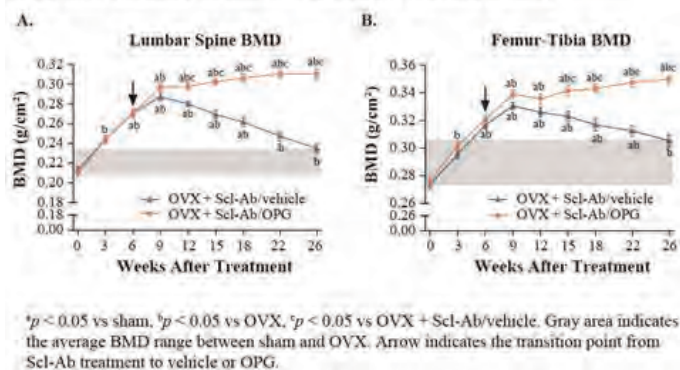
Our previous study demonstrated that some of the bone mass gained during sclerostin antibody (Scl-Ab) treatment is gradually lost after discontinuation of treatment. In the current study, we examined whether follow-up treatment with a RANKL inhibitor, OPG, would maintain the bone mass gains induced by Scl-Ab in ovariectomized (OVX) rats.

Six-month-old OVX rats (2 months post-ovariectomy) were treated with Scl-Ab (Scl-AbVI, 25 mg/kg, SC, 1x/week) for 6 weeks and then transitioned to vehicle or OPG-Fc (10 mg/kg, SC, 2x/week) for an additional 6 or 20 weeks (n=12-14/group). Vehicle-treated sham and OVX control rats were euthanized at weeks 0, 6, 12, and 26, and a group of Scl-Ab-treated OVX rats were euthanized at week 6 (n=10-12/group).

In vivo DXA analysis demonstrated that 6 weeks of Scl-Ab treatment in OVX rats increased lumbar spine and femur-tibia BMD to levels significantly above OVX and sham controls (Figure). Transition to vehicle resulted in gradual declines in BMD at both sites, to levels of sham controls, whereas transition to OPG-Fc maintained the increases in BMD at both sites. Histomorphometry revealed significant increases in vertebral trabecular bone volume (BV/TV) and tibial cortical thickness after 6 weeks of Scl-Ab treatment. Transition to vehicle led to gradual declines in these parameters, to levels that remained above OVX controls at week 26, whereas transition from Scl-Ab to OPG-Fc maintained BV/TV and cortical thickness at the peak levels achieved during Scl-Ab treatment. Six weeks of Scl-Ab treatment was associated with significant increases in trabecular, endocortical, and periosteal bone formation rates and significant decreases in trabecular and endocortical eroded surfaces. These changes were reversed upon transition to vehicle. Transition to OPG-Fc led to reductions in each of these bone resorption and formation parameters. At week 26, maximum load of lumbar vertebral bodies was significantly greater in the group transitioned to OPG-Fc than the group transitioned to vehicle.

In summary, after discontinuation of Scl-Ab treatment, bone formation returned to control levels and bone resorption increased, resulting in gradual bone loss. Transitioning to the RANKL inhibitor OPG-Fc effectively inhibited bone resorption and maintained bone mass and bone strength gains previously induced by Scl-Ab. These results support the strategy of using a RANKL inhibitor to maintain the bone mass and strength increases induced by sclerostin antibody.

Figure. OPG Maintained the Bone Mass Increased by Sclerostin Antibody



Figure

Disclosures: Xiaodong Li, Amgen Inc., 7; Amgen Inc., 3
This study received funding from: Amgen Inc. and UCB Pharma

1065

LLP2A-Alendronate, a Novel Anabolic Treatment to Reverse Bone Loss. Wei Yao¹, Min Guan², Junjing Jia³, Yu-An Evan Lay⁴, Ruiwu Liu⁵, Kit Lam⁵, Diana Olvera⁶, Robert Ritchie⁶, Jan Nolte⁷, Nancy Lane¹. ¹University of California, Davis Medical Center, USA, ²Johns Hopkins, USA, ³University of California, Davis, USA, ⁴Musculoskeletal Research Unit, Department of Medicine, University of California Davis Medical Center, USA, ⁵Department of Biochemistry & Molecular Medicine, University of California Davis Medical Center, USA, ⁶Materials Sciences Division, Lawrence Berkeley National Laboratory, USA, ⁷Stem Cell Program & Institute for Regenerative Cures, University of California Davis Medical Center, USA

Bone formation is reduced with aging due to fewer bone marrow MSCs and changes in the bone marrow microenvironment. Our research group has developed a synthetic peptidomimetic ligand (LLP2A) that has high affinity for activated $\alpha 4\beta 1$ integrin on the MSC surface, and linked it to a bisphosphonate (alendronate) that has high affinity for bone. We have previously shown that this hybrid compound, LLP2A-Alendronate (LLP2A-Ale), in vitro increased MSC migration and commitment of MSCs to osteoblast differentiation; in vivo it increased bone formation and bone mass in young immune-competent mice. In this study, we continued to evaluate the effects of LLP2A-Ale, with or without the MSC transplantation, in mice with established bone loss induced by ovariectomy or with advanced aging. Methods: C57BL/6 female mice were used in three efficacy studies. The first study used 10-week-old ovariectomized mice with established bone loss. The second study used 24-week-old adult mice and the third study used 24-month-old aged mice. LLP2A-Ale was given two monthly doses (0.9nmol IV) or in combination of mouse MSC (IV 5×10^5). Results: We found LLP2A-Ale partially prevented trabecular bone loss induced by estrogen deficiency by increasing the number of osteoblasts on the trabecular surface and the bone formation rate. MSC + LLP2A-Ale restored lost bone induced by estrogen deficiency by further increasing osteoblast surface and mineral apposition rate. The effects of LLP2A-Ale + transplanted MSCs was superior to LLP2A-Ale alone, especially at the cortical bone, where the combination treatment significantly increased cortical bone strength in all the three animal models we studied. Importantly, PTH or MSC alone failed to increase bone formation rate in 24-month-old mice. By contrast, BFR/BS was increased by 35% in LLP2A-Ale group, by 192% in MSC + LLP2A-Ale group in relative to the PBS-treated group. Only MSC + LLP2A-Ale treatment increased cortical bone maximum stress by 8% as compared to the PBS-treated group. In conclusion, LLP2A-Ale treatment increased bone mass and strength as measured by multiple outcomes in models of young adult mice, aged mice, and estrogen-deficient mice. The beneficial effects on bone formation resulted from the combination of increased homing of the transplanted MSCs to bone as well as the endogenous number of osteoblasts at the bone surface that together significantly increases the rate of bone formation. These results strongly support LLP2A-Ale as a novel therapeutic option for the treatment of bone loss related to age and hormone deficiency.

Disclosures: Wei Yao, None.

1066

An Estrogen Dendrimer Conjugate Incapable of Stimulating the Nuclear-initiated Actions of Estrogen Receptors Prevents the Loss of Cortical Bone Mass in Estrogen Deficient Mice. Shoshana Bartell¹, Aaron Warren¹, Li Han¹, Srividhya Iyer¹, Sung Kim², Benita Katzenellenbogen², Ken Chambliss³, Philip Shaul³, John Katzenellenbogen², Paula Roberson¹, Robert Weinstein¹, Charles O'Brien¹, Robert Jilka¹, Maria Jose Almeida¹, Stavros Manolagas¹. ¹Central Arkansas VA Healthcare System, Univ of Arkansas for Medical Sciences, USA, ²University of Illinois, USA, ³University of Texas Southwestern Medical Center at Dallas, USA

Loss of bone mass following estrogen deficiency is caused by increased resorption of the cancellous compartment and of the endosteal surface of the cortex, but the cellular and molecular mechanisms of the effects of estrogens in these two compartments are apparently distinct. Indeed, published genetic evidence and work reported elsewhere in this meeting have revealed that the osteoclast ER α mediates the protective effects of estrogens in the cancellous, but not the cortical, compartment. On the other hand, the ER α of osteoblast progenitors is required for normal periosteal bone accrual as well as the maintenance of cortical bone mass, but plays no discernible role in the maintenance of cancellous bone. Based on this and additional evidence that some of the effects of estrogens on bone may be mediated via non-nuclear ER α signaling, we investigated the efficacy of an estrogen dendrimer conjugate (EDC) that is not capable of stimulating the nuclear-initiated actions of ER, in preventing the effects of estrogen loss in the two bone compartments. 17-week-old C57BL/6 mice were ovariectomized (OVX) or sham-operated and implanted with mini-pumps delivering vehicle, dendrimer control (DC), or equimolar concentrations of 17 β -estradiol (E2) or the EDC for 6 weeks. In two separate experiments, the EDC was as potent as E2 in preventing loss of DEXA BMD at the spine. By μ -CT, this effect was due to the preservation of cortical but not cancellous bone. In contrast, E2 was effective in both compartments. EDC also attenuated the loss of cortical bone, the enlargement of the endosteal perimeter, and the increased cortical porosity in femurs. In addition, the EDC prevented the OVX-induced oxidative stress (as determined by ROS and glutathione levels and p66^{bac} phosphorylation) to the same extent as E2. Most importantly, the OVX-induced decrease in uterine weight was unaltered by the EDC, but restored by E2. These results demonstrate that several effects of estrogens on bone, including their protective effect on cortical bone mass maintenance and their anti-oxidant properties, are mediated by a mechanism distinct from their classical genotropic action on reproductive organs. Nonetheless, attenuation of oxidative stress by EDC, unlike the use of E2 or anti-oxidants, is not sufficient to prevent loss of cancellous bone, suggesting that nuclear actions of the estrogen-activated osteoclast ER α are also involved in the protection of this compartment.

Disclosures: Shoshana Bartell, None.

1067

A Six Year Exercise Intervention Program in 7-9 Year Old Children Improves Bone Mass and Bone Structure without Increasing the Fracture Risk – A Population-Based Prospective Controlled Study in 2395 Children. Fredrik Deter¹, Bjorn Rosengren², Jan-Åke Nilsson³, Magnus Dencker⁴, Magnus Karlsson². ¹Clinical & Molecular Osteoporosis Research Unit, Lund University, Sweden, ²Skåne University Hospital Malmö, Lund University, Sweden, ³Department of Orthopedics, Sweden, ⁴Department of Physiology, Sweden

Purpose: Pediatric exercise intervention studies that evaluate if physical activity can decrease fracture risk span at most 36 months and use bone traits as a surrogate endpoint for fractures. It is however essential to include also fractures as reports infer that a high level of physical activity is associated with higher fracture risk. We have therefore during 6 years conducted a population based controlled exercise intervention study using both bone traits and fractures as endpoint variables.

Method: During 6 years children in the intervention group received 40 minutes of daily physical education (PE) in school while those in the control group continued with the Swedish standard 60 minutes PE per week. Incident fractures were continuously registered in the total sample size of 2395 children aged 7-9 years at baseline. There were 362 girls and 446 boys in the intervention group (3515 person-years) and 780 girls and 807 boys in the control group (7628 person-years). In 78 girls and 113 boys in the intervention group and 53 girls and 54 boys in the control group, skeletal development was followed annually by dual energy X-ray absorptiometry (DXA). As to evaluate bone area (mm²), peripheral computed tomography (pQCT) measurements were done in the forearm and tibia after 5 years. Slopes and annual changes were calculated for bone mineral density (BMD; g/cm³) and femoral neck (FN) area (mm²). Data are reported as mean group difference with 95% CI within brackets.

Results: There were 20.5 fractures/1000 person-years in the intervention group and 18.8 fractures/1000 person-years in the control group, resulting in a Rate Ratio (RR) of 1.09 (0.81, 1.45) (mean (95% CI)).

The annual gain in spine BMD was higher in both girls (0.007 (0.001, 0.013)) and boys (0.004 (0.001, 0.008)) in the intervention group compared to the control group. Girls with daily PE also had higher gain in femoral neck BMD (0.006 (0.001, 0.012)) and femoral neck area (0.04 (0.01, 0.07)) and after 5 years also a larger mid

radial cross sectional area (11 (0.6, 21)) and mid tibial cortical area (17 (2, 31)) than the control girls.

Conclusions: Increased physical activity for 6 years in a population based cohort of 7-9 year old children improve the gain in bone mass, and in girls also the bone structure, without increasing the fracture risk

Disclosures: Fredrik Detter, None.

1068

Effect of Whole-Body Vibration Therapy (WBV) for Low Bone Mass in Adolescent Idiopathic Scoliosis Girls with Osteopenia: A Randomized, Controlled Trial. Tsz Ping Lam^{*1}, Bobby Kin Wah Ng², Louis Wing Hoi Cheung², Kwong Man Lee², Ling Qin³, Jack Chun Yiu Cheng².
¹Department of Orthopaedics & Traumatology, The Chinese University of Hong Kong, Peoples Republic of China, ²Department of Orthopaedics & Traumatology, The Chinese University of Hong Kong, China, ³Chinese University of Hong Kong, Hong Kong

Introduction: Adolescent idiopathic scoliosis (AIS) was associated with osteopenia which, apart from being an important health issue, was found to be a significant prognostic factor for curve progression in AIS. Although whole-body vibration (WBV) was shown to have anabolic effects on bone metabolism in animal studies, its effect on AIS subjects has not been studied before. The objective of this study was to determine whether WBV could improve low bone mineral density (BMD) and bone quality for AIS subjects with osteopenia.

Methods: This was a randomized, controlled trial with 2 parallel groups. 149 AIS girls of age 15 to 25 years old, with Cobb angle between 10 to 50 degrees and with BMD Z-scores < -1 were recruited. They were randomly assigned to either the Treatment or Control group under strict allocation concealment. In the Treatment group, subjects were treated with standing on a low-magnitude high-frequency WBV platform 20 mins a day, 5 days a week. Subjects in the Control group received observation alone. The study period was one year. Bone measurement was done at baseline and at 12-month: (1) areal BMD and BMC at bilateral femoral necks and lumbar spine using Dual-Energy X-ray Absorptiometry and (2) bone quality in terms of bone morphometry, volumetric BMD and trabecular bone micro-architecture using high-resolution peripheral quantitative computed tomography (HR-pQCT) for the non-dominant distal radius and bilateral distal tibiae according to standard protocols.

Results: The most significant findings were greater absolute and percentage increases in femoral neck areal BMD at the dominant leg (0.015 (SD=0.031)g/cm², 2.15 (SD=4.32)%) and greater absolute increase in lumbar spine BMC (1.17 (SD=2.05)g) in the Treatment group as compared with the Control group (0.00084 (SD=0.026)g/cm², 0.13 (SD=3.62)% and 0.47 (SD=1.88)g respectively, all with p < 0.05). No statistically significant difference was noted for other DXA parameters and bone quality parameters of the non-dominant distal radius and bilateral distal tibiae.

Discussion and Conclusions: WBV was effective for improving aBMD at the femoral neck of the dominant side and lumbar spine BMC in AIS subjects which might be of clinical significance in affecting curve progression in AIS. Further studies for defining the determinants that moderate the effect of WBV and its effect on curve progression in AIS subjects are warranted.

Disclosures: Tsz Ping Lam, None.

This study received funding from: General Research Fund, Research Grants Council of Hong Kong (Project no: 467808 and 468809)

1069

Effects of Aerobic Exercise on Carboxylated and Undercarboxylated Forms of Osteocalcin and their Relationship to Exercise-induced Changes in Insulin Sensitivity and Visceral and Total Body Fat in Overweight Children. Norman Pollock^{*1}, Barbara Gower², Karl Wenger¹, Jerry Allison¹, Catherine Davis¹.
¹Georgia Health Sciences University, USA, ²University of Alabama at Birmingham, USA

Although animal studies suggest that it is the undercarboxylated rather than carboxylated form of osteocalcin that affects glucose and fat metabolism, it is unclear which of the forms of osteocalcin is associated with better insulin sensitivity and fat loss in humans. This study investigated the effects of aerobic exercise on carboxylated and undercarboxylated forms of osteocalcin and their relationship to exercise-induced changes in insulin sensitivity and visceral and total body fat in children at risk for diabetes. Overweight children (n=222, aged 7-11 years, 56% female, 47% black, 86% obese) were randomly assigned to three experimental conditions: no-exercise control condition (n=78), low dose (20 min/d, n=71), or high-dose (40 min/d, n=73) aerobic exercise program for 12-weeks (5 d/wk). At baseline and posttest, an oral glucose tolerance test was used for assessment of insulin sensitivity (Matsuda index) and circulating forms of OC [total (OC_{total}), carboxylated (cOC), and undercarboxylated (ucOC)]. Given that the assay's capacity to identify ucOC depends on the concentration of OC_{total}, we also report ucOC as a percentage of OC_{total} (%ucOC). Percentage body fat (%fat) and visceral adipose tissue (VAT) were measured by DXA and MRI, respectively, at baseline and posttest. Absolute concentrations of all measures of OC showed a dose-response increase with exercise, whereas %ucOC showed a decrease (Figure). A dose-response benefit of exercise was also observed for insulin sensitivity, as indicated by a significant upward trend, and for %fat and VAT,

as indicated by significant downward trends (all P<0.04). Multiple linear regression adjusting for age, sex, and race revealed that changes in both OC_{total} and cOC were positively associated with changes in insulin sensitivity but negatively associated with changes in VAT (all p<0.05). Changes in ucOC and %ucOC were not associated with changes in insulin sensitivity, %fat, or VAT. In overweight children, circulating forms of osteocalcin are regulated by aerobic exercise in a dose-response manner. In addition, the exercise-induced changes in insulin sensitivity and visceral fat are associated with the carboxylated, rather than undercarboxylated, form of osteocalcin.

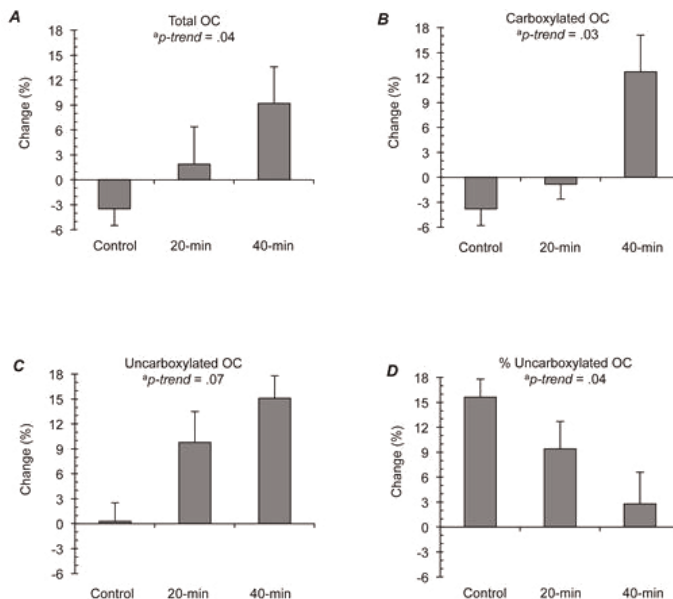


Figure. Change from baseline: total osteocalcin (A), carboxylated osteocalcin (B), undercarboxylated osteocalcin (C), and % undercarboxylated osteocalcin (D) in response to 12 weeks (5 day/wk) of either no exercise (n=78), 20 min/day of aerobic exercise (n=71), or 40 min/day of aerobic exercise (n=73). *Significant linear contrast indicates dose-response.

Disclosures: Norman Pollock, None.

1070

Effects of a Specialized School Physical Education Program on Bone Structure and Strength: A 4-year Cluster Randomised Controlled Trial. Robin Daly^{*1}, Gaelle Ducher¹, Ross Cunningham², Briony Hill¹, Rohan Telford³, Prisca Eser⁴, Geraldine Naughton⁵, Markus Seibel⁶, Ahmad Javaid⁷, Richard Telford⁸.
¹Centre for Physical Activity & Nutrition Research, Deakin University, Australia, ²Fenner School of Environment & Society, Australian National University, Australia, ³Centre for Research & Action in Public Health, Department of Health, University of Canberra, Australia, ⁴Swiss Cardiovascular Centre Bern, University Hospital (Inselspital), Switzerland, ⁵Centre of Physical Activity Across the Lifespan, Australian Catholic University, Australia, ⁶Bone Research Program, ANZAC Research Institute, University of Sydney, Australia, ⁷The Canberra Hospital, Australia, ⁸Clinical Trials Unit, The Canberra Hospital & Medical School, Australian National University, Australia

Physical activity programs incorporating specific weight-bearing exercises have proven effective for enhancing bone mineral accrual during growth, but the effects of more generalized school-based physical education (PE) on bone health remains unclear. In addition, few long-term studies have used pQCT to characterize changes in bone strength and its determinants (bone structure and volumetric BMD) in response to exercise during growth. This study investigated the effects of a specialist taught school PE program on bone mass, structure and strength and muscle mass and size in primary school aged children. This was a 4-year cluster RCT involving 365 boys and 362 girls in grade 2 aged 8 (SD 0.3) years from 29 primary schools in Canberra, Australia. All children received 150 min/week PE from classroom teachers but in 13 schools 100 min/week was replaced by two specialized PE classes that emphasized more vigorous exercise and games combined with static and dynamic postural activities involving muscle strength and function. Measurements in grades 2, 4, and 6 included DXA total body BMC and lean mass (LM), pQCT volumetric BMD, structure and strength at the radius and tibia (4% and 66% sites) and muscle CSA and pubertal development (Tanner stage). In girls, the 4-year gains in cortical area at the mid-radius and mid-tibia were on average, 9.6% (P<0.05) and 5.0% (P=0.08) greater in those who received the specialized compared to common-practice PE, with the relative increase being most apparent in the last 2 yrs. These results were independent of bone length, weight, pubertal status and the random effect of school. In boys, the only positive effect of the specialized PE was on cortical vBMD at the mid-tibia (2.4% vs 1.3%, P<0.05). However, neither of these benefits translated into significant

improvements in bone strength in the specialized PE group. There was also no evidence of any beneficial effects of specialized PE on trabecular vBMD at the distal radius or tibia or whole body LM or regional muscle CSA after 4-yrs. In conclusion, this study showed that generalized PE conducted twice weekly by specialist physical educators through grades 3-6 (age 8-12) of primary school can have some positive effects on cortical area and density, but these benefits did not translate into significant improvements in bone strength. This suggests that more specific bone loading activities may need to be incorporated into PE classes to maximize skeletal benefits during growth.

Disclosures: Robin Daly, None.

1071

Sustained Effects of Physical Activity on Bone Health: Iowa Bone Development Study. Shelby Francis*, Elena Letuchy, Steven Levy, Kathleen Janz. University of Iowa, USA

Purpose: Previous studies of young athletes and children engaged in targeted interventions have shown some maintenance of bone mineral content (BMC; g) years after cessation of training, but less is known about the sustained effects in the average child population. Using a prospective cohort, this study examined the potential effect of early childhood physical activity (PA) on BMC in adolescence.

Methods: Participants (N=156 boys, 170 girls) in the Iowa Bone Development Study had clinical exams at ages 5, 8, 11, 13, and 15 yr. Body size and somatic maturity were measured using anthropometry. Moderate to vigorous physical activity (MVPA) and vigorous PA were measured using the Actigraph accelerometer. Due to the higher fitness level in children and adolescents compared to adults, cut points were set at ≥ 4 METs for MVPA and ≥ 7 METs for vigorous PA. BMC of the lumbar spine and hip was measured using dual-energy x-ray absorptiometry. Mixed regression models were used to test whether activity level at age 5 had an effect on BMC at ages 13 and 15 after adjustment for age 13 and 15 age (yr), height (cm), weight (kg), maturity ($0 = \text{pre-peak height velocity}/1 = \text{post}$), and activity level ($\text{min} \cdot \text{day}^{-1}$). The analysis was repeated to control for BMC at age 5.

Results: On average, boys participated in 59 min, 52 min, and 38 min of MVPA at ages 5, 13, and 15, respectively. They participated in 13 min, 17 min, and 11 min of vigorous PA at ages 5, 13, and 15, respectively. MVPA and vigorous PA at age 5 predicted spine BMC at ages 13 and 15 ($p < 0.05$). MVPA at age 5 predicted hip BMC. Girls participated in 47 min, 33 min, and 26 min of MVPA at ages 5, 13, and 15, respectively. They participated in 10 min, 9 min, and 7 min of vigorous PA at ages 5, 13, and 15, respectively. Neither MVPA nor vigorous PA predicted spine BMC at ages 13 and 15. MVPA at age 5 did predict hip BMC. When the analysis was repeated to control for BMC at age 5 as well as the other covariates, the effect of MVPA and vigorous PA at age 5 remained significant for boys at the spine. For girls, neither MVPA nor vigorous PA at age 5 predicted spine or hip BMC.

Conclusions: Everyday childhood activity provides bone benefits that can be sustained into adolescence. These results, especially in boys, suggest that bone strengthening physical activity programming should begin early in childhood.

Disclosures: Shelby Francis, None.

1072

Does Stage of Sexual Maturation Determine the Relationship of Calcium Intake and Physical Activity to Bone Mass Accrual. Joan Lappe*¹, Babette Zemel², Patrice Watson³, Xiang Fang³, Vicente Gilsanz⁴, Heidi Kalkwarf⁵, Sharon Oberfield⁶, John Shepherd⁷, Karen Winer⁸. ¹Creighton University Osteoporosis Research Center, USA, ²Children's Hospital of Philadelphia, USA, ³Creighton University, USA, ⁴Children's Hospital Los Angeles, USA, ⁵Cincinnati Children's Hospital Medical Center, USA, ⁶Columbia University Medical Center, USA, ⁷University of California, San Francisco, USA, ⁸National Institutes of Health, NICHD, USA

Background: Although it is accepted that dietary calcium (Ca) and physical activity (PA) increase bone mass accrual, evidence is lacking about whether Ca and/or PA might be more important for accrual during specific stages of sexual maturation.

Aim: To describe the relationship between Ca and PA and total body bone mineral content (TBBMC) accrual by Tanner stage (TS) in a large, multi-racial cohort of children followed prospectively from early childhood until sexual maturity.

Methods: Five U.S. centers recruited 2014 healthy children (ages 5 to 19 yr) and measured them annually for up to 7 yrs. Subjects with at least 2 visits are included in this analysis (915 males, 835 females). TBBMC was assessed by dual energy x-ray absorptiometry, height (ht) with a stadiometer, and TS by endocrinologist exam. PA and Ca were assessed by self-report using the modified Slemenda questionnaire and a food frequency questionnaire, respectively.

Analyses: The relationship between PA (hrs/wk) and Ca (mg/d) and TBBMC was assessed using linear regression in a mixed model. Specifically, annualized TBBMC change (from the prior visit) was modeled as a function of prior visit TBBMC, annualized ht change, TS, and PA/Ca. Separate regressions evaluated the significance of TS by PA/Ca interactions performed on gender and racial (black, B/nonblack, NB) subgroups.

Results: Males have significantly greater average PA and Ca than females, while B have greater PA and lower Ca than NB. PA was a significant predictor of TBBMC accrual in all subgroups except B males, but no differences were seen among TS. Ca

significantly predicted accrual in NB, but not in B. When analyzing by TS, Ca was a significantly better predictor of accrual in TS 3 and 4 in NB males, in TS4 in B males, and in TS4 and 5 in NB females. When controlling for Ca, PA was associated with TBBMC accrual in all subgroups except for B males ($p < 0.08$). When controlling for PA, Ca was significantly associated with accrual only for NB.

Conclusion: PA contributes significantly to bone mass accrual in this large cohort, but has no significant association with any specific stage of sexual maturation. Overall, Ca is significantly associated with accrual in NB only, both males and females. Within subgroups, Ca appears to be more important for accrual during specific stages of sexual maturation, ie, B males, TS4; NB males, TS3 and 4, and NB females, later stages of sexual maturation.

Disclosures: Joan Lappe, None.

1073

Deletion of FoxO1, 3, and 4 from Osteoprogenitor Cells Increases Bone Mass throughout Life and Attenuates Adiposity in Aged Bone. Srividhya Iyer*¹, Elena Ambrogini¹, Li Han¹, Shoshana Bartell¹, Aaraon Warren², Julie Crawford², Paula Roberson², Robert Weinstein¹, Charles O'Brien¹, Maria Jose Almeida¹, Stavros Manolagas¹. ¹Central Arkansas VA Healthcare System, Univ of Arkansas for Medical Sciences, USA, ²Central Arkansas Veterans Healthcare System, University of Arkansas for Medical Sciences, USA

An important role of FoxO transcription factors in skeletal homeostasis has been established recently with studies of the loss or gain of FoxO function globally or selectively in osteoblasts and osteoclasts. In addition, it has been shown in many cell types, including osteoblasts, that FoxOs defend against oxidative stress or growth factor depletion and in the process divert β -catenin from Wnt/Tcf- to FoxO mediated transcription. Based on this and evidence that Wnt/ β -catenin signaling increases bone mass by promoting the progression of Osterix (Osx)-expressing cells to matrix synthesizing osteoblasts, we have deleted FoxO1,3,4 conditional alleles in committed osteoblast precursors expressing Osx1 (FoxO1,3,4flox;Osx1-Cre). At 3 months these mice exhibited a 20% increase in BMD at the spine and femur, an increase in cancellous bone volume, and increased periosteal apposition as compared to littermate controls. When the deletion was postponed until 3 months of age (by activating a Tet-off system incorporated into the Osx-Cre transgene), a very similar increase occurred in both femoral and spinal BMD, demonstrating that the phenotype was not due to developmental changes. The high bone mass was associated with increased BrdU incorporation, osteoblast number, and bone formation rate. Cultured Osx-GFP positive calvaria cells or periosteal cells from the femurs of FoxO1,3,4-flox;Osx-Cre mice exhibited higher proliferation and increased expression of the β -catenin/Tcf target genes cyclinD1, connexin43, coll6a1, and Mmp16. Consistent with the evidence that FoxOs antagonize Wnt/Tcf signaling, deletion of FoxOs by transfection of adeno-Cre in calvaria cells, increased cyclinD1 expression and proliferation, similar to treatment with Wnt3. Bone-marrow derived cells from FoxO1,3,4-flox;Osx-Cre mice also formed fewer adipocytes in response to rosiglitazone. Importantly, the high bone mass phenotype of the FoxO1,3,4-Flox;Osx-Cre mice was maintained up to 24 months of age. And at this age, FoxO1,3,4-Flox;Osx-Cre mice exhibited fewer marrow adipocytes in the femur as compared to controls. We conclude that throughout life activation of FoxOs restrains Wnt signaling by diverting β -catenin from Wnt/Tcf- to FoxO mediated transcription in osteoprogenitor cells. Thus, FoxO activation may contribute to the decreased bone mass and the increased bone marrow adiposity of the aging skeleton, perhaps while defending against oxidative stress.

Disclosures: Srividhya Iyer, None.

1074

Reciprocal Control of Osteogenic and Adipogenic Lineages by ERK/MAP Kinase Signaling and Transcription Factor Phosphorylation. Chunxi Ge*¹, William Cawthorn², Yan Li³, Guisheng Zhao³, Jennifer Westendorf⁴, Ormond MacDougald⁵, Renny Franceschi³. ¹Pom Univ of Michigan School of Dentistry, USA, ²Department of Molecular & Integrative Physiology University of Michigan, USA, ³University of Michigan, USA, ⁴Mayo Clinic, USA, ⁵Department of Molecular & Integrative Physiology University of Michigan School of Medicine, USA

Osteoblasts and adipocytes are thought to arise from a common mesenchymal stem cell. The ratio of marrow-derived osteoblasts to adipocytes decreases in osteoporosis and during skeletal unloading. Osteoblast differentiation is stimulated by ECM deposition and mechanical loading, events known to be accompanied by MAP kinase activation. Also, the osteoblast/adipocyte determination factors, RUNX2 and PPAR γ , exert reciprocal control over these 2 differentiation outcomes with RUNX2 suppressing adipogenesis and PPAR γ suppressing osteoblastogenesis. In this project, we test the hypothesis that the ERK/MAPK pathway is a major determinant of MSC lineage commitment to osteoblasts and an inhibitor of adipogenesis and that control of cell fate is achieved by phosphorylation of RUNX2 and PPAR γ transcription factors. ST2 murine MSC cells were grown in osteogenic or adipogenic medium and differentiation was measured by Alizarin Red or Oil Red O staining and expression of osteoblast and adipocyte markers. During osteoblast differentiation, ERK and

RUNX2-S319 phosphorylation increased. Interesting, PPAR γ -S112-P also increased and this was associated with decreased expression of adipocyte markers. During adipocyte differentiation, ERK activity and phosphorylation of both transcription factors decreased. Using RUNX2 and PPAR γ reporter constructs, MAPK phosphorylation was shown to directly stimulate RUNX2 transcriptional activity while inhibiting PPAR γ and this regulation was mediated by phosphorylation at S301,319 (RUNX2) and S112 (PPAR γ). Also, direct activation of MAPK signaling using an adenovirus encoding constitutively active MEK1 stimulated osteoblast differentiation and inhibited adipogenesis while DN MEK1 inhibited osteoblastogenesis and stimulated adipocyte formation. MAPK-dependent phosphorylation of RUNX2 was also shown to indirectly regulate Wnt signaling via down-regulation of the Wnt inhibitor, Axin2, leading to increased β -catenin during osteoblast differentiation. As previously reported, wild type RUNX2 is a potent stimulator of osteoblast differentiation when transfected into MSC-like cells while RUNX2 containing S301A, S319A mutations is inactive. Similarly, WT RUNX2 inhibits adipocyte differentiation while the S/A mutant is less active. Taken together, these studies show that levels of ERK/MAPK and RUNX2/PPAR γ phosphorylation are key determinants of osteoblast or adipocyte differentiation from MSCs.

Disclosures: Chunxi Ge, None.

1075

Stem Cell Antigen-1 Positive (Sca-1+) Cell-based Gene Therapy with Fibroblast Growth Factor-2 (FGF2) Promotes Robust Recruitment of Osteoprogenitors in the Bone Marrow of Recipient Mice. Susan Hall*¹, Shin Tai Chen², Kristy Howard¹, Daila Gridley³, Subburaman Mohan¹, Kin-Hing William Lau¹. ¹Jerry L. Pettis Memorial VA Medical Center, USA, ²Jerry L. Pettis VA Medical Center, USA, ³Loma Linda University, USA

FGF2 is a potent mitogenic and angiogenic protein that when administered to rodents results in large increases in osteoblast and osteoid surface at bone sites. We have shown that transplantation of Sca1+ cells expressing a modified FGF2 gene (with improved secretion and stability) provides sustained, high dose FGF2 expression, and yields rapid and robust endosteal bone formation (BF) in recipient mice. In this study, to identify the mechanism for the increased BF, we evaluated the hypothesis that the FGF2 produced by engrafted Sca1+ cells in the bone marrow (BM) acts to promote recruitment and expansion of osteoprogenitors. We employed our *ex vivo* gene therapy model to determine the effect of transplanting FGF2 overexpressing cells on the mRNA levels of putative osteoprogenitor marker genes. Sublethally irradiated stem cell-deficient mice were injected IV with Sca1+ cells transduced with MLV-based vectors expressing FGF2 or β -gal (control). At 2 and 6 weeks post transplantation, RNA was isolated from BM cells of femurs of recipient mice and evaluated for transgene expression. Aliquots of individual samples were pooled according to level of FGF2 expression (high, medium, low or control) and the mRNA levels of candidate markers of osteoprogenitors (CD29, CD44, CD90, CXCR4, nestin, PDGFR- α , PDGFR- β , Sca1, SMA- α) were assessed by qRT-PCR. At 2 weeks post transplantation, compared to controls, dramatic dose-dependent increases were observed in PDGFR- β (12-, 19- and 35-fold), SMA- α (10-, 15- and 25-fold) and nestin (7-, 9- and 11-fold) mRNA levels in the low, medium and high FGF2 pooled samples, respectively. This dose-dependent trend was also seen at 6 weeks for all three genes. Other putative osteoprogenitor markers showed small changes and/or no dose-dependent pattern. mRNA level assessment of PDGFR- β , SMA- α and nestin was repeated on individual BM samples. Linear regression analysis confirmed strong positive correlations between FGF2 mRNA levels and PDGFR- β (R=0.77, p<0.0001), SMA- α (R=0.74, p<0.0002) and nestin (R=0.83, p<0.0001). To test if the increased recruitment of osteoprogenitors is caused by increased angiogenesis, we measured mRNA levels of angiogenic marker genes (Ang1, vWF, CD31) and failed to detect consistent changes in the expression of any of gene tested. In conclusion, our findings are consistent with a model in which engrafted FGF2 expressing Sca1+ cells leads to rapid recruitment of osteoprogenitors in the BM to induce robust endosteal BF.

Disclosures: Susan Hall, None.

1076

Loss of Osteoblastic Connexin 43 Results in Delayed Bone Formation, Increased Sclerostin Expression and Attenuated Wnt Signaling During Fracture Repair. Alayna Loisel*¹, Emmanuel Paul¹, Gregory Lewis¹, Henry Donahue². ¹Penn State Hershey, USA, ²The Pennsylvania State University College of Medicine, USA

Connexin 43 (Cx43) is the predominant gap junction protein in bone, and is required for osteoblast differentiation, and bone homeostasis. We have generated mice with targeted deletion of Cx43 in osteoblasts using Col1-Cre (2.3Kb) to test the hypothesis that loss of Cx43 in osteoblasts results in decreased bone formation and mechanical properties as a result of increased Sclerostin expression, and diminished Wnt/ β -Catenin signaling. Cx43 conditional knockout mice (Cx43cKO) had significantly decreased Cx43 expression, as assessed by qPCR in the fracture callus, relative

to WT at all time-points post-fracture. Peak Cx43 expression occurred at 28 days in WT fractures (117-fold vs. WT day 3 expression, p=.001). Deletion of Cx43 in osteoblasts delayed expression of osteoblastic markers (*Col1a1*, *Osteocalcin*, *Bmp2*), suggesting a delay in the transition from cartilage to bony callus. Peak *Col1* expression occurred at 10 days (3.5-fold vs. day 3 WT, p=.02) in WT fractures, while peak *Col1* expression was delayed until 14 days in Cx43cKO fractures (3.7-fold, p=.04). Sclerostin (encoded by *Sost*), an inhibitor of bone formation and an antagonist of Wnt/ β -Catenin signaling, was significantly increased in Cx43cKO fractures at 21 days relative to WT (WT:129 \pm 13.5; Cx43cKO: 254 \pm 26.8, p=.002). Increased expression of *Wnt3a*, and Frizzled receptors were also observed, indicative of possible compensation for increased *Sost* expression. However, β -Catenin expression was significantly decreased in Cx43cKO fractures. This attenuation of β -Catenin signaling resulted in decreased BV/TV (WT:0.3 \pm 0.03 Cx43cKO:0.24 \pm 0.06 p=.03) and ultimate torque at failure (WT:21.66 \pm 4.9 N*mm, Cx43cKO:12.77 \pm 1.5, p=.009) of Cx43cKO fractures at 28 days post-repair. Loss of Cx43 during fracture healing also alters the remodeling phase of healing, with decreased *RankL* and increased *Opg* expression in Cx43cKO fractures, compared to WT at 21 days. This work identifies a novel mechanism of fracture callus mineralization via Cx43 regulation of Sclerostin and the Wnt/ β -Catenin pathway. These data suggest that targeted overexpression of Cx43 could decrease *Sost* expression, and enhance Wnt/ β -Catenin signaling to improve healing of fracture non-unions. This concept is a shift from the recognized paradigm of Cx43 as a down-stream functional target of Wnt signaling, to a role for Cx43 mediated regulation of Wnt/ β -Catenin and mineralization.

Disclosures: Alayna Loisel, None.

1077

Bone as a Site of Insulin Resistance in Type 2 Diabetes. Jianwen Wei*, Gerard Karsenty. Columbia University, USA

Type 2 diabetes is characterized by insulin resistance in insulin target cells, the classical ones being the hepatocytes, myoblasts and adipocytes. The recent realization that the osteoblast is an insulin target cell involved in the control of whole-body glucose homeostasis suggests the possibility that impaired insulin signaling in osteoblasts might contribute to the development of type 2 diabetes. Consistent with this hypothesis, we first showed that insulin resistance occurred in osteoblasts in wild type mice rendered diabetic through a high-fat-diet (HFD). Molecular evidence of insulin resistance include reduced phosphorylation of AKT at Th308 and Ser347 in bones, a decrease of bone resorption due to an increase of *Opg* expression and a decrease of the active form of osteocalcin. Next, to test if insulin resistance in osteoblasts contributes to whole-body insulin resistance, we used loss-of (*InsR_{osb}+/-* mice) and gain-of function (*$\alpha 1(1)$ -InsR* transgenic mice) models of insulin signaling in osteoblasts. Glucose tolerance tests and insulin tolerance tests showed that *InsR_{osb}+/-* mice were more severely glucose intolerant and insulin resistant than control mice fed the same HFD, in contrast *$\alpha 1(1)$ -InsR* mice were protected from insulin resistance. Accordingly, *ex vivo* cell culture experiments and *in vivo* hyperinsulinemic euglycemic clamp experiments showed that osteoblasts uptake glucose in an insulin-regulated manner and that glucose uptake in osteoblasts is decreased in mice fed a HFD. Lastly, gene profiling analysis identified *Glut1* as the main glucose transporter in osteoblasts mediating both basal and insulin-dependent glucose uptake. Accordingly, gain and loss of function experiments in the mouse showed that *Glut1* is necessary for whole-body glucose homeostasis. Taken together, this study provides evidence that insulin resistance takes place in osteoblasts in diet-induced type 2 diabetes and identifies a molecular mechanism whereby insulin favors glucose uptake in osteoblasts.

Disclosures: Jianwen Wei, None.

1078

Completing the Bone/Brain Circuit: Osteocalcin Signals within the Hypothalamus to Inhibit Bone Formation. Shu Lin¹, Ronaldo Enriquez¹, Herbert Herzog¹, John Eisman², Paul Baldock*². ¹Neuroscience Program, Garvan Institute of Medical Research, Australia, ²Garvan Institute of Medical Research, Australia

Osteocalcin (Ocn) is increasingly recognized for its endocrine actions to regulate energy homeostasis. However, despite its relatively osteoblast-specific expression, a major role for Ocn in bone has yet to be identified. Previous studies have reported a mild increase in bone mass in Ocn null mice, with elevated bone turnover and greater cortical bone formation. Thus the fundamental role of Ocn in bone is unclear.

We have examined the role of Neuropeptide Y family (NPY), which acts in the arcuate nucleus (Arc) of the hypothalamus to coordinate bone and energy homeostasis. The NPY pathway to bone is stimulated by circulating factors, such as leptin; which itself feeds back to the brain to regulate fat mass. We hypothesized that Ocn may also form a feedback loop within the brain, to regulate bone mass. Moreover, this loop may involve NPY action within the Arc of the hypothalamus.

We examined Ocn activation of hypothalamic neurons by determining c-fos expression. A Iug i.p. bolus of Ocn induced c-fos in neurons of the Arc, indicating that serum Ocn activates hypothalamic neurons. Injection of Ocn directly into the CSF circulation also activated neurons in the arcuate, as well as a number of other hypothalamic regions, indicating direct Ocn signalling in the brain.

To examine chronic Ocn supply to the hypothalamus, we injected a viral vector expressing Ocn (AAV-Ocn) into the Arc of 10 week old mice and examined bone 12 weeks later. This model mimics increased circulatory supply to the brain, as the Arc has a semi-permeable blood brain barrier. Consistent with increases in Ocn KO mice, AAV-Ocn injection significantly reduced cancellous bone volume of the distal femur (40%), compared to AAV-empty injected controls. This was associated with a significant reduction in mineral apposition rate (33%). These changes occur despite a fall in serum Ocn (AAV-empty 137 ± 7 ng/ml vs AAV-Ocn 115 ± 6 p<0.05), highlighting the importance of central signalling to the anti-anabolic effect.

This anti-anabolic Ocn effect requires intact NPY signalling, as AAV-Ocn injection did not alter bone in NPY KO or Y2 Receptor KO mice, both of which act through signalling in the Arc.

In conclusion, Ocn signals directly in neurons of the arcuate nucleus to control bone homeostasis. Chronic over supply of Ocn to these neurons inhibits bone formation and bone mass. This study defines, for the first time, a central feedback mechanism for bone mass, completing the bone-brain circuit.

Disclosures: Paul Baldock, None.

1079

No Additive Effects of In Vivo Loading and Sclerostin Antibody Treatment on Bone Anabolism in Elderly Mice. David Pflanz^{*1}, Etienne Berthet², Annette Birkhold³, Tobias Thiele², Chaoyang Li⁴, Hua Zhu Ke⁴, Georg Duda², Bettina Willie⁵. ¹Charité Universitätsmedizin Berlin, Germany, ²Julius Wolff Institute, Charité - Universitätsmedizin Berlin, Germany, ³Julius Wolff Institute, Charité Universitätsmedizin Berlin, Germany, ⁴Amgen Inc., USA, ⁵Charité- Universitätsmedizin Berlin, Germany

Bone adapts to mechanical stimuli to gain an optimized structure, although the exact mechanisms regulating this process remain unclear. The protein sclerostin, secreted by osteocytes, is thought to reduce bone formation by inhibiting Wnt signaling and decreasing osteoblast function. Recent data suggests SOST/sclerostin suppression may be at least partially responsible for the anabolic action of mechanical loading. We tested the effect of inhibition of sclerostin by sclerostin antibody (Scl-Ab) on elderly mice with or without in vivo loading.

We performed in vivo cyclic compressive loading to the left tibia of 78 week old female C57Bl/6J mice, half of which were treated with 25 mg/kg of Scl-Ab, twice a week (n=10/group). The right limb was an internal control. A peak load of -9N was applied at 4Hz for 432 cycles/day, 5days/week for 2 weeks engendering peak strains of 1200 μ e on the medial midshaft, measured by strain gauging. Longitudinal microCT at 10.5 μ m resolution was performed at day 0, 5, 10, and 15. Trabecular bone volume fraction (BV/TV), tissue mineral density (Tb vTMD, mg HA/cm³), thickness (TbTh, μ m) and separation (TbSp, μ m) were assessed in the proximal tibia. Principal moments of inertia (I_{MAX}, I_{MIN}), cortical bone area (CtAr, mm²), total cross-sectional area (TtAr, mm²), area fraction (CtAr/Tt.Ar), thickness (CtTh, μ m) and tissue mineral density (Ct vTMD, mg HA/cm³) were assessed at midshaft. An ANOVA was used to assess within-subject and between-subject effects and interactions.

By day 15, BV/TV increased significantly in Scl-Ab treated mice with (+89%) and without (+150%) loading compared to non-treated mice. Similarly, CtAr increased significantly in Scl-Ab treated mice with (+21%) and without (+27%) loading (Table 1). While Scl-Ab treated mice exhibited significant gains in bone mass, non-treated mice lost bone mass. Loading attenuated bone loss in non-treated mice; significantly greater BV/TV, TbTh, CtAr, and CtTh was measured at day 15 (loaded vs. control). No significant effect of loading was measured in Scl-Ab-treated mice at day 15. In summary, loading had a mild effect in maintaining bone mass in elderly mice, which was not observed when Scl-Ab was administered since Scl-Ab not only maintained but also increased bone mass from baseline controls. No additive effect of loading and Scl-Ab treatment on bone anabolism was observed, suggesting sclerostin may contribute to loading-induced bone gain in vivo.

| Outcome | 78 wk old | | 78 wk old + Scl-Ab | |
|---|---------------|---------------|--------------------|---------------|
| | Loaded | Control | Loaded | Control |
| Day 0 | (n=10) | (n=10) | (n=10) | (n=10) |
| Tb.BV/TV (mm ³ /mm ³) | 0.025 ± 0.010 | 0.020 ± 0.012 | 0.022 ± 0.010 | 0.022 ± 0.009 |
| Tb.Th (μ m) | 57 ± 8 | 55 ± 11 | 50 ± 10 | 51 ± 11 |
| Tb.N (1/mm) | 2.12 ± 0.74 | 2.07 ± 0.21 | 2.13 ± 0.24 | 2.16 ± 0.25 |
| Tb.Sp (μ m) | 436 ± 79 | 506 ± 55 | 491 ± 72 | 490 ± 65 |
| Tb.vTMD (mg HA/cm ³) | 967 ± 46 | 974 ± 65 | 977 ± 37 | 942 ± 34 |
| Day 5 | (n=10) | (n=10) | (n=10) | (n=10) |
| Tb.BV/TV (mm ³ /mm ³) | 0.020 ± 0.006 | 0.018 ± 0.009 | 0.023 ± 0.013 | 0.021 ± 0.009 |
| Tb.Th (μ m) | 55 ± 10 | 55 ± 11 | 54 ± 09 | 50 ± 15 |
| Tb.N (1/mm) | 2.30 ± 0.52 | 2.06 ± 0.22 | 2.21 ± 0.24 | 2.16 ± 0.24 |
| Tb.Sp (μ m) | 462 ± 85 | 505 ± 53 | 476 ± 65 | 488 ± 62 |
| Tb.vTMD (mg HA/cm ³) | 970 ± 37 | 977 ± 49 | 984 ± 33 | 946 ± 16 |
| Day 10 | (n=10) | (n=10) | (n=10) | (n=10) |
| Tb.BV/TV (mm ³ /mm ³)† | 0.018 ± 0.005 | 0.016 ± 0.006 | 0.025 ± 0.013 | 0.024 ± 0.010 |
| Tb.Th (μ m) | 57 ± 8 | 53 ± 08 | 59 ± 11 | 55 ± 19 |
| Tb.N (1/mm) | 2.24 ± 0.33 | 2.04 ± 0.19 | 2.18 ± 0.22 | 2.13 ± 0.29 |
| Tb.Sp (μ m) | 476 ± 50 | 506 ± 60 | 485 ± 47 | 475 ± 83 |
| Tb.vTMD (mg HA/cm ³) | 989 ± 49 | 976 ± 36 | 995 ± 29 | 975 ± 33 |
| Day 15 | (n=10) | (n=10) | (n=10) | (n=10) |
| Tb.BV/TV (mm ³ /mm ³)† | 0.018 ± 0.006 | 0.012 ± 0.006 | 0.034 ± 0.021 | 0.030 ± 0.013 |
| Tb.Th (μ m)† | 57 ± 10 | 47 ± 14 | 67 ± 11 | 66 ± 17 |
| Tb.N (1/mm) | 2.16 ± 0.28 | 2.27 ± 0.47 | 2.20 ± 0.29 | 2.23 ± 0.30 |
| Tb.Sp (μ m) | 484 ± 52 | 460 ± 87 | 480 ± 53 | 470 ± 70 |
| Tb.vTMD (mg HA/cm ³) | 985 ± 36 | 935 ± 103 | 1016 ± 36 | 987 ± 52 |

Table 1: Trabecular (Tb) parameters (Mean \pm SD); †treatment effect, *loading effect, p<0.05

Disclosures: David Pflanz, None.

1080

Effects of Sclerostin Antibody on Tissue Level Strength in oim Mice. Jean-Pierre Devogelaer^{*1}, Patrick Ammann², Mike Ominsky³, Catherine Behets⁴, Daniel Manicourt⁵. ¹St. Luc University Hospital, Belgium, ²Division of Bone Diseases, Switzerland, ³Amgen, USA, ⁴Université Catholique de Louvain, Belgium, ⁵Université Catholique De Louvain, Belgium, Belgium

Available treatments fail to prevent the high rate of limb fractures in children with osteogenesis imperfecta (OI) type III, a severe genetic condition with poor bone quality. A sclerostin neutralizing monoclonal antibody (Scl-Ab) markedly reduced long bone fractures in oim/oim mice, a model of OI type III; therefore, tibiae of OI mice were analyzed to test the effects of Scl-Ab on bone strength at the level of the whole bone and for the bone matrix by nanoindentation.

Wildtype (WT) and OI mice (6-week-old) were treated with either Scl-Ab at 25 mg/kg or vehicle (PBS) twice per week for 10 weeks. Bone mechanical properties of tibia midshaft were assessed using a three-point bending test as well as by nanoindentation. Statistical analysis included parametric analysis of variance (ANOVA) followed by post hoc tests. Data are provided as mean \pm SEM.

As reported previously, Scl-Ab reduced the number of fractures in upper and lower limbs in OI mice by 60% (5.2 ± 0.3 versus 2.1 ± 0.2 per mouse; p<0.001). This effect corresponded to significant improvements in tibia midshaft cortical thickness (+50%), ultimate load (+53%), and stiffness (+112%) in Scl-Ab treated OI mice compared to PBS controls (Table). Similar effects of Scl-Ab were observed in WT mice. Plastic energy, which reflects tissue brittleness, was lower in the OI mice compared to WT mice, and significantly affected by Scl-Ab treatment. At the tissue level by nanoindentation, Scl-Ab increased slightly (+4%) the elastic modulus in both OI and WT bone whereas Scl-Ab increased modestly tissue hardness (+13% versus PBS) in WT bone, but not in OI bone.

Although it was unable to change the material properties of the bone matrix in OI mice, Scl-Ab was able to reduce the rate of long bone fractures by improving bone mass and whole bone strength. These results suggest that Scl-Ab may have the potential to reduce fractures in patients with OI.

| Tibia Shaft Parameter | OI mice | | WT mice | |
|-------------------------|-------------|--------------|-------------|--------------|
| | PBS | ScI-Ab | PBS | ScI-Ab |
| Cortical Thickness (mm) | 0.18 ± 0.03 | 0.25 ± 0.02* | 0.26 ± 0.01 | 0.39 ± 0.05* |
| Ultimate Load (N) | 5.3 ± 0.8 | 8.1 ± 0.6* | 12.2 ± 1.2 | 21.3 ± 1.1* |
| Stiffness (N/mm) | 14.1 ± 2.1 | 29.9 ± 3.0* | 38.9 ± 2.2 | 61.6 ± 4.1* |
| Elastic Energy (N*mm) | 1.1 ± 0.3 | 1.0 ± 0.1 | 1.6 ± 0.1 | 3.3 ± 0.2* |
| Plastic Energy (N*mm) | 0.4 ± 0.1 | 0.9 ± 0.2* | 0.8 ± 0.1 | 1.5 ± 0.2* |
| Elastic Modulus (GPa) | 18.2 ± 0.2 | 19.3 ± 0.3* | 18.2 ± 0.2 | 19.3 ± 0.2* |
| Hardness (MPa) | 737 ± 22 | 760 ± 20 | 558 ± 13 | 628 ± 13* |

*P<0.02 versus PBS

Table Effects of Sclerostin Antibody on Tissue Level Strength in oim Mice

Disclosures: Jean-Pierre Devogelaer, None.

1081

Mechanical Loading and Intermittent Parathyroid Hormone Promote Osteoblastogenesis, Inhibit Adipogenesis, and have Opposing Effects on Osteoclast Activity In Periprosthetic Bone. Matthew Grosso^{*1}, Hayden-William Courtland¹, Xu Yang¹, James Sutherland¹, Anna Fahlgren¹, Eduardo Suero¹, F. Patrick Ross¹, Marjolein Van Der Meulen², Mathias Bostrom¹. ¹Hospital For Special Surgery, USA, ²Cornell University, USA

Mechanical loading and parathyroid hormone (PTH) administration independently stimulate bone formation, and are strong candidates for enhancing osseointegration at the bone-implant surface. An understanding of the effects of these treatments on periprosthetic bone at the cellular level is crucial to developing targeted treatment strategies for implant stability. We hypothesized that the effects of loading and PTH on periprosthetic cancellous bone are anabolic and synergistic when combined, and that these effects are mediated by enhanced osteoblast differentiation and proliferation, control of bone turnover, and inhibition of adipogenesis.

Adult rabbits (n=96) underwent surgery to insert a porous titanium implant directly on the cancellous bone beneath a mechanical loading device on the right and left distal lateral femur. The right femur was loaded daily, and the left femur received a sham loading device. Half of the rabbits received daily PTH, and half received saline. Periprosthetic cancellous bone was processed at 3, 7, 14, and 28 days for gene expression and histology.

Runx2 mRNA, a transcription factor that promotes osteoblastogenesis, increased with loading (1.5 fold, p=0.007). PTH treatment decreased SOSTmRNA, an inhibitor of Wnt signaling, (-2 fold, p=0.01), and increased β -catenin levels (1.5 fold, p=0.009). SOSTmRNA decreased and β -catenin levels increased with loading (SOST: -1.5 fold, p=0.10, β -catenin: 1.5 fold, p=0.10) but did not reach significance. PPAR γ , a transcription factor that promotes adipogenesis, decreased with PTH treatment (-2.5 fold, p=0.021) and loading (-2 fold, p=0.023), but the effect was not additive or synergistic (Fig. 1). With loading, osteoclast number decreased (-1.5 fold, p=0.007), and was supported by increased OPG levels (2 fold, p=0.02). Conversely, PTH increased RANKL levels (1.5 fold, p=0.23), and osteoclast number (2.5 fold, p=0.03) (Fig. 2).

Mechanical loading and PTH exhibit similar effects in periprosthetic bone; they promote osteoblast activity and inhibit adipogenesis, acting at least in part through the Wnt signaling pathway. Although these pathways were similar, no synergistic effect between PTH and loading was seen at the molecular or cellular level. However, we found that mechanical loading reduces osteoclast number, in contrast to the pro-resorptive PTH effects, which may allow for a net additive effect on bone formation at the tissue level in this model of implant osseointegration.

Figure 1:

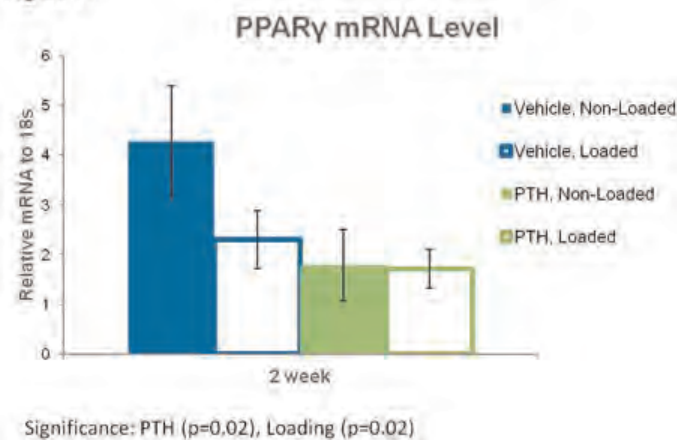


Figure 1

Figure 2:

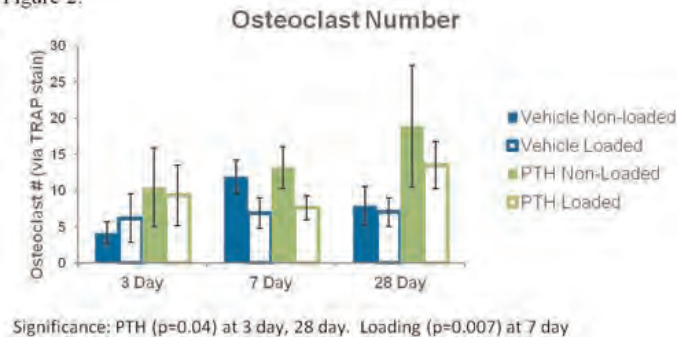


Figure 2

Disclosures: Matthew Grosso, None.

1082

Spatial Patterns of Src Activity Differ in Response to Mechanical Loading or EGF in Osteocytes. Julia Hum^{*1}, Suzanne Young², Richard Day¹, Fredrick Pavalko¹. ¹Indiana University School of Medicine, USA, ²Indiana University, USA

Mechanotransduction is the process by which a mechanical load is detected by osteocytes and osteoblasts at the cellular membrane and results in changes of gene transcription. However, the exact mechanism(s) of transmitting a physical stimulus to the nucleus is unknown. Src, a tyrosine kinase, is activated in response to mechanical loading and epidermal growth factor (EGF) treatment. We suggest that Src is an important mediator of mechanotransduction in osteocytes. To further investigate the role of Src during mechanical loading, we compared Src's pattern of activity in response to both oscillatory fluid shear stress (OFSS) and EGF treatment in live osteocytes using Förster Resonance Energy Transfer (FRET). A novel Src biosensor labeled with fluorescent probes (FP) at both C- and N-terminus was used. The activity of the Src biosensor was monitored via fluorescent lifetime imaging microscopy (FLIM). FLIM images dynamic real-time protein interactions and is capable of displaying sub-cellular locations of Src activity in live osteocytes. Src activity was assessed by measuring the FP's lifetime (nanoseconds). An inactivate Src mutant biosensor displayed no change in Src activity in response to OFSS or EGF treatment. However, in response to 5 minutes of OFSS, the Src biosensor displayed a distinct pattern of Src activity at 10, 15 and 20 minutes post OFSS. Src activity was significantly greater at the membrane after 10 minutes post OFSS as compared to static controls (p<.001). At 15 minutes post OFSS, Src activity was significantly greater in the cytoplasm (p<.001) and at 20 minutes post OFSS Src activity was significantly greater in the nuclear/perinuclear region (p<.001). In contrast, after 10 minutes of EGF treatment, Src activity significantly increased at the membrane (p<.001), but otherwise was uniformly increased throughout the osteocytes compared to static controls. Our data reveals, for the first time in live osteocytes, that OFSS and EGF treatment initially induces Src activity near the cell membrane, but with time OFSS increased Src activity in the cytoplasm and nuclear/perinuclear regions of the cell.

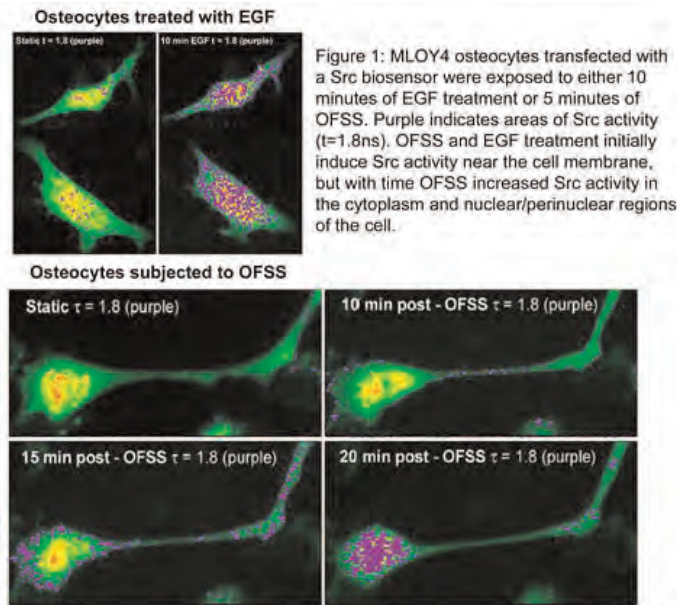


Figure 1: MLOY4 osteocytes transfected with a Src biosensor were exposed to either 10 minutes of EGF treatment or 5 minutes of OFSS. Purple indicates areas of Src activity ($\tau=1.8$ ns). OFSS and EGF treatment initially induce Src activity near the cell membrane, but with time OFSS increased Src activity in the cytoplasm and nuclear/perinuclear regions of the cell.

Spatial patterns of Src activity in osteocytes in response to mechanical loading or EGF

Disclosures: Julia Hum, None.

1083

Deletion of Sirtuin 1 in Mature Osteoblasts Increases the Anabolic Response to Mechanical Loading *in vivo*, but Inhibits Wnt Signaling *in vitro*. Nicole Fleming¹, Jonathan Gali¹, Kellen Sakala¹, Katherine Matthews¹, Jeffrey Nyman², Daniel Perrien². ¹Vanderbilt University, USA, ²Vanderbilt University Medical Center, USA

Sirtuin 1 (Sirt1) is a Class III histone deacetylase that we and others have previously shown to regulate bone homeostasis via direct actions in both osteoblasts (Ob) and osteoclasts. Sirt1 is also expressed in osteocytes (Ot) in murine bone, but its role there is unknown. Inhibition of Sirt1 has been shown to inhibit β -catenin mediated Wnt signaling, a critical mediator of mechanical adaptation in bone, via decreased expression of multiple dishevelled proteins. Hence, we sought to understand the role of Sirt1 in the *in vivo* adaptation of bone to increased mechanical load. Sirt1^{Ob-/-} and Sirt1^{Ot-/-} mice were created by crossing 2.3kb-Col1 α 1-cre mice or 10kb-DMP-cre mice, respectively, with Sirt1^{lox} mice and inbreeding. As previously described, Sirt1^{Ob-/-} mice have mild but significant low bone volume phenotype. However, neither the trabecular nor cortical phenotypes were significantly altered in Sirt1^{Ot-/-} mice. Dynamic axial loading was performed on the left tibia of 3-month old male Sirt1^{Ob-/-}, Sirt1^{Ot-/-}, or respective Sirt1^{lox} littermates 3 days per week for 3 weeks. Mechanical loading significantly increased periosteal BFR and MS/BS in the tibial diaphysis compared to the non-loaded tibia in all genotypes. Surprisingly though, the load-induced increase in bone BFR and MS/BS was significantly greater Sirt1^{Ob-/-} mice compared to both Sirt1^{lox} and Sirt1^{Ot-/-} mice ($p<0.05$). The anabolic response in Sirt1^{lox} and Sirt1^{Ot-/-} mice was not significantly different. To determine the effect of Sirt1 deletion on Wnt signaling in Ob, wild type (WT) and Sirt1^{-/-} primary calvarial Ob were treated with vehicle, Wnt3a, or LiCl for 24 hours and the expression of sFrp2 was determined by RT-qPCR as an indicator of canonical Wnt signaling. As expected, both Wnt3a and LiCl significantly decreased the expression of sFrp2 in WT Ob ($p<0.01$). However, the ability of both factors to suppress sFrp2 expression was significantly reduced in the absence of Sirt1 ($p<0.05$). While Wnt signaling is largely associated with increased osteogenesis, others have shown that Wnts inhibit late stage differentiation of and mineralization by osteoblasts. These results suggest that deletion of Sirt1 in Col1 α 1-expressing, mature osteoblasts increases the anabolic response to mechanical loading by preventing the inhibitory effects of increased Wnt signaling in mature osteoblasts.

Disclosures: Daniel Perrien, None.

1084

Lipocalin2 Is a New Osteoblast Mechano-Responding Gene That Regulates Osteoblast Differentiation and Osteoblast-Induced Osteoclastogenesis. Mattia Capulli¹, Nadia Rucci², Anna Teti². ¹Department of experimental Medicine, University of L'Aquila, Italy, ²University of L'Aquila, Italy

In a global transcriptome analysis of mouse calvarial osteoblasts subjected to simulated microgravity (0.008g), Lipocalin-2 (LCN2) was the most upregulated gene

(>8-fold) vs control (1g), suggesting a role in the response of osteoblasts to reduced mechanical loading. The enhanced expression of LCN2 correlated with an impaired osteoblast differentiation, as demonstrated by a decreased mRNA expression of Runx2, Sfrp2, Wisp2 and genes encoding for bone matrix proteins. Since the physiologic functions of LNC2 remain poorly understood and its role in bone is unknown, we transduced primary mouse osteoblasts with LCN2-expression-vector (Lcn2OBS) and investigated their phenotypic alterations. We observed that Runx2 and its downstream genes Osterix and Alp were downregulated in Lcn2OBS vs empty-vector transduced osteoblasts (emptyOBS) (-72%,-80% and -83%, respectively). Moreover, ALP activity was less prominent (-46%), thus indicating a less differentiated osteoblast phenotype. Lcn2OBS also exhibited an increase in Rankl/Opg ratio and IL-6 mRNA expression (8- and 5.3-fold increase, respectively), suggesting that LCN2 up-regulation could link poor osteoblast differentiation with enhanced osteoclastogenesis. Consistently, incubation of purified mouse bone marrow macrophages with conditioned media from Lcn2OBS, or their co-culture with Lcn2OBS, enhanced osteoclast formation compared to emptyOBS (5- and 2-fold increase, respectively). LCN2 could have an autocrine-paracrine effect given that osteoblasts expressed the LCN2 receptors, megalin and 24p3r, both at transcriptional and protein level. The mechano-responding properties of LCN2 were confirmed in three animal models of reduced mechanical loading-induced bone loss: tail suspension, treatment with the muscle paralysis inducer botox, and dystrophic MDX mice. Lcn2 mRNA was upregulated in the bones of all three models relative to controls (147-, 96- and 5.8-fold increase, respectively), with increased protein level confirmed in the botox-treated mice. Moreover, increase of mechanical loading in MDX mice, obtained by treadmill physical exercise, returned the LCN2 expression levels to those observed in WT mice. Our *in vivo* and *in vitro* data indicate that LCN2 could be a novel osteoblast mechano-responding gene and that its regulation appears to be central to the response of the bone tissue to low mechanical forces, inducing both poor osteoblast differentiation and increased osteoblast-mediated osteoclastogenesis.

Disclosures: Mattia Capulli, None.

1085

Breast Cancer-induced Osteolytic Bone Lesions are Inhibited by TGF- β Signaling in Osteoclasts, but not Inhibited when Targeted to Osteoblasts. Xiaohong Li¹, Jeffrey Nyman², Alyssa Merkel¹, Kang-Hsien Fan¹, Neil Bhowmick³, Lynn Matrisian⁴, Julie Sterling⁵. ¹Vanderbilt University, USA, ²Vanderbilt University Medical Center, USA, ³Cedars-Sinai Medical Center, USA, ⁴The pancreatic cancer action network, USA, ⁵Department of Veterans Affairs (TVHS)/Vanderbilt University Medical Center, USA

TGF- β is abundant in the bone environment and plays a critical role in the "vicious cycle" of osteolytic bone metastasis; TGF- β stimulates the cancer cells to activate osteoclasts, causing bone degradation and the release of more TGF- β from the bone matrix. Systemic delivery of TGF- β inhibitors or neutralizing antibodies has been shown to reduce tumor burden and lytic bone lesions caused by breast cancer (BCa) and melanoma cells. However, TGF- β also directly effects the proliferation and differentiation of osteoblasts and osteoclasts, and we hypothesized that cell specific TGF- β signaling in the bone microenvironment has distinct and complex roles in BCa bone metastasis.

Through both gain-of-function and loss-of-function approaches, genetically engineered mouse (GEM) models were used to delineate the role of mesenchymal cell (Mes) or myeloid cell (Mye) specific TGF- β signaling on BCa-induced osteolytic bone lesion development. Lysozyme M promoter-driven Cre was used to induce the ablation of the TGF- β type II receptor (Tgfb2) or constitutively active TGF- β type I receptor (Tgfb1) in mature macrophages, granulocytes and osteoclasts [LysM^{cre}/Tgfb2^{loxE2/loxE2}/Rosa26/Rag2^{-/-} (Tgfb_off_Mye) and LysM^{cre}/Tgfb1^{T204D}/Rosa26/Rag2^{-/-} (Tgfb_on_Mye)]. Using the ER-regulated collagen promoter, the administration of tamoxifen activates Cre in fibroblasts, osteoblasts and chondrocytes [Col^{creER}/Tgfb2^{loxE2/loxE2}/Rosa26/Rag2^{-/-} (Tgfb_off_Mes) and Col^{creER}/Tgfb1^{T204D}/Rosa26/Rag2^{-/-} (Tgfb_on_Mes)]. MDA-MB-231 BCa cells were injected into the tibiae of the GEMs and their respective Cre- controlled, immunodeficient mice. Host mice tibiae were imaged by Faxitron weekly up to 4 weeks post injection and bone lesion number and area was analyzed using Metamorph.

We found that lytic bone lesion development was significantly reduced in Tgfb_on_Mye mice compared to control mice ($p=0.007$); and correspondingly a significant increase in lytic bone lesions was observed in the Tgfb_off_Mye mice compared to control mice ($p=0.009$). In contrast, MDA-MB-231 cells induced more lytic lesions in Tgfb_on_Mes mice compared to control mice, while fewer lesion number and lesion area were observed in Tgfb_off_Mes mice. All statistics were applied by mixed effect model analysis. The results suggest that TGF- β signaling activation in osteoblasts is pro-osteolytic, but TGF- β signaling in osteoclasts is anti-osteolytic in this model of breast-to-bone metastasis.

Disclosures: Xiaohong Li, None.

1086

SOST Inhibits Prostate Cancer Invasion. Bryan Hudson*¹, Gabriela Loots², Nick Hum¹, Cindy Thomas¹. ¹Lawrence Livermore National Laboratory, USA, ²Lawrence Livermore National Laboratory, UC Merced, USA

In addition to its role in bone development, metabolism, and repair, the WNT signaling pathway is also implicated in cancer oncogenesis. Several inhibitors of WNT signaling, including dickkopf homolog 1 (DKK1), Wnt inhibitory factor 1 (WIF1), and secreted frizzled protein (sFRP), have been shown to be involved in prostate cancer (PC) metastasis; however the role of sclerostin (SOST) has not yet been explored. We examined human PC cells (PC3 and C4-2Bm) and healthy human prostate epithelial cells (HPrEC) to investigate the role of SOST in PC proliferation and invasion through the addition of recombinant proteins (rhSOST and rhDKK1) and in co-cultures with primary osteoblasts (OBs) isolated from mice lacking either the WNT co-receptor *Lrp5* (*Lrp5 KO*) or the WNT inhibitor *Sost* (*Sost KO*). We also conducted a whole-genome survey in PC3 to identify molecular changes as a function of PC3-OB co-culture. Here we report that rhSOST dramatically inhibits the invasive properties of both PC3 and C4-2Bm cells, without effecting cell proliferation or viability. In contrast, we found that rhDKK1 significantly increases invasion. Our data also shows that PC3 and C4-2Bm cells co-cultured with OBs derived from *Sost KO* mice exhibit increased invasion; an effect reversed in co-cultures with *Lrp5 KO* derived OBs. Gene expression analysis showed that major factors known to be involved in invasion, such as MMP2, are up-regulated in PC3 cells co-cultured with *Sost KO* OBs and down-regulated in *Lrp5 KO*, further implicating the direct involvement of WNT signaling in matrix degradation and cancer invasion. In support of this hypothesis, inhibition of MMP2 was sufficient to block the increased invasion of PC3 in PC3-OB/*Sost KO* co-cultures. These results were further examined *in vivo*, following intratumoral injections of PC3 cells in 8-week old control (WT), *Lrp5 KO*, and *Sost KO* mice, to determine if the host genotype alters the process of bone tumor formation. Consistent with the *in vitro* data, we found *Sost KO* mice to be more susceptible to tumor formation and growth while the *Lrp5 KO* mice showed a reduced susceptibility relative to WT. These findings support the hypothesis that the WNT signaling pathway is a critical component of prostate cancer metastasis to bone. In addition, we show that PC invasion is strongly reliant on SOST availability, where loss of SOST and hyperactive WNT activity in osteoblasts and bone tissue increases the ability of PC to invade and form tumors.

Disclosures: Bryan Hudson, None.

1087

Metformin Targets Tumor Cells and the Microenvironment to Prevent Prostate Cancer Initiation and Growth in Bone. Tunde Akinyeke*¹, Tunde Akinyeke¹, Xinying Wang¹, Satoko Matsumura¹, Himaly Shinglot¹, Rupak Bhatt¹, Anjana Saxena², Wenbo Yan³, Xin Li¹. ¹New York University, USA, ²CUNY-Brooklyn College, USA, ³Nyack College, USA

Prostate cancer is the second leading cause of cancer-related death in American men and many prostate cancer patients develop bone metastasis. Current treatment modalities for metastatic prostate cancer are mostly palliative with poor prognosis. Epidemiological studies indicated that patients receiving diabetic drug metformin have lower prostate cancer risks and better prognosis, suggesting that the metformin may have anti-neoplastic effects. However, the mechanism by which metformin impedes prostate cancer initiation and progression is unknown. The amplification of *MYC* oncogene plays a key role in early prostate epithelia cell transformation and prostate cancer growth. The objective of this study is to investigate the effect of metformin on *MYC* expression and prostate cancer progression. Our results demonstrated that: (1) Metformin selectively inhibited the growth of prostate cancer cells by stimulating cell cycle arrest and apoptosis without affecting the normal prostatic epithelial cells (RWPE-1) growth. (2) In Myc-CaP mouse prostate cancer cells, metformin decreased *MYC* protein levels by 50% through protein degradation and inhibition of de novo protein synthesis. (3) In human prostate cancer cells that either develops osteoblastic lesion (C4-2b) or osteolytic lesion (PC-3), metformin significantly decreased *MYC* at mRNA and protein levels. (4) In Hi-Myc mice which display murine prostate neoplasia and cancer highly resembling the progression of human prostate tumors, metformin (250mg/kg/d, 4wks) reduced *MYC* protein levels in prostate glands and attenuated prostate intraepithelial neoplasia (PIN, the pre-cancerous lesion of prostate). (5) In athymic mice with tumors from intra-tibia injection of C4-2b cells, metformin treated group showed a significant reduction of tumor burden in the tibia with decreased levels of serum IGF-1 (a growth factor stimulates tumor growth) and TRAP5b (a bone resorption marker). Consistently, metformin suppressed RANKL expression in primary osteoblasts indicating inhibited osteoclastogenesis. In conclusion, our novel findings demonstrate that metformin inhibits prostate cancer growth associated with down-regulation of *MYC*. Importantly metformin also alters bone microenvironment to suppress bone resorption and IGF-1 levels. Taken together, our data strongly suggest that metformin may act as a chemopreventive agent to restrict prostate cancer initiation as well as a chemotherapy agent to inhibit its growth in bone.

Disclosures: Tunde Akinyeke, None.

1088

PLCγ2/β-catenin Pathway Controls Myeloid-Derived Suppressor Cells to Promote Bone Metastasis Independent of the Osteoclasts. Aude-Helene CAPIETTO*¹, SEOKHO KIM², Deborah Novack³, Roberta Faccio². ¹Washington University School of Medicine, USA, ²Washington University in St. Louis School of Medicine, USA, ³Washington University in St. Louis School of Medicine, USA

Osteolytic bone metastases remain a clinical challenge even with anti-resorptive therapies. We have recently shown that *PLCγ2^{-/-}* mice have increased bone tumor burden despite defective osteoclasts. These findings suggest that skeletal metastases are modulated by other cells in addition to osteoclasts. Gr-1⁺CD11b⁺ Myeloid-Derived-Suppressor Cells (MDSC) promote tumor dissemination mainly by suppressing anti-tumor T-cell responses. We found aberrant expansion of MDSC and reduced T-cell activation in B16-melanoma-bearing *PLCγ2^{-/-}* mice. To determine whether MDSC promote tumorigenesis in *PLCγ2^{-/-}* mice, we adoptively transferred MDSC isolated from *PLCγ2^{-/-}* or WT mice into tumor-bearing WT mice. Animals receiving *PLCγ2^{-/-}*-MDSC displayed greater expansion of MDSC in the spleen and increased tumor burden compared to mice receiving WT-MDSC. Importantly, *PLCγ2^{-/-}*-MDSC were more efficient than WT cells to suppress CD8⁺ T-cell proliferation, via increased ROS and NO production. Thus, increased activation of MDSC promotes tumor growth in bone even in the absence of functional osteoclasts. Further confirming that MDSC expansion involves *PLCγ2* pathway, phosphorylation of PKC, a downstream target of *PLCγ2*, was decreased in MDSC isolated from tumor-bearing WT mice compared to non-tumor controls. PKC phosphorylation was further reduced in *PLCγ2^{-/-}* MDSC isolated from tumor-bearing mice. Since PKC has been shown to modulate β-catenin (β-cat) stabilization, we analyzed β-cat expression in WT and *PLCγ2^{-/-}* MDSC following tumor inoculation. *PLCγ2^{-/-}* MDSC displayed reduced β-catenin levels *in vivo* and *in vitro* compared to WT cells. Consistent with a functional role for this protein, deletion of β-catenin in myeloid cells (*LysMCre/β-cat.cKO*) led to a 2-fold increase in MDSC numbers and enhanced tumor burden. By contrast, mice expressing constitutive active β-catenin in myeloid cells (*LysMCre/β-cat.CA*) have reduced tumor growth compared to control mice.

In conclusion, our data indicate that *PLCγ2/β-catenin* pathway is critical for MDSC-mediated tumor escape from immune control. Because bone metastases are often refractory to current cancer therapies, including anti-resorptive agents, targeting MDSC and *PLCγ2/β-catenin* pathway may represent a new therapeutic avenue for bone metastases.

Disclosures: Aude-Helene CAPIETTO, None.

1089

miR-192 Impairs Osteolysis and Metastatic Angiogenesis by Novel Microvesicular Transfer Mechanisms. Karmele Valencia*¹, Diego Luis-Ravelo², Nicolas Bovy³, Susana Martinez-Canarias², Carolina Zanduetta⁴, Iker Anton¹, Ingrid Struman³, Sebastien Tabruyn³, Eva Bandrés², Fernando Lecanda¹. ¹Foundation for Applied Medical Research, Spain, ²Center for Applied Medical Research, Spain, ³GIGA Research, Molecular Biology & Genetic Engineering Unit, University of Liège, Belgium, ⁴Fima University of Navarra, Spain

Emerging evidence suggests that miRNAs (miR) can modulate a complex gene network in cell-intrinsic and extrinsic manner through their secretion into microvesicles (MV) and cargo transfer to target tissues. We previously identified miR192 as heavily downregulated in different highly metastatic subpopulations (HMS) isolated from bone metastases, but its mechanistic contribution remains unknown.

Overexpression of miR192 in HMS led to stunted decrease invasiveness and metalloproteolytic activity as compared to mock transduced cells whereas cell growth kinetics was unaltered. To delineate the pleiotropic functions of miR192 in metastatic activity, after intracardiac inoculation in nude mice, bioluminescence imaging (BLI) showed a dramatic decrease in skeletal tumor burden in mice injected with miR192 and a marked reduction in osteolytic lesions assessed by X-rays and μ CT scans. To explore its role in bone colonization, we intratibially injected (i.t.) miR192 cells. Significant decrease in BLI was associated with a decrease in osseous tumor burden in mice injected with miR192 cells. Growth kinetics and apoptosis of tumor cells were unaffected *in vivo*. Interestingly, the number TRAP⁺ cells were impaired in mice injected with miR192 cells. Transcriptomic analysis identified proosteoclastogenic factors repressed in miR192 derived tumors. Incubation with conditioned medium derived from miR192 tumor cells, but not with MV, showed a decrease TRAP⁺ cells *in vitro*. Furthermore, metastasis-induced angiogenesis was also severely deranged in mice i.t. with miR192 cells. To assess the contribution of miR192 released in MV, we isolated MV from mock and miR-192 overexpressing cells. Interestingly, miR192 was detected by qPCR in CD63-rich MV of ~100 nm in size by electron microscopy. MV transfer to endothelial cells (HUVEC) was demonstrated after MV-fluorescent labelled incubation. Cargo transfer to HUVEC was demonstrated by incubation with MV-derived from cells overexpressing a non-human miR. Incubation of HUVEC with miR192-derived MV led to decreased endothelial proliferation, migration and tubulogenesis. Moreover, miR192 in HUVEC repressed key proangiogenic IL8, CXCL1 and ICAM1 factors leading to impaired angiogenesis.

Thus, bone metastatic colonization is achieved by novel multimodal mechanisms mediated by miR192 governing tumor cell dependent functions, and non-cell

autonomously regulated tumor-induced osteolysis and angiogenesis by microvesicular transfer.

Disclosures: *Karme Valencia, None.*

1090

Measles Virus Nucleocapsid Protein (MVNP) Induction of TANK Binding Kinase 1 (TBK1) Activity Contributes to the Development of Pagetic Osteoclasts. Quanhong Sun^{*1}, Feng-Ming Wang², Benedicte Sammut³, Jolene Windle⁴, G. David Roodman², Deborah Galson¹. ¹University of Pittsburgh, USA, ²Indiana University, USA, ³University of Pittsburgh Hillman Cancer Center, USA, ⁴Virginia Commonwealth University, USA

Paget's disease (PD) is characterized by abnormal osteoclasts (OCL) with a pagetic phenotype that includes: increased sensitivity of OCL progenitors to 1,25(OH)₂D₃, RANKL and TNF α , increased OCL and nuclei/OCL, enhanced resorption capacity, increased expression of IL-6 and the transcription factors TAF12 and ATF7. We have recently reported that MVNP plays a key role in the development of abnormal OCL in PD patients expressing p62^{P392L}, the key mutation linked to PD. Further, we have also shown that MVNP can induce the pagetic OCL phenotype in vitro and in vivo in TRAP-MVNP transgenic mice. However, the molecular mechanisms by which MVNP induces a pagetic OCL phenotype have not been determined. TBK1 and IKK ϵ are IKK-related family members which physically interact with MVNP and can activate both the IRF3 and NF κ B pathways. We found that both TBK1 and IKK ϵ were increased early in OCL differentiation, suggesting a possible role in normal osteoclastogenesis. However, only TBK1 is further increased in OCL precursors from TRAP-MVNP mice compared to wildtype (WT) mice. TBK1 overexpression induced IL-6 reporter expression in both HEK293 and NIH3T3 cells, and even elevated endogenous IL-6 mRNA in both NIH3T3 and the pre-osteoclastogenic cell line RAW264.7. Knockdown of TBK1 with shRNA lentivirus impaired MVNP-induced IL-6 secretion as well as decreased TAF12 and ATF7 levels in NIH3T3 cells. The pharmacological TBK1/IKK ϵ catalytic activity inhibitor BX795 dose-dependently inhibited IL-6 RNA production in MVNP-NIH3T3 much more than in EV-NIH3T3. Further, BX795 administered after 1 day of RANKL treatment of bone marrow monocytes (BMM) also blocked the MVNP-induced increased IL-6 expression in cells from TRAP-MVNP mice compared with cells from WT mice when assayed 24 hr later. Importantly, knockdown of TBK1 in BMM from TRAP-MVNP and WT mice prior to RANKL addition impaired development of the MVNP-induced OCL pagetic phenotype, including altered IL-6 expression, TRAP-positive OCL numbers, and expression of OCL differentiation markers. Further, our study also indicated that MVNP modulates TBK1 expression by affecting the stability of both TBK1 mRNA and protein, which is dependent on IL-6, indicating a positive feedback loop. These results demonstrate that TBK1 plays a critical role in mediating the effects of MVNP on the expression of TAF12, ATF7, and IL-6, key contributors to the pagetic OCL phenotype.

Disclosures: *Quanhong Sun, None.*

1091

Ten-Year Cumulative Incidence of Second Hip fracture in Women and Men. The Norwegian Epidemiologic Osteoporosis Studies (NOREPOS). Tone Omsland^{*1}, Nina Emaus², Grethe S. Tell³, Luai Ahmed⁴, Jacqueline Center⁵, Clara Gjesdal⁶, Siri Forsmo⁷, Berit Schei⁷, Anne Johanne Sogaard⁸, Haakon Meyer⁸. ¹University of Oslo, Norway, ²University of Tromsø, 9037 Tromsø, Norway, ³University of Bergen, Norway, ⁴Faculty of Health Sciences, University of Tromsø, Norway, ⁵Garvan Institute of Medical Research, Australia, ⁶Haukeland University Hospital, Norway, ⁷Norwegian University of Science & Technology, Norway, ⁸Norwegian Institute of Public Health, Norway

Purpose: The purpose of the present population study was to examine the 10-year risk of second hip fracture by gender and investigate the impact of mortality in relation to second hip fracture risk.

Methods: All hip fractures (cervical, trochanteric or sub-trochanteric) treated in Norwegian hospitals between 1994 and 2008 were retrieved through patient administrative systems. Hip fractures sustained between 1994 and 1998 were excluded to minimize misclassifications of the second hip fractures. Thus, all subjects with a first hip fracture between 1999 and 2008 were included (n=81,867). Data were analyzed with standard Cox proportional hazard regression and re-analyzed with competing risks regression with death as the competing event of second hip fracture. Mortality following first hip fracture was analyzed by Cox regression adjusted for age. Time in the survival analyses was calculated as date of first fracture to date of event (second hip fracture or death) or censoring (emigration, end of study, (death)). Cumulative incidences were obtained from competing risks analyzes adjusted for age.

Results: A total of 6,161 women and 1,782 men, sustained a second hip fracture during the 10 years after the first hip fracture. Median time between first and second hip fracture, was 1.5 years in women and 1.2 years in men. The crude incidence rate per 10,000 person years of second hip fracture was 379 (95% Confidence Interval (CI): 370-389) in women and 333 (95% CI: 318-349) in men. The overall age-adjusted hazard

ratio (HR) of sustaining a second hip fracture in women versus men was not significant (HR = 1.03 (95% CI: 0.98-1.09)). The age-adjusted overall mortality after a first hip fracture was 77% (95% CI: 73-80) higher in men compared to women. When accounting for competing risk of death, the age-adjusted HR of a second hip fracture was 1.40 (95% CI: 1.33-1.48) in women versus men. The 10-year cumulative incidence of second hip fracture was 15% in women and 11% in men.

Conclusions: Although incidence rates of second hip fractures were almost similar in women and men, the 10-year risk of a second hip fracture was 40% higher in women compared to men when competing risk of death was taken into account. The gender difference was explained by a higher mortality in men.

Disclosures: *Tone Omsland, None.*

This study received funding from: The Research Council of Norway

1092

Contribution of Refracture to Early Fracture-Associated Mortality. Dana Bliuc^{*}, Nguyen Nguyen, Tuan Nguyen, John Eisman, Jacqueline Center. Garvan Institute of Medical Research, Australia

Background: Following an initial fracture, there is a 2-fold increased risk of re-fracture and an increased risk of premature mortality not just restricted to hip and vertebral fractures. However, the extent to which the re-fracture contributes to, and timing of, excess mortality is unknown. This study examined the additional premature mortality associated with re-fracture following all osteoporotic fractures.

Methods: 1295 subjects aged 60+ from the Dubbo Osteoporosis Epidemiology Study with initial fractures were followed for re-fracture and mortality (1989-2010). Competing risk analysis was used to examine re-fracture, mortality and mortality following re-fracture for hip, vertebral and non hip non vertebral fractures.

Results: There were 358 re-fractures and 487 deaths in women and 90 re-fractures and 206 deaths in men over 5779 p-yrs in women and 1886 p-yrs in men. Following a non-hip non-vertebral fracture in women, 52% of all subsequent fractures were either hip or vertebral. In men this fraction was 49%. Most of the re-fractures and premature mortality occurred in the first 5 years post initial fracture. Excess mortality in the first 5 yrs (above that expected for age and sex) was highest for hip fractures (8.1/100 p-yrs in women and 16.7/100 p-yrs for men). Of all the excess deaths, 25% in women and 20% in men occurred after a re-fracture. Following a vertebral fracture, excess deaths were 2.8/100p-yrs for women and 8.4/100 p-yrs for men. However, over 30% of all deaths for both women and men followed a re-fracture. For non-hip non-vertebral fractures, excess deaths were 1.8/100 p-yrs in women and 3.7/100 p-yrs in men with 30% of these deaths in women and 25% in men following a re-fracture. Population attributable risk of mortality was similar for all fracture types due to the larger number of non-hip non-vertebral fractures (13-18% in women and 25-29% in men).

Conclusion: There is a high premature mortality associated with all osteoporotic fractures occurring predominantly in the first 5 years post initial fracture. However, up to 20-30% of this early premature mortality occurs after a re-fracture with higher percentages following re-fractures after initial non hip fractures. This highlights the vital importance of re-fracture in overall fracture-associated mortality particularly in the immediate post fracture period and thus underscores the urgency for early intervention for all fracture types.

Disclosures: *Dana Bliuc, None.*

1093

Clinical Characteristics Among Patients with Different Femur Fracture Subtypes. Suzanne Morin^{*1}, Claudie Berger¹, Jacques Brown², William Leslie³, Michelle Wall⁴, Lisa Langsetmo⁵, Stephanie Kaiser⁶, Jerilynn Prior⁷, Robert Josse⁸, David Hanley⁹, Alexandra Papaioannou¹⁰, Jonathan Adachi¹¹, Christopher Kovacs¹², K. Shawn Davison¹³, W.P. Olszynski¹⁴, Tanveer Toweed¹⁵, David Goltzman¹. ¹McGill University, Canada, ²CHUQ Research Centre Laval University, Canada, ³University of Manitoba, Canada, ⁴McGill University Health Center Research Institute, Canada, ⁵Canadian Multicenter Osteoporosis Study, Canada, ⁶Dalhousie University, Canada, ⁷University of British Columbia, Canada, ⁸St. Michael's Hospital, University of Toronto, Canada, ⁹University of Calgary, Canada, ¹⁰Hamilton Health Sciences, Canada, ¹¹St. Joseph's Hospital, Canada, ¹²Memorial University of Newfoundland, Canada, ¹³Laval University, Canada, ¹⁴Midtown Professional Center (#103), Canada, ¹⁵Queen's University, Canada

Background: Variations in risk factors associated with femoral neck (FN) and intertrochanteric (IT) fractures have been well described. Similar characterization has not been carried out in individuals who sustain subtrochanteric (ST), diaphyseal (D) or periprosthetic (PP) femur fractures.

Objectives

We compared clinical and densitometric predictors associated with subtypes of femur fractures in the prospective population-based Canadian Multicentre Osteoporosis Study (CaMos).

Method: We identified all CaMos participants age 50 years and older, who sustained an incident femur fracture, as confirmed by a radiologist's report. We assessed differences in clinical variables and in bone mineral density (BMD) between

groups (FN- IT vs ST- D fractures, and PP vs non-periprosthetic (NPP)) recurrent femur fractures after initial repair. We used logistic regression analyses to determine predictors for ST-D compared to FN-IT fractures and for PP compared to NPP recurrent femur fractures.

Results: We identified 270 femur fractures in 246 participants (women: 79%; low trauma: 85%) during 14 years of follow-up. Initial fractures of the ST and D regions were infrequent (8%). There were 16 PP fractures (17%), 6 of which were D. Age, body mass index (BMI), BMD and FRAX scores at baseline were similar between groups. However, when compared to participants with FN-IT fractures, those with ST-D fractures tended to be less sedentary (1.2 hours/day less; 95% Confidence Interval [CI]: -0.1; 2.4), have lower intakes of supplemental calcium (113 mg/day less; 95% CI: -24; 249) and vitamin D (260 IU/day less; 95% CI: 35; 486) and more frequent use of bisphosphonates (Table). Among the 24 subjects with recurrent femur fractures (women: 79%, low trauma: 100%), 9 were PP (5 D) with 5 re-fractures occurring within 12 months of the index fracture. In logistic regression analyses, bisphosphonate use at the time of fracture and bisphosphonate use between cohort entry and index fracture were associated with a higher risk of ST-D fractures (Odds Ratio [OR] 3.8; 95% CI: 1.4; 10.4 and OR 3.1; 95% CI: 1.1; 9.0, respectively) compared to FN-IT fractures. Higher BMD at the femoral neck was associated with higher risk PP fracture vs NPP recurrent fractures.

Conclusion: ST-D femur fractures are infrequent but are associated with different predictors than FN-IT fractures. PP fractures, particularly of the diaphyseal region, frequently follow a recent hip fracture repair.

Table Characteristic in participants with a first femur FN- IT, D-ST fractures (isolated fractures of greater trochanter, lesser trochanter, distal femur not included: N=19)

| | Femoral Neck-Intertrochanteric N= 208 | Subtrochanteric-Diaphyseal N=19 |
|---|--|------------------------------------|
| Women, N (%) | 162 (78) | 15 (79) |
| Age (SD), years | 73.0 (8.6) | 69.8 (10.2) |
| BMD L14 (SD), g/cm ² | 0.873 (0.177) | 0.863 (0.547) |
| BMD Femoral Neck (SD), g/cm ² | 0.620 (0.108) | 0.639 (0.138) |
| BMD Total Hip (SD), g/cm ² | 0.758 (0.141) | 0.772 (0.147) |
| Sedentary hours/day, (SD) | 14.1 (3.1) | 12.9 (2.6) |
| Vitamin D, (SD) IU/day | 387 (1472) | 126 (233) |
| Calcium, (SD) mg/day | 242 (364) | 129 (283) |
| FRAX, major fracture | 16 (11) | 16 (13) |
| FRAX, hip fracture | 6 (8) | 7 (10) |
| Low Trauma (%) | 177 (87) | 15 (79) |
| Bisphosphonate use at time of fracture (%) | 75 (36) | 13 (68) |
| Cumulative bisphosphonate use at time of fracture (%) | | |
| None | 110 (53) | 5 (26) |
| 1-4 years | 51 (26) | 7 (37) |
| > 4 years | 47 (23) | 7 (37) |

Disclosures: Suzanne Morin, None.

1094

Change in Bone Mineral Density (BMD) Does Not Improve Fracture Prediction Beyond Baseline BMD. Sarah Berry*¹, Elizabeth Samelson², Robert McLean³, Kerry Broe⁴, L. Adrienne Cupples⁵, Douglas Kiel⁶.

¹Hebrew SeniorLife/Beth Israel Deaconess Medical Center, USA, ²Hebrew SeniorLife, Harvard Medical School, USA, ³Hebrew SeniorLife Institute for Aging Research & Harvard Medical School, USA, ⁴Institute for Aging Research/Hebrew SeniorLife, USA, ⁵Boston University School of Medicine, USA, ⁶Hebrew SeniorLife, USA

Purpose: Recent studies question whether a repeat BMD screening test is beneficial in older women. The purpose of our study was to examine whether change in BMD, independent of baseline BMD, predicts fracture in a population based cohort of older men and women. We further examined whether certain subgroups are more vulnerable to fracture in the setting of bone loss.

Methods: Participants included 492 women and 310 men in the Framingham Study with baseline and 4-yr follow-up BMD at the femoral neck (1987-1999) and no prior hip fracture. Hip fractures were confirmed with medical records, and non-hip fractures were self-reported. Follow-up time was calculated from time of the second BMD assessment until fracture, death, or 10 yrs. Cox regression models were used to calculate hazard ratios (HR) for the association between annual percent BMD loss and risk of fracture adjusting for baseline BMD and other covariates. We used logistic regression to calculate areas under the curve (AUCs) to determine whether a model with baseline BMD was improved by including BMD change. In secondary analyses, models were stratified by baseline age, sex, BMI, T-score, weight loss, and FRAX hip fracture risk.

Results: Mean age was 75 yrs (± 4 yrs). Twenty-one percent had a T-score >-1.0, and 54% had a T-score between -1.0 and -2.4. Mean BMD loss was 0.7% annually (± 1.8%). During follow-up, 64 hip and 121 non-hip fractures occurred. After adjusting for baseline BMD, one SD loss of BMD was associated with a 50% increased risk of hip fracture (95% CI, 1.2, 1.9; Table 1), but did not increase the risk of non-hip fracture (HR 1.0, 95% CI 0.8, 1.2). Models including baseline BMD were

not improved by including BMD change (Table 1; AUC 0.72 versus 0.73). Stratified results were similar to the overall results.

Conclusion: In community dwelling older men and women without a hip fracture, BMD loss over four years increases the risk of hip fracture, but not non-hip fracture. BMD loss did not substantially contribute to the 10 yr prediction of hip or non-hip fracture beyond baseline BMD. The contribution of BMD change to risk of fracture was similar regardless of age, sex, BMI, T-score, weight loss, or FRAX risk. Our results confirm and extend previous findings demonstrating that repeating a bone density test every two years to improve risk stratification may not be necessary in older adults provided they have a baseline assessment.

| | Baseline BMD | | | BMD change (annualized percent change) | | |
|-------------------------------------|---------------------------|--------------------------|------|--|--------------------------|------|
| | Multivariate adjusted HR* | 95% confidence intervals | AUC* | Multivariate adjusted HR* | 95% confidence intervals | AUC* |
| All participants | 1.6 | 1.2, 2.3 | 0.72 | 1.5 | 1.2, 1.9 | 0.73 |
| Age < 75 yrs | 1.8 | 1.2, 2.8 | 0.72 | 1.5 | 1.1, 1.9 | 0.72 |
| Age = 75 yrs | 1.4 | 0.8, 2.4 | 0.70 | 1.5 | 1.1, 2.1 | 0.70 |
| Men | 1.1 | 0.5, 2.3 | 0.65 | 1.5 | 0.8, 2.9 | 0.66 |
| Women | 1.8 | 1.2, 2.6 | 0.69 | 1.5 | 1.2, 1.9 | 0.70 |
| BMI < 26kg/m ² | 2.0 | 1.2, 3.0 | 0.71 | 1.5 | 1.1, 1.9 | 0.71 |
| BMI = 26kg/m ² | 1.2 | 0.7, 2.2 | 0.70 | 1.5 | 0.9, 2.5 | 0.70 |
| Weight stable or weight gain = 1lbs | 1.8 | 1.0, 3.3 | 0.67 | 1.8 | 1.2, 2.6 | 0.68 |
| Weight loss = 1lbs | 1.5 | 1.0, 2.3 | 0.76 | 1.4 | 1.0, 1.9 | 0.77 |
| T-score = -2.0 | 1.7 | 1.0, 2.7 | 0.72 | 1.5 | 1.1, 1.9 | 0.72 |
| T-score > -2.0 | 1.6 | 0.8, 3.6 | 0.68 | 1.4 | 0.9, 2.3 | 0.68 |
| FRAX hip fx risk < 3% | 1.6 | 0.7, 3.7 | 0.69 | 1.4 | 0.8, 2.4 | 0.70 |
| FRAX hip fx risk = 3% | 1.6 | 1.0, 2.6 | 0.72 | 1.5 | 1.1, 1.9 | 0.72 |

* Models include age, sex, weight, 4-year weight change, and prior history of non-hip fracture
 * Models include age, sex, weight, 4-year weight change, prior history of non-hip fracture, and baseline BMD

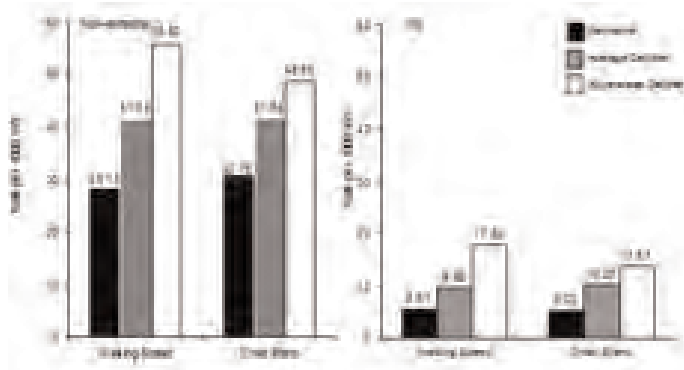
Table 1

Disclosures: Sarah Berry, None.

1095

Trajectories of change in physical function: Effects on Fractures and Mortality. Kamil Barbour*¹, Li-Yung Lui², Deborah Barnes³, Kristine Ensrud⁴, Ann Newman⁵, Kristine Yaffe³, Steven Cummings⁶, Jane Cauley⁷. ¹CDC, USA, ²California Pacific Medical Center Research Institute, USA, ³University of California San Francisco, USA, ⁴Minneapolis VA Medical Center / University of Minnesota, USA, ⁵Department of Epidemiology, University of Pittsburgh, Pittsburgh, PA, USA, ⁶San Francisco Coordinating Center, USA, ⁷University of Pittsburgh Graduate School of Public Health, USA

Prior studies have identified poor physical function as a risk factor for fractures and mortality. However, these studies did not consider change in physical function over time. We hypothesized that women who maintain their physical function would have a lower risk of non-traumatic fracture (hip and any non-vertebral) and death. We followed 9704 women enrolled into the Study of Osteoporotic Fractures at four U.S. clinical centers. Physical function was measured a maximum of 8 times over 19 years. The median (range) number of measurements for walking (m/s) and chair stand speed (time/s) were 6 (1-8) and 5 (1-8), respectively. Random slope and intercept models were used to determine a walking and chair stand speed slope for each woman, and for the entire population. Three groups were formed for walking speed: “maintainers” (slope ≥ -1 SD from 0, n=773, 8%); “average decliners” (1 SD below mean ≤ slope < -1 SD from 0, n=7676, 79%); “accelerated decliners” (slope > 1 SD below mean, n=1255, 13%). Cox proportional hazards models were used to estimate hazard ratios (HRs; 95% CI) of fracture and mortality and control for age, BMI, physical activity, falls, fracture after age 50, diabetes, stroke, hypertension, calcium intake, health status, weight change, smoking, estrogen use, and hip BMD. The HR of hip and any non-vertebral fracture was 0.64 (0.50, 0.81) and 0.76 (0.67, 0.86) for maintainers of walking speed and 1.52 (1.31, 1.76) and 1.24 (1.13, 1.36) among accelerated decliners of walking speed when compared with the average decliner group. Similar results were shown for chair stand speed. The HR of mortality was 0.49 (0.43, 0.56) for maintainers of walking speed and 0.56 (0.50, 0.64) for maintainers of chair stand speed compared with average decliner group. The HR of mortality was null for accelerated decliners of walking speed, but surprisingly 0.75 (0.70, 0.81) for accelerated decliners for chair stand speed compared with average decliners. In conclusion, women who maintained physical function up to 19 years experienced a lower risk of fractures and mortality than average decliners of physical function, suggesting that maintaining physical function may be a marker for healthy aging.



Fracture rate per 1000 women-year

Disclosures: Kamil Barbour, None.

1096

Direct Healthcare Costs for 5 Years Post Fracture in Canada: A Population-Based Assessment. William Leslie^{*1}, Lisa Lix², Greg Finlayson¹, Colleen Metge¹, Suzanne Morin³, Sumit Majumdar⁴. ¹University of Manitoba, Canada, ²University of Saskatchewan, Canada, ³McGill University, Canada, ⁴University of Alberta, Canada

Background: High healthcare costs in the 1st year post fracture are well known, but long term costs are less well studied. We estimated direct incremental healthcare costs of fracture (post- minus pre-fracture costs) in Manitoba, Canada, up to 5 years after incident fractures.

Methods: We used the comprehensive Population Health Research Data Repository for the 1.2 million residents of Manitoba, Canada, to identify incident fractures in 1997-2002 and direct healthcare costs in the year pre-fracture and 5 years post-fracture. Non-traumatic fractures (hip n=2814, spine n=1030, wrist n=3145, humerus n=1652, other n=7557) and high-trauma fractures (n=444) were identified in continuously-insured residents aged >50 years. Healthcare costs (physician visits, hospitalizations, drugs, homecare and nursing home) were converted to 2009 Canadian dollars. Data were analyzed using median values, which are less sensitive to outliers and extreme costs.

Results: Healthcare costs for all incident fractures combined showed a large increase over pre-fracture costs in the 1st year (\$120M women, \$57M men), but fell below pre-fracture costs in years 2-5 (Figure). This was attributed to higher short term mortality among higher users of healthcare. Incremental median costs (adjusted for age-related cost increases using age- and sex-matched fracture-free controls) for a hip fracture were highest in the 1st year (\$24757 women, \$20927 men), lower in the 2nd year (\$2167 women, \$844 men) and declined below pre-fracture costs by 5 years consistent with healthy survivor effect. In those who survived 5 years following a hip fracture, incremental median costs were again highest in the 1st year (\$26102 women, \$20735 men) but remained above pre-fracture costs at 5 years (\$5091 women, \$3269 men). A similar pattern was seen in 5 year survivors after non-hip fracture with the highest median incremental costs in the 1st year and costs remaining above baseline at 5 years (for women/men: spine \$2802/\$524, wrist \$259/\$382, humerus \$595/\$684, other \$206/\$529, high trauma \$667/\$805).

Conclusions: Direct healthcare costs attributable to fracture peak in the 1st year, but total costs fall below pre-fracture levels for the next 4 years. Our findings suggest that, from a societal perspective, many previous economic analyses have systematically over-estimated the economic burden of fracture. Among those who survive 5 years, however, costs remain above pre-fracture levels, especially for hip fractures.

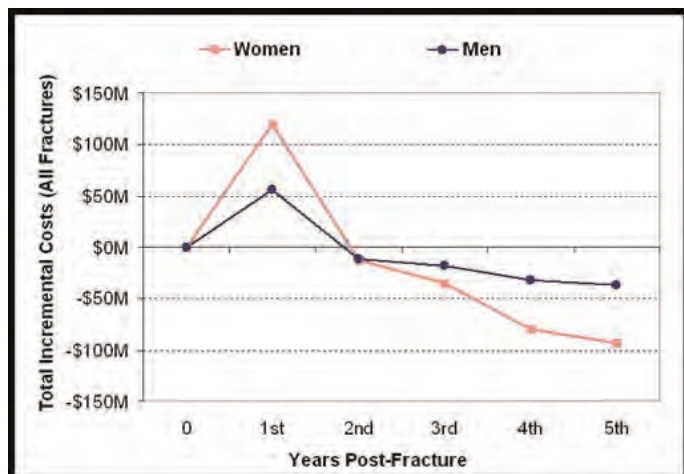


Figure: Incremental healthcare costs over pre-fracture costs for all fracture cases (million SCDN).

Disclosures: William Leslie, Amgen, 6
This study received funding from: Amgen

1097

The Effects of Combined Denosumab and Teriparatide Administration on Bone Mineral Density in Postmenopausal Women: The DATA (Denosumab And Teriparatide Administration) Study. Benjamin Leder^{*1}, Alexander Uihlein², Robert Neer³, Ruchit Kumbhani⁴, Erica Siwila-Sackman⁵, Sherri-Ann Burnett-Bowie³. ¹Massachusetts General Hospital Harvard Medical School, USA, ²Massachusetts General Hospital, USA, ³Massachusetts General Hospital, USA, ⁴Massachusetts General Hospital, USA, ⁵Massachusetts General Hospital, USA

Background: Currently approved osteoporosis medications increase BMD modestly and reduce, but do not eliminate, fractures. Combining the most commonly prescribed class of antiresorptive agents, bisphosphonates (BPs), and the anabolic agent, teriparatide (TPTD), does not increase BMD more than the respective individual therapies. Animal models suggest that the combination of the newly approved antiresorptive denosumab (DMAB) and TPTD might increase BMD more than either drug alone.

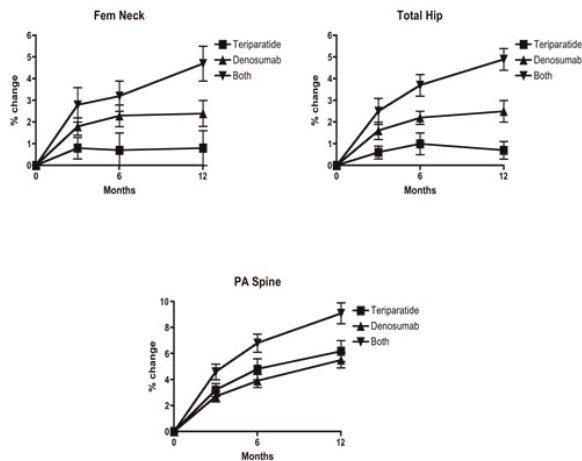
Methods: We enrolled 92 postmenopausal women at high risk of fracture (age 51-91) in a 12-month open-label RCT comparing the effects of TPTD (20 mcg SC daily, n=31), DMAB (60 mg SC Q6 mo, n=33), or both medications (n=30) on hip, spine and 1/3 radius DXA BMD. Subjects were excluded if they had used oral BPs in the past 6 months or had any prior use of strontium or IV BPs. Subjects were stratified by age and prior BP use. Between-group changes in BMD were compared by mixed-model ANCOVA.

Results: No significant between-group differences were observed at baseline (table). As shown in the figure, at 12-months, total hip BMD (mean ± SD) increased more in the combo group (4.9% ± 2.9%) than in either the TPTD (0.7% ± 2.7%), P<0.0001) or DMAB (2.5% ± 2.6%, P=0.0001) groups. Femoral Neck BMD also increased more in the combo group (4.7% ± 4.3%) than in the TPTD (0.8% ± 4.1%, P<0.001) and DMAB (2.1% ± 3.8%, P=0.013) groups. Similarly, spine BMD increased more in the combo group (9.1% ± 3.9%) than in either the TPTD (6.2% ± 4.6%, P=0.0005) or DMAB (5.5% ± 3.3%, P<0.0001) groups whereas BMD at the 1/3 radius increased similarly in the DMAB (1.7% ± 3.2%) and combo groups (2.5% ± 2.8%). These increases in radius BMD were significantly different than the decrease observed in the TPTD group (-1.8% ± 3.6%, P <0.001). DMAB alone increased BMD more than TPTD alone at the total hip (p=0.003) but TPTD and DMAB produced similar gains in the spine (P=0.7) and femoral neck (p=0.09).

Summary: Unlike the combination of TPTD and BPs, the combination of TPTD and DMAB increased BMD at the hip and spine more than either drug alone. Moreover, as DMAB-TPTD co-administration resulted in greater increases in femoral neck, total hip and spine BMD than any currently available alternatives, combined therapy with these agents may prove to be an important treatment option in patients at high risk of fracture.

| | TPTD | DMAB | Both |
|------------------------------------|------------|------------|------------|
| Age | 66 ± 8 | 66 ± 8 | 66 ± 9 |
| Previous BP use | 42% | 36% | 33% |
| Fem Neck BMD (g/cm ²) | 0.64 ± .10 | 0.64 ± .08 | 0.64 ± .07 |
| Total Hip BMD (g/cm ²) | 0.76 ± .10 | 0.77 ± .10 | 0.76 ± .07 |
| Spine BMD (g/cm ²) | 0.82 ± .10 | 0.86 ± .09 | 0.85 ± .12 |

table



figure

Disclosures: Benjamin Leder, Amgen, 2; Merck, 2
This study received funding from: Amgen, Lilly

1098

Effects of Denosumab on Fracture Risk in Japanese Patients with Osteoporosis - Results of 2-year Data from the Denosumab fracture Intervention RandomizEd placebo Controlled Trial (DIRECT). Toshitaka Nakamura^{*1}, Toshio Matsumoto², Toshitsugu Sugimoto³, Takayuki Hosoi⁴, Takami Miki⁵, Itsuo Gorai⁶, Hideki Yoshikawa⁷, Yoshiya Tanaka⁸, Sakae Tanaka⁹, Tetsuo Nakano¹⁰, Masako Ito¹¹, Teruki Sone¹², Toshiyuki Yoneda¹³, Shigeyuki Matsui¹⁴, Hideo Takami¹⁵, Masao Fukunaga¹². ¹University of Occupational & Environmental Health, Japan, ²University of Tokushima Graduate School of Medical Sciences, Japan, ³Shimane University School of Medicine, Japan, ⁴National Center for Geriatrics & Gerontology, Japan, ⁵Osaka City University Medical School, Japan, ⁶Hori Hospital, Japan, ⁷Osaka University Graduate School of Medicine, Japan, ⁸University of Occupational & Environmental Health, Japan, Japan, ⁹The University of Tokyo, Japan, ¹⁰Tamana Central Hospital, Japan, ¹¹Nagasaki University Hospital, Japan, ¹²Kawasaki Medical School, Japan, ¹³Osaka University Graduate School of Dentistry, Japan, ¹⁴The Institute of Statistical Mathematics, Japan, ¹⁵Daiichi Sankyo Co., LTD., Japan

Introduction: Denosumab increases bone mineral density (BMD) in both Japanese and Caucasian postmenopausal women with osteoporosis and was shown to reduce fracture risk in a large international study. However, the effect of denosumab on fracture risk in Japanese patients has not been evaluated.

Methods: To examine the anti-fracture efficacy and safety of denosumab (60 mg subcutaneous injection every 6 months [Q6M]) in Japanese patients with primary osteoporosis, a randomized, double-blind, placebo-controlled trial with an open-label referential comparator arm was conducted. The main eligibility criteria were age \geq 50 years, 1-4 prevalent vertebral fractures, and low BMD (L1-L4 or total hip BMD $<$ 80% of young adult mean [T-score $<$ -1.7 (L1-L4) or $<$ -1.6 (total hip)]). A total of 1262 patients were randomly assigned in a 2:2:1 ratio to the following treatment groups, respectively: double-blind denosumab injection (N=500; 25 men), double-blind placebo (N=511; 26 men), or open-label oral alendronate 35 mg weekly (N=251; 12 men) for 2 years. All patients received daily supplements of at least 600 mg calcium and 400 IU vitamin D.

Results: Denosumab significantly reduced the risk of new or worsening vertebral fractures, with incidences of 3.6% in the denosumab group and 10.3% in the placebo group at 2 years (HR, 0.343; 95%CI 0.194-0.606, P=0.0001). The alendronate group showed an incidence of 7.2% at 2 years. Denosumab also significantly reduced the risk of new vertebral fracture and multiple new vertebral fractures, compared to placebo, by 74% (P<0.0001) and 90% (P=0.0113), respectively. Denosumab significantly increased BMD compared to placebo at L1-L4, total hip, femoral neck and distal 1/3 radius by 9.04%, 5.72%, 5.11%, and 2.32%, respectively, at 2 years (all P< 0.0001). Serum CTX-1 and bone ALP levels decreased significantly in the denosumab group at month 1 and these suppression sustained throughout the study period. The incidences of hypocalcemia, cancer, infection, cardiovascular disease and hypersensitivity in the denosumab group were well balanced compared to those of the placebo group. No cases of delayed fracture healing, atypical femoral fracture or osteonecrosis of the jaw (ONJ) were observed. No patients developed a neutralizing antibody to denosumab.

Conclusion: Denosumab 60 mg Q6M for 2 years is safe and effective in reducing vertebral fracture risk in Japanese patients with primary osteoporosis.

Disclosures: Toshitaka Nakamura, Teijin Pharma, 2; Daiichi-Sankyo Co., 2; Chugai Pharmaceutical Co., 2; Asahi-Kasei Pharma Co., 2; Amgen Inc., 2
This study received funding from: Daiichi Sankyo Co., LTD.

1099

Relationship Between Changes in Bone Mineral Density and Incidence of Fracture With 6 Years of Denosumab Treatment. Paul D. Miller^{*1}, Steven Cummings², Jean-Yves Reginster³, Nathalie Franchimont⁴, Gerolamo Bianchi⁵, Michael A. Bolognese⁶, Roland Chapurlat⁷, Federico Hawkins⁸, David L. Kendler⁹, Beatriz Oliveri¹⁰, Jose R. Zanchetta¹¹, Nadia Daizadeh⁴, Andrea Wang⁴, Rachel B. Wagman⁴, Socrates Papapoulos¹². ¹University of Colorado Health Sciences Center & Colorado Center for Bone Research, USA, ²San Francisco Coordinating Center, USA, ³University of Liège, Belgium, ⁴Amgen Inc., USA, ⁵Azienda Sanitaria Genovese, Italy, ⁶Bethesda Health Research Center, USA, ⁷Hôpital Edouard Herriot, France, ⁸Hospital Universitario, Spain, ⁹University of British Columbia, Canada, ¹⁰Sección Osteopatías Médicas, Hospital de Clínicas, Universidad de Buenos Aires, Argentina, ¹¹Instituto de Investigaciones Metabólicas & University of Salvador, Argentina, ¹²Leiden University Medical Center, Netherlands

Purpose: During the first 3 years of denosumab (DMAb) treatment in FREEDOM, there were continued increases in bone mineral density (BMD) and a robust reduction in fracture risk (Cummings et al., *NEJM* 2009). The changes in total hip BMD explained a considerable proportion of the reduction in new or worsening vertebral and nonvertebral fracture risk (Austin et al., *JBM* 2011). Here, we conducted a BMD responder analysis and explored if the progressive BMD gains with 6 years of DMAb therapy continued to relate to the observed fracture incidence.

Methods: The long-term efficacy and safety of DMAb for up to 10 years is being investigated in the open-label extension of the 3-year FREEDOM trial. During the extension, all participants receive 60 mg DMAb every 6 months. For the analyses presented here, women from the FREEDOM DMAb group received 3 more years of DMAb for a total of 6 years. The percentages of women treated with DMAb who achieved BMD increases from FREEDOM baseline at the lumbar spine, total hip, and femoral neck were determined. A logistic regression model was used to examine the relationship between change in total hip BMD and new or worsening vertebral fracture. A comparable approach was employed for nonvertebral fracture using the Cox proportional hazards model.

Results: For women who received 3 additional years of DMAb treatment (N=2343 enrolled), further significant increases in BMD occurred for cumulative 6-year mean gains of 15.2% (lumbar spine), 7.5% (total hip), and 6.7% (femoral neck). At year 6, almost all women treated with DMAb had gains in BMD at the lumbar spine (98%), total hip (96%), and femoral neck (91%). Additionally, 99% of women had gains in BMD at any of these sites, and of these, the gains were $>$ 3% in 98% of women and $>$ 6% in 95% of women. Fracture incidence remained low during the extension. The relationships between total hip BMD gains and new or worsening vertebral and nonvertebral fractures with 6 years of DMAb treatment are shown in Figures 1 and 2, respectively.

Conclusion: Almost all women who received 6 years of DMAb treatment had gains in BMD at the lumbar spine, total hip, or femoral neck; and those gains were $>$ 6% in 95% of them. While on denosumab treatment, the risk of new or worsening vertebral fracture and nonvertebral fracture decreased with increasing percentage change in total hip BMD over 6 years. This association provides clinical relevance to the progressive and continued BMD gains reported with DMAb over time.

Figure 1.

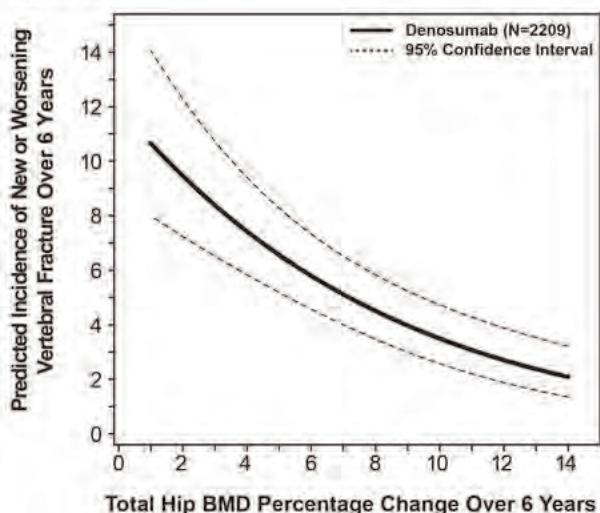
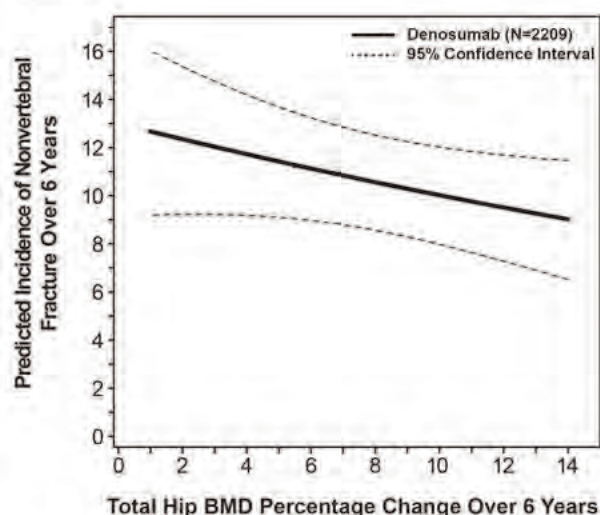


Figure 2.



Aims: To determine if strength of the spine and hip is increased from baseline by Adding and Switching to teriparatide in women on ALN and RLX and to compare the magnitude of the strength effects with these 2 approaches.

Methods: Postmenopausal women with osteoporosis pretreated for at least 18 months with ALN 70 mg/week or RLX 60 mg/day were randomized to Add or Switch to teriparatide 20 mcg administered once daily by sc injection. Quantitative computed tomography scans at baseline, 6 and 18 months were used to assess changes in volumetric BMD and estimated strength by nonlinear finite element analysis (FEA) in a blinded fashion. A plan approved prior to the completion of the assessments specified the analyses.

Results: At the spine, strength and volumetric BMD increased in all groups, and there were no significant differences between Adding and Switching (Table). In the ALN stratum, at the hip, Adding teriparatide significantly increased volumetric BMD relative to Switching at month 6 (0.9% vs -0.5%, $P=0.004$) and month 18 (2.2% vs 0.0%, $P=0.002$). Furthermore, at 18 months in the hip, significant increases in strength were only observed in the Add group (2.7%, $P<0.001$ vs baseline; between-group comparison $P=0.076$). In the RLX stratum, at the hip, both volumetric BMD and strength increased significantly at 6 and 18 months in the Add group, but only at 18 months in the Switch group.

Summary/conclusion: In postmenopausal women with osteoporosis previously treated with ALN or RLX, Adding and Switching to teriparatide conferred similar effects on the spine. In the ALN stratum at 18 months, hip strength increased significantly in the Add but not the Switch group, although the between-group difference was not significant. At 18 months, hip strength increased similarly in both RLX groups. As limitations, the study duration was 18 rather than 24 months, the study lacked power to compare fracture outcomes, and the treatment effects of prior antiresorptives on the bone tissue material properties affecting the estimation of FEA-based strength are unknown.

Median change (%) from baseline (25th, 75th IQR) for volumetric BMD (vBMD) and strength (hip for a sideways fall; spine for uniform compression) in postmenopausal women with osteoporosis previously treated with alendronate (ALN) or raloxifene (RLX) then randomized to Add or Switch to teriparatide (TPTD).

| Outcome | ALN + TPTD (Add) | ALN → TPTD (Switch) | P value ^a | RLX + TPTD (Add) | RLX → TPTD (Switch) | P value ^a |
|-----------------------|---|-------------------------------|----------------------|---|---|----------------------|
| Spine vBMD | | | | | | |
| Month 6 | 4.3* (2.1, 6.8) n=45 | 3.0* (0.8, 5.7) n=46 | 0.182 | 7.0* (3.8, 9.7) n=38 | 5.7* (1.3, 7.8) n=39 | 0.053 |
| Month 18 | 7.5* (3.7, 12.7) n=40 | 7.9* (5.3, 10.7) n=40 | 0.912 | 10.1* (6.7, 16.0) n=29 | 10.0* (6.3, 13.0) n=25 | 0.585 |
| Spine Strength | | | | | | |
| Month 6 | 6.1* (1.7, 12.4) n=45 | 7.1* (1.8, 12.6) n=46 | 0.953 | 11.4* (6.4, 17.4) n=38 | 9.7* (2.3, 13.6) n=39 | 0.082 |
| Month 18 | 13.2* (7.2, 21.4) n=40 | 15.6* (10.1, 20.7) n=40 | 0.334 | 17.5* (11.8, 27.2) n=29 | 15.7* (10.5, 25.6) n=25 | 0.521 |
| Hip vBMD | | | | | | |
| Month 6 | 0.9 [‡] (0.0, 1.7) n=42 | -0.5 (-2.1, 0.9) n=46 | 0.004 | 1.3 [‡] (-0.5, 3.0) n=40 | 0.4 (-1.0, 1.9) n=36 | 0.160 |
| Month 18 | 2.2* (0.7, 4.7) n=36 | 0.0 (-1.7, 2.6) n=39 | 0.002 | 3.2 [‡] (-0.5, 5.7) n=30 | 2.4 [‡] (1.0, 4.0) n=24 | 0.645 |
| Hip Strength | | | | | | |
| Month 6 | 0.8 (-2.4, 1.8) n=42 | -1.6 (-3.9, 1.9) n=46 | 0.101 | 1.7 [‡] (-0.5, 3.1) n=40 | -1.1 (-2.9, 3.4) n=36 | 0.048 |
| Month 18 | 2.7 [‡] (-0.5, 6.1) n=36 | 0.0 (-3.4, 4.7) n=39 | 0.076 | 2.7 [‡] (-1.1, 6.2) n=30 | 3.4 [‡] (-1.5, 5.8) n=24 | 0.951 |

Wilcoxon signed-rank test percentage change from baseline: * $P<0.0001$; [‡] $P<0.001$; [‡] $P<0.01$; [§] $P<0.05$.

^aBetween group comparison, Wilcoxon rank-sum test.

Table

Disclosures: Felicia Cosman, Lilly, Amgen, Novartis, 1; Lilly, Amgen, Merck, 2; Lilly, 9; Lilly, Novartis, 6
This study received funding from: Sponsored by Eli Lilly and Company or Lilly USA, LLC

1101

A Phase 2 Randomized Trial of Orally Administered PTH(1-31)NH₂ Tablets in Postmenopausal Women with Osteoporosis. Nozer Mehta¹, Morten Karsdal^{2*}, Roxanne Tavakkol³, William Stern³, Amy Sturmer¹, Sheela Mitta³, Kim Henriksen², Jeppe Andersen⁴, Bente Riis⁴, Peter Alexandersen⁵, Ivo Valter⁶, Bettina Nedergaard⁷, Christence Teglbiaerg⁷, Antonio Nino⁸, Lorraine Fitzpatrick⁸, Claus Christiansen², Felicia Cosman⁹. ¹Unigene Laboratories, USA, ²Nordic Bioscience A/S, Denmark, ³Unigene Laboratories, Inc., USA, ⁴Nordic Bioscience, Denmark, ⁵Center for Clinical & Basic Research A/S, Denmark, ⁶Center for Clinical & Basic Research, Estonia, ⁷Center for Clinical & Basic Research, Denmark, ⁸GlaxosmithKline Pharmaceuticals, USA, ⁹Helen Hayes Hospital, USA

Purpose: A phase 2 study was designed to test an oral tablet formulation of PTH(1-31)NH₂ as a bone anabolic agent. Background: A solid dosage enteric-coated formulation has been developed that enables oral delivery by a unique mechanism that includes an organic acid as a protease inhibitor and an acylcarnitine as a permeation enhancer. Based on results from phase 1 studies, we tested a 5 mg oral tablet dose of a

The predicted fracture incidence was estimated corresponding to the 5th through the 95th percentiles of the observed total hip BMD percentage changes over 6 years. N=number of subjects with an observed BMD value at FREEDOM extension baseline and at ≥1 follow-up visit.

Disclosures: Paul D. Miller, Procter & Gamble, SanofiAventis, Roche, Eli Lilly, Merck, Novartis, Amgen, Takeda, Radius, GE, 6; Warner Chilcott, Merck, Eli Lilly, Amgen, Novartis, Roche, GlaxoSmithKline, Baxter, Wright, 2; Warner Chilcott, Amgen, Novartis, Roche, 1
This study received funding from: Amgen Inc.

1100

Hip and Spine Strength Effects of Adding Versus Switching to Teriparatide in Postmenopausal Women with Osteoporosis Treated with Prior Alendronate or Raloxifene. Felicia Cosman^{1*}, Tony Keaveny², David Kopperdahl³, Robert Wermers⁴, Xiaohai Wan⁵, Kelly Krohn⁶, John Krege⁵. ¹Helen Hayes Hospital, USA, ²University of California, Berkeley, USA, ³O.N. Diagnostics, USA, ⁴Mayo Clinic, USA, ⁵Eli Lilly & Company, USA, ⁶Lilly USA, LLC, USA

Background: Many women treated with teriparatide for osteoporosis have previously received antiresorptive therapies. For postmenopausal women with osteoporosis previously treated with alendronate (ALN) or raloxifene (RLX), Adding versus Switching to teriparatide caused different responses in areal BMD and biochemistry (JCEM 94: 3772–3780, 2009). The effects of these approaches on bone strength are unknown.

differentiated PTH(1-31)NH₂ analog in a phase 2 proof-of-concept study. Methods: The study was a 24-week double blind, randomized, repeat dose parallel group study of rhPTH(1-31)NH₂, or placebo tablets, compared to open label Forsteo® (teriparatide) in 97 postmenopausal women with osteoporosis. The primary endpoint was to characterize percent change from baseline in BMD at lumbar spine (LS) after 24 weeks of once daily oral treatment of PTH(1-31)NH₂. Secondary endpoints included the measurement of bone markers, and measuring the exposure of oral PTH(1-31)NH₂ and teriparatide at the first and last dose. Results and Conclusions: The trial met the primary endpoint with an increase of 2.2% in LS BMD with PTH(1-31)NH₂ compared to baseline (p=0.004). Placebo had a -0.17% decrease (p=NS) and teriparatide increased LS BMD by 5.1% (p<0.001). After an initial lag, the rate of increase in BMD for oral PTH between week 12 and week 24 was comparable to teriparatide. There were statistically significant increases from baseline in the total hip BMD for PTH(1-31)NH₂ and teriparatide, with no significant differences between these two groups. In the PTH(1-31)NH₂ group, there was a minimal increase of 12.7% (p=NS) in CTx-1, a marker of bone resorption compared to a significant increase of 124.6% in the teriparatide group at week 24. Increase in the bone formation marker PINP was fairly modest in the PTH(1-31)NH₂ group, however, osteocalcin was increased 23.3% (p=0.015) compared to baseline. This is in contrast to 4.9% (p=0.87) in placebo and 172% (p<0.0001) in the teriparatide group at week 24. No clinically significant hypercalcemic events or elevated urine calcium were seen in the oral PTH(1-31)NH₂ arm. The most common adverse event in the oral PTH and placebo arms was GI pain or distress, and these events were mostly mild or moderate. The efficacy data and safety profile seen in this study demonstrate that this orally delivered PTH(1-31)NH₂ analog warrants evaluation in further late stage clinical studies.

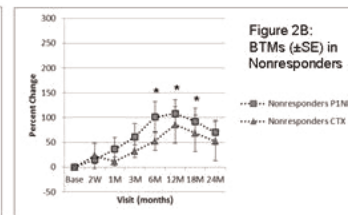
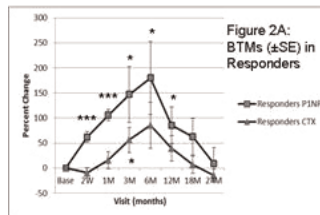
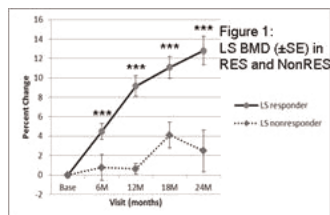
Disclosures: Morten Karsdal, Unigene Laboratories, Inc., 3
This study received funding from: Unigene Laboratories, Inc.

1102

Absence of the Anabolic Window Characterizes Premenopausal Women with Idiopathic Osteoporosis Who Do Not Respond to Teriparatide. Adi Cohen^{*1}, Polly Young², Emily Stein³, David Dempster², Hua Zhou⁴, Robert Recker⁵, Joan Lappe⁵, Chiyuan Zhang², Donald McMahon³, Serge Cremers², Alexander Zwahlen⁶, Ralph Müller⁶, Elizabeth Shane³.
¹Columbia University Medical Center, USA, ²Columbia University, USA, ³Columbia University College of Physicians & Surgeons, USA, ⁴Helen Hayes Hospital, USA, ⁵Creighton University Osteoporosis Research Center, USA, ⁶ETH Zurich, Switzerland

Idiopathic osteoporosis (IOP) in premenopausal women is characterized by cortical and trabecular microarchitectural deterioration and heterogeneous remodeling. We hypothesized that the osteoanabolic agent, teriparatide (TPTD), would improve BMD in IOP. We enrolled 21 premenopausal women with IOP (17 with fractures, age 39±6 yrs) in an open-label, 24-month pilot study of TPTD 20 mcg daily. We measured areal BMD by DXA, bone turnover markers (BTMs), and transiliac biopsy parameters. On average, there were substantial and significant (all p<0.05) 24M increases in areal BMD (±SD) at the spine (LS; 12.2±8.3%), total hip (6.4±5.6%) and femoral neck (FN; 7.8±3.4%). However, four women did not respond to TPTD (Fig 1; NonRES) defined as 12M change in BMD below least significant change at all sites). At baseline, NonRES and Responders (RES) were similar in terms of age, BMI, BMD, calciotropic and gonadal hormones, and iliac crest bone volume fraction (BV/TV). However, bone remodeling activity was lower in NonRES than RES, as evidenced by lower serum C-telopeptide (CTX; 201±160 vs 431±170 pg/mL;p=0.001), osteocalcin (OC; 12.0±1.5 vs 19.5±8.5 ng/mL;p=0.003), N-terminal propeptides of procollagen type 1 (PINP; 32±13 vs 46±17;p=0.1) and iliac crest bone formation rate (BFR/BS; 0.002±0.001 vs 0.011±0.006 mm²/mm/yr;p<0.0001). After TPTD initiation, PINP increased in RES (Fig 2A) by 1M, peaked at 180% above baseline by 6M and returned to baseline by 24M. In NonRES (Fig 2B), the PINP peak was blunted (108% above baseline) and delayed (12M). CTX rose comparably in RES (Fig 2A) and NonRES (Fig 2B) but peaked earlier in RES (6M vs 12M). In all subjects, 1M change in BTMs significantly predicted percent change in LS BMD at 12M (OC: r=0.55,p=0.02; PINP: r=0.50,p=0.04; CTX: r=0.46,p=0.046) and 24M (OC: 0.58,p=0.02; PINP: r=0.52,p=0.046) but not changes in hip BMD or BV/TV.

In summary, most premenopausal women with IOP responded to TPTD with marked increases in BMD. Those with attenuated and delayed responses to TPTD had low bone turnover at baseline and no evidence of an anabolic window, the early rise in formation markers that usually characterizes TPTD therapy. Early changes in bone formation markers predict response to TPTD in premenopausal women with IOP and may detect premenopausal women with IOP who will not experience substantial improvements in BMD in response to TPTD.



Figure

Disclosures: Adi Cohen, None.

This study received funding from: Eli Lilly

1103

Vitamin D Activation of Functionally Distinct Regulatory MicroRNAs in Primary Human Osteoblasts. Thomas Lisse^{*1}, Rene Chun², Sandra Rieger³, John Adams⁴, Martin Hewison⁴.
¹Massachusetts General Hospital, USA, ²UCLA/Orthopedic Hospital Research Center, USA, ³Mount Desert Island Biological Laboratory, Institute for Regenerative Medicine, USA, ⁴University of California, Los Angeles, USA

When bound to the nuclear vitamin D receptor (VDR), the active form of vitamin D, 1,25-dihydroxyvitamin D (1,25(OH)₂D) is a potent regulator of transcription in bone-forming osteoblasts. Less clear is the impact of 1,25(OH)₂D on post-transcriptional events in osteoblasts, such as the generation and action of microRNAs (miRNAs). Microarray analysis using replicate (n = 3) primary cultures of human osteoblasts (HOB) identified 5 human miRNAs (either registered [www.sanger.ac.uk/Software/Rfam/mirna] or proprietary) that were differentially regulated following treatment with 1,25(OH)₂D (10 nM, 6 hrs). Of these two non-proprietary miRNAs, miR-637 and miR-1228, were significantly increased following treatment with 1,25(OH)₂D. RT-PCR analyses showed that the host gene for miR-1228, low density lipoprotein receptor-related protein 1 (LRP1), was co-induced with miR-1228 in a dose-dependent fashion following treatment with 1,25(OH)₂D (0.1 – 10 nM, 6hrs). By contrast, the endogenous host gene for miR-637, death-associated protein kinase 3 (DAPK3), was transcriptionally repressed following treatment with 1,25(OH)₂D, indicating host-gene-independent regulation of miR-637. Analysis of two potential targets for miR-637 and miR-1228 in HOB, type 4 collagen (COL4A1) and bone matrix protein-2-inducible kinase (BMP2K), respectively, showed that 1,25(OH)₂D mediates suppression of these targets via distinct mechanisms. In the case of miR-637, suppression of COL4A1 appears to occur via decreased levels of COL4A1 mRNA. By contrast, miR-1228 showed no significant effect on BMP2K mRNA expression but appears to act instead by inhibition of BMP2K protein translation. In mature HOBs, siRNA inactivation of miR-1228 alone was sufficient to abrogate 1,25(OH)₂D-mediated down regulation of BMP2K protein expression. This event was associated with suppression of pro-differentiation responses to 1,25(OH)₂D in HOB, as represented by simultaneous decreases in osteocalcin and alkaline phosphatase expression. These data show for the first time that the effects of 1,25(OH)₂D on human bone cells are not restricted to classical VDR-mediated transcriptional responses but also involve miRNA-directed post-transcriptional mechanisms for regulation of gene expression.

Disclosures: Thomas Lisse, None.

1104

Transgenic Expression of the Vitamin D Receptor (VDR) Restricted to the Ileum, Cecum and Colon of VDR Knockout Mice Rescues VDR Dependent Rickets. Puneet Dhawan^{*1}, Connie Hasio¹, Ghassan Yehia¹, Liesbet Lieben², Geert Carmeliet³, Sylvia Christakos⁴.
¹UMDNJ-New Jersey Medical School, USA, ²KU Leuven, Belgium, ³Katholieke Universiteit Leuven, Belgium, ⁴University of Medicine & Dentistry & New Jersey - New Jersey Medical School, USA

The intestine plays the major role in 1,25(OH)₂D₃ action on calcium homeostasis. Yet the mechanisms involved remain incompletely understood. The established model of 1,25(OH)₂D₃ regulated intestinal calcium absorption postulates a critical role for

the duodenum. However it is the distal intestine where 70-80% of the ingested calcium is absorbed. In order to test directly the role of 1,25(OH)₂D₃ and VDR in the distal intestine, we generated mice expressing VDR exclusively in the ileum, cecum and colon by breeding VDR knockout (KO) mice with transgenic (TG) mice expressing hVDR under the control of the 9.5kb *cdx2* promoter. In adult mice from 3 independent KO/TG lines, expression of VDR was restricted to ileum, cecum and colon (highest expression was in cecum and colon). Mice from one TG line (TG [3]) showed low VDR expression in distal intestine (<30% of the levels observed in TG [1] and TG [2]). In the KO/TG mice hVDR was not expressed in duodenum, jejunum, kidney or other tissues. KO/TG mice from all 3 TG lines and VDR KO mice had alopecia. Growth arrest and hypocalcemia of the VDR KO mice were prevented in mice from KO/TG lines 1 and 2. 1,25(OH)₂D₃ treatment significantly increased serum calcium in mice from all 3 TG lines and in wild type (WT) mice (*p* < 0.05 compared to vehicle) but not in VDR KO mice. Renal calbindin-D_{9k} was similarly reduced 5-6 fold in VDR KO mice and in all 3 KO/TG lines (compared to WT). 1,25(OH)₂D₃ treatment had no effect on renal calbindin-D_{9k} expression in the KO or KO/TG mice. Although calbindin-D_{9k} was undetectable in the distal intestine of the VDR KO mice, calbindin-D_{9k} was expressed in the KO/TG [1] and [2] mice at levels equivalent to WT (in ileum and colon) or was 1.5 fold upregulated compared to WT (in cecum). In addition, μ CT analysis revealed that the expression of high levels of hVDR in the distal intestine (KO/TG mice [1] and [2]) rescued the bone defects associated with systemic VDR deficiency, including the rachitic growth plate abnormalities and the abnormal increase of bone mass in the primary spongiosa. Also, the decreased cortical thickness and increased cortical porosity were completely prevented. TG line 3 showed rickets, yet less severely compared to VDR KO mice. These findings provide evidence for the first time using VDR transgenic mice for the importance of the distal intestinal segments in vitamin D mediated calcium and bone homeostasis.

Disclosures: Puneet Dhawan, None.

1105

Blocking Osteogenic Differentiation and Mineralization: a Struggle between VDR and RUNX2 in the Mouse Mesenchymal Stem Cells. Mark Meyer^{*1}, Chang-Hun Lee², Nancy Benkuskay¹, Buer Sen³, Janet Rubin⁴, J. Pike¹. ¹University of Wisconsin-Madison, USA, ²University of Wisconsin at Madison, USA, ³University of North Carolina At Chapel Hill, USA, ⁴University of North Carolina, Chapel Hill, School of Medicine, USA

Osteogenic differentiation is believed to be primarily controlled by a master regulating transcription factor, RUNX2, and mice deficient of RUNX2 have severe skeletal defects. In the mouse, 1,25(OH)₂D₃ activates the VDR to reduce levels of RUNX2 and this in turn reduces the levels of several important osteogenic genes, blocking differentiation as well as mineralization in osteoblasts and their precursors, the multi-potential mesenchymal stem cells (MSCs). We studied this mechanism through ChIP-seq and RNA-seq of MSC cells (and MC3T3 cells) over 2 weeks of differentiation. Overlap of epigenetic markers implicated in activated enhancers, promoters and elongation (H4K5ac, H3K9ac, H3K4me1, H3K4me3, H3K36me3) revealed a modest shift in chromatin occupancy between the activated genes in the differentiation states, which may indicate a certain level of plasticity in cells with osteogenic potential. Therefore, we sought to understand the coordinated genome-wide efforts of VDR/RXR and RUNX2 (and C/EBP β) during this transition. VDR/RXR and RUNX2 overlapped significantly at 36% of sites, many of which are located within loci harboring osteogenic gene markers. Interestingly, C/EBP β , which may facilitate lineage determination, was found to be overlapped with VDR/RXR and RUNX2 binding, 52% and 45%, respectively. 1,25(OH)₂D₃ severely inhibited this differentiation and down-regulated key genes such as *Runx2* and *Osterix* (*Sp7*). We found VDR/RXR, RUNX2 and C/EBP β enhancer regions at +104kb in *Runx2* and -11kb in *Sp7* and a RUNX2 specific enhancer at +6kb within *Sp7*. siRNA knockdown of VDR reversed the 1,25(OH)₂D₃-mediated repression of these cloned enhancers and the *Runx2* mRNA. We found 1,25(OH)₂D₃ regulation of genes that modulate mineralization through the balance of pyrophosphate such as *Enpp1*, *Enpp3* and *Ank*. These genes contained intronic or intergenic distal VDR/RXR, RUNX2 and C/EBP β binding that demonstrated transcriptional response to 1,25(OH)₂D₃ after subsequent cloning and mutagenesis. Most interestingly, the regions responsive to 1,25(OH)₂D₃ in *Enpp1/3* and *Ank* were not conserved or present in our human osteoblast model lines (hOB and MG63) which may contribute to the inability of 1,25(OH)₂D₃ to inhibit *in vitro* mineralization in these cells. Overall, our studies help to define the complex arrangement of RUNX2 and VDR/RXR during the process of osteogenic differentiation and help clarify part of the mechanism by which mineralization can be blocked.

Disclosures: Mark Meyer, None.

1106

Glucocorticoid-Induced Leucine Zipper (GILZ): An Anabolic Effect Mediator of Glucocorticoids. Guodong Pan^{*1}, Kehong Ding¹, Nianlan Yang¹, Mark Hamrick¹, Carlos Isaales², Xing-Ming Shi¹. ¹Georgia Health Sciences University, USA, ²Medical College of Georgia, USA

Glucocorticoids (GCs) have both anabolic and catabolic effects on bone. However, the clinical outcome of GC therapy is a net loss of bone. Recent studies in mice have shown that the GC receptor (GR) mediates the catabolic effect and is responsible for GC-induced bone loss. However, no anabolic GC effect mediator has been identified to date. We showed previously that overexpression of glucocorticoid-induced leucine zipper (GILZ), a GC-inducible anti-inflammatory mediator, significantly enhances bone marrow mesenchymal stem cell (MSC) osteogenic differentiation *in vitro*. But the *in vivo* function of GILZ in bone is unknown. In this study we aimed to test the hypothesis that GILZ is an endogenous GC anabolic effect mediator and that bone-specific overexpression of GILZ increases bone formation in mice. We generated GILZ transgenic mice (GILZ^{Tg}) in which the expression of GILZ is under the control of a 3.6Kb type I collagen promoter. Bone-specific GILZ transgene expression was confirmed at the mRNA and protein expression levels by RT-PCR and Western blot, respectively. Bone analyses were performed using femurs of 3-month-old mice with standard bone parameter measurements. Results show that compared with their wild-type (Wt.) littermate controls, both DXA and μ CT results showed a significant bone mineral density (BMD) increase in GILZ^{Tg} mice (Tg vs. Wt: 9%, *p* < 0.05). Histology and histomorphology analyses show that the bone volume (BV/TV) and trabecular thickness (Tb.Th.) were increased significantly in GILZ^{Tg} mice (Tg vs. Wt: BV/TV 20% and Tb.Th 39% increase, respectively, *p* < 0.05). Most strikingly, the bone mineral apposition rate (MAR) was doubled in GILZ^{Tg} mice compared with the control mice (*p* < 0.01). In conclusion, our data have shown that bone-specific overexpression of GILZ can significantly increase bone formation *in vivo*, demonstrating that GILZ is an endogenous GC anabolic effect mediator and a very prominent bone anabolic drug candidate.

Disclosures: Guodong Pan, None.

1107

Osteoblast-specific Estrogen Receptor Alpha Knockout Mice Have Compromised Bone Mass and Architecture. Katherine Melville^{*1}, Timothy Bruhn¹, Sohaib Khan², John Schimenti¹, F. Patrick Ross³, Russell Main⁴, Marjolein Van Der Meulen¹. ¹Cornell University, USA, ²University of Cincinnati, USA, ³Hospital for Special Surgery, USA, ⁴Purdue University, USA

Estrogen signaling through estrogen receptor alpha (ER α) is critical to maintenance of bone mass and normal bone growth. Lack of ER α in global ER α KO female mice increases cortical and cancellous BMD in the tibia, but is accompanied by systemic increases in body mass and serum estrogen (E2) levels and decreases in uterine mass and IGF-I levels. We hypothesized that the phenotype of an osteoblast-specific ER α knockout mouse would differ from the global ER α KO mouse due to lack of systemic effects. Therefore, we generated an osteoblast-specific ER α knockout mouse (cKO) to investigate the role of ER α in osteoblasts and osteocytes in determining body and bone phenotype, while limiting the confounding hormonal systemic effects present in the global ER α KO.

Mice with a floxed ER α gene (*fl/fl*; +/+) and mice with an osteocalcin-promoter cre recombinase (+/+; oc-cre/+) were bred to generate female osteoblast-specific ER α conditional knockout mice (cKO, *fl/fl*; oc-cre/+) and littermate controls (LC, *fl/fl*; +/+). Skeletal phenotype was characterized at 12 weeks (n=7 cKO, n=6 LC) and 18 weeks (n=10/genotype). Body, ovary, and uterus mass were measured. Serum was assayed for E2, testosterone (T), IGF-I, TRACP5b, and osteocalcin (OC) levels. Cancellous and cortical regions in the tibiae and L5 vertebrae were analyzed by microcomputed tomography. Tibiae were stained for ER α immunohistochemistry. Vertebral stiffness and strength were measured in compression to failure.

ER α staining was absent from osteoblasts in cKO. In the proximal tibia, cancellous bone mass was decreased (-36%) and tissue mineral density (+5%) and trabecular separation (+54%) increased in cKO compared to LC at 12w and 18w. L5 cancellous bone volume fraction (-43%) was decreased due to decreased trabecular thickness (-11%) and increased trabecular separation (+32%) in cKO vs LC at 12w. Tibial cortical area (-7%) and tissue mineral density (-2%) were decreased in cKO vs LC at both ages. L5 strength was reduced in cKO vs LC at 12w (-11%). Body, ovary, and uterus mass, and serum E2, T, IGF-I, and OC serum levels were similar between genotypes. In contrast to the global ER α KO, cancellous and cortical mass were decreased in cKO vs LC, which likely reflects the lack of altered hormone levels in the cKO that are present in the global ER α KO.

1109

Bivariate Genome-wide Association Analysis Identifies Novel Candidate Genes for Cross-sectional Bone Geometry and Appendicular Lean Mass: The GEFOS and CHARGE Consortia. Yi-Hsiang Hsu¹, Xing Chen², Karol Estrada³, Serkalem Demissie⁴, Tamara Harris⁵, Thomas Beck⁶, Alireza Moayyeri⁷, Candace Kammerer⁸, Carolina Medina-Gomez⁹, Vilmundur Gudnason¹⁰, Tim Spector⁷, Maria Zillikens¹¹, L. Adrienne Cupples⁴, Andre Uitterlinden¹², Fernando Rivadeneira³, Douglas Kiel¹³, David Karasik^{*13}. ¹Hebrew SeniorLife Institute for Aging Research & Harvard Medical School, USA, ²Harvard University, USA, ³Erasmus University Medical Center, The Netherlands, ⁴Boston Uni Sch Pub Health, USA, ⁵Intramural Research Program, National Institute on Aging, USA, ⁶Quantum Medical Metrics, LLC, USA, ⁷King's College London, United Kingdom, ⁸University of Pittsburgh Graduate School of Public Health, USA, ⁹Erasmus Medical Center, The Netherlands, ¹⁰Icelandic Heart Association Research Institute, Iceland, ¹¹Erasmus Mc, The Netherlands, ¹²Rm Ee 575, Genetic Laboratory, The Netherlands, ¹³Hebrew SeniorLife, USA

Hip geometry and lean (muscle) mass have significant genetic correlation, indicating that genetic determinants may be shared by both bone and muscle. To identify genes with pleiotropic effects on bone and muscle traits, we performed a bivariate genome-wide association analysis (GWAS) using data from two consortia.

The Hip Structural Analysis program was used to measure the femoral neck length (FNL), neck-shaft angle (NSA), narrowest width of the femoral neck (NNW) and calculate its section modulus (NNZ), from DXA scans of GEFOS consortium participants (17,528 men and women from 10 mostly Caucasian studies). Appendicular lean mass (aLM), combining upper and lower extremities, was measured in participants of the CHARGE Musculoskeletal Consortium (22,360 Caucasian men and women from 15 cohorts).

Univariate GWAS meta-analyses of ~2.5 million autosomal SNPs (imputed based on CEU HapMap phase II panel) were first performed for hip geometry and aLM, separately. An additive genetic effect model was applied with adjustment for age, sex, height, ancestral genetic background, as well as age² and fat mass (for aLM only). We then used the univariate GWAS results to perform a bivariate analysis for each pair of HSA-aLM traits. We used the linear combination of test statistics approach with estimated variance-covariance structure, to take into account the phenotypical correlation between HSA and aLM. We considered SNPs as potentially pleiotropic if (a) they achieved genome-wide significance threshold (bivariate p-value $\leq 5 \times 10^{-8}$) and (b) the bivariate p-value was an order of magnitude lower than both univariate p-values.

For a combination NSA-aLM, there were no SNPs with genome-wide significant bivariate signal; for other pairs of phenotypes, potentially pleiotropic SNPs were mapped to regions in/near *SORCS1* (on 10q23-q25) and *C6orf223* (6p21.2) for FNL-aLM; *PPP6R3/LRP5* (11q13) for NNZ-aLM, and *ADAMTSL3* (15q25.2) for NNW-aLM pair. The potential pleiotropic genetic variants had associations in the same directions for both HSA and aLM. Notably, the same variant in *PPP6R3/LRP5* is associated at genome significant level in a bivariate GWAS of total body lean mass and BMD in children (ASBMR 2012). *LRP5*, a member of the Wnt signaling pathway, is an established locus associated with BMD and fracture risk; in contrast the role in musculoskeletal biology is less clear for *PPP6R3* (ubiquitously expressed in bone and muscle), *SORCS1*, belonging to a neuropeptide signaling pathway, and for *ADAMTSL3*, previously associated with adult height but whose *in-vivo* function is unknown.

In conclusion, using the bivariate GWAS approach, we discovered loci potentially regulating the hip geometry and muscle mass. Additional replication in independent cohorts and functional follow-up in relevant musculoskeletal tissues is needed to confirm the pleiotropic effects of these gene variants.

Disclosures: David Karasik, None.

1110

PTHrP Regulates the Modeling of Enteses During Linear Growth. Meina Wang^{*1}, Joshua VanHouten², Randy Johnson³, Arthur Broadus². ¹Yale University, USA, ²Yale University School of Medicine, USA, ³M.D. Anderson Cancer Center, USA

PTHrP is widely expressed in the fibrous periosteum (PO) and in tendon and ligament insertion sites (entheses, ENTs). In most such sites, PTHrP is mechanically-induced and is temporally associated with subjacent osteoclast (OC) and/or osteoblast (OB) populations. We tested the working hypothesis that PTHrP might regulate the modeling of cortical bone and/or ENTs using *Scx-Cre*-driven ENT-specific *PTHrP* cKO mice. Scleraxis (*Scx*) is a transcription factor that is widely expressed in the connective tissue of bone.

The *PTHrP* cKO mice display a dozen or so surface abnormalities that reflect failed development and/or modeling of ENT or PO sites. Here, we will focus on three ENTs that represent variations on a theme of load-driven PTHrP induction of ENT OCs. First, the medial collateral ligament (MCL) insertion into the proximal tibial metaphysis must migrate to accommodate linear growth, a process that is driven by OCs at the migrating edge. This process fails in the cKO mouse and is replaced by a

Proximal Tibia L5 Vertebra

LC
12w

cKO
12w



cKO vs LC Tibia and Vertebra Bone Architecture

Disclosures: Katherine Melville, None.

1108

Endocrine Actions of Parathyroid Cyp27b1 in The Ca²⁺ and Skeletal Homeostasis: Studies of Parathyroid-Specific Knockout Mice. Zhiqiang Cheng, Chia-Ling Tu, Alfred Li, Christian Santa-Maria, Hanson Ho, Michael You, Nathan Liang, Tsui-Hua Chen, Rachel Roston, Dolores Shoback, Daniel Bikle, Wenhan Chang^{*}. Endocrine Unit, VA Medical Center, University of California, San Francisco, USA

The renal 25-hydroxyvitamin D₃ 1-alpha-hydroxylase (Cyp27b1) is thought to be the major enzyme producing 1,25 (OH)₂ vitamin D₃ (1,25D), which critically modulates mineral and skeletal homeostasis. The role of extra-renal Cyp27b1 is, however, unclear. We demonstrated previously that Cyp27b1 and vitamin D receptor (VDR) constitute an autocrine/paracrine pathway to suppress PTH secretion by studying parathyroid glands from mice with homozygous Cyp27b1 (PT-Cyp27b1-KO) or VDR (PT-VDR-KO) gene KO targeted to their parathyroid cells (PTCs). In the current study, we used those mice to determine whether parathyroid Cyp27b1 contributes to circulating 1,25D levels and modulates mineral and skeletal homeostasis. Serum 1,25D (s1,25D), Ca²⁺ (sCa), phosphate (sPi), and PTH (sPTH) levels in the PT-Cyp27b1-KO and PT-VDR-KO mice and control littermates (Cont), which carry floxed alleles but no Cre, were compared as were their bone mass and structural parameters by micro-computed tomography (μCT). The specificity of excision of VDR and Cyp27b1 gene in PTCs was confirmed by PCR analyses of genomic DNA and RNA extracted from different tissues. sPTH levels increased modestly by ~80% in PT-VDR-KO mice and profoundly by ~250% in the PT-Cyp27b1-KO mice, compared to Cont mice. While sCa and sPi levels were unchanged in the PT-VDR-KO mice, PT-Cyp27b1-KO mice developed hypocalcemia and hyperphosphatemia, despite markedly elevated sPTH levels. We further found that s1,25D levels in PT-Cyp27b1-KO mice were reduced to ~30% of the level in Cont mice, even though renal Cyp27b1 RNA levels were increased by 2-3 fold (likely due to the elevated sPTH levels) along with a decrease (by ~50%) in renal Cyp24 RNA expression. These results suggest that Cyp27b1 activity in PTCs is a source of s1,25D. We examined the skeletal effects of PTC-specific gene KO on trabecular bone (Tb) parameters in the distal femurs of PT-VDR-KO and PT-Cyp27b1-KO mice. VDR KO in PTCs produced an increased Tb bone volume (BV) over total tissue volume (TV) ratio (Tb.BV/TV) and Tb number (Tb.N). These anabolic effects were, however, not evident in the Cyp27b1 KO mice, suggesting that different calcemic and phosphatemic states affect skeletal actions of PTH. Our data suggest that PTC Cyp27b1 not only exerts autocrine/paracrine actions to modulate PTH secretion but also provides an important source of s1,25D essential either directly or indirectly for maintaining mineral and skeletal homeostasis.

Disclosures: Wenhan Chang, None.

massive traction tuberosity comprising mostly mineralizing fibrochondrocytes (FCs). Second, the teres major (TM) inserts into the proximomedial humerus via a major cord-like tendon at a near-90° angle; this is anchored into a deep OC-driven cortical cave, the strength of this ENT being in the depth of its root system. Here too, OCs fail entirely in the cKO mouse, and a major FC-associated traction tuberosity forms that distorts the entire proximal humerus. Third, the latissimus dorsi (LD) inserts over a lengthy portion of the anteromedial humerus at a gentle (about 10°) angle, and its OC-driven root system resembles a saw-tooth pattern of minimal depth; here strength depends upon breadth and surface rather than depth. This ENT also fails in the cKO mouse but without a traction deformity.

The traction tuberosities are pathological structures that form because of the continued load in the absence of the normal OC modeling that the load should induce. The FCs here originate from both the tendon and cambial ENT layers as an apparent consequence of heavy loading.

These data provide the initial genetic evidence that PTHrP regulates the formation and function of membranous bone cell populations at the surface of long bones. These functions reflect the use of PTHrP as a modeling tool, in this case at three so-called fibrous insertion sites that represent forms frusts of a common strategy, presumably differing from each other as a consequence of differences in biomechanical inputs.

Disclosures: Meina Wang, None.

1111

Interactions between Periosteal Cells and Muscle-Derived Blood Vessels are Essential for Bone Autograft Healing. Nick Van Gastel*¹, Maarten Depypere², Karen Moermans¹, Ingrid Stockmans¹, Jan Schrooten³, Frederik Maes², Frank Luyten⁴, Geert Carmeliet⁵. ¹Laboratory of Clinical & Experimental Endocrinology, KU Leuven, Belgium, ²Department of Electrical Engineering (ESAT/PSI), KU Leuven, Belgium, ³Department of Metallurgy & Materials Engineering, KU Leuven & Prometheus, Division of Skeletal Tissue Engineering, KU Leuven, Belgium, ⁴University Hospitals KU Leuven, Belgium, ⁵Katholieke Universiteit Leuven, Belgium

Despite major drawbacks, autologous bone transplantation remains the therapy of choice to treat large bone defects. Cell-based bone tissue engineering seems a promising alternative, but one of the key challenges is the timely formation of blood vessels to promote survival of the cells in the implant. To gain more insight in this critical process, we examined how periosteal cells orchestrate blood vessel formation during bone autograft healing.

Using a murine segmental bone defect model, we confirmed the importance of periosteal cells in bone healing by showing that removal of the periosteum reduced the healing of autografts to the level of devitalized allografts. Implantation of autografts derived from GFP-mice further revealed that the donor periosteal cells were the main source of chondrocytes and osteoblasts in the callus. *In vitro* analysis of murine periosteum-derived cells (mPDC) indicated that they may contribute to healing not only by differentiating to osteoblasts and chondrocytes, but also by promoting endothelial cell (EC) proliferation and survival through the production of angiogenic factors such as VEGF. Ectopic co-implantation of mPDC and EC in mice proved that periosteal cells can enhance both angiogenesis and vasculogenesis *in vivo*.

The role of periosteal cells in blood vessel formation during bone repair was further shown by the observation that autografts were surrounded by a significantly higher number of blood vessels compared to allografts. In contrast to the bone-forming cells, the blood vessel network in the autograft callus was derived almost entirely from the host and was at numerous sites connected to the vessels of the adjacent muscle. The importance of the muscle vascular bed was confirmed by insertion of a membrane in between the graft and the muscle, which completely abrogated the periosteal reaction. While an angiogenic response from the host was still observed, the blood vessels could not reach the periosteum, preventing cell proliferation and callus formation.

In conclusion, our results demonstrate that periosteal cells may provide an ideal cell source for bone regeneration, not only because of their strong osteogenic and chondrogenic potential, but also by their pro-angiogenic features. In addition, we show that during bone healing the survival and function of periosteal cells drastically relies on timely interactions with blood vessels from the nearby muscle, which emphasizes the importance of the local environment.

Disclosures: Nick Van Gastel, None.

1112

Muscle Atrophy Enhances Bone Anabolism. Ted Gross*¹, Brandon Ausk¹, Steven Bain¹, Leah Downey¹, Edith Gardner¹, Ronald Kwon¹, Leah Worton², Sundar Srinivasan¹. ¹University of Washington, USA, ²The University of Washington, USA

Simultaneous atrophy or hypertrophy of muscle and bone is observed throughout life. In direct contrast to this relation, we recently observed that superimposing transient muscle paralysis upon external tibia loading elevated periosteal bone formation 2-fold compared to what the loading regimen induced without muscle paralysis. Following on this unexpected result, we designed an *in vivo* experiment to test the hypothesis that the enhanced bone anabolism associated with combined

muscle paralysis and mechanical loading requires spatial proximity between the atrophied muscle and mechanically stimulated bone. Adult female C57 mice (16 wk) each underwent a 3d/wk, 3wk external cantilever bending regimen of the right tibia (1600 µε normal strain, 100 cycles/loading bout). Mice randomly received a 0 saline injection in the right calf (R. Calf S, n=6), or BTxA (2U/100g) in the right calf (R. Calf B, n=6), left calf (L. Calf B, n=5), or the right triceps (R. Triceps B, n=5). All mice received calcein labels (d 10, 19) with p.MS, p.MAR, and p.BFR determined for the periosteal surface of left and right tibiae. No differences were noted in the contralateral left tibiae across groups. The R. Calf S tibiae demonstrated significant increases in p.MS (p<0.05), p.MAR (p<0.01), and p.BFR (<0.01) vs contralateral tibiae. Likewise, each BTxA group demonstrated significant increases in p.MS, p.MAR, and p.BFR vs contralateral tibiae (all p<0.01). p.BFR in each of the BTxA groups was significantly elevated vs the Saline group (p<0.05) but did not differ with the site of muscle paralysis. The enhanced anabolism was achieved almost entirely via enhanced p.MAR, as p.MS did not differ across groups. The lack of response in the contralateral tibiae indicate that muscle paralysis alone is not sufficient to activate a quiescent periosteum. The surprisingly equivalent anabolic benefit of L. Calf and R. Triceps muscle paralysis vs R. Calf paralysis (directly adjacent to the externally loaded tibia) demonstrates that spatial adjacency is not required as hypothesized and that reduced mechanical loading of the right tibia (which did not occur in L. Calf and R. Triceps paralysis) is not a primary underlying influence for the enhanced response. In summary, these data suggest that transient muscle paralysis results in activation of signaling pathways that, via systemic distribution, are capable of enhancing osteoblast function.

Disclosures: Ted Gross, None.

1113

Trabecular Mineralization and Muscle Fiber Growth in Response to Dynamic Fluid Flow Stimulation. Minyi Hu*¹, Robbin Yeh¹, Morgan Teeratananon¹, Yi-Xian Qin². ¹Stony Brook University, USA, ²State University of New York at Stony Brook, USA

Intramedullary pressure (ImP)-driven bone fluid flow acts as a mediator between an external load and bone cells, which then regulate bone remodeling. It is hypothesized that muscle compressions may increase vessel pressure gradient that can directly increase ImP. To establish the translational potential of ImP-induced fluid flow stimuli in bone, a dynamic hydraulic stimulation (DHS) approach has been developed to evaluate trabecular mineralization and muscle fiber growth in response to non-invasive, direct muscle compressions in a disuse osteopenia rat model. Sprague-Dawley virgin rats were randomly assigned to 5 groups: baseline control (n=15), age-matched control (n=12), hindlimb suspended (HLS, n=10), HLS+static pressure (n=10), HLS+DHS (n=14). Stimulation were given to right tibia by an inflatable cuff with 2Hz, 30mmHg static+30mmHg dynamic pressures, for 10min on-5 min off-10min on, 5d/wk for 4 wks. Two injections of calcein (10mg/kg) were given to the animals in two weeks apart during the study. The right tibiae, soleus and gastrocnemius were obtained at the animal sacrifice. The proximal tibiae were embedded with PMMA. Longitudinal sections were made to 5µm. Histomorphometric measurements were done by tracing calcein labels in the trabecular bone in the metaphyseal region using the Osteomeasure software. Muscle samples were snap-frozen, and cross-sections were made to 8µm followed by H&E staining. Muscle fiber areas were determined by the Image J software. The histomorphometry data indicated that HLS significantly reduced BV/TV, MS/BS, MAR, BFR/BS and BFR/BV compared to age-matched controls (Table 1). HLS+static pressure alone did not show a significant difference compared to HLS, except for MS/BS. However, HLS+DHS rats showed significant increases in BV/TV and all other bone formation indices, except for MAR. HLS+DHS had increases compared to the HLS group by 34% in BV/TV, 121% in MS/BS, 190% in BFR/BS, and 146% in BFR/BV. On the other hand, stimulation-induced improvements on muscle fiber growth were not shown (Figure 1). DHS did not seem to rescue muscle atrophy due to HLS. While dynamic fluid flow stimulation by DHS significantly mitigate bone loss in disuse, the current effective DHS stimuli may be suitable for bone cell responses but not for muscle fiber alterations.

| | BV/TV (Hise, %) | MS/BS (%) | MAR (mm/day) | BFR/BS (mm ³ /mm ² /day) | BFR/BV (mm ³ /mm ³ /day) |
|-------------|-----------------|-------------|--------------|--|--|
| Age-matched | 46.61±7.32 | 10.75±2.24 | 0.73±0.15 | 0.04±0.03 | 0.23±0.07 |
| HLS | 31.22±9.91* | 4.12±0.64** | 0.53±0.16* | 0.02±0.01** | 0.07±0.03** |
| HLS+Static | 40.99±18.04 | 6.53±1.18** | 0.59±0.19 | 0.04±0.01** | 0.12±0.03** |
| HLS+DHS | 44.65±3.96* | 7.09±2.50** | 0.71±0.18 | 0.05±0.02** | 0.18±0.05** |

*p < 0.05 vs. age-matched; *p < 0.05 vs. HLS; **p < 0.001 vs. age-matched; **p < 0.001 vs. HLS; †p < 0.05 vs. HLS + static

Table 1. Static and dynamic histomorphometry analysis.

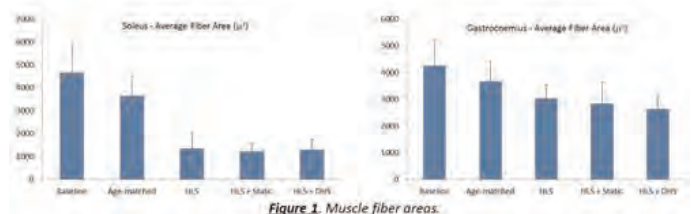


Table 1 and Figure 1

Disclosures: Minyi Hu, None.

1114

Ryanodine receptor 1 Remodeling in Cancer Associated Muscle Dysfunction. David Waning^{*1}, Khalid Mohammad², Daniel Andersson³, Sutha John⁴, Patricia Juarez-Camacho⁴, Steven Reiken³, Andrew Marks⁵, Theresa Guise². ¹Indiana University School of Medicine, USA, ²Indiana University, USA, ³Department of Physiology & Cellular Biophysics, College of Physicians & Surgeons of Columbia University, USA, ⁴Indiana University Simon Cancer Center & Indiana University School of Medicine, USA, ⁵Columbia University, USA

Muscle weakness is common in advanced cancers and is a cause of significant cancer-related morbidity and mortality. The mechanisms of cancer-associated muscle dysfunction are unknown and no effective treatment exists. Ryanodine receptor 1 (RyR1) is the skeletal muscle sarcoplasmic reticulum calcium release channel required for excitation-contraction coupling. The RyR1 channel is a macromolecular complex that is comprised of 4 RyR1 monomers and regulatory proteins that modulate channel function. RyR1 undergoes remodeling in disease states, such as muscular dystrophy and ageing, characterized by oxidation and nitrosylation of the channel and loss of the stabilizing subunit, calstabin1 resulting in leaky channels. We hypothesized that muscle weakness in cancer could be due to remodeling of RyR1 resulting in intracellular calcium leak that causes impaired muscle function.

We used a mouse model of breast cancer metastases to bone during which mice develop significant cachexia. Five-week-old female nude mice were inoculated with MDA-MB-231 breast cancer cells via intra-cardiac inoculation and compared to non-tumor bearing controls. Mice developed osteolytic lesions 12 days after inoculation. Tumor bearing mice lost significant weight by 4 weeks compared to controls (20.5±0.6 vs. 23.2±0.4; p<0.0002). This was associated with a significant reduction in total body tissue, lean mass and fat in tumor bearing mice, as assessed by DXA (P<0.01), with no difference in total body %lean mass or %fat. Muscle specific force production of the extensor digitorum longus (EDL) muscle was significantly decreased in tumor bearing mice compared to controls (p<0.001). The reduction in muscle force correlated with larger osteolytic lesions (p<0.05). Immunoprecipitation and immunoblotting of RyR1 from EDL of tumor bearing mice showed that RyR1 were oxidized, nitrosylated and depleted of calstabin1, consistent with leaky channels. Transmission electron microscopy showed dysmorphic mitochondria in tumor bearing mice.

Our data show that MDA-MB-231 bone metastases are accompanied by loss of muscle function and remodeling of RyR1 channel complex resulting in leaky channels. Similar remodeling of RyR1 has been shown to cause muscle weakness in muscular dystrophies and sarcopenia. Targeted therapy against leaky RyR1 channels improves muscle function and exercise capacity in murine models of muscular dystrophy and sarcopenia and may be an effective therapy for cancer-associated muscle weakness.

Disclosures: David Waning, None.

1115

Injury-Activated TGFβ Controls Mobilization of MSCs for Tissue Remodeling. CHANGJUN LI^{*1}, GEHUA ZHEN¹, WENYING HE¹, KAI JIAO¹, YIU-FAI CHEN², XIAOFENG JIA¹, Bing Yu³, Xu Cao⁴, Mei Wan¹. ¹Johns Hopkins University School of Medicine, USA, ²University of Alabama at Birmingham, USA, ³Johns Hopkins School of Medicine, USA, ⁴Johns Hopkins University, USA

Upon secretion, TGFβ is maintained in a sequestered state in extracellular matrix as a latent form, which is considered as a molecular sensor that releases active TGFβ in response to mechanical stress, wound repair and tissue injury. The biological implication of the temporal discontinuity of TGFβ storage in the matrix and its activation is obscure. Here, using rat and mouse models in which latent TGFβ is activated in vascular matrix in response to injury of arteries, we show that active TGFβ1 controls the mobilization and recruitment of MSCs for tissue remodeling. Active TGFβ1 was elevated in both vasculature and peripheral blood at 8 hrs after injury in both models, and the elevation sustained for 2 wks. At the same time points, Sca1⁺CD29⁺CD11b⁺CD45⁺ MSCs, in which 91% are nestin⁺ cells, were mobilized to peripheral blood and recruited to the remodeling arteries. Inhibitor of TGFβ type I receptor (TβRI) blocked the mobilization and recruitment of MSCs to the remodeling arteries. Notably, intravenously injection of rhTGFβ1 in uninjured mice rapidly mobilized MSCs into circulating blood. To confirm the MSCs feature of the mobilized cells, biotinylated rhTGFβ1 was injected i.v. and its binding to bone marrow cells was analyzed. Biotinylated rhTGFβ1 binds to bone marrow nestin⁺Sca1⁺CD29⁺CD11b⁺ cells, which have multilineage differentiation capacity and can differentiate into myofibroblast-like cells. To further investigate how injury-induced activation of TGFβ1 in vascular matrix stimulates migration of MSCs, we developed an injured aorta-conditioned medium (Aorta-CM)-based cell migration assay, in which MSCs were placed in the upper chamber and the Aorta-CM was placed in the lower chamber of a transwell. Aorta-CM prepared from *ex vivo* injured aorta significantly enhanced cell migration, and the neutralizing antibody of TGFβ1 blocked the migration. Consistently, active TGFβ1 level was significantly elevated in the injured Aorta-CM, and addition of inhibitors of either TβRI or MCP-1 in the CM blocked the migration, indicating that active TGFβ1 released from the injured vessels is a primary factor in induction of the migration of MSCs, and cascade expression of MCP1 stimulated by TGFβ amplifies the signal for migration. Collectively, the results suggest that TGFβ1

is an injury-activated messenger essential for the recruitment of MSCs to participate in vascular remodeling.

Disclosures: CHANGJUN LI, None.

1116

Hyperactive Transforming Growth Factor-beta1 Signaling Potentiates Fracture Non-union in Neurofibromatosis Type 1. Steven Rhodes^{*1}, Yongzheng He¹, Xiaohua Wu², Ping Zhang³, Shi Chen¹, Chang Jiang¹, Hiroki Yokota⁴, Xianlin Yang¹, Xianghong Peng¹, Sreemala Murthy¹, Khalid Mohammad¹, Theresa Guise¹, Feng-Chun Yang¹. ¹Indiana University, USA, ²Indiana University School of Medicine, USA, ³Indiana University – Purdue University Indianapolis, USA, ⁴Indiana University Purdue University Indianapolis, USA

Tibial pseudarthrosis, in up to 90% of cases, is associated with Neurofibromatosis type 1 (NF1). Tibial pseudarthrosis is a rare yet debilitating pediatric orthopedic condition, progressing to spontaneous fracture and subsequent fibrous nonunion. Treatment of tibial pseudarthrosis has been notoriously difficult, ultimately requiring amputation of the affected limb in many cases. Still, the molecular etiology of these pathological defects remains unclear.

Transforming growth factor-beta1 (TGF-β1) is known to be a critical factor regulating the spatiotemporal coupling of bone resorption and bone formation. Intriguingly, haploinsufficiency of *Nf1* in myeloid cells has been shown to result in hypersecretion of TGF-β1 *in vitro*. Given the fact that disruption of TGF-β signaling gradients is associated with a spectrum of osseous defects in both patients and mouse models, we sought to investigate the impact of TGF-β1 signaling in NF1 associated skeletal manifestations.

Here, we show that compared to WT mice, TGF-β1 serum levels are 5.7 fold higher in *Nf1*^{flx/flx}; *Col2.3Cre* mice, a murine model that closely recapitulates multiple NF1 skeletal defects including, short stature, osteoporosis, and mechanically induced nonunion fracture. We further found that *Nf1* deficient osteoblasts, the principal source of TGF-β1 in bone, overexpressed TGF-β1 in a gene dosage dependent fashion at both the mRNA and protein levels. Moreover, *Nf1* deficient osteoclasts and osteoblasts were hyperresponsive to TGF-β1 in tissue culture, preferentially augmenting *Nf1*^{+/-} osteoclast bone resorptive activity, while inhibiting *Nf1*^{-/-} osteoblast differentiation. These cellular phenotypes were accompanied by biochemical hyperactivation of the TGF-β1-Smad pathway. As an *in vivo* proof of concept, we found that administration of the pharmacologic TGF-β type I receptor inhibitor, SD-208, can rescue both osteoporotic and non-union fracture phenotypes in *Nf1*^{flx/flx}; *Col2.3Cre* mice, restoring bone mass and callus bone volume to WT levels. This study provides direct preclinical evidence for the critical role of *Nf1* dependent TGF-β1 signaling in the pathogenesis of NF1 associated osteoporosis and pseudarthrosis, thus implicating the TGF-β signaling pathway as a potential therapeutic target in the treatment for NF1 osseous defects.

Disclosures: Steven Rhodes, None.

1117

Metabolically Active Brown Adipose Tissue (BAT) Has Anabolic Effects on Bone Through Endocrine/Paracrine Activity Including Production of IGFBP2. Sima Rahman^{*1}, Yalin Lu², Sven Enerback³, Clifford Rosen⁴, Beata Lecka-Czernik⁵. ¹University of Toledo Health Sciences Campus, USA, ²University of Toledo Medical Center, USA, ³University of Goteborg, Sweden, ⁴Maine Medical Center, USA, ⁵University of Toledo College of Medicine, USA

Energy metabolism is tied to bone acquisition; however the role of adipose tissue in this process has not been well defined. Recently, it has been reported that in young women the volume of preformed brown adipose tissue (pBAT) directly correlated with BMD. In a mouse model, *Misty*, pBAT dysfunction was associated with very low bone mass. Forkhead protein FoxC2 represents a transcription factor which regulates mitochondrial function and increases energy production in adipose tissue. Ectopic expression of FoxC2 in adipose tissue leads to increased energy expenditure, protection from high fat-diet induced obesity and insulin resistance, and a high bone mass phenotype. At 5 mo of age, trabecular BV/TV in *aP2-FoxC2*^{Tg} mice is 3-fold higher vs. WT mice and correlates with increased osteoblast number (4-fold), increased MAR and high BFR (2- and 3- fold, respectively). The high bone mass in *aP2-FoxC2*^{Tg} mice is accompanied by increased marrow adipose tissue (MAT) which is juxtaposed in the tibia and femur. Ectopically expressed FoxC2 increases expression of UCPI, Dio2, and Prdm16 in both peripheral and marrow adipocytes suggesting acquisition of a brown-like (iBAT) phenotype. To investigate the hypothesis that iBAT has endocrine/paracrine function in the regulation of bone remodeling, the effects of conditioned media (CM) derived from iBAT represented by either epididymal fat of *aP2-FoxC2*^{Tg} mice or marrow adipocytes expressing FoxC2 on markers of osteoblast phenotype were tested. CM from iBAT significantly increased alkaline phosphatase (ALP) activity, expression of osteoblast-specific gene markers (Dlx5, osteocalcin and cyclin D), and levels of pAkt. Proteomic analysis of the secretome of FoxC2-3T3-L1 adipocytes revealed increased IGFBP2, a protein known for its insulin sensitizing properties as well as its IGF-1-independent effects on osteoblast differentiation. Serum levels of IGFBP2 protein are elevated and the

expression of IGFBP2 transcripts in WAT and MAT are also increased in aP2-FoxC2^{fl} mice. Furthermore, depletion of IGFBP2 from CM using an IGFBP2-specific antibody abrogated FoxC2-mediated increases in ALP activity in the recipient osteoblastic cells. These data suggest a role for IGFBP2 in mediating BAT's endocrine/paracrine regulation of bone mass. The role of pBAT and iBAT in the pathogenesis of osteoporosis requires further studies.

Disclosures: *Sima Rahman, None.*

1118

Overexpression of Bmi-1 in Mouse Lymphocytes Stimulates Osteogenesis by Improving the Osteogenic Microenvironment. Xichao Zhou^{*1}, Wen Sun², David Goltzman³, Andrew Karaplis³, Xiang-Jiao Yang³, Dengshun Miao⁴. ¹Nanjing Medical University, China, ²Nanjing Medical University The Research Center for Bone & Stem Cells, Peoples Republic of China, ³McGill University, Canada, ⁴Nanjing Medical University, Peoples Republic of China

Overexpression of Bmi1 in mouse lymphocytes has been shown to be important for the specification of the identity of the vertebral column, but it is unclear whether such overexpression also improves the osteogenic microenvironment and thereby stimulates osteogenesis. To investigate this, we examined the skeletal phenotype of Em-Bmi1 transgenic mice in which Bmi1 is highly expressed in lymphocytes. Western blotting confirmed a high expression level of Bmi1 protein in the thymus, spleen and bone marrow of the transgenic mice. Compared to wild-type mice, skeletal size, BMD, trabecular bone volume, osteoblast number, alkaline phosphatase (ALP)- and type I collagen-positive areas, and mRNA levels of Runx2, ALP, type I collagen and osteocalcin were all significantly increased in the Em-Bmi1 transgenic mice. Total numbers of CFU-f and ALP positive CFU-f generated by bone marrow cell cultures also increased significantly in the transgenic mice and a similar increase was observed in wild-type bone marrow cells cultured with the conditioned medium from lymphocyte cultures of the transgenic mice. In the PTHrP(1-84) knockin (*Pthrp* KI) mice that lack the nuclear localization sequence and the C-terminal region of PTHrP, Bmi1 expression is reduced and premature osteoporosis occurs. We therefore crossed Em-Bmi1 transgenic mice with *Pthrp* KI mice to generate *Pthrp* KI mice with Bmi1 overexpression in lymphocytes for comparison with the *Pthrp* KI and wild-type littermates. Lymphocytic expression of Bmi1 in the *Pthrp* KI background resulted in a longer lifespan, increased body weight, and improvement in skeletal growth and osteoblastic bone formation in the *Pthrp* KI mice, although the defects were not completely rescued. Furthermore, real-time RT-PCR revealed that levels of anti-oxidative enzymes including SOD1, 2 and 3, glutathione reductase and glutathione peroxidase 1 were up-regulated in bony tissues of the Em-Bmi1 transgenic mice, but down-regulated in the *Pthrp* KI mice; importantly, Bmi1 ectopic expression in the *Pthrp* KI mice rescued this down-regulation. Taken together, these results demonstrate that overexpression of Bmi1 in mouse lymphocytes stimulates osteogenesis and partially rescues the defects in skeletal growth and osteogenesis in the *Pthrp* KI mice by inhibiting oxidative stress and improving the osteogenic microenvironment.

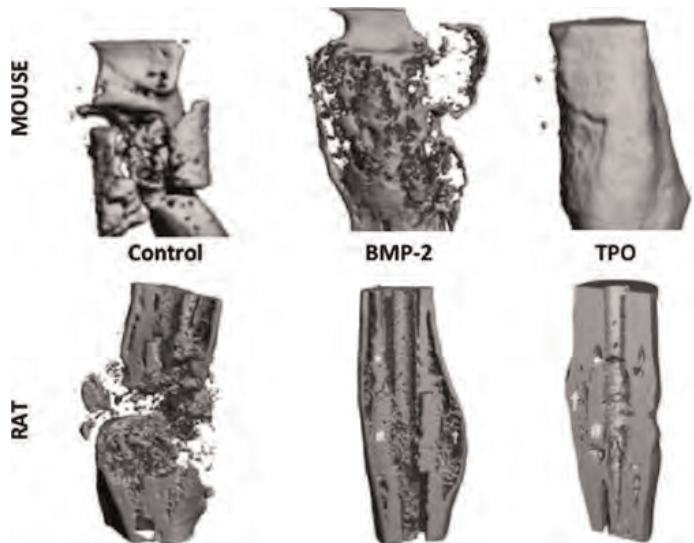
Disclosures: *Xichao Zhou, None.*

1119

Thrombopoietin: A Novel Regulator Of Bone Healing. Monique Bethel^{*1}, Patrick Millikan¹, Alexander Wessel¹, Yinghua Cheng¹, Jonathan Wilhite¹, David Burr¹, Robyn Fuchs², Tien-Min Chu³, Melissa Kacena¹. ¹Indiana University School of Medicine, USA, ²Indiana University, USA, ³Indiana University School of Dentistry, USA

Despite advances in surgical techniques and implants, orthopaedic surgeons are still challenged to obtain fracture union, spine fusion, or bridging of segmental defects. Critical-size defects in bones do not heal spontaneously and usually require the use of grafts. Unfortunately, the use of grafts poses several limitations including harvest site morbidity with autografts and concerns about disease transmission with allografts. To improve bone formation, many clinicians now use bone morphogenetic proteins (BMP), particularly in spinal fusion, fracture healing, and in critical-size defect regeneration. However, multiple side effects of BMP treatment have been uncovered including increased incidence of cancer, greater risks of radiculitis, ectopic bone formation, and osteolysis. With the high cost of BMP and concerns for side effects, there is great interest in investigating other alternatives that allow for safe and effective bone regeneration. Here we present data showing the ability of thrombopoietin (TPO), the main megakaryocyte growth factor, to heal critical-size femoral defects in both rat and mouse models. 5mm or 4mm segmental defects were created in the femur of Long Evans rats or C57BL/6 mice, respectively. The defects were filled with a novel bioabsorbable scaffold which was loaded with recombinant human TPO, BMP-2, or saline, and held stable by a retrograde 1.6mm intramedullary Kirschner wire (rats) or 23G needle (mice). Xrays were taken every 3 weeks in rats and weekly in mice. Animal were sacrificed at 15 weeks, at which time micro-computed tomography (μ CT) and histological analyses were performed. The results observed in mice and rats were similar. The saline control group did not show bridging callus at any time. Both the BMP-2 and TPO groups healed the defect, although bridging callus was evident at earlier times in the BMP-2 groups. However, the TPO groups showed a much more remodeled and physiologic contour on both Xray and μ CT. μ CT and histological analysis confirms that compared to BMP-2, TPO-treated specimens have

a thicker cortex but smaller diameter and smoother contour. TPO appears to restore the original bone contour by stimulating osteoblastogenesis, allowing for periosteal bridging and stabilization to occur, while simultaneously stimulating osteoclast formation. The therapeutic potential of TPO is high as it has already been tested in humans and could be moved into phase 2 studies quickly.



Bone healing in untreated, BMP-2-treated, and TPO-treated mice and rats 15 weeks post-surgery.

Disclosures: *Monique Bethel, None.*

1120

PTH Induce Short-Term Hemopoietic Stem Cell Expansion through T Cells. Jau-Yi Li^{*1}, Jonathan Adams¹, Laura Calvi², M. Neale Weitzmann¹, Roberto Pacifici¹. ¹Emory University School of Medicine, USA, ²University of Rochester School of Medicine, USA

Intermittent parathyroid hormone (iPTH) stimulates hemopoietic stem cells (HSCs) expansion in bone marrow (BM), but neither the involved mechanism nor the affected HSPC populations are known. Since T cells contribute the action of iPTH in bone, we investigated the role of T cells in the effects of iPTH on HSCs. iPTH (PTH 1-34, 80 μ g/kg SQ daily for 4 weeks) increased the number of HSCs (Lin-Sca-1+c-Kit+ cells) by ~2 fold and host survival after BM transplantation by ~4 fold in WT mice and T cell reconstituted-T cell deficient mice. By contrast iPTH had no effects on HSCs expansion and survival after BM transplantation in T cells deficient mice, or PPR^{T cells} mice, a strain lacking PTH receptor 1 (PPR) signaling in T cells. Thus, direct PPR signaling in T cells is required for iPTH to expand HSCs and improve post-transplantation survival. Analysis of SLAM receptor expression on HSCs and competitive repopulation assays demonstrated that iPTH specifically expands short-term HSCs (ST-HSCs) without exhausting long-term HSCs (LT-HSCs) in mice with intact PPR signaling in T cells. By contrast iPTH did not expand ST-HSCs in mice lacking T cells or PPR signaling in T cells. Since it is known that activation of Wnt and Notch signaling in HSCs is required for their expansion, we investigated the role of T cells in the iPTH-induced activation of these pathways. We found that PPR signaling in T cells increases the T cell production of Wnt ligand Wnt10b, and that Wnt10b is required for activating Wnt signaling in HSPCs and stromal cells (SCs) in response to iPTH treatment. T cell produced Wnt10b was also essential for upregulating the SC expression of Jagged1, a Notch ligand critical for HSC expansion. Accordingly, iPTH failed to expand ST-HSCs in mice with a specific deletion of T cell produced Wnt10b. Further attesting to the relevance of Wnt10b for HSCs expansion, we found that iPTH failed to promote HSCs engraftment and host survival after BM transplantation in Wnt10b null mice. In summary, these findings demonstrate that activation of PPR signaling in T cells by iPTH stimulates T cells to release Wnt10b, a factor required for activating Wnt signaling in HSCs and SCs as well as for increasing Jagged1 expression in SCs. Activation of Wnt and Notch signaling in HSCs allows iPTH to selectively expand ST-HSCs and improve host survival after BM transplantation. Thus, T cells may provide pharmacological targets for HSPC expansion.

Disclosures: *Jau-Yi Li, None.*

1121

Osterix Expressed in Chondrocytes Is Required for Skeletal Development. Shaohong Cheng^{*1}, Weirong Xing², Catrina Alarcon³, Xin Zhou⁴, Subburaman Mohan⁵. ¹VA Loma Linda Health Care Systems, USA, ²Musculoskeletal Disease Center, Jerry L. Pettis Memorial Veteran's Admin., USA, ³Jerry L Pettis VA Med Ctr, USA, ⁴MD Anderson Cancer Center, USA, ⁵Jerry L. Pettis Memorial VA Medical Center, USA

Osterix (Osx) is essential for osteoblast differentiation and bone formation as mice with targeted disruption of the *Osx* gene failed to form either intramembranous or endochondral bone. Previous studies have shown that *Osx*, a downstream target gene of Runx2, is specifically expressed in osteoblasts (Obs) and at low levels in prehypertrophic chondrocytes (CCs). Accordingly, Ob-specific ablation of *Osx* using *Col1a1-Cre* mice resulted in osteopenia, due to impaired Ob differentiation in adult mice. We found that CCs (ATDC5, RCS and primary mouse CCs) in culture expressed *Osx* at levels comparable to that of Obs, thus suggesting *Osx* expressed in CCs may also play a role in skeletal development. To evaluate the role of *Osx* expressed in CCs, we crossed floxed osterix with CC-specific *Col2a1-Cre* mice to conditionally disrupt the *Osx* gene in CCs. Surprisingly, *Cre* positive mice that are homozygous for *Osx* floxed alleles failed to survive after birth. Alcian blue and alizarin red staining of newborn *Cre* positive; *lox/lox* and corresponding wild type (WT) littermates revealed that the lengths of the total body, femur and rib were reduced by 20, 25 and 32% (all $P < 0.001$), respectively, in the knockout (KO) compared to WT mice. Besides demonstrating severely impaired mineralization of bones formed via endochondral but not intramembranous route, several bones including long bones, vertebral column and ribs were bent. In order to determine if haploid insufficiency of *Osx* in CCs influences skeletal development, we compared skeletal phenotypes of *Cre* positive; *lox* heterozygous mice with gender-matched, *Cre* negative heterozygous littermates. Body length was reduced by 6% ($P = 0.002$) in mice with conditional disruption of one allele of the *Osx* gene in CCs. PIXImus measurements revealed that BMC of total body, femur, tibia and vertebra was reduced by 17, 14, 21 and 15% (all $P < 0.01$, $n = 15-20/\text{group}$), respectively, in *Cre* positive mice compared to littermate *Cre* negative mice at 3 wks of age. BMD of total body, femur, tibia and vertebra was reduced by 4.5, 6.6, 6.0 and 9.5% (all $P < 0.05$), respectively, in the *Cre* positive; *lox* heterozygous mice. We found that expression levels of Col X, TRAP and Cathepsin K as measured by real time RT-PCR were significantly reduced (30-70%) in the femurs of *lox* heterozygous *Cre* negative mice. Conclusions: 1) *Osx* expressed in CCs is essential for survival of mice after birth. 2) Haploid insufficiency of *Osx* expressed in CCs results in reduced longitudinal growth, bone size and BMD. 3) *Osx* expressed in CCs regulates skeletal development in part by regulating CC maturation and cartilage resorption.

Disclosures: Shaohong Cheng, None.

1122

Jab1 is Required for Chondrogenesis in Embryonic Limb Development. Lindsay Bashur^{*1}, Dongxing Chen¹, Bojian Liang¹, Ruggero Pardi², Brendan Lee³, Shunichi Murakami¹, Guang Zhou¹. ¹Case Western Reserve University, USA, ²Scientific Institute San Raffaele, Italy, ³Baylor College of Medicine & Howard Hughes Medical Institute, USA

The transcriptional cofactor Jab1 controls cell proliferation, apoptosis, and differentiation in many developmental processes by regulating the activity of numerous transcription factors. However, the physiological role of Jab1 in skeletal development is still poorly understood. In this study, we utilized the *loxP/Cre* system to delineate the specific role of Jab1 in limb development. First, to determine the specific role of Jab1 in differentiating chondrocytes, we generated a chondrocyte-specific *Jab1* conditional knockout *Jab1^{fllox/lox}; Col2a1-Cre* mouse model. *Jab1^{fllox/lox}; Col2a1-Cre* mutants exhibited neonatal lethal chondrodysplasia with severe dwarfism. In E18.5 mutants, all skeletal elements developed via endochondral ossification, including the limbs, were extremely small with severely disorganized chondrocyte columns. *Jab1* mutant chondrocytes exhibited increased apoptosis and accelerated chondrocyte hypertrophy. Notably, there was a heightened expression of BMP signaling components and targets in *Jab1* mutant chondrocytes, suggesting that Jab1 is a novel inhibitor of BMP signaling in differentiating chondrocytes *in vivo*. Second, to determine the function of Jab1 in early osteochondro progenitor cells, we bred *Jab1^{fllox/lox}* mice with *Prx1-Cre* transgenes to delete *Jab1* specifically in limb buds. *Jab1^{fllox/lox}; Prx1-Cre* mutant mice displayed drastically shortened limbs starting at E14.5, mirroring the human skeletal disorder phocomelia. The E18.5 mutant limbs exhibited drastically reduced numbers of hypertrophic chondrocytes, disorganized chondrocyte columns, and increased apoptosis. To determine the underlying mechanism for the severe short-limb defect in *Jab1^{fllox/lox}; Prx1-Cre* mutants, we used a micromass culture of E11.5 *Jab1* mutant and wild-type limb mesenchyme cells to study chondrogenesis *ex vivo*. Alcian blue staining showed significantly decreased chondrogenesis in *Jab1* mutant cultures. Real time RT-PCR confirmed that the expression of chondrocyte differentiation markers, including *Sox9* and *Col2a1*, were significantly decreased in *Jab1* mutants. Furthermore, Western blot analysis revealed that the expression of BMP signaling downstream effector phospho-Smad1/5 was increased in *Jab1* mutants, suggesting that Jab1 also negatively regulates BMP signaling during early limb development. In conclusion, our study demonstrates that Jab1 is essential for successive steps of limb development *in vivo*, likely in part by inhibiting BMP signaling.

Disclosures: Lindsay Bashur, None.

1123

Inducible Conditional Inactivation of TGF-beta Type II Receptor in Prx-1 Expressing Cells in Utero and Post-natal Life Leads to Prenatal and Postnatal Growth Failure and Joint Defects. Tieshi Li^{*1}, Lara Longobardi¹, Timothy Myers², Joseph Temple³, Michael Kuijter³, Ying Li⁴, Anna Spagnoli¹. ¹University of North Carolina at Chapel Hill, USA, ²University of North Carolina, USA, ³Department of Pediatrics of UNC at Chapel Hill, USA, ⁴UNC School of Medicine, USA

The role of TGF-beta type II receptor (*Tgfr2*) signaling in skeletogenesis has been primarily studied by targeting its genetic manipulation to early embryonic mouse development. Here, to determine the need of *Tgfr2* signaling in late embryonic and postnatal skeletal growth as well as in maintaining joint integrity we have generated the *Prx1CreERT2;Tgfr2^{lox/lox}* mice to obtain temporal and limb-specific control of expression using a tamoxifen (Tam)-inducible-*Cre* system (*Prx1CreERT2*). To determine the *Prx1-Cre* inducible recombination at different prenatal and postnatal ages and to establish the optimal regimen for Tam administrations we generated the *Prx1CreERT2-LacZ-R26R* as a *LacZ-Cre* activity reporter mouse. Tam administrations ranged from E13.5 to P3, single and multiple doses were tested; mice were sacrificed 3 days after Tam. In knee and interphalangeal joints at both prenatal and postnatal stages, we found Tam-induced beta-gal activity in the perichondrium, the superficial layers of articular cartilage, tendons, ligaments and menisci. *Prx1-Cre* Tam-induced activity in these regions overlapped with but was not limited to the regions of *Tgfr2* expression that we characterized by generating *BAC-Tgfr2-LacZ* reporter mice. The lack of beta-gal activity in the *Prx1CreERT2-LacZ-R26R* not exposed to Tam confirmed the absence of *Cre*-activity leakage. We then exposed *Prx1CreERT2;Tgfr2^{fllox/lox}* mice to Tam at P3 to generate *Prx1CreERT2;Tgfr2^{lox/lox}* mice that were sacrificed at different ages. At P31, we found that compared to control (*Tgfr2^{fllox/lox}*), *Prx1CreERT2;Tgfr2^{lox/lox}* had $32.4 \pm 2.6\%$ decrease of body weight and $20.5 \pm 1.1\%$ decrease of body length. Furthermore, histological analyses of P31 *Prx1CreERT2;Tgfr2^{lox/lox}* mice showed a large number of hypertrophic chondrocytes within the knee articular cartilage as an early sign of osteoarthritis. Tam was also administered at E14.5 and *Prx1CreERT2;Tgfr2^{lox/lox}* mice analyzed at E18.5 showed growth failure ($17.1 \pm 2.2\%$ decrease) as a result of a shorter growth plate with disorganized hypertrophic chondrocytes and perichondrium. In *Prx1CreERT2;Tgfr2^{lox/lox}*, BrdU incorporation assay showed reduced proliferative activity within the superficial layer of the articular cartilage and proliferative layer of the growth plate. Our findings indicate that *Tgfr2* signaling regulates postnatal growth and is needed to maintain postnatal joint integrity by regulating chondrocyte proliferation and repressing hypertrophy.

Disclosures: Tieshi Li, None.

1124

The Skeletal Effects of Notch are Cell-Context Dependent. Stefano Zanotti^{*1}, Kristen Parker², Jian Feng³, Ernesto Canalis¹. ¹St. Francis Hospital & Medical Center, USA, ²Saint Francis Hospital & Medical Center, USA, ³Texas A&M Health Science Center, USA

Transgenic expression of Notch under the control of the *Type 1 collagen* promoter causes osteopenia, and the conditional deletion of *Notch1* and *2* in the skeleton increases bone volume and osteoblastogenesis, indicating that Notch downregulates osteoblastic differentiation/function. However, the biology of Notch is cell-context dependent. To address whether Notch has distinct effects in cells of the osteoblastic lineage at various stages of differentiation, we used the *Rosa^{Notch}* mouse model, where the Notch intracellular domain (NICD) is expressed under the control of the *Rosa* promoter following the excision of a *loxP* flanked STOP cassette between the *Rosa26* promoter and NICD. *Rosa^{Notch}* mice were crossed with transgenics expressing the *Cre* recombinase under the control of the *Osterix (Osx)*, *Osteocalcin (Oc)*, 2.3 kb fragment of *Type 1 collagen (Col2.3)* or *Dentin matrix protein 1 (Dmp1)* promoter to express Notch in osteoblast precursors, mature osteoblasts and osteocytes, respectively. Microcomputed tomography (μCT) and histomorphometry revealed that expression of Notch in undifferentiated (*Osx-Cre;Rosa^{Notch}*) or mature osteoblasts (*Oc-Cre;Rosa^{Notch}*) caused marked femoral and vertebral osteopenia due to decreased bone formation; cortical bone was porous or not present. In contrast to this osteopenic phenotype, expression of Notch in osteocytes (*Dmp1-Cre;Rosa^{Notch}*) caused a marked 3-6 fold increase in femoral and vertebral bone volume, and a pronounced increase in connectivity. The mechanism involved suppressed bone resorption due to enhanced expression of osteoprotegerin. Sclerostin mRNA was suppressed leading to enhanced Wnt signaling in osteocytes. Cortical bone thickness was increased, but the cortex was not compact and had the appearance of cancellous bone. Notch expression in osteoblasts and osteocytes (*Col2.3-Cre;Rosa^{Notch}*) caused a similar but less pronounced phenotype than that observed in *Dmp1-Cre;Rosa^{Notch}* mice. There was no sexual dimorphism in the skeletal phenotypes described. In conclusion, the skeletal effects of Notch are cell-context dependent. When expressed in osteoblasts, Notch causes osteopenia due to impaired osteoblastic differentiation/function, and when expressed in osteocytes Notch causes increased bone mass due to suppressed bone resorption. Compact cortical bone is absent in the presence of Notch suggesting that downregulation of Notch is necessary for the transition of trabecular to cortical bone.

Disclosures: Stefano Zanotti, None.

1125

Rbpj-Dependent Notch Signaling in Chondrocytes Modulates Endochondral Ossification during Osteoarthritis Development through Transcriptional Induction by Hes1. Shurei Sugita*¹, Yoko Hosaka², Taku Saito², Haruhiko Akiyama³, Ung-Il Chung⁴, Hiroshi Kawaguchi^{5, 1}, Japan, ²University of Tokyo, Graduate School of Medicine, Japan, ³Kyoto University, Japan, ⁴University of Tokyo Schools of Engineering & Medicine, Japan, ⁵University of Tokyo, Faculty of Medicine, Japan

The Notch signaling constituted of the Notch receptors, the transcriptional effector Rbpj, and the transcription target Hes/Hey family members is a potent modulator of cell differentiation in many organs. Here we examined the involvement of the Notch signaling in the endochondral ossification process which is crucial for osteoarthritis (OA) development. Intracellular domains (ICDs) of Notch1 and 2 were translocated into the nucleus of chondrocytes with their differentiation in mouse limb cartilage and in mouse and human OA articular cartilage. The tissue-specific knockout mice of Rbpj in chondroprogenitor cells (*Sox9-Cre;Rbpj^{fl/fl}*) died shortly after birth, but the embryos exhibited an impaired endochondral ossification with decreases of Mmp13 expression in the limb cartilage. We then generated the inducible conditional knockout mice (*Col2a1-Cre^{ERT};Rbpj^{fl/fl}*), inactivated Rbpj in the adult articular cartilage by tamoxifen injection to the 7-week-old mice after normal skeletal growth and joint formation, and created the surgical OA model. The *Col2a1-Cre^{ERT};Rbpj^{fl/fl}* mice showed resistance to the knee OA development as compared to the control *Rbpj^{fl/fl}* littermates. As for the underlying mechanism, Hes1 was most strongly expressed among Hes/Hey family members during differentiation of cultured mouse chondrogenic ATDC5 cells and primary chondrocytes, with Notch 1, Notch2, Rbpj, and Mmp13 expressions. Overexpression of Notch1 ICD in ATDC5 cells induced Mmp13 expression, and this induction was suppressed by the Hes1 knockdown through the siRNA transfection. Luciferase analyses revealed that the promoter activity of *MMP13* was not affected by Notch1 ICD transfection, but was enhanced by Hes1. In the *MMP13* gene between -1,000 and +1,227 bp relative to the transcriptional start site, there were six E-box motifs but no N-box motif. Deletion and mutagenesis analyses identified the core responsive region of Hes1 as an E-box at +934/+939 bp. However, the *Sox9-Cre;Hes1^{fl/fl}* mouse embryos did not show skeletal abnormality. Contrarily, the inducible conditional knockout of Hes1 (*Col2a1-Cre^{ERT};Hes1^{fl/fl}*) in adult articular cartilage by tamoxifen injection caused resistance to the knee OA development. In conclusion, Hes1, which mediates the Rbpj-dependent Notch signaling in chondrocytes, is a transcriptional inducer of endochondral ossification during OA development, representing a promising therapeutic target of OA without physiological side effects.

Disclosures: *Shurei Sugita, None.*

1126

An Appropriate Balance of Notch Signaling is Required for Articular Cartilage and Joint Maintenance. Zhaoyang Liu*¹, Anthony Mirando¹, Tyler Moore¹, Alexandra Lang¹, Anat Kohn², Alana Jesse², Regis O'Keefe², Robert Mooney¹, Michael Zuscik³, Matthew Hilton¹. ¹University of Rochester Medical Center, USA, ²UNIVERSITY OF ROCHESTER, USA, ³University of Rochester School of Medicine & Dentistry, USA

Osteoarthritis (OA) is a degenerative disease resulting in severe joint cartilage destruction and disability. While the mechanisms underlying the development and progression of OA are poorly understood, gene mutations have been identified within cartilage-related signaling molecules implicating impaired cell signaling in the pathogenesis of OA. To investigate a novel role for Notch signaling in joint cartilage development, maintenance, and the pathogenesis of OA, we first generated a *Prx1Cre;Rbpjk^{fl/fl}* (cKO RBPjk) mutant mice deleting RBPjk in mesenchymal progenitors giving rise to all synovial joint tissue. Embryonic cKO RBPjk mutants exhibit normal joint cavitation and morphogenesis, while two-week-old cKO RBPjk mutants revealed a delayed formation of the secondary ossification center. Joint integrity analysis in 2, 4, 6, and 8-month old cKO RBPjk mutants via microCT, histology, IHC, ISH, and histomorphometry showed an early onset and progressive postnatal OA-like pathology characterized by fibrosis and degeneration of the articular cartilage and meniscus, subchondral bone sclerosis, osteophyte formation, and progressive loss of extracellular matrix components. Additionally, we generated a cartilage-specific Notch gain-of-function model, *Col2Cre^{ERT2};Rosa-NICD1^{fl/+}* (cGOF NICD1), to determine whether sustained NOTCH1 signaling in postnatal chondrocytes following tamoxifen induction could promote articular cartilage maintenance. Histology, histomorphometry, IHC, and real-time RT-PCR analyses were performed on the knee joints or articular cartilage isolated from several types of cGOF NICD1 mice including mice with 3-months, 4-weeks, and 5-days of sustained NOTCH1 signaling. Interestingly, "long-term" (3-months) induction resulted in severe joint cartilage fibrosis and its own OA-like pathology, while "shorter-term" (4-weeks) induction simultaneously promoted both cartilage anabolism and catabolism, although early signs of fibrosis were also evident in this model. Finally, a brief exposure of articular chondrocytes to sustained NOTCH1 signaling (5-day induction) *in vivo* also demonstrated enhancement in both cartilage anabolic and catabolic factors without the induction of early fibrosis. Therefore, a delicate balance of Notch signaling is required for appropriate cartilage anabolism and catabolism during

postnatal joint homeostasis. Collectively, these data have implicated the Notch pathway as a novel and important therapeutic target for OA.

Disclosures: *Zhaoyang Liu, None.*

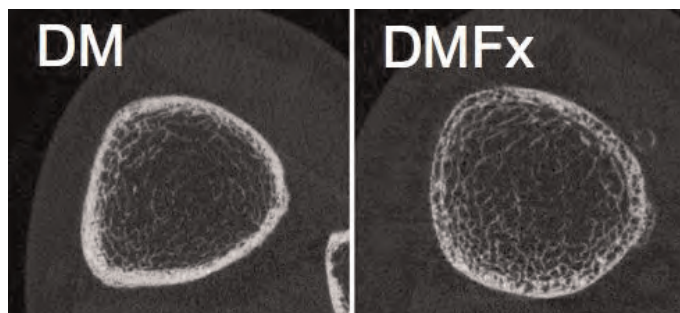
1127

Cortical Porosity as a Distinct Pathomorphology in Postmenopausal, Diabetic Women with Fragility Fractures. Janina Patsch*¹, Andrew Burghardt¹, Paran Yap¹, Thomas Baum², Ann Schwartz¹, Thomas Link¹. ¹University of California, San Francisco, USA, ²Klinikum rechts der Isar, Technische Universitaet Muenchen, Deu

Cortical porosity (Ct.Po) is increasingly recognized as a skeletal pathomorphology of potential clinical relevance. Type 2 diabetic bone disease is a metabolic bone disease with paradoxically increased fracture rates in spite of relatively high bone mineral density (BMD). The purpose of this study was to assess if Ct.Po was increased in postmenopausal diabetics with fractures when compared with non-fractured diabetics, non-diabetic controls with prevalent fragility fractures, and non-diabetic controls without fractures. All subjects (controls [Co] n=20; controls with fractures [Fx] n=20; diabetics without fracture [DM] n=20; diabetics with fracture [DMFx] n=15) underwent high resolution peripheral quantitative computed tomography (HR-pQCT; distal radius and tibia), DXA (spine, hip, radius), and a blood draw for fasting glucose, HbA1c, and c-peptide. From HR-pQCT scans, volumetric BMD, morphometric standard parameters, and extended measures of cortical bone (including Ct.Po and endocortical bone surface En.BS) [1,2] were obtained. In a 2-way ANCOVA adjusted for age, BMI, and race/ethnicity, Ct.Po was associated with fracture in DM but not controls at the ultradistal tibia (p for interaction=0.038) but not the radius. DmFx displayed the highest cortical porosity of all groups (age-, race & BMI-adjusted means +52.2% vs DM; +36.0% vs Fx; +34.2% vs Co). Coherently, DmFx also had a greater En.BS than DM (+11.12%; p=0.035). However, there were no correlations between En.BS or Ct.Po with fasting glucose, HbA1c or c-peptide. In diabetics, En.BS was significantly correlated with tibial Ct.Po (r=0.533). Compartment-specific volumetric BMD and morphometric indices by HR-pQCT (both sites) remained non-significant among the 4 groups. Patients with prevalent fractures had significantly reduced aBMD measured with DXA, but mean aBMD values remained normal to osteopenic in all patients and were particularly high in diabetics stressing the limitations of DXA. In conclusion, we found tibial Ct.Po and En.BS measured by HR-pQCT to be non-invasive surrogate biomarkers to identify type 2 diabetes mellitus postmenopausal women with prevalent fragility fractures.

References:

[1] Burghardt AJ et al. 2010; Bone 47(3):519-528. [2] Burghardt AJ et al. 2010; J Bone Miner Res 25(5):983-993.



Representative HR-pQCT scans of diabetic women with and without fragility fractures (DMFx vs. DM)

Disclosures: *Janina Patsch, None.*

1128

TBS (Trabecular Bone Score) is More Sensitive Than BMD to Diabetes-Related Fracture Risk. William Leslie*¹, Berengère Aubry-Rozier², Olivier Lamy², Didier Hans². ¹University of Manitoba, Canada, ²Lausanne University Hospital, Switzerland

Background: Type 2 diabetes (T2D) is associated with increased fracture risk but paradoxically greater BMD. TBS (trabecular bone score), a novel grey-level texture measurement extracted from DXA images, correlates with 3D parameters of bone micro-architecture. We evaluated the ability of lumbar spine (LS) TBS to account for the increased fracture risk in diabetes.

Methods: 29,407 women ≥ 50 years at the time of baseline hip and spine DXA were identified from a database containing all clinical BMD results for the Province of Manitoba, Canada. 2,356 of the women satisfied a well-validated definition for diabetes, the vast majority of whom (>90%) would have T2D. LS L14 TBS was derived for each spine DXA examination blinded to clinical parameters and outcomes. Health service records were assessed for incident non-traumatic major osteoporotic fracture codes (mean follow-up 4.7 years).

Results: In linear regression adjusted for FRAX risk factors (age, BMI, glucocorticoids, prior major fracture, rheumatoid arthritis, COPD as a smoking proxy, alcohol

abuse) and osteoporosis therapy, diabetes was associated with higher BMD for LS, femoral neck and total hip but lower LS TBS (all $p < 0.001$). Similar results were seen after excluding obese subjects with BMI > 30. In logistic regression (Figure), the adjusted odds ratio (OR) for a skeletal measurement in the lowest vs highest tertile was less than 1 for all BMD measurements but increased for LS TBS (adjusted OR 2.61, 95%CI 1.10-5.74). Major osteoporotic fractures were identified in 175 (7.4%) with and 1,493 (5.5%) without diabetes ($p < 0.001$). LS TBS predicted fractures in those with diabetes (adjusted HR 1.27, 95%CI 1.10-1.46) and without diabetes (HR 1.31, 95%CI 1.24-1.38). LS TBS was an independent predictor of fracture ($p < 0.05$) when further adjusted for BMD (LS, femoral neck or total hip). The explanatory effect of diabetes in the fracture prediction model was greatly reduced when LS TBS was added to the model (indicating that TBS captured a large portion of the diabetes-associated risk), but was paradoxically increased from adding any of the BMD measurements.

Conclusions: Lumbar spine TBS is sensitive to skeletal deterioration in postmenopausal women with diabetes, whereas BMD is paradoxically greater. LS TBS predicts osteoporotic fractures in those with diabetes, and captures a large portion of the diabetes-associated fracture risk. Combining LS TBS with BMD incrementally improves fracture prediction.

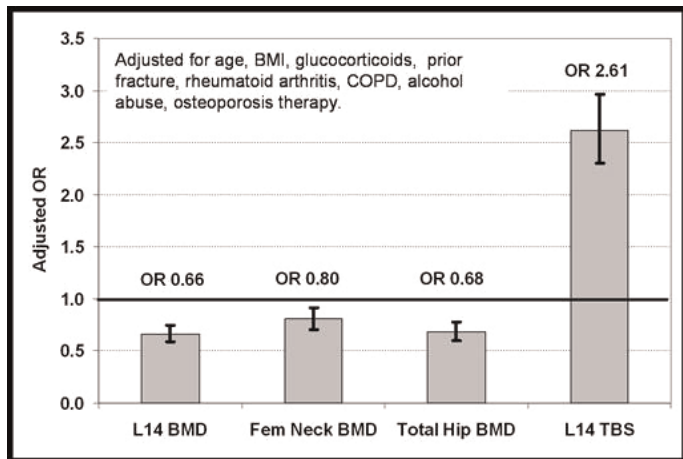


Figure: OR (95%CI) for BMD or TBS in the lowest vs highest tertile according to diabetes status.

Disclosures: William Leslie, None.

1129

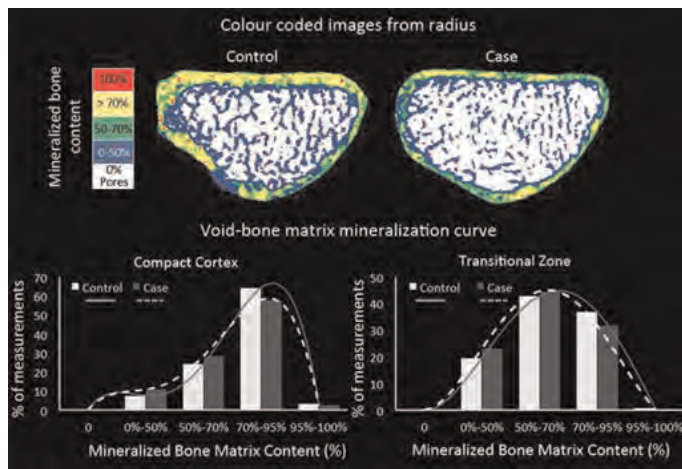
Osteoporosis is Not Enough: Cortical Porosity Identifies Women with Distal Forearm Fractures. Yohann Bala¹, Roger Zebaze², Ali Ghasem-Zadeh², James Peterson³, Shreyasee Amin³, L. Joseph Melton³, Sundeep Khosla⁴, Ego Seeman². ¹University of Melbourne, Dept. of Medicine, Australia, ²Austin Health, University of Melbourne, Australia, ³Mayo Clinic, USA, ⁴College of Medicine, Mayo Clinic, USA

Introduction: Trabecular bone loss and vertebral fractures are held to be flagships of 'osteoporosis'. However, 80% of bone is cortical, 80% of fractures are non-vertebral, 70% of all bone loss is cortical and due to intracortical resorption.¹ The resulting porosity is a quantifiable footprint of structural decay and so may predict fracture risk as resistance to bending is proportion to the 7th power cortical apparent density. We hypothesized that porosity discriminates women with distal forearm fractures better than areal BMD.

Methods: One hundred postmenopausal women with a distal forearm fracture and 105 age matched community controls from Olmsted County, Minnesota had 3D cortical imaging and aBMD (g/cm^2) assessed at the ultradistal radius by HR-pQCT and DXA.² Cross-sectional area (CSA), cortical porosity, trabecular and cortical vBMD (Ct. & Tb.vBMD, g/cm^3) were processed from HR-pQCT images using a non-threshold based image analysis, StrAx1.0, which automatically segments cortical bone into compact cortex (CC) and transitional zone (TZ). The proportion of void (porosity) was quantified as the average of void spaces in each voxel. Images were colour coded according to their mineralized matrix content. Results were expressed as a frequency or a void-bone matrix distribution curve. Due to motion artefacts, only 68 cases (63 ± 9 year-old) and 70 controls (66 ± 9 year-old, N.S.) were analysed.

Results: Among cases, 4/5 did not have osteoporosis (t-score ≤ -2.5 SD). aBMD was significantly lower in cases than in controls (0.42 ± 0.07 vs. 0.37 ± 0.08 g/cm^2 , $p < 0.001$). Ct. & Tb. vBMD were -4% and -24% lower in cases ($p < 0.018$). Porosity was higher in cases than controls (CC +11%, $p = 0.03$, TZ +3%, $p = 0.0001$). TZ porosity predicted fracture risk; each SD increase was associated with an odds ratio of 2.09 (95% CI, 1.40-3.11; $p = 0.0001$). The void-bone matrix curve in cases was shifted left in CC and TZ indicative of higher porosity.

Inference: Intracortical remodeling fragments the cortex producing porosity which allow better discriminates and so targets women with distal forearm fractures than aBMD and vBMD alone. 1) Zebaze *et al.* Lancet 2010 2) Melton III *et al.* Osteoporos Int 2010.



Figure

Disclosures: Yohann Bala, None.

1130

Postmenopausal Women with Osteopenia and Fractures Have Thin Cortices and Trabecular Plate Loss. Emily Stein¹, Xiaowei Liu², Thomas Nickolas³, Adi Cohen³, Anna Kepley⁴, X Guo⁴, Elizabeth Shane^{*1}. ¹Columbia University College of Physicians & Surgeons, USA, ²University of Pennsylvania, USA, ³Columbia University Medical Center, USA, ⁴Columbia University, USA

The majority of fragility fractures occur in women with osteopenia rather than osteoporosis by DXA. However, it is difficult to identify which women with osteopenia are at greatest risk. Abnormal microarchitecture is an important determinant of bone strength and fracture susceptibility, independent of areal BMD (aBMD) by DXA. We hypothesized that osteopenic women with fragility fractures would have abnormal microarchitecture compared to controls. We enrolled 117 women with osteopenia by DXA (age 66 ± 6 yrs, 76% Caucasian), 58 with a history of low trauma fracture after menopause (FX) and 59 non-fractured postmenopausal controls (C). All had aBMD of lumbar spine (LS), total hip (TH), femoral neck (FN), 1/3 (1/3R) and ultradistal radius (UDR) by DXA. Trabecular (Tb) and cortical (Ct) volumetric BMD (vBMD) and Tb microarchitecture were measured by high resolution peripheral computed tomography (HRpQCT, voxel size $\sim 82 \mu m$) of the distal radius and tibia. HRpQCT scans were subjected to finite element analysis (FEA) to estimate whole bone stiffness and individual trabecula segmentation (ITS) to assess plate and rod structure of Tb bone. Groups were similar with respect to age, race, BMI and years since menopause. Fracture of the forearm, spine and ankle were most common. Mean T-scores in FX (LS -1.2, TH -1.0, FN -1.6, 1/3R -0.7, UDR -1.1) did not significantly differ from those in C at any site, though they tended to be lower at the LS (0.09) and higher at the 1/3R (0.07). In contrast, there were substantial microarchitectural differences between FX and C (Table). At the radius, FX had lower Ct and Tb vBMD, thinner cortices, thinner more widely separated trabeculae and lower stiffness. By ITS, FX had fewer Tb plates, less axially aligned trabeculae and less Tb connectivity. At the tibia, differences between FX and C were limited to Ct bone. Whole bone stiffness and ITS tended to be lower. In summary, postmenopausal women with osteopenia and fractures had lower Ct and Tb vBMD, thinner, more widely separated and rod-like Tb structure, and less Tb connectivity by HRpQCT compared to controls, despite similar aBMD by DXA. At the radius, both cortical and trabecular abnormalities were associated with fractures and lower stiffness, while at the tibia, cortical abnormalities predominated. Our results suggest that trabecular and cortical bone loss as well as changes in plate and rod structure may be important mechanisms of fracture in postmenopausal women with osteopenia.

Microarchitecture in FX compared to C (% difference)

| | RADIUS | p-value | TIBIA | p-value |
|---------------------------------------|--------|---------|-------|---------|
| Ct Area (mm ²) | -8 | <0.03 | -10 | <0.03 |
| Tb Area (mm ²) | +9 | <0.02 | +8 | 0.06 |
| Total Density (mgHA/cm ³) | -12 | <0.003 | -9 | <0.01 |
| Ct Density (mgHA/cm ³) | -3 | <0.03 | -3 | 0.09 |
| Ct Thickness (mm) | -11 | <0.007 | -13 | <0.02 |
| Tb Density (mgHA/cm ³) | -12 | <0.02 | -6 | 0.14 |
| Tb Number (1/mm) | -5 | 0.10 | -1 | 0.76 |
| Tb Thickness (mm) | -6 | <0.05 | -5 | 0.16 |
| Tb Separation (mm) | +6 | 0.07 | +2 | 0.74 |
| Plate Tb Number | -8 | <0.03 | -3 | 0.08 |
| Axially aligned Tb | -14 | <0.03 | -10 | 0.06 |
| Tb Plate connectivity | -22 | <0.02 | -8 | 0.07 |
| Whole bone stiffness (kN/mm) | -10 | <0.008 | -6 | 0.07 |

Disclosures: Elizabeth Shane, None.

1131

Geometry, Density Distribution and Internal Structure of the Proximal Femur in Relation to Age and Hip Fracture Risk in Women. Julio Carballido-Gamio¹, Roy Harnish¹, Isra Saeed¹, Timothy Streeper¹, Sigurdur Sigurdsson², Shreyasee Amin³, Elizabeth Atkinson³, Terry Therneau³, Kristin Siggeirsdottir², Xiaoguang Cheng⁴, L. Joseph Melton³, Joyce Kevak⁵, Vilundur Gudnason², Sundeep Khosla⁶, Tamara Harris⁷, Thomas Lang¹. ¹University of California, San Francisco, USA, ²Icelandic Heart Association Research Institute, Iceland, ³Mayo Clinic, USA, ⁴Beijing Ji Shui Tan Hospital, China, ⁵University of California, USA, ⁶College of Medicine, Mayo Clinic, USA, ⁷Intramural Research Program, National Institute on Aging, USA

Age-related changes in hip structure are non-homogeneous. The least mechanically-stimulated regions are thought to experience the greatest bone loss, and are implicated in hip fracture because they are thought to bear the bulk of impact from lateral falls. Here we examine how the geometry, distribution of BMD, and internal structure of the hip vary with age and fracture status using inter-subject image registration, voxel-based morphometry (VBM; Ashburner 2000), and tensor-based morphometry (TBM; Ashburner 1998). A subset of 349 women representing an age-stratified, random community sample (Riggs 2004) was subdivided into young (<45 yrs; n=94), middle-age (45-59 yrs; n=98), and older (≥60 yrs; n=157) groups. A second subset of 222 age-matched (mean=79.3 yrs) women of the Age, Gene/Environment Susceptibility Reykjavik cohort (Sigurdsson 2006) was subdivided into control (no hip fracture; n=148) and fracture (incident hip fracture; n=74) groups. Using QCT scans and spatial normalization to minimum deformation templates (MDTs), global differences in bone size, and local differences in BMD (VBM) and volume (TBM) between middle-age and young, older and young, and control and fracture women were identified. Local differences were computed with voxel-wise general linear models yielding Student's t-test statistical maps (T-maps; Figure 1). Bones of older and fracture women were significantly larger than those of young and control women, respectively. In middle-age and older women, BMD was preserved in the load-bearing inferomedial and inferolateral cortices, but there were BMD deficits superiorly in the femoral neck. Fracture women had lower BMD in expected areas such as the superior cortex and trochanteric region, but differences were also seen in the inferomedial and inferolateral cortices. TBM showed volume loss in the principal compressive bands and cortices, and enlargement of the trabecular neck area in middle-age and older women compared to young women, and in fracture women compared to age-matched controls. A focal region of cortical volume loss in the superior neck of fracture women was in agreement with a study indicating cortical thinning in this area (Johannesdottir 2011). This study shows that women who sustain incident hip fracture have structural differences from age-matched controls, and a structural phenotype that is fundamentally distinct from that of normal aging, with BMD deficits in hip regions that are usually preserved with age.

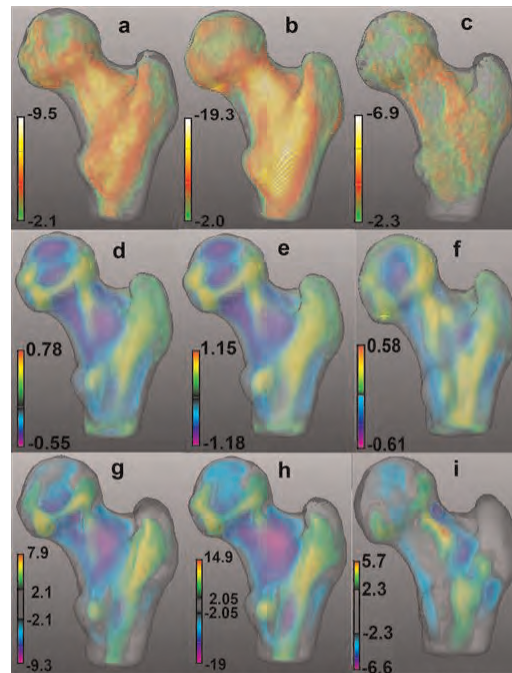


Figure 1. VBM T-maps: a) Middle-age vs Young; b) Older vs Young; c) Fracture vs Controls. Log-determinant of Jacobians showing regions of smaller (negative) and bigger (positive) volumes in the d) Middle-age; e) Older ; and f) Fracture groups than in the MDTs. TBM T-Maps: g) Middle-age vs Young; h) Older vs Young; i) Fracture vs Controls. Nonsignificant voxels after false discovery correction have been rendered semitransparent in the T-maps.

Figure-1

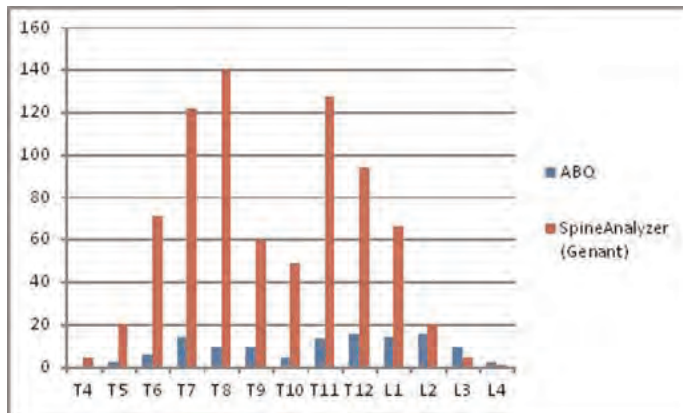
Disclosures: Julio Carballido-Gamio, None.

1132

Osteoporotic Vertebral Fracture Prevalences Vary Widely Between Radiological Scoring Methods: The Rotterdam Study. Ling Oei¹, Edwin Oei², Stephan J Breda³, Felisia Ly², Evelien van Meel³, Emma J Dogterom³, Laura GC de Kok³, Joyce BJ van Meurs³, Albert Hofman³, Huibert Pols¹, Andre Uitterlinden⁴, Maria Zillikens², Gabriel P Krestin³, Fernando Rivadeneira¹. ¹Erasmus University Medical Center, The Netherlands, ²Erasmus MC, The Netherlands, ³Erasmus MC, Netherlands, ⁴Rm Ee 575, Genetic Laboratory, The Netherlands

Global trends in ageing of populations implicate increasing numbers of osteoporotic fractures. VFX are associated with considerable morbidity and mortality. VFX are the most common fractures. Several methods for radiological assessment of VFX exist, but a gold standard is lacking. The aim of our study is to analyze differences in prevalences between methods. We applied two methods for scoring osteoporotic VFX in the population-based Rotterdam Study, an ongoing prospective cohort study (age ≥45 years). The algorithm based qualitative (ABQ) method mainly assesses endplate integrity, while quantitative morphometry (QM) based methods evaluate vertebral height loss. Trained research assistants scored lateral spine radiographs (T4-L4), using either ABQ or software-assisted QM (SpineAnalyzer, which applies Genant's classification). With ABQ, radiographs were triaged as normal, uncertain or definite fracture. Definite and uncertain VFX were re-assessed by a musculoskeletal radiologist. We compared fracture prevalences between QM and ABQ methods. Radiographs were scored for 2,475 participants (43% men) aged 46-89 years (mean 57). With QM, a prevalence of 20.8% (95% CI: 19.2%-22.4%) was found, compared to 3.2% (95% CI: 2.6%-4.1%) with ABQ. Of all individuals, 77.9% were identified as having no fractures, while 1.9% were scored fractured according to both methods. 18.9% were scored as having fractures according to QM but not ABQ; 1.3% were judged fractured according to ABQ but not QM. With ABQ, most fractures were found at the thoraco-lumbar junction, lumbar (T11-L3) and mid-thoracic (T7-T9) regions. With QM, most fractures were at the middle (T7,T8) and lower thoracic regions (T11,T12). The distribution of fracture severity was 70.8% mild, 27.1% moderate, 2.1% severe. Shape of deformity was 95.6% wedge, 2.6% biconcave and 1.8% crush. Most ABQ fractures concerned the superior endplate. The superior endplate was more frequently affected at the thoraco-lumbar junction and lumbar regions (T11-L3), while more inferior endplate fractures were seen at the mid-thoracic spine (T7-T8). In conclusion, osteoporotic VFX prevalence rates are significantly different when applying either QM or ABQ. Both QM and ABQ identify a

considerable number of deformities that were scored as normal by the other. VFX are often a first presentation of osteoporosis. Accurate VFX diagnosis is needed to identify patients with high risk for future fractures to optimize patient management.



Genent QM and ABQ fracture prevalences per vertebral level

Disclosures: Ling Oei, None.

1133

Denosumab Treatment Is Associated With Progressive Improvements in Cortical Mass and Thickness Throughout the Hip. Ken Poole¹, Graham M. Treece^{*1}, Andrew Gee¹, Jacques P. Brown², Michael R. McClung³, Andrea Wang⁴, Cesar Libanati⁴. ¹University of Cambridge, United Kingdom, ²CHUQ-CHUL Research Centre, Canada, ³Oregon Osteoporosis Center, USA, ⁴Amgen Inc., USA

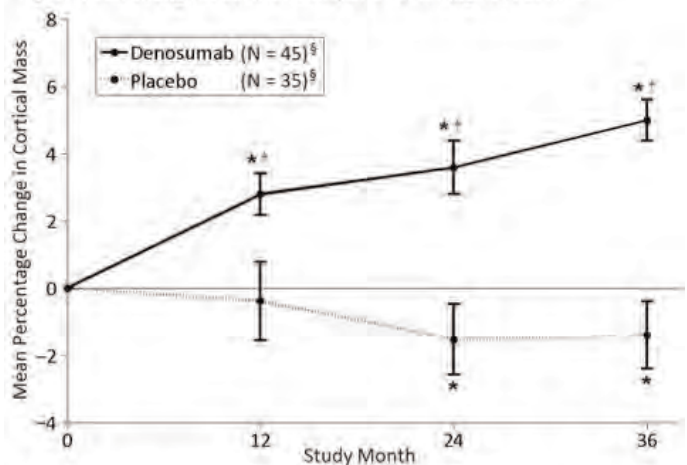
Purpose: Denosumab (a RANK ligand antibody) reduces remodeling, increases bone mineral density, and reduces cortical porosity in postmenopausal women with osteoporosis. In FREEDOM, denosumab treatment reduced the relative risk of hip fracture by 62% in those ≥ 75 years (Boonen JCEM 2011). Bone strength at the hip, estimated by FEA from QCT scans, was significantly improved from baseline and compared with placebo (Keaveny ASBMR 2010). To better characterize the changes, we used a novel cortical bone mapping technique on those same serial QCT scans, to determine the extent and distribution of mass and thickness changes at the proximal femur, a key skeletal site for fracture risk.

Methods: Eighty women age 74 ± 5 years who participated in a FREEDOM substudy underwent hip QCT scanning at baseline, and months 12, 24, and 36 during denosumab (60 mg SC Q6M) or placebo treatment; all subjects received calcium and vitamin D supplementation. For each femur, in addition to overall cortical density, the distributions of cortical mass (in mg per unit cm^2 of periosteal surface) and thickness were measured in a blinded-to-treatment manner. Distributed measures were transferred to an average femur by first registering each individual femur to this surface. Statistical parametric mapping was used to calculate significance of denosumab or placebo effects at each time point in relation to baseline, and between treatments. Distributed results were visualised as a color map over the average femur.

Results: In denosumab-treated women, there was a progressive increase in cortical mass over time, reaching a difference vs placebo of $\sim 6\%$ at 3 years ($p < 0.0001$) (Fig. 1). Approximately one-third of this increase was attributed to an increase in cortical density of $7.6 \pm 1.8 \text{ mg/cm}^3/\text{year}$ ($p < 0.0001$), which in turn remained unchanged in placebo-treated subjects ($p = 0.62$). With denosumab, cortical thickness was also significantly increased, which may represent in-filling of the cortical compartment. In contrast, average cortical mass and thickness decreased in subjects who received calcium and vitamin D alone. Mass color maps (Fig. 2) reveal the distribution of increases in cortical mass with denosumab, which were significant over an increasingly large area of the proximal femur.

Conclusion: In postmenopausal women with osteoporosis, administration of denosumab significantly and progressively increased cortical mass and thickness in regions of the proximal femur associated with hip fracture.

Fig. 1. Mean Change in Cortical Mass, as a Percentage of Baseline



Error bars show 95% confidence intervals. * $p < 0.05$ compared with baseline, † $p < 0.05$ for denosumab compared with placebo. §Not all subjects had scans at each study time point.

Fig. 1

Fig. 2. Additional Cortical Mass Increase From Baseline in Denosumab Group Compared With Placebo Group, as a Percentage of Baseline Cortical Mass

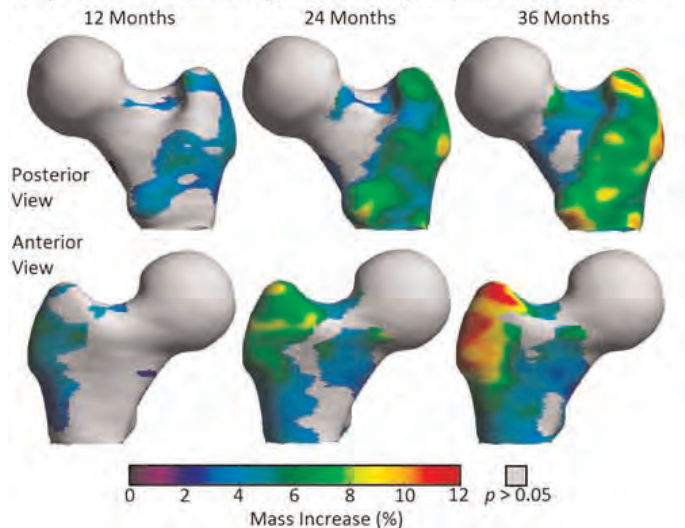


Fig. 2

Disclosures: Graham M. Treece, Amgen Inc., 6; Amgen Inc., Servier, 2; Amgen Inc., Lilly, 1
This study received funding from: Amgen Inc.

1134

Effects of 5 Years of Denosumab on Bone Histology and Histomorphometry: the FREEDOM Study Extension. Jacques Brown^{*1}, Rachel Wagman², David Dempster³, David Kendler⁴, Paul Miller⁵, Michael Bolognese⁶, Ivo Valter⁷, Jens-erik Beck Jensen⁸, Cristiano Zerbini⁹, Jose Ruben Zanchetta¹⁰, Nadia Daizadeh¹¹, Ian Reid¹². ¹CHUQ Research Centre/Laval University, Canada, ²Amgen, Incorporated, USA, ³Columbia University, USA, ⁴Associate Professor University of British Columbia, Canada, ⁵Colorado Center for Bone Research, USA, ⁶Bethesda Health Research, USA, ⁷Center for Clinical Research, Estonia, ⁸Hvidovre Hospital, Denmark, ⁹Hospital Heliopolis, Brazil, ¹⁰Instituto de Investigaciones Metabolicas (IDIM), Argentina, ¹¹Amgen Inc, USA, ¹²University of Auckland, New Zealand

Purpose: Denosumab (DMAb), a fully human monoclonal antibody to RANKL, reduces bone resorption, increases bone mineral density, and decreases risk for vertebral, nonvertebral, and hip fractures in postmenopausal women with osteoporosis.¹ Consistent with DMAB's mechanism of action, transiliac crest bone biopsies from subjects treated with DMAB for 1 to 3 years demonstrated reduced bone turnover, which was reversible with treatment cessation.^{2,3} Since long-term treatment

with DMAB has shown sustained reduction in bone turnover and low incidence of vertebral and non-vertebral fractures through 6 years,⁴ we evaluated the effects of DMAB on remodeling at the tissue level.

Methods: Transiliac crest bone biopsy assessment was conducted as a substudy of the phase 3 pivotal fracture trial (FREEDOM¹) extension

Results: A total of 41 subjects participated in the bone biopsy substudy at month 24, which corresponded to year 5 of study participation (13 cross-over and 28 long-term subjects). Demographics for this subset were comparable with that of the overall FREEDOM study extension population. Mean (SD) number of months from the last dose of DMAB to the first dose of tetracycline was 5.7 (0.5) months. Qualitative bone histology, assessed in all samples was unremarkable, showing normally mineralized lamellar bone. Five subjects in the long-term group did not have osteoid that could be visualized; samples in 4 of 5 were intact and were reported to show normal mineralization. Structural indices, including cancellous bone volume, trabecular number and surface were similar between the cross-over and long-term groups. Consistent with DMAB's mechanism of action, resorption was decreased as reflected by eroded surface in both cross-over and long-term subjects compared with placebo-treated subjects in FREEDOM (Table). A total of 10/13 (77%) cross-over subjects and 14/28 (50%) long-term subjects had specimens with double-tetracycline label in trabecular and/or cortical compartments; 5 cross-over subjects and 10 long-term subjects were evaluable for dynamic trabecular bone parameters at month 24. Dynamic remodeling indices were low for the cross-over and long-term groups, and consistent with reduced bone turnover with DMAB therapy (Table).

Conclusions: DMAB treatment through 5 years results in normal bone quality with reduced bone turnover, consistent with its mechanism of action.

1. Cummings, *NEJM* 2009
2. Reid, *JBM* 2010
3. Brown, *JBM* 2011
4. Papapoulos, *JBM* 2012

| | Pivotal phase 3 fracture trial (FREEDOM ²) | | Pivotal phase 3 fracture trial (FREEDOM ¹) study extension (at 24 months) | |
|---|--|---|---|---|
| | Placebo N=45 | DMAB N=47 | Cross-over (Placebo/DMAB) N=13 | Long-term (DMAB/DMAB) N=28 |
| Bone volume/tissue volume (BV/TV), % | Median (Q1, Q3) 12.50 (8.41, 17.41) | Median (Q1, Q3) 13.52 (10.27, 15.87) | Median (Q1, Q3) 13.94 (10.58, 18.17)* | Median (Q1, Q3) 14.24 (8.35, 20.15)* |
| Eroded surface/Bone surface, % | 1.04 (0.55, 1.88) | 0.14 (0, 0.68) | 0.15 (0, 0.44)* | 0.1 (0, 0.25)* |
| Mineral apposition rate, $\mu\text{m}/\text{day}$ | 0.75 (0.68, 0.83) | 0.30 (0.30, 0.50) | 0.59 (0.51, 0.85)* | 0.40 (0.30, 1.05)* |
| Bone formation rate, %/yr | 14.64 (8.64, 21.78) | 0.38 (0.16, 0.84) | 1.20 (0.86, 1.26)* | 2.18 (0.30, 4.87)* |
| Activation frequency, per year | 0.20 (0.12, 0.33) | 0.002 (0.001, 0.004) | 0.02 (0.01, 0.02)* | 0.03 (0, 0.07)* |
| Mineralizing surface, % | 3.08 (1.73, 6.29) | 0.12 (0.12, 0.32) | 0.28 (0.22, 0.37)* | 0.66 (0.28, 1.07)* |
| Osteoid surface, % | 6.81 (3.61, 10.10) | 0.38 (0.16, 1.22) | 0.45 (0.20, 0.72)* | 0.14 (0, 0.82)* |
| Osteoid width, μm | 8.70 (6.36, 11.00) | 5.44 (4.36, 7.43) | 5.6 (3.34, 6.57)* | 3.29 (0, 7.43)* |
| Osteoid volume, % | 0.83 (0.46, 1.33) | 0.05 (0.01, 0.11) | 0.03 (0.01, 0.06)* | 0.01 (0, 0.06)* |

Bone Histomorphometry Analysis for Subjects in FREEDOM and FREEDOM extension study

Disclosures: Jacques Brown, Amgen, Eli Lilly, Novartis, Abbott, Amgen, Bristol-Myers Squibb, Eli Lilly, Merck, Novartis, Pfizer, Roche, sanofi-aventis, Servier, Warner Chilcott, 6; Amgen, Eli Lilly, Merck, Novartis, sanofi-aventis, Warner Chilcott, 2
This study received funding from: Amgen Inc

1135

A Prospective Study of Calcium Supplement Intake and Risk of Cardiovascular Disease in Women. Julie Paik^{*1}, Gary Curhan¹, Kathryn Rexrode¹, JoAnn Manson¹, Rimm Eric¹, Eric Taylor². ¹Brigham & Women's Hospital, Harvard Medical School, USA, ²Brigham & Women's Hospital, Maine Medical Center, USA

Purpose: Previous studies on the association between calcium supplements and cardiovascular disease (CVD) in women have reported conflicting results and the relation remains unclear. A recent post-hoc meta-analysis of secondary CVD endpoints in randomized controlled trials suggested that calcium supplements increase risk of CVD, especially myocardial infarction (MI). The two observational prospective studies to date of calcium supplements and coronary heart disease (CHD) risk in women had limited follow-up (7 and 8 years, respectively); one of the two studies suggested that calcium supplements increase MI risk. No study to date has had long-term follow-up or prospectively studied cumulative average calcium supplement intake and CVD risk in women.

Methods: We conducted a prospective analysis of the relation between calcium supplement intake and the risk of CVD in a cohort of 74,272 women participating in the Nurses' Health Study (1984-2006) who were free of CVD and cancer at baseline. Calcium supplement intake was assessed every four years by semiquantitative food-frequency questionnaires. CVD outcomes were defined as CHD (nonfatal MI or fatal CHD) and stroke (nonfatal or fatal).

Results: During 22 years of follow-up, 4,857 cardiovascular events occurred (2,634 CHD and 2,223 stroke events). The age-adjusted relative risk of CVD was 0.67 (95% CI 0.62, 0.72) for women taking >500mg/day of calcium supplements (8.5% at baseline) compared to no calcium supplements. After multivariable adjustment for age, vitamin D intake, and other CVD risk factors, the relative risk of CVD for women taking >500mg/day of calcium supplements compared to no calcium supplements was 0.88 (95% CI 0.81, 0.95; p for trend <0.001). For cumulative average calcium supplement intake and CVD risk, the relative risk of CVD was 0.92 (95% CI 0.84, 1.02) for women taking >500mg/day compared to no calcium supplements. For calcium supplement use and CHD risk, the multivariable-adjusted relative risk of CHD in women taking >500mg/day compared to no calcium

supplements was 0.83 (95% CI 0.74, 0.93; p for trend <0.001). For cumulative average calcium supplement intake and CHD risk, the relative risk of CHD was 0.88 (95% CI 0.76, 1.01) for women taking >500mg/day compared to no calcium supplements.

Conclusions: In our study, calcium supplements were not associated with increased cardiovascular risk, including MI, in women.

Disclosures: Julie Paik, None.

1136

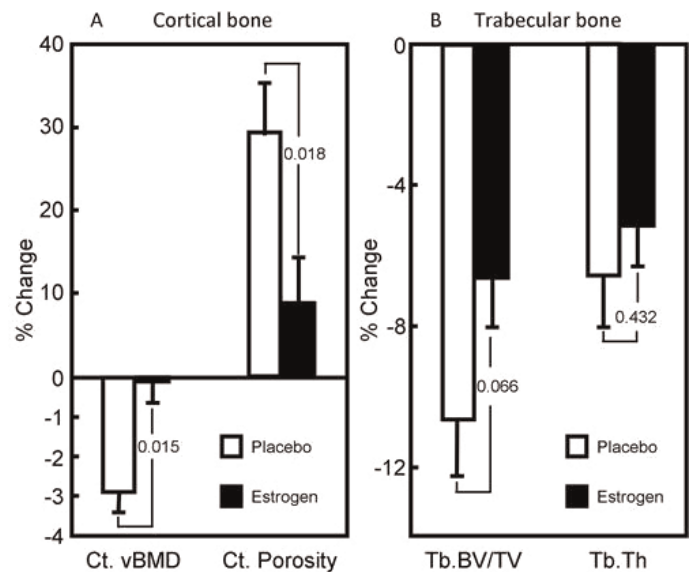
The Women's Health Initiative (WHI) Calcium plus Vitamin D Supplementation Trial: Health Outcomes 5 years after Trial Completion. Jane Cauley^{*1}, Jean Wactawski-Wende², John Robbins³, Rebecca Rodabough⁴, Zhao Chen⁵, Karen Johnson⁶, Mary Jo O'Sullivan⁷, JoAnn Manson⁸. ¹University of Pittsburgh Graduate School of Public Health, USA, ²University at Buffalo, USA, ³University of California, Davis Medical Center, USA, ⁴Fred Hutchinson Cancer Research Center, USA, ⁵University of Arizona, USA, ⁶University of Tennessee Health Science Center, USA, ⁷University of Miami, USA, ⁸Harvard Medical School, USA

The WHI Calcium plus Vitamin D supplementation trial assessed whether 1000 mg of elemental calcium with 400 IU of vitamin D₃ (CaD) versus placebo reduced the risk of hip fracture and colon cancer in 36,282 women who were age 50 to 79 yrs at study entry. After an average of 7 yrs of follow-up, modest, albeit non-significant, reductions were observed for hip, clinical vertebral and total fracture. Coronary heart disease (CHD) and cancer incidence was similar in the 2 groups. Total mortality was slightly lower in the CaD group. The objective of the current analysis was to determine the effects of CaD on outcomes over 7 yrs (trial) and 5 additional yrs of follow-up through September 2010. Follow-up continued after the planned trial completion among 86% of surviving participants, CaD, n=15025 and placebo, n=14837. Primary outcomes were identified from annual mailed questionnaires and adjudicated centrally. Hip fracture was the only fracture adjudicated in the overall period; all other fractures were self-reported. All analyses were intent-to-treat. All participants were included in the analysis according to their randomized group assignment until last contact. The post-intervention risk (annualized rate) of hip fracture among women randomized to CaD was 0.28% compared with 0.30% in the placebo group, hazard ratio (HR)=0.95; 95% confidence interval (CI) (0.78, 1.15); 0.36% vs 0.43%, respectively for clinical vertebral fractures, HR=0.83; 95% CI (0.71, 0.98); 3.31% vs 3.30%, respectively, for total fractures HR=1.00; 95% CI (0.94, 1.06), (see Table). The risk of invasive colorectal cancer was non-significantly lower among women randomized to CaD in the post-intervention period, HR=0.80; 95% CI (0.61, 1.07), while the risk of breast cancer was slightly elevated, HR=1.17; 95% CI (0.99, 1.38), p=0.06. Total cancers did not differ between the CaD and placebo groups. There was no difference in CHD and total and cardiovascular disease mortality by randomized group in the post-intervention period. In the overall period, no significant differences between treatment groups were observed except that vertebral fractures were 13% lower among women randomized to CaD vs placebo, HR=0.87; 95% CI (0.76, 0.98). In conclusion, among postmenopausal women followed for up to 12 yrs, CaD was associated with a decreased risk of vertebral fractures, but, had little effect on the other skeletal and non-skeletal outcomes.

HRpQCT Reveals That Four Years of Estrogen Therapy in Early Postmenopausal Women Prevents Cortical, but Not Trabecular, Bone Loss.
 Joshua Farr¹, Sundeep Khosla², Virginia Miller³, Ann Kearns¹. ¹Mayo Clinic, USA, ²College of Medicine, Mayo Clinic, USA, ³Department of Surgery, Mayo Clinic, USA

Cross-sectional and longitudinal studies in women have shown that cortical bone mass remains relatively stable until the menopause and then decreases significantly. By contrast, trabecular bone loss begins early in life (in the third decade) and continues throughout life, albeit with an acceleration following menopause. These observational data suggest the hypothesis that loss of cortical bone is closely tied to estrogen (E) deficiency, whereas trabecular bone loss is largely due to intrinsic age-related processes independent of E. Although a number of clinical trials of E therapy have been conducted, none could directly address this hypothesis as virtually all previous studies used DXA, which cannot separate trabecular from cortical bone or assess bone microstructure. Thus, we used HRpQCT to assess cortical and trabecular microstructure at the distal radius at baseline and at 4 years in a subset of early postmenopausal women (mean age, 53 yrs) enrolled in the Kronos Early Estrogen Prevention Study (KEEPS) in which the women were randomized to placebo, oral (0.45 mg/d conjugated equine estrogens) or transdermal (50 µg/d 17β-estradiol) E (both in combination with progesterone, 200 mg/d for 12 d each month). For this mechanistic analysis, we included women who had completed 4 years of treatment. Since the changes in bone microstructure were similar in the oral and transdermal E groups, they were combined and we report data on 31 placebo (PL) and 45 E-treated (ET) subjects. As shown in the Figure (Panel A), ET prevented the decreases in cortical vBMD and increases in cortical porosity observed in the PL group. By contrast, ET was unable to prevent decreases in trabecular bone volume fraction or trabecular thickness (Panel B). Despite these differences in cortical versus trabecular bone responses to ET observed using HRpQCT, ET consistently prevented decreases in hip, spine, and distal radius areal BMD assessed by DXA, suggesting that changes in cortical bone at these sites may have masked ongoing trabecular bone loss.

These direct interventional data thus support the observational findings showing fundamentally different regulation of cortical versus trabecular bone by E. Further animal and human studies are needed to define the mechanisms for the differential responses of trabecular and cortical bone to E as well as the underlying, E-independent processes leading to trabecular bone loss even early in life.



Figure

Disclosures: Joshua Farr, None.

What's "Normal?" Considerations in Establishing the Appendicular Lean Mass DXA Reference Population. Bjoern Buehring*, Ellen Fidler, Jessie Libber, Jennifer Sanfilippo, Brvan Heiderscheit, Diane Krueger, Neil Binklev. University of Wisconsin, Madison, USA

Sarcopenia definitions include appendicular lean mass (ALM) measurement with "low" defined as 2 SD below the young adult mean. However, population body composition continues to change over time, thereby complicating the reference standard to which DXA measurements are compared. Given this variation in "normal", a potential alternative approach is comparison with people similar to ancestral hunter-gatherers in activity as a physiologic "normal." Young athletes may represent such a population. This work compares athletes' body composition parameters with NHANES young adults and explores sarcopenia prevalence using cutpoints derived from differing reference populations.

Table: Effects of CaD compared with placebo on clinical outcomes during the intervention, post-intervention and combined phases in WHI CaD trial

| | CaD | | Placebo | | HR (95% CI) |
|-----------------------------------|---------------------|---------------------|---------------------|---------------------|-------------|
| | # events (annual %) | |
| Hip fractures | | | | | |
| Intervention | 175 (0.13) | 201 (0.15) | 0.87 (0.71, 1.07) | | |
| Post-intervention | 204 (0.28) | 212 (0.30) | 0.95 (0.78, 1.15) | | |
| Overall | 379 (0.19) | 413 (0.21) | 0.91 (0.79, 1.05) | | |
| Vertebral fractures | | | | | |
| Intervention | 182 (0.14) | 197 (0.15) | 0.90 (0.74, 1.10) | | |
| Post-intervention | 263 (0.36) | 311 (0.43) | 0.83 (0.71, 0.98) | | |
| Overall | 446 (0.22) | 508 (0.26) | 0.87 (0.76, 0.98) | | |
| Total fractures | | | | | |
| Intervention | 2103 (1.69) | 2159 (1.75) | 0.97 (0.91, 1.03) | | |
| Post-intervention | 2272 (3.31) | 2242 (3.30) | 1.00 (0.94, 1.06) | | |
| Overall | 4013 (2.20) | 4018 (2.23) | 0.99 (0.94, 1.03) | | |
| Invasive colorectal cancer | | | | | |
| Intervention | 169 (0.13) | 160 (0.12) | 1.05 (0.85, 1.31) | | |
| Post-intervention | 87 (0.12) | 107 (0.15) | 0.80 (0.61, 1.07) | | |
| Overall | 256 (0.13) | 267 (0.13) | 0.95 (0.80, 1.13) | | |
| Invasive breast cancer | | | | | |
| Intervention | 539 (0.41) | 553 (0.43) | 0.98 (0.87, 1.00) | | |
| Post-intervention | 312 (0.44) | 263 (0.38) | 1.17 (0.99, 1.38) | | |
| Overall | 851 (0.43) | 816 (0.42) | 1.04 (0.94, 1.14) | | |
| Total cancer | | | | | |
| Intervention | 1623 (1.28) | 1658 (1.32) | 0.97 (0.91, 1.04) | | |
| Post-intervention | 998 (1.39) | 1017 (1.44) | 0.97 (0.89, 1.06) | | |
| Overall | 2554 (1.34) | 2617 (1.39) | 0.97 (0.92, 1.02) | | |
| Coronary heart disease | | | | | |
| Intervention | 518 (0.40) | 488 (0.37) | 1.06 (0.94, 1.20) | | |
| Post-intervention | 374 (0.51) | 372 (0.52) | 0.99 (0.86, 1.14) | | |
| Overall | 877 (0.44) | 845 (0.43) | 1.03 (0.94, 1.13) | | |
| Total mortality | | | | | |
| Intervention | 763 (0.59) | 823 (0.64) | 0.92 (0.83, 1.00) | | |
| Post-intervention | 1012 (1.37) | 1000 (1.37) | 1.01 (0.92, 1.10) | | |
| Overall | 1775 (0.88) | 1823 (0.91) | 0.96 (0.90, 1.03) | | |
| Cardiovascular death | | | | | |
| Intervention | 240 (0.18) | 255 (0.19) | 0.94 (0.78, 1.12) | | |
| Post-intervention | 309 (0.42) | 270 (0.37) | 1.14 (0.97, 1.34) | | |
| Overall | 549 (0.27) | 525 (0.26) | 1.03 (0.92, 1.17) | | |

table

Disclosures: Jane Cauley, None.

Dose Response to Vitamin D Supplementation: Substantial Underestimate by Endocrine Society Clinical Practice Guidelines (CPG) Compared to the Institute of Medicine (IOM) Report.. Malachi McKenna*, Barbara Murray. St. Michael's Hospital, Ireland

Background: In 2011, IOM updated their *Dietary Reference Intake (DRI)* for vitamin D; they specify that 600 IU/d meets the needs of 97.5% of the population assuming minimal sunlight exposure. Shortly afterwards, the CPG for the *Evaluation, Treatment and Prevention of Vitamin D Deficiency* was published that recommends intakes up to 2000 IU/d without reference to sunlight exposure. There are at least three major differences between IOM and CPG: (1) target 25OHD (IOM noted a plateau effect at 30-to-40 nmol/L with little or no benefit above 50 nmol/L; CPG set a target of 75 nmol/L with a level below this target being labelled as "insufficiency"); (2) definition of vitamin D deficiency (IOM adopts a probabilistic approach based on 25OHD level within a range of 30-to-50 nmol/L; CPG designates vitamin D deficiency as a 25OHD <50 nmol/L); and (3) at-risk individuals (IOM specifies particular at-risk members of the general population that are addressed by their DRIs, but the same groups are considered by CPG as needing higher intakes).¹ Differences in the estimation of vitamin D dose-response may also account for the discrepancies between the two reports. The CPG states that the rate of rise of 25OHD is approximately 2.5 nmol/L/100 IU/d. The IOM dose-response is a logarithmic function that includes all oral vitamin D intake: serum 25OHD=ln(vitamin D intake IU/d). We sought to test the validity of these dose-responses by analyzing responses to vitamin D supplementation from different studies.

Methods: Studies analyzed in three reports (IOM, AHRQ-Ottawa, and AHRQ-Tufts) were selected. The ratio of observed:expected 25OHD for both IOM and CPG was calculated.

Results: Sixty studies were selected with duration ranging from 3-months to 60-months, and with daily doses ranging from 230 IU/d to 2000 IU/d, or intermittent high doses ranging from 15,000 IU/wk to 600,000 IU/6-month. The mean ratio (CI) for CPG at 1.86 (1.53-2.19) was significantly higher than for IOM at 1.13 (1.03-1.24).

Conclusion: The CPG "rule of thumb" underestimates by nearly twofold the dose response to oral vitamin D supplementation. That CPG inflates the problem of vitamin D deficiency coupled with the underestimation of the dose response means that individuals are apt to be put in harm's way if clinicians adhere to the CPG.

1. Rosen CJ, Abrams SA, Aloia JF, et al. IOM Committee Members Respond to Endocrine Society Vitamin D Guideline. *J Clin Endocrinol Metab* 2012;97:1146-52.

Disclosures: Malachi McKenna, None.

Methods: Total body DXA measurements (Lunar iDXA) were obtained in college athletes. NHANES (1999–2004) DXA body composition data (Hologic) were downloaded from the NHANES website; 20–29 year olds were used for comparison. ALM was calculated based on lean mass excluding bone values. Athlete and NHANES BMI, ALM/ht², peripheral % fat and leg fat/lean ratio were compared by t-test using JMP (SAS, Cary, NC).

Results: The mean (range) age and BMI of 313 athletes (163M/150F) and 2116 NHANES (1117M/999F) participants was 20.0 (18–24) vs. 24.3 (20–29) years and 24.5 (18.1–38) vs. 26.9 (14.4–65.0) kg/m² respectively. Athletes had lower BMI, higher ALM/height² ratios (8.58 vs. 7.85 kg/m²), lower % peripheral fat (20.5 vs. 32.4%) and leg fat/lean mass ratios (0.30 vs. 0.58, all p≤0.0001). This was also true when separated by gender (all p≤0.0001). “Low” ALM/ht² cutpoints (2 SD below young mean) differed using the athletes, NHANES and commonly utilized values (Table). Applying these cutpoints to 70–85 year old individuals in NHANES 1999–2004, sarcopenia prevalence ranged from 4% (NHANES as reference) to 32% (athletes as reference).

In conclusion, there is great variation in potential “normal” body composition data depending on the reference population used. Applying ALM/ht² cutpoints using different reference datasets results in large differences in sarcopenia prevalence; similarly, measures of body fat vary dramatically. Simplistic use of a “normal” population, (e.g., NHANES) as a reference dataset, as has been done for BMD, may not be appropriate. An alternative approach using “optimal” or “ancestral” body composition might better predict outcomes such as falls, mobility and/or fracture.

Values to define low ALM/ht² (kg/m²) using different reference data:

| Reference population | Male | Female |
|----------------------|------|--------|
| Athlete | 7.51 | 5.83 |
| NHANES | 5.76 | 4.24 |
| Baumgartner | 7.26 | 5.45 |

Disclosures: Bjoern Buehring, None.

1140

Muscle, Fat and Bone Connections: Genetic Risk Factors of Sarcopenic-Obesity and Dynapenic-Obesity and Their Consequent Risks of Osteoporotic Fractures. Yi-Hsiang Hsu*¹, Robert McLean², Elizabeth Newton³, Marian Hannan⁴, L Adrienne Cupples⁵, Douglas Kiel⁶. ¹Hebrew SeniorLife Institute for Aging Research & Harvard Medical School, USA, ²Hebrew SeniorLife Institute for Aging Research & Harvard Medical School, USA, ³Hebrew SeniorLife Institute for Aging Research, USA, ⁴HSL Institute for Aging Research & Harvard Medical School, USA, ⁵Dept Biostatistics, Sch of Public Health, Boston University, USA, ⁶Hebrew SeniorLife, USA

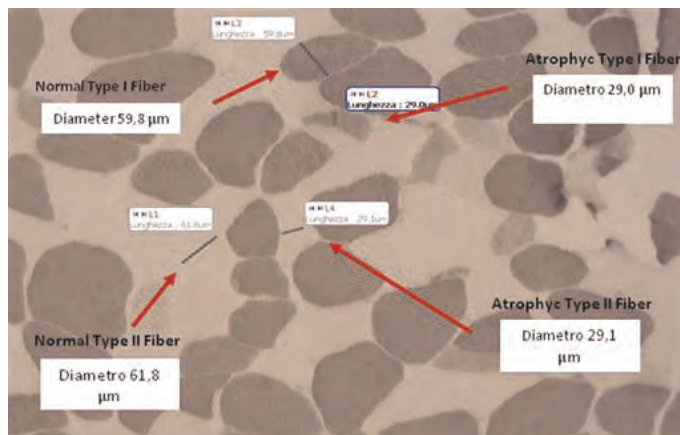
Sarcopenic-obesity (SO) and Dynapenic-obesity (DO) is characterized by excess body fat and decreased muscle mass and strength, respectively. It is common and affecting > 12% of U.S. adults aged ≥ 60 years. As a growing number of US seniors are living longer and an epidemic of obesity, SO has become a major public health burden. Although obesity is a known risk factor for major adverse health outcomes, emerging evidence shows that older adults with SO have an even greater risk on fractures, cardiovascular diseases, mobility impairment and disability compared to those with obesity or sarcopenia alone. Identifying genetic risk factors for SO and DO and their association with fracture may help to understand the underlying biology and identify new molecular targets for treatments. We performed a GWAS in 3,763 Framingham men and women participants > 50 years with 2.6 million SNPs under an additive model adjusted for potential confounders. To identify unique genetic determinants associated with SO only, we applied a mixed-effect multinomial-logit model, which accounts for the relations among obesity alone, sarcopenia alone and SO when estimating the association between SNPs and SO. We defined SO using fat and muscle mass (DXA appendicular lean mass divided by height²); and DO using fat mass and muscle strength (lowest sex-specific tertile of grip strength). Obesity was defined as total body fat % (DXA) >30 in men and >40 in women. We classified 11%, 48% and 10% of participants with SO, obesity alone and sarcopenia alone, respectively. We classified 10%, 47% and 7% of participants with DO, obesity alone and sarcopenia alone, respectively. We found SNPs significantly associated with SO only, but not obesity or sarcopenia alone, i.e. SNPs located in or near *MANBA*, *CENPE*, *PGK2* (associated with SO) and *FNI* (associated with DO) gene. Of note, a few of these SNPs were also reported to be associated with diabetes, restless leg syndrome or subclinical atherosclerosis from other GWAS. We found SNPs significantly associated with obesity alone were not found to be associated with SO (or DO). Several of the top SNPs were also found associated with osteoporotic fractures by mendelian randomization analyses. The top findings (p < 5x10⁻⁵) are further replicating in independent samples. In conclusion, our results reveal novel candidate genes associated with SO and fracture, but not with obesity or sarcopenia alone, which suggests that underlying pathophysiology of SO may be different from fatness alone and/or muscle weakness alone.

Disclosures: Yi-Hsiang Hsu, None.

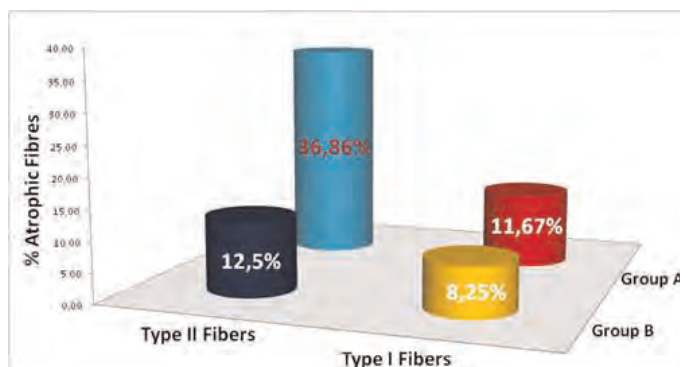
1141

Hip Fracture and Sarcopenia: A Model of Osteoporosis-related Muscle Atrophy. Umberto Tarantino*¹, Monica Celi², Jacopo Baldi³, Fabio Luigi Perrone³, Federico Maria Liuni³, Elena Gasbarra³. ¹Azienda Ospedaliera PTV, Italy, ²University of Rome Tor Vergata, Italy, ³orthopaedic Department University of Rome Tor Vergata, Italy

Osteoporosis and sarcopenia are considered two of the hallmarks of the aging process; the reduction of muscle mass and power may affect bone strength and Bone Mineral Density (BMD) by modifying loads to the skeleton. This could lead to an increased risk of fragility fracture, functional limitations and motor dependency. Aim of the study was to evaluate the degree of muscular atrophy in patients with osteoporosis and osteoarthritis and to determine the role of IGF-1/PI(3)/Akt signaling pathway in the genesis of a specific type II osteoporosis-related muscle atrophy. For this study we performed vastus lateralis biopsy in 60 women (mean age 71,53 ± 9,74) underwent orthopaedic surgery; 30 women with osteoporosis undergoing primary Total Hip Arthroplasty (THA) for hip fracture (Group A); 30 women underwent surgery for hip osteoarthritis with no significant functional limitations (Group B). Muscle fibers were measured and classified by ATPase reaction. To evaluate whether Akt and pAkt are involved in osteoporosis-related muscle atrophy, muscle homogenates of twelve patients from Group A presenting higher percentage of type II fiber atrophy and twelve age-matched control biopsies from Group B were immunoblotted. In Group A atrophic type-II fibers were 3-fold more frequent than atrophic type I fibers (36,86%; p<0.01); in Group B the same fibers atrophy were 1.5-fold more frequent than type I atrophy (12,50%; p<0.001). Muscular atrophy significantly correlates with osteoporosis degree (p<0.05) in Group A; in Group B it significantly correlates disease duration, degree of pain and functional impairment of hip joint. Furthermore patients with higher percentage of type II fiber atrophy from Group A shown values of intramuscular Akt two and a half times (60%; p<0,01) lower than the same values from Group B. Immunoblotting didn't verify the activation status of intracellular pAkt probably due to its low expression in atrophic fibers. Osteoporotic patients shown a preferential and diffuse type II fiber atrophy, that seems to be related to disease severity. On the opposite, in osteoarthritic patients, atrophy involves seems to be caused by disuse and pain. The reduction of Akt observed in the muscle of individuals from the osteoporotic group, may be one of the possible moments of compromise in intracellular IGF-1/PI(3)/Akt signaling pathway that is likely to stimulate protein synthesis and cell survival as a result of activation of the complex mTOR/p70S6K22.



Muscle histomorphometry



Rate of atrophy of Type I and Type II muscle fibers in Group A and Group B

Disclosures: Umberto Tarantino, None.

Poor Peripheral Nerve Function Is Associated with Higher Bone Marrow Fat and Skeletal Muscle Adiposity: The Osteoporotic Fractures in Men (MrOS) Study. Elsa S. Strotmeyer^{*1}, Jane Cauley¹, Yahtyng Sheu¹, Kimberly A. Faulkner², Tanushree Prasad¹, Rachel E. Ward¹, Sasa Zivkovic³, Peggy Cawthon⁴, Iva Miljkovic¹. ¹University of Pittsburgh Graduate School of Public Health, USA, ²National Institute for Occupational Safety & Health, USA, ³University of Pittsburgh School of Medicine, USA, ⁴California Pacific Medical Center Research Institute, USA

Poor peripheral nerve function has been related to lower muscle strength and lower bone mineral density, independent of diabetes, in older populations. To expand these previous findings, we investigated if peripheral nerve function was related to higher bone marrow fat or skeletal muscle adiposity. Poor sensory nerve function was assessed by lower sural nerve conduction amplitude (SNAP=amplitude in uV) from a neurodiagnostic instrument (NC-stat®, NeuroMetrix, Inc.) and lack of detection from a light touch 1.4-g and standard 10-g monofilament. Poor motor nerve function was assessed by lower peroneal nerve conduction amplitude (CMAP=amplitude in mV), using the same neurodiagnostic instrument. Poor nerve function (worse tertile vs. middle/best tertile or lack of monofilament detection) was related to outcomes from pQCT of calf intermuscular fat (IMAT) and muscle density, which reflects intramuscular fat content, in regression analyses adjusting stepwise (p<0.10 for inclusion) for age, race, diabetes, total calf fat and muscle area, height, smoking, drinking frequency, physical activity, physical function, medications/supplements and diabetes-related conditions. Participants were 613 men (77.5±5.2 years; 99% white; 21% diabetes) from MrOS in Pittsburgh, PA. Lack of monofilament detection (1.4-g for IMAT; 10-g for density) and the worst tertile of CMAP vs. middle/best tertiles were associated with higher IMAT and lower density (Table). Worst SNAP tertile vs. middle/best tertiles related to higher IMAT but not density. In a subset of 144 men, only lack of 1.4g monofilament detection was related with higher % bone marrow fat (BMF; 57.8±1.3 vs. 53.8±1.3%; p<0.05), adjusted for above but total fat and lean mass from DXA rather than pQCT body composition variables. Results indicated poor sensorimotor nerve function is associated with muscle fat infiltration independent of muscle area and poor monofilament detection is related to higher BMF in older men.

Table: Adjusted means of skeletal muscle adiposity by poor peripheral nerve function from regression analyses.

| *p-value < 0.05 | Adjusted mean ± SE | |
|---|-----------------------------|---------------------|
| | Worst tertile | Middle/Best tertile |
| Peroneal motor nerve function (CMAP) | | |
| | ≤1.63 mV | >1.63 mV |
| IMAT (mm ²) | 438.15 ± 24.17 [‡] | 343.01 ± 16.40 |
| Muscle density (mg/cm ³) | 72.93 ± 0.23 [‡] | 73.61 ± 0.16 |
| Sural sensory nerve function (SNAP) | | |
| | ≤3.22 uV | >3.22 uV |
| IMAT (mm ²) | 441.06 ± 26.70 [‡] | 358.32 ± 17.41 |
| Muscle density (mg/cm ³) | 73.16 ± 0.27 | 73.59 ± 0.17 |
| Light touch 1.4-g monofilament | No detection | Detection |
| IMAT (mm ²) | 429.53 ± 18.67 [‡] | 361.67 ± 16.78 |
| Muscle density (mg/cm ³) | 73.02 ± 0.18 | 73.35 ± 0.17 |
| Standard 10-g monofilament | No detection | Detection |
| IMAT (mm ²) | 422.58 ± 31.82 | 385.76 ± 13.42 |
| Muscle density (mg/cm ³) | 72.56 ± 0.32 [‡] | 73.32 ± 0.13 |

Table

Disclosures: Elsa S. Strotmeyer, None.

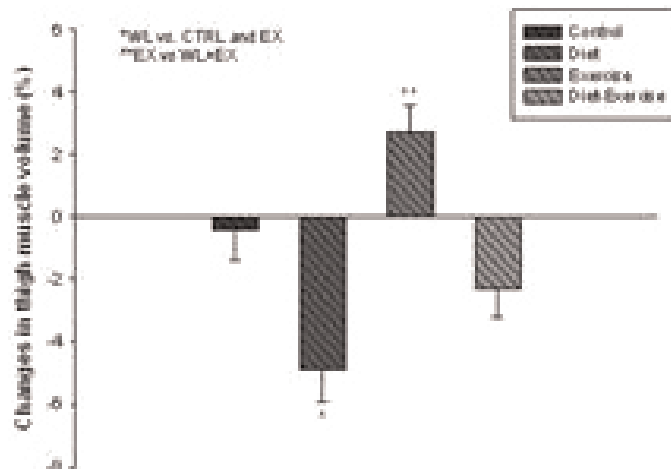
Changes in Thigh Muscle Volume Predict Changes in Femoral BMD in Sarcopenic Elderly Obese Adults Undergoing Lifestyle Therapy. Reina Armamento-Villareal¹, Nicola Napoli², Krupa Shah³, Lina Aguirre^{*4}, Tiffany Hilton⁵, David Sinacore⁶, Dennis Villareal¹. ¹University of New Mexico School of Medicine, USA, ²University Campus Biomedico, Italy, ³University of Rochester School of Medicine, USA, ⁴New Mexico VA Health Care System, USA, ⁵Ithaca College, USA, ⁶Washington University School of Medicine, USA

Purpose: Loss of femoral BMD and lean body mass are major complications of weight loss (WL) from lifestyle therapy in frail sarcopenic elderly obese (EO); but these adverse effects can be attenuated by exercise (EX). We reported that WL-induced bone loss is mediated by increase in sclerostin; however, the contribution of mechanical strain loss from muscle loss, particularly at the thigh, is poorly defined. We hypothesize that the negative effects of WL and the protective effect of exercise (EX) on femoral bone is modulated by changes in thigh muscle volume (TMV) leading to differences in mechanical strain and sclerostin production. The objective of this study is to examine changes in TMV and muscle strain and their effects on femoral BMD in EO subjects undergoing WL, EX and WL+EX.

Methods: 107 obese (BMI>30), older (age ≥ 65) subjects were randomized for 1 yr to control (CTRL) (n=27), WL (n=26), EX (n=26) and WL+EX (n=28) groups. WL was by dietary/behavioral intervention designed to induce and maintain WL of 10% of body weight; EX was by 3 supervised resistance/aerobic exercise sessions/wk and CTRL was to continue usual dietary and activity habits. TMV was measured using magnetic resonance imaging of both thighs at 0 and 12 mos; while BMD by DXA, sclerostin by Elisa, strength (knee extension and flexion by BIODEX) and physical function by Physical Performance Testing (PPT), were measured at 0, 6 and 12 mos.

Results: Data on BMD, physical function and sclerostin were reported elsewhere. Significant reduction in TMV relative to CTRL and EX was observed in the WL group while reduction in TMV in the WL+EX (Fig. 1) was not different from the CTRL. These changes followed the same pattern as the changes in total hip BMD. Both knee extension and flexion increased in the EX and WL+EX and were unchanged in the CTRL and WL (Fig. 2). TMV changes correlated with: total hip BMD changes (r=0.55, p=0.000), changes in sclerostin (r=-0.26, p=0.03) and with a borderline correlation with changes in knee flexion (r=0.23, p=0.06). Multivariate analysis showed TMV and PPT changes as predictors for hip BMD changes.

Conclusion: Changes in TMV modulate femoral BMD changes in frail EO patients undergoing lifestyle therapy. WL-induced thigh muscle loss is attenuated by EX resulting in similar improvement in strength in WL and WL+EX groups. This positive effect of EX when added to WL may in part account for the relative reduction in WL-associated bone loss in the WL+EX patients.



Changes in thigh muscle volume during lifestyle intervention in sarcopenic obese older adults

worsening fracture was estimated by logistic regression models adjusted for age, race, clinic, alcohol, smoking, BMI, diabetes, lumbar spine BMD and self-reported physical activity. Complete fracture, physical function and covariate data were available for 3,964 men (mean age: 72.8 years), of whom 444 (11.2%) had a vertebral fracture (SQ \geq 1) at baseline.

During 4.6 years of follow-up, 171 (4.3%) men had a new or worsening vertebral fracture. Weak grip strength; longer time/inability to complete the repeat chair stands; poor balance (inability to complete the narrow walk); and lower leg power were each associated with increased likelihood of new or worsening radiographic vertebral fracture (Table). Slow walking speed was not associated with vertebral fracture. Analysis of the summary physical function score indicated that each additional test with poor performance increased the likelihood of fracture by about 20% [OR: 1.2 (95% CI: 1.1, 1.4) per one unit increase in summary score]. Similar results were seen when analyses were limited to new radiographic vertebral fractures only and when results were adjusted for total hip BMD rather than lumbar spine BMD.

In summary, men with poor physical function, in particular decreased lower leg power, were more likely to develop a radiographic vertebral fracture than men with better function.

Likelihood (Odds ratio, 95% confidence interval) of new or worsening vertebral fracture, by baseline physical function

| Function category | Grip strength* | Leg Power* | Chair stands* | Narrow walk | Walking speed |
|-------------------|----------------|----------------|----------------|----------------|----------------|
| Unable | 1.8 (0.5-6.3) | N/A | 2.7 (0.9, 7.5) | 2.4 (1.3, 4.6) | N/A |
| Worst | 1.9 (1.2-3.2) | 3.7 (2.0, 6.8) | 2.0 (1.2, 3.2) | 0.9 (0.5, 1.4) | 1.6 (1.0, 2.6) |
| Poor | 1.5 (1.0-2.5) | 2.4 (1.3, 4.4) | 1.1 (0.7, 1.9) | 1.0 (0.6, 1.6) | 1.4 (0.9, 2.2) |
| Good | 1.2 (0.7, 1.9) | 2.4 (1.4, 4.3) | 1.5 (1.0, 2.5) | 1.1 (0.7, 1.8) | 1.5 (1.0, 2.4) |
| Best | 1.0 (ref) |

* p for trend across categories <0.05

Table

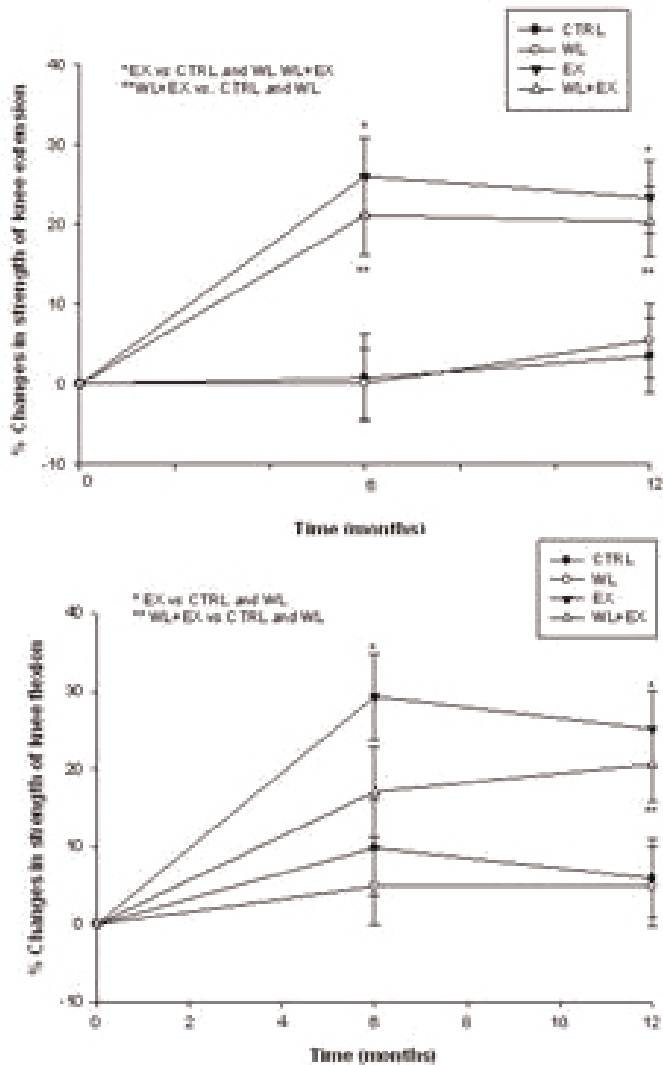
Disclosures: Peggy Cawthon, None. This study received funding from: NIH

1145

Genome-wide Profiling of DNase-Hypersensitivity during Osteoblastogenesis. Phillip Tai*, Hai Wu, Troy W. Whitfield, Jonathan Gordon, Jane Lian, Andre Van Wijnen, Gary Stein, Janet L. Stein. University of Massachusetts Medical School, USA

Gene expression during the process of osteoblastogenesis has been well-described, and multiple studies have focused on characterization of the regulatory mechanisms that define many selected bone-related genes. However, the relationship between chromatin state, bone-related gene regulation, and the cell-type specific partitioning of the genome into promoters, enhancers, silencers, insulators, and locus control regions, has yet to be fully characterized. Traditionally, DNaseI-hypersensitivity assays have been used to discover regions of chromatin that are bound by nuclear-factor complexes *in vivo* without the prior identification of the binding factor(s). The *de novo* identification of regulatory regions is possible because DNaseI preferentially digests chromatin depleted of nucleosomes - presumably due to transcription factor occupancy. We have produced unbiased genome-wide maps of regulatory regions during defined phases of osteoblastogenesis by identifying open regions of chromatin using DNaseI-hypersensitivity coupled with high-throughput sequencing (DNase-seq). Specifically, we have generated DNase-seq libraries of growth-phase MC3T3-E1, a model cell-culture system for studying osteoblastogenesis, as well as libraries of cultures subjected to differentiation conditions. We demonstrate the presence of regions exhibiting dynamic DNase-hypersensitivity at gene promoters that are known to be differentially expressed during osteoblastogenesis, as well as regions that are in close proximity to these genes. Furthermore, the comparison of DNaseI-hypersensitivity regions with the global binding of RUNX2, a master regulator of osteogenesis, as assayed by chromatin immunoprecipitation followed by high-throughput sequencing (ChIP-seq), shows interesting correlations among bone-related genes throughout differentiation. The diversity of RUNX2 enrichment that overlaps DNase-hypersensitivity regions throughout the genome implicates RUNX2 in a variety of roles: 1) its binding at far-distal regions demonstrates its role as a genome organizer, 2) enrichment of RUNX2 at exonic and intronic sequences suggests its role as a modifier of chromatin state and gene transcription, and 3) its occupancy at promoters suggests its function as an activator or repressor of gene expression. This on-going work illustrates the dynamic properties of chromatin architecture and has great potential for revealing novel regulatory regions critical for bone-related gene expression.

Disclosures: Phillip Tai, None.



Changes in knee flexion & extension during lifestyle intervention in sarcopenic obese older adults

Disclosures: Lina Aguirre, None.

1144

Physical Performance and Risk of Vertebral Fractures in Older Men. Peggy Cawthon*¹, Terri Blackwell², John Schousboe³, Lynn Marshall⁴, Howard Fink⁵, Deborah Kado⁶, Kristine Ensrud⁷, Jane Cauley⁸, Dennis Black⁹, Eric Orwoll⁴, Steven Cummings¹⁰. ¹California Pacific Medical Center Research Institute, USA, ²CPMC RESEARCH INSTITUTE, USA, ³Park Nicollet Clinic/University of Minnesota, USA, ⁴Oregon Health & Science University, USA, ⁵GRECC, Minneapolis VA Medical Center, USA, ⁶University of California, Los Angeles, USA, ⁷Minneapolis VA Medical Center / University of Minnesota, USA, ⁸University of Pittsburgh Graduate School of Public Health, USA, ⁹University of California, San Francisco, USA, ¹⁰San Francisco Coordinating Center, USA

Poor physical function has been associated with higher risk of hip and other non-spine fractures in older men, but the relation to vertebral fractures is unclear.

MrOS is a prospective cohort study of ambulatory men aged \geq 65 yrs at baseline. At baseline and again 4.6 years later, lateral spine films were reviewed using semi-quantitative (SQ) grading for new or worsening radiographic vertebral fractures (defined at follow-up as a change in SQ grade \geq 1). Physical function was assessed by walking speed (usual pace, m/s over 6 m); narrow walk (walking speed in m/s over a 6 m by 20 cm course); repeated chair stands ability (time to complete 5 stands); grip strength; and leg power (by Nottingham Power Rig). Physical function measures were analyzed as quartiles with those unable to complete the test included in a separate category (when data were available). A summary physical function score (range: 0-5) was calculated; for each of the 5 tests with poor performance (defined as in the worst performance quartile or unable to complete the measure), one point was added to the summary score; higher scores indicate worse function. Likelihood of new or

1146

miR-17-92 Cluster Critically Regulates Osteoblast Differentiation. Mingliang Zhou*¹, Junrong Ma², Xiang Chen², Meng Gong², Xijie Yu².
¹West China Hospital, Sichuan University, Peoples Republic of China,
²Laboratory of Endocrinology & Metabolism, West China Hospital, Sichuan University, China

The miR-17-92 cluster encodes six miRNAs (miR-17, miR-18a, miR-19a, miR-20a, miR-19b-1, and miR-92-1), which are highly conserved in all vertebrates. Loss-of-function of the miR-17-92 cluster resulted in smaller embryos and immediate postnatal death of all animals due to severely hypoplastic lungs and ventricular septal defects in the hearts. Germline hemizygous deletions of *MIR17HG* were accounted for microcephaly, short stature and digital abnormalities in a few cases of Feingold syndrome. These reports indicate that miR-17-92 may play important function in growth and skeletal development. However the precise roles of the miR-17-92 cluster in skeletal development and growth are largely unknown. To determine the functional roles of miR-17-92 in osteoblast differentiation, embryonic stem cells (ES cells) and bone marrow stromal cells (BMSCs) were induced to different into osteoblasts under osteogenic medium; the expression of miR-17-92 was assayed by quantitative real-time RT-PCR. The expression of miR-17-92 was down-regulated along with osteoblast differentiation, the lowest level was found in mature osteoblast. To determine the systemic function of miR-17-92 in skeleton, the bone mineral density (BMD) and bone volume were assayed in miR-17-92^{+/+} mice by DXA and micro-computed tomography (μ CT) respectively. Compared to wildtype controls, miR-17-92^{+/+} mice showed significantly lower trabecular and cortical BMD, bone volume and trabecular number at 10 weeks old. To determine the possibly direct function of miR-17-92 in bone cells, osteoblasts from miR-17-92^{+/+} mice were investigated by ex vivo cell culture, miR-17-92 was further conditionally deleted in osteoblasts by 2.3-kb *Col1a1-Cre* (miR-17-92^{ΔOB/ΔOB}). Osteoblasts from miR-17-92^{+/+} mice showed lower ALP activity and less calcification. miR-17-92^{ΔOB/ΔOB} mice demonstrated lower BMD, bone volume and trabecular number. Taken together, our results suggest that the miR-17-92 cluster critically regulates skeletal development, and this regulation is mostly through its function in osteoblasts.

Disclosures: Mingliang Zhou, None.

1147

miRNA-34c Regulates Notch Signaling during Bone Development. Yangjin Bae*¹, Tao Yang¹, Huan-Chang Zeng¹, Philippe Campeau², Yuqing Chen², Terry Bertin², Brian Dawson², Elda Munivez², Jianning Tao¹, Brendan Lee³.
¹Baylor College of Medicine, USA, ²Baylor College of Medicine, USA, ³Baylor College of Medicine & Howard Hughes Medical Institute, USA

MicroRNAs (miRNAs) are small non-coding RNAs, which mediate post-transcriptional silencing of target genes by either mRNA degradation or translational inhibition. Growing evidence indicates that miRNAs play critical roles during development, cellular differentiation, and homeostasis by regulating hundreds of targets. To date, the important roles of miRNAs in bone development and homeostasis have been suggested by excision of *Dicer* in mice using osteoblast specific *Cre* transgene. However, there are few mouse models that demonstrated either the physiological or pathological role of individual miRNAs in bone. During bone homeostasis, osteoblast and osteoclast differentiation are coupled and regulated by multiple signaling pathways and their downstream transcription factors. Here, we show that miRNA-34c (miR-34c) is significantly up-regulated in BMP2 mediated osteoblast differentiation of C2C12 cells. *In vivo*, osteoblast-specific gain of miR-34c in mice (*Coll1a1-miR34c*) leads to an age-related osteoporosis due to the defective mineralization and reduced proliferation of osteoblasts, and increased bone resorption due to increased osteoclastogenesis. This hyper-resorptive phenotype of *Coll1a1-miR34c* mice phenocopies our earlier study of the loss of Notch in osteoblasts. A transcriptome profile analysis confirmed that miR-34c indeed targets multiple components of the Notch signaling pathway including *Notch1*, *Notch2*, and *Jag1* in a direct fashion, and influences osteoclast differentiation in a non-cell-autonomous fashion. Furthermore, we showed that the defect in the osteoblast differentiation of *Coll1a1-miR34c* mice was due to the cell autonomous effect by the predicted targeting of *Satb2* and *Rumx2* rather than Notch signaling. Taken together, our study demonstrates a critical role of miR-34c in bone homeostasis by affecting both osteoblasts and osteoclasts *in vivo* via the regulation of multiple targets in osteoblasts. Furthermore, miR-34c-mediated post-transcriptional regulation of Notch signaling in osteoblasts may be targeted to antagonize the proliferative effect of Notch in the pathogenesis of osteosarcomas. Therefore, understanding the functional interaction of miR-34 and Notch signaling in normal bone development and in bone cancer could potentially lead to therapies.

Disclosures: Yangjin Bae, None.

1148

Progranulin Accelerates Bone Regeneration through Stimulating Osteoblastogenesis and Repressing Osteoclastogenesis. Chuanju Liu, Yunpeng Zhao*¹, Qingyun Tian, Brendon Richbourgh, Shuai Zhao, New York University, USA

We have previously reported that progranulin (PGRN) growth factor was expressed in the growth plate of long bone and played a critical role in endochondral ossification (Feng JQ, et al, *FASEB J.* 2010;24(6):1879-92, Bai XH, et al, *Mol Cell Biol.* 2009; 29(15):4201-19). Additionally, we recently reported that PGRN directly bound to TNF receptors, antagonized TNF-alpha activity, and protected against bone erosion in inflammatory arthritis (Tang W, *Science.* 2011; 332(6028):478-84). This study is to determine the potential role of PGRN in bone regeneration and the molecular events involved. To do so, we first established several bone defect models, including a drill-hole, a femoral segmental nonunion, and a radial non-union model, and compared the effects of the deletion of the PGRN gene and/or administration of recombinant PGRN growth factor on bone regeneration. Immunohistochemistry revealed that PGRN was clearly expressed in the newly-formed bone *in vivo*. Micro-CT and histological assays demonstrated that the deficiency of PGRN led to a significant defect in bone regeneration, whereas the administration of recombinant PGRN protein stimulated this process. PGRN acted as an important downstream mediator of BMP-2 in the course of osteogenesis since the deletion of PGRN significantly blocked BMP-2-induced osteoblast differentiation *in vitro* and ectopic bone formation *in vivo*. Importantly, the application of recombinant PGRN into PGRN knockout mice could rescue the impairment in BMP-2-triggered bone formation. Molecular studies revealed that the knockdown of PGRN using a siRNA approach in C2C12 mesenchymal precursor cells inhibited, while recombinant PGRN stimulated, the luciferase activity of Cbfa-specific reporter genes and the expressions of marker genes for osteogenesis, including osteocalcin and alkaline phosphatase (ALP). In addition to stimulating the osteoblast differentiation, PGRN was also found to function as an antagonist of TNF α and to inhibit TNF-induced osteoclastogenesis *in vitro* and in TNF transgenic mice. Furthermore, elevated osteoclast activity detected with TRAP staining was observed in the collagen-induced arthritis model of PGRN-null mice when compared with those of wild type mice. Taken together, PGRN is a novel regulator of bone remodeling and mediates this process via a dual mechanism, i.e. the stimulation of osteoblastogenesis and the suppression of osteoclastogenesis. These findings may not only provide novel insights into the role of PGRN in regulating bone regeneration and remodeling, but also present a potential therapeutic target for treating bone defects clinically.

Disclosures: Yunpeng Zhao, None.

1149

Semaphorin 3A Inhibits Osteoclastogenesis and Promotes Osteoblastogenesis Synchronously. Mikihito Hayashi*¹, Tomoki Nakashima¹, Hiroshi Takayanagi².
¹Tokyo Medical & Dental University, Japan, ²The University of Tokyo Department of Immunology, Japan

Bone homeostasis is maintained by the crosstalk between bone-forming osteoblasts and bone-resorbing osteoclasts. Osteoblasts contribute to the regulation of osteoclasts by producing anti-osteoclastogenic factors. However, an inhibitory factor of osteoclast differentiation derived from osteoblasts was not identified except for Opg, a decoy receptor for RANKL. Here we show that a conditioned medium of Opg-deficient calvarial cells contains factors that inhibit osteoclast formation. By means of functional screening and mass spectrometric analysis, we identified that one of these factors is the axon guidance molecule Semaphorin 3A (Sema3A).

Sema3a^{-/-} mice exhibited a severe low bone mass phenotype accompanied by enhanced osteoclast differentiation. Sema3A-induced inhibition is mediated by the modulation of DAP12-induced ITAM signalling. Neuropilin-1 (Nrp1), a receptor for Sema3A, competes with TREM2 for Plexin-A1, thereby functioning as a suppressor of the Plexin-A1-TREM2-DAP12-induced costimulatory signal. The inhibition of RhoA activation is also involved in the inhibitory effect of Sema3A on the migration of osteoclast precursor cells.

In addition to an osteoclastic phenotype, *Sema3a*^{-/-} mice also showed a severe defect in osteoblast differentiation and an increase in adipocyte differentiation in bone marrow. These findings suggest that Sema3A promotes mesenchymal cell differentiation toward osteoblasts, but not adipocytes. Sema3A stimulates the canonical Wnt/ β -catenin signalling pathway, at least in part, through FARP2-mediated activation of Rac1 during osteoblast differentiation. The osteopenic phenotype in *Sema3a*^{-/-} mice was recapitulated by mice in which the Sema3A-binding site of Nrp1 had been genetically disrupted.

We further investigated the therapeutic potential of Sema3A in a bone regeneration model of cortical bone defects induced by drill hole injury. The local administration of Sema3A into the injured site accelerates bone regeneration. Sema3A treatment reduced bone loss after ovariectomy by both inhibiting osteoclastic bone resorption and promoting osteoblastic bone formation synchronously. Thus, Sema3A is a promising new therapeutic agent in bone and joint diseases. This study demonstrates that Sema3A expressed by osteoblast lineage cells functions as an osteoprotective factor with the capacity to bring both osteoblasts and osteoclasts into a condition which favors bone mineral increase.

Disclosures: Mikihito Hayashi, None.

1150

Histone Deacetylase 3 Depletion in Mature Osteoblasts Promotes Apoptosis and Progressive Bone Loss With Age. Meghan McGee-Lawrence*, Elizabeth Bradley, Samuel Carlson, Qingshan Chen, Kai-Nan An, Jennifer Westendorf. Mayo Clinic, USA

Histone deacetylase 3 (Hdac3) is a nuclear enzyme that removes acetyl groups from lysine residues in histones and other proteins to epigenetically regulate gene expression. Hdac3 interacts with bone-related transcription factors and co-factors (e.g., Runx2, Zfp521), and thus is poised to play a key role in skeletal development and maintenance. We previously reported that conditional deletion of Hdac3 in osteochondral progenitor cells, using Osterix-Cre recombinase, caused severe osteopenia and increased marrow adiposity with developmental defects in both cartilage and bone. To better understand the effects of Hdac3 in bone, independent of changes in cartilage, we developed a new model where Hdac3 insufficiency was targeted to osteoblast- and osteocyte-enriched populations by driving Cre expression with the Osteocalcin promoter.

Mice deficient in Hdac3 in osteocalcin expressing cells (Ocn-Hdac3 CKO) had low cortical and trabecular bone mass compared to age-matched wildtype (WT) mice. Bone length, body size, and chondrocyte development were unaffected, confirming the bone specificity of this model. Unlike our previous Osterix-Cre Hdac3 insufficient model, changes in marrow adiposity were not observed in Ocn-Hdac3 CKO mice and primary bone marrow stromal cells (BMSC) did not differentiate into adipocytes during osteogenic culture. Bone fractures were common in the Ocn-Hdac3 CKO mice due to reduced cortical bone mineralization and material properties. Hdac3 insufficiency caused a global decrease in both bone formation and resorption. Although osteoblast activity (measured via dynamic histomorphometry) was unaffected, osteoblasts in Ocn-Hdac3 CKO mice had a flattened morphology. BMSC cultures from Ocn-Hdac3 CKO mice expressed lower levels of characteristic osteoblast genes and failed to produce WT levels of mineralized matrix. Cortical bone explants from Hdac3-insufficient mice had decreased expression of osteoblastic genes, pointing to an overall decrease in osteoblast number. Mechanistically, Hdac3 insufficiency in Ocn-expressing cells increased apoptosis both in vivo and in vitro. These data are consistent with the effects of pharmacological Hdac inhibitors on BMSC, which experience DNA damage, cell cycle arrest, and apoptosis in response to pan-Hdac inhibition during osteoblastic differentiation. Thus, Hdac3 expression in mature osteoblasts is essential for osteoblast survival and proper bone formation.

Disclosures: Meghan McGee-Lawrence, None.

1151

Regulation of Energy Metabolism by Bone Sialoprotein, a Novel Endocrine Mechanism. Jake Jinkun Chen*¹, Yuwei Wu², Liming Yu¹, Shu Meng¹, Qisheng Tu¹. ¹Tufts University School of Dental Medicine, USA, ²Tufts University, USA

Bone sialoprotein (BSP) is a major non-collagenous matrix protein in bone and other mineralized tissues that belongs to the small integrin-binding ligand, N-linked glycoprotein (SIBLING) family, whose members play multiple and distinct roles in the development, turnover, and mineralization of bone and dentin, and endocrine regulation of energy metabolism, but their functional specificities are unknown. To determine the effect of BSP in maintaining bone homeostasis through regulating bone remodeling and in regulating energy metabolism, we have first generated conditional BSP knockout mice (BSP KO) by crossing the floxed BSP mice (homozygosity) with osterix-Cre mice that specifically express Cre in osteoblasts. Although BSP KO mice were viable and bred normally, bone morphological abnormalities were clearly exhibited. When compared with wild type littermates, BSP KO mice displayed that the cartilage cells were pathologically flat and arranged disorderly in the growth plate where the number of cartilage cells decreased and no obvious hypotrophic cartilage cells were present. Histological analyses also showed that at 8 months approximately 3-4 times more megakaryocytes formed in BSP KO mice compared with wild type mice in bone marrow space. Moreover, conditional BSP knockout reduced the expression of Runx2, RANKL, NFATc1 and cathepsin K in bone tissues. Furthermore, BSP deficiency in bones decreased the expression of adiponectin in bone and fat tissues as serum BSP level decreases concomitantly. To further determine the effects of BSP on the secretion of adiponectin by adipocytes we treated 3T3-L1 preadipocyte cells with BSP (50ng/mL), which increased lipid accumulation and the expression of adiponectin, adipocyte fatty acid-binding protein (aP2), and PPAR γ messenger RNA by 3.09, 2.46 and 1.4 fold above basal values, respectively. While overexpression of BSP leads to an uncoupling of bone formation and bone resorption in mice, as shown in our previous gain-of-function study, it is interesting to find that the lack of BSP affects both osteoblast and osteoclast formation and function. For the first time, our results suggest that BSP regulates energy metabolism by modulating adipocytokine and the enzymes of lipid metabolism, aP2 and PPAR γ in an endocrine/paracrine manner and systemic pathway. Continued research and data collection will further develop our understanding of the mechanisms by which BSP contributes to bone development and energy metabolism.

Disclosures: Jake Jinkun Chen, None.

This study received funding from: NIH grants DE16710 and DE21464 to JC

1152

Hdac3 Regulates Chondrocyte Hypertrophy and Matrix Secretion by Repressing Phlpp1 Expression and Facilitating Akt Signaling. Elizabeth Bradley*¹, Lomeli Carpio¹, Meghan McGee-Lawrence¹, Alexandra Newton², Jennifer Westendorf¹. ¹Mayo Clinic, USA, ²University of California, USA

Hdacs epigenetically regulate cellular processes by modifying chromatin and influencing gene expression. Conditional deletion of Hdac3 in osterix-expressing osteo-chondroprogenitor cells causes severe osteopenia and runting because osteoblast numbers are reduced and growth plate chondrocyte maturation is disrupted. Hdac3-deficient chondrocytes enter hypertrophy sooner, but are smaller and secrete less extracellular matrix due to underphosphorylation and decreased activation of the central intracellular kinase, Akt, a crucial factor governing chondrocyte commitment, proliferation and maturation to hypertrophy. Hdac inhibitors also attenuate Akt activation by both Tgf β and Igf1, two modulators of chondrocyte differentiation. In this study we explored the mechanisms by which Hdac3 alters Akt activity in chondrocytes. Using a candidate approach, we surveyed phosphatases that were modulated by both Hdac inhibitors and Hdac3 insufficiency. The Akt phosphatase Phlpp1, but not Phlpp2 or Pp1, was expressed at higher levels both ex vivo and in vivo in Hdac-inhibited cells. Moreover, Phlpp1 expression was elevated in pre-hypertrophic chondrocytes within growth plates of Hdac3 CKO mice. Tgf β induced expression of Phlpp1, but not Phlpp2. In chromatin immunoprecipitation assays, Hdac3 associated with the Phlpp1 promoter near Smad binding elements and was released upon Tgf β exposure. Thus, Hdac3 epigenetically regulates chondrocyte hypertrophy and matrix content by directly repressing Phlpp1 levels and facilitating Akt activation. To determine the function of Phlpp1 in controlling Hdac3-mediated Akt activation, we utilized a truncated Phlpp1 protein unable to bind Akt. Truncated Phlpp1 expression rescued the effects of Hdac inhibition on Akt activation in chondrocytes. Phlpp1^{-/-} mice have shorter snout-to-tail body lengths as well as decreased femur and tibia lengths. Both the articular surface and the growth plate of Phlpp1^{-/-} mice are hypercellular. Furthermore, bone mineral density and trabecular number are decreased in Phlpp1^{-/-} mice. Together these data identify Phlpp1 as a crucial factor in skeletal development and demonstrate that Hdac3 regulates chondrocyte maturation by epigenetically repressing Phlpp1 expression.

Disclosures: Elizabeth Bradley, None.

1153

Epidermal Growth Factor Receptor Regulates Cartilage Matrix Remodeling during Endochondral Ossification through β -catenin-dependent and -independent Pathways. Xianrong Zhang¹, Ji Zhu¹, Valerie A Siclari², Motomi Enomoto-Iwamoto³, Frank Beier⁴, Ling Qin^{*2}. ¹University of Pennsylvania, School of Medicine, USA, ²University of Pennsylvania, USA, ³Children Hospital of Philadelphia, USA, ⁴University of Western Ontario, Canada

Loss of epidermal growth factor receptor (EGFR) activity in mice alters growth plate development, impairs endochondral ossification, and retards growth. However, the detailed mechanism by which EGFR regulates endochondral bone formation is unknown. We constructed a pharmacological rat model and a transgenic mouse model to study such mechanisms. Administration of an EGFR inhibitor, gefitinib, into 1-month-old rats for 7 days produced profound defects in long bone growth plate characterized by thickening of epiphyseal growth plate (2.0-fold), massive accumulation of hypertrophic chondrocytes (2.3-fold), and decreased in mineralization of hypertrophic cartilage matrix. We observed similar growth plate phenotypes along with a delayed formation of secondary ossification center (SOC) in 1-week old mice with chondrocyte-specific inactivation of EGFR (collagen2a1 promoter driven-Cre Egfr^{W⁵¹/lox}). Immunostaining for Sox9, p57 and Ki67, BrdU labeling and mRNA expression profile of chondrocyte differentiation markers revealed that EGFR inactivation did not alter growth plate chondrocyte proliferation, and differentiation, and matrix synthesis. Vascular invasion into growth plate cartilage was not impaired. However, we observed a 50% decrease in the number of TRAP-positive osteoclasts at the chondro-osseous junction, owing to decreased RANKL expression in the growth plate. Moreover, EGFR inactivation strongly inhibited the expression of matrix metalloproteinases (MMP9 and 13), increased the amount of collagen fibrils, and decreased degraded extracellular matrix products in the growth plate. At the SOC of Col-CreEgfr^{W⁵¹/lox} mice, we observed similar decreases in the chondrogenic expression of MMPs and RANKL, the number of TRAP-positive cells, and matrix mineralization, suggesting that cartilage matrix degradation was also suppressed in this region. In vitro, the EGFR ligand transforming growth factor α (TGF- α) strongly stimulated MMP9 and RANKL expression in primary chondrocytes, which was partially abolished by Wnt/ β -catenin signaling inhibitors, DKK1 and IWR-1-endo. Further study showed that EGFR signaling phosphorylated LRP6 and activated nuclear translocation of β -catenin. Since Wnt/ β -catenin signaling itself elevates these gene expression, we conclude that EGFR signaling cross-talks with Wnt/ β -catenin pathway in regulation of MMP9 and RANKL. In contrast, EGFR-induced MMP13 expression is independent of Wnt/ β -catenin pathway. Together, we demonstrated that EGFR signaling regulates matrix degradation directly by stimulating chondrocytes to express MMPs and indirectly by activating chondrogenic RANKL expression to support osteoclastogenesis. EGFR signaling plays an essential role in the remodeling

of cartilage extracellular matrix into bone through Wnt/ β -catenin-dependent and -independent pathways during endochondral ossification.

Disclosures: Ling Qin, None.

1154

Sprouty2 Regulates Skeletogenesis. Adriane Joo*¹, Roger Long², Zhiqiang Cheng¹, Wenhan Chang³, Ophir Klein¹. ¹University of California, San Francisco, USA, ²University of California, Davis, USA, ³Endocrine Unit, VA Medical Center, University of California, San Francisco, USA

Skeletal development is regulated by the cooperative activity of signaling molecules produced locally by cartilage and bone cells as well as by systemic factors. Receptor tyrosine kinase (RTK) superfamily members, including Fibroblast Growth Factor and Insulin-like Growth Factor, play critical roles in the proliferation, survival, and differentiation of chondrocytes, osteoblasts, osteoclasts, and other cells in the bone during embryonic development and postnatal bone remodeling. Recently, several molecules that inhibit RTK signaling pathways have been identified, including members of the Sprouty (Spry) family (*Spry1*, *Spry2*, *Spry3*, and *Spry4*). Spry proteins function intracellularly to antagonize RTK signaling through diverse mechanisms. By *in situ* hybridization and quantitative PCR, we found that *Spry1*, *Spry2*, and *Spry4*, but not *Spry3*, are expressed by proliferating chondrocytes, pre- and hypertrophic chondrocytes, osteoblasts, and osteocytes in adult long bones. To determine the role of Sprouty genes in skeletal development *in vivo*, we analyzed the skeletal phenotypes of Sprouty knockout (KO) mice by micro-computed tomography (μ CT). μ CT analysis showed that both the trabecular and cortical bones of *Spry2* KO mice are smaller and thinner than those of their wild-type (WT) littermates at 4 weeks, 6 weeks, and 12 weeks of age, while *Spry1* and *Spry4* KO mice showed minor to no change. In addition, static and dynamic histomorphometric analysis of global *Spry2* KO showed that both osteoblast and osteoclast activities are reduced in *Spry2* KO mice. To further investigate the function of *Spry2* in skeletogenesis, we generated (1) cartilage- or (2) bone-specific KOs of *Spry2* by crossing floxed *Spry2* mice with transgenic mice expressing Cre under (1) type II collagen- α 1 or (2) 2.3 kb fragment of the collagen I- α 1 promoters, respectively. μ CT data showed that both cartilage- and bone-specific *Spry2* KO mice had smaller and thinner trabecular bone, although their skeletal abnormalities were milder than those of the global *Spry2* KO mice. Furthermore, histological and immunohistochemical analysis of E16.5 and E18.5 limbs showed that *Spry2* mutant have smaller pre- and hypertrophic zones and increased chondrocyte proliferation compared to that of WT littermates. In both embryonic and adult bones, we detected altered expression of several molecular markers. Thus, *Spry2* regulates bone development by modulating both chondrogenesis and osteoblastogenesis.

Disclosures: Adriane Joo, None.

1155

Mice Lacking Pten in Osteoblasts Have Improved Intramembranous and Late Endochondral Fracture Healing. Travis Burgers*¹, Martin Hoffmann², Michael Morris³, Martin Alvarado⁴, Debra Sietsema⁵, Jim Mason¹, Clifford Jones⁶, Bart Williams⁷. ¹Van Andel Institute, USA, ²Grand Rapids Medical Education Partners, USA, ³Michigan State University, USA, ⁴Creston High School, USA, ⁵Orthopaedic Associates of Michigan; Michigan State University, USA, ⁶Orthopaedic Associates of Michigan, USA, ⁷Van Andel Research Institute, USA

The failure of an osseous fracture to heal (development of a non-union) is a common and debilitating clinical problem. It is estimated that 10–20% of fractures do not heal in a timely manner and progress towards non-union (Court-Brown and McQueen, 2008, and Parker et al. 2007). Mice lacking Pten in osteoblasts (*OC-cre^{tg}+*; *Pten^{fl/fl}*) have dramatic and progressive increases in bone volume and density throughout life (Figure 1; Liu et al. 2007). Since fracture healing is a recapitulation of bone development, we hypothesized that Pten mutants (*OC-cre^{tg}+*; *Pten^{fl/fl}*) would have improved fracture healing.

Mid-diaphyseal femoral fractures induced in wild-type mice and in mice lacking Pten in osteoblasts (Pten mutants) using an established technique (Bonnarens and Einhorn, 1984). They were studied via radiographs, micro-computed tomography (μ CT) scans, biomechanical testing, Western blotting and histological analysis.

Pten mutant mice had significantly stiffer and stronger intact bones relative to controls in all cohorts (Figure 2A). They also had significantly stiffer healing bones at day 28 post-fracture (PF) and significantly stronger healing bones at days 14, 21, and 28 PF (Figure 2B). Radiographs and μ CT scans showed more mineralization in the Pten mutants at the proximal and distal ends of the callus (Figure 3). Pten mutants also had larger and more mineralized calluses. The cellular composition of the callus did not differ between groups during healing, but there was less Pten and more p-Akt, indicating activated Akt signaling, in the fracture callus from the mutants late in healing (Figure 2C). Pten mutants had improved intramembranous bone formation during healing originating from the periosteum. They also had improved endochondral bone formation later in the healing process, after mature osteoblasts are present in the callus.

Our results indicate that the inhibition of Pten can improve fracture healing and that the local or short-term use of commercially available Pten-inhibiting agents may have clinical application for enhancing fracture healing.

References

Bonnarens and Einhorn. J Orthop Res. 1984;2(1):97-101.
Court-Brown and McQueen. J Trauma. 2008;64(6):1517-21.
Liu X et al. Proc Natl Acad Sci U S A. 2007;104(7):2259-64.
Parker et al. Clin Orthop Relat Res. 2007;458:175-9.

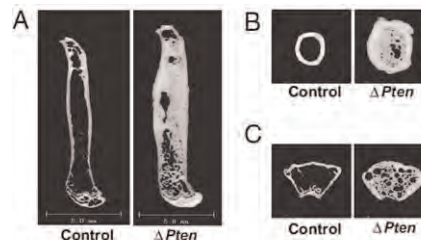


Figure 1. Osteoblast-specific deletion of Pten increases bone volume. MicroCT analysis was performed on the femur of control and Pten mutant mice at 12 months of age: A) sagittal view, B) transverse view at midshaft, C) transverse view at distal femur (Liu et al. 2007).

Figure 1

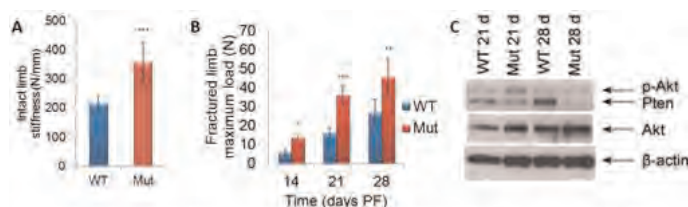


Figure 2: Pten mutants (Mut) have higher stiffness and strength in intact (A) and healing (B) femurs (* $p < 0.05$, ** $p < 0.01$, *** $p < 0.001$ WT to Mut at the time point) than the wild-type (WT) animals at each time point post-fracture (PF). Mutant animals had less Pten at days 21 and 28 PF and more p-Akt at day 21 PF (C).

Figure 2

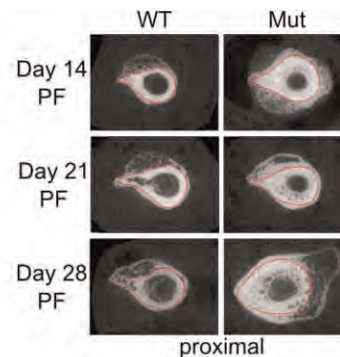


Figure 3: Representative μ CT cross sections of bone formation from the periosteum, an average of 2.7 mm proximal to the fracture. The red line indicates the transition between the existing and newly formed bone. The Pten mutants had more mineralization, especially around the existing bone, at each time point.

Figure 3

Disclosures: Travis Burgers, None.

1156

Potential Role of Periosteal Macrophages in Mediating Cathepsin K inhibition-Induced Cortical Bone Formation. Weizhong Chang¹, Shuo Liu¹, Hui Xie*¹, Maureen Pickarski², Le Thi Duong³, Xu Cao¹. ¹Johns Hopkins University, USA, ²Merck & Co., Inc., USA, ³Merck Research Laboratories, USA

Bone is composed of cortical and trabecular bone and cortical bones predominantly support the mechanical functions of bones. During growth, periosteal

cortical bone formation coordinated with endocortical bone resorption results in expansion in diameters of the long bones. Because cortical geometry is a major determining factor of bone strength, stimulation of periosteal cortical bone formation in the mature skeleton would be an effective strategy to prevent bone fracture due to bone loss disorders. Current antiresorptives, including bisphosphonates and anti-RANKL antibody have been focused on trabecular bone remodeling. Cathepsin K (CatK) inhibitor was found to stimulate cortical bone formation in various animal models and the current study is focused on the molecular mechanism of the inhibition of CatK in stimulating cortical bone formation. CatK is a major enzyme expressed by osteoclasts responsible for degradation of bone matrix during bone resorption process. In CatK KO mice or WT mice treated with a CatK inhibitor, L-006235, the number of TRAP-positive macrophages on the surface of the periosteum was increased. Nestin-positive mesenchymal stem cells (MSCs) and osteoblastic lineage cells were also increased in the periosteum of these mice. We also demonstrated that these TRAP-positive macrophages are in proximity to the Nestin-positive MSCs in the periosteal bone modeling area. Next, we prepared conditioned media with macrophages treated with a CatK inhibitor vs. vehicle. The conditioned media were then used to examine the effect on the migration of MSCs. Our results demonstrated that conditioned media from macrophages treated with L-006235 induced migration of MSCs more effectively relative to control conditioned media. The migration of MSCs was only partially inhibited by a TGF-beta1 neutralization antibody, indicating that other factor(s) are involved in the recruitment of MSCs in the periosteum in addition to TGF-beta1. Taken together, our results suggest that periosteal macrophages act as signaling cells to recruit MSCs and enhance bone formation in the periosteum.

Disclosures: Hui Xie, None.

This study received funding from: Merck & Co., Inc.

1157

Contribution of Bone Resorption to the Control of Glucose Metabolism. Mathieu Ferron*, Gerard Karsenty. Columbia University, USA

Osteocalcin is a hormone produced by osteoblasts that regulates energy metabolism by enhancing insulin secretion, insulin sensitivity and energy expenditure. While osteocalcin can exist in two forms, γ -carboxylated (GLA) and undercarboxylated (GLU), only the undercarboxylated form of this molecule appears to function as a hormone. Recent studies proposed that the osteoclast, the bone-resorbing cell, is responsible of decarboxylating and activating the osteocalcin trapped in the extracellular matrix (ECM) through the low pH generated during bone resorption. Yet direct evidence implicating osteoclasts in the maintenance of energy metabolism is still lacking. To address this question we analyzed mutant mouse strains harboring either an increase or a decrease in osteoclasts number. Osteoprotegerin (*Opg*) deficient mice are characterized by an increase in the number of functional osteoclasts. *Opg*^{-/-} mice were hypoglycemic at 1 and 3 month of age and significantly more glucose tolerant than wild type animals. Moreover, *Opg*-deficient mice were more sensitive to insulin as determined by insulin tolerance test (ITT) and had reduced fat mass. Analysis of osteocalcin carboxylation status in serum using specific ELISA assays revealed that the levels of undercarboxylated GLU13 osteocalcin was increased more than ten times in *Opg*^{-/-} mice compared to wild type. Next, to analyze the consequences on energy metabolism of a lack of osteoclasts we generated a model of conditional osteoclast-ablation through the use of the diphtheria toxin (DTA). Specifically we crossed mice that harbor a flox-stop-flox-DTA gene cassette under the control of the *Rosa26* promoter (*floxDTA*) with *Ctsk-Cre* mice, in which the Cre recombinase is expressed in mature osteoclasts only to generate osteoclast-poor (*AOsc*). As expected *AOsc* mice were severely osteopetrotic due to a decrease in osteoclasts number. These mutant mice were also characterized by a decrease in glucose tolerance, a decline in serum insulin levels and a ~50% reduction in β -cell mass. Finally, the serum levels of undercarboxylated GLU13 osteocalcin were decreased more than two fold in *AOsc* compared to control mice. Taken together, these results support the notion that osteoclasts play an important role in the control of glucose metabolism. This function occurs, at least in part, through the regulation of osteocalcin carboxylation status.

Disclosures: Mathieu Ferron, None.

1158

Targeted Expression of Catalase to Mitochondria in Cells of the Macrophage/Osteoclast Lineage Inhibits Osteoclastogenesis and Increases Bone Mass. Shoshana Bartell*, Li Han¹, Aaron Warren¹, Julie Crawford¹, Peter Rabinovitch², Stavros Manolagas¹, Maria Jose Almeida¹. ¹Central Arkansas VA Healthcare System, Univ of Arkansas for Medical Sciences, USA, ²University of Washington, USA

Mitochondrial biogenesis and reactive oxygen species generation are critical for RANKL-induced osteoclast formation, activation, and survival. Moreover, an increase in the generation of ROS has been causally linked with increased resorption in estrogen deficiency and inflammatory arthritis. Catalase is a critical enzyme for the detoxification of H₂O₂ - the most abundant of the reactive oxygen species. Based on this evidence, we have examined the role of catalase in osteoclasts. To do this, we first measured catalase levels and activity in bone marrow-derived macrophage cultures. In preparations from three different mouse strains, catalase gene expression and enzymatic activity were dramatically and consistently down-regulated during the

transition of macrophages to mature osteoclasts in the presence of M-CSF and RANKL. Encouraged by this finding, we next generated transgenic mice expressing catalase targeted to the mitochondria in cells of the monocyte/macrophage lineage, by crossing MitoCat-flox stop mice (provided by P. Rabinovitch, University of Washington) with LysM-Cre mice (MitoCat;LysM-Cre). Osteoclast cultures generated from the bone marrow of MitoCat;LysM-Cre mice exhibited 4-fold higher catalase activity than osteoclasts from control LysM-Cre mice. Bone marrow cultures from MitoCat;LysM-Cre mice exhibited a significant decrease in the number of osteoclast progenitors and in mature osteoclast formation. Moreover, the stimulation of RANKL-induced osteoclastogenesis by H₂O₂, seen in cells from control mice, was completely abrogated in cells from MitoCat;LysM-Cre mice. More important, MitoCat;LysM-Cre mice exhibited an increase in cancellous bone volume at 3 months of age as determined by micro-CT, in both the vertebrae and the femurs. These changes were associated with increased trabecular number and decreased trabecular separation. In addition, MitoCat;LysM-Cre mice had increased femoral cortical thickness. These results demonstrate that up-regulation of H₂O₂ production contributes to osteoclast generation and bone resorption. Thus, H₂O₂ production represents a rationale and appealing drug target for diseases associated with increased bone resorption, especially because targeted expression of catalase to mitochondria in mice also prevents the age-associated energy imbalance, muscle insulin resistance, and hypertensive cardiomyopathy (Cell Metab. 12, 668, 2010; Circ Res 108, 837, 2011).

Disclosures: Shoshana Bartell, None.

1159

Deletion of the Cell-adhesion Mediator PODXL in Early Osteoclast Precursors Impairs Bone Resorption and Causes a High Bone Mass Phenotype through Reduced Activation of Rac1. Megan Weivoda*, Muzaffer Cicek¹, Ashok Kumar², Larry Pederson³, Ming Ruan³, Michael Hughes⁴, Christine Hachfeld³, Rachel Davey⁵, Kelly McNagny⁶, Merry Jo Oursler¹. ¹Mayo Clinic, USA, ²Mayo Clinic College of Medicine, USA, ³Endocrine Research Unit, Mayo Clinic, USA, ⁴University of British Columbia, Canada, ⁵University of Melbourne, Australia, ⁶Biomedical Research Centre, University of British Columbia, Canada

Podocalyxin (PODXL) is a mediator of cell adhesion that is expressed by hematopoietic stem cells. We have observed that PODXL expression decreases during osteoclast differentiation *in vitro*. Because PODXL functions as an anti-adhesive in tumor progression, we hypothesized that targeted deletion of PODXL in mice would lead to increased osteoclast fusion and osteopenia. Floxed PODXL mice were crossed with Vav-Cre or Cathepsin K (Ctsk)-Cre mice to obtain mice with PODXL deleted in early hematopoietic cells (Vav/PODXL^{del}) or late osteoclast precursors (Ctsk/PODXL^{del}). Femurs were assessed by pQCT, μ CT, and histomorphometry. Bone marrow cells were examined for signaling responses, differentiation, and resorptive activity. Vav/PODXL^{del} bones displayed increased osteoclast numbers. Surprisingly, bone mineral density, bone volume, and bone formation indices were all increased. Vav/PODXL^{del} bone marrow cultured with RANKL and M-CSF produced increased osteoclast numbers *in vitro*. Although these osteoclasts adhered to bone surfaces, they did not form resorption pits. Unlike Vav/PODXL^{del} mice, Ctsk/PODXL^{del} bones did not exhibit significant changes in bone density. Ctsk/PODXL^{del} bone marrow cultures formed more and larger osteoclasts than Cre control cells, consistent with an anti-adhesive PODXL function. In contrast to Vav/PODXL^{del} osteoclasts, mature osteoclasts formed from Ctsk/PODXL^{del} marrow resorbed bone normally. These data show that late osteoclast lineage deletion of PODXL does not interfere with osteoclast function. M-CSF signaling was assessed in Vav/PODXL^{del}, Ctsk/PODXL^{del}, and control precursors. M-CSF induced ERK1/2 phosphorylation was markedly reduced in the Vav/PODXL^{del} precursors. There was also decreased Rac1 activity in Vav/PODXL^{del} osteoclasts. Constitutively active Rac1 overexpression restored bone resorption of Vav/PODXL^{del} osteoclasts *in vitro*. We conclude that PODXL is necessary for early osteoclast precursor M-CSF/ERK and Rac1 signaling and lack of PODXL in early osteoclast precursors prevents the development of functional osteoclasts due to reduced Rac1 activation. We therefore have found that mature osteoclasts that lack PODXL throughout differentiation, although able to bind to bone, cannot resorb bone whereas mature osteoclasts that lose PODXL just prior to maturity are fully functional. Resolution of these differences may provide avenues to pursue to suppress bone resorption while preserving the anabolic influences of osteoclasts.

Disclosures: Megan Weivoda, None.

1160

Ablation of Connexin 43 in Osteoclasts Leads to Decreased *in vivo* osteoclastogenesis. Mitchell Sternlieb, Emmanuel Paul, Henry Donahue, Yue Zhang*. The Pennsylvania State University College of Medicine, USA

Previous *in vitro* studies suggest that gap junction (GJ) deficiency affects osteoclastic cell formation and activity. Here, we examined the hypothesis that decreasing levels of osteoclastic connexin 43 (Cx43) the predominate Cx in bone *in vivo*, results in decreased osteoclastic bone resorption.

Mice expressing Cre recombinase under the control of the human cathepsin K promoter (ctsk-Cre; Cx43^{fl/+}) were bred with mice in which the Cx43 gene is flanked by two loxP sites (Cx43^{flx/flx}) to generate OC-Cre; Cx43^{flx/flx} (conditional Cx43

deficient) and $Cx43^{flx/flx}$ (wild type) littermate mice. Our data showed that deletion of $Cx43$ occurs during the pre-osteoclastic period. Furthermore, osteoclasts derived from osteoclast-specific $Cx43$ deficient mouse nonadhesive marrow cells (NAMCs) displayed dramatically reduced gap junctional intercellular communication (GJIC) relative to cells derived from wild type mouse NAMCs, suggesting that we had indeed reduced $Cx43$ expression in osteoclastic cells. Distal femurs from 8-week-old osteoclast specific $Cx43$ deficient mice showed a nearly significant increase in trabecular number (14.8%, $p=0.05$) and bone volume/total volume (9.2%, $p=0.05$) and a significantly reduced trabecular bone spacing (22.1%, $p<0.05$) relative to wild type mice. Femoral mid-diaphyses from osteoclast-specific $Cx43$ deficient mice displayed increased cortical bone thickness (9.1%, $p<0.05$) and reduced endosteal volume (7.9%, $p<0.05$) (Figure 1). TRAP staining revealed that the number of osteoclastic cells induced from $Cx43$ deficient NAMCs was decreased relative to those induced from wild type NAMCs. Histological examination also revealed that distal femurs from osteoclast specific $Cx43$ deficient mice had fewer osteoclasts than did femurs from wild type mice. Additionally, NFATc1 protein levels in osteoclasts from $Cx43$ deficient mice were significantly decreased, suggesting that $Cx43$ and GJIC regulate osteoclastogenesis via NFATc1.

Our data, derived using a genetic approach, reveal for the first time that $Cx43$ contributes to osteoclastogenesis both *in vitro* and *in vivo*. These results, combined with our previous studies with osteoblast/osteocyte specific $Cx43$ deficient mice, suggest that $Cx43$ mediated GJIC is critical for regulation of both bone formation and resorption *in vivo*. Furthermore, $Cx43$ -mediated GJIC in osteoclastic cells may be a novel therapeutic target for bone disease.

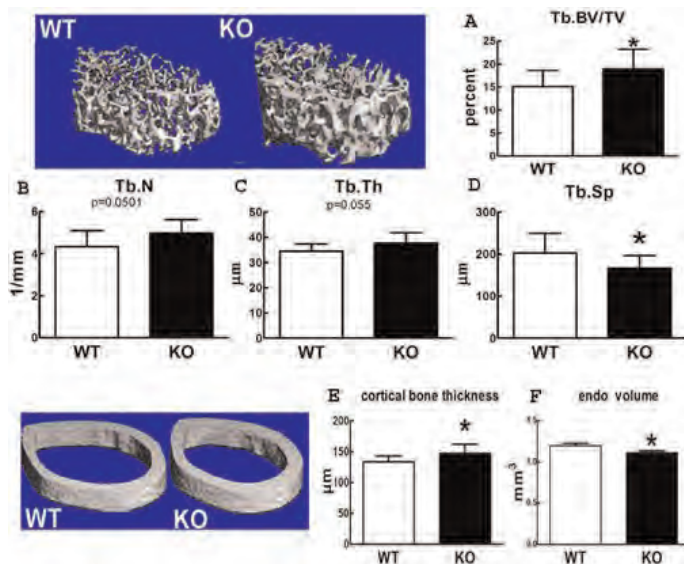


Figure 1. MicroCT reveals that osteoclast specific distal femurs from $Cx43$ deficient mice (KO) have i

Disclosures: Yue Zhang, None.

1161

The Role of Osteoclasts in Neurofibromatosis Type 1 Pseudarthrosis. Steven Rhodes*, Keshav Menon, Yongzheng He, Karl Staser, Shi Chen, Khalid Mohammad, Theresa Guise, Feng-Chun Yang. Indiana University, USA

Skeletal manifestations cumulatively affect ~70% of neurofibromatosis type 1 (NF1) patients. Tibial pseudarthrosis, the chronic non-union of a spontaneous tibial fracture, is a debilitating skeletal malady affecting children with NF1 early in life. These non-healing fractures typically respond poorly to surgical intervention and often require amputation.

Previous studies have implicated $Nf1$ deficient osteoblasts (OBLs) in the recalcitrant bone repair process. Although osteoclast (OCL) bioactivity increases during fracture repair, the role of OCLs in the pathogenesis of NF1 pseudarthrosis remains unknown. Studies have confirmed that OCLs from NF1 patients and mice exhibit multiple gain-in-functions. We recently established that transplantation of $Nf1^{flx}$ bone marrow (BM) cells to $Nf1^{flx};Col2.3Cre$ mice [carrying $Nf1^{flx}$ OBLs and wild-type (WT) background] can induce osteoporosis and severe non-union fracture healing as compared to transplantation of WT BM cells, suggesting that in concert with $Nf1^{flx}$ OBLs, $Nf1^{flx}$ BM cells play a critical role in pathogenesis of these osseous defects.

Based on these data, we hypothesized that $Nf1^{flx}$ OCLs are the key hematopoietic cell lineage contributing to the osteoporosis and impaired fracture healing in mice harboring $Nf1^{flx}$ OBLs and $Nf1^{flx}$ BM cells. To test this hypothesis, we generated $Nf1^{flx};LysMCre$ mice permitting conditional inactivation of a single $Nf1$ allele in OCLs and their progenitors. Here we report that $Nf1^{flx};LysMCre$ mice exhibit increased frequency of OCL progenitors (CFU-M), enhanced osteoclastogenesis, and accelerated bone resorption following ovariectomy induced resorptive stress. To examine the role of $Nf1^{flx}$ OCLs on fracture healing *in vivo*, lethally irradiated $Nf1^{flx};Col2.3Cre$ mice were transplanted with BM cells from WT or $Nf1^{flx};LysMCre$ mice. A fixed

tibial fracture was subsequently induced after stable reconstitution. Compared to WT BM cells, $Nf1^{flx};LysMCre$ BM cell reconstituted $Nf1^{flx};Col2.3Cre$ mice exhibited significantly reduced callus bone volume fraction (BV/TV) as determined by microcomputed tomography, revealing a substantial deficit in fracture repair. Collectively, these results suggest that in the context of $Nf1$ deficient OBLs, $Nf1^{flx}$ OCLs are the culprit hematopoietic cell lineage responsible for the pathogenesis of NF1 non-union fracture. As such, therapy targeting both the osteoclast and osteoblast lineages may be necessary to maximally augment bone healing in NF1 pseudarthrosis.

Disclosures: Steven Rhodes, None.

1162

Talin1 and Rap1 are Critical for Osteoclast Function. Wei Zou*¹, Tingting Zhu², Takashi Izawa³, Jean Chappel⁴, Susan Monkley⁵, David Critchley⁵, Brian G Petrich⁶, Alexei Morozov⁷, Mark H Ginsberg⁶, Steven Teitelbaum¹. ¹Washington University in St. Louis School of Medicine, USA, ²Washington University in St. Louis-School of Medicine, USA, ³Washington University in St. Louis, USA, ⁴Department of pathology, Washington University School of Medicine, USA, ⁵Department of Biochemistry, University of Leicester, United Kingdom, ⁶Department of Medicine, University of California, USA, ⁷Behavioral Genetics Unit, NIMH, USA

The interaction of talin1 with β -subunit cytoplasmic domains is an essential step in integrin activation. To determine talin1's role in osteoclasts, we mated $TLN1^{flx/flx}$ mice with those expressing cathepsin K-Cre (CtsK- $TLN1$) to delete the gene specifically in mature osteoclasts, or with lysozyme M-Cre (LysM- $TLN1$) mice to delete $TLN1$ in all osteoclast lineage cells. Absence of $TLN1$ impairs macrophage colony-stimulating factor (M-CSF) inside-out integrin activation and consequent cytoskeleton organization in mature osteoclasts. Talin1-deficient precursors normally express osteoclast differentiation markers when exposed to M-CSF and receptor activator of nuclear factor κ B ligand (RANKL) but attach to substrate and migrate poorly, arresting their development into mature resorptive cells. In keeping with inhibited resorptive function, CtsK- $TLN1$ mice exhibit an ~5 fold increase in bone mass. Osteoclast-specific deletion of Rap1, which in conjunction with RIAM promotes talin/ β integrin recognition, similarly yields osteopetrotic mice, which mirror CtsK- $TLN1$ animals. In keeping with osteoclast dysfunction, mice in whom talin is deleted late in the course of osteoclastogenesis are substantially protected from ovariectomy-induced bone loss and the periarticular osteolysis attending inflammatory arthritis. Thus, talin1 and Rap1 are critical for osteoclast function and their inhibition, in mature osteoclasts, may retard pathological bone loss.

Disclosures: Wei Zou, None.

1163

Lean Body Mass Mediates Associations between Physical Activity, Sedentary Behavior, and Bone Microstructure in Post-menarcheal Girls. Leigh Gabel*¹, Heather McKay¹, Lindsay Nettlefold², Douglas Race², Heather Macdonald¹. ¹University of British Columbia, Canada, ²University of British Columbia, Canada

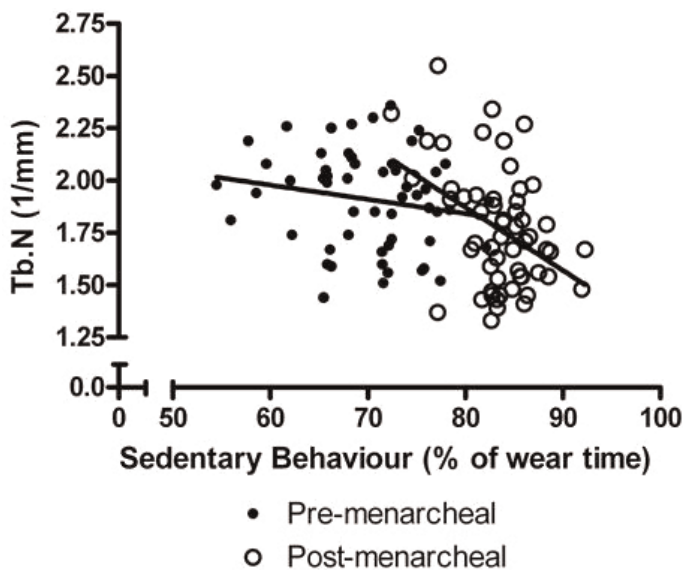
Purpose: Physical activity (PA) enhances bone accrual during growth; however, we know little about how PA and sedentary behavior (SED) influence bone microstructure during adolescence. We aimed to: 1) determine the independent contributions of moderate-to-vigorous PA (MVPA) and SED to bone microstructure and strength in pre- and post-menarcheal girls and, 2) to evaluate the role of lean mass in mediating these associations.

Methods: We used high-resolution pQCT (HR-pQCT, Scanco Medical) to measure bone microstructure and estimate bone strength at the distal tibia (8% site) in 55 pre-menarcheal (10.5 y \pm 0.6) and 56 post-menarcheal (17.7 y \pm 2.5) girls who were participants in the UBC Healthy Bones III study. Bone outcomes included total bone mineral density (Tt.BMD), total area (Tt.Ar), trabecular bone volume ratio (BV/TV), trabecular thickness (Tb.Th) and number (Tb.N), and cortical density (Ct.BMD), porosity (Ct.Po) and thickness (Ct.Th). We applied finite element (FE) analysis to HR-pQCT scans to estimate bone strength (ultimate stress). We used Actigraph GT1M accelerometers to measure MVPA and SED using 15-sec epochs and age-specific cutpoints. We included data for participants who wore the accelerometer for 3 days and at least 10 hr/day. We fit separate multivariable regression models for pre-menarcheal and post-menarcheal girls, and adjusted for age (post-menarcheal only), maturity (pre-menarcheal only), tibia length, and lean body mass.

Results: Pre-menarcheal girls accumulated significantly more MVPA and less SED than post-menarcheal girls ($p<0.001$). In pre-menarcheal girls, MVPA tended to be a positive predictor of Ct.Po and Ct.Th, accounting for 4-5% of the variance ($p=0.10$ and 0.07, respectively). In post-menarcheal girls, SED was a negative predictor of Tb.N and explained 8% of the variance ($p=0.013$). When lean mass was replaced by weight in the model, MVPA was a positive predictor of Tb.N, accounting for 5% of the variance ($p=0.048$), and SED was a negative predictor of Tb.N, accounting for 10% of the variance ($p=0.005$).

Discussion: Our findings illustrate how the skeleton responds negatively to sedentary behaviours, especially during the key period of childhood and adolescent growth. Lean body mass mediates the relation between bone microstructure and SED

and MVPA in post-menarcheal girls. The apparent maturity-specific influence of sedentary behaviour on bone microstructure is important and warrants further investigation.



Relationship between trabecular number and sedentary behaviour in pre- and post-menarcheal girls.

Disclosures: Leigh Gabel, None.

1164

Femoral Neck Cortical Thickness Declines in the Elderly Three-fold Faster Superiorly than Inferiorly: The AGES-REYKJAVIK Longitudinal Study.

Fjola Johannesdottir¹, Thor Aspelund², Jonathan Reeve³, Kenneth Poole³, Sigurdur Sigurdsson², Tamara Harris⁴, Vilundur Gudnason⁵, Gunnar Sigurdsson⁶. ¹Faculty of Engineering, University of Iceland, Iceland, ²Icelandic Heart Association, Iceland, ³University of Cambridge, United Kingdom, ⁴Intramural Research Program, National Institute on Aging, USA, ⁵Icelandic Heart Association Research Institute, Iceland, ⁶Landspítali, Iceland

Background: Marked thinning of the mid-femoral neck cortex with advancing age has been described in cross-sectional studies, both ex-vivo and in-vivo. We previously found that superior cortical thinning of the mid-femoral neck was important in determining resistance to femoral neck fracture. Therefore, we aimed to study changes in regional cortical thickness with increasing age, by using serial QCT measurements in older men and women.

Design, Setting and Participants: This is a longitudinal study of 100 men and 300 women from the Age Gene/Environment Susceptibility-Reykjavik Study (AGES-REYKJAVIK), a large prospective population-based cohort of Icelandic individuals aged 66 years and older. Segmental QCT (slice thickness 1mm) analysis of the mid-femoral neck was applied to estimate cortical thickness (CtTh) in the superior and inferior surfaces of the mid neck, using QCTPro-BIT2 (Mindways software). Participants had two measurements of cortical thickness over a median follow-up of 5.1 yr. Femoral neck (FN) areal bone density (aBMD) (DXA-like) was also measured. Relative change in cortical thickness and FN aBMD during follow-up was estimated from mixed effects regression models.

Results: The relative loss in CtTh was substantial and significantly greater in the superior surface compared to the inferior surface in both genders (see Table). Women lost relatively more cortex than men in both surfaces. The difference in FN aBMD loss was not significantly different between genders.

Conclusion: The relative age-related changes were about threefold greater in the superior surface than in the inferior surface of the mid femoral neck. Older women lost cortical thickness more rapidly than men, especially in the superior femoral neck and this is only weakly reflected in the DXA-like results. Since fractures may initiate superiorly, this increased rate of loss may contribute materially to the greater risk of femoral neck fracture in women than men.

This study was funded by NIH contract N01-AG-1-2100.

| | Age at follow-up Mean (SD) | Superior CtTh Mean % (95%CI) | Inferior CtTh Mean % (95%CI) | FN aBMD Mean % (95%CI) |
|-------|-------------------------------|---------------------------------|---------------------------------|---------------------------|
| Women | 79.5 (5.2) | -15.6 (-13.5 to -17.6) | -4.5 (-3.8 to -5.2) | -6.2 (-4.9 to -7.5) |
| Men | 78.9 (4.4) | -7.9 (-5.7 to -10.1) | -2.5 (-1.4 to -3.5) | -4.1 (-2.3 to -6.0) |

Table: Longitudinal percentage mean changes in CtTh and FN aBMD during follow-up (5.1 yrs)

Disclosures: Fjola Johannesdottir, None.

1165

Similar Effects on Cancellous Bone Matrix Mineralization by Alendronate and Two Different Doses of Odanacatib in Rhesus Monkeys. Paul Roschger¹, Phaedra Messmer¹, Nadja Fratzl-Zelman¹, Barbara M. Misof¹, Klaus Klaushofer¹, Maureen Pickarski², Le T. Duong². ¹Ludwig Boltzmann Institute of Osteology at the Hanusch Hospital of WGKK & AUA Trauma Centre Meidling, 1st Medical Department, Hanusch Hospital, Vienna, Austria, ²Bone Biology, Merck Research Laboratories, West Point, USA

Odanacatib (ODN) is a potent and selective inhibitor of cathepsin K and is currently in clinical development for the treatment of postmenopausal osteoporosis. In the present study we aimed to explore the effect of ODN treatment on the bone mineralization density distribution (BMDD) in rhesus monkeys. Ovariectomized animals treated with either vehicle (VEH, n=8), Odanacatib @ 2 mg/kg/day (ODN-L, n=8), Odanacatib @ 8 to 4 mg/kg/day (ODN-H, n=8), or alendronate @ 30mg/kg/week (ALN, n=8) for 20-months were compared. Vertebrae and diaphyseal cortex of tibiae were harvested for BMDD analyses using quantitative backscattered electron imaging (qBEI). Group comparison of BMDD variables was based on ANOVA or Kruskal-Wallis tests (Tukey's or Dunn's post-hoc analysis, respectively). In vertebral cancellous bone, average calcium concentration (CaMean +6.5%, p<0.001) was increased in ODN-L while the heterogeneity of mineralization (CaWidth -22%, p<0.001) and the percentage of low mineralized areas (CaLow -36%, p<0.01) were decreased vs. VEH. Similar BMDD differences versus vehicle were also found for ODN-H and ALN. Among the treatment groups (ODN-L, ODN-H, ALN), no significant differences could be detected. In tibial osteonal bone, CaMean was higher in the ALN group (+3.4%, p<0.01), and CaLow was decreased in the ALN (-29%, p<0.01) group all compared to VEH. No other treatment effect on osteonal bone was observed. Our BMDD findings after ODN or ALN treatment in rhesus monkeys are consistent with the previously observed antiresorptive action of ALN and other agents in postmenopausal osteoporosis. The higher CaMean is in line with an increased average tissue age due to a longer period of secondary mineralization for the bone packets. Simultaneously, CaLow, is decreased as a lesser amount of new bone is formed. Further, CaWidth is reduced, which is a typical, transient response to the bone remodeling rate reduction. Our BMDD results also indicate that vertebral bone was more responsive to treatment effects than tibial cortical bone, likely due to its higher bone turnover rates at the cancellous sites before treatment. The similarity of the vertebral cancellous BMDD for both dosages of ODN indicates that the effect on matrix mineralization had leveled off. Moreover, the overall effects of ODN and ALN was similar, though their underlying mechanisms of bone turnover rate reduction are different.

Disclosures: Paul Roschger, None.

This study received funding from: Merck & Co., Inc.

1166

Alterations in Intrinsic Bone Material Properties of Sclerosteosis Patients.

Eleftherios Paschalis¹, Paul Roschger², Antoon Van Lierop³, Rutger Van Bezooijen³, Sonja Gamsjaeger⁴, Birgit Hofstetter¹, Klaus Klaushofer⁵, Socrates Papapoulos^{3*}. ¹Ludwig Boltzmann Institute for Osteology, Austria, ²L. Boltzmann Institute of Osteology, Austria, ³Leiden University Medical Center, The Netherlands, ⁴Ludwig Boltzmann Institute of Osteology, Austria, ⁵Hanusch Hospital, Austria

Sclerosteosis (SC) is a rare, autosomal recessive, bone sclerosing dysplasia characterized by generalized osteosclerosis, caused by loss-of-function mutations in the SOST gene encoding for sclerostin, a protein produced in bone by osteocytes that decreases bone formation by inhibiting the Wnt signaling pathway in osteoblasts, resulting in unrestrained bone formation. SC patients do not sustain fractures suggesting that their bone is of good quality. To test this hypothesis we examined intrinsic material properties in bone from such patients.

Chips of compact bone obtained during surgery from 4 children (SCc; age 4-16 yrs) and 2 adults (SCa; age 24 & 43) diagnosed with SC, and 4 control subjects (CTRL; age 37-71 years), were analyzed by quantitative Backscattered Electron Imaging (qBEI) and Raman spectroscopy (RS). The former technique provides information on the bone mineral density distribution (BMDD), while the latter on the mineral/matrix ratio, proteoglycan (modulators of mineralization) content, and mineral crystallinity. Data were also compared against a historical control cohort of normal children (NC; N = 54, age 2-20 years).

qBEI analysis indicated no significant differences between the CTRL and SCa subjects in any of the outcomes. On the other hand, SCc subjects had a significantly lower CaMean (weighted mean of BMDD), CaPeak (peak position of BMDD), and CaHigh (fraction of highly mineralized bone) values compared to CTRL. CaWidth (indicative of heterogeneity of mineral distribution) in SCc was significantly higher compared to CTRL subjects. SCc had lower mineral content, and higher CaWidth and CaLow compared to NC.

RS analysis indicated that SCc subjects had lower mineral/matrix ratio compared to either CTRL or SCa while there was no difference between the CTRL and SCa values. The proteoglycan content was higher in SCc compared to either SCa or CTRL. Mineral crystallinity was lower in the SCc compared to either SCa or CTRL, while the SCa itself had lower values compared to CTRL. All outcomes were similar between SCc and NC except mineral crystallinity (significantly lower in SCc).

The results of the present study suggest that human bone formed in the absence of sclerostin has decreased mineral crystallinity, and BMDD slightly shifted to lower mineralization with higher heterogeneity. These favorable bone properties in the presence of highly increased bone mass may be responsible for the increased bone strength of patients with sclerostinosis.

Disclosures: *Socrates Papapoulos, None.*

This study received funding from: EC FP7 program; TALOS:Health-F2-2008-201099.

1167

Lower Cortical Porosity and Higher Cortical Tissue Mineral Density Help to Explain Stronger Bones in Chinese versus Caucasian Women. *Stephanie Boutroy*¹, *Marcella Walker*², *Julia Udesky*¹, *Donald McMahon*³, *George Liu*⁴, *John Bilezikian*³. ¹Columbia University Medical Center, USA, ²Columbia University, USA, ³Columbia University College of Physicians & Surgeons, USA, ⁴New York Downtown Hospital, USA

Asian women have lower rates of hip and forearm fractures compared to other racial groups despite lower areal BMD (aBMD). We have demonstrated micro-architectural differences, including greater cortical thickness (Ct.Th) and Ct volumetric BMD (Ct.vBMD), in Chinese-American (CH) versus Caucasian (CA) women. It is not known whether greater Ct.vBMD in CH women is due to greater tissue mineral density (TMD) or reduced cortical porosity (Ct.Po), both of which are being increasingly recognized as important determinants of bone strength. Using high-resolution peripheral QCT (HRpQCT, Scanco Medical AG, Switzerland), we tested the hypothesis that CH women have better cortical skeletal integrity due to lower cortical porosity and higher cortical mineral density compared with CA women.

80 CH women (46 premenopausal 36±7 yrs and 34 postmenopausal 62±2 yrs) and 82 CA women (53 premenopausal 35±4 yrs and 29 postmenopausal 63±3 yrs) were studied. Data were adjusted for height, weight and serum 25OH vitamin D.

Premenopausal CH vs. CA women had greater Ct.Th, Ct.vBMD, Ct.TMD and decreased Ct.Po at both the radius and tibia (Table). Results remained significant after adjustment except for tibial Ct.Po. A similar pattern was observed among postmenopausal women, but only Ct.Th at the radius remained significant after adjustment. As expected, postmenopausal vs. premenopausal women had lower Ct.vBMD and Ct.Th at the radius and tibia in both races. At the radius, Ct.Po more than doubled between pre- and post-menopausal women in both races (CH: 3.5±1.1% vs. 7.2±2.7%, p<0.001; CA: 4.5±1.3% vs. 9.2±4.5%, p<0.001), while Ct.TMD decreased by 3% (p<0.001) in both races. At the tibia, Ct.Po also more than doubled (CH: 6.3±1.6% vs. 13.7±3.8%, p<0.001; CA: 7.1±1.7% vs. 16.1±5.8%, p<0.001) between pre- and post-menopausal women in both races, while Ct.TMD decreased by 6-7% respectively in CA and CH women (p<0.001 for both). Age-related differences in Ct.Po and Ct.TMD did not differ by race.

In summary, both reduced Ct.Po and greater Ct.TMD explain higher Ct.vBMD in CH vs. CA premenopausal women. Thicker and preserved cortical bone structure in CH women is likely to confer greater resistance to fracture compared to CA women.

| | Percentage difference in Chinese vs. Caucasian women | | | |
|---------|--|------------|-----------|------------|
| | Radius | | Tibia | |
| | Premenop. | Postmenop. | Premenop. | Postmenop. |
| Ct.Th | 18.0***††† | 11.3**† | 8.7*† | 8.0 |
| Ct.vBMD | 2.6***††† | 3.8* | 2.3**†† | 4.8* |
| Ct.Po | -21.3***††† | -22.3* | -10.6* | -15.3 |
| Ct.TMD | 2.2***††† | 1.7 | 1.8***†† | 1.0 |

*p<0.05, **p<0.01, ***p<0.001 - non adjusted

†p<0.05, ††p<0.01, †††p<0.001 - adjusted for height, weight and serum 25OH vitamin D

Percentage difference in Chinese vs. Caucasian women

Disclosures: *Stephanie Boutroy, None.*

1168

Bone Microstructure, Serum PINP, and Plasma Osteopontin Levels are Correlated With Sympathetic Activity Measured by Microneurography in Human. *Joshua Farr*¹, *Nisha Charkoudian*², *Jill Barnes*³, *David Monroe*⁴, *Louise McCready*¹, *Elizabeth Atkinson*⁵, *Shreevasee Amin*¹, *L. Joseph Melton*¹, *Michael Joyner*³, *Sundeep Khosla*⁵. ¹Mayo Clinic, USA, ²U.S. Army Research Institute of Environmental Medicine, USA, ³Department of Anesthesiology, Mayo Clinic, USA, ⁴Mayo Foundation, USA, ⁵College of Medicine, Mayo Clinic, USA

There is increasing evidence from animal studies that the sympathetic nervous system regulates bone turnover and mass. Specifically, increased β -adrenergic activity leads to increased bone resorption, decreased formation, and decreased bone mass. In addition, osteopontin is required for β -adrenergic signaling in bone, since β -adrenergic stimulation has no effect on bone mass in osteopontin knock-out mice. There are, however, currently no data on the relationship of sympathetic activity to bone turnover or mass in humans. Thus, we used microneurography of the peroneal

nerve to directly measure sympathetic activity in 23 women aged 20 to 72 yrs (10 premenopausal [preM] and 13 postmenopausal [postM]) and correlated sympathetic activity to bone microstructure at the distal radius using HRpQCT as well as to circulating levels of bone turnover markers and osteopontin. Sympathetic activity (bursts/100 heart beats) was 2.5-fold higher in postM compared to preM women [mean (SD), 61.8 (13.4) in postM vs 24.7 (14.0) in preM, P < 0.001]. After adjusting for age, sympathetic activity was inversely correlated with trabecular bone volume fraction (Spearman $r = -0.55$, P < 0.01) and trabecular thickness ($r = -0.59$, P < 0.01), whereas positive correlations were observed for trabecular separation ($r = 0.45$, P < 0.05) and structure model index ($r = 0.46$, P < 0.05). Sympathetic activity was also negatively correlated with plasma osteopontin levels ($r = -0.43$, P = 0.045), driven mainly by the correlation in postM women ($r = -0.76$, P = 0.002). Sympathetic activity was negatively correlated with serum PINP in postM women ($R = -0.65$, P = 0.02), with a similar trend in preM women ($r = -0.58$, P = 0.08).

These findings represent the first demonstration in humans, using direct measurements of sympathetic activity, of a relationship between sympathetic activity, bone microstructure, and circulating levels of PINP and osteopontin. Given the critical role of osteopontin in mediating effects of β -adrenergic signaling in bone cells, the inverse association between sympathetic outflow and plasma osteopontin levels may reflect a negative feedback loop to limit the deleterious effects of sympathetic activity on bone metabolism. Our findings point to the need for additional human and animal studies to test this hypothesis and to further define the utility of β -adrenergic blockers (selectivity and dosage) in preventing age-related bone loss.

Disclosures: *Joshua Farr, None.*

1169

Structural and Mechanical Implications of Antiresorptive and Anabolic Treatment of Osteoporosis by In Vivo Micro-MRI Based Techniques. *Yusuf Bhagat*¹, *Maite Aznarez-Sanado*¹, *Jeremy Magland*¹, *Theresa Scattergood*¹, *Peter Snyder*¹, *Felix Werner Wehrli*². ¹University of Pennsylvania, USA, ²University of Pennsylvania Medical Center, USA

Antiresorptive and anabolic drugs hold the potential to arrest or reverse bone loss. High-resolution micro-MRI-based virtual bone biopsy (VBB) methods allow quantification of trabecular bone (TB) microarchitectural changes at peripheral skeletal locations. Here we present data from an ongoing serial translational patient study at 3 Tesla designed to evaluate the efficacy of anabolic and antiresorptive treatments in postmenopausal women (ages, 58-84) with osteoporosis. High-resolution 3D micro-MR images from the left distal tibia were acquired at baseline, 12 months (n=26) and 24 months (n=15) following randomization to either teriparatide (Forteo, Eli Lilly, 20mg daily, s.c.) or zoledronic acid (Reclast acid, Novartis, 5mg annually, i.v.), and resulted after processing in a 3D grayscale image of 137x137x410 μm^3 voxel size. Follow-up images were co-registered to the baseline grid by rigid body registration. Data were subjected to VBB processing yielding parameters of scale (bone volume fraction (BVF)) and topology (surface-to-curve (S/C) ratio and erosion index (EI)). Finite element analysis was performed on the full tibial cross section with image voxels converted to hexahedral finite elements. Axial stiffness (E_{zz}) was computed as the stress/strain ratio. Serially registered images and VBB cores (23x23x68 μm^3) from a 61-year subject are shown in Fig. 1. Most structural features are replicated in repeat VBBs and some remodeling changes upon Forteo treatment are clearly detectable as plate perforations (green arrows) observed at baseline diminishing and filing in over the duration of treatment. In both treatment arms, significant increases in spinal bone mineral density (BMD) were observed (Fig. 2). Furthermore, increases of 2.6% to 14% (p<0.001) were seen in BVF, S/C and E_{zz} over 24 months of treatment, with topology and mechanics being stronger determinants of the therapeutic efficacy in TB microarchitecture relative to BVF. The relative change in topological parameters of subjects randomized to Reclast (n=14) was similar to those in the Forteo treatment arm (n=12) over 24 months (13-14% increase in S/C and 11-12% decrease in EI, p<0.001). Axial stiffness increased by 5% (p<0.001) and 4% (p=0.07), in the Reclast and Forteo groups, respectively, with the Reclast group only eliciting a statistically significant response. Data in this ongoing treatment study demonstrated an improvement in TB microstructural parameters over a 24-month period.

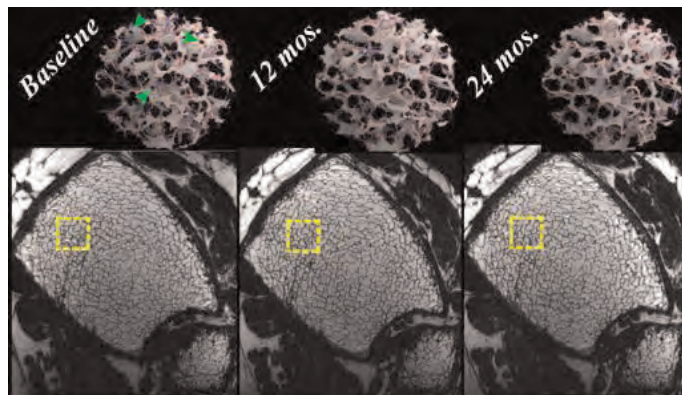


Fig. 1: Co-registered tibia TB images with VBB cores of a 61yo. woman randomized to Forteo.

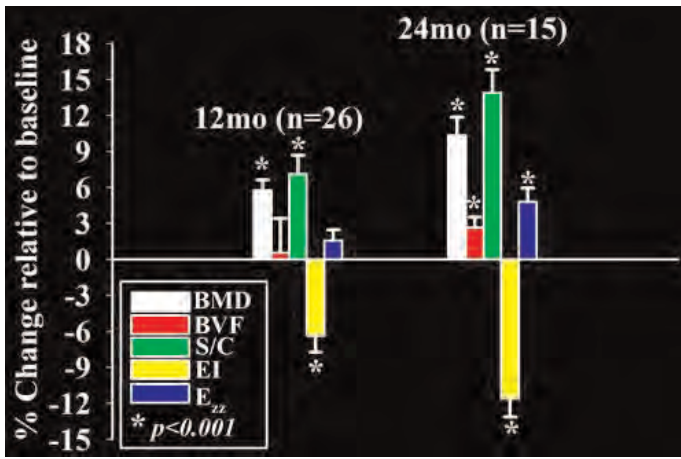


Fig. 2: Changes from baseline in the various parameters upon treatment with Reclast and Forteo

Disclosures: Yusuf Bhagat, None.

1170

Differential Effects of Teriparatide and Zoledronic Acid on the Outer and Inner Surfaces of Cortical Bone in Postmenopausal Women with Osteoporosis: Results from the SHOTZ Trial. David Dempster^{1*}, Hua Zhou², Robert Recker³, Jacques Brown⁴, Michael Bolognese⁵, Christopher Recknor⁶, David Kendler⁷, E. Michael Lewiecki⁸, David Hanley⁹, D. Sudhaker Rao¹⁰, Paul Miller¹¹, Grattan Woodson¹², Robert Lindsay², Neil Binkley¹³, Xiaohai Wan¹⁴, Valerie Ruff¹⁴, Boris Janos¹⁵, Kathleen Taylor¹⁴. ¹Columbia University, USA, ²Helen Hayes Hospital, USA, ³Creighton University Osteoporosis Research Center, USA, ⁴CHUQ Research Centre Laval University, Canada, ⁵Bethesda Health Research, USA, ⁶United Osteoporosis Center, USA, ⁷Associate Professor University of British Columbia, Canada, ⁸University of New Mexico School of Medicine, USA, ⁹University of Calgary, Canada, ¹⁰Henry Ford Hospital, USA, ¹¹Colorado Center for Bone Research, USA, ¹²USA, ¹³University of Wisconsin, Madison, USA, ¹⁴Eli Lilly & Company, USA, ¹⁵Eli Lilly Canada, Inc., Canada

Purpose: Previously, we contrasted the mechanisms of action (MOA) of teriparatide (TPTD) and zoledronic acid (ZOL) using a complete set of histomorphometric indices in the cancellous envelope of bone biopsies from postmenopausal women with osteoporosis. Recognizing the contribution of cortical bone to fracture resistance, we now extend our observations to the endocortical and periosteal envelopes.

Methods: In this randomized, double-blind, active comparator-controlled study, transiliac bone biopsies were obtained after double tetracycline labeling from 58 subjects receiving TPTD (20 µg/day, sc injection) or ZOL (5 mg/y, IV infusion). We measured a panel of dynamic and static histomorphometric indices in the cancellous, endocortical, and periosteal bone envelopes after 6 months of treatment.

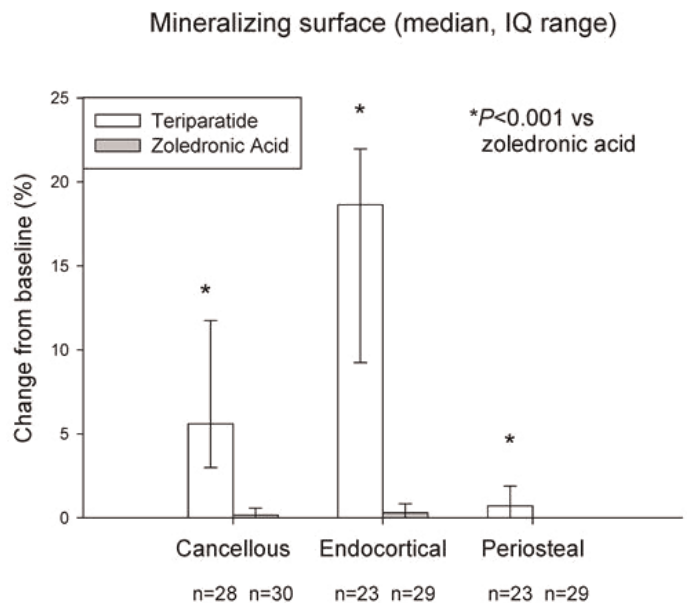
Results: The proportion of samples with tetracycline labels was significantly higher in all 3 envelopes in the TPTD group compared to the ZOL group (p < 0.001) (Table). On the endocortical surface, 100% of samples from the TPTD group displayed labels, all of which included double labels. In contrast, 52% of samples from the ZOL group had labels, 21% of which included double labels. On the periosteal surface, 70% of samples in the TPTD group displayed labels (26% with double labels) compared to 17% of samples in the ZOL group (7% with double labels). Mineralizing surface/bone surface (MS/BS), bone formation rate (BFR/BS), osteoid surface (OS/BS), osteoid thickness (O.Th), wall thickness (W.Th), and mineral apposition rate (MAR) were all significantly higher in the TPTD than the ZOL group in both cancellous and endocortical envelopes. Conversely, in both envelopes, eroded surface (ES/BS) was lower in the ZOL than the TPTD group. Periosteal MS/BS and BFR/BS were higher with TPTD than with ZOL.

Conclusions: The contrasting effects of ZOL and TPTD on bone remodeling are evident on all 3 bone envelopes with MS/BS and BFR/BS providing the most striking differentiation of the MOA of the 2 drugs. While the effect of TPTD was smaller on the periosteal than the endocortical surface, the higher values of MS/BS and BFR/BS relative to the ZOL group suggests the possibility of periosteal expansion and, therefore, an increase in bone size with TPTD. Further, in TPTD samples, MS/BS and BFR/BS were higher in the endocortical than the cancellous envelope which, coupled with an increase in wall thickness, provides a mechanism for cortical thickening with TPTD treatment.

| Number samples (%) with the following: | Cancellous | | Endocortical | | Periosteal | |
|---|-------------------------------------|------------------------------------|-------------------------------------|------------------------------------|-------------------------------------|------------------------------------|
| | TPTD | ZOL | TPTD | ZOL | TPTD | ZOL |
| Double and/or Single Labels | 28 ^a (100%) | 18 (60%) | 23 ^a (100%) | 15 (52%) | 16 ^a (70%) | 5 (17%) |
| Double Label | | | | | | |
| With Single Label | 28 (100%) | 13 (43%) | 23 (100%) | 6 (21%) | 5 (22%) | 2 (7%) |
| Without Single Label | 0 (0%) | 3 (10%) | 0 (0%) | 0 (0%) | 1 (4%) | 0 (0%) |
| Single Label Only | 0 (0%) | 2 (7%) | 0 (0%) | 9 (31%) | 10 (44%) | 3 (10%) |
| No Label | 0 (0%) | 12 (40%) | 0 (0%) | 14 (48%) | 7 (30%) | 24 (83%) |
| Indices Evaluated: | | | | | | |
| MS/BS, % | 5.60* (3.00, 11.75) n=28 | 0.16 (0.00, 0.58) n=30 | 18.64* (9.25, 21.96) n=23 | 0.30 (0.00, 0.84) n=29 | 0.71* (0.00, 1.89) n=23 | 0.00 (0.00, 0.00) n=29 |
| BFR/BS, mm ³ /mm ² /y | 0.0116* (0.0051, 0.0265) n=28 | 0.0002 (0.0000, 0.0010) n=30 | 0.0307* (0.0182, 0.0411) n=23 | 0.0003 (0.0000, 0.0014) n=29 | 0.0008* (0.0000, 0.0021) n=23 | 0.0000 (0.0000, 0.0000) n=29 |
| MAR, µm/d | 0.56** (0.48, 0.62) n=28 | 0.49 (0.37, 0.51) n=18 | 0.50* (0.43, 0.56) n=23 | 0.30 (0.30, 0.44) n=15 | 0.30 (0.30, 0.50) n=16 | 0.30 (0.30, 0.30) n=5 |
| O.Th, µm | 4.92* (4.29, 6.68) n=28 | 3.77 (3.51, 4.22) n=30 | 4.94* (4.41, 5.87) n=23 | 3.70 (2.99, 4.82) n=29 | parameter not measured | |
| W.Th, µm | 31.29*** (28.80, 33.26) n=28 | 28.63 (27.16, 30.43) n=30 | 36.30*** (34.27, 37.62) n=23 | 32.39 (29.45, 36.20) n=29 | parameter not measured | |
| OS/BS, % | 11.34* (6.58, 16.52) n=28 | 2.51 (1.27, 4.58) n=30 | 16.33* (13.57, 24.34) n=23 | 1.87 (1.08, 3.99) n=29 | parameter not measured | |
| ES/BS, % | 4.59* (3.14, 6.01) n=28 | 2.71 (1.73, 3.21) n=30 | 4.06*** (1.92, 6.32) n=23 | 1.87 (1.54, 3.33) n=29 | parameter not measured | |

*p < 0.001; **p < 0.01; ***p < 0.05. Values shown are medians (Q1, Q3).
 Statistical analyses were conducted at a 2-sided alpha level of 0.05 using Wilcoxon rank-sum test.
^aNumber of evaluable samples in the cancellous envelope was 28 for TPTD and 30 for ZOL. For the periosteal and endocortical envelopes, the number of evaluable samples was 23 for TPTD and 29 for ZOL in each envelope.
^bWhen label was absent, MS/BS was measured as zero and these values were used in the calculation of BFR/BS.
^cMAR was measured on double labels or assigned a value of 0.3 µm/d if only single labels were present; if no label was present, MAR was treated as missing.

Table



Figure

Disclosures: David Dempster, Amgen, Eli Lilly, Merck, Novartis, P&G, 1; Amgen, Merck, Novartis, P&G, 2; Eli Lilly, 6
 This study received funding from: Lilly USA, LLC

1171

Overlapping and Follow-up of Alendronate to Teriparatide Treatment Results in Maintenance of Excess BMD Gain. Christian Muschitz^{1*}, Roland Kocijan², Astrid Fahrleitner-Pammer³, Heinrich Resch⁴. ¹St. Vincent's Hospital, Austria, ²St. Vincent Hospital Vienna, Austria, ³Medical University Graz, Austria, ⁴Medical University Vienna, Austria

Purpose: After 9 months of teriparatide (TPTD) treatment the combination of alendronate (ALN) and TPTD for consecutive 9 months results in enhanced BMD gain, mostly at cortical sites, compared with 18 months of TPTD monotherapy. Administration of raloxifene (RAL) instead of ALN was less advantageous. Both antiresorptive combination therapies maintain TPTD induced bone formation to some extent, while bone resorption declines more on ALN than RAL. Our aim was to

investigate the BMD changes for the 12 months after cessation of TPTD treatment but with continuation of the respective antiresorptive treatment.

Methods: 125 postmenopausal women (mean age 71.7 ± 8.5 ys, 91.5% prevalent fractures, 95.7% prior antiresorptive treatment) were prospectively randomized after 9 months of TPTD treatment into three open-label groups for another 9 months: ALN (70 mg/week, 41 pts) or RAL (60 mg/day, 37 pts) added to TPTD treatment or no additional medication (TPTD monotherapy, 47 pts). After TPTD termination, patients were treated with the respective antiresorptive agent for another 12 months (extension phase). All subjects received 1000mg calcium and 800 IU vitamin D daily. Serum levels of intact amino terminal propeptide of type I procollagen (PINP) and type I collagen cross-linked C-telopeptide (CTX) as well as BMD measured by DXA at lumbar spine, total hip and femoral neck were evaluated at randomization, end of TPTD treatment, and at 6 and 12 months in the extension phase.

Summary: Lumbar spine BMD increased in all groups during the extension phase. Compared with values at the time of randomization, at the end of the extension phase, the increase in lumbar spine BMD was significantly higher in the ALN ($10.1 \pm 7.3\%$, $p=0.002$) and RAL ($8.4 \pm 5.4\%$, $p=0.019$) groups than in the TPTD monotherapy group ($4.5 \pm 10.3\%$). At total hip addition of RAL ($0.5 \pm 3.8\%$) did not alter the effects of TPTD monotherapy on BMD ($0.5 \pm 5.5\%$). Addition of ALN resulted in a superior increase in both total hip BMD ($8.2 \pm 5.8\%$) and femoral neck BMD ($9.1 \pm 10.1\%$, $p<0.001$ for both) compared with RAL or TPTD alone. PINP and CTX significantly declined in all groups in the extension phase reaching the lowest concentrations in the ALN combination group.

Conclusions: Our data suggest that continuation of ALN after its addition to the second 9 months of an 18-month TPTD treatment cycle resulted in a robust and enhanced BMD increase especially in the hip region.

Disclosures: Christian Muschitz, None.

1172

Genetic Variants in the Promoter of LRP5 May Be Associated with Teriparatide Response, in the Treatment of Osteoporosis. Lee O'Brien^{*1}, Haojun Ouyang², Jared Kohler³. ¹Lilly, USA, ²Eli Lilly & Company, USA, ³Biostat Solutions, Inc, USA

The goal of this study was to identify genetic markers associated with teriparatide response in patients with osteoporosis. Variants in eleven candidate genes in the Wnt (bone formation) or RANK (bone resorption) pathways were investigated in a Caucasian genetic cohort collected from a teriparatide clinical trial (NCT00035256, n = 118). Changes in bone mineral density (BMD) from baseline to 12 months was assessed in teriparatide-treated patients using ANCOVA: the model included covariate adjustments for baseline BMD, BMI, age and genotype. Results from the genetic analysis indicate that 6 genetic variants in LRP5 (total of 62 variants genotyped) were associated with a change in femoral neck BMD at 12 months (unadjusted $p = 0.01-0.03$). Average percent change in femoral neck BMD for the LRP5 genetic variant, rs312009, was 0.24, 2.54 and 3.02 for the CC, CT and TT genotypes (unadjusted $p = 0.0261$). The C allele at rs312009 disrupts a RUNX2 transcription factor binding site. In reporter-gene experiments, the C allele had poorer transcription efficacy, which may translate into less LRP5 protein and decreased Wnt pathway activation (1), resulting in decreased bone formation. Although not significant, similar directional trends were observed for teriparatide-induced changes in lumbar spine BMD (7.64, 8.29 and 10.93 for CC, CT and TT, respectively, $p = 0.4431$). Additional variants in LRP5 that were associated with teriparatide efficacy were also located in the 5' UTR, and several of these are predicted to disrupt TF binding sites including a site for a Ccaat/Enhancer Binding Protein (rs312024). These data suggest a genetic association may exist between SNPs in LRP5 and response to teriparatide treatment. Further clinical trials are needed to establish replication of these results, and to determine if these markers are associated with efficacy for other bone anabolic agents.

1) J Bone Miner Res. 2011 May;26(5):1133-44

Disclosures: Lee O'Brien, Eli Lilly and Company, 3
This study received funding from: Eli Lilly and Company

1173

Femur QCT Analysis using MIAF in Postmenopausal Women Treated with Odanacatib - Results of a 2-year Placebo-controlled Trial. Klaus Engelke^{*1}, Thomas Fuerst², Bernard Dardzinski³, John Kornak⁴, Shabana Ather⁵, Harry Genant⁶, Anne De Papp⁷. ¹University of Erlangen, Germany, ²Synarc Inc, USA, ³Merck Sharp & Dohme Corp., USA, ⁴UCSF, Dep. of Epidemiology & Biostatistics, USA, ⁵Merck & Co, Inc., USA, ⁶UCSF/Synarc, USA, ⁷Merck & Co., Inc., USA

Background: Odanacatib, a selective cathepsin K inhibitor, increases areal BMD at the spine and hip of postmenopausal women. To gain additional insight into the clinical effects in trabecular and cortical bone of odanacatib, we assessed femoral BMD by QCT in postmenopausal women treated with odanacatib.

Methods: This international, randomized, double-blind, placebo-controlled, 2-year, phase 3 trial enrolled 214 postmenopausal women with a mean age of 64 years and mean BMD T-scores of -1.8 at the lumbar spine and femoral neck. Subjects were randomized to odanacatib 50 mg weekly (ODN) or placebo (PBO); all participants received calcium and vitamin D. Hip QCT scans at 2 years were available for a subset

of these women (n=158, ODN (78), PBO (80)). BMD, BMC and volume of the integral, cortical and trabecular compartments were measured in the QCT images using MIAF (Erlangen, Germany). Subregions included the neck, trochanter and intertrochanter. Results are presented as percent change from baseline after 2 years of treatment.

Results: There were consistent and significant differential treatment effects (ODN-PBO) for integral, trabecular and cortical BMD at 24 months (see table). With no significant differential treatment effect on total femur volume, the results for BMC closely matched those of BMD for integral and trabecular compartments, respectively. However, with small but mostly significant differential increases in cortical volume (1.0-1.3%) and thickness (1.4-1.9%), the percent cortical BMC increases were numerically larger than those of BMD.

With a total femur BMC differential treatment effect (ODN-PBO) of nearly 1000mg, the proportion of BMC attributed to cortical gain was 45%, 44% 52%, 40% for the total, neck, trochanter and intertrochanter subregions, respectively.

Conclusions: In postmenopausal women treated for 2 years, odanacatib improved integral, trabecular and cortical BMD as well as BMC at all regions of the femur relative to placebo. Cortical volume and thickness significantly increased in all regions except the neck, where it was marginally non-significant. The increase in cortical volume and BMC paralleled the increase in cortical BMD, demonstrating a consistent effect of ODN on cortical bone. Approximately one-half of the absolute BMC gain occurred in cortical bone.

| Differences between weekly odanacatib 50 mg and placebo in QCT measurements at the Total Femur, Femoral Neck (FN) Trochanter Intertrochanter (IT) and Proximal Shaft after 24 months of treatment | | | |
|---|--------------|------------------------------------|---------|
| Exploratory Endpoint | 95% CI | Diff in % Change from BL (ODN-PBO) | P value |
| Total Femur Int BMD | (-2.2, -0.9) | 5.4 | <0.001 |
| Total Femur Trab BMD | (-5.4, -2.2) | 12.2 | <0.001 |
| Total Femur Cort BMD | (-1.1, 0.2) | 2.5 | <0.001 |
| FN Int BMD | (-2.0, -0.8) | 4.5 | <0.001 |
| FN Trab BMD | (-6.0, -2.4) | 9.9 | <0.001 |
| FN Cort BMD | (-0.8, 0.9) | 2.0 | 0.002 |
| Trochanter Int BMD | (-2.3, -0.8) | 7.3 | <0.001 |
| Trochanter Trab BMD | (-4.8, -1.2) | 17.2 | <0.001 |
| Trochanter Cort BMD | (-1.7, -0.4) | 4.3 | <0.001 |
| IT Int BMD | (-2.3, -0.9) | 4.6 | <0.001 |
| IT Trab BMD | (-6.1, -2.6) | 11.8 | <0.001 |
| IT Cort BMD | (-0.8, 0.5) | 1.4 | <0.005 |

Table

Disclosures: Klaus Engelke, Synarc, 7; Synarc, 3
This study received funding from: Merck

1174

Denosumab Significantly Improved Trabecular Bone Score (TBS), an Index of Trabecular Microarchitecture, in Postmenopausal Women With Osteoporosis. Michael R. McClung^{*1}, Kurt Lippuner², Maria Luisa Brandi³, Jean-Marc Kaufman⁴, Jose R. Zanchetta⁵, Marc-Antoine Krieg⁶, Henry G. Bone⁷, Roland Chapurlat⁸, Didier Hans⁶, Andrea Wang⁹, Jang Yun⁹, Carol Zapalowski⁹, Cesar Libanati⁹. ¹Oregon Osteoporosis Center, USA, ²Osteoporosis Policlinic, University of Bern, Switzerland, ³University of Florence, Italy, ⁴University Hospital of Ghent, Belgium, ⁵Instituto de Investigaciones Metabólicas, Argentina, ⁶Lausanne University Hospital, Center of Bone Diseases, Switzerland, ⁷Michigan Bone & Mineral Clinic, USA, ⁸Hôpital Edouard Herriot, France, ⁹Amgen Inc., USA

Purpose: The trabecular bone score (TBS), a novel gray-level texture index determined from lumbar spine DXA scans, correlates with 3D parameters of trabecular bone microarchitecture known to predict fracture. TBS may enhance the identification of patients at increased risk for vertebral fracture independently of bone mineral density (BMD) (Hans *JBMR* 2011; Boutroy *JBMR* 2010). Denosumab (DMAb) decreased bone turnover, increased BMD, and reduced new vertebral fractures in postmenopausal women with osteoporosis. We explored the effect of DMAb on TBS over 36 months and evaluated the association between TBS and lumbar spine BMD in women who had DXA scans obtained from eligible scanners for TBS evaluation in FREEDOM.

Methods: FREEDOM was a 3-year, randomized, double-blind trial that enrolled postmenopausal women with a lumbar spine or total hip DXA T-score ≤ -2.5 , but not < -4.0 at both sites. Women received placebo or 60 mg DMAb every 6 months. A subset of women in FREEDOM participated in a DXA substudy where lumbar spine DXA scans were obtained at baseline and months 1, 6, 12, 24, and 36. We retrospectively applied, in a blinded-to-treatment manner, a novel software program (TBS iNsite[®] v1.9, Med-Imaps, Pessac, France) to the standard lumbar spine DXA scans obtained in these women to determine their TBS indices at baseline and months 12, 24, and 36. From previous studies, a TBS >1.35 is considered as normal microarchitecture, a TBS between 1.35 and >1.20 as partially deteriorated, and ≤ 1.20 reflects degraded microarchitecture.

Results: There were 285 women (128 placebo, 157 DMAb) with a TBS value at baseline and ≥ 1 post-baseline visit. Their mean age was 73, their mean lumbar spine

BMD T-score was -2.79, and their mean lumbar spine TBS was 1.20. In addition to the robust gains in DXA lumbar spine BMD observed with DMAB (9.8% at month 36), there were consistent, progressive, and significant increases in TBS compared with placebo and baseline (Table & Figure). BMD explained a very small fraction of the variance in TBS at baseline ($r^2 < 0.07$). In addition, the variance in the TBS change was largely unrelated to BMD change, whether expressed in absolute or percentage changes, regardless of treatment, throughout the study (all $r^2 < 0.06$); indicating that TBS provides distinct information, independently of BMD.

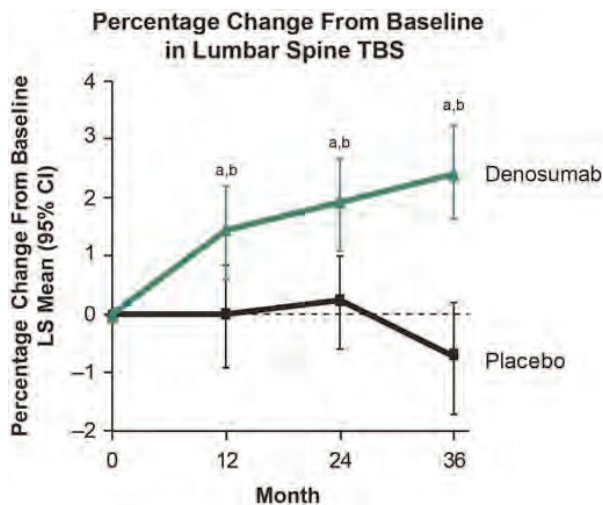
Conclusion: In postmenopausal women with osteoporosis, DMAB significantly improved TBS, an index of lumbar spine trabecular microarchitecture, independently of BMD.

Table. Lumbar Spine TBS and BMD Percentage Change From Baseline Over Time and Pearson Correlation Between TBS and BMD

| Month | Placebo (N=128) | | | Denosumab (N=157) | | |
|-------|-----------------|--------------|---------------------|--------------------|--------------------|---------------------|
| | TBS % Change | BMD % Change | Pearson Correlation | TBS % Change | BMD % Change | Pearson Correlation |
| 12 | 0.0 | -0.1 | 0.0036 | 1.4 ^{a,b} | 5.7 ^{a,b} | 0.0256 |
| 24 | 0.2 | 0.1 | 0.0004 | 1.9 ^{a,b} | 7.8 ^{a,b} | 0.0225 |
| 36 | -0.7 | 0.0 | 0.0324 | 2.4 ^{a,b} | 9.8 ^{a,b} | 0.0529 |

N=number of randomized subjects who enrolled in the DXA substudy and had observed TBS data at baseline and ≥1 post-baseline visit. ^ap<0.0144 compared with placebo. ^bp<0.0003 compared with baseline.

Table



Compared with placebo: ^ap<0.0144
Compared with baseline: ^bp<0.0003

Figure

Disclosures: Michael R. McClung, Amgen, Merck, 6; Amgen, Lilly, Merck, Novartis, 2; Amgen, Lilly, Novartis, Warner-Chilcott, 1
This study received funding from: Amgen Inc.

1175

Longitudinal Tracking of DXA Bone Measures in Children and Adolescents Over a 6-Year Period. Tishya Wren^{*1}, Heidi Kalkwarf², Babette Zemel³, Joan Lappe⁴, John Shepherd⁵, Sharon Oberfield⁶, Karen Winer⁷, Vicente Gilsanz¹. ¹Children's Hospital Los Angeles, USA, ²Cincinnati Children's Hospital Medical Center, USA, ³Children's Hospital of Philadelphia, USA, ⁴Creighton University Osteoporosis Research Center, USA, ⁵University of California, San Francisco, USA, ⁶Columbia University Medical Center, USA, ⁷National Institutes of Health, NICHD, USA

Measuring bone mass during childhood and adolescence may allow for early identification of individuals at risk for future development of osteoporosis. However, early assessment is only useful if bone measurements "track" during growth, with children who have low bone mass continuing to have low bone mass as they mature. The purpose of this prospective longitudinal multi-center study was to examine tracking of dual-energy x-ray absorptiometry (DXA) bone measures in children and adolescents over a 6-year period. The study subjects were 974 healthy boys and girls, ages 6 to 16 years, who completed 6 years of longitudinal follow-up in the multi-center Bone Mineral Density in Childhood Study (BMDCS). DXA measures of the whole body, lumbar spine, hip, and forearm were obtained annually. The correlation between baseline DXA measures and measures 6 years later was examined.

The tracking of DXA Z-scores ($r = .66$ to $.81$) was similar in magnitude to the tracking of height (Table 1). In general, tracking was better for BMD vs. BMC and for height-adjusted DXA Z-scores vs. unadjusted scores. Tracking was also slightly better for girls compared with boys. When examined as a function of sexual maturity at baseline, tracking remained strong for girls of all Tanner stages ($r = .61$ to $.89$). The weakest tracking was for Tanner stage 3, where height adjustment improved the tracking ($r = .57$ to $.76$ for unadjusted vs. $r = .69$ to $.85$ for height adjusted). Boys had poor tracking of unadjusted DXA Z-scores in Tanner stage 3 ($r = -.05$ to $.74$). Height adjustment greatly improved tracking in this group ($r > .6$ except for hip neck BMC which improved from $r = -.05$ to $r = .34$; Table 2).

In conclusion, DXA bone measures demonstrate good tracking in children and adolescents. During puberty, however, it is important to adjust DXA measures for height, particularly for boys. These results suggest that bone mass measurements during childhood may be useful for early identification of children at risk for osteoporosis later in life. This information may assist in counseling patients and initiating early interventions.

Table 1: Correlation of Z-scores between baseline and 6 years later

| | BMC | BMD | Height adjusted BMC | Height adjusted BMD |
|----------------|-----|-----|---------------------|---------------------|
| Height | .75 | --- | --- | --- |
| Weight | .68 | --- | --- | --- |
| BMI | .69 | --- | --- | --- |
| DXA whole body | --- | .66 | .71 | .66 |
| DXA spine | --- | .71 | .73 | .78 |
| DXA hip total | --- | .69 | .76 | .74 |
| DXA hip neck | --- | .69 | .74 | .72 |
| DXA forearm | --- | .74 | .72 | .78 |

Table 1

Table 2: Correlation of Z-scores between baseline and 6 years later for boys in Tanner 3

| Variable | BMC | BMD | Height adjusted BMC | Height adjusted BMD |
|----------------|-----|------|---------------------|---------------------|
| Height | .56 | --- | --- | --- |
| Weight | .60 | --- | --- | --- |
| BMI | .74 | --- | --- | --- |
| DXA whole body | --- | .33 | .30 | .65 |
| DXA spine | --- | .27 | .56 | .74 |
| DXA hip total | --- | .24 | .63 | .78 |
| DXA hip neck | --- | -.05 | .51 | .34 |
| DXA forearm | --- | .52 | .62 | .76 |

Table 2

Disclosures: Tishya Wren, None.

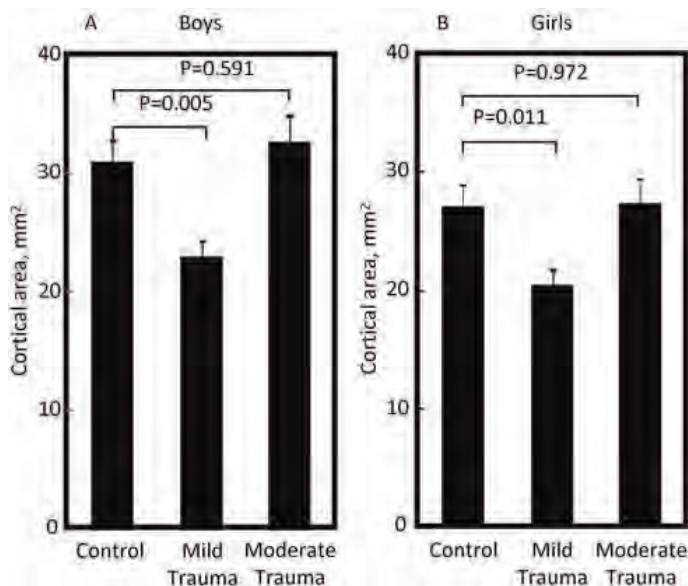
1176

HRpQCT Reveals Cortical Thinning and Deficits in Bone Microstructure in Children and Adolescents With a Distal Forearm Fracture Due to Mild but Not Moderate Trauma. Joshua Farr^{*1}, Shreyasee Amin¹, Salman Kirmani¹, Louise McCready¹, Sara Achenbach¹, L. Joseph Melton¹, Sundeeep Khosla². ¹Mayo Clinic, USA, ²College of Medicine, Mayo Clinic, USA

Distal forearm fracture (DFF) incidence peaks during growth and has increased significantly in recent years. There is mounting evidence that fractures during growth are related to skeletal fragility and some studies have shown that this relationship is independent of trauma severity. However, previous studies have been confounded by reliance on techniques (e.g., DXA) that have limitations in assessing bone mass/structure during growth, have relied on self-reported fractures, and have included subjects with miscellaneous fractures. Thus, in order to better characterize the underlying skeletal phenotype associated with DFF during growth, we used HRpQCT to determine whether a recent fracture (due to mild vs moderate trauma) is related to deficits in bone geometry and microstructure as compared to non-fracture controls. Cortical and trabecular bone parameters were assessed at the distal radius and tibia in boys ($n = 112$) and girls ($n = 96$) aged 8-15 yrs. The Landin classification (Acta Orthop Scand 202:1, 1983) was used to assign trauma levels based on medical record review and an interview. As shown in the Figure, boys (Panel A) and girls (Panel B) with a mild trauma (e.g., simple fall) DFF had significantly lower cortical area (CtA) at the radius (by 26% for both), but both boys and girls with a moderate trauma (e.g., fall from a bicycle) DFF had virtually identical CtA values as compared to controls. Cortical thickness (CtTh) at the radius was also reduced in boys and girls with a mild trauma DFF (by 14% and 13%, respectively; $P < 0.05$), with no differences in the moderate trauma DFF cases versus controls. Similar findings were noted for CtA and CtTh at the tibia. Furthermore, at the radius and tibia, boys and girls with a mild (but not moderate) trauma fracture had deficits in trabecular bone volume fraction (6-9%), although this was statistically significant only in the boys at the tibia.

Thus, a mild, but not moderate, trauma DFF during growth is associated with cortical thinning and deficits in bone microstructure not only at the distal radius, but also at the tibia. Our data suggest that DFFs during growth have two distinct

etiologies: those due to underlying skeletal deficits leading to fractures with mild trauma versus those due to more significant trauma in the setting of normal bone mass/structure. Identification of children with mild trauma fractures may be particularly important so as to target them for lifestyle and nutritional interventions.



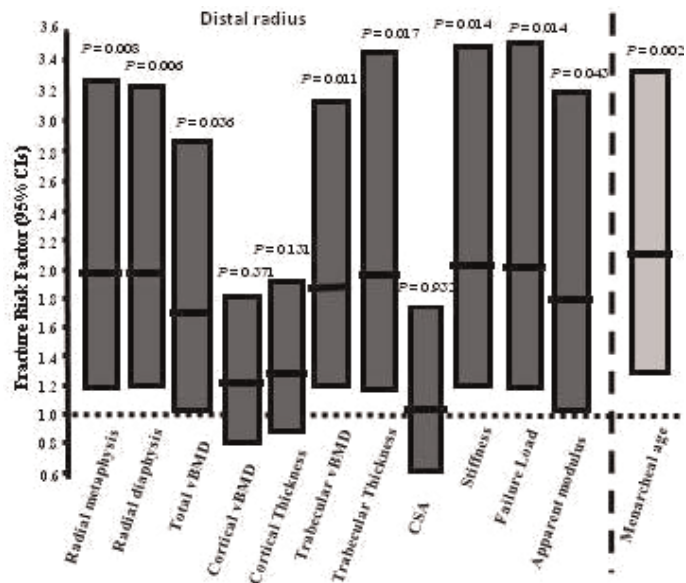
Figure

Disclosures: Joshua Farr, None.

1177

Fractures During Growth in Healthy Females: Relation with Bone Structural Alterations and Importance of Pubertal Timing. [Thierry Chevalley](#)*¹, [Jean-Philippe Bonjour](#)², [Bert van Rietbergen](#)³, [Rene Rizzoli](#)⁴, [Serge Ferrari](#)⁵.
¹University Hospitals of Geneva Division of Bone Diseases, Switzerland, ²University Hospital of Geneva, Switzerland, ³Department of Biomedical Engineering, Eindhoven University of Technology, Netherlands, ⁴University Hospital, Switzerland, ⁵Geneva University Hospital & Faculty of Medicine, Switzerland

In this study in healthy young adult women, we have assessed which bone variables are significantly associated with an increased risk of fractures during growth. Taking into account the major importance of pubertal timing in bone development, we also quantified the fracture risk related to later vs. earlier menarcheal age. We prospectively recorded fracture occurrence in healthy girls during childhood and adolescence. Healthy girls (n=124) were followed-up from the age of 7.9 ± 0.5 to 20.4 ± 0.6 (\pm SD). During the 12.5 y follow-up period, fractures, pubertal stages, menarcheal age, anthropometric variables and radius aBMD were recorded at regular intervals. At the age of 20.4 y, microstructural and strength variables of the distal radius were determined by HR-pQCT and Finite Element Analysis (μ FEA). Sixty one fractures occurred in 42 subjects. Most fractures (41%) were localized in forearm and wrist. At the age of 20.4 y mean aBMD was lower in the fracture (FX) as compared to the non-fracture (No-FX) group at both radial diaphysis ($P=0.005$) and metaphysis ($P=0.008$). Distal radius trabecular volumetric density ($P=0.010$) and thickness ($P=0.014$) were lower in the FX group. μ FEA indicated reduction in stiffness ($P=0.013$), failure load ($P=0.013$) and apparent modulus ($P=0.046$). As illustrated on the figure, calculation of Odds ratios (OR, 95% CI) revealed an increased risk of fracture for 1 SD reduction in radial aBMD diaphysis: 1.97 (1.22-3.19, $P=0.006$) and metaphysis: 1.97 (1.19-3.24, $P=0.008$), trabecular volumetric density: 1.89 (1.16-3.10, $P=0.011$) and thickness: 1.97 (1.13-3.43, $P=0.017$), stiffness: 2.02 (1.15-3.53, $P=0.014$), failure load: 2.00 (1.15-3.50, $P=0.014$) and apparent modulus: 1.79 (1.02-3.14, $P=0.043$). Menarcheal age occurred at a later age in the FX than in the No-FX group (13.5 ± 1.1 vs. 12.8 ± 1.2 y, $P=0.003$). For 1 SD (1.2 y) later menarcheal age, the risk of fracture increased twofold (OR: 2.1, 95% CI, 1.31-3.33, $P=0.002$). In conclusion, this longitudinal study with 12.5 y follow-up shows that low trabecular volumetric density and thickness in the distal radius are associated with reduced bone strength and increased risk of fractures during growth. It also documents the importance of menarcheal age on bone fragility in healthy women by demonstrating that the negative effects of later pubertal timing on bone strength is associated with increased incidence of fracture during childhood and adolescence.



Figure

Disclosures: Thierry Chevalley, None.

1178

Pre-Pubertal Bone Mass Predicts Peak Bone Mass – A 28 Year Prospective Observational Study of 214 Children. [Christian Buttazzoni](#)*, [Bjorn Rosengren](#), [Magnus Tveit](#), [Lennart Landin](#), [Jan-Åke Nilsson](#), [Magnus Karlsson](#). Skåne University Hospital Malmö, Lund University, Sweden

Purpose: There is an ongoing debate if bone mass “tracks” from growth to adulthood. We therefore undertook this prospective long-term observational study as to answer if low bone mineral content (BMC) in the pre-pubertal children is a risk factor for low BMC in young adulthood.

Methods: Distal forearm cortical BMC (g) was measured with single photon absorptiometry (SPA) in 214 children (74 recruited after a fracture, 56 with premature birth and 84 as part of a control cohort). There were 120 boys with a mean age of 9.9 years (range 3-17) and 94 girls with a mean age of 10.7 years (range 4-17). BMC was then re-measured with the same SPA apparatus in the same region mean 28 years (range 26-29) later when the boys had become mean 36.6 years (range 28-44) and the girls mean 37.4 years (range 28-44). For each individuals we calculated BMC Z-scores at childhood and adulthood, respectively, based on BMC data in the 84 controls. We used Pearssons correlation coefficient to compared baseline and follow-up Z-scores values. The proportions of children within the lower quartile of BMC, with osteopenia (BMC < -1.0 SD) and with osteoporosis (BMC < -2.5 SD) were also registered at each occasion.

Results: BMC Z-score at childhood correlated with BMC Z-score BMC in adulthood in both boys ($r=0.48$) and girls ($r=0.64$) (both $p<0.0001$). The same was found if including only children who were 10 years or older at baseline (boys $r=0.52$ and girls $r=0.73$, both $p<0.0001$) and if including only children who were below age 10 years (boys $r=0.44$ and girls $r=0.52$, both $p<0.0001$). 55% of the children in the lowest quartile of BMC were still in the lowest quartile in adulthood (57% boys and 52% girls) and 66% of the children with osteopenia still had osteopenia in adulthood (56% boys and 79% girls). The single child with osteoporosis had osteopenia in adulthood.

Conclusions: Bone mass seems to partially “track” from childhood to adulthood, so that 23% of the variance in young adult men and 41% of the variance in young adult women could be explained by the level of bone mass in childhood. Furthermore, 19% of the variance in young adult men and 27% of the variance in young adult women could be attributed to the level of bone mass before age 10 years. We infer that low bone mass in children ought to be regarded as a risk factor for low peak bone mass.

Disclosures: Christian Buttazzoni, None.

1179

Genome-wide Association Analysis of Skull BMD in Children: A Powerful Strategy to Identify Genetic Determinants of Osteoporosis-related Traits. John Kemp^{*1}, Carolina Medina-Gomez², Karol Estrada², Denise Happe², Maria Zillikens², Nicholas Timpson³, Beate St Pourcain⁴, Albert Hofman², Vincent Jaddoe², George Davey Smith⁵, André Uitterlinden², David Evans⁶, Fernando Rivadeneira², Jonathan Tobias⁷. ¹MRC Centre for Causal Analyses in Translational Epidemiology, United Kingdom, ²Erasmus Medical Center, Netherlands, ³MRC Centre for Causal Analyses in Translational Epidemiology, University of Bristol, United Kingdom, ⁴School of Social & Community Medicine, University of Bristol, United Kingdom, ⁵School of Social & Community Medicine, University of Bristol, United Kingdom, ⁶MRC Centre for Causal Analyses in Translational Epidemiology, University of Bristol, United Kingdom, ⁷School of Clinical Science at North Bristol, University of Bristol, United Kingdom

Aim: The skull is a skeletal site minimally influenced by loading, muscular activity and is less masked by environmental influences. This is reflected in the high heritability of skull BMD ($h^2=80\%$) making it a suitable trait for genetic investigations which can provide further insight into the molecular regulation of skeletal function. Yet, the relevance for osteoporosis has not been determined. We performed a genome-wide association study on skull BMD in children seeking the identification of genetic loci relevant to osteoporosis.

Methods: GWAS was performed using 9395 subjects, combining the Avon Longitudinal Study of Parents and their Children (ALSPAC, $n=5299$, mean age=9.9, SD=0.32 years) and the Generation R study (GENR, $n=4096$, mean age=6.2, SD=0.5 years), using skull aBMD from total body DXA scans, and imputed genotype data. For each cohort, association analysis was performed with MACH2QTL, using linear regression models based on an expected allelic dosage model for SNPs, adjusting for sex, age, height and population stratification. SNPs with MAF <1% and poor imputation quality ($r^2<0.3$) were excluded. After controlling for genomic inflation, we combined association data for ~2.5 million imputed autosomal SNPs into an inverse variance fixed-effects additive model meta-analysis, using METAL.

Results: SNPs in seven known BMD loci reached genome wide significance including: *WNT4* ($P=1.6 \times 10^{-12}$), *RSPO3* ($P=3.3 \times 10^{-11}$), *WNT16* ($P=2.6 \times 10^{-28}$), *TNFRSF11B* ($P=2.1 \times 10^{-11}$), *LIN7C* ($P=1.6 \times 10^{-17}$), *LRP5* ($P=1.3 \times 10^{-11}$) and *TNFRSF11A* ($P=1.8 \times 10^{-8}$). In addition, a common SNP mapping to 6q23.2 (ALSPAC: MAF=0.35; B=-0.125; P=7.7x10⁻¹⁰) and (GENR: MAF=0.31; B=-0.129; 3x10⁻⁸) upstream of the Eyes Absent 4 (*EYA4*) gene achieved genome-wide significance after meta-analysis (MAF=0.35; B=-0.1267; P=8.3x10⁻¹⁷), explaining 0.72% of the variation in Skull-BMD.

Conclusion: This study demonstrates that skull BMD assessed in children is a suitable trait for genetic investigations of osteoporosis, allowing for the dissection between bone attainment and bone loss in a setting less prone to environmental influences. Furthermore, we identified a novel locus containing a signal mapping upstream of *EYA4*. Loss of function mutations in *EYA4* are associated with sensorineural hearing loss. A link between sensorineural hearing loss and BMD has previously been identified in sclerosteosis, where skull base overgrowth occurs in the context of high bone mass, leading to cranial nerve compression.

Disclosures: John Kemp, None.

1180

Effects of Glucocorticoid Therapy on Changes in Volumetric Bone Mineral Density (vBMD) and Cortical Structure in Childhood Nephrotic Syndrome (NS). Anne Tsampalieros^{*1}, Pooja Gupta², Babette Zemel¹, Rachel Wetzsteon¹, Mary Leonard¹. ¹Children's Hospital of Philadelphia, USA, ²Emory University School of Medicine, USA

Our prior cross-sectional study in childhood nephrotic syndrome (NS) demonstrated significantly lower trabecular vBMD and greater cortical vBMD, compared with controls. However, the impact of glucocorticoids (GC) on changes in vBMD and cortical structure during growth has not been addressed.

Objectives: To examine changes in vBMD and cortical structure over one year in children and adolescents with NS and normal renal function, and to determine the longitudinal relations between GC exposure, bone outcomes, and growth.

Methods: Tibia peripheral computed tomography (pQCT) scans were obtained at enrollment, 6 and 12 months in 56 NS participants, ages 5-21 yr. Sex-, race and age-specific Z-scores were generated for trabecular BMD (TrabBMD), cortical BMD (CortBMD), and cortical dimensions based on reference data in > 650 controls. Cortical dimension Z-scores were further adjusted for tibia length. Multivariable regression models examined determinants of interval changes in Z-scores, adjusted for baseline values.

Results: 56 NS participants with a median (range) of 4 (0-16) years since diagnosis were enrolled. Mean (SD) GC doses over the first and second 6 month intervals were 0.56 (0.71) and 0.48 (0.63) mg/kg/day, respectively. Changes in TrabBMD Z-scores were not associated with GC dose. Increases in CortBMD Z-scores were independently associated with greater GC dose ($p<0.001$) and smaller increases in tibia growth ($p<0.01$). Cortical area, section modulus, and periosteal and endosteal circumference Z-scores decreased significantly over 12 months (Table). Greater increases in tibia length were associated with greater decreases in cortical dimension

Z-scores (all $p<0.01$); this association was absent in reference participants (interaction $p<0.02$). Greater GC dose was associated with decreases in height Z-score ($p<0.001$) but was not associated with changes in cortical dimension Z-scores.

Conclusions: GC therapy was associated with increases in CortBMD, potentially related to suppression of bone formation and greater secondary mineralization. Conversely, greater growth (i.e. new bone formation) was associated with declines in CortBMD. The failure to identify correlates of changes in TrabBMD may relate to the limitations of pQCT measures of trabecular compartment vBMD. The growing skeleton may be especially vulnerable to GC effects on increases in cortical dimensions. Future studies are needed to determine the fracture implications of these findings.

| Z-Scores | Enrollment | 12 Months | Change 0-12 month | 0-12 p value |
|----------------------------|---------------|--------------|-------------------|--------------|
| TrabBMD | 0.54 ± 1.32* | 0.60 ± 1.40 | -0.01 ± 0.46 | 0.76 |
| CortBMD | 0.76 ± 1.15* | 0.53 ± 1.40 | -0.20 ± 1.41 | 0.73 |
| Cortical Dimensions | | | | |
| Cortical Area | 0.25 ± 0.91* | 0.07 ± 0.92 | -0.16 ± 0.35 | 0.003 |
| Section Modulus | 0.20 ± 1.01 | 0.03 ± 0.97 | -0.19 ± 0.35 | <0.001 |
| Periosteal Circumference | 0.21 ± 1.01* | 0.05 ± 1.01 | -0.18 ± 0.30 | <0.001 |
| Endosteal Circumference | 0.07 ± 1.01 | 0.002 ± 0.95 | -0.11 ± 0.28 | 0.016 |
| Height | -0.16 ± 0.85* | -0.22 ± 0.90 | -0.05 ± 0.32 | 0.25 |

*p < 0.05 compared with reference participants

Z-scores at Enrollment and 12 Months

Disclosures: Anne Tsampalieros, None.

1181

Familial Hypocalcemic Hypercalcemia Type 3 (FHH3) is Caused by Mutation in Adaptor Protein 2 Sigma 1 (*AP2S1*). M. Andrew Nesbit^{*1}, Fadi Hannan¹, Sarah A. Howles¹, Anita A.C. Reed¹, Treena Cranston², Clare E. Thakker¹, Lorna Gregory³, Andrew J. Rimmer³, Nigel Rust⁴, Una Graham⁵, Patrick J. Morrison⁶, Steven J. Hunter⁵, Michael Whyte⁷, Gil McVean³, David Buck³, Rajesh Thakker¹. ¹Nuffield Department of Clinical Medicine, University of Oxford, United Kingdom, ²Oxford Medical Genetics Laboratories, Oxford University Hospitals NHS Trust, United Kingdom, ³Wellcome Trust Centre for Human Genetics, University of Oxford, United Kingdom, ⁴Sir William Dunn School of Pathology, University of Oxford, United Kingdom, ⁵Regional Centre for Endocrinology & Diabetes, Royal Victoria Hospital, United Kingdom, ⁶Department of Medical Genetics, Queen's University Belfast, Belfast City Hospital, United Kingdom, ⁷Shriners Hospital for Children-Saint Louis, USA

Familial hypocalcemic hypercalcemia (FHH) is an autosomal dominant disorder characterized by lifelong elevation of serum calcium concentrations with inappropriately low urinary calcium excretion. It is genetically heterogeneous with defined types referred to as FHH1, FHH2 and FHH3 whose chromosomal locations are 3q21.1, 19p and 19q13.3, respectively. FHH1, caused by mutations of the calcium-sensing receptor (*CaSR*), occurs in >65% of FHH patients, whilst the etiologies of FHH2 and FHH3 are not known. To identify the genetic defect in FHH3, we performed exome capture and high-throughput sequencing in FHH3 patients from two unrelated kindreds. Over 2,500 previously unreported non-synonymous single nucleotide polymorphisms (SNPs) were found in the whole exome of each patient, and 5 of these were non-synonymous SNPs in 5 genes from 19q13.3. Amongst these SNPs, one that involved a C to T transition that predicted occurrence of a missense mutation, Arg15Cys, in adaptor protein 2 sigma 1 (*AP2S1*), was present in the patients from both kindreds. This mutation, which altered an evolutionary conserved arginine residue, was confirmed by independent dideoxynucleotide sequencing and *HhaI* restriction endonuclease analysis which demonstrated co-segregation of the mutation with FHH3 in 32 affected members from 5 generations of the two kindreds. Wild-type (Arg15) and mutant (Cys15) AP2S1 proteins were transiently expressed in HEK293 cells stably transfected with CaSR, and an assessment of their effect on intracellular calcium in response to changes in extracellular calcium demonstrated that the mutant Cys15 AP2S1 protein shifted the dose-response curve rightward with a significantly higher EC₅₀ = 2.77mM (95% confidence interval (CI) 2.64-2.90mM) when compared to the wild-type AP2S1 EC₅₀ = 2.29mM (95% CI 2.22-2.37mM) (P<0.0001), consistent with a loss-of-function mutation. AP2S1 forms part of the AP2 complex that has a role in G protein-coupled receptor recycling, and the Arg15 residue of AP2S1 has been implicated in cargo protein acidic dileucine motif recognition. Indeed, an examination of the crystal structure of AP2 revealed that replacement of the basic, polar Arg15 residue of AP2S1 with the neutral, slightly polar Cys15 residue compromises a key contact with a polar residue found within acidic dileucine motifs.

Thus, our studies have identified the genetic defect underlying FHH3 and give important insights into calcium homeostasis.

Disclosures: M. Andrew Nesbit, None.

1182

Inactivation of SKI-1 in Osteocytes Leads to Obesity in Adult Mice and Suggests a New Bone to Brain Endocrine Pathway Regulating Body Mass.

Jeffrey Gorski¹, Nichole T. Huffman², Anne C. Breggia³, Clifford Rosen³, Sridar Chittur⁴, Amber Stern¹, Mark Dallas², Nabil G. Seidah⁵, Lynda Bonewald¹. ¹University of Missouri - Kansas City, USA, ²University of Missouri-Kansas City, USA, ³Maine Medical Center, USA, ⁴Center for Functional Genomics, Univ. at Albany, USA, ⁵Institut de Recherches Cliniques de Montreal, Canada

Obesity is a major health problem and mechanisms controlling weight gain are incompletely understood. Osteocytes are endocrine cells embedded in bone secreting sclerostin, MEPE, and FGF-23 in response to load induced strain in bone. The hypothalamus regulates body mass and bone formation via similar leptin-serotonin pathways. Inactivation of the serine protease SKI-1 in osteocytes (oscKO) by breeding [SKI-1 (fl/-) DMP1 Cre (+/-)] males with [SKI-1 (fl/fl)] females leads to a rapid increase in body mass only upon reaching skeletal maturity (Fig. 1, representative of one of three litters). Similar findings were obtained in two separate breeding programs. SKI-1 is required for activation of transmembrane bound transcription factors including ATF-6, SREBP-1, SREBP-2 and CREB-like factors. Interestingly, maturity-dependent onset of obesity is not seen in leptin-deficient ob/ob mice. At 9-11 months of age, male oscKO are significantly heavier, 44.4 +/- 6.12 gm (n=8), than control littermates, 37.9 +/- 5.17 gm (n=12) (p<0.02, t-test). Female oscKO mice (n=2) trended in the same way but did not reach significance compared with same sex littermate controls. Although heavier, male oscKO mice exhibited the same or slightly smaller femoral cortical and trabecular bone volume by microCT, and ash weight mineral content as littermate controls. Similar to ob/ob, the oscKO mouse was hyperinsulinemic yet displayed elevated blood glucose. Nesfatin1, an appetite suppressant synthesized by osteocytes and released from nucleobindin-2, was almost 20-fold higher in serum from the leanest littermate (Fig. 1). Whole genome array studies on osteocyte mRNA showed 29 genes were reduced >2-fold in oscKO compared with three control littermates, while 53 genes were increased by >2-fold in the oscKO compared to the controls. In summary, inactivation of floxed SKI-1 in osteocytes using DMP1 Cre leads to a dramatic increase in body mass only after reaching skeletal maturity, a phenotype distinct from leptin deficient ob/ob mice. We hypothesize that osteocytes, cellular endocrine sensors of load induced strain in bone, suppress appetite by release of a systemic anorexigenic factor like nucleobindin-2/nesfatin1 which is able to cross the blood brain barrier and act on the hypothalamic appetite control center. The known increase in bone stiffness occurring with skeletal maturity suggests that bone biomaterial properties also play a role in this proposed bone to brain signaling pathway.

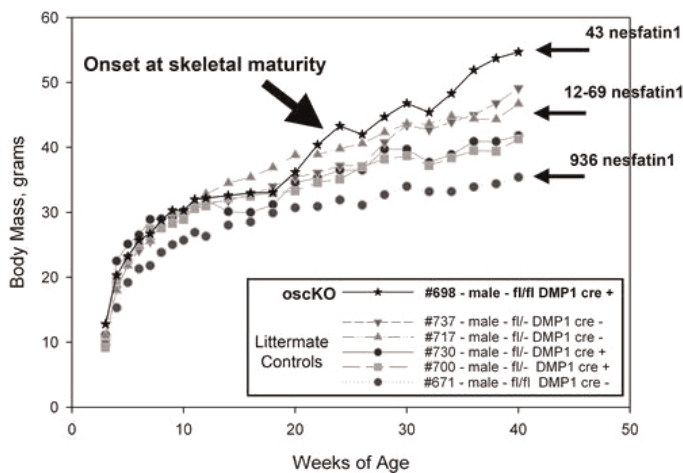


Fig 1. DMP1 Cre SKI-1 cKO mice gain weight rapidly after skeletal maturity

Disclosures: Jeffrey Gorski, None.

1183

Reverse Regulation of Ca²⁺ Signaling and NFATc1 Activity by TRPM4 Stimulates Osteoblast but Suppresses Osteoclast Differentiation and Increases Bone Mass.

Liesbet Lieben¹, Barbara Colsoul², Sophie Torrekens³, Grzegorz Owsianik², Rudi Vennekens², Geert Carmeliet⁴. ¹KU Leuven, Belgium, ²Laboratory of Ion Channel Research, KU Leuven, Belgium, ³Clinical & Experimental Endocrinology, KU Leuven, Belgium, ⁴Katholieke Universiteit Leuven, Belgium

Differentiation of osteoblasts and osteoclasts requires Ca²⁺-dependent NFATc1 activation. Regulation of [Ca²⁺]_i levels is thus crucial, but the mechanism is poorly characterized. The Ca²⁺-activated cation channel, TRPM4, controls Ca²⁺ influx in several cell types by inducing cell depolarization. TRPM4 is highly expressed in osteoblasts and osteoclasts and is therefore a likely candidate to fine-tune [Ca²⁺]_i signaling. By analyzing *Trpm4*^{-/-} mice, we show that TRPM4 regulates [Ca²⁺]_i signaling and differentiation of osteoblasts and osteoclasts in reverse direction.

First, we demonstrate that in osteoblasts, TRPM4-mediated depolarization stimulates Ca²⁺ influx via voltage-gated Ca²⁺ channels (VGCCs) which enhances NFATc1-mediated differentiation. Indeed, pharmacological activation of TRPM4 elicited a profound Ca²⁺ influx, which was suppressed by VGCC antagonists and by genetic *Trpm4* inactivation. Accordingly, *Trpm4*^{-/-} osteoblasts exhibited reduced basal [Ca²⁺]_i and *Nfatc1* mRNA levels resulting in impaired *in vitro* differentiation (mRNA differentiation markers) and mineralization.

Second, we show that osteoclasts lack VGCC activity, and as a result, the TRPM4-mediated depolarization reduces the driving force for Ca²⁺ influx and hereby smoothens the Ca²⁺ oscillations and limits NFATc1-mediated differentiation. In fact, RANKL-induced osteoclastogenesis was increased in *Trpm4*^{-/-} hematopoietic cells and was associated with an increase in the frequency and amplitude of Ca²⁺ oscillations and with enhanced NFATc1 activity. Consistent herewith, osteoclast formation was more profoundly stimulated when *Trpm4*^{+/+} osteoblasts were cultured with *Trpm4*^{-/-} vs. *Trpm4*^{+/+} hematopoietic cells. However, fewer osteoclasts were formed when *Trpm4*^{-/-} osteoblasts were used, indicating that *Trpm4*^{-/-} osteoblasts have less capacity to induce osteoclastogenesis.

These cellular effects explained the significantly reduced bone mass in *Trpm4*^{-/-} mice characterized by a manifest decrease in bone formation (serum osteocalcin, dynamic bone formation) and osteoblast differentiation (mRNA markers), with unaltered osteoclast number (TRAP, mRNA markers).

In conclusion, TRPM4-regulated [Ca²⁺]_i signaling differentially affects NFATc1 activity in bone cells, leading to stimulation of osteoblast yet suppression of osteoclast differentiation and the combined effects promote bone mass accrual.

Disclosures: Liesbet Lieben, None.

1184

Hypophosphatemic Rickets in Dentin Matrix Protein 4 (Dmp4) Knockout Mice.

Robert Brommage¹, Jeff Liu¹, Sabrina Jeter-Jones¹, David Powell¹, Andrea Thompson¹, Thomas Wronski², Peter Vogel¹. ¹Lexicon Pharmaceuticals, USA, ²University of Florida, USA

Raine syndrome (Simpson, Am J Hum Genet 81:906; 2007) in humans results from mutations in the FAM20C gene. Affected individuals usually die at birth from respiratory failure, with autopsy findings of generalized osteosclerosis.

Dmp4 is the mouse ortholog of FAM20C, with 86.5% sequence identity (Hao, J Biol Chem 282:15357; 2007) and expression in chondrocytes, osteoblasts, osteocytes, ameloblasts, odontoblasts and cementoblasts. (Wang, J Histochem Cytochem 58:957; 2010). Dmp4 knockout (KO) mice were generated by disruption of exons 1 and 2 employing homologous recombination. For all data provided below, P < 0.001 for the differences between KO and wild-type littermate mice.

Serum parameters measured in Dmp4 KO mice through weaning at 18, 22, 26 and 30 days of age (males and females combined, with Ns = 6 to 17) show modest (11%) hypocalcemia, severe (55%) hypophosphatemia and a 2.1-fold elevation of alkaline phosphatase independent of age. Newborn KO mice are normophosphatemic.

Extramedullary hematopoiesis occurs in liver and spleen. Incisors and molars are small and deformed, with degeneration and disorganization of ameloblasts and lack of mineralized enamel. The odontoblast layer is mildly disrupted with regions of dentin that contain round basophilic bodies. At 30 days of age KO mice have reduced body weight (30%), femur/tibia lengths (24%), and midshaft tibia bone diameter (22%), marrow diameter (15%) and cortical thickness (34%).

Examination of decalcified bone sections at 4 and 14 week of age shows that growth plate cartilage is thickened and disorganized in long bones, with almost total absence of cartilage cores in newly formed trabeculae. With age there is a progressive osteosclerosis affecting metaphyses of the long bones. Ribs, nasal turbinates and other bones of the skull are thicker than normal, but cortical bone in the shafts of long bones is reduced. Both nasal turbinate bones and trabeculae in the sternum are irregularly shaped.

Examination of undecalcified sections of vertebrae and femur shows extensive unmineralized osteoid, consistent with hypophosphatemic rickets and osteomalacia. Material BMD of tibial cortical bone by microCT is reduced 18%, consistent with osteomalacia.

With severe hypophosphatemia in KO mice and expression in osteocytes, FAM20C/Dmp4 is likely involved in the FGF23/DMP1/PHEX/MEPE system of phosphate homeostasis (Sapir-Koren, IBMS BoneKey 8:286; 2011).

Disclosures: Robert Brommage, Lexicon Pharmaceuticals, 3
This study received funding from: Lexicon Pharmaceuticals

1185

Pharmacological Inhibition of FGFR Signaling Ameliorates FGF23-mediated Hypophosphatemic Rickets. Simon Woehrle^{1*}, Christine Henninger¹, Olivier Bonny², Anne Thuery¹, Noemie Beluch¹, Nancy Hynes³, Vito Guagnano¹, William Sellers⁴, Francesco Hofmann¹, Michaela Kneissel¹, Diana Graus Porta¹. ¹Novartis Institutes for BioMedical Research, Switzerland, ²University of Lausanne, Department of Pharmacology & Toxicology, Switzerland, ³Friedrich Miescher Institute for Biomedical Research, Switzerland, ⁴Novartis Institutes for BioMedical Research, USA

Fibroblast growth factor 23 (FGF23) is a circulating factor secreted by osteocytes, which is essential for phosphate homeostasis. In kidney proximal tubular cells FGF23 inhibits phosphate reabsorption and vitamin D biosynthesis. Excess levels of FGF23 cause renal phosphate wasting and suppression of circulating vitamin D levels and are associated with several hereditary hypophosphatemia disorders with skeletal abnormalities, including X-linked hypophosphatemic rickets (XLH) and autosomal recessive hypophosphatemic rickets (ARHR). Currently, therapeutic approaches to these diseases are mainly limited to dietary vitamin D and phosphate supplementation, often merely resulting in partial correction of the skeletal aberrations. Here, we evaluate the use of FGFR inhibitors for the treatment of FGF23-mediated hypophosphatemia disorders using NVP-BGJ398, a novel selective, pan-specific FGFR inhibitor currently in Phase I clinical trials for cancer therapy. In two different hypophosphatemic mouse models, Hyp and *Dmp1*-null mice, resembling the human diseases XLH and ARHR, we find that pharmacological inhibition of FGFRs efficiently abrogates aberrant FGF23 signaling and normalizes the hypophosphatemic and hypocalcemic conditions of these mice. Correspondingly, long-term FGFR inhibition in Hyp mice leads to enhanced bone growth, increased mineralization and reorganization of the disturbed growth plate structure. We therefore propose NVP-BGJ398 treatment as a novel approach for the therapy of FGF23-mediated hypophosphatemia diseases.

Disclosures: Simon Woehrle, Novartis Institutes for BioMedical Research, 3
This study received funding from: Novartis Institutes for BioMedical Research

1186

Systems Genetics Identifies *Lhfp* as a Bone Mineral Density Candidate Gene and Regulator of Osteoblastogenesis. Cheryl Ackert-Bicknell¹, Daniel Gatti¹, Rachel Madenjian², John Sundberg¹, Gary Churchill¹, Charles Farber^{2*}. ¹The Jackson Laboratory, USA, ²University of Virginia, USA

It is well understood that peak bone mass is a heritable phenotype. Thus, there has been considerable effort focused on identifying and functionally characterizing the genes underlying this phenotype. Genome-wide association (GWA) and network analysis are two powerful approaches used to accomplish these goals. When used in concert, they not only identify the genes underlying a phenotype, but also aid in determining their functional role. In this study, we performed GWA for bone mineral density (BMD) using data obtained from 27 classical inbred strains of mice (i.e. not wild derived). Specifically, BMD data was collected on female and male mice at 6, 12, and 20 months of age and GWA was performed using the Efficient Mixed-Model Association algorithm. This analysis identified high-confidence BMD associations on Chromosomes (Chrs) 2, 3, and 17. To minimize false positives a second BMD GWA was performed in a partially overlapping set of 31 classical inbred strains. This replicated the association on Chr. 3. In both sets of mice the Chr. 3 association spanned a 500 Kbp genomic interval containing two annotated genes, lipoma HMGIC fusion partner (*Lhfp*) and component of oligomeric golgi complex 6 (*Cog6*). Causality modeling in a separate F2 cross was used to generate additional evidence supporting a causal role for one or both genes. These results suggested that *Lhfp*, and not *Cog6*, was a regulator of BMD. A co-expression network analysis revealed that *Lhfp* was a member of a co-expression module enriched for genes involved in osteoblast function and gene expression studies confirmed that this gene is indeed highly expressed in mouse primary calvarial osteoblasts (mOBs). Within this module, *Lhfp* was most strongly connected to genes encoding bone extracellular matrix proteins. Together, these data suggested that *Lhfp* was a regulator of osteoblast function. To test this hypothesis, we determined the effect of *Lhfp* knockdown on the differentiation of mOBs. At 10 days post-differentiation, we observed significant ($P < 0.05$) dose-dependent reductions in mineralized nodule production by cells treated with two independent *Lhfp* targeting siRNAs, substantiating our hypothesis that this gene is indeed involved in osteoblast function. In conclusion, we have used a multifaceted systems genetics approach in mice to identify *Lhfp* as a regulator of osteoblastogenesis and a promising candidate gene for BMD.

Disclosures: Charles Farber, None.

1187

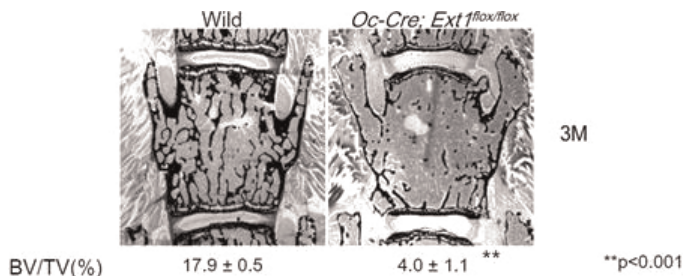
Targeted Disruption of Heparan Sulfate in Osteoblasts Leads to Severe Osteoporotic Phenotype in Mice. Satoshi Nozawa^{1*}, Fumitoshi Irie², Shinji Iizuka², Thomas Clemens³, Kazu Matsumoto⁴, Yu Yamaguchi^{2, 1}, USA, ²Sanford-Burnham Medical Research Institute, USA, ³Johns Hopkins University, USA, ⁴Gifu University, School of Medicine, Japan

Background: Although accumulating *in vitro* data suggest important roles for heparan sulfate (HS) in osteoblast differentiation, there is little information about whether and how HS is involved in bone formation *in vivo*. This study aims to determine the role of HS in the osteoblast lineage and to dissect the mechanism by which HS influences the function of these cells.

Methods: We eliminated heparan sulfate from mature osteoblasts by conditionally inactivating *Ext1*, the gene encoding an enzyme essential for heparan sulfate synthesis. Analysis of bone mass was performed by osteocalcin-Cre (Oc-Cre)-driven conditional *Ext1* mutant mice, *Oc-Cre; Ext1^{fllox/fllox}*. Standard histomorphometric variables were calculated. This was followed by initial *in vitro* investigations into the mechanism of osteogenesis and osteoclastogenesis.

Result: *Oc-Cre; Ext1^{fllox/fllox}* mice show severe osteoporotic phenotype. The reduction in bone volume observed in mutant mice was progressively more evident with increasing animal age compared with wild type. BV/TV in mutant lumbar vertebrae decreased by 52% ($p < 0.01$) at 5 weeks of age and by 22% ($p < 0.001$) at 3 months (Figure). The bone formation rates of mutants were equivalent to normal littermates. On contrast, osteoclast number (N.Oc/T.Ar, N.Oc.N/B.Pm) in mutant bones were significantly increased in the mutant mice ($p < 0.01$). Moreover, urinary deoxypyridinoline was increased in mutant mice ($p < 0.05$). As for the cause, we focused Osteoprotegerin (Opg) which contains a highly basic heparin-binding domain, suggesting that direct interaction with HS could be involved in osteoclastogenesis through the intermediary of RANK-RANKL-OPG triad. We measured cell surface-associated and soluble Opg in the NaCl extracts. We detected smaller volume of Opg on mutant osteoblast ($p < 0.05$). To elucidate the interaction with Opg and heparan sulfate, we produced recombinant Opg lacking heparin binding domain by site directed mutagenesis. The results show Opg lacking heparin binding domain could not inhibit osteoclastogenesis *in vitro* assays than the wild type Opg, which suggests heparan sulfate is required to Opg mediated osteoclastogenesis inhibition.

In summary, *Oc-Cre; Ext1^{fllox/fllox}* mice show severe osteoporotic phenotype. We suggest that HS is required for cell surface association of Opg and HS suppresses osteoclastogenesis by increasing cell surface-associated Opg, which could interfere RANK-RANKL interaction.



Oc-Cre; Ext1^{fllox/fllox} mice show severe osteoporotic phenotype.

Disclosures: Satoshi Nozawa, None.
This study received funding from: UEHARA Memorial Foundation Scholarship

1188

EphrinB2 Signaling in Osteoblasts and Chondrocytes is Required for their Differentiation and Support of Osteoclast Formation. Stephen Tonna^{1*}, Farzin Takvar², Ingrid Poulton³, Patricia Ho³, Narelle McGregor³, Carl Walkley³, Brian Liddicoat³, Liliana Tatarczuch⁴, Eleanor Mackie⁵, T. John Martin⁶, Natalie Sims⁷. ¹St Vincent's Institute, Australia, ²St. Vincent's Institute of Medical Research, Australia, ³St Vincent's Institute of Medical Research, Australia, ⁴Veterinary Science University of Melbourne, Australia, ⁵University of Melbourne, Australia, ⁶St Vincent's Institute of Medicine, Australia, ⁷St. Vincent's Institute for Medical Research, Australia

Osteoblasts express both EphB4 and its cognate ligand, ephrinB2, and treatment with PTH rapidly induces their expression of ephrinB2. Simultaneous blockade of both ephrinB2 and EphB4 signaling impedes both osteoblast differentiation and mineralization *in vitro*, while stimulation of ephrinB2 in the hematopoietic lineage inhibits osteoclast differentiation. To investigate ephrinB2 signaling within osteoblasts and chondrocytes we generated mice with conditional deletion of the ephrinB2 cytoplasmic domain in osteoblasts and sporadic hypertrophic chondrocytes (*Osx1:GFP; Cre; Efnb2^{fl/fl}*).

EphrinB2 cytoplasmic domain expression was reduced ~95% in FACS-isolated *Osx1.Efnb2^{fl/fl}* primary calvarial osteoblasts compared with *Osx1.Efnb2^{+/+}* and ~80% in *Osx1.Efnb2^{fl/fl}* primary chondrocytes. In FACS-sorted *Osx1.Efnb2^{fl/fl}* osteoblasts both early (Runx2, Osx, ALP) and late differentiation markers (OCN, PTHR1,

MEPE, SOST) were reduced by 80-90%. Similar findings were obtained when exogenous viral Cre was introduced to *Efnb2^{fl/fl}* osteoblasts. Consistent with these changes, bone formation rate was reduced by ~50% in adult *Osx1.Efnb2^{fl/fl}* mice, and late osteoblast differentiation markers were impaired by ephrinB2:ephrinB4 receptor antagonists (sEphB4 and TNYL). *Osx1.Efnb2^{fl/fl}* osteoblasts also demonstrated reduced RANKL expression (50%) and impaired support of osteoclast formation in co-culture with wild-type bone marrow precursors. This indicates that ephrinB2 signaling within the osteoblast lineage is required for appropriate differentiation and mineralization by osteoblasts and to support osteoclast formation.

Reduced support of osteoclast formation was also observed in *Osx1.Efnb2^{fl/fl}* neonates, which demonstrated high trabecular bone volume, prominent cartilage remnants, and a 75% reduction in osteoclast numbers at the growth plate; a mild osteopetrosis that resolved by 12 weeks of age. Electron microscopy revealed that the osteoclasts near the growth plate showed reduced contact with cartilage and bone, did not form ruffled borders or sealing zones and exhibited convoluted nuclei. In addition contact between osteoblasts and between osteoblasts and the bone surface was reduced and chondrocytes at all stages of maturation contained more condensed chromatin. In conclusion, these results indicate that osteoblastic ephrinB2 signaling regulates osteoblast and chondrocyte differentiation and the support of osteoclast formation by both chondrocytes and osteoblasts.

Disclosures: Stephen Tonna, None.

1189

Hypoxia-inducible Factor-1 α Restricts PTH-induced Anabolic Signals by Sequestration of β -catenin. Julie Leslie^{*1}, Thomas Clemens¹, Ryan Riddle². ¹Johns Hopkins University, USA, ²Johns Hopkins University School of Medicine, USA

The hypoxia inducible factors (Hifs) are evolutionarily conserved transcriptional factors that control homeostatic responses to low oxygen. In developing bone, Hif-1 generated signals are required for angiogenesis, which appears to be necessary for initial specification of bone-forming osteoblasts. In mature mouse bone, loss of Hif-1 α in osteoblasts resulted in a more rapid accumulation of trabecular and cortical bone. Moreover, removal of Hif-1 α from osteoblasts sensitized mature bone to load-induced bone formation by enhancing the response of osteoblasts to mechanical stimuli (Riddle, 2011 J Biol Chem 286:44449-44456). These findings suggested that Hif-1 exerts distinct developmental functions and acts in the mature skeleton as a negative regulator of bone formation. In this study, we investigated the function of Hif-1 α in osteoanabolic signaling by assessing the effect of Hif-1 α loss-of-function on bone formation in response to parathyroid hormone (PTH). Exposure of primary mouse osteoblasts to PTH resulted in the rapid induction of Hif-1 α protein levels via a post-transcriptional mechanism, but had no effect on Hif-2 α . In vivo, PTH treatment (40 μ g/kg BW/day for 6 weeks) increased trabecular bone volume to a significantly greater extent in Δ Hif1 α mice than in control littermates. To clarify the mechanism underlying increased sensitivity to PTH, we examined the activation of signaling events downstream of the PTH receptor in osteoblasts lacking Hif-1 α . The activation of cAMP and MAP kinase signaling by PTH was not significantly affected by the loss of Hif-1 α function. However, PTH induced β -catenin activity was enhanced, as evidenced by prolonged elevations in Axin2 mRNA levels in Hif-1 α -deficient cells. Further, PTH-induced occupancy of the Axin2 promoter by β -catenin (ChIP) was greater in osteoblasts lacking Hif-1 α compared to controls. Taken together, these data indicate that Hif-1 α functions in the mature skeleton to restrict osteoanabolic signaling. The availability of pharmacological agents that reduce Hif-1 α function suggests the value in further exploration of this pathway to optimize the therapeutic benefits of PTH.

Disclosures: Julie Leslie, None.

1190

Serotonin Receptor 5-HT_{2B} Controls Osteoblast Cell-cell Adhesion and Mineralization by Multiple Pathways. Yasmine Chabbi Achengli^{*1}, Jean Marie Launay², Luc Maroteaux³, Marie-Christine De Vernejoul⁴, Corinne Collet¹. ¹INSERM U606, France, ²Laboratoire de biochimie Hopital Lariboisière, France, ³INSERM UMR S-839 Institut du Fer a Moulin, France, ⁴Fédération De Rhumatologie Et INSERM U606, France

The serotonergic 5-HT_{2B} receptor is implicated in various physiological and pathological functions. Our previous in vivo results showed that in the absence of 5-HT_{2B} receptor (5-HT_{2B}^{-/-} mice) there was a decreased bone formation due to reduced mineralizing surfaces (Collet et al., 2008). In order to decipher the mechanism(s) responsible(s) for the osteoblast defect, we studied primary calvaria osteoblast cultures. Firstly, we observed that both osteoblast proliferation and mineralization were markedly impaired in 5-HT_{2B}^{-/-} cells, associated with a reduced alkaline phosphatase gene expression (-34%). Moreover, cell-cell adhesion of 5-HT_{2B}^{-/-} osteoblasts was also lower (-62%) with N-cadherin intra-cytoplasmic localization. Wnt 3a treatment induced an increase proliferation of the WT but not of the 5-HT_{2B}^{-/-} osteoblast. As multiple signaling pathways could be responsible for this phenotype we first investigated the phospholipase A2 (PLA2) pathway that has been shown to be linked to 5-HT_{2B} in an osteoprogenitor cell line. Treatment with mepacrine, a specific inhibitor of PLA2, induced a decreased cell aggregation and induced N-cadherin mislocalization. Furthermore the protein expression of COX2

was strongly decreased in 5-HT_{2B}^{-/-} culture as compared to WT. We therefore measured the level of prostaglandin E2 (PGE2) and the expression of PGE2 synthase (PGES), and we observed no differences. By contrast, the level of prostacyclin (PGI2 prostaglandin I2) was 10 fold higher and PGI synthase activity was markedly increased (WT: 11 \pm 5.2 vs 5-HT_{2B}^{-/-}: 42 \pm 6.3 p<0.0001) in absence of 5-HT_{2B} receptors. As prostacyclin is the endogenous ligand of peroxisome proliferator activated receptor β/δ (PPAR- β/δ) we hypothesized that PPAR β/δ activation could be responsible in part of the 5-HT_{2B}^{-/-} osteoblast phenotype. One of the target of PPAR β/δ is the protein convertase (PC) that is involved in N-cadherin maturation and migration to cell membrane. We showed a decrease in PC activity in 5-HT_{2B}^{-/-} osteoblasts, that was restored by treatment with GSK0660 a specific PPAR β/δ inhibitor. Treatment with GSK0660 improved 5-HT_{2B}^{-/-} osteoblast aggregation and N-cadherin localization to the membrane, and completely restored the mineralization defect of the 5-HT_{2B}^{-/-} osteoblast. In conclusion we show that osteoblast 5-HT_{2B} receptor signal mainly by the PGI2 pathway and could involve PPAR β/δ .

Disclosures: Yasmine Chabbi Achengli, None.

1191

Gli1 Participates in the Indian Hedgehog-mediated Osteogenesis during Endochondral Ossification. Hironori Hojo^{*1}, Shinsuke Ohba², Fumiko Yano³, Taku Saito⁴, Toshiyuki Ikeda⁵, Keiji Nakajima⁶, Yusuke Komiyama⁶, Naomi Nakagata⁷, Kentaro Suzuki⁷, Tsuyoshi Takato⁸, Hiroshi Kawaguchi⁹, Ung-Ii Chung¹⁰. ¹The Center for Disease Biology & Integrative Medicine, Japan, ²Division of Biotechnology, Center for Disease Biology & Integrative Medicine, Japan, ³University of Tokyo, Japan, ⁴University of Tokyo, Graduate School of Medicine, Japan, ⁵Information Technology Services, Inc., Japan, ⁶The University of Tokyo, Japan, ⁷Kumamoto University, Japan, ⁸Graduate School of Medicine The University of Tokyo, Japan, ⁹University of Tokyo, Faculty of Medicine, Japan, ¹⁰University of Tokyo Schools of Engineering & Medicine, Japan

With regard to hedgehog (Hh) signaling in mammalian skeletal development, most research has focused on Gli2 and Gli3 rather than Gli1. This is because *Gli1^{-/-}* mice do not show any gross abnormalities in adulthood, and no detailed analyses of fetal *Gli1^{-/-}* mice are available. Therefore, we aimed to determine physiological roles of Gli1 in osteogenesis. We initially examined the contribution of Gli1 to Hh signaling-mediated osteogenesis compared with Gli2 and Gli3 *in vitro* and *in vivo*. In primary perichondrial cell (PPC) cultures, wild-type (WT) cells acquired phenotypes of early osteoblasts upon Hh signaling activation by SAG, a Smoothed agonist. The SAG-mediated osteoblast differentiation was impaired in *Gli1^{-/-}* as well as *Gli2^{-/-}* cells relative to that in WT cells, whereas it was enhanced in *Gli3^{-/-}* cells. Histological analyses on *Gli1^{-/-}* mice revealed that the bone collar was absent in metatarsals of the mice at embryonic day 17.5. The *Gli1^{-/-}* perichondrium showed a decreased region of alkaline phosphatase (*Alp*)-expressing cells compared with that in the WT perichondrium, and it lacked expression of bone sialoprotein (*Bsp*). Expression of runt-related transcription factor (Runx2) or osterix was not detected in the *Gli1^{-/-}* perichondrium at this stage. In addition, *Gli1^{-/-};Gli2^{-/-}* mice showed more severely-impaired osteogenesis than either *Gli1^{-/-}* or *Gli2^{-/-}* mice, and osteoblast differentiation was impaired in *Gli1^{-/-};Gli3^{-/-}* perichondrial cells compared with *Gli3^{-/-}* cells *in vitro*. We next attempted to elucidate how Gli1 regulated osteogenesis. *Gli1* overexpression upregulated the early osteoblast markers *Alp* and *Bsp*, but not the late osteoblast marker *osteocalcin*, in PPCs and C3H10T1/2 cells. *Gli1* knockdown with shRNA inhibited the SAG-induced expressions of *Alp* and *Bsp* in C3H10T1/2 cells. *Gli1* overexpression not only rescued impaired expressions of *Alp* and *Bsp* in Indian hedgehog (*Ihh*)^{-/-} PPCs, but also upregulated their expressions in *Runx2^{-/-}* PPCs. Luciferase assay, EMSA and CHIP revealed that Gli1 transactivated *Alp* and *Bsp* via its binding to 5' regulatory regions of these genes, possibly underlying the activity of Gli1 in osteogenesis. Thus, Gli1, acting downstream of *Ihh*, contributes to early osteoblast differentiation, at least to some extent, in a Runx2-independent manner; it plays redundant roles with Gli2 and is involved in the repressor function of Gli3. We propose that Gli1 functions collectively with Gli2 and Gli3 in osteogenesis.

Disclosures: Hironori Hojo, None.

1192

Conditional Disruption of the Prolyl Hydroxylase 2 (PHD2) Gene Defines its Key Role in Skeletal Development. Shaohong Cheng^{*1}, Weirong Xing², Sheila Pourteymoor³, Subburaman Mohan⁴. ¹VA Loma Linda Health Care Systems, USA, ²Musculoskeletal Disease Center, Jerry L. Pettis Memorial Veteran's Admin., USA, ³Jerry L Pettis VA Memorial Med Ctr, USA, ⁴Jerry L. Pettis Memorial VA Medical Center, USA

Disruption of gulonolactone oxidase, a key enzyme involved in ascorbic acid (AA) biosynthesis, results in spontaneous fractures (Sfx) in mice caused by deficient osteoblast (OB) functions. Studies on the molecular mechanism for AA regulation of OBs revealed that the increase in osterix (*Osx*) expression during OB maturation is dependent on AA and that AA effects on *Osx* mRNA expression is mediated via a

novel mechanism that involves PHD2-dependent proteasomal degradation of a yet to be identified transcriptional repressor of *Osx* gene expression. Because PHD2 is strongly expressed in OBs and that inhibition of PHD2 expression using shRNA reduces AA-induced *Osx* expression and OB differentiation, we predict that PHD2 is important in the OB differentiation pathway. In order to determine if lack of PHD2 in bone cells influences the skeletal phenotype, we first generated conditional knockout (KO) of PHD2 by crossing PHD2 floxed mice with transgenic *Osx-Cre* mice. Surprisingly, none of the surviving 65 mice were *Cre* positive and homozygous for floxed PHD2 alleles. However, *Cre* positive embryos that were homozygous for floxed PHD2 alleles were detected at embryonic day 14. Since *Osx* is known to be expressed in chondrocytes besides OBs, we next crossed PHD2 floxed mice with *Coll1 α 2-Cre* mice in which expression of *Cre* recombinase is placed under the control of the procollagen type 1 α 2 promoter. Of the homozygous PHD2 floxed mice, the *Cre* positive genotype was identified in 60% fewer mice as compared to the *Cre* negative genotype. The surviving mice exhibited a 27% and a 12% reduction in body weight and femur length at 3 wks of age ($P < 0.01$). At 5 and 8 wks of age, femur and tibia BMD, measured by DXA, were reduced by $>15\%$ ($P < 0.01$) in the conditional mutants. To determine the mechanism for BMD reduction in PHD2 conditional KO mice, we measured expression levels of transcription factors, bone formation and differentiation markers using RNA extracted from femurs of conditional KO and littermate control mice. We found that mRNA levels of *Osx*, osteocalcin and ALP were reduced by 50%, 58% and 30%, respectively, in the femurs of conditional KO mice (all $P < 0.05$). In contrast, expression levels of TRAP, Runx2 and *Dlx5* were unaffected. Based on our published data and current findings, we conclude that PHD2 is critically involved in regulating OB functions and thereby bone formation in part via regulating *Osx* expression.

Disclosures: Shaohong Cheng, None.

1193

Loss of the Wnt Inhibitor Tiki2 Results in a High Bone Mass Phenotype. Bryan MacDonald¹, Alexander Robling², Xi He¹. ¹Children's Hospital Harvard Medical School, USA, ²Indiana University, USA

Activation of the Wnt/ β -catenin pathway in osteoblasts and osteocytes results in increased bone mass. Therefore therapies that target antagonists of the Wnt pathway represent promising anabolic treatments. Here we report the characterization of new antagonist of the Wnt signaling pathway and the high bone mass phenotype of the Tiki2 knockout mouse.

The TIKI gene family was identified in screen for Wnt pathway regulators in *Xenopus* embryos¹. Named after the large headed humanoid carving in Polynesian mythology; expression of TIKI resulted in embryos with enlarged heads consistent the inhibition of the Wnt/ β -catenin pathway. TIKI proteins contain an amino terminal signal sequence, a conserved TIKI domain of 330 amino acids and a carboxyl terminal transmembrane region with almost no intracellular domain. Heterologous expression shows that TIKI proteins are localized within the secretory pathway and present at the plasma membrane. Our current data indicate that TIKI acts as a protease to cleave the amino terminal residues of Wnt ligands, thereby inactivating Wnt to prevent receptor binding¹.

To analyze the role of Tiki2 in mammals we generated a Tiki2 knockout mouse. Homozygous Tiki2^{-/-} null mice are viable and fertile, and are found at the expected Mendelian frequencies on a mixed genetic background. Mouse Tiki2 is expressed in osteoblasts suggesting a role for Tiki2 in regulating bone mass. Offspring from a Tiki2^{+/-} intercross were analyzed by μ CT, and a greater amount of trabecular bone was found in Tiki2^{-/-} mice. Quantification of the trabecular bone properties revealed a significant increase in bone volume fraction (KO 0.183 \pm 0.063 BV/TV vs WT 0.099 \pm 0.038 BV/TV), trabecular number (KO 4.34 \pm 0.81 #/mm³ vs WT 3.12 \pm 0.47 #/mm³) and trabecular thickness (KO 0.0659 \pm 0.0052 mm vs WT 0.0590 \pm 0.0057 mm) in male 16 week old Tiki2^{-/-} mice (n=6) compared with +/- littermates (n=7). Our results demonstrate that genetic inhibition of the Wnt antagonist Tiki2 increases trabecular bone and suggest that inhibition of TIKI proteins may be a therapeutic option for treating low bone mass disorders.

Zhang X; Abreu JG, Yokota Y, MacDonald BT, Singh S, Coburn KL, Cheong SM, Zhang MM, Ye Q, Hang HC, Steen H, He X. Tiki1 is required for head formation via Wnt cleavage-oxidation and inactivation. Cell 2012 (in press)

Disclosures: Bryan MacDonald, None.

1194

Selective Deletion of the Soluble Colony Stimulating Factor 1 Isoform *in vivo* Eliminates Estrogen-deficiency Bone Loss in Mice. Gang-Qing Yao¹, Benhua Sun¹, Jian Jun Wu², Karl Insogna¹. ¹Yale University School of Medicine, USA, ²Yale University, USA

It has been reported that a neutralizing antibody to CSF1 completely prevents ovariectomy(OVX)-induced bone loss in mice. There are two isoforms of CSF1, soluble (sCSF1) and membrane-bound (mCSF1), but their individual biological functions are unclear. Estrogen-withdrawal increases levels of IL-1 and TNF in bone marrow, which induce the formation of a stromal cell population producing high levels of sCSF1. However, others have found that estrogen-withdrawal selectively up-regulates expression of mCSF1 and down-regulates sCSF1 expression in rat bone marrow cultures. We recently reported that one month after surgery, five month-old mCSF1 knockout (*k/o*) and wild type (*wt*) female mice experienced the same degree of

bone loss following ovariectomy (OVX). OVX induced a significant 4-fold increase in the expression of sCSF1 in the bones of *wt* mice while expression of mCSF1 was unchanged. These findings indicate that mCSF1 does not appear to be required for estrogen-deficiency bone loss but sCSF1 could play a key role in this pathologic process. To test this hypothesis we engineered sCSF1 *k/o* mice. Isoform-specific RT-PCR confirmed the absence of transcripts for sCSF1 in bone tissue isolated from these animals and no circulating CSF1 was detected in these animals when assayed with a sensitive ELISA. Surprisingly, there were no significant differences in BMD as assessed by DXA, between sCSF1 *k/o* mice and *wt* controls. To examine the effect of estrogen withdrawal in these animals 5 month-old sCSF1 *k/o* and *wt* female mice underwent ovariectomy (OVX) or sham-OVX. One month after surgery, femoral, spinal and total BMD (determined byDXA) were reduced by 7.6% and 4.9% and 6.6% respectively in OVX-*wt* animals as compared to sham-OVX *wt* mice. OVX sCSF1-*k/o* mice showed 3.8% and 6.1% and 0.89% reductions in femoral, spinal and total BMD respectively compared to sham-OVX sCSF1-*k/o* animals. MicroCT analyses demonstrated an 18% reduction of femoral trabecular bone density in OVX-*wt* animals compared to sham-OVX *wt* mice. In striking contrast, OVX sCSF1-*k/o* mice showed no reduction in femoral BV/TV. Our findings indicate important non-redundant functions for the two isoforms of CSF1. In particular, our data indicate that sCSF1 but mCSF1 plays a key role in estrogen-deficiency bone loss. However, mCSF1 is essential for normal bone remodeling.

Disclosures: Gang-Qing Yao, None.

1195

Conditional Deletion of gp130 in Osteoblasts and Osteocytes has Divergent Effects on Trabecular and Cortical Bone. Rachele Johnson¹, Holly Brennan¹, Ingrid Poulton¹, Narelle McGregor¹, Tzen Koh¹, Muhammad Zainuddin¹, Emma Walker¹, T John Martin¹, Natalie Sims². ¹St. Vincent's Institute of Medical Research, Australia, ²St. Vincent's Institute for Medical Research, Australia

Glycoprotein 130 (gp130) is a cytokine co-receptor that transduces intracellular signals in response to IL-6, IL-11, leukemia inhibitory factor (LIF) and oncostatin M (OSM). These cytokines stimulate osteoblastic RANKL expression, osteoclast formation and bone formation, but surprisingly, global deletion of gp130 resulted in enhanced osteoclast formation, while the effect of gp130 deletion on bone formation was complicated by neonatal lethality and systemic defects. To determine the role of gp130 in the osteoblast lineage, gp130 was deleted conditionally from early stages of osteoblast differentiation (*Osx1-Cre*) to late stage osteoblasts/osteocytes (*DMP1-Cre*) in C57BL/6 mice. Efficient gp130 recombination was verified by real-time PCR.

MicroCT and histomorphometry on 12-week old male mice revealed a significant reduction in trabecular bone volume (~50%) in tibiae, femora and vertebrae of *Osx1 gp130^{off}* and *DMP1 gp130^{off}* mice compared with appropriate *Cre+ wt/wt* controls. Both low bone mass phenotypes were accompanied by significant reductions (between 22-51%) in trabecular number, mineralizing surface and bone formation rate, indicating that late-stage osteoblast/osteocytic gp130 signaling is essential for normal bone formation. Although gp130-binding cytokines stimulate osteoclast formation, osteoclast number, surface and size were not changed in either KO, suggesting that while osteoblastic gp130 is critical for bone formation, it is not required for normal osteoclast formation. Even in 3-day old *Osx1* and *DMP1 gp130* KOs, no differences in osteoclast numbers were detected, indicating compensation for the lack of gp130 to support osteoclast formation in the context of normal development and remodeling.

In contrast to trabecular bone, cortical analysis by microCT revealed a significant increase in cortical thickness (4 & 12%), marrow volume (18 & 29%) and periosteal surface area (10 & 17%) in *Osx1* and *DMP1 gp130* KOs, respectively, with no change in bone length, indicating that osteoblastic gp130 may function in dramatically different ways in trabecular and cortical bone.

In conclusion, while osteoblastic gp130 is not required for osteoclast formation, its deletion may allow for osteoblast and osteocyte compensatory signaling to support osteoclast development. Furthermore, the similarity between *Osx1* and *DMP1 gp130* KO phenotypes indicates that gp130 signaling in late osteoblasts and osteocytes, but not early osteoblasts, is critical for normal bone formation.

Disclosures: Rachele Johnson, None.

1196

Macrophage Migration Inhibitory Factor (MIF) Promotes Osteoclastogenesis, RANKL Signaling and Arthritic Bone Erosion. Ran Gu¹, Julian Quim², Leilani Santos³, Eric Morand⁴, Devi Ngo⁴, Huapeng Fan⁴, Jiak Xu⁵, Richard Bucala⁶. ¹Monash Medical Centre, Australia, ²Prince Henry's Institute of Medical Research, Australia, ³Monash University, Australia, ⁴Monash Medical Centre, Australia, ⁵University of Western Australia, Australia, ⁶Yale School of Medicine, USA

In rheumatoid arthritis (RA), MIF promotes the recruitment and activation of leukocytes, but its role in bone erosion is unclear. We sought to investigate the effect of MIF on bone erosion in an *in vivo* model and *in vitro* osteoclastogenesis assays.

K/BXN serum transfer arthritis was induced in MIF^{-/-} and WT mice and characterised by scoring clinically, histologically, by TRAP staining (to identify

osteoclasts) and real time RT-PCR analysis. Osteoclastogenesis assays were performed using bone marrow (BM) cells or RAW 264.7 cells cultured with CSF-1 and RANKL. RAW264.7 cells stably transfected with NF κ B-luciferase and NFAT-luciferase reporters, and phosphorylation of ERK1/2 and p38 in bone marrow derived macrophages (BMM), were used to assess MIF effects on osteoclast signaling. RANKL-induced actin rings in bone marrow cells were stained with rhodamine-phalloidin.

Compared to WT mice, MIF^{-/-} mice with K/BxN serum induced arthritis, had significantly lower clinical scores, histological synovitis and bone damage. Significantly reduced TRAP⁺ osteoclast numbers, and OC-STAMP and DC-STAMP mRNA expression, was found in MIF^{-/-} joints. RANKL induction of osteoclastogenesis in BMM was accompanied by significant dose-dependent increases in MIF protein and mRNA expression. These findings were paralleled by the observation of significantly fewer TRAP⁺ osteoclasts, and significantly fewer large osteoclasts (>10 nuclei), in RANKL/CSF-1 stimulated cultures of MIF^{-/-} BM compared to WT. In addition, actin ring formation in response to RANKL was significantly less in MIF^{-/-} BMM. In RAW264.7 cells, RANKL-induced osteoclastogenesis, and NF κ B and NFATc1 reporter luciferase activity, was significantly abrogated by anti-MIF monoclonal antibody. In addition, reduced phosphorylation of ERK1/2, but not p38, was observed in MIF^{-/-} BMM. This was accompanied by higher expression of multiple dual specificity phosphatases (DUSP), including DUSP1,5,6,8,9,10,16 and 19, in MIF^{-/-} BMM.

In summary, MIF facilitates osteoclastogenesis *in vivo* and *in vitro*, and supports NF κ B, NFATc1 and ERK1/2 activation. These findings suggest therapeutic MIF neutralization as a potential strategy for both RA bone erosion as well as joint inflammation. The potential role of MIF in other forms of pathological bone loss is also suggested, and requires investigation.

Disclosures: Ran Gu, None.

1197

Osteoclast Specific Deletion of NEMO/IKK γ in Mice Leads to Osteopetrosis. Kyuhwan Shim¹, Manolis Pasparakis², Yousef Abu-Amer³.
¹Washington University school of medicine, USA, ²Institute of Genetics, University of Cologne, Germany, ³Washington University in St. Louis School of Medicine, USA

The transcription factor NF- κ B family is central to numerous processes including bone development. Activation of this pathway depends on degradation of I κ B upon phosphorylation by I κ B kinases. This process is tightly regulated by IKK γ (also called NEMO, NF- κ B essential modulator), the regulatory subunit of I κ B kinase. Expression and function of NEMO itself is tightly regulated by poly-ubiquitination events. Nemo is X-linked, and defects in this gene result in Incontinentia Pigmenti in human hemizygous female, yet global deficiency in mouse causes embryonic lethality. Certain clinical cases manifested skeletal defects suggesting that NEMO regulates bone metabolism. To investigate such role, we used conditional deletions of *nemo* floxed mice with cre expression driven by osteoclast specific promoters cathepsin K and lysozyme M. Micro CT analysis reveals severe osteopetrotic phenotype in trabecular region in both Cat K and Lys M cre-mediated NEMO deficient male. This phenotype is more severe in females, probably reflecting lack of dosage compensation in male. Histological analysis shows that less osteoclasts (OCs) were detected in trabeculae in KO mice consistent with defective osteoclastogenesis *in vitro*. Consistently, we show that NEMO deficiency hampered activation of IKK and phosphorylation of I κ B in OC precursors (OCPs), causing arrest of osteoclastogenesis and subsequent osteopetrosis. To further explore the underlying mechanism of this phenomenon, we examined the potential role of various NEMO ubiquitinations. To this end, several viral constructs representing strategic point mutations at key residues in coiled-coil-2 and leucine zipper domains, known to be involved in oligomerization and subsequent K63 mediated or linear ubiquitination, were utilized to examine their osteoclastogenic potential in NEMO deficient OCPs. Of these mutants, K270A-NEMO (unable to undergo SUMOylation on K270) was expressed at high levels indicating increased protein stability. Introduction of this mutant protein into NEMO-deficient cells resulted with elevated osteoclastogenesis comparable to wild type levels. In contrast, expression of the mutant K319A NEMO into NEMO-deficient cells was lower and failed to restore osteoclastogenesis, indicating that K319-modification is essential for NEMO stability and function. In summary, we provide evidence that NEMO is essential for osteoclastogenesis and bone homeostasis, and that residues K270 and K319 are crucial for these functions

Disclosures: Kyuhwan Shim, None.

1198

Ubiquitous and Osteo-chondrogenitor Specific Activation of FGFR3 Affect Endochondral and Membranous Ossification during Craniofacial Formation. Martin Biosse Duplan^{*1}, Federico Di Rocco², Catherine Benoist-Lassel², Nabil Kaci², Nadhir Litim², EMILIE MUGNIERY³, Klaus von der Mark⁴, Arnold Munnich², Laurence Legeai-Mallet⁵.
¹Faculté de Chirurgie Dentaire Université Paris Descartes AP-HP, France, ²INSERM U781, Université Paris Descartes - Sorbonne Paris Cité, Institut Imagine, Hôpital Necker-Enfants Malades, France, ³INSERM U781, France, ⁴University of Erlangen-Nürnberg, Germany, ⁵INSERM U781 - Paris Descartes university, Necker hospital, Fra

Activating FGFR3 mutations in humans result in short-limbed dwarfism and craniostenosis, implicating FGFR3 in both endochondral and membranous ossification during skeletal development. It is not well understood how FGFR3 affects the formation of the flat bone of the skull and suture homeostasis. To address this question, we generated mice expressing an activating FGFR3 mutation (*Fgfr3*^{Y367C/+}) ubiquitously (using the *CMV-cre* transgene), in osteo-chondrogenitors (*Col2al-cre*), in mature osteoblasts (*2.3kb Colla1-cre*) or in mature chondrocytes (*Coll10a1-cre*). The skull of the four mouse models were studied at 3 weeks of age using macroscopic examination of the skull after alcian blue and alizarin red staining, radiology, microCT and MRI analyses and histology of the cranial base and coronal sutures. Ubiquitous expression of the *Fgfr3*^{Y367C} resulted in dramatic morphological changes. In addition to a severe dwarfism, all mice had an impressive dome-shaped skull (33% length reduction, p<0.001), a severe malocclusion and a large midline defect. The size of nasal, frontal, interparietal and occipital bones was significantly altered. The size of the foramen magnum was reduced (38%, p<0.0001). MRI revealed significant abnormalities in the craniovertebral junction including neural compression. Most importantly both speno occipital synchondrosis and coronal sutures were prematurely fused. Targeted expression of *Fgfr3*^{Y367C/+} in osteo-chondrogenitors also induced dwarfism and morphological alterations of the skull. A brachycephalic shape (30% length reduction, p<0.0001), with a reduction of the size of the foramen (29%, p<0.0001) were observed. Neural compression was present. Fusion of the speno occipital synchondrosis and coronal suture was also present as well as defects in calvaria bones. The skull bone anomalies were less severe in these mutants. Conversely, expression of the *Fgfr3*^{Y367C} allele in mature osteoblasts or mature chondrocytes resulted in mild morphological changes. No malocclusion or anomalies of the calvarial sutures were observed. The comparative analysis of the four mouse models confirms the importance of endochondral ossification in the growth of the skull base and craniovertebral junction. These results also suggests that FGFR3 role in membranous ossification is likely mediated by early expression in a population of progenitors giving rise to osteoblast in the skull and thus affects cranial bone formation and suture homeostasis.

Disclosures: Martin Biosse Duplan, None.

1199

Hypogonadism with Estrogen Removal (HER): Differential Effects of Androgens and Estrogens on Bone Microarchitecture in Adult Men. Elaine Yu^{*1}, Alex Taylor¹, Kendra Wulczyn¹, Matthew Webb¹, Nicholas Perros¹, Mary Bouxsein², Joel Finkelstein¹.
¹Massachusetts General Hospital, USA, ²Beth Israel Deaconess Medical Center, USA

Background: Both androgens and estrogens are thought to influence bone mineral density, but the effects of testosterone (T) and estrogen (E) on bone microarchitecture are unknown.

Methods: We recruited 202 healthy men age 20-50. All men received goserelin acetate (Zoladex®, AstraZeneca LP) 3.6 mg at weeks 0, 4, 8, and 12 to suppress endogenous T and E production; anastrozole (Arimidex®, AstraZeneca LP) 1 mg daily for 16 wks to block conversion of T to E; and were randomized to treatment with 1 of 5 doses of a T gel (AndroGel®, Abbott) daily for 16 wks (Groups 1-5: placebo, 1.25g, 2.5g, 5g, 10g). Volumetric BMD (vBMD) and microarchitecture of the distal radius and tibia were assessed using high-resolution peripheral quantitative computed tomography (HR-pQCT, Scanco) in a subset of men (n=99) at wks 0 and 16. T and E levels were measured by RIA and mass spectroscopy, respectively, every 4 wks. HR-pQCT parameters were compared between groups to determine if changes occurred when T levels range from pre-pubertal to supraphysiologic while E levels are markedly suppressed in all groups. Because no important differences were seen between groups, data from all groups were then pooled to evaluate the impact of acute E suppression from wk 0 to 16. Each medication was used outside of its indications with approval.

Results: At baseline, serum levels of T and E were similar between groups (mean \pm SD for the entire cohort: T 513 \pm 158 ng/dL, E 30 \pm 10 pg/mL). Mean T levels from wk 4-16 were 43, 234, 378, 497, and 985 ng/dL in Groups 1-5, respectively and mean E levels ranged from 1.1-3.6 pg/mL. Changes in volumetric BMD and bone microarchitecture parameters were similar across groups, indicating lack of T effect on these parameters over 16 wks. In contrast, when groups were pooled to assess E effect, total, cortical, and trabecular vBMD at the radius and tibia declined from week 0 to 16 (Table). Cortical area and cortical thickness also declined while trabecular area of the radius and tibia increased.

Conclusions: In the setting of low E, short-term manipulation of T does not significantly affect vBMD or bone microarchitecture in men. Conversely, suppression

of estrogen reduces cortical and trabecular vBMD and alters cortical and trabecular architecture in a pattern consistent with "trabecularization" of the cortex. These results suggest that estrogen deficiency is the primary mediator of bone loss in hypogonadal men.

| | Radius | | Tibia | |
|----------------------|--------------|----------|-------------|----------|
| | Mean ± SD | p-value | Mean ± SD | p-value |
| Total density | -1.1 ± 1.9% | p<0.0001 | -0.9 ± 1.4% | p<0.0001 |
| Cortical density | -0.7 ± 1.3% | p<0.0001 | -0.6 ± 1.1% | p<0.0001 |
| Trabecular density | -0.7 ± 1.6% | p<0.0001 | -0.5 ± 1.5% | p=0.0009 |
| Cortical area | -2.1 ± 3.7% | p<0.0001 | -1.5 ± 2.2% | p<0.0001 |
| Cortical thickness | -2.1 ± 4.2% | p<0.0001 | -1.6 ± 2.3% | p<0.0001 |
| Cortical perimeter | 0.1 ± 1.3% | ns | 0.1 ± 0.4% | ns |
| Trabecular area | 0.3 ± 0.7% | p<0.0001 | 0.2 ± 0.4% | p<0.0001 |
| Trabecular number | -0.4 ± 10.5% | ns | -1.5 ± 8.2% | ns |
| Trabecular thickness | 0.9 ± 10.8% | ns | 1.6 ± 8.2% | ns |
| Trabecular spacing | 1.7 ± 11.3% | ns | 2.3 ± 8.5% | ns |

Percent change in HR-pQCT parameters after E suppression and variable T replacement

Disclosures: Elaine Yu, None.

This study received funding from: Abbott Laboratories.

1200

Cortical Porosity and Bone Loss Precede Menopause. Ashild Bjornerem^{*1}, Ali Ghasem-Zadeh², Roger Zebaze², Minh Bui³, Xiaofang Wang⁴, John L Hopper³, Ego Seeman². ¹University of Tromsø, Norway, ²Austin Health, University of Melbourne, Australia, ³Centre for MEGA Epidemiology, University of Melbourne, Australia, ⁴Endocrine Centre, Austin Health, University of Melbourne, Australia

In young adulthood, bone remodeling is balanced; equal volumes of bone are resorbed and replaced so no bone loss or structural decay occurs. Remodeling imbalance appears before menopause; less bone is replaced than was resorbed producing trabecular bone loss but cortical bone loss is held to begin after menopause even though the imbalance is global. An alternative explanation is that cortical bone loss occurs by intracortical remodeling creating small pores requiring sensitive methods of detection.

Images of the distal tibia were obtained using high-resolution peripheral quantitative computed tomography (HR-pQCT; Scanco Medical) in 200 premenopausal and 83 postmenopausal women participating in a cross-sectional study in Melbourne, Australia. Cortical porosity and volumetric bone mineral density (vBMD) were quantified using the manufacturers' software and StrAx1.0.

In premenopausal women aged 40 to 55 years (mean 45.7), tibia cortical porosity correlated positively with age while cortical vBMD correlated inversely; each standard deviation (SD) greater age (3.3 years) was associated with 0.20 SD higher porosity (p = 0.004) and 0.17 SD lower vBMD in the cortical transitional zone (p = 0.01) adjusted for BMI and height. These deficits were not detected using DXA as hip and spine aBMD were independent of age. In postmenopausal women aged 45 to 61 years (mean 55.0), each SD greater age (3.5 years) was associated with 0.38 SD higher porosity now in compact appearing cortex and 0.40 SD higher porosity in the transitional zone, and 0.42 SD lower cortical vBMD in the compact appearing cortex and 0.40 SD lower cortical vBMD in the transitional zone; twice that in premenopausal women (all p < 0.001, adjusted for BMI and height). Higher porosity was associated with high levels of remodeling markers in pre- and post-menopausal women.

We infer that cortical bone loss producing porosity starts before menopause in the transitional zone between compact appearing cortex and the trabecular compartment 'trabecularizing' the cortex. This finding has implications regarding the timing of treatment as the slow loss of the four-fold larger cortical bone volume than trabecular bone volume accounts for 70 percent of all bone loss and this loss, producing cortical porosity reduces cortical stiffness to the 7th power.

Disclosures: Ashild Bjornerem, None.

1201

FSH Suppression in Eugonadal Men Does Not Change Bone Turnover Markers. Alexander Uihlein^{*1}, Ruchit Kumbhani¹, Erica Siwila-Sackman¹, Joel Finkelstein¹, Hang Lee¹, Benjamin Leder². ¹Massachusetts General Hospital, USA, ²Massachusetts General Hospital Harvard Medical School, USA

Background: In-vitro and animal studies have reported conflicting results regarding an independent role for FSH in the regulation of bone turnover. Furthermore, while some epidemiologic studies have reported associations between FSH and markers of bone turnover, experimental models in postmenopausal women have not confirmed a clinically relevant, gonadal-steroid-independent role for FSH. Studies in men have not been published.

Objective: To test the hypothesis that in the setting of stable gonadal steroid levels, the suppression of FSH will alter biochemical markers of bone metabolism in eugonadal men.

Design: 62 eugonadal healthy men were assigned to the following treatment groups as part of a larger trial assessing dose-response relationships between gonadal steroids and multiple outcomes:

- 1) Goserelin acetate (Zoladex®; AstraZeneca Pharmaceuticals LP) 3.6mg SC monthly and a testosterone gel (AndroGel®; Abbott Laboratories) 5 or 10 grams daily
- 2) Placebo goserelin acetate and placebo testosterone gel

In group 1, estradiol (E2) and testosterone (T) levels are maintained in the eugonadal range whereas FSH levels are suppressed. In group 2, levels of E2, T, and FSH are unaltered.

Subjects in Group 1 were individually matched with subjects in Group 2 to ensure that the mean testosterone and estradiol levels (measured every 4 weeks during the 16 week study period) for the 2 groups were equivalent. FSH, serum CTX, and osteocalcin were measured at baseline and after 16 weeks of therapy and between group changes were compared by paired t-test. Approval was obtained to use each medication outside of its indications.

Results: As shown in the table 1, subjects were well-matched at baseline. After 16 weeks of the assigned intervention, FSH was stable in the placebo group but declined by 61% in the intervention group (P < 0.0001 for the between group comparison). Despite this change in FSH, CTX and osteocalcin did not change in the intervention group nor were any between-group differences observed (table 2).

Conclusion: In the setting of equivalent levels of T and E2, significant suppression of FSH for 16 weeks does not affect bone turnover in men. These findings suggest that FSH is not a key independent regulator of male bone metabolism.

| | Group 1- Intervention (n=33) | Group 2- Placebo (n=33) | P-value |
|-----------------------------------|------------------------------|-------------------------|---------|
| Mean Testosterone wk 4-16 (ng/dL) | 605 ± 168 | 603 ± 176 | NS |
| Mean Estradiol wk 4-16 (pg/mL) | 27 ± 8 | 28 ± 9 | NS |
| FSH (% Change) | -61.3 ± 32.0 % | -2.3 ± 17.0% | <0.0001 |
| CTX (% Change) | 9.5 ± 58.7% | 9.8 ± 78.8% | NS |
| Osteocalcin (% Change) | -3.8 ± 27.3% | 2.8 ± 22.3% | NS |

Table 2

| | Group 1- Intervention (n=33) | Group 2- Placebo (n=33) | P-value |
|-------------------------------|------------------------------|-------------------------|---------|
| Age (years) | 35 ± 7 | 30 ± 6 | 0.0013 |
| Baseline Testosterone (ng/dL) | 501 ± 149 | 583 ± 198 | NS |
| Baseline Estradiol (pg/mL) | 30 ± 8 | 30 ± 10 | NS |
| FSH (U/L) | 5.2 ± 4.5 | 4.9 ± 2.1 | NS |
| CTX (pg/mL) | 0.68 ± 0.37 | 0.73 ± 0.29 | NS |
| Osteocalcin | 14.5 ± 4.9 | 14.8 ± 4.1 | NS |

Table 1

Disclosures: Alexander Uihlein, None.

This study received funding from: Abbott Laboratories and AstraZeneca Pharmaceuticals

1202

Sclerostin/SOST, a Novel Serum and Genetic Biomarker Strongly Correlated to BMD and Fracture in Postmenopausal Women. Sjur Reppe^{*1}, Agate Noer², Runa M. Grimholt³, Bjarni V. Halldorsson⁴, Vigdis T. Gautvik², Ole K. Olstad³, Jens P. Berg³, Philippe Collas², Kaare M. Gautvik⁵. ¹Oslo University Hospital, Ullevaal, Norway, ²University of Oslo, Norway, ³Oslo University Hospital, Norway, ⁴Reykjavik University, Iceland, ⁵University of Oslo, Oslo University Hospital, Lovisenberg Deacon Hospital, Norway

Sclerostin, encoded by the *SOST* gene, is an osteocyte secreted glycoprotein that has been identified as a pivotal regulator of bone remodeling through inhibition of the anabolic Wnt signaling pathway. Mice lacking the *Sost* gene become osteopetrotic and antibodies against sclerostin (AMG 785) promote bone formation in healthy men and women.

We have analyzed *SOST* mRNA levels in iliac bone biopsies and sclerostin in serum of postmenopausal women (n=84 and 108, respectively). Furthermore, SNP analyses were performed and the genotype correlated to *SOST* mRNA/sclerostin levels. Four different areas within the *SOST* 5' upstream region were examined by bisulfite sequencing for differential CpG methylation in bone biopsies between osteoporotic (n=4) and healthy women (n=4).

Serum sclerostin and bone *SOST* mRNA correlated positively to femoral neck adjusted BMD (p<0.0001 and p=0.0003, respectively), and inversely to bone biomarker concentrations such as: bone specific ALP, BGLAP (osteocalcin), serum-1CTP and urine deoxypyrimidinium. Also, serum sclerostin levels were reduced in osteoporotic as compared to healthy women (p=0.004) corresponding to bone *SOST* mRNA changes (p< 0.0001). MicroRNA-378, has *SOST* mRNA as a putative target and was highly correlated to femoral neck BMI adjusted Z-score (r = -0.46, p=8.6E-06) as well as negatively correlated to *SOST* mRNA levels (r = -0.27, p=1.3E-02). Generally, methylation of CpG in promoter/enhancer regions leads to reduced gene expression. Analysis of CpG methylation in 4 different areas in the *SOST* upstream region showed increased methylation in one of these, closest to the *SOST* transcription start site in women with osteoporosis, concordant with their reduced

SOST mRNA levels and sclerostin serum concentrations. We also identified four different genotype markers correlating to serum sclerostin (p: 0.0016 - 0.0079) with calculated effects 0.32 to -0.42.

Serum sclerostin and *SOST* mRNA show a strong, positive correlation to age and BMI adjusted BMD. Gene heterogeneities, differential methylation patterns and miR-378 have been identified as putative regulators of *SOST* bone mRNA and sclerostin serum levels. Contrary to the current view that increased levels of sclerostin leads to osteoporosis, we propose that in humans compensatory mechanisms involving the *SOST* gene, e.g. methylation, may reduce serum sclerostin levels in situations of low BMD attempting to increase Wnt signaling and thereby promote bone formation.

Disclosures: *Sjur Reppe, None.*

1203

RANKL Derived from Mesenchymal but not Hematopoietic Cellular Sources Is Relevant for Bone Turnover in Mice. Carmen Streicher¹, Alexandra Hevny², Paul Kostenuik³, Reinhold Erben⁴. ¹University of Veterinary Medicine Vienna, Austria, ²inst. of Physiology, Pathophysiology & Biophysics, Austria, ³Amgen Inc., USA, ⁴University of Veterinary Medicine, Austria

Receptor activator of NFκB ligand (RANKL) is an essential cytokine for osteoclast differentiation and activity. RANKL can be produced by a variety of hematopoietic (e.g. T and B-cell) and mesenchymal (osteoblast lineage, chondrocyte) cell types. However, it is still controversial to what extent RANKL derived from hematopoietic vs. mesenchymal cells contributes to the physiological regulation of bone turnover. Human RANKL knock-in (huRANKL-KI) mice were used to address this question. HuRANKL-KI mice carry the human instead of the murine exon 5 in their RANKL gene, and express a chimeric RANKL protein wherein most of the RANK binding domain is human. The anti-huRANKL antibody AMG161 blocks chimeric but not murine RANKL. To establish a model for selective blockade of hematopoietic or mesenchymal cell-derived RANKL, we lethally irradiated 16-week-old female wild-type (WT) and huRANKL-KI mice on C57BL/6 genetic background, and reconstituted them with sex-matched bone marrow from hRANKL-KI or WT mice, respectively. In irradiated WT mice reconstituted with huRANKL mouse bone marrow, mesenchymal cell-derived RANKL is exclusively murine, whereas hematopoietic cell-derived RANKL is exclusively chimeric and inhibited by AMG 161. Conversely, in irradiated huRANKL mice reconstituted with WT bone marrow, hematopoietic cell-derived RANKL is exclusively murine, while mesenchymal cell-derived RANKL is exclusively chimeric and inhibited by AMG 161. To control for the effects of irradiation on ovarian function, all mice were ovariectomized (OVX) 4 weeks after irradiation, and subcutaneously received either physiological saline or AMG161 (10 mg/kg) twice weekly. Non-irradiated OVX WT and huRANKL-KI mice treated with saline or AMG161 served as controls. All mice were killed 4 weeks post-OVX. Similar to OVX huRANKL-KI mice treated with AMG161, marked increases in bone mass were observed with AMG161 treatment of OVX huRANKL-KI mice reconstituted with WT bone marrow as evidenced by pQCT and micro-CT analysis. In contrast, AMG161 failed to increase bone mass in OVX WT mice reconstituted with huRANKL-KI mouse bone marrow. Our data indicate that RANKL derived from mesenchymal, but not from hematopoietic cells, is relevant for the physiological regulation of bone metabolism in OVX mice.

Disclosures: *Carmen Streicher, None.*

1204

The ERα of Osteoblast Progenitors is Required for Normal Accrual of Cortical Bone Mass Independently of Estrogens. Srividhya Iyer¹, Aaron Warren², Martha Martin-Millan², Li Han¹, Shoshana Bartell¹, Elena Ambrogini¹, Jinhu Xiong¹, Julie Crawford², Robert Weinstein¹, Robert Jilka¹, Charles O'Brien¹, Maria Jose Almeida¹, Stavros Manolagas¹. ¹Central Arkansas VA Healthcare System, Univ of Arkansas for Medical Sciences, USA, ²Central Arkansas Veterans Healthcare System, University of Arkansas for Medical Sciences, USA

The osteoclast ERα mediates the beneficial effects of estrogens in trabecular, but not cortical bone, suggesting that other cell types mediate the effects of estrogens on the latter compartment. We tested the hypothesis that the effect of estrogens on cortical bone result from cell autonomous actions on cells of the osteoblast lineage by deleting an ERα conditional allele in pluripotent mesenchymal cells expressing Prx1 (ERα-flox;Prx1-Cre), in committed osteoblast precursors expressing Osx1 (ERα-flox;Osx1-Cre), or in mature osteoblasts and osteocytes expressing collagen 1 (ERα-flox;Col1-Cre). ERα-flox;Prx1-Cre mice exhibited a decrease in the cortical thickness of the femur after puberty in both sexes; whereas trabecular bone volume was unaffected. The cortical bone decrement was maintained with advancing age in females, but not in males, and was associated with decreased bone formation rate in the periosteum, but not the endosteum. Furthermore, ERα-flox;Prx1-Cre mice did not lose cortical bone following ovariectomy. ERα-flox;Osx1-Cre mice also had decreased cortical thickness associated with decreased periosteal perimeter and no change in cancellous bone. Periosteal cells isolated from both ERα-flox;Prx1-Cre and ERα-flox;Osx1-Cre mice exhibited decreased rate of proliferation under basal conditions. More strikingly, periosteal cells deficient in ERα failed to exhibit a Wnt3-induced

increase in proliferation and differentiation that was readily seen in cells from control mice. Importantly, estradiol had no effect on untreated or Wnt3-stimulated control cells. Cortical or cancellous bone mass or their loss following ovariectomy were unaffected in the ERα-flox;Col1-Cre mice. Elucidation of decreased periosteal bone accrual in mice lacking the ERα in osteoblast progenitors- an effect that is diametrically opposite to the effects of estrogen loss on this compartment- along with an essential role of the unliganded ERα in the potentiation of Wnt signaling demonstrate that the ERα of osteoblast progenitors is required for normal accrual of cortical bone mass, independently of estrogens. In addition, our findings establish that the ERα expressed in distinct bone cell types, periosteal osteoblast progenitors involved in modeling versus osteoclasts driving remodeling, functions to increase bone mass in cortical and trabecular bone, respectively.

Disclosures: *Srividhya Iyer, None.*

1205

Blood Circulated Catabolic and Anabolic Biomarkers Associated with Skeletal Muscle Mass in Hispanic and Non-Hispanic Postmenopausal women—an Ancillary Study of the Women's Health Initiative. Zhao Chen¹, Nicole Wright², Jennifer Bea³, Walter Klimecki³, Chengcheng Hu³, Andriene Grant³, Kamal Masaki⁴, Lihong Qi⁵, Jean Wactawski-Wende⁶, Matthew Allison⁷, Patricia Thompson³. ¹University of Arizona College of Public Health, USA, ²University of Alabama at Birmingham, USA, ³University of Arizona, USA, ⁴University of Hawaii at Manoa, USA, ⁵University of California at Davis, USA, ⁶State University of New York at Buffalo, USA, ⁷University of California at San Diego, USA

Sarcopenia (low relative skeletal muscle mass and function) is common in the elderly and it may cause poor physical function and other adverse health-related outcomes, including osteoporosis in older age. Mechanisms for sarcopenia with aging are still under investigation. The objective of this study is to examine the cross-sectional relationship between skeletal muscle mass and selected catabolic and anabolic biomarkers, which may potentially contribute to the development of sarcopenia. Participants included 318 Hispanic and 683 non-Hispanic white postmenopausal women who were between 50 and 79 years at baseline from the Women's Health Initiative Observational Study. Baseline serum samples were measured to assess inflammatory cytokines and hormones, such as interleukin (IL)-6 and tumor necrosis factor (TNF)-α, as well as insulin-like growth factor (IGF)-1 and growth hormone (GH) using the Illuminex™ multiplex platform (Rules-based Medicine). DXA-derived-lean mass measurements were used to assess total body and appendicular (arms and legs) skeletal muscle mass. Quality control on biomarkers was done using a standard protocol and biomarkers with poor quality were excluded from the final analysis. For consistency, all biomarkers were log-transformed for linear regression analysis. Linear regression models and random forest statistical techniques were used for assessing the direction and strength of the association between biomarkers and lean mass. After adjusting for multiple comparisons, a number of biomarkers were significantly associated with lean mass in either the single-biomarker or multi-biomarker models. When age, weight, height, ethnicity and percent body fat were included in linear regression models, associations between some biomarkers and lean mass were substantially attenuated. In the random forest model we identified a number of biomarkers including leptin, insulin, IL-16 and C-reactive protein as the top biomarkers associated with lean mass in addition to weight, height, age, ethnicity and percent body fat (table). In summary, a number of circulating inflammatory- and obesity-associated factors were significantly associated with lean mass after adjusting for age, height, weight, ethnicity and percent body fat. These findings have suggested a number of directions for future study to longitudinally examine these relationships and to investigate possible mechanisms underlying these associations.

Table 1: Top 15 Factors Associated with Appendicular and Total Body Lean Mass Ranked by Importance Measures in Random Forest

| | Appendicular Lean Mass ¹ | Standardized Importance ² | Total Body Lean Mass ¹ | Standardized Importance ² |
|----|-------------------------------------|--------------------------------------|------------------------------------|--------------------------------------|
| 1 | Weight | 279.5 | Weight | 323.7 |
| 2 | Appendicular Percent Fat | 231.2 | Total Body Percent Fat (Corrected) | 148.6 |
| 3 | Height | 22.1 | Height | 31.4 |
| 4 | Leptin | 17.0 | Insulin | 18.7 |
| 5 | Insulin | 16.2 | Leptin | 16.6 |
| 6 | IL-16 | 7.3 | C Reactive Protein | 6.3 |
| 7 | SHRAGE | 6.4 | Age | 5.3 |
| 8 | SHBG | 5.9 | SHRAGE | 4.7 |
| 9 | Age | 5.7 | IL-16 | 4.7 |
| 10 | C Reactive Protein | 5.7 | Direct Energy | 4.6 |
| 11 | Ethnicity | 5.0 | L ² | 4.5 |
| 12 | Creative Kinase/IB | 4.8 | Appolipoprotein A1 | 4.2 |
| 13 | Adiponectin | 4.4 | TUFAIpa | 3.9 |
| 14 | IL-16 | 4.3 | Haptoglobin | 3.4 |
| 15 | Fibrinogen | 4.3 | SHBG | 3.3 |

¹ Outcomes were log2 transformed. Biomarkers were standardized with the untransformed values included as the base value of the biomarker.
² Ranking done out of a total of 28 predictors (1) biomarkers and 3 covariates. Covariates were considered individually, and were not forced into the model for linear regression models.
³ Larger number indicates higher importance in the random forest investigation.

Table 1

Disclosures: *Zhao Chen, None.*

1206

Sarcopenia Diagnosis: Consideration of a "FRAX-like" Approach. Bjoern Buehring*, Ellen Fidler, Jessie Libber, Jennifer Sanfilippo, Bryan Heiderscheid, Diane Krueger, Neil Binkley. University of Wisconsin, Madison, USA

Sarcopenia increases falls and fracture risk. However, sarcopenia is rarely diagnosed clinically, in part because no single consensus definition exists. Current definitions are based on muscle mass alone or in combination with muscle function. However, existing definitions are imperfect in that they may not identify the same individuals as sarcopenic and do not consider fat mass. We hypothesized that an approach to sarcopenia diagnosis by combining clinically intuitive risk factors might better identify those at risk for falls and fractures. To begin evaluating this concept, this study compared sarcopenia prevalence using current definitions with that obtained using a potential alternative ("FRAX-like") scoring system based on muscle, fat and bone mass, muscle function and falls history.

Community dwelling adults age 70+ underwent DXA body composition measurement and performed a battery of muscle function tests. DXA results were used to calculate appendicular lean mass (ALM)/ht² and a potential measure of total body and muscle fat, the leg fat mass/lean mass ratio. The latter ratio is an attempt to include the effect of obesity on function (i.e. sarcopenic obesity). A fat/lean ratio ≥ 2.5 SD above the mean of 329 young athletes (178M/151F) was defined as high. Sarcopenia prevalence was determined using low ALM/ht², the European consensus approach, (low gait speed or grip strength + low ALM/ht²) and the International consensus approach (low gait speed+low ALM/ht².) An alternative ("FRAX-like") combined score with 1 point each for low ALM/ht², low grip strength or gait speed, high leg fat/lean ratio, low BMD and history falling in the last year was explored.

97 older adults (49 F/48M; mean age 81 yrs) were studied. Sarcopenia prevalence was 24%, 20% and 10% based on ALM/ht², the European and International approach respectively. Sarcopenia prevalence was 40% using a "FRAX-like" score of ≥ 3 . Percentages were significantly different ($p \leq 0.0001$).

Current approaches do not identify the same proportion of older adults as sarcopenic. A risk score combining several measures important for adverse outcomes related to sarcopenia identifies a larger proportion as potentially being at risk. As ~50% of adults over age 75 fall annually, it is possible that this "FRAX-like" approach may be a more sensitive predictor of adverse outcomes. Future research is necessary to validate proposed sarcopenia definitions.

Disclosures: Bjoern Buehring, None.

1207

Radiographic Knee Osteoarthritis is Associated with Genetic Loci Previously Associated with Bone Mineral Density. Rebecca Jackson*¹, Laura Yerges-Armstrong², Changwan Lu², Joanne Jordan³, Youfang Liu³, David Duggan⁴, Braxton Mitchell⁵, Marc Hochberg⁶. ¹The Ohio State University, USA, ²University of Maryland, USA, ³University of North Carolina, USA, ⁴Translational Genomics, USA, ⁵University of Maryland, Baltimore, USA, ⁶University of Maryland School of Medicine, USA

Risk for osteoarthritis (OA) is widely recognized to be heritable but few loci have been identified. Recently, longitudinal studies have shown that high bone mineral density (BMD) measured at the hip and/or spine is associated with the development of hip and knee OA. As 50-85% of the variance in BMD is genetically determined and GWAS have identified loci which influence BMD, we performed joint analyses across two cohorts with well-characterized measures of knee osteoarthritis: the Osteoarthritis Initiative (OAI) and the Johnston County Osteoarthritis Project (JoCo) to determine if single nucleotide polymorphisms (SNPs) previously reported to be associated with BMD at genome-wide significance are associated with radiographic knee OA.

Methods: Cases were required to have at least one knee with definite radiographic OA which was defined as the presence of definite osteophytes regardless of the presence of joint space narrowing. Controls were required to be free of radiographic evidence of disease (i.e. no evidence of osteophytes or joint space narrowing in either knee). There were 2014 and 658 Caucasian cases, respectively, in the OAI and JoCo studies, and 610 and 318 controls. The 81 SNPs selected for replication were identified through a review of the literature. Genotyping was carried out on the Illumina 2.5M and 1M arrays in GeCKO and JoCo, respectively. Association analyses for imputed SNPs (HapMap II CEU panel) were carried out separately in each cohort with adjustments for age and sex and then parameter estimates combined across the two cohorts in meta-analysis using a fixed effects model.

Results: We identified 4 SNPs significantly associated with prevalent radiographic knee OA. The strongest signal ($p < 0.01$, odds ratio = 1.17, 95% CI: [1.04-1.32]) maps to 12q3 which contains a gene coding for *SP7*. Additional loci map to 7p14.1 (*TXNDC3*), 7q31.31 (*C7orf58*) and 6q25 (*C6orf97*). For all but the SNP near *C6orf97*, the allele associated with higher BMD was associated with the higher odds of OA.

Conclusion: This large joint analysis demonstrates that several GWAS-identified BMD SNPs are associated with prevalent radiographic knee OA. These data further support the hypothesis that BMD may be a risk factor contributing to radiographic OA.

Disclosures: Rebecca Jackson, None.

1208

Vitamin D Status and Knee Pain Severity in Functionally Intact Older Adults: The Health ABC Study. Laura Tosi*¹, Robert Boudreau², Kent Kwok³, Tanushree Prasad³, Hilsa Avonayon⁴, Tamara Harris⁵, Denise Houston⁶, Stephen Kritchevsky⁶, Kushang Patel⁷, Eleanor Simonsick⁸, Jane Cauley⁹. ¹Children's National Medical Center, USA, ²University of Pittsburgh - Dept of Epidemiology, USA, ³University of Pittsburgh, USA, ⁴University of California - San Francisco, USA, ⁵National Institute of Aging, USA, ⁶Wake Forest University, USA, ⁷National Institutes of Health, USA, ⁸National Institutes of Aging, USA, ⁹University of Pittsburgh Graduate School of Public Health, USA

Background: Clinical evidence suggests that 25-hydroxyvitamin D (25(OH)D) may be important in multiple biologic processes including pain reporting, yet there exists no convincing evidence that levels of 25(OH)D are lower in individuals with chronic pain vs those pain free. The study examines the association between 25(OH)D status and reported joint pain severity in functionally intact persons aged 70-79.

Methods: Of 3,075 participants in the Health, Aging and Body Composition study, 2,793 (mean age 74.7 \pm 2.9 yrs, 51.2% women, 39.7% black) had serum 25(OH)D measures at year 2 and concurrent responses on the number of painful joints and the Modified WOMAC scale for knee pain. Quartiles of 25(OH)D were calculated based on the combined sample. Number of painful joints (0-20), joint groups (0-8: hand/wrist, hip, knee, foot/toe; left+right) and WOMAC knee pain were compared across quartiles using ANOVA and ANCOVA to adjust for covariates. The worst knee was used in the WOMAC analyses.

Results: The 25(OH)D quartile cutoffs were 18.0 ng/ml, 24.7 ng/ml and 32.3 ng/ml (min=5.0, max=186.9). The most frequently reported painful joint groups were hand/wrists (50.2%) and knees (36.2%). For both sexes, higher physical activity and dietary Vitamin-D intake were associated with higher 25(OH)D. In men, 25(OH)D status was not associated with any of the three pain measures in unadjusted or adjusted models ($p > 0.261$). For women, the highest quartile of 25(OH)D was associated with lower numbers of painful joint groups adjusted for age, race, field site, and season of serum draw ($p=0.030$), but became no longer significant ($p=0.347$) when further adjusted for education level, BMI and depressive symptoms. For WOMAC knee pain, the highest 25(OH)D quartile was strongly associated with lower knee pain in unadjusted ($p < 0.001$) and all adjusted models ($p < 0.041$). The lower three quartiles had similar WOMAC knee pain ($p=0.980$), with adjusted WOMAC knee pain of 4.05 for the lower quartiles combined vs 3.19 for the highest quartile ($p=0.004$). Dietary vitamin D attenuated this difference by 8.1%.

Conclusions: The association of 25(OH)D status with joint pain reporting is sexually dimorphic and joint specific. 25(OH)D status does not predict joint pain in men. In women, however, 25(OH)D status and WOMAC knee pain are strongly associated across all adjusted models. Clinical trials using 25(OH)D therapy to prevent/treat knee pain in women should be considered.

Table 1: Mean WOMAC across 25-hydroxyvitamin D status and sex

| | 25-hydroxyvitamin D | | | | Overall F p-value | p-trend |
|------------|---------------------|-----------------|-----------------|-----------------|----------------------|----------------------|
| | Q1 (n = 271) | Q2 (n = 369) | Q3 (n = 371) | Q4 (n = 353) | | |
| Men | | | | | | |
| Unadjusted | 1.90 | 2.11 | 1.91 | 2.17 | 0.7393 | 0.5658 |
| Model 1 | 1.85 | 2.13 | 1.94 | 2.16 | 0.7250 | 0.5300 |
| Model 2a | 2.86 | 3.20 | 3.07 | 3.43 | 0.3625 | 0.1544 |
| Model 3a | 2.75 | 3.15 | 2.91 | 3.35 | 0.2604 | 0.1748 |
| Women | | | | | | |
| Unadjusted | 3.77 | 3.49 | 3.17 | 2.10 | <0.0001 [‡] | <0.0001 [†] |
| Model 1 | 3.58 | 3.51 | 3.25 | 2.20 | 0.0007 [‡] | 0.0003 [†] |
| Model 2b | 4.03 | 4.09 | 4.03 | 3.19 | 0.0406 [‡] | 0.0324 [†] |
| Model 3b | 4.03 | 4.10 | 4.01 | 3.25 | 0.0843 | 0.0564 |

* 25-hydroxyvitamin D quartiles: Q1 (< 18.02 ng/ml), Q2 (≥ 18.02 - < 24.71 ng/ml), Q3 (≥ 24.71 - < 32.3 ng/ml), Q4 (≥ 32.30 ng/ml)

Model 1: adjusted for age, race, field site, season of HABC visit

Men:

Model 2a: adjusted for age, race, field site, season of HABC visit, education level, BMI, depressive symptoms

Model 3a: Model 2a + vitamin-D containing supplement use, vitamin D intake

Women:

Model 2b: adjusted for age, race, field site, season of HABC visit, BMI, depressive symptoms

Model 3b: Model 2b + vitamin-D containing supplement use, vitamin D intake

[‡] p-value for overall F-test < 0.05

[†] p-value for trend < 0.05

Table 2: Mean WOMAC across 25-hydroxyvitamin D status – WOMEN only

| Women | Q123 | Q4 | p-value |
|------------|------------|-----------|----------------------|
| | (n = 1084) | (n = 345) | |
| Unadjusted | 3.50 | 2.10 | <0.0001 [†] |
| Model 1 | 3.45 | 2.22 | <0.0001 [†] |
| Model 2 | 4.05 | 3.19 | 0.0041 [†] |
| Model 3 | 4.04 | 3.25 | 0.0103 [†] |

* 25-hydroxyvitamin D quartiles: Q1 (< 18.02 ng/ml), Q2 (≥ 18.02 - < 24.71 ng/ml), Q3 (≥ 24.71 - < 32.3 ng/ml), Q4 (≥ 32.30 ng/ml)

Model 1: adjusted for age, race, field site, season of HABC visit

Model 2: adjusted for age, race, field site, season of HABC visit, BMI, depressive symptoms

Model 3: Model 2b + vitamin-D containing supplement use and vitamin D intake

[†] p-value < 0.05

Tables 1 and 2

Disclosures: Laura Tosi, Society For Women's Health Research, 9

1209

Progranulin Growth Factor is Protective against Osteoarthritis through Interplay with TNF α and β -Catenin Signaling. Chuanju Liu, Yunpeng Zhao*, Qingyun Tian, Shuai Zhap, Brendon Richbrough, New York University, USA

We have previously reported that Progranulin (PGRN) regulates chondrocyte metabolism and cartilage degradation in vitro and its level is elevated in the cartilage and body fluids of patients with arthritis (Guo FJ, et al, *Arthritis Rheum.* 2010; 62(7):2023-36; Feng JQ, et al, *FASEB J.* 2010; 24(6):1879-92). Additionally, our recent findings revealed that PGRN antagonizes TNF and protects cartilage loss and bone erosion in inflammatory arthritis (Tang W, et al, *Science.* 2011; 332(6028):478-84). Furthermore, our genome-wide screen for novel, differentially expressed genes in osteoarthritis (OA) led to the isolation of PGRN as an OA-associated growth factor. This study is, thus, to determine the potential role of PGRN in the pathogenesis of OA as well as the molecular events involved. The deletion of the *PGRN* gene led to the spontaneous development of an OA-like phenotype in "aged" mice (Note that the phenotype could be observed in as early as a 6-month old). A Micro-CT of the hind knees showed osteophyte formation in aged knockout mice. Safranin O staining demonstrated a remarkable loss of proteoglycan staining and meniscus ossification. High power photography revealed clear chondrocyte clustering and migration of the irregular tide mark to the superficial zone. Surgically-induced OA models, including both DMM (destabilization of medial meniscus) and ACL (anterior cruciate ligament) transection models, demonstrated that the deficiency of PGRN accelerated the degradation of cartilage matrix molecules (e.g. Aggrecan and COMP) and OA progression, while the intra-articular injection of recombinant PGRN delayed these processes. Molecular mechanistic studies revealed that PGRN activated Akt and Erk1/2 signaling and that PGRN-induced expressions of its target genes primarily depended on TNFR in chondrocytes. In addition, PGRN inhibited TNF α -induced ADAMTS cleavage of COMP. Furthermore, the deletion of the *PGRN* gene exacerbated, whereas recombinant PGRN prevented, the loss of cartilage in TNF transgenic mice. Activation of β -catenin signaling in articular chondrocytes was reported to induce OA-like phenotype in mice (Zhu, M, et al, *JBM.* 2009, 23; 12-21), and progranulin was recently found to inhibit Wnt/ β -catenin signaling in the central nervous system (Rosen EY, et al, *Neuron.* 2011; 71(6):1030-42). We also found the mutual inhibition of PGRN and Wnt/ β -catenin signaling in chondrocytes and OA. Collectively, PGRN is a novel chondroprotective growth factor that inhibits OA development, probably through interacting with TNF α /TNFR and Wnt/ β -catenin signaling pathways. These findings not only provide novel insights into the role of

PGRN in cartilage homeostasis and arthritis in vivo, but may also lead to the development of novel therapeutic intervention strategies for osteoarthritis.

Disclosures: Yunpeng Zhao, None.

1210

Sclerostin Plays a Key Role in Abnormal Wnt/ β -catenin Signalling in Human Osteoarthritic Subchondral Osteoblasts Leading to Reduced Mineralization. Elie Abed^{1*}, Denis Couchourel², Aline Delalandre³, Daniel Lajeunesse⁴. ¹Crchum-hôpital Notre-dame, Canada, ²Danone, , ³CRCHUM, Canada, ⁴CHUM, Hôpital Notre-Dame, Canada

Objectives: Clinical and *in vitro* studies suggest that subchondral bone sclerosis due to abnormal osteoblast (Ob) function, is involved in the progression and/or onset of osteoarthritis (OA). Moreover, human OA subchondral Ob show a phenotype of very differentiated cells, however they fail to mineralize normally *in vitro* as *in vivo*. Wnt signaling plays a key role in osteogenesis by promoting the differentiation and mineralization of Ob mainly via the canonical Wnt/ β -catenin (cWnt) signaling pathway. Sclerostin (SOST) has been shown to alter cWnt signaling, however the regulation of SOST in OA Ob remains unknown. Here we investigated the role of SOST in OA Ob.

Material and Methods: We prepared primary human subchondral Ob using the sclerotic medial portion of the tibial plateaus of OA patients undergoing knee arthroplasty, or from tibial plateaus of normal individuals at autopsy. SOST expression and production were evaluated by qRT-PCR and WB analysis. The regulation of SOST expression was determined in response to transforming growth factor- β 1 (TGF- β 1) and as a function of the growth of OA Ob. SOST inhibition was performed using siRNA techniques. cWnt signaling was evaluated by measuring the activity of the TOPflash Tcf/lef luciferase reporter assay and intracellular β -catenin levels by WB. Mineralization was evaluated by Alizarin red staining. TGF- β 1 levels were determined by ELISA.

Results: SOST expression and production were elevated in OA Ob compared to normal Ob. SOST expression increased in post-confluent OA Ob and normal Ob, however its increase was more pronounced in OA Ob. SOST levels also remained always higher in OA Ob than in normal Ob. TGF- β 1 expression was high in OA Ob, and TGF- β 1 stimulated SOST expression in both normal and OA Ob whereas siRNA for TGF- β 1 reduced SOST expression about 5-fold in OA Ob. cWnt signaling and mineralization were reduced in OA Ob compared to normal Ob. SOST inhibition increased cWnt signalling, β -catenin levels and also corrected the abnormal mineralization in OA Ob.

Conclusions: This is the first demonstration of elevated SOST levels in OA Ob. High SOST levels in OA Ob are responsible, at least in part, for the reduced cWnt signaling of these cells and abnormal mineralization. As SOST is a secreted protein, this could lead to potential new avenues of treatment of OA to correct their abnormal bone phenotype and thereof contribute to reduce the burden of OA

Disclosures: Elie Abed, None.

1211

Prevention of Bone Loss during Spaceflight by Bisphosphonate. Toshio Matsumoto^{1*}, Adrian LeBlanc², Jeffrey Jones², Jay Shapiro³, Thomas Lang⁴, Linda Shackelford⁵, Scott Smith⁶, Harlan Evans⁷, Elisabeth Spector⁷, Robert Ploutz-Snyder², Jean Sibonga⁸, Toshitaka Nakamura⁹, Kenjiro Kohri¹⁰, Hiroshi Ohshima¹¹. ¹University of Tokushima Graduate School of Medical Sciences, Japan, ²Baylor College of Medicine, USA, ³Kennedy Krieger Institute, Johns Hopkins, USA, ⁴University of California, San Francisco, USA, ⁵NASA JSC, USA, ⁶Wyle/nasa Jsc, USA, ⁷Wyle, USA, ⁸NASA Johnson Space Center, USA, ⁹University of Occupational & Environmental Health, Japan, ¹⁰Nagoya City Univ, Japan, ¹¹JAXASpace Biomedical Research Office, Japan

The Mir and ISS long-duration missions documented losses in bone mineral density (BMD) from critical skeletal regions, including the most clinically important BMD losses from the hip. These studies demonstrated the wide range in individual BMD loss from -0.5% to -5.1% per a month, averaging about -1.6% per a month. A secondary consequence to uncoupled bone remodeling is hypercalciuria and the associated increase in the risk of renal stone formation.

The present study was undertaken to determine if the combination of bisphosphonate administration and an in-flight exercise regimen would have a measurable effect on preventing space flight-induced changes in bone remodeling and loss of bone mass, and reducing renal stone risk. There were a total of 10 astronauts who signed NASA consent forms to participate. One of these ultimately decided not to participate and 2 experienced stomach discomfort or dyspepsia before or during flight and did not participate or discontinued the drug. Seven crewmembers completed the protocol taking a 70-mg alendronate tablet once/week before and during flight, starting 17 days before launch. Controls are 14 previous ISS crewmembers with DXA and QCT measurements. Change in pre and post flight DXA and QCT were analyzed by random-intercept mixed-model regression analyses that included a continuously scaled covariate to accommodate flight duration (days), a group indicator for comparing the bisphosphonate cohort to controls and an interaction term to compare relative change.

The significant loss in QCT-determined bone strength and trabecular BMD in the untreated group was almost completely prevented in the treated group. Similarly, the reduction in DXA hip BMD was also prevented and lumbar BMD was significantly increased from pre-flight in the treated group (Table). Bone resorption marker, NTX, was decreased compared to preflight, in contrast to typical increases of 50% to 100% above preflight in previous crewmembers. Urinary calcium showed no increase compared to baseline levels, also distinct from the elevated levels of 50% or greater above preflight in previous crewmembers. These results are consistent with the notion that bisphosphonate administration during spaceflight will be beneficial in preventing bone loss and maintaining bone strength.

| Bone Strength | | Untreated (N=14) | Treated (N=7) | Untreated vs. Treated P |
|---------------|---------------------|------------------|---------------|-------------------------|
| | | Mean Sd ± SD | Mean Sd ± SD | |
| QCT | NI Stance Load | -14.2 ± 8.1**† | +0.80 ± 10.1 | P<0.001 |
| QCT | NI Fall Load | -10.3 ± 5.4**† | +2.3 ± 11.6 | P<0.001 |
| BMD | | | | |
| QCT | Total Hip Trab BMD | -12.7 ± 5.9** | -1.1 ± 9.8 | P<0.001 |
| QCT | Trochanter Trab BMD | -12.3 ± 5.6** | -1.9 ± 9.9 | P<0.001 |
| QCT | Femck Trab BMD | -15.4 ± 10.7** | +6.4 ± 14.8 | P<0.001 |
| DXA | Total Hip BMD | -6.1 ± 2.8** | -0.17 ± 1.5 | P<0.001 |
| DXA | Femck BMD | -6.4 ± 3.1** | -0.73 ± 1.2 | P<0.001 |
| DXA | Lumbar Spine BMD | -4.7 ± 3.1** | +2.8 ± 4.0* | P<0.001 |

table 1

| Bone Strength | | Untreated (N=14) | Treated (N=7) | Untreated vs. Treated P |
|---------------|---------------------|------------------|---------------|-------------------------|
| | | Mean Sd ± SD | Mean Sd ± SD | |
| QCT | NI Stance Load | -14.2 ± 8.1**† | +0.80 ± 10.1 | P<0.001 |
| QCT | NI Fall Load | -10.3 ± 5.4**† | +2.3 ± 11.6 | P<0.001 |
| BMD | | | | |
| QCT | Total Hip Trab BMD | -12.7 ± 5.9** | -1.1 ± 9.8 | P<0.001 |
| QCT | Trochanter Trab BMD | -12.3 ± 5.6** | -1.9 ± 9.9 | P<0.001 |
| QCT | Femck Trab BMD | -15.4 ± 10.7** | +6.4 ± 14.8 | P<0.001 |
| DXA | Total Hip BMD | -6.1 ± 2.8** | -0.17 ± 1.5 | P<0.001 |
| DXA | Femck BMD | -6.4 ± 3.1** | -0.73 ± 1.2 | P<0.001 |
| DXA | Lumbar Spine BMD | -4.7 ± 3.1** | +2.8 ± 4.0* | P<0.001 |

Table 1

Disclosures: Toshio Matsumoto, MSD, 6; Astellas Pharma, 2; Ono Pharmaceuticals, 2; Teijin Pharma, 2
This study received funding from: NASA JAXA

1212

Cortical Porosity and Estimated Bone Strength in Healthy Postmenopausal Women Treated with Exemestane for the Primary Prevention of Breast Cancer: Analyses from the nested bone strength substudy of the MAP.3 trial (MAP3BSS). Angela Cheung*¹, John Robbins², Sandhya Pruthi³, Paul E. Goss⁴, Savannah Cardew⁵, Sharmila Majumdar⁶, Sundeep Khosla⁷, Steven Boyd⁸, Andrew Burghardt⁶, Louise Bordeleau⁹, James Ingle¹⁰, Eva Szabo¹, Marta Erlandson⁵, Hanxian Hu¹, Judite Scher¹¹, Harriet Richardson¹², Karen Gelmon¹³, LIANNE TILE⁵, George Tomlinson¹. ¹University Health Network, Canada, ²University of California, Davis Medical Center, USA, ³Mayo Clinic College of Medicine, USA, ⁴Massachusetts General Hospital, USA, ⁵University of Toronto, Canada, ⁶University of California, San Francisco, USA, ⁷College of Medicine, Mayo Clinic, USA, ⁸University of Calgary, Canada, ⁹McMaster University, Canada, ¹⁰Mayo Clinic Rochester, USA, ¹¹University Health Network, Canada, Canada, ¹²Queens University, Canada, ¹³BC Cancer Agency, Canada

Background and Purpose: The MAP.3 trial, an international double-blind placebo-controlled trial of exemestane involving 4560 healthy postmenopausal women at risk of breast cancer demonstrated a 65% reduction in invasive breast cancer after a median follow-up of 35 months. Exemestane lowers circulating estrogen levels. In a nested non-inferiority bone strength substudy of the MAP.3 trial (MAP3BSS), we recently showed that exemestane reduced total volumetric BMD and decreased cortical thickness at the distal radius and distal tibia by high resolution peripheral quantitative computed tomography (HRpQCT), and areal BMD at the lumbar spine and total hip by DXA over two years. To gain further insights, we assessed the effect of exemestane on cortical porosity and estimated bone strength using finite element analysis (FEA).

Methods: We included postmenopausal women eligible for MAP.3 from 5 centers (2 US and 3 Canadian), who were not osteoporotic, not on bone medications, with baseline lumbar spine, total hip and femoral neck T-scores above -2.0. For cortical porosity, we used an automated segmentation technique to identify the periosteal and endosteal margins of the distal radius and distal tibia, and determined the intracortical pore space morphologically. For estimation of bone strength, uniaxial compression testing was performed using FEA (FAIM, Numerics88 Solutions Ltd). We performed 2 sample t-tests on the change over time. Results are presented as absolute and percent changes from baseline to one and two years.

Results: Three hundred and fifty one women participated in the MAP3BSS. At baseline, median age was 61.3 years, median areal BMD T-scores at the lumbar spine and total hip by DXA were -0.23 and 0.14, respectively, and median WHO FRAX 10-year risk for major osteoporotic fractures and hip fractures were 6.0% and 0.3%, respectively. 108 women on exemestane and 105 women on placebo had evaluable scans at 2 years. Exemestane significantly increased cortical porosity at both the distal radius and distal tibia at 1 and 2 years (Table). There is considerable heterogeneity among women. Our estimated bone strength results using FEA are pending.

Conclusions: Two years of exemestane increased cortical porosity. Taken together with the decrease in cortical thickness and the decrease in total volumetric bone density, we can conclude that exemestane has a negative effect on bone microarchitecture at the distal radius and distal tibia over the first 2 years of therapy.

| Cortical Porosity | From baseline to 1 year | | | From baseline to 2 years | | |
|----------------------|-------------------------|---------|---------|--------------------------|---------|---------|
| | Exemestane | Placebo | P value | Exemestane | Placebo | P value |
| Distal Radius | | | | | | |
| Mean Absolute Change | 0.0021 | 0.0011 | 0.09 | 0.0034 | 0.0011 | 0.007 |
| Mean Percent Change | 16.6% | 7.5% | 0.004 | 27.6% | 8.7% | <0.0001 |
| Distal Tibia | | | | | | |
| Mean Absolute Change | 0.0073 | 0.0024 | <0.0001 | 0.0129 | 0.0059 | <0.0001 |
| Mean Percent Change | 13.7% | 4.3% | <0.0001 | 24.7% | 10.0% | <0.0001 |

Changes of cortical porosity from baseline to 1 and 2 years

Disclosures: Angela Cheung, None.

This study received funding from: Canadian Breast Cancer Research Alliance, Pfizer (MAP3 study), Canadian Cancer Society (MAP3 study), NCIC-Clinical Trial Group

1213

Determinants of Low Bone Mineral Density (BMD) in Young Women with Severe Anorexia Nervosa. Karine Briot*¹, Marie-Raphael Thiebaut², Simon Paternotte³, Sami Kolta³, Nicole Barthe⁴, Alain Daragon⁵, Yves Maugars⁶, Thierry Thomas⁷, Nathalie Godart², Christian Roux³. ¹Paris Descartes University, Cochin hospital, Rheumatology Hospital, France, ²Inserm U669, Universités Paris 5 ; Psychiatry Unit, Institut Mutualiste Montsouris, France, ³Cochin hospital, France, ⁴Médecine Nucléaire, Centre Hospitalier de Bordeaux & Université de Bordeaux 2-Victor Segalen, France, ⁵INSERM U 905, France, ⁶Hôpital Dieu Et Hme, France, ⁷INSERM U1059, Service de Rhumatologie, CHU de St Etienne, France

Background: Low bone mineral density (BMD) is a known consequence of anorexia nervosa but there are few data concerning the prevalence of low BMD in young patients (adolescents and young adults) with severe disease, who require a hospitalization.

Objectives: to assess bone mineral density (BMD) at lumbar spine and hip in a large cohort of young patients with severe anorexia nervosa (AN), and to assess determinants of low BMD.

Patients and methods: the main inclusion criteria were as follows: women with severe anorexia nervosa (AN) admitted to inpatient treatment units recruited from 11 centers in France (cohort EVHAN (EValuation of Hospitalisation for AN)). Current AN diagnosis was based on the DSM-IV criteria obtained by the Eating Disorder Examination and the CIDI 3.0 with the following BMI (Body Mass Index) criteria of: BMI <10th percentile up to 17 years of age, and BMI <17.5 for 17 years of age and above. Clinical variables were assessed during the first 2 weeks after hospitalization. Lumbar spine and femoral bone mineral density (BMD), body composition (lean and fat masses) were performed during the hospitalization using dual-energy x-ray absorptiometry (DXA). Low BMD was defined by Z ≤ -2 (at least one site). Determinants associated with low BMD were tested using univariate and multivariate analysis.

Results: 150 women were the basis of this study: mean age 20.5 years, mean disease duration of 48.4 months, 90.5% were amenorrheic and mean BMI of 14.3kg/m². 34 (24.1%) reported a previous fracture. Mean Z score was -1.82 at lumbar spine and -1.34 at femoral neck; 72 (49%) had low BMD. None of them received anti-osteoporotic treatment. Univariate analysis showed that parameters significantly associated with low BMD were lifetime lowest BMI (p<.0001), BMI measured at the admission (p=0.004), low appendicular lean mass (p= p=0.034) and low appendicular fat mass (p=0.07). When using multivariate analysis, the lifetime lowest BMI remained the only determinant of low BMD (OR=1.83, CI 95% 1.40-2.50, p=0.001) while age, disease duration, amenorrhea, BMI measured at the time of admission and body composition were no longer significantly associated.

Conclusion: this study showed that 1 out of 4 patients with severe anorexia nervosa had a previous fracture, low BMD is frequent, and that among all potential risk factors tested, the lifetime lowest BMI was the only determinant.

Disclosures: Karine Briot, None.

1214

Bone Loss After Bariatric Surgery: Not Just Skeletal Unloading. Emily Stein¹, Angela Carrelli², Polly Young³, Mariana Bucovsky³, Donald McMahon¹, Chiyuan Zhang³, Bin Zhou³, Ji Wang³, X Guo³, Elizabeth Shane¹, Shonni Silverberg³. ¹Columbia University College of Physicians & Surgeons, USA, ²Columbia University Medical Center, USA, ³Columbia University, USA

The mechanism of bone loss after bariatric surgery and whether it is associated with increased skeletal fragility is unknown. We studied 22 women (age 45±10) undergoing Roux-en-Y gastric bypass (RYGB; n=14) and restrictive procedures (n=8). We measured calciotropic hormones, bone turnover markers, areal BMD (aBMD) by DXA at the lumbar spine (LS), total hip (TH), femoral neck (FN) and 1/3 radius (1/3R), and trabecular (Tb) and cortical (Ct) volumetric BMD (vBMD) and microstructure at the distal radius and tibia by high resolution peripheral quantitative CT (HRpQCT) before and 12 months after surgery. Subjects were 23% Caucasian and 59% Latina with a mean BMI of 44±5 kg/m² and normal baseline T-scores (LS:-0.1±0.2, TH:0.6±0.2, FN:0.1±0.2; 1/3R:0.1±0.2). Before surgery, average daily intake of calcium was 873 mg and vitamin D 5188 IU. Mean weight loss was 28±3 kg (Table; p<0.0001). Serum calcium fell and PTH rose despite a 50% increase in calcium (p<0.02) and stable vitamin D intake, and no change in serum 25OHD. Serum CTX increased by 136%. aBMD declined at the TH (5.4%) and FN (4.5%), but not the LS or 1/3R. By HRpQCT, Tb parameters were stable while Ct Area (CtAr), Ct thickness (CtTh) and Ct density deteriorated, particularly at the tibia. By multivariate regression, weight loss predicted 52% of variance in hip bone loss (p<0.001), while PTH increase was not a significant predictor. In contrast, PTH increase predicted the decline in Ct parameters at both radius (CtAr 26% p<0.04; CtTh 27% p<0.03) and tibia (CtAr 23% p<0.02; CtTh 16% p<0.04; Ct density 32% p<0.01), while the contribution of weight loss was less (18%, 17% and 9%, p= 0.10-0.18). RYGB patients lost more weight and had more bone loss by DXA and HRpQCT than those with restrictive procedures, which was associated with a decline cortical load share estimated by finite element analysis. In summary, our results suggest at least 2 mechanisms for bone loss after bariatric surgery. Weight loss is a more important cause of hip than tibial bone loss, likely because the load carried by the hip (2-3 x body weight) is greater than that carried by the tibia (1x body weight). In contrast, cortical losses at the tibia reflect secondary hyperparathyroidism (SHPT). In conclusion, hip bone loss after bariatric surgery reflects skeletal unloading, while deterioration of cortical microstructure is due to SHPT. The decline in cortical load share after RYGB raises concern for future increases in skeletal fragility.

Changes Following Bariatric Surgery (mean±SE)

| | Baseline | 12 months | p-value |
|--|---------------|----------------|---------|
| Weight (kg) | 115 ± 3 | 87 ± 3 | <0.0001 |
| Corrected calcium | 9.37 ± 0.01 | 9.17 ± 0.06 | <0.02 |
| PTH (pg/ml) | 37 ± 3 | 47 ± 5 | <0.05 |
| CTX (ng/ml) | 0.236 ± 0.026 | 0.562 ± 0.071 | <0.0001 |
| TH aBMD (g/cm ²) | 1.039 ± 0.024 | 0.983 ± 0.023 | <0.001 |
| FN aBMD (g/cm ²) | 0.882 ± 0.022 | 0.842 ± 0.0024 | <0.001 |
| Radius Ct Ar (mm ²) | 57.3 ± 2.5 | 56.0 ± 2.6 | <0.05 |
| Radius Ct density ((mgHA/cm ³) | 915 ± 15 | 907 ± 17 | 0.12 |
| Radius Ct Th (microns) | 892 ± 47 | 878 ± 49 | 0.14 |
| Tibia Ct Ar (mm ²) | 124.7 ± 4.6 | 122.8 ± 4.9 | <0.01 |
| Tibia Ct density ((mgHA/cm ³) | 875 ± 13 | 862 ± 14 | <0.01 |
| Tibia Ct Th (microns) | 1195±60 | 1184 ± 60 | <0.02 |

Disclosures: Emily Stein, None.

1215

Evaluation of Bone Turnover During Lactation in African-Americans: A Comparison to Caucasian Lactation. Mara Horwitz¹, Raquel Carneiro^{2*}, Linda Prebehala³, Mary Beth Tedesco³, Susan Sereika³, Caren Gundberg⁴, Andrew Stewart⁵. ¹University of Pittsburgh Div of Endocrinology - EMRC, USA, ²The University of Fortaleza, School of Medicine, Brazil, ³University of Pittsburgh, USA, ⁴Yale University School of Medicine, USA, ⁵University of Pittsburgh School of Medicine, USA

Background. Lactational bone turnover, which is mediated by PTHrP in the setting of low estrogen, has not been studied in African-American (AA) women. The AA skeleton is known to be resistant to PTH; whether it is also resistant to PTHrP and the hormonal changes of lactation are unknown. We hypothesized that AA women may be resistant to PTHrP and therefore display lower levels of bone turnover markers during lactation than Caucasians (C).

Objectives. To assess AA bone turnover during lactation and to compare this to C.

Design and Participants. This was a prospective cohort study with repeated measures of bone metabolism in 60 healthy AA women age 21-45 (three groups of 20: lactating, bottle feeding, and healthy controls) studied at 6 and 12 weeks postpartum. AA subjects were compared with a previously published identical study in C women.

Outcome Measures. Biochemical markers of bone turnover and calcium metabolism.

Results. All three AA groups displayed 30-50% lower 25OHD and two-fold higher PTH values compared to C (p<0.001, p<0.002) but similar 1,25(OH)₂D values. Formation markers (PINP and BSAP) were comparable in AA and C controls, but resorption (CTX and NTX) was lower in the AA vs. C controls (p=0.003, p<0.01). PINP and BSAP increased significantly (2-3 fold) in lactating and bottle-feeding AA women (PINP, p<0.001; BSAP, p<0.001) as did both CTX and NTX (both p<0.01). AA lactating mothers displayed quantitatively similar bone formation, but slightly lower bone resorption, compared to C women (p= 0.036).

Conclusions. Bone turnover, measured using current sensitive and specific markers, is uncoupled in favor of formation in young adult AA women when compared to C. Despite resistance of the AA skeleton to PTH, the AA skeleton appears to respond to the hormonal milieu of lactation with a robust three-fold increase in bone turnover. This is quantitatively similar to that observed in C. Whether this is associated with similar losses of bone in AA vs C during lactation has not been studied and requires further investigation.

Disclosures: Raquel Carneiro, None.

1216

The Skeletal Effects of Reducing Inflammation in Type 2 Diabetes Mellitus. Daniel Donovan¹, Serge Cremers¹, Donald McMahon², Elzbieta Dworakowski¹, Allison Goldfine³, Steven Shoelson³, Mishaela Rubin^{4*}. ¹Columbia University, USA, ²Columbia University College of Physicians & Surgeons, USA, ³Joslin Diabetes Center, USA

The skeleton is now recognized, epidemiologically, to be adversely affected in Type 2 Diabetes Mellitus (T2D), with an increased risk of fractures. Previous studies have identified reduced bone formation as a contributing factor, but the mechanisms remain speculative. One possible explanation is chronic inflammation, which negatively influences bone remodeling by reducing bone formation and increasing bone resorption. The Targeting Inflammation using SALSALATE in Type 2 Diabetes (TINSAL-T2D) trial found that a salicylate, which reduces inflammation by decreasing NF-κB, improved glycemic control in patients with T2D. We hypothesized that reducing inflammation in T2D would additionally lead to a rebalancing of the bone remodeling process. In TINSAL-T2D patients were randomized to placebo (PLB) or salsalate, at doses of 3.0, 3.5 or 4.0 g/d tid for 14 weeks. We measured markers of bone turnover (PINP, BAP, osteocalcin, s-CTX and TRAP-5b) in samples from TINSAL-T2D at 0 and 14 weeks.

76 subjects with T2D (56 ± 1yr, 51 men, BMI 33 ± 1 kg/m², 43% Caucasian, HbA1c 7.6 ± 1%; none on TZDs or insulin) were analyzed. At baseline, corrected serum calcium was 9.2 ± 1 mg/dl; PTH 35 ± 1 pg/ml; 25OHD 21 ± 2 ng/dl. Baseline PINP was 36.8 ± 2 ng/ml (nl: 16-83), BAP 28.3 ± 1 IU/L (nl: 11.6-29.6), osteocalcin 10.7 ± 1 ng/ml (nl: 8.4-33.9), s-CTX 0.29 ± 0.1 ng/ml (nl: 0.11 - 0.74) and TRAP-5b 3.2 ± 0.1 U/L (nl: 1.03-4.15). With salsalate treatment, PINP, BAP and TRAP-5b did not change, but osteocalcin increased from 0 to 14 wks at the highest dose as compared with PLB (PLB: -3% ± 9% vs. 4 mg dose: 34% ± 8%, p=0.003). Moreover, s-CTX levels increased from 0 to 14 wks at the 3.5 mg dose (PLB: 7 ± 3 vs 3.5 mg dose: 95 ± 19%, p=0.003), tending also to increase at the 4 mg dose (31 ± 22%; p=0.16 vs PLB).

These data suggest that along with reductions in inflammation and glycemic burden in TINSAL-T2D, there is an increase in bone remodeling, as reflected by increases in osteocalcin and s-CTX. Although one would not expect that bone resorption would increase with a concomitant reduction in NF-κB, there may be a coupled rise in bone remodeling in T2D as inflammation is reduced. This study provides proof of concept for a relationship between the inflammatory process and skeletal dynamics in T2D. Further studies would shed light on mechanistic approaches to the skeletal complications of T2D.

Disclosures: Mishaela Rubin, None.

FR0001

A FoxO1/ATF4 Synergism in Osteoblasts Adversely Affects Glucose Metabolism by Promoting Osteocalcin Carboxylation. Aruna Kode*, Ioanna Mosialou, Stavroula Kousteni, Columbia University Medical Center, USA

Osteoblasts beneficially regulate energy metabolism through secretion of the undercarboxylated form of osteocalcin. At the transcriptional level, *FoxO1* cooperates with *Atf4* in osteoblasts to suppress glucose metabolism, insulin production and insulin sensitivity. To understand the molecular mechanism of the insulin sensitizing properties of these two transcription factors, we examined an array of insulin regulated genes in compound mice lacking one allele of *Atf4* and *FoxO1* in osteoblasts (*FoxO1^{osb}+/-; Atf4+/-* mice). Expression of the insulin-sensitizing hormone *adiponectin* was upregulated in gonadal fat of *FoxO1^{osb}+/-; Atf4+/-* mice. In contrast, expression of *Resistin*, associated with insulin resistance, or *Leptin* were not affected. Consistent with increased adiponectin, expression of the adiponectin targets *Acyl-CoA Oxidase*, peroxisome proliferator-activated receptor- α (*Ppar α*) and Uncoupling Protein 2 (*Ucp2*) was increased in the muscle of *FoxO1^{osb}+/-; Atf4+/-* mice. Also in the muscle, expression of the insulin target *Pgcl α* and its transcriptional effectors *Nrf1* and *Mcad* was upregulated. In the liver, expression of *FoxA2* was increased whereas expression of *G6Pase* and *Pepck1* was decreased in *FoxO1^{osb}+/-; Atf4+/-* mice. The expression profiling of the metabolic phenotype of *FoxO1^{osb}+/-; Atf4+/-* mice pointed towards Osteocalcin as a potential mediator of the combined function of the 2 transcription factors. Indeed, serum levels of undercarboxylated osteocalcin were increased in *FoxO1^{osb}+/-; Atf4+/-* mice. Expression of *Esp*, the tyrosine phosphatase promoting osteocalcin carboxylation, was reduced in the bone of these animals. *FoxO1* and *Atf4* each stimulated *Esp* transcriptional activity in osteoblast cultures. Combination of both transcription factors resulted in synergistic, highly induced transcriptional activation of *Esp*. Mutation of either an *ATF4* or a *FoxO1* binding site in the *Esp* promoter abolished binding of the respective transcription factor to *Esp*. It also ablated *Esp* activation by each transcription factor. Combination of *FoxO1* and *ATF4* also failed to induce activation of *Esp* when either the *ATF4* or *FoxO1* binding site was mutated. Thus, synergistic activation of *Esp* by *ATF4* and *FoxO1* requires both factors to be bound simultaneously to DNA. Collectively, these observations indicate that *FoxO1* and *ATF4* interact in osteoblasts to control glucose homeostasis by promoting *Esp* expression and subsequent carboxylation and inactivation of osteocalcin.

Disclosures: Aruna Kode, None.

FR0002

Age-Related Impairment of the Mechanostat is Sex Specific and Associated with Impaired Cell-Cycle Progression and Decreased Mechanosensitivity. Lee Meakin*, Gabriel Galea¹, Toshihiro Sugiyama², Lance Lanyon³, Joanna Price¹. ¹University of Bristol, United Kingdom, ²Yamaguchi University School of Medicine, Japan, ³Royal Veterinary College, United Kingdom

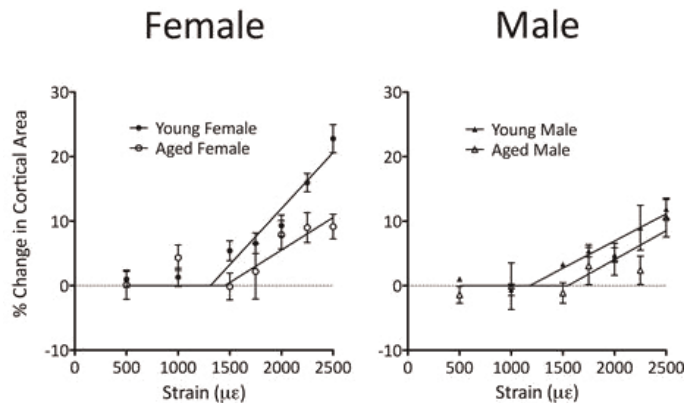
One hypothesis for the cause of age-related bone loss is decreased effectiveness of "the mechanostat". The higher prevalence of bone fragility fractures in women suggests a gender-related influence. In the present study we used the axial tibial *in vivo* loading model¹ to compare bones' adaptive responses in young and aged, male and female mice and compared the proliferative response to strain of osteoblast-like cells derived from the long bones of these mice *in vitro*.

Minimum Effective Strain (MES; x-intercept in Figure) was determined by μ CT in cortical bone and, in females, was similar in young adults (17-week) and aged mice (19-month; $p=0.54$). In contrast, in males the MES was significantly higher in aged than young mice ($p=0.04$). The slope of the strain-response curves (bone response per unit strain) was similar in young and aged males ($p=0.64$) but lower in aged than young females ($p<0.01$).

Proliferation of long bone-osteoblasts (LOBs) derived from these mice was investigated *in vitro* by Ki-67 *in situ* cell cycle analysis and showed that young male and female LOBs were recruited to the cell cycle within 1h of exposure to a single short period of dynamic strain change (peak 3400me, 600 cycles, 0.6Hz) in their substrate². Aged female LOBs were also recruited within 1h, but showed delayed progression through G2-phase with a consequential reduced increase in cell number after 48hrs. Aged male LOBs were not recruited to the cell cycle by strain. Expression of EGR2, an early marker of osteoblasts' strain responsiveness², measured by quantitative PCR, was up-regulated 1h following strain in LOBs from all groups except aged males.

In conclusion, this study demonstrates, for the first time, that ageing is associated with impaired cell cycle progression in osteoblast-like cells; in this case in response to strain. This impaired proliferative response is gender specific. *In vivo*, bones' adaptive responsiveness was less in aged than young females whereas it was similar between young and old males, although their sensitivity (MES) was different. These data implicate both age- and sex-related differences in mechano-responsiveness and sensitivity, as well as cell cycle progression. These age-related impairments of the mechanostat may be recapitulated in humans.

¹ Sugiyama et al. Bone 2011; 49: 133-9. ² Zaman et al. J Biol Chem 2012; 287: 3946-62.



Figure

Disclosures: Lee Meakin, None.

FR0004

Differential Expression of MicroRNAs in Human Mesenchymal Stem Cells with Age May Be Related to Musculoskeletal Disorders. Sudharsan Periyasamy-Thandavan*¹, Sergi Mas², Sadanand Fulzele³, Mark Hamrick³, Xingming Shi³, Carlos Isales⁴, Norman Chutkan³, Randy Ruark³, John Hinson³, Monte Hunter³, Raymond Corpe³, Hongyan Xu³, William Hill⁵. ¹Georgia Health Sciences University & Charlie Norwood VAMC, USA, ²Universitat de Barcelona, Spain, ³Georgia Health Sciences University, USA, ⁴Medical College of Georgia, USA, ⁵Georgia Health Sciences University & Charlie Norwood VAMC, USA

Age-associated osteoporosis is one of the most common and debilitating types of bone disease. Although the mechanisms involved remain poorly defined, recent studies suggest that age-associated osteoporosis is a stem cell disease. Human mesenchymal stromal/stem cells (hMSCs) are multipotent stem cells that can differentiate into osteoblasts. MicroRNAs (miRNAs), a class of short single-stranded noncoding RNAs are post-transcriptional regulators that can modulate the homeostasis of multiple genes and associated pathways simultaneously. Changes in miRNA expression have been linked to the development of numerous disorders, including musculoskeletal disorders. While miRNAs are emerging as critical modulators of cell function and phenotype development little work has been done to determine their role in hMSC differentiation or in the regulation of bone metabolism with aging. Here, we directly isolated hMSC CD271⁺ cells by using a kit (CD271 (APC) MicroBead Kit, Miltenyi Biotec Inc. CA.) from surgical bone marrow specimens of three young (under 40 yrs old) and three old (over 75 yrs old) patients, without plastic adhesion or culturing that might alter miRNA and gene expression. Total RNA was isolated from the hMSC CD271⁺ cells and microarrays were performed using an Affymetrix GeneChip[®] miRNA 2.0 Array, normalized using robust multichip average (RMA), and assessed by 2-way ANOVA analysis of young vs old hMSCs (with sex and age as the variables) using the Partek Genomics Suite. This genome-wide assessment of miRNA expression revealed multiple miRNAs whose expressions were altered with age. We identified six miRNAs (miR-579, -1244, -374ab, -671-5p, -370, -29abcd) that were significantly up-regulated in aged hMSCs. Predicted bone homeostasis targets of these miRNAs include SDF-1, BMP2, β arrestin, SOX4, Leptin, IGF-1, VEGF, Collagen type 1 $\alpha 1$ and $\alpha 2$. Similarly, we identified 11 miRNAs including miR-1231, -517-ac, -3180-5p that were significantly reduced in aged hMSCs. Predicted targets of these miRNAs included adipogenic genes such as PPAR- γ or- α , AP2- α , and CD36. These results suggest that the differential miRNA expression in hMSCs with age may regulate age-associated changes that reduce osteogenic capacity and increase the adipogenic fate of these stem cells, and may help drive the development of osteoporosis. Targeting these miRNAs may be a potential therapeutic strategy to treat age-related musculoskeletal disorders.

Disclosures: Sudharsan Periyasamy-Thandavan, None.

This study received funding from: PO1-AG036675-01 NIH

FR0005

Levels of Serum Sclerostin Are Related with Atherosclerotic Disease in Type 2 Diabetes. Rebeca Reyes-Garcia^{*1}, Pedro Rozas-Moreno², Antonia Garcia-Martin¹, Sonia Morales-Santana³, Beatriz Garcia-Fontana¹, Manuel Muñoz-Torres¹. ¹Bone Metabolic Unit (RETICEF), Endocrinology Division, Hospital Universitario San Cecilio, Spain, ²Endocrinology Division, Hospital General de Ciudad Real, Ciudad Real, Spain, ³Bone Metabolic Unit (RETICEF), Endocrinology Division, Hospital Universitario San Cecilio; Proteomic Research Service, Fundación para la Investigación Biosanitaria de Andalucía Oriental - Alejandro Otero- (FIBAO), Spain

In vitro studies have shown that calcification induces vascular smooth muscle cells (VSMCs) to undergo an osteocytic phenotype transition and *in vivo* studies in diabetic murine models have demonstrated that sclerostin, an osteocyte-derived negative regulator of bone formation, is up-regulated during calcification of VSMCs. Our aim was to explore the hypothesis that increased circulating sclerostin levels are associated with atherosclerotic disease in patients with type 2 diabetes mellitus (T2DM). We performed a cross-sectional study of 75 patients with T2DM (female: 45.3%, mean age 59±5.7 years and male: 54.7%, mean age 57.4±6.7 years) and we evaluated intima-media thickness, and the prevalence of ischemic heart disease atherosclerotic plaques and aortic calcifications. Serum sclerostin levels were determined by ELISA immunoassay.

Overall 58.6% of T2DM patients had atherosclerotic disease (AD), 37.3% had ischemic heart disease, 54.6% had abnormal intima-media thickness, 28.1% had carotid plaques and 34.7% had aortic calcifications. SMean serum sclerostin was significantly higher (P=0.006) in patients with AD (59.0±26.2 pmol/L) compared with those without AD (44.8±16.5 pmol/L). Sclerostin serum levels remained significantly higher in male patients with vs without AD (68.4±25.0 pmol/L vs 51.6±21.6 pmol/L; P=0.042). Also, higher concentrations of sclerostin were found in male patients with abnormal intima-media thickness (68.9±26.7 pmol/L vs 47.1±16.0 pmol/L; P=0.004), carotid plaques (79.0±23.7 pmol/L vs 49.0±20.5 pmol/L; P<0.001) and aortic calcifications (70.2±28.9 pmol/L vs 50.7±21.2 pmol/L; P=0.034). Serum sclerostin levels were significantly higher in female patients with vs without abnormal intima-media thickness (44.5±12.2 pmol/L vs 36.1±8.05 pmol/L; P=0.029) and aortic calcifications (48.7±13.9 pmol/L vs 36.3±7.74 pmol/L; P=0.004). In summary, serum sclerostin levels were positively related with parameters of atherosclerosis, suggesting that sclerostin is up-regulated during the progress of atherosclerotic disease in T2DM patients

Disclosures: *Rebeca Reyes-Garcia, None.*

FR0006

The Adipokine Leptin Enhances the Proliferation and Differentiation of Aged Primary Myoblasts in vitro. Matthew Bowser^{*1}, Sadanand Fulzele², William Hill³, Xingming Shi², Carlos Isaacs⁴, Mark Hamrick². ¹Georgia Health Science University, USA, ²Georgia Health Sciences University, USA, ³Georgia Health Sciences University & Charlie Norwood VAMC, USA, ⁴Medical College of Georgia, USA

The long form of the leptin receptor is abundant in human skeletal muscle, and we have previously shown that recombinant leptin therapy increases skeletal muscle mass and fiber size in aged mice. Here we sought to determine whether or not leptin may have direct effects on either the proliferation or differentiation of primary myoblasts isolated from the hindlimb muscles of young (12 mo) and aged (24 mo) mice. Primary cells were isolated and cultured and then serum-starved prior to leptin treatment (0 ng/ml, 100 ng/ml, 1000 ng/ml). MTS assays showed that leptin treatment significantly (P<.01) increased proliferation of myoblasts from both young and aged mice. Leptin did not significantly alter the expression of myogenic markers MyoD and myogenin in young myoblasts, but leptin significantly (P<.01) increased the expression of both MyoD and myogenin in myoblasts from aged mice. In addition, primary myoblasts from POUND (Lepr^{db/db}) mice, which lack both the short and long form of the leptin receptor, showed decreased proliferation and decreased expression of both MyoD and myogenin compared to myoblasts from normal mice. Together, these data provide further evidence that leptin is important for the regulation of both muscle and bone mass, and that leptin can act directly on its receptors in peripheral tissues to regulate cell proliferation and differentiation.

Disclosures: *Matthew Bowser, None.*

FR0008

The Role of Ramp3 in Development of an Aging Phenotype. Fiona McGuigan^{*1}, Kristina Akesson², Peter Grabowski³, Gareth Richards³, Timothy Skerry⁴. ¹University of Lund, Malmö, Skane University Hospital, Malmö, Sweden, ²Skåne University Hospital, Malmö, Sweden, ³University of Sheffield, United Kingdom, ⁴University of Sheffield Medical School, United Kingdom

The Receptor activity modifying proteins (RAMPs) are a group of 3 accessory proteins which interact with a number of G-protein coupled receptors (GPCR). These interactions of a RAMP with a GPCR have several roles in regulation of endocrine signalling. They alter the selectivity of a receptor for different ligands, so a calcitonin receptor (CTR) becomes a receptor for amylin when associated with a RAMP. Secondly, they are required for trafficking of the calcium sensing receptor (CaSR) and calcitonin-like receptors (CLR) to the cell surface. We have also shown that they alter the G-protein activation response of a single receptor to a single ligand. For example, a PTH1 receptor associated with a RAMP activates a different spectrum of G-proteins and second messengers from a PTH1 receptor alone stimulated by the same ligand. It is known that RAMPs associate with CTR, CLR, PTH1&2Rs, CaSR, and the glucagon, secretin and VPAC1 receptors, so effects of altered signaling in vivo are complex. Studies in RAMP3 KO mice reveal an age related phenotype with altered metabolic regulation and high bone mass. To translate these findings into a clinically relevant perspective, we investigated the relationship between RAMP3 gene variants, body composition, BMD, serum biomarkers and hormone levels in two population-based cohorts of Swedish women. Five single nucleotide polymorphisms (SNP) in the vicinity of the RAMP3 gene (rs1294935; rs11982639; rs3757575; rs12702121 and rs2074654) were genotyped in two populations; the PEAK25 cohort consisting of 1061 25 year old women and OPRA consisting of 1044 75 year-old women. BMD, fat mass and lean mass (total body; regional) were measured by DXA. Genotype distributions were the same in both cohorts (p>0.05). BMD was not significantly different between genotypes. rs2074654 showed association with body composition in older but not younger women: fat and lean mass was not significantly different in PEAK25, but 3-10% higher in OPRA women carrying the variant allele (p<0.05). In the older women this was reflected in a trend towards a lower lean/fat ratio (less-lean phenotype). After correction for covariates contributing to body composition (weight, height, smoking) the results suggest that the effect of the polymorphism is through an effect on body size. These results provide the first link between the biology of RAMPs in vitro and in mice and effects in humans.

Disclosures: *Fiona McGuigan, None.*

FR0013

Inter and Intramuscular Adiposity Explains Only a Proportion of the Association between Muscle Density and Fractures. Andy Kin On Wong^{*1}, Karen Beattie¹, Aakash Bhargava¹, Sami Shaker¹, Colin Webber², Christopher Gordon¹, Laura Pickard¹, Alexandra Papaioannou², Jonathan Adachi³, The CaMos Research Group⁴. ¹McMaster University, Canada, ²Hamilton Health Sciences, Canada, ³St. Joseph's Hospital, Canada, ⁴McGill University, Canada

Objectives:1) To determine the association between MRI-derived inter- and intramuscular fat (IMF) in the calf and fragility fractures, 2) to determine whether IMF explains part of the association between volumetric muscle density (vMD) and fractures.

Methods:A cohort of women ≥ 50 years old from the CaMos Hamilton site underwent a 1T peripheral (p) MRI (T1-weighted fast spin echo) and pQCT (20 mm/s, 38 kVp) scan of the 66% site of their calf muscle as measured proximally from the medial malleolus to the medial tibial plateau. IMF was segmented semi-automatically from muscle on single slice MR images (1.0 mm thick, 195 µm resolution) using a region-growing algorithm. Total and percent IMF area (A), as a function of muscle area, were determined. Muscles on pQCT image slices (2.3 ± 0.5mm thick, 500 µm resolution) were manually segmented from subcutaneous fat and bone using a watershed algorithm to yield a measure of vMD computed using a fixed density calibration. Number of prevalent fragility fractures (excluding skull, toes, fingers) over the last 15 years was acquired from the CaMos database. Pearson correlations determined the percentage variance of vMD and total hip aBMD explained by IMF.A. A binary logistic regression analysis measured the association between IMF.A and odds for fragility fractures. A similar model quantifying the association between vMD and prevalent fractures further adjusted for IMF.A. All models were examined with and without age, BMI and total hip aBMD as covariates. Missing values were imputed 10 times and saturated by the regression method.

Results:IMF.A explained 53.9% of the variance in vMD, with adjustment for BMI (p<0.001), and 6.7% of variance in total hip aBMD (p=0.036). Odds for fragility fractures were significantly increased with vMD alone but only marginally with IMF.A. The association with fractures remained significant for vMD after adjusting for absolute or percent IMF.A but was decreased when total hip aBMD was included in the model (Table II).

Conclusion: Visible muscle adiposity on MRI represents only a portion of muscle density. Associations of muscle density and fractures independent of inter and intramuscular fat could be explained by the quality of muscle fibres or intra/extra

myocellular lipids which cannot be quantified using the technique employed here. Variability in IMF.A could arise from partial volume effects and subjectivity in histogram-based threshold selection.

Table I. Comparison of participant characteristics between those with and without at least one fragility fracture. P-value indicates significant difference between groups from analysis of variance tests adjusted for multiple comparisons. Percent (perc) inter and intra-muscular fat (IMF) area (A) represent all visible muscle adiposity on T1-weighted MR images.

| Variable | No Fracture (N=23) | Fractured (N=47) | P-value |
|---------------------------|--------------------|------------------|---------|
| Age (years) | 67.04 ± 5.24 | 75.55 ± 8.27 | <0.001 |
| BMI (kg/m ²) | 26.31 ± 4.57 | 28.38 ± 6.26 | 0.163 |
| IMF.A (mm ²) | 601.16 ± 264.36 | 779.08 ± 410.57 | 0.063 |
| Perc IMF.A (%) | 0.163 ± 0.094 | 0.155 ± 0.076 | 0.715 |
| vMD (mg/cm ³) | 71.85 ± 1.72 | 68.76 ± 4.7 | 0.003 |

Table I

Table II. Odds for fragility fractures based on vMD and IMF information. Models were adjusted by covariates (covars): age, BMI, total hip aBMD where indicated. All odds ratios (OR) were expressed per standard deviation (SD) increase (+) or decrease (-) in the primary variable.

| Model | pMRI/pQCT Variable | OR | Lower 95% CI | Upper 95% CI | Per SD +/- |
|---------|---------------------------|-------|--------------|--------------|------------|
| Model1A | IMF.A (mm ²) | 1.84 | 0.95 | 3.57 | + |
| Model1B | Perc IMF.A (%) | 0.91 | 0.56 | 1.49 | + |
| Model1C | vMD (mg/cm ³) | 7.16 | 2.19 | 23.42 | - |
| Model2A | IMF.A + Covars | 1.63 | 0.60 | 4.44 | + |
| Model2B | Perc IMF.A + Covars | 1.08 | 0.59 | 1.95 | + |
| Model2C | vMD + Covars | 4.69 | 0.86 | 25.70 | - |
| Model3A | Model1C + Perc IMF.A | 9.83 | 2.61 | 36.76 | - |
| Model3B | Model2C + Perc IMF.A | 5.45 | 0.93 | 32.04 | - |
| Model3C | Model1C + IMF.A | 11.27 | 2.46 | 51.61 | - |
| Model3D | Model2C + IMF.A | 5.16 | 0.78 | 34.12 | - |

Table II

Disclosures: Andy Kin On Wong, None.

FR0014

Prevalent Fractures are Associated with Frailty: Baseline Data from the Canadian Multicentre Osteoporosis Study. Courtney Kennedy^{*1}, George Ioannidis¹, Jonathan Adachi², Kenneth Rockwood³, Lehana Thabane¹, Laura Pickard¹, Alexandra Papaioannou⁴. ¹McMaster University, Canada, ²St. Joseph's Hospital, Canada, ³Dalhousie University, Canada, ⁴Hamilton Health Sciences, Canada

Background: A Frailty Index is a composite measure of impairments, reflecting the concept that the more things people have wrong the more frail they are. We created a "cumulative deficits" Frailty Index utilizing baseline data from the prospective, population-based Canadian Multicentre Osteoporosis Study (CaMos) and examined the relationship with prevalent fractures, falls, and BMD. Methods: A clinical panel identified candidate Index variables (i.e., related to health status; biological plausibility) which were assessed for inclusion according to pre-defined criteria: prevalence ≥ 1% and <80%, accumulates with age, does not saturate too early, and ≤5% missing data. The final Frailty Index consisted of 31 variables. For dichotomous variables, a deficit value of "1" (present) or "0" (absent) was assigned; multi-level variables were assigned deficit values in equal cut-points. Frailty scores were computed as the sum of deficit values/total number of deficits. Osteoporosis (OP) was considered a BMD t-score ≤ -2.5. Falls (past month) and prevalent fractures were self-reported, or detected via x-ray for vertebral fractures (>3 SD below the mean normal ratio). Associations were examined with ANOVA, Dunnett's C post-hoc tests, and age-adjusted ANCOVA. Mean frailty scores (95% confidence intervals [CI]) according to prevalent fracture and falls status were graphed by 5-year age categories. Results: In CaMos men (n=2884) and women (n=6539) aged 25-103 years (mean 62.6, SD 13.4), frailty scores increased significantly with age (3.4% increase per year of age on a logarithmic scale) and were significantly higher for women than men across the life-span. In men and women ≥ 65 years: 1) Participants with a prevalent fracture had greater frailty than those without (only significant <75 years; Figure 1a); 2) Participants with a recent fall (versus non-fallers) had significantly greater frailty (Figure 1b); 3) Men with OP at the femoral neck were significantly frailer than men without. A relationship with OP was not observed for women. Conclusion: In every age decade, women had greater frailty than men. Participants with a prevalent fracture were more likely to be frail than those without, particularly at younger ages. A relationship between OP and frailty was only observed for men, which could indicate that OP has more serious consequences for men and/or is often due to secondary causes.

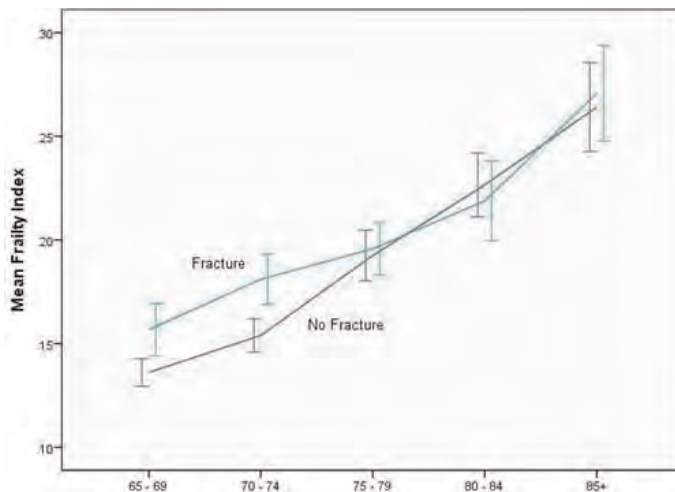


Figure 1a: Mean Frailty Score (95% CI) by Age Category, Prevalent fracture/No Fracture

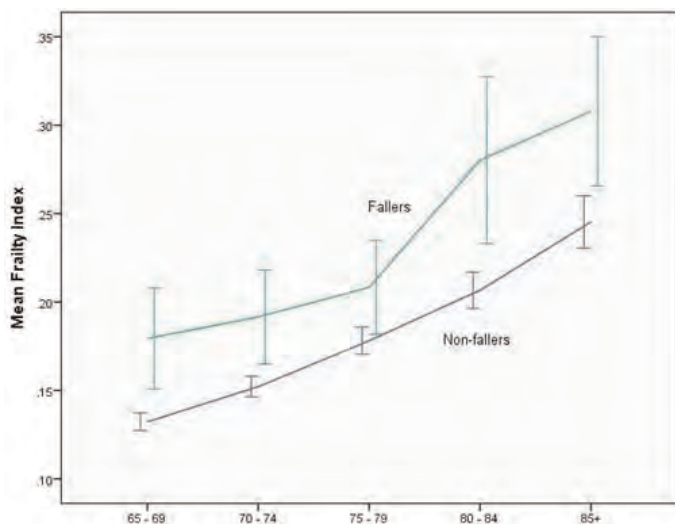


Figure 1b: Mean Frailty Score (95% CI) by Age Category, Fallers/Non-fallers

Disclosures: Courtney Kennedy, None.

FR0020

Effect of a Multifactorial Fall-and-Fracture Risk Assessment and Management Program on Gait and Balance and Disability in Hospitalized Older Adults: a Controlled Study. Andrea Trombetti^{*}, Mélanie Hars, François Herrmann, René Rizzoli, Serge Ferrari. Division of Bone Diseases, University Hospitals & Faculty of Medicine of Geneva, Switzerland

Purpose: Falls and fragility fractures among older adults are common, devastating and costly. Hospitalization affords a major opportunity for identifying high-risk individuals and for interdisciplinary cooperation to manage fall and fracture risk factors. We assessed the effects on physical performances and the level of independence in activities of daily living (ADL), of a multifactorial fall-and-fracture risk assessment and management program including targeted exercise applied in a specific geriatric hospital setting.

Methods: We conducted a controlled study among 122 geriatric in-patients (mean ± SD age, 84 ± 7 years) admitted with a fall-related diagnosis to an acute rehabilitation ward. Among them, 92 were admitted to a dedicated unit and enrolled into a multidisciplinary, multifactorial program addressing risk factors for fall and fracture, including intensive targeted exercise, who constituted the intervention group. Thirty age-matched patients who received standard usual care in a general geriatric unit formed the control group. Primary outcomes included gait and balance performances, as assessed by instrumental gait analysis and functional tests, and the level of independence in ADL, measured on two separate occasions during stay (11.6 ± 6 days apart). Secondary outcomes included length of hospital stay, incidence of in-hospital falls, hospital readmission and mortality rates.

Results: Compared to the usual care group, the intervention group improved their Timed Up & Go (P=0.017), Tinetti (P<0.001), and Functional Independence Measure (P=0.027) tests performances, as well as several gait parameters (comfortable gait velocity: adjusted mean difference, 8.6 cm/s; 95% CI, 3.0-14.1; P=0.003). Furthermore, this program favourably impacted three-month hospital readmission rate (HR, 0.30;

95% CI, 0.1-0.9; P=0.02). Three patients in both groups (10% and 3% of control and intervention patients, respectively) were readmitted for fall-related causes (P=0.14), two control patients (7%) with a fall-related fracture.

Conclusions: A multidisciplinary, multifactorial fall-and-fracture risk-based intervention program incorporating targeted exercise, delivered during hospitalization in a dedicated unit, was effective and more beneficial than usual care in improving physical parameters related to the risk of fall and reducing disability among high-risk oldest old patients.

Disclosures: *Andrea Trombetti, None.*

FR0021

Effects of High-Impact Training on Femoral Neck Structure in Postmenopausal Women with mild osteoarthritis: 12-Month Randomized Controlled Exercise Intervention (ISRCTN58314639). Ari Heinonen^{*1}, Eija Janhunen¹, Juhani Multanen², Timo Jamsa³, Urho Kujala¹, Miika Nieminen⁴, Ilkka Kiviranta⁵, Arja Häkkinen¹. ¹Department of Health Sciences, University of Jyväskylä, Finland, ²University of Jyväskylä, Finland, ³University of Oulu, Finland, ⁴Department of Medical Technology, Institute of Biomedicine, University of Oulu, Finland, ⁵Department of Orthopaedics & Traumatology, University of Helsinki, Finland

Exercise seems to be a promising action to promote bone health also in adulthood. Total bone strength is known to be a combination of material and structural properties. However, most of the exercise studies have focused on measuring only bone mineral mass as an outcome of the exercise intervention. This study evaluated the training effects of a 12-month exercise intervention on femoral neck structure in postmenopausal women who had mild knee osteoarthritis (OA).

Women with Kellgren-Lawrence (K/L) radiographic grading of knee OA 1-2 were included to the study. Eighty eligible women (mean age: 58 (SD 4) yrs, height: 165 (6) cm, weight: 72 (11) kg) were randomly assigned to undergo a supervised progressive high-impact exercise 3 times a week for 12-months (n=40) or to a non-intervention control group (n=40). At baseline and 12 months, dual-emission X-ray absorptiometry (DXA) data on 36 trainees and 40 control participants were available for hip structural analysis. The section modulus (Z), cross-sectional area (CSA), and subperiosteal width (W) at the femoral neck were analyzed from the higher K/L grade knee side. Besides the DXA scans, the dynamic balance was measured with a figure-of-eight running test, maximal isometric knee extension force was measured with a dynamometer, and cardiorespiratory fitness (VO₂ max) was evaluated by a standardized 2-kilometer walking test at baseline and 12 months. In addition, subscores for self-perceived knee pain, stiffness, and self-rated physical functioning were assessed with the Western Ontario and McMaster Universities Osteoarthritis Index (WOMAC). The univariate general linear model (GLM) was used to calculate the between-group differences at 12 months.

The baseline adjusted between-group differences were observed after the 12-month intervention in favour of trainees in Z (4.4%, p = 0.003) and CSA (1.2%, p = 0.078), while there were no change in W. The exercise group improved 7% more their isometric leg extension force (p=0.009), 3% dynamic balance (p = 0.022) and 4% estimated VO_{2max} (p=0.027) than in the control group. There were no between-group differences in WOMAC subscores.

The results of this study indicate that high-impact type of exercise can increase the femoral neck strength by improving the structural properties of bone in postmenopausal women.

Disclosures: *Ari Heinonen, None.*

FR0022

The Effects of Whole-Body Vibration and High Impact Aerobic Training on Bone Metabolism and Fall Risk in Postmenopausal Women. EKIN ILKE SEN^{*1}, Sina Esmailzadeh¹, NURTEN ESKIYURT². ¹ISTANBUL UNIVERSITY, ISTANBUL FACULTY OF MEDICINE, Turkey, ²Istanbul University, Turkey

Purpose: The aim of this study was to determine the effects of six months of supervised whole-body vibration (WBV) and high-impact aerobic (HIA) exercises on bone mineral density (BMD), serum bone turnover markers, fall risk and health-related quality of life (QoL) in postmenopausal women.

Methods: Fifty-eight eligible postmenopausal women were assigned to a WBV training group (n=19), a HIA training group (n=19), or a control group (n=20). All participants received calcium and vitamin D supplementation. The patients in both training groups participated in a supervised training program, which consisted of the one-hour exercise session three times a week for six months. The WBV groups received vibration (30–35 Hz, 2–2.8g) in five different static positions. The HIA group jumped rope (10-50 jumps/day). In all participants, baseline and six month BMD at the lumbar spine (L2-L4) and femoral neck was measured. Serum osteocalcin (OC) and C-terminal telopeptide of type I collagen (CTX) were measured at baseline, three, and six month intervals. Fall risk and health-related QoL were assessed using the Timed Up and Go (TUG) test and Quality of Life Questionnaire of the European Foundation for Osteoporosis (QUALEFFO) at baseline and sixth month of the study, respectively.

Results: At baseline, there was no significant difference between the three groups in respect to demographic and clinical characteristics of the participants (p>0.05). The BMD at the L2-L4 and femoral neck increased significantly in the WBV group (p<0.01) compared to the HIA and the control groups (p<0.05). Over six months, the serum OC significantly decreased in the WBV group and significantly increased in both HIA and control groups (p=0.001). There was no statistically significant change in serum CTx levels in the three groups (p<0.05). Finally, the TUG and QUALEFFO scores decreased in both training groups (p<0.001) compared to the controls.

Conclusions: Our data suggest that the six month supervised WBV training can be effective in the prevention of bone loss in postmenopausal women. These findings also indicate that supervised WBV and HIA training programs reduce fall risk and fractures related to osteoporosis, while at the same time improving health-related QoL in postmenopausal women.

Disclosures: *EKIN ILKE SEN, None.*

This study received funding from: Istanbul University Scientific Research Projects Unit

FR0024

Is the Relationship Between Spine Bone Mineral Density (BMD) and Prevalent Vertebral Fractures In Children Impacted by the Choice of BMD Reference Data? Leanne M. Ward^{*1}, Nathalie Alos², Stephanie Atkinson³, David Cabral⁴, Robert Couch⁵, Elizabeth A. Cummings⁶, Ronald Grant⁷, Paivi M. Miettunen⁸, Helen Nadel⁴, Celia Rodd⁹, Robert Stein¹⁰, David Stephure⁸, Shayne Taback¹¹, Mary Ann Matzinger¹, Nazih Shenouda¹, Brian Lentle⁴, Frank Rauch⁹, Kerry Siminoski⁵, and the Canadian STOPP Consortium¹². ¹University of Ottawa, Canada, ²Université de Montréal, Canada, ³McMaster University, Canada, ⁴University of British Columbia, Canada, ⁵University of Alberta, Canada, ⁶Dalhousie University, Canada, ⁷University of Toronto, Canada, ⁸University of Calgary, Canada, ⁹McGill University, Canada, ¹⁰University of Western Ontario, Canada, ¹¹University of Manitoba, Canada, ¹²Canadian Pediatric Bone Health Working Group, Canada

Background: Several reference databases are available to generate Z-scores for pediatric lumbar spine bone mineral density (LSBMD). When raw spine density for an individual is normalized on the various databases, different Z-scores are produced.

Aim: To evaluate whether the relationship between LSBMD Z-scores and vertebral fractures (VF) differs depending on the LSBMD reference database that is implemented.

Methods: VF were diagnosed by the Genant semi-quantitative method on lateral spine radiographs. LSBMD was measured by dual-energy x-ray absorptiometry with machines cross-calibrated using a spine phantom. Subjects' raw LSBMD values were converted to age-, gender-, and race-specific Z-scores for 13 sets of reference data. Various age groups were defined according to the age ranges specified by the reference databases. BMD Z-scores and the odds for VF associated with reductions in BMD Z-scores (expressed as increased odds of VF per 1 SD reduction in BMD) were compared across databases within each of the age groups.

Results: We studied 186 children through a national research program with recently diagnosed acute lymphoblastic leukemia (median age 5.3 years, range 1.3 to 17.0 years; 59% boys). Of these, 29 children (16%; 95% CI, 11% to 22%) had prevalent VF using a consensus paradigm for three experienced pediatric radiologists. The medians and ranges of the LSBMD Z-scores generated from each of the databases for the different age groups are presented in the Table. There were statistically significant differences among LSBMD Z-scores produced by the different databases within each age group. There were, however, no significant differences among the databases in the odds of VF associated with reductions in LSBMD Z-scores.

Conclusions: Although LSBMD Z-scores varied substantially among reference databases within a given age subset, the odds of VF associated with reductions in LSBMD Z-scores were similar regardless the database used to generate the Z-scores. These results highlight that the use of a LSBMD Z-score threshold as part of the pediatric osteoporosis definition is challenging, given varying results for different reference databases. On the other hand, the more consistent odds of VF in relationship to LSBMD Z-scores demonstrates that spine BMD as a risk factor for VF in children is not dependent on the choice of BMD reference database.

| Age Group (yrs) | Number of Reference Databases | LSBMD Z-score Median (range)* | Odds of VF for every 1 SD reduction in LSBMD Z-Score, Median (range)** |
|-----------------|-------------------------------|-------------------------------|--|
| 0 to 18 | 2 | -1.6 (-2.0, -1.2) | 2.2 (2.1, 2.3) |
| 0 to 5 | 2 | -1.7 (-2.0, -1.4) | 5.5 (5.1, 6.0) |
| 3 to 18 | 5 | -0.6 (-2.1, -0.3) | 2.1 (1.9, 2.1) |
| 5 to 18 | 8 | -1.0 (-2.0, -0.1) | 1.6 (1.5, 1.8) |
| 8 to 16 | 11 | -0.4 (-1.9, 0.2) | 1.9 (1.6, 2.3) |
| 9 to 14 | 13 | -0.7 (-2.0, 0.03) | 2.7 (1.7, 4.1) |

*Within each age group, LSBMD Z-scores differed significantly (p<0.001)
**Within each age group, odds ratios did not differ significantly (p>0.05)

STOPP BMD Table

Disclosures: *Leanne M. Ward, None.*

FR0031

Maternal Vitamin D Levels in Pregnancy and Offspring Bone Mass at Age 9: Findings from a UK Prospective Birth Cohort Study. Andrew Wills, Adrian Sayers*, Jon Tobias, Debbie Lawlor. University of Bristol, United Kingdom

Introduction: There is a suggestion that higher levels of maternal vitamin D (as measured by dietary intake or circulating 25(OH)D) during pregnancy are related to higher offspring bone mineral density (BMD) in later childhood, and that the 3rd trimester may be the important period of exposure. To address this question we examined whether, in the Avon Longitudinal Study of Parents and Children (ALSPAC), maternal 25(OH)D is associated with skeletal phenotypes measured by total body less head (TBLH) DXA at age 9.9 years.

Methods: Data are from 2840 mother-offspring pairs from the ALSPAC study. 25(OH)D₂ and 25(OH)D₃ were measured by HPLC on serum obtained from blood samples routinely collected during clinic attendances throughout pregnancy. Total 25(OH)D was adjusted to the respective trimester midpoint (6, 20 & 34 weeks). Whole body DXA scans were carried out in the offspring (mean age: 9.9y). The association between total 25(OH)D and TBLH bone mineral density, content, area and bone area adjusted bone mineral content was assessed using multivariable linear regression.

Results: There was no evidence for an association between maternal 25(OH)D and any of the offspring childhood DXA outcomes in minimally adjusted models (offspring age at DXA, sex, and maternal age at pregnancy) or a series of adjusted models ($p > 0.3$ for all tests). There was no evidence of non-linearity ($p > 0.05$) in these associations, or any evidence that deficient compared to replete 25(OH)D mothers had offspring with different bone outcomes. In addition we could find no evidence for an association after restricting analyses to those mothers with measures in the 3rd trimester (p for trimester 25(OH)D interactions > 0.05), or after accounting for seasonal variation in 25(OH)D in an attempt to measure habitual vitamin D levels.

Conclusion: Our study does not support the hypothesis that later childhood bone mass might be directly affected by prenatal exposure to varying levels of vitamin D.

Disclosures: Adrian Sayers, None.

FR0032

The Response of Cortical Bone to High Impact Activity is Attenuated in Girls: Findings from a Cross-sectional PQCT Study in Adolescents. Kevin Deere¹, Adrian Sayers^{*2}, Joern Rittweger³, J.H. Tobias⁴. ¹Bristol University, United Kingdom, ²University of Bristol, United Kingdom, ³Division of Space Physiology, Institute of Aerospace Medicine, Germany, ⁴Avon Orthopaedic Centre, United Kingdom

Abstract: Background: The factors which govern skeletal responses to physical activity remain poorly understood, conceivably because accelerometers measuring physical activity are calibrated against energy expenditure rather than mechanical strain. We investigated whether a more precise understanding of these factors, including gender and fat mass, can be gained based on measurement of exposure to defined levels of impact using a Newtest device (Newtest Oy, Finland).

Methods: Participants attending the ALSPAC research clinic underwent total body DXA and pQCT of the mid-tibia, and were subsequently invited to wear a Newtest accelerometer for seven days. Accelerometer results were partitioned into low (0.5-2.1g), medium (2.1-4.1g) and high (>4.1g) impact activity.

Results: 675 participants (272 boys) had valid accelerometer recordings and information on pQCT data and other covariates (mean age=17.7 years). In our fully adjusted model (for age, height, fat mass and lean mass), moderate impact activity was positively related to periosteal circumference (PC) in boys but negatively related in girls [0.039 (95%CI -0.013, 0.090, $p=0.14$) and -0.023 (-0.023, 0.017, $p=0.26$) respectively. $p=0.03$ for gender interaction, coefficient= SD change per doubling in activity]. High impact activity showed a stronger positive association with PC in boys but no association was seen in girls [0.054 (0.007, 0.100, $p=0.024$) and 0.007 (-0.028, 0.041, $p=0.707$) respectively]. In further analyses additionally stratified by fat mass, an independent interaction was observed, such that the positive relationship between high impact activity and PC was greatest in those with highest fat mass [high impact versus PC in boys: 0.01 (-0.064, 0.085, $p=0.783$), 0.045 (-0.040, 0.131, $p=0.298$), 0.098 (0.012, 0.185, $p=0.027$); high impact versus PC in girls: -0.041 (-0.101, 0.020, $p=0.187$), -0.028 (-0.077, 0.022, $p=0.271$), 0.082 (0.015, 0.148, $p=0.017$) ($p=0.01$ for fat mass interaction); lower, middle and upper fat-tertiles respectively].

Conclusions: Female gender and low body fat are associated with reduced periosteal expansion in response to high impact activity, via independent pathways. Our results suggest that skeletal response to high impacts is particularly impaired in girls with low body weight, which may partly explain the excess of stress fractures observed in this group after undergoing strenuous exercise.

Disclosures: Adrian Sayers, None.

FR0034

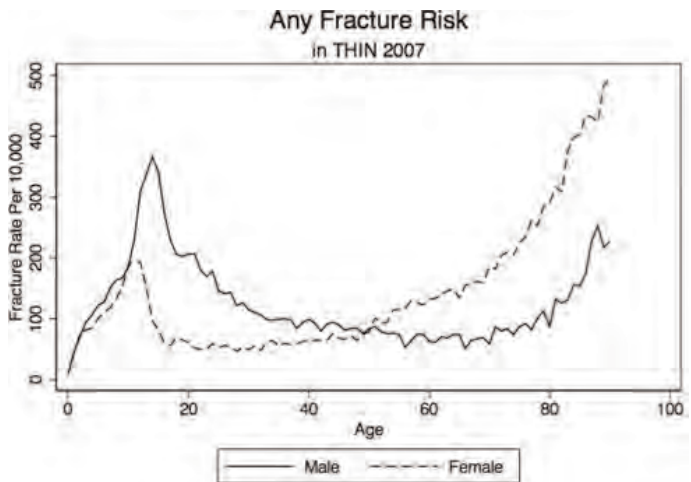
The Greater Fracture Risk in Adolescent Males Extends Through Mid-Adulthood in the United Kingdom. Kevin Haynes¹, Michelle Denburg^{*2}, Justine Shults³, Mary Leonard⁴. ¹University of Pennsylvania, USA, ²The Children's Hospital of Philadelphia, USA, ³Children's Hospital & Philadelphia, USA, ⁴Children's Hospital of Philadelphia, USA

Background: The gender differences in fracture risk in adolescent and elderly populations are well known. The greater fracture risk in adolescent males, compared with females, has been attributed to rapid growth with transitory low cortical thickness and bone density in boys but not girls. However, sex differences in fracture rates have not been evaluated in late adolescence through mid-adulthood. The objective of this study was to examine gender differences in fracture risk across the life-span in the United Kingdom.

Methods: We used The Health Improvement Network (THIN) database, which is an electronic medical record database in the United Kingdom comprising 495 General Practices. We identified 3,870,062 patients who were registered with a practice in 2007 and the 46,059 patients with a fracture code in 2007. We excluded 27,563 patients over the age of 90. We limited the study to the first fracture in 2007 in order to avoid counting follow-up visits for the same fracture as a new onset fracture. We examined incidence rates per 10,000 and determined the 95% confidence interval across all ages.

Results: The median age of the cohort in 2007 was 39 years (IQR 21-57). The Figure summarizes fracture incidence rates according to age and gender for any fracture. In patients 20 years of age, the fracture rate was 206 per 10,000 (95% CI 188, 225) for men and 61 per 10,000 (95% CI 51, 72) for women. For patients 50 years old, the fracture rate was 84 per 10,000 (95% CI 73, 95) for men and 79 per 10,000 (95% CI 68, 90) for women. For patients 80 years old, the fracture rate was 87 per 10,000 (95% CI 68, 109) for men and 290 per 10,000 (95% CI 261, 322) for women. When analyzing hip fracture separately risk began to rise after age 65 and was higher in women. In an analysis of forearm fracture both boys and girls had a similar peak childhood incidence, 71 per 10,000 (95% CI 60, 83) for girls at age 10 and 77 per 10,000 (95% CI 67, 89) for boys at age 13.

Conclusions: These data demonstrate that the greater fracture risk previously reported in the UK in adolescent boys extends into young and mid-adulthood, followed by a steady increased fracture risk in women after age 65. The results have implications to target public health interventions to both of these high risk groups. Future studies are needed to examine gender difference in bone quality, as well as behaviors that may contribute to these fracture rates across different fracture sites.



Any Fracture Risk

Disclosures: Michelle Denburg, None.

This study received funding from: The study was sponsored by an internal grant.

FR0037

Sclerostin has Differential Effects on Bone Mineral Density and Strength Parameters in Adolescent Athletes Compared with Non-Athletes. Pounch Fazeli^{*1}, Kathryn Ackerman², Lisa Pierce³, Gabriela Guereca³, Mary Bouxsein⁴, Anne Klibanski⁵, Madhusmita Misra³. ¹Massachusetts General Hospital & Harvard Medical School, USA, ²Brigham & Women's Hospital, USA, ³Massachusetts General Hospital, USA, ⁴Beth Israel Deaconess Medical Center, USA, ⁵Massachusetts General Hospital Harvard Medical School, USA

Sclerostin is a potent inhibitor of bone formation via WNT signaling inhibition and increases in hypogonadal states. In obese adults, sclerostin levels increase with diet-induced weight loss; however, this increase is not observed when weight loss is mediated by both diet and exercise. Therefore a mechanism whereby exercise may preserve bone mineral density (BMD) is by lowering sclerostin levels. Exercise is common in adolescents and we have previously shown that excessive athletic activity

causing amenorrhea leads to lower bone density and impaired microarchitecture parameters in amenorrheic athletes (AA) compared to eumenorrheic athletes (EA) and non-athletes (NA). Sclerostin has not been investigated in adolescent athletes, and its relationship to BMD, amenorrhea and exercise in this group is unknown. We hypothesized that AA would have higher sclerostin levels than EA and NA, and that higher sclerostin levels would be associated with lower BMD and strength parameters. We studied 49 adolescents 14-21 years old: 16 AA, 17 EA and 16 NA. We measured spine and hip BMD by DXA, failure load and stiffness at the radius using microfinite element analysis and measured fasting sclerostin levels (ELISA, TECO/Quidel). AA, EA and NA did not differ in bone age (AA: 17.7 ± 0.7 , EA: 17.5 ± 0.9 , NA: 17.7 ± 0.9 yrs; $p=0.25$), BMI (AA: 20.8 ± 2.2 , EA: 22.1 ± 2.2 , NA: 21.5 ± 2.4 kg/m²; $p=0.16$) or height (AA: 166.3 ± 5.6 , EA: 164.8 ± 6.7 , NA: 163.2 ± 6.2 cm, $p=0.34$). Sclerostin was higher in AA and EA compared with NA (AA: 0.42 ± 0.15 , EA: 0.44 ± 0.09 , NA: 0.33 ± 0.14 ng/ml; $p=0.047$). In NA, sclerostin was inversely associated with LBMD and its Z-score ($R=-0.61$, $p=0.01$), LBMAD ($R=-0.60$, $p=0.01$), hip BMD and its Z-score ($R=-0.55$, $p=0.03$) and stiffness and failure load ($R=-0.65$ and -0.65 , $p=0.001$ for both). However, in EA, sclerostin was positively associated with LBMD and its Z-score ($R=0.52$ and 0.55 , $p=0.03$ and 0.02) and LBMAD ($R=0.71$; $p=0.001$). The associations in EA remained significant after controlling for estradiol. Therefore sclerostin may have different effects in adolescent athletes compared to NA. In NA, sclerostin is inversely associated with BMD and strength parameters whereas in EA, sclerostin is positively associated with BMD. Sclerostin was also higher in both groups of athletes (not just AA) vs NA. Additional studies are needed to further delineate the role of sclerostin in mediating BMD and microarchitecture with exercise.

Disclosures: Pouneh Fazeli, None.

FR0040

Osteoimmunology in Adolescent Obesity: Delay of Trabecular Bone Development is Paralleled by Shift of Bone Marrow Immune Cells to Adipose Tissue. M. Ete Chan^{*1}, Danielle Green¹, Benjamin Adler¹, Gabriel Pagnotti¹, Denis Nguyen¹, Clinton Rubin². ¹Stony Brook University, USA, ²State University of New York at Stony Brook, USA

Obesity, which increases lifetime susceptibility to osteoporosis and fracture, may also confound skeletal development during adolescence, which depends on the viability of both the MSC and HSC progenitors. To determine the impact of obesity on bone development and bone marrow stem cells, this study tested the hypothesis that obesity compromises trabecular bone quantity and quality, paralleled by a disturbance in the neighboring bone marrow niche. Twenty 5 week old male C57BL/6J mice were weight matched into two groups ($n=10$). High fat diet (HF) and regular diet (RD) mice were fed with 45 and 10 kcal% fat diet, respectively, for a total of 8 weeks. At 2, 5 and 8w, proximal tibial metaphyses were scanned *in vivo* with μ CT at 17 μ m resolution (970 μ m thick region 480 μ m distal to the growth plate). At sacrifice (8w), cellular composition of bone marrow and gonadal adipose tissue were evaluated by flow cytometry. The obese phenotype was evident in HF by 2w with +7% higher body mass and +29% larger abdominal adipose tissue relative to RD ($p=0.01$). Longitudinal μ CT indicated that HF delayed trabecular bone development compared to RD (Fig. 1). Although the overall change of trabecular bone volume fraction (BV/TV) over the 8w experiment appeared similar between groups, HF showed a trend of -8% lower BV/TV at 2 weeks relative to RD ($p=0.09$), which dropped to -13% by 5w ($p<0.05$). Perhaps reflecting a compensatory mechanism, cortical volume in HF was +4% larger than RD at 5w ($p<0.05$), with consistent, but not significant, higher cortical volume at other time points. In parallel with a +152% higher adipose tissue mass ($p<0.001$) in HF at 8 w, flow cytometry analysis indicated that HF enabled infiltration of immune B-cell (+199%) and T-cells (+207%) into adipose tissue of HF relative to RD ($p<0.05$), but -15% and -31% ($p<0.01$) reductions of these immune cells in the bone marrow. In summary, these results suggest that obesity rapidly and profoundly disturbs the bone marrow niche, a consequence, perhaps, of the recruitment of immune cells into the enlarging adipose tissue from the bone marrow. Whether this shift in B- and T-cells is responsible for the delay of trabecular bone development has not yet been determined, but it does indicate that the metabolic or developmental demands of obesity put numerous systems at risk.

Differential Impacts of Obesity on Trabecular and Cortical Bone

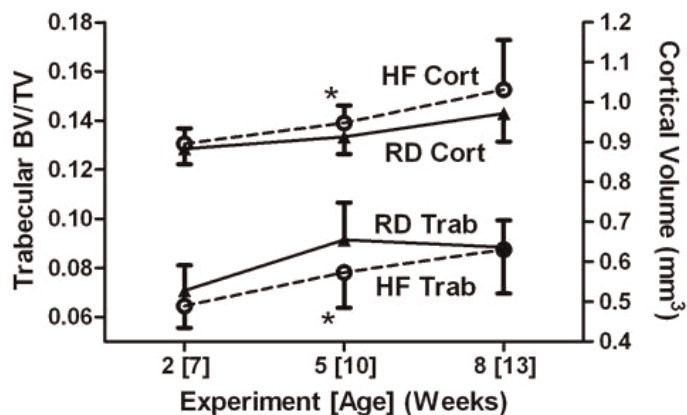


Fig. 1

Disclosures: M. Ete Chan, None.

FR0043

Pharmacological Evaluation of a CNP Analogue for the Treatment of Achondroplasia. Florence Lorget^{*1}, Nabil Kaci², Jeff Peng¹, Catherine Benoist-Lassel², Emilie Mugniery², Todd Oppeneer¹, Dan Wendt¹, Sherry Bullens¹, Stuart Bunting¹, Laurie Tsuruda¹, Charles O'Neill¹, Federico Di Rocco², Arnold Munnich², Laurence Igeai-Mallet². ¹BioMarin Pharmaceutical Inc, USA, ²INSERM, U781 - Hopital Necker-enfants malades, France

Achondroplasia (ACH), the most common form of dwarfism, is caused by a gain of function mutation in the fibroblast growth factor receptor 3 gene (FGFR3). The C-type natriuretic peptide (CNP) antagonizes FGFR3 downstream signaling by inhibiting the mitogen-activated protein kinase (MAPK) pathway. The use of CNP as a therapeutic agent for ACH is impracticable due to its short half-life. Here, we are presenting an update on the pharmacological activity of BMN 111, a novel CNP analogue with an extended plasma half-life allowing once daily subcutaneous (SC) administration. In ACH growth plate chondrocytes, we demonstrated that BMN 111 decreased MAPK pathway activation but did not affect STAT pathway activation. In *Fgfr3^{Y367C/+}* mice mimicking ACH, daily SC administration of BMN 111 led to the attenuation of the dwarfism phenotype. With 20 days of daily SC dosing of BMN 111 (800 μ g/kg) beginning at seven days of age, we observed a significant increase in the axial and appendicular skeleton length with improvements in ACH related clinical features including flattening of the skull, reduced prognathism and straightening of the tibias and femurs. The growth plate defect (reduced height of the pre-hypertrophic/hypertrophic zones and lack of columnar arrangement) was corrected along with the normalization of the size and shape of the proliferative and hypertrophic chondrocytes. A rescue of the height and architecture of the different zones of the growth plate was observed. The height of the proliferative zone was increased; the replicating chondrocytes were organized into columns parallel to the long axis of the bone. In the hypertrophic zone, the terminally differentiated chondrocytes recovered a columnar alignment. These data support further development of BMN 111 for the treatment for ACH and hypochondroplasia (HCH).

Disclosures: Florence Lorget, BioMarin, 3

This study received funding from: BioMarin Pharmaceutical Inc.

FR0045

Alendronate and PTH Dose-Dependent Improvements in Microarchitecture Lead to Improved Bone Strength despite Reductions in Tissue Material Properties. Andrea Trinward^{*1}, Steven Tommasini², Sarah Manske¹, Alvin Acerbo³, Lisa Miller⁴, Stefan Judex¹. ¹Stony Brook University, USA, ²Yale University School of Medicine, USA, ³Brookhaven National Laboratory, USA, ⁴Brookhaven National Laboratory, USA

Osteoporosis is associated with bone loss and deterioration in tissue quality. Drugs such as alendronate (ALN) and parathyroid hormone (PTH) differentially counteract bone loss, leading to drug-specific changes in measures of bone quality including bone strength. To determine how drug-induced changes in bone quality relate to mechanical strength, we subjected OVX rats to 6mo of varying doses of ALN and PTH. Morphologic (μ CT), chemical (FTIR), and mechanical properties (nanoindentation and finite element modeling) of cortical and trabecular bone in the femoral metaphysis were determined. Six mo old SD rats ($n=10$ /gp) were assigned to age-matched controls (AM), OVX controls, OVX treated with high(H), medium(M) or

low(L) doses of hPTH (75, 15, 0.3µg/kg/d), or ALN (100, 10 or 1µg/kg/2xwk). At 12mo, OVX rats had 81% less trabecular bone than AM ($p<0.001$). There were dose-dependent improvements to architecture: L-PTH had similar BV/TV as OVX, while M- and H-PTH had 2x, and 7x more BV/TV and L-, M- and H-ALN had 1x, 2x and 4x more BV/TV than OVX. Compared to AM, H-PTH and H-ALN maintained or improved both trabecular and cortical architecture, but decreased cortical tissue mineral density by 6% and 3% ($p<0.01$). There were no differences in cortical bone crystallinity, collagen cross-linking, mineralization or carbonate substitution across groups. Nanoindentation of the cortical bone showed that H-PTH and H-ALN had a 9% and 14% smaller elastic modulus and a 10% and 11% lower tissue hardness than AM ($p<0.01$). Incorporation of tissue morphology and measured elastic moduli into the finite element model demonstrated differences in structural mechanical properties. When the femoral metaphysis was subjected to a given compressive load, compared to AM, OVX had 12% lower stiffness while H-PTH and H-ALN were 46% and 18% stiffer ($p<0.05$). When combined via multiple linear regressions, CtTh, TbBV/TV and TbTh explained 91% of the variability in stiffness ($p<0.001$) while chemical or tissue mechanical properties did not enhance this association. These data show that despite deteriorated tissue properties in ALN and PTH treated rats, the improved bone architecture resulted in a structure that was able to withstand a greater mechanical load. While these results emphasize the importance of preserving bone structure during osteoporosis, the reductions in tissue material properties with ALN and PTH treatment may cause complications with long term use.

Disclosures: Andrea Trinward, None.

FR0049

Cortical Porosity and Bone Strength Assessment in Postmenopausal Women with Atypical Fractures of the Femur and Long Term Bisphosphonate Therapy. Maria Belen Zanchetta^{*1}, Vanesa Longobardi², Fernando Silveira², Maria Dielh², Mirena Buttazzoni², ANA GALICH³, Cesar Bogado⁴, Jose Ruben Zanchetta¹. ¹Instituto de Investigaciones Metabolicas (IDIM), Argentina, ²MD, Argentina, ³Instituto De Investigaciones Metabolicas, Argentina, ⁴Idim, Argentina

In recent years, concern has been raised about atypical femoral fractures of the femur (AFF) as a possible complication of long-term bisphosphonate therapy. The pathophysiology of these events remains unknown. Previously, we had assessed bone volumetric density and architectural parameters measured by HR-pQCT in 14 postmenopausal women with atypical fractures during long term bisphosphonate treatment. The purpose of the present study was to describe cortical porosity and bone strength in these patients. All major features defined by the ASBMR Task Force - subtrochanteric or femoral shaft location, transverse or oblique orientation, no trauma or comminution, a medial spike in complete fractures - were present to designate a femoral fracture as atypical. We recorded, whenever possible, all minor features.

Methods: Cortical porosity and µFE analysis were based on HR-pQCT images of distal radius and tibia (XtremeCT; Scanco Medical).HR-pQCT scans were analyzed using an automated segmentation technique developed to identify the periosteal and endosteal margins and detect intracortical pore space morphologically consistent with Haversian canals. µFE analysis assessed quantitatively the biomechanical properties that result from bone microarchitecture. We analyzed the following parameters: Cortical thickness (Ct.Th (mm)), cortical pore volume (Ct.Po.V (mm³)), intracortical porosity (Co.Po %), cortical pore diameter (Ct.Po.Dm (µm)), estimated failure load and stiffness. We compared the results with a group of 19 postmenopausal women with similar age, BMD and BMI who had never received treatment selected from our database.

Results: Minor features are described in table 1. There were no statistically significant differences in any of the parameters measured (table 2).

In this cross-sectional study, using a noninvasive and high-resolution bone imaging device, we could not find any distinctive microarchitecture deterioration in the radius and tibia of women who had suffered an atypical fracture of the femur. Our results suggest that, if there is an alteration in bone microarchitecture or strength in these atypically fractured patients, it is not generalized through the skeleton. The compromise may be specific and limited to the femoral shaft, a site of maximum tensile stress.

| Clinical Features | |
|--|------------|
| Mean treatment time (years) | 11.3 ± 5.3 |
| Only alendronate 6/14 | 43% |
| Mostly IV pamidronate 3/14 | 21% |
| Combinations 5/14 | 35% |
| Comorbidities (3/14) 2 hta; 1 celiac disease | 20% |
| Other drugs (3/14 Proton pump inhibitors) | 20% |
| Bilaterality 6/14 | 43% |
| Delayed healing 2/14 | 14% |
| Cortical thickening | 100% |
| Prodromal pain 12/14 | 80% |
| Biopsy 4/14 | |
| Result: very low bone turnover (4/4) | 18% |
| Previous osteoporotic fracture 2/14 (wrist) | 14% |
| Osteopenic by DXA at fracture time 8/14 | 57% |
| Osteoporotic by DXA at fracture time 6/14 | 43% |

Clinical Features Table 1

| | Atypical fracture and bisphosphonate treatment (n=14) | No fracture and Non treatment group (n=19) | p |
|----------------------------|---|--|--------|
| Age (years) | 71.2 ± 8.4 | 72.4 ± 4.3 | 0.35** |
| median (range) | 70.0 (57.0; 89.0) | 71.0 (68.0; 83.0) | |
| BMI (kg/m ²) | 27.1 ± 3.5 | 26.2 ± 2.8 | 0.93** |
| median (range) | 25.9 (22.6; 35.9) | 26.9 (20.1; 29.9) | |
| Years of menopause | 24.3 ± 10.3 | 24.7 ± 7.5 | 0.60** |
| T-score Femoral Neck | -1.9 ± 0.9 (n=13) | -2.3 ± 0.6 | 0.27* |
| Distal Radius | | | |
| Ct.Th (mm) | 0.67 ± 0.12 | 0.67 ± 0.08 | 0.52** |
| Ct.Po.V (mm ³) | 247.4 ± 38.8 | 256.1 ± 41.1 | 0.98** |
| Ct.Po (%) | 2.52 ± 0.89 | 2.62 ± 1.18 | 0.80* |
| Ct.Po.Dm (µm) | 165.2 ± 13.4 | 162.4 ± 15.9 (n=18) | 0.46** |
| Estimated failure load (N) | 2486.6 ± 331.4 | 2532.5 ± 347.5 | 0.70 |
| Stiffness (N/mm) | 48686 ± 6587 | 49164 ± 6674 | 0.84 |
| Distal Tibia | | | |
| Ct.Th (mm) | 0.93 ± 0.17 | 0.93 ± 0.17 | 0.90 |
| Ct.Po.V (mm ³) | 61.3 ± 21.2 | 49.8 ± 13.1 (n=18) | 0.09* |
| Ct.Po (%) | 7.95 ± 1.96 | 7.03 ± 1.98 | 0.13** |
| Ct.Po.Dm (µm) | 180.1 ± 13.5 | 186.8 ± 14.6 | 0.17** |
| Estimated failure load (N) | 6795.6 ± 888.9 (n=11) | 7175.9 ± 1147.6 | 0.35 |
| Stiffness (N/mm) | 133314 ± 17909 (n=11) | 140358 ± 23094 | 0.39 |

Results Table 2

Disclosures: Maria Belen Zanchetta, None.

This study was possible thanks to the IOF ESCOAMGEM FELLOWSHIP AWARD 2011

FR0051

Evidence of Narrower Tibiae with Increased vBMD in Stress Fractured Royal Marine Recruits Compared with Matched Controls: An Investigation of Radius and Tibia Bone Mass using pQCT. Trish Davey^{*1}, Susan A. Lanham-New², Adrian J. Allsopp¹, Pat Taylor³, Cyrus Cooper⁴, Joanne L. Fallowfield¹. ¹Institute of Naval Medicine, United Kingdom, ²Nutrition & Metabolism Department, University of Surrey, United Kingdom, ³University Hospital Southampton, United Kingdom, ⁴University of Southampton, United Kingdom

Royal Marine (RM) recruits (aged 16-32 y) undertake a strenuous 32-week military training programme. The prevalence of stress fracture (SF) is of the order of 5%. Peripheral Quantitative Computed Tomography (pQCT) provides a method of investigating structural bone parameters that may be important in the pathogenesis of SF. We have previously shown that lumbar spine and femoral neck BMD is lower in SF recruits [1]. The aim of this case-control study was to identify differences in bone structure and strength using pQCT in relation to SF during RM training as part of the UK Surgeon General's Bone Health Project. Fifty-eight SF Royal Marine (RM) recruits and 58 well-matched, un-injured RM recruits underwent pQCT scanning of the non-dominant radius and tibia. Cases and controls were matched for body weight, BMI, age and aerobic fitness. Differences between cases and controls were assessed using T-tests. At the 4% radius, SF recruits had lower total bone mineral content (BMC), trabecular BMC and trabecular volumetric bone mineral density (vBMD) than matched controls ($P<0.05$). Differences between SF recruits and controls were apparent at all slices of the tibia (4%, 16%, 38% and 66%) ($P<0.05$). SF recruits had lower: total cross-sectional area (CSA) and total BMC; cortical (cort) CSA and cort BMC; periosteal and endosteal circumferences; and polar strength-strain index (SSI)

at the 38% tibial segment than their matched controls ($P < 0.05$). Total (but not cortical) vBMD was higher in SF recruits than matched controls (38% tibia) ($P < 0.05$). There was no difference in tibial muscle area between SF recruits and controls (assessed at the 66% tibial slice). To the authors' knowledge this is the first case-control study on stress fractures within the UK military to have utilised pQCT with the close matching of injured and non-injured recruits allowing for robust comparisons to be made. Thus, narrower tibiae appear to be a risk factor for SF during military training, independent of body size; this agrees with a cohort study in military recruits using different technologies [2]. The theory of increased mineralisation as a compensatory mechanism for narrower tibiae [3] is supported by the findings from the present study, where vBMD was higher in SF recruits than matched controls.

- 1 Davey, T. et al. Osteoporosis Int 2012 (in press) [Abstract]
- 2 Beck, T.J. et al. J Bone Miner Res 1996.11 p645-53
- 3 Evans, R.K. et al. Med Sci Sports Exerc 2008.40 pS645-53

| | | Stress Fractures (n=58) Mean ± SD | Controls (n=58) Mean ± SD | P |
|--------------------|-------------------------------------|--------------------------------------|------------------------------|-------|
| Tibia 38% slice | Total CSA (mm ²) | 497.6 ± 69.9 | 553.7 ± 124.1 | 0.004 |
| | Total BMC (mg.mm ⁻³) | 416.5 ± 39.0 | 441.8 ± 51.2 | 0.014 |
| | Total vBMD (mg.cm ⁻³) | 843.6 ± 63.9 | 813.6 ± 84.4 | 0.05 |
| | Cort CSA (mm ²) | 330.2 ± 30.4 | 345.1 ± 342.4 | 0.05 |
| | Cort BMC (mg.mm ⁻³) | 376.2 ± 34.8 | 394.4 ± 42.6 | 0.03 |
| | Cort Density (mg.cm ⁻³) | 1140 ± 22.4 | 1143 ± 29 | 0.22 |
| | Periosteal Circum (mm) | 79.1 ± 5.6 | 83.0 ± 8.6 | 0.008 |
| | Endosteal Circum (mm) | 45.6 ± 7.0 | 50.4 ± 11.4 | 0.02 |
| | Polar SSI (mm ³) | 1818 ± 275 | 2005 ± 290 | 0.001 |

Bone variables assessed via pQCT of the tibia in stress-fractured RM recruits and controls

Disclosures: Trish Davey, None.

FR0056

Losing Trabecular Plates and Axial BV/TV in Hip Fractures. Bin Zhou¹, Ji Wang¹, Ian Parkinson², Xiaowei Liu³, C. David L. Thomas⁴, John G. Clement⁴, Nick Fazzalari⁵, X. Guo¹. ¹Columbia University, USA, ²SA Pathology & Hanson Institute, Australia, ³University of Pennsylvania, USA, ⁴Melbourne Dental School, Australia, ⁵Institute of Medical & Veterinary Science, Australia

Decreased bone mineral density is an important risk factor of hip fractures. However, it remains controversial regarding the relative contributions of trabecular vs. cortical components in fracture risks. Alterations in microstructures and mechanical properties of trabecular bone in the hip fracture are not well documented. We hypothesized that patients with hip fracture have distinctly weaker trabecular bone microstructure and severely compromised mechanical properties at the hip fracture site. To address this hypothesis, we applied individual trabecula segmentation (ITS) morphological analysis and micro finite element (μFE) analysis to micro computed tomography (μCT) images of inter-trochanteric trabecular bone biopsies from hip fracture patients.

Ten-mm diameter inter-trochanteric trabecular bone cores were obtained from 23 patients (age 73 ± 13, 9 male/14 female) who underwent hip replacement surgery for inter-trochanteric hip fracture. Twenty-two bone cores from cadavers (age 80 ± 11, 13 male/9 female) served as controls. Bone cores were scanned at 15 μm resolution using a μCT system (Skyscan 1174, Belgium). A cube of 4.44 × 4.44 × 4.44 mm³, corresponding to 296 × 296 × 296 voxels, was extracted from the middle of the cylinder for morphological and mechanical analysis. ITS analysis revealed interesting and distinct microstructural differences between groups (Fig. 1). The fracture group had a 33% lower plate bone volume fraction (pBV/TV) and 31% lower axial bone volume fraction (aBV/TV) than the non-fracture group (Fig. 2). The fracture group had a lower plate trabecular surface (pTb.S) and longer trabecular rods (rTb.I) than the control group. No differences were found in rod bone volume fraction (rBV/TV), plate and rod trabecular number and thickness (pTb.N, rTb.N, pTb.Th, rTb.Th). From standard μCT morphological analysis, the fracture group had 27% lower BV/TV compared with the non-fracture group. Similar results were found for Tb.N and Tb.Th, with values for the fracture group lower than the non-fracture group by 21% and 9%, respectively. Consequently, the fracture group had drastically lower Young's moduli than the control group (up to 53%) by μFE analysis.

These results suggest that there is a drastic and distinct conversion from plate-like to rod-like microstructure and a significant loss of axial trabecular bone in hip fracture patients. These microstructural changes result in a significant decrease in trabecular bone mechanical properties.

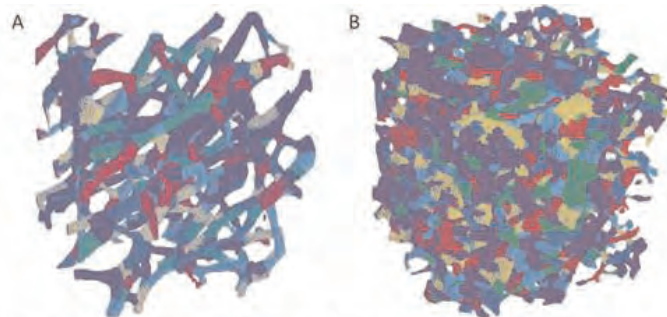


Figure 1: ITS analysis on trabecular bone from (A) fracture group, (B) control group. Different color represents individual trabeculae.

Figure1

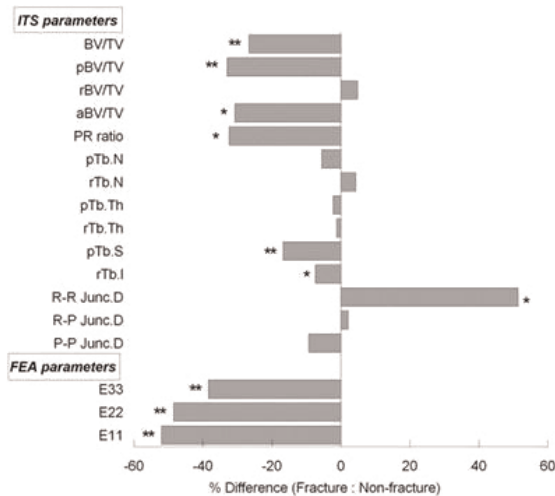


Figure 2: Difference between fracture group and control group in microstructural parameters analyzed by ITS and mechanical properties analyzed by μFE analysis. * p<0.05, **p<0.005

Figure2

Disclosures: Bin Zhou, None.

FR0057

Major Gender-related Differences in Bone Mass and Strength in Aged Sost Knockout Mice. Behzad Javaheri¹, Amber Stern^{2*}, Nuria Lara², Mark Dallas³, Alexander Robling⁴, Mark Johnson⁵. ¹School of Dentistry The University of Missouri-Kansas City, USA, ²University of Missouri - Kansas City, USA, ³UMKC School of Dentistry, USA, ⁴Indiana University, USA, ⁵University of Missouri, Kansas City Dental School, USA

Previous studies have shown that canonical Wnt signaling regulates bone mass. Sclerostin (Sost) is a negative regulator of Wnt signaling and consequently bone formation and is produced mainly in osteocytes. Mice with homozygous deletion of *Sost* (*Sost* KO or KO) have high bone mass compared with WT mice at 4-6 months of age. We recently showed greater bone mass loss in female vs. male mice with a deletion of one allele of the β-catenin gene targeted to osteocytes and that these differences increase with aging. We now address the question of whether deletion of the *Sost* gene, which causes the opposite effect of increased bone mass and strength, also displays age and gender dependence. We assessed whole body bone mineral content (wBMC) and areal bone mineral density (wBMD) using PIXImus mouse densitometry; BV/TV and other cortical and trabecular parameters by microCT, and bone biomechanical properties by 3 point bending in male and female KO and WT mice at 70-90 weeks of age. We observed no differences in body weight between male and female KO mice. wBMD and wBMC were 25% and 60% higher, respectively, in female KO compared to male KO mice (p<0.001). MicroCT analysis of the femur showed that midshaft cortical thickness was 34% higher in female KO vs. male KO mice (p<0.001) and both were higher compared to WT mice of either gender. Interestingly, no gender differences in cortical bone density or BV/TV were observed in KO mice. However, in female KO mice the proximal trabecular compartment had significantly higher BV/TV (5-fold) and trabecular thickness (70%) (p<0.001) and lower trabecular spacing compared to male KO mice. Mechanical testing of the femur showed significantly stronger bones in female KO vs. male KO mice. Both genders of KO mice were stronger than their WT counterparts. Female KO mice had significantly higher total

bone volume and cross sectional area compared to male KO, but Young's Modulus was the same between the sexes and significantly lower compared to WT. These data clearly demonstrate that the regulation of the Wnt/ β -catenin signaling pathway and its role in bone are strongly influenced by gender and aging. The mechanism(s) underlying this phenomenon are currently unknown. Importantly, these findings in *Sost* KO mice support an important role of sclerostin on bone mass that is age and sex dependent and point to the need for further studies that explore the role of sex hormones as possible mediators/regulators of sclerostin function.

Disclosures: Amber Stern, None.

FR0060

Muscle Strength Predicts Radial Bone Structure and Strength in Adolescent Boys and Girls. Vina Tan^{*1}, Heather Macdonald², SoJung Kim², Christine Voss³, Joan Wharf Higgins⁴, Patti-Jean Naylor⁴, Heather McKay².
¹Robert HN Ho Research Centre, Canada, ²University of British Columbia, Canada, ³Center for Hip Health & Mobility, Canada, ⁴University of Victoria, Canada

Muscle contractions exert the largest physiological loads on the skeleton; however, we know little about the influence of muscle on bone structure and strength in adolescent boys and girls. Thus, we aimed to determine the independent contribution of muscle strength to bone strength and structure of the radius in adolescent boys and girls. Participants in this cross-sectional study were 148 (87 boys) healthy Grade 10 students, aged 15.3 ± 0.3 yrs who volunteered for the Health Promoting Secondary Schools (HPSS) study. We obtained peripheral quantitative computed tomography (pQCT) scans at the distal (7%) and shaft (30%) sites of the non-dominant radius. Primary outcomes were: 1) bone strength index (BSI, mg^2/mm^4) at the distal radius and 2) polar strength-strain index (SSI_p , mm^3) at the radial shaft. Secondary outcomes were total bone area (Tt.Ar, mm^2), and density (Tt.BMD, mg/cm^3) at the distal radius, and cortical area (Ct.Ar, mm^2), density (Ct.BMD, mg/cm^3), and thickness (Ct.Th, mm) at the radial shaft. We measured forearm muscle strength using a maximal isometric hand-grip strength test. We assessed stretch stature, body mass and forearm length using standard anthropometric techniques. We also determined ethnicity and maturity status (boys: Tanner stage; girls: age at menarche) using self-report questionnaires. We developed sex-specific multivariable regression models to determine the independent contribution of muscle strength to each bone outcome after adjusting for forearm length, body mass, ethnicity and maturity status. In adolescent boys and girls, muscle strength was a significant predictor of BSI and SSI_p , and explained 10-19% and 18-19% of the variance ($p < 0.01$), respectively (Figure 1 & 2). At the distal radius, muscle strength predicted 9-20% of the variance in boys' and girls' Tt.Ar ($p < 0.001$). In contrast, muscle strength did not predict Tt.BMD in girls, but explained 8% ($p = 0.007$) of the variance in boys. Similarly, at the radial shaft, muscle strength explained 17-20% of the variance in Ct.Th and Ct.Ar ($p < 0.001$) in boys and girls, but did not predict Ct.BMD in either sex. Our findings are consistent with a functional model of bone development in which bone primarily adapts its cross-sectional geometry, rather than its mineral density, to withstand loads from muscle forces. The specific adaptation of bone strength to increased muscle strength achieved through an exercise-training program warrants further investigation.

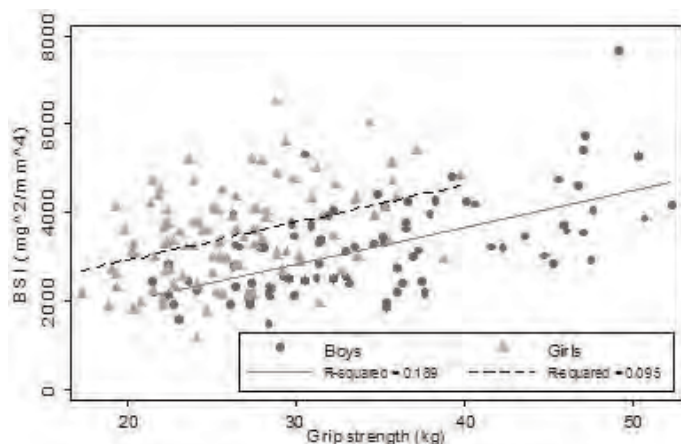


Figure 1. Relationship between bone strength index (BSI) at the distal radius and grip strength in boys and girls, $p < 0.01$.

Figure 1

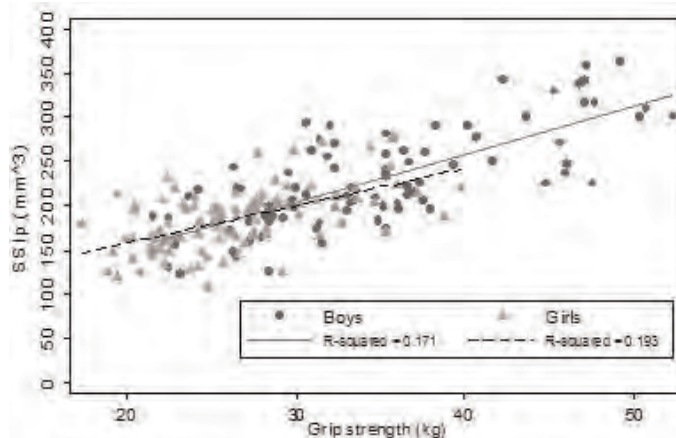


Figure 2. Relationship between polar strength-strain index (SSI_p) at the radius midshaft and grip strength in boys and girls, $p < 0.01$.

Figure 2

Disclosures: Vina Tan, None.

FR0068

Lower Osteocyte Lacunar Density in Osteons of Alendronate Treated Canine. Joseph Geissler^{*1}, Devendra Bajaj², Shahir Monsuruddin³, Matthew Allen⁴, David Burr⁴, J. Fritton⁵. ¹New Jersey Institute of Technology New Jersey Medical School, USA, ²NJ Medical School Orthopaedics, USA, ³NJ Institute of Technology Biomedical Engineering, USA, ⁴Indiana University School of Medicine, USA, ⁵New Jersey Medical School, USA

Bisphosphonates (BPs) are effective drugs that decrease fragility fracture risk through actions on decreasing individual osteoclast tunneling, and increasing and decreasing apoptosis of osteoclasts and osteocytes, respectively. The emergence of very rare, atypical fractures with their defining characteristics (long-term anti-resorptive use, low-energy cortical shaft fracture, bilaterality) has renewed interest in the effects of drugs on tissue-level mechanical properties and the mechanisms behind bone tissue damage. In canine rib bone we found that long-term alendronate (ALN) treatment reduces both stiffness (20% lower) and resistance to failure (3x fewer cycles to failure) under cyclic fatigue loading of cortical tissue beams ($1.5 \times 0.5 \times 10$ mm) at a dose associated with the treatment of Paget's. This adds to data that long-term BP treatment results in reduced toughness. This study investigated possible microstructural differences behind these mechanical differences in 3-year ALN-treated cortical tissue. Skeletally mature (1-2 yrs), female beagles ($n = 12/\text{group}$) were treated daily with ALN (1.0 mg/kg BW) or vehicle control. After 4-point bending to determine stiffness and fatigue life, beams were stained with basic fuchsin and plastic embedded. Three cross-sections from each beam were cut and polished to constant thickness, and imaged by light microscopy. Histomorphometry revealed that the average cross-sectional area of cortical osteons and their osteocyte lacunar density were lower in ALN beams by 17% and 20%, respectively ($p < 0.05$). Most interestingly, within both groups linear correlations existed between osteonal lacunar density and initial beam stiffness such that the regression equations were similar ($r = 0.54$ for combined data). This relationship might offer a means of predicting mechanical properties of osteonal bone. Reductions in osteon size are likely due to decreased individual osteoclast tunneling as recently described by Hazelwood et al. Reduced osteon size and associated lower cement line surface area may allow for larger microcracks to accumulate in interstitial spaces accounting for the reductions in mechanical properties observed. Reduced osteonal osteocyte lacunar density likely has a more purely biological origin not directly associated with the effects of BPs on osteocyte apoptosis. Since the rate of remodeling is reduced with BPs fewer osteoblasts are required to refill tunnels and available to become matrix-bound osteocytes.

Disclosures: Joseph Geissler, None.

FR0072

Mechanical Strain Downregulates C/EBP β in MSC and Decreases Endoplasmic Reticulum Stress. Maya Styner^{*1}, Mark Meyer², Kornelia Galior³, Natasha Case¹, Buer Sen⁴, Zhihui Xie⁵, William Thompson⁶, J. Pike², Janet Rubin¹. ¹University of North Carolina, Chapel Hill, School of Medicine, USA, ²University of Wisconsin-Madison, USA, ³UNC-CH School of Medicine, USA, ⁴University of North Carolina At Chapel Hill, USA, ⁵University of North Carolina, Department of Medicine, USA, ⁶University of Delaware, USA

Exercise prevents marrow mesenchymal stem cell (MSC) adipogenesis, reversing trends that accompany aging and osteoporosis. Mechanical input, analogous to exercise, limits MSC adipogenesis through activation of β -catenin, preserving MSC potential for osteogenic differentiation. C/EBP β , a transcription factor upstream of PPAR γ , is critical for adipogenesis and interestingly, has also been shown to upregulate ER stress. We thus hypothesized strain would target C/EBP β and that the targeting of this transcription factor would benefit the skeleton, not only from a lineage- perspective, but also by decreasing ER stress. Both C3H10T1/2 pluripotent stem cells as well as mouse marrow derived MSC were cultured in adipogenic medium in the presence or absence of mechanical strain applied via Flexcell device. We demonstrate herein that mechanical strain represses C/EBP β expression and activity in MSC. siRNA silencing of β -catenin prevented mechanical repression of C/EBP β . ChIP-seq demonstrated no significant association of β -catenin and its target TCF4 with the *Cehpb* gene, suggesting that mechanical repression of C/EBP β via β -catenin is indirect. Furthermore, C/EBP β overexpression did not override strain's inhibition of adipogenesis, indicating that mechanical induction of β -catenin blocks adipogenesis at multiple loci. Overexpression of C/EBP β in MSC induced a dose-dependent increase in the pro-apoptotic CHOP as well as a dose-dependent reduction in the chaperone BiP, changes consistent with increased ER stress. Application of a daily strain regimen, in addition to decreasing C/EBP β , increased ER capacity as measured by a significant increase in BiP. ChIP-seq demonstrated a significant association between C/EBP β and the *CHOP* and *BiP* genes. In conclusion, mechanical downregulation of C/EBP β not only accompanies a reduction in adipogenesis, but also limits ER stress, adding a novel mechanism whereby exercise improves MSC/skeletal health.

Disclosures: *Maya Styner, None.*

FR0073

Planar Cell Polarity Signaling directs Osteoblast Proliferation and Wolff's Law for Dynamic Strain. Gabriel Galea^{*1}, Lee Meakin¹, Hanna Taipaleenmaki², Noureddine Zebda¹, Toshihiro Sugiyama³, Gary Stein², Lance Lanyon², Andre Van Wijnen², Joanna Price¹. ¹University of Bristol, United Kingdom, ²University of Massachusetts Medical School, USA, ³Yamaguchi University School of Medicine, Japan, ⁴Royal Veterinary College, United Kingdom

Bone is a mechanically-responsive tissue with a structural hierarchy of cytoskeletal proteins, extracellular matrix proteins and minerals. The macroscopic organization of these components into a skeletal architecture occurs along the direction of load-engendered dynamic strain (Wolff's Law). Here, we investigated the cellular and molecular basis of Wolff's Law.

We first examined the direction of cell division in mouse primary osteoblasts, NIH-3T3 fibroblasts, as well as human osteoblastic SaOs-2 or chondrocytic 28I2 cells that were briefly exposed to dynamic strain by four-point substrate bending. Within 24 hrs following strain, a significantly greater proportion of osteoblastic and fibroblastic but not chondrocytic cells, divided in parallel to the strain direction, but mitotic division in unstrained cells was random. Initiating proliferation with 1 μ M estradiol before strain did not alter strain-dependent polarization of SaOS-2 division. Thus, strain orients mitotic division independently of initiating cell cycle progression.

We then addressed whether the direction of cell division is controlled by the planar cell polarity (PCP) pathway through Rho-associated coiled-coil kinase (ROCK), which mediates centriole positioning¹. ROCK-dependent centriole realignment towards the principal strain direction relative to the center of G1/S-phase nuclei was observed within 1 hr following strain as visualized by immunofluorescence microscopy for the centriole component PCM-1. ROCK blockade 1 hr before strain with the ROCK inhibitor GSK269962 prevented reorientation of division, but blockade 1 hr after strain had no effect.

Mutation of the PCP component Vangl2 (Vangl2^{-/-}), which generates loop-tail mice, alters femoral architecture (e.g., lower eccentricity, greater trabecular structure model index). The Vangl2^{-/-} mutation also compromises the polarization of long bone-derived osteoblast division in response to strain *ex vivo*.

Thus, limited acute dynamic strain influences the cell-type dependent orientation of mitotic division in osteoblasts and fibroblasts by rapid ROCK-mediated centriole realignment. These data suggest that Wolff's Law includes PCP dependent polarization of cell division as a strain-adaptive response in bone and connective tissue.¹Chevrier V et al, J Cell Biol, 2007 ;157(5):807-17

Disclosures: *Gabriel Galea, None.*

FR0076

Bone Density and Strength Differences Among Elite Female Athletes in Weight-Bearing Versus Non Weight-Bearing Sports. Brett Bruininks¹, Lesley Scibora^{*2}. ¹Concordia College (Moorhead), USA, ²University of Minnesota, USA

High-impact weight-bearing sports, generating large ground reaction forces, are positively associated with bone density and strength. Since muscle-generated forces exert the greatest physiological load on bone, sports that involve muscle contraction with little or no ground reaction forces should also be associated with enhanced strength of the loaded bone. Differences in areal and volumetric bone mineral density and parameters of bone geometry and strength were explored in elite female athletes. Fifty-three female (age 18-25 years) soccer (n=15), ice hockey (n=21), and swimming (n=17) athletes and 19 non-active controls were measured. Total body bone mineral content (BMC) and total body, lumbar spine and femoral neck areal bone mineral density (aBMD) was assessed using dual energy X-ray absorptiometry. Peripheral quantitative computed tomography was used to examine bone volumetric density (vBMD), total (ToA) and cortical bone area (CoA), and estimates of bone compressive (BSI) and bending strength (Z, SSIp) at tibia (4, 66%) and radius (4, 50%) sites. Upon adjustment for age, height/bone length and body weight, soccer and ice hockey groups exhibited significantly greater lumbar spine aBMD (both +9.6% and +8%, respectively) compared to swimmers and non-active controls. There were no significant differences among groups at the femoral neck. At the distal (4%) tibia, only soccer athletes showed 15-26% higher BSI ($p<0.05$) compared to all other groups and exhibited 13-15% greater bending strength (Z, SSIp, $p<0.05$) compared to swimmers and controls at the proximal (66%) tibia; with greater bending strength due to more robust bone geometry (CoA, +10-13%, $p<0.05$). At the distal (4%) radius only ice hockey athletes showed 24-25% greater BSI ($p<0.05$) compared to swimmers and controls. Results are consistent with previous research suggesting weight-bearing sports are associated with greater bone density and strength than non weight-bearing sports. Both elite ice hockey and soccer female athletes exhibited greater aBMD and bone strength parameters at weight-bearing sites compared to swimmers and controls. Thus, both may be bone-strength enhancing activities in females. Unexpectedly, muscle-generated forces in elite female swimmers did not appear to exert bone density or strength benefits beyond that of non-active females. Future research is needed to further investigate the role of non weight-bearing sports on bone structure and strength in females.

Disclosures: *Lesley Scibora, None.*

FR0077

Diffuse Microdamage Induced in Cortical Bone in vivo Repairs without Bone Remodeling. Zeynep Seref-Ferlengez^{*1}, Oran Kennedy², Mitchell Schaffler¹. ¹City College of New York, USA, ²The City College of New York, USA

Physiological loading produces two types of microdamage in bone: linear microcracks (LCr, ~ 50-100mm) and diffuse damage (DDx, cluster of cracks <1mm). LCr induce local osteocyte apoptosis that evokes remodeling of damaged bone. However DDx foci neither induce apoptosis nor activate resorption. The biological response of bone to DDx is unknown. Therefore we examined time-dependent changes in DDx content and bone mechanical properties after inducing DDx *in vivo*.

Methods: Under anesthesia, ulnae from 3 groups of adult (4-5 mo, n=24) female SD rats underwent creep loading to a predetermined displacement that induces only DDx. In Group 1, right ulnae were loaded on Day 0 after which rats resumed normal cage activity for 14d (Survival). On Day 14, left ulnae (Acute) were loaded identically after which rats were killed and both ulnae were harvested for histology. In Groups 2 & 3, mechanical properties of creep-loaded damaged ulnae were tested by loading to failure, either immediately after loading or after 14d (Survival) and compared to non-damaged ulnae of the same rat. DDx area fraction in Acute Loaded and Survival ulnae was measured from basic fuchsin-stained diaphyseal sections using fluorescence microscopy. DDx area fraction in Survival vs. Acute-Loaded ulnae and stiffness of creep-loaded vs. intact control ulnae were compared using paired t-tests.

Results: DDx in Survival bones was reduced ~30% compared to Acute-Loaded ulnae (Fig. 1 & 2, $p<0.02$). Moreover, no resorption or woven bone formation was seen. The stiffness of Acute-Loaded ulnae was 14% less than intact control bones ($p<0.02$) but was restored to normal levels in Survival ulnae ($p>0.6$ Fig 3).

Conclusion: These findings reveal for the first time that small crack damage in bone (DDx) undergoes some form of repair, resulting in both microscopically and mechanically demonstrable recoveries evident by two weeks after induction of DDx in living bone. This damage reduction and mechanical recovery occurred without remodeling or changes in bone architecture. These findings suggest that alternative repair mechanisms exist in bone to deal with small crack damage. The nature of such mechanisms is currently unknown, but it seems reasonable to postulate that a combination of physicochemical remineralization and/or osteocyte-mediated processes involving local production of structural or adhesive proteins play roles in such repair.

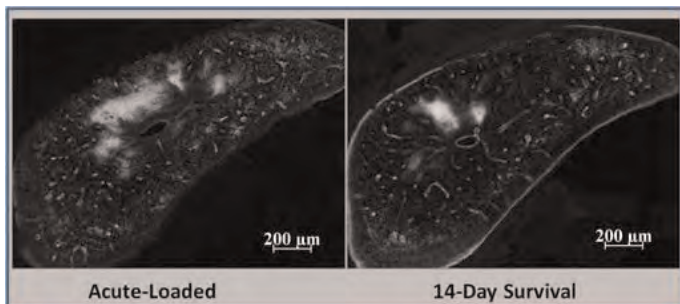


Fig.1 Fluorescence photomicrographs showing DDX of Survival and Acute-Loaded ulnae of the same rat

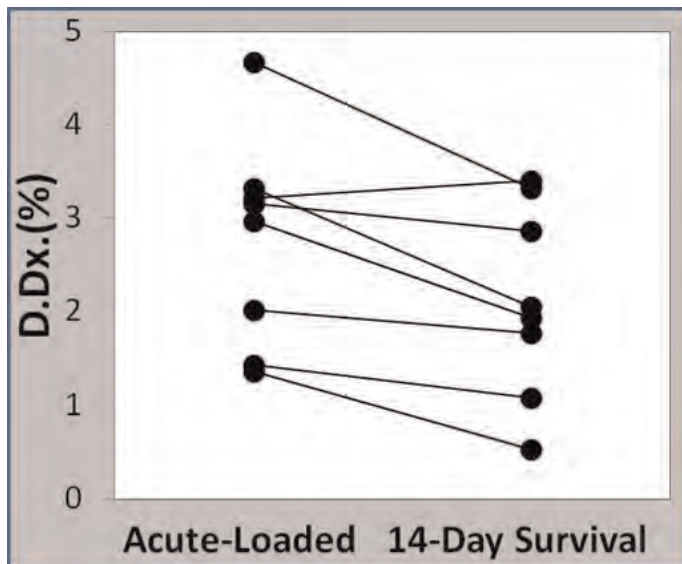


Fig. 2 Changes in DDX area fraction (%) between Acute-Loaded and Survival ulnae for each rat

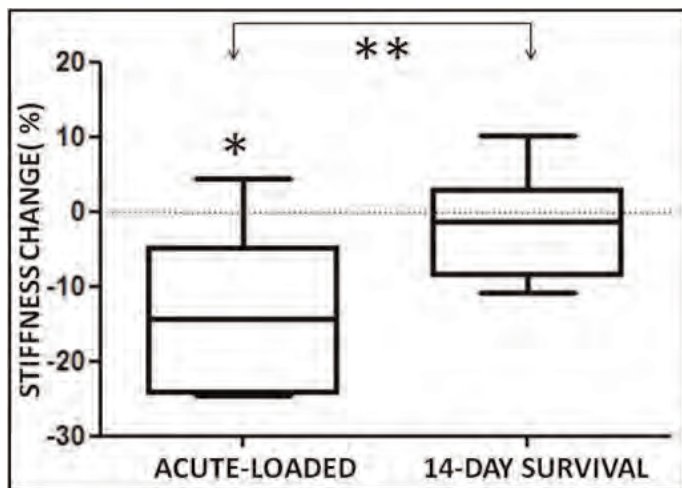


Fig. 3 %Stiffness change in Acute-Loaded and Survival ulnae relative to their non-damaged controls

Disclosures: Zeynep Seref-Ferlengez, None.

FR0079

Muscle Volume does not Affect the Osteogenic Response to Compressive Loading in the Distal Radius of Young Women. Karen Troy*, Varun Bhatia, William Edwards. University of Illinois at Chicago, USA

Bone is typically well suited for its habitual loading environment because of its ability to adapt. Although animal studies have been valuable tools for studying this process, prospective human bone adaptation data are lacking. In addition to externally applied mechanical forces, muscle forces may play an important role in bone adaptation. Greater muscle volume suggests larger habitual muscle forces

applied to the bone. Given that bone adaptation is understood to be “error signal” driven, muscle volume may be inversely related to osteogenic response magnitude. Our purpose was to use a human *in vivo* loading model to determine whether voluntary compression of the radius is osteogenic, and whether baseline muscle volume affects the response.

Eight women (20 ± 1 years) participated in an institutionally approved 28-week mechanical loading regime that targeted the distal radius. Seven women (22 ± 2 years) served as controls. Subjects applied a 300 N force by leaning onto the palm of the hand 50 cycles per day, three days per week, with each cycle being separated by two seconds. All subjects gave written informed consent prior to their participation and received QCT scans of their forearm at weeks 0, 14, and 28. Cortical, trabecular, and integral BMC, BMD, and BV in the 45 mm region proximal to the subchondral plate were computed. Muscle volume was quantified in the distal-most 10 cm region of the radius. Repeated measures ANOVAs were used to compare main effects of group and time. Pearson correlations were used to relate baseline muscle volume to 28-week changes in bone.

Loading increased the integral BMC by 54 ± 35 mg at 28 weeks. This 1.3% relative increase from baseline was significantly different from zero ($p=0.005$) and from the control group (change: -45 ± 23 mg, $p<0.001$). At 28 weeks trabecular and cortical compartments contributed 19 ± 32 and 35 ± 41 mg to the net increase, respectively. Muscle volume was not significantly correlated with changes in bone.

Compression of the radius is osteogenic in young women and can be used to prospectively study bone adaptation. In our small sample, osteogenic response was not related to muscle volume. This task can be used to determine the degree to which animal data may be translated to humans, thereby providing a validated theoretical framework within which exercise interventions to increase bone mass and prevent osteoporosis may be systematically designed and evaluated.

Disclosures: Karen Troy, None.

FR0085

Directed Differentiation of Embryonic Stem Cells to Chondrocyte and Osteoblast lineages: The Role of RhoA/ROCK Signaling. Dalea Bukhary*, Fraser McDonald², Agamemnon E Grigoriadis³. ¹King's College London/UKKing Abdulaziz University/Saudi Arabia, United Kingdom, ²King's College London Dental Institute, United Kingdom, ³Dept Craniofacial Dev & Stem Cell Biology, King's College London, United Kingdom

Treatment of bone and cartilage tissue defects caused by disease, trauma or aging is therapeutically challenging. Pluripotent stem cell-based approaches to regenerative therapies have been strengthened by a better understanding of embryonic skeletal development and how bone and cartilage lineage specification and differentiation occur. It is now well-established that *in vitro* differentiation of Embryonic Stem Cells (ESCs) and induced Pluripotent Stem Cells (iPSCs) can recapitulate embryonic development through germ layer induction followed by enrichment and expansion of specific lineages. We have developed a novel, step-wise mESC differentiation system using specific recombinant factors in the absence of serum to investigate (a) the mechanisms of pluripotent stem cell commitment to somitic mesoderm and bone/cartilage cell lineages, and (b) the role of Rho GTPase signaling in ESC-derived osteoblast/chondrocyte differentiation. Activation of the Nodal/Activin and canonical Wnt pathways together with inhibition of BMP signaling (Noggin) directed ESCs to form a primitive streak-like population expressing Brachyury, and further to somitic mesodermal subpopulations expressing PDGFR α with reduced hematopoietic/osteoclastic and cardiac potential, that subsequently differentiated efficiently in monolayer culture to osteoblast and chondroblast lineages. Inhibition of Rho/ROCK signaling using the ROCK inhibitor, Y-27632, at different developmental stages of ESC differentiation showed up to a 2 to 3-fold increase in chondrogenesis and osteogenesis, suggesting that Rho/ROCK signaling regulates the fate of bipotential chondro-osteoprogenitor cells. This was confirmed by qPCR analysis of osteoblast (Runx2, ALP, BSP) and chondrocyte (Sox9, Coll2)-specific genes, as well as by Alcian blue staining and Coll2 antibody staining of differentiated chondrocyte monolayers. Preliminary data also suggest that exposure to BMP4 together with stage-specific inhibition of ROCK signaling may play a role in maturation of hypertrophic chondrocytes. Finally, renal capsule grafting studies showed that the ESC-generated cells have endochondral ossification potential *in vivo*. Thus, the ESC model system provides defined, manipulatable and expandable chondro-osteoprogenitor populations that will provide insights into the molecular basis of bone/cartilage development and disease, as well as for generating specific populations for bone and cartilage tissue repair and replacement.

Disclosures: Dalea Bukhary, None.

FR0086

Ethanol Modulates Canonical Wnt Signaling And FoxO Activation In Acute and Chronic Binge Models of Ethanol-Induced Deficient Fracture Repair. Philip Roper*, Rachel Nauer¹, Kristen Lauing¹, John Callaci². ¹Loyola University Medical Center, USA, ²Loyola University of Chicago, USA

Alcohol abuse is a risk factor for impaired bone fracture healing, and binge drinking is the predominant alcohol abuse pattern associated with traumatic orthopedic injury. The mechanism behind this effect is unknown. The canonical Wnt signaling pathway is important in fracture healing because it drives mesenchymal

stem cell (MSC) differentiation towards osteoblasts and chondrocytes that are required for callus formation. Wnt signaling relies on activation of β -catenin to upregulate specific target genes necessary for differentiation. However, in times of increased oxidative stress, as with alcohol exposure, another family of transcription factors, the FoxO transcription factors, becomes active. Once active, FoxOs require β -catenin as a cofactor for proper function. We hypothesize that alcohol exposure may be able to activate FoxOs within the fracture callus, thereby suppressing Wnt signaling through β -catenin competition. To test this hypothesis, we devised two clinically relevant models of alcohol administration in which 7 week old male C57BL/6 mice received intraperitoneal injections of ethanol (2g/kg) or saline for three consecutive days per week for two weeks prior to injury. One hour after the last alcohol exposure, the left tibia was stabilized with an intramedullary pin and surgically fractured. Animals in the acute binge group ceased further injections, while animals in the chronic binge group continued once daily i.p. ethanol injections until the animals were euthanized. Callus tissue was examined for the effects of alcohol on tissue composition, FoxO oxidative stress signaling, and Wnt signaling. Both acute and chronic binge alcohol administration led to deficient fracture repair, however administration of alcohol during healing produced greater defects in repair as measured by decreased callus size and perturbed callus tissue composition, namely a reduction in the cartilaginous callus and the presence of mature, hypertrophic chondrocytes. FoxO1 activation was significantly increased in the fracture callus of alcohol animals as compared to saline ($p < 0.01$), with a concomitant decrease in active β -catenin ($p < 0.05$). The callus tissue of chronic binge animals also exhibited increases in total FoxO1 protein levels ($p < 0.05$). Alcohol-induced activation of FoxO signaling with the concurrent decrease in canonical Wnt signaling provides a plausible mechanistic explanation for the observed effects of alcohol on fracture healing.

Disclosures: Philip Roper, None.

FR0089

Runx2 Control Chondrocyte Proliferation through Direct Regulation of Cell Cycle Genes. Haiyan Chen^{*1}, Farah Ghori-Javed¹, Rosa Serra¹, Soraya Gutierrez², Amjad Javed¹. ¹University of Alabama at Birmingham, USA, ²Universidad De Concepcion, Chile

Runt related protein-2 (Runx2) is essential for skeletogenesis. Coordinated activity of multiple cell types including chondrocyte and osteoblast are required for skeletogenesis. To elucidate Runx2 regulatory control distinctive to chondrocyte cell population, we generated mice with a conditional ablation of Runx2 in chondrocyte. Selective deletion of Runx2 in chondrocyte by Col2a-Cre was confirmed with Rosa26-tomato mice. Homozygous mice exhibited developmentally failed endochondral ossification and dies shortly after birth. Chondroprogenitors in the hyaline cartilage of wild type mice showed uni-directional differentiation to hypertrophic chondrocytes. Runx2 deficiency resulted in disruption of chondrocyte differentiation as determined by absence of pre/hypertrophy and Collagen type X expression. To our surprise, chondrocyte proliferation which is an integral component of endochondral ossification was severely impaired. We observed a dramatic decrease (50%) in the total cell number in both proliferative and pre-hypertrophic zones of homozygous mutant compared to wild type. Similar reduction in chondrocyte cell number was noted in hyaline cartilage of trachea. Furthermore, *in vivo* BrdU labeling confirmed this reduction results from a decreased mitotic activity of chondrocyte. This unique role of Runx2 to enhance chondrocyte proliferation is consistent with the growth failure and primordial dwarfism in mutant mice. To mechanistically understand alteration in chondrocyte proliferation rate, we determined genes associated with cell cycle cascade in the Runx2 null growth plate. Our gene microarray identified 5 genes with reproducible differences in expression levels ranging from 3-50 folds. In Runx2 null chondrocytes Sfn mRNA was upregulated, while expression of Gpr132, c-Myb, cyclin A1, A2 were strongly inhibited. Interestingly, the differentially expressed gene set encompass functional grouping across cell cycle from G1/S phase to cell cycle check points and arrest. To assess if Runx2 directly regulate their transcription, we cloned 2kb promoter of all five genes. Multiple high affinity Runx recognition motifs were noted in these promoters. Chromatin immunoprecipitation revealed that in chondrocytes Runx2 is bound to these sites. Consistent with *in vivo* promoter occupancy, promoter activity of these genes was enhanced by Runx2. Our results establish for the first time that Runx2 is obligatory for chondrocyte proliferation and regulate cell cycle genes.

Disclosures: Haiyan Chen, None.

FR0090

Smad2/3 Mediated TGFbeta Signaling Regulates Chondrocyte Proliferation and Differentiation in Postnatal Growth Plate and Maintains Articular Cartilage Integrity. Weiguang Wang^{*}, Karen Lyons, Buer Song. University of California, Los Angeles, USA

Previous findings on mouse models with TGF- β type II receptor or ligand knockout revealed that TGF- β signaling plays important roles in axial skeleton formation, joint development, and long bone growth. However, it is unknown whether it is the Smad2/3 or noncanonical pathway that mediates the functions of TGF- β signaling. To study the role of Smads 2 and 3 in the process of cartilage formation and maintenance, we generated mice with conditional deletion of Smad2 in chondrocytes using Col2cre, mice with Smad3 globally deleted, and the cross of these two strains to obtain mice with both Smad2 and 3 deleted in chondrocytes (the double

mutant mice). In prenatal stages, when compared with WT littermates, none of these single and double mutant mice showed defects in axial skeleton and joint formation, but differences were observed in long bones. By P0, both *Smad2^{cko}* and *Smad3^{-/-}* mice exhibited defects in the growth plate, including an increase in proliferation of resting chondrocytes and an expansion of the hypertrophic zone. These defects were much more severe in *Smad2/3* double mutant. By 2-weeks, the double mutant mice developed a severe postnatal dwarfism, associated with a delay of secondary ossification in the resting zone, decreased proliferation in the proliferative zone, and an increase in apoptosis in the growth plate and articular chondrocytes. In addition, the double mutant mice showed a much earlier onset of an osteoarthritis-like phenotype (1 month) than previously reported for *Smad3^{-/-}* mice (Ref). Meanwhile, *Smad2^{cko}* mice showed minor but reproducible differences in growth plate morphology, demonstrating a role for Smad2 in growth plate cartilage. Analysis of articular cartilage in *Smad2^{cko}* mice is ongoing. By 4 months, the *Smad3^{-/-}* mice developed postnatal dwarfism as well as an osteoarthritis-like phenotype, as reported previously (Ref). These observations suggest that both Smad2 and Smad3 mediated TGF- β signaling is important for the regulation of postnatal growth plate chondrocyte differentiation and for maintenance of articular cartilage, and that Smad2 and 3 have overlapping function. Smad2/3 mediated signaling is not critical at prenatal stages, yet is indispensable postnatally for chondrocyte proliferation, differentiation and maintenance of cartilage in adult.

Reference: Yang et al., *J Cell Biol.* 2001 Apr 2;153(1):35-46



Figure. *Smad2/3* double mutant mice have an earlier onset and more severe OA-like phenotype than do *Smad3^{-/-}* mice. H&E staining of 1 month knee sections. Double mutants exhibit thinner superficial, middle and deep zones (yellow double head arrow) compared to *Smad3^{-/-}* null or WT mice. An increased number of hypertrophic cells are seen (blue arrow heads) in the deep zone in *Smad3^{-/-}* null mice. This is exacerbated in the double mutants (right). Chondrocyte clusters (green arrowheads) and hypercellularity are evident in the midzone of double mutants, but are not seen in *Smad3^{-/-}* null or WT mice.

Smad2/3 double mutant mice have an earlier onset and more severe OA-like phenotype than do *Smad3^{-/-}*

Disclosures: Weiguang Wang, None.

FR0091

The FOP R206H Alk2 Mutation Enhances BMP-Induced Chondrogenic Differentiation. Andria Culbert^{*}, Salin Chakkalakal, Robert Caron, Eileen Shore. University of Pennsylvania, USA

Fibrodysplasia ossificans progressiva (FOP) is a rare genetic disease characterized by heterotopic endochondral ossification within soft connective tissues and is caused by mutations in ALK2/ACVR1, a BMP type I receptor. The most common mutation, R206H, causes dysregulation of canonical BMP signaling, a key regulator of chondrocyte commitment, proliferation, and maturation. Primary mouse embryonic fibroblasts (MEFs) were harvested from wild-type and heterozygous knock-in *Alk2^{R206H/+}* embryos to examine the effects of the mutation on chondrogenic differentiation. Consistent with previous results, *Alk2^{R206H/+}* MEFs have increased canonical BMP signaling in both the presence and absence of BMP ligand, as detected by phosphorylation of Smad1/5/8. Chondrogenic media containing BMP ligand was used to induce differentiation as TGF β alone did not induce chondrogenesis of wild-type or mutant MEFs. In the absence of BMP, *Alk2^{R206H/+}* MEFs did not spontaneously differentiate, despite increased BMP signaling; however, in the presence of BMP show increased sensitivity toward chondrogenesis. *Alk2* mRNA is most abundant in undifferentiated MEFs and decreases upon differentiation, suggesting a role in early differentiation events. Consistent with our results, *Alk2^{R206H/+}* MEFs have accelerated onset and increased abundance of early chondrogenic transcripts during differentiation corresponding to the earlier appearance of chondrocyte morphology. Proliferation was quantified but showed no differences between wild-type and *Alk2^{R206H/+}* MEFs either prior to or during early chondrogenesis. Implants of MEFs into hind limbs of wild-type mice demonstrate that robust *in vivo* heterotopic endochondral ossification is induced by the combination of BMP ligand with *Alk2^{R206H/+}*, but not wild-type, MEFs. Our data demonstrate that heterozygous expression of R206H Alk2 enhances chondrogenic differentiation of progenitor cells and suggests Alk2 plays an important role early during chondrogenic differentiation. The requirement for BMP ligand to activate differentiation of *Alk2^{R206H/+}* MEFs both *in vitro* and *in vivo* suggests that an increased sensitivity to BMP signals during early stages of chondrogenesis is a critical mechanism to promote heterotopic endochondral ossification in the presence of the R206H Alk2 FOP mutation.

Disclosures: Andria Culbert, None.

FR0092

The Transcription Factor FoxC1 Regulates Chondrogenesis Together with Gli2 through Induction of PTHrP. Michiko Yoshida*¹, Kenji Hata¹, Rikako Takashima², Sachiko Iseki³, Teruko Takano-Yamamoto⁴, Riko Nishimura¹, Toshiyuki Yoneda¹. ¹Osaka University Graduate School of Dentistry, Japan, ²Osaka University, Japan, ³Section of Molecular Craniofacial Embryology, Graduate School, Tokyo Medical & Dental University, Japan, ⁴Tohoku University, Japan

Endochondral bone formation, which is an essential event for mammalian skeletal development, is regulated by various transcription factors through harmonious organization of transcriptional networks. Identification of transcription factors involved in the development of these networks would facilitate to uncover the molecular basis of endochondral ossification. Here we attempted to identify a novel transcription factor that takes a part in chondrogenesis via transcription network development. To approach this, we generated transgenic mice carrying Venus driven by Col2a1 promoter, thereby GFP is selectively expressed in chondrogenic cells. Venus-positive chondrogenic cells dissociated from E12.5 limb buds were sorted using the FACS Aria without expansion in culture. Subsequent differential microarray between Venus-positive and -negative cells led us to identify FoxC1 (Forkhead Box C1) as a candidate transcription factor. Of note, the mutation of *FOXC1* is shown to cause Axenfeld-Rieger syndrome (ARS) in human that is characterized by the anterior segment dysgenesis and diverse skeletal abnormalities. Whole mount *in situ* hybridization demonstrated evident co-expression of *FoxC1* mRNA and Col2a1 in the developing limbs. Overexpression of FoxC1 induced alcian blue-positive chondrogenesis in limb bud cells in microculture. These results collectively suggest that FoxC1 plays a role in chondrogenesis.

To further verify the functional role of FoxC1 in chondrogenesis, we searched for transcriptional target of FoxC1. FoxC1 had no effects on Col2a1 and Sox9 mRNA expression. On the other hand, FoxC1 increased PTHrP mRNA expression in conjunction with promoted chondrogenesis. Moreover, FoxC1 together with Gli2 further up-regulated PTHrP expression. IP-Western analysis revealed a physical interaction between FoxC1 and Gli2. DNA pull-down assay and ChIP experiments showed direct binding of FoxC1 to the FoxC1 binding element (CTAAATAAC) in the PTHrP gene promoter. Finally, pathogenic missense mutation (Ile126Met) of FOXC1, which is responsible for ARS, suppressed PTHrP expression induced by IHH. In conclusion, we identified a novel transcription factor FoxC1 that promotes chondrogenesis through directly up-regulating PTHrP expression in collaboration with Gli2. Further determination of FoxC1 function in transcription network and chondrogenesis should lead us to obtain deeper insights into the molecular mechanism of endochondral ossification.

Disclosures: Michiko Yoshida, None.

FR0095

Knockdown of Tribbles Homolog 3 (TRIB 3) Results in Cell and Context Specific Effects on Bone, Fat and the Hematopoietic System. Rakesh Verma*¹, Anne Breggia², Phuong Le¹, Sheila Bornstein², Donald Wojchowski¹, Clifford Rosen². ¹Maine Medical Center Research Institute, USA, ²Maine Medical Center, USA

TRIB 3 (Tribbles homologue 3 Drosophila) is a pseudokinase which regulates diverse cellular functions including insulin signaling, adipogenesis and bone formation via cell survival and stress signaling pathways. Importantly, TRIB 3 suppresses adipocyte differentiation by negative regulation of peroxisome proliferator-activated receptor gamma (PPAR γ). Bone marrow irradiation prior to transplantation induces trabecular and cortical bone loss. Interestingly, following bone marrow irradiation there is a transient period of marrow adipogenesis (days 5-10) prior to hematopoietic reconstitution and recovery of bone mass. However, the role of adipogenesis during bone marrow recovery remains unclear. In this study, we hypothesized that a reduction in TRIB 3 might promote marrow adipogenesis and alter hematopoiesis and skeletal mass. As such, we first phenotyped TRIB 3^{-/-} mice on a B6 background and B6 WT mice at 12 weeks of age by DXA and found increased % body fat, lower total body weight, decreased areal BMD, but no hematopoietic phenotype. Next we sought to investigate the role of TRIB 3 in bone marrow recovery following lethal irradiation and bone marrow transplantation. LY5.1+ WT recipient mice were lethally irradiated (10Gy) and transplanted with either LY5.2+ TRIB 3 KO or LY5.2+ WT donor cells. At 8 weeks post transplant, >90% of peripheral blood (PB) cells of all recipient mice were LY5.2+ indicating successful engraftment. Surprisingly, mice engrafted with TRIB 3^{-/-} donor cells had increases in total body weight (36%), % body fat (26%), total bone mineral density (BMD, 2%), total bone mineral content (BMC, 6%), and femoral (BMD, 7%) compared to WT receiving WT donor cells. Importantly, as compared to LY5.1 WT mice transplanted with WT donor cells, LY5.1 WT mice transplanted with TRIB 3^{-/-} donor cells exhibited marked increases in red blood cells and reticulocyte production. Interestingly, the CD11b+ myeloid population, a precursor to the osteoclast lineage, was also markedly increased in the recipient mice. Thus transplantation of donor cells without TRIB 3 led to an increase in hematopoietic elements as well as enhancement of bone mass suggesting that the target of this pseudokinase within the bone marrow includes all three major cell types. These data also highlight the cell and context specific nature of Tribbles Homolog 3 in the bone marrow and its potential role in regulating body composition and bone mass. NIH-1R24 DK092759-01

Disclosures: Rakesh Verma, None.

FR0098

HIF-1 α is Essential for the Development of the Nucleus Pulposus. Laura Mangiavini*¹, Tremika LeShan Wilson², Alexander Robling³, Irving Shapiro⁴, Makarand Risbud⁵, Ernestina Schipani¹. ¹Indiana University School of Medicine, USA, ²Department of Medicine, Indiana University School of Medicine, USA, ³Indiana University, USA, ⁴Thomas Jefferson University, USA, ⁵Department of Orthopedics Surgery, Thomas Jefferson University, USA

The intervertebral disc consists of an outer ring of fibrous cartilage called the annulus fibrosus, and an inner gelatinous structure known as the nucleus pulposus. The annulus fibrosus derives from the sclerotome, whereas it has been recently shown that the nucleus pulposus cells originate from the notochord. Notably, however, the molecular mechanisms that control differentiation of notochordal cells into cells of the nucleus pulposus are still largely unknown.

The nucleus pulposus is hypoxic and express the transcription factor Hypoxia Inducible Factor -1 α (HIF-1 α), which is a major mediator of cellular adaptation to hypoxia. In this study, we analyzed the role of HIF-1 α in the development of the nucleus pulposus by conditionally ablating HIF-1 α in the notochord. For this purpose, FOXA2-Cre transgenic mice were bred with mice homozygous for a floxed HIF-1 α allele (HIF-1 α ^{fl}) in order to generate FOXA2-Cre; HIF-1 α ^{fl/fl} mutant mice and control littermates. Mutant mice were viable with no macroscopic abnormalities. Development of the nucleus pulposus was studied from E15.5 up to 4 months. E15.5 mutant nucleus pulposus was considerably smaller than control. This phenotypic feature was not due to decreased cell proliferation or to cell death, but was, at least in part, a consequence of the reduced size of the cells forming the nucleus pulposus, which did not display the classical hypertrophic appearance shown by control cells. Our finding thus suggests that HIF-1 α deficiency had altered the differentiation of notochord cells into cells of the nucleus pulposus. Conversely, at birth, Tunel assay revealed massive cell death in the mutant nucleus pulposus. The nucleus pulposus eventually disappeared completely in postnatal mutant mice, and was replaced by cells of the annulus fibrosus. Interestingly, morphology of the vertebral bodies was normal at all time points examined, which further supported the high degree of specificity of expression of Cre recombinase in cells of the nucleus pulposus. Taken together, our findings indicate that deficiency of HIF-1 α in the notochord alters the differentiation process of notochord cells into cells of the nucleus pulposus, which then eventually die. Moreover, our study supports the notion that the nucleus pulposus originates from the notochord.

In conclusion, HIF-1 α is a differentiation and survival factors for cells of the nucleus pulposus and has an essential role in the development of the nucleus pulposus.

Disclosures: Laura Mangiavini, None.

FR0099

Manipulating the Notch Pathway to Accelerate Fracture Repair. Cuicui Wang*¹, Jie Shen¹, Kiminori Yukata², Michael Zuscik³, Regis O'Keefe¹, Hani Awad⁴, Matthew Hilton⁴. ¹University of Rochester, USA, ²University of Tokushima Graduate School, Japan, ³University of Rochester School of Medicine & Dentistry, USA, ⁴University of Rochester Medical Center, USA

Bone fractures are one of the most common problems observed in clinical orthopaedics. During fracture repair, mesenchymal stem cells (MSCs) are recruited to the fracture site and undergo differentiation to form chondrocytes and osteoblasts that aid in repairing and strengthening the bone. The process of MSC differentiation during fracture repair is reminiscent of events that occur during skeletal development. Recently, several breakthrough discoveries in our lab have identified the Notch pathway as a critical regulator of MSC differentiation during skeletal development. Specifically, our genetic data demonstrated that loss of Notch signaling accelerates cartilage and bone formation from the common mesenchymal progenitor during limb development. In our current study, we investigated whether Notch inhibition (via DAPT treatment) would accelerate and enhance fracture repair by inducing more cartilage and bone formation from MSCs recruited to the fracture site. Following the generation of an open tibial fracture in mice, DAPT (50mg/kg/day) or DMSO (vehicle) was delivered via I.P. injection for one or 4 consecutive days. Treatments began two days following fracture to ensure normal initiation of MSC recruitment and proliferation. Radiographs collected from 14 days post-fracture (14dpf) suggested greater volume of bony callus in DAPT treated mice, particularly in the 4 consecutive day treatment group. MicroCT quantification established a significant increase in mineralized callus volume in DAPT treated mice at 14dpf. Additionally, the strength of the newly formed fracture callus in DAPT treated mice, as measured by biomechanical torsion testing, was dramatically enhanced compared to controls. Histological analyses further revealed that Notch inhibition enhanced the size of the cartilage and bony callus at early time-points (4dpf and 7dpf) during fracture repair. To verify these results at the molecular level, real-time RT-PCR analyses were performed to assess changes in chondrogenic and osteogenic gene expression of callus tissue (4dpf). Consistent with our histological findings, cartilage (*Col2a1*, *Col10a1*) and bone markers (*Coll1a1*, *Bsp*, *Oc*) were significantly up-regulated. Taken together, our findings revealed that Notch inhibition accelerated fracture repair by enhancing MSC differentiation to generate a more robust cartilaginous and bony callus, therefore, the Notch pathway may serve as an important therapeutic target in the context of fracture repair.

Disclosures: Cuicui Wang, None.

FR0100**Periosteal PTHrP Regulates Cortical Bone Modeling During Linear Growth.**Meina Wang^{*1}, Joshua VanHouten², Randy Johnson³, Arthur Broadus².¹Yale University, USA, ²Yale University School of Medicine, USA, ³M.D. Anderson Cancer Center, USA

PTHrP is highly expressed in the periosteum (PO) and fibrous ligament and tendon insertion sites during linear growth. Here, we tested the hypothesis that PTHrP in the fibrous layer at the PO might regulate the modeling of cortical bone surfaces during growth. We studied this question in mice in which *PTHrP* was conditionally deleted via *sclex* (*Scx*)-Cre; *Scx* is a bHLH transcription factor that is highly expressed in the connective tissues of bone. Concordance of *Scx* and *PTHrP* expression was determined in *Scx-Cre/R26R* and *PTHrP-lacZ* reporter mice.

We focused on two regions: 1) the proximal posterolateral tibia (PL tibia), a well-known site of metaphyseal modeling or cut-back and 2) the neck and diaphysis of the fibula, chosen because it has a profoundly abnormal structure by μ CT in the *PTHrP* cKO mouse. Findings in the PL tibia included: a) abundant PTHrP expression in the fibrous PO overlying a dense population of osteoclasts (OCs) resorbing the subjacent metaphyseal cortex, b) a 75% reduction in these OCs in the *PTHrP* cKO mouse, together with a much thickened cortex in a site with concordant *R26R* and *PTHrP-lacZ* expression, and c) a striking increase in endosteal osteoblasts (OBs) at this site together with a 3-fold increase in double-label BFR by histomorphometry at 7 weeks. This thickening distorted the PL tibia on 3D μ CT in 10/10 cKO mice at 12 weeks. In the control fibular neck, we found an extraordinary rate of modeling of a curious "trabecularized cortex" that lacked a true cortical surface. Here, OCs and OBs were at work on opposing trabecular surfaces, and the entire region lit up by double label at 7 weeks. In the cKO mouse, we saw a decrease in OC bone resorption, an inside-out or endosteal pattern of double-labeling, and at 12 weeks total volumes and cross-sectional areas that were twice those seen in the control mice ($TV = 0.27 \pm 0.03$ vs 0.55 ± 0.06 mm³ and $TA = 0.17 \pm 0.02$ vs 0.33 ± 0.03 mm², $M \pm SEM$, control vs cKO/ $n = 5$ pairs, t test < 0.003). The result of this abnormal modeling was a fibular diaphysis that was markedly thickened and misshapen throughout. Clearly, the remarkable increase in the cKO fibular bone mass was the result of the uncoupling of OC and OB activities during modeling.

We conclude that PTHrP in the PO regulates cortical modeling during linear growth. Since the PO is anchored proximally in the bone collar, we propose that PO PTHrP expression may be driven in the fibrous PO by growth-induced loading.

Disclosures: Meina Wang, None.

FR0103**SULF1/SULF2 Expression in Osteochondral Cells and Their Role in Bone Development and Fracture Repair.**Gul Zaman^{*1}, Mittal Shah¹, Jaish Dudhia¹, Chantal Chenu², Andrew Pitsillides¹, Gurtej Dhoot¹. ¹The Royal veterinary College, United Kingdom, ²Royal Veterinary College, United Kingdom

Heparan sulfate 6-O-endo-sulfatases (SULF1 and SULF2) are a relatively novel family of extracellular sulfatases that selectively remove 6-O-sulfate groups from HSPGs, co-receptors for many growth factors and cytokines thereby altering their binding characteristics crucial for cell signaling. Cartilage and bone homeostasis are regulated by specific growth factors and cytokines and skeletal abnormalities have been reported in SULF1/2 double knockout mice. The role of resident osteochondral cells through SULF1/2-mediated cell signaling has not, however, been examined and the aim of this study was to examine the expression patterns of Sulfi/2 at mRNA and protein level in cartilage and bone cells during normal development and fracture repair in rat limbs using RT-PCR, immunohistochemistry and *in vitro* assays designed to determine their functional significance.

SULF1/2 expression using immunohistochemistry was observed in chondrocytes undergoing endochondral bone development in both primary and secondary ossification centres in fetal day 17 and postnatal days 5-11 rat femurs. Examination of epiphyseal growth plates revealed that compared to quiescent or hypertrophic chondrocytes, the columns of proliferating chondrocytes expressed higher levels of SULF1/2. Markedly higher levels of both SULFs, however, were expressed in osteoblasts actively forming bone when compared with proliferating pre-osteoblasts in the periosteum or the entombed osteocytes expressing the lowest levels.

A fracture model that comprised a mid-diaphyseal transverse osteotomy in the rat femur showed elevated levels of SULF1/2 in the periosteal layer adjacent to the fracture site during the early inflammatory phase. Chondrocytes, identified by Alcian blue positive staining of their extracellular matrix, were more prevalent one week after fracture and, as in growth plates, those undergoing active proliferation expressed higher SULF1/2 levels than chondrocytes exhibiting overt differentiation or hypertrophy. Active osteoblasts involved in bone accrual and osteoclasts in closely allied resorbing sites also expressed elevated levels of SULF1/2 during the fracture repair process.

Sulf1 and Sulf2 mRNA was also expressed in the osteoblast-like cell line SAOS2 and RNA extracted from calvaria, long bones and cartilage samples. In preliminary gain or loss of function analyses, the addition of SULF1 neutralizing antibodies to SAOS2 cells *in vitro* resulted in a small (15%) but significant ($p < 0.05$) increase in osteoblast-like cell (SAOS2) proliferation.

This study shows that cartilage and bone cells have distinct SULF1/2 expression profiles during development, which are recapitulated during fracture repair. Our ongoing dissection of the signaling pathways active in cells expressing these elevated

levels of SULF1/2 will provide important insight into the regulation of growth and development in osteochondral tissues.

Disclosures: Gul Zaman, None.

FR0105**Computational Simulation of Osteopontin ASARM Peptide Binding to Crystal Faces of Hydroxyapatite.**Ahmad Mansouri¹, David L. Masic², Jeffrey J. Gray², Marc McKee^{*1}. ¹McGill University, Canada, ²Johns Hopkins University, USA

Matrix extracellular phosphoglycoprotein (MEPE) and osteopontin (OPN) contain an acidic, serine- and aspartate-rich motif (ASARM) which, when phosphorylated, potently inhibits mineralization of osteoblast cultures. ASARM peptides accumulate in hypophosphatemia patients whose distinguishing clinical feature is soft bones (osteomalacia). To investigate the mechanism by which ASARM peptides inhibit mineralization, we have modeled using energy-minimization computational simulations human OPN-ASARM peptide (DDSHQSDSHHSDESDEL) binding to hydroxyapatite mineral at the atomic scale. To examine peptide binding to different hydroxyapatite atomic planes having different chemical terminations, we used RosettaSurface, a computational structure-prediction algorithm for peptide-solid surface interactions. We have determined the binding affinities, specificities and structure for ASARM-Sp0 (without phosphoserine) and two phosphorylated forms of ASARM (ASARM-Sp3 and ASARM-Sp5, with 3 and 5 phosphoserines, respectively). Peptides were constructed using PyMOL software. {100}, {001} and {010} monoclinic hydroxyapatite planar surfaces having different calcium-to-phosphate ratios were constructed using CrystalMaker software. Each surface was generated by "cutting" along a specific Miller indices (hkl) plane, and each mineral construct had a thickness of at least 8 angstroms. P-O and O-H bonds are strong and their breaking is energetically unfavorable, so we tailored the terminations to leave intact interfacial phosphate and hydroxyl ions. Different mixed-charge surfaces were constructed to reflect surfaces likely sampled during crystal growth. The RosettaSurface protocol predicted low-energy conformations for these peptides in solution and bound to mineral (adsorbed). Adsorption data revealed highly significant differences in binding energies between the 3 peptides for all crystal surfaces examined, with increased binding correlating with increased phosphorylation. All peptides were generally unstructured both in solution and upon adsorption, and phosphate and carboxylate groups coordinated with surface calcium with some degree of lattice matching. The highest binding energies were for the phosphorylated peptides on (100) and (010) terminations. In conclusion, these computational simulations provide mechanistic data on how OPN and its phosphorylated peptides act as potent biomineralization inhibitors. Support from the CIHR and the Arnold and Mabel Beckman Foundation.

Disclosures: Marc McKee, None.

FR0116**Critical Role of PTH Receptor Phosphorylation in Regulating Acute Effects of PTH on Renal Hemodynamics.**Akira Maeda^{*1}, Makoto Okazaki², Hiroko Segawa¹, Abdul Abou-Samra³, Harald Jueppner¹, John Potts¹, Thomas Gardella¹. ¹Massachusetts General Hospital, USA, ²Chugai Pharmaceutical. Co., Ltd., Japan, ³Wayne State University, School of Medicine, USA

Phosphorylation of seven serine residues on the PTHR1 C-terminal tail is thought to play a key role in controlling signaling responses induced by PTH ligands. Cells expressing a phosphorylation-deficient mutant PTHR1 (PD), having the seven serines replaced by alanine, exhibit prolonged cAMP signaling responses to PTH ligand treatment. Knock-in mice expressing this PD-PTHR1 in place of the normal PTHR1 exhibit prolonged increases in blood cAMP levels after single acute PTH(1-34) injection (Bounoutas et al., Endocrinology 2006). Last year we reported that the expected responses of decreased blood phosphate levels and increased blood 1,25(OH)₂D₃ levels following acute PTH(1-34) injection were unexpectedly blunted in the PD mice. Furthermore, whereas levels of cAMP in urine of WT mice increased robustly following PTH injection, they did not increase in urine of PD mice. These altered responses of blood and urine markers of PTH action suggested a defect in PTH function in kidneys of PD mice.

We investigated the effects of PTH injection in WT and PD mice on NaPi2a protein levels in renal brush-border membranes (BBMs) using western blot analysis. Surprisingly, NaPi2a expression was down-regulated in renal BBMs of PD mice to the same extent that it was in renal BBMs of WT mice. Moreover, real-time PCR analysis revealed that PTH injection increased 1 α -OHase mRNA expression in kidneys of PD mice to the same extent that it did in kidneys of WT mice. Thus, key molecular responses in renal proximal tubule cells were normal in PTH-injected PD mice. We then investigated effects on renal filtration. We injected (iv) WT and PD mice with FITC-inulin, along with PTH(1-34) (50 nmol/kg) or vehicle, and measured the disappearance of fluorescence from the blood over time. The values for T_{1/2} of FITC-inulin in vehicle- and PTH-injected WT mice were 17 \pm 2 and 21 \pm 5 minutes, while the corresponding values in PD mice were 14 \pm 2 and >75 minutes. Thus, renal clearance following acute PTH injection was markedly impaired in PD mice. These data show that phosphorylation of the PTHR1 plays a key role in regulating the effects of PTH on renal clearance mechanisms. Whether these effects involve direct actions of the

PTHr1 specifically within the kidney, the systemic vasculature, or elsewhere, is currently under investigation.

Disclosures: Akira Maeda, Chugai Pharmaceutical Co., Ltd., 3

This study received funding from: NIH-NIDDK DK-11794, Chugai Pharmaceutical Co., Ltd.

FR0117

Induction of Bone Marrow Apoptosis Impacts PTH Anabolic Actions in Bone. Amy Koh¹, Sun Wook Cho², Glenda Pettway¹, Laurie McCauley³. ¹University of Michigan, USA, ²Seoul National University Hospital, South Korea, ³University of Michigan School of Dentistry, USA

PTH has multifaceted effects in the skeleton, a prominent one being its potent anabolic actions. Irradiation increases bone marrow cell apoptosis, TGF β activity, and mesenchymal progenitor cell numbers which are associated with augmented PTH anabolic actions. The purpose of this study was to determine whether targeted bone marrow cell apoptosis impacts PTH anabolic actions. The pro-apoptotic agent, etoposide (ETOP) (20mg/kg) or vehicle (VEH) control, was used to treat 16wk old mice daily for 5d then 3d/wk for 6wks. PTH (50mg/kg/d) or VEH was also administered daily resulting in 4 treatment groups: VEH, PTH, ETOP and PTH+ETOP. Mice were sacrificed 24h after last injections and skeletal phenotyping, flow cytometric analyses (FACS) of the bone marrow, and serum bone turnover markers analyzed. MicroCT analysis and histomorphometry of tibiae revealed a significant increase in bone volume with PTH vs. VEH, and a significant decrease with ETOP vs. VEH. PTH administration in the ETOP treated mice had a significantly higher ratio of increase versus PTH without ETOP. At 5 days of ETOP treatment there was a significant increase in early apoptotic cells (AnnexinV+PI-) as well as MER⁺CD11b⁺F4/80⁺ and MER⁺CD68⁺F4/80⁺ cells via FACS. At 6 wks, FACS analysis revealed significantly increased percentages of CD68⁺ and Gr1⁺CD11b⁺F4/80⁺ (macrophage markers), CD45⁺ (leukocyte marker) and Lin⁺CD29⁺sca1⁺ (mesenchymal stem cell marker) cells with ETOP or PTH+ETOP treatment. Serum TRAcP5b was significantly increased with PTH and PTH+ETOP similarly whereas PINP levels were increased to a greater extent with PTH than PTH+ETOP. PTH+ETOP significantly reduced numbers of osteoclasts per bone perimeter after 6 wks of treatment when compared to VEH or ETOP but not compared to PTH alone. In another experimental model, luciferase⁺ bone marrow stromal cells (BMSCs) were implanted subcutaneously to form ectopic ossicles and their growth tracked over time using bioluminescent imaging. Mice were administered VEH, ETOP, PTH, or PTH+ETOP daily starting 7d after implantation. PTH increased BMSC luciferase signals at d6. ETOP increased signal similarly to PTH and greater than VEH while PTH+ETOP had the greatest increase in luciferase BMSC signal suggesting that the induction of apoptosis provided an environment more conducive for PTH anabolic actions. Taken together, these data suggest that targeted apoptosis augments the ability of PTH to evoke anabolic actions in bone.

Disclosures: Amy Koh, None.

FR0119

Proton Generation by Osteoblasts/Osteocytes in Response to PTH/PTHrP. Katharina Jähn¹, Matt Prideaux², Hong Zhao², Sarah Dallas¹, Lynda Bonewald¹. ¹University of Missouri - Kansas City, USA, ²University of Missouri-Kansas City, USA

PTH activates bone remodeling and elevated PTHrP during lactation has been shown to induce osteocytes to remove mineral from their perilacunar matrix (Qing *et al.* 2012). Genes associated with the production and export of protons i.e. carbonic anhydrase and ATP/H⁺ transporters, and proteins active under acidic conditions i.e. TRAP and Cathepsin K are elevated with lactation. To determine if osteocytes can acidify their microenvironment, the IDG-SW3 cell line, which recapitulates early to late osteocyte differentiation, was used. Addition of 100nM PTHrP rapidly and significantly reduced pH in the media of IDG-SW3 cultures at day 3 and 6 (representative of late osteoblasts/early osteocytes) as detected by the pH indicator dye SNARF. Similar, but less pronounced effects were observed using 100nM PTH. This effect was specific for the osteoblast lineage as similar effects were observed with osteoblastic but not fibroblastic cells. However, the effects of PTH on genes associated with proton production were dependent on stage of differentiation. PTH (50nM) treatment for 24h significantly increased gene expression of ATP6V0B, ATP6V0d2, TRAP and Cathepsin K in mature osteocyte (day15-29) IDG-SW3 cultures but not in late osteoblast/early osteocyte (day1-8) cultures. Therefore, late osteoblasts/early osteocytes are primed to release protons in response to activation by a potentially different mechanism from that of mature osteocytes. To further examine osteocyte perilacunar remodeling *in vivo*, mice expressing an α 2(I)-collagen-GFP fusion protein were allowed to lactate. The prominent green fluorescence around osteocyte lacunae and within the bone matrix in virgin mice was absent in lactating mice but reappeared with 1 week recovery after force weaning. Whereas the absence of GFP-collagen in the osteocyte perilacunar matrix with lactation may be due to proteolytic degradation of collagen, this is an unlikely explanation for the absence of fluorescence throughout the surrounding bone matrix. Using a cell lysate containing GFP, decreasing pH quenched GFP fluorescence which was partially recovered at pH>6, but not at pH<5. Therefore, recovery of GFP in the bone matrix of α 2(I)-collagen-GFP mice post-lactation suggests a reduction in pH of no more than 6 during lactation. These

data provide evidence that osteocytes may have the capacity to lower pH in their local environment, thereby affecting activation of proteases and removal of mineral.

Disclosures: Katharina Jähn, None.

FR0124

FGF23 Suppresses Chondrocyte Proliferation and Maturation in the Presence of Soluble Alpha-klotho both in vitro and in vivo. Masanobu Kawai¹, Saori Kinoshita², Yasuhisa Ohata³, Kazuaki Miyagawa⁴, Miwa Yamazaki¹, Keiichi Ozono⁵, Toshimi Michigami⁶. ¹Osaka Medical Center & Research Institute for Maternal & Child Health, Japan, ²Osaka Medical Center & Research Institute for Maternal & Child Health, Japan, ³Osaka University, Japan, ⁴Osaka Medical Center, Japan, ⁵Osaka University Graduate School of Medicine, Japan, ⁶Osaka Medical Center, Research Institute for Maternal & Child Health, Japan

Fibroblast growth factor-23 (FGF23) is well established to play a crucial role in the regulation of phosphate homeostasis. X-linked hypophosphatemic rickets (XLH) is one of the FGF23-related disorders characterized by the impaired mineralization and growth retardation. Similar to XLH, FGF23 levels are elevated in patients with chronic kidney disease (CKD) and one of the complications of childhood CKD is growth retardation. However, it remains unclear as to whether the elevated levels of FGF23 have any direct effects on chondrocyte biology with respect to the development of growth retardation. To answer this question, we performed *in vitro*, *ex vivo* and *in vivo* analyses to determine the effect of FGF23 on chondrocyte biology. *In vitro* studies revealed that FGF23 induced ERK phosphorylation and up-regulated *Egr1* expression in the presence of soluble alpha-klotho (sKL) both in ATDC5 cells and primary chondrocytes. *Ex vivo* organ culture of metatarsal rudiments showed that FGF23/sKL suppressed the linear growth of metatarsals in a dose dependent manner, which was antagonized by the co-incubation with neutralizing antibodies raised against FGF23. Calcium deposition detected by calcein labeling in the hypertrophic zone was impaired in metatarsals treated with FGF23/sKL, suggesting that chondrocyte maturation is impaired in FGF23/sKL-treated metatarsals. Histologically, the length of proliferating zone was diminished associated with decreased proliferation of chondrocytes. FGF23/sKL did not affect the expression of Sox9 and Col2a1, but significantly suppressed Indian hedgehog (Ihh) expression. Importantly, administration of Ihh protein partially rescued the suppressive effect of FGF23/sKL on metatarsal growth. *In vivo*, three-consecutive days of intraperitoneal administration of sKL in *Hyp* mice (P7) caused a decrease in the length of proliferating zone associated with a decline of proliferation of chondrocytes, but did not alter circulating phosphate levels. In adenine-induced CKD models, the length of proliferating zone was decreased in association with elevated serum FGF23 levels despite of the comparable circulating phosphate levels compared to controls. These lines of evidence suggest that FGF23 may have a direct influence on chondrocyte biology such that it suppresses proliferation and maturation of chondrocytes in the presence of sKL and blockade of FGF23 signaling could have a therapeutic potential to improve linear growth in CKD and XLH patients.

Disclosures: Masanobu Kawai, None.

FR0125

Persistent Hyperparathyroidism Is a Major Risk Factor for Fractures in the Five Years after Renal Transplantation. Rose-marie Javier¹, Peggy Perrin², Sophie Caillard², Laura Braun², Françoise Heibel², Bruno Moulin³. ¹University Hospital, France, ²Nephrology-Transplantation Department, France, ³Nephrology-Transplantation Department, Strasbourg, France

Persistent hyperparathyroidism (HPT) contributes to bone loss after renal transplantation (RT) but its impact on fracture in the early course of RT is not documented. This longitudinal study was designed to evaluate persistent HPT and its association with mineral disorders and fractures in the five years after RT.

Methods. 152 consecutive patients undergoing RT at our center between August 2004 and April 2006 were included. Bone and metabolism biochemical parameters were determined at RT, at 3, 12 and 60 months after RT (D0, M3, M12, M60). Patients characteristics, treatments and symptomatic fractures were recorded.

Results. 143 patients were analysed (age 47 ± 12 years, 59% male, 89% deceased donor, 18% RT range >1, 12% diabetic nephropathy, 37 ± 42 dialysis months, 79% haemodialysis, 17% peritoneal dialysis). Pretransplant osteopenia (BMD T-score < -1 to -2.5 at hip and/or at spine) concerned 44% of patients and osteoporosis (T-score < -2.5) 23%. At D0, intact parathormon serum concentration (PTH) was 447 ± 395 pg/mL. Incidences of persistent HPT (PTH > 130 pg/mL) at M3 and M60 were respectively 49 and 34 %, of hypercalcemia (Ca > 10.4 mg/dL) 13 and 8% and of hypophosphatemia (Ph < 2.5 mg/dL) 22 and 20 %. At M60, 12% of patients with GFR > 60 ml/min had PTH > 130 ng/L.

Recipients with PTH > 130 ng/L at M3 had decreased survival (7 vs 0, p=0.03), higher BMI, bone turnover markers (bAP, crosslaps) and calcemia and lower phosphatemia, 25OHD and GFR.

During the five post transplant years, 22 patients (15.4%) presented 30 fractures (spine:10, foot:6, forearm:6, leg:4, rib:2, hand:1, hip:1); 24 fractures were spontaneous. Mean time to first fracture was 15.9 ± 15.7 months. Six patients presented several

fractures. Fractures were significantly associated with: M3 and M12 PTH>130 pg/mL, M3 and M12 hypercalcemia, M3 hypophosphatemia, M3 albuminemia<40 g/dL and a trend for female gender and pretransplant osteopenia. Fractures were not associated with 25OHD at D0, M3 and M12 bAP, diabetes, age, M3 GFR. By ROC curve analysis, we showed that cut-off of M3 PTH of 130 pg/mL predicted fractures occurrence with a sensibility of 82% and a specificity of 58%.

Conclusion: This first longitudinal study demonstrates that persistent HPT is an important risk factor for fractures after RT. A better control of hyperparathyroidism before and after kidney transplantation should be beneficial, particularly in patients with pretransplant bone disease.

Disclosures: Rose-marie Javier, None.

FR0129

Rapid Decrease in Plasma Calcium Concentration by Treatment with ONO-5334, a Cathepsin K Inhibitor, in the Rabbit Hypercalcemia Model Induced by PTHrP. Yasuo Ochi¹, Hiroyuki Yamada², Yasutomo Nakanishi¹, Satoshi Nishikawa¹, Yasuaki Hashimoto¹, Hiroshi Mori¹, Masafumi Sugitani¹, Yutaka Shichino¹, Kazuhito Kawabata¹. ¹Ono Pharmaceutical Co., Ltd., Japan, ²ONO PHARMA UK LTD., United Kingdom

Malignancy-associated hypercalcemia is mainly caused by enhanced bone resorption associated with over-production of the parathyroid hormone-related protein (PTHrP) by tumor. ONO-5334 is a small molecule and an orally-active inhibitor of cathepsin K, which plays an important role in osteoclast-mediated bone resorption. In this study, we evaluated the effect of ONO-5334 on plasma calcium concentration (Ca) in the rabbit hypercalcemia model induced by PTHrP.

Thirty micrograms/day of PTHrP (human 1-34) or vehicle-1 (2% L-cysteine solution) was subcutaneously infused via an ALZET osmotic pump (Model 2ML1) on the back of New Zealand White rabbits (female, 11 weeks of age). On the next day, rabbits infused PTHrP were assigned to one of the following 3 groups (4-5 animals/group): PTHrP-control treated with vehicle-2 (0.5% methylcellulose solution), ONO-5334 3 or 30 mg/kg, based on plasma Ca concentration. ONO-5334 or vehicle-2 was orally administered once daily from the day following PTHrP infusion for 3 days. In separate experiments, alendronate (0.17 or 0.85 mg/kg) or zoledronic acid (0.06, 0.2 or 0.6 mg/kg) was administered intravenously in a single dose on the day following PTHrP infusion. Blood was collected over time until 4 days after beginning the PTHrP infusion, and plasma free Ca concentration was measured.

Plasma Ca concentration, at 24 hours after osmotic pump implantation, significantly increased by 4.3 mg/dL in the PTHrP-control group ($p<0.01$ vs vehicle-1-infused group), and this elevation was sustained during the study period. ONO-5334 at 3 and 30 mg/kg dose-dependently decreased plasma Ca concentration from 3 hours after first dosing and this effect was maintained by repeated dose (2.0 - 3.3 mg/dL reduction in 30 mg/kg group, $p<0.05$ vs PTHrP-control). Significant decreases in plasma Ca concentration were observed with alendronate at 0.85 mg/kg and zoledronic acid at all doses from 54 hours ($p<0.05$ vs PTHrP-control) and 24 hours ($p<0.01$ vs PTHrP-control) after dosing, respectively. The maximum reduction in Ca concentration appeared to be comparable to that of ONO-5334.

These results suggest that ONO-5334 may decrease plasma Ca concentrations much earlier than bisphosphonates in hypercalcemia patients. Rapid onset of the effect of ONO-5334 is considered to be due to direct inhibition of cathepsin K, while, for bisphosphonates, their accumulation in bone is necessary to inhibit bone resorption.

Disclosures: Yasuo Ochi, None.

FR0130

Genome Wide DNA Methylation Array in Genetic Hypercalciuric Stone-forming (GHS) Rats Reveals that Vitamin D Receptor (VDR) Regulates Crystallin Zeta (CryZ) Gene Expression through DNA Methylation. Hongwei Wang¹, Baisheng Fu¹, Jinhua wang¹, David Bushinsky², Murray Favus¹. ¹University of Chicago, Chicago, USA, ²University of Rochester, USA

Hypercalciuria is an important contributing factor in the formation of calcium oxalate kidney stones in idiopathic hypercalciuria (IH). Genetic Hypercalciuric Stone-Forming (GHS) rats are an excellent model for studies of human IH, as both form calcium-containing nephrolithiasis and have hypercalciuria and normal serum calcium. In GHS rats, hypercalciuria arises from increased intestinal Ca absorption and bone resorption, and decreased renal tubule Ca reabsorption due to elevated VDR in Ca-transporting tissues. In the present study, we investigated the role epigenetic regulation of renal Ca transport in the hypercalciuria of GHS rats. Genome wide DNA methylation array and gene microarray performed on kidneys from GHS and SD rats identified 132 gene promoter regions with hyper- or hypo- methylation in GHS rats and about 600 genes that are either enhanced or decreased. After combining the two arrays, five genes were hyper- or hypo-methylated in the GHS rats with either lower or higher gene expression respectively. In proximal and distal tubules, BSC1 transport function requires stabilization by CryZ. Loss of CryZ interrupts BSC1 mediated transport and alters pH-induced changes in ion transport including Ca. ? In GHS rats, CryZ expression is lower and the promoter region is hypermethylated. In vitro and in vivo 1,25-dihydroxyvitamin D₃ (1,25(OH)₂D₃) downregulated CryZ gene expression through binding to the same specific promoter regions. Immunocytochemistry

staining performed show VDR is mainly located the proximal and distal tubules with higher expression in GHS rats. CryZ is extensively expressed in cortex, medulla and medullary papillae. Conclusion: VDR suppresses CryZ gene expression through specific sites of hyper-methylation in GHS rat kidney. Loss of CryZ may destabilize the BSC1 transporter and thereby contribute to the hypercalciuria

Disclosures: Hongwei Wang, None.

FR0131

Increased Sost Expression in Hyp-mouse Bone: A Primary Factor Underlying Abnormal Mineralization and Osteomalacia. Baozhi Yuan¹, Stephen Bowman¹, Ying Liu², Robert Blank¹, Min Liu³, Hua Zhu Ke³, Jian Feng², Marc Drezner¹. ¹University of Wisconsin, USA, ²Texas A&M Health Science Center, USA, ³Amgen Inc., USA

A loss of function *PHEX* mutation in patients with X-linked hypophosphatemia (XLH) and in *hyp*-mice underlies the disease phenotype. Thus, targeted *PheX* deletion in osteocytes (*DMPI-Cre-PheX^{Alox/ly}*-mice) results in the *HYP* biochemical phenotype. However, Table 1 shows that *DMPI-Cre-PheX^{Alox/ly}*-mice not only manifest a mild osteomalacia compared to *hyp*-mice, but upon Pi loading restore normal bone histology, while osteomalacia persists in mutant mice. The disparate mineralization suggests osteomalacia in *hyp*-mice is due to a *PHEX* dependent variable, other than hypophosphatemia. Subsequent studies revealed bone *Sost* mRNA is increased in *hyp*-mice compared to wild type mice (11.9 ± 4.6 vs 1.1 ± 0.2 relative expression; $p<0.001$), but not in *DMPI-Cre-PheX^{Alox/ly}*-mice (1.1 ± 0.9). To determine if the suppressive effects of *Sost* mRNA/Sclerostin on mineralization contribute to the bone phenotype in *hyp*-mice, we crossed mutant and *Sost* knockout mice (*Sost^{-/-}*). The offspring *hyp^{Sost^{-/-}}*-mice had decreased serum Pi (4.61 ± 0.67 vs 10.3 ± 1.3 mg/dl; $p<0.01$) like *hyp*-mice (5.18 ± 0.14 mg/dl). The decrement is due to serum FGF23 in *hyp*- (1637 ± 781 pg/ml) and *hyp^{Sost^{-/-}}*-mice (1317 ± 522 pg/ml), which is significantly increased ($p<0.01$) above that in wild type mice (81 ± 21 pg/ml). Subsequently, we examined the effects of diminished *Sost* mRNA on bone in mice treated with a high Pi diet to eliminate any effects of hypophosphatemia. Studies in Table 2 indicate that bone from *hyp^{Sost^{-/-}}*-mice displays increased ($p<0.05$) cortical bone volume (BV/TV), but the increment fails to normalize this variable. However, the bone mineral apposition rate (MAR) increases ($p<0.01$) to a normal level. In accord, bone sections from *hyp^{Sost^{-/-}}*-mice have reduced ($p<0.01$) osteoid volume (OV), but the unmineralized matrix remains greater ($p<0.01$) than in wild type mice, reflecting inordinate stimulation of matrix formation compared to MAR. Our data demonstrate that decreased *Sost* expression normalizes the bone MAR in *hyp*-mice. However, while a reduction of *Sost* mRNA to normal in *DMPI-Cre-PheX^{Alox/ly}*-mice increases matrix formation commensurately with the MAR, rescuing the bone phenotype, an inordinate decreased *Sost* expression in *hyp^{Sost^{-/-}}*-mice excessively enhances matrix formation, resulting in increased osteoid. These observations indicate that osteomalacia in *hyp*-mice results from the cumulative effects of increased *Sost* expression and hypophosphatemia.

| Table 1 | Normal Diet | | | Phosphate Loaded Diet | | |
|-----------|-------------|------------------|----------------------|-----------------------|------------------|----------------------|
| | wt mice | <i>hyp</i> -mice | <i>DMPI-Cre-PheX</i> | wt mice | <i>hyp</i> -mice | <i>DMPI-Cre-PheX</i> |
| OV (%) | 2.7±0.3 | 38±3.4 | 14±1.7 | 2.4±0.6 | 27.2±3.5 | 3.8±0.8 |
| MAR (µ/d) | 3.0±0.4 | 0.5±0.2 | 1.5±0.3 | 3.1±0.4 | 1.4±0.16 | 2.9±0.6 |

Table 1

| Table 2 | Phosphate Loaded Diet | | |
|-----------|-----------------------|------------------|---|
| | wt mice | <i>hyp</i> -mice | <i>hyp^{Sost^{-/-}}</i> |
| BV/TV | 0.99±0.02 | 0.92±0.01 | 0.96±0.01 |
| MAR (µ/d) | 4.3±0.3 | 1.6±0.3 | 3.8±x.xx |
| OV (%) | 4.4±0.3 | 22.9±0.6 | 18.9±1.9 |

Table 2

Disclosures: Baozhi Yuan, None.

This study received funding from: Amgen

FR0132

The Effect of Antenatal Vitamin D Supplementation on Early Neonatal Calcium Homeostasis. Jennifer Harrington¹, Abdullah Al Mahmud², Rubhana Raqib², Abdullah Baqui³, Daniel Roth¹. ¹The Hospital for Sick Children, Department of Pediatrics, University of Toronto, Canada, ²ICDDR B, Bangladesh, ³The John Hopkins Bloomberg School of Public Health, USA

Antenatal vitamin D supplementation may modulate fetal and neonatal calcium homeostasis. However, the effects of high-dose maternal vitamin D supplementation on early neonatal calcium handling are not well-described. A randomized, double-blinded, placebo-controlled prenatal vitamin D trial in Bangladesh provided an opportunity to study the relationship between antenatal vitamin D status and fetal-neonatal calcium homeostasis.

Objective: In this sub-analysis we aimed to determine the effect of antenatal 3rd-trimester high-dose vitamin D supplementation on early neonatal calcium handling.

Methods: 160 women from Dhaka, Bangladesh were randomized to receive either a weekly dose of 35,000IU of oral vitamin D₃ or placebo from 26 weeks gestation. Blood and urine at time of delivery, cord blood and infant blood and urine from day 3 and 5 of life were collected. For safety monitoring, infants with calcium levels

<1.9mmol/L or >2.82mmol/L or urine calcium:creatinine ratios >2mmol/mmol had further clinical assessment, blood work and renal ultrasound.

Results: Analyses included 132 cord and maternal delivery specimen pairs as well as 74 infants. Vitamin D supplementation significantly increased cord 25(OH)D versus placebo (102.8(±28.6) vs 39.0(±18.7) nmol/L, $p<0.0001$). Maternal and cord 25(OH)D levels strongly correlated ($r=0.87$, $p<0.001$). Total serum calcium was higher in cord blood with supplementation (2.7(±0.1) vs 2.6(±0.2) mmol/L, $p=0.04$). Although hypocalcemia was not observed in either group, the infants whose mothers received vitamin D supplementation had a significant attenuation in the calcium nadir at day 3 (change in calcium from cord to day 3 -0.10(±0.17) vs -0.22(±0.18) mmol/L). Significant associations with change in calcium at day 3 included higher cord 25(OH)D ($r=0.4$, $p=0.01$) and lower cord calcium ($r=-0.57$, $p<0.001$). On multiple regression, the significant predictor for day 3 calcium level was cord 25(OH)D ($p=0.01$, $R^2=0.15$).

6 infants in both the supplemented and placebo group had evidence of transient asymptomatic hypercalcemia which spontaneously resolved, with no ultrasound evidence of nephrocalcinosis.

Conclusions: Antenatal high-dose vitamin D supplementation attenuated the early postnatal calcium nadir. While reassuring that supplementation did not result in higher rates of hypercalcemia, the clinical benefits of the observed effects on neonatal calcium handling need further exploration.

Disclosures: Jennifer Harrington, None.

This study received funding from: The Hospital for Sick Children and the Thrasher Research Fund

FR0133

Vitamin D2 and D3 Replacement Effectiveness in Patients with Chronic Liver Disease. Dorota Krajewski, Julia (Julianna) Barsony*. Georgetown University Hospital, USA

Patients with chronic liver disease (CLD) have high incidence of vitamin D deficiency and osteoporotic fractures, but vitamin D treatment guidelines have not been established in this population. We have collected data from medical records to determine the D2 and D3 doses required to normalize serum 25OHD levels (above 32 ng/ml) in vitamin D deficient patients with chronic liver disease. We selected CLD patients responding to D2 (CLD-D2, n=53) or D3 treatments (CLD-D3, n=45) and controls (C) without liver disease responding to D2 (C-D2, n=53) or D3 (C-D3, n=45) treatments. To select controls, CLD patients were matched for age, race, gender, body mass index (BMI) and baseline serum 25OHD levels. Exclusion criteria included renal insufficiency, pregnancy, hypercalcemia, recent (past year) or concurrent use of medications known to alter calcium metabolism (i.e. steroids, calcitriol, anti-seizure medications), and history of organ transplant or bariatric surgery. Liver disease severity, defined by MELD scores and serum albumin levels, were comparable between the D2- and D3-treated groups. Subgroup analysis included liver cirrhosis (LC), primary biliary cirrhosis (PBC) and non-alcoholic fatty liver disease (FLD). In responders, treatment effectiveness was characterized by calculating the daily D2 and D3 doses required to raise serum 25OHD concentration by 1 ng/ml. The results showed that effective D2 and D3 doses were both doubled in CLD compared to C ($p<0.001$). In patients with LC, effective doses correlated positively with MELD scores (D3: $r=0.705$, $p<0.005$; D2: $r=0.476$, $p<0.05$) and negatively with serum albumin (D3: $r=0.468$, $p<0.05$; D2: $r=0.464$, $p<0.05$). Effective doses of D2 were higher than D3 doses ($p<0.01$) in every group. Obesity (BMI>35) in controls increased the effective D3 doses by 42±15% ($p<0.05$) and D2 by 33±15% (NS), but FLD increased it even more: effective D3 doses increased by 135±43% and D2 doses by 83±17%. Many CLD patients (LC, n=33; PBC, n=6; FLD, n=60) were nonresponsive to weekly 50,000 IU D2 given for more than 3 months. Our findings demonstrate that patients with chronic liver disease require significantly higher vitamin D replacement doses than controls, proportionally to the severity of the liver disease, and suggest that CLD patients should be preferentially treated with D3 rather than D2.

Disclosures: Julia (Julianna) Barsony, None.

FR0136

Familial Hypocalcemic Hypercalcemia Type 2 (FHH2) Is Caused by a Mutation of G Protein Alpha 11 ($G\alpha_{11}$). Fadil Hannan^{1*}, M. Andrew Nesbit¹, Sarah Howles¹, Nigel Rust², Maurine Hobbs³, Hunter Heath⁴, Rajesh Thakker¹. ¹Nuffield Department of Clinical Medicine, University of Oxford, United Kingdom, ²Sir William Dunn School of Pathology, University of Oxford, United Kingdom, ³Core Research Facilities, University of Utah, USA, ⁴Indiana University School of Medicine, USA

The calcium-sensing receptor (CaSR), which has a central role in extracellular calcium homeostasis, is a G protein-coupled receptor that acts via the G proteins, G_q and G_{11} , that effect intracellular signalling and alterations in intracellular calcium ($[Ca^{2+}]_i$). CaSR mutations, resulting in a loss-of-function, are associated with familial hypocalcemic hypercalcemia type 1 (FHH1). However, such mutations cause FHH in ~65% of patients and two other loci for FHH have been reported on chromosome 19p and 19q13.3, and these are termed FHH2 and FHH3, respectively. The gene encoding the alpha subunit of G_{11} ($G\alpha_{11}$), referred to as *GNA11*, is located on 19p and we hypothesized that a mutation in $G\alpha_{11}$, which is abundantly expressed in the

parathyroids may cause FHH2. DNA sequence analysis of the 7 exons and 12 intron-exon boundaries of *GNA11* in a patient from the FHH2 kindred revealed a heterozygous 3-bp (CAT) deletion that led to an in-frame deletion of Ile199 (199delIle). This mutation was associated with a gain of an *XmnI* restriction enzyme site, which was used to demonstrate that the 199delIle mutation co-segregated with FHH in the kindred (10 affected and 11 unaffected family members) and not to be present in 120 alleles from 60 unrelated normocalcemic individuals, thereby indicating that it was not a common polymorphism. To investigate the functional consequences of this mutation, wild-type and mutant 199delIle $G\alpha_{11}$ proteins were expressed by transient transfection in HEK293 cells stably transfected with CaSR and assessed by measuring their $[Ca^{2+}]_i$ responses to changes in extracellular calcium ($[Ca^{2+}]_o$). The mutant 199delIle $G\alpha_{11}$ protein resulted in a rightward shift of the $[Ca^{2+}]_i$ dose-response curve with significantly higher $EC_{50} = 2.70mM$ (95% confidence interval (CI) = 2.64-2.77mM) compared to wild-type $G\alpha_{11}$ $EC_{50} = 2.33mM$ (95% CI = 2.29-2.38mM) ($p<0.0001$), consistent with this being a loss-of-function mutation. An examination of the crystal structure of $G\alpha_q$, which has 90% amino acid identity to $G\alpha_{11}$, revealed that Ile199 is located within a 13 amino acid peptide that links two functionally important domains that undergo conformational changes during activation of the $G\alpha_{11}$ protein. Thus, our study has identified the genetic abnormality causing FHH2, and this will further increase our understanding of extracellular calcium homeostasis, and the structure-function relationships of G protein alpha subunits.

Disclosures: Fadil Hannan, None.

FR0144

Modifications of Bone Material Properties Early Detected after One Year of Menopause in Women. Delphine Farlay^{1*}, Yohann Bala², Susan Bare³, Joan Lappe⁴, Robert Recker⁴, Georges Boivin⁵. ¹INSERM, UMR1033; Université De Lyon, France, ²University of Melbourne, Dept. of Medicine, Australia, ³Osteoporosis Research Center, Creighton University, USA, ⁴Creighton University Osteoporosis Research Center, USA, ⁵INSERM, UMR1033 ; Université De Lyon, France

At menopause, bone remodelling increases and becomes unbalanced leading to bone loss and fragility. However, whether modifications in bone tissue material properties (mineral and organic components) occur across menopause is still unclear. Twenty pairs of iliac bone biopsies, taken from healthy women before and after menopause [12 months after the final menses (mean interval between the two biopsies 60 ± 24 months)], were used. Impaired micromechanical properties have been previously observed at the tissue level (microhardness) in those bone biopsies. The present study thus aims to assess sub-tissue bone mineral and organic matrix composition. Sections two μm -thick were cut and analyzed by infrared microspectroscopy with a Perkin-Elmer microscope in transmission mode. Ten areas of bone matrix in each cortex (150 μm x150 μm) and 20 areas (150x50 μm) in trabecular bone were scanned, in order to observe a large area of the bone biopsy sections. After curve-fitting of infrared spectra, 5 variables were measured: mineral maturity, crystallinity index, mineralization index, carbonation and collagen maturity. Statistical analysis was performed using non parametric Wilcoxon tests. Among the 5 variables, only the mineralization index was significantly decreased after menopause in paired biopsies in trabecular bone ($p=0.0239$), and tended to decrease in cortical bone ($p=0.09$). No significant changes were observed in crystallinity index, mineral maturity, carbonation or collagen maturity, either in trabecular or in cortical bone while the activation frequency had almost doubled. This suggests that, early after menopause, trabecular bone is first affected by modification in material properties, especially by a decrease in the proportionate amounts of mineral and organic components. However, this does not yet affect the bone crystal characteristics (as crystal size, perfection, mineral and collagen maturities). The impact of the duration of menopause on the bone mineral characteristics will be further evaluated on bone biopsies taken after 14 years.

1 Recker et al 2004, J Bone Miner Res 19: 1628

2 Bala et al 2010, J Bone Miner Res 25 (Suppl 1): 1141

Disclosures: Delphine Farlay, None.

FR0145

Aortic Calcification, Arterial Stiffness, and Vascular Wnt mRNAs Are Increased In Atherosclerotic LDLR-/- Mice Lacking Smooth Muscle Cell LRP6. Jian Su Shao^{1*}, Abraham Behrmann², Karen Krehma², Su-Li Cheng¹, Linda Halstead³, Attila Kovacs², Bart Williams⁴, Dwight Towler³. ¹Washington University in St. Louis School of Medicine, USA, ²Washington University, USA, ³Washington University in St. Louis, USA, ⁴Van Andel Research Institute, USA

When male LDLR-null mice are fed high fat diabetogenic diets (HFD), osteogenic transcription factors of the Runx, Msx and Sox gene families are upregulated in the aorta with progressive calcification. Msx2 enhances mesenchymal cell mineralization in part via paracrine Wnt signals, ligands for LRP5 and LRP6. Previous studies by others indicate that global LRP5 deficiency reduces valve calcification. We wished to understand the vascular smooth muscle cell (VSMC)-autonomous roles of the related Wnt receptor, LRP6, in diabetic arteriosclerosis. Therefore, we generated and characterized SM22-Cre:LRP6(fl/fl);LDLR-/- (LRP6-CKO) mice as a model for

study, using the SM22 promoter to direct Cre expression in VSMCs. LRP6-CKO and LRP6(fl/fl);LDLR-/- control mice developed equivalent obesity (34% of body weight as fat following HFD for 3 months). No differences in bone or lean body mass – or in fasting hyperglycemia, hypertriglyceridemia, and hypercholesterolemia – were observed. However, LRP6-CKO mice exhibited increased aortic calcium accumulation (2.15 +/-0.15 ug calcium / mg aortic wet weight vs. 1.50 +/-0.12 ug/mg; p = 0.002, n =14-15 per group). Moreover, by histomorphometry, aortic valve leaflet area (1.39-fold; p = 0.03) and wall thickness (48.4 +/- 3.0 vs 41.3+/-0.4 microns; p = 0.04) were increased in LRP6-CKO mice vs. controls. Echocardiography demonstrated increased aortic pulse wave velocity in LRP6-CKO (3.40+/- 0.3 m/s) vs. controls (2.96 +/- 0.14 m/s; p = 0.035, n = 5 per genotype) , confirming the predicted increase in vascular stiffness arising from calcification and wall thickening. To begin to address mechanism, we evaluated the aortic gene expression. LRP6-CKO mice exhibited reduced aortic LRP6, with concomitant reductions in markers of VSMC differentiation (SM22, Myh11,myocardin). Aortic Sox2, a signature of proliferating multipotent mesenchymal progenitors, was increased 18-fold, but no changes were noted in aortic LRP5, Runx2, Sox9, Sox5, Sox6 or Msx2. However, aortic Wnt7b (92-fold), Wnt4 (44-fold), Wnt10a (10-fold), and Wnt3a (170-fold; all p < 0.002) were markedly and selectively upregulated in LRP6-CKO mice, mimicking the expression profile with aortic calcification arising from Mx2 transgenesis. Thus, VSMC LRP6 modulates aortic calcification in LDLR-/- mice, serving to restrain arteriosclerosis with HFD-induced disease. Secondary increases in vascular Wnt ligands with VSMC LRP6 deficiency may drive procalcific responses, presumably via LRP5.

Disclosures: Jian Su Shao, None.

This study received funding from: National Institutes of Health

FR0146

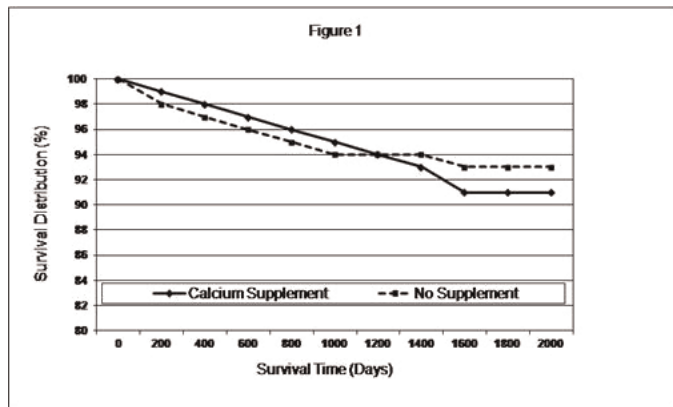
Calcium Supplementation and Cardiovascular Events. Vaishali Patel¹, James Vacek², Rajib Bhattacharya³. ¹The University of Kansas Medical Center, USA, ²KUMC, USA, ³KU Medical Center, USA

Purpose Recent reports have suggested an association between calcium supplementation and increased rate of cardiovascular events. The goal of this retrospective study was to examine the association of calcium supplements with cardiovascular disease states and survival in a large cardiovascular practice.

Methods Data was collected for 5.7 years (1/1/2004 to 10/8/2009) from the electronic medical record of Mid America Cardiology, a large cardiovascular practice at the University of Kansas Medical Center. Patients > age 50 were included in our analysis. Diagnoses were derived from the patient problem list in the patients' electronic medical record based on International Classification of Diseases, 9th Revision (ICD-9) codes. Death was determined from the Social Security Death Index.

Results The data set included 8060 subjects categorized as calcium supplement user vs. non-users. On multivariate logistic regression analysis, calcium supplementation was not an independent predictor of all-cause death. When adjusted for clinical variables and medications, calcium supplementation was not independently associated with the diagnosis of coronary artery disease. There were no significant survival differences for patients on calcium supplements vs. those who were not by product-limit survival estimate. Hazard function analysis indicated that calcium supplementation was not an independent predictor of survival when adjusted for clinical variables. (p=NS).

Conclusion Our data showed no association between calcium supplementation and coronary artery disease as well as overall survival in a large retrospective cohort of patients greater than 50 with high rates of significant cardiovascular risk factors.



Survival figure

Table 2
Proportional Hazards Analysis for Death

| Variable | Hazard Ratio | 95% Hazard Ratio Confidence Limits | P |
|--------------------|--------------|------------------------------------|--------|
| Female Gender | 0.442 | 0.344 - 0.567 | <.0001 |
| Calcium Supplement | 0.762 | 0.587 - 0.989 | .0412 |
| Age | 1.023 | 1.012 - 1.035 | <.0001 |
| Cardiomyopathy | 2.455 | 1.777 - 3.392 | <.0001 |

analysis

Table 2
Logistic regression for death as dependent variable

| Predictor | OR | CI | P |
|-------------------------|-------|-------------|--------|
| Calcium Supplement | 0.862 | 0.650-1.117 | NS |
| Coronary artery disease | 2.071 | 1.545-2.777 | <.0001 |
| Age | 1.025 | 1.013-1.036 | <.0001 |
| Diabetes mellitus | 1.523 | 1.148-2.020 | .004 |
| Cardiomyopathy | 2.821 | 1.982-4.014 | <.0001 |

variables

Table 1

| Variables | On calcium supplements | Not on calcium supplements | p Value |
|---|------------------------|----------------------------|---------|
| N (%) | 2878 (36%) | 5182 (64%) | |
| Age (years) | 67 +/- 11 | 64 +/- 10 | <.0001 |
| Women | 2402 (83%) | 3329 (64%) | <.0001 |
| Body Mass Index (kg/m ²) | 29 +/- 7 | 30 +/- 8 | <.0001 |
| Coronary artery disease (> 70% stenosis ≥1 coronary artery) | 475 (17%) | 599 (12%) | <.0001 |
| Cardiomyopathy | 159 (6%) | 176 (3%) | <.0001 |
| Hypertension | 1428 (50%) | 1767 (34%) | <.0001 |
| Diabetes Mellitus | 505 (18%) | 924 (18%) | NS |
| Valvular heart Disease | 290 (10%) | 305 (6%) | <.0001 |
| Atrial Fibrillation | 265 (9%) | 303 (6%) | <.0001 |
| Ejection Fraction (%) | 57 +/- 10 | 57 +/- 11 | NS |
| Aspirin Use | 1473 (51%) | 1469 (28%) | <.0001 |
| Angiotensin-converting enzyme inhibitor use | 1084 (38%) | 1300 (25%) | <.0001 |
| Statin use | 1582 (55%) | 1698 (33%) | <.0001 |
| Creatinine (mg/dl) | 1.19 +/- 1.01 | 1.70 +/- 3.54 | <.0001 |
| Total Cholesterol (mg/dl) | 170 +/- 45 | 166 +/- 48 | .02 |
| High-density lipoprotein cholesterol (mg/dl) | 52 +/- 18 | 46 +/- 15 | <.0001 |
| Low density lipoprotein cholesterol (mg/dl) | 95 +/- 36 | 94 +/- 39 | NS |
| Vitamin D level | 28 +/- 13 | 23 +/- 14 | <.0001 |

demographics

Disclosures: Vaishali Patel, None.

FR0148

Tissue-nonspecific Alkaline Phosphatase Upregulation in Vascular Smooth Muscle Cells Is Sufficient to Cause Medial Vascular Calcification. Campbell Sheen*¹, Wei Wang², Manisha Yadav³, Jose Luis Millan⁴. ¹Sanford Burnham Medical Research Institute, USA, ²Sanford Burnham Medical Research Institute, USA, ³Burnham Institute for Medical Research, USA, ⁴Sanford-Burnham Medical Research Institute, USA

Medial vascular calcification (MVC) is a pathological condition common to variety of diseases, including chronic kidney disease, diabetes, obesity, generalised arterial calcification of infancy, arterial calcification due to deficiency of CD73, Kawasaki Disease and Keutel Syndrome. While the genetic and physiological causes of MVC differ between these diseases, several of them share the common feature of tissue-nonspecific alkaline phosphatase (TNAP) upregulation. To investigate whether TNAP expression is sufficient to cause MVC, we developed a conditional knockin mouse model that overexpresses human TNAP under the control of the vascular smooth muscle cell specific *Tagln* promoter. As early as seven days of age, male mice showed strong alkaline phosphatase activity in the aorta and, by 14 days, distinct aortic calcification was visible by X-ray. Further X-rays and micro-computed tomography at 30 days showed extensive calcification of the aorta and renal, carotid and coronary arteries. Heart weight measurements showed cardiac hypertrophy at 14 days that became progressively worse at 30 days. Survival curves showed that most male mice died between 25 and 60 days of age. Serum alkaline phosphatase activity was approximately five and 22 times normal at days 14 and 30, respectively. No change in serum phosphate was detected at either age, and while serum calcium was normal at 14 days, it was slightly lower than controls at 30 days of age. No difference in serum pyrophosphate levels were detected at either age, implying that it is the local rather than systemic levels of pyrophosphate that are important for inhibition of calcification. Gene expression analysis showed upregulation of classical markers of MVC (*Bmp2* and *Opn*) and osteoblast markers, (*Runx2*, *Alpl*, *Phospho1*, *Pit-1*, *Enpp1*, *Ank* and *Col1a1*) and a decrease in expression of the smooth muscle marker *Tagln*. This data indicates that altering the local Pi/PPi balance is sufficient to initiate the transdifferentiation of smooth muscle cells, a hallmark of MVC. The expression levels of a variety of genes related to phosphate and pyrophosphate metabolism and/or transport were also altered. Overall, the data from this mouse model indicate that TNAP overexpression is sufficient to cause calcification and suggest that TNAP may be a critical mediator in a variety of ectopic calcification disorders.

Disclosures: Campbell Sheen, None.

FR0151

Genotype-Phenotype Correlations and Pharmacogenetic Studies in 140 Swedish Families with Osteogenesis Imperfecta. Katarina Lindahl*¹, Carl-Johan Rubin², Eva Åström³, Barbro Malmgren⁴, Andreas Kindmark⁵, Osten Ljunggren⁵. ¹Endocrinology, Sweden, ²Uppsala University, Sweden, ³Department of Woman & Child Health, Division of Pediatric Neurology, Karolinska Institutet, Sweden, ⁴Karolinska Institutet, Department of Dental Medicine, Division of Pediatric Dentistry, POB 4064 SE-14104, Sweden, ⁵Uppsala University Hospital, Sweden

Objective: Osteogenesis imperfecta (OI) is a rare heterogeneous disease of connective tissue leading to varying degrees of bone fragility. The worst form (type II) is peri-natal lethal whereas the mildest form (type I) is compatible with a normal life span and may even be diagnosed as osteoporosis in adulthood. Over 1000 mutations causing OI have been described in the genes encoding collagen type I. As *COL1A1* and *COL1A2* are large genes, there are still many codon positions where no mutations have been reported and only a fraction of theoretically possible glycine substitutions have been described. In this study the spectrum of mutations causing OI in Sweden will be investigated and genotype-phenotype correlations as well as pharmacogenetics will be studied.

Method: All patients with OI cared for at the Uppsala Osteoporosis Unit (Uppsala University Hospital) or Astrid Lindgren Childrens Hospital (Karolinska Institutet, Stockholm) were offered to enter the study. 140 families with OI accepted participation; 77 type I, 34 type IV, 20 type III, 5 without previous diagnosis and 4 with unclear OI type. Extensive clinical data is currently being collected on enrolled patients.

Exons and flanking intron sequences of *COL1A1* and *COL1A2* are being sequenced in these families.

Results: So far 133/140 families have been completely analyzed and in 27 no mutation was found. A total of 120 mutations have been detected, of which 104 are of a typical OI-type. In *COL1A1* 73 mutations were found and in *COL1A2* 31 mutations were noted. In 7 families 2 mutations were present, but only one of these was a typical OI-causing mutation. To date 16 amino acid changing mutations that were not of a typical OI-causing type have been noted, and the majority of these have an unclear significance.

Calculations of delta BMD Z-score response to bisphosphonate treatment did not show a difference in treatment response between groups with different types of OI or between patients with OI type I due to a qualitative vs. quantitative collagen defect.

Conclusion: The spectrum of mutations causing OI described in this Swedish cohort is of the expected type, with the exception of the amino acid changing mutations. It is notable that in seven patients two separate mutations were identified.

Preliminary data does not support a mutation dependent response to bisphosphonate treatment.

Disclosures: Katarina Lindahl, None.

FR0157

Osteoblast-targeted Expression of an Activating Mutation of Gsa in Mice Mimics van Buchem's Disease/Sclerosteosis rather than Fibrous Dysplasia (FD), and does not alter the Hematopoietic Microenvironment/Niche. Stefano Michienzi*¹, Isabella Saggio², Stefania Cerosimo¹, Cristina Remoli¹, Rossella Costa¹, Graham R Davis³, Alberto Di Consiglio¹, Emanuela Spica¹, Benedetto Sacchetti¹, Ana Cumano⁴, Pamela Gehron Robey⁵, Kenn Holmbeck⁶, Alan Boyde³, Mara Riminucci¹, Paolo Bianco⁷. ¹University La Sapienza, Italy, ²Sapienza University of Rome, Italy, ³Queen Mary University of London, United Kingdom, ⁴Pasteur Institute, France, ⁵NIH/NIDCR, USA, ⁶NIDCR, USA, ⁷Universita La Sapienza, Italy

To understand the role of Gsα mutations in FD, we generated lines of transgenic mice expressing GsαR201C constitutively or targeted to specific cell types. Osteoblast-targeted expression of GsαR201C (2.3COL1A1-GsαR201C) resulted in an overt high bone mass phenotype, without marrow changes and distinct from FD. Comparison of the phenotype of COL1A1-GsαR201C mice (excess Gsα signaling driven by overactivity of Gsα) and COL1A1-caPPR mice (excess Gsα signaling driven by constitutive activity of PTHR1) demonstrated that COL1A1-GsαR201C mice, but not COL1A1-caPPR, developed a deforming cortical bone excess (in addition to excess trabecular bone found in both models), suggesting Gsα-mediated effects in cortical bone not dependent on PTH. Excessive cortical bone developed by expansion of periosteal/cortical osteoblasts (Ox+/ALP+) between 2wk and 3mo of age; bone remodeling was increased, but resorption was not, relative to bone surfaces. Osteoprogenitors did not express the transgene, which was turned on in culture concurrent with mineralization and osteoblastic markers. Compared to WT, SOST expression in mature osteoblastic cells was potentially downregulated in COL1A1-GsαR201C mice, resulting in markedly enhanced Wnt signaling (increased Lef1/Axin 2 mRNAs), explaining the high bone mass phenotype. Thus, mice with osteoblast-targeted GsαR201C phenocopy human diseases caused by loss of function SOST mutations (van Buchem's disease/Sclerosteosis) rather than FD. Red and yellow marrow (femur vs. tail vertebrae, respectively) were normally distributed in COL1A1-GsαR201C mice. After 6 mo, remodeling of the massive cortices established intracortical marrow spaces populated by red or yellow marrow at respective sites. No marrow fibrosis was noted and adipocyte development was normal. Although Gsα signaling in osteoblasts is thought to affect the HSC niche and lymphopoiesis, the HSC fraction (Lin-/Sca-1+/c-kit+, LSK) was unchanged in frequency and absolute numbers. LSK/CD34- cells were also similar to WT. Numbers of CLP (Lin-/IL-7Ra+/Sca-1+/-/c-kit+/-), Pro-B (CD19+/CD43+/IgM-), Pre-B (CD19+/IgM-/CD43-) and B (CD19+/IgM+) cells were not significantly different from WT. We conclude that activating mutations of Gsα in osteoblasts do not impact on hematopoiesis, consistent with lack of expression of the transgene in bone marrow osteoprogenitors, and with preservation of a normal marrow in spite of an excess of osteoblasts and bone.

Disclosures: Stefano Michienzi, None.

FR0160

The Prostaglandin Transporter Encoding Gene *SLCO2A1* Is Mutated in Primary Hypertrophic Osteoarthropathy and Isolated Digital Clubbing. Jirko Kühnisch*¹, Wenke Seifert², Beyhan Tüysüz Tüysüz³, Christof Specker⁴, Ad Brouwers⁵, Denise Horn¹. ¹Institute of Medical & Human Genetics, Charité - University Medicine of Berlin, Germany, ²Institute for Vegetative Anatomy, Charité - University Medicine of Berlin, Germany, ³Cerrahpasa Medical Faculty, Department of Pediatric Genetics, Istanbul University, Turkey, ⁴Dept. of Rheumatology & Clinical Immunology, Centre for Internal Medicine, Kliniken Essen Süd, Germany, ⁵Department of Internal Medicine, Gelderse Vallei Hospital, Ede, Netherlands

Prostaglandin metabolism is a critical determinant of bone and cartilage function. Although the functional interaction of prostaglandin E2 (PGE2) within these tissues has been well explored its association with human monogenic disorders is still incomplete. So far, homozygous mutations within the *HPGD* gene encoding the PGE2 catabolizing enzyme 15-hydroxy-prostaglandin dehydrogenase have been identified causing primary hypertrophic osteoarthropathy (PHO). In this study we performed a mutational screen of PHO patients and individuals with isolated digital clubbing. We systematically analyzed genes encoding key proteins of the entire PGE2 pathway namely: *PTGS1*, *PTGS2*, *PTGES*, *PTGES2*, *PTGES3*, *PTGER1*, *PTGER2*, *PTGER3*, *PTGER4*, *SLCO2A1*, *SLCO3A1*, *SLCO4A1*, *PTGRI*, and *PTGR2*. We identified in three unrelated families mutations within the gene solute carrier organic anion transporter family 2A1 (*SLCO2A1*) (MIM ID *601460, chromosome 3q21). The *SLCO2A1* transcript comprises 14 exons and encodes for the 643 amino acid polytopic transmembrane protein prostaglandin transporter (PGT, *SLCO2A1*). PGT localizes to the plasma membrane and is required for internalization of extracellular

PGE2. Within the *SLCO2A1* gene we found a homozygous insertion c.830_831insT, resulting in a premature stopcodon at p.Phe276fsX18; a homozygous missense mutation c.1670T>C introducing an amino acid substitution p.Phe557Ser and a heterozygous nonsense mutation c.754C>T resulting in p.Arg252X. Homozygous mutations in PGT (Phe276fsX18 and Phe557Ser) were found to result in a PHO phenotype comprising clubbing of fingers and toes, periostosis, diaphyseal cortex expansion, swollen joints, hyperhidrosis, and seborrhic hyperplasia. In contrast, the heterozygous mutation p.Arg252X causes isolated digital clubbing, demonstrating a threshold effect by which absence of one *SLCO2A1* allele leads to isolated digital clubbing. Functionally, both stop mutations Phe276fsX18 and Arg252X result in an early translational stop which highly likely result in a loss-of-function of PGT. In summary, we identified mutations within the *SLCO2A1* gene as further molecular cause of isolated digital clubbing and PHO. Our findings suggest that apart from PGE2 degradation by 15-hydroxy-prostaglandin dehydrogenase internalization of PGE2 at the plasma membrane is critical for normal bone, joint and skin function.

Disclosures: *Jirko Kühnisch, None.*

FR0169

Bone Healing Enhancement through Inhibition of Sclerostin by Monoclonal Antibody in Rat Osteotomy Model. Pui Kit Suen^{*1}, Yixin HE², Dick Ho Kiu Chow¹, Le Huang¹, Zhong Liu¹, Chi Wai Man¹, Lizhen Zheng³, Tao Tang¹, Chaoyang Li⁴, Hua Zhu Ke⁴, Ge Zhang⁵, Ling Qin⁶. ¹The Chinese University of Hong Kong, Hong Kong, ²The Cuinese University of Hong Kong, Hong Kong, ³Prince of Wales Hospital, Hong Kong, ⁴Amgen Inc., USA, ⁵Price of Wales Hospital, Hong Kong, ⁶Chinese University of Hong Kong, Hong Kong

Introduction: Sclerostin is a negative regulator of bone formation. Previous studies demonstrated treatment with a sclerostin monoclonal antibody (Scl-Ab) significantly increased bone formation, bone mass and strength in rat closed fracture model. The objective of this study is to investigate the effects of systemic administration of Scl-Ab on fracture repair in rat femur open fracture, a more difficult-to-heal model.

Method: Ninety 6-month-old male SD rats were randomly divided into Scl-Ab group and vehicle group after a transverse osteotomy performed at the mid-shaft of right femur. One day post-surgery, rats were treated with Scl-Ab III (s.c. injection, 25 mg/kg, 2 times per week) or vehicle for 3, 6 or 9 weeks. Femora were collected and subjected to the following analyses: micro-CT, micro-CT-based angiography, four-point mechanical testing and histology. Two-way ANOVA with Bonferroni posttest was used to analyze the data.

Results: Scl-Ab treatment groups had significantly higher callus volume fraction and bone mineral density (BMD) in all 3, 6 and 9 weeks post-fracture compared to their vehicle groups (P<0.01; Figure 1). Micro-CT based angiography demonstrated increased callus vascularization in Scl-Ab group at week 3 and at week 6 (Figure 2). Hematoxylin and eosin (H&E) staining and safranin O staining showed more bony tissue in calluses at week 3 in Scl-Ab group. Four-point bending test showed significantly higher ultimate load in Scl-Ab group than vehicle group at weeks 6 (+98%, P<0.01) and 9 (+45%, P<0.05) post fracture. In addition, ultimate load at week 6 of Scl-Ab group was at the similar level as seen at week 9 of the vehicle group, indicating the increased healing by Scl-Ab in this model. Stiffness and energy to failure were also tended higher in Scl-Ab group (Figure 3).

Conclusions: This study demonstrated that Scl-Ab enhanced bone healing in rat osteotomy model, with increased bone formation, bone mass and bone strength. We observed a trend of increasing callus vascularization in the Scl-Ab group at week 3 and at week 6, based on small sample size, implying Scl-Ab induced coupling of osteogenesis and angiogenesis. Collectively, our results supported that the systemic administration of Scl-Ab enhanced open fracture healing.

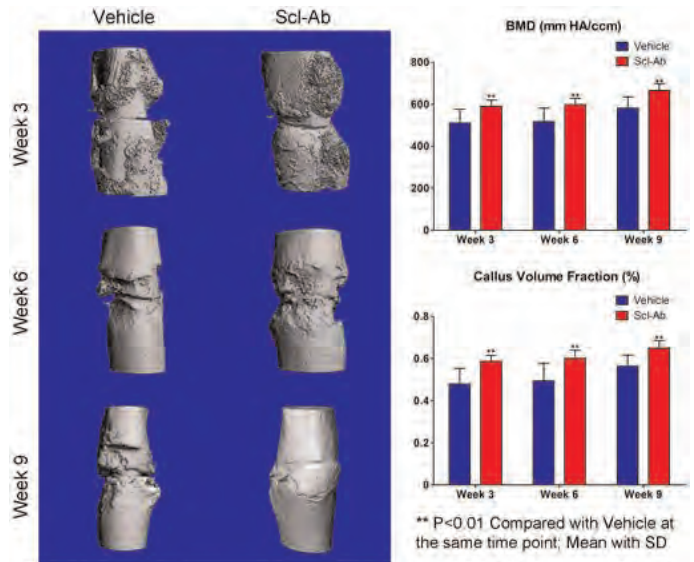


Figure 1. Micro-CT 3D images and quantitative analysis of BMD and callus volume fraction

Figure 1

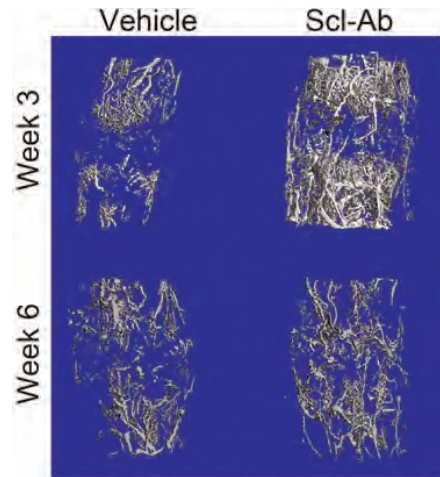


Figure 2. Micro-CT based angiography 3D images

Figure 2

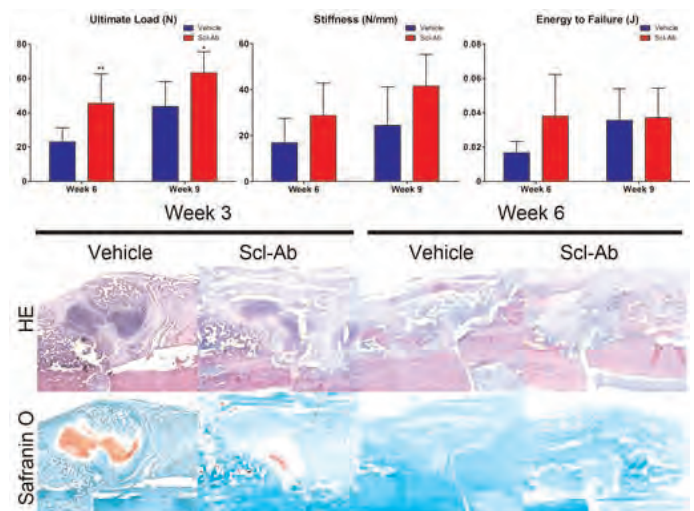


Figure 3. Mechanical Test at 6 weeks and 9 weeks post-fracture by 4-point-bending test and representative H&E and Safranin O staining of calluses at 3 weeks and 6 weeks post-fracture. ** P<0.01, *P<0.05, Compare with Vehicle at the same time point; Mean with SD

Figure 3

Disclosures: *Pui Kit Suen, None.*

This study received funding from: *Amgen Inc*

FR0170

Duffy Antigen Receptor for Chemokines (Darc) Regulates Chondrogenesis and Bone Formation During Fracture Repair. Charles Rundle*, Subburaman Mohan, Bouchra Edderkaoui, Jerry L. Pettis Memorial VA Medical Center, USA

There is now considerable experimental data to suggest that hematopoietic bone marrow cells (HBMCs) derived from both local and circulating sources participate in the healing of bone fractures. Recently, chemokine and chemokine receptor functions in the recruitment of HBMCs to the fracture site have received considerable attention. The Duffy antigen receptor for chemokines (*Darc*) is a non-classical chemokine receptor that does not signal but rather acts as a scavenger of chemokines. Based on the findings that *Darc* is expressed by inflammatory and endothelial cells and our findings that *Darc* is a negative regulator of peak bone density in mice, we hypothesized that the disruption of *Darc* would increase the bioavailability of chemokines to attract HBMCs and promote fracture healing. To test this hypothesis, we compared fracture healing in mice with a targeted disruption of *Darc* with the corresponding wild-type (WT) littermate control mice. Micro-CT examination of the fracture calluses revealed significant increases in the cross-sectional area (43%, $P=0.04$, $n=5$) and cancellous bone (30%, $P=0.03$) at the fracture site in *Darc*-knockout (KO) mice as compared to WT mice at 21 days post fracture. We then performed histomorphometric analysis of the fracture callus cartilage in *Darc*-KO mice, and determined that the area of callus cartilage at 7 days post-fracture was significantly augmented (50%, $n=5$, $P=0.02$, $n=5$) in *Darc*-KO mice as compared to WT mice. However, the ratio of cartilage area to total callus area was not different between the two strains of mice. These data suggest an early cartilage formation and more rapid conversion of cartilage to bone in the *Darc*-KO mice compared to WT mice. We determined that mRNA levels of collagen X were increased by 50% in the fracture calluses of *Darc*-KO mice as compared to WT mice at 7 days post-fracture ($P=0.05$, $n=5-6$). Taken together, these observations suggest that *Darc* gene deficiency promoted chondrocyte differentiation and cartilage maturation in the fracture callus, which subsequently resulted in increased bone formation. Based on the present findings, we conclude that the disruption of *Darc* gene expression increased the bioavailability of chemokines that then recruited HBMCs to the fracture site; these HBMCs promoted the early maturation of callus cartilage and its remodeling to bony callus.

Disclosures: Charles Rundle, None.

FR0171

Hyperactive WNT Signaling Causes Preaxial Polydactyly in *Sclerostin Sostdc1* Double Knockouts. Nicole Collette*¹, Cristal Yee², Deepa Muruges¹, Richard Harland³, Gabriela Loots⁴. ¹Lawrence Livermore National Laboratory, USA, ²University of California, Merced, USA, ³University of California, Berkeley, USA, ⁴Lawrence Livermore National Laboratory, UC Merced, USA

Sclerostin (*Sost*) is secreted by osteocytes and negatively regulates bone formation. This gene is linked to two rare skeletal dysplasias characterized by generalized increased bone density, sclerosteosis and van Buchem disease. *Sostdc1* (aka *Sostl*, *USAG-1*, *Wise*, *ectodin*) is a paralog of *Sost*, and loss of *Sostdc1* has been shown to cause supernumerary incisor development and fused molars. Both proteins function as extracellular antagonists of both BMP and WNT signaling *in vitro* and *in vivo*. However, these tissues in which gene expression was first characterized are not the sole locations of *Sost* and *Sostdc1* activity. We have shown that human *SOST* overexpression in mice causes dosage-dependent loss of distal posterior skeletal elements, resulting from altered anterior-posterior patterning of the limb bud and preferential antagonism of *Lrp5* WNT co-receptor. *Sostdc1* was shown by others to similarly affect FGF and SHH signaling in the developing tooth bud, and it binds to *Lrp4* receptors to inhibit WNT signaling, suggesting that *Sost* and *Sostdc1* may antagonize similar pathways *in vivo*. *Sost* and *Sostdc1* are expressed in complementary yet non-overlapping domains; their combined expression covers most of the ectoderm and mesenchyme of the developing limb bud prior to cartilage condensation. *Sost* knockout mice occasionally display limb defects consistent with the frequency of soft-tissue syndactyly, nail dysplasia, and radial deviation that occurs in sclerosteosis patients, while *Sostdc1* knockouts show no limb defects. Here we show that *Sost*; *Sostdc1* double mutant mice exhibit preaxial polydactyly, a common limb-associated birth defect characterized by extra digit(s) in the anterior autopod, which is often caused by ectopic sonic hedgehog (*Shh*) expression. Through a combination of skeletal stains, LacZ reporter analysis, and *in situ* hybridization, we show that *Sost* and *Sostdc1* function upstream of *Shh* to restrict *Shh* expression in the posterior limb. We find perturbed BMP signaling in the patterning limb as well. The *Sost* and *Sostdc1* null alleles release *Lrp4/5/6* receptor inhibition in the ectoderm and mesenchyme, and hyperactive BMP and WNT signaling ectopically activate *Shh* in the anterior limb bud to transform the morphology of the first digit.

This work performed under the auspices of the U.S. Department of Energy by Lawrence Livermore National Laboratory under Contract DE-AC52-07NA27344.

Disclosures: Nicole Collette, None.

FR0172

Novel Link Between CSF-1 and Lung Cancer Bone Metastasis. Sherry Abboud Werner*¹, Fermin Tio², Thomas Prihoda³, Diane Horn³, Jaclyn Hung³. ¹University of Texas Health Science Center at San Antonio, USA, ²South Texas Veterans Health Care System, USA, ³University of Texas Health Science Center, USA

CSF-1 is essential for osteoclastogenesis that, in turn, mediates osteolysis in metastatic tumors to bone. Patients with lung cancer show increased CSF-1 in serum and CSF-1 is a predictor of progression and poor survival. Adenocarcinomas metastasize rapidly and 60% of patients suffer from bone metastasis. Lung cancer stem cells sustain tumor growth and potentiate metastasis. Work in lung cancer metastasis has been hampered by the lack of animal models. The purpose of this study was to determine the role of CSF-1 in lung cancer bone metastasis and whether inhibition of CSF-1 ameliorates the disease. Human lung adenocarcinoma A549 cells were examined *in vitro* for CSF-1/CSF-1R. To establish a model of bone metastasis, A549-luc cells were injected intracardiac in SCID mice and a time course for onset and progression of metastasis was determined using x-ray, *in vivo* bioluminescent imaging and histomorphometry. To determine the effect of CSF-1 knockdown in A549 cells on bone metastasis, cells were stably transfected with a retroviral vector containing either short-hairpin CSF-1 (KD) or empty vector (CT). Mice injected with CT or KD cells were examined for incidence of tumor, tumor burden and tumor size. Results showed that A549 cells express CSF-1 and CSF-1R; CSF-1 also increased A549 proliferation and invasion, whereas soluble CSF-1R inhibited invasion. Mice injected with A549-luc cells showed osteolytic bone lesions in hindlimbs and spine after 3.5 wks, and lesions increased over 5 wks. Tumors recapitulated adenocarcinoma morphology, expressed CSF-1 and showed numerous osteoclasts along tumor/bone interface, trabecular and cortical bone loss. Analyses of KD cells showed decreased CSF-1 protein levels, reduced colony formation in agar assay and decreased fraction of stem-like cells. In mice injected with KD cells, the incidence of tumor metastasis was similar to controls, although fewer mice with KD cells had metastasis in both hindlimbs. KD tumors showed reduced CSF-1 expression, Ki-67+ cells and osteoclasts. Importantly, there was a low incidence of large tumors >0.1 cm in mice with KD cells compared to mice with CT cells (10% vs 62.5%). This study established for the first time a lung osteolytic bone metastasis model that mimics human disease and suggests that CSF-1 is a key determinant of cancer stem cell survival and tumor growth. Results may lead to novel strategies to inhibit CSF-1 in lung cancer and improve therapeutic management of bone metastasis.

Disclosures: Sherry Abboud Werner, None.

FR0174

Transgenic Overexpression of Ephrin B1 in Osteoblasts Promotes a Skeletal Anabolic Response to Mechanical Loading in Mice. Weirong Xing*¹, Chandrasekhar Kesavan², Shaohong Cheng³, Subburaman Mohan². ¹Musculoskeletal Disease Center, Jerry L. Pettis Memorial Veteran's Admin., USA, ²Jerry L. Pettis Memorial VA Medical Center, USA, ³VA Loma Linda Health Care Systems, USA

Mutation of the ephrin B1 gene in humans caused craniofrontonasal syndrome while deletion of the ephrin B1 gene in mice resulted in perinatal lethality and skull defects. Our recent findings that mice with conditional knockout (KO) of ephrin B1 in type I collagen producing osteoblasts resulted in severe calvarial defects, decreased bone size and BMD suggested that locally produced ephrin B1 is an important determinant of bone formation. To test the hypothesis that ephrin B1 overexpression promotes acquisition of peak bone mass, we generated transgenic (Tg) mice overexpressing ephrin B1 in bone cells and evaluated the consequence of ephrin B1 overexpression on the skeletal phenotype. The expression of transgene was controlled by the rat collagen 1A1 promoter/chicken beta-actin/rabbit beta-globin chimeric intron. One of the Tg mouse lines has been confirmed to express 6-fold greater levels of full-length ephrin B1 protein in calvarial osteoblasts and bone marrow stromal cells. The functionality and specificity of overexpressed ephrin B1 was confirmed by rescue of a calvarial defect in ephrin B1 conditional KO mice by crossing ephrin B1 Tg with conditional KO lines. Neither body weight nor body length was significantly different in ephrin B1 Tg vs WT mice at 8 wks of age. Surprisingly, total body BMD as measured by PIXImus was not different in the Tg mice although vertebra BMD was increased by 20% in the Tg mice at 8 wks of age. Since mechanical strain increased the expression of ephrin B receptor 2 (EphB2) in bone cells, and ephrin B1 binding to EphB2 can induce bidirectional signaling, we next evaluated if overexpression of ephrin B1 influenced the skeletal anabolic response to mechanical loading (ML). The right tibiae of Tg and WT mice (10 wks of age (N=8/group)) were loaded at 9N, 2Hz for 36 cycles per day for 2 weeks, and the left tibiae of the same mice were used as unloaded controls. A ML-induced increase in both total volume (72% vs 52%, $P<0.05$) as well as relative cortical bone volume to total volume (11% vs 5%, $P<0.01$) were significantly greater in the Tg mice compared to WT mice. In conclusion, our findings that overexpression of ephrin B1 in bone cells promotes a skeletal anabolic response to ML, thus suggesting that manipulation of ephrin B1 actions in bone may provide a means to sensitize the skeleton to mechanical strain to stimulate new bone formation.

Disclosures: Weirong Xing, None.

FR0177

Alternative Splicing, Polyadenylation, and MicroRNAs Targeting Insulin-like Growth Factor-1 in Osteoblasts. Spenser Smith¹, Catherine Kessler¹, Clifford Rosen², Anne Delany^{*1}. ¹University of Connecticut Health Center, USA, ²Maine Medical Center, USA

Insulin-like growth factor I (IGF-1) plays a critical role in skeletal growth. It is an autocrine, paracrine and endocrine regulator of bone mass. Animals and humans with deficits in IGF-1 display decreased peak bone mass and impaired linear growth. We sought to determine the post-transcriptional mechanisms regulating IGF-1 in murine osteoblasts.

IGF-1 splice variants give rise to a common mature IGF-1 peptide, but different E peptides (Ea or Eb) are encoded by inclusion or exclusion of exon 5. We identified expression of exon 4+6 (Ea) and exon 4+5+6 (Eb, mechano-growth factor) splice products, and found that the relative abundance of these variants did not change during osteoblastic differentiation *in vitro*. The IGF-1 3' untranslated region (UTR) encoded by exon 6 contains 2 alternative polyadenylation sites. Use of the proximal site gives rise to a short 3' UTR of ~195 bases, whereas use of the distal site results in a ~6300 base long UTR. The absolute level of IGF-1 mRNA did not change during osteoblastic differentiation. However, use of the distal polyadenylation site was significantly increased during this process; and the abundance of the long IGF-1 RNA increased in concert with that of osteocalcin mRNA. The long IGF-1 RNA isoform is ~50% less stable than the short isoform.

miRNAs are small non-coding RNAs that inhibit gene expression by decreasing transcript stability and/or translation. Using Luciferase-IGF-1 3' UTR reporter constructs and specific miRNA inhibitors, we found that the IGF-1 3' UTR is targeted by miR-29 and miR-365. There are 2 potential binding sites each for miR-29 and miR-365 in the long IGF-1 isoform, whereas the short isoform contains only 1 potential binding site for miR-365. Transfection of osteoblasts with inhibitors for these miRNAs caused a significant increase in IGF-1 protein levels. Further, the expression of miR-29 and miR-365 increased during osteoblast differentiation *in vitro*. The increase in miRNAs that negatively regulate IGF-1, in combination with the increased proportion of IGF-1 mRNAs containing the long 3' UTR, likely results in the down regulation of IGF-1 protein during osteoblastic differentiation. An understanding of how miR-29 and miR-365 regulate osteoblasts and the mechanisms regulating polyadenylation site usage will provide important information about the control of osteoblastic differentiation. This will allow for the identification of novel therapeutic targets.

Disclosures: Anne Delany, None.

FR0178

Conditional Deletion of IGF-I Receptor by Osterix Driven Cre-Recombinase Impairs Both Cartilage and Bone Formation. Yongmei Wang^{*1}, Hashem ElAlieh², Cha K Fong², Daniel Bikle³. ¹Endocrine Unit, University of California, San Francisco/VA Medical Center, USA, ²Endocrine Unit University of California, San Francisco/San Francisco VA Medical Center, USA, ³Endocrine Research Unit, Division of Endocrinology UCSF & VAMC, USA

Osterix (Ox) is expressed in osteoprogenitors, prehypertrophic chondrocytes (PHCs) and perichondrium in the skeleton, and is a key transcription factor for osteoblast (OB) differentiation. Ox driven cre-recombinase is widely used in manipulating genes in osteoprogenitors, but whether it also affects genes in other Ox-expressing skeletal cells remains uncertain. To investigate the role of IGF-I signaling in Ox-expressing cells in the skeleton, we generated IGF-I receptor (IGF-IR) knockout mice (^{Ox}IGF-IRKO) by crossing floxed-IGF-IR mice with mice carrying the Cre recombinase transgene controlled by a GFP labeled Ox promoter (^{Ox}GFP-cre, gift from Dr. Andrew McMahon), and monitored bone development and remodeling from 2 to 7 weeks. Compared with the control mice (floxed IGF-IR, no cre) from the same litters, the ^{Ox}IGF-IRKO mice showed significant growth retardation with smaller body size and shorter bones. At 2-7 weeks, as detected by GFP in the ^{Ox}IGF-IRKO mice, ^{Ox}GFP-cre was highly expressed in the PHCs and the inner layer of perichondral cells which give rise to trabecular OBs, but was sparsely expressed in the OBs lining the trabecular bone surface. At 3 and 7 weeks, immunohistochemistry (IHC) confirmed a marked reduction of IGF-IR expression in the cells of the prehypertrophic zone and perichondrium, but not in OBs lining the trabecular bone surface of the ^{Ox}IGF-IRKO mice. From 2 to 7 weeks, histology revealed a delayed formation of the secondary ossification center (epiphysis), irregular morphology of the growth plate (expanded hypertrophic zone) and less trabecular bone in the tibia and femur of the ^{Ox}IGF-IRKO mice when compared with the controls. Cell proliferation as assessed by the number of PCNA positive cells was reduced by 40% and 45%, respectively, in the perichondrium and in the proliferation zone of the growth plate of the ^{Ox}IGF-IRKO mice. The expression of type II collagen was not altered significantly in the chondrocytes (by IHC), whereas the mRNA level of alkaline phosphatase of the trabecular bone was decreased by 46% (by qPCR) in the ^{Ox}IGF-IRKO mice compared with the controls. Our data indicate that during postnatal bone development and remodeling, IGF-I signaling in the Ox-expressing PHC is required for chondrocyte growth and secondary ossification of the epiphysis, whereas IGF-I signaling in the Ox-expressing inner layer perichondral cells is critical for OB differentiation and maintenance of bone mass.

Disclosures: Yongmei Wang, None.

FR0179

E-selectin ligand 1 Regulates Bone Homeostasis via Modulating TGF-β Bioavailability in Bone Microenvironment. Tao Yang^{*1}, Ingo Grafe², Yangjin Bae¹, Shan Chen¹, Ming-ming Jiang¹, Terry Bertin¹, Yuqing Chen¹, Brendan Lee³. ¹Baylor College of Medicine, USA, ²Department of Molecular & Human Genetics, Baylor College of Medicine, USA, ³Baylor College of Medicine & Howard Hughes Medical Institute, USA

TGF-β is one of the most abundant growth factors in the skeletal system and plays a crucial role in skeletal homeostasis. Before TGF-β ligand can access its receptors, it must become bioavailable, a process composed of multiple steps e.g. TGF-β expression, maturation, secretion and activation from latency, etc. Although the importance of TGF-β maturation has been revealed in blood pressure homeostasis as well as in cartilage development, to date, how TGF-β maturation is involved in bone remodeling has not been fully appreciated. We previously reported that E-selectin ligand-1 (ESL-1), a Golgi apparatus localized protein, acts as a negative regulator of TGF-β bioavailability by attenuating maturation of proTGF-β during cartilage homeostasis. Our current study shows that *Esl-1*^{-/-} mice exhibit a severe and early-onset osteoporosis, suggesting that ESL-1 also plays a critical role in bone homeostasis. By bone histomorphometry, we found that OC.S/BS is markedly increased in the *Esl-1*^{-/-} bone, while the OB.S/BS is unchanged. *In vitro*, *Esl-1*^{-/-} osteoblasts show a delayed late differentiation, and an increased potency in promoting osteoclastogenesis of co-cultured osteoclast progenitors. However, the osteoclast progenitors from *Esl-1*^{-/-} mice show no difference in osteoclastogenesis under the treatment of mCSF and RANKL, implicating that ESL-1 primarily acts in osteoblasts to regulate osteoblast-osteoclast coupling in a non-cell-autonomous fashion. In addition, the molecular phenotyping of *Esl-1*^{-/-} calvarial tissue exhibits an elevated mature TGF-β/proTGF-β ratio, with a dramatic increase in TGF-β downstream targets (PAI-1, PTHrP, CTGF, etc) as well as osteoclastogenesis stimulus (RANKL). Further *in vitro* co-culture experiments demonstrate that inhibitors of TGF-β or PTHrP can effectively attenuate the osteoclastogenesis of osteoclast progenitors co-cultured with *Esl-1*^{-/-} osteoblasts, suggesting that the TGF-β/PTHrP/RANKL axis is a major mechanism acting downstream of ESL-1 and responsible for the overactive bone resorption in the *Esl-1*^{-/-} mice. In summary, our study identified ESL-1 as an important regulator of bone remodeling, and that the modulation of TGF-β maturation is pivotal in the maintenance of a homeostatic bone microenvironment and for proper osteoblast-osteoclast coupling.

Disclosures: Tao Yang, None.

FR0186

Modulation of Osteoclast Formation by Cyclically-Strained Myotubes Is Mediated by IL-6. Petra Juffer^{*1}, Richard T. Jaspers², Jenneke Klein-Nulend³, Astrid D. Bakker¹. ¹Department of Oral Cell Biology, Academic Centre for Dentistry Amsterdam (ACTA), University of Amsterdam & VU University Amsterdam, Research Institute MOVE, Amsterdam, Netherlands, ²Research Institute MOVE, Faculty of Human Movement Sciences, VU University Amsterdam, Amsterdam, The Netherlands, Netherlands, ³ACTA-VU University Amsterdam Dept Oral Cell Biology (Rm # 11N-63), The Netherlands

Skeletal muscle is an endocrine organ that produces numerous growth factors and cytokines, such as IL-6, in response to mechanical loading. In bone, these factors can affect osteoblastic bone formation, but it is unknown whether osteoclasts are also affected, and whether mechanical loading modulates the release of these factors by muscle cells. Therefore we aimed to investigate whether mechanically-loaded myotubes produce soluble factors that affect osteoclast formation, and whether IL-6 is one of these factors.

C2C12 myoblasts were seeded on laminin-coated Bioflex® 6-wells plates, and differentiated into C2C12 myotubes. C2C12 myotubes were mechanically stimulated for 1 h by applying an uni-axial cyclic strain (0-15% deformation, 1 Hz), or kept under static control conditions, and post-incubated without cyclic strain up to 24 h. Conditioned medium (CM) was collected directly after 1 h cyclic strain/static culture, and after 24 h post-cyclic strain/static culture. RNA was isolated directly after 1 h cyclic strain. IL-6 mRNA levels were measured by RT-PCR. Mouse bone marrow cells were cultured in the presence of M-CSF and RANKL, with/without myotube-CM, and with/without mouse IL-6 antibody (10 ng/mL). After 6 days of culture, osteoclast formation was quantified by counting tartrate-resistant acid phosphatase (TRAP) positive multinucleated (≥3 nuclei) cells.

CM harvested from C2C12 myotubes after 1 h static culture and 24 h post-static culture decreased the formation of TRAP⁺-multinucleated cells by 3.5-fold (1 h static) and 7.0-fold (24 h post-static) compared to non-CM. CM harvested from C2C12 myotubes after 1 h cyclic strain increased the formation of TRAP⁺-multinucleated cells by 1.7-fold compared to CM harvested after 1 h static culture. CM harvested from C2C12 myotubes after 24 h post-cyclic strain did not affect the formation of TRAP⁺-multinucleated cells. Cyclic strain increased IL-6 mRNA levels in C2C12 myotubes by 3.0-fold. Addition of IL-6 antibody to the myotube-CM nullified the effect of soluble factors produced by cyclically-strained myotubes on osteoclast formation.

Our data indicate that C2C12 myotubes secrete soluble factors that inhibit osteoclast formation, and that mechanical loading of C2C12 myotubes by cyclic strain stimulates osteoclast formation via IL-6. Since it is known that IL-6 plasma

concentrations increase substantially during muscular activity, our data suggest that muscle cells *in vivo* might affect osteoclasts via IL-6.

Disclosures: Petra Juffer, None.

FR0188

Muscle-derived Humoral Factor, Osteoglycin (OGN), Links Muscle to Bone. Ken-ichiro Tanaka*¹, Toshitsugu Sugimoto¹, Susumu Seino², Hiroshi Kajii³. ¹Shimane University School of Medicine, Japan, ²Kobe University Graduate School of Medicine, Japan, ³Kinki University Faculty of Medicine, Japan

Muscle mass is closely related to high bone mass and a decrease in fracture risk in postmenopausal women. These findings suggest that there are interactions between muscle tissues and bone metabolism. We therefore hypothesized that there might be some humoral bone anabolic factors that are produced from muscle tissues. Fibrodysplasia ossificans progressive (FOP) is a rare autosomal dominant disorder characterized by progressive heterotopic ossification in skeletal muscle. ALK2(R206H), the constitutive activating mutation of the BMP type 1 receptor is found in patients with the classic form of FOP. We performed comparative DNA microarray analysis between stable empty vector- and ALK2(R206H)-transfected mouse myoblastic C2C12 cells, since FOP and its molecular pathogenesis could be a clue to help identify some muscle-derived humoral bone anabolic factors. We hypothesized that the expression of muscle-derived bone anabolic factors might be suppressed by the conversion of muscle tissues into bone, because those factors could be predominantly expressed in muscle tissues, compared with their expressions in bone, and their systemic effects could be more important than their local effects in bone tissues. OGN was identified as one of 25 genes whose expressions were decreased <1/4 by ALK2(R206H) expression in these cells. Recombinant OGN as well as stable overexpression of OGN significantly enhanced the levels of alkaline phosphatase (ALP), type 1 collagen (Col1), β -catenin and osteocalcin (OCN) as well as mineralization in mouse osteoblastic cells (MC3T3-E1 and mouse primary osteoblasts). A reduction in endogenous OGN level by siRNA showed the opposite effects in these cells. On the other hand, OGN suppressed the levels of ALP and OCN mRNA induced by BMP-2 in C2C12 cells. OGN was detected in human serum or culture supernatant from mouse myoblasts and myotubes. Conditioned medium from OGN-overexpressed and OGN-suppressed myoblastic cells enhanced and decreased the levels of ALP and OCN in osteoblastic cells, respectively. Moreover, OGN enhanced the levels of phosphorylated ERK1/2, TGF- β -induced transcriptional activity and Col1 mRNA in MC3T3-E1 cells. ERK1/2 inhibitor antagonized the levels of Col1 mRNA enhanced by OGN, although an inhibitor of endogenous TGF- β did not affect it. These findings indicate that OGN enhances the levels of Col1 mRNA partly through ERK1/2 in osteoblasts. In conclusion, our present data suggest that OGN may be crucial factors produced by muscle-derived cells and secreted into blood that exhibits bone anabolic effects.

Disclosures: Ken-ichiro Tanaka, None.

FR0189

Physical Activity in Relation to Serum Sclerostin, Insulin-like Growth Factor-1 and Bone Turnover Markers in Healthy Young Men : A Cross-sectional and a Longitudinal Study. Mohammed-Salleh Ardawi*¹, Abdulrahman Al-Sibiany², Talal Bakhsh³, Mohammed Qari⁴. ¹Center of Excellence for Osteoporosis Research & Faculty of Medicine, Saudi Arabia, ²Center of Excellence for Osteoporosis Research & Department of General Surgery, Faculty of Medicine & KAU Hospital, King Abdulaziz University, Saudi Arabia, ³Center of Excellence for Osteoporosis Research, & Department of General Surgery, Faculty of Medicine & KAU Hospital, King Abdulaziz University, Saudi Arabia, ⁴Center of Excellence for Osteoporosis Research, and Department of Hematology, Faculty of Medicine, & KAU Hospital, King Abdulaziz University, Saudi Arabia

Background: There is no information on the interaction between sclerostin, insulin-like growth factor (IGF-1) and bone turnover markers (BTMs), in response to mechanical loading by physical activity (PA). The main objective of the present study was to study the relationships between serum sclerostin, serum IGF-1 (s-IGF-1) and BTMs and PA level in young men (age 23-34 years) and to discern how 8 weeks of PA training (PAT) affects the serum levels of sclerostin, IGF-1, and BTMs. This was a cross-sectional study with a sub-group followed longitudinally.

Subjects & Methods: A total of 816 randomly selected young men were cross-sectionally studied. Also, we followed 92 men longitudinally following the 8-week PAT (4 days/week) as compared with 88 controls. All men were medically examined and serum sclerostin, s-IGF-1, BTMs, and bone mineral density (BMD) were determined.

Results: Men with PA > 240 min per week showed significantly (vs sedentary controls) lower serum sclerostin (by 29.5 %, P<0.001) and higher s-IGF-1 (by 88.7%, P<0.001) levels, respectively. Bone formation markers were higher with increasing PA in men with PA > 240 min/week vs sedentary group. Serum sclerostin was lower (by 41.2%, P<0.0001) and s-IGF-1 rose (by 66.3%, P<0.0001) and s-OC, s-PINP, and

s-bone ALP rose by 23.5% (P<0.001), 18.6% (P<0.006) and 47.2% (P<0.001), respectively in response to 8-week PAT as compared with controls.

Conclusions: The present studies demonstrate that, in young men, even minor changes in PA are associated with clear effects on serum sclerostin, s-IGF-1 and BTMs and suggest that sclerostin could be a link between mechanical loading and disuse osteoporosis in humans.

Disclosures: Mohammed-Salleh Ardawi, None.

FR0191

The PPP6R3/LRP5 Locus Influences Lean Mass in Children of Different Ethnic Background and Highlights Pleiotropic Effects and Muscle-bone Interactions. Carolina Medina-Gomez*¹, Denise Hepppe², Karol Estrada³, Joyce Van Meurs³, Albert Hofman⁴, Yi-Hsiang Hsu⁵, David Karasik⁶, Vincent Jaddoe⁷, Maria Zillikens⁸, Andre Uitterlinden⁹, Fernando Rivadeneira³. ¹Erasmus Medical Center, The Netherlands, ²The Generation R Study Group, Erasmus Medical Center, Rotterdam, The Netherlands, Netherlands, ³Erasmus University Medical Center, The Netherlands, ⁴Department of Epidemiology, Erasmus Medical Center, Rotterdam, The Netherlands, Netherlands, ⁵Hebrew SeniorLife Institute for Aging Research & Harvard Medical School, USA, ⁶Hebrew SeniorLife, USA, ⁷The Generation R Study, Erasmus Medical Center, Rotterdam, The Netherlands, Netherlands, ⁸Erasmus Mc, The Netherlands, ⁹Rm Ee 575, Genetic Laboratory, The Netherlands

Aim: Lean and bone mass have considerably high phenotypic and genetic correlations with a shared heritability estimate ranging between 30-40% in adults. A genome-wide association study (GWAS) on total body lean mass and a bivariate GWAS on lean mass & BMD was run in a cohort of children to identify genes with pleiotropic effects on peak bone mass attainment and muscle mass. **Methods:** Subjects are part of the Generation R study, a multiethnic birth cohort in Rotterdam, The Netherlands; we included 4,096 children (mean age=6.2, SD=0.50 years) with total body DXA measurements (GE-Lunar iDXA) and genomewide genotyping (Illumina 660K). The univariate and bivariate GWAS were adjusted for age, sex, height, fat percent and 20 genomic principal components using (bivariate) PLINK. A P<5x10⁻⁸ was considered genome-wide significant (GWS). **Results:** Genomic inflation factors were close to unity indicating adequate correction for stratification. In the univariate analysis we identified a GWS association with lean mass ($\beta=0.13$, P=2.9x10⁻⁸) for a SNP mapping to 11q13.2, in the PPP6R3/LRP5 locus. The SNP explains 0.8% of the variation in lean mass and is nominally significantly associated with BMD ($\beta=0.10$, P=7.6x10⁻⁵) explaining 0.4% of BMD variation. The association with lean mass was reduced after additional correction for bone mineral content ($\beta=0.08$, P=0.001), explaining 0.2% of the phenotypic variance. In the bivariate GWAS this SNP was also associated at GWS level (P=4.8x10⁻⁸) showing positive correlations of the bivariate trait with both lean mass ($\rho=0.96$) and BMD ($\rho=0.68$). **Conclusion:** Genetic variation in the PPP6R3/LRP5 locus exerts pleiotropic effects on muscle mass and peak bone mass acquisition of children. Given the high linkage disequilibrium in the region it is difficult to establish from which gene the GWAS signal is arising. PPP6R3 is a 155 Kb gene with 23 exons of unknown function, expressed among other tissues in bone and muscle. LRP5 is ubiquitously expressed, member of the Wnt signaling pathway and shown to play a key role in skeletal homeostasis and mechanosensing. Replication in additional children cohorts is underway; while the same SNP has been found associated at genome significant level in a bivariate GWAS of bone strength and lean mass in two large consortia of adult individuals (ASBMR 2012). These pleiotropic effects on muscle mass and BMD observed in children are likely to be evident later in life.

Disclosures: Carolina Medina-Gomez, None.

FR0197

Bone Formation is Compromised by Disruption of Runx2-WW-domain Protein Interaction. Yang Lou*¹, Weibing Zhang², Marcio Beloti³, Dana Frederick⁴, Andre Van Wijnen⁴, Gary Stein⁴, Janet L. Stein⁴, Jane Lian⁴. ¹University of Massachusetts, USA, ²Univ of Massachusetts Medical School, USA, ³School of Dentistry of Ribeirao Preto, University of Sao Paulo, Brazil, ⁴University of Massachusetts Medical School, USA

The WW-domain protein (WWDP) family consists of members with one or more WW (Tryptophan-Tryptophan)-repeated motifs that are expressed in many tissues and act as co-regulatory partners of transcription factors through binding to PPxY motifs. Several WW-domain proteins, including WWP1, WWOX, YAP and TAZ, can bind to the transcription factor RUNX2 and either stimulate or suppress RUNX2 activity, dependent on the gene context, for control of skeletal development. Our earlier *in vitro* studies showed that mutation of Y433 to A433 (in the PPxY motif) in the essential NMTS domain of RUNX2 can totally or partially disrupt its interaction with these WW-domain proteins. To understand the *in vivo* significance of the cooperation of RUNX2 and WWDPs during skeletogenesis, we generated a mutant mouse model with a single amino acid substitution (Y433 to A433) integrated into the endogenous Runx2 locus. Homozygous Runx2^{Y433A/Y433A} mice exhibit developmental defects in calvaria and epiphysis of long bones at birth. The frontal calvarial sutures in

Runx2 mutant mice are not completely closed and the defect persists into adulthood. By histology the calvarial defects appear similar to RUNX2 deficient mouse models. Micro-CT bone density (BMD) and bone volume (BV) are decreased in frontal calvaria of *Runx2*^{Y433A/Y433A} mice that include the unmineralized suture area. No change in BV or BMD occurs in the parietal calvaria, suggesting commitment to osteogenesis is impaired, but mineralization is not compromised in *Runx2* mutant mice. *Ex vivo* cultures from calvaria or bone marrow of homozygous mice display delayed osteogenic differentiation at early stages. *Runx2*, *Osx*, *Col 1* and *Alk Phos* expression are reduced. Mineral deposition is moderately reduced in mutant mouse osteoblasts with delayed osteocalcin expression. Long bones of *Runx2*^{Y433A/Y433A} mice exhibit a striking disorganization of the growth plate at birth, and a thin diaphysis with weak *Alk Phos* staining on the periosteal surface. Molecular markers for chondrogenic and osteogenic differentiation are reduced. Together, the findings in calvaria and long bones indicate impairment of both intramembranous and endochondral bone formation from cell autonomous defects in the *Runx2*^{Y433A/Y433A}. We propose the mechanism for these defects is related to a critical interaction of *Runx2* with one or more positive and negative WW-domain proteins during osteogenesis.

Disclosures: Yang Lou, None.

FR0199

Characterization of the Skeletal Phenotype in Osteoactivin Transgenic Mice. Nagat Frara^{*1}, Fabiola Delcarpio-Cano¹, Robin Pixley¹, Roshanak Razmpour¹, Christina Mundy², Fouad Moussa³, Samir Abdelmagid³, Steven Popoff², Favez Safadi³. ¹Temple University, USA, ²Temple University School of Medicine, USA, ³Northeast Ohio Medical University, USA

Osteoactivin (OA), a transmembrane protein, has recently emerged as a vital glycoprotein for the differentiation and function of bone forming osteoblasts. OA expression has been shown to increase during osteoblast development with maximal expression during the final stages of differentiation. Recent studies showed that OA is also expressed by osteoclasts and plays a role in their differentiation and function. In this study, we used a transgenic mouse model over-expressing OA under the control of CMV promoter (OATg) to determine the mechanisms by which OA contributes to bone formation and remodeling *in vivo*. Western blot analysis showed a three-fold increase in OA expression in OATg compared to wild-type (WT) osteoblasts. Micro-CT analysis of femurs from 12 week-old OATg showed increased trabecular bone volume (BV/TV) in OATg mice compared to WT mice. Given that OA is also over-expressed in osteoclasts in OATg mice, we evaluated bone resorption by histomorphometry and ELISA. Serum RANK-L and CTX-1 levels were significantly decreased in OATg compared to WT mice indicative of defective osteoclast-mediated bone resorption in OATg mice. Histomorphometric analysis showed that osteoblast numbers are increased but that osteoclast numbers are dramatically reduced in OATg compared to WT mice. Next, we examined whether osteoblast differentiation is altered in OATg mice. Osteoblasts were derived from bone marrow mesenchymal stem cells of 8 week-old OATg and WT mice and from calvaria of newborn OATg and WT mice. Although proliferation was increased in OATg osteoblasts, differentiation was reduced in OATg osteoblast cultures associated with decreased alkaline phosphatase activity/staining as well as matrix mineralization compared to WT control cultures. Moreover, qPCR analysis showed that OA over-expression down-regulated mRNA expression of osteoblast markers in OATg osteoblasts compared to controls. Taken together, these data indicate that over-expression of OA *in vivo* increases bone mass by decreasing osteoclast-mediated bone resorption and enhancing osteoblast-mediated bone formation. However, OA over-expression has a negative effect on osteoblast differentiation and maturation *ex vivo*, an effect that may be dose-dependent. Additional studies are warranted to better understand the effects of OA over-expression on bone formation and remodeling *in vivo*.

Disclosures: Nagat Frara, None.

FR0201

Dlx3 Inactivation in Osteoblasts Results in Defective Endochondral Bone Formation. Juliane Isaac^{*1}, Olivier Duverger², Hong-Wei Sun³, Stacey Russell⁴, Gary Stein⁵, Jane Lian⁵, Maria I Morasso². ¹Developmental Skin Biology Section, NIAMS/NIH, USA, ²Developmental Skin Biology Section, NIAMS, National Institutes of Health, USA, ³Biodata Mining & Discovery Section, NIAMS, National Institutes of Health, USA, ⁴Departments of Cell Biology & Orthopedic Surgery, University of Massachusetts Medical School, USA, ⁵University of Massachusetts Medical School, USA

Human mutations in the homeodomain transcription factor *DLX3* gene are etiologic to Tricho-dento-osseous (TDO), an ectodermal dysplasia characterized by defects in hair, teeth and bone development. Although clinical observations and *in vitro* studies suggest that *Dlx3* plays a crucial role in bone development, the *in vivo* role of *Dlx3* in regulation of endochondral bone formation of the post natal mouse has not been elucidated. To address the mechanisms by which *Dlx3* functions during osteogenesis, we conditionally inactivated *Dlx3* in osteoblasts by crossing *osteocalcin (Oc)-Cre* mice with *Dlx3*^{fllox/LacZ} mice to generate conditional

Dlx3-deficient (*Dlx3*^{Oc-cKO}) mice. *Dlx3* is expressed in hypertrophic chondrocytes (at low levels) and continues to increase in osteoblasts and osteocytes. Micro-architectural analyses of femurs were performed on *Dlx3*^{Oc-cKO} and *Dlx3*^{+/+} males from 5 weeks to 6 months. While the bone volume and the length of the whole femur were not affected, bone mineral density (BMD) was significantly decreased in the *Dlx3*^{Oc-cKO} males in comparison to *Dlx3*^{+/+} males. Cortical bone showed a decrease in bone density and increased porosity at all ages for *Dlx3*^{Oc-cKO} males, while cortical thickness remained unchanged. In contrast, trabecular bone of the distal femur showed increases of the relative bone volume, trabeculae number and connectivity density, associated with decreased trabecular spacing and an unchanged trabecular thickness, revealing an increased bone mass density of trabeculae in the *Dlx3*^{Oc-cKO} males. These changes suggest increased bone resorptive activity in the cortical bone; however in the metaphysis, stimulated osteoprogenitor differentiation forming new trabeculae is indicated. Analysis of RNA seq obtained from mRNAs extracted from femurs of 5-week-old males identified transcripts differentially expressed in *Dlx3*^{Oc-cKO} versus *Dlx3*^{+/+} mice. Using *Ingenuity Pathways Analysis (IPA)*, we showed that differentially expressed genes were enriched in molecules involved in the differentiation of osteoblasts and in the development and function of connective tissue. These data support that conditional deletion of *Dlx3* in osteoblasts may affect bone formation through a network of Wnt, hedgehog and BMP signaling pathways contributing to an increase in trabecular bone. Overall, these data indicated a key role for *Dlx3* in endochondral bone formation of adult mice and selective functional activity of *Dlx3* between cortical and trabecular bone.

Disclosures: Juliane Isaac, None.

FR0204

Modulating Osteogenic Differentiation of Induced Pluripotent Stem (iPS) Cells Through Direct Inhibition of SOX9 by MicroRNA-335-5p and MicroRNA-342-3p. Mengqi Huang^{*}, Yuhua Hu, Qisheng Tu, Jake Jinkun Chen. Tufts University School of Dental Medicine, USA

To selectively induce the osteogenic differentiation of induced pluripotent stem (iPS) cells, it is imperative to understand the regulatory molecular mechanisms underlying the process of how these cells switch between osteogenic and chondrogenic differentiation paths. Recent studies have successfully identified SOX9, the master gene of chondrogenesis, was downregulated during osteogenic differentiation while the important factor, Osterix(OSX) was upregulated. Here we found two specific microRNAs, miR-335-5p and miR-342-3p, were upregulated after ascorbic acid treatment of iPS cells, which indicated that they may be involved in the regulation of osteogenic differentiation. To verify the pivotal roles of miR-335-5p and miR-342-3p as direct posttranscriptional regulators of SOX9 in mouse iPS cells to osteogenic lineage, we performed a series of studies including micro-RNA microarray, luciferase reporter assays, site-specific mutations, and gain- and loss-of-function analyses. Micro-RNA microarray chips showed that miR-335-5p and miR-342-3p directly repressed SOX9 expression in iPS cells through respectively unique binding sites in its 3'UTR (Fig.1,2). To investigate effects of miR-335-5p and miR-342-3p specifically targeting SOX9, we cotransfected these miRNAs into iPS cells with the cloned luciferase-SOX9/3'UTR plasmids and pMIR-REPORT beta-gal control plasmids. Luciferase activity in iPS cells stably transfected with luciferase-SOX9/3'UTR construct decreased after transfection with miR-335-5p and miR-342-3p precursor hairpins when compared with cells transfected with negative control pre-miRNAs. The effects of miR-335-5p and miR-342-3p were reversed by anti-miR-335-5p and anti-miR-342-3p treatments, which downregulated endogenous miR-335-5p and miR-342-3p (Fig.3). As a result of decreased SOX9 protein level by miRNA control, we observed that in miR-335-5p- and miR-342-3p-overexpressing iPS cells there were increased mineral nodule formation and elevated mRNA and protein levels of OSX, a key osteogenic gene (Fig.4,5). In conclusion, miR-335-5p and miR-342-3p promoted osteogenic differentiation by down regulating the expression of SOX9 in mouse iPS cells. We propose miR-335-5p and miR-342-3p to target molecules for promoting bone regeneration and wound healing. Moreover, *in vivo* experiments are ongoing to further determine the effects of iPS cells regulated by miR-335-5p and miR-342-3p in critical-size calvarial bone defects in a mouse model.

microarray at different stage of osteogenic induction

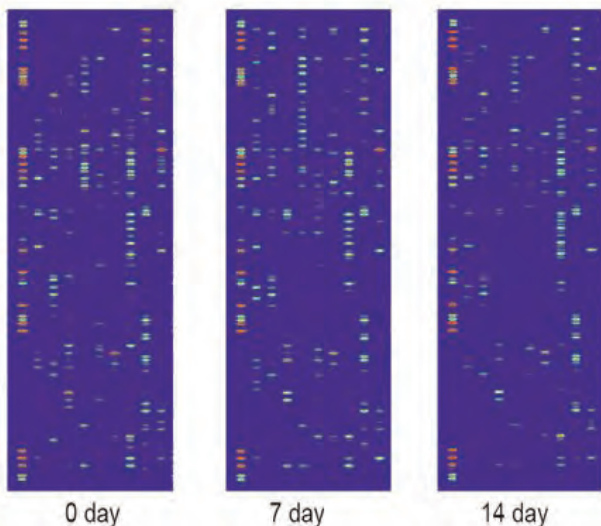
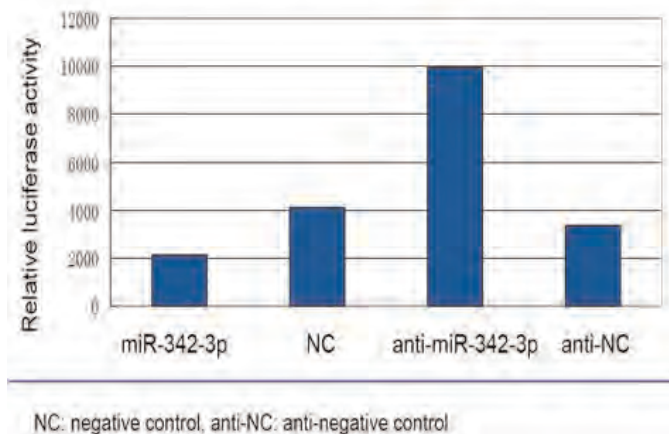


Fig.1
Signal intensity of potential miRNAs by miRNA microarray at different stage of osteogenic induction

| | 0 day | 7 day | 14 day |
|-----------------|-------|-------|--------|
| mmu-miR-101a | 4 | 5 | 6 |
| mmu-miR-101b | 1 | 11 | 1 |
| mmu-miR-1192 | 14 | 5 | 2 |
| mmu-miR-124 | 34 | 85 | 0 |
| mmu-miR-125a-3p | 11 | 68 | 21 |
| mmu-miR-128 | 58 | 119 | 116 |
| mmu-miR-129-3p | 11 | 11 | 1 |
| mmu-miR-144 | 0 | 0 | 0 |
| mmu-miR-145 | 168 | 8,085 | 757 |
| mmu-miR-155 | 11 | 207 | 8 |
| mmu-miR-194 | 1 | 1 | 14 |
| mmu-miR-186 | 27 | 128 | 119 |
| mmu-miR-217 | 17 | 2 | 9 |
| mmu-miR-30a | 99 | 292 | 87 |
| mmu-miR-30b | 66 | 337 | 168 |
| mmu-miR-30c | 197 | 334 | 498 |
| mmu-miR-30d | 137 | 422 | 225 |
| mmu-miR-30e | 14 | 27 | 9 |
| mmu-miR-335-5p | 4 | 3,430 | 41 |
| mmu-miR-342-3p | 80 | 481 | 889 |
| mmu-miR-381 | 4 | 1 | 1 |
| mmu-miR-384-5p | 4 | 1 | 1 |

Fig.2
Luciferase activity in iPS cells (ascorbic acid treated 7 days)



NC: negative control, anti-NC: anti-negative control

Fig.3

Western blot analyses indicated protein levels of SOX9 and OSX before and after transfection with miR-342-3p

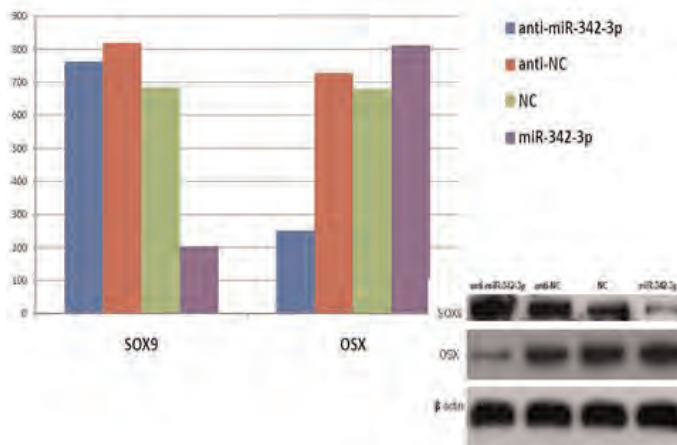
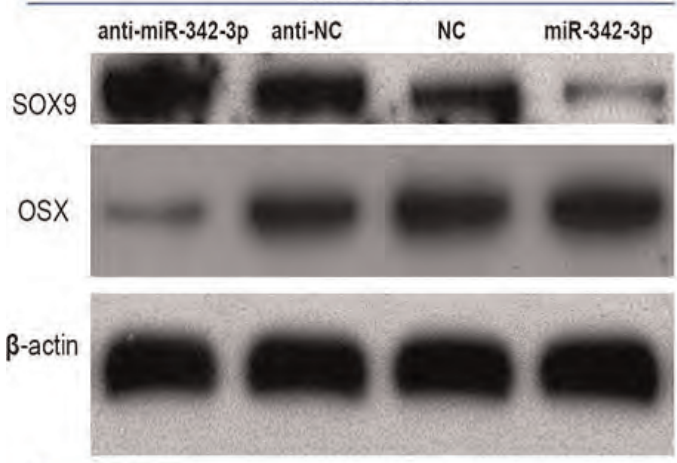


Fig.4

Western blot analyses indicated protein levels of SOX9 and OSX before and after transfection with miR-342-3p



NC: negative control, anti-NC: anti-negative control

Fig.5

Disclosures: Mengqi Huang, None.

This study received funding from: NIH grants DE16710 and DE21464 to JC

FR0209

Ubiquitin E3 Ligase Itch Negatively Regulates Osteoblast Differentiation from Mesenchymal Stem Cells. Hengwei Zhang¹, Lei Shu², Brendan Boyce², Lianping Xing³. ¹Univeristy of Rochester, USA, ²University of Rochester Medical Center, USA, ³University of Rochester, USA

Itch, a HECT family E3 ligase, affects numerous cell functions by regulating ubiquitination and degradation of target proteins. The role of Itch in osteoblasts(OBs) has not been investigated. Using 1-month-old Itch^{-/-} mice and WT littermates, we report Itch^{-/-} mice have significantly increased 1) bone volume(%BV/TV:42 ± 4vs25 ± 3.5); 2) OB numbers(#/mm:558 ± 28vs405 ± 35), and 3) bone formation rate(BFR:0.9 ± 0.1vs0.5 ± 0.04 μm³/μm²/day;MAR:1.2 ± 0.1vs0.8 ± 0.1 μm/day;MS/BS:0.75 ± 0.02vs0.63 ± 0.06% in WT mice). Compared to WT mice, bone marrow stromal cells(BMSCs) from Itch^{-/-} mice have increased OB differentiation(CFU-F colony#/well:79 ± 4vs52 ± 3; CFU-ALP+ colony#/well:63 ± 5vs38 ± 2; mineralized nodule#/well: 105 ± 7vs68 ± 8) and decreased adipogenesis (Oil red O+ cells#/well:390 ± 83vs1005 ± 71). To investigate if increased OB differentiation in Itch^{-/-} mice is due to enhanced mesenchymal stem cell (MSC) functions, we isolated CD45-enriched MSCs from BMSCs of Itch^{-/-} and WT mice and found that Itch^{-/-} CD45- cells had 1) normal MSC numbers (Sca1+/CD105+/CD11b-/CD31- cells), proliferation

and apoptosis; 2) increased OB marker gene expression (*alp*: $160 \pm 20\%$; *oc*: $180 \pm 15\%$; *runx2*: $170 \pm 15\%$ of WT cells); and 3) decreased expression of adipocyte master genes (*pparg*: $45 \pm 10\%$; *clebpa*: $55 \pm 4\%$; *clebpb*: $57 \pm 4\%$; and *clebpd*: $48 \pm 10\%$ of WT). To directly test the OB differentiation potential of *Itch*^{-/-} MSCs in vivo, we implanted *Itch*^{-/-} or WT CFU cells and decalcified bone matrix in a scaffold into tibial defects of SCID mice. *Itch*^{-/-} cells formed significantly more new bone in defects of recipient mice compared with WT cells (% BV/TV: 5.8 ± 1.9 vs 2.4 ± 0.7 ; % new bone area: 0.4 ± 0.08 vs 0.2 ± 0.05). Furthermore, over-expression of WT *Itch*, but not an *Itch* ligase-dead mutant, rescued OB differentiation defects of *Itch*^{-/-} BMSCs (%ALP+ area: 6.5 ± 1 in GFP vs 0.5 ± 0.1 in WT *itc* vs 6 ± 0.8 % in *itc* mutant). Consistent with E3 ligase function of *Itch*, the expression of known *Itch* targeting proteins, such as JunB, Runx2 and active β -catenin, was increased in *Itch*^{-/-} BMSCs. Our findings show that *Itch* negatively regulates OB differentiation from MSCs through degradation of multiple positive regulators of OBs. Thus *Itch* is a potential new target for bone anabolic drug development to treat patients with osteoporosis.

Disclosures: Hengwei Zhang, None.

FR0211

Collagen 10-Expressing Chondrocytes Have the Capacity to Become Osteoblasts In Vivo. Xin Zhou^{*1}, Klaus von der Mark², Stephen Henry³, Takako Hattori⁴, Benoit de Crombrughe¹. ¹MD Anderson Cancer Center, USA, ²Department of Experimental Medicine I, Nikolaus-Fiebiger-Center of Molecular Medicine, University of Erlangen-Nuremberg, Germany, ³University of Texas MD Anderson, USA, ⁴Department of Biochemistry & Molecular Dentistry, Okayama University Graduate School of Medicine, Dentistry, & Pharmaceutical Science, Japan

To examine whether cells derived from hypertrophic chondrocytes might contribute to the osteoblast pool in endochondral bones, we conditionally deleted an *Osx/EGFP* allele either in hypertrophic chondrocytes by *Coll10a1-Cre* or in chondrocytes by tamoxifen-induced *Agcl-CreERT2*. This *Osx* allele expresses *EGFP* only after Cre recombination and only in cells in which *Osx* is actively transcribed, namely, hypertrophic chondrocytes, osteoblast precursors, mature osteoblasts and osteocytes. Surprisingly, in addition to *EGFP*-positive (*EGFP*⁺) hypertrophic chondrocytes, abundant non-chondrocytic *EGFP*⁺ (*Osx*^{+/+}) cells were seen in the primary ossification centers. These cells were tightly associated with type I collagen, and their appearance coincided with the onset of ossification at the primary spongiosa from E15.5 until after birth. Subsequently, they were distributed throughout trabeculae surfaces, present in the endosteum, and embedded within the bone matrix. Similar results were obtained when the *Osx/EGFP* allele was inactivated in chondrocytes by tamoxifen-induced *Agcl-CreERT2*. Inactivation of the two alleles of *Osx* in hypertrophic chondrocytes by *Coll10a1-Cre* led to severely decreased bone formation selectively in the primary ossification centers due to lack of *Osx*-expressing osteoblasts, despite the presence of *Runx2*-expressing preosteoblasts in this area. Our results thus indicate that *Coll10a1*-expressing chondrocytes have the capacity to undergo transdifferentiation to become osteoblasts. In addition to cells in the periosteum, *Coll10a1*-expressing chondrocytes represent a second significant source of osteoblasts contributing to endochondral bone formation in vivo. We hypothesize that this finding represents a unique case of naturally occurring transdifferentiation in mammalian development.

Disclosures: Xin Zhou, None.

FR0212

Epigenetic Control of Osx-target Genes during Osteoblast Differentiation through NO66 Histone Demethylase. Krishna Sinha^{*1}, Hideyo Yasuda², Xin Zhou³, Benoit DeCrombrughe¹. ¹UT MD Anderson Cancer Center, USA, ²U.T.M.D. Anderson Cancer Center, USA, ³MD Anderson Cancer Center, USA

The osteoblast-specific transcription factor Osterix (*Osx*) is needed for differentiation of *Runx2*-expressing precursors into mature osteoblasts through activating a large repertoire of osteoblast genes including *Coll1a1*, *Bsp* and *Oc*. In *Osx*-null embryos, *Runx2*-positive *Osx*-null cells are arrested in their differentiation because expression of these osteoblast genes is absent. The mechanisms underlying the activation of these *Osx*-target genes in transition of preosteoblasts to osteoblasts is not very clear. We present several lines of evidence to support the hypothesis that *Osx* is indispensable for the formation of an active chromatin state of its target genes. Indeed, our results indicate that activation of the *Osx*-target genes is likely to include DNA demethylation, removal of repressor-complex from chromatin, recruitment of activators and chromatin modifying activities. With chromatin immunoprecipitation assays in *Osx*-wt and *Osx*-null calvarial cells, we demonstrate that the functional interactions of *Runx2* and *Osx* with chromatin of these genes are essential for expression of these genes in osteoblasts. Based on our findings, we conclude that in absence of *Osx*, chromatin of the *Osx*-target genes is inaccessible for the transcriptional activators including *Runx2*, *c-Myc* as well as histone modifying enzymes. We have earlier reported that NO66 is a JmjC histone demethylase specific for lysine 4 and 36 of histone H3, interacts with *Osx* and inhibits *Osx*-dependent promoter activity. Consistent with previous report, the interaction of NO66 with the chromatin of the *Bsp* and *Oc* genes is associated during repression of these genes in

Osx-null cells, indicating that NO66 might regulate histone methylation levels at the chromatin through its demethylase activity. Taken together, our results provide novel mechanistic insights in activation of *Osx*-target osteoblast genes through NO66 histone demethylase as well as DNA and histone methylation, thus adding another layer of control in chromatin architecture during transition of preosteoblasts to osteoblasts.

Disclosures: Krishna Sinha, None.

FR0217

Preconditioning Mouse Periosteal Cells to Hypoxia by Inactivation of the Phd2 Oxygen Sensor Improves In Vivo Ectopic Bone Formation. Steve Stegen^{*1}, Nick Van Gastel², Riet Van Looveren², Peter Carmeliet³, Frank Luyten⁴, Geert Carmeliet⁵. ¹Universiteit Leuven, Belgium, ²Laboratory of Clinical & Experimental Endocrinology, KU Leuven, Belgium, ³Laboratory of Angiogenesis & Neurovascular Link, Vesalius Research Center, VIB & Laboratory of Angiogenesis & Neurovascular Link, Vesalius Research Center, KU Leuven, Belgium, ⁴University Hospitals KU Leuven, Belgium, ⁵Katholieke Universiteit Leuven, Belgium

Tissue engineered constructs composed of a scaffold seeded with osteogenic cells are a promising strategy to heal osseous defects. However, the hypoxic conditions that cells encounter upon implantation can seriously impair the successful outcome and hinder bone formation. To anticipate to this detrimental environment and circumvent its negative effects, we aim at preconditioning osteogenic cells by switching on the hypoxia-inducible factor (HIF) pathway before implantation. We hypothesize that activation of this transcriptional program will not only promote angiogenesis, but will also facilitate a metabolic reprogramming which will favor cell survival in the hypoxic environment.

The HIF prolyl hydroxylase (PHD) oxygen sensors hydroxylate HIF-1 α and target it for proteasomal degradation in normoxia. In this study we genetically inactivated PHD2, the major isoform, in order to stimulate the hypoxia pathway. Murine periosteum derived cells (mPDC) obtained from *Phd2*^{lox} mice were transduced with adenovirus-Cre (Ad-Cre) or adenovirus-GFP (Ad-GFP). Within 3 days after Ad-Cre transduction, PHD2 protein levels significantly decreased (*Phd2*^{low}), leading to stabilization of HIF-1 α in normoxic conditions. As a consequence, the HIF-regulated transcriptional program was activated in the *Phd2*^{low} mPDC, which was reflected by an increased production of the angiogenic factor VEGF. In addition, mRNA levels of glucose transporters (*Glut1*) and glycolytic enzymes (*Ldh-a*, *Pdk1*) were increased, indicative of a glycolytic switch.

To investigate whether PHD2 inactivation influenced their bone forming capacity, the mPDC were seeded on a calcium phosphate-collagen scaffold and implanted ectopically in nude mice. Compared to Ad-GFP mPDC, the *Phd2*^{low} mPDCs formed significantly more new bone with osteocytes embedded in the mineralized bone, abundant osteoblasts lining the bone spicules, which surrounded islands of bone marrow. Intriguingly, the Ad-GFP mPDCs formed bone only at the periphery of the scaffold, whereas *Phd2*^{low} mPDCs formed also bone in the center, a site considered to be more hypoxic. In addition, the number and size of the blood vessels was increased in the *Phd2*^{low} condition, and these were closely associated with the sites of bone formation.

In conclusion, we show that genetic inactivation of *Phd2* activates the hypoxia signaling pathway in periosteal cells, improving their potential to form bone and attract blood vessels *in vivo*.

Disclosures: Steve Stegen, None.

FR0218

Runx2 and Osterix Molecular Complex Synergistically Regulate Osteogenic Genes. Harunur Rashid^{*1}, Haiyan Chen², Changyan Ma¹, Krishna Sinha³, Benoit DeCrombrughe³, Amjad Javed². ¹Department of Oral & Maxillofacial Surgery, University of Alabama at Birmingham, USA, ²University of Alabama at Birmingham, USA, ³UT MD Anderson Cancer Center, USA

Commitment and maturation of mesenchymal cells into osteoblast require *Runx2* and specificity protein 7 (Sp7) transcription factors. Deletion of either gene results in failed osteoblast development and bone formation. Similar skeletal phenotype by structurally unrelated proteins suggests their functional interdependence. However, molecular cross-talk between *Runx2* and Sp7 is not known. Here we investigated molecular and functional interaction between Sp7 and *Runx2* proteins. Co-IP assays revealed a physical interaction between endogenous Sp7 and *Runx2* proteins in human osteoblasts. Sp7 interacts with both isoform of *Runx2* in multiple cell types. Successful reciprocal Co-IP suggested a stable association between Sp7 and *Runx2*. Consistent with their physical interaction, a high degree of *Runx2* and Sp7 nuclear foci co-localized *in situ*. We next defined region responsible for this interaction by serial deletion mutants of both proteins. We find that DNA binding runt homology domain but not the transcriptional activation region of *Runx2* is required for this interaction. In contrast, the transactivation domain of Sp7 (89-192) but not the DNA binding Zinc fingers is necessary for *Runx2* interaction. We next tested if *Runx2*-Sp7 molecular complex differentially regulates target gene expression. Gene promoter considered markers of mature osteoblast (OC), chondrocyte (ColX), and FGF3 were

tested. Sp7 or Runx2, stimulate OC-promoter by 5 and 8 fold respectively. However, co-expression of Runx2 and Sp7 results in synergistic activation of ~70 fold. Similarly, ColX-promoter was activated by Sp7 (3 fold) and Runx2 (4 fold) but a synergistic activation of >17 fold was evident when both proteins were co-expressed. FGF3-promoter was induced ~30 fold by Sp7 or Runx2. However, a synergistic induction of 130 fold was manifested upon their co-expression. Thus Runx2 and Sp7 functionally cooperate for maximal induction of cell phenotype-restricted gene. Requirement of Runx2-Sp7 interaction for functional synergism was established by Runx2 mutant that lack activation domain but preserve Sp7 interaction. Runx2-Δ230 poorly activated (2 fold) OC-promoter but in presence of Sp7 showed synergistic response of 43 fold. Finally site-directed mutagenesis identified that functional synergism is primarily mediated through Runx responsive motif in the OC-promoter. Together, our data demonstrate that, Sp7 regulate Runx2 transcriptional activity and function through physical association.

Disclosures: Harunur Rashid, None.

FR0223

PPR-Dependent Signaling in Osteoprogenitors Regulates Bone Marrow Hematopoietic Stem Cell and Leukocyte Niches. Cristina Panaroni^{*1}, Rhiannon Chubb², Joy Wu². ¹Endocrine Unit, Massachusetts General Hospital, USA, ²Massachusetts General Hospital, USA

The signaling pathways mediating the interactions between osteoblasts and hematopoietic cells are crucial for the maintenance of hematopoietic niches. One important pathway in osteoblasts involves the PTH/PTHrP receptor (PPR). The targeted expression of constitutively active PPR to osteoblasts in mice leads to increased trabecular bone and increased numbers of hematopoietic stem cells (HSCs). Beyond support of HSCs, osteoblasts are also necessary to sustain B lymphopoiesis in bone marrow (BM). The PPR is a G protein-coupled receptor (GPCR) that signals through multiple G proteins including Gsz. We have previously demonstrated that deletion of Gsz in osteoprogenitors in mice results in reduced bone mass with fewer osteoblasts and impaired differentiation of B cell precursors blocked at the pre-pro B to pro-B transition *in vivo*. Since PTH regulates HSCs *in vivo* and enhances support of B lymphocyte differentiation by osteoblastic cells *in vitro*, we hypothesized that ablation of PPR in osteoprogenitors would negatively affect BM hematopoiesis. Osterix-Cre:PPR(fluo) conditional knockout (KO) mice were generated using the Cre recombinase under the control of the Osterix promoter to ablate PPR in osteoblast precursors. The BM cellularity is not altered in the mutant mice despite a significant reduction in body weight. As previously reported, and similar to Gsz KO mice, PPR KO mice exhibit a specific reduction in B cell precursors in the bone marrow. However, we also found higher levels of myeloid cells and a significant increase in T lymphocytes in the BM of PPR KO mice. On the contrary, in the periphery PPR KO mice exhibit severe myeloid and lymphoid deficiency, with dramatic reductions in spleen and thymus cellularity. In order to better understand the splenic and thymic failure we investigated the HSC compartment in PPR KO mice. BM and spleens of 3 week-old PPR mice showed a dramatic decrease in short term-HSCs and multipotent progenitors but not in long term-HSCs. Our results demonstrate that PPR signaling upstream of Gsz in osteoprogenitors is very important for the maintenance of specific stem cell subsets in the BM niche and plays a direct role in BM HSC and leukocyte differentiation.

Disclosures: Cristina Panaroni, None.

FR0225

The Inositol Polyphosphate/Protein Kinase Cδ Signaling Cascade is Required for the Connexin43-dependent Amplification of Runx2 Activity. Corinne Niger¹, Maria Luciotti², Atum Buo³, Carla Hebert², Vv Ma², Joseph Stains^{*1}. ¹University of Maryland School of Medicine, USA, ²University of Maryland, USA, ³University of Maryland, School of Medicine, USA

Connexin43 (Cx43) plays an important role in bone biology by enabling the cell-to-cell communication of small molecules. Yet, the identity of the second messengers shared by Cx43 and the molecular targets of these second messengers are largely unknown. In order to identify the biologically relevant second messengers being communicated by Cx43, we characterized a system in which Cx43 expression levels impact the responsiveness to FGF2 by modulating the transcriptional activity of Runx2. Here, we show the requirement of the PLCγ1/inositol polyphosphate/ PKCδ signaling cascade to the Cx43-dependent regulation of Runx2 in MC3T3 osteoblasts. Cx43 overexpression potentially enhanced the response of a Runx2-binding OSE2-luciferase reporter to FGF2. Inhibition of phospholipase C activity by U73122, ET-18-OCH3, a dominant negative PLCγ1 construct or PLCγ1-siRNA reduced this response by > 3-fold. Because PLCγ1 is classically associated with the production of DAG and InsP3, we examined the effect of a DAG lipase inhibitor (RHC-80267) and InsP3R antagonist (2-APB) on Runx2. Surprisingly, neither inhibitor had the expected effect on Runx2 activity, suggesting that an alternate pathway downstream of PLCγ1 generates the second messenger that is communicated by Cx43. Indeed, siRNA- knockdown of inositol polyphosphate multikinase (IPMK), which generates InsP4 and InsP5, and inositol hexakisphosphate kinase 1 (IP6K1), which generates inositol pyrophosphates (InsPP), prevented the Cx43-dependent potentiation of FGF2-induced signaling through Runx2, reducing transcriptional activity by ~50%. Likewise, the IP6K inhibitor TNP abolished basal and Cx43-dependent Runx2

activity, and blocked the interaction of Runx2 and PKCδ as determined by co-immunoprecipitation. This is likely due to the observation that IP6K1 but not IP6K2 siRNA prevented the nuclear accumulation of PKCδ following FGF2 treatment. To validate a role for InsPP in osteoblast function and Runx2 activity, we examined the effect of TNP on osteogenesis by real time PCR. Treatment with TNP reduced the expression of the Runx2-regulated genes, Col1a1, Osteocalcin and Osterix more than 2-fold, while Runx2 expression was unaffected. These data implicate the InsPP as mediators of the Cx43-dependent amplification of the osteoblast response to FGF2 and suggest that these low molecular weight second messengers may be biologically relevant mediators of osteoblast function that converge on Runx2 and are communicated by Cx43.

Disclosures: Joseph Stains, None.

FR0226

A FoxO1-Independent Action of Canonical Wnt signaling in Osteoblasts Regulates Bone Resorption. Aruna Kode^{*}, Ioanna Mosialou, John S Manavalan, Stavroula Kousteni. Columbia University Medical Center, USA

FoxO1 has evolved as a regulator of bone physiology that acts on osteoblasts to control their function at two levels, bone formation and whole body glucose metabolism. However, the role of osteoblast-expressed *FoxO1* in bone resorption has not been explored. We found that *FoxO1* deletion in osteoblasts increased bone resorption by increasing osteoclast numbers. Another molecule known to affect osteoclast formation through its action in osteoblasts is *b-catenin*, the canonical Wnt signaling target. In fact, *FoxO1* and *b-catenin* physically associate in osteoblasts. Therefore, we examined whether *FoxO1* affects bone resorption in association with *b-catenin*. Initial studies using a combination of cell culture assays and mouse models of *FoxO1* lack-of-function (*FoxO1^{osb/-}*) and *b-catenin* gain-of-function (*bcat(ex3)^{osb}*) mutations in osteoblasts supported this hypothesis at the transcriptional level. They showed that *FoxO1* regulates the expression of the *b-catenin* transcriptional targets, *Axin2*, *Tcf1*, *Tcf3* and *Lef1*. In contrast, expression of the *FoxO1* targets *cyclin D1*, *p27Kip1*, *Superoxide Dismutase 2*, *catalase* and *Gadd45* were not affected by *b-catenin*. A potential impact of such interaction on the skeleton was tested *in vivo*. However, genetic experiments did not support a synergism in bone mass regulation. Indeed, constitutive activation of *b-catenin* in osteoblasts (*bcat(ex3)^{osb}* mice) increased bone mass by suppressing osteoclast formation and led to osteopetrosis. This effect is mediated through upregulation of *osteoprotegerin* (*Opg*) expression. Inactivation of a single allele or both alleles of *FoxO1* in osteoblasts in compound *FoxO1^{osb/+};**bcat(ex3)^{osb}* or *FoxO1^{osb/-};**bcat(ex3)^{osb}* mice did not affect early onset osteopetrosis caused by constitutive activation of *b-catenin*. Osteoclast formation and bone volume were not reinstated in *FoxO1^{osb/+};**bcat(ex3)^{osb}* or *FoxO1^{osb/-};**bcat(ex3)^{osb}* mice. Similarly, thickening of the ribs and the formation of osteomata, benign bone tumors of the ribs, as well as the lack of tooth eruption observed in *bcat(ex3)^{osb}* mice were not affected by either *FoxO1* haploinsufficiency or by complete deletion of *FoxO1* in osteoblasts. Similar to *bcat(ex3)^{osb}* mice, normal osteoblast numbers were observed in *FoxO1^{osb/+};**bcat(ex3)^{osb}* animals. These observations identify *FoxO1* as a transcriptional potentiator for some of the TCF binding properties of *b-catenin*. However, the anti-osteoclastogenic effects of *b-catenin* occur independent of *FoxO1* activity.

Disclosures: Aruna Kode, None.

FR0227

Activated G_s Signaling in Immature Osteoblasts Alters the Hematopoietic Stem Cell Niche in Mice. Edward Hsiao^{*1}, Koen Schepers¹, Mark Scott², Trit Garg¹, Emmanuelle Passegue¹. ¹University of California, San Francisco, USA, ²Gladstone Institute for Cardiovascular Disease, USA

Adult hematopoiesis occurs primarily in the bone marrow space where blood cells closely interact with stromal niche cells, including osteoblastic lineage cells. Despite this close association, little is known about the specific roles of osteoblasts in supporting hematopoietic stem cell (HSC) function, and how conditions affecting bone formation influence hematopoiesis. Here, we use a constitutively-active engineered G_s-coupled G-protein coupled receptor (GPCR) to activate G_s-GPCR signaling in osteoblasts and assess how the concomitant increase in bone formation impacts HSC function and blood homeostasis. The Col1(2.3)^{+/Rsl1+} transgenic mouse model showed a 5-15 fold increase in trabecular bone mass with near complete loss of the normal bone marrow cavity, with histological features similar to fibrous dysplasia of the bone. The mice showed BM aplasia with progressive loss of up to 85% of HSC numbers and impaired megakaryocyte and erythrocyte development with defective recovery after myeloablation with 5FU. These blood phenotypes developed without compensatory extramedullary hematopoiesis. Surprisingly, the loss of HSCs occurs despite a large expansion of HSC-supportive niche cells, including osteoblasts, mesenchymal stem cells, and endothelial cells. Expression analysis showed that the Col(2.3)^{+/Rsl1+} osteoblasts had decreased expression of key HSC-maintenance genes, including *SDF1*, *VCAM1*, and *Angpt1*, accounting for the impaired ability to support HSC function. In addition, we observed significantly impaired HSC function in competitive transplantation experiments when naive HSCs were initially co-cultured with Col1(2.3)^{+/Rsl1+} OBCs. These findings indicate that long-term activation of G_s-GPCR signaling in osteoblasts of the HSC niche decreases HSC-supportive activity and leads to lineage-specific hematopoietic defects. Our results also suggest that long-term activation of G_s-GPCR signaling, such as in medical conditions of excess

parathyroid hormone, may lead to adverse effects on endogenous HSCs and contribute to hematopoietic disorders such as anemia and thrombocytopenia.

Disclosures: Edward Hsiao, None.

FR0229

Diet Induced Obesity Enhances Bone Marrow Myeloproliferation by Down-regulating Runx1 and Crebbp Expression. Benjamin Adler^{*1}, Danielle Green¹, M. Ete Chan¹, Clinton Rubin². ¹Stony Brook University, USA, ²State University of New York at Stony Brook, USA

Bone marrow hematopoiesis is a process which is tightly regulated by the bone marrow microenvironment to ensure lifelong hematopoietic production. Obesity increases lifetime susceptibility to a host of chronic diseases, implicating a suppressed immune system. Further, obesity biases bone marrow stromal cells (BMSCs) towards the formation of adipose tissue, compromising the bone marrow niche. Considering the consequences of obesity on immunity and the niche, we hypothesize that a high fat diet (HFD: 60% Kcal from fat) will impair bone marrow hematopoiesis. Seven week old male C57Bl/6J mice were fed either a high fat (HF) or regular chow (RD) diet. Bone marrow was analyzed using flow cytometry after 1 and 6 weeks to characterize hematopoietic cell populations. Within one week, B-cell proportions were reduced by -10% in HF compared to RD ($p < 0.05$). By 6w of HFD B-cells had collapsed by -25% and T-cells were reduced by -33%, while the myeloid cell fraction increased by +16% as compared to RD ($p < 0.01$). In RNA extracted from bone marrow at 6w, the expression of Ebf1 and Pax5, representing commitment to the B-cell lineage, were reduced by -29% and -34% in HF animals ($p < 0.01$). This response is reminiscent of hematopoietic defects in other conditions, such as aging, where excessive myeloproliferation and impairments to lymphopoiesis are seen. Interestingly the expression of hematopoietic transcription factors Runx1 and Crebbp was also decreased in HF animals by -17% and -24% ($p < 0.01$) at 6w. Hematopoietic stem cell quiescence and differentiation are balanced by several transcription factors which were first identified, in cases of extreme dysfunction, as oncogenes. Partial or complete loss of these particular transcription factors has been previously implicated in hematopoietic disorders characterized by the increased myelopoiesis and limited lymphopoiesis described here. This however is the first time that obesity has been observed to impact their expression. These data demonstrate that hematopoiesis is vulnerable to even short-term exposure to HFD, which disrupts leukocyte allocations. The data also indicate that obesity acts through a previously unrecognized mechanism in the bone marrow, down regulation of Runx1 and Crebbp, intimating therapeutic targets. These data emphasize the importance of taking a systems approach to diseases, such as obesity and osteoporosis, whose spatial co-location (bone marrow) may elucidate key pathways and interactions.

Disclosures: Benjamin Adler, None.

FR0230

Disruption of Hematopoietic Stem Cell Lineage Determination and Increased Rate of Leukemia Cell Engraftment in Mice Lacking Osteoblasts. Maria Krevvata^{*1}, Barbara Silva¹, John S Manavalan¹, Aris Economides², Ellin Berman³, Stavroula Kousteni¹. ¹Columbia University Medical Center, USA, ²Regeneron Pharmaceuticals, Inc., USA, ³Memorial Sloan-Kettering Cancer Center, USA

The fate of hematopoietic stem cells (HSCs) depends on the bone marrow niche. The osteoblast in particular, as a component of the niche, is involved in establishing homing, survival, and differentiation of HSCs. Here we examined the effect of osteoblasts on HSC function. For this purpose, we ablated osteoblasts and examined the effect on the bone marrow compartment and on extramedullary hematopoiesis. Activation of diphtheria toxin A chain (DTA) in collagen type IA1- expressing osteoblast precursors ($DTA_{osb}^{+/-}$ mice) in mice led to 50% reduction in osteoblast numbers while osteoclast surface was not affected. At 10 weeks of age $DTA_{osb}^{+/-}$ mice showed a decrease in bone marrow cellularity. In the bone marrow the hematopoietic stem and progenitor cell (HSPC) pool size, defined by Lin-Sca+c-Kit+ (LSK) cells, increased in $DTA_{osb}^{+/-}$ mice as compared to wild type littermates. The LSK+/CD150+/CD48- subset, a population with a myeloid commitment bias, was increased. The number of myeloid (CD11b+/Gr1+) cells increased in both the bone marrow and the spleen of $DTA_{osb}^{+/-}$ mice. Spleen size was not altered in 10-week old mice but increased with increasing age suggesting an age-dependent increase in extramedullary hematopoiesis in $DTA_{osb}^{+/-}$ mice. Increased myeloid activity was coupled with a reduction in B-lymphopoiesis in the bone marrow and spleen suggesting that the hematopoietic lineage progression was altered. Erythropoiesis was not affected as both the number of Ter119+ erythroid progenitors in the bone marrow and spleen as well as the number of red blood cells was not altered by osteoblast depletion. The functionality of the altered hematopoietic compartment was tested in a model of lymphoma/lymphoblastic leukemia. $DTA_{osb}^{+/-}$ mice injected with leukemic cells showed earlier tumor engraftment in the blood, bone marrow, spleen and liver as compared to wild type littermates. Total tumor burden was increased and overall survival was significantly shorter following osteoblast ablation. A 50% increase in hind-limb paralysis supported the finding of increased tumor burden at bone sites of $DTA_{osb}^{+/-}$ mice. These results indicate that osteoblast ablation alters lineage determination of HSCs by affecting the myeloid and lymphocytic compartments. Moreover, it allows for a greater engraftment of leukemia cells within the marrow

cavity. The increase in myeloid populations coupled with a decrease in B-lymphopoiesis may predispose to and increase the burden of leukemia.

Disclosures: Maria Krevvata, None.

FR0232

FGF-2 Maintains a Niche-dependent Population of Self-renewing Highly Potent non-adherent Mesenchymal Progenitors through FGFR2c. Nunzia Di Maggio^{*}, Arne Mehrkens, Adam Papadimitropoulos, Andrea Banfi, Ivan Martin. Basel University Hospital, Switzerland

Bone marrow-derived mesenchymal stem/stromal cells (MSC) are a heterogeneous population of multipotent progenitors capable of generating bone, cartilage and fat tissues and represent a fundamental tool in regenerative medicine. However, MSC are rare and require significant in vitro expansion, which is accompanied by rapid loss of differentiation capacity, limiting their potential for clinical application.

We found that primary human bone marrow (BM) cultures contain a population of intrinsically non-adherent mesenchymal progenitors (NAMP), which are distinct from the initially adhering Colony Forming Units-fibroblast (CFU-f) and are normally discarded in current culture procedures. NAMP could generate an adherent progeny with significantly greater proliferation and multilineage differentiation potential in vitro and 3-fold greater bone formation in vivo, suggesting that they represent a more primitive population. Furthermore, NAMP progeny was enriched with cells expressing CD146, SSEA-4 and SSEA-1, which have been found to mark populations of early multipotent mesenchymal progenitors. Upon serial replating, NAMP were able to regenerate and expand in suspension as non-adherent clonogenic progenitors, while also giving rise to an adherent progeny. This took place at the cost of a gradual loss of proliferative potential, shown by a reduction in colony size. However, when NAMP were expanded on the initial adherent BM fraction, they underwent significantly greater expansion than during serial replating without any loss of proliferative potential. Although not excluding cell-to-cell interactions, conditioned medium experiments showed that the adherent BM fraction positively regulates NAMP survival and proliferative potential at least in part through secreted signals. The presence of FGF-2 was critical for NAMP maintenance, but it could not induce them from the adherent fraction at any time during culture. Mechanistically, we found that NAMP function specifically depends on signaling through FGFR2c, which is expressed during osteogenesis and alterations of which have been described to affect the balance between self-renewal and differentiation of osteoprogenitors in vivo.

In conclusion, our data show that the adherent BM fraction can provide a niche function for the in vitro self-renewal of highly potent non-adherent mesenchymal progenitors and suggest potential strategies to overcome a crucial limitation in the use of MSC for regenerative medicine.

Disclosures: Nunzia Di Maggio, None.

FR0233

Generation and Characterization of Osterix-Cherry Reporter Mice. Sara Strecker^{*1}, Yu Fu¹, Peter Mave². ¹University of Connecticut, USA, ²University of Connecticut Health Center, USA

Objectives: Osterix is a zinc finger transcription factor which functions as a master regulator of osteoblast differentiation. We report here on the generation of Osterix-mCherry reporter mice. Methods: We subcloned a 40 kb region encompassing the Osterix gene from BAC clone RP24-362M3. An mCherry fluorescent reporter was then inserted into this subcloned genomic DNA region. Pronuclear injection was carried out with this construct and two founder lines were generated. Results: Preliminary characterization of reporter gene expression at early postnatal ages indicates Osterix expression is largely restricted to cells of the osteoblast lineage. Robust mCherry expression can be detected in cells of the osteoblast lineage in the skull, long bones, and axial skeleton. Reporter expression can also be detected in the kidney. At adult ages, Osterix expression is not exclusive to the osteoblast lineage and is moderately expressed in hypertrophic chondrocytes and weakly expressed in cells present within the bone marrow. Osterix expressing cells in the bone marrow appear close to, but are not on the bone surface. These cells appear similar to reticular cells with regards to their cell morphology. To validate the expression pattern of Osterix-mCherry reporter expression, we carried out immunostaining studies for endogenous Osterix protein on tissue sections. Also, qRT-PCR analysis for Osterix on FACS isolated cells from day 5 stromal cultures revealed that the mCherry positive cell fraction was approximately 35 fold higher in endogenous Osterix gene expression relative to the negative cell fraction. Conclusions: These studies substantiate that our reporter accurately represents endogenous Osterix expression in the cortical bone and cells of the bone marrow. The identity and significance of these mCherry positive cell types is currently under investigation. Future studies will further validate and characterize the mCherry + reporter expression relative to endogenous Osterix gene expression.

Disclosures: Sara Strecker, None.

FR0235

Legumain: A Novel Regulator of Human Skeletal (Mesenchymal) Stem Cell Differentiation. Diyako Qanie*¹, Abbas Jafari², Kenneth Hauberg¹, Li Chen³, Moustapha Kassem⁴. ¹University of Southern Denmark, Denmark, ²University of Southern Denmark, Denmark, ³Medical Biotechnology Center (MBC), Denmark, ⁴Odense University Hospital, Denmark

Secreted proteins of human skeletal (mesenchymal) stem cells (hMSC) may play an important role in controlling hMSC biological function via autocrine or paracrine effects. Thus, we employed quantitative proteomic analysis by Stable Isotope Labelling in Cell Culture (SILAC) and identified 315 proteins that exhibit significant (≥ 2 fold) changes during osteoblast (OB) differentiation of hMSC. Among the 14 up-regulated secreted proteins with unknown function in hMSC biology, we identified Legumain (LGMN), also called asparaginyl endopeptidase (AEP) which is a cysteine protease enzyme hydrolyzing asparaginyl bonds. Previous studies showed that LGMN exerted inhibitory effects on osteoclast differentiation via its C terminal fragment. We confirmed the production and regulation of LGMN during OB differentiation of hMSC by RT-PCR and Western blot analysis. Stable silencing of LGMN in hMSC using shRNA significantly promoted osteoblast differentiation while inhibited adipocyte differentiation. On the other hand, stable over-expression of LGMN using lentivirus vector in hMSC showed the reverse effects: significantly reduced osteoblast differentiation and enhanced adipocyte differentiation. Furthermore, conditioned medium obtained from LGMN over-expressing hMSC reduced osteoblast differentiation. In conclusion, our data demonstrated a novel autocrine/paracrine role of LGMN regulating the balance between osteoblast and adipocyte differentiation of hMSC by inhibiting osteogenesis and promoting adipogenesis of hMSC in bone marrow. Thus targeting LGMN expression could be a therapeutic drug for enhancing bone formation in bone-loss related diseases.

Disclosures: Diyako Qanie, None.

This study received funding from: Clinic for Molecular Endocrinology (KMEB)

FR0243

NF- κ B RelB Null Mice Develop Erosive Arthritis by Increasing Inflammatory Monocyte/Macrophages. Zhenqiang Yao*¹, Yanyun Li², Lianping Xing¹, Brendan Boyce². ¹University of Rochester, USA, ²University of Rochester Medical Center, USA

RelB, a NF- κ B family member, typically forms heterodimers with p52 to activate alternative NF- κ B signaling. RelB^{-/-} mice have normal basal, but impaired RANKL-induced osteoclast (OC) formation in vitro and metastasis-mediated resorption. We have found that RelB^{-/-} mice develop age-related trabecular bone gain, which we attribute to increased osteoblast (OB) functions. We generated RelB/p52 double KO (dKO) mice in a B6/129 background (BG) and found that these and RelB^{-/-} mice in this BG are more healthy than RelB^{-/-} mice in the original BG but still have impaired RANKL-induced OC formation in vitro. However, ~50% of the mice in the mixed BG develop erosive arthritis, with marked synovial inflammation (area 1.2 ± 0.4 and 1.4 ± 1 mm²/knee joint in ^{-/-} and dKO mice, respectively) accompanied by activated OCs (12.3 ± 8.3 and 16.3 ± 2.1 per knee joint) eroding bone. In contrast to the impaired RANKL-induced OC formation in vitro, the ^{-/-} mice have enhanced TNF-induced OC formation and resorption (pit area 1.1 ± 0.2 vs. 0.23 ± 0.02 mm²/slice) when we used fewer OC precursors (OCPs) because ^{-/-} mice have 5-10 fold more inflammatory monocyte/macrophages (Mon/Macs) which are mainly CD11b+Gr-1+F4/80+(M1). M-CSF, GM-CSF and TNF independently drive myeloid precursor differentiation to Mon/Macs which include 3 populations: CD11b+Gr-1+F4/80+(M1), CD11b+Gr-1-F4/80+ (M2) and CD11b-Gr-1-F4/80+ (M3) Mon/Macs. Comparing bone marrow (BM) cells cultured from WT and ^{-/-} mice, we found that M-CSF induced 86% vs 51% M2; GM-CSF induced 46% vs. 49% M1 and 14% vs. 32% of M3; TNF induced 21% vs. 61% M1 and 10% vs. 16% of M3. Notably, ^{-/-} mice have age-dependent increased TNF but not M-CSF or GM-CSF levels in serum and BM, reflecting TNF inducing its own transcription by activating RelA, and RelB forming an inhibitory complex with RelA to inhibit TNF transcription. RANKL plus either GM-CSF or TNF did not induce OC formation, consistent with RelB^{-/-} mice having more M1 Mon/Macs which form fewer OCs in vitro. However, RANKL induced significant numbers of OCs in ^{-/-} mice, suggesting that ^{-/-} myeloid precursors respond normally to RANKL in vivo. We conclude that RelB negatively regulates TNF production and the increased TNF in RelB^{-/-} mice drives myeloid precursor differentiation into inflammatory Mon/Macs (M1) which mediate joint inflammation and enhance OC function to erode bone. Development of small molecular analogs of RelB could provide a novel approach for the treatment of inflammatory arthritis.

Disclosures: Zhenqiang Yao, None.

FR0244

Osteocyte-derived RANKL in Bone Remodeling. Tomoki Nakashima*¹, Mikihito Hayashi¹, Hiroshi Takayanagi². ¹Tokyo Medical & Dental University, Japan, ²The University of Tokyo Department of Immunology, Japan

RANKL and its receptor RANK are key regulators of osteoclastogenesis. Aberrant expression of RANKL explains why autoimmune diseases, cancers, and periodontal disease are associated with systemic and local bone loss. In particular, RANKL is the pathogenic factor that causes bone and cartilage destruction in arthritis. Inhibition of RANKL function by the decoy receptor osteoprotegerin or anti-RANKL antibody prevents bone loss in postmenopausal osteoporosis, cancer metastasis and arthritis. RANKL has been postulated to be mainly expressed by osteoblasts, BMSCs and T cells, but there has been no genetic evidence regarding the major cellular source of RANKL in the bone microenvironment. We show that osteocytes embedded within the bone matrix are the critical source of RANKL in bone remodeling. Osteocytes, the most abundant cell type in bone tissue, are thought to orchestrate bone homeostasis by regulating both bone resorption and formation, but in vivo evidence and the molecular basis for the regulation has not been sufficiently demonstrated. To unambiguously isolate high purity osteocytes from bone tissue, we generated osteocyte-specific EGFP reporter mice in which osteocytes could be identified by the expression of EGFP driven by the Dmpl promoter. Using fluorescence activated cell sorting, we established a method for the isolation of high purity osteocytes from the fractions obtained by enzymatic digestion of bone. The isolated osteocytes morphologically exhibited dendritic processes and exclusively expressed Dmpl, Sost, Reln and Npy, which are well-known osteocyte-specific genes. In contrast, osteoblast-specific genes such as Kera and Fmod were strongly expressed in isolated osteoblasts. Notably, osteocytes express a much higher amount of RANKL and have a much greater capacity to support osteoclastogenesis than either osteoblasts or BMSCs. The crucial role of RANKL expressed by osteocytes was validated by the severe osteopetrotic phenotype observed in adult mice lacking RANKL specifically in osteocytes. In addition, we generated T cell-specific Tnfsf11-deficient mice, which did not exhibit any discernible osteopetrotic phenotype, indicating that the RANKL expressed on T cells does not significantly contribute to the physiological regulation of osteoclastogenesis. Thus, we provide in vivo evidence for the key role of osteocyte-derived RANKL in bone remodeling, establishing a molecular basis for osteocyte regulation of bone resorption.

Disclosures: Tomoki Nakashima, None.

FR0245

RANKL Employs Distinct Binding Modes to Engage RANK and OPG. Christopher Nelson¹, Julia Warren*², Steven Teitelbaum², Daved Fremont¹. ¹Washington University in St. Louis, USA, ²Washington University in St. Louis School of Medicine, USA

The soluble decoy receptor osteoprotegerin (OPG) plays a pivotal role in bone biology by moderating the processes that control bone mineral density. OPG binds to, and sequesters, all known forms of the TNF-related cytokine RANKL (receptor activator of NF- κ B ligand), and by doing so interferes with activation of the cell-surface receptor RANK. Here we report the crystal structures of the cytokine-binding regions of murine OPG and RANK in complex with murine RANKL. Although OPG and RANK are related members of the tumor necrosis factor receptor superfamily, the contradictory biological functions of the two receptors (soluble-decoy versus cell-surface signaling) impose different structural constraints on their binding domains. Although similar in domain organization and structure - the cytokine-binding regions of both receptors consist of four cysteine-rich domains (CRDs) linked in tandem - monomeric OPG binds RANKL with roughly 24-fold higher affinity than RANK, and inhibits RANKL-stimulated osteoclastogenesis approximately 50-times more effectively. The difference in affinity is largely attributable to a much longer off-rate of OPG compared to RANK. Several RANKL residues shift their orientation leading to rearrangement of the C-D and D-E loops. These shifts result in a much more hydrophobic binding groove for OPG than for RANK. Indeed, a tight fit of OPG with RANKL does not appear possible without significant shifts in the positions of side chains within the receptor-binding cleft. High affinity binding requires OPG^{F127}, a residue mutated in juvenile Paget's disease. These results suggest that cytokine plasticity may modulate the interactions of specific TNF-family cytokine/receptor pairs in order to fine tune receptor selectivity.

Disclosures: Julia Warren, None.

FR0246

RANKL Induces TRAF3 Lysosomal Degradation Through NF- κ B RelB, an Effect Prevented by the Lysosome Inhibitor Chloroquine. Yan Xiu*¹, Yoshikazu Morita², Chen Zhao¹, Zhenqiang Yao³, Lianping Xing³, Brendan Boyce¹. ¹University of Rochester Medical Center, USA, ²Megmilk Snow Brand Co., Ltd., Japan, ³University of Rochester, USA

TRAF3 inhibits RANKL-induced osteoclast (OC) formation through proteasomal degradation of NF- κ B-inducing kinase (NIK) and thus could limit resorption in

inflammatory bone diseases, such as rheumatoid arthritis (RA). However, RANKL also promotes TRAF3 degradation to activate NIK-induced NF- κ B canonical and non-canonical signaling, but how TRAF3 is degraded (lysosomal vs proteasomal) or how it inhibits OC formation is unclear. Hydroxychloroquine is a lysosome inhibitor, used to reduce inflammation in RA, but its effects on OCs are unknown. We report that chloroquine (CQ) reduced OC #s by 3-fold and resorption by >90% *in vitro* associated with increased TRAF3 protein levels. We generated OC-specific TRAF3^{-/-} mice and observed 2-fold more OCs in their calvarial bones vs WT mice. CQ reduced OC #s by 50% in WT mice *in vivo* but had no effect in TRAF3^{-/-} mice. CQ significantly reduced PTH-induced marrow fibrosis in WT (11 ± 1 vs 29 ± 3% with PBS), but not in TRAF3^{-/-} mice (30 ± 4 vs 28 ± 3%). Retroviral expression of TRAF3 in OC precursors (OCPs) significantly reduced RANKL-induced OC #s, associated with reduced NF- κ B RelA, RelB, and NIK protein levels and decreased p100 processing to p52, suggesting that TRAF3 suppresses canonical and non-canonical signaling to inhibit OC formation. We treated WT OCPs with RANKL and the proteasome inhibitor, MG132, the lysosome inhibitors, NH₄Cl or CQ, or the autophagy inhibitors, Bafilomycin or 3-Methyladenine, and found that only the lysosome and autophagy inhibitors prevented RANKL-induced TRAF3 degradation. We over-expressed a TRAF3-GFP fusion protein in OCPs and found that TRAF3 colocalized with the lysosomal protein LAMP2. RANKL increased co-localization of TRAF3 and LAMP2, which was prevented by CQ. Finally, we found that RANKL induced 2.5-fold more TRAF3 expression in RelB^{-/-} OCPs. Furthermore, over-expression of RelB in RelB^{-/-} OCPs reversed this reduced ability of RANKL to degrade TRAF3, indicating RelB is involved in RANKL-induced TRAF3 lysosomal degradation. Our findings indicate that RANKL induces TRAF3 lysosomal/autophagic degradation, an effect mediated by RelB, and that CQ inhibits OC formation *in vitro* and *in vivo* by preventing TRAF3 lysosomal degradation. They suggest that strategies to increase TRAF3 levels in OCPs, such as treatment with CQ or CQ derivatives, will inhibit bone resorption in conditions where RANKL is increased, such as RA.

Disclosures: Yan Xiu, None.

FR0248

Activation of the NLRP3 Inflammasome in Myeloid Cells Causes Massive Bone Resorption. Sheri Bonar¹, Cynthia Brecks², Matthew McGeough³, Susannah Brydges³, Chang Yang⁴, Deborah Novack⁵, Hal Hoffman³, Roberto Civitelli⁵, Gabriel Mbalaviele^{*5}. ¹Washington University in St. Louis, USA, ²Washington University In St. Louis, USA, ³University of California, San Diego, La Jolla, CA, USA, ⁴Washington University in St. Louis School of Medicine, USA, ⁵Washington University in St. Louis School of Medicine, USA

Nod Leucine rich Repeat with a Pyrin domain 3 (NLRP3) is a member of the NOD-like receptor family of proteins involved in innate immune responses. NLRP3 forms an inflammasome, intracellular protein complex that converts pro-IL-1 β into mature IL-1 β . We recently reported that mice globally expressing constitutively activated NLRP3 exhibit severe osteopenia stemming from abnormally accelerated bone resorption, attended by increased osteoclastogenesis. To gain insights into the cell context dependent function of NLRP3, we generated knockin mice expressing a constitutively active NLRP3 mutant in myeloid cells driven by the LysM promoter (NLRP3^{LysM}). At 2 weeks of age, NLRP3^{LysM} mice are significantly smaller and osteopenic relative to WT mice based on whole body DXA, histomorphometric and μ CT (50% lower BV/TV) analyses. FACS analysis revealed 3-fold higher number of CD11b^{low}Gr1^{low}CD117⁺ osteoclast (OC) precursors in unfractionated bone marrow cells of NLRP3^{LysM} mice relative to WT mice. Consistent with these results, the number of OC developing from unfractionated bone marrow cells or cultured bone marrow macrophages (BMMs) in the presence of M-CSF and RANKL was higher in NLRP3^{LysM} cells than in WT cells. In addition, degradation of poly(ADP-ribose) polymerase 1, a negative regulator of OC formation and substrate of the inflammasome, increased during osteoclastogenesis of NLRP3^{LysM} BMMs to a larger extent than in WT cells. Conversely, BMMs from ASC (another component of the inflammasome) or NLRP3 knockout mice formed fewer OC than WT BMMs. Thus, NLRP3 activation increases both the number of OC precursors and their sensitivity to osteoclastogenic factors. Consistent with the notion that bone degradation products might serve as endogenous activators of NLRP3, hydroxyapatite crystals (HA) induced IL-1 β production by 300-fold in BMMs, an effect that required the presence of NLRP3 and ASC. Moreover, treatment of co-cultures of WT BMMs and bone marrow stromal cells with HA led to increased OC formation. In summary, NLRP3^{LysM} mice phenocopy the severe osteopenia of mice globally expressing constitutively activate NLRP3, demonstrating that NLRP3 drives osteoclastogenesis acting directly in the myeloid lineage. Since NLRP3 activation by HA stimulates IL-1 β production and osteoclastogenesis, bone degradation products activation of the NLRP3 inflammasome in bone-resident myeloid cells may result in a positive feedback that amplifies bone resorption.

Disclosures: Gabriel Mbalaviele, None.

FR0249

Calcium/calmodulin-signaling Regulates TRPV4 Action by the Process Supporting Myosin IIA Association in Osteoclasts. Ritsuko Masuyama^{*1}, Atsuko Mizuno², Hiroshi Kaijiya³, Hideki Kitaura⁴, Koji Okabe³, Toshihisa Komori¹. ¹Nagasaki University Graduate School of Biomedical Sciences, Japan, ²Jichi Medical University, Japan, ³Fukuoka Dental College, Japan, ⁴Tohoku University, Japan

Osteoclast differentiation is critically dependent on Ca²⁺ signaling. A Ca²⁺ permeable channel, transient receptor potential vanilloid 4 (TRPV4), mediates Ca²⁺ influx in the late stage of osteoclast differentiation and thereby regulates Ca²⁺ signaling. We previously reported that *Trpv4*-null mice had increased bone mass resulting from impaired osteoclast maturation, and found that the system supplying cellular Ca²⁺ switched from Ca²⁺ oscillations to Ca²⁺ influx during osteoclast differentiation. However, the system-modifying effect of TRPV4 activity remains to be determined. To elucidate the mechanisms underlying TRPV4 activation based on osteoclast differentiation, TRPV4 gain-of-function mutants were generated by the amino acid substitutions R616Q and V620I in TRPV4 and were restrictedly introduced into osteoclast lineage in *Trpv4* null mice to generate osteoclasts *Trpv4*^{R616Q/V620I} rescue mice.

As expected, TRPV4 activation increased osteoclasts surface in tibia section (+260% vs *Trpv4*-null, +80% vs WT; $P < 0.01$), thereby resulting in bone loss (-24% vs *Trpv4*-null, -12% vs WT mice; $P < 0.05$). During *in vitro* analysis, *Trpv4*^{R616Q/V620I} osteoclasts showed activated Ca²⁺/calmodulin signaling compared with osteoclasts lacking *Trpv4* as shown by the increased *NFATc1* expression. Although the regulatory system involved with TRPV4 activation in osteoclasts remains unknown, the Ca²⁺/CaM complex has been suggested as one possible regulator because osteoclasts differentiation is accompanied by dramatic induction of calmodulin. We therefore investigated *Trpv4*^{R616Q/V620I} mice that lacked the calmodulin-binding domain (*Trpv4*^{R616Q/V620I- Δ CaM). Bone loss due to TRPV4 activation was abrogated by loss of interactions between Ca²⁺/calmodulin signaling and TRPV4 that observed in *Trpv4*^{R616Q/V620I- Δ CaM mice. Finally, modulators of TRPV4 interactions with the calmodulin-binding domain were investigated by proteomic analysis. Interestingly, non-muscle myosin IIA was identified by LC-MS/MS analysis, which was confirmed by immunoblotting following coimmunoprecipitation with TRPV4. Furthermore, myosin IIA gene silencing significantly reduced TRPV4 activation concomitant with impaired osteoclast migration examined by wound healing assay.}}

These results indicate that TRPV4 activation reciprocally regulates Ca²⁺/calmodulin signaling, which involves an association of TRPV4 with myosin IIA, and supports sufficient osteoclast function.

Disclosures: Ritsuko Masuyama, None.

FR0252

Foxp3, the Master Transcriptional Regulator in Regulatory T Cells, Controls Osteoclastogenesis and Bone Mass. Tim Hung-Po Chen^{*1}, Yousef Abu-Amer². ¹Washington University School of Medicine, USA, ²Washington University in St. Louis School of Medicine, USA

Regulatory T cells (Tregs) play an essential role in prevention of autoimmune response. Scurfy mice, which present spontaneous null mutation of the forkhead gene *foxp3*, lack Tregs and immune self-tolerance and mimic the human disease IPEX (immunodysregulation polyendocrinopathy enteropathy X-linked syndrome) which is associated with bone deformities. Despite recent research in Tregs, the mechanism of Foxp3 in bone remains unclear. In this study, we first evaluated parameters of bone in scurfy mice and found that lack of Foxp3 led to osteoporotic phenotype in mice. Histological and μ CT analyses revealed increased osteoclasts, thinner cortical bone, and reduced trabecular regions in the Foxp3 deficient scurfy mice than in wildtype controls. Taken together, Foxp3 deficient mice exhibited increased erosion and poor bone quality. We next examined gene expression of inflammatory cytokines of magnetic beads sorted CD4⁺ T cells in these mice by qRT-PCR. RANKL, TNF α and IL-17, were up-regulated. *NFATc1* mRNA and NEMO/IKK γ protein were also increased in CD4⁺ T cells. Co-immunoprecipitation assays revealed physical interaction between NEMO and Foxp3 in both primary CD4⁺ T cells and transiently transfected 293T cells, suggesting a post-translational regulatory mechanism of NEMO protein via Foxp3. The notion that expression of Foxp3 is T cell-exclusive has been recently challenged. Therefore, we tested whether in addition to extrinsic cues from Tregs, Foxp3 is also required in osteoclastogenesis in a cell intrinsic manner. We found that macrophages derived from scurfy mice generated more osteoclasts compared with wild type controls. Interestingly, flow cytometry analysis revealed that the protein expression of Foxp3 was down-regulated 7-fold in the wildtype culture during this course of RANKL treatment, suggestive of an inhibitory role of Foxp3 in RANKL induced osteoclastogenesis. These cells also showed higher proliferative activity (S-phase cells) in cultures as assessed by BrdU flow cell cycle analysis. Phenotypic analysis by flow cytometry revealed a proportion of CD11b⁺ monocyte/osteoclast precursors was markedly increased in Foxp3 deficient bone marrow, whereas a proportion of gr1⁺ granulocyte/myeloid derived suppressor cells (MDSCs) and CD11c dendritic cells were decreased. In summary, our findings suggest that Foxp3 may play a critical role in bone metabolism, not merely by its conventional function in Tregs but by directly affecting osteoclast development

Disclosures: Tim Hung-Po Chen, None.

FR0254

Impairment of Osteoclastic Bone Resorption in Rapidly Growing Female p47^{phox} Knockout Mice. Jin-Ran Chen^{*1}, Kelly Mercer², Oxana P. Lazarenko³, Thomas M. Badger⁴, Martin J. J. Ronis⁵. ¹Arkansas Children's Nutrition Center, & Department of Pediatrics, University of Arkansas for Medical Sciences, USA, ²Arkansas Children's Nutrition Center, USA, ³Arkansas Children's Nutrition Center, & Department of Physiology & Biophysics, University of Arkansas for Medical Sciences, USA, ⁴Arkansas Children's Nutrition Center. The Departments of Pediatrics, Physiology & Biophysics, University of Arkansas for Medical Sciences, USA, ⁵Arkansas Children's Nutrition Center, & Department of Pediatrics, Pharmacology & Toxicology, University of Arkansas for Medical Sciences, USA

Bone formation is dependent on the activity and differentiation of osteoblasts; whereas resorption of preexisting mineralized bone matrix by osteoclasts is necessary not only for bone development but also for regeneration and remodeling. Bone remodeling is a process in which osteoblasts and osteoclasts are coupled. It changes dramatically during the course of development as it undergoes age-dependent regulation. Accumulation of reactive oxygen species (ROS) has been suggested to inhibit bone remodeling at each life stage. Tightly controlled and cell-specific NADPH-oxidase (Nox) activities represent one of the major sources of ROS in many cell types. Here, we have utilized a p47^{phox} knockout mouse model in which the majority of Nox activity is lost as the result of loss of an essential cytosolic co-activator, and characterized bone phenotype in these mice compared to their wild type controls. We found that, in female p47^{phox} -/- mice at 6 weeks of age, bone mineral density and bone mineral content were higher in comparison to wild type controls (P < 0.05). Consistent with this, bone strength was found to be higher in femur from p47^{phox} -/- mice, compared with those from wild type controls, in three point bending tests (P < 0.05). Flow cytometric analysis showed that osteoblastic calvarial cells isolated from female p47^{phox} -/- mice had significantly lower levels of ROS. Furthermore, bone histomorphometric analysis revealed that osteoclast number was lower in p47^{phox} -/- mice compared with their wild type controls (P < 0.05). This is in agreement with reduced gene expression of bone resorption markers RANKL and TRAP in RNA isolated from both femur and bone marrow cells from female p47^{phox} -/- mice compared to their wild type controls (P < 0.05). Moreover, in *ex vivo* primary osteoblast and osteoclast precursor co-culture, TRAPase staining revealed lower numbers of mature osteoclasts (containing 3 or more nuclei) in wild type primary osteoblasts plus p47^{phox} -/- pre-osteoclast cultures compared with wild type primary osteoblasts plus wild type pre-osteoclast cultures. These data indicate that the high bone mass in 6 week old female p47^{phox} -/- mice is due to lower ROS generation leading to decreased osteoclastogenesis. *Supported in part by ARS CRIS #6251-51000-005-03S (JRC) and R01 AA18282 (MJJR).*

Disclosures: Jin-Ran Chen, None.

FR0260

Canonical Wnt Signaling Mediates an Osteoprotegerin-independent Inhibitory Effect on Osteoclastogenesis. Johannes Keller^{*1}, Michael Amling¹, Joachim Albers², Anke Baranowsky³, Thorsten Schinke⁴. ¹University Medical Center Hamburg-Eppendorf, Germany, ²Universitätsklinikum Hamburg Eppendorf, Germany, ³Universitätsklinikum Hamburg-Eppendorf, Germany, ⁴Department of Osteology & Biomechanics University Medical Center Hamburg Eppendorf, Germany

Wnt signaling plays a pivotal role in the regulation of bone remodeling, and its inhibition by specific antagonists is one of the causes for excessive bone resorption observed in individuals with multiple myeloma. Since an osteoblast-specific inactivation of β -catenin, the major intracellular mediator of canonical Wnt signaling, causes reduced expression of the osteoclastogenesis-inhibitor Opg, it appeared that this influence is solely mediated indirectly. Here we show that activating canonical Wnt signaling in murine bone marrow cells inhibits their differentiation into multinucleated osteoclasts, independent of Opg. Likewise, specific inactivation of β -catenin in the osteoclast lineage results in osteopenia due to increased osteoclastogenesis, despite normal Opg production. The same phenotypic abnormalities were observed in mice lacking the Wnt receptor Frizzled-8 (Fzd8), which was identified as a candidate regulator of bone resorption by genome-wide expression analyses. Taken together, these findings demonstrate that osteoclastogenesis is directly regulated by canonical Wnt signaling, and that this regulation is mediated, at least in part, through the serpentine receptor Fzd8.

Disclosures: Johannes Keller, None.

FR0261

Foxp3⁺ CD8 T-Cells Can Suppress Bone Turnover in Response to RANKL Administration and in Ovariectomized Mice. Reggie Aurora^{*1}, Zachary Buchwald², Jennifer Kiesel², Deborah Novack³, Richard Di Paolo². ¹Saint Louis University University, USA, ²Saint Louis University School of Medicine, USA, ³Washington University in St. Louis School of Medicine, USA

We have been previously shown that osteoclasts can cross-present antigens. Co-culturing CD8⁺ T-cells with osteoclasts induced a FoxP3⁺ regulatory phenotype *in vitro* in the presence of antigen [1]. These osteoclast-induced FoxP3⁺ CD25⁺ CD8 T-cells (OC-iT_{REG}) can suppress osteoclast activity *in vitro* in a cell-contact independent, cytokine dependent manner. To determine if OC-iT_{REG} could suppress bone turnover *in vivo* we adoptively transferred these T-cells into an OT-I transgenic mouse that lacks endogenous T_{REG}. We then injected the recipient mice with RANKL. Suppression of bone turnover (as measured by CTX) was observed in the mice that received T_{REG}. In contrast no suppression was observed in the untreated controls or in mice treated with anti-CD3/CD28 activated CD8 T-cells. We have also shown that the OC-iT_{REG} can suppress bone turnover in ovariectomized (OVX) mice, a model of post-menopausal osteoporosis. A single infusion of OC-iT_{REG} into mice two weeks post-OVX reduced bone turnover for at least 10 days. Next, to investigate whether the endogenous FoxP3⁺ CD8 T-cells could also suppress osteoclast resorption, we used the FoxP3^{GFP} reporter mouse and found that GFP⁺ but not GFP⁻ CD8 T-cells purified from the bone marrow could suppress osteoclast pitting *in vitro*. To determine whether the endogenous CD8⁺ T-cells also have bone regulatory activity *in vivo*, we performed a RANKL dose titration into wt mice and mice lacking CD8⁺ T-cells (TCR α -, b2M-). Mice lacking CD8⁺ T-cells had increased bone turnover relative to wt controls, at doses > 0.5 mg/kg RANKL. To confirm the observed suppression was due to the absence of CD8 T-cells, TCR α - mice were reconstituted with fractionated CD8 or CD4 T-cells. Mice that received CD8 T-cells showed suppression whereas the CD4 did not. Our results show that OC-iT_{REG} and endogenous CD8 T-cells can suppress osteoclast activity *in vitro* and *in vivo*.

1. Kiesel, J.R., Z.S. Buchwald, and R. Aurora, *Cross-presentation by osteoclasts induces FoxP3 in CD8+ T cells*. J Immunol, 2009.182(9): p. 5477-87.

Disclosures: Reggie Aurora, None.

FR0263

Mice with Inactivating Mutations in the RANK PVQEET⁵⁶⁰⁻⁵⁶⁵ and PVQEQG⁶⁰⁴⁻⁶⁰⁹ Motifs Exhibit Increased Bone Mass Due to Impaired Osteoclastogenesis. Zhenqi Shi^{*1}, Joel Jules², Bob Kesterson³, Dongfeng Zhao⁴, Xu Feng⁵. ¹University of Alabama, USA, ²University of Miami Miller School of Medicine, USA, ³Department of Genetics, UAB, USA, ⁴The University of Alabama At Birmingham, USA, ⁵University of Alabama at Birmingham, USA

RANKL plays a crucial role in osteoclastogenesis by activating RANK, which activates various signaling pathways including NF- κ B, JNK, ERK, p38 and Akt in osteoclast precursors by recruiting TNF receptor-associated factors (TRAFs). *In vitro* studies have identified three functional TRAF-binding motifs: PFQEP³⁶⁹⁻³⁷³ (Motif 1), PVQEET⁵⁶⁰⁻⁵⁶⁵ (Motif 2), and PVQEQG⁶⁰⁴⁻⁶⁰⁹ (Motif 3) in the RANK cytoplasmic domain. Notably, Motif 2 and Motif 3 are more potent than Motif 1 in mediating osteoclastogenesis *in vitro*, and mutation of both Motif 2 and Motif 3 dramatically impaired RANK's ability to promote osteoclastogenesis *in vitro*. To validate these findings *in vivo*, we generated knockin (KI) mice bearing inactivating mutations in Motif 2 (PVQEET to LLNDDS) and Motif 3 (PVQEQG to LLNDNA). The introduced mutations were confirmed by sequencing. Western blot and RT-PCR analyses verified that bone marrow macrophages (BMMs) from wild type (WT), heterozygous KI (RANK^{+/mut}) and homozygous KI (RANK^{mut/mut}) mice have similar levels of RANK expression. RANK^{mut/mut} mice are viable, born at the expected Mendelian frequency, and have normal tooth eruption. However, X-ray and micro-computed tomography (μ CT) analysis of femurs of 12-week old mice have revealed dramatic increases in bone mass in RANK^{mut/mut} compared to age and sex matched WT counterparts. Consistently, BMMs from RANK^{mut/mut} mice failed to form osteoclasts in tissue culture dishes and on bone slices *in vitro* in response to M-CSF and RANKL stimulation. Mechanistically, while RANKL-induced activation of the NF- κ B, ERK, p38, JNK and Akt pathways remains normal in RANK^{mut/mut} BMMs, RANKL-stimulated expression of NFATc1 is impaired in these cells. Given that TNF α - and IL-1-mediated osteoclastogenesis requires RANK signaling, we further examined the role of Motifs 2 and 3 in TNF α /IL-1-mediated osteoclastogenesis. We found that the capacity of TNF α and IL-1 to promote osteoclastogenesis from RANK^{mut/mut} BMMs in the presence of RANKL in tissue culture dishes and on bone slices is significantly impaired, indicating that Motifs 2 and 3 are integral signaling components to initiate normal RANK signaling to support TNF α - and IL-1-mediated osteoclastogenesis. These findings indicate that Motifs 2 and 3 are critical for osteoclastogenesis *in vivo* and thus they have the potential to serve as novel therapeutic targets for osteoporosis and bone erosion in rheumatoid arthritis.

Disclosures: Zhenqi Shi, None.

FR0268

Stat5 Suppresses Bone Resorption of Osteoclasts by Upregulating Expression of Dusp Family. Jun Hirose*, Hironari Masuda, Yasunori Omata, Sakae Tanaka. The University of Tokyo, Japan

Signal transducers and activators of transcription (Stats) are family of proteins which transmit the signals of various cytokines through Jak/Stat pathways. Stat5 is a member of Stat family and essential for cytokine-regulated processes such as proliferation, differentiation, and survival in hematopoietic cells. To investigate the role of Stat5 in osteoclasts, we generated mice with osteoclast-specific conditional deletion of Stat5a and Stat5b (Stat5cKO mice) by crossing Stat5a&b floxed mice and Cathepsin K-Cre mice. They grew normally without apparent morphological abnormalities, but they exhibited decreased bone mass as assessed by micro CT and DEXA, which became prominent in the course of aging. The mice exhibited an increased serum level of CTx-I, and histomorphometric analysis of proximal tibia of 8-week-old Stat5 cKO mice revealed a significant increase in the eroded surface/bone surface ratio and the osteoclast surface, but not in the osteoclast number. RANKL and M-CSF-induced osteoclast differentiation was indistinguishable between WT and Stat5 cKO cells and there was no difference in the survival of WT and Stat5cKO osteoclasts. However, bone-resorbing activity of Stat5 cKO osteoclasts was markedly promoted as compared with WT osteoclasts. To examine the mechanisms underlying, we analyzed major intracellular signaling pathways in Stat5 cKO osteoclasts, and found that Erk activity was increased in cKO osteoclasts. The expression of MAPK phosphatases Dusp (dual specific phosphatase) 1 and 2 was significantly decreased in Stat5 cKO osteoclasts as determined by DNA microarray and real-time RT-PCR analyses. Retrovirus vector-mediated overexpression of Stat5 promoted Dusp1 and 2 expression in osteoclasts. Among the known stimulators of Stat5, IL-2, IL-3, IL-5, GH and PRL, only IL-3 induced activation of Stat5 in osteoclasts, and nuclear translocation of Stat5 was observed in response to IL-3 stimulation. Rapid induction of Dusp1 and 2 expression by IL-3 was observed in WT osteoclasts but not in Stat5 cKO osteoclasts. Our results suggest that Stat 5 negatively regulates the bone-resorbing function by promoting Dusp1 and 2 expression, and IL-3 may be one of the stimulators of Stat5 in osteoclasts.

Disclosures: Jun Hirose, None.

FR0271

Evaluation of Osteocyte Dedifferentiation in vitro and in vivo. Elena Torreggiani*¹, Slavica Pejda¹, Igor Matic¹, Mark Horowitz², Ivo Kalajzic¹. ¹University of Connecticut health Center, USA, ²Yale University School of Medicine, USA

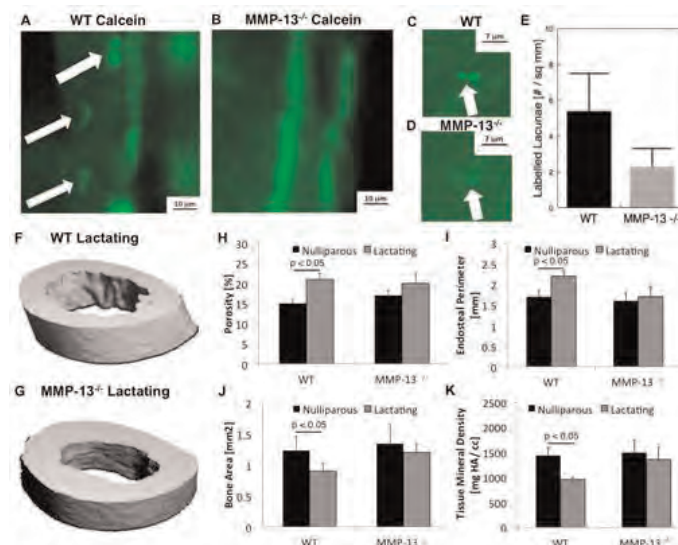
Cellular dedifferentiation has been observed in biological phenomena such as carcinogenesis, but it has been difficult to study due to a lack of experimentally traceable systems. Presently, there is no evidence for the ability of mature osteoblast lineage cells to dedifferentiate. The use of visual transgenes, such as GFP, has been instrumental for identifying cells at different stages of maturation. However, markers expressed under the control of a specific promoter are no longer expressed when promoter activity ceases. A valuable tool for lineage tracing is the Cre/loxP system. In this study we present evidence that DMP-1 expressing cells (preosteocytes/osteocytes) can undergo dedifferentiation in vitro and in vivo, accompanied by changes in gene expression. We have utilized transgenic mice in which the DMP1 promoter drives GFP expression as a visual marker of the current stage of differentiation (DMP-GFP) or drives Cre recombinase in order to activate an historical reporter in osteocytes and their progeny (DMP-Cre). Primary bone chip outgrowth cell (BCOC) cultures were prepared by enzymatic digestion (collagenase/trypsin/EDTA) to remove surface osteoblasts. When we utilized a DMP-GFP transgene, BCOC were GFP negative by epifluorescence and immunofluorescent staining for GFP. Using DMP-Cre mice bred with a Rosa-tomato reporter strain, cells that emerged from bone chips after 48-72 hours expressed Tomato. This result suggests that cells that have previously expressed the DMP promoter have the ability to dedifferentiate. Using FACS sorting we have isolated DMP-Cre/Tomato+ and DMP-Cre/Tomato- cells and shown that the positive population has the ability to redifferentiate into the osteogenic lineage, while the negative population did not mineralize, but showed some evidence of adipogenesis. BCOC cultures from DMP-GFP/DMP-Cre/Tomato mice also showed redifferentiation with the appearance of dual DMP-GFP+/Tomato+ cells. Following subcutaneous transplantation of whole bone chips derived from DMP-Cre/Tomato mice we observed formation of numerous DMP-Cre/Tomato+ osteoblasts on the surface of bone chips. Our results indicate that under certain conditions cells embedded in the matrix can grow out and begin to proliferate, suggesting that mature osteoblast lineage cells could provide an additional source of preosteoblasts capable of proliferation and differentiation. Future studies will aim to evaluate factors that affect osteocyte dedifferentiation in vivo and in vitro.

Disclosures: Elena Torreggiani, None.

FR0272

Matrix Metalloproteinase-13 is Required for Osteocytic Perilacunar Remodeling. Simon Tang*, Tamara Alliston. University of California, San Francisco, USA

Like bone mass, bone quality is specified in development, actively maintained post-natally, and disrupted by disease. The roles of osteoblasts, osteoclasts, and osteocytes in the regulation of bone mass are increasingly well defined. However, the cellular and molecular mechanisms by which bone quality is regulated remain unclear. Proteins that remodel bone extracellular matrix, such as the collagen-degrading matrix metalloproteinase (MMP)-13, are likely candidates that regulate bone quality. Using MMP-13 deficient male two-month old mice, we examined the role of MMP-13 in the remodeling and maintenance of bone matrix and subsequent fracture resistance. Throughout the diaphysis of MMP-13-deficient tibiae, we observed elevated non-enzymatic crosslinking and concentric regions of hypermineralization, collagen disorganization, and canalicular malformation. These defects localize to the same mid-cortical bone regions where osteocyte lacunae and canaliculi exhibit MMP-13 and tartrate-resistant acid phosphatase expression, as well as the osteocyte marker Sclerostin. Despite otherwise normal measures of osteoclast and osteoblast function, dynamic histomorphometry revealed that the remodeling of osteocyte lacunae is impaired in MMP-13-/- bone. While WT bone showed regular calcein incorporation in the perilacunar spaces (A, C), demonstrating osteocyte perilacunar remodeling, the loss of MMP-13 resulted in the loss of this phenomenon (B, D, E). MicroCT analysis of tibia from nulliparous and lactating WT show that lactation causes significant increases in cortical bone porosity (F; $p < 0.05$; t-test) and endosteal perimeter (I; $p < 0.05$; t-test), and decreases in cortical bone area (J; $p < 0.05$; t-test) and tissue mineral density (K; $p < 0.05$; t-test). In contrast, the cortical bone structural parameters of MMP-13-/- mice, when compared to MMP-13-/- nulliparous controls, were not significantly altered by lactation demonstrating the need for MMP-13 for osteocyte-mediated remodeling of perilacunar matrix. The loss of MMP-13, and the resulting defects in perilacunar remodeling and matrix organization, also significantly reduced MMP-13-/- bone fracture toughness and post-yield behavior. Taken together, these findings demonstrate that osteocyte perilacunar remodeling of mid-cortical bone matrix requires MMP-13 and is essential for the maintenance of bone quality.



MMP-13 is required for osteocyte perilacunar remodeling.

Disclosures: Simon Tang, None.

FR0273

Osteocyte-Produced Microvesicles: a Potential Mechanism for Communication With Osteoblasts and Osteoclasts. Pat Veno, Matt Prideaux, Vladimir Dusevich, Lynda Bonewald, Sarah Dallas*. University of Missouri - Kansas City, USA

Recent findings have highlighted the key role of osteocytes as regulators of osteoblast and osteoclast function that integrate hormonal and mechanical signals to control bone mass. However, the mechanisms by which osteocyte signals reach these bone cells are not well defined. Exosomes (50-100nm) and microvesicles (100-1000nm) are membrane-bound vesicular particles released by cells that deliver "packets" of proteins, mRNAs and microRNAs to target cells and alter their function. We have previously reported microvesicle-like particles that appear to be shed by osteocytes. To further understand their properties and function, live cell imaging and confocal and electron microscopy were used, together with microvesicle purification and analysis of their protein composition. Using transgenic mice expressing a membrane targeted GFP variant in osteocytes (Dmp1-mem-GFP), 3D confocal microscopy showed abundant spherical GFP+ve microvesicles in the bone matrix of neonatal and adult bones. Similar vesicles were seen by immunostaining for the osteocyte

membrane protein E11/gp38. GFP+ve microvesicles were also seen in marrow spaces/vascular channels in bone as well as in marrow cell suspensions from the long bones, suggesting they may be shed into the marrow space and/or circulation. Microvesicles were purified from mineralized, osteocyte-enriched primary cultures of Dmp1-mem-GFP calvarial cells and IDG-SW3 cells (a late osteoblast cell line that differentiates into mature osteocyte-like cells). Western blotting showed that several osteocyte marker proteins were present in the microvesicles, including E11, sclerostin, FGF23 and RANKL in addition to known microvesicle proteins, β -actin, fibronectin and flotillin-2. Of these, fibronectin and sclerostin were enriched in microvesicles compared to cell lysate. PTH treatment for 24h increased RANKL and E11 levels in microvesicles and decreased sclerostin. Live imaging of osteocytes from Dmp1-mem-GFP mice showed extensive membrane ruffling and shedding of vesicles from the cell body and dendrites and suggested increased microvesicle release in response to PTH. These data show that osteocytes shed microvesicles containing bone regulatory proteins which may represent a novel mechanism for cell-cell communication in bone. Release of RANKL containing microvesicles may allow osteocytes to signal to osteoclast precursors in the bone marrow and hormones such as PTH may alter microvesicle content to regulate bone remodeling.

Disclosures: Sarah Dallas, None.

FR0278

Mice Like it Hot: Housing Mice at Room Temperature Results in Cancellous Bone Loss. Urszula Iwaniec, Russell Turner*, Kenneth Philbrick, Laurence Lindenmaier, Dawn Olson, Gianni Maddalozzo. Oregon State University, USA

In contrast to humans, age-related cancellous bone loss begins in mice even as cortical bone continues to be accrued. This premature osteopenia is characterized architecturally by a pronounced decrease in trabecular number but preservation of trabecular thickness. Unlike humans who are homeotherms, the mouse is a facultative daily heterotherm and experiences cyclic changes in core temperature and bouts of torpor when subjected to cold temperature stress (temperatures below thermoneutral; ~32°C for mice) and/or caloric restriction. Activation of sympathetic signaling is important for mice to successfully adapt to low temperature and suppression of sympathetic tone has been reported to increase cancellous bone mass in mice. We therefore reasoned that premature age-related bone loss commonly seen in mice may be due to temperature stress induced by housing the animals at room temperature (20-24°C). To test this hypothesis, 1-month-old female C57BL/6J (B6) and C3H/HeJ (C3H) mice (n=20/strain) were randomized to 1 of 2 temperatures (22°C or 32°C) and maintained with no bedding for 4 months. Compared to B6 mice housed at 22°C, B6 mice housed at 32°C consumed less food (2.8±0.1 vs. 4.7±0.1 g/day; mean±SE, p<0.01). However, there was no significant effect on total body mass, lean mass, or fat mass. Furthermore, there were minimal temperature-dependent effects on cortical bone mass and architecture. In contrast, mice housed at the warmer temperature had higher cancellous bone volume/tissue volume in the distal femur metaphysis (6.6±0.4 vs. 3.0±0.2%, p<0.01), distal femur epiphysis (26.5±0.6 vs. 22.1±0.4%, p<0.01), and in the 5th lumbar vertebra (16.7±0.4 vs. 14.1±0.4%, p<0.01). The sparing effect of thermoneutral housing on cancellous bone was due to preservation of trabecular thickness. Similar temperature-dependent differences in cancellous bone mass were obtained in C3H mice (data not shown). These results support the conclusion that mild cold stress has a major negative impact on cancellous bone mass and architecture in mice and that early onset cancellous bone loss in this species is due, in part, to cold adaptation. They also suggest that studies using mice as a preclinical model to investigate interactions between energy homeostasis and bone or the etiology of age-related bone loss need to account for confounding species differences in thermo-regulation and energy metabolism.

Disclosures: Russell Turner, None.

FR0280

The Effects of Acute Hyperinsulinemia on Bone Metabolism in Healthy Adults. Kaisa Ivaska*, H. Kalervo Vaananen¹, Maikki Heliövaara², Pertti Ebeling², Heikki Koistinen². ¹University of Turku, Finland, ²Helsinki University Hospital, Finland

Recently, studies in mice have demonstrated that insulin signaling in osteoblasts stimulates bone formation and promotes the release of osteocalcin (OC) from the bone microenvironment, particularly in the uncarboxylated form. As only few studies have assessed the role of insulin signaling as regulator of bone metabolism in humans, we evaluated the effect of acute insulin infusion on markers of bone metabolism in healthy subjects. Eight subjects (51.6±10.3 yrs, BMI 31.6±3.4 kg/m²) participated in a 4-h hyperinsulinemic (40 mU/m²/min) euglycaemic (5 mM) clamp and a control 4-h saline infusion on two separate days. In addition, 12 healthy men (23.5±5.1 yrs, BMI 22.0±2.8 kg/m²) participated in a 4-h hyperinsulinemic euglycaemic clamp with a high insulin infusion rate (72 mU/m²/min). Blood samples to determine the markers of bone formation (PINP), resorption (CTX, TRACP5b) and osteocalcin (total OC, uncarboxylated OC) were collected before and at the end of infusions. During 4-h insulin infusion, the concentration of resorption marker CTX decreased by 11% (p<0.05), whereas CTX remained unchanged during saline control. Fasting CTX correlated positively with insulin sensitivity (r=0.91, p<0.01, n=8). High insulin infusion rate resulted in a more pronounced suppression of bone resorption (median decrease in CTX 32%, p<0.01). Markers of osteoblast activity (PINP, total OC)

remained unchanged during insulin and saline infusions, whereas the ratio of uncarboxylated-to-total OC significantly decreased in response to insulin (p<0.05 and p<0.01 for low and high insulin infusion rate, respectively). In summary, insulin decreases bone resorption and modulates carboxylation of osteocalcin in healthy subjects. Insulin appears to have direct effects on bone metabolism, shifting the overall balance in the favor of bone formation.

Disclosures: Kaisa Ivaska, None.

FR0281

The Sympathetic Nervous System Mediates Trabecular Bone Loss Caused by the Second Generation Antipsychotic Risperidone. Katherine Motyl*¹, Deborah Barlow², Karen Houseknecht², Clifford Rosen³. ¹Maine Medical Center Research Institute, USA, ²University of New England, USA, ³Maine Medical Center, USA

Second generation antipsychotics (SGAs) are associated with metabolic complications and reduced bone mass. Previously, we reported that risperidone (RIS) increases bone resorption and reduces bone formation in C57BL/6J (B6) mice. Molecular targets of RIS include dopamine receptor (D2R) and serotonin receptors (5HT_{2A}, 5HT_{2C}), therefore direct and/or indirect mechanisms could affect bone. First, we examined whether there is potential for RIS to act directly on bone by measuring RIS levels in bone marrow after oral gavage with 0.75 mg/kg RIS with mass spectrometry. Both RIS and its active metabolite 9-OH RIS were found in bone marrow at concentrations comparable to published brain values (0.87±0.15 ng/g and 2.29±0.55 ng/g, respectively). Consistent with the notion that RIS could act locally in bone, primary BMSC cultures treated with RIS had significantly accelerated osteoclast differentiation. Second, we hypothesized that RIS could act indirectly through inhibition of the serotonin receptor (5HT_{2C}) in the brain responsible for suppression of sympathetic signaling to bone. Therefore, we treated 8-wk old B6 female mice with 0.75 mg/kg RIS or vehicle (VEH) by daily oral gavage for 4 wks. Serum RIS and its active metabolite 9OH-RIS were within clinically relevant ranges (26±2 nM and 78±7 nM, respectively). A subset of mice from RIS and VEH groups were administered 0.5 g/L propranolol (PR, β 2AR antagonist) in the drinking water for the duration of the study. PR did not reduce the amount of RIS in serum. Neither RIS nor PR altered body composition or total aBMD by DEXA. However, RIS alone significantly lowered distal femur trabecular BV/TV, Conn.D Tb.N and increased Tb.Sp. Importantly, all of these changes were prevented by combined RIS and PR treatment. Furthermore, oral gavage alone (VEH gavage vs untreated) did not affect trabecular mCT parameters. Our findings strongly suggest that trabecular bone changes from RIS are sympathetically mediated, and likely related to its binding to 5HT_{2C}. Patients on SGAs are often prescribed β -blockers in order to combat akathisia (restlessness), thus, the clinical relevance of these findings can be readily tested. In conclusion, we have determined that both indirect (CNS mediated) and direct mechanisms likely account for trabecular bone changes from RIS. Understanding these mechanisms is crucial for developing therapeutic strategies to counteract deleterious side effects. NIH AR061932.

Disclosures: Katherine Motyl, None.

FR0288

Estrogen Regulates Physiological Bone Turnover by Targeting Mesenchymal Cells in Mice. Alexandra Heyny*¹, Carmen Streicher², Pierre Chambon³, Reinhold Erben⁴. ¹inst. of Physiology, Pathophysiology & Biophysics, Austria, ²University of Veterinary Medicine Vienna, Austria, ³Institut de Génétique et de Biologie Moléculaire et Cellulaire, France, ⁴University of Veterinary Medicine, Austria

It is well known that bone metabolism is regulated by estrogen. Estrogen acts through two receptors, estrogen receptor-alpha (ER α) and -beta (ER β). Previous studies indicated that ER α is more important than ER β for the regulation of bone metabolism. However, it is still a matter of controversy whether hematopoietic or mesenchymal cells are the main effector cells responsible for mediating the effects of estrogen on bone. To answer this question, we established a reconstitution model resulting in selective deletion of ER α in hematopoietic or mesenchymal cells. We lethally irradiated 16-week-old female wild-type (WT) and global ER α knockout mice (α ERKO) on C57BL/6 genetic background, and reconstituted them with sex-matched bone marrow from α ERKO or WT mice, respectively. In irradiated WT mice reconstituted with α ERKO mouse bone marrow, all mesenchymal cells are of recipient origin and express a functional ER α , whereas hematopoietic cells are of donor-origin and lack ER α . Conversely, in irradiated α ERKO mice reconstituted with WT bone marrow, hematopoietic cells express a functional ER α , whereas mesenchymal cells lack ER α . To control for the deleterious effects of irradiation on ovarian function, irradiated mice received physiological doses of 17 β -estradiol (10 μ g/kg) 5 times per week over 4 weeks post-irradiation. Thereafter, all mice were ovariectomized (OVX), and subcutaneously received either vehicle or 10 μ g/kg 17 β -estradiol 5 times per week. Non-irradiated sham-operated, OVX and estradiol-supplemented OVX WT and α ERKO mice served as controls. All mice were killed 4 weeks post-OVX. pQCT analysis revealed femoral metaphyseal bone loss in non-irradiated vehicle-treated WT and α ERKO OVX mice 1 month post-OVX, relative to baseline and to estradiol-supplemented OVX mice of the same genotype. Bone and uterus of OVX α ERKO mice did not respond to physiological doses of estradiol. Similar to non-irradiated

OVX WT mice, estrogen treatment of OVX WT mice reconstituted with α ERKO bone marrow fully prevented OVX-induced bone loss. In contrast, estrogen treatment failed to increase bone mass in OVX α ERKO mice reconstituted with WT mouse bone marrow. Our data indicate that cells of the mesenchymal cell lineage, but not hematopoietic cells, are mediating the effects of estrogen on bone.

Disclosures: Alexandra Heyny, None.

FR0289

A Controlled Intervention of Weight Loss and Bone Mineral Density in Older Men. Claudia Pop¹, Katherine Tomaino¹, Deeptha Sukumar¹, Yvette Schluske¹, Christopher Gordon², Robert Zurfluh¹, Xiangbing Wang³, Sue Shapses¹. ¹Rutgers University, USA, ²McMaster University, Canada, ³Robert Wood Johnson Medical School, USA

Weight loss has been shown to decrease bone mineral density (BMD) in older women and in mixed populations of older women and men (1-2). This is the first prospective controlled trial to examine the response of BMD to intentional weight (wt) loss in men. Thirty-nine overweight and obese (body mass index, 31.9 ± 4.4 kg/m²) men (58 \pm 6 years) were assigned to either weight loss (WL; n=20) or weight maintenance (WM; n=19) for six months. Men in the WL group adhered to caloric restriction (500 kcal deficit/day) and both groups were supplemented individually to meet the recommended intakes of Ca and vitamin D. Bone was measured with dual energy x-ray absorptiometry and peripheral quantitative computed tomography (pQCT) at baseline and six months. Serum was measured at baseline, 1, 3 and 6 mo for serum 25-hydroxyvitamin D, parathyroid hormone, total and free testosterone and estradiol. Steroids and pQCT are reported for a subset. In addition, physical activity levels (PAL) were recorded before and during the intervention. The WL group lost $-7.7 \pm 4.4\%$ weight and $-20.5 \pm 18.0\%$ fat mass versus $-0.2 \pm 1.3\%$ weight and $+2.2 \pm 4.6\%$ fat mass in the WM group (ANOVA). There was a greater BMD decrease in WL than WM group over six months at the femoral neck, FN, ($-0.5 \pm 2.6\%$ vs $+1.1 \pm 2.2\%$; $p < 0.05$) and total body ($-0.9 \pm 2.4\%$ vs $+1.5 \pm 2.7\%$, $p < 0.01$) but not at other bone sites (radius, lumbar spine, total hip). Tibial pQCT measurements showed that the change in cortical bone area and thickness differed between the WL compared to WM group ($p < 0.05$) with trends for other parameters. There were no differences in sex steroids at baseline, but paired t-test showed an increase in serum free testosterone and estradiol in the WM group ($p < 0.05$) and no change in the WL group after 6 months. However, the changes were not significantly different between groups (ANOVA). Additionally, PAL did not differ between groups. Others have found that wt-stable men (50-69 y), show a slight annual increase in FN-BMD (0.5%/y) (3) that appears less than the increase found in the overweight/obese men in this trial. These data show that men who lose 8% wt show a different pattern of FN and total body BMD change vs. controls. Balancing the benefits of wt loss with risk of bone loss may differ depending on age and gender. References: 1. Sukumar, J Bone Miner Res, 2011; 2. Shah K, J Bone Miner Res, 2011; 3. Melton LJ, Osteoporos Int, 2000. Support: NIH-AG12161 to SAS

Disclosures: Claudia Pop, None.

FR0290

A Critical Role for Caspase-2 in Regulating Osteoclast Numbers in Male Age-Related Osteoporosis. Ramaswamy Sharma¹, Difernando Vanegas², Daniel Victor², Marisa Lopez-Cruzan³, Diane Horn², Kathleen Woodruff², Roberto Fajardo⁴, Stephen Harris⁵, Sherry Abboud Werner⁵, Brian Herman⁶. ¹University of Texas Health Sciences Center At San Antonio, USA, ²The University of Texas Health Science Center at San Antonio, USA, ³UTHSCSA, USA, ⁴UT Health Science Center, San Antonio, USA, ⁵University of Texas Health Science Center at San Antonio, USA, ⁶UT HSC San Antonio, USA

Molecular mechanisms underlying age-dependent bone loss are not fully known. Such knowledge is critical for designing novel and safe therapies for the prevention and treatment of senile osteoporosis. Recent studies suggest that aging-related increases in oxidative stress are a major cause of SO. We have previously shown that the cysteine protease, caspase-2, is required for oxidative stress-induced apoptosis. Here, we show that caspase-2 expression in wild type (WT) mice decreased with age, correlating with a decrease in bone mineral density (BMD). Genetic ablation of caspase-2 resulted in significantly decreased BMD in old male *Casp2*^{-/-} mice, decreased bone volume, trabecular number and cortical thickness, decreased breaking force and increased total indentation distance of old *Casp2*^{-/-} bone. Together, these data suggest that loss of caspase-2 promoted bone loss. We find that lack of caspase-2 results in increased oxidative stress that may enhance differentiation of the bone-resorbing cells, osteoclasts. As expected, we found higher osteoclast numbers in *Casp2*^{-/-} mice *in vivo* and also after *in vitro* differentiation from bone marrow macrophages. Further, TRAP enzyme activity of *in vitro* differentiated *Casp2*^{-/-} osteoclasts was higher. Addition of the caspase-2 inhibitor, zVDVAD-fmk, to mature osteoclast cultures resulted in higher numbers of intact osteoclasts whereas overexpression of normal but not mutant caspase-2 resulted in decreased TRAP activity. Immunohistochemistry indicated constitutive expression of caspase-2 in bone marrow cells, osteoblasts, and lining cells. However, caspase-2 was detected in *in vitro* differentiated osteoclasts only after treatment with high levels of oxidants. Importantly, *Casp2*^{-/-} osteoclasts were less

sensitive to oxidant treatment and exhibited higher TRAP activity. Therefore, caspase-2 regulates osteoclast numbers perhaps via apoptosis. Finally, we found 2-fold higher levels of the osteoclast survival factor, Csf-1, in *Casp2*^{-/-} bone lysates, suggesting a mechanistic explanation for caspase-2-based osteoclast regulation. As proof-of-concept, we generated mice over-expressing caspase-2 selectively in osteoclasts; we observed significantly increased trabecular bone volume, trabecular number and trabecular thickness. In conclusion, our data highlight a novel role for caspase-2 in male age-dependent osteoporosis and suggest the use of caspase-2 as a diagnostic marker for osteoporosis and as a putative target for therapy.

Disclosures: Ramaswamy Sharma, None.

FR0291

Serum Sclerostin and Bone Microarchitecture – Strong Positive Association in Men from the STRAMBO Cohort. Pawel Szulc¹, Stephanie Boutry², Claudia Goettsch³, Martina Rauner⁴, Nicolas Vilyayphiou⁵, Michael Schoppet⁶, Roland Chapurlat⁷, Lorenz Hofbauer⁸. ¹INSERM UMR 1033, University of Lyon, Hopital E. Herriot, Pavillon F, France, ²INSERM UMR 1033, University of Lyon, France, ³Division of Endocrinology, Diabetes, & Bone Diseases, Dresden University, Germany, ⁴Medical Faculty of the TU Dresden, Dresden, Germany, ⁵INSERM UMR1033, Université de Lyon & Hospices Civils de Lyon, France, ⁶Philipps-University, University of Marburg, Germany, ⁷E. Herriot Hospital, France, ⁸Dresden University Medical Center, Germany

Sclerostin is secreted by osteocytes. We assessed the relation of serum sclerostin levels with bone mineral density (BMD) measured by DXA and with bone microarchitecture assessed by high resolution peripheral QCT (XtremeCT Scanco) in 1,154 men aged 20 to 87 years. After the age of 63, the association between serum sclerostin levels and age was weaker ($r=0.17$, $b=0.20 \pm 0.03SD/10$ yrs) than before this age ($r=0.55$, $b=0.43 \pm 0.03SD/10$ yrs). Further analyses are adjusted for age, weight, height, muscle strength, smoking, glomerular filtration rate, and serum levels of estradiol, parathyroid hormone, and osteoprotegerin.

Before the age of 63, men in the highest sclerostin quartile had higher BMD at the spine, hip and whole body (4-7%, $p < 0.001$) compared with the three lower quartiles combined. They had higher trabecular volumetric BMD (Tb.vBMD) at the distal radius and tibia due to higher trabecular number (Tb.N) (6 to 8%, $p < 0.001$) and less heterogeneous trabecular distribution (4 to 6% lower Tb.Sp.SD, $p < 0.001$).

After the age of 63, men in the lowest sclerostin quartile had 4 to 15% lower BMD compared with the highest quartile (0.32-0.94 SD, $p < 0.001$) at all skeletal sites. They had lower cortical thickness and density at the distal radius and tibia compared with the highest quartile (3 to 9%, 0.30-0.55 SD, $p < 0.05-0.001$). Tb.vBMD correlated positively with serum sclerostin levels, also when the central and subendocortical compartments were analyzed separately at both skeletal sites ($r=0.15$ to 0.22 , $p < 0.001$). Men in the lowest sclerostin quartile had 10% lower Tb.N (0.7 SD, $p < 0.001$) and higher Tb.Sp.SD (7 to 9%, 0.8 SD, $p < 0.001$) compared with the highest quartile. After adjustment for BMD, men in the highest sclerostin quartile had higher Tb.N (3 to 5%, 0.25-0.30 SD, $p < 0.001$) and lower Tb.Sp.SD (2 to 4%, 0.32-0.42 SD, $p < 0.001$) compared to the three lower quartiles combined.

Total cross-sectional and trabecular areas did not differ across the quartiles of sclerostin regardless of the skeletal site or age range. The differences in trabecular thickness (Tb.Th) were generally weak or non-significant.

Thus, in men, serum sclerostin levels were strongly positively associated with BMD and quality of bone microarchitecture after adjustment for potential confounders, especially after the age of 63. The association was stronger in the trabecular compartment and dependent mainly on the differences in Tb.N and Tb.Sp.SD, but not Tb.Th.

Disclosures: Pawel Szulc, None.

FR0293

Low Holotranscobalamin and Cobalamins Predict Incident Fractures in Elderly Men; The MrOS Sweden. Catharina Lewerin^{*1}, Herman Nilsson-Ehle², Stefan Jacobsson³, Valter Sundh⁴, Helena Johansson⁵, Mattias Lorentzon⁶, Magnus Karlsson⁷, Osten Ljunggren⁸, John Kanis⁹, Steven Cummings¹⁰, Claes Ohlsson¹¹, Dan Mellstrom¹². ¹Västra Götaland, Sweden, ²Section of Hematology & Coagulation, Sahlgrenska University Hospital, Sweden, ³Department of Clinical Chemistry & Transfusion Medicine, Sahlgrenska Academy at the University of Gothenburg, Sweden, ⁴Department of Community Medicine & Public Health, Geriatric Medicine, Sahlgrenska Academy at the University of Gothenburg, Sweden, ⁵Center for Bone & Arthritis Research (CBR), Departments of Internal Medicine, at the Institute of Medicine, Sahlgrenska Academy at the University of Gothenburg, Sweden, ⁶Center for Bone Research at the Sahlgrenska Academy, Sweden, ⁷Skåne University Hospital Malmö, Lund University, Sweden, ⁸Uppsala University Hospital, Sweden, ⁹University of Sheffield, Belgium, ¹⁰San Francisco Coordinating Center, USA, ¹¹Center for Bone & Arthritis Research at the Sahlgrenska Academy, Sweden, ¹²Sahlgrenska University Hospital, Sweden

Background: Subclinical cobalamin deficiency is common in the elderly and has been suggested to affect bone metabolism. However the relationship between cobalamin status and incident fractures is not clear. The aim was to determine whether serum cobalamins or holotranscobalamin (the metabolic active cobalamin) are associated with risk of developing fracture among older men.

Methods: Men participating in the Gothenburg part of the population-based MrOS (Osteoporotic Fractures in Men) Sweden cohort and without on-going B vitamin medication were included in the present study (n=790, age range 69-81 years).

Results: During an average follow up of 5.9 years, 110 men sustained one or more X-ray verified fractures including 45 men with clinical vertebral fractures. In age adjusted linear regression analysis, holoTC below the median (<51.8 pmol/L) was associated with lower lumbar spine L1-4 BMD compared to those over the median ($\beta=-0.03$, $p<0.028$), and the lowest quintile of holoTC correlated with lumbar spine L1-4 BMD ($\beta=-0.03$, $p<0.043$) compared to quintile 2-4. The risk of fracture (adjusted for age, smoking, BMI, BMD, falls, prevalent fracture, plasma total homocysteine, cystatin C, 25-OH-vitamin D, intake of calcium and physical activity), increased by 38% and 26% per each SD decrease in cobalamins (HR 1.38; 95% CI 1.11-1.72) and holotranscobalamin (HR 1.26; 95% CI 1.03-1.54), respectively. Men in the lowest quartile of cobalamins and holotranscobalamin, (age, BMI and BMD adjusted), had an increased risk of all fracture (cobalamin, HR=1.67 [95% CI 1.11-2.5]; holotranscobalamin, HR=1.76 [95% CI 1.18-2.61]) and clinical vertebral fractures (cobalamin, HR=2.42 [95% CI 1.31-4.47]; holotranscobalamin, HR=2.47 [95% CI 1.35-4.53]) compared to quartile 2-4. No associations between folate or homocysteine and incident fractures were seen.

Conclusion: We present novel data showing that low holotranscobalamin and cobalamins predict incident fracture in elderly men. This association was unaffected by adjustment for BMI, BMD, plasma total homocysteine and cystatin C.

Disclosures: Catharina Lewerin, None.

FR0294

A Comparison of Bone Turnover Markers in Hip Fracture Patients vs. a Matched Group of Non-Fractured Controls during the 12 Month Recovery Period Post-Hip Fracture. Janet Yu-Yahiro^{*1}, Jay Magaziner², William Hawkes³, Marc Hochberg⁴, Denise Orwig², Rich Hebel⁵, Anne R. Cappola⁶. ¹Union Memorial Hospital, USA, ²University of Maryland, Baltimore, USA, ³University of Maryland School of Medicine, Department of Epidemiology, Division of Gerontology, USA, ⁴University of Maryland School of Medicine, USA, ⁵University of Maryland School of Medicine, Department of Epidemiology & Public Health, Division of Gerontology, USA, ⁶Perelman School of Medicine at the University of Pennsylvania, USA

Objective: To compare levels and trajectories of serum bone turnover markers (BTMs) during the 12 months hip fracture recovery period in a cohort of hip fracture patients and age- and bone mineral density (BMD) matched non-fracture controls.

Methods: Hip fracture patients enrolled in the Baltimore Hip Studies (BHS4) (n=58) were matched by age and total hip BMD to non-fracture controls from the Baltimore cohort of the Study on Osteoporotic Fractures (SOF) (n=58). Blood was drawn from BHS4 at time of fracture and at 2, 6, and 12 months post fracture from 1998 to 2004 and from SOF subjects at Visits 2 (1988-89) and 4 (1993-1994). The mean time between these SOF visits was 42.3 months and comparison bone marker values were estimated for time points 2, 6 and 12 months using linear models. Blood was assayed for bone specific alkaline phosphatase (BSAP), C-terminal propeptide of type 1 collagen (C1CP), carboxyterminal cross-linked telopeptide of type I collagen (CTX), 25-hydroxyvitamin D (25(OH)D), and intact parathyroid hormone (iPTH). Samples from a single individual from all time points were assayed together with SOF and BHS4 samples included in each assay to control for interassay variability. Mixed

model fitting was used for repeated measures analyses with the outcome measures as dependent variables.

Results: Women in SOF and BHS4 were comparable in age 79.0 +5.6 vs. 79.4 +5.4 yrs, and total hip BMD 0.670 +0.087 vs. 0.665 +0.115 gm/cm². Over 12 months, markers of osteoblastic activity (BSAP and C1CP) were lower in hip fracture patients than controls. BHS4 subjects had significantly higher iPTH levels and significantly lower 25(OH)D levels at baseline compared to SOF controls and 25(OH)D levels remained significantly lower in hip fracture subjects compared to controls throughout the 12-mo period (Table 1).

Conclusion: Over the 12 month post fracture period, hip fracture subjects were vitamin D insufficient with secondary hyperparathyroidism and had more osteoclastic activity and less osteoblastic activity when compared to non-fracture controls. Although these results do not enable us to differentiate between the effect of vitamin D deficiency and the impact of hip fracture healing on post fracture bone markers, they demonstrate that there is a distinctly different bone metabolic profile in hip fracture patients compared to controls, which is independent of BMD and age.

Table 1 A and B

A. outcome: BAP, C1CP, CTX
comparison: SOF non-fracture controls vs Hip 4 controls
form: mean (95% CI)

| Time | BAP | | | C1CP | | | CTX | | |
|-----------|---------------------|---------------------|--------|------------------|-----------------|------|------------------------|------------------------|--------|
| | SOF | Hip 4 | p(1) | SOF | Hip 4 | p(1) | SOF | Hip 4 | p(1) |
| Baseline | 28.8 (26.8-31.1) | 16.4 (12.7-20.0) | <.0001 | 125 (112-138) | 153 (96-210) | 0.34 | 0.400 (0.347-0.454) | 0.726 (0.642-0.810) | <.0001 |
| 2 months | 29.1 (26.8-33.1) | 18.7 (15.1-21.4) | 0.24 | 123 (111-136) | 106 (91-121) | 0.09 | 0.408 (0.347-0.452) | 0.710 (0.626-0.800) | 0.67 |
| 6 months | 29.3 (27.3-31.7) | 15.3 (12.3-18.4) | 0.30 | 121 (109-132) | 95 (81-109) | 0.00 | 0.398 (0.339-0.447) | 0.662 (0.513-0.838) | <.0001 |
| 12 months | 30.2 (28.0-32.4) | 13.4 (10.6-15.6) | <.01 | 119 (108-127) | 81 (70-92) | 0.01 | 0.398 (0.350-0.448) | 0.883 (0.804-0.922) | <.0001 |

B. outcome: Vitamin D, iPTH
comparison: SOF non-fracture controls vs Hip 4 controls
form: mean (95% CI)

| Time | Vitamin D | | | iPTH | | |
|-----------|---------------------|---------------------|--------|---------------------|---------------------|--------|
| | SOF | Hip 4 | p(1) | SOF | Hip 4 | p(1) |
| Baseline | 31.6 (28.9-34.3) | 21.6 (18.4-24.7) | <.0001 | 43.9 (39.2-48.7) | 80.9 (71.9-89.9) | <.0001 |
| 2 months | 31.4 (28.8-34.1) | 24.0 (21.6-26.4) | 0.02 | 44.9 (40.2-49.6) | 86.6 (76.8-96.3) | 0.31 |
| 6 months | 31.1 (28.5-33.7) | 24.7 (22.2-27.2) | 0.02 | 46.9 (42.3-51.6) | 86.9 (76.6-97.1) | 0.54 |
| 12 months | 30.6 (28.2-33.0) | 23.8 (21.1-26.5) | 0.03 | 49.9 (45.2-54.6) | 88.7 (80.4-97.1) | 0.71 |

Notes: (1) p values refer to between-group differences at BASELINE, but comparison of mean CHANGES from baseline at 2, 6, and 12 months.

Table 1

Disclosures: Janet Yu-Yahiro, None.

FR0297

Quantification of the Circadian Modulation of the Bone Resorption Marker CTX-I in Serum and Urine under Controlled in-patient Conditions. Maria Small^{*1}, Derk-Jan Dijk², Richard Eastell³, Aldona Greenwood², John Sharpe⁴, Mikihiro Yuba⁴, Stephen Deacon¹. ¹Ono Pharma UK Ltd, United Kingdom, ²Surrey Clinical Research Centre, United Kingdom, ³University of Sheffield, United Kingdom, ⁴ONO Pharma UK, United Kingdom

Bone resorption is higher during the night compared to the daytime and is reflected in serum (s) and urine (u) CTX-I levels. However, there are a number of factors including food intake that may influence this diurnal profile. This study investigated the characteristics of the CTX-I profile over 24h in 25 post-menopausal women (PMW) (mean age +/-SD 65.3+/-6.0) in an environment minimizing confounding influences of irregular sleep, food intake and exercise. Sleep/wake disorders/complaints were excluded and a regular sleep/wake cycle (SWC) (22:30-06:30) was scheduled 7 days prior to and during the 3 day lab study (sampling on last day). Subjective sleep diaries and actigraphy were used to confirm compliance with SWC instructions and exercise restrictions. Serum sampling was obtained ~ every 2h. A longline indwelling cannula was used for overnight sampling to minimise

disturbance. Urine was collected from 08:00 ~ every 2h (4h overnight). While in clinic, meals were served at 07:00, 13:00 and 19:00 with only water at other times. Breakfast had the same nutritional content as dinner since these times were considered to influence resorption the most. Characteristics of the 24h profiles were determined by non-linear regression fitting a cosine model to the data. This gave estimates of mesor (M) (average), amplitude of the 24h variation (Amp) and time of the fitted maximum of CTX-I. Significant ($p < 0.05$) wave fits were obtained in 25 and 14 subjects for sCTX-I and uCTX-I, respectively. Each subject's Amp was > 0 ($p < 0.05$). The Amp between subjects varied and correlated with the M in both serum and urine ($r \geq 0.824$, $p < 0.001$). Mean (+/- SD) peak time and Amp estimates were 03:17 +/- 46mins and 0.187 +/- 0.078 $\mu\text{g/L}$ for sCTX-I, and 04:06 +/- 1h29mins and 33.22 +/- 12.84 $\mu\text{g/h}$ for uCTX-I. The study covered ~4m period (Jul/Aug and Nov). A significantly ($p < 0.01$) earlier peak time in sCTX-I was obtained in Nov compared to Jul/Aug. A similar effect was not observed for Amp or M. Because timing of sleep and meals was identical across the periods, this effect may be related to the change from summer to wintertime. The data show that in PMW, CTX-I has a clear circadian profile with mean peak levels at ~3am in serum and ~4am in urine. The Amp is greater in PMW with higher CTX-I levels. Circadian characteristics can be assessed at the level of the individual. These data have implications for the assessments of bone resorption status based on a single sample.

Figure 1 (24h time profiles for serum (N=25), mean +/- SE)

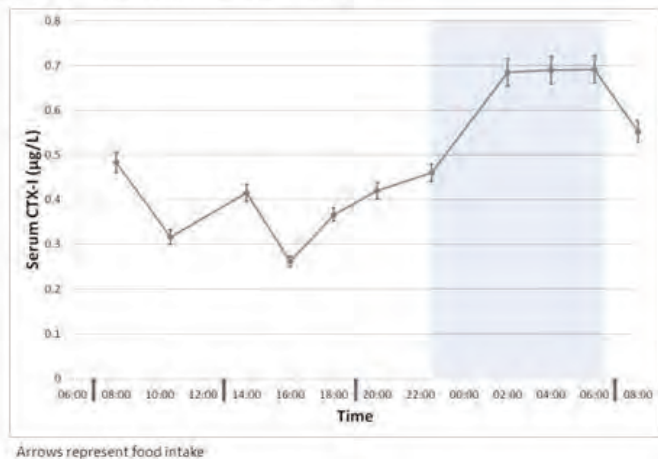


Fig1

Disclosures: Maria Small, ONO PHARMA UK LTD, 3
This study received funding from: Ono Pharmaceuticals

FR0298

Serum Sclerostin Levels are Associated with Osteoporotic Fractures in Type 2 Diabetic Patients. Masahiro Yamamoto^{*1}, Toru Yamaguchi¹, Mika Yamauchi¹, Kiyoko Nawata², Toshitsugu Sugimoto³. ¹Shimane University Faculty of Medicine, Japan, ²Department of Health & Nutrition, The University of Shimane, Junior College, Matsue Campus, Japan, ³Shimane University School of Medicine, Japan

Purpose: The patients with type 2 diabetes mellitus (T2DM) have an increased risk for vertebral fractures (VFs) compared to non-T2DM controls independent of bone mineral density (BMD) (JBMR 2009), suggesting that poor bone quality is possible cause of increased bone fragility. Low bone formation, a part of component of bone quality, is associated with VFs in T2DM women (JCEM 2012). Recent reports show that sclerostin, which is one of Wnt signaling inhibitors secreted from osteocyte, are inversely correlated with bone turnover markers. However, it is unclear whether serum sclerostin levels are correlated with osteoporotic fractures. The aim of this study is to clarify this relationship in T2DM men and women patients.

Methods: We compared parameters of bone metabolic markers including sclerostin measured by ELISA, osteocalcin, urinary NTX and spine BMD between 147 Japanese postmenopausal T2DM women (DMw) and 156 T2DM men over 50 years old (DMm), whose creatinine levels were within normal range.

Results: Sclerostin levels were significantly higher in DMw than DMm ($P < 0.01$). Stepwise regression analysis including independent variables of BAP showed that serum sclerostin was positively correlated with spine BMD and creatinine levels in both groups (DMw: $r = 0.39$, $F = 28.7$, $r = 0.30$, $F = 16.6$; DMm: $r = 0.43$, $F = 42.5$, $r = 0.17$, $F = 6.0$, respectively) and positively associated with age and HbA1c in DMm group ($r = 0.21$, $F = 9.6$, $r = 0.21$, $F = 9.4$, respectively). BAP, osteocalcin and uNTX were inversely correlated with sclerostin in DMm group ($r = -0.17$, $F = 6.8$; $r = -0.15$, $F = 4.03$; $r = -0.19$, $F = 7.6$, respectively). Multiple logistic analysis adjusted for age, BMI, HbA1c, creatinine, calcium, phosphate, and spine BMD revealed that sclerostin levels were associated with all osteoporotic fractures [DMw, 1.66 (1.08-2.55), DMm 1.54 (1.04-2.28)] and VFs [DMw, 1.59 (1.02-2.49), DMm, 1.55 (1.04-2.32)].

Conclusion: These results showed that sclerostin levels were correlated with several variables including BMD and associated with osteoporotic fractures independent of BMD. These findings suggested that increase in sclerostin level may cause bone

fragility due to poor bone quality and may explain, in part, why T2DM patients have an increased bone fragility despite their elevated BMD.

Disclosures: Masahiro Yamamoto, None.

FR0302

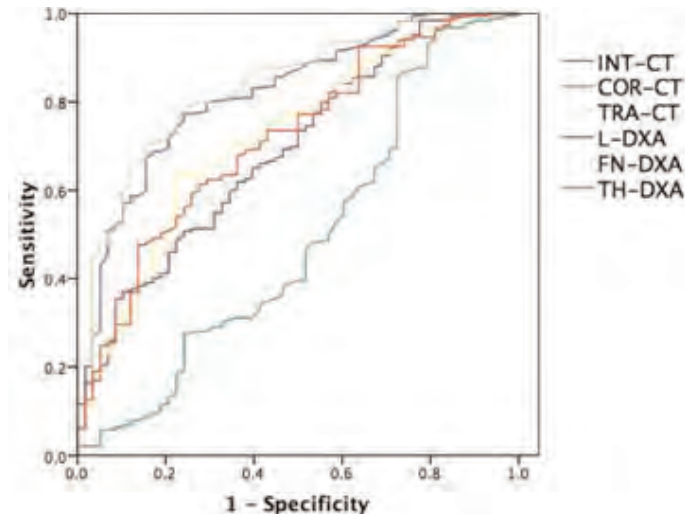
Clinical Abdominal CT can Effectively Predict the Risk for Osteoporotic Vertebral Fracture. Akifumi Nishida^{*1}, Masako Ito², Masataka Uetani¹. ¹Nagasaki University School of Medicine, Japan, ²Nagasaki University Hospital, Japan

Purpose: To evaluate the ability of clinical abdominal CT in assessing the risk for osteoporotic vertebral fractures compared with dual-energy X-ray absorptiometry (DXA).

Method and Materials: The subjects were 269 patients (108 men and 161 women, aged 56.8 ± 13.6 , 21-88 years) who underwent BMD measurement by DXA [lumbar spine (L-DXA), total hip (TH-DXA), femoral neck (FN-DXA) and vertebral morphometry] and diagnostic abdominal CT within 6 months from DXA examination. Clinical abdominal CT was performed with a 64-detector row scanner. Unenhanced axial images were obtained with a section thickness of 3 mm. The mean attenuation (in Hounsfield units) of integral, cortical and trabecular region of L2 vertebra (INT-CT, COR-CT and TRA-CT) was measured on a standard workstation (Aquarius NetStation, TeraRecon). The diagnostic ability of clinical abdominal CT and DXA with respect to discriminate prevalent vertebral fracture was assessed using receiver operating characteristic (ROC) analysis.

Results: CT attenuation measurement correlated with BMD measurement by DXA ($r = 0.202-0.687$). Seventy-three patients (27.1%) had vertebral fractures. For predicting vertebral fracture by CT attenuation measurement, ROC analysis provided area under the curve (AUC) values of 0.832 [95% confidence interval (CI) 0.773-0.891] for TRA-CT, 0.818 (95% CI 0.756-0.879) for INT-CT and 0.490 (95% CI 0.397-0.583) for COR-CT. Except for COR-CT, these values were greater than those of BMD measurement, which were 0.693 (95% CI 0.617-0.770) for L-DXA, 0.724 (95% CI 0.650-0.798) for FN-DXA and 0.715 (95% CI 0.641-0.790) for TH-DXA (Figure).

Conclusion: CT attenuation measurements of integral and cortical region of lumbar vertebra had greater discriminatory ability for vertebral fracture than DXA. CT attenuation measurements on clinical abdominal CT provide valuable data for identifying individuals at risk for fracture who would require treatment of osteoporosis, with no additional radiation or costs.



ROC curve

Disclosures: Akifumi Nishida, None.
This study received funding from: Eli Lilly

FR0303

Impact of a Reimbursement Change on Bone Mineral Density Testing in Ontario, Canada. Susan Jaglal^{*1}, Gillian Hawker¹, Ruth Croxford², Cathy Cameron³, Sarah Muncie¹, Sonya Allin⁴. ¹University of Toronto, Canada, ²Institute for Clinical Evaluative Sciences, Canada, ³Women's College Hospital, Canada, ⁴Toronto Rehabilitation Institute-University Health Network, Canada

Background: As of April 1, 2008 the physician reimbursement fee schedule for bone mineral density (BMD) testing using DXA in Ontario, Canada was revised with increased restrictions. BMD tests for patients with low fracture risk were limited to once every 36 months but prior to that, limited to once in any 24-month period. No change was made for high-risk patients who continued to be limited to one test every 12 months and a new fee code for a baseline testing with individuals being limited to

one baseline test in their lifetime. Objective: To examine the impact of the policy change for increased restrictions on BMD testing on trends in BMD testing rates, overall, by sex, risk category, age and following recent fracture. Methods: Data from the Ontario Health Insurance Plan which captures all reimbursement for DXA in the province were used to assess patterns in BMD testing from April 1, 2002 to March 31, 2011. Fractures were determined from administrative databases on physician visits, hospital discharges and emergency department visits. Joinpoint analyses were used to examine significance of trends. Results: Prior to the policy change the number and rate of DXAs were increasing steadily from 433,419 in 2002/03 to 507,658 in 2007/08 and then decreased to 422,915 in 2010 and the decrease was more pronounced for women between the ages of 50 and 79 years. The rates in men continued to increase gradually each year and levelled off after 2008. Following the policy change in 2008, the number and age-adjusted rate of BMD testing dropped particularly in the low risk group from 5.7/100 to 1.8/100 among women. More importantly, the rate of BMD testing decreased in groups at high risk for fracture after 2008. A significant decrease was seen among women who were eligible for BMD testing when they turned 65 years. Among those with fractures, overall rate of BMD testing at 6 or 12 months after fracture decreased after the policy change. Between 2002 and 2007, rates of testing following hip fractures increased by an estimated 1.68 per 100 fractures in both men and women and then fell. Conclusion: The policy change restricting access to BMD testing reduced overall testing particularly in low-risk women but also negatively affected groups at high risk for fracture, where BMD testing is indicated. This suggests that referring physicians are reducing DXA referrals across the board rather than targeting only low risk patients, thereby decreasing appropriate referrals.

Disclosures: Susan Jaglal, None.

FR0304

Management of Fragility Fractures: Impact of the Optimus Initiative on Family Physicians. Marie-Claude Beaulieu¹, Sophie Roux², Noémie Poirier³, Michèle Beaulieu⁴, François Cabana⁵, Gilles Boire³. ¹Université de Sherbrooke, Canada, ²University of Sherbrooke, Canada, ³Centre hospitalier universitaire de Sherbrooke, Canada, ⁴Merck Canada Inc, Canada, ⁵CHUS, Canada

Background: The OPTIMUS initiative was first implemented in January 2007 to educate patients and inform and empower Family Physicians (FPs) to diagnose and treat OP revealed by a Fragility Fracture (FF). In this prospective initiative, women and men over age 50 were screened for incident FF in orthopaedic clinics, and eligible outpatients were randomized to Standard Care (SC) or to either Minimal (MIN) or Intensive (INT) interventions, consisting in an initial face-to-face and phone follow-up interventions with patients by dedicated personnel and information letters with individualized recommendations to FPs. As of December 2010, 1043 outpatients (including 200 SC controls) with nonvertebral FF and 250 hip FF inpatients have been included. More than 270 of the 360 FPs from our area have been reached at least once by OPTIMUS. A better collaboration between bone health specialists, orthopaedists and FPs has taken place and treatment initiation has been improving. Initiation rates and persistence on treatment at one year after a FF event have increased from less than 20% in the control group to 43% in the MIN and 55% in the INT Intervention groups.

Objectives: To determine the factors influencing FPs' decision to treat OP
Methods: 272 FPs reached by OPTIMUS were sent a questionnaire evaluating their main reasons to start a treatment for osteoporosis, their knowledge and use of fracture risk calculators, and the potential for collaboration with nurses from Family Physician Groups (GMF), a Ministry of Health-supported grouping of FPs. One hundred and three (38%) filled questionnaires were returned.

Results: Previous FFs (100/103; 97%) and BMD results (80/103; 78%) were the two major indicators (Agree and Strongly Agree) mentioned by FPs to initiate a pharmacological treatment of osteoporosis; 10-year fracture risk (67/103; 65%) was less frequently mentioned. The FRAX and/or CAROC (Canadian Association of Radiologists and Osteoporosis Canada) tools were known by the majority (58/103; 56%), but were rarely used (FRAX by 11, CAROC by 26). Twenty-three of 30 (77%) FPs aware of CAROC found it easy to use, compared to only 14 of the 28 (50%) knowledgeable about FRAX; 9 (32%) found FRAX difficult to use. Of those FPs using FRAX and/or CAROC, 25 (68%) felt they were useful to convince patients to get treated. Two thirds (69/103) of the responding FPs already collaborated with GMF nurses to manage patients with chronic diseases, but only 6 were doing so for OP patients.

Conclusions: After 4 years of existence, the OPTIMUS initiative appears to progressively overcome the previously BMD-driven decision of FPs and to prioritize a post-FF intervention to treat osteoporosis. Fracture risk calculators remain infrequently used. There is an opportunity to integrate/systematize management of FF patients in groups of FPs with the help of GMF nurses, as these nurses are already involved in management of other chronic diseases.

Disclosures: Marie-Claude Beaulieu, None.

FR0309

Accurate and Fast Strength Predictions of Patient-specific HR-pQCT-based plate-rod Models Distinguish Women with Vertebral Fractures. Ji Wang^{*1}, Bin Zhou¹, Xiaowei Liu², Xiutao Shi¹, Emily Stein³, Elizabeth Shane³, X Guo¹. ¹Columbia University, USA, ²University of Pennsylvania, USA, ³Columbia University College of Physicians & Surgeons, USA

Deteriorating trabecular microstructure associated with aging and menopause predisposes postmenopausal women to vertebral (VB) fractures. While HR-pQCT has advanced clinical assessment of trabecular microstructure, prediction of yield strength by HR-pQCT voxel-based Finite Element Analysis (FEA) is impractical for clinical use due to its prohibitive high computational costs. Recently, a highly efficient plate-rod (PR) modeling technique based on HR-pQCT has been developed to fill the unmet clinical need to estimate bone strength. In this study, the new HR-pQCT PR models were validated against gold standard- μ CT voxel models, as well as HR-pQCT voxel models. Then, patient-specific PR models were evaluated to determine whether they discriminated VB fracture status in postmenopausal women. For validation, 19 registered μ CT (25 μ m) and HR-pQCT (82 μ m) images of trabecular sub-volumes of distal tibiae were obtained from human cadaveric samples (Fig.1A,B). For testing clinical potential of PR models, HR-pQCT images of distal radius were obtained from 20 patients with VB fractures and 30 control subjects (age-matched and no difference in aBMD by DXA except at femoral neck). After segmenting images of the trabecular microstructure into individual trabeculae, PR models were generated by modeling each rod with a 2-node beam element and each plate with multiple 3-node shell elements (Fig.1C). Both the PR models and voxel models were subjected to nonlinear FEA to estimate Young's modulus (E_y) and yield strength (σ_y). Predictions by HR-pQCT PR models strongly correlated with those of μ CT-based and HR-pQCT-based voxel models, for modulus (Fig.1D) and for strength (Fig.1E). Notably, the simplified PR models achieved both major reductions in CPU time for nonlinear FEA (64,000-fold for μ CT and 1,200-fold for HR-pQCT), and a dramatic reduction in element number (Fig.1F). Most importantly, these highly efficient patient-specific HR-pQCT PR models revealed dramatic deficiencies in modulus and strength in VB patients and demonstrated the power to discriminate VB fracture status (Fig.2). In conclusion, we thoroughly validated a novel HR-pQCT PR model of human trabecular bone against μ CT and HR-pQCT voxel models and demonstrated its ability to discriminate fracture status in postmenopausal women. An accurate nonlinear FEA of HR-pQCT PR models that requires only seconds of desktop computer time has tremendous promise as a powerful tool for clinical assessment of bone fracture risk.

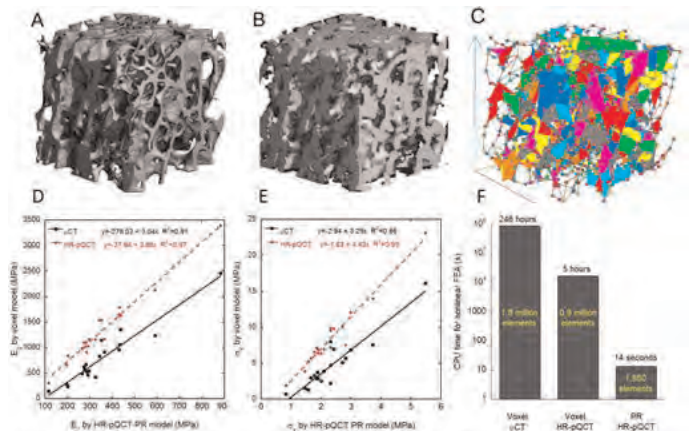


Figure 1. Registered (A) μ CT and (B) HR-pQCT images of human trabecular bone at distal tibia; (C) PR model (element thickness, red shown) based on (B), color indicates different shell and beam elements; Linear correlations of Young's modulus E_y (D) and yield strength σ_y (E) of HR-pQCT-based PR model with those of HR-pQCT and μ CT-based voxel model; (F) CPU time for nonlinear FE analysis using μ CT-based voxel model, HR-pQCT-based voxel model, and HR-pQCT-based PR model, numbers in yellow indicate the average number of elements in one FE model.

Figure 1

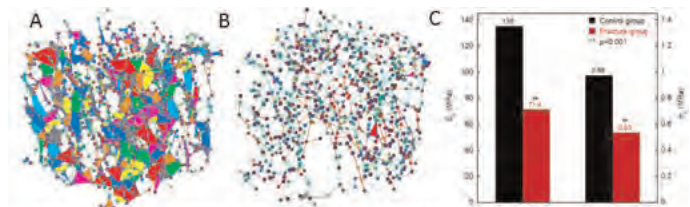


Figure 2. A HR-pQCT-based PR model for (A) the control group and (B) the fracture group; (C) Comparison of Young's modulus and yield strength between the control group and fracture group

Figure 2

Disclosures: Ji Wang, None.

FR0310

In Breastfeeding Women, Trabecular Bone Loss at the Radius, Seen by High Resolution Peripheral Quantitative CT (HRpQCT), Persists at 18 Months Postpartum. Anna Kepley¹, Stephanie Boutroy², Chiyuan Zhang¹, Mariana Bucovsky¹, Mary Beth Vrabel¹, Shannon Kokolus¹, Polly Young¹, Adi Cohen^{*2}. ¹Columbia University, USA, ²Columbia University Medical Center, USA

Lactation is associated with rapid, large decreases in lumbar spine (LS) and femoral neck (FN) BMD followed by recovery. Both human and rodent studies suggest that recovery of bone mass after weaning is site-specific, with full recovery at the spine, but only partial recovery at the femur. To characterize the site-specificity and type of bone loss (cortical versus trabecular) and recovery during lactation and weaning, we studied 15 healthy exclusively breastfeeding (BF; exclusive lactation over 8±3 mo, any lactation, 12±3 mo) and 11 healthy non-breastfeeding (nBF) women. We measured BMD by DXA (LS, FN, and the predominantly cortical 1/3 radius) and cortical (Ct) and trabecular (Tb) volumetric BMD and bone microarchitecture by radial and tibial HRpQCT (Scanco) over 18 months postpartum. At baseline (36±22 days postpartum), BF women were older (BF: 33±4, nBF: 26±4 yrs; p<0.001) and had lower BMI (BF: 24.0±3.1, nBF: 27.6±5.0 kg/m²; p=0.03) than nBF women. Return of menses occurred at 7.0±3.7 mo in BF and 1.7±0.8 mo postpartum in nBF (p<0.001). By both DXA and HRpQCT (Table), nBF women gained bone mass at most sites during the observation period. By DXA in BF women, expected BMD loss with recovery at the LS and partial recovery at the femoral neck were seen, while 1/3 radius BMD increased. In contrast, by HRpQCT, mean decreases in radial Tb vBMD, particularly at the inner Tb compartment, persisted even at 18 mo postpartum, while few changes were seen over time at the tibia (Table). Radial and tibial Ct vBMD did not change in either group. In both groups, changes in HRpQCT measures were highly variable. In BF women, timing of the baseline visit, age, time of return of menses, duration of full lactation, and time of initiation of solid food did not significantly predict DXA BMD or radial Tb vBMD changes over time. In summary, while bone loss and recovery were seen at the LS and FN in BF women, no significant changes were seen at the tibia and radial Tb bone loss persisted even at 18 months postpartum. The pattern of bone loss and recovery in breastfeeding women varies by site and type of bone.

| | Exclusively breastfeeding (n=15) | | | Not breastfeeding (n=11) | | | p: overall group*time |
|---|----------------------------------|-------------|------------|--------------------------|------------|------------|-----------------------|
| | 6 mo | 12 mo | 18 mo | 6 mo | 12 mo | 18 mo | |
| Areal BMD by DXA | | | | | | | |
| LS | -3.3±6.5*** | 0.4±7.1 | 4.0±7.5*** | 2.9±7.6** | 4.7±7.6*** | 6.8±8.1*** | p=0.001 |
| FN | -3.8±6.8*** | -4.1±7.5*** | -1.5±7.8 | -0.7±7.9 | 0.2±7.9 | -0.3±8.5 | p=0.02 |
| 1/3Radius | 2.3±4.3*** | 2.0±4.7** | 2.4±5.0*** | -0.7±5.1 | -0.9±5.1 | -1.6±5.4* | p=0.002 |
| Compartmental Volumetric BMD (vBMD) and microstructure by HRpQCT | | | | | | | |
| Radius | | | | | | | |
| Ct vBMD | 0.1±2.8 | -0.2±3.0 | 0.1±4.4 | -0.2±3.3 | 0.3±3.3 | 0.5±4.4 | p=0.6 |
| Tb vBMD | -1.5±5.8 | -1.9±6.4* | -1.7±9.6 | 1.0±6.8 | 1.5±6.8 | 2.7±9.2* | p=0.1 |
| Inner Tb vBMD | -2.7±8.1* | -4.3±9.0** | -3.8±13.5* | 0.35±9.5 | 1.7±9.5 | 3.6±13.0* | p=0.04 |
| Tb Number | -1.6±13.2 | 0.5±14.6 | 0.3±20.9 | 3.5±15.5 | 4.1±15.5* | 4.8±20.8* | p=0.4 |
| Tb Thickness | 0.2±12.4 | -2.2±13.4 | -1.9±18.3 | -1.6±14.5 | -1.9±14.5 | -1.4±18.5 | p=0.8 |
| Tibia | | | | | | | |
| Ct vBMD | -0.4±1.7 | -0.1±1.8 | -0.1±2.3 | 0.1±2.0 | 0.3±2.0 | 0.3±2.4 | p=0.6 |
| Tb vBMD | -0.5±4.6 | -0.7±4.8 | 0.1±6.4 | -0.8±5.3 | -1.0±5.3 | -1.7±6.5 | p=0.6 |
| Inner Tb vBMD | 0.1±4.9 | -0.1±7.2 | 1.1±9.6 | -1.1±8.1 | -1.2±8.1 | -2.5±9.9 | p=0.3 |
| Tb Number | 0.5±9.7 | -0.7±10.2 | 0.6±13.4 | -3.4±11.4* | -0.5±11.4 | -3.4±13.9 | p=0.02 |
| Tb Thickness | -0.8±9.9 | 0.4±10.4 | -0.6±13.6 | 3.2±11.6* | 0.2±11.6 | 2.6±14.2 | p=0.04 |

Table

Disclosures: Adi Cohen, None.

FR0311

Lower Vertebral Body Bone Strength in Subjects with Prevalent Fracture Assessed by High Resolution Axial Skeleton Quantitative Computerized Tomography. Rene Rizzoli^{*1}, Fanny Merminod¹, Mélanie Hars², Bert Rietbergen³. ¹University Hospital, Switzerland, ²Hôpitaux Universitaires De Genève, Switzerland, ³Eindhoven University of Technology, The Netherlands

Bone microarchitecture is an important determinant of bone strength, hence of fracture risk. It provides additional and complementary information to areal BMD in predicting fracture risk, when assessed by high-resolution (HR) peripheral (p)QCT. Combined with micro-finite element analyses (FEA), bone mechanical properties can be quantified. Recently HR flat-panel QCT imaging devices became available that can reveal microstructural features of the axial skeleton. We investigated if micro-FE analysis based on such HR-QCT measurements of the spine can better identify patients with prevalent fracture than density or peripheral morphology measures.

HR flat panel CT (Allura FD20 XperCT, Philips Healthcare, NL) images with a resolution of 137 microns, were created of the vertebrae T12 in vivo, in 23 patients with prevalent fracture (12 vertebral and 15 upper limb fractures) and in 17 unfractured controls, aged 66.4±1.9 (x±SD) and 66.0±1.2 years, respectively. Micro-FE models were created by converting voxels to elements with a density-dependent stiffness and comprised the vertebrae with cut-off endplates. Microstructural features and the thin cortical shell could be well represented by the models. Compression tests were simulated to determine vertebral stiffness, estimated failure load and stiffness corrected for vertebral height and cross-sectional area (modulus). In

addition, we measured spine and proximal femur areal BMD and distal radius and tibia microstructure by HRpQCT (XtremeCT, Scanco, CH).

Spine and proximal femur aBMD did not differ between fractured patients and controls. Distal radius, but not distal tibia, total density, BV/TV, trabecular number and thickness were lower in the fractured patients (p=0.044 to 0.001). At T12 level, micro-FEA revealed in the fractured group lower estimated failure load (4.5±2.0^{E3} vs 6.1±1.8^{E3} N, p=0.015) and modulus (673±257 vs 958±271 N/mm², p=0.002). When only patients with vertebral fracture were considered, none of the HRpQCT difference remained significant. In contrast, T12 stiffness (4.9±2.4^{E4} vs 7.1±2.6^{E4} N/mm, p=0.033), estimated failure load (3.9±1.9^{E3} vs 6.1±1.8^{E3} N, p=0.004) and modulus (601±268 vs 958±271 N/mm², p=0.002) were lower in the group with vertebral fracture.

These results underline the major interest of high-resolution axial QCT and FE analysis in axial skeleton fracture risk assessment.

Disclosures: Rene Rizzoli, None.

FR0312

Mechanical Implications of Subtle Changes in Trabecular Bone Estimated by MRI-Based Finite Element Modeling. Wenli Sun^{*1}, Chamith Rajapakse², X Guo³, Felix Werner Wehrli⁴. ¹University of Pennsylvania, USA, ²University of Pennsylvania School of Medicine, USA, ³Columbia University, USA, ⁴University of Pennsylvania Medical Center, USA

Early detection of changes in bone's mechanical competence is critical for the effective management of osteoporosis. Micro magnetic resonance imaging (µMRI) based finite-element (µFE) analysis can non-invasively capture temporal changes in bone strength at peripheral sites. In this study, we examined (1) the sensitivity of µMRI-based µFE analysis in detecting subtle alterations in bone stiffness, (2) the accuracy of the method, and (3) a regression model to improve the accuracy of detected changes in the limited signal-to-noise (SNR) regime of *in-vivo* µMRI.

30 human distal tibiae had previously been imaged with mCT at 25 mm isotropic voxel size. High-resolution 3D reference models were generated by extracting the trabecular bone region. The effect of bone resorption was evaluated with two modes of bone loss: homogeneous thinning (HT) and heterogeneous pitting (HP). Three levels of bone loss were implemented: 0.5%, 1%, and 2%. Micro-MR images were processed by resampling to 150-µm isotropic voxel size and superimposing Gaussian noise to reduce SNR to 20, 15, and 10. Axial stiffness was computed via simulated compressive loading in the axial direction. Paired t-tests were used to determine whether the stiffness derived from degraded and non-degraded *in-vivo* models were different. Further, the accuracy of detected differences in stiffness before and after bone loss under *in-vivo* conditions was compared to the ground truth. Finally, a linear regression model was generated to determine the dependence of mFE-derived stiffness on SNR on the basis of 15 cadavers, while the other 15 were used to test the performance of the correction algorithm based on the derived parameters.

Under *in vivo* µMR imaging conditions, 0.5 % degraded HT (and HP) models yielded 0.87% (0.67%), 0.81% (0.65%), 0.72% (0.60%) lower stiffness values than prior to bone loss at SNR=20, 15, and 10, respectively (p<0.0001). Further, the detected difference in pre- and post-bone loss stiffness under *in-vivo* MRI conditions were correlated to those derived from high-resolution reference models with R²= 0.35 (0.50), 0.26 (0.29), 0.12 (0.11) at SNR=20, 15, and 10, respectively. The error after correction in the SNR=10-20 range reached 8%-16% (12%-47%) of the high resolution reference values, it was considerably smaller than the error prior to correction. The data suggest that mechanical implications caused by subtle changes in TB density are detectable via FE analysis under *in-vivo* µMR imaging conditions. The strength of the correlation between the low and high resolution models decreased with decreasing SNR as expected. The correction model improved the accuracy of detected changes.

FR0314

Rapid Cortical Bone Loss in Patients with Chronic Kidney Disease. Thomas Nickolas^{*1}, Emily Stein², Chiyuan Zhang³, Serge Cremers³, Stephanie Boutroy¹, Xiaowei Liu⁴, Donald McMahon², Mary Leonard⁵, X Guo³, Elizabeth Shane². ¹Columbia University Medical Center, USA, ²Columbia University College of Physicians & Surgeons, USA, ³Columbia University, USA, ⁴University of Pennsylvania, USA, ⁵Children's Hospital of Philadelphia, USA

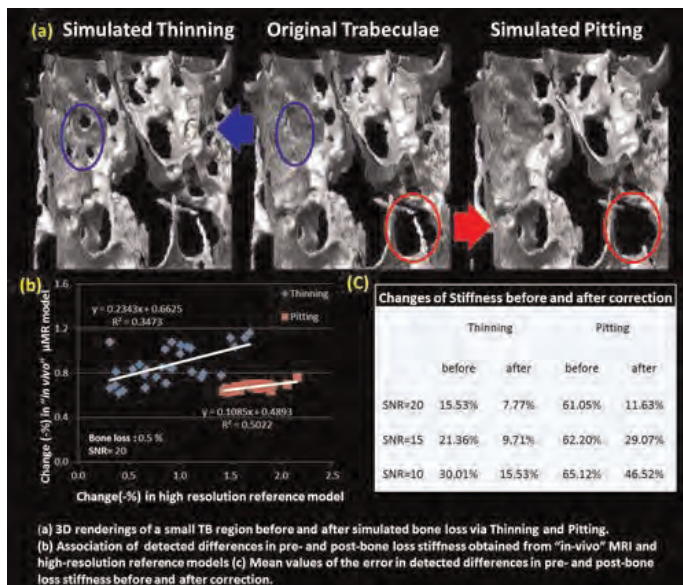
Fracture risk is elevated in patients with chronic kidney disease (CKD). We have previously reported that CKD patients with prevalent fractures have lower areal BMD (aBMD) by DXA at the ultradistal radius (UDR), and lower cortical and trabecular volumetric BMD (vBMD), thinner cortices and abnormal trabecular microarchitecture of the distal radius and tibia by high resolution peripheral computed tomography (HRpQCT). To ascertain whether microarchitectural abnormalities associated with CKD are progressive over time, we enrolled 60 patients in a longitudinal study. To date, we have measured aBMD by DXA at the lumbar spine (LS), total hip (TH), femoral neck (FN), 1/3 radius (1/3R) and ultradistal radius (UDR) and cortical and trabecular vBMD, geometry and microarchitecture of the distal radius and tibia by HRpQCT (voxel size 82 μ m) in 49 patients over a median (interquartile range) follow-up of 1.8 (1.2-2.0) years. Fasting serum was archived for batch analysis at study completion. Changes in bone parameters were annualized and compared by mixed models with adjustment for hemodialysis status and baseline measures of bone structure. Mean \pm SD age at baseline was 69 \pm 9 years; 55% were women, 37% had prevalent fractures, 16% were on dialysis. Mean GFR in non-dialyzed patients (36 \pm 17 mL/min) did not change (-0.4 \pm 6 mL/min, p=1.0). There were significant declines in aBMD at the TH (1.1 \pm 2.7%, p<0.01) and UDR (2.6 \pm 5.8%, p<0.01) but not the LS, FN or 1/3R. HRpQCT of the radius revealed significant declines in cortical area (2.6 \pm 3.8%, p<0.0001), density (1.1 \pm 1.5%, p<0.0001) and thickness (2.4 \pm 4.1%, p<0.0001). In contrast, trabecular vBMD and microarchitecture did not change, excepting a small but significant increase in trabecular area (0.7 \pm 0.7%, p<0.01). The amount, pattern and significance of changes were mirrored at the tibia. In summary, CKD is associated with progressive loss of cortical bone at both radius and tibia. The significant declines in cortical density, thickness and area, coupled with the increase in trabecular area suggest that endocortical cancellization is the primary mechanism of cortical loss. Pharmacologic interventions to decrease cortical bone loss in patients with CKD could represent a strategic therapeutic target to prevent deterioration of bone microarchitecture and lower fracture risk in this vulnerable population.

Disclosures: Thomas Nickolas, None.

FR0318

Changes in Bone Mineral Density over Time by Body Mass Index in the Health ABC Study. Jennifer Lloyd^{*1}, Dawn Alley¹, William Hawkes¹, Marc Hochberg², Shari Waldstein³, Tamara Harris⁴, Stephen Kritchevsky⁵, Ann Schwartz⁶, Elsa Strotmeyer⁷, Catherine Womack⁸, Denise Orwig¹. ¹University of Maryland, Baltimore, USA, ²University of Maryland School of Medicine, USA, ³University of Maryland, Baltimore County, USA, ⁴Intramural Research Program, National Institute on Aging, USA, ⁵Wake Forest Baptist Medical Center, USA, ⁶University of California, San Francisco, USA, ⁷University of Pittsburgh, USA, ⁸University of Tennessee, USA

Background: Cross-sectional studies have found a positive association between body mass index (BMI) and bone mineral density (BMD), but little is known about the longitudinal relationship between BMI and BMD in older adults. This relationship is important given the high prevalence of overweight and obesity. Methods: We examined average annual rate of change in BMD by initial BMI in the Health, Aging, and Body Composition Study, a cohort of White and Black well-functioning older adults age 70-79 years at enrollment. Baseline BMI (kg/m²) was categorized as normal (18.50-24.99), overweight (25.00-29.99), and obese (> 30.00). Repeated measurement of BMD (gm/cm²) was performed with DXA at baseline, and years 3, 5, 6, 8, 10. Multivariable generalized estimating equations analyses were used to predict mean BMD (femoral neck, total hip, and whole body) by baseline BMI group, adjusting for covariates. Results: The sample included 2,570 subjects [51% women] of whom 43% were overweight and 24% were obese with a mean baseline femoral neck BMD of 0.743 gm/cm² (SD=0.142), hip BMD of 0.888 gm/cm² (SD=0.169), and whole body BMD of 1.09 gm/cm² (SD=0.141). Obese older adults, compared to non-obese, had higher fat mass, higher rates of diabetes and hypertension, less physical activity, and less use of bisphosphonates, vitamin D and calcium supplements. There were no significant differences between BMI groups in the change in total hip or whole body BMD over time. However, there were significant differences between BMI groups in change in femoral neck BMD over time (p<0.001). Obese older adults lost 0.002 gm/cm² of BMD per year more compared with normal weight older adults (p<0.001). Femoral neck BMD change over time did not differ between the overweight and normal weight BMI groups (p=0.74). Indeed, obese older adults had the highest mean femoral neck BMD at baseline but had the lowest mean BMD by year 10. In year 10, mean femoral neck BMD ranged from 0.696 gm/cm² (SE=0.008) among obese, 0.719 gm/cm² (SE=0.005) among overweight, and 0.709 gm/cm² (SE=0.007) among normal weight older adults. In summary, this



Bone Loss Simulation

Disclosures: Wenli Sun, None.

This study received funding from: NIH RO1 AR 55647 K25 AR 060283

FR0313

Poor Bone Microarchitecture in Premenopausal Women with Recent Distal Radius Fracture Persists after Adjusting for Ultradistal Radius BMD.

Tamara Rozenal¹, Laura Deschamps¹, Alex Taylor², Brandon Earp³, David Zurakowski⁴, Charles Day¹, Mary Bouxsein^{*1}. ¹Beth Israel Deaconess Medical Center, USA, ²Massachusetts General Hospital, USA, ³Brigham & Women's Hospital, USA, ⁴Children's Hospital Boston, USA

Measurement of BMD by DXA combined with clinical risk factors is currently the gold standard for the diagnosis of osteoporosis and prediction of fracture risk. Yet, BMD does not always accurately reflect fracture risk as up to 50% of those who suffer fractures do not have osteoporosis by BMD testing. Advanced in vivo imaging has shown that older women and men with a history of fragility fracture have poor bone microarchitecture, often independent of their low BMD. As the origins of skeletal fragility may begin early in life, we asked whether premenopausal women with recent fracture have poor skeletal health. Thus, we recruited 40 premenopausal women with recent distal radius fracture (FX) and 80 fracture-free controls (CON). We assessed BMD of the hip, spine and radius; plus cortical (Ct) and trabecular (Tb) bone density and microarchitecture at the non-fractured/non-dominant distal radius and tibia by HR-pQCT. FX and CON did not differ with regard to age, race or BMI. BMD was similar in FX and CON at the fem neck, lumbar spine and 1/3 distal radius; but tended to be lower in the FX at the total hip and ultradistal radius (p=0.06). Ct and Tb microarchitecture differed between groups, both at the distal radius and tibia. At the distal radius, FX had lower total density, Tb density, Tb number and TbTh than CON (-6 to -14%, p<0.05 for all). Ct density and morphology at the distal radius did not differ between groups. At the distal tibia, total density, Tb density, TbTh, Ct thickness and Ct area were lower in FX vs CON (-7 to -17%, p<0.01). Conditional logistic regression showed that after adjustment for age and ultradistal radius BMD, radius Tb density, thickness, separation and distribution of Tb separation remained significantly associated with fracture (adjusted OR's: 1.94 - 2.04, p<0.05). At the tibia, after adjustment for age and femoral neck BMD, total density, Tb density, trabecular thickness, cortical area and cortical thickness remained significantly associated with fracture (adjusted OR's: 1.62 - 2.40, p<0.05). In conclusion, these findings show that despite similar BMD values, premenopausal women with recent distal radius fracture have significantly poorer bone density and microarchitecture at the distal radius and tibia compared to non-fracture controls. Early identification of women with poor bone health offers opportunities for interventions aimed at preventing further bone health declines.

Disclosures: Mary Bouxsein, None.

study found significant differences in femoral neck BMD over time by BMI groups but did not find differences in total hip or whole body BMD over time. Findings underscore the importance of looking at the longitudinal relationship between body composition and bone mineral density among older adults, indicating that weight may not be protective for osteoporosis over time.

| Adjusted Baseline BMD and Per Year Change in BMD by Body Mass Index Category, n=2,570† | | | | | | |
|--|--------|-------|------------|-------|--------|-------|
| | Normal | | Overweight | | Obese | |
| | Mean | SE | Mean | SE | Mean | SE |
| Baseline BMD (gm/cm ³) | | | | | | |
| Femoral Neck | 0.733 | 0.006 | 0.743 | 0.003 | 0.746 | 0.007 |
| Hip | 0.870 | 0.006 | 0.891 | 0.004 | 0.899 | 0.008 |
| Whole Body | 1.083 | 0.005 | 1.079 | 0.003 | 1.074 | 0.006 |
| Per Year Change in BMD (gm/cm ³) | | | | | | |
| Femoral Neck | -0.003 | 0.000 | -0.003 | 0.000 | -0.005 | 0.001 |
| Hip | -0.004 | 0.001 | -0.004 | 0.001 | -0.005 | 0.001 |
| Whole Body | -0.002 | 0.000 | -0.003 | 0.000 | -0.003 | 0.001 |

† SE= Standard error; BMD= Bone mineral density

Adjusted Baseline BMD and Per Year Change in BMD by Body Mass Index Category

Disclosures: Jennifer Lloyd, None.

FR0319

Combined Hormonal Oral Contraceptive Use and Bone Mineral Density Change in the Premenopausal Population—10-year data from the Canadian Multicentre Osteoporosis Study. Jerilynn Prior¹, Heather Macdonald¹, Wei Zhou², Claudie Berger², Christopher Kovacs³, David Hanley⁴, Tassos Anastassiades⁵, Stephanie Kaiser⁶, and CaMOS Research Group⁷.
¹University of British Columbia, Canada, ²McGill University, Canada, ³Memorial University of Newfoundland, Canada, ⁴University of Calgary, Canada, ⁵Queen's University, Canada, ⁶Dalhousie University, Canada, ⁷, Canada

Combined hormonal oral contraceptives (COC) are used by 86% of Canadian premenopausal women. Three large cohort studies suggest past COC use is associated with higher postmenopausal fracture risk (Cooper 1993; Vessey 1998; Barad 2005) although reviews routinely cite improved bone health as a non-contraceptive COC benefit. A recent large prospective cohort study of young premenopausal women showed negative BMD changes in teenagers on higher dose COC (EE 30mg) vs. teenage controls (Scholes 2011). At baseline in the Canadian Multicentre Osteoporosis Study (CaMOS), premenopausal women who had ever vs. never used COC showed significantly lower lumbar spine (L1-4) and trochanter BMD values (Prior 2001). Prospective population-based data on COC and bone mineral density (BMD) changes are lacking. The purpose of this study was to document prospective 10-year (y) BMD changes in a population-based sample of premenopausal women, ages 25-45 at baseline, stratified by whether they reported never (N-COC), intermittent (I-COC), or continuous (C-COC) use of COC based on reports at baseline, 5 and 10-y examinations. To assess between-group differences, multivariable models of BMD change of L1-L4, total hip, femoral neck and trochanter were constructed using linear regression adjusting for age, body mass index (BMI), height and baseline BMD values. Results are reported as mean ± SD and by 95%CI of differences between groups (Table). In the 227 women mean age 35 ± 5y for whom 10-y premenopausal BMD change data were available, 28 women reported never use, 170 were I-COC users and 29 were C-COC. N-COC were less likely to be white and tended to be shorter than I-COC but did not differ in age, BMI, menarche age, parity, exercise, calcium, vitamin D, cigarette or alcohol use from COC user groups. C-COC tended to be more likely than I-COC to have started COC for non-contraceptive reasons. Adjusted BMD change results (Table) showed that L1-4 change was positive in N-COC (0.007 ± 0.057) vs. negative in I-COC (-0.001 ± 0.057) and C-COC (-0.017 ± 0.060) groups although these differences were not significant. At the total hip site N-COC showed no BMD change whereas small mean positive BMD changes occurred in the I-COC and C-COC users. In summary, these data suggest that community COC use in premenopause is not associated with important BMD loss, however larger prospective population-based studies are needed—adverse BMD changes by COC use in teenagers need confirmation in population data.

| Bone site | COC use | | | Mean Difference (95% CI) |
|--------------|----------------|-----------------------|--------------------|--|
| | Never N=28 | Intermittent N=170 | Continuous N=29 | |
| | Mean (SD) | | | |
| Lumbar 1-4 | 0.007 (0.057) | -0.001 (0.057) | -0.017 (0.060) | -0.008 (-0.036; 0.019) § -0.024 (-0.060; 0.013) ‡ |
| Total hip | -0.000 (0.050) | 0.011 (0.051) | 0.007 (0.053) | 0.011 (-0.013; 0.036) § 0.006 (-0.026; 0.039) ‡ |
| Femoral neck | -0.022 (0.049) | -0.012 (0.049) | -0.009 (0.051) | 0.010 (-0.013; 0.034) § 0.013 (-0.018; 0.044) ‡ |
| Trochanter | -0.002 (0.048) | 0.012 (0.048) | 0.008 (0.050) | 0.013 (-0.010; 0.037) § 0.009 (-0.021; 0.040) ‡ |

§ Intermittent versus Never
 ‡ Continuous versus Never

TABLE - Combined hormonal oral contraceptives BMD change

Disclosures: Jerilynn Prior, None.

FR0320

Evidence for Spontaneous Recovery of Bone Mineral Density after Treatment for Cushing's Syndrome: a Long-term Follow-up Study. Anke van der Eerden¹, Martin Den Heijer².
¹Radboud University Nijmegen Medical Centre, Netherlands, ²VU Medical CenterPostbus 70571007 MB Amsterdam, The Netherlands

Introduction: Cushing's syndrome gives a high risk of osteoporotic fractures. After treatment bone mineral density (BMD) improves, but recovery lasts years and full recovery probably does not occur in all patients. We evaluated BMD of the lumbar spine and femoral neck of patients with Cushing's syndrome, measured at the time of diagnosis and during long-term follow-up.

Methods and Materials: We collected all BMD measurements of the lumbar spine and the right femoral neck performed in patients diagnosed with Cushing's syndrome in our hospital, as measured by dual-energy X-ray absorptiometry. To analyse BMD data we used a non-linear model in which individual BMD is described as an age-related deviation from the population reference value.

Results: BMD values were available for 151 patients with Cushing's syndrome. Mean follow-up time after treatment was 12.5 years (total 1888 patient years). Before treatment, patients with Cushing's syndrome had a lower BMD compared to the NHANES reference population (lumbar spine Z-score -1.8 SD (95%CI -2.1 to -1.4 SD); femoral neck -0.9 SD (95%CI -1.4 to -0.6 SD)). Recovery was complete in most patients but not in certain groups. Reaching the estimated individual final BMD took 11.0 years (95%CI 9.5 to 12.5 years, lumbar spine) and 12.0 years (95%CI 10.0 to 13.5 years, femoral neck).

Conclusion: In most patients with Cushing's syndrome, BMD improves to normal in about one decade. In 2-2.5 years BMD-loss decreases 50%, e.g. from osteoporosis to osteopenia. This supports the practice of evaluating BMD in osteoporotic Cushing patients every 2 years until reaching osteopenia.

Disclosures: Martin Den Heijer, None.

FR0321

Fracture Risk is Increased in Severe Obesity with Low Bone Mineral Density. Sarah Cawsey*, Rajdeep S Padwal, Stephanie Li, Arya M Sharma, Kerry Siminoski. University of Alberta, Canada

Purpose: The bone-protective effect of body weight is controversial and recent studies have found increased risk of some fractures in obesity. Most published research has involved individuals with modest obesity; the relationship between bone mineral density (BMD) and fracture risk has not been well characterized in severe obesity.

Methods: A cross sectional study of 400 randomly chosen female patients admitted to the Edmonton Weight Wise Regional Obesity Program (Edmonton, Alberta, Canada) from November 2008 to June 2010. Historical information including self-reported fracture history was obtained at the time of dual-energy X-ray absorptiometry (Hologic 4500A). For fracture rates, the group comprising the lowest quintile of femoral neck BMD was compared to the remainder of the population. For certain risk factors, the lowest BMD quintile was compared to an equal number (n = 75) of age- and BMI-matched controls randomly selected from the remainder of the study group.

Results: Subjects were severely obese with a mean body mass index (kg/m²) of 46.0 (SD 7.4), had an average age of 43.8 years (SD 11.1 years), and 160 (40.0%) were postmenopausal. Women in the low BMD quintile had a mean BMD Z-score of -0.1 (SD 0.4) compared to +1.6 (SD 0.9) in the rest of the population. The low BMD quintile had significantly more total fractures (50.7% vs. 18.2%, p < 0.0001), fragility-type fractures (hip, vertebral, forearm, upper arm; 14.7% vs. 5.2%, p = 0.0039), and other fractures (34.7 vs. 12.9%, p < 0.0001) compared to the remaining population.

Among other fractures, the low BMD quintile had increased rates of hand/foot fractures (16.0% vs. 5.5%, $p = 0.0019$) and ankle/lower leg fractures (17.3% vs. 7.1%, $p = 0.0051$). The low BMD quintile did not differ from control subjects for menopausal history, smoking, parental history of hip fracture, doses of calcium and vitamin D supplements, serum 25-OH vitamin D, or other lab tests. The low BMD quintile had higher risks of osteoporotic fracture (3.4% (SD 2.4%) vs. 2.5% (SD 1.6%); $p = 0.0086$) and hip fracture (0.2% (SD 0.3%) vs. 0.02% (SD 0.04%); $p < 0.0001$) according to FRAX (Canadian FRAX tool).

Conclusions: Women with the lowest BMD values among those with severe obesity have a markedly elevated risk of fracture compared to those with higher BMD values, despite the fact that their BMD Z-scores are in the "normal" range. This population may require its own reference range to define "low" density.

Disclosures: Sarah Cawsey, None.

FR0323

Race/ethnic Differences in Associations between Bone Mineral Density and Fracture History. Min-Ho Shin¹, Joseph Zmuda², Elizabeth Barrett-Connor³, Yahtyng Sheu², Alan Patrick⁴, Sun-Seog Kweon¹, Hae-Sung Nam⁵, Jane Cauley². ¹Chonnam National University Medical School, South Korea, ²University of Pittsburgh Graduate School of Public Health, USA, ³University of California, San Diego, USA, ⁴Tobago Health Studies Office, Scarborough, Trinidad & Tobago, ⁵Chungnam National University Medical School, South Korea

The aim of our study was to determine whether there are race/ethnic differences in bone mineral density (BMD) by fracture history in men aged 65 and older. We used a cross-sectional design. The datasets included the Osteoporotic Fractures in Men (MrOS) Study (5,342 White men, 243 African-American, 190 Asian, and 126 Hispanic men), Tobago Bone Health Study (641 Afro-Caribbean), Namwon Study (1,834 Korean rural), and Dong-gu Study (2,057 Korean urban). BMD was corrected according to the cross-site calibration results for all scanners. Linear regression analysis was used to estimate the difference in BMD between subjects with a positive fracture history and those without a fracture within each racial/ethnic group. Logistic regression was used to examine the association of BMD with fracture within each racial/ethnic group for fracture. In all models, we adjusted for age, body weight, height, smoking and alcohol use. Mean age (years) of the Korean combined cohorts, US white, US African-American, US Asian, US Hispanic and Afro-Caribbean were 71.2 ± 4.3 , 73.8 ± 5.9 , 71.7 ± 5.1 , 72.9 ± 5.1 , 72.0 ± 4.8 , and 72.3 ± 5.7 , respectively. The proportion with a history of non-traumatic fracture were 4.9%, 17.6%, 14.8%, 10.5%, 13.5% and 5.5% for Korean, US white, US African-American, US Asian, US Hispanic and Afro-Caribbean, respectively. The mean differences of hip and lumbar spinal BMD between subjects with fracture and without fracture were significant in all cohorts except US African American and US Asian men, Table. There was a significant race/ethnic difference in the mean lumbar spinal BMD between subjects with fracture and without fracture (p for interaction=0.049), but no difference in the mean BMD. Odds ratio (95% confidence interval) of fracture for 1 SD decrease in lumbar spine BMD were 1.37 (1.16, 1.62); 1.53 (1.41, 1.66); 1.45 (0.96, 2.19); 1.42 (0.84, 2.40); 3.34 (1.44, 7.74); and 1.96 (1.26, 3.02) for Korean, US White, US African-American, US Asian, US Hispanic and Afro-Caribbean, respectively. Our data show that BMD differences by fracture status were greatest for US Hispanic and Afro-Caribbean men with higher odds ratios of fracture for 1 SD decrease in BMD than Korean and US white, US African-American, and US Asian men. Our results suggest that there are race/ethnic differences in the association between lumbar spine BMD and fracture history.

Table. Adjusted mean and differences of BMD (g/cm³) according to history of fracture.

| | Lumbar spine BMD | | | Femoral Neck BMD | | | Total Hip BMD | | |
|----------------------|------------------|-------|---------------------------|------------------|-------|---------------------------|---------------|-------|---------------------------|
| | Fx(-) | Fx(+) | Difference(95%CI) | Fx(-) | Fx(+) | Difference(95%CI) | Fx(-) | Fx(+) | Difference(95%CI) |
| Korean cohort | | | | | | | | | |
| Dong-gu | 1.120 | 1.090 | -0.029 (-0.064 to 0.005) | 0.865 | 0.841 | -0.024 (-0.045 to -0.003) | 0.914 | 0.877 | -0.038 (-0.06 to -0.016) |
| Namwon | 1.062 | 1.014 | -0.048 (-0.088 to -0.008) | 0.851 | 0.827 | -0.024 (-0.050 to 0.001) | 0.901 | 0.879 | -0.021 (-0.048 to 0.005) |
| Combined | 1.091 | 1.056 | -0.034 (-0.061 to -0.008) | 0.858 | 0.834 | -0.024 (-0.040 to -0.008) | 0.908 | 0.877 | -0.031 (-0.048 to -0.014) |
| US | | | | | | | | | |
| White | 1.152 | 1.098 | -0.054 (-0.067 to -0.041) | 0.874 | 0.836 | -0.038 (-0.047 to -0.029) | 0.977 | 0.931 | -0.046 (-0.055 to -0.038) |
| African-American | 1.219 | 1.141 | -0.079 (-0.159 to 0.001) | 0.979 | 0.94 | -0.039 (-0.093 to 0.014) | 1.058 | 1.009 | -0.049 (-0.102 to 0.004) |
| Asian | 1.119 | 1.048 | -0.071 (-0.155 to 0.013) | 0.843 | 0.816 | -0.027 (-0.081 to 0.028) | 0.923 | 0.888 | -0.035 (-0.086 to 0.017) |
| Hispanic | 1.137 | 0.949 | -0.189 (-0.284 to -0.093) | 0.906 | 0.811 | -0.095 (-0.161 to -0.029) | 0.995 | 0.894 | -0.101 (-0.167 to -0.034) |
| Afro-Caribbean | 1.238 | 1.135 | -0.103(-0.034 to -0.172) | 1.001 | 0.932 | -0.070 (-0.120 to -0.020) | 1.181 | 1.106 | -0.076 (-0.126 to -0.026) |

Adjusted for age, weight, height, history of smoking and history of alcohol drinking.

Table

Disclosures: Min-Ho Shin, None.

FR0332

Physical Activity and Incident Fracture in Postmenopausal Women: The Women's Health Initiative Observational Study. Jean Wactawski-Wende^{*1}, Joseph C. Larson², Jane Cauley³, Zhao Chen⁴, Rebecca Jackson⁵, Andrea LaCroix⁶, Michael LaMonte¹, Meryl Leboff⁷, Judith K. Ockene⁸, John Robbins⁹. ¹University at Buffalo, USA, ²Fred Hutchinson Cancer Research Center, USA, ³University of Pittsburgh Graduate School of Public Health, USA, ⁴University of Arizona, USA, ⁵The Ohio State University, USA, ⁶Fred Hutchinson Cancer Research Center, USA, ⁷Brigham & Women's Hospital, USA, ⁸University of Massachusetts, USA, ⁹University of California, Davis Medical Center, USA

Approximately 2.0 million fractures occur annually in adult U.S. women with mortality from hip fracture approaching 20%. We assessed the role of physical activity in incident fracture in the Women's Health Initiative Observational Study (WHI-OS). The WHI-OS enrolled 71,187 postmenopausal women aged 50-79 between 1994 and 1998. Recreational physical activity and walking was self-reported at enrollment. Metabolic equivalents (MET-hours/week) were estimated for total energy expenditure as well as for sedentary, walking, and strenuous activities. Incident fractures were self-reported annually through 2005. Hazard Ratios (HR) were calculated comparing fracture incidence rates in those reporting no activity to those reporting activity, according to tertiles within those active. A total of 10,927 fractures occurred (760 hip; 2477 wrist; 1189 clinical vertebral) during an average follow-up of 7.6 years. In multivariable adjusted models, compared to those reporting no activity, those in the highest activity category (>17.5 MET-hours/week) had significantly fewer hip fractures (HR= 0.63, 95% CI: 0.48, 0.81) and significantly fewer clinical vertebral fractures (HR=0.80, 95% CI 0.66, 0.98) and marginally fewer total fractures (HR=0.95, 95% CI: 0.89, 1.02). Among those most active, wrist fracture occurred somewhat more frequently (HR=1.10, 95% CI: 0.96, 1.27). Walking and strenuous activity were similarly and significantly associated with these fracture outcomes. No evidence of effect modification by age, BMI or race/ethnicity was observed. Recreational physical activity is generally associated with fewer fractures in older women. Increased activity may be one strategy to prevent fractures in older women, especially in hip fracture where the associated morbidity and mortality are most profound.

Disclosures: Jean Wactawski-Wende, None.

FR0337

A Proposed World-Wide Gene-Environment Interaction Study of BMD and Fracture Risk: Feasibility Analysis Based on the GEFOS-GENOMOS Collaboration. Jonathan Reeve^{*1}, Stephen Kaptoge², On behalf of the GEFOS & GENOMOS consortium³. ¹University of Cambridge, United Kingdom, ²University of Cambridge Bone Research Group, United Kingdom, ³Erasmus Medical Center, Netherlands

There is widespread general and scientific interest in how to modify the genetic determinants of fracture. The GEFOS & GENOMOS consortium has just reported on the genetic determinants of BMD and fracture (Estrada K et al Nature Genetics 2012 DOI 10.1038/ng.2249). Fourteen BMD loci were associated with fracture including genes previously not known to play a role in bone biology. Our purpose is two-fold: to summarize the collection of environmental exposure data by GEFOS and GENOMOS in participating GEFOS/GENOMOS subjects; and to make the case for enlarging our planned GxE meta-analysis into a world-wide collaboration.

Fifty four European, Australasian, Far-Eastern and N American studies expressed interest in participating of which 41 were permitted by their IRBs to share individual-level environmental exposure data. This report considers data from the 27 cohorts whose phenotypic data has been cleaned and reconciled in Cambridge UK and reports on the a priori statistical power available.

Environmental exposures and plasma biomarkers were supplied as continuous or categorical variables, with almost complete data available on age, height and weight and lower levels of availability for other variables. Studies, after sample-size weighting, declared more than 50% availability of data on alcohol, smoking, fracture history, physical activity (several aspects), several diet nutrients, rural-vs-urban domicile, fall history, and exposures to glucocorticoids and exogenous estrogen. A substantial minority of studies had measured plasma biomarkers. Calculations were done to determine the a priori statistical power of the planned meta-analysis at $p < 0.001$, with testing restricted to polymorphisms reported significant by Estrada et al. Using exemplary minor allele frequencies (MAF) of 0.2 and GxE interaction coefficients of 0.03 and 0.06 per categorical exposure (or per 1 SD higher outcome in the case of continuous exposures) we report the numbers of subjects needed to achieve 80% power for the most commonly collected categorical and continuous environmental exposure or biomarker data (Table).

Conclusions. These results provide a powerful basis for investigating the interplay of genes and environment in association with fracture susceptibility and intermediate phenotypes. To achieve this goal, ensuring maximal statistical power and proper standardization of exposures, a world-wide collaboration is needed building on the current GEFOS collaboration.

| Exposure/analyte | Numbers so far available to GEFOS x 1000 | Numbers required for 80% power: GxE coefficient 0.03 | Numbers required for 80% power: GxE coefficient 0.06 |
|-----------------------------|--|--|--|
| Lifestyle: | | | |
| Smoking y/n | 39 | 260 | 65 |
| Alcohol y/n | 30 | 120 | 37 |
| Nutritional: | | | |
| Calcium/VitD/Energy/Protein | 15 | 60 | 15 |
| Plasma: | | | |
| 25(OH)D; creatinine | 15 | 60 | 15 |
| Ca++/PTH/AlkPhos | 8 | 60 | 15 |
| E2/SHP/Testo | 3 | 60 | 15 |

Power Calculations Summary

Disclosures: Jonathan Reeve, None.

FR0339

Objectively Measured Physical Activity and Bone Mineral Content from Age 5 to 15 Years: Iowa Bone Development Study. Kathleen F Janz*, Steven M Levy, Elena Letuchy, Trudy L Burns, Julie M Eichenberger Gilmore, James C Torner. University of Iowa, USA

Purpose: This study examined the longitudinal association between physical activity (PA) and bone mineral content (BMC; g) from middle childhood to middle adolescence (ages 5 to 15 yr, 10-year follow-up) and tested the premise that PA has a greater effect on BMC during specific periods of growth (window of opportunity hypothesis).

Methods: Participants in the Iowa Bone Development Study at ages 5, 8, 11, 13, and 15 yr (n = 369, 449, 452, 410, 307, respectively) were studied. Moderate-through-vigorous PA (MVPA, (min·day⁻¹) and vigorous PA (min·day⁻¹) were measured using the Actigraph accelerometer. Anthropometrics were used to measure body size and somatic maturity. BMC of the lumbar spine and hip was measured using dual-energy x-ray absorptiometry. Gender-specific multi-level models were used to create BMC growth curves for individual participants (level 1) and test the effect of PA (level 2) after considering weight (kg), height (cm) linear age (yr), non-linear age (yr²), maturity (pre peak height velocity = 0 or at/post peak height velocity = 1). To explore the possibility that bone is more sensitive to PA during certain periods of growth, we tested the interaction of PA × maturity and PA × age. The Akaike Information Criterion (AIC) was used to determine the best fitting models. Clinical significance was examined via the differences in BMC between the least (10th %) and most (90th %) active children.

Results: For boys and girls, PA added to the prediction of both spine and hip BMC throughout the 10-year follow-up (age 5 to 15 yr). There was no interaction between PA and maturity or PA and age. Models with vigorous PA had lower (better) AIC when compared to MVPA models. At age 5, the most vigorously active boys had 8.5% more hip BMC than the least active. At age 15, this difference was 2.0%. The most vigorously active girls at age 5 had 6.1% more hip BMC than the least active. The age 15 difference was 1.8%.

Conclusions: Objectively measured everyday PA, especially vigorous PA, is associated with BMC at weight-bearing skeletal sites from childhood to adolescence. Importantly, the effect of PA is the same regardless of maturity or age. The reduced contribution of PA to BMC as children age is primarily due to reductions in PA. This suggests the critical importance of early and sustained PA interventions that focus on vigorous PA. Current public health approaches focused on moderate PA may be inadequate for optimal bone health.

Disclosures: Kathleen F Janz, None.

FR0341

A Distal Forearm Fracture in Childhood Increases the Risk for Fracture during Adulthood in Men, but not in Women. Shreyasee Amin*¹, L. Joseph Melton¹, Sara Achenbach¹, Elizabeth Atkinson¹, Mark Dekutoski¹, Salman Kirmani¹, Philip Fischer¹, Sundeep Khosla². ¹Mayo Clinic, USA, ²College of Medicine, Mayo Clinic, USA

Distal forearm fractures are the most common type of fracture sustained during childhood. It remains unclear whether these fractures are related, in part, to transient bone strength deficits during growth or to deficits that may track into adulthood. If the latter, a distal forearm fracture in childhood would be expected to predict an increased risk for fractures in adulthood.

We identified 1776 Olmsted County, Minnesota residents who had sustained their first distal forearm fracture at ≤18 yrs of age between 1935 and 1992, and had available follow-up through to at least age 35 yrs. Subsequent incident fractures were identified through review of complete (inpatient and outpatient) medical records. Observed fractures (excluding pathologic fractures and those resulting from severe trauma) were then compared with the numbers expected from incidence rates in the Olmsted County population (standardized incidence ratios [SIR]). We also examined the risk for fractures at osteoporotic (OP), defined as hip, spine, wrist and shoulder, and non-osteoporotic (non-OP) sites. Analyses were stratified by sex, and then by age at the initial distal forearm fracture (<10 yrs, 11-13 yrs, 14-18 yrs).

We studied 1086 boys and 690 girls, whose mean age (± SD) at distal forearm fracture was 11 ± 4 yrs for boys and 10 ± 4 yrs for girls. Over 27,277 person-yrs of follow-up after age 35 yrs (to mean age 51 ± 11 yrs for men and 50 ± 11 yrs for women), there were 144 men and 74 women who had a fracture due to no more than moderate trauma. There was an increased risk for future mild-to-moderate trauma fractures in boys who had a distal forearm fracture, but not girls (Table). Results were similar when we considered fractures only after age 50 yrs. The increased risk was apparent irrespective of the age at initial distal forearm fracture in boys. In both men and women, the most common future fractures occurred at the spine and ribs.

A distal forearm fracture in boys may signal an increased risk for future fractures either due to persistent deficits in bone strength, continued high fracture risk activity, or both. If deficits in bone strength do track into adulthood, differences in findings between the sexes may be due to menopause in women having a greater net influence on subsequent fracture risk, but would require further study.

| | SIR (95% CI) For Future Fracture (Fx) by Age at Distal Forearm Fx | | | |
|------------------|---|----------------|----------------|----------------|
| | Any Age | <10 yrs | 11-13 yrs | 14-18 yrs |
| Men (N) | 1086 | 497 | 315 | 274 |
| Any Fx* | 1.9 (1.6, 2.3) | 1.9 (1.5, 2.5) | 1.9 (1.4, 2.5) | 1.9 (1.4, 2.6) |
| OP Fx* | 2.6 (2.1, 3.3) | 3.5 (2.5, 4.8) | 2.3 (1.4, 3.5) | 1.8 (1.0, 3.1) |
| Non-OP Fx* | 1.7 (1.3, 2.0) | 1.4 (0.9, 1.9) | 1.8 (1.2, 2.5) | 2.0 (1.4, 2.9) |
| Women (N) | 690 | 445 | 171 | 74 |
| Any Fx* | 1.0 (0.8, 1.2) | 1.1 (0.8, 1.4) | 1.1 (0.7, 1.6) | 0.5 (0.2, 1.1) |
| OP Fx* | 1.1 (0.8, 1.6) | 1.1 (0.7, 1.7) | 1.6 (0.8, 2.7) | 0.6 (0.1, 1.6) |
| Non-OP Fx* | 1.0 (0.8, 1.4) | 1.2 (0.8, 1.6) | 1.0 (0.5, 1.7) | 0.6 (0.2, 1.4) |

*excludes any pathologic or severe trauma fracture

Table

Disclosures: Shreyasee Amin, Merck & Co, 2

FR0343

BMI-Associated Increases in Proximal Femoral Volumetric BMD, Size and Strength Are Not Sufficient to Compensate for Increased Fall Forces in Obese Older Men. Jian Shen*¹, Carrie Nielson¹, Lynn Marshall¹, David Lee², Tony Keaveny³, Eric Orwoll¹. ¹Oregon Health & Science University, USA, ²O.N. Diagnostics, USA, ³University of California, Berkeley, USA

Although higher body mass index (BMI) is associated with higher bone mineral density (BMD), recent evidence indicates that obesity may not be associated with reduced hip fracture risk. Substantial proportions of hip fractures occur among overweight and obese men and women. This evidence suggests that higher BMI may have deleterious effects on bone structure or volumetric BMD, but this issue has not been studied in detail. We conducted cross-sectional analyses of baseline BMI and quantitative computed tomography (QCT)-derived femoral bone density and structural dimensions in the Osteoporotic Fractures in Men Study (MrOS). Hip QCT scans were completed in 3056 subjects (mean age: 73 y). Finite element (FE) analysis based on QCT images was further completed in a random subcohort consisting of 669 men. FE was used to assess proximal hip strength in a sideways fall orientation. Fall forces on the hip were derived, and Phi was calculated as fall force-to-strength ratio with the value ≥ 1 indicating high risk of hip fracture during a sideways fall. We used non-parametric generalized additive models to identify nonlinearity in the associations between BMI and QCT measurements, and multivariable general linear models to test the linear associations. Higher BMI was associated with slightly greater volumetric BMD and size measures at femoral neck. However, the relationship was non-linear. For men with BMI < 30 (n=2387), there was a linear relationship between BMI and QCT measurements such that higher BMI was associated with greater integral BMD, trabecular BMD, cortical thickness and cross-sectional area (Table). However, there were no significant associations among those with BMI ≥ 30 (n=669). FE analysis suggested that compared to non-obese men, obese men had higher hip strength but also higher Phi (P = 0.0001) and a higher risk of Phi-estimated hip fracture (OR: 2.14 vs non-obese men; P=0.008). These findings indicate that the relationships of BMI with femoral BMD and structure are nonlinear. In non-obese men, increased BMI is associated with increased bone size, BMD and cortical thickness. In obese individuals, there is no further improvement of those structure parameters with additional increases in BMI. FE analyses suggest that the incremental increase in strength is not proportionate with increased fall force in obese men. These results provide some insight into mechanisms underpinning fracture risk in obese men.

Table. Proximal femoral QCT and FE measurements stratified by obese status

| | BMI < 30 (n=2387) | | BMI ≥30 (n=669) | | P for Interaction* |
|---|-----------------------------|--------------------|-----------------------------|-------|--------------------|
| | SD increase per unit of BMI | P | SD increase per unit of BMI | P | |
| Femoral neck | | | | | |
| BMD (g/cm ³) | | | | | |
| Integral | 0.051 | <0.0001 | -0.017 | 0.219 | 0.0003 |
| Cortical | 0.041 | <0.0001 | -0.012 | 0.348 | 0.002 |
| Trabecular | 0.041 | <0.0001 | -0.024 | 0.089 | 0.0002 |
| Volume (cm ³) | | | | | |
| Integral | 0.026 | 0.002 | -0.015 | 0.3 | 0.013 |
| Cortical | 0.053 | <0.0001 | -0.02 | 0.163 | <0.0001 |
| Medullary | 0.005 | 0.589 | -0.009 | 0.532 | 0.314 |
| Percent cortical volume | 0.044 | <0.0001 | -0.013 | 0.336 | 0.002 |
| Cross-sectional area (cm ²) | 0.032 | 0.0002 | -0.016 | 0.254 | 0.003 |
| DXA BMD | 0.101 | <0.0001 | 0.026 | 0.019 | <0.0001 |
| | Normal (n=200) | Overweight (n=379) | Obese (n=90) | | P for trend |
| Least-squares adjusted mean | | | | | |
| Femoral strength (N) | 4694 | 5001 | 5490 | | <0.0001 |
| Fall force-strength ratio | 0.73 | 0.81 | 0.86 | | <0.0001 |

*Interaction between obese status and BMI on QCT parameters

BMI_QCT

Disclosures: *Jian Shen, None.*

FR0344

Estimated Frax[®] 10-Year Fracture Risk at the Time of Incident Fracture and Upon Refracture: Results from the Optimus Initiative. Pierre-Marc April¹, Noémie Poirier², Sophie Roux³, Marie-Claude Beaulieu¹, Michèle Beaulieu⁴, François Cabana⁵, Gilles Boire². ¹Université de Sherbrooke, Canada, ²Centre hospitalier universitaire de Sherbrooke, Canada, ³University of Sherbrooke, Canada, ⁴Merck Canada Inc, Canada, ⁵CHUS, Canada

Introduction. Identification of patients who will sustain a fragility fracture (FF) is the main objective of the WHO Fracture Risk Assessment score (FRAX[®]).

Objectives. To describe the FRAX scores at the time of an incident FF and the rates of subsequent fractures over 4 years according to FRAX category following this clinical FF.

Methods. An ongoing prospective cohort of men and women over 50 years of age was followed up in the OPTIMUS study, an intervention aimed at increasing the rate of initiation and persistence on osteoporosis treatment after an incident FF leading to an orthopaedic consultation. After inclusion, participants were counselled about osteoporosis and its relationship to FF. A letter was sent to their Family Physician (FP) to stress the importance of treating osteoporosis unmasked by a FF, with reminders to FP of patients still untreated at the time of regular phone follow-ups. At year 1, use of anti-osteoporosis medication was checked with the patients' pharmacists and confirmed in 56%. New FF were reported during phone follow-ups with patients. FRAX scores (excluding BMD) were calculated from baseline and follow-up information.

Results. From January 2007 to July 2011, 1172 patients (961 women) with FF were included. FRAX score could not be calculated in 20 patients because of missing data.

Before the incident FF, 617/1152 (53.6%) were scored at Low, 291 (25.3%) at Moderate, and only 244 (21.2%) at High risk for FF (Table). After the incident FF, 27.3% patients were still considered at Low, 40.6% at Moderate and 32.0% at High Risk. FRAX scores were still estimated Low-risk in 5.8%, 22.8%, 26.0%, 35.3%, 49.3% and 36.4% of patients with incident FF at the Hip, Proximal Humerus, Wrist, Vertebra, Ankle and Other Minor sites, respectively.

Over 2285 patient-years of follow-up, 111 recurrent FF occurred. Rates of FF were 6.71, 6.60, 4.71, 4.44, and 3.76 FF/100 patient-years after FF at Other Minor sites, Hip, Wrist, Proximal Humerus and Ankle, respectively. The estimated 10-year risk was High in 74 (66.7%) patients before the recurrent FF. Odds ratios (ORs) for recurrent FF were 4.17 [CI 2.75-6.31] for High relative to Low/Moderate risk and 3.42 [CI 2.00-5.86] for High relative to Low risk only. Rates of recurrent FF for Moderate (19/468 patients) and Low (19/315) risk groups were similar (OR 0.70 [CI 0.36-1.35]).

Conclusions. FRAX High-risk category identifies less than 25% of patients who will present an incident FF. Once a FF has occurred, a High risk score is a moderately sensitive (66%) but clinically useful (OR > 4) predictor for subsequent FF. As FRAX was designed for use in untreated patients only, High-risk scores may overestimate fracture risk in those patients becoming treated, further strengthening our observations. However, FF patients classified at Moderate and Low risks had similar rates of recurrent FF, suggesting that this subdivision may not be clinically useful after a FF.

| Site of the initial fragility fracture (FF) (Number of patients with fracture*) | 10-year fracture risk according to FRAX [®] (High Risk: ≥20% Major Fracture and/or >3% Hip FF) (Moderate Risk: ≥10% and <20% Major Fracture and <3% Hip FF) (Low risk: <10% Major Fracture and <3% Hip FF) | | | | | |
|---|---|-------------------|-------------------|-----------------------|-------------------|-------------------|
| | BEFORE the incident FF | | | AFTER the incident FF | | |
| | Low n (%) | Moderate n (%) | High n (%) | Low n (%) | Moderate n (%) | High n (%) |
| Any fragility fracture (n= 1152) | 617 (53.6) | 291 (25.3) | 244 (21.2) | 315 (27.3) | 468 (40.6) | 369 (32.0) |
| Hip (n= 225) | 49 (21.8) | 66 (29.3) | 110 (48.9) | 13 (5.8) | 71 (31.6) | 141 (62.7) |
| Vertebra (n= 17) | 9 (52.9) | 6 (35.3) | 2 (11.8) | 6 (35.3) | 7 (41.2) | 4 (23.5) |
| Wrist (n= 362) | 219 (60.5) | 86 (23.8) | 57 (15.7) | 94 (26.0) | 167 (46.1) | 101 (27.9) |
| Ankle (n= 227) | 174 (76.7) | 43 (18.9) | 10 (4.4) | 112 (49.3) | 86 (37.9) | 29 (12.8) |
| Proximal humerus (n= 202) | 92 (45.5) | 60 (29.7) | 50 (24.8) | 46 (22.8) | 87 (43.1) | 69 (34.2) |
| Other minor sites** (n= 119) | 74 (62.2) | 30 (25.2) | 15 (12.6) | 44 (37.0) | 50 (42.0) | 25 (21.0) |

*20 patients were excluded because a FRAX score could not be calculated

**Upper limb (57), Lower limb (36), Clavicle (11), Pelvis (12), Scapula (2) and Ribs (1).

Table. 10-year FRAX category before and after an incident FF

Disclosures: *Pierre-Marc April, None.*

FR0345

Fractures in Patients Diagnosed With HIV. Daniel Prieto-alhambra^{*1}, Arief Lalmohamed², Frank De Vries³, Peter Vestergaard⁴. ¹Institut Municipal D'Investigació Mèdica, United Kingdom, ²Department of Pharmacoepidemiology & Clinical Pharmacology, Utrecht Institute of Pharmaceutical Sciences, Netherlands, ³, ⁴Aarhus University Hospital, Denmark

Aim: To study the effects of a diagnosis of human immunodeficiency virus infection on fracture risk.

Subjects and methods: Case control study. From the Danish National Health Service, we identified 124,655 fracture cases and 373,962 age- and gender-matched controls. Odds ratios (OR) and 95% confidence intervals (CI) were estimated.

Results: A total of 50 patients in the fracture group and 52 in the control group had a prior HIV diagnosis, which is in the range expected in the Danish population. The risk of any fracture was thus significantly increased among HIV-infected patients (crude OR = 2.89, 95% CI 1.99-4.18). Similarly a significant increase in the risk of hip (crude OR=8.99, 95% CI 1.39-58.0), forearm (crude OR=3.50, 95 CI 1.26-9.72), and spine fractures (crude OR=9.00, 95% CI 1.39-58.1) was observed. After adjustment for alcoholism, stroke, working, co-habitation status, income, number of bed days in hospital in the previous year, number of contacts to GP or specialist in the previous year, use of anti-epilepsy drugs, use of anxiolytics or sedatives, prior fracture, and use of corticosteroids the OR for any fracture was still significantly increased (1.66, 95% CI 1.08-2.54). The trend was the same for hip fractures, but no longer statistically significant (9.93, 95% CI 0.90-109). The association with forearm (1.78, 95% CI 0.54-5.93) and spine (3.20, 95% CI 0.33-31.0) fractures was no longer statistically significant.

Conclusion: HIV infection is associated with a significant increase in the risk of fractures. Preventive measures against fractures may be considered in HIV-infected patients, especially as life-expectancy has improved significantly, and as fractures may negatively affect quality of life and increase the risk of death.

Disclosures: *Daniel Prieto-alhambra, None.*

FR0346

Iron Overload Accelerates Bone Loss in Healthy Postmenopausal Women and Middle-aged Men: a 3-year Retrospective Longitudinal Study. Beom-Jun Kim^{*1}, Seong Hee Ahn², Sung Jin Bae¹, Seung Hun Lee³, Jung-Min Koh¹, Ghi Su Kim³. ¹Asan Medical Center, South Korea, ²Division of Endocrinology & Metabolism, Asan Medical Center, University of Ulsan College of Medicine, South Korea, ³Asan Medical Center, University of Ulsan College of Medicine, South Korea

Despite extensive experimental and animal evidence about the detrimental effects of iron and its overload on bone metabolism, there have been no clinical studies relating iron stores to bone loss, especially in non-pathologic conditions. In the present study, we performed a large longitudinal study to evaluate serum ferritin concentrations in relation to annualized changes in bone mineral density (BMD) in healthy Koreans. A total of 1,729 subjects (940 postmenopausal women and 789 middle-aged men) aged 40 years or older who had undergone comprehensive routine health examinations with an average 3 years of follow-up were enrolled. BMD in proximal femur sites (i.e., the total femur, femur neck, and trochanter) was measured with dual-energy X-ray absorptiometry using the same equipment at baseline and follow-up. The mean age of women and men in this study was 55.8 ± 6.0 years and 55.5 ± 7.8 years, respectively, and serum ferritin levels were significantly higher in

men than in women ($P < 0.001$). The overall mean annualized rates of bone loss in the total femur, femur neck, and trochanter were $-1.14\%/yr$, $-1.17\%/yr$, and $-1.51\%/yr$, respectively, in women and $-0.27\%/yr$, $-0.34\%/yr$, and $-0.41\%/yr$, respectively, in men. After adjustment for potential confounders, the rates of bone loss in all proximal femur sites in both genders were significantly accelerated in a dose-response fashion across increasing ferritin quartile categories (P for trend = $0.043 < 0.001$). Consistently, compared with subjects in the lowest ferritin quartile category, those in the third and/or highest ferritin quartile category showed significantly faster bone loss in the total femur and femur neck in both genders ($P = 0.023 < 0.001$). In conclusion, these data provide the first clinical evidence that increased total body iron stores could be an independent risk factor for accelerated bone loss, even in healthy populations.

Disclosures: *Beom-Jun Kim, None.*

FR0347

Is Bisphosphonate Therapy for Benign Bone Disease Associated with Impaired Dental Healing? Gelsomina Borromeo¹, John Wark^{*2}, Caroline Brand³, Michael McCullough⁴, John Clement⁴, Lisa Crighton³, Graham Hepworth⁵. ¹The University of Melbourne, Australia, ²University of Melbourne Department of Medicine, Australia, ³Melbourne Health, Australia, ⁴Melbourne Dental School, University of Melbourne, Australia, ⁵University of Melbourne, Australia

Delayed dental healing (DDH) and osteonecrosis of the jaw (ONJ) are potentially devastating conditions associated with use of intravenous bisphosphonate therapy for oncology indications. The relationship between bisphosphonate use for non-oncology indications (benign bone disease) and these conditions has not been determined.

A case controlled study design was employed to test whether or not DDH, defined as a persistent breach in the oral mucosa and/or exposure of bone in the mandible or maxilla that fails to heal within 6 weeks, is associated with oral bisphosphonate use for a non-oncology indication.

Potential cases of DDH were identified by consecutive screening of Specialist Oral and Maxillofacial and Special Needs Dentist clinic records for patients over 50 years, during a 6-month window, in the State of Victoria, Australia. Potential cases were confirmed by a Case Adjudication Panel and then matched for age and gender (1:4, n=160 controls) and source of dental referral with controls.

Variables of interest were: precipitants (dental extractions, implant placement, denture use, none), dental clinic type (public, private), smoking history, medical comorbidities, oral hygiene habits, socio-economic status (education level, household earnings).

4212 of 22,358 patient files met inclusion criteria, of which 69 were potential cases and 40 confirmed cases.

There was an estimated 13 times increased odds of developing DDH when taking an oral bisphosphonate (OR= 13.1, 95% CI 4.4 to 39.3).

There was a modest interaction between age, gender and clinic type (public versus private). There was insufficient power to show a significant effect of smoking despite a larger number of cases being smokers. There was however a link between having another illness (such as diabetes) and developing DDH (OR=2.3; 95% CI 1.0 to 5.2). Low socio-economic status was more prevalent amongst cases; low education (OR=13.7, 5.8 to 119), low household earnings (OR=10.55, 1.2 to 93.5).

39 out of 40 cases of DDH had a dental precipitant which did not threaten the association between bisphosphonate use and DDH.

In conclusion, this study highlights an important association between bisphosphonate use and DDH in individuals with a dental precipitant and taking oral bisphosphonates in the setting of benign bone disease. The relationship with other contributing factors requires further investigation.

Disclosures: *John Wark, Novartis Pharmaceuticals, 6*
This study received funding from: Novartis Pharmaceuticals provided some financial support for the study

FR0349

Older Men with either High or Low Serum 25-hydroxy Vitamin D levels have Significantly Increased Fracture Risk: Results from the Prospective CHAMP Study. Kerrin Bleicher^{*1}, Markus Seibel², Robert Cumming³, Vasikaran Naganathan⁴. ¹University of Sydney, Australia, ²Bone Research Program, ANZAC Research Institute, University of Sydney, Australia, ³School of Public Health, University of Sydney, Australia, ⁴Centre for Education & Research on Ageing, University of Sydney, Australia

Introduction: The relationship between serum 25-hydroxyvitamin D (25OHD) and fracture risk is unclear. The aim of this study was to investigate the relationship between serum 25OHD and incident fractures in a large population based cohort of older men.

Background: As the relationship between serum levels of 25OHD and fracture risk remains unclear, we investigated this question in a large population-based cohort of older men in Sydney, Australia.

Methods: In the CHAMP study, 1705 community-dwelling men aged 70-97 years were followed for a mean of 4.4 years, during which time data on radiologically verified fractures was collected prospectively. Serum 25OHD levels were measured

using a radioimmunoassay detecting both D2 and D3 (DiaSorin). Information on potential confounders was collected at baseline using clinical measures and questionnaires. We accounted for bone mineral density (BMD), falls' history, physical activity, sun exposure, season of blood draw, country of birth, in addition to anthropometric and lifestyle factors, medical history, muscle strength, balance, and serum biochemistry. The relationship between fractures and serum 25OHD levels was analyzed using Cox's Proportional Hazard regression.

Results: There were 123 first incident fragility fractures in 1662 men with valid serum 25OHD measures. The relationship between baseline serum 25OHD and fracture risk was "U-shaped", with an increased fracture risk in men with either low or high serum 25OHD levels. In multivariate analysis, the risk of fracture was greatest in men with serum 25OHD in the lowest quintile (25OHD ≤ 36 nmol/L (14.4 ng/mL); HR= 4.5, 95% CI:2.0,10.2) and in men in the highest quintile (25OHD ≥ 73 nmol/L (29.2 ng/mL); HR=3.5, 95% CI:1.5, 8.0) compared to men in the 4th quintile (25OHD: 59 to 72 nmol/L (23.6-28.8 ng/mL)) (table 1).

Conclusion: In community-dwelling older men, fracture risk was significantly increased not only in vitamin D-deficient men, but also in men within the highest quintile of serum 25OHD. This effect was not explained by lower BMD, increased physical activity, falls' risk or other lifestyle or anthropomorphic factors.

| Serum 25OHD levels | ≤ 36 nmol/L | > 37 to ≤ 48 nmol/L | > 48 to ≤ 59 nmol/L | > 59 to ≤ 72 nmol/L | > 72 nmol/L |
|--------------------|---------------------|-------------------------------|-------------------------------|-------------------------------|------------------|
| Hazard ratio | 4.51(2.0,10.2) | 2.83(1.2,6.8) | 2.75(1.1,6.8) | Referent | 3.52(1.5,8.0) |

Table 1: Association between quintiles of serum 25OHD and risk of fracture in older men. HR(95% CI)

Disclosures: *Kerrin Bleicher, None.*

FR0350

Wrist Fracture Incidence, Risk Factors, and Associations with Subsequent Fractures in Older Men. Elizabeth Barrett-Connor^{*1}, Carrie Nielson², Kristine Ensrud³, Eric Orwoll². ¹University of California, San Diego, USA, ²Oregon Health & Science University, USA, ³Minneapolis VA Medical Center / University of Minnesota, USA

Purpose: Distal radius is one of the most common fragility fracture sites in women ages 40 to 60 years old, and history of wrist fracture is a risk factor for future osteoporotic fractures. Incidence of wrist fracture is lower in men, and its risk factors are uncertain. We analyzed risk factors for incident wrist fractures, as well as the associations between a history of wrist fracture and incident fractures, in the Osteoporotic Fractures in Men (MrOS) study.

Methods: Men ages ≥ 65 were enrolled in the MrOS cohort in 6 US cities and followed for a mean of 8.9 years. Incident fractures were ascertained by triannual postcards and confirmed by radiographic reports. Baseline data on self-reported medical conditions, history of fractures, physical activity, and difficulty with instrumental activities of daily living (IADL) were collected by questionnaire, and a medication inventory was done. Arm BMD was obtained by DXA, and blood samples were provided. Grip strength was tested by handheld dynamometer. Men with follow-up time who were not using osteoporosis medications at baseline (N=5878, 98% of the full cohort) were included in the analysis. Multivariable Cox proportional hazards models were used to identify independent risk factors for incident wrist fracture. In separate models, age-adjusted hazard ratios quantified the association between baseline history of wrist fracture and incident nonspine, wrist, and hip fracture.

Results: The incidence of wrist fracture was 1.6 per 1000 man-years overall and ranged from 1.1 among that age 65-69 at baseline to 2.3 for men ≥ 80 . Independent predictors of wrist fracture were a baseline history of fracture since age 50 (hazard ratio [HR]: 2.1, 95% CI: 1.3-3.3), difficulty with any of 5 IADLs (HR: 1.6, 95% CI: 1.0-2.7), higher serum phosphate (HR: 1.3 per SD increase, 95% CI: 1.0-1.6), and lower arm BMD (HR: 2.0 per SD decrease, 95% CI: 1.5-2.6). Baseline history of wrist fracture since age 50 was associated with an increased risk of any nonspine fracture (age-adjusted HR [AHR]: 1.8, 95% CI: 1.4-2.4) and of incident wrist fracture (AHR: 2.9, 95% CI: 1.4-5.7) and hip fracture (AHR: 1.9, 95% CI: 1.1-3.2).

Conclusions: Although wrist fractures are much less common and occur later in men compared to women, they have similar risk factors and consequences. Risks for wrist fracture in older men included age > 79 , low BMD, and/or a prior nonspine fracture. Wrist fracture predicted incident fracture, including hip fracture.

Disclosures: *Elizabeth Barrett-Connor, None.*

FR0353

Effect of Obesity on Healthcare Utilisation and Quality of Life after Fracture in Postmenopausal Women: the Global Longitudinal study of Osteoporosis in Women (GLOW). Juliet Compston^{*1}, Julie Flahive², Steven Boonen³, Adolfo Diez-Perez⁴, Stephen Gehlbach⁵, Susan Greenspan⁶, Frederick Hooven⁷, Robert Lindsay⁸, Christian Roux⁹, Philip Sambrook¹⁰, Frederick Anderson², Stuart Silverman¹¹. ¹University of Cambridge School of Clinical Medicine, United Kingdom, ²UMass Medical School, USA, ³Center for Metabolic Bone Disease & Division of Geriatric Medicine, Belgium, ⁴Autonomous University of Barcelona, Spain, ⁵University of Massachusetts, USA, ⁶University of Pittsburgh, USA, ⁷University of Massachusetts Medical School, USA, ⁸Helen Hayes Hospital, USA, ⁹Hospital Cochin, France, ¹⁰Royal North Shore Hospital, Australia, ¹¹Cedars-Sinai/UCLA, USA

Aim: Fractures in obese postmenopausal women contribute significantly to the overall fracture burden. Reduced mobility and higher rates of co-morbidity prior to fracture in obese women may adversely affect healthcare utilisation and quality of life following fracture. Obese women with fracture may also be less likely to receive anti-osteoporosis medication (AOM). We compared these outcomes in obese, non-obese and underweight postmenopausal women following incident clinical fractures.

Methods: GLOW is an observational longitudinal study of non-institutionalized women aged ≥ 55 years recruited from 723 primary physician practices in 10 countries. Self-administered questionnaires were mailed, and data collected included demographics, fracture occurrence, medication and details on hospitalization, surgery and admission to rehabilitation or nursing homes. Quality of life was assessed before and after fracture using the SF-36 and EQ-5D. Data were available over a 3-year follow-up period in 90 underweight, 3270 non-obese and 941 obese women (BMI ≤ 18.5 , 18.5–30 and ≥ 30 kg/m², respectively).

Results: Following fracture, rates of treatment at an office, hospital or nursing home were similar in the three BMI groups and similar percentages underwent surgery. Underweight women were significantly more likely to be admitted to a rehabilitation centre than non-obese and obese women (25% vs 15% and 16%, respectively). Length of stay in hospital was significantly greater in obese than non-obese women (mean 11 vs 9 days; $p < 0.05$). Changes in quality of life after fracture were generally similar between the three BMI groups, but both before and after fracture, obese women had significantly lower physical function than non-obese and underweight women and a significantly lower vitality score than non-obese women. After fracture, 63% of underweight, 46% of non-obese and 33% of obese women were taking AOM.

Conclusions: Following fracture, obese postmenopausal women require longer hospital stay than non-obese women and have lower physical function and vitality scores. Our findings suggest that the economic costs of fracture may be higher in obese than non-obese women and that although the impact of fracture on quality of life is similar, there is greater impairment both before and after in obese women. Finally, the use of AOM in obese women with fracture is low.

Disclosures: Juliet Compston, None.

This study received funding from: Warner Chilcott Company, LLC and sanofi-aventis

FR0355

Incident Bone Fracture in Men with, or at Risk for, HIV-infection in the Multicenter AIDS Cohort Study (MACS), 1996-2011. Vanessa Walker Harris^{*1}, Keri N. Althoff², Sandra Reynolds², Frank Paella³, Lawrence Kingsley⁴, Michelle Danielson⁵, Jordan E. Lake⁶, Todd Brown⁷. ¹Johns Hopkins University School of Medicine, USA, ²Johns Hopkins School of Public Health, USA, ³Northwestern School of Medicine, USA, ⁴University of Pittsburgh School of Public Health, USA, ⁵University of Pittsburgh, USA, ⁶UCLA School of Medicine, USA, ⁷Johns Hopkins University, USA

Background: Limited data are available comparing fracture incidence in HIV-infected (HIV+) and demographically similar HIV-uninfected (HIV-) persons.

Methods: Between October 1996 and 2011, fractures related to osteoporosis according to the FRAX definition (i.e. fracture of the hip, humerus, forearm, or spine) were prospectively reported or recalled during semi-annual study visits among men ≥ 30 years of age. Crude incidence rates (IR) per 100 person-years (PY), adjusted rate ratios (aIRR), and 95% confidence intervals (CI) were estimated using Poisson regression models with an interaction term for age (30-49, 50-64, ≥ 65 years) and HIV status.

Results: Among 5,106 men during 73,548 person-visits, 103 FRAX-defined fractures (53 HIV+, 50 HIV-) were reported. The crude IR of FRAX-defined fracture was 0.15 fractures/100 PY in HIV+ and 0.13 fractures/100 PY in HIV- men. After adjusting for body mass index (BMI) and race, the incidence rate of FRAX-fracture increased with age (30-49yo: reference; 50-64yo aIRR=1.19 [0.78, 1.83]; ≥ 65 yo: aIRR=2.93 [1.48, 5.80]) and HIV-infection (IRR=1.38 [0.93, 2.04]). The interaction of age and HIV status approached statistical significance ($p=0.14$). Compared to HIV-men age 30-49, the incidence rates of FRAX-defined fracture increased with age and were higher in HIV+ men compared to HIV- men, after adjustment for BMI and race (figure).

Conclusion: The rate of incident FRAX-defined, osteoporosis-related bone fractures in HIV+ and HIV- men increased with age. The increasing fracture rate is apparent in HIV+ men at younger ages as compared to HIV- men. These data provide support for recommendations for osteoporosis screening in HIV-infected men between ages 50-70 years.

Figure: Incidence rate ratios and 95% confidence intervals for FRAX-defined fractures in HIV+ and HIV- men in the Multicenter AIDS Cohort Study, by age and HIV status

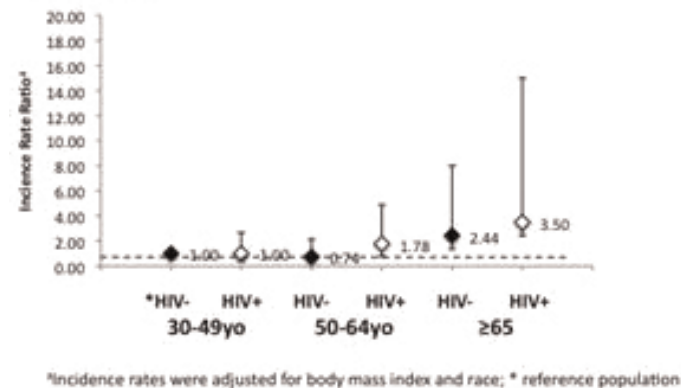


Fig 1

Disclosures: Vanessa Walker Harris, None.

FR0360

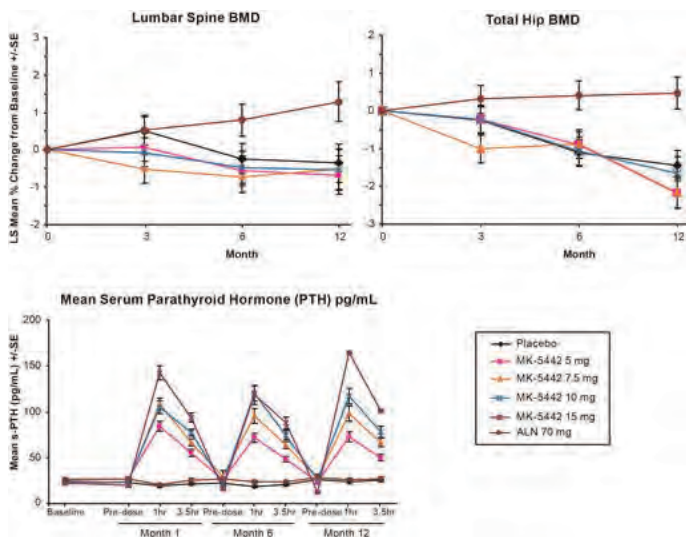
A Phase IIb Study of MK-5442 Calcium Sensing Receptor (CaSR) Antagonist in Bisphosphonate-treated Patients. Felicia Cosman^{*1}, Nigel Gilchrist², Michael McClung³, Joseph Foldes⁴, Tobias de Villiers⁵, Boyd Scott⁶, Weili He⁷, John McGinnis⁷, Norman Heyden⁷, Suvajit Samanta⁷, Annepong Pong⁷, Arthur Santora⁸, Albert Leung⁸, Andrew Denker⁶, ¹Helen Hayes Hospital, USA, ²Department of Orthopaedic Medicine & Surgery, Christchurch Hospital, New Zealand, ³Oregon Osteoporosis Center, USA, ⁴Hadassah Hebrew University Hospital, Israel, ⁵Mediclinic Panorama, South Africa, ⁶Merck & Co., Inc., USA, ⁷Merck Sharp & Dohme Corp., USA, ⁸Merck Research Laboratories, USA

MK-5442 is an orally administered, agent that stimulates the secretion of endogenous PTH by antagonism of the calcium-sensing receptor of the parathyroid gland. The resulting pulse of endogenous PTH secretion is hypothesized to stimulate bone formation thereby increasing BMD. A previous study with MK-5442 in treatment naïve osteoporotic postmenopausal women (PMW) conducted in Japan demonstrated increased BMD following 3 months of treatment. The aim of this study was to assess the effect on BMD and bone turnover of switching from long-term bisphosphonate therapy to MK-5442 in patients with persistent low bone mass on BMD and bone turnover.

This randomized, placebo (PBO) and active-controlled, dose-finding study enrolled 526 PMW who had taken alendronate (ALN) for at least 12 months preceding the trial and an oral bisphosphonate for ≥ 3 of the 4 years before the trial, and with spine or hip BMD T-scores ≤ -2.5 (or ≤ -1.5 with ≥ 1 prior fragility fracture) and ≥ 4.0 . Subjects were randomly assigned to continue ALN or switch to either PBO or MK-5442 (5, 7.5, 10 or 15 mg daily). The primary endpoint was the change from baseline in lumbar spine (LS) BMD with MK-5442 treatment compared to continued ALN at 12 months. Additional endpoints included the change from baseline in total hip aBMD, u-NTx, s-PINP, serum calcium, s-PTH, and general safety. The 15 mg group was discontinued mid-study due to the incidence of hypercalcemia observed with that dose in another study.

In patients switched from ALN to MK-5442, there was a dose-dependent pulsatile increase in PTH which resulted in increased P1NP ($\sim 125\%$ at 12 months for all MK-5442 doses) and u-NTx ($\sim 70\%$ -100%, dose dependent). However, there was no change in spine BMD in any MK-5442 group compared with a small increase in the ALN group. In the hip BMD declined in the MK-5442 group with no change in the ALN group. There was a dose-dependent increase in the incidence of hypercalcemia but other adverse events were all similar among groups.

In bisphosphonate experienced PMW with osteoporosis, switching treatment from ALN to MK-5442 resulted in a pulsatile increase in PTH and corresponding increases in biomarkers of bone formation and resorption, but a decreased BMD response compared with continued ALN therapy.



Fig

Disclosures: Felicia Cosman, Merck Sharp & Dohme Corp., 2
This study received funding from: Merck Sharp & Dohme Corp.

FR0361

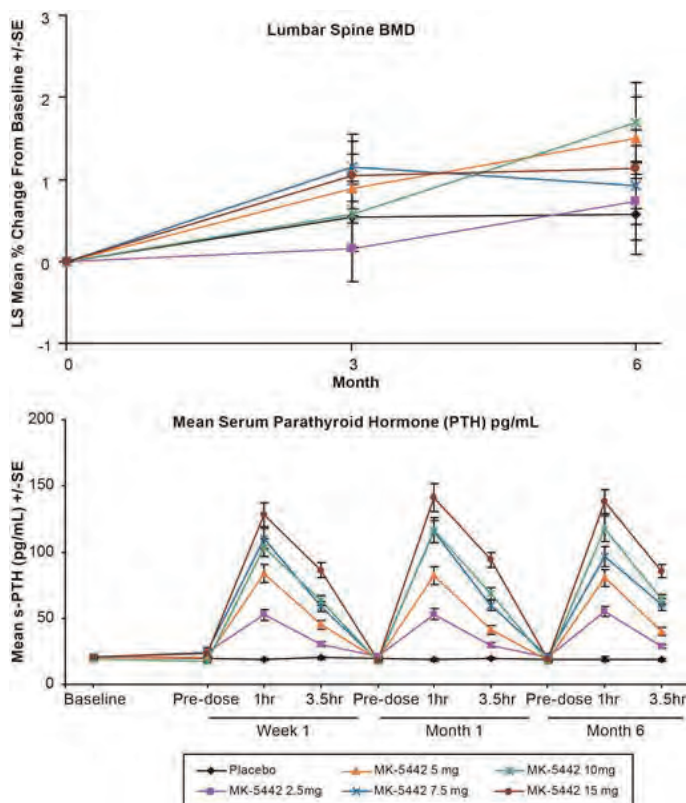
A Phase IIb, Randomized, Placebo-Controlled, Dose-Ranging Study of MK-5442 in the Treatment of Postmenopausal Women with Osteoporosis. Johan Halse^{*1}, Susan Greenspan², Felicia Cosman³, Graham Ellis⁴, Boyd Scott⁵, Norman Heyden⁶, Steven Doleck⁷, Sujavjit Samanta⁶, Weili He⁶, Arthur Santora⁷, Albert Leung⁷, Andrew Denker⁵. ¹Osteoporoseklinikken, Norway, ²University of Pittsburgh, USA, ³Helen Hayes Hospital, USA, ⁴Helderberger Osteoporosis Clinic, South Africa, ⁵Merck & Co., Inc., USA, ⁶MSD, USA, ⁷Merck Research Laboratories, USA

MK-5442 is an orally bioavailable, calcium receptor antagonist that stimulates the secretion of endogenous PTH. The resulting pulse of endogenous PTH secretion is hypothesized to stimulate bone formation and increase BMD. A previous study with MK-5442 in osteoporotic postmenopausal women (PMW) conducted in Japan demonstrated increased BMD following 3 months of treatment.

This was a multicenter, randomized, double-blind, placebo-controlled, parallel-group, dose-ranging study of MK-5442 in 383 PMW with osteoporosis defined by BMD T-Score in lumbar spine (LS), femoral neck, trochanter and/or total hip < -2.5. All had BMD \geq -3.5 at all 4 BMD sites. The objective of this Phase IIb dose-ranging study was to identify an appropriate dose of MK-5442 that would produce an osteoanabolic effect without causing excessive hypercalcemia. The effects of daily oral doses of MK-5442 (2.5, 5, 7.5, 10 or 15 mg) vs placebo (PBO) for 6 months on s-PTH, aBMD of the LS, hip sites, total body and 1/3 distal forearm, biochemical markers of bone turnover (u-NTx, s-CTX, s-BSAP, s-p1NP), serum calcium, and general safety were assessed.

A dose-dependant increase in PTH was observed at 1 hour post-dose, which resulted in increases in p1NP (20-40% at 6 months for 10 and 15 mg MK-5442), s-BSAP (4-17% at 6 months for 7.5, 10 and 15 mg MK-5442) and small decreases in uNTx (8-21%) for all doses except 15mg. There was no statistically significant difference between any of the MK-5442 doses and PBO in % change from baseline at Month 6 in LS aBMD or % change from baseline at month 6 in any other BMD endpoint. The MK-5442 treatment groups were generally similar to the PBO group regarding overall safety, with the exception of an expected dose-related increase in the incidence of hypercalcemia. (1.6%, 9.8%, 21.9%, 25.0% and 42.9% with 2.5mg, 5mg, 7.5mg, 10mg, 15mg MK-5442 respectively vs. 1.6% in PBO).

In PMW with low bone mass, treatment with MK-5442 resulted in a pulsatile increase in PTH and corresponding increases in biomarkers of bone formation however, no difference in LS BMD between MK-5442 treatment and PBO was observed.



Figure

Disclosures: Johan Halse, None.
This study received funding from: Merck Sharp & Dohme Corp.

FR0362

Pharmacokinetic Results of a Phase 2 Clinical Study of an Oral Tablet Formulation of PTH(1-31)NH₂. Amy Sturmer^{*1}, William Stern², Jenna Giacchi², Ali Bolat², Sheela Mitta², Roxanne Tavakkol², John Trang³, Jeffrey Wald⁴, Lorie Fitzpatrick⁴, Nozer Mehta¹. ¹Unigene Laboratories, USA, ²Unigene Laboratories, Inc., USA, ³PK/PD International, Inc., USA, ⁴GlaxoSmithKline, USA

Pharmacokinetic (PK) data are presented from a 24 week double blind, randomized, repeat dose parallel group study of recombinant human [rhPTH(1-31)NH₂] or placebo tablets, compared to open label Forsteo[®] (teriparatide) in 97 postmenopausal women with osteoporosis. The primary endpoint was to characterize the percent change from baseline in bone mineral density of the lumbar spine after 24 weeks of treatment with rhPTH(1-31)NH₂. Plasma samples were collected to characterize the PK profile of the oral tablets and the Forsteo[®] subcutaneous (SC) injections after the first dose and at end of treatment. Blood samples were collected pre-study and at intervals up to 5.75 hr after administration of tablets and up to 2 hr after injection. Plasma concentrations of PTH(1-31)NH₂ were determined with a validated specific sandwich ELISA that recognizes the intact molecule with a lower limit of quantitation (LLOQ) of 10 pg/mL. Plasma concentrations of PTH(1-34)OH were measured by a validated sandwich ELISA with an LLOQ of 5 pg/mL. The PK profile for the oral tablets showed a pulsatile peak with durations of at least 1 hr but less than 5 hr which is consistent with the requirement for bone anabolic activity. The mean C_{max} value for the patients receiving tablets measured at week 0 (n=32) and week 24 (n=28) was 295 pg/mL and 207 pg/mL, respectively. The mean T_{max} for both periods was 3.25 hr, which is expected for an enteric-coated tablet. The mean AUC for week 0 and week 24 were 178 pg*hr/mL and 141 pg*hr/mL, respectively. No significant differences were observed between weeks 0 and 24 in any PK parameters tested, demonstrating good reproducibility, no time-dependent changes, and little or no accumulation. Following injection, mean plasma teriparatide concentrations were observed from 0.25 hr to 2 hr at week 0 and week 24. The mean C_{max} at week 0 (n=32) was 120 pg/mL at a mean T_{max} of 0.389 hr. The mean C_{max} value in these patients measured at week 24 (n=27) was also 120 pg/mL, at a mean T_{max} of 0.34 hr. The mean AUC for weeks 0 and 24 were 122 pg*hr/mL and 123 pg*hr/mL, respectively. These results demonstrated excellent reproducibility for the PK parameters tested for teriparatide at the two PK sampling times. Oral administration of PTH(1-31)NH₂ once daily at a 5 mg dose resulted in higher mean C_{max} and AUC values and similar median C_{max} and AUC values when compared to Forsteo[®] and demonstrated the appropriate pulsatile profile for bone anabolic activity.

Disclosures: Amy Sturmer, Unigene laboratories, 7
This study received funding from: Unigene laboratories, Inc.

FR0363

Short Term Treatment with Teriparatide Stimulates Circulating Osteogenic Precursor Cells in Postmenopausal Women with Osteoporosis. Jeri Nieves*¹, Felicia Cosman², Mishaela Rubin³, Sanil Manovalen³, Marsha Zion², David Dempster³, Nancy Barbuto², Robert Lindsay². ¹Columbia University & Helen Hayes Hospital, USA, ²Helen Hayes Hospital, USA, ³Columbia University, USA

The stimulatory effects of short-term treatment with teriparatide (TPTD) on bone formation may be mediated at least in part by an increase in osteoblast number. The existence of circulating osteogenic precursor cells (COP) which are associated with bone formation has recently been demonstrated. In hypoparathyroid patients, treatment with PTH(1-84) results in an increase in the number of COP cells as well as fewer markers of immaturity (Rubin MR et al JCEM 2010), while in another study TPTD did not increase COP cells at 3 months, although there was an increase in maturation of these cells (D'Amelio et al Osteop Int 2012). In the current study, we examined the COP cell response in treatment-naïve subjects with osteoporosis (n=21) treated with daily TPTD for 3 months. At baseline and 3 months blood was collected and peripheral blood mononuclear cells (PBMCs) were obtained. Osteogenic cells were characterized using flow cytometry and antibodies against osteocalcin and stem cell markers CD34 (a marker of early hematopoietic cells) and CD146 (a marker of early mesenchymal stem cells). Serum procollagen type I N-terminal propeptide (PINP) was measured by ELECSYS. Differences in PINP and osteogenic cells from baseline to 3 months were determined with paired t-tests. The subjects were on average (mean ± standard deviation), 65 ± 7.2 years of age and 16 ± 9.5 years from menopause, had a mean spine T-score of -2.9 ± 1.0 and total hip T-score of -2.1 ± 0.8, with one-third reporting a prior fracture. There was a significant increase in PINP from 57.7 ± 27 at baseline to 117.7 ± 65 after 3 months of TPTD (p < 0.001). The % of PBMC that were OCN+ increased from 1.1 ± 0.8 at baseline (similar to previous values for postmenopausal women) to 2.0 ± 1.4 (p < 0.005) after 3 months of daily TPTD. However, the co-expression of the early cell marker OCN+/CD34+ was unchanged (43.1 ± 17.4% at baseline to 45.4 ± 18.0% at 3 months). The correlation coefficient for the change in the COP cell number and the change in PINP was 0.39 (p = 0.09). The increase in the number of COP cells signifies an increase in osteoblast proliferation and in the size of the available osteoblast pool. We hypothesize that the recruitment of a greater number of circulating osteogenic cells is a major mechanism by which TPTD stimulates new bone formation during the first three months of therapy.

Disclosures: Jeri Nieves, None.

FR0365

Treatment of Male Osteoporosis: Risedronate, Teriparatide or Both. Marcella Walker*¹, Natalie Cusano², Megan Romano², James Sliney², Chiyuan Zhang¹, Donald McMahon², John Bilezikian². ¹Columbia University, USA, ²Columbia University College of Physicians & Surgeons, USA

Most studies of combination therapy with teriparatide and bisphosphonates have not shown an advantage over monotherapy for the treatment of osteoporosis. Most combination therapeutic regimens have focused upon postmenopausal women with osteoporosis. This proof-of-concept study was directed to combination therapy of risedronate and teriparatide in men with osteoporosis. We studied 29 men with low bone mineral density (BMD) at the spine, hip, or distal 1/3 radius in a randomized, double-blinded 3-arm study. Subjects were randomized 1:1:1 to oral risedronate 35 mg weekly plus injection placebo, teriparatide 20 µg subcutaneously daily plus oral placebo, or both risedronate and teriparatide (combination) for 18 months. The primary endpoint was percentage (%) change in BMD at the lumbar spine at 18 months from baseline. Secondary endpoints included changes in BMD at other sites and at interim time points. All participants were Caucasian and age ranged from 37 to 81 years. A history of fragility fracture was present in 31% of the cohort; 24% had a history of vertebral fracture. There were no between-group differences in demographics, baseline BMD, medical or lifestyle characteristics except for history of fragility fracture, which was significantly greater in the combination therapy group vs. the risedronate group (60 vs. 0%, p < 0.05). At 18 months, lumbar spine BMD increased significantly with all 3 treatments (p < 0.05) but there were no between-group differences (p = 0.33). Total hip BMD (mean % change ± SE) increased to a greater extent in the combination group (3.86 ± 1.1%) versus teriparatide (0.29 ± 1.0%) and versus risedronate (0.82 ± 1.0%, p < 0.05 for both). Femoral neck BMD also increased to a greater extent in the combination group (8.45 ± 1.9%) versus risedronate (0.50 ± 1.7%, p = 0.002), but was not different from teriparatide alone (3.89 ± 1.7%, p = 0.07). At 18 months, there were no between-group differences in 1/3 radius BMD (p = 0.10). All therapies were well-tolerated. The results of this study indicate that 18 months of combination treatment with teriparatide and risedronate does not afford a densitometric advantage at the lumbar spine or femoral neck, but at the total hip, combination therapy shows greater improvement than teriparatide alone. Addressing the question of combination therapy in men with osteoporosis is providing new insights into this approach.

Disclosures: Marcella Walker, None.

This study received funding from: Sanofi and Warner Chilcott

FR0367

BMD Changes in Postmenopausal Women Over a 5-year Treatment-Free Period Following a 5-year Course of Alendronate. Brian McNabb*¹, Eric Vittinghoff², Ann Schwartz¹, Douglas Bauer¹, Elizabeth Barrett-Connor³, Kristine Ensrud⁴, Dennis Black¹. ¹University of California, San Francisco, USA, ²UCSF, USA, ³University of California, San Diego, USA, ⁴Minneapolis VA Medical Center / University of Minnesota, USA

Purpose: To describe bone mineral density (BMD) changes and develop a prediction model for BMD changes in postmenopausal women during a 5-year treatment-free period, following 5 years of alendronate (ALN).

Methods: We analyzed 372 postmenopausal women who had received a mean of 5 years of ALN therapy while participating in the Fracture Intervention Trial (FIT), and were then randomized to placebo and followed for 5 years while participating in the FIT Long Term Extension trial (FLEX). We describe the patterns of femoral neck, total hip, and lumbar spine BMD changes and analyze prediction of BMD changes over the 5-year treatment-free period. Predictor variables included BMD before ALN treatment, changes in BMD on ALN, BMD at the start of the treatment-free period, age, body mass index, and fracture history. Three markers of bone turnover were also analyzed as predictors in 76 women with available data. To find prediction models for the percent changes in BMD, we screened all possible linear combinations of variables, and implemented the deletion-substitution-addition (DSA) algorithm.

Results: After stopping ALN, mean femoral neck BMD losses were modest (1.4% over 5 years) with substantial variation (26% lost > 5%, and 12% gained > 5% BMD at the femoral neck). None of the variables tested were significantly predictive of percent loss over the treatment-free period. Table 1 shows the association of selected variables with the percent change in femoral neck BMD. Overall model-based prediction was poor (cross-validated R² 3.9% for best model). Results for analyses of total hip and lumbar spine BMD were similar to those for femoral neck BMD. Amongst bone turnover markers, only serum C-terminal telopeptide of type I collagen at baseline was marginally associated with percent change in BMD at the femoral neck. This weak association was not found when analyzing total hip or lumbar spine BMD, and may reflect the small sample size analyzed.

Conclusions: There was a wide range of changes in BMD over a 5-year treatment-free period, suggesting the need for a variable schedule for follow-up care and assessment of women after discontinuation of a 5-year course of ALN. We could not identify any combination of variables to predict these BMD changes. Like other candidate predictors, bone turnover markers were not convincingly associated with BMD changes, but a lack of power prevented us from ruling them out as useful predictors.

| Association of Select Predictors with the Percent Change in Femoral Neck BMD Across a 5-year Treatment-Free Period Following a 5-year Course of ALN | | |
|---|---|---------|
| Predictor of Interest | % Change in BMD with Each Increase in Predictor | |
| | Estimate (95% CI) | P-value |
| Age (5 years) | 0.22 (-0.29 to 0.74) | 0.395 |
| BMI (5 kg/m ²) | 0.66 (-0.04 to 1.35) | 0.064 |
| BMD (0.1 gm/cm ²) | | |
| At Start of ALN Treatment | 0.66 (-0.30 to 1.62) | 0.178 |
| After ALN Treatment | 0.32 (-0.53 to 1.17) | 0.464 |
| Change in BMD on ALN (1%) | -0.06 (-0.17 to 0.05) | 0.306 |
| BTM* | | |
| CTx (0.065 ng/mL)** | -1.24 (-2.48 to -0.01) | 0.049 |
| BSAP (2.86 ng/mL)** | 0.61 (-0.65 to 1.87) | 0.338 |
| PINP (11.8 ng/mL)** | 0.60 (-0.71 to 1.91) | 0.366 |

Abbreviations: BMD, bone mineral density; ALN, alendronate; 95% CI, 95% confidence interval; BMI, body mass index; BTM, bone turnover marker; CTx, serum C-terminal telopeptide of type I collagen; BSAP, bone specific alkaline phosphatase; PINP, N-propeptide of type I collagen.

* Based on data from a subset of 76 women with available data.

** One standard deviation increase.

Table 1

Disclosures: Brian McNabb, None.

FR0368

Crosstalk between Oral Microbiome and Host Innate Immune Response in the Tissues of Patients with Bisphosphonate Related Osteonecrosis of the Jaw. Smruti Pushalkar¹, Satoko Matsumura¹, Lalitha Ramanathapuram¹, Zoya Kurago¹, Kenneth Fleisher², Robert Glickman¹, Wenbo Yan³, Yihong Li¹, Xin Li⁴, Deepak Saxena*². ¹NYU College of Dentistry, USA, ²New York University College of Dentistry, USA, ³Nyack College, USA, ⁴New York University, USA

Bisphosphonates (BPs) are the standard of care for patients with metastatic cancer and multiple myeloma to prevent skeletal complications (e.g., severe bone pain, pathologic fracture, etc.) and to treat osteoporosis. The cause and effect relationship between BPs and BP-related osteonecrosis of the jaws (BRONJ) is not well established. Current research suggests that bacterial biofilms may play a significant role in the pathogenesis of BRONJ. Recently, we have shown that BRONJ lesions are heavily colonized by oral bacteria and present many clinical challenges as they are difficult to culture and antibiotic resistance may result in misguided antibiotic therapy. Here we highlight the crosstalk among the oral bacteria and host immune response in BRONJ subjects. Using 16S rDNA molecular technique we characterize the total bacterial profile of BRONJ, BP and control subjects. Denaturing gradient gel

electrophoresis cluster analysis revealed three clusters each representing the three groups, control, BP and BRONJ indicating that the microbiome present in tissue samples was distinct to each group. DGGE band pattern indicated that the BRONJ group had less bacterial diversity as compared to control indicating that high abundance of specific bacteria colonizing the BRONJ lesion. 16S sequencing and clonal analysis showed 6 phyla in all three groups. The phylum *Firmicutes* was predominant in BRONJ group (72%) followed by BP group (70%) as compared to control group (59%). The Chi-square test also showed significant differences in percent relative distribution of phyla, between control/BP groups ($p < 0.001$), control/BRONJ ($p < 0.001$) and BP/BRONJ ($p < 0.05$). There was significantly increase in the gram positive bacteria in BRONJ group. PCR Array analysis indicated that the host genes responsible for antibacterial response such as MPO, CTSG, and NOD2 were significantly down regulated. Deficient innate immune responses to microorganisms together with poor healing and repair provide continuous opportunities for expanding microbial colonization, further perpetuating the pathologic process in BRONJ. The bacterial phylotypes we identified in our studies can trigger inflammation and acute, neutrophil-dominated responses that could cause direct damage by impairment of bone remodeling processes. The study supports the hypothesis that a unique type of oral bacterial infection contributes to the pathophysiology of BRONJ and provides a target for BRONJ prevention and treatment.

Disclosures: Deepak Saxena, None.

FR0370

Effect of Zoledronic Acid on Acute Bone Loss after Spinal Cord Injury.

Thomas Schnitzer¹, Danielle Barkema¹, Kristina Herrmann¹, Ki Kim².
¹Northwestern University, USA, ²Rehabilitation Institute of Chicago, USA

Objective: To assess the efficacy and safety of zoledronic acid 5mg iv compared to placebo to prevent bone loss in patients after acute spinal cord injury.

Methods: A randomized, placebo-controlled trial of zoledronic acid 5mg was undertaken in patients who had suffered an acute spinal cord injury (SCI) within 6 months of study entry. Patients at entry had to exhibit motor loss and be non-ambulatory. Exclusion criteria included the presence of other factors that could affect bone metabolism. All subjects had normal renal function and 25-OH vitamin D at time of infusion. BMD of the spine, total hip and femoral neck was determined at baseline, 3 months and 6 months by DXA using a Hologic 4500A densitometer. Scans were done in duplicate when possible. Data affected by technical considerations (movement, heterotopic ossification) were not included. An interim analysis was done after the first 10 subjects were enrolled. An intent-to-treat analysis including all subjects receiving an infusion and having one post-baseline assessment was undertaken using a two-sample Student's T-test of BMD results. Adverse events were collected.

Results: 10 patients, all male, 6 Caucasian, 2 Latino, 2 African-American, mean age 43.6±19.7 yr signed consent and were randomized. Baseline BMD at spine (1.066 vs 1.128 gm/cm²), total left hip (1.037 vs 1.110 gm/cm²), total right hip (1.043 vs 1.124 gm/cm²), left femoral neck (0.955 vs 0.967 gm/cm²) and right femoral neck (0.957 vs 0.971 gm/cm²) were similar between the placebo and zoledronic acid group, $p > 0.05$. 6 months after infusion, the change in BMD of the group receiving placebo compared to the group receiving zoledronic acid at the spine was -2.6±1.7% vs 2.0±1.6%, $p = 0.004$; left total hip -16.3±0.3% vs -1.7±2.8%, $p = 0.002$; right total hip -11.2±8.6% vs 2.0±5.8%, $p = 0.10$; left femoral neck -14.9±12.9% vs 0.0±6.7%, $p = 0.08$; right femoral neck -21.7±4.2% vs -1.0±7.4%, $p = 0.005$. No unanticipated serious adverse events related to the study medication were reported.

Conclusion: After acute spinal cord injury, subjects receiving placebo had a significant decrease in BMD compared to those who received zoledronic acid. Zoledronic acid was effective in maintaining bone density in the lower extremities of most subjects with acute SCI for 6 months after infusion. The treatment was generally well tolerated. Although the duration of efficacy is not known, zoledronic acid may help to reduce the bone loss after acute SCI.

Disclosures: Thomas Schnitzer, Merck & Co., Inc., 6; Novartis, 6; Amgen, 6; Lilly, 6
 This study received funding from: Novartis Pharmaceuticals

FR0376

Relationship Between Change in Total Hip BMD in Response to Zoledronic Acid 5 mg and Post-treatment Change in Total Hip BMD: the HORIZON-PFT Extension Study.

Richard Eastell¹, Lisa Palermo², Brian McNabb², Steven Boonen³, Felicia Cosman⁴, Ian Reid⁵, Steven Cummings⁶, Dennis Black².
¹University of Sheffield, United Kingdom, ²University of California, San Francisco, USA, ³Center for Metabolic Bone Disease & Division of Geriatric Medicine, Belgium, ⁴Helen Hayes Hospital, USA, ⁵University of Auckland, New Zealand, ⁶San Francisco Coordinating Center, USA

There is a small mean decrease in hip bone mineral density (BMD) after stopping zoledronic acid 5 mg annually. It would be helpful to better understand the determinants of this bone loss. The purpose of this study was to determine whether greater rates of bone loss after stopping therapy are associated with greater BMD gain in response to initiation of anti-resorptive therapy or to baseline bone turnover and change in bone turnover. In the Health Outcomes and Reduced Incidence with Zoledronic acid Once Yearly-Pivotal Fracture Trial (HORIZON-PFT) Extension

study, one group of women who were randomized to receive zoledronic acid 5 mg annually for 3 years (years 0, 1 and 2) were then randomized to receive placebo annually for three infusions (at years 3, 4 and 5, Z3P3 treatment group, n=617). We measured total hip BMD by DXA at baseline, 1, 2, and 3 years after annual zoledronic acid 5 mg and at 4.5 and 6 years after annual placebo. Total PINP was measured by automated immunoassay analyser at 0, 3, 4.5, and 6 years, but results were excluded if patients had a fracture in the past year (PINP increases for up to a year following a fracture). The change in total hip BMD in years 0-3 was related to the change in total hip BMD on placebo in years 3-6 ($r = -0.15$, $P = 0.0015$). Thus, those with greater gains during years 0-3 had greater loss during years 3-6. The PINP at baseline was correlated with the change in total hip BMD in years 0-3 on zoledronic acid 5 mg annually ($r = 0.32$, $P = 0.0002$) and to the change in total hip BMD in years 3-6 after stopping treatment ($r = -0.26$, $P = 0.007$). The change in PINP (years 0-3) was correlated with the change in total hip BMD in years 0-3 on zoledronic acid 5 mg annually ($r = -0.35$, $P = 0.0003$) and the change in PINP (years 3-6) was correlated with the change in total hip BMD in years 3-6 on zoledronic acid 5 mg annually ($r = -0.18$, $P = 0.0005$). We conclude that the BMD loss after stopping zoledronic acid is greater in those with greater gains in BMD on zoledronic acid treatment. One possible mechanism for this association is that higher bone turnover before initiating treatment is associated with both greater BMD response to zoledronic acid and greater rates of loss when stopping therapy.

Disclosures: Richard Eastell, Novartis, 9

This study received funding from: Novartis

FR0377

Resolution of Effects on Bone Turnover Markers and Bone Mineral Density after Discontinuation of Long-term Bisphosphonate Use.

Bente Langdahl¹, Claude Laurent Benhamou², C. Conrad Johnston³, Kenneth Saag⁴, TOBIE DE VILLIERS⁵, Andrew Denker⁶, Annpey Pong⁷, John McGinnis⁷, Elizabeth Rosenberg⁶, Arthur Santora⁸.
¹Aarhus University Hospital, Denmark, ²CHR ORLEANS, France, ³Indiana University School of Medicine, USA, ⁴University of Alabama at Birmingham, USA, ⁵PANORAMA HOSPITAL, South Africa, ⁶Merck & Co., Inc., USA, ⁷Merck Sharp & Dohme Corp., USA, ⁸Merck Research Laboratories, USA

Background: While bisphosphonates (BP) have been well studied in long-term trials of up to 4 years' duration, relatively less is known about the immediate consequences of continuing vs. interrupting long-term treatment. This report describes changes in bone turnover and BMD in a 1-year trial of the calcium-sensing receptor antagonist MK-5442 in postmenopausal women who, after taking BP for ≥ 3 years, were randomized to continued alendronate (ALN) 70 mg weekly, switch to placebo (PBO), or switch to MK-5442. Primary results for MK-5442 are presented separately.

Methods: 526 postmenopausal women who had taken ALN for ≥ 12 months preceding the trial and an oral BP for ≥ 3 of the 4 years before the trial, with spine or hip BMD T-scores ≤ -2.5 (or ≤ -1.5 with ≥ 1 prior fragility fracture) and ≥ -4.0 , were recruited into a dose-finding study of MK-5442. Statistical tests of within-group changes and comparison between the PBO and ALN groups were performed post-hoc.

Results: At baseline, women switched from ALN to PBO (n=88) or continued on ALN 70 mg weekly (n=87) were of mean age 67 years and had mean T-scores at lumbar spine of -2.5 and total hip of -1.6, and mean baseline urine NTX/Cr= 26.6 nmolBCE/mmolCr and serum PINP= 26.0 ng/mL. Median length of previous BP use was 5.2 years. After 1 month, women switched from ALN to PBO experienced increases from baseline in urine NTX/Cr (28.4% vs. continued ALN, $p < 0.0001$), while serum PINP was unchanged. Both NTX/Cr and PINP increased by 3 months (33.7% and 37.8%, respectively vs. ALN, both $p < 0.0001$). After 12 months of PBO, least squares mean concentrations of NTX/Cr and PINP rose to 42.2 nmolBCE/mmolCr and 40.1 ng/mL (both $p < 0.0001$, Table). The markers were unchanged from baseline with continued ALN. After 12 months, the women who continued ALN had an increase in lumbar spine BMD while those switched to PBO experienced no change; total hip BMD did not change in those remaining on ALN but was reduced in women switched to PBO. BMD at both sites was significantly lower in women who switched to PBO vs. those who stayed on ALN (Table).

Conclusions: Discontinuation of alendronate after a median of 5 years resulted in an increase in NTX/Cr as early as 1 month and PINP by 3 months. After 1 year, both bone turnover markers returned to levels similar to those expected in untreated postmenopausal women. These increases were accompanied by significantly lower spine and total hip BMD vs. continued treatment with ALN.

12 Month Least Squares Mean % Change from Baseline (95% CI)

| | uNTX/Cr | sPINP | Lumbar Spine BMD | Total Hip BMD |
|-----------------------------|-------------------|-------------------|------------------|-------------------|
| Continued Alendronate 70 mg | 2.3 (-9.2, 15.3) | -5.5 (-16.7, 7.3) | 1.5 (0.3, 2.6) | 0.4 (-0.4, 1.3) |
| Switch to Placebo | 66.3 (47.3, 87.7) | 69.2 (48.6, 92.6) | -0.2 (-1.3, 0.8) | -1.4 (-2.2, -0.6) |
| p-value* | <0.0001 | <0.0001 | 0.0137 | 0.0002 |

* Continued alendronate 70 mg weekly versus switch to placebo

Table

Disclosures: Bente Langdahl, Merck Sharp & Dohme Corp, 1; Merck Sharp & Dohme Corp., 6; Merck Sharp & Dohme Corp., 2
 This study received funding from: Merck Sharp & Dohme Corp.

FR0388

A Randomized Open-Label Study to Evaluate the Safety and Efficacy of Denosumab and Ibandronate in Postmenopausal Women Sub-Optimally Treated With Daily or Weekly Bisphosphonates. Christopher Recknor*¹, Edward Czerwinski², Henry Bone³, Sydney Bonnick⁴, Neil Binkley⁵, Alfred Moffett⁶, Suresh Siddhanti⁷, Irene Ferreira⁸, Pravashi Ghelami⁹, Rachel Wagman¹⁰, Jesse Hall⁷, Michael Bolognese¹¹.

¹United Osteoporosis Center, USA, ²Medical College Jagiellonian University, Poland, ³Michigan Bone & Mineral Clinic, USA, ⁴Clinical Research Center of North Texas, USA, ⁵University of Wisconsin, Madison, USA, ⁶OB-GYN Associates of Mid-Florida, P.A., USA, ⁷Amgen, Inc., USA, ⁸Amgen Inc, United Kingdom, ⁹Ovatech Solutions, United Kingdom, ¹⁰Amgen, Incorporated, USA, ¹¹Bethesda Health Research, USA

Purpose: Denosumab, a fully human monoclonal antibody that specifically targets RANKL to inhibit osteoclast formation, function, and survival, reduces risk for vertebral, non-vertebral, and hip fractures.¹ In subjects who were treatment naïve or previously treated with alendronate, denosumab was associated with greater gains in bone mineral density (BMD) and decreases in bone turnover markers when compared with alendronate-treated subjects.^{2,3} The purpose of this open-label trial was to compare the safety and efficacy of denosumab with ibandronate over 12 months in postmenopausal women with low BMD who were sub-optimally treated with prior bisphosphonate therapy.

Methods: This was a multicenter, randomized, open-label, parallel-group study in which postmenopausal women age 55 and older were randomized 1:1 to receive open-label denosumab 60mg subcutaneously every 6 months or ibandronate 150mg orally every month for 12 months. Percent change from baseline in total hip (TH, primary endpoint), femoral neck (FN), and lumbar spine (LS) BMD at month 12, percent change from baseline in serum CTX (sCTX) at 1 and 6 months, and safety were assessed.

Results: Randomized subjects (n=833; 417, denosumab; 416, ibandronate) had a mean (SD) age of 66.7 (8.0) years and mean (SD) BMD T-score of -1.8 (0.7), -2.1 (0.7), and -2.5 (0.8) at the TH, FN, and LS, respectively. Denosumab significantly increased TH BMD compared with ibandronate at 12 months (2.2% vs 0.9%, respectively; $p<0.0001$). Denosumab also significantly increased BMD at the FN (1.7% vs 0.5%) and LS (4.1% vs 2.1%) compared with ibandronate ($p<0.0001$ at both sites). Denosumab significantly decreased sCTX at 1 month with a median change from baseline of -81.1% compared to -35.0% for ibandronate ($p<0.0001$), and sCTX remained decreased through 6 months of treatment. In this open-label study, overall adverse events were similar between groups. Reports classified as serious adverse events (SAEs) were more frequent in subjects treated with denosumab than with ibandronate. No organ system accounted for a preponderance of these reports. The incidence of SAEs involving infection and malignancy was similar between groups.

Conclusions: Denosumab treatment resulted in greater increases in BMD at all measured sites compared with ibandronate. No new safety risks were identified in this open-label study.

1. Cummings, et al. *NEJM* 2009;361:756
2. Brown, et al. *JBMR* 2009;24:153
3. Kendler, et al. *JBMR* 2010;25:72

Disclosures: Christopher Recknor, Roche, GSK, Eli-Lilly, Procter & Gamble, Merck, Novartis, Amgen, NPS, Zelos, 2; Eli-Lilly, Roche, Procter & Gamble, GSK, Merck, sonofi-aventis, 2
 This study received funding from: Amgen Inc

FR0389

Antiresorptive Action is Dependent on Access to Remodeling Upon Cortical and Trabecular Surfaces: Comparison of Denosumab and Alendronate. Roger Zebaze*¹, Cesar Libanati², Matthew Austin², John Bilezikian³, Ego Seeman¹.

¹Austin Health, University of Melbourne, Australia, ²Amgen Inc., USA, ³Columbia University College of Physicians & Surgeons, USA

Purpose: Antiresorptives differ in the extent to which they suppress remodeling. Since remodeling is surface dependent, the degree to which antiresorptives suppress remodeling could be due, in part, to differences in their accessibility to bone surfaces. Cortical bone has a low surface/bone volume configuration so accessibility to remodeling on intracortical surfaces, the main site of bone loss during aging, may be more difficult than to trabecular surfaces. Denosumab rapidly and markedly reduces remodeling and does so more than alendronate. We hypothesized that differences in distribution and mechanism of action between denosumab and alendronate will result in a greater reduction in intracortical porosity with denosumab.

Methods: Postmenopausal women aged 61 ± 5 years were randomized double-blind to denosumab 60 mg Q6M (N=83), alendronate 70 mg QW (N=82), or placebo (N=82) for 12 months. Trabecular bone volume fraction (BV/TV) and porosity in both the compact and the trabecularized cortex (outer and inner transitional zones) were measured from HRpQCT distal radius images obtained at baseline, 6 months,

and 12 months using Strax 1.0 software. Reported results are from repeated measures models fit separately for each compartment allowing for heterogeneity in variance between treatment groups.

Results: Both denosumab and alendronate improved trabecular BV/TV compared with placebo at 6 and 12 months. Alendronate reduced porosity at month 6 in the compact and trabecularized cortex compared with placebo; however, at month 12 there was no evidence of a difference with alendronate relative to placebo in any of these cortical compartments (Table). Denosumab reduced porosity at both 6 and 12 months in all cortical compartments compared with baseline and placebo. These reductions were larger than those with alendronate at month 12 in all cortical compartments (Figure). Furthermore, denosumab resulted in a more homogeneous response in the compact cortex and outer transitional zone.

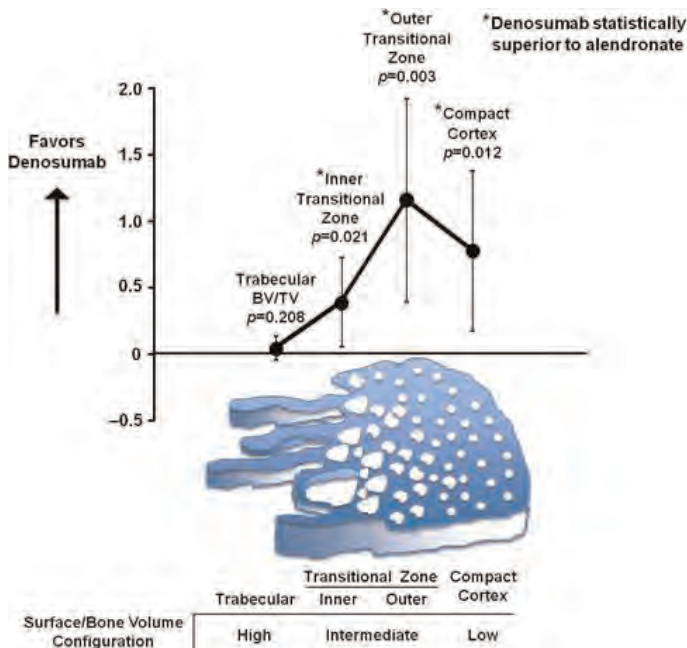
Conclusions: Cortical bone comprises most mineralized volume and increasingly determines bone strength as trabeculae disappear with aging. Access to cortical bone by therapeutic agents is a challenge because of its surface/bone volume configuration. The broader distribution of denosumab compared with alendronate is associated with greater and more uniform reductions in porosity throughout the cortex, effects likely to increase bending and compressive strength.

Table: Changes (Percentage Points Difference) From Baseline at 12 Months

| | Porosity | | | |
|-------------|------------------|-------------------------|-------------------------|----------------|
| | Trabecular BV/TV | Inner Transitional Zone | Outer Transitional Zone | Compact Cortex |
| Placebo | +0.08** | -0.54*** | -0.20 | -0.13 |
| Alendronate | +0.19***, 4 | -0.78*** | -0.81* | -0.48 |
| Denosumab | +0.25***, 4 | -1.17***, 4 | -1.97***, 4 | -1.26***, 4 |

p value relative to baseline: ***<0.001, **<0.01, *<0.025
 p value relative to placebo: 4<0.001, 4<0.025

Table



Figure

Disclosures: Roger Zebaze, Amgen, 6
 This study received funding from: Amgen Inc.

FR0391

Long-term Denosumab Treatment Maintains Low Incidence of Fracture in Postmenopausal Women ≥ 75 Years With Osteoporosis. Socrates Papapoulos^{*1}, Michael R. McClung², Nathalie Franchimont³, Jonathan D. Adachi⁴, Henry G. Bone⁵, Claude-Laurent Benhamou⁶, Jordi Farrerons⁷, J. Christopher Gallagher⁸, Johan Halse⁹, Kurt Lippuner¹⁰, Zulema Man¹¹, Salvatore Minisola¹², Ove Törring¹³, Nadia Daizadeh³, Andrea Wang³, Rachel B. Wagman³, Steven Boonen¹⁴. ¹Leiden University Medical Center, Netherlands, ²Oregon Osteoporosis Center, USA, ³Amgen Inc., USA, ⁴Charlton Medical Centre, Canada, ⁵Michigan Bone & Mineral Clinic, USA, ⁶INSERM U658, France, ⁷Hospital de la Santa Creu I Sant Pau, Spain, ⁸Creighton University Medical Center, USA, ⁹Osteoporoseklinikken, Norway, ¹⁰University Hospital, Switzerland, ¹¹Centro Tiemp, Argentina, ¹²Sapienza, Università di Roma, Italy, ¹³Karolinska Institutet Sodersjukhuset, Sweden, ¹⁴Leuven University, Belgium

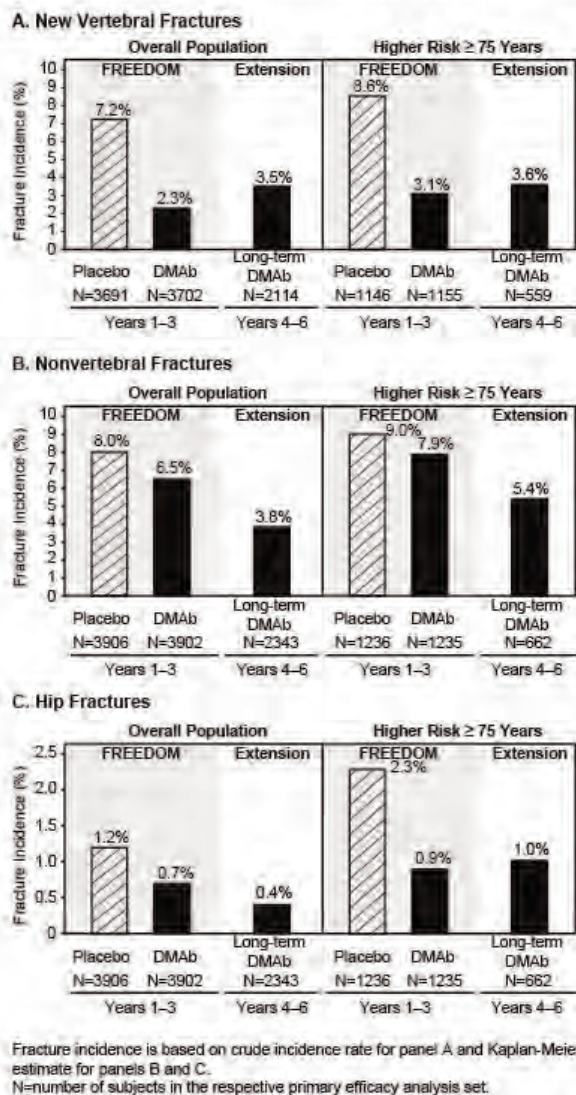
Purpose: In the pivotal fracture trial, FREEDOM, denosumab (DmAb) increased bone mineral density (BMD) and reduced the incidence of new vertebral, nonvertebral, and hip fractures in postmenopausal women with osteoporosis (Cummings 2009). In women at higher risk for fracture based on age ≥ 75 years, DmAb reduced the risk of hip fractures by 62% (Boonen 2011). The effects of long-term DmAb treatment up to 10 years are being evaluated in the FREEDOM extension study. As fracture incidence increases with age, and in particular, hip fracture in women ≥ 75 , we have further characterized the fracture incidence and BMD gains in women ≥ 75 years who have been treated with DmAb for a total of 6 years.

Methods: During the extension, each woman is scheduled to receive 60 mg DmAb every 6 months and supplemental calcium and vitamin D daily. We evaluated the fracture incidence and BMD gains in women who completed 6 years of DmAb treatment (overall long-term group) and in the subset of these women who were ≥ 75 years at FREEDOM baseline (higher-risk group).

Results: The FREEDOM baseline characteristics for the overall long-term DmAb group (N=2343) and the higher-risk group (N=662) were similar except that those subjects in the higher-risk group were older (mean age: 72 years for overall and 78 years for higher risk), and had a lower mean total hip BMD T-score (-1.9 for overall and -2.1 for higher risk). Despite the increase in age of the subjects, DmAb treatment during years 4-6 continued to be associated with a low incidence of new vertebral, nonvertebral, and hip fractures. Furthermore, the incidence of fractures in the higher-risk group during years 4-6 was similar to what was originally observed in years 1-3 in women ≥ 75 years treated with DmAb (Figure). BMD progressively increased over 6 years at the lumbar spine and total hip and was similar in women ≥ 75 compared with women in the overall long-term group. Despite advanced age, adverse events (AEs) and serious AEs in the higher-risk group in the extension were similar to the higher-risk group from FREEDOM and these events did not increase over time with DmAb treatment.

Conclusions: These results underscore the robust and consistent anti-fracture efficacy and safety profile of continued denosumab treatment over 6 years. Denosumab is a therapeutic option for women at higher risk for fracture, notably those ≥ 75 years, in whom fractures such as those at the hip increase exponentially due to cortical bone decay.

Figure. Subject Incidence of Fractures in the FREEDOM and Extension Trial



Figure

Disclosures: Socrates Papapoulos, Amgen Inc., Merck and Col., Novartis, Eli Lilly, GSK, 7

This study received funding from: Amgen Inc.

FR0392

Odanacatib Improved Estimated Femoral Strength in Postmenopausal Women - Results of a 2-year Placebo-controlled Trial. Tony Keaveny^{*1}, Kim Brixen², Roland Chapurlat³, Angela Cheung⁴, Thomas Fuerst⁵, Bernie Dardzinski⁶, Nadia Verbruggen⁷, Shabana Ather⁸, Elizabeth Rosenberg⁶, Anne De Papp⁶. ¹University of California, Berkeley, USA, ²Institute for Clinical Research, Denmark, ³E. Herriot Hospital, France, ⁴University Health Network, Canada, ⁵Synarc Inc, USA, ⁶Merck & Co., Inc., USA, ⁷Merck Sharpe & Dohme, Belgium, ⁸Merck & Co, Inc., USA

Background: In prior clinical trials, the cathepsin K inhibitor odanacatib increased areal BMD at the spine and hip of postmenopausal women. In an ovariectomized primate model, odanacatib increased cortical thickness and periosteal bone formation, and maintained normal biomechanical properties of the femoral neck and central femur. To gain additional insight into the clinical effects of odanacatib, we assessed femoral strength and geometry by QCT in postmenopausal women treated with odanacatib.

Methods: This international, randomized, double-blind, placebo-controlled, 2-year, phase 3 trial enrolled 214 postmenopausal women with a mean age of 64 years and mean BMD T-scores of -1.8 at the lumbar spine and at the femoral neck. Hip QCT scans at 2 years were available for a subset of these women (n=129). Overall proximal femoral strength was assessed as an exploratory endpoint for a simulated

sideways fall using finite element analysis (FEA). Within the femoral neck, volumetric BMD (vBMD), BMC and volume of the cortical and trabecular compartments as well as cortical thickness and cross-sectional area were assessed by morphometric analysis of the QCT images using Mindways QCTpro and BIT software (Austin, TX). Periosteal and endosteal boundaries were estimated using a global vBMD threshold and thus were sensitive to changes in vBMD with treatment. Results are presented as percent changes from baseline after two years of treatment.

Results: Treatment with odanacatib significantly increased the finite element-estimated overall femoral strength ($p < 0.001$, see Table). At the femoral neck, integral (cortical and trabecular combined) vBMD and trabecular vBMD were significantly higher in the odanacatib group, whereas cortical vBMD did not differ from placebo (Table). Estimated femoral neck cortical thickness, cortical volume, and cortical BMC were significantly higher in odanacatib-treated women; and cross-sectional area of the cortical compartment increased with odanacatib, whereas total cross-sectional area did not (Table). Taken together, these results suggest that cortical bone mass increased with odanacatib due to the accrual of bone mass at the endosteal envelope of the femoral neck.

Conclusions: In this study in postmenopausal women treated for 2 years, odanacatib appeared to improve overall proximal femoral strength by FEA, in part, by increasing cortical thickness and endosteal bone apposition along with integral and trabecular BMD at the femoral neck.

Table. Differences between weekly odanacatib 50 mg and placebo in QCT measurements at the femoral neck and total hip after 24 months of treatment

| Exploratory Endpoint: | LS Mean % Change from Baseline: | | | | Difference in % changes from baseline (ODN-PBO) | P value |
|--------------------------------|---------------------------------|---------------|-------|----------------|---|---------|
| | ODN | 95% CI | PBO | 95% CI | | |
| Femoral Neck | | | | | | |
| Integral vBMD | 2.40 | (1.61, 3.19) | -0.94 | (-1.71, -0.17) | 3.33 | <0.001 |
| Trabecular vBMD | 2.77 | (1.43, 4.12) | -0.65 | (-1.95, 0.66) | 3.42 | <0.001 |
| Cortical vBMD | 0.78 | (-0.01, 1.58) | 0.71 | (-0.06, 1.48) | 0.07 | 0.900 |
| Cortical* volume | 1.39 | (-0.27, 3.05) | -1.72 | (-3.34, -0.09) | 3.11 | 0.009 |
| Cortical* BMC | 1.15 | (-0.81, 3.11) | -2.08 | (-3.99, 0.17) | 3.23 | 0.021 |
| Cortical* Thickness | 4.11 | (2.24, 5.99) | -1.89 | (-3.72, -0.06) | 6.00 | <0.001 |
| Cortical* cross-sectional area | 3.54 | (1.69, 5.39) | -1.34 | (-3.14, 0.45) | 4.88 | <0.001 |
| Total cross-sectional area | -0.74 | (-1.80, 0.32) | 0.49 | (-0.54, 1.51) | -1.23 | 0.102 |
| Total Hip | | | | | | |
| Estimated femoral strength | 3.63 | (2.63, 4.62) | -1.92 | (-2.90, -0.93) | 5.55 | <0.001 |

* Based on BMD threshold segmentation and includes cortical and subcortical regions

Table

Disclosures: Tony Keaveny, Merck Sharp & Dohme Corp., 2; Merck Sharp & Dohme Corp., 9; Merck Sharp & Dohme Corp., 6
This study received funding from: Merck Sharp & Dohme Corp.

FR0393

The Effect of Denosumab on Bone Mineral Density (BMD) Assessed by Baseline Bone Turnover in Men With Low BMD. Paul Miller¹, Ugis Gruntmanis², Steven Boonen³, Yuqing Yang⁴, Rachel Wagman⁵, Jesse Hall⁶, Eric Orwoll⁷. ¹Colorado Center for Bone Research, USA, ²University of Texas Southwestern Medical Center, Dallas, USA, ³Center for Metabolic Bone Disease & Division of Geriatric Medicine, Belgium, ⁴Amgen Inc, USA, ⁵Amgen, Incorporated, USA, ⁶Amgen, Inc., USA, ⁷Oregon Health & Science University, USA

Purpose: Denosumab (DMAb), a fully human monoclonal RANKL antibody, has been shown to increase BMD in postmenopausal women with high and low bone turnover,¹ and reduce the risk for new vertebral, non-vertebral, and hip fractures.² ADAMO evaluated DMAB in men with low BMD and demonstrated increases in BMD at all skeletal sites measured and reductions in serum CTX (sCTX).³ We assessed the efficacy of DMAB in men across a range of baseline bone turnover in ADAMO.

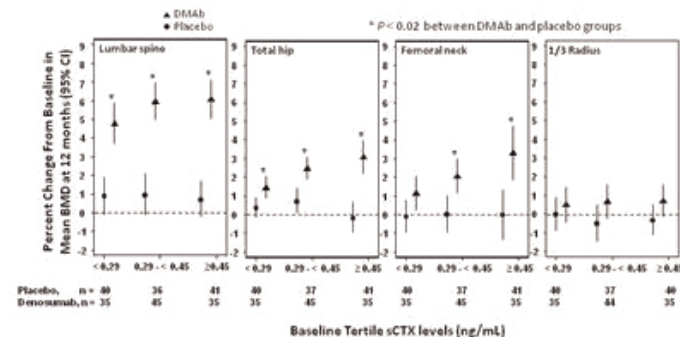
Methods: ADAMO was a multicenter, randomized, double-blind, placebo-controlled study. Subjects were randomized 1:1 to receive either 60mg DMAB or placebo administered subcutaneously once every 6 months over a 12-month period. Subjects were included if they were aged ≥ 30 and ≤ 85 yrs; had a BMD T-score ≤ -2.0 and ≥ -3.5 at the lumbar spine (LS) or femoral neck (FN), or had a prior major osteoporotic fracture and a T-score ≤ -1.0 and ≥ -3.5 at the LS or FN. Subjects received ≥ 1000 mg calcium and ≥ 800 IU vitamin D supplementation daily. Percent change in sCTX was assessed at day 15. Percent change in BMD from baseline to month 12 at the LS, total hip (TH), FN, trochanter (TR), and 1/3 radius (1/3R) BMD was assessed by tertile baseline sCTX levels.

Results: A total of 242 subjects (121, placebo; 121, DMAB) were enrolled. After 12 months of treatment with DMAB, BMD increased from baseline by 5.7%, 2.4%, 2.1%, 3.1%, and 0.6% at the LS, TH, FN, TR, and 1/3R, respectively (all $p < 0.02$ compared

with placebo and adjusted for multiplicity). sCTX was reduced by 81% (DMAB) vs 7% (placebo) from baseline at day 15. Subjects treated with DMAB, compared with placebo, demonstrated greater gains in LS and TH BMD at month 12 at each tertile of baseline sCTX (Figure). Subjects in the highest tertile of baseline resorption had numerically greatest gains in BMD when compared with the lowest tertile, although differences were not statistically significant. Associations between baseline sCTX and 12-month BMD improvements were weaker at the FN and 1/3R, sites with greater variability in measurements.⁴

Conclusions: Men with low BMD treated for one year with DMAB, compared with placebo, demonstrated greater gains in BMD independent of baseline sCTX at key skeletal sites routinely used to diagnose and manage patients with osteoporosis. The data also suggest that men at all levels of bone turnover may benefit from DMAB therapy.

1. Bone, *JCEM* 2008
2. Cummings, *NEJM* 2009
3. Gruntmanis, *ENDO* 2012
4. Brown, *ASBMR* 2009



Percent Change From Baseline in Mean BMD at 12 Months by Baseline sCTX

Disclosures: Paul Miller, Warner Chilcott, Amgen, Novartis, Roche, Procter & Gamble, sanofi-aventis, Roche, Eli-Lilly, Merck, Novartis, Amgen, Takeda, Radius, GE, 6; Warner Chilcott, Merck, Eli Lilly, Amgen, Novartis, Roche, GSK, Baskter, Wright, 2
This study received funding from: Amgen Inc

FR0400

Effects of Age and Vitamin D on Parathyroid Hormone Levels. Frank Blocki¹, Sudhaker D. Rao², Andre Valcour³. ¹DiaSorin Incorporated, USA, ²Bone & Mineral Research Laboratory, Henry Ford Hospital, USA, ³Center for Esoteric Testing, LabCorp, USA

Osteoporosis & primary hyperparathyroidism (PHPT) are two common bone & mineral disorders whose clinical expression is affected by prevailing 25OHD & calcium status. Numerous studies suggest that serum 25OHD levels supporting optimal skeletal health be defined as those where PTH declines to a minimum: results, however, are widely disparate with sufficient levels positioned anywhere from 12 to 44ng/mL. Limitations common to these studies were small sample sizes (<100 to ~30,000). Here, nearly 313,000 subjects were tested for 25OHD & PTH from July 2010 to June 2011. Median PTH values & % patients exceeding the clinical PTH threshold of 65pg/mL from groups of 6259 patients each plotted against 25OHD provided smooth, exceptionally well-fitted curves (Mean PTH=11.9+140.6(25OHD)^{-0.46}; R²=0.994 & (%High=57.2 +166.7(25OHD)^{-0.21}; R²=0.995) & evidenced no inflection points or horizontal asymptotes. Parsed across four levels (<20, 20-40, 40-60, >60 years), the same groups disclose a striking dependency upon age. Data presented here provides cause for a closer contemplation of the Institute of Medicine's recent guidance of 20ng/mL as that level assuring 25OHD sufficiency for the majority of Americans: 85,000 (27%) subjects fell below this conservative threshold. Of greater clinical relevance, 40% (27,950/70,000) & 51% (7,650/15,000) of subjects with 25OHD <20 & 10ng/mL, respectively, had biochemical hyperparathyroidism with PTH levels >65pg/mL. Despite significant limitations, several important clinical observations are germane. 1st, median PTH levels of a very large sample set plotted across the continuum of patient 25OHD levels reveals NO threshold above which increasing 25OHD fails to further suppress PTH. 2nd is the sheer magnitude of subjects >60 years old with frank deficiency whose PTH levels were above the reference range UL. This preponderance of abnormal results reinforces the 3rd International Workshop on Asymptomatic PHPT's call for 25OHD repletion (to levels minimally above 20ng/mL) of suspected PHPT subjects before consideration of elective surgery. Finally, the strong age dependency of PTH levels with 25OHD likely reflects the composite of depleted calcium stores, calcium malabsorption &/or renal malfunction. This population based study may well move the clinical community away from fixed values of 20 vs 30 vs 40ng/mL as defining vitamin D sufficiency toward patient management based upon an age dependent, PTH-25OHD continuum.

Disclosures: Frank Blocki, DiaSorin Inc, 3

FR0401

The Efficacy of High-Dose Oral Vitamin D₃ Administered Once a Year: Increased Fracture Risk Is Associated With 1,25 Vitamin D Level at 3-Months Post Dose. Kerrie Sanders*¹, Gustavo Duque², Peter Ebeling³, Thomas McCorquodale², Markus Herrmann⁴, Catherine Shore-Lorenti⁵, Geoffrey Nicholson⁶. ¹NorthWest Academic Centre, ²The University of Melbourne/Western Health, Australia, ³Ageing Bone Research Program, University of Sydney, Australia, ⁴ANZAC Research Institute, The University of Sydney, Concord, Australia, ⁵NorthWest Academic Centre, University of Melbourne, Australia, ⁶The University of Queensland, Australia

We have previously reported an increased rate of falls and fractures in a RCT using a single annual dose of 500,000IU cholecalciferol administered orally to 2,256 older women in fall or winter for 3 to 5 years¹. The increased rate of falling in the vitamin D group was higher in the first 3 months following dosing (p=0.017) suggesting an adverse mechanism in the immediate post-dose period. There was evidence of a temporal pattern of fracture risk but this was not significant. Serial biochemistry including 1,25 dihydroxyvitamin D levels (1,25D) were assessed on a sub-study of 65 randomly selected participants. Serum 25-hydroxyvitamin D (25D) and 1,25D were measured using DiaSorin immunoassays. Falls were ascertained using a monthly calendar and fractures were radiologically confirmed.

The median baseline serum 25D and 1,25D were 49nmol/L and 55pmol/L, respectively. In the vitamin D group, 25D levels at pre-dose, 1- and 3-month median post dose levels were 82, 130, and 97nmol/L, respectively and 1,25D levels were 93, 120 and 100pmol/L, respectively. Our post-hoc analysis used a binomial logistic regression with fracture (yes/no) as the outcome. The model included age and 1,25D at 3-months post-dose as the covariates. There was a 10% increased risk of fracture with increasing 1,25D levels (odds ratio {OR}: 1.10; 95% C.I: 1.02, 1.18, p<0.000). The increased risk of falls was not associated with 1,25D levels (OR: 1.02, 95% C.I: 0.98, 1.06, p=0.34). The normal range for 1,25D is 47 to 203pmol/L and may be high in hyperparathyroidism². We have previously reported evidence increased bone turnover in this group of participants³ although PTH levels were lower in the vitamin D than placebo group (3-month post-dose: 4.2 vs 5.7 pmol/L, respectively, p=0.007).

These findings suggest high 1,25D levels following a 500,000IU dose of cholecalciferol are associated with an increased fracture risk in older Caucasian women. The finding does not explain the increased risk of falls but progresses our understanding of a mechanism underlying the occurrence of increased fracture risk following annual high-dose vitamin D supplementation.

¹Sanders KM et al. JAMA 2010 ²mayomedicallaboratories.com/ ³Sanders KM et al, ANZBMS/IOF 2011

Disclosures: Kerrie Sanders, None.

FR0402

The Safety of Long-Term Use of Different Doses of Vitamin D₃ Plus Calcium in Older Caucasian and African American Women. Vinod Yalamanchili*¹, Munro Peacock², Lynette Smith³, J. Christopher Gallagher¹. ¹Creighton University Medical Center, USA, ²Indiana University Medical Center, USA, ³University of Nebraska Medical Center, USA

Background: Long-term use of vitamin D₃ and calcium supplements is common in older women. But there is no long-term data on the incidence of hypercalcemia and hypercalciuria with these supplements. In the WHI study, after seven years there was a significant increase in renal stones in the women treated with vitamin D₃ 400IU/d and 1000 mg extra calcium but no laboratory data.

Methods: 163 Caucasian and 110 African American women, ages 57-94 years, randomized to one of the doses of vitamin D₃ - 400, 800, 1600, 2400, 3200, 4000, 4800 IU/day or placebo for one year. The main inclusion criterion was vitamin D insufficiency with serum 25 hydroxyvitamin D (25OHD) < 20ng/ml (Diasorin assay). Exclusion criteria were illness or medications known to affect calcium and vitamin D metabolism. Calcium intake was increased to 1200-1400mg/d with calcium citrate. Definition of hypercalcemia and hypercalciuria was a value greater than the normal range established at baseline for each group. Serum and 24-hour urine calcium were measured at baseline and every 3 months for one year. Any abnormal event was verified after one week and if high values continued to occur then the vitamin D and calcium supplements were reduced or stopped. Multiple regression analysis was used that included the variables age, dose, calcium intake, serum 25OHD, serum and urine calcium.

Results: Mean baseline serum 25OHD for all subjects was 14.5 ng/ml, there was a curvilinear increase in serum 25OHD and reached a plateau at ~45 ng/ml. In Caucasians mean daily calcium intake at baseline was 685 mg and at the end 1230 mg; in African Americans mean baseline was 551 mg and at the end 1100 mg. The number of events of hypercalcemia and hypercalciuria are shown in table and the incidence was high. Final 24-hour urine calcium was not related to vitamin D₃ dose in both groups but was significantly related to serum 25OHD level in Caucasians only. There was no significant relationship between the events of hypercalcemia or hypercalciuria and the vitamin D₃ dose or serum 25OHD. No kidney stones were reported.

Summary: There was a high incidence of hypercalciuria especially in Caucasian women compared to African American women and both groups had events of

hypercalcemia. These events were not related to the vitamin D₃ dose. Hypercalciuria and hypercalcemia could lead to an increase in kidney stones and measurement of serum and 24-hour urine calcium is advisable with long-term use of vitamin D₃ and calcium.

Table 1. Incidence of Hypercalciuria and Hypercalcemia

| | | Hypercalcemia | Hypercalciuria |
|--|-------------------|---------------|----------------|
| Subjects (percentage with one event) | Caucasians | 11% | 33% |
| | African Americans | 15% | 11% |
| Events (percentage out of total tests) | Caucasians | 4% | 15% |
| | African Americans | 5% | 4% |

Incidence of Hypercalciuria and Hypercalcemia

Disclosures: Vinod Yalamanchili, None.

This study received funding from: National Institute on Aging

FR0406

Long-term Sclerostin Antibody Treatment in Cynomolgus Monkeys: Sustained Improvements in Vertebral Microarchitecture and Bone Strength Following a Temporal Increase in Cancellous Bone Formation. Michael Ominsky*¹, Rana Samadfam², Jacquelin Jolette³, Susan Y. Smith², Hua Zhu Ke¹, Rogely Waite Boyce⁴. ¹Amgen Inc., USA, ²Charles River Laboratories, Canada, ³Charles River Laboratories, Preclinical Services Montreal, Canada, ⁴Amgen Inc, USA

Sclerostin antibody (Scl-Ab) increases bone formation, bone mass, and bone strength in rodents and cynomolgus monkeys (cynos) in studies of up to 10 weeks duration. To investigate the long-term effects of Scl-Ab treatment, adolescent (3-5 year old) cynos were treated for 6 months with weekly subcutaneous injections of vehicle (Veh), 3, 10, or 100 mg/kg Scl-Ab (n=4/group). The data reported here are from male cynos, though similar results were observed in females.

The bone formation marker serum osteocalcin peaked within the first 3 months of Scl-Ab treatment and returned toward baseline levels at month 6, at which time the L2 vertebra bone formation rate (BFR/BS) was similar across all treatment groups. At the tibia diaphysis, endocortical BFR/BS remained dose-dependently elevated. Despite the normalization of cancellous BFR/BS at month 6, Scl-Ab dose-dependently increased DXA BMD by 15-30% at the lumbar spine compared with Veh (Table).

By ex vivo microCT, Scl-Ab resulted in dose-dependent increases in BMD at L3 vertebral bodies and L6 cancellous cores, and in bone area, cortical thickness (Ct.Th), trabecular bone volume (BV/TV), and trabecular thickness (Tb.Th) (Table). The improvements in bone microarchitecture resulted in increases in yield load for all dose levels at both L3 (+33-92%) and L6 (+83-142%) compared with Veh. Stiffness and energy to failure were also dose-dependently increased after Scl-Ab treatment at both sites. Strength properties were normalized to BV/TV to approximate material properties, and no group differences were found in yield strength, modulus, or toughness. Positive correlations between BMD and yield load were observed across all groups for both vertebral specimens, further supporting the maintenance of material properties. No group differences were found in the ratio of ash to dry weight in vertebral samples, reflecting normal matrix mineralization during Scl-Ab treatment.

These data demonstrate that 6 months of Scl-Ab treatment in cynos resulted in marked improvements in vertebral BMD, cortical and trabecular microarchitecture, and bone strength, with maintenance of bone material properties. Together, these data highlight the unique mode of action of Scl-Ab, which temporally increases cancellous bone formation, resulting in a rapid increase in bone volume of normal quality that is maintained after indices of trabecular bone formation return to baseline.

| Variable | Unit | Vehicle | 3 mg/kg | 10 mg/kg | 100 mg/kg |
|--------------------|--------------------|-----------|------------|------------|------------|
| Lumbar DXA BMD | g/cm ² | 0.62±0.02 | 0.71±0.02* | 0.74±0.03* | 0.80±0.02* |
| L3 µCT Total BMD | mg/cm ³ | 3.16±12 | 438±7* | 471±28* | 598±20* |
| L3 µCT Bone Area | mm ² | 41.3±1.7 | 60.7±2.9* | 67.04±6.5* | 83.0±8.1* |
| L3 µCT Ct.Th | mm | 0.33±0.04 | 0.38±0.01 | 0.37±0.03 | 0.61±0.05* |
| L3 Yield Load | kN | 2.20±0.19 | 2.92±0.13 | 3.48±0.37* | 4.22±0.53* |
| L6 Core µCT BMD | mg/cm ³ | 255±15 | 425±24* | 444±30* | 552±11* |
| L6 Core µCT BV/TV | % | 21.2±1.5 | 42.2±3.1 | 45.1±3.8 | 59.8±1.3* |
| L6 Core µCT Tb.Th | µm | 130±7 | 186±11* | 200±6* | 228±2* |
| L6 Core Yield Load | kN | 0.12±0.01 | 0.22±0.02* | 0.25±0.03* | 0.29±0.02* |

Mean ±SEM; *p<0.05 versus Veh by ANOVA + Dunnett's or Dunn's post test

Table

Disclosures: Michael Ominsky, Amgen, 3; Amgen, 7

This study received funding from: Amgen Inc. and UCB Pharma

FR0408

Negative Effect of N-Cadherin on the Anabolic Action of Parathyroid Hormone (PTH). Leila Revollo*¹, Jin Norris², Gabriel Mbalaviele³, Roberto Civitelli³. ¹Washington University Division of Bone & Mineral Diseases, USA, ²WASHINGTON UNIVERSITY, USA, ³Washington University in St. Louis School of Medicine, USA

Interaction between PTH/PTHrP receptor (PTH1R) and low-density lipoprotein receptor-related protein 6 (LRP6) contribute to the osteo-anabolic action of PTH through activation of β -catenin signaling. Others have shown negative regulation of canonical Wnt/ β -catenin signaling by N-cadherin interaction with LRP5/6 via axin. We previously reported that PTH1R interacts with LRP6 but not LRP5 or N-cadherin. We also find that both LRP5 and LRP6 interact with N-cadherin, but not with cadherin-11, another osteoblast cadherin; and that PTH induces rapid LRP5 and N-cadherin translocation from cytoplasmic pools to the cell surface. These results are compatible with a model whereby N-cadherin regulates PTH-PTH1R responses by sequestering LRP5/6, thus diminishing PTH-induced LRP5/6-signaling. To begin testing this model, we used mice harboring a selective deletion of the N-cadherin gene (*Cdh2*) in osteoblasts, driven by the *Osterix* promoter (*Cdh2^{fllox/flox}::Ox-Cre*: *Cdh2*-cKO). Consistent with previous models of conditional *Cdh2* ablation, *Cdh2*-cKO mice have a smaller skeleton and decreased bone mass, but normal trabecular and cortical architecture. Intermittent administration of human PTH₁₋₃₄ (80 μ g/kg bw, sc, 5x/week, 4 weeks) to 3-months-old male mice produces changes of larger magnitude in *Cdh2*-cKO (n=4) relative to control (*Cdh2^{fllox/flox}*) (n=9) mice with respect to trabecular bone volume/tissue volume (110.13 \pm 40.03% vs. 38.71 \pm 9.21% above baseline, respectively, p<0.05), and bone mineral density (31.90 \pm 8.70% vs. 12.68 \pm 3.41% above baseline, p<0.05), assessed by *in vivo* μ CT imaging. PTH treatment also increases cortical thickness in both *Cdh2*-cKO mice and control (34.14 \pm 20.18% vs. 26.28 \pm 5.90% above baseline, p>0.1), but has minimal effects on cortical tissue mineral density (3.36 \pm 0.38% vs. 2.13 \pm 1.88% from baseline, p>0.1). Cross-sectional marrow area does not change in either *Cdh2*-cKO and control group (0.58 \pm 4.68% vs. 0.35 \pm 4.97% from baseline, p>0.1). Thus, intermittent PTH administration increases trabecular bone mass and cortical thickness in mice, the latter presumably by increasing periosteal bone apposition. Osteoblast N-cadherin appears to have a restraining effect on PTH anabolic effect on trabecular but not cortical bone. We hypothesize this action of N-cadherin occurs through interference with PTH1R-LRP5/6 signaling interactions.

Disclosures: *Leila Revollo, None.*

FR0409

Treatment with an Inhibitor of Fatty Acid Synthase Reverses Bone Loss in Ovariectomized Mice. Sandra Bermeo*¹, Wei Li², Christopher Vidal³, Daniele Cultrone⁴, Mamdouh Khalil⁵, Gustavo Duque⁶. ¹PhD Student, Australia, ²University of Sydney, Nepean Clinical School, Australia, ³University of Sydney, Australia, ⁴Ageing Bone Research Program, Sydney Medical School Nepean, The University of Sydney, Australia, ⁵ANZAC Research Institute, Australia, ⁶Ageing Bone Research Program, University of Sydney, Australia

In the bone marrow, bone and fat have an antagonistic relationship with fat having a toxic effect on bone cells. This lipotoxic effect is exerted through the accumulation of fatty acids, which are synthesized by fatty acid synthase (FAS) in marrow adipocytes. In this study, we hypothesized that FAS inhibition would have a potential beneficial effect on bone mass of ovariectomized (OVX) mice. Nine-month-old C57BL/6 mice underwent OVX or SHAM surgery, and 8 wks later were treated three times a week with cerulenin (30 and 60 mg/Kg, SC) or vehicle (VEH) for 6 wks. Both SHAM and OVX mice showed a significant decrease in both body weight ($-10 \pm 2\%$) and subcutaneous fat thickness ($-25 \pm 10\%$) compared to VEH. μ CT and histomorphometry measurements indicated that trabecular bone volume/total volume (BV/TV) was significantly increased in both SHAM and OVX groups (33 \pm 10% and 52 \pm 18% respectively) as compared to VEH (p<0.001). Furthermore, treatment with low dose cerulenin induced a significant increase in mineral apposition rate (MAR) in both SHAM and OVX groups (52 \pm 8%) as compared with VEH. Overall, this anabolic effect was also associated with higher osteoblast number (~ 2 fold) with no changes in osteoclast number being observed in the OVX and SHAM groups. Changes in cell numbers corresponded with higher serum levels of P1NP (2 fold) with no changes in serum C-telopeptide in the treated groups. Additionally, *ex vivo* cultures of bone marrow stromal cells showed similar levels of osteoblastogenesis and very low levels of adipogenesis in the treated mice as compared with VEH. This evidence was supported by Western blot and RT-PCR analysis of osteogenic and adipogenic genes. Both OVX and SHAM groups showed a significantly lower expression of adipogenic genes (PPAR γ , C/EBP α and AP2, p<0.001) with no changes being observed in osteogenic genes in the treated groups. Histological quantification of marrow fat showed a significant decrease of fat volume/total volume (FV/TV) in both OVX (-26%) and SHAM (-18%) groups as compared to VEH (p<0.01). Finally, treatment of OVX mice with cerulenin improved BMD to levels equal to SHAM and VEH controls. Taken together, our results demonstrate that inhibition of FAS decreases adipogenesis and fat marrow content and stimulates bone formation by inducing an ideal marrow milieu for osteoblast function without affecting bone resorption, thus providing strong evidence that inhibition of FAS may be a novel anabolic therapy for osteoporosis.

Disclosures: *Sandra Bermeo, None.*

FR0415

A New Peptide Derived from the Matrix Protein Chondroadherin Reduces Motility of Osteoclast Precursors and Breast Cancer Cells through Inhibition of the Nitric Oxide Synthase 2 Pathway: Pre-clinical Evidence for Therapy. Nadia Rucci*¹, Mattia Capulli², Ole Kristoffer³, Kaare Gautvik⁴, Lisbet Camper⁵, Dick Heinegard⁶, Anna Teti¹. ¹University of L'Aquila, Italy, ²Department of experimental Medicine, University of L'Aquila, Italy, ³Department of Clinical Chemistry, Ullevaal University Hospital & Institute of Medical Biochemistry, University of Oslo, Norway, ⁴Oslo University Hospital, Norway, ⁵Department of Experimental Medical Science, Lund University, Sweden, ⁶Lund University, Sweden

The Nitric Oxide Synthase (NOS) 2 is implicated in many cellular functions through its ability to produce NO in an inducible manner. We isolated a cyclic peptide representing the $\alpha 2\beta 1$ integrin binding sequence of the matrix protein chondroadherin (cCHAD), which displays antiosteoclastogenic and antitumoral effects. We noted that in mouse bone marrow preosteoclast cultures cCHAD potency was greater at low cellular density suggesting an effect on cell motility. A scratch-healing assay confirmed a 88% reduction of migration in cCHAD-treated preosteoclasts vs. control. Likewise, cCHAD-treated osteotropic breast cancer cells MDA-MB231 showed reduced migration and invasion (-30% and -40%, respectively) suggesting a common mechanism of action. A real-time RT-PCR array showed that cCHAD downregulated NOS2 expression in preosteoclasts. We treated preosteoclasts with the NO donor S-nitroso-N-acetyl-D,L-penicillamine, which blocked the effect of cCHAD, rescuing normal preosteoclast motility and differentiation. In contrast, the NOS2 inhibitor N5-(1-iminoethyl)-l-ornithine mimicked the effect of cCHAD abrogating both motility and osteoclastogenesis. In healthy mice treated with cCHAD we observed dose-dependent reduction of osteoclast number and surface/bone surface (-40% and -50%, respectively) and increase of trabecular bone volume (1.55-fold), with no adverse effects. Daily treatment of ovariectomized (OVX) mice with cCHAD starting 3 days (preventive protocol) or 5 weeks (curative protocol) after OVX showed that cCHAD significantly prevented bone loss and rescued bone mass, respectively, by inhibiting osteoclast increase. *In vivo* antiresorptive effect of cCHAD was also observed in mouse models of breast cancer-induced bone metastases by intracardiac injection of MDA-MB231 cells, in which cCHAD strongly decreased the incidence of osteolytic lesions (-78%). Consistent with its antitumoral activity, cCHAD reduced visceral metastases and orthotopic tumor growth as well, confirming a direct *in vivo* effect on cancer cells. In conclusion, we provided pre-clinical evidence that cCHAD is a new potent inhibitor of the NOS2/NO pathway through which it i) increases bone mass in healthy mice, ii) counteracts bone loss in OVX-induced osteoporosis, iii) inhibits osteolytic bone metastases acting on both bone resorption and tumor expansion, iv) inhibits tumor growth. These results suggest the use of cCHAD as a new experimental therapy for bone diseases.

Disclosures: *Nadia Rucci, None.*

FR0416

Central Roles of Adiponectin on Bone Formation Through a Hypothalamic Relay. Yuwei Wu*¹, Qisheng Tu², Jin Tang², Dana Murray², Jessica Cheng², Maribel Rios³, Zhihui Tang⁴, Jake Jinkun Chen². ¹Tufts University, USA, ²Tufts University School of Dental Medicine, USA, ³Tufts University School of Medicine, USA, ⁴Peking University School of Stomatology, China

Objective: Adiponectin is an adipose tissue derived hormone. Our previous studies have shown that adiponectin inhibits osteoclastogenesis and bone resorption. Adiponectin receptors (AdipoR1, AdipoR2, T-cadherin) are expressed in the brain. However, the effects of adiponectin in the central nervous system and the underlying mechanism are still unknown. We hypothesized that adiponectin regulates bone homeostasis through hypothalamus relay in adjusting sympathetic tone.

Methods: Male C57BL/6J and adiponectin knockout mice were used in this study. A 28-gauge cannula was implanted into the third ventricle and attached with Tygon tubing to a subcutaneous micro-osmotic pump. Recombinant globular adiponectin or artificial CSF was delivered at a rate of 0.22 μ l/hr (20 ng/hr) for 28 days. The animals were sacrificed and samples were collected at the end of the experiment. The hypothalamus, brown fat tissue (BFT), bone marrow cells, and the femur without bone marrow cells were dissected for RNA or protein extraction. Genes related to bone metabolism were determined by real-time PCR and western blot.

Results: Hypothalamus APPL1 protein was decreased after the microinjection of adiponectin into third ventricle (p < 0.05). Adiponectin dramatically down-regulated the expression of BFT uncoupling protein-1 (UCP1) that was previously found to be positive correlated with sympathetic tone. Adiponectin microinjection reduced bone marrow cells RANKL and TRAP transcription, which reflected the pathway that promotes osteoclast differentiation and their capability to resorb bone was inhibited. Alternatively, adiponectin microinjection promoted femur bone NFATC1 RNA transcription and protein expression, which had been shown to promote osteoblast proliferation and bone formation.

Conclusions: For the first time, these results suggest that, in addition to its peripheral effects on bone metabolism, central administration of adiponectin can also influence hypothalamus APPL1 pathway to promote bone formation through inhibiting sympathetic tone and osteoclast activity and enhancing osteoblast activity.

Therefore, adiponectin may serve as a potential therapeutic drug to treat osteoporotic fractures, obesity, and T2DM through a combination of its peripheral and central effects in enhancing insulin sensitivity and promoting bone formation and regeneration.

Disclosures: Yuwei Wu, None.

This study received funding from: NIH grants DE16710 and DE21464 to JC

FR0417

Comparing Treatment Effects of Odanacatib and Alendronate in Lumbar Vertebrae of Ovariectomized Rhesus Monkeys using Quantitative Computed Tomography. Sangeetha Somayajula¹, Ghassan Fayad², Randolph Crawford³, Seetha R. Kummari⁴, Belma Dogdas³, Mona L Purcell⁵, Paul McCracken⁶, Jacquelyn J Cook⁵, Sherri L Motzel⁷, Le Thi Duong⁶, Don Williams⁸, Antonio Cabal⁸. ¹Merck, USA, ²Merck Research Laboratories - Modeling & Simulations, USA, ³Merck Research Laboratories - Informatics IT, USA, ⁴Case Western Reserve University, USA, ⁵Merck Research Laboratories - Imaging, USA, ⁶Merck Research Laboratories, USA, ⁷Merck Research Laboratories - Lab Animal Resources, USA, ⁸Merck & Co., Inc., USA

Clinically translatable evaluation of disease progression and treatment response is critical to the development of new therapies for osteoporosis. Quantitative computed tomography (QCT) is a clinically translatable three dimensional *in vivo* imaging modality that enables localized assessment of the effects of disease and therapy on volumetric bone mineral density (vBMD). We evaluated the effects of odanacatib (ODN) and alendronate (ALN) in comparison to Vehicle (VEH) in trabecular, endo-cortical, peripheral, and whole bone compartments within the L4 vertebra of the ovariectomized (OVX) Rhesus monkey. QCT data was obtained (in-plane spatial resolution 500 μm) for three groups (n=13 each) of OVX animals treated with VEH, 2 mg/kg ODN daily, and 15 μg/kg twice weekly ALN. Longitudinal QCT measurements are presented at 0 and 18 months post-treatment. Previous work on evaluating these therapies on Rhesus vertebrae used Mindways software for vertebra analysis in an elliptical trabecular core. Here we performed a more detailed analysis using custom software that applied image processing techniques to automatically extract 4 regions of interest (ROIs) – trabecular core, endo-cortical (a ring adjacent to the cortical bone), peripheral (a ring including cortical bone and adjacent region), and whole vertebra regions. The ROIs are shown in Fig. 1. For consistency of ROI in longitudinal vBMD measurement, we performed rigid registration of the baseline to 18 month QCT image, transformed the baseline ROIs to the 18 month QCT space, and measured vBMD in the transformed ROIs. Longitudinal percent changes in vBMD in the ROIs considered are shown in Fig 2. Both treatment groups differentiated from VEH in all the ROIs considered, demonstrating efficacy of ODN and ALN. ODN differentiated from ALN in the peripheral region (p<0.05) but not in the trabecular core, endo-cortical or whole vertebra BMD (Fig 2). The differentiation in the peripheral region could be due to an increase in cortical thickness. An increase in cortical thickness was observed in high resolution peripheral QCT of the radius and these results suggest that similar effects may be occurring in vertebra as well.

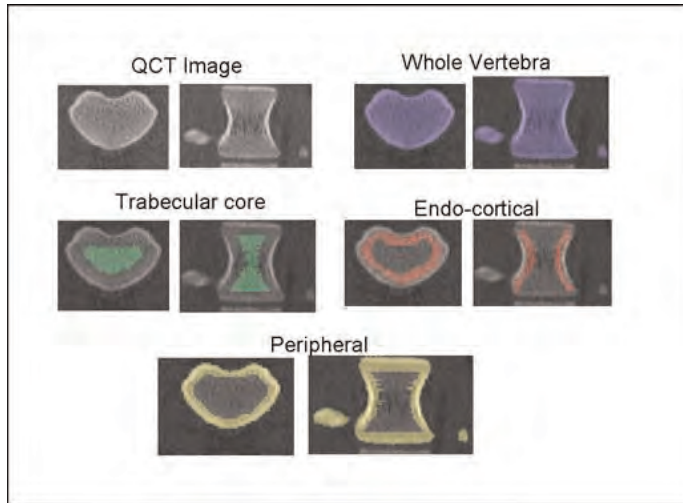


Fig 1: Regions of interest for vBMD measurement shown in transaxial and sagittal views of a subject

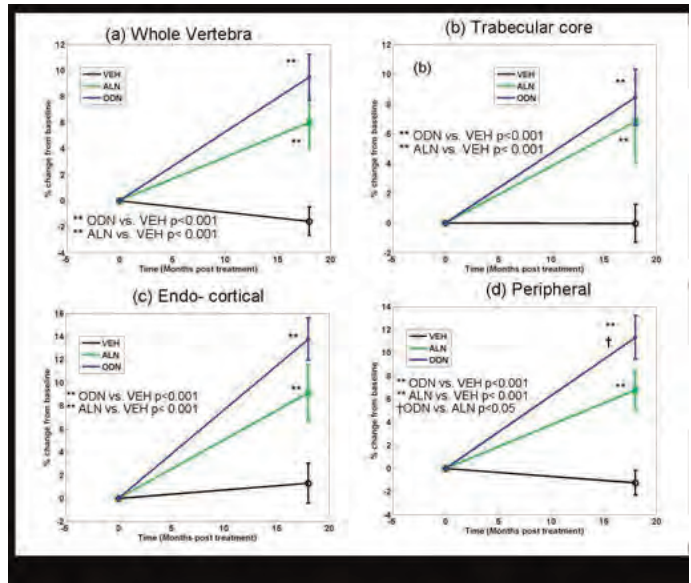


Fig 2: Percent change with respect to baseline of vBMD in the ROIs shown in Fig 1

Disclosures: Sangeetha Somayajula, None.

This study received funding from: Merck and Co., Inc

FR0418

Efficacy of Odanacatib or Alendronate following Parathyroid Hormone Treatment in Estrogen-Deficient Rabbits. Brenda Pennypacker¹, Christopher Winkelmann², John Szumiloski², Randolph Crawford², Mary Belfast³, Le Thi Duong¹. ¹Merck Research Laboratories, USA, ²Merck & Co., USA, ³Merck & Company, USA

The cathepsin K inhibitor odanacatib (ODN) and alendronate (ALN) have been shown to prevent bone loss in ovariectomized (OVX) rabbits. While ALN reduces bone remodeling, ODN preserves trabecular and cortical bone formation (BF) in this model. Intermittent administration of human parathyroid hormone 1-34 (PTH) is an approved anabolic agent for the treatment of osteoporosis. Here, we compare the effects on bone mass and remodeling in rabbits treated with ODN or ALN following PTH treatment for 6-mo, or to the respective monotherapy. Adult (7-mo) rabbits had Sham (N=20) or OVX surgery (N=120) 6-mo prior to study start. OVX-rabbits were randomized by lumbar vertebrae (LV) 5-6 into the following treatment groups: Vehicle (Veh), PTH (15μg/kg, 5x/wk), ALN (100μg/kg, 2x/wk) or ODN (~7μM·24hr, in food). After 6-mo, rabbits treated with PTH were switched to Veh (PTHswVeh), ALN (PTHswALN) or ODN (PTHswODN) for an additional 4-mo. Trabecular (Tb) vBMD by QCT of LV6 and in-life aBMD by DXA LV5-6 were determined at baseline, 3, 6 and 10-mo. Baseline Tb.vBMD in OVX decreased by 9% (p<0.05) vs. Sham. Tb.vBMD was significantly increased (p<0.001) by ODN (19%), ALN (11%) and PTH (16%) vs. Veh at 6-mo. aBMD from all groups provided similar results as Tb.vBMD measurements. PTHswVeh returned BMD to OVX levels, while switching to ODN or ALN maintained bone mass. ALN reduced mineralized surface (MS/BS) and bone formation rate (BFR/BS) of Tb.LV and CF endocortical (Ec) surfaces. Unlike ALN, the BF parameters in ODN were comparable to those in Veh. PTH significantly increased BF parameters at all sites and increased CF cortical thickness (CtTh) and area by 20% (p<0.001) and 16% (p<0.001), respectively vs. Veh. Cortical porosity (CtPo) was also increased with PTH treatment. PTHswALN and PTHswODN maintained increased CtTh and area, while switching to ALN reduced CtPo by 80% (p<0.001) and ODN by 29% (NS) compared to PTH alone. CF peak load was significantly increased by PTHswODN and PTHswALN. In LV4 and CF, positive correlations between pQCT BMC and peak load were observed (r²= 0.7318, p<0.001 and r²= 0.5386, p<0.001, respectively). In this study, ODN as follow-on treatment to PTH preserved bone mass similar to ALN in osteopenic rabbits. However, ODN maintains the window of bone formation post-PTH therapy. This supports the potential cycling usages of these agents that may offer long-term benefits to patients with severe osteoporosis.

Disclosures: Brenda Pennypacker, Merck and Co., 3

This study received funding from: Merck and Co.

FR0420

Odanacatib Treatment Reduces Remodeling and Stimulates Modeling-based Bone Formation in Central Femur and Lumbar Vertebra of Adult OVX Monkeys. Charles Chen*¹, Mei-Shu Shih², Hellen Zheng³, Le Thi Duong⁴. ¹Merck & Co., Inc., USA, ²RS Medical, USA, ³MDS, USA, ⁴Merck Research Laboratories, USA

Odanacatib (ODN), a selective and reversible Cathepsin K inhibitor has been demonstrated to reduce trabecular (Tb) and intracortical (Ic) bone turnover while preserving endocortical (Ec) and stimulating bone-site specific periosteal (Ps) bone formation in OVX-monkeys. The aim of this study is to investigate the bone site specific mechanism of ODN on bone modeling (Mo) and remodeling (Re). Adult newly OVX-rhesus monkeys (13-19 yrs, n =8-11 per group) were treated with vehicle or ODN (6 or 30mg/kg, q.d., p.o.) for 21-months. Calcein labels at 15-d interval were given at 12-mo. of dosing. Lumbar vertebrae (LV) longitudinal sections (~8-um) and central femur (CF) cross sections (50-um) were subjected to analyses for cement line and dynamic histomorphometric measures. Only newly formed hemiosteons (Ho) were evaluated. At LV Tb surface, ODN at 6 and 30mg/kg dose-dependently reduced the number of remodeling hemiosteons (Re.Ho.N) without changing the mean wall thickness (Re.W.Th) as compared to vehicle. Although modeling was very low at Tb surface of the aged monkeys, ODN did not change Mo.Ho.N/BS and Mo.W.Th. vs. Veh. Overall in Tb.LV, ODN dose-dependently reduced mineralizing surface (MS/BS), mineral apposition rate (MAR), bone formation rate (BFR/BS) and thus activation frequency (Tb.AcF). In the CF, both low and high doses of ODN also decreased Ic remodeling as in Tb LV. ODN dose-dependently reduced Ec.Re.Ho.N by 51% and 66% (p<0.05), respectively and the high dose tended to reduce remodeling formation parameters BFR/BS, MS/BS and AcF. Also similar to Tb surface, Ec.Re.W.Th was unchanged in ODN vs. Veh. Remarkably, ODN increased modeling bone formation in the CF at both Ec and Ps surfaces. ODN dose-dependently increased Ec modeling parameters, including Mo.Ho.N/BS, Mo.AcF, Mo.W.Th and bone formation parameters. At Ps surface, ODN increases all BF parameters in a dose-dependent manner. In summary, the results demonstrate that ODN reduces remodeling and stimulates modeling-based bone formation, and thus changes the ratio of modeling to remodeling hemiosteons. The findings may thus explain the bone site specific actions of ODN on trabecular and cortical surfaces. Furthermore, the dual mechanisms of ODN on bone formation clearly differentiate this agent from the standard anti-resorptives.

Disclosures: Charles Chen, Merck, 3; Merck, 7
This study received funding from: Merck

FR0422

Down-regulation of FoxO3a/SIRT1 Signaling by Measles Virus Nucleocapsid Protein is Implicated in Paget's Disease. Feng-Ming Wang*¹, Benedicte Sammut², Quanhong Sun³, Jolene Windle⁴, G. David Roodman¹, Deborah Galson³. ¹Indiana University, USA, ²University of Pittsburgh Hillman Cancer Center, USA, ³University of Pittsburgh, USA, ⁴Virginia Commonwealth University, USA

Measles virus plays an important role as an environmental factor in the pathogenesis of Paget's disease. Previous studies have shown that IL-6 is increased in the bone marrow of Paget's patients and that measles virus nucleocapsid protein (MVNP) induces IL-6 secretion by pagetic osteoclasts. Further, we have shown that IL-6 contributes to the formation of pagetic osteoclasts. However, the mechanisms regulating IL-6 production by MVNP remain unclear. Here we demonstrate that expression of MVNP resulted in a down-regulation of FoxO3a/SIRT1 signaling. The presence of MVNP impaired the expression of *Sirt1* mRNA both under basal conditions and upon activation of its upstream regulator FoxO3a by LY294002 (a PI3K/AKT inhibitor). MVNP impairment of LY294002 induction of FoxO3a-driven *Sirt1* mRNA expression is likely due to the decreased FoxO3a protein levels observed in MVNP-expressing NIH3T3 cells, and therefore the LY294002-induced nuclear accumulation of FoxO3a was attenuated. Protein stability assays revealed that FoxO3a was degraded more rapidly in MVNP-expressing cells than in control cells following the addition of cycloheximide. Similarly, co-transfection of MVNP and FoxO3a into HEK293 cells demonstrated that MVNP decreased the protein levels of the over-expressed FoxO3a in a dose-dependent manner. Luciferase activity assays showed that constitutively active FoxO3a abolished the repressive effect of MVNP on luciferase reporters driven by either FoxO3a response elements or the *Sirt1* promoter. Consistent with the high levels of IL-6 present in *Sirt1* deficient MEF cells, MVNP-expressing cells displayed increased levels of IL-6, which could be inhibited by over-expression of SIRT1 or treating the cells with the SIRT1 activator, resveratrol. Finally, activation of SIRT1 by resveratrol blocked the formation of osteoclasts in bone marrow cultures and diminished the differences in osteoclast formation between cells from wild-type and TRAP-MVNP transgenic mice. These data suggest that modulation of FoxO3a/SIRT1 signaling plays an important role in MVNP's contribution to Paget's disease through its effects on IL-6 production.

Disclosures: Feng-Ming Wang, None.

FR0424

Cushing Disease: Restoration of Bone Mass and Microarchitecture after Hypercortisolism Normalization. Eugénie Koumakis*¹, Renaud Winzenrieth², Laurence Guignat³, Catherine Cormier⁴. ¹Rheumatology Department A, Cochin Hospital, APHP, France, ²Med-imaps, Hôpital X. Arnoz, PTIB, Pessac, France, France, ³Endocrinology department, Cochin Hospital, APHP, France, ⁴AP-HP Groupe Hospitalier Cochin, France

Cushing disease (CD) is considered as a true model of a glucocorticoids (GCs) effects on bone metabolism because of the minimization of confounding factors. Hypercortisolism frequently induces bone loss which is more pronounced at the lumbar spine than at the femoral neck due to a higher content in trabecular bone. This bone loss results in osteoporosis, and leads to an increased fracture risk. Besides, several studies have shown bone mass restoration in patients with CD after treatment. The aim of our study was to examine treatment effects on bone mineral density (BMD) and on bone microarchitecture assessed by TBS in subjects with CD.

We present a longitudinal study on 11 subjects (6 women and 5 men) with CD. Mean age and BMI were 39.9 ± 12.7 years and 27.1 ± 5.0 Kg/m² respectively. Mean 24h urinary cortisol before treatment was elevated in 10 patients 326 ± 287 (149-1079) µg/24h, and one patient had very elevated levels (7268 µg/24h). All subjects were cured, i.e. 24h urinary cortisol normalization after treatment. Among these 11 subjects, 10 underwent transphenoidal surgery whereas one subject only received medical treatments. BMD and TBS were evaluated at AP Spine (L1-L4) with DXA prodigy (GE-Lunar), QDR 4500 (Hologic), and TBS iNsight® (Med-Imaps) before and after treatment. Both DXA were cross-calibrated using a custom-made phantom. Linear regression was used to evaluate TBS and BMD modifications over time. Results were normalized at 1 and 2 years after treatment. BMD and TBS gains were expressed in % in comparison to baseline.

Normalized gains in % for TBS and BMD are presented figure 1 (mean + SD). After treatment, BMD and TBS increased by 3.7 and 7.3% respectively after 1 year, and by 7.9 and 13.5% after 2 years. BMD and TBS were not correlated before (p=0.35) and after treatment (p=0.20).

To our knowledge, the present study is the first to report data on bone recovery at the spine both by DXA and TBS in cured subjects with CD. The absence of correlation between TBS and BMD and the better improvement of microarchitecture assessed by TBS than BMD suggest qualitative rather than quantitative bone alterations in hypercortisolism-induced osteoporosis. This may explain some of the discrepancies between fracture rates and relatively preserved BMD measures in GC induced bone loss. Bone microarchitecture assessment could be a useful and supplementary tool for fracture risk evaluation in GC induced bone loss.

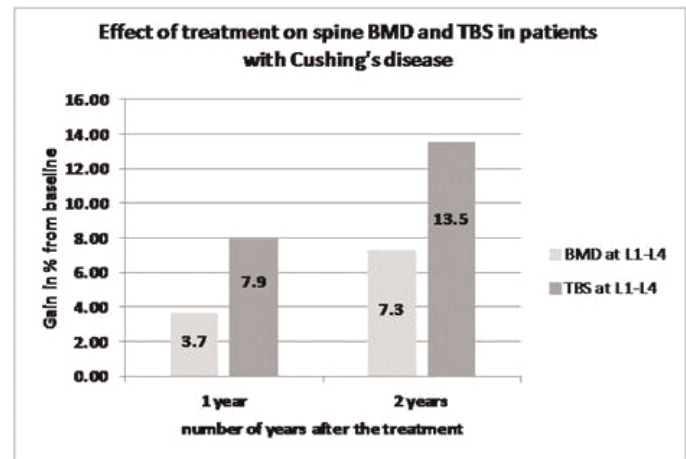


Figure 1

Disclosures: Eugénie Koumakis, None.

FR0425

Hypothalamic-pituitary-adrenal Axis is Essential for the Regulation of both Bone and Fat Metabolism via Melanocortin 2 Receptor. Tsvuyoshi Sato*¹, Dai Chida¹, Takanori Iwata², Michihiko Usui³, Yuichiro Enoki¹, Masahito Matsumoto¹, Ren Xu⁴, Satoko Sunamura⁵, Hiroki Ochi³, Toru Fukuda⁶, Shu Takeda⁷, Tetsuya Yoda¹. ¹Saitama Medical University, Japan, ²Tokyo Women's Medical University, Japan, ³Showa University Dental School, Japan, ⁴Tokyo Medical & Dental University, Japan, ⁵Keio University, Japan, ⁶Keio University School of Medicine, Japan, ⁷Keio University, Dept. of Nephrology, Endocrinology & Metabolism, Japan

The hypothalamic-pituitary-adrenal (HPA) axis is involved in maintaining homeostasis under stress conditions. Glucocorticoids (GCs) which are the end

products of the HPA axis via adrenocorticotropic hormone (ACTH) are crucial factors in the regulation of body adiposity and bone metabolism. GCs promote differentiation in adipocytes and cause glucose intolerance and central obesity. While several animal models have been developed to analyze the role of GCs in skeletal development in vivo, those results have been conflicting. Transgenic mice selectively overexpressing 11 β -hydroxysteroid dehydrogenase type2 (11 β -HSD2) within osteoblasts and osteocytes revealed that endogenous GCs are not required for normal skeletal development. Paradoxically, bone mass were lower in the transgenic mice overexpressing 11 β -HSD2 within osteoblasts and in the conditional knockout mice in which glucocorticoid receptor is specifically disrupted in osteoblasts under the control of Runx2 promoter fragments. On the one hand, the activation of the HPA axis by mental stressor has been implicated in high fat mass and low bone mass. However, the role of the HPA axis in both bone and fat metabolism is not fully elucidated. Here we characterized the bone and fat phenotype of melanocortin 2 receptor (i.e., ACTH receptor) knockout mice (MC2R $^{-/-}$ mice) disrupted of the HPA signaling pathway. We found that MC2R $^{-/-}$ mice were lean in old age and reduced fat mass. Adipose tissue weight was decreased in MC2R $^{-/-}$ mice, while adipocyte size in epididymal white adipose tissue were comparable between MC2R $^{-/-}$ mice and MC2R $^{+/+}$ controls, suggesting that white adipose cell number is decreased in MC2R $^{-/-}$ mice compared to MC2R $^{+/+}$ controls. MC2R $^{-/-}$ mice at 6 months old exhibited a high bone mineral density. Cortical thickness, bone formation rate, osteoblast surface/bone surface and serum osteocalcin were significantly increased whereas bone volume/tissue volume and osteoclast number/bone surface were normal in MC2R $^{-/-}$ mice. Accordingly, gene expression of osteocalcin in MC2R $^{-/-}$ mice was significantly increased in vivo, suggesting that the augmentation of cortical thickness was due to the enhancement of bone formation. Taken together, the HPA axis is essential for the regulation of both bone and fat metabolism through melanocortin 2 receptor. We will discuss the role of endogenous GCs and ACTH in mesenchymal stem cells differentiation and the influence of mental stress on both bone and fat metabolism.

Disclosures: Tsuyoshi Sato, None.

This study received funding from: Grants-in-aid for Scientific Research from the Ministry of Education, Science, Sports and Culture of Japan (23592941 for T.S.)

FR0426

The Role of Osteocalcin in Glucocorticoid-Induced Metabolic Dysfunction.

Tara Brennan-Speranza¹, Holger Henneicke^{*1}, Sylvia Gasparini², Caren Gundberg³, Colin Dunstan⁴, Hong Zhou¹, Markus Seibel¹. ¹Bone Research Program, ANZAC Research Institute, University of Sydney, Australia, ²Bone Research Program, ANZAC Research Institute, Australia, ³Yale University School of Medicine, USA, ⁴University of Sydney, Australia

We recently demonstrated that osteoblast-targeted disruption of glucocorticoid (GC) signaling attenuates GC-induced metabolic dysfunction and obesity, while preventing the marked decrease in circulating osteocalcin (OCN) usually seen with GC treatment. In the present study, we investigated the role of OCN in the pathogenesis of GC-induced insulin resistance, glucose intolerance and obesity.

Seven-week-old CD1 outbred mice were treated with placebo or corticosterone (1.5mg/week) for 28 days. On day 8, OCN was replaced via hepatic transfection of a non-viral DNA plasmid containing the osteocalcin gene driven by the albumin promoter (pLIVE, Mirus). We transfected either a wild-type OCN construct (wt-OCN) able to undergo gamma-carboxylation, or a mutant construct (mOCN) which cannot be carboxylated. Empty vectors were used as controls. Successful transfection was confirmed via detection of the GFP-containing pLIVE-vector in mouse hepatocytes 7 to 28 days post transfection. Insulin tolerance tests (ITT) and oral glucose tolerance tests (oGTT) were performed 0, 7, 14, 21 and 28 days into GC treatment. Body weight and composition were monitored throughout.

GC-treatment resulted in complete suppression of serum OCN levels and marked insulin resistance from day 7 onwards over the 4-week observation period. GC-treated mice receiving the wtOCN or mOCN constructs on day 8 regained their insulin tolerance in a time-dependent manner, with glucose levels falling to 60% of baseline in response to insulin on day 28. Glucose tolerance followed the same pattern (see Fig. 1). In contrast, GC-treated mice transfected with the empty vector remained insulin resistant and glucose intolerant. Furthermore, while GC-treated mice receiving the empty vector gained 60% in fat mass throughout the course of the study, hepatic osteocalcin expression attenuated the development of GC-induced obesity.

In conclusion, the adverse effects of exogenous GC on insulin sensitivity, glucose tolerance and adiposity in mice can be overcome by hepatic heterotopic expression of non-carboxylated or carboxylated osteocalcin. These data provide evidence that the osteoblast-specific peptide, osteocalcin, plays a central role mediating the effects of exogenous GC on systemic energy metabolism.

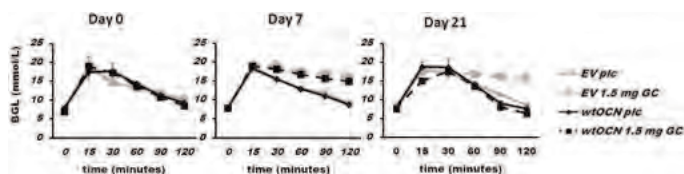


Figure 1

Disclosures: Holger Henneicke, None.

FR0427

Low Femoral and High Vertebral Bone Phenotype in α_{2C} AR Knockout Mice.

Marilia Teixeira^{*1}, Gisele M Martins², Cristiane Costa², Cecilia Gouveia³.

¹University of Sao Paulo, Brazil, ²Institute of Biomedical Science, Brazil,

³University of Sao Paulo, Institute of Biomedical Sciences, Brazil

Evidences demonstrate that sympathetic nervous system (SNS) activation causes osteopenia via β_2 -adrenoceptor (β_2 -AR) signaling. In a recent study, we showed that female mice with chronic sympathetic hyperactivity due to double knockout of adrenoceptors that negatively regulate norepinephrine release, α_{2A} -AR and α_{2C} -AR (α_{2A}/α_{2C} -ARKO), present an unexpected and generalized phenotype of high bone mass with decreased bone resorption and increased bone formation. Furthermore, we found that these animals are resistant to the thyrotoxicosis-induced osteopenia. These findings suggest that β_2 -AR is not the single adrenoceptor involved in bone mass regulation and show that α_2 -AR signaling may also mediate the SNS and thyroid hormone actions in the skeleton. To further investigate the participation of α_2 -ARs and its possible interaction with thyroid hormone in the regulation of bone mass, we are evaluating the bone phenotype of α_{2C} AR knockout mice (α_{2C} AR $^{-/-}$). A cohort of 30 day-old female congenic α_{2C} AR $^{-/-}$ mice, in a C57BL/6J background, and their wild-type (WT) controls (n=8/group) were treated with a supraphysiological dose of triiodothyronine (T3=7 μ g/100gBW/day) for 30 or 90 days. Surprisingly, a microtomography analysis showed that the trabecular bone volume (BV/TV) of the distal metaphysis of the femur and of the fifth lumbar vertebra (L5) were, respectively, 15%-45% lower and 31%-83% higher in α_{2C} AR $^{-/-}$ mice, when compared with WT animals (p<0,05 for all). Unlike the double knockout mice (α_{2A}/α_{2C} -ARKO), α_{2C} AR $^{-/-}$ mice were as sensitive to the thyrotoxicosis-induced osteopenia as WT animals. These findings suggest that α_{2C} AR may have a role in mediating the deleterious effects of the sympathetic activation in trabecular bone of vertebra and the opposite effects in the femur. In addition, these findings suggest that thyroid hormone does not interact with the SNS, via α_{2C} -AR, to regulate trabecular bone volume.

Disclosures: Marilia Teixeira, None.

This study received funding from: FAPESP - Fundação de Apoio a Pesquisa do Estado de São Paulo

FR0428

The Role of Activation Functions 1 and 2 of Estrogen Receptor- α for the Effects of Estradiol and Selective Estrogen Receptor Modulators (SERMs) in Male Mice.

Anna Borjesson^{*1}, Sara Windahl¹, Marie Lagerquist², Cecilia Engdahl¹, Helen Farman¹, Antti Koskela³, Klara Sjogren⁴, Jenny Kindblom², Alexandra Stubelius¹, Ulrika Islander¹, Maria C Antal⁵, André Krust⁵, Pierre Chambon⁵, Juha Tuukkanen³, Claes Ohlsson⁶.

¹Center for Bone & Arthritis Research, Sahlgrenska Academy, Sweden, ²Sahlgrenska University Hospital, Sweden, ³University of Oulu, Finland,

⁴Centre for Bone & Arthritis Research, Sweden, ⁵Institut de Génétique et de Biologie Moléculaire et Cellulaire, France, ⁶Center for Bone & Arthritis Research at the Sahlgrenska Academy, Sweden

Studies, in both man and mouse, show that estradiol (E2) is important for male skeletal health. The effect of E2 on bone is mainly mediated via estrogen receptor (ER)- α , as demonstrated by the findings that men with an inactivating mutation in aromatase or a non-functional ER α experience osteopenia and continued longitudinal growth after sexual maturation. To evaluate the role of different domains of ER α for the estrogenic effects on bone mass in males, we analyzed mice with a complete inactivation of ER α (ER α $^{-/-}$), a deletion of ER α activation function (AF)-1 (ER α AF-1 0) or a deletion of ER α AF-2 (ER α AF-2 0).

E2 treatment increased the amount of trabecular and cortical bone together with bone strength, and reduced the thymus weight and bone marrow cellularity in orchidectomized (orx) wild type (WT) mice. These tissues did not respond to E2 treatment in orx ER α $^{-/-}$ or ER α AF-2 0 mice. However, the effects of E2 in orx ER α AF-1 0 mice were tissue dependent, with a clear response in bone strength, cortical bone and bone marrow cellularity (68 \pm 17%, 45 \pm 6% and 33 \pm 6%, respectively, of E2 response in WT mice, p<0.05) but no significant response in trabecular bone or thymus.

To determine the tissue specific effects of selective ER modulators (SERMs) and the role of ER α AF-1 for their effects in male mice, we treated orx WT and ER α AF-1 0 mice with E2, Raloxifene (Ral), Lasofoxifene (Las), Bazedoxifene (Bza) or vehicle. Compared to the E2 response in orx WT mice, Ral, Las and Bza treatment resulted in tissue dependent effects, where the decrease in fat mass was normal after Ral and Las treatment, while the Bza treatment was less effective. The increase in trabecular bone mineral density was apparent for all SERMs, but less effective than the E2 effect. Las was the most effective SERM in increasing cortical bone mass, while none of the SERMs reduced the thymus weight. In contrast to E2, all effects of these SERMs were absent in the orx ER α AF-1 0 mice.

In conclusion, ER α AF-2 is required for the estrogenic effects on all parameters evaluated, while the role of ER α AF-1 is tissue specific. The effects of Ral, Las and Bza, in orx WT mice, are tissue dependent. In contrast to E2, all evaluated effects of these SERMs are dependent on a functional ER α AF-1. Our findings might contribute to the development of improved SERMs, with minimal side effects in males.

Disclosures: Anna Borjesson, None.

FR0431

Control of Post-Gonadarche Bone Mass Acquisition via Expression and Action of Heterogeneous Nuclear Ribonucleoprotein D (hnRNP D). Hong Chen¹, Linda Gilbert², Thomas Lisse³, Martin Hewison⁴, Mark Nanes⁵, John Adams^{*4}. ¹VA / Emory University School of Medicine, USA, ²Atlanta VA Medical Center, USA, ³Mount Desert Island Biological Laboratory, USA, ⁴University of California, Los Angeles, USA, ⁵VA Medical Center & Emory University, USA

Proteins in the hnRNP subfamily are scaffold proteins that move back and forth between the cell cytoplasm and nucleus. In the nucleus hnRNP D, also known as the estrogen response element binding protein (ERE-BP) or AUF1, interacts in trans with DNA and RNA cis elements to control gene expression by regulating chromatin remodeling, transcription, transcript splicing as well as the handling of coding and noncoding RNA. Based on the temporal sequence and configuration of hnRNP D-protein interaction, elucidated by a combination of co-immunoprecipitation and yeast two hybrid analyses in cultured cells, with the estrogen receptor alpha (ER α), the estradiol (E2) binding chaperone heat shock protein-27, and the Wnt3a signaling molecules, β -catenin and IKK α/β in the cytoplasm, hnRNP D regulates the availability of proteins (and small molecules bound to those proteins) for transnuclear transport and genomic action. Global over-expression of hnRNP D results in diminished post-gonadarche bone mass and size in vivo. This event occurs through the actions of hnRNP D to: 1) thwart movement of the E2-liganded ER α to the nucleus; 2) act in a dominant-negative mode by competing in trans with the E2-ER α binding for binding to cis-acting EREs in control of the genomic, anabolic actions of E2; and 3) operate in an E2-independent manner to promote trans-stimulation of RANKL, RANK expression and bone resorption. Here we present evidence that global knockdown or knockout of hnRNP D results in progressive increase in bone mass and size in the post-gonadarche, 7-week-old female mouse by μ CT analysis; compared to wildtype, bone mass increased by 28% and 31% in hnRNP +/- and -/- mice, respectively, and bone size by 28% and 54%, respectively. 6-month-old adult hnRNP-null mice had evidence of persistence of the anti-anabolic actions of hnRNP D, demonstrating a significant 2-4-fold increase in osteocalcin and alkaline phosphatase gene expression in primary culture of osteoblasts (OB) from hnRNP -/- compared to wildtype marrow. In conclusion, up or down regulation of hnRNP D expression in the extreme can control female bone mass and size by i) antagonizing the anabolic action of E2 on OB gene expression, ii) promoting E2-independent effects on OB-driven osteoclastogenesis, and iii) influencing the traffic of trans-acting factors from the cytoplasm to the nucleus.

Disclosures: John Adams, None.

This study received funding from: NIH NIAMS

FR0436

Transgene Expression of CYP27B1 in Osteoblasts Promotes Bone Formation without Altering Bone Resorption. Andrew Turner^{*1}, Paul Anderson², Rebecca Sawyer¹, Peter O'Loughlin¹, Gerald Atkins³, Howard Morris⁴. ¹Musculoskeletal Biology Research, Chemical Pathology, SA Pathology, Australia, ²Musculoskeletal Biology Research, University of South Australia, Australia, ³University of Adelaide, Australia, ⁴SA Pathology, Australia

The endocrine hormone 1,25-dihydroxyvitamin D (1,25D) is best known as a regulator of calcium and phosphate homeostasis, providing the necessary mineral to maintain skeletal health. Less understood are 1,25D's direct actions on bone cells, including its role in bone remodelling. In this context, it is intriguing that bone cells themselves are capable of synthesizing 1,25D by virtue of the activity of the CYP27B1 enzyme⁽¹⁾. We hypothesise that the local production of 1,25D within the osteoblast lineage serves specialized functions within the framework of bone remodelling. Moreover, we have evidence that the mechanisms that regulate Cyp27b1 gene expression in osteoblasts are specific to that lineage, and consider this key for understanding the physiological role of vitamin D activity within osteoblasts. Therefore we have adopted both in vitro and in vivo studies to investigate the regulation, as well as function, of Cyp27b1 expression within osteoblasts. We created a transgenic mouse model in which transcription of the human Cyp27b1 sequence is driven by the 3.6kb human osteocalcin promoter (OSCyp27b1) limiting the transgene expression to mature osteoblast lineage cells. In adult (20 wk) mice, BV/TV in the lumbar vertebra is 10.8% greater in OSCyp27b1 males versus wild-type littermates ($p < 0.05$, $n = 12$), and 10.1% greater in females ($p = 0.08$, $n = 15$), with similar increases in bone also observed in OSCyp27b1 femoral metaphyses. Histological analyses reveal no difference in TRAP+ osteoclast surface measures. In adult female OSCyp27b1 mice, the higher femoral BV/TV was correlated with bone formation rate ($R^2 = 0.67$, $p = 0.01$). To further pursue the effect of the OSCyp27b1 transgene on osteoblast function we have isolated osteoblasts from neonatal OSCyp27b1 calvaria. Differentiated cultures produced a mineralised extracellular matrix and expressed high levels of the human Cyp27b1 transgene, as well as osteocyte related genes such as DMP1 and SOST, suggesting that the transgene may have effects in osteocytes as well as osteoblasts. Transiently transfected deletion constructs of the CYP27B1 promoter-luciferase reporter in the osteocyte-like MLO-Y4 cells reveal an expression profile similar to that of osteoblasts⁽²⁾. Taken together, our data suggest that vitamin D metabolism within the osteoblast lineage is anabolic and is uniquely regulated.

1. Anderson PH, Atkins GJ 2008, Mol Aspects Med 29:397-406.

2. Turner AG et al, 2009, Mol Cell Endocrinol 311:55-61.

Disclosures: Andrew Turner, None.

FR0440

Parathyroid Hormone-related Protein (PTHrP) Potentiates Myeloid-Derived Suppressor Cells (MDSCs) within the Bone Marrow via Osteoblast-Derived Interleukin (IL)-6 and Vascular Endothelial Growth Factor (VEGF)-A. Serk In Park^{*1}, Amy Koh², Fabiana Soki³, Laurie McCauley³. ¹Vanderbilt University, USA, ²University of Michigan, USA, ³University of Michigan School of dentistry, USA

Bone is an essential partner for tumor progression, supplying a variety of cells critical for tumor establishment. Among bone marrow (BM)-derived cells, MDSCs, expressing CD11b and Gr1 surface markers, suppress the host immune response and infiltrate tumor tissue to promote tumor growth and angiogenesis. Much of this understanding comes from primary tumor interactions whereas regulation of MDSCs in the BM of tumor hosts remains unclear. Prostate cancer cell lines with altered levels of PTHrP were used to show that subcutaneous prostate cancer-derived PTHrP correlates with MDSC recruitment in tumor tissues and also with tumor microvessel density. MDSCs derived from the BM of mice harboring subcutaneous tumors highly expressing PTHrP and co-implanted with prostate cancer resulted in greater tumor growth and angiogenesis than MDSCs from low PTHrP tumors, suggesting PTHrP contributes to pre-metastatic microenvironment in the BM. The angiogenic effect was associated with MDSC-derived matrix metalloproteinase (MMP)-9. However, as MDSCs do not express receptors for PTHrP, subsequent studies elucidated the mechanism of MDSC activation. Osteoblasts were examined for their role in PTHrP-dependent MDSC activation. Conditioned media from saline- or PTHrP-treated primary calvarial osteoblasts were collected and added to CD11b⁺Gr1⁺ BM cells *ex vivo*, followed by quantitative PCR for *Mmp9* (a marker for MDSC activation). Additionally, mice were treated with recombinant PTHrP (1-34) 12 hours prior to flow cytometric analyses and sorting of CD11b⁺Gr1⁺ BM cells. PTHrP significantly increased *Mmp9* expression and activating phosphorylation of Src family kinases (SFKs) in MDSCs. Furthermore, CD11b⁺Gr1⁺ BM cells were isolated and treated with osteoblastic cytokines including receptor activator of nuclear factor κ B ligand (RANKL), IL-6, VEGF-A, and C-C chemokine ligand (CCL)-2. Interestingly, VEGF-A and IL-6 increased *Mmp9* expression, which was reversed by PP2, a pharmacological inhibitor of SFKs. There was no alteration in gene expression for other markers of MDSC activation including integrin β 1, CCL2, CXCR-2, or CXCR-4. In summary, tumor-derived PTHrP circulates and stimulates osteoblasts to release IL-6 and VEGF-A, contributing to activating phosphorylation of SFKs in MDSCs and subsequent expression of MMP-9. These data suggest that tumors positively regulate the bone marrow microenvironment via PTHrP expression to promote tumor angiogenesis and immune suppression.

Disclosures: Serk In Park, None.

FR0443

Thrombospondin-1 Regulates Bone Density in Healthy and Skeletal Metastatic States by Regulating Osteoclast-osteoblast Coupling. Sarah Amend^{*1}, Ozge Uluckan², Michelle Hurchla¹, Li Jia¹, William Frazier², Katherine Weilbaecher³. ¹Washington University in St. Louis, USA, ²Washington University in Saint Louis, USA, ³Washington University in St. Louis School of Medicine, USA

Thrombospondin-1 (TSP1) is a secreted ligand for 10 receptors including CD47. Under healthy remodeling, osteoclasts (OCs) and osteoblasts (OBs) are tightly regulated. In skeletal metastasis, however, tumor cells secrete factors that promote OC and OB activity, resulting in the release of growth factors that stimulate local tumor growth, leading to a vicious cycle of aberrant bone cell activation and tumor cell proliferation. We demonstrate that TSP1/CD47 ligation is essential for healthy OC/OB coupling and contributes to the vicious cycle of bone metastasis.

TSP1^{-/-} mice have 25% higher bone volume than wild type (WT) at 6 months. TSP1^{-/-} mice also show decreased serum CTX, indicative of decreased OC activity. TSP1^{-/-} OC formation and function are disrupted in culture, and OC formation is increased upon addition of CD47-binding peptide. Nitric oxide (NO) exerts a biphasic effect, with toxic effects at high and low concentrations. CD47^{-/-} mice have defective OCs rescued by inhibition of NO synthase (NOS). TSP1 antagonism in OC cultures causes 30-fold increased expression of iNOS. Pharmacological inhibition of NOS restores WT levels of serum CTX in TSP1^{-/-} mice.

TSP1^{-/-} mice also exhibit OB dysfunction. TSP1 is a component of the mineralized bone matrix. We show that OCs do not resorb TSP1^{-/-} bone normally compared to WT bone. Failure of OCs to resorb TSP1^{-/-} OB secreted matrix leads to an imbalance in remodeling, with normal OB-recruitment of OCs, but failure of the OCs to resorb the bone, leading to the TSP1^{-/-} osteopetrotic phenotype. TSP1 signaling in OC and OB coupling also plays a critical role in bone metastasis.

Contrary to their typical anti-tumor roles, TSP1 and CD47 are induced in bone metastatic cell line C42b compared to the parental non-metastatic LnCaP. We employed tumor models to uncover a paradoxical role for TSP1 in cancer progression in primary versus metastatic disease. Tumor-derived TSP1 promotes OC activity and bone cell derived TSP1 promotes tumor cell proliferation. These data indicate a role for both tumor- and host-derived TSP1 in bone metastatic tumor progression and osteolysis. These findings are especially important in light of research to develop TSP1 mimetics to treat cancer. Our data indicate that these mimetics may have detrimental effects on metastatic disease.

We show that TSP1 is a critical coupling factor, both to promote homeostatic OC/OB remodeling and to promote tumor growth and osteolysis in skeletal metastasis.

Disclosures: Sarah Amend, None.

FR0446

Inverse Biological Coupling Between the Bone-specific Transcription Factor RUNX2 and the Tumor Suppressor p53 Levels in Osteosarcoma. Hanna Taipaleenmaki*, Margaretha van der Deen, Ying Zhang, Jane Lian, Janet L. Stein, Gary Stein, Andre Van Wijnen. University of Massachusetts Medical School, USA

Osteosarcoma (OS) is the most common malignant bone tumor. RUNX2, a key regulator of osteoblast differentiation and suppressor of cell growth, is aberrantly expressed in OS. The latter suggests a context dependent function of RUNX2 as tumor suppressor or oncoprotein. We examined pathological roles of RUNX2 in OS and the mechanisms by which RUNX2 expression is deregulated to account for its tumor-related elevation. RUNX2 is expressed in OS tissue micro-arrays and positively correlates with increased staining of the proliferation marker Ki67, suggesting that RUNX2 may support osteosarcoma cell growth. Indeed, knockdown of RUNX2 inhibits cell growth in U2OS osteosarcoma cells. The frequency of RUNX2 elevation in OS (~50%) is comparable to the predisposing inactivation of tumor suppressor p53 in ~50-70% of osteosarcomas. Consistently, RUNX2 levels are elevated in the absence of p53 in distinct OS cell lines and diverse proliferating mesenchymal cells. Conversely, stabilization of p53 with the MDM2 inhibitor Nutlin-3 increases p53 protein expression, but drastically decreases RUNX2 protein levels. Thus, RUNX2 expression is inversely linked to loss of p53. The strong reduction of RUNX2 protein expression can only partially be explained by transcriptional control as indicated by the absence of p53 binding sites in the RUNX2 promoter, a less than 30% decline in RUNX2 gene promoter activity and a modest two-fold decrease in Runx2 mRNA levels after Nutlin-3 exposure. Therefore, we examined microRNA (miRNA) dependent post-transcriptional mechanisms. We monitored expression of validated miRNAs that directly target RUNX2 in human OS cells and mesenchymal progenitor cells. Elevated RUNX2 protein expression is directly linked to diminished expression of several RUNX2 targeting miRNAs, including the p53 dependent miR-34c which is the most strongly down-regulated RUNX2 targeting miRNA in OS. Ectopic expression of miR-34c markedly decreases RUNX2 protein levels, and 3'UTR reporter assays established RUNX2 as a direct target of miR-34c in OS cells. Importantly, stabilization of p53 with Nutlin-3 increases miR-34c expression while decreasing RUNX2 protein levels. We propose a novel RUNX2-p53-miRNA regulatory network that controls proliferation of osseous cells and is compromised in osteosarcoma.

Disclosures: Hanna Taipaleenmaki, None.

FR0447

Osteoclast Activation by IAP Antagonists Opposes their Potential Anti-cancer Effects and Enhances Bone Metastasis. Chang Yang*¹, Jennifer Davis², Lynne Collins³, Suwanna Vangveravong³, Robert Mach³, David Piwnicka-Worms³, Katherine Weilbaecher⁴, Roberta Faccio¹, Deborah Novack⁴. ¹Washington University in St Louis School of Medicine, USA, ²Washington University in St. Louis, USA, ³Washington University in St Louis, USA, ⁴Washington University in St. Louis School of Medicine, USA

IAP (inhibitor of apoptosis) proteins play a central role in many types of cancer, and IAP antagonists are in development as anti-cancer agents. Since IAP antagonists cause apoptosis in myeloid cells as well as tumor cells, we hypothesized that these agents might also kill osteoclasts, making the bone microenvironment less favorable for metastasis. In order to focus on the effect of these drugs on bone, we used the 4T1 mouse breast cancer line, resistant to IAP antagonist BV6 *in vitro*. BALB/c mice were treated with BV6 or vehicle weekly for 4 weeks, and 4T1 cells were injected into the tibia (IT) or left ventricle (LV) between the 3rd and 4th doses. A control set of mice received tumor cells subcutaneously (SQ). Remarkably, BV6 increased tumor growth in bone by 5.5-fold (IT) and 3.2-fold (LV) on day 10 after tumor inoculation. In contrast, there was no significant difference in the growth of SQ implanted tumor cells or in visceral tumor growth following LV injection, indicating that tumor-enhancing effects of BV6 are specific to bone. To further elucidate the effects of BV6 on bone, we treated tumor-naïve mice with BV6 for 4 weeks, and found that bone mass was decreased by 35%. Indices of both osteoclast and osteoblast activity were significantly increased, indicating high turnover osteoporosis. To determine whether osteoclasts were responsible for increased bone metastasis, we gave zoledronic acid (ZA) and BV6 prior to LV injection of 4T1 cells. In BV6-treated mice, ZA increased bone mass and decreased tumor burden in bone to the levels in mice receiving only vehicle. To expand our study to BV6-sensitive tumor cells, we inoculated human breast cancer MDA-231 cells into nude mice. BV6 strongly inhibited growth of SQ inoculated tumor cells, whereas MDA-231 cells were still able to grow in bone, indicating a site-specific reduction in anti-tumor efficacy. Other IAP antagonists, 52S and ML183, also enhanced osteoclastogenesis *in vitro* in both murine and human cells, suggesting universal osteoclast-activating effects among IAP antagonists. Mechanistically, all 3 IAP antagonists tested activate alternative NF- κ B through NIK, and NIK-deficient mice were completely resistant to BV6-induced bone loss. Thus, IAP antagonists induce high turnover osteoporosis via the osteoclast, making the bone

microenvironment favorable for metastasis. Anti-resorptive agents will likely prevent osteoclast activation and preserve the anti-tumor efficacy of IAP antagonists.

Disclosures: Chang Yang, None.

FR0448

Parathyroid Hormone-related Peptide (PTHrP) blockade Inhibits Tumor Progression in a Model of Human Melanoma. Dao Chao Huang*¹, Xian Fang Yang², Anne Camirand¹, Richard Kremer¹. ¹McGill University, Royal Victoria Hospital, Canada, ²McGill University Health Center, Canada

Parathyroid hormone-related peptide (PTHrP) is crucial to breast tumor invasion and metastasis but its role in melanoma is still obscure. We studied *in vitro* and *in vivo* effects of PTHrP in human A375 amelanotic melanoma cells by inactivating both alleles of the human *Pthrp* gene by homologous recombination, creating knock-out (KO) and wild-type (WT) A375 cells which were examined for growth, invasion and motility changes. Green fluorescent protein (GFP)-transduced KO A375 and WT A375 cells were implanted into the left cardiac ventricle (LCV) of nude mice and metastases investigated by GF imaging. A monoclonal antibody (mAb) against the N-terminus of PTHrP was used to treat mice injected (LCV) with WT A375 cells. Tumor cells were also injected s.c. and tumor growth compared between mice treated with the mAb or vehicle s.c. 3 times/wk (up to 4 wks). Compared to WT controls, homozygous KO clones (PTHrP-null), had a less transformed and less invasive phenotype, with decreased growth rate and motility, decreased anchorage-independent growth, rounder morphology and significant inhibition of Matrigel invasion. Matrix metalloproteinase-9, actin polymerization, and focal adhesion kinase expression and phosphorylation were significantly reduced in PTHrP-null cells. The more transformed and invasive phenotype was partially restored by addition of conditioned medium from WT cells. In mice sacrificed at timed intervals, disseminated GFP-expressing tumor cells were observed in liver and lungs. Osteolytic bone metastases were detected by high sensitivity X-ray analysis, and whole body scanning with GFP detection. Bone staining and osteoclast-specific TRAP staining showed that *Pthrp* blockade strongly decreased osteoclast numbers. Dissemination of GFP-labeled tumor cells was greatly reduced in mice injected with KO A375 vs controls. Total number of metastases and % of animals with metastases in each organ analyzed were markedly reduced in nude mice with KO A375 compared to WT A375 cells. Kaplan-Meier analysis showed significant survival benefit in nude mice injected with KO A375 or WT A375 cells and treated with the anti-PTHrP mAb, compared to animals injected with WT A375 cells alone or with vehicle. Overall, we provide direct evidence that PTHrP plays a major role in human melanoma tumor invasion and metastasis, and that agents aimed at suppressing PTHrP may impair melanoma progression.

Disclosures: Dao Chao Huang, None.

FR0450

The Cancer Stem Cell Marker CD44 Promotes Bone Metastasis of Breast Cancer by Enhancing Tumorigenicity, Cell Motility, and Matrix Production. Toru Hiraga*¹, Susumu Ito², Hiroaki Nakamura¹. ¹Matsumoto Dental University, Japan, ²Shinshu University, Japan

CD44, an adhesion molecule that binds to extracellular matrix, primarily to hyaluronan (HA), has been implicated in cancer cell migration, invasion, and metastasis. CD44 has also recently been recognized as a marker for stem cells of several types of cancer, including breast cancer. We found that CD44 is highly expressed in a number of cancer cell lines of different origin that preferentially metastasize to bone in a mouse model. However, the roles of CD44 in the development of bone metastasis still remain unclear. To explore this, we established the MDA-MB-231 human breast cancer cells stably expressing short hairpin RNA against CD44 (MDA/shCD44). Although there was no change in cell proliferation in monolayer culture, tumorsphere formation in suspension culture was reduced in MDA/shCD44 compared with the control cells (MDA/shLuc). Cell motility and invasion of MDA/shCD44 determined by wound healing assay and matrigel invasion assay were also significantly suppressed. Furthermore, tumorigenicity in the orthotopic site and the development of bone metastasis following intracardiac cell inoculation in nude mice were markedly decreased in MDA/shCD44. Microarray analysis revealed that the expression of HA synthase 2 (HAS2) was down-regulated by CD44 knockdown, which was confirmed by real-time RT-PCR analysis. HASs are the enzymes responsible for HA synthesis and HAS2 is the most abundantly expressed isoform in MDA-MB-231 cells. Immunohistochemical examination showed that, in the bone metastases of MDA/shLuc, HA was more densely localized in the lesions compared with surrounding bone marrow tissues and was frequently co-localized with CD44 expressed by cancer cells. In contrast, HA was sparsely distributed in the metastases of MDA/shCD44. To further study the role of HA in bone metastasis, the effects of 4-methylumbelliferone (4-MU), an inhibitor of HA synthesis, were then examined. 4-MU decreased mRNA expression of CD44 and HAS2 in MDA-MB-231 cells *in vitro* and suppressed osteoclast-like cell formation in bone marrow cultures in a dose-dependent manner. Moreover, 4-MU significantly inhibited bone metastases of MDA-MB-231 cells with reduced number of osteoclasts. These results suggest that CD44 expression in cancer cells contributes to promote bone metastasis by enhancing tumorigenicity, cell motility and invasion, and HA production. Our results also suggest the possible involvement of CD44-expressing cancer stem cells in the development of bone metastasis.

Disclosures: Toru Hiraga, None.

SA0001

See Friday Plenary Number FR0001.

SA0002

See Friday Plenary Number FR0002.

SA0003**Dietary Restriction Improves Age-related Decline of Trace Minerals in Bone.**

Keiji Kobayashi^{*1}, Hidetoshi Nojiri², Tashihiko Toda¹, Yoshitomo Saita², Daichi Morikawa¹, Masato Koike¹, Yusuke Kozai³, Isamu Kashima³, Kazuya Yoshida⁴, Mitsuru Segawa⁴, Kazuo Kaneko², Takahiko Shimizu¹.

¹Department of Advanced Aging Medicine, Chiba University Graduate School of Medicine, Japan, ²Department of Orthopaedics, Juntendo University School of Medicine, Japan, ³Division of Radiology, Department of Maxillofacial Diagnostic Science, Kanagawa Dental College, Japan, ⁴Research Laboratory, La Belle Vie Incorporated, Japan

Dietary restriction (DR) extends the lifespan of animals, but beneficial or deleterious effects of DR on bone tissue have not been fully elucidated. In this study, we investigated the bone phenotypes such as bone mass, strength and trace mineral contents in aged and DR rats.

F344 male rats were used at 4 months (young), 12 months (middle) and 25 months (aged) of age. DR male rats were restricted food by 60% until 25 months of age. We analyzed bone density and structure of femur using pQCT and 3D micro-CT, respectively. Bone strength was measured by three-point bending test. Trace mineral content in bone tissue was measured by inductively coupled plasma mass spectrometry (ICP-MS). Serum oxidative stress marker, d-ROM, was measured using a FRAS4 system in the blood

DR rats extended the mean lifespan by 124.8% and reduced body weight by 61% compared with those of *ad libitum* rats. DR treatment also normalized serum d-ROM values in aged rats, indicating that DR treatment showed anti-aging effects on aged rats. pQCT analysis revealed that DR rats showed age-related changes of cortical and trabecular bone densities as like aged rats. Micro-CT analysis also indicated that DR treatment did not normalized age-related bone atrophy of femur. In bone strength test, we did not observe the improvement of elastic modulus and maximum bending stress in aged bone by DR. These results indicated that DR did not show beneficial or deleterious effects in age-related changes of bone mass and strength. Next, we measured mineral contents in bone tissues by ICP-MS. We found that most of bone minerals were significantly decreased in an age-dependent manner. Interestingly, DR treatment significantly increased trace mineral contents, including (zinc, selenium, barium, nickel, cobalt, chromium, lead, vanadium). These results suggested that sustained trace minerals in aged bone by DR might regulate bone quality in aging.

Disclosures: Keiji Kobayashi, None.

SA0004

See Friday Plenary Number FR0004.

SA0005

See Friday Plenary Number FR0005.

SA0006

See Friday Plenary Number FR0006.

SA0007

The Effects of Simulated Microgravity on Articular Cartilage. Liliana Mellor^{*1}, Julia Oxford¹, Warren Knudson². ¹Boise State University, USA, ²East Carolina University, USA

It has been shown that astronauts experience bone density loss after space flight resembling osteoporotic conditions due to prolonged exposure to microgravity. Although bone density loss in space is a growing field of interest in space related biomedical research, little is known about the effects of microgravity on the adjacent articular cartilage. Articular cartilage is constantly exposed to mechanical forces produced by daily activities. Similar to bone, cartilage is a type of connective tissue that requires a balance between synthesis and degradation of extracellular matrix components to maintain tissue homeostasis; changes in this balance leads to cartilage degradation. Unlike bone tissue, cartilage lacks innervation, blood supply and cell-cell contact, and has a very limited regeneration capacity. Proper communication between individual chondrocytes and the extracellular matrix is crucial to maintain cartilage

homeostasis, and disruption in cell-matrix interactions can trigger cartilage degradation. Our hypothesis is that cartilage homeostasis can be disrupted by lack of gravity during space missions, resulting in early stages of arthritis. Our proposed research addresses the molecular mechanisms involved in articular cartilage loss after exposure to microgravity, which can result in impaired mobility and painful joints. We use two chondrocyte cell lines widely used in arthritis cell research, and expose them to a modeled simulated microgravity environment using a rotating wall vessel (RWV) bioreactor. Preliminary data of chondrocytes exposed to modeled microgravity for 7 days show changes in the actin cytoskeleton morphology when compared to control cells cultured under normal gravitational forces. In addition, up-regulation of IL-8, a biomarker found in sera samples of dogs with induced and natural arthritis, was also up-regulated in cells exposed to simulated microgravity. Additional genes as well as protein expression of receptors associated with extracellular matrix interactions such as CD44 will be evaluated. A better understanding of the molecular signaling pathways involved in cartilage degradation, will not only help prevent astronauts developing osteoarthritis from exposure to microgravity, but will also help us prevent further degradation in patients experiencing early stages of arthritis on Earth.

Disclosures: Liliana Mellor, None.

SA0008

See Friday Plenary Number FR0008.

SA0009

Bone Loss, not Cartilage Loss, Is Linked to Reduced Muscle Function. Shu Sun^{*1}, Anders Fabricius Nedergaard², Morten Karsdal¹, Kim Henriksen¹.

¹Nordic Bioscience A/S, Denmark, ²Nordic Bioscience, Herlev Hovedgade 207, Denmark

Introduction: Muscle loss is an important clinical problem usually manifesting as a comorbidity to metabolic or inflammatory disease or simply as a consequence of age and inadequate muscle stimulation. In both cases it leads to loss of functional capacity and operational independence and is a strong predictor of mortality and morbidity. Loss of muscle mass is associated with parallel losses of other connective tissues, e.g. bone, tendon and cartilage.

The aim of the present study was to characterize changes in different connective tissue compartments in an animal model using Botulinum toxin (botox)-induced hindlimb immobilization, and serological biomarkers.

Method: Botox was injected into the right hind limb of the Wistar rats in the Botox group. Serum were collected at the baseline and every week after the injection until the end of the study in week 4. Bone turnover biomarkers: Alkaline phosphatases (ALP), Tartrate-resistant acid phosphatase (TRACP), and C-terminal cross-linking telopeptide of collagen type I (CTX-I) were measured. In addition, C2M (MMP-cleaved Collagen II fragment, marker of cartilage degradation), C3M (MMP-cleaved Collagen III fragment, marker of tissue ECM degradation), C6M (MMP-cleaved Collagen VI fragment, marker of muscle degradation), PIIINP (Collagen III N-terminal propeptide, marker of ECM synthesis) and PVINP (Collagen VI N-terminal propeptide, marker of muscle synthesis) were measured.

Results: Botox injection resulted in increases in C6M at week 1 and 2 (p=0.05), after which it leveled off. No changes in PVINP were observed. Furthermore, CTX-I and TRACP were elevated at week 2 (p=0.03), but ALP showed a trend towards a reduction in the botox group. These effects appeared to be slightly delayed compared to the changes in muscle degradation. No changes in cartilage degradation, or connective tissue turnover C3M and P3NP no significant changes were observed.

Conclusions: In this study we showed that increasing muscle loss results in rapidly increased bone loss, through induction of bone resorption and a reduction in bone formation; however, within the short time frame no changes in cartilage degradation was observed. These data underscore that in the Botox immobilization model, the loss of muscle and bone tissue and function are quantitatively and temporally related.

Disclosures: Shu Sun, None.

SA0010

Characterising Sex- and Age-related Differences in Musculoskeletal Phenotype in Sub-Saharan Africa. Kate Ward^{*1}, Yankuba Sawo², Landing Jarjou², Ann Prentice¹. ¹MRC Human Nutrition Research, United Kingdom, ²MRC Keneba, Gambia

Low calcium intake, low BMD and high PTH are characteristic in The Gambia yet documented fragility fractures in older people are low. We reported similar or increased bone loss in Gambian compared to UK females. This cross-sectional study aimed to characterise sex differences and associations between age and bone mass and geometry, muscle area and density, using peripheral QCT.

Males (M) and females (F) aged ≥ 40 years residing in rural areas of The Gambia were recruited stratified by 5 year age-band. Outcome measures were: 4% tibia(T4)-total(tot) and trabecular(trab) BMD, total area(totA); 38% tibia(T38)-bone mineral content (BMC), cortical(cort) BMD, totA, medullary area(medA), stress-strain index(SSI); 66% tibia (T66)- muscle area(muA), muscle density(muD). The occurrence of peripheral vascular calcification (PVcal) was documented. Independent samples t-tests tested sex differences in anthropometry, ² tested differences in PVcal between M/F and age group. Univariate regression tested the relationship between age and bone/

muscle in M and F. ANCOVA tested sex differences after adjustment for age, height and weight. Sex effects are presented as % mean difference [95% CI].

Two-hundred and fifty-five individuals (120M) were recruited, mean(SD) (p<0.05 for all) age M 61.1(13.2)yrs, F 59.4(12.1)yrs, height M 1.7(0.1)m, F 1.6 (0.1)m; weight M 60.9(10.2)kg, F 56.3(10.5)kg; BMI M 21.0(3.0)kg/m², F 22.2(3.5) kg/m². Pvc occurred in 18% of scans; M/F² 0.2 NS; age gp² 173.5 p<0.001.

Age was negatively associated (R² 9-46%, p<0.001-0.06) with: T4 totBMD, trabBMD; T38 BMC,SSI; T66 muA and muD in M and F. MedA was positively, and cortBMD negatively, associated with age at T38 in F. Tota was negatively associated with age in M at T38.

M had higher tot(18%[13,22]) and trab(13%[7,20]) BMD than F at T4. At T38 M had larger bones (13%[10,16]) with higher BMC (30%[24,35]), BMD (3%[2,4]) and SSI (26%[21,30]); medA was not significantly different to F (-5%[-1,0]). At T66 muA (25%[11,19]), muD (3%[2,4]) were greater.

These data provide evidence for age-related differences in bone and muscle strength in M and F. Higher strength in M is through smaller medA and higher cortBMD, indicating thicker cortices and greater mass. Higher incidence of Pvc compared to other populations may reflect altered calcium/phosphate metabolism in The Gambia. Further exploration of musculoskeletal phenotype and the contribution of lifestyle are required.

Disclosures: Kate Ward, None.

SA0011

Early Frailty in Postmenopausal Women with Human Immunodeficiency Virus (HIV) Infection. Polly Young¹, Elizabeth Shane², Chiyuan Zhang¹, David Ferris³, Matthew Scherer⁴, Binsheng Zhao⁵, Ivelisse Colon⁶, Donald McMahon², Thuy-Tien Dam⁵, Michael Yin¹. ¹Columbia University, USA, ²Columbia University College of Physicians & Surgeons, USA, ³St Lukes-Roosevelt Hospital, USA, ⁴Columbia University, USA, ⁵Columbia University, USA, ⁶Columbia University Medical Center, USA

Aging often manifests as frailty, a syndrome predictive of falls and fractures. Studies suggest frailty occurs at a younger age in HIV+ men, but data from postmenopausal women with HIV, a group at high risk for osteoporosis and fracture, are lacking. To assess frailty prevalence, we measured frailty phenotype in a subset of 36 HIV+ and 28 HIV- postmenopausal women in a cohort study of bone metabolism. Subjects meeting 3+ criteria were classified as frail: weakness by grip strength, slow walk speed, low physical activity, unintentional weight loss, self-reported exhaustion. Appendicular lean mass was measured by dual xray absorptiometry. HIV+ women were younger (56+1 vs 59+1, p=0.03) and tended to weigh less (71+3 vs 79+3kg, p=0.08) than HIV- women, but had similar ethnicity (60% Hispanic, 40% African-American). Unadjusted results for frailty components are presented (Table). After adjustment for age and BMI, grip strength was lower in HIV+ women (p=0.015). Appendicular lean mass was similar in HIV+ and HIV- (19.4+1 vs 19.8+1kg, p=0.71). In conclusion, despite younger age, prevalence of frailty tended to be higher among HIV+ postmenopausal women than HIV- controls. Adjusted grip strength was lower in HIV+ than HIV- women despite similar appendicular mass. More challenging strength and performance measures may be necessary to detect differences in HIV+ and HIV- women. As HIV+ women age, deficits in strength may translate into frailty, falls and fractures.

| Frailty Measures | HIV+ (N=36) | HIV- (N=28) | Unadjusted p-value |
|-------------------------------|--------------|--------------|--------------------|
| Grip Strength (kg) | 22.3 +/- 3.1 | 25.2 +/- 3.5 | 0.12 |
| Walk Speed (seconds) | 5.9 +/- 0.4 | 5.9 +/- 0.8 | 0.80 |
| Physical Activity (kcal/week) | 2549 +/- 381 | 3831 +/- 501 | 0.04 |
| Weight Loss | 18% | 4% | 0.03 |
| Exhaustion | 8 (22%) | 2 (7%) | 0.03 |
| Pre-Frail (1-2 criteria) | 17 (47%) | 14 (50%) | 0.12 |
| Frail (3+ criteria) | 4 (11%) | 0 (0%) | 0.12 |

Frailty Data Table

Disclosures: Polly Young, None.

SA0012

Effects of 3 Monthly Vitamin D Supplementation Strategies among Fallers age 70 Years and Older: a Double-blind Randomized Controlled Trial. Heike Bischoff-Ferrari¹, Bess Dawson-Hughes², John E Orav³, Walter Willett⁴, Hannes Staehelin⁵, Eduard Sidelnikov⁶, Daniel Grob⁷, Robert Theiler⁸, Andreas Egli Linder⁹. ¹University of Zurich, Switzerland, ²Tufts University, USA, ³Dept. of Biostatistics, Harvard School of Public Health, USA, ⁴Dept. of Nutrition, Harvard School of Public Health, USA, ⁵Dept. of Geriatrics, University of Basel, Switzerland, ⁶University of Zurich, Switzerland, ⁷Dept. of Geriatrics, City Hospital Waid, Switzerland, ⁸Stadtspital Triemli, Switzerland, ⁹Centre on Ageing & Mobility, Switzerland

Methods: We randomized 200 seniors who had a fall in the year prior to enrollment to 3 groups with monthly oral vitamin D supplementation: (1) 24'000 IU D3 = control, (2) 60'000 IU D3, (3) 24'000 IU D3 plus 300 µg 25(OH)D (NCT01017354). Clinical visits were at baseline, 6 and 12 months, with additional monthly phone interviews to assess incident falls. The primary endpoint was the probability of reaching the 25(OH)D threshold of 30 ng/ml and the prevention of functional decline measured by the short physical performance test battery. The secondary endpoint was the risk of falling.

Results: Baseline 25(OH)D serum concentrations in 200 senior fallers (mean age = 78; 67% women) did not differ by group: mean was 18.5 ng/ml. The adjusted (age, gender, BMI, visit, baseline level) increment in 25(OH)D increase and probability of reaching the 25(OH)D threshold of 30 ng/ml in groups 1 to 3 were: (1) 10.0 ng/ml / 28%, (2) 15.3 ng/ml / 68%, (3) 25.4 ng/ml / 89% at 6 months, and (1) 9.9 ng/ml / 39%, (2) 18.3 ng/ml / 81%, (3) 25.5 ng/ml / 89% at 12 month, with significant differences between groups (2) and (3) and compared to group (1). The adjusted probability of maintained or improved function at 6 and 12 months did not differ between groups and was about 80%. In the 12 month of treatment 121 participants fell (60.5%) and reported 275 falls (141 in the first and 134 in the second 6 months of observation). The rate of falls differed by treatment group, with groups (2) and (3) having a greater risk of falling compared to group (1). In the multivariate Poisson regression model group (2) had a 58% (95% CI: 14 to 102%), and group (3) had a 45% increased rate of falls (95% CI: -2 to +92%) compared to group 1. The same pattern occurred if we analyzed fallers. Based on a Lowess plot, both low and very high achieved 25(OH)D levels at 12 month were associated with an increased risk of falling, the nadir being reached at about 30 ng/ml.

Conclusion: Our trial provides evidence that higher doses of vitamin D3 or a combination with 25(OH)D supplementation are needed to shift senior fallers to a threshold of 30 ng/ml 25(OH)D. Notably, the probability of maintained or improved function was similar for 24'000 IU vitamin D3 per month (800 IU / day) compared to the two higher dose groups. Further, fall risk may be increased with higher dose vitamin D, which in our analysis could not be explained by a toxic effect on any of the muscle / function endpoints.

Disclosures: Heike Bischoff-Ferrari, None.

This study received funding from: Funding sources: Swiss National Foundations, Velux Foundation, independent funding support by MDS, WILD, and DSM Nutritional Products

SA0013

See Friday Plenary Number FR0013.

SA0014

See Friday Plenary Number FR0014.

SA0015

Comparison of Bone Metabolism among RA Population on Chronic DMARD Therapy and Those on anti TNF Blocker, Treatment Naive RA Patients and Normal Population. Mie Jin Lim¹, Won Park¹, Seong Ryoul Kwon², Kyung Hee Jung², Kwoon Joo², Min Jung Son². ¹Inha University Hospital, South Korea, ²Inha University Hospital, South Korea

Introduction: Bone metabolism is disturbed in rheumatoid arthritis (RA) patients. Effects of oral disease modifying antirheumatic drug (DMARD) and anti tumor necrosis factor (TNF) blockers on bone metabolism are still unknown.

Objective: We sought to compare the bone metabolism among RA population on chronic DMARD, anti TNF treatment, age and sex matched naive RA patients and normal control.

Method: Thirty-three seropositive RA patients (5 male, 28 female) were enrolled. More than 90% of patients had been receiving methotrexate with or without other DMARD for more than 6 months. Etanercept was administered, twice a week. Venous blood was drawn at baseline on DMARD therapy and 12-16 weeks after etanercept use, respectively. Treatment naive RA patients who did not receive any DMARD treatment prior to the study were recruited along with normal control. Bone

metabolism was assessed using bone specific alkaline phosphatase (BSAP) and sclerostin for bone formation and c-telopeptide (CTX) for bone resorption.

Statistical differences between two groups were examined by independent samples T test. As RA on DMARD group and RA on TNF blocker group came from same population at different time point, their difference was assessed using paired samples T test. A p value of equal and less than 0.05 was denoted statistically significant.

Results: RA on DMARD group showed significantly lower level of BSAP compared to naïve RA population (p=0.044). Both BSAP and sclerostin increased after etanercept treatment, but was slightly significant only for sclerostin (p = 0.055). Serum CTX level was markedly lower in DMARD group than naïve RA population (p=0.008). It also increased after etanercept treatment which was significant (p = 0.026). Naïve RA population showed highest CTX level among all four groups.

Conclusion: In general, bone metabolism markers in RA on DMARD group showed lower serum level compared to naïve RA population which tended to increase after etanercept treatment. The normal control showed highest level of sclerostin and BSAP among all groups and those trends suggest bone metabolism might be depressed in RA patients. The bone metabolism was even more depressed after DMARD treatment and it recovered by anti TNF treatment.

| | Normal Control | Naïve RA Population | RA on DMARD group | RA on TNF blocker group |
|--|----------------|---------------------|-------------------|-------------------------|
| Patients receiving Gluco corticoid /Methotrexate | 0% / 0% | 15% / 0% | 97% / 91% | 97% / 91% |
| Prednisolone Dose (mg) | 0 | 0 ± 1.63 | 6.25 ± 2.52 | 5 ± 2.47 |
| BSAP (U/L) | 28.85 ± 6.77 | 27.7 ± 10.58 | 23.25 ± 8.02 | 24.35 ± 16.81 |
| Sclerostin (pg/mL) | 2.23 ± 2.51 | 1.56 ± 2.07 | 0.95 ± 1.75 | 1.44 ± 2.79 |
| CTX (ng/mL) | 0.38 ± 0.21 | 0.47 ± 0.68 | 0.26 ± 0.15 | 0.33 ± 0.21 |

Data are expressed as median ± standard deviation

Table 1

Disclosures: *Mie Jin Lim, None.*

SA0016

Early Increased Subchondral Bone Wnt/ β -catenin Signaling in a Murine Destabilization Osteoarthritis Model Followed by Accompanying Increased Signaling in Articular Cartilage. Danese Joiner¹, Kennen Less², Bart Williams¹. ¹Van Andel Research Institute, USA, ²Van Andel Research Institute, USA

Wnt/ β -catenin signaling is a key regulator of bone and cartilage development and homeostasis, and the degree of signaling may represent a pathological mechanism for osteoarthritis (OA) development (Zhu, M. *et al.* Arthritis Rheum. 2008; Zhu, M. *et al.* JBMR 2009). During OA progression, reduced articular cartilage and subchondral bone integrity occurs and is likely influenced by adaptive responses to altered mechanical loading (Thambyah, A. *et al.* Osteoarthr. Cartilage 2007). We hypothesized that temporal and spatial differences in Wnt/ β -catenin signaling are involved and examined articular cartilage and subchondral bone during arthritis progression post injury in mice. Ligament and meniscus transections were performed on the right knee (RK) of 8-week old WT mice (n=24). The left knees (LK) served as an untouched control. After 28 and 60 days, animals were euthanized, dissected knees micro CT scanned (Skyscan, Germany) and reconstructed onto 10 micron voxels. Knees were fixed, decalcified, paraffin embedded and sagittal sectioned at 5 um for pentachrome staining and β -catenin IHC. Knee samples were aseptically harvested from animals, homogenized, and RNA extracted with an RNeasy Mini Kit (Qiagen, Valencia, CA). Relative mRNA transcript levels of Wnt receptors and target genes were measured by RT-PCR and t-test statistics applied. Pentachrome stains showed reduced articular cartilage proteoglycan content in surgery knees at both time points (blue) and structural disorganization (Fig. 1A). Osteophytes and nuclear β -catenin (brown) in the articular cartilage and subchondral bone were present in transected knees at day 60 (Figs. 1B, 1C, 1D). Cytoplasmic β -catenin was present in subchondral bone 28 days post surgery and nuclear β -catenin, however to a lesser extent than day 60 (Figure 1D). Fold increases in Wnt receptors and target genes expressed for the RK relative to the LK occurred at day 60 and Lrp6 and cyclin D1 values were significant compared to day 28 (Fig. 2). Increased relative c-jun occurred at day 28; however was less than the day 60 value (Fig. 2). Wnt/ β -catenin signaling increased with OA progression post injury in mice and was observed early in subchondral bone and later in both subchondral bone and articular cartilage. Tissue specific therapeutics targeting regional difference in Wnt/ β -catenin signaling during injury induced OA and delivery timing could improve disease treatment.

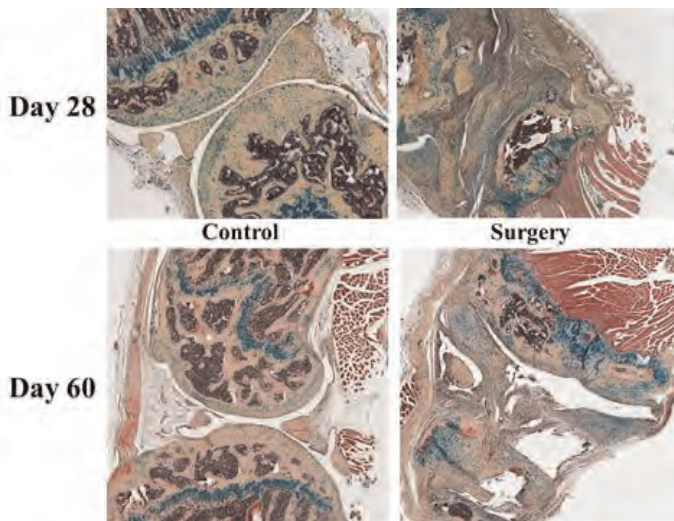


Figure 1a

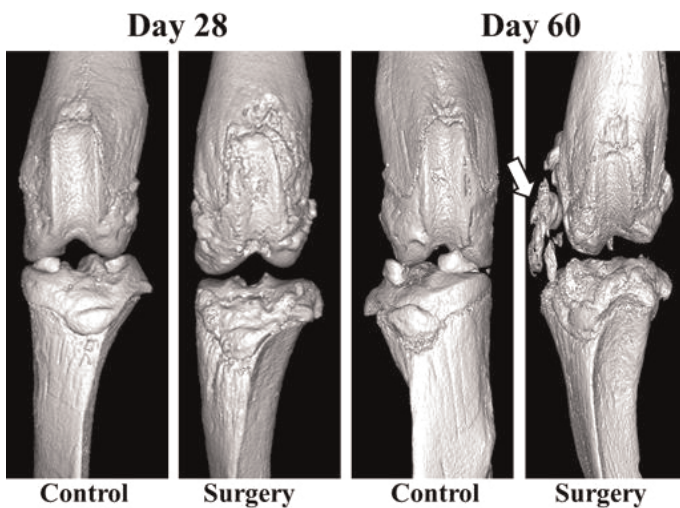


Figure 1b

Articular Cartilage

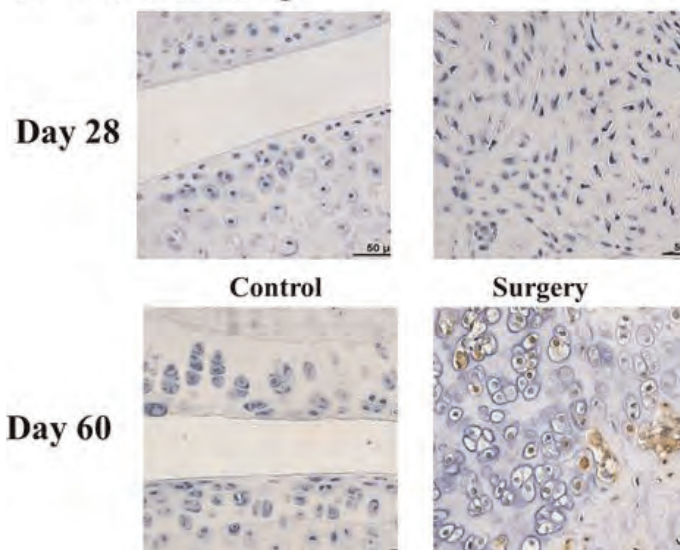


Figure 1c

Subchondral Bone

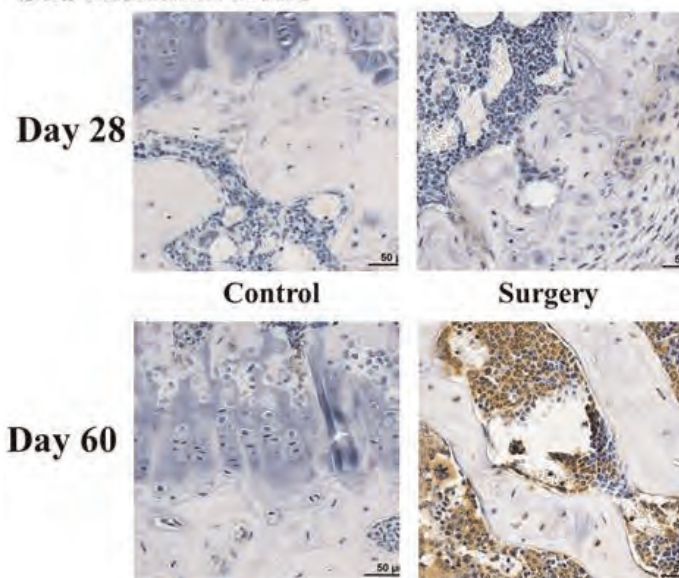


Figure 1d

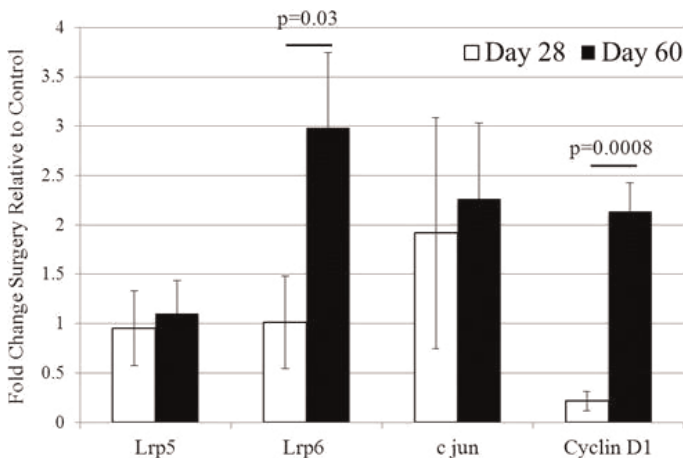


Figure 2

Disclosures: Danese Joiner, None.

SA0017

Inhibition of TGF β signaling in Nestin⁺ Stem Cells Prevents Onset of Osteoarthritis. Gehua Zhen¹, Chunyi Wen², Simon Mears³, Frederic Askin³, Xiaofeng Jia³, Frank Frassica³, Weizhong Chang⁴, Janet Crane⁴, Jie Yao⁵, Tariq Nayfeh³, Carl Johnson³, Dmitri Artemov³, Andrew Cosgarea³, John Carrino³, Mei Wan⁶, William Lu⁷, Xu Cao⁴. ¹The Johns Hopkins Hospital, USA, ²Li Ka Shing Faculty of Medicine, University of Hong Kong, Hong Kong, ³Johns Hopkins University, USA, ⁴Johns Hopkins University, USA, ⁵Hong Kong University, China, ⁶Johns Hopkins University School of Medicine, USA, ⁷The University of Hong Kong, Hong Kong

Osteoarthritis (OA) is a highly prevalent and debilitating joint disorder. There is currently no effective therapy for OA due to limited understanding of its pathogenesis. Using OA anterior cruciate ligament transection (ACLT) animal model, we demonstrate structural and histological changes indicative of uncoupled bone formation. Continuously increased total subchondral bone tissue volume with significantly altered micro-architecture was observed by μ CT scanning in ACLT mice. Histological analysis revealed that phosphorylated pSmad2/3⁺ cell number increased in a similar pattern as TRAP⁺ osteoclasts, indicating activation of TGF β 1 during continuous osteoclastic bone resorption after ACLT. Parallel to osteoid distribution, nestin⁺ stem cells and osterix⁺ osteoprogenitors were clustered in bone marrow 30 days post surgery, suggesting osteoblastic differentiation in bone marrow cavities. This phenomenon was correlated with the occurrence of intense bone marrow lesions on MRI. Significant proteoglycan loss was observed 60 days post ACLT, which is much later than when the subchondral bone micro-architectural changes began. Injection of T β R1 inhibitor (1mg/kg for 1 month) improved subchondral bone

structure and attenuated articular cartilage degeneration. Furthermore, local administration of TGF β 1 antibody in the subchondral bone reduced articular cartilage degeneration in the rat ACLT model.

To further validate the role of nestin⁺ cells in the onset of OA in the microenvironment of high level TGF β , we knocked out TGF β type II receptor (T β RII) specifically in nestin⁺ stem cells by inducible nestin-CreER after ACLT. The microarchitecture of T β RII knockout mice was significantly improved relative to WT mice once nestin⁺ stem cells no longer respond to TGF β post ACLT. Importantly, proteoglycan loss, advances of calcified cartilage zone, MMP13 and type X collagen expression in chondrocytes were prevented in ACLT T β RII knockout mice. Interestingly, the thickness of calcified cartilage zone in sham-operated T β RII knockout mice increased, suggesting a critical role of nestin⁺ stem cells in maintenance of the osteochondral junction at regular concentration of TGF β 1. This study demonstrates that high levels of active TGF β 1 in the subchondral bone contribute to the pathological changes seen at the onset of mechanically-induced OA potentially by affecting nestin⁺ stem cells. Inhibition of TGF β 1 prevented OA progression and may be a target for therapy for early stages of OA.

Disclosures: Gehua Zhen, None.

SA0018

Levels and Localization of Vitamin K2 in Subchondral Bone in Osteoarthritis Knee Joints. Yoshinori Ishii¹, Hideo Noguchi², Mitsuhiro Takeda³, Junko Sato², Noriaki Yamamoto⁴, Hirovuki Wakabayashi⁵, Junkichi Kanda⁶. ¹Ishii Orthopaedic & Rehabilitation Clinic, Japan, ²Ishii Orthopaedic & Rehabilitation Clinic, Japan, ³Ishii Orthopaedic & Rehabilitation Clinic, Japan, ⁴Niigata rehabilitation hospital, Japan, ⁵Niigata University of Pharmacy & Applied Life Sciences, Japan, ⁶Niigata University of Pharmacy & Applied Life Sciences, Japan

Objectives: The purpose of this study was to evaluate the distribution of vitamin K2 in harvested bones obtained during total knee arthroplasty in knee osteoarthritis (OA) patients. We also analyzed their characteristics of levels of vitamin K2. Our primary hypothesis was that the vitamin K2 localization would differ in subchondral bones showing different stages of OA. We also hypothesized that vitamin K2 might affect the turnover of subchondral bone in OA knees.

Methods: High-performance liquid chromatography was used to measure vitamin K2 in harvested bones obtained during 58 total knee arthroplasty procedures. Vitamin K2 levels were analyzed in the medial (FM) and lateral (FL) femoral condyles and in the medial (TM) and lateral (TL) tibial condyles. The vitamin K2 value is expressed using the median (25th percentile, 75th percentile).

Results: The median vitamin K2 values in the condyles were as follows (expressed as ng per gram of dry bone tissue): FL 87.1 (50.6, 136.4), FM 32.4 (19.8, 62.5), TM 22.7 (15.0, 52.6), and TL 50.1 (32.7, 87.7). There was significantly more vitamin K2 in the lateral femoral and tibial condyles than in the corresponding medial condyles (FL vs. FM, p<0.0001; TL vs. TM, p<0.0001). There was significantly more vitamin K2 in the FL than in the TL (p=0.003), and the FM vitamin K2 levels were higher than those of the TM, although this was not significant (p=0.212). There were no significant differences in vitamin K2 levels in men vs. women nor was there a significant correlation with age.

Conclusions: This study suggested that vitamin K2 might affect bone turnover since medial condyles showing advanced OA had lower vitamin K2 levels, while lateral condyles showing less advanced OA contained more vitamin K2. Gender and age were not correlated with vitamin K2 localization. All cases had Grade IV OA, and this study suggested that OA grade might be important in controlling the vitamin K2 levels in human bones. Animal experiments show that the vitamin K2 (MK-4) level in bone increases in a dose-dependent way, so future prospective studies should determine whether a diet rich in vitamin K or the optimal dose and preferred form vitamin K2 could be part of an effective OA treatment strategy.

Disclosures: Yoshinori Ishii, None.

SA0019

Mineral Homeostasis and Body Composition Measures in Adults with Rotator Cuff Arthropathy. Lisa Gao¹, Julie Glowacki², Lawrence Higgins¹, Meryl Leboff². ¹Brigham & Women's Hospital, USA, ²Brigham & Women's Hospital, USA

Rotator cuff arthropathy (RCA) increases with age and is associated with rotator cuff tears, cuff muscle atrophy, radiographic osteopenia, and a "soft" quality of the bone noted at surgery. We recently found increased osteoid in subjects with RCA compared to those with shoulder osteoarthritis (OA), without differences in current 25-hydroxyvitamin D levels (Glowacki J et al. ASBMR 2012). To determine the skeletal factors that may contribute to RCA, we enrolled 18 subjects with RCA and 28 controls with shoulder OA scheduled for arthroplasty for non-inflammatory disorders. All subjects signed an IRB-approved consent form. Subjects were excluded if they took any medications or had medical conditions that affect skeletal homeostasis. Prior to surgery, we measured calcium, phosphate, 25-hydroxyvitamin D [25(OH)D], bone specific alkaline phosphatase (BSAP), estimated glomerular filtration (eGFR), body mass index (BMI), bone mineral density (BMD) and body composition [lean mass index (LMI), appendicular LMI, and fat mass index (FMI)] (Table 1). The 18 RCA subjects were older than the 28 shoulder OA subjects (73.6 \pm

8.0 vs 63.3 ± 9.8 years, respectively). The RCA subjects had higher BSAP levels and marginally higher phosphate levels than those with shoulder OA. There were no significant differences between the two groups in the levels of calcium, 25(OH)D, or eGFR. Subjects with RCA tended to have lower total hip T-score; they had lower LMI and appendicular LMI, although BMIs were similar. These data show that, despite higher BSAP levels in these RCA subjects, the lack of hypophosphatemia, low vitamin D levels, or renal insufficiency is not consistent with a disorder of mineral metabolism. Because there are important relationships between muscle and bone, the lower LMI in RCA subjects may potentially contribute to the pathophysiology of RCA.

| Table 1: Clinical Parameters and Body Composition Measures | | | |
|---|--------------------------|------------------------------|------------|
| Clinical Variables (Normal Range for test) | Osteoarthritis | Rotator Cuff Arthroplasty | P Value |
| Calcium* (8.6-10.2 mg/dL) | 9.3 ± 0.5 n=28 | 9.4 ± 0.3 n=18 | 0.349 |
| Phosphate † (2.5-4.5 mg/dL) | 3.4 (2.2-3.9) n=26 | 3.7 (2.2-4.1) n=17 | 0.053 |
| 25(OH)D † (8-42 ng/mL) | 33.3 (17.6-54.0) n=27 | 34.4 (22.2-68.6) n=16 | 0.555 |
| BSAP* (Female 3.8-22.6 ug/L; Male 3.7-20.9 ug/L) | 8.5 ± 5.0 n=28 | 12.3 ± 5.8 n=16 | 0.037 |
| BMD (FN) T-Score* | -1.1 ± 0.9 n=26 | -1.2 ± 0.7 n=15 | 0.756 |
| BMD (Total Hip) T-Score* | -0.5 ± 0.7 n=26 | -1.0 ± 0.8 n=15 | 0.078 |
| BMI* (kg/m ²) | 29.8 ± 5.6 n=28 | 28.5 ± 5.0 n=17 | 0.444 |
| FMI* (fat mass/height ² - kg/m ²) | 10.9 ± 4.5 n=28 | 12.1 ± 3.7 n=17 | 0.361 |
| LMI † (lean tissue/height ² - kg/m ²) | 17.3 (13.2-22.2) n=27 | 14.3 (12.1-20.3) n=17 | 0.016 |
| Appendicular LMI † (kg/m ²) | 7.1 (5.1-9.9) n=27 | 5.7 (4.9-8.6) n=17 | 0.011 |

* mean ± SD † Median (range)

Table 1

Disclosures: Lisa Gao, None.

SA0020

See Friday Plenary Number FR0020.

SA0021

See Friday Plenary Number FR0021.

SA0022

See Friday Plenary Number FR0022.

SA0023

Tibial Response to Axial Compression in Aging C57BL/6 Mice. Nilsson Holguin^{*1}, Michael Brodt², Michelle Sanchez², Matthew Silva³.
¹Washington University Department of Orthopaedic Surgery, USA, ²Washington University Department of Orthopaedics, USA, ³Washington University in St. Louis School of Medicine, USA

Aging purportedly diminishes the ability of the skeleton to respond to mechanical loading, but recent data show that old age did not impair accrual of bone in BALB/c mice subjected to axial tibial compression. We sought to extend these findings to the commonly used C57BL/6 mice. We hypothesized that aging does not limit the response of the tibia to axial compression over a range of adult ages in C57BL/6. We subjected the right tibia of old (22 months, n=14), middle-age (12 months, n=15) and young-adult (5 months, n=15) female C57BL/6 mice to axial tibial compression (4 Hz, 1200 cycles/day, 5 days/week, 2 weeks) at 9, 10 and 10.5 N, which engendered similar peak periosteal strains of 3000 µε. The left tibia served as a contralateral control. Cortical bone measures from right and left tibias were assessed by in vivo micro-computed tomography (µCT) and by dynamic histomorphometry at 5 mm proximal of the distal tibio-fibular junction. Trabecular bone measures were determined by µCT at the proximal metaphysis, distal of the growth plate. In mice of every age, 2 weeks of tibial compression increased cortical bone volume (p<0.05, Figure 1) by increasing total volume (p<0.001) despite also increasing medullary volume (p<0.001). Compared to the increase in total and bone volume of the cortical midshaft of 5 months mice, increases were less in 12 and 22 months mice (p<0.01). Thus far, periosteal and endocortical MS/BS (n=2-3 per age) were increased in the loaded tibias of each age group compared to contralateral controls, of which 6 out of 8 of the highly strained tibias displayed some periosteal woven bone. Tibial loading increased trabecular BV/TV of 5 months mice from 0.085 to 0.010 mm³/mm³ (p<0.05) but BV/

TV did not change in 12 or 22 months mice, perhaps due to low initial values (0.032 and 0.038 mm³/mm³, respectively). By contrast, contralateral tibias from every age lost cortical bone volume and from 5 months mice lost trabecular BV/TV, suggesting a systemic effect from loading. In conclusion, these data show that while young-adult C57BL/6 mice had greater tibial bone accrual following loading than middle-age or old mice, aging did not eliminate the ability of the tibia to accrue cortical bone.

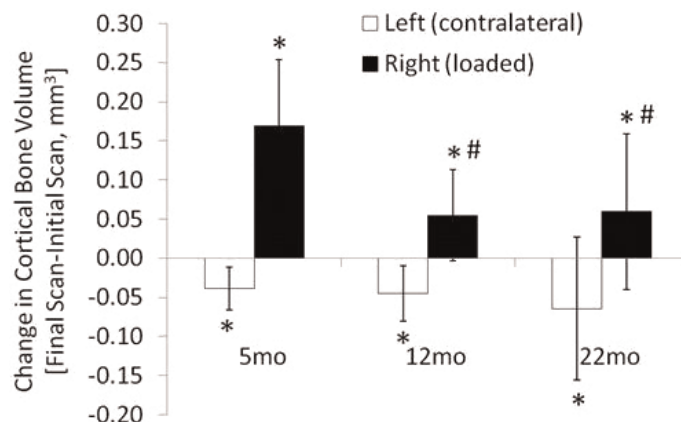


Figure 1. Cortical bone volume. * p<0.05 Final vs Initial scan, # p<0.05 vs Loaded of 5mo.

Disclosures: Nilsson Holguin, None.

SA0024

See Friday Plenary Number FR0024.

SA0025

Juvenile Paget's Disease Without Mutation of *TNFRSF11B* (OPG) or *TNFRSF11A* (RANK). Steven Mumm^{*1}, Omayma El-Shafie², Xiafang Zhang³, Samir Hussein², Deborah Novack⁴, Nicholas Woodhouse², Michael Whyte⁵. ¹Washington University School of Medicine, USA, ²Sultan Qaboos University, Oman, ³Washington University School of Medicine, USA, ⁴Washington University in St. Louis School of Medicine, USA, ⁵Shriners Hospital for Children-Saint Louis, USA

Juvenile Paget's disease (JPD) is the extremely rare heritable disorder that features the greatest rates of skeletal turnover documented in humans. In 2002, homozygous loss-of-function mutations in the *TNFRSF11B* gene that encodes osteoprotegerin (OPG) were discovered in JPD. Most JPD patients have autosomal recessive JPD that reflects remote "founders" in different geographic locations worldwide. Additionally, in 2008, we reported the JPD phenotype in a preliminary report of a Bolivian girl with a sporadic, heterozygous, 15-bp tandem duplication in exon 1 of the *TNFRSF11A* gene that encodes RANK (JBMR 23:S134, 2008). The remaining JPD patients are not understood at the molecular level. Here, we describe this type of extremely rare patient.

A 16-year-old nonconsanguineous boy from Oman had progressive skeletal deformities first noted at age 3 years. Physical examination showed macrocranium, severe and painful bony deformities, and bilateral deafness. Retinal examination showed no angioid streaks. He had 8 unaffected siblings. Radiographs and bone scintigraphy were in keeping with JPD, and showed in his skull striking expansion and sclerosis of the diploic space, basilar impression, expanded maxilla, and deformed teeth (Fig). Ribs, scapulas, and clavicles were wide and sclerotic. Severe deformities affected the femur and pelvis with loss of cortical differentiation. Fractured ribs and flattened vertebrae were also in keeping with JPD. Serum alkaline phosphatase (ALP=3,900 U/L) and other bone turnover markers (BTMs) were markedly elevated. Despite serum 25OHD=12 nmol/L ("deficient"), serum parameters of mineral homeostasis were unremarkable. He also had hyperthyroidism. Iliac crest histology [after tetracycline (TCN) labeling] revealed an irregular arrangement of trabeculae, increased osteoid, hypocellular fibrotic stroma, numerous osteoclasts in some areas, large amounts of woven bone, diffuse TCN labeling, and a very high rate of bone turnover, but without the parallel trabecular pattern identified in the OPG deficiency form of JPD (JBMR 19:695, 2004). Despite 4 mg zolendronate i.v. every month x 40, BTMs did not achieve ~1/2 peak levels.

The coding exons and adjacent mRNA splice sites of *TNFRSF11B* (OPG) and *TNFRSF11A* (RANK) were sequenced without identification of a mutation that would explain his JPD. Similarly, *TNFSF11* (RANKL), *SQSTM1*, *TGFB1*, *SFRP1*, and exons 2-4 of *LRP5* were negative. Hence, there is additional genetic heterogeneity for JPD.



Lateral skull radiograph at age 17 years shows marked expansion of the diploic space, loss of definition of the inner and outer tables, a sclerotic appearance with scattered lucencies, and platybasia.

Skull radiograph

Disclosures: Steven Mumm, None.

SA0026

Responsiveness to Pamidronate Treatment is not Related to Genotype of Type 1 Collagen in Osteogenesis Imperfecta. Junko Kanno^{*1}, Akiko Hakoda¹, Ikuma Fujiwara². ¹Department of Pediatrics Tohoku University Hospital, Japan, ²Tohoku University School of Medicine, Japan

Objective: Osteogenesis imperfecta (OI) is a heritable disorder of connective tissue characterized by bone fragility, low bone mass and short stature. Other external clinical features of OI include dentinogenesis imperfecta and blue sclerae. The majority of patients with OI have a mutation in either *COL1A1* or *COL1A2* that encode type 1 collagen. Mutation analyses of the genes have been reported, but examination of genotype-phenotype correlation in the effect of the treatment have been rarely reported. In this study, we screened *COL1A1* and *COL1A2* in OI patients and compared the results of genotype analysis with clinical examination, including increase of BMD after pamidronate treatment, in the patients.

Subjects and Methods: 22 children (9 males and 13 females) with OI types I (6), III (11), and IV (5) were analyzed. They were treated with pamidronate infusion (1mg/kg, monthly). Lumbar BMD was measured using DXA (Hologic 4500A) before and during the treatment. All exons of the *COL1A1* and *COL1A2* genes were amplified by PCR and analyzed by direct sequencing. We compared the genotype with clinical characteristics including height, blue sclerae, dentinogenesis imperfecta, fractures at birth and the Z-score of the BMD (Z).

Results: Sequencing analysis of *COL1A1* and *COL1A2* in 22 patients revealed 14 mutations in heterozygous forms; 10 missense mutations, two nonsense mutations, and two frame-shift mutations. Three mutations were novel. Each of the 14 mutations was found only in a single family even though the patients were from the same region. Glycine to serine substitutions were the most common type of mutation in both genes. Patients with serine substitutions were shorter than those with other genotype. Most of the patients had blue sclerae and dentinogenesis imperfecta. Pamidronate significantly increased Z in all the patients, though no correlation was found between the mutated gene or mutation type and increment in Z. One of the patients affecting exon 44 of the *COL1A2* suffered intracranial hemorrhage.

Conclusions: *COL1A1* and *COL1A2* mutant alleles in OI are heterogeneous. Glycine to serine substitutions tend to lead to a more severe phenotype. The genotype does not seem to be related to the effect of treatment.

Disclosures: Junko Kanno, None.

This study received funding from: Ministry of Education, Culture, Sports, Science and Technology of Japan

SA0027

Vertebral Fracture Assessment by the GE Lunar iDXA™ versus Radiographic Assessment in Children. Nicola Crabtree^{*1}, Nicholas Shaw², Wolfgang Hogler³, Natalie Bebbington³, Deirdre Chapman³, Steve Chapman³. ¹Birmingham Children's Hospital, United Kingdom, ²Birmingham Children's Hospital, United Kingdom, ³Birmingham Children's Hospital, United Kingdom

Vertebral fracture assessment (VFA) by DXA is an accepted tool for use in adults. However, its use in children has not been validated. The iDXA is a high resolution

bone densitometer capable of producing good high images with minimal radiation exposure. The aim of this study was to validate VFA using iDXA against spinal radiographic assessment (RA) for the identification of vertebral fractures in children.

Spine radiographs and VFA (L5-T2) by iDXA were acquired on the same day in 25 children. An additional 24 children had VFA alone performed. Agreement between RA and VFA was assessed by an expert paediatric radiologist and two metabolic bone specialists; agreement between raters for VFA alone was additionally assessed by an expert, an experienced and a naive DXA operator. Vertebrae were ranked as normal, mild, moderate or severe if they had <10%, 11-25%, 26-50% and >50% deformity, respectively. Levels of agreement were calculated using the kappa statistic and consistency by the intra-class correlation coefficient (ICC).

Depending on rater, 84.0-90.5% of the visible vertebrae were analysable by RA. In contrast, 97.2% of the visible vertebrae were analysable by VFA. Moderate agreement was noted between raters for RA [kappa 0.523-0.588] and between RA and VFA [kappa 0.511-0.584], substantial agreements were observed between raters for VFA assessment [kappa 0.637-0.704]. Agreement improved if the vertebral deformities were dichotomised as normal or mild versus moderate or severe, with substantial agreement observed between raters for RA and between RA and VFA and almost perfect agreement observed between raters for VFA alone [ICC ranged from 0.802-0.895, $p < 0.0001$]. Similar patterns were observed between all 6 raters for VFA with no discernable difference detected for rater experience. Poorer agreement was seen between quantitative and visual assessment [kappa 0.302-0.408], however this did improve when the classifications were dichotomised.

VFA is accurate and consistent when identifying vertebral fractures, particularly moderate and severe fractures in chronically sick children. Moreover, its accuracy appeared to be independent of reader experience. Consequently, VFA should prove to be a useful tool in the assessment of bone health in children.

Disclosures: Nicola Crabtree, None.

SA0028

Age-related Genetic Influences on Bone Traits in the Metacarpals: Evidence for Genetic Independence across the Hand. Maja Seselj^{*1}, Richard Sherwood², Dana Duren³. ¹Lifespan Health Research Center, USA, ²Division of Morphological Sciences & Biostatistics Wright State University, USA, ³Wright State University, USA

Throughout childhood, gross properties of bone (length, width, cortical thickness) are highly phenotypically correlated across the metacarpals. Early in development, patterning of the autopod is regulated by posterior genes of the *Hoxa* and *Hoxd* clusters. In this early patterning, metacarpals two (MC2) and four (MC4) are contained in separate domains of gene expression (e.g., *Hoxd11-13*), with potential differential anatomical consequences of these expression patterns. It is unclear, however, whether there remain independent genetic effects on bone properties across the hand in any post-natal period. Using a longitudinal growth series consisting of related individuals, we examined additive genetic correlations between paired bone traits of MC2 and MC4, measured from hand-wrist radiographs at ages 3 (N=197), 7 (N=293), 14 (N=400) and 18 years (N=158). Narrow-sense heritability was estimated for each trait, and genetic correlations determined for each trait pair, at each age using a maximum likelihood variance components method implemented in SOLAR. Covariates included sex, skeletal age, weight, and height (or recumbent length).

All traits were heritable at all ages. Genetic correlations between paired bone traits in MC2 and MC4 each exhibited a distinct pattern with age. First, genetic correlations for bone length of MC2/MC4 indicated incomplete pleiotropy throughout childhood, ending with complete pleiotropy ($\rho_g=1$) by age 18. Second, a high genetic correlation was found between bone widths at age 3 ($\rho_g=0.88$), tapering to moderate correlations during mid-childhood. By age 18, the shared genetic influence between MC2/MC4 bone widths was lost ($\rho_g=0$). The third pattern involves cortical thickness, where MC2 and MC4 share genetic underpinnings at ages 3 and 18 ($\rho_g=1$), but show incomplete pleiotropy at mid-childhood ages ($\rho_g=0.85, 0.68$).

Our results suggest that, despite their morphological similarity and anatomical proximity, phenotypic correlations in bone properties between individual metacarpals are not due to uniform genetic control. These patterns of genetic correlation of bone traits in the hand serve as an indicator of the changing role of genes during childhood. It is unclear whether the genetic fields established during embryogenesis continue to exert differential influence across the developed autopod, or if changes in shared genetic underpinnings reflect variation in the timing of regulation of bone growth or mitigating environmental effects.

Disclosures: Maja Seselj, None.

SA0029

Early Onset Type 2 Diabetes Impairs Skeletal Acquisition in the Tallyho Mouse. Maureen Devlin^{*1}, Miranda Van Vliet², Christine Conlon², Leeann Louis², Lamya Karim¹, Mary Boudoux¹. ¹Beth Israel Deaconess Medical Center, USA, ²Beth Israel Deaconess Medical Center, USA

The incidence of Type 2 diabetes (T2D) in children and adolescents is rising, yet it is not known whether T2D onset during peak bone mass acquisition affects bone mass, geometry or strength. Here we test effects of early onset T2D on bone mass, microarchitecture and strength in the Tallyho mouse, which develops polygenic T2D at 2-3 months of age. Methods: We compared skeletal acquisition in male

TALLYHO/JngJ and SWR/J controls (N=5/grp) fed a normal (N, 10% kCal/fat) or high fat-sucrose (HFS, 20% kCal/fat) diet from 4-16 wks of age. Outcomes included body mass, % body fat, glucose tolerance, serum leptin, whole body bone mineral content per body mass (BMC/BM), cortical (Ct) and trabecular (Tb) microarchitecture via μ CT, femoral strength by 3-pt bending, and mechanical properties of cortical bone tissue by microindentation. Results: There were no significant differences between N and HFS diet in either strain, so diet groups were pooled for analysis. Tallyho were obese and glucose intolerant, developing T2D (fasting blood glucose >250 mg/dl) by 8 wks of age. Tallyho had ~2-fold higher leptin and % body fat, with 51-64% lower BMC/BM vs. SWR at all timepoints ($p < 0.03$ for all). Tallyho had severe deficits in distal femur Tb microarchitecture: lower Tb. bone volume fraction (BV/TV) (-54%), Tb number (-27%) and connectivity density (Conn.D) (-82%) ($p < 0.01$ for all). Tallyho also had worse Tb bone in the spine: lower Tb.BV/TV (-13%, $p < 0.07$), and Conn.D (-50%, $p < 0.05$) vs. SWR. Tallyho had higher midshaft femur Ct bone area fraction, Ct. thickness, total cross-sectional area, and polar moment of inertia ($p < 0.05$ for all) vs. SWR, but these differences disappeared after adjustment for higher Tallyho body mass. 3-pt bending of the diaphysis showed Tallyho had higher maximum force but lower post-yield displacement than SWR ($p < 0.01$ for both). Cortical bone tissue properties by microindentation were worse in Tallyho, with higher indentation distances ($p < 0.05$). Conclusion: The Tallyho mouse model of early onset T2D has pronounced deficits in bone mineral content, trabecular microarchitecture, and cortical bone material properties, while cortical geometry and whole bone strength are appropriate for body mass. Biomechanical properties are consistent with bone brittleness, perhaps due to accumulation of advanced glycation endproducts. These data suggest the Tallyho mouse is a useful model for studying skeletal effects of T2D onset in adolescence.

Disclosures: Maureen Devlin, None.

SA0030

Increased Vascularity in Association with Elevated Osteoclast Precursors and Bone Resorption in the Brlm Mouse Model of Moderately Severe Osteogenesis Imperfecta. Patricia Collin-Osdoby^{*1}, Linda Rothe², Rajeev Aurora³, Joan Marini⁴, Philip Osdoby¹. ¹Washington University in St. Louis, USA, ²Washington University, USA, ³St. Louis University, USA, ⁴National Institute of Child Health & Human Development, USA

Brlm mice are a valuable model for moderately severe osteogenesis imperfecta (OI) that contain a glycine substitution (G349C) in half of their type I collagen $\alpha 1(I)$ chains, resulting in mice with a smaller body size, reduced cortical and trabecular bone volumes, abundant osteoclasts (OCs), matrix insufficiency, and brittle bones prone to fracture. Bone resorption in vivo is increased in Brlm mice and histological sections from Brlm vs. WT littermates exhibit greater numbers, sizes and TRAP stained intensities of bone-resorbing OCs. The bone vasculature is essential for normal bone development and remodeling, and it is often increased and contributes to skeletal diseases characterized by bone loss. Here, we investigated if the bone vascular network in Brlm OI mice was expanded in comparison to WT littermates (all 8 week old males). Immunostaining of bone sections showed a marked increase in PECAM-1+ stained blood vessels in Brlm vs. Wt bone, indicating greater vascularity in trabecular Brlm OI bone. Microfil injection was used to prepare bone vascular casts from Brlm and WT mice, and tibial casts were analyzed by microCT to quantify potential vascular differences. Brlm bone vascular casts demonstrated greater vessel numbers, vessel thickness, and overall vascular volumes (30% higher) compared to WT bone vascular casts, particularly in the metaphyseal region. This increased vascularity was associated with a 2-fold greater recruitment of RANK+CD11b+ OC precursors in Brlm bone marrow and the enhanced capacity of such precursors to form more bone-resorbing OCs. Increased vascularity also could provide additional potential stromal vascular niches conducive to OC stimulation, consistent with the 3-fold increase in RANKL+ mesenchymal stromal cells detected in Brlm bone marrow. We conclude that increased OC-mediated bone resorption exhibited by Brlm OI mice is associated with a notable increase in bone vascularity that may contribute to the skeletal pathology of this moderately severe OI disease through multiple mechanisms impacting on precursor cell recruitment and vascular stromal cell niches.

Disclosures: Patricia Collin-Osdoby, None.

SA0031

See Friday Plenary Number FR0031.

SA0032

See Friday Plenary Number FR0032.

SA0033

School Based Intervention Improves Fitness But Not Bone Accrual in 8-14 year old Girls. Danielle Ries^{*1}, Aaron Carrel², Sijan Wang³, Tamara Scerpella⁴. ¹University of Wisconsin School of Medicine & Public Health, USA, ²University of Wisconsin-Madison Department of Pediatrics, USA, ³University of Wisconsin-Madison Department of Biostatistics & Medical Informatics, USA, ⁴University of Wisconsin, USA

Introduction: Physical activity modulates bone growth during childhood and adolescence and may enhance lifelong bone health. However, an effective, broadly applicable activity has not been identified. Similarly, physical activity has been shown to enhance youth fitness, as assessed by body composition (BMI), V02 max testing and serologic indices of insulin sensitivity and inflammation. An ideal physical activity would improve fitness as well as skeletal health.

Purpose: To determine whether a school-based fitness-oriented curriculum known to improve V02 max, BMI, insulin sensitivity, and markers of inflammation also improves bone acquisition.

Study design: Data were evaluated from 17 elementary aged (ELEM) and 29 middle school aged (MID), non-obese girls who were enrolled in a school-based, general-fitness intervention (INT). This nine-month program consisted of 40 min of moderate to vigorous activity every other school day. All subjects underwent total body DXA scans (Norland XR-36, software version 3.7.4/2.1.0) before and after the intervention, providing total body subhead (SH) bone mineral content (BMC, g) and non-bone lean mass (LM, g). Percent change in SH BMC was calculated and compared to the same parameter in control subjects (CON) who were matched at baseline for gender, age, height and BMI. CON were enrolled in a different study and received total body scans using a Hologic Discovery A scanner (software v.12.7.3.2.3). Gynecologic age was calculated for MID as years subsequent to menarche at time of baseline scan. Multiple linear regressions were applied separately to ELEM and MID cohorts, exploring the intervention effect on SH BMC % change/month.

Results: The intervention was not a significant predictor of SH BMC % change in either age cohort, as evidenced by β coefficients: ELEM, 0.07 ± 1.83 , $p = 0.74$; MID, -0.25 ± 0.18 , $p = 0.18$. The only significant predictor was change in height for ELEM (1.62 ± 0.72 , $p = 0.033$) and gynecologic age (-0.24 ± 0.09 , $p = 0.008$) for MID.

Conclusion: Although this school-based, fitness-oriented curriculum has been shown to improve body comp, insulin sensitivity, fitness, and markers of inflammation, it did not increase the rate of bone accrual in either elementary or middle-school aged girls over a nine month period. This data demonstrates the need for alternative programs to improve fitness AND maximize bone acquisition in young females.

Subject Characteristics: Means and standard deviations for baseline characteristics and % gains

| | Age (yrs) | Gynecologic Age (yrs) | Height (cm) | Weight (kg) | BMI | SH BMC % Δ /mo | SH LM % Δ /mo |
|----------|-------------------|-----------------------|--------------------|-------------------|-------------------|-----------------------|----------------------|
| ELEM-INT | 8.8 ± 0.8 | - | 132.3 ± 9.2 | 30.1 ± 5.8 | 17.1 ± 2.1 | 1.35 ± 0.56 | 1.16 ± 0.77 |
| ELEM-CON | 9.0 ± 0.5 | - | 133.5 ± 6.6 | 31.7 ± 5.6 | 17.7 ± 2.1 | 1.35 ± 0.71 | 1.51 ± 0.62 |
| MID-INT | 12.9 ± 0.7 | 0.2 ± 1.3 | 159.6 ± 6.4 | 51.0 ± 8.4 | 19.9 ± 2.6 | 1.09 ± 0.52 | 0.79 ± 0.78 |
| MID-CON | 13.0 ± 0.7 | 0 ± 1.1 | 157.2 ± 6.9 | 48.5 ± 8.3 | 19.6 ± 3.2 | 1.38 ± 0.82 | 0.84 ± 0.68 |

table

Disclosures: Danielle Ries, None.

SA0034

See Friday Plenary Number FR0034.

SA0035

Reference Data for BMD in Children 2 – 10 Years of Age Assessed by DXL Calscan. Ann-Charlott Soderpalm^{*1}, Ragnar Kullenberg², Kerstin Albertsson Wikland³, Diana Swolin-Eide⁴. ¹Orthopedic Clinic, Sweden, ²Dept of Radiology, Sweden, ³Department of Pediatrics, Sweden, ⁴Queen Silvia Children's Hospital, Sweden

Aim: To collect normative data in order to generate pediatric reference values for calcaneal bone mineral density (BMD) in healthy 2 - 10-yr-old Swedish children.

Background: Site-specific information on bone mass development is important when investigating children with different disorders. The lower extremities e.g., are affected at an early stage in children with neuromuscular disorders such as Duchenne muscular dystrophy. Dual energy X-ray absorptiometry (DXA) in combination with a laser measurement of the heel thickness, DXL Calscan (Demetech AB), measures BMD in the heel bone and an apparent density (BMAD) is calculated. The DXL Calscan is portable, easy to use, has a short measurement time, gives a low absorbed radiation dose and the method is applicable in very young children and in individuals with disabilities.

Subjects and Method: Healthy, Swedish children were randomly included. The left foot was scanned in 117 2-yr-old, 110 4-yr-old and 107 7-yr-old children, 50% were boys, using the DXL Calscan technique. More than 35 % of the children from each age group were followed for another 2 years. A total of 645 measurements in children aged 2 – 10 yrs were performed. Height and weight were determined annually and questionnaires concerning general health were completed at every visit.

Results: The mean BMD in the 2-yr-olds was 0.17 ± 0.003 g/cm², in the 4-yr-olds 0.22 ± 0.003 g/cm² and in the 7-yr-olds 0.30 ± 0.005 g/cm². The 7-yr-old girls had a significantly higher BMD than the boys ($p=0.026$) but there were no significant gender differences in the calcaneal BMD in 2- and 4-yr-olds. BMD was significantly correlated with age ($p<0.001$, $r=0.78$). A weaker correlation was found between BMAD and age ($p<0.001$, $r=0.23$). Based on the data from the 2-yr follow-up; a total of 645 (328 girls/ 317 boys) measurements, reference curves (mean \pm 2 SD) were produced for calcaneal BMD in girls and boys aged 2 - 10 yrs according to age and height.

Conclusions: Gender differences are present in the heel bone BMD at an early age. This study presents gender specific reference curves for heel BMD for children 2-10 yrs of age. These data will be valuable in future research and for evaluating the bone health in children with different disorders and a useful complement when other bone mass measurement techniques are not possible to use, e.g. due to metallic implants. BMAD may reflect mineralization without the influence of bone size.

Disclosures: Ann-Charlott Soderpalm, None.

SA0036

Effect of Cox2 on Hypoxia-induced VEGF Expression in Cartilage During Ischemia Femoral Head Osteonecrosis. Chi Zhang^{*1}, Yang Li², Reuel Cornelia², Harry Kim³. ¹Bone Research Laboratory, Texas Scottish Rite Hospital, USA, ²Texas Scottish Rite Hospital for Children, USA, ³Scottish Rite Hospital for Children, USA

Legg-Calve-Perthes disease (LCPD) is a juvenile form of ischemic osteonecrosis of femoral head caused by blood supply disruption to the femoral head which results in the hypoxic injury. Piglet model of ischemic osteonecrosis of the femoral head involves surgically disrupting the blood supply to the femoral head. The model has been shown to have radiographic and histopathologic changes resembling LCPD. Our histological studies showed increased vessel formation in cartilage in the ischemic group. Angiogenesis is an essential component for the healing of damaged head. VEGF is an important mediator of angiogenesis. To explore the mechanism underlying this response, porcine microarray was performed to compare gene profiles of cartilage from normal and ischemic femoral heads. In the ischemic side, the expression of VEGF was upregulated along with Cox2. Microarray results were confirmed by quantitative RT-PCR. Immunohistochemistry staining demonstrated that both VEGF and Cox2 were upregulated in chondrocytes in ischemic femoral heads. To examine the coordinate expression of VEGF and Cox2 in vitro under hypoxia, pig primary chondrocytes and RCS were cultured in hypoxia station with 1% or 20% of O₂. Expressions of Cox2 and VEGF were upregulated in both RNA and protein levels. To investigate if Cox2 is involved in VEGF regulation by hypoxia, we used siRNA directed against Cox2 to knockdown Cox2 expression. We observed that expression of VEGF was increased after Cox2 siRNA transfection. Furthermore, Cox2 specific inhibitor NS-398 treatment resulted in modest upregulation of VEGF during hypoxia. Taken together, our data indicated that Cox2 is involved in VEGF regulation by hypoxia. Mechanisms of effect of Cox2 on hypoxia-induced VEGF deserve further investigation.

Disclosures: Chi Zhang, None.

SA0037

See Friday Plenary Number FR0037.

SA0038

Application of Vitamin D Status to Development of Normal Ranges for Serum Calcium Concentration in the Pediatric Population. Jeff Roizen^{*1}, Michael Levine², Dean Carlow³. ¹The Children's Hospital of Philadelphia, USA, ²Children's Hospital of Philadelphia, USA, ³The Children's Hospital of Philadelphia, USA

The recognition that vitamin D insufficiency is widespread in pediatric and adult populations raises doubts about the credibility of current reference values for serum calcium, which have been determined using uncharacterized "normal subjects." We therefore set out to determine age-adjusted normal ranges for serum calcium concentration in subjects with normal (20 – 80 ng/mL) levels of serum 25(OH)D. We reviewed clinical and laboratory data of inpatient and outpatient subjects (n = 5868) ranging from full term newborns to greater than 19 years who had a serum levels of total calcium and 25(OH)D measured in the CHOP clinical chemistry lab from 1/1/2011 to 2/16/2012. Serum calcium was measured using a colorimetric assay (VITROS 5, 1 FS automated chemistry system) and serum total 25(OH)D was determined by LS/MS/MS (analytical sensitivity of 4 ng/mL for 25(OH)D₂ and 25(OH)D₃). After excluding patients with renal or endocrine disease or who had been managed in the endocrine clinic or a critical care unit, we ascertained 4628 subjects who had serum

25(OH)D levels that were 20-80 ng/mL within 30 days of their serum calcium measurement. We used EPEvaluator v9 software (Data Innovations, Inc) in accordance with National Committee for Clinical Laboratory Standards (NCCLS) guidelines to analyze the data. We used parametric analysis to generate age-specific reference intervals for serum calcium: 0-90 day-old infants (7.2-11.1 mg/dL); 31-90 day-old infants (7.6-11.0 mg/dL); 91-180 day old infants (8.7-11.1 mg/dL), 181-365 day old children (8.4-11.1 mg/dL), 1-3 year old children (8.5-11.0 mg/dL), 4-11 year old children (8.5-10.6 mg/dL), 11-19 year old children (8.5-10.4 mg/dL) and patients greater than 19 years old (8.4-10.4 mg/dL). Non-parametric analyses yielded ranges that were within 5% of the values obtained by parametric analyses. Serum 25(OH)D levels were between 20-30 ng/mL in 27% of subjects; Wilcoxon matched-pairs signed-ranks test showed a significant (two-tailed $P < 0.03$) difference (0.35 mg/dL) between the lower limits of normal for these subjects compared to subjects with 25(OH)D levels > 30 ng/mL. In summary, we have generated normal calcium ranges for pediatric population that exclude subjects who are vitamin D-deficient. Moreover, our data indicate that many patients with serum 25(OH)D between 20-30 ng/dL have mildly depressed serum calcium levels. These new normal ranges refine previous normal ranges that likely included subjects with abnormal vitamin D status.

Disclosures: Jeff Roizen, None.

SA0039

Long-Term Evolution of a Patient with Hereditary Vitamin D-Resistant Rickets Due to a R30X Mutation in the Vitamin D Receptor. Bruno Ferraz-de-Souza^{*1}, Regina M Martin², Ana Claudia Latronico², Pedro Henrique Correa². ¹Univ of Sao Paulo School of Medicine (FMUSP), Brazil, ²Univ of Sao Paulo School of Medicine, Brazil

Background: Hereditary vitamin D-resistant rickets (HVDRR) is a rare autosomal recessive disorder characterized by end-organ resistance to calcitriol, resulting in early-onset severe hypocalcemia, rickets and secondary hyperparathyroidism. Inactivating mutations in the vitamin D receptor (VDR) are the primary molecular defect determining resistance to calcitriol. Individuals bearing heterozygous VDR mutations, including relatives of patients with HVDRR, are considered to be phenotypically normal but a heterozygous VDR mutation leading to HVDRR has been recently described.

Clinical case: In 1997, we reported a prepubertal 12-yo boy bearing a R30X nonsense mutation in VDR with severe HVDRR and alopecia (Mechica et al., J Clin Endocrinol Metab 1997). He was born to consanguineous parents and developed total alopecia at 1 mo of life followed by rickets and convulsions at 6 mo of age. Clinical diagnosis of HVDRR was made and therapy initiated at 8 mo of age. Clinical, biochemical and radiological improvement were seen with daily oral doses of 3.0 g calcium, 600,000 IU ergocalciferol and 3.0 ug calcitriol. However, hypocalcemic crisis occurring during intercurrent infections were relatively frequent until he was 11 yo. At 12 y of age, Ca serum levels stabilized leading to regression of secondary hyperparathyroidism and reduction of alkaline phosphatase levels. He developed 2ary sexual characteristics at 13 y of age and normal pubertal growth spurt. Requirements of oral calcium and vitamin D decreased slowly and progressively so that at 18 y of age he required only 1.5 g Ca/d to maintain normocalcemia. Follow-up with DXA showed normal peak bone mass and BMD accretion from 15 y of age onwards. He is now 28 yo and maintains normocalcemia without therapy. Notably, his parents and a younger sister who are heterozygous carriers of the R30X mutation are healthy and normocalcemic with mildly elevated calcitriol levels.

Conclusion: Spontaneous clinical remission of HVDRR despite the permanent molecular defect has been previously reported, occurring more commonly around puberty. Reduced calcium demand after completion of linear growth has been postulated as a mechanism to explain this observation. Nevertheless, long-term follow-up of cases such as this one indicate that remission may start early in puberty, during a period of active growth and that, therefore, yet unknown mechanisms may contribute to increase intestinal Ca absorption in these patients.

Disclosures: Bruno Ferraz-de-Souza, None.

SA0040

See Friday Plenary Number FR0040.

SA0041

Spontaneous Osteoclastogenesis in Turner Syndrome Patients with High FSH Serum Levels. Giacomina Brunetti^{*1}, Maria Felicia Faienza², Annamaria Ventura², Laura Piacente², Angela Oranger³, Flaviana Marzano², Maria Ciccarelli², Giorgio Mori¹, Luciano Cavallo², Silvia Colucci³, Maria Grano¹. ¹University of Bari, Italy, ²Interdisciplinary Department of Medicine, University of Bari, Italy, ³Department of Basic Medical Science, Section of Human Anatomy & Histology, University of Bari, Italy

Bone health is a major lifelong concern in caring for girls and women with Turner Syndrome (TS), a chromosomal aberration characterized by total or partial loss of one of the two X-chromosomes. In TS patients there is a decreased bone density and a selective reduction in cortical bone thickness that probably contributes to the

increased fracture risk. However, the mechanisms underlying the bone disease remain poorly understood. Thus, the aim of this study was to investigate the osteoclastogenic potential of unfractionated peripheral blood mononuclear cells (PBMCs) and T cell-depleted PBMC cultures from TS patients (mean age 10.44 ± 5.48 range 1.5-19 years) with high or normal FSH serum level as well as from age-matched controls. Spontaneous formation of active resorbing osteoclasts, without adding M-CSF and RANKL, occurred in PBMC cultures from TS patients with elevated FSH serum levels. Conversely, M-CSF and RANKL were essential to trigger and sustain osteoclastogenesis in PBMCs from controls as well as TS patients with normal FSH serum levels. T-cell depleted PBMC cultures from TS patients with high FSH serum level showed only a partial reduction of spontaneous osteoclast formation, suggesting that both monocytes and T cells have an important role supporting the elevated osteoclastogenesis. In fact, in these patients, monocytes express elevated c-fms, TNF α and RANK levels, whereas T cells showed high RANKL levels. Moreover, elevated amount of RANKL were also detected in PBMC culture media and sera from TS patients with high FSH circulating levels. In conclusion, the present study showed for the first time a high osteoclastogenic potential of PBMCs from young TS patients with high FSH circulating levels. This condition could contribute to the bone disease that become evident in the adult life.

Disclosures: *Giacomina Brunetti, None.*

SA0042

Dietary Calcium Restriction in Idiopathic Infantile Hypercalcemia does not Adversely Affect Spinal & Distal Radial Bone Mineral Density: Report on Nine Patients. Anjali Daniel¹, Raja Padidela^{*1}, Judith Adams², M Zulf Mughal¹. ¹Royal Manchester Children's Hospital, Central Manchester University Hospitals NHS Foundation Trust, United Kingdom, ²The Manchester Royal Infirmary, Central Manchester University Hospitals NHS Foundation Trust, United Kingdom

Idiopathic infantile hypercalcemia (IIH) (OMIM 143880) is characterised by severe hypercalcemia, failure to thrive, vomiting, dehydration and nephrocalcinosis. Laboratory evaluation of infants affected with this condition reveals hypercalcemia, suppressed parathyroid hormone and hypercalciuria. Recently loss of function mutations in *CYP24A1* gene have been found to cause IIH (N Engl J Med. 2011;365:410-21). Short-term treatment for this condition includes intravenous rehydration, furosemide, glucocorticoids, and pamidronate. Low-calcium diet and is the mainstay for managing IIH until there is resolution of hypercalcemia with age.

The aim of this study was to determine if dietary calcium restriction during infancy and early childhood adversely affected bone mineral density (BMD) in patients with IIH, when they were between 5 to 15 year old. Nine patients with IIH who were treated with dietary calcium restriction for a period ranging from 1.7 to 4 years were studied. BMD of L1-L4 was measured using the dual energy absorptiometry and data was expressed as bone mineral apparent density (BMAD; g/cm³). The lumbar spine (LS) BMAD values transformed to Z scores using the normative data [ADC;2007;92(1):53-9]. A peripheral quantitative computed tomography total and trabecular volumetric bone density (vBMD [mg/mm³]) of the distal radial metaphysis, at 4% of the non-dominant forearm length. Distal radial (DR) total & trabecular vBMD values were transformed to Z scores using the normative data [Osteoporos Int. 2009;20(8):1337-46]. A one sample t-test was used to determine if measured bone parameters were significantly different to zero.

The mean (SD) Z score of BMAD [0.09 (0.97)], DR total vBMD [0.32 (0.87)] and DR trabecular vBMD [-0.04 (0.76)] were not significantly different from zero.

From these results, we conclude that dietary calcium restriction for management of IIH during infancy and early childhood does not appear to adversely affect the distal radial and spinal BMD, when the patients were between 5 to 15 year old.

Disclosures: *Raja Padidela, None.*

SA0043

See Friday Plenary Number FR0043.

SA0044

"Distribution/Mass" and "Distribution/Quality" Relationships in Human Cortical Bone. Influence of Gender and Physical Activity. Ricardo Capozza¹, Paola Reina¹, Laura Nocciolino¹, Sara Feldman², Pablo Mortarino¹, Joern Rittweger³, Jose Ferretti^{*4}, Gustavo Cointry¹. ¹Center of P-Ca Metabolism Studies (CEMFoC), Natl Univ of Rosario (UNR), Argentina, ²LABOATEM, Faculty of Medicine, UNR, Argentina, ³Div Space Physiology, Institute of Aerospace Medicine, German Space Agency (DLR), Germany, ⁴National University of Rosario, Argentina

In a serial pQCT study (slices taken at every 5% of the tibia height throughout the bone, sites S5- S95) of sedentary and running-trained men and women aged 20-40 yr (n=10/group) we had shown that bone mass distribution along the tibia reflected a structural adaptation to the variable stress pattern imposed by the mechanical usage of the limb. Now we extend that analysis to describe the relationships between indicators of cortical bone distribution (bending and torsion cross-sectional moments

of inertia, MIs,y), mass (BMC,x₁), and "quality" (vBMD, proportional to bone tissue stiffness,x₂). Correlations between MIs and cortical BMC and between MIs and cortical vBMD were regarded as describing "distribution/mass" (d/m) and "distribution/quality" (d/q) relationships, respectively, at each studied site.

The d/m curves were all described by positive exponential functions, while the d/q curves, hyperbolically shaped, were always adjusted to negative exponential functions. All d/m and d/q correlations were significant at every site. The distributions of the r coefficients of both d/m and d/q curves, plotted by site, were described by quasi-symmetrical, bell-shaped curves, reaching a maximum toward the central region of the tibiae in every instance. Both men and trained individuals showed significantly higher MIs and BMC and lower vBMD values than women. The d/m relationships were described by unique curves for all groups, with increasing slopes from the heel to the knee. The d/q relationships were described by separate, parallel curves for men (higher ordinates, lower abscissae) and women, with little or no influence of the trained/untrained condition within sex.

Results offer original support to 4 important concepts in Bone Biology: 1. the architectural quality of diaphyseal design concerning bending and torsion strength is proportional to the relative influence of bending and torsion in the varying stress patterns along the bones (known to be maximal toward the central regions) with a significant trend to minimize bone mass; 2. there is a trade-off between cortical bone "quality" (intrinsic stiffness) and distribution, as if both variables were interrelated by a feedback control mechanism of structural diaphyseal stiffness/strength (in agreement with the mechanostat theory); 3. both d/m and d/q relationships are highly related to bone mechanical environment, and 4. the d/q relationships are also affected by sex.

Disclosures: *Jose Ferretti, None.*

SA0045

See Friday Plenary Number FR0045.

SA0046

Assessment of varying CT image resolution on Voxel-based, Subject-Specific High-throughput FEA models. David Mcerlain^{*1}, Kyle Nishiyama¹, Clara Sandino², Steven Boyd¹. ¹University of Calgary, Canada, ²Faculty of KinesiologyBone Imaging LabUniversity of Calgary, Canada

Introduction: Computed tomography (CT) is a 3D imaging modality with tremendous promise for advanced Osteoporosis diagnosis techniques. Moreover, CT data is an ideal input for creating biomechanical models using finite element (FE) analysis that simulate mechanical tests (CT-FE) to provide patient-specific estimates of bone strength. Traditional CT imaging protocols use varying voxel dimensions depending on the anatomical site and patient size, and it is likely to underestimate stress values within bone using CT-FE. Thus, the purpose of this project is to assess the optimal voxel dimensions required for subject-specific CT-FE analysis of bone strength.

Methods: Cadaveric distal tibia specimens (n=8 fresh-frozen; mean age 78) were scanned (GE Discovery CT750HD; 120 kVp, 60mA·s) and reconstructed with varied slice thicknesses (0.625mm - 2.50mm) typical in orthopaedic exams. After, all bones were scanned using micro-CT (Scanco Medical XtremeCT; 60kVp, 1.0mA; 0.082mm isotropic voxels), which acted as the over-resolved 'gold' standard. The endosteal bone surfaces were semi-automatically segmented using Stradwin (Cambridge, UK) and exported for FE model creation. In-house software converted the CT data into density units based on a phantom within the image (B-MAS200, Kyoto, Japan), which were converted to Young's modulus. Linear FE models were generated with hexahedral elements from isotropic voxels and solved using FAIM (Numerics88; Calgary, Canada). A 3-mm axial compression load was applied to each model along the articular surface.

Results: Each clinical CT-FE simulation was completed in less than 17 min (number of elements for clinical CT-FE models ranged from approximately 5800-370000). The distribution of stress appeared similar between models as the load transmitted evenly from the surface to the cortical bone, though the mean von Mises stress values decreased by 27% for the models with 2.5 mm elements versus 0.63 mm.

Discussion: This work investigates the utility and feasibility of whole bone, subjects-specific CT-FE for use in high-throughput analysis of osteoporotic patients. The bounds of solutions were determined for the resolutions tested, and these results suggest that a minimum 1mm, isotropic voxel size may be required for testing. Advanced, constitutive properties are currently under development for large-scale FE models. Future work will compare the CT-FE models to micro-CT derived FE models of the same bone.

Disclosures: *David Mcerlain, None.*

SA0047

Biomechanical Bone Testing in Cynomolgus Monkeys: Neonate, Juvenile, Young Adult and Aged Animals. Aurore Varela^{*1}, Robert Guldberg², Susan Y. Smith¹. ¹Charles River Laboratories, Canada, ²Parker H. Petit Institute for Bioengineering & Bioscience, USA

Biomechanical strength testing of bones, considered the ultimate bone quality assessment, is a critical end-point in the evaluation of the safety and efficacy of test

compounds in postnatal, juvenile, young adult and aged animals in preclinical studies. The purpose of this study was to assess precision and validate procedures for the biomechanical testing of femurs (3-point bending) and vertebral body (compression) from Cynomolgus monkeys of different ages using an MTS Servohydraulic test system, Model 242.03, using TestWorks version 3.8A for TestStar® software version 4.0C, under GLP conditions.

Femurs and lumbar vertebrae were collected from six 1-day-old, twelve 6-month-old monkeys, twenty-one 2.5-3 year-old and seventeen monkeys greater than 9 years old, and stored frozen at -20°C until pQCT scanning and testing. pQCT was measured at the expected 3-point bending fracture site (distal diaphysis). Due to the specimen size, 1-day-old femurs (~5 cm) were tested with a small fixture (rounding of 3.2 mm), bottom span of 20 mm, and 6-month-old (~8 cm) with a bottom span of 30 mm. Femurs from older animals were tested with a larger fixture (rounding of 6.35 mm), bottom span of 50 mm. Femur tests were done at a rate of 1 mm/sec, load cell 2.5kN (1-day-old and 6-month-old femurs) or 15kN (older animals). Vertebral body compression was done at a rate of 20 mm/min, load cell 2.5kN (1-day-old) or 15kN (older animals). Load and displacement data were collected and biomechanics parameters derived.

The 3-point bending tests provided the following range of results: peak load 120 to 200N, stiffness 170 to 240N/mm and area under the curve at peak load (AUC) 330 to 700N-mm as well as respective corrected parameters for specimen size, ultimate stress 115 to 150 MPa, modulus 2500 to 4000 MPa and toughness 13 to 35 MPa. In addition, using linear regression analyses, a positive relationship between femur vBMC and peak load was obtained ($r=0.90$) regardless of age, supporting the reproducibility of the procedures. %CV of peak load and stiffness was approximately 19% for 3-point-bending and 25 % for vertebral body compression regardless of age.

With respect to precision, these results were similar for bones of different size, density and age and confirm the adequacy of procedures in neonate, juvenile and adult monkeys, which support the feasibility and utility of integrating these endpoints in neonate or juvenile preclinical studies to assess potential effects on bone.

Disclosures: *Aurore Varela, None.*

SA0048

Bone Heterogeneity measured by DXA Complements aBMD for Prediction of Mechanical Behavior of Human Lumbar Vertebrae. François Duboeuf^{*1}, Jean-Paul Roux², Julien Wegrzyn³, Mary Bouxsein⁴, Roland Chapurlat⁵. ¹INSERM, UMR 1033, Université de Lyon, France, ²INSERM, UMR 1033, Université de Lyon, France, ³INSERM U1033 - Université de Lyon, France, ⁴Beth Israel Deaconess Medical Center, USA, ⁵E. Herriot Hospital, France

More than 50% of fragility fractures are not predicted by areal bone mineral density (aBMD). A previous study showed the contribution of microarchitecture heterogeneity to the mechanical behavior of human lumbar vertebrae (Wegrzyn et al. JBMR 2010: 2324-2331) in an ex-vivo study. Thus the aim of this study was to assess the contribution of bone heterogeneity measured simply by DXA to the mechanical behavior of human lumbar vertebrae.

Lumbar vertebrae (L3) were harvested fresh from 21 lumbar spines of human donors, including 11 men and 10 women, aged 54 to 93 years of age (75 ± 10 years for men and 76 ± 10 years for women). The lateral BMC (g) and aBMD (g/cm^2) of the vertebral body were measured using DXA (Delphi W, Hologic). Using subregion analysis, we measured separately anterior and posterior region from the lateral DXA view and computed the ratio of anterior to posterior DXA BMC and BMD measurements (i.e. BMC_{ratio} and BMD_{ratio}). Quasi-static uniaxial compressive testing was performed on L3 vertebral bodies under displacement control (0.5mm/min) to assess failure load (FL, N), stiffness (STF, N/mm) and Work to failure (WF, N. mm).

Anterior BMC and BMD measurements were significantly lower than posterior measures ($p<0.0001$) but no significant difference was found between the anterior and posterior areas. BMC_{ratio} was significantly correlated to FL and WF ($r=0.49$ and 0.45 ; $p=0.02$ and 0.04 respectively), but not with BMD or BMC. In addition, these correlations remained significant after adjustment with BMC or aBMD (partial correlation, $r=0.47$ and 0.46 ; $p<0.045$ for all). In multiple regression analysis the combination of aBMD and BMC_{ratio} was strongly associated with FL (multiple $R=0.75$, $p<0.001$).

In conclusion, the anteroposterior heterogeneity expressed by the BMC_{ratio} improves the prediction of bone mechanical behavior in association with aBMD in this ex vivo study, with the combination explaining up to 56% of the variability of the failure load, compared with 44% for aBMD alone. These results provide rationale for testing DXA-based heterogeneity measures as predictors of vertebral fracture in clinical studies.

Bivariate regressions

| | Failure Load (FL, N) | Work to failure (WF, N. mm) | stiffness (STF, N/mm) |
|----------------------|-------------------------|--------------------------------|--------------------------|
| | r | r | r |
| BMC | 0.53** | 0.44* | 0.42 |
| aBMD | 0.66*** | 0.58** | 0.54** |
| BMD _{ratio} | -0.03 | 0.25 | -0.35 |
| BMC _{ratio} | 0.49* | 0.45* | 0.21 |

*Pearson correlations, * $p<0.05$, ** $p<0.01$, *** $p<0.001$*

table

Disclosures: *François Duboeuf, None.*

SA0049

See Friday Plenary Number FR0049.

SA0050

Development of Functional Interactions Among Cortical and Trabecular Traits During Growth of the Lumbar Vertebral Body. Melissa Ramcharan^{*1}, Meghan Faillace¹, Zoe Guengerich², Valerie Williams², Karl Jepsen³. ¹Mount Sinai School of Medicine, USA, ²Mount Sinai School of Medicine, USA, ³University of Michigan, USA

Because variation in bone traits in the elderly is largely established by adulthood, understanding how bone function is established during growth will benefit efforts to reduce fracture risk later in life. Although skeletal structures like the vertebral body depend on both cortical and trabecular traits for whole bone function, little is known about how these traits co-develop during growth. In adults, cortical and trabecular traits are functionally related, but whether early variation in one trait is followed by adaptive changes in the other remains unclear. To study this, we examined the temporal sequence of trait maturation during growth in the vertebral body among three inbred mouse strains expressing widely varying adult vertebral traits. A/J (AJ), C57BL/6J (B6) and C3H/HeJ (C3H) mice are genetically distinct where AJ exhibits a slender (narrow relative to length) bone, B6 a robust (wide relative to length) bone, and C3H has an intermediate vertebral body size with a thick cortex and low trabecular bone mass.

Female mice from each strain were sacrificed at 7, 14, 28, and 112 days of age ($n=10$ /age/strain). The L3 and L4 lumbar vertebrae were harvested, prepared for plastic embedding, sectioned along the mid-transverse and mid-coronal plane, respectively, and then imaged using fluorescence microscopy. Morphological traits were quantified in the transverse plane by measuring relative cortical area (RCA) and, in the coronal plane by calculating trabecular bone volume/ total volume (BV/TV). Differences in traits relative to age and genotype were determined using a two-way ANOVA and Student's t-test. Overall significance was set as $p<0.05$.

At 7 days of age, BV/TV varied significantly among strains and was consistent with differences seen in adulthood (112days). For each strain, an increase in BV/TV during growth was later followed by an increase in RCA. The data suggested that early variation in trabecular BV/TV lead to an adaptive response in the cortical shell traits.

In this study, we gained a better understanding of the biological processes between cortical and trabecular bone that are essential for developing a mechanically functional vertebral body. Also, along with early established variation in trabecular traits, there was a large amount of bone resorption in the marrow space as well as an increase in anisotropy. This suggested that an increase in osteoclastic activity may regulate the initial development of genetic variation in bone traits.

Disclosures: *Melissa Ramcharan, None.*

SA0051

See Friday Plenary Number FR0051.

SA0052

Femur Strength Indices and Trabecular Bone Score (TBS) in Postmenopausal Patients With Primary Hyperparathyroidism. Elisabetta Romagnoli¹, Cristiana Cipriani¹, Claudia Castro¹, Vincenzo Carnevale², Daniele Diacinti³, Sara Piemonte¹, Jessica Pepe¹, Luigina Ostuni¹, Maurizio Angelozzi¹, Addolorata Scarpiello¹, Salvatore Minisola^{*1}. ¹Dpt of Internal Medicine & Medical Specialties, University "Sapienza", Rome, Italy, ²Dpt of Internal Medicine, "Casa Sollievo della Sofferenza" Hospital, S. G. Rotondo, Italy, ³Dpt of Radiology, University "Sapienza", Rome, Italy

Purpose: We investigated new parameters of bone strength and quality obtained from DXA-derived indices in 46 postmenopausal patients with primary hyperparathyroidism (PHPT)(mean age 64.4±11.3 yrs;BMI 24.5±4.6) and in 68 age-and BMI matched postmenopausal healthy controls (C)(61.1±6.7 yrs;BMI 24.3±3.5).

Methods: Bone mineral density (BMD) of the left hip was measured by DXA (Lunar iDXA with enCORE software version 13).Structural variables were determined using the advanced Hip Strength Analysis (HAS) program, including hip axis length (HAL,mm), cross-sectional area (CSA,mm²-an indicator of axial strength), cross-sectional moment of inertia (CSMI,mm⁴-a measure of the distribution of material around the neck axis), and femoral strength index (FSI,that indicates the risk of fracture for forces generated during a fall on the greater trochanter).In 31 patients (65±12.1 yrs;BMI 25±4.5) and 41 age-and BMI matched controls (61.2±6.8 yrs;BMI 24.7±3.7) trabecular bone score (TBS)(TBS iNspight,Med-Imaps,France) was also obtained from DXA images of the lumbar spine (LS)(Hologic QDR 4500).

Results: Table 1 reports the correlation matrix between the structural parameters studied and femoral neck BMD.In PHPT and C, both CSA and CSMI significantly correlated with HAL and BMD.No correlation was found between FSI and BMD in PHPT patients, contrary to what observed in C.Mean femoral BMD values were significantly lower in PHPT compared to C (740.7±103.2 vs 790.6±98.2 mg/cm²,p<0.02).Mean HAL,CSMI, CSA and FSI values were not significantly different between PHPT and C (Table 2). The results did not change also after adjustment for age, height, weight, HAL and femoral BMD, as appropriate.BMD at LS did not differ between groups, while mean TBS values in PHPT (1.22±0.09) were significantly lower than in C (1.26±0.08).TBS values were highly correlated with BMD at LS in both PHPT (r=0.666,p<0.0001) and C (r=0.728,p<0.0001).

Conclusion: The hip structural properties of PHPT patients, despite the lower femoral BMD, did not differ from those of C, while trabecular bone microarchitecture estimated by TBS, appeared to be compromised in PHPT patients. However, the technical limitations of these DXA-derived indices of bone strength and quality should be taken into account when interpreting the clinical significance of these results for fracture risk evaluation in patients with PHPT.

Table 1. Correlation matrix between structural parameters of femoral strength and femoral neck BMD

| | PHPT (n=46) | | Controls (n=68) | |
|------|---------------------|---------------------|---------------------|---------------------|
| | HAL | BMD | HAL | BMD |
| CSMI | r=0.652 p<0.0001 | r=0.464 p<0.01 | r=0.484 p<0.0001 | r=0.323 p<0.01 |
| CSA | r=0.490 p<0.001 | r=0.898 p<0.0001 | r=0.321 p<0.001 | r=0.835 p<0.0001 |
| FSI | r=-0.091 p=NS | r=0.220 p=NS | r=-0.203 p=NS | r=0.334 p<0.01 |

Table 1

Table 2. Mean values ± 1SD of structural indices of femoral strength

| Parameter | PHPT (n=46) | Controls (n=68) | p |
|-------------------------|---------------|-----------------|----|
| HAL (mm) | 104±6.1 | 104.2±5.3 | NS |
| CSA (mm ²) | 115.5±18.4 | 122.7±16.1 | NS |
| CSMI (mm ⁴) | 8513.6±2361.1 | 9050.8±1870.9 | NS |
| FSI | 1.48±0.33 | 1.55±0.31 | NS |

Table 2

Disclosures: Salvatore Minisola, None.

SA0053

IGF-1, PINP, CTX, Osteocalcin and 25-OH Vitamin D Stability in Human Serum under Variable Storage Conditions. Ellen McMonagle^{*1}, Elizabeth McMenamin², Anne Breggia¹, Susan Durham³, Clifford Rosen¹. ¹Maine Medical Center, USA, ²Maine Medical Center Research Institute, USA, ³Immunodiagnostic Systems, Incorporated, USA

Background: Preservation of biomarker integrity is essential for consistent and reproducible data. In this study we investigated the effects of variable storage

conditions on markers of bone metabolism including IGF-1, PINP, CTX, osteocalcin, and 25-OH Vitamin D.

Methods: Serum was separated from whole blood collected from 5 healthy volunteers, aliquoted and stored at room temperature (RT), 4°C, -20°C or -70°C. Testing time points for each storage condition included 1) immediate assay as baseline (BL) for all storage conditions; 2) storage at RT or 4°C for 4,8,24,48, or 72 hours; 3) storage at -70°C with 1 thru 6 freeze/thaw (FT) cycles; and 4) storage at -20°C until tested at 1,4,7,9, and 13 months. All immunoassays were performed using the iSYS analyzer (Immunodiagnostic Systems, Inc. Scottsdale, AZ). All statistical comparisons to BL were made using paired t tests, with two-tailed analysis and are reported as mean ± SEM.

Results: Units for all analytes are in ng/mL. CTX concentration decreased from 0.268 at BL to 0.249 (p=0.032) at RT for 4 hours; 0.217 (p=0.014) at 4°C for 24 hrs; 0.239 (p=0.018) at -70°C with 1 FT cycle and 0.222 (p=0.04) at -20°C for 1 month. Osteocalcin concentration also decreased from 17.2 at BL to 16.5 (p=0.011) at RT for 8 hrs but was not significantly affected by storage at 4°C for up to 72 hours, 6 FT cycles, or 1 year at -20°C. Conversely, the concentration of IGF-1 increased from 177 at BL to 181 (p=0.031) at RT for 4 hrs; 184 (p=0.007) at 4°C for 4 hrs; 184 (p=0.044) at -70°C with 1 FT and 216 (p=0.011) at -20°C for 1 month. 25-OH Vitamin D was stable at all time points at both RT and 4°C up to 72 hrs and also after 6 FT cycles, but increased from 22.8 at BL to 31.3 (p=0.03) after 4 months at -20°C. PINP concentration also increased from 34.3 at BL to 39.2 (p=0.003) at RT for 24 hrs; 39.2 (p=0.009) at 4°C for 4 hrs; 39.3 (p=0.0002) at -70°C with 1 FT and 39.1 (p=0.002) at -20°C for 7 months.

Conclusions: Of the 5 biomarkers tested, CTX was the most sensitive to variable storage conditions while 25-OH Vitamin D and osteocalcin appeared to be the most stable. Storage at -20°C was the most detrimental to analyte stability. This data supports the need for prompt storage of serum samples at ultralow temperatures (≤-70°C) and limited freeze-thaw cycles. An additional study of long-term storage at -70°C is currently being conducted.

Disclosures: Ellen McMonagle, None.

SA0054

Linear and Nonlinear High-Resolution Finite-Element Analysis of the Distal Tibia and Radius from in Vivo MRI. Ning Zhang^{*1}, Jeremy Magland¹, Chamith Rajapakse², Yusuf Bhagat¹, ShingChun Lam¹, Felix Werner Wehrli³. ¹University of Pennsylvania, USA, ²University of Pennsylvania School of Medicine, USA, ³University of Pennsylvania Medical Center, USA

High-resolution image-based micro-finite-element (μFE) modeling is a valuable tool for characterizing bone mechanics. Linear μFE analysis is widely utilized but can only estimate elastic moduli. Nonlinear μFE analysis is capable of predicting bone's failure strength, but is computationally far more demanding. In this study, we investigate the associations of trabecular bone yield stress and toughness with axial stiffness derived respectively from nonlinear and linear μFE modelings. In-vivo μMR images of distal tibiae of 21 women (ages 58-84) with osteoporosis and distal radii of 20 women (ages 50-75) were used as study subjects. Tibia images were previously acquired at 3T field strength and radius images at 1.5T, both with a voxel size of 137 x 137 x 410 μm³. All images were subjected to linear and nonlinear μFE simulations yielding axial stiffness and stress-strain curves. The yield stress and strain were then determined by the 0.2% offset rule (Niebur, 2000) and toughness was calculated as the area under the stress-strain curve up to the ultimate point. Sixty strain levels with a step size of 0.05% were applied to obtain each stress-strain curve (e.g., Figs. 1: radius, 2: tibia). Simulated strain maps in sagittal view (Figs. 1&2 a-c) reflecting different amounts of strain (corresponding to points on the stress-strain curve before, at and after the yield point) highlight locations where trabeculae were gradually loaded until simulated failure occurred. Figs. 3 and 4 compare yield stress (5.34 ± 0.83 MPa for tibia, 3.55 ± 0.92 MPa for radius) and toughness (45.31 ± 6.83 kPa for tibia, 38.56 ± 8.03 kPa for radius) with axial stiffness (0.81 ± 0.11 GPa for tibia, 0.57 ± 0.13 GPa for radius), respectively. Strong correlations (R²>0.97, p<0.0001) between yield stress and axial stiffness were found for both tibia and radius with similar slopes and intercepts, suggesting that (1) the axial stiffness may be able to predict trabecular bone's yield stress and (2) slopes and intercepts in the correlation may not vary much for distal tibia and radius of elderly women. Further, axial stiffness was found to explain 74% (p<0.0001) of the variation in toughness of the tibia but only 38% (p<0.005) of the radius, suggesting that nonlinear μFE analysis may provide extra information compared to linear analysis, such as fracture toughness, e.g. from the shape and trend (brittle versus ductile) of the simulated stress-strain curve.

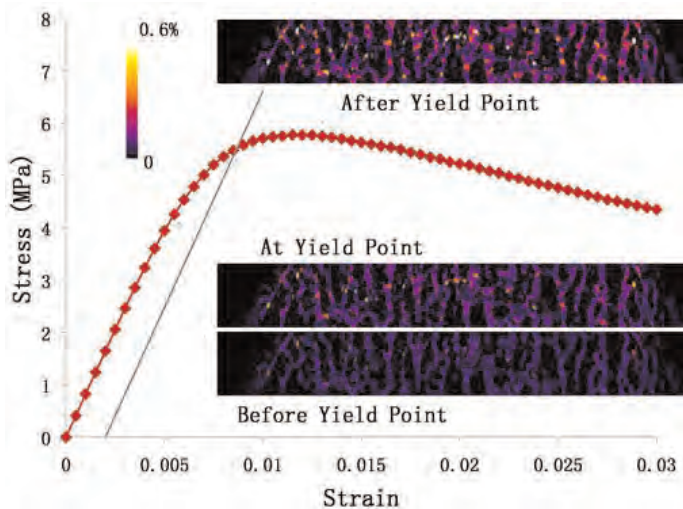


Fig. 1. Simulated stress-strain curve and strain maps based on an in vivo MR image of distal tibia.

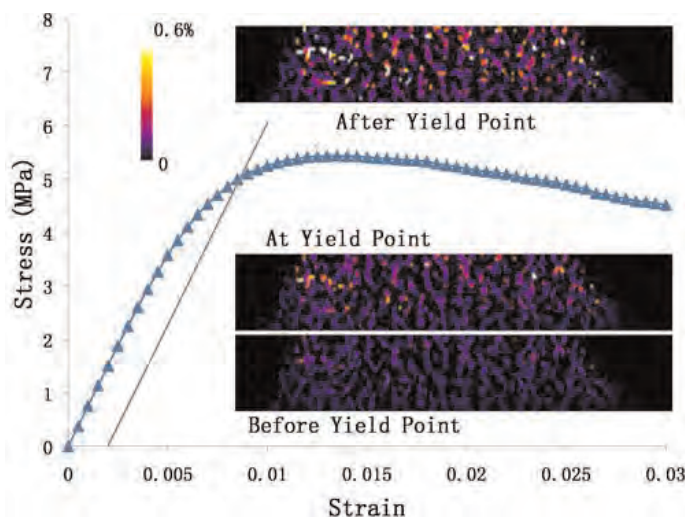


Fig. 2. Simulated stress-strain curve and strain maps based on an in vivo MR image of distal radius.

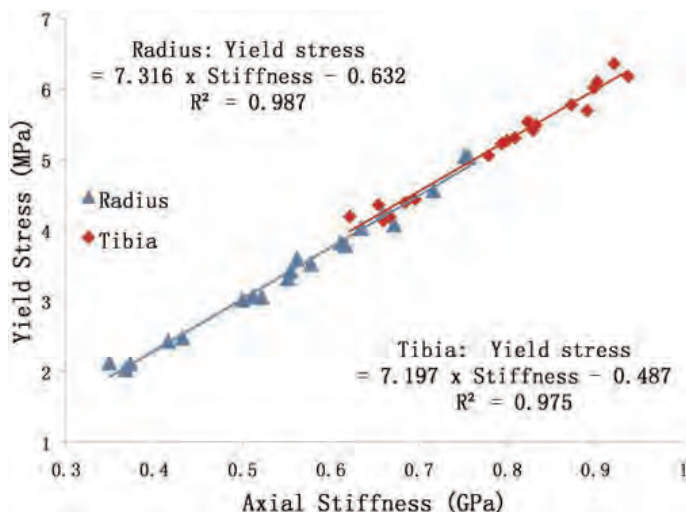


Fig. 3. Nonlinear μ FE-predicted yield stress versus linear μ FE-estimated axial stiffness.

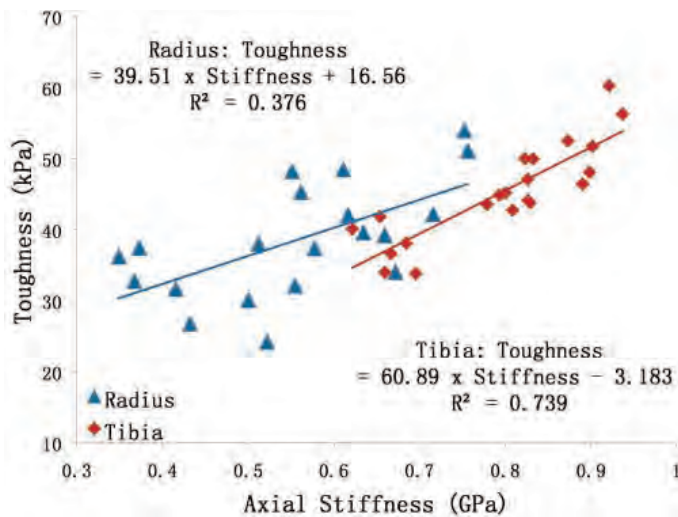


Fig. 4. Nonlinear μ FE-predicted toughness versus linear μ FE-estimated axial stiffness.

Disclosures: Ning Zhang, None.

This study received funding from: NIH

SA0055

Longitudinal Analysis of Cortical Pore Structure using HR-pQCT. Willy Tjong, Jasmine Nirody, Julio Carballido-Gamio, Andrew Burghardt, Janina Patsch, Sharmila Majumdar, Galateia Kazakia*. University of California, San Francisco, USA

Elevated levels of cortical porosity (Ct.Po) have been shown to adversely affect bone strength. Though previous cross-sectional studies have observed increased Ct.Po as a function of age, little is known on the mechanism of pore development. The purpose of this study was to characterize longitudinal changes in the cortical pore network with the goal of elucidating possible mechanisms of increased porosity. Ct.Po and pore diameter were calculated using an extended CRTX analysis previously developed in our lab. Additionally, a novel skeletonization algorithm was implemented to perform a topological analysis of the pore network. Each voxel was assigned a topological label (ie, surface, curve, junction), allowing for the classification of pores as either plate-like or rod-like. Finally, a laminar analysis was performed which quantified pore number and size in the periosteal, intracortical, and endosteal regions. Early postmenopausal women ($n = 21$, age = 57 ± 4 years) were imaged at the distal tibia at baseline and after 24 months. Ct.Po significantly increased after 24 months (+10.6%, $p < 0.001$), with both the number of plate-like canals (+14.6%, $p < 0.001$) and rod-like canals (+14.8%, $p < 0.001$) increasing. Though there was no change in the ratio of plate-like canals to rod-like canals, there was an increase in the ratio of total plate volume to rod volume (+13.8%, $p < 0.05$). This tendency toward a more plate-like pore network is confirmed by an increase in mean plate volume (+9.1%, $p < 0.05$). A corresponding decrease in mean rod volume (-3.7%, $p = 0.07$) trended towards significance. The cortical pore network also showed greater connectivity, as evidenced by an increase in the number of junctions (+25.3%, $p < 0.01$). Regional analysis indicated that increased Ct.Po was confined to the endosteal aspect of the cortex (+29.0%, $p = 0.05$; no significant changes in the other regions), and that Ct.Po increase occurred through a mechanism of increased pore size (+40.0% in the endosteal region, $p < 0.001$) rather than pore number. Based on these data, we hypothesize that age-related changes in the cortical pore network result in the preferential expansion of plate-like canals at the endosteal aspect of the cortex through a mechanism of pore merging. As cortical microstructure is linked to bone strength, the correlation between the morphological parameters presented here and the biomechanical properties of bone warrants further investigation.

Disclosures: Galateia Kazakia, None.

This study received funding from: Merck & Co., Inc.

SA0056

See Friday Plenary Number FR0056.

SA0057

See Friday Plenary Number FR0057.

SA0058

Male Obese Adolescents Have Stronger and Bigger Bones than their Normal-weighted Peers. Sara Vandewalle¹, Stefan Goemaere^{2*}, Inge Roggen³, Hans Zmierzczak⁴, Kaatje Tovey⁴, Patrick Debode⁵, Maria Van Helvoirt⁵, Youri Taes⁶, Jean-Marc Kaufman⁷, Jean De Schepper³. ¹University Hospital Ghent, Belgium, ²University Hospital, Belgium, ³University Hospital Brussels, Belgium, ⁴University Hospital Ghent, Belgium, ⁵Zeepreventorium, Belgium, ⁶Dept. Endocrinology Ghent University Hospital GhentDe Pintelaan 1859000 Gent, Belgium, ⁷University Hospital of Ghent, Belgium

Background: Recent studies have shown that obesity is associated with an increased risk of fracture. Whereas some studies report higher bone mineral density (BMD) (measured by DXA) in overweight children, other studies conclude that obesity is linked to a lower BMD. However, there are few data on bone geometry and true volumetric bone mineral density (vBMD) in obese adolescents.

Objective: To determine bone strength, bone geometry and vBMD in obese male adolescents by peripheral quantitative computed tomography (pQCT) and the relationship between muscle force and bone characteristics at the tibia in adolescents.

Methods: 51 male obese (mean BMI sds : 2.55) adolescents, aged 10-19y, recruited at the start of a residential obesity treatment program in De Haan (Belgium), and 51 healthy male controls matched for age and height (mean BMI sds: -0.17) were included in this cross-sectional study. Trabecular (4% site from distal end) and mid shaft cortical (38 % site from distal end) vBMD and bone geometry were assessed at the non-dominant leg using the Stratec XCT 2000 device. Maximal muscle force (F max) was evaluated by two leg jumping mechanography using a ground force reaction plate (Leonardo, Novotec Medical GmbH).

Results: The trabecular vBMD and area measured at the distal end of the tibia were higher in the obese group. At mid shaft, tibial cortical area, periosteal circumference and endosteal circumference were larger in the obese group. There was no significant difference in cortical vBMD between the two groups. The stress-strain index (SSI) was significantly higher in the obese group. Obese adolescents developed a significantly higher maximal force (2.1 (range: 2.8) vs 1.2 (range: 1.3) kN; p<0.001) compared to the control group. In the merged study groups significant positive associations were observed between F max and cortical bone area (β : 0.60; p<0.001), periosteal circumference (β : 0.59; p<0.001), endosteal circumference (β : 0.41;p<0.01), trabecular bone area (β :0.50; p<0.001), and trabecular vBMD (β :0.34; p=0.01), but not cortical vBMD (β :0.13; p=NS).

Conclusions: Obese adolescents have a bigger bone size and higher bone strength at the tibia compared to normal-weighted controls. They develop higher ground reaction forces and apply higher mechanical load to the skeleton.

| | Obese boys (mean±SD) | Control boys (mean±SD) | Difference between groups (%) | Significance (p) |
|---------------------------------------|----------------------|------------------------|-------------------------------|------------------|
| pQCT results T4 | | | | |
| Trabecular vBMD (mg/cm ³) | 240 ± 28 | 227 ± 28 | 5% | p<0.05 |
| Trabecular area (mm ²) | 545 ± 111 | 452 ± 87 | 20% | p<0.001 |
| pQCT results T38 | | | | |
| Cortical vBMD (mg/cm ³) | 1079 ± 57 | 1074 ± 62 | — | NS |
| Cortical area (mm ²) | 307 ± 65 | 297 ± 55 | 19% | p<0.001 |
| Periosteal circumference (mm) | 80 ± 10 | 74 ± 8 | 8% | p<0.001 |
| Endosteal circumference (mm) | 52 ± 8 | 46 ± 10 | 13% | p<0.001 |
| SSI (mm ²) | 1817 ± 460 | 1416 ± 339 | 28% | p<0.001 |

Table 1: Differences in bone size, bone strength and vBMD between the two groups

Disclosures: Stefan Goemaere, None.

SA0059

Measuring the Fracture Toughness of Mouse Bone. Alexander Makowski^{1*}, Sasidhar Uppuganti², Jeffrey Nyman³. ¹Vanderbilt University, USA, ²Vanderbilt University, USA, ³Vanderbilt University Medical Center, USA

The age-related increase in fracture risk may not be solely due to a loss in bone strength since bone matrix undergoes multiple changes independent of bone mineral density with aging and disease onset. To identify novel factors contributing to bone fracture resistance, a method was refined to quantify fracture toughness of rodent bone. This method involves generating a micro-notch in the cortex of the femur mid-shaft and loading the bone in three point bending to drive a crack from the notch through the matrix to failure. Quantifying this resistance to crack propagation as a material property known as the stress intensity factor (K_c) requires that the bone structure and the notch size be properly incorporated in the measurement. Given that the equations to do so were derived for a circular pipe and that the geometry of the mid-shaft is irregular varying across genotypes and strains, we investigated whether micro-notching the anterior vs. posterior side affects K_c using mouse strains with varying bone geometry. Femurs were harvested from nineteen 17 wk old male mice (FVB). To increase the variance in bone structure, femurs were also harvested from sixteen 11-12 wk old male, transgenic mice (on a mixed background), namely liver-specific insulin receptor knock-out (LIRKO) and cre-negative floxed mice (WT). Using a thin wafer saw and then a razor blade with μ -diamond solution, we obtained

15 anterior and 19 posterior notched bones meeting the geometry criteria. Notch angles and bone geometry were quantified from μ CT scans acquired at 6 μ m voxel size. Femurs were loaded at a rate of 0.06 mm/min to determine peak force and video was recorded (~14 μ m²/pixel; 30 fps) to track failure mode. The COV of the notch angle was lower for the posterior than for the anterior group (12.4% vs. 21.1%). Video and μ CT identified 2 specimens with deep notches and little cracking and 1 specimen with a partial notch and poor orientation. For the FVB mice, K_c is different between ant. and post. notched bones (Fig. 1). Also, K_c for post. notches differed between older FVB and younger LIRKO. Therefore, regressions to analyze independence of geometry were done separately (Fig. 1). For the ant. group, the y-intercept was not zero (95% CI: -3.97 to -0.93) suggesting a lack of independence. For the post. groups, this was not the case (FVB+WT 95% CI: -10.1 to 3.54). Further refinement of structure and notch angle analyses may help K_c become entirely independent of geometry.

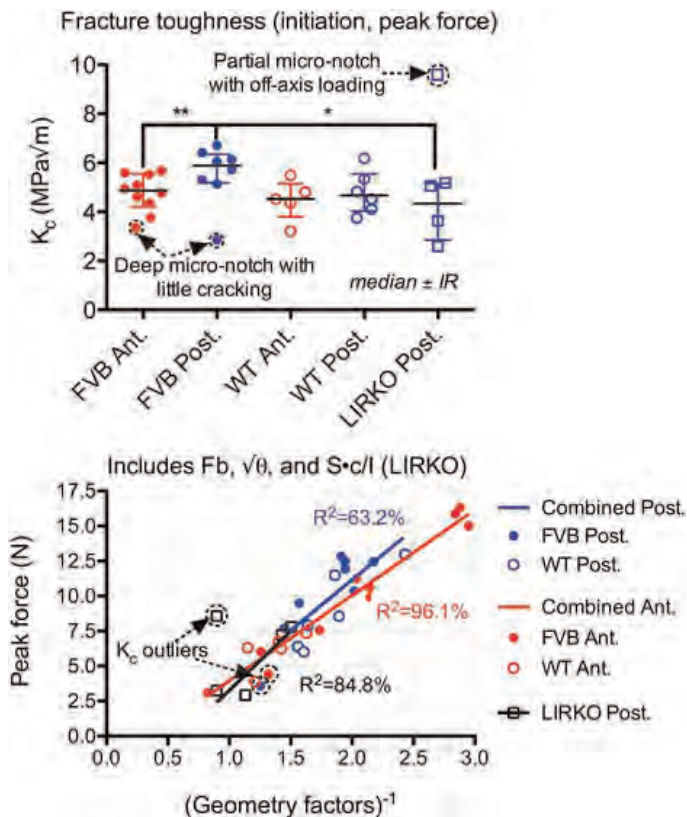


Fig 1. Fracture toughness for each group and regressions between geometry factors and peak force

Disclosures: Alexander Makowski, None.

SA0060

See Friday Plenary Number FR0060.

SA0061

Proximal Femoral Cortical Thickness in Postmenopausal Women Shows Highly Localised Significant Asymmetry. Tom Turmezei^{1*}, Graham Treece², Andrew Gee², Carol Tonkin², Madhavi Vindlacheruvu³, Karen Blesic², Kenneth Poole¹. ¹University of Cambridge, United Kingdom, ²University of Cambridge, United Kingdom, ³Cambridge University Hospitals NHS Foundation Trust, United Kingdom

Background: Establishing focal skeletal left-right difference is important for anthropological study, understanding adaptation to strain and the clinical investigation of bone. Asymmetry is not only well established in the human skeleton but, given that bone exhibits functional adaptation, is also to be expected. Differences in the lower limb are reported to be of smaller magnitude than in the upper limb, with the lower limb also mirroring the usual pattern of upper limb right-sided dominance. Until now, only selective focal or summative regions have been analysed. Dual energy X-ray absorptiometry of the proximal femora has shown either a left bias or no difference in areal bone mineral density, however individual left-right differences of up to 26% have been reported.

Method: Cortical thickness maps were created of the proximal femora from clinical CT data of 197 postmenopausal women aged 73 ± 7 yrs (mean ± sd) combined from 3 cohorts: 48 from the FEMCO study (75 ± 8 yrs), 80 from the FREEDOM study (74 ± 5 yrs) and 69 from the EUROFORS study (70 ± 7 yrs). All data were taken

from the study baseline prior to any intervention. After registration of each bone to an average (right) femur shape, statistical parametric mapping was used to determine sites of significant differences in mean cortical thickness between sides.

Results: We identified highly focal differences between left and right, including a vertical band of significantly thicker cortex along the load-bearing anteromedial aspect of the right proximal femoral shaft. Several smaller patches of cortex at the inferomedial femoral neck and the greater trochanter were also significantly different between sides, some thicker on the left (fig. 1). Results were validated across each of the study subgroups.

Discussion: Highly localised and significant left-right differences were detected in the cortical thickness of the proximal femora of postmenopausal women. The vertical band of increased thickness on the right correlates with the point of maximal stress in the early and mid-gait cycle, suggesting that side differences may be related to gait asymmetry. There is also a high thickness gradient in this region, and so findings could represent widening of thicker regions around the cortex from mineral redistribution in response to load-bearing. These results reinforce the importance of cortical thickness measurement location since dimensions derived from planar imaging can hide significant local fluctuations.

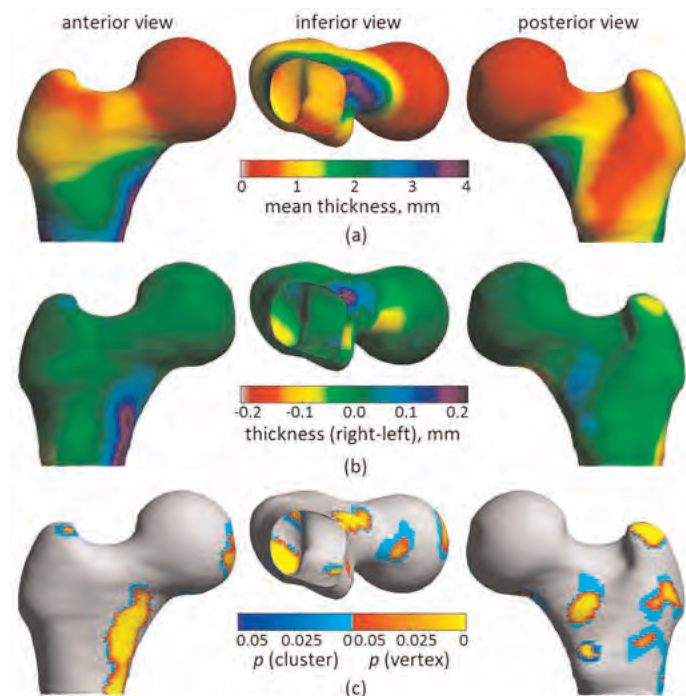


Figure 1 (a) Mean cortical thickness, (b) mean difference between left and right sides, (c) significance ($p < 0.05$) of regional (cluster) or individual (vertex) measured thickness changes. All results shown mapped to the right femur

Figure 1

Disclosures: Tom Turmezei, None.

SA0062

Solid State NMR Investigation of Bone Quality in Osteoporotic Bone: Citrate/GAGs Are Present at the Mineral-Organic Interface. Ondrej Níkel^{1*}, Deepak Vashishth¹, Danielle Laurencin², Grazyna Sroga¹. ¹Rensselaer Polytechnic Institute, USA, ²Institut Charles Gerhardt de Montpellier, UMR 5253, CNRS-UM2-ENSCM-UM1, Université? Montpellier 2, France

The Solid State Magic Angle Spinning Nuclear Magnetic Resonance (SS MAS NMR) has long been appreciated for ability to inform on mineralization¹. The SS NMR was recently shown to be useful for assessing the matrix-hydroxyapatite (HA) interface. The rotational echo double resonance (REDOR) uses dipolar interaction between ³¹P (found in HA) and ¹³C (found in the organic matrix) to probe mineral-organic interface at the scale of atoms².

To use the REDOR NMR technique on a bone, it is necessary to spin the sample at rapid rate (here 750 000RPM). This rapid rotation poses a problem for inhomogeneous material, particularly the osteoporotic tissue which has a porosity (and thus density) gradient. Most of published work to date overcomes this problem by powdering and drying, which alters the tissues³.

Instead of powdering, here, for the first time, we show the use of the ¹³C-³¹P REDOR NMR to investigate intact human osteoporotic bone. Cortical bone from mid-diaphyseal femurs of 23yr healthy and 77yr old osteoporotic donors were machined to 2x2mm cylinders. The intact bone cylinders were probed in NMR in presence of saline and ¹H, ³¹P, ¹³C Cross Polarization (CP) and ¹³C-³¹P REDOR NMR spectra were recorded at MAS.

We found that citrate⁴ and/or glucosaminoglycans⁵ (GAG) are present as the most-intimately HA-adsorbed organic species in human bone, regardless of donor's age. This finding suggests that citrate/GAG anchors the HA platelets to the organic matrix. Furthermore, the analysis of ¹³C {³¹P} REDOR NMR spectra in bone tissues with different levels of non-enzymatic glycation suggests that hydroxyproline (the outermost amino acid in the collagen triple helix) and alanine proximity to HA changed with elevated glycation level. The ¹³C and ³¹P spectra were in agreement with published literature¹⁻³ and showed no significant difference with donor age. Crystallographic environment of phosphate is thus maintained in osteoporotic bone.

- 1) Wu, Y.; Glimcher, M.J.; Rey, C.; Ackerman, J.L. *J. Mol. Biol.* 1994, 244, 423.
- 2) Jaeger, C.; Groom, N. S.; Bowe, E. A.; Horner, A.; Davies, M. E.; Murray, R. C.; Duer, M. *J. Chem. Mater.* 2005, 17, 3059.
- 3) Zhu, P.; Xu, J.; Sahar, N.; Morris, M. D.; Kohn, D. H.; Ramamoorthy, A. *J. Am. Chem. Soc.* 2009, 131, 17064.
- 4) Hu, Y. Y.; Rawal, A.; Schmidt-Rohr, K. *Proc. Natl. Acad. Sci. U.S.A.* 2010, 107, 22425.
- 5) Wise, E. R.; Maltsev, S.; Davies, M. E.; Duer, M. J.; Jaeger, C.; Loveridge, N.; Murray, R. C.; Reid, D. G. *Chem. Mater.* 2007, 19, 5055.

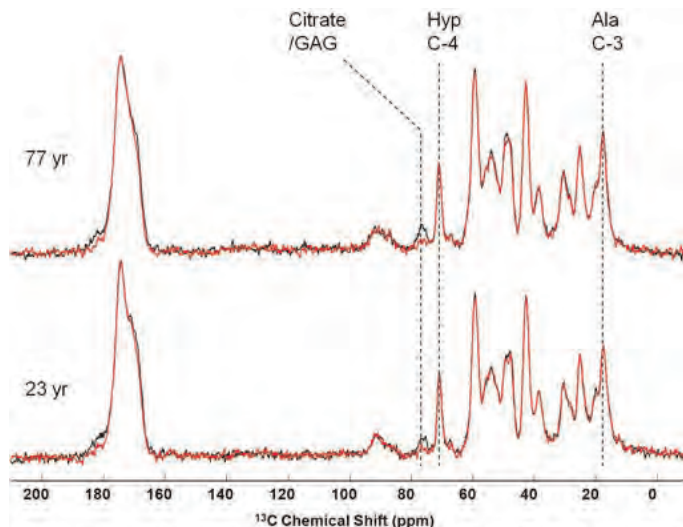


Figure 1 ¹³C-³¹P REDOR spectra of intact cortical femur from 77yr and 23yr old donors. The peaks of citrate/GAG, hydroxyproline C-4 and alanine C-3 are highlighted. Greater difference between reference (black) and REDOR (red) spectra indicates proximity to ³¹P found in mineral.

¹³C-³¹P REDOR spectra of intact cortical femur from 77yr and 23yr old donors.

Disclosures: Ondrej Níkel, None.

This study received funding from: NIH / NIAMS AR49635, Chateaubriand fellowship

SA0063

Withdrawn

SA0064

Trabecular Bone Score – TBS – a Novel Method to Evaluate Bone Microarchitecture in Primary Hyperparathyroidism. Barbara Silva^{1*}, Stephanie Boutroy¹, Didier Hans², Chiyuan Zhang³, Julia Udesky⁴, Donald McMahon⁵, Marcella Walker³, John Bilezikian⁵. ¹Columbia University Medical Center, USA, ²Lausanne University Hospital, Switzerland, ³Columbia University, USA, ⁴Columbia University Medical Center, USA, ⁵Columbia University College of Physicians & Surgeons, USA

Primary hyperparathyroidism (PHPT), a common endocrine disorder, is characterized primarily by biochemical and densitometric abnormalities. Typically, bone density by DXA is reduced at the predominantly cortical 1/3 radius while cancellous bone (e.g., lumbar spine) is generally preserved. These findings have been confirmed by bone biopsies. Since DXA does not directly assess bone microarchitecture, and bone biopsies are not routinely performed, a non-invasive approach to the evaluation of skeletal microstructure would be helpful. Trabecular Bone Score (TBS) is a novel gray-scale textural analysis to estimate trabecular microarchitecture from the AP Spine DXA. TBS correlates well with more direct measures of bone microarchitecture independent of BMD (Hans et al. 2011. *J Clin Densitom* 14:302-312). In this study, we compared TBS with High Resolution peripheral Quantitative Computed Tomography (HRpQCT, Scanco Medical AG, Switzerland), an established but not readily available approach to measuring microstructure of bone.

Materials & Method: 22 women (66.9 ± 8.6 yr) with well-characterized PHPT (elevated serum calcium and PTH levels) were studied. AP spine and hip BMD were assessed by DXA (QDR 4500, Hologic Inc, USA), and site-matched spine TBS parameters were extracted from the DXA image using TBS iNsign software (v1.9, Medimaps SA, France). Bone microarchitecture of the distal radius and tibia was

assessed by HRpQCT. Correlations between BMD, HRpQCT parameters and TBS were calculated.

Results: The mean (SD) TBS was 1.288 ± 0.123 (~ partially degraded microstructure). Correlations between TBS and BMD were positive at the lumbar spine ($r=0.39$), femoral neck ($r=0.36$) and total hip ($r=0.28$) but not significant. However, the relationships between TBS and HRpQCT parameters (Table) were positive and significant in terms of total, cortical, and trabecular volumetric BMD at both radius and tibia. After adjusting for weight, all HRpQCT parameters, except trabecular thickness, correlated significantly with TBS.

Conclusion: These data demonstrate that TBS has the potential to provide microstructure information in PHPT. The value of this approach rests with the facile availability of DXA and its routine use in PHPT. With significant correlations between TBS and microstructural indices by HRpQCT, a method that has greater resolving power but is not generally available, TBS could become a very helpful clinical tool in the assessment of skeletal involvement in PHPT.

Correlation between TBS and HRpQCT parameters:

| HRpQCT parameters | Relationship with TBS (correlation coefficient) | | |
|-------------------|---|-------|-----------------------------|
| | Radius | Tibia | Tibia (adjusted for weight) |
| Total vBMD | 0.49* | 0.61* | 0.63* |
| Ct.vBMD | 0.49* | 0.48* | 0.52* |
| Tb.vBMD | 0.48* | 0.52* | 0.49* |
| Ct.Th | 0.44* | 0.52* | 0.52* |
| BV/TV | 0.48* | 0.52* | 0.49* |
| Tb.N | 0.51* | 0.30 | 0.47* |
| Tb.Th | 0.34 | 0.04 | 0.07 |
| Tb.Sp | -0.44* | -0.35 | -0.57* |
| Tb.Sp.SD | -0.39 | -0.34 | -0.52* |

* p value < 0.05

Disclosures: Barbara Silva, None.

SA0065

Viscoelastic Mapping of Transmenopausal Bone Biopsies. Sara Campbell¹, Philip Yuya², Ben Polly³, Donna Hurley¹, Joseph Turner⁴, Joan Lappe⁵, Robert Recker⁵, Mohammed Akhter⁵. ¹National Institute of Standard & Technology, USA, ²Clarkson University, USA, ³National Renewable Energy Laboratory, USA, ⁴University of Nebraska, USA, ⁵Creighton University Osteoporosis Research Center, USA

Trabecular bone architecture has been shown to deteriorate in postmenopausal, osteoporotic women, yet the changes in the intrinsic material properties of bone during the transmenopausal period are uncertain. The general hypothesis for this work is that material properties of trabecular bone are affected by change in hormonal status at menopause soon after final menses. Here, we used atomic force microscopy (AFM) methods to measure viscoelastic properties (storage and loss modulus E' and E'' , respectively) at the nanoscale. The nanoscale spatial resolution of AFM enables measurement of material properties without the contribution of voids and pore spaces. In a previously reported study (Recker *et al.*, 2004), we obtained transilial bone biopsies from women on entry (pre-menopausal and >age 46) and at 12 months past the last menstrual period. In this preliminary work, we applied contact resonance force microscopy (CR-FM), a dynamic contact mode of AFM, on a pair of specimens from the previous study. The specimens were prepared with a flat surface (~155 nm roughness) by grinding with 600, 800, and 1200 grit sand papers and then polishing with 1 mm and 0.25 mm diamond slurry. A total of 14 point maps were acquired, each consisting of a 10 mm x 10 mm region (32 x 32 = 1024 pixels, 0.32 mm/pixel width). Absolute values of E' and E'' for the CR-FM data were obtained with use of dynamic nanoindentation values on the pre-menopausal sample as reference. Nanoindentation and CR-FM values for both E' and E'' declined in the postmenopausal bone biopsies in this pair (Table), consistent with nanoindentation results in 15 biopsy pairs (Polly *et al.*, 2012). The difference in test frequency between the two techniques (~1 MHz for CR-FM and 200 Hz for nanoindentation) likely contributes to measurement variations. Increased remodeling rates have been reported in postmenopausal women (Recker *et al.*, 2004), suggesting greater heterogeneity with respect to gradation in mineralization. Although no fractures were reported in women from the original study, the greater variation in mineralization may be responsible for lower values of E' and E'' in postmenopausal women. These results demonstrate how viscoelastic CR-FM mapping enables nanoscale characterization of material properties that may be affected by increased remodeling rates in postmenopausal women.

| sample | NI E' (GPa) | NI E'' (GPa) | CR-FM E' (GPa) | CR-FM E'' (GPa) |
|--------|---------------|----------------|------------------|-------------------|
| Pre | 18.0 ± 1.83 | 0.219 ± 0.194 | reference: 18.0 | reference: 0.22 |
| Post | 16.2 ± 1.62 | 0.154 ± 0.108 | 15.0 ± 3.0 | 0.21 ± 0.04 |

Pre-premenopausal; Post-postmenopausal; NI-nanoindentation; E' -storage modulus; E'' -loss modulus. Values represent the mean and one standard deviation of measurements.

Table

Disclosures: Mohammed Akhter, None.

SA0066

Bone Mineral and Material Properties in a Patient with Alendronate-Associated Atypical Femur Fracture Before and After Two Years Treatment with Teriparatide. Steven Ing^{*1}, Hartmut Malluche², Marie-Claude Faugere², Daniel Porter³, David Pienkowski³. ¹The Ohio State University, USA, ²University of Kentucky Medical Center, USA, ³University of Kentucky, USA

Atypical femur fractures have been reported as a potential complication of long-term alendronate treatment. We performed bone biopsies in a 62-year old white female patient after 12 continuous years of alendronate treatment, 1) at time of spontaneous atypical left femur fracture (bone pain in the left femur starting 2 years before fracture) and stress fracture of the right femur diagnosed by technetium bone scanning, and 2) 22 months after switching from alendronate to daily treatment with teriparatide.

Bone samples were processed undecalcified for bone histology and assessment of bone quality by Fourier transformed infrared spectroscopy (FTIR). Results were compared with age and gender matched controls.

The first bone biopsy showed: low cancellous bone volume, reduced trabecular thickness, low osteoblast bone interface, mildly elevated osteoclast bone interface and dystrophic osteoclasts. The second biopsy showed: high cortical porosity, a mild increase in osteoblast and osteoclast bone interface, and normal osteoclasts. Bone mineral and material properties are shown in the Table.

In conclusion, this patient with bilateral fractures after long-term alendronate treatment, had: abnormally high mineral-to-matrix ratio, abnormally low carbonate-to-phosphate ratio associated with suppressed bone turnover, and dysmorphic osteoclasts. Teriparatide treatment results in: decrease in mineral-to-matrix ratio to normal levels, increase in carbonate-to-phosphate ratio to the normal range, and decrease in collagen crosslinking within the normal range. These findings might result from: 1) cessation of alendronate use, 2) use of teriparatide, 3) changes in bone turnover, or 4) a combination of any of these.

| Table | Baseline after 12 yrs. alendronate | After 22 months teriparatide | Controls (n=12) |
|-------------------------------------|------------------------------------|------------------------------|-----------------|
| Mineral-to-Matrix Ratio | 4.54 ± 0.51* | 3.90 ± 0.41* | 3.68 ± 0.23 |
| Carbonate-to-Phosphate Ratio (x100) | 0.96 ± 0.11* | 1.10 ± 0.10* | 1.12 ± 0.07 |
| Crystal Size | 0.94 ± 0.17 | 0.86 ± 0.12 | 0.89 ± 0.04 |
| Collagen Crosslinking | 3.64 ± 0.28 | 3.34 ± 0.24* | 3.53 ± 0.27 |

* different from controls, p<0.05
*different from baseline, p<0.05

FTIR Measures at Baseline and on Teriparatide Treatment

Disclosures: Steven Ing, None.

SA0067

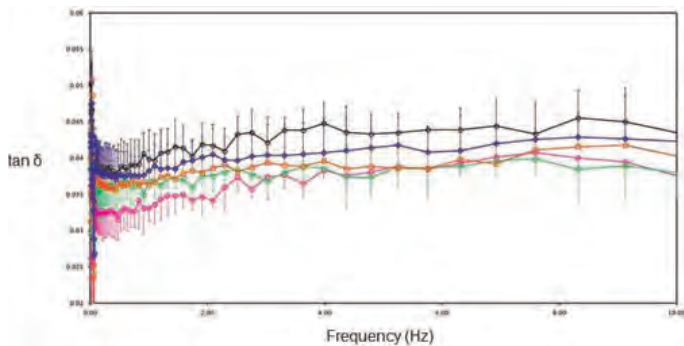
Histomorphometry and Loss Tangent Changes in OVX Rat Cortical Bone with Combination Treatment. Xiao Yang^{*}, Taeyong Lee, PADMALOSINI MUTHUKUMARAN. National University of Singapore, Singapore

Loss tangent ($\tan \delta$) has been demonstrated as an important surrogate to characterize bone strength. However, change of $\tan \delta$ in rat bone associated with ovariectomy was never studied in literature. As an effective animal model in evaluating osteoporotic drug efficacy, standardization of $\tan \delta$ measurement in SD rat is of great value. Hence, we conducted a study on the ovariectomized rat femur cortical bone to investigate the $\tan \delta$, BMD and bone area changes response to ovariectomy.

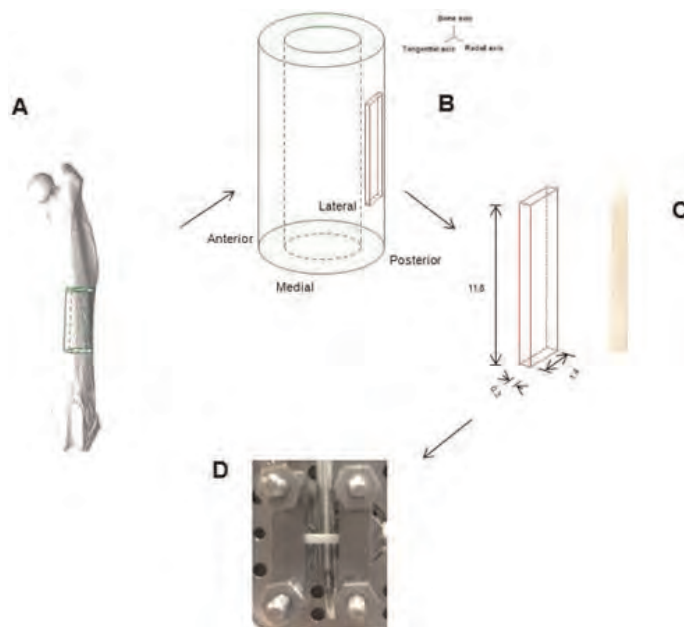
SD rats were divided into 5 groups: SHM, OVX, PTH, IBN and COM group. The rats from OVX group received ovariectomy surgery, whilst rats in SHM group received sham surgery without removing ovary organ. PTH group receive 10 µg/kg weekly PTH administrations. IBN group received 7 µg/kg ibandronate administrations. COM group received both. Rats were euthanized, 30 femurs were harvested after 3 months. $\tan \delta$ was obtained using the Dynamic Mechanical Analyzer (DMA), which produces an oscillating stress on the bone specimen so that the resultant strain can be measured. Specimens were subjected to a single cantilever bending stress (frequency range: 0.01 Hz – 15Hz) at physiological temperature (37 °C). Cortical BMD (Ct. BMD), cortical area, periosteal perimeter, endocortical perimeter, medullary area, Y-axial stress-strength indices (SSIy) was measured by pQCT.

Although there is no significant change occurred in Ct. BMD between SHM and OVX, the measured $\tan \delta$ of OVX bones was significantly lower than SHM ($p<0.001$). It worth noticing that the cortical area of OVX ($6.5 \pm 0.5 \text{ mm}^2$) was different from SHM ($7.4 \pm 0.4 \text{ mm}^2$) significantly. OVX has both larger periosteal perimeter ($14.9 \pm 0.3 \text{ mm}^2$) and endocortical perimeter ($11.8 \pm 0.6 \text{ mm}^2$) than SHM ($14.0 \pm 0.4 \text{ mm}^2$ and $10.1 \pm 0.6 \text{ mm}^2$). Among treatment groups, PTH and COM has the largest periosteal perimeter, while IBN and COM has the largest endocortical perimeter. Thus the resultant cortical area showed an additive effect in COM group. Furthermore, $\tan \delta$ of COM was significantly higher than mono treatments.

Our results suggest that, periosteal formation and endosteal resorption induced by ovariectomy surgery may cause the thinning of cortical shell in OVX rats, while the treatment can alter the configuration. In dependent of area, $\tan \delta$ of different groups varied, which suggests that there is a change in load bearing capacity between the groups.



loss tangent by frequency in different groups



sample preparation for DMA

Disclosures: Xiao Yang, None.

This study received funding from: ministry of education singapore

SA0068

See Friday Plenary Number FR0068.

SA0069

Testosterone Treatment Has Differential Effects on Trabecular and Cortical Bone Strength in Men with Hypopituitarism. Mona Al Mukaddam^{*1}, Chamith Rajapakse², Yusuf Bhagat¹, Wensheng Guo³, Jeremy Magland¹, Felix Werner Wehrli⁴, Peter Snyder¹. ¹University of Pennsylvania, USA, ²University of Pennsylvania School of Medicine, USA, ³University of Pennsylvania, USA, ⁴University of Pennsylvania Medical Center, USA

Deficiencies of testosterone (T) and growth hormone (GH) result in bone loss. Replacement of T in hypogonadal men leads to improvement in BMD, trabecular structure and bone strength. Replacement of GH in men with GH deficiency leads to improvement in BMD. The aim of this study was to determine the effects of T and GH on bone strength assessed by microMRI-based finite element analysis.

Thirty two men (age 50 ± 15 yr) with severe deficiencies of T and GH due to hypopituitarism but no prior treatment for those deficiencies were randomized to receive T alone (n=15) or T+GH (n=17) for two years. The doses of T and GH were adjusted to keep the serum concentrations of T and IGF-1 in their mid-normal ranges. MicroMRI of the distal tibia was performed at baseline and after 12 and 24 months of treatment. MicroMRI at 1.5 Tesla field strength yielded $137 \times 137 \times 410 \mu\text{m}^3$ voxels that were converted to hexahedral finite elements. Micro-finite element (μFE) models for cortical and trabecular bone were generated using an operator-guided segmentation program that delineated endosteal and periosteal boundaries. Uniaxial-simulated compression yielded axial stiffness, a marker of bone strength.

The mean serum T concentration increased from severely low before treatment to normal during months 3-24 of treatment in both the T only (67.9 to 616 ng/dL) and T+GH (91.6 to 627 ng/dL) groups. The mean serum IGF-1 concentration increased

from low before treatment to normal during months 3-24 of treatment (59.6 to 151 ng/mL) in the T + GH group and remained low in the T only group (41.7 to 47.1 ng/mL).

Both T alone and T+GH increased trabecular bone axial stiffness from 0 to 24 months (Table 1, Fig. 1a), but the increase with T+GH (10.9%; $P < 0.01$) was not significantly greater than that with T alone (8.5%; $P < 0.05$). In contrast, cortical bone axial stiffness decreased significantly in both treatment arms from 0 to 12 months (T alone, -7.3%, $P < 0.05$; T+GH, -10.2%, $P < 0.01$) and from 12 to 24 months tended to decrease further in the T only group (-1.0%, NS) but increased in the T+GH group (7.2%, $P < 0.05$) (Table 1, Fig. 1b).

We conclude that in men with hypopituitarism, testosterone treatment for two years, with or without growth hormone, significantly increased trabecular bone strength but, during the first year, significantly decreased cortical bone strength.

Table 1. Effect of testosterone and growth hormone treatment on μFE -derived stiffness in the distal tibia

| Duration of treatment | Axial Stiffness (GPa, mean \pm SE) | | | |
|-------------------------------|--------------------------------------|-----------------|-----------------|-----------------|
| | Baseline | 12 months | 24 months | |
| Testosterone | Trabecular Bone | 1.34 \pm 0.13 | 1.43 \pm 0.16 | 1.48 \pm 0.16 |
| | Cortical Bone | 0.64 \pm 0.07 | 0.60 \pm 0.07 | 0.58 \pm 0.07 |
| Testosterone + Growth Hormone | Trabecular Bone | 1.31 \pm 0.10 | 1.39 \pm 0.10 | 1.43 \pm 0.12 |
| | Cortical Bone | 0.59 \pm 0.04 | 0.53 \pm 0.05 | 0.55 \pm 0.04 |

Table 1

Figure 1a.

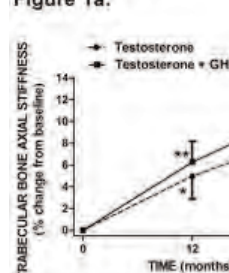


Figure 1b.

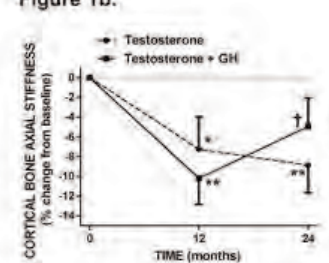


Figure 1. Percent change in axial stiffness of the distal tibia from baseline to 12 and 24 months after treatment with testosterone (N=15) or testosterone and growth hormone (N=17). Axial stiffness was determined by μMRI -based finite element analysis of trabecular bone (fig. 1a) and cortical bone (fig. 1b).

P values, vs baseline:

* $P < 0.05$

** $P < 0.01$

P value, 24 months vs 12 months:

† $P < 0.05$

‡ $P < 0.05$

Figure 1

Disclosures: Mona Al Mukaddam, None.

This study received funding from: Solvay (now Abbott), Lilly

SA0070

Effects of Spaceflight and a Sclerostin Antibody Countermeasure on the Mechanical Properties of Bone in Mice. Anthony Lau^{*1}, Alicia Ortega², Mary Bouxsein³, Ted Bateman⁴, Andrea Hanson⁵, Travis Pruitt⁶, Eric Livingston⁷, Colin Smith⁸, Angelica de Rosa⁷, Eric Lai⁷, Laura Bowman¹, Louis Stodieck⁹, Rachel Ellman³, Jordan Spatz¹⁰, Kelly Warmington¹¹, HL Tan¹¹, Dave Hill¹¹, Shweta Maurva², Andy Cureton², Sutada Lotinun¹², Chris Paszty¹³, Virginia Ferguson⁹. ¹University of North Carolina at Chapel Hill, USA, ²University of Colorado, USA, ³Beth Israel Deaconess Medical Center, USA, ⁴University of North Carolina, USA, ⁵University of Washington, USA, ⁶Clemson University, USA, ⁷University of North Carolina- Chapel Hill, USA, ⁸North Carolina State University, USA, ⁹University of Colorado, USA, ¹⁰Harvard-MIT Division of Health Sciences & Technology (HST), USA, ¹¹Amgen, USA, ¹²Harvard School of Dental Medicine, USA, ¹³Amgen, Inc., USA

Skeletal unloading from spaceflight reduces bone volume and mineral density; how this loss translates to functional change in strength and stiffness is not well known. To study this, 30 mice were flown on Space Shuttle flight STS-135 for 13-days (FL) with half treated with each vehicle (VEH, n=15) and a sclerostin antibody countermeasure (SclAb, n=15). Corresponding ground control (GC) groups were similarly treated. Bone strength was assessed through computational finite element modeling (FEM) at the proximal tibia, and mechanical testing of the femur diaphysis. FEM was created from microCT images (10 μm resolution) for a 1.0 mm thick tibial cross section just inferior to the proximal growth plate. Axial compression to 50 μm (5% deflection) of the proximal tibia was performed to determine the effective stiffness. Three-point bending the femur was performed, assessing yield and maximum forces (Pe and Pm) at the femur mid-diaphysis. Spaceflight Effects: Tibia FEA showed FL-VEH treated mice experienced declines in bone volume (BV) and bone stiffness of -17% and -35%, respectively, compared to GC-VEH mice. FEM allowed separation of trabecular and cortical compartment contributions to overall bone stiffness; FL-VEH mice had a -32% decrease in trabecular BV, which corresponded to a -45% decrease in stiffness of

the trabecular region. Three-point bending of the femur resulted in -9% and -11% declines in Pe and Pm, respectively, compared to GC-VEH. Sclerostin Antibody Effects: SclAb countermeasure increased proximal tibia BV +42% (GC), +39% (FL) and FEM stiffness +61% (GC) and +62% (FL). FEM analysis of tibial trabecular compartment shows greater effects of SclAb on BV for both GC (+88%) and FL (+96%) mice; and trabecular stiffness contribution increased +107% (GC) and +133% (FL). In femur three-point bending, SclAb treatment resulted in Pe increases of +18% (GC) and +23% (FL); while Pm increased +20% and +24% for GC and FL, respectively, with SclAb. Conclusion: The unloading environment caused a significant loss in BV, strength and stiffness in both the tibia and femur, with greater effects in trabecular bone. The SclAb largely reversed the spaceflight-mediated deterioration, with generally similar effects in GC and FL mice. Tibial FEM correlated well with femur bending strength, providing a useful, non destructive analysis technique.

Disclosures: Anthony Lau, None.

This study received funding from: Amgen

SA0071

Local Changes Due to Bone Remodelling are Triggered by Mechanical Loading. Patrik Christen^{*1}, Rafaa Ellouz², Stephanie Boutroy³, Roland Chapurlat⁴, Keita Ito⁵, Bert Rietbergen⁶. ¹Eindhoven University of Technology, The Netherlands, ²Université de Lyon, France, ³Columbia University Medical Center, USA, ⁴E. Herriot Hospital, France, ⁵Eindhoven University of Technology, Netherlands, ⁶Eindhoven University of Technology, The Netherlands

Bone has the remarkable ability to adapt to its mechanical environment in order to withstand external forces. It is generally assumed that bone achieves this in an on-going process of bone remodelling where bone cells add bone at high-load locations and remove bone at low-load locations (Wolff's law). In a recent animal experiment it was found that, indeed, a stochastic relationship between local loading conditions and bone resorption or formation at the microscopic level exists for bone adapting to higher loading (Schulte F.A., PhD Thesis ETH Zurich, 2011). With the development of high-resolution peripheral quantitative CT (HR-pQCT) imaging techniques and micro-finite element (micro-FE) analyses, it is now possible to also quantify bone microstructure and tissue loading in human bone *in vivo*. The goal of the present study was to investigate if a relationship between bone tissue loading and bone formation or resorption can be found as well for human bone during normal bone turnover.

Five postmenopausal women were measured by HR-pQCT at the distal tibia at baseline and after 6 years. Using 3D registration of baseline and follow-up images, voxels at the bone surfaces were classified as belonging either to a resorption site, a formation site, or an unchanged site. Resorption and formation were defined as a change in density exceeding 200 mg HA/cm³. Micro-FE models were created from the baseline images, and a previously developed bone loading estimation method was used to determine a realistic bone loading history for each subject (Christen *et al.*, BMMB, 2011). The bone tissue strain energy density (SED) was calculated for this loading history and histograms were made for the voxels classified as bone loss and bone gain.

The histograms showed that both bone loss and bone gain were strongly correlated with tissue loading, with bone loss decreasing and bone gain increasing with increasing tissue loading (Fig. 1). Resorption dominated over bone gain, which is in agreement with the net loss of bone found during aging in these women.

This study is the first to report such relationships for human bone. In *in vivo* human case, the resolution of the images (~82 microns) is not high enough to identify individual resorption cavities, but resulting microstructural changes could be well recognized. In conclusion: our results suggest that load-adaptive remodelling at the bone micro-level may play an important role also in humans during normal bone turnover with aging.

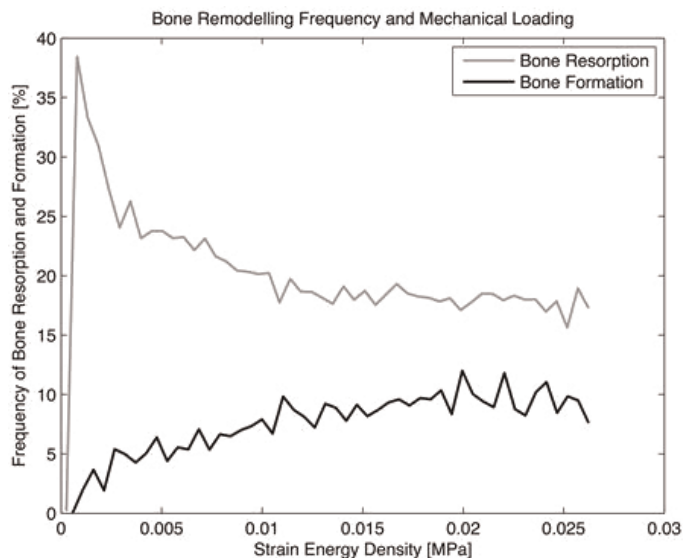


Figure 1: Frequency of bone resorption (grey) and formation (black) related to mechanical loading.

Disclosures: Patrik Christen, None.

SA0072

See Friday Plenary Number FR0072.

SA0073

See Friday Plenary Number FR0073.

SA0074

PTH Enhances Mechanical Stress-induced Osteoblast Proliferation in Calvarial Derived Osteoblasts via Up-regulation of CyclinD1 Expression. Shirakawa Jumpei^{*1}, Yoichi Ezura², Takuya Notomi³, Tadavoshi Hayata⁴, Tetsuya Nakamoto¹, Shuichi Moriya⁵, Ken Omura⁶, Masaki Noda¹. ¹Tokyo medical & dental university, Japan, ²Tokyo Medical & Dental University, Medical Research Institute, Japan, ³GCOE, Tokyo Medical & Dental University, Japan, ⁴Medical Research Institute, Tokyo Medical & Dental University, Japan, ⁵Department of Orthopaedics, Juntendo University School of Medicine, Japan, ⁶Oraland Maxillofacial Surgery of Tokyo Medical & Dental University, Japan

Mechanical stimulation regulates bone homeostasis, and increases osteoblast activity, through gene expression, protein synthesis, cell proliferation and differentiation. Exposure to mechanical forces promotes osteoblast proliferation and bone remodeling. Parathyroid hormone (PTH), a systemic factor regulating bone metabolism also stimulates osteoblast activity via intermittent administration. A positive role of PTH in the cell cycle has been observed in osteoblasts to induce a cyclin D1 expression. Relationship between PTH and mechanical stimulation has been postulated, but the molecular link between mechanical stimulation and PTH in osteoblast proliferation and osteogenesis remains unclear. We hypothesized that certain factors could affect osteoblast proliferation interactively upon mechanical and PTH stimulation. *In vitro* experiments, indicated the proliferative effects of PTH and flow-induced mechanical stress in the calvaria derived osteoblastic cell line (MC3T3E1). A trend of enhancement was observed by both treatments. To examine *in vivo* effects, we subcutaneously injected PTH(1-34) daily (40µg/kg/day) to the mice subjected to calvarial suture expansion by dental wire. The initial force was around 2 N. PTH injection tended to enhance cyclin D1 expression induced by mechanical expansion. These data indicate that mechanical stress and PTH synergistically enhance bone formation via stimulation of osteoblasts proliferation.

Disclosures: Shirakawa Jumpei, None.

SA0075

Vibration Induced Mechanical Signals that Increase Proliferation and Osteogenic Commitment of Mesenchymal Stem Cells. Gunes Uzer^{*}, Sarah Manske, Stefan Judex, Stony Brook University, USA

Human, animal and cell studies indicate that the application of vibrations can be anabolic and/or anti-catabolic to bone. The specific mechanical signal to which cells respond has not been identified, in part because the generated fluid shear is coupled with the magnitude of the applied acceleration in most *in vivo* and *in vitro* studies. We recently developed an *in vitro* model in which acceleration magnitude and fluid shear can be controlled independently. We hypothesized that vibrations in the presence of very low fluid shear conditions will enhance mesenchymal stem cell (MSC) proliferation and promote osteogenic commitment. Cells were vibrated at 100Hz, 1g acceleration magnitude for 30 minutes every day. These vibration parameters exposed cells to peak fluid shear of 0.28Pa, a level that is substantially below the threshold typically required to elicit a response in MSCs. Cells were maintained in standard culture medium or supplemented for adipogenic and osteogenic differentiation. When vibrated in standard culture medium, MSC proliferation increased by 56% ($p < 0.001$) at day three. When the differentiation mediums were used on confluent cultures, the phenotypes were not evident at the molecular level until day five. At this time point, the application of vibrations promoted transcriptional regulation towards osteogenesis. Compared to non-vibrated controls, RUNX2 expression in osteogenic cultures was 24% greater ($p < 0.01$) and PPRG expression in adipogenic cultures was 10% smaller ($p < 0.05$). Without any differentiation medium, vibrations did not induce phenotypic changes. Vibrations significantly increased the expression of c-Fos, an immediate early transcription factor, in all mediums, demonstrating that the vibration-induced accelerations were sensed by MSCs. Together, the data show that oscillatory accelerations, applied without generating significant fluid shear stresses can play a role in enhancing MSC proliferation and their osteogenic commitment at the transcriptional level. We are currently investigating whether fluid shear can contribute to this response in an additive or synergistic manner by increasing the range of fluid shear (0.05-2Pa) and acceleration (0.1-2g) magnitudes. Ultimately a better

understanding of the interactions between fluid shear and accelerations is critical for identifying and optimizing vibration regimes.

Disclosures: Gunes Uzer, None.

SA0076

See Friday Plenary Number FR0076.

SA0077

See Friday Plenary Number FR0077.

SA0078

Influence of Time and Dosing of Indomethacin on Mechanically Induced Bone Formation. Cheryl Druchok^{*1}, Kyle Eastwood², Gregory Wohl¹. ¹McMaster University, Canada, ²Department of Mechanical Engineering, McMaster University, Canada

Introduction: Prostaglandins (PGs) are important signaling factors for bone mechanotransduction. The inhibition of cyclooxygenase, responsible for the synthesis of PGs, with non-steroidal anti-inflammatory drugs (NSAIDs) has been shown to hinder bone formation induced by mechanical stimulation. However, NSAID dosing after exercise was recently shown to enhance bone formation in human subjects (Kohrt, JBMR 2010). The purpose of this pilot study was to examine the effects of Indomethacin dose and timing on bone formation in response to mechanical stimulation in a rat model of mechanical loading.

Methods: Male Sprague Dawley rats (n=20), aged four months were randomly assigned to five groups (n=4/grp) 1) low dose (0.2 mg/kg Indomethacin) administered 2 hours before loading, 2) low dose immediately after loading, 3) high dose (2.0 mg/kg) 2 hours before loading, 4) high dose immediately after loading, or 5) vehicle control. Indomethacin was delivered via a Jello® vehicle. A four-week (11 loading days) forelimb loading protocol, with recovery periods, was used. Right forelimbs were loaded to 21 N for 15 sets of 20 cycles with 20-second rest periods between each set. Left forelimbs served as non-loaded controls. To measure bone formation, fluorochrome labels were administered on day 6 (calcein green) and day 24 (alizarin complexone). Animals were sacrificed on day 27. Following dissection, right and left forelimbs were plastic embedded. Transverse forelimb sections were taken 1 mm distal to the mid-diaphysis. Images were captured by fluorescent microscope. Mineral apposition rate (MAR) was calculated for each of the medial and lateral aspects as total area of new bone encompassed between labels divided by cortical perimeter.

Results: On the lateral aspect of the ulna the group with high dose Indomethacin administered after loading had significantly greater MAR compared to all groups (p<0.05) except vehicle control (p=0.051) (Fig 1). There were no significant differences in MAR on the medial aspect (p>0.05).

Conclusions: Though NSAIDs have been shown to impair mechanically-induced bone formation, our current data in the rat model confirm recent findings in humans, that NSAID dosing after mechanical loading can enhance bone formation. These data suggest that the anti-inflammatory effects of NSAIDs after loading may be beneficial for bone formation.

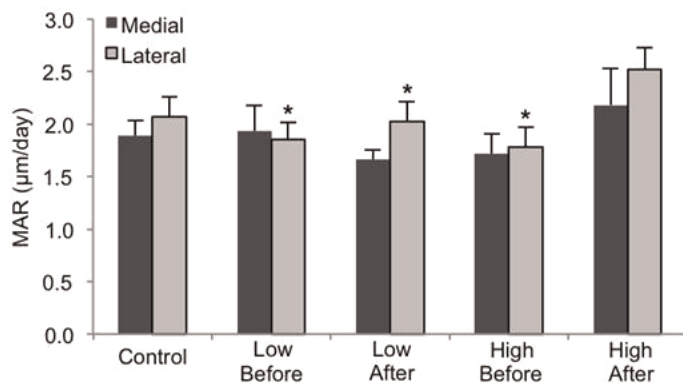


Figure 1. Average MAR on the medial and lateral aspects of the rat ulna. There were no differences in MAR between groups on the medial aspect (p>0.05). The High After group had significantly greater MAR on the lateral aspect compared to the Low Before, Low After and High Before groups. (*p<0.05 compared to High After)

Figure1

Disclosures: Cheryl Druchok, None.

SA0079

See Friday Plenary Number FR0079.

SA0080

Stepping Out: Developmental Changes in Tibial Trabecular Bone Microarchitecture and Kinematics of Early Human Walking. James Gosman¹, David Raichlen², Zachariah Hubbell^{*3}, Simone Sukhdeo⁴, Leah Souza⁴, Timothy Ryan⁴. ¹The Ohio State University, USA, ²University of Arizona, USA, ³The Ohio State University, USA, ⁴Pennsylvania State University, USA

The objective of this research is to examine how human locomotor development contributes to changes in tibial trabecular microarchitecture from homogeneous, high density morphology to one with high spatial differentiation. Of special concern is linking the kinematics of the initiation and maturation of human walking to ontogenetic changes in trabecular bone morphology. The degree of anisotropy (DA) is used as a morphological corollary to the variability of joint kinematics, representing the quality of loading as opposed to the quantity of loading. The hypothesis tested predicts that the pattern of ontogenetic within-tibial variability in the degree of anisotropy of trabecular bone in the proximal and distal tibia is associated with the age-related variability in gait kinematics. High-resolution x-ray CT scans were collected for the tibia of 70 individuals from the Norris Farms #36 skeletal collection ranging in age from neonate to adult. The entire bone was scanned with voxel dimensions less than 0.05 mm. 3D trabecular bone fabric structure was quantified for multiple cubic volumes of interest from the proximal and distal tibial metaphyses using the BoneJ plugin within ImageJ. Resolution-corrected morphometric structural analysis included bone volume fraction, trabecular number, trabecular thickness, and the degree of anisotropy (DA) from neonate to age 12. The DA was calculated using the mean intercept length (MIL) method. In addition, DA data were visualized by 3D rose diagrams generated by the Quant3D software. Gait analyses were undertaken on 16 age-grouped children between the ages of 1 and 9 years to establish new data for joint kinematics/kinetics coefficients of variation (CV) across age classes. The results of this work demonstrate that individual CVs versus age for joint angles are significant in the medial/lateral axis at the knee and ankle with the greatest variability in the youngest. Scatterplots of DA vs. age support the hypothesis of increased trabecular bone microarchitectural variability in the younger ages at the proximal, but not the distal tibia. Our conclusions from these data support the concept that the kinematic characteristics associated with the initiation of human gait contribute to intra-tibial trabecular bone microarchitectural heterogeneity and differentiation.

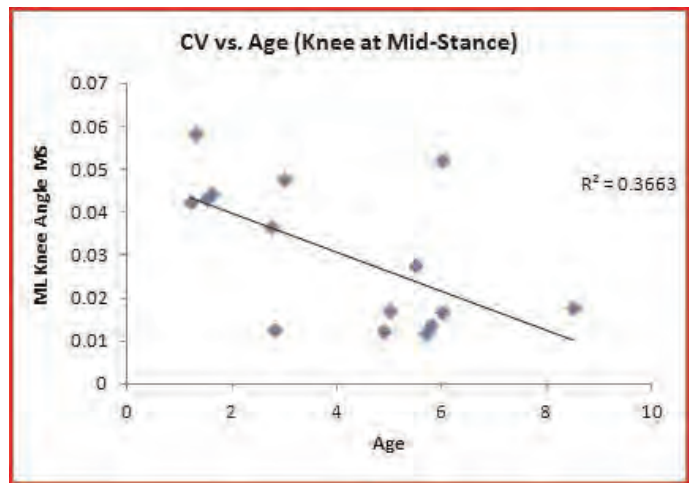


Figure 1. Coefficient of variation vs. age for medio-lateral knee angle at mid-stance.

SA0081

In-vivo Evaluation of the Progress of Bone Fracture Healing in a Rat Model: a Non-Invasive Raman Spectroscopy technique. Paul Okagbare^{*1}, Dana Begun², Francis Esmonde-Whilte³, Steven Goldstein⁴, Michael Morris².
¹Department of Chemistry, University of Michigan, USA, ²University of Michigan, USA, ³University of Michigan, USA, ⁴University of Michigan Orthopaedic Research Lab, USA

Introduction: Bone regeneration is a complex biological process. Although, the biochemical pathway of fracture healing has been intensively investigated, the mechanism of impaired healing of bone tissues remains unclear. Approximately 5 – 15% of “fractures at risk” have delayed healing, non-union and require repeated operative intervention. Where allografts are used for repair of large defects, failure rates approach 25%. Consequently there is a need for new techniques to assess and monitor progress of bone regeneration and allograft incorporation. Raman spectroscopy can complement existing techniques because it provides detailed information about the mineral and matrix composition of bone tissue. In this study, we report non-invasive Raman spectroscopy for in-vivo assessment of the progress of bone fracture healing in a rat model. The same technique can be used to study implant integration and to report on the progress of therapeutic interventions.

Methods: In an experiment approved by our institutional animal use committee, a 1.5 mm defect was created in the mid-diaphysis of a rat tibia. The defect was stabilized using a unique internal fixation plate. Following the surgery, the rats were monitored by Raman spectroscopy at two week intervals for eight weeks. Spectroscopy was performed with a fiber optic probe comprising a single laser delivery fiber and an array of signal collection fibers in contact with the skin of the rat. The fibers were mounted in a Delrin holder surrounding the tibia to allow reproducible fiber positioning.

Results: We followed the time course of fracture healing using well-established correlations between Raman spectral features for bone mineral phosphate and carbonate and for matrix collagen content. We observed callus formation during the first two weeks, followed by deposition of bone mineral and increasing mineralization with time. Mineral maturity (decreasing monohydrogen phosphate content) and increasing mineral crystallinity also increased with time.

Conclusions: This new spectroscopic methodology enables non-invasive *in-vivo* assessment of the progress of bone fracture healing and bone-graft incorporation in rodent models and is extendable to other *in-vivo* animal measurements. With current technology the technique may also be scalable for use in human subjects at anatomical sites where the periosteal surface of the bone is within about 1 cm of the skin.

Disclosures: Paul Okagbare, None.

SA0082

Studies on the Distribution of Mineral Elements in the Tooth of Zinc - deficient Rats. Yoshimi Teraki^{*}, Sagami Matsugae clinic, Japan

Abstract:Element analysis of plaque-like black deposits noted on the surface of teeth in zinc-deficient rats at necropsy was performed. Rats deficient in zinc show signs of abnormality in iron metabolism and increase of accumulation of iron in plasma and tissues.

This study was designed, therefore, to examine the plasma and salivary levels of iron and other elements and to determine the distribution of mineral elements in the dental substances of zinc-deficient rats by contact microradiography, electron probe micro-analysis (EPMA) and X-ray fluorescent element mapping spectrometry (XEMS) on ground sections of teeth. Rat tooth specimens were analyzed also for zinc, iron, copper and manganese using colorimetry and Inductively Coupled Plasma, ICP.

EPMA and XEMS analysis revealed the presence of iron on the enamel surfaces of maxillary molars teeth of zinc-deficient rats showed higher iron concentration in mixed saliva and in plasma, compared with the controls.

Thus, the sign of abnormality in iron metabolism noted in oral cavity of zinc-deficient rats was investigated by EPMA and XEMS analysis, with discussion on the origin of supradental iron deposits.

Disclosures: Yoshimi Teraki, None.

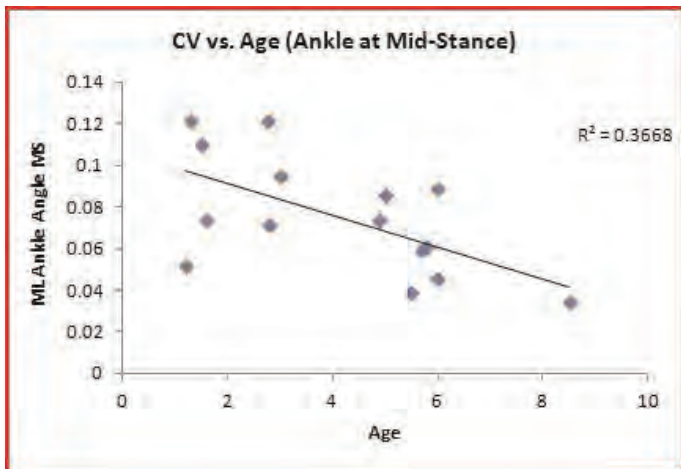


Figure 2. Coefficient of variation vs. age for medio-lateral ankle angle at mid-stance.

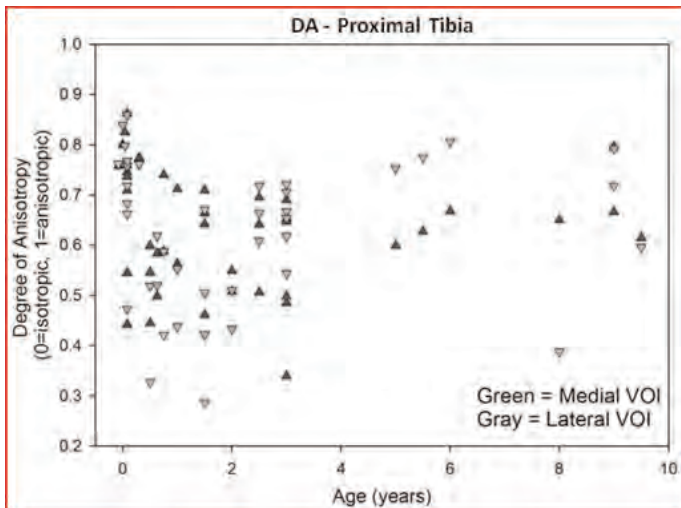


Figure 3. Degree of anisotropy by age in the proximal tibia.

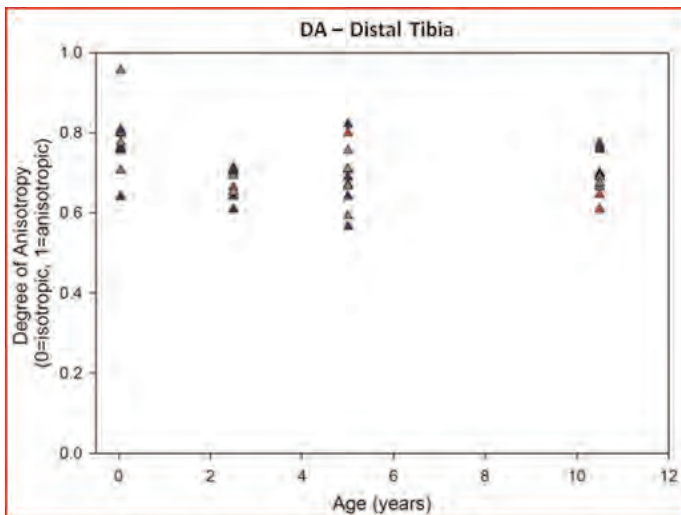


Figure 4. Degree of anisotropy by age in the distal tibia.

Disclosures: Zachariah Hubbell, None.

SA0083

Comparative Study of the Effects of Milk and Dairy Products on Bone Metabolism in Ovariectomized Rats. Rieko Tanabe^{*1}, Mayu Haraikawa², NATSUKO SOGABE³, Aoi Sugimoto², Yuka Kawamura², Satoshi Takasugi⁴, Masashi Nagata⁵, Akira Yamaguchi⁶, Tadahiro Iimura⁷, Masae Goseki-Sone⁸. ¹Department of Food & Nutrition, Faculty of Human Sciences & Design, Japan Women's University, Japan, ²Department of Food & Nutrition, Faculty of Human Sciences & Design, Japan Women's University, Japan, ³KOMAZAWA WOMEN'S UNIVERSITY, Japan, ⁴Meiji Co., Ltd., Japan, ⁵Meiji Co., Ltd., Japan, ⁶Tokyo Medical & Dental University, Japan, ⁷Tokyo Medical & Dental University, Global Center of Excellence Program, Japan, ⁸Japan Women's University, Japan

Calcium is one of the important nutrients for bone health, and the best source of calcium is food such as milk and dairy products. In this study, we compared the effect of milk, yogurt, or whey on the bone strength, body composition, and serum biomarkers using ovariectomized rats. Forty 12-week-old female Sprague-Dawley rats were ovariectomized (OVX), and another nine rats received a sham operation (Sham-Cont). After a one-week recovery period, the OVX rats were divided into 4 dietary groups: OVX-control group (OVX-Cont), 17% skimmed milk powder diet group (OVX-Milk), 17% powdered fermented milk diet group (OVX-Yogurt), and 12% whey powder and 6% whey protein extract diet group (OVX-Whey) (n=10 in each group). The calcium content was 0.5% in all 5 groups. Eighty-four days after the beginning of the experimental diet, the total bone mineral density of lumbar vertebrae was significantly higher in the OVX-Milk and OVX-Yogurt group than in the OVX-Cont group (p<0.01, respectively). Bone mineral contents of lumbar vertebrae were significantly higher in the OVX-Milk and OVX-Whey group than in the OVX-Cont group (p<0.05 and p<0.01, respectively). Interestingly, the level of serum 1 α , 25-dihydroxyvitamin D3 was significantly higher in the OVX-Cont group than in the Sham-Cont group, and significantly lower in the OVX-Milk, OVX-Yogurt, and OVX-Whey groups than in the OVX-Cont group (p<0.001, respectively). The level of serum fibroblast growth factor 23 was significantly lower in the OVX-Cont group than in the Sham-Cont group (p<0.001), and significantly higher in the OVX-Milk, OVX-Yogurt, and OVX-Whey groups than in the OVX-Cont group (p<0.05, respectively). These findings were confirmed by histological sections of the proximal tibial metaphysis. Further studies on the effects of dietary milk or dairy products on the regulation of bone metabolism would provide valuable data for the prevention of lifestyle-related disorders, including osteoporosis.

Disclosures: Rieko Tanabe, None.

SA0084

Circumferential Periosteal Division of Diaphysis of Rat Femur Stimulates Endochondral Ossification of Growth Plate. Shinjiro Takata^{*}. Institute of Health Biosciences, University of Tokushima Graduate School, Japan

Circumferential periosteal division (CPD) of diaphysis of femur of developing rat produces longitudinal overgrowth. Endochondral ossification of growth plate stimulates longitudinal overgrowth of tubular bone. Here we report the mechanisms of longitudinal CPD-induced overgrowth of femur.

Seventy-two Wistar rats aged 8 weeks were used for this study. Periosteum of diaphysis of the right femur was divided circumferentially (CPD group), and the left femur was control (Control group). Longitudinal length of CPD and Control groups 6 weeks after CPD were 41.0 \pm 0.9 and 39.4 \pm 0.7 mm (p=0.0052, n=6), respectively, indicating that overgrowth of longitudinal length reached to approximately 4.1% of Control group. Distal growth plate is responsible for approximately 91.5% of longitudinal overgrowth (n=6).

Bone histomorphometry showed that CPD increased longitudinal growth rate, mineral apposition rate, bone volume, osteoid volume, trabecular number and thickness of femur (n=6). Histological findings showed that the width of distal growth plate and the number of hypertrophic chondrocytes of CPD group were greater than those of Control group 4 weeks after CPD.

These results showed that CPD stimulates endochondral ossification of growth plate to produce longitudinal overgrowth of femur of developing rat. These facts suggest that periosteum plays an important role to regulate endochondral ossification of growth plate, and that CPD might become promising treatment to lengthen tubular bone of pediatric patients with leg length discrepancy.

Disclosures: Shinjiro Takata, None.

This study received funding from: no organization

SA0085

See Friday Plenary Number FR0085.

SA0086

See Friday Plenary Number FR0086.

SA0087

IFT80 Promotes Chondrogenic Differentiation by Regulating Hedgehog and Wnt Signal Pathways. Xue Yuan^{*1}, changdong wang², Shuying Yang³.

¹University At Buffalo, USA, ²University at Buffalo, USA, ³State University of New York At Buffalo, USA

Partial mutation of intraflagellar transport 80 (IFT80) in humans causes Jeune asphyxiating thoracic dystrophy (JATD) and short-rib polydactyly syndrome type III. These disorders have severe bone development abnormalities. However, the role and mechanism of IFT80 function in chondrogenic proliferation and differentiation remain largely unknown. We hypothesize that IFT80 is required for the formation, maintenance, and function of cilia and plays a critical role in the proliferation and differentiation of bone marrow-derived stromal cells (BMSCs) by regulating the Hedgehog (Hh) and Wnt signaling pathways. To test this hypothesis, we first analyzed the IFT80 expression pattern and found that IFT80 was predominantly expressed in bone tissue and mouse BMSCs. Silencing IFT80 caused a loss of cilia in mouse BMSCs and the promotion of cell proliferation by increased expression of Cyclin D1, Cyclin E and Cyclin-dependent kinase 1 (CDK1). Silencing IFT80 also promoted the transition of BMSCs from the G0/G1 stage to the S and G2/M stages. Moreover, silencing IFT80 in BMSCs resulted in impaired chondrogenic differentiation accompanied by the decreased expression of collagen II, aggrecan, and Gli2 and increased β -catenin expression. The overexpression of Gli2 as well as treatment with smoothed agonist (SAG), an agonist of the Hedgehog signaling pathway, in IFT80-silenced cells could rescue the chondrogenic differentiation deficiency, indicating that IFT80 regulates chondrogenic proliferation and differentiation by down-regulating the Hedgehog pathway and up-regulating the Wnt/ β -catenin signaling pathway. Overall, IFT80 functions as an inhibitor of proliferation and an activator of differentiation during the chondrogenic progress.

Disclosures: Xue Yuan, None.

This study received funding from: K08.AR055678 (S. Yang)

SA0088

Limb- and Sternum-Specific Inactivation of Dullard Gene Causes Severe Defects in Skeletal Development via Alteration of TGF- β Signaling.

Tadayoshi Hayata^{*1}, Yoichi Ezura², Makoto Asashima³, Ryuichi Nishinakamura⁴, Masaki Noda⁵. ¹Medical Research Institute, Tokyo Medical & Dental University, Japan, ²Tokyo Medical & Dental University, Medical Research Institute, Japan, ³National Institute of Advanced Industrial Sciences & Technology (AIST), Japan, ⁴Kumamoto University, Japan, ⁵Tokyo Medical & Dental University, Japan

The transforming growth factor (TGF- β) and bone morphogenetic protein (BMP) signaling pathways play important roles in endochondral bone formation, an essential process for skeletal growth. However, it has also been shown in mouse models that limit of TGF- β signaling by E-selectin-ligand-1, an inhibitor of TGF- β maturation in Golgi apparatus is of importance in endochondral bone formation as well as limit of BMP signaling by BMP inhibitors including Noggin and Smad6. Although our previous in vitro studies revealed that an intracellular factor Dullard acts as an inhibitor of both TGF- β and BMP signaling in bone cells, physiological relevance of Dullard in endochondral bone formation is unknown. In this study, we report that mice lacking Dullard in early limb and sternum mesenchyme with Prx1-Cre system exhibit retardation of ossification. Analysis of Dullard expression using Dullard LacZ knock-in mice revealed its prominent expression in the resting and proliferating chondrocytes, but not in hypertrophic chondrocytes. Although Dullard (Prx1) mutant mice were born according to Mendelian ratio, approximately 70% of the mice died 1 day after birth presumably due to defects in suckling milk, and the rest of them displayed dwarfism and defects in locomotion and died before weaning. Body weight of the Dullard (Prx1) mutant mice was reduced at birth. Soft X-ray and skeletal preparation analyses revealed that Dullard (Prx1) mice showed reduction in length of limb long bones and retardation of ossification in metatarsal and metacarpal bones as well as in sternum. Histological analysis showed occupation of hypertrophic chondrocytes in sternum of the Dullard (Prx1) mice. Luciferase reporter assay using immature murine articular chondrocytes (iMACs) isolated from P0 mice revealed that TGF- β signaling, but not BMP signaling was augmented in Dullard-deficient iMACs after 24-hour treatment. Dullard-deficient iMACs also responded to TGF- β strongly to change cell shape from round to fibroblastic. These results suggest that Dullard regulates endochondral bone formation via suppression of TGF- β signaling in chondrocytes.

Disclosures: Tadayoshi Hayata, None.

SA0089

See Friday Plenary Number FR0089.

SA0090

See Friday Plenary Number FR0090.

SA0091

See Friday Plenary Number FR0091.

SA0092

See Friday Plenary Number FR0092.

SA0093

Egr-1 Mediates the Suppressive Effect of IL-1 on PPAR γ Expression in Human OA Chondrocytes. Sarah Nebbaki*¹, Fatima Ezzahra El Mansouri², Hassan Fahmi³. ¹Research Center-Hospital Center of Montreal University, Canada, ²Research Center-CHUM, Canada, ³Research Center-CHUM, Canada

Background: Peroxisome proliferator-activated receptor gamma (PPAR γ) is a ligand activated transcription factor and member the nuclear hormone receptor superfamily. Several lines of evidence indicate that PPAR γ have protective effects in osteoarthritis (OA). Indeed, PPAR γ has been shown to down-regulate several inflammatory and catabolic responses in articular cartilage and chondrocytes and to be protective in animal models of OA. We have previously shown that IL-1 down-regulated PPAR γ expression in OA chondrocytes. In the present study we will investigate the mechanisms underlying this effect of IL-1.

Methods: Chondrocytes were stimulated with IL-1, and the level of PPAR γ and Egr-1 protein and mRNA were evaluated using Western blotting and real-time reverse-transcription polymerase chain reaction, respectively. The PPAR γ promoter activity was analyzed in transient transfection experiments. Egr-1 recruitment to the PPAR γ promoter was evaluated using chromatin immunoprecipitation (ChIP) assays. Small interfering RNA (siRNA) approaches were used to silence Egr-1 expression.

Results: We demonstrated that the suppressive effect of IL-1 on PPAR γ expression requires de novo protein synthesis and was concomitant with the induction of the transcription factor Egr-1. CHIP analyses revealed that IL-1 induced Egr-1 recruitment at the PPAR γ promoter. IL-1 inhibited the activity of PPAR γ promoter and overexpression of Egr-1 potentiated the inhibitory effect of IL-1, suggesting that Egr-1 may mediate the suppressive effect of IL-1. Finally, Egr-1 silencing with small interfering RNA blocked IL-1-mediated down-regulation of PPAR γ expression.

Conclusion: These results indicate that Egr-1 contributes to IL-1-mediated down-regulation of PPAR γ expression in OA chondrocytes and suggest that this pathway could be a potential target for pharmacologic intervention in the treatment of OA and possibly other arthritic diseases.

Disclosures: Sarah Nebbaki, None.
This study received funding from: CIHR

SA0094

GSN: A Novel Susceptibility Gene for Osteoporosis in Humans. Fei Yan Deng*¹, Wei Zhu², Yong Zeng³, Shu-Feng Lei³, Yao-Zhong Liu², Hong-Wen Deng². ¹Tulane University, USA, ²Tulane University, USA, ³Hunan Normal University, China

Osteoporosis is a public health problem, especially in the females. Low BMD is a risk factor of osteoporosis and has strong genetic determination. Genes influencing the majority of variation of BMD are largely unknown yet. Peripheral blood monocytes (PBM) can serve as progenitors of bone-resorbing osteoclasts and are involved in bone metabolism. Herein, we attempted to identify osteoporosis susceptibility gene(s), through initial proteome profiling of PBM in vivo, and using a strategy of multi-disciplinary and integrative studies.

We recruited 3 independent case-control samples (N=37, 29, 40, respectively) including premenopausal women with extremely low vs. high hip BMD from bottom 20% vs. top 20% of distribution in Caucasian population, and two population samples including 2,286 unrelated Caucasians and 1,627 unrelated Chinese, respectively. We utilized quantitative proteomics methodology to profile PBM proteomes in the 1st case-control sample to discover proteins, thus gene(s), functionally relevant to low BMD. Differentially expressed protein(s) identified were verified by western blotting (WB). Then, comparative analyses at mRNA expression level in PBM were conducted in the 2nd and 3rd case-control samples. For gene(s) also differentially expressed at mRNA level, we further tested association of gene SNPs with hip BMD in the population samples.

Among 2,117 proteins identified in PBM, gelsolin (GSN) was down-regulated 1.7-fold in subjects with low BMD in the 1st sample (p<0.05). Down-regulation of GSN gene expression in low BMD subjects were verified by WB, and further replicated at mRNA level in the 2nd and 3rd samples (p<0.05), respectively. Furthermore, seven SNPs (rs10739594, rs4837827, rs7857673, rs4837832, rs4837835, rs306761, and rs306772) within GSN locus were associated with hip BMD in the Caucasian population (p<0.05). Three of them (rs306761, rs4837827 and rs4837832) were also associated with hip BMD in the Chinese population (p<0.05), suggesting ethnic-general effect of these SNPs on hip BMD.

Based on the above integrative evidence at protein, mRNA, and DNA levels, we conclude that GSN is a significant susceptibility gene involved in the pathogenesis of osteoporosis in humans.

Keywords: Osteoporosis, BMD, monocyte, proteome, gelsolin

Disclosures: Fei Yan Deng, None.

SA0095

See Friday Plenary Number FR0095.

SA0096

The Thyroid Hormone Transporters Monocarboxylate Transporter 8 and 10 (MCT8, MCT10) Are Expressed Reciprocally in Growth Plate Chondrocytes. Noriyuki Namba*¹, Makoto Abe², Sanae Abe³, Makoto Fujiwara³, Tomonao Aikawa⁴, Mikihiro Kogo⁵, Keiichi Ozono⁶. ¹Osaka University Graduate School of Medicine, Japan, ²Osaka University Graduate School of Dentistry, Japan, ³Osaka University Graduate School of Medicine, Japan, ⁴Osaka University Graduate School of Dentistry, Japan, ⁵Osaka University Graduate School of Dentistry, Japan, ⁶Osaka University Graduate School of Medicine, Japan

Thyroid hormone transporters mediate thyroid hormone transport into the cytoplasm. Among the identified transporters, monocarboxylate transporter 8 (MCT8) has been shown to exclusively transport thyroid hormone. Since thyroid hormone is essential for the normal development of the neurons and the growth plate, untreated congenital hypothyroidism results in severe mental retardation and short stature. The Allan-Herndon-Dudley syndrome, caused by MCT8 mutations, is characterized by severe psychomotor retardation and elevated T₃ levels. Interestingly, growth is not severely retarded in these patients. This led us to hypothesize that chondrocytes utilize transporters other than MCT8 for thyroid hormone uptake. At the 2010 meeting, we reported abundant expression of monocarboxylate transporter 10 (Mct10), a transporter most homologous to Mct8 within the MCT family, in murine chondrogenic ATDC5 cells. Silencing Mct10 mRNA abrogated the effects of thyroid hormone on proliferation and differentiation in these cells. However, to date, the expression of these two transporters in the growth plate has not been clarified.

We thus utilized *in situ* hybridization to localize Mct8 and 10 *in vivo*. Pregnant C57/BL6 mice were humanely killed on embryonic day (E) 18 and humeri including the growth plate were obtained. Digoxigenin-labeled riboprobes were hybridized overnight to 14 μ m sections. Mct10 mRNA was most abundant in the resting zone (RZ) chondrocytes while the signal was weaker in chondrocytes differentiating into the secondary ossification center, the proliferating zone (PZ), as well as the hypertrophic zone (HZ) chondrocytes. In a reciprocal manner, levels of Mct8 mRNA increased with differentiation with the strongest signal observed in the HZ chondrocytes. These results were consistent with the changes in Mct8 and Mct10 mRNA levels during ATDC5 differentiation evaluated by quantitative real-time (qRT)-PCR.

The major thyroid hormone receptor in the growth plate, thyroid hormone receptor alpha 1 (TR α 1), is expressed in the RZ and PZ chondrocytes but not in HZ chondrocytes. This, in combination with the above results, indicates that Mct10 is expressed in early stage chondrocytes concomitantly with TR α 1, thus suggesting that Mct10 plays a significant role in thyroid hormone signaling in the growth plate.

Disclosures: Noriyuki Namba, None.

SA0097

Defining a Visual Marker of Progenitor Cells within the Periodontium. Hrvoje Roguljic*¹, Brya Matthews², Melissa Lacombe¹, Ivo Kalajic². ¹University of Connecticut Health Center, USA, ²University of Connecticut Health Center, USA

The periodontium is the tissue supporting the teeth including cementum, periodontal ligament (PDL) and alveolar bone. In periodontal disease, which is a major cause of tooth loss in adults, the periodontium is inflamed and cementoblasts, PDL fibroblasts and osteoblasts are affected. We have previously identified a periodontal tissue progenitor cell that resides in perivascular areas and expresses GFP under the control of the smooth muscle alpha actin (α SMA) promoter (SMA-GFP). The aim of this study is to identify and trace periodontal progenitor cells in vivo. We have generated an α SMA promoter-driven and tamoxifen inducible Cre mouse (α SMA-CreERT2) that in combination with a Rosa-tomato reporter (SMACre/Tomato) labels a defined cell population. We aimed to examine expansion and localization of these progenitor cells during normal growth and after periodontal

injury. To trace these progenitors during normal growth, tamoxifen was administered to 3-week-old SMACre/ Tomato mice on two consecutive days to label cells, and histology was performed on the second molar in mandibles after 2 and 17 days. At day 2 a small population of cells in the PDL were labeled. This population expanded by day 17, particularly in the apical region and the tension side of the root. To detect transition of SMACre/tomato labeled cells into mature phenotype we utilized a Col2.3GFP transgene. Following treatment with tamoxifen we detected a small number of SMACre/ Tomato/Col2.3GFP-expressing cells by day 17. Using a cell ablation model (Col2.3TK mice) we have established an *in vivo* injury model. Administration of ganciclovir (GCV) results in the death of cells that express the TK gene and undergo division. SMACre/ Tomato/Col2.3TK mice were treated with GCV for 16 days then SMACre-expressing cells were labeled with tamoxifen. 21 days later mice treated with GCV showed remodeling of the apical root and adjacent alveolar bone. We observed an expansion of tomato-labeled cells in the apical root region of the PDL in the GCV-treated mice compared to the untreated controls. In summary, the SMACre transgene labels a small population of cells in the PDL. These cells show expansion and differentiation into mature cells during growth, and increased expansion following cell ablation. This population of cells may represent the source of progenitors that give rise to a number of mature lineages within the periodontium that could assist tissue regeneration in periodontal disease.

Disclosures: Hrvoje Roguljic, None.

SA0098

See Friday Plenary Number FR0098.

SA0099

See Friday Plenary Number FR0099.

SA0100

See Friday Plenary Number FR0100.

SA0101

PTH in the Treatment of Non Healing Long Bones. Hans-Christof Schober^{*1}, Dirk Ganzer², Thomas Westphal³, Thomas Mittlmeier⁴, Reimer Andresen⁵, Sebastian Manzelmann⁶. ¹Klinikum Südost RostockKlinik Für Innere Medizin I, Germany, ²Orthopaedic surgery, Germany, ³orthopaedic surgery, Germany, ⁴university rostock, trauma surgery, Germany, ⁵Westküstenklinikum Heide, Germany, ⁶klinikum Suedstadt Rostock, Germany

Introduction: Teriparatide (rh PTH 1-34) a bone anabolic drug approved for the treatment of osteoporosis, has been shown to induce fracture healing in animals. Parathyroid hormone (Preotact[®]) is able to create fracture healing in patients. Non healing fractures of long bones remain a challenge to clinical practice. In desperate cases of non healing fractures, we aimed to induce fracture healing and to improve the clinical situation by short term treatment with rh PTH 1-34. So far no data are available whom to treat, how long to treat and which dosage to use. The aim of our study was to find a useful treatment period and fractures which respond to this kind of treatment.

Material and Methods: 23 patients (12 female and 11 male, age 50.4 ± 14.2yr), with non healing (average 13 ± 11months) fractures, 15 fractures of the lower leg, 6 femoral fractures, 2 fractures of the ankle joint, 2 olecranon fractures, non union for more than 3 months after repeated (in average 3,4) surgical interventions were treated. Drug administration schedule: 4 patients 60µg teriparatide daily s.c. for 6 weeks, 19 patients 20 µg daily s.c. for 8 weeks. Blood was analyzed for calcium, phosphorus, creatinine, bone specific alkaline phosphatase, alkaline phosphatase, TRAP 5b, and 25-hydroxyvitamin D. Vitamin D deficiency was treated. The callus development was evaluated by an independent radiologist.

Results: So far results are available for 20 cases. Healing took place in 17 cases (all 4 with 60µg and 13 with 20µg). All Pilon-tibial- and periprotetic fractures did heal. A functional improvement was seen in 15 cases. There were no significant differences in the calcium levels (2,4 ± 0,1 before vs. 2,5 ± 0,1 mmol/l). The increase in bone specific alkaline phosphatase and TRAP 5b reflected the action of the PTH but did not reach significance.

Conclusion: In desperate cases of non healing fractures rh PTH (1-34) Forsteo[®] may be useful. A dosage of 20µg for 8 weeks in the so called "anabolic window" seems to be adequate. Especially Pilon-tibial and periprotetic fractures might be considered. These promising results have to be evaluated in randomized controlled trials.

Disclosures: Hans-Christof Schober, None.

SA0102

Suberoylanilide Hydroxamic Acid Enhances Odontoblast Differentiation. Arang Kwon^{*1}, Kyunghwa Baek², Hye-Lim Lee¹, Joo-Cheol Park³, Jung-Wook Kim⁴, Kyung Mi Woo⁵, Hyun-Mo Ryoo⁵, Jeong-Hwa Baek².

¹Department of Molecular Genetics, School of Dentistry, Seoul National University, South Korea, ²Seoul national university, School of dentistry, South Korea, ³Departments of Oral Histology-Developmental Biology, School of Dentistry, Seoul National University, South Korea, ⁴Seoul National University, South Korea, ⁵Seoul National University School of Dentistry, South Korea

Previous studies have shown that histone deacetylase (HDAC) inhibitors stimulate osteoblast differentiation *in vitro* and bone formation *in vivo*. However, the effect of HDAC inhibitors on odontoblasts has not been elucidated. Therefore, in this study, we examined the effect of suberoylanilide hydroxamic acid (SAHA), an HDAC inhibitor, on odontoblast differentiation using a MDPC23 odontoblast-like cell line. SAHA significantly enhanced matrix mineralization and the expression levels of odontoblast marker genes. SAHA increased the expression levels of nuclear factor I/C (Nfic) and dentin sialophosphoprotein (Dspp). Nfic bound directly to the Dspp promoter and stimulated Dspp transcription. SAHA increased both basal and Nfic-induced Dspp promoter activity. SAHA-induced Dspp promoter activity disappeared when mutations were introduced within the Nfic binding element of the Dspp promoter. Nfic knockdown by siRNA blocked SAHA stimulation of Dspp expression. These results indicate that SAHA enhances odontoblast differentiation and that SAHA increases Dspp expression, at least in part, by increasing the expression level of Nfic.

Disclosures: Arang Kwon, None.

SA0103

See Friday Plenary Number FR0103.

SA0104

Calvaria Cells from Bone Sialoprotein Knockout Mice Contain Less Osteoprogenitors and Display a Cell Density-dependent Impairment of Bone Formation and Mineralization *in vitro*. Guénaëlle Bouët^{*1}, David Marchat², Blandine Merle³, Marie-Thérèse Linossier¹, Mireille Thomas¹, Wafa Boulefour¹, Laurence Vico⁴, Luc Malaval⁵. ¹INSERM U1059-Université de Lyon-Université Jean Monnet, France, ²Ecole Nationale Supérieure des Mines de Saint-Etienne, Center for Health Engineering, France, ³INSERM U1033-Université de Lyon-UCLB, France, ⁴University of St-Etienne, France, ⁵INSERM U1059-Université de Lyon-Université Jean Monnet, Saint-Etienne, France

Bone sialoprotein (BSP) is highly expressed in bone. In BSP KO (-/-) bone marrow stromal cell cultures¹, the pool of osteoprogenitor (OP) cells (CFU-F) is not reduced, nor is their early differentiation (same numbers of alkaline phosphatase positive colonies [=CFU-ALP], although they are smaller). However, the number of osteoblastic, mineralized colonies (CFU-OB) is dramatically lower¹. Because of delayed ossification of newborn BSP-/- mouse calvaria, we analysed the impact of BSP KO on *in vitro* osteogenesis in cultures of mouse calvaria cells (MCC), isolated from 6 days old mice by collagenase digestions.

In contrast to the marrow, CFU-F and CFU-ALP numbers were lower in BSP-/- MCC cultures, along with less CFU-OB. Consistent with the lack of OP, early BSP-/- cultures displayed lower proliferation and delayed population growth. Expression of osteoblast genes was analysed between day (D)3 and D17 of MCC cultures seeded at 5,000 cells/cm². Levels of most markers did not differ between BSP+/+ and -/- at D3 and D6. Periostin, however, presented a transient peak at D6 in BSP+/+ cultures, but not in the BSP-/. Starting at D14 (first CFU-OBs) expression of ALP, Col11, OSX, Runx2 as well as markers of terminal differentiation, OCN, PHEX, DMP1 and MEPE was dramatically lower in BSP-/- MCC cultures, with no mineralization. In contrast, osteopontin (OPN) and CathepsinB (CatB) were over-expressed. In high density cultures (≥25,000 cells/cm²), marker levels were similar for both genotypes, and BSP-/- cultures mineralized. PHEX binds to DMP1, MEPE or OPN, preventing cleavage by CatB and generation of free ASARM ("Acidic Serine and Aspartate Rich Motif"), a potent inhibitor of mineralization. In high density BSP-/- cultures, PHEX expression increased while CatB decreased, suggesting reduced ASARM peptide production, favoring matrix mineralization. We recently developed a long term culture system in perfused HAP/TCP cubic macroporous bone substitutes. Preliminary results in this 3D model confirm our 2D observations on BSP+/+ and -/- MCC cultures, in particular the over-expression of OPN mRNA by BSP-/- cells.

In conclusion, BSP regulates mouse calvaria osteoblast cell clonogenicity, differentiation and activity *in vitro*, consistent with low levels of bone formation *in vivo*. The BSP KO bone microenvironment may alter the proliferation/cell fate of early OP, as suggested by the smaller CFU-PAL observed in marrow cultures.

1:Malaval et al., J Exp Med, 2008, 205:1145

Disclosures: Guénaëlle Bouët, None.

SA0105

See Friday Plenary Number FR0105.

SA0106

Differential Contributions of Leprel1 to Collagen Processing. Erica Homan*¹, Caressa Lietman¹, Ingo Grafe², Roy Morello³, Dobrawa Napierala⁴, Ming Ming Jiang⁵, Elda Munivez⁵, Brian Dawson⁵, Olivier Lichtarge⁵, MarvAnn Weis⁶, David Eyre⁷, Brendan Lee⁸. ¹Baylor College of Medicine, USA, ²Department of Molecular & Human Genetics, Baylor College of Medicine, USA, ³University of Arkansas for Medical Sciences, USA, ⁴University of Alabama At Birmingham School of Dentistry, USA, ⁵Baylor College of Medicine, USA, ⁶University of Washington, USA, ⁷University of Washington Orthopaedic Research Labs, USA, ⁸Baylor College of Medicine & Howard Hughes Medical Institute, USA

Mutations in Cartilage Associated Protein (CRTAP), prolyl 3-hydroxylase 1 (P3H1), and Cyclophilin B (CypB) have been identified as causative of recessive osteogenesis imperfecta (OI). These proteins form a complex that functions to 3-hydroxylate a single proline residue on the alpha 1 chain of type I collagen as well as having cis/trans isomerase (PPIase) activity, a function essential for proper collagen folding. Recent data suggests that this 3-prolyl hydroxylation is not integral to the structural integrity of collagen; however, its absence may disrupt protein-protein interactions integral for proper collagen folding. P3H1 and CRTAP stabilize each other and when one is absent, the other is degraded. Therefore, mutations in this complex result in hypomorphic or complete loss of function alleles. It is thus unclear what roles the 3-hydroxylation function and/or the PPIase activity play in the pathogenesis of recessive OI. This project studies the contribution of P3H1 hydroxylase activity and how it pertains to the pathogenesis of recessive OI by inactivating the hydroxylase domain while maintaining the protein and complex structure.

Through evolutionary tracing we identified a residue that is considered critical for the hydroxylase function and generated a mutant P3H1 cDNA construct containing an alanine substitution at this residue. We demonstrated by immunofluorescence and Western blot that we rescued the stability of CRTAP in the loss of function cells transduced with WT or mutant P3H1 cDNA. Analysis of prolyl 3-hydroxylation by collagen mass spectrometry indicates that the enzymatic activity of P3H1 is abolished. These data suggest that the mutant can maintain the stability of the P3H1 complex, thus maintaining the PPIase function, while abolishing enzymatic activity.

To understand how the 3-hydroxylation function pertains to the pathogenesis of recessive OI, a recombinering strategy was utilized to introduce the alanine substitution into the murine P3H1 locus. Compared to control mice, the mutant mice are normal in appearance and growth. Analysis of the trabecular bone shows a reduction in BMD along with a decrease in Tb Th, an increase in Tb Sp, and a decrease in BV/TV, whereas cortical bone parameters are normal.

We have established a novel mouse model that recapitulates the bone phenotype of OI but not the cartilage phenotype of recessive OI. These observations can be attributable to the differential contributions of P3H1 to collagen processing.

Disclosures: Erica Homan, None.

SA0107

Hox Genes are Re-deployed after Development to Play Critical Roles in Adult Fracture Healing. Ilea Swinehart¹, Aleesa Schlientz², Christopher Quintanilla², Kenneth Kozloff³, Steven Goldstein⁴, Deneen Wellik*⁵. ¹University of Michigan, USA, ²University of Michigan, USA, ³University of Michigan Department of Orthopaedic Surgery, USA, ⁴University of Michigan Orthopaedic Research Lab, USA, ⁵University of Michigan Medical Center, USA

Hox genes are critical regulators of skeletal development. Loss of *Hox* function leads to regionally restricted malformations along the anteroposterior axis of the axial skeleton and the proximodistal axis of the limb. Three *Hox* genes, *Hoxa11*, *Hoxc11*, and *Hoxd11*, demonstrate functional redundancy, and loss of *Hox11* gene function leads to dramatic mispatterning of the sacrum and limb zeugopod elements (radius/ulna, tibia/fibula). Developmental expression is restricted to the perichondrium and connective tissue and expression is maintained at low levels in the periosteum through adulthood. To investigate whether *Hox11* is reactivated during bone repair, a mid-ulnar fracture was performed in adult mice. Following fracture, *Hox11* expression is highly upregulated at the site of injury as early as 3 days post-fracture. Upregulation of expression is observed during callus formation in the periphery of the callus, but is excluded from *Sox9*-expressing cells and osteoblasts. Osteoclasts in the fracture callus express high levels of *Hox11*. *Hox11* compound mutants display reduced cartilage formation after ulnar fracture and a drastically reduced ability to remodel after injury compared to controls. These data clearly highlight a post-developmental role for *Hox11* genes in skeletal repair. The mechanism of *Hox* function in fracture repair is the focus of current work in the laboratory.

Disclosures: Deneen Wellik, None.

SA0108

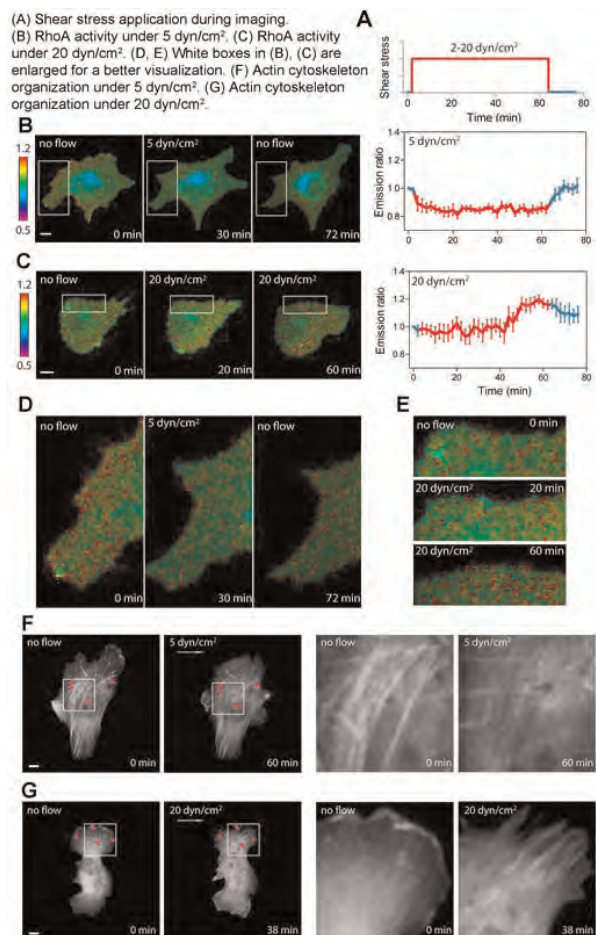
RhoA Is Differentially Regulated by Moderate and High Intensities of Shear Stress in Chondrocytes. Qiaoqiao Wan*¹, Hiroki Yokota², Sungsoo Na³. ¹Indiana University-Purdue University Indianapolis, USA, ²Indiana University Purdue University Indianapolis, USA, ³Indiana University-Purdue University Indianapolis, USA

Physical force environment is a major factor that influences homeostasis and remodeling of bone and joint tissues. It is not well understood, however, a potential role of differential intensities of shear stress in cellular mechanotransduction, in particular, shear stress-driven GTPase signaling in chondrocytes. Using a fluorescence resonance energy transfer (FRET)-based approach, we raised a question whether activities of GTPase RhoA in chondrocytes are differentially regulated depending on intensities of shear stress. RhoA is a member of the Rho GTPase, which is known to be involved in cellular migration as well as regulation of matrix metalloproteinases. We hypothesized that RhoA activities can be either elevated and/or reduced by shear stress at 2 – 20 dyn/cm².

The results revealed that C28/I2 chondrocytes exhibited an increase in RhoA activities in response to high shear stress (10 or 20 dyn/cm²), while they showed a decrease in their RhoA activities to moderate shear stress at 5 dyn/cm². No changes were observed under low shear stress (2 dyn/cm²). Shear-induced activities were closely linked to the alterations in actin cytoskeleton. In response to shear stress at 5 dyn/cm², actin stress fibers gradually disappeared but shear stress at 20 dyn/cm² resulted in the increase in their fiber formation.

To further examine the relationship of actin cytoskeleton to RhoA activity, cells were pretreated with drugs that disrupted actin filaments or inhibited pre-stress. Treatment with these drugs prevented shear-driven RhoA inhibition or activation. Shear stress of 5 dyn/cm² decreased tractions (~30%) in 20 min, while shear stress of 20 dyn/cm² substantially increased them (~70%) in 60 min. These results suggest that magnitude-dependent RhoA activities are required to achieve stress-driven strengthening and weakening of actin stress fibers. In the presence of constitutively active RhoA (RhoA-V14), intermediate shear stress was able to suppress RhoA activities, while high shear stress failed to further elevate RhoA activities.

Collectively, these results support the notion that moderate and high intensities of shear stress differentially regulate RhoA activities as well as the formation of actin stress fibers in chondrocytes.



RhoA activity and actin cytoskeleton organization are shear stress-magnitude dependent.

Disclosures: Qiaoqiao Wan, None.

SA0109

Role of Plasminogen in Bone Repair and Heterotopic Ossification. Naoyuki Kawao^{*1}, Yukinori Tamura², Katsumi Okumoto³, Masato Yano⁴, Kiyotaka Okada⁴, Osamu Matsuo⁴, Hiroshi Kajii¹. ¹Kinki University Faculty of Medicine, Japan, ²Kinki University Faculty of Medicine, Japan, ³Life Science Research Institute, Kinki University, Japan, ⁴Kinki University Faculty of Medicine, Japan

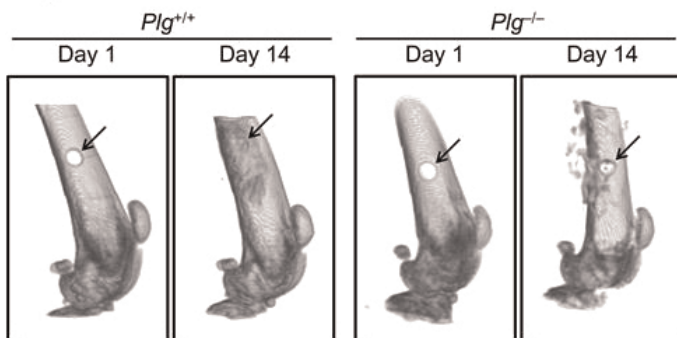
The clarification of the details in mechanism of bone regeneration is necessary to meet the clinical demand of bone generation for the treatment of bone defects. Plasminogen, a critical component of the tissue fibrinolytic system, activates tissue proteolytic system, including matrix metalloproteinases, and several reports indicate that it mediates tissue repair in skin and liver. However, the roles of fibrinolytic system in bone repair and ossification reactions still remain unknown. We therefore investigated the processes of bone repair and heterotopic ossification in mice with gene deficiency of plasminogen (*Plg*^{-/-}) and their wild-type littermates (*Plg*^{+/+}).

A hole was drilled in the femur of the 7-9 weeks old mice for the bone repair model. Heterotopic ossification was induced by the implantation of bone morphogenetic protein (BMP)-2-filled collagen sponge into the muscle. The processes of bone repair and ossification were analyzed by quantitative computed tomography (qCT) and immunohistochemistry.

The bone defect was repaired on day 14 in *Plg*^{+/+} mice, but still remained in *Plg*^{-/-} mice, as assessed by qCT (Fig. 1). In *Plg*^{+/+} mice, but not *Plg*^{-/-} mice, blood vessels were observed at the damaged site from day 4, which was associated with the expression of vascular endothelial growth factor (VEGF). The area of cartilage matrix was reduced on day 7 in *Plg*^{-/-} mice, compared with *Plg*^{+/+} mice in alcian and toluidine blue stains. Alkaline phosphatase (ALP)-positive cells as well as tartrate-resistant acid phosphatase-positive multinucleated cells were localized surrounding the bone tissue at the damaged site on day 7 in *Plg*^{+/+} mice. However, ALP-positive cells were not observed at the damaged site on day 7 in *Plg*^{-/-} mice. In contrast, the BMP-2-induced heterotopic ossification was similarly induced in both *Plg*^{+/+} and *Plg*^{-/-} mice, as assessed by qCT. Furthermore, angiogenesis and expression of VEGF were comparable between *Plg*^{+/+} and *Plg*^{-/-} mice in the heterotopic bone on day 14. These findings suggest that the presence of bone marrow is essential for the role of plasminogen in bone repair.

In conclusion, the present study indicates that plasminogen plays a key role in the processes of bone repair presumably through the expression of VEGF, but not heterotopic ossification. The modulation of the tissue fibrinolytic system might be a new strategy for the enhancement of fracture healing and the development of bone regeneration.

Fig. 1



CT images of the site of bone defect on days 1 and 14 in plasminogen gene deficient (*Plg*^{-/-}) and their wild-type (*Plg*^{+/+}) mice. The arrows indicate the site of bone defect.

Fig. 1

Disclosures: Naoyuki Kawao, None.

SA0110

A Comparison of Receptor Binding, Receptor Activation and β -arrestin Recruitment by Salmon and Human Calcitonin. Kim Andreassen^{*1}, Sara Toftegaard Petersen², Mette Grøndahl Sørensen², Morten Asser Karsdal², Kim Henriksen³. ¹Nordic Bioscience A/S, Denmark, ²Nordic Bioscience A/S, Denmark, ³Nordic Bioscience A/S, Denmark

Introduction and Aim: Salmon calcitonin (sCT) and human calcitonin (hCT) are very different pharmacologically. However, the cause of the observed difference in potency or what implications it has for future pharmacological findings remains to be elucidated. The aim of this study was to investigate whether the differences in sCT and hCT potency could be translated into differences in functional output in terms of binding kinetics and downstream signaling mediated through the calcitonin receptor (CTR).

Methods: This study was conducted on the human U2OS CALCR (U2OS) cell line over-expressing the human CTR. CTR downstream signaling was investigated with dose response profiles for cAMP induction and β -arrestin recruitment for sCT and

hCT during short term (< 2 hours) and prolonged (up to 72 hours) stimulation. CTR receptor kinetics was investigated using 125I-sCT and 125I-hCT ligands to study receptor association (up to 160 min), receptor dissociation (up to 72 hours) and competitive binding on cultured cells or isolated membranes.

Results: Short term stimulation resulted in similar cAMP and β -arrestin dose response profiles. However, hCT binding on live cells declined after 20 min, whereas sCT association on live cells continued to increase for 160 min, indicating potential differences in receptor activation. Prolonged stimulation resulted in distinct sCT and hCT dose response profiles. After 24 hours, sCT dose dependently induced a 50-200% ($P < 0.001$) and a 5-13 fold ($P < 0.001$) increase in cAMP and β -arrestin levels, respectively, compared to hCT. After 48 hours, sCT continued to induce a cAMP and β -arrestin response, whereas the hCT mediated signal ceased. Interestingly, neither sCT nor hCT dissociated appreciably from isolated membranes during 72 hours. In contrast, prolonged ligand dissociation experiments using live U2OS cells demonstrated a more than 90% release of 125I-hCT ligand after 2 hours, whereas 50% and 90% of the 125I-sCT ligand was released after 4 and 24 hours, respectively.

Conclusion: sCT promotes a prolonged activation of the CTR downstream signaling (cAMP induction and β -arrestin recruitment) compared to hCT. Our results indicate that the activity of calcitonins is linked to ligand specific differences in cellular CTR signaling and processing rather than receptor binding kinetics, which could have implications for the understanding and use of sCT in therapy of osteoporosis.

Disclosures: Kim Andreassen, None.

SA0111

Acute Exposure to Fibroblast Growth Factor 23 Increases Cardiac Contractility. Michael Wacker^{*1}, Chad Touchberry¹, Troy Green², Vladimir Tchirikov³, Lori Wetmore², Lynda Bonewald⁴. ¹University of Missouri-Kansas City School of Medicine, USA, ²William Jewell College, USA, ³University of Missouri-Kansas City, USA, ⁴University of Missouri - Kansas City, USA

Fibroblast growth factor 23 (FGF23) is a hormone secreted by bone that regulates vitamin D and phosphate metabolism. Recent clinical data shows a correlation between chronically elevated levels of serum FGF23 in patients with chronic kidney disease (CKD) and a decline in cardiac function. Our laboratory has been studying the effects of chronic FGF23 exposure in the development of cardiac hypertrophy. However, it is currently unclear if acute exposure to FGF23 contributes to changes in cardiac function. To elucidate the acute effects of FGF23 on cardiac contractility, we exposed electrically paced left ventricular muscle strips from wild-type mice (C57BL/6; n=6-9) to pathophysiological concentrations of FGF23 (90, 900, 9000 pg/ml). Treatment with FGF23 increased the magnitude of isometric force in a concentration dependent manner when compared to vehicle treatment ($p < 0.01$). Isometric force nearly doubled within 20 minutes of exposure to 9000 pg/ml with corresponding increases in the rate of force development (slope) and the area (the integral) ($p < 0.01$) associated with the contractile waveforms. However, the rate of relaxation (τ) of the left ventricular muscle strips was not affected ($p > 0.05$). Increased cardiac contractility is tightly coupled to increases in calcium-induced calcium release (CICR). Our data showing increased isometric tension and rate of force development following acute FGF23 exposure suggest that FGF23 may alter CICR mechanisms in cardiac muscle. Since calcium is involved in the induction of pathological hypertrophy, disruption of calcium homeostasis may be a common mechanism by which FGF23 increases contractility acutely and pathological hypertrophy over time. Further studies are needed to confirm this hypothesis and elucidate the specific receptor mediated mechanism for these changes in cardiac performance.

Disclosures: Michael Wacker, None.

SA0112

FGF-23 Gene Expression Increases while Bone Quality Parameters Decrease with Age in D2B6F1 Mice. Marco Loayza^{*1}, Andrew Cureton², Xiaoxin Wang¹, Ted Bateman³, Virginia Ferguson⁴, Moshe Levi⁵, Karen King⁶. ¹University of Colorado School of Medicine, USA, ²University of Colorado, Boulder, USA, ³University of North Carolina, USA, ⁴University of Colorado, USA, ⁵University of Colorado Denver, USA, ⁶University of Colorado School of Medicine, USA

Mice of the D2B6F1 strain were purchased and housed under an IACUC-approved protocol. Mice received no special treatment. Six mice per age group (12, 80 and 108 weeks) were euthanized and femurs were obtained immediately and cleaned of soft tissues and marrow. One femur was used to examine age-related alterations in bone gene expression analysis using SYBR green method. The other femur was used to examine age-related alterations bone mass, microarchitecture and strength via micro-computed tomography of the proximal tibia and three-point bending of the femur diaphysis.

Aging from 12 and 80 wks of age in D2B6F1 mice negatively influenced proximal tibia tissue density by -71.7% ($p = 0.001$) and BV/TV by -68.4% ($p < 0.01$), with no additional changes beyond 80 weeks. Reduced bone volume paralleled loss of trabecular number (Tb.N) and spacing (Tb.Sp), -65.1% and -202%, respectively ($p < 0.001$), and connectivity density by -92.6% ($p < 0.01$). Trabecular anisotropy increased by 14.4% from 12 to 80 weeks and +25% ($p < 0.001$) from 12 to 104 weeks.

There was also diminished strength in the cortical bone at the femur diaphysis in three-point bending.

The mechanism behind these age-related alterations in bone quality may be due to alterations in the gene expressions of osteoprotegerin (OPG) and RANKL. OPG expression decreased about 2-fold between 12 and 108 weeks (no change between 12 and 80 weeks), while RANKL increased about 1.5-fold between 12 and 80 weeks and 2-fold between 12 and 108 weeks. The change in the relationship between OPG and RANKL imply osteoclast activation and subsequent bone resorption.

In light of recent hypotheses that a decrease in FGF-23 may lead to a pre-mature aging-like phenotype in multiple tissues including bone (Razzaque, 2006) we measured the gene expression levels in the bone of these mice. Contrary to low FGF-23 being associated with aging hypothesis, we found a 10-fold increase in FGF-23 expression between 12 and 80 weeks (no difference between 80 and 108 weeks) that correlated significantly ($p < 0.01$) with altered bone microarchitectural metrics. FGF-23 expression appears to increase with aging and is associated with impaired bone microarchitecture.

Disclosures: Marco Loayza, None.

SA0113

Induction of the Intact and C-terminal FGF23 Levels and Its Gene Expression in Lipopolysaccharide-Induced Acute Inflammation. Shoko Ikeda^{*1}, Hironori Yamamoto², Otoki Nakahashi³, Mina Kozai⁴, Yutaka Taketani², Eiji Takeda⁵. ¹Institute of Health Biosciences, University of Tokushima Graduate School, Japan, ²University of Tokushima, Japan, ³University of Tokushima, Japan, ⁴University of Tokushima, Japan, ⁵University of Tokushima School of Medicine, Japan

Parathyroid hormone (PTH) and Fibroblast growth factor 23 (FGF23) are key regulators of inorganic phosphate (Pi) and vitamin D homeostasis. Sepsis is the systemic inflammatory response syndrome (SIRS) that occurs during severe infection and it often associated with electrolyte disorder. It has been reported that endotoxin increased plasma levels of PTH and hyperphosphaturia. However, the alteration of FGF23 during acute inflammation is still unclear. In this study, we investigated the regulation of plasma FGF23 status and its gene expression under the acute systemic inflammation using lipopolysaccharide (LPS). C57BL/6J mice were treated with LPS (E. coli 055:B5, 2-20 mg/kg, i.p.) and sacrificed at different time. Analysis of plasma parameters showed that LPS dose- and time-dependently increased the levels of plasma Pi and PTH. However, plasma intact FGF23 levels were only increased at 3hr after LPS treatment. Surprisingly, plasma levels of C-terminal FGF23 fragment were markedly increased from 1.5 to 9hr by LPS. In addition, TNF- α also increased its C-terminal levels but not intact levels in plasma. Furthermore, we revealed that the femur FGF23 mRNA expression was increased by LPS as well as FGF23 C-terminal levels. Interestingly, its increase was observed in other tissue, such as kidney, liver, lung and spleen. *In vitro* study also demonstrated that LPS directly induced FGF23 mRNA in primary osteoblast-like cells. These results suggest that acute systemic inflammation up-regulates the FGF23 gene expression in bone and other organs and increases both intact and C-terminal fragments of FGF23 in plasma. The measurement of C-terminal FGF23 may be useful as a biomarker for systemic infection like sepsis.

Disclosures: Shoko Ikeda, None.

SA0114

MEPE ASARM Motif and Age-Dependent Regulation of Fat Mass, Renal Phosphate and Bone Mass. Lesya Zelenchuk¹, Anne-Marie Hedge¹, Peter Rowe^{*2}. ¹University of Kansas Medical Center, USA, ²University of Kansas Medical Center, USA

Matrix extracellular phosphoglycoprotein (MEPE) belongs to the SIBLING protein family that includes Dentin Matrix Protein-1 (DMP1). Both proteins contain C-terminal ASARM motifs. The DMP1 ASARM-motif is capped by an additional short minifostin-motif sequence. Mutations in DMP1 cause autosomal recessive hypophosphatemic rickets with increased active FGF23. In contrast, the MEPE null mouse (Mn) has an age related increased bone mass phenotype. To determine if the free ASARM-peptide plays a role we engineered and used a murine model that expresses free ASARM-peptide on a MEPE null background (MnAt).

Wild type (WT), Mn and MnAt male mice (5 wks; N=6) were fed a normal phosphate diet to 22 wks of age. Every two weeks fat mass and aBMD were measured by DEXA and serum samples were taken for analysis. Mice were sacrificed at 22 wks after overnight metabolic-cage housing. The overnight serum plus urine was collected for further analysis. Femurs and kidneys were removed at necropsy for static and dynamic histology, micro computed tomography (μ CT) and RNA analysis. Bone dynamic histomorphometric analyses were carried following routine triple fluorescent dye labeling prior to sacrifice.

Mn mice displayed an age-dependent increase in bone mineral density (BMD), BV/TV, mineral apposition rates, osteoblast activity and trabecular number. This was accompanied by a major decrease in fat mass. In contrast the MnAt mice showed a reversed Mn phenotype and were strikingly obese (Fig 1A, B). Mn mice developed an age-dependent hyperphosphatemia whereas the MnAt mice remained hypophosphatemic (Fig 1B). Serum PTH and FGF23 levels were increased in MnAt mice relative to WT and Mn mice. No differences in PTH levels occurred between Mn and

WT mice. In contrast, Mn mice serum FGF23 levels were significantly lower than WT and MnAt mice. Serum 1,25-Vit D3 levels were increased in Mn mice relative to WT and significantly reduced in MnAt mice relative to WT and Mn mice. FGF23, Sclerostin and cystatin c expressions were increased in MnAt mice relative to WT mice. In contrast, bone mRNA expression of FGF23 and sclerostin were significantly reduced in Mn mice relative to WT mice.

In conclusion, transgenic overexpression of ASARM-peptide over corrected and reversed the age-dependent phenotypic bone, renal and fat abnormalities in MEPE null mice. This confirms processing of MEPE ASARM peptide plays a functional role in maintaining a dynamic age-dependent balance between energy metabolism and bone mass.

Fig 1.

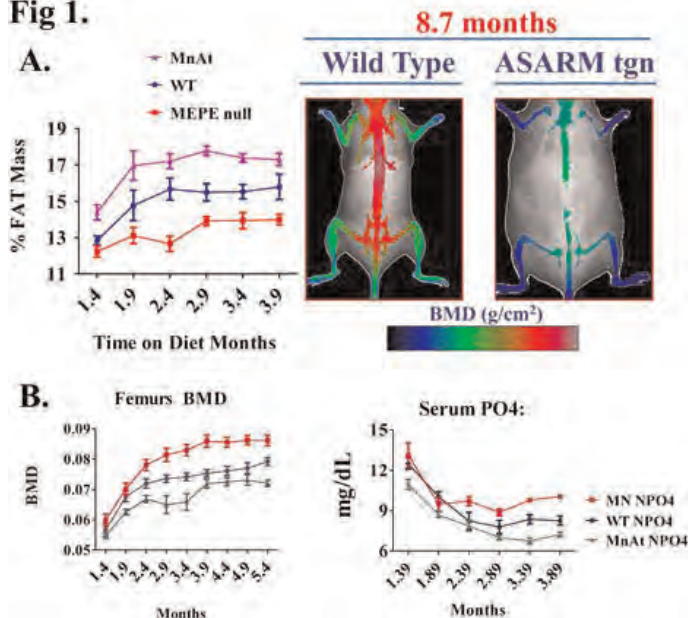


Figure 1

Disclosures: Peter Rowe, None.

SA0115

A Clinically Useful Paradigm for Optimal Interpretation of Serum 25-hydroxyvitamin D (25-OHD) Levels with Simultaneously Measured PTH Levels. Nayana Parikh^{*1}, Shijing Qiu¹, TarLisha Eskridge², Leila Idi², Sudhaker Rao¹. ¹Henry Ford Hospital, USA, ²Henry Ford Hospital, USA

A single 25-OHD level does not provide information either about the duration of vitamin D depletion or appropriate vitamin D replacement strategy in patients with low 25-OHD. Four years ago we presented a preliminary paradigm for interpretation of serum 25-OHD, the best available index of vitamin D nutrition, with concurrent PTH level in patients seeking advice for osteoporosis. We now present more detailed analysis of simultaneously measured 25-OHD and PTH levels in unselected patients seen over 5 years. We excluded patients with hypercalcemia, renal dysfunction (serum Cr >1.5 mg/dl) or with known causes of vitamin D depletion.

There were 10,310 patients, 7682 women and 6511 whites; mean age 61 \pm 14y. The mean serum 25-OHD was 24.7 \pm 12.6 ng/ml and PTH 77.2 \pm 57.3 pg/ml with the expected inverse relationship between the two. In addition, 25-OHD correlated inversely with Cr and AP, and directly with Ca and age (data not shown).

When patients were classified based on 25-OHD level (< or > 30 ng/ml), with or without high PTH (< or > 75pg/ml), 4 groups emerged that suggested different pathophysiologic basis. Group-1 (referent) had 25-OHD >30 ng/ml and PTH <75 pg/ml. Group-2 had normal 25-OHD but high PTH (>75 pg/ml) with weak relationship between the two variables. However, in the 2 groups with low 25-OHD (<30 ng/ml) with either normal (Group-3) or high (Group-4) PTH levels, there was a stronger inverse relationship between the 2 variables. Furthermore, the slope of regression was significantly steeper in Group-4 with high PTH compared to Group-3 with normal PTH (slopes: -1.76 Vs. -0.24; $p < 0.001$). This suggests that vitamin D depletion is of longer duration in Group-4 than Group-3 and thus may require aggressive pharmacologic therapy. Group-3 patients with low 25-OHD and normal PTH may represent seasonal variation, short duration vitamin D depletion or abnormal PTH response. Finally, Group-2 with normal 25-OHD and high PTH may represent patients with low calcium intake or incipient primary hyperparathyroidism and thus require further evaluation.

Conclusion: Simultaneously measured 25-OHD and PTH optimizes proper interpretation of vitamin D nutrition. The strategy offers a clinically useful tool to look for causes of high PTH in those with normal 25-OHD and reasons for lack of PTH response in those with low 25-OHD and normal PTH. We have now validated our initial proposal in a larger unselected population.

Disclosures: Nayana Parikh, None.

SA0116

See Friday Plenary Number FR0116.

SA0117

See Friday Plenary Number FR0117.

SA0118

Parathyroid Hormone Stimulates Tob1 Expression in Osteoblastic Cells *in vitro* and *in vivo*. Shuichi Moriya^{*1}, Tadayoshi Hayata², Jumpei Shirakawa³, Tetsuya Nakamoto⁴, Takuya Notomi⁵, Yoichi Ezura⁶, Kazuo Kaneko¹, Masaki Noda⁴. ¹Department of Orthopaedics, Juntendo University School of Medicine, Japan, ²Medical Research Institute, Tokyo Medical & Dental University, Japan, ³Medical Research Institute, Tokyo Medical & Dental University, Japan, ⁴Tokyo Medical & Dental University, Japan, ⁵GCOE, Tokyo Medical & Dental University, Japan, ⁶Tokyo Medical & Dental University, Medical Research Institute, Japan

In the treatment of osteoporosis, PTH is an important hormone to increase bone mass by intermittent administration. Previous studies have found that there were several early gene expressions after PTH stimulation, such as c-fos and Fra-2. Tob (transducer of erbB2) is a member of antiproliferative family proteins and acts as a bone morphogenic protein inhibitor. However, the role of Tob1 by the action of PTH in osteoblast has not fully understood. The purpose of this study was to identify the effect of PTH on gene expression of Tob1 in bone *in vitro* and *in vivo*. PTH induction of Tob1 messenger RNA (mRNA) levels in MC3T3-E1 osteoblastic cells was maximal with 100 nM human PTH (1-34). The expression of Tob1 mRNA levels *in vitro* was maximal 1 h after human PTH (1-34) addition and returned to baseline within 3 h. Time response expression of Tob1 mRNA resembled that of c-fos. The gene expression of CyclinD1, the cell cycle regulated gene, decreased after 6h of PTH treatment. Up-regulation of Tob1 mRNA expression was also noted *in vivo*, where injection of human PTH (1-34) to 4 weeks old C57/BL6 male mice resulted in about 50% increase in Tob1 mRNA expression in metaphysis of distal femur at 10 µg/kg of PTH and about 90% increase at 20 µg/kg in comparison to the injection of vehicle, after 1h of treatment. Although the expression of Tob1 mRNA increased 1h after injection, by 6h, 12h and 24h levels returned to baseline values. The expression of Tob1 mRNA *in vivo* followed a pattern similar to that of *in vitro*. Intriguingly, after daily injection of PTH for seven days, the expression of Tob1 mRNA caused about 50% increase. These results indicate that Tob1 is one of the early target genes after stimulation by PTH and PTH might regulate cell cycle via Tob1.

Disclosures: Shuichi Moriya, None.**SA0119**

See Friday Plenary Number FR0119.

SA0120

Teriparatide (PTH 1-34) Treatment Increases Peripheral Hematopoietic Stem Cells in Postmenopausal Women with Osteoporosis. Elaine Yu^{*1}, Ruchit Kumbhani², Erica Siwila-Sackman², Fred Preffer², Michelle DeLelvs², Benjamin Leder³, Joy Wu¹. ¹Massachusetts General Hospital, USA, ²Massachusetts General Hospital, USA, ³Massachusetts General Hospital Harvard Medical School, USA

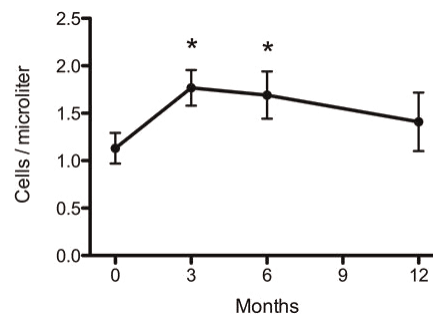
Background: Cells of the osteoblast lineage play an important role in regulating the hematopoietic stem cell (HSC) niche and early B cell development in animal models, perhaps via parathyroid hormone (PTH) dependent mechanisms. The impact of long-term daily teriparatide (PTH 1-34) treatment on cells of the hematopoietic lineage has not been investigated in human clinical studies.

Methods: We studied a subset of postmenopausal women with low bone density who were participating in the the Denosumab And Teriparatide Administration (DATA) study. Of the 36 subjects randomized to teriparatide 20 mcg SC daily, 23 women had peripheral blood leukocyte measurements at baseline, 3, 6, and 12 months, as well as DXA bone density measurements of spine and hip. Flow cytometry was performed to identify early transitional B cells (CD19+, CD27-, IgD+, CD24[hi], CD38[hi]) and HSCs (CD34+, CD45dim+; ISHAGE protocol). Data are presented as mean ± SEM.

Results: Average age of study subjects was 64 ± 5. There was an early increase in circulating HSC number of 40% ± 14% by month 3 (1.1 ± 0.2 cells/uL vs. 1.8 ± 0.2 cells/uL; p=0.004), which persisted through month 6 (1.1 ± 0.2 cells/uL vs. 1.7 ± 0.2 cells/uL; p=0.010) before declining towards baseline at month 12 (see Figure). There were no significant changes in transitional B cells or total B cells over the course of the study period. Other leukocyte lineages were also unchanged. There was no correlation between change in HSC number and changes in spine or hip bone density.

Conclusions: Daily teriparatide treatment for osteoporosis increases circulating HSCs by 3 to 6 months in postmenopausal women. This may represent a proliferation

of marrow HSCs or increased peripheral HSC mobilization. This clinical study establishes the importance of PTH in the regulation of the HSC niche within humans.



Hematopoietic stem cells during teriparatide treatment

Disclosures: Elaine Yu, None.This study received funding from: Eli Lilly, Amgen**SA0121**

Association of Serum Fibroblast Growth Factor 23 and Incident Fractures in Elderly men. Nancy Lane^{*1}, Neeta Parimi², Maripat Corr³, Jane Cauley⁴, Carrie Nielson⁵, Joachim Ix³, Gail Laughlin⁶, Eric Orwoll⁵. ¹University of California at Davis, USA, ²California Pacific Medical Center, USA, ³UCSD, USA, ⁴University of Pittsburgh Graduate School of Public Health, USA, ⁵Oregon Health & Science University, USA, ⁶University of California, San Diego, USA

Normal mineral metabolism is critical for skeletal integrity. Fibroblast derived growth factor-23 (FGF-23) is a bone derived circulating protein that is produced mainly by osteocytes and its production is stimulated by serum inorganic phosphorus and 1,25 vitamin D. Recently, serum levels of FGF-23 levels were found to be directly related to overall fracture risk in elderly Swedish Men (Mirza et al JBMR 2011). To study this association, we performed a prospective case-cohort study to understand the relation of FGF-23 and fracture risk in older Caucasian men enrolled in the MrOS study. Methods. In the cohort of 5994 men attending the baseline MrOS examination, we evaluated a subgroup of 387 men with incident non-vertebral fracture including 112 hip fractures and a sample of 1385 men randomly selected from the cohort with baseline mineral and calcium hormone measurements. FGF-23 was measured in baseline serum samples by ELISA (Millipore, Billerica, MA). All men who experienced any non-vertebral fracture from baseline until February 2007(average follow-up 4.7 years) were included in the analysis. Incident fractures were confirmed with x-ray reports. Modified proportional hazards models that account for case cohort study design were used to estimate the relative hazards (RH) of fracture in men across quartiles of FGF-23 (cutpoints 12.1, 16.6, 22.4 pg/mL). Estimates for regression models using Log transformed FGF23 were back transformed and reported as a 50% increase in FGF23. Results. Subjects with incident non-spine fractures were older, had lower total hip BMD, and higher serum phosphorus. Cases were more likely to report a history of falls and to be frail (all p<0.01). Overall, there was no difference in risk of nonspine or hip fracture by baseline FGF-23. However, in stratified analysis by subjects with eGFR < 60ml/min/1.73m² (n=54/290 non-spine fractures p for interaction=0.0047), the RH per 50% increase in FGF-23 was 1.35 (95% CI: 1.07-1.67) vs. 0.97 (95% CI: 0.87-1.08) in men with eGFR ≥60ml/min/1.73m² (324/1370 fractures) after adjustment for age, clinic site, BMI, race, total hip BMD, vitamin D and PTH. Summary. Overall, serum FGF-23 levels are not associated with incident fractures. However, higher levels of serum FGF23 are associated with fracture risk in those with GFR < 60 ml/min/1.73m².

Disclosures: Nancy Lane, None.**SA0122**

Direct *in vivo* Effects of Vitamin D Sterol Therapy on Osteocyte Viability and Wnt Signaling. Renata Pereira^{*1}, Harald Juppner², Navdeep tumber³, Barbara Gales³, Isidro Salusky⁴, Katherine Wesseling-Perry⁵. ¹UCLA, USA, ²Harvard Medical School, USA, ³UCLA, USA, ⁴University of California, Los Angeles School of Medicine, USA, ⁵UCLA Medical Center, USA

Wnt signaling is suppressed in early CKD resulting in decreased bone turnover, a phenomenon that is overcome by 2°HPT in late CKD (Sabbagh et al JBMR in press), possibly through the inhibitory actions of PTH on osteoblast/osteocyte apoptosis (Jilka et al JCI 1999). Skeletal resistance to the actions of PTH characterizes advanced CKD and is exacerbated by vitamin D sterol therapy. However, the underlying mechanisms are poorly defined and it is unknown whether impaired Wnt-signaling in osteocytes contributes to these findings in CKD. Thus, osteocyte apoptosis and Wnt signaling were evaluated in primary cultures of bone cells derived from the iliac crest of 13 dialysis patients (7M, 6F), age 16 + 1 years before and after 8 months of therapy with vitamin D sterols and phosphate binders. Apoptosis was determined by TUNEL

staining pre- and post-therapy and skeletal expression of sclerostin (SOST), a known inhibitor of Wnt signaling, was determined by immunohistochemistry; both parameters were quantified on a 3 point scale (0=none, 1=some, 2=significant amount). Table 1 displays the biochemical and bone histomorphometric data as well as the percentage of biopsies with positive staining for apoptosis and SOST before and after treatment. Both cortical and trabecular bone apoptosis were markedly decreased at baseline compared to normal controls; this abnormality was much improved after 8 months of vitamin D sterol therapy. Although biochemical values, including PTH, did not change, cortical sclerostin (but not trabecular sclerostin) expression increased significantly ($p < 0.01$) with vitamin D sterol therapy. These data demonstrate that a decrease in normal osteocyte apoptosis characterizes advanced CKD and 2^oHPT. Vitamin D sterol therapy worsens this PTH-resistance in both cortical and trabecular bone of pediatric dialysis patients while increasing suppression of Wnt signaling in cortical, but not trabecular osteocytes, independent of any changes in circulating PTH. These changes may explain, in part, differences in cortical and trabecular bone response to PTH and in the exacerbation of skeletal resistance to PTH that occurs as a result of vitamin D sterol therapy in pediatric patients treated with maintenance dialysis (Wesseling-Perry et al KI 2010).

| | Pre | Post |
|--|----------|----------|
| Biochemicals | | |
| Calcium (mg/dL) | 8.6±0.2 | 8.9±0.2 |
| Phosphorus (mg/dL) | 6.6±0.4 | 5.8±0.4 |
| Alkaline Phosphatase (U/L) | 329±50 | 301±61 |
| PTH (pg/mL) | 646±64 | 671±67 |
| 25(OH)D (ng/mL) | 23.0±2.9 | |
| Histology | | |
| BFR/BS (µm ³ /mm ³ /d) | 51.1±8.9 | 39.7±9.0 |
| OV/BV (%) | 6.7±1.0 | 4.7±0.7 |
| O.Th (µm) | 12.6±0.8 | 10.8±0.7 |
| OS/BS (%) | 39.6±3.5 | 33.2±3.4 |
| OMT (d) | 15.1±1.4 | 14.3±1.8 |
| MLT (d) | 43±10 | 57±24 |
| BVT/V (%) | 37.1±3.1 | 36.4±2.3 |
| Tb.Th (µm) | 172±16 | 163±6 |
| SOST and apoptosis (% of samples with positivity) | | |
| Cortical SOST | 27% | 85%* |
| Trabecular SOST | 27% | 31% |
| Cortical osteocyte apoptosis | 31% | 92%* |
| Trabecular osteocyte apoptosis | 8% | 69%* |

Table 1

Disclosures: Renata Pereira, None.

SA0123

Does the Activation of the FGF-23 Pathway after Living Donor Nephrectomy Increase Bone Turnover? [Anthony Hodsmann](#)¹, [Ann Young](#)², [David Goltzman](#)³, [Amit Garg](#)², [Donor Nephrectomy Outcomes Research Network](#)². ¹Western University, Canada, ²Western University, Canada, ³McGill University, Canada

Living kidney donation offers a unique setting to study changes in skeletal homeostasis attributable to mild, isolated decrements in glomerular filtration rate (eGFR). Although Living Kidney Donors (LKD) are not at short-term risk of fragility fractures (Am.J.Kid.Dis. ePub 2012), serum FGF-23 levels increase by 3.2 pg/ml per 10 ml/min/1.73 m² decline in eGFR in LKD (Am.J.Kid.Dis. ePub 2011). If bone turnover is increased after LKD, these individuals might be at long-term risk for fracture.

Methods: We performed a retrospective cohort study evaluating 2 serum biochemical markers of bone turnover (C-Telopeptide, CTX, and PINP) and other markers of the mineralizing bone disorder of chronic kidney disease (MBD-CKD) in 157 LKD and 66 Non-Donor Controls (NDC). Participants were recruited from 1140 eligible LKD and 421 potential donor-identified NDC from 9 transplant centres. Median follow-up time after donation was 5 yrs. (interquartile range: 4-8). Estimated GFR (eGFR, ml/min/1.73 m²) was calculated using the CKD-EPI formula.

Results: As expected, LKD had a lower eGFR than NDC (73 ± 15 vs. 96 ± 15 , $p < 0.0001$); they were slightly older (45 vs. 41 yr, $p < 0.01$). Within the LKD group, 68%

had eGFR levels classified as Stage II CKD, and 18% as Stage III CKD; comparable data within the NDC group were 28% and 0%, respectively. Mean serum iPTH levels remained within normal limits between groups (ns). However, serum FGF-23 ($p < 0.0001$) levels were significantly higher, whilst serum calcitriol ($p < 0.001$) levels were lower than those in NDC. Mean serum calcitriol levels were > 70 nmol/L in both groups (ns). Serum CTX ($p < 0.01$), but not PINP levels were significantly higher in LKD (Table 1) Serum CTX and PINP were strongly correlated ($r^2 = 0.74$, $p < 0.0001$) suggesting coupled bone turnover. Only serum CTX was correlated to serum PTH ($r^2 = 0.14$, $p = 0.05$) and with eGFR ($r^2 = -0.17$, $p = 0.01$). There were no significant relationships between either marker and serum FGF-23.

Conclusion: The FGF-23 pathway is activated in LKD with mild renal failure. While serum iPTH remained within normal limits, serum calcitriol was significantly lower. These early changes of MBD-CKD may have contributed to increased bone turnover and thus higher serum CTX levels in this relatively young cohort.

| Serum | FGF-23 pg/ml | iPTH pmol/L | Calcitriol pmol/L | CTX ng/L | PINP µg/L |
|-------|-----------------|----------------|----------------------|-------------|--------------|
| LKD | 38.2±15.6* | 5.7±2.5 | 63±21* | 450±229* | 46±23 |
| NDC | 29.7±10.6 | 5.1±2.2 | 77±24 | 370±161 | 45±20 |

* significantly different LKD vs. NDC

Table 1

Disclosures: Anthony Hodsmann, None.

SA0124

See Friday Plenary Number FR0124.

SA0125

See Friday Plenary Number FR0125.

SA0126

Teriparatide Treatment in a Cardiac Transplant Patient with Adynamic Bone Disease and Renal Failure – Improvement of Bone Histomorphometric Indices and Bone mineral Density. [Astrid Fahrleitner-Pammer](#)¹, [Doris Wagner](#)², [Thomas Pieber](#)³, [Alexander Rosenkranz](#)⁴, [Harald Dobnig](#)⁵. ¹Medical University Graz, Austria, ²Medical University of Graz, Austria, ³Department of Internal Medicine, Division of Endocrinology & Metabolism, Medical University of Graz, Austria, ⁴Department of Internal Medicine, Division of Nephrology, Medical University of Graz, Austria, ⁵Diagnostikinstitut Univ.Prof.Dr.H.Dobnig GmbH & Medical University Graz, Austria

Introduction: Cardiac transplantation (CTX) has a negative impact on bone metabolism. Low dose ibandronate (IBN) has been proven to prevent bone loss and fractures; however immunosuppressive therapy and decreasing kidney function may lead to Chronic Kidney Disease-Mineralizing Bone Disorders (CKD-MBD) in the long term. Adynamic bone disease and increased fracture risk are possible complications.

Case: We report a case of a CTX recipient who has received a cardiac transplant 1993 at the age of 58. He received IBN for 4 years and presented with acute back pain at the osteoporosis outpatient clinic in 2010. The patient was still on triple immunosuppressive therapy, had an impaired kidney function (CKD 4). Standardized spinal X ray showed 10 vertebral fractures. Laboratory analysis revealed elevated levels of PTH, sCTX, osteocalcin and normal 25(OH)vitamin D and bALP concentrations. Prior to initiation of osteoprotective therapy we performed an iliac crest biopsy following tetracycline double labeling which demonstrated adynamic bone disease: BV/TV 26.7% (17.8-27.4), BS/BV 17.2mm³/mm³, OS/BS 8.7% (11.5-19.1), ES/BS 2.3% (2.9-5.3), QuS/BS 89%, Tb.N 2.29 1/mm (1.3-2.1), Tb.Th 116.4 µm (127-165), Tb.Sp 319.6 µm (406-604), MS/BS 1.42%. The patient received treatment with 20 µg teriparatide daily (TPT) in combination with 500 mg calcium and 1200 IU vitamin D over 12 months. After one year a second biopsy showed high bone turnover with improved trabecular structure: BV/TV 29.9% (17.8-27.4), BS/BV 19.7mm³/mm³, OS/BS 28.7% (11.5-19.1), ES/BS 7.9% (2.9-5.3), QuS/BS 65%, Tb.N 1.98 1/mm (1.3-2.1), Tb.Th 137 µm (127-165), Tb.Sp 309.6 µm (406-604), MS/BS 1.92%. Treatment was well tolerated, the kidney function stable, PTH and 25(OH)vitamin D were within the normal range, bone turnover markers including osteocalcin, bALP and sCTX were clearly elevated, serum calcium was within the normal range and the patient felt clinically better without occurrence of new fractures.

Conclusion: Adynamic bone disease is a complex entity. Teriparatide therapy was well-tolerated and proved an very effective treatment even in a patient on triple immunosuppressive therapy and CKD 4. Controlled prospective studies are urgently needed to establish teriparatide as a treatment option in adynamic bone disease.

Disclosures: Astrid Fahrleitner-Pammer, None.

SA0127

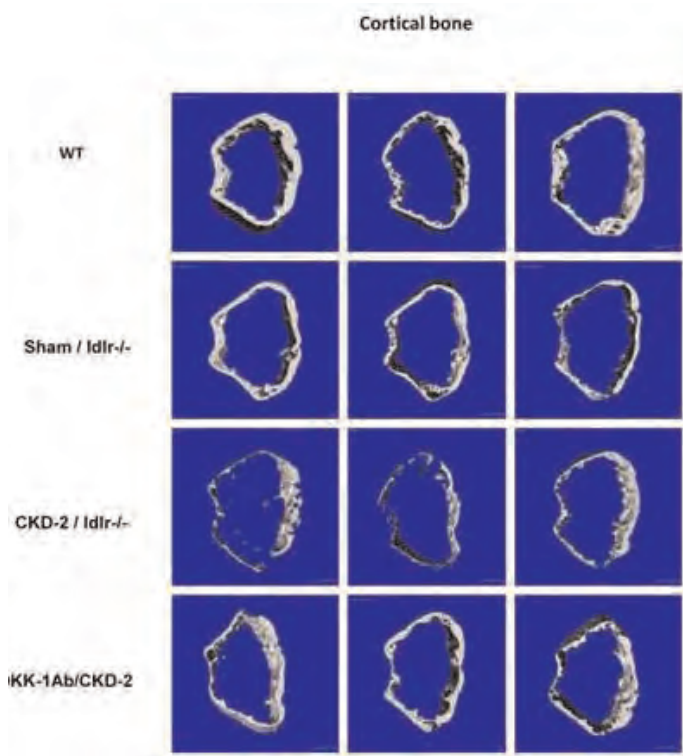
The Role of the Skeleton in the Early Chronic Kidney Disease - Mineral Bone Disorder. Yifu Fang¹, Toshifumi Sugatani², Keith Hruska^{*2}. ¹Washington University School of Medicine, USA, ²Washington University in St. Louis School of Medicine, USA

By stage 2 CKD, the CKD-MBD has been induced and the associated increase in mortality stimulated. Vascular calcification (VC) is a strong cardiovascular risk factor in CKD. The CKD-MBD in stage 2 CKD consists of stimulation of VC, the onset of osteodystrophy, and a stimulation of osteocyte secretion. While Ca, Pi and PTH levels remain normal, FGF23 and sclerostin from the osteocyte are increased. The increase in FGF23 and sclerostin serve as biomarkers of the CKD effect on the skeleton. We have linked the skeleton in CKD to stimulation of VC. The pathogenesis of the initial stimulus for osteocytic secretion of FGF23 is unclear. Early changes in phosphate homeostasis, changes in bone remodeling, and PTH are the candidate factors under investigation. We examined the actions of either modifying Pi balance through intestinal Pi binding or a skeletal anabolic factor (a neutralizing monoclonal antibody to a Wnt inhibitor, DKK1 produced by renal injury) on the early CKD-MBD.

Methods: *ldlr* deficient mice fed high fat diets were subjected to partial kidney ablation at 14 weeks of age to create an early CKD-MBD mouse model. Treatment protocols with Vehicle, CaAc, LaCO₃(3% w/w mixed in diet), or the DKK1 mab (30 mg/kg tiw IP) were conducted from 14-22 wks or 22-28 wks.

Results: Residual kidney function measured by inulin clearance was 75% of normal (stage 2 CKD). Aortic Ca levels were increased by CKD at 22 weeks of age and progressively increased to 28 wks. The serum levels of BUN, Ca, Pi and PTH were normal, but a transient elevation of PTH at 15 weeks was discovered. MicroCT of the femurs revealed cortical but not trabecular bone loss (Figure 1) which was corrected by the DKK1 mab and LaCO₃ but not by CaAc therapy. FGF23 levels were decreased by LaCO₃ and CaAc but not by the DKK1 mab. Vascular Ca levels were decreased by the DKK1 mab but not by CaAc therapy.

Conclusion: We conclude that an early osteodystrophy in CKD may be causatively associated with the stimulation of VC and that the stimulus to FGF23 secretion is independent of the osteodystrophy and may be Pi or PTH.



MicroCT

Disclosures: *Keith Hruska, None.*

This study received funding from: NIH, Fresenius, Shire

SA0128

Health Related Quality of Life in Adults with Osteogenesis Imperfecta is Impaired by Prevalence of Multiple Fractures. Jannie Hald^{*1}, Lars Folkestad², Torben Harsløf³, Malene Schmidt⁴, Hans Gjørup⁵, Dorte Haubek⁴, Kim Brixen⁶, Bente Langdahl⁷. ¹MEA Aarhus University Hospital, Tage Hansensgade 2DK-8000 Aarhus CDenmark, Denmark, ²Department of Endocrinology, Odense University Hospital; Institute of Clinical Research, University of Southern Denmark, Odense; Department of Endocrinology, Hospital of Southwest Denmark, Denmark, ³Department of Endocrinology & Metabolism, Aarhus University Hospital, Denmark, ⁴Department of Dentistry, Health, Aarhus University, Denmark, ⁵Department of Dentistry, Health, Aarhus University; Center for Oral Health in Rare Conditions, Aarhus University Hospital, Denmark, ⁶Institute for Clinical Research, Denmark, ⁷Aarhus University Hospital, Denmark

Osteogenesis imperfecta (OI) is a hereditary disease of the connective tissue (collagen type 1) with a broad clinical appearance. Common symptoms are fractures, hearing loss, dentinogenesis imperfecta (DI), growth deficiency and hypermobility.

Purpose: The aim of the present study was to determine the impact of fractures, hypermobility and DI on health-related quality of life (HRQoL) in Danish adults with OI.

Methods: A cross-sectional study of 54 Danish adult patients with OI. This investigation is part of a larger study of adult patients with OI, investigating phenotype-genotype associations. Clinical and radiographic dental examinations were performed to diagnose DI. Information about number of self reported fractures and hypermobility were collected by interviews. HRQoL was examined using the SF-36 questionnaire. The questionnaire consists of 36 questions in 8 major domains: 4 physical domains: Physical Function(PF), Role Physical(RP), Body Pain(BP) and General Health(GH) and 4 mental domains: Vitality(VT), Social Function(SF), Role Emotional(RE) and Mental Health(MH). Scores are 0-100, a higher score reflects a better self-reported HRQoL. The eight domains above were compared between OI patients with and without DI, with and without hypermobility and with less/equal to or more than 10 reported fractures.

Results: Patients with DI had impaired PF score, $p=0.04$, but similar scores for the remaining physical domains and the mental domains ($p>0.6$). Increasing number of fractures decreased the PF score ($p=0.016$), but did not affect RP, BP and GH ($p>0.2$) or the mental scores ($p>0.3$). SF-36 domains did not vary between patients reporting hypermobility and patients not reporting hypermobility, $p>0.25$.

Discussion: The phenotype of patients with OI varies considerably. We investigated HRQoL in relation to 3 phenotypical features (DI, fractures and hypermobility). The only SF-36 domain affected by DI and a high number of fractures was PF. It is not surprising that increasing number of fractures that may cause deformities and limit functionality impair the physical function score. The effect on PF seen with DI is most likely caused by the coexistence of multiple fractures and DI in severely affected patients. This needs further elucidation. Surprisingly, none of the investigated phenotypes affected the other three physical domains or mental health domains, despite severe and lifelong symptoms. This may reflect the adaptation to a congenital disease.

Disclosures: *Jannie Hald, None.*

SA0129

See Friday Plenary Number FR0129.

SA0130

See Friday Plenary Number FR0130.

SA0131

See Friday Plenary Number FR0131.

SA0132

See Friday Plenary Number FR0132.

SA0133

See Friday Plenary Number FR0133.

SA0134

Changes in Circulating Sclerostin Reflect Changes in Bone Remodeling Dynamics Induced by PTH (1-84). Aline Costa¹, Serge Cremers¹, Mishaela Rubin¹, Natalie Cusano², Elzbieta Dworakowski³, Zachary Lenane¹, Chiyuan Zhang¹, Jim Sliney Jr⁴, Donald McMahon², Marise Lazaretti Castro⁵, John Bilezikian². ¹Columbia University, USA, ²Columbia University College of Physicians & Surgeons, USA, ³Columbia University, USA, ⁴Columbia University Medical Center, USA, ⁵Escola Paulista de Medicina, Brazil

The therapeutic actions of PTH in osteoporosis reflect its ability to stimulate bone modeling initially and, more persistently, bone remodeling. In osteoporosis, these actions have been described as an "anabolic window" in which bone formation is stimulated prior to bone resorption and subsequently by bone formation exceeding bone resorption under steady state therapeutic conditions. A potential mechanism to explain these observations is a negative regulatory effect of PTH on sclerostin levels. Hypoparathyroidism (HypoPT), a disorder characterized by absent or low PTH and markedly reduced bone turnover, is associated with levels of sclerostin that are higher than healthy control subjects with normal PTH levels. Treatment of HypoPT with PTH(1-84) presents an opportunity to test how changes in sclerostin levels are related to changes in circulating markers of skeletal dynamics. In this study, we focused on bone turnover markers (BTM), P1NP (bone formation) and CTX (bone resorption), at peak responsiveness to PTH(1-84) in HypoPT, 12 mos after initiation of therapy. Fifteen HypoPT patients (6 men, 9 postmenopausal women), mean age 58 ± 7yrs, were treated for 4yrs with most receiving PTH(1-84)100 µg QOD. Sclerostin was measured at baseline and at months 12, 24, 36 and 48. Initial sclerostin levels were elevated: 1.07 ± 0.38ng/mL (ref nl: 0.61ng/mL). The cohort was divided into tertiles of BTM responsiveness. No significant changes in sclerostin levels from baseline were observed in the lowest and middle tertiles. The highest tertile, in which marked reductions in sclerostin were noted, was associated with a 6.6-fold increase in P1NP (37.7 to 247.8µg/L) and a 5.4-fold increase in CTX (0.16 to 0.87ng/mL). In these responsive groups sclerostin levels were persistently suppressed (TABLE). Reductions from baseline sclerostin values were appreciated as early as 24 mos after PTH(1-84) reaching nadirs for both P1NP and CTX at month 36. The results indicate that among the most responsive subjects with HypoPT to PTH(1-84), sclerostin levels track inversely with bone remodeling. The observations provide further evidence for a sclerostin-associated mechanism by which PTH regulates skeletal dynamics.

Table. Percentage difference in sclerostin over 4 years of PTH (1-84) treatment according to peak level of P1NP and CTX at month 12

| Highest tertile group at month 12 | Sclerostin percentage change from baseline | | | |
|-----------------------------------|--|----------|----------|----------|
| | Month 12 | Month 24 | Month 36 | Month 48 |
| P1NP (n=5) | -8 | -25** | -38*** | -30*** |
| CTX (n=5) | -6 | -20 | -32' | -34** |

*P<0.05, **P<0.005, ***P<0.0001

Table

Disclosures: Aline Costa, None.

SA0135

Differentially Expressed miRNA199b-5p in Sporadic and Hereditary Parathyroid Tumors. YOON JUNG CHUNG¹, Sena Hwang², Jong Ju Jeong³, Se Hoon Kim⁴, Yumie Rhee⁵. ¹Brain Korea 21 Project for Medical Science, Yonsei University, South Korea, ²International Clinics, Severance Hospital, South Korea, South Korea, ³Department of Surgery, College of Medicine, Yonsei University, South Korea, ⁴Department of Pathology, College of Medicine, Yonsei University, South Korea, ⁵Department of Internal Medicine, College of Medicine, Yonsei University, South Korea

Objects. The molecular mechanisms involved in parathyroid tumorigenesis are poorly understood, even in multiple endocrine neoplasia type 1 (MEN 1) which is due to germline mutation in MEN1 gene. miRNAs are interesting candidates for mediating tissue-specific regulation even in benign tumors because they are associated with cancer development and progression. The aim of this study was to identify specific miRNAs associated with parathyroid tumors either sporadically or hereditarily derived. Methods. miRNA arrays containing 887 human miRNAs with four duplicate probes per miRNA were performed on total RNA extracted from parathyroid tumor samples obtained from 6 patients (3 with primary hyperparathyroidism (PHPT) and 3 with MEN 1) and 2 normal parathyroid tissues. Differentially expressed miRNA were validated by the TaqMan real-time quantitative PCR using RNU6 as endogenous control in the tissues of 15 patients with PHPT and 10 with MEN 1. Relative quantification was performed by Livak method with 20 normal parathyroid tissues as a calibrator. Results. The circulating calcium was significantly higher in patients with parathyroid tumors; 9.3 ± 0.5, 11.4 ± 1.1 and 10.6 ± 0.9 mg/dL, respectively in normal patients, patients with tumors associated with PHPT or MEN1 (p<0.05). PTH concentration showed similar pattern as calcium; 31.7 ± 11.3, 233.0 ± 203.6, and

111.1 ± 43.4 pg/mL (p<0.05) respectively. Using FDR<0.05 from microarray data, we identified 10 differentially expressed miRNAs between normal parathyroid tissues versus those from PHPT or MEN1. Among them, putative tumor-suppressor miR-193b was significantly down-regulated in PHPT (p<0.05), but not in MEN1. It also showed similar expression profile with miRNA-365 which is known to cluster with miRNA193b. We also found that miR-199b-5p was decreased in PHPT samples (p<0.05), whereas significantly was increased in those of MEN1 when compared with normal parathyroid tissues (p<0.05). Conclusions. Down-regulation of miRNA-199b-5p seems to have a distinct role in the tumorigenesis leading to the phenotypic differences in sporadic and hereditary type of parathyroid tumors. This argues for the involvement of different miRNAs in the pathogenesis of parathyroid tumors with different genetic background.

Disclosures: YOON JUNG CHUNG, None.

SA0136

See Friday Plenary Number FR0136.

SA0137

Genetic Analyses of CDKN1B and AIP Genes in Familial Primary Hyperparathyroidism. Filomena Cetani¹, Elena Pardi², Simona Borsari², Federica Saponaro², Chiara Banti², Edda Vignali², Luisella Cianferotti¹, Gabriele Di Rosa², Mario Mastinu³, Stefano Mariotti³, Claudio Marcocci¹. ¹University of Pisa, Italy, ²Department of Endocrinology & Metabolism - Section of Endocrinology & Bone Metabolism, University of Pisa, Pisa, Italy, ³Department of Medical Sciences, Endocrinology, University of Cagliari, Italy

Primary hyperparathyroidism (PHPT) is usually a sporadic disorder, but in <10% of cases occurs as part of hereditary syndromes, including multiple endocrine neoplasia types 1 and 2A (MEN1 and MEN2A), hyperparathyroidism-jaw tumor syndrome (HPT-JT) and familial isolated hyperparathyroidism (FIHP).

MEN 1 is an autosomal dominant disorder characterized by tumours in multiple endocrine glands, most commonly parathyroid, enteropancreatic and anterior pituitary glands. To date MEN1 gene germline mutations have been identified in 70-80% of MEN1 kindreds. FIHP has a heterogeneous molecular etiology, since germline mutations of MEN1, HRPT2 and CASR genes have been reported. Recently, germline mutations of cyclin dependent kinase inhibitor 1B (CDKN1B) gene, encoding for p27 protein, have been identified in 7 kindreds with MEN1 syndrome which were negative to the MEN1 genetic screening. In addition, germline mutations of the aryl hydrocarbon receptor interacting protein (AIP) gene, responsible for 15-25% of familial isolated pituitary adenoma (FIPA) syndrome, have been recently reported in a MEN1 case.

The aim of this study was to perform a genetic screening of CDKN1B and AIP genes in patients with MEN1 syndrome (25 and 22, respectively) and in FIHP probands (15 and 14, respectively). All MEN1 kindreds were previously resulted negative for MEN1 gene mutations and all FIHP families were negative for MEN1, HRPT2, CASR mutations.

Genomic DNAs from index cases were analyzed by PCR amplification of the entire coding region and splice site and direct sequencing by a 16-capillaries automatic sequencer.

A novel frameshift germline mutation of CDKN1B gene, c.372_373delCT/p.Asn124AsnfsX2, was identified in a MEN1 proband. Two mutations in exon 1 of AIP gene were detected in two MEN1 probands, namely Arg9Gln (c.26G>A) and Arg16His (c.47G>A). Both germline mutations have already been reported, Arg9Gln in one acromegalic patient and Arg16His in several FIPA families, and patients with apparent sporadic pituitary adenoma.

Our results suggest that germline CDKN1B and AIP mutations may be partially involved in parathyroid tumorigenesis, affecting a small number of MEN1 patients.

Disclosures: Filomena Cetani, None.

SA0138

Imaging Changes in 99mTc-mibi in Patients with Primary Hyperparathyroidism Treated with Cinacalcet. Araceli Munoz-Garach¹, Diego Fernandez-Garcia², Maria Dolores Martinez del Valle-Torres³, Ana Maria Gomez-Perez², Arantazu Sebastian-Ochoa², Francisco Tinahones-Madueño². ¹, Spain, ²Endocrinologist, Spain, ³Medicine Nuclear, Spain

Introduction: Previous studies in secondary hyperparathyroidism show that treatment with cinacalcet may result in a decreased uptake of radiopharmaceutical as a result of decreased secretory activity of the parathyroid glands. However this effect has not been studied in patients with primary hyperparathyroidism (PHPT).

Objective: To assess changes in 99mTc-methoxy-isobutyl-isonitrile (MIBI) scintigraphy uptake of parathyroid adenomas in patients treated with cinacalcet.

Patients and methods: We evaluated scintigraphy changes of sixteen patients (four more patients have a negative one) treated with Cinacalcet. We determined: uptake rate (estimated as a percentage) mean and maximum uptake images obtained during both early (within 15 minutes of contrast administration) and late (an hour after dose tracer) and were reassessed after receiving treatment with Cinacalcet for a minimum

period of three months. Scintigraphy measurement was made both qualitatively and semiquantitatively. We also evaluated clinical and laboratory parameters.

Results: According to the qualitative scale 75% of analyzed patients decreased their uptake on the scan performed after a treatment period, 12% of them obtained the same results in uptake. One case out of 20 showed negative in the baseline scan but then located the adenoma in the post-treatment scan. However, in quantitative scale there is a trend to statistical significance but there are no differences between pre and post assessments, maximum and mean or early and late phase uptake.

There were no statistically significant differences between clinical parameters, biochemical and scintigraphy findings.

Conclusions: Treatment with Cinacalcet seems to decrease scintigraphy uptake of parathyroid adenomas in patients with PHPT. Further studies should evaluate the clinical relevance of this finding.

Disclosures: Araceli Munoz-Garach, None.

SA0139

Major Improvements in Quality of Life After 1 Year of PTH(1-84) Therapy in Hypoparathyroidism. Natalie Cusano^{*1}, Mishaela Rubin², Donald McMahon¹, Amanda Tulley³, Jim Sliney Jr⁴, John Bilezikian¹.

¹Columbia University College of Physicians & Surgeons, USA,

²Columbia University, USA, ³Columbia University, USA, ⁴Columbia University Medical Center, USA

Hypoparathyroidism (HypoPT) is a rare disorder characterized by low serum calcium and PTH levels for which PTH replacement is under active investigation. Patients with HypoPT often complain of compromised quality of life (QOL) and subtle neurocognitive deficits, yet virtually no data exist to define these complaints or the potential effects of PTH therapy to ameliorate them. We tested the hypothesis that HypoPT patients have a decreased QOL and that PTH therapy improves such indices. 54 HypoPT subjects [age 46±14yrs; 40 women (15 postmenopausal); etiology: 27 surgical, 26 autoimmune, 1 DiGeorge; duration 13±12yrs; calcium 8.6±0.9mg/dL; PTH 2±6pg/mL] were treated with open-label PTH(1-84) 100µg qod for 1yr. At mos 0, 1, 2, 3, 4, 5, 6, 9, and 12, subjects completed the SF-36 survey, a validated measure of health-related QOL covering elements of physical (4 domains) and mental (4 domains) health. At baseline, HypoPT subjects were lower than the normative reference range in 7/8 domains (T-scores -1.4 to -0.8; p<.05). With PTH therapy, intention-to-treat analysis showed the total score increased significantly at 1mo (434±16 to 472±15; p=.023) and remained elevated through 1yr (487±14; p=.008). The mental component summary (MCS) score improved significantly over 1yr (221±9 to 252±8; p=.01), as did 3 mental health domains, generally as early as 1mo [vitality: 35±3 to 47±2; social functioning: 63±3 to 71±3; mental health (MH): 62±2 to 70±2; T-scores improving from -1.3 to -0.8, -0.9 to -0.6, -0.8 to -0.3, respectively; p<.05 for all]. The physical component summary score increased at 6mos (210±9 to 244±8; p=.003) and remained higher at 1yr, with physical functioning (PF) improving from 65±3 to 75±3 (p=.01). Ten subjects discontinued therapy between mos 1-6: 1 for nephrolithiasis and 9 for logistics of travel/other difficulties. Subjects who discontinued PTH had significantly lower MH scores at 1mo, MCS scores at 2mos, and PF and body pain scores at 4mos. These data suggest that HypoPT is associated with QOL deficits, even in the presence of eucalcemia, and that PTH therapy significantly improves QOL indices, particularly those related to mental health. The suggestion that PTH(1-84) has direct CNS effects may account for these observations. Beyond improved biochemical control in HypoPT, these results indicate that PTH(1-84) treatment of HypoPT may lead to important improvements in QOL.

Disclosures: Natalie Cusano, None.

SA0140

Predictors of PTH and Association of PTH with Skeletal Outcomes in a Population-based Study. Claudie Berger^{*1}, Ohoud Almohareb², Lisa Langsetmo³, David Hanley⁴, Christopher Kovacs⁵, Robert Josse⁶, Jonathan Adachi⁷, Jerilynn Prior⁸, Tan Towheed⁹, K. Shawn Davison¹⁰, Stephanie Kaiser¹¹, Jacques Brown¹², David Goltzman¹.

¹McGill University, Canada, ²McGill University, Canada, ³Canadian Multicenter Osteoporosis Study, Canada, ⁴University of Calgary, Canada, ⁵Memorial University of Newfoundland, Canada, ⁶St. Michael's Hospital, University of Toronto, Canada, ⁷St. Joseph's Hospital, Canada, ⁸University of British Columbia, Canada, ⁹Queen's University, Canada, ¹⁰Laval University, Canada, ¹¹Dalhousie University, Canada, ¹²CHUQ Research Centre Laval University, Canada

We examined the potential determinants of circulating parathyroid hormone (PTH) and whether serum PTH is associated with skeletal outcomes in the Canadian Multicenter Osteoporosis Study (CaMos), a population-based prospective cohort study.

Year 10 (2005-07) blood samples (fasting) were analyzed in 1305 women and 566 men aged >35 years for PTH with a Diasorin Liaison machine (reference range of 22.2 to 108.9 pg/ml). Serum PTH values were log transformed to achieve a more normal distribution. Potential determinants of PTH considered included age group, race, season of blood draw, calcium and vitamin D intake (dietary and supplemental), body

mass index, height, corticosteroid and antiresorptive use, eGFR, 25-hydroxyvitamin D [25(OH)D], self-reported diagnosis of hypertension and kidney stones, sun exposure, cigarette smoking, and participation in a regular physical program or activity. As potential skeletal outcomes, we examined associations of (categorical) PTH with log-transformed bone-specific alkaline phosphatase (BAP), log-transformed C-terminal telopeptide of type 1 collagen (CTX) and BMD (L1-L4, femoral neck and total hip). A subgroup of 857 women and 361 men was used for CTX.

The mean (SD) and median of PTH were 61.8 (27.1) pg/ml and 57.2 pg/ml for women and 62.8 (30.4) pg/ml and 56.5 pg/ml for men. Determinants of higher PTH levels were older age, lower 25(OH)D, lower serum calcium levels and lower calcium supplement intake in both women and men. For women, determinants of higher PTH levels also included higher BMI, current use of corticosteroids, winter blood draws, and lower eGFR. Women and men in the 1st quartile (lowest values) of PTH had BAP levels lower by 11.0% (95% confidence interval: 5.1; 16.1) and 14.6% (5.2; 24.1), respectively, than those in the 4th quartile of PTH (highest PTH levels), however we did not find any association of PTH with CTX levels. Women in the 1st or 2nd PTH quartiles had total hip BMD values 0.04 (0.02; 0.06) g/cm² higher than those in the 4th quartile, whereas men in the 1st PTH quartile had total hip BMD values 0.03(-0.00; 0.06) g/cm² higher. We obtained similar results for L1-L4 and femoral neck BMD.

In this random community sample, age, 25(OH)D levels, calcium intake, BMI, renal function and corticosteroid use appeared to be determinants of serum PTH. Increasing serum PTH levels were associated with increased bone turnover, as reflected by serum BAP levels (but not CTX), and reduced hip and spine BMD values.

Disclosures: Claudie Berger, None.

SA0141

PTH (1-84) Substitution Therapy in Hypoparathyroidism: Effects on Muscle Cells, Muscle Function, Postural Stability and Quality of Life. Tanja Sikjaer^{*1}, Lars Rolighed², Niels Ortenblad³, Alexander Hess⁴, Lars Reinmark⁵, Leif Mosekilde¹.

¹Department of Medicine & Endocrinology, MEA, Aarhus University Hospital, Denmark, ²Department of Surgery P, Aarhus University Hospital, Denmark, ³Institute of Sports Science & Clinical Biomechanics, University of Southern Denmark, Denmark, ⁴Department of Clinical Neurophysiology, Aarhus University Hospital, Denmark, ⁵Aarhus University Hospital, Denmark

Myopathy and reduced quality of life (QoL) have previously been reported in patients with hypoparathyroidism (hypoPT). This may be caused by decreased activation of PTH receptors in muscle and brain.

We studied muscle function in 62 patients with chronic hypoPT randomized to 6 months of treatment with either PTH(1-84) 100 µg/d s.c. or similar placebo, administered as an add-on therapy to conventional treatment.

Mean duration of hypoPT was 12 (range: 1-37) yrs. Four subjects had idiopathic and 58 had postoperative-hypoPT. Mean age was 52±11 yrs. 85% were females.

Muscle strength was measured by an adjustable dynamometer chair. In response to PTH, Max Force Production (MFP) at elbow extension decreased significantly compared with placebo. Similarly, MFP decreased borderline significantly in response to PTH at elbow flexion, hand grip, and knee extension 60°. Moreover, hand grip Max Force (MF) and MF at elbow flexion and extension decreased borderline significantly with PTH compared to placebo.

Postural stability measured using a stadiometer in 4 different positions showed no change in response to treatment, nor did Repeated Chair Stand and Timed Up and Go tests.

Muscle biopsies obtained from the thigh showed a significantly increase in Ca²⁺ uptake and release from the sarcoplasmic reticulum in response to PTH treatment.

At baseline, needle electromyography did not show myopathy in any of the patients. Compared with placebo, PTH treatment decreased the mean duration of motor unit potentials in m. biceps brachii, in the direction towards myopathy.

The SF36v2 questionnaire showed a significantly lower baseline score, compared to the normbased population, at most subscales including the physical component score. SF36v2 and WHO-5 scores showed no changes in response to treatment.

In general, our findings suggest a slight but significant deleterious effect of PTH therapy on muscle function. Despite these findings patients did not report increased fatigue or deterioration of QoL. Accordingly, the findings are most likely of subclinical importance. During the 6-months of study, plasma calcium levels fluctuated markedly in the PTH group, until doses of calcium and active vitamin D was adjusted (down-titrated), and the large fluctuations in calcium may have compromised potential beneficial effects of PTH substitution. Accordingly, long term effects should be determined in order to evaluate whether improvements may occur in response to long term treatment.

Disclosures: Tanja Sikjaer, None.

SA0142

Skeletal Microstructural Abnormalities in Hypoparathyroidism by High Resolution Peripheral Quantitative Computed Tomography. Stephanie Boutroy^{*1}, Barbara Silva¹, Mishaela Rubin², Jim Sliney Jr¹, Donald McMahon³, Chiyuan Zhang², Natalie Cusano³, John Bilezikian³.
¹Columbia University Medical Center, USA, ²Columbia University, USA, ³Columbia University College of Physicians & Surgeons, USA

Hypoparathyroidism (HypoPT) is an uncommon disorder characterized by absent or deficient production of parathyroid hormone (PTH) and hypocalcemia. Skeletal abnormalities are described dynamically by a low turnover state and by enhanced skeletal mass by BMD. Studies by us and others have suggested that the increase in BMD is associated with hypermature bone of poor quality. High Resolution Peripheral Computed Tomography (HRpQCT; Scanco Medical AG, Switzerland) has the potential to distinguish these abnormal skeletal characteristics between trabecular and cortical compartments of bone as well as to test how a loaded site (tibia) might differ from an unloaded site (ultradistal radius).

To this end, we studied 45 women (age 45 ± 12) with well characterized HypoPT. HRpQCT female-specific Z-scores were compared to normative values from the OFELY cohort.

HRpQCT female-specific-Z-scores in HypoPT subjects were summarized in the table. Trabecular number was higher and trabecular thickness was lower at both radial and tibial sites. Trabecular separation was reduced at the tibia but not at the radius. The cortical indices as measured by cortical vBMD and cortical thickness were significantly higher than normal at the radius but not at the tibia where the values were not different from normal. The lack of PTH in HypoPT appeared to be associated with enhanced cortical parameters, but only in the radius.

The data suggested that the loaded skeletal site, as typified by the tibia, has other mechanisms by which abnormal cortical enhancement in the setting of absent PTH can be prevented.

| HRpQCT parameters | Z-score (Mean \pm SEM) | |
|-------------------------|--------------------------|----------------------|
| | Radius | Tibia |
| Total Area | 0.04 \pm 0.18 | 0.57 \pm 0.15 *** |
| Total vBMD | 0.40 \pm 0.18 * | -0.05 \pm 0.18 |
| Cortical vBMD | 0.48 \pm 0.24 * | -0.58 \pm 0.30 |
| Cortical thickness | 0.64 \pm 0.19 ** | -0.13 \pm 0.19 |
| Trabecular vBMD | 0.03 \pm 0.22 | 0.29 \pm 0.19 |
| Trabecular number | 0.89 \pm 0.28 ** | 1.53 \pm 0.21 *** |
| Trabecular thickness | -0.68 \pm 0.22 ** | -0.87 \pm 0.15 *** |
| Trabecular separation | -0.42 \pm 0.25 | -1.02 \pm 0.17 *** |
| Trabecular distribution | 0.01 \pm 0.32 | -0.61 \pm 0.20 ** |

*p<0.05; **p<0.01; ***p<0.001 versus normative values

HRpQCT female-specific Z-scores in HypoPT subjects

Disclosures: Stephanie Boutroy, None.

SA0143

Circulating Mesenchymal Stem Cells with Abnormal Osteogenic Potential in Patients with Ankylosing Spondylitis. Ki-Jo Kim^{*1}, Su-Jung Park², In-Woon Baek², Chong-Hyeon Yoon², Wan-Uk Kim², Chul-Soo Cho², Moo-Il Kang³.
¹College of Medicine, The Catholic University of Korea, South Korea, ²College of Medicine, The Catholic University of Korea, South Korea, ³Seoul St. Mary's Hospital, South Korea

Background: Ankylosing spondylitis (AS) is a chronic, progressive disease characterized by inflammation of entheses, leading to new bone formation, syndesmophytes, and ankylosis of joints, primarily in the axial skeleton. However, the mechanism of new bone formation has only partly been understood. In recent, it has been reported that alteration of osteoblastic differentiation of circulating mesenchymal stem cells (MSCs) may contribute to the pathologic change of bone.

Objectives: To evaluate a possible alteration of osteogenic potential of circulating MSCs in patients with AS

Methods: Eighty-nine consecutive patients with AS and twenty-five sex- and age-matched healthy controls were included. Baseline assessment included clinical, radiologic and laboratory data. Radiographs of the lumbar spine were used to detect syndesmophytes. Serum concentration of bone metabolic markers including bone specific alkaline phosphatase (BALP), osteocalcin and telopeptide of type I collagen were measured. Circulating MSCs were analysed and sorted by flow cytometry using four markers (CD34-/CD45-/CD13+/CD29+). The expression of transcription factors runt-related transcription factor 2 (RUNX2) and peroxisome proliferator-activating receptor γ (PPAR γ) were assessed by real-time RT-PCR.

Results: Serum BALP levels were elevated in AS patients compared with healthy subjects (26.5 ± 1.6 vs. 13.3 ± 0.8 ug/L, $P < 0.001$). Number of circulating MSCs was significantly higher in AS patients than controls (1500 ± 593 vs. 181 ± 55 /mL, $P = 0.031$) and positively correlated with serum BALP concentration ($r = 0.414$, $P = 0.002$). RUNX2 expression was upregulated in MSCs from AS patients compared with controls ($P < 0.05$), whereas PPAR γ expression was not different between two

groups. Clinically, circulating MSCs count was even more elevated in AS patients with syndesmophytes than those without (2718 ± 1287 vs. 734 ± 229 /mL, $P = 0.042$).

Conclusions: High number of circulating MSCs with osteogenic potential in AS patients was associated with the presence of syndesmophytes, suggesting a potential role of MSCs on new bone formation in AS.

Disclosures: Ki-Jo Kim, None.

SA0144

See Friday Plenary Number FR0144.

SA0145

See Friday Plenary Number FR0145.

SA0146

See Friday Plenary Number FR0146.

SA0147

Monocytic Expression of Osteoclast-associated Receptor (OSCAR) Is Induced in Atherosclerotic Mice and Regulated by Oxidized Low-density Lipoprotein in vitro. Kathrin Sinnigen^{*1}, Claudia Goetsch², Martina Rauner³, Nadia Al-Fakhri⁴, Michael Schoppet⁵, Lorenz Hofbauer¹.
¹Dresden University Medical Center, Germany, ²Brigham & Women's Hospital Cardiovascular Division, USA, ³Medical Faculty of the TU Dresden, Germany, ⁴Institute of Laboratory Medicine & Pathobiochemistry, Molecular Diagnostics, Philipps-University, Marburg, Germany, ⁵Department of Internal Medicine & Cardiology, Philipps-University, Marburg, Germany

The osteoclast-associated receptor (OSCAR), initially described as a co-stimulatory regulator of osteoclast differentiation, represents a potential link between bone metabolism and vascular biology. Previously, we identified OSCAR to be expressed on endothelial cells and vascular smooth muscle cells in response to proatherogenic factors such as oxidized low density lipoprotein (oxLDL). OSCAR expression increased in the aorta of the ApoE-knock-out (ApoE-KO) mouse, an atherogenic model compared to wild-type mice, and was further induced by a high-fat diet. Because monocytes play an important role in the progression of atherosclerosis, and OSCAR was first described on cells of the monocytic lineage, we assessed whether atherosclerosis also regulates the expression of OSCAR on monocytes and whether it is also regulated by oxLDL or other inflammatory mediators in vitro. Four weeks old male wild-type (WT) and ApoE-KO mice were fed a high-fat diet or normal chow for 6 weeks. Thereafter, peripheral blood mononuclear cells (PBMC) were isolated from the spleen by Biocoll density centrifugation to stain the cells with antibodies against CD14 and OSCAR for subsequent flow cytometric analysis. OSCAR surface expression on CD14-positive monocytes was increased 2-fold in PBMCs from ApoE-KO mice compared to WT mice. Feeding a high-fat diet further increased OSCAR surface expression up to 1.5-fold in ApoE-KO mice. In addition, we exposed a murine macrophage cell line, RAW 264.7 to oxLDL, TNF-alpha, and IL-6 for 24 and 48 hours. While IL-6 stimulation did not influence OSCAR expression, OSCAR mRNA levels were induced 3.5-fold by TNF-alpha, whereas oxLDL treated cells showed an 8-fold increase after 48 hours. In conclusion, monocytic OSCAR expression increases in a murine model of atherosclerosis and is induced by atherogenic stimuli in vitro, thus, suggesting a potential role in the process of atherosclerosis.

Disclosures: Kathrin Sinnigen, None.

SA0148

See Friday Plenary Number FR0148.

SA0149

Evaluation of Cell Therapy as a Treatment Approach for Osteogenesis Imperfecta. Penelope Armada^{*1}, Liping Wang², Elena Torreggiani³, Brya Matthews², Igor Matic², David Rowe², Ivo Kalajzic².
¹Connecticut Children's Medical Center, USA, ²University of Connecticut Health Center, USA, ³University of Connecticut health Center, USA

Osteogenesis imperfecta (OI) is a genetic disorder caused by reduced or improper type I collagen production that results in bone fragility. Recent studies have been directed at silencing or correcting the mutation in bone marrow stromal cells (BMSCs) derived from patients with OI. Despite the success of these in vitro therapeutic approaches, further development of techniques for reintroducing engineered cells back

into the patient is required. Currently, the most effective transplantation has been in the fetal period.

We aimed to evaluate whether donor cells delivered locally into femurs were able to engraft, differentiate into osteoblasts, and contribute to formation of normal bone. Donor BMSCs from mice harboring the bone-specific Col2.3GFP transgene were cultured in 5% O₂ for 7 days prior to transplant to expand undifferentiated mesenchymal progenitors (Col2.3GFP- at transplantation). The osteogenesis imperfecta murine (OIM) model was utilized as the recipient. Mice underwent irradiation, then received wild-type whole bone marrow via the retro-orbital sinus, followed by intramedullary delivery of 106 donor BMSCs in the right femur.

Histological evaluation of bones was completed one month after transplantation. We detected differentiation of donor cells into Col2.3GFP+ osteoblasts and osteocytes in cortical and trabecular bone of the transplanted femur. Col2.3GFP+ cells were not found in the contralateral femur, nor were they seen in bones from mice administered systemic BMSC transplantation. Cultures derived from transplanted femurs of mice after one month showed no Col2.3GFP+ cells after 7 days in culture, but numerous Col2.3GFP+ colonies were present by day 14 indicating the presence of donor derived progenitor cells. This was not observed in cultures from the contralateral femur or from mice that underwent systemic transplantation. To evaluate the progenitor potential of transplanted BMSCs we have performed secondary transplantation of cells recovered and expanded in vitro from recipient femurs. These cells also engrafted and differentiated into GFP+ osteoblasts and osteocytes indicating the persistence of donor stem/progenitor cells.

Our results indicate that BMSCs delivered locally in OIM femurs are able to engraft, differentiate into osteoblasts and osteocytes, and maintain their progenitor potential in vivo. Future studies will address the effects of transplantation on bone parameters and assess long-term engraftment.

Disclosures: *Penelope Armada, None.*

SA0150

Demonstration of a Bone Phenotype in a Murine PKU Model and its Attenuation with an Improved Low-Phenylalanine Diet. Patrick Solverson^{*1}, Sangita Murali², Suzanne Litscher³, Robert Blank⁴, Denise Ney². ¹University of Wisconsin - Madison, USA, ²University of Wisconsin - Madison, Department of Nutritional Sciences, USA, ³University of Wisconsin - Madison, Department of Medicine, USA, ⁴University of Wisconsin, USA

Phenylketonuria (PKU) is caused by a defect in phenylalanine (phe) hydroxylase and requires a low-phe diet plus amino acid (AA) formula to prevent cognitive impairment. Skeletal fragility has been recognized as a chronic complication of PKU, but is poorly understood. Glycomacropeptide (GMP), a low-phe protein isolated from cheese whey, provides an alternative to AA formula. Our objective was to determine how the PKU genotype and dietary protein source affect growth and the biomechanical properties of bone. Male and female PKU (Pah^{enu2}) and wild type (WT) mice, all on a C57BL/6J background, were fed low-phe GMP, low-phe AA or high-phe casein diets from 3 to 23 weeks of age. Body composition was assessed by dual-energy x-ray absorptiometry (DXA) and femur biomechanics were assessed by the 3-point bending test. Femoral diaphyseal structure and ex vivo femoral bone mineral density (BMD) were also measured. Whole bone parameters were used to perform principal component analysis (PCA). Data were analyzed by 3-way ANOVA, with genotype (2 levels), sex (2 levels), and diet (3 levels) as the main factors. Regardless of diet, PKU femora were more brittle than WT femora. Regardless of genotype, AA reduced femoral cross-sectional area with a consequent reduction of maximal load. Multiple additional differences in biomechanical performance and femoral structure were observed among the groups. For example, female, but not male, PKU mice showed reduced body growth compared to WT mice. The protective effect of GMP was more dramatic in female than male PKU mice. PCA yielded 4 PCs with Eigen values > 1, which accounted for 87% of the raw data variance. All 4 PCs displayed a genotype effect. Data are summarized in the table. In summary, the increased brittleness of PKU femora suggests that the bone matrix rather than the bone mineral is abnormal. This phenotype is significantly improved with ingestion of a low-phe diet providing GMP rather than AA as a protein source. The benefits of GMP on bone development may reflect improved collagen formation, lower dietary acid and reduced metabolic stress.

| Statistical Analysis | |
|---|---|
| Parameter | Effect (p-value) |
| Post-yield displacement(mm) | gt(0.0105) |
| Stiffness (N/mm) | gt(<0.0001), sex(<0.0001), gt*sex(0.0101), gt*sex*diet(0.0047) |
| Maximum load (N) | gt(<0.0001), sex(<0.0001), gt*sex(0.0068), diet(0.0419) |
| Energy (N-mm) | gt(0.0003) |
| Cross-sectional Area (mm ²) | sex(<0.0001), gt*sex(0.0138), diet (0.0040) |
| PC 1 | gt(<0.0001), gt*sex(0.0337), gt*diet(0.0042) |
| PC 2 | gt(<0.0001), sex(<0.0001), gt*diet(0.0340), gt*sex*diet(0.0399) |
| PC 3 | gt (<0.0001), sex(0.0044) |
| PC 4 | gt(<0.0001), sex(<0.0001), gt*diet(<0.0001) |

Table of Statistical Analysis

Disclosures: *Patrick Solverson, None.*

SA0151

See Friday Plenary Number FR0151.

SA0152

Homogeneous Mutant Collagen in Osteogenesis Imperfecta Model Mice Leads to Improved Bone Phenotype through Multiple Pathways. ADI REICH^{*1}, Wayne Cabral², Joan Marini¹. ¹National Institute of Child Health & Human Development, USA, ²Bone & Extracellular Matrix Branch, NICHD, NIH, USA

Classical osteogenesis imperfecta (OI) is caused by autosomal dominant mutations in type I collagen. The Brl knock-in mouse, with a G349C substitution in one *colla1* allele, models classical OI inheritance and bone phenotype. Brl heterozygous (HET) pups have 30% prenatal lethality; survivors have a moderate bone dysplasia. Because dominant negative disorders are typically more severe in homozygous (HZ) form, it was surprising that HZ Brl perinatal lethality was comparable to WT. Surviving HZ phenotype and bone mechanical properties were intermediate between HET and WT. We investigated two murine genotypes with homogenous mutant collagen, HZ (Brl/Brl) and Brl/mov, a compound with the null mov13 *colla1* allele. Brl/mov also have normal perinatal survival and improved bone properties. We analyzed the differentiation of cultured calvarial osteoblasts (OB) from HZ and Brl/mov mice during differentiation timecourse using Osteogenesis PCR Arrays and qPCR.

Expression of OB differentiation markers was variably altered in HZ and Brl/Mov cells, rather than restored to WT levels. HZ OB displayed increased expression of *Cdh11*, *Intga2*, and the pre-osteocyte marker *E11/Pdnp*, compared to WT and HET OB. HZ OB had blunted expression of *Dmp1*, *Sost*, *Phex*, *Colla1*, *Colla2*, *Akp*, *Runx2* and *Bmp2*. In femoral tissue RNA, HZ mice had decreased expression of *Sost*, *Osx*, *Bmp2* and *Vegfa*. Immunostaining of *Dmp1* showed lighter intensity in extracellular matrix of cortical bone, compared to HET and HZ mice. In contrast, Brl/Mov OB do not display increased expression of *E11*, *cdh11* or *Intga2*, and have increased expression of *Dmp1*, *Sost*, *Colla1*, *Colla2*, & *Akp*, compared to WT, Mov13 and Brl.

Cell-matrix exchange was performed with HZ OB to study the influence of matrix composition on OB differentiation. *Colla1*, *Runx2* and *Sost* are modulated by matrix, and WT, HET and HZ cells have normal or intermediate levels on HZ matrix. In contrast, *Alp*, *BMP2* and *Itga2* are primarily determined by cellular genotype, and are hardly altered by the matrix exchange.

HZ and Brl/mov mice achieve homogeneous mutant collagen by different mechanisms and apparently attain improved bone properties by distinct pathways.

These expression patterns suggest that several compensation mechanism involving bone mineralization and remodeling, as well as cell-matrix attachment, occur in OB on homogenous mutant matrix. These pathways function to improve OI bone phenotype and could be the basis of novel therapeutic approaches

Disclosures: *ADI REICH, None.*

SA0153

Knock-in of the p.G213R Mutation in the Mouse *Cln7* Gene Induces a Phenotype that Mimics the Human Autosomal Dominant Osteopetrosis Type II (ADO2) Disease. Evidence of Effect of Genetic Background. Imranul Alam^{*1}, Amie Gray², Shoji Ichikawa¹, Kang Chu³, Khalid Mohammad⁴, Marta Capannolo⁵, Anna Teti⁵, Michael Econs¹, Andrea Del Fattore⁶.
¹Indiana University School of Medicine, USA, ²IUPUI, USA, ³Northwestern University, USA, ⁴Indiana University, USA, ⁵University of L'Aquila, Italy, ⁶Children Hospital Bambino Gesù, Italy

ADO2 is a heritable osteosclerotic disorder that usually results from heterozygous missense mutations in the chloride channel 7 (*CLCN7*) gene. Our two labs (L'Aquila and Indianapolis) independently generated the first animal model of the disease by inserting a G-A transition at DNA position 14365 leading to Glycine-Arginine substitution at protein position 213 (analogous to a common human mutation p.G215R). Homozygous mutant mice showed lack of tooth eruption and a dramatic increase in bone mass. They died within 30 days of age with a severe osteopetrotic phenotype, thus confirming insertion of a pathogenetic mutation. Compared to WT, heterozygous B6 ADO2 mice showed significant increase of whole body aBMD (4%, $p < 0.05$) and much greater change at distal femur for BV/TV and Trab.N (75% and 65%, $p < 0.001$ and $p < 0.01$, respectively) (Table 1). In concert with ADO2 patients, bone marrow monocytes from B6 ADO2 mice, cultured with M-CSF and RANKL, showed 2-fold increase of osteoclast formation and 80% reduction of resorption pits, confirming cell autonomous impairment of bone resorption. Since the penetrance of the disorder in human is approximately 66% and severity varies considerably, we created models of phenotypic variability by cross-breeding B6 ADO2 with mice of different genetic backgrounds, namely 129, D2, Balb/c and CD1. Compared to WT, the whole body aBMD and BMC at 12 weeks of age were very high in ADO2 mice on 129 background (8% and 12%, $p < 0.0003$ and $p < 0.01$, respectively). ADO2 mice on D2 background also had significantly higher whole body aBMD (4%, $p < 0.02$). The BV/TV and Trab.N were significantly higher and Trab.Sp was significantly lower at distal femur in ADO2 mice on 129 and D2 backgrounds, while BV/TV was higher in ADO2 mice on Balb/c background and changes were not significant in CD1 ADO2 mice (Table 1). CTX/TRAcP ratio was significantly lower in all ADO2 backgrounds, except the D2 (Table 1). Our results demonstrate that we have independently generated the first bona fide mouse model of ADO2 caused by the heterozygous p.G213R *Cln7* gene mutation and that considerable variability exists for disease severity in ADO2 mice on different genetic backgrounds, consistent with the presence of genes that modify the phenotype. These mouse models will help us to identify the genes that influence penetrance and severity in human ADO2, and to test innovative therapies to treat this incurable disease.

Table 1

| Phenotypes | B6 (F1) | | | 129 (N5) | | |
|----------------|---------------|---------------|--------------|---------------|---------------|-------------------|
| | Wild | Knock-in | p-value | Wild | Knock-in | p-value |
| BV/TV (%) | 9.8 ± 3.4 | 17.2 ± 3.2 | 0.005 | 7.2 ± 0.8 | 14.1 ± 1.4 | 0.0002 |
| Trab.N. (1/mm) | 2.220 ± 0.620 | 3.700 ± 0.770 | 0.006 | 2.317 ± 0.180 | 4.009 ± 0.244 | <0.0001 |
| Trab.Th. (mm) | 0.043 ± 0.005 | 0.047 ± 0.004 | 0.27 | 0.03 ± 0.001 | 0.034 ± 0.001 | 0.03 |
| Trab.Sp. (mm) | 0.128 ± 0.049 | 0.083 ± 0.011 | 0.07 | 0.445 ± 0.050 | 0.225 ± 0.016 | 0.0005 |
| CTX/TRAcP | 1.690 ± 0.630 | 1.390 ± 0.230 | 0.6 | 1.646 ± 0.167 | 0.776 ± 0.150 | 0.0008 |

| Phenotypes | D2 (N5) | | | Balb/c (F1) | | |
|----------------|---------------|---------------|--------------|---------------|---------------|--------------|
| | Wild | Knock-in | p-value | Wild | Knock-in | p-value |
| BV/TV (%) | 6.1 ± 0.6 | 8.8 ± 0.7 | 0.008 | 13.6 ± 1.9 | 16.4 ± 2.0 | 0.03 |
| Trab.N. (1/mm) | 1.172 ± 0.154 | 2.584 ± 0.194 | 0.002 | 3.168 ± 0.345 | 4.263 ± 0.449 | 0.06 |
| Trab.Th. (mm) | 0.035 ± 0.001 | 0.034 ± 0.001 | 0.44 | 0.041 ± 0.002 | 0.038 ± 0.001 | 0.26 |
| Trab.Sp. (mm) | 0.626 ± 0.070 | 0.381 ± 0.034 | 0.007 | 0.339 ± 0.042 | 0.236 ± 0.038 | 0.09 |
| CTX/TRAcP | 1.661 ± 0.147 | 1.398 ± 0.105 | 0.17 | 3.635 ± 0.436 | 2.126 ± 0.183 | 0.005 |

| Phenotypes | CD1 (F1) | | |
|----------------|---------------|---------------|--------------|
| | Wild | Knock-in | p-value |
| BV/TV (%) | 5.3 ± 1.6 | 8.4 ± 3.6 | 0.11 |
| Trab.N. (1/mm) | 1.180 ± 0.290 | 2.210 ± 0.980 | 0.12 |
| Trab.Th. (mm) | 0.045 ± 0.002 | 0.038 ± 0.002 | 0.05 |
| Trab.Sp. (mm) | 0.191 ± 0.021 | 0.154 ± 0.035 | 0.12 |
| CTX/TRAcP | 3.489 ± 0.205 | 2.173 ± 0.160 | 0.004 |

Table 1

Disclosures: Imranul Alam, None.

SA0154

Loss of Heterozygosity of SUFU or PTCH2 Locus Associates with Keratocystic Odontogenic Tumor. Yasuyuki Shimada^{*1}, Kei Sakamoto², Kei-ichi Morita¹, Yuji Kabasawa¹, Ken Omura¹, Akira Yamaguchi².
¹Tokyo Medical & Dental University, Japan, ²Tokyo Medical & Dental University, Japan

Background and Purpose:

Gorlin-Goltz syndrome (GGS) is an autosomal dominant genetic disease characterized by multiple developmental disorders such as skeletal deformities. The patients are prone to develop basal cell carcinoma, medulloblastoma, and cystic jaw tumor called keratocystic odontogenic tumor (KCOT). About half of the patients

harbor a loss-of-function mutation in PTCH1, a receptor of sonic hedgehog, but the genetic background of the other half remains unclear. These neoplastic lesions also develop sporadically, still, only a few of them seem to be associated with PTCH1 malfunction. These suggest a possibility that other genes in the hedgehog signaling pathway may be affected. We made a hypothesis that both of Suppressor of Fused (SUFU) and PTCH2, which regulate hedgehog signaling, may be affected in GGS and also in KCOT.

This study aims to clarify the alteration of PTCH1, PTCH2 and SUFU genes in GGS patients and also in non-GGS patients who developed KCOT. Additionally, loss of heterozygosity (LOH) analysis was performed in KCOT cells to clarify the pathogenesis of KCOT.

Study Design:

DNA sequence of all the exons of PTCH1, PTCH2 and SUFU were analyzed in 31 KCOT patients (15 GGS-related and 16 sporadic) who visited the Dental Hospital of Tokyo Medical and Dental University.

DNA was extracted from buccal swab and PCR-direct sequencing was performed. KCOT cells and stromal cells were separately microdissected from formalin-fixed paraffin-embedded surgical specimens and DNA was extracted for LOH analysis using short tandem repeat polymorphic markers. Informed consent was obtained from all patients.

Results: Of all the 15 GGS cases examined, 9 (60%) had PTCH1 mutation and one had also a PTCH2 mutation. No PTCH1 mutation was found in sporadic cases. SUFU mutation was not detected.

LOH of PTCH1, PTCH2, and SUFU locus were detected in both sporadic (33.3%) and syndromic KCOT (78.6%). Although there was no distinctive predisposition of gene loci, LOH was detected more frequently in syndromic KCOTs than sporadic ones ($P = 0.018$).

Conclusions: This study indicates that acquired alteration of SUFU or PTCH2 locus may play a significant role in the development of KCOT.

Disclosures: Yasuyuki Shimada, None.

SA0155

Neurofibromin Controls Bone Mineralization by Controlling Pyrophosphate Extracellular Levels. Jean De La Croix Ndong^{*1}, Philippe Crine², Xiangli Yang¹, Florent Elefteriou¹.
¹Vanderbilt University, USA, ²Enobia Pharma, Canada

Neurofibromatosis is an autosomal dominant disease (incidence: 1/3000) caused by mutations in the *NF1* gene, which encodes the RAS/GAP neurofibromin. Patients with NF1 can present with a number of skeletal maladies, including pseudoarthrosis (PA), i.e. non-bone union following fracture, and 50-80% of patients with PA also have NF1. Despite substantial advances in the past years, the etiology of NF1 PA remains unclear, and most NF1 patients with PA still require multiple and invasive surgeries. Our goal in this study was to characterize the maturation of *Nf1*^{-/-} osteoprecursor cells using bone marrow stromal cells (BMSCs) isolated from WT and *Nf1*^{lox2}^{-/-} mice or from GFP- or cre-adenovirus infected *Nf1*^{lox/lox} BMSCs. Compared to WT BMSCs, *Nf1*^{-/-} BMSCs formed a reduced number of alkaline phosphatase-positive (cfu-AP) colonies and mineralized alizarin red-positive (cfu-Ob) colonies, which was suggestive of impaired differentiation and/or mineralization. Accordingly, the expression of osteoblast differentiation marker genes, including *Coll*, *Ocn*, *Bsp*, *Runx2*, *Osx* and *Tnsalp* was decreased in *Nf1*^{-/-} BMSCs, whereas the expression of *Rankl* was increased. BMP2 treatment was able to stimulate the differentiation of *Nf1*^{-/-} BMSCs, as measured by increased number of cfu-AP and gene expression, but was unable to correct the defective mineral deposition of *Nf1*^{-/-} cells, indicating that *Nf1*^{-/-} osteoblasts are characterized by a differentiation and a mineralization defect. Further investigations revealed that levels of extracellular inorganic pyrophosphate (ePPI), a potent inhibitor of hydroxyapatite formation and propagation, were elevated in conditioned medium from *Nf1*^{-/-} BMSCs compared to WT BMSCs. The expression of *Ank*, a transporter of extracellular inorganic pyrophosphate (ePPI), *Enpp1*, an enzyme generating PPI, and *Opn*, an inhibitor of mineral nucleation was significantly increased in *Nf1*^{-/-} immature BMSCs, whereas the expression of *Tnsalp*, whose activity is to cleave PPI, was reduced. Importantly, co-treatment of *Nf1*^{-/-} BMSCs with rBMP2 (as differentiation inducer) and a recombinant form of human TNSALP (Asfotase alpha as a mean to reduce ePPI levels) rescued both differentiation and matrix mineralization in *Nf1*^{-/-} BMSCs. Taken together, our data provide a proof of concept that pharmacological enhancements to treat NF1 PA will require both stimulation of osteoblast differentiation and inhibition of ePPI accumulation to allow proper bone healing.

Disclosures: Jean De La Croix Ndong, None.

SA0156

On the Nature of the Genetic Bases of the High Bone Mass Phenotype in Spanish Postmenopausal Women. Patricia Sarrión¹, Leonardo Mellibovsky², Roser Urreiziti¹, Maria Soler-Sala¹, Neus Cols¹, Natalia Garcia-Giralt³, Guy Yoskovitz³, Alvaro Aranguren⁴, Roberto Güerri², Xavier Nogues⁵, Adolfo Diez-Perez⁶, Daniel Grinberg^{*7}, Susana Balcells⁸.
¹Department of Genetics, University of Barcelona, CIBERER, IBUB, Spain, ²Institut Municipal D'Investigació Mèdica, Spain, ³IMIM, Spain, ⁴The University of Barcelona, Spain, ⁵Institut Municipal D'Investigació Mèdica, Spain, ⁶Parc De Salut Mar, Spain, ⁷The University of Barcelona, Spain, ⁸University of Barcelona, Spain

The purposes of this study were: to establish the prevalence of the high bone mass (HBM) phenotype in the BARCOS cohort (n=1600); to determine whether any of the HBM cases carry *LRP5* mutations that explain the phenotype; to characterize the expression pattern of osteoblast-specific and Wnt pathway genes in primary osteoblast RNA samples from two HBM cases; and to test the hypothesis of an inverse correlation between the number of common variant osteoporosis risk alleles and HBM.

Material and methods: HBM individuals within the BARCOS cohort were identified according to the criterion of a sum Zscore > 4 (total LS-Zscore + total Hip-Zscore). Relevant exons of *LRP5* were PCR-amplified and sequenced. Cosegregation analysis of markers in the *LRP5* gene region was performed in one family. Primary osteoblasts from two HBM and two control individuals were cultured and RNA was extracted. A Roche RealTime Custom Panel was used to analyse the expression of 88 osteoblast-specific and/or Wnt pathway genes. SNPs from previous GWA studies were genotyped in the HBM cases and relatives and a weighted score was obtained for each individual. These scores were plotted against BMD values.

Results: In the BARCOS cohort of postmenopausal women, 0.6% of individuals display BMD values in the HBM range. No mutations in the analysed exons of the *LRP5* gene were found in these patients. Additionally, in one familiar case in which the mother and one of the two sibs had BMD values in the range of HBM, cosegregation analysis ruled out *LRP5* involvement. Further cosegregation studies in this family allowed the exclusion of the following genes: *DKK2*, *IL6R*, *RANK*, *BMP2*, and *KRMI*. The only gene cosegregating was *RANKL*, but it was sequenced in the proband and no mutations were found. Regarding the expression analysis, five genes were found to be overexpressed in the two HBM samples: *BMP4*, *COL10A1*, *RUNX2*, *FZD3* and *SOX6*, while four were underexpressed: *DLX3*, *TWIST1*, *IL6R*, and *PPARG*.

Finally, preliminary results point to an inverse correlation between risk alleles and BMD in this group of women, although two women with the highest BMD values presented with the highest risk score. A low frequency penetrant unknown genetic variant could be a possible explanation for these cases.

Conclusions: *LRP5* is not the cause of the HBM phenotype in these cases from BARCOS cohort. The results of the expression study raise new hypotheses that should be further investigated. HBM maybe genetically heterogeneous.

Disclosures: Daniel Grinberg, None.

SA0157

See Friday Plenary Number FR0157.

SA0158

Specific Effects of Activating Gsa Mutation in Specific Compartments of the Stromal/Osteogenic Lineage in vivo Explain Pathological Features in Fibrous Dysplasia (FD) and Reveal a Novel Relationship between Fat, Bone and Gsa Signaling. Cristina Remoli^{*1}, Stefania Cersosimo¹, Emanuela Spica¹, Benedetto Sacchetti¹, Alan Boyde², Pamela Gehron Robey³, Kenn Holmbeck⁴, Isabella Saggio⁵, Mara Riminucci⁶, Paolo Bianco⁷.
¹University La Sapienza, Italy, ²Queen Mary University of London, United Kingdom, ³NIH/NIDCR, USA, ⁴NIDCR, USA, ⁵Sapienza University of Rome, Italy, ⁶University La Sapienza, Italy, ⁷Universita La Sapienza, Italy

To model FD in mice, we generated transgenic lines expressing GsαR201C either constitutively or as targeted to osteoblasts. Individual FD-defining features (enhanced osteoclastogenesis, marrow fibrosis, loss of marrow adipocytes, osteomalacia) are reproduced in mice with constitutive expression of GsαR201C (FD mice), but not in mice with an osteoblast-targeted transgene. By comparative in situ and ex vivo studies, we traced each of the non-osteoblast dependent effects of Gsα mutation to mechanisms operating in different compartments of the stromal/osteogenic lineage. 1) Enhanced osteoclastogenesis in FD mice emanates from overexpression of RANKL specifically in a compartment of ALP+/ADRB2+ perivascular stromal cells in intraosseous vascular channels. Localized overexpression of RANKL in these cells in vivo drives intracortical osteoclastogenesis and osteolysis in FD mice. Ex vivo, overexpression of RANKL is reproduced in non-differentiated stromal cells expressing GsαR201C, but not in mature transgenic osteoblasts; it is induced in cognate WT stromal cells by isoproterenol but not by PTH, consistent with the

relative abundance of ADRB2 and PTHR1 receptors. 2) Osteomalacia in FD mice reflects the ectopic expression of the mineralization inhibitor Matrix Gla Protein (MGP) in mature osteoblasts. Targeted expression of GsαR201C in mature osteoblasts, however, does not induce MGP expression or osteomalacia, indicating that MGP-expressing osteoblasts can only develop from a GsαR201C-expressing precursor. 3) Marrow adipocytes in FD mice are lost by conversion to a brown adipose tissue (BAT)-like phenotype, UCP-1 upregulation and thermogenic lipolysis, which is otherwise also induced in extramedullary WAT, and enhanced in BAT, in FD mice. 4) Committed adipogenic cells hijacked to an osteogenic fate contribute to the bulk of abnormal osteogenic cells that accumulate as "fibrosis" in murine FD bone. These cells display a phenotype (ALP+/Osx-; MGP+/PLP+/UCP1+/Oil Red O-), distinct from that of WT preosteoblasts (ALP+/Osx+/PLP-), adipocyte progenitors (Sca-1+/Osx-/PLP-/ORO-) and adipocytes (ALP-/Osx-/ORO+/PLP+), and represent the unorthodox precursor of the MGP+/PLP+ osteoblasts that deposit the dysplastic, undermineralized FD bone. Activating mutations of Gsα promote osteoclastogenesis by non-differentiated perivascular osteoprogenitors, and reprogram marrow adipocytes to an aberrant osteoblastic phenotype, thus determining the key features of the FD phenotype.

Disclosures: Cristina Remoli, None.

SA0159

The Phenotype of Subjects with Persistently Low Serum Alkaline Phosphatase in a Comprehensive Care Population. Fergus McKiernan^{*1}, Jay Fuehrer², Richard Berg². ¹Marshfield Clinic, USA, ²Biomedical Informatics Research Center, Marshfield Clinic Research Foundation, USA

Introduction: The significance of a persistently low serum alkaline phosphatase (ALP) is unknown but could indicate the presence of an inherited metabolic skeletal disorder such as Hypophosphatasia (HPP). We studied a large rural comprehensive care population to characterize the phenotype of subjects with persistently low ALP.

Methods: Our IRB approved use of Marshfield Clinic's comprehensive paper and electronic medical record (eMR) to conduct this retrospective study. The eMR was searched between 1982 and 2011 for low serum ALP values and clusters of ICD-9 diagnosis codes that pointed towards conditions known to be associated with HPP. Plots of serial ALP values were constructed for subjects with at least 2 ALP values below the lower limits of normal in adults (40-125IU/L). Subjects whose ALP was persistently ≤ 40IU/L constituted the study population. Subjects with normal ALP and sufficient meaningful clinical narrative in the eMR served as controls. Supplemental paper charts abstraction was performed when indicated and available. Confirmed cases of HPP were validated by manual chart review and excluded from this analysis.

Results: Between 1982 and 2011, 458,833 unique subjects had 2,584,751 serum ALP values. 5,190 subjects had at least 2 ALP values ≤ 40IU/L. 269 study subjects with persistently low ALP were identified and constituted the study population. Using logistic regression models, stratified by gender and including covariates for age, male study subjects appeared more likely than controls to match the ICD-9 diagnostic clusters for calcium pyrophosphate deposition disease (CPDD), abnormal dentition and myopathy. Both male and female subjects were more likely than controls to match for disorders of phosphate metabolism. Manual chart abstraction and review of available radiographs suggested that crystalline arthritis, chondrocalcinosis, calcific tendonitis and diffuse idiopathic skeletal hyperostosis (DISH) were common in subjects with persistently low ALP but that fibromyalgia and hypermobility were not. Based on this review, 17 adult subjects were suspected to have previously unrecognized HPP but this awaits confirmation.

Conclusion: Adult subjects with persistently low ALP may have excess crystalline arthritis, chondrocalcinosis, calcific tendonitis and DISH. A subset of these individuals may harbor previously unrecognized HPP. Further clinical characterization and diagnostic evaluation of this population is underway.

Disclosures: Fergus McKiernan, Enobia/Alexion, 6
 This study received funding from: Enobia

SA0160

See Friday Plenary Number FR0160.

SA0161

Polymorphisms in Wnt Antagonist Genes and Bone Mineral Density in Postmenopausal Korean Women. Dong Ock Lee¹, Hoon Kim², Seung-Yup Ku³, Seok Hyun Kim³, Jung Gu Kim^{*3}. ¹Department of Obstetrics & Gynecology, National Cancer Center, South Korea, ²Department of Obstetrics & Gynecology, Incheon Medical Center, South Korea, ³Department of Obstetrics & Gynecology, Seoul National University College of Medicine, South Korea

Objective: The purpose of this study was to investigate the association between single nucleotide polymorphisms (SNPs) in Wnt antagonist genes and bone mineral density (BMD) in postmenopausal Korean women.

Methods: The Wnt inhibitory factor-1 (*WIF-1*) c.28G>A, c.496C>A, secreted frizzled-related protein 1 (*sFRP1*) rs3242 C>T, rs16890444 C>T, *sFRP2* c.134C>T, *sFRP3* c.598C>T, c.970C>G, *sFRP4* c.958C>A, c.1019G>A, *sFRP5* c.34A>T, c.35C>A, dickkopf 1 (*Dkk1*) c.318A>G, *Dkk2* c.437G>A, *Dkk3* c.92C>G, c.147G>T and c.1003A>G polymorphisms were analyzed in 399 postmenopausal Korean women. Serum levels of osteoprotegerin (OPG), soluble receptor activator of the nuclear factor- κ B ligand (sRANKL) and bone turnover markers were measured and BMDs at the lumbar spine and femoral neck were also examined.

Results: The *Dkks* and *sFRP1* polymorphisms and the *sFRP3* c.970C>G polymorphism were not related to BMD, whereas an association between the haplotype genotype defined by the combination of the c.958C>A and c.1019G>A polymorphisms in the *sFRP4* gene and BMD at the lumbar spine were observed. The haplotype AA homozygotes showed significantly lower lumbar spine BMD and a higher serum bone alkaline phosphatase level than other genotypes. At the lumbar spine, the haplotype AA homozygote was 4.37-times more frequently observed in women with osteoporosis than in women with normal BMD. No significant differences in OPG and sRANKL were detected among single genotypes or the *sFRP4* haplotype genotype.

Conclusion: Our results suggest that the haplotype genotype of *sFRP4* c.958C>A and c.1019G>A SNPs may be genetic factors affecting lumbar spine BMD in postmenopausal Korean women.

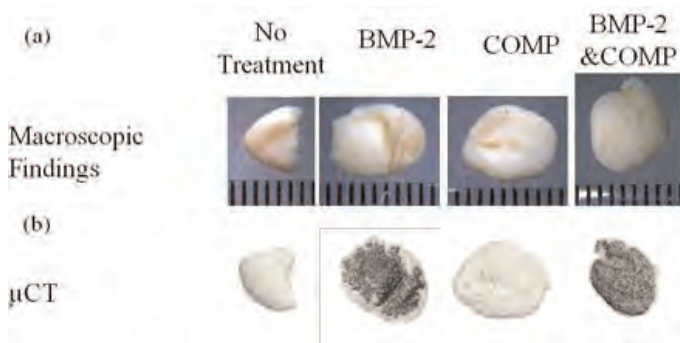
Funding support: supported by a grant (A080012) from the Korea Health Technology R&D project, Ministry of Health, Welfare & Family Affairs, ROK

Disclosures: Jung Gu Kim, None.

SA0162

COMP Enhances BMP-2 Dependent Osteogenesis via Activating BMP-2 Signaling. Kazunari Ishida^{*1}, Chitrangada Acharya², Blaine Christiansen³, Jasper Yik², Paul DiCesare², Dominik Haudenschild². ¹University of California-Davis Medical Center, USA, ²University of California-Davis Medical Center, USA, ³University of California - Davis Medical Center, USA

Introduction: High doses of BMP are clinically used to initiate bone formation in spinal fusion and fracture healing, but are associated with side-effects. We hypothesize that the high doses are required due to non-physiological presentation of free unbound BMP, and that matrix-bound BMP would be more biologically relevant and therefore more effective at lower doses. Cartilage oligomeric matrix protein (COMP) is a disulfide-bonded homo-pentameric glycoprotein located in the extracellular matrix of joint tissues. COMP interacts with other cartilage matrix components and receptor complexes at the cell surface. The repeated modular structure of COMP allows it to act as a molecular 'bridge' between these binding partners. Recently, we demonstrated that COMP has multiple binding sites for TGF- β 1, and that COMP enhanced TGF- β 1 activity. The similarity of BMP-2 to TGF- β 1 suggests that BMP-2 also binds COMP. It is our hypothesis that COMP can function as a biologically appropriate carrier to promote BMP-2 osteogenic activity. Methods: To characterize the interaction between BMP2 and COMP, ELISA-type binding assays were performed. To examine the effect of COMP on BMP signaling pathway, phosphorylation of Smad and BMP receptors protein levels were examined. To test the effect of COMP on BMP-2 dependent transcription, luciferase from a BMP-dependent promoter was assayed. BMP-2-dependent osteogenesis and matrix mineralization were measured by qRT-PCR for osteogenic genes, alkaline phosphatase enzymatic (ALP) activity, and alizarin Red S staining in C2C12 cells and human MSCs. Finally, in vivo ectopic bone formation was evaluated using a rat model, and confirmed by μ CT, ALP activity, qRT-PCR, and histology. Results: COMP directly bound BMP-2 in vitro, with a pH optimum of 5.5, which was enhanced by manganese but largely unaffected by other divalent cations or EDTA. BMP-2 treatment in the presence of COMP prolonged the phosphorylation status of Smad1/5/8 and sustained both type 1 and 2 BMP receptors protein levels out to 24 hours. COMP enhanced BMP-2-dependent transcription, osteogenesis, and matrix mineralization. Finally, COMP enhanced BMP-2-dependent in vivo ectopic bone formation. Conclusion: This study demonstrated that COMP enhances BMP-2-dependent osteogenesis via sustaining the biological activity of BMP-2. Clinically, it may be possible to use COMP as a naturally-occurring carrier to reduce the dose of BMP-2 required for bone formation.



Figure

Disclosures: Kazunari Ishida, None.

SA0163

Critical Role of ALK2 Phosphorylation at Thr203 in Activation by BMP type II Receptors. Satoshi Ohte^{*1}, Mai Fujimoto², Katsumi Yoneyama², Hiroki Sasanuma², Masashi Shin², Sho Tsukamoto³, Arei Miyamoto², Toru Fukuda², Shoichiro Kokabu², Takenobu Katagiri⁴. ¹Saitama Medical University, Research Center for Genomic Medicine, Japan, ²Saitama Medical University, Research Center for Genomic Medicine, Japan, ³Saitama Medical University RCGM, Japan, ⁴Saitama Medical University Research Center for Genomic Medicine, Japan

Bone morphogenetic proteins (BMPs) induce heterotopic bone formation in skeletal muscle through binding to type I and type II transmembrane serine/threonine kinase receptors expressed on target cells. Fibrodysplasia ossificans progressiva (FOP) is a rare autosomal dominant congenital disorder characterized by progressive heterotopic bone formation in skeletal muscle. Mutations of ALK2, a BMP type I receptor, have been found in patients with FOP. We have reported that those mutant ALK2 are moderately activated and are further activated by BMP type II receptors in C2C12 cells. In this study, we report a critical role of ALK2 phosphorylation at Thr203 in the activation by BMP type II receptors. Co-transfection of each BMP type II receptor and mutant ALK2 found in FOP induced Smad phosphorylation and osteoblastic differentiation in C2C12 cells with an increase of ALK2 phosphorylation. ALK2 has nine Ser/Thr residues in the intracellular GS domain, which is the potential phosphorylation domain by type II receptors. Substitution mutation of all of the nine Ser/Thr residues by Ala/Val (GS9AV) completely destroyed the activity of ALK2 even in the presence of type II receptors. However, substitution mutation of seven Ser/Thr residues except Thr203 and Thr209 (GS7AV) was still activated by type II receptors. A mutation at Thr203, but not Thr209, completely lost the biological activity of ALK2 in spite of co-expression of type II receptors. Moreover, the substitution at Thr203 with Val in the mutant ALK2 found in FOP completely inhibited the activities in C2C12 cells. Taken together, these findings suggest that phosphorylation of ALK2 at Thr203 plays essential role in activation by type II receptors. The activation of mutant ALK2 found in FOP may be caused through enhanced phosphorylation at Thr203 by endogenous BMP type II receptors.

Disclosures: Satoshi Ohte, None.

SA0164

High-dose BMP2 Reduces Cell Proliferation and Increases Apoptosis via DKK1 in Human Primary Periosteum-derived Cells. Nobuhiro Kamiya^{*1}, Ila Oxendine², Sasha Shafer², Harry Kim³. ¹Texas Scottish Rite Hospital for Children, USA, ²Texas Scottish Rite Hospital for Children, USA, ³Scottish Rite Hospital for Children, USA

BMP2 is a potent osteogenic factor used clinically to stimulate spinal fusion and fracture healing. Interestingly, BMP2 doses used for clinical application are much higher (500-1500 micro g/ml) than those for preclinical studies (100-300 nano g/ml) that showed positive effects of BMP2 in osteoblast differentiation and new bone formation. The effect of high-dose BMP2 on bone cells in comparison to low-dose BMP2 has not been elucidated well. The purpose of this study was to compare the effects of low and high doses of BMP2 on cell proliferation and apoptosis using human periosteum-derived cells since BMP2 is generally applied around the periosteum to stimulate osteogenesis.

We obtained human periosteum from three patients undergoing orthopaedic surgery and isolated primary periosteum-derived cells. The primary cells were treated with BMP2 in culture and cell proliferation and apoptosis were assessed by MTT and Caspase assay, respectively. MTT activity was significantly reduced with high-dose BMP2 treatment (2000 nano g/ml). In contrast, such reduction was not observed when treated with low-dose BMP2 (100 nano g/ml). Caspase activity was significantly increased with high-dose BMP2 but unchanged in the low-dose BMP2. To investigate the mechanism responsible for the alteration of cell proliferation and apoptosis, we focused on DKK1, one of well-known tumor suppressor genes while its role in bone cells is largely unknown. DKK1 expression levels assessed by qRT-PCR were dramatically increased in the high-dose group and this increase was consistent with DKK1 protein levels assessed by Western blotting. The addition of DKK1 protein to the primary cells reduced MTT activity and increased caspase activity significantly. Silencing DKK1 expression by 90% using the siRNA technique normalized cell proliferation and apoptosis in the cells exposed to high-dose BMP2. Last we examined cell cycle inhibitors that can regulate DKK1 expression. The p21 and p27 expression and p21 and p53 protein levels were all increased by BMP2 treatment. These results suggest that BMP2 has a critical role in controlling cell number via DKK1 mediated control of cell proliferation and apoptosis. In conclusion, high-dose BMP2 decreased cell proliferation and increased apoptosis. Since periosteum is important source of progenitor and osteogenic cells, further investigation on the effects of high-dose BMP2 is warranted on cell proliferation as well as differentiation.

Disclosures: Nobuhiro Kamiya, None.

SA0168

Adipocyte Lipoprotein Lipase influences Fatty Acid Composition of Bone in Mice. Brigitte Müller*¹, Alexander Bartelt², Klaus Toedter¹, Ludger Scheja¹, Joerg Heeren¹, Andreas Niemeier². ¹University Medical Center Hamburg-Eppendorf, Germany, ²University Medical Center Hamburg-Eppendorf, Germany

Objective: Dietary lipids are transported in the circulation by lipoproteins. These lipoproteins are hydrolysed by lipoprotein lipase (LPL) to release fatty acids, or can be taken up as whole particles, thereby delivering triglycerides, cholesterol and lipophilic vitamins to target cells. The contribution of the skeleton to systemic lipoprotein metabolism is poorly understood. Here we analyze the role of adipocyte-LPL in lipid uptake into bone and determine the lipid composition in mineralized bone tissue versus bone marrow.

Methods: Uptake of radiolabeled lipoproteins and fatty acids were determined in organ extracts by scintillation counting. The physiological route of dietary lipids was followed in an oral fat tolerance test with olive oil containing tracer amounts of ³H-triolein. Mice carrying adipocyte-specific lipoprotein lipase knock-out (KO) alleles were used to study pathways responsible for lipid entry into bone. Fatty acid composition was determined by gas chromatography with internal standards.

Results: In comparison to liver, muscle and brown adipose tissue, which are among the major organs involved in dietary fat clearance, lipid uptake per mg of organ weight (specific uptake) is relatively low in calvaria, femur cortex and vertebrae. Analysis of the respective bone compartments revealed that specific uptake into bone marrow was about 3x higher than into cortical bone. However, with regard to the relative contribution to the clearance of the total fat load, the skeleton (total tissue) is the fourth most important organ involved in lipid uptake. Fatty acid composition analyses in adipocyte-LPL KO mice indicated that LPL-mediated uptake of essential polyunsaturated fatty acids into cortical bone in tibia and femur was impaired to a higher degree than uptake into bone marrow. In addition, *de novo* lipogenesis fatty acid products are increased in femur cortical bone in adipocyte-LPL KO mice.

Conclusion: The majority of postprandial lipids are taken-up by initial binding of lipoproteins to endothelial cells, subsequent hydrolysis of triglycerides by lipoprotein lipase and cellular uptake of fatty acids. The current results suggest that bone marrow adipocyte-LPL is involved in fatty acid transport into matrix-associated osteoblasts and osteocytes within the cortex of long bones and thus underline the importance of the functional interplay between bone marrow adipocytes and adjacent bone cells.

Disclosures: Brigitte Müller, None.

SA0169

See Friday Plenary Number FR0169.

SA0170

See Friday Plenary Number FR0170.

SA0171

See Friday Plenary Number FR0171.

SA0172

See Friday Plenary Number FR0172.

SA0173

Oral Health and Biochemical Risk Factors for Bisphosphonate-associated Jaw Osteonecrosis. Claudine Tsao¹, Gelsomina Borromeo², Ivan Darby², Katrina Walsh², Neil O'Brien-Simpson², Eric Reynolds², Peter Ebeling*³. ¹The University of Melbourne, Australia, ²The University of Melbourne, Australia, ³The University of Melbourne, Australia

Introduction: Anti-resorptive drugs, including bisphosphonates, have been associated with jaw osteonecrosis (ONJ). Despite serum bone turnover markers (BTMs) being used in dentistry to assess ONJ risk, the relationship between serum BTMs and bone turnover in the periodontium is uncertain. In addition, the role of oral health and periodontal disease as risk factors for ONJ remains unclear and the role of surrogate measures of periodontal disease, including gingival crevicular fluid (GCF) pro-inflammatory mediators [interleukins (IL-1 β and IL-6) and tumour necrosis factor- α], has not been fully explored. If the pro-inflammatory effect of bisphosphonates translates to the periodontium, both periodontal disease and ONJ risk may increase.

Methods: Firstly, we compared levels of BTMs in GCF and serum in twenty healthy volunteers, who received oral examinations, and GCF and serum sampling. Serum was tested for the amino-terminal propeptide of Type I collagen (PINP) using automated non-isotopic immunoassays. GCF was tested for PINP using a radio-

immunoassay (RIA). Secondly, we investigated oral health risk factors for ONJ in participants with a history of bisphosphonate use. This cross-sectional study compared ONJ cases (n=22) with controls (n=41), who all received bisphosphonates. Oral examinations were conducted, and serum and GCF sampled. Serum was tested for IgG titres against four periodontopathic bacteria, biochemical parameters, BTMs, and with multiplex analysis. GCF underwent multiplex analysis and PINP RIA testing.

Results: In healthy volunteers, GCF PINP levels were 10-fold higher than in serum. A significant correlation was found between GCF and serum PINP levels ($r=0.629$, $p=0.002$), suggesting that assumptions regarding bone turnover activity in the periodontium may be inferred from serum levels, though confirmation from larger studies is required. In patients with bisphosphonate-associated ONJ, periodontal disease was associated with ONJ, as measured by three clinical parameters and the surrogate markers of serum IgG titres against *Porphyromonas gingivalis* (OR 2.72, $p=0.018$) and the GCF pro-inflammatory marker, IL-1 β (OR 24.7, $p=0.044$).

Conclusion: Bone turnover was higher in the periodontium than in the serum. Whilst the mechanism underlying the role of periodontal disease as an ONJ risk factor is uncertain, our results do also suggest that the role of oral microbes as a contributing aetiological agent may have been underestimated.

Disclosures: Peter Ebeling, None.

SA0174

See Friday Plenary Number FR0174.

SA0175

Withdrawn

SA0176

Altered Expression of Apoptosis-Associated miRNAs that Regulate IGF-1 Survival Signaling Underlies the Cell Autonomous Requirement of Cx43 for Osteocyte Survival. Rafael Pacheco-Costa*¹, Lucas Brun², David Southern³, Rejane D. Reginato⁴, Nicoletta Bivi⁵, Teresita Bellido⁵, Lilian Plotkin⁵. ¹Indiana University School of Medicine/Federal University of Sao Paulo, Brazil, USA, ²Universidad Nacional de Rosario, Argentina, ³Indiana University School of Medicine, USA, ⁴Federal University of São Paulo, Brazil, ⁵Indiana University School of Medicine, USA

Mice lacking connexin (Cx) 43 in osteocytes exhibit elevated prevalence of osteocyte apoptosis and MLO-Y4 osteocytic cells in which Cx43 is silenced exhibit spontaneous cell death; however, the basis of the cell autonomous requirement of Cx43 for osteocyte viability is unknown. We questioned whether the absence of Cx43 changes the expression of apoptosis-associated microRNAs (miRs), short RNA molecules that act as negative post-transcriptional regulators of gene expression and have profound effects on cell survival. Cx43 expression was stably silenced in MLO-Y4 osteocytic cells using shRNA. Silenced cells exhibit a decrease of more than 80% in the expression of Cx43 at the mRNA and protein levels compared to scramble shRNA-transfected control cells. miR21 and miR218 expression was altered in Cx43-deficient cells out of 47 apoptosis-associated miRs studied (Apoptosis-Associated miRNA Plate Array, Signosis). Results were confirmed by qPCR and showed that miR21 expression was decreased by 50% and that miR218 expression was increased by 500% in Cx43-deficient cells compared to control cells. A target of miR21 is PTEN, the phosphatase that inactivates the Akt-survival pathway; and a target of miR218 is IKK β kinase, which is required for NF κ B activation. Akt and NF κ B are known mediators of survival signaling activated in several cell types by insulin like growth factor-1 (IGF-1), which also inhibits apoptosis of osteoblasts and osteocytes. We therefore investigated whether the absence of Cx43 interferes with the anti-apoptotic effect of IGF-1. We found that whereas control cells were protected by IGF-1 from glucocorticoid-induced apoptosis, IGF-1 was ineffective in Cx43-deficient MLO-Y4 osteocytic cells. Moreover, whereas wild type HeLa cells that lack endogenous Cx43 were refractory to IGF-1, IGF-1 inhibited glucocorticoid-induced apoptosis in HeLa cells transfected with Cx43. Taken together, these results suggest that dis-regulation of miR21 and miR218 triggered by the absence of Cx43 causes resistance to the survival effect of IGF-1. Moreover, these findings raise the possibility that accumulation of apoptotic osteocytes in Cx43 deficient mice is due to the inability of osteocytes to respond to endogenous IGF-1.

Disclosures: Rafael Pacheco-Costa, None.

SA0177

See Friday Plenary Number FR0177.

SA0178

See Friday Plenary Number FR0178.

SA0179

See Friday Plenary Number FR0179.

SA0180

Bone and Muscle Interactions during the Progression of Nfat1 Deficiency-Mediated Osteoarthritis. Qinghua Lu¹, Brent Furomoto², H. Clarke Anderson², Jinxi Wang². ¹University of Kansas Medical Center, USA, ²University of Kansas Medical Center, USA

Purpose: Osteoarthritis (OA) is the most common form of joint disease in middle-aged and older individuals. No pharmacologic therapy is currently available to cure the disease, largely because the pathogenetic mechanisms for initiation and progression of OA remain unclear. OA involves multiple joint tissues (e.g., articular cartilage, subchondral bone, and synovium) and possible interactions between these tissues have been reported. However, it is not clear whether interactions between a joint tissue and peri-articular skeletal muscles are involved in the pathogenesis of OA. This study aimed to investigate whether metabolic interactions between the subchondral bone and peri-articular skeletal muscles play a role in the pathogenesis of OA.

Methods: Transcription factor Nfat1-deficient (Nfat1^{-/-}) mice were used in this study. Age-matched wild-type (WT) mice were used as controls. All animal procedures were approved by the institutional animal care and use committee. Joint tissues with skeletal muscles around the joint were harvested from hips, knees, and shoulders of Nfat1^{-/-} and WT mice at 1, 2, 3, 4, 6, and 12 months of age for histopathological, immunohistochemical, and gene expression analyses.

Results: At 3-6 months of age, focal loss of proteoglycan staining with chondrocyte clustering was seen in the articular cartilage of Nfat1^{-/-} joints. Chondrocyte hypertrophy occurred in the deep-calcified zones of Nfat1^{-/-} articular cartilage. Some of the subchondral bone marrow cells differentiated into chondrocytes, which subsequently underwent endochondral ossification, leading to thickening of the subchondral bone. These bony changes were accompanied by abnormal chondrocyte differentiation and endochondral ossification in the periosteum and deep layer of skeletal muscles, forming chondro-osteophytes near joint margins in the later stage. The expression of bone morphogenetic protein (BMP)-2 and (BMP)-4 was significantly increased in Nfat1^{-/-} subchondral bone than WT subchondral bone before and during the abnormal chondrocyte differentiation in peri-articular muscles.

Conclusions: During the process of Nfat1 deficiency-mediated OA, overexpression of BMP in the subchondral bone may stimulate pathological chondrocyte differentiation and endochondral ossification in periosteum and deep layer of muscles near the joint margins. This in turn compromises the function of affected joints and speeds the progression of OA.

Disclosures: Jinxi Wang, None.

SA0181

Comparison of 3D UTE (Ultrashort Time-to-Echo) MRI Versus Micro-CT For Quantitative Evaluation of the Temporomandibular Joint (TMJ) Condylar Morphology. Won Bae¹, Sheronda Statum², Daniel Geiger³, Koichi Masuda², Jiang Du¹, Christine Chung². ¹University of California, San Diego, USA, ²University of California, San Diego, USA, ³Sapienza University of Rome, Italy

Purpose: Temporomandibular dysfunction involves osteoarthritis of the temporomandibular joint, including degeneration of the mandibular condyle. Morphologic changes of the bone and fibrocartilage occurs, and it would be useful to evaluate them using non-invasive means. The purpose of this study was to determine the accuracy of novel 3D UTE MRI versus micro CT (mCT) for quantitative evaluation of mandibular condyle morphology.

Material and Methods: Three TMJ condyles specimens were harvested from cadavers. Novel 3D UTE MRI (TR=50 ms, TE=0.03 ms, voxel size=104 μm) was performed on 3-Tesla General Electric HDx, and mCT was performed using Skyscan 1076 (18 μm isotropic voxel size). MR datasets were spatially-registered with mCT dataset using FSL-FLIRT software. Bony contour of the condyles were segmented (ImageJ Segmentation Editor plugin) using global threshold (Figure 1A; mCT) or manual approach (Figure 1B; MRI, performed by two observers). Manual segmentation took less than 20 min per sample. Using Matlab, bone surface coordinates (Figure 1C,D), volume of segmented regions, and Gaussian curvature (Figure 1E,F) were determined for quantitative evaluation of joint morphology. Agreement between techniques (MRI vs. mCT) and observers (MRI vs. MRI) were determined by the means of intraclass correlation coefficient (ICC) analysis.

Results: Between MRI and mCT, the average deviation of surface coordinates (Figure 1G) was 116 μm, approximately the resolution of MRI. Average deviation (Figure 1H) of the Gaussian curvature and the volume, from MRI to mCT, was 2.2 and 4.4%, respectively. ICC coefficient for the three measures (surface, volume,

curvature) was each greater than 0.992. Between observers, the ICC coefficients were all greater than 0.997.

Conclusions: 3D UTE MR evaluation of TMJ condyle morphology including shape, volume and curvature shows high accuracy against mCT and between observers. The technique may be useful for clinical evaluation of temporomandibular joint dysfunction. Future work includes cartilage evaluation, as well as comparison of normal and degenerated mandibular condyles.

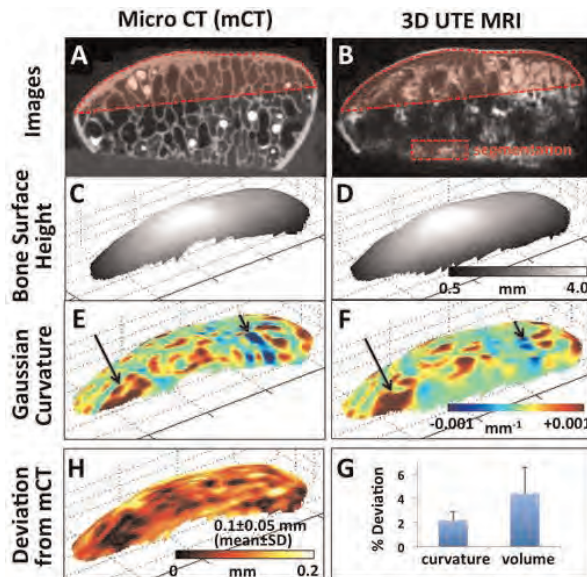


Figure 1. (A) Micro CT and (B) 3D UTE MR datasets were segmented to determine (C,D) bone surface coordinates and (E,F) Gaussian curvature in 3D. Gaussian curvature shows regions with bowl-shape (positive curvature; long arrows) and saddle-shape (negative curvature; short arrows). (G) The deviation of bone surface determined from MRI was in close agreement with that from micro CT, with a mean deviation of approximately 100 μm. (H) Deviation of the curvature and volume were small as well, showing a high accuracy of MR technique to evaluate condyle morphology.

Figure 1

Disclosures: Sheronda Statum, None.

SA0182

Cyclooxygenase-1 Plays an Important Role in C2C12 Myogenic Differentiation. Chenglin Mo¹, Orisa Igwe², Marco Brotto³. ¹University of Missouri-Kansas City, USA, ²University of Missouri, USA, ³University of Missouri-Kansas City, USA

Our previous studies have shown that prostaglandin E₂ (PGE₂) signaling through EP1 receptor is critical for myogenic differentiation in C2C12 myoblasts. Treatment with 50nM PGE₂ considerably increased myotube cell area and number of fully matured myotubes, whereas treatment with SC51322, a specific EP1 inhibitor, significantly attenuated myotube development. Cyclooxygenase-1 (COX-1) and cyclooxygenase-2 (COX-2) are the rate-limited enzymes in PGE₂ synthesis. To determine which COX is responsible for PGE₂ production in myogenesis, we first investigated the expression of COX-1 and COX-2 by Real-Time (RT) PCR and Western Blot (WB) analyses in C2C12 myoblasts. Both PCR and WB results indicated that COX-1 had higher expression than COX-2. Next, we did a time-course study of mRNA expression of COX-1, COX-2, and the three known isoforms of PGE₂ synthase (mPGES-1, mPGES-2 and cPGES) during myogenic differentiation. After the onset of differentiation, COX-1 expression was upregulated by 2-fold at 6 and 12h, and returned to baseline levels (time 0) at 24h, followed by a 2-fold downregulation at 48h. On the other hand, COX-2 expression was downregulated over this period, reaching a 5-fold downregulation at 48h. The WB results showed similar trends to those observed with RT-PCR; only COX-1 was upregulated at 12h, and returned to baseline levels at 48h. For PGES, the gene expression of mPGES-1 and cPGES did not show significant changes, but mPGES-2's profile was similar to that of COX-1, showing upregulation by 4- and 2-fold at 6 and 12h, respectively. Furthermore, the effects of the specific COX-1 inhibitor (FR122047), specific COX-2 inhibitor (NS-398), and non-specific COX-1/2 inhibitor (Indomethacin) on myogenic differentiation were tested. FR122047 (7.5 μM) and indomethacin (100 μM), but not NS-398 (50 μM), significantly decreased myotube area after 96h of differentiation (myotube area was ~45% and ~53% of control, respectively). The co-treatment with EP1 agonist 17-phenyl trinor and PGE₂ successfully rescued myotube cell area reduction that had been induced by treatments with FR122047 and Indomethacin. Our results provide

strong evidence that EP1 signaling is essential for myogenesis, and indicate that COX-1 may play a more prominent role in myogenic differentiation than COX-2.

Acknowledgements: This work was supported by NIDCR DE021888 (OJJ), and by Missouri Life Sciences Research Board and an NIH RC2 AR058962 (MB).

Disclosures: *Chenglin Mo, None.*

SA0183

Effects of Ti, PMMA, UHMWPE, and Co-Cr Particles on Differentiation and Functions of Bone Marrow Stromal Cells. Yunpeng Jiang^{*1}, Zheng Song², Paul Wooley², Shang-You Yang³. ¹Wichita State University, USA, ²Orthopaedic Research Institute, Via Christi Health, USA, ³Wichita State University, USA

Purpose:To examine variant types of orthopaedic biomaterials particles on differentiation and functions of bone MSC cell.

Methods:Bone marrow stromal cells (MSCs) were isolated from femurs of BALB/c mice by density centrifugation over Histopaque®-1083. Cells were cultured in regular culture medium or in complete-osteoblast-induction medium including 10mM β -glycerol phosphate, 100nM L-ascorbic acid, and 10nM dexamethasone. The cells were respectively co-cultured with micron-sized Ti, PMMA, UHMWPE, and Co-Cr particles at various doses. MTT assay was performed periodically for cell viability and proliferation, and immunocytochemical osteocalcin stain was also performed. Alkaline phosphatase (ALP) activities were assayed in the culture media and cell lysates; while real-time PCR performed to examine gene expression of RANKL, LRP, OSX, and Runx2.

Results:Challenge with low doses of Titanium, UHMWPE, or Co-Cr particles markedly promoted bone marrow cell proliferation while high dose of Co-Cr significantly inhibited cell growth ($p < 0.05$). Interestingly, the MSCs co-cultured with PMMA particles appeared in slow growth pattern, even at low concentration (0.63mg/ml). However, co-culturing the cells with low dose of PMMA-particles (0.63 mg/ml) in complete induction medium revealed significantly stronger ALP activity whereas Ti, UHMWPE, and Co-Cr groups showed relatively minimal ALP activity, in comparison with non-particle controls ($p < 0.05$). Further, immunocytochemistry stain exhibited considerably more osteocalcin-positive cells in PMMA-challenged cultures than other groups. Comparison of the gene expression profiles among the cells following Ti, HPE, or Co-Cr challenges did not find significant difference in LRP5, RANKL, Runx2, Osterix/Sp7; whereas all these gene expressions were elevated following PMMA challenge ($p < 0.05$).

DISCUSSION:Evidence suggests that adverse cellular responses to particulate wear debris are critical in the periprosthetic osteolysis and the pathogenesis of aseptic prosthetic loosening. While macrophage-mediated foreign body reaction and osteoclastogenesis are the major factors to resorb periprosthetic bone, wear debris-interacted bone marrow stromal cells may play an equally important role in regulation of differentiation and functions of osteoclasts and bone remodeling. The current study suggested that various types of wear debris particles behaved differently in the differentiation, maturation, and functions of osteoblasts. PMMA particles did not show marked influence on cell proliferation, unlike other types of particles which promoted cell proliferation at low concentration and resulted in accelerated cell death at high doses. Also, PMMA particles promoted the differentiation and maturation of bone MSCs with higher ALP activities, more osteocalcin+ cells and elevated expression of osteoblast markers.

Disclosures: *Yunpeng Jiang, None.*

SA0184

Genetic Variant on PLIN4 is Associated with Obesity Phenotypes and BMC in Females. Mai Abdel-Ghani^{*1}, Laura Tosi², Joseph Devaney³, Todd Spock⁴, Karin Kuhn⁴, Eric Rupe⁴, Clare Griffiths⁵, Heather Gordish-Dressman³, Eric Hoffman³, Priscilla Clarkson⁶. ¹USA, ²Children's National Medical Center, USA, ³Research Center for Genetic Medicine Children's National Medical Center, USA, ⁴George Washington University School of Medicine, USA, ⁵F. Edward Hébert School of Medicine Uniformed Services University of the Health Sciences, USA, ⁶University of Massachusetts Amherst, USA

The purpose of this study was to examine a single nucleotide polymorphism (SNP) rs8887 in Perilipin 4 (PLIN4) due to its expression in adipose tissue and its functional role in obesity and possible impact on bone mineral density. Whole blood samples were collected from 133 healthy subjects of whom 67 are males and 69 are females average age of 22.05 ± 4.82 yrs for females and 23.31 ± 5.61 yrs for males. A Dual energy xray absorptiometry (DXA)measured bone mineral density(BMD) lean mass, fat mass. Genomic DNA was extracted from blood for genotyping. Genotypes for rs8887 in PLIN4 were obtained using a TaqMan allelic discrimination assays. All PCR reactions were analyzed using an ABI 7900 Quantitative Real Time PCR system. Mean quantitative adiposity and bone measurements were compared in relation to SNP genotypes using analysis of covariance (ANCOVA) methods. Significant associations were found in both males and females. In males, significant associations with PLIN4 were seen with total fat mass ($p = 0.0136$), total lean mass ($p = 0.0268$) and lean mass of the arms ($p = 0.0097$). Males homozygous for the T allele showed increased total fat mass to males with a single copy of the C allele; TT (N=13;

21727 \pm 1269 g), CC (N=25; 17819 \pm 909 g),CT(N=29; 17187 \pm 845g).Males who were homozygous for the minor T allele had reduced total lean mass than males with a single copy of the C allele; TT (N=13; 55370 \pm 1249g), CC (N=25; 58880 \pm 894g), CT(N=29; 59450 \pm 831g).Males homozygous for the T allele showed decreased arms lean mass in contrast to males with a single copy of major C allele; TT (N=13; 6524 \pm 207g), CC (N=25; 6866 \pm 148g),and CT (N=29; 7275 \pm 137g).In females, significant associations were found with total fat mass ($p = 0.0157$) and bone mineral content ($p = 0.0216$). Females who were homozygous for the C allele showed a greater mean total fat mass in comparison to both heterozygotes and those homozygous for the T allele;TT (N=17; 20097 \pm 757g),CC (N=19; 22882 \pm 706g),CT (N=31; 20553 \pm 551g). Females homozygous for the T allele exhibited increased mean BMC in comparison to those homozygous for the T allele;TT (N=17; 2608 \pm 70), CT (N=31; 2430 \pm 52), CC (N=19; 2359 \pm 65). There was a suggestion of an association between total BMD and PLIN4, although it did not reach statistical significance ($p = 0.0523$). This study demonstrates an association between a variant in PLIN4 and adiposity phenotypes and BMC in females.

Disclosures: *Mai Abdel-Ghani, None.*

SA0185

Withdrawn

SA0186

See Friday Plenary Number FR0186.

SA0187

Muscle Derived Factor(s) Enhance the Activation of the PI3K/Akt Pathway in the Osteocyte in Response to Fluid Flow. Nuria Lara^{*1}, Leticia Brotto², Marco Brotto¹, Lynda Bonewald¹, Mark Johnson³. ¹University of Missouri - Kansas City, USA, ²UMKC School of Nursing, USA, ³University of Missouri, Kansas City Dental School, USA

Skeletal muscle is known to apply load to the skeleton. We sought to determine if muscle also secreted factors that might condition the response of the skeleton to loading. Osteocytes are the primary mechanosensory cells in bone and so we studied the effects of conditioned media (CM) from various muscle cell/fiber types on the response of the MLO-Y4 osteocyte-like cells to fluid flow shear stress (FFSS), as an *in vitro* model system for mechanical loading. C2C12 cells were induced to undergo myogenesis and CM was collected at various stages of myogenic differentiation. Also, adult mouse Soleus (Sol), an oxidative, slow twitch muscle type, and Extensor Digitorum Longus (EDL) muscle, a glycolytic, fast twitch muscle type, were isolated and stimulated *ex vivo* to produce CM for these studies. We observed that under resting conditions the addition of 10% C2C12 CM induced a rapid, but transient activation of the Akt signaling pathway, peaking at 15 minutes and returning to baseline by 2 hours in a concentration and cell type dependent manner. This activation was observed as early as Day 3 of C2C12 differentiation when myoblast fusion had started, but maximal activity was observed at day 5 coinciding with the formation of fully mature myotubes. FFSS applied to MLO-Y4 cells for 2 hours in the presence of 10% myotube CM resulted in a 6 fold increase in pAkt compared to a 3 fold increase under non-treated conditions or when 10% CM from myoblasts or blank C2C12 differentiation media was present. A similar enhanced increase in pAkt in response to FFSS was observed in the presence of EDL CM, but not in the presence of Sol CM suggesting muscle specific effects. Downstream of increases in pAkt, we observed increased β -catenin nuclear translocation in the presence of CM from myotubes in MLO-Y4 cells. We also observed activation of β -catenin only when EDL CM was present. These data provide evidence that specific muscle cell types produce soluble factors that alter the sensitivity of MLO-Y4 osteocyte like cells to fluid flow shear stress. These data support our hypothesis that beyond a mechanical interaction there is a very specific molecular coupling of muscle and bone. These data could provide a molecular basis for the high concordance between the diseases of osteoporosis and sarcopenia that exists within the aging human population.

Disclosures: *Nuria Lara, None.*

SA0188

See Friday Plenary Number FR0188.

SA0189

See Friday Plenary Number FR0189.

SA0190**Polymorphisms Associated with Physical Activity and Body Composition.**

Eric Rupe*¹, Laura Tosi², Todd Spock³, Karin Kuhn⁴, Mai Abdel-Ghani⁵, Clare Griffiths⁶, Heather Gordish-Dressman⁷, Eric Hoffman⁸, Joseph Devaney⁷. ¹The George Washington University, USA, ²Children's National Medical Center, USA, ³The George Washington University School of Medicine & Health Sciences, USA, ⁴The George Washington University School of Medicine & Health Sciences, USA, ⁵USA, ⁶Uniformed Services University of the Health Sciences, USA, ⁷Children's National Medical Center Research Institute, USA, ⁸Children's National Medical Center, USA

Objective: To explore whether six single nucleotide polymorphisms (SNPs) previously associated with leisure-time exercise behavior in an older population (mean 45.9 years) – rs12405556 (LEPR gene), rs10946904 (PRSS16 gene), rs1766581 (SIP1L2 gene), rs2762527 (PAPSS2 gene), rs9633417 (SGIP1 gene), and rs667923 (DNASE2 gene) – are associated with body and bone composition, strength, change in strength after resistance training, and physical activity in two healthy, college-aged populations of men and women.

Subjects and methods: We genotyped six SNPs in two populations. First we studied individuals enrolled in a resistance-training program of the non-dominant arm (n = 753, mean 24 years) from the FAMUSS cohort. We measured associations of the SNPs with these phenotypes: whole arm muscle (MRI), subcutaneous arm fat (MRI), bone volumes of the arm (MRI), 1-repetition max (1RM) and elbow flexion strength, before and after 12 weeks of resistance training.

Second, we examined the influence of the SNPs on physical activity levels and body measurements in the MB-UMASS cohort (n = 136, mean 22.5 years). In this study, subjects completed the International Physical Activity Questionnaire, and were measured for four criteria (by DEXA): bone mineral density, lean mass, fat mass, and percent tissue fat.

Hardy-Weinberg equilibrium was validated for each SNP. Associations and phenotypes were tested using ANCOVA. For those with a significant F-test, pair-wise comparisons were performed and p-values adjusted for multiple comparisons using the Sidak method, including appropriate covariates.

Results: We found two associations with strength/muscle measurements in the FAMUSS cohort: rs10946904 with baseline and change in 1RM in men, and rs12405556 with change in muscle volume in women. We found three SNPs to be associated with body measurements: rs12405556 with baseline total body volume, total fat, and total lean mass, all in men; rs10946904 with baseline subcutaneous fat in women; and rs1766581 with bone mineral content in women. Finally, we found two SNPs to be associated with total physical activity – rs10946904 for males and rs2762527 for females.

Discussion: We found that numerous SNPs, previously associated with physical activity in an older population, effect body composition in young individuals. We also found associations with muscle strength and response to resistance training. The same genotypes that were associated with response to training were associated with physical activity. These variants may influence skeletal muscle response to resistance training and may respond to aerobic intervention. This needs further exploration. Finally, being able to corroborate previous findings for two SNPs regarding their association with exercise behavior further supports their significance.

Disclosures: Eric Rupe, None.

SA0191

See Friday Plenary Number FR0191.

SA0192**The Relation between Age-related Declines in Hand Grip Strength and Arterial Stiffness in Korean Men. SANG HYEON JE¹, Duck Joo Lee*².**

¹Ajou University Hospital, Department of Family Medicine, South Korea,

²Ajou University School of Medicine, South Korea

Background:The hand grip strength (HGS) is an indicator of overall muscle strength as well as aging. We evaluate the associations between HGS and other clinical markers of aging in Korean men

Methods:We collected data from 5412 men who visited the Health Promotion Center in Gejeje city, Korea for health examination in 2003-2009. Tests for fasting blood sample, HGS, lipid profile, homocysteine, blood pressure and routine blood chemistry and spirometry were performed. Pulse wave velocity was used at the carotid artery level to assess arterial stiffness. Men were categorized into three HGS groups (low, medium, and high). The men also were grouped into three aged groups; young, middle and old aged groups. Odds ratio was estimated using low HGS as a reference group.

Results:Age, arterial stiffness, uric acid, homocysteine and FEV1/FVC were statistically significantly different across three HGS and aged groups (P<0.05). Compared to low HGS group, odds ratio for the arterial stiffness in medium group was 0.72 and 0.23 in high group. This finding was statistically significant in the middle aged group (P<0.05). Other clinical markers of aging in each aged group did not differ by HGS.

Conclusions: in middle aged Korean men, 40-59 years old, HGS may be related to arterial stiffness

Disclosures: Duck Joo Lee, None.

SA0193**Wnt/ Ca²⁺ Signaling Pathway Takes Shape in Muscle-bone Crosstalk.**

Sandra Romero-Suarez*¹, Cheng Lin Mo¹, Mark L Johnson², Lynda Bonewald³, Marco Brotto³. ¹University of Missouri-Kansas City, USA, ²University of Missouri-Kansas City, USA, ³University of Missouri - Kansas City, USA

Integrative biological approaches have led to the discovery of new physiological roles for bone and skeletal muscle as autocrine, paracrine, and endocrine organs. We tested the effects of conditioned media from MLO-Y4 osteocyte-like cells (MLO-Y4-CM) and primary osteocytes (PO-CM) derived from 4 months wild type mouse, and found that MLO-Y4 CM and PO-CM enhanced myogenic differentiation of C2C12 myoblasts into myotubes as detected by histomorphometric measurements. Wnt signaling is involved in various aspects of bone and skeletal muscle development and regeneration. In osteocytes, Wnts are over expressed upon fluid flow shear stress; also they are released by osteocytes. To test our hypothesis that osteocytes can biochemically signal to muscles via the Wnt pathway, we treated C2C12 muscle cells with low, physiological concentrations of Wnt3a. Wnt3a accelerated myogenic differentiation and enhanced nuclear translocation of β -catenin, which is required for transcription of the key muscle transcription factor, MyoD. This pathway showed to play a crucial role in the enhancement of myogenic differentiation produced by 10ng Wnt3a, 10% and 1% MLO-Y4 CM and PO-CM respectively. The potent effects of Wnt3a on stimulating the β -catenin signaling pathway in C2C12 muscle cells, strongly correlated with an increased sensitivity to calcium released from the sarcoplasmic reticulum by caffeine, suggesting adaptive changes of the excitation-contraction coupling machinery. These data were consistent with the upregulation of some of the essential genes related to intracellular calcium homeostasis (i.e., IP3R types 1 and 3; Stim-2; Camk2d; and SERCA-1 and 2). These findings suggest that MLO-Y4 CM and PO-CM through activation of β -catenin signaling pathway may alter intracellular Ca²⁺ release and activate an alternative Wnt/Ca²⁺ pathway that promotes or assists with myogenic differentiation. The molecular mechanisms leading to these effects of bone CM in osteocytes are currently under investigation.

Disclosures: Sandra Romero-Suarez, None.

This study received funding from: Acknowledgments: This work was supported by a Missouri Life Sciences Research Board Grant to MB and a NIAMS 1RC2AR058962-01 GO Grant to MJ, LB, MB.

SA0194**Ability of Cyclosporine to Induce Oxygen Free Radicals in a Rat Osteoblast Cell Line. Min Hyung Jung*¹, Heung Yeol Kim².**

¹School of Medicine, Kyung Hee University, Kyung Hee Medical Center, South Korea, ²School of Medicine, Kyung Hee University, Kyung Hee Medical Center, South Korea

Objective : This study examined the ability of Cyclosporine (CsA) to induce apoptosis in a rat osteoblast cell line.

Material & methods : Rat osteoblast ROS 17/2.8 cells were cultured, and treated with with 0.1-40 μ g/mL CsA for 24 hours after plating of cells. Cell viability was determined by the MTT assay. Western Blot Analysis was done with primary antibodies to caspase-3 and caspase-8. Reactive oxygen species synthesis was measured by flowcytometry.

Results: Cell viability decreased in dose-dependent manner with increasing concentrations of CsA. Treatment of ROS 17/2.8 cells with 0.1, 0.5, 1, 5, 10, 20, or 40 μ g/mL CsA caused 85%, 80%, 73%, 60%, 45%, 40%, and 27% cell viability, respectively. Western blot analysis showed reduced caspase-3 expression and induced caspase-8. The oxygen free radicals in a dose-and time-dependent manner were increased by CsA.

Conclusions : These results suggest that CsA can induce oxygen free radicals which appears to trigger apoptosis by activating pro-apoptotic signals. CsA plays a role in the post-transplantation bone diseases via the induction of apoptosis in osteoblast.

Disclosures: Min Hyung Jung, None.

SA0195

Identification of CARP-1 Target Cells in Bone and Response to PTH in Osteoblastic Cells. Sonali Sharma^{*1}, Chandrika Mahalingam¹, Shazia Zamal², Edi Levi³, Arun Rishi⁴, Nabanita Datta⁵. ¹Endocrinology, Wayne State University School of Medicine, USA, ²Oncology, VA Medical Center, USA, ³Pathology, VA Medical Center, USA, ⁴Oncology, Karmanos Cancer Institute, VA Medical Center, USA, ⁵Endocrinology, Cardiovascular Research Institute, Karmanos Cancer Institute, Wayne State University School of Medicine, USA

Bone mass is dependent on osteoblast proliferation, differentiation and life-span of osteoblasts. Intermittent administration of parathyroid hormone (PTH) increases bone mass but the mechanism of action are complex and have not been clearly established. PTH control of osteoblast cell cycle regulatory proteins and suppression of mature osteoblasts apoptosis has been previously demonstrated in the process of bone formation both in vitro and in vivo. Cell Cycle and Apoptosis Regulatory Protein (CARP)-1 (aka CCAR1) is a novel regulator of apoptosis signaling by diverse agents including cell growth and differentiation factors. Here we investigated presence of CARP-1 in bone cells, and its role in transducing PTH-dependent molecular signaling in osteoblasts. Ten to twelve-week old mice femora were immuno-stained with anti-CARP-1 polyclonal antibody. Our results demonstrate significant presence of CARP-1 in osteocytes and in osteoblasts and a minimal to absent levels are observed in the marrow cavity or in chondrocytes. Further, treatment of 7-day differentiated MC-4 (MC3T3-E1 clone-4) mouse osteoblastic cells with PTH or PTH-related peptide (PTHrP) for 30 min to 5 hr followed by Western blot analysis reveals 2-3 fold down-regulation of CARP-1 protein when compared to vehicle treated control cells. Mechanism of apoptosis by CARP-1 involves activation of p38 Mitogen Activated Protein Kinase (MAPK) and increase in p21^{WAF-1/CIP-1} protein, a cyclin dependent kinase inhibitor. Our studies further show a 3-5 fold down-regulation of pp38-MAPK and p21 protein expression with concomitant attenuation of CARP-1 abundance in differentiated MC-4 cells following PTH induction. Although PTH treatment elicited a 1.5-2 fold increase in pro caspase-9 expression, no activation of caspase 3 activity was noted pointing again antiapoptotic activity of PTH in osteoblastic cells. Our findings are indicative of a role for CARP-1 in apoptosis signaling pathways in osteoblasts and possibly in osteocytes. Taken together we propose CARP-1 as a potential regulator and may be an important target gene of the PTH and PTHrP response; hence would be a good candidate to study PTH bone anabolic action.

Disclosures: Sonali Sharma, None.

SA0196

Apolipoprotein D Deficient Mice Show Altered Bone Metabolism: A Structural and Cellular Characterization. Corine Martineau^{*1}, Quafa Najyb², Louise Martin-Falstrault³, Eric Rassart², Robert Moreau⁴. ¹Université du Québec à Montréal, Canada, ²UQAM, Canada, ³UQAM, Canada, ⁴University of Quebec At Montreal, Canada

This pilot study aimed at evaluating the impact on bone metabolism of apolipoprotein D (Apo D), a glycoprotein of the lipocalin family associated to high density lipoprotein (HDL) in mammals. Apo D is a multi-ligand, multi-functional transporter of small hydrophobic molecules namely arachidonic acid, progesterone, pregnenolone and bilirubin. Its expression is induced by several stresses such as growth arrest and inflammation. In the brain, it is thought to be involved in maintenance and repair of the nervous system although its precise role remains to be determined. To assess its potential function in bone metabolism, plasma samples were analyzed for calcemia, phosphatemia and ALP activity. Microcomputed tomography (MicroCT) and histomorphometry analyses were performed on bones harvested from ApoD-deficient or transgenic mice (overexpressing human Apo D in the brain) at different ages in both genders. Also, gene expression of Apo D, its internalization and cellular localization were determined in osteoblastic cells by RT-PCR and confocal microscopy. Plasmatic ALP activity was found to be enhanced in 9-month-old Apo D KO females ($p < 0.001$ vs WT, Bonferroni post-test), whereas calcemia and phosphatemia were normal in all groups. MicroCT data showed that Apo D-deficient females develop increasing osteopenia with age (6 month-old and 9-month-old $p < 0.05$ vs WT, Bonferroni post-test); these results were confirmed by Von Kossa staining. Histochemistry analysis of femora sections attributes the low bone mass to bone formation dysfunction with normal TRAP-positive cell distribution, yet less ALP-positive cells. No significant differences in bone status were observed in the Apo D-transgenic mice nor in the male Apo D-deficient mice. Apo D mRNA was shown to be expressed in osteoblastic cell line MC3T3-E1 and primary cultures from mouse bone marrow. Apo D added to culture medium was readily internalized by osteoblasts and recent assays also suggested that stress conditions provoke its nuclear translocation, agreeing with a stress-defense function. The sum of these results points toward a role for Apo D in osteoblastic function. In perspective, a thorough investigation of the cellular mechanisms regulating Apo D in osteoblasts under normal and stress conditions is needed to fully unravel the function of this apolipoprotein in bone metabolism, and could lead to new clinical approaches in the prevention and treatment of bone disorders.

Disclosures: Corine Martineau, None.

SA0197

See Friday Plenary Number FR0197.

SA0198

Calcium-Sensing Receptors (CaSRs) in Mature Osteoblasts Regulate Bone Formation and Maintenance of Bone Mass: Studies in Osteocalcin (OCN) Conditional Knockout Mice. Nathan Liang¹, Tsui-Hua Chen¹, Zhiqiang Cheng², Alfred Li¹, Christian Santa Maria¹, Chia-Ling Tu¹, Wenhan Chang³, Dolores Shoback^{*4}. ¹UCSF, USA, ²University of California, San Francisco, USA, ³Endocrine Unit, VA Medical Center, University of California, San Francisco, USA, ⁴VA Medical Center, USA

CaSRs play key roles in osteoblast (OB) differentiation by controlling growth, mineralization, and gene expression. Prior conditional (c) CaSR knockout (KO) models, in which the CaSR is deleted across the OB lineage [using 2.3 KB collagen 1 (Col1) Cre mice], showed early death, stunted growth, fractures and a block in differentiation in the OB lineage. To determine the role of CaSRs in cells late in OB lineage when mineralization, maturation, and transition to osteocytes occur, we bred CaSR cKO's by crossing ^{flx/flx}CaSR with OCN-Cre mice [^{OCN}CaSR (-/-)]. In contrast to ^{Col1}CaSR(-/-), ^{OCN}CaSR(-/-) mice grew as did control (cont). At 12 weeks of age, micro-CT (uCT) of trabecular (Tb) and cortical (Ct) bone and histomorphometry (HM) were performed to assess bone structure and turnover. uCT showed osteopenia of Tb bone with reduced BV/TV (bone volume/tissue volume) in male [$0.11 \pm 0.01\%$ (KO) vs $0.15 \pm 0.01\%$ (cont) ($p < 0.02$; N=12)] and female [$0.08 \pm 0.01\%$ (KO) vs $0.11 \pm 0.01\%$ (cont) ($p < 0.001$; N=13 or 15)] mice and reduced CD (connectivity density) in male [154.75 ± 19.35 (KO) vs 211.08 ± 28.25 #/mm³(cont) ($p = 0.058$) and female [107.15 ± 13.74 (KO) vs 157.30 ± 15.47 #/mm³(cont) ($p < 0.02$)] mice. Tb number (N) was significantly reduced in ^{OCN}CaSR(-/-) vs cont mice [males: 4.76 ± 0.22 vs 5.28 ± 0.19 #/mm; females: 4.22 ± 0.16 vs 4.64 ± 0.19 #/mm. ($p < 0.05$ for both)]. Tb thickness (Th) was significantly lower in female ^{OCN}CaSR(-/-) mice ($p < 0.02$) and Tb spacing (Sp) was greater in male mice ($p < 0.05$) – indicating an overall disruption of Tb microarchitecture in both genders. HM in males showed reduced BV/TV [16.57 ± 1.58 , ^{OCN}CaSR(-/-) vs $20.70 \pm 1.61\%$, cont ($p < 0.04$)], increased ES (eroded surface)/BS (bone surface) [1.39 ± 0.16 , ^{OCN}CaSR(-/-) vs $0.95 \pm 0.11\%$, cont ($p < 0.02$)], increased # osteoclasts (N.Oc)/BS [1.21 ± 0.13 , ^{OCN}CaSR(-/-) vs $0.84 \pm 0.11\%$, cont ($p < 0.02$)] and increased MAR (mineral apposition rate) [2.13 ± 0.11 , ^{OCN}CaSR(-/-) vs 1.81 ± 0.08 mcm/day, cont ($p < 0.02$)]. No significant differences were seen in TbN, TbTh or TbSp. qPCR showed reduced mRNA encoding OB genes (OCN, sclerostin, Col1) in bone from ^{OCN}CaSR(-/-). These findings are compatible with lowered bone mass in ^{OCN}CaSR(-/-) mice due to a turnover imbalance favoring resorption over formation due to loss of CaSR activation in late OB's and osteocytes.

Disclosures: Dolores Shoback, None.

SA0199

See Friday Plenary Number FR0199.

SA0200

Cytotoxic Therapies Significantly Alter the Composition of the Cells Comprising Murine Hematopoietic Stem Cell Niches. Julie Quach^{*1}, Maria Askmyr², Tanja Jovic², Hannah King², Cesar Nombela-Arrieta³, Kirby White², Emma Baker⁴, Nicole Walsh⁵, Leslie Silberstein³, Louise Purton⁶. ¹St. Vincent's Institute, Australia, ²St. Vincent's Institute, Australia, ³Joint Program in Transfusion Medicine, Children's Hospital Boston, Harvard Medical School, USA, ⁴St. Vincent's Institute, Australia, ⁵St Vincent's Institute of Medical Research, Australia, ⁶St. Vincent's Institute, The University of Melbourne, Australia

Hematopoietic stem cells (HSC) are regulated within the bone marrow (BM) in anatomical locations termed HSC niches. Cancer therapies are known to significantly impair hematopoiesis, however, their effects on HSC niche cells are largely unknown. Using adult male mice, we have extensively analyzed the effects of irradiation or chemotherapy on HSC niche cells. Our studies have focused on putative HSC niche cell types that are also important in regulating bone: endothelial cells (ECs), adipocytes, mesenchymal stem and progenitor cells (MSPCs), osteoblasts (Obs) and osteoclasts (Ocs).

We used histomorphometric analysis to quantitate the numbers of these cells in tibiae at numerous intervals up to 140 days post-therapy. Bone volume was assessed in femurs and vertebrae using microCT analysis. Fluorescence-activated cell sorting (FACS) was used to purify MSPCs and Obs for further analysis.

The earliest histological change observed was to ECs: significant vessel dilation throughout the BM was observed at early time points in response to all three therapies, although vessel number was largely unchanged. Interestingly, the vasculature changes were restricted to sinusoids, as arteries were unaltered.

Adipocytes (which are negative regulators of HSCs) significantly increased between days 7-35 post-therapy in the different treatment groups. The numbers of

MSPCs also increased at early time points post-therapy, but expressed higher levels of adipocyte-commitment genes (PPAR γ and adiponectin) compared to those critical for Ob differentiation (Runx2 and Osx). Hence the enhanced adipocyte formation observed in the mice was likely due to altered fate commitment of MSPCs.

All treatments resulted in a net bone loss with an associated increase in bone turnover (as indicated by increases in the numbers of Obs and Ocs). Inhibition of Ocs by a single dose of the bisphosphonate, zoledronic acid (ZA) prevented this bone loss, but in contrast to recent reports, did not significantly impair HSC numbers or function. A major difference in our study is that bone volume was not elevated above normal levels in response to ZA, whereas mice in the other studies were osteopetrotic when analyzed for HSCs.

In conclusion, niche cells that are important in regulating both HSCs and bone remodeling are highly susceptible to cancer therapies. Reducing damage to these niche cells may in turn improve blood cell recovery in cancer patients.

Disclosures: Julie Quach, None.

SA0201

See Friday Plenary Number FR0201.

SA0202

Does Collagen Trigger Migration of Reversal Cells into Vacated Bone Resorption Lacunae? Mohamed Abdelgawad*¹, Kent Soe², Lars H. Engelholm³, Per Kjaergaard-Andersen², Niels Behrendt³, Jean-Marie Delaisse⁴. ¹Clinical Cell Biology Department (KCB), Denmark, ²Vejle Hospital, University of Southern Denmark, Denmark, ³Finsen Laboratory, Rigshospitalet, Denmark, ⁴Vejle Hospital, IRS, University of Southern Denmark, Denmark

Bone remodelling involves bone resorption by osteoclasts, bone formation by osteoblasts, and a poorly investigated intermediate reversal phase coupling resorption to formation. The very first step of the reversal phase is the departure of the osteoclasts from the resorption lacunae and the arrival of so-called reversal cells. We previously showed that reversal cells belong to the osteoblast lineage, but the mechanism making them migrate into the resorption lacunae is not known. Our hypothesis is that collagen type I left in the lacunae by the osteoclasts exerts a haptotactic effect on these cells. Here we investigated this hypothesis as well as the underlying molecular mechanism.

We coated therefore the lower side of the membrane of transwells with native collagen or control molecules, and seeded osteoblast lineage cells in the upper chamber. Cells of two distinct origins were used: human adipocyte-derived stem cells differentiated into osteoblasts (ADSC), and primary osteoblasts obtained from outgrowths from human bone (HOB). Migration to the lower side of the membrane was quantified after an overnight culture in the presence or absence of an inactivator of urokinase plasminogen activator receptor associated protein (uPARAP), a collagen receptor involved in osteoblast migration, or of an inactivator of matrix metalloproteinases (MMPs), collagenolytic proteinases believed to be involved in uPARAP function.

Native collagen type I significantly increased the haptotactic migration of both ADSCs and HOBs, compared to collagen denatured into gelatine, vitronectine, or BSA. Inactivation of uPARAP significantly decreased their response to native collagen, and inactivation of MMPs significantly decreased that of ADSCs, the only cell type tested so far.

In conclusion, these observations support that native collagen type I left in the resorption lacunae by the osteoclast may contribute to the recruitment of reversal cells into these lacunae. This process requires recognition by the collagen receptor uPARAP. MMP-specific alterations of native collagen are likely to be involved in this mechanism, since MMP inactivators inhibit it, and since random alterations obtained through simple denaturation into gelatine results in a loss of haptotactic response.

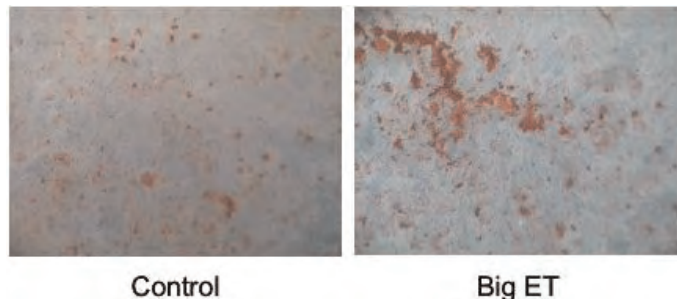
Disclosures: Mohamed Abdelgawad, None.

SA0203

Endothelin Signaling Promotes Terminal Differentiation of TMOB Cells via Increased BMP@ and Nos3 Expression. Michael Johnson*¹, Kathryn Konicke², Rachel Garbo³, Robert Blank¹, Baozhi Yuan¹, Jasmin Kristianto⁴, Suzanne Litscher³. ¹University of Wisconsin, USA, ²University of Wisconsin, USA, ³University of Wisconsin, USA, ⁴University of Wisconsin-Madison, USA

Ece1, encoding endothelin-converting-enzyme 1, is a positional candidate gene for a pleiotropic quantitative trait locus (QTL) affecting femoral size, shape, mineralization, and biomechanical performance. ECE1 is a membrane bound protease that converts biologically inert "big endothelin" (big ET) to mature endothelin 1 (ET1). ET1, in turn, is known to promote osteogenic metastases in prostate and breast cancer. In order to define the potential role of ECE1 in osteogenesis, we exposed TMOB cells to supplemental big endothelin (25ng/ml) over the course of *in vitro* differentiation, hypothesizing that this treatment would increase mineralization. Cells were grown for six days in growth medium and then switched to mineralization medium for an additional 15 days. An aliquot of cells were harvested at day 0 and

every three days thereafter and analyzed for markers of osteoblast maturation. We did not observe a difference in cell proliferation between big ET and control cells. TMOB cells exposed to big ET showed greater mineralization than control cells (Figure, N = 6, p = 0.008). In growth medium, ET-1 exposed osteoblasts showed increased expression of *Bmp2* and *Nos3* message, which persisted following the change to mineralization medium (N = 6, p = 0.008 and 0.002, respectively). Although previous work showed that ET1 exposure inhibited *Dkk1* expression, this was not the case in our experiment, as we observed transient early increases of both *Dkk1* and *Sost* message in cells treated with big ET. This disparity likely reflects differences in the cells studied. In mice, both *Ece1* and *Bmp2* expression vary concordantly as a function of *Ece1* genotype, and mirror the findings in TMOB cells. BMP2 is known to promote osteogenesis and NO production is known to be a necessary intermediate in loading-induced bone modeling. Our findings demonstrate that endothelin signaling, delivered as big ET, enhances *in vitro* mineralization of TMOB cells and suggest that this occurs in part via BMP2 and/or NO signaling.



Figure

Disclosures: Michael Johnson, None.

This study received funding from: No organization

SA0204

See Friday Plenary Number FR0204.

SA0205

Withdrawn

SA0206

Periostin Deficiency, Inhibit Beta Catenin Response to PTH and Induce Cortical Porosity through Osteocytic RANKL Expression. Nicolas Bonnet*¹, Serge Ferrari². ¹Division of Bone Diseases, Geneva University Hospital & Faculty of Medicine, S, Switzerland, ²Geneva University Hospital & Faculty of Medicine, Switzerland

Periostin is a matricellular protein expressed in osteocytes and the periosteum and mediates *Sost* in response to loading. Gene profiling in bones exposed to PTH have identified an increase of periostin (*Postn*). Since PTH inhibits *Sost* and activates β catenin, we investigated the influence of *Postn* on β catenin, osteoblastic/osteocytic genes and cortical response to PTH. To evaluate the role of *Postn* on β catenin, we used TOPGAL; *Postn*^{-/-} and *Postn*^{+/+} mice, which express a TCF β Galactosidase reporter. Activation of β catenin was evaluated by X-Gal staining on femoral sections, after intermittent PTH (iPTH). Activation of β catenin was evaluated on calvariae from these mice exposed to recombinant POSTN (rPOSTN), PTH or vehicle (Veh) followed by counting X-Gal positive cells (+). PTH effects on gene expression were evaluated on calvaria and confirm *in vivo* on osteoblastic/osteocytic fraction by qRT-PCR. Femur cortical structure in response to iPTH (40ug/kg x5weeks) was evaluated by microCT in adult *Postn*^{-/-} mice. *In vivo*, iPTH activated β catenin in TOPGAL; *Postn*^{+/+} but not in *Postn*^{-/-}. *Postn*^{-/-} cells have lower X-Gal (+) vs *Postn*^{+/+}. PTH increased the number of X-Gal (+) cells from TOPGAL; *Postn*^{+/+} (+73.1% vs Veh, p<0.0001) but not *Postn*^{-/-} (+7.9% vs Veh, NS). Moreover, rPOSTN increased the number of X-Gal (+) cells in *Postn*^{+/+} and even more so in *Postn*^{-/-} (+28.6% vs Veh, p<0.05, and +70.5% vs Veh, p<0.001). Gene expression of Runx2, Osx and Alp were all significantly lower in osteoblasts from *Postn*^{-/-} vs *Postn*^{+/+}. Moreover, PTH decreased Runx2, Osterix, OPG (-41.6%, -82.3% and -22.8% vs Veh, p<0.01) and increased RANKL (+460.0% vs Veh, p<0.01) in *Postn*^{+/+}, with no effect in *Postn*^{-/-} except for RANKL (+605.3% vs Veh, p<0.01). In osteocyte fractions, *Postn*^{-/-} have higher RANKL vs *Postn*^{+/+} (+355%, p<0.001). Moreover, PTH increased RANKL only in *Postn*^{-/-} osteocyte fractions (+596% vs Veh, p<0.01). Finally, iPTH significantly increased cortical volume (CtBV) and thickness (CtTh), but not porosity (CtPo), in *Postn*^{+/+}, whereas in *Postn*^{-/-}, iPTH increased CtPo and pores width (+126.7% and +81.5% vs Veh, p<0.05) but not CtBV nor CtTh. These results highlight the role of periostin on β catenin and PTH effects on osteocytic gene expression. They suggest that PTH-stimulated periostin expression mediates PTH anabolic effects on cortical and prevents PTH-induced porosity by reducing the osteocyte RANKL production.

Disclosures: Nicolas Bonnet, None.

SA0207

Targeting Osteoclasts to Promote Bone Regeneration; Adenosine Receptors Regulate Osteoclast Formation and Promote Bone Regeneration in a Calvarial Defect Model. Aranzazu Mediero^{*1}, Tuere Wilder², Bruce Cronstein³. ¹NYU SCHOOL OF MEDICINE, USA, ²Department of medicine, NYU School of Medicine, USA, ³NYU Medical School, USA

Various types of orthopedic procedures, including spinal fusion and repair of bone defects due to trauma, infection or metastatic disease, require formation of new bone. Adenosine, generated from the catabolism of adenine nucleotides, modulates cell function by interacting with specific cell-surface receptors (A1, A2A, A2B, A3). In previous studies we have demonstrated that adenosine A1 receptor blockade and A2A receptor stimulation diminishes osteoclast formation without directly affecting osteoblast formation or function. We therefore determined whether targeting adenosine receptors affected bone regeneration in a murine model. Male C57Bl/6 mice were anesthetized and a 3mm trephine defect was formed and covered with a collagen scaffold soaked in saline or 1 μ M adenosine receptor agonists/antagonists. Animals received the appropriate treatment daily until sacrifice. At 0, 2, 4, 6 and 8 weeks calvarias were harvested and prepared for microCT and histology. XenoLight Rediject Bone Probe 680 was injected intravenously in mice at different time points. Eight weeks after surgery microCT examination of mouse calvaria demonstrate that an A1R antagonist (DPCPX), A2AR agonist (CGS21680M) or dipyrindamole (blocks adenosine uptake and increases extracellular adenosine levels) markedly enhances bone regeneration (77 \pm 0.2%, 60 \pm 2% and 79 \pm 2% bone regeneration respectively vs 32 \pm 4% in control mice, p<0.001, n=5 mice per condition) whereas an A3R agonist (IB-MECA) had no effect (32 \pm 3% regeneration, n=5). Alkaline phosphatase and osteocalcin immunostaining at the sites of bone formation was increased in defects treated with DPCPX, CGS21680 and Dipyrindamole. In contrast, TNF α , Semaphorin4D and PlexinB1 immunostaining was diminished in DPCPX, CGS21680 and Dipyrindamole treated defects. TRAP staining revealed fewer osteoclasts in DPCPX, CGS21680 and Dipyrindamole treated defects (14 \pm 1, 17 \pm 1 and 16 \pm 1 Osteoclast/IpF respectively vs 24 \pm 1 Osteoclast/IpF for control, p<0.001) and *in vivo* imaging with a marker for new bone formation (XenoLight Rediject) showed greater bone formation in the treated mice. Targeting osteoclasts via appropriate adenosine receptor blockade or stimulation leads to increased bone regeneration in a murine model of bone regeneration. The mechanism by which adenosine receptor-mediated suppression of osteoclast function/accumulation stimulates bone regeneration likely involves suppression of semaphorin4D permitting increased osteoblast formation of bone.

Disclosures: Aranzazu Mediero, None.

SA0208

The Role of Oxygen in Blastema Formation and Skeletal Regeneration. Mimi Sammarco^{*1}, Jennifer Simkin², Ken Muneoka², Danielle Fassler². ¹Tulane University, USA, ²Tulane University, USA

One out of every 200 people in the U.S. will suffer an amputation, and this number is expected to double in the next 40 years. Amputation has protracted effects on vocational outcome, individual productivity, and personal independence far beyond the initial trauma. While complete limb regeneration in humans may someday become the ultimate therapy, the ability to coordinately control bone regeneration would reduce pain from ectopic bone spurs, and provide a better fit for prosthetics, resulting in a better quality of life in the near term. Amputation of the digit tip within the terminal phalangeal bone of rodents, monkeys, and humans results in near-perfect regeneration from a cell population called the blastema, which has been well characterized in both adult and neonatal mice. However, it remains unclear why amputations within the more proximal phalangeal elements, or within limbs, fail to produce the same regenerative result. The long term goal of this work is to understand the influence of oxygen on bone regeneration, so that these mechanisms can be exploited to confer regenerative capacity where it is lacking. The objective of this study is to gain insight into the role of oxygen in the regenerative process by manipulating oxygen within the digit tip to alter the regenerative process. Our central hypothesis is that a biphasic oxygen response facilitates the regenerative process. The basis of this hypothesis stems from the biphasic nature of the regenerative models, and oxygen's known influence in the process of wound healing. Our data shows that the highly proliferative, undifferentiated blastema initiates in a low oxygen environment. Upon exposure to increased oxygen tension, the blastema begins redifferentiation into bone, supporting the idea of a biphasic oxygen response that drives the regenerative process. Here we present a novel multi-tissue slice culture model and use our *in vitro* system to show that oxygen influence during bone regeneration is temporally specific. We propose that small increases in oxygen tension coordinately control bone ossification and directly contribute to the redifferentiation of the blastema. Research enabled by this work will lead to a defined mechanistic understanding of oxygen's role in bone regeneration and identify therapeutic targets to enhance regenerative capacity.

Disclosures: Mimi Sammarco, None.

SA0209

See Friday Plenary Number FR0209.

SA0210

Use of Vwc2 Protein as a Novel Approach to Induce Bone Formation. Ahmad Almeahmadi^{*1}, Yoshio Ohyama², Haytham Jaha², Sundharamani Venkitapathi², Reem Aljamaan², Yoshiyuki Mochida³. ¹Goldman School of Dental Medicine, Boston University, USA, ²Boston University, Henry M. Goldman School of Dental Medicine, USA, ³Boston University, Henry M. Goldman School of Dental Medicine, USA

Objective: We have recently reported that a novel secretory protein, von Willebrand domain containing 2 like (Vwc2l), promotes osteoblast mineralization *in vitro*. In the present study, Vwc2, a highly homologous protein to Vwc2l was characterized.

The objective of our study is to investigate the effect of Vwc2 on bone formation.
Methods: The expression of Vwc2 in MC3T3-E1 (MC) osteoblastic cell line was investigated by real time PCR at RNA level and by Western Blotting (WB) analysis at protein level. The presence of Vwc2 protein in bone was also examined by immunohistochemistry (IHC) and WB analysis. The effect of Vwc2 on Activin signaling was examined in MC osteoblastic cell line by WB. To characterize the function of Vwc2 protein, recombinant Vwc2 protein (rVwc2) was added into mouse calvaria *ex vivo* cultures and the extent of newly synthesized bone formation was analyzed.

Results: Vwc2 transcript is detected in MC cells with the highest expression observed at day 7 during biomineralization. The expression pattern of Vwc2 protein in the cultured media from MC cells was similar to that of Vwc2 transcript. The localization of Vwc2 protein was observed by IHC in mouse developing maxilla. The effect of Vwc2 on Activin signaling was examined and we found that Vwc2 inhibited activin initiated Smad2 phosphorylation. The effect of rVwc2 on mouse calvaria bone formation was examined and the results showed increased bone formation.

Conclusion: Our data demonstrated that Vwc2 is expressed in osteoblasts/bone and has the ability to increase bone formation. The data obtained from this study may provide insights to the biological functions of this novel protein and help to develop a new molecular design for bone loss therapies (Treatment of osteoporosis, Craniofacial reconstruction and bone regeneration).

Disclosures: Ahmad Almeahmadi, None.

SA0211

See Friday Plenary Number FR0211.

SA0212

See Friday Plenary Number FR0212.

SA0213

Frizzled Homolog 1 (FZD1) Mediates the Effect of E2F1 on Osteoblast Differentiation and Mineralization. Shibing Yu^{*1}, Laura Yerges-Armstrong², Yanxia Chu³, Joseph Zmuda⁴, Yingze Zhang⁵. ¹University of Pittsburgh Medical Center, USA, ²University of Maryland, USA, ³UPMC, USA, ⁴University of Pittsburgh Graduate School of Public Health, USA, ⁵University of Pittsburgh, USA

The mechanisms underlying transcriptional regulation of FZD1 gene expression and the roles of FZD1 in osteoblast differentiation and mineralization are not well understood. The goal of the present study was to investigate the potential roles of transcription factor E2F1 in regulating FZD1 expression and in osteoblast differentiation and mineralization. Co-transfection of an E2F1 expression plasmid and FZD1 promoter construct resulted in increased FZD1 promoter activity in an E2F1 dose dependent manner in Saos2 osteoblast-like cells. In addition, direct binding of E2F1 to the FZD1 promoter was detected using both a ChIP assay and EMSA. Consistent with these results, endogenous FZD1 mRNA and protein expression in Saos2 cells was activated by E2F1 overexpression. Increased expression of FZD1 by E2F1 subsequently promoted the expression of osteoblast markers including Osteocalcin (OCN), Alkaline phosphatase (ALP) and Collagen type I (Col I) and differentiation of Saos2 cells. Saos2 cells overexpressing E2F1 had significantly stronger Alizarin Red-S (AR-S) staining compared to control Saos2 cells when treated with osteoblast differentiation medium. Knockdown of FZD1 by siRNA significantly reduced the mineralization ability of Saos2 cells and abolished the enhanced osteoblast mineralization stimulated by E2F1 *in vitro*. Our study demonstrates that FZD1 plays a critical role in osteoblast differentiation and mineralization and that FZD1 is required for E2F1-dependent regulation of osteoblast mineralization.

Disclosures: Shibing Yu, None.

SA0214

Higher Strontium Consumption Stimulates Osteoblast Differentiation and Increase Bone Formation in Goats. Junjing Jia^{*1}, Guozhou Liao², Yueyuan Fan³, Hua Rong³, Zhiqiang Xu⁴, Xi Zhang⁵, Dahai Gu³, Qichao Huang², Zhenhui Cao³, Qiuye Lin⁶, Sizheng Gao³, Qiuye Lin³, Changrong Ge⁷, Wei Yao⁸. ¹University of California, Davis, USA, ²Faculty of Food Science, Yunnan Agricultural University, China, ³Yunnan Provincial Key Laboratory of Animal Nutrition & Feed, Yunnan Agricultural University, China, ⁴Yunnan Agricultural University, China, Peoples Republic of China, ⁵Yunnan Agricultural University, Peoples Republic of China, ⁶Yunnan Agricultural University, China, Peoples Republic of China, ⁷Yunnan Agricultural University, China, Peoples Republic of China, ⁸University of California, Davis Medical Center, USA

Many researchers have reported that strontium (Sr⁺) plays important role in increasing osteoblast differentiation and bone formation in human and in animals. In one of our previous studies, we demonstrated that higher strontium consumption increased biomarkers for bone formation, and increased bone mineral density (BMD), bone mineral content (BMC) and strength in a "red-bone" goat strain. This study was designed to investigate cellular and molecular mechanisms of strontium both in vivo and in vitro in goat.

In vivo Study: Eight six months old red-boned lambs (high bone Sr⁺ content) and eight normal lambs were sacrificed and samples from cartilage and distal tibia were taken to detect osteoblast differentiation gene markers.

In vitro Study: Periosteum-derived mesenchymal stem cells (PMSCs) were isolated from red-boned and common lambs six months of age. PMSCs were cultured in osteogenic medium containing dexamethasone, ascorbic acid and β-glycerophosphate. Goat osteoblasts were identified by ALP staining. Cells were stained with crystal violet staining for total colony forming units (CFU-F) and Alizarin Red staining for osteoblastic units (CFU-Ob). The expressions of osteoblast differentiation gene markers were detected at 14 days.

Results: In vivo study showed that red-boned goats had significantly higher alkaline phosphatase (ALP), osteocalcin (bglap) and RUNX2 genes expressions in cartilage and distal tibia. In vitro study showed that PMSCs of red-boned goat have shown higher rate of proliferation than those of common goat. PMSCs in red-boned goat can go through passage 15 compared with passage 10 in PMSCs of common goat. PMSCs in red-boned goat exhibited the greater osteogenic properties with higher activity of ALP as well as more calcium nodules than those in control group. Both ALP and osteocalcin expressions, were higher in PMSCs derived from red-boned goat compared to those derived from common goat.

In conclusion: Higher strontium consumption stimulates osteoblast differentiation and increase bone formation in goats.

Disclosures: Junjing Jia, None.

SA0215

Kinetics of Bmp2 Gene Expression in Primary Calvarial Osteoblasts: Gene Regulatory Network Constructed with ARCANe and Linked to Ingenuity Pathway Transcriptional Module. Stephen Harris^{*1}, Alexander c Lichtler², Shuo Chen³, Marie A Harris³. ¹University of Texas Health Science Center at San Antonio, USA, ²U. of Connecticut Health Center, USA, ³U. of Texas Health Science Center at San Antonio, USA

Mechanism of Bmp2 action on Osteoblasts is not well understood. There is a clear collection of genes stimulated and repressed by Bmp2 action on osteoblasts both in vivo and in vitro. For example, conditional removal of Bmp2 gene in osteoblasts results in dramatic decreased expression of Osterix and VegfA, Dlx3 and many others. We treated confluent primary calvarial osteoblasts with 100 ng/ml of recombinant Bmp2(rBMP2) and collected RNA at 1,2,4,8,16,24, and 72 hrs after this single treatment and carried out robust gene expression analysis using the Illumina Mouse W6 v2 microarray with 45,000 probes, analyzed the data with Genome Studio RNA expression module software and used a set of 1415 genes that were Bmp2 regulated at any time point, with Differential Expression Pvalue <0.005 and at least 1.7 fold change from the 0hr, 24hr, or 72 hr control time points. Using Ingenuity Pathway(IPA) and David Bioinformatic, we identified several relevant functional cluster and pathways. We used David to get a list of the transcription factor activity related genes in the 1415 geneset and used this Gene Ontology Class of 43 transcription factor(TF) dataset to construct a gene regulator network(GRN) of links between these TF and the genes they directly regulate using the reverse genetic engineering principals of the algorithms in ARCANe, implemented in the geWorkbench programs. We set the parameters at P<.05 with bootstrapping set at 20 with a consensus threshold at 0.001. We found 8 major clusters of genes around the TF Nfatc3 and Nfatc1, Alex4, Osterix, Dlx3, Egr2, Hey1, LBH, and AES. Each cluster contained from 10 to 50 candidate genes directly regulated by these TF, with some links between the clusters. Using the literature based pathway components of IPA, and the new transcriptional regulator of IPA, approximate 25% of the links identified in the GRN were supported by at least 1 reference in the IPA database. Then GRN implies that initial Bmp2 action is on increased growth related genes and Notch signaling. At later time points, the differentiation program is activated. This Bmp2 regulated GRN network will serve as a starting module for further validation and extension using whole genome sequencing and mapping of Bmp2 modulated enhancers.

Disclosures: Stephen Harris, None.

SA0216

microRNA Expression Analysis Using Next Generation Sequencing in Primary Human Bone Cells treated with Parathyroid Hormone or Dexamethasone. Navya Laxman^{*1}, Carl-Johan Rubin², Hans Mallmin³, Olle Nilsson⁴, Christian Tellgren-Roth⁵, Andreas Kindmark³. ¹Uppsala University, Sweden, ²Uppsala University, Sweden, ³Uppsala University Hospital, Sweden, ⁴Department of Surgical Sciences, Uppsala University, Sweden, ⁵Department of Immunology, Genetics & Pathology, Rudbeck laboratories, Uppsala University, Sweden

MicroRNAs (miRNAs), are a class of post-transcriptional regulators. They are naturally occurring, small non-coding RNA molecules, about 21–25 nucleotides in length. They bind to complementary sequences in the 3' UTR of multiple target mRNAs, usually resulting in their silencing.

We have previously used miRNA LNA(Locked Nucleic Acid) arrays to assess global miRNA expression in human osteoblasts(HOB), and identified approximately 90 miRNAs with significant expression levels, and also identified a subset of miRNAs exhibiting interindividual and/or gender differences. We have shown statistically significant correlations between miRNA and mRNA abundance of genes involved in bone metabolism in HOB. In the present project, we applied next generation sequencing techniques to comprehensively assess miRNA expression in HOB cells treated with parathyroid hormone (PTH) and dexamethasone (DEXA).

HOB cells were isolated from human trabecular bone collected from donors undergoing total hip replacement, and subsequently treated for 2 and 24 hours with PTH or DEXA or left untreated. Small RNA was isolated from these cells and cDNA synthesized using SOLiD library protocol. Second generation sequencing was performed using SOLiD4 on barcoded library constructs of small RNA 50bp plus barcode, at the Uppsala Genome Center. Sequence reads were aligned to a scaffold consisting of all known miRNA sequences, and number of sequence reads mapping uniquely to each miRNA were counted.

A total of 207 million reads from the small RNA library constructs was obtained, and normalized absolute expression was retrieved for the 500 most abundant miRNAs. The 75 miRNAs that exhibited the highest mean expression across the four experiments per individual were taken for downstream analyses. Expression levels were set to percent of each, and results showed a significant effect of treatment with PTH versus treatment with DEXA at 2 hours and even more pronounced at 24 hours on miRNA abundance. Interestingly, several miRNAs exhibiting significant differences in abundance have predicted mRNA targets involved in bone metabolism, e.g. miR-197 targeting Insulin-like growth factor1(IGF) and Wnt pathway members. miR-31 also showed differential expression.

miRNA absolute abundance data from next generation sequencing show that PTH and DEXA affect miRNA abundance in primary human bone cells, and that these miRNAs in turn are correlated to levels of mRNAs known to affect bone metabolism.

Disclosures: Navya Laxman, None.

SA0217

See Friday Plenary Number FR0217.

SA0218

See Friday Plenary Number FR0218.

SA0219

Sequential Expression of Sox11 and Sox4 Is Essential for Osteoblastogenesis and Bone Development. Jogeswar Gadi^{*1}, Min Jung Lee², Ajita Jami³, Kyoung Min Kim⁴, Han-Sung Jung⁵, Sung-Kil Lim⁶. ¹Yonsei University College of Medicine Seoul South Korea, South Korea, ²Department of Oral Biology, College of Dentistry, Yonsei University, South Korea, ³Division of Endocrinology & Endocrine Research Institute, Yonsei University College of Medicine, South Korea, ⁴Yonsei University College of Medicine, Republic of Korea, ⁵Department of Oral Biology, College of Dentistry, Yonsei University, South Korea, ⁶Yonsei University College of Medicine, South Korea

The high-mobility-group (HMG) domain containing transcription factors *Sox11* and *Sox4* belongs to the *SoxC* family and were found to be expressed in pre-osteoblast cells. We found that *Sox11* expression was restricted to the early stage of osteoblastogenesis by contributing in the commitment of osteoblast cells from the mesenchymal cells. *Sox11* plays an important role in the early osteoblastogenesis by regulating *Runx2* and *Osterix*. In addition to this *Sox11* involved in survival and anti apoptotic activity of MC3T3-E1 cells and primary calvaria cells. Furthermore, the induction of osteoblast differentiation inhibits the expression of *Sox11* in MC3T3-E1 cells on day7, where the *Sox4* expression was found to be sequentially increased with the progression of osteoblast differentiation at mRNA and protein levels. We also found that *Sox4* overexpression simulates the TCF/LEF reporter activity and influences the expression of Wnt signaling genes and osteoblast marker genes. All

together, we hypothesize that both the *Sox11* and *Sox4* expression was essential for the early and late stages of osteoblastogenesis respectively.

Disclosures: Jogeswar Gadi, None.

SA0220

TNF α Suppresses BMP2-induced Osteoblasts Differentiation via CREBH-mediated *smurf1* Expression. Won-Gu Jang¹, Eun-jung Kim¹, Hyuck Choi², Sin-hye Oh², Byung-Chul Jeong³, Sung-Woong Hur⁴, Jeong-Tae Koh^{*5}.
¹Korea Research Institute of Bioscience & Biotechnology (KRIBB), South Korea, ²Research Center for Biomaterialization Disorders, School of Dentistry, Chonnam National University, South Korea, ³Chonnam National University School of Dentistry, South Korea, ⁴Chonnam National University, South Korea, ⁵Chonnam National University, South Korea

Inflammation is a major risk factor for bone loss. The proinflammatory cytokine tumor necrosis factor α (TNF α) has been introduced to activate inflammatory responses via the regulated intramembrane proteolysis (RIP) of endoplasmic reticulum (ER) membrane-anchored transcription factors. cAMP response element-binding protein H (CREBH), a liver-enriched ER-bounded bZIP transcription factor, is regulated by UPR-dependent proteolytic cleavage in the liver. Here, we identified that TNF α suppresses BMP2-induced osteoblast differentiation via regulating CREBH-dependent *smurf1* expression. TNF α increased CREBH expression via NF- κ B signaling pathway, and induced the subcellular localization of CREBH to nucleus. Overexpression of CREBH suppressed BMP2-stimulated osteogenic gene expressions such as alkaline phosphatase (ALP) and osteocalcin (OC) in preosteoblast MC3T3E1 cells. TNF α induction of CREBH mRNA expression and CREBH promoter activities were significantly suppressed by BAY11-7082, an NF- κ B inhibitor. Moreover, BAY11-7082 recovered TNF α -suppressed Runx2, ALP and OC with decreased CREBH expression. In addition, inhibition of CREBH expression using siCREBH released TNF α -suppressed osteoblast differentiation. Finally, we found that TNF α or CREBH increased *smurf1* expression in MC3T3E1 cells. Moreover, CREBH-induced *smurf1* increased degradation of Smad1. Our results suggest that ER-bounded bZIP transcription factor CREBH may be a noble negative regulator of osteoblast differentiation, which induces *smurf1*-mediated Smad1 degradation. Furthermore, these provide us some information how TNF α suppresses BMP2-induced osteoblast differentiation.

Disclosures: Jeong-Tae Koh, None.

SA0221

Action of Small Molecular Inhibitors on Anabolic Effects of Intermittent PTH Treatment. Maki Uyama^{*1}, Masmitsu Kawanami¹, Masato Tamura².
¹Periodontology & Endodontics, Grad. Sch. Dent. Med., Hokkaido University, Japan, ²Biochem. & Mol. Biol., Grad. Sch. Dent. Med., Hokkaido University, Japan

Parathyroid hormone (PTH) is both anabolic and catabolic effects in bone depending on the mode of administration. Systemic intermittent administration of PTH stimulates bone formation in animals and human, and recombinant human PTH (1-34) [teriparatide] is used for the treatment of osteoporosis. Several investigations have previously shown that several molecules such as RANKL, OPG, Runx2, osterix or SOST are a target gene for PTH in bone. In vivo and in vitro studies also indicate that PTH regulated anti-apoptotic signaling, promoted osteoblast differentiation and increased the production and/or activation of osteogenic growth factors such as IGF-1 or BMP. However, up to now, the molecular mechanisms underlying bone anabolic action of PTH remain controversial. Recently, from high-throughput screening of synthetic compound libraries, a novel class of small molecule inhibitors that blocks canonical Wnt signaling or BMP/Smad signaling pathway was identified. IWP-2 prevents palmitoylation of Wnt proteins by Porcupine, thereby blocking Wnt secretion and activity. It also blocks phosphorylation of Lrp6. IWR-1 promotes β -catenin phosphorylation by stabilizing Axin-scaffolded destruction complexes, thereby blocking Wnt signaling pathway. Therefore, we investigate the effects of these small molecular inhibitors on anabolic effects of intermittent PTH treatment in order to examine target signaling pathway for intermittent PTH in osteoblasts and the level of a molecule depending on the mode of administration. In this study, osteoblastic cells were challenged with PTH intermittently or continuously with small molecular inhibitors, and then ALP activity, matrix mineralization, mRNA expression, cell number, 5-bromo-2-deoxyuridine (BrdU) incorporation were determined. Intermittent PTH(1-34) treatment of MC3T3-E1 cells caused an increase in ALP activity, whereas RANKL expression was down-regulated. In these cells, IWR-1, IWP-2 or BMP/Smad signaling inhibitor dorsomorphin regulated ALP activity and mineralization by intermittent PTH treatment. These observations indicated that involvement of canonical Wnt and BMP/Smad signaling pathway in anabolic effects of intermittent PTH treatment in osteoblasts. We also consider the anabolic effects of intermittent treatment with PTH in osteocyte.

Disclosures: Maki Uyama, None.

SA0222

Differential Effects of 1,25-dihydroxyvitamin D on *in vitro* Mineral Deposition: Interaction between Osteoblast Stage of Maturation and Culture Medium Calcium Concentration. Dongqing Yang^{*1}, Gerald Atkins², Andrew Turner³, Paul Anderson⁴, Howard Morris⁵.
¹The University of Adelaide, Australia, ²University of Adelaide, Australia, ³Musculoskeletal Biology Research, Chemical Pathology, SA Pathology, Australia, ⁴Musculoskeletal Biology Research, University of South Australia, Australia, ⁵SA Pathology, Australia

Reports of 1,25-dihydroxyvitamin D (1,25D) activity on osteoblasts include either stimulation or inhibition of mineralization. Maturation markedly influences the effects of 1,25D in culture including inhibition of proliferation, enhancing mature osteoblast mineral deposition [1] and 1,25D induction of RANKL mRNA [2]. Bone mineral deposition *in vitro* is enhanced by increasing medium calcium [3]. We now report the interaction between osteoblast maturation, the level of extracellular calcium in the culture medium and the response to 1,25D on *in vitro* mineral deposition. Confluent primary calvarial cells (C57BL/6 mouse pups 1-3 day old) (Calvarial cells) were cultured in differentiation medium for 24 days [4]. Osteoblast-like cells (isolated from 4 week-old C57BL/6 mice femoral cortices) (Cortical cells) were cultured in proliferation medium. Confluent cells were cultured in differentiation medium over 21 days. The effects of 1.8 and 2.8 mM total extracellular calcium on mineralisation (alizarin red staining) and gene expression (real-time RT PCR) were assessed. Calvarial cells exhibited properties of less mature osteoblasts than Cortical cells including reduced levels of mineral deposition (Calvarial cells 36% of Cortical cells, $p < 0.01$) and the induction of RANKL mRNA by 1,25D in Calvarial cells (Day 24, 3-fold, $P < 0.01$) but not in Cortical cells. Mineral deposition in Calvarial cultures was inhibited by 1,25D in 1.8 mM Ca²⁺-medium. (Day 24 28%, $p < 0.01$) with no effect of 1,25D in 2.8 mM Ca²⁺-medium. 1,25D in 1.8 mM Ca²⁺-medium induced the expression of both MEPE (600%, $p < 0.01$) and SOST (1300%, $p < 0.01$). In contrast, 1,25D influenced mineral deposition by Cortical cells only in 2.8 mM Ca²⁺-medium (Day 21, 120%, $p < 0.01$), without an effect on MEPE and SOST mRNA expression. Our findings indicate that 1,25D influences mineral deposition differentially according to osteoblast differentiation and perhaps also skeletal site, which may account for some of the controversy surrounding this issue. Our results suggest that the effect of 1,25D on early stage, calvaria-derived osteoblast-like cells is to inhibit mineral deposition, whereas the effect on mature, cortical bone-derived cells is to enhance mineral deposition, in particular in response to increased extracellular calcium.

1.Owen TA, et al., *Endocrinol* 1991;128:1496-504

2.Atkins GJ, et al., *JBM* 2003;18:1088-98

3.Dvorak MM, et al., *PNAS* 2004;101:5140-54.Zhou H, et al., *JBC* 2008;283:1936-45

Disclosures: Dongqing Yang, None.

SA0223

See Friday Plenary Number FR0223.

SA0224

Substrate Recognition of Human Menaquinone-4 Biosynthetic Enzyme UBIAD1. Kimie Nakagawa^{*1}, Yuri Uchino², Yoshitomo Suhara³, Toshio Okano¹.
¹Kobe Pharmaceutical University, Japan, ²Kobe Pharmaceutical University, Japan, ³Shibaura Institute of Technology, Japan

Vitamin K serves as a cofactor for vitamin K-dependent carboxylase (gamma-glutamyl carboxylase : GGCX). GGCX converts glutamate residues into gamma-carboxyglutamate (Gla) residues in vitamin K-dependent proteins, such as blood coagulation factors and bone formation factors. There are two forms of naturally occurring vitamin K, phyloquinone (PK) and menaquinones (MK-n). Moreover, menadiol or vitamin K₃ (K₃) is a synthetic compound lacking a side chain. Clinically, MK-4 the most common form of vitamin K, has been shown to prevent bone fractures. This osteoprotective effect is more pronounced in MK-4 than in PK, and hence MK-4 has been used to treat osteoporotic patients in Japan. MK-4 has been shown to act as a ligand for the steroid and xenobiotic receptor (SXR) in human osteoblastic MG-63 cells. Menaquinone-4 (MK-4) is ubiquitously present in extrahepatic tissues, with particularly high concentrations in the brain, kidney and pancreas of humans and rats. It has consistently been shown that PK is endogenously converted to MK-4. This occurs either directly within certain tissues or by interconversion to K₃, followed by prenylation to MK-4. No previous study has sought to identify the human enzyme responsible for MK-4 biosynthesis. Recently, we identified that the MK-4 biosynthetic enzyme is UbiA prenyltransferase domain containing 1 (UBIAD1) [*Nature*, 2010;468:117]. Vitamin K derivatives were converted to MK-4 by UBIAD1. In this study, we analyzed the substrate recognition and specificity of UBIAD1. We evaluated the conversion of several derivatives with 1,4-naphthoquinone structure. MG-63 cells were treated with several derivatives with 1,4-naphthoquinone structure at the concentrations of 1-100 μ M in the medium for 24hrs. The concentration of MK-4 converted from derivatives was measured by LC-APCI-MS/MS. We further evaluated inhibitory activity of derivatives against conversion of K₃ to MK-4 using deuterium-labeled compounds. As a result, 1,4-naphthoquinone

(K₃ with demethylation of 2-methyl substitute) was not converted to MK-4 in MG-63 cells. Some compounds with modification of 3-substitute did not convert to MK-4, but inhibited the conversion of K₃ into MK-4. These results showed that 2-methyl substitute of substrate for UBIAD1 required for conversion reaction, and modification of 3-substitute affect the conversion reaction of UBIAD1. These data is beneficial for the development of the ligand which controls the MK-4 biosynthetic activity of UBIAD1 in bone.

Disclosures: Kimie Nakagawa, None.

SA0225

See Friday Plenary Number FR0225.

SA0226

See Friday Plenary Number FR0226.

SA0227

See Friday Plenary Number FR0227.

SA0228

Delayed Healing and Increased Callus Adiposity in a Murine Model of Type 2 Diabetes. Matthew Brown¹, Kiminori Yukata², Regis O'Keefe³, Robert Mooney¹, Michael Zuscik⁴. ¹University of Rochester Medical Center, USA, ²University of Tokushima Graduate School, Japan, ³University of Rochester, USA, ⁴University of Rochester School of Medicine & Dentistry, USA

Introduction: Impaired healing and non-union of skeletal fractures is a major public health problem, with morbidity exacerbated in patients suffering from diabetes mellitus (DM). DM is prevalent worldwide, affecting approximately 25.8 million US adults, with >90% having obesity-related DM type 2 (DM2). While fracture healing in DM type 1 (DM1) has been studied using animal models, an investigation into the tissue and molecular basis for delayed healing in an animal model of DM2 has not yet been performed.

Methods: Male C57BL/6J mice at 5 weeks of age were placed on either a control low-fat diet or a high-fat diet (HFD) for 12 weeks. A mid-diaphyseal open tibia fracture was induced at 17 weeks and fixated using an intra-medullary spinal needle. Mice were sacrificed at days 7, 10, 14, 21, 28, and 35 for various endpoints, including micro-computed tomography (microCT), histology, and biomechanical testing.

Results: Mice provided the HFD for 12 weeks displayed increased body weight and impaired glucose tolerance, both characteristic of DM2. Compared to control mice, HFD mice administered tibia fractures showed a trend towards decreased cartilage area at days 10, 14, and 21. Woven bone area was significantly ($p < 0.05$) reduced in HFD mice at days 21 and 28. MicroCT data also showed impaired bone formation in HFD mice. Adiposity in the external callus was increased in HFD mice at later time points, achieving significance ($p < 0.05$) at days 21 and 35. Finally, HFD mice had significantly ($p < 0.05$) weakened healed fractures compared to controls at day 35, with mean torque to failure of 25 vs. 35 N*mm.

Discussion: Fracture repair studies in animal models of DM1 have demonstrated impaired chondrogenitor proliferation, premature cartilage resorption, decreased callus bone content, and biomechanically inferior fracture repair. Data from our DM2 mouse model also show delayed healing, which was distinctly characterized by increased callus adiposity in HFD mice at the end of the woven bone formation stage and during callus remodeling. This suggests altered mesenchymal stem cell (MSC) fate determination, with a shift to the adipocyte lineage at the expense of the osteoblast lineage. We hypothesize that PPAR-gamma expression is upregulated in HFD mice, driving the proposed fate switching. We further speculate that the altered callus microenvironment in HFD mice contributes to inferior fracture healing, possibly by interfering with osteoblast-osteoclast coupling.

Disclosures: Matthew Brown, None.

SA0229

See Friday Plenary Number FR0229.

SA0230

See Friday Plenary Number FR0230.

SA0231

Effects of Resveratrol on Proliferation and Differentiation of Human Bone Marrow-derived Osteoblasts. Marie Orstrup^{*1}, Torben Harsløf², Søren Kildeberg Paulsen³, Steen Bønløkke Pedersen⁴, Bente Lomholt Langdahl¹.

¹Aarhus University Hospital/MEA, Entrance 3B/Tage-Hansens Gade 28000 Aarhus C, Denmark, ²Department of Internal Medicine M, Regional Hospital Randers, Denmark, ³Department of Medicine, Regional Hospital Silkeborg, Denmark, ⁴Department of Endocrinology & Internal Medicine MEA, Aarhus University Hospital, Denmark

Background and Purpose:

Resveratrol (RSV) is a dietary supplement with anti-inflammatory effects. It inhibits NFκB, and reduces OVX-induced bone loss, and immobilization-induced bone loss in rodents. Increased levels of IL6 (thus increased inflammation) will result in increased degradation of bone and thereby decreased bone mass. RSV may alter bone turnover by affecting osteoblast and osteoclast proliferation and differentiation. In studies of hMSC-TERT cells, ST2 cells from murine bone marrow and hBMSCs from one fetal bone marrow RSV stimulates osteoblastic proliferation and differentiation dose-dependently. The aim of this study is to investigate if RSV has effects on proliferation and differentiation of bone marrow-derived osteoblasts from healthy adult human donors.

Methods: Human mesenchymal stem cells were derived from the bone marrow of 13 healthy adult human donors. Cell cultures from each donor were stimulated with different doses of RSV (10^{-8} M – 10^{-3} M)+/- vitamin D and compared with serum free (SF) conditions. Proliferation was assessed by thymidine incorporation, cell count by methylenblue (MET) assay, and differentiation by alkaline phosphatase (ALP), procollagen type1 (PINP), and osteoprotegerin (OPG), all corrected for cell number.

Results: RSV impaired proliferation, assessed by thymidine incorporation, at higher doses (0.80 ± 0.07 at 10^{-6} M compared to SF, $p < 0.02$), but with no effect on cell number. Alkaline phosphatase was reduced by RSV at higher doses (0.80 ± 0.07 at 10^{-5} M and 0.82 ± 0.07 at 10^{-6} M compared to SF, $p < 0.02$ and $p < 0.05$, respectively). At higher doses of RSV there was an increase in PINP, but only borderline significant. All doses of RSV seemed to increase OPG, but not significantly. Co-stimulation with vitamin D altered the response with respect to ALP and OPG. The reduction of ALP by RSV was neutralized, and low doses of RSV in combination with vitamin D even tended to increase ALP. Furthermore, OPG was significantly decreased.

Conclusion: Earlier studies have shown dose-dependent stimulation of proliferation and differentiation of osteoblast-like cells, without co-stimulation with vitamin D. In this first study of hBMSCs from adults RSV, in high doses, inhibited proliferation, and the effects on differentiation were ambiguous since ALP was reduced, while PINP and OPG were increased. Significant interactions with vitamin D were seen.

Disclosures: Marie Orstrup, None.

SA0232

See Friday Plenary Number FR0232.

SA0233

See Friday Plenary Number FR0233.

SA0234

Increase Rate of Osteogenic Differentiation in Human Mesenchymal Stem Cells by Low Intensity Ultrasound in Stimulated Microgravity. Sardar Uddin^{*1}, Yi-Xian Qin². ¹Stony Brook University, USA, ²State University of New York at Stony Brook, USA

Disuse osteopenia induced by microgravity (MG) during long duration space flight has been known to cause adverse effect on bone density and quality. The reduction in bone mass can be due to decreased osteoblast activity and/or decreased number of osteoblasts. Mesenchymal stem cells (MSC) are well known as progenitor cells to osteoblast, previous experiments have shown significant decrease in osteogenic differentiation of human MSCs in simulated MG [1]. Considering that the effects of MG are partially attributed to the lack of mechanical force on bone, which alters gene expression, as well as proliferation and differentiation [2], we reasoned that Low-intensity pulse ultrasound (LIPUS) provides the essential mechanical stimuli to increase the rate of differentiation of hMSC along the osteogenic lineage.

Human MSC was cultured in StemLife Media (LifeLine Cell Technology, MD) with initial seeding density of 250,000 cells per Opticell cartilage. The cells were allowed to grow to confluency and MG stimulations were started at day 7 post confluency (PC-Day 7). Cells were divided into five groups (n=4/group), MSC (Control), gravity (G), gravity + LIPUS (GU), microgravity (M) and microgravity + LIPUS (MU). Growth media changed to differentiation media (StemLife Media + 50 μg/ml ascorbic acid + 10 mM β-glycerolphosphate + 10nM dexamethasone) except for control group at PC-Day7.

Stimulated MG environment was created by putting Opticell into *in vitro* rotary system, with rotation set at 15 RPM. LIPUS groups were stimulated everyday with 30mW/cm² for 20 min. Cells were kept at 37C, in a 5% CO₂ environment during the

experiment and medium was changed every second day. Cells were analyzed for ALP activity after 7 days of stimulation and matrix mineralization (Alizarin red staining) was analyzed after 12 days of simulated MG exposure.

Alizarin red (AZ) analyses (Fig 1) shows significant increase in calcification in MU group (~50%) compare to M group. Significant decrease of calcification was also observed between G (~80%) and M group. Higher mineralization was observed in GU group (~87%) compare to G group. Furthermore, M cells show ~77% reductions in ALP activity then G cells, application of LIPUS increase ALP activity by ~32% in MU samples. GU samples also show significant increase in ALP activity by ~46% (Fig 2).

Collectively, these results strongly suggest that LIPUS increases the rate of osteogenic differentiation of hMSCs in an MG environment.

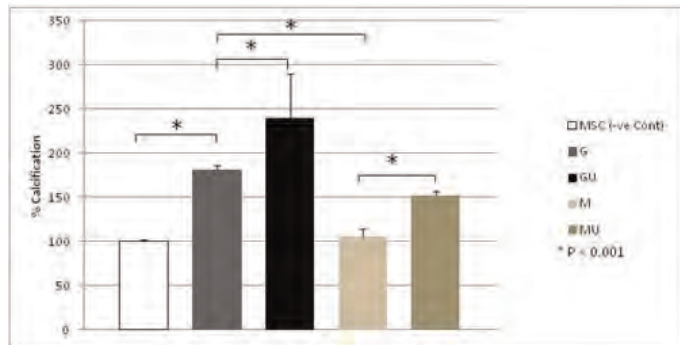


Figure 1 : Matrix calcification

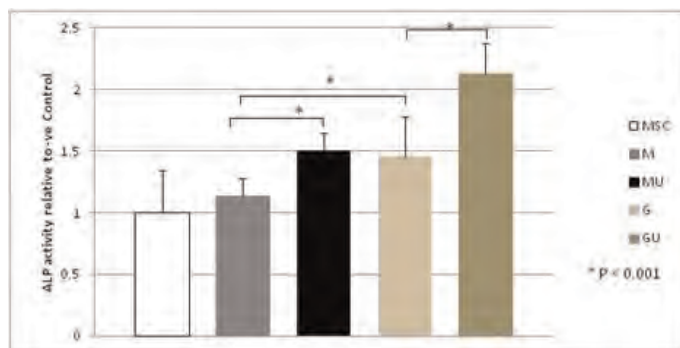


Figure 2 : ALP activity

Disclosures: *Sardar Uddin, None.*

SA0235

See Friday Plenary Number FR0235.

SA0236

Regulation of BMP/Smad Signaling and Osteoblastic Cell Differentiation by Receptor Tyrosine Kinase Pathways in Mesenchymal Stem Cells. Emmanuel Biver¹, Cvrlil Thouverev², David Magne³, Joseph Caverzasio⁴. ¹University hospital of Lille, France, ²Division of Bone Diseases, Switzerland, ³University of Lyon, France, ⁴Division Bone Diseases, Switzerland

Bone morphogenetic proteins (BMPs) are important activators of mesenchymal stem cell (MSC) differentiation into osteoblasts and are often used to improve orthopedic treatments. Mitogenic growth factors such as platelet-derived growth factors (PDGF) and fibroblast growth factors (FGF) stimulate MSC proliferation through activation of tyrosine kinase receptors (RTK) and inhibit osteoblastic cell differentiation. In this study, we investigated the effects of PDGF or FGF receptor signaling on BMP2-induced osteogenic differentiation of human MSCs and C3H10T1/2 pluripotent mesenchymal cells. Inhibition of PDGF or/and FGF receptor activity enhanced BMP2-induced MSC and C3H10T1/2 osteoblastic differentiation as shown by increased alkaline phosphatase activity, osteoblast markers expression and matrix mineralization. This effect was associated with increased Smad phosphorylation and transcriptional activity, indicating that RTK signaling interferes with Smad signaling. Since mitogen-activated protein kinases (MAPKs) ERK and JNK negatively regulated Smad transcriptional activity induced by BMP2 in MSC. Associated with these effects, BMP2-induced MSC differentiation was enhanced by the JNK inhibitor. Also, the PI3K/AKT pathway was also found to positively regulate BMP2/Smad signal through inhibition of GSK3.

In conclusion, growth factor-induced RTK signaling pathways strongly modulate BMP2/Smad signal and related MSC osteogenic differentiation. Understanding the

molecular networks by which BMPs enhance the differentiation of mesenchymal cells may help to improve the use of these cells for orthopedic treatments.---

Disclosures: *Joseph Caverzasio, None.*

SA0237

Stage-specific Embryonic Antigen-4 is a Marker of Human Deciduous Periodontal Ligament Stem Cells. Noriaki Kawanabe¹, Hiroaki Fukushima², Satoko Murata², Yoshihito Ishihara³, Takeshi Yanagita⁴, Tarek Balam², Takashi Yamashiro². ¹Okayama University Hospital, Japan, ²Okayama University, Japan, ³Okayama University, Department of Orthodontics, Japan, ⁴Okayama University Hospital, Japan

Although human deciduous teeth are an ideal source of adult stem cells, no method for identifying deciduous periodontal ligament (D-PDL) stem cells has been developed. In the present study, we investigated whether stage-specific embryonic antigen (SSEA)-4 is a marker that could be used to isolate D-PDL stem cells. Five deciduous teeth were collected from 5 healthy patients who were undergoing orthodontic treatment at Okayama University Hospital. SSEA-4 expression in D-PDL cells was detected by immunocytochemistry and flow cytometry. SSEA-4+ D-PDL clonal cells were isolated by flow cytometry. Adipogenic, osteogenic, chondrogenic, and neuronal differentiation *in vitro* was assessed to examine SSEA-4+ D-PDL cells' multipotentiality. D-PDL cells met the minimum criteria for mesenchymal stem cells (MSC): they showed plastic adherence, specific surface antigen expression, and multipotent differentiation potential. SSEA-4+ D-PDL cells were detected *in vitro* and *in vivo*. Flow cytometric analysis demonstrated that 22.7% of the D-PDL cells were positive for SSEA-4. SSEA-4+ clonal D-PDL cells displayed multilineage differentiation potential; i.e., they were able to differentiate into adipocytes, osteoblasts, chondrocytes, and neurons, *in vitro*. A clonal assay demonstrated that 61.5% of the SSEA-4+ D-PDL cells had adipogenic, osteogenic, and chondrogenic potential. Our present study demonstrated that SSEA-4+ D-PDL cells are a subset of multipotent stem cells. Hence, SSEA-4 is a specific marker that could be used to identify D-PDL stem cells.

Disclosures: *Noriaki Kawanabe, None.*

SA0238

The Notch Target Gene, Sox2, May Mediate Notch-induced Maintenance of Bone Marrow Derived Mesenchymal Stem/progenitor Cells. Teng Long¹, Cuicui Wang², Regis O'Keefe², Matthew Hilton³, Yufeng Dong². ¹University of Rochester, USA, ²University of Rochester, USA, ³University of Rochester Medical Center, USA

We previously identified the RBPjk-dependent Notch signaling pathway as an inducer of mesenchymal stem/progenitor cell (MSC) proliferation and an inhibitor of MSC differentiation during mouse bone development, although the mechanism underlying this regulation remains unknown. Since SOX2 has been identified as an important regulator of stem/progenitor cell maintenance including MSCs, we set out to demonstrate that SOX2 is important for mediating the Notch-induced maintenance of bone marrow derived MSCs *ex vivo*. We first cultured the MSCs on plates coated with recombinant protein for the extracellular domain of the Notch ligand, JAGGED1, or control protein-IgG. Gene expression analyses indicated that JAGGED1 induced Notch signaling enhanced expression of the stem cell transcriptional regulators, SOX2, OCT4 and NANOG, as well as, the Notch target gene, HES1. Cell proliferation assays using BrdU labeling also demonstrated that JAGGED1 mediated Notch signaling increased MSC proliferation by more than 20%. These data indicated that Notch activation could both enhance MSC proliferation and maintain multipotency *ex vivo*. To further identify the direct target gene(s) that contribute to the Notch-mediated maintenance of MSCs, the SOX2, OCT4 and NANOG promoters were analyzed using TESS software. Interestingly, 2 putative RBPjk binding sites were identified at -1326 to 1331 and -1233 to -1238 in the SOX2 promoter. To investigate whether SOX2 is regulated at a transcription level by Notch signaling, we cloned 2 deletion fragments of the SOX2 promoter into a luciferase vector, including a 1.8kb fragment containing both putative RBPjk binding sites and a 0.6kb fragment that lacks RBPjk binding sites. Co-transfection experiments showed that the 1.8kb promoter fragment activity was significantly induced by Notch signaling using a NICD expression plasmid, whereas the 0.6kb fragment showed no difference between control and NICD. In addition, mutation of RBPjk binding sites in the 1.8kb fragment led to a significant reduction of SOX2 promoter activity indicated that RBPjk is also involved in SOX2 transcription. Finally, ChIP assays determined that endogenous RBPjk binds to DNA fragments containing both RBPjk binding sites of the SOX2 promoter within human MSCs. Collectively, these data indicate that SOX2 is a target of RBPjk-dependent Notch signaling and may play a functional role in the Notch-mediated maintenance of MSCs.

Disclosures: *Teng Long, None.*

SA0239

Wnt-dependent Osteogenic Commitment of Mesenchymal Stem Cells Using a Novel GSK3 β Inhibitor. David Cook*¹, Simon Felgett², Mary Elizabeth Pownall², Patrick O'Shea³, Paul Genever¹. ¹University of York, United Kingdom, ²University of York, United Kingdom, ³AstraZeneca, United Kingdom

Mesenchymal stem cells (MSCs) can differentiate into multiple lineages including osteogenic, adipogenic and chondrogenic cells. Wnt signalling has been implicated in controlling MSC fate. Here we show that a novel glycogen synthase kinase 3 β inhibitor, AR28, is a potent activator of canonical Wnt signalling in vitro and in vivo. AR28 induced nuclear translocation of β -catenin in the mouse mesenchymal cell line, C3H10T1/2, and human MSCs. Western blot analyses showed that levels of active β -catenin increased up to 6-fold with AR28 administration compared to vehicle controls. Using a TCF-luciferase reporter we demonstrated that AR28 activated canonical Wnt signalling in a time- and dose-dependent manner in C3H10T1/2 cells. AR28 at 2.5 μ M increased reporter expression ~100-fold greater than 20mM LiCl and was comparable to 100ng/ml Wnt3a. AR28 induced 58% embryonal axis duplication in *Xenopus laevis* embryos, when injected into the ventral marginal zone. In-situ hybridisation confirmed secondary regions of chordin expression in 98% of AR28 injected samples, marking a second Spemann organiser region, typical of pronounced Wnt signalling.

To determine the effects of AR28 on MSC osteogenesis we used standard differentiation inducers; β -glycerophosphate, L-ascorbic acid and dexamethasone. In these conditions, AR28 caused a significant ($p < 0.05$) decrease in alkaline phosphatase activity compared to vehicle controls. However, Alizarin Red staining identified small increases in mineralisation with AR28 during early differentiation. AR28 increased mineralisation in basal conditions, which was enhanced by the addition of β -glycerophosphate and L-ascorbic acid. Increases in ALP staining could also be identified in these conditions with AR28 addition. Exposure of MSCs to AR28 for 7 days before osteogenic induction also increased mineralisation. Under adipogenic conditions, AR28 treatments at 0.05 μ M generated significant ($p < 0.05$) reductions in adipogenesis, measured by Oil Red O staining. A 10% reduction in FABP5/BODIPY positive cells was detected with as little as 63.2nM AR28 with a corresponding rescue of proliferation.

Therefore AR28 is a potent activator of canonical Wnt signalling capable of inducing time- and dose-dependent responses. Our findings indicate that potent osteo-inducers like dexamethasone can mask Wnt-dependent responses in vitro, allowing new strategies to dissect the mechanisms controlling Wnt-induced bone formation.

Disclosures: David Cook, None.

This study received funding from: AstraZeneca

SA0240

Vitamin D Metabolism and Action in Human Marrow Stromal Cells: Effects of Chronic Kidney Disease. Shuanhu Zhou*¹, Meryl Leboff¹, Sushrut Waikar², Julie Glowacki¹. ¹Brigham & Women's Hospital, USA, ²Brigham & Women's Hospital, USA

Human marrow stromal cells (hMSCs) are a target of 1,25-dihydroxyvitamin D [1,25(OH)₂D₃] action to promote their differentiation to osteoblasts, but they also participate in vitamin D metabolism by converting 25OHD₃ to 1,25(OH)₂D₃ by the 1 α -hydroxylase (CYP27B1), which we showed to be upregulated by 25OHD₃, IGF-1, and PTH, and downregulated by 1,25(OH)₂D₃ and age (Endocrinol. 151:14, 2010; J Bone Mineral Res 26:1145,2011; Aging Cell 10:962,2011). This supports an autocrine/paracrine role of vitamin D metabolism in osteoblastogenesis of hMSCs, but its clinical significance is unknown. Chronic kidney disease (CKD) is associated with impaired renal biosynthesis of 1,25(OH)₂D, low bone mass, and increased fracture risk. We tested the hypothesis that CKD influences hMSCs' production and responses to 1,25(OH)₂D. Subjects were recruited/enrolled from patients scheduled for arthroplasty for non-inflammatory osteoarthritis. The hMSCs were obtained from tissues discarded during surgery. First, there was a range of estimated glomerular filtration rates (eGFR, 30 to 145 mL/min/1.73 m²), with a significant inverse correlation with age ($r = -0.255$, $p = 0.0033$, $n = 92$). Second, there was a significant positive correlation between *in vitro* osteoblastogenic stimulation (alkaline phosphatase activity) by 1,25(OH)₂D₃ and eGFR ($r = 0.37$, $p = 0.039$, $n = 31$). In addition, we obtained hMSCs from one orthopedic patient who had been undergoing hemodialysis for 2+ years. There was decreased constitutive expression of CYP27B1 and increased CYP24A1 in hMSCs from the dialysis subject, compared with an age/gender-matched control. Nevertheless, osteoblastogenesis was stimulated in hMSCs from both the dialysis and control subjects by 1,25(OH)₂D₃ (10 mM), 25OHD₃ (100 mM), or D₃ (1000 mM); this suggests that 25OHD₃-sufficiency may play an important role in skeletal health in elders and in those with CKD. In summary, hMSCs from subjects with low eGFR and even one receiving hemodialysis synthesize 1,25(OH)₂D. Osteoblastic bone formation in CKD patients may not be optimal unless there is sufficient serum 25OHD substrate for the MSCs to synthesize and respond to local 1,25(OH)₂D.

Disclosures: Shuanhu Zhou, None.

SA0241

Localized Elevation of Cytosolic Free Calcium is Required for Uropod Retraction and Osteoclast Migration. Benjamin Wheal*¹, Natsuko Tanabe², S. Jeffrey Dixon¹, Stephen Sims³. ¹The University of Western Ontario, Canada, ²Nihon University School of Dentistry, Japan, ³The University of Western Ontario, Canada

Osteoclasts are large multinucleated cells responsible for the resorption of bone and other mineralized tissues during physiological remodeling and pathological bone loss. Active osteoclasts are highly motile and alternate between cycles of bone resorption and migration. However, little is known regarding the subcellular mechanisms that regulate osteoclast motility. We hypothesized that changes in the concentration of cytosolic free calcium contribute to the regulation of osteoclast migration. Our purpose was to characterize subcellular changes in cytosolic calcium of osteoclasts and the possible role of calcium in regulating osteoclast motility. Cytosolic calcium was monitored by digital fluorescence imaging of fura-2-loaded osteoclasts using alternating excitation wavelengths of 345 and 380 nm with emission at 510 nm. The pixel-by-pixel ratio of fluorescence intensity at 345/380 nm provided a spatial map of calcium concentration within the cell. Changes in osteoclast morphology were captured by time-lapse microscopy on an inverted phase-contrast microscope coupled to a CCD camera. Migrating osteoclasts exhibited a polarized morphology with lamellipodia extending forward at the leading edge of the cell and the uropod undergoing retraction at the rear, generating net forward movement. Migrating osteoclasts displayed a distinct spatiotemporal pattern of cytosolic calcium that consisted of a localized elevation of calcium in the uropod that lasted for up to 20 minutes and coincided with retraction of the trailing edge. A calcium gradient was observed, increasing from the cell body to the trailing edge with a significant elevation in fluorescence ratio from 0.82 ± 0.03 at the front to 1.26 ± 0.15 at the rear ($n = 6$ osteoclasts). Calcium elevation in the uropod was blocked in osteoclasts loaded with the cytosolic calcium chelator BAPTA. BAPTA-loaded osteoclasts continued to extend lamellipodia but failed to detach from the substrate, giving rise to dramatically elongated, highly branched morphologies. This highly branched morphology was unique to BAPTA-loaded osteoclasts, and the density of branching increased markedly over time. These findings reveal a novel spatiotemporal pattern of cytosolic calcium in osteoclasts, with a localized transitory elevation being required for uropod retraction – a heretofore unrecognized role for subcellular calcium signaling in the regulation of osteoclast migration.

Disclosures: Benjamin Wheal, None.

SA0242

In vitro Generation of Osteoclasts from Interleukin (IL)-3-dependent Mouse Bone Marrow Cells. HUIXIAN HONG*¹, Zhenqi Shi¹, Shunqing Wang², Xu Feng³. ¹UAB, USA, ²Department of Hematology2, First Municipal People's Hospital, Guangzhou Medical College, Guangdong, China, ³University of Alabama at Birmingham, USA

Standard methods for *in vitro* generation of osteoclasts from primary murine bone marrow cells mainly involve the use of either mononuclear cells purified by Ficoll-Hypaque density gradient centrifugations or M-CSF-dependent bone marrow cells prepared by 2- to 3-day M-CSF treatment of whole bone marrow cells. These conventional protocols are sufficient to prepare osteoclasts *in vitro* to investigate the molecular mechanism of osteoclast formation, function and survival, but they are inadequate for studies aimed at elucidating the molecular mechanism controlling differentiation and proliferation of osteoclast precursors or delineating molecular events in early osteoclastogenesis. Here, we describe an alternative method for *in vitro* generation of osteoclasts, which involves the use of interleukin (IL)-3-dependent murine bone marrow cells. Bone marrow cells, isolated from 6- to 8-week old C57BL/6 were cultured in α -MEM containing 10% FBS in tissue culture dishes overnight to remove stromal cells. Then, non-adherent bone marrow cells were harvested and continued in α -MEM containing 10% FBS without (control) or with IL-3 (1 ng/ml) for 6 days. While no cells survived in the control culture after the 6-day culturing, the IL-3-treated culture gave rise to a significant number of surviving cells. These IL-3-dependent cells were capable of differentiating into osteoclasts in response to M-CSF and RANKL stimulation. Moreover, these IL-3-dependent cells can be further expanded by plating them in non-treated plastic dishes followed with M-CSF treatment; they continued to survive and proliferate in non-treated plastic dishes in the presence of M-CSF for up to 4 days. After 4-day M-CSF treatment, these cells can be lifted by EDTA, and were still able to differentiate into osteoclasts upon subsequent stimulation of M-CSF and RANKL. Importantly, we found that IL-3 dependent bone marrow cells can be infected by retrovirus encoding GFP. In conclusion, we have developed a new strategy to generate murine osteoclasts *in vitro* using IL-3-dependent cells prepared by 6-day IL-3 treatment of murine bone marrow cells. A key advantage of this new method is the IL-3-dependent cells can be infected by retrovirus, permitting further experimental manipulations to express or knock down genes in IL-3-dependent cells for studying the molecular mechanism controlling differentiation and proliferation of osteoclast precursors or delineating molecular events in early osteoclastogenesis.

Disclosures: HUIXIAN HONG, None.

SA0243

See Friday Plenary Number FR0243.

SA0244

See Friday Plenary Number FR0244.

SA0245

See Friday Plenary Number FR0245.

SA0246

See Friday Plenary Number FR0246.

SA0247

A Network of Collagen Fibers Supporting Pre-osteoclast Trafficking from the Bone Marrow to the Bone Surface? Thomas Andersen*¹, Helene Kristensen², Jean-Marie Delaisse³. ¹Vejle Hospital, CSFU-IRS, University of Southern Denmark, Denmark, ²Vejle Hospital, Denmark, ³Vejle Hospital, IRS, University of Southern Denmark, Denmark

Differentiation of osteoclast progenitor cells into mononucleated TRAcP+ pre-osteoclasts occurs in the bone marrow. But how are these cells dispatched to the future bone resorption sites? We hypothesized that the collagen type III/I-rich reticulin network of the bone marrow might provide a structural framework for localization and migration of differentiating pre-osteoclasts towards the bone surface.

Therefore, adjacent sections from decalcified paraffin-embedded iliac crest biopsies from 11 human controls were either stained for reticular fibers, or double-immunostained for different combinations of proteins, including collagen type I and III, an endothelial cell marker (CD34), and osteoclast markers (TRAcP, cathepsin K, and OSCAR, a collagen receptor involved in osteoclast differentiation). The association between mononuclear cells positive for osteoclast markers and capillaries or collagen fibers was quantified through histomorphometry, and further analyzed by 3D-reconstructions.

Numerous mononuclear TRAcP+ cells were identified within the bone marrow. These cells showed on average 80% overlap with other osteoclast markers such as cathepsin K and OSCAR, demonstrating that they are pre-osteoclasts. Staining for reticulin, collagen type I, III, and CD34, combined with 3D-reconstructions, revealed collagen III/I-rich reticulin fibers forming a network throughout the bone marrow. These fibers were connected to the capillary network and to bone remodeling compartment canopies, forming a continuum with the collagen present in these structures. Interestingly, combining the latter stainings with staining for TRAcP or OSCAR highlighted the tight association of pre-osteoclasts with these collagen-rich structures. More precisely, double-immunostainings revealed that 93% of the TRAcP+ or OSCAR+ pre-osteoclasts were associated with collagen fibers within the bone marrow. At least 7% of the TRAcP+ or OSCAR+ pre-osteoclasts were associated with the collagen present along larger CD34+ vessels within the bone marrow.

In conclusion, the close association of pre-osteoclasts with the collagen III/I-rich reticulin and capillary networks supports the hypothesis that these linear structures provide a physical support for trafficking of differentiating pre-osteoclast towards the bone remodeling compartment canopies covering bone surfaces undergoing bone remodeling.

*Disclosures: Thomas Andersen, None.***SA0248**

See Friday Plenary Number FR0248.

SA0249

See Friday Plenary Number FR0249.

SA0250

c-Fos Plays an Essential Role in Up-regulation of RANK Expression in Osteoclast Precursors. Atsushi Arai*¹, Toshihide Mizoguchi², Suguru Harada³, Yasuhiro Kobayashi², Yuko Nakamichi⁴, Hisataka Yasuda⁵, Josef M. Penninger⁶, Kazuhiro Yamada², Nobuyuki Udagawa⁴, Naoyuki Takahashi⁷. ¹Matsumoto Dental University, Japan, ²Matsumoto Dental University, Japan, ³Chugai Pharmaceutical Co., Ltd., Japan, ⁴Matsumoto Dental University, Japan, ⁵Oriental Yeast Company, Limited, Japan, ⁶Institute of Molecular Biotechnology of the Austrian Academy of Sciences, Austria, ⁷Matsumoto Dental University, Japan

Purpose: We previously reported that RANK-positive cells were detected as osteoclast precursors in bone tissues in RANKL^{-/-} mice but not in c-Fos^{-/-} mice (J Cell Biol 184:541, 2009). It has been also shown that medullary thymic epithelial cells and intestinal antigen-sampling microfold cells are detected as RANK-positive cells. Then, we examined the role of c-Fos in the up-regulation of RANK expression in osteoclast precursors as well as medullary thymic epithelial cells and intestinal antigen-sampling microfold cells. Methods: Frozen sections of the tibia, spleen, thymus and small intestine were prepared from wild-type (WT) mice, RANKL^{-/-} mice, and c-Fos^{-/-} mice and subjected to immunohistochemistry. Splenic macrophages were prepared from WT and c-Fos^{-/-} mice, and they were cocultured with calvarial osteoblasts. Splenic macrophages were also treated with or without CSF-1. Expression of RANK was examined in those macrophages. Over-expression of c-Fos and that of RANK in c-Fos^{-/-} macrophages were examined for RANK expression and osteoclastic differentiation, respectively. Results and Discussion: (1) RANK-positive cells were similarly distributed in the thymus and intestine in WT, RANKL^{-/-} and c-Fos^{-/-} mice. In contrast, RANK-positive cells were detected in tibiae in WT and RANKL^{-/-} mice but not in c-Fos^{-/-} mice. These results suggest that c-Fos is involved in RANK expression in a cell type-specific manner. (2) CSF-1 receptor (c-Fms)-positive cells were similarly detected in tibiae of WT, RANKL^{-/-}, and c-Fos^{-/-} mice. RANK expression in WT macrophages was up-regulated by coculturing with RANKL^{-/-} osteoblasts as well as WT osteoblasts. The expression of RANK in WT macrophages was increased by the treatment with CSF-1, but not in c-Fos^{-/-} macrophages. These results suggest that CSF-1 but not RANKL expressed by osteoblasts was involved in the up-regulation of RANK expression in osteoclast precursors. (3) The over expression of c-Fos in c-Fos^{-/-} macrophages up-regulated RANK expression. However, the over-expression of RANK in c-Fos^{-/-} macrophages failed to rescue their osteoclastic differentiation potential. Conclusions: c-Fos is a transcription factor essential for osteoclasts differentiation. Our results also suggest that the up-regulation of RANK expression in osteoclast precursors which occurs in bone microenvironment is also tightly regulated by c-Fos-mediated signaling.

*Disclosures: Atsushi Arai, None.***SA0251**

Effect of Dietary Aromatic Amino Acids on Osteoclastic Differentiation. Mona El Refaey*¹, Kehong Ding¹, Qing Zhong², Jianrui Xu¹, Mark Hamrick¹, William Hill³, Xing-Ming Shi¹, Norman Chutkan¹, Monte Hunter¹, Wendy Bollag¹, Karl Insogna⁴, Carlos Isles². ¹Georgia Health Sciences University, USA, ²Medical College of Georgia, USA, ³Georgia Health Sciences University & Charlie Norwood VAMC, USA, ⁴Yale University School of Medicine, USA

Epidemiologic data shows a strong association between low protein intake and fractures in the elderly population. We have previously shown that aromatic amino acid (Phenylalanine, Tyrosine and Tryptophan) supplementation prevented bone loss in aging C57Bl6 mice placed on a low protein diet. Bone histomorphometry and markers of bone turnover demonstrated that a low protein diet suppressed bone formation and increased bone breakdown. In vitro studies with aromatic amino acids showed them to be the most potent in stimulating elevations of intracellular calcium and increases in phospho c-Raf in Bone Marrow Stromal cells (BMSCs). However, we had not previously examined the effect of aromatic amino acids on osteoclastic activity. To assess osteoclastic differentiation we examined the effects of aromatic amino acids on vitronectin, matrix metalloproteinase 9 and calcitonin receptor gene expression. We found that all aromatic amino acids downregulated vitronectin, calcitonin receptor and matrix metalloproteinase gene expression as measured by real time PCR. Taken together our data are consistent with aromatic amino acids stimulating BMSC differentiation down the osteoblastic pathway and at the same time downregulating osteoclastic differentiation by suppressing remodeling gene expression resulting in a net increase in bone mass.

*Disclosures: Mona El Refaey, None.***SA0252**

See Friday Plenary Number FR0252.

SA0253

Hsp90 Inhibitors Enhance Osteoclast Formation *in vitro* in a MITF-dependent Manner through the Induction of Stress Responses. Julian Quinn^{*1}, Ryan Chai², A. Gabrielle J. Van Der Kraan³, Matthew Gillespie¹, John Price². ¹Prince Henry's Institute of Medical Research, Australia, ²Dept of Biochemistry, Monash University, Australia, ³Prince Henry's Institute, Australia

We previously found 17-allylamino-demethoxygeldanamycin (17-AAG; an Hsp90 inhibitor and anti-cancer therapeutic) increased MDA-MB-231 breast cancer invasion of bone in nude mice, and reduced trabecular bone mass in C57black/6 mice. 17-AAG also enhanced osteoclast formation *in vitro* despite the importance of Hsp90 client proteins in osteoclast differentiation. As 17-AAG also induces stress responses via heat shock factor-1 (HSF1), we investigated whether this may underlie osteolytic actions of 17-AAG.

17-AAG and structurally unrelated Hsp90 blockers CCT018159 and NVP-AUY922 dose-dependently enhanced osteoclast formation from bone marrow and RAW264.7 cells and increased Hsp70 protein levels, indicating stress responses. C-terminal Hsp90 blockers novobiocin and coumestrolin caused neither osteoclast enhancement nor Hsp70 induction. We then employed HSF1 ablation to study 17-AAG actions. HSF1 inhibitor KNK437 did not affect RANKL-elicited osteoclast formation but blocked its enhancement by 17-AAG. pGIPZ-lentiviral shRNA knockdown of HSF1 in RAW264.7 cells reduced 17-AAG-enhanced osteoclast formation and Hsp70 levels. 17-AAG also failed to enhance osteoclast formation in RANKL-stimulated bone marrow cells from HSF1^{-/-} (but not littermate HSF1^{+/+}) mice. Overexpression of HSF1 isoforms in RAW264.7 cells by retrovirus did not enhance osteoclast formation, but made cells responsive to lower levels of 17-AAG, suggesting HSF1 is necessary but not sufficient for 17-AAG actions. Stress inducing chemotherapeutic compounds also enhanced osteoclast formation.

To investigate cellular actions of 17-AAG and HSF1 we studied RANKL-elicited intracellular factors. NFκB, p38, c-fos and NFATc1 levels were not enhanced by 17-AAG treatment, and NFκB- and NFAT-responsive luciferase assays showed no enhanced signals with 17-AAG. However, MITF protein levels were greatly enhanced by 17-AAG in RAW264.7 cells; this enhancement was blocked by KNK437. Consistent with this, 17-AAG action on osteoclast formation in RANKL-stimulated bone marrow progenitors was maximal after 3 days of culture, while TGFβ (which enhanced NFATc1 levels and was unaffected by KNK437) enhanced osteoclast formation only when present prior to day 3.

These results indicate Hsp90 blockade that induces an HSF1-dependent stress response enhances osteoclast formation in an NFATc1-independent but MITF-dependent manner. This suggests cell stress itself may enhance osteolysis by increasing progenitor responses to RANKL.

Disclosures: Julian Quinn, None.

SA0254

See Friday Plenary Number FR0254.

SA0255

Rolofylline, an Adenosine A₁R Antagonist, Inhibits Osteoclast Differentiation as an Inverse Agonist. Wenjie He^{*1}, Tuere Wilder², Bruce Cronstein³. ¹New York University Medical Center, USA, ²NYU Medical Center, USA, ³NYU Medical School, USA

Background: Previous work from our laboratory has uncovered a critical role of adenosine A₁ receptor (A₁R) in osteoclastogenesis both *in vivo* and *in vitro*. Adenosine may be generated by hydrolysis of extracellular adenosine nucleotides including CD39, ecto-5'-nucleotidase (CD73) and nucleotide pyrophosphatase phosphodiesterase 1 (NPP-1). Interestingly selective A₁R agonists neither affect basal osteoclast formation nor do they reverse A₁R-mediated inhibition of osteoclast formation. In this study, we determined whether ectonucleotidase-mediated adenosine production was required for osteoclast formation and, when we saw no effect, determined whether the A₁R was constitutively activated and the antagonist was acting as an inverse agonist to mediate its effects on osteoclast formation.

Methods: Osteoclasts were generated from bone marrow mononuclear cells (BMMs) extracted from wildtype, CD39KO, CD73KO and NPP-1KO mice using differentiation factors M-CSF and RANKL. The A₁R specific antagonist, rolofylline, was added to the culture media. TRAP+ staining was performed and Acp5 and Ctsk mRNA expression were examined to study osteoclastogenesis. Intracellular cAMP concentration was determined by ELISA.

Results: A₁R blockade inhibits osteoclast differentiation of BMMs derived from wildtype mice in a dose-dependent manner (IC₅₀=1μM p<0.05, n=3). A₁R blockade similarly inhibits osteoclast formation by BMMs from CD73KO, CD39KO and NPP-1KO mice in a dose-dependent manner (IC₅₀=1μM, 1μM, and 0.1μM, respectively, p<0.05 for all, n=3) for all three knockouts, although baseline osteoclast formation was significantly less (310 in CD73 KO vs 91 in wildtype, p<0.05, n=3) in BMMs from CD73KO mice. Moreover, in the absence of agonist rolofylline (1μM) caused an increase of cAMP content of BMMs by ~8.56 fold (p<0.05, n=3). Similarly, rolofylline (1μM) promotes increased cAMP production in normal human BMMs by ~22.3 fold, which is consistent with our findings that rolofylline inhibits human BMMs-derived osteoclast formation (p<0.001, n=3; IC₅₀=1nM).

Conclusions: Based on these findings we hypothesize that the A₁R is constitutively activated in osteoclast precursors, thereby diminishing basal adenylate cyclase activity, and that the A₁R antagonist acts as an inverse agonist to release the A₁R-mediated inhibition of basal adenylate cyclase activity. The constitutive activity of A₁R promotes osteoclast formation and downregulation of this activity blocks osteoclast formation.

Disclosures: Wenjie He, None.

SA0256

TACE Activity Regulates Osteoclastogenesis and Physiological Bone Remodeling. Kyung-Hyun Park-Min^{*}, Lionel Ivashkiv. Hospital for Special Surgery, USA

Ecotodomain shedding has been shown to be critical for the function of various membrane proteins, including TNF, Notch, and epidermal growth factor receptor (EGFR). TNF-alpha converting enzyme (TACE, also called ADAM17) is the major sheddase of TNF and releases TNF from the cell surface upon various kinds of stimulation. In addition to TNF, TACE plays a role in the shedding of more than 70 different membrane-anchored molecules, some of which are implicated in osteoclastogenesis. Since several targets of TACE are implicated in various disease conditions including rheumatoid arthritis and cancer, TACE inhibitors have been developed for therapeutic uses. However, they have failed due to low efficacy or high side-effects, creating a demand to develop highly specific TACE inhibitors. Therefore, an understanding of disease-specific TACE action will offer a more specific targeting platform for blocking TACE activity. We hypothesize that TACE activity regulates osteoclastogenesis and inflammatory bone lysis. Interestingly, we observed that TACE expression is dynamically regulated in both normal- and disease-conditioned osteoclast precursor cells by RT-qPCR. To test the role of TACE during osteoclast differentiation, we generated mice in which TACE is conditionally deleted in myeloid precursors, including osteoclast precursor cells. *In vitro* osteoclastogenesis in TACE conditional deficient mice (TACE^{ΔM}) showed delayed kinetics compared to that of littermate control mice. However, this difference *in vitro* resulted in a significant *in vivo* change in bone phenotype in TACE^{ΔM} mice. Our data show that TACE activity is required for normal osteoclast differentiation and in maintaining bone homeostasis.

Disclosures: Kyung-Hyun Park-Min, None.

SA0257

TNF and IL-1 Synergistically Promote Osteoclastogenesis in RANKL- and RANK IVVY Motif-dependent Manner. Joel Jules^{*1}, Zhenqi Shi², Monica Lewis³, Xu Feng⁴. ¹University of Miami Miller School of Medicine, USA, ²University of Alabama at Birmingham, USA, ³University of Alabama at Birmingham, USA, ⁴University of Alabama at Birmingham, USA

Tumor necrosis factor-α (TNF) and interleukin-1 (IL-1) are not only elevated in various bone diseases but are also involved in bone loss associated with these disorders. While TNF and IL-1 can enhance osteoclast survival and function, osteoclastogenesis induced by TNF or IL-1 requires the receptor activator of NF-κB (RANK) ligand (RANKL) which activates its receptor RANK. However, it is still unclear whether TNF and IL-1 together can promote osteoclastogenesis in the absence of RANKL. This study seeks to address the combined effect of TNF and IL-1 on osteoclastogenesis in relation to RANKL. We showed that TNF and IL-1 together cannot mediate osteoclastogenesis from bone marrow macrophages (BMMs) in the absence of RANKL. But, they can synergistically promote osteoclastogenesis in the presence of RANKL. Also, TNF and IL-1 can synergistically mediate osteoclastogenesis from BMMs pretreated with RANKL for as short as 18 hours. Moreover, TNF and IL-1 can still induce osteoclastogenesis synergistically 2 days after the 18-hour RANKL priming. RANK has a specific cytoplasmic motif (IVVY) which plays a critical role in osteoclastogenesis by committing BMMs to osteoclast lineage. To determine if the RANK IVVY is required for osteoclastogenesis synergistically induced by TNF and IL-1, we prepared BMMs expressing a chimeric receptor consisting of the external domain of human Fas linked to mouse RANK cytoplasmic domain (Ch1) or mouse RANK with mutated IVVY motif (Ch2). These chimeric receptors can be specifically activated by a human Fas activating antibody (hFas-AB). TNF and IL-1 can synergistically promote osteoclastogenesis from BMMs expressing Ch1 in the presence of hFas-AB, but their ability to induce osteoclastogenesis from Ch2-expressing BMMs in the presence of hFas-AB is dramatically impaired. Importantly, this finding was further recapitulated with BMMs from knockin mice bearing inactivating mutations in the IVVY motif and those from wild-type control mice. Taken together, our data indicate that TNF and IL-1 can synergistically mediate osteoclastogenesis in the presence of RANKL, and the IVVY motif is crucially required for osteoclastogenesis synergistically induced by TNF and IL-1. Significantly, these findings have revealed new insights into the regulatory mechanism of TNF and IL-1 in osteoclast biology and also support the notion that the IVVY motif has the potential to serve as a promising therapeutic target for bone loss in many bone disorders.

Disclosures: Joel Jules, None.

SA0258

Tspan4 Co-localizes with $\beta 3$ Integrin and Is Required for Osteoclast Differentiation. Loise Salles*¹, Jonah Saltzman¹, Leslie Morse², Li Zhang¹, Prateek Jha¹, Ricardo Battaglini³. ¹The Forsyth institute, USA, ²Harvard Medical School, USA, ³The Forsyth Institute, USA

The fusion of mononuclear precursors to form multinucleated cells is an essential event for osteoclast differentiation and activation. However, the molecular mechanisms involved in this process are not completely understood. In order to better understand the molecular basis of osteoclast fusion we conducted a microarray screening aimed at identifying genes specifically upregulated during the late stages of RANKL-stimulated RAW 264.7 differentiation, a time when cells begin to fuse to one another to form multinucleated osteoclasts. We identified a Tetraspanin (Tspan) family member, Tspan 4, whose expression was upregulated during the later stages of RANKL-induced osteoclast differentiation. Tetraspanins are a family of transmembrane proteins that have been shown to mediate cell fusion. In addition, members of the Tspan family can associate with other tetraspanins, with integrins and with members of the immunoglobulin superfamily of cell adhesion molecules and signaling receptors to form tetraspanin microdomains (TEMs) on the cell surface. Finally, Tspan 4 has been shown to form complexes with both $\alpha 3 \beta 1$ and $\alpha 6 \beta 1$ integrin in several cell types, but the function of these complexes remains unknown. We performed confocal microscopy analysis of differentiated osteoclasts and observed Tspan 4 and $\beta 3$ integrin co-localization to the osteoclast plasma membrane. Addition of a neutralizing human specific anti-Tspan 4 antibody significantly inhibited RANKL-induced formation of TRAP+ osteoclasts. Tspan 4 mRNA silencing in RAW 264.7 mouse monocytes had the same inhibitory effect. Accordingly, qPCR analysis of mRNA from RANKL-stimulated Tspan 4-silenced cells showed a significant reduction in the expression of Tspan 4 as well as osteoclast markers TRAP, Cathepsin K, mmp-9 and src. Conversely, overexpression of Tspan 4 in RAW 264.7 cells enhanced RANKL induced osteoclast formation. In summary, we show that Tspan 4 is upregulated during RANKL induced osteoclast differentiation. Also, we show that Tspan 4 co-localizes with $\beta 3$ integrin on the osteoclast membrane. Functional studies show that Tspan 4 is required for normal osteoclastogenesis, potentially through its interaction with $\beta 3$ integrin. Our results also suggest that Tspan 4 may be a novel therapeutic target for osteoporosis and other osteolytic diseases

Disclosures: *Loise Salles, None.*

SA0259

Anti-Resorptive Agent Modulates Mucosal Barrier Immunity of the Oral Cavity in Mouse ONJ Models. Sil Park*¹, Davood T. Quje², Ichiro Nishimura³. ¹UCLA, School of Dentistry, USA, ²UCLA, Weintraub Center, USA, ³University of California, Los Angeles, USA

Statement of problem: Anti-resorptive agents have predictably been used to treat multiple myeloma, bone metastatic cancer and osteoporosis. In spite of different pharmacological mechanisms, these drugs appear to induce abnormal responses in the oral environment and in some cases result in osteonecrosis of the jaw (ONJ). ONJ involves abnormalities of oral mucosa tissue, which is known to be one of the most efficient barrier tissues. We have hypothesized that ONJ occurs where the injury-induced mucosal barrier immunity is modulated by anti-resorptive agents.

Object: The objectives of this study were to test this hypothesis in mouse bisphosphonate-related ONJ model and to evaluate the involvement of gamma delta T cells in the pathogenesis of BRONJ using T cell receptor delta null (TCRD^{-/-}) mice.

Material and method: Female wild type and TCRD^{-/-} mice with the C57Bl6 background were treated by intravenous (retro-orbital) injection of zoledronic acid (ZOL: 540.5ug/kg; the metabolic scale equivalent dose of Reclast®) and extraction of maxillary left first molar. Control wild type mice were injected with vehicle solution and underwent the molar extraction. At 1 week and 4 weeks of tooth extraction, whole blood, maxilla, femurs, skin and intestine were harvested. The development of ONJ was determined by clinical and histological examination at week 4. Bone remodeling was characterized by serum chemistry and micro-CT analyses of maxilla and femur. Gamma delta T cells in the barrier tissues were evaluated by immunohistology.

Result: ZOL group showed the highest prevalence of BRONJ (83%) and the largest necrotic bone area, which were decreased in TCRD^{-/-} group (50%) and Control (12.3%). The anti-resorptive effect of ZOL in wild type and TCRD^{-/-} mice were equivalent at the tooth extraction site of maxilla and the distal trabecular bone of femurs. The infiltration or activation of gamma delta T cells in the barrier tissues appeared to increase by the ZOL treatment.

Conclusion: The BRONJ mouse model was established with single dose of bisphosphonate injection and dental extraction without any additional systemic alterations. The prevalence and the severity of BRONJ were decreased under the absence of gamma delta T cell. This study may suggest that stressed osteoclasts by anti-resorptive agent may abnormally modulate the oral mucosa barrier-derived cytotoxic immunity involving gamma delta T cells. This study was supported by the Investigator Initiated Studies Program (IISP-38619) of Merck & Co.

Disclosures: *Sil Park, None.*

This study received funding from: Merck & Co

SA0260

See Friday Plenary Number FR0260.

SA0261

See Friday Plenary Number FR0261.

SA0262

Importance of Proteolytic Degradation of Osteoprotegerin by Lysine-specific Gingipain in Periodontal Osteoclastogenesis. Yoichi Miyamoto¹, Masamichi Takami¹, Kentaro Yoshimura¹, Kazuyoshi Baba², Atsushi Yamada³, Ryutaru Kamijo¹, Toshifumi Maruyama¹, Kenji Mishima², Marie Hoshino², Rika Yasuhara², Tomohito Akiyama*⁴. ¹Showa University School of Dentistry, Japan, ²showa univ., Japan, ³Showa University School of Dentistry, Japan, ⁴Showa University School of Dentistry, JAPAN, Japan

Periodontitis is a chronic inflammatory disease accompanied by alveolar bone resorption by osteoclasts. Among subgingival microflora, *Porphyromonas gingivalis* is regarded as a potent etiological agent for periodontitis. *P. gingivalis* secretes the cysteine proteases called gingipains, which are classified by their cleavage site specificities, i.e., arginine-specific gingipains (HRgpA and RgpB) and lysine-specific gingipain (Kgp). While it is well known that gingipains are involved in exacerbation of periodontitis, their role in osteolysis had not been fully elucidated. We found previously that Kgp degraded osteoprotegerin (OPG), an osteoclastogenesis-inhibitory factor secreted by osteoblasts, and suppressed osteoclast differentiation induced by active vitamin D and various Toll-like receptor (TLR) ligands *in vitro* (Biochem J 419:159-166, 2009). Osteoclast differentiation is induced not only by calcium-regulating hormones and TLR ligands but also by various cytokines such as TNF α , IL-1b, and IL-17A especially in inflammatory situations including periodontitis. In this study, we investigated the effects of Kgp on osteoclast differentiation induced by these proinflammatory cytokines *in vitro*. In the co-culture system of mouse calvarial osteoblasts and bone marrow cells, differentiation of osteoclasts was induced by TNF α , IL-1b, or IL-17A in the presence or absence of Kgp. Kgp augmented the osteoclast differentiation induced by TNF α and IL-1b. On the other hand, Kgp did not enhance the osteoclast differentiation induced by IL-17A. Proteolytic degradation of these cytokines by Kgp in a cell-free system was compared with that of OPG. TNF α and IL-1b were less susceptible, but IL-17A was more susceptible to the degradation by Kgp than OPG. These results indicate that the enhancing effect of Kgp on inflammatory cytokine-induced osteoclast differentiation is dependent on the difference in the degradation efficiencies of each cytokine and OPG. Then we investigated the cleavage sites in OPG after treatment with Kgp. N-Terminal amino acid sequences of OPG fragments revealed that Kgp primarily cleaved OPG in its death domain resemble region, which might prevent dimer formation of OPG required for inhibition of RANKL. Collectively, it is suggested that degradation of OPG by Kgp is a crucial event in the osteoclastogenesis and development of bone loss in periodontitis.

Disclosures: *Tomohito Akiyama, None.*

SA0263

See Friday Plenary Number FR0263.

SA0264

Prevention of Wear Particle-induced Osteolysis by a Novel V-ATPase Inhibitor Saliphenylhalamide (SaliPhe) through Inhibition of Osteoclast Maturation and Bone Resorption. An Qin*¹, Taksum Cheng², Zhen Lin³, Lei Cao⁴, Shek Chim⁵, Nathan Pavlos⁶, Jiaki Xu⁷, Kerong Dai⁴, Ming Hao Zheng⁶. ¹School of Surgery, The University of Western Australia, Australia, ²University of Western Australia, Australia, ³Centre for Orthopaedic Research, School of Surgery, The University of Western Australia, Western Australia, Australia, ⁴Department of Orthopaedics, Ninth People's Hospital, Shanghai Jiao Tong University School of Medicine, Shanghai, P.R. China, China, ⁵School of Pathology & Laboratory Medicine, The University of Western Australia, Western Australia, Australia, ⁶University of Western Australia, Australia, ⁷University of Western Australia, Australia

Wear particle-induced peri-implant loosening (aseptic prosthetic loosening) is one of the most common causes of total joint arthroplasty. It is well established that extensive bone destruction (osteolysis) by osteoclasts is responsible for wear particle-induced peri-implant loosening. Thus, inhibition of osteoclastic bone resorption should prevent wear particle induced osteolysis and may serve as a potential therapeutic avenue for prosthetic loosening. Here, we demonstrate for the first time that saliphenylhalamide, a new V-ATPase inhibitor attenuates wear particle-induced

osteolysis in a mouse calvarial model. In vitro biochemical and morphological assays revealed that the inhibition of osteolysis is partially attributed to a disruption in osteoclast acidification and polarization, both a prerequisite for osteoclast bone resorption. Interestingly, the V-ATPase inhibitor also impaired osteoclast differentiation via the inhibition of RANKL-induced NF- κ B and ERK signaling pathways. In conclusion, we showed that saliphenylhalamide affected multiple physiological processes including osteoclast differentiation, acidification and polarization, leading to inhibition of osteoclast bone resorption in vitro and wear particle-induced osteolysis in vivo. The results of the study provide proof that the new generation V-ATPase inhibitors, such as saliphenylhalamide, are potential anti-resorptive agents for treatment of peri-implant osteolysis.

Disclosures: An Qin, None.

SA0265

Rosiglitazone Affects Osteoclast Activity in Type 2 Diabetes Mellitus. Shivani Agarwal^{*1}, Mishaela Rubin², Sanil Manavalan¹, Donald McMahon³, Antonio Nino⁴, Lorraine Fitzpatrick⁴, John Bilezikian³. ¹Columbia University, USA, ²Columbia University, USA, ³Columbia University College of Physicians & Surgeons, USA, ⁴GlaxoSmithKline Pharmaceuticals, USA

Rosiglitazone (RSG), a PPAR- activator, is associated with an increased risk of fractures in postmenopausal women with Type 2 Diabetes Mellitus (T2D), yet the mechanism for this is not well understood. Circulating osteogenic precursor (COP) cells, which contribute to bone formation, have been characterized in the peripheral circulation using flow cytometry and antibodies against osteocalcin (OCN) and early stem cell marker. Previously, we found that alterations in COP cells were present in patients treated with RSG as compared to metformin (MET), with an increase in the sub-populations of mature osteogenic cells. We hypothesized that circulating osteoclastic cells would also be affected by RSG as compared to MET.

73 subjects were randomized to RSG or MET for 52 weeks followed by an open-label period of 24 weeks of MET alone for all subjects. Osteoclast activity was measured in peripheral blood mononuclear cells by performing cell sorting for CD34+ cells, which give rise to hematopoietic stem cells and then assaying for TRAP-5b levels. We found that TRAP-5b levels in circulating sorted CD34+ cells increased between weeks 0 and 52 in both groups (RSG: 1.0 ± 3 to 10.8 ± 5 U/L; $p=0.035$; MET: 1.0 ± 3 to 13.4 ± 6 U/L, $p=0.007$). When all subjects were changed to MET, TRAP-5b levels increased further in the initial RSG group (to 23.6 ± 5 U/L, $p=0.05$ vs wk 52), but did not rise further in MET (9.7 ± 4 U/L, $p=NS$ vs wk 52) with continued MET. These data suggest that circulating osteoclast precursor cell activity increases with both RSG and MET. Contrary to our expectations, the increase was similar in both treatment groups. However, the additional increase in the RSG group after the first year, when changed to MET, suggests an initial MET-specific effect which may wane over time. It is therefore possible that RSG not only increases fracture risk by accelerating COP maturity, but by increasing osteoclast activity beyond the time of administration of the drug. Further studies of lineage allocation and bone remodeling will help to shed light on the negative impact of RSG on bone.

Disclosures: Shivani Agarwal, None.

This study received funding from: GlaxoSmithKline

SA0266

Overexpression of DRG2 Results in Increased Number and Activity of Osteoclast. Hye-Seon Choi^{*1}, Ke Ke², JW Park². ¹University of Ulsan, South Korea, ²University of Ulsan, South Korea

Small GTPases are key regulators of the actin cytoskeleton of osteoclast (OC), playing multiple roles in OC, although their functions have not been clearly defined. Developmentally regulated GTP-binding protein 2 (DRG2) is a new member of GTP-binding protein family, suggesting a possible role in OC. The role of DRG2 in bone remodeling has been examined using DRG2-transgenic (TG) mice. Overexpression of DRG2 increased OC caused increased fusion and survival of OC and elevated bone resorption on dentine slices in vitro. Mature OC from DRG2-TG mice increased large OC with actin ring by fortified M-CSF signaling via enhancing activation of ERK, Akt, c-Src, Rac1 and Rho, compared with that from wild type mice. DRG2 may form a network that generates the increased bone loss, especially associated with high level of M-CSF.

This work was supported by a KHIDI Grant (A111295), KRF Grants (BRL 2009-0087350;2010-0002644) funded by the Korean government

Disclosures: Hye-Seon Choi, None.

SA0267

Plasma Membrane Ca²⁺-ATPase-mediated Calcium Efflux Controls Osteoclast Differentiation and Survival. Youngkyun Lee^{*1}, Hyung Joon Kim², Hong-Hee Kim². ¹Kyungpook National University School of Dentistry, South Korea, ²Seoul National University, South Korea

The precise regulation of Ca²⁺ dynamics is crucial for proper differentiation and function of osteoclasts. While Ca²⁺ oscillation induced by receptor activator of NF- κ B ligand in osteoclast precursors is indispensable for osteoclastogenesis, Ca²⁺ oscillation gradually disappears in mature osteoclasts. Whereas PLC γ and IP₃ receptor have been linked to the initiation of Ca²⁺ oscillation, molecules involved in the termination of Ca²⁺ oscillation remain unidentified. In the present report, we identified expression of plasma membrane Ca²⁺ ATPase (PMCA) to be greatly increased during osteoclastogenesis. We also show that PMCA is an intrinsic negative regulator of Ca²⁺ oscillation during osteoclast differentiation. RNA interference (RNAi) studies that transiently eliminate (or knockdown) PMCA expression, as well as inhibition of PMCA using antagonists reveal significant increases in Ca²⁺ oscillation during osteoclastogenesis, both in vitro and in vivo. Interestingly, overexpression of PMCA impaired Ca²⁺ oscillation and osteoclast differentiation. The increased expression of PMCA in mature osteoclasts played an additional role in preventing osteoclast apoptosis in the face of massive Ca²⁺ entry. Thus, our results propose an updated model of Ca²⁺ dynamics during osteoclast differentiation and maturation.

Disclosures: Youngkyun Lee, None.

SA0268

See Friday Plenary Number FR0268.

SA0269

The Role of the Akt/GSK3beta/NFATc1 Axis during Osteoclastogenesis. Jang Bae Moon¹, Jung Ha Kim¹, Nacksung Kim^{*2}. ¹Chonnam National University Medical School, South Korea, ²Chonnam National University Medical School, South Korea

RANKL induces osteoclast differentiation through activation of various signaling pathways such as NF- κ B and Akt. Although the PI3K/Akt pathway has been shown to be important for osteoclastogenesis, however, the molecular events involved in osteoclast differentiation have not been revealed. Herein, we demonstrate that Akt induces osteoclast differentiation of through regulating the GSK3beta/NFATc1 signaling cascade. Inhibition of the PI3K by LY294002 reduces formation of osteoclasts and attenuates the expression of NFATc1, but not that of c-Fos. Conversely, overexpression of Akt in bone marrow-derived macrophages (BMMs) strongly induced NFATc1 expression without affecting c-Fos expression, suggesting that PI3K/Akt-mediated NFATc1 induction is independent of c-Fos during RANKL-induced osteoclastogenesis. In addition, we found that overexpression of Akt enhances formation of an inactive form of GSK3beta (phospho-GSK3beta) and nuclear localization of NFATc1, and that overexpression of a constitutively active form of GSK3beta attenuates osteoclast formation through down-regulation of NFATc1. Furthermore, BMMs from SHIP knockout mice show the increased expression levels of phospho-Akt and phospho-GSK3beta, as well as the enhanced osteoclastogenesis, compared to WT. However, overexpression of a constitutively active form of GSK3beta attenuates RANKL-induced osteoclast differentiation from SHIP-deficient BMMs. Taken together, our data suggest that the PI3K/Akt/GSK3beta/NFATc1 signaling axis plays an important role in RANKL-induced osteoclastogenesis.

Disclosures: Nacksung Kim, None.

SA0270

Changes in Gene Expression and Transcription Factor Binding Patterns in Response to 1,25-Dihydroxyvitamin D₃ and PTH During IDG-SW3 Osteocyte Progression. Hillary St John^{*1}, Kathleen Bishop², Alex Carlson², Nancy Benkusky², Mark Meyer², Lynda Bonewald³, J. Pike². ¹UW Madison, USA, ²University of Wisconsin-Madison, USA, ³University of Missouri - Kansas City, USA

Osteocytes are derived from osteoblast precursors through a process that involves the progressive secretion and mineralization of osteoid and the formation of a lacunar space occupied by individual osteocytes. Entombed cells play complex roles in bone remodeling; in bone formation and resorption under a variety of dietary, mechanical and physiologic stimuli; and in mineral homeostasis through the secretion of hormones such as FGF23 that control phosphate metabolism. Both the differentiation and mature cell function of the osteocyte are regulated by a number of systemic hormones that include 1,25(OH)₂D₃ and PTH, as well as numerous growth factors and inflammatory cytokines; the target genes and the molecular mechanisms that underlie these processes are not well defined. In the current study, we employed the mouse osteocytic IDG-SW3 cell line to explore cellular responses to both

1,25(OH)₂D₃ and PTH during the 35 day (d) program of differentiation from the cell's origin as an osteoblast to its final state as a mineralized, osteoid-surrounded osteocyte. RNA from cells treated 24 hr earlier with either vehicle, 1,25(OH)₂D₃ or PTH was isolated on d3 (osteoblastic), d14 (early osteocyte) and d35 (late osteocyte) and then subjected to direct candidate-specific qRT-PCR analysis and/or to RNA-sequencing analysis. Genome-wide ChIP-seq analysis was also conducted at these time points to correlate transcription factor activity with genes regulated by these hormones. Many genes were modulated in response to 1,25(OH)₂D₃ and/or PTH at each stage of differentiation: d3 (e.g., VDR, PTHR1, MEIS2), d14 (e.g., RUNX1) and d35 (e.g., FGF23, SOST, RANKL). With regard to 1,25(OH)₂D₃, GO term analysis of global RNA-seq results indicate that these networks include those characterized by ossification, apoptosis, vasculature development, and immune response. ChIP-seq analysis of the VDR/RXR cistromes revealed extensive overlap, as expected, and confirmed the location of 1,25(OH)₂D₃-regulated enhancers at multiple genes previously identified, including those at the VDR, RANKL, and SPP1 genes and at many additional genes as well. Most of these sites to which the VDR bound colocalized with sites containing RUNX2, C/EBPβ and/or p300. Determination of the transcriptome for PTH response and the cistrome for its CREB DNA binding factor is ongoing. These studies provide new insight into the complex and diverse actions of both 1,25(OH)₂D₃ and PTH during osteocyte differentiation.

Disclosures: Hillary St John, None.

SA0271

See Friday Plenary Number FR0271.

SA0272

See Friday Plenary Number FR0272.

SA0273

See Friday Plenary Number FR0273.

SA0274

Sclerostin Stimulation of Osteocytic Osteolysis Involves Expression of Carbonic Anhydrase II. Masakazu Kogawa¹, Asiri Wijanavaka¹, Renee Ormsby¹, Lynda Bonewald², David Findlay³, Gerald Atkins³. ¹University of Adelaide, Australia, ²University of Missouri - Kansas City, USA, ³University of Adelaide, Australia

Sclerostin (SCL) is a product of mature osteocytes embedded in mineralised bone and is a negative regulator of bone mass and osteoblast differentiation. Pre-osteocytes and osteocytes have been identified as cellular targets for SCL, and SCL by targeting these cells is an anti-anabolic agent.⁽¹⁾ SCL may also have a catabolic action through promotion of osteoclast formation and activity by osteocytes, in a RANKL-dependent manner.⁽²⁾ While osteocytes have been reported to have resorptive activity during lactation,⁽³⁾ a role for SCL in osteocytic osteolysis has not been described. To test whether SCL has direct catabolic activity via the osteocyte itself, we examined the effect of recombinant human SCL (rhSCL) on bone resorptive marker gene expression in cultures of both human primary pre-osteocytes and the mouse osteocyte-like cell line, MLO-Y4. We found that rhSCL stimulated the mRNA expression of carbonic anhydrase II (CA2), an enzyme that generates protons. rhSCL also clearly increased CA2 protein expression analysed by western blotting and immunofluorescence. Consistent with this, treatment with rhSCL significantly lowered intracellular pH (pHi) in both cell types and a similar trend was observed for extracellular pH (pHo). To investigate whether SCL-induced acidification resulted in decalcification and degradation of bone, mineralised cultures of human osteocyte-like cells were treated with rhSCL. Media from cells treated with SCL had higher total calcium concentrations compared to untreated cells; this effect was reversed with the CA inhibitor, acetazolamide (AZ). To investigate the specific importance of CA2 for the effect of SCL on osteocytes, we knocked down CA2 expression in MLO-Y4 cells using siRNA. rhSCL reduced the pHo in scramble-siRNA transfected controls but had no effect on pHo in CA2 siRNA transfected cells. AZ also abolished this activity of rhSCL. Treatment with rhSCL also resulted in a significant increase in extracellular ionised calcium levels, an effect blocked using AZ in control cells but not in CA2 siRNA transfected cells. Taken together, these results show that SCL stimulates CA2 expression in osteocyte-like cells, resulting in acidification of extracellular media and calcium release from a bone-like matrix. We conclude that SCL may have a direct catabolic action via the induction of osteocytic osteolysis.

1. Atkins GJ et al. Sclerostin is a locally acting regulator of late-osteoblast/preosteocyte differentiation and regulates mineralization through a MEPE-ASARM-dependent mechanism. *J Bone Miner Res*26:1425-1436.

2. Wijanavaka AR et al. 2011 Sclerostin Stimulates Osteocyte Support of Osteoclast Activity by a RANKL-Dependent Pathway. *PLoS One*6:e25900.

3. Qing H, et al. 2012 Demonstration of osteocytic perilacunar/canalicular remodeling in mice during lactation. *J Bone Miner Res*In Press.

Disclosures: Masakazu Kogawa, None.

SA0275

Live Imaging of Fluid Flow-induced Ca²⁺ Signaling of Osteoblasts and Osteocytes in Bone: Implications for Gap Junctional Intercellular Communication. Yoshihito Ishihara^{*1}, Yasuyo Sugawara², Hiroshi Kamioka³, Noriaki Kawanabe⁴, Keiji Naruse⁵, Takashi Yamashiro⁵. ¹Okayama University, Department of Orthodontics, Japan, ²Okayama University Graduate School of Medicine, Dentistry, & Pharmaceutical Sc, Japan, ³Okayama University Graduate School of Medicine, Dentistry, & Pharmaceutical Sc, Japan, ⁴Okayama University Hospital, Japan, ⁵Okayama University Graduate School of Medicine, Dentistry, & Pharmaceutical Sciences, Japan

Bone cells respond to mechanical stimuli by producing a variety of biological signals, and one of the earliest events is intracellular calcium ([Ca²⁺]_i) mobilization. Our recently developed *ex vivo* live [Ca²⁺]_i imaging system revealed that bone cells in intact bone explants showed autonomous [Ca²⁺]_i oscillations, and osteocytes specifically modulated these oscillations through gap junctions. However, the behavior and connectivity of the [Ca²⁺]_i signaling networks in mechanotransduction have not been investigated in intact bone. We herein introduce a novel fluid-flow platform for probing cellular signaling networks in live intact bone, which allows the application of capillary-driven flow just on the bone explant surface while performing real-time fluorogenic monitoring of the [Ca²⁺]_i changes. In response to the flow, the percentage of responsive cells was increased in both osteoblasts and osteocytes, together with upregulation of *c-fos* expression in the explants. However, enhancement of the peak relative fluorescence intensity was not evident. Treatment with 18 α-GA, a reversible inhibitor of gap junctional intercellular communication, significantly blocked the [Ca²⁺]_i responsiveness in osteocytes without exerting any major effect in osteoblasts. On the contrary, such treatment significantly decreased the flow-activated oscillatory response frequency in both osteoblasts and osteocytes. These findings indicated that flow-induced mechanical stimuli accompanied the activation of the autonomous [Ca²⁺]_i oscillations in both osteoblasts and osteocytes via gap junction-mediated cell-cell communication. Although how the bone sense the mechanical stimuli *in vivo* still needs to be elucidated, the present study suggests that cell-cell signaling via augmented gap junction-mediated [Ca²⁺]_i mobilization could be involved as an early signaling event in mechanotransduction.

Disclosures: Yoshihito Ishihara, None.

SA0276

Genetic Variants in GPR177 and LRP5 may be Association with Risk of Lumbar Spine Fracture. Lee O'Brien^{*1}, Haojun Ouyang², John Krege³, Jared Kohler⁴. ¹Lilly, USA, ²Eli Lilly & Company, USA, ³Eli Lilly & Company, USA, ⁴Biostat Solutions, Inc, USA

A genetic biomarker that can predict osteoporotic fracture risk with a high sensitivity and specificity would be clinically valuable. The goal of this study was to associate genetic variants in genes from the Wnt and RANK pathways with vertebral fracture risk, using 1111 Caucasian subjects from a carefully phenotyped cohort. Postmenopausal women with osteoporosis from the MORE trial (NCT00670319) were radiographically assessed at baseline using a visual semiquantitative scale and the semiquantitative scores for T4 to L4 were summed to generate a spinal deformity index (SDI). The SDI at baseline was assessed as an ordinal categorical variable (binned scores were 0, 1-3, 4-6, >6) using ordinal logistic regression; the model included covariate adjustments for baseline bone mineral density (BMD), age and genotype as fixed effects. GPR177 is an evolutionarily conserved transmembrane protein necessary for Wnt protein secretion, and variants in this gene have previously been associated with BMD with genome-wide significance. 14/142 variants genotyped in GPR177 were associated with SDI score. The SDI odds ratio for having two copies of the rare allele (10.5% in the genetic cohort) for rs6671127 was 0.50-0.56 (CI's 0.33-0.86, unadjusted p = 0.0063), meaning two copies of the rare allele may be protective from vertebral fracture. 16/54 variants in LRP5 may also be associated with SDI scores. The SDI odds ratio for having two copies of the minor allele (11.1% in the genetic cohort) for rs671191 was 1.68-1.90 (CI's 1.15-2.76, unadjusted p = 0.0038), meaning two copies of the rare allele may be associated with risk of vertebral fracture. One of the LRP5 variants, rs638051, may be associated with lumbar spine and femoral neck BMD (unpublished results). These findings suggest there may be value in investigating the genetic determinants of fracture in carefully phenotyped clinical trial patients and that variants of genes in the Wnt and RANK pathways might be associated with risk of vertebral fractures. Additional research including replication of these findings is required.

*Disclosures: Lee O'Brien, Eli Lilly and Company, 3
This study received funding from: Eli Lilly and Company*

SA0277**Skeletal Responsiveness to Cold Exposure: Implications for Age-Related Osteoporosis.** Casey Doucette*¹, Katherine Motyl¹, Clifford Rosen².¹Maine Medical Center Research Institute, USA, ²Maine Medical Center, USA

The sympathetic nervous system (SNS) regulates homeostatic systems including the skeleton such that activation can cause bone loss. Cold exposure is a potent stimulus for SNS activation and, in turn, an inducer of brown-like adipose tissue (BAT). In this study, we hypothesized that acute cold exposure stimulates inducible BAT in fat depots including the marrow but negatively impacts bone. To explore the role of cold exposure, we capitalized on skeletal differences between C3H/HeJ (C3H) and C57BL/6J (B6), as well as mice with a global knockout of the cold receptor (*Trpm8*^{-/-}). Male C3H mice have higher bone density and greater marrow adipose tissue (MAT) than B6. In addition, C3H mice have seasonal changes in MAT by MRI with a peak in the fall months. We studied whole bone gene expression in 6-month-old C3H and B6 male mice at 23°C and at 4°C for 6 hours. At 23°C, expression levels of *Runx2* were higher in C3H mice (1.6 fold, $p < 0.03$), consistent with earlier findings that C3H has higher bone formation. With acute cold challenge, expression of *Runx2* was decreased in C3H by 50% but was unchanged in B6. *Rankl* mRNA levels did not differ by genotype or cold exposure, but adiponectin mRNA was 2x greater in C3H at 23°C than B6. *Ucp1* transcripts were approximately 100x higher at 23°C ($p = 0.0003$) in C3H and rose further (250x, $p = 0.0007$) with cold exposure vs B6 which did not change at 4°C. *Pgc1 α* mRNA did not differ by strain at 23°C and did not increase in B6 but rose 8x in C3H at 4°C ($p = 0.0005$), suggesting that C3H marrow has thermogenic properties. *Pdk4* and *Fabp4* expression levels were also increased with cold exposure in both C3H and B6 ($p < 0.05$). Interestingly, *Adrb2* expression was higher in C3H vs B6 at 23°C, but at 4°C there was a significant increase only in B6 ($p < 0.05$). Next, we phenotyped *Trpm8*^{-/-} mice at 16 weeks. These mice lack the cold receptor globally, have reduced SNS tone, and are more susceptible to diet-induced obesity. We found slightly higher femoral areal BMD in *Trpm8*^{-/-} vs +/+ ($p < 0.08$) and significantly higher femoral %BV/TV in *Trpm8*^{-/-} (4.5%) vs +/+ (3.2%, $p = 0.04$) due to greater trabecular thickness ($p = 0.01$). Taken together, these results indicate that activation of sympathetically-mediated pathways of thermogenesis via the cold receptor affect bone mass in a strain-dependent manner. Changes in ambient temperature in the elderly may contribute to age-related bone loss. NIH AG040217, NIDDK092759

Disclosures: Casey Doucette, None.

SA0278

See Friday Plenary Number FR0278.

SA0279**Plasma Sphingosine 1-phosphate Levels and Risk of Vertebral Fracture in Postmenopausal Women.** Seung Hun Lee*¹, Beom-Jun Kim², Jung-Min Koh², Sun-Young Lee³, Young-Sun Lee⁴, Kyeong-Hye Lim⁵, Tae-Ho Kim⁶, Shin-Yoon Kim⁷, Ghi-Su Kim⁵.¹Asan Medical Center, University of Ulsan College of Medicine, South Korea, ²Asan Medical Center, South Korea, ³Asan Institute for Life Sciences, South Korea, ⁴Asan Institute for Life Sciences, South Korea, ⁵Division of Endocrinology & Metabolism, Asan Medical Center, University of Ulsan College of Medicine, South Korea, ⁶Kyungpook National University School of Medicine, South Korea, ⁷Kyungpook National University Hospital, South Korea

Background: Although sphingosine 1-phosphate (S1P) can play diverse roles in bone metabolism, the main effect seems to augment bone resorption. To investigate the possibility of S1P as a predictor for the risk of osteoporotic vertebral fractures (VFs), we performed a case-control study in postmenopausal Korean women.

Methods: Among 460 women not taking any drug and not having any disease that could affect bone metabolism, we could find 69 cases defined as subjects with radiological VFs. The controls were randomly selected from the remaining 391 subjects and matched 1:1 to cases on age and body mass index. Lateral thoracolumbar radiographs, bone mineral density (BMD), bone turnover markers, and plasma S1P levels were obtained from all subjects.

Results: S1P levels were markedly higher in subjects with VF ($7.49 \pm 3.44 \mu\text{mol/L}$) than those without VF ($5.58 \pm 2.01 \mu\text{mol/L}$; $P = 0.001$), and increased in a dose-response manner across increasing number of VF (P for trend < 0.001), even after adjustment for lumbar spine BMD as well as potential confounders. The odds ratios (ORs) for VF were marked higher in subjects in the highest S1P quartile category compared with those in the lowest S1P quartile category after adjustment for confounders (OR = 9.33, 95% CI = 2.68 – 32.49). S1P levels were inversely correlated with BMD at various sites ($P = 0.015$ to 0.044), whereas they had positive correlation with bone resorption markers ($P = 0.016$ to 0.098). **Conclusion:** These findings suggest that plasma S1P may be a potential biomarker for the risk of VFs, independent of BMD, in postmenopausal women.

Disclosures: Seung Hun Lee, None.

SA0280

See Friday Plenary Number FR0280.

SA0281

See Friday Plenary Number FR0281.

SA0282**Bone Microstructure Analysis of Femoral Head in Osteoporosis: Ex vivo HR-pQCT Study.** Ko Chiba*¹, Andrew Burghardt², Makoto Osaki³, Sharmila Majumdar². ¹Nagasaki University Hospital, Japan, ²University of California, San Francisco, USA, ³Nagasaki University, Japan

Purpose: High Resolution peripheral Quantitative CT (HR-pQCT) is a clinical high-resolution CT for peripheral skeletal sites. It is also useful as an experimental CT which can image intact bone specimens with a high spatial resolution (41 μm), sufficient to analyze trabecular bone microstructure. We imaged the femoral heads extracted from osteoporosis (OP) patients using HR-pQCT, to investigate regional differences of bone microstructure and the correlation between the OP progression and bone microstructure.

Method: Femoral heads specimens extracted from 15 OP patients with femoral neck fracture (average 85, 67-94 y.o. all female) were scanned using HR-pQCT (XtremeCT, Scanco medical) with a 41 μm voxel size. The image orientation of all femoral heads was adjusted by anatomical landmarks. The femoral head was divided into 3 longitudinal regions (superior, center, and inferior), and then 5 axial subregions (center, medial, lateral, anterior, posterior) for a total of 15 regions. Fracture regions were excluded with a 2.5 mm margin from the fracture line. As a result, 5 regions were excluded from the analysis. Thus, in 10 regions (Sup-Cen, Sup-Med, Sup-Lat, Sup-Ant, Sup-Post, Cen-Cen, Cen-Med, Cen-Ant, Cen-Post, and Inf-Med) cancellous bone microstructure was measured (TRI/3D-BON, Ratoc System Engineering, Japan). Microstructural parameters were compared between regions, and correlations between bone volume fraction and microstructural parameters were analyzed.

Results: In Sup-Cen, Sup-Post, and Cen-Cen, bone volume fraction, trabecular thickness, and trabecular number were greater, with a plate-like structure, higher connectivity, and higher anisotropy. The plate-like bone was oriented supero-inferiorly and antero-posteriorly. As bone volume fraction decreased, trabecular thickness and number decreased, with more rod-like structure, less connectivity, and higher anisotropy.

Discussion: Inhomogeneous bone microstructure in the femoral head may be derived from the weight bearing pattern in the hip joint. At Cen-Ant and Cen-Post regions, where a fixation screw is sometimes inserted erroneously, bone volume fraction was almost half of Cen-Cen region. Supero-inferior plate-like structure at central regions might be due to vertical weight bearing. In addition, daily hip flex-extension movements might cause its antero-posterior structural alignment. With the increasing severity of OP, this plate-like structure changed to rod-like structure with a loss of connectivity. Loss of horizontal connectivity and the preservation of vertical trabeculae are likely reflected by the increase anisotropy.

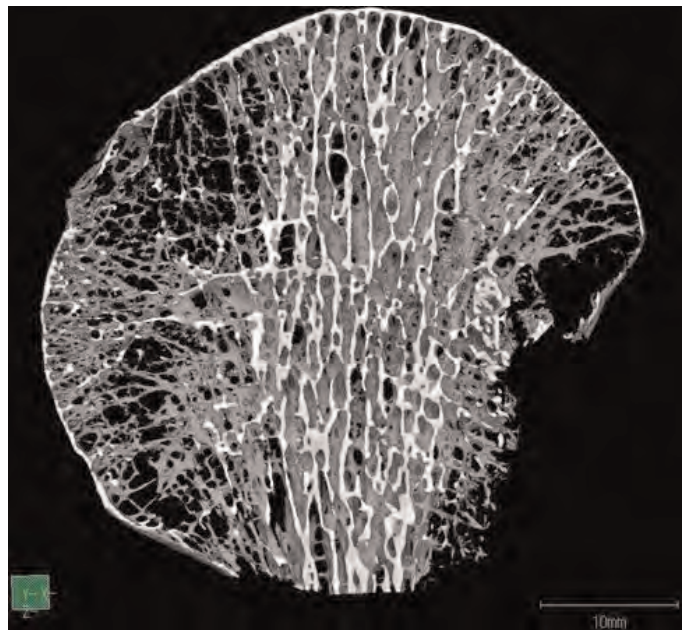


Fig.1

Disclosures: Ko Chiba, None.

SA0283

SNPs in 3'UTR RANK Gene Determine Site-Specific Low Trauma Fractures Independently of Bone Mineral Density. Natalia Garcia-Giralto¹, Guy Yoskovitz¹, Daniel Prieto-alhambra², Maria Rodriguez-Sanz³, Roser Urreizti⁴, Daniel Grinberg⁵, Robert Güerri⁶, Leonardo Mellibovsky⁷, Xavier Nogues⁸, Susana Balcells⁹, Adolfo Diez-Perez¹⁰. ¹IMIM, Spain, ²Institut Municipal D'Investigació Mèdica, United Kingdom, ³IMIM-Parc de salut Mar, Spain, ⁴Departament de genètica, Universitat de Barcelona, Spain, ⁵The University of Barcelona, Spain, ⁶Hospital Universitario Del Mar.Institut Municipal D'Investigació Mèdica, Spain, ⁷Internal medicine, Parc de salut Mar, Spain, ⁸Institut Municipal D'Investigació Mèdica, Spain, ⁹University of Barcelona, Spain, ¹⁰Parc De Salut Mar, Spain

Introduction: Bone remodelling is regulated by the RANK/RANKL/OPG system. Hence, this system would be involved in the determination of bone mineral density (BMD) and/or bone microarchitecture. In the light of the raise of miRNAs as epigenetic regulatory elements, we studied SNPs in the *RANK* 3'UTR region, which may affect miRNAs binding; secondly, we tested for an interaction between these and a previously defined BMD-related RANKL SNP (rs9594738).

Methods: Seven genetic variants were genotyped in the BARCOS cohort, and multivariable regression models were fitted to assess the association between the genotyped SNPs and both BMD and fractures.

Results: None of genotyped SNPs were significantly associated with either femoral neck or lumbar spine BMD. Two SNPs were significantly associated with clinical fractures in our cohort but even stronger evidence for an association was found when these were related to either spine or wrist/forearm fractures separately: SNP1 appeared associated with wrist/forearm fractures (Log-additive OR 3.12, (95%CI 1.69-5.75); $p = 7.16 \times 10^{-4}$), while SNP2 was related to spine fractures (Recessive OR 4.05 (1.59-10.35); $p = 8.24 \times 10^{-3}$). These associations stood for Bonferroni correction, and remained significant after further adjustment for BMD. Finally, interaction analyses between RANKL SNP rs9594738 and SNP1 on fracture produced significant results ($p = 0.039$). Accordingly, an analysis of the effect of compound genotypes of rs9594738 and SNP1 was carried out, which pointed towards increasing fracture prevalence in subjects with a higher number of unfavourable alleles, with corresponding adjusted OR 2.76 (1.30-5.81; $p = 0.007$) and OR 5.14 (1.37-15.67; $p = 0.007$) for 2 and ≥ 3 unfavourable alleles respectively compared to none/1.

In conclusion, two genetic variants in 3'UTR of RANK gene predispose to low trauma fracture in a site-dependent manner. Although this fracture association was independent of BMD, an interaction with the BMD-associated RANKL SNP rs9594738 suggests an additive effect of BMD and bone strength.

Disclosures: *Natalia Garcia-Giralto, None.*

SA0284

Space Radiation-Induced Bone Loss - Radiation Quality Response In Mice. Laura Bowman¹, Eric W. Livingston², Gregory A. Nelson³, Ted Bateman⁴. ¹University of North Carolina at Chapel Hill, USA, ²University of North Carolina at Chapel Hill, USA, ³Loma Linda University, USA, ⁴University of North Carolina, USA

Astronauts on exploratory missions will be exposed to a mixture of radiation types from solar and cosmic sources. We have shown that spaceflight relevant doses and types of radiation may cause bone loss in excess to what is already lost due to microgravity. While protons account for the majority of space radiation fluence, particles with high linear energy transfer (LET, a measure of radiation quality) are predicted to have a greater relative biological effectiveness (RBE), causing more damage. We examined bone loss of modeled space radiation representing a range of LET (protons, oxygen, silicon and iron). **Methods:** Twenty-week-old, female BALBc mice were assigned to one of four ion types: 150 MeV/amu Protons (LET = 0.6 keV/μm), 600 MeV/amu ¹⁶O (LET = 15 keV/μm), 600 MeV/amu ²⁸Si (LET = 51 keV/μm), and 600 MeV/amu ⁵⁶Fe (LET = 181 keV/μm). They were then subdivided into either irradiated (IRR) or non-irradiated (NR) groups within each ion type (n=24/group, different NR group for each ion). Irradiated animals were exposed to 50 cGy of whole body irradiation of the appropriate ion type at the NASA Space Radiation Laboratory (NSRL) at Brookhaven National Laboratory. Animals were then shipped to the University of North Carolina where they were maintained until euthanasia 14 days after irradiation. Tibiae were harvested for analysis of trabecular microarchitecture using micro-computed tomography (μCT, SCANCO Medical μCT-80). **Results:** Significant changes ($p < 0.05$) in bone trabecular volume (BV/TV) and volumetric bone mineral density (vBMD) occurred in oxygen (BV/TV, -11.1%; vBMD, -9.6%), silicon (BV/TV, -21.8%; vBMD, -18.3%) and iron (BV/TV, -11.4%; vBMD, -10.1%) irradiated groups. Connectivity density (Conn.D) and trabecular number (Tb.N) were also significant for both silicon (Conn.D, -22.6%; Tb.N, -6.4%) and iron (Conn.D, -20.1%; Tb.N, -5.2%). Silicon was the only radiation type to cause a change in trabecular thickness (Tb.Th, -4.9%) and iron caused the only change in trabecular separation (Tb.Sp, +6.1%). Proton was the only radiation type for which no significant changes were observed. **Conclusions:** Skeletal effects were observed following exposure to all ion types except proton and the changes were greatest with silicon ions. It appears LET is important in predicting the deterioration of trabecular bone and further studies should be performed with radiation species with an LET between 50 and 180 keV/μm.

Disclosures: *Laura Bowman, None.*

SA0285

Higher Strontium Consumption is Anabolic in Goats. Zhiqiang Xu¹, Dahai Gu², Zhenhui Cao², Xiaobo Chen², Hua Rong³, Guozhou Liao⁴, Qichao Huang³, Xi Zhang⁵, Shizheng Gao⁶, Qiuye Lin³, Changrong Ge⁷, Junjing Jia⁸, Wei Yao⁸. ¹Yunnan Agricultural University, China, Peoples Republic of China, ²Yunnan Provincial Key Laboratory of Animal Nutrition & Feed, Yunnan Agricultural University, China, ³Yunnan Provincial Key Laboratory of Animal Nutrition & Feed, Yunnan Agricultural University, China, ⁴Yunnan Provincial Key Laboratory of Animal Nutrition & Feed, Yunnan Agricultural University, China, ⁵Yunnan Agricultural University, Peoples Republic of China, ⁶Yunnan Provincial Key Laboratory of Animal Nutrition & Feed, Yunnan Agricultural University, China, ⁷Yunnan Agricultural University, China, Peoples Republic of China, ⁸University of California, Davis Medical Center, USA

Previous studies have reported that strontium (Sr+) plays an important role in regulating bone remodeling, and has been used as a newly drug for the treatment in osteoporosis. In 2006, our research group discovered a special goat group in a closed village (Dongshan Village) in Mile County of Yunnan Province. These goats have bright red bone including teeth and therefore are named as "red-boned goats". We performed some preliminary studies in these goats and found they had 3 folds higher strontium content and significant low calcium content in their cortical bone. The circulating alkaline phosphatase (ALP) levels were 2-fold higher than the aged-matched regular goats. The aim of study is to investigate how environmental Sr+ composition would alter bone metabolism.

Method: We collected soil, water and nature pastures samples from the Dongshan Village, in where are red-boned goats grazing. The control samples were collected from three different counties, in where are normal bone goats grazing area. Mineral compositions were measured by inductively coupled plasma mass spectrometry. Six-month-old red-boned lambs (n=10) were fed in Dongshan Village with nature pasture grazing (group I). Ten other age-matched red-boned lambs were transported to other goat farm and fed with normal pasture (group II). Total experimental period was one year. Serum ALP and bone-specific alkaline phosphatase (BSAP) were measured at 6, 12 and 18 months and femur mineral compositions were measured at 18 months.

Results: The samples of soil, water and nature pasture from Dongshan Village showed around 2-4 fold higher strontium and calcium concentration than other samples from normal bone goats grazing area. The red-boned goats in group I showed significantly higher serum ALP concentrations at three time points, and significantly higher BSAP concentrations at 6 and 12 months. Moreover, red-boned goats showed 3 fold higher strontium contents and low calcium contents in the femur at 18 months compare to group II and Control. It is interesting to note that the bone redness have dispersed from group II. There were no significant differences for serum ALP, BALP concentrations, strontium and calcium contents in the femur between group II and Control.

Conclusion and implication: Environmental strontium consumption could alter bone metabolism significantly. Higher Sr+ consumption had an anabolic action on bone.

Disclosures: *Zhiqiang Xu, None.*

SA0286

Iron Overload and Radiation Exposure Cause Oxidative Damage and Reduce Bone Density. Evelyn Yuen¹, Jennifer Morgan², Sara Zwart³, Estela Gonzalez¹, Kaleigh Camp⁴, Brandon Macias⁵, Scott Smith⁶, Susan Bloomfield⁴. ¹Texas A&M University, USA, ²ORAU, USA, ³USRA, USA, ⁴Texas A&M University, USA, ⁵Texas A&M University, USA, ⁶Wyle/nasa Jsc, USA

Astronauts on long duration space flight missions to the moon or mars are exposed to increased iron (Fe) stores and galactic cosmic radiation, both of which independently induce oxidative stress. There is growing evidence that links oxidative stress to bone loss with aging and estrogen deficiency. We hypothesized that iron overload (induced by feeding a high Fe diet) and γ radiation exposure would independently increase markers of oxidative stress and result in loss of bone mass, with the combined treatment having additive or synergistic effects.

Male Sprague-Dawley rats (3-mo-old, n=32) were randomized to receive an adequate (45 mg Fe/kg diet) or high (650 mg Fe/kg diet) Fe diet for 4 weeks and either 3 Gy (8 fractions, 0.375 Gy each) of ¹³⁷Cs radiation (γ RAD) or sham exposure every other day for 16 days starting on day 14. Serum Fe and catalase and liver Fe and glutathione peroxidase (GPX) were assessed by standard techniques. Immunostaining for 8-hydroxy-2-deoxyguanosine (8OHdG, marker of DNA adducts) quantified number of cells with oxidative damage in cortical bone. *Ex vivo* pQCT quantified volumetric bone mineral density (vBMD); bone mechanical strength (ultimate load) was assessed by 3-pt bending (midshaft tibia) and compression of the femoral neck.

High Fe diet increased serum catalase 31%, liver Fe 20%, and liver GPX 17%; high Fe diet and γ RAD increased serum Fe 20% and 25%, respectively. Preliminary data show Fe diet and γ RAD increased number of osteocytes with extensive 8OHdG staining (24% and 33%, respectively), with the combined treatment exhibiting 26% of osteocytes positively stained. γ RAD and high Fe diet lowered proximal tibial cancellous vBMD (by -15% and -12%, respectively); high Fe diet produced a small decrease in femoral neck total vBMD (-4%, $p = 0.07$). Cortical vBMD at midshaft tibia

was lower after high Fe diet, but not after γ RAD. Higher serum Fe levels were associated with lower proximal tibial cancellous vBMD ($r = -0.61$); higher liver GPX was associated with lower proximal tibial cancellous vBMD ($r = -0.60$); higher serum catalase was associated with lower vBMD at the 3 different bone sites ($r = -0.52$). No significant differences in ultimate load at mid-shaft tibia or femoral neck were detected.

High dietary iron and fractionated γ RAD cause oxidative damage in bone and are associated with decreases in bone density.

Disclosures: Evelyn Yuen, None.

This study received funding from: NASA Human Research Program and NSBRI via NASA NCC9-588

SA0287

Effect of Glucocorticoid Treatment on Wnt Signaling Antagonists (sclerostin and Dkk-1) and their Relationship to Bone Turnover and Bone Mass. Lai Gifre¹, Pilar Peris², Silvia Ruiz-Gaspà³, Ana Monegal⁴, Benet Nomdedeu⁵, Nuria Guanabens⁶. ¹Hospital Clinic Barcelona, Spain, ²Hospital Clínic of Barcelona, Spain, ³CIBERhed, Hospital Clinic of Barcelona, Spain, ⁴Rheumatology Department, Hospital Clinic of Barcelona, Spain, ⁵Hematology Department, Hospital Clinic of Barcelona, Spain, ⁶Universitat De Barcelona, Spain

Wnt-b-catenin signaling and its antagonists (sclerostin and Dkk-1) play an important role in the regulation of bone mass and osteoblastogenesis. Glucocorticoid (GCC) treatment is a well known factor related to decreased bone formation and osteoporosis development. Therefore, the aim of this study was to analyze the effect of GCC treatment on Wnt signaling antagonists (sclerostin and Dkk-1) and their relationship to bone mass and bone turnover.

Methods: Patients with recent initiation of GCC treatment were prospectively included (≥ 7.5 mg/day and ≤ 6 months on GCC treatment). Patients with associated metabolic bone diseases or on antiosteoporotic treatment were excluded. Bone turnover markers (Bone formation: PINP, bone AP; Bone resorption: CTx), Wnt antagonists (serum sclerostin and Dkk-1, determined by ELISA, Biomedica Gruppe, Austria) and bone mineral density (BMD) were assessed in all patients. The results were compared with 20 healthy individuals of similar age and sex.

Results: 21 patients (11M/10F) with a mean age of 48 ± 20 yrs and a mean GCC daily dose of 66 ± 16 mg/day were prospectively included. Idiopathic thrombocytopenic purpura (76%) and hemolytic anemia (14%) were the most frequent associated conditions. Patients on GCC treatment showed a significant decrease in bone formation compared to controls (PINP: 20 ± 9 vs. 48 ± 19 ng/ml, $p=0.001$) and an increase in bone resorption (CTx: 0.60 ± 0.23 vs. 0.35 ± 0.1 ng/mL, $p=0.006$); 20% had densitometric osteoporosis. Patients on GCC had decreased Dkk-1 levels compared to controls (31.1 ± 28.6 vs. 51.5 ± 18.2 pmol/L, $p=0.013$) with a trend to higher sclerostin values (38.6 ± 21.2 vs. 29.8 ± 13.4 pmol/L, $p=0.119$). Sclerostin levels correlated positively with GCC doses ($r=0.511$, $p=0.018$) and lumbar BMD ($r=0.573$, $p=0.008$), and negatively with bone AP ($r=-0.476$, $p=0.034$). Dkk-1 levels correlated positively with total BMD ($r=0.533$, $p=0.016$).

Conclusion: The effect of GCC treatment on the serum levels of the Wnt signaling parameters differs depending on the antagonist evaluated. Dkk-1 levels were decreased shortly after the initiation of GCC therapy whereas sclerostin values tended to increase and showed a relationship to the dose of GCC and bone formation parameters. Long-term evaluation of these parameters in this process as well as their relationship to bone turnover and bone mass evolution is clearly indicated.

Disclosures: Lai Gifre, None.

SA0288

See Friday Plenary Number FR0288.

SA0289

See Friday Plenary Number FR0289.

SA0290

See Friday Plenary Number FR0290.

SA0291

See Friday Plenary Number FR0291.

SA0292

A New Protective Function of Nell-1 Against Osteoporosis by Activation of Wnt/ β -Catenin Signaling. Aaron James^{*1}, Jia Shen¹, Mari Kim², Xinli Zhang¹, Khoi Le², Alan Nguyen², Todd Rackohn², Greg Asatrian², Donna Soffer², Cymbeline Culiati², John Adams¹, Kang Ting¹, Chia Soo². ¹University of California, Los Angeles, USA, ²University of California, Los Angeles, USA

Introduction: NELL-1 is a secreted differentiation factor, first identified to have osteogenic properties by its overexpression in human craniosynostosis. We recently described an osteoporotic phenotype of *Nell-1* haploinsufficient mice (ASBMR, 2011). While skeletally normal during development, senile *Nell-1* haploinsufficient mice manifest osteoporotic bone loss with age, with a reduction in bone-formation and concomitant increase in bone-resorption.

Methods: This study expands on this association between NELL-1 and bone maintenance. First, bone marrow mesenchymal stem cells (BMSCs) and hematopoietic stem cells (HSCs) were isolated from both wildtype and *Nell-1* haploinsufficient mice. Osteogenic differentiation or bone resorption assays were performed with BMSCs and HSCs, respectively, in the presence or absence of added recombinant NELL-1. Similar studies were performed with human BMSCs, derived from both osteoporotic and non-osteoporotic donors, assaying the effects of NELL-1 on Wnt/ β -catenin signaling.

Results: *Nell-1*^{+/-} BMSCs showed a significant reduction ($p < 0.037-0.007$) in markers of osteogenic differentiation, including alkaline phosphatase staining, Alizarin red accumulation in bone nodules and gene markers of osteogenesis (*Runx2*, *Opn*, *Ocn*). In contrast, *Nell-1*^{+/-} HSCs showed a significant increase ($p < 0.0013$) in uncoupled bone resorption, including quantification of Toluidine Blue staining, resorption 'roughness' as measured by SEM and an increase in mean resorption pit depth. These metrics of formation and resorption were all reversed by conditioning cells with recombinant NELL-1. NELL-1 dose-dependently and significantly ($p < 0.039-0.007$) increased osteogenesis and reduced bone resorption ($p < 0.026-0.0001$) in wildtype mouse BMSCs and HSCs, respectively. In human BMSCs, NELL-1-induced-osteogenesis was associated with a significant increase ($p < 0.002$) in Wnt/ β -catenin signaling. These data suggest that interaction of NELL-1 with the cellular precursors of osteoblasts and osteoclasts leads to a net increase in bone formation.

Conclusions: This study now confirms the dual roles of NELL-1 as both pro-osteogenic and anti-resorptive in bone. This new finding suggests that NELL-1 protein or *Nell-1* pathway manipulation may potentially be a future local or systematic agent for the treatment of osteoporosis.

Disclosures: Aaron James, None.

This study received funding from: CIRM, NIH/NIDCR, UC Discovery Grant

SA0293

See Friday Plenary Number FR0293.

SA0294

See Friday Plenary Number FR0294.

SA0295

Effects of Aging on Bone Turnover Markers and Bone Density Regulating Hormones in Rats. Rana Samadfam^{*}, Susan Y. Smith. Charles River Laboratories, Canada

Baseline values for bone turnover markers and hormones regulating bone density, including parathyroid hormone (PTH) and 1,25-dihydroxyvitamin D3 (VD3) in rats can vary significantly depending on diet, kit manufacturers, rat strain, time of sample collection, and/or gender. The aim of this study was to investigate the effect of aging on bone turnover markers and hormones in female and male rats of the same strain using the same time of sample collection, kit manufacturer for each analyzed parameter, and fed the same diet. Sprague Dawley rats from Charles River were fed certified rodent diet 5002. Serum and urine samples were collected from females at Months 2, 3, 7, 9, 10, 12, 13 and/or 14 for measurement of bone formation markers (total alkaline phosphatase, osteocalcin and/or PINP), PTH and/or VD3, and urinary and serum bone resorption markers (C telopeptide (CTx) and Deoxyypyridinolin (DPD)). Serum and urine was collected for males at Months 2, 3, 5, 9 and 12 for bone resorption and bone formation markers. Serum was collected from fasted animals in the morning and urine was collected overnight. Although the same manufacturers were used for each kit, the lot number was different depending on availability. The analyses for each parameter were carried out on separate occasions, months or years apart. In addition to bone turnover markers and hormones, selected serum biochemistry parameters were also evaluated. Osteocalcin and total ALP (surrogate bone formation marker) decreased with age with the sharpest declines between 2 to 6

months. Similar decreases were also noted for the bone resorption markers. PTH levels did not decline with age, however, decreases were noted for VD3. Aging had no effect on serum calcium levels, although a trend for a decline was noted for serum phosphorous. In general, the bone turnover markers and VD3 levels were higher in males compared to females, consistent with the greater bodyweight and size. In conclusion by eliminating variables the age-related decreases in serum and urinary bone turnover markers, serum phosphorous and VD3 were clearly noted for Sprague Dawley rats.

Disclosures: Rana Samadfam, Charles River, 3

This study received funding from: We are employee of Charles River

SA0296

Patients with Low-Energy Distal Radius Fracture Have Similar Bone Strength of the Femoral Neck Compared to Healthy Individuals, but Some Deviation in the Levels of Biochemical Markers of Bone Turnover. Shigeharu Uchiyama¹, Shota Ikegami², Mikio Kamimura³, Toshihiko Imaeda⁴, Kiichi Nonaka⁵, Hirovuki Kato². ¹Shinshu University, School of Medicine, Japan, ²Department of Orthopaedic Surgery, Shinshu University, School of Medicine, Japan, ³Kamimura Clinic, Japan, ⁴Department of Food & Nutritional Environment, College of Human Life & Environment, Kinjo Gakuin University, Japan, ⁵Elk Corporation, Japan

Introduction: Low-energy distal radius fracture occurs relatively earlier in life than other osteoporotic fractures, and patients with these fractures are considered to be at high risk for hip fractures. Although osteoporotic treatment for such patients is highly recommend, routine DXA examinations show that they do not always have low bone mineral density (BMD). We hypothesized that compared with age-matched healthy controls, patients with such fractures should have some risk factors for hip fractures, other than DXA-derived BMD of the proximal femur.

Methods: We enrolled 31 female patients (average age, 71 years) with a history of low-energy distal radius fracture and 82 age-matched healthy postmenopausal women without any history of fracture (controls). The BMD of the femoral neck was obtained using DXA. Data regarding geometrical parameters (hip axis length, femoral neck width, cross-sectional area, and cortical thickness), biomechanical indices (cross-sectional moment of inertia, section modulus, and buckling ratio), and bone mineral density of the femoral neck were obtained using quantitative CT and were analyzed using the Mindways QCT-PRO BIT software. The levels of biochemical markers and hormones associated with bone metabolism were compared between the patients and controls by using an unpaired t-test or Mann-Whitney U test, depending on data distribution.

Results: No significant differences were observed in the geometrical parameters and biomechanical indices between the 2 groups. DXA-derived BMD of the proximal femur; serum and urinary levels of pentosidine; and the bone alkaline phosphatase, osteocalcin, homocysteine, parathyroid hormone, and 1,25-(OH)₂ vitamin D levels did not significantly differ between the 2 groups. The patients had significantly lower serum 25-(OH) vitamin D levels, higher deoxypyridinoline levels, or lower trabecular bone mineral density (derived from quantitative CT) of the total proximal femur than the controls (p < 0.05) (Table).

Discussion: The bone strength of the femoral neck in patients with low-energy distal radius fractures may not differ much from age-matched healthy individuals. From the known risk factors for hip fracture, abnormal results for 25-(OH) vitamin D and urine deoxypyridinoline are more important risk factors for hip fractures in patients with distal radius fracture. To develop effective strategies for preventing hip fractures in such patients, further studies are required to clarify whether addressing these risk factors would be effective in such cases.

| | Fracture n=31 | Control n=82 | p value |
|---|---------------|---------------|-------------|
| Age (yrs) | 71.4 (8.4) | 72.0 (6.4) | 0.669 |
| Height (cm)/Weight (kg) | 151.9 / 52.3 | 152.9/51.5 | 0.432/0.595 |
| DXA | | | |
| Spine BMD (g/cm ²) | 0.906 (0.187) | 0.954 (0.170) | 0.192 |
| Spine T-score | -1.7 (1.57) | -1.25 (1.37) | 0.139 |
| Total Hip BMD (g/cm ²) | 0.739 (0.111) | 0.762 (0.128) | 0.381 |
| Total Hip T-score | -1.55 (0.98) | -1.35 (1.02) | 0.347 |
| FN BMD (g/cm ²) | 0.677 (0.112) | 0.696 (0.125) | 0.469 |
| FN T-score | -1.76 (0.92) | -1.58 (0.94) | 0.365 |
| Quantitative CT | | | |
| Total Hip Total Bone BMD (g/cm ²) | 0.639 (0.109) | 0.68 (0.123) | 0.105 |
| Total Hip Total Bone BMD (mg/cm ³) | 239 (40) | 251 (45) | 0.197 |
| Total Hip Cortical Bone BMD (g/cm ²) | 0.376 (0.09) | 0.400 (0.10) | 0.251 |
| Total Hip Cortical Bone BMD (mg/cm ³) | 1085 (129) | 1043 (197) | 0.084 |
| Total Hip Trabecular Bone BMD (g/cm ²) | 0.262 (0.03) | 0.280 (0.04) | 0.024 |
| Total Hip Trabecular Bone BMD (mg/cm ³) | 114 (18) | 122 (20) | 0.079 |
| FN Cross Sectional Area (cm ²) | 8.2 (1.0) | 8.4 (1.1) | 0.421 |
| FN Cross Sectional Moment of Inertia (cm ⁴) | 1.10 (0.28) | 1.14 (0.27) | 0.4 |
| FN Section Modulus (cm ³) | 0.82 (0.18) | 0.84 (0.15) | 0.477 |
| FN Cortical Thickness (mm) | 2.0 (0.7) | 2.1 (0.8) | 0.31 |
| FN Buckling Ratio | 9.9 (3.6) | 9.5 (5.2) | 0.256 |
| FN angle (degrees) | 43 (5) | 42 (5) | 0.124 |
| FN width (mm) | 27 (2) | 28 (3) | 0.456 |
| Hip Axis length (mm) | 106.0 (16.2) | 108.2 (6.3) | 0.299 |
| Serum | | | |
| Bone Alkaline Phosphatase (µg/L) | 15.2 (5.0) | 16.3 (5.5) | 0.131 |
| TRACP-5b (mU/dL) | 405 (167) | 409 (148) | 0.801 |
| Osteocalcin (ng/mL) | 6.4 (2.7) | 7.1 (2.0) | 0.1 |
| undercarboxylated Osteocalcin (ng/mL) | 4.1 (4.9) | 4.4 (2.4) | 0.52 |
| Pentosidine (µg/mL) | 0.033 (0.027) | 0.025 (0.01) | 0.298 |
| whole Parathyroid Hormone (pg/mL) | 28.7 (12.4) | 27.1 (12.5) | 0.246 |
| 1,25(OH) ₂ Vitamin D (pg/mL) | 64.5 (24.7) | 61.4 (15.3) | 0.53 |
| 25(OH)Vitamin D (ng/mL) | 18.7 (6.2) | 22.2 (6.3) | 0.011 |
| Homocystein (nmol/mL) | 8.5 (2.2) | 8.5 (2.7) | 0.783 |
| Urine | | | |
| NTx (nmolBCE/nmol.CRE) | 44.2 (22.1) | 42.8 (18.2) | 0.856 |
| Deoxypyridinoline (nmol/mmol.CRE) | 7.1 (2.4) | 5.8 (2.3) | 0.001 |
| Pentosidine (µg/mg.CRE) | 0.063 (0.097) | 0.038 (0.045) | 0.724 |

FN;femoral neck, BMD;bone mineral density.

Table

Disclosures: Shigeharu Uchiyama, None.

SA0297

See Friday Plenary Number FR0297.

SA0298

See Friday Plenary Number FR0298.

SA0299

Short-Term Effects of Anti-Catabolic and Anabolic Treatments on Bone Turnover Markers in Ovariectomized Rats. Jukka Morkko*, ZhiQi Peng, Katja Fagerlund, Mari Suominen, Jukka Rissanen, Jussi Halleen. Pharmatest Services Ltd, Finland

Short-term effects on bone turnover markers predict long-term effects on bone parameters such as bone mineral density in clinical studies and osteoporosis animal models. We have studied short-term effects of anti-catabolic and anabolic treatments on markers of bone resorption and formation in the rat ovariectomy (OVX) model. Study groups included a sham-operated group receiving vehicle, an OVX group receiving vehicle, and OVX groups receiving *s.c.* injections of 10 µg/kg/d 17β-estradiol (E2), 10 µg/kg/d alendronate (ALN), 10 µg/kg/wk zoledronate (ZOL) and 40 µg/kg/d human (1-34) parathyroid hormone (PTH). Each group contained 12 animals that were 3 months of age at the time of the operations. Dosing was started the next day after OVX and continued for 2 weeks. Procollagen I N-terminal propeptide (PINP), N-terminal mid-fragment of osteocalcin (OC), C-terminal cross-linked telopeptides of type I collagen (CTX), and tartrate-resistant acid phosphatase 5b (TRACP 5b) were determined in serum before the start of treatment and at 2 weeks. Uterine weight was decreased by OVX, demonstrating that the operations were performed successfully. OVX increased PINP values by 110%, OC values by 21% and CTX values by 49% (all with p<0.001), and decreased TRACP 5b values by 26% (p<0.01). PINP values increased 22% by PTH (not significant, ns) and decreased 72% by E2 (p<0.001), 21%

by ALN (ns) and 9% by ZOL (ns). OC values increased 29% by PTH and decreased 20% by E2, 17% by ALN and 23% by ZOL (all with $p < 0.001$). CTX values increased 5-8% by PTH, ALN and ZOL (all ns) and decreased 33% by E2 ($p < 0.001$). TRACP 5b values increased 10% by E2 (ns) and decreased 25% by PTH, 38% by ALN and 54% by ZOL (all with $p < 0.001$). We conclude that all markers showed the expected results caused by OVX and treatment by E2. Although serum CTX is a sensitive marker for monitoring efficacy of bisphosphonate treatment in clinical studies, it did not show significant effects on ALN and ZOL treatments in the rat OVX model. On the contrary, TRACP 5b showed similar significant responses to ALN and ZOL treatments as in clinical studies. Although PINP was the most sensitive marker for detecting changes by OVX and treatment by E2, it did not show significant results on PTH, ALN and ZOL treatments in this study performed in young animals. Although the changes in OC were relatively small, OC was the only marker that demonstrated significant effects on all tested therapies.

Disclosures: Jukka Morko, Pharmatest Services Ltd, 3

SA0300

Bone Shock Absorbance (BSA) Complements DXA BMD for More Accurate Discrimination of Elderly Women with and without Arm and Wrist Fractures.

Nelson Watts*¹, David Ralph², Diane Busch-James², Cyndy Cox³, Ron Schultheis², Amit Bhattacharya³. ¹Mercy Health Osteoporosis & Bone Health Services, USA, ²OsteoDynamics, USA, ³University of Cincinnati, USA

Bone Shock Absorbance (BSA) is a noninvasive and painless diagnostic technology being developed to complement dual-energy x-ray absorptiometry (DXA) determinations of bone mineral density (BMD) for more accurate evaluation of osteoporotic fracture risk. The output of a BSA test is a bone "damping value".

Arm and wrist fractures are a common type of major osteoporosis-related fragility fractures in elderly women. We report on the results of a study of 73 ambulatory white women ages 65 to 80; 30 had suffered an arm or wrist fracture in the previous 2 years (fracture cases) and 43 had no fracture at any site within 15 years (controls). The mean ages (SD) of the fracture cases and controls were 71.5 (4.2) and 71.0 (4.1) respectively. All had DXA BMD and BSA damping value determinations. DXA BMD values were evaluated as T-scores. The mean (SD) T-score at the femoral neck for the fracture cases was -1.73 (0.80) and for the fracture-free controls was -1.35 (0.75) ($p = 0.062$). Four of the fracture cases and 3 of the controls had T-scores ≤ -2.50 , indicating that they met the diagnostic criterion for osteoporosis. These DXA-derived results were consistent with expectations that while BMD is inversely correlated with osteoporotic fractures, most fractures occur in patients who do not have osteoporosis as determined by BMD. BSA-determined bone damping values were also inversely correlated with fractures. The mean (SD) bone damping values measured above the right knee for the fracture cases was 4.88 (2.33); by contrast, the mean (SD) bone damping value in the fracture free controls was 13.11 (14.38) ($p = 0.018$). Analyses with ROC curves returned AUCs of 0.65 for both T-scores ($p = 0.047$) and BSA damping values ($p = 0.040$). Interestingly and importantly, T-scores and BSA damping values were not highly correlated (Pearson Correlation Coefficient = .172; $p = .164$), suggesting that they contain independent information about fracture association. BSA damping values and DXA-derived T-scores were combined in a logistic regression model with arm and wrist fractures as the dependent variable. The output of the logistic regression model more accurately discriminated between fracture cases and controls (ROC curve AUC = 0.70, $p = .008$) than either DXA or BSA alone.

If confirmed in follow-on studies, combining BSA and DXA results may provide an improved means to identify individuals at high risk of experiencing an osteoporosis-related fragility fracture.

Disclosures: Nelson Watts, OsteoDynamics, 7

This study received funding from: OsteoDynamics

SA0301

Can Fracture Risk Calculators Help Determine Bone Density Testing Intervals in Men? Kaniksha Desai*¹, Valentina Petkov¹, Robert Adler².

¹Virginia Commonwealth University, USA, ²McGuire VA Medical Center, USA

Objectives: 1. To determine if fracture risk calculators FRAX and GARVAN can predict which men will progress from osteopenia (low bone mass by dual energy x-ray absorptiometry, DXA) to osteoporosis (OP) or have a significant decrease in bone mineral density (BMD). 2. To determine if osteopenic men should have a repeat DXA in 2-3 years.

Methods: Older men were screened for OP by DXA (of spine, hip, and forearm) in a primary care clinic program. Reports for men with osteopenia included a recommendation for a repeat DXA in 2 years. Risk factors including age, weight, alcoholism, tobacco use, previous fracture, parental hip fracture, glucocorticoid use, rheumatoid arthritis, and number of falls were assessed using CPRS (electronic medical record) and a questionnaire at DXA testing. Risk factors were used to calculate FRAX and GARVAN scores, 2 validated methods to determine 10 year fracture risk. Logistic regression models were used to determine if FRAX or Garvan at baseline can predict change in diagnosis or significant BMD loss.

Results: Osteopenic men ($n = 118$, mean age 70) had a repeat DXA 3.2 ± 0.8 years later. Only 6 had a change in diagnosis to OP, but 101 had a significant BMD loss at

one or more sites. On review of the 6 men, 2 had elevated FRAX and 4 had elevated GARVAN score at baseline. Two men were started on androgen deprivation therapy, which may have led to OP. Similar to a recent study in women, 5 out of 6 men who changed to OP had a T score worse than -2 (severe osteopenia). Overall, 14% of men with severe osteopenia progressed to OP. However, at baseline FRAX and Garvan were no different in the 14% compared with those that did not progress to OP.

Discussion: While many osteopenic men lose bone over 3 years, a repeat DXA is unlikely to show a diagnosis change. In a recent study (ML Gourlay, NEJM 366:225, 2012), older women with more severe osteopenia were more likely to develop OP than younger women with milder osteopenia. Our data in men appear to be consistent because the more severe the osteopenia, the more likely progression to OP. However, longer studies are needed to determine the appropriate DXA interval for most men. Although GARVAN and FRAX scores did not predict which men would progress, they can be used in conjunction with clinical judgment and assessment of new risks (such as androgen deprivation therapy) to determine timing of repeat DXAs.

Disclosures: Kaniksha Desai, None.

SA0302

See Friday Plenary Number FR0302.

SA0303

See Friday Plenary Number FR0303.

SA0304

See Friday Plenary Number FR0304.

SA0305

Normative Data for Bone Mineral Density and Calcaneal Ultrasound in 25-year-old Swedish Women: The Peak-25 Cohort of 1061 Women. Mattias Callréus*¹, Fiona McGuigan², Kristina Akesson³.

¹Skåne University Hospital, Sweden, ²University of Lund, Malmö, Skåne University Hospital, Malmö, Sweden, ³Skåne University Hospital, Malmö, Sweden

As bone mass later in life is largely dependent on peak bone mass achieved in young adulthood, normative values of bone mass at this age are imperative in identifying women at risk of osteoporosis. Using a population-based sample of premenopausal Scandinavian women aged 25, the aim of this study is to provide normative DXA and QUS information at an age closely representing peak bone mass.

Subjects and Methods: 1061 women were included in the Peak-25 cohort evaluating determinants of bone health. DXA (Prodigy, GE) was used to assess bone mass. Bone mineral density (BMD) and bone mineral content (BMC) were measured at; total body (TB), femoral neck (FN), trochanter (TR) and lumbar spine (LS) and Z-scores and T-scores were obtained. Quantitative ultrasound of the calcaneus (QUS) (Lunar Achilles) was also assessed: bone ultrasound attenuation (BUA), speed of sound (SOS) and stiffness index (SI). Statistical analysis (descriptives, Pearson's correlation) was performed using SPSS (SPSS Inc., Chicago, Illinois).

Results: At baseline the women were 25.5 ± 0.2 years of age, 168 ± 6 cm tall and weighed 65 ± 11 kg. DXA BMD values (g/cm^2) were 1.17 ± 0.07 (TB-BMD), 1.053 ± 0.123 (FN-BMD), 0.830 ± 0.108 (TR-BMD) and 1.217 ± 0.128 . The corresponding Z-scores were 0.63 ± 0.81 (TB), 0.54 ± 0.98 (FN), 0.38 ± 0.95 (TR) and 0.32 ± 1.03 (LS). Comparing Z-scores and T-scores, femoral neck Z-score was significantly lower in our cohort, whereas other sites showed no differences. QUS values were: BUA (117.4 ± 10.5 db/MHz), SOS (1574 ± 32 m/s) and SI (98.9 ± 14.6 %). The correlation between DXA and QUS was modest (0.44 - 0.52 ; $p < 0.001$) for SOS and SI and lower for BUA.

Conclusion: This very large cohort of exactly 25-year old women provides normative bone mass and QUS values for premenopausal young adult Swedish women and demonstrates the correlation between DXA and QUS. Interestingly, BMD values are considerably higher than those expected for age (Z-score), whereas the FN T-scores suggest that contrary to common assumption, at age 25, peak bone mass has still not been reached at the FN. How this should be interpreted is unclear; it could suggest that FN peak bone mass is reached much later in Swedish women alternatively, the reference population provided in the machine is not applicable for a Scandinavian population.

Disclosures: Mattias Callréus, None.

SA0306

Predictions of Vertebral Strength using QCT and Intra-Vertebral Heterogeneity Density vs. DXA. Amira Hussein¹, Stacyann Morgan², Glenn Barest³, Elise Morgan¹. ¹Boston University, USA, ²Boston University, USA, ³Boston University School of Medicine, Radiology, USA

Trabecular bone density and architecture are highly non-uniform throughout the vertebra. This intra-vertebral heterogeneity has often been proposed as a main reason why average measures of bone mineral density (BMD) explain only ~60% of the variance in vertebral strength. Given that spatial variations in trabecular density can be assessed non-invasively via quantitative computed tomography (QCT), the goal of this study was to determine the influence of the intra-vertebral heterogeneity in density on strength predictions.

Fresh-frozen, human, L1 functional spine units (age: 79.8+/-11.2, 15 female, 16 male) were scanned via QCT (in-plane resolution: 0.3125mm/pixel, slice thickness: 0.625mm). The volume computed tomography dose index was 96.5mGy. The vertebrae were then compressed to failure to measure the ultimate force (maximum force sustained). BMD was calculated for 5mm contiguous cubes distributed throughout the centrum. The inter-quartile range (IQR) of the cube BMD values was used as the measure of intra-vertebral variation. Average BMD and cross-sectional area (CSA) were calculated for the largest elliptical cylinder that would fit within the vertebra. The images were also used to calculate areal BMD, simulating lateral DXA (BMD_{DXA}), and to obtain an estimate of the axial rigidity (EA), the resistance to axial loading. Linear regressions were used to determine the dependence of ultimate force on each of the following combinations of explanatory variables: 1) BMD*CSA; 2) BMD*CSA and IQR; 3) BMD_{DXA}; 4) EA. A restricted vs. full F-test was used to compare regression models 1 and 2. J-tests were used to rank the four regression models from best to worst predictive performance.

Accounting for the intra-vertebral variation in density in addition to mean density significantly improved strength predictions. Including IQR in addition to BMD and CSA in the regression model improved the R² value from 0.43 (p=0.001) to 0.58 (p=0.002; F-test: p=0.038), resulting in the best regression model. Model 3 (R²=0.22, p=0.033) was inferior to model 2, and model 4 was not significant (p=0.729).

These findings show that non-invasive assessments of the intra-vertebral heterogeneity in density improve predictions of vertebral strength compared to current clinical standards that use only average BMD from QCT or DXA. The higher radiation dose incurred with QCT may thus be acceptable for certain indications when seeking more accurate assessment of bone strength and fracture risk.

Disclosures: Amira Hussein, None.

SA0307

Short Term Caloric Restriction Does Not Reduce Bone Mineral Density in Early Type 2 Diabetic Rats. Yun Kyung Jeon¹, Min Jung Bae², WON JIN Kim², YANG SEON Yi³, Sang Soo Kim², Bo Hyun Kim², Soo Hyoung Lee⁴, Yong Ki Kim⁵, In Joo Kim². ¹Pusan National University Hospital, South Korea, ²Pusan National University Hospital, South Korea, ³Pusan National University Hospital, South Korea, ⁴Kim Young Ki clinic, South Korea, ⁵Kim Yong Ki clinic, South Korea

The aim of this study is to determine short term caloric restriction (CR) alters bone mass and bone metabolism in early type 2 diabetic rat model, OLETF rats. The rats were divided into 4 groups (n=5, each): OLETF with ad libitum (AL), OLETF with CR, LETO with AL, LETO with CR. CR was practiced in male rats at 24weeks of age by 40% restriction for 4weeks until the study was terminated. The effect of CR on bone mineral density (BMD) of total femur was assessed using Dual energy X-ray absorptiometry. Serum markers were determined using immunoassay. After 4 wk CR, body weight was decreased in both species. The BMD at total femur were decreased after CR in LETO rats, but not in OLETF rats. After adjustment of body weight, BMD was still lower in LETO rats (p = 0.029), but not in OLETF rats (p = 0.262). Bone specific alkaline phosphatase decrease in LETO rats (p = 0.009), but not in OLETF rats (p=0.347). Serum leptin were lowered by CR in both species, but hyperleptinemic status maintained in OLETF rats (5.348 vs 11.770, p = 0.009). 25(OH)D were significantly increased in CR group of OLETF rats (p = 0.009), but not in LETO rats (p = 0.117). IL-6 and TNF- α were significantly decreased in OLETF rats (p=0.009), but not in LETO rats (p = 0.042) by CR. Short term caloric restriction and its related weight reduction were associated with marked decreases of BMD at femur in LETO rats, but not in OLETF rats with early type 2 diabetic status. Short term CR may not alter bone mass and bone metabolism in early type 2 diabetes.

Disclosures: Yun Kyung Jeon, None.

SA0308

Thoracic and lumbar regional differences in associations between vertebral deformity, BMD, and age in postmenopausal women. Eual Phillips¹, Chamith Rajapakse², Michael Wald³, Felix Werner Wehrli³. ¹University of Pennsylvania, USA, ²University of Pennsylvania School of Medicine, USA, ³University of Pennsylvania Medical Center, USA

Bone mineral density (BMD) is widely used to assess vertebral fracture risk. However, nearly 50% of patients with vertebral fractures have normal BMD. The goal

of this study is to examine the predictability of MRI-based vertebral deformity measures from BMD and age in the lumbar and thoracic spine.

The study comprised of 32 postmenopausal women (mean age: 71.8 years, $\sigma = 7.0$). Multi-slice sagittal MR images of the midline spine were acquired at 1.5-T (Siemens Sonata) scanner using the manufacturer's surface array coil and a turbo spin-echo sequence. Acquired spine images were taken as input to a custom software tool for quantitative VMA. Anterior, middle, and posterior heights vertebral heights were computed by taking the Euclidian distance between landmark points. Wedge (W), biconcavity (B), and crush (C) vertebral deformities were calculated for each vertebra by adapting an approach developed by Eastell. A continuous mean of each deformity class was computed for the thoracolumbar vertebral column (T4-L5). Adapted from Diacinti, vertebral height summation (VHS) was computed in the anterior (AVHS), middle (MVHS), and posterior (PVHS) regions. Genant's criteria were applied to measure for vertebral fracture frequency (FxN) and severity (FxS). Finally, intervertebral disc space summation (DSS) was also calculated for the anterior (ADSS) and posterior (PDSS) spine.

Associations between vertebral deformity, BMD, and age were found to be different in the lumbar and thoracic regions. LS-BMD demonstrated an inverse relationship with lumbar PDSS (-0.42, p < 0.05). Patient age did not express a predictive relationship with lumbar vertebral deformity. Hip BMD positively correlated with thoracic MVHS (r = 0.43, p < 0.05). Patient age conveyed an inverse relationship with thoracic MVHS (r = -0.43, p < 0.05) and a positive correlation with biconcave (r = 0.37, p < 0.05) and crush deformities (r = 0.41, p < 0.05). Age also exhibited a predictive relationship of biconcave FxN (r = 0.38, p < 0.05) and FxS (r = 0.37, p < 0.05) in the thoracic column. BMD prediction of lumbar vertebral deformity may require further investigation due to the unique shape of the lumbar spine. In conclusion, MRI-based vertebral morphometry may provide information about vertebral fracture susceptibility in addition to BMD and age.

Acknowledgements: NIH grant K25 AR 060283

Disclosures: Eual Phillips, None.

This study received funding from: NIH grant K25 AR 060283

SA0309

See Friday Plenary Number FR0309.

SA0310

See Friday Plenary Number FR0310.

SA0311

See Friday Plenary Number FR0311.

SA0312

See Friday Plenary Number FR0312.

SA0313

See Friday Plenary Number FR0313.

SA0314

See Friday Plenary Number FR0314.

SA0315

Severities of Vertebral Fractures Evaluated with Semiquantitative Analysis (SQ) in Glucocorticoid-induced Osteoporosis (GIO). Mari Ushikubo¹, Ikuko Tanaka², Shigenori Tamaki³, Harumi Kuda¹, Keisuke Izumi¹, Kumiko Akiva¹, Hisaji Oshima⁴. ¹Department of Connective Tissue Diseases, Tokyo Medical Center, Japan, ²National Center for Geriatrics & Gerontology, Japan, ³Nagoya Rheumatology Clinic, Japan, ⁴Tokyo Medical Center, Japan

Background: Although vertebral fracture is one of the major problems in treatment with glucocorticoids, severities of fractures have not been well evaluated.

Purpose: To clarify situation of severities of vertebral fractures and correlation with clinical variables.

Patients and Methods: 137 patients with connective tissue diseases other than rheumatoid arthritis were recruited and observed for 2 years (age: 61+/-15yo (mean+/-SD), disease duration; 12+/-11ys, total prednisolone (PSL) dosage: 34+/-34g, daily PSL dosage during the study period; 8+/-6mg/day). Grading with the SQ method

(Gerant et al. JBMR, 1993) was used for evaluation of severities of vertebral fractures. Bone mineral densities (BMD) were measured with DXA at the distal radius.

Results: 1) At the beginning of the observation, 42 (31%), 15 (11%), and 6 (4%) patients revealed the grade (G)1, G2, and G3, respectively. 2) Deteriorated grades during 2 years were seen in 47% of the patients. Eighty three percent of patients with incident fractures showed one-grade deterioration. In 8% and 9% of the patients, however, two- and three-grade deteriorations were detected. 3) In patients with more than the two-grade deterioration, the age and the SQ grade at the beginning were higher and the BMD was lower than those in less than one-grade deteriorated patients. Multivariable analysis with logistic regression revealed an age as a risk factor.

Conclusions: Evaluation of severities of vertebral fractures with the SQ method was suggested to be an important aspect in pathogenesis and prevention of GIO.

Disclosures: *Mari Ushikubo, None.*

SA0316

Evaluating the Effect of Osteoporosis on Femoral Cartilage Thickness using Ultrasonography in Female Patients with Knee Osteoarthritis. Levent Tekin*¹, Alparslan Bayram Çarlı², Selim Akarsu², Mehmet Zeki Kırıl².
¹Gulhane Military Medical Academy Haydarpaşa Training Hospital, Turkey, ²GMMA Haydarpaşa Training Hospital, Turkey

Introduction and Aim: Osteoarthritis (OA) and osteoporosis (OP) are diseases that significantly decrease health quality by functional loss in affected individuals and are among the most important health issues especially in the elderly population. Especially in the past 50 years, these two disorders which cause chronic pain and disability in the elderly have become a public health problem as a result of the increase in mean lifetime. Whether these two diseases affect each other is controversial in the studies that have been conducted since today. We aimed to investigate whether there is a relationship between the presence of OP and OA evaluating the femoral cartilage thickness using ultrasonography. As our knowledge, this is the first study in literature that uses ultrasonography in investigating this relationship.

Material and Methods: 80 female patients aging between 50-75, that were diagnosed as knee OA by history, physical examination and imaging methods with grade 1-3 gonarthrosis (using Kellgren-Lawrence grading Scale) were included into the study. Patients in group 1 (n=40) had a diagnosis of OP (BMD total T score lumbar or femoral <-2.5) and group 2 (n=40) had no OP (BMD total T score lumbar or femoral >-2.5). All the patients received knee joint ultrasonography. Femoral cartilage thickness was measured from three points (mid, medial and lateral femoral epicondyle) and the mean value was calculated.

Results: The mean femoral cartilage thickness in group 1 was significantly higher than in group 2 (p<0.05).

Conclusion: OP seems to be a protective factor from having OA. Nevertheless, we do not know that if this is due to the new bone formation or spurs which counts as bone mass and elevates the BMD scores in OA patients. We consider that our study will enlighten the arguments on the relationship between OP and OA and create a new horizon on this issue.

Disclosures: *Levent Tekin, None.*

SA0317

Noninvasive Prediction of Principal Trabecular Orientation Using Quantitative Ultrasound and Finite Element Analysis. Liangjun Lin*¹, Wei Lin², Yi-Xian Qin¹. ¹State University of New York at Stony Brook, USA, ²Stony Brook University, USA

Introduction: Trabecular structural alignment is heavily influenced by the particular mechanical milieu applied to it and closely related to risk of fracture¹. Quantitative ultrasound (QUS) propagation has potential to predict trabecular structural orientation and anisotropic mechanical properties². The objective of this study is to use QUS to non-invasively predict the principal structural orientation of trabecular bone, and correlate with finite element analysis (FEA) determined mechanical property.

Materials and methods: 7 trabecular bone balls (Ø 25mm) were machined from bovine femurs. Rotational QUS scanning with increment of 10° was performed around 3 anatomical axes of superior-inferior (SI), antero-posterior (AP), and medio-lateral (ML) to measure the fast wave ultrasound velocity (UV) and attenuation (ATT) (Fig. 1). The QUS data was reconstructed in a 3-D Cartesian coordinates system to predict the principal structural orientation (Fig. 2). µCT with resolution of 36.9 µm was performed on all the bone balls. Mean intercept length (MIL) tensor was calculated from the µCT images. The µCT images were then converted into mesh model of tetrahedral elements for FEA (Fig. 3). Young's modulus of 10.9 GPa and Poisson ratio of 0.3 were used in FEA. Displacement controlled loading of 1,000 µstrain was applied to each model along 6 directions: SI, AP, ML, longest vector of MIL tensor, the principal structural orientations predicted by UV and ATT.

Results: QUS was able to pick up the angle-dependent change of the trabecular structure (Fig. 4). The average angle difference between the principal structural orientations predicted by UV and the longest vector of MIL tensor is $4.45 \pm 2.20^\circ$, and the difference between ATT and MIL is $11.67 \pm 6.83^\circ$. The difference between ATT and UV is $8.96 \pm 7.48^\circ$ (Table 1).

Conclusion: The presented non-invasive QUS method was able to predict the principal structural orientation of the trabecular bone with an angle difference smaller than 10° compared to the µCT data. The ongoing FEA can validate these results and potentially predict the trabecular mechanical strength in associated orientations. These data may provide insight of the mechanism of ultrasound predictions for the structural orientation with multiple QUS parameters.

1. Martin, R.B., J Biomech, 1991.24 Suppl 1: p. 79-88. 2. Lin, W., J Acoust Soc Am, 2009.125(6): p. 4071-7.

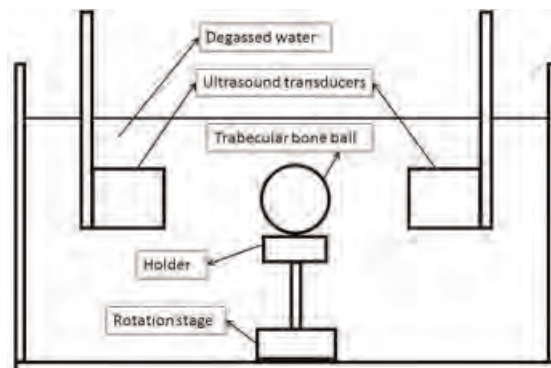


Figure 1. Schematic representation of the ultrasound measurement experiment set up.

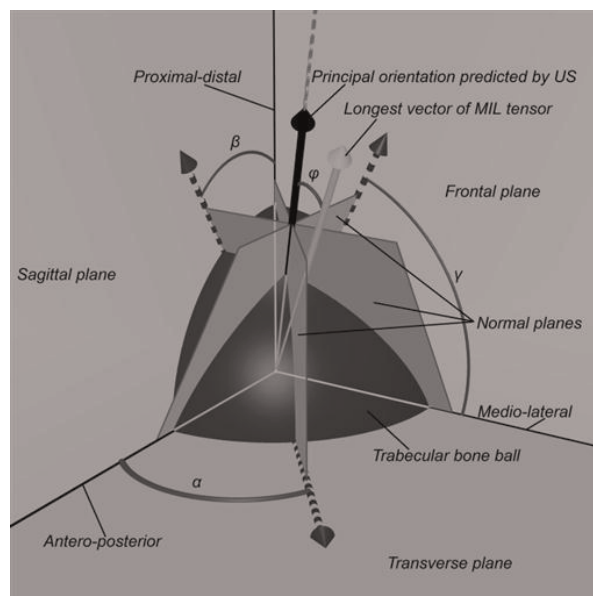


Figure 2. Representation of the mathematical model in the prediction of the structural orientation

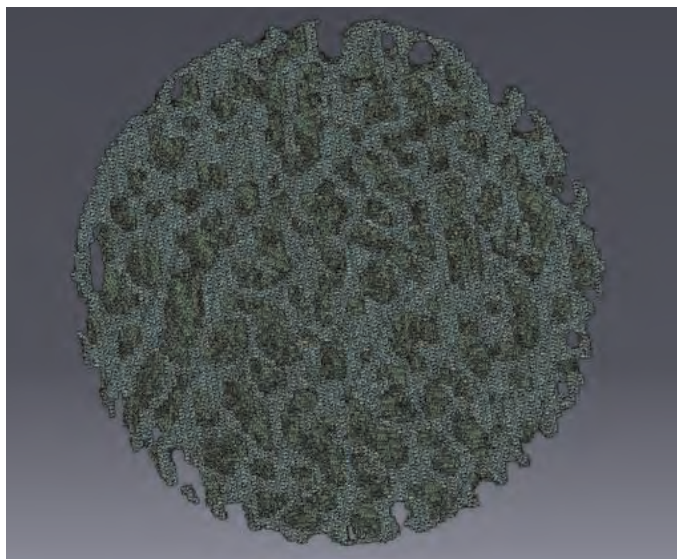
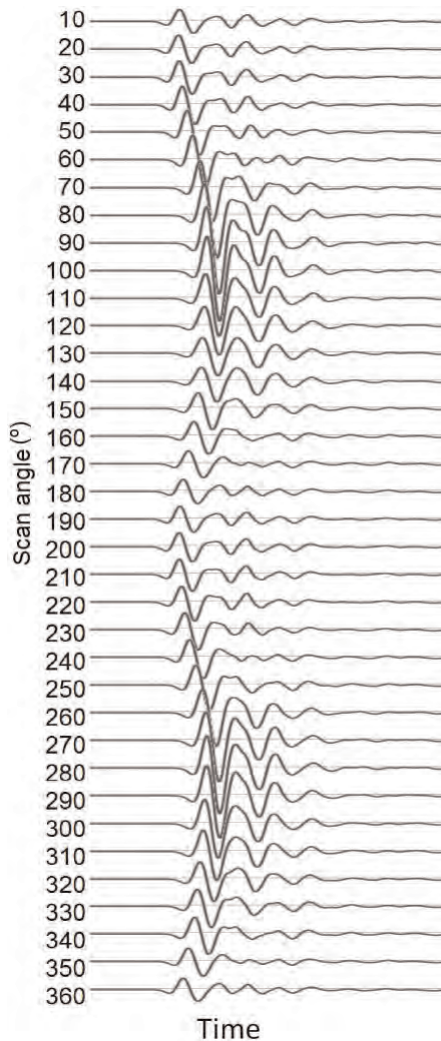


Figure 3. Tetrahedral element model of the trabecular bone ball used in FEA.



SA0319

See Friday Plenary Number FR0319.

SA0320

See Friday Plenary Number FR0320.

SA0321

See Friday Plenary Number FR0321.

SA0322

Geographic Disparities in BMD Testing and Osteoporosis Treatment for Manitoba, Canada. William Leslie*¹, Patricia Caetano². ¹University of Manitoba, Canada, ²University of Manitoba, Canada

Background: Geographic disparities in healthcare are well documented, and have recently been noted for DXA testing in the United States. The Province of Manitoba, Canada (1.2 million) has a centralized DXA testing program with testing centres in two southern urban areas (Winnipeg and Brandon). To examine regional disparities in osteoporosis care, we analyzed DXA testing and osteoporosis treatment rates for 5 fiscal years (2005/06 to 2009/10) as part of a provincial patient care initiative.

Methods: Health services are provided to virtually all Manitoban residents through a single public health care system. Manitoba Health maintains computerized databases for all residents eligible to receive health services. DXA testing was identified in a database that contains all clinical BMD results for the Province of Manitoba, Canada. Non-estrogen osteoporosis treatment (1 or more dispensations for the fiscal year) was identified in a comprehensive retail pharmacy database for the Province. Rates per 1,000 (averaged for 2005/06 to 2009/10) were computed for each of 10 provincial regional health authorities (RHAs), and for the 12 community areas (CAs) comprising the urban capital of Winnipeg. Spearman correlation coefficients were determined between the rate of BMD testing, rate of osteoporosis treatment rates, and median household income (2006 census data).

Results: BMD testing rates varied by more than two-fold between provincial RHAs (28.2 per 1,000 in Brandon to 10.3 per 1,000 in the Northern-Manitoba RHA), with a slightly smaller variation in osteoporosis treatment rates (116 per 1,000 in Brandon to 58 per 1,000 in the northern Burntwood RHA). Within Winnipeg, BMD testing rates varied by more than two-fold (maximum 32.5 per 1,000 versus minimum 12.5 per 1,000), with a large variation in osteoporosis treatment rates (maximum 116 per 1,000 versus minimum 35 per 1,000). There was a significant positive correlation between BMD testing and osteoporosis treatment rates by provincial RHA (Spearman rho=0.66, p<.05) and Winnipeg CA (Spearman rho=0.80, p<.01), but neither of these showed a significant correlation with median household income.

Conclusions: Large geographic disparities in osteoporosis care were identified in the public health care system of Manitoba, Canada. The northern regions of Manitoba, which are most distant from the DXA testing centres, have the lowest DXA testing and osteoporosis treatment rates. Targeted strategies will be required to address these disparities.

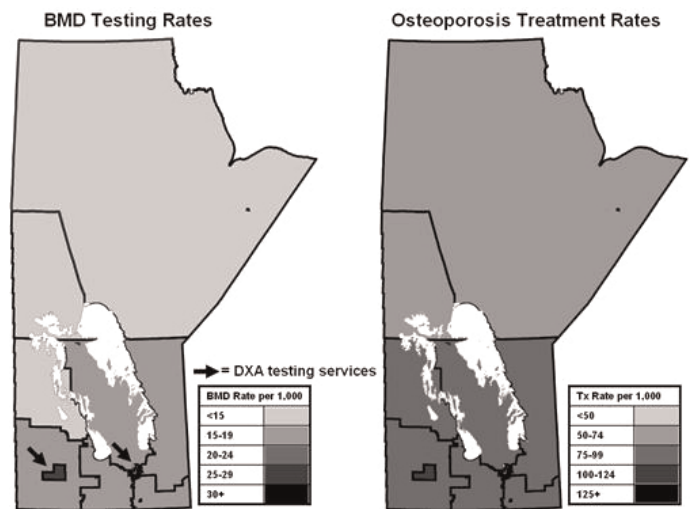


Figure: BMD testing rates (left) and treatment rates (right) for Manitoba, Canada (2005-2010)

Disclosures: William Leslie, None.

Figure 4. Typical ultrasound waves transmitted through the trabecular bone ball.

| | | Bone 1 | Bone 2 | Bone 3 | Bone 4 | Bone 5 | Bone 6 | Bone 7 | Average= standard deviation |
|-----|-----------------|--------|--------|--------|--------|--------|--------|--------|-----------------------------|
| ATT | I ₁₂ | 5.45 | 9.48 | 21.34 | 9.86 | 13.01 | 7.59 | 1.77 | 14.13±9.03 |
| | I ₁₃ | 33.34 | 24.75 | 10.56 | 8.00 | 18.32 | 6.74 | 20.18 | |
| | I ₂₃ | 29.44 | 16.73 | 9.88 | 7.72 | 25.46 | 17.76 | 4.33 | |
| UV | I | 20.52 | 16.06 | 10.74 | 3.13 | 18.61 | 5.03 | 7.65 | 11.67±6.83 |
| | I ₁₂ | 6.98 | 2.72 | 22.14 | 10.91 | 28.36 | 12.12 | 6.43 | |
| | I ₁₃ | 8.26 | 1.24 | 9.43 | 18.53 | 5.35 | 15.54 | 22.98 | |
| I | I ₂₃ | 6.22 | 4.93 | 11.49 | 12.41 | 11.73 | 16.96 | 8.73 | 4.45±2.20 |
| | I | 6.30 | 2.41 | 5.45 | 0.82 | 7.16 | 4.34 | 4.67 | |
| | I | 6.30 | 2.41 | 5.45 | 0.82 | 7.16 | 4.34 | 4.67 | |

| | Bone 1 | Bone 2 | Bone 3 | Bone 4 | Bone 5 | Bone 6 | Bone 7 | Average= standard deviation |
|---|--------|--------|--------|--------|--------|--------|--------|-----------------------------|
| Angle difference between UV and ATT (°) | 21.48 | 14.19 | 5.57 | 3.22 | 13.35 | 1.06 | 3.89 | 8.96±7.48 |

Table 1. Angle difference (°) between the principal structural orientations predicted by µCT and QUS

Disclosures: Liangjun Lin, None.

SA0318

See Friday Plenary Number FR0318.

SA0323

See Friday Plenary Number FR0323.

SA0324

Calcium and Vitamin D Intakes in a Prospective Population-based Study: the Canadian Multicentre Osteoporosis Study. Wei Zhou^{*1}, Claudie Berger¹, Lisa Langsetmo², David Goltzman¹, Suzette Poliquin³, Stephanie Kaiser⁴, Robert Josse⁵, Jerilynn Prior⁶, Tanveer Towheed⁷, Tassos Anastassiades⁸, K. Shawn Davison⁹, Christopher Kovacs¹⁰, Emmanuel Papadimitropoulos¹¹, Nancy Kreiger¹². ¹McGill University, Canada, ²Canadian Multicenter Osteoporosis Study, Canada, ³Institut national d'excellence en santé et services sociaux, Canada, ⁴Dalhousie University, Canada, ⁵St. Michael's Hospital, University of Toronto, Canada, ⁶University of British Columbia, Canada, ⁷Queen's University, Canada, ⁸Queen's University, Canada, ⁹Laval University, Canada, ¹⁰Memorial University of Newfoundland, Canada, ¹¹Lilly, Canada, ¹²University of Toronto, Canada

Calcium and vitamin D are nutrients essential for overall health, accrual of optimal bone mass, and prevention of osteoporosis and fractures in adulthood. Our objective was to estimate calcium and vitamin D intakes and their change over ten years among an adult Canadian population.

Participants in the Canadian Multicentre Osteoporosis Study (CaMos) were randomly selected from a 50 km radius of 9 cities across Canada. A short interviewer-administered semi-quantitative food frequency questionnaire was completed at baseline and Year10. Calcium intake from both diet and supplements, and vitamin D intake from milk, beverage fortification, yogurt and supplements, were estimated cross-sectionally and longitudinally, by categories of age (25-50, 51-70 and 71+) and by sex.

At baseline, the study sample included 6518 women (mean age 63 yr) and 2864 men (mean age 60 yr). Detailed intakes of calcium and vitamin D at baseline and Year 10 are shown in the Table, along with comparisons to 2010 Institute of Medicine (IOM) dietary reference intakes. The prevalence of those with intakes below the Estimated Average Requirement (EAR) ranges from 47% to 69% at baseline and 32% to 52% at Year 10 for calcium, and ranges from 72% to 83% at baseline and 42% to 76% at Year 10 for vitamin D. The calcium intake increased in all groups over 10 years with a mean change of 315 (95% confidence interval (CI): 290, 340) mg/day in women and 190 (95% CI: 154, 226) mg/day in men. Vitamin D intake increased in women, the mean change was 10.1 (95% CI: 8.7, 11.5) µg/day [405 (349, 461) IU/day] in those aged 51+ and 5.3 (95% CI: 4.2, 6.5) µg/day [214 (169, 259) IU/day] in the 25-50 group. Vitamin D intake increased by 5.3 (95% CI: 4.3, 6.4) µg/day [213(172, 254) IU/day] in men aged 51 and older, but the change was not significant in men aged 25-50. The percentage of participants reporting calcium supplements increased from 38.3% at baseline to 58.8% at Year 10, and the percentage who supplemented with vitamin D increased from 29.6% to 57.5%.

We observed a high prevalence of Canadian adults that did not meet the EAR established by the IOM for calcium and vitamin D intake. With reference to the new IOM guidelines, the present intakes are substantially below optimal intakes for bone health.

| Age (year) | n | Calcium (mg/day) | | | Vitamin D (µg/day) | | | |
|-----------------|------|------------------|------------------|-------------------|--------------------|------------|------------------|------------------|
| | | Mean (SE) | Median (IQR) | Above EAR* % (SE) | n | Mean (SE) | Median (IQR) | Above EAR % (SE) |
| Baseline | | | | | | | | |
| Women | | | | | | | | |
| 25-50 | 1040 | 961 (18) | 840 (552, 1236) | 52.9 (1.5) | 1061 | 4.9 (0.2) | 2.7 (0.5, 7.5) | 18.8 (1.2) |
| 51-70 | 3447 | 1062 (11) | 949 (602, 1374) | 46.6 (0.8) | 3499 | 7.2 (0.3) | 3.8 (1.1, 10.1) | 27.7 (0.8) |
| 71+ | 1915 | 1034 (14) | 944 (588, 1387) | 46.1 (1.1) | 1958 | 7.7 (0.4) | 3.7 (1.3, 10.1) | 27.4 (1.0) |
| Men | | | | | | | | |
| 25-50 | 735 | 918 (23) | 771 (522, 1168) | 47.5 (1.8) | 746 | 5.4 (0.7) | 2.6 (0.7, 6.3) | 17.0 (1.4) |
| 51-70 | 1345 | 908 (16) | 782 (508, 1154) | 48.6 (1.4) | 1373 | 5.1 (0.2) | 2.7 (0.8, 7.5) | 20.4 (1.1) |
| 71+ | 726 | 884 (21) | 762 (488, 1138) | 31.1 (1.7) | 745 | 5.3 (0.3) | 2.7 (1.1, 7.5) | 20.5 (1.5) |
| Year10 | | | | | | | | |
| Women | | | | | | | | |
| 25-50 | 274 | 1147 (42) | 1028 (634, 1492) | 65.7 (2.9) | 275 | 6.6 (0.5) | 3.6 (1.3, 9.8) | 24.4 (2.6) |
| 51-70 | 1623 | 1353 (18) | 1270 (821, 1772) | 64.5 (1.2) | 1624 | 13.9 (0.5) | 10.2 (2.9, 18.6) | 53.3 (1.2) |
| 71+ | 2100 | 1416 (17) | 1323 (867, 1847) | 68.3 (1.0) | 2100 | 18.8 (1.0) | 12.0 (3.8, 22.5) | 58.0 (1.1) |
| Men | | | | | | | | |
| 25-50 | 202 | 1150 (65) | 961 (595, 1370) | 60.4 (3.4) | 202 | 7.1 (0.6) | 3.9 (1.6, 10.0) | 28.2 (3.2) |
| 51-70 | 708 | 1044 (24) | 906 (574, 1427) | 57.6 (1.9) | 708 | 9.0 (0.7) | 4.2 (1.3, 12.5) | 35.2 (1.8) |
| 71+ | 660 | 1105 (25) | 971 (620, 1478) | 47.9 (1.9) | 660 | 10.9(0.7) | 6.8 (2.3, 13.9) | 42.7 (1.9) |

* EAR: Estimated Average Requirement, RDA: Recommended Dietary Allowance

[†] 1 µg = 40 International Unit (IU)

EAR for Calcium: for women age 25-50 and men age 25-70, 800 (mg/day); for women age 51+ and men 71+, 1000 (mg/day);

RDA for Calcium: for women age 25-50 and men age 25-70, 1000 (mg/day); for women age 51+ and men 71+, 1200 (mg/day);

EAR for Vitamin D for women and men age 25+: 10 (µg/day);

RDA for Vitamin D for women and men: age 25-70, 15 (µg/day); age 71+, 20 (µg/day).

Table: Calcium and Vitamin D Intake by Sex and Age Group

Disclosures: Wei Zhou, None.

SA0325

Dietary Patterns in Men and Women Aged 25 Years and Older: Relationship with Body Mass Index, 25-hydroxyvitamin D Levels, Fasting Glucose, and Risk of Diabetes Mellitus. Lisa Langsetmo^{*1}, Claudie Berger², Jerilynn Prior³, David Hanley⁴, Jacques Brown⁵, Jonathan Adachi⁶, Sophie Jamal⁷, Robert Josse⁸, Christopher Kovacs⁹, Suzanne Morin², Susan Barr¹⁰, K. Shawn Davison¹¹, David Goltzman², Nancy Kreiger¹². ¹Canadian Multicenter Osteoporosis Study, Canada, ²McGill University, Canada, ³University of British Columbia, Canada, ⁴University of Calgary, Canada, ⁵CHUQ Research Centre Laval University, Canada, ⁶St. Joseph's Hospital, Canada, ⁷The University of Toronto, Canada, ⁸St. Michael's Hospital, University of Toronto, Canada, ⁹Memorial University of Newfoundland, Canada, ¹⁰University of British Columbia, Canada, ¹¹Laval University, Canada, ¹²University of Toronto, Canada

We have previously shown younger adults are choosing a more energy-dense and less nutrient-dense diet than older adults, and that the associated dietary patterns are related to body mass index (BMI). Objectives: To determine potential relationships between dietary patterns (Nutrient-Dense and Energy-Dense) and incident diabetes mellitus, and to assess possible mediation of this relationship by BMI, fasting glucose, and/or 25-hydroxyvitamin D (25OHD).

Design: We performed a secondary analysis of a longitudinal study, the Canadian Multicenter Osteoporosis Study—a randomly selected population-based cohort. Dietary patterns were assessed by self-administered food-frequency questionnaires in year 2 (1997-99). We used principal components to derive two dietary pattern factor scores: Energy-Dense and Nutrient-Dense. Exclusion criteria were missing/incomplete questionnaires or prevalent diabetes at year 2; 3868 women and 1545 men were eligible. Clinical assessment at year 5 (2000-02) included measured height and weight. A subsample (749 women and 318 men) also had fasting serum samples analyzed at that time. Our primary outcome was self-reported diagnosis of incident diabetes (assumed to be type 2) before the 10th annual follow-up (2005-07). Regression models (Cox and multivariate) were adjusted for age, education, alcohol, smoking, physical activity, comorbidities, menopausal status, and hormone therapy.

Results: The Nutrient-Dense dietary pattern was strongly associated with intakes of fruit, vegetables, and whole grains while the Energy-Dense pattern was strongly associated with intake of soft drinks, potato chips, french fries, meats, and desserts. The Energy-Dense dietary pattern was associated with higher risk of incident diabetes, HR=1.15 (95% CI: 1.00-1.32), with this effect mediated in part by higher BMI, higher fasting glucose, and lower serum 25OHD levels. The Nutrient-Dense dietary pattern was associated with lower risk of diabetes, HR=0.85 (95% CI: 0.74-0.98), with this effect mediated in part by lower BMI values, lower fasting glucose, and higher serum 25OHD levels.

Conclusion: A diet high in vegetables, fruit, and whole grains and low in soft drinks, potato chips, french fries, meats, and desserts is associated with lower BMI, lower fasting glucose, and higher serum 25OHD values, and lower risk of incident diabetes. These results support public health measures to mitigate impact of dietary patterns prevalent in younger adults.

Disclosures: Lisa Langsetmo, None.

SA0326

Effect of Gamma-glutamyl Carboxylase gene Polymorphism on the Association between Serum Vitamin K and Gamma-carboxylation of Osteocalcin in Young Adults. Mavu Haraikawa^{*1}, Naoko Tsugawa², NATSUKO SOGABE³, Rieko Tanabe⁴, Yuka Kawamura¹, Toshio Okano⁵, Takayuki Hosoi⁶, Masae Goseki-Sone⁷. ¹Department of Food & Nutrition, Faculty of Human Sciences & Design, Japan Women's University, Japan, ²Kobe Pharmaceutical University, Japan, ³KOMAZAWA WOMEN'S UNIVERSITY, Japan, ⁴Department of Food & Nutrition, Faculty of Human Sciences & Design, Japan Women's University, Japan, ⁵Kobe Pharmaceutical University, Japan, ⁶National Center for Geriatrics & Gerontology, Japan, ⁷Japan Women's University, Japan

Osteoporosis results from complex interactions between genetic and environmental factors. Nutrition is one of the most important environmental factors in the prevention of osteoporosis. Vitamin K acts as a cofactor for gamma-glutamyl carboxylase (GGCX), which is an essential enzyme for the gamma-carboxylation of vitamin K-proteins such as osteocalcin (OC). OC is produced in osteoblasts, and fully carboxylated osteocalcin binds to the calcium ions of hydroxyapatite. The amount of OC which is not carboxylated (undercarboxylated OC: ucOC) is considered a sensitive index of the vitamin K status of bone, and an elevated ratio of ucOC to intact OC is thought to be associated with low dietary intakes of vitamin K. Recent studies demonstrated that a significantly higher association between the single nucleotide polymorphisms of GGCX (R325Q, 974G>A) is associated with the bone mineral density among postmenopausal women. In this study, we investigated the effect of GGCX polymorphism on the correlations among vitamin K intake, the level of serum vitamin K, and the ratio of ucOC to intact OC. Serum biochemical parameters, such as serum phylloquinone (PK), menaquinone-7 (MK-7), intact OC, ucOC, and bone-

type alkaline phosphatase, were measured in healthy young males (n=97, age: 22.3 ± 1.7 y, mean ± standard deviation) and females (n=92, age: 21.8 ± 1.8 y). Dietary nutrient intakes were measured based on 3-day food records before the day of blood examinations. All subjects were genotyped for polymorphism (R325Q) presence. Dietary vitamin K intake from vegetables was significantly correlated with the level of serum PK, and vitamin K intake from fermented beans, natto, was also significantly correlated with the level of serum MK-7. The ratio of ucOC to intact OC showed a negative association with the total vitamin K intake and serum MK-7 in both male (r=-0.333, p=0.001) and female (r=-0.549, p<0.001) subjects. Interestingly, on grouping by the GGCX genotype, a significant interaction between the ratio of ucOC to intact OC with serum MK-7 was observed in 325R homozygotes (r=-0.411, p=0.007, r=-0.552, p<0.001) and heterozygotes (r=-0.358, p=0.015, r=-0.540, p<0.001), but not in 325Q homozygotes in both male and female subjects. These results suggest that there is an effect of the GGCX gene polymorphism on the correlation between the levels of serum MK-7 and gamma-carboxylation of serum OC.

Disclosures: Mayu Haraikawa, None.

SA0327

Low Vitamin D Status is Prevalent among Aboriginal and Younger Women and is Related to Number of Milk Servings Consumed. Nihal A Natour*¹, John Krahn², Hope Weiler³, William Leslie⁴. ¹McGill University, Canada, ²University of Saskatchewan, Canada, ³McGill University, Canada, ⁴University of Manitoba, Canada

Background: Health disparity is a well-recognized problem among Aboriginal people in North America. Canadian Aboriginal women and men have a 2-3 fold increase in major osteoporotic fractures. The Canadian Health Measures Survey (CHMS) of plasma 25-hydroxyvitamin D [25(OH)D] concentration in white and non-white people failed to capture enough information to enable assessment according to Aboriginal ethnicity.

Data and Methods: Data from culturally appropriate surveys, a food frequency questionnaire (FFQ) and plasma 25(OH)D concentration (RIA, Diasorin) were collected from 147 urban dwelling white women and 204 urban and rural dwelling Aboriginal, First Nation (FN), women 27-75 y. Descriptive statistics (means, medians and frequencies) were used to evaluate plasma 25(OH)D concentration, according to age, ethnicity, month of blood sample collection, and servings of milk consumed. The prevalence of vitamin D deficiency and percent that met various 25(OH)D concentration cut offs were evaluated. Data was analyzed using SAS 9.2 software.

Results: First Nation women had significantly lower median plasma 25(OH)D concentration than white women (47.0 vs. 65.0 nmol/L, p<0.0001; Table 1). Plasma concentration of 25(OH)D lower than 27.5 nmol/L was present among 9.8% of FN women and 4.1% of white women. Also, plasma concentrations lower than 37.5 nmol/L were present among 20.6% of FN women and 14.9% of white women. Similar to CHMS report, our results indicate that median (IQR) of plasma 25(OH)D concentration was lower in November- March than in April-October (48.0 (13.0-83.0) vs. 57.0 (13.0-111.0) nmol/L, p=0.04). Race and number of milk servings were significant contributors to plasma 25(OH)D concentration (Table 2).

Conclusion: There is higher prevalence of vitamin D deficiency (25(OH)D <27.5 nmol) and inadequacy (25(OH)D <37.5 nmol/L) among Aboriginal FN women, and younger women 25-39 y which could have detrimental consequences to bone health.

Table1. Plasma 25(OH)D concentration (nmol/L) based on ethnicity and age

| Age | FN | | Non-FN | |
|---------|------------------|-----|-------------------|-----|
| | Median (IQR) | n | Median (IQR) | n |
| Total | 47.0 (17.0-77.0) | 204 | 65.0 (28.0-102.0) | 147 |
| 25-39 y | 46.0 (15.0-77.0) | 100 | 54.0 (1.0-107.0) | 69 |
| 40-59 y | 48.0 (14.0-82.0) | 69 | 69.0 (40.0-98.0) | 39 |
| 60-75 y | 50.0 (19.0-81.0) | 33 | 70.0 (29.0-101.0) | 39 |

P-value: FN vs Non-FN < 0.0001; interaction with age: 0.260

Table 2. Plasma 25(OH)D concentration (nmol/L) based on daily intake of milk Servings

| Age | < one milk serving/d | | one milk serving/d | | >one milk serving/d | |
|---------|----------------------|-----|--------------------|-----|---------------------|-----|
| | Median (IQR) | n | Median (IQR) | n | Median (IQR) | n |
| Total | 46.0 (15.0-77.0) | 117 | 53.0 (14.0-92.0) | 118 | 61.0 (30.0- 92.0) | 115 |
| 25-39 y | 45.0 (21.0-69.0) | 57 | 46.0 (3.0-89.0) | 55 | 55.0 (9.0-101.0) | 57 |
| 40-59 y | 45.0 (1.0-90.0) | 43 | 60.0 (23.0-97.0) | 40 | 63.0 (34.0-92.0) | 25 |
| 60-75 y | 67.0 (21.0-113.0) | 16 | 51.0 (12.0-90.0) | 23 | 65.0 (28.0-102.0) | 33 |

P-value: Milk servings P=0.02; interaction with age: 0.067

Tables

Disclosures: Nihal A Natour, None.

SA0328

Bisphosphonate Use and Increased Incidence of Subtrochanteric Fracture in South Korea: Results from the National Claim Registry. Young-Kyun Lee*¹, Yong-Chan Ha², Chan Soo Shin³, Hyun-Koo Yoon⁴, Deog-Yoon Kim⁵. ¹Seoul National University Bundang Hospital, South Korea, ²Chung-Ang University Hospital, South Korea, ³Department of Internal Medicine, Seoul National University College of Medicine, South Korea, ⁴Cheil General Hospital & Women's Healthcare Center, South Korea, ⁵Kyung Hee University Hospital, South Korea

Background: Recently, atypical hip fractures in the subtrochanteric region have been reported among patients on bisphosphonate. However, the association between atypical hip fracture and bisphosphonate is controversial. We evaluated trends in the incidences of typical and atypical hip fracture in relation bisphosphonate use in Korea from 2006 to 2010, using nationwide data obtained from the Health Insurance Review and Assessment Service (HIRA)

Methods: All new visits or admissions to clinics or hospitals for a typical and atypical hip fractures were recorded nationwide HIRA using the ICD-10 code classification. To identify hip fractures, selected ICD-10 codes and a minimum cut-off value of 50 years were used. Typical hip fracture cases were defined as those requiring hospitalization with a primary diagnosis of femoral neck fractures or intertrochanteric fracture, and atypical hip fractures as those requiring hospitalization with a primary diagnosis of a subtrochanteric fracture. We limited the cohort to those patients that underwent one of the following 7 procedures; open reduction of fractured extremity-femur, closed pinning-femur, external fixation-pelvis/femur, closed reduction of fractured extremity-pelvis/femur, bone traction, skin traction, or hemiarthroplasty-hip. To determine trends in fracture incidences, the patients were categorized by age, gender, and fracture site (typical and atypical hip fracture). Annual Percentage Change for trends was used to determine whether fracture incidences changed from 2006 to 2010. (Joinpoint Regression Program, Version 3.5.2, Statistical Research and Applications Branch, National Cancer Institute, Bethesda, USA) Age-adjusted and gender-specific incidences from 2006 to 2010 were used in this analysis.

Results: The absolute number of typical and atypical hip fracture increased during the study period. Although age-adjusted incidence rates of typical hip fractures were stable in men and women, those of atypical hip fractures in women increased 4.1 % per year during the study period (95% CI, 0.5 to 7.9) (figure 1). Nationally, the annual numbers of prescriptions of bisphosphonate also increased during the study period (figure 2).

Conclusions: The results of this study suggest a possible causal relationship between bisphosphonate use and the increased incidence of atypical hip fracture in Korea.

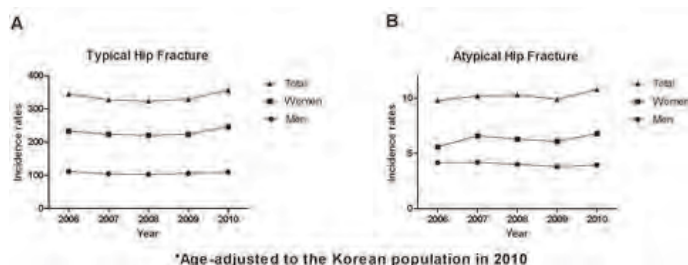


figure 1

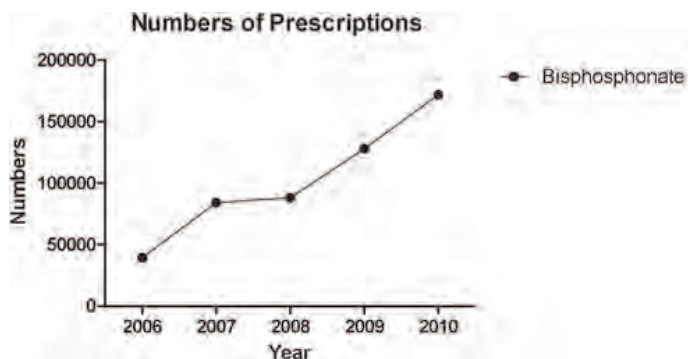


figure 2

Disclosures: Young-Kyun Lee, None.

This study received funding from: grant #11-2011-004 from the Seoul National University Bundang Hospital Research Fund

SA0329

Changes in Health Related Quality of Life (HRQoL) after non-traditional fractures. Yu Zhang*¹, Kerrie Sanders², Julie Pasco³, Mark Kotowicz⁴.
¹University of Melbourne, Australia, ²The University of Melbourne, Australia, ³Deakin University, Australia, ⁴Deakin University School of Medicine, Australia

To date studies have focused mainly on HRQoL associated with hip, spine and distal forearm fractures. HRQoL at other fracture sites have been grossly under-investigated. The aim of this study was to investigate the HRQoL related to non-traditional fractures including ribs, pelvis, clavicle, humerus, forearm (other than distal), hand, femur, tibia/fibula (other than distal), ankle (including distal tib/and fib) and foot.

Participants were recruited from the Geelong Hospital (GH), the sole provider of emergency services in a city with a population of approximately 220,000, between June 2010 and November 2011. Those aged 50+yr who had sustained a radiologically confirmed low trauma fracture (e.g. fall from standing height or less) were invited to take part. High trauma (e.g. motor vehicle accident), multiple and pathological fractures were excluded (n=92). We also excluded people with cognitive disabilities (n=65), those who were unable to understand the questionnaire (n=37) and others (n=65). Using EQ5D questionnaire within 2 weeks of fracture, HRQoL immediately before and at the time of interview was measured. EQ5D repeated 4 months post fracture. Confidence intervals were estimated using bias-corrected accelerated bootstrap. Using multiple ordinary least square regression analysis, the impact of variables on HRQoL after fracture (age, gender, fracture-related hospital admission, fracture sites, time between first interview and fracture, and pre-fracture HRQoL) was assessed.

Among the 217 participants, there were 48 humerus, 64 ankle, and 60 weight-bearing (15 pelvis, 10 femur, 18 proximal and mid tibia/fibula, 17 foot) and 45 non weight-bearing (17 rib, 8 clavicle, 16 forearm, 4 hand) fractures. Impact of fractures on HRQoL is shown in table 1. Pre-fracture HRQoL (coefficient: -0.47, p<0.01) and hospital admission (coefficient: 0.08, p<0.01) had a significant impact on loss of HRQoL 4 months after fracture.

HRQoL declines immediately after fracture. Pre-fracture HRQoL had a negative impact upon HRQoL 4 months after fracture whereas hospital admission improves the HRQoL. These short term changes in HRQoL are comparable to those reported with hip, spine and distal forearm fractures.

Table 1: Mean HRQoL (95%CI) immediately before and after fracture, and 4 months after fracture

| Fracture sites | n |
|--------------------|--------------|
| Pre-Fracture | |
| Post-Fracture | |
| 4 Months | |
| Weight Bearing | |
| 60 | |
| | 0.83 |
| | (0.78, 0.88) |
| | 0.30 |
| | (0.22, 0.38) |
| | 0.70 |
| | (0.62, 0.77) |
| Non-Weight Bearing | |
| 45 | |
| | 0.83 |
| | (0.78, 0.89) |
| | 0.49 |
| | (0.42, 0.56) |
| | 0.74 |
| | (0.66, 0.81) |
| Humerus | |
| 48 | |
| | 0.79 |
| | (0.73, 0.84) |
| | 0.28 |
| | (0.19, 0.37) |
| | 0.70 |
| | (0.66, 0.74) |
| Ankle | |
| 64 | |
| | 0.82 |
| | (0.77, 0.88) |
| | 0.32 |
| | (0.25, 0.39) |
| | 0.64 |
| | (0.59, 0.69) |
| e | |

Disclosures: Yu Zhang, None.

SA0330

Gender-Specific Hip Fracture Risk In Community-Dwelling And Institutionalized Seniors Age 65 Years And Older. Eduard Sidelnikov*¹, Michael Finsterwald², Robert Theiler³, Andreas Egli Linder⁴, Andreas Platz⁵, Hans-Peter Simmen⁶, Christian Meier⁷, Daniel Grob⁸, Sacha Beck⁹, Hannes B. Stähelin¹⁰, Heike Bischoff-Ferrari¹¹.
¹University of Zurich, Switzerland, ²Centre on Aging & Mobility, University Hospital Zurich & City Hospital Waid, Switzerland, ³Stadtspital Triemli, Switzerland, ⁴Centre on Ageing & Mobility, Switzerland, ⁵Department of Traumatology, Triemli City Hospital, Switzerland, ⁶Department of Emergency Medicine & Traumatology, University Hospital Zurich, Switzerland, ⁷Div. of Endocrinology, Diabetes & Metabolism, University Hospital Basel, Switzerland, ⁸Centre on Aging & Mobility, University Hospital Zurich & City Hospital Waid; Acute Geriatric Care, City Hospital Waid, Switzerland, ⁹Acute Geriatric Care, City Hospital Waid, Switzerland, ¹⁰Department of Geriatrics, University Hospital Basel, Switzerland, ¹¹University of Zurich, Switzerland

Background: Differences in gender-specific hip fracture risk in community-dwelling versus institutionalized seniors have not been well established.

Methods: In our primary analysis, we included 1084 hip fracture patients age 65 and older admitted to one large hospital center in Zurich, Switzerland between January 2005 and March 2010 (Triemli City Hospital). Official population statistics from the same time frame was obtained from the Statistical Bureau of the City of Zurich. Information on living conditions prior to the hip fracture (community-dwelling versus institutionalized), age, sex, body mass index (BMI), season, cognitive function, and comorbid conditions was obtained in all patients. For a sensitivity analysis, we extended to de-personalized data from 1265 hip fracture patients from the other two large hospital centers (City Hospital Waid and Zurich University Hospital) within the same time frame (2005-2009) and available data on age, living conditions, and fracture date.

Results: Hip fracture patients of the primary sample were on average 85.1 (SD = 7.1) years old and 78% of them were women. Among community-dwelling seniors, the risk of hip fracture was more than twice as high for women compared to men (RR = 2.11; 95% C.I.: 1.65 – 2.70). Among institutionalized seniors, the risk of hip fracture was 35% higher for men compared to women (RR = 1.35; 95% C.I.: 1.06 – 1.72) independent of age, BMI, season, comorbidities, and cognitive function. Consistent with the literature, age was a strong predictor of hip fracture risk: compared to seniors age 65 – 74 years, the risk of hip fractures increased more than 5 times for age 75 – 84 (RR = 5.55; 95% C.I.: 4.33 – 7.12), and 12 times for age 85-94 (RR = 12.39; 95% C.I.: 9.57 – 16.05), and more than 20 times for seniors age 95+(RR = 20.77; C.I.: 14.61 – 29.51). In the sensitivity analysis among 2349 patients of all 3 hospitals, community-dwelling women had a 67% higher risk of hip fracture than community-dwelling men (RR = 1.67; 95% C.I.: 1.43 – 1.97); and institutionalized men had 40% higher risk than institutionalized women (RR = 1.40; 95% C.I.: 1.00 – 1.85) independent of age and season.

Conclusion: It is widely believed that women have greater risk of hip fractures than men. Based on our data, that is the case for seniors living in the community, however, among nursing home patients men may be at higher risk.

Disclosures: Eduard Sidelnikov, None.

This study received funding from: City of Zurich and a Swiss National Foundations Professorship

SA0331

Occurrence of Previous Depression in Patients with Femoral Fracture in Pre-operative Phase. Fabiana Fonseca*¹, Ana Elisa Sena Klein Rosa², Segantin Bianca Isis², Priscila Primo Cáo², Thaise Arruda².
¹PUC - SP, Brazil, ²PUC-SP, Brazil

The relationship of the body in old age is very particular to each be. the objective of this study was to highlight the prevalence of depression in elderly 40 (thirty-one females and nine males) with fracture of femur in indication of surgical treatment in pre-operative stage, diagnosed with depression progresso serviced by the Hospital's Orthopedic Service of the São Paulo State Public Server. This is an observational study of cross-section. Data collection occurred with visit to patient records files and interviews structured way during the period October 2010 to February 2011. All statistical analyses were made by software Statistical Package for the Social Sciences for Windows, version 15.0. The survey was submitted to the Committee of ethics in research of Hospital Sao Paulo State civil servant and approved in April 2010. The age varied from 62 to 97 years, averaging equal to 78.9 years, dp of 9.5 years and median of 79 years, with the intention of crossing factors that concern the process of human aging, we got six seniors (15%) with a diagnosis of depression. For Gerontology, old age should be understood under different looks. With this study, we were able to note that a policy of Public Health is required to develop actions that are intended to identify situations that may be harmful to the elderly in relation to the increased risk of falls.

Disclosures: Fabiana Fonseca, None.

SA0332

See Friday Plenary Number FR0332.

SA0333

Prevalence of Fractures in Women with Rheumatoid Arthritis or Systemic Lupus Erythematosus on Chronic Glucocorticoid Therapy in Spanish Population. Maria Luz Rentero¹, Encarnación Amigo², Nicolás Chozas³, Manuel Fernández⁴, Susana Sarnago⁵. ¹Medical Department Lilly, Spain, ²Hospital de Lugo, Spain, ³Hospital Puerta del Mar, Spain, ⁴Hospital Sanitas La Moraleja, Spain, ⁵Eli Lilly & Company, Spain

Purpose: To determine the prevalence of vertebral and non-vertebral fractures in the Spanish population of women with diagnosis of rheumatoid arthritis (RA) or systemic lupus erythematosus (SLE) on chronic glucocorticoid (GC) therapy.

Methods: This is a cohort, open-label, multicentric, non-drug interventional, descriptive and cross-sectional study to assess the prevalence of vertebral and non-vertebral fractures in women ≥ 18 yrs with ≥ 1 year diagnosis of RA or SLE, on chronic GC therapy ≥ 2.5 mg of prednisone [or equivalent] for at least 3 months. Information regarding the disease, time and dose of GC treatment, prevalent vertebral and non-vertebral fractures and patients quality of life (SF-36 questionnaire) was collected. All patients had a thoracic-lumbar spine radiography and FRAX evaluation.

Results: 39 sites in Spain participated in the study (n=605 women screened from those attending the rheumatologist's office for any reason and 592 enrolled), obtaining complete data for 575 women with a mean age of 59.6+15 yrs, BMI 26.8+4.8 and 73% were postmenopausal. 83.3% (n=480) were diagnosed of RA and 16.7% (n=95) of SLE. Only 6.4% of the study population referred prevalent vertebral fractures, but in fact we confirmed by X-ray their existence in up to 18.9% of the total of patients. 9% of them stated to have suffered at least one non-vertebral fragility fracture located mainly at the distal radius and proximal femur. Mean dose of GC was 5.6 mg+3.3 of prednisone [or equivalent] for a median of 6.3 yrs. FRAX evaluation revealed the presence of any previous fracture increased by ≥ 2.5 fold the risk of ten-year probability of major osteoporotic fracture [mean (SD)=22.7+14.50 vs 8.7+8.40 respectively] or hip fracture [mean (SD)=14.8+14.1 vs 3.9+6.7 respectively]. The scores of physical component and functioning SF-36 domains were significantly lower for patients with prevalent vertebral or any fractures vs those without previous fractures. The 66.7% of the studied population was on osteoporosis treatment, out of which 43.4% were on antiresorptive therapy and 2.1% were taking anabolic treatment (49% were on calcium or Vit D). **Conclusions:** Prevalence of vertebral fractures in this setting is 3-fold greater than doctors and patient assume, so it would be very important to increase the awareness in order to enhance diagnosis and fracture prevention. AR and SLE patients with prior fractures have worse quality of life and increased risk of fracture.

Disclosures: Maria Luz Rentero, Eli Lilly and Company, 3
This study received funding from: Eli Lilly and Company

SA0334

Risk of Fracture among Treated and Untreated Men with Osteoporosis. Karen Smoyer Tomic¹, Joanne LaFleur², Liisa Palmer³, David M. Smith⁴, Carly Paoli⁵, Irene Agodoa⁶, Nicole Yurgin⁷. ¹Thomson Reuters, USA, ²University of Utah, USA, ³Thomson Reuters, USA, ⁴Thomson Reuters, USA, ⁵Amgen, USA, ⁶Amgen, USA, ⁷Amgen Inc., USA

Purpose: Osteoporosis (OP) affects an estimated 2 million men in the United States. The relationship between treatment and fracture outcomes has been reported from clinical trial populations, but little is known about the impact of treatment on fracture risk among men with OP in the real-world setting.

Methods: The *MarketScan*® Medicare Supplemental and Coordination of Benefits Database was used to identify treated (received an OP medication) and untreated (had an OP diagnosis or fragility fracture but no OP medication) men with OP between 1/1/04 and 4/30/10 and at least 12 months pre-period and 3 months post-period follow-up in the database. Patients were matched on pre-period fracture and age (± 2 years). Follow-up time was variable and ended with fracture, inpatient death, end of health plan eligibility, or on 4/30/10, whichever came first. Fracture incidence rates and time to fracture were reported. A Cox proportional hazards model was used to assess whether treated men had a lower risk of fracture compared to untreated men after controlling for demographic and clinical characteristics.

Results: Of the 3,072,696 men ≥ 65 years in the database, a total of 31,696 men met the inclusion and match criteria (15,848 in each cohort). In both cohorts, the mean age was 78 years and 55% had a pre-period fracture. 1,990 treated men had a follow-up fracture [incidence = 5.98/100 person-years (p-y)] over 33,274 p-y of follow-up, compared to 2,231 untreated men with a follow-up fracture (incidence = 8.03/100 p-y) over 27,785 p-y. Treated men also had longer mean time to fracture (588 days, SD 426) than untreated men (401 days, SD 372, $p < 0.001$). The adjusted risk of fracture was lower among treated men compared to untreated men (adjusted hazards ratio = 0.83, 95% CI: 0.78 to 0.89). Other pre-period factors associated with an increased risk of fracture were urban residence, no bone mineral density test, use of benzodiazepines, and a higher number of comorbidities and concomitant medications.

Conclusion: The fracture incidence rate was lower and time to fracture was longer for men with OP who received treatment than for those without treatment. After

controlling for prior fracture and other risk factors, treated men had a lower adjusted risk of fracture. To better characterize the benefit of OP treatment, more research is needed into the role of medication adherence and risk of fracture among men with OP.

Disclosures: Irene Agodoa, Amgen, 9
This study received funding from: Amgen

SA0335

Sex Steroid Hormones and Fracture in a Multi-ethnic Cohort of Women: The Women's Health Initiative (WHI). Jane Cauley¹, Michelle Danielson², Robert Boudreau³, Tanushree Prasad³, Douglas Bauer⁴, Rebecca Jackson⁵, Jean Wactawski-Wende⁶, Rowan Chlebowski⁷, Kristine Ensrud⁸. ¹University of Pittsburgh Graduate School of Public Health, USA, ²University of Pittsburgh, USA, ³University of Pittsburgh, USA, ⁴University of California, San Francisco, USA, ⁵The Ohio State University, USA, ⁶University at Buffalo, USA, ⁷University of California, Los Angeles, USA, ⁸Minneapolis VA Medical Center / University of Minnesota, USA

Sex steroid hormones have been linked to the risk of hip fracture. To our knowledge, however, all of these studies have been carried out in White women. The objective of the current analysis was to test the hypothesis that sex steroid hormones influence the risk of fracture across race/ethnicity. We performed a nested case-control study within the prospective WHI Observational Study. Fractures were self-reported except for hip fractures. We excluded spine, facial and digit fractures. Incident fractures were identified in 381 Black, 192 Hispanic, 112 Asian, and 46 Native American women over an average of 8.6 years. A random sample of 400 White women who fractured was chosen. One control was selected per case and matched on age, race/ethnicity, and blood draw date. Serum bioavailable estradiol (BioE₂), testosterone (BioT) and sex hormone-binding globulin (SHBG) were measured using baseline fasting serum. Conditional logistic models were used to calculate the odds ratio (OR) and 95% confidence interval (CI). Tertile cutoffs were determined in the total sample of controls. The mean age of the women across ethnicity ranged from 63-66 yrs. Comparison of median sex hormones among controls showed that BioE₂ (pg/ml) levels were lowest in Asian women (5.3) and highest in Black and Native American women (8.1). Median BioT (ng/dL) levels were also lowest in Asian women (9.5) and highest in Black women (12.1). Median SHBG (nmol/L) levels were lowest in Black women (37.9) and highest in White women (48.1). In multivariable adjusted models, higher BioE₂ was associated with a decreased risk of fracture among White and among Black women. Higher BioT was associated with a lower risk of fracture in Black women but it was not significant in White women. Increasing SHBG was associated with a lower risk of fracture in Whites but a higher risk of fracture in Blacks (p race x SHBG interaction = 0.004). There was no association between sex steroid hormones and fracture in the other ethnic groups except higher BioT was associated with a lower risk of fractures in Native American women; OR per 1 standard deviation increase in BioT = 0.20(0.05, 0.76). In conclusion, serum E₂ is an important biomarker for fracture risk in both White and Black women. Testosterone levels appear to have greater influence on fracture risk in Black and Native American women. The differential association between SHBG and fracture in Whites and Blacks needs replication.

Table: Odds ratio (95% CI) of fracture across tertiles of sex steroid hormones

| | White ^{1,2,3} | | | | | | Black ^{1,2,3} | | | | | |
|-------------------|------------------------|----------------------|----------------------|---------|----------|----------------------|------------------------|---------|--|--|--|--|
| | Tertiles | | | P trend | Tertiles | | | P trend | | | | |
| | 1 | 2 | 3 | | 1 | 2 | 3 | | | | | |
| BioE ₂ | Ref | 0.71 (0.46, 1.05) | 0.52 (0.33, 0.80) | 0.003 | Ref | 0.65 (0.40, 1.04) | 0.52 (0.32, 0.86) | 0.012 | | | | |
| BioT | Ref | 1.02 (0.76, 1.46) | 0.79 (0.54, 1.16) | 0.25 | Ref | 0.90 (0.57, 1.40) | 0.54 (0.34, 0.85) | 0.004 | | | | |
| SHBG | Ref | 0.81 (0.56, 1.16) | 0.65 (0.44, 0.96) | 0.032 | Ref | 1.60 (1.08, 2.37) | 1.51 (0.98, 2.32) | 0.039 | | | | |

¹ Matched on age, race, date of blood draw.

² WHI model: adjusted for weight, height, physical activity, calcium intake, history of fracture.

³ Tertile cutoffs: BioE₂ (pg/ml) = ≤ 4.83 , >4.83 - 8.21 , >8.21 ; BioT (pg/ml) = ≤ 8.46 , >8.46 - 13.4 , >13.4 ;

SHBG (nmol/L) = ≤ 38 , >38 - 58.2 , >58.2 .

table

Disclosures: Jane Cauley, None.

SA0336

The Contributions of First Nations Ethnicity, Income, and Delays in Surgery on Mortality Post-fracture: A Population-based Analysis. William Leslie¹, Sharon Brennan², Heather Prior³, Lisa Lix⁴, Colleen Metge¹, Brenda Elias⁵. ¹University of Manitoba, Canada, ²The University of Melbourne, Australia, ³University of Manitoba, Canada, ⁴University of Saskatchewan, Canada, ⁵University of Manitoba, Canada

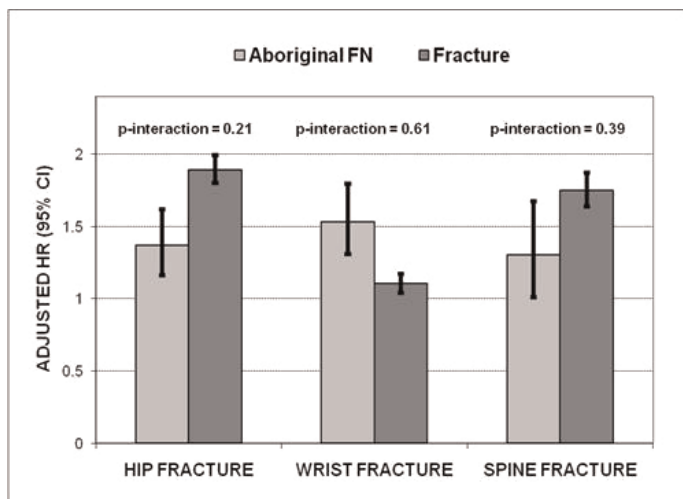
Purpose: Social determinants may influence post-fracture mortality risk. First Nations peoples are the largest group of Aboriginal (Indigenous or Native) peoples in Canada, and have a greater risk of fracture, and of mortality, than non-First Nations peoples. The purpose of this study was to examine the independent contributions of First Nations ethnicity and income to post-fracture mortality, and the association with time to surgery following hip fracture.

Methods: We used a retrospective case-control design in which non-traumatic fracture cases and fracture-free controls from Manitoba, Canada, aged ≥ 50 years

were matched for sex, age (within 5 years of birth), First Nations ethnicity, and number of co-morbid conditions. We examined differences in mortality after fracture of (i) the hip, wrist or spine between the years of 1996-2004 (Study Population 1), and (ii) the hip between the years of 1987-2002 (Study Population 2). Cox proportional hazards regression was used to model time to death. For hip fracture, logistic regression analyses were used to model the probability of death within 30 days and one year of fracture.

Results: In Study Population 1, First Nations ethnicity was associated with an increased mortality risk of 30-53% for each type of fracture, but there was no statistically significant interaction between fracture status (case-control), and First Nations ethnicity for any of the fracture types (all $p > 0.2$, Figure). Lower income was associated with an increased mortality risk of 18% for both hip and vertebral fracture, and of 26% for wrist fracture. In Study Population 2, lower income predicted mortality overall (OR 1.15, 95%CI 1.07-1.23) and for hip fracture cases (OR 1.18, 95%CI 1.05-1.32), as did older age, male sex, diabetes and >5 co-morbid conditions (all $p \leq 0.01$). Higher mortality was also seen for a pertrochanteric fracture (OR 1.14, 95% CI 1.03-1.27), surgery times of 2-3 days (OR 1.34, 95%CI 1.18-1.52) or ≥ 4 days (OR 2.35, 95%CI 2.07-2.67) after fracture.

Conclusion: Given that First Nations peoples have a higher baseline mortality compared to non-First Nations peoples, a similar relative increase in mortality associated with fracture appears to translate into a larger absolute increase in post-fracture mortality. Lower income and surgery times of >2 days are predictors of an increased mortality risk post-fracture. These data have implications regarding the prioritization of health care delivery.



No interactions between fracture status (case-control) and First Nations ethnicity

Disclosures: Sharon Brennan, None.

SA0337

See Friday Plenary Number FR0337.

SA0338

Genome-Wide Association Study Identifies the Chromosome 1q23 Gene UHMK1 as a Novel Bone Mass Density Susceptibility Gene. Hyung Jin Choi¹, Ye An Kim², Joo-yeon Hwang³, Lei Zhang⁴, Yu-fang Pei⁴, Jian Li⁵, Qing Tian⁵, Hong-Wen Deng⁶, Ah Reum Khang⁷, Jung Hee Kim⁸, Sang Wan Kim⁹, Jong-Young Lee¹⁰, Bok-Ghee Han¹⁰, Seong Yeon Kim⁷, Nam H Cho¹¹, Chan Soo Shin². ¹Chungbuk National University Hospital, South Korea, ²Department of Internal Medicine, Seoul National University College of Medicine, South Korea, ³Republic of Korea, ⁴Center of System Biomedical Sciences, University of Shanghai for Science & Technology, China, ⁵Tulane University, USA, ⁶Tulane University, USA, ⁷Department of Internal Medicine, Seoul National University College of Medicine, South Korea, ⁸Seoul National University College of Medicine, South Korea, ⁹Seoul National University Boramae Hospital, South Korea, ¹⁰Center for Genome Science, National Institute of Health, South Korea, ¹¹Department of Preventive Medicine, Ajou University School of Medicine, South Korea

Most large-scale genome-wide association studies (GWAS) of bone mineral density (BMD) have been focused on Caucasian populations. Caucasians and Asians are two distinct ethnic groups, with appreciable ethnic difference in genetic background and osteoporosis related phenotypes. To identify genetic variants that influence BMD in East Asians, we performed a quantitative trait analysis of total hip, femoral neck and lumbar spine BMD in 2729 unrelated subjects from population-based cohorts in Korea. Then, in silico replication of promising GWAS signals were performed in a Chinese Han population and two Caucasian populations (1547, 2250 and 987 subjects, respectively). We identified three BMD loci that reached

genome-wide significance ($P < 5 \times 10^{-7}$), of which one locus on 1q23 (UHMK1, rs16863247, $P = 4.1 \times 10^{-7}$ for femoral neck BMD and $P = 3.2 \times 10^{-6}$ for total hip BMD) was novel, not previously associated with bone phenotypes. Interestingly, the minor allele frequency (MAF) of rs16863247 was very low in Caucasian populations (MAF < 0.01), indicating that this association could be specific to East Asians. Two SNPs (rs9371538 and rs1856859) in the known BMD region on 6q25 (C6orf97/ESR1) were associated with lumbar spine BMD ($P = 5.6 \times 10^{-9}$ and $P = 9.4 \times 10^{-9}$, respectively). One SNP (rs7776725) in the known BMD region on 7q31 (FAM3C) was associated with total hip BMD ($P = 8.6 \times 10^{-9}$) and femoral neck BMD ($P = 1.3 \times 10^{-6}$). In gender specific analysis, one SNP (rs1160574) on 1q32 (KCNH1) was associated with femoral neck BMD ($P = 2.1 \times 10^{-7}$) and total hip BMD ($P = 2.2 \times 10^{-7}$) in female subjects. UHMK1 encodes a serine/threonine protein kinase KIS (Kinase Interacting with Stathmin). Interestingly, a recent report demonstrated that Stathmin plays an important role in the maintenance of bone mass by regulating osteoblast and osteoclast functions. Our results identify the UHMK1 gene as a candidate for East Asian specific BMD loci.

* Co-corresponding authors: Nam H Cho and Chan Soo Shin

Disclosures: Hyung Jin Choi, None.

SA0339

See Friday Plenary Number FR0339.

SA0340

The Influence of Educational Interventions on Modifiable Risk Factors for Osteoporosis After a Fragility Fracture. Louis Bessette¹, Claudia Beaudoin², Sonia Jean³, Louis-Georges Ste-Marie⁴, Jacques Brown⁵. ¹Centre Hospitalier De L'Universite Laval, Canada, ²Crchuq Research Centre-chul, Canada, ³INSTITUT NATIONAL DE SANTÉ PUBLIQUE DU QUÉBEC, Canada, ⁴CHUM, Canada, ⁵CHUQ Research CentreLaval University, Canada

Purpose: To investigate the effect of educational interventions on modifiable risk factors for osteoporosis in women (>50 old) after a fragility fracture (FF).

Methods: This study was part of the Recognizing Osteoporosis and its Consequences in Quebec (ROCQ) programme. Women who recently suffered a FF were recruited from hospitals and from an administrative database-generated list (Quebec Ministry of Health). Six to eight months after FF, women were contacted to complete questionnaires and were randomized into the control group (usual care group) or the intervention groups (written materials or videocassette + written materials). The written materials consisted of information for both the patient and their respective primary care physician regarding osteoporosis, FF and the need for treatment following FF. The 15-minute video consisted of similar information as the written materials, but went into greater depth. Women in the usual care group were told that their fracture was related to osteoporosis but did not receive the educational tools. Twelve months following randomization, follow-up questionnaires were completed. The proportion of women who improved their behavior for dietary calcium, physical activities, and alcohol and caffeine consumption 12 months after randomization were compared between usual care and intervention groups. Both intervention groups were combined for this analysis.

Results: In this analysis, we included 1,175 women (387 control, 788 interventions) with neither a diagnosis nor treatment for osteoporosis at randomization. No statistically significant difference was detected between the two groups (table).

Conclusions: When comparing the usual care group to the intervention groups, we cannot conclude that the interventions lead to statistical significant changes in the women's behavior. Therefore, a simple educational intervention on osteoporosis is not sufficient to influence life style in women who have recently suffered a FF.

| Outcome | Randomization group | % improving their behavior | P-value |
|--|---------------------|----------------------------|---------|
| Increase in dietary calcium consumption (mg/day) | Control | 45.9 | 0.142 |
| | Interventions | 50.6 | |
| Increase in time spent walking (hours/week) | Control | 24.2 | 0.686 |
| | Interventions | 25.3 | |
| Decrease in sedentary behaviors (hours/day) | Control | 37.2 | 0.392 |
| | Interventions | 34.6 | |
| Increase in level of physical activity (kcal/week) | Control | 47.5 | 0.703 |
| | Interventions | 46.3 | |
| Decrease in alcohol consumption (#/week) | Control | 32.6 | 0.278 |
| | Interventions | 29.4 | |
| Decrease in caffeine consumption (mg/day) | Control | 25.6 | 0.614 |
| | Interventions | 27.0 | |

P-value: Type 3 test from logistic regression

Proportion (%) of women who improved their behavior according to randomization group

Disclosures: Louis Bessette, Amgen, 2; Amgen, 6

This study received funding from: Amgen, Alliance for Better Bone Health (sanofi-aventis and Warner Chilcott), Eli Lilly, Merck Canada, Novartis

SA0341

See Friday Plenary Number FR0341.

SA0342

Abdominal Aortic Calcification is Associated with Vertebral Fractures Independent of Bone Mineral Density in Patients with Type 2 Diabetes. Noriko Ogawa-Furuya^{*1}, Masahiro Yamamoto², Masayuki Shinohara³, Toru Yamaguchi⁴, Toshitsugu Sugimoto⁵. ¹Shimane University Faculty of Medicine, Japan, ²Shimane University Faculty of Medicine, Japan, ³Hosogi Hospital, Japan, ⁴Shimane University Faculty of Medicine, Japan, ⁵Shimane University School of Medicine, Japan

Introduction: Meta-analyses study shows that hip fracture risk of type 2 diabetes mellitus patients (T2DM) is higher than that estimated by bone mineral density (BMD). We also reported that T2DM have an increased risk of vertebral fractures (VFs) despite increased their BMD. These results suggest that it is difficult to assess fractures risk by BMD in T2DM. Thus, investigation of other risk factors for VFs in T2DM is needed. Vascular calcification is known to be associated with osteoporosis in non-T2DM subjects. However, association between the presence of vascular calcification and VFs in T2DM still remains unclear. The aim of this study is to investigate whether or not the abdominal aortic calcification is involved in VFs in T2DM.

Methods: A total of 163 Japanese men and 196 postmenopausal women with T2DM (average age: 65 and 66; HbA1c: 8.9% and 8.9%; number of vertebral fracture: 66 and 61, respectively) were recruited. All subjects were over age 50, and whose creatinine levels were within normal range. We measured BMD at the lumbar spine, femoral neck, and radius 1/3, and evaluated VFs by thoracic and spinal radiographs. The abdominal aortic calcification scores (ACS) were assessed on lateral 1st to 4th lumbar spine radiographs by semiquantitative method of Frye et al. We analyzed a cross-sectional association between the presence of ACS and VFs.

Results: ACS of the VFs group in each sex were significantly higher than those of non-VFs group (Men: 2.7 ± 3.3 vs. 1.5 ± 2.3 , $P < 0.01$; Women: 3.1 ± 5.7 vs. 1.1 ± 2.6 , $P < 0.01$). ACS 3 or more was significantly increased risk for VFs in both genders compared with AAC 2 or less after adjustment for age, BMI, creatinine, HbA1c, duration of T2DM, LDL-cholesterol, Neck BMD, calcium, phosphate, BAP, and smoking [Men: odds ratio (OR) 2.67 (95% confidential interval (CI) 1.23-5.77), $P < 0.05$; Women: OR 2.80 (95% CI 1.14-6.87), $P < 0.05$].

Conclusions: These findings showed that ACS were associated with VFs independent of BMD in T2DM in both sexes, suggesting that abdominal aortic calcification may be linked to deteriorating bone quality and become a risk factor for VFs in T2DM.

Disclosures: Noriko Ogawa-Furuya, None.

SA0343

See Friday Plenary Number FR0343.

SA0344

See Friday Plenary Number FR0344.

SA0345

See Friday Plenary Number FR0345.

SA0346

See Friday Plenary Number FR0346.

SA0347

See Friday Plenary Number FR0347.

SA0348

Mortality of Non-respondents in a Population-based Cohort (OSTPRE) Study. Risto Honkanen^{*1}, R. Sund², Marjo Tuppurainen³, Heli Koivumaa-Honkanen⁴, Heikki Kröger⁵. ¹University of Eastern Finland, Finland, ²National Institute for Health & Welfare, Finland, ³Kuopio University Hospital, Finland, ⁴Kuopio University Hospital, lapland Hospital district, Finland, ⁵University of Eastern Finland, Finland

Nonresponse is a menace to the representativeness of a study. The Kuopio Osteoporosis Risk Factor and Prevention (OSTPRE) Study targeted to recruit all women (14220) born in 1932-41 and living in a defined geographic area in Eastern Finland in 1989. A high response (91 %) was achieved: 13100 responded. The cohort has now been followed for 20 years 1989-2009.

The purpose of this study was to compare the 20-year mortality of the non-respondents to that of the respondents. The Kaplan-Meier survival analysis was used.

A total of 1975 women died during the follow-up. The mortality of the non-respondents was double compared to that of the respondents (Figure). The most common causes of death were cancer 706 (42.9 %) vs. 89 (27.1 %), cardiovascular disease 533 (32.4 %) vs. 140 (42.7 %) and injury 110 (6.7 %) and 20 (6.1 %) for the respondents vs. non-respondents, respectively.

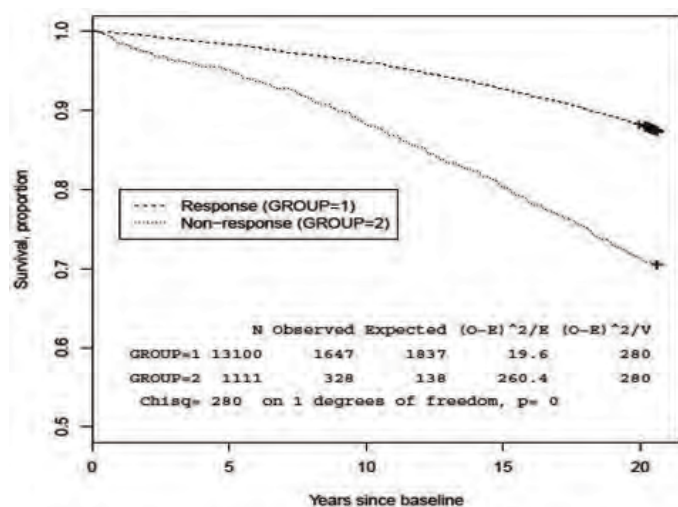


Figure 1.

Conclusions. Morbidity and mortality of non-respondents are higher than those of respondents. This may affect prevalence and risk factor effect estimates.

Disclosures: Risto Honkanen, None.

SA0349

See Friday Plenary Number FR0349.

SA0350

See Friday Plenary Number FR0350.

SA0351

Trabecular Bone Micro-Architecture during SSRI Treatment Using Multi-Detector CT Imaging and Topological Analysis on a Continuum between Plates and Rods. Punam K. Saha^{*1}, CHADI CALARGE¹, Cheng Li¹, Yinxiao Liu², Jessica Fishbaugher², Bille Tyler², Nichole Baker², Trudy Burns², Kathleen Janz¹, James Torner², Steven Levy¹. ¹University of Iowa, USA, ²University of Iowa, USA

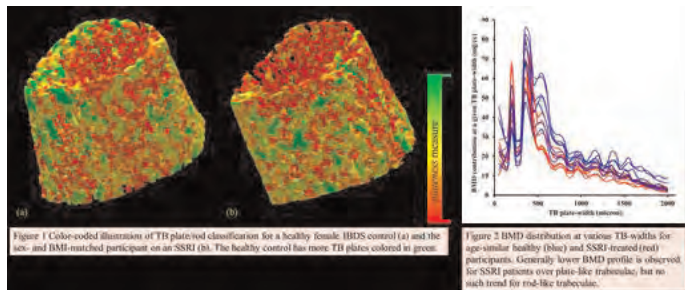
Background: Recent evidence has implicated serotonin in bone metabolism and selective serotonin reuptake inhibitors (SSRIs) in bone-loss and increased fracture-risk. Trabecular bone (TB) micro-architecture is a strong determinant of bone-strength and fracture-risk, yet, to our knowledge, it has not been characterized in SSRI-treated patients. We recently developed a peripheral high-resolution multi-detector CT (MD-CT)-based algorithm that generates unique TB micro-architectural measures by classifying individual trabeculae on a continuum between plates and rods. This algorithm was applied in a pilot study exploring TB micro-architecture in young adults receiving long-term SSRI treatment.

Methods: Seven patients (18-23 years, 2 male/5 female) on continuous treatment with an SSRI for at least one year were recruited (mean treatment duration: 3.3 ± 3.0 years; mean fluoxetine-equivalent dose: 36 ± 13 mg/day); seven sex- and body mass

index (BMI)-matched age-similar controls were selected from the Iowa Bone Development Study (IBDS) cohort. MD-CT scans of the distal tibia were acquired on a 128 slice Siemens Flash scanner at 120kV, 200mAs, pitch: 1, 0.3mm slice-thickness and 10cm scan-length (total effective dose: 0.17mSv \approx 20 days of environmental radiation). A Gammex calibration phantom was used to transform CT Hounsfield unit into BMD (mg/cc).

Results: Figure 1 compares color-coded TB plate/rod classification for a healthy female IBDS control and the matched citalopram-treated participant. It suggests that the healthy control has more TB plates (green). Figure 2 depicts BMD distribution at various TB-widths for healthy (blue) and SSRI-treated (red) participants, showing a generally lower BMD profile for SSRI patients at plate-widths greater than 400 μ m, i.e., plate-like trabeculae, but no such trend at lower plate-widths representing rod-like trabeculae. In fact, a pairwise comparison between healthy controls and matched SSRI-treated participants showed 1.7% ($p=0.017$) lower total BMD in the SSRI-treated participants. In particular, compared to controls, mean TB plate-width was 5.5% ($p=0.164$) lower and BMD at plate-like trabeculae was 24.5% ($p<0.002$) lower in the SSRI group.

Conclusion: Long-term SSRI treatment may be associated with magnified TB micro-architectural alterations. Our preliminary findings require confirmation in a larger sample, where the potential confounding skeletal effect of psychopathology is accounted for.



(1) Illustrations of TB plate/rod classification. (2) BMD distribution at various TB plate-widths.

Disclosures: Punam K. Saha, None.

This study received funding from: NIH grants: R01-AR054439, R01-DE012101, and UL1-RR024979

SA0352

Bone Health in CHARGE syndrome. Leila Khan^{*1}, Mariam Stevens², Krupa Doshi¹, Susan Williams³, Angelo Licata³. ¹Cleveland Clinic, USA, ²Cleveland Clinic, USA, ³Cleveland Clinic Foundation, USA

CHARGE syndrome first recognized in 1979 is a cluster of congenital abnormalities characterized by coloboma, heart defects, choanal atresia, growth retardation, genital hypoplasia, and ear anomalies (1). It has an estimated population-based incidence of 1/9,000 live births (2). The clinical diagnosis is made from identification of the major features of syndrome described above. Although several genetic abnormalities have been documented, a mutation on the CHD7 gene on chromosome 8q12 represents the likely cause for most affected patients (3, 4).

A 25 year old woman with CHARGE syndrome presented to endocrine clinic for evaluation of amenorrhea. Her evaluation revealed absent puberty with primary amenorrhea, complete vision loss in left eye, bilateral hearing loss, and history of surgically corrected congenital heart defects. She denied fractures and back pain, and she used no vitamin or mineral supplements. She was Tanner stage two, had scoliosis, and was short statured compared to other family members. Laboratory evaluation revealed hypogonadotropic hypogonadism with low levels of FSH and estradiol, and normal parathyroid, 25 OH vitamin D, and electrolyte levels. Calcium phosphorus product was 40 mg/dL. Bone density z-score was less than -1.5 in lumbar spine and both bilateral hips, and pelvic ultrasound revealed hypoplastic uterus and absent ovaries. Gene testing was positive for heterozygous mutation in the CDH7 gene. Other biochemical indices were normal. Treatment plan includes initiation of oral contraceptive, calcium and vitamin d replacement, and weight bearing exercise.

Individuals with CHARGE syndrome are at increased risk of developing low bone mass. In a longitudinal cohort study, questionnaires were collected from caregivers of 30 individuals with CHARGE. Results indicated that most had delayed or absent puberty with the majority not receiving hormone replacement therapy, receiving diets markedly deficient in calcium and vitamin D, and performing in less weight bearing physical activity as compared to controls (5). It is important to recognize the skeletal consequences of CHARGE since many are unaware of the risks towards poor bone health.

Disclosures: Leila Khan, None.

SA0353

See Friday Plenary Number FR0353.

SA0354

Hypophosphatasia Diagnosed in Adults: Differential Features Based on Sex, Presence of Fractures, and Symptoms at Presentation. Kathryn Berkseth¹, Peter Tebben², Matthew Drake³, Robert Wermers^{*4}. ¹University of Washington, USA, ²Mercy Clinic, USA, ³College of Medicine, Mayo Clinic, USA, ⁴Mayo Clinic, USA

Introduction: Adult hypophosphatasia (HPP) is a rare disorder characterized by low serum alkaline phosphatase (AP) levels. Limited data exists regarding the clinical presentation of HPP diagnosed in adults.

Aim: To evaluate the clinical and biochemical characteristics of adult HPP based on sex, presence of fractures, and symptoms at presentation.

Methods: Mayo Clinic Rochester patients diagnosed with HPP as adults from 1976 through 2008 were identified by diagnostic code or the medical record. Inclusion criteria were: age \geq 18 years at diagnosis; low serum AP without bisphosphonate therapy; and one additional supporting element including elevated pyridoxal 5'-phosphate (PLP) or urine phosphoethanolamine (PEA), evidence of osteomalacia (pseudofracture or stress fracture), family history, or positive genetic testing.

Results: Over the 33 year period reviewed, 22 unrelated adults were diagnosed with HPP. Median age at diagnosis was 49 years; 68% were female. Most patients (68%) were symptomatic at presentation with primary features including musculoskeletal pain (41%) or fracture (18%). Overall, 54% of patients had a history of fracture as an adult: hip/femoral neck (23%), feet (23%, all women), wrist (18%), and spine (9%, all men). Nine patients (36%) had multiple fractures, while four (all women) had subtrochanteric femur fractures. Femoral pseudofractures were observed in 2 patients; one each in a male and female. Chondrocalcinosis was only identified in women (40%). Symptomatic subjects had more fractures and chondrocalcinosis, lower median alkaline phosphatase and PLP levels, and higher median PEA levels, compared to asymptomatic patients. Clinical features seen more commonly in fracture patients included the presence of symptoms at presentation, a history of childhood rickets, dental abnormalities, lower median alkaline phosphatase levels, and higher median urine PEA levels. Conversely, median PLP levels were higher in subjects without a history of fracture.

Conclusion: Adult HPP demonstrates a wide spectrum of clinical manifestations including musculoskeletal pain, fractures, chondrocalcinosis and dental anomalies. Some overlap in laboratory characteristics exists in relationship to disease severity. In addition to genetic and environmental factors, sex may influence the clinical expression of HPP.

Disclosures: Robert Wermers, None.

SA0355

See Friday Plenary Number FR0355.

SA0356

System-level Approaches to the Secondary Prevention of Osteoporotic Fractures: A Systematic Review and Meta-analysis. Kirtan Ganda¹, Markus Seibel^{*2}, Michele Puech³, Jian Sheng Chen⁴. ¹Concord Hospital, Australia, ²Bone Research Program, ANZAC Research Institute, University of Sydney, Australia, ³Public Health Unit, Hornsby Ku-ringai Hospital, Australia, ⁴Institute of Bone & Joint Research, The University of Sydney, Australia

Introduction: Despite the availability of effective treatments that reduce re-fracture and mortality rates in patients presenting with incident osteoporotic fractures, the majority of these patients are not being assessed or treated for osteoporosis. In the past, numerous clinical care pathways have been trialed to close this treatment gap. We evaluated the effectiveness of published system-level care approaches for the secondary prevention of fractures in patients with osteoporosis.

Methods: We searched eight medical literature databases using relevant key words to identify reports published between 1996 and 2011, describing clinical or system-level care models for secondary fracture prevention. The following information was extracted from each publication by two independent researchers: Study design, patient characteristics, identification strategies, assessment and treatment initiation strategies and outcome measures (rates of BMD testing, anti-resorptive treatment initiation, re-fractures, and cost-effectiveness). The outcomes within each model of care were analysed in two ways: Firstly, we conducted meta-analyses of studies with valid control groups for two outcome measures, BMD testing and anti-resorptive treatment initiation. Secondly, we described the outcomes of studies not included in the meta-analysis, stratified by the model of care.

Results: The literature search identified 43 studies and re-grouped them into four general models of care: Type A, where patients are identified, assessed and treated as part of a fully integrated service; Type B, as in A, but the service only makes treatment recommendations (no initiation of therapy); Type C, which consists of patient education plus alerting the primary care physicians to the need for further assessment and treatment; Type D, consists of patient education only. The meta-analyses showed a trend towards better rates of BMD testing and treatment initiation with increasing intensity of intervention (table). Only five studies examined re-fracture rates but only one Type A had a control group and enough power to show a significant decrease in

re-fractures at 4 years follow-up. Type A & B services have been shown to be cost-effective.

Conclusions: Fully co-ordinated system-level approaches to secondary prevention of osteoporotic fractures appear more effective in improving patient outcomes than approaches involving alerts and/or education only, whilst still being cost-effective.

| Intervention Type | Risk Difference | 95% Confidence Interval |
|---------------------------|-----------------|-------------------------|
| Model of care 'A' (n = 8) | 0.29 | 0.19 - 0.40 |
| Model of care 'B' (n = 5) | 0.21 | 0.05 - 0.37 |
| Model of care 'C' (n = 7) | 0.16 | 0.07 - 0.25 |
| Model of care 'D' (n = 1) | 0.03 | 0.00 - 0.07 |

Summary of Meta-analyses: Treatment initiation rates by intervention type

Disclosures: Markus Seibel, None.

SA0357

Serum Sclerostin Levels Positively Correlate with the Expanded Disability Status Scale in Ambulatory Women with Multiple Sclerosis. Vit Zikan^{*1}, Ivan Raska Jr¹, Michaela Tyblová², Maria Luchavova¹, Eva Havrdova², Dana Michalska¹. ¹Department of Internal Medicine III- Department of Endocrinology & Metabolism, First Faculty of Medicine, Charles University in Prague & General University Hospital in Prague, Czech Republic, ²Department of Neurology, First Faculty of Medicine, Charles University in Prague & General University Hospital in Prague, Czech Republic

Background: The progressive immobilization, namely walking impairment is one of the most life-limiting consequences of multiple sclerosis (MS) and the most important risk factor for osteoporosis and fractures. Sclerostin, a major inhibitor of Wnt signaling and bone formation, is regulated by mechanical strain and may play a role in the pathogenesis of disuse bone loss. The aim was to evaluate the relationship between serum sclerostin levels and motor disability (assessed by Expanded Disability Status Scale, EDSS), bone mineral density (BMD) and biochemical markers of bone remodeling in ambulatory women with MS. Methods: We measured serum sclerostin levels in 120 ambulatory MS women with EDSS \leq 6.5, aged 25 to 68 years and in healthy controls. Carboxy-terminal telopeptide of type I collagen, N-terminal propeptide of procollagen type I (PINP) were evaluated by ECLIA. Sclerostin was evaluated by ELISA. Results: The ambulatory women with motor disability (EDSS $>$ 3.5) had significantly higher serum sclerostin levels than fully ambulatory women with EDSS \leq 3.5. The serum sclerostin levels correlated positively with EDSS when controlled for age in both pre- and postmenopausal women with MS ($p < 0.001$) and negatively with serum PINP ($p < 0.01$) in premenopausal women. There was no relationship between serum sclerostin and BMD after controlling for age or EDSS. Conclusion: Our results represent the first study of circulating sclerostin levels in MS. The motor disability in ambulatory women with MS is associated with a higher sclerostin levels and with reduced bone formation. Further studies are needed to evaluate the role of sclerostin on bone remodeling and bone mass in this population.

Disclosures: Vit Zikan, None.

SA0358

New Onset Diabetes Mellitus After Liver Transplantation. Relationship With 25-hydroxyvitamin D Levels And Serum Osteocalcin. Fernando Sotillo¹, Guillermo Martinez Diaz-Guerra^{*2}, Raquel Sánchez-Windt¹, Mercedes Aramendi¹, Elena García¹, Federico Hawkins³, Enrique Moreno¹. ¹University Hospital 12 de Octubre, Spain, ²University Hospital 12 Octubre, Spain, ³Hospital Universitario, Spain

Liver transplantation (LT) patients are at high risk of developing new-onset diabetes after transplantation (NODAT), but risk factors are still unknown. Experimental data have shown that Vitamin D receptors are present in pancreatic beta cell, and low levels of vitamin D have been linked with insulin resistance and metabolic syndrome. In addition, osteocalcin-deficient animals are hyperglycaemic, hyperinsulinaemic, and have decreased insulin sensitivity and increased fat mass.

The objectives of our study are firstly to investigate the prevalence of NODAT and abnormal glucose tolerance in LT patients followed up in our hospital and secondly to analyze serum osteocalcin and 25-hydroxyvitamin levels (25OHD) and their relationship with glucose tolerance and insulin resistance.

Methods: 71 patients (52 males, 19 females) with orthotopic liver transplantation without known diabetes mellitus before this procedure were studied. Mean age was 58.2 ± 11.3 years (range 21-78). Minimum time since LT was 6 months and mean time since LT was 9.2 years. An oral tolerance test with 75 g of glucose (OTTG) was performed, measuring plasma glucose, C-peptide and insulin at baseline, 60 and 120 minutes. Biochemical parameters included glycated hemoglobin (HbA1c), serum osteocalcin (total), and 25-OHD. Insulin resistance index (HOMA-IR) and insulin sensitivity index (Quicki) were calculated.

Results: Diabetes Mellitus (NODAT) was present in 19.7% (n=14), and prediabetes in 33.8% (n=24) (ADA 2011 criteria). 46.5% (n=33) had normal glucose tolerance (NGT) after LT. Vitamin D deficiency (<20 ng/ml) was present in 40%, and 70% had 25-OHD below 30 ng/ml. Serum osteocalcin and 25-OHD were not statistically different across NGT, prediabetes and NODAT patients. HOMA-IR

index was significantly higher in prediabetes ($p < 0.001$) and diabetes ($p = 0.014$) compared with NGT. Insulin sensitivity index was significantly lower in prediabetes ($p < 0.001$) and diabetes ($p < 0.01$) compared with NGT. No significant correlations between osteocalcin, 25OHD and HOMA-IR or Quicki index were found.

Conclusion: The study seems to indicate that diabetes mellitus is more prevalent in patients with liver transplantation (NODAT) than in average Spanish population and that vitamin D insufficiency is also frequent. However, no significant association has been established between serum total osteocalcin and 25OHD with diabetes mellitus or impaired glucose tolerance after liver transplantation.

Disclosures: Guillermo Martinez Diaz-Guerra, None.

This study received funding from: Fundacion Mutua Madrileña n^o 2010-016

SA0359

Study of Bone Quality at the Time of Lung Transplant in Cystic Fibrosis Patients Using Rib Specimens. Louis-Georges Ste-Marie^{*1}, Natalie Dion¹, Pasquale Ferraro², Caroline Albert¹, Nathalie Bureau², Audrav Fortin², Valérie Jomphe², Larry Lands³, Genevieve Mailhot⁴. ¹CHUM, Canada, ²CHUM, Canada, ³MUHC-Montreal Children's Hospital, Canada, ⁴Research Center CHU Sainte-Justine/University of Montreal, Canada

Nowadays, the median life expectancy of cystic fibrosis (CF) patients exceeds 45 years of age. As CF patients get older, secondary morbidities superimpose on pre-existing complications thereby worsening the patient's condition. One of the leading complications is thoracic fractures which seriously undermine the patient's quality of life. Despite its high prevalence, pathogenesis of CF related bone disease (CFBD) remains poorly understood and predicting individuals at increased risk of fracture is especially difficult given that bone mineral density (BMD) is considered a poor predictor of fractures in CF. As bone strength is determined by bone quantity and bone quality, it is reasonable to postulate that alterations in bone quality will likely contribute to the propensity to fractures in CF patients. The aim of this pilot study is to use various techniques to assess bone quality in CF patients. During lung transplantation in CF patients as well as in non-CF patients, a 2 cm segment of one rib (either the 5th or 6th) is routinely removed. These specimens were recovered to perform the following analyses: *ex vivo* BMD by DXA, high resolution micro-CT, microcrack detection and bone histomorphometry. In the last 8 months, 12 specimens were collected [6 CF: $30.3 \pm 2.1y$ and 6 non-CF (various non-CF lung diseases): $56.8 \pm 2.3y$]. There was no difference in *ex vivo* BMD (0.17 ± 0.02 vs $0.18 \pm 0.03g/cm^2$) between the two groups. However, micro-CT data in CF patients showed a significant greater BV/TV (8.79 ± 0.8 vs non-CF: $5.58 \pm 0.65\%$; $p = 0.01$) Tb.N (0.51 ± 0.06 vs non-CF: $0.3 \pm 0.03/mm$; $p = 0.007$) and Conn.D (2.76 ± 0.4 vs non-CF: $1.64 \pm 0.28/mm^3$; $p = 0.04$) whereas Tb.Sp was lower (1.06 ± 0.11 vs non-CF: $1.67 \pm 0.14mm$; $p = 0.007$). No major differences in other microstructure indices (SMI, Tb.Th) or in cortical parameters were found between CF and non-CF patients. The differences observed in trabecular bone density and microstructure are, among other factors, due to the younger age of the CF group. With a greater number of CF patients, correlations between bone parameters (density, microstructure, microcracks, bone remodeling) and clinical parameters of CFBD (fractures, BMI, bisphosphonates and glucocorticoids use) as well as biochemical indices will be investigated and data will be presented. This exploratory study has shown the feasibility of using rib specimens to assess bone quality in patients undergoing lung transplantation.

Disclosures: Louis-Georges Ste-Marie, Eli Lilly, 2; Servier, 2; Novartis, 2; Merck, 2; Alliance for better bone health, 2; AMGEN, 6; AMGEN, 2

SA0360

See Friday Plenary Number FR0360.

SA0361

See Friday Plenary Number FR0361.

SA0362

See Friday Plenary Number FR0362.

SA0363

See Friday Plenary Number FR0363.

SA0364

Evaluation of the Densitometric Response at 12 and 24 Months after Strontium Ranelate (SR) Treatment, in Patients Previously Treated with Bisphosphonates (BP). Laura Maffei¹, Maria Valeria Premrou^{*2}, Carolina Pelegrin². ¹Consultorios Asociados De Endocrinologia, Argentina, ²no, Argentina

Introduction: Many patients with severe osteoporosis need a long treatment, and frequently it is necessary to change the scheme of treatment to minimize side effects. We have already published a densitometric improvement after one year of treatment with SR in patients previously treated with BP.

Objectives: To evaluate the densitometric response after 12 and 24 months of treatment with SR. And then, if there is any difference in densitometric response between 12 and 24 months.

Material and methods: Postmenopausal patients who had received more than 3 consecutive years of BP treatment, with worsening or maintenance of bone mineral density (BMD) and requiring to continue the treatment, were studied. BMD of spine and femoral neck were performed at the baseline, 12 and 24 months after SR treatment.

Results: 63 patients were included, with a mean age of 64.83 (48-86 years). The results are expressed in the followings tables 1 and 2.

Conclusions: Spine and femoral BMD increased significantly at 12 and 24 months after SR treatment; more significant at 24 than at 12 months.

The bone turnover is very inhibited after a long use of BP; the SR would be deposited more easily in new bone. This fact could explain the improvement of the parameters with a longer treatment time.

Usually patients under a long BP treatment should make a drug holiday, however they should continue the osteoporosis therapy. This study shows that SR could be a very useful and effective alternative for these patients.

| | Baseline | | 12 months | | 24 months | |
|--------------|---------------|------------------------|---------------|------------------------|---------------|------------------------|
| | n | BMD ⁽¹⁾ | n | BMD | n | BMD |
| Spine | 59 (93.7%) | 0.813 (0.790-0.837) | 56 (88.9%) | 0.837 (0.811-0.863) | 21 (33.3%) | 0.892 (0.852-0.934) |
| Femoral Neck | 58 (92.1%) | 0.675 (0.650-0.701) | 56 (88.9%) | 0.708 (0.684-0.732) | 19 (30.2%) | 0.736 (0.692-0.782) |

⁽¹⁾ Values of BMD g / cm² (95% CI); FN: femoral neck

To compare BMD between different time points, the following results were obtained.

| | Media | % Change | P ⁽¹⁾ |
|-----------------------------|----------------|----------|------------------|
| Spine baseline vs 12 months | 0.811 vs 0.836 | 3.53% | 0.001 |
| Spine baseline vs 24 months | 0.813 vs 0.891 | 4.51% | <0.001 |
| Spine 12 vs 24 months | 0.858 vs 0.892 | 2.53% | 0.02 |
| FN baseline vs 12 months | 0.608 vs 0.705 | 3.57% | 0.001 |
| FN baseline vs 24 months | 0.667 vs 0.736 | 3.71% | 0.002 |
| FN 12 vs 24 months | 0.726 vs 0.746 | 1.37% | 0.186 |

⁽¹⁾ Paired samples t test

Table 1 and table 2

Disclosures: Maria Valeria Premrou, None.

SA0365

See Friday Plenary Number FR0365.

SA0366

Beneficial Effects of Zoledronate versus Placebo on Lumbar Spine Bone Mineral Density (BMD) and Microstructural Parameters (TBS) in Postmenopausal Women with Osteoporosis. A 3-Year Study. Albrecht Popp^{*1}, Helene Buffat², Olivier Lamy³, Romain Perrelet², Didier Hans⁴, Kurt Lippuner¹. ¹Osteoporosis Policlinic, University of Bern, Switzerland, ²Osteoporosis Policlinic, University of Bern, Switzerland, ³University Hospital, Switzerland, ⁴Lausanne University Hospital, Switzerland

Objective(s): The Trabecular Bone Score (TBS) is an index of bone micro-architecture that predicts osteoporosis fracture risk independently of bone mineral density (BMD). It is calculated from antero-posterior DXA scans of the spine. The aim of this study was to compare the effects of yearly intravenous zoledronate (ZOL) versus placebo (PLB) on spine BMD and TBS in postmenopausal women with osteoporosis.

Materials and Methods: The HORIZON trial was a randomized, double-blind, placebo-controlled study comparing the effects of once-yearly intravenous ZOL and PLB over 3 years in postmenopausal women with osteoporosis. All subjects also received adequate calcium and vitamin D3. In a subset of 98 patients (n = 49 on ZOL, 49 on PLB) retrospective analysis was performed to assess changes in lumbar spine BMD and TBS during 3 years vs. baseline. BMD was measured by DXA and TBS

parameters were assessed by TBS iNsite™ (v1.9) at baseline and 6, 12, 24, and 36 months after treatment initiation.

Results: Baseline characteristics (mean ± SD) were similar between groups in terms of age, 76.5 ± 5.1 years; BMI, 24.4 ± 4.1 kg/m²; L1-L4 T-score, -2.55 ± 1.44; and TBS 1.200 ± 0.12. ZOL induced an early and sustained significant increase in spine BMD relative to both baseline and placebo (+3.2% and +9.4% change in spine BMD with ZOL vs. corresponding -0.2% and +2.1% changes with PLB at 6 and 36 months, respectively; p < 0.01). Change in TBS was significantly greater with ZOL than with PLB at 36 months (+1.6 vs. -1.4%, respectively; p < 0.05). Spine BMD and TBS were weakly correlated (r² = 0.11), and there were no correlations between changes in BMD and TBS from baseline at any visit.

Conclusions: In postmenopausal women with osteoporosis, once-yearly intravenous ZOL therapy significantly increased lumbar BMD relative to PLB and prevented bone microarchitecture decay, as assessed by TBS, over three years. Changes in BMD and TBS were not correlated, confirming that TBS reflects bone properties other than BMD.

Disclosures: Albrecht Popp, Eli Lilly, 9; Amgen, 9

SA0367

See Friday Plenary Number FR0367.

SA0368

See Friday Plenary Number FR0368.

SA0369

Early Initiation of Bisphosphonate Does Not Affect Healing and Outcomes of Volar Plate Fixation of Osteoporotic Distal Radius Fractures. Hyun Sik Gong^{*1}, Kee Jeong Bae², Jeong Hwan Kim², Jung Eun Lee². ¹Seoul National University Bundang Hospital, South Korea, ²Seoul National University Bundang Hospital, South Korea

Background: Bisphosphonates can adversely affect fracture healing because they inhibit osteoclastic bone resorption. Given this, it is unclear whether bisphosphonate medication can be initiated safely in patients sustaining an acute distal radius fracture. The purpose of this randomized study was to determine whether the early use of bisphosphonate affects fracture healing and outcomes of osteoporotic distal radius fractures treated by volar locking plate fixation.

Methods: Fifty women older than 50 years of age who underwent volar locking plating of distal radius fractures and were diagnosed with osteoporosis were randomized to Group I (n=24, initiation of bisphosphonate at 2 weeks after operation) or Group II (n=26, initiation of bisphosphonate at 3 months). Patients were assessed for radiographic union and radiographic parameters (radial inclination, radial length, and volar tilt) at 2, 6, 10, 16, and 24 weeks, and for clinical outcomes at 24 weeks which included disabilities of the arm, shoulder, and hand (DASH) scores, wrist ranges of motion, and grip power. The two groups were compared for time to radiographic union, radiographic parameters and clinical outcomes.

Results: No significant differences were observed between the two groups with respect to radiographic or clinical outcomes. All patients achieved fracture union and mean times to radiographic union in groups I and II were similar (6.7 weeks vs. 6.8 weeks, respectively; p=0.65). Furthermore, time to radiographic union was not found to be related to osteoporosis severity or fracture type in patients treated by volar locking plate fixation.

Conclusions: In patients with an osteoporotic distal radius fracture treated with volar locking plating, the early initiation of bisphosphonate was not found to affect fracture healing or clinical outcomes. Future investigation should focus on whether the immediate initiation of medication actually results in increased osteoporosis treatment rate.

Disclosures: Hyun Sik Gong, None.

SA0370

See Friday Plenary Number FR0370.

SA0371

Effects of Bisphosphonate Alone or Combined Treatment of Bisphosphonate and Vitamin K2 on Serum Undercarboxylated-osteocalcin (ucOC) or Osteocalcin (OC) in Osteoporotic Women. Yuji Kasukawa^{*1}, Naohisa Miyakoshi¹, Toshihito Ebina², Toshiaki Aizawa³, Yoichi Shimada⁴. ¹Akita University Graduate School of Medicine, Japan, ²Dept. of Orthopedic Surgery, Kakunodate General Hospital, Japan, ³Dept. of Orthopedic Surgery, Kita-Akita General Hospital, Japan, ⁴Dept. of Orthopedic Surgery, Akita University Graduate School of Medicine, Japan

Purpose: Serum undercarboxylated osteocalcin (ucOC), which is a marker of vitamin K2 deficiency, has been considered as also a marker of bone quality

independent of bone mineral density. Its cut-off value for osteoporotic fracture is 4.5 ng/ml, however the value of uOC has been changed under treatment with bisphosphonates. The purpose of the present study was to evaluate the effects of bisphosphonate alone or combined treatment of bisphosphonate and vitamin K2 on serum uOC, osteocalcin (OC) level and the other bone metabolic markers prospectively.

Methods: Ninety-five osteoporotic women were randomly stratified into two groups: Bis-group (mean age 74-year-old, n=48), which was treated with risedronate alone (17.5 mg/week), and Bis+K2-group (mean age 76-year-old, n=47), which was treated with risedronate and menatetranone (45 mg/day). Serum uOC, OC, cross-linked N-telopeptide of type 1 collagen (NTx), and bone alkaline phosphatase (BAP) were measured before, 6-month, and 12-month after treatment, and then the change rates of these markers were evaluated.

Results: Persistence rates of treatment at 6-month and 12-month were 83% and 75% in Bis group and 74% and 68% in Bis+K2 group, respectively. The decreasing rates of uOC at 6-month and 12-month were not statistically significant between the groups (31% and 51% in Bis-group, and 34% and 56% in Bis+K2-group). However, the decreasing rates of OC in Bis-group at 6-month and 12-month (25% and 36%, respectively) were significantly higher (p<0.01) than those in Bis+K2-group (0.4% and 17%, respectively). The change rates of uOC/OC in Bis-group at 6-month and 12-month (9.3% and 23%, respectively) were significantly lower (p<0.05) than those in Bis+K2-group (36% and 48%, respectively). The decreasing rates of NTx and BAP were not statistically significant between the groups at both time points.

Conclusions: Although the decreasing rate of serum uOC level was not different between mono-therapy of bisphosphonate and combined treatment with vitamin K2, the decreasing rate of serum OC in combined treatment was significantly lower than that in mono-therapy of bisphosphonates.

Disclosures: Yuji Kasukawa, None.
This study received funding from: Akita University

SA0372

Exploration of Prognostic Factors on BMD Percent Change in Patients Administrated Risedronate -A Pooled Analysis of Clinical Trials in Japan- Ryoichi Muraoka¹, Ryo Okazaki^{2*}, ¹Ajinomoto Pharmaceuticals Co, Ltd., Japan, ²Teikyo University Chiba Medical Center, Japan

Objective : Risedronate (RIS) has been shown to inhibit osteoporotic fractures and widely used in the world. However, there are some non-responsive patients to RIS in terms of BMD increase. We performed post-hoc analyses of RIS Phase III trials conducted in Japan to explore prognostic factors associated with responsiveness to RIS.

Subjects and methods : 465 subjects whose lumbar spine BMD data were available both at the baseline and after 48 weeks of RIS treatment in Phase III trials were analyzed. In those trials vitamin D supplementation was not given. Subjects were divided into responders (N=418) by BMD percent change from baseline equal to or above 0% and non-responders (N=47) with negative BMD change. Analyses on bone turnover markers between groups were performed. Logistic regression analysis was performed in which positive BMD response to RIS as an event. Comorbid complications, demographic profiles, BMI, drug adherence, existing vertebral fracture, basal levels of serum 25(OH)D and bone turnover markers were considered as prognostic variables.

Results : In non-responders, serum bone-specific alkaline phosphatase (BAP) levels were lower at baseline (26.1 +/- 9.1U/L vs. 31.1 +/- 10.2U/L, P=0.0022) and at 4-week. The BAP value at 12, 24, 36, 48-week showed no significant differences (at 48-week, 18.2 +/- 5.6U/L vs. 19.3 +/- 6.0U/L, p=0.2773). BAP percent changes from baseline in non-responders at 12, 24, 36, 48-week were significantly lower than responders (at 48-weeks, -25.4 +/- 21.6% vs. -34.5 +/- 19.9%, p=0.0106). Compared with responders, non-responders showed blunted decreases in bone resorption markers (urinary CTX and NTX) as well. In logistic regression analysis, existing vertebral fracture, higher basal serum 25(OH)D level [above 20ng/mL (median)], and higher serum BAP level [above 28.6U/L (median)] were significantly associated with positive BMD response to RIS. Estimated odds ratio were 2.441 (P=0.0387), 2.458 (P=0.0070) and 2.310 (P=0.0092), respectively.

Conclusions : These results suggest that serum 25(OH)D level should be adequately increased prior to RIS treatment in order to ensure positive BMD response to RIS. In terms of BMD, patients with higher bone turnover markers and/or existing bone fractures are more likely to respond to RIS, suggesting RIS may be more effective in severer osteoporotic patients.

Disclosures: Ryo Okazaki, None.

SA0373

Identifying Factors Involved in Predicting Response to Intravenous Zoledronic acid in Elderly Patients with Osteoporosis. Najia Siddique^{*1}, Ng Kin Cheung², Kevin McCarroll², Nessa Fallon², Miriam C.Casey³, JB Walsh². ¹St James University Hospital, Ireland, ²St.James's Hospital, Ireland, ³Stjames's Hospital, Ireland

Introduction: IV Zoledronic acid (Zol) has been proven to increase spinal BMD in osteoporosis. However some patients may not respond to this therapy. There is limited data in the literature to identify the factors which might predict treatment

failure. This study looks at the baseline characteristics of patients who have inadequately responded to IV Zol. It also considers any significant correlation among these characteristics when compared to BMD.

Methods: This was a retrospective study. A cohort of 192 patients with post menopausal osteoporosis who were treated with IV Zol was analysed. Patients were followed up for 12-18 months after their 1st dose. From this cohort, 43 patients who had their dexa scans performed at 12-18mths post Zol infusion were selected for further analysis. All these patients were on Calcium/VitD supplements at time of infusion. These patients were divided into two main groups as Responder Vs Non responder. Patients who failed to achieve a gain of 3% or more in BMD at their lumbar spine at 12-18mth were considered as non responders. The differences in baseline characteristics between the 2 groups were compared and correlations among these characteristics were looked at. Statistical analysis was performed using T-test and Logistic regression model. A p value ≤0.05 was considered as significant.

Results: Table 1 shows baseline characteristics and lab parameters of the cohort. There was no significant difference in the general characteristics of both groups i.e. age, medical history, previous bone or other medical treatment. There was also no significant difference in their GFR, Bone markers: Ctx,P1NP, OC (table1), PTH, Vitamin D, Serum calcium and 24hr Urinary calcium. A significant difference in BMD was observed between Responders(0.76 SD ±0.13) Vs NonResponders(0.87 SD±0.19) (p0.03). A significant trend towards an increase in response with lower baseline BMD was also observed (p 0.04). Also, higher baseline BMD was observed in patients with higher baseline BMI (p0.03), higher osteocalcin p 0.029, CTX (p0.00).

Conclusion: Although this analysis couldn't identify the predictors of response, it enabled us to establish that patients who have a lower BMD at baseline show a better response to treatment and ViceVersa - so the magnitude of the response to IV Zol is increased for subjects with relatively severe osteoporosis compared to patients with less severe disease.

Table 1: General characteristics and lab results of the population at baseline.

| | |
|---|--------------------|
| Age | 71.7 (SD +/- 9.4) |
| BMI (Body Mass Index) | 23.7 (SD +/- 4.3) |
| Vitamin D nmol/l | 66.4 (SD +/- 25.4) |
| Corrected serum calcium mmol/l | 2.3(SD +/- 0.12) |
| 24 Hr Urinary Calcium | 4.5(SD +/-0.264) |
| PTH (Parathyroid hormone) | 34 (median) |
| P1NP (Procollagen Type 1 Amino-terminal Propeptide) ng/ml | 25.7 (median) |
| OC (Osteocalcin) ng/ml | 15.6 (median) |
| CTX (carboxy-terminal collagen crosslinks) ng/ml | 0.22 (median) |
| Drug Dose mg | 4 (median) |

Baseline Characteristics and Lab Parameters of the Cohort

Disclosures: Najia Siddique, None.

SA0374

Oral Sequestration Not Associated With Bisphosphonate Use. Aliya Khan^{*1}, Ed Peters², Neili Sifelddeen³. ¹McMaster University, Canada, ²University Of Alberta, Canada, ³University of Alberta, Canada

The incidence of bisphosphonate related osteonecrosis of the jaws (BRONJ) in patients taking oral bisphosphonates has been variably estimated between 0.0004% and 0.06%. The case definition in these incidence studies typically has required the presence of exposed bone for greater than 8 weeks in patients who have been treated with bisphosphonates and with no history of radiotherapy. The objective of this preliminary study was to assess the presentation profile of BRONJ type cases in the absence of bisphosphonate use. All sequestration cases, which were submitted for histopathologic exam during a 3 year period before bisphosphonates were approved for clinical use, were reviewed. 55 cases were identified. 48 cases had clinical histories indicating the suspected cause and clinical presentation and were included in the study. 34 of these cases (71%) could be attributed to a range of etiologic factors (post-surgical complication, infection, trauma, radiation, eruption) and did not match the BRONJ type profile. A further 14 cases (29%) were characterized by prolonged bone exposure in the absence of a clinically evident initiating factor. 7 of these latter cases involved idiopathic bone exposure in the posterior lingual mandible, 4 cases occurred in association with developmental exostoses and 3 cases were associated with persistent recessed gingiva. In 7 of these exposed bone cases, there was definitive information regarding lesion duration before surgical management. 3 cases (2 lingual mandible and 1 recessed gingiva) had persisted for over 8 weeks before surgical management. Thus, a minimal 6% of BRONJ type presentations could be identified from the total sequestration cases. These preliminary results indicate that studies attempting to assess BRONJ incidence need to account for the unknown incidence or "background noise" associated with BRONJ type sequestrations that occur in the absence of bisphosphonate use.

Disclosures: Aliya Khan, None.

SA0375

Pre-existing Hyperparathyroidism Affects the Anti-fracture Efficacy of Oral Alendronate in Long-term Kidney Transplantation Survivors. Atsushi Suzuki*¹, Sakura Yamamoto², Hitomio Sasaki³, Hiroyuki Hirai⁴, Yoshiteru Maeda⁵, Sahoko Sekiguchi-Ueda¹, Yasumasa Yoshino⁶, Shogo Asano⁶, Megumi Shibata⁷, Masaki Makino⁸, Nobuki Hayakawa⁹, Kiyotaka Hoshinaga³, Mitsuvasu Itoh⁵. ¹Fujita Health University, Division of Endocrinology, Japan, ²Fujita Health University, Division of Endocrinology, Japan, ³Department of Urology, Fujita Health University, Japan, ⁴Fujita Health University Division of Endocrinology, Japan, Japan, ⁵Division of Endocrinology, Fujita Health University, Japan, ⁶Toyokawa City Hospital, Japan, ⁷Fujita Health University Division of Endocrinology, Japan, ⁸Division of Endocrinology, Fujita Health University, Japan, ⁹Faculty of Pharmacy, Meijo University, Japan

Background: Post-transplantation bone diseases negatively affect the quality of life of solid organ recipients. Secondary or tertiary hyperparathyroidism is a frequent complication in kidney transplantation (KTx) recipients. Treatment with immunosuppressive agents including glucocorticoids can lead to deterioration in bone metabolism in these patients. In the present study, we explored the effects of a three-year treatment period with oral alendronate (ALN) in long-term KTx survivors.

Subjects: Post-KTx recipients were recruited (n=24, M/F=12/12, mean age 52.0 ± 7.8 years) into this study. All patients were prescribed methylprednisolone (4.07 ± 0.86 mg/day) with various immunosuppressive agents.

Results: Before treatment with oral ALN (35 mg/week), the mean concentrations of intact parathyroid hormone (iPTH) and 25-hydroxyvitamin D (25-OHD) were 139.2 ± 71.4 pg/mL and 20.8 ± 4.1 ng/mL, respectively. After 36 months of ALN treatment, mean iPTH levels increased slightly (+20.9%). Treatment with ALN reduced bone-specific alkaline phosphatase (BAP) (-35.4%), serum type I collagen N-terminal telopeptide (NTx) (-31.2%) and osteocalcin (-55.6%) levels. ALN did not increase bone mass after 24 months. Four patients suffered a clinical osteoporotic fracture during the 36-month ALN treatment period. Higher basal iPTH level and a smaller %decrease in BAP and NTx were associated with the incidence of new clinical fractures during ALN treatment.

Conclusion: Anti-resorptive therapy with ALN can suppress bone turnover even when iPTH concentration is elevated in long-term KTx survivors. Pre-existing hyperparathyroidism and a smaller decrease in bone turnover markers seem to be associated with new clinical fractures during BP treatment.

Disclosures: *Atsushi Suzuki, None.*

SA0376

See Friday Plenary Number FR0376.

SA0377

See Friday Plenary Number FR0377.

SA0378

Withdrawn

SA0379

Gastrointestinal Events and Association with Osteoporosis Treatment Initiation. Ethel Siris*¹, Shiva Sajjan², Srinivasan Rajagopalan³, Shuvayu Sen⁴, Ankita Modi⁵. ¹Columbia University College of Physicians & Surgeons, USA, ²Merck & Company, USA, ³Meddata Analytics, USA, ⁴Merck & Co., Inc., USA, ⁵Merck & Company, USA

Purpose: To examine the association of Gastrointestinal (GI) events with osteoporosis (OP) treatment initiation patterns among women after having a diagnosis of OP.

Methods: A retrospective cohort study using i3 Invision Datamart; a large U.S. claims database records from January 1, 2001 to December 31, 2010 (study period) was conducted. The index date was defined as the date of first diagnosis of OP during study period. Study included women, 55 years or older, with a diagnosis of OP based on ICD-9 codes and enrolled for at least one year before (baseline) and one year after the index diagnosis date (follow-up). Subjects were excluded if they had a diagnosis of Paget's disease, malignant neoplasm or a prescription for an OP medication anytime prior to index date during the study period. OP medications were identified based on NDC codes and included bisphosphonates (BIS) (alendronate, etidronate, ibandronate, risenedronate, zoledronic acid) and non-BIS (calcitonin, raloxifene, teriparatide). Users of estrogen therapy during the one year prior to index date were also excluded. GI events were assessed as having a GI symptom related ICD-9 diagnosis after OP diagnosis and before treatment initiation in the follow-up. The association of any GI event on OP treatment initiation was analyzed using multivariate logistic regression

model controlling for age, comorbidities, OP fracture history, glucocorticosteroid use, gastroprotective agent use and nonsteroidal anti-inflammatory drug history at baseline.

Results: 65,344 patients met the inclusion criteria with a mean age of 66 years. Almost 27.3 % of the patients had a GI event at baseline. 23.7% of patients had a GI event post diagnosis and before treatment initiation. Among patients with GI events at baseline, those who continued to have GI events in the period after OP diagnosis were less likely to be initiated with any pharmacological treatment for OP (OR: 0.20, CI: 0.19-0.22) and were less likely to be initiated with a BIS as compared to a non-BIS (OR: 0.61, CI: 0.53-0.72). Similar association was seen among subjects with no GI events at baseline and those who developed GI problems post OP diagnosis.

Conclusion: Almost 24% of women had GI events prior to treatment initiation and post OP diagnosis. Occurrence of a GI event may be associated with the likelihood of not being treated. Among patients receiving treatment, a GI event increased likelihood of being treated with a non-bisphosphonate as compared to a bisphosphonate.

Disclosures: *Ethel Siris, Amgen, Eli Lilly.; Amgen, Eli Lilly, Merck, 2 This study received funding from: Merck and Company*

SA0380

Osteoporotic Fracture Rate Among Women with at least One Year of Adherence to Osteoporosis Treatment. Adolfo Diez-Peréz*¹, Chun-Po Steve Fan², Shuvayu Sen³, Ankita Modi⁴. ¹Parc De Salut Mar, Spain, ²AsclepiusJT LLC, USA, ³Merck & Co., Inc., USA, ⁴Merck & Company, USA

Purpose: To examine the incidence of osteoporosis-related fractures over 2 years of treatment among women adherent to osteoporosis (OP) therapy for at least 1 year.

Methods: A retrospective analysis using i3 Invision Datamart (Ingenix, Eden Prairie, MN); a large U.S. claims database with records from January 1, 2001 to December 31, 2010 (study period) was conducted. Women ≥50 years old who initiated treatment with oral bisphosphonates (alendronate, risenedronate, ibandronate) during study period and were enrolled in the database for 3 consecutive years, including a baseline year before the index prescription, an adherence year (year 1), and a follow-up year (year 2). Patients were excluded if they had Paget's disease or diagnosis of malignant neoplasm. Adherence to therapy was defined as medication possession ratio (MPR) ≥0.6 during year 1 (MPR = total number of days' supply/365 days). Additional sensitivity analysis was conducted with adherence defined to be MPR ≥0.8. OP fracture incidence rate was computed as number of OP fractures per 1,000 patient-years among women adherent to osteoporosis treatment for at least one year.

Results: Among 62,446 women who met eligibility criteria, 35,737 (57%) were adherent to osteoporosis therapy (based on MPR ≥0.6) during year 1 (mean [SD] age, 60.7 [8.4] years). Among the 1-year adherent patients, OP fractures were recorded during the baseline year (before initiating therapy) for 1,507 (4.2%) patients; during year 1 for 1,397 (3.9%) patients; and during year 2 for 1,173 (3.3%) patients. There were in total 1,851 fractures in year 2 with an incidence rate of 52 per 1,000 patient-years. Hip and other non-vertebral fractures were most common, representing over two thirds of all fractures. Moreover, 2,350 (6.6%) of the 1-year adherent patients experienced a fracture in the baseline or the adherence period. 33,387 did not experience fractures in baseline or adherence period. Among 2,350 patients, 423 (18%) had fractures in the follow-up, in contrast to only 750 (2.2%) of the 33,387 patients without a fracture history had fractures in the follow-up. Similar results were obtained with sensitivity analysis of MPR ≥0.8.

Conclusion(s): Rate of osteoporotic fracture during the second year of follow-up was 3.3% despite having been previously adherent to treatment for one year. Results indicate an unmet need related to level of osteoporosis control and an opportunity for newer therapies to help address this need.

Disclosures: *Adolfo Diez-Peréz, None.*

This study received funding from: Merck and Company

SA0381

Outcomes in Patients with a Fractured Neck of Femur following the Establishment of a Fracture Liaison Service. Jude Ryan*¹, Audrey Butler², Sheila Carew³, Tina Sheehy³, Aine Costelloe³, Brian Lenehan², Declan Lyons³, Margaret O' Connor³. ¹Midwest Regional Hospital, Ireland, ²Department of Orthopaedic Surgery, Ireland, ³Clinical Age Assessment Unit, Ireland

Introduction: Fractures of the neck of femur may commonly indicate advanced osteoporosis and therapeutic interventions to slow bone loss and improve fracture risk have been shown to lead to better outcomes. We looked at the outcomes in the first eight months following the establishment of a fracture liaison service in a regional hospital.

Methods: A fracture liaison service was established in July 2011. All patients who were admitted following a fractured neck of femur were assessed in the perioperative period by a geriatric physician with a special interest in bone health and offered investigation and follow-up, excluding patients with advanced dementia. Follow-up investigations included DEXA, laboratory markers of bone health and a falls work-up. Outcome parameters included survival, re-admission rates, length of stay and

compliance with follow up. We compared length of stay to a similar period 2010 in the same unit prior to the establishment of the fracture liaison service.

Results: There were 155 patients admitted with fractured neck of femur during the 8 month study period, 111 (72%) were female. Median age was 81 (53-94) years. Length of stay was 8 (2-40) days, compared with 9 (2-56) days in 2010. The overall mortality was 10/155 and 30-day mortality was 6/155. The 30-day readmission rate was 6.5% (10/155). Follow up was offered to 112 patients to date and of these, 75 patients have attended for bone health and falls investigations (compliance rate 67%).

Conclusion: These results indicate that a fracture liaison service can reduce length of stay for patients following fractured neck of femur. Further work is needed to establish whether this service and improved compliance with follow up can influence longer term outcome measures.

Disclosures: *Jude Ryan, None.*

SA0382

Persistence With Denosumab Therapy For Postmenopausal Osteoporosis. Christine Simonelli¹, Susan Mehle², Julie Morancey³. ¹HealthEast Osteoporosis Care, USA, ²HealthEast Medical Research Institute, USA, ³HealthEast Osteoporosis Care, USA

Compliance and persistence with oral osteoporosis medications has been notoriously poor, compromising efficacy leading to more fractures and higher healthcare costs. An every 6-month subcutaneous injection option is now available with 60mg. denosumab therapy (ProliaTM) in managing postmenopausal osteoporosis. We report the persistence of this medication use over 18 months of prescribed therapy.

Consecutive patients being treated for postmenopausal osteoporosis who were felt by the clinician to be appropriate for denosumab treatment were monitored for follow-up visits. An index card was created for each patient and filed at the next 6-month time point. Patients were encouraged to set up their follow-up visit at the end of their appointment. The mean age of patients was 70.9 (39-100) and 136 (37.5%) had at least one prior fracture with vertebral fractures most common (63, 17%) and 12 (3.3%) had prior hip fracture, 31 (8.5%) prior wrist fracture. Thirty-nine (10.7%) patients had more than one prior fracture. Most patients (257, 69%) used prior osteoporosis medication with 120 (33%) using a single medication and 137 (38%) using more than one prior medication. Bisphosphonates alone were used by 122 (34%) patients, teriparatide by 36 (10%) and teriparatide and a bisphosphonate by 67 (18%). Survival of patients who had tried a previous osteoporosis medication was 88.4%, compared to 81.5% for those who had no prior osteoporosis medications. The difference was not statistically significant (Log-Rank p-value = 0.335).

Three hundred sixty-three patients received their first Prolia injection between June 2010 and January 2012 and were followed through February 29, 2012. Of 246 patients eligible for a second dose 219 (89%) received their dose and of 121 patients eligible for a third dose, 107 (88%) patients received the final dose. Reasons for using denosumab were BMD decline on prior osteoporosis medication (22.8%), adverse event on prior osteoporosis medication (25.6%), physician and/or patient preference (28.6%), history of GI disease (10.2%) and renal failure (15.4%).

Use of denosumab (ProliaTM) to manage postmenopausal osteoporosis had a high persistence with therapy in an outpatient clinical practice setting and offers an important treatment option.

Disclosures: *Christine Simonelli, Amgen, 6*

SA0383

Primary Care Providers' Management after Receipt of an Osteoporosis Electronic Consult for Patients with Recent Fracture. Richard Lee^{*1}, Karen Barnard², Kenneth Lyles³, Megan Pearson⁴, Cathleen Colon-Emeric⁵. ¹Duke University, USA, ²Duke University Medical Center, Durham VAMC, USA, ³Duke University Medical Center, USA, ⁴Durham VA Medical Center, USA, ⁵Duke University Medical Center, USA

Background: According to the Office of the Inspector General, only 45 percent of patients within the Veterans Health Administration received appropriate osteoporosis management after a fracture. An electronic consult service was implemented at a Veterans Administration Medical Center to facilitate identification of and to recommend management for patients with recent fracture.

Method: The osteoporosis electronic consult service was initiated in October 2011 at a single VAMC. The consult service coordinator identified potential osteoporotic fractures from inpatient and outpatient encounter data drawn from the central data repository. All patients with an ICD9 diagnosis code for fracture (800-829) were screened. Patients were excluded if they were deceased, receiving palliative care, under 50 years, already on treatment for osteoporosis, fracture management had been addressed by primary provider, no primary provider assigned, fracture was located in face or digits, fracture occurred in setting of high-impact trauma, suspected fracture was not seen on radiograph, or insufficient information regarding the fracture in medical record. Eligible patients were referred to a bone specialist who reviewed each medical chart. After chart review, an electronic consult note was sent to the patient's primary provider that provided recommendations for further evaluation and management of osteoporosis, consistent with current guidelines. We report the service's activity in the first 3 months after implementation and the primary providers' subsequent management.

Results: Among 986 potential fractures, 841 were excluded from further evaluation. The most common reasons for exclusion were age under 50 years (38%), fracture of the face or digits (25%), and no primary provider assigned (22%). A total of 88 fractures were reviewed by a bone specialist, and primary providers acknowledged receipt of 85 consults. Twenty seven (31%) consults recommended treatment and 40 (45%) recommended bone density assessments (DXA). The primary providers responded by referring 14 patients (35%) for DXA and prescribing bisphosphonates in 16 patients (59.3%).

Conclusion: An electronic consult service identified a number of patients with a recent fracture, who were eligible but not receiving treatment or evaluation for osteoporosis. After receipt of the consult, primary care providers referred patients for DXA in over a third and prescribed bisphosphonates in over half of the patients.

Disclosures: *Richard Lee, None.*

SA0384

Withdrawn

SA0385

Association Between Prevalent Osteoporosis (OP) and Total Health Care Costs in Managed Care Members with High Cost Chronic Diseases. Sarah Thayer¹, Gabriel Gomez Rey², Jerald Seare³, Brad Stolshek^{*4}. ¹Optum, USA, ²Optum, USA, ³Optum, USA, ⁴Amgen Inc, USA

Background: Highly prevalent or costly chronic diseases(CD) such as chronic obstructive pulmonary disease(COPD), cardiovascular disease(CVD), depression(-DEP), and diabetes mellitus(DM) and multiple CDs are of significant interest to payers. Little is known about how osteoporosis (OP) in these diseases impacts health care costs. Objective and Purpose: To examine differences in total health care costs among members with CD with or without OP, and OP only. Methods: This was a retrospective study of commercial and Medicare Advantage members aged ≥50 years continuously enrolled in a large US health plan with evidence of prevalent CD and/or OP in the identification(ID) period(01/01/07 - 10/31/09). Evidence of OP was defined as ≥1 medical claim with an ICD-9 CM diagnosis code for OP, ≥2 OP medication fills, or ≥1 medical claim for fragility fracture during the ID period. Members with Paget's disease of bone, hypercalcemia, osteogenesis imperfecta, HIV, or preventive or active breast cancer treatment were excluded. Evidence of CD was disease-specific based on medical and/or pharmacy claim algorithms during the ID period. Members were assigned to one of 11 cohorts: single or multiple CD with or without OP and OP only. Index dates were set as a random service date from medical or pharmacy claims for each disease during the ID period. Each CD with OP cohort was compared with 1) its counterpart without OP and 2) OP only. Total all-cause health care costs in a 12-month follow-up period were examined. For each CD+/-OP pairing, the association between total health care costs was assessed using a generalized linear model with a log link and a gamma distribution controlling for baseline characteristics(age group, gender, region, Quan-Charlson comorbidity score, top AHRQ comorbidities, and resource utilization). Results: A total of 422,862 members were identified with CD with prevalent OP(10.9%), CD only(84.8%) or prevalent OP only(4.3%). Each CD with OP cohort had higher mean actual costs compared with its respective CD only cohort, and the OP only cohort(p<0.001). The presence of OP was associated with higher baseline-adjusted costs in each CD cohort(p≤0.0003). Predicted mean costs were 12%-23% higher in each CD with OP cohort vs. each cohort without OP. Conclusions: Members with CD and OP had significantly higher total health care costs than those with CD only. In these members, OP should be managed closely to improve the quality of care and overall cost.

Mean total all-cause healthcare costs during follow-up by cohort

| Chronic Disease (CD) | COPD | CV | DEP | DM | ≥2 CD |
|-----------------------------------|--------|--------|--------|--------|--------|
| Actual costs US \$/year* | | | | | |
| CD + OP | 15,024 | 10,038 | 13,878 | 12,465 | 17,997 |
| CD only | 11,047 | 8,377 | 9,467 | 8,570 | 12,801 |
| OP only | 5,377 | 5,377 | 5,377 | 5,377 | 5,377 |
| Predicted costs US \$/year | | | | | |
| CD + OP | 11,953 | 9,613 | 10,259 | 9,976 | 15,119 |
| CD only | 9,930 | 8,538 | 8,310 | 8,412 | 12,741 |
| OP only | 5,740 | 6,787 | 6,592 | 7,467 | 7,313 |

*Chronic disease + OP vs without OP, all comparisons, P<0.001
Chronic disease + OP vs OP only, all comparisons, P<0.001

Total All-Cause Healthcare Costs during Follow-Up

Disclosures: *Brad Stolshek, Amgen, 6*
This study received funding from: *Amgen Inc.*

SA0386

Lack of Osteoporosis Treatment in Real World Hip Fracture Patients. Stephen Johnston¹, Yang Zhao^{*2}, Donna McMorow³, John Krege⁴, Kelly Krohn⁵, ¹Thomson Reuters, USA, ²Eli Lilly, USA, ³Thomson Reuters, USA, ⁴Eli Lilly & Company, USA, ⁵Lilly USA, LLC, USA

Purpose: National Osteoporosis Foundation guidelines recommend that postmenopausal individuals age 50 and older presenting with hip fracture should be considered for treatment with pharmacologic osteoporosis (OP) treatment. This study examined patterns of OP treatment strategies among hip fracture (HFx) patients in real world clinical practice.

Methods: Patients aged 50+ with an HFx between 1/1/2002-12/31/2010 (first observed HFx = index) were identified from a large US administrative claims database. Patients included for study had 6+ months of pre-index continuous enrollment (baseline), no baseline evidence of teriparatide (TPTD), cancer, or Paget's disease. Patients were followed for up-to 36 months post-index to observe patterns in pharmacologic OP treatments. Five cohorts were constructed based on pre- and post-index use of OP treatment: patients with no observed evidence of OP treatment pre- or post-index (N/N); new bisphosphonate (BP) initiators with no baseline BP (N/BP); BP continuers with baseline BP (BP/BP); new TPTD initiators with no baseline BP treatment (N/TPTD); TPTD initiators switching from prior BP (BP/TPTD). Demographics, clinical characteristics, and healthcare resource use were compared across the 5 cohorts.

Results: Study included 71,115 patients. The majority of the sample, 53,634 (75% of total) patients, was observed to have no OP treatment (N/N) over a median of 352 days of follow-up; 26,238 of whom had ≥ 1 year of follow-up. New BP initiators (N/BP; 9,187 patients) started BP treatment within a median of 117 days. BP continuers (BP/BP; 7,463 patients) resumed treatment within a median of 58 days. New TPTD initiators (N/TPTD; 346 patients) started TPTD treatment within a median of 138 days. TPTD initiators switching from prior BP (BP/TPTD; 485 patients) switched to TPTD treatment within a median of 64 days. Mean ages ranged from 74.0 (BP/TPTD) to 80.5 (N/N) years. The N/N cohort was the oldest (81 vs. 74-79 years), had the highest proportion of males (39% vs. 8-18%), and the lowest baseline use rates of systemic glucocorticoids (13% vs. 17-30%) and dual energy X-ray absorptiometry scans (2% vs. 5-17%).

Conclusions: In spite of a sentinel event of a hip fracture, which is a known risk factor for future fracture, 75% of patients had no evidence of OP treatment over a median follow-up of 352 days. These data provide further evidence of a substantial gap in the management of OP among patients at very high risk for fractures.

Disclosures: *Yang Zhao, None.*

This study received funding from: *Eli Lilly and Company*

SA0387

Treatment (Rx) of Post-Menopausal Women with High FRAX Scores may be Cost-Effective without First Performing Bone Densitometry. John Schousboe^{*1}, William Leslie², Brent Taylor³, Steven Cummings⁴, L. Joseph Melton⁵, Margaret Gourlay⁶, Kristine Ensrud⁷. ¹Park Nicollet Clinic/University of Minnesota, USA, ²University of Manitoba, Canada, ³University of Minnesota, USA, ⁴San Francisco Coordinating Center, USA, ⁵Mayo Clinic, USA, ⁶University of North Carolina, USA, ⁷Minneapolis VA Medical Center / University of Minnesota, USA

Background: It is uncertain whether drug Rx prevents non-vertebral fractures in postmenopausal women with femoral neck (FN) BMD T-score > -2.5 and no prevalent vertebral fracture. However, among women ≥ 65 years old, 3 of every 10 meeting FRAX treatment threshold for major osteoporotic fracture and 6 of 10 meeting FRAX treatment threshold for hip fracture have FN T-scores > -2.5 . We used a Markov microsimulation model to estimate lifetime costs, health benefits, and cost-effectiveness of Rx of older US White women with high fracture risk by FRAX without BMD compared to first obtaining a BMD test plus vertebral fracture assessment and Rx of only the subset with either FN T-score ≤ -2.5 or a prevalent vertebral fracture.

Methods: The model had states of hip, morphometric and clinical vertebral, wrist, and humerus fracture, no fracture, and death. Fracture rates, costs, and disutilities were derived from the literature. The prevalence of FN T-score > -2.5 in those with FRAX w/o BMD 10-year hip and major osteoporotic fractures risks $\geq 3\%$ and $\geq 20\%$ were from the Manitoba Bone Density database. The age-specific prevalences of vertebral fracture were from Rochester Epidemiology Project data. Models were run for women age 65, 75, or 85 until death or age 100, assuming a national health payer perspective and willingness to pay of \$75,000 per quality adjusted life year (QALY) gained. For those with FN T-score > -2.5 and no prevalent vertebral fracture, we assumed relative risks of incident clinical vertebral fracture, morphometric vertebral fracture, and non-vertebral fracture on Rx to be, respectively, 0.45, 0.64, and 1.0. (Quandt 2005; Ryder 2008). Sensitivity analyses assumed only 18% reduction of vertebral fractures on Rx in the proportion with T-score > -2.0 (Cummings 1998), or 25% of base case disutility from morphometric vertebral fractures.

Results: Table shows estimated costs per QALY gained for Rx of women with high FRAX without BMD score vs. Rx of only those with prevalent vertebral fracture or FN T-score < -2.5 .

Conclusions: Rx initiation on the basis of high fracture risk estimated by FRAX w/o BMD may be cost-effective, but this is highly sensitive to vertebral fracture disutility and to assumed vertebral fracture reduction on Rx for those with T-score > -2.0 and

no prevalent vertebral fracture. A randomized controlled trial of fracture reduction medication in this subset with preference weighted quality of life assessments is needed.

| Age | Analysis | Fracture Risk Subgroup | Drug Cost \$250/year | Drug Cost \$500/year |
|----------|--|--------------------------------|----------------------|----------------------|
| 65 Years | Base Case | $\geq 20\%$ Major Osteoporotic | \$24,504 | \$62,308 |
| | Base Case | $\geq 3\%$ Hip | \$24,858 | \$60,211 |
| 75 Years | Base Case | $\geq 20\%$ Major Osteoporotic | \$29,993 | \$98,732 |
| | Base Case | $\geq 3\%$ Hip | \$40,295 | \$97,095 |
| | Sensitivity: RR Vert Fx on Drug Rx 0.82 if T-score > -2.0 | $\geq 3\%$ Hip | \$52,162 | \$134,989 |
| | Sensitivity: Morphometric Vertebral Fracture Disutility 25% of Base Case | $\geq 3\%$ Hip | \$65,716 | \$189,907 |
| 85 Years | Base Case | $\geq 20\%$ Major Osteoporotic | \$43,928 | \$122,623 |
| | Base Case | $\geq 3\%$ Hip | \$45,847 | \$122,804 |

Disclosures: *John Schousboe, None.*

SA0388

See Friday Plenary Number FR0388.

SA0389

See Friday Plenary Number FR0389.

SA0390

Importance of Physician Communication and BMD testing in Management of Glucocorticoid-Induced Osteoporosis. Stuart Silverman^{*1}, Jeffrey Curtis², Kenneth Saag², Julie Flahive³, Adolfo Diez-Perez⁴, Jonathan Adachi⁵, Susan Greenspan⁶, Steven Boonen⁷, Cyrus Cooper⁸, Coen Netelenbos⁹, Nelson Watts¹⁰, Juliet Compston¹¹, for the GLOW investigators¹². ¹Cedars-Sinai/UCLA, USA, ²University of Alabama at Birmingham, USA, ³University of Massachusetts, USA, ⁴Parc De Salut Mar, Spain, ⁵St. Joseph's Hospital, Canada, ⁶University of Pittsburgh, USA, ⁷Center for Metabolic Bone Disease & Division of Geriatric Medicine, Belgium, ⁸University of Southampton, United Kingdom, ⁹VU Medical Center, The Netherlands, ¹⁰Mercy Health Osteoporosis & Bone Health Services, USA, ¹¹University of Cambridge School of Clinical Medicine, United Kingdom, ¹²University of Massachusetts, USA

Purpose: Guidelines recommend bone-mineral density (BMD) testing, and use of calcium (CA), vitamin D (vitD) and antiosteoporosis medication (AOM) in glucocorticoid (GC)-exposed individuals. We have reported less than optimal use of AOM, CA and vitD in such individuals in both the US and Europe (IOF/ECCEO 2012). We hypothesized that GC-exposed individuals who had a BMD test or communicated with their healthcare provider (HCP) about osteoporosis (OP) would be more likely to begin CA, vit D, and/or AOM and would be more "concerned" about their risk of fracture.

Methods: We studied the impact of BMD testing and HCP communication on medical management of GC exposure over 3 years in GLOW, a multinational prospective observational cohort of postmenopausal women (17 sites, 10 countries). Data on self-reported GC use were collected at baseline and at 1, 2 and 3 years. At baseline, participants were asked if they had ever taken GC. At both baseline and at subsequent surveys the women were asked if they had had a BMD test, had discussed OP with their HCP, and if they were taking CA, vit D and/or AOM.

Results: Of the 40,058 women with complete data over the 4 surveys, 27.4% (n=10,978) reported past/current oral GC use. Of these, 893 (2%) were current continuous users (CCU) over the past ≥ 2 years at the 3-year survey. Approximately 45% of nonusers were taking CA and VitD compared to 67% with CCU. AOM use was 22% in nonusers and 45% in CCU. Approximately 48% of nonusers had had a BMD test within the 3 years of the study, with an approximately 50% greater BMD testing in CCU. current intermittent and recent past GC users. BMD testing within the past 3 years doubled combined AOM and CA/VitD use in GC-exposed individuals compared to those who did not have a BMD. BMD testing within the 3 years of the study was associated with a 50% increase in AOM use alone in CU vs nonusers. BMD testing doubled the individual participant rating of being "very concerned" about risk of fracture in both users and nonusers of AOM. There was an almost 3-fold increase

in BMD testing among non-GC users who discussed OP with their HCP vs those who did not, and a 2-fold increase in BMD testing in GC-exposed individuals who spoke with their HCP. AOM use increased from 35% to 54% in CCU who spoke to their HCP about OP.

Conclusions: Our study confirms the importance of BMD testing and communication between patient and HCP in the management of GC-exposed individuals.

Disclosures: *Stuart Silverman, None.*

This study received funding from: Financial support from the GLOW study is provided by Warner Chilcott Company LLC and Sanofi-Aventis to the Center for Outcomes Research, University of Massachusetts

SA0391

See Friday Plenary Number FR0391.

SA0392

See Friday Plenary Number FR0392.

SA0393

See Friday Plenary Number FR0393.

SA0394

The Effect of Vitamin K₂ on Pregnancy-associated Osteoporosis: A Report of Four Patients. Hirovuki Tsuchie*¹, Naohisa Miyakoshi², Michio Hongo², Yuji Kasukawa², Yoshinori Ishikawa³, Yoichi Shimada³. ¹Akita University Graduate School of Medicine, Japan, ²Akita University Graduate School of Medicine, Japan, ³Dept. of Orthopedic Surgery, Akita University Graduate School of Medicine, Japan

Purpose: Pregnancy-associated osteoporosis is a rare disease which causes multiple vertebral compression fractures from the late gestation period to several months after delivery. Although stopping breast-feeding, wearing a corset and calcium and vitamin D intake are common treatments for this disease, there has been no report using vitamin K₂ (menatetrenone), which is one of the medicines for osteoporosis. We herein describe 4 cases showing a favorable course by prescribing vitamin K₂.

Case 1: A 30-year-old woman developed back pain 4 weeks after her first delivery. Because her back pain did not lessen by wearing a corset, we advised against breast-feeding and prescribed a daily intake of 45 mg of vitamin K₂. One year and 3 months after her delivery, her back pain had completely disappeared.

Case 2: A 31-year-old woman developed back pain 2 weeks after her first delivery. Because her back pain did not lessen by stopping breast-feeding, we instructed her to wear a corset and prescribed a daily intake of 45 mg of vitamin K₂. Nine months after her delivery, her back pain had reduced significantly.

Case 3: A second pregnant 31-year-old woman had a past history of vertebral compression fractures after her first delivery 7 years ago, and she was treated by wearing a corset and prescribing a daily intake of 45 mg of vitamin K₂. Although she had continued to take vitamin K₂ for osteoporosis treatment, she stopped to take it when she got second pregnant. We advised against breast-feeding and prescribed a daily intake of 45 mg of vitamin K₂ after her second delivery, and she did not appear any back pain and decrease of bone mineral density.

Case 4: A 30-year-old woman developed back pain 1 week after her first delivery. Because her back pain did not lessen by wearing a corset, against breast-feeding and prescribing a daily intake of nonsteroidal anti-inflammatory drugs (NSAIDs), we prescribed a daily intake of 45 mg of vitamin K₂. Eight months after her delivery, her back pain had completely disappeared.

Conclusion: Vitamin K₂ prevents fractures by improving the bone quality. Vitamin K₂ is administered safely to newborns or pregnant woman for the treatment of melena neonatorum. Although stopping lactation, corset application, and medical treatment which include calcium and vitamin D are the basis of treatment, we should consider vitamin K₂ as a choice of subsidiary treatment, because of its effectiveness and safety.

Disclosures: *Hirovuki Tsuchie, None.*

SA0395

The Efficacy of Hydroxyapatite for Screw Augmentation in Osteoporotic Patients. Jun Ho Lee*¹, Sang Hoon Jang², Ho Yeon Lee², Sang Ho Lee². ¹Wooridul Spine Hospital, South Korea, ²Wooridul Spine Hospital, South Korea

Purpose: Internal stabilization using a pedicle screw system is the gold standard for treatment of an unstable spine. Screw construct stability is of considerable importance in determining outcome, especially in spinal osteoporosis. Polymethylmethacrylate (PMMA) has been proven as an effective material for increasing the pullout strength of pedicle screws inserted into osteoporotic bones. But, it also has several disadvantages; its exothermic properties, the risk of neural injury in the event of

extravasation, and difficulties in performing revision surgery. In the current study, we used hydroxyapatite (HA) for screw augmentation in spinal osteoporosis.

Methods: From March 2002 to December 2005, 34 patients diagnosed as spondylolisthesis grade I or II with osteoporosis (T score < -2.5) underwent one level transforaminal lumbar interbody fusion (TLIF) operation. In group A (screw augmentation group), additional screw augmentation was performed with HA. In group B (control group), conventional TLIF was carried out. Clinical outcome was assessed according to the Visual Analog Scale (VAS). Radiologic outcome was assessed by repeated measurement of standing lateral radiographs obtained at postoperative day 1 and during each follow-up visit (1 month, 3 months, 6 months, and annually). To simplify the results, radiologic parameters were compared between postoperative day 1 and the 3-month follow-up, and between postoperative day 1 and the 2-year follow-up in each group.

Results: The mean age was 67.6 years in group A and 68.2 years in group B. The mean T score was -2.80 in group A and -2.68 in group B. The mean improvement in VAS pain score was 83% for back pain and 85% for leg pain in group A (p < 0.05), and 82% for back pain and 89% for leg pain in group B (p < 0.05). There were no statistically significant changes in radiological parameters in group A. However, in group B, there was a decrease in segmental lordosis (SL) to 2.57 ± 1.03 (p = 0.109) at 3 months and a significant decrease to 2.78 ± 0.67 (p = 0.003) at 2 years. There was also a significant change in screw angle (SA) to 2.50 ± 0.67 (p = 0.005) at 3 months and 3.20 ± 0.84 (p = 0.005) at 2 years in group B.

Conclusions: Our results suggest that HA cement is an useful tool for screw augmentation in osteoporotic bone and may play a role as a substitute for PMMA. It can be recommended as a promising alternative during spinal instrumentation in osteoporotic patients.

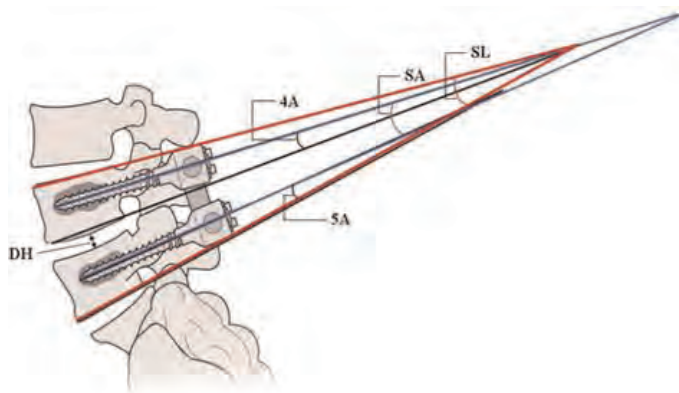


figure_1

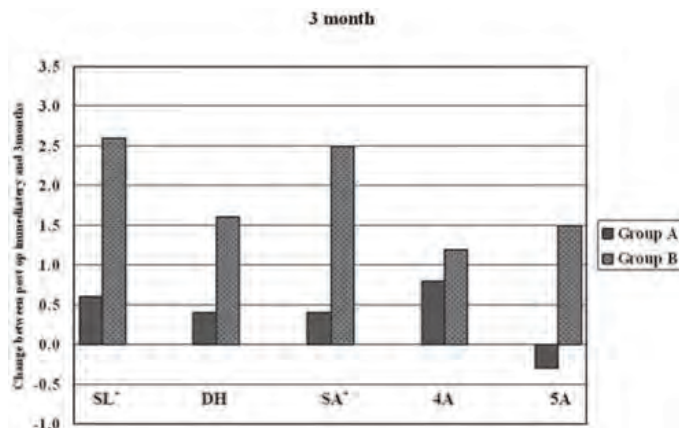


figure_2

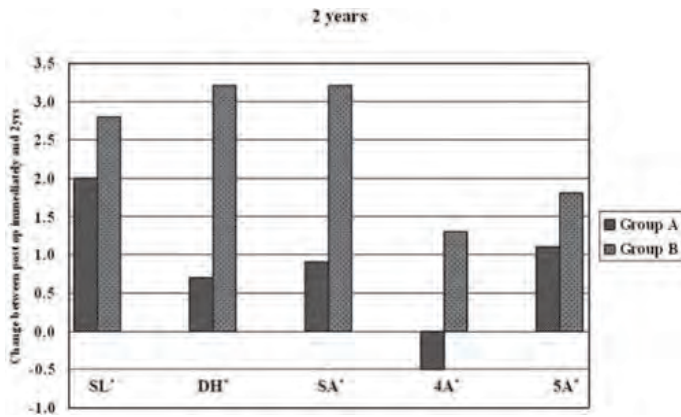


figure_3

Disclosures: Jun Ho Lee, None.

SA0396

Effects of Calcitonin on Pain, QOL, and Bone Marker in Osteoporosis Patients Suffering Vertebral Compression Fracture. Shinya Tanaka^{*1}, Akira Yoshida², Hiroaki Suzuki³, Manabu Ito⁴. ¹Saitama Medical University, Japan, ²Yoshida Orthopedic Clinic, Japan, ³Asahi Kasei Pharma, Japan, ⁴Hokkaido University Graduate School of Medicine, Japan

Objective: Many elderly individuals decrease activity of daily living (ADL) and require public nursing services due to a vertebral compression fracture associated with osteoporosis. It is important for senior citizens to prevent disuse syndrome in such senior citizens by enabling them to leave their sickbed early after suffering a fragile fracture. In patients with osteoporosis suffering fresh vertebral compression fractures, we assessed whether treatment with calcitonin was effective on improvement of the patient's quality of life (QOL) and on maintenance of bone mass, by comparison with matching patients treated with oral nonsteroidal anti-inflammatory drugs (NSAIDs) combined with an active form vitamin D3 preparation.

Method: A multicenter, open-labeled, randomized parallel-group study was conducted in female patients with primary osteoporosis aged 65 years and over complaining of dorsolumbar pain due to a fresh spinal fragility fracture(s). Patients were randomized to receive either calcitonin at 20 IU once weekly by intramuscular injection (calcitonin group) or oral NSAIDs in combination with an active form vitamin D3 preparation (NSAIDs + VD3 group).

The study treatment period lasted 6 weeks, and patients were assessed as to pain using the visual analog scale (VAS) and with respect to QOL using the Roland Morris questionnaire (RDQ) and EQ-5D. A bone resorption marker (TRACP-5b) was used to evaluate the effect of treatments on bone metabolism.

Results: At week 2 of study treatment, a relief in pain (VAS) and an improvement of QOL (RDQ and EQ-5D) were superior in the calcitonin group than those in the NSAIDs + VD3 group. The values of TRACP-5b also showed decreases at 3 months of study treatment and thereafter in the calcitonin group alone, thus suggesting greater efficacy of the calcitonin therapy as compared to the NSAIDs + VD3 therapy.

Discussion: Nasal and suppository calcitonin is evaluated as having moderate strength of recommendation in the 2010 Guideline on the Treatment Symptomatic Osteoporotic Compression Fractures published by the American Academy of Orthopaedic Surgeons (AAOS). The results of the present study also suggest that the calcitonin injectable preparation is also as effective for this disease.

Calcitonin has a mechanism of analgesic action mediated by central serotonergic neurons with a consequent relatively sustained effect unlike prompts effect of NSAIDs. In this study, the once-weekly regimen of calcitonin was effective for improving QOL and pain relief. Furthermore, since bone resorption becomes augmented after fracture and decreased ADL and sequential disuses also accelerate bone resorption, calcitonin is considered an essential drug in the treatment of early-phase vertebral compression fractures not only for relief of pain and QOL improvement but also in terms of prevention of loss of bone mass.

Disclosures: Shinya Tanaka, None.

SA0397

Unpredictable Spontaneous Fusion after Vertebroplasty and Kyphoplasty in Osteoporotic Compression Fracture. Jin Hwan Kim^{*1}, Jung Hoon Kim², Jae Hyup Lee³. ¹Inje University, Ilsanpaik Hospital, South Korea, ²Inje University, Ilsanpaik Hospital, South Korea, ³Seoul National University, College of Medicine, South Korea

Introduction: We found a spontaneous fusion after percutaneous vertebroplasty (PVP) or kyphoplasty in osteoporotic compression fractures and analyze the radiologic & clinical characteristics.

Materials & Methods: Between January 2000 and January 2011, 555 patients were treated with PVP or kyphoplasty for osteoporotic compression fracture in our department. We classified the spontaneous fusion as two groups. One is absolute spontaneous fusion group with at least three cortical continuity to adjacent vertebrae, the other is partially fusion group which progressed fusion compared to previous radiologic finding. We reviewed the plain film and analyzed the radiologic characteristics of those patients with duration of fusion, location and extent of fused segments. A clinical characteristic by visual analogue score (VAS) compared to our previous report was checked.

Results: Among them, 54 patients (9.7%) had an absolute spontaneous fusion and 43 patients (7.7%) had partially fused on plane image. In absolute fusion group, the average duration of fusion was 19 months ranged of 3 to 48 months. Forty six cases (85%) of absolute fusion patients had occurred with proximal adjacent vertebrae and 7 cases (13%) had proximal with distal adjacent vertebrae. 41 cases (76%) of spontaneous fusion occurred within 1 segment and 13 cases within multiple segments. The most cases of absolute fusion group were occurred at thoracolumbar junction (40 patients, 74%) Mean VAS score of absolute fusion group was 2.0 at final follow-up and were analyzed relatively low score compared to mean VAS of our previous report. (2.0, 2.8 respectively)

Conclusion: After percutaneous vertebroplasty or kyphoplasty in osteoporotic compression fracture, unpredictable spontaneous fusion could develop more than 10% rate, especially with proximal vertebra within 1 segment at thoracolumbar junction in radiologic aspect. Clinically, patients with spontaneous fusion had a tendency of more reduced pain than others.

Disclosures: Jin Hwan Kim, None.

SA0398

Are the IOM Vitamin D Guidelines Sufficient for Long Term Care Residents? Marv Anne Ferchak^{*1}, Carroll Lee², Gail Fiorito², Julie Wagner¹, Karen Vujevich², Subashan Perera², David Nace², Neil Resnick², Susan Greenspan¹. ¹University of Pittsburgh, USA, ²University of Pittsburgh, USA

Background: The new Institute of Medicine guidelines for vitamin D suggest a level above 20 ng/dL is sufficient for adults. However, this level may be insufficient for frail residents in long term care (LTC) facilities.

Methods: To examine the impact of vitamin D on falls, function, cognition and mental health status in LTC residents, we examined serum 25-hydroxy vitamin D levels in 181 older women (mean age 85 years) living in LTC (assisted living and skilled) enrolled in an osteoporosis clinical trial. Women were grouped as deficient (< 20 ng/dL), insufficient (20-29.9 ng/dL), or sufficient (≥30 ng/dL). At baseline, deficient women received vitamin D 50,000 IU/week for 8 weeks to achieve a level of 25-hydroxy vitamin D ≥20 ng/dL. All received vitamin D 800 IU/day as maintenance and were followed for 1 year. Outcome measures included falls (obtained from electronic surveillance and reported/document chart reviews), physical activities of daily living (PADL, eat, dress, groom, walk, transfer, bathe, get to bathroom), instrumental activities of daily living (IADL, phone, travel, shop, prepare meals, housework, handle money), physical performance test (PPT, timed sit to stand, timed walk, phone, eat), gait speed (m/sec), time to stand (sec, measure of strength), cognitive status (SPMSQ), and mental health (PHQ-9).

Results: Over 1 year, women who were deficient tended to fall more compared to the other 2 groups, but the results were not statistically significant (Table, mean ± SEM unless otherwise specified). Comparison of the 12-month continuous outcomes across the 3 vitamin D groups adjusting for baseline values using ANCOVA and pairwise comparisons, suggested that women with vitamin D deficiency had lower scores for IADL, PPT and cognitive status (p<0.05) but there was no significant difference between those with insufficiency vs sufficiency. Gait speed, IADL and cognitive status were better in women with insufficiency than deficiency (p<0.05).

Conclusions: Frail women in LTC facilities with vitamin D deficiency are at risk for functional and cognitive status impairment not readily reversed by reaching vitamin D levels above 20 ng/dL and may require levels or doses above the recommended threshold suggested by the IOM. After 1 year of maintenance with the IOM recommended dose of 800 IU/day, LTC residents with insufficient to sufficient levels (≥20ng/dL) have better functional and cognitive status than those who are initially deficient.

| Variable | Deficient (N=40) | Insufficient (N=55) | Sufficient (N=85) | P-value, 3-group comparison |
|--------------------------|------------------|---------------------|-------------------|-----------------------------|
| Incident Falls (%) | 62.5 | 52.7 | 51.8 | 0.52 |
| IADL score * | 5.1±0.5 | 6.8±0.6 * | 8.0±0.5 # | <0.0001 |
| PADL score * | 11.3±0.5 | 11.0±0.4 | 11.7±0.3 | 0.82 |
| PPT score * | 16.7±0.9 | 18.1±0.8 | 19.6±0.6 | 0.049 |
| Gait speed (m/sec) * | 0.4±0.0 | 0.5±0.0 * | 0.6±0.0 | 0.1 |
| Time to stand (sec) ^ | 4.7±0.9 | 3.5±0.4 | 3.6±0.5 | 0.38 |
| Cognitive status score ^ | 4.8±0.6 | 3.5±0.4 * | 2.9±0.4 # | 0.008 |
| Mental health score ^ | 4.8±0.7 | 3.3±0.6 | 3.2±0.4 | 0.19 |

Table

Disclosures: Mary Anne Ferchak, None.

SA0399

Effect of Daily 800 IU Versus Single Oral Bolus of 300'000 IU Vitamin D on 25-hydroxyvitamin D Serum Concentration Increase in Postmenopausal Women with Osteoporosis. Heike Bischoff-Ferrari¹, Andreas Egli Linder², Kurt Lippuner³, Albrecht Popp³, Beatrice Günther⁴, Petra Rindova⁵, Robert Theiler⁶. ¹University of Zurich, Switzerland, ²Centre on Ageing & Mobility, Switzerland, ³Osteoporosis Policlinic, University of Bern, Switzerland, ⁴Inselspital Zürich, Switzerland, ⁵Triemli City Hospital, Switzerland, ⁶Stadspital Triemli, Switzerland

Background: Correction of vitamin D deficiency among patients with osteoporosis is challenged by low adherence.

Aim: To test the efficacy of daily versus bolus vitamin D.

Methods: We randomized 99 postmenopausal women with osteoporosis treated with Zoledronate (mean age 77 years) to either daily 800 IU vitamin D3 plus 1000 mg calcium or a single oral bolus of 300'000 IU vitamin D3 plus 1000 mg calcium per day. Follow-up assessments took place at 2 weeks and 6 months.

Results: Baseline 25-hydroxyvitamin D serum concentrations (25(OH)D) did not differ between the daily (mean = 23 ng/ml) and the bolus (mean = 29 ng/ml) group. At 2 weeks, achieved mean 25(OH)D differed significantly between the daily (mean = 24 ng/ml) and the bolus group (mean = 44 ng/ml; p-value < 0.0001). At 6 months, however, achieved mean 25(OH)D were similar between the daily (mean = 29 ng/ml) and the bolus group (mean = 25 ng/ml; p-value = 0.08). At baseline, 60% in the daily and 43% in the bolus group were vitamin D replete (> 20 ng/ml; 50 nmol/l), while 23% in the daily and 28% in the bolus group had desirable 25(OH)D concentrations (> 30 ng/ml; 75 nmol/l). At 2 weeks, 71% in the daily and 96% in the bolus group were vitamin D replete (> 20 ng/ml; 50 nmol/l), while 21% in the daily and 77% in the bolus group had desirable 25(OH)D concentrations (> 30 ng/ml; 75 nmol/l). At 6 months, 61% in the daily and 83% in the bolus group were vitamin D replete (> 20 ng/ml; 50 nmol/l), while 33% in the daily and 22% in the bolus group had desirable 25(OH)D concentrations (> 30 ng/ml; 75 nmol/l).

Conclusion: Postmenopausal women with osteoporosis randomized to either 800 IU vitamin D per day versus a single oral bolus of 300'000 IU vitamin D reached similar 25(OH)D concentrations at 6 months. Notably, at 6 months, daily application leaves 39% and bolus application leaves 17% of patients in the vitamin D deficient range (< 20 ng/ml). Further, daily application shifts only 33% and bolus application shifts only 22% of patients into the desirable 25(OH)D range for fracture reduction (> 30 ng/ml) at 6 month follow-up.

Disclosures: Heike Bischoff-Ferrari, None.

This study received funding from: Funding sources: investigator initiated and independent grant by Novartis

SA0400

See Friday Plenary Number FR0400.

SA0401

See Friday Plenary Number FR0401.

SA0402

See Friday Plenary Number FR0402.

SA0403

BA058, a Novel Human PTHrP Analog, Restores Bone Density at the Spine and Femur in Osteopenic Sprague-Dawley Rats within 13 Weeks. Elisabeth Lesage¹, Aurore Varela¹, Susan Y. Smith¹, Gary Hattersley². ¹Charles River Laboratories, Canada, ²Radius, USA

BA058 is a synthetic analog of hPTHrP (1-34) currently in Phase 3 of clinical development for the treatment of post-menopausal osteoporosis. The objectives of this study were to determine the effects of BA058 on bone mass as determined by BMD in ovariectomized skeletally mature Sprague-Dawley rats. Six-month old virgin female rats (18/group) were randomly assigned to each of five groups. Four groups were ovariectomized (OVX) and one group underwent Sham surgery (ovaries remained intact). Treatment commenced following a 3-month bone depletion period. Animals received daily subcutaneous injections of vehicle (Sham and OVX controls), or BA058 at 1, 5 or 25 µg/kg/day, for a minimum 26 weeks. Blood and urine samples were analyzed for biochemical markers of bone turnover (P1NP, CTx, OC, DPD). aBMD was measured at the lumbar spine and the femur by DXA whereas vBMD was measured at the proximal tibia metaphysis by pQCT prior to surgery, at the end of the bone depletion period, and after 3 and 6 months of treatment. At the end of the bone depletion period, OVX animals showed a loss in aBMD of 6-8% at the lumbar spine and distal femur sites and a loss of 6% at proximal tibia site. Thirteen weeks of BA058 treatment restored aBMD at the lumbar spine and distal femur sites, to or above pre-OVX values at all doses. After 26 weeks of treatment at 25 µg/kg/day, lumbar and distal femur aBMD were increased by 18% and 27% compared to Sham, respectively, and 26% and 41% compared to pre-OVX,

respectively. After 13 weeks of treatment at 5 and 25 µg/kg/day, total slice vBMD and vBMC at the proximal tibia metaphysis site were restored to, or were above pre-OVX and Sham values. After 26 weeks of treatment, all BA058 treated groups showed increases in metaphyseal total slice vBMD compared to Sham, reaching 18% at 25 µg/kg/day. Increases in biochemical markers of bone turnover were also observed as compared to OVX controls, consistent with the increases in bone mass. In conclusion, BA058 potentially offers a number of important advantages as a new treatment for post-menopausal osteoporosis, including the ability to build new bone rapidly.

Disclosures: Aurore Varela, None.

This study received funding from: Radius Health

SA0404

Decreased Osteoclastogenesis in Bone Marrow Cells Derived From Ovariectomized Rats Treated With Sclerostin Antibody. Min Liu¹, Pam Kurimoto², Qing-Tian Niu², Kelly S. Warmington², Xiaodong Li², W. Scott Simonet², Hua Zhu Ke¹. ¹Amgen Inc., USA, ²Amgen Inc., USA

Inhibition of sclerostin by treatment with a sclerostin monoclonal antibody (Scl-Ab) in both animal models and humans increases bone formation and decreases bone resorption simultaneously, thereby creating the potential for a larger anabolic window with Scl-Ab treatment than other approved osteoporosis therapies. The mechanism for decreasing bone resorption by Scl-Ab is a topic of ongoing research. In the current study, we examined osteoclastogenesis in bone marrow cells derived from ovariectomized (OVX) rats treated with Scl-Ab.

Six-month-old OVX rats (2 months post-OVX) were treated with vehicle (Veh) or Scl-Ab (Scl-AbVI, 25 mg/kg, SC, 1x/week) for 6, 12, or 26 weeks. Two other groups of OVX rats were treated with Scl-Ab for 6 weeks and then transitioned to Veh for either an additional 6 or 20 weeks. Ex vivo osteoclast cultures were performed with monocytic-enriched bone marrow cells in the presence of m-CSF and RANKL for 7 days. Osteoclast formation was assessed by tartrate-resistant acid phosphatase (TRAP)-positive staining for multinucleated cells and TRAP activity was determined using the cell culture medium.

TRAP-positive cells in OVX rats were increased in size and number compared with sham controls, and these cells were decreased in size and number in OVX rats treated with Scl-Ab at both weeks 6 (Fig. 1) and 12, indicating that in vivo Scl-Ab treatment reduced the osteoclastogenesis capacity of bone marrow cells. TRAP activity in culture medium showed a significant increase in OVX rats compared with sham controls at weeks 6 (Fig. 2) and 12. Scl-Ab treatment in OVX rats for 6 and 12 weeks decreased TRAP activity to the level of sham controls. By week 26, TRAP activity in OVX controls was not significantly higher than that in sham controls, and OVX rats treated with Scl-Ab maintained TRAP activity at the level of sham controls. Discontinuation of Scl-Ab for 6 weeks increased TRAP activity to a level that was not significantly different than OVX controls. The decrease in osteoclastogenesis is consistent with the bone histomorphometric analysis from the current study that showed a decrease in bone resorption indices in vivo by Scl-Ab (data not shown).

In summary, these data suggest that decreased osteoclastogenesis may contribute to the reduction in bone resorption observed with Scl-Ab treatment, although the mechanism of action requires further investigation.

Fig. 1. Six Weeks of Scl-Ab Treatment Decreases TRAP-positive Multinucleated Cells in Bone Marrow Culture of OVX Rats (TRAP Staining)

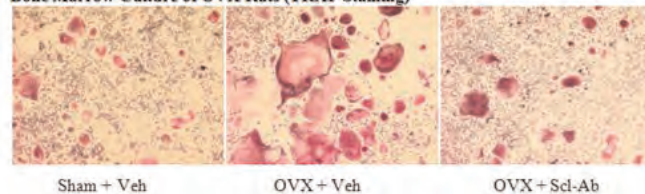
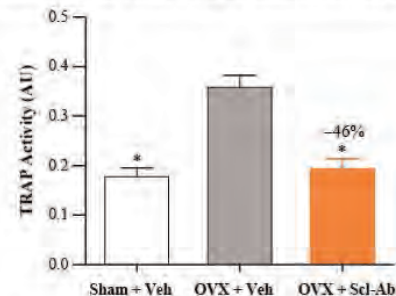


Fig. 1

Fig. 2. Six Weeks of Scl-Ab Treatment Decreases TRAP Activity in Bone Marrow Culture Medium of OVX Rats



*p < 0.05 by t-test compared with OVX + Veh
-46% change represents difference from OVX + Veh

Fig. 2

Disclosures: Min Liu, Amgen Inc., 3; Amgen Inc., 7

This study received funding from: Amgen Inc. and UCB Pharma

SA0405

In Vivo Assessment of the Calcitonin Receptor Peptide for the Treatment of Osteoporosis. David Komatsu*¹, Michael Hadjiargyrou², Srinivas Pentylala³. ¹Stony Brook University, Dept. of Orthopaedics, USA, ²State University of New York at Stony Brook, USA, ³Department of Anesthesiology, Stony Brook University, USA

Osteoporosis is the most widespread musculoskeletal disorder with a US prevalence of ~10 million. While several classes of antiresorptive drugs are clinically available to patients with osteoporosis, these agents are only able to slow disease progression. The sole approved anabolic agent, parathyroid hormone, is encumbered by several drawbacks that have limited its widespread utilization. Therefore, the development of new skeletally anabolic agents represents a major clinical need. We previously reported on the *in vitro* osteogenic activity of Calcitonin Receptor Peptide (CRP), a 12 AA-long peptide with homology to the C-terminus of the calcitonin receptor. The present study assessed the *in vivo* efficacy of CRP in normal and ovariectomized (OVX) rats to test the hypothesis that CRP is skeletally anabolic. 36 retired breeders underwent OVX at 6 months of age and after an additional month they were then divided into three groups: OVX Vehicle, OVX 15, and OVX 150. 24 aged-matched ovary intact rats (Intact) were divided into Intact Vehicle and Intact 15 groups. All rats were given 1 mL intraperitoneal injections (IP) of 50% DMSO (Vehicle) or 50% DMSO containing 15 µM (15) or 150 µM (150) 5 days/week for 5 weeks. They were then euthanized and serum, tibiae, femora, and vertebrae were collected. Femora were analyzed by microCT at the midshaft and distal metaphysis followed by 3-point bending tests. Serum samples were used for biomarker analyses. MicroCT analyses revealed significant increases in periosteal volume and periosteal surface at the midshaft, concomitant with increases in polar moment of inertia, maximum principal moment of inertia, and minimum principal moment of inertia for OVX 15 compared to Vehicle. However, subsequent biomechanical testing showed these differences were insufficient to affect femoral biomechanical integrity with no differences seen for stiffness, yield force, ultimate force, or energy to failure. Similarly, biomarker analyses failed to identify differences in bone specific alkaline phosphatase or carboxy-terminal collagen crosslinks. The completed analyses show that IP administration of CRP to rats is safe, though they provide only limited evidence that CRP is skeletally anabolic. However, histomorphometric tibial analyses, as well as microCT and biomechanical vertebral analyses remain to be completed and our hypothesis cannot be conclusively supported or refuted until these outcomes have been determined. Moreover, pharmacokinetic studies designed to establish the optimal dose, route, and frequency of CRP treatment are required for the *in vivo* anabolic potential of this peptide to be definitively assessed. In summary, these studies show that administration of CRP to ovariectomized rats results in modest improvements in midshaft femoral geometry and suggests that further study of CRP may aid in the development of new anabolic treatments for osteoporosis.

Disclosures: David Komatsu, None.

SA0406

See Friday Plenary Number FR0406.

SA0407

Manipulations of Disulfide Bonds in an Amylin Octapeptide: A Mechanism to Modify Bioactivity. Jillian Cornish*¹, Maureen Watson², Karen Callon¹, Renata Kowalczyk², Margaret Brimble². ¹University of Auckland, New Zealand, ²University of Auckland, New Zealand

Amylin, a peptide hormone co-secreted with insulin from the β-pancreatic cells, is active in fuel metabolism. We established amylin is anabolic to osteoblasts, whilst inhibiting osteoclastogenesis *in vitro* and *in vivo* thus suggesting a role in therapy of osteoporosis; although because of the peptide size and its non-osteogenic effects, it is not an ideal therapeutic agent. Previous structure-activity relationships demonstrated that an octapeptide fragment of amylin, amylin-(1-8) a ring-peptide, is inactive on fuel metabolism, but still anabolic to osteoblasts *in vivo* and *in vitro*. This small ring-peptide has thus been used as a model for the creation of orally active, non-peptide analogues, as potential candidates for the therapy of osteoporosis.

The disulfide bond in novel amylin-(1-8) analogues was modified either via macrocyclization or bridging reagent to increase potency and/or stability. A dibromomaleimide linker -analogue 1 (A1), a thiobenzyl linker (A2, A3), a thioalkyl chain of variable length (A5, A6), and a thiol-Michael modification (A7) were used to generate bridged analogues of amylin-(1-8)-NH₂. "Click chemistry" was also used to afford a triazole linked analogue. Importantly, a Nobel Prize-winning Ring Closing Metathesis (RCM) technology was used to afford chemically inert stapled analogues (A8-16).

The analogues were screened for proliferative activity in osteoblasts at physiological concentrations. Six analogues (A2, A8, A12, A13, A15, A16) significantly stimulated increases in mitogenesis (ANOVA, post hoc Dunnett) at a similar level to the native peptide with improved stability. These novel entities could lead to development of stable therapeutic compounds for use in osteoporosis treatment or for promotion of healing fractures.

Further chemical syntheses are needed to optimise these promising analogues. Subsequent synthetic modifications may further improve activity and stability.

Disclosures: Jillian Cornish, None.

SA0408

See Friday Plenary Number FR0408.

SA0409

See Friday Plenary Number FR0409.

SA0410

Effects of Alfacalcidol and ED-71/eldcalcitol Alone or in Combination with Risedronate in Ovariectomized Rats. Tetsuo Yano*¹, Mei Yamada², Makoto Shiozaki², Daisuke Inoue³. ¹Ajinomoto Pharmaceuticals Co., LTD, Japan, ²Ajinomoto Pharmaceuticals Co., LTD, Japan, ³Teikyo University Chiba Medical Center, Japan

Background/Aim: 1α,25(OH)₂D₃ and its prodrug alfacalcidol (ALF) have been used for treatment of osteoporosis, often combined with antiresorptive agents such as bisphosphonates. ED-71 is a new 1α,25(OH)₂D₃-derivative that improves calcium balance and at the same time suppresses bone resorption, and has recently been approved for treatment of osteoporosis in Japan. ED-71 has been shown to be superior to ALF in decreasing the incidence of vertebral fractures in Japanese postmenopausal women. But its efficacy in combination with bisphosphonates remains unknown. In the present study, we examined effects on BMD and bone architecture of treatment with ED-71 and ALF, each alone or in combination with risedronate using ovariectomized rats.

Methods: Female Sprague Dawley rats at 24 weeks of age were divided into one sham-operated and five ovariectomized groups (1: vehicle, 2: ED-71, 3: ALF, 4: RIS, 5: RIS + ED-71, and 6: RIS + ALF). RIS (3.5 ug/kg, s.c.) and ED-71 (0.2 ug/kg, p.o.) were given twice per week for 12 weeks. ALF (0.4 ug/kg, p.o.) was given three times per week for 12 weeks. BMD, bone architecture and bone turnover makers were measured every 4 weeks by micro CT and ELISA, respectively.

Results: BMD was significantly decreased in vehicle-treated rats compared with sham rats after 4 weeks. At 8 weeks, BMD in RIS + ALF and RIS + ED-71 was significantly increased by 55.6 and 63.9%, respectively, compared with vehicle. At 12 weeks, BMD in RIS + ALF and RIS + ED-71 significantly increased by 94.4 and 97.2%, respectively, compared with vehicle. At 12 weeks, Tb.N of ED-71, ALF, RIS, RIS + ED-71, and RIS + ALF groups significantly increased by 35.2, 42.8, 52.8, 64.8, and 57.9%, respectively, compared with vehicle. Conn.D of RIS, RIS + ED-71 and RIS + ALF significantly increased by 66.9, 68.5 and 78.4%, respectively. Bone turnover makers tended to decrease in RIS + ED-71 and RIS + ALF, but not significantly. Serum calcium concentration significantly increased in ED-71 and ALF, but decreased in RIS alone and combination of RIS + ED-71 or ALF.

Conclusions: Combination therapy with RIS and active vitamin D₃ derivatives significantly improved BMD and bone architecture greater than each alone. RIS + ED-71 was at least as efficacious as RIS+ALF in improving bone architecture, validating the combination of risedronate and the new vitamin D₃ analogue.

Disclosures: Tetsuo Yano, Ajinomoto Pharmaceuticals, 3

SA0411

Fluorescence Imaging Reveals High Bisphosphonate Delivery to the Mandible Regardless of Bone Turnover Status. Joseph E. Perosky*¹, Adrienne F. Alimasa¹, Laurie McCauley², Kenneth Kozloff³. ¹University of Michigan Department of Orthopaedic Surgery, USA, ²University of Michigan School of Dentistry, USA, ³University of Michigan Department of Orthopaedic Surgery, USA

Osteonecrosis of the jaw (ONJ) is a detrimental condition of exposed bone in the oral cavity. While associated with bisphosphonate (BP) use, it is unknown what role BPs play in the etiology of ONJ. If local BP concentration is responsible for the occurrence of ONJ, then understanding factors that regulate BP localization is of high importance. The purpose of this study was to investigate the role of bone turnover in the local accumulation of BPs at skeletal sites (mandible, femur, and tibia). High and low bone turnover states were induced by parathyroid hormone (PTH) and BP treatment, and compared to a control group (PBS) using fluorescent-labeled BPs to assess local drug concentration. Fourteen week male Balb/c mice were treated with rPTH[1-34] (80µg/kg daily), pamidronate (PAM, 1.07 mg/kg daily), or PBS injection for 1 week (n=14-16/group), after which mice were injected with a single dose of a far-red fluorescent pamidronate (FRFP, 100 nmol/kg). Twenty-four hours after injection, mice were euthanized and femora, tibiae, and mandibles were excised and imaged under fluorescence illumination to quantify average FRFP signal at anatomic sites of interest. Statistical changes were at the level p<0.05 unless otherwise noted. Serum collected at euthanasia from a subset of mice revealed the bone turnover markers, osteocalcin and TRACP5b, increased and decreased after 1 week of PTH or PAM respectively. However significant changes in bone mass or surface area by µCT were not observed at any site. FRFP signal was normalized by bone surface area (FRFP/BS) measured by µCT to compare BP delivery at multiple sites. For all treatment groups, FRFP/BS in the mandible was higher than both femur (PTH=26%, PBS=69%, PAM=39%) and tibia (PTH=99%, PBS=187%, PAM=120%). For femora and tibiae, FRFP delivery in the context of PTH-induced high bone turnover

increased compared to PBS (Femur=37%, Tibia=43%) and increased marginally, but not significantly vs. PAM low turnover groups (Femur=26%, Tibia=29%). Interestingly, mandibles were less sensitive to treatment effects, as FRFP/BS was equivalent across treatment groups. Dynamic histomorphometry revealed FRFP spatially followed calcein and alizarin labels administered 6 and 1 day prior to FRFP. These findings suggest that, at the femur and tibia, local bone turnover regulates local BP delivery, however the mandible may be particularly susceptible to high levels of BP delivery regardless of bone turnover condition.

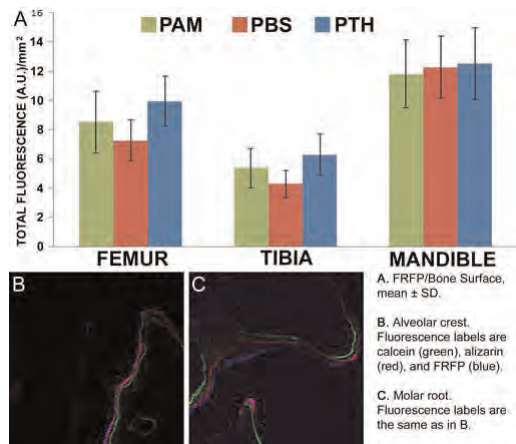


Figure: Fluorescence per bone surface area and spatial localization of fluorescence in the mandible

Disclosures: Joseph E. Perosky, None.

SA0412

Effects of Ascorbic Acid on Bone Density and Strength in Ascorbic Acid-deficient ODS Rats. Toyohito Segawa¹, Naohisa Miyakoshi¹, Yuji Kasukawa¹, Hiroyuki Tsuchie², Yoichi Shimada³. ¹Akita University Graduate School of Medicine, Japan, ²Akita University Graduate School of Medicine, Japan, ³Akita University Graduate School of Medicine, Japan

Introduction: The serum level of ascorbic acid (vitamin C) decreases with aging because of the reduction of intestinal absorptive or renal reabsorptive capacities. In recent years, it has been suggested that ascorbic acid deficiency among the elderly causes impairment of bone quality. However, the effects of this deficiency on bone mineral density or strength remain unclear. The objective of this study was to examine the effects of ascorbic acid on bone mineral density and strength in ascorbic acid-deficient rats.

Materials and Methods: Ascorbic acid-deficient rats (Osteogenic Disorder Shionogi rats) were acclimated until 4 months of age with water containing 2 mg/ml ascorbic acid; these rats were then provided with ascorbic acid-deficient water (0.5 mg/ml) for 8 weeks to create ascorbic acid-deficient rats (n = 20). Following the acclimated period, the rats were divided into the two groups (n=10 each group): 1) ascorbic acid-deficient (Aa-) group, which were provided with ascorbic acid-deficient water; and 2) ascorbic acid replenished (Aa+) group, which were given the water containing 2 mg/ml ascorbic acid. After 4 weeks treatment, bilateral femora were harvested. The right femur was used to measure bone mineral density (BMD) at the proximal end, and the left femur was used for femoral neck compression and diaphysis three-point bending tests to evaluate bone strength. BMD measurement and mechanical testing of femora were also performed for 10 Wistar rats of the same age forming the control group.

Results: BMD of the Aa- group was significantly lower than that of the control group (p<0.05). Maximum load, breaking force, and breaking energy of the femoral neck compression and diaphysis three-point bending tests of the Aa- group were significantly lower than those of the control group (p<0.05). Ascorbic acid replenishment significantly increased the parameters of bone strength in the femoral neck compression and diaphysis three-point bending tests (p < 0.05), but not BMD, as compared with those of the Aa- group. [Discussion and Conclusion] Ascorbic acid deficiency resulted in a marked decrease in bone strength rather than in bone density, suggesting that ascorbic acid may be important in maintaining bone quality rather than bone density.

Disclosures: Toyohito Segawa, None.

SA0413

Inhibition of Osteoclastic Resorption and RANKL Expression and Increase of Osteoblastic Differentiation and Extra Cellular Matrix Mineralization by Sulforaphane, a Naturally Occurring Isothiocyanate. Roman Thaler^{*1}, Monika Rumpler², Silvia Spitzer², Matteo Conti³, Klaus Klaushofer⁴, Franz Varga². ¹Ludwig Boltzmann Institute of Osteology, Austria, ²Ludwig Boltzmann Institute of Osteology at the Hanusch Hospital of WGKK & AUVA Trauma Centre Meidling. 1st Medical Department, Hanusch Hospital, Vienna, Austria, Austria, ³Istituto Scientifico Romagnolo per lo Studio e la Cura dei Tumori (I.R.S.T.), Italy, ⁴Hanusch Hospital, Austria

Sulforaphane (SFN) is abundantly present in cruciferous vegetables like broccoli or cauliflower (1). By various mechanisms SFN can prevent, delay or even reverse carcinogenesis in vivo and in vivo (2). In rheumatoid arthritis, SFN was found to inhibit synovial hyperplasia and T cell activation. Furthermore, SFN was demonstrated to inhibit osteoclastogenesis by inhibiting nuclear factor-kappaB (3).

DMSO was reported to increase differentiation and extra cellular matrix (ECM) mineralization in primary osteoblasts and in MC3T3-E1 cells (4). This may be attributed to the phenotypic shift caused by DMSO via active DNA-demethylation (5). As DMSO shares structural properties with SFN, we evaluated the effect of SFN, on bone cells and tissue.

The cell lines MC3T3-E1, RAW-264.7, MLO-Y4, mouse mesenchymal stem cells (mMSC, cultured in osteogenic medium), mouse pre-osteoclasts (mOC), newborn and adult (7 weeks old) mouse calvaria were treated with increasing concentrations of SFN for up to 6 weeks. Gene expression was measured by qRT-PCR, gene arrays and immunoblots. ECM mineralization was quantified by alizarin red staining. Osteoclastic resorption on ivory was measured and caspases 3/7 and 8 activities were evaluated. DNA hydroxymethylation was visualized by immuno-fluorescence techniques.

After 24 hours, already 3µM SFN inhibited cell proliferation and activated caspases 3/7 and 8 significantly stronger in pre-osteoclastic RAW-264.7 cells as in osteocyte-like MLO-Y4 and pre osteoblastic MC3T3-E1 cells. After 12d of 3µM SFN treatment, resorption of mOC on ivory was significantly inhibited by 40%. After 8 days and 12 days exposure to 3µM SFN, RANKL expression was significantly decreased in MLO-Y4 and in newborn and adult calvaria, respectively. SNF significantly increased the expression of *Bglp2*, *RUNX2*, *Coll1a* and *Lox* in MC3T3-E1 cells after 14 days of treatment. A similar pattern was seen after 20 days in mMSC. In both cases as well as in newborn and adult calvaria a significantly increased ECM mineralization was found after SFN exposure. Similar to DMSO (5), in MC3T3-E1 cells SFN activated genes responsible for active DNA demethylation suggesting this as cause for the effects observed.

SFN serum concentrations in the range as here used are achievable through diet. This suggests SFN as a potential regulator of bone homeostasis.

¹ Juge N, et al. Cell Mol Life Sci 2007, 2 Karmakar S et al. Neuroscience 2006, 3 Kim SJ et al. Mol Cells 2005, 4 Stephens AS et al. JBC 2011, 5 Thaler R et al. Epigenetics accepted manuscript

Disclosures: Roman Thaler, None.

SA0414

Raloxifene Prevents Skeletal Fragility in Adult Female Zucker Diabetic Sprague-Dawley (ZSDS) Rats. Kathleen Hill^{*1}, Maxime Gallant¹, Drew Brown², Amy Sato², David Burr¹. ¹Indiana University School of Medicine, USA, ²Indiana University School of Medicine, USA

In type 2 diabetes, fracture risk is increased despite normal or high bone mineral density, implicating poorer bone quality. We previously reported impaired bone material properties in the non-leptin-dependent Zucker Diabetic Sprague-Dawley (ZSDS) rat model of type 2 diabetes. Raloxifene (RAL) improves bone material and mechanical properties independent of bone mineral density, and may serve to prevent bone fragility in those with type 2 diabetes. The purpose of this study was to determine if RAL prevents the negative effects of diabetes on material properties and skeletal fragility.

24 female ZSDS rats and 24 female CD control rats were fed a high-fat diet beginning at 20 weeks of age to induce diabetes. Rats were randomized to receive daily s.c. injections of RAL (0.5 mg/kg/d) or vehicle (VEH, n = 12 ZSDS and n = 12 CD per treatment) for 12 weeks. Blood glucose was measured weekly. Diabetes was defined as blood glucose \geq 250 mg/dL. At the time of sacrifice, bones were harvested for analysis by DXA (femur, LV4), pQCT (femur mid-shaft), microCT (LV4), 3-point bending (femur) and axial compression (LV4).

RAL-treated ZSDS rats had a lower incidence of type 2 diabetes compared with VEH-treated ZSDS rats. Four of the 12 VEH-treated ZSDS rats (33%) became diabetic by study week 4 and remained diabetic throughout the 12 week study. None of the RAL-treated ZSDS rats became diabetic. RAL-treated ZSDS rats had blood glucose levels significantly lower than VEH-treated ZSDS rats that did not become diabetic, and similar to CD control rats.

Material properties were superior in RAL-treated ZSDS rats compared with both diabetic and non-diabetic VEH-treated ZSDS rats. RAL-treated ZSDS rats had greater femoral toughness than diabetic and non-diabetic VEH-treated ZSDS rats. This was due to greater energy absorption in the post-yield region. These differences

between groups were also observed for the structural (extrinsic) mechanical properties of energy-to-failure, post-yield energy-to-failure, and post-yield displacement.

RAL treatment prevented the onset of type 2 diabetes in adult female ZSD rats fed a high-fat diet and controlled blood glucose to levels similar to control rats. Additionally, RAL had beneficial effects on material-level mechanical properties in ZSD rats.

Disclosures: Kathleen Hill, None.

This study received funding from: Eli Lilly & Company

SA0415

See Friday Plenary Number FR0415.

SA0416

See Friday Plenary Number FR0416.

SA0417

See Friday Plenary Number FR0417.

SA0418

See Friday Plenary Number FR0418.

SA0419

In vivo Measurement of Bone Strontium Accumulation in Rats Using X-ray Fluorescence Spectroscopy. Gregory Wohl^{1*}, Cheryl Druchok¹, Ashlie Altman², David Chettle³, Ana Pejovic-Milic⁴, Colin Webber⁵, Jonathan Adachi⁶, Karen Beattie¹. ¹McMaster University, Canada, ²McMaster University, Canada, ³Department of Medical Physics, McMaster University, Canada, ⁴Department of Physics, Ryerson University, Canada, ⁵Hamilton Health Sciences, Canada, ⁶St. Joseph's Hospital, Canada

Introduction: Strontium ranelate is a pharmacologic treatment for osteoporosis indicated for use in Europe and Australia but not in Canada or the US. Strontium citrate is an alternative strontium (Sr) salt available as an over-the-counter nutritional supplement marketed to improve bone health. To measure *in vivo* bone Sr content, a non-invasive X-ray fluorescence spectroscopy (XRF) system has been developed and used in humans. The purpose of this study was to verify XRF measurements in a vehicle-controlled animal study comparing bone Sr levels in rats administered Sr citrate and Sr ranelate.

Methods: Female Sprague Dawley rats (n=18, 19 wk old) were randomly assigned to receive Sr ranelate (625 mg/kg/d, n=6), Sr citrate (676 mg/kg/d, n=7) or vehicle (flavoured gelatin, n=5) over 8 wks. Dosing was based on equivalent daily elemental Sr (Table 1). *In vivo* bone Sr measures were acquired at baseline, 4 and 8 wks. In acquiring XRF measurements, rats were anaesthetized (isoflurane) and the right hind limb was positioned with the anteromedial aspect of the proximal tibia 1-2 mm from the photon source (Fig 1). Backscattered X-ray spectra were measured over 900 sec, and analyzed using a nonlinear least squares, Marquardt based, fitting routine to determine Sr K_{alpha} and K_{beta} peaks (Fig 2). Rats were sacrificed at 10 wks. Group differences in bone Sr were assessed by two-way ANOVA with Bonferroni correction. Post-hoc analyses detected differences between groups (p=0.05). To verify elemental Sr content in each preparation, energy dispersive spectrometer (EDS) microanalyses were performed.

Results: In the vehicle group, bone Sr levels did not change over 8 wk and were significantly lower than bone Sr levels in Sr-dosed rats. In all Sr-dosed rats, bone Sr increased significantly (p<0.05) from baseline to 4 wk, and 4 wk to 8 wk (Table 2). However, bone Sr levels in the Sr citrate group were significantly greater (p<0.05) than the Sr ranelate group. EDS analyses revealed the Sr citrate group actually received 35% more daily elemental Sr than the Sr ranelate group (Table 1). Thus, after controlling for Sr dose, differences in bone Sr between Sr citrate and Sr ranelate groups were not significant (p>0.05).

Conclusions: Our results indicate that we can non-invasively measure bone Sr content in rats using our *in vivo* XRF system. Moreover, based on elemental Sr dose, the 8 wk accumulation of bone Sr in rats is equivalent between Sr citrate and Sr ranelate.

Table 1. Daily Sr dose

| | Molecular formula | Molecular weight [g/mol] | Dose [mg/kg/day] | Calculated† Elemental Sr [mg/kg/day] | Measured‡ Elemental Sr [mg/kg/day] |
|-------------|--|--------------------------|------------------|--------------------------------------|------------------------------------|
| Sr ranelate | C ₁₂ H ₁₆ N ₂ O ₈ SSr ₂ | 513.49 | 625 | 213 | 174.3 |
| Sr citrate | C ₈ H ₆ O ₇ Sr | 277.73 | 676 | 213 | 235.7 |

†Calculated based on molecular weight

‡Measured by energy dispersive spectrometer (EDS) micro-analysis

Table 1

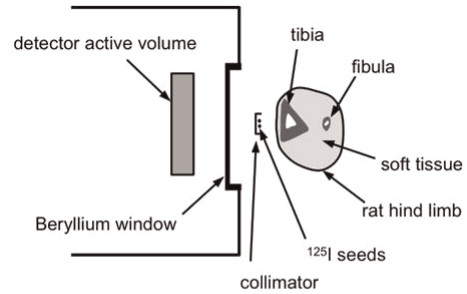


Figure 1. Position of the rat hind limb (in cross section) relative to the XRF detection system. The antero-medial aspect of the tibia was positioned perpendicular to axis of the incident photons from the ¹²⁵I seed source.

Figure 1

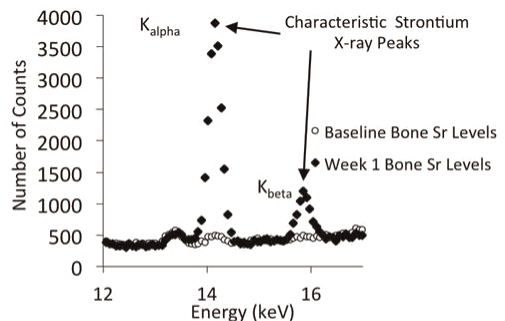


Figure 2. Characteristic Sr K_{alpha} (14.16 KeV) and Sr K_{beta} (15.8 KeV) X-ray peaks in the rat tibia at baseline and 1 wk after start of Sr dosing.

Figure 2

Table 2. Bone Sr K_{alpha} peaks (arbitrary units) at baseline, 4 and 8 wks after dosing (mean ± SD).

| Group | Baseline | Week 4 | Week 8 |
|-------------|----------|---------------------|------------------------|
| vehicle | 149 ± 24 | 250 ± 103 | 154 ± 89 |
| Sr ranelate | 145 ± 27 | a,b 5,412 ± 1,261 | a,b,d 7,052 ± 1,400 |
| Sr citrate | 141 ± 38 | a,b,c 8,221 ± 2,810 | a,b,c,d 11,785 ± 3,221 |

a significantly greater than baseline

b significantly greater than vehicle at same time point

c significantly greater than Sr ranelate at same time point

(Note: no statistical difference when Sr dose was included as a covariate at either 4 or 8 week)

d significantly greater than week 4.

Table 2

Disclosures: Gregory Wohl, None.

SA0420

See Friday Plenary Number FR0420.

SA0421

CXCL5 Stimulation of RANK Ligand Expression in Paget's Disease of Bone. Kumaran Sundaram¹, Sudhaker Rao², William Ries³, Sakamuri Reddy*¹. ¹Charles P. Darby Children's Research Institute, USA, ²Henry Ford Hospital, USA, ³Medical University of South Carolina, USA

Paget's disease of bone (PDB) is a chronic focal skeletal disorder that affects 2-3% of the population over 55 years of age. PDB is inherited as an autosomal dominant trait with genetic heterogeneity and characterized by highly localized areas of bone turnover with increased osteoclast (OCL) activity followed by an exaggerated osteoblast response. Also, pagetic OCL contains paramyxoviral nuclear inclusions and nucleocapsid transcripts. We previously detected expression of measles virus nucleocapsid protein (MVNP) transcripts in OCLs from patients with PDB. MVNP has been shown to induce pagetic phenotype in OCL. Recently, we showed that FGF-2 stimulates RANK ligand (RANKL) expression in PDB. In the present study, gene

expression profiling by Agilent microarray analysis revealed that MVNP significantly increased expression of cytokines/growth factors and signaling molecules in normal human bone marrow derived monocytes, which may play an important role in OCL development/function in PDB. We thus identified MVNP upregulation (72 fold) of the CXC chemokine ligand, CXCL5 [also known as Epithelial neutrophil activating peptide-78] mRNA expression. Bone marrow derived mononuclear cells from patients with PDB also demonstrated elevated (~180 fold) levels of CXCL5 mRNA expression compared to normal subjects. In addition, we identified a 5.0 fold increase in serum levels of CXCL5 in patients with PDB. Real time PCR analysis showed that CXCL5 stimulation (0-50 ng/ml) for 48 h increased (6.8 fold) RANKL mRNA expression in normal human bone marrow derived stromal (SAKA-T) cells. Also, CXCL5 increased (5.2 fold) CXCR1 receptor expression in SAKA-T cells. We further show that CXCL5 treatment elevated the levels of p-ERK1/2 and p-p38 in these cells. Interestingly, CXCL5 stimulation enhanced phosphorylation of CREB (cAMP response element-binding) and inhibition of p-CREB by using protein kinase (PKA) inhibitor H-89 significantly decreased CXCL5 increased hRANKL gene promoter activity. These results suggest that CREB is a downstream effector of CXCL5 signaling and that increased levels of CXCL5 contributes to enhanced RANKL expression in PDB.

Disclosures: Sakamuri Reddy, None.
This study received funding from: DOD

SA0422

See Friday Plenary Number FR0422.

SA0423

Identification and Characterization of A Novel Orally Active Calcium-Sensing Receptor Antagonist. Etsuko Fujita^{*1}, Eiji Ochiai¹, Akiko Takeuchi², Yuri Sakai³, Ryo Matsuyama³, Motoko Hamada³, Gen Unoki³, Yohei Matsueda³, Kei Yamana⁴, Hiroyuki Sugiyama¹, Yoshiaki Azuma¹. ¹Teijin Institute for Biomedical Research, Japan, ²Teijin Institute for Biomedical Research, Japan, ³Teijin Institute for Biomedical Research, Japan, ⁴Teijin Institute for Biomedical Research, Japan

Bone resorption inhibitors such as bisphosphonates are widely used for osteoporosis patients. As bone anabolic agent, intermittent administration of parathyroid hormone (PTH)(1-84) or PTH(1-34) are used and exert potent bone-forming effects in animal models and osteoporosis patients. On the other hand, continuous infusion of PTH increases bone turnover and results in bone loss. Bone anabolic agents are expected to be used for the patient with low bone turnover. Short acting calcium-sensing receptor (CaSR) antagonists are one of the promising candidates, which stimulate endogenous parathyroid hormone (PTH) transiently, mimicking teriparatide. Precedent CaSR inhibitors have failed to prove satisfied effectiveness in clinical studies probably due to prolonged PTH secretion. Here we report the pharmacological characteristics of a novel orally active CaSR antagonist TEI-A.

In human CaSR expressing cells, TEI-A inhibited the calcium stimulated intracellular Ca influx as potent as reference compound (JTT-305/MK5442). TEI-A showed almost the same inhibitory activities against rat, dog, monkey or human CaSR, indicating no species difference. Inhibitory activity of TEI-A was quite specific for CaSR and no significant inhibition was detected in a panel assay containing over 30 GPCRs and enzymes. In female rats, orally administered TEI-A induced PTH secretion in a dose-dependent manner, of which maximal level was comparable to reference compound. However, the time recovered to the basal level was shorter with TEI-A. In conclusion, TEI-A will be a promising candidate of CaSR antagonist as a bone anabolic agent with high potency, specificity and reasonable PTH stimulating activities.

Disclosures: Etsuko Fujita, Teijin Pharma Ltd., 3

SA0424

See Friday Plenary Number FR0424.

SA0425

See Friday Plenary Number FR0425.

SA0426

See Friday Plenary Number FR0426.

SA0427

See Friday Plenary Number FR0427.

SA0428

See Friday Plenary Number FR0428.

SA0429

24,25-Dihydroxyvitamin D₃ Signals through Non-vitamin D Receptor Pathways in HepG2 Cells. Kent Wehmeier^{*1}, Sarada Jaimungal², Jaisri Maharaj³, Arshag Mooradian⁴, Michael Haas⁵. ¹University of Florida, College of Medicine, Jacksonville, USA, ²Department of Medicine University of Florida -Jacksonville College of Medicine, USA, ³Department of Medicine, University of Florida-Jacksonville College of Medicine, USA, ⁴Department of Medicine, University of Florida-Jacksonville, College of Medicine, USA, ⁵Department of Medicine, University of Florida Jacksonville, College of Medicine, USA

Epidemiologic studies of cardiovascular disease risk have suggested that vitamin D may have an important role in modulating future cardiovascular events. Our lab has demonstrated that apolipoprotein A-I (apo AI) gene expression and HDL particle secretion in hepatocytes is suppressed by 24, 25-dihydroxyvitamin D₃ (24,25-[OH]₂ D₃) but not 25-hydroxyvitamin D₃. Knockdown of the vitamin D receptor (VDR) did not change the observed effects of 24,25-[OH]₂ D₃ on apo AI gene expression. Responses of resting zone chondrocytes to 24,25-[OH]₂ D₃ were mediated through non-VDR pathways based on previously published studies. Using an in vitro human hepatocyte model we investigated the ability of 24,25-[OH]₂ D₃ to modulate non-VDR signaling pathways that may affect apo AI gene expression. The activities evaluated included PKCa c-jun-N-terminal kinase (JNK) and extracellular regulated kinase ½. Treatment with 50 nM 24, 25-[OH]₂D₃ correlated with c-jun phosphorylation, down regulation of the AP-1 collagenase and apo AI gene promoter activities. Expression of peroxisome proliferator-activated receptor alpha (PPARα) and retinoid-X-receptor (RXR) were suppressed by 24, 25-[OH]₂D₃. These preliminary studies suggest the great complexity of effects of VDR ligands mediated through non-VDR signaling. Discerning effects of Vitamin D on cardiovascular risk requires dissection of the important non-VDR signaling pathways.

Disclosures: Kent Wehmeier, None.

SA0430

Bone Mineral Density in Immigrant Women Living in Stockholm with Low Vitamin D Levels Postpartum. Ingrid Bergstrom^{*1}, Ingrid Dahlman², Paul Gerdhem¹. ¹Karolinska Institutet, Sweden, ²Dept of endocrinology, metabolism & diabetes. Karolinska University Hospital Huddinge, Sweden

Introduction: A fair evidence for a positive association for 25-hydroxy vitamin D (25OHD) levels and BMD is found in older children and older adults. Not many studies are concerning women in reproductive age or in perimenopause. Aim: To find out if the bone health is affected in immigrant women in reproductive age with low levels of vitamin D compared to a Swedish control group. Subjects: We characterized a cohort of 68 pregnant immigrant women in gestational week 12 and compared their vitamin D levels with 51 nonimmigrant pregnant women. Significantly more immigrant women (77.9 %) had levels of 25OHD <25 nmol/l compared with control women, where only a minority (3.9 %) had such low level. A large proportion of the immigrant women (29.4 %) had levels <12 nmol/l compared to none of the controls. Of these women we could include forty-one immigrant women 6 to 12 months postpartum. As controls served 18 of the Swedish women. 25OHD and parathyroid hormone (PTH) levels were remeasured and DXA (hip, spine) and pQCT (radius, tibia) was performed. Neither patients nor controls received any supplementation with vitamin D. Statistical calculations were made with the Mann-Whitney U-test or the Spearman rank correlation test.

Results: Mean postpartum 25OHD was 29 nmol/L in patients and 53 nmol/L in controls. Mean postpartum PTH was 69 ng/L in patients and 38 ng/L in controls. Age in patients was 31.5 years and in controls 32.5 years, p=0.56. Mean BMI was 27.4 kg/m² in patients and 24.8 kg/m² in controls, p=0.041. Mean DXA total hip did not differ between patients and controls (1.02 and 1.00 g/cm²; p=0.78). Mean DXA spine (L1-L4) did not differ between patients and controls (1.13 and 1.17 g/cm²; p=0.26). pQCT cortical density and trabecular density of the tibia did not differ between patients and controls (p>0.61). pQCT Cortical density and trabecular density of the radius did not differ between patients and controls (p>0.59). No significant correlations were found between 25OHD or PTH and the different bone density parameters.

Conclusion: The bone health is not affected by persisting low vitamin D levels in immigrant women living in Stockholm.

| Vit D, PTH DEXA | | | |
|-----------------------|----------------------|-----------------------|-------|
| | Immigrant Women (41) | Swedish Controls (18) | P |
| Vit D nmol/L | 19,9 | 60,3 | 0,000 |
| Gestational week 12 | (11,2) | (16,7) | |
| Vit D nmol/L | 29,4 | 53 | 0,003 |
| ½ - 1 year postpartum | (17,8) | (19,2) | |
| PTH ng/L | 31,0 | 18,9 | 0,000 |
| Gestational week 12 | (18,3) | (4,8) | |
| PTH ng/L | 68,7 | 37,7 | 0,002 |
| ½ - 1 year postpartum | (35,1) | (11,2) | |
| BMD g/cm2 | 0,988 | 0,985 | 0,779 |
| Neck left | (0,138) | (0,108) | |
| BMD g/cm2 | 1,015 | 0,999 | 0,779 |
| Total hip | (0,148) | (0,093) | |
| BMD g/cm2 | 1,134 | 1,171 | 0,26 |
| L1 - L4 | (0,146) | (0,079) | |

| pQTC | | | |
|------------------------------------|----------------------|-----------------------|-------|
| | Immigrant women (41) | Swedish Controls (18) | P |
| Tibia Trabecular volume BMD g/cm3 | 221,9 | 214,05 | 0,6 |
| | (46,2) | (37,5) | |
| Tibia Cortical volume BMD g/cm3 | 1198,53 | 1197 | 0,85 |
| | (20,89) | (20,27) | |
| Tibia Cortical thickness mm | 4,6 | 4,97 | 0,051 |
| | (0,6) | (0,37) | |
| Radius Trabecular volume BMD g/cm3 | 181,83 | 176,32 | 0,58 |
| | (46,77) | (49,1) | |
| Radius Cortical volume BMD g/cm3 | 1176,32 | 1171,71 | 0,68 |
| | (28,85) | (26,2) | |
| Radius Cortical thickness mm | 2,22 | 2,34 | 0,09 |
| | (0,31) | (0,26) | |

from the Phase III Arzoxifene study (Generation) which included 1939 postmenopausal women (60 to 85 years old) with a densitometric diagnosis of osteopenia or osteoporosis. Vitamin D below 25 nmol/L was an exclusion criterion in this study. Blood was obtained at baseline between April and August (Fall and Winter). The sites included Recife, Salvador, Rio de Janeiro, São Paulo, Curitiba and Porto Alegre. Median, maximum and minimum levels of 25OHD as well as median age were calculated for each city (Table 1). Pearson correlation was used for 25OHD and latitude. Although severe Vitamin D deficiency (< 25 nmol/L) was rare (6 subjects, 0.3%), insufficiency (<75 nmol/L) was very common (1,327 subjects, 68.4%), even in those living in a tropical climate, with 56.7% in Recife (8°S) and 49% in Salvador (12°S). The prevalence of insufficiency gradually increased proportionally with latitude, reaching a prevalence of 83% in Porto Alegre (33°S) (Figure 1). On average, there was a reduction of 0.8 nmol/L for each latitudes degree south of the equatorial line. The correlation between 25OHD levels and latitude was high: r=-0.88. In conclusion, Brazil has a high prevalence of inadequacy of vitamin D, even in cities close to the Equator. Prevalence progressively increases with southward latitudes. Nevertheless, vitamin D deficiency in Brazil is clearly endemic and, in part, independent of latitude, emphasizing a multifactorial aspect of vitamin D deficiency. Greater understanding of these other factors could lead to the implementation of effective public health policies.

Acknowledgments: Bandeira F, Zerbine C, Russo L, Fernandes C, Borba V, Russo L, Brenol JC, Barbosa I.

| CITY | LATITUDE | N | AGE | 25OHD MEDIAN | 25OHD MINIMUM | 25OHD MAXIMUM |
|----------------|---------------|-----|-----|--------------|---------------|---------------|
| RECIFE | 8° 04' 03" S | 208 | 67 | 70.1 | 25.2 | 155.5 |
| SALVADOR | 12° 58' 16" S | 104 | 66 | 76.5 | 41.2 | 202.2 |
| RIO DE JANEIRO | 22° 57' S | 518 | 68 | 65.1 | 8.75 | 165 |
| SÃO PAULO | 23° 32' 51" S | 930 | 65 | 64.7 | 23 | 137.3 |
| CURITIBA | 25° 25' S | 126 | 66 | 59.9 | 25.5 | 161.1 |
| PORTO ALEGRE | 30° 05' S | 53 | 66 | 58.9 | 28 | 137.3 |

Table 1: Data from 6 Brazilian cities with age, latitude as well as median, maximum and minimum of 25OHD.

Table 1

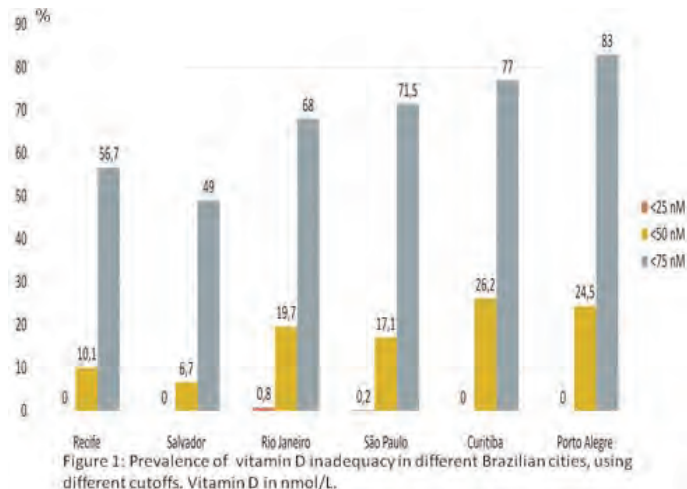


Figure 1

Disclosures: Henrique Arantes, None.

This study received funding from: Eli Lilly and Company

SA0433

Genetic Control of Serum 1,25 dihydroxyvitamin D (1,25(OH)₂D) Level Under Normal and Low Dietary Calcium (Ca) Condition. Rebecca Replogle^{*1}, Libo Wang², Min Zhang², James Fleet¹. ¹Purdue University, USA, ²Purdue University, USA

Vitamin D is integral to the regulation of Ca homeostasis and is necessary for proper bone health. There is evidence that genetic variation influences serum levels of

Disclosures: Ingrid Bergstrom, None.

SA0431

See Friday Plenary Number FR0431.

SA0432

Correlation between 25 Hydroxyvitamin D (25OHD) Levels and Latitude in a Brazilian Postmenopausal Population with Low Bone Mass: from Arzoxifene Generation Study. Henrique Arantes^{*1}, Alan Chiang², John Bilezikian³, Marise Lazaretti Castro⁴. ¹UNIFESP, Brazil, ²Eli Lilly & Company, USA, ³Columbia University College of Physicians & Surgeons, USA, ⁴Escola Paulista de Medicina, Brazil

Vitamin D is one of the major regulators of calcium homeostasis and is critically important for normal mineralization of bone. Inadequate Vitamin D, as determined by low levels of 25OH D, has become very common despite the ready availability of sunlight at some latitudes. National data from a country that spans a wide range of latitudes would help to determine to what extent latitude or other factors are responsible for vitamin D deficiency. To this end, we investigated vitamin D status in cities located at different latitudes in Brazil, a large continental country, ranging from temperate to equatorial zones. The source of the data is the Brazilian subpopulation

the vitamin D status marker, 25-hydroxyvitamin D (25(OH)D). Renal conversion of the prehormone 25(OH)D to the active metabolite 1,25(OH)₂D is increased by low dietary Ca intake. This adaptation is necessary to protect bone under periods of dietary Ca stress. However, it is unclear whether genetic effects influence the production of 1,25(OH)₂D, especially when dietary Ca is limited. We conducted a study to identify genetic loci controlling serum 25(OH)D and 1,25(OH)₂D levels in the BXD recombinant inbred panel fed either normal and low dietary Ca levels. Male mice from 51 BXD lines were placed on modified AIN93G diets containing 200 IU vitamin D and either 0.5% (the rodent Ca requirement) or 0.25% Ca from 4-12 wks of age (n=8/line/diet). Blood was collected and serum metabolites were measured using commercial RIAs. Body weight was a significant covariate influencing serum metabolites; this effect was removed and residuals were used for all further analyses. ANOVA revealed a significant main effect of genetics (p<0.01) but not diet (p=0.17) on serum 25(OH)D. Heritability (h²) of 25(OH)D on the 0.5% Ca diet was 0.49. On the 0.5% Ca diet, 25(OH)D and 1,25(OH)₂D were not correlated, suggesting novel genetic loci may control serum 1,25(OH)₂D. Main effects of genetics and diet, as well as a gene x diet interaction, were significant for 1,25(OH)₂D (p<0.01). Heritability of 1,25(OH)₂D was 0.67 and 0.65 on the 0.25% and 0.5% Ca diets, respectively. Linkage mapping was conducted using a Bayesian quantitative trait loci (QTL) method and significant loci (Bayes factor>6) were identified. Three QTL affecting 25(OH)D were identified in the 0.5% Ca group chr 1 (mid), 1 (distal), and 6. Previously identified candidate genes (e.g. VDR, GC, CUBN, or LRP2) are not located in these regions. Three unique QTL affecting 1,25(OH)₂D on the 0.5% Ca diet were identified (chr 3, 11, and 13) and 2 in the 0.25% group (chr 7 and 10). QTL on chr 9, 15, 18 were found in both diet populations. The chr 15 locus is centered 200 kb upstream of the VDR, but the other loci contain no obvious candidate genes. Our results indicate that baseline serum 1,25(OH)₂D levels are influenced by genetics and that dietary Ca restriction reveals new QTL controlling this crucial regulator of Ca homeostasis and bone health.

Disclosures: Rebecca Replogle, None.

SA0434

Identification of Cytoskeletal Binding Partners for the 1,25D₃-MARRS Receptor. Tremaine Sterling¹, Ilka Nemere^{*2}. ¹Utah State University, USA, ²Utah State University, USA

We have shown that a membrane receptor, known as the 1,25D₃-MARRS receptor, is necessary for the rapid, pre-genomic effects of 1,25D₃ on phosphate and/or calcium absorption in chick intestines. However, a clear understanding of the proteins involved in the signaling mechanisms or transduction events by which the 1,25D₃-MARRS receptor facilitates 1,25D₃-mediated phosphate or calcium uptake, as well as other cellular effects, is still under investigation. We used co-immunoprecipitation studies and mass spectroscopy to identify proteins that interact with the 1,25D₃-MARRS receptor; we have identified actin and keratin as two binding partners involved in receptor localizations in the presence or absence of 1,25D₃. Using confocal microscopy, we were able to visualize 1,25D₃-MARRS receptor localizations relative to actin and/or keratin distribution in chick enterocytes. Cells cultured in media containing phenol red had the 1,25D₃-MARRS receptor and actin localized largely in the nucleus, which was dispersed upon addition of 1,25D₃. In the absence of phenol red, staining was cytoplasmic. Addition of steroid caused diminished staining at 10 s and 30 s, with a return of intensity between 1 and 5 min. Nuclear staining was observed after 1 min. We found that F-actin concentrations are maximal when 1,25D₃-MARRS receptor localizations within enterocytes are low suggesting that cyclical conversions of F-actin to G-actin are involved in the 1,25(OH)₂D₃-mediated redistribution of the 1,25D₃-MARRS receptor within the cell. We also found that keratin distribution remains constant with 1,25(OH)₂D₃ exposure when F-actin depolymerizes into G-actin, which suggests that actin and keratin work in concert to facilitate hormone-mediated redistribution of the 1,25D₃-MARRS receptor.

Disclosures: Ilka Nemere, None.

SA0435

Role of Calbindin-D_{9k} as a Facilitator of Calcium Entry via TRPV6. Tibor Rohacs^{*1}, Puneet Dhawan², Yevgen Yudin¹, Baskaran Thyagarajan¹, Sylvia Christakos³. ¹UMDNJ-New Jersey Medical School, USA, ²UMDNJ-New Jersey Medical School, USA, ³University of Medicine & Dentistry & New Jersey - New Jersey Medical School, USA

The major role of 1,25(OH)₂D₃ is intestinal calcium absorption and calbindin-D_{9k} and TRPV6 are still being evaluated as the major intestinal targets of 1,25(OH)₂D₃. Yet studies related to the function of these proteins are limited and an understanding of the mechanisms involved in active intestinal calcium transport remains incomplete. We found that intestinal calcium absorption in response to 1,25(OH)₂D₃ still occurs in TRPV6 or calbindin-D_{9k} single knock out mice but is less efficient in the absence of both proteins [in the double KO mice 1,25(OH)₂D₃ mediated intestinal calcium absorption is reduced by 60% compared to calcium absorption in wild-type (WT) mice; p<0.05], suggesting that calbindin-D_{9k} and TRPV6 act together to affect calcium absorption. Confocal microscopy was done using WT and TRPV6 KO mice. In the duodenum of WT mice immunofluorescent staining for calbindin-D_{9k} showed discrete staining of the brush border of the enterocyte. In the TRPV6 KO mice there was loss of apical surface staining for calbindin-D_{9k}. These findings indicate that the

localization of calbindin at the brush border of the enterocyte is dependent on the presence of TRPV6. Using co-immunoprecipitation and GST pull down assays interaction between calbindin-D_{9k} and TRPV6 was observed. Calcium imaging studies in HEK cells transfected with TRPV6 showed that in response to 2 mM calcium there is an initial fast rise in the evoked calcium signal followed by a lower plateau due to calcium dependent inactivation. In cells co-transfected with calbindin-D_{9k} the plateau phase is higher (p<0.05 compared to cells co-transfected with vector). These results are consistent with calbindin-D_{9k} reducing calcium induced inactivation of TRPV6, resulting in enhanced entry of calcium via TRPV6. Calmodulin also associates with TRPV6 but unlike calbindin, calmodulin inhibits TRPV6 activity. Calmidazolium, an inhibitor of calmodulin, was found to inhibit calcium induced inactivation of TRPV6. These findings suggest novel mechanisms of enhancing intestinal calcium transport. These findings also indicate, for the first time, a functional interrelationship between calbindin-D_{9k} and TRPV6 and that calbindin-D_{9k} acts as a modulator of calcium influx via TRPV6, thus challenging the traditional model of transcellular intestinal calcium absorption and the role of calbindin as a facilitator of calcium diffusion.

Disclosures: Tibor Rohacs, None.

SA0436

See Friday Plenary Number FR0436.

SA0437

UVB Radiation Ameliorates 25 Hydroxyvitamin D Deficiency in a Gender-dependent Manner in Mice: Role of 7-dehydrocholesterol Reductase. Yingben Xue^{*1}, Lee Ying², Gordon Watson², David Goltzman³. ¹Calcium Research Lab, McGill University, Canada, ²Children's Hospital Oakland Research Institute, USA, ³McGill University, Canada

Polymorphisms in the gene encoding 7-dehydrocholesterol reductase (DHCR7), the enzyme that converts 7 dehydrocholesterol (7DHC) to cholesterol, have been associated in human genome wide association studies (GWAS) with reductions in circulating 25 hydroxyvitamin D (25OHD). Inasmuch as 7DHC is the precursor of vitamin D which is then converted to 25OHD, we examined the alterations in serum 25OHD levels in female and male mice after UVB exposure and the potential role that DHCR7 might play. Vitamin D sufficient three week old mice were maintained on a vitamin D deficient (VDD) diet for 8 wks after which serum 25OHD fell from 86.4 to 14.9 nM in females and from 78.5 to 4.4 nM in males. Although renal cyp27B1 mRNA levels were increased 250-fold in females and males on a VDD diet, serum 1,25 dihydroxyvitamin D [1,25(OH)₂D] fell from 175.3 to 25.0 pM in females and from 156.3 to 22.4 pM in males. Concomitantly, hypocalcemia, hypophosphatemia and elevated PTH were seen with skeletal evidence of secondary hyperparathyroidism and osteomalacia. Mice were then exposed to chronic UVB irradiation (2.5 kJ/m² twice weekly, for 6 wks). In females serum 25OHD rose to 53.4 nM, serum 1,25(OH)₂D rose to 139.6 pM and serum calcium, phosphorous, PTH and skeletal abnormalities were reversed. In males serum 25OHD rose only to 23.1 nM and serum 1,25(OH)₂D rose to 86.6 pM; serum calcium, phosphorus and PTH levels improved but did not quite reach levels seen on normal chow. When mice on a VDD diet were exposed to acute UVB radiation (2.5 kJ/m² once daily, for 1 week), serum 25OHD rose from 8.6 to 99.3 nM in females but only from 9.0 to 25.5 nM in males. In females 7DHC to cholesterol ratios in skin rose on the VDD diet and then fell after UVB, whereas in males the ratios remained similar on both normal chow and the VDD diet. Although protein expression of DHCR7 in skin was similar in female and male mice on normal chow, in female mice DHCR7 expression was reduced on a VDD diet but increased after UVB. Such fluctuations were not observed in the male mice. In female transgenic mice overexpressing DHCR7 in skin, reduced increases in 25OHD in response to UVB were observed. The results show gender-dependent differences in UVB-induced 25OHD levels between females and males which appear to result from increased 7-DHC in skin in female vitamin D deficient mice due to decreased expression of DHCR7, and suggest a novel mechanism for regulation of UVB induced vitamin D production in skin.

Disclosures: Yingben Xue, None.

SA0438

Differences and Similarities in Treatment Related Effects of Zoledronic Acid in Multiple Myeloma and Breast Cancer Patients with Metastasis to Bone. Kent Soe^{*1}, Jean-Marie Delaisse², Erik H. Jakobsen³, Charlotte T. Hansen⁴, Torben Plesner⁵. ¹Vejle Hospital, University of Southern Denmark, Denmark, ²Vejle Hospital, IRS, University of Southern Denmark, Denmark, ³Vejle Hospital, Department of Oncology, Denmark, ⁴Odense University Hospital, Dept. of Hematology, Denmark, ⁵Vejle Hospital, Medical Department, Denmark

Treatment frequency and duration of cancer patients with the amino-bisphosphonate zoledronic acid (Zol) is frequently debated. Both multiple myeloma (MM) and breast cancer (BC) patients with metastasis to bone receive Zol 4 mg/3-4 weeks although their bone diseases are fundamentally different. In order to get better insight we have compared MM and BC patients in regard to the effect of Zol.

In an investigator initiated phase II clinical protocol we recruited 30 MM and 30 BC patients with metastases to bone (10 Zol naive and 20 with ≥ 6 previous treatments for each disease). Blood samples from day 0 and 14 were analyzed for CTX and bALP while total 48h urine collected immediately post-infusion was used to quantify the amount of Zol excreted and determine the degree of Zol retention.

CTX levels were significantly reduced with an increasing number of Zol treatments for both MM ($p=0.0007$) and BC patients ($p=0.0241$), but the effect was more pronounced for MM. bALP levels were significantly reduced with more Zol treatments in MM ($p=0.004$) but not significantly in BC patients ($p=0.09$). If patients did not receive Zol every month then CTX levels were significantly increased in MM patients (similar trend for BC) while bALP levels significantly increased in BC but not in MM patients. This was furthermore confirmed in a multivariate linear regression analysis combined with a likelihood ratio test on the entire cohort. Treatment frequency was shown to be a highly significant predictor for CTX ($p<0.001$) and bALP levels ($p=0.01$), while the number of treatments was shown to be only a significant contributor for CTX ($p=0.015$). Multivariate linear regression combined with likelihood-ratio tests also showed that for both MM and BC patients, kidney function may be impaired by repeated treatments since the creatinine clearance decreased with the number of Zol treatments ($p=0.014$) (sex, $p=0.001$; and age, $p=0.015$ were also unsurprisingly found to affect the creatinine clearance).

Our results suggest that: 1. MM and BC do not respond in the same way to Zol treatment especially concerning the suppression of bone formation. 2. Zol must be given every month to obtain maximum suppression of bone turn-over, since CTX (for MM) and bALP (for BC) were found to increase significantly if Zol treatment was delayed beyond 4 weeks. 3. Both in MM and in BC patients the kidney function seems to be negatively affected by multiple treatments.

Disclosures: Kent Soe, Novartis, 6
This study received funding from: Novartis

SA0439

Omega 3 Fatty Acids in Fish Oil Orchestrate a Reciprocal Axis between p53-miR-200c and Zeb1 to Prevent EMT in Breast Cancer Cells. Chandi Mandal^{*1}, Goutam Ghosh Choudhury², Auriole Tamegnon², Triparna Ghosh-Choudhury³, Nandini Ghosh-Choudhury¹. ¹University of Texas Health Science Center at San Antonio, USA, ²University of Texas Health Science Center at San Antonio, USA, ³Baylor College of Medicine, USA

We have recently demonstrated efficacy of fish oil (FO) component $\omega 3$ -fatty acid (docosahexaenoic acid, DHA) to target breast cancer stem cells in preventing tumor growth and osteometastasis in mouse models. Gene expression signature of breast cancer forces the cells to undergo epithelial to mesenchymal transition (EMT) that increases the metastatic proclivity of the tumor cells. Loss of E-cadherin expression by transcriptional mechanism marks the state of EMT, which dictates tumor invasion to distant organs. We investigated the mechanism of fish oil action on EMT. Breast tumors from fish oil-fed mice showed significantly increased expression of E-cadherin mRNA. Incubation of bone metastatic MDA-MB-231 (MDA) human breast cancer cells with DHA markedly enhanced E-cadherin mRNA and protein expression, indicating reversal of EMT. Breast cancer metastasis is associated with increased expression of Zeb1, a repressor for E-cadherin transcription, and decreased levels of the tumor suppressor p53. DHA inhibited the expression of Zeb1 protein and mRNA while it significantly increased levels of p53 mRNA and protein. Importantly, tumors from FO fed mice showed significant reduction in Zeb1 mRNA expression concomitant with marked increase in p53 mRNA and protein. The mechanism by which FO regulates Zeb1 expression is not known. We considered both transcriptional mechanism and post-transcriptional regulation by microRNA (miR). Transient transfection assays using a Zeb1 promoter reporter construct in MDA cells showed significant decrease in transcription of Zeb1 by DHA. 3'UTR of Zeb1 mRNA contains recognition element for miR-200c, which is a target of p53 transcription factor. Level of mature miR-200c is significantly low in MDA cells compared to MCF10A normal breast epithelial cells. FO-fed mice tumors showed increased levels of pre-miR-200c and mature miR-200c, similar to enhanced p53 levels. Similarly, DHA markedly enhanced the expression of both pre and mature miR-200c in MDA cells. Finally, reporter assays using miR-200c promoter in MDA cells showed significant increase in miR-200c transcription in response to DHA. Together our results demonstrate a salutary effect of FO to prevent EMT of breast cancer cells by increased p53 and miR-200c, which dampens the expression of Zeb1 to upregulate E-cadherin.

Disclosures: Chandi Mandal, None.

SA0440

See Friday Plenary Number FR0440.

SA0441

PGE2 Regulates Breast Cancer Proliferation and Osteoblastic RANKL Production in a Part of Bone Metastasis through its Receptor Subtype of EP4. Satoshi Yokoyama¹, Kenta Watanabe¹, Michiko Hirata², Chiho Matsumoto³, Takayuki Maruyama⁴, Chisato Miyaura³, Masaki Inada^{*3}. ¹Tokyo University of Agriculture & Technology, Japan, ²Tokyo University of Agriculture & Technology, Japan, ³Tokyo University of Agriculture & Technology, Japan, ⁴Ono Pharmaceutical Co., Ltd., Japan

Bone metastasis of breast cancer is accompanied by severe bone destruction with increased bone resorption. We identified that prostaglandin E2 (PGE2)-induced osteoclast formation was mediated by RANKL production in osteoblasts, EP4 is the major PGE receptor in the other three EP subtypes (EP1-EP3). Here we examine the EPs antagonist, a selective inhibitor of EP signaling in metastasized breast cancer cells. When we examined the expression profiles of EPs in mouse breast cancer cell 4T1, EP1 and EP4 expression was found. PGE2-induced 4T1 proliferation was also suppressed in both EP1 and EP4 antagonist treated cells suggesting the 4T1 has a diversity to respond multiple PGE2 signaling channels for the proliferation. To examine mechanisms of 4T1 induced-bone resorption, 4T1 cells were co-cultured with bone marrow cells and osteoblasts to evaluate the supporting capacities of osteoclast formation. First we newly employed the experimental system to evaluate cell-cell interaction by the contact adhesion, co-cultured bone cells on fixated cancer cell with cell membrane. Contact with fixed-4T1 cell was strongly induced RANKL expression and PGE2 production in osteoblasts. Osteoclast formation was seen in the co-culture of bone cells on fixed-4T1 cells, only EP4 antagonist treatment completely inhibited the osteoclast formation. On the other hand, the reverse experiments of cancer cells co-cultured with fixed-osteoblasts increase the levels of PGE2 production in 4T1 cells without RANKL production. PGE2 production was perfectly attenuated by the treatment of a COX2 inhibitor NS398 suggesting the factors from osteoblast cell membrane promote PGE2 production in breast cancer. Finally, 4T1 cells were co-cultured with mouse calvaria to evaluate bone resorbing activities. 4T1 cells attachment to bone surface markedly induced the number of osteoclast and following bone resorption in organ culture, only treatment of EP4 antagonist was attenuated 4T1-induced bone resorption. 3D-micro CT analyses indicated the resorbing trail on calvarial bone surface was suppressed by the treatment of EP4. These results suggest that the interaction of breast cancer among host osteoblast, PGE2 production increased in autocrine manner. EP4 specifically regulates RANKL production in osteoblast that leads osteoclast differentiation and following osteolysis. EP4 antagonist is a candidate for the therapy of breast cancer on bone metastases.

Disclosures: Masaki Inada, None.

SA0442

Withdrawn

SA0443

See Friday Plenary Number FR0443.

SA0444

Vitamin D Strongly Influences Skeletal Metastasis Development in Breast Cancer: Comparison of Systemic Vitamin D Deficiency versus Local Ablation of CYP27B1 in Breast Tumor Cells. Aimee-Lee Luco^{*1}, Jiarong Li¹, Rene St-Arnaud², Timothy Reinhardt³, Richard Kremer⁴. ¹McGill University, Canada, ²Shriners Hospital for Children & McGill University, Canada, ³National Animal Disease Center, USDA, ARS, USA, ⁴McGill University, Royal Victoria Hospital, Canada

In advanced cases of breast cancer, the skeleton often bears the major tumor burden causing considerable suffering and morbidity. Once tumors are established in bone they are usually incurable. Vitamin D has been implicated as a possible mediator of breast tumor development and recurrence, however little is known about its possible influence on skeletal metastasis. We hypothesize that vitamin D deficiency could have a profound effect on skeletal metastasis by modulating tumor cell growth within bone directly and indirectly by enhancing bone turnover and the release of local growth factors.

Female FVB wild type mice were put on either a 1000 IU/Kg vitamin D diet or a 25 IU/Kg vitamin D diet after weaning. Six weeks after weaning, the mice (n=15/group) were injected into the right tibia with 500 000 cells suspended in 50 μ l of sterile PBS of either wild type tumor cells from PyMT breast tumors or 1 α -hydroxylase ablated breast tumor cells from PyMT 1 α -hydroxylase flox/flox cre+ mice. Three weeks following tumor cell injections the mice were sacrificed, blood collected and X-rays taken of the lower limbs. Bones were embedded in plastic for histomorphometric analysis of tumor burden. The X-rays were scored according to the following scoring method: 0 (no lesion), 1 (minor changes), 2 (small lesions), 3 (significant lesions with minor peripheral margin breaks), 4 (significant lesions with major peripheral margin breaks).

The mean weights of animals did not differ significantly. 25(OH)D levels were reduced by over 80% in animals on 25 IU/Kg diet vs. 1000 IU/Kg diet (16.7 nmol/L vs.

116 nmol/L, $p \leq 0.001$). PTH levels were significantly elevated in the low vitamin D vs. the normal vitamin D group (259 pg/ml vs. 167 pg/ml, $p = 0.05$). X-ray scores of bone lesions were as follows: 1000 IU/Kg diet injected with wild type tumor cells = 1.714 ± 1.439 , 25 IU/Kg diet injected with wild type tumor cells = 2.278 ± 1.034 , and 1000 IU/Kg diet injected with 1α -hydroxylase ablated tumor cells = 3.167 ± 0.931 . Analysis of tumor burden by histomorphometry revealed striking differences between groups, confirming the X-ray scoring. 1α -hydroxylase flox/flox cre+ tumors grew more aggressively rupturing cortical bone more frequently and invading extra-skeletal tissues. Overall, our data indicate that vitamin D regulates tumor growth within bone and that local metabolism of vitamin D by cancer cells likely plays a dominant role in this process.

Disclosures: Aimee-Lee Luco, None.

SA0445

Curcumin Induces Cell Apoptosis In Human Chondrosarcoma Through Extrinsic Death Receptor Pathway. Yi-Chin Fong^{*1}, Chih-Hsin Tang². ¹China Medical University Hospital, Taiwan, ²China Medical University, Taiwan

Chondrosarcoma is a soft tissue sarcoma with a poor prognosis that is unresponsive to conventional chemotherapy. Surgical treatment leads to severe disability with high rates of local recurrence and life threat. Curcumin, an active compound in turmeric and curry, has been proven to induce tumor apoptosis and inhibit tumor proliferation, invasion, angiogenesis, and metastasis of cancer cells. In this study, we investigated the anticancer effects of curcumin in human chondrosarcoma cells. Curcumin induced apoptosis in human chondrosarcoma cell lines (JJ012 and SW1353) but not in primary chondrocytes. Curcumin induced upregulation of Fas, FasL, and DR5 expression in chondrosarcoma cells. Transfection of cells with Fas, FasL, or DR5 siRNA reduced curcumin-induced cell death. In addition, p53 involved in curcumin-mediated Fas, FasL, and DR5 expression and cell apoptosis in chondrosarcoma cells. Most importantly, animal studies revealed a dramatic 60% reduction in tumor volume after 21 days of treatment. Thus, curcumin may be a novel anticancer agent for the treatment of chondrosarcoma.

Disclosures: Yi-Chin Fong, None.

SA0446

See Friday Plenary Number FR0446.

SA0447

See Friday Plenary Number FR0447.

SA0448

See Friday Plenary Number FR0448.

SA0449

Raman Spectroscopy Demonstrates Radiation-induced Bone Composition Changes in Murine Tibiae. Bo Gong^{*1}, Timothy Damron², Kenneth Mann², Megan Oest³, Joseph Spadaro⁴, Michael Morris¹. ¹University of Michigan, USA, ²SUNY Upstate Medical University, USA, ³SUNY Upstate Medical University, USA, ⁴State University of New York Upstate Medical University, USA

Introduction: Radiation therapy is an established method for treating human metastatic malignancies to bone and soft tissue malignancies near bone. But there are adverse sequelae including poor healing and impaired growth, reduced biomechanical competence leading to insufficiency fractures and high incidence of osteoradionecrosis. These adverse sequelae are not well detected by X-ray based techniques. We use Raman spectroscopy to characterize the chemical composition of post-irradiation murine tibia and demonstrate the presence of abnormal mineral and matrix even twelve weeks post-radiation.

Methods: Under an IACUC-approved protocol, 6 female Balb/c mice underwent radiation of the right tibiae, with a dose of 20 Gy in 4 fractions, using lead shielding to define the irradiation region. The left tibia was used as an internal control. At 12-week post-irradiation, all animals were euthanized and tibiae harvested. Thirty Raman spectra were recorded for each specimen in the region of interest (Raman microprobe, 785 nm excitation). Mineral and collagen Raman bands were analyzed using MATLAB and GRAMS/AI software. Mineral to matrix and carbonate to phosphate ratios, crystallinity (inverse FWHM of phosphate 960 cm^{-1}) and collagen cross-link ratio (amide I envelope) were used as metrics. One-way Anova was used to evaluate statistical significance ($p < 0.05$).

Results and Discussion: Irradiated tibiae exhibited lower mineral to matrix ratio, higher carbonate content and lower crystallinity. The collagen cross-link ratios were higher. The results are consistent with deposition of new mineral, indicating only

partial repair of radiation-induced damage even twelve weeks after irradiation. However, higher collagen cross-link ratio suggests that at least some mineral is deposited on a pre-existing collagen matrix. Our measurements do not establish whether the cross-links are the normal lysine-derived links or include links formed from products of radiation damage. Further measurement of the time course of radiation-induced damage and subsequent recovery is underway. This information may guide development of new dosing protocols and adjuvant therapies. Recent developments in non-invasive spectroscopy suggest it may also be useful for post-irradiation patient monitoring, at least at some sites.

Disclosures: Bo Gong, None.

This study received funding from: M.D.M. R01 AR047969 and AR055222; David G. Murray Endowment and Carol Baldwin Breast Cancer Foundation

SA0450

See Friday Plenary Number FR0450.

SA0451

The De-ubiquitinating Enzyme USP45 Is Critical to Epithelial-mesenchymal Transition (EMT) in Breast Cancer Cells Colonized Bone. Soichi Tanaka^{*1}, Toshiyuki Yoneda². ¹Osaka University, Japan, ²Osaka University Graduate School of Dentistry, Japan

Breast cancer frequently spreads to bone. Breast cancer cells disseminated in bone may acquire additional capacities that enhance their aggressiveness via interactions with bone environments. We reasoned that breast cancer cells colonized bone undergo epithelial-mesenchymal transition (EMT), an event known to exacerbate malignant phenotype of cancer cells. To test this, we investigated whether bone environments promote EMT *in vivo*. The MCF-7 human breast cancer cells stably transfected with GFP were inoculated in the mammary fat pad (MF) and tibial marrow cavity (TI). We then examined the expression of the mesenchymal marker Snail and epithelial marker E-cadherin in the tumors developed. Real-Time PCR showed increased Snail mRNA expression in MCF-7 tumors developed in TI compared with MF. In contrast, E-cadherin expression was lower in TI tumors than MF. Snail changed cell shape from epithelial to mesenchymal and reduced E-cadherin expression and induced N-cadherin and vimentin expression. These results suggest that breast cancer cells in bone show EMT and that Snail causes EMT. In search for a factor involved in EMT in bone, we found TGF β caused EMT by changing cell shape from epithelial to mesenchymal with increased Snail expression. Of interest, the bisphosphonate zoledronic acid (ZOL) inhibited TGF β -induced EMT by reversing cell shape and decreasing Snail. Proteasome inhibitor MG132 blocked these effects of ZOL, suggesting that ZOL decreases Snail via proteasomal degradation. Differential microarray between untreated and ZOL-treated breast tumors developed in tibiae identified the de-ubiquitinating enzyme 45 (USP45) as a candidate molecule involved in proteasomal degradation of Snail. USP45 expression was increased in TI tumors compared with MF. USP45 blocked ubiquitin-dependent degradation of Snail. USP45 changed cell shape from epithelial to mesenchymal, promoted cell motility, induced the expression of Snail, N-cadherin and vimentin and decreased E-cadherin expression. ZOL inhibited de-ubiquitination of Snail by USP45. Consistent with these *in vitro* effects, ZOL inhibited metastasis of breast cancer cells from tibiae to lung and liver, presumably by inhibiting EMT in bone. In conclusion, our results suggest bone environments promote EMT in breast cancer cells. ZOL may inhibit EMT in bone via stimulation of Snail degradation by preventing its de-ubiquitination by USP45, leading to the suppression of secondary metastases from bone.

Disclosures: Soichi Tanaka, None.

SA0452

The Effect of Breast Carcinoma Cells on Bone Cells: A Biomechanical Study. Xiuli Chen^{*1}, Sung Yun Park², Taeyong Lee¹. ¹National University of Singapore, Singapore, ²NUS, Singapore

Breast cancer has a strong tendency to develop bone metastases, i.e. 60-70% prevalence for patients with advanced stages of breast cancer [1]. Emerging evidence [2-3] suggests that there are more detrimental effects on osteoblasts due to metastatic cancer cells. In this paper, a biomechanical approach is used to investigate bone cells under the influence of metastatic breast cancer.

30 SD rats were inoculated with W256 breast carcinoma cells in the left femur. Primary tumor culture was isolated from 1 rat which developed a large tumor mass. Normal bone cells were isolated from SD rat bone explants harvested at 50th day. Bone cells exposed to 50% of conditioned medium from W256 and tumor cell culture were monitored for proliferation (MTT assay), alkaline phosphatase (ALP) activity (pNPP method), in-vitro mineralization (Von kossa staining), morphological (actin staining) and mechanical property changes (AFM cell indentation).

Results: Higher inhibition of proliferation, ALP activity and mineralization (Fig 1) were observed in tumor conditioned wells than in W256 conditioned wells. Changes in morphology of bone cells (Fig 1) were observed in W256 and tumor conditioned wells, with increased stretching and less detailed structure of F-actin cytoskeleton observed as compared to control wells. The changes in morphology might be also related to the decreased mineralization in ECM which can affect the cellular attachment on the substrate. Bone cells treated with W256 and tumor conditioned medium have a lower

E modulus compared to untreated cells and with the tumor conditioned bone cells exhibiting a lower E modulus. The mechanical results are likely to be related to the cytoskeletal changes since the cytoskeleton provides the basis for shape and mechanical properties.

Conclusions: Breast carcinoma cells are shown to have the effect of reducing bone cell proliferation, ALP activity and mineralization. The reduction in mineralization may have also affected the cellular attachment and morphology and indirectly, bone cell mechanical properties. Bone cell mechanical property changes may impact its mechanosensing properties and combined with reduction in functionalities, could bear consequences for tissue level changes.

References: [1]Clines G. A, Guise T.A, Expert reviews in Molecular Medicine 10 (7),2008 [2] Mastro A.M, et al. J. Cellular Biochemistry 91, 2004, [3] Dhurjati R, et al. Clinical Experimental Metastasis 25, 2008

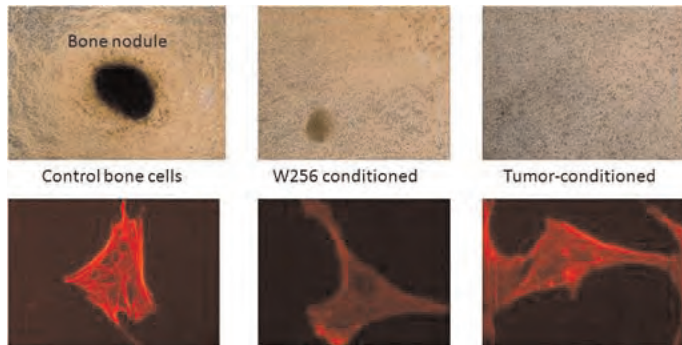


Figure 1

Disclosures: Xiuli Chen, None.

SA0453

The Therapeutic Effects of Rank-Fc Against Osteosarcoma Target not only Osteoclasts but also Osteosarcoma Cells Directly. Toru Akiyama*¹, Jonathan Clark², Peter Choong². ¹Saitama Medical Center, Jichi Medical University, Japan, ²Department of Orthopaedic Surgery, St. Vincent's Hospital Melbourne, Australia

Introduction: Osteosarcoma is the most common primary malignant bone tumor, which mainly affects adolescents and young adults. The following improvement in osteosarcoma treatment after dramatic advancement via the introduction of modern surgery and systemic chemotherapy in 70's has never been seen over the past 30 years. Thus, novel osteosarcoma therapeutic strategies are urgently required currently. We have focused on the RANKL-osteoclast system as a protagonist of osteosarcoma development. The osteoclast is the sole cell capable of resorbing bone in any bone-associated pathology, including osteosarcoma. The development in bone and metastatic lesion formation due to osteosarcoma essentially requires the induction of osteoclasts in order to degrade surrounding bone. RANKL is a critical factor for osteoclast activity. Furthermore, recent reports indicate that RANKL can support the tumorigenesis. RANK-Fc is a potent RANKL antagonist. Thus, we focused on RANK-Fc as a potent candidate of osteosarcoma therapeutic agent.

Objectives: We studied the therapeutic efficacy of RANK-Fc against osteoclast and osteosarcoma tumor cell in vitro and in vivo. Furthermore, we aimed to reveal the molecular mechanism of the RANK-Fc therapeutic efficacy.

Methods: We used our orthotopic osteosarcoma model as an in vivo treatment model. In vitro primary osteoclast study system and SaOS2 osteosarcoma cell line was used for assays of RANK-Fc efficacy on osteoclast and osteosarcoma tumorigenesis.

Results: In vivo data demonstrated that RANK-Fc suppressed tumor growth in bone with the preservation of bone structure. RANK-Fc administration prevented lung metastasis effectively, even when administered tumor - induced bone destruction started. In vitro studies revealed that RANK-Fc suppressed osteoclast formation, bone resorption activity and RANKL induced anti-apoptotic manner. Furthermore, RANK-Fc suppressed osteosarcoma cell migration, invasion ability, and anchorage-independent ability in type I collagen gel following induction of anoikis and activation of caspase-3. The anti-invasion and anti-metastasis capability of RANK-Fc is attributed to reduce ERK signaling via RANK-Fc.

Conclusions: The therapeutic effects of RANK-Fc against osteosarcoma cell are provided by its inhibition of not only osteoclast but also osteosarcoma cell itself. Our data demonstrated that RANK-Fc is a potential drug candidate for osteosarcoma with mechanisms unparalleled by current chemotherapeutic agents.

Disclosures: Toru Akiyama, None.

SU0001

Age Related Sexual Dimorphism of Trabecular Bone Loss Is Inversely Associated with Adipogenic and Osteoclastic but not Osteogenic Activities. Beth Bragdon^{*1}, Elise Morgan², Robert Burns³, Amelia Baker⁴, Anna Belkina⁴, Gerald Denis⁴, Jennifer Schlezinger⁵, Louis Gerstenfeld⁴. ¹Boston University School of Medicine Department of Orthopaedics, USA, ²Boston University, USA, ³Boston University School of Medicine, Department of Orthopaedics, USA, ⁴Boston University School of Medicine, USA, ⁵Boston University School of Public Health, USA

Bone mineral density is lower in females than males, and bone quality shows sexually dimorphic differences during aging with female animals having greater loss than males. A mechanistic molecular study was carried out to examine sexual differences in anabolic and catabolic activities during skeletal aging.

Methods: A longitudinal study from 3-18 months of male and female C57BL/6 mice (N=5-7) was carried out. PINP was assayed in serum. Cortical and trabecular bone structure was assessed in the right tibia by μ CT. Quantitative RT-PCR was used to assess the expression of three cassettes of mRNAs for osteoblasts/osteocytes (RUNX2, osterix, osteocalcin, RANKL, DMP1, FGF23), osteoclasts (cathepsin K, Trap5b) and adipocytes (PPAR γ , CEBP α , FABP4, adiponin) from both humeri. Primary bone marrow cultures were prepared from the femurs and left tibia and stimulated to undergo osteogenesis in the absence or presence of rosiglitazone; mRNA expression was assessed.

Results: μ CT showed that both males and females lose bone volume, had decreased trabecular number and had increased cortical area over time, with females having a greater bone loss than the males. qRT-PCR showed osteoblast markers, RUNX2, osterix, osteocalcin, and resorption markers were lower in the females at 3 months, but at 6 and 12 months the females had increased expression compared to the males. At 12 months, DMP1, FGF23, RANKL and SOST were all increased in females compared to males. The expression of adipocyte and osteoclast markers was constant in male mice over time but showed several fold higher expression in females at 6 months. The differences in osteoblastic metabolic activity were confirmed by assessment of serum PINP levels. Interestingly, female-derived bone marrow cultures expressed greater levels of PPAR γ , FABP4 and adiponin following 1 week of osteogenic differentiation than male-derived cultures, and induction of adipogenesis and suppression of osteogenesis by the PPAR γ ligand rosiglitazone was enhanced in female-derived cultures.

Conclusion: These findings suggest that skeletal tissue metabolism is several fold higher in females than males and males are more metabolically efficient in bone acquisition than females. In vitro studies showed the same sex dependent variation in overall metabolic activity in male and female cells even in the absence of estrogen and suggest that sexual dimorphic differences must be epigenetically imprinted within bone marrow stromal cells.

Disclosures: Beth Bragdon, None.

SU0002

Cell Signaling Pathways Regulate Postnatal Intervertebral Disc Growth and Maintenance. Chitra Dahia^{*1}, Eric Mahoney², Christopher Wylie². ¹Cincinnati Children's Hospital Medical Center, USA, ²Cincinnati Children's Hospital, USA

Degenerative disc disease afflicts 1 in 7 adults and is a major cause of lower back pain. Poor outcome of treatment combined with our limited understanding of normal disc growth and development during the postnatal stages, makes it important to design approaches for its regeneration. It is well established that cross talk between major cell signaling pathways regulates the growth and maintenance of all kinds of cells and tissues. We have previously shown using a mouse model system that the major cell signaling pathways are active in all the components of the disc during postnatal stages. The nucleus pulposus (NP), which originates from the embryonic notochord, was shown to secrete major signaling ligands including sonic hedgehog (Shh), TGF β s, BMPs and Wnts, while the annulus fibrosus (AF) and end plate (EP) surrounding the NP cells responded to these signals. However, the roles of these signaling pathways in disc growth and maintenance is not well understood. We hypothesize that Shh is a key signaling pathway that regulates other major signaling pathways in postnatal disc and that cross talk between these pathways regulates the growth and development of the disc. To test this hypothesis we have established an *in vitro* system to study the molecular control of disc growth and maintenance during the postnatal development of the mouse. Our results show that Shh signaling regulates other major cell signaling pathways like BMP, Wnt, and TGF β in controlling the various cellular functions like cell proliferation, cell differentiation, secretion of matrix and major transcription factors by the disc cells. These data also show that the roles of major cell signaling pathways in postnatal disc growth and development can be studied using specific antagonists and agonists in a simple *in vitro* culture system. It will be important in the future to identify the precise functions of each of these pathways on the growth and differentiation of the disc, the cells releasing and responding to the ligands, and the sites of interaction of the pathways in the disc cells. This will provide crucial information about molecular control of postnatal disc growth and maintenance. Identification of signals controlling postnatal intervertebral disc growth and differentiation offers the opportunity for the development of biological repair as an alternative to surgery.

Disclosures: Chitra Dahia, None.

SU0003

ERCC1 Deficiency Impairs Bone Homeostasis via an NF- κ B-dependent Mechanism. Qian Chen¹, Andria Robinson², Cheryl Clauson², Laura Niedernhofer², Paul Robbins², Hong-Jiao Ouyang^{*2}. ¹University of Missouri - Kansas City, USA, ²University of Pittsburgh, USA

Advanced age is one of the most important risk factors for osteoporosis. Accumulation of oxidative DNA damage has been proposed to contribute to age-related deregulation of osteoblastic and osteoclastic cells. ERCC1 (Excision Repair Cross Complementary group 1)-XPF (Xeroderma Pigmentosum Group F) is an evolutionarily conserved structure-specific endonuclease that is required for multiple DNA repair pathways. Inherited mutations affecting expression of ERCC1-XPF cause a severe progeroid syndrome in humans, including early onset of osteopenia and osteoporosis, or anomalies in skeletal development. Herein, we used progeroid ERCC1-XPF deficient mice, including *Ercc1*-null (*Ercc1*^{-/-}) and hypomorphic (*Ercc1*^{- Δ}) mice, to investigate the link between failure to repair DNA damage and bone development and homeostasis. Compared with their corresponding WT littermates, both *Ercc1*^{-/-} and *Ercc1*^{- Δ} mice display severe, age-dependent progressive osteoporosis in a gender-independent manner, which is reflected by significant reductions in BV/TV, Tb.Th and Tb.N, as well as an increase in Tb.Sp. The osteoporosis in *Ercc1*-deficient mice is caused by reduced bone formation and enhanced osteoclastogenesis. ERCC1 deficiency leads to atrophy of osteoblastic progenitors in the bone marrow stromal cell (BMSCs) population, increased cellular senescence, reduced cell proliferation of osteoblastic cells. Further, ERCC1 deficiency triggers permanent DNA damage and a senescence-associated secretory phenotype (SASP) in BMSCs and osteoblastic cells. The latter leads to enhanced secretion of inflammatory cytokines known to drive osteoclastogenesis, such as IL-6, TNF α , and RANKL, in BMSCs and osteoblastic cells, and thereby induces an inflammatory bone microenvironment favoring osteoclastogenesis. Furthermore, we found that NF- κ B is activated in osteoblastic and osteoclastic cells of the *Ercc1* mutant mice. Importantly, we demonstrated that p65 haploinsufficiency partially but significantly rescued the osteoporosis phenotype of *Ercc1*^{- Δ} mice. Finally, pharmacological inhibition of the NF- κ B signaling via an IKK inhibitor reversed cellular senescence and SASP in *Ercc1*^{- Δ} BMSCs. These results demonstrate that DNA damage drives osteoporosis through an NF- κ B-dependent mechanism. Therefore, the NF- κ B pathway represents a novel therapeutic target to treat ageing-related bone disease.

Disclosures: Hong-Jiao Ouyang, None.

SU0004

Fibronectin Fragments in Human Intervertebral Disc Tissue and their Effects on Disc Cells. Dessislava Markova¹, Nancy Ruel², Ana Chee², Carla Scanzello², D. Greg Anderson³, Sherrill Adams⁴, E.J. Thonar², Howard An², Yeji Zhang^{*3}. ¹Thomas Jefferson University, USA, ²Rush University Medical Center, USA, ³Rothman Institute, USA, ⁴University of Pennsylvania School of Dental Medicine, USA, ⁵Rush University Medical CTR, USA

In the degenerative intervertebral disc (IVD), increased quantities of fibronectin (FN) fragments (FN-fs) have been correlated with increasingly severe disc degeneration. A 29kDa N-terminal exogenous FN-f has been shown to disturb extracellular matrix homeostasis in vitro and in the rabbit model, suggesting that FN-fs may play a role in the pathogenesis of disc degeneration. Our current work: confirms the presence of many FN-fs in the human IVD that are similar in size to the exogenous FN-f; estimates FN-fs to be in the nanomolar range per gram of human IVD tissue by western blot; and examines the effect of the 29kDa FN-f on bovine IVD cells by gene expression level alterations. Human IVD tissues were removed during spinal surgery (n = 6, Thompson MRI grades II-V). Soluble proteins were analyzed by immunoblot with a monoclonal antibody (Ab) against the N-terminus of FN and a rabbit polyclonal Ab recognizing the FN-f neopeptide VRAA271 (kindly supplied by Pfizer, Inc.), visualized, and quantified with infra-red dye conjugated secondary antibodies by LICOR (BioSciences) infrared imager. The purified 29kDa FN N-terminal tryptic digest fragment (Sigma) was used as a positive control, and allowed estimation of the concentration of FN-fs in the samples. We have shown that normal young adult, and moderate to severely degenerative IVD tissues contain multiple smaller FN-f species. An endogenous 29kDa FN-f was observed in all diseased samples and the young adult control, but was absent from the infant tissue. Estimated in the nanomolar range per gram of tissue, there was an increase in total FN-fs detected in the moderately degenerative discs (grade IV). We examined the extracellular matrix gene expression in response to the 29kDa FN-f by real-time RT-PCR. Alginate encapsulated bovine cells were treated daily with 100nM FN-f (Sigma), or media as untreated controls. On day 6 post treatment, total RNA was extracted (Qiagen RNeasy Micro kit). Gene expression of Aggrecan, Type II Collagen, MMP-9, MMP-13, and GAPDH (as an internal control) was analyzed by the 2- $\Delta\Delta$ CT method. An inductive effect on the MMP13 gene occurred in treated annulus fibrosus cells while MMP9 and aggrecan genes were strongly induced in treated nucleus pulposus cells. In summary, we have shown the presence, and pathophysiological concentration of the 29kDa FN-f in human disc tissue. We have shown preliminary evidence that the FN-f may affect disc cell metabolism, contributing to disc degeneration.

Disclosures: Yeji Zhang, None.

SU0005

Identification of Trabecular Excrescences in Aging Bone. Adam Taylor*¹, Chris Platt², Jonathan Jarvis², Lakshminarayan Ranganath², James Gallagher², Alan Boyde³. ¹Lancaster University, United Kingdom, ²University of Liverpool, United Kingdom, ³Barts & The London School of Medicine & Dentistry, United Kingdom

Purpose: We have previously described the non-coupled formation of bone in trabecular excrescences, recognized firstly in bone samples from patients with osteoarthritis of alkaptonuria and subsequently in patients with osteoarthritis (Taylor, 2012). Three types of these structures have been identified, all of which are laid down by osteoblasts without prior preparation by osteoclasts. We aimed to determine if these novel microanatomical structures were also present in normal aged human bone samples.

Methods: Three cadaveric knees (mean = 88yrs) lacking macroscopic OA were obtained with ethical approval. Distal femur and proximal tibia were sectioned in the coronal plane. Decalcified wax embedded sections were used for analysis by routine histology (brightfield, fluorescence and polarized) and slabs for scanning electron microscopy - macerated for topographic and PMMA embedded polished block faces for compositional backscattered electron SEM imaging.

Results: All three types of previously described excrescences were found in all three samples analyzed. These structures appeared to show poor integration with the existing trabeculae. Many of the identified structures demonstrated little morphology typically of osteoclastic or osteoblastic action. Pre-existing trabeculae and the centers of excrescences showed normal levels of fluorescence but the periphery and the surfaces of contact between the excrescences and the prior trabeculae showed low levels of fluorescence. Examination by polarized light revealed normal lamellar structure throughout the existing trabeculae. This contrasted with a lack of lamellar structure seen in the excrescences. A small number of excrescences demonstrated a poorly developed lamellar structure at the centre of the excrescences but no evidence of lamellar structure at the interface with the prior trabeculae.

Conclusions: We have demonstrated that trabecular excrescences are not just present in overtly pathological bone but also in apparently normal aged human bone samples. These structures arise without previous osteoclastic action, supporting the theory that coupled remodeling is not the sole mechanism of bone internal restructuring. Ref: Taylor et al, 2012, European Cells & Materials

Disclosures: Adam Taylor, None.

SU0006

Muscle Strength of the Upper Dominant Limb in Postmenopausal Women with Primary Hyperparathyroidism. Cristiana Cipriani*¹, Elisabetta Romagnoli², Jessica Pepe³, Claudia Castro³, Antonella D'Angelo³, Addolorata Scarpello³, Maurizio Angelozzi³, Salvatore Minisola⁴. ¹University of Rome, Italy, ²Dpt of Internal Medicine & Medical Specialties, University "Sapienza", Rome, Italy, ³Department of Internal Medicine & Medical Disciplines, "Sapienza" University of Rome, Italy, ⁴"Sapienza", University of Rome, Italy

Purpose: Among neuromuscular manifestations of primary hyperparathyroidism (PHPT), a lower limb proximal myopathy has been reported. We investigated muscle strength of the upper dominant limb in a sample of postmenopausal women with PHPT (n=45, mean age 60.5±5.8 SD years; BMI 25.7±5.7 kg/m²) and in a control group of healthy age-matched women (n=38, mean age 58.3±6.46; BMI 25.2±3.6). We evaluated the association between muscle strength and both forearm bone mineral density (BMD) and phalangeal quantitative ultrasound at the same limb. The correlations between the main parameters of mineral metabolism and muscle strength were also investigated.

Methods: Maximal voluntary contraction (MVC, Newton, N) force of the upper dominant limb was evaluated using a dynamometer (Handgrip Dynamometer, Kayser Italia s.r.l.). BMD at one third of the radius (R)(Hologic QDR 4500A, Hologic Inc., USA), and phalangeal quantitative ultrasound (DBM Sonic 1200, IGEA, Carpi, Italy) were evaluated at the same limb. Ultrasonometric parameters considered were the speed of propagation of ultrasound dependent on the amplitude of the ultrasound wave crossing bone tissue (Amplitude-Dependent Speed of Sound, ADSoS) and a parameter calculated by computer analysis of dynamic parameters of ultrasound signal (Ultrasound Bone Profile Index, UBPI). Serum ionized calcium (Ca⁺⁺) and PTH were measured in both the groups. Serum phosphorus levels (P) were measured in PHPT patients. Serum 25-hydroxyvitamin D [25(OH)D] levels were assessed in the group of healthy women and in a subgroup of 35 patients with PHPT.

Results: MVC values were significantly lower in patients with PHPT, compared to the control group (186.78±57.46 N vs 233.98±57.11, respectively, p<0.001). We found a significant correlation between MVC and R-BMD in patients with PHPT (r=0.405, p<0.01) and in the group of healthy women (r=0.403, p<0.05) and between MVC and Ca⁺⁺ serum levels in PHPT patients (r=-0.32, p<0.05). No significant correlation between MVC and ultrasonometric parameters in the two groups and between MVC and P in the PHPT patients was found. The results were confirmed after adjusting for BMI and 25(OH)D values (p<0.05).

Conclusions: Our results show that there is a reduction in distal muscle strength of the upper limb in postmenopausal women with primary hyperparathyroidism. Hypercalcemia is a prominent factor influencing muscle strength in these patients.

Disclosures: Cristiana Cipriani, None.

SU0007

Ros/redox Signaling Regulates Bone Turnover in an Age-specific Manner in Female Mice. Kelly Mercer*¹, Larry Suva¹, Thomas Badger², Jin-Ran Chen³, Martin Ronis¹. ¹University of Arkansas for Medical Sciences, USA, ²Arkansas Children's Nutrition Center, USA, ³University of Arkansas for Medical Science, Arkansas Children's Nutrition Center, USA

In bone, oxidant signaling through NADPH oxidase (NOX)-derived reactive oxygen species (ROS) superoxide and/or hydrogen peroxide appears to be an important stimulus for osteoclast differentiation and activity. ROS signaling has been suggested to increase RANKL mRNA and protein expression, thus enhancing osteoclastogenic RANKL-RANK signaling between osteoblasts and osteoclast precursors. We have previously demonstrated that chronic alcohol abuse (EtOH), generates excess Nox-dependent ROS in osteoblasts, which functions to inhibit bone formation through impairment of Wnt signaling, and increases osteoclastogenesis by stimulating RANKL-RANK signaling. These effects can be blocked by the dietary antioxidant N-acetylcysteine and the pan-Nox inhibitor DPI. In the current study we utilized a well-described transgenic C57Bl/6J mouse strain which over-expresses human *catalase* (TgCAT) in all tissues to see if limiting excess hydrogen peroxide production in bone would protect against EtOH-mediated bone loss. MicroCT analysis of chow fed TgCAT mice at 6 wks revealed an osteoprotective phenotype, increased BV/TV, Tb.N. and decreased Tb.Sp., p<0.05. Six wk old, wild-type (WT) and TgCAT female mice were then given rodent chow *ad libitum*, or pair-fed (PF) liquid diets with 0% or 30% EtOH calories for 8 weeks. In WT mice at age 14 weeks, PF had no effect on bone parameters relative to *ad libitum* chow feeding but EtOH-feeding significantly reduced trabecular BV/TV, and Tb.N. and increased Tb.Sp. in tibial bone, p<0.05. EtOH consumption also decreased cortical cross-sectional area and thickness (p<0.05) in WT mice compared to PF controls, p<0.05. At 14 wks, we observed significant reductions in %BV/TV, and number, and increases in spacing and Tb.Th. in *ad libitum* chow fed and in PF TgCAT mice compared to WT chow fed and PF mice, p<0.05, suggestive of an osteoporotic phenotype associated with TgCAT overexpression later in development. EtOH-feeding had no further effect on bone parameters in TgCAT mice. In conclusion, over-expression of human catalase in TgCAT mice produced significantly greater bone mass than WT mice at 6 wks and lower bone mass at 14 wks. EtOH-feeding resulted in reductions in trabecular and cortical bone in WT mice but no additional reductions in trabecular or cortical bone parameters in TgCAT mice. These data suggest that ROS/redox signaling regulates bone turnover in an age-dependent fashion. Supported in part by R01 AA018222 (M.J.R.).

Disclosures: Kelly Mercer, None.

SU0008

The Novel Identification of CD163 Expressing Phagocytes in Joint Cartilage and its Scavenger Role in Cartilage Degradation. Kai Jiao¹, Jing Zhang¹, Mian Zhang¹, Yuying Wei¹, Yaoping Wu¹, Zhongying Qiu¹, Jianjun He¹, Yunxin Cao¹, Jintao Hu¹, Han Zhu¹, Lina Niu¹, Xu Cao², Kun Yang³, Meiqing Wang*¹. ¹Fourth Military Medical University, China, ²Johns Hopkins University, USA, ³Fourth Military Medical University, China

Cartilage degradation is the typical characteristic of arthritis. Whether there was a subset of phagocytes in cartilage expressing CD163, a specific macrophage marker, and what a role they play in degraded cartilage are attractive. Cartilage from knee and TMJs of Sprague-Dawley rats were sampled for *in vivo*, *ex vivo* and *in vitro* studies. Cartilage degradation was experimentally induced in rat's temporomandibular joints (TMJ) with our reported biomechanically dental methods. Knee osteoarthritis (OA) and normal cartilage from knee arthroplasty and amputation patients was investigated. CD163⁺ cells were identified in cartilage mid-zone, respectively occupying 3.3% and 2.6% in Col-II⁺ cells sorted from knee and TMJ cartilage, among which about 70% possessed phagocytic activity (P < 0.05). Phagocytes engulfing neighboring apoptotic and necrotic cells were found within the experimentally-induced degraded TMJ cartilage, within which there were increased expression of CD163, TNF- α and MMPs (all P < 0.05), but unchanged levels of ACP-1, NO and ROS relating to cellular digesting capability (all P > 0.05). Increased number of CD163⁺ cells with enhanced phagocytic activity were verified in Col-II⁺ cells sorted from degraded TMJ cartilage of 8-wk experimental group versus controls, and also in the isolated Col-II⁺ cells stimulated by TNF- α (all P < 0.05). Mid-zone distribution of CD163⁺ cells accompanied with increased expression of CD163 and TNF- α were further confirmed in the isolated Col-II⁺ cells from human OA knee cartilage versus controls (both P < 0.05). CD163⁺ phagocytes were identified within joint cartilage. Their increased number with enhanced phagocytic activity in degraded cartilage indicate an active capability of eliminating degraded tissues, and provide a new strategy for arthritis treatment.

Disclosures: Meiqing Wang, None.

This study received funding from: Nature Science Foundation of China (NSFC)

SU0009

Bone and Muscle Relationship in Korean Old People from KNHANES V(2010). Sangmo Hong*¹, Chang Beom Lee¹, Yong Soo Park¹, Dong Sun Kim¹, Ye Soo Pack², You Hern Ahn¹, Woong-Hwan Choi¹.

¹Endocrinology & metabolism, Hanyang University College of medicine, South Korea, ²Hanyang University College of medicine, South Korea

Background: Recently, the prevalence of osteoporosis and sarcopenia in the elderly has dramatically increased. However the relationship between these diseases is not clear.

Objective: We aimed to determine the independent relations of muscle mass to osteoporosis (femur neck) in relation to body weight, fat mass, and other confounders.

Design: We analyzed body composition and BMD data of 570 Male and 734 female who are older than 65 years from KNHANES V(2010). Body composition and bone mineral density (BMD) of femur neck were measured by DXA. Sarcopenia was defined as the appendicular skeletal muscle mass (ASM) divided by height squared (Ht²) (kg/m²) of < -1 SD below the sex-specific mean for 20 - 39 years adults.

Results: ASM/(Ht)² and BMD were positive correlated with body fat mass/(Ht)². Protein & fat, carbohydrate, calcium, phosphate, calory intake were also positive correlated with BMD. Exercise also had positive correlation with ASM/(Ht)² and BMD. However Vitamin D only positively related with ASM/(Ht)². With compound factors adjusting, ASM/(Ht)² had also positive relation with BMS in men (R²=0.171, B=0.027, p<0.001) and in women (R²=0.226, B=0.016, p=0.002). The adjusted odds ratios (95% CIs) of osteoporosis in sarcopenia patients were 1.24 (95%CI:1.47-8.15) in men and not significant in women.

Conclusions: Bone mineral density were independently associated with muscle mass. And in men, sarcopenia was independent risk factor for osteoporosis in men but not women.

Disclosures: Sangmo Hong, None.

SU0010

Changes in Lean Tissue Index, Functional Ability and Muscle Strength amongst Older Patients on Haemodialysis. Grahame Elder*¹, Avalon Moonen², Sijorjiana Green², Margaret Phillips³.

¹Westmead Hospital, Australia, ²Clinical School, University of Notre Dame, Australia, ³Department of Renal Medicine, Westmead Hospital, Australia

Sarcopenia has been defined by a number of criteria, including the lean tissue index (LTI; lean tissue mass/height²) using bioimpedance analysis or DXA, and by tests of functional ability, muscle strength, the Subjective Global Analysis (SGA) or combinations of these. Sarcopenia assessment may identify vulnerable patients and be particularly useful to target modifiable risks and to monitor for new health problems. Patients undergoing haemodialysis (HD) have chronic ill health and high mortality that may be predicted by measures of sarcopenia.

This baseline study evaluated 80 stable patients aged 60 and above on satellite HD for evidence of sarcopenia using bioimpedance analysis (Body Composition Monitor, Fresenius Medical Care). These patients were also tested for functional ability using the 6 minute walk, timed up-and-go and recurrent sit-to-stand, muscle strength using grip strength and knee extension and laboratory markers reported to predict mortality. For descriptive and comparative statistics patients were divided into 2 equal quantiles by age 60-71 and 72-86 and assessed separately by gender. Values are mean ± SD.

Patients ≥age 60 on satellite dialysis had an annual mortality of 20% in the previous year. Of the 80 prevalent patients who agreed to enter this study, 56% were male. Their LTI was 13.2 ± 2.5 kg/m² for men and 10.8 ± 2.1 kg/m² for women, with no differences between the 2 age quantiles. Tests of functional ability, muscle strength and SGA did not differ by age quantile. Amongst the laboratory biomarkers, transferrin levels were lower with age for women (p=0.047) and urea was lower for men (p=0.011).

In this cohort, patients surviving on dialysis do not show a reduction in LTI measured using bioimpedance analysis, or worsening functional ability, muscle strength or SGA scores with age. These data differ from general population and end stage kidney disease data and are consistent with selection bias for survival. However, longitudinal assessment of patients in this ongoing study will determine whether lower scores predict those patients at risk of increased mortality who could be targeted for intervention.

Disclosures: Grahame Elder, None.

SU0011

Factors Associated with 20-foot Walking Speed in the US Elderly Population.

David R Nelson¹, Lei Chen², Yang Zhao*², Zhanglin Cui², Joseph A Johnston¹. ¹Eli Lilly & Company, USA, ²Eli Lilly, USA

OBJECTIVE: To examine the relationships between physical function, as measured by walking speed, with various demographic, clinical, and muscle strength measures in the US population of age 50 years and above.

Methods: This study included individuals of age 50 and greater from the 1999-2002 waves of the continuous National Health and Nutrition Examination Survey (NHANES). The magnitude of relationships between continuous variables with physical function (i.e., 20-foot walking speed, [WS], in meters/second) were assessed using partial correlation coefficients that controlled for age and gender. The relationships between WS and demographic characteristics, vision problems, balance disorders (via Romberg tests), comorbid medical conditions, body mass index (BMI), and muscle strength via the isokinetic quadriceps strength (IQS, in Newtons) were assessed using a series of multiple regression models that utilized survey strata and weighting, with WS as the dependent variable, and age, gender, and each variable of interest (e.g., diabetes) as the independent variables. Statistical significance was assessed using p<0.05 from two-tailed tests.

Results: The study included 3960 individuals (mean age: 63.2 years; female: 53.6%). Mean WS was 1.02 meters/second and declined from 1.14 for 50-54 years old to 0.75 for those 80 and older. Similarly, mean IQS was 365.6 Newtons, declining from 426.4 for 50-54 year olds to 244.3 for those 80 and older. After adjusting for age and gender, IQS and WS were significantly correlated (partial correlation coefficient=0.27, p<0.001). In addition, increasing BMI, difficulty with balance or vision, and several medical conditions (e.g., arthritis, coronary heart disease, diabetes, stroke) were significantly related with slower 20-foot WS (p<0.01) after adjusting for age and gender, respectively.

CONCLUSION: Among individuals aged 50 and above in the US, muscle strength and 20-foot WS are positively correlated. Patients with vision or balance disorders, and certain comorbidities (e.g., coronary heart disease and arthritis) also had slower 20-foot WS. Studying the inter-relationships among these factors may help shed light on the reduction of physical function with age in the US.

Disclosures: Yang Zhao, Eli Lilly and Company, 3
This study received funding from: Eli Lilly and Company

SU0012

Gait Speed as a Measure of Frailty in Long Term Care Residents. Carroll Lee*¹, Mary Anne Ferchak¹, Julie Wagner¹, Donna Medich¹, Megan Miller², Subashan Perera¹, David Nace¹, Neil Resnick¹, Susan Greenspan¹.

¹University of Pittsburgh, USA, ²University of Pittsburgh, Division of Endocrinology, USA

Background: Because neither bone mineral density (BMD) nor FRAX adjust for the risk of falls and fractures among frail elderly with multiple comorbidity, there is need for an index/tool to characterize subjects enrolled in osteoporosis trials. Although investigators have devised a variety of complex and time intensive instruments to assess frailty and to predict adverse outcomes, these tools are challenging and often inappropriate to describe residents in long term care (LTC) facilities. Gait speed has been suggested as a quick, inexpensive, reliable method because it is associated with long term survival, function and health in ambulatory community dwelling adults. We sought to evaluate its utility in LTC.

Methods: We examined baseline walking speed (6 meter timed walk with or without an assistive device) in 181 older women (mean age 85 years) participants of a clinical trial living in LTC facilities and followed them over 1 year. Frailty was characterized as gait speed <0.6m/sec (used in community dwelling elderly). Measures included physical activities of daily living (PADL, eat, dress, groom, walk, transfer, bathe, get to bathroom), instrumental activities of daily living (IADL, phone, travel, shop, prepare meals, housework, handle money), physical performance test (PPT, timed sit to stand, timed walk, phone, eat), time to stand (measure of strength), cognitive status (SPMSQ), mental health (PHQ-9), and comorbid burden (Duke comorbidity index). At baseline we also examined hip and spine BMD and body composition (lean and fat mass).

Results: 14% were non-ambulatory. At baseline in the remaining 156, gait speed was significantly associated (all p<0.05) with PADL (r=0.51), IADL (r=0.47), PPT (r=0.63), time to stand (r=-0.43) and age (r=-0.3). Gait speed was associated (all p<0.05) with the 12 month values for PADL (r=0.50), IADL (r=0.50), PPT (r=0.54) and time to stand (r=-0.43). By gait speed criteria for community-dwelling elderly, 60% of subjects were characterized as frail (N=94). At 12 months the values for PADL, IADL, PPT and sit to stand time was worse for frail residents (Table, Wilcoxon Rank Sum test). Gait speed was not associated with cognitive status, mental health, comorbid burden, BMD or body composition.

Conclusions: Gait speed is associated with functional status but not cognitive or skeletal health in frail residents of LTC facilities and may be a simple tool to characterize vulnerable older adults in clinical trials.

| Variable | Frail Gait speed <0.6m/s | Non-frail Gait speed >0.6m/s | P-value |
|---------------------|-----------------------------|---------------------------------|---------|
| Age (years) | 86.3 ± 0.5 | 84.2 ± 0.7 | 0.029 |
| PADL score * | 11.1 ± 0.3 | 12.7 ± 0.2 | <0.001 |
| IADL score * | 6.0 ± 0.4 | 9.3 ± 0.6 | <0.001 |
| PPT score * | 17.5 ± 0.5 | 21.1 ± 0.5 | <0.001 |
| Sit to Stand (sec)* | 5.0 ± 0.5 | 2.1 ± 0.2 | <0.001 |
| Results: mean ± SEM | | | |
| * low values worse | | | |
| # high values worse | | | |

Table

Disclosures: Carroll Lee, None.

SU0013

Kyphosis and Paraspinal Muscle Composition in Older Men: Is There a Relation. Wendy Katzman¹, Dana Miller-Martinez², Lynn Marshall³, Nancy Lane⁴, Deborah Kado⁵. ¹University of California, San Francisco, USA, ²University of California Los Angeles, USA, ³Oregon Health & Science University, USA, ⁴University of California at Davis, USA, ⁵University of California, Los Angeles, USA

Hyperkyphosis is commonly observed in older men, but risk factors beyond vertebral fractures are not well established. We previously reported that poor muscle composition contributes to worse kyphosis in a cohort of both older men and women. To specifically evaluate this association in older men, we conducted a cross-sectional study to investigate differences in paraspinal muscle composition in older men depending on their degree of thoracic kyphosis. The analytic cohort included 471 randomly selected participants from the Osteoporotic Fractures in Men (MrOS) study with baseline abdominal quantitative computed tomography (QCT) scans and plain thoracic radiographs. Abdominal QCT scans were obtained using a standardized protocol that included the area between the mid-L3 and mid-L5 levels. A spline tool was used to trace the outer and inner fascial borders of the paraspinal muscle groups on each side of the vertebral body. Published Hounsfield unit ranges were applied to voxels to estimate paraspinal muscle and intermuscular adipose tissue (IMAT) volumes (cm³). Cobb angle of kyphosis was assessed from thoracic radiographs by erecting lines from the superior edge of T4 and inferior edge of T12 and calculating the angle of intersection. Multivariable linear regression was used to estimate adjusted least square means of Cobb angle within tertiles of paraspinal muscle and IMAT volumes controlling for age, height, prevalent vertebral fracture, and total hip BMD. Among men in the analytic cohort, means (standard deviation) were 74 (SD=5.9) years for age and 37.4 (SD=11.9) degrees for Cobb angle of kyphosis. Men in the lowest tertile of total paraspinal muscle volume had greater Cobb angle than men in the highest tertile (Table). There was evidence of an inverse linear trend in Cobb angle across tertiles of paraspinal muscle volume. However, Cobb angle was not associated with volume of paraspinal muscle IMAT. Results were similar among those with no prevalent vertebral fractures (Table). Moreover, among men with BMI<30, men in the lowest tertile of paraspinal muscle volume had greater adjusted mean Cobb angle (40.0, 95% CI: 37.8 - 42.2) compared to men in the highest tertile (36.1, 95% CI: 34.0 - 38.2). These results suggest that differences in body composition may potentially influence kyphosis. Further investigation in a prospective study is needed to determine if low paraspinal muscle volume contributes to worsening of kyphosis.

| Table. Adjusted mean Cobb angle of kyphosis according to volumes of paraspinal muscle and intermuscular adipose tissue among 471 men aged ≥65 years. | | | | |
|--|--|-----------------------|-----------------------|---------|
| Muscle volume tertile | Least square mean (95% CI) for Cobb angle of kyphosis within tertile of muscle measure | | | p-trend |
| | 1 | 2 | 3 | |
| Paraspinal Muscle | 38.9 (37.0 - 40.8) | 37.3 (35.5 - 39.1) | 36.1 (34.2 - 38.1) | 0.06 |
| Paraspinal Intermuscular Adipose Tissue | 37.6 (35.7 - 39.6) | 37.5 (35.7 - 39.3) | 37.2 (35.3 - 39.1) | 0.77 |
| Among those with no prevalent vertebral fracture ^b | | | | |
| Paraspinal Muscle | 38.6 (36.6 - 40.6) | 36.5 (34.6 - 38.4) | 35.9 (34.0 - 37.9) | 0.07 |
| Paraspinal Intermuscular Adipose Tissue | 36.9 (34.9 - 38.8) | 37.4 (35.6 - 39.3) | 36.8 (34.8 - 38.8) | 0.94 |

^aLeast square means and 95% CI estimated from multiple linear regression adjusted for age, height, prevalent vertebral fracture, and total hip BMD.
^bLeast square means and 95% CI estimated from multiple linear regression adjusted for age, height, and total hip BMD.

Disclosures: Wendy Katzman, None.

SU0014

Sarcopenia, Exercise and Fall Prevention in the Elderly. Eduardo Abreu¹, An-Lin Cheng¹, Leticia Brotto¹, Keyna Chertoff¹, Glenda Kinder², Elizabeth Jackson³, Tina Uridge⁴, Patricia Kelly⁵, Marco Brotto⁶. ¹University of Missouri at Kansas City, USA, ²University of Missouri Extension, USA, ³Clay County Public Health Center, USA, ⁴Clay County Senior Services, USA, ⁵University of Missouri at Kansas City, USA, ⁶University of Missouri - Kansas City, USA

Sarcopenia is defined as the age-related loss of skeletal muscle mass, strength, and function, a condition that begins in the 4th decade of life (3-5% loss of muscle mass per decade, increasing to 1-2% per year after 50 years of age). A huge disconnection between atrophy, force and power (muscles atrophy by 20-30%, force drops by 40-50%, power drops by 50-60%) suggests other factors may be involved. Overall, the loss of muscle mass and function can be both a fundamental cause and a contributor to disability and disease progression, especially when combined, as quite frequently happen, with osteoporosis. For example, weaker individuals are more susceptible to falls, which can aggravate the deleterious consequences of osteoporosis. Despite its importance, sarcopenia remains underdiagnosed. The identification of biomarkers for

sarcopenia are needed and will not only help this conditions to be better diagnosed, but also to improve our understanding of its relationship with osteoporosis and the efficacy of preventive measures (e.g., resistance training).

Sixty-three elderly individuals (ages between 64 and 94, 17 males and 56 females) were evaluated for body mass index (BMI), blood pressure, functional activities, grip strength, and serum determination of lactate dehydrogenase (LDH), muscle creatine kinase (CKM) and muscle Troponin T (TnT), before and after a 10-week exercise program designed to improve balance, strength/resistance, flexibility and endurance. Exercise resulted in a discrete but significant increase in grip strength (right hand, from 21.4 to 22.3 kg, P<0.05) and an overall improvement in the performance of functional activities. In terms of muscle biomarkers, LDH and CKM increased (from 77.1 to 83.1mU/mL, p<0.005, and from 106.9 to 114.0µg/mL, p<0.05, respectively), with TnT decreasing from 68.5 to 52.3pg/mL, p<0.05. The slight increases in LDH and CKM, two key muscle enzymes, indicate higher utilization of skeletal muscles, while the decrease in serum levels of TnT suggests a strengthening of skeletal muscles, making them less likely to be damaged.

In conclusion, a 10-week exercise program was able to help elderly individuals improve their muscle strength, which was attested by improvement in functional activities and positive changes in muscle biomarkers.

Acknowledgement: supported by grant titled "Preventing Falls in Elderly Patients" from the Department of Health Services-Clay County Senior Services, Missouri, USA.

Disclosures: Marco Brotto, None.

SU0015

Estrogen Receptor α Gene Polymorphisms in Degenerative Disease of the Temporomandibular Joint. Melissa Stemig^{*}, Shanti Kaimal, Sandra Myers, Mohammad Islam. University of Minnesota School of Dentistry, USA

Multiple studies reported a correlation between polymorphism in the estrogen receptor alpha (ER- α) gene and degenerative joint disease of the knee. This polymorphism refers to 2 point mutations (T397C, A351G) in the intron 1 of the gene. We studied presence of this polymorphism in patients affected by temporomandibular joint disease (TMJD) using xbaI and pvuII restriction fragment length polymorphisms (RFLPs). DNA samples from 42 patients who had been diagnosed with degenerative joint disease (DJD+) and 36 control patients without any DJD (DJD-) was studied. A 346 base pair long ER- α gene fragment containing the two mutation sites in intron 1, was amplified using primers that have been used in other studies. Amplified fragments were incubated for single digestion with pvuII, xbaI separately and for double digestion with pvuII and xbaI. This way presence of mutation and number of mutation in both allele could be identified. Restriction digestion was run on a 2% agarose gel at 120 volt for 30 minutes. A small volume of uncut and amplified PCR product was used for identification of digested and undigested fragments. Based on number of mutations, five different ER- α genotype was identified. These were, wild type (no mutation), homozygous (one xbaI and one pvuII point mutation in each allele), heterozygous (one wild type allele and one allele with xbaI and pvuII mutation), heterozygous with one additional xbaI mutation in the second allele and single mutation (only one xbaI mutation). Also, these five genotypes were noted in both the DJD affected and unaffected control subjects. We found higher number of homozygous and heterozygous point mutations in the DJD+ samples to DJD- samples, the difference was not statistically significant. Our findings suggest that polymorphic ER- α alone is not a risk factor for the development of degenerative changes in TMJ.

Disclosures: Melissa Stemig, None.

SU0016

Insulin Suppresses ADAMTS4 and BMP2 Expression in Osteoarthritic Fibroblast-like Synoviocytes. Daisuke Hamada^{*}¹, Haobin Ye¹, Robert Maynard², Stephen Kates², Randy Rosier², Matthew Hilton², Michael Zuscik³, Robert Mooney². ¹University of Rochester, USA, ²University of Rochester Medical Center, USA, ³University of Rochester School of Medicine & Dentistry, USA

Our recently published report established that mice fed a high fat diet, a model of type 2 diabetes, showed synovial hyperplasia and accelerated progression of posttraumatic osteoarthritis (OA). Of note, parameters of the altered metabolism in this model, not the weight gain, were associated with OA. These results, along with other published studies, suggest that systemic factors, such as the low-grade inflammation characteristic of obesity/diabetes, may be involved via effects on the synovium. Thus, we hypothesized that fibroblast-like synoviocytes (FLSs) play an important role in OA progression in the obese, diabetic state. FLSs were isolated from synovial tissue obtained from patients undergoing knee replacement surgery. FLSs were shown by western blot analysis to be insulin responsive with dose dependent phosphorylation of the insulin receptor and the downstream signaling molecule Akt. Immunohistochemistry revealed selective, strong staining for insulin receptors in mouse synovial membrane, especially in the lining layer, which mainly consists of FLSs and macrophages. As far as we know this is the first report that FLSs have insulin receptors with intact downstream signaling. To examine its potential role in regulating FLS function, the effect of insulin on responses to inflammatory cytokines was studied. As expected, TNF α and IL1 β , critical factors in OA progression,

increased FLS expression of ADAMTS4 and BMP2, molecules involved with cartilage degradation and osteophyte formation respectively. Importantly, insulin inhibited both basal and cytokine-dependent expression of these response genes by >50%. ADAMTS5 and TGF β were induced only modestly by cytokines and showed only modest suppression by insulin. TNF α induced its own expression by over 100 fold, but also showed only modest suppression by insulin. The latter suggests that pro-inflammatory cytokines initially secreted by synovial macrophages can be amplified through FLSs. In conclusion, up-regulation of ADAMTS4 and BMP2 induced by pro-inflammatory cytokines may contribute to OA progression. Insulin appears to play a selective protective role in the synovium by suppressing these responses, but insulin resistance in obesity/diabetes may impair this critical function.

Disclosures: Daisuke Hamada, None.

SU0017

Notch and Non-canonical NF- κ B Proteins Interact to Inhibit Mesenchymal Stem Cell Differentiation into Osteoblasts in Chronic Inflammation. Hengwei Zhang^{*1}, Lei Shu², Matthew Hilton², Christopher Ritchlin³, Brendan Boyce², Lianping Xing³. ¹University of Rochester, USA, ²University of Rochester Medical Center, USA, ³University of Rochester, USA

Notch signaling plays a critical role in regulating bone cell functions. But, the role of Notch in bone disorders and if Notch inhibitors can be used as bone anabolic agents is unknown. To identify pathways responsible for decreased osteoblast (OB) differentiation of mesenchymal stem cells (MSCs) in inflammatory osteoporosis, we extracted RNA from CD45-/CD105+/Sca1+ MSCs from bone marrow stromal cells (BMSCs) of TNF transgenic (TNF-Tg) mice with chronic inflammation-induced bone loss and WT littermates and subjected them to RNA sequencing and pathway analysis. Among 55 dysregulated pathways, the expression of genes encoding Notch and non-canonical NF- κ B pathway proteins was significantly elevated in TNF-Tg MSCs, which was confirmed by qPCR and Western blot. To determine if Notch inhibition affects OB differentiation from in an inflammatory environment, we treated TNF-Tg and WT mice with the Notch inhibitor DAPT (5mg/kg/day x4d). TNF-Tg MSCs formed significantly fewer CFU-ALP colonies (28 ± 8 vs 53 ± 7 in WT), had decreased expression of OB marker genes and increased Hes1 expression, which DAPT prevented. In contrast, DAPT had no effect in WT mice (colony#/well: 62 ± 10 in WT+veh; 76 ± 6 in WT+DAPT). To determine if Notch inhibition attenuates bone loss, we treated TNF-Tg mice with DAPT or vehicle for 3m. DAPT-treated TNF-Tg mice had higher bone volume and increased bone formation rate than vehicle-treated mice (BV/TV: 20 ± 3 vs 13 ± 2 ; BFR: 0.2 ± 0.03 vs 0.1 ± 0.02 $\mu\text{m}^3/\mu\text{m}^2/\text{day}$; MAR: 0.4 ± 0.02 vs 0.2 ± 0.01 $\mu\text{m}/\text{day}$), but osteoclast numbers were unaffected. In studies investigating the mechanisms involved, we found that 1) p52/RelB over-expression increased NICD-activated Notch reporter gene expression by 65-fold; 2) RelB/p52 directly bound to NICD; 3) TNF promoted RelB, p52 and NICD nuclear translocation, and binding of NICD to the RBPJ response site in the native Hes1 promoter. More importantly, MSCs from RelB/p52 double knockout mice had increased OB differentiation, decreased Hes1 levels, and did not respond to TNF-induced Notch activation. Our findings indicate 1) chronic inflammation causes persistent activation of the Notch pathway in MSCs, limiting their OB differentiation; and 2) non-canonical NF- κ B proteins potentiate Notch activation by promoting NICD nuclear translocation. They suggest that Notch inhibition is a potential new therapeutic approach for inflammatory bone loss where Notch is activated in MSCs.

Disclosures: Hengwei Zhang, None.

SU0018

Relationship between Microstructure and Degree of Mineralization of Subchondral Bone In Osteoarthritis: Synchrotron Radiation Micro CT Study. Ko Chiba^{*1}, Nobuhito Nango², Shogo Kubota², Narihiro Okazaki³, Kenji Taguchi³, Makoto Osaki³, Masako Ito¹. ¹Nagasaki University Hospital, Japan, ²Ratoc System Engineering Co., Ltd., Japan, ³Nagasaki University, Japan

Purpose: We analyzed the microstructure and degree of mineralization of the subchondral trabecular bone in hip osteoarthritis (OA) using synchrotron radiation micro CT (SRCT) to identify the relationship between bone structure and bone turnover.

Methods: Subchondral bone samples were extracted from femoral heads of 10 terminal-staged hip OA patients. The SRCT scan was performed at 30 keV energy and 5.9 mm voxel size. Trabecular bone structure, bone cyst volume, and the degree of trabecular bone mineralization were measured, and correlations between bone structure and the degree of mineralization were analyzed. In addition, the trabecular bone was divided into the area immediately surrounding the bone cyst and the remaining area, and they were compared.

Results: The average cyst volume fraction in the whole region was 31.8%, and the bone volume fraction in the bone region was 55.6%. Cyst volume was the only structural parameter that had a significant correlation with the degree of mineralization. The degree of mineralization was diminished when the bone cyst was larger ($r = -0.81$, $p = 0.004$). The trabecular bone immediately surrounding the bone cyst had a lower degree of mineralization when compared with the remaining trabecular bone ($p = 0.008$).

Conclusions: In the bone sclerosis of OA subchondral bone, there are many large and small bone cysts, which are expected to play a significant part in the high bone turnover of OA.

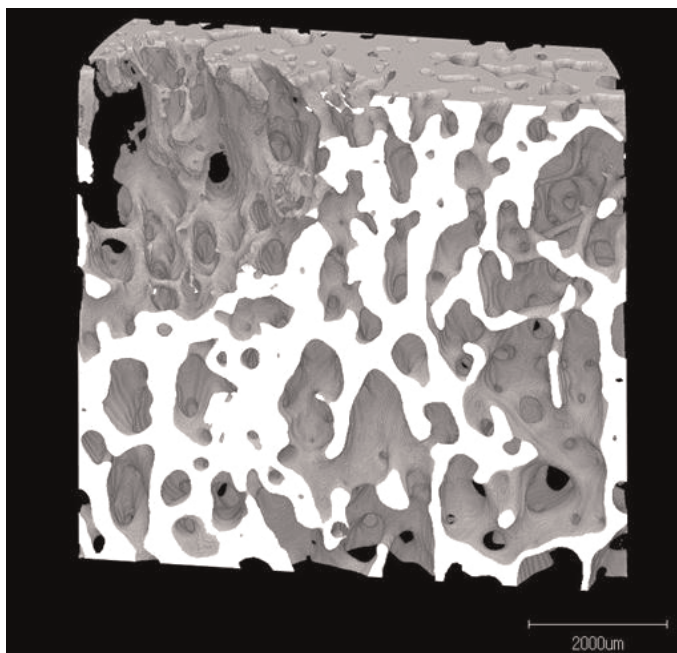


fig.1

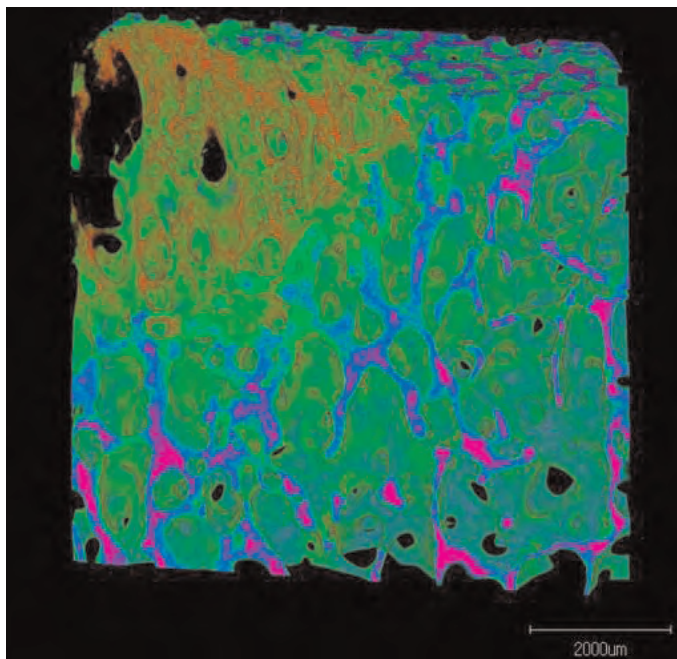


fig.2

Disclosures: Ko Chiba, None.

SU0019

Effects of Short-term Aerobic Exercise Intervention on Bone Metabolism, Physical Fitness, and Body Composition in Postmenopausal Women. Hwei-Jhen Wen^{*1}, Tsang-hai Huang², Tzai-Li Li³, Paun-Yen Chong⁴. ¹Tzu Chi University, Taiwan, ²National Cheng-Kung University, Taiwan, ³National Taiwan Sport University, Taiwan, ⁴Tzu-Chi Hospital, Taiwan

Purpose: To explore the effects of short-term aerobic exercise intervention on bone metabolism, physical function, and body composition in postmenopausal women (PMW). **Methods:** Thirty-eight healthy and sedentary PMW (age 57.76 ± 3.98 years) were recruited in the current study. Subjects attended a progressively aerobic exercise training program at high-intermediate intensity (75-85% heart rate reserve, HRR) for 10 weeks (3 days per week and 60-90 minutes each day). Blood chemistry (total cholesterol, HDL, LDL), bone biomarkers, osteocalcin (OC) and C-Terminal

telopeptide (CTX), body composition (total body fat, whole body bone mineral density, and total hip by dual-energy X-ray absorptiometry), and physical fitness (flexibility, muscular strength, and cardiovascular endurance) were measured before and after the 10-week exercise program. All data were analyzed by a paired t-test ($\alpha = .05$). Result: In bone formation marker, OC was significantly increased (15.47 ± 8.84 vs. 20.12 ± 9.11 nmol/L, $p = .00$; $\uparrow 53\% \pm 13$) while bone resorption marker as shown by CTx was significantly decreased (0.58 ± 0.24 vs. 0.51 ± 0.20 nmol/L, $p = .00$; $\downarrow 8.7\% \pm 3.9$), relative bone formation rate (OC/CTX) was significantly improved (before vs. after: 27.56 ± 12.14 vs. 45.09 ± 29.59 , $p < .01$). Moreover, total cholesterol was significantly decreased (before vs. after: 219.82 ± 41.79 vs. 208.74 ± 44.63 mg/dl, $p = .03$) after 10 weeks intervention. Hip total BMC was significantly improved (before vs. after: 22.27 ± 4.36 vs. 23.05 ± 4.23 , $p < .05$) after 10 weeks intervention. Parameters of physical fitness were significantly improved in flexibility, muscular strength, agility/dynamic balance, and cardiovascular endurance ($p < .05$). Conversely, no significant differences before and after intervention were found in total body fat percentage (before vs. after: 34.51 ± 5.60 vs. $34.38 \pm 5.15\%$). Conclusion: A 10-week aerobic training program seemed to significantly improve bone formation marker and physical fitness in PMW.

Disclosures: *Huei-Jhen Wen, None.*

This study was granted by Tzu-Chi University (TCMRC-P-99003) and National Council of Science (NSC 99-2410-H-179-015)

SU0020

High-impact Bone Exercise does not have Controversial Effects on Articular Cartilage: a Randomized Controlled Quantitative MRI Study (ISRCTN58314639). Juhani Multanen¹, Miika T Nieminen², Arja Häkkinen³, Urho Kujala⁴, Timo Jämsä⁵, Hannu Kautiainen⁶, Eveliina Lammentausta², Riikka Ahola⁷, Harri Selänne⁸, Risto Ojala², Ilkka Kiviranta⁹, Ari Heinonen⁴. ¹University of Jyväskylä, Finland, ²Department of Diagnostic Radiology, Oulu University Hospital, Finland, ³Department of Physical Medicine & Rehabilitation, Central Finland Central Hospital, Finland, ⁴Department of Health Sciences, University of Jyväskylä, Finland, ⁵Department of Medical Technology, Institute of Biomedicine, University of Oulu, Finland, ⁶Unit of Primary Health Care, Kuopio University Hospital, Finland, ⁷University of Oulu, Finland, ⁸LIKES Sports Medical Clinic, Finland, ⁹Department of Orthopaedics & Traumatology, University of Helsinki & Helsinki University Central Hospital, Finland

Osteoporosis (OP) and osteoarthritis (OA) are two common disorders, which often coexist in postmenopausal women. What is controversial and not understood is the simultaneous effect of bone favorable exercise on these two diseases. We evaluated the effects of high-impact exercise on bone mineral content (BMC) and knee cartilage biochemical composition in postmenopausal women with mild knee OA.

Eighty women aged 50-66 years with mild knee OA according the Kellgren/Lawrence radiographic severity grades 1-2 [1] were randomly assigned to undergo a supervised progressive exercise 3 times a week for 12-months (n=40) or to a non-intervention control group (n=40). The femoral neck BMC was measured by dual-energy X-ray absorptiometry (DXA). Biochemical composition of cartilage was evaluated using delayed gadolinium-enhanced MRI of cartilage (dGEMRIC) sensitive to cartilage glycosaminoglycan content, and T2 relaxation time mapping, sensitive to properties of the collagen network [2]. Perceived knee pain, stiffness, and self-rated physical functioning were assessed with the Western Ontario and McMaster Universities Osteoarthritis Index (WOMAC). As risk factors for falls, dynamic balance was measured with a figure-of-eight running test, maximal isometric knee extension force was measured with a dynamometer, and cardiorespiratory fitness was evaluated by 2-kilometer walking test.

Thirty-six trainees and 40 controls completed the study. The mean training compliance was 68%. The mean gain in femoral neck BMC in the exercise group was 0.6% (95% CI: -0.2 to 1.4) and the mean loss in the control group was -1.2% (95% CI: -2.1 to -0.4). The baseline and body mass adjusted BMC change between the groups was statistically significant ($P < 0.001$), while no changes occurred in cartilage biochemical composition. There were no between-group differences in WOMAC scored knee pain, stiffness or self-rated physical functioning. Balance, muscle force and cardiorespiratory fitness improved significantly ($p < 0.05$) more (3-7%) in the exercise group than in the control group.

Progressively implemented high-impact exercise, which improved bone integrity, did not have negative effects on cartilage biochemical composition, and may be feasible in the prevention of OP and fall risk factors in patients with mild knee OA.

REFERENCES: [1] Kellgren JH, Lawrence JS. *Ann Rheum Dis* 1957;16:494-502. [2] Nieminen MT et al. *J Magn Reson Imaging*, in press.

Disclosures: *Juhani Multanen, None.*

SU0021

Increased Cortical Thickness at the Superior Femoral Neck with Unilateral High Impact Exercise in Older Men: A Randomised Blinded Study. Sarah Allison¹, Jonathan P Folland¹, Winston J Rennie², Gregory D Summers³, Kenneth Poole⁴, Katherine Brooke-Wavell¹. ¹Loughborough University, United Kingdom, ²University Hospitals of Leicester, United Kingdom, ³Royal Derby Hospital, United Kingdom, ⁴University of Cambridge, United Kingdom

Cortical thinning at the superior femoral neck is associated with hip fracture in older men and women. Interventions that increase cortical thickness at this region would be beneficial in fracture prevention. This study evaluated the influence of a 12-month, high impact, unilateral exercise intervention on cortical thickness at the femoral neck in older men.

Healthy community-dwelling older men completed a 12-month, high impact, unilateral exercise intervention which increased to 50 multidirectional hops, 7 days a week on one randomly allocated leg. Quantitative Computed Tomography (QCT) scans of both proximal femurs were performed at baseline and after 12 months of exercise. Cortical thickness at the mid femoral neck was estimated in four anatomical quadrants (superoanterior [SA], inferoanterior [IA], inferoposterior [IP], superoposterior [SP]). Scans and analyses were conducted by observers blind to the leg allocation. Cortical thicknesses were square root transformed to achieve normal distribution prior to statistical analysis. Two-way repeated measures ANOVA was used to identify leg (exercise leg [EL] vs. control leg [CL]) x time (pre vs. post) interactions.

Thirty-six men (mean \pm SD, age 70.0 ± 3.9 yrs) exercised for 12 months. Intervention adherence was $91.1 \pm 9.1\%$ (306.2 ± 30.5 sessions completed out of 336 prescribed sessions). Fourteen men did not complete the 12-month exercise intervention due to: medical conditions or injuries unrelated to the intervention (n=9), time commitments (n=2), or discomfort during exercise (n=3). QCT data were available for thirty-two men. Cortical thickness in the SP quadrant increased more in the EL (from 0.31 to 0.47 mm) compared to the CL (from 0.36 to 0.41 mm; $P = 0.012$) as did SA quadrant cortical thickness (EL 0.84 to 0.97 mm; CL 0.85 to 0.91 mm; $P = 0.047$). IP quadrant cortical thickness also increased in the EL relative to the CL (EL 2.96 to 3.08 mm; CL 2.91 to 2.88 mm; $P = 0.039$) although IA quadrant responses did not differ between legs ($P = 0.142$).

These findings demonstrate that exercise can increase cortical thickness at the superior femoral neck, where cortical thinning is most strongly related to hip fracture. The increase in the exercise leg relative to the control leg provides strong evidence that this is a local adaptation to loading. Although high impact exercise may not be feasible for all older people, carefully targeted exercise may reduce risk of hip fracture.

Disclosures: *Sarah Allison, None.*

SU0022

Is Cross-Sectional Area of Quadriceps Muscle and Thigh Intermuscular Fat in a Single MRI Slice Representative of the Volume in Women Enrolled in the Osteoarthritis Initiative? Arpita Parmar, Karen Beattie, Ashlie Altman, Monica Malý, Norma MacIntyre^{*}. McMaster University, Canada

Purpose: Mid-thigh intermuscular fat (IMF) volume, but not quadriceps muscle (QM) volume, is related to knee strength and physical performance at a single point in time in women with or at risk for knee osteoarthritis (OA) participating in the Osteoarthritis Initiative (OAI). Our objectives were to determine if magnetic resonance imaging (MRI)-derived volumes of IMF and QM in the mid-thigh can be adequately represented by the cross-sectional area (CSA) in a single MRI slice and if 2y changes in volumes are represented by changes in single-slice CSAs.

Methods: Thirty-five women in the OAI database who were ≥ 50 y old and had baseline and 2y thigh MRI scans were randomly selected. For each woman, replicate right mid-thigh MRIs (~7.5cm stack of 15 slices taken 10cm proximal to the medial femoral epiphysis) were matched for anatomical position using 3-D image registration software (Analyze[®]) and only matched slices were included in the analyses. Segmentation software (SliceOmatic[®]) was used to quantify QM and IMF CSAs for each slice and total volumes. For cross-sectional associations, slices from only the baseline or the 2y MRI scan were included for each woman. To determine change over 2y, baseline measures were subtracted from 2y measures. Associations were described using the Pearson's product moment correlations, r , or Spearman's rank order correlations, r_s (for data not normally distributed).

Results: The women were 51 to 75y old and had symptomatic and radiographic knee OA (n = 13) or risk factors for knee OA (n = 22). QM and IMF CSAs in each slice were associated with the corresponding total volumes ($r \geq 0.975$). For example, CSA in slice 10 was associated with total volume for QM and IMF ($r = 0.998$ and 0.996 , respectively). Change in CSA in a fixed slice (both slice 10) was associated with change in volume for QM ($r_s = 0.732$) and IMF ($r = 0.861$). Change in CSA in anatomically matched slices was associated with change in QM volume ($r_s = 0.900$) and IMF volume ($r = 0.879$).

Conclusions: CSAs of QM and IMF in single MRI slices are highly representative of total volumes and can be used for cross-sectional analyses. When assessing longitudinal changes in QM and IMF, image registration to match slices anatomically appears to improve the association between QM CSA and volume. Further studies are required to determine if CSA is adequate to assess the relationships between changes in QM and IMF and physical performance or OA progression.

Disclosures: *Norma MacIntyre, None.*

SU0023

Whole Body Vibration Exercise Improves Body Balance and Walking Velocity in Postmenopausal Osteoporotic Women Treated with Alendronate: Galileo and Alendronate Intervention Trail (GAIT). Jun Iwamoto*, Tsuyoshi Takeda, Hideo Matsumoto. Keio University School of Medicine, Japan

Objectives: Recently, whole-body vibration (WBV) exercise has been developed as a new modality in the field of physiotherapy and has been used to improve physical function in the elderly. However, the effect of WBV exercise on physical function in postmenopausal osteoporotic women has rarely been investigated using randomized controlled trials. A randomized controlled trial was conducted to determine the effect of 6 months of WBV exercise on physical function in postmenopausal osteoporotic women treated with alendronate.

Subjects and Methods: Fifty-two ambulatory postmenopausal women with osteoporosis (mean age: 74.2 years, range: 51–91 years) were randomly divided into two groups: an exercise group and a control group. A four-minute WBV exercise was performed two days per week only in the exercise group. No exercise was performed in the control group. All the women were treated with alendronate.

Results: There were no significant differences in baseline characteristics including age, height, body weight, body mass index, number of fallers in the past 3 months, number of subjects with history of clinical fracture, bone turnover markers including serum alkaline phosphatase (ALP) and urinary cross-linked N-terminal telopeptides of type I collagen (NTX), and physical function parameters in terms of the indices for flexibility, body balance, muscle power, and walking velocity. After 6 months of the WBV exercise, the indices for flexibility, body balance, and walking velocity were significantly improved in the exercise group compared with the control group. The exercise was safe and well tolerated. The reductions in serum ALP and urinary NTX during the 6-month period were comparable between the two groups.

Conclusions: The present study showed the benefit and safety of WBV exercise for improving physical function in postmenopausal osteoporotic women treated with alendronate.

Disclosures: Jun Iwamoto, None.

SU0024

Cortical and Trabecular Microarchitecture and Finite Element Analysis Strength Estimates at the Ultradistal Radius Reflect Skeletal Fragility in Adolescent Girls with Anorexia Nervosa. Alexander Faje*, Lamya Karim², Alex Taylor¹, Karen Miller¹, Nara Mendes¹, Erinne Meenaghan¹, Mary Bouxsein², Madhusmita Misra¹, Anne Klibanski³. ¹Massachusetts General Hospital, USA, ²Beth Israel Deaconess Medical Center, USA, ³Massachusetts General Hospital/Harvard Medical School, USA

Introduction: Adolescents with anorexia nervosa (AN) have low bone mineral density (BMD), reduced bone turnover markers, and impaired trabecular microarchitecture independent of their abnormal BMD. Although bone strength, assessed by finite element analysis (FEA), is reduced in adult women with AN, detailed study of cortical microarchitecture and strength assessment by FEA has not been performed in adolescents with AN. Because microarchitectural abnormalities and FEA may predict fracture risk independent of BMD, these data are important to obtain in these patients.

Objective: To compare cortical and trabecular bone microarchitecture, and bone strength by FEA in adolescent girls with AN versus normal-weight controls.

Design and Methods: 44 girls (21 girls with AN and 23 normal-weight controls) 14-22 years of age were studied. Body composition and areal BMD (aBMD) were assessed by dual-energy x-ray absorptiometry. High-resolution peripheral quantitative computed tomography (HR-pQCT) was performed at the ultradistal radius of the nondominant arm to evaluate microarchitectural parameters. Extended cortical analysis was performed from HR-pQCT data, and FE models were created to estimate bone failure load and stiffness.

Results: Girls with AN and normal-weight controls did not differ for chronological age, bone age, height, sexual maturity, per design, or exercise activity. Body mass index, lean mass, percent body fat, lumbar aBMD, and total hip aBMD were significantly lower in girls with AN (p values <0.0001). Girls with AN had significantly lower total (p<0.0001) and trabecular volumetric bone density (p=0.02). Although total cross sectional area did not differ, trabecular area was higher in girls with AN (p=0.04) and cortical area and thickness lower (p=0.002 and 0.02, respectively), suggestive of increased endosteal resorption. Cortical porosity (p=0.03) and trabecular separation (p=0.04) were higher in AN. Differences in cortical area, trabecular area, total volumetric density, and cortical porosity remained significant after controlling for aBMD parameters. FEA-estimated failure load (p=0.004) and stiffness (p=0.004) were lower in girls with AN.

Conclusions: Cortical and trabecular microarchitecture are altered in adolescent girls with AN. Failure load and stiffness are also decreased, indicative of reduced bone strength.

Disclosures: Alexander Faje, None.

SU0025

Longitudinal Assessment of Bone Density and Structure in Childhood Survivors of Acute Lymphoblastic Leukemia (ALL) without Cranial Irradiation. Sogol Mostoufi-Moab*, Jill Brodsky², Babette Zemel³, Jill Ginsberg¹, Justine Shults⁴, Elizabeth Isaacoff¹, Mary Leonard³. ¹The Children’s Hospital of Philadelphia, USA, ²The Mid-Hudson Medical Group, USA, ³Children’s Hospital of Philadelphia, USA, ⁴The University of Pennsylvania, USA

Background: Children with ALL have many risk factors for impaired bone accrual. The objective of this longitudinal peripheral quantitative CT (pQCT) study was to assess changes in musculoskeletal outcomes in children and adolescents after completion of ALL treatment. Methods: Tibia pQCT was performed in 50 ALL subjects (age 5-23 yr) within 2 years of completion of therapy and reassessed in 47 subjects one year later. pQCT outcomes were converted to sex-, race-, and age-specific Z-scores for trabecular BMD (TrabBMD), cortical BMD (CortBMD), cortical dimensions and muscle area based on >650 reference participants. Cortical dimension and muscle area Z-scores were further adjusted for tibia length. Multivariable linear regression models examined determinants of changes in pQCT Z-scores. Results: ALL participants were enrolled a median of 0.8 yrs after therapy and demonstrated significantly lower mean TrabBMD and CortBMD Z-scores at enrollment, compared with reference participants (Table). Overall, CortBMD, cortical area and periosteal circumference Z-scores increased over one year. However, changes varied according to the interval since completing ALL therapy at enrollment. Among those enrolled within 6 months after therapy, cortical area and periosteal circumference Z-scores increased and CortBMD Z-scores decreased (all p<0.01). Among those enrolled after 6 months, CortBMD-Z increased (p<0.01) and cortical dimension Z-scores did not change. Overall, greater increases in periosteal circumference and cortical area Z-scores were associated with greater decreases in CortBMD Z-scores (all p<0.01). The greater cortical area and periosteal circumference Z-scores in ALL participants at 12 months, compared with reference participants, were not significant after adjustment for muscle area Z-scores. Cumulative glucocorticoid exposure during ALL therapy, leukemia risk status, and antimetabolite chemotherapy were not associated with baseline pQCT results. Conclusions: TrabBMD was low in ALL after completion of therapy and improved significantly. Early increases in cortical dimensions were associated with declines in cortical BMD; however, participants further from ALL therapy demonstrated stable cortical dimensions and increases in CortBMD. This may reflect the longer time necessary to fully mineralize newly formed bone. Failure to identify correlates of changes in TrabBMD may relate to limitations of pQCT measures of trabecular compartment BMD.

| Z-Scores | Enrollment | 12 months | Change 0-12 month | 0-12 p value |
|-----------------------------|---------------|---------------|-------------------|--------------|
| TrabBMD | -1.03 ± 1.34* | -0.58 ± 1.41* | 0.41 ± 0.72 | <0.001 |
| CortBMD | -0.84 ± 1.05* | -0.51 ± 0.91* | 0.26 ± 0.90 | 0.06 |
| Cortical Dimensions | | | | |
| Cortical Area | 0.16 ± 1.18 | 0.63 ± 1.22* | 0.48 ± 0.60 | <0.001 |
| Periosteal Circumference | 0.11 ± 0.92 | 0.45 ± 1.02* | 0.34 ± 0.36 | <0.001 |
| Endosteal Circumference | -0.07 ± 0.95 | -0.11 ± 1.00 | -0.06 ± 0.42 | 0.35 |
| Muscle Cross Sectional Area | 0.24 ± 0.93 | 0.54 ± 0.92* | 0.27 ± 0.46 | <0.001 |
| Height | 0.43 ± 0.93 | 0.42 ± 0.87 | 0.05 ± 0.33 | 0.34 |
| BMI | 0.97 ± 0.83* | 0.89 ± 0.83* | -0.04 ± 0.34 | 0.44 |

*p < 0.05 compared with reference participants

Table. Z-Scores at Enrollment and 12 Months

Disclosures: Sogol Mostoufi-Moab, None.

SU0026

Withdrawn

SU0027

Changes in Bone Mineral Density and Bone Strength from 16 to 34 Years of Age, As Assessed by High Resolution Peripheral Quantitative Computed Tomography. Lauren Burt*, Heather Macdonald², David Hanley¹, Steven Boyd¹. ¹University of Calgary, Canada, ²University of British Columbia, Canada

Peak bone mass (PBM) and bone strength are important determinants for the development of osteoporosis and fracture risk later in life. Results from dual-energy X-ray absorptiometry (DXA) studies suggest that age at PBM varies by skeletal site and occurs by the end of the second decade. Whether the same is true for bone mineral

density (BMD) or bone strength measured with high-resolution peripheral quantitative computed tomography (HR-pQCT) is unknown. We aimed to verify if PBM assessed with HR-pQCT was attained by age 19 and if BMD and bone strength remained stable through early adulthood.

We recruited 130 participants (83 women; 16-24 yrs) from Calgary, Canada, and combined this group with our first Calgary cohort (n=133, 85 women, 16-34 yrs) who were part of the Canadian Multicentre Osteoporosis Study (CaMos). Areal bone mineral density (aBMD) at the lumbar spine (LS), femoral neck (FN) and proximal femur (PF) were obtained from DXA (Hologic, USA) scans of L1-L4 and the left hip. The non-dominant radius and left tibia were scanned using HR-pQCT (Scanco Medical, Switzerland). Total volumetric BMD (Tt.BMD), cortical BMD (Ct.BMD) and trabecular BMD (Tr.BMD) were assessed using standard and automated segmentation methods. Finite element analysis estimated apparent bone strength. Sex-specific age group means were compared using a one-way ANOVA.

DXA-derived aBMD was lower in 20-24 yr old women at the FN (-8%) and PF (-7%) compared with 16-19 yr old women ($p < 0.05$). At the distal radius and tibia BMD was not significantly different between the 16-19 yr olds and 20-24 yr olds. Although not significant, Ct.BMD tended to decrease in women (range 2-3%, $p > 0.05$) and increase in men (range 1-5%, $p > 0.05$) from 16-19 yrs to 20-24 yrs. At the radius, BMD remained stable for men and women between 16-34 yrs. At the tibia, Ct.BMD was lower (-9%) in women and Tr.BMD was lower (-14%) in men and women 25-29 yrs compared with 16-19 yr olds ($p < 0.01$). Tibia bone strength was lower for 25-29 yr old men (-22%) and women (-15%) compared with 16-19 yr olds ($p < 0.05$).

Although longitudinal data are required to determine true age-related changes, our cross-sectional findings suggest that in women, PBM as measured with HR-pQCT may be achieved by age 16 or earlier. As BMD of the distal radius and tibia remained constant between 16-24 yrs, a young adult cohort may be used to establish appropriate T-score type comparisons for use with HR-pQCT.

Disclosures: Lauren Burt, None.

SU0028

Characterisation of Musculoskeletal Phenotype in Pre-pubertal Gambian Children. Kate Ward^{*1}, Landing Jarjou², Yankuba Sawo², Gail Goldberg³, Ann Prentice¹. ¹MRC Human Nutrition Research, United Kingdom, ²MRC Keneba, Gambia, ³MRC Human Nutrition Research; MRC Keneba The Gambia, United Kingdom

Gender differences in muscle and bone during development are well described in countries with moderate to high calcium intakes; there are few data from countries where children have delayed puberty and low habitual calcium intakes. This study aimed to determine whether gender differences exist in muscle and bone in pre-pubertal Gambian children and whether muscle area predicts bone phenotype.

Children aged 7.8-12.0y were recruited. Measurements were made using peripheral QCT. Volumetric total (To) and trabecular (Tb) BMD and total area were measured at 8% radius (DR) and tibia (DT). Total and medullary area, cortical content (BMC), stress-strain index (SSI) and muscle area were measured at 66% radius (R66) and 50% tibia (T50). Gender effects were tested using univariate and multiple regression adjusting for age, object length and muscle area. Data are presented as % differences [95% CI].

447 children (216M) were recruited. Mean \pm SD age M=9.3 \pm 0.1y, F=9.2 \pm 0.1y; height M=127 \pm 6cm, F=128 \pm 7cm; weight M=23.8 \pm 0.2kg, F=24.0 \pm 0.3kg. Unadjusted analyses showed M had larger bones and higher ToBMD and TbBMD at DR and DT. At R66 and T50 M had larger bones, greater muscle area and SSI, and higher BMC.

After adjustment gender differences at DR and DT remained (% value, M compared to F): ToBMD (DR 2.8/[-0.2, 5.7], DT 2.8/[-0.7, 5.0]), TbBMD (DR 8.4/[3.4, 13.4], DT 4.4/[1.1, 7.6]), total area (DR 9.7/[6.6, 12.9], DT 4.9/[2.6, 7.3]) were higher in M. BMC was higher at T50 in M (2.3/[-0.2, 4.8]). However after adjustment there were no significant gender differences in medullary (R66 2.5/[-3.2, 8.1], T50 -0.8/[-4.9, 3.4]), total area (R66 0.9/[-1.8, 3.7], T50 1.0/[-1.2, 3.1]), SSI (R66 1.9/[-1.4, 5.3] or T50 1.7/[-1.4, 6.6]). In the multiple regression models, muscle area was a significant predictor for bone geometry, the co-efficients (%) for muscle area: total area DR 9.7/[6.6, 12.9], DT 4.9/[2.6, 7.3], R66 54.0/[42.6, 65.3], T50 36.3/[29.8, 42.9]; medullary area R66 69.6/[46.7, 92.6], T50 37.8/[25.0, 50.5]; SSI R66 76.2/[62.6, 89.9] and T50 52.9/[44.1, 61.7].

Gender differences in BMD and size exist at DR and DT. After adjustment for muscle area, a proxy for muscle force, gender differences in bone shape and strength disappeared indicating the importance of muscle in the developing skeleton. Determining the contribution of muscle function and other factors to adolescent bone growth, and the timing and magnitude of peak bone strength is important in this population.

Disclosures: Kate Ward, None.

SU0029

Early-Life Exposure of Male Mice to Estrogen Alters the Trajectory of Somatic Growth and Skeletal Development. Kara Connelly^{*1}, Emily Larson², Robert Klein³. ¹Oregon Health & Science University, USA, ²Ohsu (c113), USA, ³Portland VA Medical Center, USA

Growth and maturation is governed by a complex interplay between genetic and environmental factors. Sexual dimorphism in somatic development is largely regulated by endocrine factors (e.g., growth hormone and gonadal steroids). While sex steroid hormones exert their strongest effects during puberty, there is now growing evidence that the sex steroid milieu during the neonatal period may also play a critical role in establishing the adult phenotype. To examine this question, newborn male C57BL/6 inbred mice (n = 10-14 per group) received a single subcutaneous injection of either estradiol-3-benzoate (E2; 100 mcg) dissolved in sesame oil or sesame oil alone. Body weight, body composition and bone mineral density (BMD, Piximus DXA) were measured at monthly intervals up to 4 months of age (when acquisition of adult bone mass is complete). Serum osteocalcin (a marker of bone remodeling) was determined in 4-month-old mice. At 1 and 4 months of age, circulating estradiol and testosterone levels were not affected by the treatments. As shown below, neonatal male mice exposed to E2 demonstrated significant changes in body composition and BMD throughout the study period. Despite an overall decrease in body weight, neonatal E2 exposure resulted in steadily increasing % fat mass (6-14%) over time. Consistent with the reduced body size, lean mass was reduced ~20% at all time points. Similarly, whole body BMD values of E2-treated mice were decreased (4-7%) at all time points. The single E2 treatment also resulted in increased serum osteocalcin levels (37%) a full 4 months after the original exposure. Estrogen is a determining factor in the female archetype of body growth and fat distribution as well as of a skeletal configuration that predisposes to a greater subsequent risk of osteoporosis. This study suggests that a single, brief exposure of male mice to E2 during the neonatal period can alter developmental programming to produce a female pattern of somatic growth and skeletal development. Our findings implicate neonatal estrogen exposure as a possible contributor to the development of chronic disease later in the lives of men (e.g., obesity, metabolic syndrome, osteoporosis, etc.).

| | | Body Weight, g | Lean Mass, g | % Body Fat | BMD, g/cm ³ | Osteocalcin, ng/ml |
|----------|----------|----------------|----------------|----------------|------------------------|--------------------|
| 1 month | Control | 15.7 \pm 0.4 | n.d. | n.d. | n.d. | n.d. |
| | E2 | 12 \pm 0.3 | n.d. | n.d. | n.d. | n.d. |
| | Δ | 23% *** | n.d. | n.d. | n.d. | n.d. |
| 2 months | Control | 22.4 \pm 0.4 | 18.9 \pm 0.4 | 15.7 \pm 0.2 | 46.4 \pm 0.5 | n.d. |
| | E2 | 18.7 \pm 0.6 | 15.6 \pm 0.5 | 16.6 \pm 0.3 | 44.7 \pm 0.4 | n.d. |
| | Δ | 17% *** | 18% *** | 6% * | 4% * | n.d. |
| 3 months | Control | 25.9 \pm 0.5 | 21.5 \pm 0.5 | 17.2 \pm 0.5 | 49.9 \pm 0.3 | n.d. |
| | E2 | 21.2 \pm 0.4 | 17 \pm 0.4 | 19.5 \pm 1.1 | 45.1 \pm 1.2 | n.d. |
| | Δ | 18% *** | 21% *** | 14% n.s. | 10% *** | n.d. |
| 4 months | Control | 28.3 \pm 0.7 | 23.2 \pm 0.5 | 17.9 \pm 0.5 | 52.1 \pm 0.3 | 61.5 \pm 5.6 |
| | E2 | 22.6 \pm 0.6 | 17.9 \pm 0.5 | 20.8 \pm 0.7 | 48.2 \pm 0.7 | 84.2 \pm 6 |
| | Δ | 20% *** | 23% *** | 17% * | 7% *** | 37% * |

(p values by t-test; n.s.=non-significant; * = p<0.05; ** = p<0.01; *** = p<0.001)

Disclosures: Kara Connelly, None.

SU0030

Exploring the Relationship Between Lower Extremity Muscle Work During Gait and Bone Structure in Individuals With Unilateral Cerebral Palsy. Harshvardhan Singh^{*1}, Jacques Riad², Brianne Mulrooney³, Todd Rover¹, Freeman Miller⁴, Christopher Modlesky³. ¹Department of Kinesiology & Applied Physiology, University of Delaware, USA, ²Department of Orthopedics Astrid Lindgrens Children's Hospital Stockholm, Sweden, ³University of Delaware, USA, ⁴Department of Orthopedics, AI duPont Hospital for Children, USA

Cerebral palsy (CP) is associated with underdeveloped bone structure which results in low bone strength. This may be attributed to abnormal gait; however, no studies have examined the relationship between gait and bone structure in individuals with CP. The objective of this study was to examine the relationship between interlimb differences in muscle work during gait and interlimb differences in structure and strength of the midfemur and midtibia in individuals with spastic unilateral CP. Ambulatory individuals with unilateral CP (n = 35; 13 to 24 years) and a Gross Motor Function Classification of 1 or 2 were studied. All participants were classified as type 0 or 1 using the Winters classification based on sagittal plane gait analysis. Gait analysis was performed with an 8 camera system (Vicon Motion Systems, Ltd, Oxford, UK) and with 2 force plates (Kistler, Amherst, NY) while the participants walked at a self-selected speed. Positive work was calculated as the cumulative sum of joint power generation in the sagittal plane. Magnetic resonance images of the femur and tibia (0.5 cm thick and 1.0 cm apart) were collected from both lower limbs. Images at the level of the middle-third of the femur and the middle-third of the tibia were identified and cortical volume, medullary volume, total volume and estimates of bone strength [section modulus (Z) and polar moment of inertia (J)] were determined using custom software developed with Interactive Data Language (Research Systems, Inc, Boulder, CO). The interlimb difference in muscle work at the knee joint, but not at the hip or ankle joint, was related to interlimb differences in cortical volume ($r = 0.341$, $p = 0.045$), total volume ($r = 0.403$, $p = 0.016$), Z ($r = 0.358$, $p = 0.035$) and J ($r = 0.330$,

$p = 0.053$) at the midtibia. No significant relationships were found between interlimb differences in muscle work at the hip, knee or ankle and interlimb differences in structure or strength at the midfemur ($r = -0.214$ to 0.196 , $p > 0.2$). Compared to the unaffected limb, lower work generated at the knee of the affected limb during gait may be a significant contributor to the poor structural development of the midtibia in individuals with unilateral CP. Future studies should investigate whether decreasing work asymmetry during gait leads to improved bone structure and increased bone strength in the affected limb of individuals with unilateral CP.

Disclosures: Harshvardhan Singh, None.

SU0031

Factors Affecting Timing and Tempo of BMAT Accrual May Provide a Mechanistic Link among Metabolic and Bone Health. Krista Casazza*¹, Lynae Hanks², Anna Newton¹, Stephenie Wallace¹. ¹UAB, USA, ²University of Alabama at Birmingham, USA

Investigations centered on the bone marrow compartment during growth and development represents a viable avenue in which to explore allocation of energy resources for tissue partitioning, as it is here that undifferentiated cells capable of multiple lineages meet their fate. Specifically, assessment of changes in the bone marrow cavity prior to pubertal maturation, in which peak bone mass is largely achieved, will enhance our understanding of the reciprocity between bone and fat. An emerging area of investigation is the influence of insulin/glucose homeostasis to bone (re)modeling, with considerable interest in its contribution to bone marrow adipose tissue (BMAT) accrual. Our objective was to evaluate the relationship between BMAT and total body adiposity and identify factors which may influence the relationship. Seventy two children ages 4-10y underwent MRI for assessment of femoral BMAT, DXA for assessment of body composition and venipuncture for metabolic testing. Femoral BMAT showed increases with age, and to a greater extent in girls relative to boys. BMAT was positively related to overall percent fat ($p=0.02$); however when stratified by sex and race, this relationship is only apparent in EA ($p=0.05$) and girls ($p=0.03$). When analyzed according to age, the associations were observed at ages 4y ($p=0.006$) and 10y ($p=0.04$). Insulin and BMAT were positively related ($p=0.04$); however, the relationship was only apparent in those with high adiposity ($p=0.008$). Further, controlling for insulin, the relationship between BMAT and %fat was attenuated ($p=0.07$). Although triglycerides (TG) were positively associated with BMAT ($p=0.007$), TG did not contribute to the association between BMAT and percent fat. Whereas normative BMAT accrual follows a predictable and progressive manner, metabolic perturbations may impart physiologic responses altering this process, which may be more impactful during early stages of maturation. Factors affecting timing and tempo of conversion may provide a mechanistic link among metabolic and bone health, and shed insight into the subsequent effects on energy homeostasis across the aging process, which is of particular importance in the contemporary obesogenic environment.

Disclosures: Krista Casazza, None.

SU0032

Impact of Seasonal Flux in 25-hydroxyvitamin D on Bone Turnover in Pre- and Early Pubertal Black and White Youth. Kumaravel Rajakumar*¹, Michael Holick², Charity Moore³, Elan Cohen³, Flora Olabopo⁴, Mary Ann Haralam⁴, Jaimee Bogusz⁵, Anita Nucci⁶, Susan Greenspan⁷. ¹University of Pittsburgh School of Medicine, USA, ²Boston University School of Medicine, USA, ³Center for Research on Health Care, University of Pittsburgh, USA, ⁴Department of Pediatrics, University of Pittsburgh, USA, ⁵Department of Medicine, Boston University School of Medicine, USA, ⁶Division of Nutrition, Georgia State University, USA, ⁷University of Pittsburgh, USA

Background: Seasonal fluxes in 25-hydroxyvitamin D [25(OH)D] in children can impact bone turnover, and in turn potentially affect bone accrual and peak bone mass.

Objective: To examine the effect of seasonal flux in 25(OH)D on markers of bone turnover and characterize the influence of dietary vitamin D and calcium, skin color, sunlight exposure and body-mass-index (BMI) on this relationship in 6- to 12-year-old pre- and early pubertal black and white children.

Design: Serum 25(OH)D, parathyroid hormone (PTH), osteocalcin (OC), collagen type 1 cross-linked C-telopeptide (CTX), and dietary intake of vitamin D and calcium were assessed during summer (June through September) and/or winter (December through March).

Results: A total of 138 children (mean \pm SD age: 9.1 ± 1.7 year, black: 94, male: 81) were studied. During winter, concentrations of 25(OH)D were lower and CTX were higher in all participants (Table). Furthermore, CTX levels were higher during winter in blacks. PTH was a significant predictor of serum CTX and OC after adjusting for race, season, Tanner stage, dietary calcium, skin color and BMI.

Conclusion: 25(OH)D declined significantly in both black and whites during winter despite a mean dietary intake of vitamin D >400 IU/day. CTX significantly increased during winter in blacks than whites suggesting increased rates of bone resorption in blacks during winter. Benefits of enhancement of wintertime vitamin D status on bone markers and bone mineral accrual need exploration.

| | All Participants (N=138) | | Black (N=94) | | White (N=44) | |
|-------------------------|--------------------------|-----------------|-------------------|-----------------|-------------------|-----------------|
| | Summer | Winter | Summer | Winter | Summer | Winter |
| 25(OH)D (ng/mL) | 41.2 \pm 13.0*** | 34.5 \pm 11.1 | 39.1 \pm 11.5** | 33.8 \pm 11.3 | 45.5 \pm 14.9** | 36.2 \pm 10.7 |
| PTH (pg/mL) | 37.0 \pm 25.3 | 38.6 \pm 23.7 | 38.7 \pm 22.5 | 41.9 \pm 23.5 | 33.0 \pm 30.7 | 31.8 \pm 23.1 |
| OC (ng/mL) | 17.1 \pm 10.4 | 18.0 \pm 11.2 | 17.2 \pm 11.3 | 19.0 \pm 11.3 | 16.9 \pm 8.3 | 15.8 \pm 10.9 |
| CTX (ng/mL) | 0.8 \pm 0.3*** | 0.9 \pm 0.5 | 0.7 \pm 0.3*** | 1.0 \pm 0.5 | 0.8 \pm 0.4 | 0.8 \pm 0.4 |
| Diet vitamin D (IU/day) | 430 \pm 216 | 484 \pm 307 | 421 \pm 208* | 507 \pm 331 | 449 \pm 232 | 437 \pm 244 |
| Diet calcium (mg/day) | 1114 \pm 592* | 1239 \pm 789 | 1150 \pm 577* | 1295 \pm 894 | 1037 \pm 622 | 1120 \pm 488 |

Table

Disclosures: Kumaravel Rajakumar, None.

SU0033

Maternal Diet Does Not Alter Skeletal Response to Postnatal Caloric Restriction in Female Mice. Maureen Devlin*, Leeann Louis, Christine Conlon, Miranda Van Vliet, Mary Bouxsein, Beth Israel Deaconess Medical Center, USA

The rise in osteoporosis has focused attention on environmental factors that may contribute to poor bone health, such as potential effects of maternal and postnatal diets on bone microarchitecture, geometry, and strength. Previously we showed that postnatal high fat (HF) and calorie restricted (CR) diets are deleterious to bone acquisition in male mice, and that maternal HF diet protects offspring from the harmful skeletal effects of postnatal HF diet. Here we test 1) effects of postnatal CR in female mice, and 2) whether such effects differ in mice whose mothers were exposed to CR or HF diet during gestation/lactation. **Methods:** To test the effects of postnatal CR, at 3 wks of age we weaned female C57Bl/6j mice from N diet mothers onto 30% caloric restriction (N-CR, 10% Kcal/fat) or normal diet (N-N, 10% Kcal/fat) (N=6-13/gr). To test the effect of maternal diet on response to postnatal CR, at 3 wks of age we weaned female mice from HF (45% kcal/fat) or CR mothers onto CR (HF-CR and CR-CR, N=5-10/gr). Outcomes at 6, 12 and 20 wks of age included body mass, % body fat, whole body bone mineral density (BMD, g/cm^2), and cortical (Ct) and trabecular (Tb) bone architecture at the midshaft and distal femur via μ CT. **Results:** N-CR, CR-CR, and HF-CR mice weighed less vs. N-N, with lower BMD at 6, 12, and 20 wks of age ($p < 0.05$ for all). Postnatal CR groups had lower % body fat at 6 wks vs. N-N ($p < 0.05$ for all), but not thereafter. In the distal femur, N-CR had lower Tb thickness but higher Tb number and connectivity density ($p < 0.05$ for all), such that Tb.BV/TV did not differ from N-N at 12 or 20 wks of age. HF-CR and CR-CR showed the same pattern. In the midshaft femur, all postnatal CR groups had lower bone area fraction (BA/TA, %) at 12 and 20 wks of age ($p < 0.05$ for all). Ct bone area, total cross-sectional area, and Ct thickness were also lower in N-CR, CR-CR, and HF-CR, but these differences disappeared after adjusting for their lower body mass. **Conclusion:** Compared to prior findings in male mice, CR diet has less deleterious effects on trabecular bone in females. While maternal HF was previously shown to protect offspring from deleterious effects of postnatal HF, here we found no effect of maternal diet on skeletal response of female offspring to postnatal CR. These results suggest that there are sex differences in the effects of diet on skeletal acquisition, and that in females, the response to postnatal CR is not influenced by maternal diet.

Disclosures: Maureen Devlin, None.

SU0034

Reduced Carbohydrate, Weight Loss Diet is Associated with Greater Bone Mineral Content in Early Pubertal Obese African-American Girls. Lynae Hanks*¹, Anna Newton¹, Krista Casazza². ¹University of Alabama at Birmingham, USA, ²UAB, USA

Despite consistent reports of greater bone mineral content (BMC) among African Americans (AA), fracture rate has increased exponentially among this group over recent years. A paralleled rise in metabolic disease has led to speculation of intersecting manifestations of impaired bone and metabolic health. Beyond caloric intake, macronutrient profile contributes to bone and fat mass accrual, particularly during critical periods of growth (i.e. puberty). The metabolic consequences associated with a high carbohydrate (CHO) meal challenge homeostatic mechanisms, setting a more permissive stage for adipogenesis at the expense of osteogenesis. As AA females are disproportionately affected by obesity with inherently exaggerated metabolic response to dietary CHO, it is plausible that among this group diet is particularly impactful. The objective of this study was to evaluate the association of a standard versus reduced CHO diet on BMC, with consideration of stage of development in obese AA females. A total of 26 AA girls ages eight to 15y ($\geq 96^{\text{th}}$ BMI percentile) were assigned to either a reduced- (SPEC: 42% energy from CHO, n=11) or a standard- (STAN: 55% energy from CHO, n=15) diet. All of the meals were provided and clinically tailored to meet the estimated energy requirements in a weight stable phase (five weeks), followed by a weight loss phase (1000 kcal deficit, 11 weeks). DXA was performed for body composition assessment. The contribution of diet to BMC after each diet phase was evaluated using multiple linear regression analyses in the overall sample and by pubertal status (early pubertal: Tanner 1-2; late pubertal: Tanner 3-5). BMC was greater among those on the SPEC diet only after the weight loss phase. In early pubertal subjects after the weight loss phase, those on the SPEC diet had higher BMC. Reduction in total fat was positively associated with BMC in early pubertal subjects after the weight loss phase. A reduced CHO diet to promote weight loss was associated with improved bone measures in obese AA females, which was particularly evident in those at earlier stages in pubertal

advancement. The significance of less fat gain to greater BMC in early pubertal subjects on a reduced CHO diet suggests changes in bone to some degree contrast with that of fat. These findings warrant future studies regarding assessment of changes within bone in response to dietary macronutrient profile and the reciprocity with adiposity during this critical period.

Disclosures: Lynae Hanks, None.

SU0035

Skeletal Effects of Obesity Are Prevented by a Diet Containing Soy Protein Isolate via Preservation of Insulin Signaling in Bone. Jin-Ran Chen^{*1}, Jian Zhang¹, Oxana P. Lazarenko², Jay J. Cao³, Thomas M. Badger², Martin J. J. Ronis⁴. ¹Arkansas Children's Nutrition Center, & Department of Pediatrics, University of Arkansas for Medical Sciences, USA, ²Arkansas Children's Nutrition Center, & Department of Physiology & Biophysics, University of Arkansas for Medical Sciences, USA, ³USDA, Agricultural Research Service, Grand Forks Human Nutrition Research Center, USA, ⁴Arkansas Children's Nutrition Center, & Department of Pediatrics, Pharmacology & Toxicology, University of Arkansas for Medical Sciences, USA

In both rodents and humans, excessive consumption of diets high in saturated fat and cholesterol during postnatal life is known to result in global energy imbalance, obesity and insulin resistance. However, the effects of such a "Western diet" (WD) on bone development and remodeling is poorly understood. In the current study, we show that weanling rats fed a WD containing 45% fat and 0.5% cholesterol for 6 weeks starting from post natal day 21 display obesity, reduced bone mineral density (BMD), significant increase in bone marrow adiposity, insulin resistance and impaired glucose tolerance. Substitution of dietary casein by soy protein isolate (SPI) is able to block these effects of WD in male rats. Protection of bone by dietary SPI was associated with reduced osteoblast senescence, increased undercarboxylated osteocalcin secretion and preservation of IRS1/Akt insulin signaling in osteoblasts. While WD significantly increased non-esterified free fatty acid (NEFA) levels in the rat serum, SPI was able to prevent this increase. A mixture of NEFA (individual NEFA ratio and concentration similar to their appearance in WD rat serum) accelerates entrance of osteoblasts or mesenchymal stromal ST2 cells into the senescence pathway and decreased insulin signaling. An artificial isoflavone mixture (concentrations identical to that found in SPI diet serum) increased osteoblast proliferation and blocked activation of p21/p53 and senescence associated beta-galactosidase senescence pathway and insulin resistance that occurred in osteoblasts in response to NEFA. Finally, we show that senescent osteoblastic cells *in vitro* exhibit phenotypes with reduced ability to secrete osteocalcin and decreased responsiveness to insulin/IGF1 stimulation of cell proliferation and differentiation due to cellular insulin resistance. These results suggest that the protective effects of the SPI diet on the skeleton after WD feeding are due to suppression of serum NEFA and isoflavone-mediated amelioration of osteoblastic cell senescence, increased secretion of osteocalcin and preservation of insulin signaling in bone. *Supported in part by ARS CRIS #6251-51000-005-03S (JRC).*

Disclosures: Jin-Ran Chen, None.

SU0036

A Case of Noonan Syndrome With a *SHOC2* Mutation Associated With Cortical And Trabecular Osteopenia And Early Onset Fragility Fractures. Bindu Avatapalle¹, Raja Padidela^{*1}, Jill Clayton-Smith², Tony Freemont³, Emma Burkitt Wright⁴, M Zulf Mughal¹. ¹Manchester Children's Hospital, United Kingdom, ²Genetic Medicine, Manchester Academic Health Sciences Centre, United Kingdom, ³Manchester Academic Health Sciences Centre, University of Manchester, United Kingdom, ⁴Manchester Academic Health Science, University of Manchester, United Kingdom

Introduction: Noonan syndrome (NS) (OMIM 163950) is an autosomal dominant clinically heterogeneous disorder characterised by multisystem involvement. Mutations in genes in the RAS/MAP signaling pathways are known to be responsible for approximately 70% of cases of NS. We report an infant with NS with early onset fragility fractures.

Case report: A 15 month old male infant with a history of atopic eczema, sparse hair on the scalp, slow motor development, feeding difficulties, faltering growth, congenital cardiac problems (atrial septal defect, pulmonary valve stenosis & branch pulmonary artery stenosis) and macrocephaly, presented with a painful and swollen left leg. Radiographs revealed an undisplaced spiral fracture of the mid shaft of the left femur. The skeletal survey showed generalised osteopenia and anterior wedging of T12 vertebral body. MRI of the spine showed compression fractures of multiple mid and lower thoracic vertebral bodies. His serum concentrations of calcium, phosphate, alkaline phosphatase, parathyroid hormone and 25-hydroxyvitamin D were within normal limits. With history of significant unexplained fractures child safeguarding procedures were initiated. The infant was thought to have clinical features of NS; genetic testing revealed a heterozygous mutation in *SHOC2* c.4A>G (p.ser2Gly), confirming the diagnosis of Noonan syndrome with loose anagen hair. An unlabelled trans-iliac bone biopsy revealed marked cortical and trabecular osteopenia with relatively normal

osteoblastic and osteoclastic activity. The patient has been commenced on cyclical intravenous Pamidronate therapy in order to reduce his risk of fracture.

Conclusions: Generalised osteopenia is a recognised feature in RASopathies, such as Neurofibromatosis type 1 and Costello syndrome. Stevenson and colleagues (Clin Genet. 2011;80(6):566-73) have shown that NF subjects have increased bone resorption as measured by urinary excretion of pyridinium crosslinks. However, to the best of our knowledge, osteopenia with early onset fragility fractures of axial and appendicular skeleton have not been previously described in NS.

Disclosures: Raja Padidela, None.

SU0037

Acute BMP2 Response Following Induction of Ischemic Osteonecrosis in Immature Femoral Head. Nobuhiro Kamiya^{*1}, Sasha Shafer¹, Ila Oxendine¹, Harry Kim². ¹Texas Scottish Rite Hospital for Children, USA, ²Scottish Rite Hospital for Children, USA

Juvenile ischemic osteonecrosis of the femoral head (IOFH) is one of the most serious conditions causing femoral head deformity. A lack of new bone formation following IOFH has shown to be an important contributor to the development of the deformity. Since BMP2 is a well known inducer of new bone formation, we investigated BMP2 response following IOFH in vivo (piglet, mouse models) and in vitro under hypoxic conditions (explants, primary cells).

We previously developed a piglet IOFH model by surgically disrupting the blood flow to the femoral head. In this model, RNA could be extracted from femoral head cartilage but not bone due to extensive osteonecrosis. We isolated RNA from femoral head cartilage and found a dramatic increase in BMP2 expression levels at 24h following ischemic surgery assessed by microarray and qRT-PCR, whereas BMP2 levels were normal at 2 and 4 weeks. We also established a mouse model of ischemic osteonecrosis by microsurgery and found BMP2 upregulation in articular cartilage within 48h of surgery using BMP2 reporter mice assessed by x-gal staining. In order to investigate the acute BMP2 upregulation, we cultured cartilage explants and primary chondrocytes under hypoxia (1% oxygen) and normoxia (21% oxygen) for 24h. Similar to the in vivo results, BMP2 expression levels were significantly increased under hypoxia in the cartilage explants and primary chondrocytes. Protein levels of BMP2 and its downstream signaling pSmad 1/5/8 were both increased in cartilage explants when cultured under hypoxia for 24h. Since hypoxia is known to induce the production of free oxygen radicals which is converted to H₂O₂ by superoxide dismutase 2 (SOD2), we investigated the relationship between SOD2/H₂O₂ production and BMP2 upregulation. We found a significant increase in SOD2 expression and protein levels in ischemic cartilage and hypoxic explant cartilage/primary chondrocytes. As expected, H₂O₂ production levels were significantly increased under hypoxia compared to normoxia. Interestingly, the addition of H₂O₂ to explants/chondrocytes under normoxia significantly increased BMP2 expression levels. Moreover, the addition of SOD2 protein to chondrocytes also significantly increased BMP2 expression levels. These results suggest that hypoxia induces increased H₂O₂ production via SOD2 which upregulates BMP2 expression. Further studies are required to determine why this upregulation is transient and not maintained at 2 and 4 weeks in the IOFH piglet model.

Disclosures: Nobuhiro Kamiya, None.

SU0038

Children and Adolescents with Cystic Fibrosis have Normal Volumetric BMD and Geometry at the Radius, but Low Muscle Area at the Forearm. ONDREJ SOUCEK^{*1}, Jan Lebl², Veronika Skalicka³, Dana Zemkova², Miloslav Rocek⁴, Zdenek Sumnik⁵. ¹2nd Faculty of Medicine, Charles University, Prague, Czech Republic, ²Department of Pediatrics, 2nd Faculty of Medicine, Charles University & University Hospital Motol in Prague, Czech Republic, ³Department of Pediatrics, 2nd Faculty of Medicine, Charles University & University Hospital Motol in Prague, Czech Republic, ⁴Department of Radiology, 2nd Faculty of Medicine, Charles University & University Hospital Motol in Prague, Czech Republic, ⁵University Hospital Motol, Czech Republic

Purpose

While studies in adults with cystic fibrosis (CF) showed increased fracture risk and decreased bone mineral density (BMD), the results of the pediatric studies have been contradictory. Our aims were to assess volumetric BMD, bone geometry and the muscle-bone relation at the forearm in children with CF using peripheral quantitative CT (pQCT), and to correlate these bone parameters to pulmonary function.

Method: Fifty-three patients with CF (median age 12.9 yrs, range 6.7-18.8, 29 girls) were examined by pQCT at the non-dominant forearm. Results were expressed as Z-scores using published reference data. Median forced expiratory volume in one second (FEV1, % predicted) of the spirometry examinations performed during the last year before densitometry was selected as a surrogate of pulmonary function. The differences from reference data were tested by one-sample T test, Pearson correlation coefficient was used to correlate pQCT-derived bone parameters with FEV1.

Results: Trabecular BMD was normal (mean Z-score -0.2 ± 1.3, n.s.) in children with CF. Total bone cross-sectional area, cortical bone area and cortical thickness were all normal when adjusted for height (mean Z-scores 0.0 ± 1.1, 0.0 ± 1.0 and

0.0±0.8, respectively). Cortical BMD was increased (mean Z-score 1.0±0.9, p<0.001). As a consequence of decreased muscle area (MA, mean Z-score -1.5±1.5, p<0.001) the bone mineral content to MA ratio was increased (mean Z-score 1.3±1.0, p<0.001). Whereas FEV1 was positively correlated to muscle area (R²=0.20, p<0.002) and bone geometry (i.e. cortical thickness (R²=0.24, p<0.001) and cortical bone area (R²=0.20, p<0.002)), the correlation with BMD was weak (R²=0.08, p=0.035 and R²=0.007, n.s. for trabecular and cortical BMD, respectively).

Conclusions: Children and adolescents with CF have normal volumetric bone density and geometry at the radius, but decreased muscle mass at the forearm. FEV1 seems to be a good predictor of changes in their muscle area and bone geometry at the forearm.

Disclosures: **ONDREJ SOUCEK**, None.

SU0039

Impact of the Enzymatic Crosslinking of the Collagen Matrix on the Macroscopic Mechanical Behaviour of the Cortical Bone from Children.

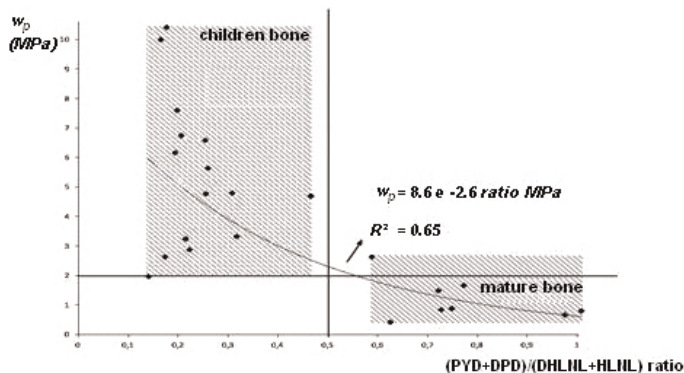
Jean-Philippe Bertheau¹, Evelyne Gineyts², Helene Follet³, Martine Pithioux⁴, Cécile Baron⁵, Philippe Lasavgues⁶, Patrick Chabrand⁵, Georges Boivin³. ¹Institut des Sciences du Mouvement ISM, CNRS UMR 6233, Université Aix Marseille, & Laboratoire de Mécanique et d'Acoustique Equipe PICNRS - UPR 7051, France, ²INSERM, UMR1033, Université de Lyon, France, ³INSERM, UMR1033 ; Université De Lyon, France, ⁴Institut des Sciences du Mouvement ISM, CNRS UMR 6233, Université Aix Marseille, France, ⁵Institut des Sciences du Mouvement ISM, CNRS UMR 6233, Université Aix Marseille, France, ⁶Laboratoire de Mécanique et d'Acoustique Equipe PICNRS - UPR 7051, Université Aix Marseille, France

Cortical bone is a material considered as quasi-fragile and showing brittle fracture in adult. However, many clinical pediatric cases show "green stick fractures" which are specific to growing bone. Elasticity of cortical bone depends on the mineral part of the matrix and the plasticity on the collagen¹ and collagen crosslink pattern of cortical organic matrix differs between adults and children. Enzymatic immature crosslinks (DHLNL+HLNL) are gradually decreased to be replaced by enzymatic mature crosslinks (PYD+DPD) in growing bone until adolescence and then remained constant throughout adult life². Our objective was to analyse the (PYD+DPD)/(DHLNL+HLNL) ratio and to correlate it with the plastic energy (*op*) of cortical bone. This study was focused on bone preferentially used for human cortical transplantation, i.e., the fibula bottom extremity. Twenty-nine bone samples were analyzed. A two-step method was developed in parallel. First, mechanical properties of children cortical bone (elasticity and plasticity) were evaluated using micro beam three points bending test until fracture, second, bone samples were powdered, demineralized and reduced to quantify the amount of collagen, to evaluate its digestibility by alpha chymotrypsin and then, to determine the (PYD+DPD)/(DHLNL+HLNL) ratio. A significant negative exponential correlation (R²= 0.65) was observed between *op* and (PYD+DPD)/(DHLNL+HLNL) ratio. A gap existed for a ratio of 0.5 (Fig.1). Above this value, corresponding to mature (adult) bone, *op* is below 2 MPa, while below this ratio and corresponding to growing (children) bone, all values were higher than 2MPa. In addition, the amount of collagen (around 22% of tissue weight) and its digestibility by alphachymotrypsin were not statistically different (T test, p >0.05) between both types of bone. In conclusion, at the subnanostructural level of organic matrix, the (PYD+DPD)/(DHLNL+HLNL) ratio was different with the age of bone and got an impact on the macroscopic mechanical behaviour of the cortical bone.

Figure1. Relationship between plastic energy and the mature/immature crosslinks ratio depending on the type of bone.

¹Bala et al *J. Mech Behav of Biomed Mater* 4 (7), 1473-1482. 2011

²Saito et al. *Osteoporos Int* 21, 195-214. 2010



Disclosures: **Jean-Philippe Bertheau**, None.

SU0040

Skeletal Findings in the First 12 Months Following Initiation of Glucocorticoid Therapy for Pediatric Nephrotic Syndrome.

Leanne M. Ward¹, Véronique Phan², Janusz Feber¹, Tom Blydt-Hansen³, Nathalie Alos², Stephanie Atkinson⁴, David A. Cabral⁵, Robert Couch⁶, Elizabeth A. Cummings⁷, Ronald Grant⁸, Paivi M. Miettinen⁹, Helen Nadel⁵, Frank Rauch¹⁰, Celia Rodd¹⁰, Robert Stein¹¹, David Stephure⁹, Shayne Taback³, Brian Lentle⁵, Mary Ann Matzinger¹, Nazih Shenouda¹, Kerry Siminoski⁶, and the Canadian STOPP Consortium¹². ¹University of Ottawa, Canada, ²Université de Montréal, Canada, ³University of Manitoba, Canada, ⁴McMaster University, Canada, ⁵University of British Columbia, Canada, ⁶University of Alberta, Canada, ⁷Dalhousie University, Canada, ⁸University of Toronto, Canada, ⁹University of Calgary, Canada, ¹⁰McGill University, Canada, ¹¹University of Western Ontario, Canada, ¹²Canadian Pediatric Bone Health Working Group, Canada

Background: Case reports suggest that children with glucocorticoid (GC)-treated nephrotic syndrome (NS) may develop symptomatic vertebral fractures (VF). However, the incidence of VF has not been documented.

Aim: To describe the incidence of VF as well as changes in lumbar spine bone mineral density (LSBMD) Z-scores after 1 year of GC therapy.

Methods: Baseline evaluation was carried out within 37 days of steroid initiation (median 18 days, range 0 to 37). VF were characterized by the Genant semi-quantitative method on baseline and 12 month spine radiographs. An incident VF was defined as an increase in the Genant grade by at least one compared to baseline. LSBMD was evaluated by dual energy x-ray absorptiometry at baseline, 3, 6 and 12 months. The children were enrolled through a national research program known as the STeroid-associated Osteoporosis in the Pediatric Population (STOPP) study.

Results: We studied 65 children to 12 months (median age 5.4 years, range 2.3 to 17.9 years; 55% boys; 80% with minimal change disease). Three of the children (5%; 95% CI, 2 to 13) had a single, asymptomatic incident VF in the mid-thoracic region at 1 year. Overall, the LSBMD Z-score was significantly lower than the healthy average at baseline (mean ± SD: -0.5 ± 1.1) and at 3 months (-0.6 ± 1; p=0.001), but not at 12 months (-0.3 ± 1.2; p=0.066). A sub-group (N=16; 25%) was identified with LSBMD Z-scores that were ≤ -1 at 12 months. In these children, the total quantity (p=0.35) and duration (p=0.33) of GC therapy were similar to those with higher LS BMD Z-scores at 1 year. However, in these 16 children each additional g/m² of cumulative GC received in the first 3 months was associated with a reduction in LSBMD Z-score of 0.48 at 12 months (95% CI, -0.83 to -0.12; p=0.008; controlling for age, gender and BMI). This relationship was not observed in the rest of the cohort (p=0.50).

Conclusions: In children with GC-treated NS, the incidence of VF was low at 12 months. Furthermore, LSBMD Z-scores were > 1.0 at this time point in the majority. However, a sub-set of children had persistent LS BMD Z-scores deficits at one year that were inversely associated with cumulative GC exposure in the first 3 months. These results suggest that some children with GC-treated NS are particularly sensitive to the deleterious effects of GC on bone development in the first few months of GC therapy.

Disclosures: **Leanne M. Ward**, None.

SU0041

Effects of Low Magnitude Mechanical Signals (LMMS) on Bone Density and Structure in Pediatric Crohn Disease: A Randomized Trial.

Mary Leonard¹, Justine Shults², Babette Zemel¹, Kevin Hommel³, Keenan Brown⁴, Sorooah Mahboubi¹, Jin Long¹, Clinton Rubin⁵. ¹Children's Hospital of Philadelphia, USA, ²University of Pennsylvania, USA, ³Cincinnati Children's Hospital Medical Center, USA, ⁴Mindways Software, USA, ⁵State University of New York at Stony Brook, USA

Introduction: Childhood Crohn Disease (CD) is associated with decreased trabecular volumetric BMD and cortical bone area. Animal and clinical studies suggest that low magnitude mechanical signals (LMMS) are anabolic to bone. The objective of this 12 month randomized double-blind placebo-controlled trial was to examine LMMS effects in pediatric CD (NCT00364130).

Methods: CD patients, ages 8-21 yr, at least 6 months since disease diagnosis, with a tibia peripheral quantitative CT (pQCT) trabecular BMD < 25th percentile for age, sex and race were eligible. Participants were randomized to 10 minutes of daily LMMS (30 Hz, 0.3 g) or a placebo device. Each device was equipped with an electronic adherence monitor. Lumbar spine QCT scans were obtained at baseline and 12 months, and tibia pQCT at baseline, 6 and 12 months. All participants were provided with cholecalciferol (800 IU/day) and calcium (1,000 mg/day). BMD results were converted to sex-specific Z-scores for age, and tibia cortical area Z-scores were further adjusted for tibia length.

Results: 138 participants were enrolled and 121 (88%) completed the 12 month visit. Baseline characteristics, including growth, Tanner stage, disease activity, medications and bone Z-scores did not differ between treatment arms (all p > 0.16). Over the study interval 28% of participants were treated with glucocorticoids and 48% with biologic agents. Mean adherence was 73% in both arms. Using an intention to treat analysis, the mean change in spine QCT trabecular BMD Z-score

was +0.13 in the active LMMS arm and -0.14 in the placebo arm for a difference in change of 0.27 (Table). LMMS had no effect on trabecular or cortical outcomes in the tibia. Similar results were obtained using an "as treated" analysis based on percent adherence. Treatment response did not vary according to baseline BMI Z-score, Tanner stage, CD severity, or concurrent medications. In the two study arms combined, pQCT trabecular BMD and cortical area Z-scores increased (both $p < 0.002$) and cortical BMD Z-scores decreased ($p < 0.0001$). Increases in cortical area Z-scores correlated with declines in cortical BMD Z-scores ($R = 0.61$, $p < 0.0001$).

Conclusions: LMMS was associated with increases in spine BMD only. The overall improvements in pQCT trabecular BMD and cortical area may be related to vitamin D and calcium supplementation, while the decline in cortical BMD may represent delayed mineralization of newly formed cortical bone.

| Z-Scores Mean \pm SD | Active LMMS (n = 60) | | Placebo (n = 61) | | Difference in Change* (95% C.I.) | P-value |
|------------------------------|-------------------------|---------------------|---------------------|---------------------|--|---------|
| | Baseline | 12 Months | Baseline | 12 Months | | |
| QCT Spine Trabecular BMD | -0.68 \pm 1.41 | -0.56 \pm 1.26 | -0.61 \pm 1.23 | -0.76 \pm 1.69 | 0.27 (0.06, 0.48) | 0.012 |
| pQCT Tibia Trabecular BMD | -1.65 \pm 0.74 | -1.44 \pm 0.98 | -1.81 \pm 0.78 | -1.58 \pm 0.90 | -0.08 (-0.28, 0.11) | 0.40 |
| pQCT Tibia Cortical BMD | -0.24 \pm 1.18 | -0.61 \pm 1.06 | -0.32 \pm 1.43 | -0.70 \pm 1.37 | -0.01 (-0.24, 0.23) | 0.97 |
| pQCT Tibia Cortical Area | -1.29 \pm 1.19 | -1.13 \pm 1.27 | -1.32 \pm 1.04 | -1.13 \pm 0.94 | -0.04 (-0.20, 0.11) | 0.58 |

Baseline and 12 Month Bone Z-scores According to Treatment Arm

Disclosures: Mary Leonard, None.

SU0042

Longitudinal follow up of clinical and radiological indices in children with Idiopathic Juvenile Osteoporosis following two years of bisphosphonate treatment. Jennifer Harrington^{*1}, Etienne Sochett². ¹The Hospital for Sick Children, Department of Pediatrics, University of Toronto, Canada, ²Hospital for Sick Children, Canada

Idiopathic juvenile osteoporosis (IJO) is an uncommon condition in children and adolescents, characterized by frequent fractures and significant bone pain in the absence of underlying systemic disease or evidence of a collagen disorder. The exact pathogenesis and optimal management strategy in IJO is still unclear, although bisphosphonates have been used in patients with significant symptoms.

Objective: To assess the clinical and radiological response following two years of bisphosphonate treatment in a cohort of children and adolescents with IJO who all had baseline histomorphometric analysis.

Results: 12 patients (6 males) aged 12.2 (± 2.5) years with IJO, had a trans-iliac bone biopsy as part of an assessment for symptomatic osteoporosis (multiple fractures and bone pain). None had a history of a significant secondary systemic disease or had abnormalities of sclera, joint hypermobility or skin laxity. Median number of previous peripheral fractures was 4(0-8) and vertebral compression fractures was 2.5(0-10). All patients had a history of bone pain. The cohort had a mean height Z score of -0.4 (± 1.4), weight Z score of -0.5 (± 1.3).

Baseline histomorphometry following tetracycline labeling showed evidence of high turnover osteoporosis in all subjects with decreased trabecular thickness 127.2 (± 33.7) μ m and increased cortical porosity. Bone formation parameters were increased such as osteoid volume /bone volume 2.3 (± 1.5)%.

Following 2 years of monthly cycles (3 months on, 1 off) of Pamidronate at a dose of 1 mg/kg, all patients had improvement in clinical symptoms. There were no new peripheral fractures, and the previous vertebral compression fractures showed evidence of either improvement (gain in vertebral height) or stabilization (no further decrease in height), with resolution or significant improvement in bone pain. Lumbar spine BMD Z scores increased post treatment (-2 (± 1.0) vs. -0.9(1.3) $p < 0.001$) and bone specific alkaline phosphatase decreased (222.9 (± 99.6) vs. 112.1 (± 82.3) U/L $p = 0.003$). There was no significant change in C-telopeptide (975.0 (± 684.9) vs. 1041.7 (± 423.2) ng/L $p = 0.7$).

Conclusions: Bisphosphonate use in children with IJO is associated with improvement in clinical symptoms and increased BMD. However further longitudinal follow up of this patient population is still needed to determine the impact of short term treatment on bone health in adulthood.

Disclosures: Jennifer Harrington, None.

SU0043

Low-amplitude, High-frequency Vibration and Musculoskeletal Health in the mdx Mouse Model of Duchenne Muscular Dystrophy. Susan Novotny^{*1}, David Nuckley¹, Gordon Warren², Dawn Lowe¹. ¹University of Minnesota, USA, ²Georgia State University, USA

Low-amplitude, high-frequency vibration appears to be most efficacious in skeletons with low bone mass. Duchenne muscular dystrophy (DMD) causes such a condition. Our previous work showed that acute vibration at 45Hz and 0.6g best amplified genes associated with osteogenesis in the mdx mouse model of DMD.

However it was unknown if chronic exposure would translate to improved bone health. Thus, the present study aimed to determine if an 8-wk vibration regimen improved skeletal health and that vibration does not further compromise muscle function or accelerate disease progression. Mdx mice, aged 3wk, received 8-wk of vibration (15min/d at 0.6g and 45Hz) and were compared to non-vibrated mdx mice. Anterior crural muscle function was assessed *in vivo* and contractility of extensor digitorum longus (EDL) muscle was analyzed *ex vivo*. Visceral and subcutaneous fat pads were isolated and weighed. μ CT of the tibia was done at the proximal metaphysis and mid-diaphysis. Dynamic histomorphometry was performed to indicate bone growth using fluorochrome labels injected 5 and 1d before sacrifice. Bone strength was assessed by 3-point bending and ultimate load and stiffness were measured. Paired t-tests were used to compare vibrated and non-vibrated mdx mice. Chronically vibrated mdx mice had up to 9% lower body and EDL masses ($p < 0.05$), as well as a trend toward lower visceral fat ($p = 0.09$) compared to non-vibrated mice. Muscle function was not compromised by vibration; isometric torque, tetanic force, specific force, and peak eccentric force were not different between groups ($p \geq 0.25$). Vibration did not improve any measure of tibial bone geometry at the midshaft or proximal metaphysis ($p \geq 0.19$). The lack of bone geometry findings was confirmed by 3-point bending and dynamic histomorphometry in which tibial strength and bone formation did not differ ($p \geq 0.19$). Despite the lack of improvements in bone health, vibration was not injurious to mdx muscle. Further, the reduction in body mass and trends toward reduced fat mass with vibration are potentially desirable in DMD. Further work is needed to determine if other vibration parameters have the capacity to improve musculoskeletal health in DMD populations. Acknowledgements: Muscular Dystrophy Association; Biomaterials Characterization & Quantitative Histomorphometry Core, Mayo Clinic, Rochester, MN; Institute for Bioengineering and Bioscience, Georgia Tech, Atlanta, GA

Disclosures: Susan Novotny, None.

SU0044

A Combinatory Biological and Physicochemical Response Lead to Bone Loss Following Radiation Exposure in Young Mice. Danielle Green^{*1}, Benjamin Adler¹, M. Ete Chan¹, Alvin Acerbo², Lisa Miller³, Clinton Rubin⁴. ¹Stony Brook University, USA, ²Brookhaven National Laboratory, USA, ³Brookhaven National Laboratory, USA, ⁴State University of New York at Stony Brook, USA

Sub-lethal doses of radiation devastate the bone marrow (BM) and bone architecture immediately following exposure. We propose a physicochemical effect contributes to bone loss rather than strictly a resorptive biological process. To test this hypothesis, 8wk old male C57Bl/6 mice were exposed to 5Gy of Cs^{137} γ -irradiation (0.6Gy/min), and compared to age-matched sham controls (AC). Mice were sacrificed at 2d or 10d following exposure (n=6-8/group/time). Radiation exposure led to drastic bone loss by 10d as shown by a -41% and -33% decline of trabecular bone volume fraction (BV/TV) and trabecular number, respectively, in irradiated mice (IRR) compared to AC ($p < 0.05$). The total number of cells in the BM for IRR declined by 65% compared to AC at 2d and showed no signs of recovery by 10d ($p < 0.05$). This indicates that the rapid decline in BV/TV seen at 10d was not solely due to a biological process aided by osteoclasts, but also a physicochemical process from radiation exposure. Osteoclast resorption has shown to contribute to bone loss, with tartrate-resistant acid phosphatase expression in the serum elevated by 43% ($p < 0.05$) at 2d following exposure compared to AC. However the compromised viability of the BM cell populations still suggests a non-biological response contributed to the rapid collapse of the bone structure. Mice tibiae were embedded in poly(methyl methacrylate), polished, and the trabecular bone's chemical composition was assessed using reflection-based Fourier transform infrared imaging (FTIR). Tissue mineralization, defined as the ratio of phosphate (900-1200 cm^{-1}) to protein (1600-1700 cm^{-1}) content, was 3.61 (-8.5% compared to AC; $p = 0.09$) and 3.30 (-15.7% compared to AC; $p < 0.05$) at 2d and 10d, respectively, in IRR. Therefore in addition to the drastic bone loss by 10d, there was also evidence of decreased mineralization in the remaining bone which was primarily caused by damage to the inorganic constituents of the matrix. The decline in mineralization was seen throughout the whole trabecular region because γ -irradiation may penetrate through the bone tissue, thereby making bone susceptible to both a biologic (osteoclastic) and non-biologic (sloughing) response. This study suggests bone loss due to radiation, whether it is from intentional exposure used for medical treatments, or accidental exposure from environmental disaster, results from both biological (cell-mediated) and physical processes (cell-independent).

Disclosures: Danielle Green, None.

SU0045

A Combined HR-pQCT and Fracture Mechanics-Based Finite Element Approach for Fracture Risk Assessment of Human Radius. Ani Ural^{*1}, Peter Bruno¹, Bin Zhou², Xiutao Shi², Elizabeth Shane³, X Guo². ¹Villanova University, USA, ²Columbia University, USA, ³Columbia University College of Physicians & Surgeons, USA

High resolution peripheral quantitative computed tomography (HR-pQCT) has recently been combined with strength-based finite element modeling (FEM) to noninvasively assess fracture risk. In this study, we aim to develop a new HR-pQCT-based FEM approach that explicitly simulates crack formation. In addition, we assess

the contribution of the cortical compartment and macroscale geometric properties to the whole bone fracture load.

Twenty distal radius images from postmenopausal women (fracture, n=10; nonfracture, n=10) were processed to obtain a cortical and a whole bone model for each subject (Fig 1a,b). Cortical and whole bone geometrical properties (thickness, area, moment of inertia at the distal, proximal and crack surfaces) for each model were assessed and the fracture load was determined under a fall loading orientation using fracture mechanics-based cohesive FEM (Fig 1c,d). Cohesive FEM simulates fracture based on a traction-displacement relationship incorporating bone fracture toughness and strength.

The simulation results showed that the cortical and whole bone fracture loads were significantly correlated for the nonfracture group and the pooled data but not for the fracture group (Fig. 2). The stepwise multiple regression analysis between the geometrical properties and the cortical and whole bone fracture loads demonstrated that cortical thickness is the best predictor for all groups except fracture group whole bone fracture load (Table 1). These results may be an evidence of the compromised cortical structure and its reduced mechanical contribution in the fracture group. The percentage of the whole fracture load carried by the cortical bone increases with the cortical fracture load and can be predicted by the ratio of cortical to whole bone geometric properties (Table 1). The ratios of cortical to whole bone geometric properties (proximal area, proximal and distal moment of inertia) between the fracture and nonfracture groups showed statistically significant differences. This information can be utilized in identification of high fracture risk groups.

In conclusion, this study introduced a new modeling approach that coupled HR-pQCT imaging with fracture mechanics-based finite element simulations and presented a systematic study on the contribution of the cortical compartment to bone fracture risk. The results demonstrated the importance of cortical geometrical properties especially the cortical thickness in predicting the whole bone fracture load.

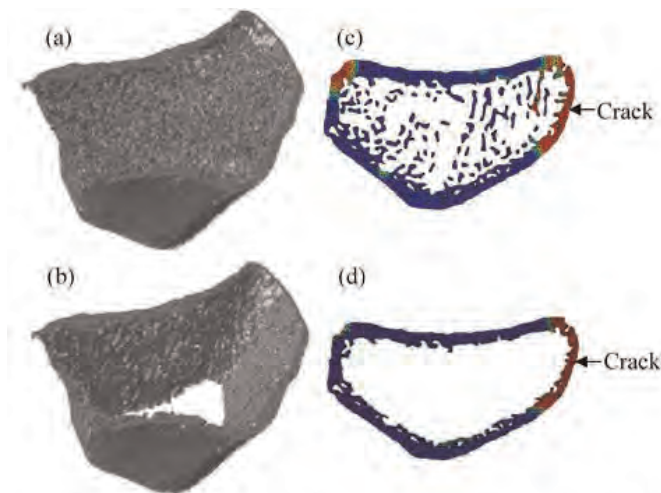


Figure 1: A sample HR-pQCT bone image from a 63-year-old subject for (a) whole bone (b) cortical bone. Finite element mesh of the crack plane tiled with cohesive elements (c) whole bone (d) cortical bone. The arrows indicate the initial location of crack formation. Red color indicates high level of damage and blue color indicates no damage.

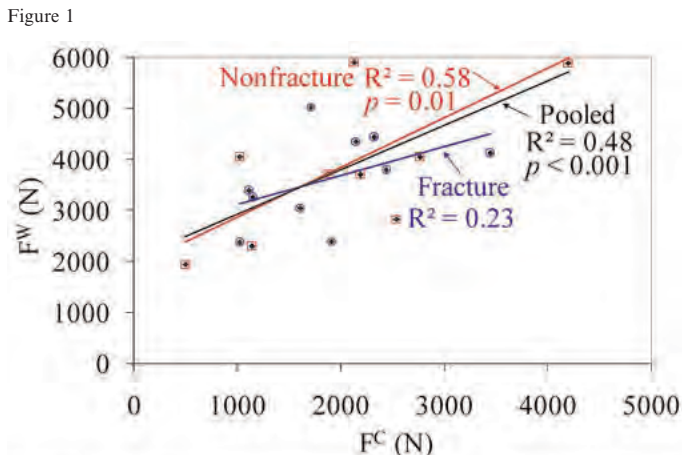


Figure 2: Cortical bone (F^C) vs. whole bone (F^W) fracture loads for fracture, nonfracture and pooled data. Note that the blue hollow circles, red hollow squares, and black diamonds correspond to fracture, nonfracture and pooled data, respectively.

Figure 2

Table 1: Stepwise multiple regression models between the fracture loads and the geometrical properties.

| Stepwise Multiple Regression Models | R^2 | p |
|--|-------|---------|
| <i>Pooled whole bone fracture load</i> $F^W = 5144.8 \text{ CTh} - 488.6$ | 0.49 | < 0.001 |
| <i>Fracture group whole bone fracture load</i> none | - | - |
| <i>Nonfracture group whole bone fracture load</i> $F^W = 5339.1 \text{ CTh} - 684.3$ | 0.52 | 0.019 |
| <i>Pooled cortical bone fracture load</i> $F^C = 4807.0 \text{ CTh} - 2.34 \text{ DJ}^C - 1017.1$ | 0.86 | < 0.001 |
| <i>Fracture group cortical bone fracture load</i> $F^C = 6815.5 \text{ CTh} - 71.6 \text{ CA}^C + 306.5$ | 0.96 | < 0.001 |
| <i>Nonfracture group cortical bone fracture load</i> $F^C = 5255.6 \text{ CTh} - 2450.4$ | 0.83 | < 0.001 |
| <i>Pooled cortical/whole bone fracture load ratio</i> $F^C/F^W = 1.30 (\text{CA}^C/\text{CA}^W) - 0.270$ | 0.47 | < 0.001 |
| <i>Fracture group cortical/whole bone fracture load ratio</i> $F^C/F^W = 1.56 (\text{CA}^C/\text{CA}^W) - 0.476$ | 0.67 | 0.004 |
| <i>Nonfracture group cortical/whole bone fracture load ratio</i> $F^C/F^W = 1.41 (\text{CI}_{xx}^C/\text{CI}_{xx}^W) - 0.474$ | 0.45 | 0.034 |

F^W = whole bone fracture load, F^C = cortical bone fracture load, CTh = cortical thickness at the crack surface, DJ^C = polar moment of inertia at the distal surface, CA^C = cortical bone area at the crack surface, CA^W = whole bone area at the crack surface, CI_{xx}^C = cortical bone moment of inertia in medial-lateral direction at the crack surface, CI_{xx}^W = whole bone moment of inertia in medial-lateral direction at the crack surface.

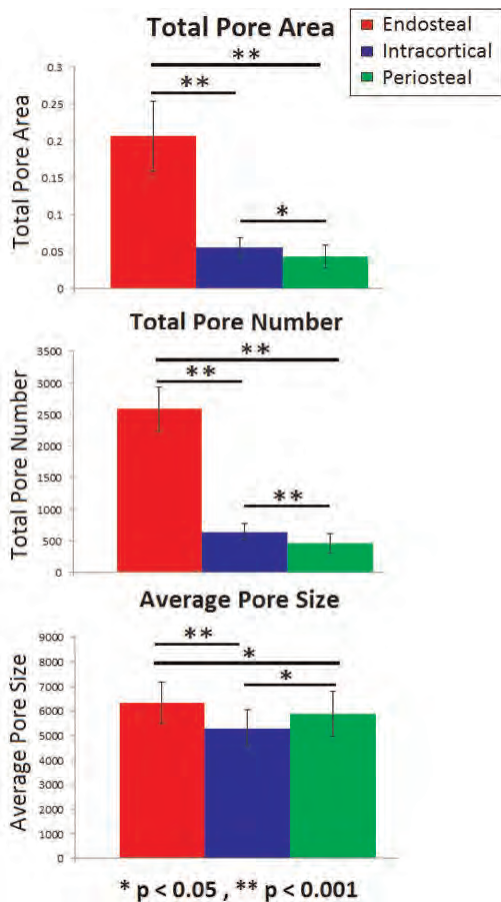
Table 1

Disclosures: Ani Ural, None.

SU0046

A Technique for Laminae Analysis of Cortical Microarchitecture in Longitudinal Studies. Jasmine Nirody*, Willy Tjong, Janina Patsch, Thomas Link, Brian Feeley, C. Benjamin Ma, Galatea Kazakia. University of California, San Francisco, USA

As the mechanical competence of long bones depends to a large degree on cortical structure, quantification of cortical parameters is vital to both fracture risk prediction and therapeutic intervention. Studies have shown that there exists considerable spatial variability in cortical microstructure, particularly porosity. The goal of this study was to develop a technique to characterize cortical microstructure variability specifically between laminae layers. Our motivation is that laminae assessment may elucidate mechanisms through which cortical porosity develops, for example expansion of the marrow space, the vascular network, or both. The cortical compartment was first segmented from high resolution peripheral QCT (HR-pQCT) images. Second, a 3D sphere-filling algorithm was used to find the cortical midline, which was then dilated in 1 deg sections by a local thickness map. This divides the cortex into three laminae corresponding to endosteal, intracortical, and periosteal regions. A skeletonization routine was then used to assign each pore to a single lamina based on the location of the pore's skeleton. Total pore area, total pore number, and average pore size were then calculated within each region. This technique was applied to a longitudinal HR-pQCT dataset obtained from the distal tibiae of individuals (n = 10, age = 34 +/- 8 yrs at baseline) undergoing knee surgery that required a 6-wk disuse period post-surgery. At baseline, the highest total pore area was found in the endosteal layer (274% and 375% higher than intracortical and periosteal respectively, p<0.001). High endosteal porosity was associated with high total pore number (304% and 461% higher than intracortical and periosteal respectively, p<0.001) rather than high average pore size. Following the disuse period, changes in cortical porosity were found in the overall cortical compartment (17.6% increase from baseline, p<0.05). Endosteally, this increase in total pore area was manifested through both increase in total pore number (+8%, p<0.05) and average pore size (+10%, p<0.05), while periosteal pores showed only significant increase in size (18% increase in average pore size, p<0.01). The application of cortical pore skeletonization and laminae evaluation of changes in porosity describe the microstructural genesis of increased porosity and suggest that unique mechanisms may be acting within endosteal and periosteal regions of the cortex in this disuse cohort.



Baseline parameter values within each lamina for disuse cohort

Disclosures: Jasmine Nirody, None.

SU0047

Assessment of Sound Wave Velocities in Osteons Reveals a Strong Correlation with Bone Matrix Mineralization Density. Stéphane Blouin¹, Stephan Puchegger², Andrea Berzlanovich³, Klaus Klaushofer¹, Paul Roschger^{*1}. ¹Ludwig Boltzmann Institute of Osteology at the Hospital of WGKK & AUVA Trauma Centre Meidling, 1st Medical Department Hanusch Hospital, Austria, ²University of Vienna, Faculty of Physics, Dynamics of Condensed Systems, Austria, ³Medical University of Vienna, Department of Forensic Medicine, Austria

The measurement of mechanical properties at tissue/material level is potentially an important parameter in prediction of the fracture risk of patients. Up to now only nanoindentation has been established to determine routinely indentation modulus and hardness of bone material. Acoustic scanning microscopy (SAM) could be an alternative approach for this purpose. This study employs SAM to measure in osteons sound wave velocities and in parallel quantitative backscattered electron imaging (qBEI) to determine mineral density. By combining velocity and density data the E-modulus of the material can be evaluated: $E = V_l^2 \cdot d \cdot 2(1+\nu)^2 / (\nu-0.5) / (\nu^2-1)$ with V_l longitudinal velocity, d density, ν Poisson's ratio (assumption 0.3). It has to be emphasized that because of the use of high frequency pulses, the E-modulus values has to be considered as dynamic elastic moduli.

Femoral diaphysis cross sections of autopsies (three bone healthy men, aged 50-59 yrs) were studied in accordance with the Institutional Ethical Review Board of the Department of Forensic Medicine of the Medical University of Vienna. Planoparallel ~30 μ m thick sections were manufactured by grinding and polishing. The exact thickness was determined using a confocal laser microscope (Leica TCS-SP5) in reflection mode. Mineralization density maps from the bone section were performed by qBEI with a spatial resolution of 1 μ m. Sound velocity maps with a scan resolution of 2 μ m were acquired from 55 osteons by a SAM (SASAM, kiberio GmbH, Saarbrücken, Germany) using short pulses (~20 ns) with a 400 MHz acoustic lens. The difference of time of flight (Δ TOF) between the echoes from front and back side of the bone sections were recorded with a time resolution of 125 ps and the velocity was calculated by division of Δ TOF by the sample thickness.

Mean velocity per osteon ranged from 3685 to 5060 $m \cdot s^{-2}$, which was strongly correlated with their mineral contents ranging from 20 to 26 weight % Ca (Pearson $r=0.713$; $p<0.0001$). In consequence the obtained E-modulus ranging from 19 and 43

GPa displayed a strong linear relationship to Ca-content too ($r^2=0.544$; $p<0.0001$; $y=2.4858x-27.472$).

The results indicate a close connection of bone mechanical properties to mineral content. Future experiments will show if the slope of the regression line is specific for healthy bone and if deviations from this are indicating diseased bone. Thus the method could be used as diagnostic and fracture risk assessment tool.

Disclosures: Paul Roschger, None.

SU0048

Association of Incident Hip Fracture with Femoral Strength Assessed by Finite Element Analysis of Dxa Scans in the Study of Osteoporotic Fracture. Lang Yang^{*1}, Lisa Palermo², Dennis Black², Richard Eastell¹. ¹University of Sheffield, United Kingdom, ²University of California, San Francisco, USA

Bone fractures only when loaded beyond its strength. The purpose of this study was to determine the association of femoral strength, as estimated by finite element (FE) analysis of DXA scans, with hip fracture in comparison to femoral neck (FN) and total hip (TH) BMD.

This prospective case-cohort study included a random sample of 1941 women at baseline (visit 2) and 668 incident hip fracture cases (373 in the cohort) occurring after visit 2 during a mean \pm SD follow-up of 10.0 ± 2.9 yrs from the Study of Osteoporotic Fractures ($n=7860$ community-dwelling women ≥ 67 yr of age). We analyzed the visit 2 DXA scans of the hip using a plane-stress, linear-elastic finite element (FE) model of the proximal femur that simulated a sideways fall [1]. The bone material properties were determined according to Morgan et al [2,3]. Femoral strength was defined as the impact force that caused the von Mises stress in 100 contiguous elements (24 mm^2 of area) to exceed the element yield stress and increased by a factor of 1.3 to account for the high loading rate during fall and associated viscoelastic strengthening. Cox regression with Prentice weighting was used to assess the association of the femoral strengths with hip fracture.

As expected, the fracture group had significantly ($p<0.05$) lower FN BMD (0.590 ± 0.095 v. 0.663 ± 0.112 g/cm^2), TH BMD (0.689 ± 0.112 v. 0.769 ± 0.129 g/cm^2) and strength (2906 ± 945 v. 3935 ± 1203 N) than the controls. The strength was highly correlated to the FN and TH BMDs (Spearman $r=0.81$ and 0.83 , $p<0.0001$). The hip BMDs and strength were significantly ($p<0.05$) associated with incident hip fracture on their own, adjusted for age and adjusted for age and BMI (see Table below). After further adjustment for BMD, femoral strength was still significantly associated with incident hip fracture and the hazard ratio was significantly ($p<0.01$) greater than that for TH BMD.

In conclusion, femoral strength derived from FE analysis of DXA scans was associated with incident hip fracture independent from age, BMI and hip BMD.

[1] Yang L et al (2009) J Bone Miner Res 24: 33-42; [2] Morgan EF, Keaveny TM (2001) J Biomech 34: 569-77; [3] Morgan EF et al (2003) J Biomech 36: 897-904.

| | Adjusted for clinical site and | | | | |
|----------|--------------------------------|-------------------|-------------------|--------------------------------|--|
| | None | Age | Age, BMI | Age, BMI, BMD | |
| TH BMD | 2.09 (1.89, 2.31) | 1.88 (1.70, 2.07) | 1.86 (1.67, 2.08) | 1.14 (0.96, 1.35) ^b | |
| Strength | 2.50 (2.22, 2.81) | 2.25 (1.99, 2.53) | 2.21 (1.95, 2.50) | 1.98 (1.64, 2.39) | |
| FN BMD | 2.27 (1.99, 2.59) | 2.07 (1.83, 2.34) | 2.04 (1.79, 2.32) | 1.40 (1.17, 1.66) ^b | |
| Strength | 2.50 (2.22, 2.81) | 2.25 (1.99, 2.53) | 2.21 (1.95, 2.50) | 1.71 (1.43, 2.04) | |

^aHR for TH BMD in the final model, significantly ($p<0.01$) lower than that for strength
^bHR for FN BMD in the final model, lower than that for strength (ns)

Hazard ratio (95% CI) for 1 SD decrease in BMD and strength

Disclosures: Lang Yang, None.

SU0049

Automatic Definition of Identical Follow-Up Volumes of Interest Using Image Registration for the Application to In Vivo Micro-CT Studies of Bone Quality. Graeme Campbell^{*1}, Friederike Grundmann², Nicolai Purcz³, Markus Boettcher³, Christian Schem², Sanjay Tiwari³, Claus-C Glueer³. ¹Christian-Albrechts Universität zu Kiel, Germany, ²University Hospital Schleswig-Holstein, Campus Kiel, Germany, ³Christian Albrechts Universität zu Kiel, Germany

The precision of repeated micro-CT measurements in mice improves with image registration (1). However, the impact of this technique on longitudinal data, in particular for studies using full body holders, has not been fully explored. Using image registration, we developed a method to define follow-up VOIs that are identical to baseline. This method was tested on longitudinal *in vivo* datasets of mouse models of osteoporosis.

Female CD1 mice were subjected to OVX at 10 wk of age followed by PTH injection at 6 mo (hPTH(1-84), $40 \mu g/kg$ s.c. 5dy/wk, $N=6$) or OVX only ($N=5$). The animals were micro-CT scanned (vivaCT 40, ScancoMedical, Switzerland) weekly for four wk in a full-body holder at a voxel size of $19 \mu m$, beginning at the time of PTH treatment in the first group and at OVX in the second. A 1.14 mm VOI of the trabecular structure beginning 0.38 mm from the proximal end of the left tibia and extending distally was defined in each scan using an automated contouring method (2) (unregistered dataset). Follow-up images were registered to baseline and the transformation matrix was inverted and used to transform the baseline VOI onto

the original follow-up images (registered dataset). To compensate for voxel 'spillover', the volume of the transferred VOI mask was adjusted until it was the same as the baseline volume. Bone architecture and mineral parameters were quantified. Repeated measures ANOVAs and paired t-tests determined time by group effects and baseline changes respectively. Significance was taken at $p < 0.05$.

Following PTH injection, increases from baseline in BV/TV (+46.7%, $p=0.004$), BMD (+19.0%, $p=0.002$) and Tb.Th (+10.8%, $p=0.002$) were observed in the registered VOIs at the end of the study. The unregistered VOIs showed similar means but only changes in BMD were significant (+18.7%, $p=0.002$). OVX resulted in decreases in BV/TV (-21.6%, $p=0.004$), BMD (-10.0%, $p=0.003$) and Tb.Th (-7.7%, $p<0.001$) in the registered VOIs. The unregistered dataset showed similar means but no significant changes were observed.

Image registration enabled the detection of changes that could otherwise not be observed. Whether the lack of observed changes in trabecular number and separation was genuine or due to limited resolution or sample size remains unclear. Future applications include studies of bone metastases in order to quantify bone loss in tumor models. (1) Nishiyama KK. et al., Bone 2009;46(1):155-61, (2) Buie HR. et al., Bone 2007;41(4):505-15

Disclosures: Graeme Campbell, None.

SU0050

Bisphosphonates Prevent the Decline in Serum TGF- β 1 Levels Following Long-Term Estrogen Deficiency. Junjing Jia^{*1}, Wei Yao², Sarah Amugongo¹, Mohammad Shahnazari³, Zhiqiang Cheng⁴, Yu-An Evan Lay⁵, Diana Olvera⁶, Robert Ritchie⁶, Tamara Alliston⁴, Nancy Lane².

¹University of California, Davis, USA, ²University of California, Davis Medical Center, USA, ³UCSF VA Medical Center, USA, ⁴University of California, San Francisco, USA, ⁵Musculoskeletal Research Unit, Department of Medicine, University of California Davis Medical Center, USA, ⁶Materials Sciences Division, Lawrence Berkeley National Laboratory, USA

Introduction: Bisphosphonates (BPs) are the most common agents prescribed for the treatment for osteoporosis. While the anti-resorptive effects of the BPs are well documented, many questions remain about their mechanisms of action, particularly following long-term use. This study evaluates the relationship between serum TGF- β 1 levels, TGF- β 1 signaling, bone mineralization and bone strength following prolonged BP treatment.

Methods: We measured serum total TGF- β 1 levels, a bone resorption marker, mineral density of bone (DBM) and biomechanical properties from cortical (tibiae) and trabecular bone (lumbar vertebral bodies) in approximately 300 rats that received BP treatments. Linear regressions were performed between serum TGF- β 1 levels and DBM or bone strength (maximum stress). TGF- β 1 expression and signaling were evaluated in vivo and in vitro.

Results: This study identified a dynamic regulation of serum TGF- β 1 following BP use. The increased serum TGF- β 1 after 60 days of OVX correlated with increased bone remodeling and was insensitive to BPs. After 120 days post-OVX, serum TGF- β 1 levels were reduced relative to sham controls. BP treatment prevented this decline in serum TGF- β 1 levels and increased the number of TGF- β 1-positive osteocytes and periosteal cells in cortical bone. Serum TGF- β 1 levels were negatively associated with cortical, but not trabecular DBM and bone strength.

Conclusions: The increased levels of serum TGF- β 1 following ovariectomy are likely due to increased osteoclast-mediated release of matrix-derived latent TGF- β 1. Long-term estrogen-deficiency results in a decline in serum TGF- β 1 levels that is prevented by BP treatment through mechanisms that are indirect. This work has implications for understanding the relationship between BPs, TGF- β 1 and bone quality.

Disclosures: Junjing Jia, None.

SU0051

Cell-independent Benefits of Raloxifene on Bone Matrix: A Novel Mechanism for Improving Mechanical Properties. Maxime Gallant^{*1}, Drew M. Brown¹, Max Hammond², Joseph Wallace³, Jiang Du⁴, Alex C. Deymier-Black⁵, Jon Almer⁶, Stuart Stock⁷, Matthew Allen¹, David Burr¹. ¹Indiana University School of Medicine, USA, ²Weldon School of Biomedical Engineering, Purdue University, USA, ³Indiana University Purdue University Indianapolis (IUPUI), USA, ⁴University of California, San Diego, USA, ⁵Department of Materials Science & Engineering, Northwestern University, USA, ⁶Advanced Photon Source, Argonne National Laboratory, USA, ⁷Northwestern University, Feinberg School of Medicine, USA

In clinical trials, raloxifene reduces vertebral fracture risk despite modest benefits to BMD. In animal studies raloxifene improves bone material-level biomechanical properties, again independently of BMD. The precise mechanisms of action underlying these mechanical benefits, which are independent of raloxifene's known anti-resorptive effects, remain elusive.

The goal of this study was to test the hypothesis that raloxifene modifies material-level properties of bone matrix through direct non-cellular physical effects on collagen and mineral. Beams were carved from canine and human cortical bone that had been frozen and thawed and therefore had no viable cells. The beams were incubated with raloxifene (2 μ M in PBS), raloxifene metabolites lacking hydroxyl groups, or PBS for 2 wks and then mechanically tested using 4-pt bending. Bone water content was assessed by gravimetric analysis and 3D ultrashort echo time (UTE) MRI. Collagen nanomorphology was analyzed using Atomic Force Microscopy (AFM).

Our results show that bone material-level toughness was greater after *ex vivo* exposure to raloxifene both in canine (+53%) and in human (+22%) cortical bone beams when compared with control beams, and this occurred within 2 days of exposure. This was driven by greater post-yield energy absorption in the raloxifene-treated specimens. Incubation with raloxifene metabolites revealed that the 2 hydroxyl groups of raloxifene were mediating this effect, as their sequential removal abolished the mechanical effect on tissue toughness. Mechanistically, raloxifene increased bone water content, quantified both by gravimetric analyses (+11%) and by UTE MRI (+17%). The latter technique also showed that the higher water content was due to greater bound water (+20% vs PBS control) within the bone, as free water content remained unchanged. Bound water was positively correlated with toughness ($r^2 = 0.75$). AFM analysis of the collagen fibril nanomorphology showed a wider distribution of collagen D-periodic spacing with raloxifene treatment, with larger D-periodic spacing compared with vehicle-treated control beams. Analyses using DXA, micro-CT and RAMAN spectroscopy showed no difference in bone density, architecture/porosity or composition between raloxifene- and vehicle-treated specimens.

Our results show for the first time that raloxifene positively affects bone matrix in a cell-independent manner through changes in both bound water content and collagen nanomorphology.

Disclosures: Maxime Gallant, None.

SU0052

Comparative Biochemical Analysis Demonstrates High Efficiency and Speed of Glucose-based in vitro Glycation Process of Bone. Grazyna Sroga^{*}, Alankrita Siddula, Deepak Vashishth, Rensselaer Polytechnic Institute, USA

Glucose and other reducing sugars react with proteins in vivo and in vitro through a slow non-enzymatic process termed glycation. As a result crosslinks, known as advanced glycation end products (AGEs), are formed within and between proteins [1, 2]. While AGEs have been shown to accumulate in a variety of collagenous human tissues and alter the tissues' functional behavior, the role of AGEs in modifying the mechanical properties of cancellous and cortical bone is not well understood.

Methods that are currently used for in vitro glycation of bone samples are based on ribose, because the time-frame of the reaction with glucose ranges from few weeks to several months due to general low reactivity of this sugar [3]. However, the use of glucose is of tremendous interest due to clinical relevance of this sugar. The goal of the current work was to develop fast and efficient in vitro glycation process of human bone samples using glucose and compare its efficiency with our formerly developed ribosylation procedure [2].

Using our new glycation process, we produced and determined the level of total AGEs in human trabecular and cortical bone. After 7 days of sample treatments followed by 7 days of dialysis, the average increase in the amount of total AGEs was approx. 5-fold for trabecular and 3-fold for cancellous human bone. These results are similar to those, which we obtained when using current golden-standard method employing ribose to produce AGEs [2, 4]. Selected fluorescent crosslinks were analyzed using ultrahigh pressure liquid chromatography (UPLC) [5].

In summary, we developed a new in vitro glycation process that significantly speeds up generation of AGEs in bone samples as compared to a standard "in solution" method using glucose, that takes over 5-9 months [3], as well as has similar efficiency as currently accepted ribosylation procedure [2, 4]. Our work opens new opportunities for studies of AGEs formation and their role in mechanical properties of bone.

[1] Bank et al, Biochem. J. 330(1998) 345-351.

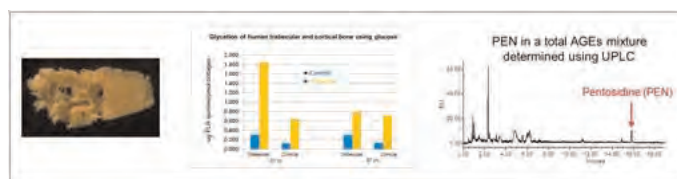
[2] Vashishth et al, Bone 28(2001) 195-201.

[3] Voziyan et al, J. Biol. Chem. 278 (2003) 46616-46624.

[4] Tang et al, Bone 40 (2007) 1144-1151.

[5] Sroga & Vashishth, J. Chromatogr. B 879 (2011) 379-385.

Acknowledgement: Funding through NIH grants AG20618 and AR49635.



Figure

Disclosures: Grazyna Sroga, None.

SU0053

Cortical and Trabecular Bone Structure Analysis at the Distal Radius – Prediction of Biomechanical Strength by DXA and MRI. Thomas Baum*¹, Melanie Kutscher², Dirk Mueller³, Christoph Raeth⁴, Felix Eckstein⁵, Eva-Maria Lochmueller⁵, Ernst J. Rummeny², Thomas M. Link⁶, Jan S. Bauer². ¹Klinikum rechts der Isar, Technische Universitaet Muenchen, Deu, ²Institut fuer Radiologie, Klinikum rechts der Isar, Technische Universitaet Muenchen, Germany, ³Institut und Poliklinik fuer Diagnostische Radiologie, Universitaetsklinikum Koeln, Germany, ⁴Max-Planck-Institute fuer extraterrestrische Physik, Germany, ⁵Institute of Anatomy & Musculoskeletal Research, Paracelsus Medical University Salzburg, Austria, ⁶Musculoskeletal & Quantitative Imaging Research Group, Department of Radiology & Biomedical Imaging, University of California San Francisco, USA

Purpose: To study whether the combination of DXA (Dual-energy X-ray Absorptiometry) derived bone mass parameters with cortical and trabecular bone structure parameters improves the prediction of radial bone strength.

Materials and Methods:

Thirty-eight left forearms were harvested from formalin-fixed human cadavers. BMC (Bone Mineral Content) and BMD (Bone Mineral Density) of the distal radius were measured by using DXA. Cortical and trabecular bone structure parameters of the distal radius were computed in high-resolution 1.5T Magnetic Resonance (MR) images. Cortical parameters included average cortical thickness and cross-sectional area. Trabecular parameters included histomorphometric and texture parameters. The forearms were biomechanically tested in a fall simulation and radial failure load (absolute radial bone strength) was measured. Relative radial bone strength was determined by dividing absolute radial bone strength separately by age, BMI (Body Mass Index), radius length, and average bone cross-sectional area.

Results:

DXA derived BMC and BMD showed statistically significant ($p < 0.05$) correlations with absolute and relative radial bone strength up to $r = 0.782$. Correlation coefficients for cortical and trabecular bone structure parameters with absolute and relative radial bone strength amounted up to $r = 0.594$ and $r = 0.738$, respectively ($p < 0.05$). In combination with the best DXA derived bone mass parameter, the best trabecular but no cortical bone structure parameter added in linear regression models significant information in predicting absolute and relative radial bone strength (up to $R_{adj} = 0.875$). Linear regression models including the best DXA derived bone mass parameter and the best trabecular bone structure parameter allowed for a significant better prediction than the bone mass parameter alone ($p < 0.05$).

Conclusion:

A combination of DXA derived bone mass parameters and trabecular but not cortical bone structure parameters most accurately predicted absolute and relative radial bone strength.

Disclosures: Thomas Baum, None.

SU0054

Effects of Age-Related Cortical Thinning and Trabecular Bone Loss on the Strain Distribution in the Lumbar Spine Following Interbody Fusion. Lillian Chatham*¹, Vikas Patel¹, Dana Carpenter². ¹University of Colorado Denver | Anschutz Medical Campus, USA, ²University of Colorado Denver, USA

The purpose of this study was to determine the effects of age, cortical thinning, and loss of volumetric trabecular bone mineral density (vBMD) on the strain distribution in the spine after lumbar interbody fusion with posterior instrumentation. Finite element (FE) models of the L4 and L5 vertebrae were developed from computed tomography data (voxel size = 0.7x0.7x2.0mm). Segmentation and meshing of the vertebrae were performed in Simpleware (Simpleware Ltd., Exeter, UK). A 27x25 mm oval spacer, pedicle screws, and 6-mm diameter rods were designed using SolidWorks (Dassault Systemes, Waltham, MA) and integrated into the models in Simpleware. For FE analysis the inferior endplate of L5 was fixed, and a 0.38 MPa pressure was applied to the superior endplate of L4 in Abaqus (Simulia, Providence, RI). A linear relationship between age and vBMD in the male lumbar spine was used to estimate vBMD loss between the ages of 30 and 90 years [1], and a linear relationship between vBMD and elastic modulus (E) was used to estimate the corresponding age-related decline in E [2]. Cortical thicknesses of 450 μ m and 200 μ m were used for the 30 and 90 year old male, respectively [3], and the cortex was assigned an E of 12 GPa [4]. A homogeneous value of E was assigned to each vertebra based on the axial rigidity of the combined trabecular and cortical compartments, and all bone tissue was assigned a Poisson's ratio (ν) of 0.3. The spacer was treated as poly(ether-ether-ketone) (E=4.6 GPa; $\nu=0.38$) [5]. The pedicle screws and rods were treated as titanium (E=110 GPa; $\nu=0.3$) [4]. Strains at the bone/spacer interface of L4 and the lateral aspect of the superior endplate of L5 were greater in the 90 year old male (Fig. 1). At the endplate of L5, the maximum strain in the 90 year old was nearly double that of the 30 year old. The results of this study demonstrate the effects of age-related cortical thinning and trabecular bone loss on the mechanical environment in bone following interbody fusion. Future analyses incorporating the effects of sex, body size, and experimental measurements of endplate material properties may provide a quantitative basis for patient-specific optimization of the osteogenic environment after spinal fusion.

References: 1. Riggs et al., J Bone Miner Res, 2004. 19: 1945-54. 2. Kopperdahl et al. J Orthop Res, 2002. 20: 801-5. 3. Mosekilde, Technol Health Care, 1998. 6: 287-97. 4. Fantigrossi et al., Med Eng Phys, 2007. 29: 101-9. 5. Rae et al., Polymer, 2007. 48: 598-615.

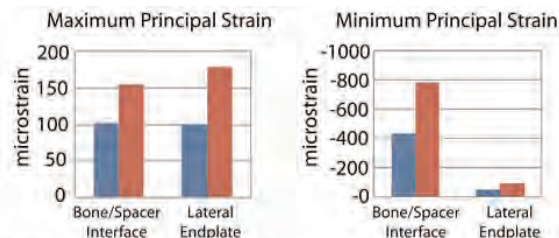


Figure 1. Mean values of maximum (tensile) principal strain and minimum (compressive) principal strain at the bone/spacer interface of L4 and the lateral aspect of the superior endplate of L5 for the 30-yr-old (■) and 90-yr-old (■) male.

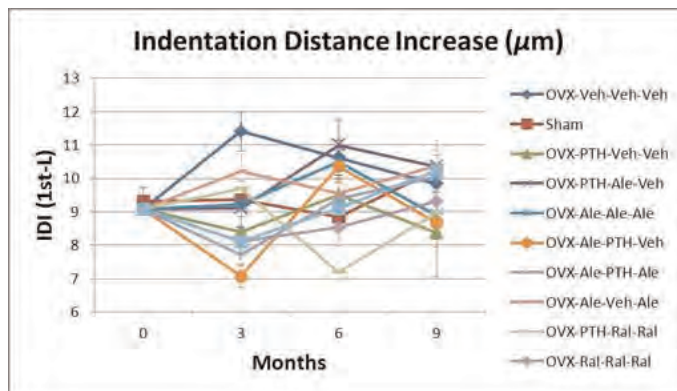
Figure 1

Disclosures: Lillian Chatham, None.

SU0055

Effects of Cyclical Treatments with Anabolic and Anti-resorptive Agents on Cortical Bone Mass and Strength. Sarah Amugongo*¹, Wei Yao², Dan Walsh³, Junjing Jia¹, Mohammad Shahnazari⁴, Diana Olvera⁵, Robert O Ritchie⁵, Nancy Lane². ¹University of California, Davis, USA, ²University of California, Davis Medical Center, USA, ³USA, ⁴UCSF VA Medical Center, USA, ⁵Materials Sciences Division, Lawrence Berkeley National Laboratory, USA

Osteoporosis is currently treated with therapies that reduce fracture risk. While the benefits of the individual agents are known, the changes that occur following long-term sequential therapies with anabolic and anti-resorptive agents on the cortical bone quantity and quality are unclear. We evaluated these changes in an ovariectomized (OVX) rat model. **Methods:** Six-month old female Sprague Dawley rats were either sham operated or OVX. The OVX rats were left untreated for two months to develop osteopenia then treated with injections of either vehicle (Veh); or hPTH (1-34) 25ug/kg/d, 5x/wk; or alendronate (Ale) 25ug/kg/d, 1x/wk, or raloxifene (Ral), 5mg/kg, po 3x/wk for three months. The three treatment regimens were either continued, switched to vehicle or other treatments for a period of three months. We monitored cortical bone architecture and mineralization by μ CT, whole bone strength and localized bone strength using Biodent Microindenter (Santa Barbara, CA). **Results:** Six months of estrogen deficiency post-OVX decreased whole bone strength (maximum stress) and increased the Indentation Distance Increase (IDI), a parameter for localized fracture resistance. Treatment with hPTH (1-34) for 3 months increased whole bone strength by 15%. This increase was rapidly lost when the treatment was withdrawn, but was maintained by switching to Ale for the next 6 months and with Ral for 3 months. PTH increased IDI during the first 3 months of treatment and did not significantly change IDI thereafter. PTH followed by Ale significantly decreased IDI by approximately 10%. Continuous Ale or Ale followed by Veh prevented the decrease in whole bone and localized cortical strength observed in OVX controls. Animals that were pretreated with Ale followed by PTH completely restored bone strength to sham levels and this was similar to a 3 month PTH treatment cycle. Continuous Ral prevented the decrease in whole bone strength, which was lower than the Ale treated groups. Ral followed by PTH also completely restored whole bone strength. **Summary:** Prolonged estrogen deficiency decreased cortical bone strength and increased indentation (fracture propagation) throughout the cortex in aged female rats. PTH both increased whole bone strength and indentation distance, possibly from new bone on periosteal surface. Sequential treatment with Ale or Ral followed by PTH might help to prevent fracture propagation. These findings warrant further evaluation in clinical trials.



Indentation Distance Increase (μ m)

Disclosures: Sarah Amugongo, None.

SU0056

Fabric Based Tsai-Wu Yield-Strength Criterion for Vertebral Trabecular Bone in Stress Space. Uwe Wolfram*¹, Thomas Gross², Dieter Pahr², Jakob Schwiedrzik³, Philippe Zysset¹. ¹University of Bern, Switzerland, ²Institute for Lightweight Design & Structural Biomechanics, Vienna University of Technology, Austria, Austria, ³Institute for Surgical Technology & Biomechanics, University of Bern, Switzerland, Switzerland

Osteoporosis related vertebral fractures are an increasing clinical problem in ageing societies. The prediction of vertebral fracture load from QCT-based finite element simulations could be very useful in the management of patients with osteoporosis. A key property to distinguish critically and non-critically loaded trabecular bone in finite element analysis is the directional dependent yield-strength. This study aimed at identifying a yield-strength criterion for vertebral trabecular bone which allows to determine patient specific direction dependent yield strength, given bone volume fraction and fabric, i.e. clinical QCT data, are known.

A fabric-dependent, orthotropic Tsai-Wu yield criterion is proposed in stress space. Nonlinear micro-finite element models of cubic vertebral trabecular bone samples with 5.62 mm edge length were generated from μ CT-scans at 36 μ m spatial resolution. Kinematic boundary conditions were imposed and the specimen were loaded force controlled beyond yield in 17 different load cases (six uni-axial, three shear and eight multi axial). The proposed yield criterion was fitted to the resulting yield data.

In axial direction, maximum yield stress 2.6 MPa in tension and 4.7 MPa in compression. Lowest shear stress was found in the transverse plane with 1.3 MPa. Multi-axial yield stresses ranged between values for uni-axial tension and compression. Yield stresses depended significantly and substantially on both volume fraction and fabric. The standard error of the estimate of the yield surface was 15.99 % and the concordance correlation coefficient between prediction and measurement was 0.95.

The results of this study are not only consistent with experimental data from the literature but also extend the current knowledge of yield to multi-axial load cases that can hardly be realised in a biomechanical experiment. Since bone volume fraction and fabric are measurable via QCT, the proposed criterion provides a yield-strength threshold to distinguish critically and non-critically loaded trabecular bone. The presented yield data and criteria will help improving the prediction of vertebral ultimate load using anatomy-specific finite element models.

Disclosures: Uwe Wolfram, None.

SU0057

Identification of Biochemical, Mechanical, and Structural Factors that Define Bone Quality. Steven Tommasini*¹, Andrea Trinward², Alvin Acerbo³, Lisa Miller⁴, Stefan Judex². ¹Yale University School of Medicine, USA, ²Stony Brook University, USA, ³Brookhaven National Laboratory, USA, ⁴Brookhaven National Laboratory, USA

Bone strength and fracture risk are highly dependent on the quantity and quality of the tissue. The aim of this study was to identify principal matrix and architectural factors that define bone quality. We hypothesized that subtle modulation of bone's matrix properties, such as chemical composition and microarchitecture, markedly influences bone quality resulting in direct effects on bone's mechanical properties. To establish a large range of micro- and macroscopic tissue properties, we examined the rat skeleton defined through estrogen withdrawal and subsequent pharmaceutical osteoporosis treatments. Six-month old female Sprague Dawley rats (n=10/group) were assigned to age-matched control, untreated OVX, OVX treated with high, medium, or low doses of either PTH or alendronate, or OVX treated with high or low doses of sodium fluoride. Treatments lasted for 6mo. Total cross-sectional area (TtAr), cortical thickness (CtTh), and tissue mineral density (TMD) of the left femoral mid-diaphysis were measured via desktop μ CT. Intracortical microporosity (e.g., lacunae number density, LcN/TV) was quantified using synchrotron μ CT (0.75 μ m resolution). Chemical indicators of bone quality were measured by FTIRI. Tissue-level mechanical properties were measured by 3-point bending of longitudinal strips from the right femoral diaphysis. Linear regression analysis of the combined dataset showed that tissue modulus correlated positively with TMD ($R^2=0.05$, $p<0.05$) and negatively with LcN/TV ($R^2=0.12$, $p<0.05$), TtAr ($R^2=0.07$, $p<0.01$), CtTh ($R^2=0.10$, $p<0.01$), and crystallinity ($R^2=0.06$, $p<0.05$). Post-yield strain correlated positively with TtAr ($R^2=0.10$, $p<0.01$), CtTh ($R^2=0.15$, $p<0.001$), and LcN/TV ($R^2=0.18$, $p<0.01$) and negatively with TMD ($R^2=0.12$, $p<0.001$). Stepwise regression analysis revealed that 26-51% of the variation in tissue-level mechanical properties was explained by a combination of chemical and architectural properties. Together, these studies identified precise interrelationships between biochemical, mechanical, and structural factors during hormone imbalances and treatments at different hierarchical levels. The results indicated that the nature of these relationships is complex and multifactorial, similar to the genetic basis of peak bone mass. Identification of these potential chemical targets is critical for improving the diagnosis, prevention, and treatment of bone quality defects induced by aging, disease, and treatment.

Disclosures: Steven Tommasini, None.

SU0058

Mechanical Competence of the Proximal Femur as Predicted from DXA, DXA-equivalent CT (CTXA) and Structure Analysis. Volker Kuhn*¹, Annemaria Leib¹, Holger Boehm², Thomas Link³, Felix Eckstein⁴. ¹Medical University Innsbruck, Austria, ²LMU Munich, Germany, ³University of California, San Francisco, USA, ⁴PMU, Austria

The purpose of this study was to compare femoral DXA and CXTA with failure loads, and to analyse the influence of neck and trochanteric structure upon the fracture type.

188 proximal femur specimens were harvested from formalin-fixed human cadavers (mean age: 79.5 \pm 10.3; ranging 52-100; 94 male; 94 female). CT images were acquired using a 16-row multislice CT scanner. DXA and CXTA (Mindways QCTPRO) included the standard regions of interest (ROIs) (total femur, trochanteric, intertrochanteric, Ward, neck). Following DXA and CT, all specimens were tested destructively in a mechanical loading device simulating a sideways fall on the greater trochanter. Structure of cross-sections within neck and trochanter was analyzed using the QCTPRO plug-in Bone Investigational Toolkit - BIT to obtain total and cortical area, BMD, cross sectional moments of inertia (CSMI) and section modulus (SM).

According T-score 20% presented normal bone, 41% osteopenic, 43% osteoporotic. Failure loads ranged from 1149N to 8146N and were 32% higher in males (4837 \pm 1465N) compared with females (3281 \pm 1064N). Fractures were comparable with types seen clinically (44% neck, 27% trochanteric, 27% subtrochanteric shaft).

Comparing the results from DXA and CXTA there were only minimal differences between aBMD and BMC. Correlations with the mechanical failure loads ranged from 0.69–0.81. However vBMD from CXTA was only moderate correlated (0.52–0.69).

For the cross-section analysis correlation with failure loads was best for cortical area (0.76), cortical and total CSMI (0.70-0.76) and cortical section modulus (0.68–0.77). Total BMD from the structure analysis was correlated only moderate (0.48–0.65), and lowest correlation was seen for cortical BMD (0.11–0.33).

For the neck fractured group nearly all parameters from BIT (neck and trochanteric) were significantly lower.

Biggest differences were presented for cortical area (-24% neck cross-section; -13% troch. cross-section) and CSMI (-32 to -38% neck; -20 to -26% troch.). However there was no significant difference for the total and cortical BMD.

Prediction of femoral strength was nearly the same for DXA and CXTA. aBMD and BMC predict failure loads better than vBMD. However cross-sectional analysis of geometric properties may improve the prediction of fracture risk and fracture type, but should be performed directly in the site of interest.

Disclosures: Volker Kuhn, None.

SU0060

Predicting Vertebral Bone Strength with a Quantitative Computed Tomography-based Finite-element Method -Creation of Strength Data According to Age Range in a Normal Population and Analysis of Factors Affecting Strength-. MASAKO KANEKO*¹, ISAO OHNISHI², Sakae Tanaka¹. ¹The University of Tokyo, Japan, ²Clinical Medical Research Center, International University of Health & Welfare, Japan

Objective(s): Spinal aBMD only explains 50-80% of vertebral strength, and the application of aBMD measurements in isolation cannot accurately identify individuals who are likely to eventually experience bone fracture, due to the low sensitivity of the test. For appropriate treatment intervention, a more sensitive test of bone strength is needed. Quantitative computed tomography based finite element methods(QCT/FEM) may allow structural analyses taking these factors into consideration to accurately predict bone strength (PBS). To date, however, basic data have not been reported regarding the prediction of bone strength by QCT/FEM with reference to age in a normal population. The purpose of this study was thus to create a database on PBS in a normal population as a preliminary trial. With these data, parameters that affect PBS were also analyzed.

Material and Methods: Participants in this study comprised individuals who participated in a health checkup program with CT and for whom scan data were available for subsequent FEM analyses. Participants included 602 men, 342 women. Exclusion criteria were provided. Scan data of L2 were isolated and taken from overall CT data for each participant with simultaneous scans of a calibration phantom. A 3-dimensional FE model was constructed from the isolated data using software. FE models were equipped with triangular shell elements for the outer surface of the cortical bone and tetrahedral solid elements with an edge size of 2 mm for the rest of the bone. A uniaxial compressive load with a uniform distribution and uniform load increment was applied.

Results: Mean PBS was lower in women than in men for all age ranges. PBS in men and women significantly decreased with age. Simple linear regression between age and PBS showed the annual rate of decline in PBS was 54N/year in men and 134 N/year in women. Mean PBS in the 70-74 year age range was

Disclosures: MASAKO KANEKO, None.

SU0061

Site Specific Micro-structural and Mechanical Properties of Human Distal Femur. Myong-Hyun Baek¹, Kwang-Kyun Kim^{*2}, Ye-Yeon Won¹, Ye-Soo Park³. ¹Ajou University Hospital, South Korea, ²Konyang University Hospital, South Korea, ³Hanyang University Hospital, South Korea

Background: Osteoarthritis (OA) is the most common form of arthritis, affecting over 20 million people in the United States alone. It is known as degenerative osteoarthritis with degeneration of articular cartilage. The aim of this study was to investigate compared in subcondral trabecular bone microstructure and mechanical properties in human distal femur with and without OA assessed by micro-CT and finite element analysis (FEA).

Methods: Ninety-six human distal cylindrical trabecular bone samples were obtained from with OA 3 and non-OA 5 cadavers. Total 6 cored trabecular bone were obtained per each distal femoral condyle (anterior, middle, and posterior). The sample size was diameter of 10 mm, height of 15 mm. All samples were scanned with a high-resolution micro-computed tomography system (micro-CT) at a spatial resolution of 24.9 μm . Based on the serial micro-CT images, a volume of interest (VOI) was selected to be 6.95 mm of diameter and 7.55 mm of side length. Based on these micro-images of trabecular bone, the finite element model was created, and the finite element analysis and the compressive test were performed sequentially.

Results: The lower microstructural and mechanical properties were lower in the OA group than non-OA group.

Conclusion: The results seem to indicate that the OA group was deterioration of microstructure and mechanical properties by reduced physical activity due to pain.

Disclosures: Kwang-Kyun Kim, None.

SU0062

The Association Between Resorption Cavities and Mechanical Failure Processes in Human Cancellous Bone. Floor Lambers^{*1}, Craig Slyfield¹, Evgeniy Tkachenko¹, Amanda Bouman¹, Tony Keaveny², Christopher Hernandez¹, Ivana Yi², Michale Jekir². ¹Cornell University, USA, ²University of California, Berkeley, USA

It is believed that resorption cavities formed during remodeling may contribute to increased fracture risk by acting as stress risers. Recently, it has been shown that, when loaded in compression, microscopic tissue damage (microdamage) forms preferentially in the vicinity of resorption cavities in human vertebral cancellous bone and that the total amount of microdamage formed by loading (DV/BV) is correlated with the percent eroded surface (ES/BS) [1]. As with any stress riser, the biomechanical effect of resorption cavities will vary based on loading mode. In the current study we test the idea that resorption cavities influence microdamage formation under loading modes other than compression by examining cancellous bone submitted to tensile loading.

Cancellous bone cores oriented in the cranial-caudal direction (8 mm diameter, 15 mm length) were collected from fourth lumbar vertebral bodies of 10 donors (8 male, 2 female, aged 47-80 years). Xylenol orange was used to stain pre-existing microdamage (caused in vivo or during specimen preparation). Specimens were then subjected to tensile mechanical loading to yield. Calcein was used to stain microscopic tissue damage caused by loading. Three-dimensional images of the bone and microscopic tissue damage were collected using serial milling, allowing visualization of the bone and microscopic tissue damage at a resolution of $0.7 \times 0.7 \times 5.0 \mu\text{m}$ (Figure 1). The results were compared to specimens tested in compression in prior work [1].

The amount of microdamage caused by tensile loading (DV/BV, $4.2 \pm 2.3\%$, mean \pm SD) was considerably greater than that generated in specimens from the same donors loaded in compression ($0.7 \pm 0.3\%$, $p < 0.01$ paired for each donor). No correlation between microscopic tissue (DV/BV) and eroded surface was found in specimens loaded in tension ($r = 0.2$, $p = 0.7$) indicating that initial regions of mechanical failure formed during tensile loading appear to be independent of resorption cavities. In contrast, our prior work showed a strong correlation between microscopic tissue damage and eroded surface ($r = 0.8$, $p = 0.01$). Our finding suggests that the influence of resorption cavities on mechanical failure processes depends on loading mode, and that cavities may have a more detrimental effect on cancellous bone biomechanics under more habitual loading modes such as compression.

[1] Slyfield, C.R. et al., Bone, doi: 10.1016/j.bbr.2011.03.031, 2012



Figure 1: Visualization of bone and microscopic tissue damage (red)

Disclosures: Floor Lambers, None.

SU0063

The Effect of Image Registration and Endocortical Segmentation Methods on Longitudinal HR-pQCT Analysis of Cortical Bone Quality. Willy Tjong, Andrew Burghardt, Janina Patsch, Sharmila Majumdar, Galateia Kazakia^{*}. University of California, San Francisco, USA

Longitudinal assessment of cortical porosity (Ct.Po) as well as geometric and densitometric measures may be influenced by: 1) image registration, and 2) endocortical boundary identification. The objective of this study was to compare cortical measures determined using three different pre-processing procedures: 1) 2D registration using endocortical boundaries defined at each time-point (2D analysis), 2) 3D registration using endocortical boundaries defined at each time-point (3D analysis), and 3) 3D registration using the baseline endosteal contour applied to follow-up time-points (3D BL analysis). Analysis was run on a dataset of post-menopausal women ($n = 12$, age = 56 ± 3 years at BL) scanned using HR-pQCT at the distal radius and tibia. Follow-up scans were conducted at 24 months. Images were registered using: 1) the default 2D algorithm (Scanco AG), which compares cross-sectional area on a slice-wise basis, and 2) a 3D algorithm based on normalized mutual information (Rview). For the 3D BL analysis, BL endosteal contours were transformed to follow-up coordinates using the transformation matrix generated from the 3D registration. Cortical measures were calculated using an extended CRTX analysis previously developed in our lab. At the radius, longitudinal significance was found only in cortical area (Ct.Ar) ($+1.7\%$ over 24 months, $p < 0.05$) using the 3D BL analysis. This response was significantly greater than that measured using follow-up endocortical contours ($p < 0.05$). No difference was found among methods for the measured response in Ct.Po. At the tibia, each method detected increased Ct.Ar (2D: $+3.1\%$, 3D: $+2.1\%$, 3D BL: $+4.4\%$; $p < 0.05$), with a significant difference between the responses measured using the 3D and 3D BL analyses ($p < 0.05$). Increased Ct.Po was detected for all methods (2D: $+9.3\%$, 3D: $+10.3\%$, 3D BL: $+11.5\%$; $p < 0.05$); responses were not significantly different from one another. A significant decrease in cortical bone mineral density (Ct.BMD) was only detected using the 3D (-1.9%) and 3D BL (-2.1%) analyses; the 2D analysis response was non-significant. Increased cortical polar moment of inertia (Ct.pMOI) was detected only using the 3D BL analysis ($+1.9\%$, $p < 0.05$). These results show that neither registration nor contouring had a significant effect on longitudinal assessment of Ct.Po for the dataset analyzed in this study. Contouring strategy, however, did affect longitudinal assessment of cortical geometry.

Disclosures: Galateia Kazakia, None.

This study received funding from: Merck & Co., Inc.

SU0064

Vertebral Deformity Fracture Number and Severity are Associated with Mechanical Competence at Peripheral Bone Derived by Micro-MRI Based Biomechanics. Chamith Rajapakse^{*1}, Eual Phillips², Wenli Sun², Michael Wald³, Peter Snyder², X Guo⁴, Felix Werner Wehrli³. ¹University of Pennsylvania School of Medicine, USA, ²University of Pennsylvania, USA, ³University of Pennsylvania Medical Center, USA, ⁴Columbia University, USA

Early detection of vertebral fractures is important because patients with such deformities are known to be at elevated risk for further fractures. Radiographic projections and DXA BMD measurements used for the assessment of vertebral deformities and fracture susceptibility have many limitations.

Advances in high-resolution imaging (e.g. μMRI and HR-pQCT) along with micro-finite-element analysis (μFEA) now permit non-invasive assessment of bone's mechanical competence at peripheral skeletal locations. Currently, however, limitations in signal-to-noise ratio in μMRI and radiation dose exposure in CT all but preclude high-resolution imaging of the vertebrae and thus their direct mechanical assessment in human subjects.

Given the systemic nature of postmenopausal bone loss, we hypothesized that the vertebral fracture status is inversely related to the mechanical competence of peripheral bone. The goal of this study was to investigate to what extent peripheral bone stiffness is predictive of vertebral deformity fractures.

This study involved sixty postmenopausal women, 60-88 years of age, with DXA BMD T-scores at either the hip or spine in the range -1.5 to -3.5. μMR images of the distal tibia and radius and sagittal images of the spine had previously been obtained on a 1.5 T clinical scanner. Axial stiffness of distal tibia and radius were computed by μFEA. Three types of vertebral deformities—wedge, biconcavity, and crush—were computed for each vertebral body visible in the spine images (Fig 1) by adapting the approach by Eastell. Number and severity of each type of deformity fractures were computed on the basis of Genant's fracture criterion (i.e. deformity > 20%) and mean deformity, respectively. Associations between vertebral fracture measures and stiffness were assessed by regression.

Tibial stiffness showed the strongest association (R² up to 0.55) with the vertebral measures (Table 1) possibly because of similarities in micro-structure at the two sites, both predominantly loaded axially. The associations between vertebral measures and stiffness of the radius (non-load bearing) were weaker (R² up to 0.18). Interestingly, spine BMD did not show any significant association with the number or severity of vertebral fractures.

In conclusion, mechanical competence of peripheral bone assessed by μMRI-based μFEA has the potential as a predictor of vertebral deformity fractures.

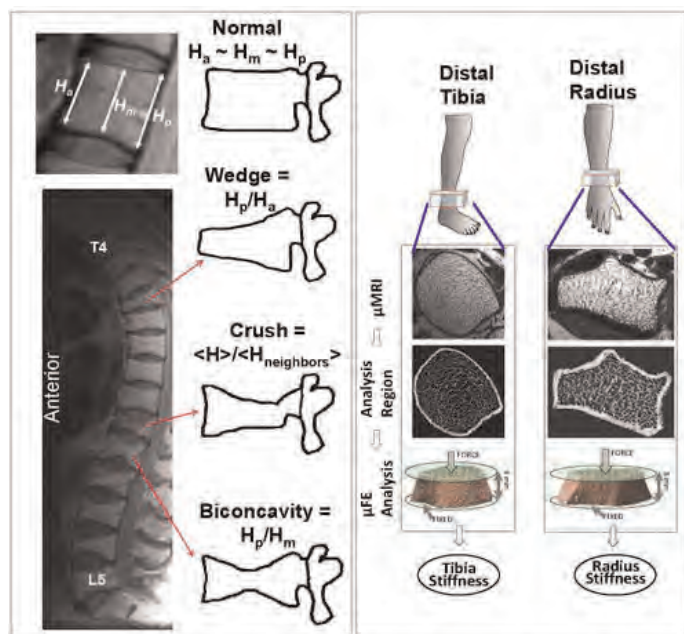


Figure 1: Illustration of vertebral morphometry and finite-element analysis.
Figure 1: Vertebral morphometry and finite-element analysis

Table 1:
R² values for the reciprocal association between FE-derived whole-section axial stiffness of distal tibia and number of vertebral fractures and their severity corresponding to three types of vertebral deformity—wedge, biconcavity, and crush.

| | Number of Fractures | Fracture Severity |
|--|---------------------|-------------------|
| Lumbar Vertebrae [L1-L5] | | |
| Wedge | 0.01 | 0.03 |
| Biconcavity | 0.12 | 0.42*** |
| Crush | 0.02 | 0.06 |
| Thoracic Vertebrae [T4-T12] | | |
| Wedge | 0.15 | 0.42** |
| Biconcavity | 0.37*** | 0.55*** |
| Crush | 0.46*** | 0.33** |
| Statistically significant (** p<0.005, *** p<0.0005) | | |

Table 1: Association Between Vertebral Deformity and FEA Measures

Disclosures: Chamith Rajapakse, None.

SU0065

Viscosity of the Organic Phase of Bone Evaluated at Bone Structural Unit Level. Pierrick Crozier¹, Insaf Hadjab², Thierry Douillard¹, Sylvain Meille¹, Georges Boivin³, Jérôme Chevallier¹, Helene Follet^{*3}. ¹CNRS, UMR5510, Université de Lyon, France, ²Université De Lyon, France, ³INSERM, UMR1033 ; Université De Lyon, France

Bone is a multi-scale composite material made of both a type I collagen matrix and a mineral phase made of crystalline apatite. The amounts, properties and organization of its constituents at tissue level influence the mechanical properties of bone. Our purpose was to study the viscosity of the organic phase at bone structural unit (BSU) level in bone. First, the effects of the embedding steps process have been studied and then, the contributions of bone mineral and organic matrix on the mechanical properties have been measured in the case of a specific bone disease: osteomalacia.

Several diaphysis femoral bone samples were taken from untreated ewes. Before embedding in PMMA, fresh and dry samples were used. Dehydration in graduated alcohol (70-100%), fluorochrome staining (calcein) and impregnation steps were tested by indentation (40 indents each test). Then, four iliac bone biopsies were taken from patient with osteomalacia and embedded in PMMA. Microradiography on 100±10μm-thick sections were taken from each biopsy and indentation tests were performed using a Berkovich indenter tip (NANOIndenter II, Nano Instruments Inc., US) to measure elastic modulus (E) (assuming a Poisson coefficient ν=0.3), contact hardness (H_c) and true hardness (H)^{1,2}. Measurements were done separately in mineralized, osteoid and resin compartments (resp 110, 111 and 22 indents per zone). Measurements were conducted in continuous stiffness measurement mode and in quasi-static mode. The second mode allowed to use a visco-elasto-plastic model (VEP)³.

Values obtained from ewes bone samples showed that embedding process increase hardness on cortical but with a gradient between periosteal and endosteal. PMMA samples values were higher (about 7.4% compared to fresh bone). On osteomalacia samples, results revealed that E, H_c and H are consistent with literature in mineralized zone⁴ (Table). Viscosity is higher in cortical bone compared to trabecular bone, and almost three times higher in mineralized tissue than in osteoid. Resin shows all the time the lowest values (Figure).

Our results show that mineral phase affects greatly viscosity however organic phase (osteoid) may play an important role in the VEP model of mechanical behavior of bone.

1. Bala 2011, J Mech Behav Biomed Mater 4:1473
2. Oliver & Pharr 1992, J Mater Res 7:1564
3. Oyen *et al.* 2003, J Mater Research 18:139
4. Zysset 2009, Osteoporos Int 20:1049

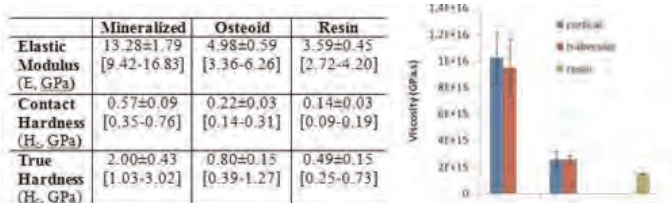


Table: Values of mechanical parameters (Mean±SD [range]) depending of the bone compartment, Figure: Example of Viscosity (Pa.s) in both cortical and trabecular bone, mineralized or osteoid zone.

Disclosures: Helene Follet, None.

SU0066

What Is the Performance in Vertebral Fracture Discrimination by Bone Mineral Density (BMD), Micro-architecture Estimation (TBS), Body Mass Index (BMI) and FRAX in Stand-alone or Combined Approaches: The OsteoLaus Study. Olivier Lamy^{*1}, Marc-Antoine Krieg², Delphine Stoll³, Berengère Aubry-Rozier³, Marie Metzger³, Didier Hans⁴. ¹Chief of the Bone Unit, Switzerland, ²University Hospital, Switzerland, ³Lausanne University Hospital - Center of Bone Diseases, Switzerland, ⁴Lausanne University Hospital, Switzerland

Introduction:Osteoporosis (OP) is a systemic skeletal disease characterized by a low bone mineral density (BMD) and a micro-architectural (MA) deterioration. Clinical risk factors (CRF) are often used as an indirect surrogate marker of MA (e.g. FRAX model). MA is yet more directly evaluable in daily practice by the Trabecular Bone Score (TBS) measure. TBS is a novel grey-level texture measurement reflecting bone micro-architecture based on the use of experimental variograms of 2D projection images. TBS has proven to have diagnosis and prognosis value, partially independent of CRF and BMD. The aim of the OsteoLaus cohort is to combine in daily practice the CRF and the information given by DXA (BMD, TBS and vertebral fracture assessment (VFA)) and FRAX to better identify women at high fracture risk.

Material and Method:The OsteoLaus cohort (1400 women 50 to 80 years living in Lausanne, Switzerland) started in 2010. CRF for OP, FRAX, lumbar spine and hip BMD, VFA by DXA and MA evaluation by TBS are recorded in OsteoLaus. Preliminary results are reported. Sensitivity and specificity in regard to vertebral fracture grade 2&3 has been calculated for all Bone modalities as stand-alone or combined approaches.

Results:We included 451 women: mean age 67.4 ± 6.7 y, BMI 26.1 ± 4.6, mean lumbar spine BMD 0.943 ± 0.168 (T-score -1.4 SD), TBS 1.271 ± 0.103. As expected, correlation between BMD and site matched TBS is low (r=0.16). Prevalence of VFx grade 2/3, is 9.3%.

See Table 1

Conclusion: BMI did not have discriminatory ability in our cohort. As in the already published studies, these preliminary results confirm the partial independence between BMD and TBS as well as with FRAX. The combination of TBS and FRAX seems to be the best comprise in sensitivity / specificity and increases significantly the identification of women with prevalent VF Fx which would have been miss-classified by BMD or FRAX or TBS alone.

| | | Sensitivity | Specificity |
|---------------------|---|-------------|-------------|
| Single modalities | FRAX All fracture (Swiss threshold as flag) | 23.6% | 92.4% |
| | FRAX All fracture (20% threshold) | 28.6% | 93.4% |
| | BMI 20 threshold | 4.8% | 93.9% |
| | Spine BMD (-2.5 T-score threshold) | 33.3% | 74.1% |
| | Spine TBS (-1.200 threshold) | 42.9% | 74.6% |
| Combined modalities | Spine BMD or TBS thresholds | 59.3% | 99.2% |
| | Spine BMD or FRAX thresholds (age)* | 45.2% | 70.4% |
| | Spine TBS or FRAX thresholds (age)* | 52.4% | 70.9% |
| | Spine TBS or BMD or FRAX thresholds (age) | 66.7% | 96.2% |

* similar results were found if FRAX All fracture threshold was used.

Table 1

Disclosures: Olivier Lamy, None.

SU0067

Early Vascular and Bone Changes after Zoledronate Treatment. Mohammed Elsalanty^{*1}, Chestine Guevarra², Nicole Howie³, Ibrahim Zakharly³, James Borke⁴. ¹Georgia Health Science University, USA, ²US Advanced Education Program in Periodontics, Fort Gordon, USA, ³Georgia Health Sciences University, USA, ⁴Western University, USA

Bisphosphonate-related osteonecrosis of the jaw (BRONJ) is a devastating adverse effect of long-term bisphosphonate use. The purpose of this study was to test the hypothesis that zoledronic acid, the most potent bisphosphonate, inhibits vascular growth in the rat's mandible following dental trauma. This inhibition will not only diminish the healing process but will initiate bone necrosis. Forty-eight Sprague-Dawley Rats were randomly divided between control (n=24) and experimental groups (n=24). Animals in the experimental group were given two IV injections of zoledronate, 4 weeks apart. The control animals were given IV saline. At the time of the second injection in both groups, the first molar tooth was extracted. Animals were sacrificed at 4, 8, or 12 weeks (8 animals in each group/time point). Extraction site was examined clinically, then mandibles were collected and the bone tissue was examined histologically as well as through microCT angiography. Results showed failure to heal in 75% of treated animals that persisted up to 12 weeks after extraction.

Vascular changes started showing as early as 4 weeks, while histologic indications of bone necrosis were detected later at 8 weeks. This study validates a BRONJ rat model and indicates that the bone necrosis is preceded by failure to elicit adequate vascular response to dental trauma.

Disclosures: Mohammed Elsalanty, None.

SU0068

In Vitro Exposure of Rat Femur to Strontium Chloride Influences Bone Material Level Properties and Increases Bone Strength. Patrick Ammann^{*}, René Rizzoli. Division of Bone Diseases, Department of Rehabilitation & Geriatrics, University Hospital & Faculty of Medicine, Switzerland

Bone microarchitecture and material level properties independently contribute to the improvement of bone strength induced by strontium (Sr) ranelate treatment as evaluated by μ CT-based finite element analysis. The influence of in vitro Sr exposure on material level properties and on bone mechanical properties is unknown. We investigated whether in vitro exposure of rat femurs to Sr is able to modify the bone mechanical properties independently of geometrical changes. One femur was exposed overnight to 1 M SrCl₂ solution and the controlateral to 1 M NaCl solution. Then 3 point-bending tests were performed allowing the determination of Maximal load, Stiffness, Energy (total, plastic) as well as post Yield behaviours i.e. post Yield load and deflection characterizing plastic phase. Similar protocol was performed using 1 M CaCl₂ solution to investigate the specificity of Sr. Bone material level properties was evaluated using nanoindentation. The total number of investigated bone samples was 32, values are means ± SEM, *p<0.05 as compared to NaCl exposure femur using a T-test. The in vitro exposure to 1 M SrCl₂ solution increased Maximal Load (+13%), Energy (+30%) but not Stiffness. In this model, modification of bone mass, geometry or micro architecture could be excluded since exposure to Sr was performed in vitro. Modification of mechanical properties could thus only be attributed to modification of bone material level properties, which were all significantly increased by in vitro Sr exposure (modulus, hardness). Furthermore, parameters characterizing plastic deformation of the femur were markedly improved by Sr exposure: plastic energy (+76%) post Yield load (+45%) and post Yield deflection (+62%). Interestingly, these results are similar to those obtained by in vivo Sr Ranelate treatment. Exposure to CaCl₂ did not affect mechanical properties underlying the selectivity of the Sr effect. These results further support the important role of bone material level properties as a determinant of bone strength

| | Maximal Load (N) | Stiffness (N/mm) | Total Energy (N*mm) | Plastic Energy (N*mm) |
|--------------------|---------------------|---------------------|------------------------|--------------------------|
| NaCl | 126.8±8.8 | 333.2±21.4 | 32.6±4.6 | 14.0±3.5 |
| Sr Cl ₂ | 143.3±8.1* | 382.6±22.0 | 42.5±6.2* | 24.7±5.1* |
| NaCl | 134.5±5.9 | 344.2±22.5 | 36.1±5.1 | 17.2±4.4 |
| CaCl ₂ | 135.0±3.8 | 354.7±18.0 | 36.2±3.0 | 19.5±3.0 |

Effects of in vitro exposure to Sr or Ca on bone mechanical properties

Disclosures: Patrick Ammann, Servier, 2

SU0069

TGF- β Suppression with a Neutralizing Antibody Increases Vertebral Body Strength in Female Mice. Alexander Makowski^{*1}, Sasidhar Uppuganti¹, Barbara Rowland¹, Alyssa Merkel¹, Daniel Perrien², Julie Sterling³, Jeffrey Nyman². ¹Vanderbilt University, USA, ²Vanderbilt University Medical Center, USA, ³Department of Veterans Affairs (TVHS)/Vanderbilt University Medical Center, USA

Transforming growth factor beta (TGF- β) is a promising target for reversing the breast cancer-induced decrease in bone's resistance to fracture. Our previous work with a neutralizing antibody to the 3 isoforms of TGF- β (1D11) found that TGF- β suppression increased trabecular bone (BV/TV) in the long bones of both young female, tumor-bearing and older male, non-tumor bearing mice with an initial low bone mass phenotype (C57BL/6). To date, TGF- β suppression has only been reported to increase lumbar vertebra (VB) strength when young male (4 wk), non-tumor bearing mice are treated with an inhibitor of the TGF- β type I receptor kinase for 6 weeks. To test the hypothesis that 1D11 could be effective in enhancing fracture resistance in female mice, we treated 13 wk old FVB mice for 4 weeks with either 13C4 (control antibody, n=5) or 1D11 (10 mg/kg, n=7) 3x per week. After euthanasia, the L6 VB was scanned at an isotropic voxel size of 12 μ m with a μ CT scanner calibrated to a hydroxyapatite phantom. Using the scanner's finite element (FE) model generator (voxel-to-brick element) and elastic solver, the failure load of each VB was predicted for high-friction, axial compression at 1% apparent strain and using failure criteria in which 2% of the model volume exceeds 0.007 equivalent strain. We selected 2 cases of material properties (v = 0.03): constant modulus (CM) of 18 GPa and VB-specific modulus (SpM) derived from the mean tissue mineral density (TMD). Lastly, each VB was subjected to axial compression at 3 mm/min in which the supporting platen had a rough surface and a moment relief to minimize slippage and off-axis loading, respectively. The strength was the peak force sustained by the VB. Mann-Whitney was used to test for differences between groups. Compared to control, 1D11-treatment increased BV/TV by 41% and TMD by 3% (p=0.0025 for both) as well as

increased the measured and predicted strengths (Fig. 1). After excluding an outlier (Fig. 1) that slipped during the compression test as observed by high magnification video, linear regression analysis found that BV/TV explained 75.8% of the variance in VB strength. Even though the μ CT-FE analysis includes the cortical shell and trabecular architecture of the VB, the CM- and SpM-predicted strength explained 63.9% and 65.6%, respectively. Thus, TGF- β suppression apparently increases VB strength by increasing BV/TV with some contribution from an increase in TMD.

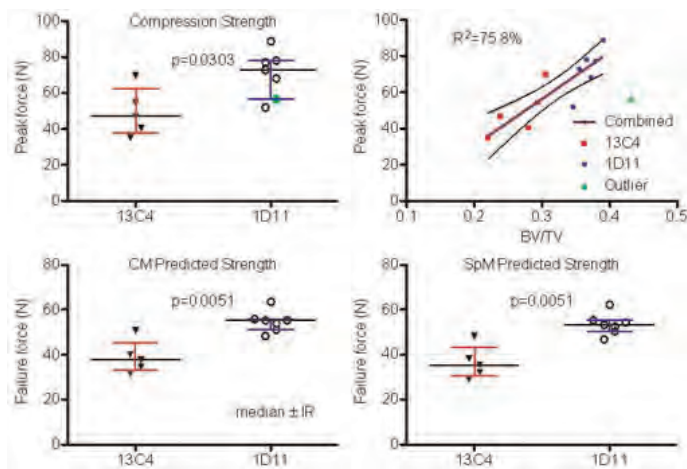


Figure 1. Vertebral body strength was greater for the 1D11-treated mice than control mice.

Disclosures: Alexander Makowski, None.

SU0070

Bone Mineral Loss at the Hip in Acute Spinal Cord Injury. William Edwards*¹, Thomas Schnitzer², Karen Troy¹. ¹University of Illinois at Chicago, USA, ²Northwestern University, USA

Bone loss following spinal cord injury (SCI) is associated with an increased risk of fracture due to minor trauma. Fractures of the hip account for approximately 10-20% of all fractures in this population and are among the most serious of injuries. DXA measurement has illustrated a 15-30% reduction in hip bone mineral during the first 6-18 months after SCI. However, there is a dearth of information regarding bone loss during the first few months after SCI, and no information regarding trabecular and cortical bone specific changes at the hip following SCI. Our purpose was to quantify changes to hip bone mineral, geometry, and structure associated with acute SCI. Ten subjects with acute SCI received clinical CT scans at baseline (within 8 weeks of SCI) and follow-up (\approx 3 months after baseline). A phantom was included in each scan to relate CT attenuation to bone equivalent density. Follow-up images were registered to their respective baseline images and CT voxels comprising the femoral neck and trochanteric region were identified for analysis. BMC and volumetric BMD (vBMD) were quantified for integral, trabecular, and cortical bone. Cross sectional area (CSA), a compressive strength index (CSI) and a bending/torsional strength index (BSI) were quantified for the femoral neck. During the 3 month period subjects experienced a 10.5% reduction in integral BMC ($p < 0.001$) and a 9.9% reduction in integral vBMD ($p < 0.001$). Trabecular BMC decreased by 15.2% ($p < 0.001$) and trabecular vBMD by 14.1% ($p < 0.001$). A 13.2% reduction was observed for cortical BMC ($p < 0.001$), while the reduction in cortical vBMD was comparatively negligible (-2.5%; $p = 0.06$). The cortical bone loss occurred primarily through cortical thinning on the endosteal surface. Femoral neck CSA illustrated a relatively small 0.9% reduction ($p = 0.03$). The observed changes in bone mineral and structure were associated with a 17.4% reduction in femoral neck CSI ($p < 0.001$) and a 16.4% reduction in femoral neck BSI ($p < 0.001$). In summary, these results illustrate that acute SCI is associated with large reductions in both trabecular and cortical bone mineral at the hip. The reductions in structural measures of femoral neck strength suggest that the reductions in bone mineral may have large mechanical consequences. These data provide a more in-depth understanding of bone loss after SCI, which ultimately may help develop targeted therapies to minimize the occurrence of SCI related fracture.

Disclosures: William Edwards, Merck & Co., Inc., 6

SU0071

Low Intensity Pulsed Ultrasound Improves Mechanical Strength and Structural Quality in a Disuse Osteopenia Model. Sardar Uddin*¹, Yi-Xian Qin². ¹Stony Brook University, USA, ²State University of New York at Stony Brook, USA

Disuse osteopenia has been known to cause adverse effect on bone mass leading to reduction of bone mineral density (BMD) and quality, particularly in weight-bearing skeletal [1]. BMD partially attributed to lack of mechanical force on bone tissue, which alters gene expression, reduction in transcription factors and growth factors. As

a mechanobiological signal, acoustic vibrations can be noninvasively applied in appropriate *in vivo* and human models at the region of interests. The objective of this study is to evaluate the local and systematic effects of low intensity pulsed ultrasound (LIPUS) on a hindlimb suspension (HLS) disused rat model.

C57BL/6 mice ($n=12$ per group, total 60) were suspended for 4 weeks via HLS. Animals were distributed into 5 groups, Age-Match (AM), Non-Suspended Sham (NS), Non-Suspended-LIPUS (NU), Suspended Sham (SS) and Suspended-LIPUS (SU). NU and SU animals' femur were exposed to LIPUS at 30mW/cm² for 20min/day for 5 days/week. After 4 weeks animals were euthanized and femur were collected. Bone mechanical strength was accessed using four-point bending test. Femur diaphysis was scanned using mCT. Bone J was used to calculated center of mass and moment of inertia.

Mechanical testing data showed that LIPUS treatment significantly improves bone elastic modulus (65%), yield strength (87%) and ultimate strength (82%) in SU group (Table 1). mCT data showed significant increase in bone mineral density (mmHg/cc), trabecular thickness in SU group and significantly reduced Bone Surface / Bone volume ratio in SU groups (Table 2). Analyses of contralateral controls showed LIPUS anabolic effects were localized and showed no systematic effects. Our preliminary histomorphometry data showed positive correlation with mCT and mechanical testing data and showed increase in bone formation both in trabecular and cortical bone (Fig 1).

| Group | Elastic Modulus (MPa) | | Yield Stress (Mpa) | | Ultimate Stress (MPa) | |
|-------|-----------------------|-------------|--------------------|--------------|-----------------------|--------------|
| | Right | Left | Right | Left | Right | Left |
| AM | 1772.12±682 | 1730.65±632 | 74.38±25.3 | 69.79±25.8 | 92.03±35.2 | 86.66±31.2 |
| NS | 1793.6±19 | 1581.32±738 | 75.52±30.9 | 74.94±27.6 | 90.39±44.7 | 88.68±32.5 |
| NU | 1881.03±643 | 1572±712 | 69.12±13 | 75.28±27.9 | 81.21±22.0 | 91.19±35.8 |
| SS | 726.47±316 | 811.86±344* | 33.07±12.2 | 41.63±12.3* | 36.42±13.3 | 47.49±25.0* |
| SU | 792.76±310 | 1407.64*† | 34.18±12.7 | 65.44±26.9*† | 45.45±15.6 | 78.08±38.8*† |

- * $P < 0.05$ relative to AM
- † $p < 0.05$ relative to contralateral control

Table 1: Effects of LIPUS on mechanical properties of mice femur.

Table 1: Effects of LIPUS on mechanical properties of mice femur.

| Groups | BMD (mmHg/cc) | | Trabecular Thickness (mm) | | BS/BV(mm ³ /mm ³) | |
|--------|---------------|---------------|---------------------------|----------------|--|-------------|
| | Right | Left | Right | Left | Right | Left |
| AM | 777.60±17.1 | 771.34±23.6 | 0.0375±0.003 | 0.0389±0.002 | 71.72±6.6 | 73.52±7.0 |
| NS | 765.20±25.6 | 762.03±21.7 | 0.0378±0.004 | 0.0379±0.003 | 73.55±7.5 | 73.94±5.6 |
| NU | 765.35±29.5 | 758.84±19.9 | 0.0377±0.003 | 0.0363±0.003 | 74.09±5.5 | 76.45±9.2 |
| SS | 754.62±18.7 | 747.86±26.5* | 0.0332±0.001 | 0.0340±0.003* | 84.31±8.9 | 85.41±6.9* |
| SU | 742.89±40.6 | 772.50±21.5*† | 0.0329±0.004 | 0.0363±0.004*† | 86.48±13.0 | 77.62±6.9*† |

- * $P < 0.05$ relative to AM
- † $p < 0.05$ relative to contralateral control

Table 2: Effects of LIPUS on mechanical properties of mice Tibia

Table 2: Effects of LIPUS on mechanical properties of mice Tibia

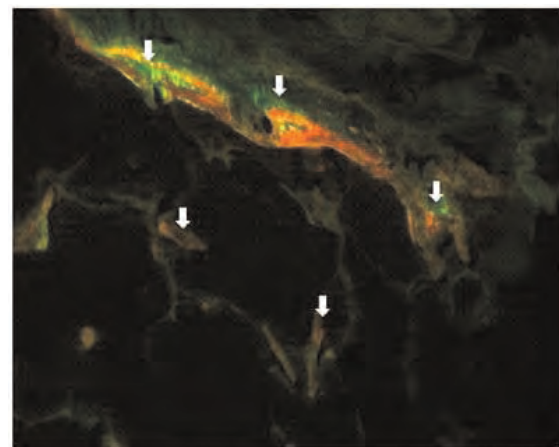


Fig 1 : Preliminary histomorphometry analyses show bone formation at different sites. Arrows indicated new formed cortical and trabecular bone.

Fig 1 : Preliminary histomorphometry analyses show bone formation at different sites

Disclosures: Sardar Uddin, None.

SU0072

Altered Bone Microarchitecture and Material Properties as Well as Reduced Osteocyte Frequency Predict Significant Changes in the Transmission of Strain to Osteocytes Within Aged Cortical Bone of Non-Human Primates. Amber Stern^{*1}, Matthew Stern¹, Branson Billings¹, Christopher Bergman², Thomas Register³. ¹University of Missouri - Kansas City, USA, ²Wake Forest University School of Medicine, USA, ³Wake Forest School of Medicine, USA

Osteocytes play an important role in the equilibrium of bone remodeling through their complex network of extracellular and intracellular communication. However, with age and osteoporotic disease state, bone becomes less responsive to strain which results in a reduced bone mass and increased risk of fracture. The purpose of this study was to use scanning electron microscopy (SEM) to quantify changes in the microarchitecture of bone that accompany the aging process. These data were then used to create representative idealized finite element models to predict the strains perceived by young and old osteocytes.

SEM imaging was used to examine the osteocyte lacunar-canalicular system of young (n=5) and old (n=5) non-human primate femurs. Images obtained at 300x magnification were collected to assess lacunar density, while osteocyte lacunar cross sectional area and the number of canaliculi per osteocyte lacuna were measured using a magnification of 3000x.

There was a significant increase (Student's T-test, p<0.05) in osteocyte lacunar cross sectional area with age (119.4±3.3 μm² for the young vs. 131.7±3.9 μm² for the old samples). The increase in cross sectional area was observed along the minor axis of the osteocyte lacuna, leading to a "fatter" lacuna in the old bones. A significant decrease in lacunar density was observed between samples from young and old bone (729.3±18.0 lacunae/mm² for the young vs. 603.7±15.2 lacunae/mm² for the old). No significant difference was observed between the number of visible canaliculi per osteocyte in young and old samples (37.1±1.1 vs. 36.8±1.2).

Representative parametric finite element models were created for the idealized young and old osteocyte lacunae based upon the results from the SEM analyses. Holding the material properties constant, there was a slight 3.2% increase in osteocyte lacunar strain with age, which was counterintuitive. However, when the material properties are taken into account (a stiffer perilacunar matrix for the old bone and a more pliable perilacunar matrix for the young bone) there was a 20% reduction in the amount of strain reaching in lacuna in the old bone when compared to the young bone.

Age-related changes in bone remodeling and osteoporosis may be due in part to a reduction in the ability of osteocytes to perceive strain due to changes in the morphology and mechanical properties of bone at the microstructural level.

Disclosures: Amber Stern, None.

SU0073

Fluid Flow Induced Osteoclast Differentiation Is Associated with Alterations in Genes Regulating Apoptosis, Necrosis and Osteoblast Differentiation. Aleksey Dvorzhinskiy^{*1}, Rune Madsen¹, Benjamin McArthur¹, Goran Andersson², F. Patrick Ross¹, Mathias Bostrom¹, Anna Fahlgren¹. ¹Hospital for Special Surgery, USA, ²Karolinska Institute, Sweden

Mechanical loading of bone is anabolic, while aseptic loosening of implants is catabolic. In our established rat model of mechanically induced prosthetic loosening, osteoclast differentiation is increased dramatically after 3 days but little is known about the underlying mechanism(s). The objective of this study was to profile signal transduction pathways in our model. Microarrays on cortical bone samples exposed to pressurized fluid flow were performed 3, 6, 12, 24 and 36 hrs, using time zero samples as controls. Of a total of 5640 genes that underwent a 1.25-fold change or greater (p<0.05) due to fluid flow only 30, mostly related to cell metabolism, were common for all time points. Gene ontology also identified significant changes in genes mediating cell death, growth and proliferation and cell-to-cell signaling. Signals linked to inflammation and apoptosis were significant up-regulated in a biphasic manner at 3 and 12 and/or 24 hrs. At the cellular level genes associated with macrophage, osteoclast and osteoblast formation and/or function were affected at the same time points. The largest differences in expression were seen after 3 hrs with increases in the interleukin (IL) family cytokines IL-6, IL-11 and leukemia inhibitory factor (LIF) and the transcription factor STAT3. In addition, levels of the pro-apoptotic factor TWEAK were higher while those of BOK, a second pro-survival molecule, were lower. There is an early and late rise in RIPK3, which stimulates a form of programmed necrosis that is suppressed by caspase 8 in response to TNFα. At later time points, osteoblast-related genes were clearly suppressed (osteocalcin, Col1a, PTHr1), while a number of those regulating macrophage and osteoclast differentiation (CSF-1, Bach1, HO-1, RANKL, RANK, OPG) were enhanced. These data suggest that mechanical loading of cortical bone stimulates complex, time-dependent changes in expression of genes regulating the survival, necrosis and/or differentiation of cells of both the myeloid and mesenchymal lineages. The net outcome, increased matrix destruction, reflects an integrated response that leads to a rapid increase in the numbers of bone-degrading osteoclasts.

Table 1. Fold change of selected genes of interests

| Signal transduction | Gene | 3 hrs | 6hrs | 12 hrs | 24 hrs | 36 hrs |
|---------------------|-------------|--------|-------|--------|--------|--------|
| IL6 cytokine family | IL-11 | 2.20* | n.d | 4.71* | n.d | n.d |
| | IL-6 | 11.98* | n.d | 2.61 | n.d | n.d |
| | LIF | 2.20* | n.d | n.d | 1.29 | n.d |
| | STAT3 | 1.39* | n.d | -1.03 | -1.06 | -1.10 |
| | | | | | | |
| Apoptosis | TWEAK | 1.65* | 1.26 | 1.48* | n.d | 1.44* |
| | RIPK3 | 1.65* | n.d | n.d | 1.67* | n.d |
| | BOK | -1.71* | -1.15 | -1.51* | -1.32* | -1.05 |
| Osteoclastogenesis | Bach1 | 1.77* | n.d | 1.56* | 1.51* | n.d |
| | HO-1 | 3.28* | n.d | 3.02* | 2.18* | n.d |
| | CSF-1 | 1.33* | n.d | 1.63* | 1.59* | 1.63* |
| | RANKL | n.d | n.d | 2.57 | n.d | 2.30 |
| | RANK | n.d | 1.08 | n.d | 1.47* | 1.58* |
| | OPG | 1.79* | n.d | -1.01 | -1.32* | 1.10 |
| Osteoblastogenesis | Osteocalcin | n.d | n.d | -1.41 | -2.92* | -3.28 |
| | Col1a1 | -1.22 | -1.19 | -1.25 | -1.50* | -1.19* |
| | PTHr1 | -1.99* | -1.31 | -1.46 | -1.64* | -1.47 |
| | | | | | | |

*= Significant fold change versus non-pressurized control (p<0.05). n.d= not detectable in the microarray.

Table 1. Fold change of selected genes of interests

Disclosures: Aleksey Dvorzhinskiy, None.

SU0074

Mechanically Activated Src Induces Activation of RhoA through mTORC2 in Mesenchymal Stem Cells. William R. Thompson^{*1}, Sherwin Yen¹, Buer Sen², Zhihui Xie¹, Natasha Case³, Maya Styner³, Christophe Guilluy¹, Keith Burridge¹, Janet Rubin³. ¹University of North Carolina, USA, ²University of North Carolina At Chapel Hill, USA, ³University of North Carolina, Chapel Hill, School of Medicine, USA

Mechanical strain directs lineage allocation of mesenchymal stem cells (MSC) by restricting adipogenesis and enhancing osteogenesis. We showed that mTORC2 is a novel mechanical target that is critical for the anti-adipogenic signal involving Akt activation, which leads to GSK3β inhibition and preserves β-catenin. How mTORC2 is activated by force is unknown, but its activation requires the presence of focal adhesions (FAs). Activation of Src and focal adhesion kinase (FAK) are some of the earliest events following integrin-FA engagement. We asked if Src/FAK signaling is involved in mTORC2 activation. Mechanical strain was applied to marrow derived MSCs (100 cycle/2%-strain) to activate mTORC2, as assessed by Akt pS473. Pharmacological inhibition of Src family kinases prevented mechanical activation of mTORC2. The strain-induced increase in pAkt was blocked in Src-depleted fibroblasts lacking isoforms Src, Yes, and Fyn, confirming the requirement for Src kinase in mechanical mTORC2 activation. Importantly, add-back of Src, but not Yes or Fyn, rescued strain Akt activation. Src and FAK associate at FAs. Strain induced FAK pY397; however, inhibition of Src failed to suppress mechanical FAK Y397 phosphorylation, suggesting that Src may be downstream of FAK in this pathway. Interestingly, Src has been shown to be involved in mechanically induced, RhoA-directed FA assembly. As mTORC2 is known to contribute to cytoskeletal architecture, we asked if Src involvement might be at the level of mTORC2 rather than directing GEF activation of RhoA. To determine a role for mTORC2 in mechanically induced RhoA activation, MSCs were treated with an mTOR or Akt inhibitor and activated RhoA was measured in lysates following strain. Full RhoA activation by strain was blocked by each inhibitor, indicating that mTORC2's effect on RhoA was mediated through its effector target, Akt. Taken together, these data show that following application of strain, Src-mediated mTORC2 activation is required for GEF-induced GDP/GTP exchange on RhoA. As such, the mechanical anti-adipogenic signal begins with Src-mediated mTORC2 activation, which distally generates both a β-catenin signal and a RhoA-induced cytoskeletal change. Interestingly, increased cytoskeletal structure is also thought to be an anti-adipogenic signal. These data suggest mTORC2 as a central signaling node in the mechanical control of MSC cell fate.

Disclosures: William R. Thompson, None.

SU0075

New Insights into Human SOST Mechanotransduction: Role of Nitric Oxide. Jesus Delgado-Calle^{*1}, Jose Riancho², Jenneke Klein-Nulend³. ¹IFIMAV-H.U. Marqués de Valdecilla-University of Cantabria, Spain, ²University of Cantabria, Spain, ³ACTA-VU University AmsterdamDept Oral Cell Biology (Rm # 11N-63), The Netherlands

Sclerostin is a Wnt signaling antagonist encoded by the SOST gene. Mechanical stimulation inhibits sclerostin expression in rodents. However, few data are available about the effect of mechanical loading in human systems. The aim of this study was to explore whether pulsating fluid flow (PFF) decreases SOST expression in a human osteoblastic cell line expressing SOST and the role of nitric oxide (NO) signaling in SOST mechanotransduction.

Human HOS-TE85 cells were exposed to 1μM AzadC to induce SOST expression. Then AzadC-treated cultures were subjected to 1h PFF (0.7±0.3 Pa, 5 Hz). The

abundance of SOST transcripts was explored by RT-qPCR. NO synthesis was determined by the Griess assay.

PPF significantly stimulated NO synthesis, while it decreased the AzadC-induced expression of SOST. Interestingly, this effect was long-lasting and in fact, SOST expression was lower at 24h post-PPF than after 1h post-PPF (0.47 ± 0.04 vs. 0.63 ± 0.03 PPF/Static ratio respectively, $p=0.03$). Interestingly, the nitric oxide synthase inhibitor 1440W, completely prevented the effect of PPF on SOST expression. On the contrary, addition of NO to AzadC-treated cells maintained under static conditions inhibited SOST expression similarly to PPF. On the other hand, the conditioned medium (CM) of cells subjected to PPF decreased SOST expression by AzadC-treated cells (0.68 ± 0.04 fold change, $p=0.03$). The CM of PPF-exposed cultures also reduced the transcriptional activity of reporter vectors containing the SOST promoter transfected into HOS-TE85 cells (CM-Static: 1.47 ± 0.10 vs. CM-PPF: 0.78 ± 0.09 , $p=0.02$).

The mechanisms by which mechanical loading down-regulates SOST expression are not completely known. The induction of SOST expression by the demethylation of its promoter provides a useful tool to study of the mechanisms involved in SOST mechanotransduction. Our results provide the first direct evidence that NO is able to decrease SOST expression in human osteoblastic cells. Nevertheless, they suggest that other soluble factors released into the medium are also involved in the PPF-related effect on SOST, presumably by decreasing the transcriptional activity of SOST promoter.

Founding: This work was supported by grants from Instituto de Salud Carlos III (PI 09/539) and FEIOMM 2011. Jesús Delgado-Calle is recipient of a fellowship from IFIMAV.

Disclosures: *Jesús Delgado-Calle, None.*

SU0076

Association between the Fracture Site and the Mechanical Axis of Lower Extremities in Patients with Atypical Femoral Fracture. Yoshitomo Saita^{*1}, Muneaki Ishijima², Atsuhiko Mogami³, Mitsuaki Kubota⁴, Takefumi Kaketa¹, Kei Miyagawa⁵, Nana Nagura³, Tomoki Wada³, Taisuke Sato⁶, Susumu Fukasaku⁶, Hogaku Gen⁵, Osamu Obayashi³, Masayuki Nemoto⁶, Kazuo Kaneko¹. ¹Department of Orthopaedics, Juntendo University School of Medicine, Japan, ²Juntendo University, Faculty of Medicine, Japan, ³Department of Orthopaedic Surgery, Juntendo Shizuoka Hospital, Japan, ⁴Department of Orthopaedics, Juntendo University School of Medicine, Japan, ⁵Department of Orthopaedic Surgery, Chiba Central Medical Center, Japan, ⁶Department of Orthopaedic Surgery, Kitanarashino Hanawa Hospital, Japan

The ASBMR task force defined the major features of atypical femoral fracture (AFF) in which AFF occurs at the subtrochanteric region or diaphysis of femoral shaft. Although there were several case series reporting the clinical features of AFF, it is still remained unclear what determines the fracture site of AFF. Based on our hypothesis that anatomical and/or biomechanical factors of lower limbs would affect the fracture site, the weight-bearing full length radiographs of lower limbs in patients with AFF were analyzed to examine whether there are relationships between the fracture site and the mechanical axis of the lower limbs.

The 8 patients with AFF (avr. 65.8 y) were analyzed. They were all female. The half of them (4 pts.) fractured at subtrochanteric region and the remaining half (4 pts.) fractured at diaphyseal region of femoral shaft. Five of 8 patients fractured their both femora. Interestingly, the bilateral AFFs were occurred almost the same region of their femoral shaft, suggesting that the individual factor(s) could affect the AFF site. We found that while the patients with subtrochanteric fracture (6 fractures in 4 pts.) tended to show genu valgus, those with diaphyseal fracture (7 fractures in 4 pts.) showed varus deformity of their lower limbs. There were significant correlations between the AFF site and the femorotibial angle (FTA) ($r=0.80$, $p=0.001$). The FTA in patients with diaphyseal fracture (avr. 182.7°) was significantly increased in comparison to that in those with subtrochanteric fracture (FTA; avr. 171.5°) ($p=0.009$). On the other hand, there were no significant difference between the fracture site and the angle of anatomical axis and mechanical axis of femora.

Although there were some reports mentioned about the shape of femora, such as lateral bowing, could be one of the risk factors of atypical diaphyseal femoral fracture, there were no report focused on the relationships between the alignment of lower limbs and AFF site. These findings suggested that fracture site of AFFs were affected by the mechanical axis of lower limbs rather than by the mechanical axis of femora *per se*. Within our knowledge, this is the first report to reveal the correlation between the biomechanical factor of lower limbs and AFF site. Our data could help physicians where to check the radiographs of patient with the risk of AFF when they complain thigh pain, and can also provide a clue to elucidate the unknown aspects of AFF.

Disclosures: *Yoshitomo Saita, None.*

SU0077

Cox-2 is Not Essential for the Bone Formation Response to Long Term Tibial Compression in Mice. Bryan Hackfort^{*1}, Gwendolin Alvarez¹, Mohammed Akhter², Diane Cullen¹. ¹Creighton University, USA, ²Creighton University Osteoporosis Research Center, USA

Mechanical loading increases bone formation acting through both the Lrp5/ β -catenin pathway and the PGE₂ pathway; however their interaction is poorly understood. The G171V mutation in the Lrp5 receptor results in a high bone mass (HBM) phenotype and increased sensitivity to forces. Low bone mass and decreased sensitivity to loading occur in Lrp5^{-/-} mice. NSAIDs inhibit Cox enzymes and Cox 2 inhibitors such as NS398 target the PGE₂ response and suppress the anabolic response to loading in rats. We have shown NS398 suppresses the bone formation rate (BFR) after a single load in mice; however, studies in two labs have shown no NS398 suppression with loading for 2-3 weeks. We hypothesize daily injections of NS398 will suppress the bone formation response to multiple, mechanical loading sessions and that suppression will be greatest in the Lrp5^{-/-} mice. Adult virgin, female HBM, WT (C57Bl6), and Lrp5^{-/-} mice were injected daily with vehicle (DMSO) or NS-398 (10mg/kg) and were injected 3 hrs prior to tibial compression (M,W,F). Sample size was 16/ drug/geno. Mice were loaded in tibial compression three days/week for a total of 10 loads over 22 days. All right tibiae were loaded for 100 cycles at 2 Hz. The left leg served as the contra-lateral control. Forces were selected to increase BFR (HBM 900 μ e, WT 1300 μ e, Lrp5^{-/-} 1950 μ e) in all mice. Calcein was injected on days 15 and 22 for histomorphometry. We found mechanical loading increased the periosteal mineralizing surface (MS/BS), mineral apposition rate (MAR), and BFR for vehicle, NS398 and all genotypes ($P < 0.05$). There were no effects due to NS398 treatment which is similar to our previous long term study where we injected only 3 days/week. When the data from both studies were combined to increase statistical power ($N = 31$), NS398 treatment, independent of load, tended to increase periosteal MAR ($P = 0.06$) and endocortical MAR ($P = 0.05$). There were no genotype differences in response. However, with post-hoc testing of the combined data, the Lrp5^{-/-} mice responded to compression in the vehicle group, but not in the NS398 group. It is possible that in the absence of Lrp5 signaling, prostaglandins play a more important role than normal. We conclude that Cox-2 inhibition with NS398 does not suppress the bone formation response to multiple loads in mice. This suggests that pathways other than Lrp5 and PGE₂ are capable of initiating a bone formation response to loading.

Disclosures: *Bryan Hackfort, None.*

SU0078

Customary Activity as a Potential Confounding Variable in Experiments on Mechanically-Adaptive Bone Remodelling Using Unilateral Loading. Lee Meakin^{*1}, Toshihiro Sugiyama², Gabriel Galea¹, Lance Lanvon³, Joanna Price¹. ¹University of Bristol, United Kingdom, ²Yamaguchi University School of Medicine, Japan, ³Royal Veterinary College, United Kingdom

In the present study we investigated the influence of different levels of normal customary activity on the adaptive response to mechanical loading in male and female C57Bl/6 mice.

Male and female 17-week-old mice were group housed and 40 cycles of non-invasive axial mechanical loading were applied to the right tibiae on alternate days for two weeks¹. Left tibiae were internal controls. Cortical and trabecular bone structure was analysed using μ CT.

While an adaptive response to loading was observed in females as previously described¹, surprisingly no response to loading was observed in males. To investigate this paradoxical result we closely observed the male animals' behaviour in their cages. This revealed that the males were much more aggressive than the females and indulged in fighting each other approximately 1.3 times per hour. In a second loading experiment we therefore housed both males and females individually. This made no difference to the females but revealed the adaptive response in males which we had always expected. Control limbs of individually housed male mice had significantly lower trabecular bone volume (-22.2%, $p<0.001$) and a lower cortical area (-10.3%, $p<0.01$) compared to group housed male mice. Loading was associated with a significant difference in trabecular bone volume (+28.3%; $p<0.001$ comparing left control with right loaded tibiae). This had been almost absent in those group-housed (+2.28%; $p=0.85$). Similarly, the loading-related increase in cortical area seen in individually housed males (+9.37%, $p<0.001$) was reduced in group housed males (5.10%, $p<0.05$).

In conclusion, these data suggest that cage activity involving fighting between group-housed males provided a higher level of natural osteogenic stimulus than that engendered by artificial loading. This led us to the initial erroneous conclusion that these animals were not responsive to loading whereas in fact they were already adapted through fighting to the high levels of strain we engendered during artificial loading. These data indicate the importance of accounting for and controlling habitual activity levels when undertaking *in vivo* loading studies.

¹Sugiyama T et al. Bone 2011; 49; 133-9

Disclosures: *Lee Meakin, None.*

SU0079

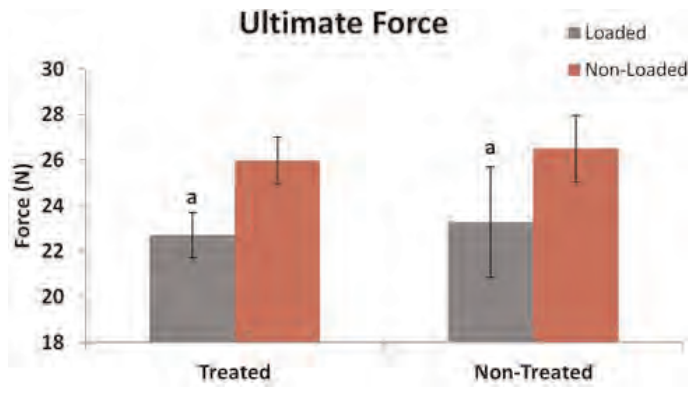
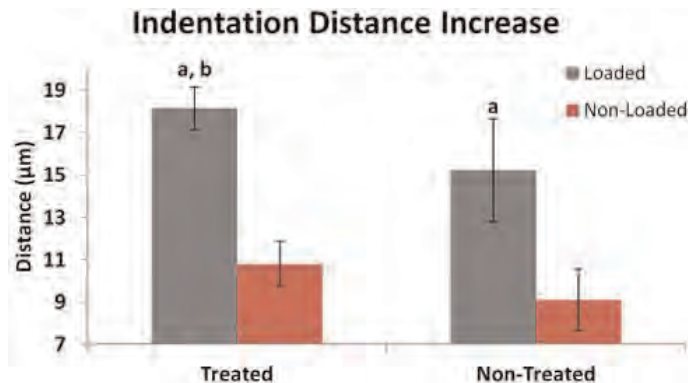
Effect of Angiogenic Inhibition on Whole Bone and Local Mechanical Properties after Damaging Osteogenic Mechanical Loading. Ryan Tomlinson^{*1}, Anne Schmieder¹, Gregory Lanza¹, Matthew Silva².¹Washington University in St. Louis, USA, ²Washington University in St. Louis School of Medicine, USA

Angiogenesis has an important role in regulating osteogenesis. Anti-angiogenic treatment has been shown to inhibit fracture healing as well as distraction osteogenesis. Previously, we have shown that inhibition of angiogenesis (using $\alpha v\beta 3$ -targeted perfluorocarbon nanoparticles) results in diminished woven bone formation following damaging osteogenic mechanical loading. Here, we extend the study to examine whole bone and local mechanical properties after loading with and without anti-angiogenic treatment.

Woven bone formation was induced at the mid-diaphysis of the ulna using an established protocol of cyclic forelimb axial compression in adult rats (n=6 per group). Right limbs were loaded while left limbs were not. Nanoparticles (treated) or saline (non-treated) was administered 2, 4, and 6 days after loading, and animals were sacrificed on day 7. Ultimate strength and stiffness were assessed on both loaded and non-loaded limbs by forelimb axial compression to failure (0.1 mm/s) immediately following sacrifice. Local mechanical properties were quantified using Biodent microindentation testing (4 N, 2 Hz, 5 cycles) immediately adjacent to the fracture site created during axial compression.

Both treated and non-treated loaded limbs had significantly reduced ultimate force and stiffness compared to non-loaded limbs, but there were no significant differences between treated and non-treated loaded limbs (Figure 1). In contrast, local bone properties measured adjacent to the fracture site were significantly different between treated and non-treated limbs. Indentation distance increase (IDI) and total indentation distance (TID) were significantly increased in treated limbs compared to both non-treated and non-loaded limbs (Figure 2).

These results indicate that the partial recovery of whole bone structural properties is not impaired 7 days after loading in treated limbs compared to non-treated limbs. However, treated limbs have significantly impaired local mechanical properties at the repair site 7 days after loading, in comparison to non-treated limbs. Since full recovery of mechanical properties occurs 14 days after loading in this model, we hypothesize that the effect of anti-angiogenic treatment on whole bone properties may be evident by day 14. However, by day 7, treated limbs already have a diminished ability to resist crack propagation compared to non-treated limbs. Further study is necessary to determine the role of angiogenesis in mechanical strength following damaging mechanical loading.

Figure 1: Ultimate Force – a: $p < 0.05$ vs. Non-Loaded.Figure 2: Indentation Distance Increase - a: $p < 0.05$ vs. Non-Loaded. b: $p < 0.05$ vs. Non-Treated.

Disclosures: Ryan Tomlinson, None.

SU0080

Stat3 in Osteocytes Is Required for Skeletal Mechanotransduction. Hongkang Zhou^{*1}, Lei Li¹, Nicoletta Bivi², Evan Himes¹, Layla Mihuti¹, Teresita Bellido², Jiliang Li¹. ¹Indiana University Purdue University Indianapolis, USA, ²Indiana University School of Medicine, USA

Signal Transducers and Activators of Transcription 3 (Stat3) is a signal transducer for the gp130 family of cytokines including IL-6, IL11 and oncostatin M, which are expressed in osteoblasts and osteocytes and play an important role in osteoblast differentiation and bone formation. IL-6 and IL-11 in bone cells have been shown to increase with mechanical stimulation. Earlier studies demonstrated that mice with lacking Stat3 in osteoblasts and osteocytes exhibit decreased bone mass and strength and a deficient anabolic response to bone loading (Bone 49:404-11, 2011). To dissect the contribution of Stat3 in osteocytes versus osteoblasts in the response to mechanical loading, we generated osteocyte-selective Stat3 knockout (KO_{Ocy}-Stat3) mice. Towards this end, Stat3 flox mice in which loxP sites flank exons 18-20 of the Stat3 gene were crossed with DMP1-8kb-Cre mice in which Cre is only expressed in osteocytes but not in osteoblasts (JBMR 27:374-389, 2012). Unlike the osteoblast/osteocyte Stat3 KO mice, KO_{Ocy}-Stat3 mice exhibited similar body mass, bone mineral content and density (BMC & BMD), and the femoral length as their sex- and age-matched littermate controls. The right ulnae of 16-week-old KO_{Ocy}-Stat3 mice and age-matched control littermate mice were loaded with peak forces of 2.5 N and 2.8 N for female and male mice, respectively, at 2 Hz, 120 cycles/day for 3 consecutive days, and mice were sacrificed 16 days later to examine the response on bone formation by histomorphometry. KO_{Ocy}-Stat3 mice were significantly less responsive to mechanical loading than littermate control mice, as indicated by decreased relative mineralizing surface compared to the respective control littermates (rMS/BS, 49 and 56%, $p < 0.001$), mineral appositional rate (rMAR, 66 and 69%, $p < 0.001$) and relative bone formation rate (rBFR/BS, 76 and 77%, $p < 0.001$) in female and male mice, respectively. We conclude that loss-of-function of Stat3 in osteocytes decrease the osteogenic response following mechanical loading. Taken together with our earlier studies, these findings demonstrate that Stat3 expression in osteoblasts is important for BMD achievement and Stat3 in osteocytes is critical for the bone response to loading.

Disclosures: Hongkang Zhou, None.

SU0081

Global Small RNA Profiling During Osteoblast Differentiation. Yukiko Maeda^{*1}, Jonathan Gordon¹, Jason Dobson¹, Carlo Croce², Janet L. Stein¹, Andre Van Wijnen¹, Gary Stein¹, Jane Lian¹. ¹University of Massachusetts Medical School, USA, ²The Ohio State University, USA

Small RNAs play an active role in modulating gene transcription and epigenetic states. Recent findings have revealed the importance of non-coding micro RNAs (miRNA) during tissue development, homeostasis, and disease. Several miRNAs have been reported to regulate osteogenesis; however, a systematic profiling of small RNAs in skeletal tissue has not been performed. Deep sequencing technology can identify all known and unknown small RNAs including novel miRNAs and non-coding (nc) RNAs such as piwi RNAs. This approach was used to analyze expression of small RNAs during the differentiation of primary calvarial osteoblasts from neonatal mice. Small RNA libraries were generated at three differentiation points of osteoblasts (i. preosteoblast, ii. osteoblast, iii. mature osteoblast). Deep sequence data from these libraries consisted of 61.8~64.8% miRNAs, 33.5~35.6% other ncRNAs and 1.3~2.2% unknown and previously unidentified small RNAs. Of the 720 known miRNAs, 32 miRNAs were up regulated and 46 miRNAs were down-regulated more than two fold during differentiation. To understand the function of miRNA expression dynamics in osteoblast differentiation, the top 100 target genes of each of the 10 most up-regulated miRNAs and 7 most down-regulated miRNAs were identified by TargetScan. Gene ontology analysis revealed that many targeted genes were involved in TGF β and Wnt signaling pathways. We then determined how these miRNAs regulate osteoblast differentiation by transfecting the miRNAs into MC3T3E1 osteoblasts. We found 5 miRNAs that up regulated the expression of Alkaline phosphatase (Alp) and Runx2 mRNA and 2 miRNAs that down regulated Alp mRNA levels. In addition, miR-199b up-regulated Wnt signaling targets Tcf and Lef (indirect effect), while miR-1983 down-regulated Tcf and Lef mRNA levels (direct effect). In summary, by using deep sequencing analysis, we have identified miRNAs that are highly up-regulated and down-regulated during osteoblast differentiation and studied several miRNAs that regulate osteoblast differentiation through modulation of Wnt and TGF β signaling.

Disclosures: Yukiko Maeda, None.

SU0082

A new FT-IR Parameter describing Acid Phosphate Substitution in Biologic Hydroxyapatite. Mila Spevak¹, Tracy Hunter¹, Carol Flach², Richard Mendelsohn², Adele Boskey^{*1}. ¹Hospital for Special Surgery, USA, ²Rutgers University, USA

Fourier Transform Infrared Spectroscopic Imaging (FTIRI) is increasing used to characterize the composition of mineralized tissues at micron and sub-micron resolutions. The purpose of this study was to validate a new parameter that provides information on the acid phosphate content in developing mineralized tissues. FTIRI spectra of bones and teeth at different developmental ages were compared by factor analysis (a chemometric technique used to condense the complex spectral data, after which multiple linear regression allows correlations to be established for a calibration set, from which properties of unknown samples can be estimated). Parameters were also confirmed by second derivative spectroscopy. Results were then validated by comparison with model compounds also analyzed by x-ray diffraction. These model compounds included hydroxyapatite prepared at three different pH's, octacalcium phosphate, etc. and mixtures thereof.

Factor analysis of FTIR images of newly formed bones (in osteons, in the periosteum, and in fracture callus) as well as in developing dentin demonstrated factors with spectral features corresponding to previously defined HPO₄ vibrations and hence higher acid phosphate content than more mature tissues in the same specimen. The use of peak height ratios 1127cm⁻¹/1096 cm⁻¹ and 1112 cm⁻¹/1096 cm⁻¹ were selected as parameters to monitor the acid phosphate content in mineralized tissues specimens evaluated by FTIRI. These were further validated by comparison with the 521 cm⁻¹ acid phosphate peaks in standard FTIR spectra of the model compounds not accessible by FTIRI. Both acid phosphate ratios showed the same trends in the mineralizing tissues. Because of the wider range of values obtained with the 1127cm⁻¹/1096 cm⁻¹ parameter, it is suggested that this should be the parameter of choice. While the acid phosphate content was generally correlated with the previously validated FTIRI crystallinity parameter (1030cm⁻¹/1020cm⁻¹) there was not a 1:1 correspondence, suggesting acid phosphate is replaced before the ripening and perfection of crystals in biologic tissues. These data indicate that FTIRI can provide additional information about the composition of mineralizing tissues during their development. Comparisons between osteons in normal and diseased tissues show a loss of acid phosphate content. It is recommended that this ratio be added to the group of parameters used to evaluate FTIRI spectra in studies of bones and teeth in health and disease.

Disclosures: Adele Boskey, None.

This study received funding from: NIH AR041325

SU0083

Trauma-induced Heterotopic Ossification In A Mouse Model. Xuhui Liu^{*1}, Heejae Kang², Hubert Kim³, Robert Nissenson⁴, Mohammad Shahnazari⁵, Olla Larm⁶, Lars Adolfsson⁶, Bernard Halloran⁷. ¹University of California, San Francisco, USA, ²San Francisco Veterans Affairs Medical Center, USA, ³University of California at San Francisco, USA, ⁴VA Medical Center & University of California, San Francisco, USA, ⁵UCSF VA Medical Center, USA, ⁶ExThera AB, Sweden, ⁷VA Medical Center (111N), USA

Introduction:

Traumatic injury of soft tissues with or without skeletal fractures is often accompanied by heterotopic ossification (HO), abnormal deposition of bone in soft tissues and in particular muscle. Battle field injuries including severe muscle damage, spinal cord injury, head trauma, neurological trauma and joint arthroplasty are frequently accompanied by HO. Heterotopic ossification has proven difficult to prevent and once developed is often extremely difficult to treat. A critical barrier to the development of more effective prevention and treatments is the lack of clinically relevant animal models. Our objective is to develop a new murine model of HO that incorporates muscle trauma as a critical component.

Methods:

12 weeks old male C57/BL6 mice received a single intramuscular injection of bone morphogenetic protein-2 (BMP-2) in a heparin-chitosan hydrogel at 0, 0.25, 0.5, 0.75, 1, 1.5 and 2 µg in the quadriceps muscles. One time muscle impaction injury was produced by dropping a metal ball of 16.3g from 100 cm high immediately after BMP-2 injection. HO was monitored using in vivo µCT scanning at 1, 2 and 4 weeks after treatment and the bones were studied histologically.

Results:

HO was observed 2 weeks after BMP-2 injection and became more condensed by 4 weeks. Without trauma, mineral deposition was only observed in mice receiving high doses (1.5 and 2 µg) BMP-2 (Figure 1). However, with trauma, HO was observed in mice receiving 1 µg BMP-2 (Figure 2). Trauma did not cause HO in mice without BMP-2 injection. Histology confirmed the µCT findings (Figure 3)

Discussion and Conclusion:

Most previous models of HO relied on the use of excessive bone morphogenetic protein-2 (BMP-2), various genetic models and growth factor-doped matrices or carriers implants, in which trauma was not involved. Muscle trauma alone has not been shown to induce HO in normal animals. In this study, we show that muscle trauma combined with a sub-threshold dose of 1 µg BMP-2, can induce HO. This novel model will serve as a powerful tool to study the mechanisms responsible for

trauma-induced HO and to devise preventative measures and effective treatments for HO.

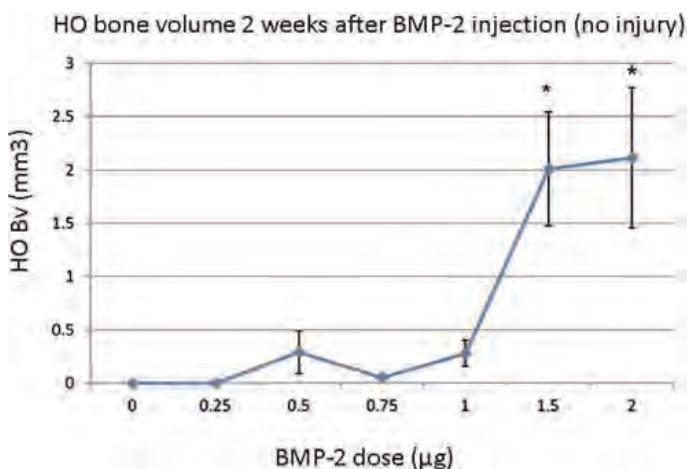


Figure 1. Dose-response curve of BMP-2 induced HO without trauma (*, P<0.05)

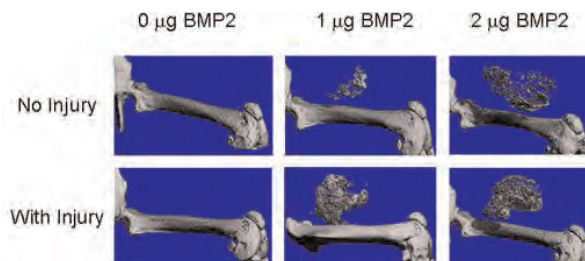


Figure 2. Typical µCT image of HO 2 weeks after BMP-2 injection with and without trauma



Figure 3. Typical H&E staining images of HO 4 weeks after BMP-2 injection with and without trauma

Disclosures: Xuhui Liu, None.

This study received funding from: Department of Defense, USA

SU0084

Cartilage-Specific Expression of Mechano-Sensitive MicroRNA-365 Affects Post-natal Skeletal Development and Bone Mass in vivo. Qian Chen^{*1}, Kun Yang². ¹Brown University School of Medicine, USA, ²Brown University, USA

MicroRNA (miRNA) is a class of noncoding RNA that negatively regulates gene expression at post-transcription level. Accumulating evidence shows that miRNAs play critical roles in cell growth, differentiation and apoptosis. However, the roles of miRNAs in mechanotransduction and skeletal development are unclear. MiR-365 was the first microRNA identified to be mechanically sensitive from microarray screening of chondrocytes. Its expression is significantly activated by cyclic loading of primary chondrocytes. MiR-365 is both necessary and sufficient for mechanical stimulation of chondrocyte proliferation and differentiation in vitro. Furthermore, the effect of miR-365 on chondrocyte proliferation and differentiation is dependent on its suppression of the levels of a target protein histone deacetylase 4 (HDAC4). To test the role of miR-365 in vivo, we generated transgenic mice that express miR-365 specifically in cartilage under the Col II Cre. Multiple transgenic lines were established in which the levels of miR-365 activation are similar to those by mechanical activation (6 to 10 fold increase) in a cartilage-specific manner. MiR-365 cartilage-specific transgenic mice were born with normal size but exhibit premature ossification as early as one week post-natally. The tibia and femur growth plates are elongated but narrower, which mimic those of Ihh cartilage-specific transgenic mice. Lack of columnar organization is apparent in the growth plate of miR-365 transgenic mice, indicating an alteration in coordinating chondrocyte differentiation. Both the skeletal size and body weight are reduced in miR-365 transgenic mice after two weeks. However, bone mineral density is significantly enhanced in miR-365 transgenic mice at 8 weeks. This suggests miR-365 promotes BMD postnatally. Therefore, cartilage-specific expression of miR-365 in vivo affects chondrocyte differentiation, skeletal growth, ossification, and BMD. It

suggests that the mechanosensitive miR-365 is a regulator of post-natal skeletal development and bone mass in vivo.

Disclosures: Qian Chen, None.

SU0085

Constitutively Active PTH/PTHrP Receptor-signaling in Bone-specific Type I Collagen-Expressing Cells Disrupts Mandibular Condyle Formation. Takeo Tsutsui^{*1}, Kenn Holmbeck², Susan Yamada², Joanne Shi³, Mara Riminucci⁴, Paolo Bianco⁵, Takeki Tsutsui¹, Pamela Robey⁶. ¹The Nippon Dental University, Japan, ²NIDCR, USA, ³nidcr.nih, USA, ⁴University La Sapienza, Italy, ⁵Universita La Sapienza, Italy, ⁶National Institute of Dental & Craniofacial Research, USA

Purpose: The developing mandibular condyle is characterized by an outermost fibrous cell layer, an underlying layer of polymorphic progenitor cells, then a zone of flattened chondrocytes, and finally a zone of hypertrophic chondrocytes. Unlike growth plates in long bones, the condyle elongates via appositional growth at the apical end through proliferation and chondrocytic differentiation of cells in the polymorphic layer. The mandibular condyle requires parathyroid hormone/parathyroid hormone-related peptide (PTH/PTHrP) signaling, yet mice expressing the PTH/PTHrP receptor (PPR) with an activating mutation (H223R, caPPR) under the control of the mouse bone-specific Col1A1 2.3 kb promoter (Col1-caPPR) present with a mandibular condyle defect. In this study, we examined changes in wildtype (WT) and transgenic (TG) condyles as a function of age.

Methods: Newborn, 4 and 10 day-old, 1 month and 3 month-old WT and TG littermates were evaluated by X-rays and microCT, and by standard histological techniques. In some cases, animals were injected with BrdU to assess proliferation, along with immunohistochemistry for the proliferation antigen Ki-67. Expression of type I collagen, type II collagen and bone sialoprotein were assessed by in situ hybridization and/or immunohistochemistry.

Results: Following birth, the TG condyle progressively displayed a major disruption in the organization and differentiation of progenitors at the apical end of the condyle, the end result of which was the lack of formation of a type II collagen-containing layer under the fibrocartilage surface, and a mass of connective cells. The disruption evolved by the continued proliferation of cells that appear to arise from the polymorphic layer in the developing condyle. These cells expressed type I collagen, and therefore express caPPR in the TG condyle. Expression of caPPR in these cells inhibited their differentiation into chondrocytes, as witnessed by their expression of type I collagen and bone sialoprotein, but lack of expression of type II collagen. These cells were unable to form a mineralized matrix in the proximal condyle, thereby explaining its concave appearance by X-ray and microCT.

Conclusions: These observations indicate that during normal development, PPR-mediated signaling is most likely transient in polymorphic cells in the mandibular condyle, and that prolonged signaling in Col1-caPPR-expressing polymorphic cells disables their ability to differentiate appropriately.

Disclosures: Takeo Tsutsui, None.

SU0086

Control of Mesenchymal Lineage Progression by microRNAs Targeting the Skeletal Gene Regulators Trps1 and Runx2. Ying Zhang^{*}, Rong-lin Xie, Jonathan Gordon, Janet L. Stein, Jane Lian, Andre Van Wijnen, Gary Stein. University of Massachusetts Medical School, USA

Mesenchymal stem cells are competent to differentiate into multiple lineages during development and tissue renewal. MicroRNAs (miRNAs) controlling biological activities of pivotal transcription factors have the ability to restrict lineage specific expression and refine regulatory options for commitment to defined mesenchymal derived phenotypes. We addressed here whether multiple miRNAs that control osteoblast lineage progression have biological potential in musculoskeletal regenerative medicine. Previously we identified multiple Runx2-targeting miRNAs that block osteoblastic differentiation. In this study, we further show that seven Runx2-targeting miRNAs (miR-23a, miR-miR-30c, miR-34c, miR-133a, miR-135a, miR-205 and miR-217) also directly regulate the chondrogenic GATA transcription factor Tricho-Rhino-Phalangeal Syndrome I (TRPS1). Mutations in the human RUNX2 and TRPS1 genes lead to craniofacial and skeletal abnormalities. Genetic interactions between TRPS1 and RUNX2 transcription factors have been established both in vitro and in vivo. Administration of exogenous Trps1/Runx2-targeting miRNAs effectively blocks differentiation of pre-committed MC3T3 osteoblasts and ATDC5 chondrocytes. Furthermore, to examine biological effects on spontaneous mesenchymal lineage progression, we administered the same panel of miRNAs to C3H10T1/2 mesenchymal stem cells. The data reveal that the regulatory network of Trps1/Runx2-miRNAs, which controls the dual osteo-chondral potential of pre-committed mesenchymal progenitor cells, redirects mesenchymal stem cells into adipogenic and myogenic cell fates with concomitant up-regulation of key lineage specific transcription factors (e.g., PPAR γ and MyoG). Thus, miRNA mediated programming of mesenchymal stem cells promotes lineage selection of either osteo-chondrogenic or adipo-myogenic cell fates to modulate musculoskeletal differentiation.

Disclosures: Ying Zhang, None.

SU0087

Estrogen Receptor Beta Increases Mandibular Condylar Cartilage Turnover. Sunil Wadhwa¹, Yosuke Kamiya^{*2}, Achint Utreja², Manshan Xu², Jing Chen¹, Hicham Drissi², Zana Kalajic². ¹Columbia University, USA, ²University of Connecticut Health Center, USA

(TMJ) disorders are the second most common musculoskeletal disease in the United States, predominantly afflicting women of childbearing ages, suggesting a role of female hormones in the disease process. However, the role of estrogen in modulating TMD is not fully understood. In long bones, estrogen via estrogen receptor Beta (ER Beta) inhibits axial skeletal growth in female but not in male mice. However the role of ER Beta in the mandibular condyle is largely unknown. We hypothesize that female ER Beta deficient mice will have increased mandibular condylar growth compared to WT female mice.

21, 49 and 120 day-old female WT (n=46) and ER Beta deficient mice (n=51) were used in this study. The mandibular condylar cartilage was evaluated by histology and the subchondral bone was evaluated by micro-CT analysis. Gene expression from both was evaluated by real time PCR analysis.

In the mandibular condylar cartilage, there was a significant increase in mandibular condylar cartilage thickness, due to increased number of cells in the superficial and polymorphic zones in the 49 day-old female ER Beta KO mice compared to WT controls. Gene expression in 49 day-old female ER Beta deficient mice revealed a significant increase in Collagen type X, Pthrp and osteopontin expression and a significant decrease in Rankl and Ihh expression compared to WT controls. Subchondral bone analysis revealed a significant increase in total condylar volume and a decrease in the number of osteoclasts in the female 49 day-old ER Beta KO compared to WT mice. There was no difference in proliferation and apoptosis in the mandibular condylar cartilage between the genotypes. However, there were differences in the expression of proteins that regulate the cell cycle. For example, we found a decrease in the expression Tieg1 and p57 and an increase in the number of cells that retained BrdU labeling after 16 hours in the mandibular condylar cartilage from the ER Beta KO compared to WT mice.

Therefore we conclude, ER Beta deficiency causes decreased resorption of the calcified matrix and a decrease in the number of cells exiting the proliferative pool in the mandibular condylar cartilage. The lower turnover state in the mandibular condylar cartilage from the ER Beta deficient mice may help decipher the sex distribution of temporomandibular joint diseases.

Disclosures: Yosuke Kamiya, None.

SU0088

Interleukin-10 Promote Chondrocyte Proliferation and Hypertrophy through Ihh and BMP-Smad Pathway. Seungwoo Han^{*1}, Hyeri Park², Eunju Lee², Younkwon Jung³, Gunwoo Kim⁴. ¹Daegu Fatima Hospital, South Korea, ²Laboratory for arthritis & bone biology, Fatima research institute, South Korea, ³ Republic of Korea, ⁴Laboratory for arthritis & bone biology, Fatima research institute, Department of Internal Medicine, Daegu Fatima Hospital, South Korea

Background and objectives: Interleukin-10 (IL-10) is a pleiotropic immunoregulatory cytokine that has been shown to be elevated in cartilage and synovium of osteoarthritis and has a chondro-protective effect. We are intended to investigate the effect of IL-10 on the endochondral ossification and the mechanisms of chondro-protective effects in osteoarthritis.

Methods: We studied the phenotypes of chondrocyte in IL-10 null mice, and the role and mechanisms of IL-10 in the differentiation, proliferation and hypertrophy with primary chondrocyte culture, tibia organ culture and micromass culture.

Results: Whole skeletal stain of E18.5 IL-10 null mice did not show significant difference in gross development compared with WT mice except a reduced temporal and occipital bone formation. The growth plate of tibia in E18.5 IL-10 null mice showed the reduced proportion of proliferating zone and increased hypertrophic zone. Immunohistochemical analysis showed a decreased expression of Sox9, PCNA, and Runx2 in growth plate chondrocytes of E18.5 IL-10 null mice. In a presence of BMP2, the primary chondrocyte from IL-10 null mice showed reduced m-RNA expression of Pthrp, the major proliferating factor for chondrocyte. IL-10 significantly increased the length of tibia organ culture compared to controls, which was responsible for the increase of both proliferating and hypertrophic layer. Mechanistically, IL-10 significantly induced Sox9, Ihh, and Runx2 in m-RNA and protein level, which was also confirmed in immunohistochemical analysis. IL-10 increased chondrocyte proliferation in MTT assay and differentiation in mesenchymal cell micromass culture, but failed to show an additive effect in response to BMP2. When we assessed IL-10-mediated chondrocyte signaling, IL-10 activated Stat3 as well as Smad1/5/8, which was major signaling molecule of BMP. Interestingly, blocking of BMP signal in ligand level with Noggin and receptor level with Dorsomorphine attenuated IL-10-mediated induction of CyclinD1 and Runx2, suggesting that IL-10-mediated chondrocyte proliferation and differentiation may be dependent to BMP-Smad pathway. However, the induction of Ihh by IL-10 was not decreased by blocking of BMP signal, suggesting direct effect of IL-10 on Ihh induction.

Conclusion: IL-10 increased chondrocyte proliferation as well as hypertrophic differentiation through Ihh and BMP-Smad pathway.

Disclosures: Seungwoo Han, None.

SU0089

Notch Gain of Function Inhibits Chondrocyte Differentiation via Rbpj-Dependent Suppression of Sox9. Shan Chen^{*1}, Jianning Tao¹, Yangjin Bae¹, Tao Yang¹, Ming-Ming Jiang¹, Terry Bertin¹, Yuqing Chen¹, Brendan Lee². ¹Baylor College of Medicine, USA, ²Baylor College of Medicine & Howard Hughes Medical Institute, USA

Notch signaling plays a critical role during development by directing the binary cell fate between progenitors and differentiated cells. Previous studies have shown sustained Notch activation in cartilage leads to chondrodysplasia. Genetic evidence indicates that Notch regulates limb bud mesenchymal stem cell differentiation into chondrocytes via Rbpj-dependent Notch pathway. However, it is still unknown how Notch signaling governs chondrogenesis of the axial skeleton where Notch signaling also serves a patterning function. We hypothesize that both Rbpj-dependent and Rbpj-independent Notch signaling mechanisms might be involved. We generated cartilage specific Notch gain-of-function (GOF) mutant mice, which displays chondrodysplasia accompanied by loss of Sox9 expression in the vertebral body. To evaluate the contribution of Rbpj-dependent Notch signaling to these phenotypes, we deleted *Rbpj* in the Notch GOF background. These mice continued to develop spine abnormalities characterized by "butterfly vertebrae" suggesting that removal of *Rbpj* does not fully rescue the axial skeleton deformities caused by Notch GOF. However, Sox9 protein level was restored in the *Rbpj* deficient Notch GOF mice compared to Notch GOF mutant, suggesting regulation of Sox9 expression is canonical or Rbpj-dependent. To further understand the molecular basis of this control, we performed ChIP assays and demonstrate direct recruitment of Rbpj/NICD transcription complex to the Rbpj-binding sites upstream of Sox9 promoter. This association of Rbpj/NICD complex to Sox9 promoter is associated with transcriptional repression in a cellular model of chondrocyte differentiation. Hence, we show that Notch negatively regulates chondrocyte differentiation in the axial skeleton by suppressing Sox9 transcription. In addition, Rbpj-independent Notch signaling mechanisms may also contribute to axial skeleton patterning.

Disclosures: Shan Chen, None.

SU0090

Proteoliposomes harboring Alkaline Phosphatase and Annexin V. Pietro Ciancaglini¹, Mayte Correia^{*2}, Ana Maria Simao², Tina Moreira³, Marc Hoylaerts⁴, Jose Luis Millan³. ¹FFCLR- USP, Brazil, ²University of Sao Paulo - Usp, Brazil, ³Sanford-Burnham Medical Research Institute, USA, ⁴Center for Molecular & Vascular Biology, University of Leuven, Belgium

The biomineralization process is initiated inside chondrocyte- and osteoblast-derived matrix vesicles (MVs). The initial crystalline hydroxyapatite (HA) generation and its deposition is accomplished by the activities of several proteins, involved in Ca²⁺ and phosphate (P_i) homeostasis, among them Annexins (AnxV), P_i-transporters, PHOSPHO1 and tissue-nonspecific alkaline phosphatase (TNAP). Anx V mediates Ca²⁺ influx. Dipalmitoylphosphatidylcholine (DPPC) and dipalmitoylphosphatidylserine (DPSP) are found in the MVs membranes and play a crucial role in the biomineralization process, regulating both Ca²⁺ entry into the MVs and formation of HA crystals. We studied the incorporation of AnxV and TNAP into DPPC:DPSP (10% molar ratio) liposomes and the ability of these proteoliposomes to transport Ca²⁺. Proteoliposomes containing TNAP and AnxV were reconstituted for 15h at 25°C, using a 1:15,000 and 1:100 protein:lipid (molar ratio), respectively. These proteoliposomes were incubated with PIPLC for 2 h at 37°C and protein concentrations were determined. The results showed that 88% of AnxV and 12% of TNAP were incorporated. Ca²⁺ influx by AnxV-containing proteoliposomes was determined by the procedure described by Garimella et al. [1]. AnxV-containing proteoliposomes (10 µg of protein) were also incubated at 37°C for 5 h in medium containing 25, 50 or 75 µCi.mL⁻¹ ⁴⁵Ca²⁺ and Ca²⁺ influx was determined by scintillation counting. We found that 16.2% of ⁴⁵Ca²⁺ was incorporated into the proteoliposomes, and the incorporation was not dose-dependent. The presence of TNAP in the proteoliposomes containing both proteins did not affect AnxV-mediated Ca²⁺ transport. We also studied the hydrolysis of PPI and ATP by TNAP-proteoliposomes and TNAP-AnxV-proteoliposomes. The V_m values for the hydrolyses of PPI decreased by around 5 times and K_{0.5} values increase 1.5 times when AnxV is present in proteoliposomes. When ATP was used as substrate, the reduction of the V_m was even great (around 7 times) and K_{0.5} values also decrease (2 times) in the presence of AnxV. Therefore, our data indicates that the presence AnxV in TNAP-proteoliposomes significantly affect the catalytic activity of TNAP. These studies will help us develop a functional synthetic MV biomimetic systems to aid in the elucidation of the mechanisms of initiation of skeletal and dental mineralization.

[1] Garimella et al., Biol. Proced Online 2004; 6: 263-267.

Disclosures: Mayte Correia, None.

SU0091

Rapid Membrane Responses of Rat Costochondral Chondrocytes to 17Beta-Estradiol Are Sex and Estrogen Receptor Alpha and Beta Dependent. Khairat ELBaradie^{*}, Barbara Boyan, Zvi Schwartz, Yun Wang. Georgia Institute of Technology, USA

Specific receptors for estrogen have been found in both male and female articular cartilage and growth plate cartilage. Our work in rat costochondral chondrocytes shows rapid responses to 17β-estradiol (E2) with increases in protein kinase C (PKC) activity in female chondrocytes but not in male chondrocytes. PKC activation is not affected by the estrogen receptor (ER) antagonist ICI 182780, but can be blocked by antibodies to ERα. The aim of the present study was to investigate which ERs are involved in sex-specific rapid membrane responses to E2 and to investigate if male and female chondrocytes have the same signaling pathway down stream of the receptor. To elucidate the pathway, PKC activity was measured in female chondrocytes that were treated with E2 ± GDPβS (G-protein inhibitor), U73122 (inhibitor of phospholipase C [PLC]) and AACOCF3 (inhibitor of cytosolic phospholipase A2 [cPLA2]). To establish the receptors involved, PKC activity was measured on male and female chondrocytes that were treated with either DPN (specific activator of ERβ), PPT (specific activator of ERα) or THC (specific activator of ERα and inhibitor of ERβ). To test the hypothesis that treatment with E2 leads to formation of a complex between ERα and ERβ, male and female chondrocytes were treated with E2 and co-immunoprecipitation followed by western blot were used to analyze the effect. To determine if the downstream signaling pathway was functional in male cells, male and female cells were treated with PLA2 activating peptide (PLAA) and the PLC activator *m*-3M3FBS and PKC activity was measured. PKC activation in female cells depended on G proteins, PLC and PLA2, based on inhibition by GDPβS, U73122 and AACOCF3. DPN and PPT induced PKC activity only in female cells, while THC had no effect in either cell type. Co-immunoprecipitation showed that there is a complex formation with E2 treatment only in female chondrocytes. Furthermore, activation of PKC by E2 was observed only in female cells, downstream activators *m*-3M3FBS and PLAA peptide induced a dose-dependent increase in PKC activity in both male and female cells. This study suggests that the rapid membrane response of female rat chondrocytes to E2 is both ERα and ERβ dependent. Male chondrocytes showed no membrane-mediated response to E2, but had the same active downstream pathway. The ability of these receptors to form a complex, might contribute to the sex-specific rapid membrane response between male and female chondrocytes.

Disclosures: Khairat ELBaradie, None.

SU0092

Crosstalk between Endothelial Progenitor Cells and Mesenchymal Stem Cells. Bettina Hafen^{*1}, Katrin Schlegelmilch², Alexander Keller², Susanne Wiesner², Norbert Schuetz³. ¹University of Wuerzburg, Orthopedic Center for Musculoskeletal Research, Germany, ²University of Würzburg, Germany, ³University of Wuerzburg, Orthopedic Center for Musculoskeletal Research, Germany

Endothelial progenitor cells (EPC) play an important role in postnatal vasculogenesis. An intact vascular system is crucial for the survival of all tissues including bone. Novel bone tissue engineering approaches using scaffolds seeded with mesenchymal stem cells (MSC) raised the idea of combining MSCs with EPCs to improve bone regeneration. For this purpose a better understanding of cell-cell interaction is needed. Thus, this study focused on changes of global gene expression patterns of human primary EPCs after receiving conditioned medium of human primary MSCs or after direct cell-cell-contact, respectively.

EPCs were isolated by Ficoll-Paque density-gradient centrifugation from Buffy Coat. For the characterization EPCs were stained with fluorescence-activated antibodies against CD34, CD31, CD45, CD133, KDR and VE-Cadherin. For the MicroArray studies EPCs were either cultured with 50% conditioned medium of MSCs for 24h or stained with CellTracker® Orange and directly cultured with green fluorescence-labelled MSCs for 24h. Subsequently cells were separated by FACS. Affymetrix GeneChip Analyses (n=4) were performed using the GeneChip® HG-U133 Plus 2.0. Results were verified by RT-PCR.

EPCs were positive for CD31 and CD45 with a fraction additionally positive for VE-Cadherin after 7 days of culture. After 14 days cells were positive for CD31, CD45 and VE-Cadherin with a fraction additionally positive for CD34. The Affymetrix GeneChip Analyses revealed 1200 regulated probe sets for the experiments with conditioned medium as well as after cell-cell-contact. GoStat analyses revealed that several signaling pathways are overrepresented due to conditioned medium of MSCs or direct cell-cell-contact, respectively, such as the cytokine-cytokine receptor interaction, chemokine signaling pathway, hematopoietic cell lineage, osteoclast differentiation and graft-versus-host disease.

Our study showed that circulating Buffy Coat-derived human EPCs are a heterogeneous population expressing expected endothelial markers. Re-evaluation of the results by RT-PCR and analyses of the MicroArray data uncovered important signaling pathways of the musculoskeletal system involved in the communication between EPCs and MSCs which will allow further functional studies. The better understanding of EPCs and therefore the more precise use of these cells opens a plethora of clinical applications especially in the field of tissue engineering.

Disclosures: Bettina Hafen, None.

SU0093

Expression profiling of miRNA-mRNA regulatory network correlated with bone mass in inbred strains of mice. Jee Hyun An^{*1}, Jae-Yeon Yang², Hyojung Park², Sang Wan Kim³, Woong-Yang Park⁴, Seong Yeon Kim², Chan Soo Shin². ¹Department of Internal Medicine, Konkuk University Hospital, South Korea, ²Department of Internal Medicine, Seoul National University College of Medicine, South Korea, ³Seoul National University Boramae Hospital, South Korea, ⁴Department of Biochemistry & Molecular Biology, Seoul National University College of Medicine, South Korea

Approximately 70% of the variability in human bone density has been attributed to genetic factors, yet its regulatory mechanism remains largely unknown. Growing body of evidence shows that microRNAs (miRNAs) play an important role in regulating bone mass. We investigated the cooperative miRNA-mRNA regulatory mechanism of peak bone mass in inbred strain of mice with different bone density using microarray analysis.

Femur and tibia of 12-week old C3H/He (high bone density) and C57BL/6 (low bone density) were harvested to extract total bone RNAs for microarray. A total of 30 miRNAs were differentially expressed between bone tissue of C3H/He and C57BL/6 mice; 16 miRNAs (miR-34c, 101a, 128, 135a, 181b, 181d, 210, 290, 296, 340, 425, 467e, 542, 582, 652, 705) were identified to be upregulated in C3H/He mice, while 11 miRNA (miR-26b, 29c, 34a, 101b, 204, 214, 219, 338, 342, 720, 801) were upregulated in C57BL/6 mice. Concomitant analysis of mRNA microarray revealed that 1,189 genes were differentially expressed between C3H/He and C57BL/6 mice. Functional clustering analysis revealed that mRNA of the genes related with the composition of extracellular matrix, microtubule, gap junction and mRNAs of Wnt and TGF- β signaling pathways were upregulated in C3H/He mice. In contrast, the mRNA of genes involved in immune and inflammatory response as well as lipid synthesis were upregulated in C57BL/6 mice. Using the integrative analysis based on computational target prediction of differentially expressed miRNAs and concomitant mRNA profiling, we found that about 20% of differentially expressed mRNAs were putative target of differentially expressed miRNAs. The candidates for miRNA-mRNA regulatory pairs include those of the component of extracellular matrix, microtubule and gap junction, indicating that peak bone mass determination in different strains of mice is at least in part mediated by differential expression of miRNA profile.

The miRNA-mRNA expression profiles reported in this study form a comprehensive transcriptome database and provide a valuable resource for understanding the role of miRNA in determining bone mass.

Disclosures: Jee Hyun An, None.

SU0094

Generation of FAM20C-GFP Transgenic Mice. Jianjun Hao^{*1}, Erxia Du², Deborah Kaback³, Wuchen Yang¹, Siu-Pok Yee³. ¹University of Connecticut Health Center, USA, ²Department of Craniofacial Sciences, Division of Orthodontics, University of Connecticut Health Center, USA, ³Department of Genetics & Development Biology, University of Connecticut Health Center, USA

Formation of calcified tissues is a well-regulated process balanced by promoters and inhibitors of biomineralization. Interruption of the balance in bone and other mineralized tissues could generate a wide range of pathologic conditions. Lethal osteosclerotic bone dysplasia (Raine syndrome), one of the neonatal osteosclerotic dysplasias, is an inherited disease clinically manifested by increased calcification and distinctive craniofacial abnormalities. Our previous study has clearly demonstrated that mutations of FAM20C gene are associated with Raine syndrome. As a first step to investigate the functional role of FAM20C, we have generated FAM20C transgenic mice to determine its spatiotemporal expression during development. To this end, we have prepared a transgene with 15 kb of FAM20C upstream promoter sequence to direct expression of the GFPtpz reporter. We anticipate that FAM20C-GFP similar to the FAM20C mRNA and protein is highly expressed in odontoblasts, ameloblasts, cementoblasts, osteoblasts and osteocytes during tooth and bone development. The FAM20C fluorescence labeled transgenic mice will provide powerful experimental models for identification and isolation of tooth and bone forming cells in mineralized tissues.

Disclosures: Jianjun Hao, None.

This study received funding from: American Association of Orthodontists Foundation

SU0095

Identification of SOX9 Target Genes and Characterization of Its Binding Sites in Chondrocytes. Chundo Oh¹, Yue Lu¹, Liang Shoudan¹, Hideyo Yasuda^{*2}, Benoit DeCrombrughe³. ¹U.T.M.D. Anderson Cancer Center, USA, ²U.T.M.D. Anderson Cancer Center, USA, ³UT MD Anderson Cancer Center, USA

The transcription factor SOX9 is a master factor regulating chondrocyte development. In order to identify the genes that are either directly or indirectly

controlled by SOX9 in chondrocytes we have performed RNA-Seq as well as ChIP-seq. For RNA-Seq the RNA expression profile of primary *Sox9^{fllox/fllox}* chondrocytes infected with Ad-*CMV-Cre* was compared with that infected with a control adenovirus. RNA-Seq indicated that the levels of *Sox9* mRNA were decreased more than 10 fold with Ad-*CMV-Cre* infection. About 200 genes showed a decrease in expression of at least 4 fold. These included many ECM genes and a number of genes for other secreted proteins, intrinsic membrane proteins, transcription factors etc. In ChIP-Seq 75% of the SOX9-interaction sites had canonical inverted repeat motif within 100 bp of the top of the peaks. SOX9 interaction sites were found in 80% of the genes whose expression was decreased more than 8 fold in SOX9-depleted cells suggesting these be direct targets of SOX9. We also examined the location and characteristics of potential SOX9-dependent enhancers in the genes identified by the ChIP-Seq data. The SOX9 binding sites in *Sox9* genes are located -80Kb upstream from the transcription initiation site. Also in *Aggrecan* and *Col2a1* genes the binding sites were detected at -30K upstream. The reporter construct containing each binding site and each promoter shows that the site has an enhancer activity dependent on SOX9.

When we focused on the SOX9 binding sites in the *Col2a1* gene, strong binding sites are found in intron 6 and -30Kb upstream and a weaker site was found in intron 1 corresponding to the SOX9 dependent enhancer, which was previously extensively characterized. By the ChIP-qPCR assay using H3 antibody the region was proven to be nucleosome depleted one in chondrogenic cells not in other cell types. Then we prepared a reporter construct that contains a 600 bp *Col2a1* promoter, intron1 with or without intron 6 and the luciferase gene. The construct that contained both intron1 and intron 6 was activated 5 to 10 fold by the SOX9/SOX5 or the SOX9/SOX6 combination in transient transfection assays using 293T or RCS (rat chondrosarcoma) cells. This enhancement was also observed in RCS cells stably expressing the construct. This finding suggests a newly found mechanism of SOX5/SOX6, that is the SOX9/SOX5/SOX6 combination enhances *Col2a1* transcription through an enhancer in intron 6 together with that in intron 1.

Disclosures: Hideyo Yasuda, None.

SU0096

Withdrawn

SU0097

Apatite-Mullite Glass-Ceramic as a Suitable Scaffold Material for Bone Tissue Engineering. Niki Gosling^{*1}, Paul Genever², David Wood³, Richard Hall³. ¹The University of York, United Kingdom, ²University of York, United Kingdom, ³University of Leeds, United Kingdom

Calcium phosphate (CaP) based ceramics are extensively used in bone replacement applications, particularly those which share chemical and compositional similarities with natural bone mineral. Fluorapatite (FA) is one such material that receives relatively little attention, despite the ability of fluoride-containing ceramics to increase osteoblast activity at the bone-biomaterial interface, stimulate cell proliferation and collagen production. Here, an apatite-mullite (AM) glass-ceramic is identified as having potential use as a bioactive FA-containing scaffold for bone tissue engineering, assessed using a human multipotent stromal/mesenchymal stem cell (MSC) population.

AM glass-ceramic scaffolds were produced with novel porous morphologies using a controlled sintering method, with compositional analysis performed via powder x-ray diffraction and differential thermal analysis. Micro-structure and cell seeding densities were determined by scanning electron microscopy (SEM). Confocal microscopy was used to determine cell viability and proliferative capacity through live/dead staining and nucleic acid incorporation assays respectively. Cell numbers were also investigated with a dehydrogenase activity colourimetric assay. The osteogenic capacity of MSCs on scaffold substrates was analysed through enzymatic activity levels of alkaline phosphatase (ALP).

SEM imaging illustrated well sintered scaffold morphology with a macro-porous structure; at higher magnifications the presence of interlocking crystalline phases with regions of micro-porosity were clearly identified. The material was shown to be a bulk nucleating system with a final composition containing both FA and mullite crystal phases with possible residual glass regions. MSC confluence at 24 hours was obtained using an initial seeding density of 6.4×10^5 cells/cm², with cells maintaining their viability up to 21 days in culture. The proliferative cell fraction was determined as $17.4 \pm 5.9\%$ of the MSC population over 24 hours and cell number increased 1.5 and 2.7 fold over 3 and 7 day culture periods respectively. ALP activity increased in both the presence and absence of osteogenic supplements by 21 days culture with 1.4 fold greater levels in osteogenic compared to control media ($p < 0.05$).

These results demonstrate for the first time the biocompatibility and osteo-supportive nature of the AM scaffold, demonstrating its capacity to function as a bone replacement material.

Disclosures: Niki Gosling, None.

SU0098

Comparison between Intramedullary Pinning and External Fixation for Mouse Tibia Fracture. Yusuke Hagiwara*, Douglas Adams, Nathaniel Dyment, Xi Jiang, David Rowe. University of Connecticut Health Center, USA

The closed long bone fracture in the mouse is widely used to study the effect of genetic and drug manipulations on the cellular basis of fracture repair. The majority of studies utilize an intramedullary pin (IMP) to stabilize the fracture, and in most cases a robust widely-spaced callus develops that includes a large cartilaginous component. While maintaining axial alignment initially, IMP fixation in the mouse typically does not provide adequate stability because the animal's size precludes the addition of transverse interlocking screws that are used clinically. The goal of this study was to develop a simple, inexpensive fixation method that provides improved fracture stability, to more closely mimic stable fixation achieved clinically. Here we report a comparison between traditional IMP fixation used by our laboratory and others versus a novel external fixation (EF) method. IMP group: a percutaneous hole was introduced manually through the tibial plateau using a 25G needle, after which a 0.011-0.015 inch stainless steel wire (sized to IM canal) was inserted into the full length of the tibia. Once in place, a controlled fracture was produced using a 3-point guillotine device. EF group: six needles (3-25G proximal and 3-28G distal) were inserted percutaneously through both cortices in a medial to lateral direction and then pushed into the barrel of a tuberculin syringe. Once in place, the fracture was induced using the guillotine. X-ray images were taken every third day and the mice were sacrificed at day 7 and 14 for histological assessment. By X-ray and photographs, the IMP group often showed tibial deformities such as fracture site angulation, shortening, or rotation, while EF demonstrated less angulation and no rotational deformity. The callus of the IMP group was larger in length and thickness while the smaller EF callus had a stronger mineralization signal. Histologically at day 14, the IMP fracture demonstrated the traditional large cartilaginous core and a callus that extended widely across the periosteal surface, while the EF repair consisted almost entirely of an early trabecular-like bone that extended from the periosteal surface through the bone marrow space to the opposite periosteal surface. This simplified, low-cost external fixation method should be helpful in understanding the contribution of the periosteal and bone marrow progenitor cells to the repair process under rigid fixation.

Disclosures: Yusuke Hagiwara, None.

SU0099

Fetal Exposure to Selective Serotonin Reuptake Inhibitors Delays Bone Growth in the Appendicular Skeleton in Rat Offspring. Zahra Hosseini¹, Maryam Badv², Nicole De Long³, Alison Holloway³, Gregory Wohl¹. ¹McMaster University, Canada, ²McMaster School of Biomedical Engineering, Canada, ³Department of Obstetrics & Gynecology, Canada

Selective Serotonin Reuptake Inhibitors (SSRIs) are a class of antidepressant drugs, which due to effectiveness and lower incidence of side effects are commonly prescribed to pregnant women. However, the use of SSRIs during pregnancy has been associated with congenital deformities such as craniosynostosis, omphalocele and heart defects. The goal of this study was to determine the effect of fetal exposure to SSRIs on skeletal growth.

Female Wistar rats were randomised to receive 10mg/kg/d sertraline orally (N=8; SSRI-Oral) or via injection (s.q., N=5; SSRI-Inj) or vehicle (VEH-Oral [N=5] and VEH-Inj [N=6]) from the confirmation of mating until parturition. One male and one female pup from each litter were sacrificed at 3 and 7 wk of age. Femurs and tibias were extracted and overall lengths were measured by caliper (± 0.01 mm). MicroCT scans (23 μ m resolution) were performed on left femurs from 3 wk rats. MicroCT data sets were analysed for lengths (total femur, diaphysis, and epiphysis), and cross-sectional area (XSA) at the mid-diaphysis. Statistical differences were assessed by ANOVA ($p = 0.05$).

At 3 wk, there was no effect of SSRI exposure on bone length in the offspring of dams given sertraline via injection. However, the femurs and tibias from male and female pups born to SSRI-Oral dams were significantly shorter than those in the vehicle treated (VEH-Oral) pups. Based on femoral microCT measures, the shorter total bone length was due to shorter diaphyseal length in the SSRI-Oral group. In female offspring, the femoral XSA at 3 wk was significantly larger in SSRI-Oral rats than all other groups, whereas there was no XSA difference between treatment groups in male pups. There were also differences in bone measures at 3 wk between delivery methods in female offspring: femoral and tibial length in the VEH-Inj rats was significantly shorter than in the VEH-Oral group. At 7 wk postnatal, femoral and tibial lengths tended to be shorter in the SSRI-Oral rats compared to VEH-Oral, but the differences were not statistically significant ($p > 0.05$).

Based on these results, the use of Sertraline during pregnancy significantly delays the growth of long bones in rats. Daily injection also had a significant detrimental effect on bone growth in female pups, suggesting a possible effect of maternal stress on bone development in this model. These data are the first to identify that maternal SSRI use has implications for bone development in the offspring.

Table1. Bone measures for males, 3 wk postnatal (mean \pm SD).

| Male | Femur length [mm] | Tibia length [mm] | Femur XSA |
|-----------|-------------------------------|-------------------------------|-----------------|
| VEH-Inj | 15.95 \pm 0.60 | 21.99 \pm 0.71 | 1.09 \pm 0.13 |
| SSRI-Inj | 15.73 \pm 0.57 | 21.64 \pm 0.88 | 1.17 \pm 0.19 |
| VEH-Oral | 16.56 \pm 0.97 | 22.54 \pm 1.02 | 1.20 \pm 0.18 |
| SSRI-Oral | 15.18 \pm 0.44 ^a | 21.04 \pm 0.39 ^a | 1.13 \pm 0.15 |

^aSignificantly less than VEH-Oral ($p < 0.05$)

Table2. Bone measures for females, 3 wk postnatal (mean \pm SD).

| Female | Femur length(Ave) | Tibia length(Ave) | Femur XSA |
|-----------|-------------------------------|-------------------------------|--------------------------------|
| VEH-Inj | 15.72 \pm 0.30 ^a | 21.11 \pm 0.82 ^a | 1.02 \pm 0.11 |
| SSRI-Inj | 15.87 \pm 0.63 ^a | 21.75 \pm 0.65 | 1.11 \pm 0.15 |
| VEH-Oral | 16.55 \pm 0.61 | 22.48 \pm 0.86 | 1.22 \pm 0.15 |
| SSRI-Oral | 15.73 \pm 0.36 ^a | 21.28 \pm 0.49 ^a | 1.37 \pm 0.17 ^{b,c} |

^aSignificantly less than VEH-Oral ($p < 0.05$)

^bSignificantly larger than VEH-Oral ($p < 0.05$)

^cSignificantly larger than VEH-Inj ($p < 0.05$)

Figures

Disclosures: Zahra Hosseini, None.

SU0100

Functional Consequences of Fibrodysplasia Ossificans Progressiva-associated Mutations ACVR1^{R206H} and ACVR1^{Q207E} in Comparison to Constitutively Active ACVR1^{Q207D}. Julia Haupt¹, Alexandra Deichsel², Katja Stange², Ekaterina Kajikhina³, Cindy Ast⁴, Naima Souidi², Frederick Kaplan⁵, Eileen Shore⁶, Petra Seemann². ¹BCRT, USA, ²BCRT, Germany, ³IMPRS-IDI, Germany, ⁴Carnegie Institute for Science, USA, ⁵University of Pennsylvania Hospital, USA, ⁶University of Pennsylvania, USA

Fibrodysplasia ossificans progressiva (FOP, MIM 135100) is a rare genetic disorder characterized by postnatal transformation of soft connective tissues into bone throughout life in a periodic and progressive manner. Mutations within the BMP type 1 receptor ACVR1 (activin A receptor, type 1; *ALK2*, *ActR1A*) were identified as the genetic cause, with R206H (c.617G>A) found to be the most frequently occurring mutation in patients. Patients with R206H develop a classic clinical FOP phenotype that is characterized by congenital great toe malformation and ectopic bone formation. Several other rare ACVR1 mutations have also been associated with an atypical FOP presentation. A patient with FOP-type ectopic ossification and atypical severe growth retardation was found to carry a Q207E (c.619C>G) mutation. We performed functional analyses to investigate differences between R206H and Q207E receptors that could reflect differences in phenotype. Viral-mediated over expression of each mutant receptor in chicken embryos induced similar skeletal abnormalities (e.g. joint fusion, formation of ectopic elements) analogous to those found in FOP patients. Effects on cell differentiation were analyzed *in vitro* using chick limb bud micromass cultures. Infection with wild-type ACVR1 did not alter cell fate decisions. By contrast, both R206H and Q207E mutations similarly enhanced chondrogenesis and osteogenesis and additionally exhibited anti-myogenic activity. Of note, a ligand-independent and strongly constitutively activating ACVR1 mutation, Q207D, has previously been identified. In all assays we found that both R206H and Q207E FOP mutations induce less severe responses compared to Q207D, an interesting result given that Q207E and Q207D affect the same amino acid residue. To examine the ligand responsiveness of R206H and Q207E, we co-expressed the BMP antagonist Noggin in micromass cultures and, in contrast to Q207D which is not inhibited by Noggin, we observed reduced chondrogenesis in cultures with R206H and Q207E, supporting that both mutant FOP receptors act in a ligand-sensitive manner. Our data show that the R206H and Q207E FOP mutant receptors have similar functional effects on cell differentiation assays, suggesting that the atypical phenotype associated with Q207E occurred coincidentally, and additionally support that FOP ACVR1 mutations are ligand-responsive and more mildly activating than the constitutively active Q207D mutation.

Disclosures: Julia Haupt, None.

SU0101

Myeloid Elf-1-Like Factor Stimulates Adipogenic Differentiation through the Induction of Peroxisome Proliferator-activated Receptor γ (PPAR γ) Expression in Bone Marrow. Kyunghwa Baek^{*1}, Je-Yoel Cho², HyoRin Hwang¹, Arang Kwon³, Hvelim Lee³, Hyun-Jung Park¹, Abdul Qadir¹, Hyun-Mo Ryoo⁴, Kyung Mi Woo⁴, Jeong-Hwa Baik¹. ¹Seoul national university, School of dentistry, South Korea, ²College of Veterinary Medicine, Seoul National University, South Korea, ³Seoul National University, South Korea, ⁴Seoul National University School of Dentistry, South Korea

Myeloid Elf-1 like factor (MEF) is one of the Ets transcription factors known to regulate cell proliferation and differentiation. A previous report has shown that osteoblast-specific MEF transgenic mice (Coll1a1-MEF-TG mice) have low bone mass but high bone marrow adiposity. In the present study, we explored a previously unappreciated mechanism whereby MEF promotes adipogenesis in bone marrow. An adipogenic colony forming unit assay showed that bone marrow cells derived from Coll1a1-MEF-TG mice had a higher adipogenic differentiation potential compared to those from wild-type. The levels of adipogenic marker genes expression in 3T3L1 cells were higher when co-cultured with Coll1a1-MEF-TG bone marrow cells than with wild-type cells. MC3T3-E1 preosteoblasts transfected with MEF secreted higher levels of 15-deoxy-delta (12, 14)-prostaglandin J2, a potent endogenous ligand of peroxisome proliferator-activated receptor γ (PPAR γ), under adipogenic conditions. MEF overexpression increased the adipogenic marker genes expression including PPAR γ and lipid droplet accumulation in MC3T3-E1 preosteoblasts and 3T3L1 preadipocytes. Endogenous MEF expression levels increased as adipocyte differentiation proceeded. Knockdown of MEF by siRNA suppressed expression levels of adipogenic marker genes including PPAR γ . MEF directly bound to the MEF binding element on the mouse PPAR γ promoter, transactivating promoter activity. Immunohistochemical staining of tibia sections demonstrated that bone lining cells and bone marrow cells express higher levels of PPAR γ protein in Coll1a1-MEF-TG mice than in wild-type mice. These results suggest that MEF transactivates PPAR γ expression, which, in turn, enhances adipogenic differentiation. Furthermore, MEF overexpressing osteoblasts secrete higher levels of adipogenic factors, creating a marrow microenvironment that favors adipogenesis.

Disclosures: Kyunghwa Baek, None.

SU0102

NELL-1 Protein as an Anabolic and Anti-resorptive Agent in an Osteoporotic Sheep Model. T. Mari Kim¹, Aaron James^{*2}, Raghav Goyal², Michael Chiang², Greg Asatrian², Xinli Zhang², Janette Zara², Alan Nguyen², Anthony Simon Turner³, Howard Seim III³, Kang Ting², Chia Soo². ¹University of California Los Angeles, USA, ²University of California, Los Angeles, USA, ³Colorado State University, USA

Introduction:

Osteoporosis causes approximately 750,000 vertebral fractures in the United States. Anti-resorptive agents such as bisphosphonates are commonly used to prevent bone fractures. Recently, anabolic agents such as anti-DKK-1 antibodies have been developed to restore bone mass.

Recombinant human Nel-like molecule-1 (rhNELL-1) has been previously shown to induce significant bone formation in multiple animal models. Here, we investigate the effect of rhNELL-1 in an osteoporotic sheep model.

Methods: Osteoporosis in sheep was induced through ovariectomy, dietary depletion, and steroid injection. Induction of osteoporosis was confirmed by DXA, Dual-energy X-ray absorptiometry.

Two methods were used to deliver rhNELL-1. For the intervertebral injection, a Hyaluronic acid (HA) paste (0.5mL) was lyophilized onto β -TCP (50mg). The lateral aspect of the lumbar vertebral body was exposed and 3.2mm holes were drilled in the cortical bone. Three different concentrations of rhNELL-1 (0.3, 0.75, 1.5mg) test articles were then injected using a luer lock syringe, and all materials were pushed into the cancellous bone of the vertebral body.

For the balloon kyphoplasty model, a large volume of HA (1.5mL) and β -TCP (150mg) were implanted for prolonged rhNELL-1 release. 2cm diameter defects were created. Two different concentrations of rhNELL-1 (0.9, 2.25mg) test articles were implanted into the cancellous portion of the vertebral body.

Assessments were performed using live-CT scans, high-resolution post-mortem microCT scans, histological staining, and histomorphometry.

Results: CT analysis showed that rhNELL-1 intervertebral injection had significant effects in increasing trabecular Bone Mineral Density (BMD) by 300% ($*p<.01$) and percent Bone Volume (BV) by over 15% ($*p=.03$). Balloon kyphoplasty increased in trabecular BMD ($*p=.003$) and BV ($*p<.001$) by 100%. Histomorphometry showed enhanced cortical and trabecular bone width in rhNELL-1 treated groups. Furthermore, number of osteoblasts significantly increased ($*p=.035$) in rhNELL-1 treated groups, whereas number of osteoclasts were either reduced or unchanged ($*p=.048$).

Conclusion: RhNELL-1 may be of clinical benefit for the osteoporotic patient, as rhNELL-1 anti-osteoclast activities may prevent vertebral subsidence or collapse. Thus, local treatments with rhNELL-1 can act as an effective anabolic and anti-resorptive agent to prevent osteoporotic bone loss or fractures.

Disclosures: Aaron James, None.

This study received funding from: CIRM, NIH/NIDCR, UC Discovery Grant

SU0103

NO66, a Jumonji Family Histone Demethylase, is a Negative Regulator of Skeletal Growth and Bone Formation. Qin Chen^{*}, Krishna Sinha, Jenny Deng, Richard R. Behringer, Benoit de Crombrugge. Department of Genetics, The University of Texas MD Anderson Cancer Center, USA

Our previous in vitro studies indicated that NO66, a jmjc-domain-containing protein, not only has histone demethylase activity, but also binds to and inhibits the activity of the osteoblast-specific transcription factor Osterix (Ox). In this study, we aimed to investigate NO66 loss- and gain-of-function in vivo using genetically engineered mouse models. Two loxp sites were introduced into the mouse genome to flank the NO66 coding region for generation of NO66lox mice. Using the Prx1 promoter directed-Cre recombination, we generated mesenchymal cell-specific NO66 knockout mice. This promoter was also used to link a flag-tagged NO66 cDNA fragment for the generation of NO66 transgenic mice. We found that during early skeleton development, deletion of NO66 gene in cells of mesenchymal lineage promotes skeletal growth and accelerates endochondral as well as intramembranous bone formation. At adult stage and with aging, deletion of NO66 gene in cells of mesenchymal lineage affects bone homeostasis and leads to high bone mass. In contrast, overexpression of NO66 in cells of mesenchymal lineage inhibits hypertrophic chondrocyte differentiation, disrupts growth plate organization, and reduces formation of both endochondral as well as intramembranous skeletal elements, and causes osteopenia at adult stages. Our results suggest an important role for NO66 in controlling skeletal growth, bone formation and bone density in vivo.

Disclosures: Qin Chen, None.

SU0104

Collagen Glycosylation and Cross-link Maturation in Bone. Masahiko Terajima^{*1}, Irina Perdivara², Kei Kaida³, Kenneth B. Tomer², Mitsuo Yamauchi⁴. ¹USA, ²Laboratory of Structural Biology, NIEHS, National Institutes of Health, USA, ³Department of Cariology, Nagasaki University Graduate School of Biomedical Sciences, Japan, ⁴North Carolina Oral Health Institute, School of Dentistry, University of North Carolina, USA

Type I collagen is the major organic component in bone providing a structural template for mineralization. During biosynthesis, specific hydroxylysine (Hyl) residues of collagen are enzymatically glycosylated forming galactosylHyl (G-Hyl) and glucosylgalactosylHyl (GG-Hyl). However, the biological significance of this modification in bone is not understood. The aim of this study was to determine the glycosylation state of Hyl residues involved in collagen cross-linking in bone obtained from fetal and mature bovine animals. Bones were demineralized, reduced with standardized NaB³H₄ and aliquots were directly analyzed for cross-links/their glycosylation. Other aliquots were trypsinized and the major cross-linked peptides were isolated by HPLC, and characterized by amino acid/cross-link analysis and nanoLC -electrospray mass spectrometry to determine the molecular loci of the cross-links and their glycosylation state. In mature bone, the major reducible/immature cross-link (dihydroxylysinonorleucine, DHLNL) was diminished with a concomitant increase of its maturational product, pyridinoline (Pyr), compared to those of fetal bone. The analyses of the cross-linked peptides revealed that, in both fetal and mature bones, the major DHLNL was derived from a1-16^C (Hyl^{ald}) X a1-87 (Hyl), and the Hyl residue was found almost entirely glycosylated in the form of GG- and G-DHLNL in a ratio of ~1:1. As a minor species, similarly glycosylated DHLNL derived from a1-16^C (Hyl^{ald}) X a2-87 (Hyl) was identified. In this locus, however, non-glycosylated DHLNL was also detected. The major Pyr in both groups was also derived from a1-16^C X a1-16^C X a1-87. However, in this mature cross-link, the predominant form was G-Pyr with minute amounts of GG-Pyr and non-glycosylated Pyr. This glycosylation pattern was essentially identical between fetal and mature bones. None of the helical a1-930 and a2-933 Hyl residues that were involved in cross-linking was found glycosylated. The differential glycosylation pattern seen in cross-linking indicates that the state of glycosylation of specific Hyl residues may modulate cross-link maturation in bone type collagen.

Disclosures: Masahiko Terajima, None.

This study received funding from: NIH grants R21 DE019569, DE020909 and AR060978.

SU0105

Further Characterization of Scoliosis-Like Vertebral Defects in Fibronectin Conditional Knockout Mice. Erica Perryn¹, Christian Richard¹, Qian Chen², Mark Dallas¹, Yixia Xie¹, Hong Zhao¹, Reinhard Faessler³, Donna Pacicca⁴, Sarah Dallas¹. ¹University of Missouri - Kansas City, USA, ²University of Pittsburgh Medical Center, USA, ³Max Planck Institute fur Biochemie, Germany, ⁴Children's Mercy Hospital, USA

Congenital scoliosis is a disease of lateral curvature of the spine that occurs due to developmental abnormalities. Fibronectin (FN) is an extracellular matrix (ECM) protein that is expressed at sites of bone formation and regulates osteoblast function. We have previously shown that conditional deletion of FN in osteoblasts using the 3.6kb COL1A1-Cre driver results in a scoliosis-like phenotype at birth that progresses with age, suggesting a potential role for FN in this disease and in vertebral development. To further understand its role in bone, FN conditional null mice (FNcKO) were generated by Cre-loxP recombination of the floxed FN allele using the 3.6kb Col1A1 Cre. As we reported previously, the mice showed a kinky tail/scoliosis-like phenotype with vertebral deformities ranging from involvement of a single to all caudal vertebrae, lumbar spine curvatures and fusion of lumbar vertebrae. Further mapping of the locations of the defects in n=39 FNcKO mice and n=40 fl/fl littermate controls showed that 70% of the FNcKO mice lacked all caudal vertebrae after CA17 and 40% were missing or had abnormalities in caudal vertebrae after CA4. 20% of the mice had a severe tail phenotype combined with fusions/curvatures in the lumbar spine. Micro CT analysis of 4 wk old FNcKO mice showed significantly reduced BV/TV in the L5 vertebra (Contr 9.66±0.74 vs FNcKO 6.54±0.76) with an even higher reduction in caudal vertebra CA5 (Contr 9.85±0.88 vs FNcKO 3.34±0.53). BV/TV was also significantly reduced in the tibia (Contr 11.53±1.54 vs FNcKO 8.13±0.82), but cortical thickness was unchanged. Histology showed abnormal vertebral segmentation, vertebral fusions, disorganized growth plates and delayed mineralization. To determine when these defects manifest, E9.5 to 14.5 embryos were examined. Curvatures in developing tail and spine structures were seen at all stages from E10.5 onwards, suggesting defective somitogenesis/resegregation. The concentration of vertebral defects in caudal regions of the embryo corresponds with early embryonic expression of the 3.6kb Col1A1 promoter in the caudal region as shown by lac Z staining. These data suggest FN is a key regulator of vertebral development. As we have previously shown that FN controls assembly of many other ECM proteins, we postulate that the defects in FNcKO mice are due to defective ECM assembly and altered ECM regulation of growth factors important in axial skeletal patterning/bone growth and development.

Disclosures: Erica Perryn, None.

SU0106

Osteogenic Effect of the Protein Component Extracted from a Hydroxyapatite-Based Product. David Musson¹, Maureen Watson², Karen Callon², Dorit Naoi², Craig McIntosh³, Jillian Cornish². ¹University of Auckland, New Zealand, ²University of Auckland, New Zealand, ³Waitaki Biosciences, New Zealand

Hydroxyapatite (HA) is a microcrystalline, mineral structure that is the primary constituent of mineralised bone. Therapeutically, HA products derived from extracellular matrices have been used extensively as "fillers" in bone and dental defects, coatings for metallic implants to promote osteoinduction, the basis for biomaterial scaffolds or as a carrier for controlled drug delivery. Here we assess what effect the protein component of a HA product has on the growth and differentiation of osteoblasts.

Using EDTA extraction, approximately 0.1mg/ml protein was extracted from bovine bone-derived MCH-CALTM, a microcrystalline HA product (Waitaki Biosciences, NZ). Levels of IGF-1, IGF-2 and osteocalcin were assessed by ELISA. Subsequently, the protein extract was used to treat primary rat osteoblasts in 2D (plastic) and 3D (within a collagen gel). Proliferation, differentiation and mineralization were assessed either through thymidine incorporation, alamarBlue®, real-time PCR and von Kossa staining. MCH-CALTM particles were also incorporated into cell-seeded collagen gels and their effect on osteoblast proliferation and differentiation were studied.

Growth factors were detected at levels similar to those found in circulation, with IGF-1 and -2 found at 230ng/g and 170ng/g, respectively. In contrast, osteocalcin was detected at 604µg/g, much higher than reported in circulation. The extracted proteins produced a significant, dose-dependent decrease in the proliferation of osteoblasts in 2D cultures, while dose-dependently increasing osteoblast mineralization. Notably, cells treated with 100µl/ml extract decreased proliferation 2.5-fold (P<0.05), yet increased mineralization 3.5-fold (P<0.05) compared to the control. Cells cultured in 3D had a similar response to those cultured in 2D, with collagen Iα1 expression levels 3-fold higher in 3D cultures treated with 100µl/ml extract, compared to untreated. The incorporation of MCH-CALTM into cell-seeded gels had no effect on cell proliferation, but did appear to increase cell differentiation.

Currently, HA based products are used to promote osteoinduction through offering structural support similar to natural bone. However, here we have demonstrated that the protein component of these products can also play a prominent role in inducing bone regeneration. This could have significant implications in the use of such products in future regenerative applications.

Disclosures: David Musson, None.

This study received funding from: Waitaki Biosciences

SU0107

In Vitro Microdistraction of Nager syndrome Dental Pulp Stem Cells: Comparison with Pre-osteoblasts and Adipose-derived Stem Cells. Joyce Yuan¹, Kenneth Fan², Daniela Bueno³, Christina Tabit¹, James Bradley¹.

¹UCLA, USA, ²University of Miami, Miller School of Medicine, USA,

³São Paulo University, Brazil, Brazil

Purpose:Stem cells induced to form bone have the potential to heal bony craniofacial defects with reduced morbidity. Our group studied the effect of linear stress exerted by a 3D microdistraction model system on the osteogenic capacity of stem cells isolated from the dental pulp of Nager syndrome (DPSCs) (a rare Craniofacial syndrome of jaw and limbs) and compared it to that of human adipose-derived stem cells (ASCs), and murine pre-osteoblasts.

Methods:The effect of linear stress on osteogenic capacity was studied by subjecting Nager DPSCs, ASCs and MC3T3 cells to two stress conditions in 3D collagen gels: gradual outward distraction at 0.5 mm/day and a static control involving no outward movement. Cells were harvested 24 hours following gel formation (day 0) and each day thereafter until day 7. The effects of stress were measured by real-time PCR for osteogenic genes (runx2, alkaline phosphatase/AP, osteonectin/ON, osteocalcin/OC, osteopontin/OP).

Results:When compared to day 0 controls, 3D static culture of Nager DPSCs for 4 days resulted in greater increases in osteogenic expression versus ASCs and MC3T3s (Nager DPSCs/ASCs/MC3T3s: AP - 49.9/0.0/1.5-fold change, OP - 30.1/2.6/1.3-fold change, OC - 9.3/0.2/1.5-fold. However, distraction of Nager DPSCs decreased expression of most osteogenic genes compared to static condition (runx-2 0.8-fold change, OP - 0.1-fold change, OC - 0.3-fold change). In contrast, distraction of ASCs increased osteogenic expression vs. static gels after 6 days (runx-2 - 46.8-fold increase, AP - 30.9-fold increase, OP - 6.7-fold increase; and ON - 5.9-fold increase at day 6). In pre-osteoblasts, distraction caused no significant change.

Conclusion:When directly compared with ASCs and pre-osteoblasts, Nager DPSCs showed the greatest osteogenesis. However, distraction stress resulted in decreased osteogenesis in Nager DPSCs, by contrast to ASCs and pre-osteoblasts.

Disclosures: Joyce Yuan, None.

SU0108

Measuring the Elastic Properties of Perlecan/HSPG2 Using Atomic Force Microscopy. Mary Farach-Carson, Jerahme R. Martinez^{*}, Kai Lou, Sitara S. Wijeratne, Ching-Hwa Kiang, Rice University, USA

Schwartz-Jampel Syndrome (SJS, MIM # 142461) is a human skeletal disorder identified in early childhood by myotonia and chondrodysplasia often with widespread musculoskeletal and joint defects. Common symptoms include a shortened stature, joint contractures and disruption of epiphyseal cartilage and bone. SJS results from mutation of the perlecan gene, HSPG2 on chromosome 1p36, that reduces the amount of normal full length perlecan deposited in the extracellular matrix (ECM); SJS thus can be considered a hypomorphic syndrome. Perlecan is a large multi-domain heparan sulfate proteoglycan (HSPG) that functions as a key structural component of the connective tissue ECM. Reduction of perlecan diminishes ECM function particularly at tissue interfaces, such as the chondro-osseous junction (COJ) of developing bones, and disrupts the lacunar canalicular system (LCS) of mineralized bone where perlecan is part of the tethering complex surrounding osteocytic processes that preserve fluid flow throughout mineralized bone. This project focuses on the physical characteristics of perlecan to better understand its role in maintaining connective tissue integrity. Our work indicates that perlecan, in addition to its role in growth factor delivery by virtue of its function as an HSPG, also serves as an elastic protein in the ECM that helps provide normal musculoskeletal tissue elasticity. One explanation for the clinical phenotype of SJS patients is the loss of perlecan's ability to mechanically support skeletal tissue. Single-molecule atomic force spectroscopy (AFM) was used to investigate the mechanical stretch properties of intact perlecan and of its individual component domains. Using AFM, we have shown that full length purified perlecan is an elastic protein that can be stretched to over 300 nm. To show that SJS mutations affect its elasticity, we have produced recombinant expressed perlecan domains containing mutations associated with SJS, focusing on domain IV of the protein that consists of 21 folded Ig modules that contain point mutations associated with SJS. AFM reveals how point mutations, linked to SJS, change the physical, elastic and mechanical properties of perlecan. This novel approach provides mechanistic data for the first time linking changes in perlecan structure and elastic properties to the symptoms of patients with SJS.

Disclosures: Jerahme R. Martinez, None.

SU0109

Selective Ablation of MT-MMP Activity in Vascular-associated Multipotent Progenitor Cells Leads to Defective Bone Formation and Disrupted Skeletal Homeostasis. Joanne Shi*¹, Susan S Yamada², Emily Purcell¹, Pamela G. Robey², Kenn Holmbeck². ¹National Institute of Dental & Craniofacial Research, USA, ²NIDCR, USA

Purpose: Membrane-type matrix metalloproteinases (MT-MMPs) exert an indispensable role in pericellular remodeling of matrix components in both skeletal and extraskeletal tissues. Previously, we have demonstrated that loss of MT1-MMP (MMP14) leads to early death with progressive fibrosis and entrapment of connective tissue cells (including osteogenic progenitors) in their extracellular matrix. These defects are partially mitigated by both extracellular compensatory proteolysis and intracellular lysosomal matrix uptake and degradation. Further ablation of MT3-MMP (MMP16) in an MT1-MMP deficient background consequently leads to perinatal death and severe developmental defects (including cleft palate). In an effort to characterize the cellular contributions to this double-deficient phenotype, we have utilized conditional ablation of MT1-MMP, here in perivascular cells and tissues, while maintaining global MT3-MMP deficiency.

Methods: A mouse line engineered to carry a conditional knock out allele for MT1-MMP was mated to mice expressing Cre-recombinase driven by the SM22 α promoter to ablate MT1-MMP gene expression in perivascular cells. This strain was subsequently crossed to an MT3-MMP deficient strain to achieve global MT3-MMP deficiency and MT1-MMP/MT3-MMP double deficiency in SM22 α -positive cells and their progeny.

Results: We show that specific ablation of MT1-MMP and MT3-MMP in the SM22 α -expressing cell population leads to a dramatic reduction of bone mass in the cranium as well as appendicular and axial bones. Cranial vault sutures were marked by matrix congestion and the bone was thinner with conspicuous fibrosis of the osteogenic tissues. In long bones, SM22 α -specific deletion of MT1-MMP/MT3-MMP caused overt diminution of trabecular bone, reduced cortical thickness and an abnormal cartilage in the epiphyseal growth plate. Vertebral segments of the spine and tail also displayed overt reduction in bone content.

Conclusion: The specific loss of MT-MMP activity in cells associated with the vasculature causes a dramatic reduction of skeletal mass in mice. Based on these findings we demonstrate that the perivascular tissue compartment is an indispensable cache of multipotent skeletal progenitor cells capable of supporting and sustaining formation of craniofacial bone, sutures, cartilages, appendicular and axial bone. These functions are critically dependent on MT-MMP-mediated pericellular proteolysis.

Funding: NIH IRP Z01 DE000676

Disclosures: Joanne Shi, None.

SU0110

Dietary Phosphorus Restriction Up-regulates the Ileal Fibroblast Growth Factor 15 Gene Expression through the Vitamin D Receptor Activation. Otoki Nakahashi*¹, Hironori Yamamoto¹, Sarasa Tanaka¹, Mina Kozai², Yutaka Taketani¹, Ken-Ichi Miyamoto³, Shigeaki Kato⁴, Eiji Takeda⁵. ¹University of Tokushima, Japan, ²University of Tokushima, Japan, ³Tokushima University School of Medicine, Japan, ⁴The University of Tokyo, Japan, ⁵University of Tokushima School of Medicine, Japan

Fibroblast growth factor (FGF) 19 subfamily including FGF23, FGF15/19, and FGF21 has a role as an endocrine factor in which the metabolism of phosphate and vitamin D, cholesterol and bile acid, and energy and lipid. Phosphorus (Pi) plays a critical role in skeletal development, mineral metabolism, and diverse cellular functions. It has been reported dietary Pi regulate the circulating FGF23. In the present study, we analyzed the effects of dietary Pi restriction on the gene expressions of ileal FGF15 and hepatic FGF21 in mice. C57BL/6J mice were given with different diets containing Pi (0.02 to 1.2%) for five days. We firstly confirmed that the plasma levels of FGF23 positively correlates with the dietary Pi amounts. On the other hand, western blots and real-time PCR analysis revealed that the gene expression of ileal FGF15, not hepatic FGF21, was increased by dietary Pi restriction. We next observed that the ileum mRNA levels of FGF15 was significantly increased by the administration of 1,25(OH)₂D₃ and decreased in vitamin D receptor knockout (VDR-KO) mice compared with the wild type mice. In addition, the luciferase assay clarified the transcriptional activation of the mouse FGF15 gene by VDR using several cell lines. Importantly, the dietary Pi restriction-induced FGF15 gene expression was prevented in VDR-KO mice. Furthermore, we found that the hepatic diurnal mRNA expression pattern of bile acid synthesis enzyme CYP7a1 as one of FGF15 negative target gene was influenced by dietary Pi. These results suggest that the dietary Pi restriction up-regulates the ileal FGF15 gene expression through VDR activation and affects the hepatic bile acid synthesis.

Disclosures: Otoki Nakahashi, None.

SU0111

Effects of Hexa-D-Arginine on Regulations of Fibroblast Growth Factor 23 and Parathyroid Hormone of Dietary Phosphate Depleted Mice. Masanori Takaiwa*¹, Kunihiko Aya², Kosei Hasegawa², Tsuneo Morishima², Youichi Kondo¹, Nobuyuki Kodani¹. ¹Dept. of Pediatrics, Matsuyama Red Cross Hosp., Japan, ²Department of Pediatrics, Okayama University Graduate School of Medicine, Dentistry & Pharmaceutical Sciences, Japan

We have previously reported a significance of PCSK in the FGF23 regulation during perinatal period. However, neither a specific PCSK nor a physiological regulation of the PCSK has been clarified. In this study, 2 groups of ten 8-week-old male C57BL/6J mice were fed either 1.5% or 0.02% Pi diet for 5days. We administered hexa-D-arginine (D6R, 3 μ mol/kg/dose, ip, tid), a PCSK3 inhibitor, to half of each groups for 3days before sacrifice. After the treatment, 4 groups of 5 mice; 1.5% Pi diet (High P), 1.5% Pi diet w/ D6R (High P+R), 0.02% Pi diet (Low P) and 0.02% Pi diet w/ D6R (Low P+R), were all healthy and serum creatinine showed no significant difference. Serum Pi of High P, High P+R, Low P and Low P+R were 8.12 \pm 0.24, 8.03 \pm 0.39, 3.36 \pm 0.33 and 5.80 \pm 0.32mg/dl, respectively. D6R increased serum Pi of Pi depleted mice concordant with significant decrements of Ca, CYP27B1 mRNA and NPT2a mRNA. Serum C-terminal FGF23 (C-FGF23) of High P, High P+R, Low P and Low P+R were 346.0 \pm 28.8, 407.8 \pm 34.4, 101.2 \pm 18.5, 198.3 \pm 20.3pg/ml, respectively. Serum intact FGF23 of these 4 groups were 247.0 \pm 19.0, 268.1 \pm 31.3, 9.6 \pm 2.6, 17.5 \pm 3.3pg/ml, respectively. Ratio between intact FGF23 and C-FGF23 (Int/C ratio) of those groups were 0.74 \pm 0.04, 0.70 \pm 0.07, 0.15 \pm 0.05 and 0.11 \pm 0.01, respectively. Additionally, FGF23 mRNA expression of the identical groups were 1.00 \pm 0.11, 0.88 \pm 0.19, 0.37 \pm 0.03 and 0.64 \pm 0.11folds of High P, respectively. Serum PTH 1-84 of High P, High P+R, Low P and Low P+R were 472.4 \pm 62.0, 236.3 \pm 60.0, 100.0 \pm 8.8 and 76.6 \pm 18.1pg/ml, respectively. Our observation regarding the Int/C ratio indicated that the FGF23 cleavage was enhanced in the Pi depleted mice. D6R seemed enough to block processing of pro-PTH by PCSK3 and subsequently suppressed the secretion of PTH1-84 in both Pi depleted and Pi loaded animals. However, although PCSK3 has been documented to cleave FGF23 in vitro, our D6R treatment to Pi depleted mice resulted in a slight decrease in the Int/C ratio in spite of the substantial increases in FGF23 mRNA and C-FGF23. This supported that FGF23 proteolysis of the Pi depleted mice was enhanced by D6R. Since D6R possesses a stimulatory effect on PCSK2 activity, further investigations would be useful to examine whether PCSK2 physiologically and specifically inactivates FGF23 in a Pi dependent manner.

Disclosures: Masanori Takaiwa, None.

SU0112

Genetic Determinants of Phosphate Response in *Drosophila*. Clemens Bergwitz*¹, Mark Wee², Sumi Sinha², Joanne Huang², Charles DeRobertis², Hway Chen², Lawrence Mensah², Adam Friedman³, Meghana Kulkarni³, Yanhui Yu³, Arunachalam Vinavagam³, Michael Schnall-Levin⁴, Harald Jueppner², Bonnie Berger⁴, Liz Perkins⁵, Stephanie Mohr³, Norbert Perrimon⁵. ¹Massachusetts General Hospital & Harvard Medical School, USA, ²Massachusetts General Hospital, USA, ³Harvard Medical School/Howard Hughes Medical Institute, USA, ⁴Massachusetts Institute of Technology, USA, ⁵Harvard Medical School/Howard Hughes Medical Institute, USA

Phosphate is required for important cellular processes and hypophosphatemia causes rickets and osteomalacia in humans. Hyperphosphatemia, on the other hand, leads to reduced lifespan due to tissue calcifications and metabolic changes by mechanism(s), which are to date poorly understood. We here used *Drosophila melanogaster* as a model organism and find that larval development depends on phosphate as a nutrient. Hemolymph phosphate concentration and adult life span are dependent on function of the Malpighian tubules. Life span furthermore is reduced when adult flies are cultured on high phosphate medium or when the Malpighian tubules are genetically ablated. To identify novel genetic determinants of phosphate response in *Drosophila* we next used S2R+ fly hemocyte cells to perform a genome-wide RNAi screen and identified 146 genes important for the cellular phosphate response with activation of ERK1/2 as readout. 103 unique and phosphate-selective genes, that did not interfere with insulin signaling, were then re-screened *in vivo* to identify genes, which regulate the effects of dietary phosphate on larval development (nutrient sensing), hemolymph phosphate concentration (endocrine sensing) and life span (phosphate toxicity) in flies. Details on the results from the validation screen will be presented.

Disclosures: Clemens Bergwitz, None.

SU0113

Metabolic Acidosis Increases Fibroblast Growth Factor 23 in Neonatal Mouse Bone. Nancy Krieger*¹, Christopher Culbertson², Kelly Kyker-Snowman², David Bushinsky¹. ¹University of Rochester, USA, ²University of Rochester School of Medicine, USA

Fibroblast growth factor 23 (FGF23) increases significantly with progressive chronic kidney disease (CKD), leading to reduced renal tubular phosphate (Pi) reabsorption, decreased 1,25(OH)₂D and increased left ventricular hypertrophy. This increase in FGF23 is associated with increased mortality. FGF23 is synthesized in osteoblasts and osteocytes, although the mechanism for its regulation is not clear. Patients with CKD have decreased renal net acid excretion leading to metabolic acidosis (MET). During MET excess acid is buffered by bone with release of mineral calcium (Ca) and Pi. MET increases not only osteoclastic bone resorption but also decreases osteoblastic bone formation. Since MET regulates osteoblast activity and osteoblasts produce FGF23, we utilized cultured neonatal mouse calvariae and primary osteoblasts to ask if a physiologic model of MET would increase FGF23. Calvariae were incubated in neutral (NTL, pH=7.46, Pco₂=38 mmHg, [HCO₃]⁻=27 mM) or acid (MET, pH=7.13, Pco₂=37 mmHg, [HCO₃]⁻=12 mM) medium or in the presence of 10 nM PTH in NTL medium as a positive control. MET significantly increased medium FGF23 protein levels at 24h (NTL=174.1±21 vs MET=379.6±36 pg/ml, p<0.05) and 48h (NTL=68±24 vs MET=328±69, p<0.05), as well as FGF23 RNA relative expression at 24h (NTL=1.64±0.3 vs MET=7.53±2.5, p<0.05) and 48h (NTL=0.93±0.1 vs MET=2.01±0.4, p<0.05). PTH stimulated FGF23 protein secretion comparably to MET at both 24 and 48h, but only stimulated FGF23 RNA at 48h. MET also induced significant Ca and Pi release. To exclude that the increased FGF23 was secondary to MET-induced release of bone Pi, primary osteoblastic cells were isolated from mouse calvariae and incubated in NTL or MET. In these cells, where there is no mineral Pi present, MET increased FGF23 RNA expression within 6h compared to incubation in NTL (NTL=1.43±0.2 vs MET=2.41±0.4, p<0.05). Thus, MET directly increases FGF23 in mouse osteoblasts. The results of this study suggest that elevated FGF23 in CKD may be due, at least in part, to MET directly stimulating osseous production of FGF23. If these results can be confirmed in humans, therapeutic interventions, including the provision of oral bicarbonate to mitigate the CKD-induced acidosis, have the potential to lower FGF23, decrease left ventricular hypertrophy and even lessen mortality.

Disclosures: Nancy Krieger, None.

SU0114

Renal and Extra Renal Regulation of the Vitamin D 1 α -hydroxylase Gene, CYP27B1, by FGF-23. Ankanee Chanakul¹, Martin Zhang¹, Harvey Armbrecht², Walter Miller¹, Anthony Portale¹, Farzana Perwad*³. ¹University of California San Francisco, USA, ²St. Louis Veterans Affairs Medical Center, USA, ³University of California, San Francisco, USA

The mitochondrial enzyme 25-hydroxyvitamin D 1 α -hydroxylase (CYP27B1), hydroxylates 25OHD to the biological active form of vitamin D, 1,25-dihydroxyvitamin D (1,25(OH)₂D), and the enzyme activity is tightly regulated by several factors. Serum 1,25(OH)₂D concentration is primarily dependent on renal 1,25(OH)₂D production. However, in extra renal tissues, CYP27B1 enzyme activity is responsible for local 1,25(OH)₂D synthesis that has important paracrine actions. We have shown that fibroblast growth factor-23 (FGF-23) directly suppresses renal CYP27B1 gene expression via activation of the extracellular signal regulated kinase 1/2 (ERK1/2) pathway. In this study, we sought to determine whether CYP27B1 gene expression is transcriptionally regulated by FGF-23 in the kidney and whether FGF-23 regulates the CYP27B1 gene in extra renal tissues. In HEK 293 cells, FGF-23 suppressed the full-length, 1.5kb human CYP27B1 promoter activity by 70%, and the suppressive effect was sustained in cells transfected with the promoter deletion constructs (-1.1kb, -926bp, -789 bp, -409bp, -200bp). This suggests that the regulatory region lies within the 200bp region. FGF-23-induced suppression of CYP27B1 promoter activity was blocked by a specific ERK1/2 inhibitor *in vitro*. To examine CYP27B1 transcriptional activity *in vivo*, we crossed *fgf-23* null mice with mice bearing the CYP27B1 promoter (1.5kb)-driven luciferase transgene (1 α -Luc). At baseline, renal CYP27B1 promoter activity was increased by 3-fold in FGF-23 null/1 α -Luc mice compared to wild-type/1 α -Luc mice. Intraperitoneal injection of FGF-23 suppressed renal CYP27B1 promoter activity, mRNA and protein expression by 26%, 93% and 55% respectively, and the suppression was blocked *in vivo* by an ERK1/2 inhibitor. These findings provide evidence that the regulation of renal CYP27B1 gene expression by FGF-23 is mediated at least in part by transcriptional mechanisms via activation of ERK1/2 signaling pathway, both *in vivo* and *in vitro*. In the heart, CYP27B1 promoter activity and mRNA were increased by 5- and 9-fold, respectively in FGF-23 null/1 α -Luc mice compared to control mice. We also observed a 3-, 9- and 10-fold increase in CYP27B1 mRNA expression in the lung, aorta and testis, respectively, but not in other extra-renal tissues. Thus, we demonstrate for the first time that CYP27B1 gene expression is regulated by FGF-23 in extra renal tissues such as the heart, lung, aorta and testis.

Disclosures: Farzana Perwad, None.

SU0115

Age Differences in the Relationship between Vitamin D and Parathyroid Hormone: KNHANES IV. Kyoung Min Kim*¹, Se Hwa Kim², Yumie Rhee³, Chang Oh Kim¹, Sung-Kil Lim¹. ¹Yonsei University College of Medicine, South Korea, ²Kwandong University College of Medicine, Myongji Hospital, South Korea, ³Department of Internal Medicine, College of Medicine, Yonsei University, South Korea

Purpose : Vitamin D deficiency is extremely common among elderly subjects, and subsequent hyperparathyroidism has been associated with poor bone health and increase of cardiovascular risk. Therefore, the ideal 25 hydroxyvitamin D [25(OH)D] concentration generally reflect the level for obtaining maximal suppression of PTH. **Methods :** A total of 3,576 adult participants aged 55 to 95 years in the Korea National Health and Nutrition Examination Surveys IV were available for analysis. We examined the relationships between 25(OH)D and parathyroid hormone in 4 aged groups. **Results :** At below a 25(OH)D of 20 ng/ml, inverse relationships between 25(OH)D and PTH were observed in all 4 age groups and the degree of these negative correlations were increased according to age ranks. However, an inverse association between 25(OH)D and PTH was only apparent in the oldest age group (85-95 years) at above a 25(OH)D level of 20 ng/ml. The incidence of secondary hyperparathyroidism was increased according to age ranks below 20 ng/ml of 25(OH)D and this increment was also observed above 20ng/ml of 25(OH)D. Whereas there were no any significant differences of bone mineral density (BMD) between hyper-parathyroidism and normo-parathyroidism groups in 55-64 years at above 25(OH)D of 20ng/ml, hyperparathyroidism group showed lower BMD of femur in 65-74 years. Moreover, hyperparathyroidism group of oldest ages (85-95 years) **Conclusion :** Elderly might need more vitamin D supplementation to produce the higher 25(OH)D concentrations required to overcome the hyperparathyroidism and subsequent bone loss.

Disclosures: Kyoung Min Kim, None.

SU0116

Bone Marrow Macrophage Cells Secrete a Factor that Inhibits PTH-Stimulated Osteoblastic Differentiation *In Vitro*. Shilpa Choudhary*, Abhijit Deb Roy, Joseph Lorenzo, Carol Pilbeam, University of Connecticut Health Center, USA

Bone marrow macrophages (BMMs) can inhibit PTH-stimulated osteoblast (OB) differentiation *in vitro*. This inhibition is blocked by the absence of cyclooxygenase 2 (Cox2) expression or activity and by osteoprotegerin, which interferes with RANKL-RANK interactions. The goal of this study was to determine if the BMM inhibition of PTH effects on OBs required cell-cell contact. We treated primary calvarial osteoblasts (POBs) from neonatal Cox2 knockout (KO) mice with PTH (10 nM) in the presence or absence of conditioned media (CM) from WT or KO BMMs, which had been cultured for 3 days with 30 ng/ml M-CSF +/- 30 ng/ml RANKL. POBs were treated for 14 days with 3 parts CM to 1 part OB differentiation media. To prevent osteoclast-like cell formation in POB cultures in response to PTH or RANKL, cultures were treated with 50 ng/ml osteoprotegerin. OB differentiation was measured by alkaline phosphatase and osteocalcin gene expression and by alizarin red staining for mineralization. PTH stimulated OB differentiation in Cox2 KO POBs cultured with no CM, with CM from Cox2 KO BMMs or with CM from WT BMMs cultured with M-CSF alone (mCM). CM from WT BMMs cultured with both M-CSF and RANKL (mrCM) blocked PTH-stimulated OB differentiation. Similar experiments were done with CM from EP2 receptor KO mice and EP4 receptor KO mice. mrCM from WT and EP2 KO (but not EP4 KO) BMMs blocked the stimulatory effects of PTH, indicating that the EP4 receptor was necessary for the inhibitory effect. Similar to PTH, forskolin (1 μ M) stimulated OB differentiation and this effect was blocked by WT mrCM. WT mrCM also blocked the stimulation of cAMP production in POBs by both PTH and forskolin. Treatment of POBs with mrCM from WT (but not Cox2 KO) BMMs abrogated the PTH stimulation of early response genes (RAMP3, Nurr1, and PTHrP) and the PTH inhibition of DKK1 gene expression. To determine if Gi/o was involved in the inhibition of PTH effects, pertussis toxin (PTx) was used. PTx (100 ng/ml) prevented the inhibitory effects of WT mrCM on both PTH-stimulated early gene expression and OB differentiation. Our results suggest that PGE₂ acts on EP4 receptors of BMM cells, which have been stimulated with RANKL, to produce a soluble factor that acts on osteoblastic cells to inhibit PTH-stimulated cAMP production and differentiation via Gi/o pathway. These studies may help to identify new pathways to improve the therapeutic potential of PTH.

Disclosures: Shilpa Choudhary, None.

This study received funding from: NIDDK

SU0117

Gender Differences in the Role of IGF-1 Signaling in Mediating the Effects of Continuous PTH on Bone. Muriel Babey^{*1}, Chak Fong², Yongmei Wang³, Takuo Kubota⁴, Elalieh Hashem², Daniel Bikle⁵. ¹UCSF, Division of Endocrinology, USA, ²UCSF, USA, ³Endocrine Unit, University of California, San Francisco/VA Medical Center, USA, ⁴Osaka University Graduate School of Medicine & Dentistry, Japan, ⁵Endocrine Research Unit, Division of Endocrinology UCSF & VAMC, USA

Intermittent administration of parathyroid hormone (PTH) has been proven a remarkably effective therapy for osteoporosis. We have found that insulin-like growth factor-1 (IGF-1) is required for these anabolic actions of PTH. However, continuous administration of PTH has been noted to increase bone resorption more than formation resulting in bone loss. Having demonstrated that IGF-1 signaling is a crucial mediator of the anabolic actions of intermittent PTH, we investigated the role of IGF-1 signaling in mediating the catabolic actions of continuous PTH.

We examined the degree to which continuous PTH (rat PTH 1-34, 60 µg/kg body weight/d) affects murine bone structure and osteoprogenitor differentiation and mineralization in FVB/N mice lacking the IGF-1 receptor in mature osteoblasts (IGF-1R OBKO, Cre-Recombinase driven by the Osteocalcin promoter) in comparison to control (ctrl) mice lacking the Cre-Recombinase. Both genders were examined. PTH infusion had net catabolic effects on trabecular bone parameters in female ctrl mice, showing a significant reduction in bone volume (BV)/ tissue volume (TV) by 31%, in trabecular number by 8% and in trabecular thickness by 11%. The catabolic effects of PTH infusion on trabecular bone parameters were blunted in female IGF-1R OBKO mice. In male PTH infused ctrl mice, the effects of continuous PTH were not catabolic for trabecular bone parameters. However, in the male IGF-1R OBKO mice PTH resulted in a non-significant trabecular bone loss of 24%. Cortical bone thickness in PTH infused female ctrl was significantly reduced by 13% which was blunted in female IGF-1R OBKO mice. The PTH infused male Ctrl mice showed no significant effect on cortical thickness but was significantly reduced by 11% in male PTH infused IGF-1R OBKO mice.

These results demonstrate that continuous PTH is catabolic for the female mouse skeleton, effects blunted by the loss of IGF-1 signaling in the mature osteoblast. In contrast, the male skeleton does not demonstrate a catabolic response to continuous PTH unless the IGF-1R is deleted from the mature osteoblast. These results are consistent with our previous results showing a greater anabolic response to PTH in the male skeleton, which is lost with deletion of IGF-1R from the mature osteoblast shifting the balance to a catabolic response. In the female, on the other hand, inhibition of the catabolic actions of continuous PTH in the IGF-1R OBKO appear to dominate the net response.

Disclosures: Muriel Babey, None.

SU0118

PTHrP Regulates Cancer microRNA Expression. Leonard Defetos^{*1}, Douglas Burton², Jessica Wang-Rodriguez³, Cheryl Chalberg², Su Tu², Kathy Smith², Rutherford Ongkeko². ¹VA San Diego Healthcare System / University of California, San Diego, USA, ²VA San Diego Healthcare System / University of California San Diego, USA, ³Veterans Administration San Diego Healthcare System, USA

Background: Parathyroid hormone related protein (PTHrP) is expressed and secreted by many malignancies, including prostate, lung, and breast. This oncoprotein is associated with regulatory effects and interactions that are important in the development and progression of these cancers, especially skeletal. However, the molecular mechanism of PTHrP's role in these cancers is not well understood. MicroRNAs (miRs) have emerged as important molecular mediators of cancer pathobiology. We posited miR regulation as a novel mechanism for PTHrP's actions in carcinogenesis. We thus explored the effects of PTHrP on the expression of oncogenic and tumor suppressor miRs using breast and prostate cancer cell lines.

Methods: Human prostate (PC-3 and DU 145) and breast (MCF-7 and MDA-MB435S) cancer cell lines were transfected with PTHrP expression plasmids or treated with PTHrP peptides; to knockdown PTHrP expression, we transfected the cells with PTHrP isoform specific siRNA oligos. Total RNAs from the cell pellets were purified and 95 separate miRs implicated in cancer, cell development, and apoptosis were analyzed using qPCR. The qPCR results from the PTHrP treated cells were compared to control cells.

Results: Significant differences in the expression of several miRs were observed when we manipulated the PTHrP expression in the cancer cells. DU 145 cells transfected with PTHrP expression plasmids upregulated miR let-7b, 30b, 92, 99a and downregulated several miRs, including 19a, 200b, 301, 370, 372, 10b, 101, 146b, 181c, 193b, 9, 124a, 127, 128a, 134, 135a, 135b, 218, 133a, and 195. When PTHrP expression was knocked down in PC-3 cells, upregulation of several miRs, including 125b and downregulation of miR 107 were observed. DU 145 cells treated with PTHrP peptides upregulated miR 19, 25, 30c, 200b, 301 and downregulated miR 92, 93, 99a, 103, 125a. Up- and downregulation of several miRs were also observed in the breast cancer cells transfected with PTHrP plasmids.

Conclusions: We have demonstrated that PTHrP regulates the expression of oncogenic and tumor suppressor miRs in breast and prostate cancer cells. The modulation of these miRs by PTHrP uncovers a key molecular pathway of oncogenesis. Furthermore, this pathway presents new treatment targets for PTHrP-expressing malignancies. Our studies provide novel insights into the molecular actions

of PTHrP as an oncoprotein and identify the PTHrP-miR pathway as a treatment target for many common cancers.

Disclosures: Leonard Defetos, None.

SU0119

Skeletal Response to Mechanical Loading and Unloading in Mice Lacking the PTH1 Receptor Expression in Osteocytes. Yili Qu¹, Yi Man², Kevin Barry¹, Jordan Spatz³, Brandon Ausk⁴, Keertik Fulzele⁵, Sutada Lotinun⁶, Roland Baron⁷, Ted Gross⁴, Paola Divieti Pajevic^{*8}. ¹Endocrine Unit, Massachusetts General Hospital, Harvard Medical School, USA, ²Endocrine Unit, Massachusetts General Hospital & Tuft School of Dental Medicine, USA, ³Harvard-MIT Division of Health Sciences & Technology (HST), USA, ⁴University of Washington, USA, ⁵Massachusetts General Hospital; Harvard Medical School, USA, ⁶Harvard School of Dental Medicine, USA, ⁷Harvard School of Medicine & of Dental Medicine, USA, ⁸Massachusetts General Hospital & Harvard Medical School, USA

Mechanical loading of the skeleton, such as during exercise, is an important anabolic signal that leads to bone formation, whereas the absence of loading, as occurs with immobilization, disuse or exposure to low gravity, causes bone loss. Despite substantial progress in characterizing the skeletal deterioration induced by disuse or microgravity, and bone formation triggered by cyclic loading, the cellular and molecular mechanisms of skeletal mechanotransduction have remained unknown. Osteocytes form a functional cellular network, which make them ideally suited to sense mechanical stimuli. To investigate the role of PTHR on osteocytes in skeletal mechanotransduction, we have subjected mice lacking the receptor specifically in osteocytes (OcyPPRKO) to hindlimb unloading as achieved by tail suspension, and tibia loading as performed by cyclic compression (100 cycles/day, 3d/wk for 3 weeks). At the end of the unloading or loading protocols, mice were sacrificed and femurs and tibia were analyzed by microCT, histology and histomorphometry. MicroCT analysis of femurs from 3 weeks unloading, revealed a significant decrease in trabecular bone (BV/TV%), trabecular thickness and increase in trabecular spacing in both OcyPPRKO and controls. Interestingly unloading induced a significant decrease in cortical thickness in both groups whereas cortical density was significantly decreased only in controls. Bone formation rate (BFR/BS; BFR/BV and BFR/TV), as assessed by histomorphometric analysis, was significantly decreased in unloaded controls whereas it was unchanged in KO mice indicating that suppression of osteoblast function during skeletal unloading is PPR-dependent. Osteoclast number (N.Oc/T.Ar and N.Oc/B.Pm) and surface (Oc.S/BS%) were increased upon unloading in OcyPPRKO mice suggesting that bone resorption is independent on PTH action on osteocytes. These data suggest that unloading induce a trabecular bone loss and trabecular thinning (possibly osteoclast-mediated) independent of PPR signaling on osteocytes. We then assess the role of PPR signaling during mechanical loading. Cyclic tibia loading stimulated bone formation in both OcyPPRKO and control mice. Interestingly KO mice displayed a significantly greater periosteal response (as assessed by BFR) compared to controls, suggesting a role of PTH signaling in regulating the rate of bone formation. Taken together these studies suggest that PPR signaling on osteocytes is involved in mechanotransduction.

Disclosures: Paola Divieti Pajevic, None.

SU0120

The Effects of Storage Temperature and Repeat Freeze-Thaw Cycles on Stability of PTH (1-34) as Determined by the IDS-iSYS Automated Analyser. Christopher Washbourne^{*1}, Jonathan Tang², William Fraser³. ¹Mr., United Kingdom, ²University of East Anglia, Norwich, UK, United Kingdom, ³University of East Anglia, United Kingdom

Endogenous PTH (1-34) is the N-terminal portion of human parathyroid hormone, formed from the cleavage of intact PTH (1-84). PTH (1-34) increases calcium absorption from the intestines and calcium reabsorption by the kidneys. Synthetic PTH (1-34) can reproduce the effects of the natural human hormone, increasing BMD in osteoporotic patients by promoting activity of osteoclasts. This is a potential target for drug treatment against the rising incidence and prevalence of metabolic bone disease.

Our aims were 1) to evaluate the IDS-iSYS PTH (1-34) kit, and 2) to investigate the effects of sample storage temperature and repeat freeze-thaw cycles on the stability of the molecule over time.

EDTA plasma samples were obtained from clinical trial subjects receiving teriparatide. Three pools containing low, medium and high concentrations of PTH (1-34) were produced; the baseline PTH (1-34) concentration was measured immediately on the IDS-iSYS platform. The pools were then aliquoted and subdivided into the following three protocols: a) stored at room temperature and measured at 30 minutes, 1, 2, 4, 8, 12, 24, 48h and 7 days; b) stored at -20°C and measured at the same time points as group a; and c) repeatedly freeze-thawed from -20°C to room temperature and measured at each cycle. This process was repeated 10 times.

The assay showed good linearity from 4–1000 pg/mL. Our precision data showed intra-assay imprecision CV of 5.4% at a concentration of 46.7 pg/mL and 7% at a concentration of 11.7 pg/mL. Inter-assay imprecision CV was 7% at a concentration of 45.1 pg/mL. The Lower Limit of Quantification (LOQ) of the assay was determined at 1.6 pg/mL, well below the lower working limit of the assay.

We compared the individual results from each time-point against the baseline [PTH (1-34)]. At room temperature we observed no decrease in [PTH (1-34)] up to 24 hours. The same trend was also observed for aliquots stored at -20°C. Our repeat freeze-thaw cycle experiment showed [PTH (1-34)] remained stable after 10 cycles.

In conclusion, EDTA plasma is a good preservative for PTH (1-34) as our results have shown no degradation up to 24 hours at room temperature, at -20°C and even after subjection to repeat freeze-thaw cycles. Our data have provided useful sample stability and storage guidelines that will allow laboratories to adopt into routine procedures, thereby improving the accuracy of analysis and ultimately improving the clinical value of results.

Disclosures: Christopher Washbourne, None.

SU0121

Changes in Bone Mass Predict Progression of Coronary Artery Calcification in Patients with Chronic Kidney Disease. Hartmut Malluche¹, Gustav Blomquist², Kimberly McLaughlin², Daniel Davenport², Marie-Claude Faugere¹. ¹University of Kentucky Medical Center, USA, ²University of Kentucky, USA

Coronary artery calcifications (CAC) and bone loss are frequently seen in patients with chronic kidney disease on dialysis (CKD-5D). The current study was designed to prospectively evaluate the relationship between changes in bone mineral density (BMD) and CAC over one year in CKD-5D patients.

At enrollment and after 1 year, CAC was assessed by Agatston scores obtained using multiple slice computed tomography. At the same times, BMD of the spine and hip was assessed by dual-energy x-ray absorptiometry (DXA) and quantitative computed tomography (QCT). Traditional cardiovascular risk factors were also recorded. Relationships between CAC and BMD at baseline and their changes after 1 year were analyzed using non-parametric tests of correlation, followed by multiple regression of log-transformed CAC differences.

At this time, there are 75 men (age 52.8 ± 12.8 yrs.) and 52 women (age 54.7 ± 13.5 yrs.) enrolled with mean dialysis vintage of 55.1 ± 54.8 mos. Thirty-eight patients have completed 1 year follow-up. Baseline BMD and CAC scores, and their changes after 1 year, are shown in the Table. Baseline CAC scores correlate inversely with QCT BMD of the hip and spine, and with DXA BMD of the hip, but not the spine. This could be explained by the known confounding of spine DXA BMD by extraosseous tissue calcifications. At one year, only changes in QCT BMD of the spine correlate with CAC progression. The very small changes in hip BMD found over 1 year provide a likely explanation for their lack of correlation with CAC progression. Multiple regression shows age and decrease in L1-L2 QCT BMD as significant predictors of CAC progression. Gender and dialysis vintage are not predictive.

In conclusion, we demonstrate in patients with CKD: 1) an inverse relationship between BMD and CAC at baseline, and 2) a relationship, after adjustment for age, between spinal bone loss and CAC progression over one year.

Table: Correlations between baseline CAC scores and QCT/DXA BMD results of the hip and spine and between changes in CAC and QCT/DXA BMD after one year.

| At Baseline | CAC | Hip QCT (g/cm ²) | Hip DXA (g/cm ²) | L1-L2 QCT (mg/cm ³) | L1-L2 DXA (g/cm ²) |
|------------------------------|--------------|--------------------------------|--------------------------------|-----------------------------------|----------------------------------|
| Median (Interquartile Range) | 203 (2-1114) | .847 (.711-.985) | .943 (.824-1.090) | 162 (131-216) | 1.230 (1.094-1.363) |
| Correlation w/ CAC | 1.000 | -.282** | -.270** | -.282** | -.064 |
| After 1 Year | Δ CAC | Δ Hip QCT (g/cm ²) | Δ Hip DXA (g/cm ²) | Δ L1-L2 QCT (mg/cm ³) | Δ L1-L2 DXA (g/cm ²) |
| Median (Interquartile Range) | 141 (3--552) | -.007 (-.032--009) | -.014 (-.028--011) | -2.85 (-13.7--8.30) | -.015 (-.060--034) |
| Correlation w/ Δ CAC | 1.000 | -.067 | .072 | -.413* | -.258 |

* p < .05; ** p < .01

Table

Disclosures: Hartmut Malluche, None.

SU0122

Characterization of Bone Quality in Rat Model with Chronic Kidney Disease. Hiromi Kimura-Suda^{*1}, Kousuke Hidaka¹, Mieko Kuwahara², Kyousuke Kanazawa¹, Hidetoshi Ueno¹, Kyouji Honma¹, Makoto Kajiwara³, Kenji Bannai², Hideyuki Yamato². ¹Chitose Institute of Science & Technology, Japan, ²Kureha Corporation, Japan, ³Kureha Special Laboratory, Japan

Kidney has several important functions in a body: removing waste products from the blood, regulating the water fluid levels, and maintaining calcium and phosphorus homeostasis. Gradual and permanent loss of kidney function, which is called chronic kidney disease (CKD), causes bone and mineral disorder (MBD). CKD-MBD patients are characterized to reduce bone strength due to abnormal bone turnover. We have previously characterized bone quality of tibia in rats at different ages using Fourier transform infrared (FTIR) imaging. FTIR images of tibia in rats indicated properties of the mineral/collagen matrix, architecture/geometry of trabecular and cortical bone. FTIR imaging is also able to detect the rate of bone turnover by comparing mineralization of normal and abnormal bone turnover. Raman spectroscopy and SEM with energy-dispersive X-ray spectroscopy (EDX) are powerful tools for both qualitative and quantitative analysis of materials without homogenization as well as FTIR imaging. We describe analysis by FTIR imaging, Raman spectroscopy and SEM with EDX to characterize bone quality of femur in rat model with CKD. Eleven-week male rats induced 5/6-nephrectomy and sham-operated rats (Sham) were kept for 16 weeks to produce rat model with CKD and control, and then each femur in rat was extirpated and embedded by poly (methyl methacrylate) (PMMA) to make longitudinal sections for the measurements. FTIR images of distribution of phosphate show both cortical and trabecular bone in CKD is reduced compared to Sham; however, visible images show only trabecular bone in severe CKD is dramatically decreased. Mineral/collagen matrix ratio using FTIR and Raman spectra indicates trabecular bone is lower than cortical bone, and center of cortical bone is calcified rather than endosteum and periosteum. These data are coincident with EDX image of calcium in femur. The mineral/collagen matrix ratio of severe CKD to Sham is reduced by 5-8%. FTIR and Raman spectra show that proportion of carbonate in severe CKD to Sham were reduced by 15-35%. Accreted bone loss is associated with high bone turnover. In high-turnover bone, proportion of carbonate accumulated in mineral matrix may be decreased. These data suggest bone quality in rat model with CKD is characterized by reduced mineral/collagen matrix ratio and carbonate/phosphate ratio in femur.

Disclosures: Hiromi Kimura-Suda, None.

This study received funding from: Takahashi Industrial and Economic Research Foundation

SU0123

Withdrawn

SU0124

Mineral Characteristics of Bone Tissue in Patients With Chronic Kidney Disease. ANNE-SOPHIE BRAVO MARTIN^{*1}, Delphine Farlay², Georges Boivin³. ¹INSERM, UMR 1033 ; Université de Lyon, France, ²INSERM, UMR1033; Université De Lyon, France, ³INSERM, UMR1033 ; Université De Lyon, France

In patients with chronic kidney disease (CKD), renal functions deterioration provokes phosphorus and calcium metabolism impairment leading to histological lesions (1). They consist generally in changes (increase or decrease) of bone remodeling level, osteoid surfaces and occurrence of mineralization disturbances. This study aims to assess in CKD patients, degree of mineralization (DMB), mineral characteristics and microhardness of bone tissue.

Iliac bone biopsies embedded in methylmethacrylate taken from 23 patients with CKD (44 ± 11 years), were used to measure DMB and heterogeneity index (HI) using quantitative microradiography (2) and Vickers microhardness (3). In 5 of the samples, mineral characteristics (crystallinity index, mineral maturity, carbonation and mineralization index) were calculated by Fourier Transform Infrared Microspectroscopy (FTIRM) (4). Data were compared to those of 43 human controls (54 ± 20 years).

DMB is significantly higher ($p < 0.05$) and HI significantly lower ($p < 0.05$) in cortical bone of CKD patients than in controls, showing a well mineralized and homogeneous bone. To the contrary, mineral maturity and mineralization index are lower in CKD than in controls. Carbonation is decreased for 4 of 5 patients whereas crystallinity varied from a patient to another. Correlations generally observed between mineral maturity and other parameters (mineralization index, carbonation, crystallinity), and between DMB and mineralization index, are not always found in patients with CKD. Results suggest a dissociation of parameters, probably due to chemical modifications of bone, caused by hyperphosphatemia and hypocalcemia related to impaired renal functions. Mineralization index is an area ratio (mineral/organic) whereas DMB is an absolute value. DMB may reflect chemical changes in apatite crystals differently than mineralization index. Finally, microhardness is significantly higher in CKD patients than in controls, both in cortical and trabecular bone ($p < 0.05$ and $p < 0.001$, respectively).

Those preliminary results have to be confirmed in a larger group of patients for whom results of biological dosages and medical history are known.

1-Lafage-Proust, 2008. *Ostéodystrophie rénale*, EMC Néphrologie 14-275-A-10;
 2-Boivin and Meunier 2002, *Calcif Tissue Int* 70:503; 3-Boivin *et al.* 2008, *Bone*
 43:532;
 4-Farlay *et al.* 2010, *J Bone Miner Metab* 28:433.

Disclosures: ANNE-SOPHIE BRAVO MARTIN, None.

SU0125

Retrospective Review of Bone Density Scans in Different Stages of Chronic Kidney Disease. Bhanu Prasad^{*1}, Siva Karunakaran¹, Mohammed Abdulhadi², Cathy Nadiger³, Cam Wilson¹. ¹University Of Saskatchewan, Canada, ²University of Saskatchewan, Canada, ³Regina Qu apelle Health region, Canada

Introduction:Our renal program undertook a retrospective chart review of all the patients who underwent a baseline Dual-energy X-ray absorptiometry(DXA) scan in our multidisciplinary chronic kidney disease clinic (CKD clinic) from Jan 2001 to Jan 2010.

Purpose of the study:To measure the mean bone mineral density,T and Z scores in prevalent CKD patients in the clinic. To determine,if there was a preferential site of bone loss in CKD patients across different disease stages.

Methods: All patients had baseline creatinine, glomerular filtration rate (eGFR)in mls/min as per the Modification of Diet in Renal Disease (MDRD) formula,renal diagnosis,and bone density measurements including, T-score and Z-scores on all patients were measured for the lumbar spine,both hips,and the one-third distal radius.

Results: Total of 410 patients were identified: For baseline characteristics and T scores: please see table 1. Analysis of variance (ANOVA) showed significant variation in BMD at the total hip and femoral neck across CKD stage(p<.001), but not for other BMD measurement sites. There was a significant positive correlation between eGFR and total hip or femoral neck BMD,and a significant negative correlation with CKD stage (all Spearman p<.05).

Conclusions:There is a demonstrable decline in total hip and femoral neckbone density with progression of CKD staging.Lumbar spine and distal radius BMD were not affected by CKD stage. Analysis of variance suggests that hip and femoral neck BMD's and T scores were significantly lower than L1-L4 and distal third of radius.

Table 1: Baseline characteristics, T scores for lumbar spine, Hip, Fem neck, Distal radius

| | CKD 2 | CKD 3 | CKD 4 | CKD 5 | ANOVA (p value) |
|-------------------------|----------|-----------|-----------|-----------|-----------------|
| Sample size | 33 | 147 | 167 | 61 | -- |
| e GFR (mean) | 69.8±9.2 | 40.9±8.5 | 22.2±4.2 | 11.8±1.9 | -- |
| Age (yrs± SD) | 62.8±9.2 | 67.2±13.7 | 68.6±13.2 | 64.3±13.8 | -- |
| L1-L4 (T score) | 0.08 | 0.02 | -0.102 | -0.429 | (0.355) |
| Hip (T score) | -0.404 | -0.822 | -1.103 | -1.422 | (0.004) |
| Fem Neck (T score) | -0.994 | -1.458 | -1.711 | -1.907 | (0.0011) |
| Distal radius (T score) | 0.664 | -0.845 | -0.913 | -1.092 | (0.353) |

Table 1 b.

| | Normal (0- <-1) | Low Bone mass (-1.0-<-2.5) | Osteoporosis (>-2.5) |
|---------------|-----------------|----------------------------|----------------------|
| Hip | 176 | 154 | 37 |
| Femoral neck | 100 | 210 | 75 |
| Distal radius | 235 | 111 | 60 |

Table 1

Disclosures: Bhanu Prasad, None.

This study received funding from: Regina Qu apelle Health region, Regina, Canada

SU0126

Osteoclast-poor Osteopetrosis in a Toddler without Mutation of the Genes TNFSF11 and TNFSFR11A that Encode RANKL and RANK, Respectively. Gary Gottesman^{*1}, Loren D. Pena², Chang Yang³, Steven Mumm⁴, Katherine Madson¹, Deborah Novack⁵, William H. McAlister⁶, Michael Whyte¹. ¹Shriners Hospital for Children-Saint Louis, USA, ²University of Illinois at Chicago College of Medicine, USA, ³Washington University in St Louis School of Medicine, USA, ⁴Washington University School of Medicine, USA, ⁵Washington University in St. Louis School of Medicine, USA, ⁶Mallinckrodt Institute of Radiology at St. Louis Children's Hospital, Washington University School of Medicine, USA

Osteopetrosis (OPT) is the rare developmental phenotype caused by failure of osteoclasts (OCs) to resorb skeletal matrix. Consequently, there is altered morphology and structure of bone. Most patients have non-functioning OCs. Rarely, OCs fail to develop because of loss-of-function mutations in TNFSF11 or TNFRSF11A encoding RANKL and RANK, respectively.

We report a 3-year-old boy with OC-poor OPT, born to consanguineous parents. At age 3 months, strabismus was attributed to septo-optic dysplasia, but no pituitary abnormalities were found. At age 2.5 years, skeletal radiographs for growth delay showed generalized increased bone density consistent with OPT – likely autosomal recessive (AR) “malignant” OPT. DXA revealed a lumbar spine Z-score of +13.4. Mutation analyses for the most likely genes, TCIRG1 and CLCN7, as well as for other AR OPT genes, PLEKHM1, OSTM1, TNFSF11, and TNFRSF11A were negative (CTGT, LLC, Allentown, PA). Duplication/deletion abnormalities were excluded by high-density targeted array analysis for the latter three genes (CTGT). We analyzed CSF1, CSF1R, TNFSF11, and TNFRSF11A with negative findings. Exome sequencing is underway.

Distal tibial metaphyseal biopsy, following tetracycline labeling, showed dense trabecular bone and retained cartilage diagnostic of an OPT. Osteoblast morphology and numbers were unremarkable, but OCs (including evaluation by TRAP staining) were absent. Fluorescence microscopy showed active bone formation.

Our patient's osteoclastogenesis was evaluated twice by differentiating peripheral blood monocytes in M-CSF and RANKL. Compared to family members and unrelated controls, only a few TRAP+ multinucleated cells formed from the patient's cells, and these failed to make actin rings on bone. RANK levels were normal on Western blots.

OC-poor OPT from RANK deficiency can be treated with bone marrow transplantation (BMT). In contrast, RANKL deficiency does not respond to BMT because the genetic defect resides in the stromal compartment rather than in the transplantable hematopoietic marrow. Our patient's failed osteoclastogenesis during *in vitro* stimulation of his monocytes suggests an intrinsic pathogenetic defect of his OC progenitors, rather than a problem with stromal-derived osteoclastogenic factors. If our patient's clinical status deteriorates, BMT could treat his osteoclast-poor OPT.

Disclosures: Gary Gottesman, None.

SU0127

Molecular Analyses of Malignant Hypercalcemia Caused by Genuine PTH, but not PTHrP, Produced in Retroperitoneal Fibrous Histiocytoma. Kosuke Uchida^{*1}, Hiroko Fujii¹, Mimi Tamamori-Adachi², Koji Morita¹, Tomoki Okazaki², Yuji Tanaka¹. ¹National Defense Medical College, Japan, ²Teikyo University School of Medicine, Japan

Ectopic production of PTH leading to malignant hypercalcemia is extremely rare, suggesting that parathyroid gland-specific PTH expression is kept under stringent control. As such, pathogenesis of ectopic PTH production is largely unknown with scattered exceptions such as large rearrangement around PTH gene locus and probable hypomethylation-related PTH gene activation. Here, we report a case of hypercalcemia due to PTH production in retroperitoneal malignant fibrous histiocytoma. Preoperative corrected Ca, iPTH and PTHrP levels in his serum were 18.2 mg/dl, 532 pg/ml, and less than 1 pmol/l, respectively. Following curative operation, whole-PTH level in tumor culture supernatant was 4830 pg/ml. Immunohistochemistry revealed clearly positive PTH staining in every tumor cell. By quantitative RT-PCR, PTH mRNA expression of correct length was confirmed and its level represented as PTH/GAPDH mRNA was so high reaching 1/20 of that in human parathyroid adenoma (hPA). Tumoral expression of HoxA3, Gcm2 and Tbx1, which are closely related to parathyroid gland organogenesis, as well as that of CaSR, were negligible. A 5.5 kb fragment of the PTH gene upstream region contains regulatory sequences necessary for parathyroid-specific transgene expression. We hypothesized that some DNA sequence within this region preferentially interacts with a silencing transcription factor(s) to prevent PTH expression in non-parathyroid tissues. On the assumption that ectopic PTH expression might be observed if such a DNA element is mutated or epigenetically modified leading to a failure to bind the above silencing factor(s), we sequenced the 5.5 kb upstream in addition to coding regions of the tumoral PTH gene. We found 4 published SNPs but no other mutation or deletion. Two distinct DNA elements within this 5.5 kb upstream region specifically interact with Ku antigen and redox factor 1 to suppress PTH promoter-driven reporter expression in various cultured cells. Aside from a role as negative calcium response element binding proteins (nCaREBs), these two proteins might function as suppressors of non-parathyroid PTH expression. Intriguingly, we found markedly lower tumoral expression of these two transcripts compared to their

expression in hPA. Currently, epigenetic difference between the tumor and hPA especially around the above upstream region is investigated.

Disclosures: Kosuke Uchida, None.

SU0128

Renal Phosphate Leak And FGF23 Variants In Patients With Recurrent Nephrolithiasis And/or Idiopathic Osteoporosis. Ranuccio Nuti¹, Daniela Merlotti¹, Teresa Esposito², Domenico Rendina³, Sara Magliocca², Riccardo Muscariello⁴, Giovanna Morello², Gianpaolo De Filippo⁴, Francesca De Pascale⁵, Fernando Gianfrancesco⁶, Luigi Gennari¹.
¹University of Siena, Italy, ²Genetic & Biophysics Institute, CNR, Italy, ³Dept. of Clinical & Experimental Medicine, University of Naples Federico II, Italy, ⁴Dept. of Clinical & Experimental Medicine, University of Naples Federico II, Naples, Italy, ⁵Dept. Clinical & Experimental Medicine, University of Naples, Italy, ⁶Institute of Genetics & Biophysics - National Research Council of Italy, Italy

A proportion of patients with calcium nephrolithiasis and/or osteoporosis show renal phosphate leak, despite normal parathyroid function. This condition is characterized by idiopathic hypophosphatemia and reduced renal phosphate threshold normalized for the glomerular filtration rate (TmPi/GFR). The aims of the present study were: 1) to assess the prevalence of renal phosphate leak and its relationship with bone loss and fractures in a population based cohort, and 2) to define the role of functional *FGF23* allelic variants in the pathogenesis of renal phosphate leak occurring in subjects with calcium nephrolithiasis and/or idiopathic osteoporosis. To fulfill these aims we recruited a population-based cohort of 1118 male and female subjects and two cohorts of 180 consecutive patients with renal phosphate leak (with or without nephrolithiasis) and 300 controls (non-osteoporotic and osteoporotic subjects with or without nephrolithiasis and normal phosphate levels). Overall, the prevalence of renal phosphate leak in the population based study was 4.2% and was higher in males than females. Moreover, subjects with renal phosphate leak showed a lower bone turnover status and an increased prevalence of symptomatic osteoporotic fractures at the hip and the vertebrae than subjects with normal phosphate levels (13.9% vs. 3.5% respectively, $p < 0.05$). Promoter and coding regions of the *FGF23* gene were sequenced in recruited cases and controls, leading to the identification of an association between renal phosphate leak and a C716T nonsynonymous change (T239M, rs7955866). In fact, the 716T allele was significantly over-represented in the 180 cases with renal phosphate leak than in controls (25% vs. 10%; $p < 0.05$). This was consistent with the analysis in the population based cohort, showing significantly lower serum phosphate and TmPi/GFR levels in *FGF23*(716T) subjects compared to *FGF23*(716C) subjects. Moreover, functional in vitro studies in HEK-293 and HK-2 cells showed that the T239M change increases *FGF23* secretion and that the *FGF23*(239M) variant induces a higher activation of the FGF receptor/ERK pathway compared to *FGF23*(239T). In summary, we provided evidence that renal phosphate leak is associated with bone fragility (in addition to nephrolithiasis) and that in a consistent proportion of cases is related to a T239M variation in *FGF23* gene.

Disclosures: Ranuccio Nuti, None.

SU0129

Acute Hypophosphatasemia; Morbidity and Mortality. Less Shrestha¹, Jay Fuehrer², Richard Berg², Fergus McKiernan¹.
¹Marshfield Clinic, USA, ²Biomedical Informatics Research Center, Marshfield Clinic Research Foundation, USA

Introduction: The differential diagnosis of low ALP is wide ranging, mostly anecdotal and infrequently discussed. The purpose of this study is to report on the conditions and circumstances associated with abrupt, dramatic lowering of ALP in patients with previously (and/or subsequently) normal ALP values.

Methods: Marshfield Clinic IRB approved use of their electronic medical record to search for subjects with at least 2 ALP values ≤ 40 IU/L (normal 40-125). 30 years of laboratory data (1982-2011) were analyzed. In conducting this analysis several patterns of low ALP became apparent. When the temporal manner of the qualifying ALP values indicated an abrupt and dramatic fall/rise in ALP from constitutively normal values the subject was deemed to have acute hypophosphatasemia. Diagnostic conditions and circumstances associated with acute hypophosphatasemia and short term mortality were recorded. Supplemental manual abstraction of paper charts was performed when indicated.

Results: 458,833 subjects had 2,584,751 serum ALP values. 13,982 subjects had at least 1 and 5,190 had at least 2 ALP values ≤ 40 IU/L of whom 191 satisfied our criteria for acute hypophosphatasemia. There were 98 men and 93 women. 189/191 were adults. Diagnostic conditions and circumstances associated with AHPP are shown in Table 1. Abrupt, dramatic lowering of ALP below the lower range of normal is often associated with transfusions (sometimes massive) or apheresis, major trauma or surgery, severe physiologic stress or disease. 22/191 (11.5%) of patients died within 1 week and 30/191 (15.7%) died within 1 month of their nadir ALP.

Conclusion: These results indicate that abrupt, dramatic lowering of ALP below the range of normal in adults is often associated with profound physiologic stress and followed by substantial short term mortality.

| | Transfusion Massive | Major Surgery | Major Trauma | GI Bleed | Apheresis | DOC Seque | Severe anemia | Acute Colonic Distention | SOB | OD |
|-------|------------------------|------------------|-----------------|----------|-----------|-----------|------------------|-----------------------------|-----|----|
| N=191 | 75 | 73 | 15 | 13 | 28 | 27 | 125 | 5 | 4 | 3 |

Table 1

Disclosures: Fergus McKiernan, None.

This study received funding from: Enobia Inc/Alexion Inc

SU0130

Bone Softening in Medieval Population: Histological Findings for Osteomalacia Diagnosis. Belén López¹, Carlos Gómez², Pablo Manrique¹, Primitiva Menéndez³, Eva Pascual⁴, Jorge Cannata Andia⁵.
¹Physical Anthropology, Systems & Organisms Biology Department, University of Oviedo, Spain, ²Bone & Mineral Research Unit. Hospital Universitario Central de Asturias, Spain, ³Department of Pathology, HUCA, Spain, ⁴Preclinic Image Laboratory, University of Oviedo, Spain, ⁵Bone & Mineral Research Unit. Hospital Universitario Central de Asturias, Spain

The diagnosis of osteomalacia, deficiency-induced or caused by other etiologies, it is especially difficult in ancient human remains. Bone deformities or pseudofractures are evidences towards the diagnosis. The aim was to study a case of osteomalacia as a part of a medieval population's Bone Health Study from northern Spain, focused in bone mass and presence of fractures.

Methods: In a population of 98 exhumed individuals, bone mass in intact femurs from 37 individuals over 20 years of age were measured by DXA (Hologic-QDR1000). Bone mass was similar in women and significantly higher in males compared to our contemporary population matched by age and sex (ASBMR 2011). Only 12 fractures were observed (not related with osteoporosis) in 11 individuals, and only one case with bone deformities was presented.

Bone deformities in the lower limbs were suggestive of bone softening: anterolateral bending femoral shafts and lateral in tibiae-fibulae (Figure 1). Studies were conducted with Micro-CT (SkyScan 1174) and conventional histology (decalcified and undecalcified techniques) on iliac crest fragments. A specimen from similar age and sex without deformities was used as control.

Results: The women with bone softening was 37 years old, her height was of 136cm, below the population mean (152 ± 6 cm), with 0.932gr/cm^2 ($T = -0.95$, $Z = -1.04$) of lumbar spine bone mass and 0.724gr/cm^2 ($T = -1.064$, $Z = -0.865$) at femoral neck. The bone radiological examination didn't objectify pseudofractures, and she had a wedge fracture (Genant's grade I) in Th-11 vertebrae. No rickets related changes (like epiphyseal abnormalities or cranial deformity) were observed. Micro-CT analysis showed a greater heterogeneity in the mineralization of both, cortical and trabecular bone. Goldner's trichromic stain showed focal areas of normal mineralization on a background of mosaic appearance in both trabecular and cortical undecalcified bone, whereas Haematoxylin-Eosin stain showed intra-trabecular loss of tissue in the same corresponding areas (Figure 2).

Conclusions: The histological findings support an osteomalacia diagnosis, in which the poorly calcified osteoid suffered protein degradation whereas the well mineralized protein matrix was preserved. In this population, the prevalence of osteomalacia ($\approx 1\%$) is lower than that reported in other similar populations. A rural population lifestyle and an isolated case leads us to think it was a not deficiency-induced osteomalacia.



Figure 1. Lower extremities long bones X-Ray view.

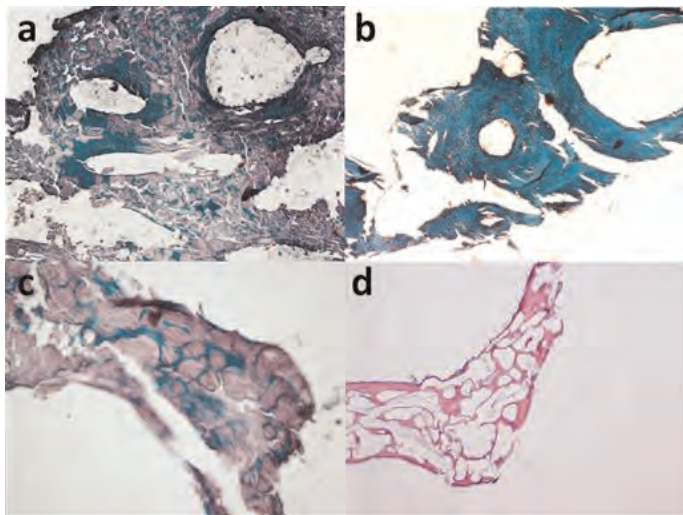


Figure 2. A (propositus Goldner st., 10X), B (control Goldner st., 10X), C (propositus Goldner st., 4), D (control Goldner st., 4)

Disclosures: Carlos Gómez, None.

SU0131

Occult Hyperosteoidosis in Rotator Cuff Arthropathy. Julie Glowacki*, Sherwin Erfani, Shuanhu Zhou, Laurence Higgins, Thomas Thornhill, Meryl Leboff. Brigham & Women's Hospital, USA

Although there is growing awareness of vitamin D-deficiency, there is little information about prevalence of bone mineralization defects. Rotator cuff arthropathy (RCA) is a disorder associated with rotator cuff tear, "soft" quality of the humeral bone noted at the time of arthroplasty, fatty infiltration of shoulder muscles, and radiographic osteopenia. We tested the hypothesis that osteoid is increased in subjects with RCA, compared with shoulder Osteoarthritis (OA). We evaluated bone that was discarded during arthroplasty for shoulder or hip disorders, either from enrolled subjects consenting for additional research tests or as de-identified material. Subjects were eligible if they required a joint prosthesis for non-inflammatory disorders; there were 39 subjects with RCA, 73 with shoulder OA, and, for comparison, 38 subjects with hip OA. We excluded subjects taking medications or with co-morbid conditions that could affect skeletal metabolism. Portions of trabecular bone from the discarded humeral or femoral head were prepared for non-decalcified histology; they were graded for osteoid relative to bone surfaces on an Osteoid Index (OI) scale of 0-3, without knowledge of diagnoses. For subjects with available serum levels, there was an inverse correlation between 25(OH)D and PTH ($p=0.0036$). With the shoulder cohorts, there was a significant 1.7-fold higher OI for subjects with RCA (1.2 ± 0.1 , $n=39$) than for subjects with shoulder OA (0.7 ± 0.1 , $p=0.011$, $n=73$). Likewise, for a subgroup of shoulder subjects for whom serum 25(OH)D levels were available, there was a significant 2.3-fold higher OI for RCA (1.2 ± 0.2 , $n=11$) than for shoulder OA (0.5 ± 0.2 , $n=21$, $p=0.039$), despite no differences in current serum 25(OH)D levels. In contrast, for hip OA subjects, there was a significant correlation between OI and serum 25(OH)D (Spearman $r=-0.35$, $p=0.033$). The hip OI was 2.6-fold higher in vitamin D-deficient (<20 ng/ml 25OHD) subjects (1.3 ± 0.2) than in non-deficient subjects (0.5 ± 0.1 , $p=0.007$). In sum, hyperosteoidosis was evident in RCA and in hip OA subjects with vitamin D-deficiency.

Disclosures: Julie Glowacki, None.

SU0132

The Expression of CD73 and Osteoblast/osteocyte Specific Genes in Causative Tumors of Oncogenic Osteomalacia. Yuki Nagata*¹, Yasuo Imanishi¹, Jun Hashimoto², Akimitsu Miyauchi³, Hiroshi Kajii⁴, Katsuhito Mori¹, Keisuke Kobayashi¹, Masaaki Inaba¹. ¹Osaka City University Graduate School of Medicine, Japan, ²National Hospital Organization, Osaka Minami Medical Center, Japan, ³Miyauchi Medical Center, Japan, ⁴Kinki University Faculty of Medicine, Japan

Background: Oncogenic osteomalacia (OOM) is a rare disease characterized by renal phosphate wasting and hypophosphatemic osteomalacia due to the secretion of fibroblast growth factor 23 (FGF-23) from causative mesenchymal tumors. OOM tumors express phosphate-metabolism related factors such as FGF23, DMP1, MEPE and FRP-4, which are reported to be physiologically expressed in osteogenic lineages, suggesting that OOM tumors have osteogenic characteristics. To determine whether mesenchymal stem cells differentiate toward osteoprogenitor cells in the generation of

OOM tumors, the expressions of surface marker profiles for stem cell differentiation were examined.

Methods: DNA microarray analysis of global gene expression was performed in the tumor compared between OOM and non-OOM, which histopathologic classification was matched (giant cell tumor). Seventeen causative OOM tumors and 6 histopathologic classification-matched non-OOM tumors were analyzed by quantitative real-time RT-PCR and immunohistochemistry.

Results: In DNA microarray, 1432 genes in OOM tumor were up-regulated compared to non-OOM tumor. In these genes, osteoblast/osteocyte specific genes such as Runx2, osterix, osteocalcin, and sclerostin were elevated as well as phosphate-metabolism related factors such as FGF23, DMP1, MEPE and FRP-4. The expression of an osteoprogenitor gene, CD73, also increased. To evaluate the elevation of these genes in OOM tumors, real time RT-PCR analyses were performed on osteoblast/osteocyte specific genes, genes for phosphate-metabolism related factors, and osteoprogenitor genes. The expressions of these genes were elevated in OOM tumors compared to non-OOM. Interestingly, enhanced expression of CD73 was observed in OOM, however, other mesenchymal stem cell markers such as CD105, CD166, and Stro1 did not elevate. Immunohistochemical analyses also confirmed the elevated expressions of these osteoblast/osteocyte specific genes, and genes for phosphate-metabolism related factors.

Conclusion: The expression of CD73 may play a role in osteogenic differentiation and may give osteogenic characteristics to OOM tumors differentiated from mesenchymal cells. CD73 may have a role in the differentiation of OOM tumor to obtain osteoblast/osteocyte characteristics and the expressions of phosphaturic factors.

Disclosures: Yuki Nagata, None.

SU0133

Acute and Chronic Effects of PTH (1-84) on Circulating Sclerostin Levels in Hypoparathyroidism. Aline Costa*¹, Serge Cremers¹, Mishaela Rubin¹, Zachary Lenane¹, Elzbieta Dworakowski¹, Chivuan Zhang¹, Donald McMahon², Jim Sliney Jr³, Marise Lazaretti Castro⁴, John Bilezikian². ¹Columbia University, USA, ²Columbia University College of Physicians & Surgeons, USA, ³Columbia University Medical Center, USA, ⁴Escola Paulista de Medicina, Brazil

The regulatory effect of PTH upon transcription of the sclerostin gene (SOST) is seen clinically by a decline in circulating sclerostin levels. However, the mechanism of this negative regulatory effect and the time course of PTH's suppression of sclerostin have not yet been elucidated. PTH replacement therapy in hypoparathyroidism (HypoPT), a disorder characterized by hypocalcemia and absent or inappropriately low levels of PTH, is an ideal clinical venue to study the regulatory effects of PTH on sclerostin. We investigated the acute and chronic effects of PTH (1-84) administration on circulating sclerostin in HypoPT subjects. Four subjects (2 men, 2 postmenopausal women) with postoperative HypoPT (mean age 54 ± 11 yrs) were treated for 6 months with daily PTH (1-84) 50mcg subcutaneously. The PTH administration regimen was not changed during this 6-month period. Initial sclerostin levels were above normal: 1.396 ± 0.62 ng/mL (Reference norm: 0.61 ng/mL). Acute changes in circulating serum sclerostin [ELISA (TECOMedical)] were measured at months 1 (at the onset of PTH therapy) and 6 of the treatment period. Serum samples were obtained immediately before PTH injection and at 30, 60, 120 and 240 minutes thereafter. After the first PTH injection, at month 1, there was a 16% decline ($p < 0.05$) in sclerostin at 120 min. At month 6, pre-injection sclerostin levels were already lower than the preinjection baseline values at month 1 by 25% ($p < 0.05$). Sclerostin levels fell further by 34% ($p < 0.05$) at 60 min after PTH injection and remained suppressed for up to 2 hours. These results indicate that PTH chronically and acutely regulates the circulating concentration of sclerostin in human subjects. Responsiveness to the regulatory actions of PTH is even greater with its chronic administration. The results suggest that the source of sclerostin is associated with a sensitive skeletal compartment of bone that becomes even more responsive to PTH over time. We propose that this is a novel example of time-dependent progressive PTH sensitivity in a human model of a PTH-sensitive target gene.

Disclosures: Aline Costa, None.

SU0134

Biochemical Response to Cinacalcet Treatment in Patients with Primary Hyperparathyroidism. Araceli Munoz-Garach*¹, Diego Fernandez-Garcia², Maria Dolores Martinez del Valle-Torres³, Ana Maria Gómez-Perez², Pedro Moya-Espinosa², Arantzazu Sebastian-Ochoa², García José Manuel Jiménez-Hoyuela⁴, Francisco Tinahones-Madueño². ¹Spain, ²Endocrinologist, Spain, ³Nuclear Medicine, Spain, ⁴Endocrinologist, Spain

Introduction: Parathyroidectomy is nowadays the first treatment option in patients with primary hyperparathyroidism (PHPT). However, not all patients are candidates for surgery or refused it. Thus, treatment with calcimimetics has proven to be a good alternative in selected patients.

Objective: To evaluate the clinical experience of treatment with Cinacalcet in patients with PHPT.

Patients and methods: We collected data from patients treated with Cinacalcet between years 2009-2012. We evaluated demographic and analytical parameters. We determined: glucose profile, lipids, and level of calcium, phosphorus, vitamin D and PTH.

Results: Twenty-seven patients are receiving treatment with Cinacalcet, 10 were men and 17 women, with a mean age at diagnosis of 65 years. The mean profile in calcium-phosphorus is: initial serum calcium 11.34 ± 1.12 mg/dl, phosphorus 2.62 ± 0.38 mg/dl and PTH 260.96 ± 190.04 pg/ml. Dose of Cinacalcet was 30 mg in 80% of patients and 60 mg in 20% of them. Treatment with these doses of cinacalcet produced a significant decrease in calcium levels ($p < 0.001$) and PTH levels ($p < 0.05$). After treatment, the mean calcium levels were 9.62 ± 1.19 mg/dl, phosphorus 2.77 ± 0.63 mg/dl; PTH $i \pm 119.9$ 179.41 pg/ml. There were no significant relationships between clinical or laboratory parameters both at baseline and while taking treatment. Only one patient had to discontinue treatment because of intolerance.

Conclusions: Treatment with Cinacalcet is effective on reducing calcium levels in patients with PHPT who are not candidates for surgery for their clinical characteristics or comorbidities.

Disclosures: Araceli Munoz-Garach, None.

SU0135

Chronic Kidney Disease in Primary Hyperparathyroidism. Marcella Walker^{*1}, Polly Chen², Nicole Weber², Anna Kepley², Chiyuan Zhang¹, Donald McMahon², Shonni Silverberg¹. ¹Columbia University, USA, ²Columbia University College of Physicians & Surgeons, USA

Although current guidelines for parathyroidectomy (PTX) in primary hyperparathyroidism (PHPT) include an estimated glomerular filtration rate (eGFR) < 60 ml/min, data regarding the effect of chronic kidney disease (CKD) on bone and mineral metabolism in PHPT are limited. In a convenience sample of 29 postmenopausal women with PHPT, we measured bone turnover markers, dual-x-ray absorptiometry (DXA) and high-resolution peripheral quantitative computed tomography (HRpQCT). We report differences in skeletal health in PHPT with and without CKD. Participants were typical of those with mild PHPT: age \pm SD 65 \pm 12 yrs, serum calcium 10.9 ± 0.8 mg/dl, PTH 88 ± 46 pg/ml. Mean eGFR was 89 ± 33 ml/min and 5 individuals had eGFR < 60 ml/min (mean eGFR 49 ± 7 ml/min; all CKD3). There were no between group differences in age, race/ethnicity, weight, kidney stones or fragility fracture between those with and without CKD. There were no differences in serum calcium, PTH, FGF-23 or phosphate, but 25OHD was higher in those with CKD (41 ± 8 vs. 28 ± 12 ng/ml, $p=0.03$; vitamin D supplement intake 1001 ± 645 vs. 748 ± 1080 IU daily, $p=0.062$). Bone turnover markers (BSAP and CTX) and DXA T- and Z-scores did not differ, nor did total volumetric BMD (vBMD), cortical vBMD, or cortical thickness (Ct.Th.) by HRpQCT at the radius. Trabecular (Tb) vBMD (147 ± 14 vs. 115 ± 35 , $p=0.054$) and Tb number (2.1 ± 0.3 vs. 1.7 ± 0.3 , $p=0.07$) tended to be higher in those with CKD, while Tb heterogeneity was lower. Tb thickness and spacing did not differ. A similar pattern was apparent at the tibia. eGFR positively correlated with cortical measures at the radius and tibia respectively (vBMD: $r=0.38-0.49$, $p=0.02$ and $p=0.003$; Ct.Th.: $r=0.39$, $p=0.02$ for both). In a small group of women with PHPT, lower eGFR was associated with worse cortical density and thickness, while trabecular features were maintained in those with CKD. The data suggest that mild renal dysfunction affects bone quality in PHPT. These data provide some support for current guidelines that set a glomerular filtration rate of 60 ml/min as a threshold for concern. Further work is needed to confirm and extend our understanding of the effect of CKD on the skeleton in PHPT.

Disclosures: Marcella Walker, None.

SU0136

Four-Year Effects of PTH(1-84) on Cortical Bone in Hypoparathyroidism. Stephanie Boutrouy^{*1}, Mishaela Rubin², Natalie Cusano³, Aline Costa², Zachary Lenane², Jim Sliney Jr¹, John Bilezikian³. ¹Columbia University Medical Center, USA, ²Columbia University, USA, ³Columbia University College of Physicians & Surgeons, USA

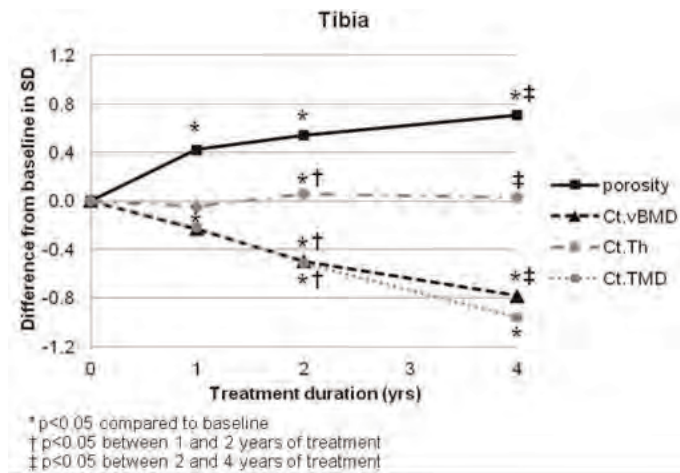
Hypoparathyroidism (HypoPT), a disorder characterized by hypocalcemia and low PTH levels, is associated with bone mineral density (BMD) that typically is not reduced. With PTH treatment, we have observed an increase in areal BMD at the lumbar spine (cancellous bone) and a decrease in areal BMD at the 1/3 radius (cortical bone), yet it is not known to what extent bone microstructure and other aspects of bone quality might be affected.

To this end, we studied 30 patients (25 women/5 men, baseline serum calcium 8.6 ± 1.0 mg/dl and PTH 3.1 ± 2.3 pg/ml) with HypoPT who were treated at least 2 years and up to 4 years with PTH(1-84) [PTH], 100 mcg SC qod. We analyzed volumetric BMD (vBMD) and microstructure by high resolution peripheral quantitative computed tomography (HRpQCT, Scanco Medical AG, Switzerland) at the distal radius and tibia. Additional parameters of cortical bone were performed with an advanced algorithm (Burghardt, JBMR 2009 and Nishiyama, JBMR 2009). Data were analyzed by paired non-parametric testing.

At the tibia, total and trabecular (Tb) vBMD did not change, whereas Tb.vBMD slightly increased at the radius after 1 and 2 years of treatment (1.8% and 1.2% respectively, $p < 0.05$), without change in total vBMD. Throughout the 4 years of treatment, cortical thickness remained stable at both skeletal sites, with differences

from baseline ranging from -2.1% to 1.1% (-0.11SD to 0.06SD). Cortical vBMD fell after 1 year of treatment at the tibia and after 2 years of treatment at the radius; a continuous decrease was observed at the tibia (-1.14% (-0.24 SD), $p=0.013$ between 1 and 2 years and -0.86% (-0.18 SD), $p=0.028$ between 2 and 4 years). In parallel, cortical porosity increased from baseline up to 4 years of treatment (35.2% (0.90 SD) at the radius and 20.1% (0.71 SD) at the tibia, $p < 0.001$). Cortical Tissue Mineral Density (Ct.TMD) decreased significantly after 2 years at the tibia but remained unchanged at the radius.

The results provide new insight into how de novo PTH exposure to a skeleton deprived of PTH affects skeletal microstructure over a 4-year period of time.



Effects of PTH(1-84) on tibial cortical bone in Hypoparathyroidism

Disclosures: Stephanie Boutrouy, None.

SU0137

Hyperparathyroidism-Jaw Tumor Syndrome: A Novel Mutation in HRPT2. Alison Matthews^{*1}, Michaela Koontz¹, Laura Konczal², Mark Weidenbecher³, James Arnold³, Teresa Zimmerman¹. ¹Department of Pediatrics, Rainbow Babies & Children's Hospital, Case Western Reserve University, USA, ²Center for Human Genetics, University Hospitals Case Medical Center & the Department of Pediatrics, Rainbow Babies & Children's Hospital, USA, ³Department of Otolaryngology-Head & Neck Surgery, Case Western Reserve University School of Medicine, University Hospitals Case Medical Center, USA

Introduction: Hyperparathyroidism-Jaw Tumor syndrome (HPT-JT) is a rare familial syndrome that is characterized by tumors of the parathyroid glands, maxillary and mandibular bones. Mutations in the HRPT2 gene have been identified as a cause for HPT-JT.

Case presentation: A 13-year-old African-American male presented to the emergency department with homicidal and suicidal ideation. Screening laboratory tests were significant for serum calcium of 13.3 mg/dL (8.5-10.7 mg/dL). Further investigations revealed significantly elevated PTH at 328 pg/mL (14-72 pg/mL). Thyroid ultrasound showed a cystic mass in the region of the left inferior parathyroid gland measuring 14.5 x 6.9 x 7.8 mm. Smaller masses were also noted in the regions of the left and right superior parathyroid glands. Maternal family history identified deaths in the 4th decade of life due to unspecified cancer in a 3rd degree relative, fatal premature cardiovascular disease in the mother and another 3rd degree relative, with the latter also affected by an upper thoracic cancer of unknown tumor type. There was no known family history of hyperparathyroidism, endocrine neoplasias or jaw tumors. After parathyroidectomy of the left upper and lower glands, intraoperative PTH and postoperative calcium levels normalized. Histopathological examination of the surgical specimens showed a 5.7 gram left inferior parathyroid with foci of vascular invasion and oncocytic features; and a 0.3 gm left superior parathyroid gland had histological features of parathyroid adenoma. Panorax x-ray of the jaw identified a compound odontoma of the left mandible. Genetic testing on peripheral leukocytes revealed a splice-site mutation denoted as c.131+1 G>C in CDC73 (HRPT2) that to our knowledge has been previously unreported though another nucleotide substitution at the same position (c.131+1 G>A) has been reported in association with familial isolated hyperparathyroidism and HPT-JT¹⁻³

Conclusion: This is a case of hyperparathyroidism-jaw tumor syndrome with a novel mutation in HRPT2.

1. Cetani F et al. J Clin Endocrinol Metab. 2004;89:5583.
2. Bradley KJ et al. J Med Genet 2005;42: e51.
3. Newey PJ et al. Human Mutation 2010;31(3): 295-307.

Disclosures: Alison Matthews, None.

SU0138

PTH(1-84) in Hypoparathyroidism: Course as Determined By Changes in Bone Turnover Markers After 4 Continuous Years of Treatment. Natalie Cusano^{*1}, Mishaela Rubin², Donald McMahon¹, Elzbieta Dworakowski², Serge Cremers¹, Amanda Tulley¹, Jim Sliney Jr³, John Bilezikian¹.
¹Columbia University College of Physicians & Surgeons, USA, ²Columbia University, USA, ³Columbia University Medical Center, USA

Hypoparathyroidism (HypoPT) is a rare disorder characterized by reduced bone remodeling. PTH treatment has significant early salutary effects on bone remodeling, but whether these benefits persist is unknown. We previously described the effect of PTH(1-84) on biochemical markers of bone turnover in 64 HypoPT subjects over 2 yrs. Bone turnover markers (BTM) increased significantly with PTH(1-84), and generally remained higher than baseline at 2 yrs. We now extend our findings to report a unique experience of 4 yrs of PTH(1-84).

HypoPT subjects (n=27; age 51 ± 12 yrs; 20 women (10 postmenopausal); etiology: 16 postoperative, 10 autoimmune, 1 DiGeorge; duration 20 ± 15 yrs; serum calcium 8.5 ± 1 mg/dl; PTH 5 ± 4 pg/ml) were treated with PTH(1-84) with most receiving 100 µg every other day for 4 yrs. P1NP, BAP, OCN, CTX, and TRAP were measured at baseline and months 6, 12, 18, 24, 30, 36, 42, and 48. Z-scores were calculated with normal ranges for men and pre- and postmenopausal women.

All BTM at baseline were in the low- to mid-normal range (Z-score range -1.7 to +0.3). With PTH(1-84), all BTM increased significantly, peaking up to 3-fold from baseline values at 6-12 months (Table). Thereafter, BTM declined to a new steady state at 30 months. The new steady state was higher than the pre-treatment values for all BTM (Z-score -0.7 to +2.0). For the next 18 months, BTM were constant at these higher new baseline values.

The results indicate that long-term treatment with PTH(1-84) normalizes BTM in HypoPT but not before the skeleton has first experienced a salutary recovery of abnormally low bone remodeling. The second phase, namely normalization of BTM after 30 months, suggests that long-term treatment of HypoPT with PTH(1-84) leads to a normalization of bone metabolism. The results are likely to be applicable to skeletal dynamics upon direct examination of bone tissue itself.

Table. Changes in markers of bone formation (P1NP, BAP, OCN) and resorption (CTX, TRAP) over 4 yrs of PTH(1-84).

| Time | P1NP (µg/L) | BAP (U/L) | OCN (ng/mL) | CTX (ng/mL) | TRAP (U/L) |
|---------------------------|------------------------------|---------------------------|----------------------------|--------------------------------|----------------------------|
| Normal range ^a | 19-83 | 11.5-29.6 | 8.4-33.9 | 0.112-0.738 | 1.03-4.15 |
| Baseline | 41.2±17 | 25.6±2 | 18.1±5 | 0.184±0.07 | 3.1±0.5 |
| Peak (6-12 mos) | 140.3±17 ^b (361%) | 41.6±2 ^b (83%) | 43.7±5 ^b (242%) | 0.444±0.07 ^b (314%) | 5.8±0.5 ^b (94%) |
| 30 mos | 78.7±17 (132%) | 28.6±2 (25%) | 27.0±5 (135%) | 0.239±0.07 (110%) | 4.8±0.5 ^b (61%) |
| 48 mos | 73.3±17 (148%) | 26.6±2 (20%) | 23.9±5 (88%) | 0.342±0.07 (105%) | 4.6±0.5 ^b (56%) |

Means±SE (% change from baseline)
^aAll normal ranges for premenopausal women
^bp<0.05 from baseline

Table

Disclosures: Natalie Cusano, None.

SU0139

Skeletal Microstructural Abnormalities in Primary Hyperparathyroidism by High Resolution Peripheral Quantitative Computed Tomography. Stephanie Boutroy^{*1}, Barbara Silva¹, Natalie Cusano², Donald McMahon², Chiyuan Zhang³, Julia Udesky⁴, John Bilezikian².
¹Columbia University Medical Center, USA, ²Columbia University College of Physicians & Surgeons, USA, ³Columbia University, USA, ⁴College of Physicians & Surgeons, Columbia University Medical Center, USA

Primary Hyperparathyroidism (PHPT) is characterized primarily now as an asymptomatic disorder, but skeletal abnormalities have been well described densitometrically by us and others. High Resolution peripheral Computed Tomography (HRpQCT; Scanco Medical AG, Switzerland) has promise to provide additional information about cortical and trabecular compartments of bone in PHPT at ultradistal radial (unloaded) and tibial (loaded) sites. To this end, we studied 38 women (age 67 ± 10) with well characterized asymptomatic PHPT. HRpQCT female-specific Z-scores were compared to normative values from the OFELY cohort.

HRpQCT female-specific-Z-scores in PHPT subjects were summarized in the table. At the radius, in 4 of 9 indices: total vBMD, trabecular (Tb) vBMD, thickness, and heterogeneity of the Tb distribution, subjects with PHPT were significantly impaired compared to normal. At the tibia, however, in addition to significant reductions in Total vBMD and Tb.vBMD, the following other abnormalities were noted: total area (increased), trabecular number (increased) and trabecular thickness (decreased). While no abnormalities in cortical parameters were seen in the radius, cortical vBMD, and cortical thickness were both markedly reduced at the tibia.

The results indicated in one of the first applications of HRpQCT to skeletal imaging in PHPT that both trabecular and cortical abnormalities are seen, the latter being only detected in a site that is regularly subjected to load-bearing. The results suggested that PTH differentially affects skeletal microstructure in a manner that is site and load-dependent.

| HRpQCT parameters | Z-score (Mean ± SEM) | |
|-------------------------|----------------------|------------------|
| | Radius | Tibia |
| Total Area | -0.31 ± 0.19 | 0.67 ± 0.20 ** |
| Total vBMD | -0.45 ± 0.20 * | -0.82 ± 0.16 *** |
| Cortical vBMD | -0.24 ± 0.18 | -1.13 ± 0.21 *** |
| Cortical thickness | -0.23 ± 0.17 | -0.78 ± 0.17 *** |
| Trabecular vBMD | -0.78 ± 0.20 *** | -0.49 ± 0.17 ** |
| Trabecular number | 0.04 ± 0.25 | 0.71 ± 0.26 * |
| Trabecular thickness | -1.54 ± 0.13 *** | -1.19 ± 0.17 *** |
| Trabecular separation | 0.37 ± 0.29 | -0.16 ± 0.28 |
| Trabecular distribution | 0.82 ± 0.39 * | 0.35 ± 0.37 |

*p<0.05; **p<0.01; ***p<0.001 versus normative values

HRpQCT female-specific Z-scores in PHPT subjects

Disclosures: Stephanie Boutroy, None.

SU0140

Suboptimal Vitamin D Levels Affect Both Cortical and Trabecular Bone in Primary Hyperparathyroidism. Marcella Walker^{*1}, Polly Chen², Nicole Weber², Anna Kepley², Chiyuan Zhang¹, Donald McMahon², Shonni Silverberg¹.
¹Columbia University, USA, ²Columbia University College of Physicians & Surgeons, USA

Suboptimal vitamin D (25OHD) levels are common in primary hyperparathyroidism (PHPT), but data regarding the skeletal consequences of low vitamin D are limited. In 43 patients with mild PHPT (81% female, age ± SD 65 ± 13yrs; serum calcium 10.9 ± 0.8mg/dl, PTH 116 ± 65pg/ml) we measured bone markers BSAP & CTX, BMD by DXA and high resolution peripheral quantitative CT (HRpQCT). Mean 25OHD was 28 ± 12ng/ml. Low 25OHD was common (25% <20ng/ml; 51% <30ng/ml). Levels of 25OHD were inversely associated with PTH levels (r=-0.39, p=0.02) and GFR (-0.43, p=0.009), and correlated with serum phosphate (r=0.33, p=0.05) and FGF-23 (r=0.40, p=0.02). 25OHD was not associated with serum calcium (r=0.19, p=0.25), bone markers, BMD by DXA or microarchitecture on HRpQCT. Those with 25OHD <30ng/ml vs. ≥30ng/ml were older (69 ± 11 vs. 61 ± 13yrs, p=0.05) and had higher BMI (30.3 ± 5.8 vs. 26.7 ± 5.5kg/m2, p=0.05), but did not differ by race, gender, PHPT duration, kidney stones, fracture, or meeting surgical guidelines. In those with 25OHD <30 vs. ≥30ng/ml, PTH (130 ± 72 vs. 97 ± 52pg/ml, p=0.12) and calcium levels did not differ, but phosphate (2.9 ± 0.4 vs. 3.2 ± 0.4mg/dl, p=0.01) and FGF-23 (81 ± 46 vs. 119 ± 63pg/ml, p=0.04) levels were lower. Bone markers, age/BMI-adjusted lumbar spine, total hip and femoral neck BMD did not differ. Those with 25OHD <30ng/ml had lower 1/3 radius BMD (0.621 ± 0.06 vs. 0.672 ± 0.07g/cm2, p=0.03), and worse age/BMI-adjusted trabecular (Tb) microarchitecture on HRpQCT (Table). Total bone area, Dcomp, Ct. thickness, TbN and TbSp did not differ. Radius BMD and Tb differences were no longer significant after adjusting for PTH level. In those with frankly deficient 25OHD levels, PTH levels were higher (<20 vs. ≥20ng/ml: 150 ± 58 vs. 103 ± 64pg/ml, p=0.04; <20ng/ml vs. ≥30ng/ml [97 ± 52pg/ml], p=0.02) and similar trends were seen on DXA and HRpQCT. In summary, low 25OHD is common in PHPT, and PTH is highest in those with lowest 25OHD levels. Suboptimal vitamin D in PHPT is associated with cortical abnormalities (DXA at the highly cortical 1/3 radius site) and trabecular microarchitectural deterioration (HRpQCT). These effects on BMD and microarchitecture appear to be mediated by higher PTH levels. Further work is needed to determine whether vitamin D treatment improves skeletal health in PHPT.

| HRpQCT Index | 25OHD <30 ng/ml | 25OHD ≥ 30 ng/ml | P value |
|--------------------------------|-----------------|------------------|---------|
| Dtrab (mg HA/cm ³) | 113 ± 29 | 134 ± 32 | 0.04 |
| BV/TV | 0.094 ± 0.02 | 0.111 ± 0.03 | 0.04 |
| TbTh (µm) | 0.053 ± 0.009 | 0.059 ± 0.009 | 0.02 |
| Outer/Inner Tb density | 3.98 ± 1.6 | 2.11 ± 1.8 | 0.02 |

Table

Disclosures: Marcella Walker, None.

SU0141

Usefulness of Ultrasound Elastosonography in Primary Hyperparathyroidism. Federica Saponaro^{*1}, Valeria Loiacono², Gabriele Di Rosa¹, Maria Scutari², Luisella Cianferotti¹, Silvia Chiavistelli¹, Paolo Vitti², Teresa Rago², Claudio Marcocci¹, Filomena Cetani¹. ¹Department of Endocrinology & Metabolism - Section of Endocrinology & Bone Metabolism, University of Pisa, Pisa, Italy, ²Department of Endocrinology & Metabolism, University of Pisa, Pisa, Italy

Preoperative localization of parathyroid lesions is very important in patients with primary hyperparathyroidism (PHPT), particularly when surgery is performed by a minimally invasive approach. Parathyroid imaging is generally performed by B-mode conventional ultrasonography (CUS) and TC99-MIBI scintigraphy, but both procedures may give false positive results. Ultrasound elastosonography (USE), a new diagnostic technique that assesses hardness/elasticity of tissue, has been recently applied in the presurgical evaluation of thyroid nodule.

The aim of this study was to investigate the usefulness of USE in the evaluation of parathyroid lesions.

Eightyone consecutive patients (13 males and 68 females) with PHPT were prospectively enrolled in this study. All patients underwent CUS and USE.

Parathyroid stiffness/elasticity was classified using the following USE score: 1=high elasticity, 2=intermediate elasticity, and 3=low elasticity.

We report the results of USE examination in 43/81 patients who underwent parathyroidectomy (PTX) and the USE scores were correlated with the histological diagnosis.

At histology 36 patients had parathyroid adenoma (29 chief cells adenoma and 7 oxyphil cells adenoma), 6 hyperplasia, with prevalence of chief cells, and one atypical adenoma (a lesion with histological features worrisome of carcinoma, without clinical evidence of malignancy).

The USE score was 1 in 32 adenomas, 5 hyperplasia and in the atypical adenoma; 2 in 2 adenomas and one hyperplasia; and 3 in 2 adenomas.

In conclusion, a score of 1 characterizes the majority of benign parathyroid lesions in patients with PHPT, independently of histology. Further studies in a larger series, including patients with parathyroid carcinoma, are necessary to establish the usefulness of USE in the diagnostic evaluation of parathyroid lesion, particularly in the preoperative identification of patients with parathyroid malignancy.

Disclosures: Federica Saponaro, None.

SU0142

Effect of Higher Strontium Consumption on the Bone Mineral Density, Content and Strength in Goats. Changrong Ge¹, Zhiqiang Xu¹, Yueyuan Fan², Zhenhui Cao², Dahai Gu^{*2}, Hua Rong², Guozhou Liao², Weizhong Wang³, Linli Tao², Xi Zhang⁴, Shizheng Gao², Queye Lin², Junjing Jia², Wei Yao⁵. ¹Yunnan Agricultural University, China, Peoples Republic of China, ²Yunnan Provincial Key Laboratory of Animal Nutrition & Feed, Yunnan Agricultural University, China, ³Yunnan Provincial Key Laboratory of Animal Nutrition & Feed, China, ⁴Yunnan Agricultural University, Peoples Republic of China, ⁵University of California, Davis Medical Center, USA

It has been previously reported that strontium ranelate significantly reduce the risk of bone fractures in postmenopausal osteoporosis. Strontium (Sr⁺) was reported to play dual roles in increasing bone formation and decreasing bone resorption in human and animals. In our previous studies, we demonstrated that higher strontium consumption in goats induced redness bone and increased biomarkers of bone formation. This study evaluated how Sr⁺ (SrSO₄ or SrCl₂) consumption from water, plants and soil affect bone mineral density (BMD), bone mineral content (BMC) and strength in goats.

Forty eight 1-month-old red-boned lambs were fed in a village (Dongshan Village) with nature grazing that was high in strontium content for 18 months. Forty eight age-matched normal boned lambs were fed in normal environmental strontium content village with nature grazing for 18 months as Control. Eight goats from each group were sacrificed at 1, 6, 12 and 18 months to measure bone mineral density (BMD), bone mineral content (BMC) in femur and tibia using bone dual X-ray absorptiometry (DEXA), tibia minerals composition using inductively coupled Plasma mass spectrometry and femur strength by compression testing.

Result: Red-boned goats had significantly higher strontium content at four time points and lower calcium content in femur and tibia at 12 and 18 months with significantly higher BMD and BMC in femur and tibia as well as femur strength at 1 and 6 months compare to the Control group. No significant difference was found for BMD and BMC between two groups at 12 months. In contrast, femur strength in red-boned goats was somewhat lower than Control at 12 months (P<0.07). The red-boned goats had significantly lower BMD, BMC and strength compare to control at 18 months.

In conclusion, we found that strontium consumption from environment increased BMD, BMC and strength at early experimental periods. Prolong strontium consumption reduced BMD and BMC in tibia and femur, and reduced femoral strength in goats. Our results in goats implicated that high dose and long-term strontium ranelate treatment may have negative effects on the bone mass and strength.

Disclosures: Dahai Gu, None.

SU0143

Increased Bone Loss with Sustained Disease Duration in HLA-B27 Transgenic Rats Is Associated with Altered Osteoblast Function. Martina Rauner^{*1}, Sylvia Thiele², Peggy Benad³, Christine Hamann⁴, Ricardo Bernhardt⁵, Ingrid Fert⁶, Luiza Krause⁶, Maxime Breban⁶, Lorenz Hofbauer². ¹Medical Faculty of the TU Dresden, Germany, ²Dresden University Medical Center, Germany, ³Department of Medicine III, TU Dresden, Germany, ⁴Dresden Technical University Medical Center, Germany, ⁵Technische Universität Dresden, Germany, ⁶Institut Cochin, France

Spondyloarthritis (SpA) encompasses a group of HLA-B27-associated diseases characterized by inflammation of the axial skeleton, systemic bone loss, and the appearance of spondylophytes. While the effects of inflammation on bone loss are well understood, mechanisms that induce aberrant bone formation remain poorly defined. In this study, we used the HLA-B27 transgenic rat, which develops a multisystemic inflammatory disorder similar to SpA, to study the dynamics of bone remodeling during the course of SpA. The bone phenotype was assessed in HLA-B27 transgenic (B27) and control non-transgenic (NTG) and HLA-B7 (B7) rats at disease onset (2 months old) and after disease progression, at 6 and 12 months of age. At 2 months of age, no apparent changes were observed in the cortical bone of either genotype as assessed by pQCT. However, at 12 months, cortical thickness of B27 rats decreased by 55% vs. NTG and 40% vs. B7 and led to a decreased moment of inertia (-56% vs. NTG and -40% vs. B7). At the trabecular compartment, B27 rats had a lower BMD at all ages compared to NTG and B7 rats with the decrease becoming more pronounced towards the more advanced disease group (-25% (2 months), -34% (6 months), -50% (12 months) vs. NTG). Of note, B7 rats also displayed a 20% lower BMD at 2 months of age as compared to NTG, which did not progress further. Thus, while the trabecular BMD of B27 rats did not differ from B7 rats at disease onset, a significant decrease in BMD was observed after 6 (-20%) and 12 months (-35%). Similar results were obtained by μ CT analysis. Trabecular bone mass was decreased by 49% vs. NTG and 37% vs. B7 rats at 12 months. At this age, trabecular thickness was significantly decreased in B27 rats compared to both genotypes, leading to an increase in trabecular separation. Despite the profound bone loss of B27 rats, serum bone resorption markers (TRAP and CTX) did not differ at any age between the genotypes. However, the ex vivo potential to form osteoclasts and mRNA levels of OSCAR and TRAP were increased in B27 rats. The bone formation marker PINP was markedly decreased at 2 and 6 months of age in B7 and B27 rats compared to NTG (35-40%) but did not differ at 12 months of age. In conclusion, B27 rats lose bone during disease progression which is specific for the SpA-associated B27 transgene and associated with altered osteoblast function.

Disclosures: Martina Rauner, None.

SU0144

KLF10 is a Critical Mediator of Wnt Signaling in Valve Interstitial Cells. Muzaffer Cicek¹, Malavannan Subramaniam¹, John Hawse², Thomas Spelsberg¹, Nalini Rajamannan^{*3}. ¹Mayo Clinic, USA, ²Mayo Clinic College of Medicine, USA, ³Northwestern University Medical School, USA

We have previously demonstrated that β -catenin plays important roles in valve calcification with a specific osteogenic phenotype defined by increased bone mineral content and overall valve thickening. Recent studies indicate that KLF10 may be involved in mediating the Wnt signaling pathway in bone, which is known to play critical roles in osteoblast differentiation and bone mineralization. Therefore, we sought to test the role of KLF10 in mediating Wnt signaling, as well as differentiation and mineralization, in valve interstitial cells (VICs). Therefore, we analyzed the Wnt pathway genes in valve interstitial cells (VICs) isolated from porcine valves. Exposure of VICs during the course of differentiation, led to increased the expression of Runx2, Sox9 and osteocalcin consistent with endochondral gene activation. Differentiated cells also stained positive with Von Kossa while undifferentiated cells stained negative confirming the induction of an osteogenic phenotype were increased. As expected, expression of both Lef1 and Co-expression of both β -catenin and LEF1 led to co-activation of the top-flash reporter when transfected into VICs. However, when KLF10 was co-expressed with LEF or β -catenin, there was a significant decrease in reporter activity was observed. These data suggested that KLF10 regulates, LEF and β -catenin to form a transcriptionally active protein complex leading to enhanced Wnt signaling in VICs. This possibility was further confirmed by the observation that KLF10 and β -catenin co-localize with one another in the nucleus of VICs following stimulation with LiCl and/or TGF- β treatment. Taken together, these data implicate an important role for KLF10 in mediating Wnt signaling and LEF transcriptional activity in VICs, and implicate in an important role for canonical the Wnt signaling pathway in the observed osteogenic bone phenotype of cardiac aortic valves.

Disclosures: Nalini Rajamannan, None.

SU0145

Lineage Switching by Mouse and Human Smooth Muscle Cells *In Vitro* Results in Phenotypic Osteoblast-like Cells That Are Responsive to 1,25-Dihydroxyvitamin D₃. Sohel Shamsuzzaman*, J. Pike. University of Wisconsin-Madison, USA

Atherosclerosis is a complex disease that involves focal formation of aberrant collections of cell types within vessel walls that adversely affect vascular function. Despite the pathology, it is perhaps the tendency for these sites to undergo calcification that is most closely associated with cardiovascular disease mortality. As osteoporosis and vascular calcification frequently co-exist, this relationship suggests the possibility of a common underlying mechanism. In support, studies over the past decade have suggested that vascular smooth muscle cells (VSMC) are capable of phenotype switching in response to disease-related signals into cell types that can potentiate and accelerate vascular plaque formation and may be responsible for calcification. To explore this cellular transition, we examined the changes in gene expression that occur in mouse and human aortic smooth muscle cells cultured over time in the presence of osteogenic medium (OM). We also assessed their cellular ability to produce an alizarin red-positive calcified matrix as well. Both *RUNX2* and *SP7* expression were rapidly increased in response to OM, as were genes responsible for the osteoblast phenotype, among them *COL1A1*, *ALPL*, *BGLAP* and the mineralization regulators *MGP*, *ENPP1* and *3*, and *ANK*. *RANKL* and *OPG* were expressed in both cell types. *NTSE* (CD73) and its receptors *ADORA2A* and *ADORA2B*, on the other hand, were suppressed during the transition. Interestingly, differentiated osteoblast-like cells also expressed markers of the osteocyte phenotype, including *DMP-1* and *E11*. Surprisingly, classic VSMC markers such as SM- α actin, SM2 α and SM-MHC were also expressed in *bona fide* mouse and human osteoblasts and were not downregulated during osteoblast-like phenotype switching. As the vitamin D receptor was present in both cell types, we also examined the ability of 1,25(OH)₂D₃ to regulate genes found in both VSMCs and in OM-derived osteochondroprogenitors. In addition to the classic vitamin D target *CYP24A1*, 1,25(OH)₂D₃ also modulated many of the genes noted above including *ALPL*, *BGLAP*, *OPN*, *MSX2*, *ENPP3*, *ANK*, *NTSE*, *ADORA2A*, *ADORA2B*, *OPG* and *RANKL*. Our ChIP-seq analyses have pinpointed the regulatory regions that mediate their induction by 1,25(OH)₂D₃ and its receptor. We conclude that VSMCs manifest an ability to differentiate into vitamin D responsive osteoblast-like cells with matrix synthesizing and calcifying properties that are consistent with those of authentic bone cells.

Disclosures: Sohel Shamsuzzaman, None.

SU0146

Serum 25-hydroxy-vitamin D is an Independent Risk Factor for Abdominal Aortic Calcification. Lisa Langsetmo*¹, Brian Lentle², Sophie Jamal³, Christopher Kovacs⁴, David Hanley⁵, Susan Whiting⁶, Claudie Berger⁷, Stephanie Kaiser⁸, Robert Josse⁹, Jerilyn Prior², Jonathan Adachi¹⁰, Anthony Hodzman¹¹, K. Shawn Davison¹², Suzanne Morin⁷, Jacques Genest⁷, Nancy Kreiger¹³, David Goltzman⁷. ¹Canandian Multicenter Osteoporosis Study, Canada, ²University of British Columbia, Canada, ³The University of Toronto, Canada, ⁴Memorial University of Newfoundland, Canada, ⁵University of Calgary, Canada, ⁶University of Saskatchewan, Canada, ⁷McGill University, Canada, ⁸Dalhousie University, Canada, ⁹St. Michael's Hospital, University of Toronto, Canada, ¹⁰St. Joseph's Hospital, Canada, ¹¹Western University, Canada, ¹²Laval University, Canada, ¹³University of Toronto, Canada

Cardiovascular disease is a leading cause of morbidity and mortality in the industrialized world. The relationship between risk factors for osteoporosis and aortic calcification has not been fully elucidated. Objectives: 1. To determine the association between specified risk factors (age, sex, smoking, diabetes) and aortic calcification; 2. To assess serum 25-hydroxy-vitamin D (25OHD) as an independent risk factor for aortic calcification; 3. To determine mortality risk attributable to aortic calcification.

Methods: We scored abdominal aortic calcification (AAC) on lateral spine x-rays (L1-L4) using the Framingham method in a sub-cohort of the Canadian Multicenter Osteoporosis Study at baseline (214 men, 589 women). At Year 10, a second sub-cohort (187 men, 485 women) had measurement of AAC, fasting serum glucose, and 25OHD. We used logistic regression to determine risk factors for presence of aortic calcification, and Cox proportional hazards to determine the association between baseline Framingham AAC score and all-cause mortality over 10 years. We tested for 25OHD threshold effects at cut-offs of 30, 50, 75, 100 nmol/L.

Results: Age was strongly associated with the presence of aortic calcification with prevalence increasing from 20% of 50-year olds to 80% of 80-year olds; age-specific prevalence was similar in men and women. The associations between other risk factors and aortic calcification adjusted for age and sex were: diabetes (OR=2.60; 95% CI: 1.20-5.67), smoking (OR= 5.03; 95% CI: 2.93-8.64, current vs. never smoker and OR= 1.85; 95% CI: 1.31-2.61, former vs. never smoker). In women, low serum 25OHD (OR=1.91; 95% CI: 1.09-3.35 for 25OHD<50 nmol/L versus 25OHD≥50 nmol/L) was a risk factor for AAC after adjusting for age, smoking, heart disease, glucose, and diabetes, while in men, the results were inconclusive. Framingham AAC score was a risk factor for all-cause mortality over 10 years after adjustment for age, sex, heart disease, diabetes, and smoking. Those with mild scattered aortic calcification

(scores=1-4) had higher risk of mortality (hazard ratio/HR=2.02; 95% CI 1.10-3.71) compared with those with no aortic calcification and those with extensive aortic calcification (scores>13) had much higher risk (HR=4.21; 95 CI: 1.85-9.58).

Conclusion: In women, low serum 25OHD was found to be an independent risk factor of aortic calcification. Furthermore, aortic calcification was an independent predictor of all-cause mortality.

Disclosures: Lisa Langsetmo, None.

SU0147

Serum Osteocalcin is Associated with Severe Abdominal Aortic Calcifications Progression in Older Men: the MINOS Study. Cyrille Confavreux*¹, Pawel Szulc², Stephanie Boutroy³, Annie Varennes⁴, Nicolas Vilayphiou⁵, Joelle Goudable⁶, Roland Chapurlat⁷. ¹INSERM U1033 - Universite de Lyon, France, ²INSERM UMR 1033, University of Lyon, Hopital E. Herriot, Pavillon F, France, ³Columbia University Medical Center, USA, ⁴Hospices Civils de Lyon, France, ⁵INSERM UMR1033, Université de Lyon & Hospices Civils de Lyon, France, ⁶Université de Lyon - INSERM U1060, France, ⁷E. Herriot Hospital, France

Introduction. Diseases characterized by insulin resistance, such as type 2 diabetes and metabolic syndrome (MetS), are associated with elevated cardiovascular mortality. In mice, osteocalcin is a hormone secreted by osteoblast and regulating energy metabolism through its action on insulin secretion, insulin resistance and fat mass. The *osteocalcin* deficient mice phenotype recapitulates characteristics of the MetS. Interestingly, severe abdominal aortic calcification (AAC) is predictive of cardiovascular mortality. Thus our primary aim was to assess prospectively the association of the serum total osteocalcin level with the AAC progression.

Methods. The MINOS cohort consists of 798 older men followed-up prospectively for 7.5 years. Kauppila's abdominal aortic calcification score was assessed from lumbar spine radiographies. AAC progression was calculated as the difference between AAC on the last available radiographs and AAC at baseline divided by follow-up duration. MetS diagnosis relies on the presence of three criteria among the following five: elevated blood fasting glucose, high blood pressure, elevated serum triglycerides, elevated waist circumference and reduced serum HDL-cholesterol.

Results. At baseline, the lowest osteocalcin concentrations were associated with increased severity of MetS. Osteocalcin decreased across tertiles of AAC. In logistic regression model, higher osteocalcin was significantly associated with a lower prevalence of high calcification (OR=0.78 per SD increase 95%CI:0.64-0.94; p=0.01) whereas age, hypertension, tobacco consumption and serum phosphorus were associated with increased prevalence of high calcification. AAC progression was faster in men in the lowest osteocalcin quartile and risk of severe AAC progression was higher in this quartile (OR= 2.27 [1.35-3.81]; p<0.005). In stepwise logistic regression analysis including other bone turnover markers (BSAP, CTX, PINP), osteocalcin was the only marker associated with AAC score (OR=0.80 [0.65-0.77] per SD increase; p=0.02).

Conclusion. In older men, the lowest osteocalcin concentrations were associated with higher prevalence of MetS and high AAC score and with severe AAC progression. This study suggests that serum total osteocalcin level might be an independent indicator of cardiovascular risk.

Disclosures: Cyrille Confavreux, None.

SU0148

The Presence and Severity of VFA detected Aortic Calcification is Strongly Associated with Cardiovascular Disease in Rheumatoid Arthritis. Ausaf Mohammad*¹, Diane Bergin², Derek Lohan², Sarah Mooney², John Newell³, Martin O'Donnell³, Robert J Coughlan⁴, John J Carey⁴. ¹Rheumatology Unit Merlin Park University Hospital, Ireland, ²Radiology, Galway University Hospitals, Ireland, ³HRB Clinical Research Facility, NUI Galway, Ireland, ⁴Rheumatology, Galway University Hospitals, Ireland

Introduction: Patients with rheumatoid arthritis (RA) are at increased risk of osteoporosis and cardiovascular disease (CVD), and have increased cardiovascular mortality. Traditional clinical prediction tools for CVD perform poorly in RA populations. Reliable CVD risk stratification remains an unmet need in this population. Aortic calcification (AC) can be detected and assessed using modern DXA technology, and is an important marker of prevalent and incident CVD in other populations. It is unknown whether DXA detected AC is a useful marker of CVD in RA populations, many of whom have scans as part of their usual clinical care.

Objectives: To determine the prevalence of AC in a cohort of RA patients, and to evaluate whether the presence and severity of AC could help identify those most likely to have CVD. Methods: We conducted a cross-sectional study of our RA cohort ≥40 years of age. Risk factors and details of CVD were recorded on those who met 1987 ACR criteria for RA classification, and had a DXA and VFA (GE Lunar, USA) scan available for analysis. The study was approved by our local I.R.B. Two blinded Consultant musculoskeletal radiologists examined all VFA scans to determine the presence and severity of AC using a previously validated 24-point scale. We compared the prevalence and severity of AC between RA patients with and without CVD, and

determined if AC was independently associated with prevalent CVD using multi-variable logistic regression.

Result: 1330 patients with inflammatory arthritis were screened. 603 met the inclusion criteria: 74% were female, 76% were sero-positive, 43% were smokers and the mean age was 56 years. 230 RA subjects had ≥ 1 documented CVD event. Overall AC was present in 211 of subjects: 11% was mild (< 9 points), 57% moderate (9-16) and 32% severe (> 16 points). Aortic calcification was significantly more common in those with CVD (76% Vs 10%) than those without CVD ($p < 0.001$). In multivariable analyses both the presence and severity of AC was significantly and independently associated with prevalent CHD (OR = 2.70; 95% CI 1.8 to 3.2).

Conclusion: Aortic calcification is common in patients with RA, and several fold more frequent among those with CVD. The presence and severity of VFA-detected aortic calcification should alert physicians to the presence of CVD in patients with RA.

Disclosures: Ausaf Mohammad, None.

SU0149

An Inheritable, Direct Replica of Human Fibrous Dysplasia (FD) of Bone Generated through Constitutive Expression of Gs α R201C in the Mouse.

Isabella Saggio¹, Cristina Remoli¹, Stefania Cersosimo¹, Stefania Piersanti¹, Stefano Michienzi¹, Manuela Spica¹, Pamela G. Robey², Kenn Holmbeck³, Ana Cumano⁴, Alan Boyde⁵, Mara Riminucci⁶, Paolo Bianco⁷. ¹Sapienza University of Rome, Italy, ²NIDCR, NIH, USA, ³NIH/NIDCR, USA, ⁴Pasteur Institute, France, ⁵Queen Mary University of London, United Kingdom, ⁶University La Sapienza, Italy, ⁷Universita La Sapienza, Italy

Mouse models of FD of bone, a crippling skeletal disease, have been missing, hampering the understanding of the disease and the development of effective treatment. FD is caused by non-inherited, postzygotic mutations of Gs α , thought to be embryonic lethal if germline transmitted. We have generated multiple lines of transgenic mice, which develop an inherited, exact histopathological replica of human FD in postnatal life, independent of genetic mosaicism. Gs α R201C under the control of 2 different constitutive promoters (EF1 α , PGK) was inserted into 3rd generation LV vectors, which were used for perivitellic injection in 1-cell embryos (FVB or B6). Founders (chimeric and non-chimeric) developed a polyostotic skeletal phenotype, and germline-transmitted both the transgene (TG) and the phenotype. Multiple lines were established, which continue to transmit the disease after > 7 generations (with a Mendelian pattern of inheritance and evidence of 1 copy of the TG in 1 line). The TG was expressed in embryonic and neonatal tissues; self-renewal and differentiation in vitro and in vivo of TG-expressing ES cells were unaltered; the phenotype developed postnatally. TG expression and cAMP overproduction across the skeleton were robust, both at lesional and non-lesional sites. Monthly X-rays of > 100 mice/genotype in each of 4 lines for 24 months documented the onset and evolution of bone lesions. Subtle changes first became apparent at 2 months. The tail was the earliest and the only obligate site of skeletal lesions. Further focal lesions developed over time in long and short bones, skull, axial skeleton, with a recurrent spatial and temporal pattern. Initial, pre-FD lesions in different bones were histologically identified as ectopic foci of intracortical remodeling: tunneling resorption cavities were filled with accumulating osteogenic cells (nascent fibrosis) and scant amounts of nascent dysplastic bone. Extension of pre-FD lesions caused progressive deformity, spontaneous fracture, osteomalacia, osteolysis/sclerosis, leading to a full-blown histological replica of human FD by ~ 1 year: at this time, all histological hallmarks of human FD ("Chinese writing," fibrosis, Sharpey fibers, etc.) were reproduced in murine lesions, which could be "mock-diagnosed" as FD by physicians knowledgeable in the area, and blinded to the murine origin of tissue samples. These lines represent the first mouse model of human FD and highlight critical aspects of its natural history.

Disclosures: Isabella Saggio, None.

SU0150

Bone Marrow Transplantation Reduces Inflammation and Inflammation-Induced Bone Loss in Cherubism Mice. Teruhito Yoshitaka¹, Shu Ishida²,

Tomoyuki Mukai³, Yasuyoshi Ueki⁴. ¹University Missouri-Kansas City School of Dentistry, USA, ²University Missouri-Kansas City School of Dentistry, USA, ³University of Missouri - Kansas City, USA, ⁴University of Missouri-Kansas City School of Dentistry, USA

Cherubism is a genetic disorder caused by mutations in SH3BP2, which is typified by jaw bone destruction. We had previously created a mouse model of cherubism and discovered this condition to be a hematopoietic disorder where myeloid lineage cells are highly activated. These cells are primarily responsible for the TNF-dependent systemic inflammation resulting in bone erosion and joint destruction. In this study, we have investigated whether transplantation of bone marrow from wild-type (WT) mice will rescue the inflammation in homozygous cherubism mutants (mutant). Whole bone marrow cells collected from 6 weeks old WT or mutant mice were intravenously injected into the myelo-ablated homozygous cherubism mice pre-treated with busulfan. Ten weeks after transplantation, tissues of recipient mice were subjected to histological analysis to evaluate inflammation. MicroCT analysis was performed to

assess the calvarial and jaw bone loss as well as joint bone destruction. Histological analysis showed that inflammatory area in liver was significantly decreased in homozygous mutant mice transplanted with WT bone marrow cells ($0.6 \pm 0.3\%$) compared to the control homozygous mutant mice transplanted with the cells from homozygous mutants ($15.6 \pm 3.6\%$). In lung, inflammatory area was also reduced in homozygous mutant mice transplanted with WT bone marrow cells ($1.6 \pm 1.5\%$) compared to those mice treated with bone marrow cells from mutant mice ($13.4 \pm 7.0\%$). Consistent with the rescue of systemic inflammation in liver and lung, bone loss area at the top of calvarial bone along the parietal suture in mutant mice treated with WT bone marrow cells was significantly decreased to $6.9 \pm 1.8\%$, which is comparable to that of untreated WT mice ($6.1 \pm 0.5\%$), while homozygous mutants transplanted with bone marrow cells from mutants exhibited $10.4 \pm 2.8\%$ bone loss. In the oral cavity, the linear distance between the cemento-enamel junction and the alveolar bone crest at the proximal end of first molar was also improved to $263 \pm 24 \mu\text{m}$ in mutant mice transplanted with WT cells, comparable to the WT mice ($239 \pm 26 \mu\text{m}$), as compared to the homozygous mutant mice transplanted with mutant cells ($402 \pm 40 \mu\text{m}$). In summary, bone marrow replacement in homozygous cherubism mutant mice with WT bone marrow cells improved the tissue inflammation and inflammation-induced bone loss. These results suggest that bone marrow transplantation could be a novel option for the treatment of cherubism patients.

Disclosures: Teruhito Yoshitaka, None.

This study received funding from: RO1DE02835

SU0151

C-mpl is Expressed on Osteoblasts and Osteoclasts and is Important in Regulation of Skeletal Homeostasis. Tomas Meijome¹, Jenna Baughman¹,

Adam Hooker², Yinghua Cheng², Brahmananda Chitteti², Pierre Eleniste³, Edward Srouf², Robyn Fuchs⁴, Angela Bruzzaniti³, Melissa Kacena².

¹Indiana University-Purdue University Indianapolis, USA, ²Indiana University School of Medicine, USA, ³Indiana University School of Dentistry, USA, ⁴Indiana University, USA

There are a number of hematologic disorders in which megakaryocyte number and/or function is altered and in which a skeletal phenotype is observed. C-mpl is the cell surface receptor for the main megakaryocyte growth factor, thrombopoietin, which makes it crucial in megakaryocyte development and proliferation. As megakaryocytes have been previously shown to enhance bone formation, it may be expected that reduced megakaryocyte numbers would lead to decreased bone formation. However, in c-mpl^{-/-} mice which have a drastic 90% reduction in megakaryocyte numbers, our group and others observed a similar or higher bone mass compared to controls. Here we show that c-mpl is expressed on osteoblasts and osteoclasts and begin to identify how c-mpl regulates bone. Static and dynamic bone histomorphometry parameters suggest that c-mpl deficiency results in a high bone turnover state with a net balance or gain in bone volume. Bone volume/total volume was elevated 2.2-3.4 fold in c-mpl^{-/-} mice compared to controls as measured by static histomorphometry ($p=0.005$) and microCT ($p<0.001$), respectively. Static bone histomorphometry showed a 1.6 fold increase in the number of osteoblasts/tissue area ($p=0.05$) and a 2 fold increase in the number of osteoclasts/tissue area ($p=0.003$) in c-mpl^{-/-} femurs compared to control femurs. Dynamic bone histomorphometric analyses revealed no differences between c-mpl and control femurs with respect to bone formation rate/total volume (354 ± 22 vs. 317 ± 43 , $p=0.5$) or mineral apposition rate (1.9 ± 0.1 vs. 1.7 ± 0.2 , $p=0.3$). In vitro, a higher percentage of c-mpl^{-/-} osteoblasts were in active phases of the cell cycle, leading to an increase in osteoblast number. No differences in osteoblast differentiation were observed in vitro as examined by Real-Time PCR and functional assays. In co-culture systems, which allow for interactions between osteoblasts and osteoclast progenitors, c-mpl^{-/-} osteoblasts enhanced osteoclastogenesis. The MCSF/OPG/RANKL axis, a major path by which osteoblasts regulate osteoclastogenesis, was however unaffected in c-mpl^{-/-} osteoblasts. Taken together, these findings not only reaffirm the importance of megakaryocytes in skeletal homeostasis but also shed light on the effects of c-mpl expression on bone cells and bone regulation. Further clarifying how c-mpl regulates bone formation may provide insight into the homeostatic regulation of bone mass as well as bone loss diseases such as osteoporosis.

Disclosures: Tomas Meijome, None.

SU0152

Identification of the PolyA Mutation (c.*231A>G) in the PHEX 3'UTR in Five Boys with X-linked Hypophosphatemia (XLH). Steven Mumm¹,

Margaret Huskey¹, Valerie Wollberg¹, Katherine Madson², Deborah Wenkert², Gary Gottesman², William McAlister¹, Michael Whyte².

¹Washington University School of Medicine, USA, ²Shriners Hospital for Children-Saint Louis, USA

Heritable forms of hypophosphatemic rickets (HR) include X-linked dominant HR (XLH, caused by de-activating mutations in the PHEX gene), autosomal recessive HR (ARHR, caused by de-activating mutations in the DMP1 gene), and autosomal dominant HR (ADHR, caused by activating mutations in the FGF23 gene). Over the past 28 years, we have cared for 284 pediatric HR patients. We are investigating 30 of the 72 sporadic HR patients (those for whom DNA is available) to identify their

genetic defects causing rickets. For these 30 patients, we have previously reported PHEX coding region or splice site mutations in 9 patients and larger genomic disruptions in PHEX for 2 patients. The remaining 19 patients lack coding region or splice defects in PHEX, DMP1, or FGF23.

Previously, a novel single base change near the polyadenylation (polyA) signal in the 3' UTR of the PHEX gene has been reported as the cause of XLH in a small number (7) of patients (Ichikawa et al. Bone 43: 663-6, 2008). This c.*231A>G mutation is located 3 bp upstream of the putative polyA signal (AATAAA). Accordingly, we investigated whether this defect accounts for some of our 19 enigmatic sporadic XLH patients who do not have mutations in the coding region or splice sites of PHEX, DMP1, or FGF23. We analyzed the PHEX 3' UTR containing the polyA signal by PCR amplification and sequencing of the region in all 30 sporadic patients. We found the defect in 5 unrelated boys. All had the identical mutation as previously reported (c.*231A>G); none showed other changes near the polyA site. Our cohort of 30 sporadic XLH patients included 20 girls and 10 boys—consistent with having twice as many girls as boys affected by this X-linked dominant disease. Finding 5 boys but no girls with the polyA defect suggests a gender bias for this mutation. For three of the boys, parental DNA was available and for all cases, the mother showed the mutation. To determine if this unique PHEX mutation arose in a distant founder, we established a haplotype for the 5 boys using 6 SNPs that span ~2.5 Mb in and around the PHEX gene. We found that 3 boys shared a common haplotype suggesting they are distantly related, while 2 boys each had a different haplotype, suggesting that this unique mutation has arisen independently in these individuals.

Disclosures: Steven Mumm, None.

SU0153

Mineralizing Enthesopathy is a Common Feature of Renal Phosphate Wasting Disorders Attributed to FGF23 and is Exacerbated by Standard Therapy in Hyp Mice. Carolyn Macica*¹, Xiuying Bai², Jean-Pierre Falet³, Emily Walters⁴, Andrew Karaplis³. ¹Yale University School of Medicine, USA, ²Lady Davis Institute, Canada, ³McGill University, Canada, ⁴Yale University, USA

Enthesopathy is a common feature of X-linked hypophosphatemia (XLH). We have previously shown that the enthesopathy is recapitulated in Hyp mice, a murine model of XLH, and is characterized by significant hyperplasia of mineralizing fibrochondrocytes (FCs) that co-express FGFR3/klotho. It is unclear however whether it occurs in other forms of renal phosphate wasting disorders attributable to high FGF23 levels and what is the underlying pathophysiology. Here, we describe two brothers of Lebanese origin with autosomal recessive hypophosphatemic rickets (ARHR) due to the Met1Val (M1V) mutation in dentin matrix acidic phosphoprotein 1 (DMP1). In addition to the biochemical and skeletal features of long-standing rickets with elevated FGF23 levels, these individuals exhibited severe, debilitating, generalized enthesopathy. These data suggest that mineralizing enthesopathy is a feature common to phosphate wasting disorders mediated by FGF23. To address this possibility, we examined a murine model of FGF23 overexpression using a transgene encoding the secreted form of human FGF23 (R176Q) cDNA (FGF23-TG mice). Mice have a biochemical profile and phenotypic traits akin to phosphate-wasting disorders attributed to FGF23. We report that FGF23-TG mice display a similar mineralizing enthesopathy of the Achilles and plantar facial insertions evident by 12 wks, the period of developmental maturity. The enthesopathy (expressed as a percentage of total enthesis area) is characterized by an expansion of alkaline phosphatase-positive FCs embedded in a mineralized matrix (wild-type mice, 0.75 ± 0.5%; FGF23-TG mice, 15.1 ± 3.4%, p<0.01; Hyp mice, 21.1 ± 2.1%, p<0.01). The standard therapy for phosphate-wasting disorders is oral phosphate and calcitriol. However, the impact of treatment on enthesophyte progression is unknown. We thus treated Hyp mice with phosphate (1.93 g phosphate/L water) and calcitriol (0.175 µg/kg/day) from wks 3 to 12. We found that the mineralizing enthesopathy persisted despite improving bone mass. In addition, treatment had the untoward effect of further exacerbating mineralization of FCs with a significant reduction in the area of unmineralized matrix surrounding the cell (untreated Hyp, 59.1 ± 21.2 µm²; treated Hyp, 32.4 ± 12.4 µm²). These studies support the need for newer interventions targeted at limiting the actions of FGF23 while minimizing both the toxicities and potential morbidities associated with standard therapy.

Disclosures: Carolyn Macica, None.

SU0154

Osteopetrosis, Osteopetrorickets and Hypophosphatemic Rickets Differentially Affect Dentin and Enamel Mineralization. Thorsten Schinke¹, Till Koehne*². ¹Department of Osteology & Biomechanics University Medical Center Hamburg Eppe, Germany, ²Department of Osteology & Biomechanics, University Medical Center Hamburg-Eppendorf, Germany

Osteopetrosis (OP) is an inherited disorder of defective bone resorption, which can be accompanied by impaired skeletal mineralization, a phenotype termed osteopetrorickets (OPR). Since individuals with dysfunctional osteoclasts often develop osteomyelitis of the jaw, we have analyzed, if dentin and enamel mineralization are differentially affected in OP and OPR. Therefore, we have applied non-decalcified histology and quantitative backscattered electron imaging (qBEI) to compare the dental phenotypes of *Src*^{-/-}, *ocloc* and *Hyp*^{fl/fl} mice, which serve as models for OP, OPR

and hypophosphatemic rickets, respectively. While both, *Src*^{-/-} and *ocloc* mice, were characterized by defects of molar root formation, only *ocloc* mice displayed a severe defect of dentin mineralization, similar to the *Hyp*^{fl/fl} mice. Most importantly, while enamel thickness was not affected in either mouse model, the calcium content within the enamel phase was significantly reduced in *ocloc*, but not in *Src*^{-/-} or *Hyp*^{fl/fl} mice. Taken together, these data demonstrate that tooth eruption, dentin and enamel mineralization are differentially affected by disturbances of osteoclast function, calcium and phosphate homeostasis. Moreover, since defects of dental mineralization may trigger premature tooth decay and thereby osteomyelitis of the jaw, they further underscore the importance of discriminating between OP and OPR in the respective individuals.

Disclosures: Till Koehne, None.

SU0155

Withdrawn

SU0156

Serum Serotonin is Elevated in Osteoporosis Pseudoglioma Syndrome (OPPG) and Inversely Related to Muscle Mass and Bone Quality. Elizabeth Streeten*¹, D Holmes Morton², Erik Puffenberger², Sheila Ramirez³, Sruti Chandresakaran¹, Kathleen Ryan¹, Rita Herskovitz⁴, Mary Leonard⁵. ¹University of Maryland School of Medicine, USA, ²The Clinic for Special Children, USA, ³University of Maryland, USA, ⁴Childrens Hospital of Philadelphia, USA, ⁵Children's Hospital of Philadelphia, USA

Purpose: OPPG is an A.R. disorder of childhood osteoporosis and blindness, due to inactivating mutations in *LRP5*. Correlations reported in some (but not all) studies between high serum serotonin and OPPG suggest that serotonin-lowering may be a treatment option, but the relation of OPPG to serotonin remains unclear given the small sample sizes of past studies and the lack of clear mechanistic evidence in humans. The aims of this study were to measure serotonin in OPPG patients and controls and to evaluate for associations between serotonin and bone quality.

Methods: Fasting serum serotonin (5-HT) was measured in 54 participants (mean age in yrs±SD): 10 with OPPG (12+7), 10 heterozygotes (Hets) (23+16), and 34 controls (20+14.0). OPPG participants were off osteoporosis medications for at least 6 months. Tibial pQCT was performed in 15 participants who also had 5-HT measured: 6 with OPPG, 8 Hets, 1 with no mutation; data were compared to a normal database. The study was IRB approved. Participants signed informed consent or assent.

Results: In the 54 participants with 5-HT measured, 5-HT was higher in OPPG 213.3±84 ng/ml than in unaffecteds (Hets + controls) 121±66 (p=0.0009; after age adjustment p=0.003); 5-HT was not different in Hets vs controls. OPPG patients were shorter (p=0.05) and had similar BMI (p=0.14) to unaffecteds. By pQCT, the 6 OPPG patients vs 9 unaffecteds had lower trabecular density (TD), lower periosteal circumference (PC) and lower section modulus (SM) (p=0.004, 0.03, 0.02), similar fat Z-score (p=0.39) but a trend toward lower muscle Z-score (p=0.09). 5-HT was inversely related to Z-scores for muscle area, TD, CD, PC and SM (Table below).

Conclusions: Serum serotonin was higher in OPPG participants than in Hets and those with no *LRP5* mutation. We believe this is the largest study on serum serotonin in OPPG. Higher serotonin levels were associated with lower muscle mass, lower volumetric bone density and deleterious bone quality, supporting earlier studies in the mouse model of OPPG that serotonin is involved with the pathophysiology of OPPG and suggesting that serotonin lowering may be an effective treatment for OPPG.

Table: Correlation between serum 5-HT and tissue/bone phenotype on pQCT (n=6 OPPG, n=9 unaffected).

| | BMI | Fat Z-score | Muscle Z-score | TD Z-score | CD Z-score | PC Z-score | SM Z-score |
|----------------|------------|-------------|----------------|--------------|-------------|-------------|-------------|
| r ² | 0.14 | 0.07 | 0.40 | 0.38 | 0.29 | 0.49 | 0.48 |
| B coeff. | -7.6 ± 5.2 | 19.2 ± 16.9 | -31.5 ± 10.7 | -42.4 ± 15.0 | 31.3 ± 13.6 | -27.4 ± 7.8 | -28.2 ± 8.2 |
| p-value | 0.17 | 0.33 | 0.01 | 0.01 | 0.04 | 0.004 | 0.004 |

Table

Disclosures: Elizabeth Streeten, None.

SU0157

Skeletal Analysis of the Tc1 Mouse Model of Down Syndrome Suggests a Limited Region of Human Chromosome 21 is Involved in Low Bone Mass. Tristan Fowler^{*1}, Nisreen Akef¹, Jaclyn Vander Schilden², Robert Skinner², Frances Swain², Shane Shelton², William Hogue², Kent McKelvey³, Dana Gaddy¹, Larry Suva¹. ¹University of Arkansas for Medical Sciences, USA, ²Department of Orthopaedic Surgery, Center for Orthopaedic Research, USA, ³Department of Genetics, University of Arkansas for Medical Sciences, USA

Down Syndrome (DS), trisomy of chromosome 21, is one of the most common congenital disorders leading to a wide range of health problems in humans, including low bone mass. The Tc1 mouse carries a significant part of human chromosome 21 (Hsa21) in addition to the full set of mouse chromosomes and shares many phenotypes observed in humans affected by DS. However, it is unknown whether Tc1 mice also exhibit low bone mass and might thus represent a good model for understanding the skeletal phenotype that is common in DS. In this study we carried out a structural and functional assessment of the skeleton of Tc1 mice. Animals were received at 8 weeks old and followed for 4.5 months before sacrifice. DEXA analysis revealed no differences between WT and Tc1 BMD or BMC at any age examined. Tc1 mice at 4 months of age developed a significant decrease in whole body weight. However, the whole body % body fat was significantly increased when compared to WT. MicroCT analysis of the tibia at 5.5 months of age revealed a significant increase in cortical thickness and significant decreases in total cortical diameter, medullary area, and medullary diameter, but no significant differences in any trabecular bone parameters were observed in tibia or femur. Blood collected at sacrifice was screened by ELISA for markers of bone formation and bone resorption, PINP and CTX, respectively. Tc1 mice had significantly decreased markers suggesting a net low bone turnover. Surprisingly, when *ex vivo* bone marrow cultures were assessed, there were significant increases in osteoblast recruitment and the number of mineralized bone nodules, suggesting increased osteoblast progenitors and differentiation capacity of bone forming cells. Furthermore, whole bone marrow cultures stimulated toward osteoclastogenesis, and purified bone marrow macrophages, had significantly increased numbers of TRAP+/MNC, indicating enhanced osteoclastogenesis in the presence of stromal cells and when cultured as a purified population. The skeletal phenotype in the Tc1 mouse is in stark contrast to the Ts65Dn model of DS that we characterized as having a dramatically low bone mass phenotype accompanied by decreased osteoblast and osteoclast differentiation and function. These results suggest that genes that are only present in two copies in the Tc1 mouse model and three copies in Ts65Dn mouse model may predispose to low bone mass when an additional copy is active

Disclosures: Tristan Fowler, None.

SU0158

Targeted Sequencing of Previously Identified Loci Associated with BMD. Douglas Kiel¹, Yi-Hsiang Hsu^{*2}, Ching-Ti Liu³, John Robbins⁴, Adrienne Cupples³, Serkalem Demissie³, David Karasik¹, Jennifer Brody⁵, Guo Li⁵, Yanhua Zhou⁶, Bruce Psaty⁵, Tamara Harris⁷. ¹Hebrew SeniorLife, USA, ²Hebrew SeniorLife Institute for Aging Research & Harvard Medical School, USA, ³Boston University School of Public Health, USA, ⁴University of California, Davis Medical Center, USA, ⁵University of Washington, USA, ⁶Boston University, USA, ⁷Intramural Research Program, National Institute on Aging, USA

Genome wide association studies (GWAS) have identified disease-related genomic regions, but the majority of identified common SNPs are in introns or intergenic regions which may not be functional but which may be in linkage disequilibrium with causal variants. In the largest GWAS meta-analysis of spine (LS) and femoral neck (FN) BMD, the GEFOS Consortium identified and replicated 56 genome-wide significant loci associated with BMD. We followed up 4 of these loci (chr1p31.3: *WLS*, 5q14.3: *MEF2C*, 11p11.2: *LRP4*, 20p12.2: *JAG1*) using next-generation sequencing to identify potential causal variants associated with BMD. Participants from the Framingham Heart Study (n=920 M&W) and the Cardiovascular Health Study (n=366 M&W) underwent targeted sequencing of these 4 regions, including 100 from each cohort with extreme low FNBM (T-score<-2.0 & Z-score<-1.5). 10,931 sequence variants were observed: 9% analyzed in our previous GEFOS meta-analysis; 14% not previously tested but reported in "dbSNP"; 77% novel variants in the study populations. Within each class of variants (e.g., non-synonymous, splicing, intronic,

etc), ≥90% were rare (MAF<0.1%). SNP-phenotype association analyses were separately performed for common and rare variants. For "common" variants (MAF≥1%), a regression model adjusted for age, sex, wt and ancestral genetic background was used in each study, followed by fixed-effects inverse-variance meta-analyses. We excluded SNPs that only produced results in one study, had heterogeneity p-values<0.0001, and heterogeneity I²>50. We identified a common variant associated with FN BMD (p=7.8x10⁻⁵) not previously identified as a GWAS signal in the *WLS* region. In each study we collapsed the rare variants (MAF<1%) within each locus using inverse-allele frequency weighting (Madsen-Browning procedure). Individual study results were combined using a fixed-effects weighted-Z meta-analysis. The most significant association with LS BMD for rare variants was found within a sub-region of the chr11p11.2 locus (near *LRP4*) (p-value=1.1x10⁻⁷). In conclusion, targeted resequencing of previously identified GWAS loci yielded novel findings in the *WLS* gene for common variant association with FN BMD. The majority of newly identified variants were rare. We found potential causal variants near the *LRP4* locus associated with LS BMD. Sequencing of GWAS loci may identify new information to improve our understanding of the genetic associations with BMD.

Disclosures: Yi-Hsiang Hsu, None.

SU0159

Teriparatide Improves BMD and Bone Strength in Adults with Osteogenesis Imperfecta: A Randomized, Blinded, Placebo Controlled Trial. Eric Orwoll^{*1}, Sandra Veith¹, Ying Wang¹, Jodi Lapidus¹, Tony Keaveny², David Lee³, Sandesh Sreenath-Nagamani⁴, Jay Shapiro⁵, Brendan Lee⁶. ¹Oregon Health & Science University, USA, ²University of California, Berkeley, USA, ³O.N. Diagnostics, USA, ⁴Baylor College of Medicine, USA, ⁵Kennedy Krieger Institute, Johns Hopkins, USA, ⁶Baylor College of Medicine & Howard Hughes Medical Institute, USA

There have been very few studies of the treatment of adults with osteogenesis imperfecta (OI) and effective drug therapies have not been identified. Anabolic agents may be useful to increase bone mass, but have not been evaluated. We performed a randomized, double blind, placebo controlled trial of teriparatide in 77 adults with OI (33 men, 44 women). The mean age was 41 years (range 18-75). 51 were judged to have osteogenesis imperfecta type I, 14 had type III and 12 had type IV. None had received recent pharmacological therapy for their bone disease. Participants were treated for 18 months with teriparatide (20 ug/day) or placebo. All received calcium and vitamin D supplements. We obtained baseline and q 6month measures of areal BMD (DXA), and vertebral QCT scans were obtained at baseline and 18 months. Incident fractures at any site were assessed by self report.

Areal BMD increased more in the teriparatide treated group than in the placebo treated group at the total hip (2.7% vs -0.6%; p= 0.007) but not at the spine (5.3% vs 3.1%; p= 0.18) or total body (-0.1% vs 1.0%; p= 0.32). However, volumetric trabecular spine BMD by QCT increased by 13% in the teriparatide treated group and decreased 6% in the placebo group (p= 0.03). Vertebral strength estimated by non-linear finite element analysis (calculated using either conventional or reduced tissue-level material properties) increased 13% in the treated group and decreased 2.4% in the placebo group (p= 0.003). The proportion of patients with clinical fractures was lower in the teriparatide treated than in the placebo group (29 vs 36%) but the difference was not significant (RR 0.8; 0.42, 1.55). The rate of adverse events was similar in the two groups; there were no drug related serious adverse events.

In conclusion, therapy with teriparatide in adults with osteogenesis imperfecta was well tolerated and resulted in an increase in areal hip and volumetric spine BMD, as well as an increase in estimated vertebral strength.

Disclosures: Eric Orwoll, Merck, Lilly, Amgen, 6; Merck, Wright, 2
This study received funding from: Lilly

SU0160

Genetic Determinants of Trabecular and Cortical Volumetric Bone Mineral Densities and Bone Microstructure. Claes Ohlsson^{*1}, Lavinia Paternoster², Terho Lehtimäki³, Joel Eriksson⁴, Mika Kähönen⁵, Olli Raitakari⁶, Marika Laaksonen⁷, Vera Mikkilä⁷, Jorma Viikari⁸, Leo-Pekka Lyytikäinen³, John P Kemp², Adrian Sayers⁹, Maria Nethander¹⁰, Liesbeth Vandenput¹¹, David M Evans², Mattias Lorentzon¹², J.H. Tobias¹³. ¹Center for Bone & Arthritis Research at the Sahlgrenska Academy, Sweden, ²MRC Centre for Causal Analyses in Translational Epidemiology, University of Bristol, BS8 2BN, UK, United Kingdom, ³Department of Clinical Chemistry, University of Tampere & Tampere University Hospital, Tampere, Finland, 33521, Finland, ⁴Center for Bone & Arthritis Research, Institute of Medicine, Sahlgrenska Academy, University of Gothenburg, Sweden, Sweden, ⁵Department of Clinical Physiology, University of Tampere & Tampere University Hospital, Tampere, Finland, 33521, Finland, ⁶Research Centre of Applied & Preventive Cardiovascular Medicine, University of Turku & the Department of Clinical Physiology, Turku University Hospital, Turku, Finland, 20521, Finland, ⁷Department of Food & Environmental Sciences, University of Helsinki, Helsinki, Finland, Finland, ⁸Department of Medicine, University of Turku & Turku University Hospital, Turku, Finland, 20521, Finland, ⁹School of Social & Community Medicine, University of Bristol, Bristol BS8 2PS, UK, United Kingdom, ¹⁰Genomics Core Facility, University of Gothenburg, Gothenburg, Sweden, Sweden, ¹¹Sahlgrenska University Hospital, Sweden, ¹²Center for Bone Research at the Sahlgrenska Academy, Sweden, ¹³Avon Orthopaedic Centre, United Kingdom

Previous studies using dual-energy X-ray absorptiometry have demonstrated that age is a major predictor of fracture risk independent of areal bone mineral density (aBMD). Although this aBMD-independent effect of age has been attributed to poor bone "quality", the structural basis for this remains unclear. Computer tomography (CT) analysis has the capacity to reveal unique information about bone quality. The objective of the present study was to identify genetic determinants of trabecular and cortical volumetric bone mineral density (vBMD) and bone microstructure as analyzed by peripheral quantitative CT (pQCT).

Separate genome-wide association (GWA) meta-analyses were performed for cortical and trabecular vBMDs of the tibia. The cortical vBMD analysis (n= 6930) included three discovery (*ALSPAC*, *GOOD*, and *YFS*) and one replication (*MrOS Sweden*) cohort, while the trabecular vBMD analysis (n= 3522) included two discovery (*GOOD* and *YFS*) and one replication (*MrOS Sweden*) cohort. Inverse variance weighted fixed-effect model meta-analyses of study-specific results were performed. The cortical vBMD GWA meta-analysis identified genetic variants in four separate loci reaching genome-wide significance (*RANKL*, rs1021188, p=3.6x10⁻¹⁴; *LOC285735*, rs271170, p=2.7x10⁻¹²; *OPG*, rs7839059, p=1.2x10⁻¹⁰ and *ESRI*, rs6909279, p=1.1x10⁻⁹). Together, these four SNPs explained 5.8% of the variation in cortical vBMD in the GOOD cohort. The trabecular vBMD GWA meta-analysis identified one locus reaching genome wide significance (*FMN2*, rs9287237, p=1.9x10⁻⁹). This SNP explained 1.7% of the variation in trabecular vBMD in the GOOD cohort.

High resolution pQCT analyses (XtremeCT) of the distal tibia were available in a subset of the GOOD cohort (n= 729), providing bone microstructure data. rs1021188, the SNP most strongly associated with cortical vBMD, was significantly associated with cortical porosity (Fig 1). The trabecular vBMD SNP rs9287237 was significantly associated with trabecular BV/TV (effect size 0.29 SD per allele, p=1.8x10⁻⁵), trabecular number and trabecular thickness (Fig 1).

In conclusion, a genetic variant in the *RANKL* locus influences cortical vBMD partly via an effect on cortical porosity whereas a variant in the *FMN2* locus influences trabecular vBMD via effects on both trabecular thickness and number. The genetic variants associated with cortical and trabecular bone parameters differed, underscoring the complexity of the genetics of bone parameters.

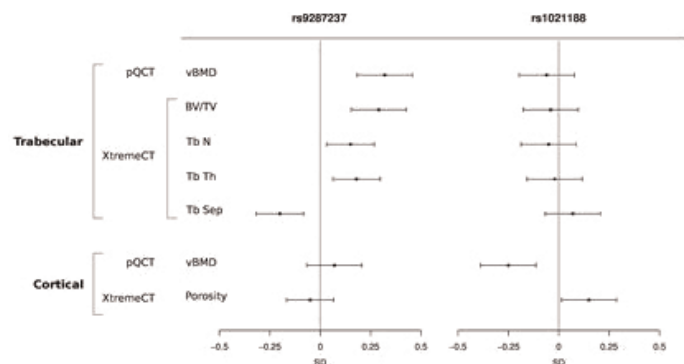


Fig 1

Disclosures: Claes Ohlsson, None.

SU0161

Identification of Sex-specific Genetic Loci for Bone Fragility Phenotypes in Heterogeneous Stock Rats. Imranul Alam^{*1}, Daniel Koller¹, Qiwei Sun², Toni Cañete³, Gloria Blázquez³, Regina López-Aumatell⁴, Esther Martínez-Membrives³, Elia Vicens-Costa³, Carme Mont³, Sira Diaz³, Adolf Tobeña³, Alberto Fernández-Teruel³, Adam Whitley⁴, Pernilla Stridl⁵, Margarita Diez², Martina Johannesson⁴, Amelie Baud⁴, Jonathan Flint⁴, Michael Econs¹, Charles Turner², Tatiana Foroud². ¹Indiana University School of Medicine, USA, ²IUPUI, USA, ³Autonomous University of Barcelona, Spain, ⁴Wellcome Trust Center for Human Genetics, United Kingdom, ⁵Karolinska Institutet, Sweden

Osteoporosis is a common bone disease with reduced bone mineral density (BMD) and increased susceptibility to fracture at multiple skeletal sites. BMD, structure and strength are the primary skeletal determinants of osteoporotic fracture risk and are under substantial genetic control. Previously, using a highly informative heterogeneous stock (HS) rat model, we identified several chromosomal regions with evidence of linkage to bone density, structure and strength phenotypes. The purpose of this study is to identify sex-specific genetic loci and potential candidate genes underlying these chromosomal regions that contribute to bone fragility phenotypes in HS rats. We used a total of 1734 rats (836 males and 898 females) and measured bone geometry, density and strength phenotypes at multiple skeletal sites (mid- and distal femur, femoral neck and lumbar vertebrae). Genotyping for 70,000-high quality SNPs were obtained from an Affymetrix custom SNP array. Haplotypes were constructed for each rat using the multipoint HAPPY method. A genome-wide empiric significance threshold was computed for each bone phenotype. We identified a total of 30 (16 male and 14 female) sex-specific QTLs meeting these thresholds, including 7 QTLs for BMD and 23 for structure. In addition to many novel genes, we also identified several genes underlying these QTLs (*Bmp5*, *Ccna1b*, *Dpp4*, *Grb2*, *Il6ra*, *Map3k7*, *Ptgs1* and *Tbrg1*) that have been previously shown to have a role in skeletal development and homeostasis. Importantly, we identified sex-specific QTLs contributing to different bone phenotypes in these rats within very narrow chromosomal regions, which will greatly facilitate the identification of causative genes for osteoporosis. Future studies involving the genes identified in this study in human populations will provide insights into the sex-specific genetic determinants of bone fragility.

Disclosures: Imranul Alam, None.

SU0162

Adverse Effects of BMP2 on Bone Formation and Osseointegration. Sharon Hyzy^{*1}, Rene Olivares-Navarrete², Barbara Bovan², Zvi Schwartz². ¹Georgia Tech, USA, ²Georgia Institute of Technology, USA

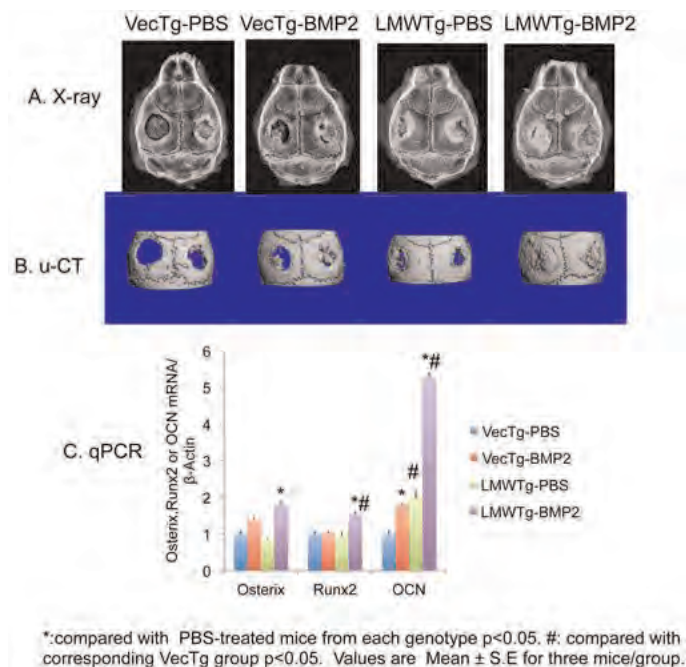
Bone morphogenetic proteins (BMPs) induce cartilage and bone formation in embryonic and adult processes. Clinically, large bolus doses of BMP2 are used for orthopaedic and dental applications to induce bone formation, and in combination with biomaterials to increase peri-implant bone. Inflammatory (swelling/seroma) and bone-related (ectopic bone/bone resorption) complications are reported after BMP2 treatment in addition to bone formation. The purpose of this study was to investigate potential deleterious effects of BMP2 on inflammation and apoptosis in osteoblasts. Effects on peri-implant inflammation were examined by quantifying secreted inflammatory interleukin (IL) production of osteoblast-like MG63 cells on tissue culture polystyrene (TCPS) or titanium substrates: smooth (PT) [Ra<0.4µm], sandblasted/acid etched (SLA) [Ra=3.2µm], or hydrophilic-SLA (modSLA) after 24 hour incubation ± 40 ng/ml BMP2. Apoptosis was assessed in confluent human mesenchymal stem cells (hMSCs) and normal human osteoblasts (NHOst) on TCPS treated with 50-200 ng/ml BMP2. Apoptosis was measured by quantitative *in-situ* TUNEL, caspase-3 activity, and BAX/BCL2 expression. Data are mean±SEM of n=6 cultures/variable (ANOVA/Bonferroni). Surface roughness and energy decreased pro-inflammatory and increased anti-inflammatory interleukin production by osteoblasts. In contrast, exogenous BMP2 abolished the surface effect, increasing pro-inflammatory IL6, IL8, and IL17 in a surface roughness-dependent fashion and decreasing anti-inflammatory IL10 on rough surfaces. BMP2 had little effect on apoptosis in hMSCs. In contrast, BMP2 increased TUNEL, caspase-3, and BAX/BCL2 in NHOst in a dose-dependent manner. The results suggest that while surface features direct an initial controlled inflammatory response, the addition of BMP2 induces a pro-inflammatory response. The apoptotic effects of BMP2 on apoptosis depend on cell maturation state, inducing apoptosis in committed osteoblasts. Addition of BMP2 to microtextured orthopaedic and dental implants may increase inflammation and possibly delay bone formation. Dose, location, and delivery strategies are important parameters to consider when using BMP2 as a therapeutic and must be optimized to minimize complications.

Disclosures: Sharon Hyzy, None.

SU0163

BMP-2 Synergizes the Bone Healing Effect of Low Molecular Weight FGF-2 on Calvarial Defects in Mice. Liping Xiao^{*1}, Sylvain Catros², Daisuke Ueno³, Lyndon Charles¹, Liisa Kuhn¹, Marja Marie Hurley⁴. ¹University of Connecticut Health Center, USA, ²University of Bordeaux Segalen, France, ³Tsurumi University, Japan, ⁴University of Connecticut Health Center School of Medicine, USA

Repair of calvarial bone defects remains a significant clinical problem. BMP-2 is FDA approved for fracture healing but is expensive. Targeted overexpression of the low molecular weight (LMW) FGF-2 isoform in osteoblasts resulted in increased bone mass in mice via Wnt signaling. We reported that targeted overexpression of LMW FGF-2 in osteoblastic lineage directly enhanced the healing of calvarial defects in mice, partially due to increased osteoblast activity. In this study we determined whether low concentrations of BMP-2 would be additive or synergistic with overexpression of LMW FGF-2 on calvarial bone defect healing. Two-month-old male LMWTg and VecTg mice were utilized. Bilateral calvarial defects (3.5 mm) were created in parietal bones of LMWTg and VecTg mice. A scaffold that was the same size as the defect and made of 70% type I collagen and 30% hydroxyapatite was placed in each defect and delivered either 0.5µg/5µl/scaffold rhBMP-2 or PBS. Mice were sacrificed 4 wks post surgery. Calvarial BMD was measured by DXA. Digital x-rays and micro-CT were performed to compare healing among groups. RNA was extracted from the defect area to examine by qPCR, genes that are important for bone formation. Two-way ANOVA was used to assess differences between genotypes and treatment groups. BMD was significantly increased in LMWTg compared with VecTg $p < 0.0001$. Consistent with previous findings, digital x-ray and micro-CT analysis (Figure A & B) showed enhanced calvarial defect healing in LMWTg mice. However, this healing was incomplete. BMP-2 treatment alone at this low dose resulted in incomplete healing of the defect in VecTg mice compared with vehicle. However, BMP-2 treatment of LMWTg mice completely healed the defect. Osterix mRNA was not different between VecTg and LMWTg, however BMP-2 significantly increased osterix in both genotypes $p < 0.0001$ (Fig C). Runx2 mRNA was significantly increased in LMWTg compared with VecTg $p < 0.051$. BMP-2 caused a further significant increase in RUNX2 in LMWTg. OCN mRNA was significantly increased in LMWTg compared with VecTg $p < 0.0001$; BMP-2 treatment significantly increased OCN in VecTg $p < 0.0001$. There was a synergistic increase in Osteocalcin (OCN) mRNA in BMP-2 treated LMWTg mice $p < 0.0001$. These studies demonstrate that BMP-2 synergistically increased the bone healing effect of LMW FGF-2. This provides a rationale for the clinical application of low dose combinations of two growth factors to augment bone defect healing.



Representative x-ray, micro-CT images and gene expression by qPCR

Disclosures: Liping Xiao, None.

SU0164

Endogenous BMP7 Activity is Prerequisite for Postnatal Joint Homeostasis. Kahaer Abula^{*1}, Takeshi Muneta¹, Kazumasa Miyatake¹, Jun Yamada¹, Yu Matsukura¹, Mika Yamaga¹, Ichiro Sekiya¹, Aris Economides², Vicki Rosen³, Kunikazu Tsuji¹. ¹Tokyo Medical & Dental University, Japan, ²Regeneron Pharmaceuticals, Inc., USA, ³Harvard School of Dental Medicine, USA

While the osteo- and chondro-inductive activities of recombinant bone morphogenetic protein 7 (BMP7) are well established, evaluation of the role of endogenous BMP7 in bone and cartilage homeostasis has been hampered by perinatal lethality in BMP7 knockout mice. To overcome these problems, we employed conditional deletion of BMP7 from the embryonic limb prior to the onset of skeletogenesis to create limb skeletons lacking BMP7. We have reported that the absence of locally produced BMP7 had no effect on postnatal limb growth, articular cartilage formation, maintenance of bone mass, or fracture healing. In this study, to evaluate the roles of endogenous BMP7 in postnatal joint homeostasis, we performed detailed histological analyses of the knee joint in adult BMP7 conditional knockout mice and found the accelerated degeneration of articular cartilage in the absence of endogenous BMP7. Safranin O staining of sagittal sections of the knee joint from 24 week-old mice revealed the significant loss in proteoglycan contents in articular cartilage matrix in the absence of endogenous BMP7. In this region, extensive proliferation of articular chondrocytes and ectopic expression of type III collagen were observed, suggesting the progression of osteoarthritis in these mice. Extensive degeneration of meniscus was also observed in BMP7 conditional knockout mice. We observed meniscal lesions in all the BMP7 conditional knockout mice at 24 weeks. Interestingly huge numbers of synovial fibroblasts were migrated on the surface of meniscus in these mice. These cells looked highly proliferative and expressed type III collagen. We observed less severe but similar results in the growing BMP7 conditional knockout mice (8 week-old). These data strongly suggest that endogenous BMP7 activity is involved in the mechanical properties of meniscus, proliferation and migration of synovial fibroblasts, and maintenance of hyaline cartilage in the articular joint.

Disclosures: Kahaer Abula, None.

SU0165

Loss of BMPR2 Leads to High Bone Mass Due to Increased Osteoblast Activity. Jonathan Lowery^{*1}, Giuseppe Intini¹, Karen Cox², Laura Gamer¹, Sutada Lotinun¹, Kunikazu Tsuji³, Roland Baron⁴, Vicki Rosen¹. ¹Harvard School of Dental Medicine, USA, ²Department of Developmental Biology, Harvard School of Dental Medicine, USA, ³Tokyo Medical & Dental University, Japan, ⁴Harvard School of Medicine & of Dental Medicine, USA

Canonical BMP signaling occurs through complexes of type 1 and type 2 receptors that lead to activation of the downstream effectors SMAD1/5/8. While the type 2 BMP receptor BMPR2 predominantly binds to BMPs, the other type 2 BMP receptors, ACVR2A and ACVR2B, have significantly lower affinity for BMPs than for Activin-like ligands. The binding of ACVR2A/B to Activin-like ligands leads to activation of a different class of downstream effectors, SMAD2/3. Multiple genetic studies in mice have shown that BMP signaling is required for normal endochondral ossification and osteoblast function; conversely, sequestration of Activin-like ligands leads to increased bone mass, implicating signaling through SMAD2/3 as a negative regulator of bone formation. These findings suggest that BMPR2 is the major type 2 receptor for BMP signaling in osteoprogenitors, chondrocytes and osteoblasts (OBs). Surprisingly, conditional deletion of *Bmpr2* in early limb mesenchyme using *Prx1-Cre* (*Bmpr2*-cKO mice) had no effect on limb skeletal development (Gamer et al., 2011), likely due to compensation by ACVR2A/B. In contrast, here we report that *Bmpr2*-cKO mice develop high bone mass postnatally. Micro-CT analysis revealed an increase in proximal tibia trabecular BV/TV in both male ($p < 0.01$) and female ($p < 0.001$) *Bmpr2*-cKO mice at 8-10 weeks of age when compared to littermate Cre-negative *Bmpr2*-floxed mice. Additional analysis using dynamic histomorphometry showed increased trabecular thickness ($p = 0.012$), mineral apposition rate ($p = 0.019$) and bone formation rate ($p = 0.002$) in the proximal tibia of *Bmpr2*-cKO mice. However, as there was no difference in OB or osteoclast number between *Bmpr2*-cKO mice or littermate controls, our findings suggest that loss of BMPR2 in the *Prx1*-Cre expression domain leads to increased bone mass due to an overt increase in OB activity. This is a distinctly different phenotype than the high bone mass associated with loss of the type 1 BMP receptor *Alk3* in osteoblasts, which causes decreased osteoblast activity but results in high bone mass due to a secondary defect in osteoclastogenesis. As BMP signaling is essential for OB function, we hypothesize that the absence of BMPR2 in osteoblasts requires ACVR2A and/or ACVR2B to transduce signals from both BMP and Activin-like ligands. We predict this change in receptor usage leads to a net decrease in SMAD2/3 signaling relative to SMAD1/5/8 signaling in these cells, resulting in enhanced osteoblast activity.

Disclosures: Jonathan Lowery, None.

SU0166

Recombinant Human BMP-2 Induces a Transient Dose Response for Bone Repair in Critical Sized Long Bone Defects. Kenneth Kozloff*¹, Joseph S. Tramer¹, Ed Berryman², Joseph E. Perosky¹, Eric Vanderploeg², Steven A. Goldstein¹, Cedo M. Bagi². ¹University of Michigan Department of Orthopaedic Surgery, USA, ²Pfizer, Inc., USA

Recombinant human BMP2 (rhBMP2) is a potent anabolic agent that induces bone repair. However, supra-physiologic doses required may limit application safety. The purpose of this study was to monitor rhBMP2 dose response in a critical long bone defect through longitudinal imaging and functional gait testing to determine minimal effective dosing over 8 weeks of bone repair. Adult male Sprague-Dawley rats were grouped as follows: sham-operated; absorbable collagen sponge (ACS)+PBS control; ACS+low rhBMP2 (0.75µg), ACS+high rhBMP2 (3.75µg). A unilateral 5mm mid-diaphyseal femoral defect was stabilized with a custom PEEK fixation plate and ACS constructs were implanted. Sham rats received incision with no fixator. Rats returned to normal cage activity for 4 or 8 week recovery. All changes are $p < 0.05$ unless noted, $n=8$ /group. Dynamic weight bearing tests observed a decrease in % body mass placed on operated limbs 2 days post-surgery compared to baseline in empty (-16%) and low BMP (-13%) rats with a corresponding shift to the contralateral limb in rats with empty defects (+13%). By 3 weeks, hindlimb gait patterns did not differ from baseline, though a gradual transition in mass distribution from hind to forelimbs was observed in sham and empty groups. In vivo μ CT quantified regenerate bone mineral content (BMC) during healing. At 2 weeks, high BMP induced 232% increase in BMC over ACS alone, while low BMP showed a modest (73%) but not significant increase. By 4 weeks, BMP induced a dose dependent increase in BMC (163% low, 315% high) and this response continued through 6 weeks (242% low; 342% high). Ex vivo μ CT at 4 weeks confirmed a dose response with significant increase in BMC (194%, 482%), bone volume (252%, 730%), and bone volume fraction (193%, 436%) in low and high BMP respectively compared to ACS alone. Between 4 and 8 weeks, low BMP induced increases in BMC from 19 mg to 34 mg to reach high BMP levels which remained unchanged over the same period (38mg vs. 39 mg). Qualitative observation of ex vivo μ CT images suggests reorganization of bone from 4 to 8 weeks at both BMP doses from a woven to lamellar appearance. Empty sites remained unhealed at 8 weeks. In summary, rhBMP2 induced an early dose dependent response that equilibrated by 8 weeks in a critical sized rat femoral defect. These data suggest that similar regenerate bone volumes can be accomplished with smaller doses of rhBMP2 in the long-term healing environment.

Disclosures: Kenneth Kozloff, Pfizer, Inc., 6
This study received funding from: Pfizer, Inc.

SU0167

Fgf-23: The Untold Regulator of Hematopoiesis. Lindsay Coe*¹, Sangeetha V.M.², Despina Sitara¹. ¹New York University College of Dentistry, USA, ²New York University, USA

Fibroblast growth factor-23 (FGF-23) is a bone-derived hormone which regulates phosphate homeostasis and bone mineralization. Mice deficient in Fgf-23 (Fgf-23^{-/-}) exhibit significantly elevated levels of serum phosphate and vitamin D, reduced bone mineralization and severe growth retardation. Impaired bone mineralization and changes in the bone marrow microenvironment are reported to disrupt normal hematopoiesis in mice. Our current study examines a novel role for Fgf-23 as a key regulator of hematopoiesis. Here, we analyzed 6-week-old Fgf-23^{-/-} and wild-type (WT) littermate mice and characterized their hematopoietic cellular composition using automated complete blood counts and flow cytometry in peripheral blood and bone marrow. Hematology data revealed increased numbers of red blood cells and decreased numbers of white blood cells in peripheral blood of Fgf-23^{-/-} mice. Moreover, flow cytometry analysis showed a reduction in B-lymphopoiesis in peripheral blood and bone marrow of Fgf-23^{-/-} mice compared to WT littermates. Our recent findings furthermore suggest that Fgf-23^{-/-} mice exhibit changes in T-lymphocytes, erythrocytes, and hematopoietic stem cell progenitors (HSC) in the bone marrow. *In vitro* colony-forming unit assays support changes in HSC function in the bone marrow of our Fgf-23^{-/-} mice. In addition, we have found that exogenous administration of FGF-23 protein in WT mice results in opposite hematopoietic changes than in Fgf-23^{-/-} mice. We are currently investigating the mechanisms mediating the effects of Fgf-23 on hematopoiesis. Our preliminary data on fetal liver hematopoiesis indicate that the hematopoietic changes in Fgf-23^{-/-} mice are most likely due to a direct effect of Fgf-23 on HSCs rather than the result of altered bone marrow niche alone. This is the first report suggesting that Fgf-23 is directly associated with changes in hematopoiesis. Since *in vivo* ablation of Fgf-23 results in hypervitaminosis D, we are currently investigating whether the effects of Fgf-23 in hematopoiesis are vitamin D-mediated. To address this question, we are generating a mouse model deficient in both Fgf-23 and 1- α -hydroxylase (the enzyme responsible for converting vitamin D to its active form) genes. Taken together, our studies demonstrate a novel role for FGF-23 in hematopoiesis that is beyond its involvement in phosphate homeostasis and bone mineralization.

Disclosures: Lindsay Coe, None.

SU0168

A Case Report of the Percutaneously Injection of Platelet-rich Plasma (PRP) to Accelerate Fracture Healing in an Athlete. YOHEI KOBAYASHI*¹, Yoshitomo Saita¹, Masashi Nagao², Hiroki Nakajima¹, Hiroshi Ikeda¹, Kazuo Kaneko¹. ¹Department of Orthopaedics, Juntendo University School of Medicine, Japan, ²Juntendo University Nerima Hospital, Japan

Background: Platelet rich plasma (PRP) is a treatment used in many fields including orthopedics, cosmetics surgery and sports medicine. As PRP contains growth factors such as TGF-beta, b-FGF, PDGF and VEGF, injection of PRP would stimulate and enhance the process of tissue healing. Although many animal studies suggested that the efficacy of PRP therapy for bone regeneration, the efficacy of PRP injection for the fracture repair in human remained unclear. Here we report a case of professional soccer player using PRP for complete fibula fracture. Bridging of callus was observed from two weeks after the fracture and he could start running four weeks after the fracture without operative treatment.

case
A 23-year-old professional soccer player sustained a closed complete transverse fracture at the distal part of the fibula. Since the fracture was minimally displaced, we chose the conservative care. The leg was immobilized in an aircast brace. We performed two times of PRP treatments during his treatment course (three days and two weeks after the injury). For the preparation of PRP, we used autologous platelet preparation kit (MyCellsR), and purification of PRP was performed as manufacturers' protocol. In short, 20 ml of peripheral blood was taken and then centrifuged for 8 minutes (3,500 rpm), erythrocytes and white blood cells were removed and 2ml of PRP was obtained. PRP is then percutaneously injected multiply around the fracture site guided with ultrasonography. Callus formation was observed at two weeks after the injury. The brace was removed two weeks after injury and partial weight-bearing was started. Since vigorous callus formation was observed in X-ray at four weeks after the injury, he began running. At six weeks after the injury, almost complete bone union was observed in the X-ray.

Conclusion: Athletes desire a rapid return to their preinjury level of function, and PRP may have certain applications that will facilitate bone healing. Further investigations will be needed to confirm PRP efficacy and to elucidate its mechanism of action.

Disclosures: YOHEI KOBAYASHI, None.

SU0169

Angiogenesis with Bone Malignant Melanoma Induces Production of Prostaglandin E2 in Host Stromal Cells. Kenta Watanabe, Statoshi Yokoyama, Chiho Matsumoto, Michiko Hirata, Chisato Miyaura, Masaki Inada*. Tokyo University of Agriculture & Technology, Japan

Bone metastasis of malignant melanoma is accompanied by severe bone destruction with increased bone resorption. We recently reported that bone destruction was blunted in mPGES-1-null mice injected by mouse malignant melanoma cells. Prostaglandin E2 (PGE2) is a part of the key signal on bone metastasis mediated by osteoclast, the supportive factors of its differentiation such as RANKL was expressed in host stromal cells. In this study, we examined the PGE2 promoted melanoma growth and supportive angiogenesis in the models of bone malignant B16. When B16 cells were implanted subcutaneously into wild-type mice, B16 cells grew rapidly to form solid tumor with angiogenesis. In mPGES-1-null mice, the growth of B16 solid tumor was blunted to compare with experimental wild-type mice. When *in vivo* fluorescent imaging reagent AngioSense applied to the experimental group of mPGES-1-null mice, angiogenesis in skin around B16 was dramatically blunted suggesting melanoma growth in skin is depending on PGE2 related angiogenesis. In intra-vein injection of B16 cells into wild type mice, B16 cells were metastasized to all kinds of bone systemically, cortical and cancerous bone, such as vertebra, mandible, femur, tibia and its angiogenesis was occurred close to B16 metastasized area. In mPGES-1-null mice, B16 metastasis was perfectly suppressed to compare in wild type mice, angiogenesis was also dramatically suppressed in femur and tibiae. *In vitro*, when dermal fibroblasts derived from wild-type mice were co-cultured with fixed-B16 cells, production of PGE2 was markedly increased in the conditioned medium, while dermal fibroblasts derived from mPGES-1-null mice were produced much less amounts of PGE2. When the treatment of PGE2 to dermal fibroblasts derived from wild-type mice, production of vascular endothelial cell growth factor (VEGF)-A and basic fibroblast growth factor (bFGF) was increased in the conditioned medium, while dermal fibroblasts derived from mPGES-1-null mice were produced much less amounts of VEGF-A and bFGF. These results suggest that PGE2 produced by host stromal cells promotes VEGF-A and bFGF production leads angiogenesis at the site of melanoma metastasized. PGE2 receptors antagonist could be a possible candidate for the upstream therapy of bone cancer proliferation associated with angiogenesis.

Disclosures: Masaki Inada, None.

SU0170

Chondrogenic and Osteogenic Effects of Wnt Proteins on Human Chondrocytes, Osteoblasts and Mesenchymal Stem Cells. Rene Olivares-Navarrete^{*1}, Sharon Hyzy², Christine Wasilewski¹, Caitlin Cundiff¹, Zvi Schwartz¹, Barbara Bovan¹. ¹Georgia Institute of Technology, USA, ²Georgia Tech, USA

Wnt proteins regulate patterning, proliferation, differentiation, and apoptosis in diverse tissues. Wnts act in both an autocrine and paracrine fashion. They bind to specific Frizzled receptors and trigger signaling according to the specific ligand-receptor combination. Wnts activate 3 main signaling pathways, canonical Wnt/ β -catenin-dependent, Wnt/calcium-dependent, and Wnt/planar cell polarity pathways. Wnts are involved in bone and cartilage development and growth; however, the role of Wnts in bone and cartilage regeneration is poorly understood. The aim of this study was to elucidate the possible regenerative effect of Wnt proteins on human chondrocytes (CH), osteoblasts (OB), and mesenchymal stem cells (MSC). All cell types were treated with canonical (Wnt1, Wnt3a, Wnt7a) or calcium-dependent (Wnt5a, Wnt5b, Wnt11) Wnt ligands. mRNA levels of integrin subunits and chondrogenic and osteogenic markers were measured after two treatment strategies: (1) throughout culture period; (2) last 12 hrs of culture. Data are mean \pm SEM (n=6 cultures/variable, ANOVA/Bonferroni's Student's t-test). In MSCs, Wnt1, Wnt5a, and Wnt11 increased osteogenic markers RUNX2, ALP, and BGLAP, with Wnt5a inducing the most robust response. Chondrogenic markers SOX9, ACAN, COMP, and COL2 increased in MSCs after Wnt5a, Wnt5b, and Wnt11 treatments. In CH, Wnt5a, Wnt5b, and Wnt11 strongly increased SOX9, ACAN, COMP, COL2, while Wnt1, Wnt3a, and Wnt7a increased COL1 and decreased SOX9 and COL2. In OB, all Wnts tested increased ALP. Wnt5a and Wnt11 increased RUNX2 and BGLAP, while Wnt7a increased RUNX2. Interestingly, Wnt5a, Wnt5b, and Wnt11 decreased ITGA5 in all cell types, but increased collagen receptors ITGA1, ITGA2, and ITGB1. Wnt3a increased ITGA5 in all cell types and decreased ITGA2 in OB and ITGA1 in CH. The effect of Wnts on integrins was more robust in MSCs. Canonical Wnt activators decreased chondrogenic markers and collagen receptors, suggesting the ligands tested are not involved in adult chondrogenesis or osteogenesis. The results indicate that Wnts have similar effects on MSC, CH, and OB. Wnt5a, Wnt5b, and Wnt11, activators of the Wnt/calcium-dependent pathway, increased chondrogenic and osteogenic markers in MSCs, increased chondrogenic expression in CH, and increased osteogenic expression in OB. This suggests that Wnts induce chondrogenesis and osteogenesis in undifferentiated cells and maintain the phenotype of mature chondrocytes or osteoblasts.

Disclosures: Rene Olivares-Navarrete, None.

SU0171

Dual Effects of Adiponectin During Osteoblast Differentiation Through pSmad1/5/8 Signaling Pathway. Liming Yu^{*}, Qisheng Tu, Jake Jinkun Chen. Tufts University School of Dental Medicine, USA

Adiponectin (APN) is an adipokine associated with insulin resistance and obesity. However, its effects on osteogenesis remain controversial and unclear. The present study aims to determine the signaling pathways and transcriptional regulators in adiponectin-enhanced osteoblast function and its crosstalk with the bone morphogenic protein (BMP) transduction pathway. Cultured MC3T3-E1 cells were treated with ascorbic acid (AA) and globular adiponectin. The signaling pathway of adiponectin in osteoblastic differentiation was investigated through BMP signaling pathway by real-time quantitative PCR and western blot analysis. The osteogenic mRNA gene expression and SMAD1/5/8 phosphorylation were detected. Following AA induction for 0d, 3d, and 7d, SMAD1/5/8 phosphorylation was upregulated at 10, 20, and 30 min after globular adiponectin treatment. There was peak activation after 30 min of adiponectin treatment, especially at a low dose, while pSMAD1/5/8 was down-regulated when stimulated with globular adiponectin after 14d of induction, specifically at a high dose (Figure 1). The osteogenic genes, specifically BSP (bone sialoprotein) and OCN (osteocalcin), mRNA expression significantly increased in the early osteoblastic induction stage and decreased at the late stage. Runx2, a key transcriptional regulator in osteogenesis, was not significantly increased or decreased during globular adiponectin treatment. The mRNA expression of Osterix and Satb2 were decreased when stimulated with globular adiponectin at the late stage. We concluded, for the first time, that globular adiponectin has a positive effect of osteoblast differentiation in the early stage, while having a negative effect at the late stage. The dual effects of adiponectin on osteoblastic differentiation are through the pSMAD1/5/8 signaling pathway.

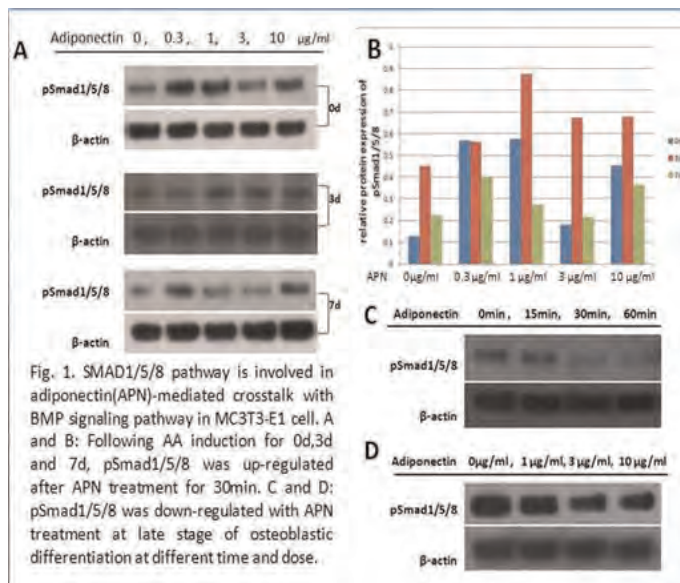


Figure 1

Disclosures: Liming Yu, None.

This study received funding from: NIH grants DE16710 and DE21464 to JC

SU0172

Immunological Phenotype in a Mouse Model of Osteogenesis Imperfecta. Thomas Lisse^{*1}, Svetoslav Kalaydjiev², Dirk Busch², Martin Hrabec de Angelis². ¹Mount Desert Island Biological Laboratory, USA, ²Helmholtz Zentrum Munich, Germany

Osteogenesis imperfecta (OI) is an inherited disorder characterized by increased bone fragility, fractures, and osteoporosis, and most cases are caused by mutations affecting the type I collagen genes. Inflammation is a complex cellular and humoral response against trauma and infection, and its presence leads to destruction of tissue in humans. Here we describe the immunological differences in a mouse model for OI termed *Aga2* (abnormal gait 2) that was isolated from the Munich N-ethyl-N-nitrosourea mutagenesis program. *Aga2*⁺ animals had markedly increased activated T helper (CD4⁺ ~60% increase) and regulatory (CD4⁺/CD25⁺) and B (CD19⁺/CD5⁺) cells suggesting an adaptive immune response to potential soluble or infectious factors. ELISA for IgG isotypes confirmed the B cell response. Furthermore, *Aga2*⁺ animals showed a pronounced NK/T cell (CD3⁺ DX5⁺) response suggesting suppression of a potent immune response during disease progression. Interestingly, the myeloid precursor (CD11b⁺/Gr⁻) population was decreased in *Aga2*⁺ mice, suggesting the differentiation of more professional macrophages such as osteoclasts during inflammation. These observations were more prevalent in female animals. Collectively, these results suggest a potent inflammatory response in the OI animal model. Further detailed immunological analysis in this OI animal model may provide molecular insights into the complex nature of inflammatory diseases and the relationship between inflammation and bone metabolism.

Disclosures: Thomas Lisse, None.

SU0173

Intermittent in vivo Parathyroid Hormone (PTH) Treatment Decreases Apoptotic Rates of Hematopoietic Stem Cells (HSCs) Prior to Expanding Their Numbers. Isamat Shafiq¹, Benjamin Frisch^{*1}, Rebecca Porter¹, Julianne Smith¹, Olga Bromberg¹, Miles Basil¹, Robinder Dhillon², Edward Schwarz², Laura Calvi³. ¹University of Rochester School of Medicine & Dentistry, USA, ²University of Rochester, USA, ³University of Rochester School of Medicine, USA

HSCs are rare primitive cells capable of reconstituting all blood cell lineages throughout the life of an individual. Our group and others have established that activation of osteoblastic cells by PTH increases HSCs. Apoptosis is an important HSC fate choice, and thus, could cause the PTH-dependent HSC expansion. To determine if in vivo PTH treatment decreases HSC apoptosis rate, C57B/6 mice were treated intermittently with saline or PTH (40ug/Kg) for 28 days. Flow cytometric analysis can enumerate the HSC-enriched lineage *Sca-1*⁺ *c-kit*⁺ (LSK) cell pool as well as subsets: long term HSCs (LT-HSCs), short-term HSCs (ST-HSCs), and multipotent progenitors (MPPs). PTH significantly increased LSK cells and all 3 subsets in the marrow by the 10th day of treatment through day 28. Despite a lack of increased HSCs by phenotypic analysis at 7 days of treatment, marrow from PTH treated mice displayed an increase in LT-HSC function as measured by competitive

repopulation assays with superior engraftment through 16 weeks. Therefore we determined to measure the effect of PTH on apoptotic rates of HSCs using Annexin V membrane expression. By the 7th day of PTH treatment, LT-HSC apoptotic rates were decreased in the PTH treated group compared to vehicle (VEH/ PTH 10.482+ 2.25 vs. 6.27+ 1.93, $p \leq 0.01$) suggesting that changes in LT-HSC apoptosis precede the HSC increase. These results were confirmed by flow cytometric measurement of activated caspase 3. PTH treatment decreased the percentage of LT-HSCs that were positive for activated caspase 3 (VEH/ PTH 4.3+ 0.5 vs. 2.4+ 0.3, $p \leq 0.01$). Both Annexin V as well as caspase 3 analyses revealed that PTH treatment also significantly reduces the rates of apoptosis in both ST-HSCs and MPPs. PTH induced micro-architectural changes in trabecular bone at day 7 of treatment suggesting bone involvement despite the lack of an increase in bone volume. These results suggest for the first time that PTH may exert its beneficial effect on bone marrow reconstitution at least in part by decreasing apoptosis of HSCs. PTH induced survival of HSCs may be mediated by secondary factors such as prostaglandins as PTH is known to increase the expression of cyclooxygenase. Additionally, since stressful manipulation of HSCs *ex vivo* is essential for their use in transplantation, defining factors regulating and decreasing their apoptosis may dramatically improve their engraftment efficiency, expanding their clinical use when their numbers are limited.

Disclosures: Benjamin Frisch, None.

SU0174

Non-canonical Wnt5a and Secreted Frizzled Related Protein-1 (sFRP1) Stimulate Expression of CXCL5 and CXCL8 Chemokines in Part via Bone Morphogenetic Protein (BMP) and Mitogen-activated Protein Kinase (MAPK) Signaling in Human Mesenchymal Stem Cells (hMSCs). David Bischoff*, Jian-hua Zhu, Weibiao Huang, Nalini Makhijani, Dean Yamaguchi. VA Greater Los Angeles Healthcare System, USA

We had previously demonstrated that CXC chemokines such as CXCL1 and CXCL8 are elaborated from hMSCs during osteogenesis and may be involved in angiogenic stimulation during bone repair. Differentiation of hMSCs with osteogenic differentiation medium (OGM) and dexamethasone (DEX), an OGM component, also increased CXCL5 mRNA expression 8- and 5-fold, respectively, compared to HMSCGM control medium (OGM: 17.11+/-0.78; DEX: 11.23+/-2.10, n=4 vs HMSCGM: 2.06+/-0.78, n=8 $p < 0.001$). RoR2, a co-receptor for non-canonical Wnt signaling was also significantly up-regulated by OGM and DEX approximately 12-fold compared to HMSCGM. Ru486, a glucocorticoid receptor antagonist completely inhibited the OGM- and DEX-stimulated increases in RoR2 (Ru486+OGM: 0.88+/-0.63 vs Ru486+DEX: 1.40+/-0.56 n=3). Thus it was tested if the non-canonical Wnt pathway was involved in the stimulation of CXCL5 in OGM. Conditioned medium (CM) from L-cells expressing Wnt5a, a non-canonical Wnt, stimulated a 3-fold increase in CXCL5 mRNA expression (6.93+/-3.53 vs 2.35+/-2.16, n=16, $p < 0.001$) and an increase in CXCL5 protein secretion (2.01+/-0.24 vs 1.32+/-0.40 pg/ml n=3, $p < 0.05$) in comparison to control L-cell CM. sFRP1, which should inhibit both canonical and non-canonical Wnt signaling enhanced the expression of CXCL5 at 7 days of culture (control: 1.71+/-0.85, sFRP1: 6.22+/-1.36, n=6, $p < 0.001$) and 10 days of culture (control: 0.88+/-0.66, sFRP1: 5.50+/-1.02, n=6, $p < 0.001$), and CXCL8 at 7 days (control: 0.31+/-0.22, sFRP1: 17.74+/-0.62, n=6, $p < 0.001$). Dkk-1, an inhibitor of canonical Wnt signaling did not inhibit CXCL5 induction. sFRP1 stimulated phosphorylation of extracellular signal-regulated kinase (ERK) in hMSCs with maximum stimulation at approximately 5 minutes after sFRP1 addition. BMPs are known to induce osteogenesis; noggin, a BMP inhibitor, was found to decrease the expression of sFRP1-stimulated CXCL5 and CXCL8 mRNA by approximately 50% at 7 days of culture (CXCL5: 7.01+/-2.86 vs 3.98+/-0.79, n=6 $p < 0.05$; CXCL8: 11.80+/-4.38 vs 6.48+/-0.69, n=6 $p < 0.01$) but not at 10 days. Conclusions: 1) the expression of the CXC chemokine, CXCL5, was enhanced in hMSCs undergoing osteoblastogenesis; 2) the non-canonical Wnt pathway appears to be involved in CXC chemokine expression during osteogenic differentiation; 3) sFRP1 which further stimulated CXCL5 and CXCL8 mRNA expression in OGM may do so independently of the non-canonical Wnt pathway and in part via BMP and MAPK signaling.

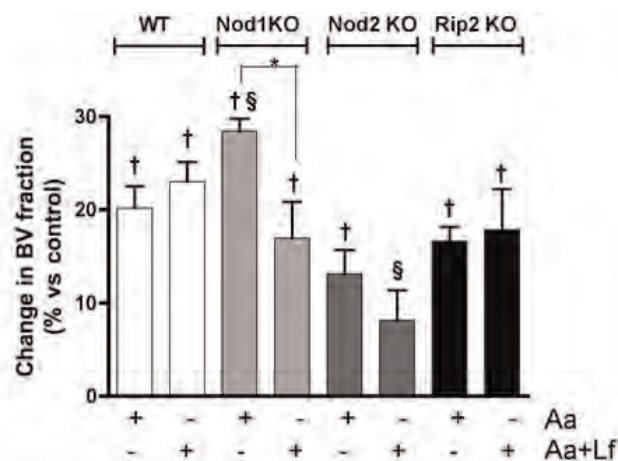
Disclosures: David Bischoff, None.

SU0175

Role of Nod Signaling on Bone Resorption in Experimental Periodontal Disease. Joao A C de Souza¹, Marcell C Medeiros¹, Sabrina C T Frasnelli¹, Fernanda R G Rocha², Mario J Avila-Campos³, Dario S Zamboni⁴, Carlos Rossa⁵. ¹Sch of Dentistry at Araraquara-Univ Estadual Paulista (UNESP), Brazil, ²School of Dentistry at Araraquara-Univ Estadual Paulista (UNESP), Brazil, ³Biological Sciences Institute-Univ de Sao Paulo (USP), Brazil, ⁴Sch of Medicine of Ribeirao Preto-Univ de Sao Paulo (USP), Brazil, ⁵School of Dentistry at Araraquara - Univ Estadual Paulista (UNESP), Brazil

Recognition of pathogenic bacteria by the host is initially mediated by the innate immune response through detection of pathogen-associated molecular patterns by Toll-like receptors and Nucleotide-oligomerization domain (Nod) proteins. There is lack of information on the *in vivo* role of Nod signaling in the modulation of host-bacteria interactions in the oral mucosa. Our hypothesis is that Nod proteins play an

important role in the modulation of the immune response and the resultant bone resorption associated with periodontal disease. We used Nod1, Nod2 and Rip2 knockout mice in a C57/Bl6 background and also wild-type mice of the same strain as controls. Periodontal disease was induced by injections of PBS suspensions of heat-killed Gram-negative *Aggregatibacter actinomycetemcomitans* (Aa) (3×10^6 UFC) or of Aa associated with Gram-positive *Lactobacillus fermentans* (Lf) (1.5×10^6 UFC of each) in the palatal mucosa adjacent to the first molar. Controls received injections of the same volume of PBS diluent. Injections were performed 3x/week under inhalation anesthesia and all animals were killed after 15 days (6 injections). Maxillae were dissected, fixed in 10% buffered formalin for 24 h and transferred to 70% ethanol. Bone resorption was assessed by microcomputer tomography using 18 μ m slices. A standardized region of interest (ROI) of 2 mm² (2 mm in mesio-distal width and 1 mm in the apico-coronal direction) was created on the middle section between the buccal and lingual aspects of the first molar. This ROI included the teeth plus 180 μ m towards the middle of the palate, in a total volume of 3,200 μ m³. In WT mice, injections of Aa produced significant bone resorption, which was discretely increased when Aa+Lf were injected. A significantly greater severity of bone loss was observed in Nod1 KO animals injected with Aa alone, whereas in the presence of Lf bone resorption was significantly inhibited. Nod2 signaling is also relevant to the alveolar bone loss, as significant decreases on the severity of bone resorption was observed in Nod2 KO animals, especially in the presence of Lf. In Rip2 KO animals, representative of simultaneous deficiency of both Nod1 and Nod2 signaling, bone resorption was attenuated but with a similar pattern observed in WT animals. We conclude that Nod1 and Nod2 signaling play important and non-redundant roles in the microbial-induced alveolar bone resorption associated with experimental periodontal disease.



† : $p < 0.05$ vs PBS-injected control in the same genotype

§ : $p < 0.05$ vs same stimulus in WT animals

* : $p < 0.05$ for the difference between Aa and Aa+Lf stimulation

Figure μ CT data

Disclosures: Carlos Rossa, None.

This study received funding from: Fundacao de Amparo a Pesquisa do Estado de Sao Paulo (FAPESP) - 2010/05783-5

SU0176

Estrogen by Genotype Interactions Define Bone Mass and Body Composition in Female *Igfbp2*-/- Mice. Victoria Demambro¹, Casey Doucette¹, Phuong Le¹, David Clemmons², Clifford Rosen³. ¹Maine Medical Center Research Institute, USA, ²University of North Carolina, USA, ³Maine Medical Center, USA

We previously reported that global KO of *Igfbp2* (-/-) leads to a sexual dimorphic phenotype such that the male -/- mice have low bone mass and increased adiposity whereas female -/- have normal bone mass and weight. To elucidate if this dimorphism was due to an interaction between IGFBP-2 and estrogen we ovariectomized (OVX) and sham operated 8wk -/- and +/+ mice. We also performed *in vitro* MC3T3E1 studies with escalating doses of estradiol and *ex vivo* metatarsal cultures treated with estradiol. OVX caused significant weight gain in both genotypes; however, OVX -/- mice gained less body weight ($p = 0.04$) and % fat ($p = 0.03$) compared to OVX +/+ mice. Analysis of the intra-abdominal fat compartment by *in vivo* μ CT confirmed these differences ($p = 0.007$). Sham -/- femurs had increased marrow adiposity (MAT) compared to +/+, but OVX on the other hand, caused a decrease MAT in the -/- mice, but an increase in the OVX +/+ femurs. Inguinal fat pad gene expression following OVX showed increases in "brown-like" adipogenic genes including *Ucp1* in both genotypes although the -/- mice exhibited the greatest rise. OVX caused decreases in aBMD and aBMC in both genotypes, with the greatest decrease in the OVX -/- vs. +/+. MicroCT of the femoral midshaft confirmed these changes with an 11.5% loss of cortical thickness in the OVX -/- vs. a 5.5% loss in the OvX +/+. In the distal femur there were significant decreases in %BV/TV with OVX in the -/- that were greater than

+/- controls ($p=0.01$), including changes in trabecular number ($p=0.03$) rather than trabecular thickness ($p=0.4$). Serum CTx was higher in OVX -/- vs. OVX +/- ($p=0.001$), as was serum adiponectin ($p=0.06$). Following OVX in the +/- mice, there was a marked decrease in serum levels of IGFBP-2 ($p=0.003$). MC3T3 cells cultured with estradiol secreted higher levels of IGFBP-2 in the culture media vs. MC3T3 alone. Furthermore, ex vivo +/- metatarsals cultured in the presence of estrogen had increases in length ($p=0.05$) and levels of IGFBP-2 ($p=0.02$). These data suggest a positive interaction between estrogen and IGFBP-2. Removal of IGFBP-2 alone is not sufficient to recapitulate the male -/- phenotype, yet when both estrogen and IGFBP-2 are removed, there is heightened bone loss. However, OVX in -/- mice also increased sympathetic tone, which can explain the reduced adiposity and may contribute to the increased bone loss in the female -/- mice following OVX.

NIH-R01 AR061164-01A1

Disclosures: Victoria Demambro, None.

SU0177

Matrix IGF-1 Regulates Bone Mass by Activation of mTOR in Mesenchymal Stem Cells. Lingling Xian*¹, Xiangwei Wu¹, LIJUAN PANG¹, Michael Lou¹, Clifford Rosen², Tao Qiu¹, Janet Crane³, Frank Frassica¹, Liming Zhang¹, Juan Pablo Rodriguez⁴, Xiaofeng Jia⁵, Shoshana Yakar⁶, Argiris Efstratiadis⁷, Shouhong Xuan⁸, Mei Wan¹, Xu Cao³. ¹Johns Hopkins University School of Medicine, USA, ²Maine Medical Center, USA, ³Johns Hopkins University, USA, ⁴The University of Chile, Chile, ⁵Department of Biomedical Engineering, Johns Hopkins University School of Medicine, USA, ⁶New York University COLLEGE OF DENTISTRY David B. Kriser Dental Center, USA, ⁷Department of Genetics & Development, Columbia University, USA, ⁸Columbia Univ. Medical Center, USA

IGF-1 is known in regulation of animal size and longevity. It is the most abundant factor deposited in the bone matrix and regulates skeleton growth and peak bone mass. We investigated the mechanism of IGF-1 in maintenance of bone mass. We found that IGF-1 stimulates phosphorylation of IGF1R, IRS1, PI3K, Akt and mTOR in Sca-1⁺ MSCs. IGF-1-induced osteoblastic differentiation of Sca-1⁺ MSCs and mineralization were inhibited by PI3K inhibitor or rapamycin (mTOR inhibitor). Furthermore, siRNA knockdown of IRS1 inhibited phosphorylation of PI3K, Akt and mTOR induced by IGF-1. Rapamycin inhibited IGF-1-induced expression of osteix, Runx2, alkaline phosphatase, osteocalcin, osteoglycin and osteonectin. Sca-1⁺ *Igf1r*^{-/-} or *Igf1r*^{fl/fl} MSCs were transplanted underneath the renal capsule of immuno-deficient *Rag2*^{-/-} mice with injection of rapamycin or vehicle daily for 4 weeks. Rapamycin inhibited mineralization and differentiation of MSCs in histological analysis. Moreover, subcutaneous injection of rapamycin in wild-type mice showed that osteocalcin-positive osteoblasts decreased significantly at the bone surface trabecular bone deficits, indicating that the IRS1-Akt-mTOR activation is essential for MSC differentiation in bone formation.

We then examined IGF-1 levels in bone matrix and found that the decrease of IGF-1 levels in the bone matrix correlates with decrease of bone mass during aging of rats. Osteoporotic patients with hip fractures were also found to have 40% lower IGF-1 levels in bone marrow serum relative to controls. To assess whether IGF Binding Protein 3 (IGFBP3) regulates IGF-1 activity in bone, we injected IGF-1/IGFBP3 into the distal femur cavity of aged rats once a week for 4 weeks. Co-injection with IGF-1/IGFBP3 produced a higher level of IGF-1 in the bone matrix along with improvement in trabecular mass and micro-architecture. Furthermore, we investigated whether systemic IGF-1 and IGFBP3 can target and become immobilized in the bone matrix. IGF-1/IGFBP3 was delivered for 4 weeks via osmotic pumps embedded subcutaneously into IGF-1 gene deletion liver-induced-deficient (LID) mice. Infusion of IGF-1/IGFBP3 significantly increased both IGF-1 and IGFBP3 in the bone matrix and enhanced trabecular bone formation relative to LID mice infused with vehicle or IGF-1 alone. Thus, IGF-1 released during bone resorption from matrix activates mTOR to induce osteoblast differentiation of MSCs in maintaining bone micro-architecture and mass.

Disclosures: Lingling Xian, None.

SU0178

FSH Limits Osteon Size and Regulates Development of Osteoblasts in a Process that also Responds to High Levels of HCG. Harry Blair*¹, Irina Tourkova¹, Li Liu¹, Li Sun², Lisa Robinson¹, Mone Zaidi³. ¹University of Pittsburgh, USA, ²Mount Sinai School of Medicine, USA, ³Mount Sinai Medical Center, USA

Previously we showed that osteoclast development, survival, and activity are enhanced by FSH, via receptors expressed in pre-osteoclastic cells and in osteoclasts. The effect is mediated by a non-cAMP dependent alternative FSH receptor complex. Here we report that FSH receptors also occur in mesenchymal stem cells (MSC) and to a lesser extent in osteoblast precursors. We studied the role of FSH in regulating these bone forming cells. Using FSH- β negative mice, we demonstrate dysregulated osteon activity with very long unbroken fronts of bone formation and dual calcein labels. In isolated human MSC, or in the hOB osteoblast precursor fraction, we also demonstrate response to FSH. This response is mediated by an alternative receptor

complex with an FSH splice variant which, by PCR, is identical to the form missing exon 9 that we previously characterized in human osteoclasts. The receptor responds to FSH at physiological levels (25 ng/ml) via MAP kinase intermediate signals including phospho-Erk1/2, at times as short as 10 minutes. This response occurs without detectable cAMP signaling, a hallmark of the classical FSH receptor response. Other changes in response to FSH include ~ 2 fold upregulation of NO synthase activity in hOBs, where NO can downregulate proliferation and promotes maturation of the cells, suggesting that this is a component of the process that limits the bone forming unit when FSH is present, particularly at high levels. In carrying out this work, we used, as a control, HCG. Surprisingly, at high concentrations of HCG (1000 ng/ml) hOB cells showed response at 10 min in Erk1/2 phosphorylation that was similar to that induced by 25 ng/ml of FSH. This suggests that HCG at high levels signals by a similar process, possibly by variant FSH-R itself. This in turn might account for findings using biological assays in human pregnant serum of "FSH like" activity, while molecular assays, done by others, showed that no meaningful amount of FSH exists in pregnant serum. Our findings show that bone formation responds to FSH to limit the size of bone forming units and are consistent with the role of FSH in promoting bone turnover by osteoclasts that we previously defined. Our findings are also consistent with changes in bone mass in FSH-R or FSH deficient animals, and the incidental finding of response to high levels of HCG may help explain puzzling physiological changes noted during pregnancy as a result of very high HCG levels.

Disclosures: Harry Blair, None.

SU0179

Effects of Activin A and Follistatin on the Differentiation of Aged Primary Bone Marrow Stromal Cells (BMSCs) and Primary Myoblasts in vitro. Xingming Shi*¹, Matthew Bowser², Nianlan Yang¹, Linlin He¹, Samuel Herberg¹, Sadanand Fulzele¹, William Hill³, Carlos Isales⁴, Mark Hamrick¹. ¹Georgia Health Sciences University, USA, ²Georgia Health Science University, USA, ³Georgia Health Sciences University & Charlie Norwood VAMC, USA, ⁴Medical College of Georgia, USA

The activin A-follistatin system is thought to play an important role in the regulation of muscle and bone mass throughout growth, development, and aging. We have previously found that activin protein levels are increased in bone marrow supernatant of aged mice relative to its antagonist follistatin, whereas follistatin levels are significantly decreased in skeletal muscle of aged mice. In order to better understand the effects of these factors on osteogenesis, adipogenesis, and myogenesis we isolated primary bone marrow stromal cells (BMSCs) and myoblasts from the hindlimbs of young (12 mo) and aged (24 mo) mice. BMSCs cultured in adipogenic or osteogenic medium were treated with increasing doses of either activin A or follistatin, and myoblasts cultured in myogenic medium were also treated with either activin A or follistatin. Oil Red O staining of BMSCs cultured in adipogenic conditions demonstrate that activin is a potent inhibitor of adipogenic differentiation in vitro, whereas alizarin red staining of BMSCs in osteogenic conditions shows that activin A is mildly osteogenic. Follistatin did not have a marked effect on either adipogenic or osteogenic differentiation of BMSCs. Activin and follistatin both increased proliferation of myoblasts in vitro. Activin A decreased expression of myostatin (GDF-8) and increased expression of IGF-1 in aged myoblasts, whereas follistatin increased myostatin expression and decreased IGF-1 expression in both young and aged myoblasts. Together these findings suggest that activin A has significant effects on the differentiation of both BMSCs and myoblasts, and that age-associated changes in the activin signaling network may impact the repair and regeneration of muscle and bone tissue.

Disclosures: Xingming Shi, None.

SU0180

Adult Patients With Cerebral Palsy Show Negative Bone Balance Specifically More In Spastic Type. Won Jin Kim*¹, Sung-Rae Cho², Yumie Rhee¹. ¹Department of Internal Medicine, College of Medicine, Yonsei University, South Korea, ²Department of Rehabilitation Medicine, Yonsei University, College of Medicine, South Korea

Patients with cerebral palsy (CP) patients are known to have low bone mass with increased risk of fragility fracture. CP is classified into four major types: spastic, ataxic, dyskinetic and mixed. Spastic CP is the most common type which is characterized by hypertonicity and impaired neuromuscular mobility. In comparison, dyskinetic CP shows mixed muscle tone with involuntary motions. The aim of this study is to discover the relationship between bone mineral density (BMD) by dual X-ray absorptiometry according to the type of CP. Fifty four patients with CP (age 19 to 60 years, mean age 36.4 y.o., 29 males and 25 females) were included for this cross-sectional analysis. Lumbar spine (LS) and femoral BMD Z-score were measured. Bone markers, including C-telopeptide (CTx) and osteocalcin (OCN), were also analyzed. Among these patients, there were 22 spastic and 32 dyskinetic type of CP. Z-score of LS BMD was not different between two types of CP. Meanwhile, Z-score of total hip and trochanteric BMD were significantly lower in spastic type than dyskinetic type (-1.62 ± 0.25 vs. -1.06 ± 0.19, -1.64 ± 0.23 vs. -0.95 ± 0.20, respectively, $p < 0.05$). As their ambulatory ability varied, all patients were sub-classified into 3 groups: totally dependent non-ambulatory group, wheelchair-bound group, and independently ambulatory group. Totally dependent ambulatory patients showed

significantly lower BMD in hip including trochanteric and total region in spastic CP patients ($p < 0.05$), but not in patients with dyskinetic type. More than half of the patients with either type of CP showed abnormally elevated CTx but about 90% of patients showed normal OCN level compared to the normal control range. These results reveal that reduced weight bearing and immobilization of CP patients cause negative bone balance due to increased bone resorption leading to lower bone mass. Hypertonicity with clonus and muscle spasms of affected limbs in spastic CP patients resulted in more deteriorated bone mass compared with dyskinetic CP type. In conclusion, different type and degree of activity or ambulation in CP patients should be considered as important factors affecting bone metabolism.

Disclosures: Won Jin Kim, None.

SU0181

Withdrawn

SU0182

Evaluation of α SMA Expressing Cell Contribution To Muscle Heterotopic Ossification. Elena Torreggiani¹, Danka Grcevic², Brya Matthews¹, Ivo Kalajzic¹. ¹University of Connecticut Health Center, USA, ²University of Zagreb, USA

Heterotopic ossification is characterized by the formation of bone in atypical locations including muscle and subcutaneous tissues. Enormous progress has been made in understanding the identity of the cells that participate in the lesion formation, and molecular mechanisms underlying the induction of the osteogenic commitment. Several studies addressed to identify the role of BMP signaling in the heterotopic ossification have been performed. However, the identity of progenitor cells that contribute to BMP-induced heterotopic ossification is still unknown.

The aim of our current work is to evaluate whether the cells that reside in the perivascular niche can actively contribute to the bone formation. We have observed the expression of a smooth muscle α -actin promoter directed green fluorescent promoter (α SMA-GFP) in the perivascular location in both muscle and subcutaneous tissue. The critical evidence of the transition of the cellular phenotype can be obtained by combinatorial approach of using visual markers for transgene expression and Cre/loxP recombination system that will allow for the lineage tracing. Therefore we have bred α SMACreERT2 mice with reporter mice in which RFP Tomato expression is controlled by ubiquitous promoter and dependent on Cre activation by tamoxifen. To assess the transition of the α SMA expressing cells to osteoblast lineage we have used a bone specific Col2.3 promoter driving GFP. These mice were intercrossed to generate a triple transgenic model α SMACreERT2/Ai9/Col2.3GFP.

Heterotopic ossification was induced by intramuscular injection of 2.5 μ g of BMP2/Matrigel. The formation of bone ossicles was evaluated by x-ray analysis and mice were sacrificed at different time points. The contribution of α SMACreERT2/Ai9 labeled cells to bone was evaluated using fluorescence microscopy. Our results suggest that α SMA expressing cells can give rise to a population of mature osteoblasts present within heterotopic lesions. Currently, we directed our efforts to better define the cellular phenotype of the α SMACreERT2/Ai9 labeled progenitor cells. We plan to evaluate the α SMACreERT2/Ai9 expression to the presence of endothelial (CD31), hematopoietic (CD45), satellite cells (SM/C2.6) and mesenchymal stem cells (PDGFR α , PDGFR β and Sca1) markers by flow cytometry. This study provides new insight into the cellular identity of cells that participate in the formation of the heterotopic ossification.

Disclosures: Elena Torreggiani, None.

SU0183

Glucocorticoids Induce Atrophy of Bone and Muscle by FoxO- and ATF4-dependent Mechanisms. Nicoletta Bivi¹, Naomie Olivos², Amy Sato¹, David Southern¹, Teresita Bellido¹. ¹Indiana University School of Medicine, USA, ²IUPUI, USA

Excess of glucocorticoids (GC), either endogenous GC as in aging, or due to GC administration as immunosuppressants, leads to loss of bone (osteopenia) and muscle (sarcopenia). Muscle weakness, in turn, reduces body balance and increases the risk of falls and thus of bone fractures, making osteopenia and sarcopenia a public health concern. We hypothesized that the damaging effects of GC in bone and muscle arise from activation of a common pathway. We found that the loss of bone mass induced by GC administration for 14d to C57/Bl6 mice is accompanied by muscle atrophy. GC-treated mice exhibited a significant loss of total lean muscle mass by PIXImus, and reduced weight of the tibialis anterior (TA) muscle, composed mainly of typeII-fast twitch fibers. In contrast, the weight of soleus (SOL) muscle, known to be resistant to GC effect and composed mainly of typeI-slow twitch fibers, remained unchanged compared to placebo control mice. The loss of bone and muscle mass in GC-treated mice was accompanied by enhanced protein degradation machinery, as evidenced by increased expression of the FoxO-target genes E3 ubiquitin ligases Atrogin1 and MuRF1 in vertebral bone as well as in TA muscle, but not in SOL muscle. Atrogin1 and MuRF1 expression was also elevated in MLO-Y4 osteocytic cells by 2- and 60-fold and in C2C12 myotubes by 7- and 3.5-fold, respectively, after 24h treatment with dexamethasone (Dex, 10⁻⁶M). Furthermore, in MLO-Y4 and OB6 osteoblastic cells, GC decreased the expression of genes regulated by ATF4, a

transcription factor controlling protein synthesis and amino acid transport. Thus, Dex decreased by 30-50% the expression of enzymes involved in the synthesis of nonessential amino acids including glycine and proline (Asns, Mthfd2, Phgdh, Pycr1, and Psat1); and reduced the expression of transporters of essential amino acids (Slc1a4, 7a5, and 7a1). The combination of increased degradation and decreased synthesis resulted in a progressive decline in total protein content per cell, which became significantly reduced by 30% at 72h in Dex-treated MLO-Y4 cells. Taken together, these findings demonstrate that GC favor protein degradation over protein synthesis leading to atrophy of bone and muscle, in vivo in a recognized model of GC excess, and in vitro in osteocytic, osteoblastic and muscle cells. Interventions that interfere with the atrophy pathway might prove beneficial in preventing and treating simultaneously GC-induced osteopenia and sarcopenia.

Disclosures: Nicoletta Bivi, None.

SU0184

Improved Osteochondral Allograft Preservation using Serum-free Chemically-defined Media. Joseph Garrity*, James Cook, Aaron Stoker. University of Missouri, USA

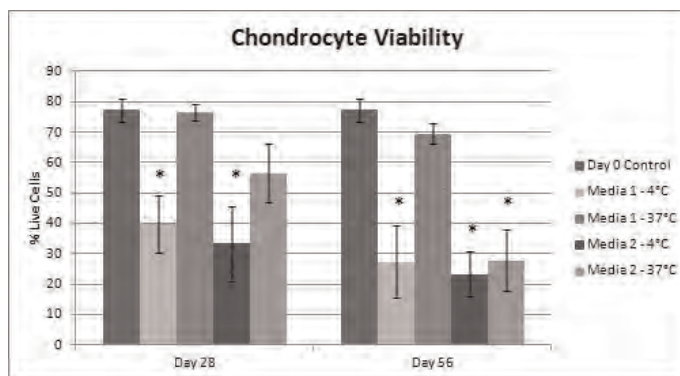
Purpose: Osteochondral allografts (OCAs) are currently preserved at 4°C and used within 28 days of donor harvest. The window of opportunity for implantation is limited to 14 days due to a two week disease testing protocol. This study was performed to assess the effects of storage up to 56 days in a serum-free chemically defined media at 37°C.

Methods: OCAs from 15 adult canine cadavers were aseptically harvested within four hours of death. Medial and lateral femoral condyles were stored in Media 1, a basic media similar to the current standard, or Media 2, an anti-inflammatory and chondrogenic media containing dexamethasone and TGF β 3, at 4°C or 37°C for up to 56 days. Chondrocyte viability, proteoglycan (GAG) and collagen (HP) content, biomechanical properties, and collagen II and aggrecan content were assessed at Days 28 and 56. Five femoral condyles were stored overnight and assessed the next day to serve as controls.

Results: Storage in Media 1 at 37°C maintained chondrocyte viability at significantly higher levels than in any other media temperature combination and at levels not significantly different from controls. OCAs stored in either media at 4°C showed a significant decrease in chondrocyte viability throughout storage. Glycosaminoglycan (GAG) and hydroxyproline (HP) were maintained through 56 days of storage in OCAs in Media 1 at 37°C. There were no significant differences in elastic or dynamic moduli among groups at Day 56. Qualitative immunohistochemistry demonstrated the presence of collagen II and aggrecan throughout all layers of cartilage.

Conclusions: OCA viability, matrix content and composition, and biomechanical properties were maintained at "fresh" levels through 56 days of storage in media 1 at 37°C. OCAs stored at 4°C were unable to maintain viability or matrix integrity through 28 days of storage. These findings suggest that storage of OCAs in a defined media at 37°C is superior to current protocols (4°C) for tissue preservation prior to transplantation. Storage of OCAs in a serum-free chemically-defined media at 37°C can "increase the window of opportunity" for implantation of optimal tissue from 14 days to 42 days after disease testing clearance.

The use of tissues from dogs that have been humanely euthanized for unrelated reasons with documented consent for disposal at the university is allowed by the general rules and regulations of the IACUC.



Chondrocyte viability

SU0186

Withdrawn

SU0187

Muscle-myopathy & X-linked Hypophosphatemic rickets (HYP). Lesya Zelenchuk¹, Anne-Marie Hedge¹, Peter Rowe*². ¹KUMC, USA, ²University of Kansas Medical Center, USA

Hypophosphatemia, rickets, myopathy, muscle-pain, increased bone-cell cathepsin-D and PHEX-related proteases (Nephrilysin, ECEL1/DINE) occur in PHEX-defective mice (HYP). The increased proteases accelerate the release of protease-resistant ASARM-peptides from up regulated bone-SIBLING proteins (MEPE for example). Here we use several murine models and osmotic pump-infusion experiments to unravel the role of cathepsin D, Nephrilysin-like activity and cystatin-C (a serine protease inhibitor) in the pathology of HYP.

HYP mice and "MEPE-null/ASARM-peptide" transgenic mice (MnAt) were used as ASARM-peptide over expressing groups. Wild type (WT) and MEPE null mice (Mn) were used as normal and reduced ASARM-peptide groups respectively. WT and HYP mice were infused with vehicle (VE), ASARM-peptide or a synthetic peptide (SPR4-peptide) that binds and neutralizes ASARM activity (WT-VE, WT-ASARM, HYP-VE and HYP-SPR4 respectively). Serum-urine chemistries were measured and protein/mRNA expressions calculated from femurs and kidneys. Bone marrow stem cell cultures were used to calculate cathepsin D and B enzyme activities. Femurs and kidneys were scanned by micro computed tomography (μ CT).

HYP mice, MnAt mice, and WT-ASARM mice had hypophosphatemia with increased fractional excretion of phosphate (FEP), serum FGF23 and mineralization defects. Bone cultures from HYP mice and WT-ASARM mice displayed increased cathepsin D & B activities. Increased expression of sclerostin occurred with HYP, MnAt and WT-ASARM mice compared with WT mice. Increased cystatin-c expression occurred in HYP mice and MnAt mice compared to WT mice. SPR4 peptide infusion prevented the increased cystatin c expression and suppressed sclerostin expression.

In conclusion, loss of PHEX in HYP-mice results in increased expression of PHEX-related proteases (ECEL1/DINE) and cathepsin D activity. Cathepsin D then activates cathepsin B and inactivates cystatin-C, a serine-protease inhibitor. The resulting increased protease activity degrades matrix SIBLINGs including MEPE and releases protease-resistant ASARM-peptides. The increased acidic ASARM-peptide levels and protease activity likely contributes to the myopathy and bone defects. Also, cystatin-C is a TGF β responsive protein that influences matrix-metalloproteinase 2 (MMP2) and SPARC regulation of myogenesis. Further studies of HYP muscle pathology will increase our understanding of musculoskeletal physiology in disease and health.

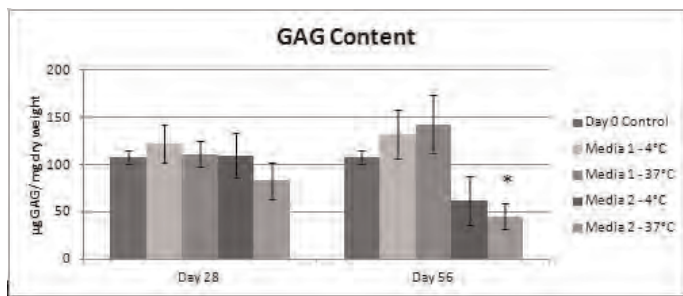
Disclosures: Peter Rowe, None.

SU0188

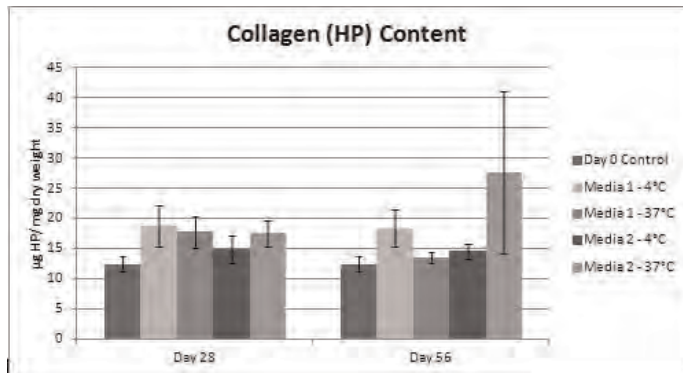
Risk Factors, Frequency and Treatment of Bone Mineral Loss in Survivors of Childhood Allogeneic Bone Marrow Transplantation: A Single Institution Review. Carla McCrave*, Celia Gonzales, Nancy Shreve, Rukhsana Rahmetulla. Children's Mercy Hospital, USA

Recent data from the International Bone Marrow Transplant Registry reported that 14,309 persons less than 21 years of age are alive after undergoing allogeneic bone marrow transplantation (allo BMT) between 1968 and 2002. As a result of the growing success of pediatric allo BMT, an increasing number of long-term survivors are at risk for disease-and-therapy-induced adverse effects, including diminished bone mineral density and osteonecrosis. Little is known about what factors contribute to bone loss in the pediatric allo BMT patient and limited guidelines are available to direct management of these patients. Purpose: evaluate risk factors, frequency, severity and management of bone mineral loss in survivors of pediatric allo BMT. Methods: we will conduct a retrospective review of bone mineral loss in survivors of pediatric allo BMT at Children's Mercy Hospital from 1997 to 2011 to evaluate the following variables: demographic information, bone mineral density using dual photon x-ray absorptiometry (DEXA), parameters significant to bone metabolism (calcium, phosphorus and vitamin D), contributing factors associated with bone loss, and management strategies of bone mineral loss. Summary: investigation of decreased bone mineral density in children who have undergone an allogeneic BMT is needed to determine risk factors, long-term implications, appropriate preventive measures and potential interventions.

Disclosures: Carla McCrave, None.



GAG Content



HP Content

Disclosures: Joseph Garrity, None.

SU0185

Influence of Different Exercise Loading Histories on Bone Marrow Adiposity and Its Relationship to Bone Structure and Strength in Young Female Athletes. Timo Rantalainen*¹, Riku Nikander², Ari Heinonen³, Tomas Cervinka⁴, Harri Sievanen⁵, Robin Daly⁶. ¹Lappeenranta University of Technology, Finland, ²Metropolia University of Applied Sciences, Helsinki, Finland, ³Department of Health Sciences, University of Jyväskylä, Finland, ⁴Department of Biomedical Engineering, Tampere University of Technology, Tampere, Finland, ⁵UKK Institute, Finland, ⁶Centre for Physical Activity & Nutrition Research, Deakin University, Australia

Since osteoblasts and adipocytes share a common bone marrow progenitor cell, it has been suggested that increased loading may bias the cell differentiation towards osteoblastogenesis rather than adipogenesis. This study examined whether marrow adiposity: 1) differs between young female athletes with differing loading histories; and 2) is an independent predictor of cortical density, structure and strength. 179 female athletes involved in high impact (HI: volleyball, hurdling, triple & high jump), odd impact (OI: soccer, tennis, squash, badminton), repetitive, low impact (RL: endurance running), high magnitude (HM: power lifting) and repetitive, non-impact sports (RN: swimming) and 41 controls (CON) were studied. Athletes and controls were aged 17-40 yrs (mean \pm SD: 23 \pm 5 yrs). pQCT was used to assess mid-tibial marrow density (MaD), as an estimate of marrow adiposity, bone geometry, cortical density (CoD) and the strength strain index (SSI). Radial CoD of three concentric rings [endo- (EndoD); mid- (MidD) and peri-cortical (PeriD)] was also assessed. HI, OI and RL groups had 11-31% larger CortAr and SSI (both $P < 0.001$) than HM, RN and CON. In contrast, HI, OI and RL groups had 0.8-2.2% lower total, MidD and PeriD than CON ($P < 0.05$ - < 0.001); there were no differences in EndoD. MaD was lowest in the CON, indicating increased adiposity, but there were no significant differences between the athletic groups and CON ($P = 0.20$). Secondary analysis showed that MaD was higher in the combined impact [HI, OI, RL] versus non-impact groups [HM, RN, CON], indicating lower marrow adiposity [net difference 0.5% (95% CI: 0.2-0.8, $P < 0.05$)]. Multivariate analysis showed that MaD was positively associated with SSI, CoA and PeriD ($P < 0.05$ - < 0.001) and inversely related to EndoD ($P < 0.001$) after adjusting for age, bone length, loading groups, MedAr, muscle CSA and fat%. Overall, MaD explained an additional 1.2% to 4.8% of the variance in these bone traits. In conclusion, female athletes involved in impact sports that increased bone strength had also reduced marrow adiposity compared to athletes involved in non-impact sports and controls. The finding that lower marrow adiposity was also independently associated with greater CortAr and SSI supports the notion that reduced marrow adipocyte infiltration is associated with increased osteoblastogenesis at the expense of adipogenesis.

Disclosures: Timo Rantalainen, None.

SU0189**The Direct and Indirect Costs of Long Bone Fractures in a Working Age US Population.** Machaon Bonafede¹, Derek Espindle¹, Anthony Bower^{*2}.¹Thomson Reuters Healthcare, USA, ²Amgen, USA

Background: Information is limited regarding the costs associated with long bone fractures in a working age population, particularly around lost productivity.

Objective: To estimate the direct and indirect costs associated with long bone fractures in a working age population.

Methods: Adult patients with long bone fractures between 1/1/2001 and 12/31/2008 were identified in the MarketScan Commercial and Health Productivity Management Databases. Costs and utilization, including workplace absenteeism and short term disability, were compared in the 6 months before and after a fracture. Observed incremental costs (i.e., the difference in costs before and after a fracture) were reported in mutually exclusive fracture cohorts. Multivariate adjusted costs were calculated using GLM with fracture type as dummy variables.

Results: A total of 208,094 patients met the study inclusion criteria for the following fracture types: tibia shaft (n=49,839), radius (n=97,585), hip (n=11,585), femur (n=6,788), humerus (n=29,884) and multiple fractures (n=12,413). The average observed direct costs in the 6-months prior to a long bone fracture were as follows: radius (\$3,291), tibia (\$4,175), multiple fractures (\$5,291), humerus (\$5,457), femur (\$8,147) and hip (\$12,923). The average incremental direct cost increase in the 6-months following a fracture ranged from \$5,707 for radius fractures to \$18,965 for femur fractures; observed incremental direct medical costs were \$39,041 for patients with multiple fractures. Incremental observed absenteeism costs ranged from \$886 for radius fractures to \$2,478 for femur fractures and \$3,337 for multiple fractures while incremental short term disability costs ranged from \$1,820 for radius fractures to \$4,131 for hip fractures and \$6,177 for multiple fractures. Multivariate adjustment yielded substantively similar results for both direct and indirect costs outcomes.

Conclusion: Long bone fractures are costly, both in terms of direct medical costs and lost productivity; lost productivity represents a significant portion of the burden of long bone fractures.

Disclosures: Anthony Bower, None.

This study received funding from: Amgen, Inc.

SU0190**The Effect of Sex, Age, and Race on Body Composition.** Lan-Juan Zhao^{*}, Ming-Yi Wei, Yumei Tian, Hong-Wen Deng. Tulane University, USA

Few study estimated the sex effect on body composition in a wide age span in different races. The aim of the study was to estimate how sex and age affect body composition among African American, Caucasian, and Asian population.

A total of 14,356 participants (Age 20-95 years, 2,601 Africa American, 5,167 Caucasian, and 6,588 Asian subjects) were recruited in US and in China. Trunk fat mass (a main obesity phenotype), and limb lean mass (a main phenotype of sarcopenia, a health problem characterized by a decrease in muscle) were measured by Dual-emission X-ray absorptiometry (DXA). Percentage trunk fat mass (PTFM) and percentage limb lean mass (PLLM) were calculated.

For all the three races, before age 75, the females always has lower PLLM and higher PTFM compared to the males (p < 0.001). For both genders, PLLM slowly and steadily decreases with age in all the three races. PTFM increases with age in both genders before age 65. After age 65, the age effect on the body compositions varies with gender and races. African American women decrease their PTFM after age 65.

Racial effect on body composition was more evident in the females than the males. Compared to Caucasian and Asian women, African-American women always had the highest PTFM and lowest PLLM from age 20 to 65. In this age span, Asian women always had the lowest PLLM. The racial effect on body composition varies with age in the males.

In summary, our large sample size study suggested a significant age, race, and sex effect on body composition.

Disclosures: Lan-Juan Zhao, None.

SU0191**Withdrawn****SU0192****The Role of the Proteins of the Nuclear Envelope in the Pathophysiology of Osteosarcopenia.** Sandra Bermeo^{*1}, Christopher Vidal², Wei Li³, Diane Fatkin⁴, Gustavo Duque⁵. ¹PhD Student, Australia, ²University of Sydney, Australia, ³Ageing Bone Research Program, Sydney Medical School Nepean, The University of Sydney, Australia, ⁴Victor Chang Institute, Australia, ⁵Ageing Bone Research Program, University of Sydney, Australia

INTRODUCTION: Sarcopenia and osteopenia are two components of the frailty syndrome that could share common underlying mechanisms. Recently, we have reported that lamin A/C deficient mice (*Lmna*^{-/-}) show both osteo and sarcopenia together with fat infiltration of muscle and bone (*Tong et al, Mech Ageing and Develop, 2011*). This evidence suggests that the proteins of the nuclear envelope, particularly in the inner nuclear membrane (INM), could play a role in the pathogenesis of osteosarcopenia and frailty. Since all the proteins of the INM are interconnected, in this study we assessed whether changes in lamin A/C expression in *Lmna*^{-/-} mice also affect other proteins of the INM in muscle and bone. METHODS: Sections of the middle of the thigh and total proteins from femoral bone marrow and muscle were obtained from wild type (WT) and *Lmna*^{-/-} mice tested by western blotting and immunofluorescence respectively. Expression of the three major proteins of the INM (Emerin, MAN1 and nesprin-1) were compared between wild type and *Lmna*^{-/-} mice using immunofluorescence and western blotting. RESULTS: Our results showed that *Lmna*^{-/-} mice had a decreased MAN1 expression in both bone and muscle (71 and 83%, respectively) as compared to WT controls (p<0.01). Conversely, there was an increase (~2 fold) of both nesprin-1 and emerin in bone of *Lmna*^{-/-} mice, whereas in muscle we observed no change in the expression of emerin with nesprin-1 being significantly lower in *Lmna*^{-/-} mice (-49%) as compared with their WT controls (p<0.01). CONCLUSION: Absence of lamin A/C is associated with major changes in the expression of other proteins of the INM in muscle and bone. Whereas MAN1 expression is decreased in both tissues, an increase in nesprin-1 and emerin in bone happened concomitantly with stable emerin and lower nesprin-1 in muscle. In conclusion, our results suggest that both, lamin A/C and MAN-1, could play an important role in the pathogenesis of osteosarcopenia while the role of high emerin and nesprin-1 in osteopenia and low nesprin-1 in sarcopenia remains to be elucidated. In conclusion, we report that the proteins of the INM could play different roles in the pathogenesis of osteosarcopenia. The characterization of their specific role and targeted interventions to increase their expression and function could become an effective therapy for frailty in the near future.

Disclosures: Sandra Bermeo, None.

SU0193**Wnt Canonical and Non-canonical Signaling Pathways are Involved in Muscle-Bone Crosstalk.** Sandra Romero-Suarez^{*1}, Mark L Johnson², Lynda Bonewald³, Marco Brotto³. ¹University of Missouri, Kansas City, USA, ²University of Missouri- Oral Biology, USA, ³University of Missouri - Kansas City, USA

Wnt/ β -catenin and Wnt/ Ca^{2+} have been implicated in a variety of developmental processes such as cell differentiation, cell polarity and cell proliferation. We have previously shown, using histomorphometric measurements and gene expression, that 1% and 10% conditioned media from MLO-Y4 osteocyte-like cells (MLO-Y4-CM) and primary osteocytes derived from 4-month wild type mice (PO-CM) enhanced the myogenic differentiation of C2C12 myoblasts into myotubes. This result demonstrated that osteocytes signal to muscles biochemically in a manner never before appreciated (ASBMR, 2011). Wnts are released by bones during mechanical loading. To test our hypothesis that osteocytes can biochemically crosstalk to muscles via Wnts-related signaling, we treated C2C12 muscle cells with 10ng Wnt3a. At this physiological concentration, Wnt3a accelerated myogenic differentiation and enhanced nuclear translocation of β -catenin, which is required for transcription of the key muscle transcription factor MyoD. Wnt/ β -catenin pathway showed to play a crucial role in the enhancement of myogenic differentiation produced by 10ng Wnt3a, MLO-Y4 CM and PO-CM. The potent effect of Wnt3a on stimulating the activation of the β -catenin signaling pathway in C2C12 muscle cells strongly correlated with an increased sensitivity to calcium released from the sarcoplasmic reticulum via IP3 that manifested in the form of calcium oscillations and enhanced response to caffeine in releasing calcium from the sarcoplasmic reticulum. This correlation suggests adaptive changes of the excitation-contraction coupling machinery, which is further supported by robust upregulation of some of the essential genes related to intracellular calcium homeostasis (i.e., IP3R types 1 and 3; Stim-2; Camk2d; and SERCA-1 and 2). We postulate that these changes likely reflect adaptation to enhanced myogenic differentiation and/or that calcium homeostasis modulation is directly linked to transcriptional regulation. In summary, these findings suggest that MLO-Y4 CM and PO-CM through activation of β -catenin signaling pathway modifies intracellular Ca^{2+} release/homeostasis to promote myogenic differentiation. The molecular mechanisms leading to these effects of bone CM in skeletal muscle C2C12 cells are currently under investigation.

Acknowledgments: This work was supported by Missouri Life Sciences Research Board Grants and a NIAMS 1RC2AR058962-01 GO Grant to MJ, LB, andMB.

Disclosures: Sandra Romero-Suarez, None.

SU0194

A Mechanistic Approach to Prevent Palmitate-Induced Lipopoptosis in Human Osteoblasts. Krishanthi Gunaratnam^{*1}, Christopher Vidal², Gustavo Duque³. ¹Sydney Medical School-Nepean Level 5 South Block, Australia, ²University of Sydney, Australia, ³Ageing Bone Research Program, University of Sydney, Australia

Lipopoptosis is defined as an overload of lipids in non-adipose tissues, which induces apoptosis of the cells in their vicinity. In bone, lipopoptosis has been associated with either the presence of fatty acids (FA) (mostly palmitic acid [PA]) or adipokines, which are secreted by adipocytes into the bone marrow milieu in an autocrine manner. However, the mechanisms by which FA trigger osteoblast apoptosis remain unclear. Initially, we assessed the mechanism of lipopoptosis in bone cells *in vitro* by exposing normal human osteoblasts (Ob) (Lonza, Switzerland) to PA (100, 250 and 500uM) at different timed intervals (24, 48 and 72h). Cell survival was quantified by MTS (Promega). Apoptosis was identified by TUNEL assay and electron microscopy. Additionally, the apoptotic pathways were identified using proteomic analysis of 43 apoptosis proteins (RayBio). Proteins showing a significant change were confirmed by Western blot. TUNEL assay showed an increase in DNA fragmentation in PA-treated cells in a dose- and time-dependant manner ($p < 0.05$). Electron microscopy showed nuclear fragmentation, which was more prevalent at higher concentrations of PA. Proteomic analysis identified 4-fold increase in Fas ligand with concomitant increase in the expression of the mitochondrial apoptotic proteins Bax (10%), Bad (2 fold), Cytochrome C (30%) and p53 (1.5 fold) ($p < 0.01$). Furthermore, after identification of the apoptotic pathways, we attempted to rescue Ob from apoptosis by using SP600125, an inhibitor of c-Jun N-terminal kinases (JNK), an essential upstream step in the mitochondrial apoptotic pathway. Cells were treated as previously described in the presence or absence of JNK inhibitor (10uM). JNK inhibitor-treated cells showed a significant and dose-dependant decrease in cytochrome C expression both by Western blot (~ -80%, $p < 0.05$) and immunofluorescence analyses (~ -16%, $p < 0.01$). Finally, at 72h TUNEL assay showed a significant decrease in the number of apoptotic cells in the JNK inhibitor-treated cells. In summary, we have identified that lipopoptosis of Ob is induced through the activation of mitochondrial apoptotic pathways. In addition, regulating the activation of mitochondrial apoptotic pathways could prevent this type of lipopoptosis. The regulation of FA secretion and the inhibition of lipopoptosis would protect Ob against fat and could become a potential therapeutic target for osteoporosis in the future.

Disclosures: Krishanthi Gunaratnam, None.

SU0195

The Effects of Extracellular pH on Proliferation and Differentiation of hBMSCs. Yea Leem^{*1}, Jae-Suk Chang², Dong Yeon Lee³, Kang-Sik Lee⁴. ¹Seoul Asan Hospital, South Korea, ²Ulsan University, Asan Medical Center, South Korea, ³Kangwon National University Hospital, South Korea,

Objective: Extracellular surroundings such as pH can affect activity, morphology, and function of various cells including osteoblast. Change of pH by metabolic process, fracture, and implantation may effect on proliferative and differential capacity of osteoblast. The purpose of the current study is to identify whether the change of pH affects the proliferation and the differentiation of human Bone Marrow Stem cells (hBMSCs) and what mechanism is involved with.

Methods: To achieve objective of the current study, hBMSCs were cultivated in the conditioned media adjusted to pH ranging from 6.4 to 8.0 using addition of HCl and NaOH. The ratio of proliferation of hBMSCs with pH was measured for 24h, 48h, and 72h using WST-8 method. To elucidate the underlying mechanism involved, hBMSCs was subjected to blocking ERK and CaSR activation. The Osteogenic-related genes and ALP activity were tested under the conditioned media.

Results: The proliferation of hBMSCs was promoted under extracellular alkali conditions (pH 7.6-8.0) via CaSR/ERK pathway evidenced by increased Runx2, Alkaline phosphatase, and Osteocalcin expression concomitant with CaSR and ERK activation. On the other hand, the differentiation was inhibited/delayed via decreased ALP activity besides gene expression at pH 8.0.

Conclusion: Extracellular alkali or acidic surrounding according to pH alteration can play a crucial role in hBMSC behavior including the proliferation and the differentiation.

Disclosures: Yea Leem, None.

This study received funding from: This work was supported by Korean Ministry of Health, Welfare, and Family Affairs (MHWFA grant A084697)

SU0196

Adherent Bacterial Lipopolysaccharide Inhibits the Osseointegration of Orthopaedic Implants. Lindsay Bonsignore^{*}, Joselyn Tatro, Goldberg Victor, Edward Greenfield. Case Western Reserve University, USA

Osseointegration is the process by which an orthopaedic implant makes direct bone-to-implant contact (BIC) and is crucial for the long-term function of the implant. Contaminants, such as bacterial debris and manufacturing residues, can remain on orthopaedic implants after sterilization and impair osseointegration. For example, a specific lot of implants that was associated with impaired osseointegration and high failure rates was discovered to have contaminants including lipopolysaccharide (LPS). In addition, LPS adheres to implant surfaces sterilized and packaged by an orthopaedic implant manufacturer. LPS on implants may inhibit osseointegration because soluble LPS and LPS adherent to implant surfaces inhibits osteoblast differentiation in cell culture. We therefore, tested the hypothesis that adherent LPS inhibits the osseointegration of orthopaedic implants using our murine model of osseointegration. Titanium alloy implants, used clinically for craniofacial surgery, were implanted into a unicortical pilot hole in the mid-diaphysis of the femur and osseointegration was analyzed by histomorphometry and biomechanical pullout testing. We found that the percentage of BIC was inhibited in a dose dependent manner in mice with implants with adherent LPS. Thus, 200 EU/m² of LPS inhibited BIC by 15% at one week after implantation, 1200 EU/m² inhibited by 39% ($p = 0.017$), and 8500 EU/m² inhibited by 47% ($p = 0.003$). This inhibition of BIC by LPS was maintained throughout a four week time course ($p < 0.001$). Adherent LPS also significantly inhibited biomechanical pullout measures of ultimate force and stiffness at two weeks after implantation. Adherent LPS inhibited osseointegration by signaling through its cognate receptor TLR4 because adherent LPS did not affect BIC in TLR4-/- mice and TLR4-/-/TLR2-/- mice but inhibition by adherent LPS was similar in wild-type mice and TLR2-/- mice ($p < 0.05$). Our results may reflect cell autonomous effects on osteoblasts because we have previously shown that LPS adherent to implant surfaces inhibits osteoblast differentiation in cell culture. These results provide further rationale for development of better detection and removal methods for LPS on orthopaedic implants.

Disclosures: Lindsay Bonsignore, None.

SU0197

Arl6ip5 Controls Rankl Intracellular Trafficking in Osteoblasts and Thereby Suppresses Osteoclast Formation. Yu Wu^{*1}, Jun Fan¹, Ying Peng¹, Yuedi Ding¹, Runlin Yang¹, Lili Deng¹, Jianwei Zhou², Dengshun Miao³, Qiang Fu⁴. ¹Jiangsu Institute of Nuclear Medicine, China, ²Nanjing Medical University, China, ³Nanjing Medical University, Peoples Republic of China, ⁴Institute of Nuclear Medicine, Peoples Republic of China

The expression of Rankl in osteoblastic cells is stimulated by locally acting or circulating osteotropic cytokines and hormones such as interleukins, PTH, and 1,25-(OH)₂-D₃ during the bone remodeling process. However, mechanisms that control subcellular trafficking events, membrane expression, and extracellular secretion of the newly synthesized Rankl, which are essential for the communication between osteoblastic cells and osteoclastogenic cells, are still unclear. It has been shown previously that intracellular Rankl is mainly localized to the lysosome in osteoblast-like cell ST2 cells and primary osteoblasts. Here we found that Arl6ip5 (ADP-ribosylation-like factor 6 interacting protein 5), an endoplasmic reticulum (ER)-localized protein belonging to the prenylated rab-acceptor-family interacting with small Rab GTPases, regulates intracellular trafficking of Rankl. After reduction of Arl6ip5 protein levels in UAMS32 stromal/osteoblastic cells by RNA interference, Rankl protein was mainly localized at the plasma membrane but not in the endoplasmic reticulum (ER) or in the lysosome. The amount of soluble Rankl in UAMS32 culture supernatant was increased after PTH treatment. Similar results were obtained in primary osteoblasts extracted from *Arl6ip5* knockout mice (*Arl6ip5*^{fl/fl;E11a-Cre}). The over-expression of hemagglutinin (HA)-tagged Arl6ip5 in UAMS32 cells increased Rankl retention in the ER and decreased its presence at the cell surface. Co-cultured of UAMS32 cells with reduced Arl6ip5 levels, or *Arl6ip5* knockout primary osteoblasts, with non-adherent bone marrow cells from normal mice increased the formation of mature osteoclasts, compared with cells expressing Arl6ip5, and the results were reversed after re-express of Arl6ip5 in osteoblastic cells. Immunoprecipitation assays revealed that Arl6ip5 directly interacts with Rankl and the interaction was decreased when the cells were treated with PTH. In addition, *Arl6ip5* knockout mice had decreased body weight and reduced bone mass, which was reflected by μ CT analysis. In summary, our results indicate that Arl6ip5, as a negative regulator of Rankl intracellular trafficking, plays a crucial role for osteoclastogenesis.

Disclosures: Yu Wu, None.

SU0198

Deletion of the Rho-GEF Kalirin decreases bone formation, bone length and trabecular bone mass in female mice. Su Huang¹, Pierre Eleniste², Neelam Shah¹, Matthew Allen³, Angela Bruzzaniti¹. ¹Indiana University School of Dentistry, USA, ²Indiana University-Purdue University Indianapolis, USA, ³Indiana University School of Medicine, USA

Bone homeostasis is maintained by a balance between the activity of osteoclasts and osteoblasts, which in turn, is regulated by local and systemic factors, and by intracellular signaling proteins. Kalirin is a novel GTP-exchange factor protein that has been shown to play a role in cytoskeletal remodeling and dendritic spine formation in neurons. However, its function in non-neuronal cells is largely unknown. We found by Western blotting and real time PCR that Kalirin is expressed in osteoclasts and osteoblasts, suggesting it may be important in bone remodeling. We therefore examined the role of Kalirin in regulating bone cell function and bone mass using 14 wk global Kalirin knockout (Kal-KO) mice. MicroCT analyses revealed a 44% lower bone volume/trabecular volume in Kal-KO female mice and 20% lower BV/TV in males, relative to wild-type littermates. Consistent with the BV/TV results, bone formation rate and mineralizing surface/bone surface were lower in female mice, but not male mice, compared to sex-matched littermates. Although cortical bone parameters were significantly reduced in Kal-KO mice, the differences were similar between males and females. Histological analyses also revealed a significant 47% increase in osteoclast surface/bone surface in female mice *in vivo*. Moreover, we found an increase in osteoclast differentiation as well as an increase in the ratio of secreted RANKL to osteoprotegerin by osteoblasts *in vitro*. Finally, we found a sex-specific decrease in tibial bone length (5.5%, $p < 0.02$) in female mice, and a corresponding 18% decrease in serum levels of insulin like growth factor-1 (IGF-1) in Kal-KO female mice, compared to controls. Our studies demonstrate that Kalirin is an important regulator of longitudinal bone growth, trabecular bone mass and bone remodeling in female mice, and may regulate paracrine and/or endocrine signaling of IGF-1 and estrogen, and the function of bone cells.

Disclosures: Angela Bruzzaniti, None.

SU0199

Development and Characterization of a Total Osteocalcin ELISA that Detects the Intact and N-Mid Carboxylated, Undercarboxylated, and Uncarboxylated Forms. Russell Jarres, Elizabeth Weiss, Bethany Salerni*, Peter Wunderli. ALPCO Diagnostics, USA

Osteocalcin, or bone gla-protein, is the most abundant non-collagenous protein found in bone. Produced by osteoblasts, osteocalcin is a useful biomarker in the study of bone formation and turnover. More recent evidence suggests uncarboxylated osteocalcin serves an endocrine role involved in a bone to β -cell feed-forward loop that helps to maintain glucose homeostasis. Current reference levels of osteocalcin are in debate, as most of the commercially available assays for human osteocalcin detect some, but not all, of the forms present in circulation.

A novel assay has been developed to detect all fragments and carboxylation states of human osteocalcin. Cross-reactivity was determined for intact (1-49) and N-mid (1-43) fragments at all possible carboxylation states; for reference, a similar analysis was conducted on 4 commercially available ELISAs. The assay described herein was the only assay to detect all forms of osteocalcin present in circulation. The performance characterization for the assay is as follows. As a likely result of the increased detection of all forms, the range of osteocalcin concentrations observed in freshly frozen samples collected from normal donors is higher (15-30 ng/mL) than that generally reported. 40 μ l of serum is required per duplicate determination, and the assay has a run time of 135 minutes. The standards span a range of 1.25 – 80 ng/ml, with a LoD of 0.12 ng/ml, LLoQ of 2.5 ng/ml and LLoQ >70 ng/ml. Intra-assay precision, evaluated across 4 samples (n = 20), gave a range of 1.7 – 3.6% CV across a concentration range of 10.1 – 52.2 ng/ml. Inter-assay precision, evaluated across 4 samples and 10 assays (n = 20), gave a range of 4.3– 6.8% CV across a concentration range of 14.0 – 68.2 ng/ml. Parallelism was determined by diluting 10 samples 1:2, 1:4, and 1:8; the mean recovery range was 92 – 109%, with no dilutions exceeding +/- 20% of the expected value. Spike & recovery was determined through spikes of calibration material at 5, 15, and 30 ng/ml into 10 samples; the mean recovery range was 98 – 108%, with no spike level exceeding +/- 20% of the expected value. Plasma samples were tested and shown to have a strong correlation to matched serum values; EDTA-plasma (n = 13) $r^2 = 0.97$ with a slope of 0.73, and Heparin-plasma (n = 13) $r^2 = 0.97$ with a slope of 0.75.

Disclosures: Bethany Salerni, ALPCO Diagnostics, 3
This study received funding from: ALPCO diagnostics

SU0200

Establishment and Maintenance of Human Osteoblasts in 2D and 3D *in vitro* Without the Use of Animal-derived Materials. Carole Elford, Deborah Mason, Jim Ralphs, John Gregory, Alastair Sloan, Bronwen Evans*. Cardiff University, United Kingdom

Musculoskeletal replacement therapies require the use of media not containing animal-derived materials. It is also important to advance and implement the 3Rs

(replacing, reducing, refining the use of animals in research and testing). We have developed an 'animal-free' protocol to establish/maintain human osteoblasts *in vitro*, and applied this to 2D and 3D cultures.

Human tibial explants were set up in non-FCS containing media - 1) and 2) α -MEM plus human serum (pooled and AB respectively; Lonza), 3) α -MEM plus K/O serum replacement (Invitrogen), 4) TheraPEAK (defined medium; Lonza), 5) Stempro (defined medium; Invitrogen). α -MEM plus FCS was used as control. Osteoblasts established in this control medium were also maintained in test media and cell numbers (MTS), differentiation (qRT-PCR, ALP activity) and mineralisation (Alizarin red) measured. We also investigated methods of osteoblast maintenance in 3D human collagen gels.

The best 'animal-free' supplement/medium for establishing osteoblasts was human serum, although osteoblast outgrowths in this medium appeared later than with FCS. No osteoblasts were observed with K/O. When osteoblasts from explants grown in FCS were maintained in test media, TheraPEAK increased ($133.8\% \pm 1.72$ (SEM); $p < 0.001$) whereas all other media decreased cell numbers to a similar extent (e.g. $85.6\% \pm 1.21$; $p < 0.001$ in human serum). All media increased ALP although the increase with TheraPEAK ($997.8\% \pm 44.26$; $p < 0.001$) was higher than with the other test media (e.g. human serum $232.7\% \pm 10.2$; $p < 0.001$). Type I collagen expression was also significantly reduced in the presence of TheraPEAK, and no mineralisation was observed. All other test media resulted in good mineralisation *in vitro*. The osteoblasts were also successfully maintained in human collagen (97% type I, 3% type III) gels for 10 days. It was possible to induce mineralisation in these gels and confocal microscopy showed that the cells formed communicating networks indicating possible differentiation towards the osteocytic lineage.

The following protocol establishes and maintains human osteoblasts in an 'animal-free' environment *in vitro*: i) explants in α -MEM plus pooled human serum (1–2 weeks), ii) seed and maintain osteoblasts in TheraPEAK (2 weeks) and iii) maintain osteoblasts in α -MEM plus pooled human serum (1 week) prior to setting up assays. We are currently using this protocol to study the differentiation of primary human osteoblasts to osteocytes in 3D collagen gels.

Disclosures: Bronwen Evans, None.

SU0201

Increased total vBMD at the hypoxia prone site of the juxta-articular metacarpal bone. Valeria Heise¹, Jolanda Widmer², Prisca Eser², Peter M Villiger², Daniel Aeberli³. ¹Medical faculty of the University of Bern, Switzerland, ²Department of Rheumatology & Clinical Immunology/Allergology University Hospital Berne, Freiburgstrasse 18, 3010 Bern Switzerland, Switzerland, ³Dept. of Rheumatology & Clinical Immunology/Allergology University Hospital, Switzerland

Background: scleroderma is characterized by a triad of microangiopathy, activation of humoral and cellular immune responses and tissue fibrosis, affecting the skin as well as a variety of internal organs. The pathogenesis of scleroderma is unknown, but vascular alterations have been suggested to play an important role in this condition. The current understanding is that low levels of oxygen (below 5%) lead to an accumulation of Hypoxia-inducible factor (HIF)1 alpha and multiple angiogenic mediators such as VEGF. Very recently, regulation by HIF1alpha and VEGF was not only suggested in hypoxia induced angiogenesis but also in osteogenesis, particularly in bone repair. It is therefore presently unknown whether hypoxia leads to osteogenesis at the hypoxia prone skeletal sites. Using peripheral quantitative computed tomography (pQCT), the aim of the present study was to determine the total and trabecular volumetric BMD (vBMD) at the hypoxia prone site of the juxta-articular metacarpal bone.

Methods: Consecutive female patients with diagnosed localized scleroderma (anti-centromere antibodies positive) seen at the Department of Rheumatology of the Inselspital Bern were recruited. Additionally, a group of healthy controls was recruited from hospital staff and through locally distributed flyers. pQCT measurements were performed at the third metacarpal bone and the tibia. Scans were placed at 4% of the distal epiphyses. Measured parameters were cross-sectional area (CSA), total BMD and trabecular BMD (of the central 45% of total CSA). Disease severity was measured by modified Rodnan Skin Score.

Results: A total of 30 patients were recruited, of whom 10 were excluded due to comorbidities and medications. Mean age was 60 years (range 52-68 years), and mean disease duration was 45 months (range 4-156 months). Age, height and weight were comparable between patients and healthy controls. The scleroderma group had 6.9 % resp. 7.8% higher total vBMD resp. trabecular vBMD at the distal metacarpal bone ($p=0.037$ and 0.042 , respectively). Total vBMD at 4% of the distal metacarpal epiphyses was positively related to total vBMD at the distal tibia in scleroderma and healthy controls ($r_2=0.235$, $p=0.03$ and $r_2=0.218$, $p=0.05$, respectively). No significant correlation between total vBMD at the 4% distal metacarpal site and disease duration or Rodnan Skin Score was found.

Conclusion: This cross-sectional pQCT study of patients with localized scleroderma supports the hypothesis that low levels of oxygen may induce osteogenesis at the hypoxia prone site of the juxta-articular metacarpal bone.

Disclosures: Daniel Aeberli, None.

SU0202

Inner Ear Vestibular Signals May Contribute to Bone Loss in Microgravity Conditions. Guillaume Vignaux^{*1}, Stéphane Besnard², Pierre Denise², Florent Elefteriou¹. ¹Vanderbilt University, USA, ²Université de Caen, France

Microgravity conditions during long-term spaceflights induce bone loss and increase risk of fracture. The vestibular system in the inner ear is dysfunctional under microgravity and is known to regulate autonomic outflow. Since sympathetic nerve activation induces bone loss, we hypothesized that microgravity-induced bone loss in space may be, at least in part, caused by disturbance in vestibular signals.

To address this hypothesis, a vestibular lesion (VBX) was performed by transtympanic bilateral injection of sodium arsenite in 3-months old rats. A control group (Sham) was also analyzed following transtympanic and bilateral injection of PBS. Two additional sham or VBX groups received the beta-blocker propranolol in drinking water for one month. Horizontal locomotor activity was evaluated by a continuous recording telemetric system 3 days before lesion, 3 days after and the 3 last days of the study. One month after VBX, DXA measurements were performed in whole body, spine and femurs, and micro-CT and histomorphometry analyses were performed on the right femur.

No difference in locomotor activity was observed between Sham and VBX rats before vestibular lesion and 3 days post-lesion. Unexpectedly, during the last 3 days, locomotor activity increased 2 times in VBX rats compared to control.

DXA analyses indicated a highly significant and selective bone loss in VBX rats on distal femoral epiphyses (-13.0% vs Sham) whereas no change in bone mineral density was observed in the whole body and spine. This vestibular-related bone loss was confirmed by micro-CT analyses, by a significant reduction in trabecular Bone Volume/Tissue Volume, trabecular thickness and trabecular number in the VBX group versus Sham group. This phenotype was accompanied with a significant decrease in osteoblast surface/bone surface ratio but no change in osteoclast surface/bone surface ratio. Propranolol treatment had no effect in the Sham group but completely blunted the vestibular-related bone loss in the VBX group, restoring all bone microarchitecture and cellular parameters.

We conclude that vestibular signals, possibly transmitted via sympathetic nerves, modulate bone remodeling, and that vestibular dysfunction in space may contribute to microgravity-induced bone loss, along with the lack of proper mechanical stimulation of bone cells. These results offer a new approach to study and prevent space-related bone loss.

Disclosures: Guillaume Vignaux, None.

SU0203

Loss of Sc65 and its Consequences on Osteoblast Secreted Proteins and Bone Homeostasis. Roy Morello^{*1}, Larry Suva¹, Dana Gaddy¹, Patrizio Castagnola², Katrin Gruenwald¹, Brittany Hendrix¹. ¹University of Arkansas for Medical Sciences, USA, ²IRCCS Azienda Ospedaliera Universitaria San Martino - IST - Istituto Nazionale per la Ricerca sul Cancro, Italy

The Leprecan family of genes comprises five members: *Leprel1*, *Leprel2*, *Leprel3*, *Crtap*, and *Sc65*. Mutations in 3 of these genes cause diseases such as osteogenesis imperfecta (OI) and severe myopia. *Leprel2*, encoding prolyl 3-hydroxylase 3, and *Sc65* are the least well-understood. Here we have characterized the function of *Sc65*, a protein with over 50% amino acid identity to *Crtap*. We found that *Sc65*, like all other Leprecans, is localized to the rough endoplasmic reticulum (rER) and is highly expressed during cartilage and bone formation. More important, mice homozygous for a mutant *Sc65* allele that do not express *Sc65* protein have significant lower bone mass compared to their WT littermates. These changes were associated with decreased trabecular architecture and cortical geometry. Although bone formation rate was not affected there was an increase in the serum levels of CTX, suggesting excessive bone resorption. Osteoclasts and their precursors do not express *Sc65*. Yet *in vitro* assays demonstrated increased osteoclastogenesis, suggesting a non-cell autonomous defect. Osteoblasts express high levels of *Sc65* and normally secrete a wealth of factors that are important for bone formation and resorption, including type I collagen, osteopontin, osteoprotegerin, RANKL, among others. Importantly, these proteins must be correctly modified, folded and chaperoned outside the cell to perform their proper biological function. We, therefore, hypothesized that *Sc65*, like *Crtap*, represents an interacting partner for specific ER resident enzymes and participates in the modification/secretion of molecules that regulate osteoclast activity. To elucidate potential mechanism(s) that could account for the increased bone resorption, we collected serum free medium from primary calvarial *Sc65* mutant and WT osteoblasts and performed a detailed proteomic analysis. Several differentially expressed targets were identified and sequenced by mass spectrometry. Consistent with our hypothesis, we identified approximately forty proteins that were differentially secreted in WT vs *Sc65* mutants. These include several secreted osteoblastic proteins that are known to affect osteoclast maturation. These findings, coupled with ongoing efforts aimed at identifying *Sc65* protein interactors, should allow a better understanding of the *Sc65* functional network.

Disclosures: Roy Morello, None.

SU0204

Mechanism Analysis of a Novel Bone Anabolic Peptide. YURIKO FURUYA^{*1}, Yutaka Yoshihara¹, Kahn Masud², Atsushi Inagaki¹, Kaoru Mori¹, Kazuhiro Aoki³, Keiichi Ohya², Kohji Uchida¹, Hisataka Yasuda⁴. ¹ORIENTAL YEAST CO.,LTD, Japan, ²Pharmacology Department of Hard Tissue Engineering Division of Bio-Matrix, Japan, ³Tokyo Medical & Dental University, Japan, ⁴Oriental Yeast Company, Limited, Japan

In the previous meeting, we reported that a peptide known to abrogate osteoclast (Oc) differentiation by binding RANKL surprisingly exhibited bone anabolic effect in mice through increment of MAR and BFR in cortical area with unknown mechanisms. The peptide (W9) increased alkaline phosphatase (ALP) activity and stimulated mineralization in MC3T3-E1 (E1) cells. Increases in ALP activity and mineralization were similarly observed in human mesenchymal cell culture under osteoblastic conditions.

To clarify the mechanisms of W9, we investigated its signaling pathway in osteoblast (Ob) differentiation/mineralization. Addition of BMP-2 synergistically increased ALP activity and mineralization in E1 cells in the presence of W9. Recombinant soluble BMP receptor (sBMPR) suppressed an increase in ALP activity in E1 cells treated with W9. In addition, anti-BMP2/4 neutralizing antibody suppressed the increase in ALP activity. In ectopic bone formation, W9 increased bone mineral content in collagen pellet containing BMP-2. These results suggested the involvement of BMP-2/4 in the Ob differentiation by W9. Consistent with these results, increases in mRNA expression of BMP-4, CTGF, IGF-1, IGF-2, ALP, and osteocalcin were observed in E1 cells treated with W9 for 96 hr in GeneChip analysis. Addition of p38 MAP kinase inhibitor blocked the increase in ALP activity by W9, suggesting the involvement of a signal through p38 activation in the mechanisms. Phosphorylation of smad1/5/8 known as BMP signal also was enhanced by addition of W9 in E1 cells. On the other hand, W9 did not accumulate beta-catenin in E1 cells, suggesting Wnt canonical signaling pathway was not involved in the mechanisms. W9 was known to bind RANKL or TNF-alpha. RANKL knock-down partially blocked the increase in ALP activity in E1 cells treated with W9, raising the possibility that RANKL was a target of the peptide.

Taken together, W9 stimulated Ob differentiation/mineralization through p38 and smad1/5/8 activation in synergy with BMP-2/4.

Disclosures: YURIKO FURUYA, Oriental Yeast Co., Ltd, 3

SU0205

Monoosteophil Derived from LL-37 Treated Monocytes and Their Role in Accelerated Bone Repair. Zhifang Zhang^{*}, John E. Shively. City of hope, USA

Background: Bone generation and maintenance involve osteoblasts, osteoclasts, and osteocytes. However, an incomplete understanding of bone forming cells during wound healing has led to an unfilled clinical need such as nonunion of bone fractures. Furthermore, ectopic calcification, which arises in soft tissues in a variety of diseases, for example atherosclerosis and tuberculosis, also suggests the existence of an unknown type of bone forming cell. We have previously shown that LL-37 treated human monocytes survive for up to a year in culture and generate a novel lineage of bone forming cells we have termed monoosteophils to reflect their origin and bone forming function. We have hypothesized that monocytes may be critical responders to bone injury in which LL-37 produced in the surrounding inflammatory milieu generates monoosteophils that repair the injury. Here, we tested this hypothesis in a bone repair model (Monfoulet and Rabier, 2010) and investigated the unique markers of monoosteophil differentiation.

Results: We treated human monocytes *in vitro* for one day with human LL-37 and implanted them in Matrigel over a freshly drilled hole (0.9 mm) in mid diaphyseal femurs of NOD/SCID mice. In untreated or control monocyte treated mice, bone repair required at least 28d as described by Monfoulet and Rabier. However, bone repair was complete in 14d for the monoosteophil treated group as determined by visual analysis (below) and low resolution μ CT compared to the other two groups. Monoosteophils, differentiated from LL-37 treated monocytes, were identified by up-regulation of integrin α 3 and α 3b1 and down-regulation of CD14, CD16, and CD163 on cell surface. Microarray analyses indicated the differential expression of 206 genes in the formation of monoosteophils. Among these genes, the top up-regulated genes include SPP1 (osteopontin), GPNMB (osteonectin), CHI3L1 (cartilage glycoprotein-39), CHIT1 (Chitinase 1), MMP-9 and MMP-7. ELISA results confirmed that the levels of above proteins in the culture media are significantly higher than controls.

CONCLUSION: Monoosteophils may represent a novel method for using readily available autologous cells to accelerate bone repair. Integrin α 3 and α 3b1, CD14, CD16, and CD163 can be used as differentiation markers of monoosteophils differentiated from LL-37 treated monocytes. Furthermore, monoosteophils may have wide ranging applications in the clinic including repair of broken bones, treatment of osteoporosis, and even prevention of ectopic mineralization by blocking its differentiation and function.

Disclosures: Zhifang Zhang, None.

SU0206

Osteoclasts Exert Anabolic Stimuli on Osteoblasts Independent of their Resorption Capability, while Increasing Cartilage Turnover. Karoline Natasja Stæhr Gudmann*¹, Kim V. Andreassen², Christian Thudium³, Anne-Christine Bay-Jensen¹, Morten Karsdal³, Kim Henriksen³. ¹Nordic Bioscience, Denmark, ²Nordic Bioscience.com, Denmark, ³Nordic Bioscience A/S, Denmark

Osteoarthritis (OA) is a disease known to have a high bone turnover both at the osteoclast and osteoblast level, and anti-resorptive compounds have shown potential as treatments of OA. This indicates that osteoclasts may affect cartilage turnover either directly through the secretion of cytokines or indirectly via modulation of osteoblasts/osteocytes and through these the cartilage. The aim of this study was to investigate the role of osteoclasts in the joint turnover more into details. We looked into how bone formation by the osteoblasts and cartilage turnover were affected by exposure to conditioned medium (CM) from macrophages, resorptive and non-resorptive osteoclasts.

Osteoclasts were obtained by isolating monocytes from human peripheral blood and differentiated into osteoclasts with RANKL and M-CSF. CM was collected and pooled from macrophages and 4 groups of osteoclasts: functional, from osteopetrotic patients, inhibited by drugs (diphyllin, E64 and GM6001), and osteoclast precursors, or the corresponding non-CM (no cells). To assess the effect of osteoclasts on cartilage, explants from bovine knees were cultured in the presence of CM from functional osteoclasts.

The presence of mature osteoclasts was verified by TRACP activity. Non-resorbing osteoclasts had decreased levels of CTX-I and calcium release. Both resorbing and non-resorbing osteoclasts but not precursors, macrophages and non-CM induced bone formation when treating the osteoblastic cell line 2T3 with 50% of CM analyzed by Alizarin Red extraction. In supernatant from cartilage explants, it was shown that CM caused a decrease in the cartilage formation marker PIINP and an increase in aggrecan degradation as visualized by safranin-O.

Our results showed that anabolic factors secreted from different subtypes of osteoclasts were able to induce bone formation by osteoblasts relying both on resorption dependent and independent processes. Furthermore, CM from osteoclasts had the opposite effect on cartilage, and seemed to reduce collagen formation and accelerate aggrecan degradation.

In conclusion, this illustrates that osteoclasts preserve their anabolic capacity on osteoblasts independently of their bone resorption capacity whereas the effect of CM from osteoclasts appears catabolic on chondrocytes. Further studies will show whether the catabolic effect on chondrocytes is dependent on osteoclasts functionality.

Disclosures: Karoline Natasja Stæhr Gudmann, None.

SU0207

Over-expression of Connective Tissue Growth Factor Enhances Bone Formation. Christina Mundy*, Alex Lambi, Robin A. Pixley, Roshanak N. Razmpour, Mary Barbe, Steven Popoff. Temple University School of Medicine, USA

Connective Tissue Growth Factor (CTGF) is a matricellular protein, which serves an important role in osteogenesis. We have previously shown that CTGF is expressed in active osteoblasts lining the bone surfaces during postnatal bone growth and fracture repair, and addition of exogenous CTGF results in enhanced osteoblast proliferation and differentiation. To investigate the effects of CTGF on bone development in vivo, we generated transgenic (TG) mice that over-express CTGF under the control of truncated mouse 3.6kb type I collagen promoter. This promoter is preferentially expressed in cells of the osteoblast lineage at earlier stages of their differentiation. Quantification of CTGF mRNA and protein expression levels confirmed a modest (3-5-fold) over-expression of CTGF in bones from TG compared to wild-type (WT) mice. To investigate the effect of CTGF over-expression on postnatal skeletal development, we performed microCT scans of the distal femoral metaphysis from age-matched TG and WT mice. This analysis revealed a significant increase in trabecular bone volume (BV/TV) in TG compared to WT mice. Moreover, findings from histomorphometric analysis of the distal femora confirmed enhanced bone formation in the TG mice. To examine the effect of CTGF over-expression on osteoblast differentiation in culture, we isolated calvarial osteoblasts from TG and WT mice. Proliferation was significantly increased in TG osteoblasts. Additionally, TG osteoblasts displayed increased alkaline phosphatase staining and activity, indicative of increased osteoblast differentiation. Taken together, these results suggest that modest increases in CTGF expression can positively regulate bone formation in vivo and osteoblast proliferation/differentiation in vitro.

Disclosures: Christina Mundy, None.

SU0208

Oxy133 Promotes Osteogenic Differentiation In Vitro and Spine Fusion In Vivo: A Potential Therapeutic Molecule for Stimulation of Bone Formation. Scott Montgomery*¹, Vicente Meliton², Taya Nargizyan², Frank Stappenbeck², Michael Jung², Kamran Movassaghi², Jared Johnson¹, Bayan Aghdasi², Haijun Tian², Yanlin Tan², Hirokazu Inoue², Elisa Atti², Sotirios Tetradis², Renata Pereira², Jeffrey Wang², Farhad Parhami². ¹UCLA, USA, ²University of California, Los Angeles, USA

Purpose: Osteogenic factors are often used in orthopedics to improve fracture healing and induce spine fusion. We previously reported the osteogenic activity of specific oxysterols and investigated their potential for use in clinical applications requiring bone formation. Here we identify a more potent and easily synthesized osteogenic oxysterol analogue, Oxy133, and evaluate its ability to promote osteogenesis in vitro and spine fusion in a rat model in vivo.

Methods: Mouse C3H10T1/2 (C3H) embryonic fibroblasts, M2-10B4 (M2) multipotent bone marrow stromal cells, and primary human mesenchymal stem cells were treated with Oxy133 and the expression of osteogenic differentiation markers alkaline phosphatase (ALP), bone sialoprotein (BSP), Ostrix (OSX), and osteocalcin (OCN) was measured by Q-RT-PCR. Role of Hedgehog (Hh) pathway was assessed by examining: 1) activation of a Gli-dependent luciferase reporter, 2) expression of Hh target genes Patched1, Gli1, and HIP, and 3) inhibition by the Hh pathway inhibitor, cyclopamine. For in vivo studies, 8-week old male Lewis rats underwent posterolateral L4-L5 spine fusion using collagen sponges to deliver DMSO control, 5µg BMP2, or 0.2, 2, or 20 mg Oxy133. Bone formation and fusion were measured radiographically at 4, 6, and 8 weeks and confirmed by micro-CT, manual palpation, and histology at sacrifice eight weeks after surgery.

Results: Oxy133 induced the in vitro expression of Hh target genes and osteogenic markers, which was inhibited by cyclopamine. EC50 for the induction of ALP activity in C3H and M2 cells was 0.5mM, which is lower than the EC50 reported for other osteogenic oxysterols. Oxy133 activated a Gli-dependent luciferase reporter, and together with the induction of Hh pathway target genes and the inhibitory effects of cyclopamine demonstrated the role of Hh signaling. In vivo, bilateral bone formation was observed on radiographs at 4 weeks and fusion was confirmed with micro-CT at 8 weeks in all (8/8) animals treated with 20 mg Oxy133 or BMP2, compared to 50% (4/8) of animals treated with 2 mg Oxy133. No fusion was observed in the control or Oxy 133 0.2 mg groups although new bone formation was observed in some animals in the latter group.

Conclusions: Treatment of osteoprogenitor cells with Oxy133 in vitro caused robust osteogenic differentiation and induced spine fusion in vivo. Oxy133 is a potent, novel, easy to synthesize osteogenic oxysterol suitable for further therapeutic development.

Disclosures: Scott Montgomery, None.

SU0209

Study on the Mechanism of Action of Aendronate in Osteoblast Differentiation. Hoon Choi¹, Ari Kim*². ¹Inje University Sanggyepaik Hospital, South Korea, ²Sanbon Hospital, College of Medicine, Wonkwang University, South Korea

Objectives: To investigate the effect of alendronate on osteoblast proliferation and differentiation using mouse preosteoblast cell line, MC3T3-E1 and myoblastic cell line, C2C12.

Material & Methods: C2C12 and MC3T3-E1 cell lines were cultured in DMEM media with various concentrations (10-9 M, 10-8 M, 10-7 M, 10-6 M, 10-5 M, 10-4 M) of alendronate for one, two, or three days. After the indicated culture times, MTT assay and ALP activity were examined. The expression of genes for ALP, osteocalcin (OCN), collagen I $\alpha 1$ (Col 1), inhibitor of differentiation (Id) and cathepsin K (CTSK) were examined by RT-PCR method. Transcription factors related to the increased expression of Id genes were identified with TRANSFEC program. The effect of these transcription factors on the expression of Id genes were tested by promoter assay.

Result: Alendronate had no cytotoxicity regardless of the concentrations used. ALP activity in C2C12 cells was increased in alendronate treated group compared to the control group before 24 hours of treatment, but decreased rapidly after 24 hours of treatment. In MC3T3-E1, it was increased greatly at 10-8 M before 48 hours of treatment and it was decreased rapidly at more than 10-8 M concentration regardless of times of treatment. Expressions of ALP, Col 1 and OCN genes had a tendency to increase with decreasing of alendronate concentrations before 24 hours of treatment in both cell lines. The expression of Id-1 gene began to increase from 10-6 M of alendronate compared to the control group and kept to 10-8 M. However, Id-2 gene expression was increased gradually with increasing of alendronate concentrations. Among transcription factors related to the promoter of Id genes, CREB and C/EBP β increased promoter activity of Id genes to 2-fold and 4-fold, respectively. Co-treatment of C/EBP β and alendronate resulted in a significant increased promoter activity of Id genes compared to each single treatment.

Conclusion: This study shows that alendronate has a dose-dependent effect in osteoblast differentiation. The effect may be associated with the increased expression of Id genes via a synergistic interaction with C/EBP β .

Disclosures: Ari Kim, None.

SU0210

Withdrawn

SU0211

Comparative Osteogenic Capacities of MSCs Isolated from Equine Bone Marrow, Synovium and Adipose Tissue. Antonella Andrietti, Yuwen Chen, Sushmitha Durgam, Matthew Stewart*. University of Illinois, USA

Purpose: To compare the osteogenic capabilities of donor-matched putative stem cell populations from bone marrow (BM), synovium (SYN) and adipose tissue (ADI). The results were analysed to determine whether any of these cell populations were 'predisposed' to the osteogenic pathway under basal conditions, and to identify populations that are particularly able to undergo osteogenesis for clinical applications.

Methods: Specimens were collected from six healthy adult horses. BM aspirates were collected from the tuber coxae. Adipose tissue was collected from the fat depot adjacent the tail butt and synovium was collected from the dorsal surface of the carpal joints. Primary BM cultures were seeded into T75 culture bottles. Adipose tissue and synovium were digested in collagenase and the primary isolates were seeded at 5,000 cells/cm². Cells were passaged twice, and the third passage cells were transferred to osteogenic medium (DMEM, 10% FBS, β -glycerophosphate, dexamethasone and ascorbic acid). Phenotypic changes were assessed after 7 and 14 days. Matrix mineralization was monitored by Alizarin Red (AR) staining and by alkaline phosphatase (ALP) localization. Bulk ALP activity was also measured. Up-regulation of ALP, Runx2, Osterix (OSX), Osteonectin (OSN) and osteomodulin (OSM) mRNAs was assessed by QPCR.

Results: Under basal conditions, there were no significant differences between the cell populations in expression of osteogenic markers. This suggests that no population was 'pre-committed' to the osteogenic lineage. BM monolayers developed multicellular aggregates that stained strongly with AR by day 7. Mineralization of cell aggregates was further increased by day 14. Aggregate staining was apparent by day 14 in SYN and ADI cultures, but aggregate numbers and staining intensities were markedly less than in BM cultures. BM cells significantly increased ALP activity and mRNA levels, concurrent with upregulation of Runx2 and Osx expression. Neither OSN nor OSM mRNA levels were altered during osteogenesis. Although ADI cells did increase ALP activity, neither these cells nor SYN cells significantly up-regulated any other indicator of osteogenic differentiation.

Conclusions: The results indicate that BM cells are far superior for osteogenic applications and suggest that SYN and ADI cells in osteogenic culture conditions are unable to increase expression of Runx2 and OSX; transcription factors mandatory for osteogenesis.

Disclosures: Matthew Stewart, None.

SU0212

Dynamin GTPase Activity is critically required for Osteoblast Migration and Differentiation. Pierre Eleniste*¹, Su Huang², Angela Bruzzaniti³. ¹Indiana University-Purdue University Indianapolis, USA, ²Indiana university, USA, ³Indiana University School of Dentistry, USA

Osteoblasts are essential for maintaining bone mass and bone quality. The dynamin GTPase controls endocytosis and actin remodeling in a number of cells, and its activity is stimulated by tyrosine phosphorylation. However, the phosphatase leading to dynamin inactivation, and the role of dynamin in osteoblasts is unknown. In this study, we examined the function of dynamin in osteoblasts, and dynamin dephosphorylation and inactivation by the PTP-PEST phosphatase. We co-expressed dynamin with the phosphatase PTP-PEST and then quantified dynamin phosphorylation and activity by immunoprecipitation and chemical GTPase assays. PTP-PEST decreased dynamin phosphorylation and activity in a dose-dependent manner. In addition, amino acids Y231 and Y597 were important for the effects of PTP-PEST since mutant dynY231F and dynY597F decreased GTPase activity and phosphorylation by 40-60%, compared to dynamin. Next, calvarial osteoblasts were treated with dynasore, a chemical inhibitor of dynamin GTPase activity, and osteoblast morphology, migration and alkaline phosphatase (ALP) activity were examined. Dynasore-treated osteoblasts exhibited a 40% increase in the number of actin-rich focal adhesions and a 70% decrease in actin stress fiber formation. Consistent with increased focal adhesions, dynasore decreased osteoblast migration by 62%, compared to controls. Finally, inhibition of dynamin with dynasore significantly decreased osteoblast ALP expression. These studies suggest that dynamin regulates focal adhesion turnover as well as osteoblast migration and differentiation.

Disclosures: Pierre Eleniste, None.

SU0213

Effect of Adiponectin on the Expression of its Specific Receptor 1/2 in Osteoblasts and Osteoclasts Under Inflammatory Conditions. Lan Zhang*, Qisheng Tu, Shu Meng, Jake Jinkun Chen. Tufts University School of Dental Medicine, USA

Adiponectin, an adipocyte-derived cytokine, can promote bone formation, inhibit bone resorption, and function as an anti-inflammatory mediator. Hence it is a potential therapeutic molecule to treat inflammation-mediated periodontitis where excess bone resorption takes place. However, the decrease of adiponectin receptor (adipoR1/R2) induced by inflammation restricts its use in inflammatory bone diseases. This study investigated the effect of adiponectin on the expression of adipoR1/R2 in osteoblasts and osteoclasts under inflammatory conditions.

MC3T3-E1 and RAW 264.7 cells were cultured in α -MEM and RPMI 1640 with 10% fetal bovine serum (FBS) respectively. After confluence, the cells were starved with culture medium containing 1% FBS for 24h, then 100 ng/ml *E. coli* lipopolysaccharide (LPS) was used to stimulate cells for 24h, and 50 ng/ml sRANKL was simultaneously added to induce osteoclastogenesis in RAW 264.7 cells. Adiponectin (0.5 μ g/ml or 1 μ g/ml) was used to treat MC3T3-E1 and RAW 264.7 cells, respectively. After 24h of adiponectin treatment, the mRNA expression levels of adipoR1/R2 and a transcription factor, forkhead box O1 (FoxO1), were determined in MC3T3-E1 (Figure 1) and RAW 264.7 cells (Figure 2) using real-time RT-PCR.

The mRNA expressions of adipoR1/R2 were down-regulated by LPS stimulation in both MC3T3-E1 and RAW 264.7 cells. However, the treatment of adiponectin reversed LPS-induced reduction of adipoR1/R2. FoxO1 promoted the expression of adipoR1 by binding to its promoter. We determined the mRNA expression level of FoxO1 and found that similar to affecting adipoR1/R2, LPS stimulation down-regulated FoxO1, but adiponectin reversed the effect of LPS.

It was summarized that adiponectin may have a positive effect on the expression of adipoR1/R2 through FoxO1 in osteoblasts and osteoclasts under inflammatory conditions. These findings for the first time provide the insight into the cellular mechanisms of the therapeutic effects of adiponectin in treating periodontitis.

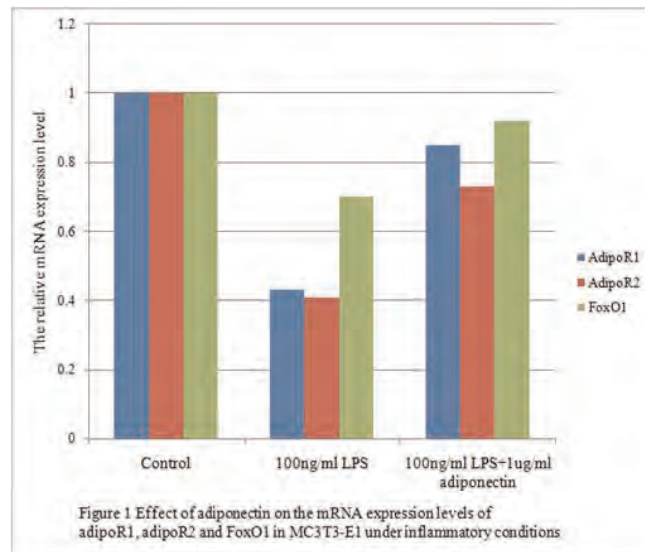


Figure 1

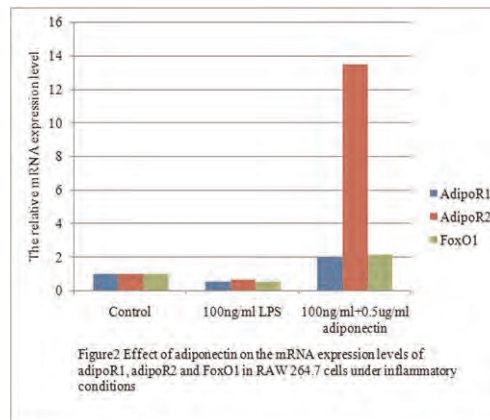


Figure 2

Disclosures: Lan Zhang, None.

This study received funding from: NIH grants DE16710 and DE21464 to JC

SU0214

Epigenetic Regulation of Osteogenic Transcription Factor SATB2 by PHF8, a Jumonji Family Histone Demethylase. Qisheng Tu^{*1}, Yuwei Wu², Shu Meng¹, Liming Yu¹, Dana Murray¹, Jake Jinkun Chen¹. ¹Tufts University School of Dental Medicine, USA, ²Tufts University, USA

Epigenetic regulation of gene expression is a central mechanism that governs cell stemness, determination, commitment, and differentiation. It has been recently found that PHF8, a major H4K20/H3K9 demethylase, plays a critical role in craniofacial and jaw bone development. As a nuclear matrix protein, special AT-rich sequence-binding protein 2 (SATB2) is expressed in branchial arches and in cells of the osteoblast lineage, and required for preventing craniofacial abnormalities and defects. However, the lack of the understanding the epigenetic modulation of SATB2 impedes our further insight into this important osteogenic transcription factor. In this study, our hypothesis to be tested is that PHF8 converts SATB2 chromatin into a transcriptionally active conformation and subsequently SATB2 orchestrates multiple molecular mechanisms in osteoblastogenesis. We performed a series of studies including quantitative RT-PCR, Western blot, site-specific mutations, gain- and loss-of-function analyses, mineralization assays and conventional ChIP assays. Our results showed that expression levels of PHF8 and SATB2 in preosteoblast MC3T3-E1 and bone marrow stem cells (BMSCs) increased simultaneously during osteogenic differentiation. PHF8 expression level was increased as early as 3 days after osteogenic induction, and was sustained at a high expression level throughout the 14-day experimental period. The SATB2 mRNA levels were also increased in parallel. Overexpressing PHF8 in BMSCs and MC3T3-E1 cells with wild type PHF8 upregulated the expression of SATB2, Runx2 and osterix, and bone matrix proteins, while mutant PHF8 did not show this enhancement, which was dependent on its H3K4me3-binding PHD and catalytic domains. PHF8 also promoted osteoblastic differentiation and mineralization *in vitro*. Moreover, knockdown of PHF8 reduced the expression of SATB2 and other bone markers. Furthermore, we found PHF8 binding near TSS of the *Satb2* gene in our ChIP assays. Taken together, our results suggest, for the first time, that PHF8 enhances osteogenic differentiation via regulation of the SATB2 expression pattern by modulating histone methylation states. We expect that epigenetic regulation of BMSCs during osteogenic differentiation will promote SATB2-dependent activation and facilitate bone tissue engineering and regeneration.

Disclosures: Qisheng Tu, None.

This study received funding from: NIH grants DE16710 and DE21464 to JC

SU0215

Genetic Evidence for a PTH-PKA- α NAC Signalling Cascade in Bone. Martin Pellicelli^{*1}, Alice Arabian², Joy Wu³, Henry Kronenberg³, Rene St-Arnaud⁴. ¹Shriners Hospital for Children - Canada, Canada, ²Shriners Hospital for Children, Canada, ³Massachusetts General Hospital, USA, ⁴Shriners Hospital for Children & McGill University, Canada

Daily injection of parathyroid hormone (PTH) is the only approved anabolic treatment for osteoporosis. The binding of PTH to its receptor induces *G α s*-mediated activation of adenylyl cyclase, which stimulates cAMP production to turn on effector kinases. In turn, these phosphorylate downstream targets to mediate the PTH signal. PTH-induced cAMP production was shown to be sufficient to provoke its bone-forming effects. A predominant effector pathway downstream from cAMP accumulation is the activation of protein kinase A (PKA). To further characterize *G α s*-mediated signalling downstream from PTH in bone cells, mice with osteoblasts specifically deficient for *G α s* have been generated (Wu, JY et al. 2011. J Clin Invest 121: 3492). These mice exhibit reduced bone mass, decreased expression of the osteoblastic marker *Osteocalcin* (*Ocn*), and abnormal persistence of immature, woven bone with increased numbers of osteocytes. These traits are a remarkable phenocopy of the traits characterized in mice that we generated with a knock-in mutation that prevents the Nascent polypeptide associated complex And Coactivator alpha (α NAC) to efficiently transfer from the cytosol to the nucleus of osteoblasts (Meury, T et al. 2010. Mol Cell Biol 30: 43). The phenotypic similarities suggest that *G α s* and α NAC form part of a common genetic pathway. To test this hypothesis, we have altered gene dosage for *G α s* and α NAC in compound heterozygous mice. Compound *G α s*; α NAC heterozygotes have a reduced bone mass phenotype and show increased numbers of osteocytes per surface area, as well as enhanced expression of osteocytic differentiation markers. Moreover, treatment of osteoblasts with PTH, forskolin or the PKA-selective activator 6-Bnz-cAMP lead to translocation of α NAC to the nucleus. Purified PKA phosphorylates α NAC *in vitro*, and we have identified the PKA phosphoacceptor site within α NAC as residue serine 99. Mutation of this residue affects subcellular localization of α NAC, with a serine-to-alanine (S99A) mutation reducing nuclear entry, while a phosphomimetic S99D alteration translocates the mutant α NAC protein to the nuclear compartment. The S99A mutation also abolishes α NAC-mediated forskolin-dependent transcriptional activation of the *Osteocalcin* (*Ocn*) gene promoter. Taken together, our results support the existence of a signalling cascade that initiates with PTH binding to its receptor, activation of *G α s* to stimulate cAMP accumulation and effector kinase activity, thus sending α NAC to the nucleus to regulate *Ocn* gene transcription.

Disclosures: Martin Pellicelli, None.

SU0216

Odd-skipped Related2 Regulates Wnt Signaling Pathway. Shinji Kawai^{*1}, Atsuo Amano². ¹Osaka University Graduate School of Dentistry, Japan, ²Osaka University, Japan

Odd-skipped related 2 (Osr2) zinc finger transcription factor is one of the factors which participates in osteogenesis. We previously reported on the function of Osr2 by using the transgenic mice of dominant negative Osr2. In this transgenic mice, delayed mineralization in calvarial and cortical bone tissues, distinctly increased radiolucency in soft X-ray analysis, reduced staining intensities with alcian blue and alizarin red in the skull and skeletal elements, and markedly thinner parietal and cortical bones are observed. The proliferation and differentiation of calvarial osteoblast decreased. Moreover, Osr2-deficient mice revalidated that Osr2 play a critical role in secondary palate and teeth development. On the other hand, Wnt family is secreted type protein, Wnt is related with embryogenesis, oncogenesis, etc. and Wnt plays the important role in bone formation and cartilage formation. In this study, we aim at clarifying the correlation of Osr2 and Wnt signal pathway. Osr2 was over-expressed in the cells and expression profile related to signal pathway was analyzed by DNA microarray. As a result of clustering analysis, Wnt signal pathway was most controlled among various kinds of signal pathways. Moreover, Osr2 regulated TopFlash activity. From these results, it is suggested that Osr2 participates in bone formation or joint formation via Wnt signal pathway.

Disclosures: Shinji Kawai, None.

SU0217

Osteoblast-specific Transcription Factor Osx Controls VEGF Expression in Osteoblasts. Chi Zhang^{*1}, Wanjin Tang², Fan Yang², Yang Li², Benoit de Crombrughe³, Hongli Jiao⁴, Guozhi Xiao⁵. ¹Bone Research Laboratory, Texas Scottish Rite Hospital, USA, ²Texas Scottish Rite Hospital for Children, USA, ³University of Texas M.D. Anderson Cancer Center, USA, ⁴University of Pittsburgh, USA, ⁵University of Pittsburgh School of Medicine, USA

Bone formation is a developmental process involving the differentiation of mesenchymal stem cells to osteoblasts. Angiogenesis and osteogenesis are tightly coupled during bone formation. Vascular endothelial growth factor (VEGF) is involved in both angiogenesis and osteogenesis. Relatively little is known about the transcriptional regulation of VEGF expression in osteoblasts. Osterix (Osx) is an osteoblast-specific transcription factor required for bone formation. In this study, we examined VEGF regulation by Osx. Microarray was carried out to compare the RNA expression profiles of wild type and Osx-null calvarial cells at E18.5 in mouse embryos. Our results revealed that VEGF expression was downregulated and that osteoblast marker osteocalcin (OC) was absent in Osx-null calvarial cells, which were confirmed by quantitative real-time RT-PCR. Overexpression of Osx in stable C2C12 mesenchymal cells using Tet-off system resulted in upregulation of both VEGF and OC expression. The inhibition of Osx by siRNA led to repression of VEGF and OC expressions in osteoblasts. These results suggest that Osx controls VEGF expression while Osx induces OC expression. Transfection assays demonstrated that Osx activated both VEGF and OC promoter activities. A series of VEGF promoter deletion mutants were examined and the minimal Osx-responsive region was defined to the proximal 140bp of VEGF promoter. Additional point mutant studies were used to identify two GC-rich regions that were responsible for VEGF promoter activation by Osx. Gel Shift Assay showed that Osx bound to the VEGF promoter sequence directly. Chromatin immunoprecipitation assays indicated that endogenous Osx associated with native VEGF promoter in primary osteoblasts. To examine the effect of Osx on VEGF protein level in osteoblasts *in vivo*, we used Osx conditional knockout mice. Immunohistochemistry staining showed decreased VEGF protein levels in tibiae of mice in which Osx was inactivated postnatally. Hypoxia has been reported to couple angiogenesis to osteogenesis, and hypoxia-inducible factor-1 α (HIF-1 α) upregulates VEGF. Synergistic interplays were observed between Osx and HIF-1 α in VEGF promoter activation in transfection assays. In conclusion, we provide the first evidence that Osx controlled VEGF expression in osteoblasts, suggesting a potential role of Osx in coordinating osteogenesis and angiogenesis.

Disclosures: Chi Zhang, None.

SU0218

Role of Brd2 Gene in the Regulation of Sex Linked Bone Loss and its Association with Adipocyte Differentiation. Beth Bragdon¹, Robert Burns², Amelia Baker², Anna Belkina³, Gerald Denis², Elise Morgan⁴, Louis Gerstenfeld², Jennifer Schlezinger^{*5}. ¹Boston University School of Medicine Department of Orthopaedics, USA, ²Boston University School of Medicine, USA, ³Boston University School of Medicine, USA, ⁴Boston University, USA, ⁵Boston University School of Public Health, USA

Prior studies have shown that mice that have one functional copy of the double bromodomain protein (*brd2*) gene become obese as they age but remain insulin sensitive. These mice provide a model to assess the effects of obesity on bone loss in the absence of insulin resistant diabetes.

Methods: A longitudinal study of 3-18 month old male and female WT and *brd2lo* mice on a C57BL/6 background (N=5-7) was carried out. Cortical and trabecular bone structure was assessed in the right tibia by μ CT. Quantitative RT-PCR was used to assess the expression of three cassettes of mRNAs for osteoblasts/osteocytes (RUNX2, osterix, osteocalcin, RANKL, DMP1, FGF23), osteoclasts (cathepsin K, Trap5b) and adipocytes (PPAR γ , CEBP α , FABP4, adiponin) from both humeri. Primary bone marrow cultures were prepared from the femurs and left tibia and stimulated to undergo osteogenesis, and mRNA expression was assessed.

Results: μ CT showed that only the female *brd2lo* mice had a statistically greater bone loss compared to WT counterparts. qRT-PCR showed that the female *brd2lo* mice had decreased RUNX2, osterix, and osteocalcin expression compared to the WT females while the male *brd2lo* mice showed increased expression levels compared to the WT. In contrast, the adipocyte-associated genes all showed elevated expression in both male and female *brd2lo* mice, with expression in females being the highest. While younger *brd2lo* males and females had increased expression of the osteoclast markers compared to their WT counterparts, this difference was lost with age. In primary bone marrow cultures stimulated to undergo osteogenesis, those derived from *brd2lo* mice showed decreased PPAR γ expression and activation with concomitant suppression of Runx2 expression in female-derived cultures, but not in male-derived cultures.

Conclusions: Loss of *brd2* expression led to rapid and selective age-dependent osteoporosis in female mice but not male mice. Molecular assessments suggested that while diminished *brd2* expression increased adipocyte differentiation in both males and females, it altered osteogenesis primarily in female mice. The maintenance of sex-dependent variation in osteoblastic and adipogenic gene expression in primary bone marrow cultures suggests that some sexual dimorphic differences must be epigenetically imprinted within bone marrow stromal cells. While loss of *brd2* expression leads to obesity in both male and female mice, this contrasts with effects on osteogenesis and bone.

Disclosures: Jennifer Schlezinger, None.

SU0219

The Transcription Factors, Mef2c and Zfp521, Participate in PTH Stimulated MMP-13 Gene Expression in Osteoblastic Cells. Teruyo Nakatani^{*1}, Emi Shimizu², Nicola Partridge². ¹New York University College of Dentistry, USA, USA, ²New York University College of Dentistry, USA

Parathyroid hormone (PTH) regulates the transcription in the osteoblast of many genes. One of these genes is matrix metalloproteinase-13 (MMP-13), which is involved in bone remodeling and early stages of endochondral bone formation. Previously we reported that PTH induces MMP-13 transcription by regulating histone deacetylase 4 (HDAC4). HDAC4 interacts with Runx2, bound to the MMP-13 promoter, and suppresses basal MMP-13 gene transcription. In the rat osteoblastic cell line, UMR 106-01, after PTH treatment, HDAC4 dissociates from Runx2, which is then free to recruit histone acetyl transferases (HATs), especially p300, to the MMP-13 promoter. It is known that as well as Runx2, HDAC4 associates with the transcription factor, Mef2c, and represses its activity. It has been reported that zinc finger protein 521 (Zfp521) associates with Runx2 in chondrocytes, leading to a repression of Runx2 activity via an HDAC4-dependent mechanism. To determine whether Mef2c or Zfp521 are involved in the transcriptional regulation of MMP-13, their expression was transiently knocked down in UMR 106-01 cells by siRNA transfection. Knockdown of Mef2c repressed MMP-13 mRNA expression and promoter activity with or without PTH treatment. To determine whether Mef2c associates with the MMP-13 gene, we performed ChIP assays after 4 h of PTH treatment. The binding of Mef2c to the MMP-13 promoter was increased after PTH treatment. In addition, PTH treatment caused Mef2c protein to migrate more slowly at 2-4 h (indicating phosphorylation) and later degradation in the nucleus. On the other hand, knockdown of Zfp521 enhanced MMP-13 mRNA expression and promoter activity. To examine if Zfp521 is necessary for binding of HDAC4 on the MMP-13 promoter, we performed ChIP assays and found that depleting Zfp521 prevented HDAC4 binding. Immunoprecipitation showed that Mef2c interacts with Zfp521 and after PTH treatment the binding was decreased. Mef2c also binds to Runx2 and this binding was increased by PTH treatment. In conclusion, Mef2c is necessary for MMP-13 gene expression at the transcriptional level and may participate in PTH stimulated MMP-13 gene expression by increased binding to the MMP-13 promoter. Zfp521 suppresses MMP-13 gene expression at the transcriptional level and is necessary for HDAC4 to bind to the MMP-13 promoter. Many factors participate in MMP-13 promoter activity and PTH regulates the association and dissociation of HDAC4 and HATs.

Disclosures: Teruyo Nakatani, None.
This study received funding from: NIH

SU0220

Transactivation of BMP2 Expression by the Wnt Pathway in Osteoblasts. Ming Zhao^{*1}, Rongrong Zhang¹, Shuai Liu¹, Babatunde Oyajobi², Di Chen³, Hong-Wen Deng¹. ¹Tulane University, USA, ²University of Texas Health Science Center at San Antonio, USA, ³Rush University Medical Center, USA

The BMP and Wnt signaling pathways tightly regulate each other to control osteoblast differentiation and bone formation. Multiple mechanisms associated within the two signaling cascades are involved in the functional communication between the pathways. While BMP signaling has been shown to regulate expression of the Wnt pathway and its target genes, however, on the other hand, little is known whether Wnt signaling controls BMP expression in osteoblasts. BMP2 is a prototype of BMP family that plays a critical role in osteoblastogenesis. Given the putative Tcf/Lef response elements (TREs) in the BMP2 promoter, we hypothesize that the Wnt signaling pathway functions as a stimulator of BMP2 transcription in osteoblasts. First, we confirmed the signaling activity of the Wnt/b-catenin pathway in various osteoblast or osteoblast precursor cell lines, including MC3T3-E1, 2T3, C2C12 and C3H10T1/2 cells. Then, we determined the effects of interaction between the BMP and Wnt pathways on BMP signaling activity and consequent osteoblast differentiation. The data suggest that Wnt signaling is an upstream activator of the BMP signaling pathway. Next, we examined the role of the Wnt pathway in regulation of BMP2 expression by altering Wnt signaling activity in these osteoblast cells. We found that activation of Wnt signaling by either treatment with Wnt3a or overexpression of b-catenin/TCF4 complex stimulated BMP2 transcription at both promoter and mRNA levels. In contrast, blockage of the Wnt pathway by either incubation with Wnt antagonists DKK1 and sFRP4, or inhibition of b-catenin/TCF4 activity with E3 ubiquitin ligase b-TrCP or ICAT and DTCF4, reduced BMP2 transcription in these cells. Lastly, using a site mutation approach, we have identified the functional TREs in the BMP2 promoter, suggesting that Wnt activation of BMP2 expression in osteoblasts is mediated through direct b-catenin/Tcf/Lef transactivation of BMP2 promoter. Together, these results demonstrate that the Wnt signaling pathway is an upstream activator of BMP2 expression in osteoblasts, which provides novel insights into the functional cross-talk between the BMP and Wnt pathways in osteoblasts.

Disclosures: Ming Zhao, None.

SU0221

Circulating Sclerostin Levels Are Reduced During Gestation And Differ Between Women With Gestational Diabetes And Controls In The 3rd Trimester. Luigi Gennari^{*1}, Elisa Guarino², Daniela Merlotti¹, Elena Ceccarelli², Dorica Cataldo², Konstantinos Stolkis³, Stella Campagna², Beatrice Franci², Barbara Lucani², Ranuccio Nuti¹, Francesco Dotta².

¹University of Siena, Italy, ²Dept. Internal Medicine Endocrine Metabolic Sciences & Biochemistry University of Siena, Italy, ³Dept. Internal Medicine Endocrine Metabolic Sciences & Biochemistry University of Siena, Italy

Different observations showed a condition of low bone turnover and decreased osteoblast activity in type 1 or 2 diabetes. Sclerostin is a secreted Wnt antagonist produced by osteocytes that regulates osteoblast activity and thus bone turnover. Its levels increase with age and are negatively regulated by estrogen and PTH. In a previous study we demonstrated that circulating sclerostin is increased in patients with type 2 diabetes than in age-matched controls despite slightly increased PTH levels, suggesting that the transcriptional suppression of sclerostin production by PTH may be impaired in diabetes. The aim of the present study was to evaluate the relationship between sclerostin levels and glucose or bone homeostasis in women with gestational diabetes. To this aim we recruited 47 women with gestational diabetes (GDM) and 103 pregnant women with normal glucose homeostasis (GCT) undergoing an oral glucose tolerance test between the 12th and the 36th gestational week (mean 26.7 \pm 3.5). A control group of 30 age-matched non-pregnant women was also recruited as reference population. Women with GDM had fasting glucose levels within the reference range, but significantly higher than GCT women or non-pregnant controls. Overall, circulating sclerostin levels did not significantly differ between GDM and GCT groups (14.7 \pm 9 vs. 13.4 \pm 7 pmol/l, respectively), while were significantly decreased in both groups compared to non-pregnant controls (29.9 \pm 11 pmol/l; p < 0.01). Moreover, sclerostin levels progressively decreased by gestational age in GCT (r = -0.24; p < 0.05) but not GDM, so that in women in the 3rd trimester of gestation sclerostin was significantly increased in GDM than GCT groups (16.1 \pm 9 vs. 11.3 \pm 5 pmol/l, p < 0.05, respectively). Of interest maternal circulating sclerostin positively correlated with the weight (r = 0.19, p = 0.08) and the height (r = 0.22, p < 0.05) at birth of the newborn (data available for 82 cases). In conclusion, our data suggest that serum sclerostin is reduced during pregnancy in normal and GDM females, but significantly decreases by gestational age only women with normal glucose homeostasis. Further studies are required to assess the potential implications of variations in circulating sclerostin on bone health of the newborn and the mother under normal or impaired glucose homeostasis.

Disclosures: Luigi Gennari, None.

SU0222

Protein Kinase C α Deletion Age-dependently Alters Bone Architecture in Female Mice, Impairs Osteoblast Responsiveness to Estrogen and Strain and Replicates Features of Gaucher Disease. Gabriel Galea^{*1}, Toshihiro Sugiyama², Lee Meakin¹, Christopher M Williams¹, Sarah Curtis¹, Lance Lanyon³, Alastair W Poole¹, Joanna Price¹. ¹University of Bristol, United Kingdom, ²Yamaguchi University School of Medicine, Japan, ³Royal Veterinary College, United Kingdom

Protein kinase C (PKC) regulates osteoblast activity *in vitro*¹ and plays a role in the pathogenesis of several major diseases, including Gaucher disease² which is associated with impaired bone structure and increased fracture risk. This led us to investigate the effects on bone regulation *in vivo* of deleting PKC α in mice.

Bones from female and male PKC α ^{-/-} (KO) mice and wild type (WT) littermates were analyzed by μ CT and histomorphometry. The effect of 17 β -estradiol (E2), mechanical strain and Wnt3a on the proliferation of long bone-derived osteoblasts (LOBs) from KO and WT mice was determined by Ki-67 *in situ* cell cycle analysis. Differentiation of cultured LOBs was analyzed by alkaline phosphatase activity, mineralized nodule formation and expression of osteoblast markers (by QPCR). Selected osteoblast and adipocyte markers and Wnt target genes were measured in bone marrow from KO and WT mice by QPCR. Gaucher correlates analyzed were spleen weight and marrow expression of the GBA1 enzyme which is mutated in human patients.

Between 12 and 22 weeks of age, female, but not male, KO mice developed extensive diaphyseal intra-medullary bone due to active formation. WT LOBs proliferated in response to E2, strain and Wnt3a. Cells from KO mice proliferated similarly to WT cells in response to Wnt3a, but showed no response to E2 or strain. All measures of differentiation were greater in KO LOBs compared to WT cells. This correlated with higher levels of expression of osteoblast markers (Runx2, Osterix, Col1A1) and Wnt target genes (cMyc, Axin2, Wisp2, Cyr61³) in KO marrow. In contrast, adipocyte marker (PPAR γ , C/EBP α) expression was lower in marrow from KO mice. KO mice also had progressive splenomegaly, lower levels of GBA1 and 'Gaucher-like' cells in marrow.

In conclusion, this study demonstrates that deletion of PKC α leads to an age-related, gender-specific abnormality in bone formation in mice which also has features of Gaucher's disease. The requirement of PKC α for the proliferative response of osteoblasts to estrogen and mechanical strain and its inhibitory effect on differentiation, potentially via altered Wnt signaling³, may contribute to the mechanisms behind increased fracture risk in Gaucher patients.¹Nakura A et al., Bone 2011;48(3):476-84. ²Mistry PK et al., Proc Natl Acad Sci U S A. 2010;107(45):19473-8. ³Si W et al., Mol Cell Biol. 2006;26(8):2955-64.

Disclosures: *Gabriel Galea, None.*

SU0223

PTH Targets MKP-1 and pp38-MAPK Pathway in The Regulation of Osteoblast Mineral Homeostasis. Chandrika Mahalingam¹, Bharat Sampath¹, Rashmi Patil¹, Abdul Abou-Samra², Nabanita Datta^{*3}. ¹Endocrinology, Wayne State University School of Medicine, USA, ²Endocrinology, Wayne State University School of Medicine, USA, ³Endocrinology, Cardiovascular Research Institute, Karmanos Cancer Institute, Wayne State University School of Medicine, USA

We have recently reported that MAPK phosphatase (MKP) -1 deletion in mice regulates osteoblast gene expression and skeletal responsiveness to PTH. MKP-1 knockout (KO) osteoblasts exhibited attenuated PTH inhibition of *in vitro* mineralization and no change in matrix Gla protein (MGP) expression compared to wild type (WT) cells. Here we studied the role of pERK and pp38-MAPK cascade, the downstream effector of MKP-1, in the response of osteoblasts to PTH. Primary cultures of WT and MKP-1 KO calvarial osteoblasts were differentiated with media containing ascorbic acid and beta glycerophosphate. The cells were incubated with PTH(1-34) either alone or in combination with U0126, MEK1/2 inhibitor, or SB203580, pp38 inhibitor, from day 1 to day 14-17. Von Kossa assay of mineralization was performed. Results show that blocking pERK does not block mineralization of differentiated osteoblasts from either WT or KO mice. In contrast, blocking the pp38 MAPK pathway attenuates mineralization (by 25-50%) in both genotypes. PTH inhibition (>90%) of mineralization in WT osteoblasts is not influenced by SB203580. In the KO osteoblast PTH treatment alone continues mineralization, and PTH in presence of SB203580 blocks mineralization (>95%). We next asked whether PTH signaling on mineralization differs in mature versus early osteoblastic cells. Osteoblasts were differentiated for 7-10 days and then treated with PTH alone or in combination with the inhibitors for additional 8-10 days. Notably, in contrast to early osteoblasts exposure of mature WT osteoblasts to PTH continues mineralization (40-60%) in the presence or absence of SB203580. MKP-1 KO osteoblasts shows similar responses to PTH as observed in less mature cells. Real-time PCR analysis reveals that MGP expression in WT cells are significantly less following PTH treatment with either inhibitors compared to PTH alone (approx. 2-fold vs. 6-fold). In KO osteoblasts PTH alone does not show any change in MGP expression but PTH increases MGP expression 3-4 fold in the presence of the inhibitors, suggesting a distinct role for MKP-1 in PTH control of MGP. These data support to a notion that MKP1-plays a key role in osteoblast mineral homeostasis and in transducing PTH signal differently from early to late osteoblasts, targeting pp38 MAPK pathway.

Disclosures: *Nabanita Datta, None.*

SU0224

Sphingosine-1-phosphate Regulates Osteoblast Maturation and Mediates Some Estrogen Effects on Bone. Duangrat Songsawad¹, Pawinee Piyachaturawat¹, Harry Blair², Lisa Robinson^{*2}. ¹Mahidol University, Thailand, ²University of Pittsburgh, USA

Estrogen is a major positive regulator of skeletal mass, with well-established inhibitory effects on osteoclastic bone resorption. Evidence of direct estrogen actions on osteoblasts have also been reported, but the effects are complex and the underlying mechanisms unclear. Past studies have suggested both transcriptional and non-transcriptional mechanisms for estrogen modulation of osteoblasts. Sphingosine-1-phosphate (S1P) signaling was recently identified as an important skeletal regulator. As in other cell types, estrogen might act in bone through stimulation of sphingolipid signaling: in such cells, estrogen treatment increases sphingosine kinase production of S1P that, after export, binds cell surface receptors to exert autocrine/ paracrine effects. We investigated the role of S1P using non-transformed primary human osteoblasts in culture. Addition of S1P reproduced key effects of estrogen treatment. Osteoblast differentiation was enhanced with increases in alkaline phosphatase activity and mRNA, as well as up-regulation of Osterix and Runx2. Similar effects were observed with SEW-2871, an agonist selective for the S1P receptor 1 (S1PR1). We confirmed osteoblast expression of S1P receptors, in particular S1PR1, and also found expression of sphingosine kinase 1, using quantitative real-time PCR corroborated by immunoblot results. To test whether estrogen may act through S1P in bone, we evaluated the effects of the sphingosine kinase 1 inhibitor, SK1-I, on osteoblast response to estrogen. Treatment with SK1-I inhibited estrogen induction of alkaline phosphatase, Osterix and Runx 2. SK1-I also inhibited osteoblast production of osteoprotegerin and enhanced their expression of RANKL, suggesting that S1P may also be important to inhibitory effects of estrogen on osteoclastogenesis. Estrogen increased the expression of sphingosine kinase 1 in osteoblasts, consistent with a transcriptional mechanism for estrogen actions through S1P signaling. But we also found evidence of acute, non-genomic estrogen effects: as early as 15 minutes after treatment with estrogen, osteoblast sphingosine kinase activity more than doubled. The results overall indicate that S1P can modulate osteoblast differentiation, and through both acute activation of sphingosine kinase enzyme activity and induction of its expression, may mediate estrogen effects on bone. These studies thus suggest that the sphingosine-1-phosphate pathway may represent a novel target for anti-osteoporotic therapy.

Disclosures: *Lisa Robinson, None.*

SU0225

Withdrawn

SU0226

Blockade of Endogenous Gi Signaling in Osteoblasts Accelerates Bone Fracture Healing. Liping Wang^{*1}, Dylan O'Carroll², Richard Kao³, Lalita Wattanachanya⁴, Robert Nissen⁴. ¹VA Medical Center, San Francisco, USA, ²SF VAMC, USA, ³UCSF/VAMC, USA, ⁴VA Medical Center & University of California, San Francisco, USA

G protein-coupled receptors (GPCRs) regulate skeletal homeostasis. We previously demonstrated that activation of endogenous Gi signaling using engineered GPCRs targeted to osteoblasts (OBs) resulted in osteopenia due to suppressed bone formation. Recently, we found that blockade of Gi signaling in OBs prevented age-related bone loss by increasing bone formation in both trabecular and endocortical surfaces in female mice in which expression of pertussis toxin (PTX) gene, under the control of 2.3 kb Collagen I α 1 promoter (Col1(2.3)), was regulated via a tetracycline responsive promoter. We therefore hypothesized that blockade of Gi signaling in OBs may accelerate fracture (FX) healing. Closed, non-stabilized tibial FXs were created in 3 and 6 month old transgenic and littermate control mice, and PTX gene expression was activated by withdrawal of doxycycline 2 weeks before FX. The healing process was evaluated 28 days post-FX by μ CT, histomorphometry, and gene expression. We found an age-related decrease in bone formation rate (BFR) and bony callus (BV/TV) in both transgenic and control mice. Although FXs, regardless of age and genotype, were completely bridged after 28 days, μ CT demonstrated a 21.4% (p<0.05) increase in callus BV/TV and a 28.5% (p<0.05) increase in trabecular thickness (Tb.Th) in 3 month old Col1 (2.3).PTX mice and a 58.4% (p<0.05) increase in callus BV/TV and a 25.5% (p<0.05) increase in Tb.Th in 6 month old transgenic mice. Furthermore, with histomorphometry, we found in the callus, a 40.8% (p<0.01) and a 45% (p<0.05) increase in trabecular BV/TV and a 76.1% (p<0.01) and a 129.4% (p<0.05) increase in BFR in the 3 and 6 month old transgenic mice, respectively. In addition, the Col1(2.3).PTX mice showed decreased mRNA expression of alkaline phosphatase, collagen type I, osterix, and DKK1 in the callus. The finding of decreased expression of DKK1 in Col1(2.3).PTX mice suggests that endogenous Gi signaling serves to maintain DKK1 expression thereby suppressing WNT signaling during bone healing. Collectively, our findings demonstrate that endogenous Gi signaling in OBs restrains FX healing and blockade of Gi signaling in OBs promotes FX healing by accelerating bone formation and mineralization in the callus. Further studies are needed to identify the Gi-GPCRs in OBs that constrain bone formation during FX repair.

Disclosures: *Liping Wang, None.*

SU0227

Bone Sialoprotein Is Essential for Osteoblastic Differentiation and Maturation of Osteoprogenitor Cells. Jinxi Wang*, Qinghua Lu, M. Kareem Shaath, James Bernard, University of Kansas Medical Center, USA

Bone sialoprotein (BSP) is an extracellular matrix protein highly expressed in developing and postnatal regenerating bone. Its biological function in bone formation remains unclear. Our recent *in vivo* studies demonstrated that implantation of BSP stimulated new bone formation in the central regions of rat/mouse critical-size cranial bone defects. BSP-responsive cells were primarily derived from the dura mater, where Runx2-expressing cells were detected in non-operated normal rodents. Runx2 has been identified as a key transcription factor for activation of osteoblast differentiation. It is not clear why these Runx2-expressing cells in the dura do not differentiate into osteoblasts and form ectopic bone in normal rodents. To test our hypothesis that BSP is essential for differentiation and maturation of Runx2-expressing osteoprogenitor cells, we performed loss- and gain-of-BSP function analyses in cell cultures. Primary cells isolated from the dura or calvaria of young adult mice were cultivated separately in α -MEM media. When the cells reached ~80% confluence, they were cultured in osteogenic differentiation media with ascorbic acid (50 μ g/ml) and 5 mM β -glycerophosphate and treated as follows: Dural cells were treated with or without BSP, while calvarial cells were transduced with BSP RNAi lentivectors (to knockdown BSP expression) or scrambled lentivectors (negative controls). The results revealed that: 1) In dural cells, mineralized bone-like nodules were formed in BSP-treated, but not in untreated cultures; expression level of osteocalcin (a marker of mature osteoblasts) was significantly higher in the BSP-treated than the untreated cultures. 2) In calvarial cells, mineralized bone-like nodules were formed in cultures without knockdown of BSP, but not in cultures with knockdown of BSP; expression level of osteocalcin was significantly higher in the cultures without BSP knockdown than the cultures with BSP knockdown. The results indicate that BSP is essential for differentiation and maturation of Runx2-expressing osteoprogenitor cells in mouse dura and calvaria. Thus, Runx2-expressing cells in the dura normally do not spontaneously differentiate into functional osteoblasts without BSP. The data also suggest that knockdown of BSP suppresses osteoblast maturation in calvarial cells which normally differentiate into osteoblasts and form bone nodules in the presence of endogenous BSP and osteogenic media.

Disclosures: Jinxi Wang, None.

SU0228

Characterization of a Periosteal Mesenchymal Progenitor Cell Population Involved in Fracture Healing. Brya Matthews*¹, Danka Grcevic², Liping Wang¹, David Rowe¹, Douglas Adams¹, Ivo Kalajic¹. ¹University of Connecticut Health Center, USA, ²University of Zagreb School of medicine, Croatia

Fracture healing is a complex process that involves many cell lineages. Studies of gene expression in whole fracture callus do not distinguish contributions from different cell lineages. Previously we showed that α -smooth muscle actin (SMA) is a marker of progenitor cells that expand rapidly following fracture. We aimed to characterize this population during its commitment to callus formation. To identify and trace cells in periosteum and bone marrow (BM) we used SMA promoter-driven inducible Cre expression (SMA-CreERT2) combined with a Cre-activated TdTomato reporter A19 to generate SMA9 mice. Tibias were fractured in 3-4 month old SMA9 mice pretreated with tamoxifen. Periosteum/soft callus and BM were collected 2 days after treatment (unfractured), and 2 and 6 days after fracture.

The majority of SMA9+ cells in unfractured periosteum are CD45-, 10% express Sca1, and 30% express CD51, a marker of committed osteoprogenitors. SMA9+ BM cells show quite different surface marker profiles, with 80% CD45+. In addition, microarray analysis revealed over 3000 genes differentially regulated between these two cell populations. Histology indicated that SMA9+ cells form chondrocytes and osteoblasts in a fracture callus, indicated by concomitant expression of Col2.3GFP and Col2A1GFP. FACS analysis showed that SMA9+ cells comprised 0.8% of cells in unfractured periosteum, and 1.2% and 3.5% 2 and 6 days after fracture, respectively, and 0.09%, 0.3% then 1.6% in BM. These SMA9+ cells were selectively isolated by FACS sorting and microarray analysis was performed.

Two days after fracture many upregulated genes in periosteum were associated with mitosis or immune response (e.g. chemokines Cxcl2 and Ccl9). By day 6, upregulated genes were associated with bone and cartilage, with >50-fold increase in Acan and Col2a1, and elevated Ibsp and osterix. Numerous downregulated genes were associated with vascular and muscle development, including an expected decrease in SMA. Notch signaling components were decreased in SMA9+ cells following fracture, including Notch1, 3, 4, Hes1 and Hey1. These changes were confirmed by real time PCR.

In summary, this is the first study to characterize gene expression in a defined subset of cells involved in fracture healing. After fracture, proliferation is stimulated in SMA9+ periosteal progenitor cells followed by differentiation into chondrocytes and osteoblasts. Downregulation of Notch signaling may be important in this process.

Disclosures: Brya Matthews, None.

SU0229

Effects of Auraptene on Osteoblast Differentiation. Takayuki Yonezawa*¹, Ayaka Hibino², Toshiaki Teruya², Byung-Yoon Cha², Kazuo Nagai², Ung-Il Chung³, Je-Tae Woo². ¹The University of Tokyo, Japan, ²Chubu University, Japan, ³University of Tokyo Schools of Engineering & Medicine, Japan

In the treatment of osteoporosis, anti-resorptive drugs have been mainly used to suppress bone loss but anabolic drugs are needed to effectively increase bone mass. Parathyroid hormone (PTH) has been developed clinically as anabolic drug for osteoporosis and shows a superior effect on bone formation, however, it has some drawbacks such as limitation of administration and high costs. Auraptene is a natural coumarin derivative isolated from the peel of Citrus fruits. Several pharmacological properties such as chemoprevention were reported in recent years. To develop the agent for the treatment of bone-decreasing diseases, natural compounds which promote osteoblast differentiation were screened using mouse preosteoblastic MC3T3-E1 cells. As a result, we found that auraptene increases the activity of alkaline phosphatase (ALP), a marker of early osteoblast differentiation. Auraptene also increased the mRNA and protein expression of osteocalcin, a late-stage osteoblast differentiation maker, and promoted osteoblastic mineralization. The promotion of ALP activity by auraptene was abolished by the treatment of bone morphogenetic protein (BMP) signal inhibitors. Auraptene increased the mRNA expressions of BMP-2. In addition, BMP-responsive reporter activity was enhanced by auraptene. These results indicate that auraptene promotes osteoblast differentiation probably by inducing the expressions of BMP and activating BMP signaling pathways. Structure-activity relationship study using auraptene derivative compounds indicated that geranyl group is important for the promoting activity of osteoblast differentiation. Thus, auraptene is expected to possess bone anabolic property and be applied for its use in the treatment of bone-decreasing diseases and bone regeneration.

Disclosures: Takayuki Yonezawa, None.

This study received funding from: Erina Co Inc.

SU0230

Effects of Quercetin on the Differentiation of Mesenchymal Stem Cells to Osteoblasts and Adipocytes. Antonio Casado-Diaz*¹, Raquel Santiago-Mora², Jaouad Anter¹, Jose Manuel Quesada Gomez³. ¹IMIBIC Hospital Universitario Reina Sofia, Spain, ²Universidad De Córdoba, Spain, ³Quesper R&D, Spain

Quercetin is a natural flavonoid found abundantly in many fruits, vegetables, grapes, red wine and other food products. Flavonoids display antioxidant and free radical scavenging activity and their consumption has been proposed as chemopreventive agent against degenerative diseases such as cancers, cardiovascular diseases, osteoporosis and diabetes.

The aim of this work was the study of the effects of quercetin (10⁻⁷ – 10⁻⁵ M) in mesenchymal stem cells induced to differentiate to osteoblasts and adipocytes. Endpoints related to cell proliferation, activity of alkaline phosphatase (ALP) in osteoblasts, formation of lipid droplets in adipocytes and mRNA levels of osteoblastogenic and adipogenic gene markers were studied. The expression of the osteoblastogenesis-related genes ALP, type 1 collagen and osteocalcin was markedly down-regulated when osteoblasts were treated with 10⁻⁵ M quercetin. Quercetin inhibits cell viability and ALP activity on osteoblasts mainly at high concentrations (10⁻³ M).

Cell viability on adipocytes was not affected by quercetin, even at high concentrations. Quercetin enhances adipocytes differentiation but does not increase the formation of lipid in mature adipocytes. 10⁻⁵ M quercetin increased the mRNA levels of PPAR γ 2 and FABP-4, despite LPL expression was down-regulated after 14 days treatment.

Quercetin inhibits differentiation of MSCs to osteoblasts and up-regulates adipogenic gene markers at high concentrations. Molecular studies are needed to understand the exact mechanisms of its action. These data support caution in recommending the intake of flavonoids such as quercetin in large quantities because of its potential detrimental effect on the bone.

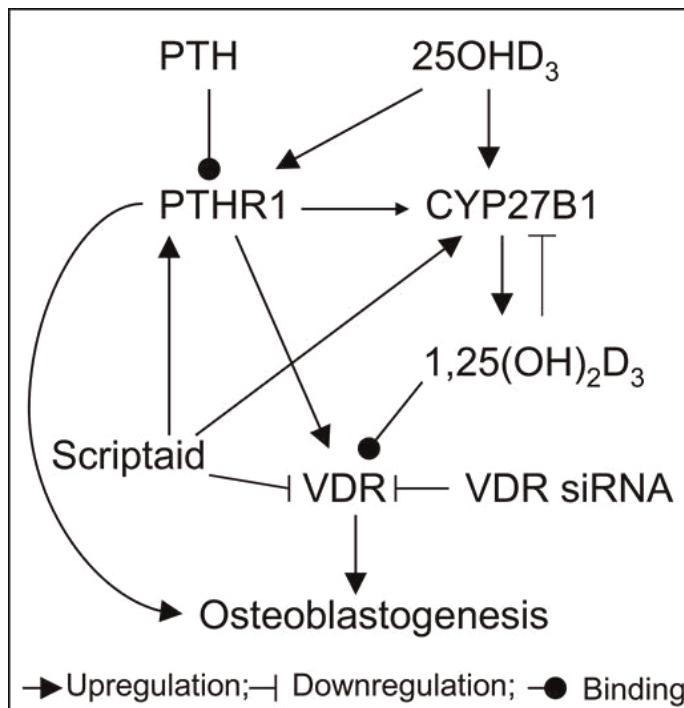
Disclosures: Antonio Casado-Diaz, None.

SU0231

Histone Deacetylation Mediates the Rejuvenation of Osteoblastogenesis by the Combination of PTH and 25(OH)D in hMSCs from Elders. Shuanhu Zhou*, Shuo Geng, Julie Glowacki, Brigham & Women's Hospital, USA

Skeletal aging is characterized as a gradual loss of bone mass due to an excess of bone resorption that is not balanced by new bone formation. Vitamin D metabolites are important effectors of bone and mineral homeostasis. Human bone marrow stromal cells (hMSCs) are a target of 1 α ,25-dihydroxyvitamin D (1,25(OH)₂D) action to promote their differentiation to osteoblasts, but also participate in vitamin D metabolism by converting 25-hydroxyvitamin D (25OHD₃) to 1,25(OH)₂D₃ by the 1 α -hydroxylase (CYP27B1) (Endocrinol. 151:14-22, 2010; JBMR 26:1145-53, 2011). This supports an autocrine/paracrine role of vitamin D metabolism in osteoblastogenesis of

hMSCs. There are age-related decreases in expression of PTHR1 and CYP27B1 and action of 25(OH)D₃ in hMSCs, but osteoblastogenesis is rejuvenated by synergy between PTH(1-34) and 25(OH)D₃ (Aging Cell 10:780-8, 2011; Aging Cell 10:962-71, 2011). In this study, we assessed the mechanisms of that rejuvenation. The hMSCs were obtained from tissue discarded during orthopedic surgery; osteoblastogenesis was assessed by Alkaline Phosphatase (AlkP); gene expression was determined by PCR; and gene silencing was used to knock-down the VDR. First, 1,25(OH)₂D₃ had no effect on AlkP activity in hMSCs that had been transfected with VDR siRNA; thus VDR was required. Second, PTH upregulated VDR, and 25OHD₃ upregulated PTHR1 receptor in hMSCs. We tested the effects of the epigenetic modulation drug Scriptaid, an inhibitor of histone deacetylase (HDAC) on these outcomes. In hMSCs from a 76-year-old male subject, 100 nM PTH1-34 (*p<0.05 vs. control, ANOVA) and 100 nM 25OHD₃ (**p<0.01) significantly stimulated AlkP activity, with greater effect when combined (***p<0.001). Scriptaid inhibited the stimulation of PTH and 25OHD₃ on osteoblastogenesis. Scriptaid alone downregulated VDR, but upregulated CYP27B1 and PTHR1. In summary, our data demonstrated that chromatin deacetylation is required for the synergistic effect of PTH and 25OHD₃ on osteoblastogenesis in hMSCs. Epigenetic regulation of the VDR may be central to rejuvenating osteoblastogenesis.



Figure

Disclosures: Shuanhu Zhou, None.

SU0232

Identification of Novel Runx2 Target Genes in Osteoblastic Differentiation. Jianning Tao¹, Yangjin Bae¹, Alison Roos¹, Terry Bertin¹, Jason Yustein¹, Lawrence Donehower¹, Brendan Lee². ¹Baylor College of Medicine, USA, ²Baylor College of Medicine & Howard Hughes Medical Institute, USA

Runt-related transcription factor 2 (Runx2) is a master transcription factor required for osteoblastic differentiation, proliferation, and metabolic function. Mutations in the human Runx2 gene result in Cleidocranial dysplasia (CCD), an autosomal dominant skeletal disease. Although upstream signaling regulators of Runx2 have been well studied, its direct downstream target genes have not been in an un-biased analysis during osteoblast differentiation. In this study, we examined recruitment of Runx2 to murine genomic proximal promoter using chromatin immunoprecipitation (ChIP)-on-chip analysis in MC3T3-E1 cells. We found that among 19,489 transcripts represented in the array, high-confidence binding sites of RUNX2 were found in 1125, among them, including 225 unknown and 900 known functional genes. Through gene ontology analysis, we found that the functions of these genes belong to a diverse group of categories, such as cell division, apoptosis, mineralization, cell motility and adhesion. Among these genes, many are known direct targets of Runx2, including Bone Gamma-carboxyglutamate protein (OC), Osteoprotegerin (OPG), and RUNX2 itself. In addition, we found that many potential direct targets of Runx2 are components of the evolutionally-conserved signaling

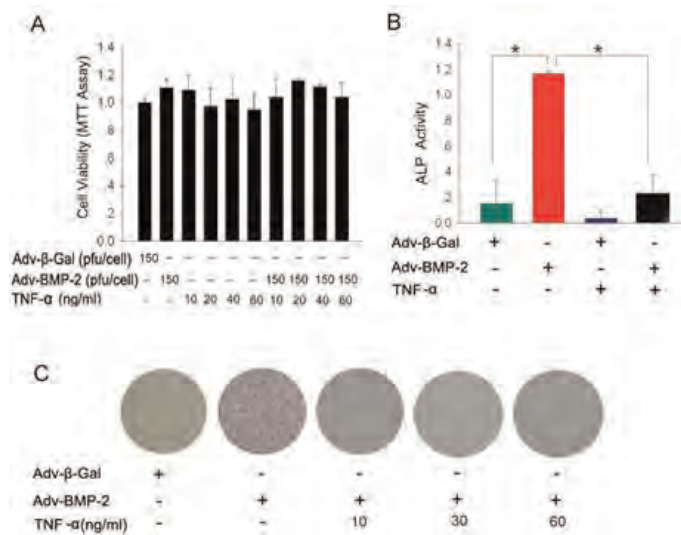
pathways such as TGFβ, Wnt, and Notch. Moreover, our results from shRNA-mediated knock-down or overexpression of Runx2 in osteoblasts demonstrate that Runx2 directly regulates components of TGFβ pathway including TGFβ1, TGFβR2, Id3, Gdf6, and Glg1. This suggests that Runx2 can execute a feedback to regulate its upstream regulators. Thus, identification of novel target genes of Runx2 will further our understanding of the Runx2 transcriptional network and possibly reveal new susceptibility markers for bone disorders such as osteosarcoma.

Disclosures: Jianning Tao, None.

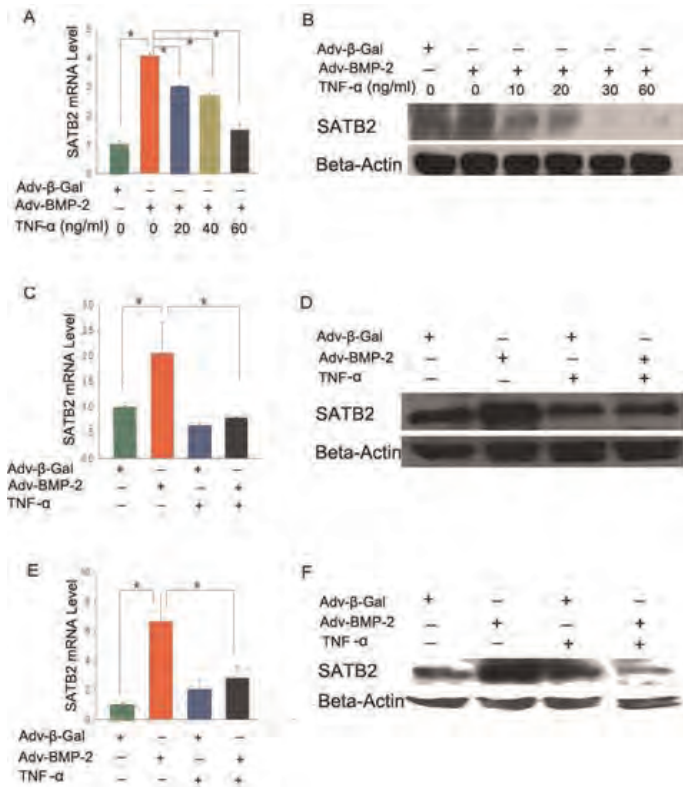
SU0233

Inhibition of SATB2 Expression by Tumor Necrosis Factor through NF-κB and Mitogen-Activated Protein Kinase Pathways. Xiaoling Zhang^{*1}, Chijian Zuo², Yu Shi², Xiaoying Zhao², Ning Zhang², Kerong Dai², Jiake Xu³. ¹Institute of Health Sciences, Shanghai Jiao Tong University School of Medicine (SJTUSM) & Shanghai Institutes for Biological Sciences (SIBS), Chinese Academy of Sciences (CAS), Shanghai 200025, China, ³University of Western Australia, Australia

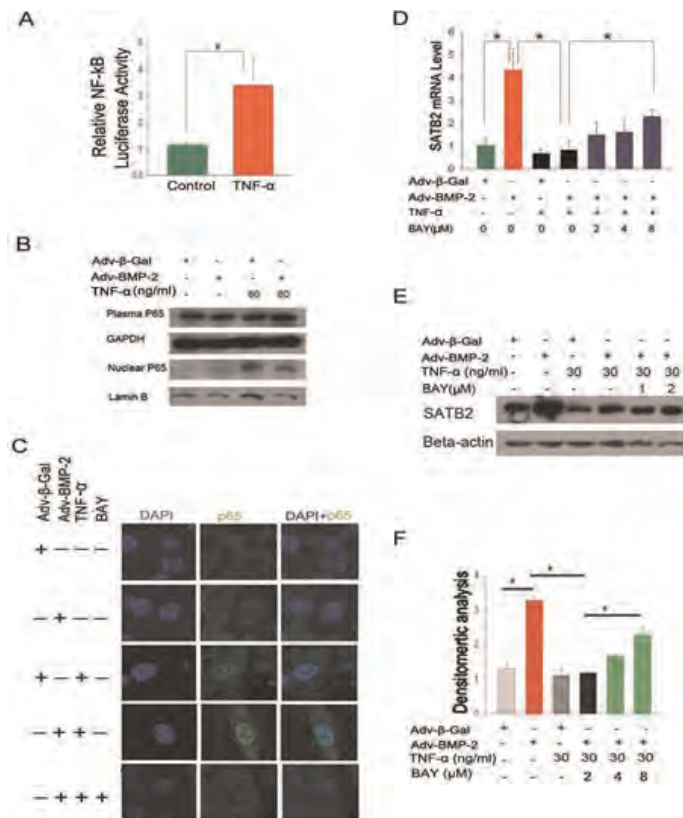
Tumor necrosis factor alpha (TNF-α) plays an important role in the pathogenesis of osteoporosis, which results from the imbalance between bone resorption and formation. TNF-α induces bone loss by stimulating osteoclastic resorption and reducing osteoblastic bone formation. Although the TNF-α mechanism of facilitating RANKL-induced osteoclast differentiation and bone resorption is well known, the mechanisms behind the suppression of the osteoblast differentiation from mesenchymal stem cells are still poorly understood. SATB2 was recently discovered to be a key transcription factor for osteoblast differentiation, but its regulation by osteoblast-related signals remains to be elucidated. We hypothesized that SATB2 expression was suppressed by TNF-α and that this effect contributed to the inhibition of osteoblast differentiation. Using an *in vitro* osteoblast differentiation model, we treated mesenchymal cell line C2C12 with Adenovirus-BMP-2, which induces the cells to undergo osteoblast differentiation. SATB2 expression was significantly increased when the BMP signaling was stimulated. TNF-α treatment inhibited C2C12 cell differentiation and sharply decreased BMP-induced SATB2 expression. Considering that SATB2 is a critical transcription factor for osteoblast differentiation, our findings suggest that its reduced expression contributed to the inhibitory effect of TNF-α on osteoblast differentiation. As signal mediators of TNF-α, the nuclear factor-κB (NF-κB) and mitogen-activated protein kinase (MAPK) signaling pathways and their role in the regulation of SATB2 expression were investigated. Upon TNF-α treatment, the NF-κB signaling pathway in C2C12 cells was significantly activated and the NF-κB inhibitor, BAY11-7082, blocked the inhibition of SATB2 expression mediated by TNF-α. The activity of extracellular signal-regulated kinase-1/2 (ERK1/2) and P38, but not c-Jun NH(2)-terminal kinase (JNK), was increased by the treatment of TNF-α in C2C12 cells. Furthermore, the inhibitor of ERK1/2, U0126, was found to abrogate the TNF-α inhibition of SATB2 expression. These results suggest that TNF-α suppresses SATB2 expression through NF-κB and MAPK signaling pathways.



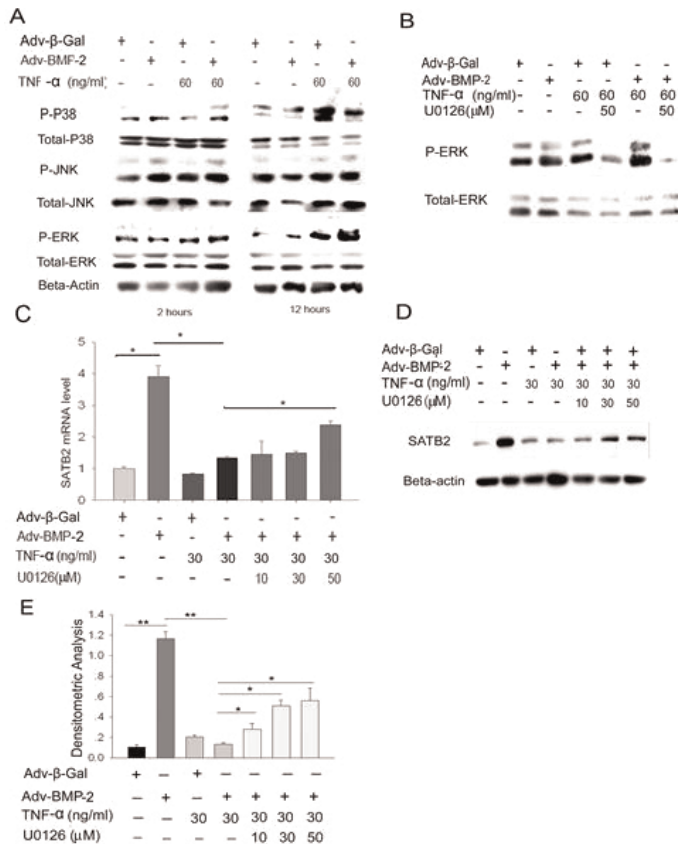
TNF-α inhibits C2C12 cell osteoblastic differentiation



TNF-alpha inhibits SATB2 gene expression



TNF-alpha inhibits SATB2 expression by activating NF-?B



TNF-alpha inhibits SATB2 expression by activating the ERK signaling pathway

Disclosures: Xiaoling Zhang, None.

SU0234

LMP-1 Regulates Osteoblast/Adipocyte Lineage Commitment of Mesenchymal Stem Cells (MSCs). Manjula Viggaswarapu¹, Maggie Bargouti², Mesfin Teklemariam³, Scott Boden⁴, F. Louisa Titus^{*3}. ¹Emory University School of Medicine, USA, ²AREF/ VAMC, USA, ³Emory University, USA, ⁴Emory Spine Center, USA, ⁵VA Medical Center, Decatur, USA

Osteoporosis is associated with increased osteoclast mediated bone resorption, and is also associated with increased adipocytes and decreased osteoblasts in bone marrow. These cells share a common progenitor and the proportion of each cell type is determined by factors that regulate lineage determination of the progenitors. LIM Mineralization Protein-1 (LMP-1) is an intracellular protein whose overexpression stimulates differentiation of preosteoblasts and enhances BMP-2-induced differentiation of human MSCs. Here we report that LMP-1 also inhibits the adipogenic pathway in hMSCs.

Human MSCs overexpressing LMP-1 were grown under adipogenic conditions for 17d prior to analysis of lipid accumulation or osteogenic conditions for 21d prior to silver staining. LMP-1 cDNA was delivered using a modified Type 5 adenovirus at 10 moi. The control construct delivered GFP cDNA. LMP-1 reduced the lipid content of the adipogenic cultures and also reduced expression of adiponectin. Under osteogenic conditions, hMSCs expressing LMP-1 induced nodule formation and bone sialoprotein (BSP) expression compared with control cells. Since b-catenin activation enhances osteogenesis and decreases adipogenesis, we measured the effect of LMP-1 on b-catenin reporter activation. Reporter activity increased 2-3 fold compared to control and b-catenin protein accumulation was measurable 24h after LMP-1 treatment in cells grown under adipogenic and osteogenic conditions. Further, PPARg activity decreased 50-70% 48h after treatment with LMP-1 in cultures grown under adipogenic conditions; this decrease was blocked by inhibiting b-catenin activity, suggesting that b-catenin is required for LMP-1 inhibition of PPARg activity. Expression of BSP was decreased by inhibiting b-catenin activity, suggesting that LMP-1 induction of osteoblastogenesis requires b-catenin activity. Since canonical activation of b-catenin requires Wnts, we applied Wnt inhibitors to LMP-1 treated hMSCs and measured b-catenin reporter activity. Blocking Wnt 10b activity prevented the LMP-1-induced increase in reporter activity under both growth conditions, suggesting that Wnt 10b is required for LMP-1-induced b-catenin reporter activation. We conclude that LMP-1 inhibits lineage commitment of hMSCs toward adipocytes and enhances commitment to osteoblasts through canonical activation of b-catenin. Thus, increasing LMP-1 influence on hMSC lineage determination represents a novel bone anabolic therapeutic strategy

Disclosures: F. Louisa Titus, None.

SU0235

Released Proteins from Demineralized Bone Enhance the Osteogenic and Angiogenic Potential of Primary Progenitor Cells. Peter Supronowicz^{*1}, Scott Tran², Mick Popp². ¹RTI Biologics, USA, ²RTI Biologics, Inc, USA

Demineralized bone matrix (DBM) is routinely utilized as an orthopedic implant for bone void filler and/or extender applications. The complex collections of extracellular matrix proteins contained within are exploited for their osteoinductive properties to recruit and differentiate the host's progenitor cell populations in an effort to enhance the bone repair process. The purpose of the study was to examine the release of select extracellular matrix proteins from DBM while concurrently evaluating the matrix deposition and protein production by progenitor cells cultured in proximity to the allograft in vitro. Proteins were selected based on their relevance to new matrix synthesis as well as angiogenesis.

Primary progenitor cells isolated from human bone marrow were plated in 24-well plates for 24 hours. Transwell inserts containing 50mg of DBM were placed over the cell layers (Figure 1A); the system was cultured in osteogenic media for 14 days under standard cell culture conditions. Cells and DBM were also cultured separately under the same conditions. Supernatants were collected after 3, 7, 10, and 14 days and analyzed by ELISA for BMP-2, BMP-7, OPN, CXCL5, and VEGF; lysates and hydrolysates were collected after 14 days and assayed for alkaline phosphatase and calcium-containing mineral, respectively.

In the presence of DBM, progenitor cells exhibited a 67% reduction in AP activity while concurrently producing significantly ($p < 0.05$) more calcium-containing mineral deposits (Figure 1B). BMPs and OPN were only present in DBM while CXCL5 and VEGF were exclusive to cell supernatants. However, while the increase in Ca^{2+} persisted through two separate donors, one source of DBM did not release detectable amounts of BMP-2 past the third day. Furthermore, cell proximity to the DBM resulted in a significantly ($p < 0.05$) synergistic increase in VEGF production (Figure 2).

The findings in this study suggest that progenitor cells produce calcified matrix more rapidly in the presence of DBM, attributable to a bone morphogenetic protein but not necessarily exclusive to BMP-2; the argument can also be made for VEGF. This can have beneficial implications for not only cells in the recipient, but cells that could be delivered alongside the allograft as well. In addition, the elicited effects can be credited to levels of proteins in the picogram per milliliter concentrations as opposed to the typical hundreds of nanograms commonly used in in vitro studies.

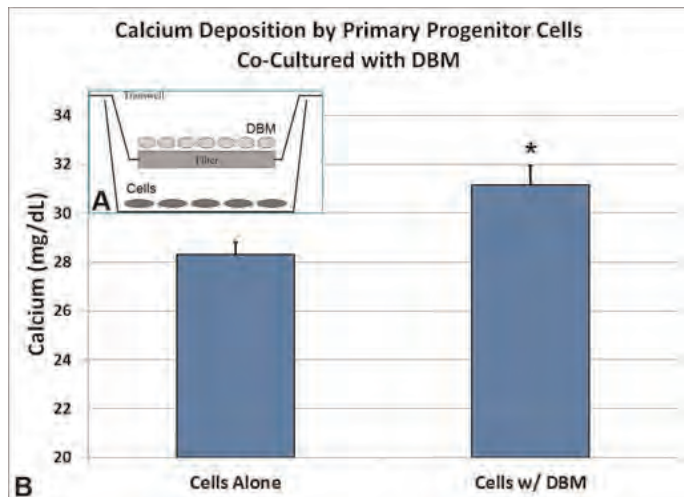


Figure 1

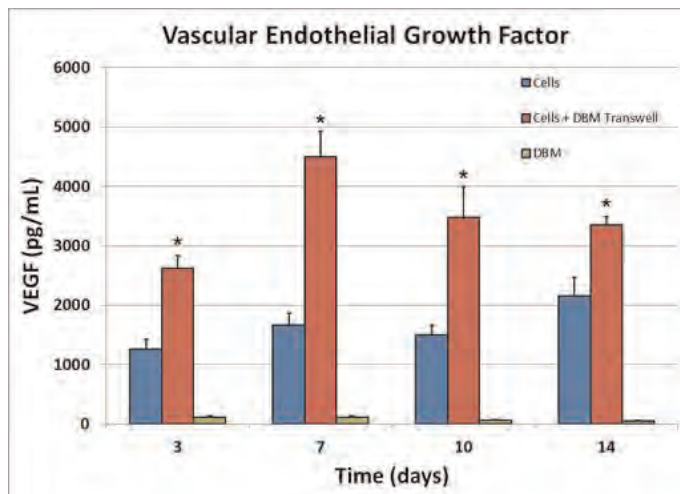


Figure 2

Disclosures: Peter Supronowicz, RTI Biologics, 3

SU0236

Short (15 Minutes) BMP-2 Treatment Stimulates Osteogenic Differentiation of Human Adipose Stem Cells Seeded on Calcium Phosphate Scaffolds.

Janice R. Overman¹, Elisabet Farre-Guasch², Marco N. Helder³, Christiaan M. ten Bruggenkate⁴, Engelbert A.J.M. Schulten⁵, Jenneke Klein-Nulend^{*6}. ¹ACTA-University of Amsterdam & VU University Amsterdam, Dept Oral Cell Biology, Research Institute MOVE, Netherlands, ²International University of Catalunya, Dept Basic Sciences, Faculty of Medicine & Health Sciences, Spain, ³VU University Medical Center, Dept Orthopaedic Surgery, Research Institute MOVE, Netherlands, ⁴VU University Medical Center/ACTA, Dept Oral & Maxillofacial Surgery, Research Institute MOVE, Netherlands, ⁵VU University Medical Center/ACTA, Dept Oral & Maxillofacial Surgery, Research Institute Amsterdam, Netherlands, ⁶ACTA-VU University Amsterdam Dept Oral Cell Biology (Rm # 11N-63), The Netherlands

A one-step concept for bone regeneration has been postulated in which human adipose tissue-derived mesenchymal stem cells (hASCs) are harvested, triggered to differentiate, seeded on biosynthetic substitute carriers, and implanted in the same operative procedure. Toward this goal it was investigated whether short (minutes) incubation with a physiological dose of BMP-2 suffices to trigger osteogenic differentiation of hASCs seeded on calcium phosphate carriers.

hASCs were isolated from subcutaneous abdominal wall adipose tissue. hASCs were treated with/without BMP-2 (10 ng/ml) for 15 min, and seeded on β -tricalcium phosphate granules (β -TCP; sized < 0.7 mm or > 0.7 mm) or biphasic calcium phosphate (BCP; 60%/40% or 20%/80% hydroxyapatite/ β -TCP). Attachment was determined after 10-30 min. After 4, 14, and 21 days of culture, proliferation (DNA content), and osteogenic differentiation (alkaline phosphatase (ALP) activity; osteogenic gene expression of CBFA1, collagen-1, osteonectin, and osteocalcin), as well as expression of the adipogenic marker PPAR- γ were analyzed. Gene expression was determined by real-time PCR.

hASC attachment to the different β -TCP and BCP scaffolds was similar, and unaffected by BMP-2. BMP-2 increased the DNA content of hASCs seeded on the scaffolds by 2.1-fold (day 14) and 2.7-fold (day 21) compared to untreated controls. ALP activity increased in time on both scaffold types, but this was not affected by BMP-2. ALP gene expression was increased (3.0-fold) by BMP-2 on BCP scaffolds only at day 14. In hASCs seeded on BCP and β -TCP, BMP-2 also stimulated gene expression of the osteogenic markers CBFA1 by 4.9-fold (BCP) and 3.7-fold (β -TCP), collagen-1 by 6.8-fold (BCP) and 8.9-fold (β -TCP), osteonectin by 8.6-fold (BCP) and 7.3-fold (β -TCP), and osteocalcin by 1.9-fold (BCP) and 2.2-fold (β -TCP) at day 21. In contrast, BMP-2 treatment inhibited expression of the adipogenic marker PPAR- γ by 4.5-fold (BCP) and 4.0-fold (β -TCP) at day 21.

In conclusion, this study revealed that 15 minutes incubation with a physiological dose BMP-2 had a long-lasting stimulating effect on osteogenic differentiation of hASCs after culturing on BCP or β -TCP scaffolds. Our findings indicate that this short pre-treatment with BMP-2 is a very promising tool for its use in a clinical one-step surgical procedure, and strongly support a one-step clinical concept for bone regeneration.

Disclosures: Jenneke Klein-Nulend, None.

SU0237

TLE3 Switches Cell Fate between Osteoblast and Adipocyte in Bone Marrow Stromal Cells. Shoichiro Kokabu¹, Takenobu Katagiri², Vicki Rosen¹.
¹Harvard School of Dental Medicine, USA, ²Saitama Medical University Research Center for Genomic Medicine, Japan

Osteoblast lineage cells and marrow adipocytes come from common progenitors, which are bone marrow stromal cells (BMSCs). In senile osteoporosis and some pathological conditions, the balance of osteoblastogenesis and adipogenesis in this cell population is disrupted so that adipogenesis is increased with respect to osteoblastogenesis, and as a consequence, bone mass is decreased. While the molecular mechanisms controlling the balance between osteoblastogenesis and adipogenesis in adult bone are of great interest, the exact nature of the signals regulating this process remains to be determined. Recently transducin-like enhancer of split 3 (TLE3) was reported to enhance adipogenesis in adipose tissue (Villanueva CJ et al., 2011). Here we report that TLE3 not only enhances adipocyte differentiation in BMSCs but also suppresses osteoblast differentiation, suggesting it may be a physiological regulator of cell fate decisions. We first examined the expression of TLE3 in adult bone (10-wk-old femur) using immunohistochemistry and found that bone marrow contains a wealth of TLE3 positive bone marrow stromal cells. Next using W20-17 mouse bone marrow stromal cells as a model (Thies RS et al., 1992), we found that over-expression of TLE3 induced adipocyte differentiation and suppressed ALP activity and mRNA levels of Osterix and Osteocalcin induced by treatment with BMP2. To examine the mechanism by which TLE3 is able to suppress osteoblast differentiation while inducing adipogenesis, we focused on Runx2, a transcription factor essential for osteoblast differentiation by BMSC that is regulated, in part, by BMP signaling. We found that while TLE3 strongly suppressed ALP activity and OSE2-luciferase activity induced by Runx2 it did not affect phosphorylation of Smad1/5/8 or suppress the induction of the BMPs early response genes ID1 and ID3. Introduction of a point mutation in the WD40 domain of TLE3 diminished the ability of TLE3 to affect adipocyte and osteoblast differentiation in W20-17 cells, suggesting TLE3 interacts with Runx2 via WD40 domain to modulate transcriptional activity. In conclusion, we identify TLE3 as a transcriptional regulator of BMSC differentiation into osteoblasts and adipocytes in vitro. We also confirm the expression of TLE3 by bone marrow stromal cells resident in adult bone. Taken together, our data suggest that TLE3 activity may be key in balancing adipocyte and osteoblast differentiation in the adult bone marrow microenvironment.

Disclosures: Shoichiro Kokabu, None.

SU0238

Total-Body Irradiation promotes Engraftment and New Bone Formation upon Local Injection of Mesenchymal Stem Cells in a Murine Tibial Transplant Model. Samuel Herberg¹, Galina Kondrikova¹, Khaled Hussein¹, Mohammed Elsalanty², Xing-Ming Shi¹, Mark Hamrick¹, Carlos Isales³, William Hill⁴.
¹Georgia Health Sciences University, USA, ²Georgia Health Science University, USA, ³Medical College of Georgia, USA, ⁴Georgia Health Sciences University & Charlie Norwood VAMC, USA

Purpose: The effectiveness of cell therapy for the treatment of bone diseases remains uncertain. Successful engraftment following transplantation of total bone marrow (TBM) or bone marrow-derived mesenchymal stem cells (BMSCs) in mouse and human subjects have been reported, albeit at low levels. Improved outcomes have been achieved using (sub)-lethal doses of total-body irradiation (TBI) to ablate host stem cell populations prior to systemic or local injection of TBM or BMSCs in young and old recipients. However, radiation exposure is known to negatively impact normal bone growth. Here, we tested the hypothesis that a lethal dose of TBI promotes cell engraftment and new bone formation following intramedullary tibial transplantation of BMSCs in young mice. Methods: 6-month-old C57BL/6 male mice were divided into 2 groups. Animals were left untreated or received a single lethal dose of 8.25 Gy TBI without shielding followed by retro-orbital injection of rescuing TBM 24 h later. The next day, mice received GFP+ BMSCs at 1.3×10^5 , 1.3×10^6 , 6.6×10^6 , or 1.32×10^7 cells/ml via intramedullary injection into left tibias. Right tibias served as vehicle controls. After 4 weeks, animals were euthanized and tibias harvested for BMD analysis and 3-D morphometry with μ CT (BV/TV, Tb.N, Tb.Th, Tb.Sp) followed by processing and sectioning at 8 μ m for histology and immunohistochemistry. Results: No differences in BMD or 3-D morphometric parameters were found among transplanted groups or between experimental and control tibias in non-irradiated animals. Radiation exposure caused significant bone loss in control tibias compared to non-irradiated controls ($p < 0.01$). However, new bone formation was promoted following TBI in experimental groups relative to controls. BMD, BV/TV, and Tb.N were significantly increased ($p < 0.0001$), and Tb.Th and Tb.Sp decreased ($p < 0.001$) in treated groups compared to vehicle controls and non-irradiated transplanted groups. This effect highly correlated with the number of transplanted BMSCs per tibia. Histology confirmed the μ CT results and immunohistochemistry revealed GFP+ cells integrated in the newly formed trabecular network as well as lining the endosteal surface. Conclusion: These data suggest that TBI prior to intramedullary tibial transplantation of BMSCs promotes cell engraftment and new bone formation in young mice. Future studies aim to clarify the mechanisms of BMSC engraftment without exposure to irradiation.

Disclosures: William Hill, None.
This study received funding from: NIA

SU0239

Wnt Signaling Regulates Glucose Metabolism During Osteoblast Differentiation. Emel Esen¹, Courtney Karner², Fanxin Long², Adewole Okunade³, Bruce Patterson⁴.
¹Washington University in St. Louis, USA, ²Washington University School Of Medicine, USA, ³department of internal medicine, USA, ⁴internal medicine, USA

Wnt signaling has emerged as an important regulator of osteoblast differentiation and function. However, the molecular mechanisms underlying these regulations are not fully understood. In particular, genetic manipulations of Lrp5 versus b-catenin in osteoblasts and osteocytes appear to differentially affect osteoblasts or osteoclasts in postnatal mice, raising the possibility that b-catenin independent mechanisms may contribute to Wnt/Lrp5 signaling in the regulation of osteoblast number and function. Here we report that Wnt signaling acutely induces glucose consumption and appears to promote glycolysis over oxidative metabolism in a variety of osteoblast-lineage cell lines. Mechanistically, Wnt-induced reprogramming of glucose metabolism requires Lrp5 signaling independent of b-catenin, and is associated with upregulation of the protein levels of key glycolytic enzymes. Importantly, disruption of metabolic reprogramming by knocking down the induced glycolytic enzymes impairs osteoblast differentiation in response to Wnt. Thus, Wnt signaling regulates osteoblast differentiation in part through direct reprogramming of cell metabolism.

Disclosures: Emel Esen, None.

SU0240

Transgenic Disruption of Glucocorticoid Signaling in Osteoblasts Attenuates Inflammation and Bone Loss in Collagen Antibody-Induced Arthritis. Jinwen Tu¹, Yaqing Zhang¹, Julian Kelly¹, Cornelia Spies¹, Frank Buttgerit², Colin Dunstan³, Markus Seibel¹, Hong Zhou¹.
¹Bone Research Program, ANZAC Research Institute, University of Sydney, Australia, ²Department of Rheumatology & Clinical Immunology, Charité University Medicine, Germany, ³University of Sydney, Australia

Background: Transgenic (tg) overexpression of the glucocorticoid (GC) inactivating enzyme, 11beta-hydroxysteroid dehydrogenase type 2 (HSD2), under the control of a 2.3Kb collagen type I promoter (Col2.3-HSD2), abrogates intracellular GC signalling exclusively in mature osteoblasts and osteocytes. Using the T cell-independent K/BxN serum transfer model of autoimmune arthritis, we previously reported that osteoblast-targeted disruption of endogenous GC signalling attenuated arthritis in Col2.3-HSD2-tg mice. In the present study, we aimed to further elucidate the role of endogenous GCs in a T cell-dependent model of inflammatory joint disease, namely collagen antibody-induced arthritis (CAIA). Methods: CAIA was induced in 6-week-old male Col2.3-HSD2-tg mice (tg-CAIA, n=8) and their wildtype (WT) littermates (WT-CAIA, n=10). Eight tg and 8 WT mice receiving carrier only served as controls (CTR). Body weight and the degree of arthritis (clinical score of paw swelling) were measured daily from induction to endpoint (day 14). Skeletal changes were determined by micro-CT and histomorphometry of the tibia. Results: Both tg-CAIA and WT-CAIA mice developed acute arthritis with significant swelling and redness of all paws. However, based on clinical scores, the inflammatory response was significantly blunted in tg-CAIA mice from day 9 onward ($p < 0.05$). Histologically, synovial inflammation was less pronounced in the wrist and ankle joints of tg-CAIA compared to WT-CAIA mice. As for micro-CT analysis, tibial trabecular separation was significantly increased ($p < 0.05$) with lower trabecular number ($p = 0.05$) in WT-CAIA but not tg-CAIA (compared to WT-CTR), consistent with accelerated bone resorption. In contrast, trabecular thickness was increased in WT-CAIA ($p < 0.05$) but not tg-CAIA mice. Similar results were obtained by tibia histomorphometry, were significantly increased osteoclast surface in WT-CAIA mice ($p < 0.01$ compared to tg-CAIA) confirmed the known effects of inflammation on systemic bone turnover. At the same time, inflammatory activity was found attenuated in tg-CAIA compared to WT-CAIA mice ($p = 0.05$), with lesser effects on bone structural parameters. Conclusions: Our results demonstrate that disruption of GC-signalling in mature osteoblasts attenuates arthritis not only in T cell-independent but also in T cell-dependent models of arthritis. 1. Arthritis and Rheumatism, 60: 1998-2007, 2009

Disclosures: Hong Zhou, None.

SU0241

Distinct Roles of Cathepsin K and MMPs in Osteoclastic Bone Resorption. Ditte Marie Merrild¹, Kent Soe², Jean-Marie Delaïsse³.
¹Vejle Hospital, Denmark, ²Vejle Hospital, University of Southern Denmark, Denmark, ³Vejle Hospital, IRS, University of Southern Denmark, Denmark

Bone matrix degradation by the osteoclast (OC) requires solubilization of mineral and of collagen. Two distinct types of collagen solubilizing proteases are generated by the OC: (i) cathepsin K (catK) which is well-known to be the main responsible for collagen solubilization by OCs, and (ii) matrix metalloproteinases (MMPs). It remains unknown which role MMPs play in the resorption process.

In order to address this question, we generated OCs from blood donors and cultured them on bone discs in the presence or absence of inhibitors of catK (E64) and

MMPs (GM6001). We quantified resorption by measuring eroded surface, erosion depths, and CTX collagen fragments in the conditioned medium. We also analyzed whether excavations occurred as individual round pits or as elongated trenches. This parameter is usually not taken into account, although pits reflect the classical OC resorption cycle made of alternating resorption and migration episodes, whereas trenches reflect "continuous" resorption without interruption by migration. Furthermore, we quantified catK and MMPs expression through PCR.

We found that catK inhibition, but not MMP inhibition, strongly reduced CTX and excavation depths compared to controls. This confirmed that catK and not MMPs are the major players in bone matrix solubilization. CatK and MMP inhibition did not significantly affect total eroded surface, but MMP inhibition reduced significantly the proportion of pits at the expense of an increase of trenches, whereas catK inhibition had the opposite effect. These same opposite effects were also seen when correlating pits and trenches with expression levels of catK and MMP14, which happen to vary naturally in the OCs generated from different donors. Our interpretation is that low MMP activity tends to maintain OCs in the active mode of the resorption cycle, because of inhibition of the migration episodes necessary to allow the generation of successive pits. This view is in accordance with earlier observations that MMPs are required for OC migration.

In conclusion, our observations indicate that in contrast with catK, MMPs do not play a major role in the solubilization of collagen from bone matrix, but that they play a regulatory role allowing migration episodes interrupting active bone resorption, whereas catK rather promotes continuous resorption. This subtle action of MMPs may have important effects on the geometry of excavations, likely to affect micro-architecture and bone strength.

Disclosures: Ditte Marie Merrild, None.

SU0242

Tks5-Dependent Formation of Circumferential Podosomes/Invadopodia Mediates Cell-Cell Fusion. Tsukasa Oikawa^{*1}, Masaaki Oyama², Hiroko Kozuka-Hata², Shunsuke Uehara³, Nobuyuki Udagawa⁴, Hideyuki Sava⁵, Koichi Matsuo⁶. ¹School of Medicine, Keio University, Japan, ²Medical Proteomics Laboratory, Institute of Medical Science, University of Tokyo, Japan, ³Department of Biochemistry, Matsumoto Dental University, Japan, ⁴Matsumoto Dental University, Japan, ⁵Division of Gene Regulation, Institute for Advanced Medical Research, School of Medicine, Keio University, Japan, ⁶School of Medicine, Keio University Laboratory of Cell & Tissue Biology, Japan

Osteoclasts fuse to form multinucleated cells during osteoclastogenesis. This process is mediated by dynamic rearrangement of the plasma membrane and cytoskeleton, and it requires numerous factors, many of which have been identified. The underlying mechanism remains obscure, however. Here we show that Tks5, a master regulator of invadopodia in cancer cells, is crucial for osteoclast fusion downstream of phosphoinositide 3-kinase and Src. Expression of Tks5 was induced during osteoclastogenesis, and prevention of this induction impaired both the formation of circumferential podosomes and osteoclast fusion without affecting cell differentiation. Tyrosine phosphorylation of Tks5 was attenuated in *Src*^{-/-} osteoclasts, likely accounting for defects in podosome organization and multinucleation in these cells. Circumferential invadopodia formation in B16F0 melanoma cells was also accompanied by Tks5 phosphorylation. Coculture of B16F0 cells with osteoclasts in an inflammatory milieu promoted the formation of melanoma-osteoclast hybrid cells. Our results thus reveal an unexpected link between circumferential podosome/invadopodium formation and cell-cell fusion in and beyond osteoclasts.

Disclosures: Tsukasa Oikawa, None.

SU0243

Characterization of the Formation and Progression of Periapical Lesions induced in Teeth of TLR-2 Knockout Mice. Raquel Silva^{*1}, Andiara De Rossi², Léa Silva³, Paula Ferreira³, Paulo Nelson-Filho³. ¹School of Dentistry of Ribeirão Preto - University of São Paulo, Brazil, ²Faculty of Dentistry of Ribeirão Preto, University of São Paulo, Brazil, ³School of Dentistry of Ribeirão Preto - University of São Paulo, Brazil

The aim of this study was to characterize the formation and progression of experimentally induced periapical lesions in TLR2 knockout (TLR2 KO) mice. Periapical lesions were induced in molars of 28 wild type (WT) and 27 TLR2 KO mice. After 7, 21 and 42 days, HE-stained sections were evaluated for description of pulpal, apical and periapical features, and neutrophils numbers (conventional light microscopy) and for determination of periapical lesion size (fluorescence microscopy). Sections were also evaluated by TRAP histochemistry (osteoclasts), immunohistochemistry (osteoclastogenesis markers RANK, RANKL and OPG), Data were analyzed by Mann-Whitney and Kruskal-Wallis tests ($\alpha=0.05$). Wild type group showed significant differences ($p<0.05$) in periapical lesion size and osteoclast number between 7 and 42 days and between 21 and 42 days. In TLR2 KO group, significant differences ($p<0.05$) in periapical lesion size and osteoclast number were found between 7 days and the other periods. There was significant difference ($p<0.05$) between the two types of animal with respect to periapical lesion size, which was larger in the TLR2 KO animals. No significant differences ($p>0.05$) were found between WT

and TLR2 KO mice related to: pulpal, apical and periapical features, and immunohistochemical results (except for RANK expression). Number of neutrophils on TLR2 mice increased from day 7 to 21, also with a decrease on day 42. Statistically significant differences were found among all time points ($p<0.05$). Comparing the two types of animals, there was a significant difference regarding all time points ($p<0.05$) with a larger number of neutrophils in TLR2 mice. Knockout animals developed larger periapical lesions with greater number of osteoclasts, indicating the importance of this receptor in the host's immune and inflammatory response to root canal and periradicular infection.

Disclosures: Raquel Silva, None.

SU0244

Gain or Loss of FoxO Function in Osteoclasts alter Bone Mass in Mice. Shoshana Bartell^{*}, Elena Ambrogini, Li Han, Aaron Warren, Julie Crawford, Srividhya Iyer, Joseph Goellner, Haibo Zhao, Charles O'Brien, Stavros Manolagas, Maria Jose Almeida. Central Arkansas VA Healthcare System, Univ of Arkansas for Medical Sciences, USA

Reactive oxygen species (ROS) are a critical requirement for RANKL-induced osteoclast generation, activation, and survival; and an increase in ROS generation has been implicated in the increased resorption associated with estrogen deficiency as well as the decreased bone formation associated with advancing age. However, unlike the effects of acute estrogen deficiency, the age-associated increase in ROS production is accompanied by decreased, rather than increased, osteoclast numbers in cancellous bone. Based on this and evidence that global combined deletion of FoxO1,3,4 - an important transcriptional defense mechanism against oxidative stress - leads to an increase in ROS and osteoclast progenitor number, we hypothesized that FoxO activation is responsible for the dampening of osteoclast generation in aged mice. To this end, we generated mice in which FoxO1,3,4 were specifically deleted or FoxO3 was overexpressed in the osteoclast lineage (using the LysM-Cre mouse), designated FoxO1,3,4⁰Oc and FoxO3TgOc, respectively. FoxO1,3,4⁰Oc mice exhibited decreased vBMD and cancellous bone volume in vertebrae and femora, associated with decreased trabecular number and thickness and increased trabecular separation. FoxO1,3,4⁰Oc mice also had decreased femoral cortical thickness and higher serum levels of CTx. In line with this, bone marrow cultures from FoxO1,3,4⁰Oc mice maintained in the presence of M-CSF and RANKL exhibited an increase in the number of osteoclast progenitor and in mature osteoclast formation. Furthermore, macrophages and osteoclasts exhibited decreased expression of the FoxO-target gene catalase and higher ROS levels in response to RANKL. Administration of the antioxidant NAC to FoxO1,3,4⁰Oc mice prevented the decrease in bone mass. FoxO3TgOc mice had an exactly opposite phenotype to that of the FoxO1,3,4⁰Oc mice: increased bone mass, decreased osteoclastogenesis and serum levels of CTx, as well as higher catalase expression and lower ROS levels in response to RANKL. These results demonstrate that FoxOs inhibit osteoclast generation by attenuating ROS and support the hypothesis that increased FoxO activation with age decreases osteoclast numbers and thereby the rate of bone remodeling. Nonetheless, an even greater decline in osteoblast supply and survival, the two key culprits of the age-associated decline in cancellous bone mass, tilt the balance between formation and resorption toward the latter.

Disclosures: Shoshana Bartell, None.

SU0245

Identification and Analysis of a Novel Splicing Variant of Mouse Receptor Activator of NF- κ B. Riko Kitazawa^{*1}, Satomi Mukai², Junko Ishii², Kiyoshi Mori³, Takeshi Kondo³, Ryuma Haraguchi¹, Sohei Kitazawa¹. ¹Ehime University, Japan, ²Kobe University, Japan, ³Kobe University Graduate School of Medicine, Japan

Receptor activator of NF- κ B (RANK) is a member of the tumor necrosis factor receptor (TNFR) family expressed in osteoclast precursors, and RANK-RANK ligand (RANKL) signaling is a key system for differentiation, activation and survival of osteoclasts.

We have identified a novel alternative splicing variant of mouse RANK gene (vRANK) that contains a new intervening exon between exon 1 and exon 2 of mouse full-length RANK (fRANK) mRNA. Since this novel exon contains the stop codon, vRANK encodes truncated amino acids that have a portion of the signal peptide of fRANK and an additional 19 amino acids that show no homology to previously reported domains.

By transient transfection studies with vRANK-GFP and -Flag expressing constructs, vRANK was found localized mostly in the cytoplasm and partly in the cell membrane, but was not secreted into the culture supernatant. Under the stimulation of various factors, the expression of vRANK mRNA was almost parallel to that of fRANK in RAW264.7 cells not treated with M-CSF. Overexpression of vRANK, on the other hand, decreased TRACP mRNA expression as well as the number of NFATc1-positive multinucleated giant cells. While the mRNA expression levels of NFATc1, a master transcriptional factor of the osteoclast differentiation program, were not affected, apoptotic cells increased significantly in vRANK-transfected cells treated with sRANKL.

Taken together, these results suggest that vRANK may be a novel osteoclast suppressor that reduces the number of RANKL-induced mature osteoclasts mainly by negating the anti-apoptotic effect of RANKL.

Disclosures: Riko Kitazawa, None.
This study received funding from: Ehime University

SU0246

IL-4 Inhibits TNF- α -mediated Osteoclast Formation by Inhibition of RANKL Expression in TNF- α -activated Stromal Cells and Direct Inhibition of TNF- α -activated Osteoclast Precursors. Hideki Kitaura¹, Toshiya Fujii², KEISUKE KIMURA³, Masahiko Ishida², Zaki Hakami², Teruko Takano-Yamamoto¹. ¹Tohoku University, Japan, ²Division of Orthodontics & Dentofacial Orthopedics, Department of Translational Medicine, Tohoku University Graduate School of Dentistry, Japan, ³, Japan

It has been reported that osteoclastogenesis is induced by TNF- α . IL-4 is most important cytokine involved in humoral immunity. TNF- α as pro-inflammatory cytokine also exist in inflammatory site. In this study, we investigated whether IL-4 inhibits TNF- α -mediated osteoclast formation *in vivo*. TNF- α was administered with and without IL-4 into the supracalvaria of mice. The numbers of osteoclasts and the levels of mRNA for cathepsin K and tartrate-resistant acid phosphate (TRAP), which are osteoclast markers, in mice administered both TNF- α and IL-4 were lower than those in mice administered TNF- α alone. The levels of tartrate-resistant acid phosphate 5b (TRACP 5b) as a marker of bone resorption in mice administered both TNF- α and IL-4 was also lower. Next, we investigated whether IL-4 inhibited TNF- α -mediated osteoclast formation in mouse bone marrow derived macrophages (BMMs). When BMMs were cultured with TNF- α , osteoclasts were formed. When they were cultured with both TNF- α and IL-4, osteoclast formation was suppressed by IL-4. Furthermore, we investigated whether IL-4 inhibit the production of RANKL with the stromal cell induced by TNF- α *in vitro*. Stromal cells incubated with TNF- α , expression level of RANKL mRNA was increased in comparison with control, but not treated with TNF- α and IL-4. Furthermore, we investigated whether IL-4 effects both stromal cell and BMMs in TNF- α -mediated osteoclast formation *in vivo*. We administered TNF- α and IL-4 to chimeric mice which WT marrow is transplanted into lethally irradiated WT (WT>WT), WT marrow is transplanted into lethally irradiated TNFRs KO (WT>KO), TNFRs KO marrow is transplanted into lethally irradiated WT (KO>WT) and TNFRs KO marrow is transplanted into lethally irradiated TNFRs KO (KO>KO). WT>WT, WT>KO and KO>WT mice, the number of osteoclasts and level of RANKL mRNA in mice administered both TNF- α and IL-4 were lower than those in mice administered TNF- α alone. IL-4 also inhibited TNF- α -induced osteoclast formation in mice whose T cells were blocked by anti-CD4 and anti-CD8 antibodies. We conclude that IL-4 inhibits osteoclast formation that is related to both physiological bone resorption induced by RANKL and pathological bone resorption induced by TNF- α via a T cell-independent mechanism *in vivo*.

Disclosures: Hideki Kitaura, None.

SU0247

Ameloblastin Modulates Osteoclastogenesis through Calcium-NFAT Pathway. Xuanyu Lu^{*}, Yoshihiro Ito, Xianghong Luan. University of Illinois at Chicago, USA

Osteoclastogenesis, ameloblastin, calcium, NFATc1

Proteins of the extracellular matrix often have multiple functions to facilitate complex tasks ranging from signaling to structural support. Here we have focused on the function of one of the matrix proteins expressed in bones and teeth, the matrix adhesion protein ameloblastin (AMBN). Transgenic mice with 5-fold elevated AMBN levels in mandibles suffered from root cementum resorption and delamination and reduced alveolar bone thickness. *In vitro* application of AMBN doubled bone marrow monocyte (BMMC) adhesion, elevated ERK1/2 and AKT phosphorylation and enhanced RhoA expression. AMBN also triggered osteoclast differentiation, podosome belt formation and osteoclast spreading. Following induction with RANKL and CSF-1, AMBN dramatically increased osteoclast numbers and resorption pits. The effect of AMBN on osteoclastogenesis was accomplished through an increase in Ca²⁺ influx and NFATc1 nuclear translocation. Together, our data suggest that AMBN regulates osteoclast differentiation as well as mineralized tissue resorption by promoting calcium-NFATc1 dependent extracellular matrix signaling cascades.

Disclosures: Xuanyu Lu, None.

SU0248

Cnot3 (Ccr4-not complex subunit3), a Regulator of mRNA Stability, Regulates Bone Mass and Gene Expression Related to Osteoclast Formation. Chiho Watanabe^{*1}, Masahiro Morita², Yoichi Ezura³, Tetsuya Nakamoto¹, Tadayoshi Hayata⁴, Takuya Notomi⁵, Keiji Moriyama¹, Tadashi Yamamoto², Masaki Noda¹. ¹Tokyo Medical & Dental University, Japan, ²Division of Oncology, Institute of Medical Science, University of Tokyo, Japan, ³Tokyo Medical & Dental University, Medical Research Institute, Japan, ⁴Medical Research Institute, Tokyo Medical & Dental University, Japan, ⁵GCOE, Tokyo Medical & Dental University, Japan

Posttranscriptional gene regulation such as mRNA stability is important for the gene expression. However, contribution of mRNA stability in bone metabolism is barely understood. Ccr4-not complex is a deadenylase and enhances mRNA degradation. Cnot3 is one of the Ccr4-not complex subunits and regulates stability of specific mRNAs in liver, but its role in bone is not known. We found that Cnot3 is expressed in bone *in vivo* and in osteoblasts and osteoclasts *in vitro*. To determine the function of Cnot3 in bone mass regulation, bone structure of the Cnot3^{+/-} mice were examined (as -/- is lethal) with DXA and microCT. Bone mineral density of the femur of Cnot3^{+/-} mice was reduced in comparison to wild-type mice. In the distal femur, bone volume per tissue volume (BV/TV) was suppressed compared to wild-type mice and this indicated Cnot3^{+/-} mice exhibited low bone mass. When we compared mice about 14 weeks to 2 years old mice, base line levels of BV/TV decreased with age. Reduction levels due to the Cnot3 deficiency was more than that due to age-dependent decrease. Cortical bone thickness was more decreased in aged Cnot3^{+/-} mice in comparison to wild-type mice. These results suggest that there is a relationship between aging and Cnot3. We performed bone histomorphometry using calcein labeling of femur and TRAP staining of tibia. Mineralized surface and osteoclast number were increased in Cnot3^{+/-} mice. These data suggest that Cnot3^{+/-} mice show osteoclast dominant high-turnover type osteopenia. Bone marrow cells culture with M-CSF and RANKL showed higher level of TRAP positive multinuclear cells in 14 weeks old Cnot3^{+/-} mice. However, osteoclast formation by co-culture system with osteoblast induced by dexametazone and vitD showed similar levels compared to wild type. This suggests that Cnot3 deficiency in osteoclasts enhances its formation, but inhibits osteoclast formation via osteoblast partially. Interestingly, in 2 years old Cnot3^{+/-} mice, osteoclast formation was increased even in co-culture system. This indicates that effect of Cnot3 deficiency in osteoclast was upregulated by aging. Osteogenic medium (beta-glycerophosphate and ascorbic acid) showed similar levels of mineralized nodule formation. Expression levels of genes related to bone resorption were up-regulated in osteoblasts(M-CSF and Opg) and osteoclasts(Rank) where Cnot3 was knocked down. In conclusion, our data indicate that Cnot3 is required for the osteoclast function and maintain the bone mass.

Disclosures: Chiho Watanabe, None.
This study received funding from: GCOE program

SU0249

Cot Kinase Promotes Ca²⁺ Oscillation/Calcineurin-independent Osteoclastogenesis by Stabilizing NFATc1 Protein. Yukiko Kuroda^{*1}, Chihiro Hisatsune², Akihiro Mizutani³, Katsuhiko Mikoshiba², Koichi Matsuo⁴. ¹Laboratory of Cell & Tissue Biology, Japan, ²Laboratory for Developmental Neurobiology, Japan, ³Department of Pharmacotherapeutics, Japan, ⁴School of Medicine, Keio University Laboratory of Cell & Tissue Biology, Japan

Osteoclasts are multinuclear bone resorbing cells formed by fusion of monocyte/macrophage lineage precursor cells. Activation of the transcription factor nuclear factor of activated T cells c1 (NFATc1) by the receptor activator of NF- κ B ligand (RANKL) is critical for osteoclast differentiation. In our previous report, we demonstrated that osteoblasts induce osteoclast differentiation via Ca²⁺ oscillation/calcineurin-dependent and -independent NFATc1 activation pathways; however, the mechanism underlying the latter remained unclear. Here we show that Cot, a serine/threonine kinase also known as tumor progression locus 2 (Tpl-2), directly phosphorylates all Ca²⁺/calcineurin-regulated NFAT family members (NFATc1 through NFATc4) and increases their protein levels. Moreover, Cot activity in osteoclasts was enhanced via cell-cell interaction with osteoblasts, and Cot promoted Ca²⁺ oscillation/calcineurin-independent osteoclastogenesis by increasing NFATc1 stability through phosphorylation. Our findings propose an NFAT activation mechanism involving phosphorylation-induced protein stabilization, which operates *in vivo* even in the absence of Ca²⁺ oscillation and calcineurin activity.

Disclosures: Yukiko Kuroda, None.

SU0250**Different Influences of Hypoxia between Osteoclastogenesis and Osteoclastic Bone Resorption.** SEONG SIK KIM^{*1}, Yong-Deok Kim², Lexie Holliday³.¹Pusan National University, USA, ²Pusan National University, South Korea, ³University of Florida College of Dentistry, USA

Osteoclasts are the primary mediators of pathological bone resorption including rheumatoid arthritis, pathological fracture, and primary bone tumors. Hypoxia is known to act as a major stimulator of osteoclastogenesis. However, it has unclear how hypoxia acts for osteoclastic bone resorption. This study was initiated to test effects of hypoxia during osteoclastogenesis and osteoclastic bone resorption. We used RAW264.7 cell for osteoclastogenesis and mouse bone marrow derived cells for osteoclastic bone resorption on the dentin slices.

By quantitative immunoblotting, we found that hypoxia inducible factor 1 alpha increased during osteoclastogenesis but not osteoclastic bone resorption under hypoxia in both RAW 264.7 cell and mouse bone marrow derived cells.

With TRAP staining, we compared osteoclastogenesis between hypoxia and normoxia. Many TRAP-positive osteoclasts were observed under hypoxia than normoxia. In osteoclastic bone resorption, however, more TRAP-positive osteoclasts were observed in normoxia than hypoxia on the dentin slices. Scanning electron microscopic observation of resorption pits on the dentin slices confirmed that osteoclastic bone resorption was more stable in normoxia state than hypoxia.

For detection of osteoclast polarization, we performed immunostaining of osteoclasts and resorption pits. We used rhodamine-conjugated phalloidin immunostaining of F-actin ring, which included in ruffled membrane, for attachment structure on the bone surface during osteoclast polarization.

Distribution of actin rings showed same field with scanning electron microscopic observation of resorption pits.

These results suggest that hypoxia inducible factor 1 alpha is associated with early osteoclast formation, but not osteoclastic bone resorption. Understanding influences of hypoxia during osteoclast formation and polarized activation helps to control the pathological bone disease.

Disclosures: SEONG SIK KIM, None.

SU0251**Glyceollin, a Selective Estrogen Receptor Modulator, Preserves Bone Mass by Inhibition of Osteoclast Differentiation.** Min-Su Han^{*1}, Gyoung-Ho Cho¹, Kyung Eun Lim¹, Na-Rae Park¹, Xiangguo Che¹, Jae-Hwan Jeong¹, In-Kyu Lee², Hyun-Ju Kim³, Shin-Yoon Kim³, Je-Yong Choi⁴. ¹1,2,3, South Korea, ²3, South Korea, ³2, South Korea, ⁴1Dept. of Biochemistry & Cell Biology, School of Medicine, 2Skeletal Diseases Genome Research Center, 3World Class University Program, Kyungpook National University, South Korea

Glyceollin has been known as a phytoestrogen with anti-estrogen effects on breast and ovarian cancer. Glyceollin may not be a good candidate to preserve bone mass because of its anti-estrogen effect. However, the effect of glyceollin on bone has not been elucidated yet. To explore the effect of glyceollin on bone, we used high-dose vitamin D injection mouse model showing significant bone loss in skeleton. The local calvarial injection or systemic subcutaneous injection of glyceollin (0.5 - 100 µg/kg) once a day for 9 days protected high-dose vitamin D mediated bone loss. Glyceollin treated calvaria or long bone exerted low tartrate resistant acid phosphatase activity compared to control group. To elucidate molecular mechanism of the protective effect of glyceollin on bone, osteoclastogenesis was evaluated using mouse primary cultured bone marrow macrophages (BMM) and osteoblasts. Glyceollin increased BMM proliferation, but it had no effect on osteoblasts proliferation. Glyceollin inhibited the expression of osteoclast markers including OSCAR, NFAT-c1, DC-STAMP, alpha V integrin, and cathepsin K in M-CSF/RANKL-mediated osteoclastogenesis of BMM. Indeed, glyceollin inhibited osteoclast resorption activity. Besides, glyceollin decreased RANKL expression together with the increase of osteoprotegerin (OPG) expression, which resulted in decrease of RANKL/OPG ratio in primary cultured calvarial osteoblasts. Collectively, these results indicate that glyceollin, a good therapeutic drug candidate as anti-estrogen effect on breast and ovarian cancer, preserves bone mass through the inhibition of both osteoclast differentiation and osteoclastogenic function of osteoblasts.

Disclosures: Min-Su Han, None.

SU0252**HDAC7 Regulates Osteoclastogenesis by Repressing MITF Activity.** Eric Jensen^{*1}, Lan Pham¹, Ann Emery¹, Melissa Stemig², Raj Gopalakrishnan¹, Kim Manskyl¹. ¹University of Minnesota, USA, ²University of Minnesota School of Dentistry, USA

Osteoclast differentiation requires stringent control of gene activation and repression in response to physiological cues. Transcriptional repression is mediated by corepressors including histone deacetylases (HDACs), a large diverse group of proteins. Non-selective inhibition of HDAC activity has been reported to inhibit osteoclast differentiation. However, the role of individual HDACs in osteoclasts

remains poorly understood. The goal of this study was to characterize the role of individual HDACs in differentiation of osteoclasts. We have identified Histone Deacetylase 7 (HDAC7) as a novel regulator of osteoclast formation.

To characterize the role of HDAC7 in osteoclast differentiation, we created osteoclast-specific HDAC7 knockout mice using LysM-Cre. µCT data from 1 and 3 months old animals indicate that the HDAC7 conditional knockout mice are osteopenic compared to their wild type littermates, exhibiting a 50% reduction of BV/TV. In vitro osteoclastic cultures of bone marrow monocytes from the HDAC7 conditional knockout mice form larger osteoclasts than control cultures, have increased expression of genes such as OCSTAMP, c-fos and Nfatc1, form larger resorption pits on dentine discs, and are hypersensitive to RANKL stimulation. Confirming the in vivo phenotype, we show that shRNA suppression of HDAC7 in wild-type osteoclastic cultures enhanced their differentiation of, while overexpression of HDAC7 inhibited their formation. These observations suggested an inhibitory role for HDAC7 in osteoclasts. Further in vitro studies indicate that this effect is mediated by repressive interactions of HDAC7 towards microphthalmia-associated transcription factor, MITF. HDAC7 inhibits MITF-dependent transcription, and the physical interaction between MITF and HDAC7 is attenuated by stimulation with RANK Ligand (RANKL), a factor that enhances MITF activity.

Collectively, our data indicate that HDAC7 expression negatively regulates osteoclast differentiation and suggest a model in which HDAC7 maintains transcription repression of MITF target genes until this repression is relieved by stimulation with RANKL, allowing for expression of essential osteoclast genes.

Disclosures: Eric Jensen, None.

SU0253**Lysosomal Calcium Channel, TPC2, Regulates Osteoclastogenesis via Generation of Intracellular Ca²⁺ Response and Subsequent NFATc1 Localization: A Novel Mechanism of Osteoclastic Ca²⁺ Signaling.** Takuya Notomi^{*1}, Yoichi Ezura², Masaki Noda³. ¹GCOE, Tokyo Medical & Dental University, Japan, ²Tokyo Medical & Dental University, Medical Research Institute, Japan, ³Tokyo Medical & Dental University, Japan

Intracellular Ca²⁺ controls multiple cellular functions and is regulated by the Ca²⁺-release from internal stores. Osteoclast differentiation is promoted by the receptor activator of NF-κB ligand (RANKL)-induced intracellular Ca²⁺ levels ([Ca²⁺]_i) and the subsequent nuclear factor-activated T cells c1 (NFATc1) activation. Although osteoclasts are lysosome-rich cells, current studies of intracellular Ca²⁺ in osteoclast have been focusing on molecules of endoplasmic reticulum (ER) and/or plasma membrane rather than lysosome. Here, we show that a lysosomal calcium channel, Two Pore Channel2 (TPC2), regulates RANKL-induced osteoclast differentiation through the modulation of [Ca²⁺]_i.

TPC2 knockdown (TPC2-KD) by lentivirus system in precursor cells (RAW267.4 and primary mice bone marrow macrophage) suppressed RANKL-induced differentiation into multinucleated osteoclasts evaluated by TRAP activity and the number of TRAP+ multinucleated osteoclasts (more than 80% reduction in comparison to control, respectively). TPC2-KD also suppressed osteoclastic resorption activity based on pit formation assay (over 80% reduction compared to control).

Quantification of the number of cells having NFATc1 in nuclei revealed that TPC2-KD suppressed the level of nuclear NFATc1 by more than 70%, suggesting the presence of TPC2 promotes nuclear localization of NFATc1. The population of RANKL-responding cells (RC) which show dynamic [Ca²⁺]_i response was suppressed by TPC2-KD in osteoclast precursors (34% versus 2% for control and TPC2-KD respectively). To examine lysosome-dependent [Ca²⁺]_i, bafilomycin A1 (Baf), a specific inhibitor of lysosomal Ca²⁺ release, was used to deplete lysosomal store. Baf treatment suppressed the levels of RC. This reduction was similar to that in the cells treated with thapsigargin, a specific inhibitor of ER Ca²⁺ store, to deplete ER-Ca²⁺ store. These results indicate that Ca²⁺-release from lysosomal store is a key event in the RANKL-induced [Ca²⁺]_i dynamic response. By analyzing [Ca²⁺]_i and integrated peak curve area in more than 800 osteoclast precursors, we confirmed that lysosomal-dependent [Ca²⁺]_i consistently exists independently of ER store in RANKL-treated osteoclast precursors. We conclude that TPC2 is a critical molecule for osteoclastogenesis and Ca²⁺ signaling. The osteoclastic lysosome function would be a target to develop novel therapeutic agents for skeletal disorders.

Disclosures: Takuya Notomi, None.

SU0254**MIF Down-regulates the RANKL-RANK Signaling Pathway by Activating Lyn Tyrosine Kinase.** Se Hwan MUN^{*1}, Sun-Kyeong Lee². ¹Department of Medicine, University of Connecticut Health Center, USA, ²University of Connecticut Health Center, USA

We previously reported that the cytokine macrophage migration inhibitory factor (MIF) down-regulated osteoclastogenesis in bone marrow cultures. Furthermore, we found that the number of osteoclasts formed in cultures from MIF KO mice was greater than those from WT. We also reported that CD74 is a receptor for MIF in bone marrow cells. However, the mechanism by which MIF down-regulates osteoclastogenesis is unknown. We now report that the tyrosine kinase, Lyn is activated when MIF binds to its receptor, CD74. Activated Lyn then down regulates the RANKL-mediated signaling cascade by suppressing NFATc1 protein. In the

current study, we examined if MIF modulates Lyn phosphorylation, if it associates with CD74, a MIF receptor, and if it down-regulates RANKL-mediated signaling. These studies were carried out in bone marrow macrophage cell culture system. Osteoclast-like cells (OCL) were identified as TRAP(+) and multinucleated.

We previously reported that MIF down-regulated RANKL-induced NFATc1 and AP-1 expression in BMM cultures. Lyn is a member of the src family kinases and was previously shown to be a negative regulator of osteoclastogenesis. We found that MIF treatment enhanced Lyn phosphorylation in RANKL induced BMM cultures and that CD74 and Lyn co-immunoprecipitated in these cells. MIF down-regulated RANKL-induced phosphorylation of Gab2, JNK1 and c-jun, which are pathways that regulate osteoclast differentiation via NFATc1 activation. In addition, MIF down-regulated RANKL-induced calcium signaling pathways including the phosphorylation of Syk and PLC γ . In order to confirm our hypothesis that the MIF-CD74 complex activates Lyn tyrosine kinase and in turn down-regulates RANKL-induced signaling pathways, WT BMM cells were transfected with small interfering RNA specific for Lyn. Neither cell cultures from CD74 KO mice nor the Lyn siRNA transfected cells had a decrease in osteoclastogenesis with MIF treatment. Furthermore, OCL formation was increased by 23% in cells transfected with Lyn siRNA compared to cells that were treated with a negative control siRNA.

This study is the first to report that the MIF-CD74 complex associates directly with Lyn in osteoclasts and that MIF phosphorylates Lyn to activate it. These results argue that MIF activates Lyn through CD74 and, in turn, down-regulates RANKL-mediated osteoclast differentiation pathways by suppressing NFATc1 and AP-1 activation.

Disclosures: Se Hwan MUN, None.

SU0255

miR-29 Regulates Osteoclastogenesis. Tiziana Franceschetti^{*1}, Catherine Kessler², Sun-Kyeong Lee², Anne Delany². ¹UCHC, USA, ²University of Connecticut Health Center, USA

Osteoclast differentiation is an intricate process, subject to epigenetic, transcriptional, and post-transcriptional regulation. microRNAs (miRNAs) are key post-transcriptional regulators of gene expression, playing a fundamental role in physiological and pathological conditions. miRNAs important in osteoblasts have been identified, and among these is the miR-29 (a/b/c) family. miR-29a and c differ by 1 base, and are functionally redundant. In osteoblasts, miR-29 regulates matrix synthesis and differentiation, but its role in osteoclasts remained undefined.

Here, we investigated the role of miR-29 in osteoclast differentiation, using primary cultures of mouse bone marrow-derived macrophages (BMMs). We observed that retroviral-mediated miR-29 knock-down results in diminished formation of TRAP (tartrate-resistant acid phosphatase)-positive multinucleated osteoclasts. Further, miR-29 inhibition is associated with a reduction in osteoclast size.

qRT-PCR showed that miR-29c expression increases in the early phases of osteoclast maturation, in concert with mRNAs for osteoclast markers including TRAP and Cathepsin K. miR-29c then decreases in terminally differentiated cells. In contrast, miR-29a expression presents a modest upregulation in the late stages of osteoclast maturation. To better understand how miR-29 regulates osteoclast function, we identified miR-29 target genes using Luciferase-3' UTR reporter assays and specific miR-29 inhibitors. We demonstrated that miR-29 negatively regulates the expression of Calcitonin Receptor, a marker of mature osteoclasts, and Jun Dimerization Protein 2 (JDP2), which positively mediates RANKL-induced osteoclast differentiation. Moreover, we found miR-29 targets RNAs critical for cytoskeletal organization, including Cell Division Control protein 42 (CDC42), SLIT-ROBO Rho GTPase activating protein 2 (SRGAP2), and G protein-coupled receptor 68 (GPR68). Importantly, these RNAs are upregulated in differentiated osteoclasts.

In summary, our data indicate that miR-29 regulates osteoclast formation. miR-29c expression is downregulated in late osteoclasts, and it targets genes important for cytoskeletal remodeling, motility and survival. A comprehensive understanding of how miRNAs regulate osteoclast formation and activity will lead to identification of new therapeutic targets for the treatment of bone diseases. Our study provides important information about the role of miR-29 in osteoclasts.

Disclosures: Tiziana Franceschetti, None.

SU0256

Mutation in OA/GPNMB Inhibits Bone Resorption *in vivo* and Osteoclast Differentiation *in vitro*. Samir Abdelmagid^{*1}, Joyce Y Belcher², Carlynn A Fulp¹, Fouad M Moussa¹, Roshanak Razmpour³, Fabiola Del-Carpio Cano³, Steven Popoff⁴, Fayez Safadi¹. ¹Northeast Ohio Medical University, USA, ²University of Pennsylvania, USA, ³Temple University, USA, ⁴Temple University School of Medicine, USA

Our lab was the first to report a key role of osteoactivin (OA/GPNMB) in osteoblast differentiation and bone formation. We reported that OA/GPNMB is expressed during osteoblast differentiation *in vitro*. We also showed that injection of recombinant (r) OA into the femur medullary space stimulated osteogenesis *in vivo*. Recent report showed that OA/GPNMB is expressed in osteoclasts (OC). In this study, we were interested to examine the functional role of OA/GPNMB during osteoclastogenesis. Immunofluorescent localization of OA/GPNMB in multinucleated osteoclasts (mOC) (≥ 3 nuclei) showed co-localization of OA/GPNMB protein with

actin ring and $\beta 3$ integrin. In addition, we tested the effects of rOA on osteoclastogenesis using bone marrow-derived hematopoietic cells. rOA protein enhanced RANKL-mediated osteoclastogenesis in a dose dependent manner measured by TRAP activity, total number and size of OC. Our laboratory obtained a mouse model with a natural mutation in the OA/GPNMB gene encoding a truncated protein with defective function and skeletal phenotype. Characterization of the bone phenotype by micro-CT analysis showed decreased bone volume and trabecular number in 8-week old mutant compared to wild-type (WT). Histomorphometric analysis showed no difference in the total number of TRAP-positive OC; however, mOC were significantly increased in number in OA/GPNMB mutant compared to WT. Although, the size of mOC was not changed; however, the mOC surface over bone surface was decreased in the mutant compared to WT, suggesting defective bone resorption in OA/GPNMB mutant mice. Transmission electron microscopy analysis demonstrated an abnormality in the ruffled border of mOC in OA/GPNMB mutant compared to WT. Defective OC function was confirmed by decreased levels of CTX in sera from OA/GPNMB mutant compared to WT. Next, we examined OC differentiation derived from OA/GPNMB mutant and WT mice *ex vivo*. TRAP-positive mOC number and activity were dramatically reduced in OA/GPNMB mutant compared to WT. Next, we examined adhesion of OA/GPNMB mutant and WT mOC over vitronectin. Interestingly, we found decreased adhesion of mOC and focal adhesion kinase (FAK) activity in OA/GPNMB mutant mOC compared to WT. Collectively, our data suggest that defective mOC in OA/GPNMB mutant mice is mediated at least in part, by OC adhesion and FAK activation pathway. Further studies are warranted to investigate the mechanism(s) of OA/GPNMB in osteoclastogenesis and bone remodeling.

Disclosures: Samir Abdelmagid, None.

This study received funding from: NIH

SU0257

Suppressive Effects of BRD4 Inhibitor on Inflammatory Cytokine Expression and RANKL-Induced Osteoclastogenesis. Shu Meng^{*}, Lan Zhang, Qisheng Tu, Jake Jinkun Chen. Tufts university School of Dental Medicine, USA

Bromodomain-containing protein 4 (BRD4), formerly named MCAP (mitotic chromosome-associated protein), belongs to BET family that carry two tandem bromodomains and an extraterminal domain. BRD4 is ubiquitously expressed in the cell nucleus of various tissues where it binds to acetylated chromatin and positively regulates RNA polymerase mediated transcription. BRD4 suppression by a synthetic bromodomain inhibitor, JQ1, decreased oncogene MYC transcription and significantly reduced tumor growth in animal models. This study investigated the effects of BRD4 inhibitor on inflammatory cytokine expression and receptor activator of nuclear factor kappa-B ligand (RANKL)-induced osteoclastogenesis *in vitro*.

RAW264.7, a mouse macrophage-like cell line, was purchased from ATCC and cultured in RPMI 1640 with 10% FBS, 0.1mg/ml streptomycin and 100U/ml penicillin. Cells were treated by 100ng/ml lipopolysaccharide (LPS) of *E. coli* with or without 250nM JQ1 for 1, 4, 24 and 48 hours, respectively, and were harvested at the indicated time. During RANKL-induced osteoclast differentiation, cells were treated with 250nM JQ1 on day 1, 2 and 3, respectively, and were collected after 5 days. Total RNA was extracted and reverse transcribed into cDNA. The mRNA expression levels of inflammatory cytokine genes and osteoclast specific genes were examined by real time PCR.

LPS stimulation increased expression of interleukin-1beta (IL-1 β), interleukin-6 (IL-6), and tumor necrosis factor alpha (TNF- α) in RAW264.7 cells. BRD4 inhibitor significantly suppressed LPS stimulated inflammatory cytokine expression (Fig 1). Compared with RANKL-induced osteoclast differentiation, the osteoclast-specific gene expressions, such as c-Fos, NFATc1, TRACP, cathepsin K and TRAF6, were blocked by BRD4 inhibition in mouse macrophages (Fig 2).

Macrophages play crucial roles in both inflammation and osteoclastogenesis that associate immunity with bone metabolism. Various bone resorption disorders are now recognized as inflammation induced, such as rheumatoid arthritis, osteoporosis, and periodontitis. The present study demonstrated that BRD4 inhibition significantly suppressed inflammation cytokine expression and osteoclastogenesis in mouse macrophages. These results provide the potential for a novel therapeutic strategy in clinical treatment of bone destruction diseases and pave the way for future animal studies that focus on the effects of BRD4 inhibition on inflammation and bone resorption.

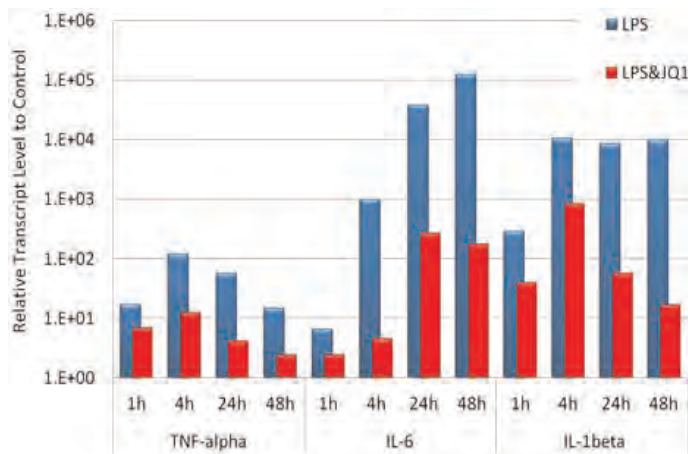


Figure 1. Real-time PCR mRNA expression levels of inflammatory cytokine genes in LPS stimulated RAW264.7 w/o BRD4 inhibitor, JQ1.

Figure 1

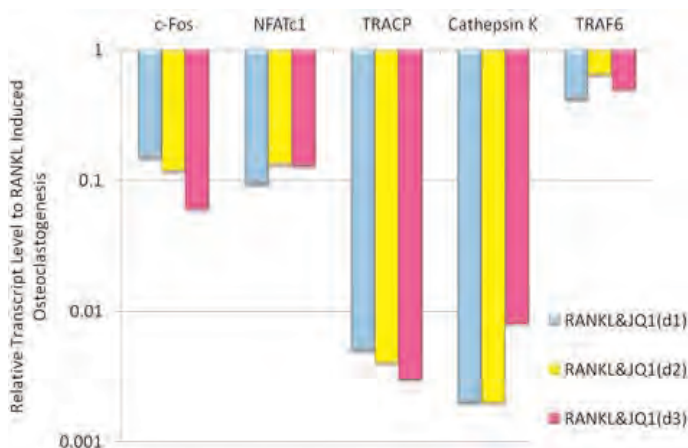


Figure 2. Real-time PCR mRNA expression levels of osteoclast specific genes in RANKL-induced RAW264.7 with JQ1 treatment, compared with RANKL-induced osteoclastogenesis without JQ1.

Figure 2

Disclosures: *Shu Meng, None.*

This study received funding from: NIH grants DE16710 and DE21464 to JC

SU0258

Tetracyclines Inhibit Osteoclast Differentiation by Converting the Differentiation Pathway from Osteoclasts to Dendritic Cells. Masanori Koide*¹, Sava Kinugawa², Yasuhiro Kobayashi², Toshihide Mizoguchi², Akihiro Muto², Tadashi Ninomiya², Ichiro Kawahara², Midori Nakamura², Hisataka Yasuda³, Naoyuki Takahashi², Nobuyuki Udagawa².
¹Matumoto Dental University, Japan, ²Matsumoto Dental University, Japan, ³Oriental Yeast Company, Limited, Japan

Tetracyclines such as doxycycline and minocycline are widely used to suppress the growth of bacteria in patients with inflammatory diseases. Tetracyclines have been shown to prevent bone loss, but the mechanism involved is not known. We have previously reported that tetracyclines inhibited RANKL-induced osteoclastogenesis of bone marrow-derived macrophages (BMMs), but had no effects on cell growth and phagocytic activity. Tetracyclines impaired osteoclast differentiation through the inhibition of MAPK signals (J. Bone Miner. Res. 22 (suppl 1): M106, 2007). It is known that osteoclasts and dendritic cells (DCs) are derived from common progenitors such as BMMs. In this study, we show that tetracyclines convert the differentiation pathway from osteoclasts to DCs. Treatment of BMMs with minocycline increased expression of DC markers such as CD11c and CD86 in the presence of RANKL. GM-CSF is known to induce DC differentiation through STAT5. We then examined whether STAT5 is involved in minocycline-induced DC differentiation. GM-CSF induced the phosphorylation of STAT5 in BMMs, but minocycline did not. Midostaurin, a STAT5 signaling inhibitor, suppressed the differentiation induced by GM-CSF but not by tetracyclines. These results indicate that the DC differentiation induced by tetracyclines is independent of STAT5

signaling. Finally, we examined whether tetracyclines suppress osteoclast differentiation and induce DC differentiation using RANKL-transgenic mice, a constitutively enhanced bone resorption model. The injection of tetracyclines into the subcutaneous tissue overlying calvariae of RANKL-transgenic mice suppressed RANKL-induced osteoclastogenesis and promoted the concomitant appearance of CD11c-positive cells. Taken together, our results suggest that the local administration of tetracyclines inhibit bone resorption through the conversion from osteoclast to DC differentiation. Tetracyclines may be a useful drug for preventing bone loss induced by local inflammation including periodontitis.

Disclosures: *Masanori Koide, None.*

SU0259

Bisphosphonates Alter the Number and Distribution of Osteoclasts and the RANKL Expression During Tooth Eruption of Rats. Vivian Bradaschia-Correa¹, Tais Oliveira², Lorraine Ferreira², Victor Arana-Chavez*².
¹Universidade de São Paulo, Brazil, ²University of São Paulo, Brazil

The bisphosphonates are drugs with known capability to inhibit clastic activity, and were employed in the present study with the purpose of interfering in the resorption of the alveolar bony crypt that occurs physiologically during the formation and eruption of rat molars. The objective of the present study is to evaluate the effect of the bisphosphonates alendronate and etidronate on the number of osteoclasts in the occlusal portion of the alveolar crypt during the formation of the eruptive pathway, as well as the protein expression of RANK, RANKL and OPG. Newborn Wistar rats were daily treated with 2.5 mg/kg alendronate (ALN) or 8 mg/kg etidronate (ET) during 4, 8, 14, 21 and 28 days. The controls (CON) received sterile saline solution. In the time points cited, their maxillae were fixed under microwave irradiation, decalcified and embedded in Spurr or JB-4 resin. The ultrathin sections were examined in a transmission electron microscope. JB-4 semi-serial sections were incubated for TRAP histochemistry, the osteoclasts in the occlusal half of the bony crypt surface were counted. Additional ALN and CON rats had the occlusal bone that covers the upper first molar removed and submitted to protein extraction, SDS-PAGE and Western Blotting and the membranes were incubated for RANK, RANKL, OPG and actin antibodies. ALN inhibited tooth eruption, while ET delayed it. The TRAP-positive osteoclasts were more numerous in the alveolar crypt surface of ALN specimens; however, they presented more latent osteoclasts at all time points. The ET presented reduced number of osteoclasts, but they were mostly activated. Ultrastructural analyzes confirmed the latent phenotype of osteoclasts of ALN specimens, while CON and ET osteoclasts presented typical activated phenotype. RANKL protein expression was inhibited at all time points in the ALN specimens, while OPG and RANK were not affected. The reduced number of osteoclasts in the ET specimens may have delayed the eruptive process. The decreased expression of RANKL may have inhibited the activation of osteoclasts and consequently inhibited the eruptive process in ALN specimens.

Disclosures: *Victor Arana-Chavez, None.*

This study received funding from: Grants 06160094-5 and 09154853-9 (FAPESP, Brazil)

SU0260

Calcitonin Inhibits SDCP-induced Osteoclast Apoptosis and Increases its Efficacy in a Rat Model of Osteoporosis. Jia-Fwu Shyu*¹, Yi-Jie Kuo², Chin-Bin Yeh³, Jui-Lin Chien¹, Chuan-Jen Wang¹, Wen-Hui Chan¹, Ni-Ko Wei¹, Ying-Jui Lu¹, Chi-Hung Lin⁴.
¹National Defense Medical Center, Taiwan, ²Taipei Medical University Hospital, Taiwan, ³Tri-Service General Hospital, Taiwan, ⁴National Yang Ming University, Taiwan

Although calcitonin has been clinically used for nearly 30 years, its role in calcium homeostasis and bone remodeling remains controversial; discrepant effects of calcitonin on bone cells have been reported. Because calcitonin may prolong osteoclast survival through inhibition of apoptosis, this study aimed to analyze the mechanism by which calcitonin influences osteoclast apoptosis induced by a bisphosphate analog, sintered dicalcium pyrophosphate (SDCP). As determined by a caspase-3 activity assay, annexin-V staining, and TUNEL analysis, calcitonin inhibited SDCP-induced apoptosis in primary osteoclast cultures. Western blot analysis along with studies using pharmacological inhibitors revealed that calcitonin increased Bcl-2 and Erk activity, and SDCP decreased Mcl-1 activity. A pit formation assay and tartrate-resistant acid phosphatase (TRAP) staining showed that calcitonin alleviates the decreased osteoclast survival but not resorption induced by SDCP. In vivo histomorphometric analysis of the tibia in ovariectomized rats revealed increased bone formation, and microcomputed tomography of the fifth lumbar vertebrae showed an additive effect of calcitonin and SDCP on bone volume. Finally, analysis of the serum bone markers, CTX-I and PINP, suggests that the increased bone volume induced by cotreatment with calcitonin and SDCP may be due to decreased bone resorption and increased bone formation. Therefore, calcitonin reduces SDCP-induced osteoclast apoptosis and increases its efficacy in an in vivo model of osteoporosis.

Disclosures: *Jia-Fwu Shyu, None.*

SU0261

Deletion of Connexin37, a Connexin Preferentially Expressed in Osteocytes versus Osteoblasts, Increases Bone Mass and Reduces Osteoclasts by Regulating Osteocytic Expression of RANKL and OPG. Rafael Pacheco-Costa^{*1}, Nicoletta Bivi², Jennifer S. Fang³, Keith Condon², Janis Burt³, Matthew Allen², Teresita Bellido², Rejane D. Reginato⁴, Lilian Plotkin².
¹Indiana University School of Medicine/Federal University of Sao Paulo, Brazil, USA, ²Indiana University School of Medicine, USA, ³University of Arizona, USA, ⁴Federal University of São Paulo, Brazil

Connexin (Cx) 43, the most abundant Cx expressed in bone, is required for osteoblast differentiation and bone mass acquisition, for the response of osteoblastic cells to bisphosphonates and PTH, and for osteocyte survival. A polymorphism in the gene encoding Cx37, another member of the α family of Cxs, has been associated with high BMD in a Japanese population. Yet, Cx37 expression in the skeleton and its potential function in bone cells have not been examined. We found that Cx37 is expressed in bone at about 5-times lower levels than Cx43; and that it is preferentially expressed in osteocytes. Thus, osteoblasts were separated from osteocytes by fluorescence activated cell sorting in digested neonatal calvaria from DMP1-8kb-GFP mice, in which osteocytes are fluorescent. Cx37 mRNA expression was 3-fold higher in GFP positive osteocytes than in GFP negative osteoblasts; whereas Cx43 mRNA expression was 1.7-fold higher in osteoblasts compared to osteocytes. Cx37 null mice are viable and their body weight is comparable to their wild type littermates (wt). Cx37^{-/-} females are sterile due to impaired ovarian follicle development, but males breed normally. We then examined the skeletal phenotype of male mice to avoid the potential contribution of hormonal alterations in females. Three-month-old male Cx37^{-/-} mice exhibit 20 and 25 % higher femoral and lumbar spine BMD, respectively, compared to wt littermates (by DEXA, n=3,4). μ CT revealed 56 % (17.8 \pm 3.5 vs. 11.4 \pm 1.8 %) and 22 % (27.4 \pm 1.8 vs. 21.5 \pm 2.3 %) higher cancellous bone volume; and 25 % (0.5 \pm 0.02 vs. 0.4 \pm 0.04 cm) and 11 % (0.50 \pm 0.020 vs. 0.45 \pm 0.008 cm) higher trabecular thickness in distal femur and 6th lumbar vertebra, respectively for Cx37^{-/-} vs. wt mice. Bone material density was increased (46.8 \pm 5.26 vs. 37.5 \pm 3.05 pixel), suggesting reduced resorption; and, accordingly, histomorphometric analysis showed a significant reduction (-37 %) in osteoclast surface (Oc.S/BS) in the distal femur of Cx37^{-/-} mice vs. wt (4.0 \pm 1.2 vs. 6.4 \pm 1.0 %). Consistent with these *in vivo* findings, MLO-Y4 osteocytic cells in which the expression of Cx37 was reduced by 82 % using shRNA exhibited a 50 % decrease in RANKL expression and a 200 % increase in OPG expression, resulting in 80 % lower RANKL/OPG ratio. We conclude that Cx37, a Cx preferentially expressed in osteocytes, controls bone mass by affecting osteoclast formation through the regulation of osteocytic pro- and anti-osteoclastogenic cytokines.

Disclosures: Rafael Pacheco-Costa, None.

SU0262

Effects of Azithromycin on Osteoclast Formation and Activation. Hitoshi Amano^{*1}, Kakei Ryu², Shinichi Iwai², Katsuji Oguchi², Shoji Yamada³.
¹Showa University School of Dentistry, Japan, ²Showa University, School of Med, Japan, ³Showa University, School of Dentistry, Japan

Azithromycin (AZM), a member of the macrolide group of drugs, is an antibiotic, and function as an anti-inflammatory drug.

Materials and Methods

Bone marrow cells from femur and tibia of ddY four/five-week-old mice passed Sephadex G10. The cells were cultured with pH7.0 α MEM, which include CSF-1 (25ng/ml) and RANKL (100ng/ml), with or without AZM (0 - 10 μ g/ml). RAW264.7 cells for this experiment are the same as before, using only RANKL. An *in vivo* experiment was performed using ddY 5-week-old mice. The experimental group was injected with AZM (10 mg/kg), and after 30 minute 0.9% acetic acid was injected intraperitoneally. The control group was only injected with acetic acid and the stretching number of both group. On day4 and day7, both groups were injected with only acetic acid.

Results: After 6 days, both cells were differentiated to TRAP positive multinucleated osteoclasts. The number of osteoclast decreased as the AZM dose increased. In the *in vivo* experiment, the stretch number of the experimental group was higher on day7 then it was on day0.

Discussion: Differentiation of hematopoietic stem cells and RAW264.7 cells into mature osteoclasts decreased as a result of AZM treatment. Injection of dilute acetic acid solution intraperitoneally caused a writhing response in the control group. This reaction was significantly reduced by pretreatment with AZM.

Conclusion: These results provide evidence for the important finding that AZM effects osteoclast differentiation and possesses anti-inflammatory properties.

Disclosures: Hitoshi Amano, None.

SU0263

Investigation of the *in vivo* Osteoclast Dependent and Independent Bone Formation. Christian Thudium^{*1}, Carmen Flores², Ilana Moscatelli³, Karoline Natasja Støhr Gudmann⁴, Annemarie Brüel⁵, Jesper Skovhus Thomsen⁶, Morten Karsdal¹, Johan Richter², Kim Henriksen¹.
¹Nordic Bioscience A/S, Denmark, ²Department of Molecular Medicine & Gene Therapy, Lund Strategic Center for Stem Cell Biology, Sweden, ³Lund University, Sweden, ⁴Nordic Bioscience, Denmark, ⁵University of Aarhus, Denmark, ⁶Institute of Anatomy, University of Aarhus, Denmark

Patients and mice with mutations inhibiting osteoclasts by either function (osteoclast-rich) or differentiation (osteoclast-poor) have osteopetrosis, a disease characterized by increased bone volume. Studies show that while both disease variants result in increased bone volume, the osteopetrotic phenotype is more severe in osteoclast-rich osteopetrosis likely due to maintained osteoclast derived anabolic signaling.

To investigate osteoclast dependent and independent bone formation we compared *ocloc* transplanted mice (acidification and resorption impaired) head to head with mice receiving stem cells from the *RANK KO* mice, which do not develop osteoclasts. Changes in bone turnover and structure were investigated in detail during a four month period.

Adult mice were irradiated and transplanted with fetal liver cells from *wt*, *ocloc* or *RANK KO* mice (Ly5.2) by IV injection into *wt* mice (Ly5.1). Serum samples were collected every two weeks for measurement of bone turnover markers (CTX-I, TRACP 5b). At 14 weeks the animals were euthanized and bones were collected for histomorphometry, μ CT and mechanical tests.

An engraftment level of approx. 97% was obtained. The resorption biomarker CTX-I was reduced to the same extent in both *ocloc* and *RANK KO* transplanted mice, while TRACP5b was increased 50% in the *ocloc* and decreased 50% in *RANK KO* mice compared to their respective control groups. *In vitro* osteoclast differentiation from splenocytes developed morphologically normal in *ocloc*, while no osteoclasts could be obtained from *RANK KO* transplanted mice. Both cell populations failed to resorb bone *in vitro*.

μ CT analyses of femurs showed an increase in cortical bone and a decrease in marrow space and trabecular thickness in both *ocloc* and *RANK KO* transplanted groups compared to controls. Furthermore, mechanical testing showed significant increase in bone strength in 3-point bending test.

In summary, we here show that adult mice transplanted with *ocloc* or *RANK KO* stem cells both have increased bone volume and strength with similar bone characteristics in femur compared to *wt* controls. In these mature osteopetrotic mice data suggests that bone formation exists both with and without osteoclasts. Further analysis will determine to which extent the presence of osteoclasts mediate an additional anabolic response. Although, the clinical phenotypes of these types of osteopetroses strongly support that the non-resorbing osteoclasts in the *ocloc* mice have this capacity.

Disclosures: Christian Thudium, None.

SU0264

The Rac Exchange Factor Dock5 is Necessary for Bone Resorption by Osteoclasts: Physiological Implications and Therapeutic Applications. Anne Blangy^{*}, Gaëlle Cres, Virginie Vives. CRBM - CNRS Montpellier University, France

Bone is a highly dynamic tissue that undergoes permanent remodeling throughout life. Bone dynamics is ensured by the osteoclasts, multinucleated macrophages specialized for bone resorption, and the osteoblasts, cells derived of mesenchymal origin, specialized for bone formation. During bone resorption, actin cytoskeleton in osteoclasts undergoes extensive reorganization to assemble the sealing zone, the podosome-based adhesion organelle essential for bone resorption and typical of osteoclasts. RhoGTPase signaling pathways, as major regulators of actin organization and then of cell adhesion and morphology, have essential functions in osteoclast biology. It is of particular importance for the assembly of the sealing zone.

We identified Dock5 as an activator of the GTPase Rac essential for bone resorption (Vives et al. J Bone Miner Res. 2011 May;26(5):1099-110). In the absence of Dock5, osteoclasts exhibit an important drop in Rac activity accompanied with a very low capacity to resorb bone. We identified C21 as a chemical inhibitor of Rac activation by Dock5 that hinders the resorbing activity of osteoclasts in culture. The differentiation process induced by RANKL is mostly unaltered in the absence of Dock5. Dock5^{-/-} mice have high bone mass and normal osteoclast numbers, confirming *in vivo* that Dock5 is essential for bone resorption but not for osteoclast differentiation. Dock5 expression is mainly restricted to osteoclasts in the mouse. In particular, it is not expressed in osteoblasts, the bone forming cell. These properties characterize Dock5 as a potential novel target against osteoporosis.

To challenge this hypothesis, we tested if C21 could prevent bone loss in two models of exacerbated osteolysis in the mouse: ovariectomy and collagen-induced arthritis. We found that daily injection of C21 (5 mg/d/kg) efficiently prevented trabecular bone loss in ovariectomized mice suggesting that the inhibition of Dock5 can prevent bone loss consecutive to estrogen deficiency. We further found that C21 did not affect the inflammatory response of mice injected with bovine collagen. Mice have similar levels of anti-collagen antibody and arthritic scores. Interestingly, C21 injection protected mice against cortical joint bone erosion induced by collagen

injections, suggesting that the inhibition of Dock5 can also prevent bone loss stimulated by inflammation.

Taken together, our observations characterize Dock5 as a novel target to develop anti-osteoporotic treatments.

Disclosures: Anne Blangy, None.

SU0265

Adenosine A_{2A} Receptor Stimulation Inhibits Osteoclast Formation by Suppressing NFκB Translocation to the Nucleus by a PKA-mediated Mechanism. Aranzazu Mediero^{*1}, Bruce Cronstein². ¹NYU SCHOOL OF MEDICINE, USA, ²NYU Medical School, USA

Adenosine, a nucleoside released at sites of injury and hypoxia, mediates its physiologic and pharmacologic effects via activation of G-protein-coupled receptors (A1, A2A, A2B, A3). Previously we reported that the A2AR agonist CGS21680 inhibited osteoclast differentiation in a dose-dependent manner so here we determined which intracellular pathways are involved in A2AR-mediated regulation of osteoclast differentiation. Osteoclast morphological characterization was studied in M-CSF/RANKL-stimulated murine marrow osteoclast precursors in the presence/absence of CGS21680 (A2A agonist) and ZM241385 (A2A antagonist) stained with AlexaFluor555-Phalloidin. Osteoclast differentiation in the presence/absence of CGS21680, ZM241385 and PKA/EPAC activators/inhibitors was further studied by TRAP staining. Signaling events (PKA/EPAC, NFκB and MAPK) were studied by Western Blot in PKA knockdown (lentiviral shRNA for PKA or scrambled) RAW264.7 cells. Osteoclast marker expression was studied by RT-PCR. Cytokine expression was assayed by ELISA. A2AR stimulation increases cAMP which activates protein kinase A (PKA) and direct activation of PKA inhibits osteoclast differentiation by $40.1 \pm 4.3\%$ ($p < 0.001$, $n = 5$). Interestingly, cAMP also stimulates EPAC activation and direct EPAC activation increases osteoclast formation by $6.8 \pm 3.2\%$ ($p < 0.001$, $n = 5$). PKA activation increased over time in the presence of CGS21680 with no change in EPAC activation. A2AR activation inhibits NFκB nuclear translocation in scrambled shRNA but not PKA knockdown cells ($p < 0.001$, $n = 4$). CGS21680 activates MAPK (pERK1/2, p-p38 and pJNK) and pre-treatment with ZM241385 reversed this activation; ERK1/2 was activated scrambled but not PKA-knockdown cells. A2AR activation inhibits the expression of osteoclast differentiation markers (Cathepsin K and Osteopontin) by a PKA-dependent mechanism. Finally, A2AR activation decreases IL-1β/TNFα secretion during osteoclast differentiation and these cytokines reverse the A2AR effect. Adenosine, acting at A2AR, inhibits osteoclast differentiation and regulates bone turnover mainly by the activation of PKA and the inhibition of NFκB translocation to the nucleus. Because adenosine mediates the anti-inflammatory effects of methotrexate we speculate that the capacity of methotrexate to inhibit bone erosion in Rheumatoid Arthritis may be mediated by increases in adenosine which inhibit osteoclast formation and function.

Disclosures: Aranzazu Mediero, None.

SU0266

c-Src Links a RANK/αvβ3 Integrin Complex to the Osteoclast Cytoskeleton. Takashi Izawa^{*1}, Wei Zou², Jean Chappel¹, Xu Feng³, Steven Teitelbaum². ¹Washington University in St. Louis, USA, ²Washington University in St. Louis School of Medicine, USA, ³University of Alabama at Birmingham, USA

RANK ligand (RANKL), by mechanisms unknown, directly activates osteoclasts to resorb bone. Because c-Src is key to organizing the cell's cytoskeleton, we asked if the tyrosine kinase also mediates RANKL-stimulated osteoclast activity. RANKL induces c-Src to associate with RANK³⁶⁹⁻³⁷³ in an αvβ3-dependent manner. Furthermore, RANK³⁶⁹⁻³⁷³ is the only one of six putative TRAF binding motifs sufficient to generate actin rings and activate the same cytoskeleton-organizing proteins as the integrin. While c-Src organizes the cell's cytoskeleton in response to the cytokine, it does not participate in RANKL-stimulated osteoclast formation. Attesting to their collaboration, αvβ3 and activated RANK co-precipitate, but only in the presence of c-Src. c-Src binds activated RANK via its Src homology (SH) 2 and αvβ3 via its SH3 domain suggesting the kinase links the two receptors. Supporting this hypothesis, deletion or inactivating point mutation of either c-Src SH2 or SH3 domain obviates RANK/αvβ3 association. Thus, activated RANK prompts two distinct signaling pathways; one promotes osteoclast formation and the other, in collaboration with c-Src-mediated linkage to αvβ3, organizes the cell's cytoskeleton.

Disclosures: Takashi Izawa, None.

SU0267

Orai1-Deficient Mice Develop Osteopenia Due to Impaired Functions of Osteoblasts and Osteoclasts. Sung-Yong Hwang^{*1}, Julie Foley², Wei Zou³, Steven L. Teitelbaum³, Gary S. Bird², James W. Putney². ¹Washington University in St. Louis School of Medicine, USA, ²NIEHS, USA, ³Washington University in St. Louis, USA

Store-operated Ca²⁺ entry (SOCE) is a major Ca²⁺ influx pathway in most non-excitable cell types and Orai1 was recently identified as an essential pore-subunit of SOCE channels. Orai1-mediated SOCE has been shown to play a critical role in the activation of hematopoietic cells including T cells. We previously reported that silencing of Orai1 inhibits osteoclast differentiation from RAW264.7 cells, resulting from impaired cell fusion. Here we investigate the physiological role of Orai1 in bone homeostasis using Orai1-deficient mice (Orai1^{-/-}). Orai1^{-/-} mice developed osteopenia with decreased bone mineral density and trabecular bone volume. There was no difference in the number of TRAP-positive osteoclasts *in vivo*. Consistent with the Orai1 knockdown study in RAW264.7 cells, osteoclastogenesis *in vitro* from Orai1^{-/-} bone marrow-derived monocyte/macrophage cells yielded fewer and smaller osteoclasts due to a defect in cell fusion of preosteoclasts. Induction of two osteoclastic fusion genes, *ATP6v0d2* and *DC-STAMP*, was impaired in Orai1^{-/-} osteoclasts. Resorption activity *in vitro* was also impaired in Orai1^{-/-} osteoclasts. To assess the role of Orai1-mediated SOCE in osteoblastogenesis, SOCE in MC3T3-E1 preosteoblastic cells was inactivated by lentiviral overexpression of a pore-dead Orai1 mutant. Lack of SOCE in MC3T3-E1 had no effect on ALP stain and expression but substantially inhibited mineralized nodule formation. Induction of bone matrix proteins, collagen type 1 a1 and 2, was significantly reduced in MC3T3-E1 cells lacking SOCE. Accordingly, bone marrow derived-stromal cell culture from Orai1^{-/-} mice showed impaired mineral deposition. We found that expression of collagen type 1 a2 was significantly decreased in Orai1^{-/-} osteoblasts despite an increase in the expression of ALP and osteocalcin. This indicates that Orai1 is involved in the function but not differentiation of osteoblasts. Together, these results suggest that Orai1 plays a critical role in bone homeostasis by regulating both osteoblasts and osteoclasts.

Disclosures: Sung-Yong Hwang, None.

SU0268

Regulation of Bone-resorption and Sealing Zone Formation in Osteoclast through Akt-mediated Microtubule Stabilization. Sakae Tanaka¹, Naoto Tokuyama^{*2}, Takumi Matsumoto¹, Yuhō Kadono¹. ¹The University of Tokyo, Japan, ²University of Tokyo, Japan

Objective. Akt, downstream effector of PI3K, are known to associate with various cellular processes. In osteoclasts, its involvement with differentiation and its limited contribution to survival are known, however its roles in bone-resorbing activity of mature osteoclasts remain elusive.

Methods. For functional analyses, we used osteoclasts differentiated from murine bone marrows using co-culture system with Akt inhibitor or adenoviral overexpression of constitutively active Akt1. We also generated mice with osteoclast-specific conditional deletion of Akt1 and Akt2 (referred to herein as DKO mice) by crossing Akt1 flox mice, Akt2 flox mice and cathepsin K-cre knockin mice.

Results. Treatment with Akt inhibitor disrupted sealing zone formation and decreased bone-resorbing activity of osteoclasts. Regular structure of microtubules were lost and acetylated tubulins, which reflect stabilized microtubules, were reduced, whereas mandatory Akt activation produced the opposite effect. Mandatory Akt activation increased the binding of microtubule-associated protein APC, APC-binding protein EB1, and Dynein activator complex Dynactin with microtubules. Depletion of Akt1 and Akt2 resulted in disconnection of APC/EB1 and decrease of bone-resorbing activity with reduced sealing zone formation, which were recovered with addition of LiCl, GSK-3β inhibitor. DKO mice showed mild osteosclerosis due to reduced bone resorption.

Conclusion. Our findings indicate that Akt controls the bone-resorbing activity of osteoclasts by stabilizing microtubules through regulating the bindings of microtubule associated proteins.

Disclosures: Naoto Tokuyama, None.

SU0269

Serum Calcium-decreasing Factor, Caldecrin, Inhibits RANKL-mediated Ca^{2+} Signaling and Actin Ring Formation in Mature Osteoclasts via Suppression of the Src Signaling Pathway. Akito Tomomura^{*1}, Hiroya Hasegawa², Naoto Suda³, Hiroshi Sakagami⁴, Mineko Tomomura⁵. ¹Meikai University, School of Dentistry, Japan, ²Div. of Orthodont. Meikai Univ. School of Dentistry, Japan, ³Div. Orthodont. Meikai Univ. School of Dentistry, Japan, ⁴Meikai Pharm.-Med. Lab. Meikai Univ. School of Dentistry, Japan, ⁵Div. Biochem. Meikai Univ. School of Dentistry, Japan

We have purified and cloned the serum calcium-decreasing factor, caldecrin, from the pancreas. Caldecrin is a secretory-type serine protease, which has chymotryptic activity and is also known as chymotrypsin C. We originally reported that the administration of caldecrin decreases mouse serum calcium concentration without protease activity. Recently, we reported that caldecrin inhibits osteoclast differentiation by inhibition of RANKL-mediated Ca^{2+} oscillation, leading to suppression of NFATc1 activation. The inhibitory effect of caldecrin on osteoclast differentiation does not depend on its protease activity (Hasegawa *et al. J Biol Chem* 2010). We have also demonstrated that caldecrin suppresses bone resorption by mature rabbit osteoclasts. These results, including the previous *in vivo* finding of rapid serum calcium decrease after intravenous injection of caldecrin, suggest that caldecrin may be functional not only in the osteoclast differentiation step but also in the bone resorption step of mature osteoclasts. Here, we investigated the effects of caldecrin on the function of mature osteoclasts by treatment with RANKL. Caldecrin inhibited the RANKL-stimulated bone resorptive activity of mature osteoclasts. Furthermore, caldecrin inhibited RANKL-mediated sealing actin ring formation, which is associated with RANKL-evoked Ca^{2+} entry through transient receptor potential vanilloid channel 4. The inhibitors of PLC γ , Syk, and c-Src, suppressed RANKL-evoked Ca^{2+} entry and actin ring formation of mature osteoclasts. Interestingly, caldecrin significantly inhibited RANKL-stimulated phosphorylation of c-Src, Syk, PLC γ 1, and γ 2, SLP-76, and Pyk2, but not those of ERK, JNK, or Akt. Caldecrin inhibited RANKL-stimulated c-Src kinase activity and c-Src-Syk association. These results suggest that caldecrin inhibits RANKL-stimulated calcium signaling activation and cytoskeletal organization by suppression of the c-Src-Syk pathway, which may in turn reduce the bone resorptive activity of mature osteoclasts. Thus, caldecrin is capable of acting as a negative regulator of osteoclastogenesis and osteoclast function of bone resorption.

Disclosures: Akito Tomomura, None.

This study received funding from: Ministry of Education, Culture, Sports, Science, and Technology of Japan

SU0270

Autophagy Protects Osteocytes through Preconditioning Mechanism. Rekha Kar^{*1}, Manuel Riquelme², Jean Jiang³. ¹The University of Texas Health Science Center, USA, ²University of Texas Health Science Center, USA, ³University of Texas Health Science Center at San Antonio, USA

Autophagy has been proposed as a double edged sword conferring protective or detrimental effect on cells depending on the cellular context and degree of removal of cytoplasmic materials and damaged organelles. Basal level of autophagy has been detected in primary osteocytes and in the osteocyte cell line MLO-Y4. We have shown that glucocorticoid, dexamethasone (Dex) induces autophagy in osteocytes. Furthermore, osteocytes in murine and human cortical bone displayed punctuate distribution of microtubule associated light chain 3 (LC3) suggestive of autophagy. This study was conducted to determine the role of autophagy in regulating the susceptibility of osteocytes to cell death. We show here that oxidative stress induced cell death of MLO-Y4 cells. The treatment of oxidant, H_2O_2 decreased autophagy as evidenced by decrease in LC3 expression. GFP LC3 punctate staining and red fluorescent acridine orange staining. To elucidate the role of autophagy during oxidative stress-induced cell death, we preincubated cells with the autophagy inhibitor chloroquine. Oxidative stress induced cell death of osteocytes is exacerbated by the autophagy inhibitor, suggesting protective function of basal level of autophagy against oxidative stress-induced cell death. To further confirm the protective function of autophagy, we pretreated cells with Dex to enhance the development of autophagy in osteocytes. Interestingly, preincubation with Dex protected osteocytes from oxidative stress-induced cell death. Furthermore, we showed that pre-treatment with Dex not only reduced susceptibility of osteocytes to oxidative stress-induced cell death but also conferred protection against TNF α and cycloheximide-induced cell death. Taken together, our results suggest that autophagy developed leads to the preconditioning of osteocytes and conveys novel cell protective function against oxidative stress and other insults.

Disclosures: Rekha Kar, None.

SU0271

Mechanical Vibration Induces Differential Frequency-Dependent Responsiveness in Osteocytes versus Cementoblasts. Dawei Liu^{*1}, Chao Liu², Lidan You³. ¹Marquette University School of Dentistry, USA, ²University of Toronto, Canada, ³Mechanical & Industrial Engineering, University of Toronto, Canada

Objective: To explore differential biological responses of cementoblasts versus osteocytes to mechanical vibration **Materials and Methods:** Mouse osteocyte cell line MLO-Y4 and cementoblastic cell line OCCM.30 cells were cultured in α -MEM supplemented by 2.5% FBS and 2.5% CS (for MLO-Y4), and 10% FBS (for OCCM.30). The cells (up to the 10th passage) were seeded in 6-well plates coated with type I collagen and grew to 70% (for MLO-Y4) and 100% (for OCCM.30) confluency. Completely filled up with α -MEM with 0.5% FBS and sealed, the 6-well plates were subjected to a low-magnitude (0.3g) and high-frequency (30, 60 and 90Hz respectively) mechanical vibration for 1 hour. To explore the possible involvement of MAPK signaling pathway, a specific MEK1 inhibitor - PD98059 (15 μ M) was added in designated groups during the vibration. After vibration, the cells were lysed to collect total RNA. Total RNA was extracted and reverse-transcribed to synthesize cDNA. For the genes of RANKL, OPG, and 18S, quantitative PCR was used to amplify the cDNA of the samples using gene-specific primers and SYBR Green I. The copy numbers of RANKL and OPG for each experimental group were normalized to 18S (housekeeping gene) rRNA. Each experiment was repeated at least 3 times, and 3-6 samples for each group. One-way ANOVA with Tukey's post hoc test was used to compare the results among the groups, with *p* value being set at 0.05. **Results:** Among the 4 experimental groups (0, 30, 60, 90Hz), LMHF mechanical vibration significantly reduced the RANKL/OPG ratio specifically at 60Hz for MLO-Y4 cells (45% down, *p*<0.01, *n*=6) and 30Hz for OCCM.30 cells (35% down, *p*<0.05, *n*=5). When PD98059 was added during vibration, the vibration-induced reduction of RANKL/OPG ratio was obliterated only in MLO-Y4 cells. **Conclusions:** LMHF mechanical vibration induces differential biological responses in osteocyte and cementoblasts by different specific frequencies, which is partially mediated by MAPK signaling pathway.

Disclosures: Dawei Liu, None.

This study received funding from: NIDCR

SU0272

Novel Osteocytic Cell Lines to study RANKL, FGF23, and SOST/Sclerostin Regulation. Jordan Spatz^{*1}, Yili Qu², Kevin Barry², Chris Adamson³, Lowell Misener³, Paola Divieti Pajevic⁴. ¹Harvard-MIT Division of Health Sciences & Technology (HST), USA, ²Endocrine Unit, Massachusetts General Hospital, USA, ³Calm Technologies, Canada, ⁴Massachusetts General Hospital & Harvard Medical School, USA

Although it is known bone responds to its mechanical environment, the mechanisms underlying skeletal mechano-transduction are poorly understood. Osteocytes, the most abundant yet least understood bone cell type, are thought to be the mechanosensors of bone. To date, studies of osteocytes' have been limited by the lack of osteocytic cell lines. To this end, mice expressing the green-fluorescent protein (GFP) under the control of Dentin Matrix-Protein 1 (8KbDMP1-GFP) were mated with mice carrying a ubiquitously expressed SV40Ag (Immortomouse Charles River) and osteocytes were isolated from long bones of double transgenic offspring. Cells were subjected to sequential collagenase digestions followed by FACS sorting for intrinsic GFP expression. Sorted immortalized cell displayed the dendritic morphology and expressed genes characteristic of an osteocytic population such as, SOST, DMP1, FGF23, RANKL, and had low levels of genes characteristic of osteoblasts, such as Kera. Clones were then selected on the basis of their high expression of SOST mRNA and their responsiveness to PTH treatment. Two clones, namely Ocy454 and Ocy491 were further analyzed. Notably, after two weeks in culture, one cell line, Ocy454 expressed levels of SOST mRNA that were 72-fold higher than wild type osteoblasts, as assessed by qPCR. Furthermore, in 2D culture Ocy454 increased RANKL, decreased SOST/Sclerostin, and showed no change in FGF23 expression upon treatment with 100nMPTH(1-34) for 4 hrs. To test the effects of a 3D culture environment on expression and regulation of osteocyte-specific genes, Ocy cells were seeded at 4 million cells/ml onto collagen coated Alvetex scaffolds and cultured for an additional 7 to 14 days. Interestingly, under 3D culture conditions, Ocy454 showed a five-fold increase in FGF23 expression that was not observed in 2D culture conditions. In addition, we evaluated the effects of simulated microgravity, as achieved by the NASA rotating wall bioreactors, on the regulation of RANKL and SOST mRNA expression in these cells. Ocy454 increased SOST by 24% and RANKL by 300% under NASA bioreactor simulated microgravity conditions resembling *in vivo* unloading in murine models. In summary we have established novel DMP1/SOST enriched osteocytic cell lines from long bones and importantly show the benefit of a 3D culture environment to understanding osteocytic regulation of FGF23, *in-vitro*.

Disclosures: Jordan Spatz, None.

SU0273

THE Role of RPTP μ and Sclerostin in Bone Mechanosensing and Regulation of Bone Formation. Martijn Van Der Velde^{*1}, Jessica Theeuwse², Marc Jamon³, Laurence Vico⁴, Norbert Laroche⁴, Clemens Löwik⁵, Karien De Rooij⁶. ¹Leiden University Medical Centre, The Netherlands, ²Leiden University Medical Centre, Netherlands, ³Faculté de Médecine de La Timone, France, ⁴University of St-Etienne, France, ⁵Leiden University Medical Center, Netherlands, ⁶Leiden University Medical Center, The Netherlands

In search for treatments of osteoporosis, proper control of bone formation has gained increasing attention. Sclerostin has proven to be a potent and specific target, since it is exclusively expressed in mature osteocytes and suppresses bone formation by antagonizing Wnt-signaling. In addition, mechanical stimulation of bone inhibits sclerostin expression, suggesting a functional coupling between these pathways, but the exact mechanisms remain elusive.

RPTP μ , a transmembrane protein involved in cell-cell interactions, is expressed in cells responding to mechanical forces. In bone, we show specific expression of RPTP μ in osteocytes and postulate a similar role.

To elucidate the roles of RPTP μ and sclerostin in mechanosensing and the regulation of bone formation, we performed two experiments:

1. Bone marrow obtained from WT, RPTP μ ^{-/-}, human sclerostin overexpressing (hSOST^{+/tg}) and RPTP μ ^{-/-}hSOST^{+/tg} mice was cultured under osteogenic conditions. Differentiation, mineralization and osteocyte formation were determined by measuring ALP activity in culture medium, Alizarin Red staining and expression of the osteogenic differentiation markers osteocalcin, DMP-1 and sclerostin.

2. In WT mice subjected for 3 weeks to 3G gravitation by centrifugation, the expression of sclerostin and RPTP μ was determined by immunohistochemistry performed on long bone sections and compared to those of stationary controls.

Experiment 1 shows that RPTP μ ^{-/-}-derived cultures have increased osteogenic differentiation, mineralization and osteocyte formation, while hSOST^{+/tg} cultures show opposite effects. Interestingly, over-expressing human sclerostin in RPTP μ ^{-/-} mice completely overruled the effects of RPTP μ deficiency since RPTP μ ^{-/-}hSOST^{+/tg} cultures were similar to hSOST^{+/tg} cultures.

Experiment 2 demonstrates that RPTP μ and sclerostin are expressed in different types of osteocytes. Moreover, centrifugation increased the expression of sclerostin, while it decreased the expression of RPTP μ .

Together, our results demonstrate that both RPTP μ and sclerostin are involved in the regulation of bone formation and osteocyte formation. In addition, they are expressed in a reciprocal fashion, both in terms of tissue distribution and responsiveness to mechanical loading, implicating a functional interaction between RPTP μ and sclerostin in the regulation of bone formation in response to mechanical loading.

Disclosures: Martijn Van Der Velde, None.

SU0274

Tracking Transcriptomic and Transcription Factor Cistromic Changes During Osteoblast to Osteocyte Differentiation. Kathleen Bishop^{*1}, Hillary St. John², Nancy Benkusky¹, Mark Meyer¹, Lynda Bonewald³, J. Pike¹. ¹University of Wisconsin-Madison, USA, ²University of Wisconsin-Madison, USA, ³University of Missouri - Kansas City, USA

Osteocytes are terminally differentiated osteoblasts that become fully embedded in bone as a result of osteoid secretion and mineralization. These cells are highly abundant, reside in specialized bone lacunae and communicate via an extensive dendritic-like canalicular network. Despite emerging understanding of these cells, however, little is known of the determinants that promote osteocyte differentiation from its cellular precursors. We used the mouse osteocytic IDG-SW3 cell line together with RNA- and ChIP-seq methods to identify changes in gene expression patterns that occur on a genome-wide scale during this cell's maturation and to characterize the transcription factor programs that are responsible. IDG-SW3 cells undergo a differentiation program that proceeds over 35 days (d), beginning as an osteoblast and progressing to a mineralized, matrix-embedded early (d14 to 21) and then late osteocyte (by d35). RNA was harvested on d3 and weekly to d35 and then subjected to RNA sequencing. Cells were also harvested at d3, d14 and d35 and subjected to ChIP-seq analysis using antibodies to RUNX2, C/EBP β and the coregulator p300. Cluster analysis revealed multiple programs of gene expression that included genes that were rapidly suppressed after d3 or were strongly upregulated, peaking at either the early (e.g., DMP1, RANKL, E11, ANK) or the late (e.g., PTHR1, VDR) stage of osteocyte differentiation. A gene network was also upregulated only at the late osteocyte stage (e.g., SOST, FGF23, MEPE, ALPL) as well. GO term analysis of these clusters suggested a temporal-specific modulation of multiple transcription factors including RUNX2, SATB2, SP7, MEF2c, GR and ER α , and also gene networks associated with skeletal homeostasis, osteoblast differentiation, and muscle and neuronal development/function. ChIP-seq analysis revealed an extensive genome-wide RUNX2 DNA binding cistrome; this cistrome overlapped extensively with the cistromes for C/EBP β and p300, thereby identifying key regulatory regions for multiple gene targets and suggesting the existence of a novel regulatory complex associated with the osteoblast/osteocyte phenotype. These complexes also assembled near genes considered classic markers of osteocytes including SOST, FGF23 and MEPE, thus identifying locations of key enhancers. These and additional data provide new molecular insight into the

differentiation program and the mechanisms that describe the osteoblast to osteocyte transition.

Disclosures: Kathleen Bishop, None.

SU0275

Osteocytes Dissolve Mineral through Canaliculi via a Diffusion-limited Process. Nobuhito Nango^{*1}, Shogo Kubota¹, Wataru Yashiro², Atsushi Momose³, Koichi Matsuo⁴. ¹Ratoc System Engineering Co., Ltd., Japan, ²Graduate School of Frontier Sciences, The University of Tokyo, Japan, ³Institute of Multidisciplinary Research for Advanced Materials, Tohoku University, Japan, ⁴School of Medicine, Keio University Laboratory of Cell & Tissue Biology, Japan

It is postulated that osteocytes could function in bone remodeling through perilacunar and canalicular remodeling. At the last meeting, we reported that osteocytes dissolve mineral via canaliculi (average diameter, 0.26 μ m) in a wide area within bone. Here we report the mechanism of mineral dissolution based on analysis of tibial diaphyseal cortical bone from wild-type and c-Fos-deficient mice, which lack osteoclasts. A multi-scan X-ray microscope with an effective pixel size of 0.22 μ m was constructed in a synchrotron radiation facility (Spring-8, Japan). We employed a two-step method to scan a single area of the specimen. To measure the absolute value of bone mineral around canaliculi, we applied differential phase imaging. We then used X-ray microscopy under defocus conditions to detect canaliculi by enhancing their edges. Alignment of resultant 3D images revealed osteocyte canaliculi and the mineral density of their surroundings, which was further analyzed in cross-sections orthogonal to the orientation of canaliculi.

When we examined low and high mineral zones of a specimen from a 4 week-old wild-type mouse (Fig. a, b), both showed V-shaped reduction in mineralization levels around canaliculi (Fig. c). The reduction in mineralization levels was greatest at each canalculus in the center, and mineralization levels were gradually elevated around the canalculus reaching background levels at 1.5 μ m away from the canalculus. The background mineralization levels were lower by 32% in the low mineral zone compared to the high mineral zone in this sample (Fig. c). Mineralization levels were normalized to background, and a demineralization graph around canaliculi (n=5 for each zone) was generated for both low and high mineral zones (Fig. d, e). Experimental data points closely fit a theoretical Gaussian curve ($r^2=0.99$).

These results suggest that unknown materials spread from canaliculi to bone matrix via diffusion and dissolve minerals. Estimated diffusion constants of the hypothetical materials were similar between low and high mineral zones. Analysis of 14 and 28 week-old wild-type and c-Fos-deficient mice revealed comparable results. Lactating and non-lactating mice are being compared. Overall, these data are consistent with the view that a transition from high to low mineral zones occurs by continuous emission from canaliculi of materials that promote mineral dissolution.

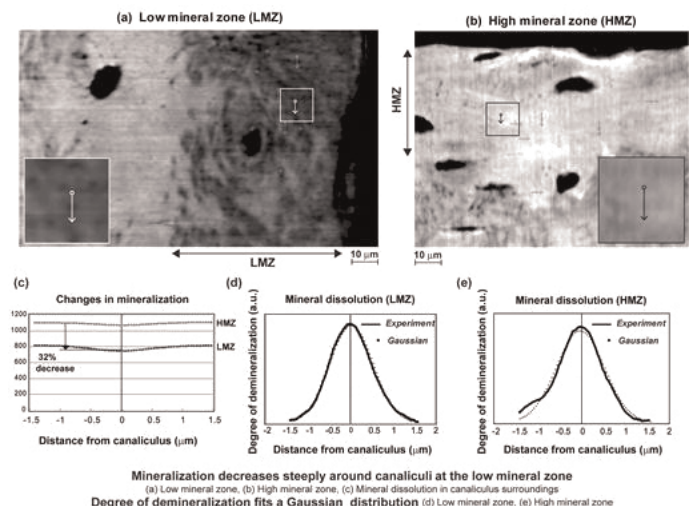


Fig.1

Disclosures: Nobuhito Nango, None.

SU0276

Bone Loss after Bariatric Surgery: Discordant Results between DXA and QCT Bone Density. Elaine Yu^{*1}, Chantel Baldwin¹, Mary Bouxsein², Abby Cange¹, Lee Kaplan¹, Joel Finkelstein¹. ¹Massachusetts General Hospital, USA, ²Beth Israel Deaconess Medical Center, USA

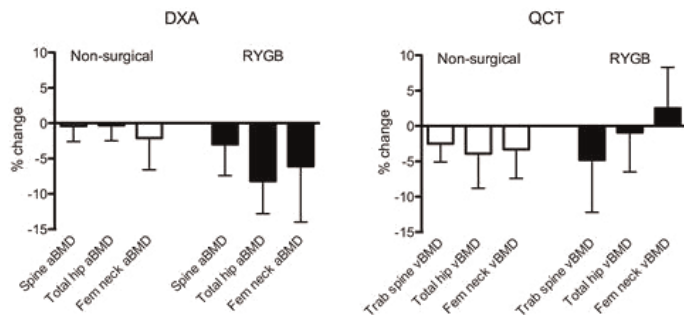
Purpose: Several studies have suggested that dramatic bone loss occurs in the first year after bariatric surgery. Studies-to-date have relied upon dual-energy x-ray absorptiometry (DXA), even though it may be subject to artifact with changing body

composition. Quantitative computed tomography (QCT) bone imaging techniques may be more accurate in obese patients who are undergoing profound weight loss.

Methods: We enrolled 50 adults with severe obesity into a prospective longitudinal study, including 30 subjects undergoing Roux-en-Y gastric bypass (RYGB) and 20 matched non-surgical controls. Lumbar spine and proximal femur areal bone mineral densities (aBMD) were measured by DXA and volumetric bone mineral densities (vBMD) were measured by QCT at 0 and 12 mo. Poor quality DXA and QCT scans were excluded from the analysis. One-year data are presented for the first 34 subjects (25 RYGB, 9 controls). Paired t-tests were used for within-group comparisons, and independent t-tests were used for comparisons of RYGB and controls.

Results: Baseline gender (86% female), age (mean \pm SD: 47 ± 16 y), weight (266 ± 41 lbs), and BMI (45 ± 7 kg/m²) were similar in the RYGB and control groups as were baseline areal and volumetric BMDs. At one year, weight loss was significantly greater in the RYGB group vs. controls ($30 \pm 9\%$ vs. $0 \pm 5\%$, $p < 0.0001$). DXA aBMD and QCT vBMD were stable in the control group after one year. In contrast, aBMD by DXA decreased $2.9 \pm 4.3\%$ at the spine ($p = 0.002$), $8.5 \pm 4.6\%$, at the total hip ($p < 0.0001$), and $6.2 \pm 6.7\%$ at the femoral neck ($p < 0.0001$) compared to baseline in subjects who had RYGB, although only bone loss at the total hip significantly exceeded that of the control group ($-8.5 \pm 4.6\%$ vs. $-0.2 \pm 2.1\%$, $p < 0.0001$). Trabecular spine vBMD by QCT decreased $4.8 \pm 7.4\%$ in the RYGB group ($p = 0.006$), but this change was not significantly different from the change in controls ($-4.8 \pm 7.4\%$ vs. $-2.5 \pm 2.6\%$, $p = 0.239$). There were no changes in total hip or femoral neck vBMD by QCT in the RYGB group. In the RYGB group, weight loss was significantly associated with change in total hip aBMD ($r = 0.28$, $p = 0.046$), but not with change in total hip vBMD ($r = -0.06$, $p = 0.826$).

Conclusions: Striking declines in DXA aBMD were observed after RYGB but similar patterns were not seen by QCT vBMD. These discordant results suggest that imaging artifacts from large changes in body weight after bariatric surgery may lead to overestimation of bone loss by DXA, particularly at the hip.



Change in bone density at 1 year

Disclosures: Elaine Yu, None.

SU0277

Functional Study of BMD-Associated rs9594738 in the RANKL gene context. Guy Yoskovitz¹, Natalia Garcia-Giralt², Maria Rodriguez-Sanz³, Roser Urreiziti⁴, Robert Guerri Fernandez⁵, Sergi Ariño-Ballester³, Daniel Prieto-alhambra⁶, Leonardo Mellibovsky⁷, Daniel Grinberg⁸, Susana Balcells⁹, Xavier Nogues¹⁰, Adolfo Diez-Perez¹¹. ¹IMIM, Parc de salut Mar, RETICEF, Spain, ²IMIM, Spain, ³IMIM, Parc de Salut Mar, Barcelona, Spain, Spain, ⁴Department of Genetics, University of Barcelona, Spain, ⁵Fundacio IMIM, Spain, ⁶Institut Municipal D'Investigació Mèdica, United Kingdom, ⁷Hospital del Mar, Parc de Salut Mar, Spain, ⁸The University of Barcelona, Spain, ⁹University of Barcelona, Spain, ¹⁰Institut Municipal D'Investigació Mèdica, Spain, ¹¹Internal Medicine, Hospital del Mar, Parc de Salut Mar, RETICEF, Spain

Introduction: Over the past decade, many genome-wide association studies (GWA) and meta-analyses were performed to identify genes and regions involved in bone metabolism and in the osteoporotic phenotype. Nevertheless, the grand majority of these GWAs results were not tested at any functional level. This study aimed to reveal the functionality of bone mineral density (BMD) associated SNP rs9594738 which lies ~184kb upstream to the RANKL gene. This SNP and its surrounding previously suggested it may act as a distal RANKL regulatory region.

Methods: The proximal 2015 bp region of the RANKL promoter was cloned into pUC19 vector and subsequently into pGL3 basic vector and a total of 4 structures were designed: P1 (-2015 bp promoter), P2 (-1347 bp), P3 (-1038 bp) and P4 (-330 bp). These structures were transfected into human osteosarcoma cell line (U2OS) with and without an 835bp region which includes the SNP rs9594784, which was named distal region (DR). Second phase was to test the effect of known cytokines, hormones and growth factors (TGF- β , vitamin D, 17 β -Estradiol, Dexamethasone, rHTNF α , PTH and IL-1) 6 hours after transfection followed by a 16 hours incubation period. *In silico* study, intended to identify the differences between the two alleles was performed, followed by electrophoretic mobility shift assay (EMSA) and supershift experiments. Finally, to achieve a comprehensive view of the DR in the osteoblast context, we

performed an expression analysis using osteoblast mRNA extraction to test if this region is expressed.

Results: Functional experiments exploring this RANKL distal region (DR) harboring rs9594738 demonstrated the region's capacity to inhibit the RANKL basal promoter in reporter gene assays. Moreover, DR includes vitamin D response element(s) which activate the reporter gene expression. On the other hand, we also demonstrated the existence of RNA transcribed from part of DR, suggesting alternative regulation mechanisms.

Conclusion: our results demonstrate a DR functionality in the RANKL gene context with a vitamin D involvement.

Disclosures: Guy Yoskovitz, None.

SU0278

MiR-422a in Human Circulating Monocytes is a Potential MicroRNA Biomarker Underlying Postmenopausal Osteoporosis. Yang Wang^{*1}, Benjamin Moore², Xian-Hao Peng², Xiang Fang¹, Joan Lappe², Robert Recker², Peng Xiao². ¹Creighton University, USA, ²Creighton University Osteoporosis Research Center, USA

MicroRNAs (miRNAs) are a class of short non-coding RNA molecules that regulate gene expression by targeting mRNAs. Recently, miRNAs have been shown to play important roles in the etiology of various diseases. However, little is known about their roles in the development of osteoporosis. Circulating monocytes are osteoclast precursors that also produce various factors important for osteoclastogenesis, such as IL-1, IL-6, TNF- α and IGF-1. Therefore, in this study we aimed to find significant miRNA biomarkers in human circulating monocytes underlying postmenopausal osteoporosis. We used ABI TaqMan[®] miRNA array followed by qRT-PCR validation in human circulating monocytes to identify miRNA biomarkers between 10 high BMD and 10 low BMD postmenopausal Caucasian women. MiR-422a was up-regulated with marginal significance ($P = 0.065$) in the low compared with the high BMD group in the array analysis. However, a significant up-regulation of miR-422a was identified in the low BMD group by qRT-PCR analysis ($P = 0.029$). We also performed bioinformatic target gene analysis and found several potential target genes of miR-422a, which are able to inhibit osteoclastogenesis. Further qRT-PCR analyses of the target genes in the same study subjects showed that the expression of five of these genes (CBL, CD226, IGF-1, PAG1, and TOB2) correlated negatively with miR-422a expression. Only one study demonstrated that miR-422a was down-regulated in osteoblast-like cell line (MG-63) treated with peptide-15. However, our study suggests for the first time that *in vivo* miR-422a in circulating monocytes (osteoclast precursors) is a potential miRNA biomarker underlying postmenopausal osteoporosis.

Disclosures: Yang Wang, None.

This study received funding from: The State of Nebraska (LB692 and LB595) and NIH (R01AR04054496-02S1)

SU0279

Bone Turnover Markers and Response to Oral Bisphosphonates in Patients with Type 2 Diabetes. Dong Jin Chung^{*}, Jin Ook Chung, Dong Hyeok Cho, Min Young Chung. Chonnam National University Medical School, South Korea

The bone mass is known to be decreased in patients with type 1 diabetes, and this is primarily due to osteoblastic dysfunction. The data on bone mineral density (BMD) in patients with type 2 diabetes has been inconsistent. However, many recent epidemiologic studies have shown that the osteoporotic fracture risk is also increased in patients with type 2 diabetes, and even in patients with normal or higher BMD. In this study, we compared the levels of bone turnover markers in type 2 diabetic postmenopausal women (n=161) with those of non-diabetic postmenopausal women (n=467). Furthermore, we investigated the change of bone turnover markers to oral bisphosphonates (alendronate or risedronate) in both diabetic (n=48) and non-diabetic postmenopausal women (n=87). Serum CTX, osteocalcin, blood glucose and glycosylated hemoglobin levels were measured after overnight fasting. The duration of diabetes was 9.9 years and the level of glycosylated hemoglobin was 8.2%. Both serum osteocalcin and CTX were significantly lower in type 2 diabetes (19.7 ± 11.0 ng/ml and 0.476 ± 0.250 ng/ml) than those of non-diabetic women (24.8 ± 10.9 ng/ml and 0.533 ± 0.227 ng/ml). Although the serum CTX level in type 2 diabetes was not significantly different from that of non-diabetics after adjustment by age and BMI, the serum osteocalcin level was still significantly lower than that of non-diabetic women even after adjustment by age and BMI ($p < 0.05$). The osteocalcin level showed significant negative correlation with fasting blood glucose ($p < 0.05$) and glycosylated homeoglobin level ($p < 0.05$). Meanwhile, the duration of oral bisphosphonate use were 26.6 ± 22.0 and 30.7 ± 23.7 months in non-diabetic and diabetic groups. However, both serum osteocalcin and CTX levels after bisphosphonate use were not significantly different between diabetic (11.7 ± 4.8 ng/ml and 0.155 ± 0.137 ng/ml) and non-diabetic groups (13.0 ± 6.7 ng/ml and 0.132 ± 0.091 ng/ml). In summary, bone formation marker, osteocalcin, was significantly decreased in type 2 diabetic women compared to non-diabetics, and it was significantly associated with glucose metabolism showing inverse relationship. These results show that low bone formation and poor glycemic control status might be important contributing factors for increase

in fracture risk in type 2 diabetic women. In regards to response to bisphosphonate, further studies with large sample size would be needed.

Disclosures: Dong Jin Chung, None.

SU0280

Increased Bone Mass in Mice Lacking the Adipokine Apelin. Lalita Wattanachanya^{*1}, Wei-Dar Lu², Liping Wang², Dylan O'Carroll², Ramendra K. Kundu³, Thomas Quertermous³, Robert Nissenson⁴. ¹King Chulalongkorn Memorial Hospital The Thai Red Cross Society, Thailand & VA Medical Center & University of California, San Francisco, USA, ²VA Medical Center, San Francisco, USA, ³Stanford University School of Medicine, USA, ⁴VA Medical Center & University of California, San Francisco, USA

Adipose tissue plays an important role in skeletal homeostasis and there is interest in identifying adipokines that have negative effects on bone mass. We have previously demonstrated that blockade of G protein coupled receptor (GPCR)-induced Gi signaling in osteoblasts (OBs) in vivo suppressed bone formation. However, the identity of the ligands and OB Gi-GPCRs that are responsible for negatively regulating bone formation is unclear. Apelin, an adipokine, is a ligand for the Gi-GPCR APJ and has been shown to be involved in many physiological and pathological conditions. Apelin is reported to enhance mitogenesis as well as suppress apoptosis in MC3T3-E1 cells and human primary osteoblast cells in vitro. However, it is unclear whether apelin plays a physiological role in regulating skeletal homeostasis in vivo. In this study, we compared the skeletal phenotype of apelin knock-out (APKO) and wild type (WT) mice using uCT and histomorphometric analysis and also investigated the direct effect of apelin on bone cells in vitro. APKO mice showed increased fractional cancellous bone volume (BV/TV) at the distal femur at 20 weeks of age ($10.43 \pm 1.36\%$ in male KO vs. $7.17 \pm 1.50\%$ in male WT and $9.24 \pm 0.30\%$ in female KO vs. $6.91 \pm 0.78\%$ in female WT, $p < 0.05$). Cortical bone thickness at the femoral midshaft was increased by 12% ($p < 0.01$) in males and was unchanged in females. Expression levels of OB marker genes were significantly increased in these mice, correlated with an increase in bone formation marker, serum procollagen 1N-terminal peptide (PINP). Markers of osteoclastogenesis (RANK and calcitonin receptor mRNA expression) and bone resorption (serum pyridinoline) were also increased in APKO male mice. Apelin, when added to primary culture media on the third day of culture for 24 and 48 hour, increased proliferation in MC3T3 (+25%, $p < 0.01$) and primary calvarial osteoblasts (COBs) (+41%, $p < 0.01$) in a dose dependent manner with the maximum effect at 5nM. However, apelin had no effect on the formation of mineralized nodules when added continuously to COBs under osteogenic conditions. Moreover, addition of apelin to primary mouse bone marrow stromal cells did not affect their ability to undergo osteoclastogenesis. Taken together, our results indicate that apelin has negative effects on bone probably through activating of Gi signaling in OBs. Further studies are warranted to determine the possible role of apelin as an "anti-anabolic" adipokine.

Disclosures: Lalita Wattanachanya, None.

SU0281

Mice with Brown Fat Dysfunction are Resistant to High Fat Diet Induced Obesity but Susceptible to Impaired Bone Remodeling after Acute Cold Exposure. Phuong Le^{*1}, Katherine Motyl¹, Victoria Demambro¹, Leeann Louis², Masanobu Kawai³, Sheila Bornstein⁴, Kathleen Bishop⁵, Mary Bouxsein⁶, Clifford Rosen⁴. ¹Maine Medical Center Research Institute, USA, ²Center for Advanced Orthopedic Studies, Beth Israel Deaconess Medical Center, USA, ³Osaka Medical Center & Research Institute for Maternal & Child Health, Japan, ⁴Maine Medical Center, USA, ⁵University of Wisconsin-Madison, USA, ⁶Beth Israel Deaconess Medical Center, USA

Fat mass is highly regulated by brown-like adipocytes in white adipose tissue (WAT) in both humans and rodents. Bone remodeling is dependent on systemic energy metabolism and, with age, bone remodeling becomes uncoupled and brown adipose tissue (BAT) function declines. We have found that *Misty* (*mlm*) mice have accelerated age-related trabecular bone loss that is accompanied by changes in BAT, including reduced temperature (by infrared imaging), lower expression of *PGC1 α* , and less sympathetic innervation compared to wildtype (+/+). Despite impaired BAT function, *mlm* mice have normal core body temperature, suggesting heat is produced from other sources. Indeed, upon acute cold exposure (4°C for 6 hr), inguinal WAT from *mlm* mice compensated for BAT dysfunction by increasing expression of *Ucp1*, *PGC1 α* , *Dio2* and other thermogenic genes. This was accompanied by increased appearance of brown-like adipocytes in WAT. Browning of WAT is under the control of the sympathetic nervous system (SNS) and, if present even at room temperature, would cause resistance to high fat diet induced obesity. Thus, we treated *mlm* and +/+ with 58% fat/kcal diet (Hfd) for 13 wks. Despite weight gain in +/+, *mlm* mice on Hfd had no change in body mass. In fact, *in vivo* μ CT demonstrated significantly lower visceral and subcutaneous fat in *mlm* compared to +/+ fed a Hfd. However, Hfd did not alter trabecular BV/TV in either genotype. The resistance to Hfd induced obesity supports the notion that SNS tone is elevated in *mlm*. To test if SNS activity could be

in part responsible for accelerated age-related trabecular bone loss, we treated +/+ and *mlm* mice with the β -blocker, propranolol. As predicted, propranolol slowed trabecular BV/TV loss in the distal femur of *mlm* mice without affecting +/+. Interestingly, acute cold exposure decreased *Runx2* and increased *Rankl* expression in *mlm* bone, but only *Runx2* was decreased in +/+. Finally, the *mlm* mutation (a truncation of DOCK7) also has a significant cell-autonomous role. We found *Dock7* expression in whole bone and MC3T3-E1 cells. Primary osteoblast differentiation from *mlm* BMSCs was impaired while osteoclast differentiation was accelerated, demonstrating a novel role for DOCK7 in bone remodeling. Despite the multifaceted effects of the *mlm* mutation, we have shown that impaired BAT function leads to altered SNS activity and bone loss, and for the first time that cold exposure negatively affects bone remodeling. AG040217.

Disclosures: Phuong Le, None.

SU0282

Analysis of Intracellular Calcium Fluxes in Human Bone Cells from Osteoporotic and Osteoarthritic Patients. Monica Celi^{*1}, Elena Gasbarra², Claudio Frank³, Giovanna D'Arcangelo⁴, Alessandro Cutarelli⁵, Mario Marini⁴, Virginia Tancredi⁴, Umberto Tarantino⁶. ¹University of Rome Tor Vergata, Italy, ²Orthopaedic department, University of Rome "Tor Vergata", Italy, ³ISS National Center for Rare Disease, Italy, ⁴Department of Neuroscience, University of Rome Tor Vergata, Italy, ⁵ISS National Center for Rare Disease, Italy, ⁶Orthopaedic Department, University of Rome Tor Vergata, Italy

We studied changes in intracellular Ca²⁺ concentration in bone cell cultures obtained from human subjects with osteoporosis and osteoarthritis, to evaluate differences between these patients and healthy subjects. We enrolled 36 patient: 12 undergoing primary total hip arthroplasty (THA) for osteoporotic femoral fractures (group A, mean age range 57-80), 12 for hip osteoarthritis (group B, mean age range 57-80) and 12 healthy subjects who suffered a high-energy trauma fracture (group C, mean age range 18-30) as controls. All patients gave informed consent for using bone samples as a source of bone cells. DXA at lumbar spine and femur, in terms of BMD, were performed. Measurement by microfluorimetric techniques of the intracellular calcium concentration was done by using the calcium indicator dye fura-2. Cultures of osteoblastic cells in monolayers adherent to non coated glass coverslips were incubated at 37 °C in medium containing 5 microM fura-2/AM for 30 min and then incubated for an additional 20 min in medium without dye. Imaging was performed with the Argus 50 system (Hamamatsu) with excitation wavelengths of 340 and 380 nm for acquiring ratio images of fura-2. ATP and Thapsigargin, an inhibitor of the calcium-ATPase of the endoplasmic reticulum, were added during the experiments. Group A reported a BMD value of 0.673 ± 0.196 g/cm², group B 1.005 ± 0.194 g/cm² and group C 1.179 ± 0.259 g/cm². Application of ATP (1mM) induced in osteoblastic cultures from control patients a fast and transient increase (ratio value from 0.67+0.01 to 1.74+0.13) in intracellular calcium concentration [Ca²⁺]_i. When a partial recovery was reached, further addition of Thapsigargin (100nM) to the cells induced an additional increase of [Ca²⁺]_i (ratio value 0.85+0.03) due to release from intracellular calcium stores. In osteoblastic cultures (B) ATP significantly increased [Ca²⁺]_i (ratio value from 0.67+0.01 to 1.53+0.19) but in lower amount than control cells. In this experimental group Thapsigargin induced a [Ca²⁺]_i increase (ratio value 0.98+0.05) slightly stronger than the control. In osteoblastic cultures (A), ATP stimulation exhibited a significantly lower increase in [Ca²⁺]_i (ratio value from 0.67+0.01 to 1.21+0.09), while the effect of Thapsigargin was similar to control cells (ratio value 0.87+0.06). Our data coming from osteoporotic patients indicate an impairment of intracellular calcium influx. P2 receptors may be important drug targets for the modulation of bone turnover.

Disclosures: Monica Celi, None.

SU0283

Radiation-Induced Osteoporosis – Dose and Dose Rate Response to Protons. Laura Bowman^{*1}, Eric W. Livingston¹, Gregory A. Nelson², Ted Bateman³. ¹University of North Carolina at Chapel Hill, USA, ²Loma Linda University, USA, ³University of North Carolina, USA

Exposure to solar and cosmic radiation presents a significant risk to the health of an astronaut's skeletal system, in addition to bone loss caused by reduced loading conditions. Protons constitute 80-90% of deep space radiation and are therefore a source of significant concern. Galactic cosmic rays (GCRs) give a continuous low dose rate exposure, but the greater danger comes from solar particle events (SPEs). Over the course of a 6-8 month lunar mission, SPEs resulting in doses of 1 Gy are realistic with rare events reaching 2 Gy. This report presents two studies with the following aims: 1) determine an approximate dose threshold for proton irradiation causing bone loss two weeks after exposure (dose response), and 2) examine the effect of dose rate on bone loss caused by a single 2 Gy dose of protons (dose rate response). Methods: Seventeen-week-old, female C57BL/6 mice were divided into six groups (n=25/group, similar masses between groups) and assigned to one of the following radiation profiles: 1) 0.5 Gy (acute, 0.2 - 0.5 Gy/min), 2) 0.75 Gy (acute), 3) 1 Gy (acute), 4) 2 Gy (acute), 5) 2 Gy (0.5 Gy/hr), 6) 2 Gy (0.25 Gy/hr). An additional control group (n=25) was not irradiated. All exposures were conducted using 150 MeV protons at

LL University. Two weeks after irradiation, hind limbs were collected for analysis using micro-computed tomography (μ CT, SCANCO Medical μ CT-80). Results: Significant differences ($p < 0.05$) in trabecular bone volume fraction (BV/TV) were reported relative to control for all irradiated groups (0.5 Gy, -9.7%; 0.75 Gy, -11.7%; 1 Gy, -15.9%; 2 Gy, -21.0%). All doses but 0.5 Gy caused a reduction in the trabecular number (0.75 Gy, -8.2%; 1 Gy, -10.0%; 2 Gy, -10.0%). Trabecular connectivity (Conn.D) and volumetric bone mineral density (vBMD) were decreased at both 1 Gy (Conn.D, -23.8%; vBMD, -13.4%) and 2 Gy (Conn.D, -42.8%; vBMD, -23.3%). Decreases in BV/TV, connectivity density, trabecular number, and mineral density relative to control were observed for all 2 Gy irradiated groups. All dose rates demonstrated a similar degree of bone loss. Conclusions: Skeletal effects were demonstrated in mice irradiated with acute, whole-body doses of protons as low as 0.5 Gy. Mice irradiated to 2 Gy of protons lost similar amounts of bone regardless of dose rate. Levels of radiation below those predicted for lunar missions lead to deterioration of bone and represent a significant risk for decreased skeletal health.

Disclosures: Laura Bowman, None.

SU0284

Taller Women Have Thinner and More Porous Cortices to Fall Harder upon and Fracture. Ashild Bjornerem¹, Roger Zebaze², Ali Ghasem-Zadeh², Minh Bui³, Xiaofang Wang⁴, John L Hopper³, Ego Seeman². ¹University of Tromsø, Norway, ²Austin Health, University of Melbourne, Australia, ³Centre for MEGA Epidemiology, University of Melbourne, Australia, ⁴Endocrine Centre, Austin Health, University of Melbourne, Australia

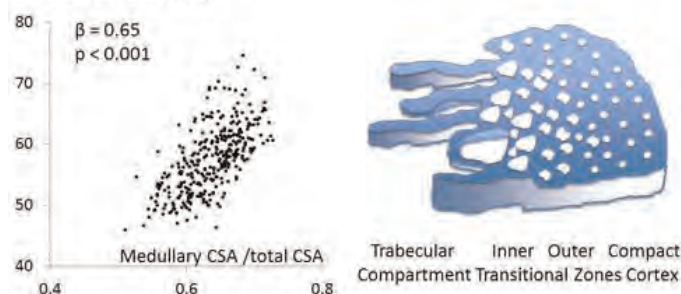
Taller individuals are at increased risk for fracture even though their long bones are built with a larger total cross sectional area (CSA). As the cortex is further from the neutral axis, its mass is minimized, cortical area, bending and compressive strength are conserved, by assembling a thinner cortex (relative to the total CSA) by greater endocortical resorption than periosteal apposition. We proposed that as the intracortical (haversian canal) surface is contiguous with the endocortical surface, minimizing mass is also achieved by assembling the thinner cortices with higher porosity.

We obtained images at distal tibia using high-resolution peripheral quantitative computed tomography (HR-pQCT; Scanco Medical) and quantified micro-architecture including cortical porosity using StrAx1.0 for 185 pairs of female twins aged 40 to 61 years, 93 of whom had had fractures in a cross-sectional study in Melbourne, Australia.

Each standard deviation (SD) greater height (6 cm) was associated with a 0.72 SD larger tibia total CSA, 0.69 SD larger medullary CSA, 0.46 SD thinner cortices relative to bone size (Medullary CSA/Total CSA) and 0.41 SD higher porosity (age, BMI adjusted, all $p < 0.001$). For each SD thinner cortex (larger medullary CSA/total CSA), porosity was 0.65 SD higher ($p < 0.001$, fig 1). These results were confirmed in a within-twin pair analysis; a larger within-twin pair difference in height was associated with a larger within-pair difference in porosity ($p = 0.03$). Each SD greater porosity at all the cortical compartments was associated with 36% to 79% higher risk of prevalent fracture; at the compact appearing cortex (OR 1.36; 95% CI 1.03-1.80), outer (OR 1.38; 95% CI 1.01-1.88) and inner (OR 1.79; 95% CI 1.06-3.02) transitional zones adjusted for age and BMI (fig 2).

We infer that taller women have thinner and more porous cortices, which may contribute to risk for fracture because cortical bone stiffness is proportional to the 7th power of its apparent density (inverse of porosity).

Cortical Porosity (%)



Disclosures: Ashild Bjornerem, None.

SU0285

A High Calcium Diet Failed to Rescue the Osteopenia Phenotype in Claudin-18 Knockout Mice. Fatima Alshbool¹, Catrina Alarcon¹, Jon Wergedal², Subburaman Mohan². ¹JL Pettis VA Med Ctr, USA, ²Jerry L. Pettis Memorial VA Medical Center, USA

We recently demonstrated that mice with targeted disruption of Claudin-18 (Cldn-18) exhibit osteopenia due to increased bone resorption (BR). In addition, Cldn-18 knockout (KO) mice exhibited abnormalities in the gastric mucosa consistent with atrophic gastritis. Since Cldn-18 is the predominant Cldn expressed in stomach and

since Cldns have been predicted to play an important role in regulating paracellular transport of small molecules including H^+ across the epithelial barrier, we evaluated if lack of Cldn-18 influences gastric pH. We found that the gastric pH was significantly less acidic ($pH 6.1 \pm 0.18$ vs 2.6 ± 0.25 , $P < 0.001$) in Cldn-18 KO mice compared to littermate wild type (WT) control mice at 10 wks of age. Because the deleterious effects of decreased gastric pH on calcium (Ca) absorption has been well documented in clinical studies, we considered the possibility that increased BR and decreased bone mass in the Cldn-18 KO mice fed with a normal Ca diet is a consequence of impaired Ca absorption caused by a lower stomach pH. To test this possibility, we subjected Cldn-18 KO and WT mice to either a normal Ca (0.6%) or a high Ca (2%) diet at birth. PIXImus revealed that the high Ca diet increased lumbar BMD by 22% but had no effect on femur or tibia BMD at 3 wks of age in WT mice compared to normal Ca diet. As expected, total body, femur, tibia and lumbar BMD were reduced significantly in Cldn-18 KO mice at 3 wks of age compared to WT mice on the normal Ca diet. Treatment of Cldn-18 KO mice with a high Ca diet also increased lumbar BMD by 32% but had no effect on femur or tibia BMD. Comparison of the skeletal phenotype of Cldn-18 KO and WT mice on a high Ca diet revealed that the osteopenia phenotype was still maintained at different skeletal sites in the KO mice at 3 wks of age. Furthermore, the osteopenia phenotype in the Cldn-18 KO mice was retained even after maintaining Cldn-18 KO mice for 12 weeks on a high Ca diet. Conclusions: 1) A high Ca diet increased vertebra BMD in both WT and Cldn-18 KO mice but lumbar vertebra in Cldn-18 KO mice was still osteopenic compared to WT mice despite the response. 2) The failure to rescue the osteopenia phenotype in Cldn-18 KO mice with a high Ca diet suggests that increased BR is likely to be due to direct effects of lack of Cldn-18 on osteoclasts and not due to gastric pH changes caused by lack of Cldn-18 in the stomach.

Disclosures: Fatima Alshbool, None.

SU0286

The Effects of Weight Loss and Changes in Fat and Lean Tissue on Bone Mineral Density in Women and Men – Results of a Randomized Controlled Trial. Amir Tirosh¹, Russell de Souza¹, Frank Sacks¹, George Bray², Steven Smith², Meryl Leboff¹. ¹Brigham & Women's Hospital, USA, ²Pennington Biomedical Research Center of the Louisiana State University System, USA

The Preventing Overweight Using Novel Dietary Strategies (POUNDS LOST) is a randomized controlled trial of 811 overweight and obese adults assigned to one of 4 weight loss diets differing in fat, protein, and carbohydrates (NEJM.360:859, 2009). We recently showed that participants on these weight loss diets lost more fat than lean mass, without differences among the 4 diets (AJCN. 95:614, 2012). The impact of these changes on bone mineral density (BMD), however, is uncertain. In 424 participants (mean age 52 ± 9 years, 57% females) from 2 centers (Boston and Baton Rouge), we measured BMD at the spine, total hip (TH) and femoral neck (FN), and quantified fat and lean mass by DXA (QDR 4500A, Hologic, Bedford MA) at baseline, and at 6 months and 2 years following the dietary interventions. These studies showed that at baseline, there was a stronger correlation between BMD and body composition measurements in women than in men, with the lean body mass compartment exhibiting the strongest correlation with BMD ($r = 0.419, 0.507$ and 0.523 for spine, FN and TH, respectively, all $p < 0.001$). In men, only lean body mass correlated with hip BMD ($r = 0.298$ between lean body mass and TH BMD, $p < 0.001$).

The overall average weight loss was 7.9% after 6 months and 6.9% after 2 years. Following this significant weight loss, the change in BMD from baseline to 6 months was 0.0005 gm/cm^2 ($p = 0.07$) at the spine, -0.001 gm/cm^2 ($p < 0.001$) at the TH and -0.0007 gm/cm^2 ($p = 0.016$) at the FN. From baseline to 2 years, these changes were 0.005 ($p = 0.04$), -0.014 ($p < 0.001$), and -0.014 gm/cm^2 ($p < 0.001$), respectively. Loss to follow-up was 22% at 6 months and 44% at 2 years.

Changes in spine, FN and TH BMD following 2 years of dietary intervention, directly correlated with changes in lean body mass in women ($r = 0.200, 0.324$ and 0.260 for spine, FN and TH, respectively), whereas changes in fat mass correlated only with changes in TH BMD (0.274 , $p < 0.001$) but not with change in spine or FN BMD. In men, changes in lean or fat mass were not associated with changes in FN and TH BMD, whereas the changes in lean body mass (-0.323 , $p < 0.001$) and in fat mass (-0.213 , $p = 0.027$) were negatively correlated with change in BMD at the spine.

In conclusion, weight loss results in gender-specific effects on BMD. While men exhibited an increase in spine BMD and no change in hip BMD, women tended to decrease BMD at all sites regardless of the diet to which they were assigned.

Disclosures: Amir Tirosh, None.

SU0287

11- β -hydroxysteroid Dehydrogenase Type 1 Overexpression Increases Adipogenic Differentiation in Mesenchymal Progenitor Cells by Increased Endogenous Cortisol Production. Johannes Beismann^{*1}, Regine Koepp¹, Martina Blaschke², Nicolai Miosge³, Vera Ritz¹, Volker Bähr⁴, Frank Streit⁵, Heide Siggelkow⁶. ¹University Medicine of Goettingen, Department of Gastroenterology & Endocrinology, Germany, ²University Medicine of Goettingen, Department of Gastroenterology & Endocrinology, Germany, ³Tissue Regeneration Group, Medical Faculty, Department of Prosthodontics, University Medicine, Germany, ⁴Department of Endocrinology, Diabetes & Nutrition, Charité-University Medicine Berlin, Germany, ⁵Department of Clinical Chemistry, Georg-August University, Germany, ⁶University Medicine of Goettingen, Dep. of Gastroenterology & Endocrinology, Germany

Introduction The differentiation of mesenchymal progenitor cells (MSCs) to the osteoblastic or adipogenic phenotype is thought to be an important pathophysiological mechanism for bone diseases. Dexamethasone induced adipogenesis in MSCs by decreasing osteogenic differentiation.

The internal cortisol metabolism in bone seems to be mainly regulated by the enzyme 11- β HSD1, a key enzyme converting cortisone to active cortisol or vice versa.

Material and methods Human primary MSCs were transfected for 6 h at confluence using lipofectamine and a pcDNA3.1 plasmid for 11- β HSD1 overexpression. MSCs were further cultured for either 48 hours, 7 days or up to 28 days. mRNA was analyzed by PCR and protein by western blotting. Cortisol and cortisone synthesis was determined by lc-ms/ms.

Results After transfection 11- β HSD1 expression increased 10 to 1000 fold depending on the individual experiment. Expression remained stable over 7 days and decreased thereafter. Osteoblastic differentiation using dexamethasone 10-8M decreased 11- β HSD1 expression independent from transfection. 11- β HSD1 protein was detectable by western blotting after 28 days. Without addition of external cortisone, cortisol was detectable in 11- β HSD1 transfected MSCs at very low levels only. Even so, the adipogenic differentiation measured by aP2 and C/EBP alpha was clearly induced after 7 days, still to be seen at day 28. In addition, RANKL expression was induced with maximal levels seven days after transfection suggesting an osteoclast inducing effect by endogenous cortisol. After addition of cortisone for 48 hours cortisol synthesis doubled after transfection with 11- β HSD1.

Discussion Our results show, that in human primary MSCs the synthesis of cortisol relies exclusively on 11- β HSD1. Plasmid overexpression is followed by a functional protein converting cortisone to cortisol. Hence, also by increased internal cortisol synthesis adipogenesis is induced in MSCs. We suggest, that our model represents the increase in 11- β HSD1 during aging and that cortisol increase in bone is a pathogenetic factor for age-related osteoporosis.

In part this work was supported by Elsbeth-Bonhoff Foundation

Disclosures: Johannes Beismann, None.

SU0288

Disruption of the Claudin-18 Gene Diminishes Ovariectomy-induced Bone Loss in Mice. Ha Young Kim^{*1}, Catrina Alarcon¹, Sheila Pourteymoor¹, Subburaman Mohan². ¹Jerry L Pettis VA Med Ctr, USA, ²Jerry L. Pettis Memorial VA Medical Center, USA

Claudin-18 (Cldn-18) is a member of the tight junction family of proteins and we recently showed that targeted disruption of Cldn-18 decreases trabecular bone volume (Tb.BV) by increasing bone resorption (BR). Since estrogen deficiency decreases Tb.BV in part by a RANKL-mediated increase in BR and Cldn-18 negatively modulates RANKL-induced osteoclast differentiation, we evaluated if estrogen deficiency induced bone loss is further exacerbated by disruption of Cldn-18 in mice. Cldn-18 knockout (KO) and littermate wild type (WT) mice were ovariectomized (OVX) or underwent a sham operation (sham) at 6 wks of age and the skeletal phenotype was evaluated at 14 wks of age. PIXImus revealed that total body, femur and lumbar BMD were reduced by 8, 11 and 13% respectively (all P<0.05) after 8 wks of OVX compared to sham in WT mice. As expected, total body, femur and lumbar BMD were reduced 14, 15, and 21% (all P<0.05) in Cldn-18 KO sham mice compared to sham WT mice. However, OVX failed to induce significant changes in total body, femur or vertebra BMD in the Cldn-18 KO mice. Micro-CT analysis of distal femur revealed that Tb. BV/TV was decreased by 50% in the OVX WT compared to sham mice, that was caused by a 26% decrease in Tb. number and a 30% increase in Tb. separation (all P<0.05). By contrast, none of the Tb. parameters were significantly different in OVX KO mice compared to sham KO mice. The diminished OVX response in Cldn-18 KO mice cannot be explained on the basis of a 50% reduction in Tb.BV/TV in these mice as we have found that calcium deficiency caused a further loss of Tb. bone in the KO mice. We next tested the possibility that Cldn-18 is downstream of estrogen signaling by evaluating estrogen regulation of Cldn-18 expression in bone. We found that mRNA levels of Cldn-18 was reduced by >80% (P<0.05) in the bones of OVX mice compared to sham mice. Accordingly, treatment of primary cultures of mouse calvarial osteoblasts with 10 nM estrogen for 24 hours increased Cldn-18 expression by 2.9 fold (P<0.05) over vehicle control. Conclusions: 1) OVX induced bone loss in WT but not Cldn-18 KO mice. 2) Estrogen effects on osteoclasts may in part be mediated via regulation of Cldn-18 signaling.

Disclosures: Ha Young Kim, None.

SU0289

Prevalence of Low BMD and Osteoporosis in Male Hypogonadisms. Mário Rui Mascarenhas^{*1}, Ana Paula Barbosa², Ana Gonçalves³, Vera Simões⁴, António M. Gouveia Oliveira⁵, David Santos Pinto⁶, Manuel Bicho⁷, Isabel do Carmo⁸. ¹Lisbon's Faculty of Medicine, Santa Maria University Hospital, CHLN,EPE, Portugal, ²Endocrinology, Santa Maria Hospital & Faculty of Medicine, Portugal, ³Endocrinology, Diabetes & Metabolism Department, Santa Maria Hospital, CHLN-EPE, Portugal, ⁴Endocrinology & Metabolism Center - Genetics Lab (Lisbon's Faculty of Medicine), Osteoporosis Unit - CEDML, Lda, Portugal, ⁵Biostatistics Department, FCMUNL, Portugal, ⁶Osteoporosis Unit, CEDML, Lda, Portugal, ⁷Endocrinology & Metabolism Center - Genetics Lab (Lisbon's Faculty of Medicine), Portugal, ⁸Endocrinology, Diabetes & Metabolism Department, Santa Maria University Hospital, CHLN-EPE, Portugal

Male hypogonadism is a condition in which there is not enough testosterone synthesis by the testes, sperm or both. Normal sex steroids levels are essential for optimizing peak bone mass and their deficiencies during adulthood may modify the maintenance of the bone mass and may be associated with fragility fractures.

AIMS -Prospective study for evaluation of the bone mineral density (BMD) in hypogonadal males without therapy as compared with a group of normal men.

MATERIAL AND METHODS -A group of 230 men was divided in a group of 115 men, 51.2(\pm 19.3) years old, with hypogonadisms (hypergonadotropic, hypogonadotropic and eugonadotropic hypogonadisms) without treatment which was compared to a group of 115 normal men, 50.9(\pm 18.0) years old (control group). The BMD at the lumbar spine, at the hip, at the distal radius (1/3 or 33%) and at the whole body, as well as the total fat and lean body masses, were evaluated by DXA with the QDR Discovery-W densitometer (Hologic Inc.). Fasting peripheral blood was collected for LH, FSH, PRL, estradiol and total testosterone plasma measurements. The weight, the height and the BMI were also determined. Descriptive, Anova and regression analysis statistical tests were used; statistical significance was considered for P<0.05.

RESULTS -The mean age, weight, BMI and total fat body mass were identical between the groups, but the mean height and total lean body mass were decreased in the hypogonadisms group. The mean BMD, T-scores and Z-scores were lower in the hypogonadisms group at every skeletal regions, as compared with the control group. The BMD qualification is presented in Table 1. Significant correlations were detected between the BMD at the lumbar spine and at the femoral neck vs. the height, the total fat body mass and the total lean body mass, in the hypogonadal men.

CONCLUSIONS -The results of this study suggest that in the hypogonadisms of the males, the prevalence of low bone mass is elevated (>65%) and of osteoporosis about 40%. The BMD is positively influenced by the height, body fat mass and BMI which may have clinical relevance, because the shortest height and lowest corpulence hypogonadal patients may have a major indication for a DXA scan, as it is important to detect precociously hypogonadal men with low and/or osteoporosis in order to begin a replacement therapy as soon as possible, in order to reduce the future osteoporotic fracture risk.

| | GROUP | HYPOGONADISM | CONTROL |
|---------------------|------------|----------------|----------------|
| | | n = 115 (100%) | n = 115 (100%) |
| BMD | | | |
| Normal | 37 (32.2%) | 79 (68.7%) | |
| Low | 31 (27.0%) | 29 (25.2%) | |
| Osteoporosis | 47 (40.8%) | 7 (6.1%) | |

TABLE 1. The prevalence of low BMD and osteoporosis in the hypogonadisms and in the control groups.

Disclosures: Mário Rui Mascarenhas, None.

SU0290

Bone Marrow Fat Is Metabolically Distinct Fat Depot. Riku Kiviranta^{*1}, Tam Pham², Jarna Hannukainen², Anna Karmi², Heidi Immonen², Minna Soivio³, Pauliina Salminen⁴, Pirjo Nuutila². ¹Medical Biochemistry & Genetics & Turku PET Centre, University of Turku, Finland, ²Turku PET Centre, Finland, ³Department of Medicine, Turku University Hospital, Finland, ⁴Department of Surgery, Turku University Hospital, Finland

In adults, majority of bone marrow space of long bones is filled with fat tissue. Adipocytes are also present within trabecular bone areas such as vertebral bodies. Very little is known about bone marrow fat or its glucose metabolism. To characterize bone marrow metabolic activity we measured regional glucose uptake in femoral and vertebral bone marrow during fasting and insulin stimulation in normal weight healthy subjects.

Nine healthy adults (BMI 23.7 \pm 1.9 kg/m²) volunteered for the study. The subjects were imaged with positron emission tomography (PET) using ¹⁸F-fluorodeoxyglucose (¹⁸F-FDG) tracer to measure glucose uptake (GU) in skeletal muscle, abdominal subcutaneous (c) fat, abdominal visceral fat and vertebral and femoral bone marrow. PET imaging was performed at fasting state and during hyperinsulinemic euglycemic clamp to measure basal and insulin-stimulated GU.

Fasting GU in femoral bone marrow that consists mainly of fat was significantly higher than in sc fat (4.93 ± 1.58 mmol/l/min vs 2.82 ± 0.38 mmol/l/min, respectively, $p < 0.05$) but did not significantly differ from visceral fat. Skeletal muscle GU was 56% higher than that of femoral bone marrow ($p < 0.01$). Interestingly, glucose uptake in vertebral bone marrow that contains bone and hematopoietic cells and adipocytes, was five-fold higher than in femur ($p < 0.001$). Insulin stimulation during clamp induced a four-fold increase in femoral bone marrow GU (20.43 ± 6.00 mmol/l/min, $p < 0.001$ vs. fasting state), which remained higher than that of sc and visceral fat. Skeletal muscle showed an expected nine-fold increase in GU to 69.73 ± 34.42 mmol/l/min. Surprisingly, insulin did not stimulate glucose uptake in vertebral bone marrow (25.98 ± 3.46 clamp vs 24.78 ± 4.59 mmol/l/min at fasting) demonstrating that vertebral and femoral bone marrow compartments differ in the regulation of their metabolic activity.

This study shows that glucose metabolism differs significantly between vertebral and femoral bone marrow. GU in vertebral bone marrow cells appears to be insulin independent. Conversely, insulin stimulates GU in the mainly fatty femoral bone marrow to similar extent to brown fat. Moreover, the overall GU in femoral bone marrow both in fasting state and during hyperinsulinemic euglycemic clamp is higher than in other fat depots. Thus, our data supports the hypothesis that bone marrow fat is functionally distinct yellow fat.

Disclosures: Riku Kiviranta, None.

SU0291

High Serum Cystatin C Predicts Incident Hip Fracture in Elderly Men. MrOS Sweden. Ewa Waern¹, Osten Ljunggren², Ulf Lerner³, Catharina Lewerin⁴, Helena Johansson⁵, Kristine Ensrud⁶, Magnus Karlsson⁷, Eric Orwoll⁸, Mattias Lorentzon⁹, Hans Herlitz¹⁰, Claes Ohlsson¹¹, Dan Mellstrom¹. ¹Sahlgrenska University Hospital, Sweden, ²Uppsala University Hospital, Sweden, ³University of Umea, Sweden, ⁴Västra Götaland, Sweden, ⁵Swedish University of Agricultural Sciences, The Biomedical Center, Sweden, ⁶Minneapolis VA Medical Center / University of Minnesota, USA, ⁷Skåne University Hospital Malmö, Lund University, Sweden, ⁸Oregon Health & Science University, USA, ⁹Center for Bone Research at the Sahlgrenska Academy, Sweden, ¹⁰Department of Nephrology Institute of Medicine at the Sahlgrenska Academy, University of Gothenburg, Sweden, ¹¹Center for Bone & Arthritis Research at the Sahlgrenska Academy, Sweden

Serum cystatin C is widely used as a serum marker for renal function. High values are related to poorer kidney function. In contrast to serum creatinine, cystatin C is not related to body mass index. Earlier studies of postmenopausal women have indicated a higher risk of hip fracture in women with high serum cystatin C. However in elderly men there are few data showing that increased risk of hip fracture is related to high cystatin C. The aim of this study was to examine the association of high cystatin C and incident hip fractures in men. We used the MrOS, Sweden cohort (n=3014) of men aged 69-80 years who were recruited from a national population register. Bone mineral density (BMD) was measured with Lunar and Hologic DXA and standardized BMD was estimated. All incident fractures were collected from national X-ray registers during the 7 years following baseline. A total number of 388 men sustained one or more fractures, including 90 hip fractures. 206 of 1299 men (16%) had a baseline X-ray verified vertebral fracture. Cystatin C was measured by immunoturbidimetry with polyclonal antibodies against human cystatin C (cystatin C immunoparticles, Dako A/S, Glostrup, Denmark). Serum cystatin C increased with age ($p < 0.001$). The mean value of cystatin C was 1.138 mg/l (0.30). Estimated GFR was below 45 ml in 7.9% and 27.1 % had GFR below 60 ml. There was a linear association with serum cystatin C and all types of fractures (GR 1.14(CI 1.1-1.2) adjusting for BMI, hip BMD, age, previous fracture and general health. Cystatin C (per SD increase) predicted hip fracture [HR 1.26(CI 1.03-1.54)]. A multivariate model including hip BMD, BMI, age and center showed increased hip fracture risk [HR 1.71 (CI 1.10-2.65)] when comparing quartile IV against quartile I-III of cystatin C. The multivariate hip fracture risk adjusted for age, hip BMD, BMI and center for men with GFR below 45 ml was HR 2.6 (CI 1.5-4.4) and below 60 ml HR 1.8 (CI 1.1-2.7). Men with estimated GFR

below 60 ml had an increased risk for prevalent vertebral fractures OR 1.42 (CI 1.01-1.99) adjusting for age, BMI, lumbar spine BMD, site and PTH.

We conclude that high cystatin C is related to increased risk of incident hip fractures and prevalent vertebral fractures in elderly men.

Disclosures: Ewa Waern, None.

SU0292

Hyperthyroidism Affects the Bone Mineral Density and the Total Lean Body Mass in Young Men. Ana Paula Barbosa^{*1}, Mário Rui Mascarenhas², António M. Gouveia Oliveira³, Vera Simões⁴, Ana Gonçalves⁵, David Santos Pinto⁴, Manuel Bicho⁶, Isabel Do Carmo⁵. ¹Endocrinology, Santa Maria Hospital & Faculty of Medicine, Portugal, ²Lisbon's Faculty of Medicine, Santa Maria University Hospital, CHLN,EPE, Portugal, ³Biostatistics Department, FCMUNL, Portugal, ⁴CEDML - Endocrinology, Diabetes & Metabolism Clinic, Lda, Portugal, ⁵Endocrinology, Diabetes & Metabolism Department, Santa Maria Hospital, CHLN-EPE, Portugal, ⁶Metabolism & Endocrinology Center, Genetics Laboratory (FMUL), Portugal

The peak bone mass is usually acquired in the third decade of life; nevertheless, some endocrine diseases like hyperthyroidism may affect it. After that age, this disease is one of the most important causes of the loss of the acquired bone mass. In the young adult, the ISCD recommends that, in the absence of osteoporotic fracture, the diagnosis of osteoporosis should be done by the association of the risk factors for osteoporosis with the qualification of bone mineral density (BMD) by DXA. The changes in the lean and fat masses that occur in hyperthyroidism may also contribute to the fragility fractures.

OBJECTIVES- To evaluate the changes of the body composition in young men with hyperthyroidism.

MATERIAL AND METHODS- In a group of 38 men aged < 40 years, the total body soft tissues composition (lean and fat masses, Kg) and the BMD (g/cm²) at the lumbar spine (L₁-L₄), at the proximal femur, at the distal radius and at the whole body were evaluated by dual X-ray absorptiometry, using the Hologic QDR Discovery W densitometer.

These men were paired in hyperthyroid (n=19) and control (n=19) groups. No patient was previously treated for hyperthyroidism and/or OP.

In the controls, the BMD was qualified using the Z-score, according to the ISCD guidelines.

Descriptive and comparative tests were used and statistical significance was considered for P<0.05.

RESULTS- The mean of the age and the height were identical between the groups, but the mean of the total lean body mass and of the BMD at the femur neck and at the whole body were significantly reduced in the group of the hyperthyroidism, as compared with the control group (Table 1).

CONCLUSIONS- The data of this study may suggest that hyperthyroidism in young adult men may have significant impact in the body composition, namely in the total body lean mass and in the bone mass, thus predisposing such men to an increased bone fragility fractures risk in their future.

| Variables | GROUPS | CONTROL | HYPER THYROIDISM | P |
|---------------------------------------|--------|-------------|------------------|--------|
| Age (years) | | 31.9(±0) | 31.6(±0.2) | NS |
| Height (cm) | | 176.2(±4) | 175.5(±6) | NS |
| Total Lean Mass (kg) | | 62.5(±7.5) | 54.9(±7.1) | 0.0035 |
| BMD femoral neck (g/cm ²) | | 0.934(±0.1) | 0.843(±0.2) | 0.0487 |
| BMD total body (g/cm ²) | | 1.230(±0.1) | 1.111(±0.1) | 0.0008 |

Table 1. The mean (±SD) of the total lean body mass and of the BMD at several skeletal sites.

Disclosures: Ana Paula Barbosa, None.

SU0293

The Relationship between Inhibitors of the Wnt-signalling pathway (Dickkopf-1 and Sclerostin), Bone Mineral Density, Vascular Calcification and Arterial Stiffness in Post-Menopausal Women. Geeta Hampson^{*1}, Sylvie Edwards², Soraya Conroy³, Glen Blake⁴, Ignac Fogelman⁵, Michelle Frost⁴. ¹St. Thomas' Hospital, United Kingdom, ²osteoporosis screening unit, Guy's hospital, Kings College London, United Kingdom, ³department of clinical chemistry, St Thomas' Hospital, kings college london, United Kingdom, ⁴King's College London, United Kingdom, ⁵Guy's Hospital, United Kingdom

Epidemiological studies have shown an association between bone loss/osteoporosis and vascular calcification (VC). Recent studies have implicated the Wnt signalling pathway in the pathogenesis of VC. Wnt-signalling inhibitors, Dickkopf-1 (DKK1), sclerostin (SCL) are up-regulated in areas of VC. We hypothesize that the Wnt-signalling pathway may provide a common mechanistic link between bone loss and VC. The aim of the study was to investigate the possible association between circulating concentrations of DKK1 and SCL with bone mineral density (BMD), abdominal aortic calcification (AAC) and arterial stiffness in post-menopausal women. One hundred and forty six post-menopausal women aged (mean [SD] 61.5[6.5] years were studied. SCL, DKK1, total cholesterol, HDL-cholesterol were measured in serum. BMD was measured at the lumbar spine (LS), femoral neck (FN), total hip (TH). AAC was detected by lateral DXA imaging and quantified using the 8- and 24- point score. Arterial stiffness was determined by analysis of pulse wave

velocity (PWV) which measures the transit time of the pulse waves between the carotid and femoral artery. In univariate analyses, a significant positive correlation was observed between SCLE and BMD at the FN ($r=0.166$, $p=0.043$) and TH ($r=0.165$, $p=0.044$). The association remained significant at the FN ($p=0.045$) and TH ($p=0.026$) following correction for confounders such as age, BMI, smoking habits, physical activity. No significant correlation was observed between DKK1 and BMD. In contrast, in univariate analysis, there was a significant negative correlation between log DKK1 and AAC (24-point score: $r=-0.25$, $p=0.008$ and 8-point score: $r=0.21$, $p=0.024$). Following multi-linear regression analysis and correction for age, blood pressure, total and HDL-cholesterol, BMI, DKK1 remained negatively associated with AAC (24-point score: $p=0.017$, 8-point score: $p=0.044$). In contrast, SCLE was positively associated with AAC (24-point score: $p=0.048$, 8-point score: $p=0.031$). The mean PWV was 8.8 [1.5] m/s in the whole study population. Subjects with a PWV >9 m/s had significantly higher SCLE (PWV <9 m/s: 23.8[12.3], PWV ≥ 9 m/s 29.7 [14] pmol/L, $p=0.03$). No association was observed between DKK1 and PWV. Our data suggest that DKK1 and SCLE may play a part in VC. Future longitudinal studies are needed to establish the role of SCLE and DKK1 in the pathogenesis of VC.

Disclosures: Geeta Hampson, None.

SU0294

Changes in Bone Turnover Markers by Treatment with Human PTH(1-34) and Zoledronate in Young and Adult Ovariectomized Rats. Jukka Morko*, ZhiQi Peng, Katja Fagerlund, Mari Suominen, Jukka Rissanen, Jussi Hallee. Pharmatest Services Ltd, Finland

Bone turnover markers are predictive tools for long-term bone effects in clinical studies and osteoporosis animal models, and they are widely used for monitoring the efficacy of anabolic and anti-catabolic treatment of osteoporosis. We have studied short-term effects of bone turnover markers on anabolic treatment with human (1-34) parathyroid hormone (PTH) and anti-catabolic treatment with zoledronate (ZOL) in young (3 months of age) and adult (6 months of age) ovariectomized (OVX) rats. Study groups included a sham-operated control group receiving vehicle, an OVX-operated control group receiving vehicle, and OVX-operated groups receiving s.c. injections of 10 $\mu\text{g/kg/wk}$ ZOL and 40 $\mu\text{g/kg/d}$ PTH. Each group contained 12 animals. Dosing was started the next day after OVX and continued for 2 weeks. Procollagen I N-terminal propeptide (PINP), N-terminal mid-fragment of osteocalcin (OC), C-terminal cross-linked telopeptides of type I collagen (CTX), and tartrate-resistant acid phosphatase 5b (TRACP 5b) were determined in serum before the start of treatment and at 2 weeks. Uterine weight was decreased by OVX, demonstrating that the operations were performed successfully. OVX increased PINP values by 103% in young rats and 138% in adult rats (both with $p<0.001$), OC values by 24% in young rats and 30% in adult rats (both with $p<0.001$), and CTX values by 51% in young rats ($p<0.05$) and 65% in adult rats ($p<0.001$), and decreased TRACP 5b values by 24% in young rats ($p<0.01$) and 10% in adult rats (not significant, ns). PINP values decreased 3-5% by ZOL in young and adult rats (ns) and increased 19% by PTH in young rats (ns) and 48% in adult rats ($p<0.05$). OC values decreased 30% by ZOL in young rats and 34% in adult rats, and increased 24% by PTH in young rats (ns) and 63% in adult rats (all with $p<0.001$). CTX values increased 4% by ZOL and 5% by PTH in young rats and decreased 11% by ZOL and 5% by PTH in adult rats (all ns). TRACP 5b values decreased 57% by ZOL in young rats and 68% in adult rats (both with $p<0.001$) and decreased 25% by PTH in young rats ($p<0.01$) and 22% in adult rats ($p<0.05$). We conclude that adult rats are more optimal for PTH treatment, demonstrating higher changes in the bone formation markers. Serum CTX showed no treatment responses, while TRACP 5b decreased by both treatments in both young and adult animals. OC was the only marker that demonstrated highly significant effects (with $p<0.001$) on both treatments in both young and adult animals.

Disclosures: Jukka Morko, Pharmatest Services Ltd, 3

SU0295

Does Hypocalcemia Diagnose Low Calcium Absorption? Karen Hansen*¹, Nelson Watts², Nick Keuler¹, Rachael Erin Johnson¹. ¹University of Wisconsin, USA, ²Mercy Health Osteoporosis & Bone Health Services, USA

Twenty-four hour urine calcium (24HUC) levels are often recommended in the initial evaluation of patients with osteoporosis in order to diagnose hypercalcemia. Low urine calcium values might indicate low calcium absorption. To our knowledge, the diagnostic performance of 24HUC levels in detecting calcium malabsorption has not been published. In a post-hoc analysis of three separate studies, we evaluated whether 24HUC <150 mg could diagnose low TFCA or low milligrams of calcium absorbed (MGCA), defined as TFCA times total daily calcium intake from all sources.

Postmenopausal women were admitted for 24 hours to measure TFCA using dual stable isotopes. The dose-corrected ratio of two calcium isotopes in a 24-hour urine collection was used to calculate TFCA. Dietary and supplemental calcium intake was duplicated during each TFCA study using 4-7 day food records. Associations between 24HUC, TFCA and MGCA were assessed using Pearson correlation coefficients. Sensitivity, specificity, positive (PPV) and negative predictive value (NPV) were calculated for the ability of 24HUC values <150 mg to diagnose low calcium absorption.

47 women with a mean \pm SD age of 60 ± 8 years, serum 25(OH)D of 37 ± 19 ng/mL, and habitual intake of 1300 ± 620 mg calcium per day from all sources (diet: 950 ± 300 mg, supplement: 360 ± 500 mg) completed 109 TFCA studies. There was no correlation between 24HUC and TFCA ($r=0.14$, 95% CI -0.05-0.32, $p=0.15$) but a moderate correlation between 24HUC and MGCA ($r=0.38$, 95% CI 0.21-0.53, $p<0.0001$). A threshold of <150 mg of calcium in a 24-hour urine collection showed acceptable sensitivity and NPV but lower specificity and PPV for low calcium absorption, defined as <100 mg, <120 mg or <150 mg of calcium absorbed in 24 hours (Table).

A 24-hour urine calcium value <150 mg, based on a urine collection under ideal research conditions, demonstrates reasonable sensitivity but low specificity for diagnosing calcium malabsorption in a cohort of postmenopausal women. We suggest the need for larger studies in other patient populations to further evaluate these findings.

| Low Calcium Absorption Defined as: | Prevalence | 24-Hour Urine Calcium <150 mg | Sensitivity | Specificity | PPV | NPV |
|------------------------------------|------------|---------------------------------|-------------|-------------|------|------|
| <100 mg Calcium Absorbed | 0.055 | 4 of 6 subjects | 0.67 | 0.55 | 0.08 | 0.97 |
| <120 mg Calcium Absorbed | 0.101 | 8 of 11 subjects | 0.73 | 0.57 | 0.16 | 0.95 |
| <150 mg Calcium Absorbed | 0.147 | 11 of 16 subjects | 0.69 | 0.58 | 0.22 | 0.92 |

Table 1

Disclosures: Karen Hansen, None.

This study received funding from: National Institute of Health- NIA and NIAMS

SU0296

Nutritional Status of Calcium and Other Bone-related Nutrients in Adult Post-kidney Transplantation Recipients. Hiroyuki Hirai*¹, Atsushi Suzuki², Hitomi Sasaki³, Midori Hasegawa⁴, Yoshiteru Maeda⁵, Sahoko Sekiguchi-Ueda², Megumi Shibata⁶, Yukio Yuzawa³, Kiyotaka Hoshinaga⁷, Kazuhiro Uenishi⁸, Mitsuyasu Itoh⁶. ¹Fujita Health University Division of Endocrinology, Japan, Japan, ²Fujita Health University, Division of Endocrinology, Japan, ³Department of Urology, Fujita Health University, Japan, ⁴Division of Nephrology Fujita Health University, Japan, ⁵Fujita Health University, Division of Endocrinology, Japan, ⁶Fujita Health University Division of Endocrinology, Japan, ⁷Division of Urology, Fujita Health University, Japan, ⁸Kagawa Nutrition University, Japan

Background: Kidney transplantation (KTx) is an established therapy for end-stage renal diseases (ESRD), and the progress of immunosuppressive therapy improved survival rate of KTx recipients. Despite KTx could restore many disorders in ESRD patients, pre-existing chronic kidney disease-mineral and bone disease (CKD-MBD) and other clinical risk factors such as hyperparathyroidism and glucocorticoid therapy would make osteoporosis as a serious problem in post-KTx patients. Because of glucocorticoid therapy and co-existence of diabetes mellitus, KTx recipients often need to restrict their calorie intake. However, the strict control of food intake leads to the reduction of their calcium (Ca) intake, which could deteriorate bone strength in KTx recipients. The aim of this study is to estimate nutritional status of Ca and other nutrients which could affect bone and Ca metabolism in post-KTx recipients.

Subjects and Methods: Post-KTx recipients in outpatient clinic of FujitaHealthUniversityHospital were recruited ($n=84$, M/F=50/34, age, 53.4 ± 12.2 years old). Median serum albumin and creatinine levels were 4.3 g/dL (3.4-5.0) and 1.19 mg/dL (0.58-2.89). We estimate intake of nutrients including Ca, vitamin D and other nutrients by simple food frequency questionnaire by Uenishi et al (J Nutr Sci Vitaminol 2008; 54:25-29). Data are median (25th-75th) and 95% cut-off index (CI).

Results: Median body mass index of KTx recipients was 20.4 kg/m² (15.9-29.1). Median total energy in KTx recipients was 1558 kcal/day (705-2182). Their daily intake of Ca, vitamin D and vitamin K were 398 mg (142-764), 10 mg (6.5-16.0), and 140 mg (36-551), respectively. Subjects whose daily Ca intake was more than 600 mg/day was only 16.7%. Protein and salt intake were 66.4 g/day (33.1-99.8) and 8.4 g/day (7.0-11.4).

Discussion: Our findings suggest that post-KTx recipients in Japan seemed to restrict their calorie intake for the prevention of their overweight and metabolic disorder. On the contrary, their daily Ca intake was insufficient, though most of them could take vitamin D and K more than recommended adequate intake (A.I.) (A.I in Japan: vitamin D, 5.5 mg/day and vitamin K, 65-75 mg/day).

Conclusion: Nutritional intervention should be considered to ameliorate Ca homeostasis and bone metabolism in post-KTx recipients in Japan.

Disclosures: Hiroyuki Hirai, None.

SU0297

Relationship Between Glucose Metabolism and Undercarboxylated Osteocalcin: Cross-sectional Study in Community-dwelling Population (Shimane Community-based Health Research and Education, COHRE Study). Shozo Yano*¹, Toru Nabika¹, Atsushi Nagai¹, Tsuvooshi Hamano², Masayuki Yamasaki¹, Minoru Isomura¹, Kuninori Shiwaku¹, Shuhei Yamaguchi¹, Toru Yamaguchi¹, Toshitsugu Sugimoto³. ¹Shimane University Faculty of Medicine, Japan, ²Shimane University, Japan, ³Shimane University School of Medicine, Japan

Objectives: Undercarboxylated osteocalcin (ucOC) is known as a bone metabolic marker. Recently, ucOC has been found to play hormonal roles in regulating insulin and adiponectin secretion. Thus, we performed a cross-sectional study to examine relationships between ucOC levels and glucose and/or lipid metabolism.

Subjects and Methods: We included 1,870 subjects (M; 774, F; 1,096) aged over 50, who took health examination. According to the current medication and past history, 605 subjects (M; 245, F; 360) have hypertension (HT), 316 (M; 70, F; 246) have dyslipidemia (DL), and 182 (M; 98, F; 84) have type2 diabetes mellitus (DM). In this study, we excluded subjects using insulin. Fasting blood samples were collected after we confirmed their consent. The concentration of ucOC and TRACP5b were measured by ECLIA and FAICEA, respectively. Smoking, exercise, and life style (standing or sedentary) were asked.

Results: Serum ucOC level was higher in female than male (5.9 vs 3.8 ng/ml). It was significantly lower in DL(+) than DL(-) only in female (5.4 vs 6.0 ng/ml). It was significantly lower in DM(+) than DM(-) in both male (3.0 vs 3.9 ng/ml) and female (4.5 vs 6.0 ng/ml). In logistic regression analysis, low level of ucOC was significantly associated with the presence of DM in both male and female after adjusting for covariates including age, BMI, serum Cr, HDL-C, TG, smoking, life style, exercise and TRACP5b. No significant association was found between ucOC and the presence of dyslipidemia after adjusting for HbA1c. These findings suggest that the presence of DM, but not DL, had an intense association with low serum ucOC level. Next, multiple regression analysis showed that ucOC and BMI had negative and positive associations with HbA1c and fasting plasma glucose, respectively, while no association was found between TRACP5b and these indices. Serum ucOC had a positive association with insulin level, whereas TRACP5b had no association, suggesting a strong relationship between high level of ucOC and insulin secretion as well as better glycemic status.

Conclusions: Our findings suggest an interrelationship between ucOC and glucose metabolism in both male and female in community-dwelling Japanese people.

Disclosures: Shozo Yano, None.

SU0298

Sclerostin is Associated with Quantitative Bone Ultrasound and Bone Turnover in Female Nursing Home Residents. Karin Amrein¹, Harald Dobnig², Stefan Pilz³, Andreas Tomaschitz³, Doris Wagner³, Karl Heinz Fenzl⁴, Thomas R. Pieber³, Astrid Fahrleitner-Pammer*¹. ¹Medical University Graz, Austria, ²Diagnostikinstitut Univ.Prof.Dr.H.Dobnig GmbH & Medical University Graz, Austria, ³Medical University of Graz, Austria, ⁴Roche Austria, Austria

Introduction: Sclerostin, a protein produced by osteocytes, inhibits bone formation. Serum levels correlate with age and bone mineral density (BMD, measured with dual X-ray absorptiometry) in osteoporosis and in healthy subjects. In elderly nursing home residents whose mobility is limited, BMD assessment with quantitative bone ultrasound (QUS) is easily available and might add additional valuable information on bone microarchitecture and fracture risk. Only recently, it was shown that community dwelling elderly women with higher sclerostin levels have a greater hip fracture risk.

Objective: We aimed to evaluate the association of circulating sclerostin levels with results of QUS, fracture risk and mortality in a cohort of 539 institutionalized elderly women.

Methods: In a prospective cohort study among elderly female patients recruited from 95 Austrian nursing homes, sclerostin levels were measured with a quantitative sandwich enzyme-linked immunosorbent assay. Calcaneal stiffness, radial speed of sound (SOS), and phalangeal SOS were measured at baseline. Patients were followed for hip fractures and survival status.

Results: We examined 539 study participants aged 84 ± 6 years. The mean serum sclerostin level was 24.6 ± 13.0 pmol/L (range 6.6 to 97.3). Partial correlation analysis adjusted for age and kidney function revealed a significant positive correlation of sclerostin levels with calcaneal stiffness, radial and phalangeal SOS (correlation coefficients 0.301, 0.228 and 0.207 respectively, all $p < 0.01$) and a significant negative correlation with osteocalcin and serum crosslaps (correlation coefficients -0.202 and -0.133 $p < 0.05$). After a mean follow-up of 27 ± 8 months, 139 patients had died and 30 suffered a hip fracture. Sclerostin levels did not differ between survivors and nonsurvivors (24.2 ± 12.3 vs. 25.7 ± 14.9 pmol/L, $p=0.224$) or patients with and without a hip fracture (22.1 ± 10.2 vs. 24.8 ± 13.4 pmol/L, $p=0.294$).

Conclusions: In institutionalized elderly women, there is a significant relationship of serum sclerostin levels with BMD indices measured with QUS. The strongest correlation was evident for calcaneal stiffness which has been proven to be predictive for hip and nonvertebral fractures in this population. However, higher sclerostin were not associated with hip fracture or survival status in our study. Thus, sclerostin serum

levels may not predict outcome, at least in a nursing home population with impaired mobility.

Disclosures: Astrid Fahrleitner-Pammer, None.

SU0299

Unsaturation Level Decreased in Bone Marrow Lipids of Postmenopausal Women with Low Bone Density Using High Resolution HRMAS NMR. Xiaojuan Li*¹, Keerthi Shet¹, Juan Pablo Rodriguez², Ana Maria Pino², John Kurhanewicz¹, Ann Schwartz¹, Clifford Rosen³. ¹University of California, San Francisco, USA, ²The University of Chile, Chile, ³Maine Medical Center, USA

Bone marrow adiposity may play a critical role in affecting both bone quantity and quality. Increased bone marrow adiposity measured by in vivo proton magnetic resonance (¹H-MRS) has been associated with decreased bone mineral density (BMD). However, only very limited studies have investigated whether the composition of marrow adipose tissue (MAT) changes as bone density declines, and these studies have provided mixed results. We recently showed preliminary evidence that less unsaturated and more saturated fatty acids in MAT, as measured by in vivo MRS, predicted fractures in postmenopausal women with or without type-2 diabetes. The goal of this study was to quantify MAT composition of marrow samples from postmenopausal women using ex vivo high-resolution magic angle spinning (HRMAS) NMR spectroscopy.

Twenty-four bone marrow samples were harvested from iliac crest during surgeries from postmenopausal women (65-89 years) who had bone fracture or arthroplasty. HRMAS data was acquired using a 500 MHz Varian INOVA spectrometer while samples were spun at a rate of 2.25 kHz. Lipid peaks were quantified from the resulting HRMAS spectra (Figure 1). The triglyceride composition, specifically the mono-unsaturation level (MUL), double-unsaturation level (DUL), total unsaturation level (UL=MUL+DUL, assuming little poly-unsaturated lipids) and total saturation level (SL=1-UL) was determined using the method described in the literature, Figure 1.

Significant decrease of MUL was observed in samples from subjects with low bone density (based on L2-L4 DXA t-score) compared to controls, Table 1. Decrease of UL and increase of SL were also found in subjects with low bone density, but the difference was significant only in subjects with osteopenia. Samples from four subjects who had hip fracture showed lower MUL compared to those without a fracture, but the difference was not significant with this small cohort ($13.0\% \pm 5.2\%$ non-fracture vs. $10.7\% \pm 7.2\%$ with-fracture).

The high resolution ex vivo spectral results demonstrated decreased unsaturation level and increased saturation level in marrow samples from subjects with low bone density, confirming previous in vivo observations. This result suggested not only the amount but more importantly the MAT composition changed during the disease. MAT composition quantification may help identify non-invasive and novel markers for bone quality and potentially for fracture.

Table 1. Demographic and HRMAS measures of control, osteopenia and osteoporotic samples.

| | Age (years) | BMI (kg/m ²) | L2-L4 t-score | UL | DUL | MUL | SL |
|------------------------------|-------------|--------------------------|---------------|--------------|--------------|--------------|--------------|
| Control (n=7) | 70.7±5.1 | 27.4 ± 5.0 | 0.6 ± 1.5 | 25.2% ± 6.9% | 7.5% ± 2.5% | 17.8% ± 4.8% | 74.8% ± 6.9% |
| Osteopenia (n=9) | 72.2 ± 5.6 | 26.5 ± 3.2 | -1.7 ± 0.3 | 18.0% ± 2.2% | 7.7% ± 2.6% | 10.3% ± 3.0% | 82.0 ± 2.2% |
| Osteoporosis (n=8) | 77.1 ± 9.0 | 24.2 ± 3.0 | -3.1 ± 0.5 | 20.5% ± 6.9% | 10.0% ± 5.5% | 10.6% ± 5.6% | 79.5 ± 6.9% |
| P (control vs. Osteoporosis) | 0.1 | 0.2 | 0.0004 | 0.211 | 0.269 | 0.019 | 0.211 |
| P (control vs. Osteopenia) | 0.6 | 0.7 | 0.007 | 0.024 | 0.731 | 0.006 | 0.024 |

UL: unsaturation level; DUL: double-unsaturation level; MUL: mono-unsaturation level; SL: saturation level

Table 1

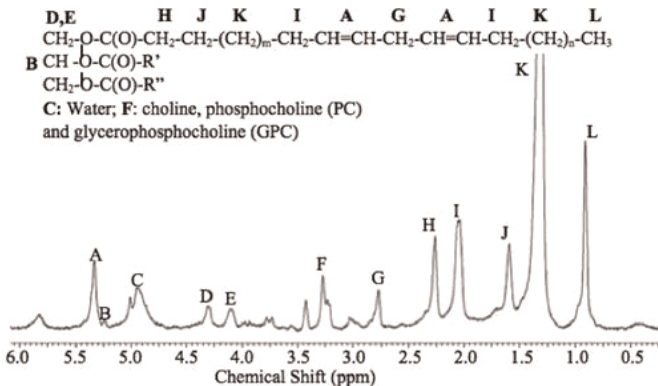
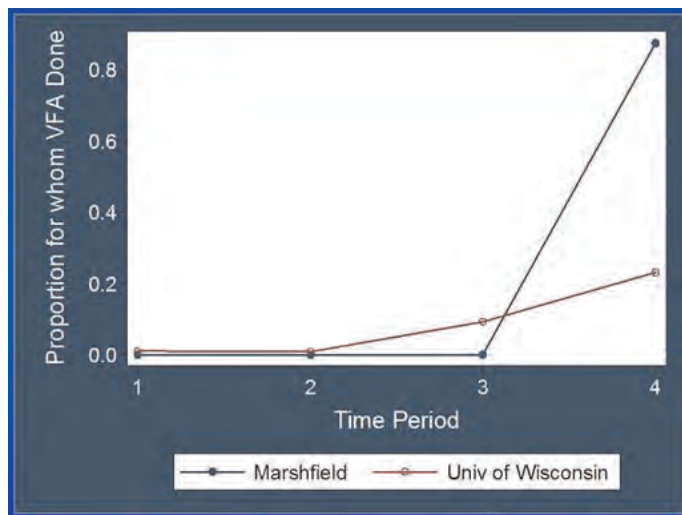


Figure 1. Representative bone marrow HRMAS NMR spectroscopy. Unsaturation Level = A/L; Double-unsaturation level (DUL) = G/L; Mono-unsaturation level (MUL) = UL - DUL (assuming little poly-unsaturated lipids); Saturation level (SL) = 1-UL

Figure 1

Disclosures: Xiaojuan Li, None.



Disclosures: John Schousboe, None.

SU0300

A Performance Algorithm Improves Appropriate Vertebral Fracture Assessment Use Among Those Referred for DXA and Improves Utilization of Fracture Prevention Medication for those with Prevalent Vertebral Fracture. John Schousboe¹, Fergus McKiernan², Neil Binkley³. ¹Park Nicollet Clinic/University of Minnesota, USA, ²Marshfield Clinic, USA, ³University of Wisconsin, Madison, USA

Background: Vertebral fracture assessment (VFA) identifies prevalent vertebral fracture and improves fracture risk estimation but is under-utilized in clinical practice. A performance algorithm implemented by DXA technologists at Park Nicollet Health Services, a large urban community health care delivery organization, increased appropriate VFA use over 7 years. The objectives of this study were to a) assess how well DXA technologists implemented a VFA performance algorithm over a 5 year period and b) assess VFA use following implementation of similar performance algorithm at a large rural multispecialty community health care organization and a university health center, and c) assess the effect of identifying prevalent vertebral fracture using this algorithm on physician prescription of fracture prevention medication.

Methods: We devised a physician order option simplified from the ISCD 2007 Position Statement for VFA indications to specify that VFA is appropriate for those patients whose worst T-score (lumbar spine, femoral neck, total hip) is ≤ -1.5 PLUS either age ≥ 65 years OR height loss ≥ 1.5 inches OR current glucocorticoid use. The order option was introduced at the other 2 institutions in January 2011 with the revision that the T-score criterion was changed to between -1.5 and -2.5. VFA utilization among those with the aforementioned criteria for the 8-month period following performance algorithm implementation was compared to the 3 preceding 8 month periods by χ^2 statistic.

Results: At Park Nicollet, 72% of those who met the performance algorithm criteria had VFA whereas 92% of those lacking an indication did not. Following implementation 23% of patients meeting the performance algorithm criteria at study center 1 and 86% at study center 2 had VFA appropriately performed (p-value for trend < 0.0001 ; Figure). Among those who had a VFA, the odds ratio of starting or intensifying fracture prevention therapy was 3.2 (95% C.I. 2.1 - 5.1) for those with VFA positive for fracture compared to VFA negative for fracture, adjusted for bone density, prior clinical fracture, age, sex, glucocorticoid use, and study site.

Conclusions: DXA technologists can successfully identify patients for whom VFA is indicated using a VFA performance algorithm. VFA results appropriately and positively influence physician prescribing behavior for fracture prevention medication.

SU0301

Fat tissue Measurements by Dual-Energy X-Ray Absorptiometry: Cross-Calibration of Three Different Fan-Beam Instruments. Jorge Malouf¹, Silvana Di Gregorio², Luis Del Rio², Ferran Torres³, Ana Marin⁴, Jordi Farrerons⁴, Silvia Herrera⁴, Pere Domingo⁵. ¹Hospital de la Santa Creu i Sant Pau, Spain, ²Cetir Centre Medical, Spain, ³Biostatistics & data management platform, Institut d'investigacions biomèdiques Agust Pi Sunyer, Universitat de Barcelona., Spain, ⁴Mineral Metabolism Unit. Hospital de Sant Pau, Spain, ⁵Infectious diseases Unit. Hospital de Sant Pau, Spain

Analysis of total tissue composition and, particularly, body fat measurements has become progressively important in the diagnosis and follow-up of patients with different clinical conditions. Dual-energy X-ray absorptiometry (DXA) fan-beam scanners are widely used to measure body composition but the development translational equations to be able to compare data of different scanning systems is necessary. The aim of this study was to assess the extent of agreement for regional measurements of body composition between the following three fan-beam DXA scanners: (i) Hologic Discovery, (ii) Lunar iDXA, and (iii) Lunar Prodigy Advance. The study population consisted of 91 adult healthy volunteers (40 males, 51 females; mean age 48.5 ± 14.4 years) who underwent DXA evaluation of the lumbar spine, hip, and whole body in each machine on the same day. Agreement between the three scanners was evaluated according to the Bland-Altman method and Lin's concordance correlation coefficient. Results showed a better agreement and concordance for the Lunar iDXA scanner than for any of them with the Hologic scanner. Differences were higher for any tissue or region than for the whole tissue mass. Translational equations were developed to ensure comparability of body composition measurements obtained with each of these three scanners.

Table. Formulas of prediction of DXA, Prodigy and Hologic for the estimation of fat, after the use of fractional polynomials.

| | Hologic | Prodigy |
|----------------------|---|---|
| DXA | | |
| Task activation rate | $1.02 + 1.01 \cdot 10^{-10} \cdot \text{Weight} + 1.01 \cdot 10^{-10} \cdot \text{Weight}^2 + 1.01 \cdot 10^{-10} \cdot \text{Weight}^3$ | $0.58 + 1.01 \cdot 10^{-10} \cdot \text{Weight} + 1.01 \cdot 10^{-10} \cdot \text{Weight}^2 + 1.01 \cdot 10^{-10} \cdot \text{Weight}^3$ |
| Task age rate | $0.58 + 1.01 \cdot 10^{-10} \cdot \text{Weight} + 1.01 \cdot 10^{-10} \cdot \text{Weight}^2 + 1.01 \cdot 10^{-10} \cdot \text{Weight}^3$ | $0.77 + 1.01 \cdot 10^{-10} \cdot \text{Weight} + 1.01 \cdot 10^{-10} \cdot \text{Weight}^2 + 1.01 \cdot 10^{-10} \cdot \text{Weight}^3$ |
| Area Fat | $917 \cdot \text{Age} + 1.01 \cdot 10^{-10} \cdot \text{Weight} + 1.01 \cdot 10^{-10} \cdot \text{Weight}^2 + 1.01 \cdot 10^{-10} \cdot \text{Weight}^3$ | $462 \cdot \text{Age} + 1.01 \cdot 10^{-10} \cdot \text{Weight} + 1.01 \cdot 10^{-10} \cdot \text{Weight}^2 + 1.01 \cdot 10^{-10} \cdot \text{Weight}^3$ |
| Leg Fat | $102 \cdot \text{Age} + 1.01 \cdot 10^{-10} \cdot \text{Weight} + 1.01 \cdot 10^{-10} \cdot \text{Weight}^2 + 1.01 \cdot 10^{-10} \cdot \text{Weight}^3$ | $171 \cdot \text{Age} + 1.01 \cdot 10^{-10} \cdot \text{Weight} + 1.01 \cdot 10^{-10} \cdot \text{Weight}^2 + 1.01 \cdot 10^{-10} \cdot \text{Weight}^3$ |
| Total Fat | $466 \cdot \text{Age} + 1.01 \cdot 10^{-10} \cdot \text{Weight} + 1.01 \cdot 10^{-10} \cdot \text{Weight}^2 + 1.01 \cdot 10^{-10} \cdot \text{Weight}^3$ | $267 \cdot \text{Age} + 1.01 \cdot 10^{-10} \cdot \text{Weight} + 1.01 \cdot 10^{-10} \cdot \text{Weight}^2 + 1.01 \cdot 10^{-10} \cdot \text{Weight}^3$ |
| Total Fat | $1134 \cdot \text{Age} + 1.01 \cdot 10^{-10} \cdot \text{Weight} + 1.01 \cdot 10^{-10} \cdot \text{Weight}^2 + 1.01 \cdot 10^{-10} \cdot \text{Weight}^3$ | $1717 \cdot \text{Age} + 1.01 \cdot 10^{-10} \cdot \text{Weight} + 1.01 \cdot 10^{-10} \cdot \text{Weight}^2 + 1.01 \cdot 10^{-10} \cdot \text{Weight}^3$ |
| Total mass | $176 \cdot \text{Age} + 1.01 \cdot 10^{-10} \cdot \text{Weight} + 1.01 \cdot 10^{-10} \cdot \text{Weight}^2 + 1.01 \cdot 10^{-10} \cdot \text{Weight}^3$ | $176 \cdot \text{Age} + 1.01 \cdot 10^{-10} \cdot \text{Weight} + 1.01 \cdot 10^{-10} \cdot \text{Weight}^2 + 1.01 \cdot 10^{-10} \cdot \text{Weight}^3$ |
| Prodigy | | |
| Task activation rate | $0.742 + 1.01 \cdot 10^{-10} \cdot \text{Weight} + 1.01 \cdot 10^{-10} \cdot \text{Weight}^2 + 1.01 \cdot 10^{-10} \cdot \text{Weight}^3$ | $0.742 + 1.01 \cdot 10^{-10} \cdot \text{Weight} + 1.01 \cdot 10^{-10} \cdot \text{Weight}^2 + 1.01 \cdot 10^{-10} \cdot \text{Weight}^3$ |
| Task age rate | $0.742 + 1.01 \cdot 10^{-10} \cdot \text{Weight} + 1.01 \cdot 10^{-10} \cdot \text{Weight}^2 + 1.01 \cdot 10^{-10} \cdot \text{Weight}^3$ | $0.677 + 1.01 \cdot 10^{-10} \cdot \text{Weight} + 1.01 \cdot 10^{-10} \cdot \text{Weight}^2 + 1.01 \cdot 10^{-10} \cdot \text{Weight}^3$ |
| Area Fat | $1102 \cdot \text{Age} + 1.01 \cdot 10^{-10} \cdot \text{Weight} + 1.01 \cdot 10^{-10} \cdot \text{Weight}^2 + 1.01 \cdot 10^{-10} \cdot \text{Weight}^3$ | $500 \cdot \text{Age} + 1.01 \cdot 10^{-10} \cdot \text{Weight} + 1.01 \cdot 10^{-10} \cdot \text{Weight}^2 + 1.01 \cdot 10^{-10} \cdot \text{Weight}^3$ |
| Leg Fat | $2078 \cdot \text{Age} + 1.01 \cdot 10^{-10} \cdot \text{Weight} + 1.01 \cdot 10^{-10} \cdot \text{Weight}^2 + 1.01 \cdot 10^{-10} \cdot \text{Weight}^3$ | $1074 \cdot \text{Age} + 1.01 \cdot 10^{-10} \cdot \text{Weight} + 1.01 \cdot 10^{-10} \cdot \text{Weight}^2 + 1.01 \cdot 10^{-10} \cdot \text{Weight}^3$ |
| Total Fat | $101 \cdot \text{Age} + 1.01 \cdot 10^{-10} \cdot \text{Weight} + 1.01 \cdot 10^{-10} \cdot \text{Weight}^2 + 1.01 \cdot 10^{-10} \cdot \text{Weight}^3$ | $632 \cdot \text{Age} + 1.01 \cdot 10^{-10} \cdot \text{Weight} + 1.01 \cdot 10^{-10} \cdot \text{Weight}^2 + 1.01 \cdot 10^{-10} \cdot \text{Weight}^3$ |
| Total Fat | $526 \cdot \text{Age} + 1.01 \cdot 10^{-10} \cdot \text{Weight} + 1.01 \cdot 10^{-10} \cdot \text{Weight}^2 + 1.01 \cdot 10^{-10} \cdot \text{Weight}^3$ | $672 \cdot \text{Age} + 1.01 \cdot 10^{-10} \cdot \text{Weight} + 1.01 \cdot 10^{-10} \cdot \text{Weight}^2 + 1.01 \cdot 10^{-10} \cdot \text{Weight}^3$ |
| Total mass | $469 \cdot \text{Age} + 1.01 \cdot 10^{-10} \cdot \text{Weight} + 1.01 \cdot 10^{-10} \cdot \text{Weight}^2 + 1.01 \cdot 10^{-10} \cdot \text{Weight}^3$ | $410 \cdot \text{Age} + 1.01 \cdot 10^{-10} \cdot \text{Weight} + 1.01 \cdot 10^{-10} \cdot \text{Weight}^2 + 1.01 \cdot 10^{-10} \cdot \text{Weight}^3$ |
| Hologic | | |
| Task activation rate | $0.817 + 1.01 \cdot 10^{-10} \cdot \text{Weight} + 1.01 \cdot 10^{-10} \cdot \text{Weight}^2 + 1.01 \cdot 10^{-10} \cdot \text{Weight}^3$ | $0.822 + 1.01 \cdot 10^{-10} \cdot \text{Weight} + 1.01 \cdot 10^{-10} \cdot \text{Weight}^2 + 1.01 \cdot 10^{-10} \cdot \text{Weight}^3$ |
| Task age rate | $0.817 + 1.01 \cdot 10^{-10} \cdot \text{Weight} + 1.01 \cdot 10^{-10} \cdot \text{Weight}^2 + 1.01 \cdot 10^{-10} \cdot \text{Weight}^3$ | $0.822 + 1.01 \cdot 10^{-10} \cdot \text{Weight} + 1.01 \cdot 10^{-10} \cdot \text{Weight}^2 + 1.01 \cdot 10^{-10} \cdot \text{Weight}^3$ |
| Area Fat | $710 \cdot \text{Age} + 1.01 \cdot 10^{-10} \cdot \text{Weight} + 1.01 \cdot 10^{-10} \cdot \text{Weight}^2 + 1.01 \cdot 10^{-10} \cdot \text{Weight}^3$ | $533 + 1.01 \cdot 10^{-10} \cdot \text{Weight} + 1.01 \cdot 10^{-10} \cdot \text{Weight}^2 + 1.01 \cdot 10^{-10} \cdot \text{Weight}^3$ |
| Leg Fat | $262 \cdot \text{Age} + 1.01 \cdot 10^{-10} \cdot \text{Weight} + 1.01 \cdot 10^{-10} \cdot \text{Weight}^2 + 1.01 \cdot 10^{-10} \cdot \text{Weight}^3$ | $638 \cdot \text{Age} + 1.01 \cdot 10^{-10} \cdot \text{Weight} + 1.01 \cdot 10^{-10} \cdot \text{Weight}^2 + 1.01 \cdot 10^{-10} \cdot \text{Weight}^3$ |
| Total Fat | $462 \cdot \text{Age} + 1.01 \cdot 10^{-10} \cdot \text{Weight} + 1.01 \cdot 10^{-10} \cdot \text{Weight}^2 + 1.01 \cdot 10^{-10} \cdot \text{Weight}^3$ | $368 \cdot \text{Age} + 1.01 \cdot 10^{-10} \cdot \text{Weight} + 1.01 \cdot 10^{-10} \cdot \text{Weight}^2 + 1.01 \cdot 10^{-10} \cdot \text{Weight}^3$ |
| Total Fat | $802 \cdot \text{Age} + 1.01 \cdot 10^{-10} \cdot \text{Weight} + 1.01 \cdot 10^{-10} \cdot \text{Weight}^2 + 1.01 \cdot 10^{-10} \cdot \text{Weight}^3$ | $368 \cdot \text{Age} + 1.01 \cdot 10^{-10} \cdot \text{Weight} + 1.01 \cdot 10^{-10} \cdot \text{Weight}^2 + 1.01 \cdot 10^{-10} \cdot \text{Weight}^3$ |
| Total mass | $131 \cdot \text{Age} + 1.01 \cdot 10^{-10} \cdot \text{Weight} + 1.01 \cdot 10^{-10} \cdot \text{Weight}^2 + 1.01 \cdot 10^{-10} \cdot \text{Weight}^3$ | $267 \cdot \text{Age} + 1.01 \cdot 10^{-10} \cdot \text{Weight} + 1.01 \cdot 10^{-10} \cdot \text{Weight}^2 + 1.01 \cdot 10^{-10} \cdot \text{Weight}^3$ |
| Total mass | $380 \cdot \text{Age} + 1.01 \cdot 10^{-10} \cdot \text{Weight} + 1.01 \cdot 10^{-10} \cdot \text{Weight}^2 + 1.01 \cdot 10^{-10} \cdot \text{Weight}^3$ | $1164 \cdot \text{Age} + 1.01 \cdot 10^{-10} \cdot \text{Weight} + 1.01 \cdot 10^{-10} \cdot \text{Weight}^2 + 1.01 \cdot 10^{-10} \cdot \text{Weight}^3$ |

The coefficients in the current table have been rounded to three decimal digits, unless the coefficient was smaller than that value in absolute terms. The formulas with the rounded coefficients are available in the supplementary information published in the web as supplementary file.

The Hologic, DXA, and Prodigy terms in the formula refer to each machine observed values; gender is 0 for females and 1 for males; height should be filled in centimeters and height in kg.

Translational equations

Disclosures: Jorge Malouf, None.

SU0302

High Prevalence of Vertebral Deformities in Patients with a Recent Symptomatic Fracture and Osteopenia. Etienne Stegeman¹, Irene Bultink¹, Willem Lems^{*2}. ¹VU University Medical Center, The Netherlands, ²Vrije Universiteit Medical Centre, The Netherlands

Background: The 2011 Dutch ‘‘CBO guideline for osteoporosis and fracture prevention’’ advocates bisphosphonate treatment not only for patients with osteoporosis (T-score <-2.5) but also for patients with osteopenia and a vertebral fracture, because prevalent fractures are an independent risk factor for future fractures. Nowadays, the measurement of vertebral height can easily be performed with a Vertebral Fracture Assessment (VFA), in addition to a DXA measurement. However, data from VFA are slightly less reliable than conventional radiographs, which are regarded as gold standard. Therefore, a height loss of at least 25% was regarded as a fracture threshold, instead of the 20% height loss that is usually incorporated in phase III trials.

Objective: To determine the prevalence of vertebral fractures assessed by VFA in patients aged 50 years and older with a recent symptomatic fracture and diagnosed with osteopenia.

Patients, methods

Patients aged \geq 50 years who visited the emergency room with a symptomatic fracture, were invited to the outpatient clinic for a fracture risk assessment by DXA and additional VFA. In 2011, 203 consecutive visitors of the fracture risk outpatient clinic were included.

Results: Of the patients in the study group, 139/203 (68%) were female, 64/203 (32%) were male, with a mean age of 67.2 years. The DXA results showed that 55/203 patients (27%) had a normal BMD, 96/203 (47%) had osteopenia and 52/203 (26%) had osteoporosis.

The osteopenia subgroup consisted of 64/96 (67%) females and 32/96 (33%) males, with a mean age of 67.8 years. The VFA results are demonstrated in Table 1. In 53/96 (55%) patients at least one vertebral deformity with \geq 20% reduction of vertebral height was detected. Of those, the height loss was \geq 25% in 31/96 (32%) patients and \geq 40% in 10/96 (10%). Conclusion: In patients with a symptomatic fracture and osteopenia, roughly one third has at least one vertebral fracture with a height loss of \geq 25%. Since vertebral fractures are a strong predictor of future vertebral and nonvertebral fractures, treatment of this patient group deserves serious consideration. Additional VFA measurement enables the detection of vertebral fractures in osteopenic patients, which can be decisive in assigning treatment to this patient group. These data support the additional use of VFA in patients aged 50 years and older with a symptomatic fracture.

| | | Vertebral height loss | | | |
|--------------|-----|-----------------------|-----------------|-----------------|------------|
| | | < 20% | \geq 20 - 25% | \geq 25 - 40% | \geq 40% |
| Normal BMD | 55 | 28 (51%) | 12 (22%) | 13 (24%) | 2 (4%) |
| Osteopenia | 96 | 43 (45%) | 22 (23%) | 21 (22%) | 10 (10%) |
| Osteoporosis | 52 | 25 (48%) | 7 (13%) | 16 (31%) | 4 (8%) |
| | 203 | | | | |

Table 1 - VFA Results

Disclosures: *Willem Lems, None.*

SU0303

How Primary Care Physicians Assess Postmenopausal Women Following Education on the 2010 Osteoporosis Canada Guidelines (OC CPG). Alexandra Papaioannou¹, Jonathan Adachi², Cheryl Colizza³, David Hanley^{*4}, Stephanie Kaiser⁵, David Kendler⁶, Peter Lin⁷, Marla Shapiro⁸, Suzanne Morin⁹. ¹Hamilton Health Sciences, Canada, ²St. Joseph’s Hospital, Canada, ³Amgen, Canada, ⁴University of Calgary, Canada, ⁵Dalhousie University, Canada, ⁶Associate Professor University of British Columbia, Canada, ⁷Canadian Heart Research Centre, Canada, ⁸University of Toronto, Department of Family & Community Medicine, Canada, ⁹McGill University, Canada

Objectives: To determine in a prospective practice assessment how Canadian physicians stratify and treat postmenopausal women at risk of fracture after training on the OC CPG

Methods: Following accredited education, primary care physicians (PCPs) were invited to participate in a practice assessment regarding patients at risk of postmenopausal osteoporosis (PMO). Physicians were asked to assess 20 postmenopausal patients with available BMD data, currently not treated for PMO. Patients were 50+ years and had T-score < -2.0 or prior fracture after age 40. Physicians received a hand-held device that prompted them for patient data, perceived fracture risk and treatment choice, and that calculated absolute fracture risk using the CAROC model.

Results: • 69 PCPs from across Canada participated, assessing 872 patients

- Patient characteristics:
 - o 73% assessed at routine visit or visit unrelated to PMO
 - o Prior fracture in 20%
 - o 21% had experienced height loss

- o \geq 1 comorbidity in 53%
- o \geq 1 key PMO risk factor in 48%
- o 66% taking calcium, 74% vitamin D
- 49/183 (27%) patients with height loss vs. 36/689 (5%) without had prior spine fracture
 - Per CAROC, 10-year fracture risk of each patient was low in 305 (35%), moderate in 378 (43%) and high in 189 (22%) (Table):
 - o PCP evaluation agreed with CAROC in 65% of cases
 - o PCPs overestimated risk in 24% and underestimated risk in 11% of cases
 - PCPs chose pharmacotherapy for 60% (227/378) of moderate-risk patients:
 - o 49% of these patients had \geq 1 risk factor vs. 29% of those not recommended therapy
 - o Age did not appear to factor into the decision to treat
 - For moderate-/high-risk patients, the most common treatment choices followed OC CPG first-line treatment recommendations:
 - o Moderate-risk: 78% bisphosphonates (BPs) (5% daily, 45% weekly, 22% monthly, 6% yearly); 21% RANKL inhibitor; 2% other
 - o High-risk: 71% BPs (4% daily, 39% weekly, 21% monthly, 7% yearly); 35% RANKL inhibitor; 13% other

Conclusion: Most of these untreated postmenopausal women were at moderate/high risk for fracture per CAROC assessment. Physician-perceived assessment agreed with CAROC in 65% of cases, with the remainder possibly subject to over- or under-treatment. Choice of pharmacologic treatment varied with risk group, with greater use of weekly BPs and less use of RANKL inhibitor in moderate-risk patients, 40% of whom received no pharmacotherapy.

Conflict Statement: This research was sponsored by Osteoporosis Canada. Financial support was provided by Amgen Canada.

| Physician Perceived Assessment (n, %) | CAROC Actual Risk Assessment (n) | Patients Inaccurately Assessed (n) |
|--|----------------------------------|------------------------------------|
| Low 243 (28%) | Low* | 190 |
| | Moderate | 52 |
| | High | 1 |
| Moderate 385 (44%) | Low | 105 |
| | Moderate* | 236 |
| | High | 44 |
| High 244 (28%) | Low | 10 |
| | Moderate | 90 |
| | High* | 144 |
| Total patients inaccurately assessed (n, %) | | 302 (35%) |

*Correct answer

Table

Disclosures: *David Hanley, Amgen, Novartis, 1; Amgen, Novartis, Eli Lilly, Warner-Chilcott, 2; Amgen, 6*
 This study received funding from: *Amgen*

SU0304

Osteoporosis-Related Knowledge among Older Patients Undergoing DXA and its Association to Bone Density. Stephanie Edmonds^{*1}, Xin Lu², Peter Cram¹, Kenneth Saag³, Douglas Roblin⁴, Fredric Wolinsky⁵. ¹University of Iowa, USA, ²University of Iowa, Department of Internal Medicine, Division of General Medicine, USA, ³University of Alabama at Birmingham, USA, ⁴Kaiser Permanente of Atlanta, USA, ⁵University of Iowa, College of Public Health, Department of Health Management & Policy, USA

Purpose: To examine whether prior history of osteoporosis or low bone density predicts osteoporosis-related knowledge level.

Methods: We administered the 10-item ‘Osteoporosis and You’ knowledge questionnaire to consecutive adults 50 years old or older presenting for DXA at three sites in the United States. The scale’s summary score ranges from 0 to 10 reflecting the number of correct responses. Using self-reported history of DXA results, patients were classified as having 1) normal bone density or 2) abnormal bone density (those with low bone density or osteoporosis). Using linear regression we compared the mean number of correct responses among the two bone-density groups.

Results: We administered the ‘Osteoporosis and You’ scale to 205 participants who previously underwent DXA. The mean age was 66.7 (\pm 8.4), 93.2% were women, 86.3% were white, 10.7% were African-American, and 79.5% had at least some college education. There were 87 participants with normal bone density and 118 with abnormal bone density (60 with low and 58 with osteoporosis). In the unadjusted regression analysis we found that having a diagnosis of osteoporosis or low bone density was associated with a significantly higher knowledge score compared to having normal bone density by 0.6 correct answers (p=0.01). However, after adjusting for age, sex, race, and education, the association between having a prior diagnosis of low bone density or osteoporosis, knowledge became marginally insignificant (p=0.08).

Conclusion: Patients with abnormal bone density did not have significantly higher scores on the ‘Osteoporosis and You’ knowledge scale after adjusting for other

characteristics. Future research needs to be done to learn how osteoporosis-related knowledge could be increased in patients at risk for fracture.

Disclosures: *Stephanie Edmonds, None.*

SU0305

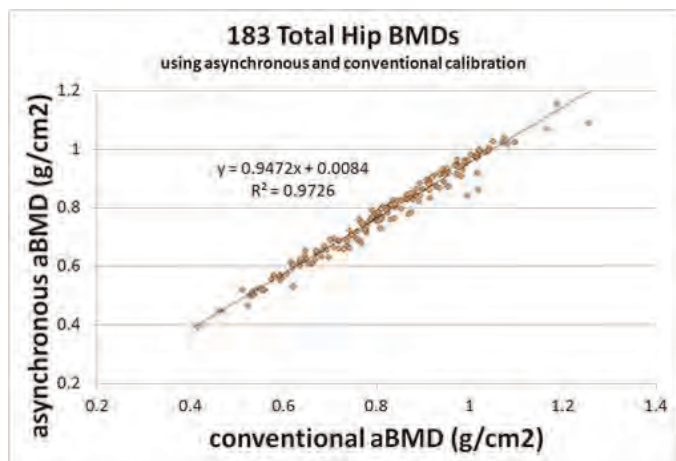
Preliminary Investigation of Quantitative CT (QCT) Bone Densitometry using Asynchronous Calibration. Keenan Brown^{*1}, Gabriel Bodden¹, Alan Brett². ¹Mindways Software, USA, ²Mindways Software, Inc., USA

Objective(s): Asynchronous calibration for quantitative CT (QCT) bone densitometry permits extracting QCT measurements from other abdominal or pelvic CT procedures with zero additional radiation dose. Accuracy and precision in CT bone densitometry have previously relied on simultaneous scanning of a calibration phantom with the patient. We report here assessments of systematic and random measurement differences between a prototype commercial QCT device using asynchronous calibration and a commercially available conventional QCT device.

Material and Methods: Our retrospective cohort included 146 femoral scans from 73 subjects, ages ranged 3 to 97; the scans were acquired with solid phantoms using multiple scanner models from each of four major manufacturers. A second cohort included 220 femoral measurements from 110 subjects, ages ranged 19 to 73; the scans were acquired with liquid CT calibration phantoms using two scanner models from one major manufacturer. BMD for each femur was measured using QCT PRO Version 5.0 (Mindways Software, Austin, TX, USA) in its conventional mode and a new mode for asynchronous calibration using independently acquired, scanner-specific QA scans.

Results: Regression analysis of the first cohort resulted in correlation coefficients above 0.97 between asynchronously and conventionally calibrated BMD estimates. The slope of the regression line was close to unity with a consistent bias wherein asynchronously calibrated BMD estimates averaged 5.8% less than conventionally calibrated measurements. An SEE of 0.021 g/cm² was found for data ranging from 0.335 to 1.254 g/cm². In addition, we assessed correlations of the BMD measurement bias to CT manufacturer, X-ray energy, and patient size. These revealed no statistically significant trends. Substantially similar results were observed with the second cohort involving the use of liquid CT calibration phantoms except that asynchronously calibrated BMD estimates average 3.4% less than the conventionally calibrated estimates.

Conclusion(s): The high correlations of asynchronously calibrated BMD estimates with conventional BMD estimates suggest this approach has substantially equivalent accuracy in reproducing T-Scores and that the asynchronous calibration method is robust with respect to variations in CT equipment, kVp, patient size and phantom type. This approach may provide new clinical utility in dual-use and retrospective CT BMD screening.



Total hip area density for combined cohorts.

Disclosures: Keenan Brown, Mindways Software, 3; Mindways Software, 8
This study received funding from: Mindways Software

SU0306

Risk of Fracture in Sarcoidosis Is High Despite not Low BMD, Implication of Serum 25(OH) Vitamin D Level. Nathalie Saidenberg-kermanac'h^{*1}, Hilario Nunes², Luca Semerano³, Danielle Sadoun², Xavier Guillot⁴, Marouane Boubaya⁴, Nicolas Naggara⁵, Dominique Valeyre², Marie-Christophe Boissier⁶. ¹Avicenne hospital (AP-HP), France, ²Department of pneumology, Avicenne Hospital (APHP), France, ³Department of rheumatology, Avicenne Hospital (APHP) & EA4222 Paris13 University, France, ⁴Department of rheumatology, Avicenne Hospital (APHP), France, ⁵Department of radiology, France, ⁶Department of Rheumatology, Avicenne Hospital (APHP) & EA4222 Paris 13 University2, France

Background The prevention of fragility fractures in patients with sarcoidosis (Sa) is a serious concern since risk factors are poorly understood and vitamin D (vitD) or calcium prescription is a matter of hesitation in these patients.

Objectives To evaluate factors increasing the risk of osteoporosis (OP) in Sa.

Methods We prospectively included 142 consecutive patients with histologically proven Sa. Biological and clinical parameters of Sa activity and severity, BMD (DXA, Lunar Prodigy) and vertebral fracture prevalence on lumbar and thoracic spine (with Genant's semi-quantitative method of) were assessed.

Results: 80 women (51 post-menopause) and 62 men, (age 51 ± 11.9), with a mean Sa duration of 9.5 ± 7 years were included. 28 patients had never received corticosteroids (CCS), 33 had received vitD supplements, and 46 bisphosphonates, within the 6 months preceding the study. Fragility fractures had occurred in 23.5 % of the patients, (vertebral fractures in 13.7%). 40.1% had BMD T-score < -1DS in at least one site, (20 patients with OP). Nevertheless, the average BMD was not low (mean Tscore -0.44DS at the lumbar spine). VitD supplementation significantly increased serum 25(OH)vitD (p<0.0001) without any significant variation of the calcemia. In multivariate analysis, fracture (OR:3.69, 95%IC, 0.96-14.21, p=0.098), low calcium intake (OR:5.79, 95%IC, 1.82-18.42, p=0.001), and menopause (OR:3.32,95%IC, 0.67-16.47, p=0.068), were predictive of a low BMD. Age (OR:1.09 95%IC, 1.0-1.18, p=0.021), the NYHA score (OR:3.28 95%IC, 0.79-13.61, p=0.089), the cumulative dose of CCS (OR:1.48, 95%IC, 1.06-2.05, p=0.023), and low BMD (OR:3.75, 95%IC, 0.91-15.36, p=0.093), were predictive of fracture. VitD showed a protective effect on BMD for serum levels between 10 and 15.5ng/ml (low BMD OR:0.17, 95%0.04-0.83 p=0.028). In a surprising way, values above this threshold were associated with an increased risk of fracture (OR:4.71,95%IC,1.01-22.01, p=0.052). Low 25(OH)vitD and not 1.25(OH)2vitD, was significantly correlated with disease activity parameters (disease flare, ACE, severity of lung involvement, erythrocyte sedimentation rate).

Conclusions: Sa patients have a high risk of fracture despite not lowered BMD. There could be a bimodal relationship between VitD levels and fracture risk. Predictive factors of fracture, independent from BMD and reflecting the severity of Sa, should be considered when a preventive treatment of OP is planned.

Disclosures: Nathalie Saidenberg-kermanac'h, None.

SU0307

The Effect of IV Contrast on Apparent Vertebral Bone Mineral Density Measured with Multi-detector Computed Tomography can be Reliably Determined Regardless of Phase of Enhancement. Kevin Hoover^{*1}, Susan J. Back¹, Qin Wang¹, Curtis Hayes². ¹Virginia Commonwealth University, USA, ²Virginia Commonwealth University School of Medicine, USA

Purpose: To quantify the effect of intravenous (IV) contrast on vertebral bone mineral density (vBMD) as measured in Hounsfield units (HU) on clinical multi-detector computed tomography (MDCT) scans.

Introduction: Computed tomography is routinely used to evaluate pathology in the abdomen and pelvis. Soft tissues are routinely inspected on IV contrast enhanced MDCT scans as contrast can be helpful in evaluating both benign and malignant pathologies. Attenuation values of bone are used in evaluating vBMD using quantitative CT (qCT). qCT uses specific technical parameters without the use of intravenous and oral contrast. In order to determine if MDCT can be used to evaluate vBMD, the effect of contrast must be determined.

Methods: 114 MDCT scans with four phases (pre-contrast, arterial, portal-venous, and delayed IV contrast) performed to evaluate hepatic disease were measured for apparent vBMD in HU using regions of interest (ROI) within the mid-vertebral body at the T12-L4 levels. HU measurements were also performed using ROI in the IVC, aorta, retroperitoneal fat, liver and the psoas muscle. 25 four phase MDCT scans were used to test the predictive ability of the models to determine both the phase of enhancement and the pre-contrast vBMD.

Results: MDCT vBMD measurements for the T12-L4 levels demonstrate there is a specific pattern of cancellous bone enhancement that mirrors that of the liver. There are predictable vBMD ratios for each phase of enhancement to the pre-contrast phase without overlapping 95% confidence intervals: 1.0774 for arterial, 1.1932 for portal venous and 1.1221 for delayed. Inverting these values allows the identification of correction factors to remove the effect of contrast on vBMD: 0.928 for arterial, 0.838 for portal-venous and 0.891 for delayed. Determining the phase retrospectively is necessary to use the appropriate correction factor. All five of the soft tissues assessed show a close correlation with the phase of enhancement (P < .005). The aorta and IVC measurements are the most predictive of the phase.

Conclusion: Normative data for pQCT utilize values derived from specifically acquired CT scans without intravenous and oral contrast. In a highly reproducible manner, non-contrast HU values for measurement of vBMD can be predicted from post-contrast MDCT examinations suggesting these may provide useful values to screen for osteoporosis.

Disclosures: Kevin Hoover, *Bioclinica*, 2

SU0308

The Relationship between Pulmonary Function and Bone Mineral Density in Health Subjects in Korea. Yun Kyung Jeon¹, Min Jung Bae², WON JIN Kim², YANG SEON Yi², Bo Hyun Kim¹, Sang Soo Kim¹, Soo Huoung Lee³, Yong Ki Kim³, In Joo Kim¹. ¹Pusan National University Hospital, South Korea, ²Pusan National University Hospital, South Korea, ³Kim Yong Ki clinic, South Korea

Introduction: There are many reports that osteoporosis incidence is higher in patients with pulmonary diseases. But there are little study about the relationship between pulmonary function and bone mineral density (BMD) in healthy subjects. To investigate, we enrolled healthy subjects with 86 males, 123 postmenopausal women, and 341 premenopausal women.

Method: We analyzed the pulmonary function test (PFT) and BMD in 500 subjects >19 years old who were registered for the Korean National Health and Nutrition Examination Survey, 2008-2009. The individuals were non-smokers, and had screened for routine health checkup. None of the subjects had pulmonary or metabolic disease or medication which can affect pulmonary function or BMD test. The individuals who had smoked < 6 packs of cigarettes during their lifetime were defined as non-smokers.

Results: In postmenopausal women, forced vital capacity (FVC) and forced expiratory volume in 1s (FEV1) were significantly related with lumbar spine (LS) BMD and femoral neck (FN) BMD (r=0.420 r=0.390, p < 0.001, respectively and r=0.420, r=0.433, p<0.001, respectively). In premenopausal women and men, FVC and FEV1 were significantly associated with FN BMD(r=0.223, r=0.185, p<0.001 respectively and r=0.422, r=0.495, p<0.001 respectively), but not with LS BMD (r=0.140; p=0.009, r=0.105;p=0.052 and r=0.137; p=0.209, r=0.159;p=0.145). After adjustment of age and body mass index, FEV1 was significantly correlated with FN BMD (standardized β = 0.505, p<0.001)

Conclusion : FN BMD was related with pulmonary function in healthy subjects, especially with FEV1. More studied are needed to evaluated the relationship between BMD and PFT which is associated with life style activity.

Disclosures: Yun Kyung Jeon, *None*.

SU0309

Bone Mineral Density (BMD) Combined with the Trabecular Bone Score (TBS) Significantly Improves the Identification of Women at High Risk of Fracture: The SEMOF Cohort Study. Albrecht Popp¹, Salome Meer¹, Marc-Antoine Krieg², Romain Perrelet¹, Didier Hans³, Kurt Lippuner¹. ¹Osteoporosis Policlinic, University of Bern, Switzerland, ²University Hospital, Switzerland, ³Lausanne University Hospital, Switzerland

Introduction: Trabecular Bone Score (TBS) is a novel grey-level texture measurement reflecting bone micro-architecture (MA) based on the use of experimental radiograms of 2D projection images. The aim of this analysis was to investigate whether combining quantitative and qualitative (i.e. BMD and TBS) information obtained from DXA scans performed on a single device contributed to better identification of women at high fracture risk.

Methods:In the prospective SEMOF study, women were randomly selected from official state registries between January 1998 and April 2000. Only women from the Center for Bern, Switzerland, with no history of hip fracture, between 70 and 80 years of age, independent for their daily activities were included in the present analysis. Lumbar spine and hip BMD assessed by DXA (Hologic, USA) and MA evaluation by TBS (Medimaps, France) were recorded. After checking for normal distribution, results of all parameters were expressed as means and SD. The hazard of the first clinical fracture was calculated by using the age and BMI adjusted proportional hazards model of Cox.

Results: The necessary information was available for 557 out of 701 women (79%) with the following baseline characteristics (mean ± SD): age 76.1 ± 3.0 years, BMI 25.6 ± 3.9 kg/m², lumbar spine and hip BMD, 0.863 ± 0.174 and 0.771 ± 0.121 g/cm², respectively, and TBS 1.195 ± 0.115. As expected, correlation between lumbar spine BMD and site matched TBS was low (r²=0.25). After 2.72 ± 0.77 years of follow-up, the incidence of fragility fracture was 9.4%. Age- and BMI-adjusted ORs (per SD decrease) were 1.6 (1.1-2.1) (AUC = 0.68), 1.8 (1.4-2.3) (AUC = 0.66), 1.7 (1.2-2.3) (AUC = 0.61) for spine, total hip, and femoral neck BMD, respectively, and 1.9 (1.4-2.5) (AUC = 0.73) for TBS. TBS remained significant after adjustment of any of the BMD values. When using a triage approach, 57% of fragility fractures had a BMD T-score below -2.5 and 75% of fractures had a TBS < 1.200. Combining BMD < -2.5 SD at any site or TBS < 1.200 identified 85% of all women with an osteoporotic fracture.

Conclusion:As in the already published studies, these preliminary results confirm the partial independence between BMD and TBS. More importantly, combining TBS and BMD values improved fracture prediction. Thus TBS added to BMD information may become an important parameter for further refining individual fracture risk.

Disclosures: Albrecht Popp, *None*.

SU0310

Comparison of Bone Quality on 1T pMRI, pQCT and hr-pQCT: Precision, Least Significant Change & Cross-Calibration. Andy Kin On Wong¹, Karen Beattie¹, Aakash Bhargava¹, Colin Webber², Dean Inglis¹, Laura Pickard¹, Angela Cheung³, Alexandra Papaioannou², Jonathan Adachi⁴, The CaMos Research Group⁵. ¹McMaster University, Canada, ²Hamilton Health Sciences, Canada, ³University Health Network, Canada, ⁴St. Joseph's Hospital, Canada, ⁵McGill University, Canada

Objectives:To determine 1) short-term, one-year precision for each modality; 2) cross-calibration equations for bone structure from 1T peripheral(p) MRI and pQCT relative to hr-pQCT.

Methods:Women ≥ 50 years old had their non-dominant wrist scanned once at baseline on each modality, and twice a year later. The standard hr-pQCT protocol was used. A region of interest (ROI) 9.5 mm proximal to the radial inclination, spanning 9.02 mm was identified (82 μm isotropic). To align within the same ROI, a single-slice (2.3 ± 0.5mm, 200 μm in-plane) pQCT scan was prescribed at 11.5 mm proximal to the same landmark. On 1T pMRI at the same 9.5 mm ROI, an axial spoiled 3D gradient echo sequence acquired 10 contiguous slices (1.0 mm, 150 μm in-plane). Tb.Sp, BV/TV and Tb.N were computed on all images. Linear regression analyses determined slope and intercepts for cross-calibrating pMRI and pQCT against hr-pQCT-derived measures. Root-mean square coefficients of variation (RMSCV) and standard deviations (RMSSD) assessed precision error of short- and long-term test-retests. Least significant change (LSC) was calculated as per ISCD guidelines. Secondary analyses included those without fractures and not taking antiresorptives.

Results: 62 women (mean age: 74.6 ± 8.8 years; BMI: 27.3 ± 6.2 kg/m², 22 with a fracture, 22 on antiresorptive therapy) completed at least two scans, 37 completed all three and at least 34 completed follow-up scans on each modality. pMRI systematically yielded larger Tb.Sp compared to both CT modalities overall. Hr-pQCT yielded lower BV/TV compared to both pMRI and pQCT (Tables I and II). The relationship between pMRI and hr-pQCT Tb.Sp was closest to unity. One-year LSCs were generally similar to short-term LSCs. Except for MRI-derived Tb.Sp (5.31%), short-term RMSCV for all other variables were within 5% for all modalities in participants not on antiresorptive therapy without a fracture. Precision error was increased by 1.2-2.0 fold when all participants were included.

Conclusion: 1T pMRI and pQCT provide valid and precise measures of bone structure acceptable for use in longitudinal studies. These data provide a means for cross-calibrating measurements across modalities. Susceptibility artifact between the anterior bone-muscle boundary (MRI, Figure 1) and elaborate cavities in certain participants (all modalities) introduce variability in bone structural data.

Table I. Comparison of hr-pQCT, 1T pMRI and pQCT-derived bone structure values. Values expressed in median ± standard deviation. Friedman's tests showed significant differences across modalities for all variables (p<0.001). ^a Indicates significant difference compared to hr-pQCT measure at the 95% confidence level.

| Modality | Hr-pQCT (N=37) | MRI (N=37) | pQCT (N=35) |
|------------------|----------------|----------------------------|----------------------------|
| BV/TV (fraction) | 0.120 ± 0.038 | 0.498 ± 0.049 ^a | 0.447 ± 0.130 ^a |
| Tb.N (units/mm) | 1.98 ± 0.44 | 0.89 ± 0.12 ^a | 1.14 ± 0.24 ^a |
| Tb.Sp (mm) | 0.446 ± 0.254 | 0.558 ± 0.174 | 0.475 ± 0.354 |

Table I

Table II. Cross-calibration linear equations comparing 1T pMRI and pQCT against hr-pQCT. Slope with 95% confidence intervals (CI) and intercept was obtained by linear regression analysis as per the ISCD guidelines. BMI was not a significant covariate.

| Modality | Variable | N | Slope | Lower 95%CI | Upper 95%CI | Intercept | R ² | P-value |
|----------|----------|----|-------|-------------|-------------|-----------|----------------|---------|
| pQCT | BV/TV | 42 | 0.290 | 0.269 | 0.311 | -0.010 | 0.952 | <0.001 |
| pMRI | BV/TV | 49 | 0.548 | 0.403 | 0.693 | -0.152 | 0.551 | <0.001 |
| pQCT | Tb.N | 42 | 1.584 | 1.210 | 1.959 | 0.111 | 0.647 | <0.001 |
| pMRI | Tb.N | 49 | 2.486 | 1.709 | 3.263 | -0.300 | 0.469 | <0.001 |
| pQCT | Tb.Sp | 42 | 0.576 | 0.442 | 0.710 | 0.194 | 0.653 | <0.001 |
| pMRI | Tb.Sp | 49 | 1.171 | 0.975 | 1.366 | -0.193 | 0.756 | <0.001 |

Table II

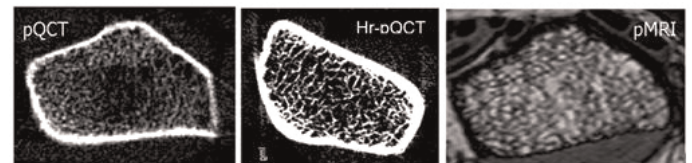


Figure 1. Comparison of single-slice images from pQCT, hr-pQCT and 1T pMRI.

Figure 1

Disclosures: Andy Kin On Wong, *None*.

SU0311

Cortical Porosity in Humans with Type 1 Diabetes Mellitus and Fractures: A Preliminary Study. Laura Armas^{*1}, Mohammed Akhter², Robert Recker².
¹Creighton University, USA, ²Creighton University Osteoporosis Research Center, USA

Patients with Type 1 diabetes mellitus (T1DM) have a 7-12 times greater fracture risk than healthy adults. While lower BMD accounts for a small percentage of this increased risk, other factors related to bone quality also increase fracture risk. We report here preliminary results of 5 patients with T1DM (3 females, 2 males, ages 21-46), who have sustained a fragility fracture while diabetic, and 2 healthy controls (1M, 1F, ages 37, 45 yr). The subjects were healthy without diabetic complications and the females were premenopausal. A transiliac bone biopsy was obtained after tetracycline labeling. The biopsy specimens were fixed, embedded and the intact specimens were scanned (16 micron resolution) using compact cone-beam type tomography in a desktop micro-CT (micro-CT-40, Scanco Medical AG, Bassersdorf, Switzerland). The measured BV/TV (bone volume to total volume ratio) variable from the cortex of each bone biopsy was used to calculate the cortical porosity (1-BV/TV) %. Calculated cortical porosity was 19% greater in the fracturing diabetic group compared to the control group (Table). While cortical BV/TV parallels the cortical porosity, it also agrees with the trabecular BV/TV (Table) which was 13% lower in the fracturing diabetics..

| (Mean ± SD) | Trab-BV/TV (%) | Cort-BV/TV (%) | Cort-Porosity (%) |
|--|----------------|----------------|-------------------|
| Control | 20.9 ± 0.1 * | 80.4 ± 5.0 | 19.5 ± 5.0 |
| Fracture T1DM | 18.3 ± 0.1 * | 76.8 ± 4.5 | 23.2 ± 4.5 |
| Trab- Trabecular bone; Cort- Cortical bone; *Armas et al. Bone, 2012 | | | |

Table

Disclosures: Laura Armas, None.

This study received funding from: NIH - grant 1K23AR055542 - 01A1

SU0312

Efficacy of Osteoporotic Agents in Trabecular Microstructure. Kenichiro Matsuzaki^{*1}, Masako Ito², Hironori Kaneko³, Masanori Kato⁴, Tomohiro Hikata⁴, Nobuhito Nango⁵, Morio Matsumoto⁴, Yoshiaki Toyama⁴.
¹National Hospital Organization Tokyo Medical Center, Japan, ²Nagasaki University Hospital, Japan, ³Keio University, Japan, ⁴Keio University School of Medicine, Japan, ⁵Ratoc System Engineering Co., Ltd., Japan

We investigated the efficacy of drugs for osteoporosis treatment analyzing trabecular microstructure with clinical multi-detector row CT (MDCT) in 4 randomly allocated groups in a double-blind manner.

184 postmenopausal women (mean age 69.9yrs) with BMD < 80%-YAM were randomly allocated into 4 groups of Risedronate (RIS), Alfacalcidol (ALF), RIS+ALF and Raloxifen (RLX)+ALF in a double-blind manner, and 67 patients were followed for 2 years. There were 18 in RIS, 13 in ALF, 19 in RIS+ALF and 17 in RLX+ALF. CT scanning was performed to measure the same vertebra under the same condition at baseline and 6, 12, 18 and 24 months after administration. Microstructures were analyzed with a 3D image analysis system.

QCT-BMD markedly increased in RIS+ALF group and was maintained in ALF group and the values were between them for the other two groups. BV/TV, TbN and TbSp were significantly improved in RLX+ALF group. They deteriorated in RIS+ALF group at month 6 and maintained thereafter. They were largely maintained in RIS group and ALF group. Improvement in trabecular shape was observed in RIS group and RIS+ALF group at month 6. Significant improvement in trabecular connectivity was observed in RLX+ALF group.

The change in trabecular microstructure and QCT-BMD indicate an increase in mineralization in RIS group and RIS+ALF group. Microstructure was improved in RLX+ALF group. It is suggested that Bisphosphonate and SERM may have different effects on trabecular microstructure.

Disclosures: Kenichiro Matsuzaki, None.

SU0313

Evaluation of Cortical Porosity from HR-pQCT at the Tibia: Comparison with Synchrotron Radiation Micro-computed Tomograph. Agnes Ostertag¹, Sylvie Fernandez², Francoise Peyrin³, Marie-Christine De Vernejoul⁴, Christine Chappard^{*5}.
¹U606 INSERM, France, ²Rhumatisme et Travail Association, France, ³CREATIS ID 19 ESRF, France, ⁴Fédération De Rhumatologie Et INSERM U606, France, ⁵UMR 7052 CNRS, France

The HR-pQCT (XtremeCT Scanco®) with a voxel size at 82 (µm³) is carried out routinely in clinical research protocols. Micro-computed tomography (micro-CT) has

become a standard tool for examination of trabecular and cortical bone in 3 dimensions (3D). The purpose of this study is to evaluate the accuracy and precision of cortical measurements derived from HR-pQCT images using a local comparison with morphological measurements from synchrotron radiation (SR) micro-CT. Thirty tibia specimens (mean age 82.2±9.7) were scanned at 3.5 cm from the tibial pilon. The acquisition and analysis protocols provided by the manufacturer were used. Fourteen samples were scanned twice to calculate the Root Mean Square Coefficient of Variation (RMSCV,%). The usual outcomes include: volumetric bone density (gHA/cm³) for entire (Dtot) and cortical (Dcomp) regions, cortical thickness (Ct.Th,mm). New features as cortical porosity (Ct.Po) and mean pore diameter (mPo.Dm) were measured with manual correction of the endosteal contour. In a site matched region of HR-pQCT images, bone samples were taken at the posterior part of the tibia and imaged on beamline ID19 (ESRF,Grenoble). The acquisition parameters used were 30 keV, 3500 views over 360°, the exposure time for each view was 0.3s. The voxel size is 7.5 (µm³). Ct.Th_SR was manually measured. A unique threshold was used for the whole dataset. Using the CTAn Skyscan® software, the following parameters were obtained: Pore volume/Bone volume (PoV/TV_SR %), pore diameter (Po.Dm_SR,mm), pore spacing (Po.Sp_SR,mm), pore number (Po.N_SR,mm⁻¹) and the degree of anisotropy (DA,no unit). Maps of linear attenuation coefficient were converted into degrees of mineralization of bone (DMB) with data expressed in g/cm³. Pearson correlation coef. (r) between Ct.Th vs Ct.Th_SR was r=0.58**. Correlation coef. were not significant for Dcomp vs DMB and for mPo.Dm vs Po.Dm_SR and PoV/TV_SR. Significant correlation coef. between PoV/TV_SR and cortical parameters from HR-pQCT are shown in Table 1. To explain Dcomp in multivariate analysis, the determination coef (r²) was 0.80 with a combination of PoV/TV_SR, Po.N_SR and Po.Sp_SR instead of 0.77 with PoV/TV_SR alone. In conclusion, Dcomp from HR-pQCT images is the most pertinent parameter reflecting with a good precision cortical porosity measured from SR micro-CT images. Dcomp was not better explained by a combination of morphological parameters from SR micro-CT images.

| Table 1 | PoV/TV_SR | |
|---------|-----------|-----------|
| | (r) | RMSCV (%) |
| Dtot | -0.52** | 0.32 |
| Dcomp | -0.83¥ | 0.20 |
| Ct.Th | -0.68¥ | 0.43 |
| Ct.Po | 0.52** | 3.86 |
| mPo.Dm | 0.30 | 1.86 |

* p<0.05, ** p<0.01, ¥ p10⁻⁴

Table1

Disclosures: Christine Chappard, None.

SU0314

Significance of the Proximal and Distal Parts of the Neck for the Discrimination of Hip Fracture: Results from the Prospective European Femur Fracture Study (EFFECT). Oleg Musevko¹, Valérie Bousson², Judith Adams³, Jean-Denis Laredo⁴, Klaus Engelke^{*1}.
¹University of Erlangen, Germany, ²Hôpital Lariboisière, France, ³Manchester Royal Infirmary, United Kingdom, ⁴Assistance Publique-Hôpitaux de Paris, Hôpital Lariboisière, France

Purpose: The aim of the cross sectional prospective EFFECT study was the discrimination of subjects with and without fresh osteoporotic hip fractures. Earlier, the discriminative power of BMD and cortical thickness as measured by QCT in different VOIs was shown [1]. Here we analyzed the usefulness of additional strength related parameters in the neck.

Methods: 101 women were enrolled in two imaging centers, 44 women with fresh hip fractures (mean age, 81.6 years) and 57 female controls (mean age, 73.4 years). In the 44 fractured women measurements were performed of the non-fractured hip; in the controls the left hip was investigated. In 19 slices perpendicular to the neck axis, which were spaced 1 mm apart (Figure), the following parameters were analyzed using MIAF-Femur: integral and cortical area, buckling ratio (BR), cortical thickness, and integral and polar polar moments of inertia (PMIA). Slice number 0 was centered at the smallest neck cross section, slice numbering increased (decreased) towards the head (trochanter). Between group differences were compared by Student's t-tests. Adjustments were made for age, height and weight.

Results: Consistent with the earlier 3D analysis, in all slices integral and trabecular but not cortical BMD were significantly lower in the fractured group. For none of the slices, integral and cortical area differed between the two groups. Cortical thickness and buckling ratio were also not significantly different between the two groups in the distal part of the neck. However, in slices 7-9, i.e. those closest to the head significant differences, after adjustment for age, height and weight, between fractured and

unfractured subjects were found (see table). The cortical polar moment of inertia values were significantly different close to the center of the neck in slices -1 to -4.

Conclusions: This study confirms the importance of the BMD distribution throughout the neck for hip fracture discrimination but indicates a more important role of proximal femur with respect to cortical thickness and buckling ratio.

This project was in part supported by the German Federal Ministry of Education and Research (BMBF, project BioAsset 01EC1005D).

[1] V. D. Bousson, J. Adams, K. Engelke et al. 2011, JBMR, 26, 881-93



Fig.: location of analyzed slices in the neck

| Significant slices | Parameter | Range of p-values for significant slices (adjusted) | Mean Values Control | Mean Values fractured subjects |
|--------------------|-----------|---|---------------------|--------------------------------|
| 7 to 9 | CortThick | 0.002-0.005 (0.031-0.049) | 2.8-2.7 | 2.61-2.52 |
| 7 to 9 | BR | <0.002 (0.023-0.053) | 1.16-1.28 | 1.26-1.39 |
| -4 to -1 | PMIACort | 0.02-0.19 (0.018-0.048) | 6.71-4.54 | 5.5-4.29 |

table

Disclosures: Klaus Engelke, None.

SU0315

The Suppression Ratio: A MRI Biomarker of Cortical Bone Porosity. Yusuf Bhagat*¹, Cheng Li¹, Shing Chun Benny Lam², Felix Werner Wehrli³.
¹University of Pennsylvania, USA, ²Laboratory for Structural NMR Imaging University of Pennsylvania, USA, ³University of Pennsylvania Medical Center, USA

Cortical bone water, which consists of water bound to collagen and mobile water in the lacuno-canalicular spaces and Haversian pores, can be detected and quantified by ultra-short echo-time (UTE) MRI [1]. The mobile water fraction bears strong clinical relevance as it scales with the expanding pore volume in aging and mainly in osteoporosis. Although impossible in vivo, the quantification of pore water would permit an indirect estimation of porosity. In this UTE-MRI study of the mid-diaphyseal tibia of 32 healthy females (27-81 y.o.) scanned at 3T, we propose to obtain a surrogate measure of porosity in the form of the suppression ratio (SR), i.e. a ratio of the unsuppressed to the soft-tissue suppressed UTE signal intensity. The rationale is that the water in larger pores has longer T2* and will experience a reduction in signal intensity by suppression schemes used to attenuate soft-tissue protons. SR parametric images were obtained via inversion recovery (IR) nulling and dual-band (DB) saturation at 0.35x0.35x5 mm³ voxel size as previously described [2]. The periosteal and endosteal cortical boundaries were segmented to generate a cortical bone mask that yielded mean SR values, cortical thickness and normalized cortical area. Preexisting subject bone water concentration (BWC) and volumetric BMD data [1] were used to determine associations with SR. Axial mid-tibia IR-based SR parametric colormaps and corresponding histograms from young (33 y.o., Fig.1A), middle-aged (55 y.o., Fig.1B) and elderly (74 y.o., Fig.1C) subjects enable visualization of the distribution of SR values per individual. SR histograms were relatively symmetric in the young, and contrasted with those from older subjects becoming increasingly asymmetric with long tails toward high SR values, signifying the presence of large pores. Both methods demonstrated an increase in SR with age (Fig.2), with mean DB-based SR 12% lower than mean IR (p<0.001). Strong inverse associations were seen between SR and cortical BMD, cortical thickness and normalized cortical area (Table), indicating that increased porosity is a consequence of osteoid loss and given a

constant mineralization density, scales with volumetric BMD. BWC was weakly correlated with SR (Table), given that in the young, majority of bone water is collagen-bound. These data suggest that the suppression ratio serves as an in vivo biomarker of cortical porosity.

[1] Rad H. NMR Biomed 24:855 (2011); [2] Li C. Magn Reson Med (in press)

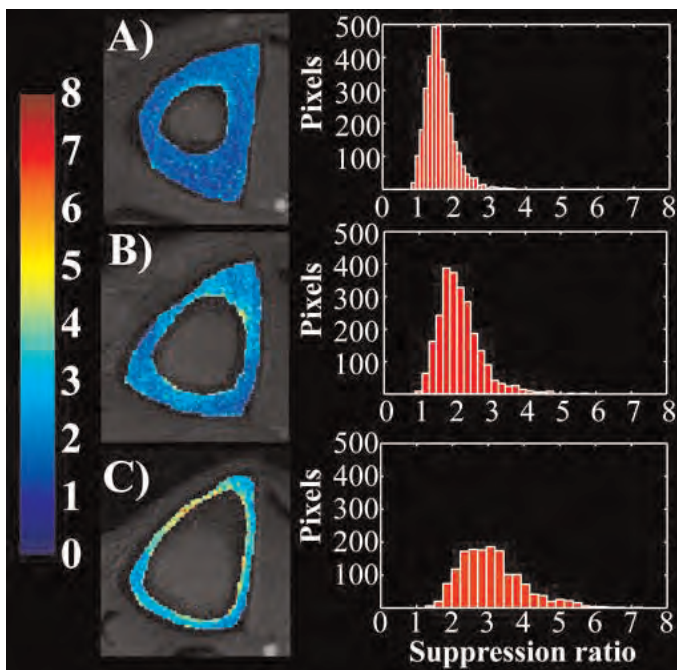


Figure 1: IR-based SR cortical bone water colormaps and histograms

Parameters Suppression Ratio

IR DB

Bone Quality

Cortical BMD (mg/cm³) 0.43 0.44

Bone water conc. (%) 0.27 0.25

Geometry

Cortical thickness (mm) 0.49 0.47

Normalized cortical area 0.58 0.56

Table: Correlations (R², p<0.01) between (IR and DB) and bone quality and geometric parameters

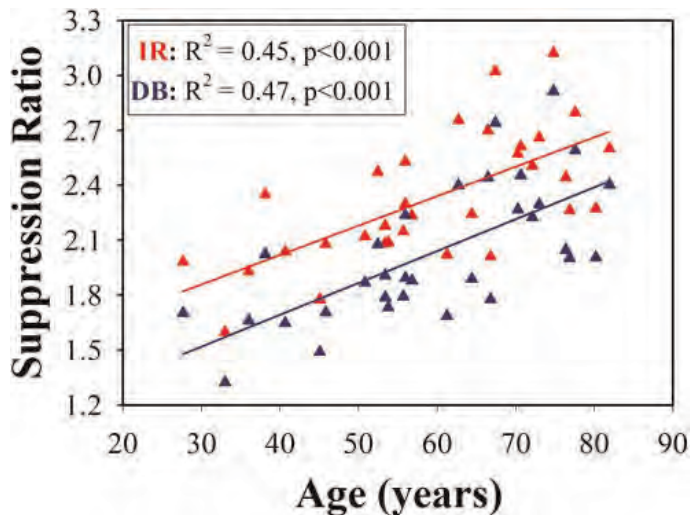


Figure 2: Plot of age vs. suppression ratio for IR and DB-based suppression techniques in 32 women

Disclosures: Yusuf Bhagat, None.

SU0316

Clinical Assessment of the 1/3rd Radius Using a New Desktop Ultrasonic Bone Densitometer. Emily Stein¹, Fernando Rosette¹, Polly Young², Mafo Kamanda-Kosseh², Donald McMahon¹, Gangming Luo³, Jonathan Kaufman³, Elizabeth Shane¹, Robert Siffert⁴. ¹Columbia University College of Physicians & Surgeons, USA, ²Columbia University, USA, ³CyberLogic, Inc., USA, ⁴The Mount Sinai School of Medicine, USA

The objective of this study was to evaluate the capability of a novel ultrasound device (*UltraScan 650*, CyberLogic, Inc., New York, NY, USA) to estimate clinically bone mineral density (BMD) at the 1/3rd radius. The device (Fig. 1) rests on a desktop and is portable, and permits real-time evaluation of the radial BMD. The device measures two (2) net time delay (NTD) parameters, NTD_{DW} and NTD_{CW} . NTD_{DW} is defined as the difference between the transit time of an ultrasound pulse through soft-tissue and cortex only, and the transit time through soft-tissue, cortex and medullary cavity, and the transit time through soft tissue only of equal overall distance. NTD_{CW} is defined as the difference between the transit time of an ultrasound pulse through soft-tissue and cortex only, and the transit time through soft tissue only again of equal overall distance. The square root of the product of these two parameters is a measure of the radial BMD at the 1/3rd location as measured by dual-energy x-ray absorptiometry (DXA). A clinical IRB-approved study measured ultrasonically 49 adults at the 1/3rd radius. The study group consisted of 18 men (mean age 31, range 23-60) and 31 women (mean age 51, range 21-83). BMD was also measured at the same site and time using DXA. The measured mean (standard deviation) BMD was 0.70 g/cm^2 (0.12 g/cm^2) with a range of $0.45 - 0.92 \text{ g/cm}^2$. Linear regression between BMD and the square root of the product $NTD_{DW} * NTD_{CW}$ produced a linear correlation coefficient of 0.93 ($P < 0.001$). These results are consistent with previous computer simulation and *in vitro* studies. In conclusion, although x-ray methods are effective in bone mass assessment, osteoporosis remains one of the largest undiagnosed and under-diagnosed diseases in the world today. The research described here should enable significant expansion of diagnosis and monitoring of osteoporosis through a desktop device that ultrasonically assesses bone mass at the 1/3rd radius.



Fig. 1. UltraScan 650 Bone Densitometer

Disclosures: Jonathan Kaufman, None.

This study received funding from: CyberLogic, Inc., which would like to gratefully acknowledge the support of the National Institute on Aging of the NIH through SBIR Grant No. AG036879.

SU0317

Novel Ultrasound Method for Osteoporosis Screening and Diagnostics. Janne Karjalainen¹, Ossi Riekkinen², Heikki Kroger³, Jukka Jurvelin¹. ¹University of Eastern Finland, Finland, ²Finland, ³Kuopio University Hospital, Finland

As we lack effective screening or diagnostic devices at primary healthcare, over 75% of osteoporotic patients are not diagnosed nor receive treatment for their pathological condition¹. In this study, a novel small size pulse-echo (PE) ultrasound (US) device is introduced for fast single-site US measurements to screen osteoporosis, as well as for multi-site measurements to diagnose osteoporosis

Elderly Caucasian woman ($n = 141$, age = 72.9 ± 6.6 years) were examined using PE US measurements (2.5MHz) of cortical bone thickness in proximal and distal tibia, and distal radius (Bone Index Finland Ltd., Kuopio, Finland). Further, bone mineral density in the femoral neck (BMD_{neck}) and total hip (BMD_{total}) was determined by using axial DXA. Based on DXA, osteoporosis was diagnosed in individuals with T-Score lower than -2.5 in total hip or in femoral neck. US results were combined with the subject characteristics to provide a parameter, Density index, DI^2 (patent pending). Thresholds for DI were determined to reach 90% sensitivity and specificity in diagnostics of osteoporosis^{3,4}. For purpose of screening, the DI was determined by using a single-site US measurement. When the DI was low, below the threshold for healthy human, multi-site measurements were conducted.

A total of 31 subjects were diagnosed to be osteoporotic by DXA. Firstly, by using a single-site US measurement, 56 subjects (40%) were diagnosed to be healthy with no need for additional measurements. Second, by using multi-site US measurements for 85 subjects (60%), 47 subjects (33%) were diagnosed to be non-osteoporotic or osteoporotic (DI was over the healthy or below the osteoporotic threshold, respectively). 38 subjects (27%) were found to require additional DXA measurement to verify the diagnosis. DI, as determined with the multi-site US measurement, provided a significant estimate of BMD_{neck} and BMD_{total} ($r = 0.72-0.74$, $p = 0.001$, $n = 141$).

The present results are encouraging and suggest that the small-size portable US instrument may provide a fast method for osteoporosis screening (< 1 minutes) and the multi-site method (approximately 10 minutes) for diagnostics of osteoporosis at primary healthcare. However, a higher number of subjects should be examined to validate the thresholds with 90% sensitivity and specificity for DI^2 .

[1] Nguyen, Med J Aust 180:2004, [2] Karjalainen, Osteoporos Int, 23:2012, [3] Hans, J Clin Densitom 11:2008, [4] Blake, Osteoporos Int. 16:2005.

Disclosures: Janne Karjalainen, Bone Index Finland Ltd., 3
This study received funding from: Bone Index Finland Ltd.

SU0318

MEF2C is associated with Forearm Bone Mineral Density but not Forearm Osteoporotic Fractures. Hou-Feng Zheng^{*1}, Laura Yerges-Armstrong², Joel Eriksson³, Paul Leo⁴, Ulrica Bergström⁵, William Leslie⁶, David Goltzman¹, Braxton Mitchell⁷, Ulrika Pettersson⁸, Emma Duncan⁹, Mattias Lorentzon¹⁰, Elizabeth Streeten¹¹, Claes Ohlsson¹², Brent Richards¹. ¹McGill University, Canada, ²University of Maryland, USA, ³University of Gothenburg, Sweden, ⁴University of Queensland Diamantina Institute, Australia, ⁵Ortopedkliniken, Sweden, ⁶University of Manitoba, Canada, ⁷University of Maryland, Baltimore, USA, ⁸Clinical Pharmacology, Sweden, ⁹Royal Brisbane & Women's Hospital, Australia, ¹⁰Center for Bone Research at the Sahlgrenska Academy, Sweden, ¹¹University of Maryland School of Medicine, USA, ¹²Center for Bone & Arthritis Research at the Sahlgrenska Academy, Sweden

Background: Forearm fractures affect 1.7 million individuals worldwide each year and most often occur earlier in life than hip fractures. While the heritability of forearm bone mineral density (BMD) and fracture is high, their genetic determinants are largely unknown. Aim: To identify common genetic variants associated with forearm BMD and forearm fractures. Methods: We recently conducted a meta-analysis for forearm BMD, which comprised of 5,371 subjects from 5 cohorts. In current study we conducted conditional and joint analysis of multiple SNPs in genome-wide suggestive region with program GCTA v0.93.9 (<http://gump.qimr.edu.au/gcta/massoc.html>). We then tested the BMD-associated SNPs in 2,023 forearm fracture cases and 3,740 controls. Results: 8 SNPs in or near MEF2C gene showed genome-wide suggestive association with forearm BMD ($1.1 \times 10^{-6} < P < 1.5 \times 10^{-7}$), with the most significant SNP at rs12521522 (-0.20 standard deviations [SD] per A allele, $P = 1.5 \times 10^{-7}$). The joint analysis in 10M region around MEF2C showed that the effect of rs12521522 increased to genome wide significance (-0.43 SD per A allele, $P = 9.0 \times 10^{-19}$). However, this locus was not associated with increased risk of forearm fracture (SNP rs12521522: Odds Ratio = 1.14 [95% CI: 0.92-1.35], $P = 0.14$). Conclusion: Common genetic variation at MEF2C is associated with forearm BMD but not forearm osteoporotic fractures. These findings increase our understanding of the etiology of osteoporosis-related phenotypes.

Disclosures: Hou-Feng Zheng, None.

SU0319

Bone Mineral Density and Other Factors Associated with Incident Fracture among Afro-Caribbean Men. Yahtyng Sheu^{*1}, Jane Cauley¹, Clareann Bunker¹, Alan Patrick², Victor Wheeler², Joseph Zmuda¹. ¹University of Pittsburgh Graduate School of Public Health, USA, ²The Tobago Health Studies Office, Trinidad & tobago

Few studies have examined the risk factors for fracture among African ancestry men. Therefore, we used data from the Tobago Bone Health Study to investigate factors associated with incident fracture among 2,527 Afro-Caribbean men aged 40 and older (mean age, 57 ± 11 years). Demographic information, anthropometric measurements, medical and fracture history, lifestyle factors, and BMD (measured by dual-energy X-ray absorptiometry) were assessed at study entry. Incident fracture was defined if men reported any fracture between the baseline and a follow-up visit that occurred after an average of 4.4 ± 0.8 years. At baseline, 496 men experienced at least one fracture prior to enrollment, of which 74% were due to traumatic events. At follow-up, 28 men reported at least one new fracture. Fracture types included 3 wrist, 4 shoulder, 1 upper arm, 4 rib, 14 ankle, 3 hand and 1 skull fracture. There were no significant differences in age, body weight, height, weight change, body mass index, grip strength, smoking and drinking status, physical activity level, and prevalence of diabetes, cardiovascular disease and falls between men with and without incident fracture. However, those with fractures were less likely to work as farmers ($p=0.036$) and more likely to have had a past history of fracture ($p<0.0001$). In addition, men with incident fracture had lower BMD at the femoral neck (0.94 ± 0.15 vs. 0.99 ± 0.15 g/cm², $p=0.085$) and total hip (1.15 ± 0.15 vs. 1.09 ± 0.15 g/cm², $p=0.018$) than those without a fracture. From age-adjusted logistic regression models, every 1 standard deviation decrease in femoral neck and total hip BMD was associated with a 61% ($p=0.029$) and 75% ($p=0.09$) greater risk of incident fracture. Men with a prior fracture history were also 4 times (odds ratio=4.1; 95% confidence interval=1.9-8.7) more likely to experience a new fracture during follow-up. Working as a farmer was associated with 55% lower risk of incident fracture ($p=0.049$). Consistent with previous findings among other racial/ethnic groups, lower hip BMD and previous fracture history were associated with higher risk of fracture in Afro-Caribbean men.

Disclosures: Yahtyng Sheu, None.

SU0320

Cortical Bone Changes with Aging among Men of African Descent. Yahtyng Sheu^{*1}, Clareann Bunker¹, Christopher Gordon², Alan Patrick³, Victor Wheeler³, Joseph Zmuda¹. ¹University of Pittsburgh Graduate School of Public Health, USA, ²McMaster University, Canada, ³The Tobago Health Studies Office, Trinidad & tobago

Age-related differences in cortical bone geometry have been measured using 3-dimensional imaging techniques primarily in cross-sectional studies and in Caucasians. There are limited data on age-related changes in cortical bone among African ancestry men. Therefore, our study evaluated the patterns and correlates of longitudinal changes in cortical bone geometry among 648 Afro-Caribbean men aged 40 years and above (mean= 59 ± 9 years) recruited from the Tobago Bone Health Study. Peripheral quantitative computed tomography (pQCT) was used to measure total and cortical volumetric bone density (vBMD, mg/cm³) as well as cortical thickness (THK, mm) at the radius and tibia. Demographic information, anthropometric measurements and medical history were assessed at study entry. After approximately 6 years of follow-up (range, 5-7 years), the overall decline in total vBMD, cortical vBMD, and THK were 1.54%, 0.62% and 2.22% at the radius, and 1.92%, 0.76% 2.93% at the tibia (all $p<0.001$). Age was associated with a statistically significant acceleration in the decline in cortical bone parameters, except cortical vBMD at the radius. Every 10 year increase in age was associated with a 0.45% ($p=0.0011$), 0.04% ($p=0.4359$) and 0.90% ($p=0.0009$) greater decline in radius total vBMD, cortical vBMD and THK, respectively. The corresponding decline per 10 years at the tibia was 0.33% ($p<.0001$), 0.29% ($p<.0001$) and 0.32% ($p=0.0101$). Furthermore, men aged 70 years and older were more likely to experience an accelerated rate of decline in vBMD and THK at both skeletal sites compared to those aged 40-49 years, except for cortical vBMD at the radius (Table). In addition to older age, lower lean mass (measured by dual-energy x-ray absorptiometry) and grip strength were also associated with a greater decline in all cortical parameters except radius cortical vBMD. Androgen deprivation treatment for prostate cancer also had a strong and detrimental impact on cortical geometry changes with age (0.83% to 3.9% greater decline for all parameters). Our preliminary longitudinal data document an accelerated decline for cortical bone parameters in older black men compared to their middle aged counterparts and identify several factors associated with these changes.

Table: Percent change in cortical bone parameters over an average of 6 years in youngest and oldest age groups.

| | Age 40-49 (n=95) | Age 70+ (n=98) | p-value |
|---------------|------------------|----------------|---------|
| Radius | | | |
| Total vBMD | -0.63** | -2.08* | 0.0013 |
| Cortical vBMD | -0.52* | -0.69* | 0.3258 |
| THK | -0.37 | -3.40* | 0.0005 |
| Tibia | | | |
| Total vBMD | -1.56* | -2.61* | <0.0001 |
| Cortical vBMD | -0.48* | -1.08* | <0.0001 |
| THK | -2.62* | -3.60* | 0.0140 |

* denoted age-specific changes with $p<0.0001$

** denoted age-specific changes with $0.05 < p < 0.001$

Disclosures: Yahtyng Sheu, None.

SU0321

Dental Factors Predicting Systemic Osteoporosis: Alveolar Bone Mineral Density (al-BMD) and Microdamage Compared with Lumbar Bone Mineral Density (LBMD). Yoshitomo Takaishi^{*1}, Takashi Sugishita¹, Aiko Kamada², Takashi Ikeo², Takami Miki³, Takuo Fujita⁴. ¹Takaishi Dental Clinic, Japan, ²Osaka Dental University, Japan, ³Osaka City University Medical School, Japan, ⁴Katsuragi Hospital, Japan

Background: Osteoporosis and periodontal diseases both affect a large proportions of the population. Jawbone supporting the teeth is affected by osteoporosis just like other bones, and characterized by its reflection of the process of periodontal disease. However, the relationship between periodontal disease and osteoporosis has not been established.

Purpose: Extending our observation on the association of osteoporotic fracture with al-BMD and alveolar bone microdamage demonstrated by computerized radiogrammetry and stereoscopically magnified X-ray film (Bone Right), contributions of dental and periodontal factors to systemic fracture were analyzed in detail by logistic regression analysis.

Materials and Methods: In 31 subjects consulting dental clinics for oral care to prevent periodontal disease, al-BMD and number of microdamages were measured by Bone Right method along with number of teeth lost, pocket depth, attachment level, markers of bone turnover such as bone specific alkaline phosphatase (BAP) and deoxypyridinoline (DPD) and urine Ca/Cr, in addition to LBMD by DXA. Correlation coefficient diagram was constructed and multiple logistic regression analysis was performed, using these dental factors and age and years after menopause as independent variables and fracture in other parts of the skeleton as the dependent variable.

Results: Systemic fracture was positively correlated with number of teeth lost and DPD. Positive correlation was found between alveolar bone microdamage and years after menopause or BAP. Multiple regression analysis using age, LBMD, al-BMD, BAP as independent variables and fracture as dependent variable indicated a significant contribution of al-BMD ($p=0.0109$), number of microdamage ($p=0.0045$) and pocket depth ($p=0.0492$), but not LBMD ($p=0.1563$), age ($p=0.2524$), BAP ($p=0.9646$), DDP ($p=0.4048$), and attachment level ($p=0.7496$).

Conclusion: Dental factors including al-BMD, alveolar bone microdamage and to a lesser extent, pocket depth appeared to predict fracture at site other than jaw bone, but LBMD failed to do so.

Disclosures: Yoshitomo Takaishi, None.

SU0322

Predicting Onset of Transmenopausal Bone Mineral Density (BMD) Loss in Study of Women's Health Across the Nation (SWAN). Gail Greendale¹, Arun Karlamangla¹, Shinya Ishii^{2*}. ¹University of California, Los Angeles, USA, ²Department of Geriatric Medicine, University of Tokyo, Japan

Background: A period of rapid BMD loss brackets the final menstrual period (FMP), starting ~1 year before it and lasting for ~2 years after it. To be able to prevent this rapid bone loss, we must know when its onset is approaching. Objective: To establish whether (and how well) we can determine if a woman is approaching or has crossed the time when trans-menopausal BMD loss typically starts (1 year prior to FMP). Methods: The study sample included 1777 observations from 446 women, pre- or early peri-menopausal at baseline, who had annual BMDs for up to 1 year after they experienced an FMP and contemporaneous serum samples. Candidate primary predictors for having reached 1 year prior to the FMP were current measurements of serum estradiol [E2] and follicle stimulating hormone [FSH] and creatinine-normalized urinary N-telopeptide [NTX], relative to each woman's measurements of the same analytes during pre- or early perimenopause when she was at least 2 years prior to the FMP. Covariates added to augment prediction were age, race/ethnicity, body mass index, current smoking and menopause transition stage. We used modified Poisson regression to model the probability of having crossed the typical rapid bone loss onset point (1 year prior to FMP), and employed generalized estimating equations to account for within-woman correlations in repeated measures. Candidate models were compared for discrimination ability using the area under the Receiver Operating Curve (AUC). Parallel analyses were conducted to predict timing (before vs. after) relative to 2 years prior to FMP. Results: Current values of E2 and FSH (expressed as fraction or multiple of each woman's own baseline value, log-transformed) predicted timing relative to both 1 and 2 years prior to the FMP well (Table). Adding NTX and previous year values of E2 and FSH did not improve prediction. Conclusion: The ratio of current to baseline E2 and FSH along with 5 clinical variables can predict if a woman is 1 year prior to her FMP. Support: NIH/ DHHS, through the NIA, NINR and the NIH ORWH (Grants NR004061; AG012505, AG012535, AG012531, AG012539, AG012546, AG012553, AG012554, AG012495).

| Candidate Models | AUC for 2y prior to FMP | AUC for 1y prior to FMP |
|-----------------------|-------------------------|-------------------------|
| E2 + FSH | 0.773 | 0.826 |
| NTX | 0.592 | 0.613 |
| E2 + FSH + NTX | 0.774 | 0.827 |
| E2 + FSH + covariates | 0.892 | 0.927 |

Table

Disclosures: Shinya Ishii, None.

SU0323

Vertebral Bone Marrow Fat Associated with Lower Trabecular BMD and Prevalent Vertebral Fracture in Older Adults. Ann Schwartz^{1*}, Trisha Hue¹, Thomas Lang¹, Sigurdur Sigurdsson², Tamara Harris³, Clifford Rosen⁴, Vilundur Gudnason², Eric Vittinghoff¹, Kristin Siggeirsdottir², Gunnar Sigurdsson⁵, Keerthi Shet¹, Lisa Palermo¹, Xiaojuan Li¹. ¹University of California, San Francisco, USA, ²Icelandic Heart Association Research Institute, Iceland, ³Intramural Research Program, National Institute on Aging, USA, ⁴Maine Medical Center, USA, ⁵Landspítali, Iceland

Previous studies in women have reported a negative correlation between vertebral bone marrow fat (BMF) and bone density (BMD). This may result from a direct local effect of marrow fat on bone cells and/or from a shift in stem cell lineage allocation towards adipogenesis and away from osteoblastogenesis. Little is known about the separate associations of marrow fat with trabecular and cortical bone. To assess these relationships in older adults, we used data from the AGES-Reykjavik cohort.

Vertebral BMF was measured in 302 participants. Quantitative computed tomography (QCT) and dual x-ray absorptiometry (DXA) scans of the hip and spine, including DXA assessments of vertebral fracture, were also obtained. BMF (ratio of fat to water plus fat, %) was measured with magnetic resonance spectroscopy (MRS) (1.5 Tesla) at L1 through L4. Participants with recent use of a bone-active medication (N=44) were excluded from these analyses. The relationships between average BMF (L1-L4) and log-transformed bone outcomes were assessed using linear regression models, adjusted for age ($X=79 \pm 3.8$ years), body mass index (BMI) ($X=27.7 \pm 3.8$ kg/m²), and diabetes status (5%). Mean BMF (L1-L4) was $53.5 \pm 8.1\%$ in men and $55.0 \pm 8.4\%$ in women. Those with prevalent vertebral fracture (32 women, 21 men) had higher mean BMF (56.3% vs 53.4%, $p=0.025$) in models adjusted for age, sex, diabetes and trabecular spine vBMD. BMF was associated with QCT-derived trabecular BMD in the spine for men and women and in women with femoral neck trabecular BMD (results in table below.) Total hip aBMD (DXA) (-0.3% for each 1% increase in BMF, $p=0.037$), but not spine aBMD (DXA), was negatively correlated with BMF in women only. In conclusion, we observed correlations with marrow fat and trabecular, but not cortical, bone. Higher marrow fat was associated with prevalent vertebral fracture, even after adjustment for trabecular spine BMD.

Table. Percent difference* in QCT outcome for each 1% increase in vertebral marrow fat

| QCT measurement | Men (N=118) | | Women (N=140) | |
|--------------------------------|--------------|--------------|---------------|--------------|
| | % difference | 95% CI | % difference | 95% CI |
| Spine | | | | |
| Trabecular BMD | -1.18 | -2.11, -0.23 | -2.07 | -3.15, -0.98 |
| Integral BMD | -0.16 | -0.59, 0.27 | -0.70 | -1.11, -0.29 |
| Vertebral compressive strength | -0.65 | -2.05, 0.78 | -2.58 | -3.83, -1.33 |
| Femoral neck | | | | |
| Trabecular BMD | 0.73 | -0.10, 1.58 | -0.87 | -1.60, -0.13 |
| Cortical BMD | 0.04 | -0.16, 0.24 | -0.04 | -0.20, 0.13 |
| Integral BMD | 0.16 | -0.25, 0.57 | -0.27 | -0.64, 0.10 |

*Adjusted for age, BMI, diabetes status

Table

Disclosures: Ann Schwartz, None.

SU0324

Higher Plasma Methylmalonic Acid (MMA) Concentration is Associated with Lower Bone Volumetric Density, Size and Strength: The Framingham Osteoporosis Study. Robert McLean^{1*}, Paul Jacques², Jacob Selhub², Kerry Broe³, Xiaochun Zhang⁴, Marian Hannan⁵, Mary Bouxsein⁶, Douglas Kiel⁷. ¹Hebrew SeniorLife Institute for Aging Research & Harvard Medical School, USA, ²Jean Mayer US Dept of Agriculture Human Nutrition Research Center on Aging at Tufts University, USA, ³Institute for Aging Research Hebrew SeniorLife, USA, ⁴Institute for Aging Research Hebrew SeniorLife, USA, ⁵HSL Institute for Aging Research & Harvard Medical School, USA, ⁶Beth Israel Deaconess Medical Center, USA, ⁷Hebrew SeniorLife, USA

Low vitamin B12 status has been associated with increased fracture risk, yet it is unclear whether this relation is due to effects on BMD. Our previous work in the Framingham Offspring cohort suggested lower plasma vitamin B12 concentration may be associated with worse spinal QCT bone measures, yet effects were small and not statistically significant. Because B12 circulates in an inactive form, plasma vitamin B12 has limited sensitivity and specificity to identify poor vitamin B12 status. Plasma MMA is a specific marker of functional vitamin B12 status and elevated concentration is a sensitive indicator of B12 inadequacy. To further test the hypothesis that lower vitamin B12 is associated with worse bone health in a larger sample and using a more sensitive indicator of B12 status, we determined the cross-sectional association between plasma MMA concentration and QCT measures of spinal bone density, size and strength among 3,162 community-dwelling men and women from the Framingham Offspring and 3rd Generation cohorts. Plasma MMA (pmol/mL) was measured via LC/MS (inter-assay CV=5.5%) from fasting blood samples obtained in 1998-2001 (Offspring) and 2002-05 (3rd Generation). QCT scans of the lumbar spine ascertained in 2002-06 were used to measure trabecular volumetric BMD (Tb.vBMD, g/cm³), integral volumetric BMD (Int.vBMD, g/cm³), cross-sectional area (CSA, cm²) and estimated compressive strength (N) at L3 using custom software. Quartiles of MMA suggested a threshold, thus analysis of covariance compared adjusted least squares mean QCT bone measures in the upper quartiles combined (Q3-Q4) to the lower quartiles combined (Q1-Q2), adjusting for sex, age, height, and BMI. Mean age of participants was 52 yrs (range 31-86) and 48% were female. Tb.vBMD, Int.vBMD and estimated strength in Q3-Q4 were significantly ($P<0.05$) lower (2.1-3.4%) compared to Q1-Q2 (Table). CSA in Q3-Q4 was 0.9% lower ($P=0.04$) compared to Q1-Q2. Results were similar after further adjustment for cigarette smoking, alcohol consumption, physical activity, and estrogen use and menopause status in women. Using a more functional measure of vitamin B12, our results suggest that lower B12 status is associated with worse volumetric bone density, size and strength in the lumbar spine, though the effect may be modest. Because vitamin B12 status is easily modified, longitudinal studies are needed to support vitamin B12 supplementation as a potential measure for maintaining bone health.

| QCT bone measure | MMA quartile ^b | | P-value |
|-------------------------------|---------------------------|---------------|---------|
| | Q1-Q2 | Q3-Q4 | |
| Tb.vBMD (g/cm ³) | 0.145 (0.001) | 0.140 (0.001) | 0.003 |
| Int.vBMD (g/cm ³) | 0.190 (0.001) | 0.186 (0.001) | 0.006 |
| CSA (cm ²) | 11.4 (0.03) | 11.3 (0.03) | 0.04 |
| Compressive strength (N) | 4510.1 (26.4) | 4377.8 (26.5) | 0.0007 |

^aAdjusted for sex, age, height, BMI
^bMMA (pmol/mL) range for quartiles: Q1-Q2, 45-141; Q3-Q4 142-6225

Table

Disclosures: Robert McLean, None.

SU0325

Increased Dietary Calcium Intake Is Not Associated With Coronary Artery Calcification. Jung Hee Kim^{*1}, Eu Jeong Ku¹, Ah Reum Khang¹, Ji Won Yoon¹, Kyung Won Kim¹, Eun Jung Lee², Whal Lee³, Sang-Heon Cho¹, Chan Soo Shin⁴. ¹Seoul National University College of Medicine, South Korea, ²Seoul National University Healthcare System Gangnam Center, South Korea, ³Department of Radiology, Seoul National University Hospital, South Korea, ⁴Department of Internal Medicine, Seoul National University College of Medicine, South Korea

Purpose Adequate calcium intake has long been recommended for the prevention and treatment of osteoporosis; however, a recent study reported that calcium intake increased cardiovascular risk. Coronary artery calcification is a reliable predictor of cardiovascular events. We investigated the relationship between dietary calcium intake and coronary artery calcification.

Methods From 2006 to 2009, we recruited 2,710 men and 1,143 women (postmenopausal women, 626) aged 30 years or older and presenting at Healthcare System Gangnam Center of Seoul National University Hospital. We excluded subjects who were taking calcium supplements and those who were seriously ill. Coronary artery calcium scores were measured by using a 16-row multi-slice computed tomography scanner, and dietary calcium intake was assessed using a 24-hour recall diary.

Results Coronary artery calcification did not differ among tertiles of dietary calcium intake. Blood pressure, fasting glucose level, and homeostasis model assessment of insulin resistance were not also different according to dietary calcium intake and In addition, dietary calcium intake did not impact on serum calcium or phosphate level. High serum phosphate level raised the risk for coronary artery calcification.

Conclusion High dietary calcium intake was not associated with coronary artery calcification, but the effect of calcium supplementation on coronary artery calcification requires further study.

Disclosures: Jung Hee Kim, None.

This study received funding from: The Korea Healthcare technology R&D Projects of the Ministry for Health, Welfare & Family Affairs (A110948 and A100675)

SU0326

Nutritional Factors and Osteoporosis at Each Skeletal Site in Korean Adults Aged 50 Years or Older: The Korea National Health and Nutrition Examination Survey 2008-2009. Yong Jun Choi^{*1}, Bu Kyung Kim², So-Yeon An², Yoon-Sok Chung². ¹Ajou University Hospital, South Korea, ²Ajou University School of Medicine, South Korea

Introduction: It has been reported that the vertebral fracture rate is higher in Asians than Caucasians. It is well known that Asians and Caucasians have different life styles, especially in diet. In this study, we calculated the proportion of older adults who have osteoporosis at each skeletal site and investigated if nutritional factors affect osteoporosis at each skeletal site.

Method: We used data from the Fourth Korea Health and Nutrition Examination Surveys (KNHANES) to examine the prevalence of osteoporosis according to the skeletal sites in adults aged ≥ 50 years. We excluded the subjects with comorbidities affecting bone metabolism and divided the subjects with osteoporosis into three groups, spine (osteoporosis only at the spine), femur (osteoporosis only at the femur), and spine and femur osteoporosis (at both spine and femur) groups. The 24-h dietary recall method was used to collect data on food items consumed by participants during the previous 24 h. Information on supplement use was also collected. We compared nutritional factors between the spine and femur groups.

Results: In men, 4.6% had osteoporosis only at the lumbar spine, 1.4% only at the femur and 1.5% at both the spine and femur. In women, 13.2% had osteoporosis only at the lumbar spine, 7.7% only at the femur and 14.1% at both the spine and femur.

The mean age of the spine osteoporosis group was younger than the femur group. After adjustment for age and body mass index, there were no significant differences in nutritional factors between the two groups in men and women. There was also no significant difference in vitamin D level between two groups. After adjustment of age, BMI, vitamin D level, energy intake; protein intake was significantly associated with the lumbar spine bone mineral density (BMD) ($P=0.003$); carbohydrate intake was significantly associated with the total hip ($P=0.007$) and femur neck ($P=0.018$) BMD; calcium intake was associated with the total hip ($P=0.023$) and lumbar spine ($P=0.004$) BMD in women. In men, only calcium intake was associated with femur neck BMD ($P=0.002$).

Conclusion: More Korean older adults had osteoporosis only at the lumbar spine. There were no significant nutritional differences between the spine and femur osteoporosis group. Protein, carbohydrate and calcium intake were associated with BMD in women; only calcium intake was associated with BMD in men.

Disclosures: Yong Jun Choi, None.

SU0327

Social Disadvantage, Bone Mineral Density and Vertebral Wedge Deformities in the Tasmanian Older Adult Cohort. Sharon Brennan^{*1}, Tania Winzenberg², Julie Pasco³, Anita Wluka⁴, Amelia Dobbins³, Graeme Jones⁵. ¹The University of Melbourne, Australia, ²Menzies Research Institute Tasmania, Australia, ³Deakin University, Australia, ⁴Monash University & Alfred Hospital, Australia, ⁵Menzies Research Institute, Australia

Purpose: The relationship between social disadvantage and bone mineral density (BMD) appears complex and remains unclear, and little is known about the association between social disadvantage and vertebral wedge deformities. We aimed to examine the relationship between social disadvantage, BMD and wedge deformities in older adults from the Tasmanian Older Adult Cohort.

Methods: BMD and wedge deformities were measured by dual energy x-ray absorptiometry and associations with extreme social disadvantage was examined in 1,074 randomly-recruited population-based adults (51% female). Socioeconomic status was assessed by Socio-Economic Indexes For Areas values derived from residential addresses using Australian Bureau of Statistics 2001 census data. Lifestyle variables were collected by self-report. Regression models were adjusted for age, body mass index (BMI), dietary calcium, serum vitamin D (25(OH)D), smoking, alcohol, physical inactivity, calcium/vitamin D supplements, glucocorticoids, and hormone therapy (females only).

Results: Compared to other males, socially disadvantaged males were older (65.9yr versus 61.9yr, $p=0.008$), and consumed lower dietary calcium and alcohol (both $p \leq 0.03$). Socially disadvantaged females had greater BMI (29.9 ± 5.9 versus 27.6 ± 5.3 , $p=0.002$) and consumed less alcohol ($p=0.003$) compared to other females. Socially disadvantaged males had fewer wedge deformities compared to other males (33.3% versus 45.4%, $p=0.05$). After adjustment, social disadvantage was negatively associated with hip BMD for females ($p=0.02$), but not for males ($p=0.70$), and showed a trend for positive association with wedge deformities for males ($p=0.06$), but not for females ($p=0.85$).

Conclusions: Social disadvantage appears to be associated with BMD for females, independent of BMI and other osteoporosis risk factors. A lower prevalence of vertebral deformities was observed for males of extreme social disadvantage. Further research is required to elucidate potential mechanisms for these associations.

Disclosures: Sharon Brennan, None.

SU0328

Bone Area of the Radius Contributes to Fracture Risk Independently of Bone Mineral Density. Helena Johansson^{*1}, Anders Odén², Magnus Karlsson³, Eugene McCloskey⁴, John Kanis⁵, Dan Mellström². ¹Swe, ²Centre for Bone & Arthritis Research (CBAR), Sahlgrenska Academy, University of Gothenburg, Sweden, Sweden, ³Skåne University Hospital Malmö, Lund University, Sweden, ⁴University of Sheffield, United Kingdom, ⁵University of Sheffield, Belgium

Bone mineral density (BMD) is calculated from bone mineral content and the bone area of its determination. BMD is known to be associated with fracture risk and osteoporosis is defined using BMD. The aim of the present study was to determine if the bone area as an estimate of bone size was associated with fracture risk independently of BMD.

We studied the relationship between bone area and the risk of hip fracture in 11,179 Swedish women recruited at mammography, a routine screening tool offered to all women. The cohort comprised women aged 45-70 years screened during the years of 1992-1997. Baseline data included general health and life-style questionnaires and measurements of weight, height, body mass index (BMI), BMD and area of the radius measured with Osteometer DTX 200. Incident hip fractures were captured during an average of 13 years follow up (maximum 16 years) from a national register of all hip fractures using a unique personal registration number held by all Swedish citizens. During follow up, 305 women sustained one or more hip fractures. An extension of Poisson regression was used to investigate the relationship between bone area, other

risk variables and the risk of hip fracture. All associations are adjusted for age and time since baseline.

Mean distal radial bone area was 4.1 cm² (range 2.6-5.7) and mean BMD was 0.45 g/cm² (range 0.10-0.80). Bone area rose with age ($r=0.19$, 95% CI: 0.18-0.21) whilst BMD decreased with age ($r=-0.52$, 95% CI: -0.53-0.50). The risk of fracture increased with each SD of lower BMD (hazard ratio per SD 1.35; 95% CI: 1.19-1.52). The risk of fracture increased with each SD of higher bone area, hazard ratio per SD 1.12 (95% CI: 1.00-1.26) and persisted when adjusted for BMD (HR/SD 1.12, 95% CI: 1.00-1.25). When additionally adjusted for BMI the hazard ratio was unchanged (HR/SD 1.14, 95% CI: 1.02-1.28) but when BMI was replaced by height the association between bone area and hip fracture was no longer significant (HR/SD 1.07, 95% CI: 0.95-1.20). When other risk factors such as previous fracture, smoking, BMI and BMD was adjusted for, bone area remained a significant predictor of hip fracture risk but when BMI was replaced by height the association was no longer significant. There was no interaction between age and bone area ($p=0.16$) and neither between age and BMD ($p=0.28$).

These results suggest that the predictive value of radial BMD for hip fracture risk may be enhanced by the adjustment of bone area or height.

Disclosures: Helena Johansson, None.

SU0329

Characteristics and Medication Use Among Women with Osteoporosis Fracture: Analysis of a United States Managed Care Population. Ankita Modi¹, Amber Wilk², Shiva Sajjan³, Panagiotis Mavros³. ¹Merck & Company, USA, ²Virginia Commonwealth University, USA, ³Merck & Co., Inc., USA

Purpose: The study aims to describe characteristics and treatment history of women with osteoporotic fractures in a large managed care population in the US.

Methods: A retrospective analysis using i3 Invision Datamart, a large U.S. claims database, from January 2001 to December 2010 (study period) was conducted. Women 50 years or older who had an osteoporotic fracture during the study period with two years continuous enrollment prior to index date (first fracture date) and one year after index date were included. Women with Paget's disease were excluded. ICD-9 codes were used to identify osteoporotic hip, vertebral and non-vertebral fractures. Osteoporosis therapies included oral bisphosphonates (aendronate, etidronate, ibandronate, risedronate) and non-bisphosphonates (calcitonin, raloxifene, and teriparatide). Characteristics of women included age at fracture, fracture site, Charlson comorbidity index, falls history, use of corticosteroid, estrogen, and nonsteroidal anti-inflammatory drugs. Osteoporosis medication adherence defined as Medication Possession Ratio (MPR) $>=0.80$ during baseline was also assessed.

Results: 193,836 (6.3%) of all women 50 years or older had an osteoporotic fracture during the study period. 49,469 women met eligibility criteria. The mean age at fracture was 66 years. Only 12,724 (25.7%) women had osteoporosis diagnosis history. Osteoporotic index fractures included 12.0% women with hip fractures, 23.4% vertebral fractures, 67.6% non-vertebral fractures, and 3% multiple fractures. At baseline, only 8.2% of women were treated (6.4% with oral bisphosphonate treatment and 1.8% with non-bisphosphonate therapy). 4,043 (37.2 %) of the women were adherent to osteoporosis therapy at baseline. Among those women with osteoporosis diagnosis history, only 2,578 (20.3%) were on osteoporosis medication during 12 months prior to index fracture.

Conclusions: Osteoporosis disease awareness as evidenced by prior diagnosis was low among patients experiencing osteoporotic fractures. A significantly lower proportion, 20.3% of women diagnosed with osteoporosis prior to having a fracture received treatment. Women with fractures should be evaluated for appropriate osteoporosis management to prevent future fractures.

Disclosures: Ankita Modi, Merck & Co., Inc., 7

This study received funding from: Merck & Co., Inc.

SU0330

Differences in Bone Resorption during Royal Marine Training and in Relation to Stress Fracture. Trish Davey¹, Susan Lanham-New², Adrian J. Allsopp¹, Mark Hajjawi³, Timothy Arnett³, Joanne L. Fallowfield¹. ¹Institute of Naval Medicine, United Kingdom, ²University of Surrey, United Kingdom, ³University College London, United Kingdom

Royal Marine (RM) training is recognised as one of the toughest military training programmes in the world. Stress fracture (SF) prevalence is of the order of 5%. Markers of bone turnover provide a method of investigating changes in bone that may progress our understanding of stress fracture pathogenesis and the effects of military training on bone. Previous studies in the military have yielded conflicting results with regards to changes in bone turnover across military training [1-3]. However, bone metabolism in relation to SF during military training has never been investigated. As part of the UK *Surgeon General's Bone Health Project*, the aim of the present study was to compare bone turnover across training, and between recruits who suffered a SF during training and those who did not. Non-fasted venous blood samples were collected for analysis of serum C-telopeptide of collagen cross-links (CTX) as a marker of bone resorption at the start, middle and end of the 32-week RM training programme. Differences between SF and non-SF recruits were investigated by ANCOVA, with age, body weight, and fitness as co-variables. Differences across

training were assessed by repeated measures ANOVA with Tukey's post-hoc test. Serum CTX was lower at the end of training (mean 0.42 \pm SD 0.19 ng.ml⁻¹) compared with the start (0.54 \pm 0.27 ng.ml⁻¹) and middle of training (0.57 \pm 0.29 ng.ml⁻¹) (n=36) ($P<0.001$). CTX did not differ between SF and non-SF recruits at any stage of training. The lower bone resorption at the end of training is contradictory to the literature, where bone resorption markers were elevated at the end of military training programmes [2, 3]. Bone and energy metabolism are closely linked [4], such that the energy-depleted state of recruits following completion of the *Commando Tests* in week-31 may result in a temporary reduction in bone remodelling. The lack of difference in bone resorption between SF cases and controls is consistent with findings in athletes [5]. In conclusion, serum CTX was not useful in predicting SF during military training. The lower bone resorption seen at the end of training warrants further investigation.

1 Etherington, J. et al. *Calcif Tissue Int*, 1999,64 p 389-93

2 Evans, R.K. et al. *Med Sci Sports Exerc*, 2008,40 p S660-70

3 Sheehan, K.M. et al. *Mil Med*, 2003,168 p 797-801

4 Confavreux, C.B. et al. *Mol Cell Endocrinol*, 2009,310 p 21-9

5 Bennell, K.L. et al. *Calcif Tissue Int*, 1998,63 p 80-5

| Stage of Training | Stress fractures | Controls |
|-------------------|-------------------------|-------------------------|
| | Mean \pm SD | Mean \pm SD |
| Start | 0.56 \pm 0.36 n=66 | 0.50 \pm 0.23 n=71 |
| Middle | 0.61 \pm 0.33 n=49 | 0.54 \pm 0.24 n=48 |
| End | 0.42 \pm 0.23 n=14 | 0.43 \pm 0.16 n=22 |

CTX in Stress Fractured Recruits and Controls across RM Training

Disclosures: Trish Davey, None.

SU0331

Explaining the Sex Difference in Fracture Risk: The Role of Muscle Quality. Nguen Nguen, Tuan Nguen*, Dana Bliuc, Jacqueline Center, John Eisman. Garvan Institute of Medical Research, Australia

While it is well-known that men have greater risk of fracture than women, it is not clear which underlying factors are responsible for the difference. Skeletal muscle is one of the most powerful determinants of bone strength. This study was designed to test the hypothesis that measures of skeletal muscle mass account for the sex difference in fracture risk.

The study was designed as a population based prospective investigation, which involved 779 women and 354 men aged 50 or above at baseline. Baseline body composition measures included fat mass, lean mass, and BMD were measured by DXA (GE-Lunar Prodigy). From the whole body scan, we extracted the amount of fat-free mass at the left and right arms, left and right legs. Appendicular muscle mass was estimated as kilograms of fat-free soft tissue in the upper plus lower extremities. Sarcopenia was defined as appendicular skeletal muscle mass/height² less than 2 standard deviations below the mean for young, healthy reference populations. Muscle strength of upper and lower limb is measured using a dynamometer. Muscle quality (MQ) was defined as muscle strength per unit of mass.

During the 10 year median duration of follow-up, 238 women (31%) and 67 men (19%) had sustained a low-trauma fracture. The prevalence of sarcopenia was 21% in men and 20% in women. Increased fracture risk was associated with sarcopenia, but the association was not independent of BMD. Muscle quality in men was not significantly different from women. In either sex, each standard deviation lower in muscle quality was associated with ~30% increased risk of fracture (95% CI: 1.10 to 1.56). In the model with age, BMD and sex, women had greater risk of fracture than men (HR 1.5; 95% CI 1.1 to 2.2). However, when muscle quality was added to the model, the effect was no longer statistically significant, but muscle quality remained an independent predictor.

These results suggest that muscle quality is a predictor of fracture risk, and that the sex difference in fracture risk could be in part explained by the association between muscle quality and fracture.

Disclosures: Tuan Nguen, None.

SU0332

Incidence and Characterization of Fractures in Men Under 65 Years Old with Osteoporosis. Angelika Manthripragada¹, Cynthia D. O'Malley², Ugis Gruntmanis³, Jesse Hall⁴, Rachel Wagman⁵, Paul Miller⁶. ¹Amgen, USA, ²Amgen Inc., USA, ³University of Texas Southwestern Medical Center, Dallas, USA, ⁴Amgen, Inc., USA, ⁵Amgen, Incorporated, USA, ⁶Colorado Center for Bone Research, USA

Purpose: Since there are few epidemiologic data in young men with osteoporosis (OP) we conducted a study to estimate fracture incidence rates (IR) in this population. We characterized fractures by age, type, timing in relationship to diagnosis/treatment, and evidence of related trauma.

Methods: Using claims data from the MarketScan® database, we identified men age 30 to 64 years with an OP diagnosis or related prescription claim between 1/1/2005 and 12/1/2009. The index date was defined as first occurrence of either the OP diagnosis or prescription claim. Men were followed for a minimum of 12 months post-index date, and censored at the earliest of fracture, disenrollment, or 12/1/2010. We estimated fracture IRs by age and fracture type (closed fractures of the hip, pelvis, shaft/distal femur, humerus, distal radius/ulna, proximal radius/ulna, and pathologic and closed fractures of the spine), 6 months prior to the index date, and during the entire study period (pre and post index date). We also estimated the number of fractures associated with trauma, identified by e-codes or the presence of multiple concurrent fractures.

Results: We identified 21,617 men, of whom 50.2% were categorized by OP treatment, 47.6% by OP diagnosis, and the remainder by both. The majority (76.8%) were in the 50-64 years age group, with 6% in the 30-39 year (youngest) age group. Of the 1,800 fractures identified during the study period, 58.6% occurred in the 6 month period before diagnosis/treatment. We determined 302 (16.8%) of all identified fractures were associated with trauma; 59.9% of these occurred prior to diagnosis/treatment. Fracture IRs during the entire study period were highest for spine [IR=16.7 per 100,000 person-years (95% CI 15.7, 17.7)], followed by hip [IR=4.1 per 100,000 person-years (95% CI 3.6, 4.6)]. While fracture rates for spine, hip, and humerus increased with age, fractures of the distal and proximal radius/ulna and shaft/distal femur decreased with age. However the differences across age groups were not significant.

Conclusion: The IR of fractures in young men diagnosed with or treated for OP varies by type, with no significant difference by age, perhaps as a result of limited power or the younger age range within the study population. The majority of fractures occur prior to OP diagnosis/treatment, suggesting that osteoporosis in young men is frequently identified via fracture.

Disclosures: Angelika Manthripragada, Amgen Inc, 7; Amgen Inc, 3
This study received funding from: Amgen

SU0333

Osteoporosis Treatment Following Fragility Fracture Remains Unaddressed Despite Available Therapies and Established Recommendations. Cynthia O'Malley¹, Akhila Balasubramanian², Douglas Dirschl³, Pei-Ran Ho⁴, Joseph Lane⁵, Laura Tosi⁶. ¹Amgen Inc, USA, ²Amgen Inc., USA, ³The University of North Carolina at Chapel Hill, Department of Orthopaedics, USA, ⁴Amgen, Inc, USA, ⁵Hospital for Special Surgery, USA, ⁶Children's National Medical Center, USA

Purpose: Clinical practice recommendations state patients with fragility fracture should be evaluated and treated for osteoporosis (OP) as they are at high risk for future fractures. To determine conformity with these recommendations we assessed the use of pharmacologic OP treatment in a large population cohort of patients with fragility fractures.

Methods: This retrospective database analysis used 2000-2010 data from a large commercially-insured population. Community-dwelling individuals aged ≥ 50 years with a newly diagnosed fragility fracture and no evidence of OP treatment, malignancy, or Paget's disease in 12 months pre-fracture were included. OP treatment (including oral and parenteral bisphosphonates, raloxifene, teriparatide and calcitonin) rates in the 12 months post-fracture were evaluated descriptively with Pearson's chi-squared tests and Cochran-Armitage tests for significance of trends.

Results: The cohort included 88,571 women and 41,984 men with mean ages of 72.3 yrs and 70.5 yrs, respectively. A minority of patients, 18.6% of women and 9.6% of men, initiated OP treatment post-fracture. Treatment rates increased with age, being highest in the 75-84 age group and then declining in the 'oldest old' individuals aged ≥ 85 yrs. Yet even in the 75-84 age group, only 23% of women and 13% of men were treated. The exception to this peak in the 75-84 age group was in women with hip fractures, where rates were consistently 20-22% for all ages except the oldest old. Rates declined to 17% for women ≥ 85 , who accounted for 34% of female hip fractures. For both genders, OP treatment initiation was highest following vertebral fracture, intermediate following hip and lowest following wrist and humerus fractures ($p < 0.0001$). OP treatment rates declined during the study period (Figures 1A, 1B). For women, this was observed across all age groups with treatment rates declining steadily by 6-8% between 2001 and 2010 ($p < 0.0001$). The already low treatment rates among men declined steadily over time for those < 65 yrs while the decline was less pronounced for older men.

Conclusion: OP pharmacotherapy is severely underutilized following fragility fracture, regardless of patient age or fracture site. Treatment rates appear to have declined over the last decade, despite greater emphasis on recommendations for OP treatment following fragility fracture and despite the known increased risk of future fracture conferred by fracture occurrence.

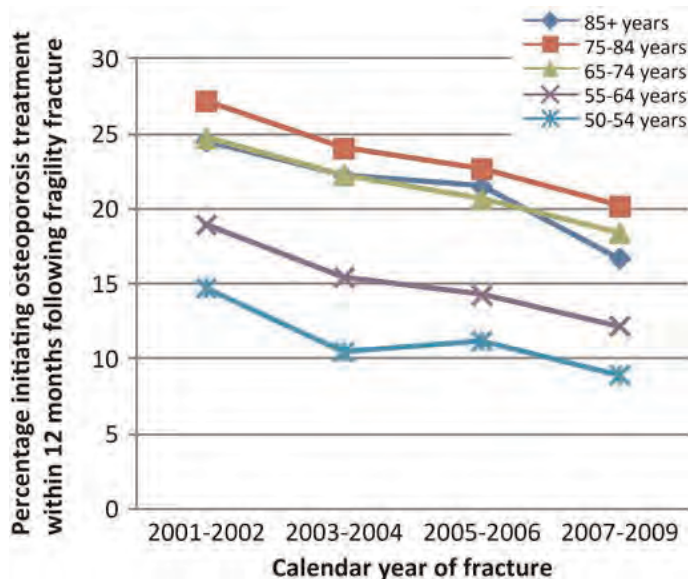


Figure 1A: Time trends in osteoporosis treatment rates following fragility fracture among women

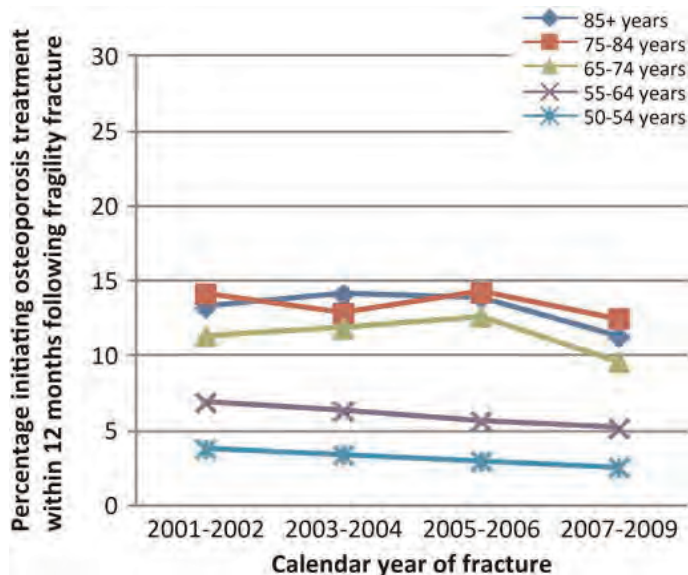


Figure 1B: Time trends in osteoporosis treatment rates following fragility fracture among men

Disclosures: Cynthia O'Malley, Amgen Inc, 7; Amgen Inc, 3
This study received funding from: Amgen Inc

SU0334

Steeply Increase of Hip Fracture Incidence Rate in Jeju Island, South Korea: A Prospective Cohort Study(2002-2011). Yong-Taik Lim^{1*}, Yong-Chan Ha², Young-Kyun Lee³, Jae-Suk Chang⁴, Deog-Yoon Kim⁵. ¹Department of Obstetrics & Gynecology, College of Medicine, the Catholic University, South Korea, ²Chung-Ang University College of Medicine, South Korea, ³Seoul National University Bundang Hospital, South Korea, ⁴Ulsan University, Asan Medical Center, South Korea, ⁵Kyung Hee University Hospital, South Korea

Background: Recently, Some studies reports that incidence of hip fracture in some advanced countries shows steady or decreasing. However, there is no report of long-term trend of hip fracture incidence in developing countries. This prospective longitudinal cohort study was performed to estimate the ten-year hip fracture incidence rate trend of people over 50 years of age in South Korea. **Methods:** Informations of patients over 50 years of age who sustained a hip fracture were obtained from the records of eight hospitals in Jeju Island between 2002 and 2011 to calculate the incidence of hip fractures in this age group. The exclusion criteria were: nonresidents of Jeju Island, patients who sustained traffic accident or major trauma, fractures of the pathologic bone (metastasis), isolated fractures of greater trochanter or lesser

trochanter, and fractures of the subtrochanteric region. Results: There were 2055 hip fractures during the study period. Annular number of hip fractures rose from 151 in 2002 to 304 in 2011. The crude fracture incidence in woman also increased remarkably from 165.4/100,000 to 245.5/100,000. However, the crude fracture incidence in man was steady during ten years (71.3/100,000 in 2002 and 83.7/100,000 in 2011). Conclusion: The total number of hip fracture increase twofold and incidence rate of hip fracture in women also steeply increase during ten-year study period. Therefore, hip fractures in developing country is raising socioeconomic concern with the rapid aging of the population in South Korea.

Disclosures: Yong-Taik Lim, None.

SU0335

The Association between Fracture Site and Obesity in Men: a Population-based Study. Melissa Premaor^{*1}, Juliet Compston², Daniel Martinez-Laguna³, Xavier Nogues⁴, Adolfo Diez-Perez⁵, Daniel Prieto-alhambra⁶. ¹Federal University of Santa Maria, Brazil, ²University of Cambridge School of Clinical Medicine, United Kingdom, ³Primary Care Department, Institut Català de la Salut, Spain, ⁴Institut Municipal D'Investigació Mèdica, Spain, ⁵Parc De Salut Mar, Spain, ⁶Institut Municipal D'Investigació Mèdica, United Kingdom

Background: Our group has previously reported a site-dependent association between obesity and fracture in women, with an increased risk of proximal humerus fractures and a decreased incidence of hip, clinical spine, wrist/forearm, and pelvic fractures in obese women. In this study we evaluated the relationship between body mass index (BMI) and fracture site in men aged ≥ 65 .

Methods: We carried out a population-based cohort study using data from the SIDIAP^Q (Sistema d'Informació per al Desenvolupament de l'Investigació en Atenció Primària) database. SIDIAP^Q contains the primary care computerized medical records of >1,300 GPs in Catalonia (North-East Spain), with information on a representative 30% of the population (>2 million people). SIDIAP^Q is further linked to the official hospital discharge database. In 2009, 186,171 men ≥ 65 were eligible, of whom 139,419 (74.9%) had an available BMI measurement. For this analysis men were categorized as underweight/normal (2, n=26,298), overweight (25 - 2, n=70,851), obese 1 (30 - 2, n=35,142), and obese 2 (≥ 35 kg/m², n=7,128). Fractures were ascertained using ICD codes. We estimated adjusted rate ratios (RR; adjusted for age, smoking, alcohol drinking, use of oral corticosteroids and Charlson co-morbidity index) to compare the categories using Poisson Regression.

Results: A statistically significant reduction in clinical spine and hip fractures [Figure] was observed in obese 2 (RR [95% CI] 0.65 [0.44,0.96] and 0.50 [0.35,0.72]), obese 1 (0.65 [0.52,0.81] and 0.65 [0.55,0.77]), and overweight men (0.77 [0.64,0.92] and 0.63 [0.55,0.72]) when compared with underweight/normal men. Additionally, obese 1 men had fewer wrist/forearm (RR 0.76 [0.60,0.97]) and pelvic (RR 0.39 [0.23,0.66]) fractures than underweight/normal men. Conversely, multiple rib fractures were more frequent in overweight (RR 3.42 [1.03,11.37]) and obese 2 men RR 7.39 [1.84,29.77]), and a borderline significant (p=0.07) increased risk was seen in the obese 1 (RR 3.22 [0.90-11.46]). Proximal humerus and tibia fracture incidence was similar across all BMI categories.

CONCLUSION: In these older men, being obese or overweight was associated with significantly lower risk of hip, clinical spine, wrist/forearm and pelvic fracture. Increased risk was only seen for multiple rib fractures, suggesting gender-related differences in the effects of obesity on fracture risk.

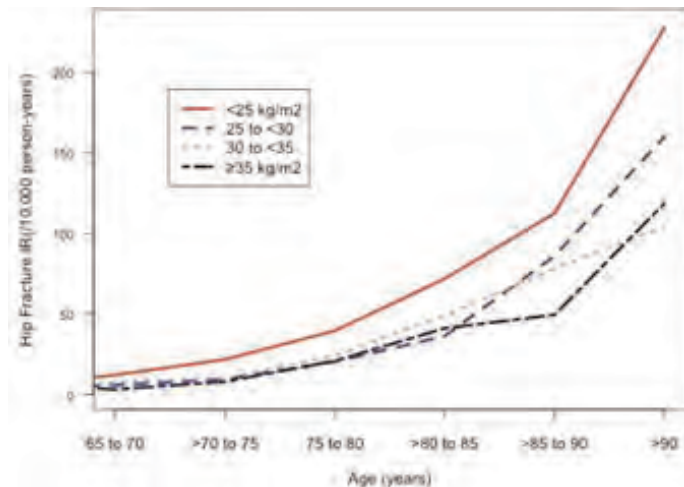


FIGURE. Age-specific hip fracture Incidence Rates (/10,000 person-years) in men aged 65 and older fo

Disclosures: Melissa Premaor, None.

SU0336

Use of Administrative Data for National Surveillance of Osteoporosis and Related Fractures in Canada: Results from a Feasibility Study. William Leslie^{*1}, CCDSS Canadian Chronic Disease Surveillance System Osteoporosis Working Group². ¹University of Manitoba, Canada, ²Public Health Agency of Canada, Canada

Purpose: To evaluate the feasibility of using administrative data to identify diagnosed osteoporosis and the most common sites for fractures due to osteoporosis (hip, forearm, vertebra, humerus and pelvis) for national monitoring through the Canadian Chronic Disease Surveillance System (CCDSS).

Methods: Five provinces (British Columbia=BC, Alberta=AB, Manitoba=MB, Ontario=ON and Quebec=QC) carried out population-based record linkage analyses to test multiple algorithms combining hospitalizations (H), physician visits (P) and use of osteoporosis prescription drugs. International Classification of Diseases (ICD) 9th Revision and 10th Revision in addition, drug identification number (DIN) codes were used. The adopted algorithm for osteoporosis (ICD-9-CM: 733.x and ICD-10-CA: M80, M81) was based on 3 years of data while the algorithms for fractures were based on 1 year of data. Osteoporosis prevalence and fracture incidence estimates (age-standardized to the 1991 Canadian population) were disaggregated by sex and province from 1995/96 to 2007/08.

Results: The age-standardized prevalence of diagnosed osteoporosis in those 65+ increased over time: 1H or 1P in 3 years produced estimates ranging from 8.4 to 14.6% for 2007/08. All provinces demonstrated consistency in age and sex patterns with prevalence of diagnosed osteoporosis being higher in women and increasing with age. These results are consistent with previous validation work (Leslie et al: Osteoporos Int 2011). While adding drug data produced higher estimates compared to the corresponding algorithm without drug data, these data are not available in all jurisdictions. The age-standardized incidence of fractures in those 40+ showed similar sex and age patterns in all provinces. The highest level of agreement across jurisdictions was among hip and humerus fracture rates, with wider regional variation for forearm, vertebra and pelvis fractures.

Conclusions: The algorithms adopted by the CCDSS will be suitable for the national monitoring of diagnosed osteoporosis, hip and non-hip fractures. Physician coding practices likely contribute to the provincial variations observed in forearm, vertebra and pelvis fracture rates given the highly consistent hip fracture rates which are predominately derived from hospitalization data. Diagnosed osteoporosis is dependent on bone mineral density testing and differences in access likely contribute to the provincial variations observed in osteoporosis prevalence.

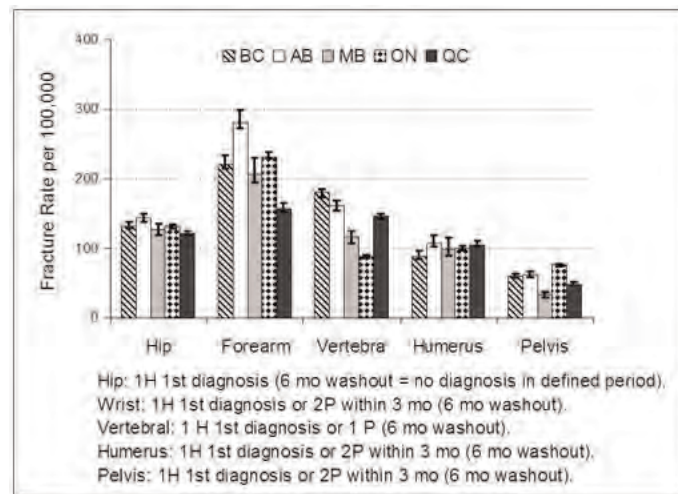


Figure: Age-standardized fracture rates (95% CI) for women and men combined (age 40+), 2007/2008.

Disclosures: William Leslie, None.

SU0337

Genetic Influence of Age-Specific Factors on Bone Traits: Results From a Linkage Analysis of an Australian Cohort. Sing Nguyen^{*}, Jacqueline Center, John Eisman, Tuan Nguyen. Garvan Institute of Medical Research, Australia

Though genome-wide association studies have been largely successful in identifying the common variants associated with diseases such as osteoporosis, they are quickly facing the limitations posed by issues such as numbers needed to detect, missing heritability, and the prevalence of rare variants. There is therefore merit in returning to methods such as linkage analysis, which are able to avoid these issues.

The Dubbo Osteoporosis Genetics Study is a large multi-generational family study aimed at identifying the genes influencing measures of osteoporosis such as bone mineral density (BMD) and quantitative ultrasound (QUS) measures. We previously performed a variance components linkage analysis using SOLAR on a discovery set of

500 related individuals, finding a novel loci associated with femoral neck BMD, as well as multiple suggestive linkage signals for lumbar spine and total body BMD at previously identified loci.

We have since increased the number of genotyped individuals and have extended the analysis to include a further 500 related individuals. Initial linkage analysis of this extended cohort failed to replicate our previous results for BMD, but did reveal multiple suggestive linkage signals for QUS measures. In order to identify potential age- and sex-specific linkage, we stratified our data and performed further linkage analyses. Whilst sex-specific analyses failed to identify any significant linkage, we were able to identify in our age-specific cohorts several suggestive linkage signals for femoral neck BMD not previously identified in either the discovery or extended cohort. This suggests the presence of genes which may act upon bone at different stages of life.

Disclosures: Sing Nguyen, None.

SU0338

Genome-Wide Mapping of Promoter Methylation in Osteoporotic Bone Tissue. Jesus Delgado-Calle¹, Agustín F. Fernández², María Teresa Zarrabeitia³, Carolina Sañudo¹, María Isabel Pérez-Nuñez⁴, Manuel Sumillera⁴, Jesús Sainz⁵, Mario F. Fraga², Jose Riancho*⁶. ¹IFIMAV-H.U. Marqués de Valdecilla-University of Cantabria, Spain, ²Cancer Epigenetics Laboratory. Instituto Universitario de Oncología del Principado de Asturias (IUOPA), HUCA, University of Oviedo., Spain, ³Unit of Legal Medicine, University of Cantabria, Spain, ⁴Department of Orthopaedic surgery & Traumatology. Hospital U.M. Valdecilla, Spain, ⁵IBBTEC, University of Cantabria, Spain, ⁶University of Cantabria, Spain

Environmental influences induce epigenetic marks, and specifically DNA methylation that, in turn, lead the differentiation programs for cell fate. We hypothesized that methylation marks could contribute to the pathogenesis of osteoporosis and explored the methylation profile of osteoporotic bone.

DNA was isolated from femoral bone samples obtained from patients with osteoporotic hip fractures (FRX; 27 women, age 80±4 y) and controls with osteoarthritis (OA; 26 women, age 75±6 y). Genomewide profiling of DNA methylation was performed with the Illumina Infinium 27k arrays which analyze 26300 CpG sites. Beta values, which are proportional to the methylation rate (range 0-1) were estimated for each CpG site. The methylated/unmethylated ratios were computed, log-transformed, quantile-normalized and compared by t-tests, with multiple test correction by the Benjamini method (FDR). Genomewide transcriptome was analyzed by ultra-sequencing of reverse-transcribed RNA isolated from pools of FRX and OA bone samples.

The average methylation level was similar in both groups (beta 0.273 in FRX and 0.276 in OA), with a strong correlation between them (r=0.989). There was a marked inverse correlation between methylation and gene transcription (r=-0.32 in FRX and -0.30 in OA; both p<0.0001). The comparison of beta values in both groups revealed statistically significant differences (FDR<0.05) in 241 loci. Most of these differentially methylated regions (DMR) were part of true CpG islands, located within 600 kb of the TSS. In 217 loci methylation levels were higher in OA than in FRX. In 128 loci the differences in beta values between FRX and OA was >0.05, and in 45 they were >0.10. Pathway analysis with DAVID webtool showed that DMRs were over-represented in glycoprotein signaling, neuronal differentiation, adherence, homeobox proteins and cell proliferation. Text-mining analysis with GRAIL software (restricted to the 45 genes with beta value differences >0.1) revealed underlying connections between 13 genes (p<10E-5), including IRX2, IRX4, TLX3, FGF4, HOXA9 and SOX1.

In conclusion, analysis of bone DNA from patients with osteoporotic fractures and osteoarthritis reveals a number of differentially methylated sites. Unexpectedly, most of them do not include classical bone candidate genes and may point to new gene pathways playing a role in common skeletal disorders.

Founding: Instituto de Salud Carlos III (PI 09/539). JDC has a grant from IFIMAV.

Disclosures: Jose Riancho, None.

SU0339

Population Differences in Rates of Change for pQCT Measures at the Radius in Adult Males. Howard Wey*¹, Teresa Binkley¹, Maggie Eilers², Lee Weidauer¹, Bonny Specker¹. ¹South Dakota State University, USA, ²Creighton University, USA

We previously described differences in cross-sectional pQCT measurements of BMC, vBMD, and bone size at the radius between populations living in rural (Hutterite and non-Hutterite) and non-rural settings (Bone 35: 1389-1398, 2004). Both Hutterite and rural men have greater total bone area at the 20% site than non-rural men, and Hutterite men have smaller cortical thickness than both rural and non-rural men. We report here on rates of change for pQCT measurements at the 20% radius for these male populations. The data include body composition and pQCT measurements on these individuals collected every 18 months for up to 5 years of this ongoing study. Linear mixed models are used to estimate rates of change in bone measures and include baseline age, height, lean mass, fat mass, group (H, R, or NR), time (since

baseline), and interactions of time with age with time and group. Significant associations with group were found for cortical thickness, cortical area, cortical BMC, and cortical vBMD that depended on age. For cortical thickness in young males (20-25 years), the rate of change for H was positive and greater than both R (zero rate) and NR (negative rate); as populations aged, the rate of change became negative and not significantly different among populations. For cortical area, BMC, and vBMD in young males (20-25 years), the rate of change for H was positive and greater or equal to R (positive rate), but greater than NR (zero rate) for all bone measures. As populations aged, the rates became negative and the order reversed (NR and R a smaller negative rate than H). Inclusion of grip strength eliminated significant group differences in rates of change for cortical thickness and vBMD, but not cortical area and BMC. Addition of a physical activity measure did not further change the significance of group effects. For all three populations, the rate of change in total area at the 20% radius was significantly greater than zero up to age 60 years of age (except 20-25 years for R: p=0.1). The continued increase in total area at older ages (40-50 years) suggests all populations may adapt to decreasing vBMD at these ages by increasing bone size. Furthermore, the lack of population differences in total area at any age suggests that the difference in bone size that exists in cross-sectional samples may result from population difference bone growth during adolescence.

Disclosures: Howard Wey, None.

SU0340

The Impact of Educational Interventions for Osteoporosis on Calcium and Vitamin D Supplementations After a Fragility Fracture. Louis Bessette*¹, Claudia Beaudoin², Sonia Jean³, Louis-Georges Ste-Marie⁴, Jacques Brown⁵. ¹Centre Hospitalier De L'Université Laval, Canada, ²Crchuq Research Centre-chul, Canada, ³INSTITUT NATIONAL DE SANTÉ PUBLIQUE DU QUÉBEC, Canada, ⁴CHUM, Canada, ⁵CHUQ Research CentreLaval University, Canada

Purpose: To investigate the impact of educational interventions on consumption of calcium (Ca) and vitamin D (D) supplement in women (>50y old) after a fragility fracture (FF).

Methods: This study was part of the Recognizing Osteoporosis and its Consequences in Quebec (ROCQ) programme. Women who recently suffered a FF were recruited from hospitals and from an administrative database-generated list (Quebec Ministry of Health). Six to eight months after FF, women were contacted to complete questionnaires and were randomized into one of three groups: 1) usual care (UC), 2) written materials (WM) or 3) videocassette and written materials (VC). The WM consisted of information on FF, osteoporosis and the need for treatment following FF, and were provided to the patient and their primary care physician. The 15-minute video consisted of similar information, but went into greater depth. Women in the UC group were told that their fracture was related to osteoporosis but did not receive the educational tools. Groups were compared for difference change distributions in consumption of Ca and D supplement before randomization and 12 months afterwards, and for proportions of women improving their consumption.

Results: Tables 1 and 2 present the results of the analyses among 1) women without diagnosis and treatment for osteoporosis and 2) women taking no supplement at randomization. For women without diagnosis and treatment, the mean increase in Ca supplement in the UC, WM, and VC groups was 33, 93, and 91 mg/day, respectively (p-value: WM vs UC=0.163, VC vs UC=0.026, WM+VC vs UC=0.038). For D supplements, the mean increase in the UC, WM, and VC groups was 58, 105 and 118 IU/day, respectively (p-value: WM vs UC=0.214, VC vs UC=0.012, WM+VC vs UC=0.029). The proportion of women who increased their Ca and D intake by supplements was similar in all 3 groups (Ca: 19 to 25% and D: 23 to 29%). For women taking no supplement at randomization, results showed a greater impact of the intervention: 30%, 28%, and 21% started taking Ca in WM, VC and UC group, respectively; 33% started taking D in both intervention groups and 24% in the UC group.

Conclusions: Educational interventions on osteoporosis improved Ca and D supplement consumption in women who have recently suffered a FF, principally in the subgroup of women who were not taking supplement at randomization.

| Group | Without diagnosis and treatment for osteoporosis at randomization (N=1,175) | | | Without consumption of calcium supplement at randomization (N=637) | | |
|-------|---|---------|----------------------|--|---------|----------------------|
| | Δ | p-value | % who ↑ their intake | Δ | p-value | % who ↑ their intake |
| UC | 33.0 | Ref | 19.4 | 162.6 | Ref | 21.1 |
| WM | 92.6 | 0.163 | 24.6 | 248.7 | 0.024 | 30.4 |
| VC | 90.5 | 0.026 | 23.0 | 215.6 | 0.104 | 27.8 |
| WM+VC | 91.5 | 0.038 | 23.8 | 230.6 | 0.030 | 28.9 |

UC: Usual care, WM: Written materials, VC: Videocassette

Δ: Mean difference change in consumption (mg/day)

p-value: Results of nonparametric tests

Ref: Each difference change distribution was compared to that of the UC group

Table 1: Impact of educational interventions on consumption of calcium supplement

| Group | Without diagnosis and treatment for osteoporosis at randomization (N=1,175) | | | Without consumption of vitamin D supplement at randomization (N=637) | | |
|-------|---|---------|----------------------|--|---------|----------------------|
| | Δ | p-value | % who ↑ their intake | Δ | p-value | % who ↑ their intake |
| UC | 58.4 | Ref | 23.1 | 137.0 | Ref | 23.9 |
| WM | 104.8 | 0.214 | 27.9 | 202.5 | 0.038 | 32.9 |
| VC | 118.3 | 0.012 | 28.6 | 196.5 | 0.030 | 33.6 |
| WM+VC | 111.8 | 0.029 | 28.3 | 199.3 | 0.016 | 33.3 |

UC: Usual care, WM: Written materials, VC: Videocassette
 Δ: Mean difference change in consumption (iU/day)
 P-value: Results of nonparametric tests
 Ref: Each difference change distribution was compared to that of the UC group

Table 2: Impact of educational interventions on consumption of vitamin D supplement

Disclosures: Louis Bessette, Amgen, 6; Amgen, 2
 This study received funding from: Amgen, Alliance for Better Bone Health (sanofi-aventis and Warner Chilcott), Eli Lilly, Merck Canada, Novartis

SU0341

Total Energy Expenditure (EE) by Accelerometry: Relationship to Macrostructural and Mechanical Properties of Bone. Jane Cauley^{*1}, Kathy Wilt Peters², Yahtyng Sheu¹, Peggy Cawthon³, Stephanie Harrison⁴, Kristine Ensrud⁵, Andy Kin On Wong⁶, Dawn Mackey⁷. ¹University of Pittsburgh Graduate School of Public Health, USA, ²California Pacific Medical Centre, San Francisco, USA, ³California Pacific Medical Center Research Institute, USA, ⁴San Francisco Coordinating Center, USA, ⁵Minneapolis VA Medical Center / University of Minnesota, USA, ⁶McMaster University, Canada, ⁷CPMC Research Institute, USA

Physical activity (PA) has been linked to improvements in areal bone mineral density (aBMD) at both the hip and spine. However, little is known about the association of PA and bone strength and size parameters measured by peripheral quantitative computed tomography (pQCT). In addition most previous studies of PA relied on self-report of primarily leisure time activity. Lower intensity activities and unstructured activities which account for the majority of total energy expenditure (EE) in older adults are more difficult to quantify by self-report. The objective of the current analysis was to test the hypothesis that higher total EE is associated with better macrostructural and mechanical properties of bone in older men. Total EE was measured using the multi-sensor SenseWear Pro Armband(SWA). Older men participating in the Osteoporotic Fracture in Men Study (MrOS) in Pittsburgh wore the SWA for at least 5 days. pQCT was measured at the 4% and 33% radius and 4% and 33% tibia using the Stratec XCT-2000 (Germany). Least square mean pQCT parameters were computed across quintiles of total EE in models adjusting for age. Analyses were confined to 308 men who wore the SWA >90% of the time. The mean age of the men was 78.7 ± 4.6 years; mean BMI, 28.1 ± 4.1kg/m². There was no association either at the radius or tibia between total EE and trabecular or cortical volumetric BMD or with endosteal circumference. However, total EE was associated with greater bone size, specifically, larger cross-sectional area and periosteal circumference and greater strength of bone at the 33% site of the tibia, Table. Cortical cross-sectional area, periosteal circumferences, polar moment of inertia, section modulus, and strength strain index increased with increasing total EE. Comparing quintile 5 with quintile 1 of total EE, there was 3.8% to 11.9% higher bone strength or bone size, corresponding to differences of 0.45 to 0.91 standard deviation units. Similar results were observed at the 33% site of the radius. Further adjustment for BMI and season had little effect. In conclusion, our results suggest superior bone strength and bone geometry but not vBMD in older men across increasing total EE. This could contribute to our previous observation that men with higher total EE have a lower risk of fracture.

Table: Age-adjusted least square mean pQCT parameters at tibia (33%) across quintiles of total EE.

| Total EE Quintile (kcal/d) | Cortical cross-sectional area (mm ²) | Periosteal circumference(mm) | Polar moment of inertia (mm ⁴) | Section modulus (mm ³) | Stress strain index (mm ²) |
|----------------------------|--|------------------------------|--|------------------------------------|--|
| 1481.20 <= Q1 < 2022.80 | 300.8 | 74.5 | 30214 | 1927 | 1237 |
| 2022.80 <= Q2 < 2235.17 | 320.3 | 76.2 | 33217 | 2065 | 1311 |
| 2235.17 <= Q3 < 2433.20 | 323.8 | 75.9 | 33205 | 2075 | 1284 |
| 2433.20 <= Q4 < 2704.80 | 333.7 | 77.5 | 35779 | 2196 | 1352 |
| 2704.80 <= Q5 < 4272.20 | 336.7 | 77.2 | 35948 | 2196 | 1346 |
| P trend | <0.0001 | 0.005 | 0.0005 | 0.0004 | 0.03 |

Q5 vs Q1:

Table
Disclosures: Jane Cauley, None.

SU0342

Effects of Calcium and Vitamin D Supplementation on Bone Health Status in Patients with Chronic Obstructive Airway Diseases. Yi-Chin Lin^{*1}, Y-T Lai², T-C Wu³, S-L Yeh². ¹Chung Shan Medical University, Taiwan, ²Chung Shan Medical Univ., Taiwan, ³Chung Shan Medical Univ. Hospital, Taiwan

Osteoporosis is one of the most common complications in patients with chronic obstructive airway diseases. The current study was carried out to investigate the effects of calcium and vitamin D supplementation on bone status in patients with chronic obstructive airway diseases using glucocorticoids. Patients were recruited from outpatient department of chest medicine in a medical university hospital, Taichung, Taiwan. The subjects were randomly assigned to either experimental (calcium 550 mg plus 200 IU of vitamin D per day) or placebo group. The duration of intervention was 12 months. Measurements and blood samples were collected for analyses at baseline and 6 months and 12 months post-intervention, respectively. The results showed that changes in bone mineral density (BMD) at total body, lumbar spine, and femoral neck did not significantly differ between groups. Percent changes of BMD in 6 months and 12 months were 0.42 ± 0.28% and 0.05 ± 0.26% at total body, 1.06 ± 0.81% and 0.77 ± 0.59% at lumbar spine, and -0.05 ± 1.07% and 0.25 ± 0.85% at femoral neck in the experimental group vs. -0.61 ± 0.39% and -0.78 ± 0.56% at total body, -0.33 ± 0.80% and -0.36 ± 1.29% at lumbar spine, and -1.14 ± 1.05% and -1.67 ± 1.12% in the placebo group, respectively. Results of multiple regression showed that group (beta=1.494, p<0.01) and change in serum level of 25(OH)D (beta=0.022, p<0.01) positively predicted percent change in total body BMD, whereas change in serum level of bone resorption marker ICTP (beta=-0.001, p<0.01) was a negative predictor. Change in serum level of bone formation marker osteocalcin (beta=-0.037, p<0.05) negatively predicted percent change in lumbar spine BMD, whereas gender (beta=2.910, p<0.05) and change in urinary ratio of calcium to creatinine (beta=0.013, p<0.05) were positive predictors for percent change in femoral neck BMD. It appears that supplementation of calcium and vitamin D may decrease bone loss at lumbar spine and femoral neck in patients with chronic obstructive airway diseases using glucocorticoids. Intervention for longer period or with higher dosages may be necessary for observing significant changes in bone measurements.

Disclosures: Yi-Chin Lin, None.

SU0343

Fracture Risk According to the FRAX Algorithm in Postmenopausal Women with a Recent Clinical Fracture. Piet Geusens^{*1}, Tineke Van Geel², Sandrine Bours³, John Eisman⁴, Jacqueline Center⁴, Joop Van Den Bergh⁵. ¹Maastricht UMC & UHasselt, Netherlands, ²Maastricht University, The Netherlands, ³Maastricht University Medical Centre, The Netherlands, ⁴Garvan Institute of Medical Research, Australia, ⁵VieCuri MC Noord-Limburg & Maastricht UMC, The Netherlands

Objective: The use of the FRAX fracture risk algorithm has widespread interest, but its use in daily practice is still a matter of debate. We assessed fracture risk based on the FRAX algorithm in postmenopausal women older than 50 years at the time they present with a clinical fracture.

Method: In 362 out of 672 consecutive patients, presenting with a clinical fracture, their 10-year fracture risk was calculated using FRAX, calibrated for the Netherlands. We analyzed how many patients had a FRAX risk ≥ 20% (FRAX ≥ 20%) for major fractures (clinical vertebral, wrist, humerus, hip) and ≥ 3% for hip fractures (hip FRAX ≥ 3%), with and without including femoral neck T-scores (TFN), and excluding the current fracture.

Results: FRAX ≥ 20% was found in 17% of patients without BMD and in 10% with BMD, hip FRAX ≥ 3% in 51% without BMD and in 38% with BMD (Figure 1). These percentages were lower in patients without a prior fracture (n=218) (7%, 4%, 38% and 27% respectively), and in patients younger than 70 years (n=198) (1%, 0%, 13% and 10%). In patients with TFN -1 to -2.5 these percentages were 11%, 1%, 43% and 23% respectively, and, in patients with TFN ≤ -2.5, 30%, 24%, 72% and 71%.

Conclusions: Most postmenopausal women presenting with a clinical fracture did not have FRAX ≥ 20% or hip FRAX ≥ 3%, especially those without a prior fracture and who were younger than 70 years. Most patients with TFN ≤ -2.5 were not identified using FRAX ≥ 20%, however >70% had hip FRAX ≥ 3%. These results draw attention to the high percentage of postmenopausal women below these fracture thresholds who actually present with a clinical fracture.

Figure 1. The individual values of FRAX according to age in patients without a prior fracture (circles) and in patients with a history of prior fracture (triangles). A/ FRAX for major fractures without BMD. B/ FRAX for hip fractures without BMD. Horizontal lines indicate fracture thresholds of FRAX ≥ 20% for major osteoporotic fracture and of FRAX ≥ 3% for hip fracture. Curved lines indicate mean values of FRAX in patients with a prior fracture according to age (solid lines for patients with a history of prior fracture, dotted lines for patients without a prior fracture).

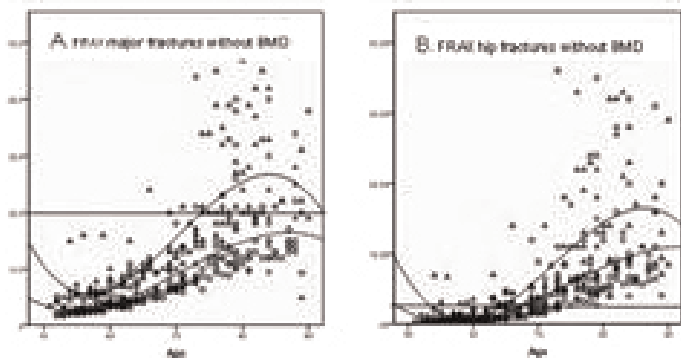


figure 1

Disclosures: Piet Geusens, None.

SU0344

Fracture Risk Is Increased by the Complication of Hypertension and Treatments with Calcium Channel Blockers in Postmenopausal Women with Type 2 Diabetes. Toru Yamaguchi¹, Shin Takaoka², Ken-ichiro Tanaka³, Miwa Morita², Masahiro Yamamoto¹, Mika Yamauchi¹, Shozo Yano¹, Toshitsugu Sugimoto³. ¹Shimane University Faculty of Medicine, Japan, ²Internal Medicine 1, Shimane University Faculty of Medicine, Japan, ³Shimane University School of Medicine, Japan

OBJECTIVE: Patients with type 2 diabetes mellitus (T2DM) are known to have an increased risk for fracture compared to non-T2DM controls, despite their higher bone mineral density. T2DM patients frequently have other common diseases such as hypertension (HT), dyslipidemia (DL), and cardiovascular disease (CVD). However, it is unknown whether or not the complication of these diseases would affect fracture risk in T2DM.

RESEARCH DESIGN AND METHODS: We examined the association between prevalent morphometric vertebral fractures (VFs) or prior non-VFs versus HT, DL, or CVD in T2DM patients (VF: 137 men over 50 years old and 158 postmenopausal women; non-VF: 204 men and 202 women).

Results: VF, non-VF, HT, DL, and CVD were found in 30 (22%), 10 (5%), 106 (52%), 106 (52%), and 50 (25%) men, and in 56 (35%), 23 (11%), 136 (67%), 127 (62%), and 42 (21%) women, respectively. Comparison between subjects with and without fractures showed that the presence of DL or CVD did not affect fracture risk in T2DM men or women. In contrast, the presence of HT was significantly associated with VFs ($P=0.0041$) as well as non-VFs ($P=0.0333$) in women. Treatments with calcium channel blockers (CCBs) tended to be associated with VFs ($P=0.0504$), and were significantly associated with non-VFs ($P=0.0102$) in the population. Multivariate logistic regression analyses showed that the presence of HT significantly increased VF risk in women after adjustments for age, body mass index (BMI), and serum creatinine [odds ratio (OR) 4.74, $P=0.0100$]. This result was still significant after additional adjustments for treatments with anti-hypertensive medications or the histories of falls. CCB treatments significantly increased VF and non-VF risks in women after adjustments for age, BMI, and serum creatinine (OR 2.35, $P=0.0240$ and OR 3.33, $P=0.0213$, respectively), while the significance for non-VFs but not VFs disappeared after an additional adjustment for the histories of falls.

Conclusions: These findings suggest that in T2DM postmenopausal women, the presence of HT increases VF risk independent of anti-hypertensive medications or falls, and that CCB treatments increase non-VF risk possibly via falls.

Disclosures: Toru Yamaguchi, None.

SU0345

High Serum Total Bilirubin as a Protective Factor against Hip Bone Loss in Healthy Middle-aged Men: A Three-year Retrospective Longitudinal Study. Seong Hee Ahn¹, Jung-Min Koh¹, Beom-Jun Kim¹, Seung Hun Lee², Sung Jin Bae¹, Ghi Su Kim². ¹Asan Medical Center, South Korea, ²Asan Medical Center, University of Ulsan College of Medicine, South Korea

Introduction Bilirubin is known to have a physiologic role as an antioxidant that efficiently scavenges peroxyl radicals and suppresses oxidation. Since oxidative stress has detrimental effects on bone metabolism, we hypothesized that bilirubin may function as a protective predictor against future bone loss. In the present study, we performed a large longitudinal study of healthy middle-aged men investigating the association between serum total bilirubin concentrations and annualized changes in bone mineral density (BMD).

Methods The study enrolled a total of 917 Korean men aged 40 years or older who had undergone comprehensive routine health examinations with an average follow-up interval of 3 years. BMD in proximal femur sites was measured with dual-energy X-ray absorptiometry using the same equipment at baseline and follow-up.

Results The overall mean annualized rates of bone loss in the total femur, femur neck, and trochanter were $-0.25\%/yr$, $-0.34\%/yr$, and $-0.44\%/yr$, respectively. After adjustment for age, weight, height, baseline BMD, lifestyle-relating factors, and hepatic markers, the rates of bone loss in all proximal femur sites were significantly attenuated in a dose-response fashion across increasing bilirubin quartile categories. Consistently, compared with subjects in the lowest bilirubin quartile category, those in the highest bilirubin quartile category showed significantly diminished bone loss in all proximal femur sites after adjustment for the confounding factors.

Conclusions This study provides the first clinical evidence that serum total bilirubin may have an endogenous beneficial effect on bone metabolism through antagonism of oxidative stress, especially in subjects without liver diseases.

Disclosures: Seong Hee Ahn, None.

SU0346

HIV Infection Is Strongly Associated with Increased Risk of Hip Fracture: a Population-based Study. Daniel Prieto-alhambra¹, Cristina Carbonell², Francesc Fina-Aviles³, Alberto Soria-Castro³, Robert Güerri⁴, Xavier Nogues⁵, Adolfo Diez-Perez⁶. ¹Institut Municipal D'Investigació Mèdica, United Kingdom, ²Facultat de Medicina Universitat de Barcelona, Spain, ³Institut Català de la Salut, Spain, ⁴Hospital Universitario Del Mar, Institut Municipal D'Investigació Mèdica, Spain, ⁵Institut Municipal D'Investigació Mèdica, Spain, ⁶Parc De Salut Mar, Spain

PURPOSE

The increasing effectiveness of anti-retroviral therapies is related to increased number of survivors, and to older HIV-infected populations. Due to both the direct effects of the virus on bone and to side effects of some anti-retroviral drugs, osteoporosis and fragility fractures need further consideration in this scenario. We studied the association between HIV infection and risk of major fractures.

Method: -Study Design: population-based cohort study.

-Population of study: we screened the SIDIAP-Q database to identify anyone with a prevalent diagnosis of HIV infection (ICD-10 codes B20, B22 and B24), and ascertained incident major fractures (hip, clinical spine, wrist/forearm, pelvis and proximal humerus) in the population aged 40 years or older in the period 2007-2009. SIDIAP-Q contains the computerized medical records of >1,500 General Practitioners in Catalonia (North-East Spain) with information on a representative >2.1 million people. To complete data on fracture we further linked to the official Hospital Discharge Episodes database.

-Measurements: Main exposure was a prevalent diagnosis of HIV/AIDS. Main outcome was incidence of major fractures.

-Statistical analyses: we used Poisson regression to model the effect of HIV/AIDS on fracture risk. Multivariate models were adjusted for age, gender, smoking, alcohol drinking, oral glucocorticoid use, and co-morbidities (as listed in the Charlson Index).

Results: Among 1,118,225 eligible participants, we identified 2,143 (0.2%) subjects with a prevalent diagnosis of HIV/AIDS, who were observed for a median (interquartile range) of 2.997(2.995-2.998) years. HIV-infected patients presented 43 major fractures in the study period (12 hip), corresponding to an incidence rate of 76.69/10,000 person-years [95%CI 56.88-103.4]. Age, gender and BMI-adjusted Rate Ratios (RR) for HIV/AIDS were 2.32 [1.73-3.11]; $p<0.001$ and 4.80 [95%CI 2.65-8.68; $p<0.001$] for any major and hip fracture respectively; this remained significant after further adjustment for co-morbidities: RR 1.47 [1.01-2.15; $p=0.047$]; 3.46 [1.64-7.28; $p=0.001$] respectively.

Conclusion: HIV-infected patients are at increased risk of fractures, with more than three-fold higher hip fracture rates. Further studies are needed to identify predictors of fracture and potential interventions to prevent osteoporosis in this population.

Table. Fracture incidence rates in HIV infected and non-infected participants in SIDIAP, and fracture rate ratios.

| Fracture site | HIV non-infected | | HIV infected | | Rate Ratio | |
|---------------|------------------|---------------------|--------------|---------------------|------------------------------|---------------------------|
| | N FX | IR/10,000 (95%CI) | N FX | IR/10,000 (95%CI) | Age, gender and BMI-adjusted | Multivariate adjusted* |
| Any clinical | 24,549 | 78.94 [77.96-79.94] | 43 | 76.69 [56.88-103.4] | 2.32 [1.73-3.11]; p<0.001 | 1.72 [1.22-2.41]; p=0.002 |
| Hip | 7,307 | 23.50 [22.97-24.04] | 12 | 19.62 [10.86-35.42] | 4.80 [2.65-8.68]; p<0.001 | 3.46 [1.64-7.28]; p=0.001 |
| Non-hip | 17,242 | 57.77 [56.93-58.62] | 31 | 60.64 [43.33-84.86] | 1.91 [1.36-2.67]; p<0.001 | 1.47 [1.01-2.15]; p=0.047 |

FX = Fracture; IR = Fracture Incidence Rate

* Further adjusted for smoking, alcohol drinking and co-morbidities.

Figure. Age-specific incidence rates (/100 person-years) of major fracture in HIV-infected vs HIV-infection-free controls.

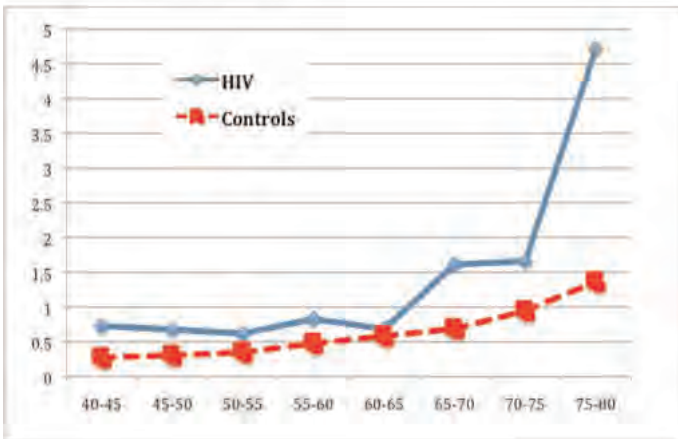


Table and Figure

Disclosures: Daniel Prieto-alhambra, None.

SU0347

Rheumatoid Arthritis Patients Have Equivalent Fall Risk but Higher Vertebral Fracture Risk Compared to Healthy People -TOMORROW Study- Tatsuya Koike¹, Yuko Sugioka², Tadashi Okano¹, Kenji Mamoto¹, Masahiro Tada¹. ¹Osaka City University Medical School, Japan, ²Osaka city University Medical school, Japan

[Background and Objectives] Rheumatoid arthritis (RA) is a representative disease causing secondary osteoporosis. The causes of osteoporosis are multifactorial. Accelerated generalized bone loss leads patients often to increase risk of vertebral fractures. Furthermore, patients with RA who have muscle weakness and stiff or painful joints may be at increased risk of falling. The aim of this study was to use a prospective design to investigate the prevalence and the risk factors of vertebral fractures and the incidence of falls and their risk factors in RA (TOMORROW study, clinical trial registration number: UMIN000003876).

[Methods] The participants in the study were consisted 202 RA patients (54% using biological agents) and 202 age- and sex-matched healthy volunteer (HV). We evaluated bone metabolic markers, muscle volume, bone density, thoracolumbar spine X-ray, disease activity. The occurrences of falls for 1 year and the prevalence of vertebral fracture were assessed.

[Results] Prevalence of vertebral fractures was 45.5% in RA group and 30% in volunteer group. In the RA group bone mineral density, urine pentosidine, homocysteine and bone specific alkaline phosphatase (BAP) showed a significant correlation with presence of the vertebral fractures. Eighteen percent of RA patients and 16% of volunteer reported one or more falls during the previous 1 year. There is no difference in occurrence of falls between RA patients and volunteer. After adjusting for risk factor of falls such as history of falls, age, gender, smoking and BMI, multiple logistic regression analysis identified that history of falls was the most significant parameter associated with falls (odds ratio: 2.71, p<0.001). The RA group also had lower whole muscle volume (RA: 37.2 vs HV: 39.6 kg; p=0.001), leg bone

mineral density (RA: 0.967 vs HV: 1.031 mg/cm²; p<0.001) and shorter exercise time than volunteer, but there is no relation with rate of falls.

[Conclusion] We concluded that fall rate in RA patients was not higher than in volunteer and that only history of falls may play a role in increasing the risk of falls. However, RA patients have many vertebral fractures compared to volunteers. It was suggested that the bone quality marker and the presence of vertebral fractures is closely involved in RA patients. We will continue to investigate prospectively the incidence of new vertebral fractures and the progression of osteoporosis.

Disclosures: Tatsuya Koike, Abbott Japan, 1; Takeda Pharmaceutical, 6; Ono Pharmaceutical, 1; Chugai Pharmaceutica, 1; Mitsubishi Tanabe Pharma Corporation, 1; Teijin Pharma, 6; Bristol Myers Squibb, 1; Janssen Pharma, 1; Mitsubishi Tanabe Pharma Corporation, 6

SU0348

The Association of Fasting Urinary Calcium Excretion with Bone Mineral Density and Fracture Risk in Older Men: the Osteoporotic Fractures in Men Study. Jian Shen¹, Carrie Nielson¹, Lynn Marshall¹, Areef Ishani², Douglas Bauer³, Jane Cauley⁴, Elizabeth Barrett-Connor⁵, Eric Orwoll¹. ¹Oregon Health & Science University, USA, ²Veterans Affairs Medical Center, USA, ³University of California, San Francisco, USA, ⁴University of Pittsburgh Graduate School of Public Health, USA, ⁵University of California, San Diego, USA

Increased calcium excretion is particularly common in men and has been associated with low bone mineral density (BMD) and risk of fractures. Calcium excretion is conventionally measured with 24-hr urine specimens, which are practically difficult. The association between fasting urine calcium excretion and skeletal outcomes is less well understood. The objective of this study was to examine fasting urinary calcium associations with BMD and fracture risk in older men participating in the Osteoporotic Fractures in Men Study (MrOS). Methods: We assessed the associations between baseline fasting urinary calcium and BMD in 1076 men (mean age: 73 y) randomly chosen from the MrOS cohort; 810 men had repeat BMD at an average 4.6 years after baseline. A fracture case-cohort design included a random subcohort (N= 1076) and 310 additional validated cases of non-spine fracture occurred over the next 7 years after baseline. We calculated fractional excretion of calcium (FEca) using the equation: (fasting urinary calcium × plasma creatinine) / (plasma calcium × urinary creatinine). General linear models were used to compare baseline and annualized percent change in hip BMD across quartiles of FEca. We used Cox proportional hazard models with appropriate weights for case-cohort analysis of fracture. All models included age, clinic site, race and weight. Additional potential confounders included serum vitamin D, PTH, renal function and dietary calcium. Results: Higher FEca was associated with slightly lower baseline total hip BMD (Table), however, it was not associated with subsequent rate of change in BMD. While there appeared some evidence of an association between higher FEca and increasing risk of hip fracture (P for trend = 0.08), this association was markedly attenuated after adjustment for hip BMD. We found no evidence of an association with risk of any non-spine fracture. Conclusions: In spite of a cross-sectional association with lower hip BMD, fasting urinary calcium was not associated with higher rates of bone loss. Higher fasting urinary calcium may be associated with an increased risk of hip fracture, but this association is explained by lower BMD among those men with higher excretion. Our findings require further investigation of clinical utility of fasting urinary calcium for the prediction of bone loss and fracture risk in older men.

Table. FEca associations with baseline DXA-BMD, BMD loss and incident fractures

| | Quartile 1 (n=271) (< 0.004) | Quartile 2 (n=270) (0.004-0.007) | Quartile 3 (n=272) (0.007-0.011) | Quartile 4 (n=263) (≥ 0.011) | P for trend |
|---|------------------------------|----------------------------------|----------------------------------|------------------------------|-------------|
| Least-squares adjusted mean | | | | | |
| Total hip BMD (g/cm ³) ¹ | 1.016 | 0.989 | 0.989 | 0.969 | <0.0001 |
| Total hip BMD loss (%/yr) ² | -0.397 | -0.265 | -0.278 | -0.251 | 0.089 |
| | Quartile 1 (n=346) | Quartile 2 (n=347) | Quartile 3 (n=347) | Quartile 4 (n=346) | P for trend |
| Hip fractures | | | | | |
| Fracture cases | 15 | 18 | 25 | 26 | |
| Adjusted hazard ratios (95% CI) | | | | | |
| Age, race, weight and site | ref | 1.31(0.62-2.80) | 1.59(0.79-3.20) | 1.81(0.89-3.71) | 0.08 |
| Age, race, weight, site and baseline hip BMD | ref | 0.85(0.39-1.84) | 1.08(0.53-2.20) | 1.18(0.57-2.44) | 0.48 |

¹ adjusted for age, site, race and weight

² adjusted for age, site, race, weight and weight change

Calcium excretion and BMD

Disclosures: Jian Shen, None.

SU0349

The Relationship between Functional Capacity of Muscle and Fracture Risk Determined by Korean FRAX model: The Chungju Metabolic Disease Cohort (CMC) Study. Kyunghee Kim*¹, Moo-Il Kang², Sun Hee Ko³, Eun Hee Jang⁴, Ki-Hyun Baek⁵. ¹The Catholic University of Korea, Seoul, Korea, South Korea, ²Seoul St. Mary's Hospital, South Korea, ³The Catholic University of Korea, South Korea, ⁴St. Mary's Hospital, South Korea, ⁵department of internal medicine, the Catholic University of Korea., South Korea

BACKGROUND It has been demonstrated that there is a positive correlation between functional capacity of muscle and bone mineral density(BMD). It is also well known that muscle weakness contributes to an increased risk of falling. This study was attempted to clarify the relationship between functional capacity of muscle measured by several related tests and the fracture risk calculated by the Korean FRAX model.

MATERIALS AND METHODS We conducted a population-based and cross-sectional survey to 472 men and 821 post menopausal women aged 50 years and older in a rural area of Chungju, Korea. Bone mineral density was measured by DXA (Hologic QDR4500). Muscle strength and balance performance were measured by the handgrip strength test(HGS), tandem standing test(TST), and timed up and go test(TUG). Clinical information for incorporation into the FRAX model was collected by an interviewer-administered standardized questionnaire.

RESULTS Higher BMD of femur neck and total hip was significantly associated with greater muscle functional status after adjusting age and body mass index. Of the participants, 7.2 % of men and 18.5% of women experienced an osteoporotic fracture. That incidence significantly increased with higher quartile of TUG in women, especially after adjusting other clinical risk factors(age, body mass index, parental hip fractures, current smoking, oral glucocorticoid use, rheumatoid arthritis, secondary osteoporosis and alcohol intake). The 10-year probability of major osteoporotic fractures and hip fractures calculated by the Korean FRAX model were 4.5±2.0(%) and 2.1±1.7(%) in men, and 9.2±4.1(%) and 3.7±2.7(%) in women respectively. The functional capacity of muscle was negatively correlated with the fracture risks in both men and women(P<0.05).

CONCLUSION The results of this study suggest that it may be important for the elderly to maintain their functional capacity of muscle for preventing osteoporotic fractures. Those tests assessing muscle function may be helpful for stratification of osteoporotic fracture risk.

Disclosures: Kyunghee Kim, None.

SU0350

Vertebral Body Morphology is Associated with Incident Lumbar Vertebral Fracture in Postmenopausal Women. The OFELY Study. Jean-Paul Roux*¹, Safaa Belghali¹, Elisabeth Sornay-Rendu², Roland Chapurlat³. ¹INSERM, UMR 1033, Université de Lyon, France, ²INSERM UMR1033, Université de Lyon, France, ³E. Herriot Hospital, France

Vertebral morphology may be associated with further risk of fracture, independently of prior vertebral fracture. The aim of our study was to analyze vertebral anterior cortical curvature (Ct.curv) and body height heterogeneity, in post menopausal women before incident vertebral fracture.

Our nested case-control study within the OFELY cohort has included 29 postmenopausal women with incident lumbar vertebral fractures (mean age 71±9 years, mean time to fractures 9±4 years), age-matched with 57 controls without incident fracture. Body height at baseline was not significantly different between groups. Digital scans were performed on lateral X-rays of lumbar spine (T12 to L4) at baseline with a spatial resolution of 0.26mm/pixel. From these radiographs, the following parameters were measured from six digitized points: 1) the posterior, middle and anterior vertebral height, 2) the heterogeneity of heights evaluated by the coefficient of variation of these three values, 3) the anterior cortical radius of curvature. All measurements were done by two observers, intra and inter observers reproducibility were excellent with an ICC of 0.99, 0.97 and 0.61 respectively.

Mean vertebral heights were significantly lower among women who fractured subsequently than in those who would not. The posterior heights did not differ between these two groups, but the anterior and middle heights were significantly lower at L4 and L3 vertebrae in women with subsequent fracture. No significant differences were found at L1-L2 and T12. The mean heterogeneity of vertebral height was significantly greater in the fracture group. In addition, fractured patients had a significantly higher radius of curvature at baseline.

To conclude, women who will fracture have shorter vertebral height, greater heterogeneity of vertebral height than those who will not fracture, and their anterior vertebral body edge is less concave.

| | Mean vertebral heights (mm) | Mean heterogeneity of heights (CV%) | L4/L3 | | | Ct.curv |
|-----------|-----------------------------|-------------------------------------|---------------|---------------|---------------|-----------|
| | | | ant. height | mid. Height | post. Height | |
| Fractures | 33.43 | 6 | 35.89 / 36.21 | 33.56 / 32.71 | 34.17 / 35.89 | 88 / 82 |
| Controls | 34.53 | 5 | 36.75 / 37.11 | 34.68 / 34.07 | 34.93 / 36.43 | 77 / 58 |
| p* | 0.049 | 0.003 | NS / 0.02 | 0.02 / 0.03 | NS / NS | NS / 0.04 |

*Mann Whitney test.
No significant differences were found in L1-L2-T12.

table

Disclosures: Jean-Paul Roux, None.

SU0351

The History of Fractures in 186 Swiss Women with Anorexia Nervosa. Sigrid Jehle-Kunz*¹, Markus Wegmüller², Romain Perrelet², Kurt Lippuner². ¹Osteoporosis Policlinic, University of Bern, Switzerland, Switzerland, ²Osteoporosis Policlinic, University of Bern, Switzerland

Introduction: Bone health is a major concern in women with anorexia nervosa (AN). This study aimed at describing the epidemiological characteristics of fractures in all women with presumed AN referred for bone health assessment to the Osteoporosis Policlinic of the University Hospital of Bern, Switzerland, between 1994 and 2011.

Methods: A retrospective analysis of the fracture history in 186 female patients with AN was performed. Fractures were categorized as major osteoporotic fractures (MOF; clinical spine, hip, distal radius, and proximal humerus fractures), and other fractures (non-MOF). Patients were categorized into three age groups: before peak bone mass (PBM) acquisition (Group I, age ≤ 20 years), during the plateau phase of PBM (Group II, 21-50 yrs), and postmenopausal (Group III, > 50).

Results: (are summarized in Table1)

Conclusion: As evidenced by fracture history, fractures of any type, including MOF, are very frequent in women with AN, at any age, justifying encompassing diagnostic work-up with regard to bone health and full assessment of individual fracture risk.

Table 1.

| | Group I (≤ 20 yrs) | Group II (21-50 yrs) | Group III (> 50 yrs) |
|---|--------------------|----------------------|----------------------|
| Nr of women with AN | 36 | 120 | 30 |
| Median Body Mass Index in kg/m ² (range) | 16.0 (12.3 - 19.5) | 16.6 (11.5 - 19.6) | 17.5 (12.9 - 19.6) |
| Median age in years (range) | 17 (10 - 20) | 31 (21 - 50) | 56 (51 - 77) |
| Median age at menarche in years (range) | 12 (10 - 16) | 14 (11 - 19) | 14 (11 - 22) |
| Total nr of previous (MOF + non-MOF) Fx | 9 (100.0%) | 116 (100.0%) | 35 (100.0%) |
| Total nr of MOF | 5 (55.6%) | 32 (27.6%) | 12 (34.3%) |
| Hip | 0 | 9 | 1 |
| Clinical spine | 0 | 4 | 2 |
| Distal radius | 4 | 15 | 6 |
| Proximal humerus | 1 | 4 | 3 |
| Total nr of non-MOF | 4 (44.4%) | 84 (72.4%) | 23 (65.7%) |
| Tibia / Fibula / Lower leg | 1 | 20 | 4 |
| Rib | 0 | 17 | 4 |
| All other | 3 | 47 | 15 |
| Nr (%) of patients ≥ 1 Fx | 8 (22.2%) | 84 (63.3%) | 19 (63.3%) |

Table1

Disclosures: Sigrid Jehle-Kunz, None.

SU0352

Hip Fracture Incidence Is Much Higher in Hong Kong Chinese Women than Beijing Chinese Women Despite Higher Bone Density in Hong Kong Women : Major Implications for Hip Fracture Prevention. Rick Chung*¹, HAI TANG², PengCheng Ha³, Pansy Tse⁴, Yan Lam⁴, George Qin³, Carol Chan⁴, Edith Lau¹. ¹Center for Clinical & Basic Research (CCBR) (Hong Kong), Hong Kong, ²BEIJING FRIENDSHIP HOSPITAL, China, ³CCBR(Beijing), China, ⁴CCBR(Hong Kong), Hong Kong

Back ground and objectives

Hong Kong has the highest incidence of hip fracture in Asia, while mainland China still has very low incidence of hip fracture. However, it has been predicted there will be a major epidemic of hip fracture in China. The objective of the current study is to compare the bone mineral density at the hip between a large population sample of Hong Kong and mainland Chinese women, so that insight can be gained into the etiology of hip fracture.

Subjects and methods

7130 ambulatory Hong Kong Chinese women and 7037 mainland Chinese women living in Beijing (aged 50 to 96) were recruited from the community. They volunteered for the study. BMD was measured by Lunar Prodigy Advance Whole Body Bone Densitometers. Cross calibration was carried out by a phantom. The prevalence of osteoporosis was calculated according to the World Health Organization criteria. BMD at the total spine and femoral neck were adjusted for age, height and weight and compared between the 2 populations.

Results: According to published data, the incidence rate of hip fracture was 465/100,000 in Hong Kong Chinese women and 229/100,000 in Beijing Chinese women. The prevalence of osteoporosis at the total hip in our study was 24.8% in Hong Kong Chinese women and 20.0% in Beijing Chinese women, but these did not account for difference in weight and height. After adjustment for age, height and weight, the BMD of Hong Kong Chinese women was 2.8% higher at the hip and 1.5% higher at the femoral neck than Beijing Chinese women. This implies that BMD is a poor

measurement of bone strength, and also that there are many extraskeletal factors causing hip fracture.

Conclusion: The difference in hip fracture incidence between Hong Kong Chinese and Beijing Chinese women cannot be explained by difference in BMD. Further research should focus on better measurement of bone strength in Chinese women, as well as extraskeletal factors for hip fracture, so that recommendations can be made to prevent the imminent epidemic of hip fracture in mainland China.

| Total hip | Age group | Mean (g/cm ²) | | P Value by t-test |
|------------------|-----------|---------------------------|------------------|-------------------|
| | | Hong Kong (n=7130) | Beijing (n=7037) | |
| | 50-64 | 0.907 | 0.886 | <0.05 |
| | ≥65 | 0.806 | 0.780 | <0.05 |
| | All | 0.838 | 0.815 | <0.05 |
| Femoral neck BMD | 50-64 | 0.834 | 0.824 | <0.05 |
| | ≥65 | 0.737 | 0.722 | <0.05 |
| | All | 0.767 | 0.756 | <0.05 |

Bone mineral density (BMD) with adjustment for age, height and weight at the hip in subjects from Beijing and Hong Kong.

Disclosures: Rick Chung, None.

SU0353

Is There an Increased Risk of Hip Fracture in Multiple Sclerosis (MS)? Analysis of the Nationwide Inpatient Sample (NIS). Rajib Bhattacharya¹, Richard Dubinsky². ¹KU Medical Center, USA, ²University of Kansas, USA

Objective: To determine if people with MS have a higher rate of hip fractures and to explore the discharge disposition of MS patients with acute hip fracture.

Background: Impaired ambulation, frequent falls, and prolonged immobilization combined with the high rate of vitamin D deficiency in people with MS could lead to an increased risk of hip fracture.

Methods: Retrospective cohort analysis of 20 years of the NIS (HCUP, AGRQ.gov), a 20% stratified sample of US hospital admissions. Admissions with a primary diagnosis of acute hip fracture were identified, as was the subset with a secondary diagnosis of MS. Indirect adjustment was used to compare the prevalence of MS in this population, to that of the US (Noonan, Neurology, 2002). Because of the large number of records and multiple comparisons, p was set a priori at < .0001.

Results: 0.25% of 1,063,726 hip fracture admissions were for MS. Over the 20 years of this dataset the proportion with MS increased from 0.21% to 0.31%. There was a trend for lesser mortality for MS (0.25 vs. 2.97%, p < .0001) yet discharge to nursing home or rehabilitation was less for MS (69.25% vs. 72.17%, p < .0001). When compared to the population prevalence the prevalence of MS among the patients with hip fracture was 2.844 (95% confidence interval; 2.841, 2.852) predicted when age adjusted and 2.505 (2.499, 2.512) when adjusted for gender and age. When adjusted for race (white, black) the prevalence was 2.175 (2.168, 2.182). Race was specified for 65% of the sample.

Conclusions: In this nationwide sample of 20 years of US hospital admissions the rate of hip fracture for people with MS was more than twice predicted. While the risk of falls can be partially mitigated through physical therapy and fractures with vitamin D, bisphosphonates are less effective pre-menopause.

Disclosures: Rajib Bhattacharya, None.

SU0354

Role of TLR 4 in the Dysregulation of Skeletal Metabolism Associated with Type 2 Diabetes. Elizabeth Rendina¹, Yan Wang², Kelsey Hembree³, McKale Davis³, Jennifer Graef³, Sandra Peterson³, Katie Clark³, Stephen Clarke¹, Edralin Lucas¹, Brenda Smith¹. ¹Oklahoma State University, USA, ²Department of Plant & Soil Sciences, Oklahoma State University, Oklahoma State University, USA, ³Department of Nutritional Sciences, Oklahoma State University, USA

Type 2 diabetes (T2DM) is a major public health problem affecting ~25 million Americans and if current trends continue this number is projected to double in the next 40 years. Although fracture incidence has not been classically associated with T2DM, recent evidence has shown that these patients have an increased risk of fracture 5-10 years post diagnosis, independent of bone mineral density (BMD). Previous studies in animal models with mutations in toll-like receptor (TLR)-4 (i.e., C3H/HeJ and TLR-4^{-/-} mice) have suggested that inflammatory signaling via TLR-4 may be involved in the initiation and progression of T2DM. Since TLR-4 and inflammation are known to negatively affect bone metabolism, the increase in fracture incidence associated with T2DM may be in part explained by this pathway. The current study aimed to investigate the role TLR-4 plays during the initiation and progression of T2DM, and to correlate changes in glucose homeostasis with skeletal alterations over time. Four-week old male C57BL/6 and C3H/HeJ mice (n=10 mice/

group) were randomly assigned to a control (CON=10% kcal fat) or high fat (HF=60% kcal fat) diets for either 2, 8, or 16 wks. Body weight and fasting blood glucose were monitored over time, and an intraperitoneal glucose tolerance test (IGTT) and whole body dual energy x-ray absorptiometry (DXA) scans were performed at each endpoint. As anticipated, mice on the HF diet, both the C57BL/6 and C3H/HeJ strains, had greater body weight ($P<0.05$) than their control counterparts beginning at 2 weeks and throughout the remainder of the study. Fasting blood glucose was elevated in both strains on the HF diet after 2 and 8 weeks, however, the increase in glucose was only observed in the C57BL/6 strain at 16 weeks. Impaired glucose tolerance occurred in both strains on the HF diet at 2, 8, and 16 weeks, while plasma insulin was increased only after 16 wks. The C57BL/6 mice on the HF diet experienced a decrease in whole body BMD by 8 and 16 wks, but this effect on bone was delayed until 16 wks in the C3H/HeJ strain. The delayed skeletal effects observed in the C3H/HeJ mice suggest that TLR-4 may contribute to the skeletal phenotype in T2DM. Further investigation is needed to understand the effects of TLR-4 signaling on osteoblasts and osteoclasts, and the resulting changes in bone microarchitectural and biomechanical properties in the context of T2DM.

Disclosures: Elizabeth Rendina, None.

SU0355

Serum 25-Hydroxyvitamin D Level and Incident Type 2 Diabetes in older men, the Osteoporotic Fractures in Men Study (MrOS). Nicola Napoli¹, Anne Schafer², Christine Lee³, Jane Cauley⁴, Elsa Strotmeier⁵, Andrew Hoffman⁶, Erin Le Blanc⁷, Ann Schwartz⁸, Dennis Black⁸. ¹University Campus Biomedico, Italy, ²University of California, San Francisco & the San Francisco VA Medical Center, USA, ³Oregon Health & Science University, USA, ⁴University of Pittsburgh Graduate School of Public Health, USA, ⁵University of Pittsburgh, USA, ⁶Stanford University, USA, ⁷Center for health research, Kaiser permanente, USA, ⁸University of California, San Francisco, USA

Several studies have found an association between vitamin D levels and risk of developing diabetes. Even if the mechanism through which vitamin D regulates pancreatic function is still unclear, immunomodulation and effects of vitamin D on insulin resistance may play a main role. However, the effect of vitamin D levels on diabetes risk has not been consistent among observational studies, and also vitamin D intervention studies in diabetic patients have yielded varying results. In the present study we have investigated the effect of vitamin D on incident Type 2 diabetes in men (>65 years of age) who participated in the multisite Osteoporotic Fractures in Men (MrOS) study from March 2000 to March 2009.

After excluding 369 subjects with diabetes at baseline, 2477 subjects had baseline Vitamin D levels. Clinical information, BMI and other factors related to type 2 diabetes were assessed at baseline visit while incident diabetes was determined at a follow-up visit 8.7 years later by self-report and medication use. Cox proportional hazards regression models were used to determine the relationship between 25(OH)D concentration and subsequent risk of a incident diabetes, with adjustment for covariates.

At baseline patients were on average 73.5 years old (± 5.9), had a BMI in the overweight range (27.1 ± 3.1) and total 25(OH)D of 24.5 ng/ml (± 7.8). Incident diabetes was diagnosed in 120 subjects.

Analysis adjusted for clinic site and age (model 1) showed that vitamin d levels were associated with lower incidence of type 2 diabetes (HR=0.80 (see table)). After a further adjustment for BMI (model 2), the relationship was attenuated and no longer statistically significant. Further adjustments had little effect.

In conclusion, vitamin D levels are not associated with lower Type 2 diabetes incidence in older males. Body fat is a depot of vitamin D and it may explain the key role played by BMI.

| | HR(95% CI) for diabetes, per 1 SD increase in 25(OH)D |
|--|---|
| Model 1: Adjusted for age and site | 0.80 (0.65 – 0.97) |
| Model 2: Adjusted for age, site and BMI | 0.86 (0.70 – 1.05) |
| Model 3: Adjusted for age, site, race, month, History of congestive heart failure, Smoking, PASE score & BMI | 0.88 (0.71 – 1.09) |

Risk of incident Type 2 Diabetes and 25(OH)D

Disclosures: Nicola Napoli, None.

SU0356

Trabecular Bone Score in Rheumatoid Arthritis and Ankylosing Spondylitis and Changes during Long Term Treatment with TNF α Blocking Agents. Eric Toussiroot^{*1}, Laurent Mourot², Daniel Wendling¹, Gilles Dumoulin³, Clinical Investigation Center Biotherapy⁴. ¹University Hospital Minjoz, France, ²University of Franche Comté, France, ³Physiology, France, ⁴University Hospital, France

Inflammatory rheumatic diseases (IRD) such as rheumatoid arthritis (RA) and ankylosing spondylitis (AS) are associated with osteoporosis. Bone mass in RA and AS has been well evaluated by measuring areal bone mineral density (BMD) with DXA. Trabecular bone score (TBS) is a new method evaluating bone microarchitecture by assessing pixel gray-level variations in DXA images from lumbar spine.

In a case-control study, TBS was evaluated in patients with RA or AS and healthy controls (HC). Changes in LS and hip BMD and TBS score during anti-TNF α treatment were also examined in a prospective study.

In the case control study, 30 patients with RA (ACR criteria, 19 F; 12 post menopausal women; age [mean \pm SD]: 56.9 \pm 9.7 yrs; disease duration: 11.7 \pm 8.8 yrs; 26 under low dosage corticosteroids [CTC]) and 30 patients with AS (NY criteria, 27 M, age 43.8 \pm 13.4 yrs; disease duration: 13.0 \pm 11.1 yrs; no CTC) were evaluated and compared to 50 HC (29 F, 12 post menopausal women, age: 46.6 \pm 11.1 yrs). LS BMD and hip BMD were measured by DXA (Lunar GE iDXA). TBS was calculated from L2-L4 BMD images (TBS insight[®], Med-Imaps). In the prospective study, a group of 20 patients requiring anti-TNF α (6 F; 12 AS, [age: 40.7 \pm 16.1 yrs] and 8 RA [age 60.5 \pm 9.7 yrs]; disease duration: 9.6 \pm 9.8 yrs; 9 under low dose CTC) were followed for 2 years. LS BMD, hip BMD and TBS score were measured at baseline and after 6, 12 and 24 months.

- Case control study: RA patients had lower BMD and T score at the hip ($p < 0.005$) compared to HC. Hip T score in patients with AS was also decreased ($p = 0.02$). LS BMD did not differ between patients and HC. TBS was lower in RA and AS compared to HC: 1.242 \pm 0.16 and 1.282 \pm 0.13 vs 1.365 \pm 0.14, respectively ($p = 0.005$).

- Prospective study: under anti-TNF α , LS and hip BMD at M24 increased (+ 6.3% and + 2.4% respectively), with significant changes at the spine ($p < 0.001$). In the whole group, TBS score did not change. However, in patients with RA, TBS score decreased (baseline to M24: 1.362 \pm 0.048 to 1.308 \pm 0.07) ($p = 0.032$) while in patients with AS, TBS remained stable.

TBS score is decreased in IRD, especially in RA, suggesting alterations of bone micro architecture. Long term anti TNF α treatment is associated with a positive effect on (LS) bone mass but no changes in TBS score. On the contrary of AS, TBS score decreased in RA under anti-TNF α , suggesting different influences on the bone of this drug's class.

Disclosures: Eric Toussiroot, None.

SU0357

Differential Diagnosis Marfan Syndrome, Ehlers-Danlos Syndrome and Osteogenesis Imperfecta. Vaclav Vyskocil^{*1}, Tomas Pavelka². ¹Center for Metabolic Bone Diseases, Czech Republic, ²Department of Orthopaedic Surgerz, Czech Republic

900 patients with inherited connective tissue diseases and bone dysplasias were examined by means of a diagnostic system based on revised criteria for Marfan and Ehlers-Danlos syndromes as well as for osteogenesis imperfecta, benign joint hyperelasticity and juvenile osteoporosis of the youth. In 541 patients all data necessary for differential diagnostics were obtained: 200 patients met the criteria for Marfan syndrome (MFS), 92 patients for Ehlers Danlos syndrome (EDS) and 73 persons for osteogenesis imperfecta (OI). 211 patients had benign joint hyperelasticity (BJH) and the remaining patients demonstrated other diagnoses. Examined biochemical parameters e.g. osteocalcin OC was significantly increased in patients with type IV of OI when compared with type I and significantly lower level of PICP in patients with OI when compared to other groups. Crosslinks were significantly higher in patients with OI as well as in patients with Marfan syndrome up to 13 years, but in older children no difference was found. The highly specific marker for Marfan syndrome was bird chest and thumb test. On the other hand in osteogenesis imperfecta drum chest and larger head circumference were typical. Decreased vital pulmonary capacity was found in all severe chest deformities and in scolioses greater than 25 degrees Cobb angle. Patients with Marfan syndrome were tall and had longer extremities to trunk, the highest incidence of hernias and in addition to that, they had also longer anteroposterior bulbous length measured by ultrasonography. Acetabulum protrusion or spondylolisthesis also occur only in MFS patients. Recurrent luxations, varicose veins and chronic pains were observed only in Ehlers-Danlos syndrome. The presented diagnostic system including clinical, biochemical, densitometric, radiologic and ultrasonic parameters seems to be adequate for differential diagnosis of connective tissue diseases. Molecular genetic examination was indicated only in few unclear cases.

Disclosures: Vaclav Vyskocil, None.

SU0358

Low Bone Density of Spine in Patients with Lumbar Spinal Stenosis. Reza S Roghani^{*1}, Mansoor Ravegani², Ahmad Delbari³, Shahab Tabatabaei⁴, Mehrsheed Sinaki⁵. ¹Iran, ²Shahid Beheshti University, Iran, ³Sabzevar University, Iran, ⁴University of welfare & rehabilitation, Iran, ⁵Mayo Clinic, USA

Background: Recent advances in imaging techniques has made it possible to address new challenges related to aging osteoporotic spine and choice of proper exercise program. With aging combination of osteoporosis (OP) & osteoarthritis (OA) may result in back pain, in the setting of spinal stenosis. Degenerative disorders of lumbar spine such as Lumbar canal stenosis usually are managed through lumbar flexion bias strengthening exercises. This may, increase risk of vertebral fractures in case of Spinal OP.

Material and Methods: A cross sectional study was conducted on eighty five elderly patients who referred to affiliated clinics of the Iranian research center of aging (IRCA) with low back pain related to ambulatory activities. Lumbar spinal stenosis was suspected on the basis of clinical evaluations. The study was carried out from January 2008 to December 2009, Tehran, Iran. IRCA Ethical Committee of approval was obtained and Informed consents were obtained prior to study.

Procedure: After clinical evaluation those patients who had clinical diagnosis of lumbar spinal stenosis (LSS) were referred for MRI. After the diagnosis was substantiated by MRI, they were referred for BMD evaluation on DEXA.

Results: 37(43%) of LSS patients had spinal osteoporosis, 42(49%) had spinal osteopenia. Totally 79 out of 85 (93%) patients had below normal BMD.

Comparing BMD of this group with the value of Spine BMD in elderly population of Iran, (33% of osteoporosis and 50% of osteopenia of spine) there was no statistically significant difference.

Discussion and conclusion: Although there is no statistically significant difference in spinal BMD between LSS patients and general elderly population of Iran, significant bone loss in more than 90% of patients with LSS needs to be addressed. This is of great concern as decision making related to prescribing the appropriate exercise program. Prevention of further vertebral fracture necessitates impimention of our modified spinal extension exercise program.

Disclosures: Reza S Roghani, None.

SU0359

Early Corticosteroid Withdrawal after Kidney Transplantation: Paradoxical Effects on the Central and Peripheral Skeleton. Sapna Iyer^{*1}, Lucas Nikkel², Chiyuan Zhang³, Donald McMahon⁴, Stephanie Boutrov², Xiaowei Liu⁵, X Guo³, Sharmila Majumdar⁶, David Wojciechowski⁷, Elizabeth Shane⁴, Thomas Nickolas². ¹University of California San Diego, USA, ²Columbia University Medical Center, USA, ³Columbia University, USA, ⁴Columbia University College of Physicians & Surgeons, USA, ⁵University of Pennsylvania, USA, ⁶University of California, San Francisco, USA, ⁷University of California San Francisco, USA

Fracture risk is increased in kidney transplant (KTx) recipients. In the first year after KTx patients receiving corticosteroid-based immunosuppression experience significant loss of areal bone mineral density (aBMD) and high fracture rates. In some studies, early corticosteroid withdrawal (ECSW) is associated with lower rates of bone loss, though its effects on fracture risk and bone quality are unclear. We enrolled 48 adult KTx recipients, mean age 50 \pm 14 years, in a prospective study to quantify the effects of ECSW on bone mass and microarchitecture of the central and peripheral skeleton. We measured aBMD by dual energy X-ray absorptiometry (DXA) of the lumbar spine (LS), total hip (TH), femoral neck (FN), 1/3 radius (1/3R) and ultradistal radius (UDR) at baseline, 3, 6 and 12 months after KTx. We used high resolution quantitative computed tomography (HRpQCT) to assess volumetric bone mineral density (vBMD), bone geometry and microarchitecture at the distal radius and tibia. Comparisons were made using mixed models adjusted for baseline bone measures; results are expressed as Means \pm SD. To date, 39, 40 and 32 patients have completed 3-, 6- and 12- month follow-up, respectively. At KTx, BMI was 28 \pm 6 Kg/m²; 28% were women and 72% were white. Over 12 months, LS aBMD did not change significantly. TH and FN aBMD declined at 3 months (-1.3 \pm 3.7%, $p < 0.05$ and -1.4 \pm 5.9%, $p < 0.01$, respectively), but recovered to levels not significantly different from baseline by 12 months. In contrast, 1/3R and UDR aBMD declined over 12 months (-1.9 \pm 7.0%, $p < 0.01$ and -3.2 \pm 9.8%, $p < 0.001$, respectively). By HRpQCT at the radius, cortical (Ct) area and Ct and trabecular (Tb) vBMD declined over 12 months (-4.9 \pm 11.8%, -2.0 \pm 5.5% and -4.7 \pm 7.8%, $p < 0.001$, respectively). In contrast, Tb area and microarchitecture did not change significantly. The pattern and significance of changes were mirrored at the tibia, though the amount of loss was smaller. There were no clinical features to distinguish KTx recipients who experienced significant bone loss from those with stable aBMD by DXA. In summary, 12 months after KTx, recipients managed with ECSW do not sustain bone loss at the central skeletal. However, there is progressive bone loss at the radius and less pronounced, but still significant, bone loss at the weight-bearing tibia that appears to be due to losses in both the Ct and Tb compartments.

Table 1: Bone Changes over 12 Months

| | Baseline | 3m % Change (±SD) | p | 12m % change (±SD) | p |
|---------------------------------------|----------|-------------------|--------|--------------------|--------|
| aBMD (g/cm²) | | | | | |
| LS | 1.115 | -0.1±6.6% | NS | +1.2±10.5% | NS |
| TH | 0.981 | -1.3±3.7% | <0.01 | +0.1±6.3% | NS |
| UDR | 0.501 | -0.6±6.3% | NS | -3.2±9.8% | <0.001 |
| Radial vBMD (g/cm³) | | | | | |
| Ct | 865 | -0.7±3.1% | <0.05 | -2.0±5.5% | <0.001 |
| Tb | 172 | -2.1±4.5% | <0.001 | -4.7±7.8% | <0.001 |

Table 1

Disclosures: Sapna Iyer, None.

SU0360

Acute Effect of Anti-Osteoporotic Therapies on Bone Turnover Markers in Recent Vertebral Compression Fractures. Costantino Corradini¹, Alessio Maione², Calogero Crapanzano³, Fabrizio Ferrara², Wilfried Stuflesser², Cesare Verdoia². ¹State University of Milan, Italy, ²Orthopaedic Clinic, State University of Milan, Italy, ³Clinical Pathology Unit, AO Orthopaedic Institute G.Pini, Italy

Introduction:In postmenopausal women with femoral and/or vertebral fractures an anti-osteoporotic treatment is indicated for a remarkable increase in lumbar spine BMD and significant reduction of new fracture. The objective of this prospective study was to evaluate the acute effect on bone turnover markers and bone mineral density of risedronate, strontium ranelate or teriparatide in osteoporotic women during one or more vertebral compression fractures (VCF).

Materials and methods:62 compliant women (age 63.1 +/- 5.6 years) with recent osteoporotic VCF verified with magnetic resonance were recruited. They were undergone to conservative treatment with brace and an anti-osteoporotic therapy following guidelines of Italian regulatory agency. So a single VCF was assigned to receive risedronate (RIS group) 35 mg once weekly or strontium ranelate (SR group) 2gr once daily while with a second or two contemporary VCF was prescribed teriparatide (TPTD group) 20 microg once daily. All patients received a supplementation of vitamin D3 100000 UI once monthly. Serum and urinary bone turnover markers and lateral thoraco-lumbar spine X-rays were obtained from all women before, 1, 3 and 6 months after treatment initiation. Lumbar BMD was measured by DEXA before and 6 months after treatment initiation.

Results:The three groups were homogeneous for number, age, body mass index and baseline biochemical bone turnover markers, lumbar BMD. 25-OH vitaminD was at lower levels at the beginning but the supplementation was sufficient to normalize in 6 month. PTH was increased in few patients and were quickly reduced in those of TPTD group. Serum total Calcium were increased within range of normality in TPTD group in 6 month. The high values of DPD observed at the beginning were significantly and constantly reduced in 6 month. Osteocalcin were increased significantly between first and third month only in TPTD group. The healing were detected with radiograms. A light and inconstant progression in VCF were detected in RIS and SR groups. At 6 month follow-up all patients live, but 2 in RIS and SR group were afflicted by new vertebral or non vertebral fracture.

Conclusions:In recent osteoporotic VCF osteoanabolic therapy with TPTD results in acute increase in serum bone formation markers levels, that may reflect an increase in the number of active osteoblasts with acceleration of healing process.

References:Fahrleitner-Pammer A. Osteop Int 2011, 2709; Chevalier Y Bone 2010, 41

Disclosures: Costantino Corradini, None.

SU0361

Comparative Effects of Teriparatide and Ibandronate on Spine Bone Mineral Density (BMD) and Microarchitecture (TBS) in Postmenopausal Women with Osteoporosis. Christoph Senn¹, Sabina Guler¹, Albrecht Popp¹, Delphine Stoll², Berengère Aubry-Rozier², Romain Perrelet¹, Didier Hans³, Kurt Lippuner¹. ¹Osteoporosis Policlinic, University of Bern, Switzerland, ²Center of Bone Disease, Lausanne University Hospital, Switzerland, ³Lausanne University Hospital, Switzerland

Objectives:The trabecular bone score (TBS) is an index of bone microarchitecture, independent of BMD, calculated from antero-posterior spine DXA scans. Although already well validated for fracture discrimination and prediction, there is yet almost no study which investigated TBS's ability to monitor treatment response. The aim of this study was to compare the effects of teriparatide, recombinant human 1-34 parathyroid hormone (PTH (1-34)) and the bisphosphonate ibandronate (IBN), on lumbar spine (LS) BMD and TBS in postmenopausal women with osteoporosis.

Materials and Methods:Two patient groups matched for age, BMI, and baseline LS BMD, treated with either subcutaneous PTH (1-34) 20 micrograms subcutaneous daily (N=70) during 18 months or intravenous IBN 3mg every 3 months (N=105) during 2 years were compared. TBS was calculated retrospectively at baseline and after 24 months using TBS iNsite Software (v1.9; Medimaps, France) using ISCD

rules for individual vertebrae exclusion. Changes in BMD and TBS between baseline and 2 years were expressed as percentage change and differences between groups over 24 months were tested for statistical significance.

Results:Baseline characteristics (overall mean ± SD) were similar between groups in terms of age 68.0 ± 7.1 years; body mass index, 23.8 ± 3.8 kg/m² and BMD L1-L4, 0.739 ± 0.115; but TBS was lower in the PTH (1-34) group (1.192 ± 0.10 vs. 1.230 ± 0.09; p < 0.02). Over 24 months, PTH (1-34) induced a significantly larger increase in BMD than IBN (+7.13% vs. +1.64% p < 0.0001) and the change in TBS was significantly greater with PTH (1-34) than with IBN (+4.30 vs. -0.95%, p < 0.0001). Spine BMD and TBS were only weakly correlated at baseline (r² = 0.06) and there was no correlation between the changes in BMD and TBS over 24 months (r² < 0.01).

Conclusions:In postmenopausal women with osteoporosis, treatment with PTH (1-34) led to a significantly higher increase in LS BMD and TBS than IBN, suggesting that teriparatide had more pronounced effects on bone microarchitecture than IBN. Effects on TBS were independent of the effects on BMD.

Disclosures: Christoph Senn, Novartis, 7

SU0362

Effect of Teriparatide on Fracture Healing in Patients with Non-Displaced Incomplete Atypical Femur Fractures. Angela Cheung¹, LIANNE TILE², R Bleakney³, Aliya Khan⁴, Savannah Cardew², Rowena Ridout⁵, Heather McDonald-Blumer², Khalid Syed¹, Jessica Chang¹, Hanxian Hu¹, Suzanne Morin⁶, Alexandra Papaioannou⁷, Robert Josse⁸, Earl Bogoch⁹, Jonathan Adachi¹⁰. ¹University Health Network, Canada, ²University of Toronto, Canada, ³Mount Sinai Hospital, Canada, ⁴McMaster University, Canada, ⁵Toronto Western Hospital, Canada, ⁶McGill University, Canada, ⁷Hamilton Health Sciences, Canada, ⁸St. Michael's Hospital, University of Toronto, Canada, ⁹St. Michael's Hospital, Canada, ¹⁰St. Joseph's Hospital, Canada

Purpose: With the increased awareness of atypical femur fractures (AFFs), incomplete non-displaced fractures associated with bisphosphonate therapy are diagnosed more frequently, but optimal therapy for these fractures is unclear. We describe a case series of 13 patients with incomplete AFFs who have been treated with teriparatide therapy.

Methods: Thirteen patients who sustained an incomplete non-displaced AFF according to the criteria set forth by ASBMR were included. We assessed radiographic fracture healing using CT scans and plain radiographs, measuring the depth of the lucency line through the cortex and the degree that it extends around the circumference every 6 months. We also measured areal BMD at the total hip, femoral neck, lumbar spine and forearm by DXA (Hologic Discovery A, Hologic Inc.) every 6 months. Outcomes, such as pain, mobility, and progression or regression of incomplete fracture as well as need for surgical intervention, were also noted.

Results: All 13 patients were postmenopausal women (69.2% Caucasians, 15.4% Southeast Asians, 15.4% South Asians) with mean age of 68.6 (range 57.5- 81.0) years, mean BMI of 27.5kg/cm² and mean serum 25-hydroxyvitamin D of 116.9 nmol/L at the time of diagnosis of incomplete AFF. All had normal ionized calcium and intact PTH. Eight out of thirteen had a previous complete AFF. Average duration of bisphosphonate use was 12.6 years (range 3.0-28.0 years). Mean BMD T-scores at the lumbar spine, total hip and femoral neck at the time of diagnosis of incomplete AFF were -1.87, -1.14 and -1.85, respectively. As of March 5, 2012, average duration of teriparatide therapy was 13.4 months (range: 1.4 to 20.2 months). Out of the 13 patients, 3 had to have prophylactic surgical repair for their incomplete AFFs (2 for debilitating pain and progression of incomplete fracture and 1 because of patient / physician preference). For the other 10 patients, 5 had radiographic improvement, 4 had no change and 1 progressed despite teriparatide. Improvement in pain corresponded to radiographic healing, but often preceded it. Of the 13 patients at last follow-up, only 2 did not require the use of an assistive device for mobility.

Conclusions: Based on limited observational data without a control group for comparison, it is unclear whether teriparatide improves fracture healing in patients with incomplete non-displaced AFFs. A randomized controlled trial examining the use of teriparatide in this population is urgently needed.

Disclosures: Angela Cheung, Eli Lilly, 2

SU0363

Qualification of a Physiologically-Based Model for Predicted Bone Marker and Bone Mineral Density Changes Associated with Denosumab Treatment. Matthew Riggs, Kyle Baron^{*}, Elodie Plan, Marc Gastonguay. Metrum Research Group LLC, USA

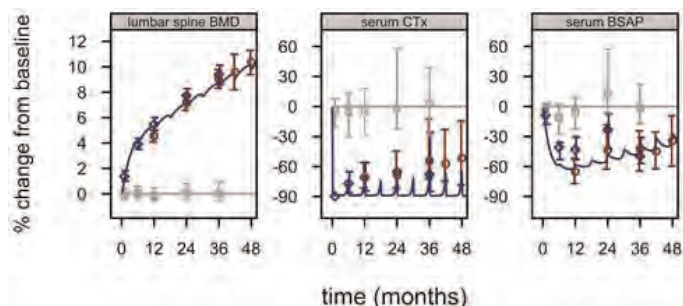
The goal of this investigation was to qualify the predictive performance of an existing physiologically-based, multiscale systems pharmacology model (MSPM) using data external to those used to develop it. The MSPM was initially developed to describe longitudinal bone marker (BM) changes affected by both teriparatide and denosumab (dmab) treatment (Bone. 2010;46:49-63) and includes other relevant factors (e.g., calcium, PTH, calcitriol) and cellular and organ-level regulations, e.g., PTH control of urinary calcium excretion, RANK-RANKL-OPG system in bone, and differentiation and apoptosis controls for osteoclasts and osteoblasts. In the model, RANKL depletion affects an immediate decline in osteoclasts due to increased

apoptosis and a later, less pronounced, decline in osteoblast function regulated by PTH and TGF- β change. Development of this model included earlier dmab trial data (NCT00043186). A further extension of this model, using the earlier dmab data along with clinical manifestations associated with estrogen loss and during CKD-MBD (J Clin Pharmacol. 2012;52:45S-53S), linked bone markers with BMD change.

The external data used for the current evaluation were digitized from FREEDOM trial (NCT00089791) reports: serum C-terminal telopeptide (CTX) and bone specific alkaline phosphatase (BSAP) (J Bone Miner Res. 2011;26(3):530-7) and lumbar spine (LS) BMD (NEJM. 2009;361(8):756-765). BM and BMD model predictions over time were obtained for placebo (no intervention) and dmab 60 mg Q 6 months (for up to 4 years) and compared to the corresponding observed data.

Model predicted changes in LS BMD following dmab 60 mg Q6 months were: 1.1, 4.0, 5.2, 6.1, 6.9, 8.5, 9.2, and 9.8% at 1, 6, 12, 18, 24, 36, 42 and 48 months, respectively, and were in close agreement with observed data: mean absolute percentage error=9.1%; mean percentage error=-7.9%. The model also predicted the nearly complete decline in osteoclast function with a slight increase in pre-dose (6 months after previous dose) CTX and BSAP with continued administration.

The use of external data to qualify the performance of the existing MSPM for prediction of BM and BMD changes associated with dmab treatment indicated that the model predictions can be generalized across data sets. These results provide further confidence in model-based predictions of physiologic changes due to modulation of the RANK-L system and related decision-making in drug development and clinical practice.



NCT00089791: placebo(gray); dmab 60mgQ6m(blue) and NCT00043186(red); Solid lines=model predictions.

Disclosures: Kyle Baron, Amgen, Inc. 2

SU0364

Sex-specific Effects of DHEA Supplementation on Bone Mineral Density and Body Composition: A Pooled Analysis of Four Randomized Controlled Trials.

Vanessa Sherk¹, Catherine Jankowski², Sundeep Khosla³, Donna Kritz-Silverstein⁴, Gail Laughlin⁴, K. Sreekumaran Nair⁵, Krupa Shah⁶, Dennis Villareal⁷, Denise Von Muhlen⁸, Edward Weiss⁹, Pamela Wolfe², Wendy Kohrt². ¹University of Colorado - Denver, USA, ²University of Colorado Denver, USA, ³College of Medicine, Mayo Clinic, USA, ⁴University of California, San Diego, USA, ⁵Mayo Clinic, USA, ⁶University of Rochester School of Medicine, USA, ⁷University of New Mexico School of Medicine, USA, ⁸University of California San Diego, USA, ⁹Saint Louis University, USA

Dehydroepiandrosterone (DHEA) supplementation in older adults has inconsistent effects on bone mineral density (BMD) and body composition. Although older women appear to have more favorable responses to DHEA therapy than older men in some trials, the potential sex-specific effects of DHEA have not been fully examined. Therefore, pooled data from four randomized, double-blinded placebo-controlled trials (Mayo Clinic, UC San Diego, UC Denver, Washington Univ) were analyzed to determine whether the effects of DHEA on BMD and body composition differ between women and men. Results are reported for women (n=283) and men (n=282) aged 55 y or older who completed a 1-year intervention of DHEA (50 mg/d or, in men at one site, 75 mg/day) or placebo. Serum hormone levels, lumbar spine and proximal femur (total hip, femoral neck, trochanter, subtrochanter) BMD, and body composition were measured at baseline and at 12 months. Serum DHEA sulfate (DHEAS) and estradiol (E₂) levels increased (all p<0.001) over 12 months in women (mean±SD: 231.2±164.0 µg/dL and 8.7±11.0 pg/mL) and men (269.4±177.2 µg/dL and 4.8±12.2 pg/mL) taking DHEA relative to those taking placebo (women: 0.5±27.2 µg/dL and -0.6±4.1 pg/mL; men: -6.7±38.5 µg/dL and -0.5±6.5 pg/mL). Total testosterone (T) increased in women on DHEA (18.6±20.9 vs 0.4±14.2 µg/dL in placebo; p<0.001), but not in men (-25.8±107.1 vs -6.9±90.5 µg/dL in placebo; p=0.11). DHEA supplementation improved lumbar spine BMD in women (1.0±3.4% vs -1.0±3.8%; p<0.001), but not men (1.0±3.5% vs 0.4±4.2%; p=0.18). Women taking DHEA also had favorable changes in total hip (0.0±2.8% vs -0.8±2.7%; p=0.007) and trochanter (0.4±3.8% vs -0.8±3.1%; p=0.008) BMD and fat-free mass (0.5±1.4 kg vs 0.0±1.3 kg; p=0.002). Men taking DHEA had greater decreases in fat mass than those on placebo (-0.4±2.3 kg vs 0.4±2.6 kg; p=0.02). In conclusion, the benefits of DHEA therapy on BMD and body composition in older adults are sex-specific. The reasons for this are not clear, but may be related to the loss of gonadal steroids in women at an earlier age than in men and the associated reliance on

prohormones, such as DHEA, for the synthesis of biologically active androgens and estrogens.

Disclosures: Vanessa Sherk, None.

SU0365

Vasodilation of the Bone Resistance Vasculature in Rats Is More Robust to PTHrP than to PTH 1-84 and PTH 1-34. Rhonda Prisby¹, Tyler Benson^{*1}, Thomas Menezes¹, Jeremiah Campbell², Enoch Samraj¹. ¹University of Texas at Arlington, USA, ²University of Texas at Arlington, USA

Parathyroid hormone (PTH) 1-84 is produced by the parathyroid gland, while parathyroid hormone-related peptide (PTHrP) is produced in a variety of tissues and cells. Further, PTH 1-34 is administered exogenously as a treatment for osteoporosis. Previously, we have shown that PTH 1-84 directly stimulates vasodilation of the femoral principal nutrient artery (PNA; the primary conduit for blood flow to long bones) via two pathways that resulted in NO-mediated signaling. In addition, both PTH 1-84 and PTH 1-34 decreased mean arterial pressure in rats; whereby a bolus injection of PTH 1-84 was a less potent, but not less efficacious, hypotensive agent. Similarly, PTHrP is a vasorelaxant in several tissue beds (e.g., the pulmonary and coronary circulation). We sought to 1) compare vasodilator responses of the femoral PNA to PTH 1-84, PTH 1-34 and PTHrP and 2) determine the signaling mechanism(s). **METHODS:** Right femoral PNAs were dissected from male Wistar rats (536 g) and cannulated to assess vasodilation to PTH 1-84 (10⁻¹³ - 10⁻⁸ M; n=10), PTH 1-34 (10⁻¹³ - 10⁻⁸ M; n=10) and PTHrP (10⁻¹³ - 10⁻⁸ M; n=6). Inhibition of nitric oxide (NO) via L-NAME and prostacyclin (PGI₂) via indomethacin were used to determine the signaling pathways involved. **RESULTS:** Vasodilation peaked at 47%, 43% and 74% of maximum to the cumulative doses of PTH 1-84, PTH 1-34 and PTHrP, respectively; whereby, vasodilation to PTHrP was significantly (p < 0.05) higher than to PTH 1-84 and PTH 1-34. Further, vasodilation to PTH 1-84 tended (p = 0.07) to be higher than that to PTH 1-34. Inhibition of NO with L-NAME reduced vasodilation by 81%, 92% and 54% with PTH 1-84, PTH 1-34 and PTHrP, respectively. The addition of indomethacin to L-NAME treated vessels did not further inhibit vasodilation vs. L-NAME alone. **DISCUSSION:** These data demonstrate a more potent bone vasodilator responsiveness to PTHrP as opposed to the full length protein (i.e., PTH 1-84) and the commonly prescribed medication for osteoporosis (i.e., PTH 1-34). Moreover, these data demonstrate that the production of NO is critical for vasodilation. Such results indicate that PTH 1-84 and PTH 1-34 may enhance skeletal blood flow, particularly during clinical treatment. However, since PTHrP is expressed in >90% of breast cancer carcinoma cases that are metastatic to bone tissue, such robust responsiveness of the bone resistance vasculature to PTHrP may also serve to detrimentally augment blood flow to tumors.

Disclosures: Tyler Benson, None.

SU0366

Characteristics of Initiators of Different Osteoporosis (OP) Medications among Women with Postmenopausal Osteoporosis (PMO) in The Health Improvement Network (THIN) in the UK. Fei Xue^{*1}, Chuck Wentworth², Victor Gastanaga¹, Cathy Critchlow¹. ¹Amgen Inc., USA, ²Analytic Consulting Solutions, Inc, USA

Background: Observational studies have suggested that different OP medications for the treatment of PMO, e.g., bisphosphonates (BPs) vs. other medications, may have dissimilar effectiveness and safety profiles. It is unclear to what extent such discrepancies are attributable to confounding by indication due to different baseline patient characteristics, such as age, comorbidities and concomitant medications.

Objectives: Describe PMO patients who initiated treatment with BPs or other OP medications.

Methods: Women ≥55 years with ≥12 months of data in the THIN database were included as PMO patients if they had received a diagnosis of OP, a diagnosis of osteoporotic fracture or treatment with OP medications, and did not have a cancer diagnosis in the period up to 5 years prior to cohort entry from 1995 to 2008. A woman with PMO was included in the BP initiator cohort if she received a BP and did not receive any OP medication in the prior 12 months. Women in the initiator cohort of other OP medications (calcitonin, parathyroid hormone and SERMs) were identified in the same manner. Each cohort was described with regard to demographic factors, comorbidities and concomitant medications based on the 12-month baseline period prior to drug initiation.

Results: In 114,760 women with PMO, 60,954 (53.1%) initiated treatment with BPs and 2,648 (2.3%) with other OP medications. Relative to initiators of other OP medications, initiators of BPs were older (mean age=73.1 vs. 66.7 yrs), and tended to have a higher prevalence of OP (17.4% vs. 15.4%), osteoporotic fracture (11.4% vs. 4.5%), hypertension (14.0% vs. 8.8%), diabetes (10.7% vs. 6.5%), heart failure (1.4% vs. 0.7%), atrial fibrillation (1.8% vs. 0.6%), coronary heart disease (5.1% vs. 3.6%), asthma (7.9% vs. 4.4%), COPD (5.0% vs. 2.0%), hypercholesterolemia (1.1% vs. 0.9%), kidney failure (0.5% vs. 0.2%), stroke (2.1% vs. 0.7%), obesity (0.5% vs. 0.3%), and anti-diabetics treatment (5.7% vs. 2.5%).

Conclusion: Our results suggest patients who initiated treatment with BPs tended to be older and have more baseline comorbidities than initiators of other OP medications, likely reflecting physician preferences when deciding whom to treat with BP, the standard of care for PMO during the study period. Such discrepancies should

be taken into consideration when comparing the post-treatment efficacy and safety profile of these medications.

Disclosures: Fei Xue, Amgen, Inc. , 7
This study received funding from: Amgen Inc.

SU0367

Clinical Results of Nonunion after Atypical Femoral Fracture. Kyu Hyun Yang*¹, Chang-Wug Oh². ¹Gangnam Severance Hospital, South Korea, ²Kyungpook National Univeristy, South Korea

Purpose: Task force of ASBMR reported the concurrent evidences regarding atypical femoral fracture (AFF) in 2010. One of them is high incidence of delayed union or nonunion up to 26% after surgical fixation. However, clinical report after surgical treatment of nonunion is still missing. We performed a retrospective study to review the clinical results of nonunion treatment in AFF.

Patients and method: Nonunion developed after surgical fixation for AFF in fifteen patients (seventeen femora) and were treated by additional intervention(s) until union. Number of subtrochanteric fracture nonunion was 10 and shaft nonunion 7. We reviewed the medical records and radiographs of these patients and compared the results of subtrochanteric nonunion with shaft nonunion.

Results: All AFF nonunion was developed in female patients. Patients of subtrochanteric nonunion group were younger than shaft nonunion group. Femoral bowing was noted in shaft fracture group only. Eleven out of 17 cases of AFF showed lateral cortical hypertrophy at the time of initial fracture. Effect of autogenous bone graft was acceptable in both groups. Average total numbers of operation were same in both groups.(Table 1)

Conclusion: Even though the incidence of nonunion after atypical femoral fracture is high compared to other low energy trauma, a proper treatment after development of nonunion resulted in good clinical outcomes by single intervention in most of the cases. Healing speed of this nonunion was slow and it took long times to be united.

| | subtrochanteric nonunion | shaft nonunion | Remarks |
|-----------------------------|--------------------------|----------------|---------|
| Cases (number) | 10 | 7 | |
| Gender | all female | all female | |
| Age(years) | 69.8 | 76.4 | p=0.033 |
| BP over 2 years (patients) | 7 | 5 | |
| Mean BP(years) | 5.3 | 3.3 | p=0.211 |
| Femoral bowing | 0 | 6 | p<0.001 |
| Local cortical hypertrophy | 7 | 4 | p=0.339 |
| Fracture age until nonunion | 7 months | 9.7 months | p=0.088 |
| Union time after nonunion | 11.6 months | 24.2 months | p=0.414 |
| total number of ORIF | 2.2 | 2.2 | |
| Autogenous bone graft | 8 | 5 | |

Characteristics of subtrochanteric and shaft nonunion patients

Disclosures: Kyu Hyun Yang, None.

SU0368

Comparative Effectiveness of Oral Bisphosphonates in Reducing Hip Fracture Risk. Suzanne Cadarette*¹, Linda Levesque², Muhammad Mamdani¹, Sylvie Perreault³, David Juurlink¹, J Michael Paterson⁴, Greg Carney⁵, Nadia Gunraj⁴, Milica Nikitovic¹, Gillian Hawker¹, Colin Dormuth⁵. ¹University of Toronto, Canada, ²Queen's University, Canada, ³University of Montreal, Canada, ⁴Institute for Clinical Evaluative Sciences, Canada, ⁵University of British Columbia, Canada

Background: Oral bisphosphonates are effective in reducing vertebral fracture risk, however, only alendronate and risedronate have proven efficacy in reducing hip fracture risk.

OBJECTIVES: To examine the comparative effectiveness of cyclical etidronate and risedronate versus alendronate in reducing hip fracture risk among older men and women.

Methods: We examined the comparative effectiveness of oral bisphosphonates in reducing hip fracture risk among new users aged 66 or more years in British Columbia (BC) and Ontario, 2001/02-2008/09. BC data included all drugs dispensed in community pharmacies. Ontario data included drugs covered through the public plan with unrestricted coverage of etidronate therapy, yet restricted access to treatment with alendronate and risedronate to those with low bone mineral density. Sex- and province-specific Cox-proportional hazards models, matched on propensity score derived from healthcare utilization data-based risk factors for fracture, were used to compare 1-year hip fracture rates between drug exposures. Alendronate was the referent in all comparisons.

Results: We identified little difference in fracture rates between etidronate or risedronate and alendronate among men and women in BC, or among women in Ontario. We similarly identified little difference in fracture rates between risedronate and alendronate (HR=0.94; 95%CI=0.79-1.16) among men in Ontario. However,

lower hip fracture rates were observed among men in Ontario treated with etidronate vs. alendronate (HR=0.75; 95%CI=0.59-0.95).

INTERPRETATION: We identified little difference in the effectiveness of alendronate or risedronate in reducing hip fracture risk among men or women. Despite being matched on measured risk factors for fracture, results suggest that residual confounding persisted with fracture rates lower among men in Ontario treated with etidronate compared to alendronate. Careful attention to province-specific drug restriction policies in Canada is important when examining the comparative safety and effectiveness of medications. Results support little difference between alendronate and risedronate in reducing hip fracture risk among men or women, with similar drug access to these agents in both provinces, and results corroborate prior findings among women. Further evidence is needed to support our findings of little difference between etidronate and alendronate, with clear policy-induced selection bias noted in Ontario, and possible residual confounding in BC.

Disclosures: Suzanne Cadarette, None.

SU0369

Correlations Between 25(OH)D and BMD Change in Postmenopausal Osteoporotic Women and other Secondary Analyses of a 1-year Trial of Weekly Alendronate (ALN) Plus Vitamin D₃ 5600 IU vs. Standard Care. Neil Binkley*¹, Steven Boonen², Douglas Kiel³, Stuart Ralston⁴, Jean-Yves Reginster⁵, Christian Roux⁶, Annpey Pong⁷, Elizabeth Rosenberg⁸, Arthur Santora⁹. ¹University of Wisconsin, Madison, USA, ²Katholieke Universiteit Leuven, Belgium, ³Hebrew SeniorLife, USA, ⁴University of Edinburgh, United Kingdom, ⁵University of Liege, Belgium, ⁶Hospital Cochin, France, ⁷Merck Sharp & Dohme, USA, ⁸Merck & Co., Inc., USA, ⁹Merck Research Laboratories, USA

Objective: Vitamin D supplements are recommended as adjunctive therapy with anti-osteoporotic drugs. In this international, randomized trial, women receiving single tablet alendronate/vitamin D₃ 5600 IU (ALN/D) for 1 year had higher 25(OH)D, higher BMD, and lower bone turnover markers than women receiving Standard Care (prescribed by patients' personal physicians who were not investigators in the trial), even though a majority of Standard Care participants took a bisphosphonate (most often ALN) plus varying doses of vitamin D. Subgroup analyses and determination of correlations between serum 25(OH)D and BMD change in patients treated with alendronate were performed.

Methods: Participants were postmenopausal women ≥65 years old with BMD T-scores at spine or hip of ≤-2.5 (or ≤-1.5 with prior fragility fracture), 25(OH)D 8 to 20 ng/mL, and increased risk of falls. The primary study endpoint was proportion of participants with 25(OH)D <20 ng/mL.

Results: Participants (n=515) were of mean age=73 years, 72% Caucasian, with mean baseline 25(OH)D=14.8 ng/mL. After 1 year, fewer women taking ALN/D than Standard Care had 25(OH)D <20 ng/mL among all trial participants and in the following : baseline 25(OH)D ≤ or >15 ng/mL, age ≤ or >75 years, and European or non-European residence. Among Standard Care women receiving ALN, end-of-study 25(OH)D levels correlated positively with percent increase from baseline in lumbar spine and femoral neck BMD (Table, Pearson correlation coefficients (95% CI)=0.23 (0.02, 0.41) and 0.24 (0.03, 0.41), respectively). Baseline 25(OH)D levels correlated with increases in only lumbar spine BMD (Table, Pearson correlation coefficient (95% CI)=0.22 (0.01, 0.40)).

Conclusions: In osteoporotic postmenopausal women with low 25(OH)D, the increase in lumbar spine and femoral neck BMD during treatment with alendronate was positively correlated with serum 25(OH)D. This parameter could be a determinant to optimize the BMD response to alendronate.

Correlations between Tertiles of 25(OH)D and % Change from Baseline in BMD in Standard Care Patients Receiving ALN

| | Increasing Tertiles of Baseline 25(OH)D | | | Increasing Tertiles of 1 year 25(OH)D | | |
|---|---|-----------|-----------|---------------------------------------|-----------|-----------|
| | 1 | 2 | 3 | 1 | 2 | 3 |
| Mean 1-year % change in LUMBAR SPINE BMD (SE) | 3.7 (0.8) | 5.2 (0.7) | 5.9 (0.8) | 3.9 (0.7) | 4.9 (0.8) | 5.8 (0.8) |
| [Range of 25(OH)D (ng/mL)] | [5-11] | [11-16] | [16-38] | [6-22] | [22-29] | [29-47] |
| Mean 1-year % change in FEMORAL NECK BMD (SE) | 2.1 (0.7) | 1.9 (0.6) | 2.3 (0.8) | 1.3 (0.6) | 2.4 (0.7) | 2.9 (0.8) |
| [Range of 25(OH)D (ng/mL)] | [5-12] | [12-16] | [16-38] | [6-22] | [22-29] | [29-47] |

Table

Disclosures: Neil Binkley, Merck Sharp and Dohme, 6; Merck Sharp and Dohme, 2
This study received funding from: Merck Sharp & Dohme Corp.

SU0370

Evaluation of 42 Cases of Subtrochanteric Fractures using the ASBMR Taskforce Criteria for Atypical Femoral Fractures. Angela Juby*, Sean Crowther. University of Alberta, Canada

Purpose

The purpose of this study was to evaluate the radiographs of cases of subtrochanteric fracture identified in a database search, and see whether they fulfilled the ASBMR taskforce criteria for atypical femoral fracture.

Method: Data was obtained from a retrospective chart review of all cases with an ICD 10 code for subtrochanteric fracture or unspecified hip or femur fracture, referred to two tertiary care hospitals over a seven year period (2002-2009), in Edmonton, Alberta, Canada. 50 cases of isolated subtrochanteric fracture or femoral shaft fracture were identified after chart review, out of 232 probable cases suggested by coding alone. A radiologist independently reviewed all 50 cases using the ASBMR Taskforce criteria to assess for atypical femoral fracture. Ethics approval was obtained from the regional ethics review board.

Results: Radiographic films were available for review in 42 cases. In 8 cases (4 each from 2002 and 2003) films were not available. Of those 42, 19 fulfilled the criteria for atypical fracture, that is, they all had the five major features: location; appropriate history; transverse or short oblique; non-comminuted; and a possible medial spike. 7 of these cases also had radiological minor features (cortical thickening, delayed healing or bilaterality). Clinical data review identified a further 11 cases with positive minor features, bringing 18/19 cases having all five major and some minor features. The clinical minor features included prodromal symptoms (5 cases), comorbidities (4), bisphosphonate use (13), glucocorticoid use (4), anticonvulsant use(1). Of interest, the 5 previously reported cases based on general X ray reports and prodromal symptoms, 3 did not meet the new criteria for atypical femoral fracture.

Conclusions: Atypical femoral fractures are rare fractures. Over a seven year period, from two major referral hospitals servicing Northern Alberta (a catchment area of approximately 2 million people), only 50 possible cases were identified from general radiographic reports. However, only 19/42 (45%) of these were true atypical femoral fractures based on the ASBMR criteria. During the study period, approximately 21 000 typical osteoporotic hip fractures would have occurred, highlighting the much greater risk of typical versus atypical fractures in osteoporotic patients.

Disclosures: *Angela Juby, None.*

SU0371

Is Bisphosphonate Use Associated with Atypical Humeral Diaphyseal Fractures? Debra Sietsema¹, Clifford Jones*¹, Martin Hoffmann². ¹Orthopaedic Associates of Michigan; Michigan State University, USA, ²Grand Rapids Medical Education Partners, USA

Introduction: A number of recent case series and retrospective reviews have identified a subgroup of atypical fractures of the femoral shaft associated with bisphosphonate use. These case series have suggested that long-term bisphosphonate use may ultimately alter bone strength, most likely due to suppression of bone turnover. The purpose of this study was to determine whether there was an association between bisphosphonate use and atypical humeral diaphyseal fractures.

Methods: From 2003-2010, a retrospective review of patients with humeral fractures was completed.

Results: 71 humeral diaphyseal fractures with low energy mechanism of injury were identified in 50 (70%) females and 21 (30%) males with an average of 74 (50-96). 13 of 71 (18.3%) had current or prior bisphosphonate usage. A statistically significant difference (p=0.001) occurred in the incidence of atypical fractures between prior bisphosphonate use 8 of 13 (61.5%) as compared to 9 of the 54 (16.7%) without bisphosphonates. The "atypical" diaphyseal humeral patterns were: 1 transverse or short oblique with cortical thickening (type I), 13 lateral bending wedge (type II), and 3 severely comminuted (type III). Patients with "atypical" fracture patterns had bisphosphonate usage for an average of 5.6 years (0.4-12 years) compared to 2.4 years (0.4-4.8 years) of bisphosphonate usage for those without these fracture patterns. Additionally, worsening atypical fracture pattern type corresponded to duration of bisphosphonate usage.

Conclusion: Multiple case series have demonstrated that bisphosphonate usage is associated with atypical subtrochanteric femoral fractures. This is the first case series report to associate atypical diaphyseal humeral fractures with prolonged bisphosphonate use. Additionally we recommend a classification scheme. Further analysis and prospective studies to more fully delineate the association between bisphosphonate usage and atypical fractures in the humerus and other parts of the skeleton are recommended.

Disclosures: *Clifford Jones, Eli Lilly, 2; Eli Lilly, 1*

SU0372

Is Zoledronic Acid Retention onto Bone Different in Multiple Myeloma and Breast Cancer Patients with Bone Metastasis? Kent Soc*¹, Torben Plesner², Erik H. Jakobsen³, Charlotte T. Hansen⁴, Henrik B. Jorgensen⁵, Jean-Marie Delaisse⁶. ¹Vejle Hospital, University of Southern Denmark, Denmark, ²Vejle Hospital, Medical Department, Denmark, ³Vejle Hospital, Department of Oncology, Denmark, ⁴Odense University Hospital, Dept. of Hematology, Denmark, ⁵Vejle Hospital, Dept. of Nuclear Medicine, Denmark, ⁶Vejle Hospital, IRS, University of Southern Denmark, Denmark

The bone seeking bisphosphonate zoledronic acid (Zol) is given as a monthly dose (although this may vary) of 4 mg to both multiple myeloma (MM) and breast cancer pts with bone metastasis (BC). However, bones of MM and BC pts show a difference in retention of the bisphosphonate probe used for bone scintigraphy. Therefore we hypothesized that disease-specific factors may differently influence Zol retention in MM and BC pts.

In order to test this hypothesis, we established an investigator initiated phase II clinical protocol on 30 MM and 30 BC patients (10 Zol naive and 20 with ≥ 6 previous administrations for each disease). The degree of Zol retention was determined by quantifying the amount of Zol in 48h post infusion urine. Serum levels of CTX and bALP at day 0 and 14 were also measured to evaluate bone resorption and formation, respectively. Bone scintigraphy was also conducted.

On average, 2.5 mg Zol was retained in the skeleton of both MM and BC after each administration, and around 24 mg accumulated after one year of treatment. In MM multiple administrations did not result in saturation, but in BC a negative linear correlation (p=0.018) was found between the average mg Zol dose per month and the amount of Zol retained at next infusion. This suggests that there is some degree of saturation in BC. Zol retention did not correlate with CTX levels. Using linear regression analyses, Zol retention correlated with bALP levels in BC (p=0.001) but not in MM, whereas correlation with CTX/bALP ratio was significant for Zol naive MM (p=0.012) and nearly significant for all MM (p=0.066) but not for BC pts. Multivariate linear regression analyses combined with likelihood-ratio tests on the entire cohort demonstrated that Zol retention was best predicted by the average mg Zol dose/month (p=0.005), age (p<0.001) and number of metastases/lesions (p=0.001)(R²=0.97). The bisphosphonate probe used in scintigraphy bound in general more weakly to sites of high bone turn-over in MM compared to BC, and 20% of MM pts showed "cold" lesions.

In conclusion, MM and BC pts retain similar amounts of Zol. Most of the binding appears to be determined by similar factors in MM and BC, incl. administration frequency, age and number of metastasis/lesions. However, our data also suggest that some of the site-specific binding might be determined by disease-specific factors that can be critical for Zol activity at sites of bone destruction, as expected from bone scintigraphy.

Disclosures: *Kent Soe, Novartis, 6*

This study received funding from: Novartis

SU0373

Ocular Inflammatory Reactions in Patients treated with Osteoporosis Medications – Cohort Analysis using a National Prescription Database. Michael Pazianas¹, Kim Brixen², Pia Eiken³, Emma Clark⁴, Bo Abrahamson*⁵. ¹University of Oxford, United Kingdom, ²Institute for Clinical Research, Denmark, ³Hilleroed Hospital, Denmark, ⁴University of Bristol, United Kingdom, ⁵Copenhagen University Hospital Gentofte, Denmark

Ocular inflammatory reactions have been described in patients on bisphosphonate (BP) treatment. We estimated the incidence rate of ocular inflammation at 3 and 12 months in patients treated for osteoporosis using a register based cohort linked to prescription data (hospitals and private practice) and hospital data. Between Jan 1, 1997 and Dec 31, 2007, a total of 88,202 patients beginning osteoporosis therapy were identified. Of those patients, 82,404 (93%) began oral BPs and 5798 (7%) non-BPs.

Topical eye steroids (TES): Within the first year of treatment, 4,769 (5.4%) filled one or more prescriptions for TES. More subjects on alendronate or etidronate used TES in the first year of treatment, compared to the year before (5.9% vs 5.1%, p<0.05; 5.5% vs 4.7%, p<0.05 respectively). The difference in ibandronate users was of similar magnitude but did not reach statistical significance (6.3% vs 3.8%, p=0.07). TES treatment rates (per 1000 patient years) in the first year of osteoporosis treatment were 44 (95% CI 42-46) for alendronate, 40 (38-43) for etidronate, 45 (35-57) for risedronate, 32 (27-37) for raloxifene and 64 (49-83) for strontium ranelate. After adjustment for age, Charlson index, and the number of co-medications, pulmonary disease in men was associated with an increased risk (1.48; 1.17-1.86, p=0.001). In women, malignant disease (OR 1.27; 1.02-1.60, p=0.04) and pulmonary disease (1.32; 1.07-1.62, p=0.01) were significant predictors at 3 months and rheumatic diseases at 12 months (1.20; 1.10-1.31, p<0.001). There was no significant difference between the different drug classes (BPs vs non-BPs, alendronate vs non-alendronate-BPs) for risk of ocular inflammation, with age and the number of co-medications being the only significant predictors.

Hospital treated uveitis: Hospital treated uveitis occurred in 48 subjects (0.05%) with no significant difference between the different drug classes. Age and the number of co-medications were the only significant predictors.

In conclusion, following initiation of treatment for osteoporosis, the risk of inflammatory eye reactions requiring TES is relatively low and not significantly different between BP and non-BP users. Patients with a rheumatic or pulmonary disease are at increased risk.

Disclosures: Bo Abrahamsen, Warner-Chilcott, 2

SU0374

Osteonecrosis around Dental Implants in Patients with Bisphosphonate Treatment. Tae-Geon Kwon^{*1}, Je-Yong Choi², Hong-In Shin³.
¹Kyungpook National University, School of Dentistry, South Korea, ²Kyungpook National University, School of Medicine, South Korea, ³Dept. of Oral Pathology, School of Dentistry, Kyungpook National University, Samduck 2 Ga, Jung Gu, South Korea

Background: The prognosis of dental implant placed in patients covering bisphosphonates (BP) remained uncertain. Bisphosphonate-related jaw necrosis (BRONJ) associated with dental implant is a rare but continuously reported. To verify related risk factors and clinical characteristics of BRONJ, the present study analyzed the patients with the osteonecrosis of the jaw around dental implant following the BP administration. **MATERIAL & METHODS:** The 17 patients with osteonecrosis of the jaw associated with dental implant were diagnosed and treated at our institute from 2008 to 2011. Patients' medical histories, demographic features, histo-pathological, radiographic and laboratory findings were documented with information of BP administration. **RESULTS:** Of the BRONJ patients associated with dental implants, 52% (n=9) had mandibular development, seven had maxillary involvement and one had maxillo-mandibular involvement. Oral BP users were dominant (n=13, 76.5%) than intravenous BP. Four patients developed osteonecrosis within 6 months after the surgery, which suggests surgical process during the dental implant procedure can be a contributing factor. However, other 11 patients showed successful osteointegration after the fixture installation for average 23 months (12~53 months) until the development of osteonecrosis. Moreover, two patients successfully maintained implants over than 2 years and BRONJ developed after BP administration and not by the implant surgery. Therefore, only 23.5% of the patients could be regarded as "surgically-triggered" BRONJ. Non-decalcified section of en-bloc osseous sequestration with implant showed that the osseointegration were partially remained around the implants. **CONCLUSION:** Considering the time between implant placement and BP administration, our results and those of others imply that already osseointegrated dental implant also can cause the osteonecrosis around the implant after BP administration. Potential risk of BRONJ need to be explained to patients before or after the dental implant installation if intravenous BP or long term oral BP administration is indicated.

Disclosures: Tae-Geon Kwon, None.

SU0375

Rapid Resolution with Teriparatide in Delayed Healing of Atypical Fracture Associated to Long-Term Bisphosphonate Use. Silvina Mastaglia^{*1}, Gabriel Aguilar², Beatriz Oliveri³. ¹SECCIÓN OSTEOPATÍAS MÉDICAS, HOSPITAL DE CLÍNICAS, Argentina, ²Centro de Diagnóstico Dr. Enrique Rossi, Argentina, ³Centro De Osteopatías Médicas, Argentina

Bisphosphonates (BF) are the drugs most widely used to treat osteoporosis due to their efficiency in reducing osteoporotic fractures and improving bone mineral density (BMD). However, recent reports associate long-term bisphosphonates (BF) use with low-impact atypical fractures and prodromal pain¹. Delayed fracture healing was observed in 26% of the cases¹. Teriparatide is an anabolic drug which has shown to be effective in stimulating bone formation. **Purpose:** Description of the evolution of a right femoral diaphyseal fracture developed in a patient while taking her long term BF treatment. Her fracture suffered a delay in its healing and it rapidly healed with teriparatide treatment. **Case Report:** A 57-yr-old postmenopausal Caucasian female, with a delayed healing of her right femoral diaphyseal fracture, after 10 months, despite of an orthopedic treatment. Her fracture had been preceded by a 9-month progressive, bilateral and severe pain in thighs. Her medical history included a vulvar cancer at 44, osteoarthritis and osteopenia treated with alendronate over 7 yrs. Menopause at 49. Her family history did not include any a maternal fragility fracture. She never smoked or consumed alcohol excessively. In first visit, she was using a walking-stick. It was considered as an atypical right femoral fracture associated to long-term alendronate use. According to this information alendronate was suspended. The following studies were performed: bone densitometry [(DXA, Lunar Prodigy, Madison, USA): Lumbar Spine (L2-L4): 0.912g/cm²; T-score: -2.4 and Left Total Femur: 0.805g/cm²; T-score: -1.6]; mineral metabolism laboratory iPTH: 40ng/ml (rv:10-65ng/ml), 25OHD: 40ng/ml (rv:>30ng/ml); sCTX: 318 ng/ml (rv:80-590ng/ml), BSAP: 76UI/l (rv:31-95UI/L)] and a left femur magnetic resonance imaging (MRI) which revealed a diaphyseal fracture from stress. Prescription: 20µg daily of subcutaneous teriparatide (recombinant human PTH1-34; Forteo; Eli Lilly & Co., IN). After a 10-day treatment, the patient expressed a significant pain reduction, no longer requiring any device to walk. In 3 months, a CT scan showed the healed fracture, thus the patient could return to her usual activities. **Conclusion:** Atypical

fracture healing associated to a long-term alendronate use was accelerated by 20µg daily subcutaneous teriparatide, leading to a fast recovery of her mobility and quality of life.

¹ J Bone Miner Res. 2010; 25:1-28.

Disclosures: Silvina Mastaglia, None.

SU0376

Use of Bisphosphonates and Risk of Atypical Femur Fracture: a Systematic Review and Meta-analysis. Seouyoung Kim¹, Lydia Gedmintas^{*1}, Daniel Solomon². ¹Brigham & Women's Hospital, USA, ²Harvard Medical School, USA

Background: Bisphosphonates are the most commonly used drugs for the prevention and treatment of osteoporosis. Although there have been an increasing number of studies reporting a link between use of bisphosphonates and atypical femur fracture (AFF) in the subtrochanteric or diaphyseal region as a consequence of over-suppression of bone resorption, there is still limited data available.

Objectives: We aimed to conduct a systematic review and meta-analysis of published studies to evaluate risk of AFF associated with bisphosphonate use.

Methods: A comprehensive search in MEDLINE and EMBASE was performed using a combination of the Medical Subject Headings and keywords (January 1st, 1990 to December 26th, 2011). Our search was limited to English language articles. Case series or reports were excluded. We calculated pooled risk ratios (RR) using a random-effects model and examined between study heterogeneity with the I-squared statistic.

Results: Eleven eligible studies including 2,203,178 patients were identified. One reported the results of secondary analyses of randomized clinical trials, plus 5 cohort and 5 case-control studies. Across all studies, bisphosphonate exposure was associated with an increased risk of AFF [pooled RR: 2.71; 95%CI: 1.42-5.21]. Large heterogeneity was noted (I-squared= 92%). Stratified analyses by study design showed a RR of 3.48 (95%CI 1.11-10.95) for case-control studies. Subgroup analysis of 6 studies including data regarding long-term use of bisphosphonates yielded a RR of 3.70 with a wide 95%CI (0.35-38.81). After limiting the analysis to 2 studies that confirmed the characteristics of AFF in the long-term users of bisphosphonates, the RR was 13.79 (95% CI 1.46-130.40).

Conclusions: Our study found an elevated risk of AFF associated with bisphosphonate exposure. A more pronounced risk was observed in long-term users of bisphosphonates and in studies that confirmed the type of fracture. Given the heterogeneity between the studies and the known benefit of bisphosphonates on osteoporosis, these results should be interpreted with caution but suggest that bisphosphonate use is associated with an increased risk of relatively rare femoral fractures.

Disclosures: Lydia Gedmintas, Pfizer, 6; Takeda Pharmaceuticals North America, 6

SU0377

What Predicts Osteoporosis Treatment in Nursing Home Residents: Baseline Data from the ViDOS Cluster Randomized Controlled Trial. Courtney Kennedy^{*1}, Alexandra Papaioannou², George Ioannidis¹, Lora Giangregorio³, Lehana Thabane⁴, Irenea Soles¹, Suzanne Morin⁵, Richard Crilly⁶, Susanne King⁷, Mary-Lou van der Horst¹, Lisa Dolovich⁷, Ravi Jain⁸, Jonathan Adachi⁹. ¹McMaster University, Canada, ²Hamilton Health Sciences, Canada, ³University of Waterloo, Canada, ⁴McMaster University, Dept. Clinical Epidemiology & Biostatistics, Canada, ⁵McGill University, Canada, ⁶University of Western Ontario, Canada, ⁷Dept Family Medicine, McMaster University, Canada, ⁸Osteoporosis Canada, Canada, ⁹St. Joseph's Hospital, Canada

Background: Previous studies indicate that non-profit long-term care (LTC) homes perform better on a variety of quality of care measures than for-profit LTC homes, however few studies have examined facility characteristics other than their profit status. Prescribing-related outcomes as a measure of quality of care have also not been well-examined. The Vitamin D and Osteoporosis (ViDOS) study is a cluster randomized controlled trial to improve evidence-based osteoporosis (OP)/fracture prevention strategies in LTC homes in Ontario, Canada. Using baseline data from 40 LTC homes (n=19 intervention, n=21 control), we report osteoporosis medication prescribing in all residents and for those at high-risk because of a prior hip fracture. We also examined the relationship between facility characteristics and the use of OP medication. **Methods:** De-identified clinical/prescribing data was downloaded from the database of the pharmacy provider that services all study homes. Information about fractures was gathered from Medication Administration Records. The facility's characteristics were collected from LTC administrators/care directors or via publicly available information on the health ministry web-site: size of LTC home (small: < 100; medium: 100-199; large ≥ 200 beds); community size (small: <30,000; medium: 30,000-99,999; large: ≥100,000 people); profit status (non-profit/profit); and chain affiliation (chain/non-chain). The generalized estimating equations technique, assuming an exchangeable correlation structure, was used to examine associations between facility characteristics and OP medication prescribing. The LTC home was used as the clustered variable in all analyses. **Results:** Overall, there were 5454 residents [71% women, mean age=82.8 (standard deviation [SD] 10.8) years] residing

in the 40 ViDOS study homes. The mean facility size was 142 residents (SD 79.5, range 43-378). At baseline, 6.5% (n=355) of residents had a documented hip fracture. Prescribing rates for OP medications were 20% for all residents and 35% for residents with a documented hip fracture. The table below presents the OP medication prescribing rates according to facility characteristics. Conclusion: OP medication use was higher in residents with hip fractures. Prescribing rates were significantly higher as home size increased and in non-profit homes.

| | % (n/N) | Odds Ratio (95% Confidence Intervals) |
|--------------------------|-----------------|---------------------------------------|
| Size of home | | |
| Small (n=14) | 16.2 (141/872) | 0.65 (0.43, 0.97) |
| Medium (n=16) | 18.6 (409/2202) | 0.82 (0.56, 1.19) |
| Large (n=10) | 22.1 (525/2380) | Reference |
| Community size | | |
| Small (n=16) | 18.9 (254/1345) | 0.88 (0.64, 1.25) |
| Medium (n=4) | 24.7 (98/397) | 1.45 (0.71, 2.99) |
| Large (n=20) | 19.5 (723/3712) | Reference |
| Profit Status | | |
| Non-profit (n=5) | 25.0 (285/1142) | 1.49 (1.16, 1.91) |
| For-profit (n=35) | 18.3 (790/4312) | Reference |
| Chain affiliation | | |
| No (n=8) | 22.2 (318/1434) | 1.07 (0.73, 1.57) |
| Yes (n=32) | 18.8 (757/4020) | Reference |

Residents Taking Osteoporosis Medication

Disclosures: Courtney Kennedy, None.

SU0378

Are there Racial and Ethnic Differences in Weighting of Patient Preferences about Osteoporosis Medication Attributes? Stuart Silverman^{*1}, Andrew Calderon², Deborah Gold³. ¹Cedars-Sinai/UCLA, USA, ²OMC Clinical Research Center, USA, ³Duke University Medical Center, USA

Introduction: Decision-making about osteoporosis (OP) medication-related behavior relies heavily on patient preferences about specific medication attributes. Patients may decide to initiate, change, or stop therapies based on ranking of perceived attributes of the therapy and their personal attitudes toward those attributes. We used Max-Diff, a form of conjoint analysis, to understand patient weighting of attributes across four racial/ethnic groups at two sites in the United States.

Methods: Using qualitative interviewing, we identified four basic osteoporosis medication attributes: efficacy, safety, cost and convenience. We then recruited a sample of 367 PM women at risk of OP fractures in Los Angeles, CA and Durham, NC belonging to four racial/ethnic groups: Caucasian (n=100), African-American (n=100), Asian-American (n=82), and Hispanic-American (n=85). Respondents completed a laptop-based questionnaire that included a demographic questionnaires; they also weighted 39 statements about these four attributes from least important to most important. Based on the weighting of these statements, MaxDiff analyses were then done to evaluate the relative weight of each attribute.

Results: Overall, our participants in all four groups rated efficacy > safety > cost > convenience. Although there were no differences between the racial/ethnic groups on overall ranking of attributes, subgroup analyses revealed significant (p<0.05) effects of age, education, and income on ranking of attributes.

Conclusions: The findings of this study confirm that individual postmenopausal women differ in their rankings of osteoporosis medication attributes. Differences by race and ethnicity may be less important than differences by age, education, and income. Healthcare providers must account for individual patient preferences as they communicate about and prescribe osteoporosis medications.

Disclosures: Stuart Silverman, None.

This study received funding from: Novartis Pharmaceuticals

SU0379

Association of Gastrointestinal events and Osteoporosis Treatment Persistence in a Managed Care Setting. Ethel Siris^{*1}, Tao Fan², Chun-Po Steve Fan³, Shiva Sajjan⁴, Shuvayu Sen⁵, Ankita Modi⁴. ¹Columbia University College of Physicians & Surgeons, USA, ²Merck, USA, ³AsclepiusJT LLC, USA, ⁴Merck & Company, USA, ⁵Merck & Co., Inc., USA

Purpose: To examine the association between gastrointestinal (GI) events developed after initiation of osteoporosis (OP) therapy and treatment persistence.

Method: A retrospective cohort study using i3 Invision Datamart; a large U.S. claims database from January 2001 to December 2010 (study period) was conducted. Women 50 years or older, who had a prescription of an oral bisphosphonate (BIS) (alendronate, ibandronate, risedronate) during study period with continuous enrollment 1 year prior to (baseline) and after (follow-up) the first BIS prescription date (index date) were included. Women with Paget's disease or malignant neoplasm in baseline or follow-up were excluded. Four mutually exclusive treatment patterns (Persistent, Switcher, Discontinuer, and Augmenter) were created based on the first treatment change experienced in the follow-up. Gastrointestinal events were identified using ICD-9 diagnoses codes for GI symptoms in follow up. GI events could be new, recurrent or pre-existing (i.e., present prior to the study period) during the follow up period after OP treatment initiation. The study design does not ascribe causality of GI events. Cox models were used to assess the association of GI events in the follow-up period (post-treatment GI) with treatment patterns adjusting for age, OP-related fractures at baseline, and Charlson comorbidity index. Time to first treatment change (i.e., either discontinuation, switching or augmentation) was analyzed using cox models with post-treatment GI as a time-varying covariate and baseline GI as stratifying variable.

Results: 99,788 women met inclusion criteria. Of these women, 39,166 (39.2%) persisted, 545 (0.5%) switched, 59,843 (60.0%) discontinued, and 234 (0.2%) augmented therapy. The mean time to switch, discontinuation, and augmentation were 103.8 days, 115.9 days, and 106.9 days respectively. 27,455 (23.2%) experienced post-treatment GI events. Compared to patients without a post-treatment GI event, women with post-treatment GI events were associated with a 35% increased likelihood of switching or discontinuing treatment [HR (95% CI): 1.35 (1.32, 1.39), p<0.05] in reference to those who persisted on therapy.

Conclusion: Patients who experienced GI events while on therapy were significantly more likely to discontinue or switch their initial OP treatment as compared to those without GI events. Study results have implications for further improving OP disease management among patients with gastrointestinal problems.

Disclosures: Ethel Siris, Amgen, Lilly, 1; Amgen, Lilly, Merck, 2
This study received funding from: Merck and Company

SU0380

National Bone Health Alliance: A Multi-Sector Public-Private Partnership Working Together to Improve America's Bone Health. David Lee^{*}. National Bone Health Alliance, USA

The U.S. National Bone Health Alliance (NBHA) is a public-private partnership launched in 2010 that brings together the expertise and resources of its member organizations to collectively promote bone health and prevent disease; improve diagnosis and treatment of bone disease; and enhance bone research, surveillance and evaluation.

NBHA membership currently includes 41 members (28 non-profit organizations and 13 companies) as well as liaisons representing the CDC, FDA and NIH (ASBMR is among the founding members of the NBHA).

The concept for NBHA stems from two major activities:

1. The 2004 *Bone Health and Osteoporosis: A Report of the Surgeon General* called for bone health stakeholders to join forces to develop a National Action Plan.
2. The *Summit for a National Action Plan for Bone Health*, convened in June 2008, involved more than 150 individuals representing an array of stakeholders.

The recommendations contained in the summit report focused on four priority areas: develop a bone health alliance; promote bone health and prevent disease; improve diagnosis and treatment; and enhance research, surveillance and evaluation.

NBHA provides a platform for its collective voice to weigh in on subjects important to bone health, particularly vitamin D, calcium, DXA reimbursement and utilization and the risks and benefits of use of bisphosphonates and other bone health therapies; ongoing communication among individuals and organizations interested in bone health; shared priorities and projects to become reality through pooled funding; and stakeholders to work together towards the goals and recommendations of the *National Action Plan on Bone Health*.

The operations and major activities of NBHA are funded through financial support from its members, which may include but are not limited to corporations, academic and medical institutions, professional and membership organizations, associations, advocacy groups and non-profit and philanthropic organizations. The members of the Alliance are working from a shared vision: to improve the overall health and quality of life of all Americans by enhancing their bone health.

NBHA is implementing three major initiatives in 2012:

1. Secondary Fracture Prevention Initiative;
2. 2 Million 2 Many Public/Health Professional Awareness Campaign
3. Bone Turnover Marker Standardization Project

In addition to these projects, NBHA is identifying additional project areas and activities to pursue (and also convenes a rare bone working group).

Disclosures: David Lee, None.

SU0381

Predictors of Non-adherence to Bisphosphonates for Male Veterans with Osteoporosis and/or Osteoporotic Fracture: Importance of Mental Health Conditions. Lewis Kazis^{*1}, Austin Lee², Mingfei Li³, Joanne LaFleur⁴, Steven C. Vlad⁵, Kathleen Carey⁶, Priscilla Chew⁷, David Chandler⁸, Nicole Yurgin⁹, Robert Adler¹⁰. ¹Boston University School of Public Health, Boston, MA, USA, ²Boston University, USA, ³Bentley University, USA, ⁴University of Utah, USA, ⁵Boston University School of Medicine, USA, ⁶Boston University School of Public Health, USA, ⁷Edith Nourse Rogers VA Medical Center, USA, ⁸Amgen Inc, USA, ⁹Amgen Inc., USA, ¹⁰McGuire VA Medical Center, USA

Background:In women, adherence of $\geq 80\%$ to long-term bisphosphonate therapy is required to demonstrate fewer osteoporotic fractures, fewer hospitalizations, and lower costs. There are few studies of bisphosphonate adherence in men, and reasons for non-adherence are unknown. The objective of this study was to assess the determinants of adherence among male veterans diagnosed with osteoporosis and/or osteoporotic fracture who were receiving bisphosphonate therapy.

Methods:A retrospective analysis of a cohort of veterans treated during fiscal years 2005 to 2009 was performed using the Department of Veterans Affairs' (VA) administrative databases. The VA Decision Support System (DSS) was used to identify men with a diagnosis of osteoporosis and/or osteoporotic fracture who had received prescriptions for alendronate (10 mg or 70 mg), risedronate (5 mg, 30 mg, or 150 mg), or ibandronate (150 mg). The medication possession ratio (MPR) was defined as the dependent variable and was computed as the ratio of total supply of bisphosphonate prescription dispensed (days) divided by the total prescription period (days). Independent variables included age, marital status, medical co-morbidities (a count based on the established Selim index ranging from 1 to 30), and mental co-morbidities (specifically depression, anxiety, post-traumatic stress disorder [PTSD], alcohol abuse, and schizophrenia). Multivariable logistic regression was conducted with MPR dichotomized as $< 80\%$ (non-adherent) vs. $\geq 80\%$ (adherent). Results are reported as odds ratios (ORs) with 95% confidence intervals. A separate logistic model was used to analyze the interaction of depression and alcohol abuse with adherence.

Results:In total, 77,370 subjects met the inclusion criteria with a mean age of 72 years, 34% were not married, and they had a mean of 3 co-morbidities. Of the mental co-morbidities, 16% had depression, 6.6% had anxiety, 5.8% had PTSD, 4.4% had alcohol abuse, and 1.5% had schizophrenia. The most significant ORs for non-adherence ($< 80\%$) were alcohol abuse (1.57 [1.46, 1.69]) and depression (1.21 [1.16, 1.27]). Another logistic regression model showed that patients with both depression and alcohol abuse have a higher OR 2.47 [2.21, 2.76] ($P < 0.001$) compared with those without depression and alcohol abuse.

Conclusion:In male veterans with osteoporosis and/or osteoporotic fracture, adherence to bisphosphonate therapy was lowest in those who had a diagnosis of depression and alcohol abuse.

Disclosures: Lewis Kazis, Amgen Inc., 6
This study received funding from: Amgen Inc.

SU0382

Variation in the Days Supply Field for Osteoporosis Medications in Ontario. Andrea Burden^{*1}, Angie Huang², Mina Tadrous¹, Suzanne Cadarette¹. ¹University of Toronto, Canada, ²Institute for Clinical Evaluative Sciences, Canada

Purpose:Pharmacy claims data are commonly used to examine patterns of drug utilization and to classify drug exposure in postmarketing research. However, the accuracy of the days supply field has not received great attention. We sought to describe the days supply reported for osteoporosis drugs (bisphosphonates, calcitonin, raloxifene) by dosing regimen and examine if the days supply reported matched the typically expected dosing interval.

Methods:We used data submitted to the Ontario Drug Benefits program for residents aged 65 or more years to examine the variation in days supply reported for osteoporosis medications, 1997-2011. The number and proportion of days supply values submitted were summarized by dosing regimen (daily-, weekly-, and monthly-oral; nasal spray; cyclical - 14 days active drug + 76 days calcium; and yearly infusion), and residence status (community vs. long-term care [LTC] resident). We defined "typically expected" days supply by the dosing regimen: daily in 7-, 30-, or 100-day intervals, weekly in 7- or 30-day intervals, monthly and nasal spray in 28- or 30-day intervals, and cyclical as 90-day supply.

Results:We identified 17,615,364 osteoporosis prescriptions dispensed to community (78%) or LTC. Most daily oral prescriptions (97%) were dispensed for a typically expected days supply. However, distinct differences were observed for other regimens with the typically expected days supply more common in community vs. LTC: cyclical etidronate (86% community vs. 40% LTC), weekly oral (91% community vs. 60% LTC), and monthly oral (94% community vs. 35% LTC) or nasal spray (84% community vs. 40% LTC). In both settings, annual zoledronic acid infusion was most commonly dispensed as 1-day supply (62%).

Conclusions:Results suggest that there may be reporting errors in the days supply field in Ontario pharmacy claims, particularly among prescriptions dispensed in LTC. The variation noted for osteoporosis medications in Ontario are likely indicative of similar reporting errors for other drugs and in other regions. Errors in the days supply

field may have significant implications for drug exposure misclassification in pharmacoepidemiologic studies.

Disclosures: Andrea Burden, None.

SU0383

Effects of Bazedoxifene on Intervertebral Disc Height and Association With Incident Vertebral Fractures in Postmenopausal Women. Nancy Lane^{*1}, Thomas Fuerst², Amy B. Levine³, Teresa Hines³, Robert Williams³, Santosh Sutradhar³, Arkadi Chines⁴. ¹University of California at Davis, USA, ²Synarc Inc, USA, ³Pfizer Inc, USA, ⁴Amgen Inc., USA

Purpose: Reduced intervertebral disc height (DH) has been associated with a risk of incident vertebral fractures (Sornay-Rendu et al, *Arthritis Rheum.* 2006). Interestingly, estrogens preserve intervertebral disc space in postmenopausal women. Bazedoxifene (BZA), a selective estrogen receptor modulator, prevents and treats postmenopausal osteoporosis. This exploratory analysis determined the effects of BZA on intervertebral DH and its association with incident vertebral fractures.

Methods: Lateral spine radiographs were obtained from subjects (N = 3,886) enrolled in a 3-year, phase 3 study in postmenopausal women with osteoporosis. Point placement for vertebral body quantitative morphometry was re-used to calculate intervertebral DH in the thoracic (T7-T10) and lumbar (L1-L4) regions. Association of DH with fracture was evaluated by a logistic regression model that included treatment, age, and baseline DH and lumbar bone mineral density (BMD) T-score as covariates. Percent change from baseline in DH was evaluated by an ANCOVA model that included age, treatment (placebo, BZA 20 and 40 mg), and baseline DH and BMD T-score as covariates.

Results: For BZA and placebo subjects, logistic regression showed a significant association between higher baseline lumbar anterior DH and lower new vertebral fracture incidence (odds ratio [95% confidence interval], 0.81 [0.66-0.98]; $P=0.03$). In contrast, higher baseline thoracic anterior and middle DH were significantly associated with higher new vertebral fracture incidence (1.45 [1.06-1.98]; $P=0.02$ and 1.52 [1.06-2.18]; $P=0.02$, respectively). In the lumbar region, BZA was associated with a reduction from baseline in individual DH vs placebo, but the finding was not consistent over 3 years. In the thoracic region, BZA 20 and 40 mg were associated with significantly reduced anterior and middle DH from baseline at Months 24 and 36 ($P<0.05$); BZA 40 mg was associated with significantly reduced middle DH at Month 12 ($P<0.01$) and posterior DH at Month 24 ($P<0.05$).

Conclusions: There was no clear association between new vertebral fractures and baseline intervertebral DH in this population. BZA 20 and 40 mg were associated with small reductions from baseline in anterior and middle DH in the thoracic, but not lumbar, region. Increased thoracic spine DH may be on the biological pathway for incident vertebral fractures, though a random effect cannot be excluded. Additional studies in other data sets are warranted.

Table. ANCOVA Analysis of Percent Change in DH

| Month | Lumbar region | |
|---------------------|--|-----------------------------------|
| | Difference in least-squares means (95% CI) | |
| | BZA 20 mg vs placebo | BZA 40 mg vs placebo |
| <i>Anterior DH</i> | | |
| 6 | -0.66 (-1.50; 0.18) | -1.16 ^a (-2.00; -0.33) |
| 12 | -0.19 (-1.40; 1.03) | -1.06 (-2.28; 0.17) |
| 24 | -0.13 (-1.56; 1.29) | -0.63 (-2.07; 0.81) |
| 36 | -0.26 (-1.83; 1.31) | 0.17 (-1.43; 1.76) |
| <i>Middle DH</i> | | |
| 6 | -0.32 (-1.13; 0.48) | -0.31 (-1.11; 0.49) |
| 12 | -0.75 (-2.06; 0.56) | -0.74 (-2.06; 0.58) |
| 24 | -0.91 (-2.26; 0.45) | -0.55 (-1.91; 0.82) |
| 36 | -0.37 (-1.96; 1.23) | -0.42 (-2.04; 1.20) |
| <i>Posterior DH</i> | | |
| 6 | -0.35 (-1.98; 1.29) | 1.64 ^b (0.01; 3.26) |
| 12 | -1.30 (-4.42; 1.83) | 0.37 (-2.78; 3.52) |
| 24 | -2.02 (-5.17; 1.12) | -1.17 (-4.35; 2.01) |
| 36 | -0.67 (-4.00; 2.66) | -0.40 (-3.79; 2.98) |
| Month | Thoracic region | |
| | Difference in least-squares means (95% CI) | |
| | BZA 20 mg vs placebo | BZA 40 mg vs placebo |
| <i>Anterior DH</i> | | |
| 6 | -0.45 (-1.78; 0.87) | -0.47 (-1.80; 0.86) |
| 12 | -1.26 (-3.53; 1.00) | -1.66 (-3.94; 0.63) |
| 24 | -2.34 ^a (-4.59; -0.09) | -2.76 ^b (-5.04; -0.49) |
| 36 | -2.98 ^b (-5.42; -0.53) | -2.73 ^b (-5.19; -0.27) |
| <i>Middle DH</i> | | |
| 6 | 0.21 (-0.92; 1.35) | -0.07 (-1.20; 1.07) |
| 12 | -1.93 (-4.00; 0.15) | -2.77 ^a (-4.86; -0.68) |
| 24 | -2.51 ^b (-4.53; -0.50) | -2.93 ^a (-4.96; -0.90) |
| 36 | -3.17 ^a (-5.31; -1.02) | -3.24 ^a (-5.40; -1.08) |
| <i>Posterior DH</i> | | |
| 6 | -0.16 (-1.70; 1.37) | -0.44 (-1.98; 1.10) |
| 12 | -1.89 (-4.91; 1.13) | -3.55 (-6.59; -0.50) |
| 24 | -1.08 (-3.75; 1.59) | -2.72 ^b (-5.41; -0.02) |
| 36 | -1.59 (-4.27; 1.10) | -1.50 (-4.21; 1.20) |

ANCOVA, analysis of covariance.

^a $P<0.01$.

^b $P<0.05$.

Table

Disclosures: Nancy Lane, Pfizer InclWyeth, 2
This study was supported by Pfizer Inc.

SU0384

Variation in Vitamin D-Related Genes and Reduction of Hip Fractures with Postmenopausal Hormone Therapy: The Women's Health Initiative. Rebecca Jackson^{*1}, Andrea Lacroix², Aaron Aragaki³, David Duggan⁴, Chris Carlson², Charles Kooperberg². ¹The Ohio State University, USA, ²Fred Hutchinson Cancer Research Center, USA, ³Fred Hutchinson Cancer Research Center, USA, ⁴Translational Genomics, USA

Observational and clinical studies have suggested that the effect of hormone therapy (HT) on bone mineral density is enhanced by concomitant vitamin D with or without calcium. Recent data have identified variation in genes responsible for cholesterol synthesis (DHCR7), vitamin D hydroxylation (CYP2R1), and transport (GC) that influence vitamin D status. We tested the hypothesis that variation in these vitamin D-related genes is associated with the impact of postmenopausal HT on reducing risk of hip fracture. We performed an evaluation of variation in GWAS-identified variants near these genes that influence vitamin D status, in relation to hip fracture risk in response to HT using genome-wide association study (GWAS) data from 357 incident hip fracture cases in European American participants in the WHI randomized clinical trials of estrogen-alone [0.625 mg/day conjugated equine estrogen (CEE)] and estrogen plus progestin [(E+P) CEE+2.5 mg medroxyprogesterone/d]. Participants were genotyped on the Illumina 550 or 610 platforms. Unconditional logistic regression was performed to estimate relative risk (RR) and 95% confidence intervals (CIs) for the interaction of CEE, E+P or both combined with each SNP on risk for hip fracture by using an additive model for each SNP and adjusted for age, BMI and first 4 principal components. We identified two significant interactions of E+P and SNPs related to GC (rs1155563 and rs2282679) on reduction in hip fracture risk. The RRs (95%CI) associated with 0, 1 and 2 minor alleles (MA) of rs1155563 were 0.60 (0.40, 0.90), 1.18 (0.74, 1.88) and 1.16 (0.44, 3.02) (p=0.04). Similar results were seen associated with rs2282679 (p=0.05). There was a trend towards replication of this interaction with CEE (0 MA RR 0.48 (0.29, 0.80) and 1-2 MA 0.95 (0.54, 1.67) (p=0.08). In combined analyses, the RR (95%CI) associated with 0 and 1 or 2 MA was 0.55 (0.42, 0.78) and 1.14 (0.82, 1.59) (p=0.003). Findings from our study suggest that the benefit of postmenopausal HT (CEE or E+P) in reducing hip fracture is greatest for women with zero minor alleles of variants associated with GC which encodes vitamin D binding protein, with no benefit for women with one or more minor alleles. As previous studies suggest that women with 0 MA for the GC gene have the highest levels of vitamin D, these data suggest that HT benefits women with the highest levels of 25-hydroxyvitamin D.

Disclosures: Rebecca Jackson, None.

SU0385

Cost-Effectiveness of Denosumab versus Zoledronic Acid in a Population 75 years or Older in the US. Anju Parthan^{*1}, Morgan Deffin¹, Nicole Yurgin², Joice Huang³, Pei-Ran Ho⁴, Andrea Wang³, Douglas Taylor¹. ¹OptumInsight, USA, ²Amgen Inc., USA, ³Amgen Inc, USA, ⁴Amgen, Inc, USA

Purpose: Hip fracture incidence rises with age and the number of hip fractures peaks after the age of 75; however, few studies addressed clinical and economic benefits of treating fractures in this group. We examined cost-effectiveness of denosumab (DMAB) vs zoledronic acid (ZA) in post menopausal women with osteoporosis (PMO) who were 75 years and older in the US.

Methods: A lifetime cohort Markov model was developed from a US third party payer perspective. In the model, patients may transition every 6 months between 7 health states: well, hip fracture, vertebral fracture, other osteoporotic fracture, post hip fracture, post vertebral fracture, and death. Background fracture risks, mortality rates, utilities and medical and drug costs were derived using published data sources. Fracture relative risk reduction vs placebo at 3 years was estimated from the subgroup of age ≥ 75 years in FREEDOM trial for DMAB^{1,2} (hip, 62%; new vertebral, 64%; nonvertebral, 16%) and in HORIZON trial for ZA³ (hip, 18%; clinical vertebral, 66%; nonvertebral, 27%).

Patient characteristics in the older subgroups in both trials were different; therefore, we also examined an alternate subgroup in FREEDOM⁴ (age ≥ 75 , FN BMD T-score ≤ -2.5 , or previous hip or vertebral fracture), which was more comparable to the older population in HORIZON. Expected costs and quality-adjusted life years (QALYs) were estimated for DMAB and ZA and discounted at a rate of 3% per year. In addition, extensive sensitivity analyses were conducted.

Results: In the PMO population age ≥ 75 years, total lifetime healthcare costs (i.e., drug and PMO related medical costs) for DMAB and ZA were \$52,000 and \$57,800, respectively. Total QALYs were 6.37 and 6.34, respectively. DMAB dominated ZA by having lower costs and more QALYs due to fewer hip fractures. Similarly, in the alternate scenario, the total healthcare costs were \$51,600 and \$57,800 and the total QALYs were 6.37 and 6.34, for DMAB and ZA, respectively. Results from the deterministic sensitivity analyses were robust when selected variables were varied $\pm 25\%$ from their base-case estimate. At \$60,000/QALY willingness-to-pay, DMAB is cost-effective in 98% of the probabilistic simulations compared to ZA.

Conclusion: In this population with increased likelihood of hip fracture, DMAB represented better value than ZA. This was driven by greater hip fracture prevention with DMAB compared to ZA, which led to lower healthcare costs and more QALYs.

¹Boonen et al. *JCEM* 2011;96: 1727

²McClung et al. *JBM* 2011. DOI 10.1002/jbmr.536

³Boonen et al. *J Am Geriatr Soc* 2010;58:292

⁴Amgen data on file. High risk criteria: Age ≥ 75 AND baseline femoral neck BMD T-score ≤ -2.5 or prevalent vertebral or hip fracture

Disclosures: Anju Parthan, Amgen Inc, 2

This study received funding from: Amgen Inc

SU0386

Individual Derived Quality of Life Changes Over 12-months following Fracture. Kerrie Sanders^{*1}, Geoffrey Nicholson², Sandra Iuliano-Burns³, Ego Seeman³, Richard Prince⁴, Gustavo Duque⁵, Tania Winzenberg⁶, Marita Cross⁷, Lyn March⁷, Peter Ebeling⁸, Fredrik Borgstrom⁹. ¹NorthWest Academic Centre The University of Melbourne Western Health, Australia, ²The University of Queensland, Australia, ³Austin Health, University of Melbourne, Australia, ⁴Sir Charles Gairdner Hospital, Australia, ⁵Ageing Bone Research Program, University of Sydney, Australia, ⁶Menzies Research Institute Tasmania, Australia, ⁷Royal North Shore hospital, Australia, ⁸The University of Melbourne, Australia, ⁹LIME/MMC Karolinska Institute, Sweden

AusICUROS is the Australian arm of the International Costs and Utilities Related to Osteoporotic fractures Study initiated through the IOF. Using a uniform study design to estimate costs and quality of life (QoL) related to fractures, AusICUROS is being conducted at eight centres across Australia. Prospective data are collected from patients with recent fracture (Fx) at four timepoints: Phase 1 collects information within two weeks of Fx and documents QoL before (recollected) and immediately after Fx and phases 2 to 4 collect data 4-, 12- and 18-months post-fracture. Data are primarily collected by personal interview at phase 1 and telephone interview at phases 2 to 4. Eligibility includes diagnosis of a low energy Fx and age at least 50 years. Recruitment occurs largely through acute hospitals' emergency departments and orthopaedic wards.

We report on individual derived health-related QoL changes following Fx using time trade off (TTO: 1=perfect health, 0=death) and visual analogue scale (VAS; 'thermometer' 100=perfect health, 0=death) and changes in ICECAP index (total score out of 20) of capability for older people as an estimate of 'non health-specific' QoL, assessing attributes of attachment (friendship), role (purpose), enjoyment and security (not having to worry) and control (make one's own decisions).

Results from the first 564 participants (80% women, 95% living at home) are presented with 12-month data for 312 of these participants. Median and interquartile range is reported for age and mean values for all QoL indices with 25% unable to answer the TTO.

These results suggest that at 12-month post Fx, many aspects of QoL including those not directly health-related, have not returned to pre-Fx status in patients with hip and vertebral Fx. Throughout the 12-month post fracture period, self-rated health (VAS) and ICECAP attributes were similar in vertebral and hip Fx patients (Phases 1^{a,b}; 2 & 3; p value for difference range 0.2 to 0.8). Although there is a recruitment bias towards more serious vertebral Fx patients, the impact of vertebral Fx on QoL is likely to be currently underestimated compared to hip Fx. The work is novel in addressing both the health and non-health related attributes of QoL following Fx.

Table: QoL scores immediately before^a and after^b fracture; 4- & 12 months later

| Fracture | phase 1 ^{a,b} , 2 & 3 | TTO | VAS | ICECAP* |
|-----------|------------------------------------|------------------------|----------------|----------------|
| Hip | N=182, 135, 93 Age 79 (71, 86) | 0.83; 0.71; 0.79; 0.78 | 78; 52; 72; 73 | 17; 13; 15; 16 |
| Wrist | N=302, 262, 181 Age 66 (59, 75) | 0.94; 0.87; 0.92; 0.90 | 84; 68; 81; 81 | 18; 14; 17; 17 |
| Vertebrae | N=80, 58, 38 Age 71 (61, 79) | 0.85; 0.76; 0.83; 0.85 | 73; 47; 71; 68 | 18; 12; 15; 15 |

*Unweighed total ICECAP score.

Disclosures: Kerrie Sanders, None.

SU0387

Yield of Electronic Medical Records Screening in Identifying Patients Eligible for Osteoporosis Treatment after Recent Fracture. Cathleen Colon-Emeric^{*1}, Richard Lee², Karen Barnard³, Megan Pearson⁴, Kenneth Lyles¹. ¹Duke University Medical Center, USA, ²Duke University, USA, ³Duke University Medical Center, Durham VAMC, USA, ⁴Durham VA Medical Center, USA

Background: Electronic medical record systems can rapidly identify fracture patients so that healthcare systems can target osteoporosis treatment programs. However, it is not clear what proportion of such patients are actually eligible for treatment.

Method: In a Veterans Affairs Medical Center, a secondary fracture prevention electronic screening protocol was developed and proceeded in 3 stages. First, all patients with an ICD-9 code for fracture (800-829) over the preceding 6 months were identified using the electronic medical record. Additional data was obtained automatically at this stage, and patients were excluded if they were already on

bisphosphonate, their fracture was facial or digital, they did not have a primary care provider, they were under age 50 years, or had died.

In a second stage, chart abstraction was completed by the project director. Patients were excluded if their fracture occurred after high-impact trauma, the coded fracture was not confirmed on radiograph, the fracture occurred more than 10 years previously, bone density screening had already been obtained, the fracture was pathologic, the patient was receiving palliative care, or the patient had been offered and declined therapy.

In the final stage, remaining patients were referred to a bone specialist who reviewed the medical record and generated an electronic consult to the primary provider that gave recommendations for further evaluation and management consistent with current guidelines.

Results: Among 986 veterans with ICD9 fracture code within the study period, 841 (85%) were ultimately excluded from further intervention. A majority (n=574, 68%) were excluded in the first, automated screening stage [no primary provider (22%), age under 50 years (38%), already on a bisphosphonate (12%), fracture facial or digital (25%), patient had died (3%)]. Chart abstraction was required to exclude 267 (32%) prior to physician review [high trauma (37%), remote injury or no evidence of fracture (36%), palliative care (9%), other reasons (18%)] Eighty-eight physician consults were completed, with 67 (76%) recommending osteoporosis treatment or BMD testing.

Conclusion: An electronic screening tool was effective at the healthcare center level in identifying recent fracture patients for secondary osteoporosis intervention, but most (85%) are ultimately not eligible for additional interventions. Most exclusions (68%) can be made without additional chart abstraction.

Disclosures: Cathleen Colon-Emeric, None.

SU0388

Change in uOC/OC Ratio with use of Teriparatide in Treatment of Vertebral Compression Fracture. Yoichi Kishikawa*. Kishikawa Orthopedics, Japan

Background: Teriparatide as a daily injection (FORTEO) has an excellent bone formation-promoting effect, and is known to promote the healing process of fracture. While remarkable increase in bone mineral density is reported for vertebral bodies rich in cancellous bone, its bone union-promoting effect in the treatment of compression fracture is unproven. In conservative management of vertebral compression fracture, rest level varies from case to case, posing a major bias in the evaluation of therapeutic effect of drugs; however, our previous report showed the preventive effect of non-weight-bearing rest therapy against vertebral collapse in the initial phase of treatment of vertebral compression fracture.

Method: The bone union-promoting effect of teriparatide was verified using teriparatide in patients with vertebral compression fracture having the same rest level. In addition, TRAP5b, OC, and uOC were measured as bone metabolism markers to determine the changes in bone metabolism when teriparatide was used for vertebral fracture healing, based on which the quality of the bone formed was estimated. Furthermore, alfacalcidol (0.25 mg) was used as a concurrent drug.

Results: With regard to fracture healing, a callus appeared to form approximately in the second week on X-ray examination. While the callus started to form in the posterior part of vertebral body, the overall impression was that the callus formation started early. The callus seemed more osteoblastic, and bone union seemed to be achieved earlier than usual. Remodeling after bone union were observed. The changes in bone mineral density apparently did not increase after 4 months, during which time the data of bone metabolism markers before and after the administration were obtained for 26 patients (4 men, 22 women; average age: 78 years). In most of the patients, TRAP5b, OC, and uOC all increased. TRAP5b/OC ratio decreased (N=26, Wilcoxon test, P=0.0016), suggesting the changes in bone metabolism were driven by bone formation. uOC/OC ratio increased (N=26, Wilcoxon test, P=0.0005). Since the bone metabolism turnover was enhanced, and the uOC values relatively increased, it is possible that bone of distinct quality was formed.

Discussion: With respect to the bone formed when teriparatide was used in the treatment of vertebral fracture, it is possible that bone with relatively increased uOC was formed. It is expected that bone of better quality can be formed using vitamin-K as a concurrent drug.

Disclosures: Yoichi Kishikawa, None.

SU0389

Effects of Combination Treatment with Raloxifene and Alfacalcidol in Postmenopausal Women. Noriaki Yamamoto*, Naoto Endo², Hideaki Takahashi¹. ¹Niigata rehabilitation hospital, Japan, ²Niigata University, Japan

Background: The purpose of this study is to determine the effects of combination treatment with raloxifene and alfacalcidol in postmenopausal women for 1 year.

Methods: We conducted a randomized, open-labeled, multicenter study with 36 postmenopausal women. All subjects were divided into 3 subgroups. Group A: 12 women (69.4 ± 8.0) take 1 μg/day alfacalcidol, Group B: 12 women (68.3 ± 6.8) take 60 mg/day raloxifene, and Group C: 12 women (71.0 ± 8.3) both of raloxifene and alfacalcidol for 12 months. Bone mineral density of lumbar spine (L-BMD) and proximal femur (F-BMD), Serum Ca and bone metabolic markers (urinary NTX, intact PTH) were assessed at beginning, 6, and 12 months of this study. As physical evaluation, one leg standing time was assessed at beginning and 12 months.

Results: Comparing to the baseline, L-BMD no significant increased in A-group +2.0 ± 1.3%, B-group +1.9 ± 1.0%, C-group +3.9 ± 2.2% at 12 month. u-NTX changes demonstrated +13.8 ± 18.3%, -10.1 ± 22.1%, -37.9 ± 5.6% (p < 0.001) at 6 months, +3.6 ± 10.5%, -19.7 ± 15.9%, -36.0 ± 8.5% (p < 0.05) at 12 months respectively. I-PTH slightly increased in group B +9.7 ± 11.8%, but decreased in group C -20.8 ± 7.9% not significantly. One leg standing time increased in group A +39.6 ± 29%, in group C +42.8 ± 37.3%, but the changes did not reach a significant level.

Conclusion: Combination treatment with raloxifene and alfacalcidol demonstrated better effects on bone metabolism comparing to raloxifene alone treatment in postmenopausal women. Also it might be possible that the supplementation of alfacalcidol improved physical function in osteoporosis patients.

Disclosures: Noriaki Yamamoto, None.

SU0390

Morning Administration of the New Cathepsin K Inhibitor, ONO-5334, Causes Greater Suppression of Bone Resorption Markers Compared with Evening Administration. Richard Eastell¹, Derk-Jan Dijk², Maria Smal³, Aldona Greenwood², John Sharpe⁴, Mikihiro Yuba⁴, Stephen Deacon³. ¹University of Sheffield, United Kingdom, ²Surrey Clinical Research Centre, United Kingdom, ³Ono Pharma UK Ltd, United Kingdom, ⁴ONO Pharma UK, United Kingdom

Bone resorption is highest at night, thus it would seem preferable to administer anti-resorptive drugs in the evening. Evening administration of the cathepsin K inhibitor, ONO-5334, has been shown to increase BMD at least comparably to alendronate in patients with osteoporosis in the Phase II OCEAN study. This study was designed to investigate the effects of morning (M) (8am) versus evening (E) (8pm) dosing of multiple doses of 150 mg ONO-5334 on bone resorption markers in healthy post-menopausal women. The study had a randomized, single-blind, 2 period crossover design. Subjects were randomised to 1 of 2 different dosing sequences, either to E active dose in the first period and M active dose in the second period, or to M active dose in the first period and E active dose in the second period. Subjects received 2 doses per day (one active, one placebo). There was at least 10 days washout between periods. All subjects were dosed in the fed condition 30 minutes after a standard meal. 14 subjects were enrolled and 11 subjects completed and were eligible for the per protocol set. There was a marked difference in effect between M and E administration on the serum CTX profile across 24h (time-matched against individual's own D-1 24h baseline), Figure 1. Although E administration showed a larger suppressive effect this appeared less sustained. M dosing showed a more consistent suppressive effect across 24h. Summarising over the whole 24h using area under the curve (AUC) analysis, the effect appeared to be of a lesser magnitude although significant differences were still observed. M dosing achieved a 5.9% greater suppression of serum CTX (24h AUC) compared with E dosing (p < 0.05) (LS means % change from baseline (CFB), M=68.8% and E=62.9%). With urine CTX/Cr (24h AUC), M dosing showed 6.8% greater suppression compared with E dosing (p < 0.01) (LS means %CFB, M=92.6% and E=85.8%). Whether suppressing CTX levels consistently for longer across 24h is clinically meaningful compared to a shorter but equally or more potent suppression with a once daily regimen remains to be proven with ONO-5334. The study highlights that time of administration may be important when administering ONO-5334 (at least at 150mg) and this may be PK related. E administration of ONO-5334 has been shown to significantly improve BMD. It remains to be seen whether M administration would show increased efficacy (on BMD) and whether the M vs E effect is observed with higher doses of ONO-5334.

Figure 1. Serum CTX after 5 days of dosing with ONO-5334 (Time-matched % change from baseline)

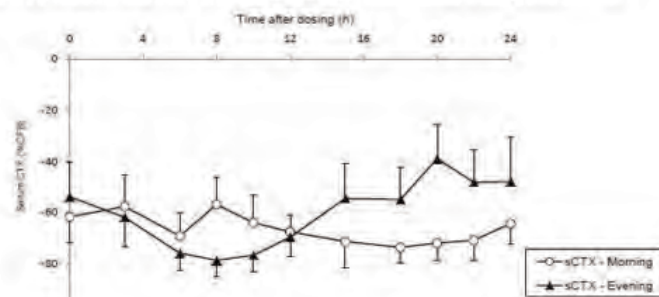


Fig1

Disclosures: Richard Eastell, ONO PHARMA UK LTD, 2
This study received funding from: Ono Pharmaceuticals

SU0391

Positive Effects of Dried Plum on Bone may be due in part to Suppression of Sclerostin Levels. Shirin Hooshmand^{*1}, Marcus Elam², Sheau Ching Chai³, Raz Saadat², Bahram Arjmandi³. ¹San Diego State University, USA, ²Florida State University, USA, ³Florida State University, USA

Several animal studies and two clinical trials have repeatedly confirmed that dried plum (*Prunus domestica* L.) has positive effects on bone turnover biomarkers and bone mineral density (BMD). Recent studies have shown that osteocytes actively participate in almost every phase of mineral handling by bone and may independently control bone resorption and bone formation via production of sclerostin. To further investigate the effects of dried plum on osteocytes, we measured the serum sclerostin levels in osteopenic postmenopausal women (n=236) not on hormone therapy or any other prescribed medication known to influence bone metabolism. Participants were randomly assigned to one of the two treatment groups: dried plum (100 g/d) or a comparative control fruit regimen (dried apple) for one year. All participants received 500 mg Ca/400 IU vitamin D daily. Bone mineral density of lumbar spine, forearm, hip, and whole body were assessed at baseline and at the end of the study using DXA. Blood and 24-hr urine samples were collected at baseline and after 12 months to assess bone biomarkers. Physical activity recall and food intake were monitored throughout the study. Dried plum significantly increased BMD of ulna and spine in comparison to the control group. In comparison with corresponding baseline values, dried plum significantly decreased serum levels of bone turnover markers including bone-specific alkaline phosphatase and tartrate resistant acid phosphatase-5b. Changes from baseline levels for serum sclerostin in dried plum group were -1.1% vs. +3.9% in control group. The decrease in sclerostin levels as a result of dried plum treatment is of great importance since recent studies have shown that sclerostin not only inhibits bone formation but also that higher serum sclerostin levels are associated with a greater risk of hip fractures in women. Hence, these preliminary data indicate that the positive effects of dried plum on bone are likely in part due to inhibition of sclerostin.

Disclosures: Shirin Hooshmand, None.

SU0392

Sclerostin and DKK1 in Postmenopausal Osteoporosis treated with Denosumab. Luca Idolazzi^{*1}, Helal Mahamid¹, Maria Rosaria Povino¹, Carmela Dartizio¹, Elisabetta Vantaggiato¹, Alessandro Giollo¹, Gaia Tripi¹, Davide Gatti¹, Maurizio Rossini², Silvano Adami³. ¹Rheumatology Section, Department of Medicine, University of Verona, Italy, ²Verona University, Italy, ³University of Verona, Italy

INTRODUCTION: The bone mass benefits associated with long-term treatment of postmenopausal osteoporosis with anti-resorbers are limited by the rapid coupling of decreasing bone resorption with bone formation. The Wnt signaling appears to be involved in this coupling process during treatment with bisphosphonates, while its role during treatment with the anti receptor activator of nuclear factor kappa B ligand (RANKL) antibodies Denosumab is unknown.

Methods: We measure the serum levels of Dickkopf-1 (DKK1), sclerostin and bone turnover markers in patients participating to from our centre in a multicenter placebo controlled trial lasting 36 months: 19 women were on placebo and 24 on Denosumab 60 mg subcutaneous every 6 months.

Results: All measured parameters (serum C-terminal telopeptide of type I collagen [sCTX], serum bone alkaline phosphatase [bAP], DKK1 and sclerostin remained unchanged during the observation period in the placebo group. sCTX and bAP were significantly suppressed by denosumab treatment over the entire follow-up. Denosumab treatment was associated with significant increases in serum sclerostin within the first 6 months (+29%) and these were maintained over the entire study period while serum DKK1 significantly decreased versus baseline within the first 6 months with a trend for further continuous decreases which reached statistical significance versus the placebo group from the 18th month onward. The changes in DKK1 were significantly and positively related with the changes in sCTX and bAP while those of sclerostin were significantly and negatively related only with those of bAP.

CONCLUSION: the changes in bone turnover markers associated with denosumab treatment of postmenopausal osteoporosis are associated with significant increase in sclerostin similar to those seen after long term treatment with bisphosphonates, and significant decrease in DKK1. This latter observation might be put in the perspective of the continuous increase over 5 years in BMD observed during treatment of postmenopausal osteoporosis with denosumab.

Disclosures: Luca Idolazzi, None.

SU0393

The Dynamic Profile of CTX Observed With Denosumab Is Maintained Over 6 Years of Treatment: Results From the First 3 Years of the Pivotal Phase 3 Fracture Trial (FREEDOM) Extension. Christian Roux^{*1}, Michael R. McClung², Nathalie Franchimont³, Silvano Adami⁴, Peter R. Ebeling⁵, Ian R. Reid⁶, Heinrich Resch⁷, Georges Weryha⁸, Nadia Daizadeh³, Andrea Wang³, Rachel B. Wagman³, Richard Eastell⁹. ¹Paris Descartes University, France, ²Oregon Osteoporosis Center, USA, ³Amgen Inc., USA, ⁴University of Verona, Italy, ⁵University of Melbourne, Australia, ⁶University of Auckland, New Zealand, ⁷St Vincent Hospital, University of Vienna, Austria, ⁸Hôpitaux de Brabois, CHU de Nancy, France, ⁹University of Sheffield, United Kingdom

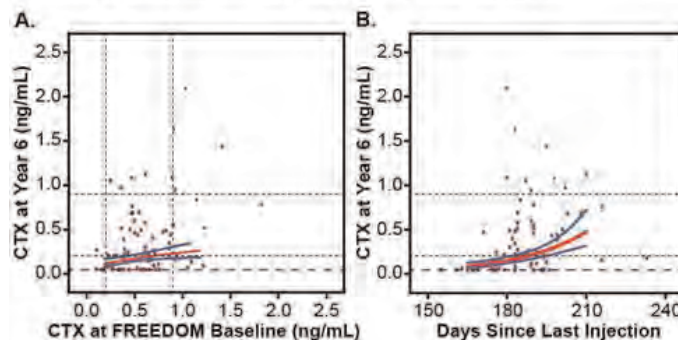
Denosumab (DMAB) is associated with a unique profile of bone resorption inhibition: a rapid decrease in CTX by 3 days and a release of inhibition at the end of the 6-month dosing interval when DMAB serum levels decrease (McClung *NEJM* 2006). This dynamic profile of CTX inhibition is sustained with continued treatment. In FREEDOM, CTX values at 6 months were influenced by baseline CTX values and days since the 1st injection (Eastell *JBMR* 2011). The 3-year FREEDOM study has been extended, and 3 additional years of data are available. Here we explore whether the rapid and dynamic inhibition of CTX continues to be observed, and whether CTX values after 6 years of continued DMAB treatment remained highly predicted by pre-treatment CTX values as well as by the days since last injection.

During the FREEDOM extension, subjects received 60 mg DMAB every 6 months and daily supplemental calcium/vitamin D. CTX was measured in fasting serum samples by ELISA (Nordic Bioscience). We evaluated the dynamic profile of CTX in 50 subjects from the long-term group (3 years DMAB in FREEDOM, 3 years in extension) who had CTX measurements at 10 days and 6 months following the 1st DMAB dose in the extension. To determine if pre-treatment CTX values and days since last injection continued to predict CTX values over time, data were assessed from 79 subjects who had also received 6 years of DMAB and had CTX measurements available at FREEDOM and extension baseline and year 6. A Tobit-style model was used to handle the censoring of the CTX values below the quantification limit at year 6 and to evaluate its relationship with days since the last injection, and the FREEDOM and extension baseline CTX values.

Ten days after the 1st DMAB dose in the extension, CTX values were decreased with a median reduction of 91%, and at 6 months after DMAB administration, CTX values were reduced by 77% (n=50). At the end of the dosing interval at year 6, the median reduction in CTX was 57% (n=79). CTX values at year 6 were significantly correlated with CTX values at FREEDOM baseline ($p<0.01$) and time since the last DMAB dose at year 5.5 ($p<0.0001$) (Fig.). CTX values at year 6 also were significantly correlated with CTX values at the extension study baseline (after 3 years of DMAB in FREEDOM, $p<0.0001$).

Long-term DMAB treatment is associated with a dynamic profile of CTX reduction. Pre-treatment CTX values and time since the last DMAB injection continue to be significant predictors of the CTX values at year 6.

Fig. Relationship Between CTX at Year 6 and (A) CTX at FREEDOM Baseline and (B) Days Since Last Injection



Red lines represent the fit from a Tobit-style model and blue lines represent the 95% confidence bands; dotted lines represent the premenopausal reference range (0.2 to 0.9 ng/mL); dashed lines represent the lower limit of quantification (0.049 ng/mL).

Fig.

Disclosures: Christian Roux, Amgen Inc., Lilly, MSD, Novartis, Roche, 2; Amgen Inc., MSD, Bongrain, 6
This study received funding from: Amgen Inc.

SU0394

The Results of a Double-blind, Randomized, Phase 2 Dose-finding Study of Odanacatib, a Potent Cathepsin-K Inhibitor, in Japanese Patients with Osteoporosis with a Model-based Pharmacokinetic (PK) Analysis. Shinji Uchida^{*1}, Masataka Shiraki², Masao Fukunaga³, Tatsushi Tomomitsu³, Go Fujimoto⁴, Mariko Nakagomi⁴, Albert Leung⁵, Stefan Zajic⁵, Arthur Santora⁵, Julie Stone⁶, Julie Passarelli⁷, Toshitaka Nakamura⁸. ¹MSD K.K., Japan, ²Research Institute & Practice for Involuntal Diseases, Japan, ³Kawasaki Medical School, Japan, ⁴MSD KK, Japan, ⁵Merck Research Laboratories, USA, ⁶Merck Sharp & Dohme Corp., USA, ⁷Cognigen Corp, USA, ⁸University of Occupational & Environmental Health, Japan

Purpose: To assess the efficacy and safety of oral odanacatib (ODN) 10, 25, or 50 mg or placebo (PBO) once-weekly (OW) for 52 weeks in a double-blind, randomized, multi-center study in Japanese female and male (4%) patients with osteoporosis, and to characterize the pharmacokinetic profile.

Methods: The primary efficacy endpoint was the % change from baseline at 52 weeks in lumbar spine (L1 - L4) BMD. Secondary endpoints included % changes in total hip, femoral neck, trochanter BMD and bone biomarkers after 52 weeks. A model-based population-PK analysis was conducted as an exploratory endpoint using odanacatib concentration-time data from this study. The subsequent population-PK model was used to estimate predicted steady-state patient exposures.

Results: 287 patients were randomized to PBO (n=73) or ODN 10 mg (n=74), 25 mg (n=71), or 50 mg (n=69). The least-squares (LS) mean % changes from baseline in lumbar spine BMD were 0.5%, 4.1%, 5.7% and 5.9% in the PBO or ODN 10 mg, 25 mg and 50 mg groups. The LS mean % changes from baseline in total hip BMD were -0.4%, 1.3%, 1.8% and 2.7% with PBO or ODN 10 mg, 25 mg and 50 mg. The changes in femoral neck and trochanter BMD were similar to those at the total hip. Odanacatib reduced bone markers of resorption in a dose-dependent manner. The absolute magnitude of the % change in bone formation markers was smaller than of the resorption markers. After 52 weeks, for patients receiving ODN 50 mg OW, geometric mean % changes from baseline (SE) were -58.6 (3.3) for urine NTX/creatinine (n=51), but only -25.9 (3.2) for serum BSAP (n=54). The tolerability and safety profiles were similar among all treatment groups, and there was no numerical difference in the AE reporting between the 25 mg and 50 mg. The pop-PK model-based AUC estimates were similar in Japanese patients relative to non-Japanese patients at the same doses, with considerable overlap in individual predicted exposures. Covariate analysis suggested that race/ethnicity does not substantially influence odanacatib pharmacokinetics.

Conclusions: Treatment with odanacatib for 52 weeks once weekly increased lumbar spine and all hip site BMD in a dose-dependent manner and was well-tolerated in Japanese patients with osteoporosis. Pop-PK analysis suggests that there is little difference in pharmacokinetics between Japanese and non-Japanese patients. Taken together, the data from this study support the choice of the 50 mg weekly dose in Japanese patients.

Disclosures: Shinji Uchida, Merck Sharp & Dohme Corp., 3
This study received funding from: Merck Sharp & Dohme Corp.

SU0395

CT-assisted Balloon Sacroplasty for the Treatment of Insufficiency Fractures Considering Individual Approaches Adapted to the Course of the Fracture Type Denis I, II and III. Reimer Andresen^{*1}, Sebastian Radmer², Peter Kamusella³, Christian Wissgott⁴, Jan Banzer⁵, Hans-Christof Schober⁶.

¹Westküstenklinikum Heide, Germany, ²Center of Orthopedics, Germany, ³Institute of Diagnostic & Interventional Radiology/Neuroradiology, Westküstenklinikum Heide, Germany, ⁴Institute of Diagnostic & Interventional Radiology/Neuroradiology, Westküstenklinikum Heide, Germany, ⁵Charité Universitätsmedizin Berlin, Germany, ⁶Klinikum Südstadt RostockKlinik Für Innere Medizin I, Germany

Introduction: In elderly patients with reduced bone quality, insufficiency fractures of the sacrum are relatively common and are typically associated with intense, debilitating pain. The objective of our study was to determine the practicability of cement augmentation using a balloon catheter via individual approaches taking into consideration the complex anatomy of the sacrum and the course of the fracture, as well as the postinterventional determination of leakages and representation of the outcome pain.

Material and methods

In 30 patients with severe osteoporosis (23 women with an average age of 72.4 years, 7 men with an average age of 68.7 years), a sacral fracture was detected by CT and MRT. This fracture was unilateral in 17 women and bilateral in the other patients. In order to achieve a cement distribution longitudinally in relation to the fracture, the balloon catheter was inserted into the sacrum via a hollow needle either from caudal to cranial, from dorsal to ventral or from lateral transiliac to medial. The balloon catheter was then inflated and deflated 1-3 times along the fracture in the respective direction, and the hollow space created was then filled with PMMA cement using a low-pressure procedure. A conventional radiograph in two planes and a control CT were then performed. Pain intensity was determined pre-intervention, on

the 2nd day post-intervention and 6 and 12 months post-intervention, using a visual analogue scale (VAS).

Results: The balloon sacroplasty was performed successfully from a technical point of view in all patients. The radiographic and CT control showed sufficient cement distribution in the sacrum along the course of the fracture, whereby leakage could be ruled out. According to the VAS, the mean value for pain was 8.8 pre-intervention, there was a significant reduction in pain on the 2nd postoperative day, with an average value of 2.7 (p<0.001), which was stable at 2.5 after 6 months and 2.3 after 12 months.

Discussion: Approaches that take into account the anatomy of the sacrum and the course of the sacral fracture enable reliable augmentation with an optimum amount of cement. This makes balloon sacroplasty an effective treatment that has few complications for rapid and significant pain reduction in patients with a sacral fracture.

Disclosures: Reimer Andresen, None.

SU0396

Mechanical Vibration Improves Neuromuscular Parameters and Preserve Bone Mass in Postmenopausal Osteopenic Women. Mônica Oliveira¹, Hellen Rodrigues², Rosângela Marin², Orivaldo Silva³, Marise Lazaretti Castro^{*4}. ¹University Federal of São Paulo Brazil, Brazil, ²Unifesp, Brazil, ³USP, Brazil, ⁴Escola Paulista de Medicina, Brazil

It is generally agreed that physical exercise is important for women with osteopenia, for helping to maintain and improve bone mass in this population. In addition, the vibratory stimulus through the vibrating platforms is also being studied as a resource for the prevention of osteoporosis. This study developed a vibrating platform of low intensity and low frequency (60Hz, i = 0.6 g) in order to study the effects of mechanical vibration on bone mass as well as agility, flexibility, balance and muscle strength in osteopenic women postmenopause. The longitudinal study was conducted with 109 women, 5 years postmenopausal, diagnosed with osteopenia by bone densitometry. The women were divided into: group Platform (GP=52) and Control Group (CG=57) matched for age, weight and height. The GP the volunteers were standing on the vibrating platform without the exercises for 20 minutes, 5 twice per week for 12 months. Densitometry and physical assessment were performed at the beginning and at 12 months of study. As the result, in the lumbar spine (L1-L4) was a significant increase in BMC of the two groups. In the femoral neck and total femur was a maintenance of bone mass compared to the control group that lost 2.3% of bone mass in femoral neck and -1.06% in the total femur. Flexibility was a gain of 11.5% in GP and GC -6.4% worsened, the static balance improved 15% as well as walking speed and maximum gait speed also improved 4% and 9% respectively in the GP. The functional mobility, the GP twice improved: 85.2%, compared to GC which improved 41.7% in the GP. STEP improved 12.5%, while the CG -4.1% worsened. There was a significant increase in muscle strength in the GP as : 46.81% in the hip flexors, extensors 56.4% in the column, 26.6% of elbow flexors and 5% in right hand grip compared to the CG that no significant change in any of these parameters, with a loss of muscle strength of -23.6% in the knee extensor muscles, and -3% in the left hand grip compared to the GP. In this study from these findings, we conclude that the vibrating platform maintained bone mass, improved agility, flexibility, balance and increased muscle strength all parameters who also collaborate in the prevention of falls and fractures due to bone fragility.

Disclosures: Marise Lazaretti Castro, None.

SU0397

Treatment of Osteoporotic Vertebral Body Fractures by Means of Percutaneous Balloon Kyphoplasty. Long Term Results of a Prospective, Clinical Trial. Thomas Blattert^{*}. Orthopaedische Fachklinik Schwarzbach, Germany

Balloon kyphoplasty is a minimally-invasive, percutaneous surgical technique for reduction and stabilization of osteoporotic vertebral body fractures. However, there is no prospective, clinical trial on long term results concerning the safety and efficacy of the method so far.

This prospective, clinical trial investigated both safety and efficacy of percutaneous Balloon kyphoplasty. All vertebrae were stabilized with Polymethylmethacrylate (PMMA). Pre- and postoperatively, the following data were acquired: subjective rating of pain (Visual Analog Scale, VAS), bisegmental endplate-angle (EA2), anterior and posterior height of vertebra. Inclusion criteria were osteoporotic fractures of vertebral bodies in the thoracolumbar spine, patient age \geq 65 years, fracture age \leq 4 months, and t-score \leq -2.5 (DEXA). Exclusion criteria were tumor lesions and additional posterior instrumentation.

442 vertebrae of 407 patients suffering from acute pain could be included with a minimum-follow up of five years. The average patient age was 78 years (61-93). Average t-score was -2.6. (-3.2 to -2.5). 346 patients suffered from pain for two weeks on average, whereas 96 patients were not able to recall the onset of pain. Fractures were only localized within the thoracolumbar spine with only A type of injuries occurring. 389 of 407 patients experienced marked pain-relief as expressed on the VAS (8.1 \pm 1.7 to 1.8 \pm 1.4; 0 "best" to 10 "worst"). Average correction of EA2 was 7.1°. The anterior vertebral height could be restored by 7.7 mm on average, posterior height by 3.2 mm. There were no neurological complications. In 40 (9.0%) vertebrae, we saw

intraoperative leakage of cement (7 (1.6%) out of these with epidural leakage), however, no clinical consequences had to be noted. There were 6 (1.4%) cases of intraoperative balloon-perforation, and 14 (3.2%) cases of subsequent vertebral body fractures in the adjacent level.

Balloon-kypoplasty is an efficient, and minimally-invasive therapeutic option for the treatment of painful vertebral body fractures having its focus on cases with underlying osteoporosis. Depending on the age and type of fracture, this treatment can obtain a significant rate of fracture reduction. Compared to current literature on vertebroplasty, this technique presents fewer leakage complications at equal success in reducing pain.

Disclosures: Thomas Blattert, AOSpine, Biomet, Medtronic, Spontech, Synthes, 2

SU0398

Withdrawn

SU0399

Intermittent Megadose Treatment with Vitamin D₃ is not Optimal to Keep Serum 25OHD Levels at or over the Target of 75 nmol/l - Placebo-Controlled, One-Year Study with 100 000 and 200 000 IU Three Monthly. Ville-Valtteri Vålímäki¹, Tuula Pekkarinen², Eliisa Löytyntyniemi³, Matti J. Vålímäki⁴. ¹Department of Orthopaedics & Traumatology, University of Helsinki & Helsinki University Central Hospital, Finland, ²Department of Internal Medicine, Helsinki University Central Hospital, Finland, ³Department of Statistics, University of Turku, Finland, ⁴Division of Endocrinology, Department of Medicine, Helsinki University Central Hospital, Finland

This study was aimed at studying the efficacy and safety of intermittent megadose treatment with vitamin D₃ (cholecalciferol). Sixty elderly (mean age 75.0 yrs) women were randomized to receive placebo (group A) or 100 000 IU (group B) or 200 000 IU (group C) cholecalciferol orally every 3 months for 1 year. Blood and urine was collected at baseline, 3, 6, 9, 10 and 12 months and 1 week after every treatment bolus. The primary endpoint was the percentage of serum 25OHD measurements reaching or exceeding the target of 75 nmol/l. In comparison to placebo both vitamin D₃ doses increased ($p < 0.001$) 25OHD to the same extent. After baseline serum 25OHD was > 75 nmol/l in 15.4% of 162 measurements in group A, in 51.2% ($n=162$) in group B, and in 57.7% ($n=162$) in group C. Serum PTH was reduced only with the dose of 200 000 IU ($p=0.053$). Serum ionized calcium was similar in all the groups, but the highest vitamin D₃ dose increased urinary excretion of calcium 1 week after every bolus ($p < 0.001$). Creatinine clearance decreased similarly in the study groups over time. Serum C-terminal type 1 collagen telopeptide remained unchanged but some tendency to increased levels of serum procollagen type 1 N-terminal propeptide was found in vitamin D₃ groups. Serum 1,25(OH)₂D measurements are under process. We conclude that 3-monthly treatment with vitamin D₃ is too infrequent to keep 25OHD levels at or over 75 nmol/l. To optimize this treatment modality more frequent administration with smaller boluses is suggested.

Disclosures: Ville-Valtteri Vålímäki, None.

SU0400

The Influence of Vitamin D Supplementation on Mean Changes in Serum 25(OH)D: a Meta-analysis. Sakineh Shab Bidar¹, Sandrine Bours², Piet Geusens³, Joop Van Den Bergh⁴. ¹Maastricht University, Netherlands, ²Maastricht University Medical Centre, The Netherlands, ³University Hasselt, Belgium, ⁴VieCuri MC Noord-Limburg & Maastricht UMC, The Netherlands

Background: Vitamin D deficiency is widespread. Supplementation is recommended widely but, the optimal dose to apply in daily practice is not clear.

Aim: To review the factors that influence mean changes in serum 25(OH)D by giving vitamin D supplement

Methods: A comprehensive search for trials published from PubMed up to November 2011 was performed. We selected all randomized placebo-controlled clinical trials with vitamin D supplementation with $n \geq 30$. The studies were evaluated for publication bias and heterogeneity. Pooled difference mean (DM) and 95% CIs were calculated using the random-effects models. Subgroup, sensitivity, and meta-regression analyses were also conducted.

Results: 51 RCTs of vitamin D supplementation with 72 comparison groups with changes of serum 25(OH)D₃ contributed to the analysis and doses between 400 and >2000 IU/d ($n=6658$). A univariate analysis of all 51 studies and 72 time points documents the effect of pre-specified sex, age, trial duration and baseline values of serum 25(OH)D₃ on changes of serum 25(OH)D₃ levels. Vitamin D supplement was associated with a positive treatment effect in most studies 38.8 (34.7 to 42.9; $p < 0.001$) nmol/L. Subgroup analysis showed a statistically significant dose-response effect when studies were grouped by daily vitamin D dose with a plateau in increase in serum vitamin D levels from 800 IU/day on. The increase reached a plateau at 6 months. Treatment effect also was statistically different across clinical and demographic variables with largest increase in elderly >80 years old, women and with lower

baseline levels of serum 25(OH)D₃ ≤ 50 nmol/L. The meta-regression analysis indicated that age of study participants, trial duration, dosage of vitamin D and baseline levels of serum 25(OH)D₃ independently influenced treatment effect.

Conclusions: This meta-analysis indicated a mean increase of 48 nmol/L in serum 25(OH)D₃ with daily dose of 800 after >6 months, without higher increases with higher dose or longer duration. The mean increase was highest in elderly (>80 years old) and with lower baseline levels of serum 25(OH)D.

Disclosures: Sandrine Bours, None.

SU0401

The Vitamin D Dose Response in Obesity. Mageda Mikhail*, John Aloia, Ruban Dhaliwal, Martin Feuerman. Winthrop University Hospital, USA

Background: Obesity is widespread among the general population. The same can also be said about the inadequacy of vitamin D status. Determining the response of serum 25(OH)D to vitamin D₃ supplementation in the obese with BMI >35 kg/m² and comparing it to individuals with a BMI < 35 kg/m² may lead to concurrent recommendations for optimal vitamin D intake in the obese population and general public.

OBJECTIVE: To determine the dose response of vitamin D₃ in a group of participants with BMI >35 kg/m².

DESIGN: Randomized, double-blind, placebo-controlled study. It is an extension of our prior study of vitamin D dosing in healthy adults in whom the BMI cut-off was below 35 kg/m² (reference indicated below). Participants were randomized during the winter months, after an assessment of baseline 25(OH)D levels, to a vitamin D supplementation arm (100 mcg daily if baseline 25(OH)D was below 50 nmol/L, or 50 mcg daily if baseline 25(OH)D was >50 nmol/L) or placebo arm. Subjects with baseline 25(OH)D level >80 nmol/L were excluded from the study. After 8 weeks, a repeat 25(OH)D measurement was done and the study medication was stopped.

Results: A total of 39 subjects were randomized. At two months, there were 25 subjects remaining in the study (14 placebo, 11 active). 25(OH)D concentration increased to a mean of 75 nmol/L in the active group at the end of the study. The mean slope (i.e. vitamin D₃ response) at 2 months [defined as 25(OH)D change/baseline dose] was 0.398 nmol/L/mcg/d.

CONCLUSION: The dose response of vitamin D₃ (slope) in subjects with BMI >35 kg/m² was significantly lower at 0.398 nmol/L/mcg/d compared to the slope in the previous study in subjects with BMI < 35 kg/m² which was at 0.66 nmol/L/mcg/d (40% reduction in the slope).

Reference: Aloia JF, Patel M, DiMaano R, Li-Ng M, et al. Vitamin D intake to attain a desired serum 25-hydroxyvitamin D concentration. Am J Clin Nutr 2008; 87(6):1952-8.

Disclosures: Mageda Mikhail, None.

SU0402

Vitamin D Status and Response to Additional Vitamin D in Korean Women with Osteoporosis. Sung Soo Kim*, Seok Joon Yoon². ¹School of Medicine Chungnam National University, South Korea, ²Chungnam National University Hospital, South Korea

Background: The aim of this study is to evaluate the extent of vitamin D inadequacy in women being treated for osteoporosis.

Methods: This was a prospective, open-label study. The osteoporotic patients with medication (included daily vitamin D 1000 IU) were recruited in outpatient clinic. Serum 25-hydroxyvitamin D₃ (25OHD) status was divided into deficiency (less than 20 ng/dL), insufficiency (20 to 30 ng/dL) and sufficiency (more than 30 ng/dL). Serum 25OHD was measured at baseline and after additional vitamin D supplementation for 12 months. Deficient and insufficient patients received additional vitamin D 1000 IU per day (total 2000 IU per day).

Results: Of the 108 patients included, 61 patients (56.5%) completed the study. At baseline, mean (SD) serum 25OHD concentrations was 23.2 (9.7) ng/dL and the proportion of patients with deficient, insufficient and sufficient 25OHD levels were 24.1% (26/108), 32.4% (35/108) and 43.5% (47/108) respectively. After additional supplementation, 25OHD levels increased by 45.4% to 51.1 (25.4) ng/dL ($P < 0.001$) and the proportion of patients with deficient, insufficient and sufficient 25OHD levels were 4.9% (3/61), 14.8% (9/108) and 80.3% (49/61) respectively.

Conclusions: About a half of osteoporotic patients being treated with medication have inadequate vitamin D status. Additional vitamin D supplementation significantly increased serum 25OHD levels, and 80.3% achieved optimal levels. These results suggest that about a half of osteoporotic women receiving pharmacologic therapy may require twice the recommended dose of vitamin D (2000 IU per day) in South Korea.

Disclosures: Sung Soo Kim, None.

SU0403

3D Architectural Developmental Patterns of Primary and Secondary Spongiosa at the Proximal Tibia of Young Rats in Response to Daily Parathyroid Hormone (PTH) Administration. Shenghui Lan, Abhishek Chandra, Ling Qin, Xiaowei Liu*. University of Pennsylvania, USA

Intermittent PTH increases bone volume and improves bone structure, and the magnitude and rate of responsiveness are greater in young rats than mature rats. We hypothesized that PTH directly affect the primary spongiosa (I SP) and quickly translated the increased bone mass into the secondary spongiosa (II SP) in growing rats. To address this, we monitored the longitudinal changes in tibial trabecular bone microstructure of young rats by registered in vivo μ CT scans. Saline (n=5) or PTH (80 μ g/kg, n=3) was injected daily to 1-month-old rats for 12 days. A 4mm axial section below growth plate of the right proximal tibia was scanned every other day by Scanco vivaCT 40 at 10.5 μ m resolution for PTH group. Scans were less frequent in vehicle group (d0 and d12) to prevent radiation-induced bone loss while PTH exerts a protective effect against radiation to allow multiple scans. PTH-treated bone images at 4, 8, and 12 days were registered to those obtained 4 days earlier. A 2mm bone section in the II SP was compared to the corresponding volume in the I SP in the 4-day-earlier scan. As shown in Fig A3, periosteal resorption (red) and endocortical formation (green) occurred in 4 days while major trabecular pattern between I SP remained in the II SP. Rapid bone growth caused I SP translate into II SP toward diaphysis at a rate of 0.25mm/day and resulted in decreases in both periosteal and endosteal perimeters (Fig A). There were increases of 74% in bone volume fraction (BV/TV) and 39% in trabecular number (Tb.N), and a 67% decrease in spacing (Tb.Sp) in the I SP at day 8 compared to day 0. Consistently, the corresponding volume in II SP at day 12, which was translated from I SP at day 8, caused increases of 86% in BV/TV, 46% in Tb.N and 17% in trabecular thickness (Tb.Th) than the II SP at day 4 (translated from I SP at day 0). Furthermore, we found decreases of 22-24% in Tb.N but increases of 13-21% in Tb.Th in the II SP at day 4, 8, and 12 compared to the corresponding volume in the I SP 4 days earlier. There were also increases in tissue mineralization in the II SP of 10% at day 4 and 7% at day 12 compared to I SP at day 0 and day 8 (Fig B). We conclude that PTH directly affected I SP and fast growth rate in young rats mediated the translation of improved bone volume and structure into II SP. This explained the rapid response of growing rats to PTH that achieved significant increases in BV/TV, Tb.N and Tb.Th compared to vehicle-treated controls (Fig C).

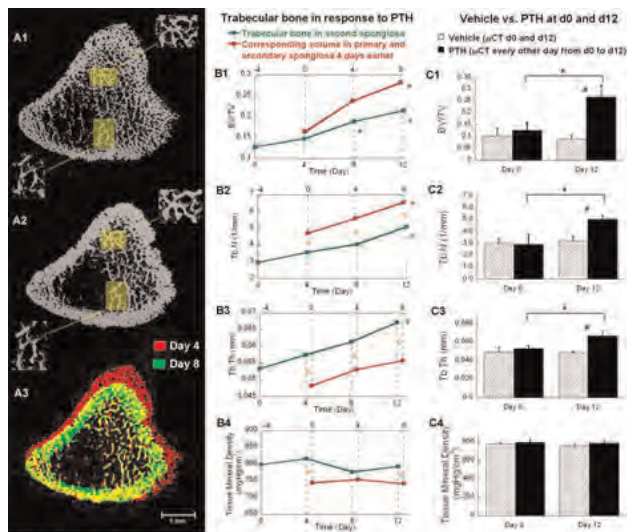


Fig A 1) 3D bone structure of proximal tibia at day 4 with daily PTH injection. 2) the registered bone structure at day 8; similar trabecular patterns were enlarged in the insets. 3) overlapped 2D registered bone structure images of day 4 (red) and day 8 (green), yellow represents common bone tissue.
Fig B Longitudinal changes of trabecular bone in the secondary spongiosa and the registered primary spongiosa (4 days earlier) in response to PTH. Green (red) asterisk indicates significant difference in the secondary spongiosa from day 0 (primary spongiosa from day 4); yellow number sign indicates significant difference in translation of primary to secondary spongiosa in 4 days.
Fig C Comparisons of bone volume and structure at the secondary spongiosa of vehicle and PTH-treated rats at day 0 and day 12.

Figure 1

Disclosures: Xiaowei Liu, None.

SU0404

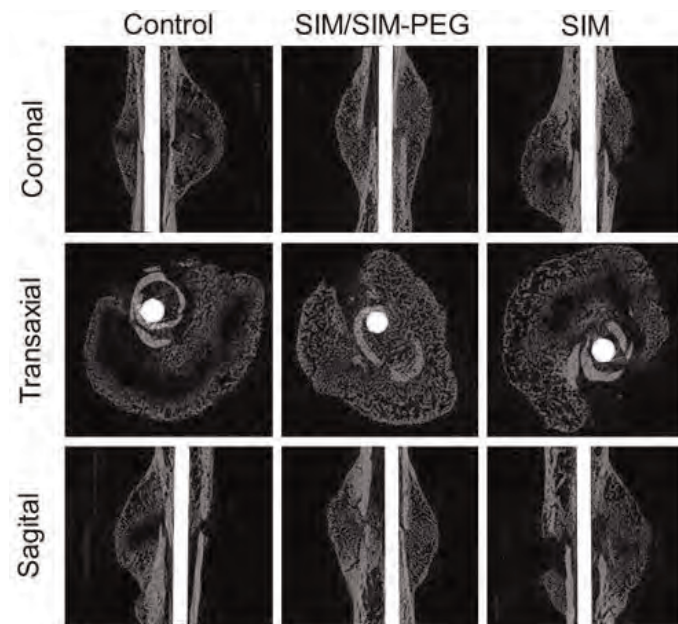
A Novel Macromolecular Prodrug of Simvastatin Promotes Bone Fracture Repair in Mice. Yijia Zhang*¹, Zhenshan Jia¹, Anand Dusad¹, Aaron Daluiski², Edward Fehringer¹, Steven Goldring², Dong Wang¹. ¹University of Nebraska Medical Center, USA, ²Hospital for Special Surgery, USA

Purpose. Fractures are a significant and increasing health burden to our society. Aging and the incipient risk of osteoporosis result in loss of bone mass and deterioration of bone quality predisposing to fracture. This study was undertaken to test the efficacy of a novel micelle-forming macromolecular prodrug of simvastatin (SIM) in localizing to a fracture site and augmenting fracture repair.

Method. By conjugating three SIM molecules to the chain terminus of methoxy polyethylene glycol (mPEG), an amphiphilic macromolecular prodrug, SIM-PEG was synthesized and further formulated into micelles loaded with free SIM (SIM/SIM-PEG). Unilateral transverse femoral fractures were created by osteotomy. Eighteen 10-week-old male Swiss Webster mice were osteotomized and randomly assigned into three groups (n = 6): SIM/SIM-PEG (equiv. SIM 6 mg/kg/d, weekly i.v.), SIM (equiv. SIM 6 mg/kg/d, daily i.p.) and vehicle treated control group (CON). The treatments were initiated on day 8 post osteotomy and the mice were euthanized on day 22. The fractured femurs were collected and processed for micro-CT analysis. The data were reconstructed and analyzed to evaluate the morphology of the longitudinal fracture callus.

Results. Micro-CT imaging showed that SIM/SIM-PEG treated mice exhibited extensive consolidated calcified callus formation, while CON and SIM exhibited foci of immature callus with relatively low density. Moreover, the histomorphometry parameters, e.g. callus volume and callus thickness of the SIM/SIM-PEG treated mice were both higher (+28.6%, p=0.149 and +9.1%, p=0.009 respectively) than the CON mice, while the ratio of callus surface to volume for SIM/SIM-PEG group was remarkably lower than the CON group (-13.5%, p=0.014), suggesting that the SIM/SIM-PEG formulation enhanced callus formation, calcification and organization. No statistical significance was found in quantitative comparison between SIM and CON groups.

Conclusions. The popular cholesterol-lowering drug, SIM is known to exert anabolic effects on bone but its potential efficacy in promoting fracture repair is limited by its lack of selective targeting to skeleton/fracture sites. To address this challenge, we synthesized SIM-PEG in a micelle formulation loaded with free SIM and showed that it selectively localizes to the fracture site during the initial inflammatory phase of fracture repair where it exerts a potent and locally sustained bone anabolic effect.



MicroCT imaging of the fracture callus of osteotomized mice

Disclosures: Yijia Zhang, None.

SU0405

Inhibition of BMP-2 Signaling Using a Soluble Form of BMPRIA Increases Bone Mass in Aged Mice. Aaron Mulivor*, Denise Barbosa, Ravi Kumar, R. Scott Pearsall. Acceleron Pharma, USA

Bone Morphogenetic Proteins (BMPs) induce endochondral bone formation and regulate osteoblastogenesis and osteoclastogenesis. Recently, it was shown that targeted inactivation of the BMP receptor BMPRIA (ALK3) in osteoblasts or osteoclasts causes an increase in bone formation. To investigate new therapeutic strategies for skeletal fragility indications, a soluble BMPRIA receptor-Fc fusion protein (RAP-661) was generated to inhibit BMP signaling through the endogenous receptor.

In order to assess the effects of BMPRIA inhibition, mice aged, 6, 12 and 104 weeks received either twice weekly injections of RAP-661 (10 mg/kg, IP) or vehicle (PBS, IP) for six weeks. DEXA and microCT were used to evaluate the effect of RAP-661 on bone.

DEXA measurements after 6 weeks of treatment revealed increases in total BMD in the 6 week old mouse cohort of 27% (RAP-661) and 16% (PBS), 9% (RAP-661) and 3% (PBS) in the 12 week old mice and 9% (RAP-661) and -2% (PBS) in the 104 week old mice compared to baseline values measured at study day 0 prior to the initial treatment. All BMD increases in the RAP-661 treated cohorts were statistically significant compared to PBS treated cohorts (p < 0.05)

Serum biomarker and bone histomorphometry analysis demonstrated RAP-661 treatment was both antiresorptive and anabolic. RAP-661 treatment increased serum OPG 56% ($p < 0.05$), BSALP 37% ($p < 0.01$), osteocalcin 61% ($p < 0.01$) mineralizing surface 115% ($p < 0.05$) and bone formation rate 80% ($p < 0.05$) and decreased RANKL 52% ($p < 0.05$), TRAP5b levels 67% ($p < 0.01$), eroded surface 36% ($p < 0.05$), and osteoclast surface 44% ($p < 0.05$) after treatment.

These preclinical results demonstrate RAP-661 increases bone mass in young, growing mice and older, osteopenic mice. Bone biomarker analysis suggests that RAP-661 leads to new bone formation by both inhibiting osteoclast activity and increasing osteoblast activity. Therefore, inhibition of BMP signaling using a soluble form of BMPRI1A represents a promising new therapeutic approach for the treatment of bone loss.

Disclosures: Aaron Mulivor, Acceleron Pharma, 3

SU0406

Short- and Long-term Effects of Sclerostin Antibody in an Ovariectomized Rat Model. Xiaodong Li*, Qing-Tian Niu, Kelly S. Warmington, Frank J. Asuncion, Denise Dwyer, Mario Grisanti, Chun-Ya Han, Marina Stolina, Paul J. Kostenuik, W. Scott Simonet, Michael S. Ominsky, Hua Zhu, Ke, Amgen Inc., USA

Short-term treatment with sclerostin antibody (Scl-Ab) increases bone formation, bone mass, and bone strength in various animal models of bone loss and bone repairs. In this study, we characterized the effects of short- and long-term Scl-Ab treatment in an ovariectomized (OVX) rat model.

Six-month-old OVX rats (2 months post-OVX) were treated with vehicle or Scl-Ab (Scl-AbVI, 25 mg/kg, SC, 1x/week) for 6, 12, and 26 weeks (n=12 per group).

In vivo DXA analysis demonstrated that BMD increased significantly at lumbar spine (Figure 1) and femur-tibia after 3 weeks of Scl-Ab treatment and increased progressively up to week 26. Vertebral trabecular bone volume and tibial cortical thickness increased significantly after 6 weeks of Scl-Ab treatment, and continued to increase up to week 26. Dynamic histomorphometric analysis showed that trabecular, endocortical, and periosteal bone formation rates (BFR/BS) increased and peaked at week 6 in the Scl-Ab-treated group (Figure 2). Thereafter, trabecular and endocortical BFR/BS in the Scl-Ab group gradually declined but remained significantly greater than OVX controls at weeks 12 and 26, while periosteal BFR/BS returned to the level of OVX controls at week 26. Serum osteocalcin gradually declined in OVX controls and in the Scl-Ab-treated group during the study. However, serum osteocalcin was significantly greater at weeks 3, 6, and 9 in the Scl-Ab group compared with OVX controls, and no significant difference was found thereafter. Eroded surface, a bone resorption index, on lumbar vertebral trabecular bone was significantly lower in Scl-Ab-treated rats compared with OVX controls at all time points. A three-point bending test at week 26 demonstrated that the maximum load of femoral shafts was significantly greater in the Scl-Ab-treated group than both sham and OVX controls. There was a strong correlation between femoral bone mass and maximum load, and neutral-to-positive effects on calculated cortical bone material properties, indicating that newly formed bone from Scl-Ab treatment had good bone quality.

In summary, short-term Scl-Ab treatment resulted in rapid increases in bone formation and decreases in bone resorption that led to a significant increase in bone mass. Long-term Scl-Ab treatment continuously increased bone mass while bone formation returned toward the OVX control level and bone resorption remained at the same lower level observed with short-term treatment.

Figure 1. Effects of Scl-Ab on Lumbar Spine BMD

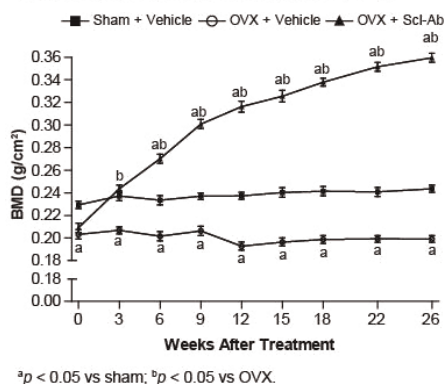


Figure 1

Figure 2. Effects of Scl-Ab on Trabecular Bone Formation

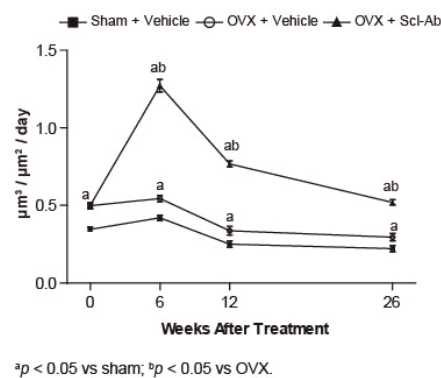


Figure 2

Disclosures: Xiaodong Li, Amgen Inc., 3; Amgen Inc., 7

This study received funding from: Amgen Inc. and UCB Pharma

SU0407

The Effects Of Parathyroid Hormone And Bisphosphonate Treatment On The Local Mechanical Control Of Bone Formation And Resorption. Friederike Schulte*, Claudia Weigt¹, Davide Ruffoni², Floor Lambers³, Alina Levchuk¹, Duncan Webster¹, Gisela Kuhn¹, Ralph Müller¹. ¹ETH Zurich, Switzerland, ²ETH Zürich, Switzerland, ³Cornell University, USA

The mechanical environment in trabecular bone triggers local formation and resorption both under controlled loads and after ovariectomy. Osteoporotic bone loss can be counteracted by pharmacological therapies such as parathyroid hormones (PTH) or bisphosphonates (BIS). Here, we hypothesized that the underlying local mechanoregulation is disturbed by PTH but not by BIS, since PTH shows synergistic effects with loading, but BIS does not.

15-week old B6 mice were ovariectomized. 11 weeks later, the 6th caudal vertebra was loaded (8N, 3000 cycles, 10 Hz, 3/week) and either PTH (daily, PTH, n=9) or bisphosphonate (once, BIS, n=10) treatment was started. Loaded controls received vehicle in both studies (VEH, n=9 and n=8). At weeks 26 and 30, *in vivo* micro-CT scans were taken. Registration allowed the assessment of formation and resorption rates and the division of the surface into 3 clusters: formed, quiescent or resorbed. The strain energy density (SED) distribution at week 26 was determined and the mean SED value in each cluster was calculated for all animals. Pairwise paired Student's t-test with Bonferroni correction was used between clusters and unpaired t-test between control and treatment groups. Furthermore, linear regression analysis was performed between the amount of formed or resorbed areas and the corresponding mean SED.

After 4 weeks, loading increased bone volume fraction by 22%, concurrent PTH (BIS) treatment added another 38% (4%). PTH induced primarily an increase in mineralizing surface while BIS reduced mineral resorption rate ($p < 0.05$). In the VEH groups, mean SED values at formation (resorption) surfaces were higher (lower) than at quiescent surfaces ($p < 0.05$). A similar pattern was found in the BIS group, with no significant differences compared to VEH. Conversely, in the PTH group, mean SED values at quiescent sites were shifted downwards, leading to a lack of significant difference in SED values between quiescent and resorption sites. No correlation was found between the amount of formed or resorbed areas and mean SED in any group except in the formation cluster of PTH ($R = -0.66$).

These results indicate that PTH induces formation at formerly quiescent sites on the bone surface by shifting SED values needed for quiescence to a lower level. This assumption is supported by the finding that the larger the formed areas, the lower the mean SED value. BIS, on the other hand, does not alter the sites but only the amount of bone resorption.

Disclosures: Friederike Schulte, None.

SU0408

Validation of Urinary ⁴⁵Ca Excretion from Deep-Labeled Bone for Screening Anabolic Osteoporosis Therapies in Rats. Emily Hohman*, George McCabe, Connie Weaver. Purdue University, USA

Urinary excretion of calcium tracers from deep-labeled bone offers a rapid and sensitive method to screen potential osteoporosis therapies. Subjects are given an IV dose of a Ca isotope (⁴¹Ca in humans or ⁴⁵Ca in animals), which equilibrates with (deep-labels) Ca in all bone compartments. Changes in urinary Ca tracer in response to dietary or drug interventions reflect changes in net bone turnover. We have previously utilized this method to screen anti-resorptive therapies (Weaver et al. 2009 J. Clin. Endocrinol. Metab. 94: 3798-3805), but the effect of anabolic therapy on tracer excretion is unknown. Mathematical modeling suggests that anabolic therapy decreases urinary Ca tracer appearance (Lee et al. 2011 Anal. Bioanal. Chem. 399: 1613-1622). We used teriparatide, an anabolic agent, in rats to confirm our model. 8-month-old female Sprague Dawley rats (n=11) were given a bolus dose of ⁴⁵Ca via tail

vein catheter. After a one-month equilibration period, multiple 24-hour urine samples were collected to determine baseline ^{45}Ca and total Ca excretion, and baseline total BMD by DXA was measured. Rats were then treated with 30 $\mu\text{g}/\text{kg}$ teriparatide (PTH 1-34, provided by Eli Lilly, Indianapolis, IN) sc/day for 3 months. Urine was collected throughout the study and analyzed for ^{45}Ca and total Ca. Prior to sacrifice, total BMD was measured again. Baseline $^{45}\text{Ca}/\text{total Ca}$ ratios were used to generate predicted values for $^{45}\text{Ca}/\text{total Ca}$ throughout the study period. Observed $^{45}\text{Ca}/\text{total Ca}$ was compared to the predicted values to determine relative reduction of bone loss (RR), a measure of net bone turnover. Teriparatide treatment decreased urinary $^{45}\text{Ca}/\text{total Ca}$ ratio (Fig. 1), and increased BMD by 19.8%. In the first 10 days of treatment, teriparatide reduced RR by an average of 13%. Maximal suppression of RR occurred during days 41-60 (Fig. 2), when RR was reduced by 47%. Average RR during the first 10 days was predictive of change in BMD ($R^2 = 0.28$, $p=0.09$). This study confirms that anabolic therapy decreases RR, and that acute changes in RR in response to treatment are predictive of long-term changes in BMD. These results suggest that monitoring urinary excretion of calcium tracers is an effective method to screen potential osteoporosis therapies that may act through anabolic as well as antiresorptive mechanisms.

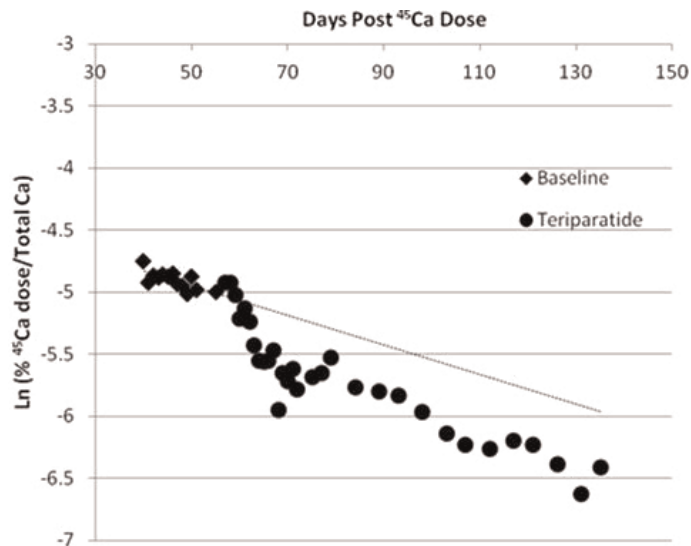


Figure 1: Urinary $^{45}\text{Ca}/\text{total Ca}$ curve for one rat. The dotted line represents the predicted values based on baseline $^{45}\text{Ca}/\text{total Ca}$ excretion

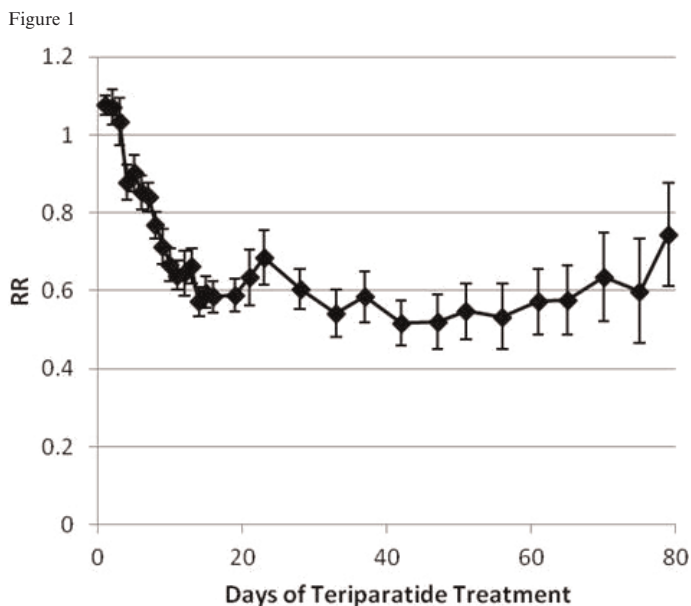


Figure 2: Average RR throughout teriparatide treatment. Baseline RR=1. Values are mean \pm SEM.

Figure 2

Disclosures: Emily Hohman, None.

SU0409

Analgesic Effects of Minodronate on Formalin-induced Acute Inflammatory Pain in Rats. Naohisa Miyakoshi*, Toyohito Segawa, Yuji Kasukawa, Hiroshi Aonuma, Hirovuki Tsuchie, Yoichi Shimada. Akita University Graduate School of Medicine, Japan

Introduction: Recent reports have shown that bisphosphonates exert analgesic effects in patients with osteoporosis. Minodronate, a third-generation bisphosphonate, is expected to show greater analgesic effects than other bisphosphonates, as previous reports have shown that among bisphosphonates, only minodronate has P2X2/3 receptor antagonistic actions and exhibits analgesia in mice. However, studies on analgesic effects of minodronate compared with morphine as a positive control for analgesia against formalin-induced acute inflammatory pain in rats have not yet been conducted.

Methods: Four-month-old female Wistar rats were divided into a minodronate group, a morphine group, and a vehicle control group ($n=10$ each). Rats then received a single injection of minodronate (50 mg/kg), morphine (10 mg/kg), or vehicle. Thirty minutes after this injection, all rats received an injection of formalin into the right hind paw to induce acute inflammatory pain. Behaviors after formalin injection in phase 1 (0-5 min) and phase 2 (10-30 min) were monitored according to nociceptive responses and a foot stamp test. Numbers of paw licking and paw lifting behaviors were counted as parameters of nociceptive response. As a foot stamp test, rats were allowed to ambulate on white paper after sponges were glued to bilateral soles and soaked with different colored ink for each side (red for right; black for left). Limb usage was evaluated by counting foot stamps on the paper, and percentage limb usage of the formalin-injected side (number of stamps of formalin-injected right side/number of stamps of left side $\times 100$) was calculated.

Results: The minodronate group showed significantly lower nociceptive responses and significantly higher percentage limb usage compared with the vehicle group in phase 2 ($p<0.05$). However, no significant differences were observed in any parameters between the minodronate group and vehicle group in phase 1. The morphine group showed significantly lower nociceptive responses and significantly higher percentage limb usage compared to the other two groups in both phase 1 and phase 2 ($p<0.05$).

Conclusions: For this pain model in rats, minodronate showed significant analgesic effects in phase 2 of formalin-induced acute inflammation. Minodronate may be beneficial for patients with osteoporosis accompanying acute pain, including fractures.

Disclosures: Naohisa Miyakoshi, None.

SU0410

Effects of Zoledronic Acid and Fracture on the ex vivo Proliferation and Osteoblastic Differentiation of Rat Mesenchymal Stem Cells. Terhi Heino*¹, Heikki Halkosaari¹, Jessica Alm², Ville-Valtteri Valimäki³. ¹Department of Cell Biology & Anatomy, University of Turku, Finland, ²Orthopaedic Research Unit, Finland, ³Helsinki University Central Hospital, Finland

While bisphosphonates mainly target bone-resorbing osteoclasts, they have also been suggested to affect osteogenic cells. We hypothesized that zoledronic acid (ZA) treatment in vivo would systemically enhance bone marrow mesenchymal stem cell (MSC) proliferation and osteoblastic differentiation ex vivo and that this effect could be modulated by fracture. The study comprised 50 female rats (16-23 wk, 224-351 g) divided into six groups: Fracture and weekly ZA ($n=9$); Fracture and bolus ZA ($n=8$); Fracture and weekly placebo (saline) ($n=13$); Intact and weekly ZA ($n=6$); Intact and bolus ZA ($n=7$); Intact and weekly placebo ($n=6$). A right-sided closed femoral fracture was induced and after 1 wk s.c. ZA or placebo injections were initiated. The ZA doses (0.1 mg/kg for bolus group and 0.014 mg/kg/wk for weekly group) were comparable to the annual 5 mg dose used to treat osteoporosis in humans. Fracture healing was monitored with x-ray imaging at 0, 4 and 8 wk and with uCT at 8 wk. Rats were sacrificed at 8 wk. Bone marrow MSCs were isolated from the intact femur and tibia by plastic adherence. Proliferation was evaluated over 7 passages. Osteoblastic differentiation was induced by dexamethasone, ascorbic acid and β -glycerophosphate and assayed by quantification of alkaline phosphatase (ALP) activity and ALP stained area. Mineralization was quantified by von Kossa stained area. Results were statistically analyzed using Mixed Models. MSCs isolated from ZA groups showed significantly enhanced proliferative capacity ($p=0.002$) but no difference was observed between bolus and weekly groups. No difference was observed between ZA and placebo groups in osteoblastic differentiation or mineralization. Interestingly, in cultures without osteoblast induction, basal ALP activity ($p=0.024$) and ALP stained area ($p=0.015$) were significantly higher in ZA groups than in placebo groups. No statistically significant difference was observed in MSC proliferation but osteoblastic differentiation was significantly enhanced in fractured vs. intact groups ($p=0.003$). In contrast, MSCs from fractured animals showed lower level of mineralization than MSCs from intact animals ($p=0.043$). In conclusion, ZA treatment in vivo stimulates MSC proliferation and induces spontaneous osteoblastic phenotype ex vivo. Furthermore, fracture can modulate the osteoblastic differentiation and mineralization of MSCs ex vivo. These effects appear to be systemic and long-lasting after in vivo exposure.

Disclosures: Terhi Heino, None.

This study received funding from: -

SU0411

Induction of Antral Ulcers by Alendronate, A Nitrogen-Containing Bisphosphonate, in Rat Stomachs. Koji Takeuchi*, Daisuke Hara, Avano Imasato, Misato Oka, Kikuko Amagase. Kyoto Pharmaceutical University, Japan

Background/Aim: Bisphosphonates (BPPs) are a class of compounds that have been developed as an anti-resorptive agent for treating the bone diseases. Clinical studies, however, showed that these drugs caused the untoward effects on the upper gastrointestinal tract. In the present study, we demonstrated the development of antral ulcers induced in rats by alendronate and investigated the pathogenic factors involved in this model. **Methods:** Male SD rats fasted for 18 h were given alendronate (100-600 mg/kg) PO as a single injection. Then, they were re-fed normally and killed on various days up to 7 days later. Omeprazole (30 mg/kg) was given p.o. once daily after alendronate while indomethacin (1 mg/kg) or rebamipide (30, 100 mg/kg) was given p.o. twice daily. **Results:** Alendronate caused non-hemorrhagic damage in both the corpus and antrum of fasted rats, but after refeeding for 3 days the lesions in the corpus healed completely, while those in the antrum developed into large ulcers with increased vascular permeability. Acid secretion was decreased after alendronate treatment. The development of antral ulcers was accompanied by an increase in MPO activity and lipid peroxidation as well as a decrease in SOD activity and GSH content in the mucosa. Histologically, the damage did not penetrate the muscularis mucosa, yet severe edema and neutrophil infiltration were observed in the submucosa. Neither omeprazole nor indomethacin had any effect, while all opurinol and SOD reduced the severity of these ulcers. Likewise, gastroprotective drugs, such as rebamipide, teprenone or irsogladine significantly suppressed the ulcerogenic response in the antrum with a concomitant reversal of the increased vascular permeability, MPO activity and lipid peroxidation as well as the reduced SOD activity and GSH content. **Conclusions:** These results suggest that alendronate did not cause gross damage in the stomach of fasted rats, yet produced large ulcers in the antrum with severe edema after refeeding. The pathogenesis of these ulcers may be explained by impairment of the mucosal anti-oxidative system and does not involve acid/peptic digestion and deficiency of prostaglandins. This lesion model would be useful for screening of the mucosal protective drugs against antral lesions in the stomach.

Disclosures: Koji Takeuchi, This study received funding from: Ajinomoto Pharma, 6

SU0412

Preservation of the Bone Structure and Function in Mice on a Western-Style Diet by Mineralized Red Algae. Muhammad Aslam*, James Varani. University of Michigan, USA

The purpose of this study was to determine whether a mineral-rich extract derived from the red marine algae, *Lithothamnion calcareum*, could be used as a dietary supplement for prevention of bone mineral loss. A cohort of C57BL/6 mice (300 males and females) was equally divided into four groups based on diet. One group received a low-fat rodent diet (AIN76A). The second group received a high-fat western-style diet (HFWD). The third and fourth groups were fed the same AIN76A and HFWD respectively along with the mineral-rich extract. Mice were maintained on the respective diets for 5, 12 and 18 months. Then, long bones (femora and tibiae) and a subset of C8 vertebrae were analyzed by three-dimensional micro-computed tomography and concomitantly assessed for bone strength. Tartrate-resistant acid phosphatase (TRAP) and N-terminal peptide of type I procollagen (PINP) were assessed in plasma obtained at the time of sacrifice. Bone mineral analysis was performed using inductively coupled plasma optical emission spectrometry. To summarize, female mice on the HFWD had reduced bone mineralization and reduced bone strength relative to female mice on the low-fat diet as early as at five months; male mice showed relatively less effect at earlier stages but bone loss and reduced bone strength was evident at 18 months. The bone defects in female mice on the HFWD were overcome in the presence of the mineral-rich supplement. In fact, female mice receiving the mineral-rich supplement in the HFWD had better bone structure/function than did female mice on the low-fat diet. Female mice on the mineral-supplemented HFWD had higher plasma levels of TRAP than mice of the other groups. Mice on HFWD had slightly higher PINP levels than other groups. Bone mineral analysis showed that bones of mice on the HFWD had higher levels of barium, iron, manganese, silicon and zinc. Bones from supplemented diets had significant higher levels of strontium and sulfur. Calcium, magnesium and phosphorus levels were similar in all bone samples with slight reduction in bones of mice on the HFWD. These data are consistent with the suggestion that osteoporosis is an early age phenomenon and can be prevented with a multi-mineral diet starting at young age. They also suggest that mineralized red algae can overcome the adverse effect of high-fat diet and protect mice from bone loss. Based on these results, it would be worthwhile to undertake a long-term comprehensive prospective study in human volunteers.

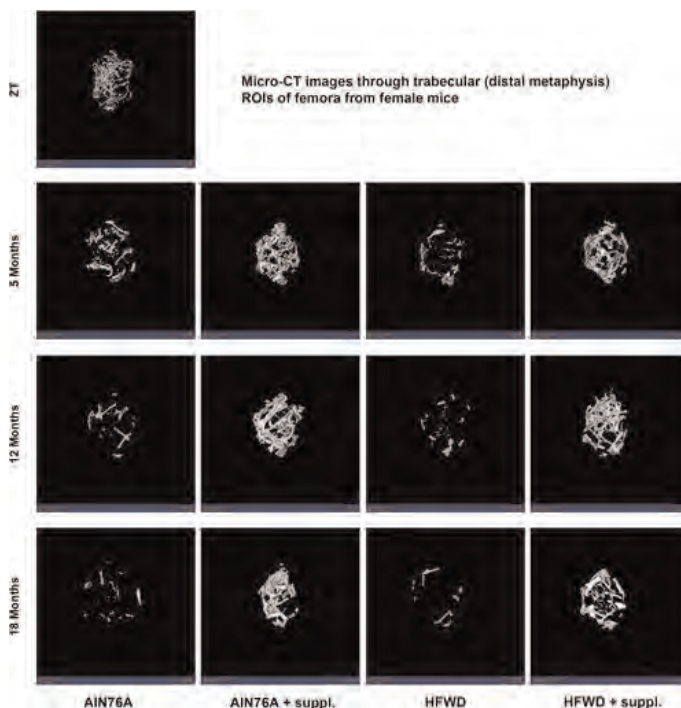


Figure 1. Trabecular ROIs in female femora.

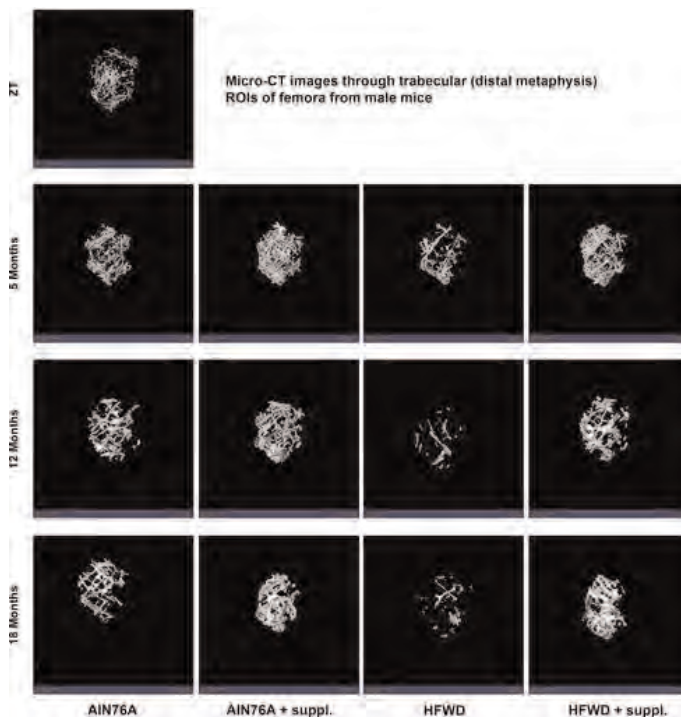


Figure 2. Trabecular ROIs in male femora.

Disclosures: Muhammad Aslam, None.

This study received funding from: 1-Grant CA140760 from the National Institutes of Health, Bethesda, MD. 2- Grant 11-0577 from the Agency for International Cancer Research, St. Andrews, Fife, Scotland.

SU0413

Withdrawn

SU0414

Endoxifen Differs From Other Selective Estrogen Receptor Modulators *in vitro* and Enhances Bone Mass In Ovariectomized Mice. Anne Gingery*¹, Malayannan Subramaniam², Muzaffer Cicek², Kevin Pitel², Urszula Iwaniec³, Russell Turner³, James Ingle², Matthew Goetz², Thomas Spelsberg², John Hawse⁴.
¹Mayo Clinic School of Medicine, USA, ²Mayo Clinic, USA, ³Oregon State University, USA, ⁴Mayo Clinic College of Medicine, USA

Endoxifen is a selective estrogen receptor modulator (SERM) that is currently being developed as a novel drug for the treatment of breast cancer. Since SERMs have been indicated for the treatment of osteoporosis, we sought to characterize the effects of endoxifen on bone. To understand endoxifen's mechanism of action, we compared the gene expression profiles of estrogen receptor alpha (ER α) and ER beta (ER β) expressing MC3T3 osteoblast (OB) cells, treated with endoxifen to those treated with estradiol (E2), tamoxifen, raloxifene or lasofoxifene. Interestingly, there was little overlap in the genes regulated by these agents in ER α or ER β expressing OBs. At the level of OB proliferation, all of the SERMs and E2 suppressed the proliferation rates of ER α expressing cells to varying degrees. In ER β expressing cells, endoxifen increased cell proliferation while E2 and all other SERMs had no significant effect. Mineralization assays revealed that E2 treatment enhanced the differentiation of ER α expressing OBs while the SERMs had little to no effect. In contrast, the differentiation of ER β expressing OBs was induced by SERM treatment with endoxifen having the greatest effect. These observations correlated well with the expression levels of Runx2, osterix, osteocalcin and alkaline phosphatase throughout the course of differentiation. The *in vivo* effects of endoxifen on the mouse skeleton were examined in 3 month ovariectomized C57BL/6 mice treated with endoxifen (50mg/kg/day) or vehicle control for 45 days. DXA analysis revealed significant increases in BMD and BMC throughout the skeleton following endoxifen treatment. Increased trabecular density, cortical content, area and thickness were observed by pQCT in the tibial metaphysis and diaphysis. Micro-CT analysis of the femoral metaphysis revealed increases in bone BV/TV, trabecular number and thickness, as well as decreased trabecular spacing. In addition, serum markers of bone formation and resorption were increased in endoxifen treated animals indicating active bone remodeling. Taken together, our *in vitro* data indicate that endoxifen functions differently through the actions of both ER α and ER β to elicit unique effects on bone relative to that of other SERMs and E2. These studies are the first to examine the *in vivo* impact of endoxifen on the skeleton and suggest that it may ultimately have utility for the prevention and/or treatment of osteoporosis.

Disclosures: Anne Gingery, None.

SU0415

Effects of Ethanol and Water Extracts of *Fructus ligustri Lucidi* on Vitamin D Metabolism and Intestinal Calcium Absorption in Mature Ovariectomized Rats. Xiaoli Dong*¹, Sasa Gu¹, Quangui Gao¹, Ming Xian Ho¹, Haotian Feng², Man Sau Wong¹, Liva Denney³.
¹Department of Applied Biology & Chemical Technology, The Hong Kong Polytechnic University, China, ²Nestlé Research Centre Beijing, China, ³Nestlé Research Centre, Switzerland

Previous studies indicated that ethanol extract of *Fructus Ligustri Lucidi* (FLL), a Chinese herb could increase the circulating levels of 1,25(OH)₂D₃ in aged female rats by directly stimulating 25-dihydroxyvitamin D₃-1 α -hydroxylase (1-OHase) activity. To further explore the potential of the herb for bone protection, the present study aimed to investigate the effects of FLL ethanol (EE) or water extract (WE) as supplemental food constituents on 1,25(OH)₂D₃ production and intestinal calcium (Ca) absorption in 6-month-old ovariectomized (OVX) rats. Treatment diets were prepared by mixing different herbal extracts with basal medium Ca powder diet (MCD, 0.6% Ca, 0.65% P). Six month-old female Sprague Dawley rats were subjected to bilateral ovariectomy (OVX) or sham-operation and randomly assigned to 5 groups, i.e., sham rats fed with MCD; OVX rats fed with MCD; OVX rats fed with MCD and injected by β -estradiol (200ug/kg, weekly injection); OVX rats fed with MCD supplemented with EE (700 mg/kg/d); OVX rats fed with MCD supplemented with WE (700 mg/kg/d). Rats were administered with different treatment diets at the dosage of 15g/rat/day for 12 weeks. At the end of experiment, rat serum, urine, feces were collected for detection of 1,25(OH)₂D₃ production and intestinal Ca absorption in rats. In addition, human proximal tubule (HKC-8) cells were chosen for *in vitro* investigation of the direct actions of EE and/or WE on 1,25(OH)₂D₃ synthesis. Our results showed that EE, but not WE, treatment significantly elevated serum 1,25(OH)₂D₃ levels by 45.2% (P<0.05) in 6-month-old OVX rats. *In vitro* study indicated that EE, but not WE, significantly enhanced renal 1-OHase mRNA expressions directly in HKC-8 cells. In contrast, our results also showed that WE, but not EE, could significantly improve intestinal Ca absorption rate in 6-month-old OVX rats by 21.2% (P<0.05). The increase in intestinal Ca absorption rate in 6-month-old OVX was not associated with an increase in circulating levels of 1,25(OH)₂D₃. Our results showed that EE increased circulating 1,25(OH)₂D₃ levels in OVX rats and stimulated renal 1-OHase mRNA expression in HKC-8 cells; whereas WE increased intestinal Ca absorption rate in OVX rats possibly via 1,25(OH)₂D₃-independent manner. Further work is needed to evaluate closely the potential of different FLL extracts for bone protection.

Disclosures: Xiaoli Dong, None.

This study received funding from: Nestlé Research Centre Beijing

SU0416

Efficacy of Switching Alendronate and Odanacatib Treatments on Bone Mass, Mechanical Properties and Bone Remodeling in the Lumbar Spine of Ovariectomized Rabbits. Kevin Scott*¹, Michael Gentile², Carlyle Horrell³, Christopher Winkelmann³, Randolf Crawford³, John Szumiloski³, Rana Samadfam⁴, Susan Y. Smith⁴, Le Thi Duong⁵.
¹Merck & Company, USA, ²Merck & Co., Inc., USA, ³Merck, USA, ⁴Charles River Laboratories, Canada, ⁵Merck Research Laboratories, USA

Odanacatib (ODN), a selective and reversible inhibitor of cathepsin K (Cat K) is currently in development for treatment of postmenopausal osteoporosis. Here we evaluated BMD, bone strength and remodeling in the lumbar spine (LV) of OVX rabbits comparing ODN and alendronate (ALN) monotherapies to ALN and ODN switch treatment paradigms. NZW rabbits (age 13 mo) were ovariectomized 6 mo prior, then assigned to respective treatment groups: 1) OVX-Vehicle, 2) ODN (~7 μ M 24 hr, p.o., in food), 3) ALN (0.3 mg/kg/wk.s.c.), 4) ODN switch to ALN (ODNswALN) and 5) ALNswODN. Total treatment duration for all groups was 16 mo and therapeutic agents were switched in groups 4 and 5 at 8 mo. Longitudinal assessments of LV bone mineral density (aBMD) were made at 4 mo intervals by DXA (LV5-6) and QCT (LV6, trabecular, vBMD). Histomorphometric (LV4) and combined strength data (LV5-6) were determined at 16 mo. Treatment with ODN for 8 mo increased aBMD by 11% (p \leq 0.01) and vBMD by 18% (p \leq 0.001) vs. baseline, while ALN increased aBMD by 7% and vBMD by 6% vs. baseline. ODN treatment continued to further increase aBMD by 8% and vBMD by 4% from 8 to 16 mo (p \leq 0.01). In the ODNswALN group bone mass gain is maintained up to 8 mo then decreased slightly to study end, -2% for aBMD and -2% for vBMD. In the ALNswODN group, LV BMD further increased by 7% and 11%, respectively. Peak load and yield load were significantly increased in ODN, ALN and the switch groups (p \leq 0.05 vs. OVX-Veh). Stiffness was significantly increased in ODN and in switch groups (p \leq 0.05 vs. OVX-Veh). Peak load correlated positively with aBMD (R = 0.6954, p \leq 0.0001) and aBMC (R = 0.6879, p \leq 0.0001) in all groups. The bone formation rate (BFR) was unchanged in ODN (4%) and decreased in ALN (-50%, p \leq 0.05) vs. OVX-Veh. BFR was lower in ODNswALN (-50%, p \leq 0.05) but trended higher in ALNswODN (+16%) at study end. In summary, treatment with ODN or ALNswODN increased bone mass and strength in the LV. These gains are supported by higher BFR from the respective groups vs. ALN. Conversely, switching from ODN to ALN protected bone mass gained with ODN by reduced remodeling. The data demonstrates that switching treatment from ALN to ODN has a positive effect on the lumbar spine bone mass and strength by re-activating bone formation. The preclinical results suggest that ODN may offer an alternative treatment option for patients on long-term therapy with bisphosphonate(s).

Disclosures: Kevin Scott, Merck, 3

This study received funding from: Merck

SU0417

Green Tea Polyphenols Improve Bone Microarchitecture and Quality in Obese Female Rats Fed with High-fat and Restricted Diets. Chwan-Li Shen*¹, Jay Cao², James Yeh³, Ming-Chien Chyu⁴.
¹Texas Tech University Health Sciences Center, USA, ²USDA ARS, USA, ³Winthrop University Hospital, USA, ⁴Texas Tech University, USA

We have previously demonstrated that green tea polyphenols (GTP) mitigate trabecular bone loss in various bone loss models. This study further investigates the efficacy of GTP on bone microstructure and quality in obese rats fed high-fat diet and restricted diets. Forty-eight 3-month-old SD rats were fed a high-fat diet at libitum for 4 months. After 4 months, the animals were assigned to a 2 (high-fat diet vs. restricted diet with 35% caloric deficit) \times 2 (no GTP vs. 0.5% GTP in drinking water) factorial design for another 4 months. Efficacy was evaluated by dual-energy absorptiometry, micro-CT, histomorphometric analysis, and 3-point bending test. Data were analyzed by two-way ANOVA followed by Fisher's LSD test. The results show that the restricted diet lowered bone mineral content, density, and strength at femur, trabecular bone volume at tibia and lumbar vertebrae, trabecular thickness, number and cortical thickness of tibia. The restricted diet also increased trabecular separation and eroded surface, periosteal formation rate, as well as endocortical formation rate and eroded surface at tibia. Supplementation of GTP into the drinking water for 4 months resulted in increases in rats fed both high-fat and restricted diets in bone mineral content, density, and strength at femur, trabecular bone volume at tibia and lumbar vertebrae, trabecular thickness and number, and cortical thickness of tibia. GTP supplementation also lead to a decrease in trabecular separation, trabecular bone formation rate and eroded surface, periosteal formation rate, endocortical formation rate and eroded surface. This study demonstrates that GTP supplementation in drinking water can increase bone mineral density, strength, and microstructure through suppressing bone turnover rate in rats fed both high-fat and restricted diets.

Disclosures: Chwan-Li Shen, None.

SU0418

Halofuginone Protects from Ovariectomy-Induced Bone Loss. Carl DeSelm*, Steven Teitelbaum. Washington University in St. Louis School of Medicine, USA

Halofuginone (HL) is a small molecule inhibitor of TGF-beta signaling and IL-17 production, with a favorable safety profile in humans. As both IL-17 and TGF-beta contribute to bone destruction in various circumstances, and molecular TGF-beta inhibition has a favorable effect on baseline murine bone density, we tested the effects of HL on bone loss in ovariectomized (ovx) mice. Femora of eight-week-old mice were analyzed by *in vivo* microCT before ovx, and two and four weeks after ovx. Beginning the day of the procedure, mice were injected with 2 ug/day of intraperitoneal HL or an equivalent volume of DMSO-PBS control. Two independent *in vivo* studies using two different HL manufacturers from the USA and China yielded similar results, demonstrating HL has a protective effect on BV/TV, trabecular thickness, trabecular space, connectivity density, and BMD as measured by microCT. Serum CTx, a surrogate measure of bone resorption, is significantly elevated in control treated mice, but not HL treated mice. These data demonstrate that in the acute ovariectomized, low estrogen state, HL is protective against bone loss.

Disclosures: Carl DeSelm, None.

SU0419

The Influence of Therapeutic Radiation on the Patterns of Bone marrow in Ovary-Intact and Ovariectomized Mice. Susanta Hui*¹, Leslie Sharkey², Louis Kidder³, Yan Zhang³, Gregory Fairchild¹, Kavti Coghill⁴, Corv Xian⁵, Douglas Yee⁶. ¹University of Minnesota, USA, ²Department of Veterinary Clinical Sciences, College of Veterinary Medicine, University of Minnesota, USA, ³Masonic Cancer Center, University of Minnesota, USA, ⁴Department of Therapeutic Radiology, University of Minnesota, USA, ⁵University of South Australia, Australia, ⁶Department of Medicine, Medical School, University of Minnesota, USA

Purpose: To characterize the radiation-induced damage on a medically relevant model of the integrated regulation of the tissue components of the bone-marrow system (bone, hematopoietic, stromal/adipose) in the presence or absence of ovarian function.

Methods: Single fractional 16 Gy radiation was delivered to the caudal skeleton of ovary-intact (I±R) and ovariectomized (OVX±R) mice. Marrow fat, hematopoietic cellularity, and cancellous bone volume fraction (BV/TV%) were assessed.

Results: Ovariectomy alone did not significantly reduce Day 30 marrow cellularity in non-irradiated mice (OVX-R vs. I-R, $p=0.8445$); however it impaired the hematopoietic recovery of marrow following radiation exposure (OVX+R vs I+R, $p=0.0092$). The combination of radiation and OVX dramatically increases marrow fat compared to either factor alone ($p<0.0001$ for both). The synergistic effect was also apparent in the reduction of hematopoietic marrow cellularity; however this synergistic effect was absent in BV/TV. The expected inverse relationship between marrow adiposity vs. hematopoietic cellularity and bone volume was observed. However compared with OVX mice, intact mice demonstrated twice the reduction in hematopoietic cellularity and a tenfold greater degree of bone loss for a given unit of expansion in marrow fat as shown in figure 1.

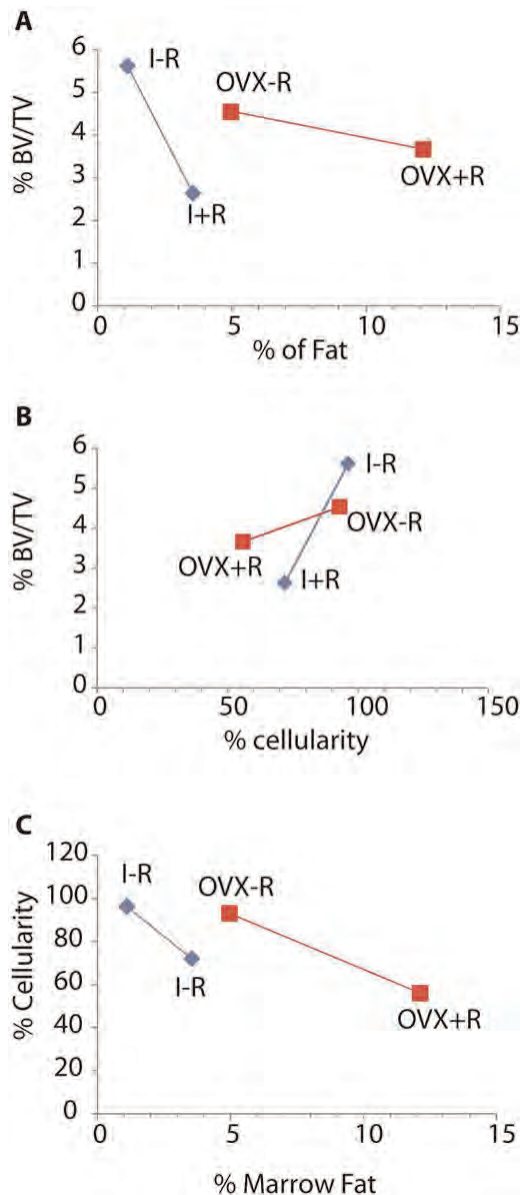
Figure 1. Ovariectomy influences the relationships between bone volume (BV/TV), adipogenesis (% marrow fat), and hematopoiesis (% cellularity) at Day 30 with or without 16 Gy radiation to the hind limb in mice. Data of every two measurements are represented as least squares mean values for the group.

Panel A: OVX results in a 10 fold reduction in the rate of bone volume loss per unit increase in marrow fat after radiation treatment compared with intact mice.

Panel B: OVX blunts the rate of bone volume loss relative to reduced hematopoietic cellularity after radiation compared with intact mice by a factor of 6.

Panel C: OVX halves the reduction in hematopoietic cellularity compared with increased marrow fat after radiation treatment compared with intact mice.

Conclusion: Prior ovariectomy exacerbated adipose accumulation in the marrow space in mice after delivery of a clinically-relevant focal radiation exposure, but blunted bone loss and hematopoietic suppression. In the normally coupled homeostatic relationship between the bone and marrow domains, OVX appears to alter feedback mechanisms. Confirmation of this non-linear phenomenon and multiple interactions in light of the differing radiosensitivities of the participating tissues is warranted.



Multivariate Interactions

Disclosures: Susanta Hui, None.

SU0420

The Reversibility of the Cathepsin K Inhibition in Osteoclastic Bone Resorption in vitro. Ya Zhuo*¹, Le Thi Duong². ¹Merck & Co., Inc., USA, ²Merck Research Laboratories, USA

Odanacatib (ODN) is a selective and potent cathepsin K inhibitor (CatKi) currently developed for the treatment of postmenopausal osteoporosis. We previously demonstrated that ODN reduced efficiency of osteoclastic (Oc) bone resorption by blocking degradation of demineralized collagen in resorption lacunae and transcytosis. Here, we examine the kinetics of reversibility of CatKi in blocking Oc function in vitro. First, enzyme engagement in active Oc is tracked by bодipy-labeled CatKi (B-CatKi) on bone slices using confocal microscopy. B-CatKi readily binds to active CatK in transcytotic vesicles and resorption lacunae. Incubation with L-873724 an analog of ODN for 5min, displaces B-CatKi from CatK pool in resorption lacunae, without fully displacing it in intracellular vesicles. Next, mature human Oc on bone slices are pre-treated with either vehicle, ODN or Alendronate (ALN) for 2 days. The culture media are then replaced with either vehicle only or the same respective treatment for another 4 days. The collagen degradation marker CTx is measured in the media at 1hr, 4hr, day1, 2, 3 and 4. TRAP-positive Oc and resorption pits are stained on day 4. Pre-treatments with ODN and ALN for 2 days significantly reduce CTx to the same extent. After the media are changed, CTx is barely detectable at 1 or 4 hr in all groups. After 1 day, while ODN continuously reduces CTx release, discontinuation of ODN results in rapid time-dependent increase of CTx vs. ODN controls ($p<0.001$), leading to full reversal of Oc activity by day 4. On the other hand, vehicle switched to ODN treatment also quickly reduces CTx release and Oc

functions. As expected, discontinuation of ALN does not change CTx level or reverse Oc activity. Discontinued ODN or ALN does not change Oc numbers compared to respective continuous treatment. Furthermore, ODN significantly increases TRAP(+) Ocs, maintains the numbers of shallow pits accompanied with reduced pits area; whereas discontinued ODN returns pits numbers and area to vehicle levels. Both ALN regimens maintain Oc numbers and reduce pits numbers well below to that in vehicle. In summary, our results highlight the basic mechanism of ODN differentiated from bisphosphonates at cellular levels. ODN displays fast kinetics of inhibitory and resolution of effects on osteoclastic bone resorption; while discontinuation of ALN did not reverse its treatment effects in the same time frame.

Disclosures: *Ya Zhuo, Merck, 7; Merck, 3*
This study received funding from: Merck

SU0421

Increased Expression of IL-6 and the p62 P392L Mutation are Sufficient to Induce Pagetic OCL in Mice. Noriyoshi Kurihara¹, Jumpei Teramachi¹, Jolene Windle², G. David Roodman¹. ¹Indiana University, USA, ²Virginia Commonwealth University, USA

The primary cellular abnormality in Paget's disease (PD) resides in the osteoclast (OCL). PD OCL express measles virus nucleocapsid protein (MVNP), form increased number of OCL that are increased in size, contain increased nuclei/OCL, have increased bone desorbing capacity/OCL, increased 1,25-(OH)₂D₃ and RANKL responsiveness. In addition, PD is characterized by abnormal OCL that secrete high IL-6 levels and induce exuberant bone formation. We reported that MVNP expression and the SQSTM1 (p62) mutation in OCL both contribute to the increased OCL activity in PD, and that p62 P394L knockin mice (p62KI) do not develop pagetic lesions but rather develop osteopenia. Although, OCL numbers in p62KI mice were increased, OCL morphology was a normal. In addition, stromal cells from p62KI mice produced high levels of RANKL when treated with 1,25-(OH)₂D₃. However, bone marrow cultures from p62KI mice produce much lower levels of IL-6 than bone marrow cultures from mice with targeted expression of MVNP in OCL (MVNP mice). Therefore, production of low levels of IL-6 may contribute to the lack of a pagetic phenotype in p62KI mice. To test this hypothesis, we generated p62KI/IL-6 transgenic mice by breeding p62KI mice to TRAP-IL-6 mice in which overexpression of IL-6 is driven by the TRAP promoter, and characterized their OCL. OCL precursors from p62KI/IL-6 and MVNP mice were hyper-responsive to 1,25-(OH)₂D₃ and formed OCL at low concentrations (10⁻¹⁰M) of 1,25-(OH)₂D₃ compared to WT. OCL formation in marrow cultures from p62KI/IL-6 mice was increased but to a lesser extent than in cultures of MVNP marrow. OCL formation from pure populations of OCL precursors of p62/IL-6 mice and TRAP-IL-6 mice were hyper-responsive as were TRAP-IL-6 mice. RANKL production in whole bone marrow culture of p62KI/IL-6 treated with 1,25-(OH)₂D₃ was increased compared to transgenic lines (p62/IL-6: 40 pg/ml, p62KI: 20 pg/ml, TRAP-IL-6: 15 pg/ml, MVNP and WT<10pg/ml). 1,25-(OH)₂D₃ increased bone resorption in marrow cultures from the three transgenic mouse lines compared to WT with the percent of area of bone resorption increased in p62KI/IL6(26±3) and MVNP (32±2) compare to WT (3±1), p62KI (22±3), IL-6 (8±2) mice. Thus p62KI/IL-6 mice develop OCL with an intermediate pagetic phenotype in vitro. These data demonstrate that high IL-6 level are required for p62KI mice to form Paget's like OCL.

Disclosures: *Jumpei Teramachi, None.*

SU0422

Study of the Sequestosome 1 Gene Copy Number in Paget's Disease of Bone. Sabrina Guay-Bélanger¹, Edith Gagnon², Jean Morissette², Jacques Brown³, Laetitia Michou⁴. ¹Centre de recherche du CHUQ-CHUL, Canada, ²CHUQ (CHUL) Research Centre, Canada, ³CHUQ Research Centre/Laval University, Canada, ⁴Centre De Recherche Du CHUQ - CHUL, Canada

Purpose: Paget's disease of bone (PDB) has an autosomal-dominant mode of inheritance with incomplete penetrance in approximately one-third of cases. To date, only the Sequestosome 1 (SQSTM1) gene has been linked to PDB, with more than 20 reported mutations. The SQSTM1/P392L mutation was the first described and remains the most common mutation in PDB. Recently, a new prevalent form of genomic variation has emerged. Copy number variation (CNV) is described as a segment of DNA that is 1 kb or larger and is present in variable copy numbers in comparison with a reference genome. Three CNVs have already been reported in the SQSTM1 gene region. The objective of this study was to determine if one CNV of the SQSTM1 gene was associated with PDB.

Methods: This investigation focussed on the CNV_0068 since it covers the whole SQSTM1 gene, including exons 7 and 8, where mutations are located. We analysed 277 PDB-affected patients, of whom 38 were carriers of a P392L mutation, 16 healthy individuals carrier of a P392L mutation, and 298 healthy controls. We used the TaqMan Copy Number Assays according to the manufacturer's protocol. We performed case-control comparisons of individuals with loss of copy (i.e. less than two copies) of the SQSTM1 gene or with gain of copy (i.e. more than two copies), to individuals with two copies, who were considered the reference. Furthermore, the subgroups of patients carrying a P392L mutation were compared to healthy controls. Finally, phenotype-genotype correlations were performed. Statistical analyses included Student T test,

Fisher's exact test, odds ratio (OR) and 95% confidence interval calculations. Differences were considered statistically significant when $p < 0.05$.

Results: Comparisons of subgroups to healthy controls demonstrated that gain in SQSTM1 copy number was significantly more frequent in individuals carrying a P392L mutation, PDB-affected (39.5% versus 23.5%, $p = 0.051$, OR = 2.036 [0.988; 4.196]) or not (50.0% versus 23.5%, $p = 0.028$, OR = 3.619 [1.213; 10.801]). However, no phenotype-genotype correlation was found.

Conclusion: This study suggests that a gain of SQSTM1 copy number is associated with the presence of the P392L mutation, whether mutation carriers were PDB-affected or not.

Disclosures: *Sabrina Guay-Bélanger, None.*

SU0423

Withdrawn

SU0424

Osteoblasts Mediate Glucocorticoid-Induced Metabolic Dysfunction. Holger Henneicke¹, Tara Brennan-Speranza¹, Frank Buttgerit², Colin Dunstan³, Hong Zhou¹, Markus Seibel¹. ¹Bone Research Program, ANZAC Research Institute, University of Sydney, Australia, ²Department of Rheumatology & Clinical Immunology, Charité University Medicine, & Deutsches Rheumaforschungszentrum, Germany, ³University of Sydney, Australia

Background: Osteoblasts have been shown to be involved in the regulation of energy metabolism.¹ This study aimed to establish whether the effects of glucocorticoids (GC) on systemic fuel metabolism (glucose intolerance, insulin resistance, obesity) are mediated via the osteoblast.

Methods: We used a transgenic mouse model in which the GC-inactivating enzyme, 11 β -hydroxysteroid-dehydrogenase type 2, has been targeted exclusively to mature osteoblasts and osteocytes to disrupt pre-receptor GC-signalling in these cells. The transgene is not expressed in any other tissue, including fat, pancreas, liver, muscle or the CNS. Transgenic (tg) mice and their wild type (WT) littermates received either corticosterone 1.5mg/week (CS) or placebo (PLC) via s.c. pellets for 28 days. We have previously shown that this dose results in significant suppression of bone formation.² Body weight and composition (by PIXImus) were measured at baseline and 7, 14, 21 and 28 days into GC treatment. Serum total osteocalcin (OCN) and uncarboxylated OCN (uOCN), blood lipids, glucose tolerance (via oGTT) and insulin sensitivity (via ITT) were monitored throughout the 4-week observation period.

Results: In WT mice, GC-treatment led to a profound decrease in serum total and uOCN levels from day 7 onwards ($p < 0.001$ vs. baseline). Tg mice exposed to exogenous GCs also displayed a reduction in serum OCN and uOCN levels, but maintained higher concentrations than WT animals at all time points. In WT mice, exogenous GCs led to the development of complete insulin resistance and glucose intolerance from day 7 onwards, while tg mice remained sensitive to insulin and displayed normal glucose tolerance over 4-weeks (Fig. 1). Compared to GC-treated WT mice, tg animals maintained lower serum cholesterol and triglyceride levels during GC treatment. At endpoint, total body fat mass in GC-treated WT and tg mice differed by 4g (WT: 12.1±0.8g; tg: 8.1±0.5g, $p < 0.01$), with no appreciable difference between PLC-treated WT and tg mice.

Conclusion: Osteoblast-targeted disruption of GC-signalling significantly attenuates both the suppression of serum OCN concentrations as well as the effects of GCs on systemic fuel metabolism and body composition in mice. These data suggest that the effects of GCs on energy metabolism may be mediated via the osteoblast and its specific product, osteocalcin.

(1) Lee et al. Cell 2007;130(3):456-69

(2) Henneicke et al. Bone 2011;49(4):733-42

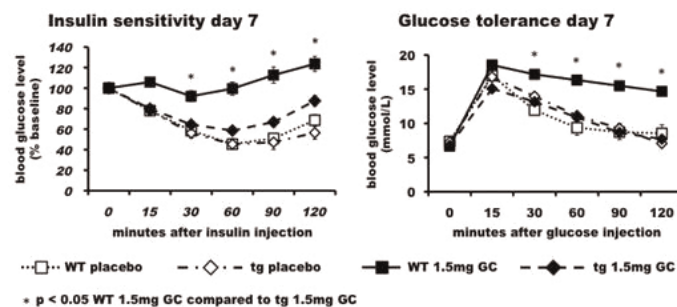


Figure 1

Disclosures: *Holger Henneicke, None.*

SU0425

Serum Sclerostin Level in Patients with Endogenous Cushing's Syndrome. Zhanna Belaya*¹, Liudmila Rozhinskaya², Ntalia Dragunova¹, Alexander Ilijin¹, Galina Melnichenko¹. ¹The National Research Center for Endocrinology, Russia, ²The National Research Centre for Endocrinology, Russia

Endogenous Cushing's syndrome (CS) is a rare endocrine disorder with the excess of glucocorticoids (GC) which influence the bone metabolism without other confounding factors: the disease itself, the dose and type of GC, the compliance.

The purpose was to estimate the serum levels of sclerostin (SCL), secreted frizzled related protein 1 (sFrz1) and dickkopf 1 (Dkk1) in patients with CS

Methods: We recruited 40 (34 female), Me 30 y.o. [Q25-Q75 26-40] consecutive patients with active CS (24 h urinary free cortisol (UFC) 2575 [1184-4228], reference range 60-413 nmol/24 hours; 18 patients sustained low traumatic fractures; and 40 age, sex, BMI matched healthy individuals. All participants provided fasting blood samples (0800-1000h) for bone turnover markers (osteocalcin (OC), carboxyterminal cross-linked telopeptide of type I collagen (CTX)), Insulin-like growth factor 1 (IGF-1), Dkk1, SCL, sFrz1. Blood samples were centrifuged and stored at -70°C. Serum SCL, sFrz1, Dkk1 were measured by an enzyme immunoassay using commercially available reagents (Biomedica Medizinprodukte GmbH & Co KG with rev.no. 100728, Usen Life Science Inc. E95880Hu and Enzo Life Sciences ADI-900-151. consequently). Serum samples on OC, CTx, IGF1 were assayed by ECLIA Cobas e601 Roche. UFC was measured by an immunochemiluminescence assay (extraction with diethyl ether) on a Vitros ECI.

Results: SCL level was significantly higher in patients with CS- 392,4 [346,5 – 421,0] versus control - 340,0 [280,8-414,6] pmol/l p=0.032. Notably, the difference was in medians and the lower quartiles, reflecting the lack of SCL suppression, but not the increased upper level. It might be the cause of absence of any correlations of SCL with UFC, IGF1 or OC. Dkk1 and sFrz1 did not differ from healthy control. We have found a marked suppression of OC in patients with CS versus healthy individuals, the CTx level did not differ from the control subjects. A negative correlation was found between the 24 h UFC level and OC R=-0.47 (p<0,05), but not with CTx R=0,22 (p>0,05). Patients with CS and fractures had lower OC level (p=0.15) and higher UFC (p=0.001).

Conclusion: patients with CS have higher serum SCL level that can be explained by the lack of suppression, but not the increased level of SCL above upper limit. As compared to sFrz1 and Dkk1, SCL seems to be the most promising target molecule for intervention to treat osteoporosis in patients with CS.

Disclosures: Zhanna Belaya, None.

This study received funding from: Presidential Grant AA-6978.201

SU0426

ER α 36 is Expressed in Estrogen Receptor Negative and Triple Negative Breast Tumors and Mediates Anti-apoptosis, Angiogenesis, and Metastasis. Reyhaan Chaudhri*¹, Agreen Hadadi¹, Natalia Cuenca¹, Ruth O'Regan², Zvi Schwartz¹, Barbara Boyan¹. ¹Georgia Institute of Technology, USA, ²Winship Cancer Institute of Emory University, USA

Estrogen signaling through ER α 36, a novel ER α variant, enhances protein kinase C (PKC) activity in triple negative breast cancer cells through a membrane-associated mechanism. We have shown that PKC activity positively correlates to breast tumor aggressiveness, and estradiol(E2)-dependent PKC activation leads to downstream effects such as anti-apoptosis, angiogenesis, and metastasis of triple negative breast cancer cells in vitro. However, the mechanism by which this occurs is unclear. Therefore, the purpose of this study was to determine if ER α 36 is found in breast tumors and if its presence depends on receptor status and second, to examine the mechanism by which E2 enhances breast cancer aggressiveness, particularly in regards to anti-apoptosis and angiogenesis. Using immunohistochemistry on a breast cancer tissue microarray, we found that approximately 44% of tumors were ER α 36-positive, of which 5 were classified as luminal A(ER+/PR+/HER2-), 4 were triple negative(ER-/PR-/HER2-), 3 were ER-(ER-/PR+/HER2+), 2 were luminal B(ER+/PR+/HER2+), and 2 were HER2+(ER-/PR-/HER2+). We observed non-nuclear staining of ER α 36. In addition, in many samples exhibiting vasculature, red blood cells were strongly positive, further supporting our *in vitro* data that ER α 36 functions primarily as a membrane receptor. *In vitro*, we found that ER α 36 antibodies blocked E2's ability to prevent taxol-induced apoptosis, measured by MTT and caspase-3 activity, implicating ER α 36 as the membrane receptor responsible. Inhibition of phospholipase C(PLC) and phosphoinositide-3-kinase(P13K) also prevented E2's anti-apoptotic effect suggesting a mechanism involving PLC, P13K, and PKC. HCC38 cells treated with increasing concentrations of E2-BSA, an E2 conjugate that activates membrane signaling only, increased production of vascular endothelial growth factor (VEGF) and basic fibroblast growth factor (FGF2) as measured by ELISA. In conclusion, ER α 36 is present in triple negative and ER-negative tumors and our data shows that E2 signaling through membrane-associated ER α 36 activates a specific signaling mechanism that leads to cancer cell aggressiveness in vitro. These data indicate that ER α 36 plays a major role in enhancing breast cancer severity and provides a novel target for chemotherapeutic drug design in patients with ER-negative or triple negative breast cancer that may benefit from therapies that target ER α 36.

Disclosures: Reyhaan Chaudhri, None.

SU0427

Examination of ER α Signaling Pathways in Cortical Bone of Mutant Mouse Models Reveals the Importance of ERE-dependent Signaling. Kumar Chokalingam*¹, Matthew Roforth¹, Kristy Nicks¹, Ulrike Moedder (McGregor)², Sundeep Khosla³, David Monroe⁴. ¹Mayo Clinic, USA, ²King's College, London UK, United Kingdom, ³College of Medicine, Mayo Clinic, USA, ⁴Mayo Foundation, USA

Estrogens play vital roles in the function and remodeling of bone. The mechanisms of estrogen receptor-alpha (ER α) action can be categorized into those involving direct binding to estrogen response elements (ERE; classical) or indirect DNA binding (non-classical, via protein-protein binding). The generation of non-classical ER knock-in (NERKI) mice provides a unique opportunity to define these pathways in bone. To better understand the role of these ER α signaling pathways *in vivo*, we examined the gene expression patterns of both complete ER α knockout (ERKO) and NERKI mice, compared to wildtype (WT) controls. Since both models exhibit high circulating estrogen levels, we ovariectomized 3 month old mice and replaced them with a low dose estrogen pellet for 4 weeks to fix estrogen levels between genotypes (n=13). Whole transcriptome analysis of RNA isolated from the flushed long bones (cortical bone) revealed 763 and 284 differentially expressed genes in ERKO and NERKI compared to WT, respectively (q \leq 0.1; fold-change \geq 1.5). Interestingly, 28% of the 763 affected genes in ERKO mice (210) were also affected in NERKI mice, demonstrating ERE-dependence. Gene ontology analysis of these genes revealed regulation of pathways involved in focal adhesion and extracellular matrix interactions, suggesting the regulation of these pathways are ERE-dependent in bone. However, a majority of genes regulated in ERKO mice (553; 72%) were unique, suggesting these genes are regulated by non-classical mechanisms. To further explore the biological pathways affected in ERKO mice, we performed custom QPCR arrays for known genes involved in bone physiology. Specifically, mRNA levels for select bone formation genes (alkaline phosphatase, bone sialoprotein, osterix and Dmp1) were suppressed in ERKO cortical bone. Interestingly, genes involved in the induction of senescence, apoptosis and autophagy were significantly increased. In summary, using ERKO and NERKI mouse models where systemic estrogen levels have been fixed, we found that the majority of the genes regulated by ER α in bone are via non-ERE pathways. However, since NERKI mice display an osteoporotic phenotype, it can be deduced that the minority of the ERE-dependent genes/pathways play a critical role in the regulation of bone physiology. Collectively, these data demonstrate the importance of ER α signaling and specifically, ERE-dependent pathways, in regulating bone metabolism.

Disclosures: Kumar Chokalingam, None.

SU0428

TGF- β Inducible Early Gene-1 Mediates both Estrogen and Canonical Wnt Signaling Pathways in Bone. John Hawse*¹, Muzaffer Cicek², Anne Gingery³, Kevin Pite², Sarah Grygo², Urszula Iwaniec⁴, Russell Turner⁴, Malayannan Subramaniam², Thomas Spelsberg². ¹Mayo Clinic College of Medicine, USA, ²Mayo Clinic, USA, ³Mayo Clinic School of Medicine, USA, ⁴Oregon State University, USA

TGF- β Inducible Early Gene-1 (TIEG) is known to play important roles in regulating bone physiology. Previous studies have demonstrated that TIEG knockout (KO) mice exhibit a gender specific osteopenic phenotype affecting females only. Ovariectomy and estrogen replacement studies have demonstrated that TIEG expression is essential for maximal estrogenic activity in the skeleton. Specifically, the skeletal response to estrogen was approximately halved in TIEG KO mice relative to wildtype (WT) littermates as determined by DXA, pQCT and micro-CT analyses. In order to better understand the molecular mechanisms responsible for this defective estrogenic response, we performed gene expression profiling studies on the cortical shells of long bones isolated from WT and TIEG KO mice. This analysis identified sclerostin as one of the most differentially expressed genes as its mRNA levels were elevated approximately 12-fold in KO animals relative to WT controls. Serum sclerostin levels were also significantly elevated in KO mice suggesting that TIEG may regulate sclerostin expression. This possibility was further supported by the fact that TIEG over-expression resulted in suppression of sclerostin promoter activity *in vitro*. Since sclerostin is a potent inhibitor of Wnt signaling, we next utilized the TOPGAL reporter mouse model to determine if loss of TIEG expression altered the activity of the canonical Wnt pathway in the skeleton. LacZ staining of the L5 vertebrae revealed a 40% decrease in Wnt pathway activity in TIEG KO mice relative to WT controls. Since TIEG was shown to regulate both estrogen and canonical Wnt signaling, and since estrogen is known to inversely affect sclerostin levels, we sought to further examine TIEG's potential role in mediating cross-talk between these two pathways in bone. Interestingly, treatment of MLOA5 osteocyte cells with estrogen resulted in increased expression of TIEG with a concomitant decrease in sclerostin mRNA levels. These effects were completely blocked by the potent estrogen receptor antagonist, ICI 162,780, revealing a direct role for the estrogen receptors in regulating both TIEG and sclerostin expression. Taken together, these studies reveal important roles for TIEG in regulating estrogen and Wnt signaling in bone and suggest that TIEG may be a key factor in mediating cross-talk between these two pathways in part by suppressing sclerostin expression following estrogen exposure.

Disclosures: John Hawse, None.

SU0429

1 α ,25-Dihydroxyvitamin D₃ Regulates Multiple Novel Metabolic Pathways in Developing Zebrafish. THEODORE CRAIG^{*1}, Yuji Zhang¹, Melissa McNulty¹, Sumit Middha¹, Andrew Magis², Cory Funk³, Nathan Price³, Stephen Ekker¹, Rajiv Kumar⁴. ¹Mayo Clinic, USA, ²University of Illinois, USA, ³Institute for Systems Biology, USA, ⁴Mayo Clinic College of Medicine, USA

Theodore A. Craig^a, Yuji Zhang^b, Melissa S. McNulty^a, Sumit Middha^b, Andrew T. Magis^c, Cory Funk^d, Nathan D. Price^d, Stephen C. Ekker^e and Rajiv Kumar^{a,c,e,1}

^aNephrology and Hypertension Research, Department of Internal Medicine, ^bDivision of Biomedical Statistics and Informatics, Department of Health Sciences Research, Mayo Clinic, 200 First St. SW, Rochester, MN 55905, ^cCenter for Biophysics and Computational Biology, University of Illinois – Urbana-Champaign, 156 Davenport Hall MC-147, 607 South Mathews Avenue, Urbana, IL 61801, ^dInstitute for Systems Biology, 401 Terry Avenue North, Seattle, WA 98109-5234, ^eDepartment of Biochemistry and Molecular Biology, Mayo Clinic, 200 First St. SW, Rochester, MN 55905.

The biological role of vitamin D receptors (VDR) which are abundantly expressed in developing zebrafish prior to the development of a mineralized skeleton, intestine and kidney, is unknown. We probed the role of VDR in developing zebrafish biology by examining changes in expression of RNA by whole transcriptome shotgun sequencing (RNA-seq) in fish treated with picomolar concentrations of the VDR ligand and hormonal form of vitamin D₃, 1 α ,25-dihydroxyvitamin D₃ (1 α ,25(OH)₂D₃). We observed significant changes in RNAs of transcription factors, leptin, peptide hormones, and RNAs encoding proteins of fatty acid, amino acid, xenobiotic metabolism, receptor-activator of NF κ B ligand (RANKL), and calcitonin-like ligand receptor pathways. Early highly restricted, and subsequent massive changes in >10% of expressed cellular RNAs were observed. At day 2 (24h 1 α ,25(OH)₂D₃-treatment), only 4 RNAs were differentially expressed (hormone vs. vehicle). On day 4 (72h-treatment), 77 RNAs; on day 6 (120h-treatment) 1039 RNAs; and on day 7 (144h-treatment), 2407 RNAs were differentially expressed in response to 1 α ,25(OH)₂D₃. Fewer RNAs (n = 481) were altered in day 7 larvae treated for 24h with 1 α ,25(OH)₂D₃ vs. those treated with hormone for 144h. At 7 days, in 1 α ,25(OH)₂D₃-treated larvae, pharyngeal cartilage was larger and mineralization was greater. Changes in expression of RNAs for transcription factors, peptide hormones, and RNAs encoding proteins integral to fatty acid, amino acid, leptin, calcitonin-like ligand receptor, RANKL and xenobiotic metabolism pathways, demonstrate heretofore unrecognized mechanisms by which 1 α ,25(OH)₂D₃ functions *in vivo* in developing eukaryotes.

Disclosures: THEODORE CRAIG, None.

SU0430

Comparison of Two Oral Vitamin D₂ Supplementation Doses in Maintaining Optimal Vitamin D Level in Children and Adolescents with Inflammatory Bowel Disease. Helen Pappa^{*1}, Paul Mitchell², Hongyu Jiang³, Rajna Filip-Dhima³, Sivan Kassifi⁴, Catherine Gordon⁵. ¹Children's Hospital Boston, USA, ²Clinical Research Program, Children's Hospital Boston, USA, ³Clinical Research Program, Children's Hospital Boston, USA, ⁴Division of GI & Nutrition, Children's Hospital Boston, USA, ⁵Children's Hospital Boston & Harvard Medical School, USA

Background: Vitamin D is important for bone metabolism and immunoregulation. Both properties may be important for pediatric patients with inflammatory bowel disease (IBD). Hypovitaminosis D is prevalent among children and adolescents with IBD, and risk factors for this condition include impaired vitamin D homeostasis due to an inflamed intestine. In a prior study, we found that large doses of vitamin D₂ are needed to treat vitamin D insufficiency in this population. In the present study, we aimed to compare the efficacy and safety of two regimens of vitamin D supplementation in the maintenance of optimal serum vitamin D concentration [25-hydroxyvitamin D (25OHD) \geq 32 ng/mL] in this population.

Method: From January 2008 to April 2010, 63 patients with the diagnosis of IBD, age 7-20 years, and serum 25OHD concentration > 20 ng/mL were enrolled into an unblinded, randomized, controlled clinical trial. They were randomized to receive orally either: A) 400 IU vitamin D₂/day (N=33) or B) 2,000 IU vitamin D₂/day from November through April and 1,000 IU/day from May through October (N=30) for 12 months, in addition to age appropriate calcium supplementation. Serum 25OHD concentration, inflammatory cytokines, and measures of calcium homeostasis were collected every 3 months. The study was approved by the local institutional review board.

Results: Among the 48 subjects who completed all 4 follow up visits, 6 (13%) achieved and maintained a serum 25OHD concentration \geq 32 ng/mL at all visits (arm A = 3 (11%) vs. arm B = 3 (14%); $P = 1.0$), and 26 (54%) maintained serum 25OHD concentration > 20 ng/mL (arm A = 16 (59%) vs. arm B = 10 (48%); $P = 0.6$). Compliance with the study medication (% of the doses taken) was similar (arm A = 75% vs. arm B = 73%; $P = 0.4$). Interleukin - 6 (pg/mL), a cytokine associated with intestinal inflammation in patients with IBD, was higher in arm A than arm B during follow-up: median (IQR) arm A = 2.3 (1.3, 3.6) vs. arm B = 1.4 (1.1, 2.5); $P = 0.06$. No serious adverse events were noted.

Conclusions: Daily oral doses of vitamin D₂ of up to 2,000 IU appear to be inadequate to maintain optimal vitamin D level in children and adolescents with IBD.

Daily oral doses of 2,000 IU/day are safe in this patient group. Further studies are needed to define the vitamin D supplementation doses that would achieve and maintain optimal vitamin D status, as well as to uncover any effect of vitamin D on the immune system in this population.

Disclosures: Helen Pappa, None.

SU0431

Deletion of VDR in Mature Osteoblasts results in Increased Cancellous Bone Volume. Paul Anderson^{*1}, Gerald Atkins², Howard Morris³, Rachel Davey⁴. ¹Musculoskeletal Biology Research, University of South Australia, Australia, ²University of Adelaide, Australia, ³SA Pathology, Australia, ⁴University of Melbourne, Australia

Direct actions of active vitamin D, 1,25(OH)₂D₃ on the skeleton have previously been reported to include both anabolic and catabolic activities. Over-expression of VDR in mature osteoblasts and osteocytes increases trabecular bone volume due to the combined effects of increased bone formation and reduced osteoclastic bone resorption. Thus we hypothesise that the role for VDR in mature osteoblasts/osteocytes is to mediate osteoblastic activity of bone formation and a subsequent signalling of osteoclastogenesis and bone remodelling. To address this hypothesis, we genetically inactivated the VDR in the mature osteoblastic lineage (ObVDRKO), by crossing floxed-VDR (flVDR) mice with Osteocalcin-Cre mice (Ocn-Cre). Young (6w) male and female ObVDRKO mice demonstrate significant increases in total femoral bone volume as well as trabecular BV/TV (23% increase in male ObVDRKO $p < 0.05$, 28% increase in female ObVDRKO $p < 0.05$) without a change in body weight or total femur length when compared to flVDR control littermates. This increase in bone volume is due to a significant increase in trabecular number (Tb.N) (16% increase in male ObVDRKO $p < 0.05$, 29% increase in female ObVDRKO $p < 0.01$) with no significant change in trabecular thickness (Tb.Th). No changes to growth plate width or TRAP positive osteoclasts/bone surface (OcS/mm) occurred in ObVDRKO mice when compared to flVDR control littermates suggesting that the increased bone volume is not due to either increased primary spongiosa mineral deposition or reduced bone resorption in the secondary spongiosa. Preliminary data suggest that mineralising surface/bone surface is significantly increased in female ObVDRKO mice compared to flVDR mice (19%, $p < 0.05$) as assessed by the extent of double fluorochrome labelled surfaces. Such data suggest that a major role of VDR in mature osteoblasts/osteocyte in actively growing mice mediates osteoblastic activity to limit osteoblast proliferation thus limiting bone formation and bone mineral accrual. Further investigations will help elucidate this novel activity of VDR in mature osteoblasts to modulate osteoblast proliferation and bone mineral accrual, rather than a secondary effect on bone resorption. These data demonstrate the necessity for VDR in osteocalcin expressing cells to regulate osteoblast activities.

Disclosures: Paul Anderson, None.

SU0432

Differential Effects of 1,25-dihydroxyvitamin D₃ and 25-hydroxyvitamin D₃ on Protein Expression in Primary Human Muscle Cells versus Mesenchymal Stem Cells from Bone Marrow (MSCBM). A Quantitative Proteomics Analysis. Astrid Stunes¹, Milajm Pepaj², Unni Syversen³, Erik Fink Eriksen^{*4}. ¹Norwegian University of Science & Technology, Norway, ²Department of Endocrinology, Section Hormone Laboratory, Oslo University Hospital, Aker, Norway, ³University Hospital, Trondheim, Norway, ⁴Oslo University Hospital, Norway

Calcitriol, 1,25-dihydroxyvitamin D₃ (1,25(OH)₂D) is considered to be the physiologically active form of vitamin D. However, it is circulating levels of the precursor calcidiol, 25-hydroxyvitamin D₃ (25(OH)D) which correlate significantly to osteomalacia, bone mineral density (BMD), fracture risk and muscle function. Cells in bone, bone marrow and muscle are all capable of hydroxylating 25(OH)D to 1,25(OH)₂D, but 25(OH)D could also act directly via binding to nuclear 1,25(OH)₂D receptors. If intracellular hydroxylation were the dominating pathway one would expect the cellular effects of 25(OH)D and 1,25(OH)₂D to be the same, - if not significant differences would be expected. In order to test this hypothesis we investigated protein expression in bone and muscle cells after stimulation with either of the two vitamin D analogues.

Protein expression was examined using stable isotope labeling by amino acids (SILAC) in bone and muscle cell cultures. Proteins in cell samples and medium were digested to peptides using trypsin, and relative quantification and identification of proteins were analyzed by high-pressure liquid chromatography-mass spectrometry (HPLC-MS, LTQ XL-Orbitrap). Regulated proteins were annotated using the Universal Protein Resource Database.

In bone cells, 25(OH)D stimulation induced significant up-regulation of three proteins and down-regulation of 27 proteins compared to untreated cells. Exposure to 1,25(OH)₂D, however, caused significantly down-regulation of only two proteins, in contrast to muscle cells where 1,25(OH)₂D caused an up-regulation of 23 proteins. With respect to number of regulated proteins, the effects of 25(OH)D in muscle cells were similar to that of bone cells with up-regulation of four, and down-regulation of 36 proteins.

Proteins up-regulated by 25(OH)D in both bone- and muscle cells, were mainly members of the heat shock protein 70 group, suggesting a stress response in both cell types. Proteins up-regulated by 1,25(OH)₂D in muscle cells were mainly structural proteins and proteins involved in motility and binding.

In conclusion, our data show that 25(OH)D stimulation exerts significant impact on the proteomic profile in both bone and muscle cells. While significant in muscle cells, the effects of 1,25(OH)₂D are negligible in bone cells. The diverging effects of 25(OH)D and 1,25(OH)₂D suggest that other pathways than intracellular hydroxylation are responsible for cellular actions of 25(OH)D in the two cell types.

Disclosures: Erik Fink Eriksen, None.

SU0433

Phospholipids Cause Significant Matrix Suppression and Loss of Assay Sensitivity when Measuring 25 Hydroxyvitamin D by Isotope-dilution, Liquid Chromatography-tandem Mass Spectrometry. Paul Glendenning^{*1}, Brian Cooke², Carla D'Orazio¹. ¹Royal Perth Hospital, Australia, ²PathWest Royal Perth Hospital, Australia

Inter-method automated immunoassay disagreement is a recognised problem for 25-hydroxyvitamin D methods (25OHD). Automated immunoassay disagreement has been attributed to differences in extraction efficiency from vitamin D binding protein (DBP), variation in metabolite recognition (25OHD₂ compared with 25OHD₃) and possible heterophilic antibody interference with some methods. These problems along with immunoassay insensitivity have stimulated the development of a number of reference based isotope dilution, liquid chromatography tandem mass spectrometric (LC-MSMS) methods for 25OHD analysis. LC-MSMS requires careful sample extraction which resolves DBP issues, allows separate quantification of 25OHD₂ and 25OHD₃ and since measurement is dependent on specific mass:charge ratio measurements, is not subject to heterophilic antibody problems. Whilst acknowledging some problems with epimeric and isobaric interference, LC-MSMS methods have generally offered improved assay specificity and the recent introduction of reference standard materials are likely to improve 25OHD accuracy. However, apparent recovery values used in the evaluation of LC-MSMS methods have obscured the insensitivity of current reference based LC-MSMS methods. We identified matrix suppression issues with many different LC-MSMS methods in current use. We identified significant quantities of endogenous phospholipid co-elute at the same time as 25OHD under the gradient conditions in use by such methods. Matrix suppression of LC-MSMS methods are in most cases reduced by the use of de-lipidised stripped serum. Endogenous phospholipid concentration, quantified by immunoassay, correlates closely with the degree of matrix suppression of LC-MSMS methods. Phospholipid effects on 25OHD analysis using LC-MSMS results in significant matrix suppression with resultant loss of assay sensitivity. The selection of extraction methods plus solvent choice require further optimisation to resolve this important issue.

Disclosures: Paul Glendenning, None.

SU0434

Polymorphisms in the CYP2R1 Gene Present in the General Population Affect 25-hydroxylase Activity. Jeff Roizen^{*1}, Jingman Zhou², Michael Levine³. ¹The Childrens Hospital of Philadelphia, USA, ²Intrexon, USA, ³Children's Hospital of Philadelphia, USA

Activation of vitamin D requires two enzymatic steps: first, hydroxylation by 25-hydroxylase (CYP2R1) in the liver to form 25-(OH)vitamin D₃ (25OHD), and second, hydroxylation by 1 α -hydroxylase (CYP27B1) in the kidney to generate calcitriol, the fully active form of vitamin D. 25OHD is the principle circulating vitamin D metabolite and low levels indicate vitamin D insufficiency. Our current understanding of vitamin D homeostasis suggests that serum 25OHD levels solely reflect vitamin D intake from the diet or produced in the skin after UVB irradiation. However, recent genetic association studies have identified an association between SNPs in or near the CYP2R1 gene and serum 25OHD concentrations, thus raising the possibility that CYP2R1 polymorphisms influence serum 25OHD concentrations. To test this hypothesis we assessed the function of four (E104K, D108G, Q274R and T383A) of 17 CYP2R1 polymorphisms (www.ncbi.nlm.nih.gov/project/SNP) plus one missense mutation (L99P) found in patients with genetic deficiency of 25-hydroxylase. Each amino acid change was introduced into a FLAG-tagged wild type human CYP2R1 cDNA. Transient transfection of HEK293 cells showed that all variants were expressed similarly to wild type CYP2R1. To determine 25-hydroxylase activity, wild type and variant CYP2R1 cDNAs were used to transfect HEK293 cells stably expressing a fusion protein consisting of the ligand binding domain of the VDR fused to yeast GAL4 DNA binding domain plus a reporter containing destabilized firefly luciferase under the control of nine copies of the yeast Gal4 Upstream Activator Sequence. Cells were incubated with varying concentrations (0 to 100 μ M) of 1 α (OH)cholecalciferol and luciferase activity was determined. The T383A variant had similar Km (18.3 μ M) and Vmax as the wild type CYP2R1 protein (Figure 1). By contrast, both Q274R (37.3 μ M) and D108G (51.5 μ M) had increased Km relative to wild type (18.1 μ M) CYP2R1 (Figure 1). Finally, the E104K variant had a reduced Km (4.5 μ M) relative to the wild type CYP2R1 enzyme. In summary, we developed a novel mammalian one-hybrid assay for CYP2R1 activity and demonstrated that non-synonymous CYP2R1 polymorphisms possess variable 25-hydroxylase activities. Our

results indicate that polymorphic alleles of CYP2R1 that are present in the general population may contribute to the variable responsiveness of serum 25OHD levels in normal subjects after oral vitamin D supplementation and UVB exposure.

Enzymatic Assay of CYP2R1 Activity

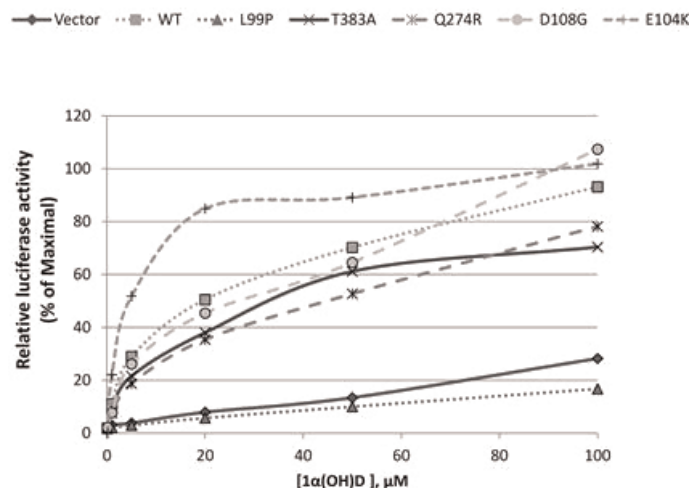


Figure 1.

Disclosures: Jeff Roizen, None.

SU0435

The Association of Vitamin D Status and Fasting Plasma Glucose according to Body Fat Mass in Thai Adults. Hataikarn Nimitphong^{*1}, La-or Chailurkit¹, Suwannee Chanprasertyothin², Piyamit Sritara¹, Boonsong Ongphiphadhanakul¹. ¹Department of medicine, Ramathibodi Hospital, Mahidol University, Thailand, ²Ramathibodi Hospital, Mahidol University, Thailand

Vitamin D affects beta cells proliferation and survival which might underlie the reported relationship between vitamin D status and human glucose homeostasis. However, results thus far are inconclusive and other factors including adiposity might confound the relationship between vitamin D and glucose homeostasis. Moreover, such studies from countries in the tropics are scarce. The purpose of the present study was to investigate the relationship between vitamin D status and fasting plasma glucose (FPG) according to body fat in young Thai adults.

This study was a part of the health survey of the employees of the Electricity Generating Authority of Thailand (EGAT). Subjects consisted of 1990 adults, 72.8% males, aged 25-54 years. Total body fat was measured by bioelectrical impedance analysis. Serum 25-hydroxyvitamin D₂ [25(OH)D₂] and 25-hydroxyvitamin D₃ [25(OH)D₃] were analyzed by LC-MS/MS and total 25(OH)D was used as a marker of vitamin D status [25(OH)D of less than 20 ng/mL was defined as vitamin D deficiency].

Males had significantly higher BMI, waist circumference (WC), FPG, muscle mass and lower total body fat mass when compared with females. 25(OH)D concentrations in females were significantly lower than those in males (21.39 \pm 0.22 vs. 26.03 \pm 0.16 ng/mL, $p < 0.001$). Accordingly, females had higher prevalence of vitamin D deficiency than males (43.07% vs. 13.87%, $p < 0.01$). Univariate analyses revealed that age ($p < 0.001$) and FPG ($p < 0.001$) were positively correlated to 25(OH)D levels while female gender ($p < 0.001$) and total body fat mass ($p = 0.03$) were negatively correlated to 25(OH)D levels. FPG was no longer correlated to 25(OH)D levels after controlling for age, gender and body fat. However, when subjects were stratified into tertiles according to body fat mass, 25(OH)D levels of subjects in the lowest body fat mass tertile was positively associated to FPG ($p = 0.01$) after controlling for age and gender. No relationship between 25(OH)D and FPG was detected in the middle and the highest body fat mass tertile.

In conclusion, our finding in this relative young population goes in the opposite direction of most studies where a relationship between low vitamin D status and diabetes has been demonstrated. Age as well as adiposity might influence the relationship between vitamin D status and glucose homeostasis.

Disclosures: Hataikarn Nimitphong, None.

SU0436

The Homeobox Proteins PBX1 and MEIS2 Participate in Enhancer Function at Vitamin D Target Genes and Highlight a New Regulatory Region Downstream of *Cyp24a1*. Paul Goetsch^{*1}, Nancy Benkusky², Erin Riley², Seong Min Lee², Mark Meyer², J. Pike². ¹University of Wisconsin - Madison, USA, ²University of Wisconsin-Madison, USA

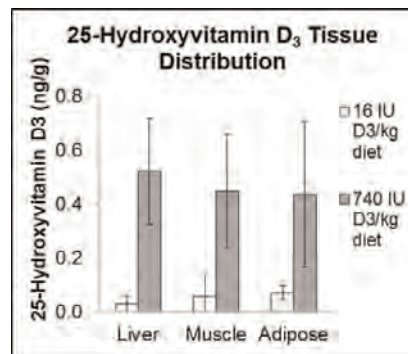
Newer models of mammalian transcriptional regulation describe a complex network of transcription factors that utilizes combinatorial sets of distal enhancers to direct the tissue specificity of transcriptional responses. For inducible hormonal systems such as response to 1,25-dihydroxyvitamin D₃ (1,25(OH)₂D₃), almost nothing is known of the networks that direct target gene hormone sensitivity. Evidence suggests target gene enhancers assemble permissive regulatory complexes prior to the binding of the hormone activated vitamin D receptor (VDR) and retinoid X receptor (RXR) heterodimer. In fact, the quintessential 1,25(OH)₂D₃ target, *Cyp24a1*, which encodes the cytochrome P450 enzyme that inactivates the hormone, exhibits such functional preformed regions that directly mediate 1,25(OH)₂D₃ induction of the gene. This suggests 1,25(OH)₂D₃-mediated activation of *Cyp24a1* represents a good model to study the contribution of additional transcriptional regulators to VDR transcriptional activity. Here, we report the contribution of two previously uncharacterized VDR target associated homeodomain factors, PBX1 and MEIS2, to the VDR transcriptional response using *Cyp24a1* as a model gene. In MC3T3-E1 cells, ChIP-seq experiments indicate both PBX1 and MEIS2, which are reported functional partners, bind in the absence of hormone to a new element 27kb downstream of the *Cyp24a1* transcriptional start site (+27kb) and are induced at the +37kb *Cyp24a1* enhancer as well. Importantly, neither of these factors are detected at the *Cyp24a1* proximal promoter region. RNAi of each factor suggests these binding activities culminate in modulating the transcriptional output of the VDR-mediated *Cyp24a1* induction. More generally, genome-wide occupancy identified by ChIP-seq analysis indicates co-binding of these factors to at least ~30% of VDR binding regions. Since both PBX1 and MEIS2 are also known tissue development factors, we verified co-localization of these factors with VDR *in vivo* in representative 1,25(OH)₂D₃ target tissues including duodenum, kidney, and calvaria. Together, these data suggest that developmental regulatory networks directed by transcription factors such as PBX1 and MEIS2 contribute to the regulation of 1,25(OH)₂D₃ sensitive genes. Discovery of such components of the vitamin D *cis*-regulatory network and transcriptional analysis of model genes such as *Cyp24a1* offer potential insights into the genesis and maintenance of gene hormone sensitivity.

Disclosures: Paul Goetsch, None.

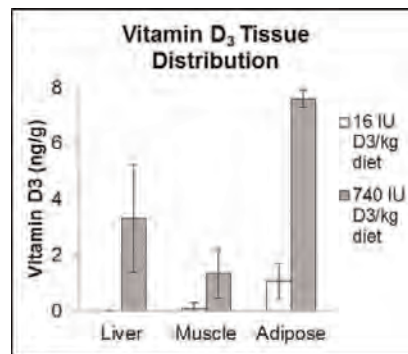
SU0437

Validation of an Analytical Method for the Quantification of Vitamin D and 25-Hydroxyvitamin D in Soft Tissues. Tristan Lipkie^{*}, Amber Jannasch, Bruce Cooper, Emily Hohman, Connie Weaver, Mario Ferruzzi. Purdue University, USA

Inadequate data on tissue distribution of vitamin D and its metabolites remains a barrier to defining health outcomes of vitamin D intake and 25-hydroxyvitamin D status. While advances have been made on analytical methods for serum/plasma 25-hydroxyvitamin D status, analysis of other biological tissues remains under-developed. The purpose of this study was to develop a method for the analysis of vitamin D₂/D₃ and 25-hydroxyvitamin D₂/D₃ in tissues, and determine their distribution in select tissues from a dose-response study. Sprague-Dawley rats were fed a vitamin D-deficient diet for 7 weeks followed by diets containing 25 to 1000 IU vitamin D₂ or vitamin D₃/kg feed for 8 weeks. Liver, gastrocnemius muscle, and epididymal fat homogenates (n=4) were analyzed by high-pressure liquid chromatography-tandem mass spectrometry (HPLC-MS/MS) with electrospray ionization (ESI) following liquid-liquid extraction (LLE), solid-phase extraction (SPE), and derivatization with 4-phenyl-1,2,4-triazoline-3,5-dione (PTAD). Recovery of heavy isotope internal standards was lower for vitamin D (25-60%) than for 25-hydroxyvitamin D (100-120%), possibly because of ion suppression from co-eluting lipids. Accuracy of calibration, determined by analysis of NIST standard reference material 1950 metabolites in human plasma, was -21% for 25-hydroxyvitamin D₃ and +15% for 25-hydroxyvitamin D₂. Inter-day coefficient of variation for the plasma reference material was 6 to 8%. Intra-day coefficient of variation for plasma was 10-15%, which estimates analytical repeatability. Intra-day coefficient of variation for tissue homogenates was larger, 5 to 44%, suggesting some inhomogeneity within tissues and/or tissue sampling. Biological variation between tissues in the same group ranged from 4 to 66%. A dose-response was observed in all tissue pools for both vitamin D and 25-hydroxyvitamin D. This method is well suited to more complete studies of vitamin D metabolite bioavailability and tissue distribution.



25-Hydroxyvitamin D Tissue Distribution



Vitamin D₃ Tissue Distribution

| Method Validation Data | | | | |
|---------------------------------------|-------|--------|---------|--------|
| | Liver | Muscle | Adipose | Plasma |
| Recovery d6-D ₃ (%) | 38.6 | 35.2 | 25.2 | 59.3 |
| Recovery d6-25(OH)D ₃ (%) | 100.3 | 114.1 | 121.8 | 109.2 |
| Intra-day CV D ₃ (%) | 5.4 | 26.6 | 43.5 | 15.1 |
| Intra-day CV 25(OH)D ₃ (%) | 39.8 | 34.8 | 26.6 | 10.0 |
| Inter-day CV D ₃ (%) | - | - | - | 6.5 |
| Inter-day CV 25(OH)D ₃ (%) | - | - | - | 7.8 |

Method Validation Data

Disclosures: Tristan Lipkie, None.

SU0438

Bone Biomarkers Associate with Osteolysis in a Bisphosphonate-Treated Model of Prostate Cancer Metastasis. Marta Martin-Fernandez^{*1}, Karmele Valencia², Carolina Zanduetta², Susana Martinez-Canarias², Cristina Quicios³, Carmen Gonzalez-Enguita³, Fernando Lecanda⁴, Concepcion De La Piedra Gordo⁵. ¹Spain, ²Fima University of Navarra, Spain, ³Urology, Fundacion Jimenez Diaz, Spain, ⁴Foundation for Applied Medical Research, Spain, ⁵Instituto de Investigación Sanitaria Fundación Jiménez Díaz, Spain

Skeleton is one of the most common sites of metastasis in a variety of solid tumors including prostate. Bone metastasis development can produce an increase in biochemical markers of bone turnover. Bisphosphonates, as zoledronic acid (ZA), are potent inhibitors of osteoclastic activity, and are currently used in the follow-up of the treatment of bone metastasis. The aim of this study was to investigate the sensitivity of serum biomarkers in the development of osteolytic lesions during treatment with bisphosphonates.

Luciferase transduced PC-3M human prostate cancer cells were injected directly into the proximal tibia (i.t.) of 48 male athymic nude mice. Twenty-four mice were treated with zoledronic acid one week after i.t. at a single dose of 70 µg/kg. Twelve animals per group were sacrificed at days 28 and 38 postinjection. Tumor burden was assessed by bioluminescence imaging. Osteolytic lesions were monitored by X-ray image analysis. Bone remodelling markers, 5b Isoenzyme of tartrate resistant acid phosphatase (TRAP 5b), aminoterminal propeptide of procollagen I (PINP),

osteocalcin (BGP) and C-telopeptide of collagen type I (CTX)) were determined in serum.

Tumor burden increased over time. However, no differences in tumor burden were detected between 28 and 38 days. ZA administration diminished the increase of bioluminescence observed in tumoral non-treated animals. X-ray analysis showed a significant increase of metastasis area in non-treated group. ZA treatment avoided partially the increase of bone lesion area. Interestingly, bone formation markers such as PINP and BGP were significantly lower ($p < 0.05$) in ZA-treated animals in comparison to vehicle control mice. Moreover, bone resorption markers CTX and TRAP5b showed decrease in ZA treated mice ($p < 0.05$). Comparative analysis showed a positive correlation between bone osteolytic area (X-rays) and tumor burden (bioluminescence) with BGP ($p < 0.05$) and TRAP5b ($p < 0.05$ and $p < 0.01$, respectively) remodeling biomarkers.

These studies suggest the validity of these biomarkers to monitor the degree of osteolysis during ZA- treatment.

Disclosures: *Marta Martin-Fernandez, None.*

This study received funding from: Spanish Urology Association

SU0439

Breast Cancer and Bone Quality Issues: Effects of Exemestane and Tamoxifen Treatments. Peyman Hadji¹, M kalder², Annette Kauka², M Bauer², M Ziller², Didier Hans³. ¹Philipps-University of Marburg, Germany, ²Department of Gynaecological Endocrinology, Reproductive Medicine & Osteoporosis, Philipps-University of Marburg, Germany, ³Lausanne University Hospital, Switzerland

Aim: We analyzed effects of Exemestane (EXE) and Tamoxifene (TAM) on bone quantity and quality of a sub-group of the randomized Tamoxifene Exemestane Adjuvant Multinational (TEAM) trial.

Methods: Patients recruited in this study were postmenopausal women with hormone sensitive primary breast cancer. Patients received randomly Exemestane or Tamoxifene (1:1) as adjuvant therapy for hormone receptor-positive breast cancer. Patients had a T-score > -2.5 at baseline. Patients developing a T-score of ≤ -2.5 during treatment were withdrawn from the study. Patients included had no metabolic disease affecting bone and did not take any drugs affecting bone. Bone mineral density (BMD) was assessed at baseline and after 6, 12 and 24 months of treatment on a GE-Lunar Prodigy densitometer. Bone quality, as expressed as bone microarchitecture status, was evaluated by Lausanne University Hospital without knowing the clinical status/treatments of the patients, using TBS at lumbar spine L1-L4. TBS (TBS iNsight[®], v1.9, Med-Imap, Pessac, FRANCE) is a grey-level texture measurement, which correlates with 3D bone microarchitecture parameters, regardless of BMD. TBS and BMD were evaluated on the same region of interests.

Results: Study groups were composed of 17 and 17 women taken TAM and EXE respectively. Patients receiving TAM showed a mean increase from baseline in lumbar spine BMD of 0.7, 2.9 and 4.0% and in TBS of 2.8, 3.2 and 3.5% at 6, 12 and 24 months treatment respectively. Conversely, patients receiving EXE showed a mean decrease from baseline in BMD of 2.7, 3.7 and 4.7% and in TBS of 1.3, 1.9 and 3.1% at 6, 12 and 24 months treatment respectively. No significant correlations were obtained between TBS and BMD at spine or at total hip at baseline and during the follow-up. There were significant differences in the changes in lumbar spine BMD and at total hip between treatment groups ($P < 0.005$ at any time points). Changes in TBS from baseline at spine were also significantly different between EXEM and TAM: $p = 0.015$, 0.008 and 0.002 at 6, 12 and 24 month respectively.

Conclusions: Exemestane resulted in decreases in bone quantity and quality whereas Tamoxifene induced and increase in bone quantity and quality and independently from each other. The rapid influence of Tamoxifene on TBS should be further investigated and might be related to temporally bone quality status of the patient related to the chemotherapy.

Disclosures: *Peyman Hadji, None.*

SU0440

Interleukin (IL)-11 Promotes Osteoclastogenesis by Stimulating Differentiation and Survival of Osteoclast Progenitor Cells. Erin McCoy¹, HUIXIAN HONG², Xu Feng¹. ¹University of Alabama at Birmingham, USA, ²UAB, USA

Bone metastases occur in more than 80% of patients with advanced breast cancers and are responsible for the worst morbidities of the disease. The cytokine interleukin (IL)-11, which is known to be produced by breast cancer, has been shown to promote osteoclast formation, allowing for excessive bone resorption. The actions of IL-11 in the osteoclast formation process have not been fully elucidated, with some groups suggesting a receptor activator of NF- κ B ligand (RANKL) – independent role in osteoclast formation, while others show that osteoclast formation is enhanced by IL-11 only when osteoblasts are present in the culture. We sought to further investigate the role of IL-11 in supporting osteoclast formation, function, and survival. To this end, we first determined whether IL-11 was sufficient to support RANKL-independent osteoclast formation using murine bone marrow macrophages and found that IL-11 as high as 100ng/ml was unable to induce osteoclast formation. Given that several other cytokines such as IL-1 and tumor necrosis factor α (TNF- α) can promote osteoclastogenesis in the presence of permissive levels of RANKL, we

next investigated whether IL-11 can do so, too. Our data indicate that, unlike IL-1 and TNF- α , IL-11 failed to enhance osteoclast formation in the presence of permissive levels of RANKL. We then pretreated bone marrow macrophages with either macrophage-colony stimulating factor (M-CSF), PBS, or IL-11 for 4 days prior to treatment with RANKL and MCSF. We found that while freshly isolated murine bone marrow cells treated with only PBS died by day 5, IL-11 was capable of supporting survival of a small population of bone marrow cells. Importantly, the IL-11-dependent cells formed osteoclasts upon treatment with RANKL and MCSF. These data suggest that IL-11 plays an important role in osteoclastogenesis by stimulating survival and/or differentiation of osteoclast progenitor cells. These studies have revealed a new mechanism by which IL-11 exerts its impact on osteoclast formation/function. Secondly, these findings have laid a foundation for future investigations to clarify IL-11's specific role in breast cancer bone metastasis, which may provide novel insights into the development of breast cancer bone metastasis but also address therapeutic potential of IL-11 for treating and preventing breast cancer induced osteolysis.

Disclosures: *Erin McCoy, None.*

SU0441

Osseous Metaplasia in Breast Tumors: Rare but Deadly. Janine Danks¹, Kristi Milley², Samantha Richardson¹, John Slavin³, Judith Nimmo⁴. ¹School of Medical Sciences, RMIT University, Australia, ²Rmit University, Australia, ³Anatomical Pathology, St Vincent's Hospital, Australia, ⁴Australian Specialist Animal Pathology, Australia

Breast cancer with osseous and/ or cartilaginous metaplasia is very rare in humans (0.2% of all cases (Huvos et al NY State J Med, 73:1078, 1973)). Patients with this tumor do not have a good prognosis and there is no specific treatment regime because of the infrequency of these tumors.

The aim of this project was to demonstrate key cell types required for cartilage and bone formation in this breast tumor. Osseous metaplasia appears to be more common in dogs with more than 50% of canine tumors being benign mixed tumors (Merck Veterinary Manual). Only some of these have osseous or cartilaginous metaplasia. Our group are using canine mammary tumors (Rivera et al, Cancer Res. 69:8770, 2009) as model of human breast cancer. Dogs suffer from natural occurring breast cancer and live in the same environment as humans and epidemiological, clinical, morphologic and prognostic features similar to human breast cancer.

In our studies canine mixed mammary tumors (CMT) have been collected from specialist veterinary pathologists and veterinary surgeons. In this study there are 11 benign complex, 26 benign mixed, five malignant complex and three malignant mixed tumors with osseous and/or cartilaginous metaplasia.

These tumours were classified histopathologically and the ductal portion was subtyped using a panel of six antibodies using immunohistochemistry (IHC). Molecular subtyping has five subtypes: Luminal A, Luminal B, Basal-like, HER2+ and Normal-like. The antibodies are estrogen receptor (ER), progesterone receptor (PR), epidermal growth factor receptor (HER2), p63, CK5, vimentin, Ki67. These molecular subtypes have been suggested to better reflect patient prognosis (Perou et al, Nature 406:747, 2000) than the current typing by ER/PR status.

Apart from the tumor typing, IHC with antibodies to Runx2, osteocalcin, sclerostin and collagen type 2 has been carried out on these canine mixed mammary tumors to classify the metaplastic tissue as cartilage or bone using bone or cartilage markers. In these canine tumors the cartilage and bone appear independently of one another. Further research is required to identify the origin of the cells that produce this ectopic bone and cartilage.

Disclosures: *Kristi Milley, None.*

SU0442

Osteocytic Connexin 43 Hemichannels in Prevention of Bone Metastasis. Jade Zhou¹, Jean Jiang². ¹The University of Texas Health, USA, ²University of Texas Health Science Center at San Antonio, USA

Bone metastases are major, potentially fatal complications in patients with advanced cancers including breast, prostate and lung cancers. The gap junction-forming protein connexin 43 (Cx43) has been known to inhibit primary tumor cell growth. In addition to gap junctions, Cx43 also forms halves of gap junctions known as hemichannels which allow communication between the intracellular and extracellular environments. Cx43 hemichannels in osteocytes have been shown to open when induced by mechanical stimulation as well as by treatment with alendronate (AD), an efficacious and commonly used bisphosphonate drug. The opening of hemichannels is known to release small molecules important for bone formation and remodeling. To confirm the opening of Cx43 hemichannels in the presence of AD, we measured uptake of ethidium bromide (EtBr) in MLO-Y4 cells after the addition of AD. An increase in Cx43 hemichannels EtBr uptake was observed after AD treatment. To elucidate the effect(s) of osteocyte Cx43 hemichannels on cancer cell growth and migration, we treated MLO-Y4 osteocytes with AD. Conditioned media (CM) was collected after treatment and were used to incubate with metastatic MDA-MB-231 breast cancer cells and PC3 prostate cancer cells. Cell migration was measured using wound healing and transwell migration assays, and cell proliferation was measured using the soft agarose anchorage-independent growth assay. The CM collected from MLO-Y4 osteocytes treated with AD reduced cancer cell migration and proliferation in a dose-dependent manner.

However, direct treatment with AD had no effect on the cell migration or proliferation of the MDA-MB-231 cells. These data validated that the decrease in migration and proliferation was not a result of direct action by AD on the cancer cells. In order to elucidate the direct functional involvement of Cx43 hemichannels in cell migration, we treated the MLO-Y4 cells with Cx43 (E2) antibody, a specific antibody which blocks hemichannel activity but not gap junction channels formed by Cx43. The inhibitory effect of the CM on the migration and proliferation of MDA-MB-231 and PC3 cells was diminished. Interestingly, the inhibitory effects of osteocytes on cancer cell migration were not observed when using osteoblasts. Together, these results suggest the functional importance of osteocytic Cx43 hemichannels in attenuating cancer cell migration and growth.

Disclosures: Jade Zhou, None.

SU0443

TGF β -Mediated Alteration in Sphingolipid Metabolism as a Potential Determinant in Osteolytic Bone Metastasis. Keith Stayrook^{*1}, Yong Wei², Donna Cerabona¹, Pierrick Fournier¹, Daniel Edwards¹, Maryla Niewolna¹, Khalid Mohammad¹, Yibin Kang², Theresa Guise¹. ¹Indiana University, USA, ²Princeton University, USA

Bone metastasis is the ultimate and incurable step of malignancy for many solid tumor types resulting in severe consequences including pain, hypercalcemia, fractures and nerve compression syndromes that drastically reduce quality of life. Bone metastases locally disrupt bone remodeling and are classified by radiographic appearance as osteolytic or osteoblastic. Mechanistic understanding of the preferential homing of tumor cells to bone and their behavior within the tumor-bone microenvironment remains poorly understood. Recent evidence suggests that sphingolipid metabolism may be a key regulatory pathway in tumor progression, metastasis and normal bone homeostasis. In this study, we queried microarray gene expression changes from previously described MDA-MB-231 breast cancer cell metastatic sub-lines (Kang et al, Cancer Cell 2003) to identify any changes in genes involved in sphingolipid metabolism upon TGF β 1-stimulation and their metastatic capacity. Sphingosine kinase-1 (SphK-1) and UDP-glucose ceramide glucosyltransferase (UGCG) mRNAs were found to be significantly ($p < 0.05$) increased by TGF β 1 treatment in the various sub-lines tested. Furthermore, highly metastatic sublines feature significantly ($p < 0.01$) higher induction of SphK-1 by TGF β 1 as compared to low metastatic sub-lines. Additional qRT-PCR screening of a panel of human tumor cell lines with various capacity for bone metastasis revealed that only the osteolytic human MDA-MB-231 breast cancer and melanoma 1205Lu cells display significant SphK-1 upregulating capacity (~ 2 to 5 fold) upon TGF β 1 stimulation. We demonstrate that SphK-1 upregulation is both dose and time dependent and blocked by co-treatment with the Alk4/5 inhibitor SD-208. To probe the functional significance of this upregulation, we found that co-treatment MDA-MB-231 cells with TGF β 1 +/- SPHK-1 inhibitors significantly ($p < 0.05$) impairs the ability of TGF β -stimulated MDA-MB-231 conditioned media to enhance the chemotaxis/migration of pre-osteoclast-monocytic RAW264.7 cells. Our data suggests that SphK-1 expression and its subsequent production of sphingosine-1-phosphate (S1P) may be a potential key determinant in metastatic capacity and/or osteolytic behavior of human tumor cells.

Disclosures: Keith Stayrook, Eli Lilly & Company, 3

SU0444

The miR-218-Wnt Axis Promotes Osteomimicry of Osteolytic Breast Cancer Cells that Home to Bone. Hanna Taipaleenmaki^{*1}, Mohammad Hassan², Yukiko Maeda¹, Carlo Croce³, Janet L. Stein¹, Andre Van Wijnen¹, Jane Lian¹, Gary Stein¹. ¹University of Massachusetts Medical School, USA, ²University of Alabama, USA, ³The Ohio State University, USA

Signaling pathways that are crucial in bone development, including Wnt and BMP, are also upregulated in breast cancer cells that grow aggressively in the bone microenvironment. Homing of breast cancer cells to bone is facilitated by their ability to express many osteoblast related genes ("osteomimicry"). Here, we tested whether osteogenic miRNAs are aberrantly expressed in tumor cells metastatic to bone to support the osteomimetic properties.

miR-218 is highly expressed in osteoblasts and promotes bone marrow stromal cell commitment and osteogenic differentiation, thus serving as a potential "osteomiR". We find that miR-218 expression is significantly up-regulated in highly metastatic MDA-MB-231 breast cancer cells and is not detectable in normal MCF-10A mammary epithelial cells. Wnt signaling is known to promote metastatic activity, and we demonstrate that the aberrant miR-218 expression positively correlates with high endogenous Wnt signaling activity as detected by the Wnt responsive Top Flash reporter assay and by expression of the Wnt transcriptional mediators *LEF1* and *TCF4*. Mechanistically, miR-218 directly targets several inhibitors of Wnt and BMP signaling including *SOST*, *DKK2*, *sFRP-2* and *TOB1*, which were validated by several approaches. Ectopic expression of miR-218 further increases Wnt activity in MDA-MB-231 cells while inhibition of miR-218 decreases Wnt signaling. By using ectopic expression of miR-218 or miR-218 inhibitor we addressed whether miR-218 also affects genes related to osteomimicry. Bone sialoprotein (*BSP*) and osteopontin (*OPN*), both reported to be elevated in serum of breast cancer patients and, *CXCR-4*, a chemokine receptor directly linked to bone metastasis, are all upregulated in the

presence of miR-218. We conclude that miR-218 activates Wnt signaling to enhance osteomimetic properties of bone metastatic MDA-MB-231 cells.

Disclosures: Hanna Taipaleenmaki, None.

SU0445

Axl is a Novel Therapeutic Target for Osteosarcoma. Ashley Rettew^{*1}, Eric Young², Dina Lev², Patrick Getty¹, Edward Greenfield¹. ¹Case Western Reserve University, USA, ²The University of Texas MD Anderson Cancer Center, USA

Osteosarcoma is the most common primary bone sarcoma and the eighth most common childhood malignancy. The receptor tyrosine kinase Axl contributes to the progression of many cancers. While Axl has not been extensively investigated in osteosarcoma, expression is significantly upregulated in metastatic osteosarcoma cell lines (M112 and M132) compared to their genetically related parental Hu09 cells (Nakano, T. et al. 2003). We hypothesize that Axl contributes to the progression of osteosarcoma. Our phosphoproteomic screening showed that Axl was phosphorylated in all 5 human osteosarcoma cell lines tested. Moreover, siRNA screening of the metastatic 143B cells showed that Axl knockdown by a pool of four siRNA duplexes inhibited invasion, motility and colony formation. We began to examine the possibility of off-target effects by individually testing the four siRNA duplexes to validate the screening results. In 143B cells, each duplex knocked down Axl expression by >90% and inhibited invasion, motility and colony formation by ~30%, thereby making it unlikely that the results are due to off-target effects. Furthermore, shRNA targeting Axl showed similar results. BGB324 (BerGenBio AS), a small molecule inhibitor specific for Axl, rapidly reduced Axl phosphorylation in a dose-dependent manner in 143B cells. Colony formation and motility were also significantly inhibited in 143B cells in a dose-dependent manner with the maximal dosage of BGB324 (10 uM) inhibiting colony formation by 100% ($p < 0.001$) and motility by 54% ($p < 0.001$). In the metastatic M112 and M132 osteosarcoma cells, BGB324 significantly inhibited colony formation, motility and cell growth in a dose dependent manner ($p < 0.008$). Moreover, 10 uM of BGB324 caused cell death of preformed colonies in all three cell lines. Finally, immunostaining demonstrated medium to strong staining for total Axl and phospho-Axl on 5 of 6 osteosarcoma patient samples. Taken together, our results demonstrate that Axl promotes the *in vitro* phenotype of metastatic osteosarcoma cells and is expressed and activated in human patient samples. Furthermore, the small molecule inhibitor BGB324, which is well tolerated in mice, may be a valuable translational compound for the development of patient therapies. Ongoing studies will determine whether Axl is important to *in vivo* tumorigenesis and metastasis and whether expression/activity levels correlate with patient outcomes.

Disclosures: Ashley Rettew, None.

SU0446

CCL3/MIP-1 α Overexpression Induces Diffuse Bone Loss in a Mouse Model of Human Multiple Myeloma. Wei Zhang^{*1}, David Dingli¹, Stephen Russell¹, Matthew Drake². ¹Mayo Clinic, USA, ²College of Medicine, Mayo Clinic, USA

Multiple myeloma (MM) is an incurable clonal plasma cell malignancy and the second most common hematologic malignancy worldwide. The vast majority of MM patients develop bone disease with lytic lesions. Less well-recognized is the diffuse osteoporosis affecting nearly all MM patients, leading to an increased risk of osteoporotic-type fractures. Animal models can assist both to expand our understanding of disease pathogenesis and in the evaluation of new therapies. We developed a new model of myeloma based on a well-characterized human myeloma cell line (KAS-6/1). Injected cells proliferate in the murine bone marrow leading to increased circulating human IgG levels. However, mice injected with KAS-6/1 cells do not develop focal osteolytic lesions. Serum levels of CCL3/MIP-1 α have been correlated with bone disease in both monoclonal gammopathy of undetermined significance (MGUS) and MM. KAS-6/1 cells were transduced with a lentiviral vector coding for MIP-1 α to establish KAS-MIP cells which express high MIP-1 α levels and have growth kinetics similar to the parental KAS-6/1 cell line. CB17 scid/scid mice injected via the tail vein with KAS-MIP cells (1×10^7 cells) were monitored daily for onset of hind limb paralysis, and euthanized as planned 38 days following injection. Relative to the control groups, KAS-MIP mice had marked bone loss by DXA at the lumbar spine, femur, and tibia within two weeks of cell injection ($p < 0.05$ at all time points). At euthanasia, microCT analysis (Panel A) showed that relative to control mice, KAS-MIP mice had significantly lower femoral relative bone volume (BV/TV; Panel B), trabecular number and thickness, with corresponding increases in trabecular separation and structure model index ($p < 0.05$ for all microCT parameters). Histomorphometry to evaluate these findings is ongoing. Our study demonstrates KAS-MIP-1 α overexpression recapitulates many MM features including the diffuse osteoporosis that is frequently a prominent disease component, but does not result in focal osteolytic lesion development. Further, the elevated MIP-1 α levels with diffuse bone loss are consistent with the biochemical findings and skeletal phenotype we have recently shown by HRpQCT imaging to be present in humans with the MM precursor condition MGUS. This is the first mouse MM model with diffuse osteoporosis, and will serve as a platform to study the role of MIP-1 α in monoclonal gammopathy-associated bone loss.

SU0448

Factors Driving Osteolytic and Osteoblastic Lesions in Murine Models of Medulloblastoma Skeletal Metastasis. Jessica Grunda*, James Mobley, Gregory Clines. University of Alabama at Birmingham, USA

Purpose: Recent meta-analyses indicate that bone metastases significantly diminish medulloblastoma patient survival, response to therapy, and quality of life. However, no studies exist investigating mechanisms underlying the development or treatment of these skeletal metastases, highlighting the critical need for research in this area. The purpose of this study was to characterize recently generated murine models of medulloblastoma bone metastasis and identify factors potentiating the development of osteolytic and osteoblastic lesions.

Methods: The human D283 Med and DAOY medulloblastoma cell lines were injected into the intratibial medullary space of athymic nude mice and the development of bone lesions and tumor burden were monitored through radiographic imaging. Control and tumor-bearing femora and tibiae were excised, formalin fixed, decalcified, paraffin embedded, and subjected to histomorphometric analysis to assess pathological bone remodeling and osteoclast numbers. Potential bone metastasis factors were explored through immunohistochemistry (IHC), enzyme-linked immunosorbent assay (ELISA), and mass spectrometry proteomic profiling.

Results: A primarily osteolytic and mixed osteolytic / osteoblastic radiographic phenotype was seen for DAOY and D283 Med injected mice respectively. These radiographically observed bone phenotypes were confirmed by histomorphometric analysis. Both DAOY and D283 Med tumors expressed CXCR4, a cancer to bone homing factor. Consistent with the observed bone phenotypes, DAOY tumors displayed higher levels of the osteolytic factors RANK ligand (RANKL), PTH-related protein (PTHrP) and tumor-necrosis factor-alpha (TNF α), whereas higher levels of the osteoblastic factor, endothelin-1 (ET-1), were observed in D283 Med tumor tissues. *In vitro* mass spectrometry proteomic profiling of medulloblastoma cell conditioned media also identified macrophage migration inhibitory factor (MIF) as a potential factor driving medulloblastoma skeletal metastasis.

Conclusions: Investigation of these newly developed mouse models of medulloblastoma osseous metastasis uncovered potential signal-transduction pathways involved in the metastasis of medulloblastoma to bone. Information gleaned from these studies may aid in the future development of targeted treatment modalities for bone metastases and may also help uncover previously unknown signaling pathways potentiating the development of this childhood brain neoplasm.

Disclosures: Jessica Grunda, None.

SU0449

Giant Cell Tumour Successfully Treated by Denosumab. Berengere Aubry-rozier*, Stephane Cherix, Hannes Rudiger. Lausanne University Hospital, Switzerland

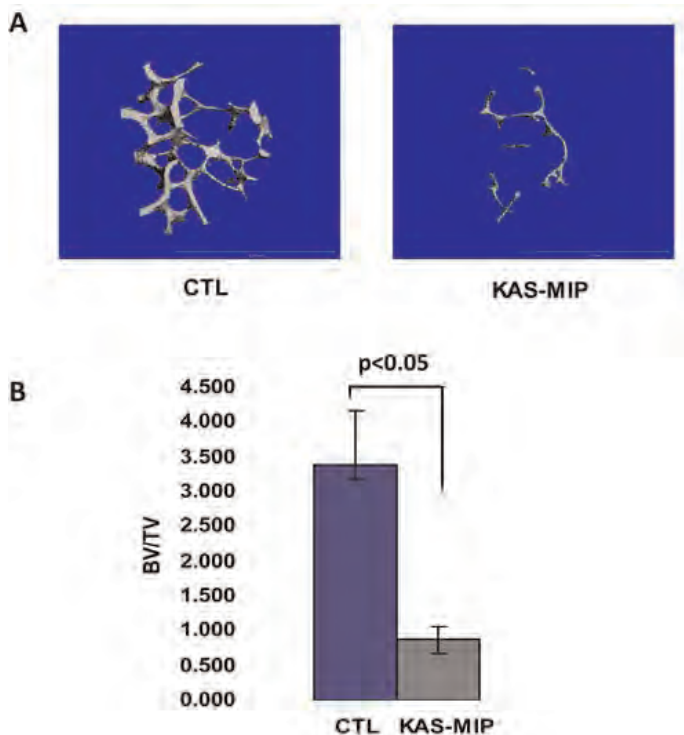
Introduction: Giant cell tumour (GCT) is a benign but locally aggressive primary osteolytic bone tumour, associated with skeletal morbidity and rare metastatic potential. Bone destruction by osteoclast-like giant cells is induced by an over-expression of RANK ligand (RANKL) by tumour cells. The efficacy of denosumab, a fully human monoclonal antibody against RANKL, has been described in GCT¹. We report the case of a patient with GCT in the distal radius, successfully treated by denosumab.

Clinical case: A 28 years old carpenter male, good health, presented with a painful swollen left wrist. We observed swelling of the dorsal wrist, limitation of function, without neurovascular problem. X ray revealed an osteolytic lesion in the distal left radius. Biopsy confirmed the diagnosis of GCT, grade 3 according to the Enneking classification. Osteolytic progression was dramatically in 4 months time. Due to the proximity to the radio-carpal joint with advanced scalloping of subchondral and metaphyseal cortical bone, joint-salvage surgery was not possible. We initiated a treatment with denosumab (XGEVA), 120mg/ week for 1 month, followed by monthly injections. At 6 weeks, a significant decrease of pain and swelling was observed. A beginning recorticalization of eroded bone without progression of the size of the lesion was clearly noted on the X-Ray. No local or systemic side effects were observed. As a consequence, appropriate surgery is now possible.

Discussion: While surgery remains the treatment of choice for GCT, joint-salvage may not always be possible in cases with extensive epiphyseal involvement. The presence of osteoclast-like giant cells seems to make those lesions prone to the specific anti-RANKL treatment with denosumab, which is generally well tolerated. Denosumab appears to slow down tumour growth and promotes recorticalization of eroded bone. It might allow less aggressive and joint-salvage surgery in selected cases.

¹D. Thomas and al. Denosumab in patients with giant-cell tumour of bone: an open-label, phase 2 study. *Lancet Oncol* 2010; 11: 275-80

Disclosures: Berengere Aubry-rozier, None.



Control vs KAS-MIP

Disclosures: Wei Zhang, None.

SU0447

ErbB3 Silencing Inhibits Osteosarcoma Cell Proliferation and Tumor Growth In Vivo. François-Xavier Dieudonné*, Nicolas Jullien, Nadia Habel, Caroline Marty, Dominique Modrowski, Nicolas Sévère, Olivia Fromigüé, Pierre J. Marie. Inserm UMR-606 & University paris Diderot, France

Osteosarcoma is the most common primary bone tumor in children and adults. Despite improved prognosis, resistance to chemotherapy remains responsible for failure of osteosarcoma treatment. The identification of the molecular signals that contribute to the aberrant osteosarcoma cell growth may provide clues to develop new therapeutic strategies for chemoresistant osteosarcoma. The ErbB family of receptor tyrosine kinase plays an important role in the growth of various organs. ErbB3 lacks an intrinsic kinase activity and forms preferred heterodimerisation with ErbB2 to activate signaling. The role of ErbB2/ErbB3 in osteosarcoma cell growth and tumorigenesis is unknown. Here we investigated the implication of ErbB3 in bone tumor cells using short hairpin RNA (shRNA)-mediated inhibition of ErbB3. We found that silencing ErbB3 using lentiviral infection decreased cell growth by 50 % in K7M2 murine osteosarcoma cells. In contrast, ErbB3 silencing did not significantly increase cell apoptosis in these cells. Using standard *in vitro* assays, we showed that ErbB3 silencing reduced cell migration by 40 % and decreased cell invasion by 30 % in K7M2 cells which are highly metastatic. These results indicate that ErbB3 plays an important role in bone tumor cell growth and invasiveness *in vitro*. We therefore investigated whether ErbB3 silencing may reduce tumor progression in a mouse model. In this assay, parental and shErbB3-transduced murine K7M2 cells were injected in BALB/C mice and tumor growth was determined after 5 weeks. In this murine bone tumor model, ErbB3 silencing in K7M2 cells strikingly reduced tumor growth and number compared to control tumors. Histological analysis of the developing ectopic bone tumors showed that shRNA-targeted ErbB3 expression decreased cell replication by 40% as determined by Ki67 staining, whereas cell apoptosis evaluated by TUNEL staining was not increased. Taken together, our results indicate that ErbB3 plays an essential role in bone tumorigenesis. The finding that ErbB3 depletion greatly reduces bone tumor cell growth and invasiveness *in vitro* and *in vivo* raises the potential therapeutic interest of targeting ErbB3 to impact bone tumors in which ErbB3 is highly expressed. Since our data indicate that inhibition of ErbB3 expression exerts anti-cancer effects in osteosarcoma, the use of specific ErbB3 antagonists such as therapeutic antibodies in conjunction with other therapies may prove to be useful for reducing osteosarcoma cell growth and malignancy.

Disclosures: François-Xavier Dieudonné, None.

SU0450

Identification of miR-326 as a Novel Biochemical Marker of Bone Metastasis in a Lung Cancer Model. Karmele Valencia^{*1}, Marta Martin-Fernandez², Carolina Zanduetta³, Cristina Ormazabal⁴, Susana Martinez-Canarias⁴, Eva Bandres⁴, Concepcion De La Piedra Gordo⁵, Fernando Lecanda¹.
¹Foundation for Applied Medical Research, Spain, ², Spain, ³Fima University of Navarra, Spain, ⁴Center for Applied Medical Research, Spain, ⁵Instituto de Investigación Sanitaria Fundación Jiménez Díaz, Spain

Bone metastasis of non-small cell lung cancer (NSCLC) is an incurable condition that often remains undetected until advanced stages. Patients diagnosed with NSCLC benefit from the use of antiresorptive agents such as bisphosphonates (ZA) that delay the apparition of skeletal related events. The diagnosis is usually performed with bone scintigraphy screening and confirmed by radiography and/or computed tomography or magnetic resonance. During the clinical course, response to treatment that relies on serial radiographs to evaluate bone changes is often confronted by limitations. This is mainly due to the slow detectable changes, and the confounding appearance of lesions containing mixed and/or osteosclerotic areas. Thus non-invasive methods would be useful in the clinical practice for early detection and monitoring treatment response. Emerging evidence suggest that miRNAs (miR) associate with tumor and metastasis progression. Moreover, miR are stabilised and released to the extracellular milieu into microvesicles which can be detected in the circulation.

The aim of this study was to identify novel serum markers and investigate their sensitivity when compared to clinical serum biomarkers during the development of metastases. Tumor burden and osteolytic lesions were evaluated by bioluminescence imaging (BLI), X-Ray and μ CT image analysis, after intracardiac inoculation of metastatic A549M1 in athymic nude mice. Animals were treated with ZA or the vehicle. We measured biochemical markers TRAP5b, BGP, PINP and CTX and we performed screening of miR in serum associated with tumor burden and response to ZA treatment. We identified miR-326 that showed robust correlation with BLI ($r=0.603$, $p<0.001$) only in control animals. In contrast, PINP was highly associated with BLI in vehicle ($r=-0.723$ and $p<0.001$) and ZA-treated mice ($r=-0.608$ and $p<0.001$) as well as with tumor burden in both groups as assessed by X-ray imaging. As a consequence, a robust correlation between miR-326 and PINP ($r=-0.59$ and $p<0.001$) and BGP ($r=0.529$, $p<0.005$) was detected in vehicle treated animals. Moreover, miR193b was the only miR that correlated with BGP, CTX and PINP only in ZA-treated animals.

In conclusion, miR-326 and PINP showed strong correlation with tumor burden in untreated animals, whereas monitoring treatment response to ZA could be better achieved with miR193b. Thus, miR326 represents a potential novel biochemical marker for monitoring bone metastatic progression.

Disclosures: Karmele Valencia, None.

SU0451

RANKL, OPG, and Denosumab in Fibrous Dysplasia. Jeffrey TSAI^{*1}, Nisan Bhattacharyya¹, William Chong², Alison Boyce³, Rachel Gafni³, Alfredo Molinolo¹, Pamela Robey⁴, Michael Collins³.
¹NIDCR, NIH, USA, ²National Institute of Health, USA, ³National Institutes of Health, USA, ⁴National Institute of Dental & Craniofacial Research, USA

Purpose: Fibrous dysplasia (FD) is a skeletal disease caused by constitutive Gs α activation. Receptor activator of nuclear factor kappa-B ligand (RANKL) is a key factor in osteoclast differentiation and also plays a role in tumorigenesis. Osteoprotegerin (OPG), a RANKL decoy receptor, inhibits RANKL signaling. It was reported that RANKL mRNA expression is upregulated in FD, and that treatment of an FD subject with a rapidly expanding lesion with anti-RANKL antibody (denosumab) reduced the rate of expansion. This study examines RANKL expression in FD tissue, RANKL and OPG levels in sera and primary bone marrow stromal cells (BMSCs) from FD subjects, and effects of denosumab on serum RANKL and OPG.

Methods: FD and control tissue (bone), sera, and BMSCs were studied. The presence and level of Gs α mutation load in FD BMSCs was assessed by sequencing. RANKL immunohistochemistry (IHC) was performed on tissue. RANKL expression in BMSCs was analyzed by RT-PCR. Levels of circulating RANKL and OPG in sera, and shed/soluble RANKL and OPG in BMSC conditioned media were measured by ELISA.

Results: FD tissue showed robust RANKL expression by IHC. FD BMSCs expressed more RANKL mRNA than control BMSCs by RT-PCR. In conditioned media from BMSCs, RANKL expression, both basal and stimulated with 1,25-(OH)₂ Vit D₃ and PGE₂, was higher in FD vs. control cultures. Relative to controls, RANKL and OPG levels were elevated in FD sera: 194.6 ± 4.7 vs. 14.2 ± 10.6 pg/ml, and 196.4 ± 48.5 vs. 49 ± 19.9 pg/ml, $n=10$ and $p<0.05$ for both. There was a trend toward a higher RANKL/OPG ratio in FD vs. control sera ($p=0.15$). In a FD subject treated with denosumab, bone turnover markers CTX and PINP decreased during six months of treatment. Surprisingly, circulating RANKL levels increased (51.6 vs. 3627.2 pg/ml, pre vs. during treatment), while OPG levels decreased (236.0 vs. 52.4 pg/ml, RANKL/OPG ratio 0.2 vs. 69.2). Upon denosumab discontinuation there was a rebound in bone turnover markers and evidence of bone resorption (hypercalcemia).

Conclusions: These data are consistent with a role of RANKL in FD. RANKL inhibition with denosumab may affect circulating RANKL levels and the RANKL/OPG ratio in FD subjects. The mechanism and significance of increased RANKL and RANKL/OPG ratio with denosumab treatment is unclear and requires further study.

Disclosures: Jeffrey TSAI, None.

SU0452

Regulation of PTHrP Expression in Bone Invasive Oral Squamous Cell Carcinomas. Cara Gonzales¹, Alyssa Merkel², Shelless Cannonier², Julie Sterling^{*3}.
¹University of Texas Health Science Center San Antonio, USA, ²Vanderbilt University, USA, ³Department of Veterans Affairs (TVHS)/Vanderbilt University Medical Center, USA

Oral Squamous Cell Carcinoma (OSCC) is an aggressive cancer that kills 50% of patients within five years of initial diagnosis. Although many advances have been made in treating early staged OSCC, none have reduced the death rate of this rapidly fatal disease in over 30 years. Invasion of the mandible by OSCC has been correlated to a significantly decreased disease-free survival period. However, it is unclear why some OSCC patients develop mandibular invasion while others do not. Through micro-array analysis we found that OSCC over-express parathyroid hormone-related protein (PTHrP) and confirmed by qPCR, similar to other tumors that metastasize to bone. Recently, other groups have confirmed PTHrP expression in feline OSCC samples and in some human mandibular biopsies. Since our previous studies have indicated that PTHrP is regulated by the Hedgehog (Hh) transcription factor, Gli2, and Transforming growth factor beta (TGF- β), we reasoned that these factors may regulate PTHrP and mandible invasion in OSCC. Furthermore, others have recently demonstrated that Gli2 is over-expressed in OSCC patients by immunohistochemistry. After determining that the Cal27 and SCC4 OSCC lines expressed components of the Hh signaling pathway (Gli1, Gli2, Gli3, Smo), we transiently transfected the SCC4 cells with a Gli2 repressor construct and found that this reduced PTHrP expression significantly. Additionally, we treated 3 cell lines with GANT58 (a Gli antagonist) to inhibit Gli2 function and found that it reduced PTHrP expression in multiple OSCC by 40-fold (SCC4) and 2-fold (Cal27 and HSC3). Since our previous data have demonstrated that TGF- β regulates Gli2 expression, we hypothesized that the increase in Gli2 was likely mediated through TGF- β signaling. Therefore, we treated cells with 5ng/ml of TGF- β and found that this increased expression of PTHrP by 40 fold (SCC4), 2.3 fold (HSC3), and 4-fold (Cal27). These increases were completely blocked by GANT58 treatment. Additionally, we were able to reduce PTHrP expression in OSCC cells by approximately 50% using a TGF- β inhibitory antibody. This study demonstrates that PTHrP is expressed in OSCC and that this expression is regulated by Gli2 through TGF- β signaling. These findings support the notion that PTHrP over-expression gives primary OSCC the capacity to locally invade bone, and suggests that Gli2 or TGF- β inhibition may be novel therapeutic targets for the treatment of invasive OSCC.

Disclosures: Julie Sterling, None.

SU0453

Restoration of Bone Formation in Myeloma Osteolytic Lesions by the Cathepsin K Inhibitor KK1-300-01. Keiichiro Watanabe^{*1}, Masahiro Abe², Ryota Amachi², Masahiro Hiasa², Takeshi Harada², Shiro Fujii², Shingen Nakamura², Hirokazu Miki², Kumiko Kagawa², Hiroshi Mori³, Itsuro Endo⁴, Eiji Tanaka², Toshio Matsumoto⁴.
¹Tokushima University Hospital, Japan, ²University of Tokushima, Japan, ³ONO PHARMACEUTICAL CO., LTD., Japan, ⁴University of Tokushima Graduate School of Medical Sciences, Japan

Multiple myeloma (MM) markedly enhances osteoclast (OC) formation while suppressing stromal cell differentiation into osteoblasts (OBs) to cause devastating bone destruction with rapid loss of bone. Cathepsin K inhibitors have unique actions to suppress bone resorption without impairing the viability of OCs. In the present study, we aimed to clarify the therapeutic potential of the cathepsin K inhibitor KK1-300-01 (KK1) on MM bone disease. MM cells enhanced pit formation as well as osteoclastogenesis in cocultures with rabbit bone cells on bone slices. KK1 potently suppressed the pit formation by MM cells, but not osteoclastogenesis nor MM cell growth. Mouse and rabbit bone marrow-derived OCs facilitated in vitro mineralized nodule formation by MC3T3-E1 cells in the presence of KK1, suggesting the KK1-irrelevant direct effects of OCs on osteoblastogenesis. We next examined the effects of KK1 in human INA6 MM-bearing SCID-rab models. KK1 was administered orally via chow after confirming MM growth. MicroCT images showed MM tumor expansion in and outside the rabbit bones with marked osteolytic destruction in control mice. Treatment with KK1 prevented bone destruction and increased bone trabeculae in size with, to our surprise, marked tumor reduction within the bone marrow cavity but not outside the bone. Histomorphometric analyses also showed elevated trabecular bone volume/total volume ratios with a marginal change in OC numbers in the treated mice. These results demonstrate that KK1 has a potential to prevent bone destruction and restore bone formation in MM bone lesions. We previously reported that extensive osteoclastic bone resorption in MM bone lesions

releases and activates TGF-beta from bone to suppress the terminal OB differentiation, and that bone-forming mature OBs are able to suppress MM tumor growth within bone (PLoS One, 2010). Given OC-derived "coupling factors", KK1 is suggested to spare the damage in OCs while inhibiting bone resorption to retain the "coupling factors" for bone formation together with reducing the release from bone of anti-anabolic factors such as TGF-beta, leading to robust bone formation and resultant tumor contraction in bone. The combinatory treatment with KK1 of anti-MM agents such as the proteasome inhibitor bortezomib is warranted for further study to improve the efficacy of tumor suppression along with rebuilding bone in MM lesions with bone defect.

Disclosures: Keiichiro Watanabe, None.

This study received funding from: ONO PHARMACEUTICAL CO.

MO0001

Absence of Functional Leptin Receptor Isoforms in the POUND (Lepr^{db/db}) Mouse is Associated with Decreased Femoral Bone Volume, Increased Femoral Bone Marrow Adipogenesis, and Muscle Wasting. Phonepasong Arounleut¹, Mohammed Elsalanty², Khaled Hussein¹, Carlos Isaacs³, Alexis Stranahan¹, Mark Hamrick¹. ¹Georgia Health Sciences University, USA, ²Georgia Health Science University, USA, ³Medical College of Georgia, USA

Functional leptin receptors are expressed in a variety of musculoskeletal tissues including bone, cartilage, and skeletal muscle, and congenital absence of leptin in the ob/ob mouse is associated with increased bone marrow adipogenesis, reduced hindlimb bone mass, and decreased muscle mass. In order to better define the role of leptin signaling in musculoskeletal physiology we examined the muscle-bone phenotype of the POUND mouse, a mouse lacking all functional leptin receptor isoforms. This model differs from the db/db mouse, which expresses the short form but not the long form of the leptin receptor. Consistent with a complete loss of functional leptin signaling, POUND mice are similar in body weight to ob/ob mice and weigh approximately 20% more than db/db mice at four months of age. MicroCT data show that bone volume fraction (BV/TV) in femora from POUND mice is reduced more than 50% compared to wild-type controls, with a 20% reduction in trabecular thickness and 40% reduction in trabecular number. Histomorphometry reveals a marked increase in marrow fat in the distal femora of POUND mice relative to wild-type controls. Mass of the tibialis anterior muscle is reduced approximately 40% in POUND mice relative to controls, and fiber size of the predominantly fast-twitch extensor digitorum longus muscle is also reduced ~30% in POUND mice. These data provide additional evidence that leptin signaling plays a key role in the regulation of both muscle and bone mass.

Disclosures: Phonepasong Arounleut, None.

MO0002

Dlx5 Inhibits Adipogenic Differentiation through the Down-Regulation of Peroxisome Proliferator-Activated Receptor γ (PPAR γ) Expression. HYELIM LEE^{*1}, Kyung-Mi Woo¹, Hyun-Mo Ryoo², Jeong-Hwa Baek³. ¹SEOUL NATIONAL UNIVERSITY, South Korea, ²Seoul National University School of Dentistry, South Korea, ³Seoul National University, School of Dentistry, South Korea

Dlx5 is a positive regulator of osteoblast differentiation that contains a homeobox domain. Because there are possible reciprocal relationships between osteogenic and adipogenic differentiation of bone marrow mesenchymal stem cells, we examined the regulatory role of Dlx5 in adipogenic differentiation in this study. Adipogenic stimuli suppressed the expression levels of Dlx5 mRNA. Over-expression of Dlx5 inhibited adipogenic differentiation, whereas knock-down of Dlx5 enhanced adipogenic differentiation in a 3T3-L1 preadipocyte cell line. Over-expression of Dlx5 suppressed the expression of adipogenic marker genes, including C/EBP α and PPAR γ . Dlx5-mediated suppression of adipogenic differentiation was overcome by over-expression of PPAR γ but not by that of CREB or C/EBP α . Dlx5 decreased the transcriptional activity of CREB and C/EBP α in a dose-dependent manner. Dlx5 directly bound to CREB and C/EBP α and prevented them from binding to and subsequently transactivating the PPAR γ promoter. These results suggest that Dlx5 plays an important regulatory role in fate determination of mesenchymal stem cells toward the osteoblast lineage through the inhibition of adipocyte differentiation as well as the direct stimulation of osteoblast differentiation.

Disclosures: HYELIM LEE, None.

This study received funding from: the National Research Foundation of Korea (NRF) funded by the Ministry of Education, Science and Technology

MO0003

Dynamics of Post-transplantation Bone Marrow Adiposity: A Model for Understanding Bone-Fat Interactions. Puong Le^{*1}, Eliza Grlickova-Duzevik², Anne Breggia³, Kathleen Bishop⁴, Clifford Rosen³, Mark Horowitz⁵. ¹Maine Medical Center Research Institute, USA, ²University of Maine, USA, ³Maine Medical Center, USA, ⁴University of Wisconsin-Madison, USA, ⁵Yale University School of Medicine, USA

Bone marrow (BM) adiposity is noted with aging, estrogen deficiency, calorie restriction, immobilization, and anorexia nervosa. There is a transient phase of BM adiposity after bone marrow transplantation (BMT) following whole body irradiation in humans and mice. In these states, there is an inverse association between the total number of marrow adipocytes and trabecular bone volume fraction. We hypothesized that marrow adiposity induced by BMT was a useful model for understanding the cellular aspects of bone-fat interactions. We studied C57BL/6J (B6) and C3H/HeJ (C3H) mice that were lethally irradiated (10Gy) and then transplanted with syngeneic BM cells to delineate the time course and function of marrow fat after injury. Between 5-10 days post BMT, the BM repopulates with cells having the morphologic characteristics of adipocytes. After day 10, adipocytes disappear and are replaced by

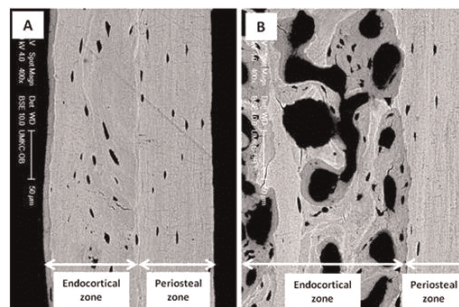
hematopoietic elements that repopulate the marrow. Using osmium tetroxide staining with μ CT, we found extensive uptake of osmium in areas where adipocytes resided histologically, i.e. the secondary center of ossification and below the growth plate extending into the diaphysis. To address the origin of these 'transient' adipocytes, we transplanted BM cells from GFP expressing B6 mice into irradiated B6 recipients. At days 5-9, a significant proportion of the adipocytes were GFP+ suggesting donor origin. We next asked whether there were strain differences in the marrow response to BMT between B6 and C3H males and females. BMSCs were obtained from the femurs and tibias of ten-week-old control and BMT B6 and C3H mice. Following red blood cell lysis, the cell suspension was centrifuged and the surface fat layer was collected. The magnitude of fat in both transplanted and non-transplanted mice was as follows: C3H males > C3H females > B6 males > B6 females. Consistently, *in vitro* adipogenic colony formation was greater in C3H vs B6 mice. qPCR of the isolated fat demonstrated greater detectable mRNA levels of aP2 and adiponectin in C3H vs B6 female control and BMT groups. Additionally, aP2 and adiponectin levels were greater in C3H BMT males vs C3H BMT females. In conclusion, there is significant marrow adiposity between days 5-10 post BMT. The adipocytic response to injury is strain and gender specific. However, the lineage of the adipocyte precursor and the functional significance of these cells have yet to be determined. NIH-1R24DK092759-01

Disclosures: Puong Le, None.

MO0004

Dysfunctional Osteocytes Increase RANKL and Promote Cortical Pore Formation in Their Vicinity: a Mechanistic Explanation for the Development of Cortical Porosity with Age. Robert Jilka^{*1}, Annick DeLoose², Leslie Climer², Lynda Bonewald³, Robert Weinstein¹, Charles O'Brien¹, Stavros Manolagas¹. ¹Central Arkansas VA Healthcare System, Univ of Arkansas for Medical Sciences, USA, ²Central Arkansas Veterans Healthcare System, Univ of Arkansas for Medical Sciences, USA, ³University of Missouri - Kansas City, USA

Cortical porosity is an important contributor to the increased skeletal fragility associated with aging, but the underlying cellular and molecular mechanisms responsible for this pathology are unknown. Osteocytes are an important source of RANKL, and recent evidence indicates that osteocyte apoptosis induced by fatigue-loading of cortical bone is associated with increased synthesis of RANKL by viable neighboring osteocytes. Since osteocyte apoptosis increases with advancing age, we investigated whether osteocyte death is associated with cortical porosity using mice in which osteocytes are resistant to apoptosis due to deletion of Bak and Bax – two proteins essential for apoptotic death. Cortical porosity in the distal half of the femur of wild type controls increased from 1.5% to 6.0% between 3 and 22 mo of age, as quantified by microCT. Cortical porosity in 22 mo mice lacking Bak and Bax was 7-fold higher as compared to the controls. The increased porosity in the Bak/Bax-deficient mice was associated with a 2-3 fold increase in the expression of RANKL, as measured by quantitative PCR using RNA from osteocyte-enriched humeral bone shafts. The rate of bone remodeling within the porous areas of 22 mo old control and Bak/Bax-deficient mice was 2-3 fold higher than that of cancellous bone, measured in the same section. However, the total intracortical remodeling area in Bak/Bax-deficient mice was significantly higher than in controls. The porous areas of 22 mo old normal and Bak/Bax-deficient mice were confined to the inner endosteal portion of the cortex, as determined by backscatter scanning electron microscopy (see Figure). In both wild type and Bak/Bax-deficient mice, the density of osteocytes with pyknotic nuclei and condensed cytoplasm was increased by approximately 2-fold in periosteum adjacent to porous endosteal bone, as compared to the periosteum adjacent to intact cortical bone. We propose that the age-related increase in cortical bone remodeling and development of porosity is due to stress signals produced by dysfunctional osteocytes of the periosteal cortex, leading to increased local RANKL production by viable neighboring osteocytes. Abrogation of apoptosis by deletion of Bak and Bax increases the duration and/or intensity of these stress signals, and thereby magnifies RANKL production and cortical porosity.



Backscatter scanning electron microscope images of the diaphyseal cortex of femurs from 22 mo old mice. The cortical bone is composed of a lamellar periosteal zone and a less orderly endocortical zone separated by a highly mineralized boundary. (A) The cortex of the wild type animals shows 6% porosity. (B) In Bak/Bax-deficient mice, the porosity is 7-fold higher and erosion cavities perforate the endocortical zone.

Porosity Figure

Disclosures: Robert Jilka, None.

MO0005

Pb Treatment Generates Reactive Oxygen Species in Articular Chondrocytes and Results in Osteoarthritis-like Changes to the Oxidant Scavenging Milieu. Tzong-Jen Sheu¹, Shen-chin Hsu^{*2}, Shanshan Shi³, J. Edward Puzas³, Min-jon Lin⁴, Jonathan Holz¹. ¹University of Rochester, USA, ²Chung Shan Medical University Hospital Dept of Pharmacy, Taiwan, Taiwan, ³University of Rochester School of Medicine, USA, ⁴Chung Shan Medical University, Taiwan

The risk of Pb exposure remains high. The association of Pb exposure with joint degeneration and the joint's susceptibility to oxidative damage present it as a likely target of Pb toxicity. Our lab has previously demonstrated that Pb exposure disrupts normal articular chondrocyte phenotype. Therefore, we hypothesize that this change is mediated, in part, by the generation of reactive oxygen species (ROS).

Results: Pb treatment generated ROS in a dose-dependent manner, *in vitro*. Hydrogen peroxide and superoxide levels were significantly elevated at 24hrs. At 48hrs, hydrogen peroxide levels remained significantly elevated. Pb treatment increased oxygen consumption, elevated levels of SOD1, and reduced levels of SOD2, glutathione peroxidase, and catalase in a dose-dependent manner. Exogenous catalase ameliorated Pb inhibition of TGF- β signaling; hydrogen peroxide reduced TGF- β and increased Smurf2 and type X collagen gene expression. In the joint, Pb-treated mice showed increases in lipid peroxidation and SOD1, and a mouse model of osteoarthritis also displayed elevated SOD1.

Conclusions: Pb treatment elevated ROS, specifically H₂O₂ and superoxide. Pb-induced changes in cellular respiration and ROS scavenging may account for this. The ability of H₂O₂ to disrupt TGF- β signaling and elevate type X collagen production, in conjunction with the ability of catalase to prevent Pb's inhibition of TGF- β signaling, demonstrate that the effects of Pb on articular chondrocytes may be mediated by H₂O₂. Furthermore, the generation of ROS by Pb, the ability of Pb and ROS to disrupt components of cell signaling, and alterations in ROS scavenging all parallel changes observed in OA.

Disclosures: Shen-chin Hsu, None.

MO0006

Withdrawn

MO0007

Suppression of Autophagy in Osteoblasts and Osteocytes Increases Oxidative Stress and Recapitulates the Effects of Aging on the Murine Skeleton. Melda Onal, Jinhua Xiong, Shiqiao Ye, Li Han, Robert Jilka, Robert Weinstein, Maria Jose Almeida, Haibo Zhao, Stavros Manolagas, Charles O'Brien*. Central Arkansas VA Healthcare System, Univ of Arkansas for Medical Sciences, USA

Cancellous bone turnover declines with age in mice, but, because the balance between bone resorption and bone formation favors resorption, bone mass also declines. The mechanisms responsible for the decline in bone turnover are unclear. Autophagy is an intracellular process in which organelles and proteins are delivered to lysosomes for degradation and recycling of their components. Moreover, suppression of autophagy in long-lived cells such as neurons and myocytes leads to increased numbers of damaged mitochondria, oxidative stress, and cell death or dysfunction. Therefore, a reduction in autophagy has been proposed as a mechanism underlying cell and tissue aging. Consistent with this, we found that expression of the autophagy-related genes BNIP and LC3 is lower in the cortical bone of 20-month-old, compared with 6-month-old, C57BL/6 mice. This was associated with an increase in the amount of mitochondrial DNA, which has been demonstrated to be a consequence of reduced autophagy in other systems. To examine the role of autophagy in osteoblasts and osteocytes, we deleted a conditional allele for ATG7, a gene essential for autophagy, using a DMP1-Cre transgene. Lipidation of LC3 was reduced, and mitochondrial DNA was elevated, in the bones of conditional knockout (KO) mice, confirming suppression of autophagy. Spinal and femoral bone mineral density was lower, compared to littermate controls, in both male and female conditional KO mice beginning at 4 months of age and continuing to at least 12 months of age. Micro-CT analysis revealed low cancellous bone volume, low cortical thickness, and high cortical porosity in 6-month-old conditional KO mice compared with control littermates. At this age, osteoclast number, osteoblast number, bone formation rate, and wall width were also lower in the conditional KO mice. In addition, oxidative stress was higher in the bones of conditional KO mice as measured by reactive oxygen species levels in the bone marrow of the femur and by p66shc phosphorylation in L4 vertebra. Strikingly, each of these changes parallels changes that occur in aged wild type mice. These results demonstrate that suppression of autophagy in osteoblasts and osteocytes mimics the impact of aging on the skeleton and suggest that a decline in autophagy with age contributes to the low bone mass associated with aging.

Disclosures: Charles O'Brien, None.

MO0008

T Lymphocytes and Osteoclast Precursors in Early Rheumatoid Arthritis. Patrizia D'Amelio^{*1}, Francesca Sassi¹, Iliaria Buondonno¹, Guido Rovera², Raffaele Pellerito², Giancarlo Isaia¹. ¹University of Torino, Italy, ²Mauriziano Hospital, Italy

Purpose: Rheumatoid arthritis (RA) is an immune-mediated disease characterized by articular inflammation and tissue damage, which lead to disability and increased mortality. The pathogenesis of this disease has been sought in the imbalance between different T cells subset that leads to autoimmune activation, anyway no definitive data has been obtained in humans.

The aim of this study is to evaluate differences in immuno phenotype between patients with early RA and healthy controls and to evaluate the possible effect of colecalciferol in these subjects.

Methods: We enrolled in the study 16 female patients affected by early phase RA not previously treated, and 25 healthy controls, age matched. Patients were randomized to receive 300000 UI of colecalciferol per os (8) or placebo (8) (all the patients were treated with MTX 15 mg/week im and metilprednisolone per os 2-4 mg/day).

At baseline in all the subjects we measured osteoclast precursors and T cells subsets in peripheral blood by flow cytometry, patients were recalled at center after three months of therapy.

Results: We observed an increase in osteoclast precursors (OCP) in peripheral blood of RA patients, in particular OCP from RA patients expressed high level of CD 16 on cell surface.

We also found increased number of T regulatory cells (Tregs) in healthy subject; whereas T cells producing IFN gamma and IL-17 are more present in RA patients.

The administration of colecalciferol does not affect OCP, whereas it seems to modify T cells subset, in particular we observed a significant decrease in Th 17 cells in patients treated with colecalciferol.

Conclusion: These preliminary data confirms previous data on the presence of a sub population of monocytes able to differentiate into osteoclasts in patients affected by inflammatory disease, these cells express high level of CD 16 on cell membrane and seem to have a peculiar role in bone erosions. We also suggest a possible role for decrease in Tregs in the pathogenesis of RA, this decrease could lead to a break in self-tolerance and an increase in the pro-inflammatory T cells subset that produce high amount of INF gamma and IL-17. As regards colecalciferol it acts reducing Th17 and have no effect on OCP.

Disclosures: Patrizia D'Amelio, None.

MO0009

Dual Energy X-ray Absorptiometry Body Composition: A New Phantom for Clinical Trials. Colin Miller^{*1}, Blaine Horvath², Hui Jing Yu², Stuart Jackson³, Neil Binkley⁴. ¹BioClinica, Inc., USA, ²BioClinica, USA, ³University of Alberta, Canada, ⁴University of Wisconsin, Madison, USA

Background: Dual energy X-ray absorptiometry (DXA) instruments are established as a method for body composition measurement because of their ease of use and low radiation dose. However, longitudinal variation is observed in DXA measurements and a phantom is needed to monitor and calibrate such drift. Phantoms are available to monitor bone mineral density. However, there has been no phantom available for the monitoring of body composition in clinical trials. A BioClinica Body Composition (BBC) phantom was developed for quality control and monitoring machine drift within major DXA manufacturers. The unique phantom design measures 36 cm in width and 61 cm in length and weighs 29 kg. The phantom contains high-density polyethylene, polyvinyl chloride and aluminum plates for simulation of bone. The goal of this study is to evaluate the precision of this new BBC Phantom.

Methods: Part of the development process, a beta version of the phantom was evaluated by GE Lunar and Hologic. To examine the stability of this new phantom, a total of 10 BBCs were scanned on a GE Lunar Prodigy; each was scanned 5 times on separate days. To compare measurement variability between two manufacturers, 1 of these 10 BBCs was also scanned 5 times on a Hologic Discovery A. Multiple additional scans will be performed on a GE Lunar Prodigy and GE Lunar iDXA densitometer.

Results: Precision of 5 consecutive phantom scans, expressed as the coefficient of variation, for all 10 phantoms ranged from 0.14% to 0.31% for total body BMC, 0.30% to 0.92% for total body fat, 0.13% to 0.59% for total body lean tissue, and 0.31% to 0.93% for total percent fat. For a given phantom, the average (SD) values for total body BMC, total body fat, total body lean and total percent fat were estimated as 610g (3), 7000g (22), 10619g (44) and 38% (0.15) from Hologic scans, and as 616g (1), 6263g (35), 10913g (20), and 36% (0.13) from GE Lunar scans. All preliminary data are summarized in Table 1.

Conclusion: Data from total body DXA scans of this new phantom showed high precision for lean, fat and bone mineral compartments. This semi-portable phantom may prove to be appropriate in clinical trials for the evaluation of body composition.

Table 1. Phantom Body Composition Analysis Summary (%CV)

| Manufacturer | BBC # | WBOT_BMC [g] | WBOT_FAT [g] | WBOT_LEAN [g] | WBOT_PFAT [%] |
|--------------|-------|--------------|--------------|---------------|---------------|
| GE (Lunar) | 1 | 0.25% | 0.39% | 0.22% | 0.40% |
| GE (Lunar) | 2 | 0.22% | 0.40% | 0.31% | 0.46% |
| GE (Lunar) | 3 | 0.14% | 0.84% | 0.45% | 0.85% |
| GE (Lunar) | 4 | 0.31% | 0.92% | 0.52% | 0.93% |
| GE (Lunar) | 5 | 0.19% | 0.30% | 0.13% | 0.31% |
| GE (Lunar) | 6 | 0.29% | 0.83% | 0.59% | 0.87% |
| GE (Lunar) | 7 | 0.22% | 0.69% | 0.40% | 0.66% |
| GE (Lunar) | 8 | 0.14% | 0.85% | 0.48% | 0.80% |
| GE (Lunar) | 9 | 0.20% | 0.66% | 0.40% | 0.74% |
| GE (Lunar) | 10 | 0.21% | 0.56% | 0.18% | 0.38% |
| Hologic | 10 | 0.50% | 0.31% | 0.42% | 0.39% |

*WBOT = Whole Body Total

Table 1

Disclosures: Colin Miller, BioClinica, 3
This study received funding from: BioClinica

MO0010

Muscle Assessment by HRpQCT: A Preliminary Assessment of its Potential Utility. Marta Erlandson¹, Andy Kin On Wong², Eva Szabo³, Martin Zulliger⁴, Aakash Bhargava², Karen Beattie², Jonathan Adachi⁵, Angela Cheung³. ¹University of Toronto, Canada, ²McMaster University, Canada, ³University Health Network, Canada, ⁴Scanco Medical AG, Switzerland, ⁵St. Joseph's Hospital, Canada

Purpose: To determine how well HRpQCT muscle measures obtained at the distal tibia using an experimental algorithm compare to standard pQCT measures at the commonly reported 66% calf site.

Methods: Women ≥ 50 years from the Hamilton cohort of the Canadian Multicenter Osteoporosis Study (CaMos) completed a single slice (2.3 ± 0.3 mm thick) pQCT scan (XCT 2000, Stratec) at the 66% site of the tibia as measured from the distal malleolus to the medial tibial plateau. Total bone area was segmented using contour mode 1 and peel mode 2 with a threshold of 280 mg/cm³ and 400 mg/cm³. Limb area was analyzed using contour mode 3 and peel mode 2 with a threshold of 40 mg/cm³. A filter was applied to smooth the segmented limb area. pQCT-derived muscle cross-sectional area (MCSA) was calculated by subtracting total bone area from limb area. Muscle density (MD) was computed by taking the quotient of the corresponding muscle mass and MCSA. Standard HRpQCT scans (Xtreme CT, Scanco) were also acquired at the distal tibia and bone was segmented from the images using standard contouring. HRpQCT-derived MD and MCSA were then calculated using a newly developed algorithm in which tight thresholding limits (34.22-194.32 mg HA/cm³) were used to identify muscle seed volumes which were then iteratively expanded. A short band of grayscale values between the fat and muscle was left open as undetermined into which the seed volumes expand to encompass the entire muscle tissue volume. Bland-Altman plots were used to assess the agreement between pQCT and HRpQCT MD and MCSA. Pearson correlation coefficients were calculated to assess the relationship between pQCT and HRpQCT measurements.

Results: 45 women had a pQCT-derived mean MD at the mid-calf (69.9 ± 4.9 mg/cm³) that was significantly lower than the HRpQCT-derived MD at the more distal site (71.2 ± 4.0 mgHA/cm³) ($p=0.025$). The Bland-Altman analyses revealed no evidence of directional bias for MD; however, MCSA varied according to magnitude such that a larger MCSA increased the discrepancy between the two modalities. MD was moderately correlated between the two modalities ($r=0.64$, $p<0.01$); there was no relationship between MCSA measured by pQCT at the mid-calf and the MCSA measured at the distal site ($r=0.24$, $p=0.12$).

Conclusions: These preliminary findings suggest that lower leg MD obtained from HRpQCT images may provide 41% of the information obtained from pQCT. Further testing and optimization of the HRpQCT algorithm may improve these correlations.

Disclosures: Marta Erlandson, None.

MO0011

Patterns of Major Osteoporotic Fractures in the Very Old. Bjorn Rosengren¹, Magnus Karlsson¹, Ingemar Peterson², Martin Englund². ¹Skåne University Hospital Malmö, Lund University, Sweden, ²Musculoskeletal Sciences, Department of Orthopedics, Clinical Sciences Lund, Lund University, Sweden

Fractures in very old individuals are associated to high post fracture morbidity and even mortality. Even though life expectancy is generally increasing in western countries and it has been estimated that 50% of the children of today are going to celebrate their 100th birthday specific interest in fracture patterns of the very old has been low. Description of disease including time trends is necessary.

Methods: Through the Skåne Health Care Register, a diagnosis-based register covering all in- and outpatient health care data of residents in the County of Skåne, Sweden (1.2 million inhabitants), we registered all major osteoporotic fractures (hip, forearm, spine and shoulder) in individuals aged ≥ 90 years from year 1999 to 2010

(119 000 person-years). We calculated gender-specific age-standardized incidence rate for each fracture type using one-year age- and sex-specific population figures from the population register, where the average population of the examined years was used as the standard population. Trends of incidence were evaluated by linear regression, and we present data as mean annual change per 10 000 and year with 95% confidence interval (95% CI) with two-tailed α -level set to 0.05.

Results: During the examined 12 years there were 9 466 fractures (83% in women and 17% in men) corresponding to a rate of 792 per 10 000 person-years (883 in women and 533 in men). In women the most common fracture site was the hip followed by (in order) forearm, spine and shoulder. For men the most common fracture site was the hip followed by spine, shoulder and forearm.

The annual rate of major osteoporotic fractures in total was increasing in women (+ 9.3 per 10 000 and year (95% CI 1.9, 16.7)) but not in men (+5.2 (-3.5, 13.8)). Time trends however differed depending on specific fracture type. Hip and forearm fracture rates were stable in both women and men while spine fracture rates were increasing in both women (+8.5 (6.4, 10.5)) and men (+6.6 (3.6, 9.7)). Shoulder fracture rate was increasing in women (+2.8 (0.2, 5.4)) but was stable in men (+0.3 (-2.4, 3.0)). Changes were generally most evident in the age-strata 90-94 years (data not shown).

Conclusion: Rates of major osteoporotic fractures in the very old are high and are increasing. As this population will further grow in the future the resulting fracture burden will become a major clinical concern. We must hence try to find fracture preventive strategies affecting also the very old.

Disclosures: Bjorn Rosengren, None.

MO0012

pQCT Derived Lower Leg Muscle Density as a Predictor of Fall Status in Community-dwelling Adults: A Logistic Regression Analysis of the Saskatoon CaMos Cohort. Andrew Frank¹, Jonathan Farthing², Philip Chilibeck², Cathy Arnold³, W.P. Olszynski⁴, Saija Kontulainen¹. ¹University of Saskatchewan, Canada, ²College of Kinesiology, University of Saskatchewan, Canada, ³School of Physical Therapy, University of Saskatchewan, Canada, ⁴Midtown Professional Center (#103), Canada

Over 90% of hip fractures are attributed to falls, and muscle function is a major factor contributing to fall incidence. Poor lower extremity performance, the development of mobility impairments, frailty, and fracture are all associated with muscle adiposity. However, lower leg muscle adiposity has not been investigated as a determinant of fall status in community-dwelling older adults.

Our objective was to determine the ability of peripheral quantitative computed tomography (pQCT) derived lower leg muscle density (an imaging surrogate of muscle adiposity) to predict the fall status of community-dwelling older adults. It was hypothesized that fallers would be more likely to have lower muscle density after accounting for age, sex, body mass index (BMI), and health status.

Women (n=143), and men (n=43) age 60 or older (mean 74.2, SD 7.7y; and 74.6, 8.4y) were recruited from the Saskatoon CaMos Cohort. Fallers (≥ 1 fall/y) and non-fallers were grouped using a 12-month retrospective falls survey. Participant age, sex, BMI, SF-36 health status, a timed up and go test score (TUG), and grip strength were recorded. A pQCT scan was acquired at 66% of tibia length to determine lower leg muscle density. Missing data were assessed by Little's Missing Completely At Random (MCAR) test. Bivariate relationships with fall status were analyzed for each variable. A Multivariable model containing muscle density, age, sex, BMI and health status was generated to test our hypothesis. Sample descriptive statistics, Odds ratios (OR), and 95% confidence intervals (95% C.I.) were reported.

The sample included 54 Fallers (1) and 129 Non-fallers (0). Little's MCAR indicated that missing data were completely at random ($\chi^2_{513}=536$, $P=0.227$); therefore a pairwise deletion analysis was utilized. Bivariate ORs were found for muscle density, SF-36 general health, SF-36 physical function, 0.85, 0.96, 0.98, ($P<0.01$), and TUG 1.14, ($P<0.05$) respectively. Our multivariable model indicated that if age, sex, BMI and general health were held constant in the model, a 1mg/cm³ increase in leg muscle density (less adipose content) reduced the odds of being a faller by 17% (OR 0.83, 95% C.I. 0.72 to 0.92).

Higher leg muscle density reduces the odds of falling in community-dwelling adults after accounting for variability in age, sex, BMI, and general health.

Disclosures: Andrew Frank, None.

MO0013

Relationship Between Skeletal Muscle Mass, Strength And Physical Performance In Elderly Men With Sarcopenia. Marija Tamulaitiene¹, Asta Mastaviciute², Vidmantas Alekna³, Arvydas Laurinavicius⁴, Donatas Petroska⁴, Vaidile Straziene⁵. ¹Vilnius University, Faculty of Medicine; National Osteoporosis Center, Vilnius, Lithuania, ²Vilnius University, Faculty of Medicine; National Osteoporosis Center, Lithuania, ³Vilnius University, Lithuania, ⁴Vilnius University, Faculty of Medicine; National Center of Pathology, Lithuania, ⁵State Research Institute Centre for Innovative Medicine; Vilnius University, Lithuania

Background: The relation between muscle mass and muscle strength, and physical performance is not clear in sarcopenia.

Purpose: To analyze the relationship between muscle mass, muscle strength and physical performance in sarcopenic men.

Methods: This was a case-control study on ambulatory men aged 70 years and older. DXA was used to measure muscle mass, leg and arm muscle mass separately, body fat percentage (%BF), fat mass (iDXA, GE Lunar). The subjects performed three maximum attempts for dominant handgrip strength measurements with dynamometer and the mean value of these trials was recorded in kilograms (kg). Physical performance was assessed by short physical performance battery (SPPB): standing balance tasks, five repeated chair stands test and the 4-m walk test. Sarcopenia was defined when appendicular skeletal muscle mass divided by stature squared was less than 7.26 kg/m². Skeletal muscle needle (16 gauges) microbiopsy from vastus lateralis femoris was performed in 10 sarcopenic men using standard histo-morphological methods.

Results: Twenty six sarcopenic men and 49 controls (mean age 78.9±6.4 y and 77.8±4.8 y, p=0.45) were included. Sarcopenic men were smaller (169.1±5.9 cm vs 172.1±5.9 cm, p=0.036), lighter (69.3±8.4 kg vs 83.6±11.2 kg, p<0.001) than controls. Fat mass was lower in sarcopenic men than in controls (19.5±6.2 and 25.5±7.9 kg, p<0.001) although there were no differences in % BF, android fat, gynoid fat. Leg muscle mass (14.9±1.5 kg vs 18.1±1.9 kg, p<0.001) arm muscle mass (5.5±0.6 kg vs 6.9±0.8 kg, p<0.001) and muscle strength (24.6±7.7 kg vs 30.1±9.0 kg, p<0.001) were lower in sarcopenic men. No differences were in all tests of SPPB in both groups. There was correlation between muscle strength and arm muscle mass (r=0.6, p=0.002) in sarcopenic men. There was correlation between muscle strength and arm muscle mass (r=0.4, p=0.016), leg muscle mass (r=0.3, p=0.038) in controls. Qualitative morphological-histochemical analysis revealed regular distribution of myocytes I and II type in majority of samples, and focally increased number of lysosomes were found in 2 cases.

Conclusion: Sarcopenic men had lower leg and arm muscle mass and lower muscle strength, although physical performance did not differ between age- and sex-matched persons. Muscle strength was associated only with arm muscle mass in sarcopenic men.

Disclosures: Asta Mastaviciute, None.

MO0014

Thoracic Kyphosis Is More Strongly Associated with the Size and Density of the Thoracic Spinal Extensor Muscles than Lumbar Spinal Extensor Muscles. Dennis Anderson^{*1}, Alexander Bruno², Brett Allaire¹, Yoo Mee Kim³, Serkalem Demissie⁴, Mary Bouxsein¹, Elizabeth Samelson⁵. ¹Beth Israel Deaconess Medical Center, USA, ²Harvard-MIT, USA, ³Division of Endocrinology, MizMedi Hospital, South Korea, ⁴Boston University School of Public Health, USA, ⁵Hebrew SeniorLife, Harvard Medical School, USA

A healthy spine displays congruency between the posterior curvature of the lumbar spine (lordosis) and the forward curvature of the thoracic spine (kyphosis) which allows a person to easily assume an upright posture. While degree of kyphosis varies widely in healthy individuals of all ages, exaggerated kyphosis (hyperkyphosis) is common in older adults and associated with negative health outcomes. Multiple factors may contribute to increased kyphosis with aging, including vertebral fractures (VFX), disc degeneration and spinal extensor muscle weakness. Reduced lumbar spinal extensor muscle density from CT scans, which indicates increased fat content of muscle tissue, is also associated with increased hyperkyphosis in older adults, as well as back pain and loss of functional capacity. However, thoracic spinal extensor muscles may more directly affect kyphosis than lumbar muscle density, as an individual with weak thoracic muscles might be unable to fully extend the thoracic spine and maintain an upright posture with a normal degree of kyphosis.

We conducted a cross-sectional study to determine the association of kyphosis with thoracic and lumbar spinal extensor muscle size and density in a convenience sample of 110 women and 75 men (mean age 62 years, range 31-87) from the community-based Framingham Heart Study CT Study. We measured kyphosis (Cobb angle) from T4-T12 and lordosis angle from L1-L4 from CT lateral scout views, and spinal extensor muscle cross-sectional area (CSA, cm²) and density (in Hounsfield Units) from axial CT scans at T8 and L3. Correlation coefficients (r) were calculated for the association between kyphosis and T8 and L3 muscle CSA and density, adjusted for sex, age, prevalent VFX (T4-T12), and lumbar lordosis.

Cobb angle averaged 34.6±11.0°, increased with age, and was larger in women and those with prevalent VFX. Increased Cobb angle was associated with reduced muscle density, but only in thoracic muscle in the fully adjusted model (Table). Increased Cobb angle was associated with smaller thoracic muscle CSA (not statistically significant when adjusted for fracture and lordosis), but not with smaller lumbar muscle CSA. Thoracic spinal extensor muscle CSA and density are reduced in women and men with increased kyphosis, likely indicating reduced muscle strength. Thoracic muscle is more strongly associated with thoracic spinal curvature than lumbar muscle, and may play an important role in preventing hyperkyphosis.

Table: Correlations for associations between thoracic kyphosis and thoracic and lumbar spinal extensor muscle CSA and density.

| | Unadjusted | | Adjusted for sex, age | | Adjusted for sex, age, VFX, lordosis | |
|------------------------|------------|-------|-----------------------|-------|--------------------------------------|-------|
| | r | p | r | p | r | p |
| Thoracic Muscle | | | | | | |
| CSA | -0.31 | <0.01 | -0.26 | <0.01 | -0.13 | 0.07 |
| Density | -0.30 | <0.01 | -0.24 | <0.01 | -0.27 | <0.01 |
| Model R ² | 0.22 | | 0.24 | | 0.51 | |
| Lumbar Muscle | | | | | | |
| CSA | -0.05 | 0.53 | 0.12 | 0.11 | 0.06 | 0.42 |
| Density | -0.34 | <0.01 | -0.23 | <0.01 | -0.12 | 0.12 |
| Model R ² | 0.15 | | 0.18 | | 0.47 | |

Table

Disclosures: Dennis Anderson, None.

MO0015

Alendronate Protection Against Articular Cartilage Erosion in OVX Rats Supports a Role of Subchondral Bone Loss in Osteoarthritis Pathogenesis.

Jing Hu¹, Songsong Zhu^{*2}. ¹Sichuan University, Peoples Republic of China, ²Sichuan University, China

Objective: Osteoporosis (OP) and osteoarthritis (OA) are major health problems in the increasing elderly population, but their relationship remains unclear. The present study was to investigate whether alendronate (ALN), a potent inhibitor of bone resorption, could protect articular cartilage from degeneration in a combined animal model of OP and OA induced by ovariectomy (OVX).

Methods: Seventy-eight OVX rats were divided into five groups: OVX with either vehicle treatment, early ALN treatment at OVX, or late ALN treatment at 8 weeks after OVX and sham-operated with either vehicle or ALN treatment. Cartilage and subchondral bone changes were evaluated by histology and micro-CT. Osteoprotegerin (OPG) and receptor activator of nuclear factor-κB ligand (RANKL) in the cartilage and subchondral bone were examined by RT-PCR and immunohistochemistry analysis. Matrix metalloproteinase 9 (MMP-9) and MMP-13 was also determined by immunohistochemistry.

Results: Early ALN treatment completely prevented both subchondral bone loss and cartilage surface erosion caused by OVX, as determined by histology, micro-CT and urine collagen degradation markers. Late ALN treatment inhibited subchondral bone loss and significantly reduced cartilage erosion, although they did not recover to normal levels. This protective effect of ALN was due to increased ratio of OPG/RANKL, possibly via inhibition of up-regulated MMP9 and MMP-13 expression.

Conclusion: The subchondral bone plays a critical role during the interplay between OP and OA. Treatment for OP with inhibitors of bone resorption reduces articular cartilage degeneration when OP and OA coexist in same individuals.

Disclosures: Songsong Zhu, None.

This study received funding from: NSFC, China

MO0016

Chondrocyte Metabolism in Inflammatory Arthritis is regulated by CIZ.

Tetsuya Nakamoto^{*1}, Takayuki Motoyoshi¹, Tasuku Hada¹, Makiri Kawasaki¹, Tomomi Sakuma², Tadayoshi Hayata³, Yoichi Ezura⁴, Masaki Noda¹. ¹Tokyo Medical & Dental University, Japan, ²Tokyou Medical & Dental University, Japan, ³Medical Reserach Institute, Tokyo Medical & Dental University, Japan, ⁴Tokyo Medical & Dental University, Medical Research Insititute, Japan

Chondrocyte metabolism is a critical issue to maintain normal joint function as deterioration of its homeostasis leads to destruction of cartilage in joints that is a critical organ for locomotion. Arthritis is a rapidly increasing health problem in modern societies where aged population is soaring. However, the mechanism of chondrocyte metabolism in arthritis is still incompletely understood. Cas interacting zinc finger protein (CIZ) is a transcriptional regulator that controls the activity of the promoters for the matrix metalloproteinases (MMPs) including MMP-3, an enzyme considered to be implicated in joint destruction in arthritis. CIZ is also known as nuclear matrix protein 4 (Nmp4) or zinc finger protein 384 (Zfp384). CIZ is expressed in skeletal cells and suppressive roles of CIZ in bone formation were reported previously. However, the role of this transcription factor in pathophysiology of chondrocyte metabolism has not been elucidated. K/BxN serum transfer model of inflammatory arthritis is induced by the autoantibodies that interact with the antigen on the surface of the cartilage and the pathology of this arthritis resembles that of human rheumatoid arthritis. By using K/BxN arthritis model in mice, we reported that CIZ is induced in chondrocytes upon arthritis in wild type mice and that CIZ

deficiency suppresses arthritis phenotype. In this model, arthritis-induced proteoglycan loss in articular cartilage was suppressed. As a mechanistic base, we observed that IL-1 β was induced by arthritis and increases CIZ expression in chondrocytes. CIZ itself transcriptionally activates IL-1 β expression in chondrocytes. In contrast, TNF induction by arthritis was not suppressed by CIZ deficiency. Moreover, CIZ also activates RANKL in chondrocytes and deficiency of CIZ suppresses osteoclast activation in arthritis model. Furthermore, CIZ deficiency suppresses MMP-3 expression in arthritic chondrocytes. These results indicate that CIZ is a critical regulator of chondrocyte metabolism in arthritis.

Disclosures: Tetsuya Nakamoto, None.

MO0017

Effects of Teriparatide on Bone Metabolism of Patients with Rheumatoid Arthritis and Osteoarthritis. Daihei Kida*. National Hospital Organization Nagoya Medical Center, Japan

Objectives: To evaluate change in bone quality in patients at high risk of fracture by quantification of several bone biochemical markers and bone mineral density (BMD), before and after teriparatide (TPD) treatment. **Methods:** fifty-seven female patients with rheumatoid arthritis (RA; mean age 70.8 \pm 8.0 yrs, and eighteen female patients with osteoarthritis (OA; mean age 69.9 \pm 10.9) were assessed. Levels of serum osteocalcin (OC), serum undercarboxylated osteocalcin (ucOC), serum bone specific alkaline phosphatase (BAP), procollagen type I N-terminal propeptide (PINP) serum tartrate resistant acid phosphatase isoform 5b (TRAP-5b), urinary N-teropeptide of type I collagen/creatinine (NTx), serum calcium (Ca), serum phosphorus (P), vitamin D metabolites 1,25-dihydroxyvitamin D3 (1,25D3), intact parathyroid hormone (iPTH), calcitonin (CT) and BMD at the lumbar spine (LS) and total hip (TH) were measured at baseline and 6 months after TPD by subcutaneous injection (20 microg once a day). Statistical analysis also performed. **Results:** Levels of biochemical markers before and after TPD are summarized in Table 1a and 1b. Although no additional vitamin D supplementation intake were recommended, significant increasing was found in level of 1,25D3 in both RA and OA groups. Significant differences between RA group and OA group were found on mean serum Ca levels before and after treatment. TPD administration significantly stimulated bone formation and bone resorption and increased BMD after 6 months in both OA and RA groups (data not shown). **Conclusions:** Therefore, ucOC levels were significantly higher and CT levels were significantly lower after 6 months, it is possible that beneficial reactivation of the osteoblast system by TPD administration might require high amounts of vitamin K and/or calcitonin.

Table 1a. Levels of biochemical markers before TPD administration

| | RA Group (n=57) | OA Group (n=16) | P-Value (RA vs OA) |
|--------------|-----------------|-----------------|--------------------|
| ucOC (ng/mL) | 5.65 \pm 5.73 | 6.95 \pm 5.27 | NS |
| CT (pg/mL) | 33.6 \pm 12.8 | 36.1 \pm 11.1 | NS |
| VitD (mg/mL) | 58.7 \pm 25.6 | 58.8 \pm 21.5 | NS |
| Ca (mg/dL) | 9.66 \pm 0.33 | 9.96 \pm 0.26 | <0.001 |

Table 1b. Levels of biochemical markers after TPD administration

| | RA Group (n=57) | OA Group (n=16) | P-Value (RA vs OA) |
|--------------|--------------------|--------------------|--------------------|
| ucOC (ng/mL) | 19.83 \pm 19.00‡ | 21.27 \pm 16.90‡ | NS |
| CT (pg/mL) | 23.0 \pm 10.9‡ | 20.5 \pm 8.3‡ | NS |
| VitD (mg/mL) | 84.3 \pm 64.5‡ | 105.9 \pm 53.1‡ | <0.01 |
| Ca (mg/dL) | 9.79 \pm 0.33‡ | 10.1 \pm 0.35 | <0.001 |

Two-sided P-value for the comparison between RA Group and OA Group are determined by Mann-Whitney test. Two-sided P-value for the comparison between baseline and 6 months in each group are determined by Wilcoxon signed rank test. †:P<0.05, ‡:P<0.01, §:P<0.001vs before.

Table 1a and 1b

Disclosures: Daihei Kida, None.

MO0018

Treatment of Murine Osteoarthritis by Cartilage Matrix Preservation and Reducing Inflammation by Gene-Transfer. Zhechao Ruan*¹, Ayelet Erez¹, Kilian Guse¹, Brian Dawson¹, Yuqing Chen¹, Brendan Lee². ¹Baylor College of Medicine, USA, ²Baylor College of Medicine & Howard Hughes Medical Institute, USA

Osteoarthritis (OA) is a chronic debilitating disease characterized by degeneration of articular cartilage, subchondral bone, and intraarticular inflammation. To date, different treatment approaches have resulted in limited success. Here, we report novel effective gene transfer as treatment for mice with trauma-induced OA by cartilage matrix preservation and decreased inflammation.

Proteoglycan 4, (*PRG4*), is one of the few genes known to be associated with OA and its loss of function mutation results in early onset OA in both humans and mice. In addition, interleukin 1 receptor antagonist (*IL1Ra*) has been shown in several studies to alleviate OA in different models. Hence, we hypothesized that gene transfer of *PrG4* and *IL1Ra* to the intra-articular space would be beneficial in OA. To test our hypothesis, we generated a transgenic mouse over-expressing *PrG4* under the bone specific promoter, *collagen 2a1* (*Col2a1*). Using a modified surgical OA model, involving cruciate ligament transection, we recapitulated the post-traumatic human OA in a mouse model. Our results show that *PRG4* transgenic mice are protected against the development of OA as compared to WT mice. Moreover, to evaluate the potential synergistic therapeutic effects of *PRG4* and *IL1Ra*, we injected helper-dependent adenoviral vectors expressing *PRG4* (HDAd-*PRG4*) and *IL1Ra* (HDAd-*IL1Ra*) separately or in conjunction to wild type mice after induction of post-traumatic OA. Injections of either HDAd-*PRG4* or HDAd-*IL1Ra*, resulted in a protective effect against OA while co-injection of the both had a positive synergistic protective effect.

In summary, we identified *PRG4* as a novel target for OA chondroprotection. The successful gene delivery of *PRG4* and *IL1Ra* using HDAd could potentially have therapeutic implications for OA.

Disclosures: Zhechao Ruan, None.

MO0019

Bone Changes in Athletes throughout a Competitive Season. Lee Weidauer*¹, Maggie Eilers², Teresa Binkley¹, Matt Vukovich¹, Howard Wey¹, Bonny Specker¹. ¹South Dakota State University, USA, ²Creighton University, USA

The purpose of this study was to investigate bone changes in athletes from pre- to post-season. Female D1 collegiate athletes (ATH; aged 20y) and 12 inactive controls (NON; aged 19y) had DXA and left distal 4%, 20%, and 66% tibia scanned by pQCT prior to and within 2 months after their competitive season. Soccer players (n=12) were considered as odd-impact loading (ODD), cross-country athletes (n=15) as low-impact loading (LOW), and volleyball and basketball players (n=12) as high-impact loading groups (HIGH). **Results:** Mean hip and femoral neck aBMD were lower at baseline in NON vs. ATH (0.99 vs. 1.10, p=0.03 and 0.92 vs. 1.01, p=0.06). Hip aBMD changes differed between NON and ATH (0.2 vs. -0.4, p=0.01) which could be attributed to changes in hip BMC (p=0.01) rather than bone area (NS). Changes in trabecular area at the 4% (defined using vBMD <170mg/cm³) differed with a 14% and -5% change in NON and ATH respectively (p=0.04), resulting in lower trabecular content among ATH than NON (p=0.003). Change in cortical area and bone content differed between NON and ATH (both p=0.001), with a loss in cortical bone content among ATH (-17mg, p<0.05) compared to gains in cortical area and bone content among NON (38mm² and 42mg, both p<0.05). Loss of cortical bone among ATH appeared on the periosteal surface (decreased 2.3mm) rather than a loss at the endosteal surface (no change). NON had a significant increase in periosteal expansion (6.2mm, p<0.05). Changes in cortical area and bone content differed among athletes with gains among LOW (14mg & 11mm²) and losses in HIGH and ODD (-38mg & 35mm² and 39mg & 33mm², respectively). A difference in change of cortical thickness was observed with a loss in ODD (-0.5mm, p<0.05) and gain in LOW (0.3mm, p<0.05). In summary, athletes lost a significant amount of bone mass at the hip throughout the competitive season. Differences in trabecular area and content can be explained by an increase in vBMD along the endosteal surface among athletes, leading to an apparent decrease in area and content compared to non-athletes. Changes in cortical area, thickness, and bone content were similar among HIGH and ODD athletes, while changes among LOW athletes were similar to NON. However, decreases in cortical content and periosteal circumference may put them at a greater risk of stress fracture as the season progresses.

Disclosures: Lee Weidauer, None.

MO0020

FRAX without BMD has Low Predictive Value of Low BMD in Older People. Charles Inderjeeth¹, Van Victoria², Foo Brendan², Anupam Chauhan², Antonia Petta². ¹University of Western Australia, Australia, ²SCGH, Australia

Osteoporosis is common and increases with ageing. BMD is a useful tool to identify people with osteoporosis. However access to BMD in older frail populations makes it difficult to screen this high risk population. Fracture risk assessment tools, like FRAX have been considered as options to identify this high risk group to better target groups at risk.

AS part of a routine screening program utilising a mobile DXA BMD service in older populations who would not have easy access to DXA, we also assessed risk based on FRAX without BMD. The main objective was to assess the predictive value of FRAX in identifying people with osteoporosis on BMD.

To date 442 people included, mean age 80.3 (SD 6.35), 56% female. 160 had history of minimal trauma fracture and 22 previous hip fracture. A FRAX (without BMD) calculated 10 year Hip Fracture risk of above 25% was over 90% sensitive in identifying people with a T score below -2.5. However specificity was 6% or less and PPV of 16%. The negative predictive value of low FRAX was equally unhelpful. The results were no different even when using a T -3.0 as the cut off to predict risk.

The search for tools to identify older frailer populations who may not have access to BMD for risk of osteoporotic fracture continues. Unfortunately FRAX was not useful in this cohort in substituting for BMD assessment.

Disclosures: Charles Inderjeeth, None. This study received funding from: NIL

MO0021

Higher Bone Mineral Content at Superior as well as Inferior Femoral Neck in Older Adults Habitually Participating in Multidirectional Loading Activities. Katherine Brooke-Wavell¹, Rachel Duckham², Hannah Carpenter³, Rachael Taylor⁴, Richard Morris⁵, Tahir Masud⁴, Steve Liffie⁵, Denise Kendrick³. ¹Loughborough University, United Kingdom, ²UMASS, USA, ³Nottingham University, United Kingdom, ⁴Nottingham University Hospitals NHS Trust, United Kingdom, ⁵University College London, United Kingdom

The age related decrement in bone is disproportionately greater at the superior femoral neck, where thinning of the cortex is associated with hip fracture. It is thus important to identify factors that preserve bone at the superior aspect of the femur. This study aimed to evaluate differences in bone mineral content (BMC) and density (BMD) at upper and lower femoral neck according to habitual physical activity type in older adults.

Participants were men and women aged over 65 years, recruited through primary care. Those with medical conditions or medications substantially affecting bone metabolism were excluded. Participants had dual X-ray absorptiometry measurements of body composition, BMC and BMD, a questionnaire on health status, smoking and medication and a telephone interview on the type, frequency and duration of physical activity. BMC and BMD were compared according to physical activity participation using a general linear model, with age, gender, weight, %fat, smoking status and comorbidities as covariates.

Participants were 104 men and 148 women with mean \pm SD age 71.7 ± 5.2 y, height 1.65 ± 0.10 m and weight 76.6 ± 15.0 kg. The activity types participants reported practising at least once in a typical week included: group exercise (e.g. tai chi; 8.5%), swimming (7.2%), cycling (3.1%), odd-impact exercise (dancing, aerobics; 13.9%), leg weight-lifting (4.5%), other home exercises (18.5%), walking for exercise (71.2%), gardening (82.5%) and home maintenance (e.g. painting; 38.4%). Femoral neck BMC and BMD were higher in participants than non-participants in odd-impact exercise (by 6.3 and 5.1% respectively, both $P < 0.05$). Increments were of similar magnitude at upper and lower femoral neck (BMC 6.0% and 6.5% respectively, both $P < 0.05$; BMD 4.8%, $P = 0.07$ and 5.3%, $P = 0.01$ respectively). Participants in home maintenance had higher femoral neck BMD (by 5.9% and 4.2% at upper and lower femoral neck respectively, both $P < 0.05$), but not BMC, than other men and women. BMC and BMD did not differ significantly according to participation in other physical activities.

Habitual participation in activities involving multidirectional loads was associated with higher femoral neck BMC and BMD, with benefits evident at both superior and inferior regions. Activities such as dancing, aerobics and home maintenance may preserve bone at both superior and inferior aspects of the femoral neck in older adults, potentially reducing hip fracture risk.

Disclosures: Katherine Brooke-Wavell, None.

MO0022

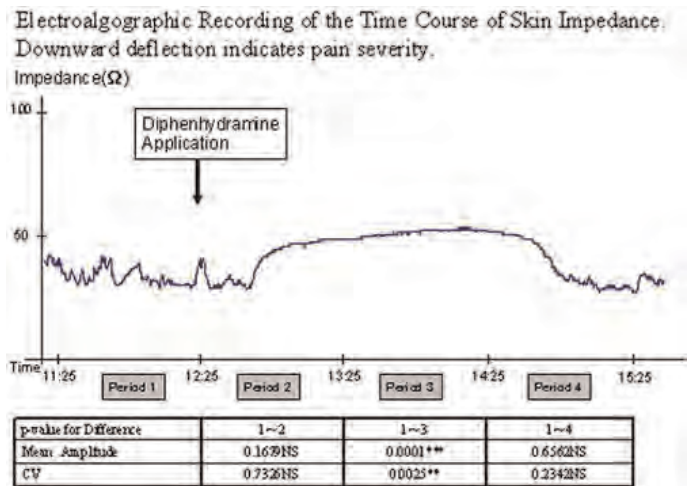
Prompt Analgesic Effect of Diphenhydramine Ointment on Bone, Muscle and Joint Pain Assessed by Electroalgometry. Takuo Fujita¹, Mutsumi Ohue¹, Mikio Nakajima², Yoshio Fujii³, Akimitsu Miyauchi⁴, Yasuyuki Takagi⁵. ¹Katsuragi Hospital, Japan, ²Dept of Orthopedic Surgery, Osaka Medical College, Japan, ³Calcium Research Institute Kobe Branch, Japan, ⁴Miyauchi Medical Clinic, Japan, ⁵National Hyogo Chuo Hospital, Japan

Purpose In view of the role of histamine in pain sensing mechanism along with cytokine and transmitter on muscle fatigue pain frequently occurring in seniors, diphenhydramine, a classical anti-H₁ receptor agent, was tested for pain due to degenerative bone and joint disease with muscle strain.

Methods Pain in response to exercise loading was assessed by electroalgometry (EAM) utilizing % fall of skin impedance as a pain index, along with recording of subjective pain by VRS system dividing the distance between no pain and unbearable pain into 100 equal parts, before and after application of 1% diphenhydramine ointment. After a preliminary study on a 82 year old subjects with osteoarthritis of the fingers, time course of diphenhydramine effect was compared with that of indometacin and placebo in a crossover system in 5 subjects with degenerative joint disease. The response to diphenhydramine and indometacin was then compared in 13 postmenopausal women with mean age of 72 ± 7 year before and 30 minutes after application again by crossover.

Results Diphenhydramine markedly inhibited the fall of % skin impedance and pain induced by exercise ($p = 0.0066$ and 0.0008). Basal level of skin impedance rose 20 minutes after application lasting about 2 hours. The amplitude and frequency of downward deflections indicating spontaneous pain markedly decreased ($p = 0.0001$ and 0.0025) (Fig 1). Diphenhydramine showed significantly higher analgesic effect than indometacin and placebo 10~360 minutes by EAM and 30~180 minutes by VRS. In 13 postmenopausal women diphenhydramine decreased the degree of pain from 31.6 ± 12.3 to $15.1 \pm 11.1\%$ ($p = 0.0001$) by EAM and from 9.6 ± 4.6 to 5.0 ± 3.6 ($p = 0.0002$) by VRS 30minutes after application.

Conclusion Diphenhydramine showed a highly significant analgesic effect on topical application in subjects with chronic bone, joint and muscle pain in elderly subjects



Electroalgographic Recording

Disclosures: Takuo Fujita, None.

MO0023

Site Specificity of Physical Activity and its Effect on Long-Term Risk of Fracture: Spine vs. Hip. Mehrsheed Sinaki, Morgan Brubaker*, Paul Limburg. Mayo Clinic, USA

Physical activity can have a positive effect on bone mass, but the effect on incidence of hip fracture is controversial. The types of daily activity shown to be protective include household chores, leisure activities, standing, walking, and stair-climbing. Significant morbidity and mortality are associated with sustaining a hip and/or vertebral fracture. Mortality rate within a year of hip fracture is reportedly 20-24%. In this study, we analyzed the effect of improving back extensor strength on the risk of vertebral vs. hip fractures. It has been previously reported in the same study group that increasing back extensor strength decreased the risk of vertebral fracture after 10 years. We reviewed these 50 subjects' detailed evaluations 18 years after the 10-year follow-up of the randomized, controlled trial to determine if it had the same protective effect at 28 years. The original study included 50 healthy, white, postmenopausal women who had evaluations every 4 weeks for 2-years, then a follow-up at 10-years. The evaluations included an activity questionnaire, measurement of back extensor strength, and review of good posture and lifting principles. The exercise group performed a progressive weight-lifting program for back extensor muscles. While prone, wearing a weighted backpack (30% of maximal isometric strength), they lifted

the backpack 10 times, 5 days a week. As their strength increased, the weight could be increased up to a maximum of 50 lbs. At the end of the 2-year trial, the exercise group had significantly stronger back extensor muscles when compared to the control group. Our review of subjects' charts 18 years after the 10-year follow-up revealed 0 (0%) vertebral compression fractures and 5 (18.5%) hip fractures in the exercise group. In the control group, there were at least 6* (26%) vertebral compression fractures and 1 (4%) hip fracture. Fisher's Exact Test revealed a significant difference in vertebral fracture rate ($p < 0.05$), but no significant difference in hip fracture rate ($p = 0.199$) at 28 years. Our long-term follow up data demonstrates that to prevent fractures, the muscular support of the site of interest needs to be strengthened. After 28 years, the 2-year back strengthening exercise program significantly reduced the risk of vertebral fracture, but did not reduce the risk of hip fracture. *In the subjects' charts, vertebral fractures listed as "multiple" were counted as 2 fractures in our statistical analysis.

Disclosures: Morgan Brubaker, None.

MO0024

Successful Management of Headaches Related to Occipito-Cervico-Thoracolumbar Malposture of Osteopenia/Osteoporosis: Significance of Axial Proprioception in Headaches. Mehrsheed Sinaki*¹, Ivan Garza¹, Eiji Itoi², Michio Hongo³, Mansoor Ravegani⁴, Reza Roghani⁴, Bart Clarke⁵.
¹Mayo Clinic, USA, ²Tohoku University School of Medicine, Japan, ³Akita University Graduate School of Medicine, Japan, ⁴Shahid beheshti University, Iran, ⁵Mayo Clinic College of Medicine, USA

Axial posture is not static, but rather a dynamic process affected by orientation of different anatomical units in relationship to one another at any given time. Posture can affect the muscles recruited for static upright position as well as locomotion. Posture can be influenced by multiple factors; i.e. aging, gender, bone loss, muscle strength, and occupation. The most disfiguring effect of axial loss of muscle strength and bone is the anterior wedging of the thoracic spine due to the contributing effect of gravity on the natural thoracic kyphosis and forward head position. In our outpatient clinic, we see patients with or without osteopenia/osteoporosis for neck pain and/or headache. In this communication, we report cases of headache and neck pain in the setting of hyperkyphosis (thoracic kyphosis > 50°), who had tried other measures including pharmacotherapy for relief of their headache without success. All had neurological and musculoskeletal evaluations and full assessment of gait and physical activity.

Intervention: All subjects, after full evaluations, were provided with instructions to improve their occipito-cervico-thoracolumbar malposture through specific postural exercises. Our mechanical intervention included posture training through re-education of axial muscles and joint proprioception with or without use of weighted orthotics. All patients reported substantial improvement. Our figures depict the kinesiology and efficacy of these techniques.

Conclusion: Headaches can be complex and their etiology needs elaborate work-ups. In this presentation, we discuss the headaches related to overuse of posterior cervical muscles in the setting of malposture related to axial bone loss.

Disclosures: Mehrsheed Sinaki, None.

MO0025

Hypophosphatasia: Diagnosis Missteps. Katherine Madson*¹, Karen Mack¹, William McAlister², Michael Whyte¹. ¹Shriners Hospital for Children-Saint Louis, USA, ²Mallinckrodt Institute of Radiology, Washington University School of Medicine, USA

We report a 3½ year old boy whose hypophosphatasia (HPP) diagnosis was delayed by 2 years through a series of instructive errors searching for the clinical, laboratory, and radiographic characteristics of this inborn-error-of-metabolism. HPP features rickets with paradoxically low serum alkaline phosphatase (ALP) activity due to deactivating mutation(s) within the gene that encodes the cell surface "tissue nonspecific" isoenzyme of ALP (TNSALP). Consequently, several phosphocompounds accumulate extracellularly including pyridoxal 5'-phosphate (PLP), inorganic pyrophosphate, and phosphoethanolamine.

He developed bowed legs at age 1 year after weight bearing for 1 month. His pediatrician diagnosed "physiologic bowing". At age 17 months, non-traumatic loss of a central mandibular incisor occurred with root intact. His pediatric dentist said this was abnormal. At age 1½ years, a 2nd tooth was lost without trauma and if he shed additional teeth "he should enter a research study". The dentist mentioned *acid phosphatase* deficiency as a possible etiology.

Subsequently, mother searched the internet using keywords "bowing and tooth loss" and found HPP. She requested testing for HPP and an orthopedist for her child's bowing. The orthopedist's radiographs were "normal" at age 20 months, and "did not suggest Blount's Disease". Four months later knee radiographs showed "metaphyseal spurs" diagnosed as Blount's Disease, and he was given orthotics.

During the pediatrician's evaluation for HPP, serum *acid phosphatase* was ordered twice. Serum ALP of 90 U/L on a metabolic panel reviewed by a pediatric geneticist was judged "normal", but used an adult normative range (50-136 U/L); the pediatric range was not provided. For HPP substrate testing the clerks ordered *Vitamin B1*, rather than *Vitamin B6 (PLP)*, and *phosphotidylethanolamine auto-antibodies*, rather than phosphoethanolamine. The diagnosis of HPP by the geneticist was finally made

when a heterozygous mutation on exon 10 c.1034C>T (p.Ala345Val) was found [Connective Tissue Gene Tests (Allentown, PA)].

On referral to us, we documented low serum ALP for age, elevated plasma PLP, and typical radiographic metaphyseal changes consistent with mild childhood HPP. Typically, the diagnosis of HPP can be made from the disorder's characteristic clinical, biochemical, and radiographic features.

Disclosures: Katherine Madson, None.

MO0026

Reliability of Lateral Distal Femur DXA Measures. Nicole Mueske¹, Cassie Nguyen², Tishya Wren*¹. ¹Children's Hospital Los Angeles, USA, ²University of Southern California, USA

Bone mineral content (BMC) and density (BMD) are commonly assessed using dual-energy x-ray absorptiometry (DXA). However, standard DXA measures are often difficult to obtain in certain clinical populations, such as children with cerebral palsy or spina bifida, due to metal implants and joint contractures. Lateral DXA of the distal femur has been suggested as an alternative for these patients. The purpose of this study was to evaluate the reliability of lateral distal femur DXA measures.

Five children with spina bifida and 5 controls (age 9.5 ± 2.1 yrs; 4 males, 6 females) had DXA scans bilaterally, with each scan being analyzed 3 times by 2 raters. Five healthy young adults had unilateral DXA scans 3 times with repositioning between scans. DXA imaging was performed on the lateral distal femur with the subject lying on the side being measured. Regions of interest (ROI) were defined in the anterior distal metaphysis (R1), metadiaphysis (R2), and diaphysis (R3) as described by Henderson et al. [1]. An additional region (R4) was defined in the metaphysis similar to R1, but aligned with the medullary canal to better represent cancellous bone. Coefficients of variation (CV) were calculated for BMC, BMD, and projected area in regions R1-R4.

Variability was consistently lower for BMD than for BMC and area (Table 1). The CVs for BMD were under 1.5% for within rater variability and under 4% for total inter- and intra-rater variability. For the repeated scans, CVs were below 4.5% except for R1 BMC and area. In general, CVs were higher for R1 than R4. CVs were also higher for patients compared with controls. These results suggest that DXA measures of the lateral distal femur are reliable and may be useful when standard DXA measures cannot be obtained. However, it is recommended that the original methodology be modified to use a central, rather than anterior, ROI in the metaphysis because R1 can be difficult to position and encompasses the anterior cortex, increasing variability of the DXA measures in this region. With this modification, lateral distal femur DXA provides a reliable option for bone mass assessments in pediatric patient populations that have a high risk for fracture but are unable to undergo DXA at standard sites due to their orthopaedic issues.

Acknowledgements: Support provided by NIH-NICHD Grant # 5R01HD059826. **References:** 1. Henderson et al. (2002). *Am J Roentgen* 178: 439-443.

Table 1: Coefficients of variation (%), mean \pm SD

| | R1 | R2 | R3 | R4 |
|-------------------------------|----------------|---------------|---------------|---------------|
| Intra-Rater | | | | |
| Area | 5.3 \pm 2.3 | 1.6 \pm 0.5 | 1.5 \pm 0.4 | 2.4 \pm 0.3 |
| BMC | 5.0 \pm 1.6 | 1.5 \pm 0.3 | 1.4 \pm 0.3 | 3.0 \pm 0.1 |
| BMD | 1.3 \pm 0.9 | 0.4 \pm 0.0 | 0.4 \pm 0.0 | 0.9 \pm 0.1 |
| Inter- and Intra-Rater | | | | |
| Area | 9.2 \pm 3.4 | 4.5 \pm 3.1 | 5.2 \pm 3.4 | 6.8 \pm 3.7 |
| BMC | 10.7 \pm 5.6 | 5.2 \pm 3.6 | 5.4 \pm 3.4 | 9.7 \pm 6.2 |
| BMD | 3.8 \pm 2.6 | 1.4 \pm 0.9 | 1.6 \pm 0.9 | 3.8 \pm 2.6 |
| Repeat Scans | | | | |
| Area | 6.8 \pm 4.5 | 2.4 \pm 1.1 | 3.2 \pm 2.1 | 3.1 \pm 2.0 |
| BMC | 8.1 \pm 5.0 | 3.0 \pm 1.9 | 3.4 \pm 1.6 | 4.4 \pm 1.1 |
| BMD | 3.4 \pm 2.5 | 1.0 \pm 0.8 | 3.9 \pm 3.9 | 1.5 \pm 1.1 |

Table 1

Disclosures: Tishya Wren, None.

MO0027

Vitamin D Status in Healthy 2-4 Month Old Infants in New York City. Tulasi Ponnappakkam*¹, Ranjitha Katikaneni², Robert Gensure³.
¹Childrens Hospital at Montefiore, New York/Albert Einstein College of Medicine, USA, ²Childrens Hospital at Montefiore/Albert Einstein College of Medicine, USA, ³Children's Hospital at Montefiore, Albert Einstein College of Medicine, USA

Vitamin D is very important for normal bone health in children; deficiency causes rickets. At the Children's Hospital at Montefiore, we routinely see several cases per year of vitamin D deficiency leading to rickets and/or hypocalcemic seizure. The American Academy of Pediatrics has recently revised its guidelines for vitamin D

supplementation in the first 6 months of life, recommending infants receive at least 400 IU/day. Of note, neither breast milk nor fortified formulas provide this amount of vitamin D, suggesting that all infants should receive supplements. We are conducting a cross sectional study to assess vitamin D status in 2-4 month old infants in New York City in an effort to provide more specific supplementation recommendations in this region. A total of 96 healthy 2-4 month-old infants will be recruited over the course of 1 year. After obtaining an informed consent, we administer a short (1 page) questionnaire regarding type of feeding and vitamin D supplementation, and obtain a 1 ml blood sample for measurement of 25-D and alkaline phosphatase. We have completed recruiting for two seasons, 23 in fall and 22 in winter, the season where vitamin D levels would be expected to be lowest. Average Vitamin D levels for the fall season were 35.0 ± 8.9 ng/ml (19.3-51.8). Average vitamin D levels for the winter were 20.5% lower ($p < 0.01$), but most were still above goal levels (> 20 ng/ml). Infants receiving additional supplementation showed increased vitamin D levels (29.2%, $p = 0.01$), as expected. Average Alkaline Phosphatase Levels were 304 ± 83 U/L (172-522) in fall and 293 ± 68 in winter, both in the normal range for age. Importantly, the only subjects with vitamin D levels below 20 ng/ml were exclusively breastfed over the winter season, receiving no vitamin supplements, and most with mothers reporting that they were not taking prenatal vitamins and were probably vitamin D deficient themselves. These subjects showed very low (< 10 ng/ml) vitamin D levels, much different from the rest of the study cohort, and in the rachitic range. None had clinical signs of rickets or elevations in alkaline phosphatase, suggesting that the vitamin D deficiency developed recently. These results suggest that rather than emphasizing universal supplementation, efforts should be made to identify and treat individuals at risk to develop vitamin D deficiency, at least in the New York City area.

Disclosures: Tulasi Ponnappakkam, None.

MO0028

Adenovirus 36, Adiposity and Bone Strength in Late-Adolescent Females.

Emma Laing^{*}, Ralph Tripp¹, Norman Pollock², Clifton Baile³, Mary Anne Della-Fera¹, Srujana Ravalam¹, Stephen Tompkins¹, Deborah Keys⁴, Richard Lewis¹. ¹The University of Georgia, USA, ²Georgia Health Sciences University, USA, ³University of Georgia, USA, ⁴Independent Statistical Consultant, USA

Our previous studies in adolescent females suggest that excess weight in the form of fat mass is associated with lower cortical bone strength. Adenovirus 36 (Ad36) is the only adenovirus to date that has been linked with obesity in humans. The purpose of this study was to assess the relationship between Ad36-specific antibodies, adiposity and bone strength in our sample of late-adolescent females. A cross-sectional study of 115 females aged 18-19 years was performed. Participants were classified according to adiposity by dual energy X-ray absorptiometry [body fat percentage as normal-fat ($< 32\%$ body fat; $n = 93$) or high-fat ($\geq 32\%$ body fat; $n = 22$)], and according to the presence of Ad36-specific neutralizing antibodies as assessed by Adenovirus plaque reduction assay [Ad36+ (≥ 0.4 OD 450nm; $n = 62$) and Ad36- (< 0.4 OD 450nm; $n = 53$)]. Peripheral quantitative computed tomography measured bone geometrical properties at the 4% and 20% sites, and muscle cross sectional area (MCSA) at the 66% site, from the distal metaphyses of the radius and the tibia. After controlling for MCSA and limb length, significant adiposity x Ad36 interactions were observed, such that total area (at the 4% and 20% sites), as well as cortical bone mineral content, cortical area, endosteal circumference, periosteal circumference, and polar strength strain index of the 20% radius were all significantly lower in Ad36+ vs. Ad36- subjects from the high-fat group, but not the normal-fat group ($P < 0.03$). No adiposity x Ad36 interactions were observed at the tibia. These data support an association of adiposity and bone strength at the radius with the presence of neutralizing antibodies to Ad36 in late-adolescent females.

Disclosures: Emma Laing, None.

MO0029

Bone Structure Abnormalities in Children With Osteogenesis Imperfecta.

Christopher Modlesky^{*}¹, Brianne Mulrooney¹, Lauren Davey², Michael Bober². ¹University of Delaware, USA, ²A.I. duPont Hospital for Children, USA

Osteogenesis imperfecta (OI) is a genetic disorder in which type I collagen production is deficient. The result is low bone mass and a high rate of fracture in children with OI. There is also evidence of a compromise in bone structure that contributes to their bone fragility. However, the structural compromise in the lower extremities of children with OI is poorly studied. The aim of this study was to examine the cortical bone macrostructure and trabecular bone microstructure in the femur of children with type I OI, the mildest form of the disorder. Seven children with Type I OI (5-10 y) and 15 typically developing children in the same age range and between the 5th and 95th age-based percentiles for height and body mass were studied. Measures of cortical bone macrostructure and strength [i.e., cortical bone volume, polar moment of inertia (J), and section modulus (Z)] at the middle third of the femur and trabecular bone microstructure [i.e., apparent trabecular bone volume to total volume (appBV/TV), trabecular number (appTb.N), trabecular thickness (appTb.Th) and trabecular separation (appTb.Sp)] at the distal end of the femur were estimated using magnetic resonance imaging. Areal bone mineral density (aBMD), bone mineral content (BMC) and bone area in the distal femur were assessed using dual-energy

X-ray absorptiometry. There was not a group difference in age but children with OI vs. control children had lower height and body mass ($p < 0.05$). Children with OI vs. controls also had 34 % lower cortical volume, 44 % lower J and 38 % lower Z in the mid femur (all $p < 0.05$). Interestingly, children with OI vs. controls had 22 % higher appBV/TV and 30 % higher appTb.Th, but 6 % lower appTb.N in the distal femur (all $p < 0.05$). On the other hand, aBMD was 27 % lower ($p < 0.001$), BMC was 27 % lower ($p = 0.005$) and bone area was not different ($p = 0.895$) in the distal femur of children with OI vs. controls. The findings suggest that children with type I OI have a compromised cortical bone macrostructure in the femoral shaft. The findings also suggest that children with type I OI have fewer trabecular structures than normal in the distal femur; however, the structures are thicker resulting in a greater concentration of trabecular bone. The mechanisms underlying this altered trabecular structure and its effect on fracture incidence requires further investigation.

Disclosures: Christopher Modlesky, None.

MO0030

Compromised Bone-Muscle Unit in Boys with Duchenne Muscular Dystrophy. Diane Visy^{*}¹, Wendy King², John Kissel², Prem Goel², Velimir Matkovic². ¹University of Zagreb, Croatia, ²The Ohio State University, USA

Bone mineral density (areal and volumetric) and body composition have been evaluated in 93 boys with Duchenne Muscular Dystrophy (DMD) and its healthy controls (ages 5-30 y). Each participant had a DXA measurement of the whole body and various skeletal regions of interest, and peripheral quantitative computerized tomography (pQCT) measurement of the proximal and distal radius and tibia. The results of the research study indicate that DMD boys (steroid treated) do not go through normal puberty and have delayed skeletal maturation affecting longitudinal bone growth and periosteal envelope expansion (bone geometry/bone volume). A phase of rapid skeletal modeling seems to be decreased in Duchenne boys due to steroids and/or the lack of biomechanical forces exerted on the bone-muscle unit leading to a reduced peak bone mass formation. R^2 for regressing total body bone mineral content (TBBMC) of DMD boys and its controls on lean body mass (LBM) was 93.4% ($p < 0.0001$). However, the range of TBBMC and LBM in the controls was between 655-3943 g, and 14892-73314 g, respectively, while the same in the Duchenne boys was between 459-2067 g, and 13060-39347 g, respectively. The ratio of TBBMC/LBM was the same between the groups: 0.047 ± 0.009 in DMD, and 0.049 ± 0.005 in controls ($p = 0.09$). Duchenne boys have a comparable or higher endosteal bone accretion (mass per volume ratio) in the shaft regions of the long bones, as compared to the controls. However, the bones remain smaller and narrower, which by itself can contribute to abnormal bone quality at these sites. The reduced bone mass and volumetric density at the trabecular bone structures predisposes DMD boys to a higher rate of bone fragility fractures. The study provided significant new information about the skeletal mineralization and its structure in DMD boys as relates to lean body mass, indicating compromised bone-muscle unit.

Disclosures: Diane Visy, None.

This study received funding from: Muscular Dystrophy Association

MO0031

Femoral Neck Development in 4- to 10-year-old Precompetitive Gymnasts: a 4-year Longitudinal Study. Adam Baxter-Jones^{*}¹, Rita Gruodyte¹, Stefan Jackowski¹, Marta Erlandson². ¹University of Saskatchewan, Canada, ²University of Toronto, Canada

In young children, it has been demonstrated that regular participation in physical activity is associated with greater bone strength at the femoral neck. Gymnastics, a high-impact weight-bearing physical activity, has been shown to be highly osteogenic. We have shown previously in this cohort that bone mass development, indexed by bone mineral content (BMC) accrual, is positively affected by low-level (recreational) gymnastics exposure (1 to 2 hrs per week). However, BMC is only one single component of bone strength. Bone strength is influenced not only by bone mineralization but also bone geometry, bone architecture and the imposing loads on the bone. The aim of this study was to investigate whether low-level gymnastics training effected the estimated structural geometry development of the proximal femur. 163 children (30 gymnasts, 61 ex-gymnasts, and 72 non-gymnasts) between the ages of 4 and 6 years were recruited into this study and assessed annually for 4 years. A dual-energy X-ray absorptiometry (DXA) image of their hip was obtained. Values of cross-sectional area (CSA), section modulus (Z) and cortical thickness (CT) at the narrow neck (NN), intertrochanter (IT), and shaft (S) were estimated using the hip structural analysis (HSA) program. Multilevel random-effects models were constructed and used to develop bone strength development trajectories (Estimate \pm SE). Once the confounders of size and lifestyle were controlled it was found that gymnasts had 6% more NNCSA than non-gymnasts (0.09 ± 0.02 cm², $p < 0.05$), 7% more NNZ (0.04 ± 0.01 cm³, $p < 0.05$), 5% more ITCSA (0.11 ± 0.04 cm³, $p < 0.05$), 6% more ITZ (0.07 ± 0.03 cm³, $p < 0.05$), and 3% more SCSA (0.05 ± 0.02 cm³, $p < 0.05$). These results suggest that early exposure to low-level gymnastics confers benefits related to geometric and bone architecture properties. Continuous participation in recreational gymnastics offers important benefits for bone strength development in childhood and if maintained it is suggested will improve bone health in adolescence and adulthood.

Disclosures: Adam Baxter-Jones, None.

MO0032

High Fructose and Low Calcium Diet Diminish the Quality of Circumferential Long-Bone Growth. Edek Williams*¹, Devendra Bajaj², Veronique Douard³, Ronaldo Ferraris³, J. Fritton⁴. ¹UMDNJ Graduate School, USA, ²NJ Medical School Orthopaedics, USA, ³NJ Medical School Pharmacology & Physiology, USA, ⁴New Jersey Medical School, USA

High fructose (HF) intake is a public health problem and we recently showed that HF consumption inhibits adaptive increases in intestinal calcium (Ca) transport. However, little is known about effects of HF intake on bone quality during growth. Greater data exists for low calcium (Ca). Three-wk-old male mice were fed for 5 wk with 40% glucose or fructose diets containing normal (0.5%) or low (0.02%) Ca (n=9/group). Weight and long-bone lengths were not affected. Consistent with literature, low-Ca diet resulted in less stiff (~40%; p<0.01) long bone with increased post-yield displacement (>65%, p<0.05) by mid-shaft, 3-point bending. The most striking biomechanical difference with the combined feeding of low Ca plus fructose was loss of the normal linear relationship between stiffness and maximum load sustained (n.s. vs. r > 0.6 for the other 3 groups). By histomorphometry, low Ca resulted in decreased (>20%, p<0.05) cortical width, partially explaining the bending results. Only the glucose-fed group exhibited compensation to maintain outside circumference and diameter by increased periosteal bone formation rate; p.BFR by calcein labels was 3-fold greater vs. each of the other 3 groups (p<0.05). One plausible mechanism for poor circumferential growth involves the deleterious effect of fructose on intestinal Ca transport and the renal step of 1,25(OH)2D3 synthesis. Compared to glucose, the fructose diet completely prevented both adaptive increases in Ca transport, and 1 α -hydroxylase-mediated synthesis of 1,25(OH)2D3 levels; 1 α -hydroxylase protein expression was reduced by 60% (p<0.05). Previously, the serum level of FGF-23, an inhibitor of 1 α -hydroxylase and produced by osteocytes, was demonstrated inversely proportional to 1,25(OH)2D3 serum level. Interestingly, FGF23 level increased in fructose-fed growing male rats compared to glucose. Together these data suggest that HF inhibits Ca reabsorption in the gut via an inhibition effect of FGF23 on 1,25(OH)2D3. With normal Ca diet there is little effect of fructose on intestinal Ca transport and renal 1,25(OH)2D3 synthesis. However, when challenged with low-Ca diet, circumferential bone growth suffers and the type of sugar consumed matters. With HF, compensation to circumferential growth by increased periosteal bone formation is less effective than for equivalent calories of glucose and bone quality may be more adversely affected.

Disclosures: Edek Williams, None.

MO0033

Lack of Association of Fluoride Intake with Girls' Childhood Bone Development Assessed by Dual-Energy X-ray Absorptiometry (DXA). Steven Levy*¹, John Warren², Barbara Broffitt², Elena Letuchy³, Trudy Burns¹, Julie Eichenberger Gilmore¹, James Torner¹, Kathleen Janz¹, Kathy Phipps⁴. ¹University of Iowa, USA, ²University of Iowa College of Dentistry, USA, ³University of Iowa College of Public Health, USA, ⁴University of Oregon, USA

Childhood bone development is important, because early adult peak bone mass is an important determinant of later bone health. Little is known about the possible associations of fluoride intake and childhood bone development and there are no longitudinal studies. Purpose: To assess associations between estimated fluoride (F) intake and dual-energy x-ray absorptiometry (DXA) outcomes in girls at ages 8, 11, 13 and 15. Methods: Prospective cohort study of participants in the Iowa Fluoride Study/Iowa Bone Development Study. The setting was in the general community. Babies without major health problems were recruited at birth from 8 Iowa hospitals (95% white and mostly middle/high SES). Mailed questionnaires and assay of water and beverage sources of participants were used to assess F intake from birth. DXA bone densitometry assessments were conducted at ages 8, 11, 13, and 15. Estimates of fluoride intake were: area-under-the-curve (AUC) of fluoride for: a) approximately 3 years before each bone assessment (n=213), b) birth to 5 years (n=217), and c) birth to DXA scan age (n=237). Physical activity (non-sedentary movement counts per minute) was measured using ActiGraph uniaxial accelerometers. Regression models using SAS PROC MIXED for growth models were developed with random intercept and slope (to allow individual growth trajectories) and were adjusted for height, weight, Tanner stage, maturation offset, and age and maturation offset interaction. The outcome measures were bone mineral content (BMC) of whole body, hip, and lumbar spine and bone mineral density (BMD) of hip and lumbar spine. Due to the multiple hypothesis tests, p<0.01 was considered statistically significant. Results: Approximately 70% received optimally fluoridated water (0.7-1.2 mg/L). There were no statistically significant relationships between fluoride AUC for the approximate 3 years before each scan, the period from birth to 5 years, or birth to scan age and DXA bone outcomes. Results were not changed when adjusted for average physical activity. Conclusions: Results suggest that fluoride intake within the range of intake represented in the study is not associated with normal childhood bone development of girls.

Disclosures: Steven Levy, None.

This study received funding from: NIH (R01-DE09551, R01-DE12101, M01-RR00059, and UL1-RR024979)

MO0034

Pre-menarcheal Development of Vertebral Body Geometry, Density and Strength in Relation to Loading. Jodi Dowthwaite*¹, Paula F. Rosenbaum², Tamara Scerpella³. ¹SUNY Upstate Medical University; Syracuse University, USA, ²SUNY Upstate Medical University, USA, ³University of Wisconsin, USA

Introduction: Maturity-specific bone growth in relation to loading is poorly understood; in particular, lumbar spine studies have been confounded by posterior element BMC and failure to account for 3D geometry. This preliminary longitudinal analysis used paired posteroanterior (PA) and supine lateral (LAT) lumbar spine DXA scans to evaluate growth in L3 vertebral body geometry, density and theoretical strength in relation to physical activity, maturity and height velocity.

Methods: Girls, age 8-16, were recruited for annual paired PA/LAT DXA scans. Annual mean non-aquatic physical activity exposure (PAL, h/wk, including gymnastics) was calculated based on semi-annual questionnaires; gymnasts (GYM) were defined based on gymnastics training \geq 6 h/wk. Physical maturation (MAT) represented pre-puberty (Tanner breast stage I, both scans), pre-puberty/puberty transition (Scan 1= Tanner I, Scan 2= Tanner II+), puberty (Tanner II+, both scans). Data inclusion criteria were: 1) pre-menarcheal data only; 2) 0.85 to 1.15 year inter-DXA intervals (annualized); 3) GYM trained \geq 8/12 months between scans. Analyses evaluated 1 year of pre-menarcheal growth for 56 girls. Isolating vertebral body L3, paired scans yielded: LATBMC, indices of bone geometry (LATheight, PAwidth, LATdepth, PALATvolume, PALATCSA, PAwidth/LATdepth ratio (WDRatio)), density (-PALATBMAD) and strength (PALATIBS (compressive strength), FRI (fracture risk index)). Multiple regression analysis tested height (or height velocity), MAT, PAL and GYM as predictors of vertebral properties at Scan 2, assessing annualized growth velocities over the inter-DXA interval.

Results: Within girls, relative PAL was similar prior to each DXA (pre-Scan 1 vs. inter-scan interval: rho=0.85). Scan 2 height predicted Scan 2 bone geometry (p<0.001). Accounting for height and MAT, GYM predicted Scan 2 LATBMC, BMAD, IBS, FRI (no height) and WDRatio (p<0.05); baseline value entry weakened GYM prediction of LATBMC, BMAD, WDRatio (p=0.05-0.08). Vertebral growth velocities were predicted by height velocity, not PAL or GYM; MAT predicted LATBMC and PALATvolume velocities (p<0.05).

Conclusion: These results suggest that in pre-menarcheal subjects, activity-related vertebral body differences were established during earlier loading/development. Continued exposure to similar relative loading dose maintained activity-related vertebral differences in relation to height velocity/pubertal status.

Disclosures: Jodi Dowthwaite, None.

MO0035

Skeletal Effects of Fat Mass Loss in Obese Adolescents. Brittney Bernardoni*¹, Aaron Carrel², Sijan Wang³, Tamara Scerpella⁴.

¹University of Madison School of Medicine & Public Health, USA,

²University of Wisconsin-Madison Department of Pediatrics, USA,

³University of Wisconsin-Madison Department of Biostatistics & Medical Informatics, USA, ⁴University of Wisconsin, USA

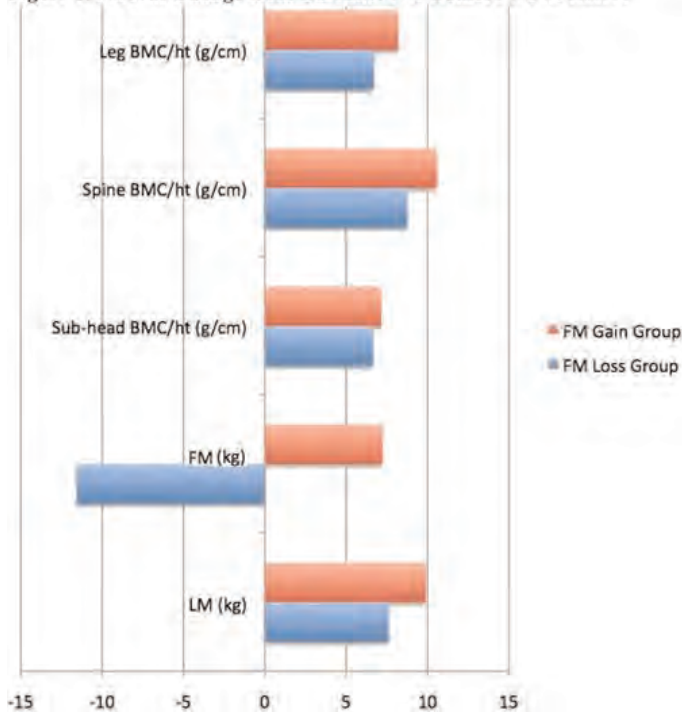
INTRODUCTION: Enhancement of peak bone mass is protective for osteoporosis and nearly half of adult bone mineral content (BMC) is accrued during puberty. As adolescent obesity continues to rise, the effect of excess fat mass (FM) on bone acquisition has become an important area of research. In particular, the effects of weight and FM loss on bone acquisition are unknown. Existing research has shown conflicting evidence, with FM negatively, positively, and not correlated with total BMC.

Purpose: To longitudinally examine the effects of FM loss on BMC acquisition in obese adolescents.

Methods: 55 obese adolescents from a single middle school participated in a randomized controlled study evaluating the effects of a 9-month school-based exercise program. The intervention consisted of 40 minutes of moderate to vigorous activity every other school day; control students continued normal physical education classes. Non-bone lean mass (LM), FM, sub-head BMC, leg BMC, and lumbar spine BMC were assessed pre- and post-intervention using whole-body dual energy x-ray absorptiometry (DXA, Norland XR-36, software version 3.7.4/ 2.1.0). Multiple linear regression analyses explored the effect of the intervention, FM change and LM change on change in BMC/ht at sub-head, spine, and leg regions; other variables included pre-BMC/ht, gender, chronologic age, pre-height, change in height and pre-LM.

Results: Participants included 23 boys and 24 girls, aged 12.8 \pm 0.7 at baseline. From the group as a whole, 23 participants (12 control/11 intervention subjects; 10 males/13 females) lost FM (3.76 \pm 2.47 kg) over the course of the intervention. Gain in FM was positively correlated with gain in BMC for all sites (p<0.005). Neither the intervention nor LM gain was significantly correlated with BMC acquisition. In addition, change in height and pre-LM predicted sub-head and leg BMC acquisition; baseline BMC also predicted leg BMC acquisition.

Conclusions: In this cohort of obese adolescents, bone acquisition was positively correlated with fat mass gains, independent of lean mass gains. Thus FM losses during adolescence may limit bone acquisition and reduce peak mass, with detrimental long-term skeletal health implications. Future research is required to elucidate the relationship between FM and BMC change and to identify interventions that decrease FM while maintaining or increasing BMC.

Figure 1. Percent Change from Baseline: FM Gainers v. FM Losers

figure

Disclosures: *Brittney Bernardoni, None.***MO0036**

The Relationship Between Prepubertal Adiposity, Age of Peak Height Velocity and Bone Strength in Adolescence. Natalie Glass¹, Kathleen Janz¹, James Torner¹, Elena Letuchy¹, Trudy Burns¹, Julie Eichenberger Gilmore¹, Janet Schlechte², Steven Levy¹. ¹University of Iowa, USA, ²University of Iowa Hospital, USA

Purpose: To determine whether prepubertal adiposity in girls is associated with an earlier age of maturation and greater bone mineral content and strength in adolescence.

Methods: 198 girls from the Iowa Bone Development Study, a population-based, longitudinal study, who underwent whole body DXA scans at age 8, height measurements and radial and tibial pQCT scans at age 15 were included in the analyses. Adiposity was defined as fat mass index (FMI, total body fat mass/height²). Tertiles of age 8 FMI were assigned and age 15 bone parameters were compared between tertiles unadjusted and adjusted for age of peak height velocity, height, lean mass and physical activity level.

Results: The highest compared with the lowest age 8 FMI tertile had a significantly younger age of peak height velocity (11.36 ± 0.49 vs. 12.12 ± 0.44 , $p < 0.0001$). In unadjusted analyses, age 15 cortical bone mineral content (BMC), cortical thickness, periosteal circumference, endosteal circumference and strength strain index were higher in the the highest compared with the lowest FMI tertile at the tibia (all $p < 0.05$) and radius except for cortical thickness, which did not significantly differ between groups ($p = 0.0898$). Significant differences were no longer present after adjusting for age of peak height velocity, height, lean mass and physical activity level (all $p > 0.05$).

Conclusions: Prepubertal adiposity is associated with an earlier age of peak height velocity in girls and higher cortical BMC and strength in adolescence. However, adjusted analyses suggest that the higher cortical BMC and strength in adolescence in girls with higher prepubertal FMI may be due to age of peak height velocity, lean mass, physical activity level or other unmeasured factors.

Disclosures: *Natalie Glass, None.*

This study received funding from: NIH, grant #s: R01-DE09551, R01-DE12101, M01-RR00059, and ULI-RR024979

MO0037

Reduced Bone Mass Acquisition in a Mouse Model of Post-Traumatic Stress (PTS). Hongrun Yu^{*}, Heather Watt, Chandrasekhar Kesavan, Jon Wergedal, Subburaman Mohan. Jerry L. Pettis Memorial VA Medical Center, USA

Post-Traumatic Stress Disorder (PTSD) is an anxiety disorder that develops after exposure to life threatening events such as threat of death, serious illness or natural

disasters that evoke intense fear, helplessness and horror. Because post-traumatic stress (PTS) influences the hypothalamic-pituitary-adrenal (HPA) axis, and because of the established role for HPA hormones in regulating bone metabolism, we propose that PTS, which may lead to PTSD, has a negative impact on bone formation. To test this hypothesis, we employed a modified single prolonged stress model in which several stressors such as restraining, forced swimming and electric shock were applied in sequence at one time (within 3 hours) to three week old pre-pubertal C57BL/6J mice. Behavioral change of the animals was monitored by their freezing response to audio cues associated with electric shocks, which is a measure of conditioned fear memory, one of component indicators of PTSD symptoms. Weekly freeze tests indicated that the stressed mice froze significantly longer than the control mice throughout the experiment (average 3.6 vs. 1.7 sec, $p < 0.05$). Evaluation of skeletal phenotypes by PIXImus 2 weeks after the stress treatment revealed that total body bone mineral content (BMC), bone area (B area) and bone mineral density (BMD) were reduced by 10%, 7% and 4%, respectively (all $p < 0.05$) in the stressed mice compared to the control mice. At 3 weeks, BMC and B area were reduced by 13% and 8%, respectively in the lumbar vertebrae, and by 9% and 11%, respectively in the femur. Micro-CT measurements of excised tibia 6 weeks after PTS revealed decreased trabecular bone density (19%) and trabecular number (12%), and increased trabecular spacing (14%) in the stressed vs. control mice (all $p < 0.05$). Based on these data, we conclude that PTS in pre-pubertal mice had a negative impact on bone mass acquisition.

Disclosures: *Hongrun Yu, None.***MO0038**

Circulating Parathyroid Hormone as an Important Determinant on Peripheral Bone Density and Osteoprotegerin in Healthy Korean Adolescents. Wonjin Kim¹, Dong Phil Choi², Hyeon Chang Kim², Yumie Rhee³. ¹College of medicine, Yonsei university, South Korea, ²Department of Preventive Medicine, College of Medicine, Yonsei University, South Korea, ³Department of Internal Medicine, College of Medicine, Yonsei University, South Korea

INTRODUCTION: Bone mineral accretion during adolescent is a critical determinant of low bone mass later in life. Bone mass in this period is known to increase due to the effects of growth and sex hormones. The aim of this study was to find out significant factors associated with bone mass and markers of bone metabolism in a well-designed Korean adolescent cohort group. **METHODS:** Three-hundred one healthy freshmen (aged 15 to 17, mean age 15.4 years old, 153 males and 148 females) from Jangseong high school were recruited in summer of 2008. Heel and forearm bone mineral density (BMD) were measured by dual-X ray absorptiometry (DXA, Osteosys Inc. Seoul, Korea). Meticulous measurement of weight, height, hip and thigh circumference was done. Blood chemistry and hormones such as serum calcium, 25-hydroxy vitamin D₃ (VD), parathyroid hormone (PTH), osteoprotegerin (OPG), osteocalcin (OCN), leptin were measured. **RESULTS:** Boys were 15.5 years old in average, and girls were 15.4 years old. Boys showed higher BMD than girls in both heel and forearm ($p < 0.01$, respectively). Therefore, we analyzed gender-specifically afterwards. In all genders, body mass index (BMI), hip and thigh perimeter showed all significantly positive relation with both heel and forearm BMD ($p < 0.05$ in each parameter). However, regarding biochemical factors, VD positively correlated with peripheral BMD only in male even after adjustment with BMI, hip/thigh circumferences, and all other parameters. In females, BMI independently correlated positively with forearm BMD only, while PTH negatively with heel BMD only after the adjustment ($p < 0.05$, respectively). Interestingly, PTH was positively associated with OPG in both genders ($r = 0.212$ and $r = 0.218$, male vs. females, respectively, $p < 0.05$). However, the significant correlation only remained in males after adjustment with BMI, BMD and VD ($p < 0.05$). **Conclusions:** This study with adolescents in a narrow range of age around 15 revealed that PTH is positively associated with OPG in males and is negatively correlated with heel BMD in females, respectively. VD showed significant positive correlation with BMD at both regions only in males. In conclusion, there are certain gender-specific factors affecting bone accrual in adolescence probably in relation to sex hormones, therefore, exact knowledge of critical factors would be important for the understanding underlying mechanism of peak bone mass.

Disclosures: *Wonjin Kim, None.***MO0039**

Gut-bone Signaling: A Link between Type 1 Diabetes and Osteoporosis. Jing Zhang^{*}, Regina Irwin, Robert Britton, Narayanan Parameswaran, Laura McCabe. Michigan State University, USA

Osteoporosis and fractures are serious complications of type 1 diabetic (T1D) patients. By using pharmacologic (streptozotocin-induced, STZ mice) as well as spontaneous (Ins2^{+/+} mice) T1D adolescent and adult mouse models, we demonstrate that T1D induced bone trabecular and cortical bone loss. Serum osteocalcin and vitamin D levels are decreased while TRAP5 levels are increased in young T1D mice indicating reduced bone formation and elevated bone resorption. The underlying mechanisms for T1D bone loss can be multifaceted. Given the important role of the intestine and calcium absorption in regulating bone density we examined intestinal calcium binding protein (CaBP) expression in the jejunum. Consistent with vitamin D

deficiency, vitamin D regulated genes such as CaBP9K, CaBP28K and TRPV6 (calcium channel) were suppressed, which would impair calcium absorption. Next, we examined the intestinal microbiota which has been demonstrated to alter vitamin D and intestinal calcium binding protein expression. We found that T1D increases jejunal levels of firmicute bacteria while bacterioidete bacteria levels are decreased compared to the control mice. Regional microbial community changes could affect the gut and also modify gut-bone signals. FACS and cytokine analyses support a role for altered gut and bone inflammation with increased T-cells in the marrow of T1D mice. Taken together, we have identified an alternative mechanism of T1D bone pathology, gut-bone signaling, that could provide the basis for therapeutic targets approaches to improve T1D patient bone health.

Disclosures: Jing Zhang, None.

MO0040

Leptin but not Osteocalcin relates to Insulin Resistance in Early Pubertal Children. Kathleen Hill^{*1}, Emma Laing², Ashley Ferreira², Berdine Martin³, Anthony Acton⁴, Connie Weaver³, Richard Lewis², Munro Peacock⁵. ¹Indiana University School of Medicine, USA, ²The University of Georgia, USA, ³Purdue University, USA, ⁴Indiana University, USA, ⁵Indiana University Medical Center, USA

Purpose: Lower serum osteocalcin in obese children and inverse associations between leptin and osteocalcin and osteocalcin and insulin resistance in children have been reported (Reinehr 2010 Int J Obes 34:852), which suggests that osteocalcin may link fat, bone and energy metabolism. The purpose of this study was to investigate the relationship among serum leptin, osteocalcin, and glucose and insulin in early pubertal children.

Methods: Baseline data from 318 healthy black and white boys and girls (pubertal stage 2 or 3) who participated in a 12-week oral vitamin D intervention study were analyzed. Height and weight were obtained and body composition determined by DXA. Fasting serum insulin, glucose, leptin, osteocalcin, bone alkaline phosphatase (BAP) and urine N-telopeptides of type I collagen (NTX) were measured. Homeostasis Model of Assessment (HOMA) estimate of insulin resistance was calculated (fasting glucose mg/dL x fasting insulin μ U/mL/405). Non-normal data were transformed. Mean differences between obese ($\geq 95^{\text{th}}$ BMI percentile, n = 68) and non-obese (n = 250) children were evaluated by ANCOVA (covariates of age, pubertal stage, and race were included when significant). Relationships among variables were evaluated using linear regression.

Results: Obese children had higher BMI (27 vs. 18 kg/m²), %body fat (39 vs. 26%), and leptin (18 vs. 6 ng/mL). Osteocalcin was lower in obese children (27 vs. 33 ng/mL, p < 0.01), but other measures of bone turnover, NTX and BAP, were not different. Obese children had greater insulin resistance (HOMA-IR = 5.3 vs. 3.7, p < 0.01) and fasting insulin (25 vs. 17 μ U/mL, p < 0.01), but fasting glucose was not different between obese and non-obese (both 89 mg/dL, p = 0.8). Leptin was positively associated with % body fat, insulin resistance, fasting insulin, and fasting glucose (r=0.88, 0.54, 0.55, 0.13, respectively, p < 0.05). Leptin was negatively associated with osteocalcin (r = -0.17, p < 0.01), but not with BAP or NTX; however, there was no relationship between osteocalcin, insulin resistance, fasting insulin, or fasting glucose.

Conclusions: These data confirm that obese children have lower osteocalcin than non-obese children and there is a negative association between leptin and osteocalcin. However, the data do not support a clinically relevant osteocalcin-mediated pathway between bone and energy metabolism.

Disclosures: Kathleen Hill, None.

MO0041

Serum Homocysteine Levels in Children with Fractures and Low Bone Mineral Density. A Pilot Study. Stepan Kutilek^{*1}, Vladimir Nemecek², Petra Rehackova³. ¹Pardubice Hospital; Faculty of Health Studies; University of Pardubice, Czech Republic, ²Consultant; Head of Pediatric Dept., Czech Republic, ³Study Coordinator, PhD Student, CCBR Czech Republic, Czech Republic

Background: High serum homocysteine (S-Hcy) levels are associated with low bone mineral density (BMD) and increased fracture risk in postmenopausal women. So far, data on S-Hcy and bone health are lacking in children and adolescents.

Patients, Methods: We assessed S-Hcy levels in 19 children and adolescents (12 boys and 7 girls; mean age 14.9 \pm 3.3 years) with prevalent low-energy trauma fractures (mean 4 \pm 2.6 per patient) and/or low spinal L1-L4 BMD (below -2SD Z-score; DXA Lunar GE). Other assessments included serum alkaline phosphatase (S-ALP) and serum CrossLaps. At the time of assessment, the children were not taking any drugs known to influence bone metabolism. To eliminate the influence of age, the obtained results were expressed as Z-scores \pm SD.

Results: S-Hcy Z-score was significantly higher (1.4 \pm 1.8; p=0.001) and L1-L4 BMD Z-score was significantly lower (-2.1 \pm 1.3; p=0.0001), respectively, in comparison with reference values. S-ALP did not differ from reference values (p=0.91), while S-CrossLaps were higher (1.5 \pm 1.9; p=0.001). S-Hcy was inversely correlated to L1-L4 BMD (r = -0.66; p=0.01) and S-ALP (r = -0.56; p=0.03) and not related to number of prevalent fractures (r=0.11) or S-CrossLaps (r = -0.14). These results suggest negative influence of elevated S-Hcy on bone formation and BMD in children with fractures, while bone resorption was increased in this group of pediatric

patients. In conclusion, our results suggest that elevated S-Hcy is a risk factor of impaired bone health in children and adolescents. Further studies are necessary for more detailed clarification of these issues.

Disclosures: Stepan Kutilek, None.

MO0042

Impact of Vitamin D Supplementation on Gross Motor Development: The Result of a Randomized Dose-response Trial in Canada. Brandy Wicklow^{*1}, Sina Gallo², Annette Majnemer², Catherine Vanstone², Sherry Agellon², Kathryn Comeau², Glenville Jones³, Mary L'Abbe⁴, Ali Khamessan⁵, Atul Sharma², Hope Weiler², Celia Rodd². ¹University of Manitoba, Canada, ²McGill University, Canada, ³Queen's University, Canada, ⁴University of Toronto, Canada, ⁵EURO-PHARM INERNAIONAL CANADA INC, Canada

Evidence suggests vitamin D plays an important role in skeletal muscle development in addition to its role in calcium homeostasis and bone mineralization. Profound deficiency has been associated with lower muscle mass, increased body sway, and features of proximal myopathy. To date there is little data assessing the effect of vitamin D on muscular development and motor function in typically developing infants.

Objective: To determine the effect of plasma 25-OH-D3 status on gross motor development in healthy term infants.

Study Design: This was a prospective cohort sub-study of 55 healthy infants randomized at 1 month of age to 400 IU (n=19), 800 IU (n=18) or 1200 IU (n=18) vitamin D3/d consecutively recruited from a larger clinical trial (ClinicalTrials.gov #NCT00381914). Motor performance at 3 and 6 months of age was quantified by the Alberta Infant Motor Scale (AIMS). Plasma vitamin D metabolites were measured by tandem mass spectrometry (LC-MS/MS, Warnex Inc, Laval, Qc). Data were analyzed by factorial analysis of variance using SPSS 19.0.

Results: Infants did not differ in plasma 25-OH-D3 concentrations or anthropometry. AIMS scores did not differ at the 3 month assessment, but total scores and sitting sub-scores were significantly higher at the 6 month assessment in infants receiving 400 IU vitamin D3 compared to the 800 IU and 1200 IU supplement groups, p<0.005. Prone sub-scores were higher in infants receiving 400 IU compared to the 800 IU group. (Table 1). This translates to developmental advancement of approximately 1month in infants receiving 400 IU/d, particularly in the sitting position despite all infants having normal 6 month AIMS scores. At 6 months, anthropometry did not differ significantly among treatment groups; as expected plasma concentrations of 25-OH-D3 and the C-3 alpha epimer of 25-OH-D3 differed significantly between the 400 IU and both 800 IU and 1200 IU groups (Table 1). Preliminary analyses suggested that higher concentrations of 25-OH-D3 or C-3 alpha epimer of 25-OH-D3 were associated with lower AIMS scores.

Conclusions: Although all infants had normal gross motor development at 6 months, development in those infants receiving the recommended 400 IU/d dose was significantly enhanced. While the search for explanatory confounders continues, it remains unclear why the recommended 400 IU/day vitamin D supplementation is associated with better acquisition of developmental milestones and skeletal muscle function.

Table 1. Characteristics of infants at 6 months of age receiving 400 IU, 800 IU or 1200 IU daily of vitamin D3 supplementation.

| | Gender (% male) | Age (days) | 25-OH-D ₃ (nM) | 3-epi-25-OH-D ₃ (nM) | 24,25 (OH) ₂ D ₃ (nM) | AIMS Prone | AIMS Supine | AIMS Sit | AIMS Total |
|----------------|-----------------|------------|---------------------------|---------------------------------|---|------------------------|-------------|------------------------|-------------------------|
| 400 IU (n=19) | 47 (9/19) | 187 (8.3) | 81.3 (25.5) | 12.4 (7.4) | 10.8 (5.6) | 10.5 (2.3) | 7.7 (1.1) | 6.6 (1.8) | 27.5 (4.6) |
| 800 IU (n=18) | 61 (11/18) | 183 (4.4) | 100.5 (25.7) | 17.0 (11.9) | 12.2 (6.0) | 8.8 [†] (1.7) | 7.0 (0.6) | 5.4 [†] (1.4) | 23.9 [†] (2.7) |
| 1200 IU (n=18) | 61 (11/18) | 184 (7.1) | 115.7 [†] (40.6) | 24.4 [†] (14.0) | 15.6 (7.1) | 9.0 (2.0) | 7.3 (0.8) | 5.3 [†] (1.1) | 24.2 [†] (3.1) |

Data are presented as means (standard deviation) or percent (proportion). [†] p value < 0.005 compared to the 400 IU group.

Table

Disclosures: Brandy Wicklow, None.

MO0043

Therapeutic Effects of Hematopoietic Stem Cell Transplantation in Osteogenesis Imperfecta. Meenal Mehrotra^{*1}, Makio Ogawa², Amanda LaRue³. ¹Research Services, Ralph H Johnson VAMC & Medical University of South Carolina, USA, ²Department of Pathology & Laboratory Medicine, medical university of South Carolina, USA, ³Ralph H. Johnson VAMC Medical University of South Carolina, USA

Osteogenesis Imperfecta (OI), a genetic disorder resulting from the abnormal amount and/or structure of Type I collagen, is the most common hereditary bone disease. It is characterized by fragile bones that fracture upon little or no trauma and skeletal deformities. Presently there is no cure for OI. Ideally, therapy should be directed towards improving the production and integrity of the secreted collagen. Clinical trials using bone marrow stem cells in a small number of children with severe forms of OI have shown promising results with increased growth velocity, total body

mineral content and fewer fractures. Although bone marrow transplantation shows potential, there is a controversy regarding the cell involved. While current dogma states that bone marrow contains two types of stem cells, hematopoietic stem cells (HSCs) and mesenchymal stem cells (MSCs), recent studies have begun to question this distinction. Our preliminary data shows that osteoblasts can also be derived from the HSC. Therefore, we hypothesize that HSC transplantation should lead to replacement of affected osteoblasts with normal cells in turn correcting collagen defects in bone and preventing OI pathologies. We tested this hypothesis using transplantation of bone marrow cells highly enriched for HSCs from transgenic enhanced green fluorescent protein (EGFP) mice into irradiated homozygous OI mice (*oim*; B6C3Fe *ala-Coll1a2^{tm1/J}*). After confirming multilineage engraftment, bone parameters were temporally analyzed using longitudinal micro-computed tomography (micro-CT). Dramatic improvements were observed in 3D micro-CT images which correlated with histomorphometric assessment of bone parameters including an increase in bone volume, trabecular number and trabecular thickness with a concomitant decrease in trabecular spacing. Longitudinal analysis of control mice showed continued deterioration in bone parameters. Engrafted mice gained weight and became less prone to spontaneous fractures while the control mice worsened clinically and eventually developed kyphosis. Paraffin sections of decalcified bones showed the presence of numerous EGFP⁺ cells within the bone. The majority of the EGFP⁺ cells stained positive for Runx-2, demonstrating that they were osteoblasts and osteocytes as well as their origin from the HSC. Long term, these findings have the potential to identify HSC transplantation as the therapy of choice for this collagen disorder.

Disclosures: Meenal Mehrotra, None.

MO0044

In vivo Precision of Magnetic Resonance Imaging based Measures of Bone Structure and Strength at the Femoral Neck. James Johnston*, Leina Liao, Nguyen Nguyen, David Leswick, Saija Kontulainen, University of Saskatchewan, Canada

Purpose: The femoral neck is a common site of hip fracture. Currently available clinical imaging techniques used to assess femoral neck strength, including dual energy x-ray absorptiometry (DXA) and computed tomography (CT), are limited. DXA is a 2D imaging technique which cannot measure 3D bone structure. CT can measure 3D bone structure but both CT and DXA are radiological techniques which expose subjects to ionizing radiation. Magnetic resonance imaging (MRI), a 3D imaging technique offering non-ionizing radiation, has potential for assessing 3D bone properties at the femoral neck. The objective of this study was to determine the in vivo precision of MRI-based measures of bone geometry and strength at the femoral neck.

Methods: Left femoral neck region of 14 subjects (5M:9F; age:21-68) were scanned 3 times using a 1.5T MRI (MAGNETOM Avanto, Siemens) with a T1-weighted spin-echo sequence (parameters: TR=12.7 ms, TE=7.14ms, 3 excitations, 10° flip angle, 0.49x0.49x5mm voxel size). Participants were positioned in a supine position with legs extended and externally rotated 15°. Participants were repositioned after a short walk between scans. Image processing software (ANALYZE 10, Mayo Foundation) was used to semi-automatically delineate the endosteal and periosteal boundaries of the femoral neck. Using custom algorithms (MATLAB, Mathworks, Inc.), bone structural properties were derived from the images, including: total area (TotA), cortical (CorA) and trabecular (TrabA) area, and cortical wall thickness (Cwt) (Figure 1). Bone strength parameters were also derived from images, including maximum and minimum principal moment of inertia (Imax and Imin), which indicate bending resistance of the femoral neck (Figure 1). Short-term in vivo precision of bone geometry and strength properties was assessed using root mean square coefficient of variation (CVrms%).

Results: Descriptive statistics (mean, standard deviation and range) and precision errors of MRI-based measures of bone geometry and strength are reported in Table 1. For geometrical properties, precision errors ranged between 1.8% (TotA) and 9.2% (CorA). For strength properties, precision errors were 10.4% (Imin) and 10.8% (Imax).

DISCUSSION AND CONCLUSION: MRI-based measures of bone at the femoral neck demonstrated in vivo precision errors < 11%. MRI is a promising 3D technique for monitoring changes in bone structure and strength at the clinically important femoral neck.

Table 1. Descriptive statistics (mean, standard deviation (SD), range) and precision errors (CV%) with respect to derived geometrical and strength properties.

| Bone Variable | TotA, mm ² | CorA, mm ² | TrabA, mm ² | Cwt, mm | Imax, mm ⁴ | Imin, mm ⁴ |
|---------------|-----------------------|-----------------------|------------------------|-----------|-----------------------|-----------------------|
| Mean | 698 | 124 | 569 | 1.49 | 15420 | 12540 |
| (SD) | (114) | (16.6) | (106) | (0.17) | (3968) | (4402) |
| Range | 510-984 | 93.5-159 | 397-839 | 1.12-1.87 | 10440-25420 | 7109-23330 |
| CV% | 1.8 | 9.2 | 2.3 | 8.7 | 10.4 | 10.8 |

Table 1

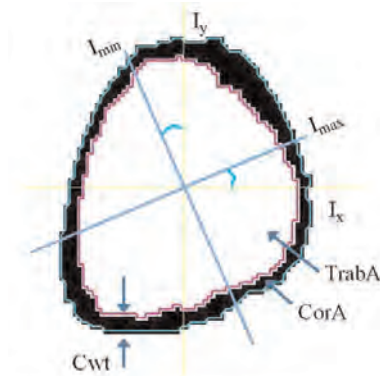


Figure 1: Illustration of bone geometrical parameters (trabecular area – TrabA; cortical area – CorA; cortical wall thickness – Cwt) and strength parameters (maximum area moment of inertia – Imax, minimum area moment of inertia – Imin) derived from magnetic resonance images of the femoral neck.

Figure 1

Disclosures: James Johnston, None.

MO0045

Association of Prevalent Vertebral Fractures with Bone Density and Strength at the Thoracic and Lumbar Spine in Men and Women. Mary Bouxsein^{*1}, Alexander Bruno², Qiong Louie-Gao³, Dennis Anderson¹, Brett Allaire⁴, Douglas Kiel⁵, Tony Keaveny⁶, Serkalem Demissie³, David Kopperdahl⁷. ¹Beth Israel Deaconess Medical Center, USA, ²Harvard-MIT, USA, ³Boston University School of Public Health, USA, ⁴Center for Advanced Orthopedic Studies, Beth Israel Deaconess Medical Center, USA, ⁵Hebrew SeniorLife, USA, ⁶University of California, Berkeley, USA, ⁷O.N. Diagnostics, USA

Vertebral fractures (Vfx) occur most commonly in the mid-thoracic and thoraco-lumbar regions. Yet most spinal imaging for BMD measurements is done in the lumbar spine as the overlying ribs interfere with 2D measurements in the thoracic spine. In a cohort with QCT scans of the lumbar and thoracic spine, we asked whether bone density or strength measurements at the thoracic spine were more strongly associated with Vfx than measures at the lumbar region. We studied 40 subjects (22 M, 18 W) with moderate or severe prevalent Vfx (25 Vfx in thoracic, 14 in lumbar, 1 in both) and 80 age- and sex-matched controls with no Vfx (2:1 matching). Mean age of subjects was 67.8 ± 9.3 yrs. We used conditional logistic regression to determine the association between prevalent Vfx and integral (IntBMD), trabecular (TbBMD) and cortical (CtBMD) bone density; total, trabecular and cortical strength estimated by finite element analysis; and the compressive load:strength ratio (L:S) for anterior flexion with 10 kg weights in the hand at lumbar (L3) and thoracic (T10) vertebrae. We found that prevalent Vfx were more strongly associated with lumbar than thoracic bone measures (Table). For example, odds ratio (OR, per 1 SD decline) for density variables ranged from 3.7 – 3.9 at L3 compared to 1.7 – 2.6 at T10; and for FE-derived strength variables from 2.8 – 4.5 for L3 vs. 1.7 – 2.6 at T10. We also found that associations between prevalent Vfx and bone density or FE-estimated bone strength were stronger in women than men at both spine regions. Thus, in women the highest ORs occurred for FE-estimated strength of the L3 Tb centrum (OR=11.8) and whole vertebrae (OR=10.7), but the corresponding OR were not significant in men. Acknowledging the small number of Vfx cases, we conclude that bone density and strength measures in the lumbar spine are more sensitive in discriminating prevalent Vfx than those in the thoracic spine despite many Vfx occurring in the mid-thoracic and thoraco-lumbar regions. Further, the association between prevalent Vfx and both density and strength may be different in men and women. In contrast to women, in men prevalent Vfx were less strongly associated with low bone density and strength, suggesting that these fractures may be due to prior traumatic loading events rather than skeletal fragility. A better understanding of the origins of these sex-differences in factors related to Vfx may improve assessment of future fracture risk.

Risk of prevalent VFX, expressed as odds ratio (OR, 95% CI) per 1 SD decrease in all subjects, men only and women only.

| | Combined (40 VFX, 80 Cont) | Men (22 VFX, 44 Cont) | Women (18 VFX, 36 Cont) |
|----------------|-------------------------------|--------------------------|----------------------------|
| L3 | | | |
| IntBMD | 3.9 (1.9 – 8.2) | 2.7 (1.1 – 6.4) | 5.3 (1.7 – 17.1) |
| TbBMD | 3.9 (1.8 – 8.2) | 2.5 (1.1 – 5.8) | 6.0 (1.8 – 20.3) |
| CtBMD | 3.7 (1.8 – 7.8) | 2.8 (1.1 – 6.9) | 4.3 (1.5 – 12.6) |
| Strength_FE | 3.5 (1.5 – 8.2) | 1.9 (0.9 – 4.1) | 10.7 (1.8 – 64.1) |
| TbStrength_FE | 2.8 (1.3 – 6.2) | 1.7 (0.9 – 3.3) | 11.8 (1.8 – 79.3) |
| CtStrength_FE | 4.5 (1.7 – 12.2) | 2.5 (0.9 – 7.2) | 6.8 (1.6 – 29.1) |
| Load:Strength* | 2.8 (1.5 – 5.5) | 1.8 (0.9 – 3.4) | 4.0 (1.4 – 11.6) |
| T10 | | | |
| IntBMD | 2.3 (1.3 – 4.1) | 1.9 (0.9 – 3.9) | 2.5 (1.1 – 5.8) |
| TbBMD | 2.6 (1.4 – 4.9) | 2.1 (1.0 – 4.3) | 3.1 (1.3 – 7.8) |
| CtBMD | 1.7 (1.0 – 2.9) | 1.6 (0.9 – 3.0) | 1.8 (0.9 – 3.6) |
| Strength_FE | 2.0 (1.1 – 3.7) | 1.6 (0.9 – 2.9) | 2.4 (1.0 – 5.8) |
| TbStrength_FE | 1.9 (1.0 – 3.4) | 1.5 (0.9 – 2.7) | 2.6 (1.0 – 6.6) |
| CtStrength_FE | 2.0 (1.1 – 3.5) | 1.7 (0.9 – 3.2) | 2.1 (0.9 – 4.6) |
| Load:Strength* | 2.2 (1.2 – 3.8) | 2.0 (0.9 – 4.5) | 2.2 (1.0 – 4.6) |

Bold indicates significant OR (p<0.05); * per 1SD increase

Table

Disclosures: *Mary Bouxsein, None.*

MO0046

Association of Trabecular Bone Score (TBS) with Mechanical Behavior of Human Lumbar Vertebrae. Jean-Paul Roux^{*1}, Julien Wegrzyn², Stephanie Boutroy³, Mary Bouxsein⁴, Didier Hans⁵, Roland Chapurlat⁶. ¹INSERM, UMR 1033, Université de Lyon, France, ²INSERM U1033 - Université de Lyon, France, ³Columbia University Medical Center, USA, ⁴Beth Israel Deaconess Medical Center, USA, ⁵Lausanne University Hospital, Switzerland, ⁶E. Herriot Hospital, France

The measurement of areal bone mineral density (aBMD) does not predict at least half of fragility fractures, but assessment of bone microarchitecture may improve this prediction. The trabecular bone score (TBS) is a grey-level measure of texture using a modified version of experimental variogram and can be extracted from DXA images (Pothuaud L. et al., Bone 42, 2008: 775-787). The aim of the current study was to assess whether the TBS is associated with the mechanical behavior of human lumbar vertebrae.

Lumbar vertebrae (L3) were harvested fresh from 16 human donors (7 men, 9 women, age: 82 ± 8 yrs for men and 72 ± 11 yrs for women). The antero-posterior and lateral BMC (g) and aBMD (g/cm²) of the vertebral body were measured using DXA (Delphi W, Hologic) and then the TBS was extracted using TBS iSight software (Medimaps SA, France). The trabecular bone volume (Tb.BV/TV), trabecular thickness (Tb.Th), degree of anisotropy (DA), and structure model index (SMI) were measured using μ CT with a 35- μ m isotropic voxel size (Skyscan1076). Quasi-static uniaxial compressive testing was performed on L3 vertebral bodies under displacement control (0.5mm/min) to assess failure load (FL, N) and stiffness (STF, N/mm).

The TBS was significantly correlated to Tb.BV/TV, SMI and stiffness (r=0.58, -0.62 and 0.64; p<0.02 for all), borderline not significant with FL but not with BMC or BMD. In bivariate regressions, STF was associated with TBS (r=0.64), lateral BMD (r=0.53) and apBMC (r=0.49)(all p<0.05). FL was associated with SMI (r=-0.56, p=0.03) and lateral BMD (r=0.49, p=0.05) and TBS (r=0.46, p=0.07). Using stepwise regressions, the combination of TBS (first step, p=0.003), Tb.Th (second step, p=0.002) and apBMC (third step, p=0.008) was strongly associated with STF (multiple R=0.89, p<0.001). There was no other significant predictor of bone stiffness.

In conclusion, the TBS was significantly correlated to the most relevant microarchitectural parameters associated with vertebral biomechanical properties (i.e. Tb.BV/TV and SMI). In addition, the combination of TBS, Tb.Th and BMC explained up to 79% of the variability of the stiffness. These initial results suggest that TBS might improve assessment of vertebral strength in combination with standard DXA measurements.

Disclosures: *Jean-Paul Roux, None.*

MO0047

Biological Co-adaptation of Morphological and Composition Traits in Weight-bearing and Non-weight Bearing Bones of Baboons. Lynn Copes^{*1}, Steven Tommasini², Tarjit Patel³, Steven Leigh⁴, Robin Bernstein⁵.

¹George Washington University, USA, ²Yale University School of Medicine, USA, ³Department of Orthopaedics, Washington University, USA, ⁴Department of Anthropology, University of Illinois, USA, ⁵Department of Anthropology, George Washington University, USA

Having a slender bone (narrow width relative to length) has been shown to be a major predictor of fracture and fragility. Recent work examining mouse femora and human tibiae demonstrated that slender bones relative to length had thicker cortices and higher tissue mineral density, whereas relatively robust bones had thinner cortices and lower tissue mineral density. This project examined the relationship between morphology and tissue quality in weight-bearing and non-weight bearing bones in adult male (n=13) and female (n=21) captive baboons (*Papio anubis*) as part of a larger study investigating the role hormones may play on the co-variation of these traits. If the co-adaptation of shape and tissue mineralization is a mechanism by which bone genetically programmed to be slender achieves functionality, it is expected that the correlation between bone shape and quality will be higher in weight-bearing relative to non-weight bearing bones. Tissue mineral density (TMD), cortical thickness (CtTh), and two measures of bone slenderness: total subperiosteal area / length (TtAr/Le) and polar moment of inertia / length (J/Le) of the midshafts of the right femur, tibia, humerus, radius, ulna and clavicle, as well as single right rib from each baboon was measured via μ CT. In the case of the ribs, length was replaced with maximum height of the area scanned. We found that the co-adaptation of traits was site-specific, and in some cases, sex-specific. For example, in the tibia and radius, the expected inverse relationship between CtTh and TtAr/Le exists in both sexes and the combined sample, but in the femur and humerus, no such relationships were found, indicating proximal and distal elements may coordinate variables differently. The ulna, clavicle, and rib showed significant positive (rather than inverse) relationship between J/Le and TMD and CtTh, but the three bones have three different patterns of relationship between TtAr/Le and bone quality (ulna: positive; clavicle: none; rib: inverse). The variation between patterns of biological co-adaptation in bones with similar morphology and function (i.e., radius and ulna) indicates that there may be more than one mechanism responsible for the coordination of bone robusticity and tissue quality across the skeleton. Our findings have broad application for both clinicians interested in predicting fracture risk and to anthropologists attempting to reconstruct the physiological environments in which humans evolved.

Disclosures: *Lynn Copes, None.*

MO0048

Bone Marrow Edema and Structural Alterations in Bone Microarchitecture. Afrodite Zendeli^{*1}, Christian Muschitz², Roland Kocian³, Heinrich Resch⁴. ¹Austria, ²St. Vincent's Hospital, Austria, ³St. Vincent Hospital Vienna, Austria, ⁴Medical University Vienna, Austria

Background: Bone marrow edema (BME) is a localised painful bone lesion which is diagnosed by MRI. Ischemia, osteoarthritis, local osteoporosis and bone bruise/stress fractures are possible pathophysiological pathways. Less data are available on bone micro structure of cortical and trabecular sites measured by high-resolution peripheral quantitative computed tomography (HR-pQCT). The aim of this cross-sectional pilot study was to investigate bone mineral density (BMD) measured by DXA, bone micro structure and serum BTM values in patients with BME compared to age matched healthy controls (HC). Methods: We compared 11 non osteoporotic patients (mean 50.2 ± 12 ys) with MRI diagnosed atraumatic BME of lower limb (2 femoral head, 4 proximal tibia, 5 foot) to 22 age matched healthy controls. All subjects had DXA of spine/hip, a HR-pQCT examination of distal radius and tibia as well as serum examinations of fasting intact amino terminal propeptide of type I procollagen (PINP), type I collagen cross-linked C-telopeptide (CTX), 25OH vit D3, intact parathyroid hormone (iPTH). Results: All subjects presented osteopenic BMD values measured by DXA at spine and hip without statistical difference between the groups. BTMs of formation and resorption did also not differ from HC. In the HR-pQCT measurements BME patients compared to HC had increased total bone area (TotalArea) at the radius (285.7 ± 55 vs 248 ± 48 mm², p<0.05) and at the tibia (744.3 ± 242 vs 655.3 ± 122.1 mm², p=0.08) as well as a significantly increased cortical perimeter (Ct.Pm) and trabecular area (TrabArea) at the radius (p<0.05 for both), but a reduced density of inner trabeculae (Dinn) and trabecular separation (Tb.Sp) (0.42 ± 0.15 vs 0.51 ± 0.07 mm, p<0.05). At the tibia the trabecular thickness (Tb.Th) (0.07 ± 0.01 vs 0.08 ± 0.01 mm, p<0.05) and the density of the compacta (Dcomp) (799.9 ± 69.8 vs 835.9 ± 72.7 mgHA/ccm, p=0.092) was lower, but trabecular number (Tb.N) exceeded controls (1.81 ± 0.3 vs 1.67 ± 0.24 I/mm, p=0.084). Conclusions: Our data show no predictive value of BMD measurements by DXA or serum BTMs. HR-pQCT measurements detect a pattern of structural differences at cortical, but to a greater extent at trabecular sites of radius and tibia with an increased number, but thinner structure of trabeculae. This distinction in microarchitecture could trigger the susceptibility to local bone marrow edema.

Disclosures: *Afrodite Zendeli, None.*

MO0049

Bone Quality by TBS, BMD and Sex Steroids Levels in Normal Men. Mário Rui Mascarenhas¹, Ana Paula Barbosa², Vera Simões³, Ana Gonçalves⁴, David Santos Pinto⁵, Manuel Bicho⁶, Didier Hans⁷, Isabel do Carmo⁴.

¹Lisbon's Faculty of Medicine, Santa Maria University Hospital, CHLN,EPE, Portugal, ²Endocrinology, Santa Maria Hospital & Faculty of Medicine, Portugal, ³Endocrinology & Metabolism Centre (Genetics Lab) of Lisbons Faculty of Medicine, Osteoporosis Unit - CEDML, Lda, Portugal, ⁴Endocrinology, Diabetes & Metabolism Department, Santa Maria University Hospital, CHLN-EPE, Portugal, ⁵CEDML - Lisbon's Endocrinology, Diabetes & Metabolism Clinic (Osteoporosis Unit), Portugal, ⁶Metabolism & Endocrine Centre (Genetics Lab) of Lisbons Faculty of Medicine, Portugal, ⁷Lausanne University Hospital, Switzerland

Rational: The bone mass and the sexual steroids, in adult males, seem to decline slowly with the aging process. The impact of the androgens on the age-related BMD alterations in the male is still controversial. The bone strength is mostly dependent on BMD and bone structure. The trabecular bone score (TBS) is determined from grey-level variation analysis of the DXA images using the experimental variogram method to estimate bone micro-architecture. Although many studies are available in women, the data about the bone micro-architecture are very scarce in men. The aim of this study is to evaluate the relationship between the lumbar spine bone quality as assessed by TBS, the spine and hip BMD as well as the total testosterone levels in a group of normal adult men.

Materials and Methods: In a group of 80 normal adult men (53.5 ± 16.6 years old), the lumbar spine and hip BMD (g/cm²) were evaluated by DXA (Discovery W, Hologic Inc., USA). Site matched spine TBS was derived for each spine DXA scan (TBS iNsite software, Medimaps SA, France). Fasting blood collection was also performed to measure the total testosterone and sex hormone binding globulin (SHBG) plasma levels. Free androgen index (FAI) and the BMI (kg/m²) were calculated. Adequate statistical tests were used.

Results: In this group of men, the obtained means (±SD) were: height=1.719(±0.07) m, weight=82.7(±14.1) kg, BMI=27.9(±4.4) kg/m² lumbar spine BMD=1.065(±0.2) g/cm², femoral neck BMD=0.903(±0.2) g/cm², lumbar spine TBS=1.351(±0.1), total testosterone=5.5(±1.7) ng/ml, SHBG=31.3(±15.8) nmol/l and FAI=21.7 (±7.8). The correlation coefficients between spine TBS and other parameters are in the Table 1.

Conclusions: The weak correlation between spine TBS and BMD confirms that TBS is measuring other bone properties than BMD. The results of this study suggest that bone quality assessed by TBS is marginally influenced by height, weight and BMI and to a larger extent by age. In addition, it seems that the total testosterone levels are also playing a role on bone quality (TBS). Indeed, normal men with a low total testosterone plasma levels may tend to have diminished BMD and bone quality and thus weaker bone strength.

Acknowledgements: Medimaps (Medimaps, Bordeaux, France) and Radilan (Lisboa, Portugal) for the kind free access and use of the TBS iNsite software for this study

| Spine TBS vs. | CC | P |
|--------------------------------|---------|--------|
| Age years | -0.3342 | 0.0024 |
| Height m | 0.3349 | 0.0024 |
| Weight kg | -0.2380 | 0.0335 |
| BMI kg/m ² | -0.4417 | 0.0000 |
| Spine BMD g/cm ² | 0.1989 | NSD |
| Femoral neck g/cm ² | 0.2458 | 0.0279 |
| Total testosterone ng/ml | 0.2400 | 0.0320 |
| FAI | 0.2272 | 0.0427 |

NSD = Non significant difference

Table 1. Correlation coefficients between spine TBS and other parameters.

Disclosures: Mário Rui Mascarenhas, None.

MO0050

Changes in Cortical Density and Microstructure in Pre- and Post-menarcheal Girls: A 12-month HR-pQCT Study. SoJung Kim¹, Heather Macdonald¹, Lindsay Nettlefold², Leigh Gabel¹, Heather McKay¹. ¹University of British Columbia, Canada, ²Centre for Hip Health & Mobility, Canada

Rising estrogen levels at menarche are associated with reduced bone turnover that in turn, leads to decreased rates of intracortical remodeling and increased cortical bone mineral density (BMD). However, we know little about changes in both cortical and trabecular bone microstructure in post-menarcheal girls. Therefore, we describe 12-month changes in bone microstructure, BMD and estimated bone strength in pre- and post-menarcheal girls; participants in the ongoing Healthy Bones III Study. We assessed 52 pre-menarcheal (PRE, 10.4 ± 0.6 yrs) and 86 post-menarcheal girls (POST, 17.6 ± 2.4 yrs), measured in spring, 2009 and spring, 2010. We measured height, weight and forearm length using standard methods and assessed menarche status, physical activity (PA), and calcium intake (Ca²⁺) by self-report questionnaire.

We used high-resolution peripheral quantitative computed tomography (HR-pQCT, Scanco Medical, Switzerland) to assess BMD, bone microstructure and strength at the non-dominant distal radius (7% site). We performed a standard morphologic analysis to determine total BMD (Tt.BMD), trabecular bone volume fraction (BV/TV), trabecular number (Tb.N), thickness (Tb.Th) and separation (Tb.Sp). We used a customized automated segmentation algorithm to determine cortical BMD (Ct.BMD), porosity (Ct.Po), and thickness (Ct.Th), and we applied finite element (FE) analysis to HR-pQCT scans to estimate bone strength (ultimate stress). We fit multivariable regression models to compare 12-month change in bone variables between PRE and POST girls adjusting for baseline age, weight, lean mass, average PA, Ca²⁺, and change in forearm length. Over 12 months, POST girls had greater gains in Tt.BMD (9%) and Ct.BMD (3%) compared with PRE girls (Tt.BMD, -2%; Ct.BMD, 1%; p<0.001, Table). POST girls also had a greater increase in Ct.Th (17%) and a decrease in Ct.Po (-10%) compared with PRE girls (Ct.Th, 4%; Ct.Po, 7%). Changes in trabecular microstructure were small (-1-4%) in PRE and POST girls, and did not differ between groups. Gains in bone strength were also similar between groups (15-16%). Our findings indicate that menarche influences microstructure of cortical bone to a larger degree than trabecular bone. Decreased cortical porosity, increased tissue density and thicker cortices in post-menarcheal girls may be necessary to consolidate cortical bone for later reproductive needs.

Table. Baseline and 12-month change in BMD, bone microstructure and strength at the distal radius in pre- and post-menarcheal girls.

| | Baseline | | 12-month change | |
|---------------------------------|-----------------------|------------------------|------------------------|------------------------|
| | Pre-menarcheal (n=52) | Post-menarcheal (n=86) | Pre-menarcheal (n=52) | Post-menarcheal (n=86) |
| Tt.BMD (mg HA/cm ³) | 252.3 (33.8) | 344.8 (62.7) | -9.9 (-23.4, 3.6) | 31.0 (22.2, 39.8)* |
| Ct.BMD (mg HA/cm ³) | 524.7 (50.1) | 799.3 (92.3) | -43.9 (-70.2, -17.7) | 47.8 (30.8, 64.8)* |
| BV/TV | 0.140 (0.019) | 0.141 (0.030) | -0.003 (-0.008, 0.002) | 0.000 (-0.003, 0.003) |
| Tb.N (1/mm) | 2.07 (0.21) | 1.90 (0.26) | -0.10 (-0.19, -0.01) | -0.01 (-0.07, 0.04) |
| Tb.Th (mm) | 0.068 (0.007) | 0.074 (0.011) | 0.001 (-0.002, 0.005) | 0.001 (-0.001, 0.003) |
| Tb.Sp (mm) | 0.420 (0.053) | 0.463 (0.079) | 0.028 (0.005, 0.052) | 0.002 (-0.014, 0.017) |
| Ct.Th (mm) | 0.28 (0.12) | 0.86 (0.22) | -0.07 (-0.12, -0.02) | 0.14 (0.10, 0.17)* |
| Ct.Po (%) | 4.9 (1.8) | 1.6 (1.4) | 0.01 (0.01, 0.02) | -0.01 (-0.01, -0.00)* |
| Ultimate stress (MPa) | 19.2 (6.5) | 35.3 (9.5) | 1.06 (-1.83, 3.96) | 5.39 (3.51, 7.28) |

Data are presented as the adjusted mean (95% CI). *p<0.001

Table

Disclosures: SoJung Kim, None.

MO0051

Comparison of CT-scan-based and 2D-BMD-based Vertebral Finite Element Models for Vertebral Strength Evaluation. Christophe Travert¹, Nicolas Vilayphiou², Helene Follet³, Wafa Skalli¹. ¹Arts et Metiers ParisTech, France, ²INSERM UMR1033, Université de Lyon & Hospices Civils de Lyon, France, ³INSERM, UMR1033 ; Université De Lyon, France

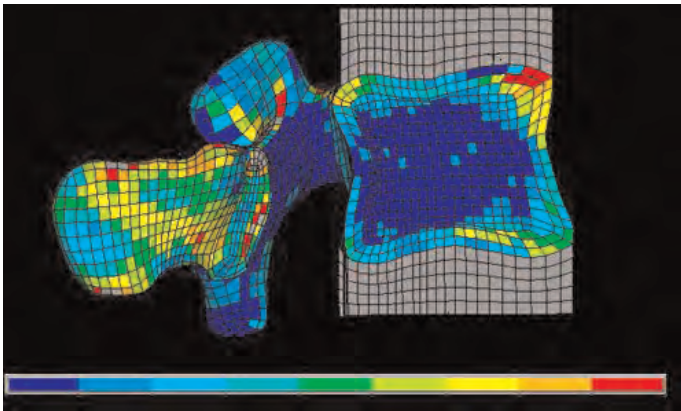
CT-scan based Finite Element Models (FEM) have been proposed to evaluate vertebral strength, and fracture risk. However, the main limitation of such approach in routine osteoporotic diagnosis is the cost and radiation exposure of the CT-scan. Developing an accurate FEM which is deployable at a large scale is still a challenge. Other approaches have been proposed to build a vertebral FEM using only 2D Bone Mineral Density (BMD) measurements, such as DXA or the dual energy EOS system. These models are limited by two factors: the approximation of geometry resulting from a pair of 2D X-ray, and the limited information on Bone Mineral Density (BMD) distribution within the vertebra.

The objective of this study is to compare the modeling approaches used in CT-based FEM and in 2D-BMD-based FEM.

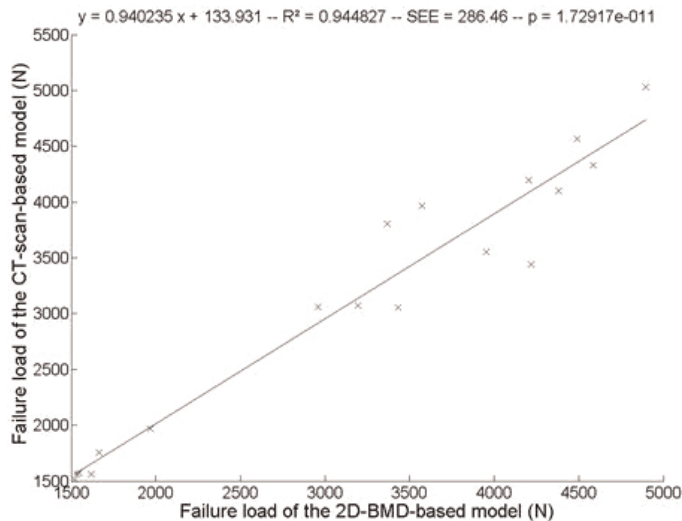
18 ex-vivo vertebrae (L1-L4, 6 donors, age 80 ± 9 years) have been scanned alongside a calibration phantom to build CT-based FEM. To simulate the effect of using 2D-BMD-based input, a pair of Digitally Reconstructed Radiographs (DRR) has been generated from these CT-scans. Different modeling approaches have been compared. In the CT-scan-based FEM, the geometry is obtained by segmentation of the CT-scan images, and material properties are assigned to each element of the model according to the BMD value measured in the corresponding voxels of the calibrated CT-scan. In the 2D-BMD-based FEM, the geometry is reconstructed using the pair of DRR only, and a BMD distribution is estimated from the lateral DRR to personalize the material properties. This BMD distribution is derived from a generic BMD distribution obtained on a different scanned vertebra. The element's BMD values are adjusted to fit the DRR. Vertebral strength has been estimated in anterior compression on each model.

The estimated load to failure in the CT-based and 2D-BMD-based model were 3117 ± 1184 N and 3172 ± 1223 N respectively. Linear regression shows that 2D-BMD-based model estimated very well the failure load of the CT-based model (R²=0.94, SEE=286N). Results from additional intermediate models shows error in the geometric reconstruction were compensated by the estimation of the BMD distribution.

Although these preliminary results are on theoretical data, 2D-BMD-based models appears as a good alternative to CT-scan-based models. Further work will address the issue of using 2D-BMD images from actual dual energy EOS, rather than DRR from CT-scan.



Finite element model configuration



Comparison of the two models

Disclosures: *Christophe Travert, None.*

MO0052

Computational Trabecular Microarchitecture Quantification with 3D texture analysis as a Marker to Differentiate Postmenopausal Women with and without Fractures. Alexander Valentintsch¹, Janina Patsch², Andrew Burghardt², Thomas Link², Sharmila Majumdar², Lukas Fischer³, Claudia Schueller-Weidekamm⁴, Heinrich Resch⁵, Franz Kainberger⁶, Georg Langs¹. ¹Medical University of Vienna, Austria, ²University of California, San Francisco, USA, ³Medizinische Universität Wien, Austria, ⁴Medical University of Vienna, Austria, ⁵Medical University Vienna, Austria, ⁶Medical University of Vienna, Division of Muskuloskeletal Radiology & Neuroradiology, Austria

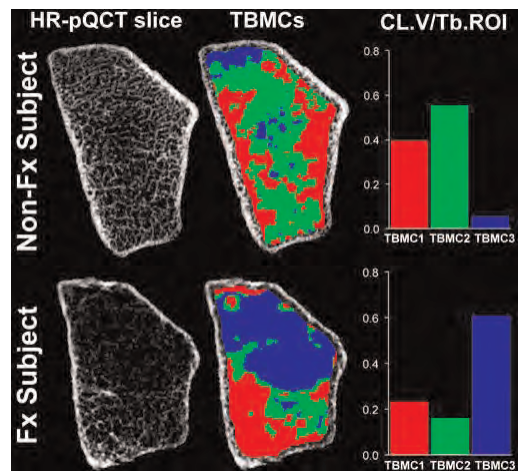
High resolution peripheral quantitative computed tomography (HR-pQCT) permits the non-invasive assessment of cortical and trabecular bone density, geometry, and microarchitecture. Although researchers have developed and applied various post processing algorithms to quantify image properties, 3D-texture analysis has not yet been utilized in HR-pQCT research. Motivated by high isotropic spatial resolution and the information density provided by HR-pQCT scans we propose a post-processing algorithm that quantifies trabecular bone microarchitecture characteristics via three-dimensional texture features in HR-pQCT scans beyond standard morphometry.

During a training phase, the computational method identified feature clusters that reflected trabecular bone regions with specific texture found across the entire training set, or *trabecular bone microarchitecture classes (TBMC)*. After training, new data could be analyzed by automatically segmenting the trabecular bone corresponding to the trained cluster features. The trabecular bone was then described by the histogram of relative trabecular bone volume covered by each cluster. We evaluated intra- and inter-scanner repeatability of the analysis on 14 distal radius samples scanned repeatedly.

TBMCs identified in repeated measurements exhibited an overlap of 0.922 to 0.974 (Dice), across site repeatability was 0.812 (Dice). The TBMC histograms are expressed as cluster volume fraction (CL.V/Tb.ROI). The TBMC algorithm differentiates three morphological bone classes that are based on distinct, three-dimensional character-

istics in trabecular bone microarchitecture: Thick, homogenous trabeculae with low intertrabecular spacing are predominant in TBMC 1 (red). On the contrary, TBMC 3 (blue) is filled with much thinner, inhomogenous trabecular structures that are poorly connected. Separating TBMC 1 and TBMC 3, TBMC 2 (green) represents zones of intermediate morphometric quality. In a second experiment the TBMC histograms showed significant differences between postmenopausal women with (n=18) and without (n=18) prevalent fragility fractures.

We demonstrated that 3D-texture analysis and feature clustering is a promising new HR-pQCT post-processing option with good cross-site reproducibility and high differentiating power between fracture subjects and non-fracture controls.



Representatives of differences in TBMCs between Fx and Non-Fx Subjects

Disclosures: *Alexander Valentintsch, None.*

MO0053

Correlation between Fracture Strength and Imaging endpoints: Radiography, pQCT and Micro-CT. Aurore Varela*, Susan Y. Smith, Charles River Laboratories, Canada

Predicting fracture healing clinically is challenging, subjective and susceptible to individual variability. Can multiple imaging techniques provide a better fracture healing assessment? The objective of this study was to correlate biomechanics strength data to pQCT, micro-CT and X-Ray datasets from a rat fibula osteotomy model. Male rats (18/group) were treated with vehicle, PTH 1-34, Alendronate or Diclofenac and terminated 15 or 29 days after surgery. X-Rays were taken on Days 14 and 28 post-surgery, and Faxitron was done ex vivo. Callus area, BMC and BMD were measured by pQCT and micro-CT *in vivo*; total, mature and immature callus were segmented. Fibulae were tested to failure in 4-point bending. PTH and Alendronate treatment improved bone healing and Diclofenac delayed bone healing¹. All data were included in order to use a broad dataset for the correlation analysis.

Correlations between radiological scoring and strength parameters (Peak load and stiffness) were modest (r=0.55) with the strongest correlations noted for callus size (the extent of periosteal and endosteal reactions, r=0.61). Results were similar in vivo or ex vivo, at Days 14 or 28. For pQCT, callus area and BMC showed a strong correlation at Day 14 (r=0.81) with no correlation for BMD (r=0.06). At Day 14, correlations were strongest for the immature callus parameters, consistent with the healing stage. Inversely, as callus matured at Day 28, correlations were stronger for callus BMD (r=0.61), but weak for area and BMC. At this stage of healing, correlations were stronger for the mature callus parameters. Results were generally similar for the micro-CT parameters.

pQCT and micro-CT parameters generally correlated well with strength parameters (between 0.5 to 0.83); however, the strongest correlations changed depending on the stage of the healing. A combination of X-rays, pQCT and/or micro-CT evaluations at specific stages of healing may provide additional and more appropriate criteria to non-invasively assess bone healing and fracture strength. These data confirm that a combination of multiple modalities can successfully assess bone healing outcome and be used to characterize the effects of pharmacological compounds.

¹A. Varela, L. Chouinard, Y. Trudel, C. Ruh, I. Primakova, G. Boyd, KJ. Escott, SY. Smith. Fibula Osteotomy Model in the Sprague-Dawley Rat: Radiology, Densitometry, Biomechanics and histological characterization. Poster presented at Annual ASBMR meeting, San Diego, 2011

Disclosures: *Aurore Varela, None.*

MO0054

Distinct tissue mineral density (TMD) distribution in human trabecular plates and rods. Ji Wang^{*1}, Galatea Kazakia², Bin Zhou¹, Xiutao Shi¹, X Guo¹.¹Columbia University, USA, ²University of California, San Francisco, USA

A newly developed Individual Trabecular Mineralization (ITM) technique provides unique measures of individual trabecular (Tb) plate or rod mineralization—one of the critical determinants of bone strength. A previous μ CT-based ITM study has demonstrated novel and distinct distributions of individual trabecular TMD (Tb.TMD) with Tb types and orientations. However, the inherent limitation of TMD evaluation using a polychromatic μ CT (e.g. beam hardening effect) calls for more rigorous verification of the new technique. In this study, we performed ITM analyses on human Tb bone images scanned by BOTH conventional μ CT and SR μ CT- gold standard for evaluating TMD. 14 Tb bone cylinders were harvested from femoral heads, vertebrae, and proximal tibiae, and imaged by μ CT at 8 μ m (Scanco μ CT40). Images were reconstructed and beam hardening corrected (BHC) based on hydroxyapatite (HA) wedge phantom of 200 or 1200 mg HA/cm³. SR μ CT imaging was performed at 7.5 μ m at the National Synchrotron Light Source. Attenuation values were converted to HA density by phantom calibration (Fig 1A). The microstructure of a cubical sub-volume of each bone core was segmented into individual trabeculae (Fig 1B), and Tb.TMD was calculated for each trabecula. Mean Tb.TMD of Tb plates and rods were examined, as well as stratified to various orientations. SR μ CT-based ITM measurements showed that Tb plates were 1.0% more mineralized than rods (Fig 1C), which was consistent with the previous μ CT-based study with 63 samples. However, SR μ CT and μ CT of current 14 Tb samples showed significantly different Tb.TMD measurements. μ CT with BHCs resulted in the plate and rod Tb.TMD lower than SR μ CT values by 12.2-17.0% and 11.4-16.2%, respectively. Due to more underestimated plate Tb.TMD, the plate vs. rod Tb.TMD difference was diminished in μ CT-based measurements. Results also suggested that plate Tb.TMD varied with Tb orientations in a consistent pattern: transverse>oblique>longitudinal, which was not influenced by μ CT artifacts (Fig 1D). Interestingly, axially aligned plates were less mineralized than plates along other directions, though they account for the majority of bone volume and predominate mechanical properties. In conclusion, the Tb type and orientation-associated heterogeneous TMD distribution in Tb bone is confirmed by SR μ CT-based ITM analysis. Tb plates, particularly transverse plates, are most highly mineralized. μ CT-based ITM analysis is feasible with adequately large sample size and appropriate BHC.

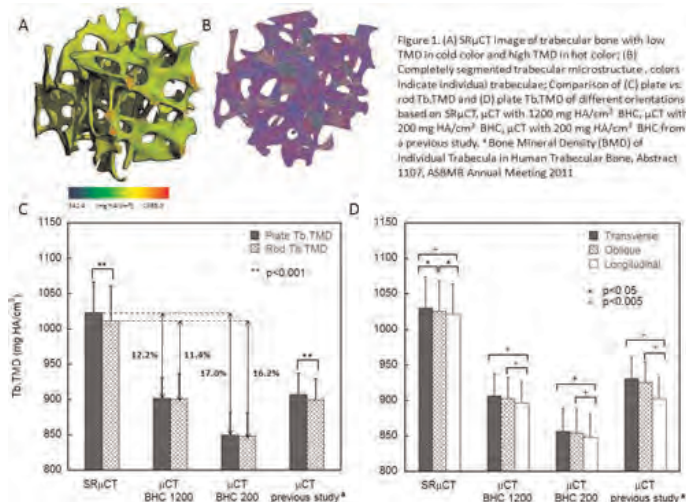


Figure 1

Disclosures: Ji Wang, None.

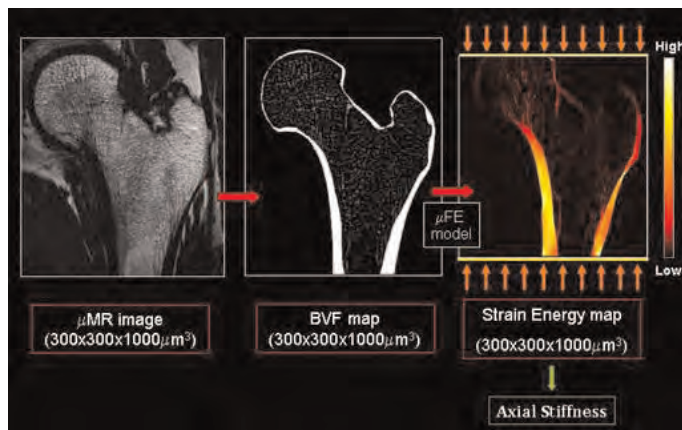
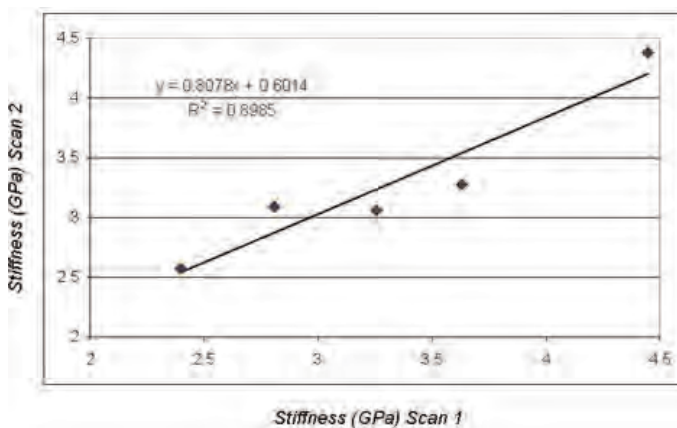
MO0055

Finite-Element Analysis based on In Vivo Micro MR Images of the Proximal Femur. Maite Aznarez-Sanado^{*1}, Chamith Rajapakse², Jeremy Magland¹, Ning Zhang¹, Felix Werner Wehrli³. ¹University of Pennsylvania, USA, ²University of Pennsylvania School of Medicine, USA, ³University of Pennsylvania Medical Center, USA

Assessment of fracture risk at the proximal femur on the basis of in vivo images is of considerable clinical interest. Micro-Finite-Element Analysis (μ FEA) is a promising tool for the evaluation of bone strength and fracture risk [1,2]. Here, we examined the reproducibility of FEA on the basis of in vivo μ MR images of the proximal femur. 5 subjects (mean=32.2 y.o., range=24-48 y, 3 males) were scanned at 3T twice using the same imaging protocol and with complete repositioning in between. High-resolution images (300x300x1000 μ m³, FLASE sequence [3]) were acquired for the purpose of generating finite-element models. A second dataset acquired at lower resolution allowed distinction between cortical bone and surrounding ligamentous and

cartilaginous structures. This image was used for the purpose of segmenting the cortex, which was performed manually. Grayscale MR image intensities were normalized to the mean signal values of pure marrow, with pure bone and pure marrow having values of 0 and 100%. Subsequently, contrast of the resulting images was inverted to generate bone-volume fraction (BVF) maps (Fig. 1). μ FE models were generated for each dataset [4]. First, each bone voxel in the BVF map was directly converted to a hexahedral finite element with dimensions equal to the voxel size. Bone tissue was assumed to be isotropic and linearly elastic. The elastic modulus of pure bone was set to 15 GPa and the actual modulus of each element was computed as BVF¹⁵ GPa. Poisson's ratio was kept constant at 0.3. Axial stiffness was computed via simulated compressive loading in the axial direction (Fig. 1). Since the load was applied along the infero-superior axis, axial stiffness corresponded to the stance-phase loading. Computed axial stiffness showed good reproducibility. Fig. 2 displays the consistency of the measurements obtained for each of the subjects. Mean coefficient of variation for axial stiffness across subjects was 4.9%, ranging from 1.1 to 7.3%. Intraclass correlation coefficient was 0.97. The data suggest that serial assessment of mechanical competence of the proximal femur via MRI-based μ FEA may be feasible.

References: [1] Boutroy et al, JBMR, 2008; [2] Vilyaphiou, Bone, 2010; [3] Magland et al, MRM, 2009; [4] Zhang, Proc. ISMRM, 2011

Processing steps necessary to determine FEA derived-axial stiffness based on in vivo μ MR images

Test-retest plot for axial stiffness evaluated in five different subjects

Disclosures: Maite Aznarez-Sanado, None.

MO0056

Fracture Healing in Postmenopausal Women with a Distal Radius Fracture Monitored by High-Resolution Peripheral Quantitative Computer Tomography (HRpQCT): A Pilot Study. Sandrine Bours^{*1}, Joost De Jong², Paul Willems³, Chris Arts³, Peter Brink³, Bert Rietbergen⁴, Tineke Van Geel⁵, Piet Geusens⁶, Joop Van Den Bergh⁷. ¹Maastricht University Medical Centre, The Netherlands, ²Eindhoven Technical University, Netherlands, ³Maastricht University Medical Centre, Netherlands, ⁴Eindhoven University of Technology, The Netherlands, ⁵Maastricht University, The Netherlands, ⁶University Hasselt, Belgium, ⁷VieCuri MC Noord-Limburg & Maastricht UMC, The Netherlands

Background: Fracture healing is a dynamic process, in which an inflammatory reaction induces bone resorption and formation in order to repair the fracture and restore bone strength. In contrast to plain radiographs, high-resolution (HR) pQCT allows to visualize trabecular and cortical bone three dimensionally. From these 3D images bone strengths can be calculated.

Objective: To assess changes in bone morphology and strength *in-vivo* during fracture healing over time.

Method: The fracture region of eight postmenopausal women with a stable distal radius fracture was imaged using HRpQCT (Xtreme CT, Scanco, Switzerland) at 1-2 weeks post-fracture (baseline) and 3-4, 6-8 and 12 weeks post-fracture (follow-up). Morphology parameters were measured and follow-up overlay images were used to identify regions of bone gain and loss exceeding 300 mgHA/cm³. Finite element models were created based on the HRpQCT images and bone stiffness in compression was calculated.

Results: The overlay image revealed bone resorption sites developing mainly in the trabecular bone that accounted for a bone loss of up to 10% over time (p<0.05). At the same time, bone apposition sites developed mainly at the endocortical side of the fracture and accounted for a bone gain of up to 17% over time (p<0.05). The net 7% gain is correlated to increase in volumetric bone density, vBMD (r>0.79). Compared to baseline, bone stiffness increased up to 38% (p<0.05) over time (figure 1). The change in stiffness after 12 weeks correlates to the net increase in vBMD (r=0.89, p=0.018 at 12 weeks). No changes were found at the contra-lateral wrist.

Conclusions: This is the first pilot study to analyse *in vivo* changes in bone structure and biomechanical competence at the site of fracture using HRpQCT in humans. Significant changes were detected in concomitant bone loss and gain and in increase of compression stiffness.

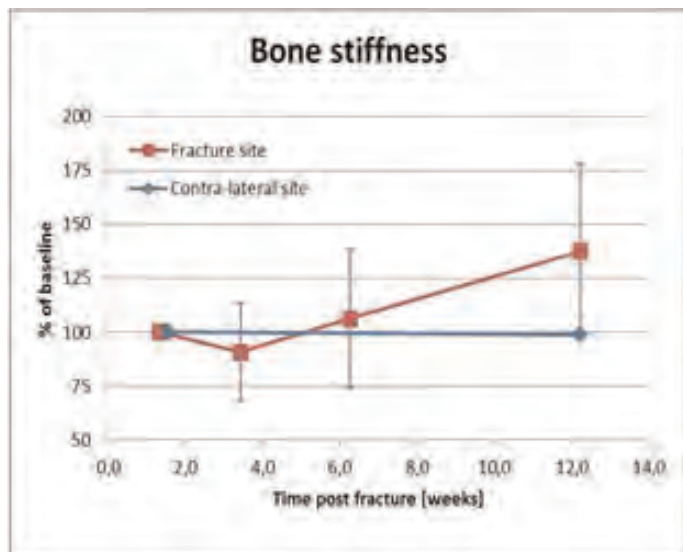


figure 1. Changes of bone stiffness at fracture site and contra-lateral radius

Disclosures: Sandrine Bours, None.

MO0057

Hip Structural Analysis of Patients with Atypical Femur Fractures: Data from the Ontario AFF Cohort. [Angela Cheung](#)^{*1}, [George Tomlinson](#)¹, [LIANNE TILE](#)², [Aliya Khan](#)³, [Robert Josse](#)⁴, [Earl Bogoch](#)⁵, [Heather McDonald-Blumer](#)², [Rowena Ridout](#)⁶, [Savannah Cardew](#)², [Moiria Kapral](#)¹, [K. Shawn Davison](#)⁷, [Robert Bleakney](#)⁸, [Khalid Syed](#)¹, [Jessica Chang](#)¹, [Queenie Wong](#)¹, [Hanxian Hu](#)¹, [Suzanne Morin](#)⁹, [Jacques Brown](#)¹⁰, [Alexandra Papaioannou](#)¹¹, [Jonathan Adachi](#)¹². ¹University Health Network, Canada, ²University of Toronto, Canada, ³McMaster University, Canada, ⁴St. Michael's Hospital, University of Toronto, Canada, ⁵St. Michael's Hospital, Canada, ⁶Toronto Western Hospital, Canada, ⁷Laval University, Canada, ⁸Mount Sinai Hospital, Canada, ⁹McGill University, Canada, ¹⁰CHUQ Research Centre Laval University, Canada, ¹¹Hamilton Health Sciences, Canada, ¹²St. Joseph's Hospital, Canada

Purpose: To better understand the etiology of atypical femur fractures (AFFs), we explored whether there were hip or femoral shaft structural differences between patients on bisphosphonates with AFFs and those with severe osteoporosis (SO), those with osteopenia (Op), and those in the Toronto Canadian Multicentre Osteoporosis Study (CaMOS).

Materials and Methods: We conducted a cross-sectional study to examine the Ontario AFF cohort and compared them to the Toronto CaMOS, SO and Op cohorts. All AFF patients were assessed by an osteoporosis specialist, and their X-rays were reviewed by a musculoskeletal radiologist to confirm the diagnosis of atypical femur fracture based on the ASBMR diagnostic criteria. Women in the SO cohort were participating in a teriparatide trial and women in the Op cohort were participating in an osteoporosis prevention trial. We performed hip structural analysis (HSA) on the femur scans acquired at baseline using DXA in all these populations. We used ANCOVA for comparison and controlled for age.

Results: Of the 67 AFF patients in the Ontario cohort, 63 were postmenopausal women and 4 were men. Mean age was 68.3 years. 61% were Caucasians, 27% were South East Asians and 12% were South Asians. 63% had fractures prior to their AFFs and 58% had bilateral AFFs. Of those with bilateral fractures, 11 (28%) had bilateral subtrochanteric fractures, 18 (46%) had mid-diaphyseal fractures, and 10 (26%) had one of each. Of those with unilateral AFFs, 12 (43%) had subtrochanteric fractures and 16 (57%) had mid-diaphyseal fractures. Average duration of bisphosphonate use was 9.2 years (range 1.9 - 28.7 years). Mean serum 25-hydroxyvitamin D level was 100 nmol/L. Areal BMD T-scores ranged from 0.84 to -3.95 for lumbar spine, 0.82 to -3.53 for total hip, and 0.33 to -3.79 for femoral neck. They were significantly higher in the AFF cohort than in the SO cohort, and lower than in the Op cohort. Those with AFFs had statistically significant differences in femoral shaft BMD, cross-sectional area, cross-sectional moment of inertia, section modulus, width, buckling ratio and femoral shaft to neck angle than the other cohorts (Table), but these cohorts overlap substantially for all parameters.

Conclusions: It is difficult to identify specific hip and femoral shaft structural characteristics that differentiate patients on bisphosphonates with atypical femur fractures from other cohorts.

| | AFF vs CaMOS | AFF vs SO | AFF vs Op |
|--------------------|--------------|-----------|-----------|
| FS BMD | 0.0004 | <0.0001 | 0.0001 |
| FS CSA | <0.0001 | 0.002 | <0.0001 |
| FS CSMI | 0.002 | 0.22 | 0.017 |
| FS Section Modulus | 0.024 | 0.26 | 0.099 |
| FS width | 0.0007 | 0.052 | 0.004 |
| FS Buckling Ratio | 0.027 | 0.0001 | 0.002 |
| FS: FN angle | 0.0008 | 0.019 | 0.0009 |

P-values for the comparisons of HSA parameters between different cohorts

Disclosures: Angela Cheung, Novartis, 2; Warner Chilcott, 2; Merck, 2; Merck, 6

MO0058

In Vivo Microindentation for the Assessment of Bone Material Level Properties. [Patrick Ammann](#)^{*1}, [Robert Güerri](#)², [Paul Hansma](#)³, [Xavier Nogues](#)⁴, [Adolfo Diez-Perez](#)⁵. ¹Division of Bone Diseases, Switzerland, ²Hospital Universitario Del Mar. Institut Municipal D'Investigació Mèdica, Spain, ³University of California, Santa Barbara, USA, ⁴Institut Municipal D'Investigació Mèdica, Spain, ⁵Hospital del Mar-IMIM-Universitat Autònoma, Barcelona, & RETICEF, Instituto Carlos III, Spain., Spain

Intrinsic bone tissue quality is an important determinant of bone fragility but its assessment is invasive. A novel micro-indentation technology is available and can be performed *in vivo*. Preliminary studies confirm its ability to discriminate patients with and without fracture, but the significance of the parameters investigated is still unclear. Since protein malnutrition affects bone material level properties, -geometry and -strength-, rats were fed a normal or an isocaloric low-protein diet. Both femurs were collected and measurements of geometry using micro CT (diameter, cortical thickness), material level properties using nanoindentation (modulus, hardness and working energy), micro indentation (indentation distance increase (IDI), unloading stiffness and average energy dissipated) and bone mechanical properties (maximal load, stiffness and energy) using a three points bending test were determined. To better understand the clinical significance of micro-indentation values, parameters of micro-indentation were correlated with parameters of bone strength and bone material level properties. Values are expressed as means ± SEM. Student's t-test for testing differences and regressions analysis were performed. Protein malnutrition affects bone strength decreasing maximal load, stiffness, energy and plastic energy. Determinants of bone strength were also altered: like geometry (decreased cortical thickness) and bone material level properties (decreased modulus, hardness and working energy). Parameters of micro-indentation were affected on the same direction; IDI was significantly increased and unloading stiffness and average energy dissipated were significantly decreased. The values of micro-indentation were systematically correlated with the other measurements. The best significant correlations were observed between indentation distances and hardness (nanoindentation) and between average energy dissipated and plastic energy (biomechanics); for all the significant correlation r2 are ranged between 0.5 and 0.327. These observations indicates (i) that microindentation is enough sensitive to detect effect of a low protein diet on bone material tissue quality and (ii) that parameters of microindentation predict values of material level properties measured by nano-indentation and plastic energy (characterizing plastic deformation of the sample and indirectly material properties) using biomechanics. These observations open large possibilities to investigate *in vivo* material level properties.

| Casein | Normal | Low |
|----------------------------------|---------------|-----------------|
| IDI (µm) | 10.86 ± 0.59 | 13.17 ± 0.56** |
| Unloading Stiffness (N/µm) | 0.921 ± 0.045 | 0.753 ± 0.033** |
| Average Energy Dissipated (N*µm) | 39.28 ± 1.62 | 34.62 ± 0.79** |

Effects of a low protein diet : micro-indentation

Disclosures: Patrick Ammann, None.

MO0059

Intra and Inter-individual Variation in Tissue Type as a Reflection of Suppressed Remodeling Rate in Slender Tibiae. Naomi A. Hampson*¹, David Lin², Karl Jepsen³, Haviva Goldman². ¹Drexel University, USA, ²Drexel University College of Medicine, USA, ³University of Michigan, USA

Purpose: Previous research has shown that individuals with more slender (narrow relative to length) tibiae are at higher risk for stress fracture possibly due to compensatory increases in tissue stiffness needed to increase bending strength. Based on our previous study of porosity, ash content and geometry interactions, we hypothesized that slender bones increase tissue stiffness by suppressing remodeling relative to robust bones. Specifically, we investigated whether slender tibiae have less secondary (osteonal and interstitial) tissue than robust tibiae. We studied two locations along the length of the tibia to determine whether more slender locations (e.g. distal tibia) remodeled less than more robust ones.

Materials and Methods: Cross sections of 10 human tibiae (age 37 +/- 8 yrs) were obtained from 38% and 66% from the distal articular surface, embedded in PMMA and cut/ground to 100 µm. Sections were imaged in their entirety by transmitted and circularly polarized light using a 5x objective. 12 regions of interest (ROIs) were extracted as shown in Figure 1. Primary and secondary bone areas (including pores) were hand traced for each ROI, to calculate a % area for each.

Results: The cortices of slender individuals (at both 38% and 66%) contained significantly (p<0.05) less secondary tissue relative to robust individuals, and periosteal sites were generally less remodeled than the mid-cortex. There was significant regional variation around the cortex at both 38% and 66% locations, such that the anterior cortex contained the most secondary tissue, followed by the posterior cortex. The antero-medial cortex contained the least secondary tissue. On average, 38% did not contain a lower % secondary tissue relative to 66%, though a few individual ROIs did significantly differ.

Conclusions: Our results suggest that slender individuals have significantly less remodeled bone relative to robust individuals. The proportion of remodeled bone is not uniform around the tibia, likely reflecting local loading and growth history of the bone. These local issues need to be considered in addition to global regulators of remodeling such as robustness. This is illustrated in the complex results of our study of 38% vs. 66% sites. Since the distal site is subject to higher strains than the 66% site, both local and global regulators may be affecting overall remodeling rates and need to be teased apart in future studies.

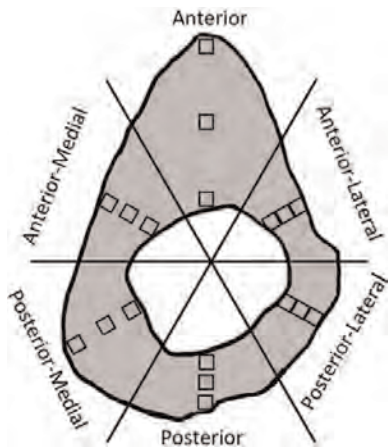


Figure 1: ROI Locations

Disclosures: Naomi A. Hampson, None.

MO0060

Local Topological Analysis applied to HR-pQCT images of the Distal Radius and the Distal Tibia in the OFELY Study. Jean-Baptiste Pialat*¹, Stéphanie Boutroy², Pierre-Jean Gouttenoire³, Rafaa Ellouz⁴, Nicolas Vilayphiou⁵, Elisabeth Sornay-Rendu⁶, Roland Chapurlat⁷, Françoise Peyrin³. ¹INSERM U1033, Team1, Université de Lyon & Hospices Civils de Lyon, France, ²INSERM UMR1033 & Université de Lyon, France, ³CREATIS, CNRS UMR 5220, INSERM U1044 & Université de Lyon, France, ⁴INSERM UMR 1033 & Université de Lyon, France, ⁵INSERM UMR1033, Université de Lyon & Hospices Civils de Lyon, France, ⁶INSERM UMR1033, Université de Lyon, France, ⁷INSERM UMR 1033, Université de Lyon & Hospices Civils de Lyon, France

Purpose: Local Topological analysis (LTA) was developed for high resolution imaging (1). However, we showed in a preliminary study including 33 women with wrist fracture and age-matched controls that this technique was feasible at 82µm resolution and could improve the microarchitectural description (2). The aim of the present study was to assess whether this technique could be associated with all prevalent fractures in a larger sample of patients. Methods: 101 women from the OFELY cohort (mean age 72.7 ± 8.5) with prevalent vertebral and non vertebral fractures were compared with 101 age-matched controls without fracture. Bone microarchitecture was assessed by High Resolution peripheral Quantitative Computed Tomography (HR-pQCT, XtremeCT, Scanco Medical AG, Switzerland) at the distal radius and tibia. Areal (a)BMD was assessed by DXA at the ultra distal radius and total hip. Finite element analysis (FEA) was computed to determine trabecular bone stiffness based on HR-pQCT images. LTA was applied to label each bone voxel as rod, plate or node (1). The bone volume to total volume (BV/TV), the node, rod and plate ratio over total volume (NV/TV, RV/TV, PV/TV) and the plate over rod volume (PV/RV) were calculated. Associations between LTA parameters and fractures were computed in a conditional logistic regression model, with and without adjusting for aBMD. Correlations between variables were calculated at each site and between anatomical sites. Results: All topological parameters differed between women with prevalent fractures and controls at both sites. Most of them remained significantly different after adjustment for ultradistal radius aBMD or total hip aBMD (Table1). PV/RV was positively correlated with trabecular thickness (r= 0.71 at the radius and 0.80 at the tibia, both p<0.0001), negatively correlated with structural model index (r= -0.60 and -0.59 at the radius and tibia, p<0.0001) and positively correlated with Trabecular Stiffness (r= 0.46 at the radius, 0.40 at the tibia, both p<0.0001). Correlations between anatomical sites ranged from r= 0.58 for PV/RV to 0.75 for BV/TV. Conclusion: Topological parameters assessed at the distal radius and tibia were associated with vertebral and non vertebral fractures, partially independently from aBMD.

1. Peyrin F et al. Med Phys 2010;37: 4364-76.
2. Pialat JB et al . Osteoporos Int (2011) 22 (Suppl 1):S97-S117.

| | Distal Radius | | Adjusted for UDR BMD | |
|-------|---|--|----------------------|---------|
| | % difference (fracture-control) / control | without adjustment OR [95% CI] p value | OR [95% CI] | p value |
| PV/RV | -6.8% | 1.76 [1.16 ± 2.4] 0.006 | 1.4 [0.95 ± 2.06] | 0.09 |
| NV/TV | -19.8% | 2.44 [1.54 ± 3.86] <0.0001 | 2.39 [1.25 ± 4.56] | 0.008 |
| PV/TV | -19.2% | 2.39 [1.54 ± 3.72] <0.0001 | 2.22 [1.21 ± 4.07] | 0.01 |
| RV/TV | -13.5% | 2.14 [1.42 ± 3.24] <0.0001 | 1.84 [1.07 ± 3.17] | 0.027 |
| BV/TV | -16.0% | 2.34 [1.52 ± 3.61] <0.0001 | 2.18 [1.19 ± 4] | 0.01 |

| | Distal Tibia | | Adjusted for Total Hip BMD | |
|-------|---|--|----------------------------|---------|
| | % difference (fracture-control) / control | without adjustment OR [95% CI] p value | OR [95% CI] | p value |
| PV/RV | -11.8% | 1.54 [1.11 ± 2.14] 0.005 | 1.73 [1.05 ± 2.81] | 0.027 |
| NV/TV | -15.4% | 2.07 [1.37 ± 3.12] 0.001 | 1.71 [1.01 ± 2.91] | 0.048 |
| PV/TV | -16.0% | 2.28 [1.48 ± 3.52] <0.0001 | 2.05 [1.21 ± 3.48] | 0.007 |
| RV/TV | -6.1% | 1.43 [1.04 ± 1.97] 0.028 | 1.13 [0.77 ± 1.66] | 0.54 |
| BV/TV | -11.1% | 2.02 [1.36 ± 3] 0.001 | 1.7 [1.05 ± 2.77] | 0.03 |

Table 1: Association between topological parameters and prevalent fractures

Disclosures: Jean-Baptiste Pialat, None.

MO0061

Non-invasive Imaging of Human Bone Turnover - A Longitudinal Pilot Study in Lung Transplant Recipients with Severe Bone Loss. Lukas Fischer*¹, Alexander Valentinitzsch², Barbara Zweytick², Claudia Schüller-Weidekamm², Peter Pietschmann³, Franz Kainberger⁴, Georg Langs⁴, Janina Patsch². ¹Medizinische Universität Wien, Austria, ²Medical University of Vienna, Austria, ³Institute fuer Pathophysiologie, Austria, ⁴Medical University of Vienna, Austria

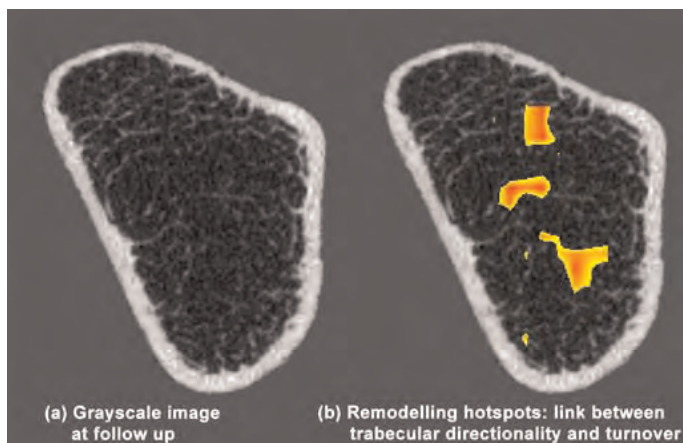
Secondary osteoporosis is a severe but poorly understood problem in lung transplant (LuTX) recipients. In research settings, high resolution peripheral quantitative computed tomography (HR-pQCT) can be used for the non-invasive

assessment of changes in bone microarchitecture over time. The aims of this pilot study were to develop an optimized, threshold-independent tool for the quantification of trabecular dynamics beyond standard morphometry and to investigate the relation between trabecular dynamics and serum markers of bone turnover.

We used HR-pQCT baseline and follow-up scans of the distal radius (n=11 patients; interval=6 months). All scans were analysed with the standard software provided by the manufacturer. In addition, data were rigidly registered and trabecular reorganization was quantified by three dimensional texture analysis (i.e. optical-flow algorithm). We obtained color-coded deformation-maps for each case. Changes were described by measures of entropy (e.g. directional dominance) and the combination of microarchitectural and directional dynamics by Kullback-Leibler-Divergence (KLD). In general, KLD indicates if structural changes occur preferentially at/along trajectory-like structures instead of a more homogenous spatial distribution of trabecular dynamics. Serum markers (CTX, OCN) were measured at each time point. DXA was performed at baseline.

By DXA, mean T-Scores (spine & hip) were osteopenic/osteoporotic. 77 % of LuTX patients exhibited increased CTX and decreased OCN at baseline. Mean trabecular density (D_{trab}) and peripheral trabecular density (D_{meta}) decreased significantly over time (-1.8%, p=0.046; -1.8%, p=0.006). The remaining HR-pQCT standard parameters did not change significantly. Global KLD was significantly correlated with CTX at baseline (r=0.62) and the OCN/CTX ratio after 6 months (r=-0.64). These results were confirmed by local (voxelwise) analysis which additionally yielded regional turnover maps (see figure).

Our pilot data indicate that visualization and quantification of local trabecular dynamics is feasible on longitudinal HR-pQCT data. We further conclude that in LuTX patients trabecular directionality is linked to local and systemic bone turnover. This preliminary finding seems plausible as osteoporosis does not only impair bone density and microstructure but also leads to reorganization of the trabecular network with reinforcement and increased structural directionality.



HRpQCT: link between trabecular directionality and turnover

Disclosures: Lukas Fischer, None.

MO0062

Osteocalcin and Osteopontin Regulate Bone Mineralization by Controlling Bone Magnesium Levels. Atharva Poundarik¹, Caren Gundberg², Deepak Vashishth³. ¹Rensselaer Polytechnic University, USA, ²Yale University School of Medicine, USA, ³Rensselaer Polytechnic Institute, USA

Bone mineral quality is critical to bone health. Whilst non-collagenous proteins like osteocalcin (OC) and osteopontin (OPN) are associated with bone mineral [1], their exact role remains poorly understood. Ionic impurities like magnesium (Mg), sodium (Na), fluorine (F), etc., influence the crystallinity and quality of bone apatite. It has been hypothesized that presence of Mg may inhibit transformation of amorphous calcium phosphate to calcium rich hydroxyapatite [2]. Studies demonstrate that destabilization of the apatite crystal structure by Mg is accompanied by a decreased Ca/P molar ratio and reduction in crystal size. Hence, removal of Mg from apatite during calcification is necessary for incorporating Ca into mineral [3]. Here, we report the presence of increased quantities of Mg in OC^{-/-} and OPN^{-/-} bones suggesting a new functional role for OC and OPN in bone mineralization.

Energy dispersive x-ray spectroscopy (EDXS) was performed on carbon-coated fracture surfaces of WT, OC^{-/-} and OPN^{-/-} bones at an operating voltage of 10kV. Spectra were acquired (5 regions per bone) for a live time of 300 seconds. Principal peaks corresponding to Ca, P, Mg and Na were identified. Elemental quantification was done after calibration with a silicon standard. Ca/P and Mg/Ca molar ratios were computed and statistically analyzed using ANOVA. Our results show that magnesium levels, as measured by the Mg/Ca ratio, are greater in the OC^{-/-} (0.033±0.004, p<0.001) and OPN^{-/-} (0.032±0.001, p<0.001) mice bones than in WT (0.024±0.001). Consistent with previous studies, we also observed a significantly lower Ca/P molar ratio in the OC^{-/-} (1.305±0.108, p<0.05) and OPN^{-/-} (1.349±0.009, p<0.05) mice bones as compared to WT (1.393±0.015). These findings suggest that OC and OPN facilitate the precipitation of a stable hydroxyapatite mineral phase by removal of Mg during mineralization. In absence of OC and OPN, Mg is not effectively removed leading to the formation of smaller

mineral crystals with lower Ca/P molar ratio. Our previous study also shows a reduction in size of mineral crystals in OC^{-/-} and OPN^{-/-} mice bones [4]. Thus, the removal of Mg may be a mechanism by which OC and OPN increase Ca uptake and control crystal size and maturity.

Acknowledgements: NIH Grants AR49635, AR38460

References:

- [1] Wiesmann et al. Int. Rev. Cytol. 242: 2005
- [2] Nielson, Calcif. Tiss. Res. 11: 1973
- [3] Bigi et al. Calcif. Tiss. Int. 50: 1992
- [4] Poundarik et al. Presentation No. 1103, ASBMR 2011

Disclosures: Atharva Poundarik, None.

MO0063

Reference Point Indentation Measures Are Associated with Whole Bone Mechanical Properties Independent of Geometry. Lamya Karim^{*}, Leeann Louis, Christine Conlon, Mary Bouxsein, Beth Israel Deaconess Medical Center, USA

Whole bone mechanical behavior is determined by bone mass, geometry, and material properties. Until recently, there has been no method available to assess bone material properties in patients. Newly developed reference point indentation (RPI) allows assessment of cortical bone indentation properties in vivo and ex vivo, and may be useful for assessing skeletal fragility [1]. However, the extent to which RPI measures are associated with traditional biomechanical properties is unknown.

Thus, we extracted 40 radii from 20 adult rats, measured polar moment of inertia (pMOI) and tissue mineral density (TMD) by μ CT at the mid-diaphysis, and performed RPI (Biodent, Active Life Scientific) using a maximum force of 9 N at 2 Hz for 10 cycles. Radii were randomly divided into groups for 3-point bending or fracture toughness tests. Radii selected for fracture toughness tests were notched on the anterior side of the mid-diaphysis before testing.

RPI measures were not associated with pMOI or TMD. For 3-point bending, pMOI correlated positively with whole bone stiffness (STF, r=0.48, p<0.05) and failure load (FL, r=0.56, p<0.05), and had a negative trend with post-yield displacement (PYD, r=-0.39, p=0.10). STF and PYD were also correlated (r=-0.61, p<0.05). Indentation distance (ID) and total ID (TID) were positively correlated with each other (r=0.96, p<0.05) and STF, but negatively with work-to-failure and PYD (Table 1). Creep ID (CID) was the only variable associated with fracture toughness (Table 1). Stepwise multiple regression for STF and FL showed that addition of TID to pMOI significantly improved r² from 0.37 to 0.54 and from 0.53 to 0.65, respectively.

Results indicate that RPI measures are independent of structural properties and hence, assess purely material behavior. Stiffer bones underwent less plastic deformation and were therefore more brittle. Consequently, they experienced greater indentation distances. Also, bone requiring less energy to fail experienced deeper indentation distances. Furthermore, tougher bone may have greater ability to undergo creep deformation before reaching failure. As bone's organic matrix determines creep [2], CID and toughness are likely influenced by protein matrix changes. In conclusion, we found for the first time that RPI measures reflect several whole bone mechanical properties as assessed by traditional mechanical tests.

1. Diez-Perez et al, J Bone Miner Res, 2010
2. Bowman et al, J Biomech Eng, 1999

Table 1. Correlation coefficients between several RPI measures and whole bone material properties are shown. Asterisks denote significant differences (p<0.05).

| | Work-to-failure [N*mm] | Stiffness [N/mm] | Post-yield displacement (mm) | Initiation toughness [Pavim] | Propagation toughness [Pavim] |
|----------------|------------------------|------------------|------------------------------|------------------------------|-------------------------------|
| CID (μ m) | -0.00 | -0.03 | 0.28 | 0.46* | 0.51* |
| TID (μ m) | -0.65* | 0.58* | -0.50* | 0.31 | 0.18 |

Table 1

Disclosures: Lamya Karim, None.

MO0064

Site-specific Associations Between BMI and Bone Content and Density in Healthy Adults: A pQCT Study. Amanda Lorbergs^{*}, Stefan Jackowski², Andrew Frank², Ashlee McLardy², Lauren Sherar³, Adam Baxter-Jones², Saija Kontulainen². ¹McMaster University, Canada, ²University of Saskatchewan, Canada, ³Loughborough University, United Kingdom

The effect of being overweight and/or obese on bone structure is controversial. This is in part because of the paucity of research concerning the site-specific effects of increased body mass index (BMI) on bone structure in males and females. The purpose of this cross-sectional study was to compare the radius and tibia content and density of normal, overweight, and obese adult males and females.

One hundred and fifty one healthy adults (79 males, 72 females; aged 24-53 years) from the Saskatchewan Growth and Development Study (SGDS) and the Saskatchewan Pediatric Bone Mineral Accrual Study (PBMAS) were separated into normal weight (NW), overweight (OW), or obese (OB) groups according to the World Health Organization criteria. Distal and shaft bone properties of the radius and tibia were measured using peripheral quantitative computed tomography (pQCT). Sex-specific MANCOVAs controlling for age, height, and limb-specific muscle cross-sectional area (MCSA) were used to assess BMI group differences in bone variables.

There were no significant differences in adjusted bone variables observed at the radius between BMI groups in either males or females ($p > 0.05$). Male and female OW and OB groups had significantly greater adjusted total content (mg/mm; males: NW (mean \pm SD) 401.4 ± 15.5 , OW 429.3 ± 15.5 , OB 448.9 ± 22.5 ; females: NW 293.2 ± 6.1 , OW 313.2 ± 7.7 , OB 317.7 ± 13.0) and adjusted total density (mg/cm³; males: NW 319.4 ± 8.7 , OW 341.1 ± 6.9 , OB 352.5 ± 12.6 ; females: NW 283.7 ± 6.3 , OW 305.1 ± 8.0 , OB 310.1 ± 13.4) at the distal tibia ($p < 0.05$). Respectively, OW and OB groups had greater adjusted cortical content (mg/mm; males: NW 440.5 ± 9.9 , OW 461.3 ± 7.9 , OB 466.2 ± 14.4 ; females: NW 354.4 ± 5.9 , OW 361.2 ± 7.4 , OB 366.6 ± 12.4) at the tibia shaft ($p < 0.05$).

Being overweight and/or obese in adulthood may confer skeletal benefits to total bone density and cortical content at the weight-bearing tibia, but not at the non weight-bearing radius. These skeletal site-specific differences may be pertinent to fracture risk.

Disclosures: Amanda Lorbergs, None.

MO0065

Structural-Functional Imaging of Bone Quantity and Quality Measures and Bone Marrow Fat and Blood Perfusion in Axial and Appendicular Skeletons.

H van Holsbeeck^{*1}, T Chenevert¹, M Feng¹, D Hamstra¹, J Jacobson¹, S Lee¹, C Van Poznak¹, Yebin Jiang². ¹University of Michigan, USA, ²Osteoporosis & Arthritis Lab, Department of Radiology, University of Michigan, USA

Bone quality, including measures of 3D bone mineral density, bone geometry, bone microstructures, and mechanical properties, can better predict osteoporotic fracture as well as monitor treatment responses than standard 2D DXA measures of bone quantity. There are considerable controversial findings of aging changes in bone mineral and structures between the axial and appendicular skeletons. There are little data addressing osteoporosis in men. Changes in bone and bone marrow are closely related, such as shift of differentiation of bone marrow-derived mesenchymal stem cells from osteoblasts to adipocytes in aging and in osteoporosis. We studied changes in bone quality and bone marrow, using structure function imaging, in male axial and appendicular skeletons.

Twelve male volunteers were recruited, with age of 53-70 years old (mean 61 years, SD 6 years). DXA 2D projectional BMD, and 3D volumetric BMD and geometry of vertebral bodies and femoral neck were measured using quantitative CT. The distal radius and distal tibia were scanned using micro CT (Xtreme CT) with isotropic resolution of 82 micrometers. Finite element analysis was used to determine the mechanical properties. Magnetic resonance (MR) spectroscopy and MR perfusion were performed to determine vertebral body bone marrow fat and bone marrow blood perfusion.

There are strong correlations between bone quantity and quality parameters and bone marrow fat ($r: -0.72 \sim -0.82$, $p < 0.05$), and between bone quality parameters and bone marrow blood perfusion ($r: 0.68 \sim 0.74$, $p < 0.05$). There are moderate correlations among bone mineral and structure and biomechanical properties ($r: 0.52 \sim 0.62$, $p < 0.05$) in the axial skeleton, among bone mineral and structure and biomechanical properties ($r: 0.58 \sim 0.69$, $p < 0.05$) in the appendicular skeleton, and mild to moderate correlations in bone mineral and structure and biomechanical properties between the axial and appendicular skeletons ($r: 0.44 \sim 0.58$, $p < 0.05$).

High correlations are found between structural and functional parameters in bone quantity and quality including 2D and 3D bone mineral measures, bone structures and geometry, and biomechanical properties, and in bone marrow including bone marrow fat and blood perfusion, while moderate correlations are found between the axial and appendicular skeletons.

Disclosures: H van Holsbeeck, None.

MO0066

The Role of Bone Intrinsic Properties on the Mechanical Behavior of Lumbar Vertebrae: Organic rather than Inorganic Bone Matrix?

Julien Wegrzyn^{*1}, Jean-Paul Roux², Delphine Farlay³, Roland Chapurlat⁴, Mary Bouxsein⁵. ¹INSERM U1033 - Université de Lyon, France, ²INSERM, UMR 1033, Université de Lyon, France, ³INSERM, UMR1033; Université De Lyon, France, ⁴E. Herriot Hospital, France, ⁵Beth Israel Deaconess Medical Center, USA

Engineering principles dictate that the whole bone strength is determined by the bone mass, microarchitecture and intrinsic properties to the bone matrix. However, few studies have directly investigated the contribution of bone tissue material properties or bone matrix composition on whole bone strength in humans. This study aimed to assess the influence of characteristics of the organic and inorganic bone matrix on the mechanical behavior of human lumbar vertebrae.

We obtained 17 fresh frozen lumbar spines (8 W, 9 M, aged 76 ± 11 years). L3 bone mass was measured by DXA and microarchitecture by μ -CT (Skyscan 1076[®] with a 35 μ m-isotropic voxel size). Microarchitectural parameters were directly measured: Tb.BV/TV, SMI, Tb.Th, DA, Ct.Th, Ct.Po and radius of anterior cortical curvature. Quasi-static uniaxial compressive testing was performed on L3 vertebral bodies under displacement control at 0.5mm/min until failure occurred. Failure load (N), stiffness (N/mm) and work to failure (N.mm) were extracted from the load/

displacement curves. FTIRM analysis was performed on 2 μ m-thick sections from L2 trabecular cores, with a Perkin-Elmer GXII Auto-image Microscope equipped with a wide band detector (MCT, 7800-400cm⁻¹). Twenty measurements per sample were performed at 30*100 μ m of spatial resolution. Each spectrum was collected at 4cm⁻¹ resolution and 50 scans in transmission mode. Mineral and collagen maturity, and mineralization and crystallinity index were measured.

There was no association between the vertebral trabecular bone matrix characteristics and bone mass or microarchitecture. Mineral maturity, mineralization and crystallinity index were not related to whole vertebrae mechanical properties. However, collagen maturity was positively correlated with vertebral failure load and stiffness ($r=0.64$, $p=0.005$ and $r=0.54$, $p=0.025$, respectively). In addition, these correlations remained significant after adjustment with aBMD ($r=0.65$, $p=0.006$ and $r=0.50$, $p=0.048$, respectively) and BMC ($r=0.71$, $p=0.002$ and $r=0.58$, $p=0.019$, respectively).

In conclusion, independently of aBMD, collagen maturity explained more than one third of the variability in mechanical behavior of lumbar vertebrae. No role of mineralization on vertebral mechanical behavior was found in this study focused on an elderly patients' cohort, though additional studies are needed to confirm these initial results.

Disclosures: Julien Wegrzyn, None.

MO0067

Tissues with Low and Abnormally High Mineral Content but Normal Crystal Size Coexist in Children with Osteogenesis Imperfecta Type VI.

Nadja Fratzl-Zelman^{*1}, Paul Roschger¹, Ingo Schmidt², Francis Glorieux³, Klaus Klaushofer¹, Peter Fratzl², Frank Rauch³, Wolfgang Wagermaier².

¹Ludwig Boltzmann Institute of Osteology at Hanusch Hospital of WGKK & AUA Trauma Centre Meidling, 1st Med. Dept. Hanusch Hospital, Austria, ²Max Planck Institute of Colloids & Interfaces, Dept. of Biomaterials, Germany, ³Genetics Unit, Shriners Hospital for Children & McGill University, Canada

Recessive osteogenesis imperfecta (OI) type VI is caused by mutations in *SERPINF1* that lead to a loss of function of pigment epithelium-derived factor, a potent antiangiogenic factor¹. Affected individuals develop a severe OI phenotype and have striking bone histological findings, characterized by accumulation of osteoid and a prolonged mineralization lag time, suggesting a distinctive mineralization defect².

To assess bone material quality, we used quantitative backscattered electron imaging to evaluate bone mineralization density distribution in iliac bone biopsy samples from children with OI type VI ($n=7$, age: 2.3-9.1 years). Compared to age-matched controls³, patients with OI type VI had significantly higher mean and most frequent mineral concentrations in both cancellous (CaMean +4.6%, CaPeak +11.7%) and cortical bone tissue (CaMean +11.5%, CaPeak +22.9%). The fractions of bone matrix with high and with low mineral content were both remarkably increased, indicating an extreme heterogeneity of bone tissue mineralization (cancellous bone: CaHigh +4625%, CaLow +195%, CaWidth +35%; cortical bone: CaHigh +10480%, CaLow +64%, CaWidth +32%). Synchrotron small angle x-ray scattering ($n=3$) showed that the thickness parameter of mineral crystals was numerically smaller or similar in the younger OI type VI patients than in age-matched controls, despite a much higher mineral fraction in patients with OI type VI.

Taken together, these results suggest that highly mineralized areas of the OI type VI bone matrix contain mineral particles that are not larger but are more densely packed. Despite the unique etiology of OI type VI with intact collagen synthesis and distinctive bone histology, mean bone matrix mineralization density is enhanced to values similar or even above those found in OI patients with collagen type I gene mutations.

References: ¹Homan EP et al., JBMR 26 (2011) ²Glorieux FH et al., JBMR 17 (2002) ³Fratzl-Zelman, N et al., Bone 44 (2009)

Disclosures: Nadja Fratzl-Zelman, None.

MO0068

Age-Specific Bone Microarchitecture values at Lumbar Spine in US Caucasian Women Derived from DXA: TBS Normative Data.

Christine Simonelli^{*1}, Edward Leib², Renaud Winzenrieth³, Didier Hans⁴.

¹HealthEast Osteoporosis Care, USA, ²University of Vermont, USA, ³Med-imaps, Hôpital X. Arnoz, PTIB, Pessac, France, France, ⁴Lausanne University Hospital, Switzerland

Trabecular Bone Score (TBS,Med-Imaps,France) is an index of bone micro-architecture extracted from antero-posterior spine DXA. Previous studies reported the ability of spine TBS to differentiate between women with and without fractures from age- and BMD-matched controls as well as its ability to predict future fracture. In this cross-sectional analysis from two facilities in the U.S., we have investigated the age related changes of the lumbar vertebrae micro-architecture assessed by TBS in a cohort of US Caucasian women.

Subjects in the study were Non-Hispanic US white women aged 30 and older with a BMD Z-score at spine L1-L4 within ± 2 SD. Individuals were excluded if they had fractures or were on any osteoporosis treatment and/or had any illness that would be expected to impact bone metabolism. All data have been obtained from Prodigy DXA

devices (GE-Lunar, Madison, WI, USA). Cross-calibrations between the two centers were performed for TBS and BMD. BMD and TBS were evaluated at spine L1-L4 but also for all possible vertebrae combinations. To validate the cohort, a comparison between BMD normative data of our cohort and US Caucasian Lunar data provided by the manufacturer was done.

A database of 427 Caucasian US women ages 30 to 90 years was created. BMD normative f obtained from this cohort were not statistically different from the US Caucasian Lunar normative data provided by the manufacturer ($p=0.83$). This outcome therefore validates indirectly our cohort. TBS values at L1-L4 were poorly correlated with BMI ($r=-0.10$) and with height ($r=-0.29$) and not correlated with weight. TBS values obtained for all lumbar vertebral combinations (L1, L2, L3, L4) decreased significantly with age (see figure 1). There was a linear decline of 16.2% (~ 2.8 T-score) in the micro-architecture at L1-L4 between 45 and 90 years of age (vs. -3.2 for BMD). The micro-architecture loss rate increases after the age of 65 years by 50% (-0.004 to -0.006). Similar results were obtained for other ROIs of the lumbar spine.

In conclusion, the decrease seen in lumbar TBS reflects age-related micro-architecture changes at spine. This age-related micro-architectural modification is similar to that obtained for French Caucasian women population ($r^2>0.99$). These findings suggest that TBS normative data can be used in clinical practice to assess bone micro-architecture deterioration over time and improve patient management.

Age-related TBS curve at L1-L4 for US Caucasian women

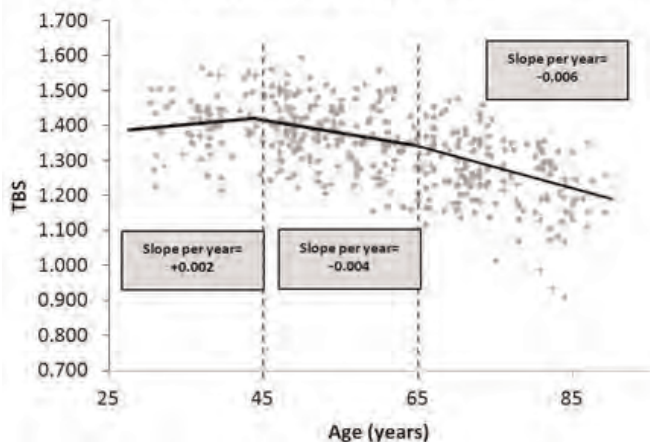


Figure 1

Disclosures: Christine Simonelli, None.

MO0069

Intravenous Ibandronate Treatment of 24 Months Increases Cancellous and Cortical Bone Mineralization Density in Male Patients with Idiopathic Osteoporosis. Barbara Misof^{*1}, Janina Patsch², Paul Roschger¹, Christian Muschitz³, Eleftherios Paschalis¹, Eva Prokok¹, Klaus Klaushofer¹, Peter Pietschmann⁴, Heinrich Resch³. ¹Ludwig Boltzmann Institute of Osteology at the Hanusch Hospital of WGKK & AUVA Trauma Centre Meidling, 1st Medical Department, Hanusch Hospital, Heinrich Collin Str. 30, Vienna, Austria, ²Department of Radiology, Medical University of Vienna, Waehringer Guertel 18-20, Vienna, Austria, ³II. Medical Department with Osteology/Rheumatology & Gastroenterology, KH Barmherzige Schwestern (St. Vincent Hospital) Vienna, Academic Teaching Hospital of the Medical University Vienna, VINforce study group, Stumpergasse 13, Vienna, Austria, ⁴Department of Pathophysiology & Allergy Research, Center for Pathophysiology, Infectiology & Immunology, Medical University of Vienna, Waehringer Guertel 18-20, Vienna, Austria

Therapeutic options and clinical trials for men with osteoporosis are still limited. We aimed to study the effect of 24 months ibandronate (IBA) treatment (3mg/3ml intravenous) in 19 male subjects with idiopathic osteoporosis within an open-label, single-center, prospective Phase III study. Patients (aged 36-80 yrs) were included if they had low BMD (fem. neck T-score lower -2 and lumbar spine T-score lower -1) and/or prevalence of at least one low trauma fracture and no secondary cause of osteoporosis. Primary endpoint was to evaluate the effect of treatment on bone mineralization density distribution (BMDD) based on quantitative backscattered electron imaging (qBEI) analysis of paired biopsy samples (baseline, after 24 months of IBA).

IBA caused significant changes in cancellous (Cn.) and cortical (Ct.) BMDD variables. Wilcoxon signed rank comparison to baseline revealed significant increases in average calcium concentrations (Cn.CaMean $+2.4\%$, p lower 0.001; Ct.CaMean $+3.0\%$, $p=0.002$) and in mode calcium concentrations (Cn.CaPeak $+3.1\%$, $p=0.027$; Ct. CaPeak $+2.3\%$, $p=0.030$). The heterogeneity of mineralization (Cn.CaWidth -14% , $p=0.044$; Ct.CaWidth -16% , $p=0.001$) and the proportion of low mineralized bone areas (Cn.CaLow -28% , Ct.CaLow -45% , both p lower 0.001) were reduced. We found

a strong dependency of the absolute treatment induced changes in Cn. and Ct.CaMean on the baseline values of Cn. and Ct. CaMean respectively (linear regression $R=0.68$ for Cn. and $R=0.82$ for Ct. bone, both p lower 0.001). Absolute changes in CaMean for cancellous vs. cortical bone were similar ($p=0.465$) but correlated well with each other (Spearman coefficient $R=0.78$, p lower 0.001).

Our findings are in line with the antiresorptive/anticatabolic effect of IBA and with previously observed bisphosphonate effects on BMDD in postmenopausal osteoporosis: Less bone is formed and the existing bone packets have prolonged time for secondary mineralization, causing an increase in average and mode mineralization densities, together with a decrease in the proportion of low mineralized areas and the well known transient reduction in the heterogeneity of calcium concentrations. The dependency of the treatment induced change in CaMean on its baseline value suggests that the patients with very low mineralization densities at baseline are having the largest increase during treatment. The similarity of changes in Cn. and Ct. bone indicates that IBA exerts treatment effects in both compartments.

Disclosures: Barbara Misof, None.

This study received funding from: Roche Austria

MO0070

Radiographic Characteristics of Prodromal Bone Deterioration (PBD) at the Lateral Femur in Patients with Long-term BP Treatment. Shijing Qiu^{*1}, Mahalakshmi Honasoge¹, Saroj Palnitkar², Sudhaker Rao¹, Sanjay Reddy¹. ¹Henry Ford Hospital, USA, ²Henry Ford Health System, USA

Despite increased attention and wide publicity, very little is known about the pathogenesis of atypical femoral fracture (AFF) following long-term BP therapy. We have found that a prodromal bone deterioration (PBD) usually precedes the occurrence of AFF. In the recent 2 years, we encountered 13 postmenopausal women who received BP therapy for 5-13 years with or without mid thigh pain. The x-rays showed focal cortical thickening with a bump on the lateral femoral diaphysis (Fig 1A), which we refer to as PBD. The bone damage was confirmed by isotope bone scan. Tomosynthesis of X-ray image can reveal a fracture line that may not be visible on conventional X-ray image (Fig 1B). PBD occurred at the junctions of the upper 1/3rd and lower 2/3rds of the femoral diaphysis, sometimes bilaterally and sometimes with AFF in one femur and asymptomatic PBD in the other. When bilateral it was symmetrical in the individual patient. BP therapy was discontinued for patients with PBD. Prophylactic internal rod fixation was performed in 3 patients. Another interesting, but distressing, finding was that x-ray of the femurs in an osteoporotic patient on prolonged BP therapy showed typical PBD that was characterized by focal cortical thickening at the lateral femoral diaphysis associated with an incomplete fracture line (Fig 2A) and positive bone scan (Fig 2B). Seven days later, AFF occurred at the site of PBD (Fig 2C). This strongly suggests that PBD is necessary for the development of AFF. Recently, X-rays of both femurs were taken in 25 consecutive patients on long term BP treatment. Three patients (12%) had the signs of PBD, suggesting the prevalence of PBD may be significantly higher than currently recognized.

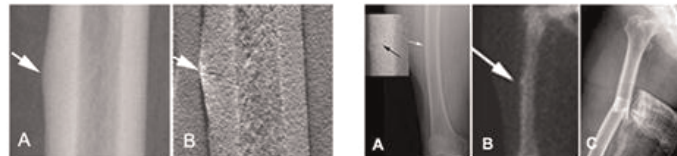


Fig 1. PBD on lateral cortex of the femur. (A) Note the focal bump-cortical thickening (arrow). (B) The fracture line that is unclear on the X-ray can be shown with tomosynthesis.

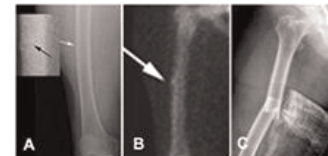


Fig 2. A BP treated patient with PBD at the lateral femur (A, arrow) and positive bone scan (B, arrow). Seven days later, AFF occurred at the site of PBD (C).

Figures

Disclosures: Shijing Qiu, None.

MO0071

Bone Remodeling is Linked to Vessel Remodeling in Femoral Head and Neck. Ping Zhang^{*1}, Hiroki Yokota². ¹Indiana University - Purdue University Indianapolis, USA, ²Indiana University Purdue University Indianapolis, USA

Osteoporosis and osteonecrosis are serious orthopedic problems. Mechanical loading prevents bone loss and disuse induces osteopenia. To our knowledge, however, the role of blood circulation in the femoral head and neck for disuse osteopenia has not been fully investigated. The object of this study is to examine if blood circulation is involved in bone remodeling in the proximal femur.

Thirty-six C57/BL/6 mice (~ 14 wks) were divided into three groups such as loading, unloading, and age-matched control. The loading group received knee loading, in which 0.5 N loads were laterally applied to the knee at 15 Hz for 5 min/day for 5 consecutive days. In the unloading group, animals were subjected to tail suspension for 2 weeks. Microfil infusion was performed to evaluate blood supply and vessel remodeling.

The loading group presented an increase in bone mass in the proximal femur. Compared to the control group, knee loading increased cortical thickness in the mid- ($p<0.05$) and proximal diaphysis ($p<0.01$), as well as the femoral neck ($p<0.01$). It also elevated cortical area in the mid- ($p<0.001$) and proximal diaphysis ($p<0.01$), and

increased cortical bone volume (BV/TV) in the mid- ($p<0.01$) and proximal diaphysis ($p<0.05$) together with femoral neck ($p<0.05$).

The unloading group exhibited a significant deficit in bone remodeling. Compared to control, it reduced cortical cross area ($p<0.05$), bone area fraction ($p<0.01$), cortical thickness ($p<0.01$), and cortical BV/TV ($p<0.01$) in the mid-diaphysis. Micro CT images of a whole head and neck showed that unloading decreased BV/TV ($p<0.001$), and reduced the trabecular number ($p<0.001$) and trabecular thickness ($p<0.01$), while it increased trabecular separation ($p<0.001$). Histological analysis revealed that unloading reduced cortical thickness by 21% ($p<0.05$) and BV/TV by 48% ($p<0.01$) in the femoral head. Furthermore, in the loaded samples we observed vessel networks around the proximal femur with several branches extending toward the femoral head and neck. Unloaded samples, however, decreased the number and size of blood vessels with a fewer number of microfil stained regions.

This study demonstrates that loading enhances bone mass and vessel networks in the proximal femur, while unloading reduces them. The results show that an appropriate supply of blood is associated with bone remodeling, indicating that enhancing blood circulation to the proximal femur may suppress disuse driven bone loss in the femoral head and neck.

Disclosures: Ping Zhang, None.

MO0072

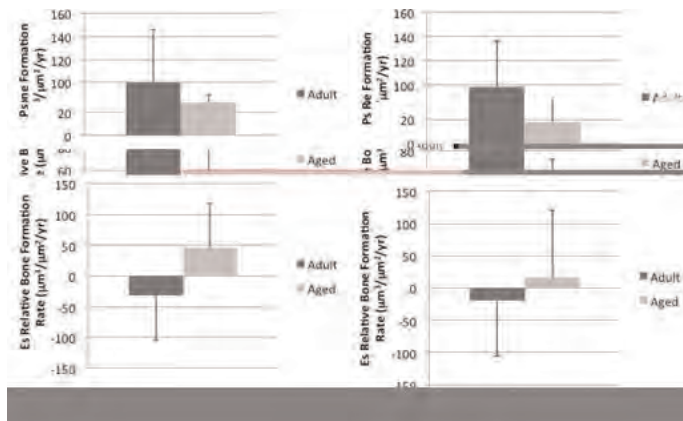
Aging Mice Exhibit Reduced Periosteal and Greater Endosteal Mechano-responsiveness Following Two Weeks of Axial Compressive Loading. Alesha Castillo, Ian Mahaffey*, Whitney Cole. VA Palo Alto Health Care System, USA

Introduction: Mechanical loading is a potent regulator of bone mass. Although results are mixed, data suggest that aging bones are less responsive to anabolic mechanical stimuli [1, 2, 3, 4]. With regard to studies in aging mice, background strain, gender, and loading protocol all affect load-induced osteogenesis. Furthermore, data in long bones suggest an envelope-specific (corticoperiosteal, corticoendosteal, trabecular) and site-specific (% of total length) response, which can have a significant effect on changes in bone strength. The purpose of this study was to determine the effects of aging on the mechano-responsiveness of adult and aging C57BL/6 female mice in an envelope- and site-specific manner using the *in vivo* tibial axial compressive loading model [5].

Methods: The right tibia in 16-wk-old (adult) and 52-wk-old (aging) C57BL/6 female mice was subjected to axial compressive loading (5 N, 2 Hz, 60 cyc, 3 d/wk for 2 wks). The left tibia served as nonloaded internal control. All mice were given *in vivo* fluorochrome bone labels. Cortical (Ct) geometry, and periosteal (Ps) and endosteal (Es) bone formation rates were calculated [6] at 45% and 50% of the total tibial length (TL). Relative (r) values (right minus left) were calculated. Trabecular (Tb) bone microarchitecture in the proximal tibia was characterized by microCT analysis.

Results: Aging mice had a smaller Ct thickness at 45% TL ($p<0.05$) and 50% TL ($p<0.001$), and greater minimum moment of inertia ($p<0.05$) at 50% TL, compared to adult mice. Loading did not affect Ct geometric properties at either site. Aging mice had lower Ps MS/BS and BFR, and Es MS/BS at 45% TL, and lower Ps MS/BS and Es MS/BS at 50% TL in the non-loaded tibia. Es rMS/BS was higher at 45% TL ($p<0.05$), and Ps rBFR was lower ($p<0.05$) at 50% TL, in aging versus adult mice. Aging mice had lower BV/TV ($p<0.001$) and Tb.N ($p<0.001$), and higher Tb.Sp ($p<0.01$), in the non-loaded tibia versus adult mice. The short-term loading regimen did not affect Tb bone architecture in either group.

Conclusions: Our data suggest that aging female C57BL/6 mice can respond to mechanical stimulation at the Ps and Es envelopes in a site-specific manner, although the Ps response is significantly attenuated in aging versus adult mice. Aging mice appear to be more responsive at the Es surface. Greatest effects were observed in MS/BS, which points to differences in number or activity of osteoblasts in adult versus aging animals.



Periosteal and Endosteal Relative Bone Formation Rates

Disclosures: Ian Mahaffey, None.

MO0073

Gene Expression in Corticocancellous Tissue is Altered Following Cyclic Tibial Loading in Adult Female Mice. Whitney Bullock*, Russell Main, Daniel Duffy, Philip DeShield, Purdue University, USA

Mechanical stimulation of bone can have protective effects against skeletal wasting diseases by increasing bone mass. The skeletal response to mechanical stimulation is regulated by a complex interaction of genetic factors that are still poorly understood. Previous studies in mice have examined gene expression in whole bones, but have not focused specifically on genetic regulation of skeletal mechanotransduction at corticocancellous sites, which are most susceptible to age-related bone loss in humans. Evidence from knockout models suggests that cortical and cancellous tissues may be regulated differently in response to mechanical stimuli. Therefore, the objective of this study is to examine how mechanical stimuli affect gene expression at corticocancellous sites. Given the age-related reduction in estrogen and concomitant decrease in adaptive skeletal response to mechanical stimuli, we are particularly interested in the role of estrogen receptor alpha (esr1) in the skeleton's genetic response to mechanical stimuli.

Female, 16-week old C57Bl/6 mice were subjected to cyclic axial compression of the tibiae for a single loading event (432 load cycles, 4Hz, ~5min/d) and euthanized either 3hr or 24hr following the loading event. At each time point, mice (n=12/group) had a 3.5N, 5.2N, or 7.0N (Low, Medium, High) compressive load applied to the left tibiae, while the right tibiae served as contralateral controls. Following loading, control and loaded tibiae were isolated, divided into diaphyseal and metaphyseal sections and flash frozen. RNA was isolated, reverse transcribed and analyzed by qPCR. We examined Sost, Esr1 and Runx2. β -actin was used as a housekeeping control gene. Statistical analyses were performed using linear mixed models with repeated measures and statistical significance indicated at $\alpha=0.05$.

Gene expression was significantly altered 24hr following loading, but did not differ between the loaded and control limbs at any load level. Sost and Runx2 were down-regulated more in the High load group compared to the Low load group 24 hours following a single compressive loading event, while Esr1 was up-regulated more in the High load group relative to the Low load group. Future work will examine additional loading protocols involving multiple-day loading events, and comparison of gene regulation in corticocancellous and diaphyseal cortical bone.

Disclosures: Whitney Bullock, None.

MO0074

The Role of Endothelial BMP2 in Osteogenesis of the Mouse Forelimb. Jennifer McKenzie*¹, Sarah McBride², Vicki Rosen³, Matthew Silva⁴.

¹Washington University in St. Louis, USA, ²Clemson University, USA, ³Harvard School of Dental Medicine, USA, ⁴Washington University in St. Louis School of Medicine, USA

BMP2 is essential for post-natal skeletal homeostasis and is required for fracture healing. BMP2 may also play a role in stress fracture healing, a process characterized by rapid increases in vascularity followed by non-endochondral woven bone formation. Recently, we observed early upregulation of BMP2 after creation of a stress fracture, with the unexpected finding that BMP2 expression occurred first in vascular cells then in bone cells. To investigate the role of BMP2 in endothelial cells we created a conditional knockout by crossing VE-cadherin-Cre with BMP2^{fllox/fllox} mice. The skeletal phenotypes of control (Cre-negative; BMP2^{fllox/fllox}) and conditional knockout (cKO) mice were assessed by DXA and *in vivo* microCT from 1-6 months of age in male and female mice. Deletion of endothelial BMP2 did not result in any gross phenotype. Bone density, mineral content and morphology as measured by whole-body DXA and tibial microCT were not different between control and cKO mice (n=4-5/group). The right forelimbs of additional mice aged 6 mo were subjected to a loading protocol that creates a stress fracture and triggers woven bone formation. There were no differences in bone formation parameters between control and cKO as measured by microCT (woven bone extent/volume) or dynamic histomorphometry (mineral apposition rate, mineralizing surface) 10 days after loading (n=11-12/group). Thus, conditional deletion of endothelial BMP2 does not alter skeletal development or homeostasis. Our data indicate that loss of endothelial BMP2 alone does not influence non-endochondral, woven bone formation in a murine stress fracture model.

Disclosures: Jennifer McKenzie, None.

MO0075

Withdrawn

MO0076

Exposure to Big Endothelin-1 in Bovine Sternal Cores Mimics Some Aspects of Mechanical Loading. Luisa Meyer¹, Michael Johnson², Juan Vivanco³, Robert Blank², Heidi Ploeg³, Everett Smith². ¹University of Wisconsin - Madison, USA, ²University of Wisconsin, USA, ³University of Wisconsin Madison, USA

It is well established that mechanical loading increases bone strength by inducing bone remodeling. Endothelin-1 (ET-1), a ubiquitous autocrine/paracrine signaling molecule, is known to promote osteogenesis in the setting of breast and prostate cancer. It was hypothesized that ET-1 acts synergistically with mechanical loading to increase the apparent stiffness of bovine trabecular bone cores. In a 2x2 factorial trial of daily compressive loading and 25 ng/ml big ET-1, 48 bovine sternal cores were maintained in individual polycarbonate chambers. The cores were tested in compression with a piezoelectric controlled axial loading system with measurements of force and displacement. Apparent stiffness was calculated from the slope of the force-displacement data and apparent elastic modulus was determined assuming Hooke's Law and the bulk dimensions of the bone core. The cores in the "load" groups were subjected to dynamic loading once a day of -2000 microstrain for 120 cycles at a frequency of 2 Hz. Apparent elastic modulus was determined from a quasistatic measurement at baseline and on days 15, and 23. Culture media were changed daily and collected at baseline and every three days thereafter. Prostaglandin E2 production was measured by ELISA. Loading of the bone cores significantly ($p < 0.05$) increased the mean percent change in apparent elastic modulus (+26% in "load+ET-1" and +17% and in the "load" groups). Exposure to ET-1 contributed to an increase in stiffness from baseline to day 23 in both the "load" and "no load" groups, 26% and 13% respectively. The effect of ET-1 alone (+13%) and exercise alone (+17%) were not significantly different. In all treatment groups prostaglandin production began at 8 days post osteotomy and continued throughout the remainder of the experiment, while in the control group prostaglandin production began to decrease at day 12 and by day 15 was 70% of the treatment groups. The study results suggest that exposure to ET-1 mimicked exercise induced strain.

Disclosures: Everett Smith, None.

MO0077

Mechanotransductive Stimulation using LIPUS Accelerates Fracture Healing in a Disuse Osteopenia Model. Yi-Xian Qin¹, Long Bi², Maria Pritz². ¹State University of New York at Stony Brook, USA, ²Stony Brook University, USA

Introduction: Mechanical wave induced by low-intensity pulsed ultrasound (LIPUS) treatment has been proven to have a therapeutic role in promoting mineralization and decreasing the duration of fracture healing. Similar effect of LIPUS on accelerating fracture healing on disuse osteopenia was therefore hypothesized, using a rat hind limb suspension (HLS) femoral fracture model with LIPUS intervention.

Method: Closed femoral fracture procedures were performed on thirty-six Sprague-Dawley rats after they were randomly divided into three groups. In group FSU, the rats were disuse-induced by HLS, and LIPUS treatment was administered daily to the fractured femur; in group FSC, the rats were HLS but without LIPUS treatment; in group NFC, no HLS and LIPUS treatments were applied after fracture. *In vivo* mCT was used to exam the fractured femur immediately and two weeks after fracture. Five weeks later, femurs of fracture were harvested and subjected to *ex vivo* mCT evaluation and four-point bending to assess morphometric and mechanical properties. Undecalcified samples of fracture healing areas were embedded by polymethylmethacrylate and sectioned and stained with Von Kossa and hematoxylin-eosin.

Results: Although there were no significant changes of morphometric properties proved by *in vivo* mCT among the three groups at the 0 and 2 weeks ($P > 0.05$), *ex vivo* mCT showed 30% ($p < 0.05$) bone volume increase in treated group than the control in 5 weeks (Fig. 1). 4-pt mechanical bending test showed 5-week ultrasound treated group was 48% ($p < 0.05$) higher than the sham control in Young's modulus (Fig. 2). Histological staining showed a higher ratio of lamellar bone formed in the fracture areas of FSU (36%), compared to control groups (20%) (Fig. 3). In contrast, only cartilage-like tissues and wove bone formed in the fracture areas in the NFC and FSC groups.

Conclusion: These comparable results on healing responses imply that LIPUS can accelerate fracture healing in a disuse osteopenia condition.

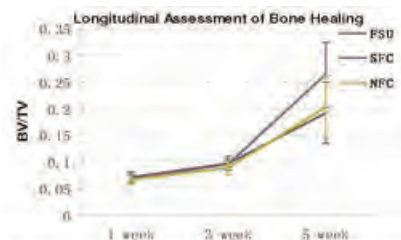


Fig. 1. MicroCT bone volume fraction in ultrasound treated group (FSU) indicated 30% increase compared to control groups.

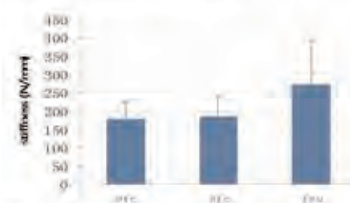


Fig. 2. 4-pt bending test showed 48% stiffness increase in the ultrasound treated group compared to the controls.

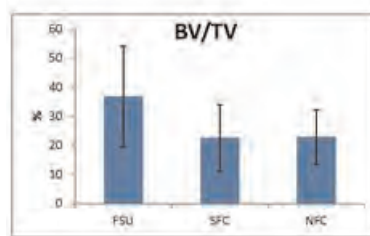


Fig. 3. Histology results (2-D) showed bony ingrowth and mineralization increased in fracture callus.

Figure 1-3

Disclosures: Long Bi, None.

This study received funding from: National Space Biomedical Research Institute through NASA Cooperative Agreement NCC 9-58; NIH (R01 AR052379 and R01 AR049286); and NYSTAR

MO0078

Physical Activity in Adolescence may be Associated with Larger Total and Cortical Area and Greater Bone Strength. Rachel Duckham^{*1}, Adam Baxter-Jones², Donald Bailey², Robert Faulkner², James Johnston², Saija Kontulainen². ¹UMASS, USA, ²University of Saskatchewan, Canada

Introduction: Previous reports from the Pediatric Bone Mineral Accrual Study (PBMAS) indicated that physical activity (PA) in adolescence is beneficial to bone accrual in adolescence (Bailey et al. J Bone Miner Res 1999) and adult bone mineral mass (Baxter-Jones et al. Bone 2008). However it is unclear whether these benefits result in greater bone strength.

Purpose: To investigate whether physical activity (PA) levels in adolescence results in greater bone size, density and estimated bone strength in adulthood.

Methods: Peripheral quantitative computed tomography (pQCT) was used to assess the weight-bearing tibia and clinically relevant radius in 92 young adults in 2010 (53 females, 39 males), who had participated in the PBMAS since 1991. Total area (ToA), cortical density (CoD) and area (CoA), and estimated bone strength (SSI_p) were measured at the diaphysis and total density (ToD), trabecular density, (TrD) and bone strength (BSI) at the metaphysis. Lower leg and forearm muscle cross sectional area (CSA) were also assessed. Participants were grouped by their adolescent PA levels (inactive, average and active) based on mean PA z-scores obtained from questionnaires completed during adolescence. Analysis of variance adjusting for adult height and muscle CSA was used to compare bone parameters between groups. Alpha was set to 0.05.

Results: At the tibia, adult males who were more physically active than their peers in adolescence had 13% greater bone strength (SSI_p, $p=0.02$), and 10% greater ToA ($p=0.03$) compared to their inactive peers. Adult females, who were more active in adolescence, had 9% larger CoA ($p=0.02$) at the tibia when compared to their inactive peers. At the radius, adult males who were more active in adolescence had 17% greater bone strength (SSI_p, $p=0.05$) and 13% greater ToA ($p=0.03$) compared to their inactive peers. No other significant differences in bone properties or estimated strength were found at the weight-bearing tibia or at the clinically relevant radius in adult males or females according to adolescence PA.

Conclusion: PA in adolescence maybe associated with greater total and cortical bone area, and bone strength in adulthood at the tibia and radial diaphysis. Further research should consider the role of adult PA levels in this association.

Disclosures: Rachel Duckham, None.

MO0079

Physical Activity is Associated with Improved Cortical Microstructure at the Ultradistal Tibia in Young Men. Martin Nilsson*¹, Robert Rudäng¹, Claes Ohlsson², Mattias Lorentzon³. ¹Centre for Bone & Arthritis Research At the Sahlgrenska Academy, Sweden, ²Center for Bone & Arthritis Research at the Sahlgrenska Academy, Sweden, ³Center for Bone Research at the Sahlgrenska Academy, Sweden

Purpose: We have previously reported an association between physical activity, trabecular microstructure and cortical bone geometry in young adult men (Nilsson, M. et al. J Clin Endocrinol Metab. 2010 Jun;95(6):2917-26). The aim of this study was to investigate if physical activity was associated with cortical microstructure and estimated failure load in weight-bearing bone in young men.

Methods: Micro-CT-based evaluation of cortical microstructure and finite element analysis of the ultradistal tibia was performed, using measurements from a high resolution 3D pQCT device (XtremeCT, Scanco Medical AG, Switzerland) in 828 men, 24.1 ± 0.6 yrs old. A standardized questionnaire was used to collect information about current physical activity duration (years), level (recreational/competitive/elite), and type (strain score 0-3, based on ground reaction force for each type of physical activity).

Results: A linear regression model (including age, height, weight, calcium intake, smoking, and alcohol intake as covariates) revealed that physical activity duration, level, and degree of mechanical loading (strain) were all independently associated with mean cortical pore diameter (duration B=-0.4 (µm/year), p<0.001; level B=-3.4 (µm/category), p<0.001; strain B=-4.0 (µm/strain score category), p<0.001), periosteal circumference (duration B=0.2 (mm/year), p<0.001; level B=1.8 (mm/category), p<0.001; strain B=1.4 (mm/strain score category), p<0.001), and total bone strength (estimated ultimate failure load) (duration B=99 (N/year), p<0.001; level B=794 (N/category), p<0.001; strain B=720 (N/strain score category), p<0.001) at the ultradistal tibia. Physical activity variables were not associated with cortical porosity index. Men with the highest degree of mechanical loading (strain score 3, e.g. basketball) had 8.0% smaller cortical pore diameter than men with the lowest weight-bearing physical activity strain (strain score 1, e.g. jogging; Figure 1).

Conclusion: In this large cohort of young men, increasing physical activity duration and loading were independently associated with lower cortical pore diameter, larger periosteal circumference, and higher bone strength at the ultradistal tibia, indicating that physical activity can modulate the cortical bone structure and increase bone strength.

Figure 1. Physical Activity and Cortical Pore Diameter at the Ultradistal Tibia

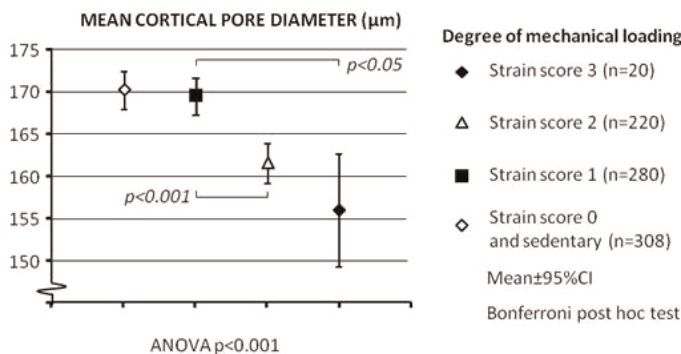


Figure 1

Disclosures: Martin Nilsson, None.

MO0080

Identification of Bone-Derived Binding Partners of Human Phosphate Regulating Endopeptidase Mutated in X-Linked Hypophosphatemia (PHEX). THEODORE CRAIG*¹, Rajiv Kumar². ¹Mayo Clinic, USA, ²Mayo Clinic College of Medicine, USA

Background: PHEX, a membrane associated endopeptidase mutated in X-linked hypophosphatemia, is known to bind proteins such as sclerostin that are important in bone mineralization. Other substrates for PHEX are unknown. To identify novel substrates for PHEX, we investigated the interaction of the extra cellular domain of PHEX with rat bone proteins.

Methods: PHEX, amino acid residues 50-749, was synthesized as a maltose binding protein-PHEX construct. The MBP-PHEX construct was bound to an

amylose column and washed extensively with low ionic strength buffer. Rat bone proteins were decalcified with EDTA over 72 hours at 4 °C. The decalcified protein extract was applied to MBP-PHEX amylose columns. As control, MBP was bound to amylose and bone proteins were applied to the MBP column. The MBP-PHEX-amylose and MBP-amylose columns were washed extensively with low ionic strength buffer and bound proteins were eluted with 1.5 M sodium chloride. The eluted proteins were separated by SDS-polyacrylamide gel electrophoresis. Bands and interband regions were cut out and proteins within the gel slices reduced, carboxymethylated, trypsinized and analyzed by mass spectrometry.

Results: Several novel proteins were identified bound to MBP-PHEX but not to MBP alone. Novel proteins binding to PHEX include peptidyl-prolyl cis-trans isomerase, chondroadherin, serpin B, S-100 protein, heparin co-factor 2, moesin, radixin and ezrin. Chondroadherin is a secreted cartilage protein that influences chondrocyte attachment and the interaction between PHEX and this protein could conceivably be important in chondrogenesis. Moesin, radixin and ezrin are gap junction proteins abundantly expressed in chondrocytes.

Conclusion: The association of PHEX with proteins important in cartilage function suggests novel mechanisms by which PHEX functions in bone.

Disclosures: THEODORE CRAIG, None.

MO0081

Inactivation of Nedd4 Enhances Vascular Cell Mineralization through Stabilizing a Smad1 in Human Vascular Smooth Muscle Cells. Je-Yoel Cho¹, Ji-Hyun Lee^{2*}, Xiangguo Che³, Jae-Jin Cho², Je-Yong Choi⁴. ¹College of Veterinary Medicine, Seoul National University, South Korea, ²Seoul National University, South Korea, ³Kyungpook National University, South Korea, ⁴Kyungpook National University, School of Medicine, South Korea

Vascular calcification is associated with atherosclerosis, diabetes and chronic kidney disease and it has been suggested to be similar to bone mineralization. However, the mechanism is poorly understood. Neural precursor cell expressed developmentally down-regulated protein 4 (NEDD4) is an ubiquitin-protein ligase containing a calcium/lipid-binding domain, multiple WW domains and a C-terminal HECT domain. We previously reported that Nedd4 could be a modulator to Smad1 in BMP2/TGFβ1 signaling. Thus, we assessed the effect of Nedd4 on the human vascular smooth muscle cell (hVSMCs) calcification. Knockdown of Nedd4 using Nedd4 siRNA increased the bone related gene expression levels and the formation of mineralized nodules in hVSMCs. Nedd4 knockdown also up-regulated p-Smad1 levels in hVSMCs. Nedd4 transfection decreased p-Smad1 levels. Nedd4 was phosphorylated on its Ser/Thr residues by TGFβ1 treatment. Moreover, the NEDD4 protein expression was lower on the calcified aorta where the p-Smad1 levels were high. These results showed that Nedd4 knockdown repressed the inhibition effect of osteoblastic differentiation in calcifying hVSMCs through the Nedd4/Smad1 signaling pathway. These results provide evidences for the hypothesis that Nedd4 plays a protective role against vascular calcification.

Disclosures: Ji-Hyun Lee, None.

This study received funding from: No. 20110019355 & 20100026741

MO0082

Mineralization Is Supported by Regulated Transport of H⁺ out of the Osteon. Li Liu^{1*}, Irina Tourkova¹, Lida Guo¹, Paul Schlesinger², Peter Friedman³, Harry Blair¹. ¹University of Pittsburgh, USA, ²Washington University, USA, ³University of Pittsburgh School of Medicine, USA

Mineralization of cartilage and of bone requires a high-phosphate environment, provided by phosphate carriers and by phosphatase activity. In cartilage, diffuse mineralization occurs in acellular matrix solely by this mechanism. In bone, however, mineralization is dense, vectorial, and occurs in a cell-bound structure. Deposition of bone mineral evolves ~1.5 moles of H⁺ per mole of Ca²⁺, suggesting that an ion transport system drives vectorial mineral deposition that is enabled by phosphate production and matrix protein synthesis. We previously showed that mineralizing osteoblasts have very high expression of Na⁺/H⁺ transporters by which they extrude massive acid loads, and that pH_i of mineralizing cells, when Na⁺ is removed, rapidly acidifies. In mice with the Na⁺/H⁺ regulatory factor-1 knocked out, with dietary compensation for renal phosphate loss, we show a mineralization defect causing wide calcine labels in bone formation, but greatly reduced mineral production, in keeping with regulated Na⁺/H⁺ extrusion from the osteon of H⁺. It remained unclear how osteocytes/osteoblasts within bone forming units might accomplish vectorial uptake of H⁺. Using membrane vesicles from mineralizing osteoblasts, acridine quenching fluorometry showed high capacity, low gradient H⁺ uptake. These membranes are characterized also by high alkaline phosphatase activity. H⁺ uptake was not dependent on ATP or any other demonstrable energy source, but was dependent on an inside to outside K⁺ gradient. An active membrane K⁺ conductance was shown by bilayer clamping. Osteoblast and osteocyte membranes were also characterized by very high expression of two Cl⁻/H⁺ exchangers, CLCN3 and CLCN5. The CLCN3 exchanger is predominant, accounting for ~80% of CLCN mRNAs. It is strongly expressed on osteocyte/osteoblast processes in bone. Expression of CLCN3 and CLCN5 increase ~10 fold during transition to mineralization in culture. We hypothesize that Cl⁻ (out) H⁺ (in) transport by CLCN3 mainly balances K⁺ voltage,

with net uptake of H^+ by osteoblasts and allowing the high volume acid excretion that occurs at the basolateral surface of the osteon via Na^+/H^+ exchange. This hypothesis further supported by the CLCN3 deficient mouse, which is osteoporotic; its detailed characterization is ongoing. Our data define an acid extrusion mechanism supporting rapid vectorial bone mineralization, permitting efficient capture of phosphate as mature mineral of PO_4^{3-} and OH^- calcium salts.

Disclosures: Li Liu, None.

MO0083

Cbfb Deficiency in Mesenchymal Stem Cell Provides Insight into Pathogenesis of Cleido Cranial Dysplasia and Mechanism of Cartilage Development. Mengrui Wu^{*1}, Fei Tian², Junging Ma³, Wei Chen⁴, Guochun Zhu⁵, Bo Gao⁵, Wang Lin³, Lianfu Deng⁶, Yi-Ping Li⁴. ¹The University of Alabama at Birmingham, USA, ²Department of Pathology, University of Alabama at Birmingham, USA, ³Institute of Stomatology, Nanjing Medical University, China, ⁴University of Alabama at Birmingham, USA, ⁵Department of Pathology, University of Alabama at Birmingham, USA, ⁶Shanghai Institute of Traumatology & Orthopaedics, Shanghai Key Laboratory for Prevention & Treatment of Bone & Joint Diseases with Integrated Chinese-Western Medicine, Ruijin Hospital, Jiao Tong University School of Medicine, China

Core binding factor beta (Cbfb) forms heterodimer with core binding factor alpha (Cbfa1) and the human gene mutation of Cbfa1 or Cbfb resulted in cleidocranial dysplasia (CCD) (Khan A. et al, 2006). Cbfb^{-/-} was embryonic lethal and Cbfb GFP/GFP and Cbfb^{-/-}Tg mice died at birth. The role of Cbfb in skeletal cells and in postnatal skeletal development remains unclear. To examine the function of Cbfb in skeletal development and in the pathogenesis of CCD, mesenchymal-cell-specific Cbfb-deficient mice [Cbfb^{fl/fl} Prx1-cre mice] were generated and characterized. Cbfb^{fl/fl} Prx1-cre mice survive to adult with skeletal defects, resembling CCD features, including short stature, delayed closure of cranial sutures, and defects in clavicle. Long bones from 4-week old Cbfb^{fl/fl} Prx1-cre mice were examined by histological analysis. Chondrocyte proliferation in Cbfb^{fl/fl} Prx1-cre mic was inhibited according to PCNA stain. Structure of growth plates in mutant mice was disrupted with elongated resting zone, shortened proliferative zone and disappeared columnar organization in proliferative zone. Chondrocyte hypertrophy in mutant mice was also retarded according to reduced Collagen X expression. The expression of Indian hedgehog (Ihh), cyclin D1, and was dramatically reduced in Cbfb^{fl/fl} Prx1-cre mice. However, the expression of parathyroid hormone-related protein receptor (PTHrP-R) was increased. The expression of osteopontin and osteocalcin in trabecular bone was reduced. Osteoblastogenesis of calvarial cells derived from Cbfb^{fl/fl} Prx1-cre mice was inhibited as well. Interestingly, though was recognized as 'stabilizer' of Cbfa1, there was no significant change of Cbfa1 expression in Cbfb^{fl/fl} Prx1-cre mice either in vivo or in vitro. Our studies provided insight into pathogenesis of CCD and demonstrated the essential role of Cbfb in chondrocyte proliferation, hypertrophic zone maturation and trabecular bone formation through up-regulation Indian hedgehog and down regulation PTHrP-R in postnatal mice.

Disclosures: Mengrui Wu, None.

MO0084

Choline Kinase Beta is an Important Regulator of Endochondral Bone Formation. Zhuo Li^{*1}, Gengshu Wu¹, Roger Sher², Kayla Rumack³, Gregory Cox², Michael Doschak¹, Monzur Murshed⁴, Frank Beier³, Dennis Vance¹. ¹University of Alberta, Canada, ²The Jackson Laboratory, USA, ³University of Western Ontario, Canada, ⁴McGill University, Canada

Choline kinase is the first enzyme in the choline pathway to generate phosphatidylcholine and converts choline to phosphocholine. Choline kinase has two isoforms encoded by the genes *Chka* and *Chkb*. Inactivation of *Chka* results in embryonic lethality, whereas *Chkb* mutant mice display neonatal forelimb bone deformation. To understand the mechanisms of the bone deformation phenotype, we characterized the major long bones in the forelimb. We found that the deformation is specific to the radius and ulna and the deformation occurs during the late embryonic stage. We also found that the radius and ulna in mutant mice display abnormal chondrocyte cell morphology, unorganized proliferative columns and expanded hypertrophic zones in their growth plates as well as delayed formation of primary ossification centers. To further understand these phenotypes, we examined chondrocyte apoptosis, cartilage extracellular matrix (ECM) degradation and mineralization events. We found that mutant hypertrophic chondrocytes have a decreased rate of apoptosis. In addition, the cartilage in mutant mice has diminished ECM degradation by matrix metalloproteinase 9 and 13. Moreover, matrix of mutant chondrocytes shows impaired mineralization both *in vivo* and *in vitro*. Taken together, our data suggests that choline kinase beta plays an important role in endochondral bone formation through regulation of growth plate chondrocyte physiology.

Disclosures: Zhuo Li, None.

MO0085

Identification of Signature Genes Selectively Expressed in Mesenchymal Stem Cells Derived from Synovial Joint Tissues. Yoichi Ezura^{*1}, Tadayoshi Hayata², Tetsuya Nakamoto³, Takuya Notomi⁴, Takeshi Muneta³, Ichiro Sekiya⁵, Masaki Noda³. ¹Tokyo Medical & Dental University, Medical Research Institute, Japan, ²Medical Research Institute, Tokyo Medical & Dental University, Japan, ³Tokyo Medical & Dental University, Japan, ⁴GCOE, Tokyo Medical & Dental University, Japan, ⁵Tokyo Medical & Dental University, Japan

Stromal progenitor cells existing in various adult tissues possess multi-potency to differentiate into various cell types, and thus called as mesenchymal stem cells (MSCs). Basic characterization of these cells indicated that common features are shared. However, detailed comparison also indicated that there are consistent differences among them. Synovium derived human MSCs are most potent for *in vitro* chondrogenesis, whereas bone marrow derived MSCs are more potent for osteogenesis. Gene expression and epigenetic status of these cells appeared to be different at some important loci (1, 2). Here, to investigate further the basic differences among MSCs derived from different tissues, we compared the gene expression profiles of human MSCs obtained from bone marrow, synovium, adipose tissue, skeletal muscle, as well as other connective tissues, including meniscus, cruciate ligaments, and articular cartilage as sources for MSC isolation. As previously indicated, expression profiles of hMSCs derived from intra synovial-joint tissues (is-MSCs), that are synovium, meniscus and cruciate ligaments had similar profile, when compared with extra synovial-joint tissue derived MSCs. However, even among the genes selected as highly expressed in is-MSCs, many genes showed different expression patterns among these cell types. The comparison identified 23 genes specifically expressed in meniscus derived MSCs, 8 genes specifically expressed in ligament derived MSCs, and 22 genes specifically expressed in synovium derived MSCs. Functional analysis of these specific genes in chondrogenic and ligamentous differentiation potentials would clarify the developmental and adoptive regulation of stromal progenitor cell differentiation to cells contribute to cartilaginous and fibrous tissue formation.

(1) Segawa, Y. et al., Journal of Orthopaedic Research 27: 435-441 (2009)(2) Ezura, Y. et al., ASBMR 2011 Annual Meeting

Disclosures: Yoichi Ezura, None.

MO0086

Loss of Stk11 (Lkb1) in Chondrocytes Delays Chondrocyte Hypertrophy Resulting in a Chondrosarcoma-like Overgrowth in the Postnatal Skeleton. Lick Pui Lai^{*}, Andrew McMahon. Harvard University, USA

Stk11 (also known as liver kinase b1 (Lkb1)) is a serine-threonine protein kinase that acts upstream of the AMP-activated protein kinase (AMPK) family in coupling energy homeostasis to cell growth, proliferation and survival. Through chondrocyte specific removal of Stk11 activity, we show that Stk11 is required for the normal switch of mitotic chondrocytes to a post-mitotic hypertrophic chondrocyte fate. To determine the molecular mechanisms underlying Stk11 action, we examined the mTOR pathway, which is inhibited by AMPK in growth regulation. Strikingly, rapamycin treatment of the pregnant mouse was able to rescue the delay in chondrocyte hypertrophy in Stk11 mutant embryos, suggesting that Stk11 inhibition of mTOR signaling is critical for the switch in chondrocyte fate. To determine the consequences of Stk11 removal in the postnatal skeleton, we examined long bones following chondrocyte specific removal of Stk11 at embryonic stages. Removal of Stk11 led to chondrosarcoma-like overgrowth phenotype in the Stk11 mutant skeletal elements. Furthermore, in contrast to wild-type chondrocytes isolated from the postnatal day 30 growth plate, Stk11 mutant chondrocytes proliferated and formed colonies in monolayer and anchorage-independent agar cultures, indicative of a neoplastic transformation. Gene Ontology analysis of gene expression profiles indicated an augmented activity of cell proliferation and cell cycle regulators within the chondrosarcoma-like population compared to chondrocytes in the normal growth plate. Taken together, these data demonstrated an unexpected role of Stk11 in balancing proliferative and non-proliferative hypertrophic states of chondrocyte development through the regulation of mTOR signaling. Stk11 is a known tumor suppressor; our findings raise the possibility that loss of Stk11 may play a role in human chondrosarcoma, a possibility that we are investigating.

Disclosures: Lick Pui Lai, None.

MO0087

Mitochondrial Superoxide Produced by Sod2 Deficiency Suppresses Proliferation of Chondrocytes. Masato Koike^{*1}, Hidetoshi Nojiri², Yoshitomo Saita², Daichi Morikawa¹, Keiji Kobayashi¹, Kenji Watanabe¹, Kazuo Kaneko², Takahiko Shimizu¹. ¹Department of Advanced Aging Medicine, Chiba University Graduate School of Medicine, Japan, ²Department of Orthopedics, Juntendo University School of Medicine, Japan

Osteoarthritis (OA) is known as a progressive and degenerative joint disease in elderly people. It has been reported that mitochondrial SOD2 was significantly

down-regulated in the superficial layer of OA cartilage (Ruiz-Romero et al. *Mol. Cell. Proteomics*, 2009, Scott et al. *Ann Rheum Dis*, 2010). *Sod2* protects cells and tissues from mitochondrial oxidative stress. However, it has been unclear how *Sod2* insufficiency affected physiological functions of chondrocytes. To clarify the biological consequences of *Sod2* deficiency in chondrocytes, we generated *Sod2*-deficient chondrocytes using tamoxifen-inducible cre-loxp system (*Rosa26-CreERT2^{flwt}*, *Sod2^{fllox/lox}*).

At first, we isolated costal chondrocytes from newborn mice and evaluated *Sod2* gene ablation and SOD2 protein content. Tamoxifen treatment completely deleted *Sod2* gene and depleted SOD2 protein in mutant chondrocytes at culture day 6. Dihydroethidium staining revealed 2.5-fold increase of intracellular superoxide production in mutant chondrocytes compared with wild-type ones. In the growth analysis, we found that cell numbers of *Sod2*-deficient chondrocytes were significantly suppressed by 60% after 6 days of culture. Moreover, proliferation of mutant chondrocytes were also decreased by 65% as determined in BrdU incorporations. Next, we analyzed apoptosis with annexin-V and propidium iodide staining and cleaved caspase-3 proteins. Interestingly, double positive stained cells and cleaved caspase-3 proteins were not increased in mutant cells, indicating that *Sod2* deficiency in chondrocytes did not induce apoptosis. Finally, cell cycle analysis revealed an increase of G2 phase in *Sod2*-deficient chondrocytes compared with control, suggesting that *Sod2* plays a pivotal role in regulating cell proliferation of chondrocytes.

These results indicated that excessive mitochondrial superoxide by *Sod2* deficiency suppressed growth ability of chondrocytes.

Disclosures: Masato Koike, None.

MO0088

Phosphate-mediated Activation of Hypertrophic Chondrocyte Apoptosis is modulated by PTHrP and 1,25-dihydroxyvitamin D. Eva Liu^{*1}, Eric Zhu², Francesca Gori², Marie Demay³. ¹Endocrine Unit, Massachusetts General Hospital, Brigham & Women's Hospital, Harvard Medical School, USA, ²Endocrine Unit, Massachusetts General Hospital, Harvard Medical School, USA, ³Massachusetts General Hospital & Harvard Medical School, USA

Circulating phosphate is a critical determinant of growth plate maturation. Hypophosphatemia impairs hypertrophic chondrocyte apoptosis, leading to the development of rickets in growing animals. Phosphate induction of Erk1/2 phosphorylation is required for phosphate-mediated hypertrophic chondrocyte apoptosis. Activation of the PTH/PTHrP signaling pathway impairs Erk1/2 phosphorylation. Studies in cultured metatarsals and in the growth plates of the hypophosphatemic Hyp mice demonstrate that phosphate restriction induces expression of PTHrP mRNA. Because 1,25-dihydroxyvitamin D suppresses PTH/PTHrP expression and prevents rickets in hypophosphatemic Npt2a null mice, investigations were undertaken to determine whether PTHrP and 1,25-dihydroxyvitamin D modulate the effects of phosphate on activation of Erk1/2 in hypertrophic chondrocytes and to identify signaling molecules activated by phosphate upstream of Erk1/2.

Costal chondrocytes were isolated from neonatal mice and cultured under conditions that promote hypertrophic differentiation. Pretreatment of hypertrophic chondrocytes with the C-Raf inhibitor GW5074 impaired Erk1/2 phosphorylation in response to phosphate, placing C-Raf upstream of Erk1/2 phosphorylation. Twenty four hours pretreatment of hypertrophic chondrocytes with 10-8 M 1,25-dihydroxyvitamin D led to an increase in both basal and phosphate-induced Erk1/2 phosphorylation, without altering C-Raf phosphorylation, demonstrating that 1,25-dihydroxyvitamin D enhances the effects of extracellular phosphate on activation of the Erk1/2 signaling pathway in hypertrophic chondrocytes, acting downstream of C-Raf. Two hours pretreatment of hypertrophic chondrocytes with 10-6 or 10-7 M PTHrP impaired both basal and phosphate-induced C-Raf and Erk1/2 phosphorylation. Thus, these investigations demonstrate that activation of C-Raf by phosphate is required for Erk1/2 phosphorylation in hypertrophic chondrocytes and that this signaling pathway is modulated by 1,25-dihydroxyvitamin D and PTHrP.

Disclosures: Eva Liu, None.

MO0089

Response of GFP Reporters Expressed in the TMJ Condylar Cartilage to Mechanical Loading. Achint Utreja^{*1}, Sumit Yadav², Xi Jiang¹, Ravindra Nanda³, David Rowe¹. ¹University of Connecticut Health Center, USA, ²University of Connecticut Health Center, USA, ³Craniofacial Sciences, USA

The temporomandibular joint (TMJ) is a fibrocartilaginous joint that bears the forces of the mandible during mastication. In the process of developing GFP reporters for studying the fracture callus, we have come to realize that the TMJ utilizes the same lineage as the fibrocartilage that is formed in a fracture and which responds to mechanical loads imposed by an unstable fixation. The only striking difference is that the fracture resorbs but the fibrocartilage of the TMJ remains intact. As the cellular organization of the TMJ is highly reproducible and loads can be administered in a controlled manner, it can be a useful model for exploring the cellular response to mechanical loading. The GFP reporters that have proven to be useful in following the

progression of cells that form the TMJ are: SMAA -> Dkk3 -> Col1A1-3.6 -> Col2A1 -> Col10A1. The Dkk3 cells are located in the proliferative (outer) zone. Differentiation progresses inward toward the tidemark, which is formed by the most superficial zone of the Col10A1 cells as labeled by alizarin complexone (AC) when injected 24 hours prior to sacrificing the animals. Experimental mice carrying the Dkk3-eGFP x Col1A1-3.6-GFPcy transgenes underwent forced jaw opening with a custom spring exerting 50 grams force for 1 hour/day for 5 days whereas the controls did not receive any force. AC and EdU (a BrdU analog) were injected on day four; 24 hours prior to sacrificing the mice, and the animals were harvested on day 5. Serial sagittal cryosections of the non-decalcified mandibular condyle were compared to assess the differences between experimental and control groups. The loading regimen significantly increased the number and depth of Dkk3-GFP cells as well as the number of EdU-positive cells without a noticeable change in the Col1A1-3.6 cells. In addition, the intensity of the tidemark labeling diminished in the loaded animals. Although the interpretation of these findings will require more investigation, the model does show a cellular response to a non-destructive and tolerated load that suggest an activation of the progenitor population and a reduction of the barrier that separates the cartilage from the underlying bone. These changes may reflect enhanced remodeling of the cartilage. Knowing the extent of the normal cellular response to loading will be essential to appreciate when the capacity of the response is exceeded and leads to cartilage destruction.

Disclosures: Achint Utreja, None.

MO0090

TGF- β 1 Decreases Ift88 Expression in Chondrocytic Cell Line ATDC5. Makiri Kawasaki^{*1}, Tetsuya Nakamoto¹, Takuya Notomi², Tadayoshi Hayata³, Yoichi Ezura⁴, Masaki Noda¹. ¹Tokyo Medical & Dental University, Japan, ²GCOE, Tokyo Medical & Dental University, Japan, ³Medical Research Institute, Tokyo Medical & Dental University, Japan, ⁴Tokyo Medical & Dental University, Medical Research Institute, Japan

Chondrocytes sense mechanical loadings in our daily activities and this mechanostimulation is required for cartilage homeostasis. Primary cilium, a projection from cell surface, presents on most of the mammalian cells. This small organelle has been reported to coordinate several cell signaling pathways, and also it is thought to be an effective candidate as a mechanosensor in chondrocytes. But the molecular mechanism of mechanotransduction through primary cilium in chondrocytes is largely unknown.

Intraflagellar transport (IFT) system plays an essential role in the formation and maintenance of primary cilium. Ift88 is one of the IFT particles moving anterogradely along the primary cilium, and its lack causes defective ciliogenesis in articular chondrocytes in vivo. It has been reported that the cKO mouse lacking Ift88 specifically in early limb bud mesenchyme exhibited defects in endochondral bone formation and ectopic chondrocytes development in perichondrium. Recently it was reported that the mutant mice lacking Ift88 specifically in chondrocytes presented OA symptoms. But the involvement of Ift88 and its role in the proliferation and the differentiation of chondrocytes remain elusive. Therefore in this study, we examined the expression pattern of Ift88 in chondrogenic cell line ATDC5 when cells were treated with BMP2 and TGF- β 1.

We showed that Ift88 is expressed in ATDC5 and its expression was increased in the differentiation of ATDC5. The expression pattern of Ift88 was corresponding to that of type 2 collagen. The expression of Runx2 and Osterix was increased in the late stage of culture. When ATDC5 was treated with 100ng/ml BMP2 for 24h and 72h, the expression of Ift88 was comparable with the control, while when treated with 2ng/ml TGF- β 1 for 24h, the expression of Ift88 was significantly decreased compared with the control. TGF- β 1 is important for the proliferation and the differentiation of chondrocytes and it is reported to inhibit terminal hypertrophic differentiation of chondrocytes. Consistent with these preceding reports, the expression of Col2a1 was dose-dependently increased with TGF- β 1 treatment, and the expression of Col10a1 tended to be decreased by TGF- β 1 treatment. These results suggest that Ift88 participates in the proliferation and the differentiation of ATDC5 and may be involved in the late stage of the differentiation of ATDC5 through TGF- β 1 signaling.

Disclosures: Makiri Kawasaki, None.

This study received funding from: Global COE

MO0091

Dual Role of the Trps1 Transcription Factor in the Mineralization Process. Lauren Stevenson¹, Callie Mobley², Manisha Yadav³, Tony Winters², Anne Poliard⁴, Odile Kellermann⁵, Brendan Lee⁶, Jose Luis Millan⁷, Dobrawa Napierala^{*8}. ¹University of Alabama, USA, ²University of Alabama at Birmingham, USA, ³Burnham Institute for Medical Research, USA, ⁴Faculté de Chirurgie Dentaire, et UMR-S 747, Université Paris Descartes, France, ⁵INSERM UMR-S 747, Université René Descartes, France, ⁶Baylor College of Medicine & Howard Hughes Medical Institute, USA, ⁷Sanford-Burnham Medical Research Institute, USA, ⁸University of Alabama At Birmingham School of Dentistry, USA

TRPS1 is a transcriptional repressor that belongs to the GATA family of transcription factors. In humans either *TRPS1* deficiency (tricho-rhino-phalangeal

syndrome, TRPS) or dysregulated *TRPS1* expression (Ambras syndrome) results in skeletal and dental abnormalities, demonstrating the *TRPS1* involvement in endochondral bone formation and tooth development. Moreover, TRPS patients frequently present with the low bone mass phenotype indicating its involvement in bone homeostasis. These and our previous data demonstrating accelerated mineralization of the perichondrium in *Trps1* mutant mice and impaired dentin mineralization in *Coll1a1-Trps1* transgenic mice implicate *Trps1* in the mineralization process. To understand the role of *Trps1* in differentiation and function of cells producing mineralized matrix, and to identify *Trps1* molecular networks in these cells we used the 17IIA11 preodontoblastic cell line, a cellular model of mineralization. We generated both *Trps1*-deficient and *Trps1*-overexpressing stable cell lines, and analyzed their mineralization by alkaline phosphatase and alizarin red staining. As predicted, based on our previous *in vivo* data, delayed and decreased mineralization of *Trps1*-overexpressing cells was observed when compared to control cells. This was associated with downregulation of genes regulating phosphate homeostasis. Interestingly, *Trps1*-deficient cells lost the ability to mineralize and demonstrated decreased expression of several genes critical for the initiation of the mineralization process, including *Akp2* and *Phospho1*. Based on these data we have concluded that *Trps1* serves two critical and context-dependent functions in cells producing mineralizing matrix: 1) *Trps1* is required for their maturation by supporting expression of genes crucial for the initiation of the mineralization process, 2) *Trps1* represses the function of mature cells and restricts the extent of extracellular matrix mineralization.

Disclosures: Dobrawa Napierala, None.

MO0092

Enhanced Expression of miRNA-424 during Osteogenic Differentiation in Human Skeletal Muscle-derived Stem Cells. Teruyo Oishi*¹, Akiyoshi Uezumi², Arihiko Kanaji³, Kunihiro Tsuchida², Harumoto Yamada⁴.

¹Department of Orthopaedic Surgery, Fujita Health University School of Medicine, Japan, ²Division for Therapies against Intractable Disease, Institute for Comprehensive Medical Science, Fujita Health University, Japan, ³Department of Orthopaedic Surgery, Keio University, Japan, ⁴Department of Orthopaedic Surgery, Fujita Health University School of Medicine, Japan

Objective: MicroRNAs (miRNAs) comprise a group of non-coding small RNAs and are involved in the post-transcriptional regulation of various mRNAs. Past studies have demonstrated that miRNAs play essential roles in the regulation of stem cell self-renewal and de-differentiation *in vivo*. We have previously reported that murine platelet derived growth factor- α positive (PDGFR α +) cells in the muscle tissue have a capacity for both adipogenic and osteogenic differentiation *in vitro*, suggesting that PDGFR α cells in the muscle have the property as mesenchymal stem cells (Nat Cell Biol. 2010). The purpose of this study is to examine the osteogenic differentiation capacity of human PDGFR α cells *in vitro* and to evaluate the expression pattern of miRNAs during osteogenic differentiation of the human PDGFR α mesenchymal stem cells. **Methods:** In the present study, we used the muscular tissues obtained from the patients underwent hip surgery. Informed consent was obtained from all the patients prior to the surgery. After enzymatic digestion of the tissues, PDGFR α cells were isolated using flow cytometry and cultured in the osteogenic medium for 7 and 14 days. After the incubation, the cells were fixed and stained with NBT/BCIP to detect alkaline phosphatase and with alizarin-red. To evaluate the expression profile of miRNAs during osteogenic differentiation, we performed a miRNA profiling assay using the cells incubated with osteogenic medium for 10 days. The levels of miRNAs, which showed significant change during osteogenic differentiation, were also confirmed by quantitative RT-PCR. **Results:** Positive staining for alkaline phosphatase and for alizarin-red was observed 7 and 14 days after the osteogenic induction, respectively. The miRNA profiling analysis and quantitative RT-PCR showed a significant increase in the expression levels of miRNA-424 during osteogenic differentiation. **Conclusion:** Our finding showed that miRNA-424 expression was increased during the osteogenic differentiation in human PDGFR α cells, suggesting that the upregulation of miR-424 is potentially involved in the osteogenic differentiation of human skeletal muscle-derived stem cells.

Disclosures: Teruyo Oishi, None.

MO0093

Identification of Novel Transcription and Epigenetic Factors in Chondrocytogenesis. Yuan SI*¹, Min-Young Youn², Kazuki Inoue³, Yoko Yamamoto², Yuuki Imai⁴. ¹Tokyo University, Japan, ²University of Tokyo, Japan, ³university of Tokyo, Imcb, Nuclear Signaling, Japan, ⁴The University of Tokyo, Japan

Chondrocytogenesis is the process by which cartilage is formed from condensed mesenchyme at growth plate. This process originates from mesenchymal stem cell with subsequent formation of proliferative chondrocyte and then differentiation into hypertrophic chondrocyte. This sequential differentiation is regulated by well-known transcription factors, such as Sox9 and Runx2. However, the involvement of other factors, especially epigenetic regulators, in chondrocytogenesis remains elusive. Thus, the purpose of this study is identification of transcription and/or epigenetic novel

factors in chondrocytogenesis and their underlying molecular mechanism *in vitro* and *in vivo*.

Based on the establishment of the chondrocyte differentiation model *in vitro*, via mass cultured C3H10T1/2 (10T1/2) cell line treated with BMP2, differentiation stage dependent gene expression profiles of the mass cultured chondrocytes was analyzed by gene expression microarray. From the identification of the differentially expressed candidates among differentiation stages and followed by validation through qRT-PCR analysis, we focused on Aire, which mutation causes the reversible metaphyseal dysplasia, and Dot1, which is known as a methyltransferase towards histone H3 Lys79. Dot1 is highly expressed in bone and cartilage, which indicated that they may take function during chondrocyte differentiation.

As the results of Aire knockdown by shRNA, mRNA expression levels of chondrocyte-marker genes, such as Col2a1 and Col10a1 were decreased. This data suggested that Aire might work as a novel active regulator of chondrocytogenesis. To further confirm the functional and molecular mechanism of Aire, the physical interaction between Aire and known transcription factors, such as Sox9 and Runx2, Co-IP will be performed. On the other hands, Dot1 knockdown lead the decreased expression of chondrocyte-marker genes and Sox9. To define the molecular mechanism of Dot1, the modification status of H3K79me3 on Sox9 promoter regions was detected with CHIP assay, indicating that Dot1 might activate the chondrocyte differentiation via alteration of methylation status of H3K79.

Taken together, Aire could be regarded as a novel active regulator, while, Dot1 could be considered as a novel epigenetic activator during the chondrocytogenesis. Generation of the chondrocyte-specific Aire and Dot1 knockout mice should be required to clarify the physiological function of these novel factors in bone growth *in vivo*.

fig.1 The establishment of chondrocytogenesis in 10T1/2 cell line. The expression of col2a1, the proliferative chondrocytes marker gene, was obvious at day5 of micro mass cultured 10T1/2 cell line, while, at day10 10T1/2 cell was differentiated into hypertrophic chondrocytes.

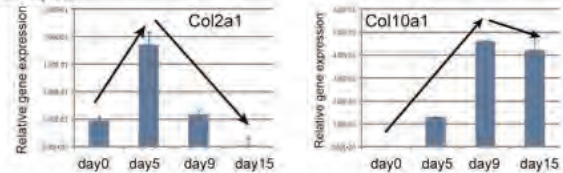


fig.2 Aire increased the expression of Col2a1 and Col10a1 in Aire stable knockdown cell line

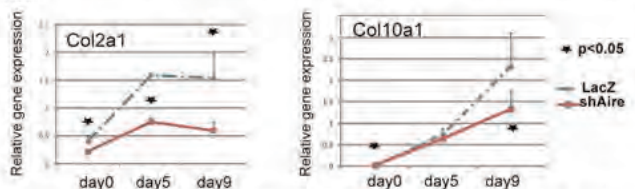


Fig.3 chondrocyte marker genes and Sox9 were up-regulated by Dot1 in Dot1 stable knockdown cell line

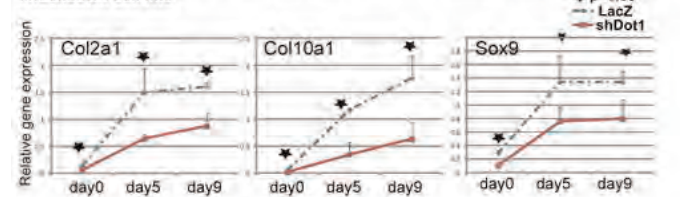
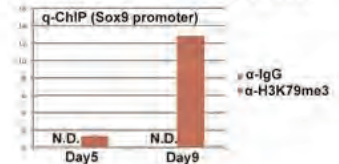


Fig.4 the modification status of H3K79me3 on Sox9 promoter regions was detected during chondrocytogenesis



Disclosures: Yuan SI, None.

MO0094

The Role of Lysyl Oxidase-like Protein 2 in Mineralization of Human Dental Pulp Stem Cells.. Je-Yoel Cho¹, Joohyun Kim*², Hye-Jeong Park².

¹College of Veterinary Medicine, Seoul National University, South Korea, ²Seoul National University, South Korea

Tooth development is a complex process of reciprocal interactions between oral epithelium and mesenchyme during mouth development, beginning early in mammalian embryogenesis (Thesleff et al., 1995). Human adult dental pulp stem

cells (hDPSCs) are a unique precursor population isolated from postnatal dental pulp and have the ability to differentiate into a variety of cell types for formation of a reparative dentin-like complex. In previous study, we identified expressional changed proteins by analysis of secretome during hDPSC differentiation into odontoblast-like cells using LC-MS/MS. In analyzed data list, the LOXL2 (lysyl oxidase homolog 2) was one of the down-regulated proteins during hDPSC differentiation into odontoblast-like cells. Furthermore, the LOXL2 is not reported in dental research field yet. Therefore, we studied the expression pattern of the LOXL2, a dentin matrix protein during odontogenic differentiation of DPSCs, showed that mRNA level of the LOXL2 were reduced at the all stages - we examined 3, 5, 7, 14, 21 days - of differentiation of hDPSCs in osteogenic / odontogenic media. The expression pattern of the LOXL2 in total cell lysate protein is also decreased by time course - 3, 5, 7, 14, 21 days -. These results might be proposed that the LOXL2 acts in the mineralization of human dental pulp stem cells.

Disclosures: Joohyun Kim, None.

This study received funding from: No. 2006-2004608

MO0095

Characterisation of Inflammatory Murine Fibroblast-like Synoviocytes. Rowan Hardy¹, Claudia Huelso¹, Yingling Liu¹, Shihani Stoner¹, Mark Cooper², Markus Seibel¹, Hong Zhou^{*1}. ¹Bone Research Program, ANZAC Research Institute, University of Sydney, Australia, ²University of Birmingham, United Kingdom

Fibroblast-like-synoviocytes (FLS) have been shown to contribute to juxta-articular osteoporosis during inflammatory joint diseases through the production of multiple secreted factors that drive osteoclast activity and suppress osteoblast differentiation. Despite a growing use of FLS isolated from murine inflammatory models to examine their signalling with osteoblasts and osteoclasts, a robust characterisation of these cells has not been performed. In this study, FLS were isolated from inflamed joints of K/BxN mice and their purity in culture determined by immuno-fluorescence and RT-PCR. Basal expression of pro-inflammatory genes was determined by Real-Time PCR. Secreted IL-6 was measured by ELISA, and its regulation by TNF α and corticosterone (the major glucocorticoid in rodents) measured relative to other cell populations including FLS isolated from non inflamed tissues and the cell lines C2C12 and MC3T3-E1. Purity of FLS culture was identified by positive expression of fibronectin, prolyl-4-hydroxylase, CD90.2 and CD248 in greater than 98% of the population. FLS isolated from K/BxN mice possessed significantly greater basal expression of the inflammatory markers IL-6, CCL-2 and VCAM-1 when compared to FLS isolated from non-inflamed tissue (IL-6, 3.6 fold; CCL-2, 11.2 fold; VCAM-1, 9 fold; P<0.05). This elevated expression was abrogated in the presence of corticosterone at 100 nmol/L. TNF α significantly increased expression of all inflammatory markers to a much greater degree in K/BxN FLS relative to other mesenchymal cell lines (K/BxN; IL-6, 40.8 fold; CCL-2, 1343.2 fold; VCAM-1, 17.8 fold; ICAM-1, 13.8 fold; P<0.05), with secreted IL-6 mirroring these results (K/BxN; Con, 169 + 29.7 versus TNF α , 923 + 378.8 pg/ml/1x10⁵ cells; P<0.05). Dose response experiments confirmed effective concentrations between 10 and 100 nmol/L for corticosterone, and 1 and 10 ng/ml for TNF α . Further analysis of the inflammatory phenotype over prolonged passage revealed that it remained stable between passages four and seven, deteriorating from passage eight onwards. This study justifies the use of murine FLS as a suitable model of inflamed human synovial fibroblasts for the future investigation of their signalling with both osteoblasts and osteoclasts. Furthermore, we have established a well characterised inflammatory profile in FLS that provide guidelines on their pro and anti-inflammatory responses as well as their effective culture duration.

Disclosures: Hong Zhou, None.

MO0096

Effect of Negatively Charged Oligo(polyethylene glycol) Fumarate on Periosteal Chondrogenesis. Michelle Casper^{*1}, Mahrokh Dadsetan², Michael Yaszemski³. ¹Author, USA, ²Co-author, USA, ³Mayo Clinic College of Medicine, USA

Introduction: Periosteal tissue is used clinically to repair cartilage with good to excellent results because of its chondrogenic properties¹. One technique for cartilage engineering is using hydrogels. Oligo(polyethylene glycol) Fumarate (OPF) is an injectable, photo-crosslinkable, biodegradable hydrogel². It can be predictably manipulated to suit the needs of developing cells. OPF hydrogels support chondrocyte proliferation and growth³. We investigated the effect of negatively charged OPF hydrogels on periosteal chondrogenesis.

Method: Periosteal disks were harvested from rabbits. Explants were separated into 3 groups: 1) agarose culture (control), 2) neutral OPF hydrogel, and 3) negatively charged OPF hydrogels. The agarose culture was supplemented with TGF- β for the first 2 days of a 6 week culture. Hydrogels received no supplementation. OPF was synthesized. Explants were placed in hydrogel and hydrogel was polymerized using UV light, cut into disks with explants at center. Widths and lengths of explants were measured; explants were weighed and analyzed for aggregate moduli and GAG content. Samples were embedded for histology.

Results: Explants in charged hydrogels were significantly larger than neutral and statistically similar to agarose group (Fig 1). Explants in the negative group were

stiffer than the agarose group, not significantly. There was not enough tissue in neutral group to assess stiffness. GAG production was significantly highest in agarose. The neutral group was the lowest with the negative group almost producing significantly more GAG (p =0.085). Wet and dry weights of the negative group were significantly higher than the other groups.

Discussion: Periosteal chondrogenesis occurs in an agarose culture with TGF- β supplementation⁴. In this study, we investigated the effect of negative charge in OPF hydrogels on periosteal chondrogenesis through encapsulation without TGF- β supplementation. When negative charge was present, explants were statistically similar in size and GAG production to the standard agarose culture and were stiffer than the other groups. This demonstrates that negatively charged OPF hydrogels are capable inducing a chondrogenic response in periosteal explants.

1. O'Driscoll SW, Fitzsimmon JS, *Clin Orthop*, 2001; S190.
2. Dadsetan M et al. *Biomacromolecules* 2007;8(5):1702-9.
3. Dadsetan M et al. *Acta Biomaterials* 2011;7(5):2080-2090.
4. Miura Y et al. *Clin Orthop Relat Res* 1994 Apr;(301):271-80.

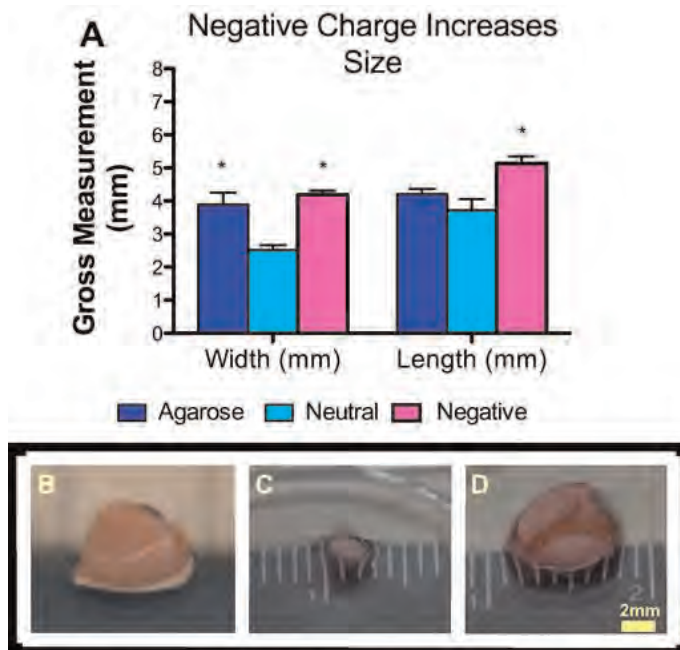


Figure 1. Gross Analysis. A) Comparison of measured widths and lengths * indicates significantly higher than neutral. Gross view of tissue groups at harvest from: B) agarose culture, C) neutral OPF hydrogel culture, D) negatively charged OPF hydrogel culture.

Figure 1 Gross Analysis

Disclosures: Michelle Casper, None.

MO0097

Gender-dependence of Bone Materials Properties in *Colla2* deficient mice (*oim*). Xiaomei Yao^{*1}, Carleton Stephanie², Charlotte Phillips², Yong Wang¹. ¹University of Missouri-Kansas City, USA, ²University of Missouri-Columbia, USA

Purpose: Osteogenesis imperfecta (OI) is a dominant skeletal disorder characterized by bone fragility and deformities. This study aimed to define the structural, biomechanical, and chemical basis for *oim* mice on the gender differences.

Methods: The left tibiae from 4-month-old of wild type +/+ (*wt*, 8 females, 8 males), heterozygous (+/*oim*, 8 females, 8 males), and homozygous (*oim/oim*, 7 females, 6 males) mice were used in this study. The cortical and trabecular bone morphological parameters were evaluated using micro-computed tomography (μ CT). Following the μ CT analysis, the bones were loaded to failure using three-point bending to acquire the mechanical properties. The chemical compositions of the cortical bone were analyzed using Raman microscopy on the fractured surface. The differences between the female and male were evaluated by two-tailed Student's *t*-test. The differences among *wt* controls, +/*oim*, and *oim/oim* mice were evaluated by one-way analysis of variance (ANOVA) with Tukey's post test. Differences with *P* < 0.05 were considered significant.

Results: Dramatic gender dependence was observed by μ CT for both cortical and trabecular bone. Tibial cortical bone width of female *wt* mice was 8.5% thinner than male *wt*. Across all the genotypes, female tibiae, in comparison to male tibiae, exhibited significantly lower trabecular BV/TV (-134.64% for *wt*, -131.88% for +/*oim*, and -76.26% for *oim/oim*), number of trabeculae (-71.64% for *wt*, -87.26% for +/*oim*, and -37.96% for *oim/oim*), and trabecular connectivity (-596.91% for *wt*, -381.47% for +/*oim*, and -259.39% for *oim/oim*), as well as significantly increased trabecular separation (47.23% for *wt*, 49.29% for +/*oim*, and 26.25% for *oim/oim*). There were

also significant decreases in the biomechanical properties of female tibias compared to male tibias, further indicating increased fragility in female bone. The moment of inertia and ultimate force in female tibias relative to male tibias had lower values (-97.54% for *wt*, -50.72% for *+loim*, and -66.68% for *oimloim*) and (-41.12% for *wt*, -26.57% for *+loim*, and -14.46% for *oimloim*), respectively. There was no significant difference in gender based on the Raman results.

Conclusion: Gender dependence of cortical and trabecular bone properties and biomechanical integrity profoundly exists in the *oim* mice, with *oim* female bones exhibiting more compromised biomechanical properties.

Disclosures: Xiaomei Yao, None.

This study received funding from: NIH

MO0098

Inverted Osteon: a Novel Bone Superstructure Emerging from Tumor Chaos. Edward Mertz^{*1}, Emmanouil Saloustris¹, Sisi Liu¹, Constantine Stratakis², Sergej Leikin¹. ¹National Institutes of Health, USA, ²NICHD, National Institutes of Health, USA

To make tough bone, osteoblasts organize themselves and extracellular matrix in highly ordered superstructures, which are usually formed by apposition on preexisting bone surfaces. Here we report unusual, trabecular-like bone spicules that grow *de novo* and exhibit a novel type of bone superstructure. These spicules occur within tail-vertebrae tumors of mice that have heterozygous gene deletions of different regulatory subunits of protein kinase A (PKA). We used polarized and confocal fluorescence microscopies, Raman micro-spectroscopy and *in vivo* labeling of bone forming surfaces to characterize collagen and cell organizations, mineral and organic matrix composition as well as growth mode of the spicules. Most bone material within the tumors is poorly organized and undermineralized. However, we also observed cylindrical spicules that have composition and mineralization typical of normal bone. Their osteocytes and collagen matrix are highly-organized in circumferential lamellae resembling secondary osteons in cortical bone. In a secondary osteon, the circumferential superstructure emerges when osteoblasts lay bone on the inner surface of a cylindrical tunnel dug by osteoclasts, filling up the channel from its periphery to the center, where a thinner channel is left for a blood capillary. The osteon-like spicules within the tumors show an inverted pattern of bone growth and mineralization. The central core of the spicule is filled with a well-organized and mineralized bone, in which the collagen matrix is oriented perpendicular to the spicule axis. This core matrix is deposited at the growing tip of the spicules and provides a template for lateral apposition of collagen lamellae and their mineralization in the center-to-periphery direction. Thus, such "inverted osteons" grow axially without a preexisting guiding template. The rates of their axial and lateral growth and the resulting aspect ratio depend on which regulatory subunit of PKA is deleted, suggesting that there might be ways to induce and control formation of well-organized *de novo* trabeculae. It remains to be seen whether the inverted osteon can also occur in other pathological or normal conditions.

Disclosures: Edward Mertz, None.

MO0099

Proliferation, Colony Formation and Trilineage Differentiation of White-tailed Deer Antlerogenic Progenitor Cells and Animal-Matched, Marrow-Derived Mesenchymal Stromal Cells. Ethan Daley^{*1}, Andrea Alford¹, Steven Goldstein². ¹University of Michigan, USA, ²University of Michigan Orthopaedic Research Lab, USA

Cervid antler is the only adult mammalian bony tissue capable of complete, repeated regeneration. Distal regrowth is rapid (up to 1in/day) and achieved via endochondral ossification. Once initiated, growth is maintained by antlerogenic progenitor cells (APC) in the antler's reserve mesenchyme (RM.) Though antler's potential as a model of bone regeneration is clear, we lack basic knowledge of the APC phenotype and how it compares with other cervid mesenchymal stromal cells (MSC). Here, we present data regarding *in vitro* APC proliferation, self-renewal capacity and trilineage differentiation relative to animal-matched, marrow-derived MSC.

APC were harvested from the RM and MSC from the phalanges of wild, mature white-tailed bucks (*Odocoileus virginianus*, n=3 unless noted.) Assays used 3 or more replicates; means were compared using paired t-tests.

Proliferation: relative passage 1 cell numbers were estimated daily for 192hrs using a DNA-binding dye. MSC number was greater than APC at all time points after 24hrs ($p < 0.05$). **Colony formation:** no difference was found in passage 1 colony counts (APC:24±22; MSC:26±4.6, $p=0.88$.)

Adipogenesis: MSC showed oil-red O-positive lipid droplets; none were apparent for APC. **Chondrogenic micromass culture:** Acid fuchsin staining indicated collagen formation in all masses. Cell viability was assessed with TUNEL and Hoechst staining. No difference was found in matrix area per non-apoptotic cell (APC:0.12±0.02; MSC:0.13±0.03, $p=0.19$, n=2) but APC had greater mean (APC:135±18; MSC:51±4, $p=0.06$, n=2) and peak (APC:2598±98; MSC:1146±54, $p=0.02$, n=2) TUNEL grayscale signals. **Osteogenesis:** At 7 days APC alkaline phosphatase activity exceeded MSC (APC:9.4±2.6; MSC:5.3±1.1 pmol/ug-min, $p=0.05$), but declined to parity through days 10, 14 and 22. There was no difference in 22 day alizarin red optical density (APC:0.1±0.02; MSC:0.24±0.33, $p=0.38$.)

This is the first comparison of APC and cervid MSC proliferation, colony formation and trilineage differentiation. Preliminary data suggest that compared to MSC, RM APC may be more committed chondrocyte/osteoblast progenitors. Rapid APC proliferation is thought to foster fast antler growth; our results suggest proliferation is highly variable or abetted by other processes *in vivo*. APC micromass results recall the antler tip, in which robust apoptosis colocalizes with, and may regulate, proliferation.

Disclosures: Ethan Daley, None.

MO0100

Role of ALK5, a TGF-beta type I Receptor, in preventing abnormal lateral expansion of growth plate cartilage. Tomoya Matsunobu^{*1}, Kiyoyuki Torigoe², Muneaki Ishijima³, Ashok Kulkarni², Yukihide Iwamoto⁴, Yoshihiko Yamada². ¹Graduate School of Medical Sciences, Kyushu University, Japan, ²Laboratory of Cell & Developmental Biology, National Institute of Dental & Craniofacial Research, NIH, USA, ³Juntendo University, Faculty of Medicine, Japan, ⁴Department of Orthopaedic Surgery, Graduate School of Medical Sciences, Kyushu University, Fukuoka, Japan, Japan

Transforming growth factor-beta (TGF-beta) exerts its diverse activities during development and pathogenesis. Previously, we demonstrated that mice lacking ALK5, a type I TGF-beta receptor, in skeletal progenitor cells using *Dermo1-Cre* ($ALK5^{Dermo1CKO}$) are perinatally lethal, and display short-limb dwarfism with abnormal cartilaginous protrusions in developing limbs. Chondrocyte-specific conditional ALK5 mutant mice mediated by *Col2a1-Cre* ($ALK5^{Col2CKO}$), on the other hand, exhibited no obvious defects in limbs. In $ALK5^{Dermo1CKO}$ growth plates, although chondrocytes proliferate and differentiate, perichondrial cell proliferation and differentiation to osteoblasts are severely inhibited, suggesting that ALK5 is required for the progenitor cell commitment to osteoblast differentiation. In this study, we characterized the abnormal cartilaginous protrusions in $ALK5^{Dermo1CKO}$ mutant mice to investigate the role of ALK5 in cartilage integrity. Most of the protrusions occurred from both proximal and distal metaphyses of E18.5 $ALK5^{Dermo1CKO}$ femurs, and serial axial sections showed that the protrusions originated from the cartilage region adjacent to the ossification groove of Ranvier. Chondrocytes in the protrusions proliferated and expressed aggrecan and Sox9. They were differentiated to hypertrophic chondrocytes and eventually mineralization occurred. These results indicate that ALK5-deficient chondrocytes at the periphery of the cartilage expand and differentiate horizontally. Expression of ALK5 in control E18.5 femurs were observed in the perichondrium, particularly in the groove of Ranvier, and in a thin chondrocyte layer at the periphery of cartilage located adjacent to the perichondrium. ALK5-deficient growth plates had a thin perichondrium, and chondrocytes at the tip of the protrusions in E18.5 $ALK5^{Dermo1CKO}$ femurs invaded into the perichondrium. Since $ALK5^{Col2CKO}$ mice did not show abnormal cartilaginous protrusions, TGF-beta signaling in the perichondrium but not in the cartilage may play an important role in cartilage integrity. It is possible that the perichondrium may interact with chondrocytes at the periphery of the cartilage to regulate transverse expansion of the growth plate through TGF-beta signaling, and that ALK5-deficiency in the perichondrium could not prevent chondrocytes from lateral expansion. Our results suggest that TGF-beta signaling in the perichondrium plays a critical role in regulating cartilage integrity and normal longitudinal expansion of the growth plate.

Disclosures: Tomoya Matsunobu, None.

MO0101

The Role of Hox11 Genes in Musculoskeletal Patterning in the Limb. Ilea Swinehart¹, Aleesa Schlientz¹, Christopher Quintanilla¹, Deneen Wellik^{*2}. ¹University of Michigan, USA, ²University of Michigan Medical Center, USA

Development of the vertebrate musculoskeletal system requires precise coordination between muscles, tendons and bones to form an integrated and functional system. Recent data from our lab suggests that Hox genes play a key role in this process *in vivo*. Hox genes are well known regulators of skeletal development and function in a region-specific manner along the anteroposterior axis of the axial skeleton and proximodistal axis of the limb. The three members of the Hox11 paralogous group, Hoxa11, c11 and d11, demonstrate overlapping functionality in the sacrum and limb zeugopod. Loss of function of Hox11 genes leads to dramatic mispatterning of the sacrum and zeugopod skeletal elements (radius/ulna, tibia/fibula). Utilizing a Hoxa11eGFP knock-in allele our lab has demonstrated that Hox11 expression in the developing limb is expressed in multiple tissues including the perichondrium, tendons and muscle connective tissue, however, expression is largely excluded from skeletal elements. As suggested by the expression patterns, Hox11 mutants also have severe defects in the formation and patterning of zeugopod muscle groups and the associated tendons. Using expression analyses, three-dimensional reconstruction on serial sections of the limb to clearly define the muscle and tendon phenotype in Hox11 mutants, and conditional deletion approaches our goal is to determine the functional contribution of Hox11 genes in musculoskeletal integration during development. Elucidating the *in vivo* factors required for musculoskeletal development is a key goal

of our research. Regeneration and repair mechanisms often closely mirror developmental pathways and, given the clear role for Hox genes in the patterning of many organ systems, especially the developing skeleton, our work may have important implications for tissue engineering strategies.

Disclosures: Deneen Wellik, None.

MO0102

Alkaline Phosphatase Modulation of Preosteoblasts by Different Salts of Fluoride. Kellen Gasque*, thamara frascarelli alberconi, Ana Flávia Soares, Marilia Afonso Rabello Buzalaf, ana carolina Magalhães, rodrigo cardoso de oliveira. Bauru Dental School, Brazil

Fluorides cause chemical and biological changes in the bone tissue, depending on the dosage and the exposure duration to this element. Important clinical conditions, such as osteoporosis, osteopetrosis, and bone sclerosis, may be modulated by the intake of fluoride (NaF). Results on the usage of NaF for the treatment of bone diseases remain controversial and sometimes hampered by toxic complications. Aluminum fluoride was tested by MTT and Neutral Red assays as an attempt to find an alternative source to NaF. Alkaline Phosphatase (AP) activity was evaluated on MC3T3-E1 preosteoblastic cells treated with different concentrations of AlF₃ (5µM, 10µ, 100µ e 1mM) and assessed at 24, 48, 72 and 96 hours. Data were tested for One-Way Anova, and Tukey post test (if p<0,05). Significance level at p<0,05. All concentrations of AlF₃ decreased the production of AP, compared to no treated group (p<0,001), but only 24h group presented significant statistical difference among all concentrations (p<0,001). There was not significant statistical difference among groups comparing NaF and AlF₃ treatments. Our results demonstrated AlF₃ produced Alkaline phosphatase levels similar to NaF. Thus, it could be a fluoride alternative source to bone disease treatments; nevertheless, further studies are still required. Financial Support: Fapesp 2009/07289-0 and 2010/18934-1.

Disclosures: Kellen Gasque, None.

MO0103

Defective Craniofacial Development and Bone Formation in CTGF Knockout Mice. Alex Lambi*¹, Christina Mundy¹, Talia L. Pankratz², Joan T. Richtsmeier², Steven Popoff¹. ¹Temple University School of Medicine, USA, ²Pennsylvania State University, USA

Connective tissue growth factor (CTGF/CCN2) is a member of the CCN protein family, a group of matricellular proteins whose shared multi-modular structure affords them roles in normal and pathologic scenarios. CTGF is produced by osteoblasts and has been shown to stimulate their matrix production and differentiation. The importance of CTGF in skeletal development has been demonstrated in CTGF knockout (KO) mice that exhibit numerous defects in bone and cartilage, the severity of which results in neonatal lethality. Previous studies have noted gross differences in CTGF KO craniofacial bones and an inability of osteoblasts obtained from KO calvariae to differentiate in culture. In this study, we performed an in-depth characterization of the CTGF KO skull phenotype using micro-CT and craniofacial landmark analyses. These analyses demonstrated significant differences in the size and shape of skulls from CTGF KO mice compared to their wild-type (WT) littermates. We also found differences in the morphology of the three skull regions – cranial vault, cranial base, and facial skeleton. CTGF KO skulls also invariably presented with unique, non-parametric traits including changes in the nasal bones, mandibles, palate and vomer, and pterygoid plates of the sphenoid bone. To elucidate potential mechanisms responsible for the phenotypic differences seen in CTGF KO skulls, we performed quantitative PCR (qPCR) using RNA from CTGF KO and WT calvariae. We found decreased expression of the osteoblast differentiation/function-related genes Runx-2, type I collagen, alkaline phosphatase, and osteocalcin, as well as decreased expression of the CCN family members Cyr61/CCN1 and Nov/CCN3. Additionally, we found alterations in the ligand and receptor expression levels of the TGF-β1 and BMP-2 signaling pathways. Lastly, we analyzed the differentiation of calvaria-derived primary osteoblasts *in vitro* and showed that CTGF KO osteoblasts have decreased proliferation compared to WT osteoblasts, but that there is no inherent defect in the ability of KO osteoblasts to properly differentiate under unstimulated, osteogenic culture conditions. In conclusion, CTGF KO mice demonstrate a unique array of defects in craniofacial development that appear to be linked to aberrant bone formation and dysregulation of TGF-β and BMP receptor signaling *in vivo*.

Disclosures: Alex Lambi, None.

MO0104

Glycosaminoglycans Modulate Osteoclast Development and Functions Depending on their Sulfation Pattern. Juliane Salbach*¹, Martina Rauner², Claudia Goetsch³, Stephanie Möller⁴, Matthias Schnabelrauch⁴, Vera Hintze⁵, Dieter Scharnweber⁵, Lorenz Hofbauer¹. ¹Dresden University Medical Center, Germany, ²Medical Faculty of the TU Dresden, Germany, ³Brigham & Women's Hospital/Cardiovascular Division, USA, ⁴Biomaterials Department, INNOVENT, Germany, ⁵Max Bergmann Center for Biomaterials, Technische Universität Dresden, Germany

Bone mass and strength are maintained by the coordinated actions of bone-resorbing osteoclasts and bone-forming osteoblasts. Since the incidence of bone loss disorders is increasing in our aging population, the development of new adaptive biomaterials is important. The extracellular matrix (ECM) affects differentiation of bone cells and is critical for bone regeneration. An ideal artificial ECM used for implant materials should slightly repress osteoclastogenesis and concurrently increase osteoblast functions. Here, we assessed the role of glycosaminoglycans (GAGs), natural occurring components of the bone ECM, and their sulfated derivatives on osteoclast functions. Osteoclasts were differentiated from human peripheral blood mononuclear cells with RANKL (50 ng/ml) and M-CSF (25 ng/ml) for 21 days on cell culture plates coated with artificial ECMs containing rat collagen type I (Coll)/hyaluronan (HA) or Coll/chondroitin sulfate (CS). Coatings with Coll alone served as control. One hour after seeding, the adhesion rate was measured using crystal violet. Cell viability was determined at day 5. Following differentiation, cells were fixed and stained for tartrate-resistant acid phosphatase (TRAP). The number of osteoclasts was determined by counting multinucleated (≥3 nuclei) TRAP-positive cells. Osteoclast precursors seeded on aECMs were affected at all stages of differentiation. While native, unmodified GAGs (HA, CS) had no effect on adhesion, their sulfoderivates significantly increased osteoclast precursor attachment up to 60%. Viability was not (CS) or negatively (HA) regulated by native GAGs. The introduction of sulfate groups significantly increased viability to control levels. Differentiation of precursors on CS or HA led to reduced osteoclast numbers with intact morphology, whereas the degree of sulfation dose-dependently increased the number of TRAP-positive osteoclasts accompanied by a loss of osteoclast-specific sealing zone structures and resorptive activity based on immunofluorescence and resorption studies. These effects were paralleled by a decrease in the osteoclastic markers cathepsin K, TRAP, OSCAR and the osteoclast cytoskeleton regulator SWAP-70. In summary, artificial ECMs containing GAGs with optimized sulfur content modify osteoclastogenesis and may represent a useful tool to control bone remodelling processes on implant surfaces.

Disclosures: Juliane Salbach, None.

MO0105

Integrin-Mediated Osteoblast Adhesion to CTGF (CCN2) Induces Activation of Intracellular Kinases, Cytoskeletal Reorganization and Differentiation. Honey Hendsi*¹, Christina Mundy², Alex Lambi², Robin A. Pixley², Steven Popoff². ¹Temple University, USA, ²Temple University School of Medicine, USA

Connective Tissue Growth Factor (CTGF) is a matricellular protein that has been shown to mediate cell adhesion, and thereby regulate cell proliferation, migration and differentiation. Previous studies have shown that integrins serve as functional signaling receptors for CTGF and that the specific integrin(s) involved are cell-type dependent. To date there is no information concerning CTGF/integrin interactions in osteoblasts. To determine whether osteoblasts can adhere to immobilized recombinant CTGF (rCTGF), we conducted adhesion assays using the MC3T3-E1 osteoblastic cell line. Osteoblasts adhered to rCTGF in a concentration-dependent manner similar to other known extracellular matrix (ECM) components (e.g. fibronectin). Next we used an array of blocking antibodies directed against individual α and β integrin subunits known to be on the osteoblast surface. Osteoblast adhesion was significantly decreased using anti-α_v or β₁ blocking antibodies. Subsequent co-immunoprecipitation analyses demonstrated that CTGF interacts with α_v and β₁ integrins in osteoblasts. Furthermore, the specificity of this CTGF/integrin interaction occurs in the C-terminal domain of CTGF. Immunofluorescent staining of cells cultured on substrates of rCTGF, fibronectin (positive control) or BSA (negative control) demonstrated that osteoblast adhesion to rCTGF resulted in changes in cell shape, cytoskeletal reorganization and the formation of focal adhesions. Western blot analysis revealed that adhesion of osteoblasts to rCTGF leads to activation of FAK and ERK1/2. Osteoblast differentiation was also enhanced when cells were cultured on rCTGF-covered plates compare to controls. These experiments establish CTGF as an ECM-associated adhesion protein and demonstrate that the integrin α_vβ₁ is a functional signaling receptor for CTGF in osteoblasts. In another series of experiments, we isolated osteoblasts from CTGF KO mice and their unaffected (WT) littermates to compare their ability to adhere to substrates composed of CTGF and other common bone matrix components (e.g. type I collagen). In all cases KO osteoblasts were defective in their ability to adhere to any of the substrates used in our experiments. These results suggest that integrin/matrix interactions are impaired in CTGF KO osteoblasts, and confirm a proposed role for CTGF acting as a molecular bridge to enhance interactions between osteoblast integrins and other bone matrix components.

Disclosures: Honey Hendsi, None.

MO0106

Mechanically Stressed Osteoblasts Secrete Soluble Factors that Activate Early Stage Osteoarthritis in Chondrocytes. Padma Pradeepa Srinivasan*, Andris Kronbergs, Randall Duncan, Catherine Kirn-Safran, University of Delaware, USA

Osteoarthritis (OA) is the most common chronic degenerative disease of cartilage associated with subchondral bone thickening and osteophyte formation. The role of subchondral bone in the etiopathology of OA is irrefutable yet unclear. Identifying the various soluble factors released by the subchondral osteoblasts (OB) in response to mechanical stress and altered knee loading following trauma or during aging is crucial to develop disease modifying drugs for OA. Here, we propose that mechanical stimulation of OB via specific calcium channels induces leptin secretion that, in turn, stimulates catabolic pathways in chondrocytes. Targeting these calcium channels or leptin secretion would slow/prevent progression of OA. We demonstrated that T-type voltage sensitive calcium channels (T-VSCC) are essential for the anabolic response of subchondral bone following load using a mice carrying null mutation for the $\alpha 1H$ subunit of Cav3.2, the pore forming subunit of T-VSCC. We have also shown that shear stress induces a significant increase in leptin secretion in the conditioned media (CM) of osteoblasts by performing ELISA. Using real-time RT PCR, we demonstrate that the addition of the CM from the sheared OBs on primary mice chondrocytes causes an increase in collagen X (a marker of hypertrophy and early OA) and a decrease in both aggrecan and collagen II mRNA steady-state levels. Similarly, exogenous addition of leptin to primary mouse chondrocytes stimulates the synthesis of mRNA levels of collagen X and matrix metalloproteinases (MMPs) that cause degradation of the cartilage matrix components leading to OA. We are currently demonstrating that calcium channel and leptin signaling inhibitors can reverse the changes induced by the CM from stressed OBs *in vitro*. In future studies we will perform DMM surgery (Destabilization of Medial Meniscus) in Cav3.2 knock-out mice and WT mice and also test the efficacy of leptin inhibitors as intra-articular injections. We predict that these studies will show that loss of function of the T-VSCC will attenuate the local metabolite production by OBs and slow the progression of OA. The translational objective of this project is to show that local application of leptin inhibitor can be used as potential and novel medical remedy for OA.

Disclosures: Padma Pradeepa Srinivasan, None.

MO0107

Systemic Administration of an Antagomir Designed to Inhibit miR-92, a Regulator of Angiogenesis, Failed to Modulate Skeletal Anabolic Response to Mechanical Loading. Anthony Sengul¹, Subburaman Mohan², Jon Wergedal², Joe Rungaroon³, Chandrasekhar Kesavan^{2*}. ¹University of Riverside, USA, ²Jerry L. Pettis Memorial VA Medical Center, USA, ³JLP VA Medical Center, USA

Mechanical loading (ML) is a powerful stimulator of new bone formation. The importance of blood vessels in the formation of skeleton and in fracture repair has been well documented. Since ML influences expression of angiogenic marker genes, we proposed that stimulation of angiogenesis may provide a means to promote skeletal anabolic response to ML. To evaluate this prediction, we determined if promotion of angiogenesis by systemic treatment with an antagomir against miR-92a, a well established inhibitor of angiogenesis, will increase bone formation response to mechanical strain. We subjected 10 week old C57BL6/J (B6) mice to two weeks of external load by four point bending (9N load, 2Hz frequency, 36 cycles, once per day). During the first week of ML, mice were injected with antagomir (50µg/dose) against miR-92 or control antagomir (3 alternate days via retro-orbital). No difference in tissue weights (heart, kidney, liver) were found in mice treated with miR-92 vs. control antagomir suggesting no side effects. Two weeks of ML increased tibia cross sectional area (CSA) and BMD by 15% and 6%, as expected, in the control antagomir treated mice. Similar increases in CSA (16%) and BMD (7%) were found in mice treated with miR-92 antagomir. To determine if systemic administration of miR-92 antagomir was effective in reducing levels of miR-92, real time RT-PCR was performed in RNA samples of heart and skeletal muscle. The results from our study revealed a 5-14 fold decrease in miR-92 levels in the heart and skeletal muscles of mice treated with miR-92 antagomir compared to control antagomir. In contrast, expression levels of two other MicroRNA's miR-93 and -20a were not different between the two groups of mice, thus suggesting specificity of the antagomir used. Surprisingly, we failed to detect significant changes in the expression levels of vascular genes (VEGF, CD31 and Tie2) in heart or skeletal muscle at the time point examined. Based on our findings, we conclude that systemic administration of antagomir against miR-92, while it reduced expression levels of miR-92 in the skeletal muscle and heart; it did not significantly alter either angiogenic or osteogenic response, thus suggesting possible redundancy in miR-92 regulation of angiogenesis.

Disclosures: Chandrasekhar Kesavan, None.

MO0108

Proteolytic Processing of Osteopontin by PHEX and Accumulation of Osteopontin Fragments in Hyp Mouse Bone, the Murine Model of X-linked Hypophosphatemia. Nilana Barros^{1*}, Betty Hoac², Raquel Neves¹, William Addison³, Diego Assis¹, Monzur Mursheed², Adriana Carmona¹, Marc McKee². ¹UNIFESP, Brazil, ²McGill University, Canada, ³Harvard University, USA

X-linked hypophosphatemia (XLH/HYP) – showing renal phosphate wasting, hypophosphatemia, osteomalacia and tooth abscesses – is caused by mutations in the zinc-metalloproteinase PHEX gene (phosphate-regulating gene with homologies to endopeptidase on the X chromosome). PHEX is expressed by mineralized tissue cells and inactivating mutations in PHEX lead to distal renal effects (implying accumulation of a secreted, circulating phosphaturic factor) and accumulation in bone and teeth of mineralization inhibiting ASARM-containing (acidic serine- and aspartate-rich motif) peptides which are proteolytically derived from the mineral-binding matrix proteins of the SIBLING family (small, integrin-binding ligand N-linked glycoproteins). While the latter observation suggests a local, direct matrix effect for PHEX, its physiologically relevant substrate proteins have not been identified. Here, we investigated two SIBLING proteins containing the ASARM motif – OPN (osteopontin) and BSP (bone sialoprotein) – as potential substrates for PHEX. Using cleavage assays, gel electrophoresis and mass spectrometry, we report that OPN is a full-length protein substrate for PHEX. Degradation of OPN was essentially complete, including hydrolysis of the ASARM motif, resulting in only very small residual fragments. Western blotting of Hyp (the murine homolog of human XLH/HYP) mouse bone extracts having no PHEX activity clearly showed accumulation of ~35 kDa OPN fragment that was not present in wild type mouse bone. Immunohistochemistry and immunogold labeling (electron microscopy) for OPN in Hyp bone likewise showed an accumulation of OPN and/or its fragments as compared to normal wild type bone. Incubation of Hyp mouse bone extracts with PHEX resulted in the complete degradation of these fragments. In conclusion, these results identify full-length OPN and its fragments as novel, physiologically relevant substrates for PHEX, suggesting that accumulation of mineralization inhibiting OPN fragments may contribute to the mineralization defect seen in the osteomalacic bone characteristic of XLH/HYP.

Disclosures: Nilana Barros, None.

This study received funding from: Canadian Institutes of Health Research (CIHR); Fundação de Amparo à Pesquisa do Estado de São Paulo (FAPESP)

MO0109

FGF-23 Gene Variation Associates with Phosphate Homeostasis and Bone Health in Finnish Children and Adolescents. Minna Pekkinen^{1*}, Christine Laine¹, Riikka Mäkitie¹, Elisa Saarnio², Christel Lamberger-Allardt³, Heli Viljakainen⁴, Outi Mäkitie⁵. ¹Folkhälsan Institute of Genetics, University of Helsinki, Finland, ²Calcium Research Unit, Department of Food & Environmental Sciences (Nutrition), University of Helsinki, Finland, ³University of Helsinki, Finland, ⁴Helsinki University Central Hospital for Children & Adolescents, Finland, ⁵Hospital for Children & Adolescents, Helsinki University Hospital, Finland

Fibroblast growth factor 23 (FGF-23), synthesized by osteoblasts and osteocytes, is part of hormonal bone-parathyroid-kidney axis, which is modulated by PTH, 1,25(OH)₂-vitamin D, diet and serum phosphorus levels. Several hereditary disorders with inappropriately high serum FGF-23 levels are associated with phosphate wasting and impaired bone mineralization. In the present study we investigated the genetic variation in the *FGF-23* gene and its association with parameters of phosphate homeostasis and bone health in Finnish children and adolescents.

This school-based study included 183 healthy children and adolescents (110 girls, 73 boys) aged 7-19 years (median 13.2 years), who were assessed for bone health and its determinants. The genetic variation was detected by direct sequencing of *FGF-23* coding exons with flanking intronic regions. The haplotype analysis were performed with Haplowiew 4.2. The concentrations of plasma/serum Ca, Pi, 25-hydroxyvitamin D (25-OHD), PTH, FGF-23 and the bone formation and resorption markers PINP and ICTP, as well as urine Pi and Creatinine concentrations were determined. Bone mineral density (BMD) was assessed with DXA (Hologic Discovery A). Statistical analyses were performed with PASW18.

We detected three different *FGF-23* polymorphisms: c.212-37insC (rs3832879) in intron 1 and two SNPs in exon 3, rs7955866 (p.T239M) and rs11063112 (p.P241P). Genotypes among the 183 subjects were for rs3832879 -/- (78%) and -/C (22%); for rs7955866 G/G (80%) and G/A (20%); and for rs11063112: A/A (47%), A/T (45%) and T/T (8%). Four different haplotypes were observed: AG- (58.1%), TG- (20.8%), AGC (10.9%), TA- (9.8%). The variation in *FGF-23* gene was significantly associated with P-Pi (p=0.043), S-ICTP (p=0.029) and U-Ca/U-Crea (p=0.014) in both pubertal boys and girls. In boys, but not in girls, *FGF-23* gene variation associated with S-25-OHD concentrations (p=0.032). In both genders, *FGF-23* gene variation was independently associated with femoral BMD Z-score in multivariate regression models (other variables in the model were weight, height, fat and lean mass, serum 25-OHD concentration and physical activity, p=0.001), but not with lumbar spine or whole body BMD.

The observed associations between *FGF-23* haplotypes and plasma Pi, urine Ca, serum 25-OHD and femoral BMD suggest that genetic variation in the *FGF-23* gene may play a role in mineral homeostasis and bone remodeling.

Disclosures: Minna Pekkinen, None.

MO0110

Osteoclastic Bone Resorption might be Involved in the Secretion of FGF23 into Circulation. Miwa Yamazaki^{*1}, Kazuaki Miyagawa², Yasuhisa Ohata³, Masanobu Kawai¹, Keichi Ozono⁴, Toshimi Michigami⁵. ¹Osaka Medical Center & Research Institute for Maternal & Child Health, Japan, ²Osaka Medical Center, Japan, ³Osaka University, Japan, ⁴Osaka University Graduate School of Medicine, Japan, ⁵Osaka Medical Center, Research Institute for Maternal & Child Health, Japan

FGF23 is a circulating phosphaturic factor that plays a critical role in phosphate (Pi) homeostasis. FGF23 produced by bone acts mainly in kidney. Despite of its endocrine function, the precise mechanisms by which the circulating levels of FGF23 are controlled remain unclear. A recent clinical study demonstrated the rapid decrease in serum FGF23 following bisphosphonate infusion in osteogenesis imperfecta, which brought us to hypothesize that FGF23 embedded in bone might be released into circulation through osteoclastic bone resorption. To test this notion, we have investigated the effects of rapid bone resorption on the secretion of FGF23, using a mouse model established by Boyce, et al. (*Endocrinol*, 1989), where IL-1 injection into subcutaneous tissue over calvariae stimulates bone resorption both locally and systemically and induces hypercalcemia. C57BL/6J mice (10-wk-old, male) were administered daily for 4 days with either IL-1 β (2.5 μ g/day) or vehicle (saline). The injection was performed into the left side of the calvariae once a day, and the mice were sacrificed 24 hours after the last injection to harvest blood and calvarial bone. Serum calcium (Ca) levels were significantly increased in the mice injected with IL-1 β compared with the control mice (10.9 \pm 0.25 mg/dl vs. 9.40 \pm 0.18 mg/dl; $p < 0.0001$), suggesting the increased bone resorption. Serum levels of intact FGF23 also were significantly elevated in the IL-1 β -injected group compared with the control group (221.25 \pm 33.36 pg/ml vs. 120.70 \pm 32.74 pg/ml; $p < 0.001$). There was no significant difference in serum Pi levels. Then, real-time PCR was performed using RNA extracted from the calvariae to examine the mRNA expression of *Rankl*, *Opg* and *Fgf23*. The expression ratio of *Rankl* to *Opg* was increased in the calvariae of IL-1 β -injected group compared with the control group, confirming the increased bone-resorbing activity. Interestingly, the *Fgf23* mRNA was rather decreased in the calvariae of IL-1 β -injected group, although there was no obvious difference in the immunostaining using anti-FGF23 antibody. Elevated serum FGF23 despite of the decrease in its mRNA level suggested its accelerated secretion from the bone matrix. These results indicate the involvement of osteoclastic bone resorption in FGF23 secretion into circulation. During bone resorption, the increase in serum Pi might be prevented by the simultaneous release of FGF23 from bone.

Disclosures: Miwa Yamazaki, None.

MO0111

Phosphate Sensing in Osteocytes: Extracellular Phosphate Induces FGF23 Expression in IDG-SW3 Osteocyte-Like Cells. Nobuaki Ito^{*1}, David Findlay², Renee Ormsby², Paul Anderson³, Lynda Bonewald⁴, Gerald Atkins². ¹The university of Adelaide, Australia, ²University of Adelaide, Australia, ³Musculoskeletal Biology Research, University of South Australia, Australia, ⁴University of Missouri - Kansas City, USA

FGF23 is a critical osteoblast/osteocyte-derived hormone that acts on the kidney to regulate phosphate (Pi) homeostasis. FGF23 binds to its specific receptor comprising canonical FGF receptor, FGFR1(IIIa) and Klotho, and down-regulates the expression of sodium-phosphate co-transporter NaPi-IIa, IIc and CYP27b1. Several reports indicate that *in vivo*, Pi and 1,25(OH)₂ vitamin D (1,25D) stimulate the production of FGF23. 1,25D is also reported to up-regulate FGF23 expression in mouse primary osteoblasts *in vitro*, an effect enhanced in concert with extracellular Pi⁽¹⁾. This indicates that osteoblasts and/or osteocytes can sense Pi, although the way, in which they do so has not been elucidated. Further, little is known about the effect of Pi on bone formation or resorption-related genes in either osteoblasts or osteocytes. In this study, the mouse osteocyte-like cell line, IDG-SW3 was differentiated for 35d, giving rise to a mature osteocyte-like phenotype⁽²⁾. A particular advantage of this cell model is that it is the only known cell line to produce FGF23⁽²⁾. The expression level of several bone-related genes was then evaluated in response to varying concentrations of extracellular Pi (1, 4, 10mM), in the presence or absence of 1,25D (10nM). Pi dose-dependently increased the expression of FGF23 mRNA (up to 40-fold), as well as genes associated with bone formation and mineralisation, including OCN, SOST, PHEX, DMP1 and MEPE, and key genes related to bone resorption, OPG and RANKL. 1,25D further up-regulated the mRNA expression of OCN and RANKL, and down-regulated that of OPG, SOST, PHEX, DMP1, MEPE. Additionally, 1,25D decreased CYP27b1 mRNA levels in the presence of Pi at 10nM. Interestingly, the prominent induction of CYP24 mRNA by 1,25D was attenuated by high levels of Pi. These findings provide strong evidence that osteocytes can sense the extracellular concentration of Pi. Our results indicate that a variety of osteoblast-osteocyte specific genes are regulated in response to Pi. They also demonstrate the interaction between

1,25D and Pi acting at the level of the osteocyte. Furthermore, some of these genes affected by extracellular Pi are possibly involved in the cascade between Pi sensing and FGF23 production.

1. Yamamoto et al. 2010 J Endocrinol206:279-286.
2. Woo et al. 2011 J Bone Miner Res26:2634-2646.

Disclosures: Nobuaki Ito, None.

MO0112

Transient but not Constitutive Activation of ERK Is Necessary for the Unique Action of FGF23 in Bone. Tomoko Minamizaki^{*1}, Yukiko Konishi², Hirotaka Yoshioka¹, Katsuyuki Kozai¹, Yuji Yoshiko¹. ¹Hiroshima University Institute of Biomedical & Health Sciences, Japan, ²Hiroshima University Graduate School of Biomedical & Health Sciences, Hiroshima

Fibroblast growth factor 23 (FGF23) primarily expressed in osteoblasts/osteocytes targets renal tubules to suppress phosphate reabsorption and vitamin D activation. Membrane protein Klotho forms a complex with FGF23-FGF receptor (FGFR)1, which appears to be necessary for FGF23-specific signaling. Recently, we showed that FGF23 and the truncated form of the extracellular domain of Klotho (soluble Klotho, sKL) cooperatively inhibit bone mineralization independently of serum phosphate levels in klotho-deficient mice, suggesting that FGF23 may directly play a role in bone mineralization. Amongst canonical FGF signaling involved in bone formation, the physiological and/or pathological significance of FGF23 in bone remains unclear. In comparison to FGF family members including FGF2, the most common member of FGFs involved in bone formation, FGF23 was abundant in mouse/rat osteoblasts/osteocytes, especially when treated with 1 α ,25(OH)₂D₃ *in vitro* and *in vivo*. Although FGF2 was only faintly detected in rat osteoblasts/osteocytes, FGF23/sKL actions during matrix mineralization *in vitro* could be mimicked by addition of FGF2. However, unlike FGF23/rKL, FGF2 constitutively activated the ERK-MAPK pathway and irreversibly inhibited matrix mineralization with the up- and down-regulation of ankylosis gene and alkaline phosphatase, respectively. In contrast, FGF23/sKL did not increase osteoprogenitor cell proliferation, while FGF2 did. Pretreatment with not only FGFR1a(IIIc) chimera but also SU4502, an inhibitor of FGFR1 phosphorylation blocked any of these effects. DNA microarray analysis of rat osteoblast/osteocyte cultures revealed that FGF2 altered expression of a large number of genes, whereas FGF23 regulated only about 50 genes including PheX. FGF23/sKL but not FGF2 increased Sprouty homolog (Spry)1 and 4, which are expressed in mesenchymal tissues and acts as antagonists of Ras-Raf-ERK signaling downstream of FGFR. RNAi knockdown of Spry1/4 in rat osteoblast/osteocyte cultures increased the duration of ERK activation by FGF23/sKL, with resultant changes in gene expression profiling. Thus, amongst FGF family members expressed in bone, 1 α ,25(OH)₂D₃-induced FGF23 plays a role to regulate bone mineralization via its unique pathway which is characterized by transient ERK phosphorylation.

Disclosures: Tomoko Minamizaki, None.

MO0113

Analysis of Relationships between intact PTH and 25-hydroxy vitamin D (25OHD) and its Fractions as Measured by LC-MS/MS. Adam May^{*1}, Earle Holmes², Pauline Camacho¹. ¹Loyola University of Chicago, USA, ²Loyola University Medical Center, USA

Purpose: Measurement of 25OHD by liquid chromatography tandem mass spectrometry (LC-MS/MS) provides concentrations of total 25OHD, 25OHD3, 25OHD2. However, the clinical significance of these fractionated values remains unclear. The aim of this study was to investigate determinants of total 25OHD, 25OHD3 and 25OHD2 with intact PTH in a patient sample lacking medical conditions known to affect vitamin D physiology.

Methods: We studied 4842 patients that were evaluated for 25OHD by liquid chromatography tandem mass spectrometry (LC-MS/MS) (Quest Diagnostics, Wood Dale, IL, 60191) between 3/1/2011 and 9/29/2011. The population of interest was adults with unknown vitamin D status undergoing their first evaluation with paired 25OHD and intact PTH assays. Patients with hypercalcemia, renal insufficiency (eGFR < 60), elevated ALT, abnormal TSH levels, cirrhosis, chronic kidney disease including renal transplantation, and recent Vitamin D supplementation and/or hydrochlorothiazide use were excluded from analysis. A total of 215 patients met selection criteria. Key analytic variables were patient age, gender, race, BMI, total 25OHD, 25OHD2, 25OHD3, intact PTH, total calcium, and ionized calcium. Relationships between these variables were characterized by regression analysis and ANOVA. A multivariate logistic regression was used to identify predictors of serum PTH > 65 ng/mL. Statistical analysis was performed using SYSTAT (Systat Software, Inc., Chicago, IL, 60606).

Results: The mean 25OHD3 levels were higher among Caucasians (33.6 μ g/mL) than non-Caucasians (22.0 μ g/mL) ($f = 14.3$, $p = 0.000$), and lower in patients with BMI ≥ 25 (28.9 μ g/mL) than patients with BMI < 25 (36.6 μ g/mL) ($f = 12.9$, $p = 0.000$). Univariate comparisons by regression analysis showed significant correlations between logPTH and log25OHD3 ($r = -0.284$, $p = 0.000$), log total 25OHD ($r = -0.227$, $p = 0.001$), and BMI ($r = 0.176$, $p = 0.018$). No significant correlation was seen between logPTH and other analytic variables including 25OHD2. Statistically significant predictors of serum PTH > 65 ng/mL in a stepwise logistic regression

identified a 2-parameter model that included log25OHD3 ($p = 0.000$, $OR = 0.059$, $CI 0.286-0.012$) and $BMI < 25.0$ ($p = 0.018$, $OR = 0.304$, $CI 0.816-0.113$).

Conclusion: Among patients lacking confounders of normal vitamin D physiology, 25OHD3 is a strong predictor of elevated PTH, and is more closely correlated to PTH than total 25OHD or 25OHD2.

Disclosures: Adam May, None.

MO0114

Cinacalcet Single Dose Fast Test can Foresee Therapeutic PTH-response in Primary Hyperparathyroidism (PHP)? Alessandra De Remigis¹, Luigi Vianale², Pierluigi De Remigis², Giorgio Napolitano³. ¹Johns Hopkins University, USA, ²General Hospital Chieti Italy, Italy, ³University of Chieti, Italy

Cinacalcet is a calcimimetic that increases a sensitivity of calcium-sensing receptor (CaRs) on parathyroid cells, reducing PTH secretion and than serum calcium in PHP; therefore it has been proposed as medical therapy in PHP. However a CaRs polymorphism has been showed, can explain different responses to cinacalcet.

A cinacalcet single dose fast test was implemented in PHP in order to identify responders from non-responder subjects to the calcimimetic drug.

10 subjects (8 female and two male, aging 20-80 yr) were taken in consideration with PHP diagnosis. In fact all presented high serum PTH (commercial chemiluminescent assay, normal range from 6,5 to 36,8 pg/ml) and calcium, low serum phosphorus and low vitamin D levels. We succeeded to localize an image attributable to parathyroid (probably adenoma in all cases), by neck ultrasound and sestamibi scintiscan.

We evaluated repeatedly the reduction of serum PTH and calcium, starting from 8 in the morning (baseline) and then hour intervals for 3 hours after cinacalcet single oral dose (60 mg).

In 7 of 10 subjects (70%) a significant decreasing of PTH was showed, with a percentage of PTH reduction variable from maximum of 78% (from 438 pg/ml to 92 pg/ml) to a minimum of 18,6% (from 150 pg/ml to 122 pg/ml), three subjects were non-responders (two male and one female) (see table).

Time course of PTH curves (figure 1) are characteristic in 7 subjects, who experienced hormone decline: a very significant reduction ($p < 0,001$) of PTH levels happened at the first hour, than the curve flattens.

All were put on cinacalcet chronic therapy and two male subjects continued to be unresponsive both for PTH and serum calcium levels.

The others responded reaching normal calcium levels, even the only female subject non responder to single dose fast test.

In conclusion in our experience we demonstrate cinacalcet single dose with 60mg could be a good fast test to discriminate responder and non responder to chronic therapy in 90 % of cases of PHP.

| Subj sex | PTH 0 pg/ml | PTH 60 | PTH 120 | PTH 180 | <PTH % | Ca % |
|----------|-------------|--------|---------|---------|--------|------|
| 1 f | 438 | 92 | 65,5 | 114 | -78 | -5,8 |
| 2 m | 42,7 | 41,3 | 40,9 | 42 | -3 | -1,7 |
| 3 f | 50,2 | 38,8 | 27,5 | 28,2 | -22,7 | -0,7 |
| 4 f | 55,4 | 18,8 | 13,2 | 10,2 | -66 | -2,3 |
| 5 m | 97,3 | 104 | 102 | 102 | 6 | 0,3 |
| 6 f | 63,1 | 38,8 | 42,8 | 27 | -59,3 | -6,9 |
| 7 f | 150 | 122 | 92,5 | 81,6 | -18,6 | -1,8 |
| 8 f | 167 | 130 | 41,6 | 45 | -22,1 | -0,9 |
| 9 f | 210 | 197 | 239 | 220 | -6,1 | -0,3 |
| 10 f | 180 | 90 | 85 | 88 | -50 | -1,7 |
| mean | 141 | 87 | 73 | 74 | 52 | |

Table PTH levels in 10 subjects before and after cinacalcet 60mg

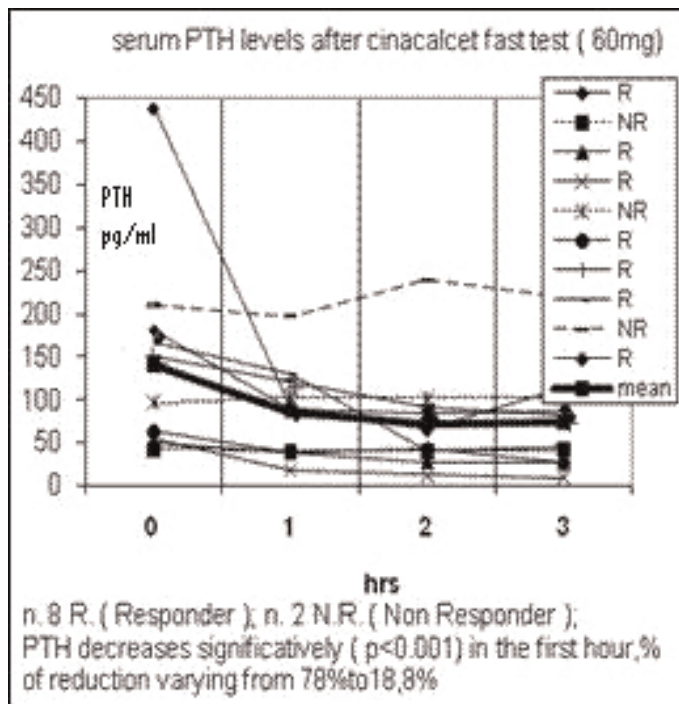


Figure time-course of serum PTH curves after cinacalcet fast test

Disclosures: Alessandra De Remigis, None.

MO0115

Crosstalk Between Parathyroid Hormone Related Proteins And Minor Fibrillar Collagens.. Minoti Hiremath^{*}, Neda Shefa, Julia Oxford. Boise State University, USA

The aim of our study is to determine if PTHrP regulates bone growth during endochondral ossification by regulating the expression of minor fibrillar collagens. Based on abundance, collagens are classified as major collagens, including type 1 and 2, and minor collagens including type 5 and 11. Minor collagens regulate the formation of major collagen fibrils and dictate the quality of the ECM that is synthesized. In humans, heterozygous mutations in the COL11A1 gene cause chondrodysplasia with eye and ear defects designated as Stickler syndrome type II or Marshall syndrome. Collagen 11 is expressed at the periphery of the cartilage underlying the bone collar, distal to the hypertrophic zone. Based on the human diseases caused by mutations of COL11A1 and the expression profile, Collagen XI appears regulate bone growth.

Parathyroid hormone related protein (PTHrP) also regulates bone growth by binding to its cognate G-protein coupled receptor, PTHR1. PTHR1 maintains columns of proliferating chondrocyte and delays their differentiation into prehypertrophic chondrocytes, preventing premature ossification. Loss of PTHR1 results in Bloomstrand's osteo-chondrodystrophy characterized by short bones, small ribcage and domed skulls, and is phenocopied by *PTHrP^{-/-}* mice.

We hypothesized that one of the mechanisms by which PTHR1 regulates endochondral ossification is by regulating expression of minor fibrillar collagens or their isoforms. We used C2C12 cells treated with Bmp2, as a model of osteoblasts. After 5 days of Bmp2 treatment, PTHR1 was added for 24 hours and control plates were left untreated. Using semi-quantitative RT-PCR, we observed that PTHR1 regulates expression of COL11 isoforms V1b and V1bV2 in C2C12 cells. This result is intriguing because we found that V1b isoforms of COL11 were expressed adjacent to the bony collar and distal to the hypertrophic zone. Moreover, these isoforms decrease mineralization in MC3T3-E1 and in Bmp2-treated C2C12 osteoblasts. We also tested regulation of minor collagens COL5A1, COL5A3 and COL11A2 by PTHR1, in C2C12 cells, using RT-PCR. Our results indicate that PTHR1 reduces COL5A1 and COL11A2 and increases COL5A3 expression in C2C12 cells. Thus, we demonstrate that PTHR1 regulates minor collagens in myogenic and osteoblastic cell lines. We are currently examining the expression of minor collagens to determine if they are absent or mislocalized in the developing long bones *PTHrP^{-/-}* mice.

Disclosures: Minoti Hiremath, None.

MO0116

Histomorphometric Analysis of Marrow Adipocytes after Treatment with Cinacalcet or Parathyroidectomy for Renal Hyperparathyroidism. Aiji Yajima*¹, Yasuo Imanishi², Masaki Inaba², Yoshihiro Tominaga³, Shigeru Satoh⁴, Akemi Ito⁵, Sharon Martin Moe⁶. ¹Akita University, School of Medicine, USA, ²Osaka City University Graduate School of Medicine, Japan, ³Nagoya 2nd Red Cross Hospital, Japan, ⁴Division of Renal Replacement Therapeutic Science, Department of Urology Akita University, Japan, ⁵Ito Bone Histomorphometry Institute, Japan, ⁶Indiana University, USA

Purpose: Marrow cellular differentiation may be altered by changes in PTH. We hypothesized that PTH lowering by either parathyroidectomy or cinacalcet would alter marrow adipocytes. Methods: In the 45 hemodialysis (HD) patients with secondary hyperparathyroidism, marrow adipocytes were evaluated by histomorphometric analysis of transiliac bone biopsy before and after treatment with cinacalcet (Cin; n=12 with baseline and 1 year, Age=59 ± 6, HD duration=10 ± 5 years) or total parathyroidectomy with reimplantation (PTX, n= 16 at 4 weeks, n = 4 at one year; Age=57 ± 9, HD duration=16 ± 7 years). Serum intact PTH was measured on the day of bone biopsy. Adipocyte volume (Ad.V/Ma.V; %), adipocyte number (N.Ad/Ma.V; N/mm³) and mean adipocyte volume (Ad.V/N.Ad; × (10⁻³)/mm³) were calculated as the secondary parameters. Results: The PTH dropped in the PTX group at 4 weeks from 1070 to 11.5 pg/ml. At 4 weeks in these patients, there was improvement in the parameters of osteitis fibrosa, and an increase in the marrow adipocyte volume (Adv/MaV; 20 ± 12 vs. 31 ± 15%, p < 0.001) and the number of adipocytes/marrow volume (N.Ad/Ma.V; 143 ± 86 to 189 ± 76, p = 0.001). At one year, both treatments improved PTH (PTH decreased by 1162 ± 338 in PTX vs. 649 ± 326 pg/ml in the Cin groups), with a final PTH was 20 ± 15 in the PTX group vs. 100 ± 50 pg/ml in the Cin group, p = 0.006). The histologic parameters of osteitis fibrosis improved with marked decrease in osteoclast surface, osteoblast surface, and fibrosis in both treatments. However, after one year, the patients who underwent a PTX had no osteoclast surface Oc.S/BS of 0.03 ± 0.05 % vs. those treated with cinacalcet (1.4 ± 1.9 %; p = 0.023) and no osteoblast surface Ob.S/BS (0 ± 0 vs. 12.3 ± 0.1%, p 0.004). After one year, there was a difference in the proportion of marrow filled with adipocytes in the PTX group (28.9 ± 14.4%) compared to the Cin group (44.4 ± 12.3%, p = 0.054). The number of adipocytes normalized by marrow volume in the PTX group was greater than the Cin group (91 ± 104 vs. -12 ± 62, p = 0.03). Conclusion: An acute reduction of iPTH increased marrow adipocytes 4 wks after parathyroidectomy. However at one year, this effect was lessened and no different than a more gradual reduction of iPTH with cinacalcet.

Disclosures: Aiji Yajima, Kirin Co Ltd, 2

MO0117

LIAISON® 1-84 PTH Reference Ranges for Healthy Subjects and CKD stage 5 Patients in Comparison to LIAISON® N-tact™ PTH assay. Zlata Fejfarkova*¹, Daniel Rajdl², Roman Cibulka², Richard Pikner³, Hana Novotna⁴. ¹Klatovská Nemocnice, A.s., Czech Republic, ²Institute of Clinical Biochemistry & Hematology, Faculty of Medicine Pilsen, Charles University, Czech Republic, ³Department of Clinical Laboratories & Bone Metabolism, Klatovská nemocnice, Czech Republic, ⁴Dept. of Nephrology, Klatovská Nemocnice, Czech Republic

Our aim was to establish reference ranges for 1-84 PTH LIAISON®, 3rd generation, in blood donors and patients with CKD stage 5 on dialysis and afterwards to compare them with LIAISON® N-tact™ PTH assay. Methods: Blood donors (N=96); inclusion criteria were both 25(OH) Vitamin D >12 ng/ml, total calcium: 8.4– 10.8 mg/dl. CKD patients on dialysis (N=350), sampled prior dialysis. In both groups we measured 1-84 PTH and N-tact PTH in EDTA samples DiaSorin, USA. 1-84 PTH has 0% cross-reactivity with fragment 7-84 PTH while N-tact™ PTH has 52% cross-reactivity with fragment 7-84 PTH. Material: EDTA plasma were separated within 60 minutes and immediately frozen at -80 Celsius degrees until determination. Reference ranges were established as 2.5 and 97.5 quantiles of blood donors distribution. Recommended range for CKD stage 5 patients was determined as 1-84 PTH values (N=54) matched with N-tact values between 169-288 pg/ml, that correspond with 150-300 pg/ml (1) PTH Allegro® Nichols Institute Diagnostics.(2)

Results: 1-84 PTH provides significantly lower values than N-tact PTH, 28-43% (90% CI) of N-tact PTH in blood donors and 28-62 % in CKD patients respectively. We found reference range of 1-84 PTH within 8.2-28.5 pg/ml and 22.3-76.5 pg/ml for N-tact PTH for healthy subjects. In CKD stage 5 patients we found 1-84 PTH levels between 49-158 pg/ml correspond with 169-288pg/ml of N-tact PTH. This range is recommended for maintaining normal bone turnover. In general, there exists very good correlation between these two methods (Spearman corr. coef. 0.976) there, but in subgroup of values from 49 -158 pg/ml Spearman correlation is only 0.550 with N-tact PTH.

Conclusions: We have established acceptable reference ranges 1-84 PTH assay for both healthy subjects and patients with CKD stage 5. 1-84 PTH LIAISON assay provides true measurement of intact 1-84 PTH. Despite very good general correlation we found higher percentage levels of 1-84 PTH in CKD patients with N-tact PTH levels above 300 pg/ml. Further evaluation is needed to establish clinical value of new 1-84 PTH LIAISON mainly in CKD patients.

1. Souberbiell J-C., et. al. Assay-Specific Decision Limits for Two New Automated Parathyroid Hormone and 25-Hydroxyvitamin D assays. *CLinical Chemistry* 51, No. 2,2005

2.K/DOQI Clinical Practice Guidelines for Bone Metabolism and Disease in Chronic Kidney Disease. *American Journal of Kidney Diseases*, Vol 42, No 4, Suppl 3 October, 2003

Disclosures: Zlata Fejfarkova, None.

MO0118

PTH Prevents the Deterioration of Trabecular Bone Architecture Induced by Localized Radiation. Abhishek Chandra*¹, Shenghui Lan², Xianrong Zhang³, Ji Zhu³, Xiaowei Liu¹, Ling Qin¹. ¹University of Pennsylvania, USA, ²Department of Orthopaedics, Union Hospital, Tongji Medical College, Huazhong University of Science & Technology, China, ³University of Pennsylvania, School of Medicine, USA

Localized radiation therapy is one of the most common treatments for cancer patients. However, it has inevitable adverse effects on the bones close to the irradiated region, leading to reduced bone density, fractures and osteoradionecrosis. To date, there is no preventive or curative treatment for radiation-induced bone damage. Parathyroid hormone (PTH) has potent anabolic effects on bone with great stimulation of bone turnover. Here we investigated whether PTH had radioprotective effects on rat trabecular bone focally radiated by longitudinal micro-computed tomography (μCT) scans. One-month-old rats (n=6/group) received either saline or PTH (80 microgram/ kilogram) daily injections for 12 days and the right tibiae were scanned every other day by Scanco vivaCT40 with an effective dose of 0.4 Gy/scan on the right tibia and undetectable level on the left. At day 12, the left tibiae were scanned as non-irradiated controls. Blood chemistry analyses demonstrated the effectiveness of PTH actions and neither PTH nor multiple scans altered the axial bone growth rate. We observed a gradual decrease in bone volume fraction (BV/TV, 43% d12 vs d0), trabecular number (TbN, 53%) and connectivity density (ConnD, 66%) and an increase in trabecular separation (TbSp, 88%) in the irradiated vs. contralateral tibiae in vehicle group. In contrast, PTH-treated irradiated tibiae exhibited a significant increase in BV/TV(110% d12 vs d0), due to increases in TbN (27%), trabecular thickness (TbTh, 37%) and ConnD (73%). A 46% decrease in structure model index indicated a greatly improved plate-like trabecular structure by PTH. Moreover, at d12, accumulated radiation dosage (2.4 Gy) resulted in a 44% reduction in BV/TV in irradiated vs. contralateral tibia, while no difference was found in PTH group. Overall, bone structures in both tibiae from PTH group were greatly improved compared to vehicle-treated tibiae. Histomorphometry analysis revealed significant decreases in osteoblast number, mineral apposition rate and bone formation rate in the irradiated tibia at d12 while all these parameters were greatly elevated in both tibiae in the PTH group. Although radiation increased levels of free radicals in bone marrow in both vehicle and PTH groups, the increased apoptosis rate caused by DNA damage was only observed in vehicle but not PTH group. Hence, our data are first to demonstrate a strong radioprotective effect of PTH on bone and suggest a potential clinic application of PTH in radiotherapy.

Disclosures: Abhishek Chandra, None.

MO0119

Defective Glomerular Maturation in the Ebf1-Deficient Mouse Underlies the Disconnect Between High Circulating Osteocalcin and Decreased Osteoblast Maturation in These Animals. Jackie Fretz*¹, Tracy Nelson², Heino Velazquez³, Yougen Xi², Gilbert Moeckel⁴, Mark Horowitz¹. ¹Yale University School of Medicine, USA, ²Department of Orthopaedics & Rehabilitation, Yale University School of Medicine, USA, ³Department of Internal Medicine- Nephrology, Yale University School of Medicine, New Haven, CT 06520, USA, USA, ⁴Department of Pathology, Yale University School of Medicine, USA

Multiple coordinated signaling pathways, cytokines, and transcription factors have been identified as integral to maturation of the nephron from its mesenchymal progenitors. We present here a completely novel role for Early B cell Factor 1 (Ebf1) as a transcription factor required for proper glomerular maturation. Using the Ebf1-null mouse as a model we characterized the biochemical, metabolic, and histological abnormalities in renal development that arise in the absence of this transcription factor. The expression of Ebf1 is both spatially and temporally regulated within the developing cortex and glomeruli. In the absence of Ebf1, developing kidneys show thinned cortices, reduced cortical glomerular maturation, and nephrogenic blastema that persists into adulthood. The glomeruli that form after postnatal day 14 exhibit defective tuft formation that is mediated through reduced expression of podocyte-derived VEGF-A. The mice exhibit early albuminuria, elevated blood urea nitrogen (BUN) levels, and their glomerular filtration rate(GFR) is reduced by >66%. We have reported previously on a defect in late osteoblast maturation that arises through cell autonomous functions and is also present in the Ebf1-knockout mice. These phenotypes are separable, and the reduction in GFR explains the disconnection in these mice between the circulating levels of osteocalcin (twice that of their littermates) despite markedly reduced bone density and >80% reductions in osteocalcin production from osteoblasts *in vitro* and *in vivo*. Taken together these results present

the first report of a significant and novel role of Ebf1 in glomerular development, podocyte maturation, and maintenance of kidney integrity and function.

Disclosures: Jackie Fretz, None.

MO0120

ELISAs for Biomarkers of Bone and Mineral Disorders of Patients with Chronic Kidney Disease. Daniel-Sebastian Karau¹, Wolfgang Woloszczuk^{*2}, Thuy Oanh Ho Thi³, Rainer Oberbauer⁴, Roelf Datema⁵.
¹Biomarker Design ForschungsGmbH, Austria, ²Biomedica Medizinprodukte GmbH & CoKg, Austria, ³Biomedica, Austria, ⁴Medizinische Universitätsklinik Wien, Austria, ⁵Biomarker Design, Austria

We develop ELISAs for evaluation of blood parameters in patients with chronic kidney disease-bone & mineral disorder (CKD-BMD). Six biomarkers have been selected: FGF23 as an early marker related to phosphate homeostasis, sclerostin as an osteocyte marker, sRANKL as a key player in calcification processes, endostatin and NT-proCNP as markers of different aspects of vascular injury, and SPARC because of its known role in bone remodeling. ELISA tests for these proteins (except the one for SPARC) fulfill the requirements of a robust ELISA suitable for routine use. Median reference levels were 16 pg/ml for C-terminal FGF23, 23 pM for sclerostin, 200 fM for sRANKL, 116 ng/ml for endostatin and 2 ng/ml for NT-proCNP. Median levels were elevated in patients before and after hemodialysis (N=26): FGF23 (75- resp. 35-fold), sclerostin (3.5- resp. 2.3-fold), endostatin (6- resp. 4-fold), and NT-proCNP (50- resp. 16-fold). The only significant correlation between any of these parameters was between levels after dialysis of endostatin and NT-proCNP, both related to endothelial function.

In these patient samples, no consistent changes were observed for sRANKL or OPG. Measurements of SPARC were confounded by SPARC release from thrombocytes during preparation of EDTA plasma. Interestingly, we found a significant correlation between sclerostin and big-endothelin, a marker of severe cardiac insufficiency, post, but not before dialysis. The main challenge remaining is to assign specific parameters to defined pathologies within CKD-BMD.

Supported by funding from the European Community's Seventh Framework Programme under grant agreement number 241544 (SysKid).

Disclosures: Wolfgang Woloszczuk, None.

MO0121

Increased Bone Density in Mice Lacking the Proton Receptor OGR1. Nancy Krieger^{*1}, Zhenqiang Yao¹, Kelly Kyker-Snowman², Brendan Boyce³, David Bushinsky¹.
¹University of Rochester, USA, ²University of Rochester School of Medicine, USA, ³University of Rochester Medical Center, USA

Chronic metabolic acidosis, a systemic increase in proton (H⁺) concentration, stimulates net calcium (Ca) efflux from bone mediated primarily through increased osteoblastic cyclooxygenase 2, leading to prostaglandin E₂-induced stimulation of RANKL and subsequent increased osteoclastic bone resorption. Osteoblasts express the H⁺-sensing G-protein coupled receptor, OGR1, which activates IP₃ mediated intracellular Ca (Ca_i) release. We have shown that H⁺-induced Ca_i signaling in the osteoblast requires OGR1, suggesting that OGR1 is the H⁺ sensor activated by metabolic acidosis to initiate its response in bone. To determine the role of OGR1 in early bone development, a time when large amounts of metabolic acid are generated, we obtained mice with a genetic null mutation in OGR1 (KO, provided by K. Seuwen, Novartis). Although these mice have no gross phenotype when compared to wild type C57/Bl6 mice (WT), μ CT and histologic data show clear abnormalities in bone. By μ CT, vertebrae from 8 wk old KO mice have significantly increased bone volume, increased trabecular thickness and number and decreased trabecular spacing compared to WT. Tibia from these mice also have increased trabecular bone volume, trabecular thickness and number in the KO mice compared to WT (Table 1). Histomorphometric analysis with Visiopharm software of bone sections from the tibial diaphysis, scanned with an Olympus VS110 virtual slide scanning system on TRAP-fast green stained slides, showed increased bone volume (WT=7.47 \pm 0.66% vs KO=11.22 \pm 0.96%, p<0.05) and decreased trabecular spacing (WT=67.0 \pm 4.9/mm² vs KO=45.0 \pm 2.6, p<0.05) in OGR1 KO vs WT mice. Osteoclast number was increased in KO tibiae; however, there appeared to be decreased TRAP⁺ staining indicating a decrease in the number of active osteoclasts. These data suggest that in rapidly growing mice, which generate considerable amounts of metabolic acid, lack of the H⁺ receptor OGR1, is associated with increased trabecular bone, as well as changes in osteoclast number and activity.

| μ CT results | BV/TV | Tb.N | Tb.Sp. | Tb.Th. |
|------------------|------------------|----------------|--------------------|--------------------|
| WT vertebrae | 0.28 \pm 0.01 | 6.2 \pm 0.1 | 0.151 \pm 0.004 | 0.047 \pm 0.001 |
| KO vertebrae | 0.38 \pm 0.02* | 7.3 \pm 0.2* | 0.127 \pm 0.003* | 0.054 \pm 0.001* |
| WT tibia | 0.15 \pm 0.01 | 5.2 \pm 0.1 | 0.185 \pm 0.005 | 0.046 \pm 0.001 |
| KO tibia | 0.23 \pm 0.01* | 7.2 \pm 0.1* | 0.128 \pm 0.003* | 0.047 \pm 0.001 |

Data are mean \pm SE for 11-12 bones/group. *p<0.05 compared to WT at same location.

Table 1

Disclosures: Nancy Krieger, None.

MO0122

Klotho Gene Ablation Alters Hematopoiesis. Sangeetha V.M^{*}, Lindsay Coe, Despina Sitara. New York University College of Dentistry, USA

Klotho, the anti-aging hormone, is primarily expressed in kidney and is known to control mineral ion homeostasis. Genetic inactivation of klotho in mice results in a complex phenotype including significant reduction in bone mineral density and osteoblast numbers. Mineralization and bone remodeling substantially contribute to the establishment of the marrow environment and the importance of osteoblasts in hematopoiesis is well supported. The current study was designed to address the role of klotho in hematopoiesis *in vivo*. To test this hypothesis, we compared changes in blood cell production and differentiation in 6-week old klotho^{-/-} and wild-type littermates. Complete automated blood count was carried out in peripheral blood. The phenotypic analysis of hematopoietic cells was assessed by flow cytometry and the colony forming potential was evaluated using methylcellulose based colony assay. Here we identified a novel function of klotho in the regulation of hematopoiesis as klotho^{-/-} mice exhibit severe hematopoietic defects. Peripheral blood and bone marrow from klotho^{-/-} mice display a significant increase in erythroid populations paralleled by a consistent decrease in B-lymphocytes and changes in granulocyte/monocyte populations. Interestingly, klotho^{-/-} mice show higher levels of circulating hematopoietic stem cells (HSCs) indicating an apparent defect in either the HSCs or in the bone marrow niche. We have further observed that the bone marrow compartment of klotho^{-/-} mice indeed harbors very low HSCs as compared to the wild type littermates. The changes in erythropoiesis and granulopoiesis are reflected in their ability to form colonies *in vitro*. Our observations suggest that regulation of bone and mineral metabolism by Klotho may modulate adult steady-state hematopoiesis. As klotho^{-/-} mice exhibit hypervitaminosis D and vitamin D receptor is known to control klotho, we are currently investigating whether vitamin D plays any role in the regulation of hematopoiesis by klotho. Furthermore, our preliminary data on fetal liver hematopoiesis also indicate that klotho^{-/-} mice have altered pre-natal hematopoietic development. Further studies are underway to confirm these findings as our observations raise the possibility of a broader functional significance of klotho. Taken together, our study demonstrates a novel function of klotho which may establish a close regulatory network between kidney, bone, and the hematopoietic environment.

Disclosures: Sangeetha V.M, None.

MO0123

Osteoprotegerin is Associated with Fractures in Men and Women with Stage 3-5 Chronic Kidney Disease. Sarah West^{*1}, Charmaine Lok², Sophie Jamal³.
¹University of Toronto, Canada, ²Toronto General Hospital, Canada, ³The University of Toronto, Canada

Purpose: Men and women with chronic kidney disease (CKD) are at extremely high fracture risk, but the best method to evaluate fracture risk in CKD is unknown. High levels of osteoprotegerin (OPG) are associated with fractures in postmenopausal women. The association between OPG and fracture status in men and women with stage 3-5 CKD is unknown.

Methods: We used baseline data from an ongoing prospective study of adult subjects with stages 3-5 CKD (based on estimated glomerular filtration rate using the MDRD formula) to determine if serum OPG (EIA, Biomedica Gruppe) could discriminate among those with and without fractures (self-reported low trauma fractures after age 40 and/or prevalent vertebral fractures by morphometry). Results are expressed as odds ratio (OR) of fracture per standard deviation increase in OPG with 95% confidence intervals (CI).

Results: Data was available for 163 subjects (95 men). Overall, most subjects were Caucasian (74%), with a mean age of 63.6 \pm 15.6 years and a mean weight of 79.1 \pm 19.0 kg. Subjects were evenly distributed by stage of CKD (39% stage 3, 35% stage 4, 27% stage 5), and 27% of subjects had diabetes. Mean serum calcium was 2.36 \pm 0.13 mmol/L, phosphate was 1.30 \pm 0.31 mmol/L, and parathyroid hormone (PTH) was 24.1 \pm 25.9 pmol/L. Compared to those without fractures (n=107), those with fractures (n=56) were older (61 \pm 16 vs. 69 \pm 14 years, p=0.001), had higher levels of serum PTH (18.6 \pm 15.2 vs. 35.3 \pm 37.7 pmol/L, p<0.001), were more likely to self-report a fall in the past year (26% vs. 50%, p=0.002), and cause of CKD was more often diabetes (24% vs. 32% p=0.02). The mean level of OPG was 8.56 \pm 3.53 pmol/L,

and OPG levels increased with stage of CKD (stage 3: 7.94 ± 3.18 , stage 4: 8.29 ± 3.63 , stage 5: 9.82 ± 3.64 pmol/L). Mean OPG was elevated in those with fractures compared to those without (9.37 ± 4.23 vs. 8.13 ± 3.04 pmol/L, $p=0.03$). Further, after adjusting for stage of CKD, OPG was associated with fractures (OR: 1.12, 95% CI: 1.01-1.23).

Conclusions: OPG is associated with fractures in men and women with stage 3-5 CKD. Our data suggests that OPG may be useful in discriminating fracture status in this cohort. However, further prospective studies are needed to confirm this finding.

Disclosures: Sarah West, None.

MO0124

Sclerostin and Bone Turnover Markers in Adult Patients with Different Types of Osteogenesis Imperfecta. Roland Kocijan^{*1}, Christian Muschitz², Karin Amrein³, Astrid Fahrleitner-Pammer³, Peter Pietschmann⁴, Judith Haschka¹, Sebastian Dinu⁵, Heinrich Resch⁶. ¹St. Vincent Hospital Vienna, Austria, ²St. Vincent's Hospital, Austria, ³Medical University Graz, Austria, ⁴Institute fuer Pathophysiologie, Austria, ⁵Central Laboratory St. Vincent Group, Vienna, Austria, ⁶Medical University Vienna, Austria

Purpose: Sclerostin is a key regulator, expressed by osteocytes, that inhibits osteoblast differentiation and bone formation. Sclerostin is a glycoprotein that negatively regulates the WNT-pathway. Currently no reliable biochemical bone markers are available for osteogenesis imperfecta (OI), an inherited disorder characterized by increased bone fragility.

The aim of our study was to evaluate the role of sclerostin, as an inhibitor of bone formation in the regulation of bone metabolism in adult patients with OI.

Methods: Serum sclerostin levels (quantitative sandwich ELISA assay - Biomedical, Austria) and bone turnover markers (BTM) including intact amino terminal propeptide of type I procollagen (PINP), type I collagen cross-linked C-telopeptide (CTX), intact PTH and vitamin D (25-OH) were assessed in 23 adult patients with OI (OI total, mean age 45.4 ± 16.7). OI total was divided into the mild OI I and the moderate and severe OI III/IV group, according to the Sillence classification. Patients using bisphosphonate therapy within the last five years were excluded from the calculations.

All data were compared to a healthy age and gender matched control group (CO, n=46, mean age 40.6 ± 7.2).

Correlations between sclerostin, BTM and BMD, measured by DXA, were carried out.

Results: Sclerostin was significantly decreased in OI I (17.9 ± 12.5 pmol/l) and OI III/IV (13.3 ± 10.0 pmol/l) when compared to CO (42.3 ± 14.5 pmol/l, $p<0.001$), however, within the OI subgroups Sclerostin levels were similar.

Additionally, PINP and CTX as well as PTH were decreased in all types of OI ($p<0.05$ - $p<0.001$).

Vitamin D levels were slightly decreased (26.6 ± 13.4 ng/ml) but similar in all OI subgroups and controls (28.1 ± 10.2 ng/ml).

Calcium and phosphate were in normal range and did not differ from CO. There was a statistically significant positive correlation between Sclerostin and age ($p<0.05$), but no correlations were found between sclerostin and any of the bone turnover markers, vitamin D or BMD at lumbar spine and hip.

Conclusion: Sclerostin is decreased in patients with OI, independently from type of OI or other BTM.

Our data strongly suggest low bone resorption in all types of OI, reflected by decreased Sclerostin, PTH and CTX, indicating an uncoupling of bone metabolism in OI. Alternatively CTX and PINP values may be decreased due to the pathophysiology of the collagen disease.

Disclosures: Roland Kocijan, None.

MO0125

The Effects of Idiopathic Hypercalciuria on Bone Mineral Mass and Bone Geometry in Postmenopausal Women: A Tibia pQCT Study. Konstantinos Stathopoulos*, Ilias Bournazos, Eleutheria Metania, Pelagia Katsibri, Andonis Partinevelos, Erato Atsali, Panagiotis Papageorgopoulos, Grigoris Skarantavos. Bone Metabolic Unit, 1st Department of Orthopedics, University of Athens, School of Medicine, "Attikon" University General Hospital, Greece, Greece

Aim: We assessed the effects of Idiopathic Hypercalciuria (IH) on bone mineral mass and bone geometry in different age groups using pQCT of the tibia

Material and Methods:

We reviewed medical records of 41 postmenopausal women with IH who presented as outpatients in our department. Inclusion criteria: 1) Recently (<6 months) diagnosed and untreated IH 2) postmenopausal status >2y 3) Normal renal function (normal serum Creatinine, eGFR) Exclusion criteria: 1) Diseases causing hypercalciuria other than IH (granulomatous and endocrine diseases, malignancies) 2) Other Bone metabolic disorders 3) Drug-induced hypercalciuria 4) use of any medication for osteoporosis during the last 12 months. The patients were assigned in 3 different age groups: 48-59y (N=15), 60-69y (N=21), 70-79y (N=5). All patients underwent pQCT of the tibia (XCT2000 scanner, Stratec Medintechnik, Germany) and 3 slices were obtained at the 4% (trabecular bone), 14% (subcortical and cortical) and 38%

(cortical) of tibia length sites. For each site we estimated bone mineral content, bone areas, cortical thickness, periosteal and endosteal circumference and we compared results with our published tibia pQCT database of 219 age-matched healthy postmenopausal women. We performed statistical analysis and data is expressed as mean \pm standard deviation (S.D.) Results: There were no statistical differences between patients with IH and healthy subjects in all age-groups concerning variables of trabecular bone. Concerning cortical bone (38% slice) we found statistical differences only in the younger (48-59y) age group between patients with IH vs age-matched controls: patients with IH had lower cortical bone mineral mass (256.54 ± 39.95 vs 282.63 ± 38.63 mg/cm, $p=0.019$), cortical area (220.4 ± 33.34 mm² vs 246.85 ± 32.85 , $p=0.005$) and cortical thickness (3.90 ± 0.81 vs 4.53 ± 0.57 mm, $p=0.0005$), while they had greater endosteal circumference (45.27 ± 8.11 vs 40.34 ± 4.51 mm, $p=0.001$). Conclusions: Early (48-59y) postmenopausal women with IH have lower values of cortical bone mass, cortical area, cortical thickness and greater endosteal circumference vs age-matched controls. Older women with IH were not found to have statistical differences on bone measurements vs age-matched controls using pQCT of the tibia.

Disclosures: Konstantinos Stathopoulos, None.

MO0126

Evolution of Hypovitaminosis D Prevalence in a Swiss Rheumatology Outpatient Population: a pre-post Information Study. Berengere Aubry-rozier*, Delphine Stoll, Olivier Lamy, Marc-Antoine Krieg, Didier Hans. Lausanne University Hospital, Switzerland

Introduction: Vitamin D reduces the risk of fall and fracture in elderly. Hypovitaminosis D is highly prevalent in our outpatient population (86% in 2009¹). We evaluated the evolution of vitamin D status in a similar population 2 years later, in a pre-post information study.

Method: One month-screenings were proposed in November 2009¹ and 2011 to all outpatients in our clinic. During this 2 year-period, an implementation about the benefits of vitamin D was diffused by medical grandrounds. 25-OH vitamin D level was categorized as deficient ($30 \mu\text{g/l}$). Patients who received any high dose of vitamin D 3 months before each screening period were excluded. Subanalysis per type of disease (inflammatory rheumatic disease (IRD), degenerative disease (DD), osteoporosis (OP)) was also performed.

Results: In 2011, 299 patients were included with a mean vitamin D level $24.2 \mu\text{g/l}$ (4-79). 4.7% had deficiency, 65.9% insufficiency, 29.4% normal results. 111 patients were on daily oral vitamin D, of which 1%, 47% and 52% had deficiency, insufficiency and normal results respectively. In the non vitamin D users the corresponding percentages were 7%, 77% and 16%. In IRD (N=202) and DD (N=41), the mean level of vitamin D was similar ($22.7 \mu\text{g/l}$) out of which 23% were normal. In OP (N=89) the mean vitamin D was higher ($27.9 \mu\text{g/l}$) as the percentage of normal (45%).

Compared to 2009, the rate of patients with normal vitamin D level had both increased in OP (31% to 45%) and in IRD (12% to 23%) while stable in DD, although the percentage of patients with daily vitamin D decreased by ~10%.

Conclusion: After information on guidelines, the prevalence of normal vitamin D level increased in two years. It could be related to higher number of prescriptions of high doses of vitamin D3 (e.g. every 3-6 months) and better adherence to daily supplements.

1. Stoll D et al. High prevalence of hypovitaminosis D in a Swiss rheumatology outpatient population. Swiss medical weekly, 2011. 141: p. w13196.

Disclosures: Berengere Aubry-rozier, None.

MO0127

HMWFGF2 Isoforms Regulate Bone Mineralization via Modulation of Pyrophosphate Genes in Mouse Bone Marrow Cultures. Marja Marie Hurley*¹, Liping Xiao². ¹University of Connecticut Health Center School of Medicine, USA, ²University of Connecticut Health Center, USA

Overexpressing FGF2 high molecular weight isoforms (HMW) in osteoblastic lineage cells induced hypophosphatemia, osteomalacia, increased FGF23 in serum and bones of HMWtg mice (Xiao and Hurley 2010). HMW also induced defective mineralized bone formation in phosphate replete bone marrow cultures (BMSC) via abnormal FGF23/FGFR/Receptor/MAPK signaling. Although neutralizing FGF23 antibody, FGF Receptor and MAPK/ERK inhibitors partially rescued the mineralization defect in vitro, the rescue was incomplete. Other investigators using osteoblastic cell lines reported that FGF2 impairs mineralization via pyrophosphate (PPI), however the FGF2 isoform(s) involved were not identified. We speculated that HMW modulate PPI genes. The elaboration and transport of PPI into the extracellular matrix and its hydrolysis to phosphate is critical for mineralization. Nucleoside triphosphate pyrophosphatase (ENPP1 or PC-1) catalyzes ATP to generate PPI. ANK decreases intracellular PPI and increases extracellular PPI, tissue nonspecific alkaline phosphatase (TNAP) hydrolyses PPI to phosphate that is necessary for crystal generation. The Sodium-dependent Pi co-transporter Slc20a1 (Pit-1) that regulates phosphate homeostasis in bone. Was also examined. To determine whether HMW regulates mineralization via PPI and whether this regulation is dependent or independent of FGFR/MAPK pathway, BMSCs harvested from Vector and HMW mice were cultured in osteogenic medium for 21 days with or without FGFR tyrosine kinase inhibitor SU5402 (25uM) or the MAP kinase inhibitor PD98059 (25uM). Mineralized nodule formation was determined by Alizarin Red

staining and gene analysis by qPCR. Mineralized nodules were significantly decreased in HMW cultures and the inhibition was partially rescued by FGFR and MAPK inhibitors. mRNAs for Enpp1, Ank, Slc2a1 were significantly increased while Tnap mRNA was significantly decreased in HMW cultures. SU5402 caused a marked reduction in Enpp1, Ank, Slc2a1 mRNAs and a marked increase in Tnap mRNA in HMW cultures. There was a basal increase in pERK42/44 that was blocked by PD98059, however Enpp1, Ank, and Slc2a1 mRNA were further increased in PD98059 HMW cultures and there was no increase in Tnap mRNA. These data suggests that HMW increases PPI and decreases TNAP via FGFR but not MAPK/ERK signaling. We conclude that HMW signals via FGFR but not MAPK to regulate PPI accumulation and bone mineralization in vitro.

Disclosures: Marja Marie Hurley, None.

MO0128

LC-MS/MS for Vitamin D Analysis. Much more than a Single Analytical Technique. Caje Moniz^{*1}, Lewis Couchman², Christopher Benton², Julia Jones³, Graham Carter³. ¹King's College Hospital, United Kingdom, ²Kings College Hospital, United Kingdom, ³Charing Cross Hospital, United Kingdom

Accurate measurement of 25-hydroxyvitamin D (25OHD) is important to determine status and supplementation protocols. Currently, LC-MS/MS is favoured as the method of choice for the analysis of total 25OHD in serum, but measurement is not straightforward. Importantly, LC-MS/MS is not a single technique: variables such as sample preparation, chromatography and ionization/fragmentation should each be considered. We therefore analysed the results from a survey of LC-MS/MS users, organized by the international vitamin D external quality assessment scheme (DEQAS), to determine the influence of such variables on the reported results for two DEQAS distributions (10 samples, July and October 2010).

Completed questionnaires were returned by 65 laboratories. For analysis, individual laboratory results for each of the 10 samples were divided by the corresponding LC-MS/MS method mean results. Of the 605 results submitted, 346 (57%) were from laboratories using electrospray ionization (ESI), and 259 (43%) from laboratories using atmospheric pressure chemical ionization (APCI). Although the mean ratio of results was not significantly different between ESI and APCI ($P > 0.5$), there was significantly more variation ($P < 0.001$) in the results obtained by laboratories using ESI. Regarding fragmentation, there was significantly greater variation ($P < 0.001$) observed between results from laboratories where a non-specific water-loss transition (loss of 18 m/z units) was monitored. 52% of laboratories using ESI used a method which monitored a water-loss transition, compared to only 22% of laboratories using APCI.

Only 3 laboratories (5%) were able to resolve the isobaric metabolite 3-epi-25OHD (present in neonates, but also in some of the adult population) from 25OHD. 41 (63%) laboratories were unable to resolve this metabolite, and 21 (32%) laboratories did not know whether their method could distinguish it from 25OHD.

LC-MS/MS offers increased specificity over many immunoassay-based methods for the measurement of 25OHD, but there are many variables which must be considered. Assay standardisation and calibration must always be considered, but so too must the LC-MS/MS conditions. MS/MS is an achiral technique, and so cannot distinguish some isobaric metabolites, such as 3-epi-25OHD, but also can suffer from interference if non-specific transitions are used. Further harmonisation is necessary, along with similar analysis of sample preparation techniques used.

Disclosures: Caje Moniz, None.

MO0129

Usefulness of Serum Fibroblast Growth Factor 23 Levels in the Diagnosis and Management of Vitamin D-Deficient Rickets. Takuo Kubota^{*1}, Taichi Kitaoka², Yasuhisa Ohata³, Makoto Fujiwara², Kohji Miura², Yoko Miyoshi², Noriyuki Namba², Shinji Takeyari⁴, Takehisa Yamamoto⁴, Keiichi Ozono². ¹Osaka University Graduate School of Medicine & Dentistry, Japan, ²Osaka University Graduate School of Medicine, Japan, ³Osaka University, Japan, ⁴Minoh City Hospital, Japan

Vitamin D-deficient rickets (DDR) has recently reemerged among developed countries. However, the diagnosis of vitamin D deficiency is occasionally not easily made because of preexisting hereditary hypophosphatemic rickets (HHR) and/or the controversial reference range of serum 25 hydroxyvitamin D (25OHD) levels. Fibroblast growth factor 23 (FGF23) is a newly discovered hormone which inhibits renal phosphate reabsorption and suppresses 1-alpha hydroxylase activity. The usefulness of serum FGF23 levels in the diagnosis and management of DDR has not been fully elucidated. In the present study, we evaluated serum FGF23 concentrations and other mineral metabolism-related laboratory data in children with DDR and compared with those of HHR patients. This study group comprises 21 children with DDR at the mean age of 18 months and 8 patients with HHR at the mean age of 21 months. Serum concentrations of FGF23 (mean, 8.4; min. - max., 0 - 18 pg/ml), 25OHD (8.9; 3.0 - 17.1 ng/ml) and calcium were lower in DDR patients than those in HHR ones (FGF23, 70.8; 58 - 84 pg/ml; 25OHD, 15.8; 8.2 - 25.2 ng/ml), whereas serum levels of phosphate, intact parathyroid hormone (PTH) and 1,25(OH)₂D were higher in DDR patients. Although the biochemical data above were significantly different between DDR and HHR, all the values overlapped between DDR and

HHR, except for serum FGF23 levels, suggesting that the serum FGF23 level is the most critical biochemical marker to distinguish DDR from HHR. In addition, serum FGF23 concentrations were increased following one to three-month treatment compared to those before the treatment, while serum concentrations of PTH and alkaline phosphatase were reduced after the treatment. Serum phosphate and calcium levels were not significantly increased at that moment. These results suggest that serum FGF23 levels may be an early marker for the recovery of serum phosphate levels, similar to serum PTH concentrations for the restoration of serum calcium levels. Collectively, this study suggests that serum FGF23 level is a useful parameter for the diagnosis and management of DDR.

Disclosures: Takuo Kubota, None.

MO0130

Association of Primary Hyperparathyroidism with Sarcoidosis.. Bart Clarke¹, Vivien Lim^{*2}. ¹Mayo Clinic College of Medicine, USA, ²Khoo Teck Puat Hospital, Singapore

Primary hyperparathyroidism (PHPT) and sarcoidosis (S) are both relatively common disorders that may separately contribute to abnormal calcium and phosphate metabolism via different mechanisms. We evaluated the clinical and laboratory characteristics of patients diagnosed with both disorders at our institution between January 1998 and December 2011, and examined the effects of these disorders on calcium and phosphate metabolism and mineral supplementation requirements. A total of 26 subjects with both disorders were identified, of which 22 (81.4%) were female, with mean BMI 30.3 ± 6.4 kg/m². The mean age at diagnosis of PHPT was 61.3 ± 13.0 years, while that for S was 54.6 ± 16.1 years. Subjects were diagnosed with S first in 54% of cases, and with PHPT first in 7% of cases, and with both disorders within 6 months of each other in 35%. In one case, the order of diagnosis was unclear. For subjects whose S was diagnosed first, the mean interval between the two diagnoses was 18.7 ± 17.5 years. For those subjects whose PHPT was diagnosed first, the mean interval between the two diagnoses was only 0.8 years. At the time of diagnosis of PHPT, mean total calcium was 10.9 ± 1.0 mg/dL, phosphate 3.0 ± 0.6 mg/dL, PTH 79 ± 43 pg/mL, 25-hydroxyvitamin D 27 ± 9 ng/mL, 1,25-dihydroxyvitamin D 54.1 ± 18 pg/mL, and 24-hour urine calcium 341 ± 277 mg. For those cases where PHPT and S were diagnosed simultaneously, mean serum total calcium was 11.0 ± 0.6 mg/dL, phosphate 2.6 ± 0.7 mg/dL, PTH 56 ± 15 pg/mL, 25-hydroxyvitamin D 28 ± 6 ng/mL, 1,25-dihydroxyvitamin D 71 ± 22 pg/mL, and 24-hour urine calcium 632 ± 361 mg. For those cases where S was diagnosed first, mean serum total calcium at time of diagnosis of S was 11.6 ± 2.5 mg/dL, phosphate 3.6 ± 0.6 mg/dL, PTH 15.5 ± 5.5 ng/mL, and 1,25-dihydroxyvitamin D 106 ± 43 pg/mL. At the time patients were first seen for S in our institution, mean ACE level was 52 ± 45 U/L. Differences between the latter two groups were statistically significant ($P < 0.05$) for phosphate and PTH values. Of these patients, 88.5% were not taking calcium and/or vitamin D supplementation at the time of diagnosis. Of subjects with PHPT, 62% underwent surgery at a mean of 6.0 ± 4.8 months after diagnosis, and one subject had surgery 4.3 years later. In conclusion, S and PHPT may occur in the same patient. Patients with PHPT may be diagnosed with S soon after PHPT is recognized, but the converse may not be true. Lower serum phosphate and higher serum PTH may help distinguish patients with concomitant disease.

Disclosures: Vivien Lim, None.

MO0131

Does an Elevated Serum Parathyroid Hormone Increase Cardiovascular Risk? Comparison of Coronary Artery Calcification in Patients with Primary Hyperparathyroidism versus Normocalcemic Hyperparathyroidism in the Dallas Heart Study. Naim Maalouf^{*1}, Colby Avers², Natalie Cusano³, Shonni Silverberg⁴, John Bilezikian³. ¹University of Texas Southwestern Medical Center, Dallas, USA, ²UT Southwestern Medical Center, USA, ³Columbia University College of Physicians & Surgeons, USA, ⁴Columbia University, USA

Background: The relative contributions of high serum calcium (sCa) vs. high serum parathyroid hormone (sPTH) to increased cardiovascular (CV) risk in primary hyperparathyroidism (PHPT) is unclear. Normocalcemic hyperparathyroidism (NCHPT) is characterized by normal sCa and high sPTH in the absence of a definable 2ry hyperparathyroid disorder. To assess the contribution of high sPTH vs. high sCa on CV risk, we compared coronary artery calcification (CAC) scores among 3 groups: classic PHPT (high sCa and sPTH); NCHPT (normal sCa and high PTH) and controls (normal sCa and sPTH), all from the Dallas Heart Study, a multiethnic, population-based cohort study of Dallas county residents.

Methods: Serum creatinine, Ca, PTH, 25OHD and CAC (by electron beam CT) were measured. NCHPT subjects had 25OHD > 20 ng/ml, no current lithium or hydrochlorothiazide use, and eGFR > 60 ml/min. We compared the unadjusted and adjusted prevalence of CAC > 10 Agatston units in PHPT and NCHPT vs. controls and assessed the impact of sCa, PTH, 25OHD on CAC in a multivariable (MV) model that included traditional CV risk factors (CVRF).

Results: Subjects included 20 PHPT, 108 NCHPT and 3,077 controls (Table). The PHPT group had higher age and sCa, a greater proportion of women, Blacks and smokers, higher median CAC score, and greater prevalence of CAC > 10 than the other 2 groups. The NCHPT group had higher sPTH and 25OHD. Compared to

controls, the likelihood of having a CAC>10 was greater in PHPT subjects [unadjusted odds ratio (OR): 3.9 (95% CI: 1.3-11.1); adjusted for age, gender, race, CVRF OR: 2.58 (95% CI: 0.79-8.49)], and lower in NCHPT subjects [unadjusted OR: 0.50 (95% CI: 0.26-0.97); adjusted for age, gender, race, CVRF OR: 0.46 (95% CI: 0.22-0.995)]. In a MV model including sCa, PTH, phosphorus, 25OHD, age, gender, race, BMI, smoking, diabetes, hypercholesterolemia and low HDL in the entire population, increasing sCa was associated with a greater likelihood of CAC>10 [OR: 1.70 (95% CI: 1.21-2.38) per 1 mg/dL] while increasing sPTH was associated with lower likelihood of CAC>10 [OR: 0.992 (95% CI: 0.986-0.998) per 1 pg/mL].

Conclusion: In this population-based study, PHPT was associated with higher CAC and NCHPT with lower CAC than controls. Increasing serum calcium was associated higher CAC and increasing serum PTH with lower CAC. These findings suggest that hypercalcemia is a more important factor in CV risk as measured by CAC than hyperparathyroidism in PHPT.

| | PHPT | NCHPT | Controls |
|---|--------------------|--------------------|-------------------|
| Number of Subjects | 30 | 108 | 9,977 |
| Age (years) | 50.1 (9.6) | 42.9 (10.9) | 43.7 (10.0) |
| Women - % | 70% | 50% | 57% |
| Black - % | 85% | 23% | 51% |
| White - % | 10% | 45% | 29% |
| Hispanic - % | 5% | 25% | 18% |
| Body Mass Index (kg m ²) | 29.6 (6.6) | 28.2 (5.0) | 29.7 (7.0) |
| Smoking - % | 43% | 12% | 28% |
| Diabetes - % | 10% | 8% | 11% |
| Hypercholesterolemia - % | 10% | 12% | 13% |
| Low HDL - % | 43% | 42% | 41% |
| Serum Calcium (mg/dL) | 10.4 (0.5) | 9.2 (0.3) | 9.2 (0.3) |
| Serum Ca corrected for albumin (mg/dL) | 10.7 (0.7) | 9.2 (0.3) | 9.3 (0.3) |
| Serum Phosphorus (mg/dL) | 3.0 (0.4) | 3.1 (0.5) | 3.2 (0.6) |
| Serum Creatinine (mg/dL) | 0.9 (0.2) | 0.9 (0.2) | 0.9 (0.2) |
| Serum PTH (pg mL) - median (IQR) | 33.9 [15.6, 64.3] | 65.7 [59.8, 79.5] | 36.9 [28.0, 48.8] |
| Serum 25-OH-vit D (ng/mL) - median (IQR) | 12.4 [9.9, 18.5] | 23.4 [21.4, 27.6] | 16.5 [11.9, 23.4] |
| EBCT-CAC score - Median (IQR) | 22.2 [0, 272.3] | 0 [0, 2.3] | 0.5 [0, 4.8] |
| EBCT-CAC >10 - % | 50% | 11% | 21% |
| Odds Ratio for CAC>10 (unadjusted) | 3.88 [1.35, 11.11] | 0.50 [0.26, 0.97] | Reference |
| Odds Ratio for CAC>10 (age, sex, race-adjusted) | 2.71 [0.85, 8.64] | 0.37 [0.17, 0.78] | Reference |
| Odds Ratio for CAC>10 (Multivariable-adjusted*) | 1.58 [0.70, 3.49] | 0.46 [0.22, 0.995] | Reference |

* adjusted for age, sex, race, body mass index, smoking, diabetes, hypercholesterolemia, and low HDL -cholesterol
 Data shown as Mean (Standard Deviation) unless indicated otherwise
 EBCT: Electron Beam Computed Tomography; CAC: Coronary Artery Calcium; IQR: Interquartile Range

Table

Disclosures: Naim Maalouf, None.

This study received funding from: National Institutes of Health

MO0132

Effect of Recombinant Human Parathyroid Hormone (rhPTH[1-84]) on Skeletal Dynamics and BMD in Hypoparathyroidism: the REPLACE study. John Bilezikian¹, Bart Clarke², Michael Mannstadt³, Tamara Vokes⁴, Dolores Shoback⁵, Hjalmar Lagast⁶, Roger Garceau⁷. ¹Columbia University College of Physicians & Surgeons, USA, ²Mayo Clinic College of Medicine, USA, ³Massachusetts General Hospital Harvard Medical School, USA, ⁴University of Chicago, USA, ⁵VA Medical Center, USA, ⁶NPS Pharmaceuticals, USA

Hypoparathyroidism (HypoPARA) is a rare disorder characterized by PTH deficiency and low serum calcium (Ca) with a wide range of clinical manifestations. Skeletal analysis shows increased cancellous bone volume and reduced bone turnover. Therapy for HypoPARA usually involves large amounts of Ca and active vitamin D (calcitriol). A phase 3, randomized, double-blind, placebo (PLB)-controlled, 24-week study assessed whether therapy with rhPTH(1-84) reduced Ca and calcitriol requirements, while normalizing or maintaining albumin-corrected total serum Ca (the REPLACE study). In the study, 134 patients were randomized [daily subcutaneous injections of rhPTH(1-84) (n=90) or PLB (n=44)]. Ca and calcitriol doses were reduced $\geq 50\%$ in 53.3% of those receiving rhPTH(1-84) compared to 2.3% who received PLB (P<0.001). We now report effects of rhPTH(1-84) on bone turnover markers (BTMs) and BMD in HypoPARA.

The study design allowed for the initial 50 µg rhPTH(1-84) dose to be increased to 75 or 100 µg while reducing Ca and calcitriol supplementation to maintain pre-randomization optimized serum Ca levels of 8.0-9.0 mg/dL. Serum levels of bone specific alkaline phosphatase (BSAP), N-terminal propeptide of type 1 collagen (P1NP), osteocalcin (OC), and C-telopeptide (CTX) were obtained throughout the study. Lumbar spine (LS), femoral neck (FN), total hip (TH), and distal one-third radius (DR) BMD were obtained at baseline and week 24.

Baseline BTM (mean ± SD) for PLB vs rhPTH(1-84) were 4.4 ± 4 vs 3.9 ± 3 µg/L for OC; 35.1 ± 18 vs 34.8 ± 24 µg/L for P1NP; 9.0 ± 3 vs 8.9 ± 3 µg/L for BSAP; 237 ± 170 vs 233 ± 211 ng/L for CTX. Change from baseline between treatment groups was significantly different at weeks 8 and 24 (P<0.001 for both times; Figure).

BMD (mean ± SD; g/cm²) at baseline for PLB and rhPTH(1-84) was 1.2 ± 0.3 and 1.2 ± 0.2 (LS); 1.0 ± 0.2 and 1.0 ± 0.2 (FN); 1.1 ± 0.2 and 1.1 ± 0.2 (TH); 0.8 ± 0.1 and 0.8 ± 0.1 (DR). The % changes in BMD from baseline [PLB vs rhPTH(1-84)] in FN (-0.3 vs -2.5) and TH (-0.3 vs -2.1) were significantly different at week 24 (P<0.001); differences in LS and DR BMD were not significant. Z-scores (mean ± SD) at week 24 for PLB and rhPTH(1-84) were 1.7 ± 2 and 1.4 ± 1 (LS); 1.0 ± 1 and 1.0 ± 1 (FN); 1.2 ± 1 and 1.0 ± 1 (TH); 0.5 ± 1 and 0.4 ± 1 (DR).

Patients with HypoPARA, often having reduced bone turnover and increased BMD, respond to 24-weeks of rhPTH(1-84) with significant increases in BTMs and mild decreases in hip BMD.

Figure. Mean Percentage Change from Baseline for Bone Turnover Markers

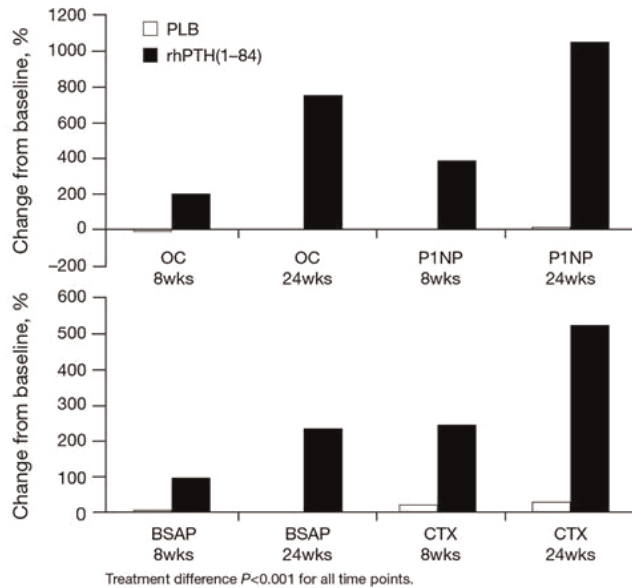


Figure 1

Disclosures: John Bilezikian, NPS Pharmaceuticals, 6; NPS Pharmaceuticals, 2
 This study received funding from: NPS Pharmaceuticals

MO0133

Efficacy and Safety of Low Dose Recombinant Parathyroid Hormone (rhPTH[1-84]) in Hypoparathyroidism: The RELAY Study. Tamara Vokes¹, Dolores Shoback², Bart Clarke³, Michael Mannstadt⁴, John Bilezikian⁵, Jolene Berg⁶, Hjalmar Lagast⁷, Roger Garceau⁷. ¹University of Chicago, USA, ²VA Medical Center, USA, ³Mayo Clinic College of Medicine, USA, ⁴Massachusetts General Hospital Harvard Medical School, USA, ⁵Columbia University College of Physicians & Surgeons, USA, ⁶Cetero Research, USA, ⁷NPS Pharmaceuticals, USA

Hypoparathyroidism (HypoPARA) is a rare disorder characterized by low serum calcium (Ca) and low PTH. Current management of HypoPARA consists of large amounts of Ca and active vitamin D (calcitriol). Maintaining normal serum Ca level can be challenging. rhPTH(1-84) at 50-100 µg/day is effective in maintaining target Ca levels; 53% of patients with HypoPARA reduced Ca and/or calcitriol doses by $\geq 50\%$ compared with 2% who received placebo (P<0.001) in the REPLACE study. Due to the potential for hypercalcemia in patients who may be exquisitely sensitive to PTH, the current study examined the efficacy of lower dose of rhPTH(1-84).

This dose-blind, multicenter study randomized 47 patients with HypoPARA (85% female; mean age 48 ± 10 y; BMI 31 ± 7; 72% postsurgical; 38% with duration of HypoPARA <10 y) to 25 (n=23) or 50 µg (n=24) rhPTH(1-84) subcutaneously once daily for 8 weeks. At baseline, Ca supplementation was >2000 mg/day in 26% and calcitriol was >0.5 µg/day in 30% of the study population.

Primary endpoint was the percentage of responders at Week 8 with response defined as reduction in supplement doses to ≤ 500 mg Ca/day and ≤ 0.25 µg calcitriol/day, while maintaining serum Ca levels between 7.5 mg/dL and the upper limit of normal (ULN). Secondary endpoint was the percentage of responders at Week 8 with $\geq 50\%$ reduction in Ca and calcitriol intake, while maintaining serum Ca between 7.5 mg/dL and ULN.

In intent to treat analysis, 18% (25 µg; 95% CI; 5, 40) and 25% (50 µg; 95% CI; 10, 47) of patients were responders (P=0.725). A $\geq 50\%$ reduction in Ca/calcitriol occurred in 9% (25 µg; 95% CI; 1, 29) and 29% (50 µg; 95% CI; 13, 51) of patients (P=0.139).

Adverse events (AEs) were reported in 65% (25 µg group) and 75% (50 µg group) of patients, with paresthesia and muscle spasms as the most common treatment-emergent AEs in both groups. AEs were similar to those reported previously. One patient discontinued due to arthralgia deemed unrelated to study medication.

Thus, some patients with HypoPARA receiving lower doses (25 or 50 µg) of rhPTH(1-84) see improved mineral homeostasis and decreased need for large doses of supplements. The response rate differences, 7% and 20% for primary and secondary endpoints, respectively, between the 2 dose groups favored the 50 µg dose; however, the differences were not statistically significant. These results indicate that doses as low as 25- and 50-µg/day of rhPTH(1-84) are adequate for the treatment of a subset of patients with HypoPARA.

Disclosures: Tamara Vokes, NPS Pharmaceuticals, 2
 This study received funding from: NPS Pharmaceuticals

MO0134

Epidemiology and Natural History of Normocalcemic Primary Hyperparathyroidism and Normocalcemic Hypoparathyroidism. Natalie Cusano*¹, Naim Maalouf², Elzbieta Dworakowski³, Chiyuan Zhang³, Serge Cremers³, John Bilezikian¹. ¹Columbia University College of Physicians & Surgeons, USA, ²University of Texas Southwestern Medical Center, Dallas, USA, ³Columbia University, USA

Primary hyperparathyroidism (PHPT), a common endocrine disorder, is defined by hypercalcemia and high PTH. A variant of PHPT has been described, normocalcemic PHPT (NPHPT), in which serum calcium (Ca) is normal (nl) and PTH is high, in the absence of secondary (2β) causes. Hypoparathyroidism (HypoPT) is characterized by hypocalcemia and low PTH. Loss of parathyroid function may occur over time. As is the case for NPHPT, there may be a phase of normocalcemic HypoPT (NHypoPT) in which the serum Ca is maintained but the PTH is low. The epidemiology and natural history of these diseases remain poorly understood. We hypothesize that asymptomatic individuals with NPHPT and NHypoPT can be identified epidemiologically. The Dallas Heart Study (DHS) is a multiethnic, community-dwelling study of Dallas county residents (30-65 yrs). DHS (DHS1) became longitudinal when laboratory/other data were collected 8 yrs later (DHS2). We measured intact PTH (nl: 14.3-55.0 pg/ml) in 3446 subjects from DHS1, 2035 of whom had follow-up in DHS2. NPHPT was defined as PTH > 55 pg/ml with nl albumin-adjusted serum Ca, excluding all common 2β causes. 652 subjects had high PTH and normal Ca. All common 2β causes of high PTH were excluded: low vitamin D (< 20 ng/mL, 476), renal failure (GFR < 60 cc/min, 55), and thiazide/lithium use (10). NPHPT was identified in 111 (3% prevalence). In 66 subjects who had follow-up in DHS2, 1 developed hypercalcemic PHPT (2%) and 15 continued to show evidence of NPHPT (1 high Ca/low GFR/thiazide, 19 high PTH/low D or low GFR, 30 normal PTH). NPHPT subjects were more likely to be black (47% vs. 25%; p < .001), had lower corrected Ca (9.3 vs. 9.4 mg/dl; p < .001), lower phosphorus (P) (3.1 vs. 3.2 mg/dl; p = .01), and higher CTX (0.413 vs. 0.358 μ g/L; p = .008). There were no differences in age, gender or BMI. NHypoPT was defined as PTH < 14.3 with normal adjusted Ca. 68 (2%) with NHypoPT were identified. Of the 26 subjects with follow-up in DHS2, 0 developed overt HypoPT and 2 remained with NHypoPT. NHypoPT subjects were more likely to be men (69% vs. 31%; p < .001), have lower BMI (25.8 vs. 28.9; p < .001), higher Ca (9.5 vs. 9.4; p < .001), higher P (3.4 vs. 3.2; p = .003), and a trend towards lower CTX (0.310 vs. 0.358; p = .065). There was no difference in age or ethnicity. This is the first study to track patients with apparent NPHPT and NHypoPT over time, providing new insights into the epidemiology and natural history of these two subclinical disorders in a community-dwelling population.

Disclosures: Natalie Cusano, None.

MO0135

Further Insights into the Pathogenesis of Primary Hyperparathyroidism: A Nested Case-Control Study. Lars Rejnmark*¹, Anne Kristine Amstrup¹, Charlotte Mollerup², Niels Fogh-Andersen³, Lene Heickendorff⁴, Leif Mosekilde¹. ¹Aarhus University Hospital, Denmark, ²Department of Endocrine Surgery, Copenhagen University Hospital, Rigshospitalet, Denmark, ³Department of Clinical Biochemistry, Copenhagen University Hospital Herlev, Denmark, ⁴Dept. of Clinical Biochemistry, Aarhus University Hospital, Denmark

Background: the pathogenesis of primary hyperparathyroidism (PHPT) is largely unknown.

Objective: to ascertain plasma levels of calcium, PTH, and 25-hydroxyvitamin D (25OHD) as measured prior to a clinical diagnosis of PHPT.

Study subjects: within three population based cohorts, we identified participants diagnosed with PHPT (cases) after their inclusion. Cases (n=117) were compared with controls (n=233), matched on age, gender, and time of year of blood sampling.

Results: time from inclusion until a clinical diagnosis of PHPT was median 5.6 years. Parathyroidectomy was performed in 97% of the cases. At cohort inclusion, undiagnosed hyperparathyroid hypercalcemia (PHPT) was present in 63% of the cases. Among the remaining cases without PHPT at inclusion, 55% had normocalcemic hyperparathyroidism (vs. 21% in the matched controls, p < 0.01), and 31% had normoparathyroid hypercalcemia. Overall, 25OHD levels were lower in cases compared with controls. Compared with their matched controls, 25OHD levels were decreased in normocalcemic hyperparathyroidism, but not in normoparathyroid hypercalcemia. An adenoma was subsequently removed from 78% of the cases with normocalcemic hyperparathyroidism, whereas 39% of the cases with normoparathyroid hypercalcemia had parathyroid hyperplasia (p=0.02). Overlap performance analyses showed a positive predictive value (PPV) for later PHPT of 95% for plasma calcium levels > 2.52 mmol/l. Excluding cases with vitamin D insufficiency, the PPV for later PHPT was 82% for PTH levels > 5.5 pmol/l.

Conclusion: years prior to a clinical diagnosis of PHPT, calcium homeostasis shows signs of perturbations. Latent PHPT may be characterized by either normocalcemic hyperparathyroidism or normoparathyroid hypercalcemia. Such patients should be offered long-term follow-up in order to assess whether their biochemical profile represents an early state of PHPT.

Disclosures: Lars Rejnmark, None.

MO0136

Parathyroid Atypical Adenomas: Mutational Screening of CDC73/HRPT2 Gene. Claudio Marcocci*¹, Simona Borsari¹, Elena Pardi¹, Chiara Banti¹, Federica Saponaro¹, Antonella Picone¹, Gabriele Di Rosa¹, Liborio Torregrossa², Filomena Cetani¹. ¹Department of Endocrinology & Metabolism - Section of Endocrinology & Bone Metabolism, University of Pisa, Pisa, Italy, ²Department of Surgery, Division of Pathology, University of Pisa, Italy

Atypical parathyroid adenomas represent a subset of tumors with histological features worrisome for carcinoma (PC), such as trabecular growth, fibrous bands and increased mitotic activity without unequivocal criteria of malignancy (local recurrence and/or metastasis). The question of whether these lesions might represent an anticipation of an aggressive clinical behavior that overtime may acquire the full blown features of malignancy remains to be established. *CDC73/HRPT2* tumor suppressor gene mutations have been reported in up to 80% of sporadic metastatic PC, mainly associated with reduced expression or loss of the encoded protein parafibromin. With the exceptions of some studies on parafibromin expression, there are no genetic studies of *HRPT2* gene in atypical adenomas.

In this study we collected 15 parathyroid atypical adenomas from patients with sporadic primary hyperparathyroidism (PHPT), obtained at the time of surgery or retrieved from paraffin embedded sections. All, but one, patients, 8 males and 7 females, with a mean age at diagnosis of 47.5 years (range 16-68 yrs), were submitted to a single parathyroidectomy (PTX). At histology no specimen showed cystic features. Familial history of PHPT was negative in all patients. Follow-up after surgery ranged from 6 months to 9 years. Thirteen patients were cured by surgery, and two had persistent PHPT.

All specimens were screened for *HRPT2* mutations. The entire coding region of the gene was sequenced with a BigDye chemistry.

A heterozygous mutation in the donor splice site of intron 1 (c.131G>T) was identified in one adenoma. Unexpectedly, this was a germline mutation, carried by the youngest patient, aged 16 years, of our series. This patient has a remission of PHPT 12 years after PTX. No kidney or jaw lesions have been detected up to date. This mutation was also found in the patient's healthy father. All the remaining tumors were negative.

Our results suggest that the involvement of *HRPT2* gene in parathyroid atypical adenoma is rare. However, the genetic screening of *HRPT2* gene can be suggested in young patient with PHPT and a single gland involvement.

Disclosures: Claudio Marcocci, None.

MO0137

Primary Hyperparathyroidism and Hypoparathyroidism Show Major Microstructural Differences from Each Other by High Resolution Peripheral Computed Tomography. Stephanie Boutroy*¹, Barbara Silva¹, Mishaela Rubin², Jim Sliney Jr¹, Julia Udesky¹, Donald McMahon³, Chiyuan Zhang², Natalie Cusano³, John Bilezikian³. ¹Columbia University Medical Center, USA, ²Columbia University, USA, ³Columbia University College of Physicians & Surgeons, USA

The two disorders of PTH function characterized by excessive secretion, primary hyperparathyroidism (PHPT) or deficient production, hypoparathyroidism (HypoPT) present an opportunity to attribute differences in microstructure to PTH. With the non-invasive technique of High Resolution peripheral Quantitative Computed Tomography (HRpQCT; Scanco Medical AG, Switzerland), we could differentiate among measurements made at a loaded (tibia) or unloaded (radius) site.

To this end, we studied 38 (PHPT, age 67 ± 10) and 45 (HypoPT, age 45 ± 12) women. Each group of patients had well-documented disease with either hypocalcemia and low PTH (HypoPT) or hypercalcemia and high PTH (PHPT). HRpQCT female-specific Z-scores were compared to normative values from the OFELY cohort.

Differences in HRpQCT female-specific Z-scores in HypoPT compared to PHPT subjects were summarized in the table. For the trabecular (Tb) indices, Tb.vBMD, number and thickness, HypoPT subjects demonstrated significantly higher values than in PHPT. PHPT subjects had significantly higher Tb separation and a more heterogeneous Tb network. These differences were observed at both the radius and the tibia, with the exception of Tb thickness that was similar at the tibia between PHPT and HypoPT. The cortical indices, cortical vBMD and thickness, at both the radius and the tibia, were significantly greater in HypoPT than in PHPT. The results suggested that microstructural differences can be seen in virtually all trabecular indices at both the radius and tibia between PHPT and HypoPT. While there were individual differences from normal between loaded (tibial) and unloaded (radius) bone for both HypoPT (cortical bone enhanced at the radius but not at the tibia) and PHPT (cortical bone impaired at the tibia but not at the radius), when the two disorders of PTH function were compared to each other, site no longer was a differential determinant.

The results emphasized the importance of PTH in helping to regulate microstructure of bone.

Main Outcome Measures: Clinical manifestations, biochemical abnormalities in PHPT patients, and copy number variations of candidate genes in benign and malignant parathyroid tumors were analyzed.

Results: In the past 10 years, 2/3 of PHPT patients were still symptomatic, but the percentage of asymptomatic cases has been increasing and reached up to 48.5% in recent 2-3 years. Serum PTH levels above 317.8 pg/dl have the capacity to define the symptomatic cases with AUC 0.84 ($P < 0.001$). Malignant PHPT had a shorter course of the disease [$0.33 (0.5-6)$ vs $1.08 (0-12.67)$ year, $P = 0.004$], higher albumin-corrected serum calcium (3.28 ± 0.32 vs 2.89 ± 0.33 mmol/l, $P < 0.001$), and PTH levels [$1643 (285.2-2974.9)$ vs $351.4 (103.1-2250.0)$, $P < 0.001$], and larger tumor size (3.57 ± 1.30 vs 2.50 ± 1.19 cm, $P = 0.037$), as compared with benign ones. A copy number gain of CCND1 was present in 5 out of 7 malignant tumors and in only 3 out of 14 benign ones (71% vs 21%, $P = 0.026$). The cyclinD1 mRNA expression was 3-fold increase in malignant tumor samples ($p = 0.003$).

Conclusion: The general clinical and biological features of PHPT in Chinese patients in the past 10 years are still classical, but there is a trend to have more asymptomatic cases. Gain of copy number of CCND1 gene may be one of the mechanisms underlying parathyroid cancer.

Disclosures: Jian-min Liu, None.

MO0140

The Epidemiology of Hypo- and Pseudohypoparathyroidism in Denmark.

Line Underbjerg¹, Tanja Sikjaer², Leif Mosekilde³, Lars Rejnmark³.
¹Department of Medicine & Endocrinology, MEAAarhus University Hospital, Denmark, ²Department of Medicine & Endocrinology, MEAAarhus University Hospital, Denmark, ³Aarhus University Hospital, Denmark

Background: Hypoparathyroidism (HypoPT) and pseudohypoparathyroidism (Ps-HypoPT) are relatively rare diseases, characterized by low levels of parathyroid hormone (PTH) and plasma calcium or high plasma PTH and low plasma calcium, respectively. Most common, chronic HypoPT is due to complications following neck surgery. Rare causes include congenital HypoPT and autoimmune destruction of parathyroid glands. The rare cases of Ps-HypoPT are caused by inherited resistance to PTH in the target organs. Only few data are available on the prevalence of HypoPT. Recently, a survey from the Mayo Clinic in Minnesota, USA identified 54 cases with HypoPT equal to a prevalence of 37/100,000.

AIM: The aim of the study is to identify the total number of patients in Denmark with HypoPT incl. familial/idiopathic causes and Ps-HypoPT.

METHOD: The study is conducted as a case-finding study in order to identify patients with possible HypoPT or Ps-HypoPT. Data were extracted from The Regional and The National Patient Registry on hospital discharge diagnoses and compared with pharmacies prescription databases. The identified potential patients were all subsequently validated by reviewing their medical charts.

Results: Within a population of 3,861,241 persons, we identified 1,003 living patients with chronic HypoPT (prevalence=26/100,000; 81% women). 899 had postoperative HypoPT (prevalence=23/100,000; 83% women), 33 had Ps-HypoPT (1/100,000; 64% women), and 71 familial/idiopathic HypoPT (2/100,000; 61% women). Mean age at time of diagnosis was 44 ± 15 years for postoperative cases. Most patients (98%) received treatment with alphacalcidol. Mean daily dose was significantly ($p = 0.01$) higher among patients with familial/idiopathic HypoPT (1.8 ± 1.2 µg) compared with patients with postoperative HypoPT (1.4 ± 1.1 µg), whereas patients with Ps-HypoPT received a significantly higher daily dose (2.3 ± 1.9 µg) than the patients with postoperative ($p < 0.001$) and familial/idiopathic ($p = 0.03$) HypoPT.

In conclusion: Our data covering a population of app. 3.8 million citizens suggest a slightly lower prevalence than previously reported. This may be due to geographical differences regarding surgical intervention or different methodology applied to identify patients.

Disclosures: Line Underbjerg, None.

MO0141

Bioactive PLGA/TCP/Icaritin Composite Scaffolds Reduce Collapse Incidence of Femoral Head in a Bipodal Emu Model of Steroid-Associated Osteonecrosis. Lizhen Zheng¹, Zhong Liu², Ming Lei³, Le Huang², Yixin HE⁴, Ge Zhang⁵, Ling Qin².
¹Prince of Wales Hospital, Hong Kong, ²Chinese University of Hong Kong, Hong Kong, ³Shenzhen Second People's Hospital, China, ⁴The Chinese University of Hong Kong, Hong Kong, ⁵Price of Wales Hospital, Hong Kong

Icaritin is a novel bioactive and osteogenic phytochemical found in serum as a metabolite of phytoestrogenic herbal epimedium. Bioactive porous PLGA/TCP/Icaritin was fabricated using our established rapid prototyping technique. We have established a bipodal emu model of steroid-associated osteonecrosis (SAON), induced by a combination of methylprednisolone and Lipopolysaccharide, with hip joint collapse similar to humans that is desirable for preclinical research of osteonecrosis and subsequent joint collapse. This study is to evaluate treatment efficacy of PLGA/TCP/Icaritin scaffolds implanted for repairing steroid-associated osteonecrosis in emu femoral head after core decompression.

| HRpQCT parameters | Difference between Z-score (in SD) HypoPT - PHPT | |
|-------------------------|---|----------|
| | Radius | Tibia |
| Total Area | 0.35 | -0.10 |
| Total vBMD | 0.85 ** | 0.77 ** |
| Cortical vBMD | 0.72* | 0.55 ** |
| Cortical thickness | 0.87 *** | 0.64 * |
| Trabecular vBMD | 0.81 ** | 0.78 ** |
| Trabecular number | 0.85 * | 0.82 * |
| Trabecular thickness | 0.85 ** | 0.32 |
| Trabecular separation | -0.79 * | -0.86 ** |
| Trabecular distribution | -0.81 * | -0.96 ** |

* $p < 0.05$; ** $p < 0.01$; *** $p < 0.001$

Differences in HRpQCT female-specific Z-scores in HypoPT compared to PHPT subjects

Disclosures: Stephanie Boutrou, None.

MO0138

Serum Dkk1 and Sclerostin Levels in Parathyroid Disorders. Giuseppe Viccica¹, Luisella Cianferotti², Simona Borsari¹, Elena Pardi¹, Roberta Centoni¹, Silvia Chiavistelli¹, Sonia Albertini¹, Edda Vignali¹, Antonella Meola¹, Filomena Cetani², Claudio Marcocci².
¹Department of Endocrinology & Metabolism - Section of Endocrinology & Bone Metabolism, University of Pisa, Italy, ²University of Pisa, Italy

The "canonical" Wnt/ β -catenin pathway plays an important role in the development and patterning of bone. Dkk1 (Dickkopf1) and sclerostin are competitive soluble inhibitors of this pathway through their binding to LPR5/6 coreceptors of Wnt/Frizzled complex. In vitro studies have shown that PTH decreases Dkk1 and sclerostin expression in osteoblasts and osteocytes. Aim of this study was to evaluate serum Dkk1 and sclerostin levels in patients with primary hyperparathyroidism (PHPT) and patients with hypoparathyroidism (HypoPT), and to compare the results with those of a healthy control group. The study group consisted of 32 patients with PHPT, 6 patients with HypoPT and 24 healthy controls. Serum Dkk1 concentration was lower in PHPT (6.8 ± 2.7 pmol/L, $P < 0.0001$) and HypoPT patients (8.3 ± 2.5 pmol/L, $P = 0.047$) compared to healthy subjects (11.0 ± 2.9 pmol/L), whereas no difference was found between PHPT and HypoPT patients ($P = 0.24$). No significant correlation was found between Dkk1 and PTH, bone turnover markers and bone density in PHPT patients. Serum sclerostin concentration in PHPT patients (17.1 ± 7.5 pmol/L) was lower than in subjects with HypoPT (25.5 ± 5.4 pmol/L, $P = 0.013$) and controls (22.1 ± 5.8 pmol/L, $P = 0.009$), whereas no difference was found between HypoPT patients and controls ($P = 0.20$). No significant correlation was found between sclerostin and PTH, bone turnover markers and bone density in PHPT patients. In summary, in patients with PHPT both serum levels of Dkk1 and sclerostin are decreased compared to controls; the limited number of patients with HypoPT does not allow to draw any definitive conclusion.

Disclosures: Giuseppe Viccica, None.

MO0139

The Clinical Features of Primary Hyperparathyroidism in Chinese Patients in the Past 10 Years. Jian-min Liu¹, Lin Zhao², Li-hao Sun³, Xiao-yan He³, Hong-Yan Zhao³, Bei Tao³, Xi Chen⁴, Guang Ning³.
¹Rui-jin Hospital, Shanghai Jiao-tong University School of Medicine, Peoples Republic of China, ²Department of Endocrinology, Rui-jin Hospital, Shanghai Jiao-tong University School of Medicine, China, ³Department of Endocrine & Metabolic Disease, Rui-jin Hospital, Shanghai Jiao-Tong University School of Medicine, China, ⁴Department of Surgery, Rui-jin Hospital, Shanghai Jiao-Tong University School of Medicine, China

Context: It is not known whether the Chinese primary hyperparathyroidism (PHPT) patients are still symptomatic or have transitioned into asymptomatic in recent years. The gene(s) involved in the molecular pathogenesis of parathyroid cancer has not been clearly identified.

Objective: The objective of this study was to describe the uniqueness and the changing pattern of the clinical, biochemical profiles of sporadic Chinese PHPT patients in the past 10 years and identify gene(s) responsible for malignant parathyroid tumors.

Design and Setting: This was a retrospective study conducted in a clinical center. Subjects: A total of 249 PHPT patients were studied.

SAON was induced on 15 adult male emu (30 hips). 12 weeks after SAON induction, core decompression (bone tunnel) of a 6mm in diameter was created at proximal femur. A custom-made PLGA/TCP/Icaritin cylinder composite was implanted into the drill bone tunnel (P/T/I group, n=10), respectively. PLGA/TCP was used as vehicle control (P/T group, n=10) and no scaffold implanted group was used as empty control (Control group, n=10). 12 weeks after implantation, femora were collected and microCT was used to evaluate the collapse and local osteogenesis within volume of interests (the entire tunnel of 6mm diameter and the centre tunnel of 4mm diameter).

No animal died after SAON induction. Femoral head collapse incidence was 70% in the Control group, 30% in the P/T group and 10% in the P/T/I group. (Fig.2-A). Within the bone tunnel, newly formed bone was found in P/T/I group and P/T group while almost no new bone formed in Control group in micro-CT images (Fig.1). Micro-CT quantitative analysis showed that the BMD and BV/TV of newly formed bone in tunnel in the P/T/I group were both significantly higher than those in the P/T group (Fig.2-BC), indicating that PLGA/TCP/Icaritin composite scaffolds reduced incidence of collapse in femoral head by enhancing the repair of SAON lesions in femoral head in bipedal emu. No pathological changes were observed macroscopically.

This was the first efficacy study using bipedal emu model for prevention of joint collapse after core-decompression. Clinical trial registration is on the way before applying for SFDA approval for clinical research and applications. The innovative and bioactive PLGA/TCP/Icaritin porous scaffolds were able to reduce incidence of joint collapse in steroid-associated osteonecrotic femoral head of bipedal emu.



Figure 1: Representative 3-D micro-CT images of Control group (A), P/T group (B) and P/T/I group (C).

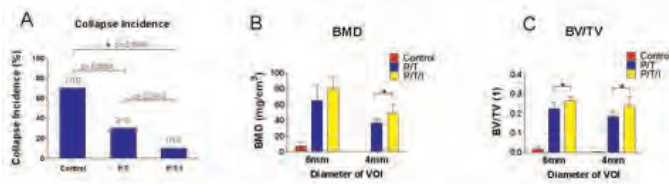


Figure 2: collapse incidence in each group (A), BMD (B) and BV/TV (C) in each group. (*P<0.05)

Figures

Disclosures: Lizhen Zheng, None.

MO0142

Osteoporosis and Vertebral Fractures are Independent Predictors of Cardiovascular Disease in Rheumatoid Arthritis, and Outperform Traditional Risk Factors and Disease Activity Scores. Ausaf Mohammad^{*1}, Diane Bergin², Derek Lohan², Sarah Mooney², John Newell³, Martin O'Donnell³, Robert J Coughlan⁴, John J Carey⁴. ¹Rheumatology, Unit1, Merlin Park University Hospital, Ireland, ²Radiology, Galway University Hospitals, Ireland, ³HRB Clinical Research Facility, NUI Galway, Ireland, ⁴Rheumatology, Galway University Hospitals, Ireland

Introduction: Rheumatoid arthritis (RA) patients are at increased risk of cardiovascular disease (CVD), and have 2-3 fold increased cardiovascular mortality. Traditional risk factors and risk prediction tools for CVD perform poorly in RA populations. Novel biomarkers and better tools are needed. Recently a strong association between osteoporosis and CVD has been recognised. RA patients are also at increased risk of osteoporosis, thus many undergo DXA scanning as part of their ongoing care. DXA technology can diagnose osteoporosis by measuring BMD or detecting vertebral fractures (VF).

Objectives: To determine the prevalence of osteoporosis and VF in a cohort of RA patients and how well they predict CVD compared to traditional CVD risk factors and RA disease activity. **Methods:** We conducted a cross-sectional study of our RA cohort. We evaluated risk factors for, and details of CVD among patients' ≥ 40 years who met 1987 ACR criteria for RA classification. Only those with a prior DXA and VFA scan available for analysis were included. Study was approved by local I.R.B. All scans were evaluated by two blinded Consultant musculoskeletal radiologists to determine the prevalence, number and severity of VF using Genant criteria. Patients were diagnosed as 'normal', 'osteopenia' or 'osteoporosis' using WHO DXA criteria for the purposes of the study. We compared the prevalence of osteoporosis and VF between RA patients with and without CVD, and using multivariate logistic regression analyses assessed whether fractures, osteoporosis traditional CVD risk factors and RA disease activity were independently associated with prevalent CVD.

Result: 603 patients met study inclusion criteria: (74%) female, mean age 56 years, 76% sero positive. 230 subjects had 1 or more documented CVD event: MI: 45, stent: 145, CHF: 33, and stroke: 7. Subjects with CVD were more likely to have VF (24% Vs

12%) and osteoporosis (60% Vs 15%) compared to those without CVD ($p < 0.001$). Low BMD and VF were independently associated with CVD in multivariate regression analyses ($P < 0.001$), and outperformed traditional risk factors for CVD and RA disease activity scores (table 1).

Conclusion: The presence of low BMD and VF among RA patients should alert physicians not just to the presence of osteoporosis, but also to the possibility of CVD. Interventions to reduce the development of CVD in RA patients with osteoporosis may be warranted.

Table 1: Association between Osteoporosis, Vertebral Fractures, Traditional Risk factors for CVD and RA Disease Activity Scores in study population*

| Variable | Odds Ratio (95% Confidence Interval) |
|--------------------|---|
| Diabetes Mellitus | 1.61 (1.04-2.48) |
| Smoking | 1.18 (1.10-1.27) |
| Hypertension | 1.58 (1.12-1.89) |
| Hyperlipidemia | 1.02 (1.00-1.05) |
| CRP | 1.73 (1.41-2.12) |
| DAS28 | 1.63 (1.30-2.03) |
| Vertebral fracture | 2.70 (1.50-4.75) |
| Osteoporosis | 2.67 (1.87-3.91) |

* Adjusted for age, gender

Table 1

Disclosures: Ausaf Mohammad, None.

MO0143

Association of Cortical Volumetric Bone Mineral Density with Arterial Calcification in African Ancestry Men. Allison Kuipers^{*1}, Joseph Zmuda¹, J. Jeffrey Carr², J. Greg Terry², Clareann H Bunker¹, Alan L. Patrick³, Victor W. Wheeler³, Iva Miljkovic¹. ¹University of Pittsburgh Graduate School of Public Health, USA, ²Wake Forest University of Health Sciences, USA, ³Tobago Health Studies Office, Trinidad & Tobago

Osteoporosis and cardiovascular disease (CVD) are common age-related conditions, but the link between them cannot be explained by age alone. Subclinical measures of osteoporosis and CVD, such as bone mineral density (BMD) and arterial calcification, have been correlated in population-based studies. However, this association is less well defined in African ancestry individuals and, to our knowledge, has not been studied using measures of cortical bone separately. Therefore, we tested the association of cortical BMD captured by peripheral quantitative computed tomography (pQCT) with aortic and coronary artery calcification (AC and CAC, respectively) in preliminary analysis of 175 men of African ancestry aged 40 and older from the Tobago Bone Health Study. Cortical BMD was assessed at the non-dominant radius and left tibia. Calcification measures were assessed using computed tomography of the lower abdomen between L3 and S1 (AC) and of the chest starting at the carina and through the entire heart (CAC). Scans were scored for calcification using the Agatston method and presence of any calcification was defined by a score ≥ 10 in order to exclude false positives. Odds ratios were expressed as the effect of a 1 SD increase in BMD in age and multivariable adjusted models using logistic regression. The prevalence of AC and CAC were 69% and 28%, respectively. After adjustment for age, greater radius cortical BMD was associated with decreased odds of AC (OR=0.58; 95% CI: 0.37-0.99; P=0.014). This association remained significant after adjustment for standing height, body weight, hypertension, diabetes and current smoking (OR=0.52; 95% CI: 0.32-0.83; P=0.006). Results were similar at the tibia. There was no significant association between cortical BMD and CAC in any models. In these African ancestry men, we identified a novel association of cortical BMD with aortic calcification. These findings will need to be expanded upon in a larger sample to better understand the shared physiology between skeletal and arterial calcification.

Disclosures: Allison Kuipers, None.

MO0144

Regional Up-regulation of 25-hydroxyvitamin D 1alpha-hydroxylase (CYP27B1) Gene Is Associated with the Pathogenesis of Ectopic Calcification in the Alpha Klotho Mutant Mice. Hironori Yamamoto^{*1}, Ayako Otani¹, Nozomi Yokoyama¹, Rina Onishi¹, Yuichiro Takei², Yutaka Taketani¹, Ken-Ichi Miyamoto³, Eiji Takeda⁴. ¹University of Tokushima, Japan, ²The University of Tokushima School of Medicine, Japan, ³Tokushima University School of Medicine, Japan, ⁴University of Tokushima School of Medicine, Japan

Alpha klotho plays an essential role in the signaling pathway of fibroblast growth factor (FGF) 23, which is a critical regulator of the phosphate and vitamin D metabolism in kidney. Alpha klotho mutant (*kllkl*) mice have hyperphosphatemia, hypercalcemia and hypervitaminosis D, and develop ectopic calcification, together with short lifespan. It has been reported that these disorders are caused by over-production of 1,25-dihydroxyvitamin D through the renal up-regulation of 25-hydroxyvitamin D 1alpha-hydroxylase (CYP27B1) gene. In the present study, we investigated the relationship between the expression of CYP27B1 and the pathogenesis of ectopic calcification in *kllkl* mice. Real-time PCR analysis confirmed that renal cortex CYP27B1 mRNA expression was up-regulated in *kllkl* mice compared with wild type mice. Surprisingly, immunohistochemical analysis and von Kossa staining revealed that the regional high-expressed CYP27B1 in kidney cortex from 3-week-old mice without ectopic calcification, in other hand, in 6-week-old mice, its localization merged with calcifying renal arterioles and tubular cells. Importantly, we found that the CYP27B1 was also co-localized with the calcified lesions of heart and aorta in *kllkl* mice. In addition, its colocalization was also seen in heart of CKD rats with hyperphosphatemia. *In vitro* analysis using rat aortic vascular smooth muscle (A-10) cells, inorganic phosphate (Pi) loading did not increase the CYP27B1 mRNA levels, however, promoted its protein accumulation in mitochondria. These results suggest that the regional up-regulation of CYP27B1 expression by abnormality of FGF23-klotho signaling is implicated with the pathogenesis of ectopic calcification.

Disclosures: Hironori Yamamoto, None.

MO0145

Relationships between Serum Adiponectin and Bone Density, Adiposity and Calcified Atherosclerotic Plaque in African Americans. Thomas Register^{*1}, Jasmin Divers¹, Donald Bowden¹, J. Jeffrey Carr¹, Leon Lenchik², Lynn Wagenknecht¹, R. Caresse Hightower¹, Jianzhao Xu¹, Carrie Smith¹, Keith Hruska³, Carl D. Langefeld¹, Barry Freedman¹. ¹Wake Forest School of Medicine, USA, ²Wake Forest University, USA, ³Washington University in St. Louis School of Medicine, USA

Background: Circulating adiponectin concentrations are negatively associated with volumetric bone mineral density (vBMD) and visceral adiposity in European Americans (EA). We sought to clarify relationships between serum adiponectin and vBMD, adipose tissue volumes, and calcified atherosclerotic plaque (CP) in African Americans (AA).

Methods: Serum adiponectin concentrations were assessed in relation to quantitative computed tomography-derived measures of vBMD in thoracic and lumbar vertebrae, adipose tissue volumes, and CP in coronary and carotid arteries and infra-renal aorta in 479 unrelated AAs with type 2 diabetes. Generalized linear models were fitted to test for associations between adiponectin and measured phenotypes.

Results: Participants were 57% female with mean±SD (median) age 55.6±9.5 (55.0) years, diabetes duration 10.3±8.2 (8.0) years, serum adiponectin 8.26±7.41 (6.10) ug/ml, coronary artery CP mass score 280±634 (14), carotid artery CP 47±133 (0), and aortic CP 1616±2864 (319). Women had significantly higher BMI and adiponectin concentrations, and lower coronary and carotid artery calcium than males (all p<0.05). Adjusting for age, sex, BMI, mean arterial pressure, hemoglobin A_{1c}, and LDL-cholesterol, adiponectin was inversely associated with thoracic and lumbar vertebral vBMD (parameter estimates [PE] -0.0716 and -0.0621, respectively; both p<0.0001), visceral adipose tissue (PE -0.0169; p<0.0001) and C-reactive protein (CRP, PE -0.0284; p=0.019), and positively associated with albuminuria (PE 0.0524; p=0.0011). Significant associations were not observed between adiponectin and CP in any vascular bed or with pericardial adipose tissue.

Conclusions: Serum adiponectin levels were inversely associated with cross-sectional measures of thoracic and lumbar vertebral vBMD, visceral adiposity and CRP in AAs, but not with pericardial adipose tissue or vascular CP. The data support a regulatory role for adiponectin in modulation of bone density.

Disclosures: Thomas Register, None.

MO0146

Lentiviral Rescue of TCIRG1 Expression in IMO Osteoclasts Restores Resorptive Function in a Lineage Specific Manner. Christian Thudium^{*1}, Ilana Moscatelli², Carmen Flores³, Karoline Natasja Staehr Gudmann⁴, Anders Fasth⁵, Ansgar Schulz⁶, Oscar Porras⁷, Anna Villa⁸, Morten Karsdal¹, Kim Henriksen¹, Johan Richter³. ¹Nordic Bioscience A/S, Denmark, ²Lund University, Sweden, ³Department of Molecular Medicine & Gene Therapy, Lund Strategic Center for Stem Cell Biology, Sweden, ⁴Nordic bioscience, Denmark, ⁵University of Gothenburg, Sweden, ⁶University Medical Center Ulm, Germany, ⁷National Children's Hospital, Costa Rica, ⁸Milan Unit, Istituto di Ricerca e Genetica Biomedica, CNR, Italy

Infantile malignant osteopetrosis (IMO) is a rare hereditary bone disease characterized by inability of the osteoclasts to resorb bone. In more than 50% of cases the disease is caused by pathological deletion mutations in TCIRG1, a gene encoding the osteoclast specific V-ATPase subunit a3. Due to the severity of IMO and the issues of allogenic marrow transplantation, gene therapy is an attractive alternative.

The aim of the study was to rescue the function of IMO patient derived osteoclasts through insertion of TCIRG1 using lentiviral vectors, with the future purpose of autologous stem cell transplantation treatment.

CD34⁺ cells from peripheral blood of 5 IMO patients and from normal cord blood were transduced with SIN lentiviral vectors expressing endogenous TCIRG1 and GFP under a SFFV promoter. The cells were expanded for 2 weeks, during which they were transduced. Cells were then differentiated for 10 days on bone slices with M-CSF and RANKL to mature osteoclasts, and osteoclastogenesis, activity and expression of TCIRG1 investigated.

The transduction efficiency after 2 weeks was approximately 40%. qPCR analysis and western blot revealed increased mRNA and protein levels of TCIRG1 compared to GFP transduced controls. TCIRG1 protein was, however, only expressed at late stages of osteoclast differentiation, but not late stages of macrophages not incubated with RANKL, whereas GFP was seen throughout both the expansion and osteoclast differentiation period. Furthermore, this regulation seemed isolated to the hematopoietic lineage as TCIRG1 was readily expressed in HT1080, a non-hematopoietic control cell line. Vector corrected IMO osteoclasts generated increased Ca²⁺ release and CTX-1 into the media, and showed clearly visible resorption pits, while non-corrected IMO osteoclasts developed normally but failed to resorb bone. Rescue resorption was approximately 70% of that of osteoclasts generated from normal CD34⁺ cord blood cells.

In conclusion, we provide the first *in vitro* evidence of lentiviral-mediated correction of a genetic disease involving the osteoclast lineage, supporting further development of gene therapy of IMO and other diseases affecting these cells. In addition, we observed a differentiation dependent regulation of TCIRG1 using a viral promoter, suggesting a novel regulatory mechanism for TCIRG1, which could prove beneficial from a gene therapy perspective.

Disclosures: Christian Thudium, None.

MO0147

A Limited Number of Mutations in MAFB, a Negative Regulator of RANKL-induced Osteoclastogenesis, Cause Idiopathic Multicentric Osteolysis with Nephropathy. Steven Mumm^{*1}, Margaret Huskey¹, Deborah Wenkert², Gary Gottesman², Katherine Madson², William McAlister¹, Michael Whyte². ¹Washington University School of Medicine, USA, ²Shriners Hospital for Children-Saint Louis, USA

Idiopathic multicentric osteolysis with nephropathy (IMO) is typically a sporadic, but sometimes an autosomal dominant, disorder that features carpal-tarsal lysis and nephropathy leading to renal failure. At Shriners Hospital for Children, St. Louis, we have cared for 6 children with IMO during the past 28 years. This year, mutations in the single exon MAFB [v-maf musculoaponeurotic fibrosarcoma oncogene ortholog B (avian)] gene were reported in 11 patients with IMO (also called multicentric carpotarsal osteolysis) (Zankl et al. AJHG 90:494-501, 2012). We investigated whether our IMO patients had mutations in the MAFB gene.

Our six patients with IMO presented with pain starting between birth and 3 years, most were initially diagnosed with juvenile idiopathic arthritis. The appropriate diagnosis of IMO for 5/6 patients was made between the ages 1-5 years based on radiographs showing dissolution of carpals and tarsals. Additional bones showed lysis. Proteinuria presented from ages 1 – 12 years in 5/6 patients; one required renal transplantation. We analyzed the MAFB gene by PCR amplification and sequencing of the region where mutations were previously reported. We found four different heterozygous defects in five of our IMO patients: c.176C>T, p.Pro59Leu; c.206C>T, p.Ser69Leu; c.209C>T, p.Ser70Leu; c.211C>T, p.Pro71Ser. These four mutations, localized within an 18 amino acid stretch of the transactivation domain of the 323 amino acid MAFB protein, were identical to ones previously reported, suggesting a limited set of mutations that cause IMO. The lack of nonsense or other truncating mutations suggest a dominant negative mechanism. Our sixth patient appears to have a unique mutation in the same region; this finding needs to be verified. None of the parents are clinically affected. DNA samples were available for some parents, each unaffected, and without their child's MAFB mutation. Hence, although the defects

likely arose spontaneously in all of our patients, each appeared to be within an 18 amino acid region and four mutations were identical to those carried among the previously reported 11 patients. Our results validate our phenotypic characterization of IMO, are consistent with the molecular results of Zankl et al., and suggest a limited set of defects within MAFB cause IMO.

MAFB is a negative regulator of RANKL-mediated osteoclastogenesis. Therefore, MAFB mutations would enhance RANKL-mediated osteoclastogenesis to cause IMO.

Disclosures: Steven Mumm, None.

MO0148

A Non-synonymous Coding Variant in Frizzled-1 is Associated with Enhanced Wnt Signaling and Mineralization of Saos2 Osteoblast-like Cells. Yingze Zhang*¹, Shibing Yu², Allison Kuipers³, Yanxia Chu¹, Joseph Zmuda³. ¹University of Pittsburgh, USA, ²University of Pittsburgh Medical Center, USA, ³University of Pittsburgh Graduate School of Public Health, USA

Frizzled-1 (FZD1) is a coreceptor for Wnt ligands. We have previously reported that a novel non-synonymous coding variant (c.190G>A/p.A64T) in the FZD1 gene enhances canonical Wnt signaling in osteoblasts. This genetic variant was also associated with increased bone mineral density among Afro-Caribbean men. The goal of current experiments was to further characterize the functional consequences of this FZD1 protein variant on mineralization of Saos2 osteoblast-like cells. We first established Saos2 cells stably expressing A64T allele specific cDNA clones. Cells were then cultured in osteoblastic differentiation medium containing 50 ug/ml ascorbic acid and 7.5 mM β -glycerophosphate for 14 days, fixed and stained with 0.5% Alizarin Red-S (AR-S) and the mineralization area quantified. We detected significantly higher mineralization for FZD1-64T expressing cells (79.7%) compared to both FZD1-64A wild type expressing cells (45.8%) and Saos2 cells only (7.7%). Down-regulation of endogenous FZD1 gene expression in Saos2 cells using siRNA resulted in approximately 50% reduction in mineralization area compared to cells treated with scrambled siRNA. Subcellular localization experiments further demonstrated allele specific up-regulation of cell surface FZD1 expression for the 64T variant compared to the 64A allele. Our data collectively suggests that the common A64T variant is associated with increased FZD1 receptor on the cell surface, enhanced Wnt signaling and up-regulation of osteoblast mineralization.

Disclosures: Yingze Zhang, None.

MO0149

A Novel TMEM41B Mutation Causes Autosomal Recessive Syndromic Acro-osteolysis with Recurrent Infections, Sensory Neuropathy and Mental Retardation. Bram CJ van der Eerden*¹, Pietro Chiurazzi², Sigrid Swagemakers³, Marijke Schreuders-Koedam⁴, Giovanni Neri², Peter J van der Spek³, Johannes Van Leeuwen⁵. ¹Department of Internal Medicine, Erasmus MC, Netherlands, ²Istituto di Genetica Medica, Università Cattolica del Sacro Cuore, Italy, ³Department of Bioinformatics, Erasmus University Medical Center, Netherlands, ⁴Department of Internal Medicine, Erasmus University Medical Center, Netherlands, ⁵Erasmus University Medical Center, The Netherlands

Acro-osteolysis refers to the progressive osteolysis of phalanges in the hands and feet associated with recurrent ulcers of the fingers and soles, usually resulting in loss of toes or fingers. We set out to clinically, genetically and molecularly characterize an Italian family with autosomal recessive transmission of acro-osteolysis, short stature, mental retardation, sensory neuropathy and recurrent infections.

Both patients (brother and sister) had a history of fractures and low BMD at several sites (sister: femoral neck T-score -2.9, proximal femur -3.3, lumbar spine L2-L4 -3.2; brother: femoral neck -1.3, proximal femur -2.0). Laboratory tests indicated increased bone turnover (increased beta cross-laps and relatively high osteocalcin) and hypogonadism (increased FSH in both probands) with increased LH and low estradiol in the sister. Interestingly, both patients had extremely low 25(OH)₂D₃ (~4 ng/ml), while 1,25-(OH)₂D₃ was normal in the brother but low in the sister.

The clinical symptoms in the patients overlapped partly with both Hajdu-Cheney syndrome and Hereditary sensory and autonomic neuropathy type II but mutations in the corresponding genes (*NOTCH2*, *WNK1*, *FAM134B*) were excluded by SNP haplotyping as well as by complete genome sequencing. Instead, we identified a novel homozygous missense mutation (D107G) in the *TMEM41B* gene localized in 11p15.4, which encodes a SNARE-associated Golgi protein.

Finally, we tested the functional relevance of the *TMEM41B* mutation in peripheral blood mononuclear cells-derived osteoclast of both patients, their parents and control individuals. *TMEM41B* mRNA was markedly elevated after 21 days in culture when mature osteoclasts appear and immunofluorescence with specific antibodies parallels this observation. Importantly, the number of mono- and multinuclear osteoclasts was significantly elevated, which was corroborated by a 2-fold increase in bone resorption activity of patients' osteoclasts compared to normal controls as well as to the heterozygous parents.

In conclusion, we identified *TMEM41B* as a gene involved in the pathogenesis of a new syndromic condition with recessive inheritance characterized by acro-osteolysis,

sensory neuropathy, hypogonadism and intellectual disability. In addition, our experiments indicate a gain-of-function effect of the D107G mutation leading to an increase in bone resorption activity in these patients with acro-osteolysis.

Disclosures: Bram CJ van der Eerden, None.

MO0150

Abnormal Type I Collagen Folding and Matrix Deposition in a Cyclophilin B KO Mouse Model of Recessive Osteogenesis Imperfecta. Wayne Cabral*¹, Elena Makareeva², MaryAnn Weis³, Sergey Leikin², David Eyre³, Joan Marini¹. ¹Bone & Extracellular Matrix Branch, NICHD, NIH, USA, ²Section on Physical Biochemistry, NICHD, NIH, USA, ³Orthopaedic Research Laboratories, University of Washington, USA

Osteogenesis Imperfecta (OI) is a heritable osteochondrodysplasia characterized by bone fragility and growth deficiency. Absence of proteins involved in collagen post-translational interactions results in recessive forms of OI; most cases involve components of the collagen prolyl 3-hydroxylation complex, CRTAP, P3H1 and PPIB/CYPB (OI types VII-IX, respectively). The α 1(I) Pro986 3-hydroxylation was speculated to play a role in collagen alignment and cross-linking in fibrils. PPIB, a prolyl cis-trans isomerase, is thought to be the major PPIase responsible for the rate-limiting step in collagen helix formation. To further characterize the role of 3-hydroxylation complex components in collagen folding, Ppib-null mice were generated using a gene-trap ES cell clone with a β -geo reporter construct inserted in the first intron of *Ppib*. Homozygous *Ppib* knockout mice were verified by RT-PCR to have complete absence of *Ppib* transcripts in skin, fibroblasts, femora and calvarial osteoblasts. *Ppib*^{-/-} mice weigh 33% less than WT littermates and have reduced femoral and L1-L2 vertebral DXA. Ppib protein was absent and P3h1 reduced 50% on western blots of *Ppib*^{-/-} cultured fibroblast and osteoblast lysates. In agreement with some previously described patients with PPIB mutations, α 1(I) P986 3-hydroxylation of fibroblast and osteoblast collagen was severely reduced (11 and 5% of WT, respectively). Direct intracellular collagen folding assays and broadened appearance of steady-state collagen alpha chains from *Ppib*^{-/-} cells on SDS-Urea PAGE support delayed folding of the collagen helix. In contrast, collagen thermal stability, 5-lysyl and 4-prolyl hydroxylation of α 1(I) chains, as well as gel migration of α 1(I) CNBr peptides were normal, consistent with normal post-translational modification, but unexpected in the context of delayed collagen folding. Inhibiting hydroxylation of fibroblast collagen with α , α -dipyridyl resulted in *Ppib*^{-/-} collagen alpha chains with faster migration than WT chains on SDS-Urea PAGE, suggesting altered conformation due to loss of peptidyl-prolyl isomerization or altered glycosylation of hydroxylsyl residues. In *Ppib*^{-/-} fibroblast cultures collagen deposition was 30% of WT, despite minimally delayed secretion. These data suggest unique roles for Ppib in collagen post-translational processing, trafficking and extracellular matrix incorporation in addition to its role as a folding chaperone.

Disclosures: Wayne Cabral, None.

MO0151

Cause of Death (COD) in Patients with Osteogenesis Imperfecta (OI) in Denmark. Lars Folkestad*¹, Jannie Hald², Jeppe Gram³, BENTE LANGDAHL⁴, Bo AbrahamSEN⁵, Kim Brixen⁶. ¹Osteoporose Klinikken Odense University Hospital, Denmark, ²MEA Aarhus University Hospital, Tage Hansensgade 2DK-8000 Aarhus C Denmark, Denmark, ³Hospital of Southwest Denmark, Denmark, ⁴AARHUS UNIVERSITY HOSPITAL, Denmark, ⁵Copenhagen University Hospital Gentofte, Denmark, ⁶Institute for Clinical Research, Denmark

Introduction: The phenotype of OI is heterogeneous ranging from perinatally lethal to increased fracture risk in otherwise healthy individuals, however, little is known regarding COD in patients with OI. We aimed to chart CODs in the Danish OI population.

Methods: Patients with OI were identified from hospital contacts with the ICD-8 code 756.59 or ICD-10 code DQ 78.0 in the Danish National Patient Registry (DNPR) while data regarding date of birth, sex, time of death and the primary COD were retrieved from the Danish Register of Causes of Death. Data regarding COD in the Danish general population were identified from the online recode Statistics Denmark.

Results: During the period from the 1th of Jan 1977 until 31 Dec 2009, a total of 609 patients with OI diagnosis (57% female) were identified and 140 of these were deceased at the time of data extraction. The leading COD in the Danish OI cohort were cardiovascular disease and OI *per se*. When excluding the patients that died prior to their 10th year of life, cardiovascular disease were still the leading COD. Age at death for the Danish population in 1977, 2009 and the Danish OI Cohort are listed in table 1, whereas CODs can be seen in table 2.

Discussion: There are several limitations to this study. Firstly the accuracy of the CODs registered relies on the physicians' judgment and coding. Secondly, the deaths in the Danish OI cohort occurred over 32 years and the population COD may have changed over time. Thirdly, it is likely that only the severest cases of OI is known and thus registered in the DNPR. Furthermore, our study cannot address the possible correlation between the clinical severity of OI and the COD.

Conclusions: The leading COD in the Danish OI cohort were cardiovascular disease and OI *per se*. To clarify any differences in COD between the Danish OI cohort and the Danish population a case-control study is needed. Most deaths from OI *per se* occurred before the age of 10 years, indicating more severe phenotypes of OI in these patients.

| Table 1: Age at death (years) | 1977 Danish Population (n(%)) | 2009 Danish Population (n(%)) | OI Cohort (n(%)) |
|-------------------------------|-------------------------------|-------------------------------|--------------------|
| 0-9 | 789 (1.6) | 261 (0.5) | 21 (15.0) |
| 10-19 | 344 (0.7) | 131 (0.2) | 7 (5.0) |
| 20-29 | 603 (1.2) | 234 (0.5) | 2 (1.4) |
| 30-39 | 879 (1.7) | 573 (1.0) | 4 (2.8) |
| 40-49 | 1.806 (3.6) | 1.570 (2.9) | 14 (10.0) |
| 50-59 | 4.705 (9.4) | 4.038 (7.4) | 15 (10.7) |
| 60-69 | 9.800 (19.4) | 851(15.6) | 20 (14.3) |
| 70-79 | 15.424 (30.6) | 12.675 (23.1) | 22 (15.7) |
| 80+ | 16.134 (32.2) | 26.776 (48.8) | 35 (25.0) |
| Total | 50.485 (100.0) | 54.895 (100.0) | 140 (100.0) |

Table 1: Age at death

| Table 2: Cause of death | Danish Population 1977 (n(%)) | Danish Population 2009 (n(%)) | Danish OI Cohort (n(%)) |
|--|-------------------------------|-------------------------------|-------------------------|
| Cerebrovascular | 4.813 (9.5) | 3.800 (6.9) | 7 (5.0) |
| Cardiovascular | 16.472 (32.6) | 8.656 (15.8) | 29 (20.7) |
| Malignancy | 12.719 (25.2) | 14.888 (27.1) | 24 (17.1) |
| COPD, asthma or respiratory tract infections | 3.102 (6.1) | 5.564 (10.1) | 9 (6.4) |
| Mental illness | - | 3.076 (5.6) | 3 (2.1) |
| Accidents or suicide | 3.300 (6.5) | 2.061 (3.8) | 6 (4.3) |
| OI | - | - | 26 (18.6) |
| Other | 9.766 (19.3) | 18.224 (33.2) | 32 (22.6) |
| Unknown | 313 (0.6) | 380 (0.7) | 4 (2.8) |

Table 2: Cause of Death

Disclosures: Lars Folkestad, None.

MO0152

Withdrawn

MO0153

Enzyme Replacement Therapy Prevents Enamel Defects in Hypophosphatasia Mice. Manisha Yadav¹, Rodrigo Cardoso de Oliveira², Brian Foster³, Hanson Fong⁴, Esther Cory Burak⁵, Sonoko Narisawa⁶, Robert Sah⁵, Martha Somerman⁷, Michael Whyte⁸, Jose Luis Millan⁹. ¹Burnham Institute for Medical Research, USA, ²University of São Paulo, Bauru Dental School, Department of Biological Sciences, Brazil, ³National Institute of Arthritis & Musculoskeletal & Skin Diseases (NIAMS), USA, ⁴University of Washington School of Dentistry, USA, ⁵Department of Bioengineering, UCSD, USA, ⁶Sanford Burnham Medical Research Institute, USA, ⁷NIDCR, USA, ⁸Shriners Hospital for Children-Saint Louis, USA, ⁹Sanford-Burnham Medical Research Institute, USA

Hypophosphatasia (HPP) is the inborn error of metabolism characterized by deficiency of alkaline phosphatase activity leading to rickets or osteomalacia and to dental defects. HPP occurs from loss-of-function mutations within the gene that encodes the tissue-nonspecific isozyme of alkaline phosphatase (TNAP). TNAP knockout (*Alpl*^{-/-}, a.k.a. *Akp2*^{-/-}) mice closely phenocopy infantile HPP, including the rickets, vitamin B6-responsive seizures, improper dentin mineralization, and lack of acellular cementum. Here, we report that lack of TNAP in *Alpl*^{-/-} mice also causes severe enamel defects, which are preventable by enzyme replacement with mineral-targeted TNAP (ENB-0040). Immunohistochemistry was used to map the spatiotemporal expression of TNAP in the tissues of the developing enamel organ of healthy mouse molars and incisors. We found strong, stage-specific expression of TNAP in ameloblasts. In the *Alpl*^{-/-} mice, histological, μ CT, and scanning electron microscopy analysis showed reduced mineralization and disrupted organization of the rods and inter-rod structures in enamel of both the molars and incisors. All of these abnormalities were corrected in mice receiving from birth daily subcutaneous injections of mineral-targeting, human TNAP (sALP-FcD₁₀, a.k.a. ENB-0040) at 8.2 mg/kg/day for up to 44 days. These data reveal an important role for TNAP in enamel mineralization, and demonstrate the efficacy of mineral-targeted TNAP to prevent enamel defects in HPP.

Disclosures: Manisha Yadav, None.

MO0154

High-Throughput Bone Phenotyping of 100 Knockout Mouse Lines Identifies 9 New Genes That Determine Bone Strength. John Bassett¹, Apostolos Gogakos², Jacqueline White³, Holly Evans⁴, Richard Jacques⁵, Anne Van der Spek², Alan Boyde⁶, Michael Campbell⁵, Peter Croucher⁷, Graham Williams². ¹Imperial College London, United Kingdom, ²Molecular Endocrinology Group, Dept Medicine, Imperial College London, United Kingdom, ³Wellcome Trust Sanger Institute, United Kingdom, ⁴The Mellanby Centre for Bone Research, University of Sheffield, United Kingdom, ⁵School of Health & Related Research, University of Sheffield, United Kingdom, ⁶Institute of Dentistry, Queen Mary University, United Kingdom, ⁷Garvan Institute of Medical Research, Australia

Osteoporosis is a common polygenic disease but its genetic basis is poorly defined. The majority of the variance in bone mineral density is genetically determined yet only a small proportion is accounted for by known genetic variation, suggesting many genes remain to be identified. We hypothesised that a bone-specific extreme phenotype screen in unselected knockout mice would rapidly identify new genetic determinants of bone strength. We report a high-throughput multi-parameter screen to identify abnormal and functionally significant skeletal phenotypes in mice generated by the International Knockout Mouse Consortium.

We analyzed 100 consecutive knockout mouse strains from the Sanger Institute Mouse Genetics Project. Bone length, cortical thickness and bone mineral content (BMC) were determined by Faxitron digital x-ray microradiography, and trabecular bone volume, thickness and number by micro-CT. Reference data were derived from 77 wild-type mice. Individuals with values >2SD outside the normal range were considered outliers. Mahalanobis statistical analysis identified outliers not apparent from a single variable but anomalous when covariance with all variables was considered. Functional significance was confirmed by biomechanical testing.

10 strains had significant abnormalities in structural parameters and bone strength. One of the strains, *Spare*, has been described previously. 9 new genes, not previously implicated in skeletal homeostasis were identified. These included, *Bbx*, a transcription factor, *Slc38a10*, an amino acid transporter, *Cadml*, an adhesion molecule, *Setdb1*, a histone methyl transferase, *Spns2*, a sphingosine-1-phosphate transporter, *Asxl1*, a chromatin-binding Polycomb protein and 3 genes of unknown function *Fam73b*, *Trim45* and *Prpsap2*. Eight of the 10 lines were still identified when statistical stringency was increased from >2 to >3SD. Multi-parameter analysis revealed a new functional classification of bone structure. Bones were either weak but flexible with low BMC (*Bbx*, *Cadml* and *Fam73b*), weak and brittle with low BMC (*Prpsap2*, *Slc38a10* and *Spare*) or strong but brittle with high BMC (*Asxl1*, *Setdb1*, *Spns2* and *Trim45*).

These data demonstrate that rapid unbiased screening allows identification of new genetic determinants of bone structure and strength that could not otherwise be predicted using candidate gene approaches or existing disease models.

Disclosures: Peter Croucher, None.

MO0155

Muscle-Bone Interaction in Hypophosphatemic Rickets : A Mechanostat-Based Assessment. Louis-Nicolas Veilleux^{1*}, Moira Cheung², IBTIHEL MOUNA BEN AMOR³, Francis Glorieux⁴, Frank Rauch⁵. ¹McGill University, Canada, ²Imperial College, United Kingdom, ³SHRINERS HOSPITAL FOR CHILDREN, Canada, ⁴Shriners Hospital for Children & McGill University, Canada, ⁵Shriners Hospital for Children, St. Louis, Canada

Context: The mechanostat model proposes that bone tissue constantly monitors the deformations (strains) which result from mechanical forces. It is thought that the highest bone strains are induced by muscle contractions. In hypophosphatemic rickets (HPR) mineralization defect persists despite treatment, leading to softer bone material. A given mechanical load on HPR bones will therefore lead to a larger than normal deformation. According to the mechanostat model, this should result in increased bone mass. Objective: The goal of the present study was to assess the muscle-bone relationship in the lower extremities of HPR patients and of healthy controls. Patients and Other Participants: 31 individuals with HPR (6 to 60 years; 9 males) and 31 age- and gender-matched controls. Main Outcome Measures: Calf muscle cross-sectional area (mm²) and muscle density (mg/mm³) and tibia bone mineral content (BMC; mg/mm) were measured by peripheral quantitative computed tomography. Lower extremity peak force (kN) was measured by jumping mechanography through the multiple two-legged hopping test. Results: Compared to age- and gender-matched controls, patients with HPR had normal muscle cross-sectional area (HPR = 5561 ± 1340 mm²; Controls = 5382 ± 1727 mm²; P = 0.58) but lower muscle density (HPR = 68.5 ± 4.2 mg/cm³; Controls = 71.3 ± 3.5 mg/cm³; P = 0.005) and lower peak muscle force (HPR = 2.0 ± 0.6 kN; Controls = 2.5 ± 0.9 kN; P < 0.001). BMC was not significantly higher in HPR patients (HPR = 227 ± 66 mg/mm; Controls = 216 ± 54 mg/mm; P = 0.27). However, after adjustments for muscle force, tibial BMC was 21% higher in HPR patients than in controls (P < 0.001). When adjusted for muscle cross-sectional area instead of muscle force, tibial BMC was 12% higher in HPR patients than in controls (P = 0.01). Conclusions: The present study supports the prediction from the mechanostat model and shows that for a given local muscle force, HPR patients have higher bone mass in the tibia than controls.

Disclosures: Louis-Nicolas Veilleux, None.

MO0156

The Low Bone Mass in Genetic Hypercalciuria Stone-forming (GHS) Rats Is Due to the Enhanced Bone Resorption and Decreased Bone Formation.

Hongwei Wang¹, Honggang Ye¹, Jinhua Wang¹, Sooyoung Park¹, Baisheng Fu¹, David A. Bushinsky², Murray J. Favus^{1*}. ¹University of Chicago, USA, ²University of Rochester, USA

Hongwei Wang¹, Honggang Ye¹, Jinhua Wang¹, Sooyoung Park¹, Baisheng Fu¹, David A. Bushinsky², Murray J. Favus^{1*}

1. Section of Endocrinology, University of Chicago Pritzker School of Medicine, Chicago, Illinois 60637, USA

2. Division of Nephrology, University of Rochester School of Medicine and Dentistry, Rochester, New York 14642, USA

Genetic Hypercalciuria Stone-Forming (GHS) rats are a useful model for human idiopathic hypercalciuria (IH), as both form Ca kidney stones and have low bone mass through increased intestinal Ca absorption and bone resorption, and decreased renal tubule Ca reabsorption. The low bone mass is accompanied by a defect in cortical bone that is more brittle and fracture-prone. Histomorphometry indicates that bone resorption is increased and bone formation may be decreased. This study investigates the molecular mechanisms that may mediate low bone mass in GHS rats. Gene microarray analysis on bone marrow stromal cells reveal that the genes related to bone resorption including RANKL, RANK, GM-CSF, TNF α , and IL1 are increased, while genes related to bone formation (BMP2, Spp1, Sost) are decreased in GHS rats compared to normocalciuric Sprague Dawley (SD) rats. Gene array analysis on splenic CD14⁺ cells from GHS and SD rats indicate that some genes including VDR, TNF, IL-17 pathways, CEPBP, CAMP, TNFR1 and IL-17R α are upregulated. Real-time PCR results confirm the microarray analysis. Serum RANKL and BMP2 levels are increased and decreased, respectively in GHS rats (both P<0.05). In addition, immunostaining demonstrated greater RANKL expression in bone marrow stromal cells from GHS rats. GHS bone marrow monocytes cultured in vitro with RANKL (100ng/ml) showed greater stimulation of expression of osteoclastic genes such as integrin β , CAII, cathepsin K and TRAP. The mature osteoclast cell number increased at different dosage of RANKL. Mature osteoclasts are also individually larger in dimensions in GHS rats. The bone marrow stromal cells cultured in the presence of BMP2 induced greater osteoblastic gene expression such as ALP, and RUNX2 as well as greater alkaline phosphatase (ALP) activity and matrix mineralization in SD rats compared to GHS rats. In conclusion, our results demonstrate that the reduction in osteoblast-mediated bone formation is reduced and contributes to low bone mass in GHS rats. Enhanced bone resorption is also a cause of low bone mass.

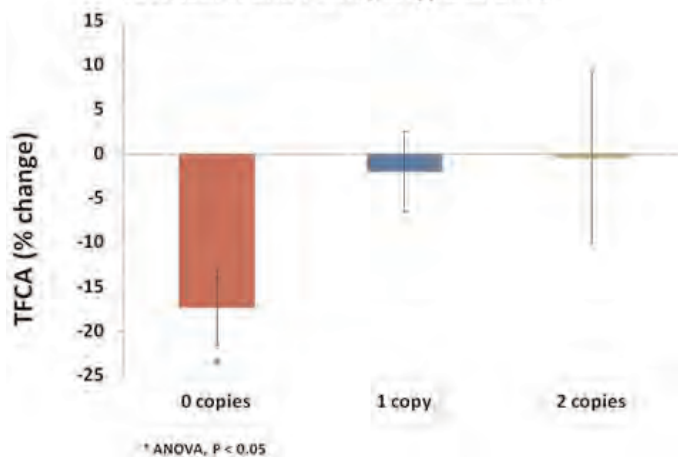
Disclosures: Hongwei Wang, None.

MO0157

Estrogen Receptor- α Gene Haplotypes Influence Calcium Absorption during Caloric Restriction. Brian Chang^{*}, Deeptha Sukumar, Hasina Ambia-Sobhan, Muhammad Naem, Derek Gordon, Sue Shapses. Rutgers University, USA

It is estimated that greater than 70% of the variance in calcium absorption is due to genetic variation. There is evidence that vitamin D receptor (*VDR*) gene polymorphisms will influence absorption during low Ca intake, yet the influence of estrogen receptor- α (*ESR1*) gene polymorphisms on Ca absorption has not been extensively examined. Ca absorption is attenuated during caloric restriction and our primary goal was to determine whether haplotypes of the *ESR1* and *VDR* gene polymorphisms influence the response. Body composition, bone mineral density (BMD using dual energy x-ray absorptiometry), serum parathyroid hormone (PTH), 25-hydroxy vitamin D (25OHD), estradiol and true fractional calcium absorption (TFCA using dual stable isotopes) were measured in 211 women (ages 36-75 y; BMI: 31.8 \pm 7.4 k/m²) and in a subgroup of postmenopausal women (n = 46) after 6 weeks of caloric restriction. Genotypes for the *VDR* (*BsmI*, *ApaI*, *TaqI*) and the *ESR1* (*XbaI*, *PvuII*) polymorphisms were determined through PCR-RFLP analysis and the common *VDR* (BaT, baT, baT) and *ESR1* (px, Px, PX) haplotypes were reconstructed using PHASE v2.1.1. We used 1-way ANCOVA, including age, body mass index, and serum 25OHD levels as covariates with post-hoc analyses to determine how the *VDR* and *ESR1* haplotypes predicted the variations in fractional Ca absorption (dual stable isotopes), PTH, and BMD. In the entire population, there was lower BMD at the femoral neck and total body (p < 0.05) in women with 2 copies of the baT allele. Serum PTH was higher (p < 0.05) and TFCA was higher, but not significantly, in women with two copies of the *ESR1* PX allele. After 6 weeks of caloric restriction, ANCOVA (Δ weight covariate), showed that women without copies of the PX allele (p < 0.05) have the largest decrease in TFCA (Figure). Overall women with the baT allele (2 copies) have lower BMD at multiple bone sites which is consistent with previous studies. In addition, only those women without copies of the *ESR1* PX allele reduce TFCA in response to caloric restriction. This could suggest the need for higher dietary calcium or vitamin D depending on the presence of the PX allele. Support: NIH-AG12161

Calcium absorption change with caloric restriction and PX haplotype of *ESR1*



Postmenopausal women

Disclosures: Brian Chang, None.

MO0158

OPG Gene Polymorphisms 1181G>C and 245T>G Associated with Vertebral Fractures in a Community-dwelling Elderly: The Sao Paulo Ageing & Healthy Study (SPAHS). Rosa Pereira^{*1}, Valéria Caparbo², Soledad Matamouros², Caroline Cha², Jaqueline Lopes¹, Camille Figueiredo², Isac Castro³, Ricardo Oliveira⁴, Luiz Onuchic², Ciro Martinhago⁴. ¹Faculdade de Medicina da Universidade de São Paulo, Brazil, ²Faculdade de Medicina da USP, Brazil, ³Nephrology, Faculdade de Medicina da USP, Brazil, ⁴RDO Diagnósticos Médicos, Brazil

Introduction: Osteoprotegerin (OPG), a secreted member of the tumor necrosis factor receptor family, is a potent inhibitor of osteoclast activation and differentiation. With this key role in the control of resorptive activity, OPG is a candidate gene for genetic control of bone mass and fractures. Vertebral fractures have important clinical implication for future fracture risk, including hip fractures and are associated with an increase of mortality in the following decades. There are no studies analyzing OPG gene polymorphism in a Brazilian community-dwelling elderly.

Objective: To evaluate the OPG gene polymorphism and OPG serum levels and its association with vertebral fractures in a Brazilian community-dwelling elderly.

Material and methods: 815 elderly subjects (510 women and 305 men) living in São Paulo, Brazil were genotyped for the presence of OPG gene polymorphism 1181G>C (rs2073618), 245T>G (rs3134069), 163C>T (rs3102735), 209G>A (rs3134070). OPG serum levels were measured by ELISA (Biomedica, Vienna, Austria). Vertebral fractures (VF) were evaluated by thoracic and lumbar spine radiographs using Genants semiquantitative methods (Grade 0 - no fracture, Grade 1 - reduction of 20-25% of anterior, mild and/or posterior height, Grade 2 - reduction of 26-40% in any height; Grade 3 - reduction of over 40% in any height).

Results: Vertebral fractures were found in 32.9% of subjects (14.6% Grade 1, 14.5% Grade 2, 3.4% Grade 3). The prevalence of genotypes containing the 1181 C allele (CG and CC) was lower in the group of patients with vertebral fractures (Grade 2 or 3) compared to the group of subjects without vertebral fractures (Grade 0) (52.1 vs. 63.0%, p=0.017). Moreover, the frequency of the genotypes containing the 245 G allele (GC and GG) was higher in the patients with vertebral fractures (Grade 2 or 3) comparing to patients with vertebral fractures (Grade 1) (22.6 vs. 12.2%, p=0.026). No difference was found regarding 163C>T and 209G>A OPG polymorphisms and the presence of vertebral fractures (p>0.05). Concerning osteoprotegerin serum levels, all OPG gene polymorphisms studied did not influence these levels (p>0.05).

Conclusion: Our data demonstrate that 1181 C is a protector allele against development of VF and 245 G allele consists in a risk factor for the severity of VF development in a Brazilian community-dwelling elderly.

Disclosures: Rosa Pereira, None.

This study received funding from: #09/11755-7

MO0159

Linker Regions of Smad1/5/8 Regulate Bone-inducing Activity of BMPs. Sho Tsukamoto^{*1}, Satoshi Ohte², Katsumi Yoneyama¹, Mai Fujimoto¹, Arei Miyamoto¹, Eiko Murata³, Ejiro Jimi⁴, Takenobu Katagiri⁵. ¹Saitama Medical University RCGM, Japan, ²Saitama Medical University, Research Center for Genomic Medicine, Japan, ³Saitama Medical University, Faculty of Health & Medical Care, Japan, ⁴Kyushu Dental College, Japan, ⁵Saitama Medical University Research Center for Genomic Medicine, Japan

Smads are critical transcription factors for the TGF-beta family. Smad proteins consist of conserved MH1 and MH2 domains, which are required for DNA binding and interaction with other proteins, respectively. The linker region flanked these N- and C-terminal domains to regulate their functions. BMP and TGF-beta/Activin receptors phosphorylate Smad1/5/8 and Smad2/3, respectively, at two Ser residues in the Ser-Val/Met-Ser (S-V/M-S) motif of the MH2 domains. We have shown that a substitution mutation of the S-V-S motif in Smad1 with D-V-D activated constitutively the transcription of a target gene and osteoblastic differentiation of C2C12 cells. The constitutively activated Smad1 allowed us to elucidate its specific role in BMP signal transduction without activating other signaling pathways. In the present study, we examined the roles of each Smad in BMP/TGF-beta signaling by establishing constitutively active Smad1/2/3/5/8. The mutant Smad5 was active equivalent to mutant Smad1 in the activation of BMP-specific luciferase reporters and osteoblastic differentiation of C2C12 cells, although mutant Smad8 was much weaker than Smad1/5. In contrast to Smad1/5/8, mutant Smad2/3 did not activate osteoblastic differentiation of C2C12 cells and activated only TGF-beta/Activin-specific reporters. Smad8 has more than 90% homology with Smad1/5 in both MH1 and MH2 domains but only 40% homology in the linker region. Substitution of the linker region of Smad8 with that of Smad1 or Smad5 increased the transcriptional activity of Smad8. Taken together, these findings suggest that the bone-inducing activity of BMPs may be transduced via Smad1/5, but less via Smad8. The structural difference in linker region between Smad1/5/8 regulates their biological activities.

Disclosures: Sho Tsukamoto, None.

MO0160

LPS Inhibits Ectopic Bone Formation Induced by BMP-2 plus TGF-β1 in Mice. Akifumi Matsumoto^{*1}, Masamichi Takami², Arei Miyamoto³, Keita Tachi², Tetsuo Suzawa², Kazuyoshi Baba², Ryutaru Kamijo². ¹Showa University, Japan, ²Showa University School of Dentistry, Japan, ³Saitama Medical University, Research Center for Genomic Medicine, Japan

We previously reported that TGF-β1 strongly enhances ectopic and orthotopic bone formation induced by BMP-2, which would be beneficial for performing bone regenerative treatments such as alveolar bone reconstruction in periodontitis patients. However, affected patients often have bacterial infection in periodontal tissues that may affect bone regeneration induced by BMP-2 and TGF-β1. To examine the effects of bacterial infection on bone formation, we implanted collagen sponges containing BMP-2 (5 mg/sponge), TGF-β1 (50 ng/sponge), and various amounts of LPS (0, 0.5, 1.0, 3.0 mg/sponge) under the fascia of the latissimus dorsi muscles of mice (male, 6 weeks old). After 14 days, LPS reduced the volume of ectopic bone formed in a dose-dependent manner. The total volume of ectopic bone induced by BMP-2 + TGF-β1 with administration of 1 mg of LPS was less than 25% of that induced in the control group, while LPS also reduced the volume of ectopic bone induced by BMP-2 alone (5 mg/sponge). Histological analysis of ectopic bone tissue formed in the presence of LPS (1 mg/sponge) revealed that bone volume/tissue volume (BV/TV) and trabecular bone thickness (Tb.Th) were significantly decreased, while trabecular spacing (Tb.Sp) was significantly increased. Interestingly, osteoblast number (N.Ob/BS) and osteoid volume (OV/BV) were significantly increased, while osteoclast number (N.Oc/TV) did not change. Since LPS induces production of TNF-α, which is known to inhibit chondrogenesis and osteoblast differentiation, we implanted collagen sponges containing BMP-2 (5 mg/sponge), TGF-β1 (50 ng/sponge), and LPS (1 mg/sponge) into TNF-α deficient mice. However, LPS reduced the volume of ectopic bone in both the wild-type and TNF-α deficient mice. These results suggest that LPS suppresses ectopic bone formation induced by BMP-2 and TGF-β1 in mice independent of TNF-α production.

Disclosures: Akifumi Matsumoto, None.

MO0161

Mesenchymal Stem Cell-derived BMP2 Regulates Endosteal SDF1-Cell Osteoblastic Differentiation. Timothy Myers^{*1}, Lara Longobardi², Tieshi Li², Ying Li³, Joseph Temple¹, Anna Spagnoli². ¹University of North Carolina, USA, ²University of North Carolina at Chapel Hill, USA, ³UNC School of Medicine, USA

We and others have consistently reported that bone marrow (BM) mesenchymal stem cells (MSC) transplanted into fracture mouse models improve healing and thus provide a potential therapy to treat fracture non-unions. However, the healing

mechanism remains unknown. Although transplanted MSC engraft within the fracture site only a small fraction differentiate into repairing cells. This suggests that the more substantial effect of MSC is due to the release of paracrine-acting factors such as BMP2. BMP2 is expressed early in fracture healing and mice lacking BMP2 in mesenchyme limb progenitor cells lack fracture repair. Here we show that mice haploinsufficient for BMP2 in early limb mesenchyme using Prx1Cre-mediated recombination (BMP2^{+/-}) with a stabilized tibia fracture had smaller calluses, less soft tissue, less new bone and weaker biomechanical properties than control mice (BMP2^{+/lox} or BMP2^{lox/lox}). When BM-MSC obtained from control littermates were transplanted into BMP2^{+/-} mice, formation of new bone, soft tissue and biomechanical strength were returned to wild type levels. Histological and BMP2 reporter imaging analyses revealed that transplanted MSC express BMP2 at the site of injury and uniquely along the endosteum. Furthermore, BMP2-expressing cells localized adjacent to SDF1-expressing cells along the endosteum. This is consistent with our previous work showing that MSC homing to the fracture site is dependent on the CXCR4-SDF1 signaling axis. To determine whether MSC-derived BMP2 regulates SDF1 expression and differentiation of SDF1-expressing cells into osteoblasts, we isolated SDF1-mRFP-expressing endosteal cells from hindlimb long bones of transgenic BAC mice encoding a SDF1-mRFP fusion protein. SDF1-mRFP-expressing endosteal cells were treated with either osteogenic differentiation medium with or without exogenous BMP2 or conditioned media (CM) from control MSC or MSC with shRNA targeted to BMP2. FACS analyses showed that the number of SDF1-mRFP positive cells decreased when cells were cultured with either BMP2-containing CM from MSC or exogenous BMP2 compared to controls. RT-PCR analyses for osteoblastic markers showed that this decrease was associated with an increase of marker expression. These results suggest that MSC-derived BMP2 is sufficient to restore fracture healing in BMP2-deficient mice through the paracrine regulation of endogenous SDF1-expressing pre-osteoblastic cells leading to increased new bone formation.

Disclosures: Timothy Myers, None.

MO0162

Stromal Cell-derived Factor-1β mediates Bone Morphogenetic Protein Receptor Signaling, Chemotaxis, and Apoptosis-Resistance via Enhancing Autophagy in Murine Mesenchymal Stem Cells *in vitro*. Samuel Herberg^{*1}, Xing-Ming Shi¹, Wendy Bollag¹, Mark Hamrick¹, Carlos Isales², William Hill³. ¹Georgia Health Sciences University, USA, ²Medical College of Georgia, USA, ³Georgia Health Sciences University & Charlie Norwood VAMC, USA

Purpose: Increasing evidence suggests that stromal cell-derived factor (SDF)-1 is involved in bone formation. The underlying molecular mechanisms, however, have not yet been fully elucidated. Recently, we described genetically engineered bone marrow-derived mesenchymal stem cells (BMSCs) that conditionally overexpress SDF-1b, the less abundant but more potent splice variant compared to SDF-1a. We showed that SDF-1b enhances *in vitro* mineralization and increases mRNA and protein levels of key osteogenic markers during bone morphogenetic protein (BMP)-2-stimulated osteogenic differentiation of BMSCs. In this study, we tested the hypothesis that SDF-1b mediates BMP receptor signaling, chemotaxis, and apoptosis-resistance of BMSCs *in vitro*.

Methods: BMP receptor signaling was assessed by Western blot. Serum-starved BMSCs were pretreated with 600 μM AMD3100, 50 μM U0126, or vehicle for 4 h prior to stimulation with 300 ng/ml BMP-2 for 30 min. Whole cell lysates were subjected to SDS-PAGE, electroblotted onto PVDF membranes, and probed for (p)Erk1/2 and (p)Smad1/5/8. Transwell migration assays were performed using conditioned media from genetically engineered BMSCs in lower chambers. Serum-starved Jurkat cells or BMSCs at 5.0-8.0x10⁵ cells/ml in upper chambers were allowed to migrate across the 8-μm membranes for 4-8 h prior to quantifying total DNA with CyQuant GR dye at 485/535 nm. Apoptosis was induced with 1.0 mM H₂O₂ for 6 h. Cell death was quantified by trypan blue staining and Western blot analysis of cleaved caspase-3 and PARP. Autophagy was evaluated by Western blot for LC3-II.

Results: SDF-1b significantly potentiated Smad1/5/8-mediated BMP-2 signal transduction in genetically engineered BMSCs via Erk1/2 phosphorylation (p<0.05). Pretreatment with the CXCR4 antagonist AMD3100 or the specific MEK1/2 inhibitor U0126 abolished this effect. SDF-1b, independent of SDF-1a, significantly promoted the migratory response of CXCR4-expressing Jurkat cells and BMSCs (p<0.01). SDF-1b mediated significant apoptosis-resistance in genetically engineered BMSCs (p<0.001). The greater number of surviving cells was found to be a result of enhanced autophagy.

Conclusion: These data suggest that SDF-1b may exert its biological activities during osteogenic differentiation of BMSCs in both an autocrine and paracrine fashion. Future studies will examine the use of these genetically engineered BMSCs in acute and chronic bone injury models.

Disclosures: Samuel Herberg, None.

MO0163**Trends in Nonunion Incidence and Correlation with NSAID Use in the United States from 1996 to 2009.** John Wang*¹, Timothy Bhattacharyya².¹Intramural Research Program, NIAMS/NIH, USA, ²Intramural Research Program, NIAMS/NIH, USA

Background: Surgical care for bone fractures has improved in the last decade. We sought to ascertain if there were any changes in the incidence or treatment of nonunions and whether such changes were correlated with NSAID use.

Methods: The Nationwide Inpatient Sample (NIS) was used to estimate the number of patients hospitalized for surgical treatment of a nonunion from 1996 to 2009. We calculated age and population adjusted rates and compared overall and fracture-site-specific trends. We then used segmented regression time-series analysis to correlate quarterly estimates in nonunions with changes in the use of NSAIDs, particularly COX-2-inhibitors as measured using Medical Expenditure Panel Survey (MEPS).

Results: Nonunions in the U.S. declined significantly from a peak of 25,426 in 2003 to 20,984 in 2009 (p=0.007). Similar declining patterns were observed for tibia, humerus and femur, whereas nonunions at the radius and spine declined markedly. Use of autograft for nonunions declined somewhat while BMP use rose markedly. Between 2000 and 2004, there was a significant peak in nonunion incidence that correlated strongly with the introduction and withdrawal of COX-2 inhibitors (p<0.0001). Overall, the rate of nonunions per 100 fractures has declined from 2.5% in 1996 to 2.2% in 2009 (p<0.0001).

Conclusions: From 1996 to 2009, a steady and significant decline in incidence of nonunions in the United States was interrupted by an increased trend from 2000 to 2004, which correlated significantly with the introduction and later withdrawal of COX-2 inhibitors.

Disclosures: John Wang, None.

MO0164**Selective Knockout of HMWFGF2 Isoforms in Mice Increases Serum Phosphate and Increases Bone Formation In Vivo and In Vitro.** Liping Xiao*¹, Thomas Doetschman², Marja Marie Hurley³.¹University of Connecticut Health Center, USA, ²University of Arizona, USA, ³University of Connecticut Health Center School of Medicine, USA

HMWFGF2 transgenic mice (HMWTg) were created by overexpressing nuclear high molecular weight isoforms of FGF2 (HMW) in osteoblastic lineage (Xiao and Hurley, J. Biol Chem, 2010). The phenotype of HMWTg mice includes reduced bone mineral density (BMD) hypophosphatemia and increased serum FGF23 as well as increased Fgf23 mRNA and protein in bone. Decreased mineralization was also observed in vitro in bone marrow stromal cell (BMSC) cultures from HMWTg mice compared with VectorTg mice. Since we observed abnormalities in bone mineralization both in vivo and in vitro in HMWTg mice, we hypothesized that knockout of HMW isoforms (HMWKO) should modulate the phenotypic changes observed in HMWTg mice. The generation of HMW-deficient (HMW^{-/-}) mice was previously described (Azhar and Doetschman Dev. Dyn 2009). In order to determine the phenotypic effects of HMW deficiency, BMD, in vitro bone formation and serum phosphate were determined in 2-month-old male HMW^{-/-} mice versus WT littermates. BMD was assessed by DXA. To determine mineralized bone formation in vitro, BMSCs from both genotypes were cultured under osteogenic conditions. The cells were harvested on day 7, 14 and 21 to assess early osteoblastic differentiation by alkaline phosphatase (ALP) staining and mineralized nodule formation by von Kossa staining. To determine whether there were alterations in biochemical markers, serum was collected from WT, heterozygote (HMW^{+/-}) and HMW^{-/-} mice to measure serum phosphate and calcium. In contrast to HMWTg mice, which had decreased BMD, DXA analysis showed that HMW^{-/-} mice have significantly increased femoral BMD by 15% compared with WT. In vitro bone formation studies showed that, in contrast to decreased mineralized bone nodule formation observed in HMWTg BMSC cultures, there was a significant increase in ALP positive colony area of 28% at 1 week of culture in HMW^{-/-} cultures compared with WT. By 3 weeks of culture, mineralized area was significantly increased by 25% in BMSC cultures from HMW^{-/-} mice compared with WT. In contrast to the hypophosphatemia observed in HMWTg mice, we observed a progressive increase in serum phosphate in HMW^{+/-} and HMW^{-/-} mice compared to WT. Similar to our finding in HMWTg mice, there was no change in serum calcium between WT and HMW^{-/-} mice. Our data in HMWKO mice are consistent with the corresponding HMWTg mouse phenotypes suggesting that HMWFGF2 isoforms have negative biological functions in bone and phosphate homeostasis in mice.

Disclosures: Liping Xiao, None.

MO0165**Disruption of PTH/PTHrP Receptor in Osteocytes does not Affect Hematopoiesis.** Keertik Fulzele*¹, Cristina Panaroni², Vaibhav Saini³, Xiaolong Liu⁴, Kevin Barry⁴, Joy Wu⁴, Paola Pajevic Divieti⁵.¹Massachusetts General Hospital; Harvard Medical School, USA, ²Endocrine Unit, Massachusetts General Hospital, USA, ³MGH, Harvard Medical School, USA, ⁴Massachusetts General Hospital, USA, ⁵MGH- Harvard Medical School, USA

The two major branches of hematopoietic cells, lymphoid and myeloid cells, are continuously replenished through lineage commitment of hematopoietic stem cells. These events are coordinated by intrinsic as well as extrinsic factors from cells of the bone marrow (BM) microenvironment. Dominant myeloid lineage commitment and expansion, sometimes at the cost of lymphoid lineage, occurs during 'emergency granulopoiesis' in response to infection or a disease condition such as myeloproliferative syndrome (MPS). Very little is known about the contribution of the cells of BM microenvironment in such lineage commitment and disease progression. Previously we have demonstrated that osteocytes lacking the stimulatory subunit of G-proteins (G α) secrete factors that promote preferential myeloid lineage commitment and expansion. Most notably, mice lacking Gsa in osteocytes (OCY-G α KO) showed a dramatic increase in myeloid cells in peripheral blood, bone marrow and spleen, a phenotype resembling that of MPS. Microarray analysis has shown that osteocytes express more than 150 G-protein coupled receptors (GPCR). Among these receptors, PTH/PTHrP receptor (PPR), which signals through Gsa, is the most well studied GPCR in osteocytes. Here we hypothesized that PPR signaling is responsible for the osteocyte-mediated myeloid cell expansion. To test this, we engineered mice lacking PPR in osteocytes (OCY-PPRKO) by mating PPR-floxed mice with DMPI-Cre mice. In contrast to the complete blood count profile of peripheral blood from OCY-G α KO mice, OCY-PPRKO mice showed no changes in the numbers of leukocytes, neutrophils, lymphocytes, and platelets as compared to controls (p=NS, N \geq 8). Immunophenotypic analysis of mature hematopoietic cells by flow cytometry analysis of bone marrow and spleens of control and OCY-PPRKO mice showed no difference in the percentage of granulocytes, monocytes, macrophages, erythrocytes, B-cells, and T-cells (p=NS, N \geq 8). The addition of conditioned media from 7-day cultures of osteocyte-enriched bone explants (OEBE) from control mice onto bone marrow cells increased myeloid colonies (p<0.01, N=3). However, in contrast to OCY-G α KO mice, OEBE conditioned media from OCY-PPRKO mice did not further increase myeloid colony formation (p=NS, N=3). Taken together, these results show that PPR signaling in osteocytes is not responsible for myeloproliferative factors secreted by G α -deficient osteocytes.

Disclosures: Keertik Fulzele, None.

MO0166**Increased Activity Is Associated with Higher Osteocalcin in Children and Adolescents.** Saydi Chahla*¹, William Thomas², Brigitte Frohner², Aaron S. Kelly², Brandon Nathan², Lynda E. Polgreen².¹University of Minnesota Medical School, USA, ²University of Minnesota, USA

Background. The mechanisms for the protective effects of physical activity on obesity and insulin sensitivity are not fully characterized. One potential mediator is osteocalcin (OCN), a protein secreted from osteoblasts. Like physical activity, increased OCN is associated with increased insulin sensitivity and decreased adiposity. Therefore the goal of this study was to determine the associations between physical activity and OCN.

Methods. Healthy children, aged 9-17 years, were recruited for the study. General physical activity score was measured by the Physical Activity Questionnaire for Older Children (PAQ-C) for participants age 8-13 years and the Physical Activity Questionnaire for Adolescents (PAQ-A) for participants age 14-17. Serum total intact osteocalcin (iOCN), bone-specific alkaline phosphatase (BSAP) and N-telopeptide (NTx) were measured by EIA. Percent body fat was measured by dual-energy x-ray absorptiometry (DXA).

Results. 49 healthy participants (55% female) age 9-17 years with mean BMI SDS 1.1 (range -1.5 to 2.8) participated. General physical activity score was positively associated with iOCN (r=.46, p=.001) but not associated with BSAP or NTx. This association remained significant after adjustment for percent body fat, age and gender (r=.31, p=.04).

Conclusions. Increased physical activity was specifically associated with increased OCN, but not another marker of bone formation (BSAP) or a marker of bone resorption (NTx). Direct measures of physical activity and insulin resistance are needed to further explore the role of OCN in the protective effects of physical activity on obesity and insulin sensitivity.

Disclosures: Saydi Chahla, None.

MO0167

Intercellular Adhesion Molecule 1 Deficiency Leads to Impaired Neutrophils Recruitment and Increased Tissue Destruction in Endodontic Infection. Andiara De Rossi¹, Raquel Silva², Sandra Fukada³, Lea Assed Bezerra da Silva¹, Marcos Antonio Rossi⁴. ¹Faculty of Dentistry of Ribeirão Preto, University of São Paulo, Brazil, ²School of Dentistry of Ribeirão Preto - University of São Paulo, Brazil, ³Faculty of Pharmaceutical Sciences of Ribeirão Preto, University of São Paulo, Brazil, ⁴ Faculty of Medicine of Ribeirão Preto, University of São Paulo, Brazil

Intercellular adhesion molecule-1 (ICAM-1) plays important role in several inflammatory skeletal diseases, by mediating transmigration of inflammatory cells to the sites of infection, and osteoclastogenesis, by providing adhesion between osteoblasts and osteoclast precursors. Aiming to investigate the specific role of ICAM-1 in modulation of host immune response to endodontic infection, we used a well-established model of endodontic disease in mice. Periapical lesions were induced in wild-type and ICAM-1 knockout mice by occlusal crown access and root canal exposure from the mandibular first molars, which were left open to the oral environment. The obtained lesions were evaluated at different stages of development by conventional and fluorescence microscopy, immunohistochemistry (inflammatory cells), immunofluorescence (RANK, RANKL and osteoprotegerin - OPG) and enzyme histochemistry (osteoclasts). Our results show that at days 21 and 42 following pulp infection ICAM-1 knockout mice presented significantly greater bone resorption than WT mice, quite similar to the increase observed in the number of osteoclasts and in the expression of RANK/RANKL/OPG. The recruitment of neutrophils to periapical inflammatory tissues was lower in ICAM-1 than WT mice. Overall, the data demonstrate that ICAM-1 play a protective role in endodontic infection, at least partially associated with neutrophils recruitment to the sites of infection.

Disclosures: Andiara De Rossi, None.

MO0168

Myeloid-derived Suppressor Cells as Key Immune Regulators of Non-union Fractures. Seth Levy¹, anadi sawant², Selvarangan Ponnazhagan¹. ¹The University of Alabama At Birmingham, USA, ²University of Alabama at Birmingham, USA

Every year in the United States there are more than 6 million fractures; approximately 10% of fractures demonstrate delayed healing or develop into non-union fractures. The event of osteogenesis following fractures depends on, and is influenced greatly by associated vasculogenesis and stimulatory signals in the bone microenvironment, including an influx of immune cells in the fracture site. The hypoxic microenvironment aids in the survival of many immune cell types, demanding understanding of the role of infiltrating immune cells in non-union fractures and possibly targeting them if found they are involved in the cascade of signaling leading to non-union fractures. To better understand the significance of immune cells in fracture healing, we have evaluated the immune cell populations that play a key role during stages of fracture healing in an immunocompetent mouse model of femoral fracture. Results of these studies so far indicate that during the initial phase of fracture healing there is a dramatic increase in the number and percentage of myeloid-derived suppressor cells (MDSC) in the fracture area followed by a decrease in the number of MDSC as the fracture heals. MDSC are a heterogeneous subpopulation of immune cells that are known to survive in hypoxic environment, promote angiogenesis, and suppress a variety of lymphocyte populations. These data suggests that MDSC may play a significant role in regulating the activity of many infiltrating immune cells and their impact on bone biology. Comparative studies have been performed utilizing gemcitabine to selectively decrease the levels of MDSC present in the bone marrow and results of this study indicate that mice with MDSC ablation show delayed healing, confirming that MDSC indeed play a vital role in normal fracture healing. The effect of lymphocytes on bone growth after fracture is well documented; however, there is still a lack of understanding in how these cells are regulated to either aid in healing or how those immune cells which negatively affect bone growth are suppressed. This study may will not only lead to an understanding of how regulatory immune cells help delineate those fractures that heal versus which fractures form non-union, but may also lead to novel therapeutic targets that may increase fracture healing, preventing the formation of non-unions.

Disclosures: Seth Levy, None.

MO0169

Myostatin Serum Concentrations are Decreased with Vitamin D Supplementation in Black, but not White, Children. Paige Berger¹, Norman Pollock², Emma Laing¹, Matthew Bowser³, Mark Hamrick², Carlos Isaacs⁴, Stephanie Foss¹, Connie Weaver⁵, Munro Peacock⁶, Stuart Warden⁷, Kathleen Hill⁸, Richard Lewis¹. ¹The University of Georgia, USA, ²Georgia Health Sciences University, USA, ³Georgia Health Science University, USA, ⁴Medical College of Georgia, USA, ⁵Purdue University, USA, ⁶Indiana University Medical Center, USA, ⁷Indiana University, USA, ⁸Indiana University School of Medicine, USA

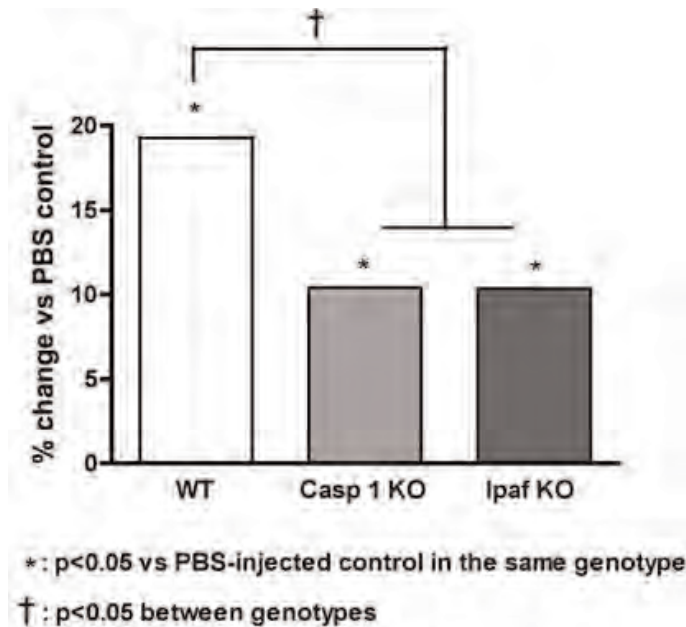
Myostatin inhibits muscle differentiation and growth, while follistatin is an antagonist to myostatin. Animal and cell culture data have identified a vitamin D-regulated pathway for muscle regulation via myostatin and follistatin; however, no interventions have been conducted regarding vitamin D and these proteins in humans. This study investigated the effect of vitamin D supplementation on serum concentrations of muscle-related outcomes [i.e., myostatin, follistatin, insulin-like growth factor-I (IGF-I)], 1,25(OH)₂D and parathyroid hormone (PTH) in youth. A sample of black and white children (N=40, aged 9-13 years, 50% female) received either placebo (n=20) or 4,000 IU vitamin D₃ (n=20) per day for 12 weeks. Serum myostatin, follistatin, and IGF-I were measured using ELISA, and PTH and 1,25(OH)₂D were measured using IRMA and RIA, respectively. Because of racial differences in 25(OH)D concentrations, analyses were conducted separately for black and for white participants. Analyses of covariance tested group differences on outcome variables at posttest, adjusting for pubertal stage, sex and baseline value. In black children, myostatin and PTH were lower and 1,25(OH)₂D was higher following supplementation with the 4,000 IU dose vs. placebo (all p<.02). These changes in myostatin concentrations in black children were positively associated with changes in PTH (r=.41) and negatively with 1,25(OH)₂D (r=-.40; both p<.05). No effect of supplementation was observed for follistatin or IGF-I in the black children, and there was no effect of vitamin D supplementation on the muscle-related outcomes, PTH or 1,25(OH)₂D in the white children. Results from this vitamin D intervention suggest a role for myostatin suppression in black children, which may be explained via actions of PTH and 1,25(OH)₂D.

Disclosures: Paige Berger, None.

MO0170

NLR4 Inflammasome and Bone Loss in Experimental Periodontal Disease. João Chave De Souza¹, Marcell Costa de Medeiros¹, Fernanda Regina Godoy Rocha¹, Sabrina Cruz Tfaile Frasnelli¹, Morgana Rodrigues Guimarães¹, Mario Julio Ávila Campos², Dario Simões Zamboni², Carlos Rossa³. ¹UNESP, Brazil, ²USP, Brazil, ³School of Dentistry at Araraquara - Univ Estadual Paulista (UNESP), Brazil

Periodontal disease is the most prevalent lytic disease of bone in humans. It is initiated and maintained by microorganisms in the dental biofilm, but most of the tissue damage is mediated by the immune response to these microorganisms. Inflammasomes are multi-protein complexes that include a nucleotide-oligomerization domain leucine-rich repeat containing receptor (NLR), caspase-1 and an adaptor protein. These complexes participate in the sensing of microbial (MAMPs) and tissue damage (DAMPs)-derived molecular patterns by the innate immunity. Caspase-1 is the central effector molecule in these protein complexes and participates in the processing of inflammatory cytokines and apoptosis. NLR4 (Ipaf) inflammasome is expressed in myeloid cells and participates in the immune response to Gram-negative bacteria presenting a type III or IV secretory system; but its role on the bone resorption associated with periodontal infection has not been investigated. Our hypothesis is that the NLR4 inflammasome has an important role in the immune response associated with destructive periodontal disease and affects alveolar bone resorption. We used mice genetically deficient for Ipaf and Caspase-1 in a C57/Bl6 background and also wild-type mice of the same strain as controls. Periodontal disease was induced by injections of PBS suspensions of heat-killed Gram-negative *Aggregatibacter actinomycetemcomitans* (Aa) (3x10⁶ UFC) in the palatal mucosa adjacent to the first molar. Controls received injections of the same volume of PBS diluent. Injections were performed 3x/week under inhalation anesthesia and all animals were killed after 15 days (6 injections). The maxillae were dissected, fixed in 10% buffered formalin for 24 h and transferred to 70% ethanol. Bone resorption was assessed by microcomputer tomography using 18 µm slices. A standardized region of interest (ROI) of 2 mm² (2 mm in mesio-distal width and 1 mm in the apico-coronal direction) was created on the middle section between the buccal and palatal aspects of the first molar. This ROI included the teeth plus 180 µm towards the middle of the palate, in a total volume of 3,200 µm³. In WT mice injections of Aa produced significant (p<0.05) bone loss, which was markedly reduced in NLR4 and Caspase-1 KO knockout mice. We conclude that NLR4 inflammasome and Caspase-1 have important roles in the bone resorption associated with periodontal infection.



Disclosures: João Chave De Souza, None.

MO0171

Osteocalcin Is Associated with Adiposity but not Insulin Sensitivity as Measured by IVGTT in Healthy Children and Adolescents. Lynda E. Polgreen^{*1}, William Thomas¹, Brigitte Frohnert¹, Saydi Chahla², Aaron S. Kelly¹, Brandon Nathan¹. ¹University of Minnesota, USA, ²University of Minnesota Medical School, USA

Background. Osteocalcin (OCN) has been positively associated with insulin sensitivity (Si) in adults and children. However, such studies have used surrogate measures of Si (i.e. HOMA) rather than direct measures, such as frequently sampled IV glucose tolerance testing (IVGTT), leaving some doubt to this association. The goal of this study was to determine if OCN was associated with Si measured by IVGTT.

Methods. Healthy children, aged 9-17 years were recruited for the study and underwent an IVGTT and dual-energy x-ray absorptiometry (DXA). Serum total intact osteocalcin (iOCN), carboxylated osteocalcin (gla-OCN), bone-specific alkaline phosphatase (BSAP) and N-telopeptide (NTx) were measured by EIA. Percent body fat was measured by DXA.

Results. 46 children and adolescents (54% female) with a wide range of BMI SDS (-1.5 to 2.8) participated. Gla-OCN was positively associated with Si ($r=.32$, $p=.03$); iOCN trended toward positive association with Si ($r=.26$, $p=.09$). After adjustment for percent body fat, there was no association between either gla-OCN or iOCN with Si. BSAP and NTx were not associated with Si or percent body fat. Percent body fat was negatively associated with gla-OCN ($r=-.44$, $p=.003$), iOCN ($r=-.39$, $p=.008$) and Si ($r=-.73$, $p<.001$).

Conclusions. Gla-OCN was associated with insulin sensitivity; however this association was dependent on adiposity. As HOMA is known to be strongly associated with adiposity, previously described relationships may reflect a strong association of OCN with adiposity rather than insulin sensitivity. Percent body fat was not associated with other markers of bone remodeling, suggesting a unique regulatory pathway between OCN and adiposity.

Disclosures: Lynda E. Polgreen, None.

MO0172

PDGFBB Promotes PDGFR Alpha-positive Cell Migration into Artificial Bone in vivo. Shigeyuki Yoshida^{*1}, Ryotaro Iwasaki², Hiromasa Kawana², Taneaki Nakagawa², Takeshi Miyamoto³. ¹Keio University, Japan, ²dentistry & oral surgery, Japan, ³Keio University School of Medicine, Japan

[Purpose] Bone defects caused by traumatic bone loss or tumor dissection are now treated with auto- or allo-bone graft, or sometime artificial bone transplantation. Large bone defects often cause difficulties in providing auto- or allo-graft bones and thus artificial bones are used to fulfill the bone defects. Implantation of artificial bones often results in bone affinity failure likely because the artificial bones contain no mesenchymal stem cells/pre-osteoblastic cells. Growth factors may induce cell migration into artificial bones, however, several growth factors are known to inhibit osteoblastogenesis. Thus we searched a growth factor, which induce cell migration but

not inhibit osteoblast differentiation. [Methods] Mouse osteoblastic cell line, MC3T3-E1, cells were seeded in 96-well tissue culture plates at a density of 1×10^4 cells/well. On achieving confluence, cells were cultured in α -MEM containing 10% FBS in the presence or absence of bone morphogenetic protein-2 (BMP-2) (300 ng/ml) with or without platelet derived growth factor BB (PDGFBB) (10 ng/ml), hepatocyte growth factor (HGF) (10ng/ml), fibroblast growth factor (FGF2) (10 ng/ml) and Transforming growth factor-beta1 (TGF-b1) (10ng/ml) for 72 hours. Thereafter, cells were subjected to realtime PCR. β -TCP was impregnated with or without 2 ug of PDGFBB, followed by implantation into hamstring muscles of mouse hind paws. At 3 and 7 days post-implantation, mice were euthanized by cervical dislocation, and β -TCP were dissected and subjected to histological analyses. [Results] We found that PDGFBB did not inhibit or even stimulated osteoblast differentiation shown by Alkaline Phosphatase (ALP), osteocalcin (OCN), Runt-related transcription factor 2 (RUNX2), and Osterix (OSX) expression compared with TGF β , HGF, and FGF. PDGFBB also promotes significant increase in migration of PDGF receptor alpha (PDGFR α)-positive mesenchymal stem cells/pre-osteoblastic cells into artificial bones *in vivo*. [Conclusion] These results suggest that combination of artificial bones and PDGFBB is of benefit to promote host cell migration into artificial bones without inhibiting osteoblastogenesis.

Disclosures: Shigeyuki Yoshida, None.

MO0173

Growth Hormone Deficiency and Bone. Peter Jackuliak¹, Martin Kuzma^{*2}, Juraj Payer³, Zdenko Killinger⁴, Peter Vanuga⁵, Zuzana Homerova², Tomas Koller², Sona Tomkova⁶, Ivica Lazurova⁷. ¹Slovakia, ²University Hospital Bratislava, Slovakia, ³University Hospital, Ruzinov, Slovakia, ⁴University Hospital, Slovakia, ⁵National Institute of Endocrinology & Diabetology, Slovakia, ⁶Nemocnica Kosice - Saca a.s., Slovakia, ⁷University Hospital Kosice, Slovakia

Background: Growth hormone deficiency (GHD) influences many of body functions, such as reduced bone mineral density (BMD), which leads to increased risk of osteoporotic fractures. Except its effect on longitudinal bone growth has growth hormone (mediated by IGF-I) potential to regulate bone remodeling.

Objectives: Prospective multicentre study to asses bone status after two years of recombinant growth hormone treatment.

Methods: 147 patients (84 men), age 18-61 yrs, 104 patients with adult onset of growth hormone deficiency (AO-GHD), 43 patients with childhood onset deficiency (CO-GHD). Patients had 6 etiologic types: after surgery, posttraumatic, idiopathic, and congenital, after radiotherapy and post inflammatory. Patients were treated with human recombinant growth hormone applied daily subcutaneously. IGF-I levels were in reference ranges. We assessed BMD (g/cm²) of lumbar spine, femoral neck and whole body by using conventional densitometry (device: Hologic Discovery) and laboratory markers of bone remodeling (osteocalcin – bone formation, CTx – bone resorption). Periods of measurement were at the baseline, at 3., 6., 12. and 24. month of treatment.

Results: The highest increase of BMD was recorded by L-spine (increase 13.7%, $p<0.0001$), preferably in men (14.6%, $p=0.037$). BMD of femoral neck increased about 13 % in patients with CO-GHD ($p=0.004$). Significant difference ($p<0.05$) in BMD based on number of other pituitary differences was confirmed by whole body BMD (the highest increase by patients with 1 more pituitary deficiency – increase 21 %). Both bone markers were increasing during whole 12 months of treatment. After that CTx (osteoresorption marker) has started to decline ($p<0.0001$). Positive correlation was observed between BMD and IGF-I ($R=0.319$; $p=0.0018$).

Conclusion: Two year therapy with recombinant human growth activated bone remodeling, what leads to increase of BMD in patients with adult GHD.

Disclosures: Martin Kuzma, None.

MO0174

Integrin Signaling Regulates the Skeletal Response to IGF-1. Candice GT Tahimic^{*1}, Roger K. Long², Takuo Kubota³, Chak Fong⁴, Alicia T. Menendez⁴, Hashem Elalieh⁴, Yongmei Wang⁵, Daniel Bikle⁶. ¹Endocrine Unit, San Francisco Veterans Affairs Medical Center / UCSF, USA, ²Department of Medicine, University of California, Davis, USA, ³Osaka University Graduate School of Medicine & Dentistry, Japan, ⁴Endocrine Unit, University of California, San Francisco / SF Veterans Affairs Medical Center, USA, USA, ⁵Endocrine Unit, University of California, San Francisco/VA Medical Center, USA, ⁶Endocrine Research Unit, Division of Endocrinology UCSF & VAMC, USA

Skeletal unloading pertains to the loss of weight bearing functions during prolonged injury or microgravity conditions of spaceflight. The profound effects of skeletal unloading include osteopenia resulting from diminished proliferation of osteogenic precursors and increased apoptosis of osteoblasts. We have proposed that disruption of the IGF-1 signaling pathway is one of the underlying causes of bone loss during skeletal unloading. We base this proposition on our observations that IGF-1 infusion fails to stimulate bone formation in unloaded bones and that bone marrow stromal cell (BMSC) cultures from unloaded bone fail to phosphorylate the IGF-1

receptor following IGF-1 administration and is incapable of activating downstream signaling pathways such as Akt and MAPK. In this current study, we postulate a critical role for integrin signaling in the response to IGF-1 in that these cells have significantly reduced levels of multiple integrin subunits, that pretreatment of BMSC cultures from loaded bones with echistatin, an antagonist of beta 1 and beta 3 integrins, recapitulates the unloading-induced resistance to IGF-1, and that siRNA knockdown of beta 1 and beta 3 integrins blocks IGF-1 signaling. Moreover, inhibition of Fak and Pyk2, non-receptor kinases that function in integrin signaling, result in a blunted phosphorylation response of the IGF-1 receptor following IGF-1 treatment and diminished Akt and MAPK phosphorylation. Taken together, our results show that integrin signaling regulates the response of osteogenic cells to IGF-1. Hence, interventions to maintain integrin signaling may be efficacious in preventing the loss of skeletal responsiveness to IGF-1 associated with skeletal unloading.

Disclosures: Candice GT Tahimic, None.

MO0175

A 220 Kb DNA Segment Spanning the Mouse *Tnfsf11* Transcription Unit and Its Upstream Regulatory Control Region Rescues the Pleiotropic Biologic Phenotype of the RANKL Null Mouse. Kathleen Bishop^{*1}, Erin Riley¹, Seong Min Lee¹, Joseph Goellner², Charles O'Brien³, J. Pike¹. ¹University of Wisconsin-Madison, USA, ²University of Arkansas for Medical Sciences, USA, ³Central Arkansas VA Healthcare System, Univ of Arkansas for Medical Sciences, USA

RANKL is a TNF α -like cytokine that is produced by mesenchymal lineage cells such as chondrocytes, osteoblasts and osteocytes and plays an essential role in bone development and remodeling. It is regulated by local inflammatory mediators such as TNF α , IL-1 and IL-6 and by systemic regulators such as 1,25(OH)₂D₃ and PTH. Recent studies suggest that RANKL also plays a role in the immune system and in mammary gland development, cardiovascular function, and thermoregulation. Aberrant RANKL expression also underlies bone loss diseases of various etiologies and is involved in breast cancer. These diverse biological roles suggest that expression of *Tnfsf11* (the RANKL gene) is exquisitely regulated. Our recent work *in vitro* and *in vivo* highlights this hypothesis; a complex set of at least ten distal *Tnfsf11* enhancers and other elements located up to 173 kb upstream of the gene's transcriptional start site integrates both cell-specific and factor-dependent regulation. To establish groundwork for further study of this gene *in vivo*, we used a recombineering method to fuse two large DNA segments that together contain both the *Tnfsf11* transcription unit and its control regions, introduced a luciferase reporter into the final 3' exon and created two transgenic strains of mice; both strains expressed RANKL in the appropriate tissues. Each strain was then crossed into the RANKL null mouse to assess the transgene's ability to rescue the null phenotype. RANKL null pups were born with and without the transgene in the expected ratios. RANKL null mice without the transgene were toothless and displayed a reduced growth pattern, closed marrow cavities, high BMD, and severe osteoporosis. They also exhibited defective lymph node organogenesis and hypertrophic spleen and thymus weights. Females were fertile but unable to lactate. RANKL null mice containing the *Tnfsf11* transgene derived from either of the two strains were normal and without any of the biological defects associated with the RANKL null phenotype. Indeed, pregnant female transgene-rescued mice exhibited appropriate mammary gland development as they were capable of normal lactation and mobilized sufficient calcium and phosphorus levels to produce viable healthy litters. We conclude that the mouse *Tnfsf11* gene locus identified originally through unbiased Chip-chip analysis can function as a transgene to fully restore tissue-wide and regulated expression of RANKL to the RANKL null mouse.

Disclosures: Kathleen Bishop, None.

MO0176

A Muscle Specific Factor Increases Survival of Dexamethasone-Stressed Osteocytes. Katharina Jähn^{*1}, Leticia Brotto¹, Nuria Lara¹, Chenglin Mo², William Guthel³, Mark Johnson⁴, Marco Brotto¹, Lynda Bonewald¹. ¹University of Missouri - Kansas City, USA, ²University of Missouri-Kansas City, USA, ³University of Missouri Kansas City, USA, ⁴University of Missouri, Kansas City Dental School, USA

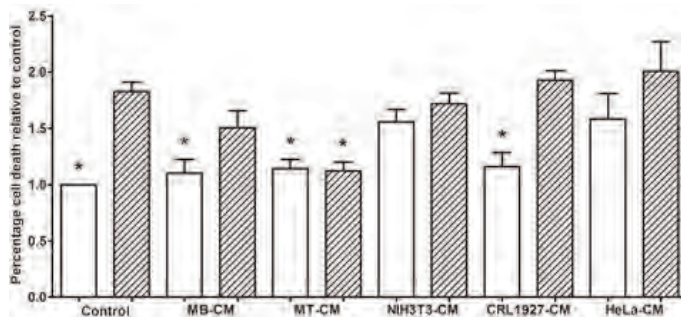
Exercise is beneficial for maintaining health, potentially through loading of both muscle and bone. We showed previously that mechanical loading induces the production of prostaglandin E₂ (PGE₂) by osteocytes, which protected these cells from glucocorticoid-induced apoptosis. Muscles have been shown to produce factors termed 'myokines' that are released into the muscle interstitial space and the global circulation. The hypothesis for the present studies is that muscle may also produce factors that would promote osteocyte viability. Osteocyte viability has been shown to be important for skeletal maintenance and function. In this study, MLO-Y4 osteocyte-like cells and primary osteocytes were exposed to conditioned media (CM) from C2C12 myotubes (MT), myoblasts (MB) or *ex vivo* working EDL and Soleus muscle that were electrically stimulated to produce either a twitch (1Hz) or tetanic force (80Hz). Cell death was quantified using Trypan Blue exclusion assay and cell apoptosis was determined using the nuclear fragmentation assay. MT-CM but not MB-CM protected against dexamethasone-induced MLO-Y4 apoptosis. EDL CM

from muscle stimulated at 80Hz was more potent than soleus CM stimulated at the same frequency and several magnitudes greater than CM from muscles stimulated at 1Hz.

Next we determined if the effects of the muscle CM were tissue specific. CM from MTs was compared to CM from HeLa epithelial cells, NIH3T3 fibroblasts, and CRL-1927 kidney mesangial cells for their ability to maintain osteocyte survival. Cell number/media volume was controlled for each cell type. No significant protective activity was found using non-muscle CM.

PGE₂ was not responsible for the protective effects of the muscle CM as muscle produces very low amounts that are insufficient to block apoptosis in this assay. In order to identify the active factor in MT-CM, we conducted experiments that indicate the active factor(s) is smaller than 10kDa, soluble in ethyl acetate and volatile. High pressure liquid chromatography (preparative C18 column, acetonitrile gradient) of ethyl acetate extracted CM showed active fractions could be collected. Mass spectrometric analysis of these fractions revealed peaks of 344, 353, 355 and 357 m/z that were only apparent in the MT not in the MB-CM.

These results support the concept that healthy, mature skeletal muscle promotes osteocyte survival upon exposure to dexamethasone through the secretion of muscle-specific factor(s).



MT-CM but not MB, NIH3T3, CRL or HeLa-CM protects against dexamethasone-induced cell death in MLO-Y4

Disclosures: Katharina Jähn, None.

MO0177

Animal Models of Sarcopenia: Orchidectomized Rat and Monkey Models. Aurore Varela^{*1}, Elisabeth Lesage¹, Nancy Doyle¹, Solomon Haile¹, Joseph Arezzo², Susan Y. Smith¹. ¹Charles River Laboratories, Canada, ²Albert Einstein College of Medicine, USA

Sarcopenia with aging is devastating for quality of life, and related healthcare expenditures are enormous. Androgens may indirectly affect musculoskeletal homeostasis through interaction with body composition and the GH-IGF-I axis. In aging humans, abnormalities in GH/IGF1 signaling may contribute to reduced functional efficiency in the muscle-bone system. This study evaluated the effects of orchidectomy (ORX) and testosterone depletion on muscle in aged Sprague-Dawley rats and cynomolgus monkeys (NHP).

Animals (10 six month-old male rats or 20 male NHP aged \geq 9 years old randomized by body weight (BW) or BMC) were ORX or Sham operated. In rats, fat/lean analysis by pQCT was measured at 0, 6 and 13 weeks at the proximal tibia metaphysis and diaphysis. Muscle weights were recorded at necropsy after 13 weeks. Conduction velocity was recorded in the mixed caudal nerve, the sensory digital nerve, and the distal motor branches of the tibial nerve innervating plantar muscles of the foot at 0, 6 and 12 weeks. In NHP, muscle mass was assessed by DXA, pQCT at 4, 8, 12 and 16 months post-ORX. Another subgroup of NHP (n=7) was used for muscle weight at necropsy 10 weeks post-ORX: tibialis cranialis, gastrocnemius, EDL (extensor digitorum longus), biceps brachii.

In rats, muscle area by pQCT was decreased 6% and 13% at Weeks 6 and 13, respectively, with no significant changes in muscle density or fat area. Paired muscle weights showed consistent trends for lower gastrocnemius and EDL weights by 4%. The induced changes in muscle were not associated with slowing of either sensory or motor nerve conduction velocity. In NHPs, BW decreased by 20% during the first 4 months after ORX and then stabilized. Muscle area decreased 18% compared to pre-ORX. There was no effect on % body fat. After 10 weeks, paired muscle weights showed lower biceps, gastrocnemius and EDL weights by 23, 25 and 21%, respectively, for ORX NHPs compared to shams.

The ORX rat and NHP are established models of osteoporosis with bone loss associated with increased bone turnover; the present study indicates that these models can also be valuable to evaluate androgenic compounds and agents that may modify androgen deprivation-induced sarcopenia. Associated with muscle biomarkers and muscle histomorphometry, these tests provide a comprehensive evaluation of muscle mass and function for preventing and treating muscle loss.

Disclosures: Aurore Varela, None.

MO0178

Withdrawn

MO0179

Burden and Medical Needs In Older Patients with Total Hip Arthroplasties and Muscle Atrophy or Weakness. Lindsay Hallett¹, Julia Green¹, Julie Birt², Yang Zhao³, Talia Foster¹, Russel Burge^{*2}. ¹United Biosource Corporation, USA, ²Eli Lilly & Company, USA, ³Eli Lilly, USA

Purpose: Incidence of total hip arthroplasties (THA) increased by 25-50% since the early 1990s in developed countries. Among patients undergoing these invasive operations, preoperative muscle atrophy/weakness is associated with poor post-operative function. Our systematic review assessed disease burden and medical needs related to muscle atrophy/weakness in older patients with THA in US, Canada, Australia, and five major countries in Europe.

Methods: Using keywords for muscle atrophy/weakness and THA, we systematically searched English-language, MEDLINE- and EMBASE-indexed literature published 5/2001 - 5/2011 and materials available from governmental or professional organizations. Included articles related to treatment, economic, humanistic, and epidemiologic burden of muscle atrophy/weakness (defined as evaluations of muscle atrophy, strength, or performance) in THA patients aged 50+ years. Genetic and molecular biology studies, case reports, and articles evaluating muscle atrophy/weakness in <20 patients were excluded.

Results: Forty articles were identified. While changes may not occur in the early postoperative period, strength improves from preoperative levels two years after THA. Treatment guidelines for THA, available only from France, recommended postoperative physical therapy (PT) to strengthen weakened muscles; however did not specify the type and frequency of PT. Postoperative PT and exercise improve muscle strength and function, but not compared with healthy controls. Intensive PT, weight-bearing exercises, aquatic PT, electric muscle stimulation, or preoperative exercise and education do not reduce hospital LOS compared with usual care in THA patients in Australia and France. Our review did not identify estimates of prevalence or incidence, productivity or work loss, or societal or treatment costs of muscle strength or functional deficits in older THA patients.

Conclusions: The epidemiologic and economic burden of muscle atrophy/weakness in THA is unclear, and few interventions can fully restore strength and function. The influence of muscle atrophy/weakness on overall THA disease burden remains ill-defined; therefore, future studies are warranted.

Disclosures: Russel Burge, None.

This study received funding from: Eli Lilly and Company

MO0180

Cellular Mechanisms of Tendon-muscle Crosstalk. Janalee Isaacson¹, Sandra Romero-Suarez², Leticia Brotto³, Chenglin Mo⁴, Marco Brotto⁵, Eduardo Abreu^{*3}. ¹Student, SON PhD Program, USA, ²University of Missouri, Kansas City, USA, ³School of Nursing, Muscle Biology Research Group, University of Missouri-Kansas City, USA, ⁴University of Missouri-Kansas City, USA, ⁵University of Missouri - Kansas City, USA

Tendons are mechanosensitive tissues responsible for the transmission of force between bones and muscles, as evidenced by tendon injuries that occur from overuse and by the careful progression of exercises designed to promote tendon healing in the rehabilitative phase. In addition to the mechanical load, practitioners recognize many other factors that may affect the patient's recovery course, including their age, nutrition, level of activity, genetic, and epigenetic factors. Intriguingly, a more elementary aspect of tissue biology (i.e., tissue to tissue crosstalk) has not been considered as a major factor for the healing process. Due to the spatial and functional relationship between muscles, bones and tendons, it is reasonable to expect interaction between these tissues. Although transmission of mechanical load is the most obvious relationship between muscles, tendons and bones, new evidence has shown that these tissues might also communicate through biochemical factors. In fact, previous results from our lab suggest the existence of crosstalk from bone to muscle cells and vice-versa. To investigate a possible crosstalk between tendons and muscles, we tested the hypothesis that conditioned media from tenocytes (CM-T) would exert noticeable effects on myogenic differentiation. Myoblasts (C2C12) were treated either with the differentiation media (DIFF, DMEM + 2.5% horse serum + 1% antibiotic), control group, or with DIFF plus 10% CM-T media, treatment group, for up to 7 days. Tenocytes were obtained from explants of C57Bl6 WT mouse flexor digitorum brevis (FDB) tendon. CM-T was obtained from 90% confluent tenocytes cultures. Results revealed CM-T had a profound effect to promote myogenic differentiation. There were significant increases in mean myotube area and fusion index, but not in number of myotubes. Furthermore, CM-T caused the upregulation of myogenic regulatory factors (MRF), including MyoD1, and of genes related to the Calcineurin-NFAT pathway.

These findings provide further evidence that tenocytes are able to biochemically signal to muscle cells. The potential clinical implications for patients suffering from musculoskeletal disorders compel our group to continue work understanding the biochemical communication between muscles and tendons. Uncovering these signaling mechanisms that underlie tendon to muscle crosstalk might lead to a better

understanding of the bone-muscle-tendon unit, which is a major focus of our current studies.

Disclosures: Eduardo Abreu, None.

This study received funding from: Missouri Life Sciences Research Board Grant to MB and a NIAMS IRC2AR058962-01 GO Grant to MB

MO0181

Change of Muscle Strength, Muscle Mass, Muscle Related Markers in Rheumatoid Arthritis Patients Treated with Tocilizumab. Akihide Nampei^{*1}, Makoto Hirao², Hideki Tsuboi³, Shosuke Akita³, Kosuke Ebina⁴, Kenrin Shi⁵, Hideki Yoshikawa⁵, Jun Hashimoto⁶. ¹Osaka Rosai Hospital, Japan, ²Osaka University, Graduate School of Medicine, Department of Orthopedics, Japan, ³National Hospital Organization, Osaka Minami Medecel Center, Japan, ⁴Osaka University, Graduate School of Medicine, Japan, ⁵Osaka University Graduate School of Medicine, Japan, ⁶National Hospital Organization, Osaka Minami Medical Center, Japan

Background: Rheumatoid arthritis (RA) patients appear decreased muscle mass and muscle strength. The reason was considered as reduced physical activity from joint pain and stiffness, and increased resting energy expenditure from excess produced inflammatory cytokines. Previous reports showed that muscle related markers, such as serum creatine kinase (CK) and creatinine (Cr) were low level in RA patients.

Hypothesis: Does strong medication, such as potent biologic cytokine antagonists, improve the decreased muscle mass and the low level of muscle related markers in RA patients?

Objectives: To investigate the muscle strength, muscle mass and muscle related markers sequentially against RA patients treated with tocilizumab (IL-6 receptor antibody).

Methods: Eleven RA patients treated with tocilizumab were enrolled. Disease activity score (DAS28CRP), C-reactive protein (CRP), matrix metalloproteinase-3 (MMP-3), modified health assessment questionnaire (MHAQ), grip strength, pinch strength, lean body mass, CK, Cr, Cystatin-C were measured before and 1, 3, 6 months after tocilizumab treatment.

Results: Mean age was 51.1 years. Disease duration was 7.7 years. Baseline CRP was 2.3 ± 2.2 mg/dl, MMP-3 was 321 ± 202 ng/ml, DAS28CRP was 4.3 ± 0.5 . DAS, MMP-3 decreased immediately at 1 month and MHAQ at 3 months. Grip and pinch strength were increased significantly at 3, 6 months ($p=0.003$, 0.001) and 6 months ($p=0.019$) respectively. Lean body mass tended to increase at 6 months, but not significantly ($p=0.055$). CK was not changed during 6 months, Cr was elevated significantly at 6 months ($p=0.012$), and Cystatin C was not changed during 6 months. The ratio of Cr/CystatinC was increased at 1 month significantly ($p=0.045$) and persisted until 6 months.

[Discussion]

Previous reports showed that grip and pinch strength were improved in RA patients treated with TNF antagonists, but lean body mass was not significantly changed at 12 weeks. Our results were consistent with these anti TNF reports. The reason of unchanged muscle mass might be that observation period was too short. Our results also showed CK was not changed, but Cr was elevated significantly. Since Cystatin C was not increased, the meaning of Cr elevation might not be the deterioration of renal function, but the early response of muscle mass increase

[Conclusion]

It might be possible that tocilizumab not only suppress the inflammation, but also improve the muscle metabolism.

Disclosures: Akihide Nampei, None.

MO0182

Discordant Bone and Muscle Adaptation to Multiple Microgravity Exposure with Interposed Resistance Exercise. Yasaman Shirazi-Fard^{*}, Kevin Shimkus, Jacqueline Perticone, Derrick Morgan, Joshua Davis, James Fluckey, Susan Bloomfield, Harry Hogan. Texas A&M University, USA

Bone and muscle responses to repeated exposures to microgravity remain a concern for astronaut health. Previously, we showed that incorporating resistance exercise during recovery from disuse not only provides benefits to bone during reloading but also for subsequent exposure to disuse even with cessation of exercise. This study focuses on primary muscle outcomes as well as the bone-muscle relationship.

Adult male Sprague-Dawley rats (6mo.) were assigned to age-matched cage controls (CC) and hindlimb unloaded (HU) groups by body weight and total (integral) vBMD. HU animals were exposed to 28d of hindlimb suspension, followed by 56d of recovery, and then a 2nd HU exposure (2HU). HU animals also performed squat jumping resistance exercise protocol during recovery (2HU+EX). Animals were operantly conditioned, then trained over 6 weeks (3d/wk) with exercise intensity increasing weekly. At baseline and then every 28 days, longitudinal *in vivo* pQCT scans were taken at proximal tibia metaphysis (PTM) and a group (n=15) was euthanized. The soleus, plantaris, and gastrocnemius muscles were excised, weighed, and snap-frozen in liquid nitrogen. Rates of muscle protein synthesis were assessed by

deuterium oxide incorporation and measured via gas chromatography-mass spectrometry.

Exercise led to a significant increase in relative muscle mass (i.e., normalized by body weight) in the soleus (91%) and gastrocnemius (24%), but it did not protect against muscle loss during the 2nd HU exposure. Rates of protein synthesis were depressed due to unloading in soleus (-10%, n.s.) and gastrocnemius (-18%). Resistance exercise did not alter rates of protein synthesis after the 2nd HU as 2HU+EX was not different from 2HU or age-matched control. However, 2HU was significantly lower than CC, which suggests beneficial effects of exercise. Considering the ratio of PTM total BMC to total muscle mass (MM), bone and muscle recovers with a constant upward trend for 2HU+EX ratio during exercise, which is significantly higher than the declining trend for 2HU ratio. During the 2nd HU, BMC/MM for 2HU+EX increases significantly and at a higher rate than 2HU. These data suggest that there is a mismatch between bone and muscle adaptation to microgravity or recovery therefrom; interestingly, moderate resistance exercise prior to a subsequent bout of unloading is more beneficial to bone than to muscle.

Disclosures: Yasaman Shirazi-Fard, None.

MO0183

Does Vitamin D Supplementation Affect Body Composition and Strength?

Violet Lagari*¹, Orlando Gomez-Marin², Silvina Levis². ¹University of Miami, USA, ²University of Miami School of Medicine, USA

Purpose: Few prospective studies have examined the association between vitamin D and muscle mass or strength. The aim of this study is to investigate if vitamin D supplementation is associated with improvements in lean mass, fat mass, and strength.

Methods: Body composition [BC] measurements were obtained on 86 subjects at baseline and 6 months using dual-energy x-ray absorptiometry as part of a single site, double-blind, randomized clinical trial enrolling subjects aged 65 and older to receive 400 (low dose) or 2,000 (high dose) IU vitamin D₃ daily, regardless of their current 25(OH) vitamin D [25(OH)D] level. Preliminary multivariate analyses revealed a significant gender x treatment interaction. Thus, within gender, separate correlation and regression analyses were performed to assess different interrelationships and the effect of treatment on relative changes in 25(OH)D, total lean mass, total fat mass and grip strength, an indicator of muscle strength.

Results: Gender-specific comparisons yielded no significant differences between treatment groups with respect to baseline characteristics such as age, BMI, race, ethnicity, smoking status, alcohol use, grip strength, weight, height, 25(OH)D, calcium and vitamin D supplements, grip strength, and total lean and fat mass. Among women, some relative changes (%) for the low and high dose groups, respectively, included: total lean mass, 0.56 ± 2.6 and 0.36 ± 2.9 ; grip strength, -5.6 ± 11.0 and -3.2 ± 12.6 ; total fat mass, 0.08 ± 5.6 and -0.85 ± 5.4 ; 25(OH)D, -6.3 ± 28.1 and 24.6 ± 51.2 . Also among women, significant inverse correlations were found between relative changes in total lean mass and relative change in grip strength ($p = 0.035$); and between relative change in total fat mass and relative change in 25(OH)D ($p=0.014$). The latter relationship remained significant after adjusting simultaneously for treatment, age, and BMI. Among men, there were no significant correlations between relative changes in total lean, fat mass, grip strength, and 25(OH)D.

Conclusions: The significant inverse correlation between relative changes in total fat and 25(OH)D, support the evidence that higher supplemental doses are needed in persons who are overweight. The results of this clinical trial assessing the effects of vitamin D supplementation on BC and muscle strength do not show an effect of vitamin D supplementation on changes in total lean mass or grip strength.

Disclosures: Violet Lagari, None.

This study received funding from: Merck & Co. and the Marjorie Cowan Family Foundation

MO0184

Improving Outpatient Follow-up for Osteoporosis Management After a Hip Fracture. Anika Alarakhia*¹, Robert Quinet². ¹Ochsner Medical Center, USA, ²Ochsner Medical Center-New Orleans, USA

Purpose: Patients who are hospitalized for hip fractures are asked to follow-up with Rheumatology in 6-8 weeks after their hospitalization to assess their risk of osteoporosis and their need for a bisphosphonate and/or other approved treatments. Outpatient follow-up in our clinic after being hospitalized for a hip fracture has notoriously been poor. The purpose of this study was to determine the rate of outpatient follow-up of patients after a hip fracture and then to implement an intervention to increase the follow-up rate.

Methods: We conducted a chart review involving 50 hospitalized hip fracture patients prior to intervention, and 50 hospitalized hip fracture patients after intervention. The intervention included an informational handout which explained the risk of osteoporosis and risks that can lead to further fractures, the importance of receiving a bone density scan, and different treatments to help prevent further fractures that can be implemented as an outpatient. This informational handout was given to the patient and/or family prior to hospital discharge. The results were documented comparing clinic follow-up rates prior to intervention and follow-up rates after intervention.

Results: After retrospectively reviewing fifty charts from July 2006 to March 2011 of hospitalized hip fracture patients, it was noted that only 3/50 (6%) of patients followed up to the Rheumatology clinic after their hospitalization. A prospective

review is currently being done on charts from May 2011, and is still ongoing. Out of the patients who received intervention, 15/41 (36.5%) of patients have followed up to the Rheumatology clinic after their hospitalization. This shows a significant increase in follow-up rates after the intervention was initiated.

Conclusion: We believe that outpatient follow-up for a patient after being hospitalized for a hip fracture is extremely important to prevent further fractures which can increase a patient's morbidity and mortality. After receiving an informational handout while in the hospital regarding osteoporosis and treatment options that can be provided as an outpatient, we found that the follow-up rate increased dramatically. It is concluded that once patients and their families fully understood the importance of seeing a Rheumatologist to assist in preventing further fractures, they were more willing to make a follow-up appointment with a Rheumatologist in the outpatient setting.

Disclosures: Anika Alarakhia, None.

MO0185

Withdrawn

MO0186

Relationship between Regional Bone Mineral Density and Muscle Mass in Elderly Men with Sarcopenia. Vidmantas Alekna*¹, Asta Mastaviciute², Arvydas Laurinavicius³, Marija Tamulaitiene⁴, Donatas Petroska³, Vaidile Strazdiene⁵. ¹Vilnius University, Lithuania, ²Vilnius University, Faculty of Medicine; National Osteoporosis Center, Lithuania, ³Vilnius University, Faculty of Medicine; National Center of Pathology, Lithuania, ⁴Vilnius University, Faculty of Medicine; National Osteoporosis Center, Vilnius, Lithuania, ⁵State Research Institute Centre for Innovative Medicine, Lithuania

Background: The relation between regional muscle mass and bone mineral density in sarcopenia is still unclear.

Purpose: To analyze the relationship between regional bone mineral density (BMD) and muscle mass in sarcopenic men.

Methods: This was a case-control study on ambulatory men aged 70 years and older. The exclusion criteria were: conditions known to affect muscle and fat tissue metabolism; taking any medication known to affect muscle or lipid metabolism. Dual-energy X-ray absorptiometry (iDXA, GE Lunar) was used to measure BMD and body composition. Sarcopenia was defined when appendicular skeletal muscle mass divided by stature squared was less than 7.26 kg/m². The legs muscle mass/total body lean mass ratio was calculated. Skeletal muscle needle (16 gauges) microbiopsy was performed in 10 sarcopenic men – the samples were taken from vastus lateralis femoris muscle and standard histo-morphological methods were used.

Results: Twenty six men with sarcopenia and 49 controls (mean age 78.9±6.4 y and 77.8±4.8 y, p=0.45) were included. Sarcopenic men, comparing to the controls, were smaller (169.1±5.9 cm vs 172.1±5.9 cm, p=0.036), lighter (69.3±8.4 kg vs 83.6±11.2 kg, p=0.0001) and had lower body mass index (24.2±2.3 vs 28.2±3.8, p=0.0001). Total fat mass was lower in sarcopenic men than in controls (19.48±6.2 and 25.48±7.9 kg, respectively; p=0.0001) but there was no difference in % body fat. BMD was lower in sarcopenic men both at total body (1.104±0.2 g/cm² vs 1.211±0.1 g/cm², p=0.003) and at total hip (0.918±0.2 g/cm² vs 1.035±0.2 g/cm², p=0.007) comparing to controls, and there was no difference in lumbar spine BMD. The ratio of leg muscle mass with total lean mass was lower in sarcopenic group than in controls – 0.31±0.1 and 0.33±0.2, respectively (p=0.009). The analysis of data revealed the correlation of leg muscle mass with lumbar spine BMD (r=0.5, p=0.006), total body BMD (r=0.5, p=0.005) and with total hip BMD (r=0.4, p=0.02) in men with sarcopenia. There was no such correlation in controls. Qualitative morphological-histochemical analysis revealed regular distribution of myocytes I and II type in majority of samples, and focally increased number of lysosomes were found in 2 cases.

Conclusion: This study showed that total body BMD as well as regional BMD at hip and spine is associated with leg muscle mass in sarcopenic men.

Disclosures: Vidmantas Alekna, None.

MO0187

The characterization of Effects of Low Intensity Vibration on Bone and Muscle in the Rat Model of Acute Spinal Cord Injury. Helen M. Bramlett¹, W. Dalton Dietrich¹, Lana Jones Mawhinney¹, Alex Marcillo¹, Ofelia Furonos-Alonso¹, Amade Bregy¹, William A. Bauman², Christopher Cardozo², Weiping Qin^{*3}. ¹University of Miami Miller School of Medicine, USA, ²James J. Peters VA Medical Center, USA, ³Bronx Veterans Affairs Medical Center, USA

Introduction: Following spinal cord injury (SCI), sublesional bone is rapidly and extensively lost. Low intensity vibration (LIV) has been suggested to reduce bone loss. It has been suggested to reduce loss of bone in children with cerebral palsy and osteoporotic women, but its efficacy in SCI-related bone loss is unclear. The purpose of this study was to perform an initial characterization of the effects of LIV on bone and bone cells in an animal model of SCI.

Methods: Female rats with contusion injuries of the spinal cord after a 12.5 mm weight drop at T10, resulting in motor-incomplete SCI, were studied. Beginning 28 days post-SCI, LIV was administered for 15 minutes twice daily for 35 days.

Results: LIV appeared to be tolerated well by the animals. LIV did not attenuate the significant 5% decline in bone mineral density (BMD) at the distal femur and proximal tibia, determined by dual energy x-ray absorptiometry. LIV did not reduce the 37% elevation of levels of a plasma bone resorption marker, type I collagen cross-linked C-telopeptide. However, LIV did reduce by 68% the 2-fold increase in osteoclast numbers observed in ex-vivo osteoclastogenesis assays performed using marrow hematopoietic stem cells obtained from the tibia and femur. Gene expression analysis after osteoblastic differentiation of marrow stromal cells from the femur and tibia were also performed. LIV completely reversed the 2-fold elevation in mRNA levels for SOST in osteoblasts, and it more than reversed the 40% reduction in mRNA levels for Runx2, an osteoblast differentiation factor. Following SCI, gastrocnemius muscle weights were reduced by 13% and were not significantly increased by LIV. SCI-mediated reduction of the mRNA levels in gastrocnemius were mitigated by LIV for PGC-1 α , an activity sensitive gene, and for MCIP1.4, a transcript regulated by NFAT and sensitive to calcineurin signaling, and, consequently, to neuromuscular activity, although these changes did not reach statistical significance.

Conclusion: In this rodent model of neurologically motor-incomplete SCI, LIV did not reduce bone loss but did significantly reduce osteoclastogenesis in ex-vivo cultures and expression of SOST. These preliminary results are quite encouraging concerning the effect of LIV on bone resorption. Perhaps, a longer duration of LIV after SCI, or a more severe model of injury, would have resulted in noticeable and favorable changes to BMD.

Disclosures: Weiping Qin, None.

MO0188

Whole Body Metabolic Changes Impact Lactation-Induced Bone Loss Through FGF-21 and IGFBP-2. Sheila Bornstein^{*1}, Phuong Le², Victoria Demambro², Katherine Motyl², Sue Brown³, Sutada Lotinun⁴, Roland Baron⁵, David Clemmons⁶, Mark Horowitz⁷, Mathieu Ferron⁸, Gerard Karsenty⁸, Clifford Rosen¹. ¹Maine Medical Center, USA, ²Maine Medical Center Research Institute, USA, ³University of Virginia, USA, ⁴Harvard School of Dental Medicine, USA, ⁵Harvard School of Medicine & of Dental Medicine, USA, ⁶University of North Carolina, USA, ⁷Yale University School of Medicine, USA, ⁸Columbia University, USA

Lactation is associated with bone loss due to high calcium demand. Trans-differentiation of adipocytes into epithelial cells and milk production also lead to high substrate demand. Because the skeleton is closely linked to global fuel homeostasis, we hypothesized that circulating factors associated with maternal metabolic changes contributed to skeletal loss during lactation. To test this, we performed an observational study of lactating and non-lactating women (n=56), n=44 lactating >5 mos; n=12 non-lactating. There was significant bone loss from both the spine (-6.2%, p<0.001) and hip (-3.8%, p<0.001) by 3 mos that was restored 12 months after return of menses. NTx and osteocalcin increased markedly at 3 mos of lactation (p<0.001), as did serum IGFBP-2 (p=0.004) which correlated with bone turnover markers (p<0.05) and insulin sensitivity. To test whether IGFBP-2 or other factors independent of estrogen and PTHrP were related to bone turnover we performed a longitudinal study of 12-20 week old lactating C57BL6 mice (n=10). There was a 33% decline in %body fat (p<0.01) at d7 of lactation that was also associated with a profound reduction in marrow fat as measured by osmium-CT of the femur. Day 21 of lactation was the nadir of cortical bone loss (p<0.001) with increased cortical porosity and enhanced insulin sensitivity. Cortical bone was fully recovered by 21 days post-lactation, but in contrast trabecular BV/TV remained low vs. age-matched non-lactating controls (2.5% vs. 5%) despite a 30% increase in BFR (p<0.05) and a decrease in osteoclasts and eroded surfaces (p<0.05). Three insulin sensitizers: IGFBP-2, FGF-21 and Glu 13 OCN were increased at d7 of lactation (p<0.01) and correlated with a marked rise in serum CTx. Gene expression in the inguinal fat pad showed 70% suppression of "brown like" adipocyte markers (UCP-1, DiO2, FGF-21, Pgc1a) (p<0.02) consistent with low sympathetic tone. In contrast, PDK4 mRNA increased two fold at d7 and 7.7 fold at d21 (p<0.02). During lactation there are profound energy demands for nutrients to meet mammary needs. Increases in FGF-21 and IGFBP-2 with lactation may contribute to high bone resorption and these factors plus a marked increase in Glu13 osteocalcin contribute to enhanced insulin sensitivity. Understanding lactation-induced bone loss requires careful analysis of whole body metabolic changes that impact bone remodeling. NIH-1R24 DK092759-01

Disclosures: Sheila Bornstein, None.

MO0189

Glucose-Dependent Insulinotropic Peptide Prevents Serum Deprivation-Induced Apoptosis In Both Human Mesenchymal Cells And Osteoblasts. Joanne Rasschaert¹, Jessica Berlier^{*2}, Ilham Kharroubi³, Jing Zhang³, Céline Gillet³, Myrielle Mathieu³, Valerie Gangji⁴. ¹Laboratory of Bone & Metabolic Biochemistry, Belgium, ²Laboratory of Bone & Metabolic Biochemistry - Université Libre de Bruxelles, Belgium, ³Laboratory of Bone & Metabolic Biochemistry, Université Libre de Bruxelles, Belgium, ⁴Hôpital Erasme, Université Libre de Bruxelles, Belgium

Human mesenchymal stem cells (MSC) are able to differentiate into cells of connective tissue lineages, including bone and cartilage. Hence, MSC-based therapies are promising for the treatment of bone and cartilage diseases. One of the major issues in regenerative cell therapy is the biosafety of fetal calf serum (FCS) and human serum used for cell culture. Therefore, development of a culture medium preserving MSC viability, differentiation and expansion without the use of serum will be of clinical value.

Glucose-dependent insulinotropic peptide (GIP) is an incretin exerting beneficial effects on bone turnover in mice through its action on osteoblasts and osteoclasts.

To optimize MSC culture in the absence of serum, we evaluated the ability of GIP to protect MSC from serum deprivation-induced apoptosis. The capacity of GIP to induce proliferation and osteoblastic differentiation and the signaling pathway involved were examined.

MSC isolated from bone marrow of healthy donors and SaOS-2 cells, an osteoblastic cell line, were pre-cultured in standard culture condition (10% FCS) and then further cultured in the presence or absence of FCS and/or GIP (0.1-1 μ M). To induce osteoblastic differentiation, cells were cultured in an osteogenic medium. Cell proliferation was evaluated by BrdU incorporation. Gene expressions of apoptotic and osteoblastic markers and of GIP receptor (GIPR) were analyzed by qPCR. Cell viability was evaluated by Annexin/FACS and fluorescent microscopy. Activation of pro-survival kinases was quantified by Western blot and intracellular cAMP levels were determined by RIA.

Activation of GIPR increased intracellular cAMP levels in MSC and SaOS-2, indicating that GIPR is functional in both cell types. Serum deprivation induced apoptosis in both MSC and SaOS-2. Addition of GIP prevented serum deprivation-induced apoptosis by 48% and 33% for SaOS-2 and MSC, respectively. This effect was exerted partially through the PKB/Akt signaling pathway. GIP also increased the ratio of anti-pro-apoptotic genes expression. However, GIP did not prevent the decrease of cell proliferation induced by serum deprivation.

These findings demonstrate that GIP exerts a protective action against apoptosis on human MSC and suggest a novel approach to culture MSC without serum but preserving cell viability and differentiation. Moreover, this observation could improve the biosafety of regenerative cell therapy.

Disclosures: Jessica Berlier, None.

MO0190

Anabolic and Anti-resorptive Effects of Colforsin Daropate Hydrochloride, a Water-soluble Derivative of Forskolin. Jiwon Lim^{*1}, Young-Ae Choi¹, Hong-In Shin¹, Eui Kyun Park². ¹Kyungpook National University, South Korea, ²Kyungpook National University School of Dentistry, South Korea

Intracellular cyclic adenosine monophosphate (cAMP) plays significant role in bone homeostasis. Here, we examined effects of colforsin, a water soluble derivative of forskolin, on osteoblastic differentiation of mesenchymal cells, osteoclast differentiation and bone loss prevention. Colforsin compared to forskolin substantially promoted mineralization of mouse calvarial cells and increased expression of osteogenic markers such as alkaline phosphatase (ALP) and osteopontin (OPN) in a dose dependent manner. Increased ALP expression was consistent with elevated ALP activity and staining. Colforsin compared to forskolin dramatically induced intracellular level of cAMP and H89, a protein kinase A inhibitor, also significantly suppressed colforsin-induced mineralization and ALP expression, indicating that colforsin may stimulate osteoblastic differentiation and mineralization through cAMP/PKA pathway. In addition, osteoclastic differentiation of murine bone marrow mononuclear cells and marker expression was dose-dependently suppressed by colforsin. These results suggest a positive effect of colforsin on bone remodeling. Consistently colforsin prevented bone mineral density decreases induced by ovariectomy with a dose dependent manner. Taken together, our data suggest that colforsin may have both anabolic and anti-resorptive effect on bone.

Disclosures: Jiwon Lim, None.

This study received funding from: Ministry for Health, Welfare & Family Affairs, Republic of Korea

MO0191

Anti-Diabetic Drug Rosiglitazone Inhibits Bone Regeneration and Causes Massive Accumulation of Fat at Sites of New Bone Formation. Lichu Liu^{*1}, James Aronson², Piotr Czernik³, Shilong Huang⁴, Yalin Lu³, Sima Rahman⁵, Vipula Kolli⁶, Larry Suva², Beata Lecka-Czernik⁷. ¹Arkansas Children's Hospital Research Institute, USA, ²University of Arkansas for Medical Sciences, USA, ³University of Toledo Medical Center, USA, ⁴Huazhong University, China, ⁵University of Toledo Health Sciences Campus, USA, ⁶NICHD/NIH, USA, ⁷University of Toledo College of Medicine, USA

Thiazolidinediones (TZDs) are peroxisome proliferator-activated receptor gamma (PPAR γ) activators and insulin sensitizers that represent a class of drugs used to treat hyperglycemia in diabetic patients. In bone, PPAR γ controls mesenchymal stem cell (MSC) lineage allocation, and its activation with TZDs commits MSCs toward the adipocytic lineage while suppressing osteoblast differentiation. Clinically, bone homeostasis and bone repair is affected in patients with type 2 diabetes mellitus (T2DM). Indeed, T2DM is associated with a two-fold increase in fracture risk, and TZDs use increases this risk an additional two-fold. Although the detrimental effects of TZDs on bone mass and increased fracture rate are now well documented, surprisingly there is a paucity of evidence describing the effect of TZDs on bone healing. In this study, we determined the effect of systemic administration of the TZD rosiglitazone on new bone formation in two models of bone repair *in vivo*; 1.) drilled bone defect regeneration (BDR) and 2.) distraction osteogenesis (DO a model of extended bone formation). Rosiglitazone significantly inhibited new endosteal bone formation in both models. The effect of rosiglitazone treatment was correlated with a massive accumulation of fat cells at sites of new bone formation. Although rosiglitazone treatment increased the total amount of fat in the non-operated tibia, the number of adipocytes at sites of new bone formation in both BDR and DO models exceeded this amount by many folds. The diminished bone regeneration induced by DO in rosiglitazone-treated animals was associated with a significant decrease in cell proliferation, measured by the number of PCNA-positive cells. There was also a significant decrease in neovascularization, as measured by both the number and area of vascular sinusoids, as well as the number of VEGF-positive cells. In summary, TZDs decrease new bone formation in these models of bone repair *in vivo*. The mechanisms for the diminished bone repair include intrinsic changes in mesenchymal stem cell (MSC) proliferation and differentiation, as well as changes in the local environment supporting bone regeneration. These studies suggest that new bone formation may be significantly compromised in T2DM patients on TZD therapy.

Disclosures: Lichu Liu, None.

MO0192

Ca²⁺/Calmodulin-Dependent Protein Kinase Kinase 2 as a Novel Modulator of Bone Remodeling. Uma Sankar^{*1}, Rachel Carv², Michael Voor¹, Deborah Novack³. ¹University of Louisville, USA, ²Owensboro Cancer Research Program, University of Louisville, USA, ³Washington University in St. Louis School of Medicine, USA

Imbalances in bone remodeling result in pathological conditions such as osteoporosis. Our studies reveal a key role for Ca²⁺/calmodulin (CaM)-dependent protein kinase (CaMK) kinase 2 (CaMKK2) in both the anabolic and catabolic pathways of bone remodeling. Micro-computed tomography and histological analyses reveal a significant increase in trabecular bone volume coupled with the presence of significantly higher numbers of cuboidal and columnar osteoblasts in the long bones of *Camkk2*^{-/-} mice, in comparison to age- and sex-matched wild-type (WT) mice. Further, mesenchymal stem cells derived from *Camkk2*^{-/-} mice yield four times more alkaline phosphatase positive osteoblasts that express higher levels of osterix and osteocalcin than WT. In contrast, *Camkk2*^{-/-} femurs possess fewer multinuclear osteoclasts that stain weakly for tartrate-resistant acid phosphatase activity and display impaired attachment to the bone surface, indicating that loss of CaMKK2 also affects osteoclast differentiation and/or function. Finally, inhibition of CaMKK2 by its selective cell permeable inhibitor STO-609 offers protection from ovariectomy-induced osteoporosis.

Following its binding to Ca²⁺/CaM, CaMKK2 phosphorylates and activates downstream targets such as CaMKIV, which in turn phosphorylates and activates transcription factors including cyclic adenosine mono phosphate (cAMP) response element binding protein (CREB). However, we found Ser¹³³ phosphorylated form of CREB to be markedly elevated in osteoblast progenitors deficient in CaMKK2 or CaMKIV. This suggested the involvement of other CREB kinases such as cAMP-protein kinase (PKA), a central mediator of parathyroid hormone-stimulated osteoblast differentiation. Indeed, phospho-PKA levels are elevated in CaMKK2-deficient osteoblasts. It is well documented that the CaMK and cAMP-PKA pathways negatively regulate each other in several cell types. Further, *Camkk2*^{-/-} osteoblasts also possess significantly higher levels of the Wnt co-receptor lipoprotein related protein 5 and osteoprotegerin (OPG), a decoy receptor for RANKL. Taken together, these results suggest that the loss or inhibition of CaMKK2 results in the de-repression of the PKA-Wnt-OPG pathway that positively impacts osteoblast differentiation and bone growth and negatively impacts osteoclast differentiation and bone loss. Inhibition of CaMKK2 could therefore be explored as a novel therapeutic strategy in combating osteoporosis.

Disclosures: Uma Sankar, None.

MO0193

Cysteine Mutants of Sclerostin Retained a Comparable Inhibitory Potency on Wnt/ b-Catenin Signaling Despite of Inappropriate Folding. Ajita Jami^{*1}, Eun Jin Kim², Jogeswar Gadi³, Kyoung Min Kim², Hyo jin Cho⁴, Sihoon Lee⁵, Sung-Kil Lim². ¹Yonsei University College of Medicine, South Korea, ²Yonsei University College of Medicine Seoul South Korea, South Korea, ³Division of Endocrinology, South Korea, ⁴Gachon University School of Medicine, South Korea

Sclerosteosis is a very rare recessively inherited high-bone-mass disorder. The first identified case was caused by mutations in a single gene (*Sost*) encoding a novel secreted protein, Sclerostin. Sclerostin encodes a 213 amino acid, secreted protein containing a leader sequence and a cysteine-rich protein domain like its closest family member, Wise. The cystine-knot domain is the only recognizable motif found in the Sclerostin/Wise, Norrie, and DAN subfamilies. However, the importance of cystine knot in *Sost* has never been studied. In this study, we made mutations in the cysteine residues of cystine-knot motif of *Sost* by site-directed mutagenesis. We found that secretion of all cysteine mutants was partially impaired, and mutant mouse Sclerostin was retained in ER. This indicates that the cysteine residues forming disulphide bridges are important for keeping a rigid molecular scaffold that owes its exceptionally high stability through appropriate folding. However, cysteine mutants including Cys165Arg mutant mouse Sclerostin synthesized in *E-coli* revealed a comparable potency to the wild type Sclerostin in inhibition of Wnt/ b-catenin signaling unexpectedly. Meanwhile, C165R synthesized in *E-coli* was unstable and more vulnerable to degradation after binding to MC3T3E1 cells. Taken together, breaking the disulfide bond through point mutation at cysteine residues leads to instability of Sclerostin without deteriorating the inhibitory potency of Wnt/b-catenin signaling.

Disclosures: Ajita Jami, None.

MO0194

Deciphering the Role of Parafibromin in Bone Development. Casey Droscha^{*1}, Bart Williams², Travis Burgers¹, Cassandra Diegel¹. ¹Van Andel Institute, USA, ²Van Andel Research Institute, USA

Hyper-parathyroidism-jaw tumor (HPT-JT) syndrome is an autosomal dominant disorder in which patients present with parathyroid tumors and fibro-osseous tumors of the maxilla or mandible. Mutational studies have linked HPT-JT to the hyperparathyroidism type 2 gene (*HRPT2*) which encodes the protein parafibromin. Parafibromin is a nuclear protein which binds β -catenin and mediates Wnt/ β -catenin signaling by recruiting chromatin modifiers while also facilitating transcription as a member of the PAF complex. The importance of Wnt/ β -catenin signaling as a positive regulator of bone development has been clearly shown by many researchers. To this end, we are interested in learning how parafibromin affects Wnt target genes responsible for osteoblast differentiation and fate. To evaluate parafibromin regulation of Wnt/ β -catenin signaling, we have generated a conditional mouse model of *Hrpt2* where parafibromin is eliminated specifically in mature osteoblasts using Osteocalcin-cre. Loss of parafibromin within osteoblasts results in a statistically significant increase in bone mineral density and thickness of cortical bone as compared to wildtype littermates by 3 months of age as determined by dual energy x-ray absorptiometry (DXA). Additionally, loss of parafibromin within osteoblasts increases femoral stiffness and increased femoral maximum load as determined by four-point bending. We are currently looking at how the loss parafibromin *in vitro* affects cell proliferation, apoptosis, and differentiation of osteoblasts.

Disclosures: Casey Droscha, None.

MO0195

Development of a Novel Tetrapod-shaped Drug-eluting Artificial Bone. Yujiro Maeda^{*1}, Shinsuke Ohba², Hironori Hojo³, Nobuyuki Shimohata⁴, Fumiko Yano¹, Kenichi Yamamoto⁵, Noriko Hatano⁶, Tsuyoshi Takato⁶, Ung-Il Chung⁷. ¹University of Tokyo, Japan, ²Division of Biotechnology, Center for Disease Biology & Integrative Medicine, Japan, ³The Center for Disease Biology & Integrative Medicine, Japan, ⁴Center for Disease Biology & Integrative Medicine, Faculty of Medicine, University of Tokyo, Japan, ⁵Tokyo university, Japan, ⁶Department of Sensory & Motor System Medicine, Faculty of Medicine, University of Tokyo, Japan, ⁷University of Tokyo Schools of Engineering & Medicine, Japan

Artificial bones are known to fail in a certain percentage of cases, because of inferiority of mechanical strength and substitution for bones, compared to autologous bone transplantation. Therefore, there is a clear need for osteoinductive bone implants acting on host cells in less invasive and safer manners. This study aimed to develop a small compound-based bone implant system by loading a smoothed agonist (SAG) and a helioxiantin derivative (TH), an osteogenic compound that we previously identified, on newly-developed tetrapod-shaped calcium phosphate granules (Tetra-bone[®]).

To confirm osteogenic activities of the two compounds, we cultured C3H10T1/2 cells for 14 days with either of the two compounds or both. Real time RT-PCR analysis showed that SAG and TH induced expression of *alkaline phosphatase (Alp)* and *osteocalcin (Oc)*, respectively, suggesting that the two compounds promoted different stages of osteogenesis. The combination of SAG and TH induced expression of both *Alp* and *Oc* more strongly than either of them; von Kossa staining revealed extensive calcification in the combination. We then monitored release of SAG or TH from SAG- or TH-loaded Tetrabones by examining expression of osteoblast marker genes in C3H10T1/2 cells or pre-osteoblastic MC3T3-E1 cells cultured with the compound-loaded Tetrabones. SAG-loaded one had induced *Alp* expression for 12 days in C3H10T1/2 cells, and TH-loaded one did *Oc* expression for more than 35 days in MC3T3-E1 cells. These data indicate that the two compounds loaded on Tetrabones can be released in a controlled manner and act to differentiate progenitor cells into osteoblastic ones.

To evaluate bone regeneration by the compound-loaded Tetrabones, we implanted them into 2.2 mm-cylinder-shaped bone defects created in femur shafts of 11-week-old rats. Fourteen days after implantation, bone regeneration areas were assessed by histological analyses and 3-D quantitative analyses using micro CT-scanned images. The areas were significantly increased in the combinational use of SAG- and TH-loaded Tetrabones, compared to either of them; the combination regenerated not only trabecular bones but also cortical ones.

Thus, we created a novel tetrapod-shaped drug-eluting artificial bone, which locally acted on host cells to induce bone regeneration, by taking advantage of tetrapod-shaped calcium phosphate granules and the combinational use of two different compounds, SAG and TH, acting on different stages of osteogenesis.

Disclosures: Yujiro Maeda, None.

MO0196

Droplets versus Injection: Simple Methods of Loading Stem Cells into Biomaterials that Generate Different Outcomes in Bone Regeneration..

Luciane Capelo¹, Bruno Pimenta², Eliandra de Souza³, Roberto Fanganiello⁴, Maria Rita Passos-Bueno². ¹Federal University of Sao Paulo, Brazil, ²University of Sao Paulo, Brazil, ³UNIFESP, Brazil, ⁴Institute of Biosciences, University of Sao Paulo, Brazil

There is a trend in the bone engineering field of using bioreactors to add cells into biomaterials to have a homogeneous cell distribution. Here we report two simple and non-expensive methods of loading cells into biomaterials that promote differential distribution of the cells and creates a diverse microenvironment/compartimentalization that can be useful to facilitate guided bone regeneration in different bone sites.

Stem cells isolated from human dental pulp (DPSC) were added to CellCeram (Scaffdex)-a bioabsorbable ceramic composite scaffold that contains 60% hydroxyapatite and 40% β -tricalciumphosphate-only using two different methods: a drop of media containing 1×10^6 cells on the top of the 0.5mm disc or multiple injections all over the CellCeram disc (n=5). Discs were implanted in 0.5mm calvarial defects made in rats. Controls were made with empty discs (no cells; n=5).

In a second set of experiments, cell distribution in the biomaterial was evaluated in vitro using a similar biomaterial and fluorescent HEK293 cells added in a droplet or injections. The droplet clearly restrains the cells mainly in the surface area, forming a cone of penetration through the biomaterial. The injections promote a homogeneous distribution of cells.

The results obtained 50 days after implantation revealed a polarized bone formation on the side that received the drop of media (40ul) containing SHEDs. Bone islands, formed in every pore of the biomaterial at that side were well organized with lamellae formed around a central channel containing a blood vessel, similar to a Havers or Volkman channel. On the other side of the disc, where no human cells were detected, loose connective tissue was observed. The biomaterial that received multiple injections containing the same cells at the same initial concentration had a more homogeneous human cell distribution, bone islands were observed all over the biomaterial, well formed, but not all pores contained bone tissue. This distribution promoted a more fragile looking graft where the bone islands were diffused in the biomaterial and not interacting with the host.

Our study shows that (1) the distribution of cells can be controlled in order to modulate bone formation outcome; (2) heterogeneous or homogeneous distribution could be aimed in accordance to the type of bone or bone compartment intended to be regenerated; (3) loading methods can be useful to create compartments in the biomaterial to facilitate bone regeneration.

Disclosures: Luciane Capelo, None.
This study received funding from: FAPESP

MO0197

Effects of Dried Plum Supplementation on Bone Metabolism. Brenda Smith¹, Thomas Wronski², Jennifer Graef¹, Elizabeth Rendina¹, Katie Clark¹, Stephen Clarke¹, Edralin Lucas¹, Bernard Halloran³. ¹Oklahoma State University, USA, ²University of Florida, USA, ³VA Medical Center (111N), USA

Age-related osteoporosis is a significant public health problem. Despite advances in therapeutic options over the past two decades, the search continues for more effective, low-cost treatment strategies. Dietary supplementation with dried plums

(DP) has been shown to prevent and reverse age-related bone loss, but the underlying alterations in bone metabolism have remained in question. The purpose of this study was to determine the effects of DP consumption on bone metabolic activity over time. Adult (6 mo) male C57BL/6 mice (n = 40) were assigned to the control (CON) or 25% (w/w) DP diets for 4 or 12 wks. Bone densitometry, microCT and bone histomorphometry were used to assess bone mass, volume, structure and metabolic activity. As early as 4 wks, animals consuming the DP supplemented diet had a higher whole body bone mineral density (BMD) and vertebral trabecular bone volume (BV/TV) compared to the CON animals, 4.6% and 25%, respectively. BV/TV at the distal femur metaphysis was increased in the DP-treated animals, but only after 12 wks. The increases in BV/TV with DP in the spine and femur metaphysis occurred in conjunction with a greater trabecular number (TbN) and no change in trabecular thickness (TbTh). Cortical area and thickness were also increased (p<0.05) in the femur of the DP group. Bone histomorphometric analyses at 4 wks revealed that DP decreased (p<0.001) osteoblast surface (67%) and osteoclast surface (62%), although the osteoclast surface did not reach the level of statistical significance (p<0.10). Both the osteoblast and osteoclast surfaces normalized to the CON animals by 12 wks. Coincident with the alterations in osteoblast and osteoclast parameters, the mineralizing surface (MS/BS) and bone formation rate (BFR/BS) were reduced at 4 wks (p<0.05). Interestingly, by 12 weeks of DP supplementation, BFR/BS (~3-fold) and MS/BS (~1.7-fold) tended to be increased (p<0.10) compared to the CON animals. These results suggest that supplementing the diet with 25% DP initially suppresses cancellous bone turnover in the distal femur metaphysis, but a rebound effect is observed by 12 weeks. More rapid improvement in trabecular bone observed in the vertebra suggests that site-specific responses should be considered. Further investigation is warranted to understand the mechanisms involved in DP's alterations in bone formation.

Disclosures: Jennifer Graef, None.

MO0198

Lamin A/C Acts as an Essential Transcriptional Regulator of Mesenchymal Stem Cell Differentiation by Controlling the Dynamics of the Wnt/ β -catenin Pathway. Christopher Vidal¹, Sandra Bermeo², Hong Zhou³, Gustavo Duque⁴. ¹University of Sydney, Australia, ²PhD Student, Australia, ³Bone Research Program, ANZAC Research Institute, University of Sydney, Australia, ⁴Ageing Bone Research Program, University of Sydney, Australia

Changes in the expression of lamin A/C, an integral protein of the inner nuclear membrane, are associated with the cellular features of age-related bone loss. Reduced expression of lamin A/C inhibits osteoblastogenesis while facilitates adipogenic differentiation of mesenchymal stem cells (MSC) *in vitro*. *In vivo*, lamin A/C null mice exhibit decreased bone mass, lower osteoblast number and higher fat infiltration in muscle and bone. In this study we investigated the role of lamin A/C in MSC differentiation focusing on the Wnt/ β -catenin signaling. We hypothesized that lamin A/C plays a regulatory role in the nuclear translocation of the essential elements of this pathway. Human MSC were transfected with either 0.2 μ g of pcDNA-LMNA construct or LMNA siRNA in MSC medium. After 24h, medium was changed to osteoblast induction medium (OIM) with the addition of 20mM Lithium Chloride (LiCl). Nuclear and cytoplasmic proteins were extracted and immunoblotted for lamin A/C and β -catenin. Expression of lamin A/C was increased 36 fold in the transfected cells. Nuclear β -catenin was significantly higher (~2 fold) in MSC expressing higher levels of lamin as compared to control (p<0.05). Conversely, nuclear β -catenin was significantly lower (~ -42%) in siRNA-treated MSC. Immunofluorescence for β -catenin confirmed the nuclear accumulation of β -catenin in MSC over-expressing lamin A/C. Furthermore, to assess β -catenin transcriptional activity in lamin A/C transfected cells we used the TOP/FOPFLASH plasmid system. Cell lysates were analysed for luciferase activity, which was significantly higher in cells over-expressing lamin (p<0.05). Finally, to assess the effect of lamin A/C over-expression on MSC differentiation, we transfected osteogenic- and adipogenic-differentiating MSC with pcDNA-LMNA construct as previously described. Transfected cells showed higher osteogenic and lower adipogenic differentiation potential as indicated by high alkaline phosphatase (ALP) and low oil red O staining respectively. Gene and protein expression of ALP was higher (2 fold) in lamin A/C transfected MSC as compared to control (p<0.05). Conversely expressions of PPAR γ and lipoprotein lipase were significantly lower in lamin A/C transfected cells (p<0.05). In conclusion, our studies demonstrate that lamin A/C plays a significant role in the differentiation of both osteoblasts and adipocytes by regulating the nuclear translocation of the elements of the Wnt/ β -catenin signaling during early MSC differentiation.

Disclosures: Christopher Vidal, None.

MO0199

Molecular Clock Regulates Calcification in Developing Murine Calvaria. John-David McElderry*, Guisheng Zhao, Renny Franceschi, Michael Morris. University of Michigan, USA

Further development of anabolic therapies for skeletal disorders depends in part upon more complete understanding of the mechanism of osteogenesis. The calcification process in bone involves osteoblast-secreted proteins that regulate mineral formation. Osteoblasts contain a fully functioning molecular clock that controls the scheduled expression of many genes both directly and through downstream pathways. We hypothesize that the molecular clock regulates calcification timing and therefore is a key element in directing osteogenesis. To test this hypothesis, we have developed bioluminescence/Raman spectroscopic methodology for time-resolved measurement of gene expression and mineral deposition in cultured neonatal murine calvaria (D0). We measured expression of the molecular clock and formation of mineral with hourly sampling. We tracked molecular clock component Period 1 (Per 1) using a Per1/Luciferase transgene reporter and tracked newly deposited mineral in the fontanel space using Raman spectroscopy. Calvaria in culture show oscillatory expression of Per1, thus demonstrating a peripheral clock functionality which persisted up to 7 days after harvest. Within the posterior fontanel, mineral is deposited at the interparietal bone edge in a stair-step fashion consistent with periodic mineralization events. Analysis of the time-resolved mineralization data reveals oscillatory activity similar to Per1 expression, with peak mineralization occurring at 26.5 ± 10 hour intervals and lasting up to 5 cycles. Over time, cultured calvaria show an increase in cycle duration indicating a loss in functionality, analogous to a mechanical clock winding down. Although the complexity of interaction remains unknown, we conclude that protein-mediated mineral formation is regulated in a time dependent fashion by the local circadian pathway.

Disclosures: John-David McElderry, None.

MO0200

Plasminogen Activator Inhibitor-1 Is Involved in Streptozotocin-induced Diabetic Bone Loss in Female Mice. Yukinori Tamura*¹, Naoyuki Kawao¹, Kiyotaka Okada¹, Masato Yano¹, Katsumi Okumoto², Osamu Matsuo¹, Hiroshi Kaji¹. ¹Kinki University Faculty of Medicine, Japan, ²Life Science Research Institute, Kinki University, Japan

Fracture risk is increased mainly due to the impaired bone formation in diabetes. However, details of mechanisms for diabetic osteoporosis still remain unclear. Plasminogen activator inhibitor-1 (PAI-1), a primary inhibitor of fibrinolysis, is produced by various cells, including endothelial cells and adipocytes, and it contributes to several metabolic disorders, such as diabetes and cardiovascular disease. Although the fibrinolytic system has been suggested to be associated with the bone metabolism, the role of PAI-1 in the pathogenesis of diabetic osteoporosis is unknown. We therefore examined the effect of PAI-1 deficiency on the streptozotocin-induced diabetic osteoporosis using PAI-1-deficient mice.

Streptozotocin (50mg/kg body weight) or saline was injected into the abdominal cavity of both male and female wild-type (WT) and PAI-1-deficient (PAI-1^{-/-}) mice for 4 days.

After streptozotocin-induced hyperglycemia for a month, body weight was equally decreased in WT and PAI-1^{-/-} mice of both genders. Although blood glucose levels were markedly increased in diabetic mice, there were no differences in their levels between WT and PAI-1^{-/-} mice. Cortical and trabecular bone mineral density values in tibia, assessed using quantitative X-ray computed tomography (CT) were significantly decreased in both male and female diabetic WT mice, compared with those in control WT mice. However, PAI-1 deficiency prevented the streptozotocin-induced bone loss in female, but not in male mice. Likewise, the impairment of mechanical property (second moment of minimum and polar areas assessed using CT) by diabetes was suppressed by PAI-1 deficiency only in female mice. Furthermore, the gene expression analysis showed that the mRNA levels of osteogenic markers, such as Runx2 and Osterix, suppressed by diabetes were reversed by PAI-1 deficiency in tibia of female mice, but not in male mice. Moreover, the mRNA level of PPAR γ , an adipogenic marker, enhanced by diabetes was markedly suppressed by PAI-1 deficiency only in female mice.

In conclusion, our study demonstrated that PAI-1 deficiency protected against the streptozotocin-induced diabetic bone loss presumably through the preservation of osteogenesis and the suppression of adipogenesis in female mice. These data suggest that PAI-1 plays an important role in the pathogenesis of diabetic osteoporosis, and this pathological importance may be a gender-dependent.

Disclosures: Yukinori Tamura, None.

MO0201

Post-lactation Bone Formation may be Driven by Downregulated Sclerostin, Cathepsin K, and DKK1, and Upregulated Hematopoietic Factors, which Stimulate Osteoblast Proliferation and New Bone Formation. Jillian Collins*¹, Beth J. Kirby¹, Robert Gagel², Christopher Kovacs¹. ¹Memorial University of Newfoundland, Canada, ²University of Texas M.D. Anderson Cancer Center, USA

The maternal skeleton resorbs during lactation to provide calcium to milk; post-weaning, osteoclast number rapidly declines while osteoblasts proliferate and promptly restore the skeleton to baseline or above. Rodents lose 25% of bone mineral content (BMC) during 3 weeks of lactation and regain it fully in 2-3 weeks, while mice lacking the gene for calcitonin and calcitonin gene-related peptide- α (*Ctgrp* null) lose 55% of spine BMC and recover fully post-weaning.

Previous work has shown that post-weaning recovery does not require PTH, PTHrP, calcitriol, vitamin D receptor (VDR), calcitonin, or estradiol. Therefore, unknown factors must be responsible for stimulating bone formation during post-weaning.

We hypothesized that the genes responsible for regulating post-weaning bone formation will be differentially regulated in bone or adjacent marrow, and may show more marked differential regulation in *Ctgrp* nulls as compared to wt. We carried out genome-wide microarray analyses on RNA obtained from tibias of sister mice: virgin and at day 7 of postweaning. RNA was extracted from bone with marrow intact, run on the Affymetrix Mouse Gene 1.0 ST array, and analyzed by local pooled error test. False discovery rate was controlled by examining only genes with adjusted p-value <0.01.

At day 7 post-weaning vs virgin in wt, over 600 genes (many from bone marrow) showed differential expression as compared to about 300 genes in *Ctgrp* null. These include significant fold reductions of sclerostin (-1.65), DKK1 (-1.87), cathepsin K (-1.61), and VDR (-1.52); and 2-3-fold upregulation of voltage-dependent calcium channels. The most marked changes are in factors not previously associated with bone metabolism, including upregulation of melanoma-associated antigen (MAGE) which potently inhibits p53 and regulates cell proliferation and apoptosis (29-fold in wt and 105-fold in *Ctgrp* null), and 8-fold elevations of many Major Urinary Proteins (MUPs) which increase metabolism and energy expenditure. Comparing *Ctgrp* null to wt during post-weaning, 13 genes show differential expression with a 6.5-fold increase of MAGE being the most marked change.

In conclusion, microarray analysis reveals alterations in sclerostin, cathepsin-K, and DKK1 which should stimulate bone formation. MAGE, MUPs, and other differentially expressed marrow genes will be assessed to determine if they stimulate proliferation of osteoblasts or induce apoptosis of osteoclasts during post-weaning.

Disclosures: Jillian Collins, None.

MO0202

Regulation of Osteoclast formation by Toll-like receptors 2 and 5. Ali Kassem*¹, Ulf Lerner², Pernilla Lundberg¹, Pedro PC Souza³, Catharina Lindholm¹. ¹Umeå University, Sweden, ²University of Umea, Sweden, ³University of São Paulo State, Brazil, ⁴Gothenburg University, Sweden

Infections within or in the vicinity of the skeleton induce osteolytic diseases such as periodontitis, arthritis, osteomyelitis, peri-implantitis. Although host production of osteotropic cytokines is crucial, the precise mechanism by which pathogen associated molecular patterns induce osteoclastogenesis and bone loss is not fully understood. Recognition of these patterns by members of the toll-like receptor (TLR) family may be important. We have studied how activation of TLR2 and 5 affects bone resorption, osteoblasts and osteoclast progenitors. Activation of TLR2/1 or TLR2/6 dimers with either LPS from *P. gingivalis*, heat killed *Listeria monocytogenes* (HKLM), Pam₂CSK₄ (ligand for TLR2/6), Pam₃CSK₄ (ligand for TLR2/1) or FSL1 increased the release of ⁴⁵Ca from mouse calvarial bones. This response was associated with increased expression of the osteoclastic genes *Acp5*, *Ctsk* and *Oscar*, as well as of *c-Fos* and *Nfatc1* mRNA, enhanced degradation of bone matrix as assessed by release of the collagen fragment CTX and increased number of cathepsin K⁺ osteoclasts. TLR2 agonists also increased the mRNA and protein expression of RANKL without affecting OPG mRNA or protein. Recombinant OPG inhibited ⁴⁵Ca release triggered by TLR2 ligands. All TLR2 agonists increased mRNA expression of *Il-1b*, *Tnf- α* , *Il-6* and *Cox-2*. Anti-IL-1b and anti-TNF α did not affect LPS *P.g.* induced *Rankl* mRNA. Indomethacin (inhibitor of prostaglandin synthesis) reduced *Rankl* mRNA but did not affect ⁴⁵Ca release in bones stimulated by LPS *P.g.* or Pam₂CSK₄. Osteoblasts isolated from the periosteum of calvarial bones expressed TLR1, 2, 5 and 6. LPS *P.g.*, HKLM, FSL1, Pam₂CSK₄ and Pam₃CSK₄ induced *Rankl* mRNA, without affecting *Opg* mRNA in isolated osteoblasts. Activation of TLR5 by ST-FLA (Flagellin from *S. typhimurium*) also enhanced ⁴⁵Ca release and increased *Rankl* mRNA in calvarial bones without affecting *Opg* mRNA, a response seen also in calvarial osteoblasts. In contrast to periosteal osteoclast formation, all TLR2 agonists, but not the TLR5 agonist, robustly inhibited RANKL stimulated osteoclast formation in mouse bone marrow macrophage cultures. These data show that TLR2- and TLR5-signaling stimulates periosteal osteoclast formation and bone resorption by enhancing RANKL/OPG ratio in osteoblasts, but that TLR2 agonists inhibit RANKL signaling in early osteoclast progenitor cells in bone marrow

Disclosures: Ali Kassem, None.

MO0203

Regulator of G Protein Signaling Protein 12 Regulates the Coupling between Osteoblasts and Osteoclasts during Bone Remodeling. Tongjun Liu*¹, Xiaoning He², Yi-Ping Li³, Jay Cao⁴, Xinping Zhang⁵, Chunyi Li², Shuying Yang⁶. ¹The University At Buffalo, USA, ²University at Buffalo, USA, ³University of Alabama at Birmingham, USA, ⁴USDA ARS, USA, ⁵University of Rochester Medical Center, USA, ⁶State University of New York At Buffalo, USA

The imbalance of osteoblasts and osteoclasts plays a central role in the pathogenesis of osteoporosis and other bone diseases including Paget's disease and osteogenesis imperfect, etc. To develop new and efficient therapeutic strategies for these often-debilitating diseases, it is crucial to identify the molecular mechanisms of bone remodeling. In recent years, strong evidence has shown that RANKL-evoked Ca²⁺ oscillations play a switch-on role in NFATc1 activation and osteoclast differentiation. Our recent investigations suggested that Regulator of G-protein signaling protein (RGS) plays an essential role in Ca²⁺ oscillations and osteoclast differentiation. Despite these new insights, it is still largely unknown biological functions of RGS proteins after birth. To investigate the role of RGS12 during bone remodeling, we generated a postnatal inducible disruption of RGS12 in mice. Mutant mice were smaller than the controls up to 4-5 months after birth. Deletion of RGS12 inhibited osteoclast differentiation and the ability of the mutant osteoblasts to form mineralized nodules in culture. Wild type osteoblast can partially rescue the deficiency of osteoclast differentiation resulted from mutant BMMs; while mutant osteoblasts significantly inhibited osteoclast differentiation in co-culture system. Interestingly, Micro-CT and histological results showed that bone mass was increased which could overcome age caused bone resorption. These results demonstrate an important coupling and age-dependent role of RGS12 in osteoclasts and osteoblasts for bone remodeling.

Disclosures: Tongjun Liu, None.

This study received funding from: K08AR055678 (S. Yang)

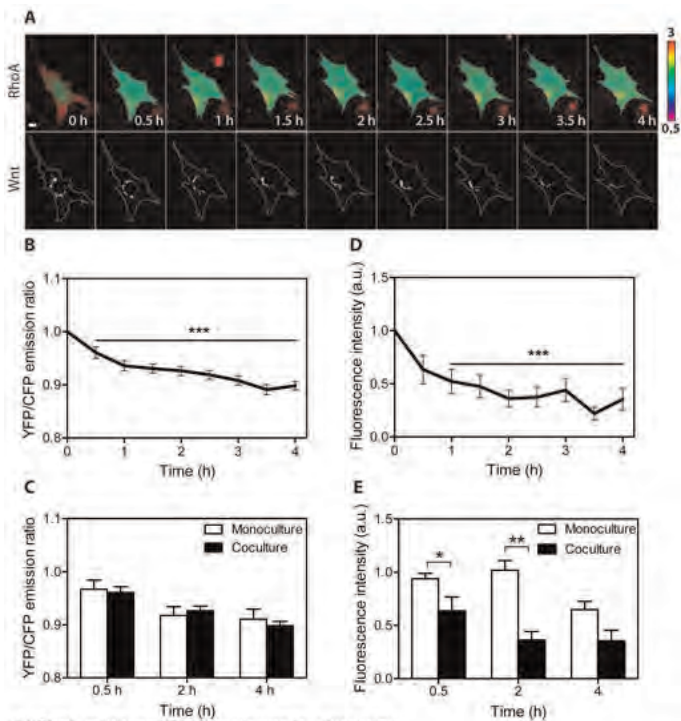
MO0204

RhoA Activity and Wnt Signaling are Suppressed in Clinorotated Osteoblasts. Eunhye Cho*¹, Qiaoqiao Wan¹, Hiroki Yokota², Sungsoo Na¹. ¹Indiana University-Purdue University Indianapolis, USA, ²Indiana University Purdue University Indianapolis, USA

Bone is a dynamic tissue under constant remodeling in response to various signals including mechanical loading. A lack of proper mechanical loading induces disuse osteoporosis. Wnt signaling together with a network of GTPases is known to play a primary role in load-driven bone formation, but little is known about their role in bone loss under a weightless condition. In this study, we addressed a question: Does weightlessness suppress an activation level of RhoA GTPase and Wnt signaling? We focused on RhoA activity since it is known to be elevated by fluid flow induced shear stress and reported to be linked to Wnt signaling. Our hypothesis is that osteoblasts under clinorotation reduce RhoA activity as well as b-catenin linked transcription in Wnt signaling. Using a fluorescence resonance energy transfer (FRET) technique with a biosensor for RhoA together with a fluorescent Wnt reporter, we examined the effects of clinostat-driven simulated weightlessness. As a control, we employed shear stress induced by an oscillatory fluid flow.

The results revealed that both RhoA activity and Wnt signaling were down-regulated by clinorotation in osteoblasts. In an osteocyte-osteoblast co-culture system, Wnt signaling was further decreased (~70%) by clinorotation. The reduction in RhoA activity was correlated to a decrease in cytoskeletal organization of actin filaments. To test interactions of RhoA and Wnt signaling, we employed two RhoA mutants (constitutively active and dominant negative) as well as a pharmacological inhibitor to Wnt signaling. First, transfection of a constitutively active RhoA mutant enhanced suppression of Wnt signaling. Compared to control cells, the reduction in Wnt signaling with the constitutively active RhoA mutant took place earlier (1.5 vs. 3.5 h) and the reduction level was deeper. Second, a pharmacological inhibitor to Wnt signaling completely blocked RhoA activity. Third, osteoblasts, which were transfected with a dominant negative RhoA mutant, exhibited a rapid and transient increase in Wnt signaling in response to shear stress.

Collectively, the results suggest that clinorotation decreases Wnt signaling and RhoA activity in osteoblasts. Furthermore, Wnt signaling stimulates activities of RhoA that in part inhibits Wnt signaling through a feedback mechanism.



(A) RhoA activity and Wnt signaling under clinorotation. (B) Time course of RhoA activity. (C) RhoA activity is not different between monocultures and osteoblast-osteocyte cocultures. (D) Time course of Wnt signaling. (E) Wnt was significantly suppressed in cocultures.

RhoA and Wnt are suppressed in clinorotated osteoblasts.

Disclosures: Eunhye Cho, None.

MO0205

The Effects of Micro-Spatial Environment for Osteoblast Osteogenesis. Mirei Chiba*¹, Ryosuke Miyai², Takeru Ota², Haruhide Hayashi². ¹Tohoku University Graduate School of Dentistry, Japan, ²Graduate School of Dentistry, Tohoku University, Japan

Objectives: Various biomaterials have been developed to regenerate bone. One of the most important influences on osteoblast reactivity is the three-dimensional morphology of the substrate, which includes the size, shape, and surface texture of the material. Many studies have demonstrated that cell shape and orientation are related to gene expression, and cells may change shape after adhering to a material surface, leading to different cell phenotypes as well as cytoskeletal changes that may affect cellular metabolism. The size and shape of particles used in biomaterials affect osteoblast proliferation and differentiation.

Although the characteristics of the biomaterials used in osteoblast scaffolds have been investigated, the effects of the amount of micro-space available have not. Therefore, in the present study, we investigated the effects of the micro-spatial environment on osteoblast proliferation and differentiation using a photolithographic technique.

Materials and Methods: MC3T3-E1 osteoblastic cells were cultured on culture plates with a micro-box-patterned surface that consisted of squares with sides 100 to 200 μm in length and heights ranging from 50 to 100 μm . Cell growth was observed and a cell viability assay, alkaline phosphatase (ALP) activity assay, and quantitative real-time PCR were performed. Cytoskeleton staining (actin filaments), DAPI, and ALP staining were also investigated.

Results: MC3T3-E1 cells were cultured and cell growth was observed. Micro-pattern did not affect cell proliferation. The cells gathered at the junction of the base and the wall of the box, and then proliferated towards the center. In addition, the actin filaments of the cells were aligned in a ring. mRNA expression was assessed by quantitative real-time RT-PCR. The micro-pattern significantly upregulated gene expression related to osteoblast differentiation. Osteocalcin gene expression was also upregulated in the MC3T3-E1 cells. Furthermore, alkaline phosphatase activity increased.

Conclusion: The amount of micro-space available to osteoblasts affected their proliferation and differentiation, demonstrating the importance of having optimal space for osteogenesis. The molecules involved in extracellular environment recognition might participate in micro-space-induced osteogenesis.

Disclosures: Mirei Chiba, None.

MO0206

Computational Systems Biology of Osteoblasts. Cheryl Ackert-Bicknell*, Karen Dowell, Catherine Sharpe, Allen Simons, Matthew Hibbs, The Jackson Laboratory, USA

The reductionist approach of studying a single gene or protein in isolation is unable to recapitulate all aspects of polygenic diseases such as osteoporosis. Increasing evidence suggests that suites or pathways of proteins, RNAs, lipids, and other small molecules work together to perform normal cellular functions. High-throughput measurement techniques, such as microarrays, next generation sequencing, mass spectrometry, etc., have enabled the preliminary study of entire pathways of genes simultaneously. This wealth publically available data can be used in gene network modeling to produce highly accurate predictions of protein function. As such, we have developed a Bayesian network machine learning methodology that takes advantage of these data to generate a predictive network of gene-gene interaction in the osteoblast. To construct our network, we first assembled an extensive compendium of high-throughput expression data specific to primary osteoblasts and selected osteoblast-like cell lines. We then integrated this expression data, with other types of data sets (sequence similarity, physical interaction, and regulatory datasets) to construct an osteoblast-specific functional relationship network. Our machine-learning algorithm was trained against a "gold standard" set of gene-gene interactions, known to occur in osteoblasts based on literature reports. The integrated networks confirm many well-characterized genes and proteins important for osteoblast development and bone biology, and predict many novel players. For example, from our network, we observed that *Serpinf1* is highly associated with *Coll1a1* expression. Very recently, loss-of-function mutations in *SERPINF1*, were shown to cause Osteogenesis Imperfecta Type VI. We are currently validating predictions from our network through traditional laboratory experiments. Unlike prior efforts to integrate mammalian high-throughput data, which often treat an organism as "one giant homogenous cell", we emphasize the vital role of cellular context (i.e. cell type, tissue niche, developmental stage, etc.) on molecular functions. As our network was constructed using diverse data specific to the osteoblast, we demonstrate that our network will be useful for the study osteoblast maturation and function.

Disclosures: Cheryl Ackert-Bicknell, None.

MO0207

Foxp1/2/4, New Transcriptional Regulators for the Chondrocyte Hypertrophy and Osteoblast Differentiation during Skeletal Ossification. Xizhi Guo¹, Haixia Zhao^{*1}, Wenrong ZHOU². ¹Shanghai Jiao Tong University, Peoples Republic of China, ²Shanghai JiaoTong University, Peoples Republic of China

Great progress has been achieved in the past years in understanding the transcriptional regulation of skeletal ossification, especially the activator for chondrocyte and osteoblast differentiation, such as Runx2, Osterix, etc. Yet the scenario of the transcriptional complexes for osteoblast differentiation is still not well-defined. Here we discovered that Foxp1/2/4, transcriptional factors of the forkhead gene family, contributed to the transcriptional control of osteochondrogenic differentiation. Through in situ hybridization and IHC, very specific and similar expression of Foxp1, Foxp2 and Foxp4 were detected in the perichondrium of skeleton during embryonic development. To understand the function of the Foxp1/2/4 proteins in bone development, genetic approaches were used including transgenic or gene knockout mice. Overexpression of Foxp1, Foxp2 or Foxp4 in the chondrocytes driven by Col2a1 promoter inhibited chondrocyte maturation in mice. Conversely, conditional inactivation of Foxp1 or Foxp2 promoted the hypertrophy and apoptosis in the chondrocytes. The double knockout of Foxp1 and Foxp2 exhibited additive defects in chondrocyte differentiation compared to the single knockout mice. These results are in line with the report that Foxp1/2/4 acts as homo- or heterodimer complex. Meanwhile, overexpression or inactivation of Foxp1/2 in osteochondrogenic progenitor cells both inhibited osteoblast differentiation. Molecularly, Foxp1/2/4 proteins repressed the transcriptional activity of Runx2 via directly binding to the Runt domain. Thus we concluded that Foxp1/2/4 proteins regulate the multiple steps of skeletal ossification, including chondrocyte hypertrophy, survival and osteoblast differentiation.

Disclosures: Haixia Zhao, None.

MO0208

Genome-Wide Analysis of H4 Acetylation in Osteoblasts. Amel Dudakovic*, Jared Evans, Ying Li, Sumit Middha, Meghan McGee-Lawrence, Jennifer Westendorf, Mayo Clinic, USA

Epigenetic events alter the phenotype, exome, and heritable state of the genome without changing DNA sequences. Posttranslational histone acetylation is an epigenetic event that relaxes chromatin structure and promotes gene expression. It is regulated by the opposing activities of acetyltransferases and deacetylases. Histone deacetylase (Hdac) inhibitors such as vorinostat and valproate are therapeutic options for cancer, epilepsy and several other diseases because of their ability to induce expression of silenced genes. Hdacs are required for proper skeletal development and

regeneration but Hdac inhibitors promote terminal osteoblast maturation. The goal of this study was to understand how Hdac inhibitors influence genome-wide histone acetylation patterns in differentiating osteoblasts. Chromatin immunoprecipitation was coupled with high-throughput sequencing (ChIP-Seq) to profile histone 4 acetylation (H4-Ac) across the genome of MC3T3 sc.4 cells during early osteoblast maturation in the presence of vehicle or vorinostat. Thus, after 4 days in osteogenic medium MC3T3 cells were exposed to vehicle or 20 μ M vorinostat for 2 hours. Chromatin was immunoprecipitated with anti-H4-Ac or control IgG. Sequencing libraries were prepared and massively parallel high throughput sequencing was performed on Illumina HiSeq2000 system. Data sets were analyzed with Useq, MACS and CEAS software. An overall increase in H4-Ac was observed within genes that are associated with osteoblast differentiation (e.g., Runx2, osterix, osteocalcin, alkaline phosphatase, collagen type I) and Wnt signaling pathways (e.g., SOST, Lrp5, Lrp6, Wnt10b) in the presence of vorinostat. At a genome-wide scale, the most extensive H4-Ac occurred within 2 kB of transcription start sites in the vehicle treated group. Vorinostat increased and expanded H4-Ac throughout active genes (i.e., within exons, introns, transcription termination sites) except within 500 base pairs upstream and downstream of transcription start sites. These data indicate that Hdac inhibitors may enhance the existing gene expression program of committed osteoblasts by extending the range and extent of H4-Ac in active genes.

Disclosures: Amel Dudakovic, None.

MO0209

Ift88 Functions in Osteoblast Differentiation. Courtney Haycraft*, Sarah Joseph, Medical University of South Carolina, USA

Primary cilia are formed and maintained through a conserved process termed Intraflagellar Transport (IFT). The process of IFT requires the coordinated movement of large protein particles along the ciliary axoneme. The proteins that make up the IFT particle are highly conserved across ciliated eukaryotes and loss of one of the components leads to disruption in ciliary structure and function. Ift88 is a component of the IFT particle and its loss leads to loss of all ciliary structures and subsequent mid-gestational lethality. Work from several groups over the last decade has demonstrated that cilia play diverse roles throughout the mammalian body and their subsequent loss results in pathologies including polydactyly, renal cysts, obesity and skeletal defects. Our previous work has demonstrated that disruption of Ift88 in the developing limb using Cre-loxP technology results in severe disruption of endochondral bone formation including loss of the bone collar. Cilia are highly expressed in the perichondrium and periosteum of the developing skeleton and we have begun to examine their localization within the tissue and surrounding matrix. Our preliminary findings demonstrate the cilia are localized parallel to the longitudinal axis of the developing bone in the fibrous region of the periosteum but assume a more perpendicular orientation within the cambic region. These findings are currently being verified. We have isolated preosteoblast cell lines from the calvaria and periosteum of Ift88 conditional mutant mice. For both cell types, disruption of Ift88 leads to decreased osteoblast differentiation and matrix mineralization in vitro. We have begun to examine the gene expression profile of the Ift88 mutant cell lines to determine at which point osteoblast differentiation is disrupted. While our previous work has shown that Ihh signaling is disrupted in the developing long bones, we have begun to use our in vitro culture system to determine if reactivation of Ihh signaling within the Ift88 mutant cells is sufficient for differentiation into osteoblasts or if additional pathways are disrupted.

Disclosures: Courtney Haycraft, None.

MO0210

Intramembranous Bone Formation in a Transgenic Model of Constitutive Gs-G Protein Signaling in Osteoblasts. Lalita Wattanachanya^{*1}, Liping Wang², Richard Kao³, Dylan O'Carroll², Wei-Dar Lu², Edward Hsiao⁴, Bruce R. Conklin⁵, Robert Nissenson⁶. ¹King Chulalongkorn Memorial Hospital The Thai Red Cross Society, Thailand & VA Medical Center, San Francisco, USA, ²VA Medical Center, San Francisco, USA, ³UCSF/VAMC, USA, ⁴University of California, San Francisco, USA, ⁵Gladstone Institute of Cardiovascular Disease, University of California, San Francisco, USA, ⁶VA Medical Center & University of California, San Francisco, USA

G protein coupled receptor (GPCR) signaling in osteoblasts (OBs) is an important regulator of bone formation. We have previously described a mouse model expressing Rs1, an engineered constitutively active Gs-coupled receptor, under the control of the 2.3 kb-Col I promoter. Rs1 mice showed a dramatic age-dependent increase in trabecular bone with features resembling fibrous dysplasia. These changes were accompanied by an increase in OB lineage cells, especially immature OBs, indicated by an expansion of cells expressing osterix and runx2 in the femur. This result suggested the role of paracrine mediators, secreted from mature OBs, influencing early OB commitment, differentiation, and/or proliferation. In this study, we evaluated how Gs signaling affects intramembranous bone formation by characterizing the Rs1 calvarial bone phenotype at 1 and 9-weeks of age. We also analyzed the effect of altered OB G protein signaling on the OB transcriptome in vivo from calvariae of 1 week old Rs1 mice to identify candidate paracrine mediators of the effects of Rs1. The Rs1 calvariae were composed of trabecular-like and bone marrow-like structures. Histomorphometric analysis revealed an increase in calvarial thickness; a dramatic

increase in TV; and an increase in trabecular BV with partial loss of cortical structure. These phenotypes became more severe with age. By immunohistochemistry, osterix was detected in cells throughout the intertrabecular space while osteocalcin was expressed predominantly in cells along bone surfaces. Rsl1 was detected only in osteocalcin expressing cells. These findings in calvariae were similar to the changes seen in femurs. We further identified candidate paracrine mediators by determining the effect of Rsl1 on the expression level of genes encoding secreted proteins. We identified and validated 10 genes (up-regulated: Lipi, Figf, Sipi, Rbp4 and Mfge8; down-regulated: Chad, Fgf9, Car2, Thbd and Ostn) whose expression was significantly altered in Rsl1 expressing OBs compared to control (real time PCR, $p < 0.05$). All except Lipi have been shown to be involved in skeletal homeostasis; however, none has previously been reported to be related to OB-specific Gs signaling. In summary, our results document that the effects of constitutive Gs-GPCR signaling in mature OBs in calvarial bone closely resembles the effects seen previously in endochondral bone. They further identify a series of candidate paracrine mediators of the effects of Gs signaling in OBs.

Disclosures: Lalita Wattanachanya, None.

MO0211

Nuclear Receptor Ror β Is a Novel Regulator of Runx2 Activity in Osteoblasts. Gang Liu¹, Matthew Roforth¹, Sundeep Khosla², David Monroe³. ¹Mayo Clinic, USA, ²College of Medicine, Mayo Clinic, USA, ³Mayo Foundation, USA

The regulation of osteoblastic differentiation requires the coordinate activities of numerous transcription factors. Although a few are essential, such as Runx2 and osterix, others serve the purpose of fine-tuning in response to various environmental and hormonal cues. In a previous screen designed to assess the expression patterns of the nuclear receptor superfamily during osteoblastic differentiation, we identified retinoic acid receptor-related orphan receptor beta (Ror β) as potentially suppressed throughout differentiation. Ror β expression was detected in whole bone, primary bone marrow stromal cells, calvarial cells, and osteocytes, but not in osteoclast cultures, suggesting Ror β expression is limited to the mesenchymal osteoblastic lineage. We also demonstrated that Ror β inhibited mineralization of MC3T3-E1 cells, suppressed a Runx2-dependent reporter and inhibited production of the Runx2-dependent genes osteocalcin and osterix. These data strongly suggest that Ror β suppresses bone formation through inhibition of Runx2; however, the mechanisms involved remain unknown. In this study, we employed whole transcriptome profiling using a MC3T3 cell model where Ror β is modestly overexpressed (2.5-fold), in order to further understand the role of Ror β in osteoblast differentiation. We identified 317 Ror β -regulated genes (≥ 1.5 -fold; $q \leq 0.05$) when compared to control MC3T3 cells. Gene ontology analysis indicated that Ror β regulated genes involved in Mapk signaling, Wnt signaling, proliferation and matrix-integrin interactions. Interestingly, a number of regulated genes identified were also known Runx2 targets (i.e. Mgp, Dcn, Pdgfr1, Grh), demonstrating a more generalized modulation of Runx2 by Ror β . Coimmunoprecipitation assays revealed that Ror β and Runx2 interact and that the suppression of Runx2 activity requires an intact DNA binding domain (DBD) of Ror β . This occurs through protein-protein interactions with Runx2 rather than through DNA binding of adjacent sites, since a Ror β DBD double-point mutant that specifically inhibits DNA binding was still capable of repressing Runx2 activity. These data suggest that Ror β may suppress osteoblast differentiation through molecular interactions with Runx2 leading to the modulation Runx2 target genes. Further characterization of Ror β function in osteoblasts may define it as a potential clinical target to treat age-related bone loss.

Disclosures: David Monroe, None.

MO0212

Parathyroid Hormone Regulates Dissociation of HDAC4 from Runx2 on the MMP-13 promoter by PKA Phosphorylation in Osteoblastic Cells. Emi Shimizu^{*1}, Zui Pan², Teruyo Nakatani¹, Nicola Partridge¹. ¹New York University College of Dentistry, USA, ²UMDNJ-Robert Wood Johnson Medical School, USA

Histone deacetylases (HDACs) are crucial regulators of gene expression in transcriptional co-repressor complexes. Previously, we reported that HDAC4 was a basal repressor of matrix metalloproteinase-13 (MMP-13) transcription and parathyroid hormone (PTH) regulates HDAC4 to control MMP-13 promoter activity through causing its dissociation from Runx2. The aim of the present study was to determine the mechanism and signal transduction pathway by which this occurred. We found that PTH induces the protein kinase A (PKA)-dependent phosphorylation of HDAC4 in the nucleus of cells of the rat osteoblastic cell line, UMR 106-01. In contrast, PKA is necessary for the translocation of HDAC4 into the nucleus. We demonstrated that PKA-dependent phosphorylated HDAC4 is released from Runx2 on the runt domain of the MMP-13 promoter in these cells. Point mutations of serines at 355, 576, 740 or threonine at 815 in rat HDAC4 showed that only mutation at serine 740 prevented the release of HDAC4 from Runx2 on the MMP-13 promoter and also the PTH stimulation of MMP-13 transcription. Using antibodies to the equivalent phosphorylation site in human HDAC4 (serine 632), we found that PTH transiently stimulated phosphorylation of this residue and this was abolished when PKA was inhibited. Thus, PTH-induced PKA phosphorylation of serine 740 in rat

HDAC4 is crucial for regulating MMP-13 transcription in osteoblasts. The protein 14-3-3 beta is associated with the shuttling of HDAC4 between nucleus and cytoplasm. Co-localization of 14-3-3 beta and HDAC4 is increased after PTH stimulation and both accumulate in the cytoplasm. These mechanisms regulating HDAC4 and their roles in such processes are crucial for bone and chondrocyte development. Our data support a link between PTH regulating HDAC4 phosphorylation by PKA and trafficking and the control of MMP-13 transcription through association with Runx2.

Disclosures: Emi Shimizu, None.

MO0213

Single Cell Gene Expression Profiling of Mature Murine Primary Osteoblasts. Simon Melov, James Flynn^{*}. Buck Institute for Research on Aging, USA

In tissues with complex histological architecture such as bone, it is often difficult to isolate and molecularly characterize specific cell populations. This difficulty is partially due to isolation of the cells from the tissue of interest, and secondly defining cells with markers that are amenable to additional profiling such as gene expression. To further define molecular characteristics of defined cell types from intact bone, we have developed a protocol to isolate pure cortical osteoblasts, and carry out gene expression analysis on the purified individual cells. Briefly, mouse femurs were isolated from C57BL/6 mice and the bone shaft was dissected, marrow flushed out, and pre-digested to remove periosteal tissue. The remaining tissue was pulverized and collagenase digested to release cells from the bone matrix. The resulting cell population was then further purified using FACS sorting for the canonical mature osteoblast signature of cells that are CD31 and CD45 negative and alkaline phosphatase positive. These targeted cells in addition to randomly selected cells from the total cell population were then prepared for quantitative PCR and assayed with a panel of 89 genes of interest in bone using nanofluidic qPCR on a microfluidic PCR system (Biomark).

We show here that robust gene expression profiling is possible from individual isolated osteoblast cells from adult bone. This approach will facilitate the identification of transcriptional profiles that can identify novel subpopulations within cells identified as osteoblasts by FACS. Single cell expression profiling provides a new dimension to the transcriptional profile of the primary osteoblast population, thereby expanding our understanding of how these cells may function in normal and diseased states.

*Disclosures: James Flynn, Merck, 6
This study received funding from: Merck*

MO0214

The Effect of the Light/Dark Cycle, Hormone Replacement Therapy (HRT), and Melatonin on Bone Physiology in a Blind, HER2+neu Mouse Model. Paula Witt-Enderby^{*1}, John Slater², Nakpangi Johnson², Corry Bondi², Balasunder Dodda³, Mary Kotlarczyk³, William Clafshenkel⁴, Shalini Sethi², Suzanne Higginbotham⁵, James Rutkowski⁶, Vicki Davis⁷. ¹Duquesne University, School of Pharmacy, USA, ²Duquesne University School of Pharmacy, Division of Pharmaceutical Sciences, USA, ³Duquesne University Graduate School of Pharmaceutical Sciences, USA, ⁴Graduate School of Pharmaceutical Sciences, Duquesne University, USA, ⁵Duquesne University School of Pharmacy, Division of Clinical, Social & Administrative Sciences, USA, ⁶Clarion Research Group, USA, ⁷Clarion University, USA

Melatonin release from the pineal gland is regulated by the light/dark cycle and by an endogenous pacemaker; blind women without light perception maintain a melatonin rhythm but one that is out of sync with the light/dark cycle. Melatonin levels begin to rise at dusk and peak around 2 AM. Melatonin is an entraining molecule for most of our physiological systems, including bone; disruption in the rhythm of these systems, for example, by light at night, increases one's risk of cancer and hip and wrist fracture. Understanding the role of endogenous circadian rhythms on bone physiology may help explain the negative consequences of disrupted light/dark rhythms on bone health resulting in novel therapeutic interventions to counteract these effects. We investigated the effects of the light/dark cycle and 9-month treatment with hormone replacement therapy (HRT; 0.5 mg E2/50 mg P4 per 1800 Kcal diet) and/or nocturnal melatonin (15 mg/L water) on serum melatonin levels and on Runx2, BMP-2, BMP-6, Bglap (osteocalcin; OC) and Per2 mRNA levels in bone in a blind HER2+neu mouse model using RIA and real-time RT-PCR, respectively. The effects of chronic HRT (\pm melatonin) on bone quality and density were also assessed by histomorphometry and micro CT, respectively. The results of our study show that melatonin levels in the blind mice fluctuate in a diurnal manner when housed in a 12:12 hour light:dark cycle. Runx2, BMP-2, BMP-6, Bglap (OC) and Per2 mRNA levels are coincident with melatonin levels. Treatment with HRT or nocturnal melatonin increased bone density. HRT increased surface bone, decreased trabecular space and decreased the number of osteoclasts without affecting osteoblast numbers. Melatonin plus HRT did not significantly increase bone density even though this combination significantly increased Bglap (OC) mRNA levels. These data suggest that endogenous melatonin rhythms modulate markers important to bone physiology.

HRT with and without nocturnal melatonin in cycling mice produces unique effects on bone markers and bone density. The effects of these therapies alone and combined may improve bone health in women with low nocturnal melatonin levels from too little sleep, too much light, or age and with low estrogen levels after menopause.

Disclosures: Paula Witt-Enderby, None.

MO0215

Ucma, an unique Cartilage Matrix-associated Protein, as a Common Target of Runx2 and Osterix during Osteoblast Differentiation. Yeon Ju Lee^{*1}, Wook-Young Baek², Eun-Hye Lee¹, Jung-Mi Lee¹, Jung-Eun Kim².

¹Department of Molecular Medicine, Cell & Matrix Research Institute, Kyungpook National University School of Medicine, South Korea, ²Kyungpook National University School of Medicine, South Korea

Runx2 and Osterix (Osx) have been known as the master transcription factors for bone formation. However, genes that act downstream of both Runx2 and Osx have not been well studied. To investigate downstream target genes of Runx2 and Osx, DNA microarray was conducted in calvaria of Wildtype (WT), Runx2^{AC/+} (Runx^{het}), Osx^{+/-} (Osx^{het}), and Runx2^{AC/+};Osx^{+/-} double heterozygous (Double^{het}) mice. During osteogenesis, many genes were up- and down-regulated by both Runx2 and Osx. Compared to WT, in particular, the expression of Ucma (unique cartilage matrix-associated protein) was decreased in Runx^{het} or Osx^{het} and it was more decreased in Double^{het}. Reduced expression of Ucma was confirmed by RT-PCR in calvaria of Runx^{het}, Osx^{het}, and Double^{het}. Ucma was increased by the overexpressed Runx2 and Osx alone and it was further increased by the co-overexpression of Runx2 and Osx. During MC3T3-E1 osteoblastic cell differentiation, Ucma expression was gradually increased in a middle stage following expression of Runx2 or Osx. To analyze whether Runx2 and Osx modulate the transcriptional activity of Ucma, Ucma reporter construct was co-transfected with Runx2 and/or Osx expression plasmid into MC3T3-E1 osteoblastic cells. Either Runx2 or Osx directly activated a 980 bp fragment of the Ucma promoter in a dose-dependent manner. To define the region of the Ucma promoter that was responsive to Runx2 and Osx, a series of Ucma promoter deletion constructs were examined and the Runx2- and Osx-responsive region was refined to between -222 to -41 bp of the Ucma promoter. Collectively, this study suggests that Ucma might be a novel downstream target gene regulated by both Runx2 and Osx in osteoblast differentiation and bone formation.

Disclosures: Yeon Ju Lee, None.

MO0216

BMP-2 Promotes Osteoclast Differentiation by Enhancing the Activity of Smad1. Yoshihiro Yoshikawa^{*}, Aiko Kamada, Isao Tamura, Seiji Goda, Eisuke Domae, Takashi Ikeo. Osaka Dental University, Japan

It is well established that Bone morphogenetic protein 2 (BMP-2) has crucial role in osteoblast differentiation, but it has also been suggested to promote osteoclast differentiation. However the mechanisms by which BMP-2 promotes osteoclast differentiation are not known.

To exam the effects of BMP-2 on osteoclast differentiation, we used primary osteoblasts isolated from calvaria of new born mice. At first, we evaluated expression of genes by real-time PCR and proteins by Western Blot and immunofluorescence in the presence of 10⁻⁸ M 1,25(OH)₂D₃ and 100 ng / ml BMP-2. In addition, we used a proximity ligation assay (PLA) for detecting protein-protein interaction.

In this report, we showed that only BMP-2 has no effect by itself, but BMP-2 upregulated the expression of receptor activator of nuclear factor-κB ligand (RANKL) and vitamin D receptor (VDR) by treatment with 1,25(OH)₂D₃ in primary osteoblasts for 6 and 24 hours. Cycloheximide didn't affect BMP-2-enhanced gene expression of RANKL for 6 hrs. However the expression was suppressed for 24 hours. These observations suggest the effects of BMP-2 on primary osteoblasts result from directly and indirectly accelerating osteoclast differentiation. The stimulatory action of BMP-2 on RANKL expression was suppressed by Smad1 siRNA with 1,25(OH)₂D₃. BMP-2 signaling is mediated by phosphorylation of Smad 1, 5, and 8 which then translocates into the nucleus. We detected interaction between VDR and Smad1 by PLA in situ.

We suggest that BMP-2, not only promotes osteoblast differentiation, but promotes osteoclast differentiation by enhancing the activity of Smad1 and interacting between VDR and Smad1 with 1,25(OH)₂D₃.

Disclosures: Yoshihiro Yoshikawa, None.

MO0217

Involvement of GPR30-mediated Signaling in the Estrogenic Effects of Flavonoids on Rat Osteoblastic UMR106 Cells. Ming Xian Ho^{*1}, Xiaoli Dong¹, KA CHUN Wong¹, Man-Sau Wong². ¹The Hong Kong Polytechnic University, Hong Kong, ²Hong Kong Polytechnic University, Hong Kong

Flavonoid compounds from natural sources, including Naringin from citrus fruits, Icarin from Herba Epimedii and Genistein from legumes have been shown to

improve bone properties by exerting estrogen-like effects on osteoblasts. Our previous studies on Naringin and Icarin revealed their abilities to activate estrogen receptors(ER) ligand-independently without inducing ERE-dependent transcription in rat osteoblastic UMR106 cells, suggesting that a distinct signaling mechanism from classical ER-mediated genomic pathway might be involved. The present study intends to investigate the effects of Naringin, Icarin and Genistein on UMR106 cells and the involvement of GPR30, a novel membrane ER in exerting their effects. The basal gene expression of GPR30 in UMR106 cells was detected by RT-PCR and gel electrophoresis. The effects of these 3 flavonoids on cell proliferation and differentiation were assessed by MTS assay and alkaline phosphatase (ALP) activity, respectively. The results indicated that UMR106 cells express GPR30 endogenously at mRNA level. Upon treatment at a wide range of concentrations, naringin (10-10 M to 10-7M) and icarini (10-12M to 10-6M) significantly increased cell proliferation and ALP activity in UMR106 cells in a dose-dependent manner. In contrast, genistein exerted stimulatory effect only at lower concentrations (10-9M to 10-8M) but demonstrated inhibitory effect at higher concentrations (10-5M) on cell proliferation and differentiation. Co-treatment with ER antagonist ICI182780 (10-6M) as well as with specific GPR30 antagonist G15(10-6M) was able to abolish the promoting effects of all 3 compounds at their most potent dosages on UMR106 cell proliferation and ALP activity. Together, these findings imply that naringin, icarini and genistein exert their stimulatory effects on osteoblasts proliferation and differentiation via signaling pathway which involves both ER and GPR30.

Disclosures: Ming Xian Ho, None.

MO0218

PTH Induces Osteocyte Dedifferentiation, Changes in Morphology and Reverts Embedding Osteocytes to a More Motile Phenotype. Matt Prideaux^{*1}, Erica Perryn², Sarah Dallas³, Lynda Bonewald³. ¹University of Missouri-Kansas City, USA, ²University of Missouri Kansas City School of Dentistry, USA, ³University of Missouri - Kansas City, USA

Although most studies examining PTH effects on bone remodeling have focused on the osteoblast, recent studies have suggested that osteocytes may be a major target cell for the actions of PTH in bone. To identify mechanisms responsible for these effects, primary osteoblasts/osteocytes and the IDG-SW3 cell line, which recapitulates early to late osteocyte differentiation, were utilized. The effect of 50nM PTH (1-34) was examined using osteoblast and osteocyte-enriched cell populations isolated from murine long bones, and ex-vivo collagen digested bone fragments containing mainly mature osteocytes. IDG-SW3 cells were cultured over 30 days and treated with a single administration of PTH at day 0, 7, 14, 21 and 28. Cell morphology and movement were analyzed and RNA and protein were harvested 24 and 48h after treatment.

Expression of the osteocyte marker genes Sost, Dmp1, Phex and Mepe, which increase during IDG-SW3 cell maturation, was significantly reduced after a single treatment with PTH, particularly at the later time points. RANKL expression was enhanced by PTH. A similar decrease in these osteocyte marker genes and increase in RANKL was seen in the bone fragments cultured with PTH. Forskolin and 8-bromo-cAMP mimicked the effects of PTH, but these effects were not blocked with the PKA inhibitor PKI (5-24). Surprisingly, increased expression of the late osteoblast marker Keratocan and the early osteocyte marker E11 was observed with PTH treatment in mature IDG-SW3 cells and bone fragments, suggesting dedifferentiation of mature osteocytes to a more immature phenotype.

Live cell imaging of mature IDG-SW3 cells showed that PTH treatment resulted in profound changes in cell morphology from dendritic to elongated cells together with a dramatic increase in cell motility. Similar effects were seen in cultured calvarial explants from Dmp1-GFP mice, whereby PTH treatment altered the morphology of embedding osteocytes and appeared to revert them to a more motile phenotype.

These data suggest that PTH acts to downregulate mature osteocyte markers and upregulate early osteocyte/osteoblast markers, thereby inducing dedifferentiation of mature osteocytes. In addition, E11 is a novel target of PTH and its upregulation may induce the striking change in morphology and increased motility in the GFP-positive cells as they revert back to a more osteoblastic phenotype. These observations suggest that accelerated movement/motility may play a role in PTH induced bone remodeling.

Disclosures: Matt Prideaux, None.

MO0219

Statins and Bisphosphonates Inhibit Menaquinone-4 Biosynthesis in Bone. Toshio Okano^{*1}, Kimie Nakagawa¹, YOSHIHISA HIROTA¹, Yoshitomo Suhara², Naoko Tsugawa¹. ¹Kobe Pharmaceutical University, Japan, ²Shibaura Institute of Technology, Japan

Introduction: We have recently identified a novel human enzyme, UBIAD1, responsible for the conversion of phyloquinone(PK) to menaquinone-4(MK-4) that is a cofactor for g-glutamyl carboxylase(GGCX) involved in the activation of vitamin K-dependent proteins such as blood clotting factors in the liver and osteocalcin in bone (*Nature*, 2010;468:117). MK-4 is also known to be an active ligand for steroid and xenobiotic receptor(SXR) and modulates the expression of various genes related to osteoblastic functions via binding to SXR. The aims of the present study were to characterize the enzymatic properties of UBIAD1 and to examine the effects of statin,

bisphosphonates and warfarin on the MK-4 biosynthesis by UBIAD1 in bone of animals and human osteoblast-like MG-63 cells.

Methods: Lovastatin(LOV) and Simvastatin(SIM) as lipophilic statins and Pravastatin(PRA) as a hydrophilic statin were used in this study. Etidronate(ETI) as a FPP synthase inhibitory activity negative bisphosphonate, and Alendronate(ALN) and Zoledronate(ZOL) as FPP synthase inhibitory positive bisphosphonates were used in this study. MG-63 cells were treated with either statins at the concentrations of 0.5 to 10 mM or with bisphosphonates at the concentrations of 5 to 100 mM in the medium for 24hrs, and thereafter incubated with 1mM deuterium-labeled phyloquinone(PK-d₇) for further 24hrs. After incubation, the amounts of MK-4-d₇ generated from PK-d₇ were measured by LC-MS/MS. Mice were singly orally given warfarin at the dose of 5 mg/kg body weight, and the concentrations of MK-4 in bone were periodically measured by LC-MS/MS after administration.

Results: LOV and SIM significantly inhibited the MK-4 biosynthesis by UBIAD1, but PRV did not influence MK-4 biosynthesis. ALN and ZOL significantly inhibited MK-4 biosynthesis, but ETI did not influence MK-4 biosynthesis. The concentrations of MK-4 in bone of mice were remarkably reduced at 1 day after warfarin administration, and thereafter the MK-4 concentrations gradually increased to the normal level at 10 days after administration. The MK-4 biosynthesis in MG-63 remarkably reduced by warfarin treatment, but warfarin did not directly inhibit MK-4 biosynthesis by UBIAD1 in a cell-free system.

Conclusion: Statins with lipophilic property and bisphosphonates with FPP synthase inhibitory activity appear to inhibit MK-4 biosynthesis in bone probably due to inhibition of geranylgeranyl pyrophosphate in a mevalonate pathway, and lead to lack of vitamin K action on bone. Therefore, it is suggested the combination use of statins and bisphosphonates with vitamin K during the treatment of osteoporosis.

Disclosures: Toshio Okano, None.

MO0220

Undercarboxylated Osteocalcin Predicts Beta-cell Function in Adult Men and Women with Impaired Fasting Glucose. Barbara Gower^{*1}, Caren Gundberg², Norman Pollock³, Thomas Clemens⁴, Laura Lee Goree⁵, Wesley Granger⁵. ¹University of Alabama at Birmingham, USA, ²Yale University School of Medicine, USA, ³Georgia Health Sciences University, USA, ⁴Johns Hopkins University, USA, ⁵Univ. Alabama at Birmingham, USA

Animal studies indicate that osteocalcin (OC), particularly the undercarboxylated isoform, affects insulin sensitivity and secretion. No clinical study has examined associations of OC isoforms with beta-cell function using robust measures, or determined whether OC is associated with skeletal muscle or hepatic insulin sensitivity. The objective of this study was to test the hypothesis that undercarboxylated osteocalcin (unOC) would be positively and uniquely associated with skeletal muscle insulin sensitivity and beta-cell function in overweight/obese adults under energy balance conditions. Participants were 63 non-diabetic, overweight or obese men and women, 24 of whom had impaired fasting glucose (IFG; fasting glucose of >100 mg/dL). Diet was controlled 3 d prior to testing to ensure energy balance. Serum concentrations of total OC and unOC were measured by RIA, with hydroxyapatite absorption used to separate carboxylated from undercarboxylated OC. Concentrations of type I procollagen (PINP) were assessed to gauge bone formation. Insulin sensitivity (S_I) was determined by three methods to examine associations of OC with measures that reflect primarily skeletal muscle insulin action (intravenous glucose tolerance test, IVGTT-S_I), vs those that primarily reflect hepatic (fasting insulin and glucose concentrations, HOMA-IR) and whole-body (meal tolerance test, Meal-S_I) insulin action. β-cell response to glucose (basal, PhiB; dynamic, PhiD; static, PhiS; and total, PhiTOT) was determined using C-peptide modeling of meal test data. Intra-abdominal adipose tissue (IAAT) was assessed with computed tomography scanning. In all participants combined, total OC was independently and positively associated with S_I-IVGTT (standardized regression coefficient 0.45, P<0.01), after adjusting for IAAT and PINP. OC was not associated with Meal-S_I or HOMA-IR. In participants with IFG, unOC was independently and positively associated with PhiS and PhiTOT, after adjusting for insulin sensitivity (standardized regression coefficient for PhiTOT 0.44, P<0.05). In conclusion, unOC may be uniquely associated with beta-cell function in individuals with dysregulated glucose metabolism. In overweight/obese subjects, OC appears to be associated with skeletal muscle, rather than hepatic, insulin action. Further research is needed to verify this hypothesis using clamp methodology, and to probe the cause-and effect nature of these relationships.

Disclosures: Barbara Gower, None.

MO0221

Anti-Hypertensive Drug Telmisartan Is a Selective PPAR γ Agonist with Anti-Diabetic but Not Anti-Osteoblastic Activity. Vipula Kolli^{*1}, Yalin Lu², Piotr Czernik², Sima Rahman³, Beata Lecka-Czernik⁴. ¹NICHD/NIH, USA, ²University of Toledo Medical Center, USA, ³University of Toledo Health Sciences Campus, USA, ⁴University of Toledo College of Medicine, USA

Anti-diabetic drug rosiglitazone (RSG) improves insulin sensitivity by activating PPAR γ nuclear receptor, however its prolonged use causes bone loss and increases fracture risk in part due to suppression of osteoblast differentiation from marrow mesenchymal stem cells (MSCs). Telmisartan (TEL), the anti-hypertensive drug and angiotensin receptor blocker, also acts as a selective PPAR γ agonist. *In vitro*, in a model of MSC differentiation under the control of PPAR γ 2, TEL inhibited cell proliferation and induced brown-like adipocyte phenotype typified by significant increase in expression of FoxC2, UCP1 and Dio2, however and in contrast to RSG, TEL did not affect osteoblast phenotype as assessed by an alkaline phosphatase (ALP) activity and expression of Runx2 and Dlx5. Moreover, TEL did not suppress the expression and activity of TGF β /BMP signaling pathway, and even prevented RSG negative effect on the expression of members of this signaling pathway. *In vivo*, in a murine model of Type 2 diabetes, yellow agouti A^{vy/a} mice, at the dose which normalized glucose levels and glucose tolerance, TEL did not affect bone mass and body weight, and did not increase marrow fat. In contrast, a dose of RSG, which equally to TEL normalized diabetic phenotype, resulted in 60% loss of trabecular bone, significant increase in body weight, and massive accumulation of fat in bone. Simultaneous treatment with RSG and TEL of A^{vy/a} mice partially prevented bone loss and decreased levels of RSG-induced bone turnover markers, but did not counteract RSG effect on body weight. These results indicate that TEL may be a safe for bone alternative to treat hyperglycemia and provide *in vivo* evidence that the anti-diabetic and the anti-osteogenic activity of PPAR γ may be differentially activated by selective agonists.

Disclosures: Vipula Kolli, None.

MO0222

Aromatic Amino acids Combinations Are Not More Potent Than Single Amino Acids in Activating the MAPK Pathway in BMSCs. Mona El Refaey^{*1}, Kehong Ding¹, Qing Zhong², Jianrui Xu¹, Mark Hamrick¹, William Hill³, Xing-Ming Shi¹, Norman Chutkan¹, Monte Hunter¹, Wendy Bollag¹, Karl Insogna⁴, Carlos Isles². ¹Georgia Health Sciences University, USA, ²Medical College of Georgia, USA, ³Georgia Health Sciences University & Charlie Norwood VAMC, USA, ⁴Yale University School of Medicine, USA

Epidemiologic data demonstrates an association between low protein intake and fractures in the elderly population. The term 'entero-osseous' axis was coined by our lab to describe the relationship between nutrient stimulated gut hormone release and bone formation. However these nutrient effects on bone turnover are indirect, mediated by gut hormones. Little is known about direct nutrient effects on osteoprogenitor / bone marrow stromal cells (BMSC). Since BMSCs differentiate into bone forming or osteoblastic cells they would appear to be natural targets for ingested nutrients. Conigrave et al (2000) demonstrated that L-type amino acid bind to the extracellular calcium receptor. We have previously shown that individual aromatic amino acids (Phenylalanine, Tyrosine and Tryptophan at 100mM) were the most potent amino acids in increasing intracellular calcium and in addition Tryptophan and Tyrosine induced the largest increase in phospho c-Raf. However *in vivo* these amino acids would normally be ingested together. Thus we wished to determine whether combinations of these amino acids were more potent than individual amino acids in activating the MAPK pathway in BMSCs. BMSCs were isolated from C57Bl6 mice and stimulated with single aromatic amino acids or various combinations of two or all three members of this family. We found that Tryptophan was the most potent aromatic amino acid in increasing ERK phosphorylation compared to any aromatic amino acid by itself or even when all three were added; results showed no dose dependent effect. Taken together our data are consistent with individual amino acids as key nutrients in maximizing BMSC proliferation and potentially resulting in a net increase in bone mass.

Disclosures: Mona El Refaey, None.

MO0223

Bone Loss Following Stabilization of Beta-Catenin in *mTert*-Expressing Mesenchymal Stem Cells. Diana Carlone^{*}, Rebecca D. Riba, Dana M. Ambruzs, Samantha Stewart, David T. Breault. Children's Hospital Boston, USA

Proper development, remodeling and regeneration of bone are dependent on the activity of multipotent mesenchymal stem cells (MSCs). Establishing the tools to identify and study these cells will greatly advance our understanding of their role in bone biology, which will lead to improved treatment options for bone diseases.

Telomerase (Tert) activity prevents cellular senescence and is required for maintenance of stem cells in regenerative tissues. We have generated transgenic mouse lines (mTert-GFP and mTert-rtTA) that allow for the identification, isolation and genetic manipulation of mTert-expressing cells. Previously, we showed that mTert-GFP expression marks telomerase-expressing ES cells, iPSC cells and self-renewing tissue stem cells. To investigate whether mTert expression marks MSCs, we isolated GFP+ and GFP-ve cells from the non-hematopoietic fraction of bone marrow using flow cytometry and assayed their ability to form fibroblastic-colony forming units (CFU-Fs), a characteristic of MSCs. Fifteen percent of GFP+ cells gave rise to colonies compared with only 0.5% of GFP-ve cells. These results demonstrate that mTert-GFP+ cells exhibited a 30-fold enrichment in their capacity to form CFU-Fs and indicate that nearly all of the mesenchymal stem cell activity is found within the GFP+ cell population. Current lineage-tracing studies demonstrate that mTert+ cells are present within long bones and contribute to both cartilage and bone lineages. In addition, consistent with our observations in other tissues, the relative number of telomerase-marked cells appears to decrease with age. Finally, the canonical Wnt/ β -catenin signaling pathway has been shown to play an important role in stem cell self-renewal and bone homeostasis. To investigate the effect of this pathway on MSCs, we stabilized β -catenin in mTert+ cells and assessed their colony-forming capacity. While short-term exposure to Wnt signaling increased CFU-Fs (2-3 fold), prolonged activation resulted in an 80% depletion in CFU-Fs and a corresponding decrease in osteoblast differentiation, *in vitro*. In addition, we observed a decrease in both cortical and trabecular bone and overall body length. These studies indicate that mTert expression is a biomarker for MSCs and that Wnt signaling regulates MSC self-renewal and function. Further analysis of these cells may translate into new therapeutics for bone abnormalities.

Disclosures: Diana Carlone, None.

MO0224

Characterization of Progenitors with the Potential to Differentiate into Mesenchymal and Hematopoietic Lineages. Danka Grcevic*¹, Brya Matthews², Sanja Ivcevic¹, Hector Aguila², Ivo Kalajzic². ¹University of Zagreb School of Medicine, Croatia, ²University of Connecticut Health Center, USA

Within the bone marrow (BM) microenvironment mesenchymal and hematopoietic cells are anatomically and functionally related. In our previous study we confirmed that cells expressing smooth muscle α -actin promoter (SMA) directed transgene represent mesenchymal progenitors with the potential for terminal differentiation into mature osteoblast lineage cells *in vitro* and *in vivo*. We now proposed that SMA+ cells also comprise hematopoietic progenitors. This is in line with recent studies that identified progenitor cells expressing both mesenchymal and hematopoietic markers, challenging the long-existing postulation of early separation between those two lineages. In order to trace phenotypic and functional characteristics of SMA+ cells, we generated SMACreERT2 transgenic mice and characterized its expression by crossing it with the Ai9 reporter transgenic line to generate SMACreERT2/Ai9 (SMA9) mice. In a time-course of *in vivo* tamoxifen induction we were able to identify SMA+ cells within BM compartment, comprising less than 0.1% of BM cells 4 days and reaching approximately 0.3% among BM cells 65 days after the first injection. Flow-cytometric analysis confirmed that majority of cells expressed CD45 together with other hematopoietic markers, such as CD11b, Gr-1, Ter119, B220 or CD3. However, around 10% of cells were CD45+ but negative for all other lineage markers. Three weeks after tamoxifen induction those cells expressed immature markers Sca-1 and CD34, but were negative for endothelial markers CD106 and CD31. In addition, they were released into circulation, since we found 0.15% SMA+ cells in the peripheral blood, all expressing mature hematopoietic markers. Moreover, sorted SMA+ cells gave rise to myeloid/monocyte colonies in the methylcellulose cultures. In the parabiotic pair of wild-type and transgenic SMA9 mouse, we detected SMA+ cells in circulation and, occasionally, within the spleen of the wild-type counterpart. On the other hand, CD45- BM population expressed mesenchymal markers such as PDGFB and leptin receptor, increasing in the percentage with the time after tamoxifen induction. Interestingly, some CD45low BM cells also expressed mesenchymal markers together with Sca-1. Our findings provide evidence that SMA+ population gave rise to mature mesenchymal as well as hematopoietic cells. In further experiments we aimed to identify intracellular signaling molecules that control the commitments of progenitors to those lineages.

Disclosures: Danka Grcevic, None.

MO0225

Col2.3GFP Marked Human Embryonic Stem Cells (hESC) Demonstrate Osteoblast Specific Reporter Expression in a Mouse Calvarial Defect Model. Xiaonan Xin*, Xi Jiang, Liping Wang, Mary Louise Stover, Shuning Zhan, Jianping Huang, I-Ping Chen, Ernst Reichenberger, David Rowe, Alexander Lichtler. University of Connecticut Health Center, USA

The use of hESC and induced pluripotent stem cells (iPSC) for study and treatment of genetic bone diseases, such as craniometaphyseal dysplasia (CMD) and osteogenesis imperfecta (OI), and traumatic bone injuries requires efficient protocols to differentiate hESC/iPSC into cells with osteogenic potential, and to isolate differentiated osteoblasts for analysis. We have reported immunohistochemical

methods for identification of human osteoblasts in mouse calvarial defects, however these methods require multiple steps and do not allow convenient isolation of pure osteoblasts. We have established zinc finger nuclease (ZFN) technology to increase the efficiency of homologous recombination at AAVS1 site (referred to as a "safe haven" site), and have delivered a construct containing Col2.3 promoter driven GFPemerald to human embryonic stem cells (H9Zn2.3GFP) to mark the cells in the osteoblast lineage. In a teratoma formed using these cells, we identified GFP positive cells specifically associated with bone. We also differentiated the cells into a mesenchymal stem cell population with osteogenic potential for mouse calvarial defect model implantation. We observed GFP positive cells associated with alizarin complexone (AC) labeled newly formed bone surfaces. This bone showed a similar distinctive pattern of AC labeling and bone structure as was seen with human bone in teratomas, which was different from mouse bone. The GFP positive cells were also alkaline phosphatase (AP) positive, and immunohistochemistry with human specific bone sialoprotein (BSP) antibody has indicated that the GFP positive cells are also associated with human BSP containing matrix. Therefore, we believed that our Col2.3GFP is marking the cells in the osteoblast lineage. The drug selection method generated mixed cell population with about 30% Col2.3GFP targeted cells, so we performed single cell cloning to generate a 100% Col2.3GFP positive cell population, which was confirmed by FISH using a GFP probe. The karyotype was normal. We demonstrated the pluripotency of this clonal line by Tra1-60 immunostaining, pluripotent low density RT PCR array and embryoid body (EB) formation. We are testing these cells by forming teratomas and differentiating the cells *in vitro* and implanting them in the calvarial defect model. We expect that these cells will be useful to develop optimal osteogenic differentiation protocols, and to isolate osteoblasts from normal and diseased iPSC for analysis.

Disclosures: Xiaonan Xin, None.

MO0226

Effect of High Calcium Environment on Proliferation and Survival Activity of BMSCs *in vitro*. EunAh Lee*¹, HyunJi Cho², Jong Kuk Park³, WheeMoon Cho², Youngsook Son². ¹Kyung Hee University, South Korea, ²Lab of Tissue Engineering, College of Life Science, Kyung Hee University, South Korea, ³Korea Institute of Radiational & Medical Science, 215-4 Gongneung-dong, Nowon-gu, South Korea

Bone remodeling sites are known to have locally elevated high calcium concentration. Even though osteoclasts resorb bone tissue debris, many cells residing near the bone remodeling units are inevitably exposed to high calcium concentration. To test the effect of high calcium concentration on hBMSCs, hBMSCs and human dermal fibroblasts (hDFs) were exposed to media with various concentrations of calcium. The viability of hBMSCs were significantly higher than that of hDFs in all ranges of calcium concentrations tested. When calcium concentrations were higher than 5mM, a increase of calcium concentration reduce the number of both hBMSCs and hDFs. When apoptosis was determined by FACS analysis of propidium iodide-incorporated fraction of cells, proportion of apoptotic cells slightly increased as the calcium concentration elevated which indicated that declined cell number in high calcium media was due to cell apoptosis. Although environment of high calcium concentration severely induced growth arrest of hDFs, this tendency was weakly shown in hBMSCs. Rather, the growth of hBMSCs was accelerated when calcium concentrations were between 3 to 5mM. Our results suggest that high calcium media exert less stress on hBMSCs compared to hDFs, and this may explain their survival mechanism in endosteal micro-environment. This research was supported by a grant from Korean Ministry of Health and Welfare given to Youngsook Son (A040003) and a grant from National Research Foundation of Korea given to EunAh Lee (2011-0009391).

Disclosures: EunAh Lee, None.

MO0227

Effect of Strontium Ion on *in vitro* Proliferation and Osteogenic Differentiation of PA20-h5, a Clonal Mesenchymal Stem Cell Line Derived from Subcutaneous Adipose Tissue. Simone Ciuffi*, Valeria Nardone, Sergio Fabbri, Francesca Marini, Roberto Zonefrati, Carmelo Mavilia, Gianna Galli, Barbara Pampaloni, Annalisa Tanini, Anna Maria Carossino, Maria Luisa Brandi. University of Florence, Italy

Introduction:

Strontium ion (Sr²⁺) acts on bone metabolism uncoupling bone remodelling and favoring bone formation. The human adipose tissue derived mesenchymal stem cells (hAMSCs) are able to differentiate into osteoblasts producing alkaline phosphatase (ALP) and calcified nodules. These characteristics, combined with the great achievable quantity and the low invasivity in tissue sampling, make the adipose tissue an optimum source of stem cells for bone regeneration. The aim of our study was to evaluate the effects of Sr²⁺ on proliferation and osteogenic differentiation of a clonal cell line, named PA20-h5, obtained from a primary culture of AMSCs.

Methods: PA20-h5 is derived from a healthy 45 years old female. Cell proliferation was evaluated in the presence of Sr²⁺ at concentrations from 5 to 400 mM in culture medium containing 1.5% FCS, for times ranging from 0 to 12 days. Osteogenic differentiation was induced by culturing the cells in osteogenic medium (OM) [Ham's F12 Coon's modification medium supplemented with 10% FCS, 10 nM

dexamethasone, 10 mM β -glycerophosphate, 0.2 mM sodium L-ascorbyl-2-phosphate, 1% antibiotics] and different Sr^{2+} concentrations from 2.5 μM to 2 mM for times ranging from 7 to 35 days. The osteogenic differentiation was evaluated by quantitative fluorometric assay for ALP and HA and analysis of *ALP*, *RUNX2*, *SMAD1*, *OCN*, *OPN*, *OPG*, *LRP5*, *RUNKL*, *COL1A1* and *DKK1* genes expression by qPCR.

Results: Growth curves showed a significant increase of proliferation [200%] for the 100 μM Sr^{2+} concentration compared to the untreated control. Significant increases of ALP activity and HA production were observed, respectively, for concentrations of Sr^{2+} from 100 to 2000 μM , and for 2.5 to 50 μM , for induction times between 14 and 35 days. The 100 μM Sr^{2+} concentration induced the early (already after 6 days of treatment) increase of expression of *ALP* and *RUNX2*, if compared to cell cultured only in OM, while all the other genes were not affected in their expression.

Conclusions: These findings demonstrate that 100 μM Sr^{2+} stimulates hAMSCs growth. At higher concentrations [100-2000 μM] Sr^{2+} promoted the expression of early markers of osteogenic differentiation as ALP, while at lower doses [2.5-50 μM] Sr^{2+} induced *in vitro* bone mineralization. In conclusion, Sr^{2+} could play a role in the therapy of bone disorders also promoting osteogenic cells proliferation and differentiation.

Disclosures: Simone Ciuffi, None.

MO0228

Effect of Strontium Release from Amidated Carboxymethyl Cellulose Hydrogel on the Osteoinduction of a Clonal Cell Line Obtained from Human Adipose Tissue-Derived Mesenchymal Stem Cells. Valeria Nardone*, Sergio Fabbri, Cecilia Romagnoli, Gaia Palmi, Elisa Bartolini, Gianna Galli, AnnaMaria Carossino, Annalisa Tanini, Maria Luisa Brandi. University of Florence, Italy

Introduction:

In the recent years, there has been an increasing interest in interactive application principles of biology and engineering, for the development of valid biological systems for bone tissue regeneration, such as for the treatment of bone fractures or skeletal defects. The application of stem cells together with biomaterials releasing bioactive factors promotes the formation of bone tissue by inducing proliferation and/or cell differentiation. The aim of our study was that to evaluate the effect of strontium (Sr^{2+}) released from amidated carboxymethylcellulose hydrogel (CMCA) on the osteoinduction of PA2-E12, a clonal cell line obtained from human adipose tissue-derived mesenchymal stem cells (hADSCs).

Materials and Methods:

PA2-E12 clonal cell line, previously characterized for its multi-potency in our laboratory, was plated on tissue culture polystyrene (tPS) substrate in Ham's F12 Coon's medium +10% fetal calf serum (FCS) and, reached the semiconfluence, differentiated by osteogenic medium (OM): Ham's F12 Coon's medium +10% FCS with 10nM dexamethasone, 10mM β -glycerophosphate and 200mM sodium L-ascorbyl-2-phosphate, or by OM with scalar concentrations from 3 μM to 3mM Sr^{2+} , or, alternately, in OM in presence of transwell containing CMCA enriched with the same Sr^{2+} concentrations. Osteoinduction was evaluated quantitatively by fluorometric assays for alkaline phosphatase (ALP) and hydroxyapatite (HA) production during 1-42 days of induction.

Results: A preliminary observation has shown a limited adhesion of PA2-E12 to the CMCA, associated to a maintenance of round morphology. Significant increases of ALP activity compared to control were observed in cells cultured in OM in presence of Sr^{2+} released from CMCA enriched with 3mM Sr^{2+} after 7 and 14 days, and in cells cultured in OM with 300 μM and 3mM Sr^{2+} after 14 days. Significant increases in the formation of HA deposits compared to control were observed after 14 days both for cells cultured in presence of Sr^{2+} released from CMCA enriched with 3mM Sr^{2+} and for cells cultured in OM with 30 μM Sr^{2+} .

Conclusions: Our results have shown that CMCA enriched with Sr^{2+} at concentrations 100 times higher than those used in OM, is able to promote the osteoinduction of PA2-E12 probably thanks to a release of Sr^{2+} in the culture medium, as shown both by increased ALP (until 99%) and HA (until 169%) differentiation markers compared to control at 14 days.

Disclosures: Valeria Nardone, None.

MO0229

Effects of Cytoskeletal Manipulation on Mechanotransduction in Mesenchymal Stem Cells. Petra Müller, Anne Langenbach, Joachim Rychly*. University of Rostock, Germany

Biological responses, including multipotent differentiation of mesenchymal stem cells depend on mechanical properties of the environment. Mechanotransduction into the cell is mediated by integrins which are able to form a physical connection to the actin cytoskeleton. To analyze the role of the cytoskeleton in mechanically induced activation of human mesenchymal stem cells (MSC) more in detail, we asked whether modification of the cytoskeleton using three different agents affects the activation of intracellular signaling proteins. In addition we asked, whether differentiation to adipocytes is controlled by changes in the cytoskeletal organization.

Integrin mediated mechanical loading was applied by drag forces using magnetic microbeads attached to β 1-integrin receptors. Cellular responses were detected by measuring phosphorylation of Erk and Akt using Western blot or the Bioplex technique. To modify the actin cytoskeleton, MSC were preincubated using depolymerizing (cytochalasin D (CyD), latrunculin A (Lat-A)) or polymerizing (jasplakinolid (Jas)) drugs.

Mechanical stress applied to β 1-integrin receptors induced a significant activation of Erk and Akt. Incubation of the cells with CyD, Lat-A, and Jas at subtoxic concentrations induced a partial fragmentation, contraction, or irregular organization of the cytoskeleton, respectively. In the presence of the polymerizing drug Jas the activation of Erk and Akt by mechanical integrin stress remained unaffected. Using the depolymerizing drugs, CyD reduced the activation of Akt with little effect on Erk activation, whereas treatment of the cells with Lat-A completely blocked the mechanically induced activation of Erk and Akt. Adipogenic differentiation of MSC remained unaffected by treatment with the depolymerizing drugs, but was impaired when the polymerizing drug Jas was applied.

In conclusion, although all three actin inhibitors significantly affected the structure of the cytoskeleton, only Lat-A, which blocks the formation of F-actin from G-actin, strongly impaired the mechanotransduction to activate cell signaling. The results revealed an inverse relationship between adipogenic differentiation and activation of Akt and Erk, when modifying the actin cytoskeleton.

Disclosures: Joachim Rychly, None.

MO0230

Hypoxia Disrupts Osteoblast Proliferation and Mineralization in Rats with High Intrinsic Aerobic Capacity. Jacqueline Cole*, Lauren G. Koch¹, Steven L. Britton¹, Ronald Zernicke¹, Kenneth Kozloff². ¹University of Michigan, USA, ²University of Michigan Department of Orthopaedic Surgery, USA

Exercise alters organism aerobic capacity directly via mechanical loading. Aerobic exercise also alters cellular aerobic capacity in muscle via mitochondrial biogenesis, but the effect on bone cells is unknown. We previously found greater potential for osteoblast mineralization in rats selectively bred as high capacity runners (HCR) than in low capacity runners (LCR). Our objective was to examine if HCR and LCR osteoblasts have a differential response to hypoxia during differentiation and mineralization. We hypothesized differences would be more apparent with hypoxia.

Female HCR and LCR rats were matched for age (2.2 mo) and body mass (173 g). HCR females in this generation had an 8-fold farther untrained treadmill run to exhaustion than LCR females (2228 vs. 269 m). Our cohort was euthanized, and femora and tibiae were excised and used for *in vitro* (n=3 per group) or biomechanics (n=15 per group) assays. Marrow stromal cells were harvested, cultured in triplicate using standard procedures, differentiated using osteogenic medium, and exposed to normoxic (20% O_2) or hypoxic (1% O_2) conditions. Cell proliferation and mineralization were assessed on days 0, 3, 7, 10, and 14. For biomechanics, femora were examined with micro-computed tomography and 3-point bending to failure (right) and dynamic histomorphometry (left).

On average across differentiation, HCR cells proliferated more than LCR for both normoxia and hypoxia ($p < 0.0001$). HCR cells also mineralized more per cell than LCR for normoxia ($p = 0.003$) and hypoxia ($p = 0.001$). HCR cultures were more detrimentally affected by hypoxia than LCR for mineralization ($p = 0.01$) and cell count ($p = 0.006$) but not for mineralization/cell (Fig 1-4). Femoral cortical tissue mineral density (TMD) showed modest increases in HCR vs. LCR (1.3%, $p = 0.07$). Compared with LCR at femoral distal metaphysis, HCR had lower trabecular TMC (42%) and TMD (3%), bone volume fraction (39%), trabecular thickness (35%) and number (9%), and higher trabecular separation (87%). HCR had lower energy to failure (16%) but higher estimated elastic modulus (14%) than LCR.

Both cellular and tissue mineralization were enhanced in HCR vs. LCR. Hypoxia substantially disrupted HCR proliferation and mineralization, which was unexpected given the superior HCR response to fracture and ovariectomy observed previously. This differential response may result from impaired HCR glycolytic capacity. Mechanisms will be explored in upcoming gene expression assays.

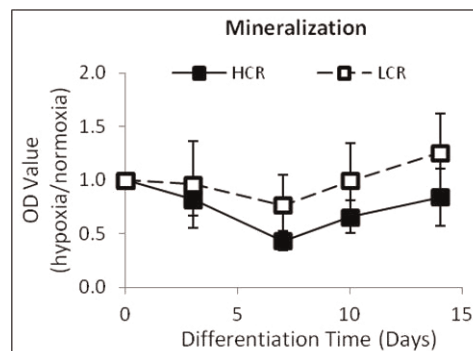


Fig. 1. HCR cultures were more detrimentally affected by hypoxia than LCR cultures for mineralization.

Figure 1

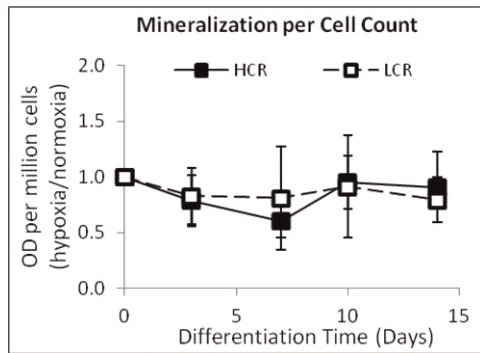


Fig. 2. HCR and LCR cultures were affected similarly by hypoxia for mineralization per cell.

Figure 2

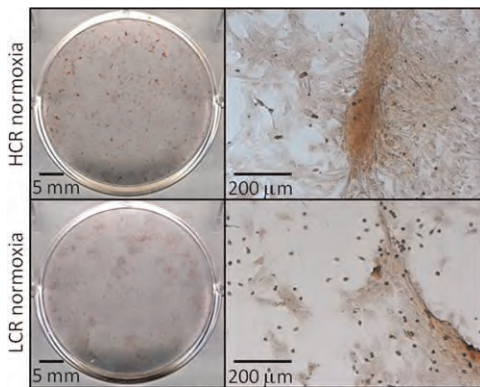


Fig. 3. Mineral nodules for normoxia cells at day 10 with magnification at 0X (left) and 10X (right).

Figure 3

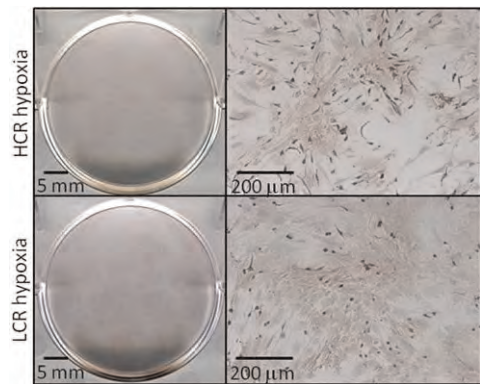


Fig. 4. Mineral nodules for hypoxia cells at day 10 with magnification at 0X (left) and 10X (right).

Figure 4

Disclosures: Jacqueline Cole, None.

MO0231

Osteoprotegerin (OPG) Secreted from Osteoblasts Stimulates Human Mesenchymal Stem Cells for Osteogenesis. SunMi Palumbo*, Wan-Ju Li. University of Wisconsin-Madison, USA

Osteoblasts play a critical role in maintaining bone homeostasis by producing bone matrix and regulating osteoclastogenesis. Previous studies have shown that conditioned medium (CM) from osteoblast culture enhances osteogenesis (OG) of mesenchymal stem cells (MSCs), indicating that osteoblasts secrete soluble factors that regulate MSC differentiation. In this study, we aim to identify OG factors in CM produced by osteoblasts and to investigate the underlying molecular mechanism mediated by these OG molecules to determine how osteoblasts regulate OG of human MSCs (hMSCs).

We prepared CM from the MG-63 osteoblast-like cell culture and tested whether the CM affects differentiation of hMSCs and whether the regulation is associated with the differentiation status of hMSCs by culturing hMSCs with or without CM for 2

passages, and then inducing for osteogenesis with or without CM. Our results showed that both the levels of *osteocalcin* (OC) mRNA transcript and ALP activity significantly increased in the cells treated with CM prior to and/or during differentiation (+/-, -/+, +/+), and the +/- group showed the greatest increase of these osteogenic markers among all the tested groups (Fig. 1). To identify OG factors in the CM, we performed a comparative protein assay and an ELISA to analyze the culture supernatants of the MG-63 cells and hMSCs, and found that the level of osteoprotegerin (OPG), known as a potent anti-osteoclastogenic protein, was 5.5 times higher in the MG-63 cell culture than the reference MSC culture. Based on the concentration detected by the ELISA, we treated hMSCs with 40 ng/mL OPG prior to and/or during osteogenic differentiation (Fig. 2) and found that both the levels of OC mRNA transcripts and calcium deposits significantly increased in the cells treated with OPG prior to but not during OG (+/-), suggesting that OPG is one of the key soluble molecules capable of priming undifferentiated hMSCs to enhance subsequent OG. Furthermore, we observed that NF-κB p65 was greatly activated in the OPG-treated hMSCs. By regulating NF-κB activity using its inhibitor, we demonstrated that NF-κB is one of the regulators mediating the OPG-induced OG (Fig. 3). Taken together, our results demonstrate that OPG increases the osteogenic capacity of undifferentiated hMSCs through the activation of NF-κB, and the findings can be used to create a model elucidating the interaction between osteoblasts and MSCs.

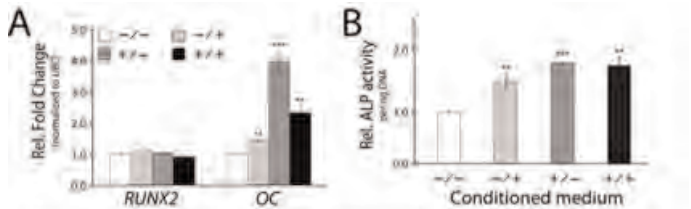


Figure 1. Effect of the MG-63 cell CM on osteogenesis of hMSCs. Undifferentiated hMSCs were treated with (+) and without (-) CM for 2 passages prior to osteogenic differentiation, and then differentiated in osteogenic medium supplemented with (+) and without (-) CM. (A) Real-time-PCR analysis detecting mRNA transcripts of osteogenic markers, and (B) quantitative assay to measure ALP activity showed that CM addition enhanced osteogenesis of hMSCs. RUNX2: Runx-related transcription factor 2, OC: Osteocalcin, and ALP: Alkaline phosphatase. ** p < 0.005, *** p < 0.0005. n = 3.

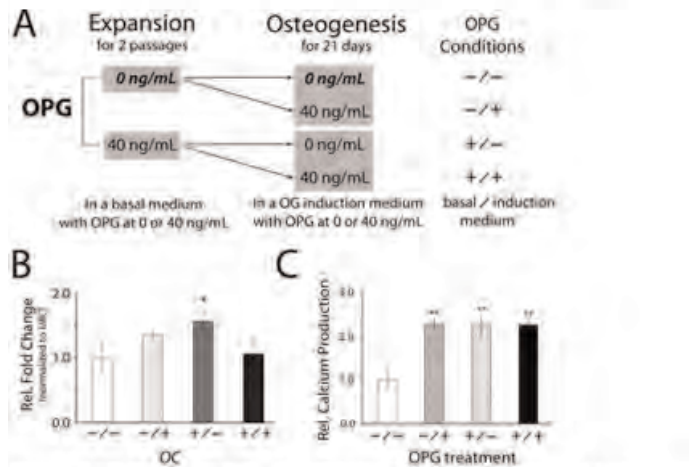


Figure 2. Effect of OPG on the regulation of hMSC osteogenesis. (A) Experimental design. Human MSCs were cultured in basal medium with (+) or without (-) 40 ng/mL osteoprotegerin (OPG) for 2 passages prior to osteogenesis and then induced for differentiation in osteogenic medium with (+) or without (-) 40 ng/mL OPG. The control group is denoted in bold and italic. (B) Real-time PCR analysis and (C) calcium mineral production assay showed that OPG increased both the levels of OC mRNA transcripts and mineralization in the cells treated with OPG prior to but not during differentiation (+/-). * p < 0.05, ** p < 0.005, n = 3.

Figures 1 and 2

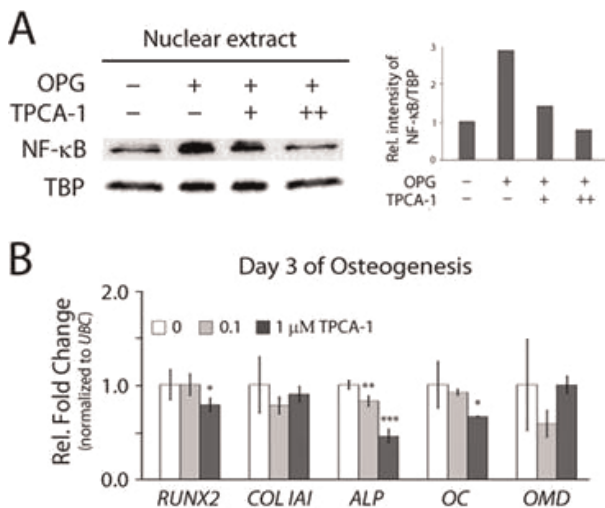


Figure 3. Effect of NF- κ B inhibition on osteogenesis of hMSCs treated with OPG. Human MSCs were treated with both 40 ng/mL OPG and a NF- κ B inhibitor, TPCA-1, for 2 passages prior to osteogenesis, and then were induced for osteogenesis without OPG and TPCA-1. (A) The nuclear levels of NF- κ B were decreased in a TPCA-1 dose-dependent manner. (B) The mRNA expression of osteogenic markers showed that TPCA-1 inhibited the OPG-mediated osteogenic induction. *COL1A1*: Collagen type I, α 1, *OMD*: Osteomodulin. * $p < 0.05$. ** $p < 0.005$. *** $p < 0.0005$. $n = 3$.

Figure 3

Disclosures: SunMi Palumbo, None.

MO0232

Protein Kinase Inhibitor γ (PKI γ) Conversely Regulates Osteogenesis and Adipogenesis by Inactivating Protein Kinase A. Xin Chen¹, Bryan Hausman¹, Janet Rubin², Guangbin Luo¹, Shunichi Murakami¹, Guang Zhou¹, Edward Greenfield¹. ¹Case Western Reserve University, USA, ²University of North Carolina, Chapel Hill, School of Medicine, USA

The PKI gene family inactivates nuclear PKA and thereby terminates PKA-induced gene expression. We previously showed that PKI γ is the primary PKI expressed in calvarial osteoblasts, murine femoral metaphyses, and osteoblastic cell lines. We also showed that PKI γ knockdown significantly increases the effects of PTH or forskolin (FSK) on PKA activation, immediate-early gene expression, and inhibition of apoptosis. PKA signaling stimulates both osteogenesis and adipogenesis; however, the two lineages are often conversely regulated. Our goal was therefore to determine which of the two mechanisms predominates. Murine embryonic fibroblasts (MEFs) from PKI γ KO mice generated in our lab were compared with wild type MEFs. As expected, PKA signaling was substantially increased in PKI γ KO MEFs. To determine whether PKI γ KO simultaneously regulates osteogenesis and adipogenesis, MEFs were cultured in a 1:1 mixture of osteogenic and adipogenic media. PKI γ KO increased alkaline phosphatase (ALP) activity by 3.4 fold ($p < 0.05$) and substantially increased ALP staining. Moreover, PKI γ KO increased mineralization as assessed by Alizarin Red S (ARS) staining by 10-fold ($p < 0.05$) and inhibited adipogenesis as assessed by oil red O (ORO) staining by 30% ($p < 0.05$). Co-staining for ALP and ORO confirmed that the PKI γ KO MEFs are substantially more osteogenic and substantially less adipogenic than the wild type MEFs. To confirm above results, lineage-specific media were used to further examine the role of PKI γ . PKI γ KO increased ALP and osteocalcin (OC) mRNAs by 5.3 and 16.5 fold, respectively ($p < 0.05$) after 7 days of culture in osteogenic medium supplemented with FSK. PKI γ KO also increased ALP activity and mineralization ($p < 0.05$). Similarly, siRNA-mediated knockdown of PKI γ in a murine MSC cell line increased FSK-induced ALP and OC mRNAs by 2.6 and 2.1 fold, respectively ($p < 0.05$). In contrast, adipogenesis was inhibited by PKI γ KO as both ORO staining and PPAR γ , C/EBP α , Adiponectin, and Leptin mRNAs were decreased by 20-52% ($p < 0.05$). These results show that PKA activation by PKI γ KO simultaneously increases osteogenesis and inhibits adipogenesis. Therefore, inhibition of PKI γ might be a novel therapeutic option to increase the PKA-mediated anabolic effects of PTH in osteoporotic patients.

Disclosures: Xin Chen, None.

MO0233

Rodent Trabecular Bone Marrow Is Enriched with a Highly Proliferative, Immunosuppressive, and PTH-responsive Population of Mesenchymal Progenitors. Valerie Siclari¹, Ji Zhu², Kentaro Akiyama³, Fei Liu⁴, Xianrong Zhang², Abhishek Chandra¹, Songtao Shi³, Ling Qin¹. ¹University of Pennsylvania, USA, ²University of Pennsylvania, School of Medicine, USA, ³University of Southern California, USA, ⁴Shanghai Ninth People's Hospital, China

The traditional method for harvesting rodent bone marrow (BM) by simply flushing long bones yields mesenchymal stem cells (MSC) from the diaphyseal (central) bone but not those residing in the trabecular (endosteal) bone. We have developed a unique method based on enzymatic digestion of rat or mouse bone tissues to harvest BM cells and generate MSCs from the endosteal and central marrow regions. Endosteal BM from one-month-old rats formed 3-fold more and 1.7-fold larger CFU-F colonies with a similar percentage of alkaline phosphatase (ALP)-positive colonies compared to the central BM. Similar results were observed with mice and isolation of endosteal BM cells from mice expressing GFP under a 2.3kb collagen 1 promoter confirmed that the GFP+ osteoblasts, released by digestion into the endosteal BM, were not the source of the endosteal CFU-F colonies. Endosteal MSCs generated by this method expressed traditional BM MSC surface markers and were capable of multi-lineage differentiation and in vivo bone formation. Interestingly, they exhibited accelerated growth rate with a doubling time of about 20 hr compared to central MSCs (~48 hr), which is likely due to the decreased expression of the cell cycle inhibitor p21. Moreover, they showed greater immunosuppressive activity in an in vitro T cell apoptosis assay and a dextran sulfate sodium-induced acute colitis mouse model. Further experiments revealed a 2-fold decrease in endosteal CFU-F colony number in aging mice compared to young mice, which is consistent with a 5-fold decrease in the percentage of Sca1high+CD29high+CD45- mesenchymal progenitors in the endosteal BM in aging mice. No decrease was observed in the central BM MSCs numbers from aging mice. Parathyroid hormone (PTH) injection is the only approved anabolic therapy for osteoporosis and it greatly stimulates bone formation. A single PTH injection significantly increased the number (3-fold) of CFU-F colonies and the size (2.1-fold) of CFU-ALP-negative colonies formed from the endosteal BM with no effect on those from the central BM. Taken together, we have provided strong evidence that endosteal MSCs from bone have distinct functional characters from the traditional central MSCs and that they are more metabolically active and relevant to physiological bone formation.

Disclosures: Valerie Siclari, None.

MO0234

ER α and ER β differentially regulate the effects of estradiol and mechanical strain on proliferation and *Sost* expression. Gabriel Galea¹, Lee Meakin¹, Toshihiro Sugiyama², Andre Van Wijnen³, Lance Lanyon⁴, Joanna Price¹. ¹University of Bristol, United Kingdom, ²Yamaguchi University School of Medicine, Japan, ³University of Massachusetts Medical School, USA, ⁴Royal Veterinary College, United Kingdom

Estrogen Receptor (ER) signaling mediates anabolic effects of mechanical strain and estrogens on bone, partly through osteoblast proliferation¹ and down-regulation of the osteocyte-specific Wnt antagonist *Sost*/sclerostin². We sought to establish commonalities and differences in the ER-related mechanisms by which 17 β -estradiol (E2) and strain regulate *Sost* and osteoblast proliferation.

Proliferation and *in situ* cell cycle analysis was by Ki-67 staining of human SaOs-2 cells and osteoblasts from long bones of adult mice (LOBs). *Sost* expression, not detected in LOBs, was assessed in SaOs-2 cells by qPCR. Strain was by four-point bending³ of the cells' substrate. ER signaling was interrogated by non-selective inhibition with fulvestrant or with selective agonists (PPT for ER α , DPN for ER β) and antagonists (MPP against ER α , PTHPP against ER β) (all 0.1 μ M). *Sost* was measured in bones of adult female ER α ^{-/-} mice and vehicle- or tamoxifen-treated WT.

Strain recruited quiescent LOBs to the cell cycle within 1h. Equally rapid recruitment of quiescent SaOs-2 cells followed exposure to strain or E2. Proliferation was increased by ER β blockade, strain and E2, but these increases were prevented by ER α blockade. Sclerostin pre-treatment had no effect on proliferation following E2, but prevented that following strain. Strain and E2 both down-regulated *Sost* in SaOs-2 cells within 8hrs. Neither PTHPP nor PPT altered *Sost* expression but DPN down-regulated it, as did MPP. *Sost* levels were lower in ER α ^{-/-} bones than in WT. Tamoxifen down-regulated *Sost* in bones from OVX mice, in which it enhanced the osteogenic effects of loading. In SaOs-2 cells fulvestrant and blockade of ER β , but not ER α , prevented *Sost* down-regulation by strain or E2.

In conclusion, in osteoblastic cells, ER α maintains basal *Sost* expression and enables rapid induction of proliferation following exposure to strain or E2, but does not mediate *Sost* down-regulation by strain or E2. ER β opposes ER α by inhibiting basal proliferation and mediates *Sost* down-regulation following strain or E2. ER β -mediated down-regulation of *Sost* by strain relieves inhibition of ER α -mediated proliferation. The proliferation-related effects of E2 are independent of sclerostin.¹Cheng et al, J Bone Miner Res, 2002;17(4): 593-602. ²Modder UI et al, J Bone Miner Res, 2011;26(1):27-34. ³Galea et al, FEBS Letters, 2011;585(15):2450-4.

Disclosures: Gabriel Galea, None.

MO0235

Influence of Estradiol on the Mechanical Response of Human Fetal Osteoblasts Cells *in Vitro*. PADMALOSINI MUTHUKUMARAN*, Chwee Teck Lim, Taeyong Lee. National University of Singapore, Singapore

Aim Post menopausal osteoporosis primarily occurs due to estrogen deficiency. The influence of estrogen on the cellular and molecular aspects osteoblasts and osteoblasts-like cells has been extensively studied. However, the influence of estrogen on mechanical aspects of osteoblasts cells has not yet been studied. The aim of this study is to investigate the direct effect of estradiol on the structural and mechanical properties human fetal osteoblasts (hFOB1.19) and its response to fluid shear stress (FSS).

Methods The hFOB cells were grown to confluency and then grown with either medium alone or medium with 10nM and 100nM β -Estradiol. Atomic Force Microscopy indentation was used to determine the apparent elastic modulus (E^*) using Hertz's contact equation. The cells were stained with TRITC-Phalloidin for f-actin and imaged using confocal microscope. To analyze the cells response to FSS, the cells were grown in fluid channel made of PDMS and subjected to 1 Pa FSS. The cells were stained with Fluo-3AM for intracellular calcium. The increase in intracellular calcium level following FSS was monitored using fluorescence microscope. The cells were also tested for alkaline phosphatase (ALP) activity, mineralization and proliferation.

Results The cells treated with estradiol showed significantly lower E^* (0.3kPa for both 10nM and 100nM) as compared to the control cells (0.58kPa) [Fig1]. The confocal images showed that the altered mechanical properties were associated with changes in the density of the actin filaments [Fig2]. Flow induced increase in intracellular calcium level is higher in estradiol treated cells as compared to control cells. The quantified mineralization of all groups remained the same. The ALP activity of estradiol treated cells significantly increased.

Conclusions The results suggest that during the pathogenesis of osteoporosis the estrogen deficiency can not only cause the changes in the molecular mechanism in osteoblasts cells but is also associated with changes in their elasticity. The confocal images showed that the changes in mechanical properties are due to changes in density of actin filaments and not due to difference in mineralization of the cells. Thus, this study shows that estradiol influences the mechanical properties of osteoblasts primarily through cytoskeletal changes of the cells. The changes in the mechanical property of the cells were also associated with changes in its response to mechanical stress.

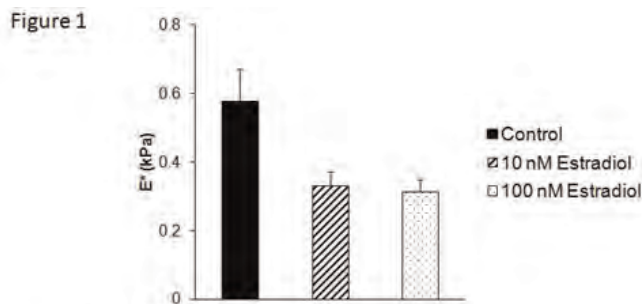


Figure 2

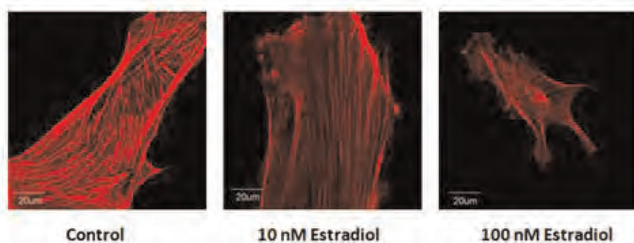


Figure 1 and 2

Disclosures: PADMALOSINI MUTHUKUMARAN, None.

MO0236

Inhibition of Lipopolysaccharide Induced Osteoclast Formation And Bone Resorption *In Vitro* In Mice By Cystatin C. Fredrik Stralberg*¹, Anders Grubb², Ulf Lerner³. ¹Molecular Periodontology, Umeå University, Sweden, ²Lund University, Sweden, ³University of Umea, Sweden

We have found that RANKL induced osteoclast formation in cultures of mouse bone marrow macrophages (BMM) and human CD14⁺ monocytes is inhibited by i) cystatin C, ii) a peptidyl derivative (Z-RLVG-CHN₂) based on the sequence of a cystatin C domain crucial for its cysteine proteinase inhibitory activity, and iii) the

fungal cysteine proteinase inhibitor E-64. The inhibitory mechanism is due to RANKL facilitated uptake of cystatin C and is associated with decreased signaling downstream RANK, suggesting that intracellular cysteine proteinases play a prominent role in osteoclast differentiation (ASBMR 2011).

In the present study, we demonstrate that osteoclast formation stimulated by lipopolysaccharide (LPS) *e.coli* (10mg/ml) in RANKL-primed (4ng/ml RANKL for 24h) purified BMMs is inhibited by cystatin C. The inhibitory effect was associated with decreased LPS-induced mRNA expression of osteoclast-specific genes such as *Acp5* (TRAP), *Ctsk* (cathepsin K), *Calcr* (Calcitonin Receptor), *Cfos* (c-Fos), and *Nfatc1* (NFATc1). Cystatin C decreased LPS-induced protein of NFATc1 and c-Fos as assessed by Western Blot. Cystatin C also abolished LPS-stimulated osteoclast formation of TRAP⁺MuOCL cells, resorption pits, and release of CTX when BMM were cultured on bone slices. The two other cysteine proteinase inhibitors Z-RLVG-CHN₂ and E-64, also inhibited osteoclast differentiation of RANKL-primed LPS-stimulated BMM. In contrast, the MMP inhibitor TIMP-1 did not affect LPS stimulated TRAP⁺MuOCL formation. Furthermore, semi-quantitative RT-PCR show that cystatin C inhibited LPS induced upregulation of *JunB*, *Fra-2*, *p52*, *RelB*, and *Ikbα* mRNA. Together, the data suggest that cystatin C inhibits osteoclast formation by inhibiting LPS-induced differentiation of mononuclear osteoclast progenitor cells. The effect is due to inhibition of signaling pathways downstream TLR-4 known to be important in RANKL-induced osteoclastogenesis, like NfκB, AP-1, and NFATc1. These data indicate that cysteine proteinases seem to be important in both LPS- and RANKL-induced osteoclastogenesis.

Disclosures: Fredrik Stralberg, None.

MO0237

Paxillin Contracts the Osteoclast Cytoskeleton in a myosin IIA-dependent manner. Wei Zou*¹, Carl DeSelm¹, Thomas Broekelmann², Robert Mecham³, Scott Vande Pol⁴, Kyunghee Choi⁵, Steven Teitelbaum¹. ¹Washington University in St. Louis School of Medicine, USA, ²Washington University School of Medicine, USA, ³Washington University School of Medicine, USA, ⁴Department of Pathology, University of Virginia, USA, ⁵Department of pathology, Washington University School of Medicine, USA

Osteoclastic bone resorption depends upon the cell's ability to organize its cytoskeleton via the $\alpha v \beta 3$ integrin and osteoclastogenic cytokines. Since paxillin is a key cytoskeleton-organizing adaptor protein which associates with $\alpha v \beta 3$, we asked if it participates in skeletal degradation. Exploration of the role of paxillin in osteoclast function is compromised by the fact that mice deleted of the protein die in early embryogenesis. To circumvent this difficulty, we generated Pax^{-/-} and Pax^{+/-} osteoclasts from murine embryonic stem cells (ESCs). Unlike deletion of other $\alpha v \beta 3$ -associated cytoskeleton-regulating molecules, which impairs the cell's ability to spread, paxillin-deficient (Pax^{-/-}) osteoclasts "superspread" in response to RANK ligand (RANKL) and form large, albeit dynamically atypical, actin bands. Despite their increased size, Pax^{-/-} osteoclasts resorb bone poorly, excavating pits approximately 1/3 normal depth. Ligand-occupied $\alpha v \beta 3$ or RANKL promotes paxillin serine and tyrosine phosphorylation, the latter via c-Src. The abnormal Pax^{-/-} phenotype is rescued by WT paxillin but not that lacking its LD4 domain. In keeping with the appearance of mutant osteoclasts, WT paxillin, overexpressed in WT cells, impairs their spreading capacity. Most importantly, the abnormal phenotype of Pax^{-/-} osteoclasts likely represents failed RANKL-mediated delivery of myosin IIA to the actin cytoskeleton via the paxillin LD4 domain but is independent of tyrosine phosphorylation. Thus, in response to RANKL, paxillin associates with myosin IIA to contract the osteoclast cytoskeleton thereby promoting its bone-degrading capacity.

Disclosures: Wei Zou, None.

MO0238

Resorption Capacity of Osteoclasts Predefined by Surface Porosity of Ceramic Biomaterials. Kanthi Lewis*¹, Gerald Zimmer², Astrid Rohrhofer¹, Oskar Hoffmann¹. ¹University of Vienna, Austria, ²Baxter Innovations AG, Austria

The importance of pore size in bone biomaterials for osteoblast migration and bone formation has been well studied, however little is known about the effect on osteoclast (OC) function. As bone repair is dependent on resorption of graft material prior to new bone formation, the rate of remodeling by OC is an important consideration. Thus the effect of porosity on OC activity is the focus of this work.

The effect of biomaterial porosity on OC was evaluated using commercially available beta-tri-calcium phosphate (β -TCP) powder. Disks were prepared and sintered at nine temperatures from 900°C to 1280°C yielding different surface porosities. Materials were evaluated via scanning electron microscopy and porosity quantified via image J software. Disk compositions were confirmed via X-ray diffraction to rule out phase changes during sintering. Rabbit OC were cultured on disks for 48h and the number of viable OC was determined via TRAP staining. F-actin proteins of the cytoskeleton were stained with Alexa Fluor Phalloidin to evaluate resorption activity. Actin rings indicate actively resorbing OC.

Material surface porosity ranged from 41.3% (900°C) to 1.6% (1280°C) as a function of sintering temperature. While no significant differences were observed in

the number of mature OC adhered to ceramic disks of varying porosity, as measured by TRAP staining, increasing the porosity decreased the resorption ability of the OC. Actin staining confirmed that porosity between 41.3% and 32.9% inhibited actin ring development, indicating no resorption took place. A porosity of 20.8% gave rise to a slight increase in resorption activity, and significant increases were observed with porosities $\leq 15.6\%$ with maximum resorption on disks with a porosity of 1.6%. Thus OC resorption of a biomaterial is dependent on the biomaterial porosity, while initial attachment of mature OC is not.

It is shown that for ceramic β -TCP disks a lower porosity supports the formation of actin rings and OC activation, with 1.6% the most optimal for OC to establish the sealing zone on the material surface, required for actin ring formation and bone resorption. It is believed that when the surface interaction is insufficient due to high porosity, the osteoclast attachment is incomplete and subsequent remodeling and formation of new bone may be delayed. These findings should be taken into consideration whenever biomaterials intended as bone graft substitutes are designed.

Disclosures: *Kanthi Lewis, None.*

MO0239

A T-box Family Transcription Factor may Mediate CSF1-induced JDP2 Gene Transcription. Chen Yao*, Gang-Qing Yao, Karl Insogna. Yale University School of Medicine, USA

CSF1 has a non-redundant role in osteoclastogenesis and is reported to promote osteoclast progenitor survival. We wondered if there were also pro-differentiation actions of the cytokine. In a microarray screen designed to identify CSF1 targets in osteoclasts, expression of Jun dimerization protein 2 (JDP2) was significantly induced by CSF1. JDP2 has a critical role in osteoclastogenesis since suppressing its expression blocks osteoclast differentiation. We previously reported cloning of a 3297 bp fragment of the JDP2 gene from -2612 to +682 bp (relative to the transcription start site). A CSF1 response element was found in the sequence -191 to -141 bp. Using this 50 bp sequence as labeled probe, competition studies were performed by EMSA using a panel of cold probes derived from the original 50 bp sequence. These studies localized the cis-element to the first 35 bp of the 50 bp construct. In subsequent competition tests, mutated oligos derived from this 35 bp sequence were used. These revealed that mutation of the 3 thymidines in the sequence TGGGTGTGAA, to adenines, completely abolished the ability of the mutant 35 bp oligo to compete in an EMSA. Introducing the same mutation into a functional 200 bp JDP2 promoter completely abrogated CSF1 activity in a luciferase-based JDP2 reporter assay using pZen cells, a murine cell line expressing c-fms. A database search initially suggested a brachyury-binding site overlapping the region of the mutated thymidine bases. However brachyury-specific antibodies were unable to supershift the target band in an EMSA. It has also been reported that this sequence represents a putative binding site for the T box superfamily of transcription factors, which are highly homologous to brachyury. To identify which T-box member is expressed and responsive to CSF1, we used a pair of degenerate primers designed to amplify the conserved T-box domain in murine T-box family members. RT-PCR was performed using cDNA derived from pZen cells and osteoclast like cells generated in vitro (OCLs). PCR products were cloned and sequenced and revealed that OCLs only express T-box 3 while pZen cells express T-box 1, 2 and 3. We conclude that CSF1 stimulates JDP2 expression via a TGGGTGTGAA motif, which could be a binding site for T-box proteins. T-box 3 is a candidate for mediating the effects of CSF1 on JDP2 expression in osteoclasts.

Disclosures: *Chen Yao, None.*

MO0240

IFN- γ Inhibits Mechanical Stress-induced Osteoclastogenesis and Bone Resorption. Haruka Kohara*¹, Hideki Kitaura², Masako Yoshimatsu¹, Yuji Fujimura¹, Yukiko Morita¹, Toshiko Eguchi¹, Noriaki Yoshida¹. ¹Nagasaki University, Japan, ²Tohoku University, Japan

The focus of this experiment is to detect expression of Interferon- γ (IFN- γ) and to define the effect of IFN- γ on tooth movement and mechanical stress-induced osteoclastogenesis in mouse tooth movement model. Orthodontic force initiates an inflammatory response, resulting in bone resorption, which causes tooth movement. Several studies have shown that orthodontic force induces expression of tumor necrosis factor- α (TNF- α), an inflammatory cytokine, and suggested an important role for TNF- α in orthodontic tooth movement. IFN- γ , another inflammatory cytokine, is expressed on the pressure side of teeth in a rat tooth movement model. In this study, we investigated the effects of IFN- γ on experimental tooth movement in mice. A Ni-Ti closed coil spring was worn between the upper anterior alveolar bone and the upper left first molar in mice. First, we evaluated expression level of mRNA of IFN- γ at local site on orthodontic tooth movement. In addition, IFN- γ was injected into a local site adjacent to the first molar every other day during the tooth movement. After 12 days, the amount of tooth movement was measured. Tissue surrounding the first molar was removed for histological observation. The number of tartrate-resistant acid phosphatase (TRAP)-positive cells at the pressure side of experimental tooth was counted as osteoclasts. This experimental appliance moved the first molar to mesial side. IFN- γ mRNA expression level at local site was increased on orthodontic tooth movement. The number of TRAP-positive cell was increased at the pressure side of the first molar. On the other hand, the amount of the tooth movement and the number of TRAP-positive cell at the pressure side in IFN- γ -injected mice were less than that of control mice. IFN- γ was induced on experimental tooth movement. IFN- γ could

inhibit mechanical force loaded osteoclastogenesis and tooth movement. The results suggested that IFN- γ might inhibitory affect excessive osteoclastogenesis during orthodontic tooth movement, and that IFN- γ might be useful for control of orthodontic tooth movement.

Disclosures: *Haruka Kohara, None.*

MO0241

Manipulation of the RANKL/RANK/OPG Axis Using Structure-based Design and Yeast Surface Display. Julia Warren*¹, Christopher Nelson², Daved Fremont², Steven Teitelbaum¹. ¹Washington University in St. Louis School of Medicine, USA, ²Washington University in St. Louis, USA

The interaction between Receptor Activator of NF- κ B Ligand (RANKL) and its receptor RANK is key to the differentiation and function of the osteoclast, the sole bone resorbing cell. Osteoprotegerin (OPG), a soluble homodimer, acts as a decoy receptor for RANKL. RANK and OPG contain four similar cysteine-rich repeat domain (CRD) regions, but OPG binds RANKL with greater affinity and markedly different kinetics. An imbalance in the RANKL/RANK/OPG axis with decreased OPG and/or increased RANKL is associated with diseases that favor bone loss, including osteoporosis. To explore the structural basis of RANK versus OPG binding to RANKL, we designed 34 RANKL mutants. Our initial screens have identified six candidate RANKL mutants, all of which contain CD loop insertions, which retain variable levels of OPG binding (including normal) but show no detectable binding to RANK. These findings are also in accordance with the co-crystal structures which demonstrate a dramatic rearrangement of the RANKL CD loop when bound to RANK versus OPG and may explain the observed differences in affinity despite the similar footprints of the interfaces. Using similar methods, we were not able to design mutations that abolish binding to OPG while leaving binding to RANK intact. Therefore, we have established a yeast surface display system to screen libraries of randomly mutated RANKL proteins and select for these properties. RANKL is expressed on the surface of yeast fused to the C-terminus of an inducible yeast mating protein, Aga2p. Using flow cytometry, we can detect a dose-dependent increase in OPG and RANK binding to surface displayed wild-type RANKL, indicating functionality of our system. After multiple rounds of sorting randomly mutagenized RANKL libraries, we appear to have enriched for RANKL mutants that have lost the ability to bind OPG while still retaining the ability to bind RANK. We are now in the process of screening individual clones to identify novel mutations in RANKL with these properties. Once identified, we will analyze recombinant proteins using biophysical and biological read-outs of function.

Disclosures: *Julia Warren, None.*

MO0242

Prostaglandin D₂ Induces Apoptosis of Human Osteoclasts Through the Activation of Akt and ERK Signaling Pathways. Artur De Brum-Fernandes¹, Li Yue*¹, Sophie Roux², Stephen McManus². ¹Universite De Sherbrooke, Canada, ²University of Sherbrooke, Canada

Prostaglandin D₂ (PGD₂) is a lipid mediator, which functions by activating two specific receptors: the D-type prostanoid (DP) receptor and chemoattractant receptor homologous molecule expressed on T-helper type 2 cells (CRTH2). Our previous findings showed that PGD₂ induces osteoclast (OC) apoptosis through the activation of CRTH2-dependent intrinsic apoptotic pathway. The objective of this study is to determine which signaling mediates PGD₂-induced OC apoptosis. Human OCs were generated through the differentiation of human peripheral blood mononuclear cells in the presence of rhRANKL (60 ng/ml) and M-CSF (10 ng/ml) for 21 days, and then treated with PGD₂ as well as its agonists/antagonists. Caspase-3 fluorogenic substrate assay and immunoblotting were performed to determine caspase-3 activity and key proteins involved in phosphatidylinositol3-kinase (PI3K)/Akt, mitogen-activated protein kinase (MAPK)/extracellular-signal-regulated kinase (ERK) and NF- κ B signalling pathways. Human differentiated OCs were pretreated with a specific PI3K inhibitor (LY294002, 1 μ M) and a specific inhibitor of MAPK/ERK kinase (MEK)-1/2 (U0126, 1 μ M) for 30 min prior to the treatment of PGD₂ as well as its agonists/antagonists for 24 h. We found that 10 nM of both PGD₂ and CRTH2 agonist (DK-PGD₂) treatments decreased the phosphorylation of Akt at Ser473, whereas the phosphorylation of Akt (Ser473) was augmented by CRTH2 antagonist CAY10471 (10 nM) in OCs. Treatment of OCs with a PI3K inhibitor LY294002 further reduced Akt phosphorylation, but increased caspase-3 activity caused by PGD₂. A significant decrease in the phosphorylation of ERK (Tyr204) was also observed in OCs after treatment with 10 nM of PGD₂ or CRTH2 agonist (DK-PGD₂). Moreover, the treatment of OCs with a specific MEK-1/2 inhibitor (U0126) further reduced ERK phosphorylation at Tyr204, but increased caspase-3 activity in the presence of PGD₂ incubation. Interestingly, treatment with DP agonist (BW 245C, 10 nM) or DP antagonist (BW A868C, 10 nM) did not have any effect on either Akt or ERK phosphorylation in OCs. Furthermore, the treatment of OCs with 2 nM and 10 nM of PGD₂, DP agonist (BW 245C), CRTH2 agonist (DK-PGD₂), DP antagonist (BW A868C), or CRTH2 antagonist (CAY10471) did not alter the phosphorylation of RelA/p65 on Ser536. These results suggest that PGD₂ promotes CRTH2-dependent apoptosis in human differentiated OCs by activating the PI3K/Akt and MEK/ERK, but not NF- κ B signaling pathways.

Disclosures: *Li Yue, None.*

MO0243

Comparative analysis of Osteoclast Differentiation from Red-boned and Common Goats. Qiuye Lin¹, Zhenhui Cao¹, Hua Rong¹, Zhiqiang Xu², Dahai Gu¹, Guozhou Liao¹, Qichao Huang¹, Xiaobo Chen¹, Xi Zhang³, Shizheng Gao¹, Zhe Wang⁴, Changrong Ge², Junjing Jia¹, Wei Yao⁵.
¹Yunnan Provincial Key Laboratory of Animal Nutrition & Feed, Yunnan Agricultural University, China, ²Yunnan Agricultural University, China, Peoples Republic of China, ³Yunnan Agricultural University, Peoples Republic of China, ⁴College of Animal Husbandry Veterinary, Jilin University, China, ⁵University of California, Davis Medical Center, USA

In the previous study, red-boned goats with six months age have shown higher bone mineral density and contents in femur and tibia than common goats of same age. Bone metabolism results from a balance between osteoclast-driven bone resorption and osteoblast-mediated bone formation. Little is known about osteoclast behavior of red-boned goats. Therefore, we investigated the osteoclast differentiation of red-boned goats. Bone marrow cells obtained from the femurs of red-boned goats or common goats (n=4, aged 6 months) and were cultured for 72 h in α -minimal essential medium supplemented with 10% fetal bovine serum and 50 ng/ml macrophage-colony stimulating factor (M-CSF). Adherent cells were used as bone marrow macrophages (BMMs) and were incubated for 6 days with 50 ng/ml M-CSF in the presence of 25 ng/ml receptor activator of NF- κ B ligand (RANKL). The medium was replaced with fresh medium containing these reagents every 48 h. The adherent cells were fixed and stained for tartrate-resistant acid phosphatase (TRAP), and the number of TRAP-positive multinucleated cells was counted. Total RNA was isolated and receptor activator of NF- κ B (RANK) gene expression was assessed using Real-time RT-PCR. BMMs were plated onto dentine slices and cultured with 50 ng/ml M-CSF and 25 ng/ml RANKL for 14 days. At culture termination, the slices were rinsed with phosphate-buffered saline (PBS) and left overnight in 1 M ammonium hydroxide to remove all attached cells. The slices were then washed in PBS and examined for formation of resorption pits with a scanning electron microscope. BMMs from red-boned goats and treated with M-CSF and RANKL suggested less potential to differentiate into osteoclasts than did those from common goats, as evaluated by the number of TRAP-positive multinuclear cells. Furthermore, decreasing resorption activity was observed in BMMs from red-boned goats. Gene expression level of RANK, which is expressed on the surface of osteoclast progenitors, was shown to reduce during differentiation of BMMs from red-boned goats compared to those from common goats.

Disclosures: Qiuye Lin, None.

This study received funding from: Joint Funds of the National Natural Science Foundation of China and Yunnan Provincial Government (U0836601)

MO0244

Differential Regulation of Osteoclast Precursor Migration by Activin A and RANKL. Tristan Fowler^{*}, Richard Kurten, Larry Suva, Dana Gaddy.
 University of Arkansas for Medical Sciences, USA

The early recruitment of osteoclast (OC) precursor cells involves a variety of coordinated steps, including migration, which represents an important regulatory step in bone resorption. RANKL and Activin A (ActA) are potent stimulators of osteoclastogenesis in murine bone marrow cultures. Interestingly, ActA does not induce osteoclastogenesis in isolated murine bone marrow macrophages (BMM), but inhibits RANKL-induced OC development. We hypothesized that these factors might also exhibit differential regulation of OC precursor migration, and tested their effects *in vitro* on normal BMM motility and migration using time-lapse video microscopy. BMMs were plated onto culture dishes and cultured with 25 ng/ml mCSF alone for 24hrs, prior to the addition of RANKL (100 ng/mL) or ActA (50 ng/mL), alone or together, for up to 4d. Cells were imaged using Scion imaging software at 60 images/hour and the cells maintained at 37°C and 5% CO₂/Air. The 4hr movement of ten individual motile OC precursors were tracked and analyzed with NIH ImageJ MTrackJ. Motility parameters calculated for each individual cell track included cumulative track length, migration rate, maximum instantaneous velocity, range of velocity, and percent total displacement. BMMs cultured with mCSF alone migrated at a constant velocity and distance from d1-d4. RANKL treatment significantly increased motility rate, cumulative track length, and maximum instantaneous velocity on days 2 & 3, an effect that was lost by d4. In contrast, ActA treatment caused a significant decrease in motility rate, cumulative track length, and maximum instantaneous velocity on d1-4. Surprisingly, when added together, ActA treatment completely blocked all RANKL stimulated OC precursor motility. To determine if the effects on OC precursor migration were consistent with motility, cells were treated for 6hr with different combinations of mCSF, ActA, and RANKL in transwell dishes, and the number of migrating cells across the transwell membrane determined. Although RANKL significantly increased migration, ActA alone had no effect. However, when added together, ActA prevented the RANKL-induced increase in OC precursor migration. Together, these data provide the first evidence of ActA inhibition of RANKL. The data strongly support the hypothesis that ActA suppression of RANKL-stimulated OC precursor motility and migration, both of which are critical for OC differentiation and function, is dominant over the pro-OC activity of RANKL.

Disclosures: Tristan Fowler, None.

MO0245

Gender-Based Differences in RANKL Induced Osteoclastogenesis Through MKP-1 Signaling. Michael Valerio^{*}, Keith Kirkwood. Medical University of South Carolina, USA

Osteoclasts (OC) arise from hematopoietic progenitor populations in response to M-CSF and RANKL. RANKL signals through its cognate receptor RANK, activating NF- κ B and MAPK pathways, leading to translocation of OC-specific transcription factors (TF). Regulation of these pathways is partially dependent on phosphatases such as MAPK phosphatase-1 (MKP-1), which deactivates TF translocation. Recent preliminary evidence from our lab showed that ablation of Dusp-1 (gene for MKP-1) results in increased osteoclastogenesis (OCgen) within progenitor sub-populations in female mice. Additionally, we and others have noted phenotype differences in male and female *Dusp-1*^{-/-} (KO) mice, including reduced size in female. Based on these observations, we hypothesize that MKP-1 differentially regulates RANKL induced OCgen in male vs. female mice. To test this, 8-12 week old age-matched male and female WT and *Dusp-1*^{-/-} mice were sacrificed and OC progenitor cells were flushed from BM, sorted into CD11b^{high} (Macrophage (M Φ)), CD11b^{low} (M Φ /OC lineage), and CD11b⁻ (non-M Φ) populations, then stained for M-CSF Receptor (CD115) and stem cell marker c-kit (CD117). Defined populations were plated and treated with M-CSF or M-CSF + RANKL for up to nine days. TRAP assay was used to assess morphology following treatment. qPCR was utilized for RNA expression of early (DAP12, FLT3, PU.1), mid (NFATc1, DC/OC-STAMP) and late (Calcitonin Receptor, Cathepsin K) OC genes for 3, 5, 7 and 9 days. Initial sort results indicated no significant differences between the percent distribution of sub-populations. Conversely, our data indicates that female KO have significantly more expression of both CD115 and CD117, but less dual expression with CD11b compared to male counterparts and WT. TRAP assay data suggests that within each sub-population, *Dusp-1* KO male mice have 48% less OC than WT counterparts. Moreover, OC size compared to WT was negligible. In contrast, female KO have 30% more OC and CD11b^{low} cells are about 5.5-fold larger than male WT counterparts. In accordance with these data, qPCR data indicates male KO mice express OC-specific markers close to WT levels. Conversely, female KO RANKL-treated cells expressed higher levels of OC-specific genes including a 6-fold increase in master OC TF NFATc1. Collectively, our results support the hypothesis that MKP-1 differentially regulates RANKL induced OCgen in males vs. females through regulation of OC number, size and gene expression.

Disclosures: Michael Valerio, None.

MO0246

Lis1 Regulates Osteoclastogenesis through Small GTPase Cdc42. Shiqiao Ye^{*}, Stavros Manolagas, Haibo Zhao. Central Arkansas VA Healthcare System, Univ of Arkansas for Medical Sciences, USA

Haploinsufficiency of LIS1, also known as platelet-activating factor (PAF) acetylhydrolase isoform 1b subunit 1 (PFAH1b1), causes lissencephaly, a severe human developmental brain disorder due to impaired neuronal migration. LIS1 has been shown to regulate microtubule dynamics, PAF, and Cdc42 in neurons. Since these molecules/pathways are critical for osteoclast differentiation, survival, and/or function it is likely that LIS1 regulates osteoclastic bone resorption. To test this hypothesis, we have generated LIS1 macrophage conditional knockout (cKO) mice by crossing LIS1-floxed mice with LysM-Cre mice. LIS1 expression was abolished in macrophages and osteoclasts from LIS1 cKO mice but not in those from control mice, as shown by western blots. LIS1 cKO mice had no gross skeletal abnormality during development, but at 5-month old of age, they exhibited increased bone mass measured by micro-CT, as compared to their control littermates. The level of serum TRAP5b, an *in vivo* marker of osteoclast number, was decreased in cKO mice, indicating that loss of LIS1 impairs osteoclastogenesis. Consistent with this finding, macrophages isolated from cKO mice had intrinsic defects in osteoclast differentiation as revealed by a decreased number of TRAP+ osteoclasts and reduced level of TRAP 5b in culture medium. The attenuated osteoclast formation in LIS1-null macrophages was associated with a significant decrease in macrophage proliferation, osteoclast differentiation and survival, due to reduced activation of ERK and AKT by M-CSF and prolonged RANKL-induced JNK activation. These defects were cell autonomous because reconstitution of wild type LIS1 in cKO macrophages by retroviral transduction rescued osteoclastogenesis and M-CSF/RANKL signaling. Next, we searched for downstream pathway(s) of LIS1 critical for osteoclast formation. Neither ectopic PAF nor overexpression of NDE1 and NDEL1, two LIS1 binding partners in regulating microtubule dynamics, rescued the osteoclast formation defect in cKO cultures. On the other hand, expression of a constitutively active form of Cdc42 dramatically increased osteoclastogenesis in cKO macrophages. Moreover, M-CSF- and RANKL-stimulated Cdc42 activation was blunted in cKO pre-osteoclasts as measured by a GST-pull down assay. We conclude that LIS1 regulates bone remodeling in mice and is an essential molecule for the activation of Cdc42 during osteoclast differentiation.

Disclosures: Shiqiao Ye, None.

MO0247

Liver X Receptor Activation Suppresses Osteoclastogenesis via the Down-regulation of c-Fos Expression and Promotes Apoptosis in Mature Osteoclast. Hyun-Ju Kim*, Hye Jin Yoon, JungMin Hong, Shin-Yoon Kim. Kyungpook National University Hospital, South Korea

Liver X receptors (LXRs) are nuclear receptors that play important roles in lipid homeostasis and inflammatory response. LXRs have been known to play a role in RANKL-induced osteoclast development. However, the precise mechanisms by which LXRs regulate osteoclast formation and the effects of LXRs on osteoclast survival and inflammation-mediated bone destruction remains unclear. In this study, we show that the LXR ligands, T0901317 and GW3965, suppressed osteoclast formation from primary bone marrow macrophages (BMMs) in a dose-dependent manner. While the RANKL-induced p-38 phosphorylation was not altered, the JNK activation was strongly inhibited by T0901317. Furthermore, T0901317 and GW3965 significantly suppressed both mRNA and protein expression of c-Fos, which is a key transcription factor for osteoclast differentiation. The inhibitory effect of LXR ligands on osteoclast formation was reversed by c-Fos overexpression, suggesting that c-Fos is a downstream target for anti-osteoclastogenic action of LXRs. Additionally, T0901317 induced apoptosis in mature osteoclast. Confirming the in vitro effect, LXR ligand protected lipopolysaccharide (LPS)-induced bone loss in vivo. Taken together, our results demonstrate that LXRs inhibit RANKL-mediated osteoclastogenesis by suppressing c-Fos expression and induce osteoclastic cell death.

Disclosures: Hyun-Ju Kim, None.

MO0248

Magnesium Deficiency Results in an Increased Formation of Osteoclasts. Marina Belluci¹, Ton Schoenmaker², Carlos Rossa-Junior³, Silvana Orrico³, Teun De Vries⁴, Vincent Everts⁵. ¹Department of Diagnosis & Surgery, School of Dentistry at Araraquara – UNESP-Univ. Estadual Paulista, Araraquara, Brazil, ²Dept Periodontology, ACTA, Netherlands, ³Department of Diagnosis & Surgery, School of Dentistry at Araraquara, Brazil, ⁴ACTA, University of Amsterdam & VU University, The Netherlands, ⁵Department of Oral Cell Biology Academic Centre of Dentistry Amsterdam (ACTA), The Netherlands

Magnesium (Mg^{2+}) deficiency is a frequently occurring disorder that leads to loss of bone mass, abnormal bone growth and skeletal weakness. Until now, it is not clear whether Mg^{2+} deficiency affects the formation and/or activity of osteoclasts. We evaluated the effect of Mg^{2+} restriction on these parameters. Bone marrow cells from long bone and jaw of mice were seeded on plastic and on bone in medium containing different concentrations of Mg^{2+} (0.8 mM which is 100% of the normal value, 0.4, 0.08 and 0 mM). The effect of Mg^{2+} deficiency was evaluated on cell viability after 3 days and proliferation rate after 3 and 6 days, as was mRNA expression of osteoclastogenesis-related genes and Mg^{2+} -related genes. After 6 days of incubation, the number of tartrate resistant acid phosphatase-positive multinucleated cells (TRACP⁺-MNCs) was determined, and the TRACP activity of the medium was measured. Osteoclastic activity was assessed at 8 days by resorption pit analysis. Mg^{2+} deficiency resulted in increased numbers of osteoclast-like cells; a phenomenon found for both types of marrow. Mg^{2+} deficiency had no effect on cell viability and proliferation. Increased osteoclastogenesis due to Mg^{2+} deficiency was reflected in higher expression of osteoclast-related genes. However, resorption per osteoclast as well as TRACP activity were lower in the absence of Mg^{2+} . In conclusion, Mg^{2+} deficiency augmented osteoclastogenesis but appeared to inhibit the activity of these cells. Together, our in vitro data suggest that altered osteoclast numbers and activity may contribute to the skeletal phenotype as seen in Mg^{2+} deficient patients.

Disclosures: Vincent Everts, None.

MO0249

Osteoclasts Support Angiogenesis in vitro. Mohammad Islam*, Melissa Stemig. University of Minnesota School of Dentistry, USA

Multiple studies have reported proangiogenic function of osteoclasts. However, the relationship between osteoclasts and angiogenesis is poorly understood. We hypothesized that osteoclast secreted molecules support endothelial cell growth, differentiation and their angiogenic function. We used human umbilical vein endothelial cells (HUVEC) and CD14⁺ human peripheral blood mononuclear cells and used osteoclast culture media to study HUVEC cell growth, differentiation and function. HUVEC cells express endothelial specific marker CD31, develop specific morphology and angiogenic function. CD14⁺ cells, in presence of macrophage colony stimulating factor (m-CSF) and receptor activator of nuclear factor kappa B ligand (RANKL), differentiate into functional osteoclasts. Differentiated osteoclasts secrete enzymes and cytokines in the culture medium. CD14⁺ cells were plated for osteoclast differentiation. RANKL and m-CSF were added for their differentiation into osteoclasts. At D3, media was replaced and old media (OCLCM) was collected and filtered to use in D1 HUVEC culture. HUVEC cells were analyzed at D7 for CD31 expression, angiogenic function and mRNA expression of endothelial genes. HUVEC cultures using endothelial growth media supplemented with endothelial growth

factors (EGM2) and cytokines were used as positive control and HUVEC cultures using α -modified eagle medium (α -MEM supplemented with 10% FBS) was used as negative control. We found that differentiated osteoclasts express angiogenic genes including angiopoietin 2, β 3 integrin, sphingosine kinase. Preliminary results show that use of α -MEM in the culture reduces CD31 expression in HUVEC cells, cause increase cell death and loss of endothelial specific functions. However, use of α -MEM based OCLCM prevented loss of CD31 expression in HUVEC cells. Our findings demonstrate supportive roles of osteoclast secreted molecules in endothelial cell survival and differentiation.

Disclosures: Mohammad Islam, None.

MO0250

PDF Suppresses Osteoclast Differentiation, Bone Resorption Activity and Survival via Osteoprotegerin Induction. Toru Akiyama*¹, Jonathan Clark², Peter Choong². ¹Saitama Medical Center, Jichi Medical University, Japan, ²Department of Orthopaedic Surgery, St. Vincent's Hospital Melbourne, Australia

Background: Pigment epithelium-derived factor (PEDF) has been shown to be one of the most potent inhibitors of angiogenesis. Previously, we demonstrated a therapeutic effect of PEDF on osteosarcoma, which is the most common primary malignant bone tumor. Interestingly, the activity of PEDF against osteosarcoma is strictly limited to a bone milieu. Furthermore, a novel disease locus responsible for osteogenesis imperfecta, SERPINF1, coding for PEDF has been found recently. Although the involvement of PEDF in bone homeostasis has not been suggested previously, it was reported that a relationship between bone resorption and angiogenesis exists in erosive bone pathologies such as bone metastasis and rheumatoid arthritis. Vascular endothelial growth factor (VEGF), a potent pro-angiogenic factor, facilitates OCL bone resorption activity and elongates OCL survival. To grow in bone, osteosarcoma has to induce osteoclast (OCLs). Moreover, VEGF receptor-1 signaling is essential for OCL development in M-CSF deficient mice. OCL formation is mediated by RANKL and M-CSF. Hence, angiogenesis correlates with osteolytic lesion formation through OCL induction. However, the relationship between PEDF and OCL function has not been revealed precisely yet.

Objectives: We aimed to study the effects of PEDF on several osteoclast functions and its molecular mechanism.

Methods: In vitro osteoclast assay system is utilized to study osteoclast differentiation, bone resorbing activity and survival.

Results: OCL differentiation and bone resorption activity were inhibited by PEDF in a dose-dependent manner, although osteoclast survival was not affected by PEDF. RT-PCR data demonstrated that PEDF upregulated osteoprotegerin (OPG) and suppressed RANKL in primary osteoblast (POB). OPG is an antagonist of RANKL. RANKL and the osteoclast marker, TRAP, in OCL were suppressed by PEDF.

Conclusions: These results suggest that PEDF may inhibit osteoclast differentiation and bone resorption activity via controlling OPG expression. Further studies are required to reveal the linkage between angiogenesis and bone homeostasis.

Disclosures: Toru Akiyama, None.

MO0251

Pre-adipocytes Support Osteoclastogenesis through RANKL Expression. Sunao Takeshita*, Toshio Fumoto, Kyoji Ikeda. National Center for Geriatrics & Gerontology, Japan

Bone marrow is progressively replaced with adipose tissue with aging, concomitantly with a decline in bone mass as well as strength. The mechanism underlying proliferating fatty marrow and the development of osteoporosis is not fully understood. Although recent studies point to matrix-embedded osteocytes as a new source of RANKL, it remains to be determined whether and how RANKL derived from other cell types in the bone marrow contributes to osteoclastogenesis. We reported in ASBMR 2009 that adipogenic cultures of mouse bone marrow induced robust formation of extremely long-lived osteoclasts, even in the absence of RANKL, and they revealed high expression of RANKL by themselves. When primary stromal cells from mouse bone marrow or the stromal cell line ST2 were stimulated by dexamethasone and IBMX for adipogenic differentiation, RANKL expression was induced transiently and concomitantly with down-regulation of OPG, prompting us to hypothesize that cells at a pre-adipocyte stage express RANKL, thereby supporting osteoclastogenesis. This concept was further supported by the findings that the early adipogenic transcription factors C/EBP β and C/EBP δ , but not the late PPAR γ , bind to RANKL promoter and transactivate RANKL transcription, suggesting that an early stage of adipocyte differentiation is linked to osteoclastogenesis through RANKL expression. In fact, when bone marrow cells from aged mice were analyzed by flow cytometry, we found that RANKL expressing cells were positive for the pre-adipocyte marker Pref-1 and were also weakly positive for B220, that the number of these cells were higher than younger mice, and most importantly, that these RANKL/Pref-1/B220-positive marrow cells were capable of generating osteoclasts from bone marrow macrophages. Thus, the capacity of cells at a pre-adipocyte stage to express RANKL and support osteoclastogenesis may account for the concomitant progression of bone destruction and fatty marrow with aging.

Disclosures: Sunao Takeshita, None.

This study received funding from: National Center for Geriatrics and Gerontology

MO0252

The Farnesoid X Receptor Negatively Regulates Osteoclast Formation. Mijung Yim¹, Ting Zheng*². ¹Sookmyung Women's University, South Korea, ²College of Pharmacy, Sookmyung Women's University, South Korea

Farnesoid X receptor (FXR, NR1H4) is a member of the nuclear receptor superfamily of ligand-activated transcription factors. Initially cloned and named as the farnesoid X receptor in 1995, as a metabolic regulator, it plays key roles in bile acid, cholesterol, lipid, and glucose metabolism. By regulating the expression of genes involved in diverse metabolic pathways, such as controlling bile acid homeostasis, lipoprotein and glucose metabolism, hepatic regeneration, intestinal bacterial growth and the response to hepatotoxins, FXR is becoming an attractive drug target for different metabolic diseases. The hydrophobic BA chenodeoxycholic acid (CDCA) is the most effective natural activator of FXR. It is synthesized in the liver from cholesterol and is conjugated at the carboxylic acid carbon with either glycine or taurine. Since the function of FXR on bone metabolism is not clear, we investigated the biologic significance of FXR in osteoclast formation using CDCA, which facilitate FXR function by binding to the FXR ligands. First, CDCA was shown to inhibit RANKL-induced osteoclast formation without cytotoxicity in vitro. The mRNA levels of osteoclastogenic markers were decreased with the treatment of CDCA. In experiments to elucidate its mechanism of action, CDCA was found to significantly inhibit RANKL-induced gene expression of c-fos and nuclear factor of activated T-cells (NFATc1), two essential transcription factors for osteoclast development. Moreover, the inhibitory effect of CDCA on osteoclast formation was rescued by retroviral NFATc1 over-expression. Therefore, the anti-osteoclastogenic effect of CDCA is likely to be elicited by interference with RANKL signaling to the induction of c-fos and subsequently that of NFATc1. Next, we investigated the effect of FXR on osteoclast formation using bone marrow-derived macrophages (BMMs) from FXR knockout mice in vitro. As expected, FXR deficiency markedly accelerated RANKL-induced or LPS-induced osteoclast formation. RT-PCR and Real-time PCR analysis revealed that the mRNA levels of osteoclastogenic genes were increased in FXR knockout mice. In consistent with these data, FXR deficiency induced osteoclastic pit formation on dentin slices by bone resorption assay. Be corresponded to the mechanism of CDCA, FXR deficiency was found to significantly increase the expression of RANKL-induced c-fos and NFATc1. Further study verified that FXR deficiency in BMMs may modulate the signaling pathways of IL-6. Finally, we investigated the effect of FXR deficiency on bone loss in vivo. In accordance with in vitro study, FXR deficiency accelerated LPS-induced osteoclast formation in vivo. Taken together these results indicate that FXR exert a new inhibitory role on RANKL-induced osteoclast formation. Thus FXR could be useful target for the treatment of bone diseases associated with excessive bone resorption.

Disclosures: Ting Zheng, None.

MO0253

TMEM178 Is a Novel Negative Regulator of Inflammatory Cytokine Production and Osteoclastogenesis during Rheumatoid Arthritis. Corinne Decker*¹, Deborah Novack², Roberta Faccio³. ¹Washington University in St. Louis, USA, ²Washington University in St. Louis School of Medicine, USA, ³Washington University in St Louis School of Medicine, USA

Pathological bone loss in human disease such as rheumatoid arthritis is largely due to excessive osteoclast (OC) activation as a consequence of local inflammation. We have previously reported that phospholipase C gamma-2 (PLC γ 2) deficient mice are osteopetrotic due to defective OC formation and are protected from inflammatory bone loss due to impaired innate immune responses. In fact, PLC γ 2^{-/-} neutrophils and bone marrow macrophages (BMM) display reduced NF κ B activation and reduced IL-1, IL-6 and TNF- α mRNA levels following integrin-mediated adhesion in vitro, suggesting that PLC γ 2 controls the development of inflammation by regulating the transcription of NF κ B-dependent genes. To determine which NF κ B target genes are modulated by PLC γ 2, we performed a gene array comparing WT and PLC γ 2^{-/-} BMM lifted and re-plated on the integrin substrate pRGD for 0, 2, and 4 hours. Transmembrane protein 178 (TMEM178), an integral membrane protein of unknown function, was highly induced in adherent WT cells but diminished in PLC γ 2^{-/-} cells. Furthermore, we found that TMEM178 mRNA expression was also dependent on the NF κ B subunit cRel, confirming that TMEM178 is a PLC γ 2-dependent NF κ B target. To gain insight into the role of TMEM178 in the innate immune inflammatory response, we turned to the TMEM178 knockout mouse. Surprisingly, IL-1, TNF- α , and IL-6 mRNA levels in TMEM178^{-/-} BMM were dramatically upregulated compared to WT cells following adhesion on pRGD. This heightened inflammatory response also occurred in TMEM178^{-/-} BMM stimulated with the TLR agonists LPS or zymosan. Because inflammatory cytokines stimulate osteoclastogenesis (OCG), we next asked if TMEM178 modulates OC formation. Strikingly, TMEM178^{-/-} BMM cultured with M-CSF and RANKL display accelerated OCG (OC/well day 4 KO=90 \pm 9, WT=18 \pm 3; p<.0002) and elevated mRNA levels of OC markers NFATc1, TRAP, β 3 integrin, DC-STAMP, calcitonin receptor, and cathepsin K. The addition of LPS or TNF to OC precursors further enhanced OC formation in TMEM178^{-/-} cultures compared to WT. To investigate the in vivo role of TMEM178, we utilized the K/B x N serum transfer arthritis model and found that TMEM178^{-/-} mice display enhanced bone loss and increased IL-1 mRNA levels in inflamed paws. Taken together, these findings characterize TMEM178 as a negative regulator of the innate

immune response and OC formation and activation, thus positioning TMEM178 as a potential therapeutic target in inflammatory arthritis.

Disclosures: Corinne Decker, None.

MO0254

Dynasore Rapidly Disrupts Podosome Belts in Polarized Osteoclasts. Shunsuke Uehara*¹, Takahiro Nakayama¹, Toshihide Mizoguchi², Teruhito Yamashita³, Yasuhiro Kobayashi², Nobuyuki Udagawa³, Naoyuki Takahashi³. ¹Department of Biochemistry, Matsumoto Dental University, Japan, ²Institute for Oral Science, Matsumoto Dental University, Japan, ³Matsumoto Dental University, Japan

Dynamins (Dyn), a GTPase protein, is involved in endocytosis. It has been reported that (1) Dyn 2 is localized to podosome belts (the ring-like structure of actin, actin rings) in osteoclasts (OCLs), and (2) overexpression of the dominant-negative mutant of Dyn (K44A) leads to shrink OCLs, which in turn inhibits their bone-resorbing activity. These results suggest that Dyn is involved in the bone-resorbing process of OCLs. However, it remains to elucidate how Dyn regulates the bone-resorbing activity. Then we investigated the effect of dynasore, an inhibitor of the GTPase-activity of Dyn, on actin ring and pit formation in OCL in vitro and in vivo. OCLs were obtained from cocultures of calvarial osteoblasts and bone marrow cells in the presence of 1 α ,25(OH) $_2$ D $_3$ in collagen gel-coated dishes. OCLs were seeded on dentin slices (dentin) and cultured for 48 hr in the presence or absence of dynasore. Cells were stained for F-actin and TRAP activities. After removal of cells from dentin, dentin was stained with Mayer's hematoxylin to observe resorption pits. Dynasore showed no effects on OCL number on dentin. However, dynasore dose-dependently inhibited formation of actin rings and resorption pits by OCLs. We previously showed that polarized OCLs put marks stained for TRAP activities (TRAP-marks) on dentin (Bone 49:1331, 2011). Then, those dentins were stained for TRAP. TRAP-marks also disappeared by the addition of dynasore. We examined the time course of changes in the dynasore-induced disappearance of actin rings and TRAP-marks in osteoclasts that had polarized on dentin. Most actin rings and TRAP-marks disappeared within 30 min and 60 min, respectively, by the addition of dynasore. Disappearance of actin rings preceded that of TRAP-marks. Fluorescent immunostaining showed that Dyn 2 was co-localized with actin rings. Dyn 2 was diffused throughout the cytoplasm of OCLs by the addition of dynasore. Finally, we examined whether dynasore disrupts actin rings of OCLs in vivo. Dynasore was administered i.p. to 7-day-old mice. After 60 min of the injection, calvariae were dissected and stained for F-actin. Many actin rings were observed near sutures of calvariae in control mice. Actin rings disappeared in calvariae of mice injected with dynasore. Taken together, these results suggest that the GTPase-activity of Dyn is involved in the maintenance of actin rings in OCLs, and dynasore suppresses bone resorption due to disruption of actin rings in OCLs.

Disclosures: Shunsuke Uehara, None.

MO0255

Effects of IL-12 on Mechanical Loading Induced Bone Resorption. Masako Yoshimatsu*¹, Hideki Kitaura², Yuji Fujimura¹, Haruka Kohara¹, Yukiko Morita¹, Toshiko Eguchi¹, Noriaki Yoshida¹. ¹Nagasaki University, Japan, ²Tohoku University, Japan

We previously reported that IL-12 inhibits tumor necrosis factor (TNF)- α mediated osteoclast formation by inducing apoptosis. We also reported that TNF- α plays an important role in mechanical loading-induced osteoclast formation and bone resorption. With respect to bone resorption, IL-12 has been studied by several research groups, but no studies have investigated the effects of IL-12 on mechanical loading induced bone resorption. The aim of this study is to investigate whether IL-12 inhibits bone resorption on mechanical loading.

We established a mechanical loading model in mice using orthodontic tooth movement. Briefly, a Ni-Ti closed coil spring was inserted between the upper incisors and the upper left first molar to move the molar in the mesial direction. Recombinant mouse IL-12 was injected locally adjacent to the first molar every other day during the experimental period, at doses varying from 0 to 1.5 μ g/day. After 12 days, the animals were killed and the tooth movement was evaluated by measuring the distance between the first and the second molars. After that, their jaws were processed for histological evaluation using tartrate-resistant acid phosphatase (TRAP) and TdT-mediated dUTP-biotin nick end-labeling (TUNEL) staining. In other jaws, the first molars were carefully extracted and the root surface was observed under a scanning electron microscope.

In the IL-12-treated mice, tooth movement and root resorption appeared to be reduced. The number of TRAP positive cells around the root of the first molar was reduced in the IL-12-treated mice. In TUNEL-stained sections, many apoptotic cells were recognized around the root of the first molar in the IL-12-treated mice.

Our findings suggest that IL-12 inhibits not only alveolar bone resorption but also root resorption during mechanical loading. These findings may arise through apoptosis induced by IL-12.

Disclosures: Masako Yoshimatsu, None.

MO0256

Efficient Blockade of NADPH Oxidase-mediated Osteoclastogenesis and Bone Resorption by Insect-derived Low Molecular Agenet 5-S-GAD. Masakazu Kogawa¹, Nobuko Akiyama², Naoki Kato³, Tsuyoshi Sato³, Koji Hisatake³, Masafumi Tsujimoto⁴, Masahito Matsumoto³.
¹University of Adelaide, Australia, ²RIKEN Wako Institute, Japan, ³Saitama Medical University, Japan, ⁴RIKEN Advanced Science Institute, Japan

Reactive oxygen species (ROS) play critical roles for various physiological function and cell differentiation as an intracellular signal mediator. However, the molecular mechanism by which ROS is involved in osteoclast differentiation and bone resorption is needed to be elucidated. Here, we show that treatment of BMM with 5-S-GAD, an insect-derived antibacterial compound, inhibits RANKL-induced ROS production and osteoclast differentiation in a dose dependent manner. Remarkable reduction of osteoclast lineage marker gene expression such as *TRAP*, *Cathepsin K*, *Calcitin receptor*, *OSCAR* and master regulator *NFATc1* was observed by the treatment with 5-S-GAD. In the process of osteoclastogenesis, we found that 5-S-GAD inhibits not only NADPH oxidase (Nox)-mediated H₂O₂ production but also phosphorylation of p38 MAP kinase. Mutant mice of p38 we have generated represented increased trabecular bone in femur due to loss of osteoclasts, supporting our first observation as far as we know that p38 is essential for osteoclastogenesis *in vitro* (Matsumoto *et al.*, (2000) *JBC*, 275, 31155-61) and *in vivo*. Moreover, pit formation assay showed bone resorption by osteoclasts abrogated by the treatment of 5-S-GAD. In fact, formation of actin ring in osteoclasts reduced in the presence of the agent compared with that of control. These results suggest that 5-S-GAD is an attractive candidate for curing bone loss diseases including osteoporosis as targets of both osteoclast function and differentiation triggered by Nox family at the initial stage of the intracellular signaling pathway. (Ochiai Memorial, Kanzawa Medical and Kowa life science Foundations)

Disclosures: Masahito Matsumoto, None.

MO0257

Neutralization of Macrophage Colony-stimulating Factor Inhibits Lipopolysaccharide-induced Osteoclastogenesis In Vivo. KEISUKE KIMURA^{*1}, Hideki Kitaura², Toshiya Fujii³, Masahiko Ishida⁴, Zaki Hakami⁴, Teruko Takano-Yamamoto².
¹, Japan, ²Tohoku University, Japan, ³Division of Orthodontics & Dentofacial Orthopedics, Tohoku University Graduate School of Dentistry, Japan, ⁴Division of Orthodontics & Dentofacial Orthopedics, Department of Translational Medicine, Tohoku University Graduate School of Dentistry, Japan

Lipopolysaccharide (LPS) is a major component of cell wall of gram-negative bacteria and is well known as a potent inducer of inflammation and a pathogen of inflammatory bone loss. The formation of osteoclasts depends on macrophage-colony-stimulating factor (M-CSF) and receptor activator of necrosis factor- κ B ligand (RANKL). It has recently been reported that administration of an antibody of the M-CSF receptor c-fms completely blocked osteoclastogenesis and bone erosion induced by TNF administration or inflammatory arthritis. This study aimed to examine the effect of neutralization of M-CSF on LPS-induced osteoclastogenesis *in vivo*. C57BL/6J mice were injected LPS as a positive control, LPS and anti-c-fms antibody, anti-c-fms antibody or PBS as a negative control into supracalvariae. Animals were sacrificed, and fixation and demineralization were performed. Histological sections of calvaria were stained for tartrate-resistant acid phosphatase (TRAP), and osteoclast numbers were determined. The level of tartrate-resistant acid phosphatase 5b (TRACP 5b), which is a bone resorption marker, in mice serum was determined according to the protocol of the Mouse TRAP Assay kit. The expression levels of M-CSF, cathepsin K, TRAP and RANK mRNA in mice calvariae were quantified by real-time RT-PCR. Microfocal computed tomography was used to clarify the bone resorption pit in the calvariae. The number of osteoclasts in the suture of the calvaria in mice and TRACP 5b in mice serum administered both LPS and antibody were lower than those in mice administered LPS alone. The expression levels of Cathepsin K and TRAP mRNA were also reduced in mice administered LPS and antibody compared with mice administered LPS. Many radiolucent spots on calvariae were observed in microfocal computed tomography images in the LPS-administered group but not in the group administered both LPS and anti-c-Fms antibody. The results suggested that M-CSF and its receptor are potential therapeutic targets in bacterial infection-induced osteoclastogenesis, and that anti-c-Fms antibody might be useful for inhibition of infection-induced bone erosion.

Disclosures: KEISUKE KIMURA, None.

MO0258

RANKL-mediated Lineage Commitment Dictates the Effect of Thiazolidinediones (TZDs) on Osteoclastogenesis. Dongfeng Zhao^{*1}, Zhenqi Shi², Amy Warriner³, yongjun wang⁴, Xu Feng³.
¹The University of Alabama At Birmingham, USA, ²University of Alabama, USA, ³University of Alabama At Birmingham, USA, ⁴Research Institute of Spine, Longhua Hospital, Shanghai University of Traditional Chinese Medicine, China

Thiazolidinediones (TZDs), synthetic peroxisome proliferation-activated receptor γ (PPAR γ) agonists, are drugs currently used for treating Type 2 Diabetes Mellitus (T2DM). Emerging evidence indicates that TZD treatments increase the risk of bone fractures in patients with T2DM. PPAR γ induces bone loss in part, if not primarily, by regulating osteoclastogenesis. However, the effect of TZDs on osteoclastogenesis remains controversial; while numerous groups demonstrated that TZDs inhibit osteoclastogenesis, one recent study showed that TZDs promote osteoclastogenesis. Given that we have recently revealed that RANKL-mediated osteoclast lineage commitment of bone marrow macrophages (BMMs) plays a crucial role in osteoclastogenesis mediated by various factors such as lipopolysaccharide, TNF α and IL-1, we hypothesize that RANKL-mediated lineage commitment may also determine the effect of TZDs on osteoclastogenesis. In the current work, we have carried out several *in vitro* studies to address this possibility. First, we found that neither rosiglitazone nor pioglitazone can promote osteoclast formation in tissue culture dishes or on bone slices in the presence of M-CSF but without RANKL. Moreover, we demonstrated that both rosiglitazone and pioglitazone dose-dependently inhibit osteoclastogenesis in tissue culture dishes and on bone slices from BMMs freshly isolated from 6- to 8-week old C57BL/6 mice with complete inhibition of osteoclastogenesis at 40 μ M/ml of either TZD. Importantly, we found that the inhibitory effect of rosiglitazone and pioglitazone on osteoclastogenesis was significantly impaired when BMMs were pretreated with 100ng/ml RANKL for as short as 24 hours. Taken together, these data indicate the effects of TZDs on osteoclastogenesis are determined by RANKL-mediated lineage commitment of osteoclast precursors. Furthermore, we determined whether rosiglitazone and pioglitazone can exert effects on osteoclast survival. Our data indicate that both rosiglitazone and pioglitazone can extend the lifespan of osteoclasts *in vitro*. In summary, we have revealed important new insights into the actions of TZDs in osteoclast biology. Importantly, our current studies have laid a foundation for future studies to further elucidate the molecular mechanism by which PPAR γ controls osteoclast formation and survival, which may guide future development of new therapeutics (PPAR γ agonists) with fewer adverse side effects for treating T2DM.

Disclosures: Dongfeng Zhao, None.

MO0259

Withdrawn

MO0260

Detection of Adiponectin Receptors in Multinucleated Osteoclast-like Cells *in vitro* by Immunofluorescence and qPCR. Elda Pacheco-Pantoja^{*1}, Victoria Waring-Green², Peter Wilson³, Lakshminarayanan Ranganath³, William Fraser⁴, James Gallagher³.
¹Universidad Anahuac Mayab, Mexico, ²Royal Veterinary College, United Kingdom, ³University of Liverpool, United Kingdom, ⁴University of East Anglia, United Kingdom

The discovery of adipokines has had a major impact on adipose tissue research and its potential involvement in bone metabolism. Some adipokines are proposed as modulators of bone homeostasis and therefore in this study we searched for the presence of adipokine adiponectin receptors in osteoclasts. Since published data on adiponectin receptors (AdipoR1, -R2) in osteoclasts have shown discrepancies we decided to investigate these receptors using two different techniques: immunofluorescence and qPCR. In this study we performed observations of AdipoR1, -R2 in peripheral blood mononuclear cells (PBMC) that were induced to differentiate.

PBMCs were isolated and stimulated to differentiate using M-CSF and RANKL and relative expression of AdipoR1, -R2 was screened using reverse transcription and quantitative PCR (qPCR) at 1, 7 and 14 days. Acid phosphatase (TRACP5) and Cathepsin K (CTSK) were evaluated as osteoclastic markers at the same time points. Results showed that TRACP5 was expressed from day 1 and CTSK from day 7, with the highest expression level at day 14 for both markers. AdipoR1 and -R2 also showed the highest levels at day 14, with greater expression for AdipoR1 at all three point times.

Cells were harvested at different stages of development and the immunofluorescent observations were carried out at 2, 7, 14 and 21 days using anti AdipoR1 and -R2 antibodies. The cells were cultured in three different conditions: non-supplemented medium, medium with added M-CSF, or medium with the two differentiation factors for osteoclastic precursors, M-CSF, and RANKL. The non-supplemented control did not display fluorescence whereas at day 2 specific but weak signals were detected only in cells cultured with M-CSF and RANKL. At days 7, 14 and 21, cells incubated with M-CSF and RANKL displayed specific strong signal detected mainly at the periphery of the cells, and in the cytoplasm, showing a localized patchy pattern for both receptors. In contrast, a diffuse fluorescent pattern was detected in the cytoplasm of the cells with M-CSF alone.

In summary, AdipoR1 and -R2 were detected by qPCR and immunofluorescence. The immunofluorescence patterns suggest that those receptors are located, or re-located, in the plasma membrane with distribution in the cytoplasm when PBMC are committed to differentiate to osteoclasts. These findings provide an explanation for the controversy found in the published literature regarding the role of adiponectin in bone metabolism.

Disclosures: *Elda Pacheco-Pantoja, None.*

MO0261

Down-regulation of MicroRNA-21 Biogenesis by Estrogen Action Contributes to Osteoclastic Apoptosis. Toshifumi Sugatani*, Keith Hruska, Washington University in St. Louis School of Medicine, USA

A decrease in estrogen levels at menopause contributes to rapid loss of bone mineral density and an increase in fracture risk. Estrogen inhibits osteoclastogenesis and induces osteoclastic apoptosis; however, the molecular mechanisms remain controversial. Recently, a group has demonstrated that estrogen enhances the expression of Fas Ligand (FasL) in osteoclasts which in turn causes cell death through an autocrine mechanism. In contrast, other groups have shown that estrogen stimulates the transcription of the FasL gene in osteoblasts, but not in osteoclasts, and FasL acts in a paracrine fashion to induce osteoclastic apoptosis. Thus, two quite different molecular mechanisms have been suggested to explain the effects of estrogen in osteoclastic apoptosis. Here we show that the proapoptotic effect of estrogen during osteoclastogenesis is regulated by a posttranscriptional increase in FasL production by down-regulated microRNA-21 (miR-21) biogenesis. We have demonstrated that miR-21 is highly expressed in osteoclast precursors and mature osteoclasts. We found that estrogen down-regulates miR-21 biogenesis and stimulates caspase-3 activity via estrogen receptor α (ER α), which is expressed in osteoclast precursors and osteoclasts, because those effects were absent in ER α -null osteoclast precursors and osteoclasts. We were unable to confirm enhanced-FasL levels by estrogen action at mRNA levels in RANKL-induced osteoclastogenesis. Instead, estrogen enhanced FasL levels posttranscriptionally. The molecular mechanisms is that estrogen down-regulates miR-21 levels, which targets FasL, so that FasL protein levels are up-regulated and apoptosis is induced in a autocrine fashion during RANKL-induced osteoclastogenesis. In fact, gain-of function of miR-21 prevented the apoptosis by estrogen action in the cells. Thus, osteoclastic survival is controlled by autocrine actions of FasL regulated by estrogen and miR-21 plays a central role during osteoclastogenesis.

Disclosures: *Toshifumi Sugatani, None.*
This study received funding from: NIDDK R01

MO0262

Isoporsalen Inhibits RANKL-Induced Osteoclastic Differentiation of RAW264.7 Cells by Suppressing c-fos-NFATc1. Jin Zhang*¹, Shu Meng¹, Yuwei Wu², Liming Yu¹, Lan Zhang¹, Mengqi Huang¹, Qisheng Tu¹, Jake Jinkun Chen¹. ¹Tufts University School of Dental Medicine, USA, ²Tufts University, USA

Isoporsalen is the main part of *Malaytea Scurfpea Fruit*, a Chinese herb used for thousands of years to strengthen bone, and is commonly used to enhance bone healing and treat ageing related osteoporosis. In this study, we examined the effect and detailed mechanisms by which isoporsalen regulates receptor-activated nuclear factor κ B ligand (RANKL)-induced osteoclast differentiation.

RAW264.7 cells were exposed to isoporsalen (at a concentration of 10^{-5} M) in the presence or absence of RANKL for 1, 3, and 5 days. The mRNA expression was studied by real-time PCR. Isoporsalen reduced the RANKL-induced gene expressions and osteoclast formation without inhibiting the cell viability. After treatment with isoporsalen (10^{-3} M), the key transcription factors of osteoclast differentiation, c-fos and nuclear factor of activated T cells c1 (NFATc1), were significantly inhibited at 1d and 3d. Osteoclast differentiation marker, tartrate resistances acid phosphatase (TRAP) and cathepsin K, decreased to 15-30% at 3d and 5d. Isoporsalen significantly inhibited c-fos expression while having no effect on Jun, NF-B, and AKT1 pathway.

In conclusion, we demonstrated that isoporsalen has an inhibitory effect on differentiation of RAW264.7 cells *in vitro*. Isoporsalen inhibited RANKL-induced osteoclastogenesis by suppressing the RANKL-c-fos- NFATc1 pathway.

Disclosures: *Jin Zhang, None.*
This study received funding from: NIH grants DE16710 and DE21464 to JC

MO0263

Microgravity Control of Autophagy Modulates Osteoclastogenesis. Yuvaraj Sambandam*¹, Molly Townsend², Srinivasan Shanmugarajan³, Jason Pierce², Sakamuri Reddy³. ¹Medical University of South Carolina, USA, ²MUSC, USA, ³Charles P. Darby Children's Research Institute, USA

Long term space flight has been hampered due to the physiological stresses that the weightlessness/microgravity (μ Xg) environment has imposed on the astronauts. Evidence indicates that astronauts experience 13-20% of bone loss during space flight.

Recently, we used the NASA developed rotary cell culture system (RCCS) to simulate μ Xg conditions and showed increased osteoclastogenesis in murine bone marrow cultures. Autophagy is a cellular self-consumption process for degradation of damaged/dysfunctional cellular organelles, protein aggregates to recycle the nutrients in starvation, metabolic stress, hypoxia and radiation exposure conditions for cellular survival and function. Therefore, we hypothesize that μ Xg control of autophagy modulates osteoclastogenesis. Real-time PCR analysis of total RNA isolated from mouse bone marrow derived non-adherent cells subjected to μ Xg for 24 h demonstrated a significant increase in autophagic markers LC3, Atg16L and Atg5 mRNA expression compared to ground based control (Xg) cultures. Furthermore, Western blot analysis of total cell lysates obtained from the ground based and μ Xg subjected RAW 264.7 cells showed 8.0 fold and 7.0 fold increases in the Atg5 and LC3-II expression, respectively. Confocal microscopy identified elevated levels of autophagosome formation as evident from LC3-II expression in μ Xg conditions compared to ground based control RAW 264.7 cells. Super array screening of autophagy related genes by real-time PCR identified elevated levels of Atg16L, Atg9, Cathepsin-S, GAA, IFN- γ , IGF1, TNFSF10, TRP73, PRKAA1, RSP6KB1 and IRGM1 mRNA expression in μ Xg subjected RAW 264.7 cells. Autophagy inhibitor, 3-methyladenine (3-MA) treatment (200 μ M) to mouse bone marrow derived mononuclear cells showed a significant decrease in μ Xg induced LC3 and Atg5 mRNA expression. Interestingly, 3-MA potentially inhibits osteoclast formation in mouse bone marrow cultures. In summary, μ Xg induced autophagy plays an important role in modulation of osteoclasts differentiation and could be a potential therapeutic target to prevent bone loss in astronauts during space flight missions.

Disclosures: *Yuvaraj Sambandam, None.*
This study received funding from: NASA REAP grant, South Carolina

MO0264

T-reg/Th17 Cells and TGF- β /SOCS3 Signaling Regulate Dendritic Cell-derived Osteoclastogenesis and Bone Loss. Andy Y-T Teng*¹, Yen-Chun Grace Liu². ¹School of Dentistry, Kaohsiung Medical University, Kaohsiung, Taiwan, Taiwan, ²Kaohsiung Medical University, Taiwan

RANKL/RANK-OPG axis is known as the central triad that regulates the osteoclastogenesis in bone remodeling. Inflammation-induced bone loss is associated with elevated osteoclast (OC) activity & function wherever reported the development of functional OC derived from CD11c⁺ dendritic cells (called: DDOC) in response to RANKL plus inflammatory stimuli (i.e., *Aggregatibacter actinomycetemcomitans*-Aa; J. Immunol. 2006 & Blood 2009). In the present study, we investigated how the signal interactions between DDOC/T-cells (i.e., T-reg & Th17 cells) and osteotropic cytokines that modulate DDOC-mediated osteoclastogenesis. Our resulting data showed that: i) neutralization of TGF- β activity by mAb abolished DDOC development in co-cultures, based on TRAP & resorptive-pit assays *in-vitro* ($p < 0.03$) & *in-vivo* ($p < 0.02$); ii) transfection of dominant-negative SOCS3 molecules into CD11c⁺DDOC (via sh-RNA or adenovirus) and subsequent adoptive-transfer study yielded a significant inhibition of osteoclastogenesis and bone resorption *in-vitro* & *in-vivo* ($p < 0.05$); iii) addition of Foxp3⁺CD4⁺T-reg cells into CD11c⁺DC with sonicated Aa in co-cultures resulted in significantly reduced SOCS3 & TRAP expressions and osteoclastogenesis vs. bone resorption assays *in-vitro* & the calvarias in NOD/SCID mice, respectively ($p < 0.05$). iv) IL-17 may signal with other cytokines in a positive (i.e., RANKL, TGF- β) or negative (i.e., IL-1, TNF- α) fashion, yielding different mTRAF6 transcriptome activities for osteoclastogenesis. Conclusion: These findings suggest that: i) TGF- β /SOCS-3 signaling is involved in regulating the development of DDOC function & activity; ii) Foxp3⁺T-reg/Th17 cells may be a potentially integral player underlying the inflammation-induced osteoclastogenesis & bone loss through DDOC/T-cell interactions at the osteo-immune interface. Project supported by NIH-DE018356 & -015786, USA; University of Rochester, National Health Research Institute EX100-S34199N & National Science Committee NSC-100-2314-B037-050-MY3, Taiwan.

Disclosures: *Andy Y-T Teng, None.*

MO0265

ERK Signaling Protects Osteocytes against Oxidative Stress-induced Cell Death through the regulation of Connexin 43 Hemichannels. Manuel Riquelme¹, Rekha Kar², Jean Jiang³. ¹University of Texas Health Science Center, USA, ²The University of Texas Health Science Center, USA, ³University of Texas Health Science Center at San Antonio, USA

Subthreshold oxidative stress (OS) activates cellular protective mechanisms by increasing the resistance to subsequent injury. This mechanism depends on connexin (Cx) 43 hemichannels (HC) activity. HC are transmembrane channels that allow the flux of small metabolites and ions (< 1 kDa) through plasma membrane. Little is known about how HC are regulated in response to acute injury. By time lapse ethidium bromide (EtBr) uptake, molecule that do not cross the plasma membrane, we corroborated that OS induced a transient increase of Cx43 HC activity in MLO-Y4 osteocytic cells, which was prevented by cell permeable reducing agent and Cx43(E2) antibody, specific Cx43 HC blocker. ERK pathway known to be activated under stress conditions was activated after 15 min, with a maximum at 60 min after H₂O₂ exposure. Increased cell surface expression of Cx43 at earlier time points correlated with increased HC activity. Furthermore, we also observed increased phosphorylation

of Cx43 specifically at MAPK site at a time when the Cx43 HC had lower activity. Preincubation with MAPK and ERK inhibitors, PD98059 and U0126, respectively, further enhanced effect of H₂O₂ on HC activity. In contrast to HC activity, inhibition of ERK by U0126 reduced cell surface expression of Cx43. This result indicates that the decrease of HC activity is likely caused by the increased phosphorylation of Cx43 by ERK, but not through the reduction of Cx43 on the cell surface. Furthermore, the inhibition of ERK signaling also increased the intracellular calcium levels and exacerbated OS induced cell death of MLO-Y4 cells. In conclusion, OS increased the Cx43 HC activity in osteocytes, a process regulated by ERK phosphorylation in Cx43 MAPK consensus site. The inhibition of ERK signaling induces a transient increase in cell surface expression of Cx43 and deregulated opening of HC, leading to augmentation of H₂O₂-induced cell death.

Disclosures: Jean Jiang, None.

MO0266

Osteocytes in situ Produce Nitric Oxide in Response to Mechanical Stimulation: A Novel *ex vivo* Mechanical Loading Model for Murine Fibulae.

Rishikesh Kulkarni¹, Leo van Ruijven², Rommel Bacabac³, Jenneke Kleinf-Nulend¹, Astrid Bakker^{*1}. ¹Department of Oral Cell Biology, Academic Centre for Dentistry Amsterdam (ACTA), University of Amsterdam & VU University Amsterdam, Research Institute MOVE, Netherlands, ²Department of Functional Anatomy, Academic Centre for Dentistry Amsterdam, University of Amsterdam & VU University Amsterdam, Netherlands, ³Medical Biophysics Group, Department of Physics, University of San Carlos, Philippines

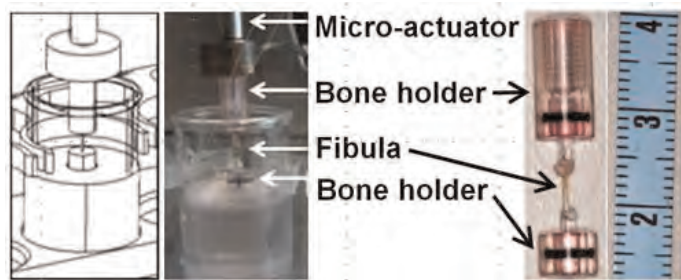
Lack of physical activity causes bone loss and fractures in elderly people and in bedridden or otherwise inactive youth. Osteocytes stimulate bone degradation when experiencing a lack of mechanical stimuli, but how they sense mechanical stimuli is not fully understood. Studies using osteocytes cultured on flat substrates provide valuable insight into which molecules are produced by these cells, but they may be less useful for unraveling the mechanism behind osteocyte mechanotransduction. We developed a novel *ex vivo* mechanical loading model to study the response of individual osteocytes residing in isolated murine fibulae. This model was validated by determining whether mechanical loading increases nitric oxide (NO) production by osteocytes in situ.

Freshly isolated mouse fibulae (length 5 mm) were incubated with DAR-4M AM chromophore, and mechanically stimulated by dynamic axial compression using a novel micro-actuator (Fig. 1). Mechanical stimulation consisted of sinusoidal compression of fibulae (amplitude 12.5, 25, or 100 μ m, frequency 5 Hz) for 5 min. Global bone strains were measured using strain gauges. Micro-CT scans of fibulae were made at a voxel size of 6 μ m, and converted into finite-element models to calculate strain distributions over compressed fibulae. NO production was semi-quantified by confocal microscopy in the same osteocytes before and after mechanical stimulation and after saturation with the NO donor SNAP.

Finite-element modeling predicted that strains were on average 5-fold higher on the medial side of the fibulae vs. the lateral side. Compression with amplitudes of 12.5, 25, and 100 μ m resulted in global strains of 3×10^3 , 10×10^3 , and 40×10^3 μ e. Fluorescence intensity in non-stimulated osteocytes was 40% of the intensity measured after saturation with SNAP. Placing fibulae in the micro-actuator without application of compression did not enhance osteocyte fluorescence intensity. Mechanical stimulation increased fluorescence intensity of osteocytes by 1.3-fold to 1.6-fold (12.5 and 100 μ m displacement).

In conclusion, we demonstrated enhanced NO production by single murine osteocytes in situ by using a novel *ex vivo* mechanical loading model. This may enable detailed investigations into the mechanism behind osteocyte mechanotransduction by e.g. using fibulae derived from knock-out mice with osteocyte phenotypes.

Fig. 1. Setup with fibula glued to bone holder attached to micro-actuator (scale, cm).



Disclosures: Astrid Bakker, None.

MO0267

Osteocytes Inhibit Osteoblast Differentiation by Cell-cell Contact: Potential Implications for the Regulation of Bone Remodeling. Koji Fujita^{*1}, David Monroe², Matthew Roforth¹, James Peterson³, Sundeep Khosla⁴. ¹Mayo Clinic, USA, ²Mayo Foundation, USA, ³Endocrinology Research Unit, Mayo Clinic, USA, ⁴College of Medicine, Mayo Clinic, USA

There is increasing evidence that osteocytes regulate multiple aspects of bone remodeling, including bone formation. Given their embedded location in bone, osteocyte regulation of osteoblasts could be via secreted factors or by direct cell-cell contact, the latter likely through their dendritic processes. Thus, we used a novel transwell system whereby osteoblastic MC3T3 cells were either physically separated but co-cultured with MLO-A5 cells (co-culture) or both cell types were cultured on two sides of a permeable membrane that allowed for direct cell-cell contact (co-culture + cell contact). In this experimental design, both conditions permit cross-talk between the osteoblastic and osteocytic cells via secreted factors, with the cell-cell contact conditions allowing, in addition, for direct cellular cross-talk. Compared to co-culture alone, 7 days of co-culture + cell contact led to a marked suppression in the expression (by QPCR, n = 4-6, all P < 0.05) of osteoblast differentiation marker genes in the osteoblastic MC3T3 cells. Specifically, mRNA levels for runx2 decreased by 78%, osterix by 93%, osteocalcin by 97%, alkaline phosphatase by 99%, col1 α by 77%, and PTHr1 by 99%. Interestingly, as compared to co-culture alone, co-culture + cell contact led to a marked increase (>300%) in SOST expression in the osteocytic MLO-A5 cells. Since clinical studies have shown that estrogen reduces circulating sclerostin levels, we also examined effects of estradiol (10⁻⁸ M). Under co-culture + cell contact conditions, estradiol significantly suppressed SOST mRNA levels in MLO-A5 cells (by 80%).

In summary, using experimental conditions that mimic the potential cross-talk between osteocytes and osteoblasts in vivo, we found that direct cellular interactions between osteocytic and osteoblastic cells leads to a profound inhibition of osteoblastic differentiation. The marked upregulation of SOST expression following cell-cell contact in the osteocytic cells indicates that local control of bone formation may be an important physiological function of sclerostin. These findings further suggest the hypothesis that, as osteoblasts lay down mineralized bone in the basic multicellular unit (BMU) and themselves transition to osteocytes, these accumulating newly embedded osteocytes may, by direct cellular interactions with the incoming wave of osteoblasts, limit bone formation and thereby lead to a controlled re-filling of the space excavated by osteoclasts.

Disclosures: Koji Fujita, None.

MO0268

Parathyroid Hormone-Related Protein is Involved In Cell Protection Conferred By Hypotonic Shock In Osteocytic MLO-Y4 Cells. Marta Maycas^{*1}, Luis Fernandez De Castro², Beatriz Bravo³, Pedro Esbrit², Arancha Gortazar⁴.

¹Universidad San Pablo CEU, Spain, ²Fundacion Jimenez Diaz, Spain, ³Universidad San Pablo CEU School of Medicine, Spain, ⁴Universidad San Pablo-CEU School of Medicine Madrid Spain, Spain

Parathyroid hormone (PTH)-related protein (PTHrP) is an important modulator of bone formation and bone remodeling. It has also been shown that PTHrP is overexpressed after mechanical stimulation of osteoblasts and osteocytes in vitro. Recent data demonstrate that transgenic mice expressing a constitutively active PTH type 1 receptor (PTH1R) – recognizing both PTH and PTHrP – in osteocytes display increased bone mass. In fact, a role of the PTHrP system in osteocyte function has recently been suggested. In the present study, we aimed to explore the possible involvement of PTHrP in osteocyte survival induced by mechanical stimulation. MLO-Y4 cells were subjected to either mechanical strain by hypotonic shock or stimulation with PTHrP (1-36) (100 nM) for 1 h. Cell viability was assessed by trypan blue exclusion after incubation with 50 μ M etoposide for 6 h. Changes in PTHrP protein expression, and localization of β -catenin were examined by Western blot. Hypotonic shock stimulated β -catenin stabilization related to an increased nuclear and membrane localization within 1 h; this was followed by an increase in PTHrP protein and cell survival. Pre-treatment with either an N-terminal PTHrP antiserum or the PTH1R antagonists, PTHrP (7-34) and JB4250, at 1 μ M, or transfection with PTH1R siRNA all decreased the mechanical stimulus-related cell protection, associated with β -catenin destabilization (mainly in the cell membrane). On the other hand, PTHrP (1-36) stimulation mimicked these events triggered by mechanical stimulus. In summary, these in vitro findings indicate that the PTHrP system is involved in osteocyte protection conferred by mechanical stimulus. This might contribute to the anabolic actions of PTHrP in bone.

Disclosures: Marta Maycas, None.

MO0269

The Mineralization Kinetics of Endocortical Bone is Altered in *Sost* Knockout Mice. Andreas Roschger^{*1}, Nadja Fratzl-Zelman¹, Barbara M. Misof¹, Ina Kramer², Klaus Klaushofer¹, Paul Roschger¹, Michaela Kneissel².

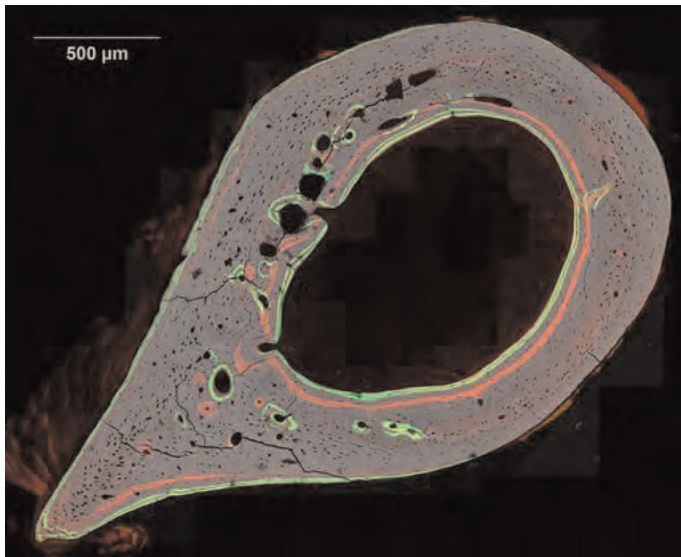
¹Ludwig Boltzmann Institute of Osteology at Hanusch Hospital of WGKK & AUA Trauma Centre Meidling, 1st Medical Department; Hanusch Hospital Vienna, Austria, ²Musculoskeletal Disease Area, Novartis Institutes for BioMedical Research, Basel, Switzerland

Sclerostin, encoded for by the *SOST* gene, is an osteocyte secreted negative regulator of bone formation. It antagonizes WNT signaling by binding to the WNT co-receptors LRP 5/6. In humans absence of sclerostin expression in bone gives rise to bone overgrowth (Sclerosteosis, Van Buchem disease). Consistently *Sost* knockout (KO) mice present with a tremendous increase of cortical and cancellous bone mass and strength. This phenotype is related to elevated lamellar bone formation. Though the phenotype is well documented, no studies have assessed so far the mineralization profile of the excessively formed bone.

We analyzed longitudinal (n=9) and transversal (n=9) sections of the femur diaphysis of *Sost* KO mice and corresponding sections of wildtype mice (n=11 and, n=10, respectively) by quantitative backscatter electron imaging (qBEI). The animals, from which transversal sections were investigated, had received fluorescent double labels (10 days interval) at 8 weeks of age and again at 16 weeks of age prior to sacrifice. The undecalcified samples were processed for qBEI measurements as published previously, thus allowing for determination of local Ca concentration (wt% Ca) with a spatial resolution of about 1µm and of bone mineralization density distribution (BMDD). Superposing qBEI and fluorescent images in the transversal section samples facilitated the measurement of the mineral content of cortical bone at defined tissue ages (between the double labels).

We detected at the endocortical envelope a significantly lower degree of mineralization in the *Sost*-KO mice at the 8 week and 16 week time point (-1.9 % (p<0.001) and -1.5 % (p<0.05) respectively) compared to wildtype. This was consistent with BMDD data from the entire cortical bone in the longitudinal sections, where we observed a reduction of the mean Ca content by -1.9 % (p<0.05). Interestingly at the subperiosteal bone envelope no differences were detectable at either time point between genotypes, indicating diverging mineralization dynamics at the different cortical envelopes.

In conclusion the data suggest that sclerostin deficient mice have altered mineralization kinetics at the endocortical bone envelope accounting for the shift of the BMDD to lower mineral content. This observation may relate to recent in vitro findings implicating sclerostin in physiologic bone mineralization.



qBEI image of a transversal femur cross-section of a *Sost*-KO mouse with superposed fluorescent image

Disclosures: *Andreas Roschger, None.*

MO0270

Nck, an Actin Cytoskeleton Modulator, Controls Expression of Osteocytic Genes, Phosphate Homeostasis by Regulating FGF 23 Expression in Bone and Maintains Bone Mass. Smriti Aryal A.C^{*1}, Kentaro Miyai², Yoichi Ezura³, Tadayoshi Hayata⁴, Takuya Notomi⁵, Tetsuya Nakamoto², Tony Pawson⁶, Masaki Noda². ¹Department of molecular pharmacology, Tokyo medical & dental university, Japan, ²Tokyo Medical & Dental University, Japan, ³Tokyo Medical & Dental University, Medical Research Institute, Japan, ⁴Medical Research Institute, Tokyo Medical & Dental University, Japan, ⁵GCOE, Tokyo Medical & Dental University, Japan, ⁶Mount Sinai hospital, Samuel Lunenfeld Research Institute, Canada

Ncks (non catalytic region of tyrosine kinase) are adaptor proteins that play a major role to regulate actin cytoskeleton. Mammals carry two Nck genes; Nck1 and Nck2 (collectively termed as Nck). Previous study reported that genetic deletion of individual Nck genes did not result in any significant phenotype (Bladt F., et al Mol cell Biol, 2003) while in kidney Nck conditional double knock-out mice showed defects in foot processes of kidney podocytes (Jones N., et al Nature, 2006). However the role of Nck in bone metabolism has not been understood clearly. We have observed that osteoblast specific Nck conditional double knock-out mice (Ob-Nck-dko) generated under the control of 2.3 kb type I collagen promoter showed significant reduction in trabecular bone volume (BV/TV) and trabecular number (Tb.N/BS), an increase in the cortical bone thickness and volume, reduction in the number of osteocytes, deformation in lacunar-canalicular network, defect in primary osteoblast migration and reduction of BMD of newly formed bone in Ob-Nck-dko mice compared to the wild type (Wt). Further study was designed to find the underlying mechanism of different phenomenon between cortical and trabecular bone in the Ob-Nck-dko mice compared to Wt littermates. Bone histomorphometry revealed that the mineral apposition rate (MAR), bone formation rate (BFR) and mineralized surface per bone surface (MS/BS) were significantly reduced in the trabecular bone of Ob-Nck-dko mice compared to Wt suggesting that the individual osteoblast activity and function were affected in the trabecular bone in the absence of Nck. Quantitative real time PCR analysis (qRT-PCR) showed a decrease in mRNA levels of osteocyte marker genes such as *Sost*, *Dmp1* and proliferation marker, *cyclinD1* in the cortical bone of Ob-Nck-dko compare to Wt. Moreover, the mRNA expression of fibroblast growth factor 23 (*FGF23*) was also reduced in the cortical bone of Ob-Nck-dko mice compared to Wt. This reduction in *FGF23* mRNA expression was accompanied by an increase in the serum phosphate levels in Ob-Nck-dko mice compared to Wt. Considering all the results of this study, it can be concluded that Nck controls the expression of osteocytic genes that are involved in the formation of canalicular network, Wnt signaling and phosphate homeostasis by regulating *FGF23* expression in bone and maintains bone mass.

Disclosures: *Smriti Aryal A.C, None.*

MO0271

Association Study of Polymorphisms in the *OPG* Gene with BMD and Fractures in BARCOS Cohort. Natalia Garcia-Giralt^{*1}, Laura De-Ugarte², Guy Yoskovitz¹, Maria Rodriguez-Sanz², Roser Urreiziti³, Susana Balcells⁴, Robert Güerri⁵, Leonardo Mellibovsky⁶, Adolfo Diez-Perez⁷, Daniel Grinberg⁸, Xavier Nogues⁶. ¹IMIM, Spain, ²IMIM-Parc de salut Mar, Spain, ³Departament de genètica, Universitat de Barcelona, Spain, ⁴University of Barcelona, Spain, ⁵Hospital Universitario Del Mar. Institut Municipal D'Investigació Mèdica, Spain, ⁶Internal medicine, Parc de salut Mar, Spain, ⁷Parc De Salut Mar, Spain, ⁸The University of Barcelona, Spain

INTRODUCTION Osteoporosis is a complex disease defined by reduced bone mineral density (BMD). Numerous genome wide association studies (GWAs) have been performed, identifying single nucleotide polymorphisms (SNPs) associated with osteoporotic phenotypes, including variants in the osteoprotegerin (OPG) gene. The aim of this study was to broaden our knowledge over the *OPG* gene in association with fractures and BMD (lumbar spine (LS) and femoral neck (FN)).

METHODS Eight SNPs in the *OPG* gene were genotyped in the 825 postmenopausal women with Spanish ancestry which were recruited from Hospital del Mar, Barcelona (BARCOS cohort). Six SNPs were selected in continuous to a previous published study which was performed in our group and 2 SNPs in the distal promoter were replicated from other studies. The polymorphism genotyping was carried out using the SNPlex System (Applied BioSystem) at the CEGEN platform (Barcelona, Spain). Statistical analysis was performed using R software version 2.13.2. For BMD association analysis, multivariate linear regression was adjusted by body mass index (BMI), age at menarche, years since menopause at the time of densitometry, and months of breast feeding for all models. For outcome fractures, logistic regression was adjusted by BMI and age for all models.

RESULTS Two pairs of SNPs were found to be in linkage disequilibrium: rs11573878 and rs11573898 ($r^2=0.94$) and rs1564858 and rs2228568 ($r^2=0.96$). No association was found with fractures. Four SNPs yielded significant results for BMD: rs6469804 (FN, dominant model, $p=5.1 \times 10^{-3}$, β -coefficient=-0.019, 95% CI [0.006 to 0.033]) and rs6993813 (FN, dominant model, $p=0.014$, β -coefficient=-0.017, 95% CI [0.004 to 0.031]) both located in the distal promoter(-80kb and -88kb upstream

respectively), rs7820642 (LS, log-additive model, $p=0.018$, β -coefficient=-0.020, 95% CI [-0.037 to -0.004]) and FN, dominant model, $p=0.039$, β -coefficient =-0.015, 95% CI [-0.030 to -0.001]) located in the promoter region (-3571pb upstream) and finally, rs1564858 (LS, recessive model, $p=0.012$, β -coefficient=0.103, 95% CI [0.022 to 0.184]) in the intron 2. Only rs6469804 stood for Bonferroni multiple testing (p target= 8.3×10^{-3}).

CONCLUSIONS Four SNPs in the *OPG* gene were found associated with BMD in the BARCOS cohort. This is the first time that SNPs rs7820642 and rs1564858 are associated with LS BMD while SNPs rs6469804 and rs6993813 are replicated from previous GWAS.

Disclosures: *Natalia Garcia-Giralt, None.*

MO0272

Changes of microRNA Profile and microRNA-mRNA Regulatory Network in Ovariectomy-induced Bone Loss in Mice. Jee Hyun An^{1*}, Jung Hun Ohn², Jung Ah Song², Jae-Yeon Yang², Hvung Jin Choi³, Ae Kyung Park⁴, Sang Wan Kim⁵, Woong-Yang Park⁶, Seong Yeon Kim², Chan Soo Shin². ¹Department of Internal Medicine, Konkuk University Hospital, South Korea, ²Department of Internal Medicine, Seoul National University College of Medicine, South Korea, ³Chungbuk National University Hospital, South Korea, ⁴Sunchon National University College of Pharmacy, South Korea, ⁵Seoul National University Boramae Hospital, South Korea, ⁶Department of Biochemistry & Molecular Biology, Seoul National University College of Medicine, South Korea

MicroRNAs (miRNAs) have emerged as important regulators in various developmental, physiological, and pathological conditions, and growing evidence shows the possible role of miRNAs in regulating bone mass. We investigated the change of miRNAs and mRNA expression profiles in bone tissue of ovariectomized mice model and evaluated regulatory mechanism of bone mass mediated by miRNAs in estrogen deficiency state. Eight-week old female C3H/He mice underwent ovariectomy (OVX) or sham operation (Sham-op), and their femurs and tibias were harvested to extract total bone RNAs after 4 weeks for microarray analysis.

Eight miRNAs (miR-127, -133a, -133a*, -133b, -136 -206, -378, -378*) were identified to be upregulated after OVX while one miRNA (miR-204) was down-regulated. Concomitant analysis of mRNA microarray revealed that a total of 658 genes were differentially expressed between OVX and Sham-op mice. Computational target prediction of differentially expressed miRNAs identified potential targets and integrative analysis using concomitant mRNA microarray results showed that genes of PPAR γ and CREB pathways were activated and mitochondria OXPHOS, stress response, and apoptosis were upregulated in skeletal tissues after ovariectomy. We further studied the role of miR-127 in vitro, which exhibited the greatest changes after OVX. When C3H10T1/2 cells were transfected with miR-127 inhibitors, alkaline phosphatase activities and mRNA expression of osteoblast-specific genes, Col type 1, ALP, Runx2, and osteocalcin were significantly increased. Furthermore, transfection of miR-127 inhibitors enhanced the osteocyte-like morphological changes of MLO-Y4 cells and their survival in apoptosis assay. In addition, miR-127 inhibitors have significantly inhibited osteoclastic differentiation of bone marrow macrophage.

Taken together, these results suggest novel insight into the role of distinct miRNAs profile and miRNA-mRNA regulatory network in the pathogenesis of estrogen deficiency induced osteoporosis.

Disclosures: *Jee Hyun An, None.*

Disclosures: *Jee Hyun An, None.*

MO0273

Greater Bone Density in Obese Individuals is Not a Result of DXA Artifact: a High Resolution Peripheral Quantitative Computed Tomography (HR-pQCT) Study. Amy Evans^{1*}, Richard Eastell², Jennifer Walsh². ¹Academic Unit of Bone Metabolism, University of Sheffield, United Kingdom, ²University of Sheffield, United Kingdom

Obesity is associated with increased bone mineral density (BMD) at the hip and lumbar spine. Measurements of BMD by dual x-ray absorptiometry (DXA) may be confounded by soft tissue effects. To avoid this issue, we used high resolution peripheral quantitative computed tomography (HR-pQCT) to study how obesity affects BMD and bone microstructure.

We studied individually matched pairs of lean (BMI 18.5 to 24.9 kg/m²) and obese (BMI >30 kg/m²) individuals, aged 55 to 75 years (21 male pairs and 21 female pairs). DXA was used to determine hip and lumbar spine areal BMD. HR-pQCT was used to determine volumetric BMD and microarchitectural parameters at the distal radius and distal tibia.

Obesity was associated with greater BMD at each site in women (all $p<0.01$) and men (all $p<0.05$ except tibia; $p=0.1$). At the radius and tibia, higher BMD in obesity was due to greater cortical area and thickness (and density in women) and greater trabecular number (all $p<0.05$, men and women). At the radius, trabecular density was also greater in obese subjects ($p<0.001$, men and women). Bone size (total area and cortical perimeter) did not differ between lean and obese subjects.

The difference in distal radius and distal tibia BMD observed in obesity is of a similar magnitude to that of the lumbar spine and total hip. Whilst DXA-measured BMD in obesity may be unreliable, these results suggest that such increases may not

be artifactual. Obesity is associated with structural differences such as greater cortical thickness and trabecular number, without any difference in bone size.

| Mean Absolute and Percentage Difference in BMD Between Lean and Obese Individuals | | | |
|---|-----------|---------------|---------------|
| Site | | BMD | |
| | | Male | Female |
| Lumbar spine g/cm ² | Mean (SD) | 0.12 (0.18) | 0.21 (0.18) |
| | % | 13.5* | 25.6** |
| Total hip g/cm ² | Mean (SD) | 0.14 (0.18) | 0.21 (0.13) |
| | % | 16.5* | 26.5** |
| Distal radius mg/cm ³ | Mean (SD) | 46.08 (56.48) | 55.94 (91.95) |
| | % | 19.5* | 29.1* |
| Distal tibia mg/cm ³ | Mean (SD) | 21.22 (58.94) | 52.57 (62.67) |
| | % | 9.3 | 22.6** |

* $p<0.05$, ** $p<0.001$ lean vs obese by paired samples t-test

Table 1

| Mean Absolute and Percentage Difference in Cortical Thickness and Trabecular Number Between Lean and Obese Individuals | | | | | |
|--|-----------|--------------------------|-------------|---------------------------|-------------|
| Site | | Cortical Thickness mm | | Trabecular Number 1/mm | |
| | | Male | Female | Male | Female |
| Distal radius | Mean (SD) | 0.12 (0.23) | 0.16 (0.29) | 0.24 (0.33) | 0.37 (0.47) |
| | % | 30.4* | 56.2* | 13.7* | 25.2* |
| Distal tibia | Mean (SD) | 0.14 (0.29) | 0.32 (0.25) | 0.33 (0.29) | 0.19 (0.39) |
| | % | 15.2* | 46.1** | 18.07** | 13.6* |

* $p<0.05$, ** $p<0.001$ lean vs obese by paired samples t-test

Table 2

Disclosures: *Amy Evans, None.*

MO0274

Adipose Tissue In OVX Animals Is Associated With Lower Osteocyte Density, Decreased Bone Formation And Trabecular Microarchitecture Deterioration. Helder Fonseca^{1*}, Daniel Moreira-Goncalves², Maria Fernandes³, José Duarte². ¹CIAFEL, Faculty of Sport Sciences, University of Porto, Portugal, ²CIAFEL, Faculty of Sport, University of Porto, Portugal, ³Faculty of Dental Medicine, University of Porto, Portugal

The relation between body fat and skeletal health remains controversial. Our purpose was to investigate the long-term effects of estrogen loss on body fat and determine if adipose tissue, particularly in the bone marrow, is associated with femur bone quality. Female Wistar rats were either ovariectomized (OVX, n=13) or sham-operated (SHAM, n=12) at 5 months of age. Following 9 months (at 14 months of age), they were sacrificed and their intra-abdominal fat content dissected and weighed. Serum was collected for assaying estrogen and CTX (bone resorption) concentration (ELISA). Left femora were dissected for histological assessment of osteocyte oxidative damage (carbonyl group immunohistochemistry), osteocyte density, dynamic histomorphometry, trabecular microarchitecture and bone marrow fat content. At sacrifice OVX animals were heavier ($384 \pm 38.3g$ vs $313 \pm 40.2g$, $p<0.01$), had a higher intra-abdominal ($32.5 \pm 9.2g$ vs 17.9 ± 11.2 , $p<0.01$) and bone marrow fat content ($52.5 \pm 4.7\%$ vs $20.3 \pm 10.8\%$, $p<0.01$) than SHAM. Moreover, these variables were shown to be highly correlated. Histological analysis to the femur mid-diaphysis also revealed a lower osteocyte density ($605 \pm 50/\mu m^2$ vs $648 \pm 47/\mu m^2$, $p<0.05$) and higher number of osteocytes displaying signs of oxidative stress damage ($46.5 \pm 5.8\%$ vs $33.7 \pm 8.9\%$, $p<0.01$) in OVX. Notoriously, body weight and bone marrow fat content correlated positively with empty osteocyte lacunae numbers ($r=0.394$, $p<0.05$; $r=0.386$, $p<0.05$, respectively) and with the number of osteocytes displaying signs of oxidative stress damage ($r=0.622$, $p<0.01$; $r=0.562$, $p<0.01$, respectively). Serum CTX was also higher in OVX animals ($13.4 \pm 1.8ng/mL$ vs $10.9 \pm 1.9ng/mL$) and correlated with bone marrow fat content ($r=0.468$, $p<0.01$). Conversely, bone formation rate and mineral apposition rate correlated both inversely with body weight ($r=-0.626$, $p<0.01$; $r=-0.517$, $p<0.05$, respectively) and bone marrow fat content ($r=-0.564$, $p<0.05$; $r=-0.555$, $p<0.05$, respectively). Body weight and bone marrow fat content were also directly correlated with distal femur Tb.Sp ($r=0.709$, $p<0.01$; $r=0.846$, $p<0.01$) as well as inversely correlated with BV/TV ($r=-0.663$, $p<0.01$; $r=-0.840$, $p<0.01$) and Tb.N ($r=-0.766$, $p<0.01$; $r=-0.916$, $p<0.01$). Our results suggest that higher body weight and most importantly bone marrow fat are associated with increased osteocyte damage and bone resorption and with decreased osteocyte density, bone formation and trabecular microarchitecture deterioration.

Disclosures: *Helder Fonseca, None.*

This study received funding from: Fundação para a Ciência e Tecnologia (FCT) grants SFRH/BPD178259/2011 and PTDC/IDES/103047/2008

MO0275

qBSE-SEM Study of Femoral Midshaft Mineralization Density in People with HIV/AIDS. BIN HU*¹, Tina Gulati², Yusuf M. Juwayeyi³, John E. Chisi⁴, Alan Boyde⁵, Timothy Bromage¹. ¹New York University College of Dentistry, USA, ²NYU college of dentistry, USA, ³Department of Anthropology, Long Island University, USA, ⁴Department of Anatomy, University of Malawi College of Medicine, Malawi, ⁵Institute of Dentistry, Barts & The London School of Medicine & Dentistry, Queen Mary University of London, United Kingdom

Aim: Low bone mineral density and fragility fracture risk are said to be increased in HIV patients, yet the mechanism of action are unclear, in part because of limitations imposed by the non-invasive diagnostic methods employed. We aim to determine if there are bone mineral density and remodeling differences in midshaft femurs posthumously extracted from sub-Saharan Africans of Bantu origin with and without HIV/AIDS.

Methods: 12 midshaft femurs derived from sub-Saharan Africans of known life history with (n=8) and without (n=4) HIV/AIDS were embedded in polymethyl-methacrylate and sectioned. Quantitative backscattered electron microscopy (qBSE) in the scanning electron microscope (SEM) was performed with a Zeiss EVO 50 SEM. Contrast, and brightness conditions were standardized against two novel halogenated resins with mean atomic numbers bracketing the known low and high mineralization densities of bone. From 256 gray level images, bone mineral density variability was partitioned into eight equal grey-level bins and measured in proportion to the detected bone area using Leica Quantimet 550 image analysis software.

Results: Contrary to previous studies, there is a tendency for increased bone mineral density around the midshaft femur cross section of individuals with HIV/AIDS, but this does not reach statistical significance in the small sample presently. However, the subpopulation of low density actively infilling osteons is low in HIV/AIDS individuals. Gray values between 0-160 reflect newly mineralizing low density bone, the proportion of which is reduced on average by 10% in the HIV/AIDS group. Mineral densities in the gray level range of 160-256 indicate older and more mineralized bone in remaining areas, which average 10% higher in the HIV/AIDS group.

Conclusions: Bone remodeling is suppressed at the midshaft femur in HIV/AIDS individuals. The formation of new matrix is inhibited and bone packets are allowed to age and increase in mineral density, a phenomenon that we suggest may be linked to leptin inhibition of bone formation. Such skeletal impairment in HIV/AIDS individuals would increase the probability of fragility fractures. Regions that have significant numbers of HIV infected people and whose health care systems are unfamiliar with bone loss diseases – e.g. sub Saharan Africa – may be witnessing a crisis in the making. This is the first study of actual bone tissues of HIV/AIDS individuals, and as we continue to increase the sample size in this ongoing project, further study may lead to enhanced understanding of the mechanisms and the development of drugs specifically designed to reduce the risk of fracture for those infected with the HIV virus.

Disclosures: BIN HU, None.

MO0276

Relationship Between Serum Sclerostin and Sex Steroids in Prostate Cancer Patients. Antonia Garcia-Martin*¹, Mariela Varsavsky², Rebeca Reves-Garcia¹, Beatriz Garcia-Fontana³, Sonia Morales-Santana⁴, Manuel Muñoz-Torres³. ¹Bone Metabolic Unit, Endocrinology, Hospital Universitario San Cecilio., Spain, ²Endocrinology Division, Hospital Sant Pau i Santa Tecla, Spain, ³Bone Metabolic Unit (RETICEF), Endocrinology Division, Hospital Universitario San Cecilio, Spain, ⁴Bone Metabolic Unit (RETICEF), Endocrinology Division, Hospital Universitario San Cecilio; Proteomic Research Service, Fundación para la Investigación Biosanitaria de Andalucía Oriental -Alejandro Otero-(FIBAO), Spain

Recent studies have evaluated serum sclerostin levels in bone diseases as osteoporosis, but there are no data on prostate cancer (PCa) patients. Our aims were to compare serum levels of sclerostin in PCa patients and healthy controls, and to evaluate their relationship with sex steroids and bone metabolism in these patients. A cross-sectional study of 65 subjects including 20 patients with PCa treated with androgen deprivation therapy (ADT), 23 patients with untreated PCa, and 22 healthy controls was performed. We measured serum sclerostin levels, sex steroids levels, bone turnover markers, and bone mineral density (BMD). Serum sclerostin levels were significantly higher in PCa patients compared to control subjects: ADT: 73.7±25.3 pmol/L; non ADT: 56.14±16.45 pmol/L; healthy controls: 45.52±11.98 pmol/L, p<0.05 for both comparisons. Furthermore, in PCa group, ADT treated patients had significantly higher sclerostin levels than PCa patients without treatment (p<0.05). In ADT PCa patients, there was a negative relationship between serum sclerostin levels and estrogens after adjusting by BMI (Biodisponible estradiol: r=-0.560, p=0.037; Free estradiol: r=-0.537, p=0.047). There was a positive correlation between serum sclerostin and TRAP in ADT PCa patients (r=0.486, p=0.048). Finally, there was no relationship between serum sclerostin levels, androgens and BMD in PCa patients. In summary, serum sclerostin levels are increased in patients with prostate cancer compared to healthy control. Moreover, ADT treated patients had higher sclerostin

concentrations compared to patients without treatment. Estrogen deficiency plays a key role in elevation of sclerostin serum levels in the group with hypogonadism due to TDA.

Disclosures: Antonia Garcia-Martin, None.

MO0277

Bone Microarchitecture Assessment by High-resolution Peripheral Quantitative Computed Tomography (HR-pQCT) in Pregnancy and Lactation-Associated Osteoporosis. Maria Belen Zanchetta*¹, Armando Negri², Fernando Silveira², Rodolfo Guelman³, Jose Ruben Zanchetta¹. ¹Instituto de Investigaciones Metabolicas (IDIM), Argentina, ²MD, Argentina,

Pregnancy and Lactation-Associated Osteoporosis (PLAOs) is a rare condition characterized by the occurrence of fragility fractures - most commonly vertebral - in late pregnancy or during the postpartum period. The etiology and pathogenesis of these conditions are not completely clear.

Our aim was to evaluate cortical and trabecular volumetric and architectural parameters in women who had suffered a fragility fracture during late pregnancy or postpartum.

We took HR-pQCT measurements (Xtreme CT; Scanco Medical AG, Bassersdorf, Switzerland) of the radius and tibia in 5 women. We compared these results with healthy premenopausal women with similar age and BMI selected from our database. Secondary causes of Osteoporosis were ruled out in all patients but one (a woman who had hipercalciuria, kidney stones, history of anorexia nervosa, hiperprolactinemia and history of 12-month lactation without calcium intake previous to her second pregnancy when she fractured her hip).

Clinical characteristics of our patients were similar to those described in literature (table 1): most fractures occurred during first pregnancy and various risk factors were present in all women (family history, very low calcium intake, low normal BMI, late menarche). Lumbar spine Z-scores were severely diminished (below minus 2) in all of them. The mean time between the fracture occurrence and the Xtreme measurement was 24 months (Range: 2 months to 4 years). There were statistically significant differences in almost every volumetric and architectural parameter (table 2). Trabecular bone was the most affected (trabecular density and trabecular bone volume were 45% lower and trabecular number and thickness were 26% lower) but cortical bone was also compromised (cortical area and thickness were 22% lower). The results were similar but less pronounced in tibia.

Conclusion: In these women with PLAO we found a profound deterioration of bone microarchitecture in peripheral sites. Probably they had begun their pregnancies with some alteration in bone microarchitecture due to acquired or inherited factors. The physiological decrease that took place during pregnancy and lactation was not resisted by their already decreased bone mass and therefore, fractures occurred. Prospective studies are necessary to determine whether women affected by this condition would be able to recover or at least improve their trabecular and cortical microarchitecture.

| Clinical Features | |
|---|------|
| Post partum vertebral fractures | 4/5 |
| Hip fracture during pregnancy | 1/5 |
| Median number of vertebral fractures | 2.8 |
| Median time between delivery and fractures (days) | 60 |
| Median menarche age (years) | 14.1 |
| Regular menses | 3/5 |
| Other drugs (corticoids) | none |
| Primiparous | 4/5 |
| Smoker | 1/5 |
| Very poor calcium intake | 3/5 |
| Family history of Osteoporosis | 1/5 |
| Previous fragility fracture | none |
| Median historical minimum BMI (3-5) | 17.4 |

Clinical features Table1

| | FL-Osteoporosis (n=3) | Healthy Control (n=12) | P |
|------------------------------------|--------------------------|---------------------------|--------|
| Age (years) | 71.0 ± 5.2 | 52.6 ± 4.1 | 0.07 |
| BMI (kg/m ²) | 23.4 ± 2.8 | 22.2 ± 2.1 | 0.11 |
| Z-score L3 | -1.4 ± 0.4 | -1.4 ± 0.6 | <0.001 |
| Z-score FN | -1.4 ± 0.3 | -1.1 ± 0.7 | <0.001 |
| Distal Radius | | | |
| Cortical Area (mm ²) | -411 ± 65 | 522 ± 65 | 0.002 |
| Trabecular Area (mm ²) | 2221 ± 40.9 | 1993 ± 29.6 | 0.19 |
| DIOP (mg HA/cm ²) | 2452 ± 88.5 | 3413 ± 42.9 | 0.001 |
| Deloop (mg HA/cm ²) | 127.0 ± 37.4 | 309.7 ± 34.1 | 0.004 |
| Ca (D) (mg) | 0.434 ± 0.118 | 0.799 ± 0.110 | 0.007 |
| Dist (mg HA/cm ²) | 97.1 ± 11.1 | 172.8 ± 46.5 | 0.061 |
| BV/TV (%) | 8.1 ± 2.4 | 14.7 ± 3.8 | 0.041 |
| Tb-N (1/mm) | 1.47 ± 0.24 | 2.40 ± 0.31 | 0.002 |
| Distal Tibia | | | |
| Cortical Area (mm ²) | 84.2 ± 18.5 | 112.8 ± 10.0 | 0.004 |
| Trabecular Area (mm ²) | 646.7 ± 110.0 | 1192 ± 78.1 | 0.02 |
| DIOP (mg HA/cm ²) | 2243 ± 86.2 | 3044 ± 41.7 | 0.018 |
| Deloop (mg HA/cm ²) | 174.3 ± 54.5 | 290.7 ± 23.5 | 0.023 |
| Ca (D) (mg) | 0.180 ± 0.248 | 1.143 ± 0.178 | 0.007 |
| Dist (mg HA/cm ²) | 112.9 ± 16.2 | 152.4 ± 23.5 | 0.014 |
| BV/TV (%) | 9.1 ± 1.0 | 13.8 ± 1.0 | 0.014 |
| Tb-N (1/mm) | 2.43 ± 0.23 | 3.78 ± 0.25 | 0.018 |

Microarchitecture Table2

Disclosures: Maria Belen Zanchetta, None.

MO0278

Caloric Restriction Attenuates Bone Loss during Hypothalamic Suppression.

Kathryn Mitchell, Megan Lunny, Vanessa Yingling*. Temple University, USA

Low energy availability and hypothalamic amenorrhea are both risk factors for developing insufficient bone mineral density in an estimated 22-50% of young physically active women. However, caloric restriction has also been associated with increased life span and increased mitochondrial biogenesis. We set out to determine the effect of both caloric restriction and hypothalamic suppression on bone strength and geometry. 30 female Sprague-Dawley rats, age day 23, were randomly assigned to a control (C, n=8) group that received daily saline injections (.2cc), or two experimental groups; delayed puberty (GnRH-a, n=14) or food restricted and delayed puberty (FR-G, n=8). Delayed puberty was achieved through daily injections of gonadotropin releasing hormone antagonist (GnRH-a, .2cc, dosage .2mg*kg⁻¹) and the food restriction was a 30% caloric restriction (no micronutrient deficit) based on the C group's average daily consumption. All protocols lasted 27 days and animals were sacrificed at 50 days of age. Body weight at sacrifice for the FR-G was significantly lower than C (15%, p<0.001) while GnRH-a was higher than C (8%, p=0.013). The GnRH-a treatment successfully suppressed hypothalamic function as evidenced by lower uterine and ovary weights in both the FR-G and GnRH-a groups (p<0.001). FR-G animals lost primarily body fat indicated by the higher percent muscle per fat compared to control (64%, p=0.038). Bone strength was similar between groups, however when normalized by body weight the FR-G and GnRH-a groups had higher peak moments than control (19%, p=0.004 and 20%, p<0.001 respectively). Micro CT analysis of the femur indicate a lower polar moment of inertia in FR-G compared to control and GnRH-a, however there was an increase in average cortical thickness in the FR-G group. The BV/TV of the distal femur was lower in both FR-G and GnRH-a compared to control. When normalized by body weight, FR-G had significantly higher BV/TV compared to GnRH-a. Caloric restriction combined with hypothalamic suppression increased femoral strength relative to body weight compared to control, potentially due to an increased cortical thickness. Caloric restriction seemed to provide a protective effect on trabecular bone from the significant decrease in bone volume resulting from the GnRH-a injections. The maintenance of lean body mass, slower growth rate or increased mitochondrial efficiency associated with caloric restriction may benefit bone strength and structure.

Disclosures: Vanessa Yingling, None.

MO0279

Microfractures in the Femoral Head of Patients with Osteoporosis: Analysis of Microcallus by Synchrotron Radiation Micro-CT. Narihiro Okazaki*, Ko Chiba¹, Kenji Taguchi¹, Nobuhito Nango², Masako Ito¹, Makoto Osaki³. ¹Nagasaki University Hospital, Japan, ²Ratoc System Engineering Co., Ltd., Japan, ³Nagasaki University, Japan

Introduction: A microfracture is a tiny fracture that occurs in trabecular bone, and a microcallus is a small callus formed at a microfracture. The occurrence of extensive microfractures is thought to be a cause of insufficiency fractures in patients with osteoporosis (OP), but the mechanism of microfracture formation is not well known.

Synchrotron radiation micro-computed tomography (SRCT) is a high-resolution micro-CT with high quantitative performance using a synchrotron radiation X-ray, which can perform three-dimensional bone microstructure analysis as well as identify trabecular bone mineralization.

To understand the mechanism of microfracture formation, microcalluses were analyzed in subchondral trabecular bone of osteoporotic femoral heads by SRCT.

Materials and methods

The subjects were 7 female patients with a femoral neck fracture (FNF) who had undergone bipolar hip arthroplasty (mean age 75 ± 9 years, range 65-92 years).

Using a coring reamer, subchondral bone columns 10 mm in diameter and 10 mm in height were extracted from the center of the weight-bearing part of the femoral head. SRCT scanning was performed at the BL20B2 beamline in the SPring-8 synchrotron radiation facility (Hyogo, Japan).

The measurement region was a 5-mm³ cube located 1 mm beneath the subchondral bone plate. The number of microcalluses, trabecular structure in the measurement region, and the degree of mineralization of microcallus were measured using bone microstructure measurement software TRI/3D-BON (Ratoc System Engineering, Tokyo, Japan). The correlation between the number of microcalluses and bone trabecular structure was analyzed by Spearman's rank correlation coefficient test.

Results: Microcalluses were observed in 6 of 7 cases (86%), with a mean of 5 microcalluses (range, 4-12). The number of microcalluses had a significant negative correlation with bone volume fraction and trabecular thickness. The degree of mineralization was lower in microcalluses than in other trabecular bone.

Discussion: Most OP patients with FNF had several microcalluses in subchondral trabecular bone in the femoral head. Microcalluses were more prevalent in patients with thinner trabecular thickness. Microfractures might occur commonly in OP patients due to the normal impacts of daily activities and increase with OP progression. The degree of mineralization of microcalluses was low, indicating that a microcallus consists of immature woven bone.

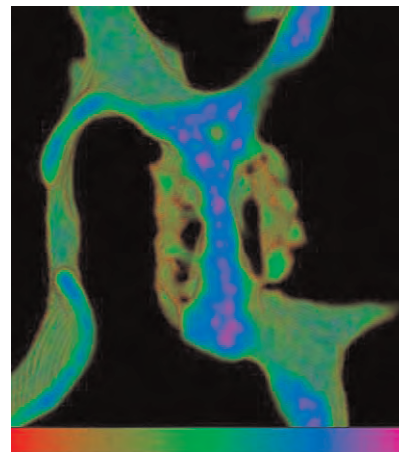


Fig. 1 Microcallus

Disclosures: Narihiro Okazaki, None.

MO0280

The Impact of Low Activity Crohns Disease (CD) and Ulcerative Colitis (UC) in Calcium Metabolism, Bone Mass and Marrow Adiposity. Clara Bastos¹, Marcello Nogueira-Barbosa¹, Carlos Salmon², Francisco Jose De Paula³, Luiz Troncon¹. ¹School of Medicine of Ribeirao Preto, USP, Brazil, ²University of Sao Paulo, Brazil, ³School of Medicine of Ribeirao Preto - USP, Brazil

Introduction: Bone loss has been established as an important complication of inflammatory bowel diseases (IBD). The consequences of IBD on the skeleton of young and middle aged patients (excluding postmenopausal women) in remission or exhibiting low IBD activity have not been extensively evaluated. Our target was to evaluate the bone mass, alterations in mineral metabolism and marrow adiposity in this group of patients. **Methods:** The study comprised 19 CD, 14 UC and 40 control (C) individuals paired by age, weight, BMI and gender. They were submitted to the calcium absorption test, bone mineral density by DXA, MR spectroscopy for marrow adiposity in L3 vertebral body (1.5 Tesla, ACHIEVA, Philips Medical System) and blood was drawn for determinations of calcium, albumin, PTH, osteocalcin and inflammatory parameters. **Results:** Age and BMI were similar in the three groups (DC: 38.7 ± 10.6 years; 24.6 ± 5.1 kg/m² vs UC: 41.7 ± 14.3 years; 25.8 ± 3.9 kg/m² vs C: 35.9 ± 9.3 years; 26.0 ± 4.3 kg/m²). BMD was slightly lower in CD in comparison to the other two groups (e.g. L1-L4: CD=0.965 ± 0.111 vs UC=1.036 ± 0.180 vs C=1.041 ± 0.147 g/cm²). Additionally, the frequency of low T-Score was higher in the CD group in total hip and L1-L4 (e.g. DC=58% vs RCU 36% vs C 40%). The serum levels of PTH were higher in UC patients in comparison to controls (CD=55.6 ± 19.8 vs UC=66.8 ± 31.0 vs C=45.9 ± 20.6 pg/ml, p<0.05). The calcemic response to oral calcium load was similar in the three groups. However, considering only controls and patients exhibiting osteopenia and osteoporosis the calcemic response was increased in the UC group (UC=1.8 ± 0.2 vs C=1.2 ± 0.1 mg/dl, p=0.01; CI 95% 0.11-1.09). In addition, UC patients showed higher calcemic response to oral calcium than the C group (CD=0.09 ± 0.06 vs UC=0.16 ± 0.11 vs C=0.10 ± 0.05 mg/dl, p=0.02; CI 95% 0.007-0.112). There was no difference between the three groups concerning the fat fraction in L3 through MR spectroscopy (CD=44.7 ± 15.3 vs UC=38.2 ± 16.8 vs C=42.4 ± 17.0%). **Conclusion:** Our results show that different operative mechanisms are involved in the regulation of mineral metabolism in IBD patients. UC patients exhibit increased calcium absorption, which might protect the bone mass of this group. CD has greater impact in bone than UC. Marrow adiposity is not increased in these well nourished, low activity IBD patients.

Disclosures: Francisco Jose De Paula, None.

MO0281

Bone μ CT and Histomorphometric Responses to a 19-week Obesogenic Diet Program in Growing and Mature Wistar Rats. CEDRIC LAVET*¹, Norbert Laroche¹, Arnaud Vanden Bossche¹, Marie therese Linossier¹, Maude Gerbaix², Marie-Helene Lafage-Proust³, Daniel Courteix⁴, Laurence Vico⁵. ¹Lyon University- INSERM U1059 -LBTO, France, ²Clermont University, France, ³INSERM Unit 890, France, ⁴Universite Clermont Ferrand Laboratoire De Biologie Des APS, France, ⁵University of St-Etienne, France

Obesity-related mechanical loading is thought to enhance bone formation. Fat accumulation leads to a chronic inflammation through proinflammatory cytokines and can increase bone resorption. The relationships between obesity and bone remodeling are still poorly understood.

It is established that high fat/high sucrose diet (HF/HS) leads to obesity and associated metabolic disorders. Mature (M) and growing (G) males Wistar rats 6 and 1 mo-old (n=105, respectively) were exposed to a HF/HS diet whereas 2 other groups (n=2x15) were assigned to an iso-caloric control diet during 19 weeks.

HF/HS diet induces obesity with greater body weight (M:+10%;G:+15%,p<0.001), visceral fat mass (M:+15%;G:+19%,p<0.001), and waist circumference (M:+6%;G:+11%,p<0.001) in rats submitted to HF/HS diet (Obese,Ob) as compared to control (Ctr). MicroCT analysis at the tibia trabecular proximal metaphysis demonstrates that BMD in M is slightly lower (-1.5%,p<0.01) in Ob as compared to Ctr, while microstructural parameters do not show any difference. In G, Tb.N is higher (+13%,p<0.01) in Ob vs. Ctr while BMD remains unchanged. At the tibia cortical diaphysis, BMD is similar between M Ob and M Ctr while it decreases (-1.3%,p<0.01) in G Ob compared to G Ctr. Same analyses were performed at L3 trabecular and cortical levels: no alteration are seen between Ob and Ctr in both M and G. Histomorphometric analysis performed at proximal tibia secondary spongiosa and L3 vertebral body shows the same obesity-related changes in M and G: a marked decrease of the OS/BS-70%, and Os.Th-50% (p<0.001) and of the Oc.S/BS-70% (p<0.001) is seen in both Ob groups and at both bone sites. In vertebrae, MS/BS and MAR are decreased in M and G Ob groups vs. Ctr (respectively -60% & -35%,p<0.001). In tibia, they remain unchanged in Ob groups. The density of adipocytes in proximal metaphyseal tibia stands constant between all groups.

We demonstrated that, in this model, obesity dramatically reduces bone resorption and osteoid formation and impaired mineralization in both M and G. These cellular activity impairments result however in different BMD and structural adaptations according to the axial or peripheral skeleton, to the bone compartment and age of the animals. Analyses of insulin, glycemia, lipid profile, bone markers, adipokines, and proinflammatory cytokines are in progress and will allow a better understanding of the underlying mechanisms of bone adaptation to obesity.

Disclosures: CEDRIC LAVET, None.

This study received funding from: Fondation pour la Recherche Médicale

MO0282

Distal Radius and Tibia Bone Microstructure is Positively Correlated to Dietary Protein Intakes in both Women and Men Aged 65 Years. Claire Durosier*¹, Thierry Chevalley², Fanny Merminod³, Serge Ferrari⁴, Rene Rizzoli³. ¹Hopitaux Universitaires De Geneve, Switzerland, ²University Hospitals of Geneva Division of Bone Diseases, Switzerland, ³University Hospital, Switzerland, ⁴Geneva University Hospital & Faculty of Medicine, Switzerland

Areal BMD is positively correlated to dietary protein intakes (DPIs), which accounts for 1 to 8% of BMC/BMD variance (Darling et al, systematic review, 2009). However, the relationship between bone microstructure, an important determinant of bone strength, and DPIs, is still unknown. We measured distal radius and tibia bone microstructure by HRpQCT (XtremCT, Seanco Co, Bruttisellen, CH) and evaluated dietary protein and calcium intakes, using a food frequency questionnaire, in 759 women and 196 men, aged 65±1 years (x±SD). This tight age range allowed us to neglect the influence of age in the bone microstructure analysis.

There were highly significant positive correlations (p<0.001 for all) between bone microstructure variables and DPIs, such as in distal radius cross-sectional area (adjusted-r²=4.3%), cortical area (adj.r²=4.5%), cortical thickness (adj.r²=1.5%), BV/TV (adj.r²=1.5%), trabecular number (adj.r²=1.8%), but not thickness. At distal tibia, the corresponding adj.r² (p<0.001 for all) were 3.2, 5.5, 2.7, 2.3 and 3.0%, respectively. Bone remodeling markers CTX and P1NP were inversely correlated to DPIs (adj.r²= 1.0 and 0.6%, respectively, p<0.01). After adjustment for dietary calcium intakes, distal radius and tibia microstructure and DPIs adj.r² for the positive correlations became (p<0.001 for all) 4.4 and 3.1% for total cross-sectional area, 5.1 and 5.9% for cortical area, 1.9 and 3.1% for cortical thickness, 1.7 and 2.3% for BV/TV, and 1.7 and 3.0% for trabecular number, respectively. There was no association between remodeling markers and DPIs anymore.

These results recorded in a very homogeneous population of healthy 65-year old subjects of both sexes underline the calcium-independent positive correlations between bone microstructure in both compartments and dietary protein intakes, with a possible influence on the modeling process as well.

Disclosures: Claire Durosier, None.

MO0283

Evaluation of Semiquantitative Analysis (SQ) for Vertebral Fractures in Glucocorticoid-Induced Osteoporosis (GIO). Ikuko Tanaka*¹, Shigenori Tamaki², Mari Ushikubo³, Harumi Kuda³, Keisuke Izumi³, Kumiko Akiya³, Hisaji Oshima⁴. ¹National Center for Geriatrics & Gerontology, Japan, ²Nagoya Rheumatology Clinic, Japan, ³Department of Connective Tissue Diseases, Tokyo Medical Center, Japan, ⁴Tokyo Medical Center, Japan

Background) Evaluation of fracture in GIO is crucial for analysis of pathogenesis and prevention of the osteoporotic fracture.

Purpose) To clarify usefulness of the SQ method (Gerant et al. JBMR, 1993) for evaluation of vertebral fractures in GIO.

Patients and Methods) Patients (n=137) with connective tissue diseases other than rheumatoid arthritis were recruited and observed for 2 years. The means of age, disease duration, total prednisolone (PSL) dosage, and daily PSL dosage during the study period were 61±15 (SD), 12±11 years, 34±34g, and 8±6mg/day, respectively. Prevalent vertebral fractures were seen in 44% of the patients. Agents used for prevention and treatment of GIO were bisphosphonates (54%), active vitamin D3 (7%), vitamin K2 (6%). Bone mineral densities (BMD) were measured with DXA at the distal radius.

Results) 1) Incident vertebral fractures determined with deteriorating grades by the SQ method were seen in 64 patients (47%). 2) Logistic regression analysis showed the age (1.43 (OR)/5yo), total PSL dosage (1.09/5g), daily PSL dosage (2.36/5mg), and BMD (1.25/5% decrease) as independent risk factors, and treatments with bisphosphonates (0.02) and vitamin K2 (0.06) as preventing factors (P<0.05).

Conclusions) The SQ method was suggested to be useful for analyzing incident vertebral fractures in GIO.

Disclosures: Ikuko Tanaka, None.

MO0284

Associations between pQCT Derived Bone and Muscle Properties and FSH, LH, AMH, Inhibin A and B, Estradiol and Progesterone Concentrations during one Interovalary Interval in Women. Saija Kontulainen*¹, Heidi VandenBrink², Chizen Donna², David Robertson³, Georgina Hale⁴, Angela Baerwald². ¹University of Saskatchewan, Canada, ²Department of Obstetrics, Gynecology, Reproductive Sciences, University of Saskatchewan, Canada, ³Prince Henry's Institute of Medical Research, Monash Medical Centre, Australia, ⁴Department of Obstetrics & Gynecology, University of Sydney, Austria

The relationship between cortical and trabecular bone and reproductive hormone production during perimenopausal transition is poorly understood. Our objective was to characterize associations between hormone production and radius and tibia bone and surrounding muscle properties in women.

A prospective, observational pilot study was conducted in 30 healthy women (age 18-55 yrs). Concentrations of Follicle Stimulating Hormone (FSH), Luteinizing Hormone (LH), AntiMullerian Hormone (AMH), Inhibin A and B, Estradiol, and Progesterone were measured every 1-3 days during one interovalary interval (IOI). Concentrations were recorded as the mean, minimum and maximum over the follicular and luteal phases and entire IOI, and mean day 2-4. Peripheral Quantitative Computed Tomography (pQCT) images were obtained to determine radius and tibia properties: trabecular bone area, content and density at the distal sites; cortical and marrow cavity (MC) areas, cortical content and density, muscle area and density (estimate of muscle fatness) at the shaft sites. Significant associations (p<0.05) between endocrine and pQCT outcomes were determined using Spearman rank correlation coefficients (rho).

In radius, FSH was positively associated with trabecular area and content (rho: 0.37-0.40). AMH correlated negatively with trabecular area and content (-0.34 to -0.45). Inhibin B was negatively associated with trabecular area and content (-0.37 to -0.43). Forearm muscle density was positively associated with AMH (0.38) and Inhibin A and B (0.38 to 0.52). Progesterone correlated positively with cortical content and area (0.38-0.47). In tibia, FSH correlated positively with trabecular and MC areas (0.36 - 0.53) and negatively with muscle area (-0.49). LH was positively associated with trabecular content and area, and MC area (0.37 - 0.55). AMH correlated negatively with trabecular area (-0.36 to -0.49). Inhibin B was negatively associated with trabecular content and area (-0.37 to -0.43). Calf muscle density correlated positively with Inhibin A and B (0.39 - 0.52). No relationships were noted between bone/muscle properties and estradiol.

Elevated FSH was related to greater trabecular area and content while the opposite was observed for AMH and Inhibin A/B concentrations in radius and tibia. Associations between muscle properties and FSH, AMH, Inhibin A and B concentration suggest that the relationships between these hormones and bone properties may be influenced by muscle size and density.

Disclosures: Saija Kontulainen, None.

MO0285

Association between Low Bone Mass with Arterial Stiffness in Healthy Korean Adult Males. Hee-Jeong Choi*¹, Byung-yeon Yu², Han Jin Oh³.
¹Department of Family Medicine, Eulji University School of Medicine, South Korea, ²Konyang University Hospital, Republic of Korea, ³Kwandong University, College of Medicine, South Korea

Background Previous data have shown consistent relationships between osteoporosis and arterial stiffness in postmenopausal women. These results suggest that low bone mass and arteriosclerosis are closely linked pathological conditions. The aim of this study was to assess the association between low bone mineral density (BMD) and arterial stiffness in healthy adult males.

Methods Data was gathered from 166 adult males who visited the health promotion centre for a routine check-up, after excluding participants who had medical history of cardiovascular disease; taking medications for diabetes, hypertension, dyslipidemia, or osteoporosis. Lumbar spinal BMD (L1-4) was measured by dual-energy X-ray absorptiometry. Cardiac-ankle vascular index (CAVI) was measured using a Vasera VS-1000 vascular screening system (Fukuda Denshi, Tokyo, Japan). Multivariate logistic analyses were done to identify the association of the low bone mass (T-score ≤ -2.5 in males ≥ 50 years or Z-score ≤ -2.0 in males).

Results The mean age of the subject was 45.5 ± 9.5 years. Twenty-eight percent of the subjects had metabolic syndrome. The mean LS BMD was 1.188 ± 0.158 g/cm² in normal CAVI group and 1.108 ± 0.120 g/cm² in high CAVI group (P=0.003). Percentage of low BMD in normal- and high CAVI group were 24.4% and 45.2%, respectively (P=0.003). LS BMD was negatively correlated with CAVI after adjusting for age (r=-0.19, P=0.013). In multiple logistic regression analysis, high CAVI was independent predictor of low LS BMD (OR=3.63, 95% CI, 1.47-8.95) after adjusting for age, body mass index, smoking, alcohol drinking, exercise, and metabolic syndrome.

Conclusions In apparently healthy adult males, a high CAVI was associated with low bone mass. This finding suggests that males with arteriosclerosis should be considered for further evaluation of low bone mass.

Disclosures: Hee-Jeong Choi, None.

MO0286

Blood Flow and Vascular Conductance to Bone and Marrow of the Hindlimb Are Reduced in Obese Zucker Diabetic Fatty Rats. John Stabley*, Robert Davis, Bradley Behnke, Michael Delp. University of Florida, USA

Ambiguity surrounding the detrimental impact of type 2 diabetes mellitus on bone persists. Obese Zucker diabetic fatty (ZDF) rats are a widely utilized animal model of type 2 diabetes mellitus that display many of the symptoms of type 2 diabetes in humans, such as obesity, high blood pressure, and abnormal blood cholesterol levels. Several mechanical bone properties (e.g., stiffness, ultimate load, etc.) are decreased in 20-wk old obese ZDF rats versus their lean counterparts. An enhanced vasoconstrictor responsiveness of isolated resistance arteries from hindlimb skeletal muscle of the same rats is also evident, suggesting similar alterations in the bone resistance vasculature may occur in type 2 diabetes mellitus. The present study investigated the effects of diabetes mellitus on blood flow to the bone and marrow compartments of the hindlimb in the 20-wk old obese ZDF rat. Radioactive microspheres (15.5 ± 0.1 μ m diameter) were infused via a catheter implanted into the left ventricle of the heart while 20-wk old male lean (n=11) and obese (n=7) ZDF rats stood quietly. Regional bone and marrow tissue radioactivity were measured in the femur, tibia, and fibula bones. Body mass was greater in the obese vs. lean ZDF rats (lean: 367 ± 30 , obese: 422 ± 75 g). Fasting (12 hr) blood glucose was greater in obese ZDF rats (lean: 95.5 ± 10.1 , obese: 208.7 ± 86.8 mg/dl, p<0.001), thus confirming diabetes in obese animals. Blood flow (ml/min/100 g) and vascular conductance (ml/min/100 g/mmHg) in obese ZDF rats were decreased in all regions analyzed with the exception that vascular conductance to both the diaphysis of the femur and the distal metaphysis of the tibia were not different between lean and obese ZDF rats. Diabetes-induced reductions in hindlimb bone and marrow perfusion may compromise medullary fluid pressures and decrease both bone interstitial fluid flow and bone interstitial shear stress, thus impairing a critical stimulus of bone formation.

Table 1. Blood flow in lean and obese ZDF rats.

| | Blood Flow (ml/min/100 g) | |
|----------------------------|---------------------------|-------------------|
| | ZDF Lean | ZDF Obese |
| Femoral neck | 37.5 \pm 8.4 | 21.8 \pm 12.4** |
| Femur, distal metaphysis | 61.3 \pm 15.4 | 37.1 \pm 16.1** |
| Femur, diaphyseal marrow | 83.7 \pm 29.5 | 55.2 \pm 33.9* |
| Femur, diaphysis | 10.9 \pm 4.6 | 5.2 \pm 2.8** |
| Fibula | 44.3 \pm 11.6 | 19.6 \pm 10.0† |
| Tibia, proximal metaphysis | 64.8 \pm 16.5 | 33.8 \pm 15.3† |
| Tibia, distal metaphysis | 31.0 \pm 17.2 | 17.8 \pm 12.1* |
| Tibia, diaphyseal marrow | 111.8 \pm 34.6 | 60.7 \pm 41.1** |
| Tibia, diaphysis | 12.9 \pm 3.8 | 6.1 \pm 2.9† |

*p<0.05, different from ZDF lean mean. **p<0.01, different from ZDF lean mean.
 †p<0.001, different from ZDF lean mean.

Table 1. Blood flow in lean and obese ZDF rats.

Disclosures: John Stabley, None.

MO0287

Nocturnal Oxytocin Secretion Is Lower in Young Female Athletes Compared with Non-athletes and Is Associated with Bone Microarchitecture Parameters. Elizabeth Lawson*¹, Kathryn Ackerman², Nara Mendes Estella³, Gabriela Guereca³, Lisa Pierce³, Mary Boussein⁴, Anne Klibanski¹, Madhusmita Misra³. ¹Massachusetts General Hospital/Harvard Medical School, USA, ²Brigham & Women's Hospital, USA, ³Massachusetts General Hospital, USA, ⁴Beth Israel Deaconess Medical Center, USA

Oxytocin (OT) is a hormone produced in the hypothalamus and secreted into the peripheral circulation. Preclinical data indicate that OT is anabolic to bone. OT knockout mice have severe osteoporosis, and administration of OT improves microarchitecture. Postmenopausal women with osteoporosis have lower OT levels than those without. OT increases acutely after exercise, but baseline OT secretion in athletes is not well-defined. We recently reported impaired microarchitecture in normal-weight amenorrheic athletes (AA) vs. eumenorrheic athletes (EA) and non-athletes (NA). Estradiol stimulates OT secretion. We therefore hypothesized that nocturnal OT levels in AA would be low and associated with impaired bone microarchitecture. We studied 45 women (15 AA, 15 EA, and 15 NA) ages 15-21 of comparable bone age and BMI cross-sectionally. We used high-resolution peripheral quantitative CT to assess microarchitecture at the weight-bearing distal tibia and non-weight-bearing ultradistal radius. Serum samples were obtained every 60min, 11pm-7am, and pooled for an integrated measure of nocturnal OT (enzyme immunoassay; Assay Designs). Nocturnal OT was lower in AA (245 ± 22 pg/ml) and EA (344 ± 53 pg/ml) vs. NA (446 ± 40 pg/ml, p<0.04), but comparable between AA and EA. At the tibia, AA had higher %trabecular (Tb) area and Tb spacing (TbSp), and lower Tb number (TbN), %cortical (cort) area, and total density than NA. At the radius, AA had higher %Tb area and lower Tb density, %cort area and cort thickness (Th) than NA. In AA, at the tibia, OT levels were positively associated with cort density (r=0.57, p=0.03); whereas at the radius, OT levels were positively associated with TbTh (r=0.52, p=0.049), %cort area (r=0.64, p=0.01), cort density (r=0.60, p=0.02) and cort Th (r=0.67, p=0.006), and negatively with %Tb area (r=-0.62, p=0.01). In all subjects, at the tibia, OT secretion was positively associated with TbN (r=0.32, p=0.03) and negatively with TbSp (r=-0.30, p=0.04). At the radius, OT was associated with %cort area (r=0.30, p=0.04) and cort Th (r=0.30, p=0.04). Conclusions: 1) nocturnal OT secretion is low in both AA and EA vs. NA, and 2) OT levels are associated with specific site-dependent microarchitectural parameters. Notably, in AA but not EA, low OT levels are strongly correlated with decreased trabecular and cortical bone measures at the non-weight-bearing radius, suggesting that OT may contribute to hypostrogenic bone loss.

Disclosures: Elizabeth Lawson, None.

MO0288

Polyethylene Particles Placed Over the Calvarium Reduce Cancellous Bone Formation in the Femur. Kenneth Philbrick*, Lindsay Wagner, Dawn Olson, Russell Turner, Urszula Iwaniec. Oregon State University, USA

Particles generated from wear of prosthesis joint bearing surfaces induce inflammation and promote pathological periprosthetic bone resorption (osteolysis). The effect of particle-induced osteolysis on distant skeletal sites is much less well defined. However, based on previous studies we hypothesize that local inflammation inhibits bone formation at distant skeletal sites. We therefore investigated whether placement of particles over the calvarium (particle challenge) affects bone formation in the femur in mice. To accomplish this, female C57BL/6 mice (N=10), age 4 weeks, were randomized to no-treatment and particle-treatment groups (N=5/group). Polyethylene particles, 2.5 mg, were surgically implanted on top of the calvarial periosteum. Fluorochrome labels, calcein 15 mg/kg, were administered 3 and 1 days prior to sacrifice to label mineralizing bone. Mice were sacrificed 2 weeks after induction of particle challenge. Calvaria and femur were excised and analyzed using μ CT and histomorphometry. A one-tailed t-test was used to determine if particles placed over the calvarium resulted in lower bone volume and bone formation in the distal femoral metaphysis. As expected, particle challenge induced calvarial osteolysis (Figure 1). There were no effects of short-term particle challenge on cancellous bone architecture or mineral apposition rate (MAR) in the distal femur (Table 1). However, calvarial particle challenge reduced mineralizing bone perimeter (M.Pm/B.Pm) and bone formation referenced to bone perimeter (BFR/B.Pm) and bone area (BFR/B.Ar). These findings suggest that osteolysis induced by orthopedic debris particles may contribute to systemic osteopenia by decreasing bone formation.

MO0290

The Influence of Mechanical Stress to the Osteoporotic Pain-related Property in Osteoporotic Rats with Compressed Caudal Vertebrae. Miyako Suzuki¹, Gen Inoue², Seiji Ohtori², Sumihisa Orita², Masayuki Miyagi², Tetsuhiro Ishikawa², Hiroto Kamoda², Yoshihiro Sakuma², Yasuhiro Oikawa², Go Kubota², Kazuyo Yamauchi², Kazuhisa Takahashi². ¹, Japan, ²Department of Orthopaedic Surgery, Graduate school of medicine, chiba university, Japan

Introduction: We have previously reported that the expression of calcitonin gene-related peptide (CGRP), a marker of inflammatory pain, is increased in dorsal root ganglia (DRG) neurons innervating lumbar vertebrae of osteoporotic rats. In addition, we have sought to determine whether osteoporotic pain is simply derived from inflammatory pain or includes any other pain-related factors. We focused on the possibility that osteoporotic pain is exacerbated by mechanical stress on the vertebral bodies. The purpose of this study was to examine the effect of mechanical stress on osteoporotic pain using a caudal vertebrae compression model in rats.

Materials and methods: As an osteoporosis model, we used female rats ovariectomized (OVX) at 5 weeks (n = 24). Fluoro-Gold (FG), retrograde neurotracer, was applied on the periosteal surface of a caudal vertebra to detect DRG neuronal cells innervating the caudal vertebra. After the FG-labeling, they were divided into two groups: OVX+CMP group (n=12) with longitudinally-compressed caudal vertebra using wires and rubber bands and OVX group (n =12) without compression. One, 2, 4 and 8 weeks after the FG-labeling, the vertebra applied FG and bilateral S1 to S3 DRGs were resected. In the caudal vertebra and FG-labeled DRG neurons, expression of CGRP and activating transcription factor 3 (ATF3), a marker for neuronal injury, were compared between the two groups using immunohistochemistry.

Results: In the vertebrae, ATF3 immunoreactive(-ir) nerve fibers were observed only in the OVX+CMP group at 8 weeks. In DRGs, the proportions of FG-labeled CGRP-ir DRG neurons in the OVX+CMP group were significantly elevated at 4 and 8 weeks compared with the OVX group (p < 0.05). The proportion of FG-labeled ATF3-ir DRG neurons was also significantly increased at 8 weeks (p <0.05).

Discussion: More ATF3 immunoreactivity was observed in both DRG neurons and the caudal vertebra in the 8-weeks OVX+CMP group besides the increased CGRP expression. The result of this study implies that some factors of nerve injury might be involved in sensory neurons innervating caudal osteoporotic vertebra, which suggests that the osteoporotic pain might include an element of neuropathic pain in addition to one of inflammatory pain. Our results demonstrated that the compression stress onto the vertebrae increased the biomarker for neuronal injury. These findings imply that mechanical compression stress onto vertebrae may exacerbate osteoporotic pain.

Disclosures: Miyako Suzuki, None.

MO0291

Development of Point of Care Testing for N-telopeptide and C-telopeptide using Nanotechnology. Kyoung Min Lee¹, Chin Youb Chung¹, Ki Hyuk Sung¹, Min Ho Lee², Moon Seok Park¹. ¹Seoul National University Bundang Hospital, South Korea, ²Korea Electronics Technology Institute, South Korea

Study Design: Reliability of measuring serum CTx and urine NTx level using nanotechnology and correlation with ELISA measurements

Objective. To investigate the feasibility of point of care testing for serum CTx and urine NTx level in terms of reliability and correlation with ELISA measurements

Summary of Background: Measuring bone turnover marker is an useful tool for follow up evaluation in the treatment of osteoporosis. NTx and CTx have been known to be bone resorption marker and usually measured by ELISA method. However, ELISA test is a time consuming and complex procedure. If we could measure NTx and CTx using nanotechnology, it would be a useful tool as a point of care testing because it is more economic and less time consuming.

Methods: Monoclonal antibodies for NTx and CTx, strips for photoscan were developed using nanotechnology. Blood and urine samples were collected from patients undergoing examination and laboratory tests for osteoporosis. Repeated measurements of serum and urine NTx, CTx concentration three times and reliability of measurements were evaluated using intraclass correlation coefficients (ICCs). Correlation between nanotechnology measurements and ELISA measurements were analyzed, and multiple regression analysis was performed.

Results: Reliabilities of measurements using nanotechnology were 0.997 and 0.964 for serum CTx and urine NTx, respectively. Correlation between nanotechnology measurements and ELISA measurements were r=0.994 (p<0.001) and r=0.975 (p<0.001) for serum CTx and urine NTx, respectively.

R² values were over 0.8 for both of serum CTx and urine NTx measurements using nanotechnology.

Conclusions: Serum CTx and urine NTx measurements using nanotechnology are believed to show the possibility for point of care testing in the follow up of osteoporosis. Improvement of monoclonal antibody production, refinement of strip for photoscan and photosensing system could improve the accuracy and reliability of nanotechnology measurements.

Disclosures: Kyoung Min Lee, None.

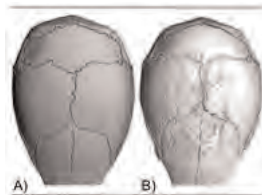


Figure 1: Representative μCT reconstructions of C5/TL6 mouse calvaria from A) no-treatment and B) particle-treatment groups. Surgical implantation of polyethylene particles induced osteolysis at the calvaria in mice.

Table 1: μCT and histomorphometric parameters of the distal femoral metaphysis

| | No Treatment | Particles | P-Value |
|-----------------------------------|--------------|------------|---------|
| | N = 5 | N = 5 | |
| μCT | | | |
| BV/TV (%) | 12.2 ± 1.2 | 10.4 ± 1.1 | 0.151 |
| Tb.N (mm ⁻¹) | 5.8 ± 0.3 | 5.3 ± 0.3 | 0.114 |
| Tb.Th (μm) | 39 ± 0.8 | 38 ± 0.7 | 0.145 |
| Histomorphometry | | | |
| M.Pm/B.Pm (%) | 10.9 ± 2.1 | 6.4 ± 1.1 | 0.048 |
| MAR (μm/d) | 3.8 ± 0.3 | 3.4 ± 0.1 | 0.070 |
| BFR/B.Pm (μm ³ /μm/yr) | 160 ± 37 | 79 ± 12 | 0.035 |
| BFR/B.Ar (%/yr) | 987 ± 265 | 464 ± 58 | 0.045 |

Data: Mean ± SE

Table 1 and Figure 1

Disclosures: Kenneth Philbrick, None.

MO0289

Subclinical Hyperthyroidism in the Postmenopause may not Influence Bone Mineral Density and Soft Tissue Composition. Ana Paula Barbosa¹, Mário Rui Mascarenhas², António M. Gouveia Oliveira³, Vera Simões⁴, Ana Gonçalves⁵, David Santos Pinto⁶, Manuel Bicho⁷, Isabel Do Carmo⁵. ¹Endocrinology, Santa Maria Hospital & Faculty of Medicine, Portugal, ²Lisbon's Faculty of Medicine, Santa Maria University Hospital, CHLN,EPE, Portugal, ³Biostatistics Department, FCMUNL, Portugal, ⁴Metabolism & Endocrinology Centre (Genetics Lab) of Lisbons Faculty of Medicine, CEDML - Lisbon's Endocrinology, Diabetes & Metabolism Clinic (Osteoporosis Unit), Portugal, ⁵Endocrinology, Diabetes & Metabolism Department, Santa Maria University Hospital, CHLN-EPE, Portugal, ⁶CEDML - Lisbon's Endocrinology, Diabetes & Metabolism Clinic (Osteoporosis Unit), Portugal, ⁷Metabolism & Endocrinology Centre (Genetics Lab) of Lisbons Faculty of Medicine, Portugal

Subclinical hyperthyroidism is a relatively frequent silent condition in the elderly people and has been associated to BMD reduction and/or osteoporosis and even to bone fragility fractures. The pathophysiology includes both bone formation and resorption inhibition by the TSH independently of the thyroid hormones effects. Also, the reduction in the lean mass can be present and worsening the risk of falls.

OBJECTIVES- To evaluate the effects of subclinical hyperthyroidism in the bone mineral density (BMD) as well as in the soft body composition of elderly women.

MATERIAL AND METHODS- A total of 78 postmenopausal women was divided and paired in subclinical hyperthyroidism (n=39) and control (n=39) groups.

The BMD (g/cm²) at the lumbar spine (L₁-L₄), at the hip, at the distal radius (1/3 or 33%) and at the whole body, as well as the total body soft tissue composition (lean and fat masses, kg) were evaluated by dual X-ray absorptiometry, using the Hologic QDR Discovery W densitometer.

Fast blood collection was also performed to measure the TSH, FT4, FT3, the pituitary hormones levels, osteocalcin, PINP, CTX and alkaline phosphatase (APH).

No patient was previously treated for hyperthyroidism or low bone mass/osteoporosis.

The BMI (kg/m²) also was calculated.

Descriptive, Anova and regression analysis statistical tests were used.

RESULTS- The anthropometric, TSH and DXA data are described in Table 1.

Significant correlations were detected between the BMD at the femoral neck vs. the bone alkaline phosphatase in the subclinical hyperthyroidism group: CC=-0.3905 (R²=15.2505;p=0.0399).

CONCLUSIONS- The results of this study strongly suggest that the BMD measured at several skeletal regions and the total fat and lean masses in a group of subclinical hyperthyroid postmenopausal women are not significantly different from those without thyroid dysfunction. If in the clinical hyperthyroidism there is a diminished BMD and soft tissues amount, it is possible that in the subclinical hyperthyroid postmenopausal patients the duration of this illness is not long enough to induce BMD changes, that can be measured by a DXA scan.

| Variables | Groups | CONTROL | SUBCLINICAL HYPERTHYROIDISM | P |
|--|--------|---------------|-----------------------------|-------|
| Age years | | 66.3 (±10.7) | 66.4 (±11.4) | N/D |
| Weight kg | | 69.2 (±9.9) | 69.3 (±11.0) | N/D |
| Height m | | 1.543 (±0.05) | 1.548 (±0.06) | N/D |
| BMI kg/m ² | | 29.1 (±3.9) | 28.9 (±4.3) | N/D |
| TSH μIU/ml | | 1.87 (±0.8) | 0.09 (±0.1) | 0.000 |
| APH IU/l | | 63.5 (±12.7) | 75.5 (±21.5) | 0.014 |
| Total body lean mass kg | | 40.2 (±5.1) | 38.9 (±4.9) | N/D |
| Total body fat mass kg | | 27.8 (±6.7) | 28.2 (±6.9) | N/D |
| BMD L ₁ -L ₄ g/cm ² | | 0.928 (±0.1) | 0.886 (±0.1) | N/D |
| BMD hip (total) g/cm ² | | 0.875 (±0.1) | 0.873 (±0.2) | N/D |

Table 1. The mean anthropometric, TSH, APH and BMD in both groups.

Disclosures: Ana Paula Barbosa, None.

MO0292

Is Urinary Pentosidine Level a Predictive Marker for the Severity of Osteoporotic Vertebral Fracture? Koji Nozaka*, Naohisa Miyakoshi, Michio Hongo, Yuji Kasukawa. Akita University Graduate School of Medicine, Japan

Background:To date, there have been numerous reports on adverse prognostic factors for osteoporotic vertebral fracture. Various factors based on imaging diagnostics, such as a low anterior vertebral body height at time of injury (%), large local kyphosis angle (°), injury of posterior wall of vertebral body, a broad range of low signal intensity on T1-weighted MRI, and localized high signal intensity on T2-weighted MRI, are being tested, but there is not yet a consensus on their utility. Although "high urinary pentosidine (Pen) level" is a useful surrogate marker for detecting bone-quality-deterioration types of osteoporosis, reports comparing osteoporotic vertebral fracture severity according to urinary Pen values are unclear.

Objective:To compare osteoporotic vertebral fracture severity according to urinary Pen level.

Subjects and Methodology:Subjects consisted of 23 patients with fresh osteoporotic vertebral fracture, among the 160 of 3051 patients who underwent bone mineral density analysis at our hospital in 2009-2010, who also consented to urinary Pen analysis (standard range: 0.019 to 0.07 µg/mg Cr). Results showed Pen level above the standard range (High Pen group) for 13 subjects and Pen level below the upper limit of the standard range (Normal Pen group) for 10 subjects. Endpoints were bone mineral density measured as YAM (%), anterior vertebral body height at time of injury (%), and local kyphosis angle (°).

Results:Mean age and YAM were not significantly different between the High Pen group (77.1 years and 50.0%) and the Normal Pen group (73.5 years and 55.5%). Anterior vertebral body height at time of injury (%) was significantly lower ($p < 0.05$) in the High Pen group (59.9%) than in the Normal Pen group (76.1%). Local kyphosis angle was significantly greater ($p < 0.05$) in the High Pen group (14.0°) than in the Normal Pen group (4.5°).

Discussion:These findings suggest that spinal alignment may be worse and osteoporotic vertebral fracture more severe in patients with high urinary Pen levels (bone-quality-deterioration types of osteoporosis) than in patients with normal urinary Pen levels (non-bone-quality-deterioration types of osteoporosis). Although investigations are currently being conducted with greater numbers of cases, and other additional factors such as MRI, and pseudarthrosis rate, it is believed that urinary pentosidine level can be a predictive marker for the severity of osteoporotic vertebral fracture.

Disclosures: *Koji Nozaka, None.*

MO0293

Measurement of Sclerostin in the Circulation: Validation and Comparison of Two Commercially Available ELISAs for Circulating Sclerostin. Aline Costa*¹, Serge Cremers¹, Elzbieta Dworakowski¹, Thomas Nickolas², Mishaela Rubin¹, Marcella Walker¹, Emily Stein³, Marise Lazaretti Castro⁴, Shonni Silverberg¹, John Bilezikian³. ¹Columbia University, USA, ²Columbia University Medical Center, USA, ³Columbia University College of Physicians & Surgeons, USA, ⁴Escola Paulista de Medicina, Brazil

Measurement of circulating sclerostin levels may be useful in a number of metabolic bone diseases. Recent work indicates that results of sclerostin assays may be different depending on assay manufacturer and type of sample (serum vs plasma) used. We compared two different ELISAs for sclerostin from TecoMedical (Sissach, Switzerland) and from Biomedica (Vienna, Austria). Both assays have undergone protocol adjustments since they were commercially launched. Twenty anonymous paired patient samples of serum, EDTA plasma and heparin plasma were tested in both assays, along with serum from 10 patients with CKD and 34 patients with a variety of metabolic bone diseases. The average serum level of all patients was 0.713 ± 0.58 ng/mL with the Biomedica assay and 0.734 ± 0.43 ng/mL with the TECO assay ($p = .002$). For the 20 paired samples, from serum, EDTA plasma and from heparin plasma, levels were 0.743 ± 0.72 , 1.011 ± 0.75 , and 0.911 ± 0.72 , respectively for Biomedica; and 0.725 ± 0.46 , 0.948 ± 0.52 , and 0.900 ± 0.52 for TECO. There was a strong correlation between sclerostin in plasma and serum with the Biomedica ELISA (EDTA plasma vs serum: $r = 0.940$, $p < .0001$; heparin plasma vs serum: $r = 0.968$, $p < .0001$) and with TECO (EDTA plasma vs serum: $r = 0.911$, $p < .0001$; heparin plasma vs serum: $r = 0.915$, $p < .0001$). Intra- and inter-assay precision ($n = 6$) were 3.2% and 9.4% for TECO, respectively and 13.6% and 18.4% for Biomedica. Samples were stable for the TECO assay with an average level after 72 hrs of 115% at 4°C, 108% at room temperature (RT) relative to pre-treatment. Samples were stable after 3 cycles of freeze-thaw with a mean level of 110%. Stability data showed more variability for the Biomedica assay with an average concentration after 72 hrs of 98% at 4°C and 78% at RT. The mean concentration after 3 cycles of freeze-thaw was 95%. The mean recovery of added sclerostin to serum samples (1 and 2 ng/mL) was 96% of the expected sclerostin concentration with TECO and 146% with Biomedica. Upon dilution (1:2 and 1:4) serum sclerostin concentrations were 96% and 88% of the expected for TECO, and 139% and 118% for Biomedica. The two assays showed a strong correlation in all serum samples ($n = 64$; $r = 0.901$, $p < .0001$) with no apparent influence of disease. Overall, the two assays correlated well with each other. Subject to further

studies, the TECO assay appears to have less variability with regard to stability, dilution, recovery, inter- and intra-assay variability.

Disclosures: *Aline Costa, None.*

This study received funding from: TECO Medical

MO0294

Prognostic Value of Serum Osteocalcin and Undercarboxylated Osteocalcin Levels on Vascular Complications in Type 2 Diabetes. Megumi Shibata*¹, Atsushi Suzuki², Junnichi Ishii³, Fumihiko Kitagawa³, Toshiaki Sakuishi³, Takashi Fujita³, Takashi Ishikawa³, Ikuko Tanaka³, Hirovuki Hirai⁴, Yoshiteru Maeda⁵, Sahoko Sekiguchi-Ueda², Yasumasa Yoshino⁶, Shogo Asano⁷, Masaki Makino⁸, Nobuki Hayakawa⁹, Mitsuyasu Itoh¹⁰. ¹Fujita Health University Division of Endocrinology, Japan, ²Fujita Health University, Division of Endocrinology, Japan, ³Department of Joint Research Laboratory of Clinical Medicine Fujita Health University, Japan, ⁴Fujita Health University Division of Endocrinology, Japan, ⁵Fujita Health University, Division of Endocrinology, Japan, ⁶Toyokawa City Hospital, Japan, ⁷Division of Endocrinology Toyokawa City Hospital, Japan, ⁸Division of Endocrinology Fujita-health University, Japan, ⁹Faculty of Pharmacy, Meijo University, Japan, ¹⁰Fujita Health University, Division of Endocrinology, Japan

Background: Osteocalcin (OC) and its inactive form, undercarboxylated osteocalcin (uOC) have been reported to affect insulin secretion and sensitivity under both physiological and pathological conditions. We have previously reported that both OC and uOC levels are affected by renal function, and OC and uOC levels were higher in the patients with the past history of cardiovascular disease, even in CKD stages 1 and 2. In the present study, we evaluated their prognostic value on vascular complications in type 2 diabetes patients.

Results: We enrolled 341 type 2 diabetes outpatients (M/F=203/138; Mean age, 65.5 ± 11.4 years). Mean serum OC and uOC levels were 4.1 ± 3.5 ng/ml and 3.3 ± 3.7 ng/ml at baseline, respectively. Both OC and uOC levels were closely related to estimated GFR and urinary albumin concentration (UAE), but not with HbA1c. OC and uOC levels were associated with the existence of micro- and macrovascular diseases. Follow-up periods were 727 ± 244 days. During follow-up period, 8 cases died mainly due to macrovascular diseases and cancer. Macrovascular diseases (defined as acute myocardial infarction, unstable angina with percutaneous coronary intervention, peripheral arterial diseases with percutaneous intervention, apoplexy, or hospitalized heart failure) were occurred in 21 cases. In addition, apparent microvascular event such as hemodialysis due to diabetic nephropathy and/or unstable proliferative diabetic retinopathy were found in 12 cases. Serum OC or uOC level at baseline did not predict future death in this population, and were not related to new onset of macrovascular diseases or cancer. uOC was weakly associated with microvascular event, while OC was not. Conclusion: Although serum OC and uOC levels were associated with pre-existing micro- and macrovascular diseases, their predictive values for future vascular events were not apparent during short-term follow-up.

Disclosures: *Megumi Shibata, None.*

MO0295

Reference Intervals for Bone Turnover Markers in Younger and Older Women: the OPUS Study. Fatma Gossiel*¹, Judith Finigan², Richard Jacques³, David Reid⁴, Dieter Felsenberg⁵, Christian Roux⁶, Claus-C Glueer⁷, Richard Eastell². ¹The University of Sheffield, United Kingdom, ²University of Sheffield, United Kingdom, ³School of Health & Related Research, University of Sheffield, United Kingdom, ⁴University of Aberdeen, United Kingdom, ⁵Charité - Campus Benjamin Franklin, Germany, ⁶Hospital Cochin, France, ⁷Christian Albrechts Universitaet zu Kiel, Germany

In order to interpret bone turnover markers (BTM) in clinical practice we need to establish reference intervals for young women to identify targets for treatment and for older women to identify high bone turnover that might indicate secondary osteoporosis. It is difficult to establish reference ranges for older women because they commonly suffer from diseases or take drugs that affect bone turnover. The aims were 1) to identify diseases and drugs that have a substantial effect on BTM so that they can be used as exclusion criteria; 2) to establish reference intervals in younger and older women and test if they are different. We studied younger women ages 30 to 39 ($n = 258$) and older women aged 55 to 79 years ($n = 2419$) from the OPUS study, a 5-European centre population-based study. We administered a questionnaire and obtained non-fasting serum and second morning void urine samples, and measured β CTX, intact PINP, bone ALP and 25(OH)D using the IDS-ISYS, osteocalcin using the Roche Elecsys 2010, and NTX using the Vitros Ortho-Clinical Diagnostics, all automated immunoassays as well as routine biochemistry panel and BMD spine and hip by DXA. Bone turnover markers had a skewed distribution, so they were log-transformed. Based on a multiple linear regression analysis, at least one BTM was

affected by vitamin D insufficiency (25(OH)D<50nmol/L), stage 4 or 5 chronic kidney disease(eGFR < 30 mL/minute/1.73m2), osteoporosis (spine or hip BMD T-score ≤ -2.5), estrogen replete, or drugs or diseases known to affect bone turnover. These were then used as exclusion criteria for selecting the populations for the reference intervals (geometric mean +/- 1.96 SD), table. There are several diseases and drugs that influence bone turnover markers in older women that need to be excluded for reference intervals. Reference intervals need to be determined separately for older and younger women because they differ.

| BTM | Older women (n=343) | Younger women (n=58) |
|----------------------|----------------------|----------------------|
| βCTx ng/ml | 0.31 (0.10 - 1.00) | 0.19(0.05 - 0.63)* |
| NTX nmol BCE/mmol Cr | 49.7 (21.2 - 116.4) | 38.1 (15.0 - 97.0)* |
| Intact PTH ng/ml | 40.6 (15.9 - 103.4) | 30.1 (4.2 - 74.5)* |
| Bone ALP ng/ml | 14.1 (7.2 - 27.6) | 9.8 (5.2 - 18.6)* |
| Osteocalcin ng/ml | 24.5 (12.7 - 47.4) | 17.9 (8.8 - 36.4)* |

*P<0.05 in dependent sample t-test

Table

Disclosures: Fatma Gossiel, None.
This study received funding from: IDS

MO0296

A Descriptive Study of Adult Patients with Idiopathic Hypercalciuria. Vidhya Illuri^{*1}, Alicia Stapleton², Pauline Camacho¹. ¹Loyola University of Chicago, USA, ²Loyola University Medical Center, USA

Purpose

Idiopathic Hypercalciuria(IH) is a very common finding in patients with osteoporosis and kidney stones. IH is defined as 24 hour urine calcium excretion > 250 mg/d in women and 300 mg/d in men that is not associated with conditions known to increase calcium elimination. Hypercalciuria has been described in as high as 10% of patients with secondary osteoporosis and 50-60% of patients with nephrolithiasis are due to this condition. We aimed to study patients with primary diagnosis of IH detected in the workup for osteoporosis or osteopenia and characterize them retrospectively.

Method: We included all adult male and female patients seen at Loyola University Medical Center with urinary calcium > 300 mg/24 hours from 2008-2011. Patients who had other causes for hypercalciuria such as primary hyperparathyroidism and vitamin D excess were excluded. 49 patients were included in the study. We reviewed each patient's initial history and biochemical findings, including, 24 hour urine calcium, urine creatinine, urine sodium, age, gender, race, weight, height, serum calcium, ionized calcium, vitamin D, intact PTH, BMD score, T score and Z score, as well as their personal and family history of kidney stones, fractures, and osteoporosis.

Results: The study population consisted of 5 males (5%) and 44 females(95%) of predominately Caucasian race(94%), all of whom were diagnosed with idiopathic hypercalciuria as part of a workup for secondary causes of bone loss. The mean age of the population was 58.4 years. 18.4% of patients had a family history of kidney stones, 53.1% had a family history of osteoporosis, 16.3% of patients had a personal history of kidney stones, 42.9% had diagnosis of osteopenia, 53.1% had a diagnosis of osteoporosis, and 46.9% had a history of fragility fractures. The mean lumbar spine T score was -2.14(+/- 1.13) and mean lumbar spine Z score was -1.0(+/- 1.37). The mean femoral neck T score was -1.54(+/-0.92) and mean femoral neck Z score was -0.53(+/-0.63).

Conclusion: Idiopathic hypercalciuria is more common in women in the 6th decade of life. The majority patients with IH did not present with a personal history of kidney stones. Bone density is often lower than age matched controls, evidenced by lumbar spine Z scores at -1 SD or lower. Bone loss appears to be more prominent in trabecular bone. Our results suggest that all patients with osteoporosis, and particularly those with premature osteoporosis should be screened for idiopathic hypercalciuria because most patients do not have clinical manifestations of the disease. In most cases, idiopathic hypercalciuria was easily corrected by thiazide diuretics.

Disclosures: Vidhya Illuri, None.

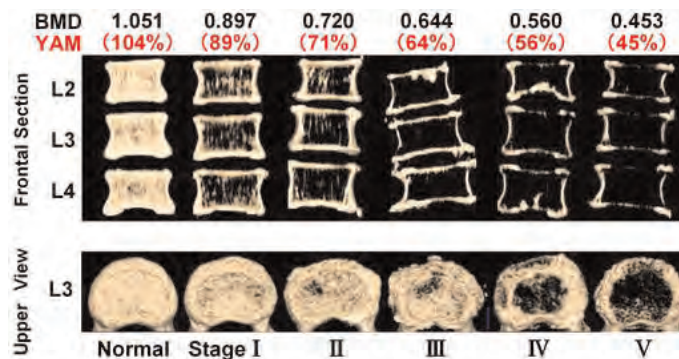
MO0297

Withdrawn

MO0298

Comparison of 3D-CT Images for Osteoporotic vertebra and Lumbar BMD in Elderly Women. Sumiaki Okamoto^{*1}, Hitoshi Noguchi², Hiroyuki Suzuki³, Sumitada Okamoto¹, Akira Itabashi⁴. ¹Okamoto Clinic SORF, Japan, ²Noguchi Thyroid Clinic & Hospital Foundation, Japan, ³Suzuki Orthodontic office, Japan, ⁴Saitama Center for Bone Research, Japan

We have previously reported porosity of vertebral endplates appear early in the progression of osteoporosis and may present a reliable indicator of bone loss. In our current study, we graded the CT images into 6 stages and compared the coronal and sagittal CT sections of the vertebra in an attempt to propose a grading scale for the progression of osteoporosis. We created computerized 3-D renderings by Helical CT (Asteion Super 4 edition Toshiba). We then grouped the results into 6 stages and compared them to conventional BMI. Stage 1 is normal vertebrae of pre-menopausal women aged between 20 and 50. The endplates were not porous in transverse sections and the vertebral bodies appeared solid with little or no space between the intravertebral trabeculae in coronal and sagittal sections. The cortex could not clearly be discerned from the marrow. Stage 1 is equivalent to vertebral BMD of 1.051g/cm². Stage 2 is the vertebrae of women 5 years post-menopause. The endplates are coarse but minimally porous. Intravertebral trabeculae appear intermittently in coronal and sagittal sections and the marrow appears framed in thick cortex. Stage 2 is equivalent to vertebral BMD of 0.897g/cm². Stage 3 is the average vertebrae of women 90 years old. The endplates are porous with large pores. Intravertebral trabeculae appear sparse in coronal and sagittal sections and the marrow is framed in thick cortex that is easily discernable from the interior of the bone. Stage 3 is equivalent to vertebral BMD of 0.720g/cm². Stage 4 is vertebrae with BMD 100mg/cm² lower than the average 90 year old woman. Intravertebral trabeculae cannot be observed. The cortex frames an empty void. Endplates are obviously porous with connecting pores. Sclerotic bone formation can be observed at the vertebral rims. Stage 4 is equivalent to vertebral BMD of 0.644g/cm². Stage 5 is vertebrae with BMD 200mg/cm² lower than the average 90 year old woman. The cortex forms a crooked and intermittently broken frame. The endplates have large voids. Stage 5 is equivalent to vertebral BMD of 0.560g/cm². Stage 6 is vertebrae with BMD 300mg/cm² lower than the average 90 year old woman. The cortex frame is absent at the midline in coronal and sagittal sections. The endplates appear ringed by the vertebral cortex. Stage 6 is equivalent to vertebral BMD of 0.453g/cm². We have found that the staging by CT images rarely contradicts the BMD and vice versa. This may be a useful scale for staging severity of osteoporosis.



Stage classification of 3D CT Findings

Disclosures: Sumiaki Okamoto, None.

MO0299

CTXA Hip - An Extension of Classical DXA Measurements Using QCT. Christopher Cann¹, Judith Adams², Keenan Brown³, Alan Brett^{*4}. ¹University of California, San Francisco, USA, ²Manchester Royal Infirmary, United Kingdom, ³Mindways Software, USA, ⁴Mindways Software, Inc., USA

Introduction: Bone mineral density (BMD) estimates for the proximal femur using DXA are currently considered the standard for making a diagnosis of osteoporosis in an individual patient using BMD alone. We have compared BMD results from a commercial QCT BMD analysis system, CXTX Hip (see Figure 1), which provides clinical data for the proximal femur, to results from DXA. We have also used CXTX Hip to determine cortical and trabecular contributions to total BMD.

Material and Methods: Sixty-nine patients were scanned using 3D QCT and DXA. CXTX Hip BMD measurements for Total Hip and Femoral Neck were compared to DXA results. Twenty-two women were scanned at 0,1,2 years and CXTX Hip and DXA results analyzed for long term reproducibility.

Results: Reproducibility was 0.011 g/cm² for CTXA Total Hip and 0.012 g/cm² for CTXA Femoral Neck compared to 0.012 g/cm² and 0.013 g/cm² respectively for DXA (see Table 1). The correlation of Total Hip BMD CTXA vs. DXA was R=0.97, and for Femoral Neck (see Figure 2) was R=0.95 (SEE 0.044 g/cm² in both cases). Cortical bone comprised 62 ± 5% (mean ± SD) of total hip bone mass in osteoporotic women.

Conclusion: CTXA Hip provides substantially the same clinical information as conventional DXA, and in addition provides estimates of volume-derived parameters which may be useful in evaluation of bone strength.

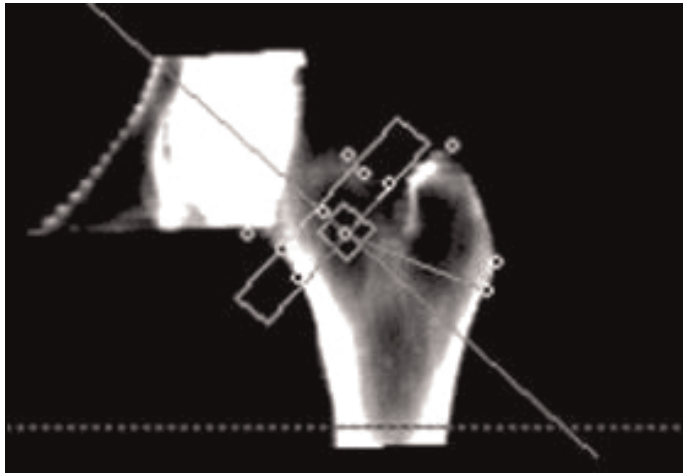


Figure 1. CTXA projected image with standard regions of interest used for BMD calculations.

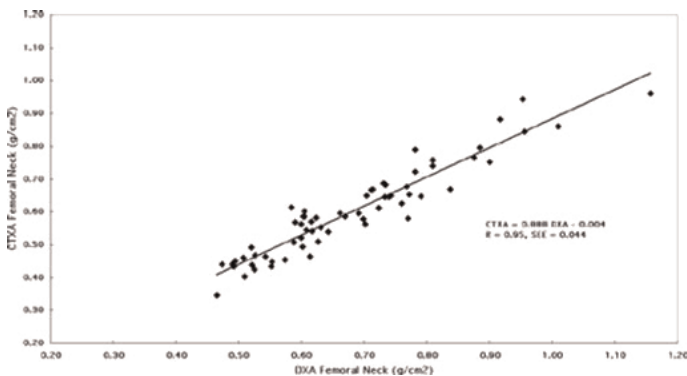


Figure 2. Correlation of area BMD for CTXA and DXA for femoral neck region of interest.

| | Total Hip | | Femoral Neck | |
|------------------------------------|-----------|-------|--------------|-------|
| | CTXA | DXA | CTXA | DXA |
| Areal Density (g/cm ²) | 0.645 | 0.700 | 0.551 | 0.598 |
| Precision (g/cm ²) | 0.011 | 0.012 | 0.012 | 0.013 |
| CV (%) | 1.7 | 1.7 | 2.1 | 2.1 |

Table 1: Summary of Long-Term In Vivo Precision, CTXA vs. DXA, in Osteoporotic Subjects

Disclosures: Alan Brett, Mindways Software, Inc., 7

MO0300

Differences in Mineralization between Cortical and Trabecular Bone in Human Proximal Femur. Xiutao Shi*, Bin Zhou, Ji Wang, X Guo. Columbia University, USA

Recent clinical studies have rejuvenated research interests in cortical bone such as increased cortical porosity in diabetes or osteoporotic fractures. Similar to trabecular bone, both microstructure (such as porosity) and mineralization play important roles in determining the mechanical integrity of cortical bone. For example, human cortical bone tissue has been assumed to be more mineralized than trabecular bone tissue. However, direct comparison of the tissue mineralization of cortical and trabecular bone of human proximal femur as determined by micro computed tomography (μCT) has rarely been reported. In this study, we performed μCT scanning of human femoral bone samples that included both cortical and trabecular bone compartments from three important anatomic regions: femoral neck (FN), greater trochanter (GT), and lesser trochanter (LT). We then directly compared the tissue mineralization density (TMD) between cortical and trabecular bone tissue.

Fifteen FN, 17 GT, and 16 LT samples that contained both cortical and trabecular bone compartments were collected from the femurs of 15 donors (8M/7F, 73 ± 14 years) depending on availability at the corresponding regions (Fig. 1A). After

scanning via a μCT system (vivaCT 40, Scanco Medical AG) at 15 μm resolution, images of cortical and trabecular bone compartments were segmented for separate analysis. Using standard hydroxyapatite (HA) phantoms, bone TMD (mg HA/cm³) was determined (Fig. 1B-D).

The TMD of cortical bone was higher than that of trabecular bone for all three anatomic regions (Fig. 2, p < 0.001). The average TMD of cortical bone was 1049 ± 53 mg HA/cm³, compared to that of trabecular bone, which was 929 ± 38 mg HA/cm³. No difference was observed for the TMD of cortical bone across anatomic regions (Fig. 2, p > 0.14). In contrast, the TMD of trabecular bone was dependent on the anatomic region (Fig. 2, p < 0.05), with that of LT the highest and that of GT the lowest.

The TMD of femoral cortical bone does not depend on the anatomic region. Trabecular bone from different anatomic regions in the proximal femur has different TMDs. The implications of heterogeneity in TMD of trabecular bone in the proximal femur should be of great interest in the etiology of osteoporotic hip fractures.

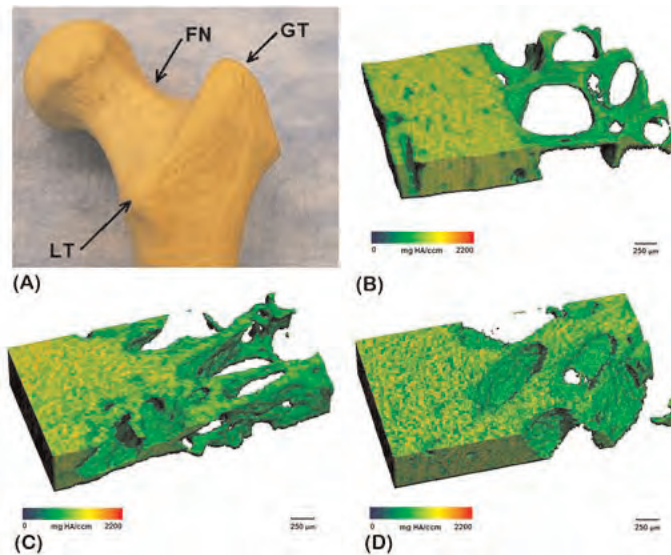


Fig. 1. Illustration of anatomic regions (A) and TMD distributions at FN (B), GT (C), and LT (D).

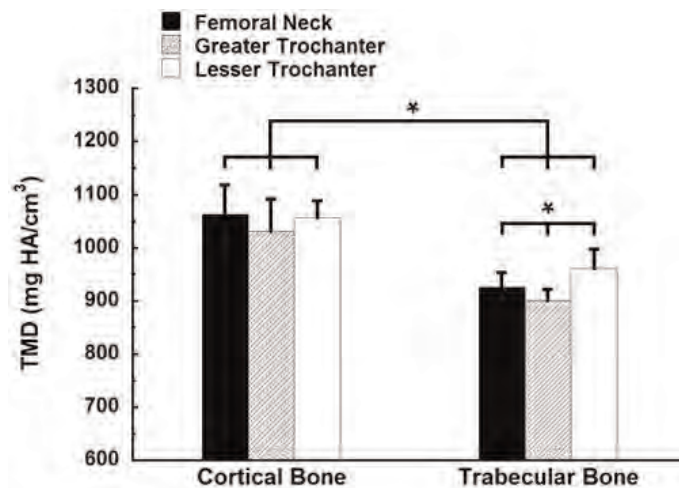


Fig. 2. Comparison of TMD between cortical and trabecular bone at FN, GT, and LT.

Disclosures: Xiutao Shi, None.

MO0301

Evaluation of Norland Illuminatus Applications Software When Operating Under a Windows XP or Windows Seven System. Tom Sanchez*¹, Chad Dudzek², Mark Thomas³, Terry Schwalenberg², Rick Olaszewski⁴, Debbie Thomas³. ¹Norland - A Cooper Surgical Company, USA, ²Norland-a CooperSurgical Company, USA, ³SouthTech Medical Electronics, USA, ⁴CooperSurgical Company, USA

Evaluation of bone or soft tissue assessments by DXA can be compromised by differences in software. While differences in Applications Software are usually carefully validated differences can also be brought about by changes in the Operating System. This study compared phantom based assessments under tightly controlled

conditions when carrying out DXA studies using the Windows® XP or Seven based Operating System.

The studies reported here were performed on the Norland XR-800 operating with Illuminatus Applications Software under either a Windows® XP or Seven Operating System. Scans were performed on anatomical phantoms for the AP Spine, Lateral Spine, Hip, Heel (Research Scan) and two different Whole Body Phantoms. Scans were performed using standard scan setting with 25 repeated scans of each phantom (except the whole body phantoms which had 10 repeated scans) under each operating system.

As noted in the table below precision for studies done under Windows® XP or Seven were similar and within the expected range. Similarly, the ratio of the Windows® XP value to the Windows® Seven value proved to be near unity indicating the scanner produced similar results with either operating system.

Examination of studies performed on the various phantoms indicates that studies performed under the Windows® XP Operating System show similar precision to studies performed under the Windows® Seven Operating System. Furthermore, the studies show that the absolute results obtained with the two operating systems were similar. The results as a whole support a conclusion that results obtained using a Windows® XP or Windows® Seven Operating System are compatible.

| | Precision Windows® XP (%) | Precision Windows® 7 (%) | XP/7 |
|--------------|---------------------------|--------------------------|---------|
| AP Spine | 0.4 | 0.7 | 101.60% |
| Lat Spine | 0.6 | 0.6 | 100.16% |
| Total Hip | 0.4 | 0.7 | 101.82% |
| Heel | 0.4 | 0.4 | 100.40% |
| Midi BMC | 0.8 | 0.9 | 99.08% |
| Midi Lean | 2.0 | 2.8 | 100.18% |
| Midi Fat | 1.3 | 1.8 | 101.01% |
| Crystal BMC | 1.0 | 1.2 | 99.98% |
| Crystal Lean | 2.1 | 1.1 | 99.00% |
| Crystal Fat | 1.6 | 0.8 | 100.82% |

Results Obtained with Windows XP or Seven

Disclosures: Tom Sanchez, None.

MO0302

Femoral Neck Buckling Ratio, Gender Differences and Associations to Proximal Femoral Fractures. Arne Hoiseth¹, Knut Strømsoe². ¹Curato Rtg., Norway, ²none, Norway

Buckling ratio is the ratio between wall thickness of a tube and the tube diameter. Applied on bones it is the ratio of cortical thickness (CoTh) over bone diameter. By using multi slice-CT we assessed this ratio in the middle portion of femoral necks at right angle to the neck axis. The neck diameter (ND) was calculated as the mean of 4 manual measurements at 45 degrees to each other. CoTh was the mean of 8 manual measurements at the points where the 4 diameters intersected the cortex. This ratio is denoted BR1. On the same CT-slices cortical volume (or area in the slices) and cortical bone mass (calculated as the product of cortical volume and cortical density) were assessed by a semiautomatic program. We thus defined two additional buckling ratios: BR2 as (cortical volume/ND) and BR3 as (cortical mass/ND). 34 Males and 79 females having suffered a proximal femoral fracture and age and sex matched non fractured cases (23 males and 50 females) were included in this study. The purpose was to determine the differences in BR1, BR2 and BR3 between genders and between fractured and non-fractured cases. For all three definitions of BR we found statistically significant gender differences in the non-fractured cases. For fractured cases there was a clear difference between males and females, but the differences were not statistically significant for BR1, while for BR2 these differences were highly significant. For females and males separated the differences for fractured and non-fractured cases did not reach significance for BR1, while for BR2 and BR3 the differences were highly significant. We performed this study as an exploratory investigation. The results indicate that all three definitions of buckling ratio is strongly associated to gender both in fractured and non-fractured cases, although these differences were less among the fractured cases, buckling ratio does not appear as a common fracture denominator for males and females. BR1 gave a weaker differentiation in the fracture assessments compared to integrating cortical volume (BR2) and cortical bone mass (BR3) into the computation. This may be due to a less precise measurement of cortical thickness, being done manually. We hypothesize, however, that BR3 has a stronger association to bone strength than BR1 and than BM2, integrating cortical bone mass rather than just dimensions.

Disclosures: Arne Hoiseth, None.

MO0303

Has Primary Care Physicians' (PCPs) Understanding and Use of the 2010 Osteoporosis Canada Clinical Practice Guidelines (OC CPG) Increased Since Publication? Suzanne Morin^{*1}, Alan Bell², Daniel Ngui³, Robert Josse⁴, Heather Frame⁵, Jacques Brown⁶, Angela Cheung⁷, Bridget Burns⁸, Alexandra Papaioannou⁹. ¹McGill University, Canada, ²University of Toronto, Canada, ³University of British Columbia, Canada, ⁴St. Michael's Hospital, University of Toronto, Canada, ⁵Assiniboine Medical Clinic, Canada, ⁶CHUQ Research Centre Laval University, Canada, ⁷University Health Network, Canada, ⁸Amgen Canada, Canada, ⁹Hamilton Health Sciences, Canada

Objective: To compare the awareness, use and understanding of the 2010 OC CPG by PCPs at two time points following guideline dissemination

Methods: Two online surveys (May 2011 and January 2012) were conducted with the same group of Canadian PCPs to assess change in their understanding and use of the OC CPG. To gauge their understanding, respondents in each survey evaluated fracture risk of three hypothetical patients.

Results: • 304/2100 physicians completed the first survey (S1); 150 of whom completed the second survey (S2)

- Prior to the S1, 32% (97/304) (95CI: 27, 37) of PCPs attended ≥1 educational event on the 2010 OC CPG vs. 43% (65/150) (35, 51) in S2
- Comparing responses between surveys for the 150 PCPs that completed both:
 - o The proportion reporting use of the OC CPG increased from 62% (54/70) to 89% (84, 94)
 - o The proportion relying primarily on CAROC tool for evaluating postmenopausal osteoporosis remained unchanged (18%); FRAX[®] use increased slightly from 12% to 15%
 - o Many physicians (48%) (38, 55) in the S2 continued to obtain the 10-year fracture risk assessment from the DXA report, vs. 59% (48/64) in S1
 - o Despite indicating they understood how risk assessment is calculated, PCPs listed a diverse set of parameters not included in the models
- Evaluation of risk category of three hypothetical patient cases in the two surveys (Table) revealed that:
 - o The proportion who correctly assessed all three patients' risk category remained low; S1 4% vs. S2 8%
 - o PCPs who correctly assessed the high-risk patient decreased from 93% to 72%
 - o Most PCPs assessed the two moderate-risk patients incorrectly
- Contrary to OC CPG recommendations, PCPs in S2 identified etidronate (43%) and calcitonin (13%) as first-line therapies, similar to findings in S1

Conclusions: In sequential surveys to assess PCPs' use and understanding of the 2010 OC CPG, the proportion indicating they used the guidelines increased. However, PCPs still had difficulty assessing fracture risk. Assessment of hypothetical cases yielded inconsistent results, providing no clear evidence of improvement with time. Also, prescribing habits appear to be independent of CPG recommendations in some cases. Further strategies are necessary to improve guideline uptake and increase use of the CAROC or FRAX tools for risk assessment.

Conflict Statement: This research was sponsored by Osteoporosis Canada. Financial support was provided by Amgen Canada.

| % (95 CI) | 58 year old female with vertebral compression fracture identified on x-ray | | 60 year old female with lumbar spine T-score: -2.5, femoral neck T-score: -2.2, glucocorticosteroid use for 6 months at 10 mg daily | | 65 year old female with femoral neck T-score: -1.9, wrist fracture 3 years prior | |
|-----------|--|-------------------|---|-------------------|--|-------------------|
| | Survey 1 | Survey 2 | Survey 1 | Survey 2 | Survey 1 | Survey 2 |
| Low | 0% | 1% | 0% | 2% | 9% | 11% |
| Moderate | 5% | 21% | 17% (11 to 23) | 29% (22 to 36) | 29% (22 to 36) | 47% (39 to 55) |
| High | 93% (89 to 97) | 72% (65 to 79) | 82% | 67% | 61% | 40% |
| Not sure | 1% | 6% | 1% | 2% | 1% | 2% |

Shaded box are the correct answer.

Table – PCP Response to Three Patient Cases (n= 150)

Disclosures: Suzanne Morin, Amgen, 6; Amgen, Novartis, 1; Amgen, Novartis, Eli Lilly, Wamer-Chilcott, 2
This study received funding from: Amgen

MO0304

Sensitivity of Locating Routines in Identifying the Ward's Region in a DXA Hip Scan. Jing Mei Wang^{*1}, Jiachang Liu², Tom Sanchez³. ¹Norland-a CooperSurgical Company, Peoples Republic of China, ²304 PLA Hospital, China, ³Norland - A Cooper Surgical Company, USA

The Ward's Region of Interest in the proximal hip region is reported to be an area that may be less sensitive to mechanical load and may indeed reflect changes in calcium balance. While DXA hip studies do evaluate a Ward's region a consensus of how to use the result has not developed, in part, because different manufacturers locate the region in different ways. This study compares if search based routines or routines based on placement of region of interest markers generate truly different results and, if so, which method more effectively locates a Ward's-like region.

Hip scans from a population of 25 females between 41 and 76 years of age were analyzed using a search routine to locate the Ward's Region (Norland Search) or setting the Ward's Region centered on the intersection of the lower femur neck cursor and the neck bisection line (Centered Method) or centered on the neck bisection line and resting on the lower femur neck cursor line (Lower Neck Method).

Significant positive regressions demonstrate that the Centered Method ($y=0.9337x + 0.0866$; $r=0.9602$) or Lower Neck Method ($y=0.9376x + 0.1337$; $r=0.8693$) showed higher Ward's densities than seen in the Norland search method. The clinical magnitude of those differences is reflected in the mean group t-scores—the Norland Search Method being -1.68, the Centered Method being -1.26 and Lower Neck Method being -0.85. When mean group densities were compared by a Newman-Keuls One-way Analysis of Variance the mean densities were found to be different [$F(2,72)=3.14$, $p<0.05$]. When Norland Search Method results were compared by paired t-tests to the results obtained by the Centered Method ($t = 6.7470$, $p<0.001$) or the Lower Neck Method ($t = 6.7236$, $p<0.001$) results proved to be significantly different.

This study confirms that indeed different methods of placing the location of a Ward's Region do result in significantly different results. The study also shows that if we believe that the Ward's Region is likely to be characterized by a lower density then methods based on search routines will perform better than methods that set the region based on landmark placed cursors.

Disclosures: Jing Mei Wang, None.

MO0305

The Influence of Type 2 Diabetes on Bone Health in Native American Women. Misti Levva^{*1}, Yan Wang², Stephens Lancer¹, Mary Zoe Baker³, Mark Payton², Brenda Smith². ¹University of Oklahoma Health Sciences Center, USA, ²Oklahoma State University, USA, ³University of Oklahoma College of Medicine, USA

Recent evidence suggests that people with type 2 diabetes, especially diabetes duration > 10 yrs, have an increased risk of fracture. Native Americans are known to have a prevalence of type 2 diabetes that is ~2X the national average, but the availability of evidence regarding their bone health is limited. This study, evaluating a subset of participants from the Oklahoma Native American Women's Osteoporosis Study, was designed to examine the extent to which type 2 diabetes affects BMD and bone metabolism in Native American women. Participants included women (n=123), 50 years of age and older, who were eligible to receive services at area Indian Health Clinics and completed a baseline and one year follow-up visit. At each visit, participants underwent DXA scans (whole body, hip, spine and forearm) and anthropometric measurements, and completed questionnaires to ascertain information related to their medical history, calcium intake and tribal heritage. Participants also had the option to provide a blood sample for measures of bone biomarkers, 25-hydroxyvitamin D3, and inflammatory indicators. Thirty six percent of the participants (n=44) reported a diagnosis of type 2 diabetes (DM). For the purpose of data analysis, comparisons were made between DM and non DM groups, and the DM group was subsequently stratified by years post-diagnosis (<10 yr or >10 yr) to determine the influence of diabetes duration on outcome measures. DXA results revealed a greater BMD in the hip regions of the DM group and more specifically the DM<10 yr group. In contrast, the hip BMD in the DM>10 yr group was similar to that of the non diabetic controls suggesting a biphasic effect in the early phase of diabetes compared to diabetics >10 yr post diagnosis. Moreover, the percent change in BMD was significantly lower in the DM>10 yr group than in the DM<10 yr group. No differences in BMD were observed in the spine or forearm regions. Analysis of bone metabolic markers revealed a decrease ($P<0.05$) in serum C-telopeptide in the DM group and no alterations in bone alkaline phosphatase. DM>10 yr tended ($P<0.10$) to have an elevated serum interleukin-6, but no other differences were observed between groups in inflammatory indicators or 25-OH vitamin D status. These findings suggest a need to further investigate the factors that contribute to this biphasic effect of type 2 diabetes on BMD and its impact on long-term fracture risk in Native American women.

Disclosures: Misti Levva, None.

MO0306

Assessing Efficacy of Osteoporosis Drugs: A Three-Year Finite Element Analysis Study of the Femoral Neck. Taeyong Lee, Anitha D^{*}. National University of Singapore, Singapore

Introduction: Osteoporosis remains prevalent amongst the elderly and is known to vary from 10-20% in patients aged 50 years and older, depending on race and assessment methods. [1] Following osteoporosis therapy, increases in BMD can be deceptive. While commercially available drugs seemingly counteract bone loss and consequently reduce fracture risk, the efficacy of these drugs in treating osteoporosis is still unclear. [2] Therefore, we aim to compare drug influences, mainly ibandronate, risedronate and raloxifene, on BMD, peak fracture load (F_{cr}) and buckling ratio (BR) at the femoral neck.

Method: This study used data from existing quantitative computed tomography (QCT) in the period 2008-2010 of females who are 50 years of age or older and had been diagnosed with osteopenia or osteoporosis.

From the patients' QCT scan data, BMD was categorized into osteopenic, osteoporotic and normal groups. Geometric analysis is done by reslicing perpendicular to the femoral neck axis. The cortical thickness and radius is obtained by averaging all the profile ray values and BR is calculated. Structural analysis is performed by use of finite element analysis (FEA) software. With the use of appropriate boundary conditions [3], F_{cr} is obtained from force versus displacement curves.

In our preliminary results, we have first analyzed three patients from the ibandronate (IBN) group (62-66 years in 2008), all of whom are diagnosed as osteopenic over three successive years.

Results: Figure 1 shows F_{cr} for three patients for three successive years (2008 being base year). For patient 1, F_{cr} showed an increase of 1.48 in 2009 and 1.89 in 2010. Similarly, patient 3 showed an increase to 1.14 (2009) and to 1.21 (2010). Patient 2, however, showed a slight decrease from 1.70 (2009) to 1.66 (2010). This decrease is however statistically insignificant.

Discussion: From Figure 1, it is seen that the F_{cr} had increased over the three successive years, for the three subjects. This implies that the bone is becoming progressively stronger, meaning that it fails at higher loads.

However, changes in BR did not show any particular trend, meaning that while IBN effected improvements on the structural strength of the femoral neck, geometrical properties remained considerably unaffected.

References

Martien, J.M. et al, Osteoporos Int, 15:120-124

Seeman E, Nature, doi:10.1138/2001012

Keyak JH, Med Engng & Phys, 23:165-173

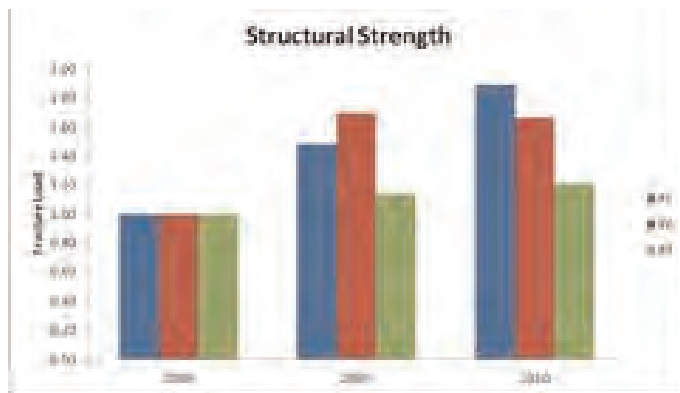


Figure 1 - F_{cr} versus year of assessment (2008 being base year)

Disclosures: Anitha D, None.

MO0307

fineSA, a New Magnetic Resonance Technique, can Accurately Distinguish Normal from Osteopenic or Osteoporotic Trabecular Bone Structure in a Clinical Trial. Amanda Cox^{*1}, Michael Stone², Jane Turton², Irene DeBiram³, Kristin James⁴, Juliet Compston³. ¹Acuitas Medical, United Kingdom, ²University Hospital Llandough, United Kingdom, ³University of Cambridge School of Clinical Medicine, United Kingdom, ⁴OsteoTronix Ltd., United Kingdom

Purpose: Quantitative, non-invasive, radiation-free, *in vivo* analysis of trabecular bone structure in the central skeleton of humans is currently unavailable. We have previously shown in a preclinical study that *fineSA*[1] a new magnetic resonance-based technique, provides measurements of trabecular structure that correlate significantly with μ CT derived trabecular separation (Tb.Sp) [2]. The aim of this study was to evaluate the use of *fineSA* in the quantification of trabecular structure *in vivo* in the human proximal femur and spine.

Method: Signal analysis of a finely sampled, 1-D, spatially-encoded echo from a selectively excited volume within the bone provides a high-resolution measure of the characteristic repetitive spacing (wavelength) of trabecular elements present in the

sampled volume, analogous to the histomorphometric measure of Tb.Sp. This analysis, repeated on echoes from successive excitations, yields a spectrum defining a characteristic structural wavelength, a distribution width, and a measure of noise and confidence interval. We have applied the *fineSA* technique in three anatomical directions in the L1 vertebra and the femoral neck in 20 postmenopausal women. Seven had normal BMD (T-score ≥ -1), 11 had osteopenia (T-score -1 to -2.5) and 2 had osteoporosis (T-score ≤ -2.5) at the hip and/or spine. *fineSA* data acquired in this study were correlated with bone mineral density (BMD) measured by dual energy X-ray absorptiometry (DXA) at the same skeletal sites.

Results: Clear differences were seen between the spectra from women with normal BMD and those with osteopenia or osteoporosis (Figs 1 and 2). Data acquired in the hip in the ML (medial/lateral) and AP (anterior/posterior) direction showed the best correlation with BMD T-score (Table 1).

Conclusion: *fineSA* enables quantitative assessment of trabecular bone structure in the lumbar spine and proximal femur *in vivo*. The results showed good correlation with BMD measured by DXA at the same skeletal site as the *fineSA* analysis, the best correlation ($r=0.579$, $p=0.008$) being obtained by application of *fineSA* in the hip, as this enabled the largest region of homogeneous bone to be sampled.

References:

- 1) Compston, J, et al., ISMRM Annual Meeting, May 2012
- 2) Stone, M, et al., 2009; Available from: <http://www.acuitasmedical.com/images/downloads/news/ASBMR09.pdf>

| | Hip M/L <i>fineSA</i> | Hip A/P <i>fineSA</i> | Spine S/I <i>fineSA</i> | Spine M/L <i>fineSA</i> |
|--------------------------|---------------------------|---------------------------|----------------------------|----------------------------|
| Correlation with T-Score | $r=-0.5316$ $p=0.0192$ | $r= 0.5787$ $p=0.0075$ | $r= 0.4705$ $p=0.0363$ | $r=0.5318$ $p=0.0158$ |

Table 1

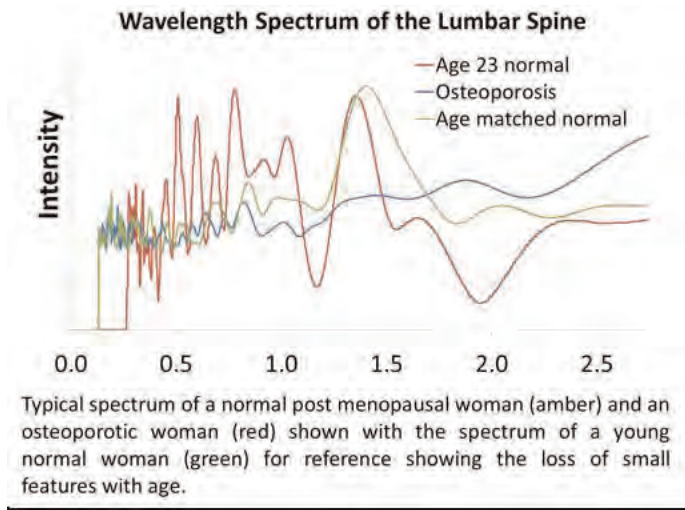


Figure 1

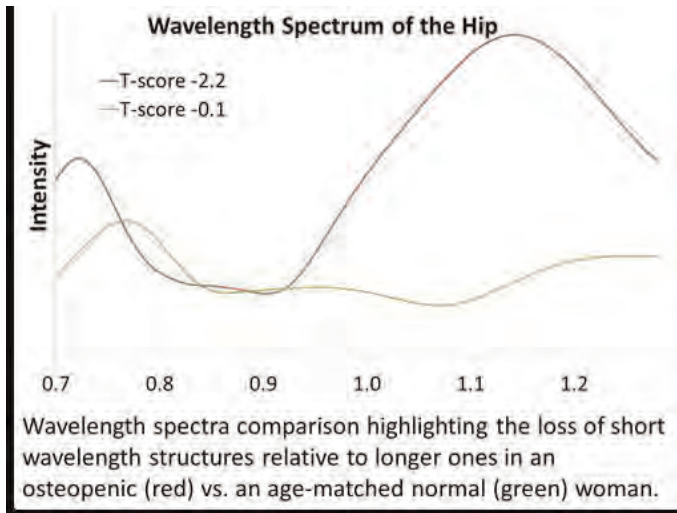


Figure 2

Disclosures: Amanda Cox, Acuitas Medical, 3

MO0308

Short-term *in vivo* Precision of Bone Density and Microarchitecture at the Distal Radius and Tibia Using HR-pQCT: A Comparison Between Young and Older Aged Adults. Chantal Kawalilak¹, James D Johnston², David Leswick³, Saija Kontulainen². ¹College of Kinesiology, Canada, ²University of Saskatchewan, Canada, ³University of Saskatchewan & Saskatoon Health Region, Canada

Objective. To compare short-term precision of 3-dimensional (3D) bone density and microarchitecture between young and older aged adults. Further, to determine the least significant change (LSC) and the 95% limit of agreement (LOA) for all bone outcomes in these two groups.

Methods. Distal radius and tibia of 64 participants were measured at 2 time points with an isotropic resolution of 82µm, using high-resolution peripheral quantitative computed tomography (HR-pQCT). Young adults (n=30; mean age (SD): 27 (9) years) were measured within 24 hours of the first scan, while older adults (n=34; 74 (7) years) were measured within 1 week of the first scan. Standard protocols were used to acquire the following bone variables: cortical area, cortical density, cortical thickness (CtTh), trabecular area, trabecular density, bone volume fraction (BV/TV), trabecular number (TrN), trabecular thickness (TrTh), trabecular separation (TrSp), and trabecular heterogeneity (TbI/N.SD). Precision error (CV%_{RMS}), LSC and LOA were calculated (Glüer et al. Osteoporosis Int., 5:262-270, 1995; Glüer. JBMR, 14(11):1952-1962, 1999). MANCOVA (adjusted for time interval) was used to compare precision between the two groups. Significance was set at $p<0.05$.

Results. No significant differences were found between the young and older adult cohorts for precision error of bone variables at the radius (Table 1a/b) or tibia (Table 2a/b).

Conclusion. There was no difference in the precision between young adults and older adults, indicating that HR-pQCT can be operated to measure bone density and structural parameters with similar precision in healthy adults. Our lab precision seems to be within the same range as previously reported (Boutroy et al. J. Clin. Endocrinol. Metabol., 90(12):6508-6515, 2005).

| Table 1. Radius Measures | | | | | | |
|---|-----------------|------------------|--------------|------------|---------|-------------|
| (a) Young Adults (n=30) | First Scan ± SD | Second Scan ± SD | Mean ± SD | %CVrms (%) | LSC (%) | 95% LOA |
| Area | | | | | | |
| Cortical (mm ²) | 62.6 ± 18.3 | 61.5 ± 17.6 | 62.1 ± 18.0 | 3.1 | 8.5 | 2.6 ± 2.5 |
| Trabecular (mm ²) | 270.0 ± 64.0 | 270.1 ± 64.0 | 270.4 ± 64.0 | 0.6 | 1.8 | 2.8 ± 2.6 |
| Density | | | | | | |
| Total Density (mg HA/cm ³) | 332.1 ± 54.3 | 328.7 ± 52.9 | 330.4 ± 53.5 | 1.6 | 4.5 | 7.9 ± 7.2 |
| Cortical Density (mg HA/cm ³) | 872.4 ± 54.5 | 865.3 ± 59.0 | 867.8 ± 56.4 | 1.2 | 3.3 | 15.9 ± 12.5 |
| Trabecular Density (mg HA/cm ³) | 193.1 ± 45.7 | 192.1 ± 45.0 | 192.6 ± 45.3 | 0.9 | 2.6 | 3.0 ± 2.4 |
| Structure | | | | | | |
| Ct.Th (mm) | 0.81 ± 0.19 | 0.79 ± 0.18 | 0.80 ± 0.18 | 3.3 | 9.1 | 0.04 ± 0.03 |
| BV/TV (%) | 16.1 ± 3.8 | 16.0 ± 3.8 | 16.1 ± 3.8 | 0.9 | 2.5 | 0.2 ± 0.2 |
| TbN (1/mm) | 2.2 ± 0.3 | 2.2 ± 0.3 | 2.2 ± 0.3 | 6.7 | 18.7 | 0.2 ± 0.2 |
| TbTh (mm) | 0.07 ± 0.01 | 0.07 ± 0.01 | 0.07 ± 0.01 | 6.7 | 18.7 | 0.01 ± 0.01 |
| TbSp (mm) | 0.39 ± 0.07 | 0.40 ± 0.06 | 0.39 ± 0.06 | 6.7 | 18.8 | 0.04 ± 0.04 |
| TbI/N.SD (mm) | 0.15 ± 0.03 | 0.16 ± 0.03 | 0.16 ± 0.03 | 9.3 | 26.0 | 0.02 ± 0.02 |

Table 1a - Young Adult Radius Parameters

| 1b) Older Adults (n=34) | First Scan± SD | Second Scan± SD | Mean± SD | %CVrms (%) | LSC (%) | 95% LOA |
|---|----------------|-----------------|-------------|------------|---------|-----------|
| Area | | | | | | |
| Cortical (mm ²) | 38.8±14.5 | 38.8±14.8 | 38.8±14.6 | 2.8 | 7.8 | 1.6±0.9 |
| Trabecular (mm ²) | 239.9±47.1 | 239.8±47.0 | 239.9±47.0 | 0.4 | 1.2 | 1.4±1.2 |
| Density | | | | | | |
| Total Density (mg HA/cm ³) | 246.4±54.0 | 246.6±55.3 | 246.6±54.6 | 1.4 | 3.9 | 5.1±5.1 |
| Cortical Density (mg HA/cm ³) | 778.7±102.8 | 776.4±104.9 | 777.6±103.7 | 1.5 | 2.9 | 12.1±10.3 |
| Trabecular Density (mg HA/cm ³) | 127.5±38.8 | 127.9±38.2 | 127.7±38.5 | 2.1 | 5.9 | 2.7±2.5 |
| Structure | | | | | | |
| Ct.Th (mm) | 0.54±0.21 | 0.54±0.21 | 0.54±0.21 | 3.0 | 8.4 | 0.02±0.02 |
| BV/TV (%) | 10.7±3.3 | 10.7±3.2 | 1.7±3.3 | 2.0 | 5.6 | 0.2±0.2 |
| Tb.N (1/mm) | 1.8±0.5 | 1.8±0.4 | 1.8±0.4 | 6.7 | 18.7 | 0.2±0.1 |
| Tb.Th (mm) | 0.06±0.01 | 0.06±0.01 | 0.06±0.01 | 5.6 | 15.7 | 0.01±0.01 |
| Tb.Sp (mm) | 0.59±0.40 | 0.57±0.31 | 0.58±0.35 | 6.8 | 19.1 | 0.08±0.14 |
| Tb.N/SD (mm) | 0.33±0.34 | 0.32±0.26 | 0.33±0.30 | 7.4 | 20.7 | 0.05±0.12 |

Table 1b. Older Adults Radius Parameters

| 2a) Young Adults (n=30) | First Scan± SD | Second Scan± SD | Mean± SD | %CVrms (%) | LSC (%) | 95% LOA |
|---|----------------|-----------------|-------------|------------|---------|-------------|
| Area | | | | | | |
| Cortical (mm ²) | 151.3±40.0 | 150.6±39.0 | 150.9±39.5 | 0.9 | 2.5 | 2.4±2.6 |
| Trabecular (mm ²) | 626.7±132.9 | 627.3±133.2 | 627.0±133.0 | 0.2 | 0.5 | 1.7±1.9 |
| Density | | | | | | |
| Total Density (mg HA/cm ³) | 350.8±56.8 | 349.6±55.7 | 350.2±56.2 | 0.7 | 2.0 | 3.9±3.9 |
| Cortical Density (mg HA/cm ³) | 919.5±33.6 | 918.9±33.3 | 919.2±33.4 | 0.4 | 1.1 | 5.5±4.4 |
| Trabecular Density (mg HA/cm ³) | 212.8±48.4 | 212.1±47.6 | 212.5±48.0 | 0.8 | 2.3 | 2.6±2.8 |
| Structure | | | | | | |
| Ct.Th (mm) | 1.38±0.29 | 1.38±0.28 | 1.38±0.28 | 0.9 | 2.6 | 0.02±0.02 |
| BV/TV (%) | 17.7±4.0 | 17.7±4.0 | 17.7±4.0 | 0.9 | 2.4 | 0.2±0.3 |
| Tb.N (1/mm) | 2.1±0.4 | 2.1±0.4 | 2.1±0.4 | 3.9 | 11.0 | 0.1±0.1 |
| Tb.Th (mm) | 0.09±0.01 | 0.09±0.01 | 0.09±0.01 | 3.7 | 10.3 | 0.005±0.004 |
| Tb.Sp (mm) | 0.41±0.10 | 0.42±0.09 | 0.42±0.09 | 4.0 | 11.2 | 0.01±0.01 |
| Tb.N/SD (mm) | 0.18±0.05 | 0.18±0.05 | 0.18±0.05 | 4.9 | 13.8 | 0.01±0.01 |

Table 2a. Young Adult Tibia Parameters

| 2b) Older Adults (n=34) | First Scan± SD | Second Scan± SD | Mean± SD | %CVrms (%) | LSC (%) | 95% LOA |
|---|----------------|-----------------|-------------|------------|---------|-----------|
| Area | | | | | | |
| Cortical (mm ²) | 85.3±26.6 | 85.1±26.3 | 85.2±26.4 | 1.2 | 3.2 | 1.6±1.1 |
| Trabecular (mm ²) | 621.4±103.9 | 621.9±103.9 | 621.6±103.9 | 0.1 | 0.4 | 1.3±0.7 |
| Density | | | | | | |
| Total Density (mg HA/cm ³) | 244.8±48.12 | 244.1±47.50 | 244.4±47.78 | 0.9 | 2.6 | 3.2±3.7 |
| Cortical Density (mg HA/cm ³) | 777.6±77.09 | 778.5±76.04 | 778.1±76.49 | 0.3 | 0.9 | 7.5±6.1 |
| Trabecular Density (mg HA/cm ³) | 155.6±41.65 | 155.2±41.03 | 155.4±41.31 | 1.4 | 3.8 | 3.1±3.4 |
| Structure | | | | | | |
| Ct.Th (mm) | 0.81±0.26 | 0.81±0.26 | 0.81±0.26 | 1.4 | 4.0 | 0.02±0.01 |
| BV/TV (%) | 13.0±3.5 | 12.9±3.4 | 13.0±3.4 | 1.4 | 3.8 | 0.3±0.3 |
| Tb.N (1/mm) | 1.7±0.4 | 1.7±0.4 | 1.7±0.4 | 6.8 | 19.0 | 0.2±0.2 |
| Tb.Th (mm) | 0.08±0.02 | 0.08±0.02 | 0.08±0.02 | 6.3 | 17.5 | 0.01±0.01 |
| Tb.Sp (mm) | 0.55±0.18 | 0.55±0.17 | 0.55±0.17 | 6.9 | 19.3 | 0.05±0.05 |
| Tb.N/SD (mm) | 0.30±0.23 | 0.31±0.23 | 0.30±0.23 | 6.5 | 18.1 | 0.02±0.02 |

Table 2b. Older Adult Tibia Parameters

Disclosures: Chantal Kawallak, None.

MO0309

The Impact of Glucocorticoid Therapy on Trabecular Bone Score in Older Women. Margaret Paggiosi¹, Richard Eastell². ¹Sheffield Teaching Hospitals NHS Foundation Trust, United Kingdom, ²University of Sheffield, United Kingdom

Glucocorticoid therapy is associated with increased fracture risk that cannot be fully explained by decreased bone mineral density (BMD); this may be a consequence of alterations in bone quality. Trabecular Bone Score (TBS) has been developed as a tool with which to study bone microarchitecture.

We assessed the ability of TBS to discriminate between (i) glucocorticoid-treated women, (ii) women who had sustained a recent fracture, and (iii) healthy women. Older women (n=576, ages 55-79 years) were recruited from the local population. Women had either (i) taken prednisolone 5 mg/day (or equivalent) for >3 months (n=64) or (ii) sustained a recent fracture of the distal forearm (n=46), proximal humerus (n=37), vertebra (n=30) or proximal femur (n=28), or (iii) were healthy population-based individuals (n=371). We measured lumbar spine BMD by DXA (Hologic QDR 4500A) and calculated TBS by examining pixel variations within the DXA images to produce grey-level texture measurements (TBS – Clinical Data Analysis software v1.6, Med-Imaps).

In the healthy, population-based cohort, associations between BMD and age, and TBS and age, were evident and therefore simple linear regression was performed and used to calculate Z-scores adjusted for age (Table 1). BMD and TBS were significantly lower for the fracture groups than for healthy individuals. Both variables displayed similar performance, however TBS, but not BMD, was significantly lower in glucocorticoid-treated women (p=0.0004).

We conclude that (i) women with fractures have lower than expected BMD and TBS, and (ii) there is a significantly greater decrease in TBS than BMD for glucocorticoid-treated women. TBS, when used in combination with BMD, may be a useful tool for the further study of glucocorticoid-induced osteoporosis.

Table 1. Z-scores (95%CI) for BMD and TBS

| Group | BMD Z-score (95%CI) | TBS Z-score (95%CI) |
|---------------------------|---------------------------------------|-------------------------------------|
| Glucocorticoid | -0.13 (-0.40 to 0.15) [#] | -0.80 (-1.09 to -0.51) [#] |
| Forearm fracture | -0.34 (-0.67 to -0.01) | -0.38 (-0.69 to -0.07) [#] |
| Humerus fracture | -0.57 (-0.86 to -0.27) [#] | -0.87 (-1.12 to -0.51) [#] |
| Vertebral fracture | -1.38 (-1.69 to -1.07) ^{###} | -1.04 (-1.40 to -0.68) [#] |
| Femoral fracture | -0.77 (-1.13 to -0.41) ^{##} | -0.64 (-1.05 to -0.24) [#] |
| Healthy, population-based | 0.00 (-0.10 to 0.104) | 0.00 (-0.10 to 0.11) |

[#] = different from healthy, individuals (p<0.001)
^{##} = different from other fracture groups (p<0.001)
^{###} = different from vertebral fracture and glucocorticoid group (p<0.001)
^{####} = different from femoral and vertebral fractures (p<0.001).

Table 1

Disclosures: Richard Eastell, Med-Imaps, 9

MO0310

The Impact of TBS in the Analysis of Gender Specific Differences in Bone Microarchitecture in Females and Males with Fragility Fractures. Heinrich Resch¹, Angela Trubrich², Christian Muschitz³, Roland Kocjan⁴, Judith Haschka⁴, Afrodite Zendeli², Philippe Zysset⁵, Didier Hans⁶. ¹Medical University Vienna, Austria, ²Austria, ³St. Vincent's Hospital, Austria, ⁴St. Vincent Hospital Vienna, Austria, ⁵University of Bern, Switzerland, ⁶Lausanne University Hospital, Switzerland

Rational: Biomechanical competence of bone is only partly explained by bone mass. Apart from material properties, microarchitecture is an important determinant of bone strength, which is assessed by invasive methods like transiliac biopsies. Alternatively Trabecular Bone Score (TBS) is a novel grey-scale textural analysis to estimate trabecular microarchitecture from the AP Spine DXA. TBS correlates well with more direct measures of bone microarchitecture independent of BMD (Hans JCD 2011). The aim of the study was to compare gender specific structural characteristics with different imaging modalities.

Materials and Methods: In this retrospective study we evaluated gender specific structural characteristics by micro-tomographic imaging system (µCT40, Scanco, Switzerland) in transiliac bone biopsies of 22 males and 14 females of similar age between 18 and 61 years having sustained fragility fractures but otherwise healthy. Furthermore AP spine was assessed by DXA (QDR 4500, Hologic Inc, USA), and site-matched spine TBS parameters were extracted from the DXA image using TBS insight software (v1.9, Medimaps SA, France).

Results: Laboratory tests did not reveal any evidence of metabolic disorder in any of our subjects. Most of the 3D parameters measured with µCT were significantly correlated with the Spine TBS with correlations which tended to be higher in female than in male. BMD of the lumbar spine (0.966±0.15 vs 0.973±0.138 g/cm2) was similar in both gender groups. On a structural level analysis of trabecular bone by µCT we did not observe, gender specific differences in the parameters of microstructure like BV/TV, ConnD, SMI, Tb.N, Tb.Th, Tb.Sp, Tb.(1/N).SD. However, mean TBS of the spine was significantly higher in females than in males (1.288 ± 0.133 vs 1.165 ± 0.119; p<0.005).

Conclusions: Correlations between 3D parameters as assessed by 40µCT and TBS are mostly significant. In younger individuals with primary osteoporosis there are no significant differences between DXA BMD and 3D parameters between the two genders but with TBS, TBS being higher in female than in male while it tends to be the opposite for BV/TV or ConnD parameters. Would it mean that at equivalent quantity, the texture of man is more based on thick trabeculae but in women more pattern? Or just that iliac crest may have a different pattern than the spine? Further analyses are nevertheless required to better characterize this finding as it may relate to fracture incidence difference.

Disclosures: Heinrich Resch, None.

MO0311

Validation of an Automatic Vertebral Prevalent Fracture Classifier Based Upon Full Vertebral Shape. Jane Haslam¹, Joes Staal², Klaus Engelke³, Bernd Stampa⁴, Harry Genant⁵, Thomas Fuerst⁶, Peter Steiger^{*7}. ¹Optasia Medical Ltd, United Kingdom, ²Optasia Medical, United Kingdom, ³University of Erlangen, Germany, ⁴Synarc A/S, Germany, ⁵UCSF/Synarc, USA, ⁶Synarc Inc, USA, ⁷Optasia Medical, USA

Background: We previously presented initial results for a prevalent vertebral fracture classifier, which used full vertebral shape information annotated on lateral spinal radiographs to determine fracture/no-fracture status of vertebral bodies between T4 and L4. The current study reports the classifier performance on an independent test-set.

Methods: The test-set consisted of standard lateral spinal radiographs for 200 subjects, for whom 2590 evaluable vertebral bodies between T4 and L4 of a total possible 2600 were Genant Semiquantitative (SQ) scored by a radiologist, giving 164 mild fractures, 70 moderate fractures and 0 severe fractures. Full vertebral shape plus standard 6-point morphometry for each vertebra was annotated semi-automatically using the SpineAnalyzer vertebral deformity assessment workflow software (Optasia Medical, Cheadle, UK) by an experienced radiographic technician blinded to the SQ scores. The classifier then used the full vertebral shape to determine fracture/no-fracture status for each vertebra, and the results were compared against those obtained assessing fracture status on the basis of QM wedge, bi-concave and crush deformities, thresholding maximum deformity % according to the Genant criteria: normal <20% , fractured ≥20%. Agreement with 'gold-standard' fracture status according to SQ score was calculated using Cohen's kappa (and 95% confidence intervals) for i) normals (SQ=0) vs. all fractures (SQ=1,2) and ii) normals (SQ=0) vs. definite fractures (SQ=2).

Results:**Standard QM results:**

- i) Normals (SQ=0) vs. all fractures (SQ=1,2): kappa=0.41(0.33, 0.49)
- ii) Normals (SQ=0) vs. definite fractures (SQ=2): kappa=0.56(0.46, 0.67)

Classifier results:

- i) Normals (SQ=0) vs. all fractures (SQ=1,2): kappa=0.56(0.49, 0.62)
- iii) Normals (SQ=0) vs. definite fractures (SQ=2): kappa=0.70(0.60, 0.79)

Conclusions: In the 200 subjects only moderate inter-rater agreement was found between fracture status assessed by QM and corresponding 'gold-standard' SQ-score fracture status. Using the classifier trained on a vertebral body shape description to assess fracture status gave improved results; in the case of normals vs. all fractures this improvement was significant. This work demonstrates that using a full description of vertebral shape enables us to make a significantly better determination of vertebral fracture status than using QM alone.

Disclosures: Peter Steiger, Optasia Medical Ltd., 3

MO0312

Vertebral Microarchitecture and Fragility Fracture in Men: a Trabecular Bone Score (TBS) study. Edward Leib^{*1}, Berengere Aubry-rozier², Renaud Winzenrieth³, Didier Hans². ¹University of Vermont, USA, ²Lausanne University Hospital, Switzerland, ³Med-imaps, Hôpital X. Arnoz, PTIB, Pessac, France, France

Introduction: Around 25% of individuals with osteoporosis are men. BMD measurement by DXA is the gold standard used to diagnose osteoporosis and assess fracture risk. However, BMD does not take into account microarchitecture alterations. TBS is an index of bone microarchitecture extracted from spine DXA. Previous studies have reported the ability of TBS to discriminate and predict osteoporotic fractures in women. The aim of this study is to evaluate the potential diagnostic value of TBS as a complement to bone mineral density (BMD) for predicting fractures in men.

Methods: To be eligible for this study, subjects had to be US white men aged 40 and older. Furthermore, subjects were excluded if they had any treatment or illness that may influence bone metabolism. Fractured subjects were included if the presence of at least one fracture were confirmed. Cases were matched for age (± 3 years) and BMD (± 0.04 g/cm²) with three controls. BMD and TBS were first retrospectively evaluated at AP Spine (L1-L4) with Prodigy densitometer (GE-Lunar, Madison, USA) and TBS iNsite® (Med-Imaps, France) in Lausanne University Hospital blinded from clinical outcome. Inter-group comparisons were undertaken using Student's t-tests or Wilcoxon signed ranks tests. Odds ratios were calculated per one standard deviation decrease as well as areas under the receiver operating curve (AUC).

Results: After applying inclusion/exclusion criteria, a group of 184 male subjects was obtained. This group consists of 46 fractured subjects (age=63.9±13.1 years, BMI=27.2±4.4 kg/m²) and 138 control subjects (age=63.2±12 years, BMI=26.7±3.8 kg/m²) matched for age (p=0.75) and BMD (p=0.35). A weak correlation was obtained between TBS and BMD and between TBS and BMI (r=0.27 and r=-0.29, respectively, p<0.01). TBS value between the control and fractured group was significantly different (p=0.007; Δ TBS=-0.062), whereas no differences were obtained for BMI, height and weight (p=0.41, 0.15 and 0.12 respectively). The odds ratio (OR) per standard deviation and the AUC were OR=1.60[1.13-2.27] and AUC=0.620[0.546-0.690] for TBS, respectively.

Conclusion: This study shows the potential use of TBS in men. TBS revealed a significant difference between fractured and age- and spine BMD-matched non

fractured subjects. This result is consistent with those previously reported demonstrating the ability of TBS to identify and predict fracture.

Disclosures: Edward Leib, None.

MO0313

Ultrasound Based Tomographic Imaging Device for Musculoskeletal Health. Shiva Kotha, James Macione^{*}. Rensselaer Polytechnic Institute, USA

Ultrasound is uniquely suited to revolutionize imaging, diagnostics, and treatment of musculoskeletal ailments, very inexpensively. Through integration of a conformable ultrasound systems with modern smart phones, massive amounts of data can be generated, which can be analyzed through cloud based applications, in order to determine subtle factors that contribute towards musculoskeletal health, among many others. As a first step, we demonstrate the generation of a tomographic image based on reflection (B-mode) images obtained using a commercial ultrasound unit (GE RT 3200, 3.5MHz transducer, 1-D linear curved array with 128 elements – which gives roughly 0.5mm axial and 1mm transverse resolution). All studies were performed using IRB or IACUC approvals, as appropriate. Briefly, the specimen was placed in a water bath and held stationary. An ultrasound probe was rotated around the specimen and B-mode images were obtained at intervals of 1.118 degrees. Tomographic reconstruction was performed using a sub-set of 100 images using different compounding algorithms. Tomographic reconstructions are shown for an excised sheep femoral bone and for a human forearm. Results demonstrate that it is possible to identify the surfaces of bone and its thickness. Moreover, it is possible to identify structures such as muscles, as well as blood vessels. The structures are clearer in the sheep femur compared to human bones, possibly, because the dimensions of the sheep bone are smaller – enabling reflection mode images to be obtained from the thickness of the entire bone. This suggests that the quality of reflected images – especially for the human bone, can be significantly improved by using new transducers that collect data from more angles relative to the origin of the ultrasound pulse. It is noted that using complimentary imaging modalities incorporated into the ultrasound device (tomographic imaging, time-of-flight, to name a few), it will become possible to improve the quality of the images – while providing information about bone integrity.

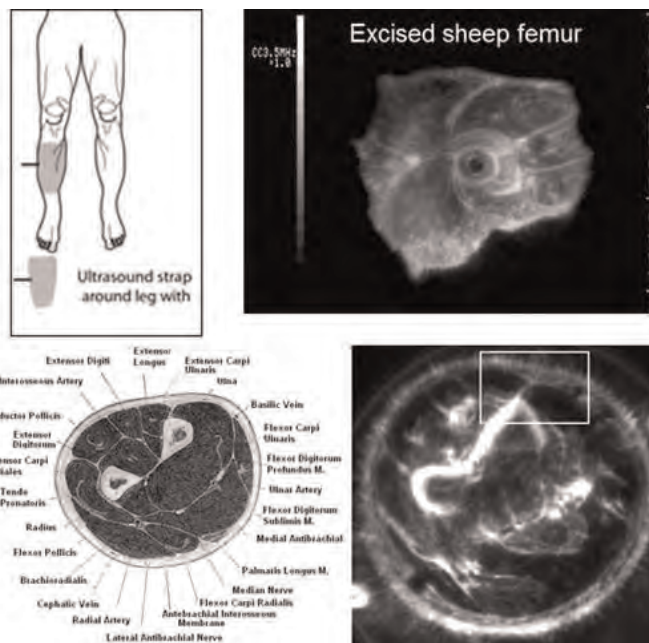


Figure demonstrating ultrasound tomographic reconstruction

Disclosures: James Macione, None.

MO0314

Age-related Loss of Cortical Bone Mass and Fragility Fractures in Women from Roman Britain. Simon Mays^{*}. English Heritage, United Kingdom

This work investigates age-related loss of cortical bone mass and the prevalence of fragility fractures in a series of female skeletons from an archaeological site in Roman Britain (3rd-4th century AD). Results are compared with modern reference data.

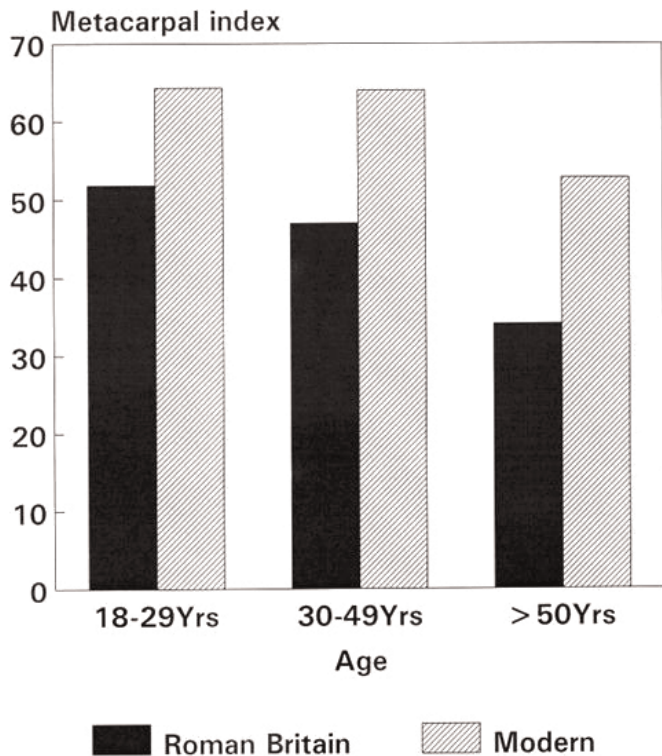
Metacarpal cortical index (thickness of cortical bone normalised by total bone width), measured using radiogrammetry, was used as a measure of bone mass. Fragility fractures (wrist, hip, or vertebral body) were identified by gross and radiographic examination of skeletons.

Results show that peak thickness of metacarpal cortical bone in young adults was less than in modern women (p < 0.01). Mean cortical thickness in the > 50yr cohort (taken to be post-menopausal) differed significantly (p < 0.05) from that in younger adults but there is no significant variation in cortical thickness in younger age classes.

Metacarpal cortical bone thickness in the > 50yrs cohort is only 66% of the young adult value, suggesting greater post-menopausal loss of bone mass than in a modern European reference group. There was a high prevalence of fragility fractures. For example, the estimated population prevalence of Colles' fracture in the over 50 yr cohort was 0.084-0.581 (95% confidence intervals), which exceeds that in a modern reference population (p < 0.05).

Poor nutrition during the growth period is likely a factor in the low peak bone mass in the Romano-British group, although other as yet unidentified factors may also be involved. The severity of post-menopausal loss of bone mass is more puzzling. Excess caffeine intake, corticosteroid use and tobacco smoking have been associated with increased loss of bone mass in women, but none of these substances was available in Roman Britain. Sedentary lifestyle, another risk factor for increased loss of bone mass, is unlikely: given the absence of mechanical labour saving devices at the time there would have been an emphasis on physical labour. Preliminary results of a histological study of the skeletal remains indicate that vitamin D deficiency may have been a problem in some older females. Perhaps this played a part in the severity of post-menopausal loss of bone mass seen in women in this group, but further work is needed to confirm this.

The work demonstrates the value of studying osteoporosis in archaeological populations for shedding light on the history of the disease.



Metacarpal cortical index versus age in a Romano-British skeletal population

Disclosures: Simon Mays, None.

MO0315

Improvement in Femoral Neck BMD in Older Women between 2002 and 2010. Kirsti Uusi-Rasi*, Saija Karinkanta, Harri Sievänen. UKK Institute for Health Promotion Research, Finland

The number of hip fractures among Finns over 50-years of age rose constantly between 1970 and 1997, but since then, there has been a nationwide decline in incidence of hip fractures. One possible explanation, although not the only one, for the declining fracture rates, could be improved bone mineral density (BMD).

The aim of this study was to evaluate changes in femoral neck BMD (fn BMD) among older Finnish women. We compared the baseline data of two cohorts of home-dwelling women, who were recruited in exercise intervention studies. The first study cohort from the year 2002 included data of 217 women, the second cohort from the year 2010 included 400 women. The inclusion criteria in both studies were age between 70-80 years, moderate to vigorous exercise no more than 2 hours per week and no contraindication to supervised exercise. However, the exercise program for the first cohort was more demanding (including jumping exercise), while in the second cohort the exercise was based on balance and resistance type and exclusion criteria were not so strict. The women in the cohort 2 had to be fallen at least once during the previous year, while the cohort 1 did not have this criterion.

Dual-energy X-ray absorptiometry was used to measure fn BMD. We scanned 50 volunteers for cross-calibration between the two scanners and applied a linear regression equation to compare BMD measurements collected with Norland XR-26 (cohort 1) and Lunar Prodigy Advance (cohort 2). Between-cohort differences were evaluated with analysis of covariance using age, height and weight as covariates.

Characteristics of the study cohorts are listed in Table. Cohort 2 was somewhat older and taller than Cohort 1. Adjusted mean difference (95% CI) in fn BMD

between the cohorts was 0.054 g/cm² (0.034 to 0.074) corresponding mean difference of 0.5 in T-score in favour of the cohort 2.

This observation suggests that femoral neck BMD has improved among older Finnish women, but reason for improvement is unclear.

| | Cohort 1, n=217 | Cohort 2, n=400 |
|-------------------------------------|-----------------|-----------------|
| Femoral neck BMD, g/cm ² | 0.804 (0.125) | 0.854 (0.126) |
| Age, y | 73.0 (2.4) | 74.2 (3.0) |
| Height, cm | 159.0 (5.5) | 159.8 (5.7) |
| Weight, kg | 70.2 (10.6) | 72.1 (11.6) |
| BMI | 27.8 (3.9) | 28.3 (4.5) |
| Calcium intake, mg/d | 938 (319) | 1060 (465) |

Table. Baseline characteristics (mean, sd) of the study cohorts

Disclosures: Kirsti Uusi-Rasi, None.

MO0316

Psychological Well-Being is Positively Associated with Adult Bone Mineral Density. Findings from the Study of Midlife in the United States (MIDUS). Arun Karlamangla¹, Carolyn Crandall¹, Carol Ryff², Neil Binkley³, Dana Miller-Martinez⁴, Gail Greendale¹, Teresa Seeman⁴. ¹University of California, Los Angeles, USA, ²University of Wisconsin, USA, ³University of Wisconsin, Madison, USA, ⁴University of California, USA

Background: Depression in adults is associated with low bone mineral density (BMD) and increased fracture risk. Little is known about the bone-protective effects, if any, of positive affect and psychological well-being. Just as positive affect is more than merely the absence of negative affect, psychological well-being is more than the absence of psychiatric illness.

Objective: To determine if positive aspects of psychological health are associated positively with adult BMD.

Methods: The Study of Midlife in the United States interviewed a national sample of adults (25-75 years old) in 1995-96 (wave 1), and again 9-10 years later (wave 2), at which time lumbar spine and femoral neck BMD (by dual-energy x-ray absorptiometry) were also measured in 720 participants. Eight positive dimensions of psychological health: positive affect, life satisfaction, and 6 dimensions of psychological well-being, were assessed in both waves. We examined associations of each of the 8 positive psychological health measures (averaged over the 2 waves) with BMD measured in wave 2, and adjusted for age, gender, race, education, financial advantage, clinic site, body weight, menopause stage (in women), smoking status, and physical activity.

Results: Four of eight dimensions of positive psychological health were significantly associated positively with femoral neck BMD, and one (purpose in life) was also associated positively with lumbar spine BMD (See table). These effects were not modified by either gender or race.

Conclusions: Positive aspects of psychological health are associated with higher BMD. Future research will examine the physiological pathways through which positive psychological health may influence adult bone strength and fracture risk

| | Femoral Neck BMD | Lumbar Spine BMD |
|--------------------------------|----------------------|----------------------|
| Average positive affect | 0.069 (.001, .137)* | 0.023 (-.042, .088) |
| Average life satisfaction | 0.060 (-.011, .131) | 0.008 (-.066, .081) |
| Average well-being scales | | |
| Positive relations with others | 0.069 (.003, .136)* | 0.041 (-.032, .115) |
| Self-acceptance | 0.063 (.000, .126)* | 0.015 (-.044, .094) |
| Autonomy | 0.031 (-.029, .091) | 0.032 (-.037, .102) |
| Personal growth | 0.018 (-.046, .083) | -0.004 (-.070, .063) |
| Environmental mastery | 0.019 (-.043, .082) | -0.024 (-.091, .044) |
| Purpose in life | 0.113 (.049, .176)** | 0.080 (.008, .152)* |
| *p < .05; **p < .01 | | |

Table

Disclosures: Arun Karlamangla, None.

MO0317

The Relationship between Nonalcoholic Fatty Liver Disease and Metabolic Bone Disease in Korean Men. Eun Jung Rhee*¹, Hyung-Geun Oh².
¹Kangbuk Samsung Hospital, Sungkyunkwan University School of Medicine, South Korea, ²Department of Neurology, Soonchunhyang University College of Medicine, Cheonan, Korea, South Korea

Background: Osteoporosis is a disease associated with aging and obesity. Nonalcoholic fatty liver disease (NAFLD) is a common metabolic disease increasing prevalence of obesity. However, there are not much known about the association of the two diseases. We aimed to analyze the relationship between NAFLD and metabolic bone disease in Korean men.

Methods: In 411 Korean men who participated in health screening program, metabolic and anthropometric parameters were measured. Abdominal ultrasonograms were performed and the presence of NAFLD was assessed. Lumbar spine bone mineral density (BMD) was performed in every subject. The presence of metabolic bone disease was assessed according to the T score: osteoporosis (lower than or same as -2.5), osteopenia (-2.5~-1.0) and normal (higher than -1.0). Subjects who responded to drink alcohol were excluded from the participants.

Results: Mean age of the participants is 50 years old and mean body mass index (BMI) is 24.4 kg/m². Among the participants, 137 (33.3%) subjects had NAFLD. 310 subjects (75.2%) were normal, 94 subjects (22.8%) were osteopenic and 8 subjects (1.9%) were osteoporotic. Osteoporotic group showed the lowest mean BMI and waist circumference compared to osteopenic and normal subjects (<0.01). When the proportion of NAFLD was assessed according to metabolic bone disease status, proportion of subjects with NAFLD was the highest (35.8%) in the normal subjects compared with osteopenic (27.7%) or osteoporotic (0%) subjects.

Conclusions: Proportion of the subjects with NAFLD was higher in subjects with normal BMD compared with metabolic bone disease in Korean men.

Disclosures: Eun Jung Rhee, None.

MO0318

The Worldwide Impact of Osteoporosis on the Burden of Hip Fractures. Helena Johansson*¹, Anders Oden¹, Eugene McCloskey², John Kanis³.
¹University of Gothenburg, Sweden, ²University of Sheffield, United Kingdom, ³University of Sheffield, Belgium

The aim of this study was to determine the number of hip fractures in men and women aged 50 years or more in 2010 in all countries for which there was information on hip fracture risk and the proportion attributable to osteoporosis. Hip fracture rates were identified by a systematic review in 61 countries representing 82 % of the world population. The number of incident hip fractures in one year in countries for which data were available was calculated from the population demography in 2010 and the age- and sex-specific risk of hip fracture. The number of hip fractures attributed to osteoporosis was computed as the number of hip fractures saved assuming that all individuals with a femoral neck T-score of <-2.5 SD had a T-score at the threshold of osteoporosis (= -2.5 SD). The total number of new hip fractures for the 61 countries was 2.32 million (743,223 in men and 1,586,603 in women) with a female to male ratio of 2.13. Of these 1,165,178 (50%) would be saved by uplifting BMD in individuals with osteoporosis to a T-score of -2.5 SD. The majority (83%) of these 'prevented' hip fractures were found in men and women at the age of 70 years or more. Extrapolation to the world population using age and sex specific rates gave an estimated number of hip fractures of approximately 2.8 million in 2010 of which 1,369,093 were preventable with the avoidance of osteoporosis (264,747 in men and 1,104,346 in women). If there were strategies eliminating osteoporosis without affecting the distribution of BMD above -2.5 SD they could save 49% of all hip fractures.

Disclosures: Helena Johansson, None.

This study received funding from: University of Sheffield

MO0319

Three Dimensional Structural Analysis of the Proximal Femur Reveals Differing Patterns of Age-related Changes in Trabecular Versus Cortical Bone in Women. Kristy Nicks*¹, Shreyasee Amin¹, L. Joseph Melton¹, Sara Achenbach¹, Louise Mccready¹, B. Lawrence Riggs¹, Klaus Engelke², Sundeep Khosla³.
¹Mayo Clinic, USA, ²University of Erlangen, Germany, ³College of Medicine, Mayo Clinic, USA

Studies using quantitative computed tomography (QCT) have demonstrated that in women, decreases in trabecular volumetric bone mineral density (vBMD) begin in the 3rd decade, whereas decreases in cortical vBMD begin in midlife, coincident with the menopause. However, these studies have been limited by the fact that cortical bone was assessed principally at peripheral sites, while trabecular bone was assessed at both central and peripheral sites. In addition, although QCT measures vBMD in 3-dimensions (3D), the analyses to date have used a 2D approach. Therefore, we sought to determine the changes in proximal femur vBMD with age and menopausal status in an age-stratified population of 358 women (20-97 yrs) using 3D analysis that allows for the determination of changes in bone geometry and vBMD in different volumes of interest (VOIs) (Medical Image Analysis Framework-Femur Option [MIAF-F]). We

assessed cross-sectional changes in trabecular and cortical vBMD in the femoral neck (FN), trochanter (FT), and intertrochanteric region (FIT), and cortical vBMD at the femur shaft (FS). Consistent with previous data, MIAF-F analysis demonstrated a 2-3 fold greater decrease in trabecular (62-74%) than cortical (16-28%) vBMD with increasing age. At the FN, cortical vBMD decreased more in the superior quadrants (39-42%) than the inferior quadrants (13-22%) with increasing age. Moreover, as shown in the Table, the slopes of the regression lines of trabecular vBMD vs. age at the FN, FT, and FIT were clearly different from zero for both pre- and postmenopausal women and very similar between the two groups. By contrast, these slopes in premenopausal women were not different from zero for cortical vBMD vs. age at any site measured, but more than 2-fold greater at each site in the postmenopausal women. Bone volume increased significantly with increasing age in all measured VOIs by 15-23% (P < 0.01), consistent with ongoing periosteal apposition with aging.

In summary, these data represent the first application of 3D volumetric analysis to define regional changes in femoral trabecular and cortical bone with age in a population-based sample of women. The underlying mechanisms responsible for the differential losses of trabecular vs cortical bone and the implications of the greater losses of cortical bone in the superior vs inferior FN for hip fracture risk warrant further investigation

Slopes of vBMD vs age in pre- versus postmenopausal women; ***P < 0.001 versus 0.

| | Premenopausal | Postmenopausal |
|---------------------------|---------------|----------------|
| Trabecular | | |
| Neck | -3.2*** | -2.7*** |
| Trochanter | -1.5*** | -1.4*** |
| Inter-trochanteric region | -2.0*** | -2.3*** |
| Cortical | | |
| Neck | -1.1 | -2.2*** |
| Trochanter | 0.0 | -3.2*** |
| Inter-trochanteric region | -1.0 | -2.8*** |
| Shaft | -1.1 | -2.4*** |

Table

Disclosures: Kristy Nicks, None.

MO0320

25-OH Vitamin D and PTH Levels in Patients Population at Bone Centre in Southwest Bohemia Region of the Czech Republic. Richard Pikner*¹, Zlata Fejfarkova², Michaela Heidenreichova¹, Miroslav Zabransky¹.

¹Department of Clinical Laboratories & Bone Metabolism, Klatovska nemocnice, Czech Republic, ²Klatovská Nemocnice, A.s., Czech Republic

The aim was to evaluate distribution of 25 OH vitamin D and elevated PTH levels according to season and calcium and vitamin D supplements usage. **Methods:** We evaluated in total 2908 patients during 2009-2010. This patients population included both untreated and vitamin D and calcium supplemented patients. We evaluated only their first visit at Bone Centre during which blood samples for 25 OH vitamin D, PTH and bone markers were taken. 25 OH vitamin D and N-tact PTH were measured using immunoassay on the automated system LIAISON, DiaSorin USA. We excluded patients with primary hyper or hypoparathyroidism, renal bone disease and patients on active vitamin D or parathormone treatment. We divided patients according to their 25 OH vitamin levels into 3groups: Deficient = up to 10ng/ml; Insufficient = 10-25ng/ml; Sufficient = above 25 ng/ml, and by season into 2 groups: May-September (SS) and October-April(WS). In these subgroups we evaluated frequency of PTH elevation (above 77 pg/ml) in relation to calcium and vitamin D supplementation. **Results:** We found vitamin D deficiency in 12% of untreated and 5.2% of supplemented patients during SS; 30.5% and 9.2% in WS respectively. We found vitamin D sufficiency in 14% of untreated and 27.7% of supplemented patients in SS; 5.5 %and 15.6% in WS respectively. Most of the patients were vitamin D insufficient: 74% of untreated and 67.1% of supplemented in SS; 64%and 75.2% in WS. In vitamin D deficient patients we found PTH elevation in 48.5% of untreated and in 32% of supplemented patients in SS; 56.2% and 63% in WS respectively. In vitamin D sufficient patients the rate of PTH elevation was 10.6% of untreated and 20.1% of supplemented patients in SS; 26.3% and 30.8%in WS. **Summary:** We found important influence of season on 25 OH vitamin D levels and frequency of PTH elevation both in untreated and supplemented patients. Only 56.5 % in SS and 65.2% supplemented patients had adequate dosing of vitamin D (at least 400IU daily). There was an evident correlation between low 25 OH vitamin D levels and the frequency of PTH elevations and we found relatively high frequency (10.6.-30.8%) of patients having sufficient vitamin D levels and PTH elevation, which might be caused by low calcium intake. **Conclusion:** 25 OH vitamin D and PTH measurement is of high importance as it helps to individualize vitamin D and calcium supplementation dosing and to normalize calcium and vitamin D homeostasis.

Disclosures: Richard Pikner, None.

MO0321

Associations among Total and Food Additive Phosphorus Intake, Forearm Bone Mineral Density and Bone Mineral Content in 37-to-47-Year-Old Population – the PHOMI Study. Suvi Itonen¹, Virpi Kemi¹, Elisa Saarnio², Merja Kärkkäinen¹, Heini Karp¹, Minna Pekkinen³, Harri Sievanen⁴, Kalevi Laitinen⁵, Christel Lamberg-Allardt¹. ¹University of Helsinki, Finland, ²University of Helsinki, Finland, ³Folkhälsan Institute of Genetics, University of Helsinki, Finland, ⁴UKK Institute, Finland, ⁵Helsinki University Central Hospital, Finland

Dietary phosphorus (P) intake in Western countries is 2-3-fold higher than recommended. It has been shown in experimental human and animal studies that high dietary P intake, especially as food additives, has negative effects on or associations with calcium and bone metabolism. The effect differs among different dietary P sources, as absorption is poor from some sources (e.g. cereals), and some contain calcium (e.g. milk), which has positive effects on bone. P intake has increased because of the expanding use of P salts as food additives. P salts are well absorbed and may thus be more deleterious to calcium and bone metabolism than natural sources. The aim of the study was to investigate the associations among total and food additive P intake, forearm bone mineral content (BMC) and density (BMD) in a cross-sectional study.

573 subjects (185 men, 388 pre-menopausal women) aged 37-47 years participated in the study. BMC and BMD were measured from distal and proximal sites of the non-dominant radius with peripheral quantitative computed tomography (pQCT). Total dietary P intake was assessed by 3-day food records. Food additive P intake was calculated from food frequency questionnaires which included widely food additive P containing foodstuffs. Fasting blood samples and background data were collected. The data was analyzed statistically by partial correlations and multivariate linear regression models.

Median P intake in females was 1489 mg/d (range 670-2763 mg/d) and in males 1754 (range 804-3493 mg/d). There were no statistically significant correlations ($p > 0.05$) among total or food additive P intake and distal or proximal radius BMC or BMD neither in males nor females when adjusted for age, height, weight, serum 25-hydroxy vitamin D concentration, smoking, physical activity, calcium intake and contraceptive use. In multivariate backward regression models with above-mentioned covariates neither total or food additive P intake were statistically significant ($p > 0.05$) factors for explaining BMC or BMD and they were excluded from the models.

Neither total nor food additive P intake were associated with forearm BMC or BMD in the current study. However, the data should be studied further by structural equation models taking into account the metabolic pathways in calcium and bone metabolism.

Disclosures: Suvi Itonen, None.
This study received funding from: -

MO0322

Positive Association of Dairy Intake with Bone Mineral Density (BMD) Depends on Vitamin D Intake: The Framingham Original Cohort. Shivani Sahni¹, Katherine Tucker², Douglas Kiel³, Lien Quach⁴, Virginia Casey⁴, Marian Hannan⁵. ¹Hebrew SeniorLife, Institute for Aging Research, USA, ²Northeastern University, USA, ³Hebrew SeniorLife, USA, ⁴IFAR, Hebrew SeniorLife, USA, ⁵HSL Institute for Aging Research & Harvard Medical School, USA

Objective: Health effects of dairy foods may be due to more than a single nutrient. We evaluated the association of intake of milk, yogurt, cheese, cream and total dairy intake (with/without cream, due to its high fat content) with BMD at femoral neck-FN, trochanter-TR and lumbar spine-LS in the Framingham Cohort. We further examined if total vitamin D intake modified the associations as it affects calcium absorption from dairy products.

Methods: 831 men and women completed a food frequency questionnaire (FFQ) in 1988-89 and BMD assessment (hip, spine) in 1988-89 using Lunar DP3 dual-photon absorptiometer. Dairy intake variables (servings/week) were log transformed to achieve normal distribution. We used linear regression to calculate beta estimates and P values adjusting for age, sex, energy intake, weight, height, estrogen use in women, calcium supplement use and vitamin D supplement use. These associations were further examined by low total vitamin D intake (< 242 IU/d, median intake) versus higher intakes.

Results: Mean age was 76.8 y (SD:4.9, range:68-96), milk intake was 5.9 servings/week (SD:6.5) and total vitamin D intake was 335 IU/d (SD:287). In bivariate analyses, milk, yogurt and dairy (with cream) intakes were positively associated with multiple BMD sites (P range:0.006-0.05). In Model 1 (adjusted for age, weight, height, sex and total energy intake), most of the associations became non-significant except for yogurt intake ($P=0.04$) and total dairy (with cream; $P=0.05$). Full models showed no significant associations (P range:0.41-0.99).

After stratification by vitamin D intake, in the low vitamin D group, milk intake was positively associated with hip BMD (P range:0.04-0.05) and dairy intake (without cream) was positively associated with LS-BMD ($P=0.04$) in Model 1. Full models showed no significant associations. However, in the high vitamin D group, yogurt, cream and dairy (with cream) intakes were positively associated only with LS-BMD both in Model 1 (P range:0.004-0.02) and full-models (Table 1). For hip BMD, Model 1 and full models showed no significant associations (P range:0.09-0.93).

Conclusion: In this population of older adults with low vitamin D intakes, dairy intake was associated with LS-BMD in those with vitamin D > 242 IU/d but not in those with lower vitamin D. Thus, the association of dairy intake with BMD seemed to be dependent on vitamin D intake level, perhaps due to its role in the absorption of calcium from dairy products.

Table 1. Association of dairy intake with LS-BMD in the Framingham Original Cohort.

| Servings/week | Low Vitamin D (n=307) | | | High vitamin D (n=299) | | |
|------------------------|-----------------------|-------|---------|------------------------|-------|---------|
| | Beta | SE | p-value | Beta | SE | p-value |
| Milk | 0.00603 | 0.003 | 0.11 | 0.00092 | 0.001 | 0.52 |
| Yogurt | 0.01523 | 0.014 | 0.30 | 0.01502 | 0.007 | 0.03* |
| Cheese | 0.00187 | 0.003 | 0.61 | 0.00434 | 0.003 | 0.24 |
| Cream | -0.00124 | 0.002 | 0.53 | 0.00560 | 0.002 | 0.009* |
| Dairy without cream | 0.00442 | 0.002 | 0.10† | 0.00199 | 0.001 | 0.13 |
| Total Dairy with cream | 0.00079 | 0.001 | 0.62 | 0.00287 | 0.001 | 0.009* |

Full models were adjusted for age, weight, height, sex and total energy intake, estrogen use in women, calcium supplement use and vitamin D supplement use. * $P < 0.05$, † $P < 0.1$.

Table 1

Disclosures: Shivani Sahni, The General Mills Bell Institute of Health and Nutrition, 6
This study received funding from: The General Mills Bell Institute of Health and Nutrition

MO0323

The Effects of Low-methionine Diets and Endurance Exercise on Bone Metabolism, Histomorphometry and Biomaterial Properties in Growing Male Rats. Tsang-hai Huang¹, Liang-tong Kuo², Shen-Yu Hsieh³, Ming-Shi Chang², Rong-Sen Yang⁴. ¹National Cheng-Kung University, Taiwan, ²National Cheng Kung University, Taiwan, ³National Taiwan Normal University, Taiwan, ⁴National Taiwan University Hospital, Taiwan

Purpose: To investigate the effects of low-methionine (MET) diets and endurance exercise (EXE) on bone metabolism, histomorphometry and biomaterial properties in growing male rats.

Methods: Seventy-two male SD rats (7 weeks old) were randomly assigned to six groups, which were the 0.86%MET, 0.52%MET, 0.17%MET, 0.86%MET+EXE, 0.52%MET+EXE and 0.17%MET+EXE groups (n=12 for each). Control animals were fed with a purified diet containing 0.86% methionine while 0.52% and 0.17% MET-fed animals were set as the low MET diet groups. For the EXE groups, animals were subjected to treadmill running training by a protocol of 22 m/min, 60 min/day and 5 days/week for 8 weeks. After the end of eight-week intervention, all animals were sacrificed under deep anesthesia. Serum samples and bone tissues were collected and stored for analyses of serum bone markers, histomorphometry and biomaterial. Statistical analysis was processed by using two-way(MET*EXE)ANOVA ($\alpha = 0.05$).

Results: In serum markers assay, 0.17%MET rats were significantly lower in serum osteocalcin, CTX-1, IGF-1 and IGFBP-3. In addition, exercise rats showed significantly lower serum CTX-1, IGF-1 and IGFBP-3. In histomorphometry, main effect of MET was shown in spongy bone structure that 0.17%MET rats were significantly lower in BV/TV (%) and trabecular number whereas higher in trabecular separation as compared to that of 0.86%MET and 0.52%MET rats. Additionally, in the main effect of exercise, exercise rats were higher than non-exercise rats in trabecular thickness. In biomaterial properties, femora of 0.17%MET rats showed significant lower whole bone strength and bending energy. Conversely, in tissue-level bone material properties, 0.17%MET rats revealed a significant increase in yield stress and Young's modulus.

Conclusions: Low-methionine diets seemed to down-regulated bone turnover rate and negatively affected the whole bone strength. However, a lower bone turnover rate might be potential in preventing aging related bone loss (e.g. osteoporosis). And, tissue-level bone material properties showed significantly benefits resulted from low-methionine diets. Moreover, endurance exercise showed some modification or synergistic effects for low-MET diets.

Disclosures: Tsang-hai Huang, None.

MO0324

A 12-year Longitudinal Study of the Influence of Vertebral Fracture on Spinal Configuration and Vice Versa. Tetsuya Kobayashi^{*}. Asahikawa Medical University, Japan

[Background/Purpose] Vertebral compression fracture (VCF) is the most frequent outcome of osteoporosis, and modification in sagittal spinal alignment (SSA) after VCF is one mechanism of fracture cascade. Purpose of this study is to investigate 1) longitudinal SSA changes before and after VCF, and 2) the association between baseline SSA and incidence of VCF among subjects without baseline fractures. [Methods] 228 community-based female volunteers aged over 40 years were recruited from population register and were followed with upright serial entire spine radiograms for a mean 12.1 years. SSA was evaluated by thoracic kyphosis (TK), lumbar lordosis (LL), and sagittal balance measured by C7 sagittal vertical axis (SVA). Radiological grade of osteoporosis was recorded and VCF was identified by both quantitative and semi-quantitative method. 198 subjects without baseline VCF were further classified as standard SSA (TK and LL within 1SD of mean value), decreased SSA (more than 1SD decrease in TK or LL), and increased SSA (more than 1SD increase in TK or

LL). [Summary of the results] New VCF occurred in 30 subjects at 52 vertebrae during observation. SSA in subjects with VCF and without VCF changed in the same direction; TK in increase, LL in decrease, and SVA in forward shift. Thoracolumbar kyphosis and SVA change became significant not with the first VCF but after second VCFs (Figure 1). VCF occurred mostly at thoracolumbar junction, however, VCF at L3-5 level were associated with more forward shift of SVA than fractures above L2 vertebra (111.0 vs. 35.3mm, $p=0.0323$). Among 198 subjects without baseline VCF, univariate Cox proportional hazards analyses revealed baseline age, grade of osteoporosis, 1 SD decrease in TL and LL were identified as risk factors of VCF. In multivariate analyses, 1 SD decrease in LL (RR 3.106, 95% CI 1.193-8.084, $p=0.0202$) was an independent predictor of VCF, as well as the grade of osteoporosis. [Conclusions] Single VCF induced segmental kyphosis and SSA remained identical to normal subjects. Two or more VCFs induced significant spinal kyphosis. Decreased SSA without fracture was associated with increased risk of VCF by more than three-fold compared with standard SSA. Importance of evaluating SSA should be emphasized especially among unestablished osteoporosis in order to prevent 1st VCF, which is a strong predictor of subsequent fractures.

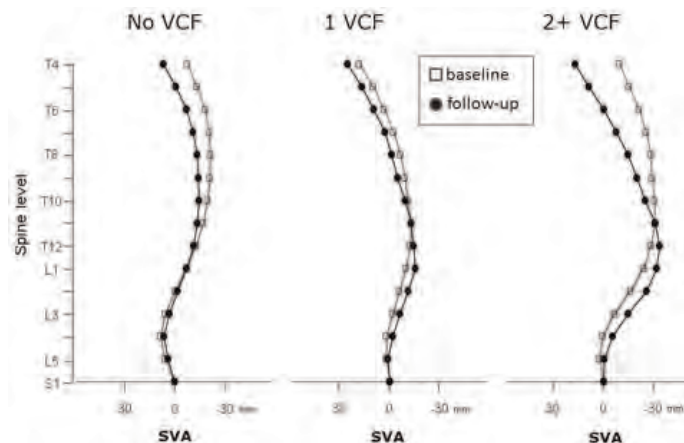


Figure. Longitudinal changes in gross SSA with/without VCF

Disclosures: Tetsuya Kobayashi, None.

MO0325

Withdrawn

MO0326

Association of Plasma Vitamin D or Vitamin K Concentration with Fracture Incidence in Elderly Women; 10 Years Cohort Study. Naoko Tsugawa*¹, Masataka Shiraki², Yuri Uchino¹, Maya Kamao¹, Toshio Okano¹. ¹Kobe Pharmaceutical University, Japan, ²Research Institute & Practice for Involuntal Diseases, Japan

Low vitamin K (VK) and vitamin D (VD) status associate with low BMD or fracture. Serum concentration of undercarboxylated osteocalcin (ucOC) or parathyroid hormone (PTH) is considered to be a sensitive marker of VK or VD status in the bone, respectively. However, previous studies have not established a method to set the cut off value predicting VK or VD status in bone using these sensitive markers. We have recently reported that a novel method based on curvature analysis for estimating the vitamin K requirement in bone using serum ucOC concentration (*Clinical Nutr.* 2012, 31, 255-260). In present study, we evaluated the cut off values of serum VK (phyloquinone: K₁) and VD (25-hydroxyvitamin D: 25-D) concentrations by a new curvature method, and confirmed that these cut off values could be a predict marker of fracture in 10 years cohort study. Subjects were 159 post-menopausal women (≥ 60 y, average: 70.7y) who participate Nagano cohort. Serum ucOC or PTH concentration was significantly and negatively correlated with K₁ or 25-D concentration, respectively. Cut off value of serum K₁ or 25-D concentration was approximately 1 ng/mL or 20 ng/mL, respectively. When subjects were divided into low and high K₁ (LK and HK) groups by K₁ 1 ng/mL, the incidence of clinical fracture in LK group was significantly higher than that in the HK group in Kaplan-Meier analysis. On the other hand, subjects were divided into low and high VD (LD and HD) groups by 25-D 20 ng/mL, the incidence of clinical fracture in LD group was significantly higher than that in the HD group. Moreover, when subjects were divided into 4 groups (LK-LD, LK-HD, HK-LD, HK-HK), the incidence of clinical fracture was highest in LK-LD group, and lowest in HK-HD group. In conclusion, these results suggest that the cut off values of serum K₁ and 25-D concentration which were evaluated by the novel method based on curvature analysis could be a predict marker of clinical fracture.

Disclosures: Naoko Tsugawa, None.

This study received funding from: No organization

MO0327

Bisphosphonate Treatment and Mortality Rate after a Hip Fracture in Patients Participating in a Secondary Prevention Program. Maria Diehl*¹, Andrea Beratarrechea², Natalia Pace³, Javier Saimovic⁴, Adriana Trossero², Gaston Perman², Luisa Plantalech⁵. ¹Metabolic Bone Disease Unit, Endocrinology Department, Argentina, ²Medical Programs Area, Internal Medicine Department, Argentina, ³Medical Program Area, Internal Medicine Departments, Argentina, ⁴Home Medicine Section, Internal Medicine Department, Argentina, ⁵Metabolic Bone Disease Unit, Endocrinology Department, Hospital Italiano de Buenos Aires, Argentina

Hip fracture (HF) is associated with high long-term mortality. The percentage of patients treated for osteoporosis after a HF is low. The aim of this study was to analyze the impact on osteoporosis treatment and mortality rates of a secondary prevention program in patients admitted for HF.

Two cohorts consisting of all the patients (>50 years) admitted for a HF in 07/01/05 to 12/31/06 (historical cohort HC) and in 07/01/08 to 12/31/09 (intervention cohort IC) were selected.

A multidisciplinary prevention program was created in July 08. All patients in IC were invited to participate. Emphasis was made in treatment with calcium, vitamin D and bisphosphonates (BP). Data on vital status, Charlson Index and treatment were obtained from electronic health records. Both cohorts were followed for a mean time of 2 years with regards to mortality.

We compared three groups: IC who agreed with the program (ICP), IC who did not participate (ICNP) and HC. Mortality ratios and Cox hazard regression models were computed to identify predictive factors.

We included 252 patients in HC and 252 in IC (44% ICP), average age 79.5 ± 8.1 and 81.5 ± 7.2 years ($p=0.040$), 78.9% and 83.3% female, respectively. Basal differences in clinical fracture, BP treatment, Charlson index were not significant between HC and IC. The loss of cases was 4.37% in HC vs 0.79% in IC ($p=0.010$). The proportion of patients who received BP post-HF was 38.4% in HC vs 54.7% in IC ($p < 0.001$).

Survival at 12 months in ICP vs ICNP and HC was: 97.2 (CI 91.7-99.1), 90 (83.7-93.9), 89.9% (85-93) and at the end of follow up: 94.2 (87.5-97.3), 78.7 (69-85.7), 81.4% (75.7-85.9) respectively ($p=0.005$).

Patients treated with BP after HF in both cohorts had a survival rate of 88.6% (83.4-92.3) vs 79.6% (73.7-84.3) in those without BP ($p=0.008$).

Factors associated with mortality in multivariate analysis were: age increase per year HR 1.06 (CI 1.02-1.1 $p < 0.001$), diabetes HR 1.96 (1.09-3.52 $p=0.024$) dementia HR 2.17 (1.36-3.49 $p=0.021$) and BP after HF, HR 0.09 (0.03-0.26 $p < 0.001$).

Mortality was lower in patients participating in the program. Treatment with BP after HF was associated with reduced risk of mortality in both cohorts. Osteoporosis treatment in HF patients increased after the implementation of a multidisciplinary program. Elderly population with dementia and diabetes was the highest risk group. We consider important to develop strategies to improve osteoporosis treatment after a HF.

Disclosures: Maria Diehl, None.

MO0328

Differences in Fracture Associated Complications in Men and Women. Hans-Christof Schober*¹, Kathrin Baessen², Patrick Haar³, Thomas Westphal³, Thomas Mittlmeier⁴. ¹Klinikum Südstadt Rostock Klinik Für Innere Medizin I, Germany, ²klinikum Suedstadt Rostock, Germany, ³Dept. trauma & orthopaedic surgery, Germany, ⁴Dept. trauma & orthopaedic surgery Univ. Rostock, Germany

Introduction: Osteoporosis associated fractures represent a major health problem. Furthermore these fractures have a large economic effect. Main associated fractures are those of the proximal femur and humerus. The incidence of surgical and medical complications after fractures of the proximal femur and the proximal humerus is difficult to evaluate. The aim of the study presented was to assess medical and surgical complications of proximal femur and humerus fractures in comparison to the fracture incidence of a well defined population.

Methods: Between October 2008 and October 2009 we prospectively collected all patients sustaining a fracture of the proximal femur and proximal humerus, presenting to all health care institutions in the city of Rostock (200 413 inhabitants). For every patient the type of fracture was ensured by X-Ray. All of the health care reports were reviewed. Complications (anaemia with the need of transfusion, pneumoniae, urinary tract infection, death, non healing, wound infection, screw cut out) were collected.

Results: In female patients we detected 134 fractures of the proximal femur and 91 of the proximal humerus. In male patients the numbers were 60 and 38. The most common complications in femur fractures were in anaemia with a need of transfusion (47.6% in female compared to 26.6% in male patients ($p < 0.05$)). In male patients a significant higher rate of pneumoniae (10.0% vs. 4.14%, $p < 0.01$) were found. In humerus fractures the number of complications was one third of these in femur fractures.

Conclusion: Concerning the femur fractures women suffered more severe bleeding than men whereas the rate of pulmonary infections and the death rate is twice as high in male than in female. Concerning the surgical complications no difference could be detected. Due to these results the number of complications and the resulting medical costs might be higher than expected. In order to improve the outcome special attention has to be drawn to the medical complications.

Disclosures: Hans-Christof Schober, None.

MO0329

Does Accounting for Bone Mineral Density Alter the Association between Body Mass Index and Fracture? Nicole Wright*¹, Silvina Levis², Jennifer Bea³, Laura Carbone⁴, Jane Cauley⁵, Zhao Chen³, Carolyn Crandall⁶, Jeffrey Curtis¹, Rebecca Jackson⁷, Karen Johnson⁸, Andrea Lacroix⁹, John Robbins¹⁰, Marcia Stefanick¹¹, Nelson Watts¹², Jean Wactawski-Wende¹³.
¹University of Alabama at Birmingham, USA, ²University of Miami School of Medicine, USA, ³University of Arizona, USA, ⁴University of Tennessee Health Science Center, USA, ⁵University of Pittsburgh Graduate School of Public Health, USA, ⁶University of California, Los Angeles, USA, ⁷The Ohio State University, USA, ⁸University of Tennessee, USA, ⁹Fred Hutchinson Cancer Research Center, USA, ¹⁰University of California, Davis Medical Center, USA, ¹¹Stanford University, USA, ¹²Mercy Health Osteoporosis & Bone Health Services, USA, ¹³University at Buffalo, USA

Background & Objective: Higher body weight or body mass index (BMI) may be protective against fractures. However, the relationship between BMI and fracture is influenced by bone mineral density (BMD). Using the Women's Health Initiative BMD (WHI-BMD) sub-cohort (n=11,020), the primary objective of this study was to examine the association between BMI and fracture risk by fracture type with and without adjustment for BMD.

Methods: We used Cox-proportional hazard models to test the association between BMI and fracture risk before and after adjustment for hip BMD. Incident self-reported fractures of interest included all fractures combined (total fracture), clinical spine, upper limb (hand, lower arm, elbow, and upper arm), lower limb (foot, lower leg, knee, and upper leg), and adjudicated hip fractures.

Results: The proportion of women within the normal BMI range (18.5-24.9 kg/m²) was 32.2%; 35.3% were overweight (25.0-29.9 kg/m²), 20% were in obesity category 1 (30.0-34.9 kg/m²), and 12.6% were in obesity category 2 (≥ 35.0 kg/m²). A total of 1706 fractures were identified in the study population, of which 32%, 38%, 18%, and 12% were in the normal weight, overweight, obese I and obese II groups. The association between BMI and fracture risk changed with adjustment for BMD at all fracture sites (Table). With adjustment of clinical factors only, no significant association between BMI and fracture risk was observed for total fractures and both upper and lower limb fractures, and a protective effect of obesity was seen for clinical spine and hip fractures. However, after the addition of hip BMD, the total fracture risk increased by 59%. Similarly, risk for upper and lower limb fractures increased by 2.14-fold and 1.49-fold. The significant protective effect of BMI on hip fractures disappeared after adjustment for BMD.

Conclusion: BMD modifies the association between body mass and fracture, supporting the hypothesis that the added bone mass in those with higher BMIs may not equate to higher bone strength; the key determinant in fracture risk.

Table: Association between BMI and Fracture With and Without Adjustment for Hip Bone Mineral Density

| | No BMD* HR (95% CI) | Hip BMD** HR (95% CI) |
|--------------------------------|------------------------|--------------------------|
| Total Fracture (n=1706) | | |
| Overweight (25.0-29.9) | 1.10 (0.91 1.33) | 1.27 (1.05 1.54) |
| Obese I (30.0-34.9) | 0.93 (0.73 1.17) | 1.23 (0.96 1.57) |
| Obese II (≥ 35.0) | 1.07 (0.83 1.39) | 1.59 (1.21 2.11) |
| Clinical Spine (n=234) | | |
| Overweight (25.0-29.9) | 0.60 (0.37 0.96) | 0.67 (0.41 1.09) |
| Obese I (30.0-34.9) | 0.61 (0.34 1.08) | 0.84 (0.45 1.54) |
| Obese II (≥ 35.0) | 0.69 (0.34 1.37) | 0.93 (0.43 1.98) |
| Upper Limb (n=736) | | |
| Overweight (25.0-29.9) | 1.28 (0.95 1.72) | 1.57 (1.16 2.13) |
| Obese I (30.0-34.9) | 1.09 (0.76 1.57) | 1.60 (1.09 2.34) |
| Obese II (≥ 35.0) | 1.31 (0.88 1.95) | 2.14 (1.39 3.30) |
| Lower Limb (n=842) | | |
| Overweight (25.0-29.9) | 1.08 (0.82 1.41) | 1.20 (0.91 1.58) |
| Obese I (30.0-34.9) | 0.95 (0.69 1.33) | 1.21 (0.85 1.71) |
| Obese II (≥ 35.0) | 1.03 (0.71 1.48) | 1.49 (1.01 2.21) |
| Hip (n=156) | | |
| Overweight (25.0-29.9) | 0.78 (0.45 1.35) | 1.12 (0.63 1.99) |
| Obese I (30.0-34.9) | 0.25 (0.09 0.68) | 0.46 (0.15 1.43) |
| Obese II (≥ 35.0) | 0.35 (0.11 1.08) | 1.05 (0.32 3.39) |

*Adjusted for Age, Race, current HT, CT flag, Osteoporosis, General Health Status, number of falls, diabetes treatment, RA, total vitamin D, total calcium, age at menopause, physical activity, Glucocorticoids, Osteoporosis medications, PPI, Thiazide diuretics, Loop diuretics, Statins and NSAIDs; **Adjusted for previous model + Hip BMD

Table

Disclosures: Nicole Wright, Amgen, 6

MO0330

Micro Finite Element Analysis Derived Biomechanical Properties of the Trabecular Bone, and Not Cortical Porosity, Is Associated With Prevalent X-ray Verified Fractures In Young Adult Men. ROBERT RUDANG*¹, Anna Darelid², Martin Nilsson³, Dan Mellstrom⁴, Claes Ohlsson⁵, Mattias Lorentzon⁶.
¹INSTITUTE OF MEDICINE, SAHLGRENKA ACADEMY, Sweden, ²Gothenburg University, Sweden, ³Centre for Bone & Arthritis Research At the Sahlgrenska Academy, Sweden, ⁴Sahlgrenska University Hospital, Sweden, ⁵Center for Bone & Arthritis Research at the Sahlgrenska Academy, Sweden, ⁶Center for Bone Research at the Sahlgrenska Academy, Sweden

We have previously reported that fracture prevalence in young men is associated with reduced trabecular volumetric BMD and to a lesser extent with reduced cortical volumetric BMD (Darelid, A.J Bone Miner Res. 2010 Mar;25(3):537-44). The aim of this study was to investigate the biomechanical properties, as derived by micro-CT-based finite element (μ FE) analysis, of the trabecular and cortical compartment, as well as cortical porosity, and their association with prevalent distal forearm fractures in young adult men. In this cross-sectional, population-based study, including 557 young adult men (24.1 \pm 0.6 yr), we performed HR-pQCT scanning at the metaphysis of the non-dominant radius to obtain trabecular bone volume fraction (BV/TV) and trabecular number. By ultra-distal cortical evaluation we obtained cortical porosity (%), and by μ FE analysis we obtained estimated ultimate failure load (F.ult(N)). F.ult was subdivided into the load distributed in the trabecular (F.ult.Trab(N)) and cortical (F.ult.Cort(N)) bone. A standardized questionnaire was used to obtain information about calcium intake, smoking, physical activity and fracture prevalence. Reported fractures were verified in local hospital X-ray records and national health care registers. In all, 93 subjects had at least one prevalent distal forearm fracture, while 464 subjects had no fractures. Men with at least one prevalent distal forearm fracture had lower F.ult at the radius (4.6%, p=0.02) and a reduced F.ult.Trab. (7.2%, p<0.01), while no significant differences were seen for F.ult.Cort nor cortical porosity. Using a logistic regression model (including calcium intake, smoking, physical activity, age, height and weight as covariates), we found that the prevalence of distal forearm fractures increased for every SD decrease in F.ult (Odds Ratio (OR) 1.28 (1.00-1.64)) and F.ult.Trab (OR 1.36 (1.06-1.75)). Using the same covariates, also trabecular BV/TV (OR 1.46 (1.14-1.87)) and trabecular number (OR 1.36(1.08-1.71)) were associated with prevalent distal forearm fractures. In conclusion, young men with prevalent distal forearm fractures have a smaller estimated ultimate failure load distributed in the trabecular bone of the radius, due to reduced BV/TV and trabecular number, than men without fracture, indicating that the trabecular microstructure rather than the cortical microstructure or geometry, is of greater importance for fracture risk at this bone site in this population.

Disclosures: ROBERT RUDANG, None.

MO0331

Mortality Following Lower Extremity Fractures in Men with Spinal Cord Injury. Laura Carbone*¹, Amy Chin², Stephen Burns³, Jelena Svircev³, Helen Hoenig⁴, Michael Heggenes⁵, Frances Weaver⁶.
¹University of Tennessee Health Science Center, USA, ²Edward J. Hines, Jr. VA Hospital, USA, ³VA Puget Sound Health Care System / University of Washington-Rehabilitation Medicine, USA, ⁴Durham Veterans Affairs Medical Center, USA, ⁵Baylor College of Medicine, USA, ⁶Edward J. Hines, Jr. VA Hospital / Stritch School of Medicine, Loyola University, USA

Context: In the United States there are over 200,000 men with Spinal Cord Injuries (SCI) who are at markedly increased risk for lower limb fractures. Increased mortality following hip fractures has been well described in men without SCI, but the risk of mortality following fractures in the SCI population is unknown.

Objectives: To determine whether lower extremity fractures are associated with an increased risk for mortality in men with SCI.

Design, Setting, and Patients: A population-based, nested, case-control study of male Veterans enrolled in the VA Spinal Cord Dysfunctions Registry from FY2002-2007 to determine the association between lower extremity fractures and mortality. Each fracture case (n=1028) was matched to a fracture-free control using propensity scores (n=1028).

Main Outcome Measures: Mortality rates for up to five years.

Results: The lower extremity fracture rate was 2.72 per 100 patient-years at risk. Among fracture cases, mortality was more common in older men (\geq age 65) compared with younger men (p<0.001), but did not differ by site of lower extremity fracture (P=0.26). There were no significant differences in unadjusted mortality rates in fracture cases (7.17 per 100 patient-years at risk) compared with controls (6.33 per 100 patient-years at risk) (P=0.81). Cases and controls were matched on propensity scores adjusting for demographic (age, race), SCI-related injury factors (level/completeness of SCI), socioeconomic status and comorbidities. There was no significant difference in survival time in fracture cases compared with non-fracture controls [HR 0.89 (95% CI 0.72-1.11)].

Conclusions: Lower extremity fractures were frequent events in men with SCI. Although mortality was higher in older compared with younger men following these fractures, it did not differ by site of lower extremity fracture. Compared to non-

fracture controls, mortality in male veterans with SCI was not differentially affected by the presence of a lower extremity fracture.

Disclosures: Laura Carbone, None.

This study received funding from: Veterans Affairs Medical Center, grant IR06-212-2

MO0332

Obese and Overweight Patients Have Reduced Mortality after a Hip Fracture: the Latest Obesity Paradox. Daniel Prieto-alhambra*¹, Melissa Premaor², Francesc Fina Aviles³, Xavier Nogues⁴, Muhammad Javaid⁵, Nigel Arden⁵, Cyrus Cooper⁶, Juliet Compston⁷, Adolfo Diez-Perez⁸.

¹Institut Municipal D'Investigació Mèdica, United Kingdom, ²Federal University of Santa Maria, Brazil, ³Institut Catala de la Salut; SIDIAP-IDIAP Jordi Gol, Spain, ⁴Institut Municipal D'Investigació Mèdica, Spain, ⁵University of Oxford, United Kingdom, ⁶University of Southampton, United Kingdom, ⁷University of Cambridge School of Clinical Medicine, United Kingdom, ⁸Parc De Salut Mar, Spain

PURPOSE

Despite the increasing prevalence of overweight and obesity, data on the impact of obesity on mortality post-fracture is lacking. We aimed to study the association between obesity and mortality following fractures at the hip and other osteoporotic site.

Method: -Study Design:population-based cohort study.

-Population of study:we screened the SIDIAP-Q database to identify anyone who suffered either a hip or a non-hip osteoporotic fracture at age 45 years or older between 1/1/2007 and 31/12/2009. Participants were followed up to the end of 2009. SIDIAP-Q contains the computerized medical records of >1,500 General Practitioners in Catalonia (North-East Spain) who achieve high coding quality standards. It contains information on a representative 35% of the population (>2.1 million people). Death status is provided to SIDIAP-Q by the national death registry and data on inpatient diagnosis are obtained for SIDIAP-Q from the official Hospital Episodes Database. In the study period, 959,242 patients aged ≥45 were eligible.

-Measurements:Main exposure was the most recent body mass index (BMI) measurement prior to fracture. This was categorized in four WHO categories: underweight (

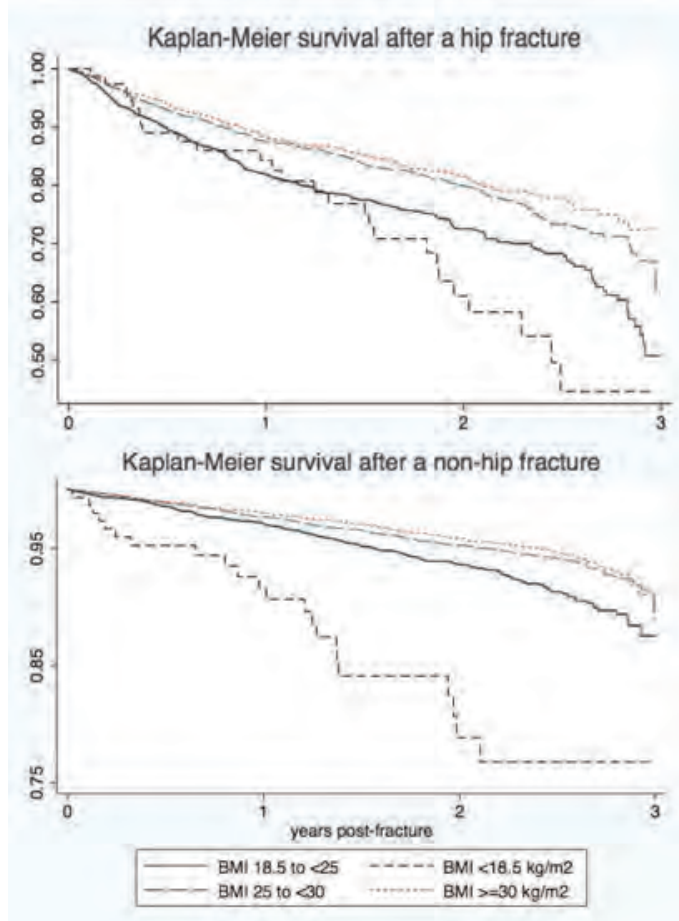
-Statistical analyses:we modelled the effect of BMI on mortality using Cox regression, where normal weight was the reference category.

Results: We identified 6,988 and 29,372 subjects with a hip and a non-hip osteoporotic fracture within the study period followed for a median (inter-quartile range) of 1.17(0.53-2.02) and 1.36(0.65-2.15) years respectively. Adjusted Hazard Ratios (HR) for overweight and obesity on mortality were 0.74 (95%CI 0.62-0.88; p=0.001) and 0.74 (0.60-0.91; p=0.004) after hip and 0.50 (0.32-0.77; p=0.002), 0.56 (0.36-0.87; p=0.010) after non-hip fracture (Table). Kaplan-Meier estimates of mortality for each BMI group are shown (Figure).

Conclusion: Obese patients survive longer following a hip and non-hip osteoporotic fracture. This surprising finding is consistent with other chronic conditions like COPD or heart failure, but the reasons for reduced mortality remain unknown and need further research.

TABLE. Results of Cox regression on the effect of BMI on mortality post-fracture

| | HIP FRACTURE | | | NON-HIP OP FRACTURE | | |
|------------------|--------------|---------------------------|---------------------------|---------------------|---------------------------|---------------------------|
| | N(%) deaths | Unadjusted HR (95%CI) | Adjusted HR (95%CI) | N(%) deaths | Unadjusted HR (95%CI) | Adjusted HR (95%CI) |
| Normal (n=) | 308 (22.8%) | REF | REF | 233 (4.9%) | REF | REF |
| Underweight (n=) | 26 (32.9%) | 1.36 [0.91-2.02]; p=0.137 | 0.98 [0.64-1.50]; p=0.92 | 22 (14.2%) | 2.87 [1.85-4.44]; p<0.001 | 2.19 [1.36-3.52]; p=0.001 |
| Overweight | 309 (16.3%) | 0.70 [0.59-0.81]; p<0.001 | 0.74 [0.62-0.88]; p=0.001 | 321 (3.5%) | 0.71 [0.60-0.84]; p<0.001 | 0.67 [0.55-0.81]; p<0.001 |
| Obese | 187 (14.2%) | 0.62 [0.51-0.74]; p<0.001 | 0.74 [0.60-0.91]; p=0.004 | 247 (3.2%) | 0.64 [0.54-0.77]; p<0.001 | 0.73 [0.59-0.89]; p=0.002 |



Disclosures: Daniel Prieto-alhambra, None.

MO0333

Prevalence and Risk Factors for Vertebral Fractures among Asian Indians >50 Years of Age-Delhi Vertebral Osteoporosis (DEVOS) Study. Raman Marwaha¹, Nikhil Tandon², Yashdeep Gupta², Kunal Bhadra¹, Archana Narang³, Kalaivani Mani⁴, Ambrish Mithal⁵, Subhash Kukreja*⁶.

¹Institute of Nuclear Medicine & Allied Sciences, India, ²AII India Institute of Medical Sciences, India, ³Dr B.R.Sur Homeopathic Medical College Hospital & Research Centre, India, ⁴AII Institute of Medical Sciences, India, ⁵Medanta Medicity, India, ⁶University of Illinois, USA

India has a population of over 1.2 billion and with improvement in life expectancy, the proportion of older individuals is increasing. There is paucity of data on the prevalence and risk factors for osteoporotic fractures in this population. Morphometric vertebral fractures are common, are associated with significant morbidity and predict the occurrence of future vertebral and non-vertebral fractures. In the present

study, we evaluated the prevalence and risk factors for morphometric vertebral fractures among older Asian Indian men and women.

Methods: We recruited 808 healthy subjects aged 50 years or older, residing in 3 residential colonies in Delhi, India who volunteered to participate in this study. All subjects underwent lateral X-rays of the lumbar and thoracic spine according to standardized protocol. All X-rays were evaluated by a single trained person by an advanced semi-automated SpineAnalyzer® software (Optasia Medical). Recruited subjects underwent anthropometric, biochemical, and hormonal evaluation. Forty five subjects (5.6%) were excluded from final analysis due to technical/quality issues with the obtained radiographs.

Results: 348 males and 415 females, with mean age of 64.9 (6.7) years were evaluated. Vertebral fractures were present in 17.9% subjects (Males-18.8%, Females-17.1%). Prevalence of fractures increased with age in females from 14.7% in 50-60 years age group to 22.4% in >70 years age group, but not in males (21.6% in 50-60 years age group to 20.3% in >70 years age group). Among the risk factors only body weight was protective against fractures. All other factors, including prior history of self-reported fractures, calcium vitamin D supplementation and serum 25 OH vitamin D level were not significantly associated with fracture risk. The prevalence of vertebral fracture in the present study is similar to that reported in other population-based studies in the literature. The lack of increased risk for vertebral fracture with increasing age in men is also similar to that reported for other populations suggesting that the vertebral fractures in men may have a traumatic etiology.

Conclusions: A high prevalence of vertebral fractures was observed in older Asian Indian subjects but the overall rates are similar to those reported for other populations. Higher body weight was the only risk factor which was significantly associated with lower fracture risk.

Disclosures: Subhash Kukreja, None.

MO0334

Identification of New MicroRNA Binding Site Polymorphisms for Bone Mineral Density in Meta-Analysis of Genome-Wide Association Studies. Tianhua Niu^{*1}, Lei Zhang², Shu-Feng Lei³, Jian Li², Yu-Fang Pei², Yongjun Liu², Hui Shen⁴, Yaoshong Liu⁴, Hong-Wen Deng⁴. ¹Tulane University School of Public Health & Tropical Medicine, USA, ²Center for Bioinformatics & Genomics, Department of Biostatistics & Bioinformatics, Tulane University School of Public Health & Tropical Medicine, USA, ³College of Life Sciences, Hunan Normal University, China, ⁴Tulane University, USA

Aim: MicroRNAs (miRNAs) are pivotal post-transcriptional regulators of gene expression, and molecular variants at miRNA binding sites could influence complex human traits. Our aim was to identify novel miRNA-binding site polymorphisms for human bone mineral density (BMD) phenotypes.

Methods: We performed a systematic, three-stage meta-analysis of genome-wide association (GWA) studies for lumbar spine, hip, and femoral neck BMD phenotypes. After analyzing 32,811 miRNA binding site single nucleotide polymorphisms (SNPs) in 11,038 individuals of various ancestries (Stage I), top 20 miRNA-binding site SNPs were selected for *in silico* replication in 3 GWA studies in Australian, Dutch, and Korean populations respectively (Stage II). Six SNPs, i.e., rs4647940 (*FGFRL1*, 4p16.3), rs3213550 (*PRR5-ARHGAP8*, 22q13.31), rs1057392 (*PTH2R*, 2q34), rs6904261, rs11155801, and rs9479085 (all 3 are in *C6orf97-ESR1*, 6q25.1), were further examined in *de novo* genotyping replication in a cohort comprising a sample of 3,923 unrelated European individuals (CEU3) and a sample of 2,740 unrelated Chinese Han individuals (CHI2) (Stage III).

Results: In combined meta-analysis across all stages, rs4647940 and rs3213550 were found significantly associated with femoral neck BMD ($P = 8.87 \times 10^{-12}$ and 1.17×10^{-5} , respectively) and hip BMD ($P = 4.76 \times 10^{-9}$ and 5.06×10^{-3} , respectively) phenotypes, and suggestive associations for rs6904261, rs11155801, and rs9479085 with spine BMD ($P = 2.70 \times 10^{-3}$, 3.23×10^{-3} , and 9.20×10^{-3} , respectively) were revealed.

Conclusion: genetic variants at miRNA-binding sites located in *FGFRL1*, *PRR5-ARHGAP8* and *C6orf97-ESR1* gene regions may play important roles in BMD variation, which merit further studies in development of osteoporosis.

Disclosures: Tianhua Niu, None.

MO0335

Replication of European Loci Associated with Bone Mineral Density in Koreans. Ye An Kim^{*1}, Hyung Jin Choi², Eu Jeong Ku¹, Sang Wan Kim³, Jong-Young Lee⁴, Bok-Ghee Han⁴, Seong Yeon Kim¹, Chan Soo Shin¹, Nam H Cho⁵. ¹Department of Internal Medicine, Seoul National University College of Medicine, South Korea, ²Chungbuk National University Hospital, South Korea, ³Seoul National University Boramae Hospital, South Korea, ⁴Center for Genome Science, National Institute of Health, Osong Health Technology Administration Complex, South Korea, ⁵Department of Preventive Medicine, Ajou University School of Medicine, South Korea

Most genome-wide association studies (GWAS) have reported bone mineral density (BMD) related variations in European populations. This study was designed to investigate whether the BMD loci discovered in European BMD GWAS were also associated with BMD in East Asian ethnic samples. We include genetic markers at genome-wide significance (GWS, p value less than 5×10^{-8}) levels and variants with suggestive significance in recent European GWAS. A total of 2729 unrelated Korean individuals from a population-based cohort were analyzed. For the replication study, we selected a total of 671 SNPs from previous European studies (474 GWS SNPs from 24 loci which previously reached GWS and 197 suggestive SNPs which showed weaker association with BMD). Among 474 GWS SNPs from 24 loci, 255 SNPs from 14 loci were replicated. Replicated loci were as follows; 1p31.3 (GPR177, $P = 0.016$), 1p36 (ZBTB40, $P = 0.038$), 3p22 (CTNBN1, $P = 0.002$), 5q14 (MEF2C, $P = 0.008$), 6q25 (ESR1, $P = 0.009$), 7p14 (STARD3NL, $P = 0.001$), 8q24 (TNFRSF11B, $P = 0.0004$), 11p14.1 (DCD5, $P = 0.013$), 11p15 (SOX6, $P = 0.0009$), 12q13 (SP7, $P = 0.048$), 13q14 (AKAP11, $P = 0.002$), 17q21 (HDAC5, $P = 0.030$), 18q21 (TNFRSF11A, $P = 0.020$), and 20p12 (JAG1, $P = 0.016$). Nine loci which previously showed association with BMD at GWS level were not replicated; 2p21 (SPTBN1), 4q21.1 (MEPE), 7q21.3 (FLJ42280), 11p12 (ARHGAP1), 11q13.4 (LRP5), 14q32 (MARK3), 16q24 (FOXL1), 16q23 (ADAMTS18), and 17q21 (SOST). GWS SNPs were replicated in Korean population with the replication rate of 53.8%. Among these loci, two loci (2p21 and 7p21.3) showed considerable differences in effective allele frequency (0.35 vs. 0.03 and 0.32 vs. 0.13, respectively). Among 197 suggestive variants, 12 SNPs with significant associations were included for meta-analysis. Four markers reached a significant combined p value (less than 7×10^{-5}). One marker (rs7543680) is located near ZBTB40 gene. The other variants are rs11711157 in the CPN2 gene, rs11599750 in CPN1 gene, and rs3783833 in RPS6KA5 gene. The result of our study illustrates the effect of ethnic differences in BMD susceptibility genes, and underscores the need for further genetic studies for each ethnic group.

* Co-corresponding authors: Chan Soo Shin and Nam H Cho

Disclosures: Ye An Kim, None.

MO0336

Vitamin D Binding Protein Genotype Is Associated with Serum 25-hydroxyvitamin D Concentration and Bone Traits in Finnish Adults – the PHOMI study. Elisa Saarnio^{*1}, Minna Pekkinen², Virpi Kemi³, Suvi Itkonen³, Outi Makitie⁴, Heini Karp³, Merja Kärkkäinen³, Harri Sievanen⁵, Christel Lamberg-Allardt³. ¹University of Helsinki, Finland, ²Folkhälsan Institute of Genetics, University of Helsinki, Finland, ³University of Helsinki, Finland, ⁴Hospital for Children & Adolescents, Helsinki University Hospital, Finland, ⁵UKK Institute, Finland

Vitamin D binding proteins (DBP, Gc) are polymorphic carriers of vitamin D and its metabolites. There are three common phenotypes of DBPs, which differ by their amino acid composition. Serum 25-hydroxyvitamin D (S-25OHD) concentration varies between DBP phenotypes. Furthermore, DBP isoforms have been associated with decreased bone mineral density and increased fracture risk.

Our aim was to study the associations among DBP genotypes, S-25OHD and bone traits in a cohort in Finland. We investigated 596 Caucasian subjects (378 premenopausal women, 218 men) aged 37-47 years in the cross-sectional PHOMI study. Dietary intakes of vitamin D and Ca including supplements were calculated with a validated food frequency questionnaire. The concentrations of S-25OHD and parathyroid hormone (S-PTH) were determined. DNA was isolated from blood samples. Bone traits were analyzed from distal and proximal sites of non-dominant radius and tibia with pQCT. Background data was collected with a questionnaire. Genotyping was performed with a Taqman method based on a single nucleotide polymorphism (rs4588=Thr420Lys) in the DBP gene (homozygote Gc 1-1, heterozygote Gc 1-2, homozygote Gc 2-2).

The distribution of the SNP among the subjects was: Gc 1-1 64%, Gc 1-2 31% and Gc 2-2 4%. There was a significant difference in 25OHD levels in women between the genotypes, the concentration being highest in Gc 2-2 (59.5 nmol/L), intermediate in Gc 1-1 (57.6 nmol/L) and lowest in Gc 1-2 (51.6 nmol/L) based on a covariance analysis (covariates: vitamin D and Ca intake, PTH and sunlight exposure) ($p=0.008$). Gc genotype was associated with bone mineral content (BMC) (Gc 1-1: 631, Gc 1-2: 615; Gc 2-2: 600 mg, $p=0.037$), total area of the bone (Gc 1-1: 358; Gc 1-2: 348, Gc 2-2: 344 mm², $p=0.037$) and SSI (stress and strain index) (Gc 1-1: 1378; Gc 1-2: 1319; Gc 2-2: 1295, $p=0.020$) of proximal tibia (covariates: age, height, weight, S-25OHD, PTH, physical activity, vitamin D and Ca intake and use of contraceptives). In men no association were found among DBP genotypes, 25OHD and bone traits.

S-25OHD concentrations are associated with genetic variation in the DBP gene in women. The results differ from our previous preliminary study with adolescents but this may be due to differences in vitamin D intake between the genotypes in the adult subjects. DBP genotype is related to BMC, bone area and bone strength in women.

Disclosures: *Elisa Saarnio, None.*

MO0337

Physical Activity as Determinant of Femoral Neck Strength in Adult Women. Findings from the SWAN Hip Strength Across The Menopausal Transition Study.. Takahiro Mori¹, Shinya Ishii², Gail Greendale³, Jane Cauley⁴, Barbara Sternfeld⁵, Weijuan Han³, Arun S. Karlamangla³. ¹West Los Angeles Veterans Health Administration, USA, ²University of Tokyo, Japan, ³University of California, Los Angeles, USA, ⁴University of Pittsburgh Graduate School of Public Health, USA, ⁵Division of Research, Kaiser Permanente, USA

Although areal bone mineral density (BMD) is widely used for the assessment of bone strength, it alone is not sufficient to assess fracture risk. For instance, BMD is higher in Caucasian than Asian women and in diabetics than non-diabetics, although the incidence of fractures is also higher in Caucasian women and in diabetics. Composite indices of femoral neck strength integrate body height and weight with femoral neck BMD, femoral neck width (FNW), and femoral neck axis length (FNAL) to gauge bone strength relative to loads borne during falls. These indices are inversely associated with incident fractures, and unlike BMD, are consistent with fracture risk differences between Asians and Caucasians, and between diabetics and non-diabetics.

To examine the associations of self-reported physical activity with the composite indices of femoral neck strength, we analyzed data from 1921 women (from 4 ethnic groups: 962 Caucasian, 501 African American, 238 Japanese, 220 Chinese) from the baseline visit of the Study of Women's Health Across the Nation (SWAN), when participants were in pre- or early peri-menopause. Composite indices of femoral neck strength in different failure modes were created as: BMD*FNW/weight for compression strength, BMD*(FNW)²/(FNAL*weight) for bending strength, and BMD*FNW*FNAL/(height*weight) for impact strength. Physical activity was assessed with the Kaiser Physical Activity Survey (range, 1 for low to 5 for high) in four domains: sport, work (among those employed), home, and active living. We used multiple linear regression to separately examine the associations between physical activity in each domain and the strength indices, controlling for age, menopause state, race/ethnicity, and SWAN study site.

Sport activity (standard deviation (SD), 1.03), active living (SD, 0.78), and total activity score (excluding work; SD, 1.77) were each positively associated with each of the strength indices (Table). Neither work activity (SD, 0.73) nor home activity (SD, 0.83) was associated with any strength index. Sport activity and active living may positively impact bone strength relative to load, but physical activity at home and at work appear to have no influence on bone strength relative to load, highlighting the importance of regular physical activity outside of home and work routines to bone health.

| | Compression Strength Index | Bending Strength Index | Impact Strength Index |
|------------------------|----------------------------|------------------------|-----------------------|
| Sport Activity Score | 0.199 | 0.165 | 0.202 |
| Active Living Score | 0.194 | 0.169 | 0.193 |
| Total Activity Score** | 0.228 | 0.194 | 0.233 |

* Units: Strength index standard deviation (SD) per SD increment in activity score
 ** Excluding work, since many in sample did not work outside the home
 All p values < 0.0001

Table: Adjusted associations* of domain-specific physical activity level with strength indices

Disclosures: *Takahiro Mori, NIH, 6*

This study received funding from: NIH/ DHHS through grants NR004061, AG012505, AG012535, AG012531, AG012539, AG012546, AG012553, AG012554, AG012495.

MO0338

Age Modifies Hip Fracture Risk Associated with Risk Factors and Functional Status: The Global Longitudinal study of Osteoporosis in Women (GLOW). Frederick Hooven^{*1}, Julie Flahive², Steven Boonen³, Stephen Gehlbach⁴, Ethel Siris⁵, Susan Greenspan⁶. ¹University of Massachusetts Medical School, USA, ²UMass Medical School, USA, ³Leuven University Center for Metabolic Bone Diseases, Belgium, ⁴University of Massachusetts, USA, ⁵Columbia University College of Physicians & Surgeons, USA, ⁶University of Pittsburgh, USA

Purpose: Predicting fractures among postmenopausal (PM) women at younger ages is challenging, as younger age is strongly associated with lower fracture risk. Although older PM women fracture more frequently than younger PM women, one large cohort study estimated that 20% of hip fractures and 37% of all osteoporosis-associated fractures occur in women from 50–64 years of age. We investigated whether the relationship between established risk factors and other characteristics and hip fracture was modified by age.

Methods: GLOW is an observational longitudinal study of non-institutionalized women aged ≥55 years recruited from 723 primary physician practices in 10 countries. Self-administered questionnaires were mailed; data collected included demographics, fractures, and risk factors. Measures of physical function and vitality were derived using items from the SF-36. Means and frequencies of risk factors for fracture were calculated for women in 3 different age categories who experienced a hip fracture over 3 years of follow-up. P-values for interaction were calculated.

Results: Forty three women in the 55–64-years age group (n=21,281) reported hip fractures, as did 84 women in the 65–74-years category (n=19,462) and 226 women aged ≥75 years (n=13,212). Mean weight was significantly lower among women who fractured only in the oldest age group (≥75 years). The interaction of physical function (PF) and age was significant (p=0.001), and the magnitude of the difference in PF between women ages 55–64 who fractured (mean PF=63) and those who did not (mean PF=81) was substantially greater than for women ≥75 years (mean PF, fracture=53; mean PF, no fracture=60). Interaction between age group and vitality index was also significant (p=0.03). The difference in frequency of fracture history between those who fractured their hip and those who did not was substantially higher for the youngest women (hip fracture, 40%; no hip fracture 14%), than for the oldest (hip fracture, 47%; no hip fracture 37%) (Figure). Interaction between age group and history of fracture was also significant (p=0.01).

Conclusions: Prior fracture may be more important, and low weight less important, for predicting hip fractures in younger PM women than in older PM women. Low physical function and vitality may also be important predictors of hip fracture specifically in younger PM women.

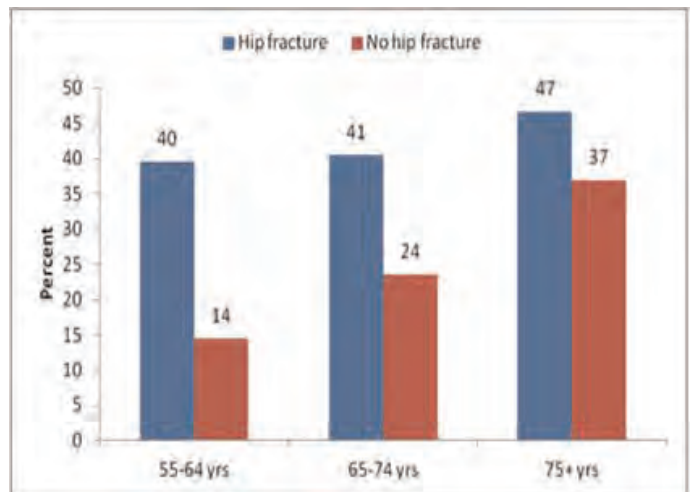


Figure. Rates of any prior fracture according to age group and hip fracture incidence (n=53,955)

Disclosures: *Frederick Hooven, None.*

This study received funding from: Sanofi-Aventis and Warner Chilcott Company LLC

MO0339

C-Reactive Protein, Femoral Neck Strength, and Fracture Risk: Data from Study of Women's Health Across the Nation (SWAN). Shinya Ishii*¹, Jane Cauley², Gail Greendale³, Carolyn Crandall³, Michelle Danielson⁴, Yasuyoshi Ouchi⁵, Arun Karlamangla⁶. ¹Graduate School of Medicine, University of Tokyo, Japan, ²University of Pittsburgh Graduate School of Public Health, USA, ³University of California, Los Angeles, USA, ⁴University of Pittsburgh, USA, ⁵Department of Geriatrics, University of Tokyo, Japan, ⁶Division of Geriatrics, David Geffen School of Medicine at UCLA, USA

Background: Higher levels of C-Reactive Protein (CRP), an inflammatory marker, are associated with greater fracture risk. However, some studies have found CRP to be positively associated with dual energy x-ray absorptiometry-derived areal bone mineral density (BMD).

Objective: To test the hypothesis that composite indices of femoral neck strength, which integrate femoral neck BMD, femoral neck width (FNW) and femoral neck axis length (FNAL) with body size, better explain the positive association between CRP and fracture risk than does BMD.

Methods: Study sample included 1872 women from 4 race/ethnic groups (931 Caucasians, 501 African Americans, 213 Chinese and 227 Japanese), pre- or early peri-menopausal at baseline. Serum CRP was measured and composite indices for femoral neck strength in 3 failure modes were created from baseline data as BMD*FNW/weight for compression strength, BMD*(FNW)²/(FNAL*weight) for bending strength, and BMD*FNW*FNAL/(height*weight) for impact strength. Incident non-digital, non-craniofacial fractures were ascertained annually over median follow up of 9 years. The functional form of the associations of log(CRP) with fracture hazard were assessed using restricted cubic splines and linear splines (with fixed knots) were fit as necessary.

Results: During the follow-up, 194 women (10.4%) had fractures. In analyses adjusted for age, race/ethnicity, diabetes, menopause transition stage, body mass index, smoking, physical activity, medications, and study site, log(CRP) was associated inversely with each of the composite strength indices (-0.06 to -0.07SD per doubling of CRP, all p<.0001), but not associated with femoral neck BMD. Adjusted for the same covariates in proportional hazards analyses, fracture hazard increased linearly with baseline log(CRP), only for CRP levels => 3 mg/L. Addition of femoral neck BMD to the model did not attenuate the CRP-fracture association. However, addition of any of the femoral neck composite strength indices attenuated the CRP-fracture association and made it statistically non-significant.

Conclusion: For serum CRP values above 3 mg/L, fracture risk increases with increasing CRP. Unlike BMD, composite strength indices are inversely related to CRP levels, and partially explain the increased fracture risk associated with inflammation.

Supported by NIH/ DHHS, through the NIA, NINR and the NIH ORWH (Grants NR004061; AG012505, AG012535, AG012531, AG012539, AG012546, AG012553, AG012554, AG012495).

| Table: Adjusted relative hazard for fracture per doubling of CRP level above 3 mg/L | | |
|---|---|------|
| | Relative Hazard (95% Confidence Interval) | p |
| Fully adjusted model | 1.28 (1.04, 1.58) | 0.02 |
| Full model + BMD | 1.29 (1.05, 1.58) | 0.02 |
| Full model + compression index | 1.22 (0.99, 1.51) | 0.06 |
| Full model + bending index | 1.24 (1.00, 1.53) | 0.05 |
| Full model + impact index | 1.23 (0.99, 1.52) | 0.06 |

Table

Disclosures: *Shinya Ishii, None.*

MO0340

Withdrawn

MO0341

Different Cardiovascular Risk Factor Pattern for Osteoporotic Fractures in Middle Aged Icelandic and Swedish Women. Anna Holmberg*¹, Kristin Siggeirsdottir², Thor Aspelund³, Gunnar Sigurdsson⁴, Kristina Akesson⁵, Vilmundur Gudnason². ¹Skane University Hospital, Malmö, Sweden, ²Icelandic Heart Association Research Institute, Iceland, ³Icelandic Heart Association, Iceland, ⁴Landspítali, Iceland, ⁵Skåne University Hospital, Malmö, Sweden

Introduction: Cardiovascular disease (CVD) and osteoporotic fractures are well known causes of morbidity and mortality. The conditions have many common risk factors, suggesting a possible common pathogenesis. This study examined possible associations between CVD risk factors and osteoporotic fractures in women at middle age, comparing their impact in two cohorts.

Material and methods: The Malmo Preventive Project (MPP) Sweden, and the Reykjavik Study (RS) Iceland are cardiovascular prevention studies with a long time follow-up regarding CVD and fractures. Subjects between 45 and 60 years of age were selected, 7791 women from the MPP and 3165 women from the RS, mean age 53 and 54 years, mean follow-up 21 and 20 years. Baseline descriptives were similar, with a higher systolic blood pressure (131 vs. 127 mm Hg) and s-cholesterol (6.5 vs. 6.0 mmol/L) in the Icelandic women. Clinically relevant CVD risk factors were analyzed for each database in a multi-variable Cox proportional hazard model with osteoporotic fractures (wrist, proximal humerus, vertebral, hip) as end points. The included risk factors were age, heredity for CVD, BMI, diastolic blood pressure, s-cholesterol, s-triglycerides, smoking, physical activity and diabetes.

Results During follow-up 1129 (14%) and 1017 (32 %) of the women in MPP and RS suffered osteoporotic fractures.[A1] In both cohorts age (HR 1.04-1.08, CI95%1.03-1.10), BMI (HR 0.97-0.98, CI95% 0.96-1.00) and smoking (HR 1.15-1.22, CI95% 1.00-1.39) were significantly associated with fracture. The strongest risk factor in the MPP was diabetes (HR 1.86, CI95% 1.19-2.91), whereas physical activity had a protective effect (HR 0.81, CI95% 0.70-0.93). In the RS elevated triglycerides (HR 0.88 CI95% 0.82-0.95 per 0.5 mmol/L) was significantly protective, independent of the protective effect of BMI. Adding cardiovascular events as a risk factor in the multi-variable analysis only marginally effected the results, but was in the MPP a significant risk factor for fracture (HR 1.55 CI95% 1.23-1.94).

Conclusions: Common CVD risk factors were significantly associated with fracture risk in middle aged women in both cohorts with a few unique risk factors in either cohort. The risk factor impact was different in the two cohorts, possibly a result of slight differences in the study cohorts, or reflecting that CVD risk factors have different impacts in different communities. Our study emphasizes the need for further research.

[A1]Ta fram siffror

Disclosures: *Anna Holmberg, None.*

MO0342

Incident Fall Rate is Associated With Higher BMI In Older Men: The Osteoporotic Fractures in Men (MrOS) Study. Smriti Shrestha*¹, Carrie Nielson¹, Melanie Abrahamson¹, Kristine Ensurd², Marcia L Stefanick³, Tien Dam⁴, Eric Orwoll¹. ¹Oregon Health & Science University, USA, ²University of Minnesota Medical School, USA, ³Stanford University, USA, ⁴Columbia University Medical Center, USA

The risk of falling increases with age, and the majority of the hip fractures result from falls. We have observed after BMD adjustment there is an increased risk of hip fracture among older obese men. In this analysis, we evaluated the effect of BMI category on 1) incident fall rates and 2) the association between falls and hip fracture.

Between March 2000 and April 2002, 5994 community-dwelling men aged ≥65 yrs were enrolled in the MrOS study. Baseline BMI was categorized according to the WHO guidelines (18.5-24.9, normal, 25-29.9, overweight, 30-34.9, obese I, ≥35, obese II and III). Fall information was collected over an average follow up of 8.7 yrs using tri-annual questionnaires. Physical function was measured with six meter walk pace, narrow walk pace, grip strength, chair stand time and leg extension power. The probability of a fall was modeled using Generalized Estimating Equations. Several potential confounders were tested, and age was considered as a potential effect modifier of the BMI-falls association. Cox proportional hazard regression models were used to analyze the association between incident falls and hip fracture, and the interaction between BMI and fall rate was tested.

The average fall rate was 0.76 per person-year (ppy). Fall rate increased with age and was 1.17 ppy in ≥80 age group. Among the overall cohort, fall rates in obese men were higher compared to normal weight men. The BMI-falls association differed by age group (p for interaction= 0.007). Compared to normal weight men, the risk of falls was higher in obese men between the ages of 65-79, but not among those ≥80 (Table 1). Narrow walk pace appeared to mediate some of the effect of obesity on falls; adjustment for narrow walk pace attenuated the BMI-falls association among men in obese II and III group by 11%. However, history of diabetes, history of arthritis, use of medication (statin, anticonvulsant and analgesic) did not substantially alter the associations. For each additional fall in a year, the risk of hip fracture increased by 14% (HR 1.14 95% CI: 1.09-1.20). However, this association did not differ by BMI category (p for interaction= 0.67).

The risk of falls was higher in obese men under 80 yrs. The higher fall rate with higher BMI and the association between fall rate and hip fracture is a potential explanation for the previously observed association between obesity and BMD-adjusted hip fracture risk in this cohort of older men.

Table 1. BMI and risk of falls among older men, the Osteoporotic Fractures in Men (MrOS) Study

| | Normal {18-24.9 kg/m ² } n=1602 | Overweight {25-29.9 kg/m ² } n=3004 | Obese I {30-34.9 kg/m ² } n=1012 | Obese II and III {35-50 kg/m ² } n=231 | | |
|---------------------------|---|---|--|--|------------------|--------|
| Fall rate per person-year | 0.76 | 0.72 | 0.84 | 1.02 | | |
| Age (years) | Fall rate | Relative Risk * (95% confidence interval) | | | P trend | |
| 65-69 | 0.57 | Ref | 1.01 (0.85-1.21) | 1.35 (1.12-1.64) | 1.56 (1.16-2.08) | 0.0001 |
| 70-74 | 0.70 | Ref | 0.93 (0.80-1.08) | 1.25 (1.05-1.49) | 1.35 (1.03-1.75) | 0.004 |
| 75-79 | 0.86 | Ref | 1.16 (1.02-1.33) | 1.18 (0.98-1.42) | 1.68 (1.25-2.26) | 0.003 |
| ≥80 | 1.17 | Ref | 0.86 (0.75-0.98) | 0.86 (0.67-1.07) | 0.95 (0.63-1.44) | 0.08 |

*Adjusted for study site

Table 1

Disclosures: *Smriti Shrestha, None.*

MO0343

Musculoskeletal Changes in Women Have Accompanied an Increase in BMI during the Obesity Epidemic. Julie Pasco¹, Haslinda Gould², Sharon Brennan^{2*}, Mark Kotowicz³. ¹Deakin University, Australia, ²The University of Melbourne, Australia, ³Deakin University School of Medicine, Australia

Introduction: The obesity epidemic has been monitored in terms of increasing body mass index (BMI) but this measure masks changes in the components of body composition, namely body fat mass, lean mass and bone. The aim of this study was to determine how body composition has changed over a decade among women living in south-eastern Australia.

Methods: Body composition (fat, lean and bone) was evaluated among women in the Geelong Osteoporosis Study (GOS) using DXA (Lunar DPX-L) during two time periods, a decade apart. DXA was performed for 1433 women (aged 20-94 years) during 1993-7 and for 1002 women (aged 20-93 years), 2004-8. Fat mass and lean mass were divided by the square of height (kg/m²) and bone was expressed as whole body BMD (g/cm²). Linear regression models were used to determine time-related differences; models were adjusted for age and checked for interaction terms.

Results: Mean BMI increased from 26.2 kg/m² (95%CI 25.9-26.5) in 1993-7, to 26.9 kg/m² (95%CI 26.6-27.2) in 2004-7; mean fat mass increased 4.6%, from 10.11 kg/m² (95%CI 9.91-10.31), to 10.58 kg/m² (95%CI 10.34-10.81); mean lean mass increased 0.6%, from 14.84 kg/m² (95%CI 14.77-14.91), to 14.94 kg/m² (95%CI 14.86-15.02); and mean BMD increased from 1.152 g/cm² (95%CI 1.146-1.158), to 1.184 g/cm² (95%CI 1.178-1.190) (all p<0.05). These increases were observed for all ages.

Conclusions: Our findings reveal that over the period of one decade, accompanying increases in fat mass, increases in the musculoskeletal components of body composition have also contributed to the increase in BMI.

Disclosures: *Sharon Brennan, None.*

MO0344

Predictive Value of Historical Height Loss and Current Height/knee Height Ratio for prevalent Vertebral Fracture. Akiko Kuwabara^{1*}, Kiyoshi Tanaka², Kousei Yoh³. ¹Osaka Shoin Women's University, Japan, ²Kyoto Women's University, Japan, ³Hyogo Medical College, Sasayama Medical Center, Japan

Purpose: Height loss (HL), an important signs of vertebral fracture (VFX), can be a good indicator for the presence of VFX. Further evaluations such as BMD measurement or X-ray examination is recommended to those with HL. Much remain to be studied regarding HL. First, data from non-Caucasians are quite limited. Second, HL can be evaluated in two ways. Serial height measurement and historical HL (HHL) are useful for incident and prevalent VFX, respectively. Although the latter would be preferred for the case finding of subjects with VFX, these two methods have not been well distinguished. HHL, however, is sometimes unknown or unreliable, since it depends on the patients' recall. Then we have made a hypothesis that current height/knee height (CH/KH) ratio could be a good alternative to HHL, since KH is little affected by aging or VFX.

Subjects and methods: Study subjects were 154 patients visiting the outpatient orthopedic clinic (age 69.8±9.6 years). Current height was measured with a wall-mounted stadiometer. VFX was radiographically confirmed. HHL was defined as the difference between the patients' recalled maximal height and the current height.

Results: Patients with VFX had significantly larger HHL compared with those without it (median 7.0 cm vs 2.0 cm). The positive likelihood ratio (LR+) for VFX was flat at HHL less than 6.0 cm, and it was 5.3 (95%CI; 1.7-17.3) and 6.3 (95%CI; 2.9-14.2) for HHL from 6.1 to 8.0cm and >8.1 cm, respectively. In receiver operator characteristics analysis, the area under the curve (AUC) for the ability of HHL to detect VFX was 0.84 (95%CI; 0.77-0.90). When HHL>6.0 cm was adopted as the cut-off value for VFX, sensitivity was 59% (95%CI; 51-65%), and specificity was 90% (95%CI; 85-94). The LR+ for detecting multiple fractures was also high at HHL>6.0

cm. CH/KH ratio was significantly lower in patients with VFX than in those without it (3.2±0.1 vs 3.4±0.1). AUC for detecting VFX in CH/KH ratio was 0.73 (95%CI; 0.65-0.82). At CH/KH ratio < 3.2, sensitivity was 59% (95%CI; 51-65%), and specificity was 90% (95%CI; 85-94). According to the multiple regression analyses, HHL and CH/KH ratio were both significant predictors for VFX.

Conclusions: The appropriate threshold value detecting VFX for HHL was considered to be 6.0cm in Japanese population. Additionally, CH/KH ratio can also be a marker for VFX prediction, when data on the HHL are unavailable.

Disclosures: *Akiko Kuwabara, None.*

MO0345

The Associations between Serum Lipids and Bone Turnover Markers in Men Aged 45 Years and Over: Analysis of NHANES 1999-2002 Data. Maryam Hamidi^{1*}, Shabbir Alibhai², Moira Kapral², LIANNE TILE³, Angela Cheung². ¹University of Toronto/University Health Network-TGH, Canada, ²University Health Network, Canada, ³University of Toronto, Canada

Purpose: Recent data suggest that serum lipids may be associated with bone mineral density and bone turnover markers. Very few studies have examined these relationships with bone turnover markers. The objective of our study was to examine the associations between serum total cholesterol, high-density lipoprotein cholesterol (HDL), low-density lipoprotein cholesterol (LDL), and triglycerides, and serum bone-specific alkaline phosphatase (BAP, a biomarker of bone formation) and urinary N-Telopeptides/Creatinine (uNTx/Cr, a biomarker of bone resorption) in a population-based cohort.

Methods: We used cross-sectional data from the National Health and Nutrition Examination Survey 1999-2002 cycles. We included men aged ≥ 45 years who were not taking steroids, osteoporosis treatment medications and statins; were free from kidney and liver disease, cancer, rheumatoid arthritis; and were fasting ≥ 8.5 hours prior to examination. Natural logarithmic transformation of serum lipids and bone turnover markers was performed to reduce the within sample variability and to avoid inappropriate exclusion of outliers. Weighted multiple regression models with adjustments for relevant confounders were used to examine the relationship between serum lipids and bone turnover markers.

Results: 723 men were eligible and included in the analysis. The mean age was 57.6±0.4 years. We found significant quadratic relationships between LDL and BAP (p= 0.048) and total cholesterol and BAP (p=0.028). HDL had an inverse linear association with BAP (p=0.0025), while triglycerides had a positive linear association with BAP (p=0.0003). Adjustments for age, ethnicity, physical activity, BMI, dietary supplement intake, alcohol intake and nicotine exposure did not change these results. There were no associations between serum lipids and uNTx/Cr.

Conclusions: We found that higher HDL concentrations were associated with lower bone formation, whereas higher triglycerides concentrations were associated with higher bone formation. Based on our results, the relationships between LDL and bone formation, and total cholesterol and bone formation are not linear in men aged 45 and over. Further studies are needed to confirm these findings and to explore the underlying reasons for such associations.

Disclosures: *Maryam Hamidi, None.*

MO0346

The Frindex Model: High-Risk Patients Based on FRAX Cut-off Points From A Cohort Of Spanish Women Followed For 10 Years. Enrique Casado^{1*}, Rafael Azagra², Gloria Encabo³, Amaya Aguvé⁴, Jesús Pujol-Salud⁵, Juan Carlos Martín-Sánchez⁶, Emili Gené⁷, Marta Zwart⁸, Francesc López-Expósito⁹, Genís Roca¹⁰, Silvia Güell¹¹, Núria Puchol¹². ¹University Hospital Parc Taulí, Spain, ²Clinical Pharmacology, Health Centre Badia del Vallés, Universitat Autònoma de Barcelona, USR MN-IDIAP Jordi Gol, Spain, ³Nuclear Medicine, Hospital Vall d'Hebron, Spain, ⁴Health Centre EAP Granollers Centre, Spain, ⁵Health Centre EAP Balaguer, Universitat de Lleida, Spain, ⁶Bioestatistics, Universitat Internacional de Catalunya, Spain, ⁷Emergency, University Hospital Parc Taulí, Spain, ⁸Health Centre, EAP Girona-2, Spain, ⁹Health Centre, EAP Bon Pastor, Spain, ¹⁰Health Centre EAP Sant Llàtzer, Spain, ¹¹Health Centre EAP Montcada, Spain, ¹²Clinical Pharmacology, Health Centre Badia del Vallés, Spain

Purpose: To develop an accurate model of fracture risk assessment based on FRAX, using a cohort of Spanish women followed for 10 year and to establish the best thresholds for indication of DXA and treatment (high-risk patients).

Methods: Longitudinal multicenter study. Women between 40-90 years from FRINDEX cohort (35,000 people in Barcelona) had completed a DXA and an extensive questionnaire on risk factors for fracture at baseline, who had been followed for 10 years and who had not received any treatment for osteoporosis were selected. New self-reported osteoporotic fractures contrasted with electronic or clinical reports were collected. The risk of major osteoporotic fracture for Spanish population based on FRAX (with and without DXA) was assessed in all women. We

calculated the Area Under the curve (AUC) for both DXA and 10-year risk of major fracture by FRAX, to determine the best cut-off point to indicate DXA or establish osteoporotic treatment.

Results: We selected 816 women, mean age 56.8 ± 8.2 years. After 10 years, 76 women (9.3%) had suffered 95 osteoporotic fractures, of which 49 (6%) were major (15 hip, 4 vertebral, 13 humerus and 17 distal radio). Women who suffered a major osteoporotic fracture during the follow-up were significantly older ($p < 0.001$), had more previous fractures ($p < 0.001$), had suffered more falls ($p = 0.016$), and had a higher prevalence of osteoporosis by DXA (60% vs 15%) ($p < 0.001$). The AUC-ROC for predicting future fracture was better for FRAX major fracture without and with BMD (0.736 and 0.733 respectively) than for DXA using T-score of femoral neck (0.697). The FRIDEX model was created selecting the best cut-off point for the 10-year absolute risk of major fracture by FRAX without BMD. This model classifies women as a low risk of fracture (10-year risk or major fracture $< 5\%$), intermediate risk (5-7.5%) and high risk (7.5%). In women with intermediate risk the model reassess the probability of fracture including the T-score of femoral neck by DXA in the FRAX tool and classify these patients as low or high risk for fracture. The application of this model could save 82% of DXA scans and avoid up to 31% of unnecessary treatments.

Conclusions: The FRIDEX model based on FRAX cut-off points, compared with DXA based model, has a better or equal discriminative ability to detect women who will suffer osteoporotic fractures over a 10-year period. This model could save unnecessary DXA and osteoporotic treatments.

| Risk of fracture according FRIDEX Model | 10-year absolute risk of major fracture (FRAX) | Women with major fracture after 10 years of follow-up in FRIDEX cohort | Women with major fracture/Total women |
|---|--|--|---------------------------------------|
| Low | $< 5\%$ | 3,6 % | 24/673 |
| Intermediate | $\geq 5\% y < 7,5\%$ | 13,7 % | 10/73 |
| After DXA...Low | $< 7\%$ | 10,7 % | 6/56 |
| After DXA...High | $\geq 7\%$ | 23,5 % | 4/17 |
| High | $\geq 7,5\%$ | 21,4 % | 15/70 |

Table 1: FRIDEX Model

Disclosures: Enrique Casado, None.

This study received funding from: Sponsored by FEDER, IS Carlos III Grant. Science Ministry of Spain. IDIAP Jordi Gol, Department of Health, Government of Catalonia, Spain

MO0347

The Incorporation of Support Vector Machines and Hip Geometric Structure Assessments in the Development of Hip Fracture Risk Prediction Model. Zhao Chen^{*1}, Peng Jiang², Chengcheng Hu², Leslie Arendell³, John Robbins⁴, Samy Missoum². ¹University of Arizona College of Public Health, USA, ²University of Arizona, USA, ³University of Arizona Mel & Enid Zuckerman College of Public Health, USA, ⁴University of California, Davis Medical Center, USA

Background: Hip fracture prediction models, such as FRAX, have been developed and widely used. Robbins and colleges (Robbins et al 2007) have shown that in the Women's Health Initiative (WHI), collectively, 11 predictors including general health, height, weight, fracture after age 55 years, race/ethnicity, physical activity, currently smoking status, corticosteroid use, diabetes, age, and parents have had a history of a broken hip, may generate a prediction with area under the curve (AUC) being 80% for 5-year hip fracture risk. The prediction property of this model was less accurate (AUC% = 71%) in the participants of the WHI bone mineral density (BMD) cohort but when BMD was added into the model, AUC% reached 80%.

Objectives: The purpose of this study was to investigate the utility of support vector machines (SVM) technique and hip geometric structure assessments in predicting 5-year and 10-year hip fracture risk in the participants of the WHI bone mineral density cohort.

Methods: SVM was used to develop the prediction models. SVM is a powerful classification technique that is able to extract, in a high dimensional space, complex nonlinear "decision functions" between two classes of data, such as fractured and non-fractured hips. It does not have any model assumptions and is often referred as a machine learning approach. Hip geometric structures were assessed on hip scans from the Dual-energy X-ray Absorptiometry using T. Beck's hip structure analysis (HSA) approach. Cross-sectional areas, bone width, section-modulus, cortical thickness and buckling ratio were assessed in three regions: femoral neck, intertrochanter and shaft. The participants in the WHI observational study were used to develop the model and women from the WHI clinical trials were used as the validation group. The 11 predictors in the WHI model and measurements from HSA were used to develop SVM models for hip fracture prediction.

Results: Preliminary results from the validation suggest that the 11 predictors plus HSA model from SVM may generate a good 5-year hip fracture prediction (AUC% = 0.82), and an even better 10-year hip fracture prediction (AUC% = 0.86).

Conclusion: The preliminary study findings suggest that the SVM approach is an alternative method that should be further explored and HSA may be considered in hip fracture prediction. Comparisons should be done to see if the accuracy of hip fracture prediction can be improved by the SVM approach and the HSA measurements.

Reference: Robbins J et al. Factors associated with 5-year risk of hip fracture in postmenopausal women. JAMA 2007, 298 (20): 2389-2398.

Disclosures: Zhao Chen, None.

MO0348

Prevalence of Low Bone Mineral Density (BMD) in 186 Swiss Women with Anorexia Nervosa. Sigrid Jehle-Kunz^{*1}, Markus Wegmüller², Romain Perrelet², Kurt Lippuner². ¹Osteoporosis Policlinic, University of Bern, Switzerland, Switzerland, ²Osteoporosis Policlinic, University of Bern, Switzerland

Introduction: Guidelines regarding the assessment of bone health in the work-up of Anorexia Nervosa (AN) differ among centers and countries. This study aimed at describing the BMD characteristics in all patients with presumed AN referred for bone health assessment to the Osteoporosis Policlinic of the University Hospital of Bern, Switzerland, between 1994 and 2011.

Methods: All female patients with presumed AN and available BMD results (N=186) were retrospectively analyzed. BMD was measured by DXA at the lumbar spine (LS) and the femoral neck (FN) in all patients and at distal tibial epiphysis (TEPI) and tibial diaphysis (TDIA) in a subset of patients. Patients were categorized into three age groups: before peak bone mass (PBM) acquisition (Group I, age ≤ 20 years), during the plateau phase of PBM (Group II, 21-50 yrs), and postmenopausal (Group III, > 50). As recommended, a Z-score ≤ -2.0 SD (1) and a T-score ≤ -2.5 SD (2) were used as thresholds for pathologically low BMD before and after the age of 50 years, respectively.

Results: (summarized in attached Table1)

Conclusion: In women with AN, low BMD was highly prevalent at all sites and at any age, suggesting that these women should deserve encompassing bone health diagnostic work-up for the assessment of their individual fracture risk, including BMD measurements at all sites.

References:

- 2007 ISCD Official Positions (www.ISCD.org).
- Assessment of fracture risk and its application to screening for postmenopausal osteoporosis. Report of a WHO Study Group. Geneva, World Health Organization, 1994 (WHO Technical Report Series, No. 843).

Table 1.

| | Group I (≤ 20 yrs) | Group II (21-50 yrs) | Group III (> 50 yrs) |
|---|--------------------------|--------------------------|--------------------------|
| Nr of women with AN | n=36 | n=120 | n=30 |
| Median age in years (range) | 17 (10 - 20) | 31 (21 - 50) | 56 (51 - 77) |
| Median Body Mass Index in kg/m ² (range) | 16.0 (12.3 - 19.5) | 16.6 (11.5 - 19.6) | 17.5 (12.9 - 19.6) |
| Median duration of AN in months (range) | 24 (1 - 96) | 144 (9 - 420) | 420 (132 - 660) |
| Percentage of patients with low BMD at | (Z-score ≤ -2.0 SD) | (Z-score ≤ -2.0 SD) | (T-score ≤ -2.5 SD) |
| LS | 50.0% | 60.0% | 40.0% |
| FN | 36.1% | 53.3% | 30.0% |
| TDIA | 10.0% | 12.5% | 23.3% |
| TEPI | 20.0% | 45.0% | 43.3% |
| At any site | 50.0% | 75.8% | 63.3% |

Table 1

Disclosures: Sigrid Jehle-Kunz, None.

MO0349

Bone Mass and Vitamin D Levels in Women with a Diagnosis of Fibromyalgia. Francisco Mateos¹, Carmen Valero², Jose Manuel Olmos², Julio Castillo³, Benigno Casanueva⁴, Jesús González-Macías^{*2}.

¹Department of Internal Medicine, University Hospital Marqués de Valdecilla, University of Cantabria, RETICEF, IFIMAV., Spain, ²Department of Internal Medicine, Hospital Universitario Marqués de Valdecilla-IFIMAV, Universidad de Cantabria, RETICEF., Spain, ³Centro de Salud "José Barros". Camargo. University of Cantabria., Spain, ⁴Rheumatology, Santander, Spain

Introduction: Several studies have described an association between fibromyalgia, on the one hand, and osteoporosis and/or hypovitaminosis D on the other. This association, however, has not been confirmed by other studies. Of note, the studies have usually been carried out in small size samples and they have excluded postmenopausal women.

Objective: To study this association in a larger sample of fibromyalgia patients including both pre and postmenopausal women.

Material and Methods: 205 patients and 205 healthy controls were included in the study. Patients were recruited from a private clinic specializing in fibromyalgia. Controls were enrolled from a Primary Care Center; they were matched with patients by age and by the moment of inclusion in the study, to avoid seasonal vitamin D differences. BMD (DXA, Hologic QRD 4500) and serum 25OHD, iPTH, P1NP and CTX (Elecys 2010) were measured.

Results: Mean age was 55.5 ys. Two thirds were postmenopausal. Mean time since diagnosis was 5.4 ± 6.4 ys. BMD at the lumbar spine was 0.971 ± 0.146 g/cm² in patients and 0.970 ± 0.132 g/cm² in controls; the corresponding figures at the femoral neck were 0.780 ± 0.122 g/cm² and 0.785 ± 0.117 g/cm² respectively (ns). Adjusting for

potential confounders did not alter the lack of differences. 25OHD levels were 23.0 ± 9.5 ng/ml in patients and 24.1 ± 9.6 ng/ml in controls (ns). A different seasonal 25OHD pattern was seen in patients and controls, with a significant increase in July-September in the latter (up to 26.9 ± 9.7 ng/ml.) but not in patients (23.2 ± 7.3 ng/ml.), so that differences in this term were significant ($p=0.03$). PTH concentration was 51 pg/ml in patients and 48 pg/ml in controls ($p=0.034$). This difference was greater in postmenopausal women: 54 ± 17 and 48 ± 16 pg/ml; $p=0.008$. No seasonal change in PTH was seen in patients, while a decline was observed in controls. In fact, PTH differences between groups were only appreciated in the central months of the year. P1NP or CTX were similar in both groups.

Conclusions: No differences in BMD or 25OHD were seen between patients and controls. Our results suggest that the association previously reported between fibromyalgia and either osteoporosis or hypovitaminosis D is not due to intrinsic mechanisms linking these disorders. Rather, they are probably due to lifestyle differences.

Disclosures: *Jesús González-Macías, None.*

MO0350

Cross Sectional Study of Bone Health in Children with Cystic Fibrosis in Quebec, Canada. Isabelle Rousseau-Nepton^{*1}, Catherine St-Laurent Lemerle², Marc Fillion³, Marcel Milot⁴. ¹Montreal Children's Hospital, Canada, ²Centre Hospitalier Universitaire de Québec, Canada, ³Hôpital Maisonneuve-Rosemont, Canada, ⁴Centre de Santé et de Services Sociaux de Chicoutimi, Canada

Background: Controversy exists regarding bone health status of children with cystic fibrosis (CF). Our objective was to assess bone density and fracture rates within a genetically heterogeneous population in the province of Quebec. **Methods:** All children followed in 2 CF clinics (Quebec City and Chicoutimi) were invited to take part of the study. Lumbar and total body bone mineral densities (BMD) were examined using dual energy x ray absorptiometry (Hologic QDR 4500 and LUNAR). Determinants of bone health were collected including, but not limited to, mutations in the CFTR gene, corticosteroid exposure, calcium and vitamin D intakes, level of physical activity, anthropometrics and serum and urine minerals and 25-OH-D. In addition, a thoracolumbar spine anteroposterior radiograph was done for each child. **Results:** To date, about 100 children have been recruited and data on 19 children from 1 centre (Chicoutimi) are presented. The cohort was constituted of Caucasians, 63 % of girl and 37 % of boys, with ages ranging from 6 and 16 years old (mean 10 years). Mutations analysis revealed that 3 patients were homozygote $\Delta F508$, 9 patients were heterozygote $\Delta F508$ and 7 patients had different mutations. The majority of the children had a mild pulmonary disease (15/19), a normal weight and an insufficiency in vitamin D (14/19). Bone ages were concordant with chronological ages. The BMD Z scores were all normal except for one case; the mean was negative (-0.74) and values ranged from -2 to 1.2. BMD were corrected for height. Bone mineral apparent densities (BMAD) were calculated. No patients presented spine fractures on thoracolumbar spine radiographs, but 3 reported fractures of superior extremities. **Conclusions:** To date, we report a normal bone health status in this subsample of children with a mild CF. No fragility fractures were described. Future analysis will be done with the entire cohort to identify the best predictors of BMD in CF children. Moreover, a link between BMD and CF mutations will be sought.

Disclosures: *Isabelle Rousseau-Nepton, None.*

MO0351

Erythropoiesis Alters Mesenchymal Differentiation and Decreases Osteogenesis in a Thalassemia Mouse Model by Mechanisms that Involve Interactions with Hematopoietic Progenitors and Erythropoietin Signaling. Maria Vogiatzi^{*1}, Zhiwei Yang², Adele Boskey³, F. Patrick Ross³. ¹New York Presbyterian Hospital, Weill Cornell Medical College, USA, ²Weill Cornell Medical College, USA, ³Hospital for Special Surgery, USA

Thalassemias are chronic congenital anemias caused by a defect in hemoglobin synthesis that results in increased erythropoietin (EPO) levels due to anemia and expansion of defective erythroids. Thalassemias are associated with high rates of osteoporosis as a result of decreased bone formation. To determine mechanisms by which erythropoiesis leads to bone loss in thalassemia, we studied changes in mesenchymal stem cell (MSC) commitment using the *th3/+* mouse model of β thalassemia intermedia, which has the hematological and bone abnormalities seen in patients.

Mesenchymal stem cells (MSC) cultures from wild type (wt) and *th3/+* under osteogenic or adipogenic media. MSC cocultures with hematopoietic progenitors (HP) from wt and *th3/+*. Changes in osteogenesis or adipogenesis were determined by CFU numbers and qPCR for Runx2, bone sialoprotein, osterix, osteocalcin and PPAR γ .

i) Decreased osteogenesis and increased adipogenesis was seen in MSC cultures from *th3/+* compared to wt. ii) Decreased osteogenesis in *th3/+* was reversed when MSC cultures were treated with either a monoclonal EPO antibody (EPOA) or soluble EPO receptor (EPOR). iii) Using qPCR, EPO expression was increased in MSC from *th3/+* compared to wt, while EPOR was expressed in low levels in MSC. iv) To determine the role HP on MSC differentiation, we co-cultured MSC from wt and *th3/+* with HP from wt and *th3/+*, and identified that Lin-Sca+ckit+ (LSK) cells from *th3/+* alter MSC fate and decrease osteogenesis compared to wt. Further studies are under

way to determine if erythroid progenitors also affect MSC fate. v) Non Adherent BM cells (NABMC), which include a wide range of progenitors, from wt and *th3/+* were then co-cultured with wt MSC in the presence of EPOA and its control. NABMC from *th3/+* decreased osteogenesis, and their effect was reversed by EPOA treatment, suggesting that EPO can also alter MSC differentiation in *th3/+* through interactions with HP.

Thalassemia is a disease model of chronic stress erythropoiesis. Using the *th3/+* thalassemia mouse, we observed that LSK alter MSC commitment resulting in decreased osteogenesis, while the role of erythroid progenitors is under investigation. HP-stroma interactions are regulated at last in part by EPO. Finally, our data indicate that EPO produced by thalassemia MSC alters osteogenesis via direct EPOR signaling on MSC.

Disclosures: *Maria Vogiatzi, None.*

MO0352

Longitudinal Changes in Trabecular Bone Microarchitecture in Postmenopausal Women With and Without Type 2 Diabetes. Janet Pritchard^{*1}, Lora Giangregorio², Stephanie Atkinson¹, Karen Beattie¹, Dean Inglis¹, George Ioannidis¹, Hertzel Gerstein¹, Zubin Punthakee¹, Jonathan Adachi³, Alexandra Papaioannou⁴. ¹McMaster University, Canada, ²University of Waterloo, Canada, ³St. Joseph's Hospital, Canada, ⁴Hamilton Health Sciences, Canada

Purpose: Women with type 2 diabetes (T2D) experience a greater loss of bone mineral density (BMD) compared to controls. How trabecular bone microarchitecture changes in the face of greater BMD loss in women with T2D is unknown. We aimed to quantify and compare 2-year changes in trabecular bone network hole number and size, apparent trabecular thickness (Tb.Th), number (Tb.N) and separation (Tb.Sp), and network connectivity in women with and without T2D.

Methods: Postmenopausal women ≥ 65 years who were not taking medications known to affect bone were enrolled. A 1-T peripheral MRI scanner (OrthOne, GE) was used to acquire axial scans of the distal radius (resolution $195\mu\text{m} \times 195\mu\text{m} \times 1000\mu\text{m}$). Scans were analyzed for trabecular bone microarchitecture outcomes listed above using in-house software (OsteoQ). Baseline scans were matched to followup scans using registration software (Analyze, Mayo Clinic). DXA (Hologic, Discovery) was used to obtain proximal femur and lumbar spine BMD. We report the percent change in all of the above variables for the two groups. Multivariable linear regression models were used to assess associations between group and percent change in microarchitecture variables. Covariates included ethnicity, history of an osteoporotic fracture and change in the number of medications since baseline. An alpha level <0.05 was considered significant.

Results: Of the participants enrolled in the study at baseline, 15/30 participants with T2D (mean \pm SD age at baseline 71.1 ± 4.8 years), and 22/30 participants without T2D (age at baseline 70.7 ± 4.9 years) completed the followup visit. After adjustment for covariates, women with T2D had a significantly higher percent increase in the number of holes in the trabecular bone network (mean \pm SD $7.9 \pm 4.5\%$) compared to controls ($-6.2 \pm 3.9\%$, $p=0.036$). There was no difference in the change in hole size in women with and without T2D (mean \pm SD $-0.5 \pm 4.6\%$, vs. $2.3 \pm 4.0\%$, $p=0.680$). Changes in BMD and other microarchitecture variables were not different between groups.

Conclusions: In this study, changes in the size of trabecular bone network holes in women with T2D were not different than in women without T2D, but there was a greater increase in the number of trabecular bone network holes in women with T2D. Our study is limited by small sample size and larger studies should investigate whether trabecular bone loss is accelerated in women with T2D.

Disclosures: *Janet Pritchard, None.*

MO0353

Renal Safety of 2-hour Pamidronate (PAM) Infusion for Osteogenesis Imperfecta (OI) Patientes. Telma Oliveira^{*1}, Maria Cristina Andrade², Barbara Peters¹, Fernanda Reis³, João Thomás Carvalhaes², Marise Lazaretti-Castro¹. ¹Bone & Mineral Unit, Division of Endocrinology-UNIFESP, Brazil, ²Department of Pediatric Nephrology-UNIFESP, Brazil, ³Department of Radiology-UNIFESP, Brazil

The most widely used treatment schedule with cyclic intravenous PAM in OI patients has been done for 3 days in a 3-4 hour infusion. The aim of this study is to demonstrate that 2-hour and 1-day infusion may be safe. A single center prospective trial was carried out to examine the renal safety of 2-hour intravenous PAM infusion. A total of 18 children and adolescents with OI type I, III and IV were included. The average age was 8.89 ± 4.12 years and 55.6% were female and 44.4% male. The kidney function was done before and during the treatment with serum creatinine, urine microalbuminuria sample, urine protein, kidney ultrasound examination and glomerular filtration rate (GFR). A total dose of 2mg/Kg of PAM every 4 months (a total of 2 doses) was administered on these patients. The kidney function was monitored for 0, 2, 8, 24 hours and 7-day after the PAM infusion. During this monitoring time it was observed no renal deterioration in these patients. In the first infusion, the average serum creatinine baseline was 0.38 ± 0.12 and 0.37 ± 0.11 mg/dl after a 7-day period ($p=0.53$). There was a slight transitory increase on the creatinine

between baseline and 8-hour (0.38 ± 0.12 vs. 0.43 ± 0.12 , $p=0.014$). However, the creatinine level was recovered from 8-hour to 7-day (0.43 ± 0.12 vs. 0.37 ± 0.11 , $p=0.001$). In the second infusion, there were no significant changes in creatinine level between the baseline and 7-day (0.38 ± 0.14 vs. 0.40 ± 0.14 , $p=0.56$). It was also found lower level of baseline creatinine in all OI patients. GFR followed the same pattern, there was a slight transitory decrease, but still in the normal range and it was recovered in a 7-day period in both infusions. The GFR average rates of the first infusion between baseline to 8-hour and 7-day were 167.82 ± 31 vs. 147.67 ± 28 vs. 170.44 ± 34 ml/min/1.73m², $p=0.02$ e $p=0.004$). The highest individual variation in baseline creatinine was an increase of 67.68% in 8 hours followed by a reduction of 61.9% in an 8-24-hour period. No significant differences were observed in microalbuminuria, urea, sodium, potassium. These results suggest that there were no events of renal deterioration with 2-hour PAM infusion in OI patients. Regarding safety, short PAM infusion was generally well tolerated and the incidence of clinical or laboratory adverse experiences were similar to 4-hour PAM infusion described in the literature. The low level of baseline creatinine should be related with low lean body mass found in OI patients.

Disclosures: *Telma Oliveira, None.*

MO0354

Serum 25 Hydroxyvitamin D and Bone Mineral Density in Patients with Erythropoietic Protoporphria. Gonzalo Allo¹, Guillermo Martinez Diaz-Guerra¹, Rafael Enriquez de Salamanca², Federico Hawkins³. ¹University Hospital 12 Octubre, Spain, ²Research Center, University Hospital 12 de Octubre, Spain, ³Hospital Universitario, Spain

Background: Erythropoietic protoporphyria (EPP) is a rare inherited photodermatosis with severe painful cutaneous photosensitivity. Patients must avoid sun exposure and they must use adequate clothing and sunscreens. Vitamin D is mostly synthesized within the skin under the influence of ultraviolet B radiation. The objective of our study is to show evidence of vitamin D deficiency/insufficiency in a Spanish EPP population, and evaluate the impact of these levels in serum mineral metabolism and bone mineral density.

Methods: In a cross-sectional study of 10 EPP patients (median age 25; range 22-55, 4 male and 6 female), we assessed: Clinical features, biochemical values (including serum 25 hydroxyvitamin D) and bone mineral density measurements by dual x-ray absorptiometry. Statistical analyses were performed using Wilcoxon signed-rank test and Spearman's rho correlation.

Results: Median serum 25(OH)D level was 19.65 ng/ml [17.50;24.80]. 4 patients had 25(OH)D in insufficiency range (20-30 ng/ml) and 5 patients in the deficiency range (<20 ng/ml). Lumbar T-score median levels were in the osteopenia range in both females

(-1.50 [-2.30;-1.0]) and males (-1.90 [-2.40;-0.70]). Also in the female group femoral neck T-score were in the osteopenia range (-1.20 [-1.60;-0.60]). There were no significant differences in DXA values between 25(OH)D deficient patients (n=5) and those who had values above 20 ng/ml (n=5).

Conclusions: Low bone mass and vitamin D deficiency are frequently found in patients with EPP. Bone metabolism studies should be recommended in these patients, as well as calcium and vitamin D supplementation.

Table 1. Clinical characteristics. Data are given as median [IQR] or n (%).

| Characteristic | All patients (n=10) | Females (n=6) | Males (n=4) |
|--|---------------------|---------------|---------------|
| Age | 25 [22, 55] | 25 [23, 34] | 42 [14.5, 62] |
| Duration of the disease (years) | 15 [10, 22] | 16 [14, 19] | 12 [3, 42] |
| Family History | 3 (30%) | 2 (33.3%) | 1 (25%) |
| Osteoporosis | | | |
| Calcium and vitamin D previous treatment | 1 (10%) | 1 (16.6%) | 0 (0%) |
| sunlight exposure (minutes) | 10 [5, 17.5] | 22 [21, 24] | 12 [5, 19] |

Table 1. Clinical Characteristics

Table 2. Biochemical values. Data are given as median [IQR].

| Biochemical values | All patients (n=10) | Females (n=6) | Males (n=4) |
|------------------------------|--------------------------|--------------------------|--------------------------|
| Calcium (mg/dl) | 9.50 [9.20; 9.60] | 9.60 [9.40; 9.80] | 9.20 [8.80; 9.40] |
| 25(OH)D (ng/ml) | 19.65 [17.50, 24.80] | 19.50 [17.50; 24.00] | 21.55 [14.65; 29.05] |
| iPTH (pg/ml) | 41.60 [29.60; 51.00] | 33.50 [18.40; 41.60] | 70.40 [51.00; 71.80] |
| Osteocalcin (ng/ml) | 21.55 [14.60; 44.91] | 21.55 [13.22; 44.91] | 25.60 [16.51; 40.95] |
| BAP (ng/ml) | 19.25 [15.60; 21.75] | 19.00 [14.80; 21.80] | 19.49 [16.39; 21.70] |
| β-CTX (ng/ml) | 0.36 [0.28; 0.63] | 0.34 [0.20; 0.63] | 0.45 [0.30; 0.78] |
| FEP (µg/dl) | 719.00 [455.00; 1207.00] | 774.00 [455.00; 1207.00] | 719.00 [469.00; 1156.50] |
| Serum protoporphyrin (µg/dl) | 19.00 [13.00; 39.00] | 19.50 [16.00; 39.00] | 15.00 [8.50; 39.50] |

- Abbreviations: iPTH: intact parathyroid hormone; BAP: bone alkaline phosphatase; β-CTX: Beta-crossLaps; FEP: Free erythrocyte protoporphyrin.

Table 2. Biochemical values

Table 3. Lumbar spine, femoral neck and total hip DXA values. Data are given as median [IQR].

| DXA values | All patients (n=10) | Females (n=6) | Males (n=4) |
|---------------------------------------|----------------------|----------------------|----------------------|
| Lumbar spine BMD (g/cm ²) | 0.85 [0.80; 0.94] | 0.85 [0.80; 0.94] | 0.86 [0.71; 0.93] |
| Lumbar T-score | -1.70 [-2.35; -0.85] | -1.50 [-2.30; -1.0] | -1.90 [-2.40; -0.70] |
| Lumbar Z-score | -1.15 [-2.10; 0.60] | -1.25 [-2.10; 0.10] | -0.15 [-1.80; 1.20] |
| Femoral neck BMD (g/cm ²) | 0.71 [0.64; 0.83] | 0.69 [0.64; 0.78] | 0.83 [0.53; 0.93] |
| Femoral neck T-score | -0.90 [-1.75; -0.10] | -1.20 [-1.60; -0.60] | -0.20 [-3.00; 0.00] |
| Femoral neck Z-score | -0.4 [-1.65; 0.60] | -0.60 [-1.40; -0.20] | 0.00 [-2.00; 1.20] |
| Total hip BMD (g/cm ²) | 0.85 [0.77; 1.01] | 0.84 [0.80; 0.86] | 0.96 [0.38; 1.07] |
| Total hip T-score | -0.75 [-1.40; 0.25] | -0.80 [-1.10; -0.70] | -0.50 [-2.90; 1.00] |
| Total hip Z-score | -0.65 [-1.20; 0.60] | -0.80 [-1.10; 0.00] | -0.50 [-1.30; 2.20] |

- Abbreviations: DXA: Dual X-Ray Absorptiometry; BMD: Bone mineral density.

Table 3. Lumbar spine, femoral neck and total hip DXA values

Disclosures: *Gonzalo Allo, None.*

MO0355

Associations Between Bone Density and Geometry and Prevalent Fractures Among Individuals with Spinal Cord Injury. Deena Lala¹, B. Catharine Craven², Lehana Thabane³, Alexandra Papaioannou⁴, Jonathan Adachi⁵, Milos Popovic⁶, Lora Giangregorio^{*1}. ¹University of Waterloo, Canada, ²Toronto Rehabilitation Institute, Canada, ³McMaster University, Canada, ⁴Hamilton Health Sciences, Canada, ⁵St. Joseph's Hospital, Canada, ⁶University of Toronto, Canada

Objectives: Low areal bone mineral densities (aBMD) of the hip and knee regions are associated with lower extremity fracture risk in individuals with spinal cord injury (SCI); however, the contribution of trabecular BMD (TbvBMD) and cortical bone

geometry to fracture risk is unclear. We examined whether indices of bone density and geometry measured via peripheral quantitative computed tomography (pQCT) can discriminate between SCI participants with or without a prior lower extremity fragility fracture.

Methods: A nested case-control study was performed using data from a two-year prospective cohort study (CIHR #86521). Adults with chronic [duration of injury (DOI) \geq two years] traumatic SCI (C1-T10 AIS A-D) were included. The cause, location, and date of post injury lower extremity fragility fractures were obtained and verified. DXA was used to measure aBMD of the distal femur and proximal tibia, while pQCT was used to measure TbvBMD, cortical thickness (CTh), buckling ratio (BR), cross-sectional moment of inertia (CSMI), and polar moment of inertia (PMI). Univariate analysis determined correlates of prevalent fragility fractures (age, gender, motor complete injury, DOI, and past bisphosphonate use). Odds ratios (OR) per standard deviation (SD) decrease in bone density and geometry and 95% confidence intervals (CI) relating bone density and geometry to fracture prevalence were obtained with logistic regression analysis.

Results: Among 68 adults (mean age 49.2 ± 11.4 ; 19 females; 43 AIS A-B) with SCI, there were 18 cases with fractures and 49 controls without fracture. Individuals without prevalent fractures had significantly greater aBMD ($p < 0.0001$) and bone geometry ($p < 0.05$) than those with fractures. Every SD decrease in aBMD and TbvBMD was significantly associated with increased fracture prevalence after adjusting for motor complete injury (see Table). However, after adjusting for aBMD at the distal femur and motor complete injury, all the indices of bone geometry were no longer significantly correlated with fracture status.

Conclusion: Indices of bone density and geometry are associated with prevalent fractures; however bone density may be the strongest correlate of prevalent fracture in individuals with SCI when controlling for motor complete (AIS A-B) impairment. Fracture risk prediction models require further validation in a larger sample and should control for impairment.

Table: Odds ratios for indices of bone strength and prevalent fractures in individuals with SCI

| | Fractures (Unadjusted) | | Fractures (Adjusted) | |
|--|------------------------|---------|----------------------|---------|
| | OR (95% CI) | P-Value | OR (95% CI) | P-Value |
| aBMD Distal Femur (g/cm ³) | 0.20 (0.06-0.49) | 0.003* | 0.19 (0.05-0.55) | 0.006* |
| aBMD Proximal Tibia (g/cm ³) | 0.16 (0.05-0.42) | 0.011* | 0.17 (0.04-0.50) | 0.004* |
| TbvBMD (mg/cm ³) | 0.15 (0.03-0.44) | 0.004* | 0.14 (0.03-0.53) | 0.013* |
| CTh (mm) | 0.35 (0.15-0.72) | 0.008* | 0.45 (0.18-0.96) | 0.056 |
| BR | 1.91 (1.06-3.81) | 0.041* | 1.52 (0.81-3008) | 0.203 |
| CSMI (mm ⁴) | 0.40 (0.14-0.88) | 0.048* | 0.50 (0.17-1.12) | 0.138 |
| PMI (mm ⁴) | 0.28 (0.08-0.71) | 0.020* | 0.34 (0.10-0.90) | 0.053 |

Areal bone mineral density, aBMD; Trabecular volumetric bone mineral density, TbvBMD; Cortical thickness, CTh; Buckling Ratio, BR; Cross-sectional moment of inertia, CSMI; Polar moment of inertia, PMI

*Odds ratio per SD decrease (all variables except BR which is per SD increase), adjusted for motor complete injury

* $P < 0.05$

Table

Disclosures: *Lora Giangregorio, None.*

MO0356

The Proinflammatory Cytokine TNF- α Modifies the Resorptive Behaviour of Newly Generated Osteoclasts in vitro from Patients with Acute Charcot Foot.

Nina Petrova^{*1}, Peter Petrov², Michael Edmonds¹, Catherine Shanahan³.
¹Diabetic Foot Clinic, King's College Hospital, United Kingdom,
²Department of Materials, Imperial College, United Kingdom, ³King's College London, United Kingdom

Aims: To investigate the role of TNF- α as a modulator of osteoclastic activity in vitro in patients with acute Charcot foot.

Material and methods: Peripheral blood mononuclear cells were isolated from 9 patients with Charcot foot, 7 diabetic and 6 healthy controls and cultured in vitro on bovine disks for 21 days in the presence of (1) macrophage-colony stimulating factor (M-CSF) and receptor activator of nuclear factor κ B ligand (RANKL) and (2) M-CSF, RANKL and neutralising antibody to TNF- α (na-TNF- α). Bovine discs were stained with toluidine blue. Resorption was measured by two methods: (1) median area of resorption at the surface by image analysis (%) and (2) median area of resorption under the surface (μ m²) measured by Dektak 150 Surface Profiler and calculated using Origin Pro 8.6. Five scans per disc were carried out. On average, 60 pits per condition per subject were analyzed.

Results: The newly generated osteoclasts in Charcot patients exhibited increased resorbing activity in cultures with M-CSF+RANKL. The percentage of osteoclastic resorption was significantly greater in Charcot compared with diabetic patients (40.1% (10.6) vs 12.3% (17.9), median (interquartile range); $p = 0.004$) and also greater in Charcot patients compared with healthy subjects (40.1% (10.6) vs 20.4% (12.7), $p = 0.014$). Similarly, the median area of disc erosion under the surface was significantly greater in Charcot compared with diabetic patients (9.1 μ m² (6.3) vs 4.3 μ m² (3.3), $p = 0.022$) and also in Charcot patients compared with healthy subjects (9.1 μ m² (6.3) vs 3.3 μ m² (2.4), $p = 0.002$).

The addition of na-TNF- α to cultures with M-CSF+RANKL led to marked decrease in the osteoclastic resorption only in Charcot patients (from 40.1% (10.6) to 28.2 (14), $p = 0.035$) but not in diabetic patients (from 12.3% (17.9) to 13.3% (15.2), $p = 0.902$) nor in healthy subjects (from 20.4% (12.7) to 19.7% (9.6), $p = 0.818$).

Similarly, the median area of disc erosion was significantly reduced only in Charcot patients (from 9.1 μ m² (6.3) to 4.1 μ m² (5.5), $p = 0.05$) but not in diabetic patients (from 4.3 μ m² (3.3) to 2.9 μ m² (3.3), $p = 0.456$) nor in healthy subjects (from 3.3 μ m² (2.4) to 3.5 μ m² (1.8), $p = 0.818$).

Conclusion: In acute Charcot foot, TNF- α modifies the resorptive behaviour of newly generated osteoclasts in vitro. The active mode of their resorption cycle is maintained and this results in large and deep bone erosions.

Disclosures: *Nina Petrova, None.*

MO0357

Osteoporosis and Osteopenia after the Solid Organ Transplantation. Jana Brunova^{*1}, Simona Kratochvilova². ¹Institute for Clinical & Experimental Medicine, Czech Republic, ²IKEM, Czech Republic

Background: Osteoporosis is a frequent complication in patients after the transplantation (Tx) of solid organs. The contributing factors include disturbances of bone metabolism due to end-stage organ failure and intensive immunosuppressive therapy and use of corticosteroids after the transplantation.

Patients and methods: We investigated the prevalence of osteoporosis and osteopenia in 304 diabetic patients after the kidney Tx for renal failure due to diabetic nephropathy, in 986 non-diabetic patients after the kidney Tx and 567 patients after the liver Tx. The bone loss was diagnosed with densitometry (DEXA) using Lunar Prodigy apparatus. In diabetic patient we investigated characteristics of bone metabolism: Ca, P, parathormone (PTH), osteocalcin, 1, 25(OH)₂ D₃, 25OHD₃, ICTP, and bone ALP (BALP).

Results: In diabetic patients after the kidney Tx osteopenia was present in 50 % and osteoporosis in 28 %. Patients with Tx for non-diabetic nephropathy had osteopenia in 45 % and osteoporosis in 27 %. Patients after liver Tx showed osteopenia in 45 % and osteoporosis in 18 %. The proximal femurs were affected mainly in diabetic patients and L spine in patients after the liver Tx. Low levels of 25OHD₃ were found in 63 % of diabetic patients after Tx and elevated levels of osteocalcin in 58 % and very high levels of osteocalcin in 15 %. Mild elevation of PTH values was present in 72 % patients and significantly increased (2-3times) levels were in 17 % of patients. The BALB levels were elevated in 64 % Tx diabetic patients and ICTP in 78 %. The mean creatinine level was 121.3 ± 39.4 mmol/l; mild elevation creatinine was found in 55 % but higher levels (200-275 mmol/l) were present only in 6% of patients.

Conclusions: Patients with organ transplantation display a high prevalence osteopenia and osteoporosis. The highest percentage of reduced bone density cases was present in transplanted diabetics patients (78 %), followed by non-diabetic patients after kidney Tx (72 %) and lowest among patients after liver Tx (63 %). Diabetic patients had frequently impaired characteristics of bone metabolism and low D vitamin levels despite of organ transplantation.

Disclosures: *Jana Brunova, None.*

MO0358

¹⁸F-fluoride PET as a Non-invasive Imaging Biomarker Tool for Determining Treatment Efficacy at the Hip: a Prospective, Randomised, Controlled Clinical Study. Michelle Frost^{*1}, Amelia Moore¹, Muhammad Siddique¹, Glen Blake¹, Didier Laurent², Babul Borah², Ursula Schramm², Theodore Pellas², Paul Schlever¹, Paul Marsden¹, Ignac Fogelman³. ¹King's College London, United Kingdom, ²Novartis Pharma AG, Switzerland, ³Guy's Hospital, United Kingdom

With the development of therapies for osteoporosis with novel mechanisms of action and methods of delivery there is an increasing need for a biomarker of treatment efficacy at clinically relevant skeletal sites to accelerate drug development, particularly during early phase trials. The functional imaging technique of ¹⁸F-fluoride positron emission tomography (¹⁸F-PET) allows the non-invasive quantitative assessment of regional bone metabolism at any skeletal site, including the lumbar spine and proximal femur. The aim of this study was to determine if ¹⁸F-PET can be used as an early biomarker for determining treatment efficacy at the hip using the anabolic agent teriparatide. Twenty-seven treatment-naive postmenopausal women with osteopenia were randomised to receive teriparatide and calcium and vitamin D (TPT group, n=13) or calcium and vitamin D only (control group, n=14). Subjects in the TPT group were treated with 20 μ g/day teriparatide for 12 weeks. ¹⁸F-PET scans of the proximal femur (bilateral hips), pelvis and lumbar spine were performed at baseline and 12-weeks. The plasma clearance of ¹⁸F-fluoride to bone, K_i, a validated measurement of bone formation, was estimated at 6 regions of the hip and the pelvis using Patlak analysis and at the spine using a modified two-point Patlak method. A significant increase in K_i was observed at all ROIs at the hip including the total hip (+27%, $p = 0.002$), femoral shaft (+48%, $p = 0.001$), intertrochanter (+28%, $p = 0.001$), femoral neck (+25%, $p = 0.040$), and purely cortical (+51%, $p = 0.001$) and trabecular ROIs (+21%, $p = 0.017$) in the TPT group. Significant increases in K_i in response to TPT were also observed at the lumbar spine (18%, $p = 0.001$) and pelvis (42%, $p = 0.001$). No significant changes in K_i at any of the hip ROIs, spine or pelvis were observed for the control group. Areal BMD measured at baseline and 18-weeks increased significantly at the lumbar spine (+2.6%, $p = 0.012$) and total hip (+0.9%, $p = 0.012$) in the TPT group only. In conclusion, this is the first study demonstrating that ¹⁸F-PET can be used as an imaging biomarker for determining treatment effect

on bone formation rate at the hip and other skeletal sites as early as 12-weeks following initiation of therapy.

Disclosures: Michelle Frost, Novartis Pharma, 6
This study received funding from: Novartis Pharma

MO0359

Change in Serum Sclerostin after 24 Months of Teriparatide or Alendronate.

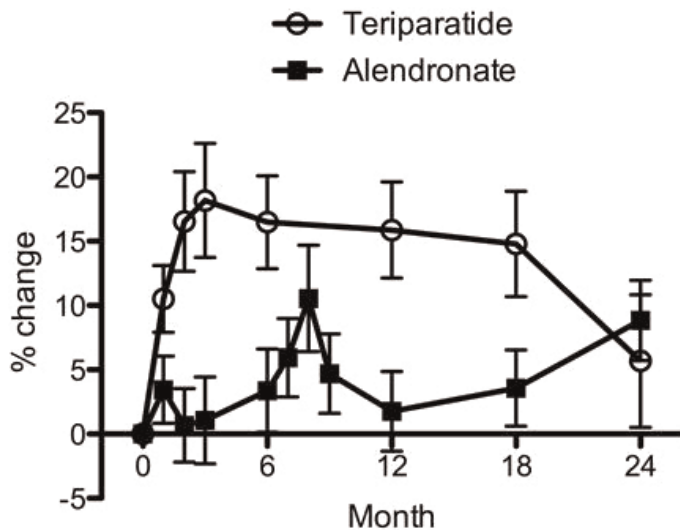
Elaine Yu*, Elizabeth Schindler, Jason Wyland, Robert Neer, Joel Finkelstein, Massachusetts General Hospital, USA

Purpose: It has been postulated that sclerostin is a mediator of the skeletal anabolic actions of parathyroid hormone (PTH). Serum sclerostin decreases acutely in response to either continuous PTH infusions or a 2-wk course of once-daily subcutaneous teriparatide (PTH 1-34, abbreviated TPT). In contrast, two studies did not find any significant change in serum sclerostin levels with 6- or 18-months of once-daily sc TPT therapy.

Methods: We assessed changes in serum sclerostin (Biomedica, Austria) in 41 men and 35 women with osteoporosis who had been randomized to TPT 40 mcg SC daily (n=31) or alendronate (ALN) 10 mg daily (n=45) for 24 months. Serum sclerostin was measured in a single assay in sera collected immediately before and at multiple timepoints during therapy, and compared against baseline within groups. Cumulative changes in sclerostin were analyzed by area-under-the-curve (AUC) and compared between groups. Correlations were assessed between sclerostin and previously reported simultaneous levels of bone turnover markers (osteocalcin, P1NP, and N-telopeptide) and DXA BMD at the lumbar spine and total hip.

Results: TPT treatment increased circulating sclerostin levels modestly. Levels peaked at 3 months (mean \pm SEM: 18.2 \pm 4.4%, p=0.004), and began to wane at 18 months. In contrast, serum sclerostin did not change appreciably in the ALN group. Cumulative changes in sclerostin throughout the study were greater in subjects treated with TPT than with ALN (p=0.040). Patterns of response to treatment were similar in men and women. Baseline sclerostin levels were significantly associated with spine BMD (r=0.45, p<0.001) and hip BMD (r=0.36, p=0.001), but not with OC, P1NP, or NTX. Changes in sclerostin were not associated with changes in BMD at any site or with changes in any bone turnover marker.

Conclusions: Daily injections of TPT caused modest but clear increases in serum sclerostin levels over a 24-month period, and the pattern was distinctly different from that seen with ALN treatment. The observed increase in circulating sclerostin after TPT was unexpected, and its relation to the anabolic effects of PTH are unclear.



% change in sclerostin

Disclosures: Elaine Yu, None.
This study received funding from: NIH

MO0360

Effects of Baseline Status of Bone Turnover Markers and Vitamin D Sufficiency on Efficacy of Teriparatide Once-a-day Subcutaneous Injection in Japanese Patients with Osteoporosis. Takanori Yamamoto*¹, Mika Tsujimoto², Etsuro Hamaya³, Hideaki Sowa⁴. ¹Eli Lilly, , ²Eli Lilly Japan K.K., Japan, ³Eli Lilly, Japan, ⁴Lilly Research Laboratories Japan, Eli Lilly Japan K.K., Japan

Purpose: It is known that the baseline status of biochemical markers for bone turnover (bone turnover markers) and vitamin D sufficiency affect changes in bone mineral density (BMD) and bone turnover markers during osteoporosis treatment. The purpose of this study is to examine the effect of these factors on BMD and bone turnover markers after administering teriparatide 20 µg/day.

Methods: A randomized clinical trial of teriparatide 20 µg/day was previously conducted in Japanese patients with osteoporosis at high risk of fracture (ClinicalTrials.gov identifier: NCT00433160). This study consisted of a 12-month placebo-controlled, double-blinded period and a 12-month treatment period in which all patients received open-label teriparatide. Vitamin D (cholecalciferol) and calcium were also administered throughout the study period. Patients in each treatment group (placebo-TPTD group [n=67] and TPTD-TPTD group [n=136]) were stratified into 3 subgroups by the tertile values of serum procollagen type I N-terminal propeptide (P1NP) or serum type I collagen cross-linked C-telopeptide (CTX) at baseline, and changes in lumbar spine (LS) BMD was evaluated by subgroup. Changes in LS BMD, serum P1NP and serum CTX were also evaluated by subgroup of serum 25-hydroxyvitamin D (25OHD) at baseline (<20 ng/mL, ≥20 ng/mL). Percent change from baseline to 24 months for BMD in TPTD-TPTD group was analyzed using a mixed effect model on repeated measurements (MMRM) with fixed effects of subgroup, and a random effect of subject.

Results: LS BMD increased by 10% or more after the 24-month treatment, with statistically significant increases from baseline, in every subgroup of P1NP, CTX and 25OHD. Subgroups with a higher baseline P1NP or CTX had greater percent change in LS BMD after the 24-month treatment; however, the baseline status of vitamin D sufficiency did not affect the percent change of LS BMD, P1NP nor CTX after the 24-month treatment.

Conclusion: These results suggested that increase in BMD can be expected with teriparatide 20 µg/day treatment regardless of baseline status of bone turnover markers, and that the higher the bone turnover markers are at baseline, the more BMD-increasing effect can be achieved. In addition, it was suggested that, when vitamin D and calcium are appropriately supplemented, clinically significant increase in BMD and changes in bone turnover markers by teriparatide 20 µg/day treatment can be expected regardless of baseline vitamin D insufficiency.

Disclosures: Takanori Yamamoto, Eli Lilly Japan K.K., 3
This study received funding from: Eli Lilly Japan K.K.

MO0361

P1NP as an Aid for Monitoring Patients Treated with Teriparatide: Canadian Pilot Study. Jacques Brown*¹, Louis-Georges Ste-Marie².

¹CHUQ Research Centre Laval University, Canada, ²CHUM, Canada

Purpose: Type I collagen is abundant in osteoblasts and secreted as procollagen into the extracellular space where it is cleaved at both its amino-terminal and carboxy-terminal ends to give rise to N-terminal (P1NP) and C-terminal propeptides of Type I collagen. P1NP is released into circulation as a trimeric form which is unstable at 37°C and is rapidly converted to its monomeric form. P1NP has several practical advantages including its low diurnal variability and stability at room temperature. Its circulating levels are not significantly influenced by food intake and, consequently, patients do not need to be fasting. P1NP is primarily metabolized by the liver and its clearance is unaffected by renal dysfunction. P1NP may be a useful aid for monitoring response to teriparatide treatment.

Methods: We conducted a prospective, open-label, 6-month pilot study in 17 women and 2 men with established osteoporosis who have previously received bisphosphonates for 5 to 10 years. This population reflects the vast majority (> 90%) of the patients treated with teriparatide in Canada. All patients had normal renal function and 25-OH vitamin D levels > 75 nmol/L prior to teriparatide treatment. Blood samples were collected at home by the Forteo Customer Care visiting nurse at baseline and month 3 in all patients and at month 1 and/or month 6. P1NP were measured by a single independent lab using an automated analyzer and results were reported within 4-6 weeks to the ordering physician. This pilot study aimed to test the feasibility of the program.

Results: All patients were sampled at the exact time point requested by the ordering physician and results were sent within 4-6 weeks. As expected in this population previously treated with bisphosphonates, the mean baseline P1NP value was low at 34.4 ng/L (SD 18.5 ng/L). Most patients (14/19) increased their respective P1NP values by more than 100% from baseline at all time points. The mean percent changes from baseline were 153%, 178% and 300% at months 1, 3 and 6 respectively.

Conclusions: The feasibility of P1NP program linked to the Canadian Forteo Customer Care program has been successfully tested and it is currently offered to Canadian physicians prescribing teriparatide and willing to participate.

Disclosures: Jacques Brown, Eli Lilly, 6; Eli Lilly, 2; Eli Lilly, 1
This study received funding from: Eli Lilly

MO0362

Supplemental Collagen with Calcium Improves Bone Health in Part by Attenuating Sclerostin. Marcus Elam*¹, Shirin Hooshmand², Jennifer Gu³, Bahram Arimandi¹. ¹Florida State University, USA, ²San Diego State University, USA, ³AIDP Inc., USA

In vivo evidence suggests that supplemental collagen is an effective modality for the treatment of ovariectomy-induced bone loss. However, in clinical trials involving postmenopausal women, results vary. The purpose of this study was to investigate the bone loss reversal effects of a collagen supplement with the addition of calcium for the reversal of bone loss in osteopenic postmenopausal women. Women 1 to 5 years postmenopausal, not on hormone replacement therapy or any other prescribed medication known to influence bone metabolism were randomized among two

treatment groups to receive as a dietary supplement intervention daily for three months of either of the following: 500 mg of calcium carbonate and 5 µg vitamin D (control), or 5 g of hydrolyzed collagen containing 500 mg elemental calcium and 5 µg vitamin D. Bone mineral density of the lumbar spine and whole body were assessed at baseline and the end of the study using dual-energy x-ray absorptiometry. Blood samples were collected at baseline and after 3 months to assess bone biomarkers of bone metabolism. Physical activity recall and three-day food frequency questionnaire were completed to examine physical activity and dietary confounders as potential covariates. The collagen supplement significantly increased total body BMD in comparison to the control group (1% vs. baseline; $P = 0.021$). Compared to corresponding baseline values, collagen tended to increase bone-specific alkaline phosphatase activity and decrease tartrate resistant acid phosphatase-5b. Mean serum values of sclerostin, an osteocyte-originated molecule, was decreased by 11%, further indicative of the collagen supplement's bone forming ability. The results of this pilot study suggested that supplemental collagen, when combined with calcium, enhances bone mass by increasing bone formation and suppressing bone resorption.

Disclosures: Marcus Elam, None.
This study received funding from: AIDP Inc.

MO0363

Atypical Femoral Fractures: Radiographic and Histomorphometric Features in 12 Patients. Aliya Khan^{*1}, Angela Cheung², Adil Zaidi¹, Nazir Khan¹, Ken Pritzker³, Bryan Lentle⁴. ¹McMaster University, Canada, ²University Health Network, Canada, ³University of Toronto, Canada, ⁴University of British Columbia, Canada

Purpose: This study describes characteristics and histomorphometric and radiographic features of atypical femoral fractures (AFF) as seen in 12 cases referred for evaluation.

Methods: All patients referred for evaluation of AFF were reviewed. Patients meeting the ASBMR criteria for AFF were further evaluated and tetracycline labelled bone biopsies were completed. Radiographs were reviewed by a musculoskeletal radiologist.

Results: All fracture lines were transverse or short oblique with thickened cortices. We report 12 cases of AFF in patients on long term bisphosphonate (BP) therapy. 7 of 12 fractures occurred without a fall or direct trauma to the femur with 5 cases occurring after a fall from standing height. All patients were female; average age was 66 years (range 54-80 years). 4 of the 12 cases were of Chinese descent, 3 were East Indian with 5 being Caucasian. Average BP durations of use was 8.1 years (range 7-14 years). 8 of 12 patients were on alendronate alone, 4 patients were on risedronate. 1 patient had received 18 months of teriparatide, 3 years prior to AFF and had received a total of 10 years of BP use prior to teriparatide. Prodromal thigh or groin pain was seen in 9 of the 12 patients for 3 to 12 months prior to fracture. Proton pump inhibitor use was present in 1 patient for the previous 2 years. 2 patients were on prednisone for rheumatoid arthritis.

Summary: A large number of the patients with radiographic features of an AFF had evidence of mineralization abnormalities on tetracycline labelled bone biopsy. These women had normal or mildly reduced serum vitamin D levels. Decreased bone formation was seen in 3 patients. A significant number of these women were of Asian descent (7 of 12). 7 of the 12 AFF occurred in the absence of a fall. Prodromal pain was commonly seen. Proton pump inhibitors were used in only 1 patient.

Conclusion: Histomorphometric features seen on bone biopsy in women sustaining an AFF in association with long term bisphosphonate use included evidence of mineralization abnormalities and decreased bone formation. Improved understanding of the pathophysiology leading to these fractures may be gained with further histomorphometric data in larger numbers of patients. A significant number of women were of Asian descent and further evaluation of all AFF with identification of predisposing key clinical risk factors is needed.

Disclosures: Aliya Khan, None.

MO0364

Atypical Femoral Fractures-a Single Center Data. Elena Segal^{*}, Daniela Militianu, Marina Nodelman, Doron Norman, Michael Soudry, Sophia Ish-Shalom. Rambam Health Care Campus, Israel

Introduction: Since the initial case reports in 2005, atypical femoral shaft fractures (AF) have aroused continuous medical concern. Data about prevalence of AF is still uncertain and causal relationship to bisphosphonate treatment has not been established. Observations suggest that the risk increases with duration of exposure. Underreporting might mask the true incidence of the problem. Evaluation of x-ray films by radiologist specialized in bone diseases is not a part of routine evaluation in the Department of the Orthopedic surgery.

Study aims: To evaluate AF prevalence in our institution; to establish the feasibility of AF case identification by existing ICD-9 codes; to review AF patients' clinical and radiological characteristics and duration of bisphosphonate exposure.

Methods: We identified patients discharged during 2007 – 2010 with Subtrochanteric, Supracondylar, Femoral shaft fractures (ICD-9 codes 820.22; 821.23; 821.33; 821.01; 821.11), who met criteria of AF. Patients younger than 50 and those with major trauma were excluded. Admission femoral x-rays were examined by a senior radiologist. The fractures were classified as atypical or not-atypical according to the published criteria. Hospital files of patients with AF were reviewed: age, prefracture

functional status, medications. Later, community medical records were reviewed, when available, for current and past medication exposure.

Results: 1568 hip fracture patients were admitted to the hospital during four years period, of them 108 with relevant ISD-9 codes; 14 (0.89%) answered criteria of AF. All AF patients were women, aged 66-94, mean age 78 ± 5.6 . All were independently walking before hospitalization, while 2 used walking sticks. 3 (21%) had no trauma; 11 (78.6%) – fell from standing height, 1(7%) had prodromal pain; 11 were exposed to bisphosphonates for 4-9 years. No patient was diagnosed as having AF during hospitalization.

Conclusion: Atypical fractures are rare (0.89%), and our data are consistent with the published data. Case identification could represent some difficulties. Case-identification based solely on ICD codes, without radiological evaluation, leads to significant over-estimation and can't be appropriate. Most patients in our analysis were exposed to bisphosphonates for more than 4 years.

Disclosures: Elena Segal, None.

MO0365

Atypical Subtrochanteric and Diaphyseal Femoral Fractures Associated with Long-term Bisphosphonate use in Postmenopausal Osteoporosis – A Case Study. Oliver Bock^{*}, Uta Stege, Dieter Felsenberg, Charité - Campus Benjamin Franklin, Germany

Objectives: The incidence of atypical femoral fractures (AFF) associated with the use of bisphosphonates (BP) for the treatment of patients with osteoporosis appears to be very low. Moreover, a causal association between BP and AFFs has not been clearly established. However, recent observations suggest that the risk rises with increasing BP exposure, and there is concern that lack of awareness and under-reporting may mask the true incidence of the problem. Despite their relative rarity, AFF, if occurring in individual patients, are of great challenge for further medical management.

Patients and methods: We report here on five patients with altogether eight BP-associated AFF who were identified in or referred to our osteoporosis outpatient clinic since November 2009. This case study follows the recommendations given by the ASBMR for AFF reports. We provide detailed information on individual risk patterns and treatment considerations as well as on different therapeutic outcomes.

Results: All five AFF patients in our case study were treated with BP for postmenopausal osteoporosis (including one case with primary hyperparathyroidism occurring later during BP treatment). Their mean age at the time of (first) AFF was 75 years (range: 66-86 years), the mean duration of BP treatment was 7 years (range: 3-11 years). Two patients suffered from bilateral, complete subtrochanteric AFF followed by delayed healing after osteosynthesis – both these patients had a medical history with long lasting rheumatoid arthritis, glucocorticoid and proton-pump inhibitor treatment. The other four AFF occurred in three patients without any additional clinical risk factors recently discussed in the pathogenesis of AFF and showed the radiological patterns of incomplete diaphyseal insufficiency fractures with involvement of the lateral cortex only. Otherwise, our patients with complete or incomplete AFF and with subtrochanteric or diaphyseal AFF, respectively, did not differ in prior fracture, BMD and BTM history.

As for the moment of abstract submission, one out of three patients treated with teriparatide showed after two years clinical and radiographic evidence for improved fracture healing. On the other hand, in a case with assumed contraindications for teriparatide one complete diaphyseal AFF developed from an originally incomplete insufficiency fracture.

Disclosures: Oliver Bock, None.

MO0366

Beneficial Effect of Strontium Ranelate Compared to Alendronate on Trabecular Bone Score in Post Menopausal Osteoporotic Women: A 2 Year Study. Didier Hans^{*1}, Marc-Antoine Krieg², Olivier Lamy³, Dieter Felsenberg⁴. ¹Lausanne University Hospital, Switzerland, ²University Hospital, Switzerland, ³Chief of the Bone Unit, Switzerland, ⁴Charité - Campus Benjamin Franklin, Germany

Objective(s): Trabecular Bone Score (TBS, Med-Imaps, France) is an index of bone architecture independent of BMD calculated by quantifying local variations in grey level from antero-posterior spine DXA scan and reported to be associated with fracture in prior case-control and prospective studies¹. We compared the effects of strontium ranelate (SrRan) and alendronate (ALN) on spine architecture patterns as assessed by TBS in women with postmenopausal osteoporosis.

Material and Methods: A post-hoc analysis was performed on DXAs (Hologic and GE Lunar Devices) from 79 women out of 189 included in a double blind, double dummy study and randomized to SrRan 2g/day or ALN 70mg/week during 2 years². Spine TBS parameters were assessed by TBS iNsite (v1.9) at the spine after 12 and 24 months of treatment. We applied ISCD rules for individual vertebrae exclusion independently for BMD and TBS respectively. Since duplicate measurements were performed at baseline, precision were calculated as CV%.

Results: Baseline characteristics (mean \pm SD) were similar between groups in term of age, 69.2 ± 4.4 years; BMI, 23.8 ± 4.4 kg/m²; L1-L4 T-score, -2.9 ± 0.9 and TBS 1.230 ± 0.09 . As expected, the correlation between Spine BMD and TBS was very low with $r^2 = 0.12$. Precision errors were 1.1% and 1.6% for Spine BMD and TBS

respectively. Over 1 and 2 years, L1-L4 BMD increased significantly by 5.6% and 9% in SrRan group and by 5.2% and 7.6% respectively in ALN group. Similarly, Spine TBS increased by 2.3% (p<0.001) and 3.1% (p<0.001) in SrRan group and by 0.5% (ns) and 1.0% (ns) respectively in ALN group with a significant between-group difference in favor of SrRan (p=0.04 and p=0.03). There were no correlation between delta BMD and TBS at 1 year or at 2 years. The two treatments were well tolerated.

Conclusion(s): Strontium ranelate has greater effects on bone architecture index at the spine compared to alendronate in women with postmenopausal osteoporosis after two-year treatment. These results consolidate previous studies supporting a benefit of strontium ranelate on bone architecture.

1. Hans D. et al. J Bone Miner Res. 2011 Nov;26(11):2762-9; 2. Felsenberg D., et al. Osteoporosis Int 2011;22(suppl. 1):S102

Disclosures: **Didier Hans**, medimaps, 8; medimaps, 7
This study received funding from: Servier

MO0367

Comparative Effectiveness and Safety of Generic Versus Branded Alendronate Among Medicare Beneficiaries. Huifeng Yun^{*1}, Elizabeth Delzell¹, Jeffrey Curtis¹, Lingli Guo¹, Pradeep Sharma¹, Meredith Kilgore², Paul Muntner¹, Amy Warriner¹, Kenneth Saag¹. ¹University of Alabama at Birmingham, USA, ²University of Alabama At Birmingham School of Public Health, USA

Background: The availability of low cost generic alendronate may facilitate access to anti-osteoporosis pharmacotherapy. However, it is not clear if generic and branded alendronate products are equivalent in terms of effectiveness and safety.

Objective: To evaluate the incidence of fractures (effectiveness outcome) and upper gastrointestinal (GI) conditions (safety outcome) among Medicare beneficiaries initiating generic versus branded alendronate during 2007-2009.

Methods: From the national random 5% sample of Medicare beneficiaries, we selected subjects who were >=65 years of age; continuously enrolled in Medicare parts A, B and D and not in a Medicare Advantage plan; and newly treated with alendronate during 2007-2009 (no prior use of any osteoporosis medication during the 12-month baseline period preceding the index prescription fill). We identified outcomes using claims data on diagnoses and procedures. Fractures included for hip, spine, humerus and distal radius/ulna. GI conditions included hospitalized upper GI bleeding and other upper GI disease and GI symptoms, defined as a physician evaluation and management claim on at least two days with the same diagnosis code. Follow-up continued through the earliest of loss of Medicare coverage, switching from branded to generic alendronate or vice versa, 90 days after the last alendronate prescription refill, death or 12/31/2009. Cox proportional hazards models evaluated the association between generic, compared to branded, alendronate and each outcome. Sensitivity analyses excluded subjects with any diagnosis of an upper GI condition or symptom during baseline.

Results: Of the 8,903 new users of branded alendronate and 15,575 new users of generic alendronate, 1061 had a fracture, 116 had upper GI bleeding, 756 had other upper GI disease, and 1546 had upper GI symptoms. After multivariable adjustment, hazard ratios for generic compared to branded alendronate were 0.96 (95% confidence interval (CI): 0.77-1.21) for fractures, 1.21 (95% CI: 0.53-2.75) for hospitalized upper GI bleeding, 1.11 (95% CI: 0.86-1.45) for other upper GI disease and 1.23 (95% CI: 1.02-1.49) for upper GI symptoms (Table 1).

Conclusions: Compared to branded alendronate, generic alendronate appeared to have similar anti-fracture effectiveness and comparable GI safety in a large cohort of new users enrolled in Medicare. Further studies are needed to evaluate the safety of generic alendronate.

| | Hospitalized Upper GI Bleeding | | | Other Upper GI Disease | | | Upper GI Symptoms | | |
|---|--------------------------------|----------------|-----------------|------------------------|------|-----------------|-------------------|------|-----------------|
| | N | R [†] | HR (95% CI) | N | R | HR (95% CI) | N | R | HR (95% CI) |
| Overall cohort | | | | | | | | | |
| Branded | 85 | 0.40 | Ref | 361 | 2.58 | Ref | 663 | 4.91 | Ref |
| Generic | 53 | 0.40 | 1.21(0.53-2.78) | 395 | 3.11 | 1.11(0.86-1.43) | 885 | 7.15 | 1.23(1.02-1.49) |
| Cohort limited to beneficiaries without any diagnosis of upper GI problem at baseline | | | | | | | | | |
| Branded | 50 | 0.35 | Ref | 223 | 1.65 | Ref | 500 | 3.82 | Ref |
| Generic | 39 | 0.34 | 1.34(0.51-3.49) | 245 | 2.14 | 1.21(0.87-1.69) | 596 | 5.58 | 1.20(0.97-1.49) |

* Adjusted for baseline demographic factors, comorbidities and medications. Comorbidities included glucocorticoid-related disease, bone disease, diabetes, renal disease, fall-related conditions, depression, stroke, chronic obstructive pulmonary disease; medications included anticonvulsants, antidepressants, antipsychotics, antiemetics, lipid-lowering drugs, non-steroidal anti-inflammatory drugs, and steroids.
[†] Number of events
[‡] Absolute incidence rate

Table 1
Disclosures: **Huifeng Yun**, Amgen, 6

MO0368

Effects of Combined Treatment with Alendronate and Alfacalcidol Comparing with other Bisphosphonates and Alfacalcidol in BMD Changes at Postmenopausal Osteoporotic Women. Corina Galesanu^{*1}, Alexandru Florescu², Andra Iulia Loghin², Ilinka Grozavu², Petronela Ancute², Valentin Zaharia², Veronica Mocanu². ¹University of Medicine & Pharmacy, Romania, ²University of Medicine & Pharmacy "Gr.T.Popa", Romania

Purpose. Postmenopausal osteoporosis is an important health problem. The spectrum of osteoporosis therapy is extended; the bisphosphonates by inhibiting bone resorption, increase bone mineral density (BMD) at different skeletal sites and reduce fracture incidence. D-hormone analogs (Alfacalcidol) have been proven to be potent in increasing BMD. Two hundred fifty four postmenopausal osteoporotic women were enrolled in a prospective randomized, open-label study of 12 months duration to compare the efficacy Alendronate (generic) +Alfacalcidol + Calcium (group A) with other bisphosphonates +Alfacalcidol + Calcium on BMD change.

Material and Methods. Postmenopausal osteoporotic women eligible were between 40 and 80 years old with BMD at lumbar spine or total hip, T-score <-2.5. From October 2009 to April 2011 a total of 254 patients were randomized in a 3/1 fashion: Alendronate (generic) 70 mg/wk + Alfacalcidol 1µg/d+Calcium 1000 mg/d=200 women (group A) and Bisphosphonates+Alfacalcidol 1µg/d+Calcium 1000mg/d=54 women (group B) followed 12 months. BMD was measured by Dual Energy X-ray Absorptiometry (DXA-BMD Hologic) at baseline and after 12 months at lumbar spine L1-L4 and total hip. For statistical analysis we used t-test (p=0.005) for all group A and B and for subgroups of ages.

Results. The baseline characteristics of the patients were well balanced between the two groups. The mean age of the patients in each group was 62.5 +/- 8.7 years. After 12 months in a group A, BMD at lumbar spine was statistically significant changed at the subgroups of ages 50-54 and 65-69 years and for total hip at the subgroups of ages 50-59 and 60-64 years. In the group B statistically significant difference was in the subgroups 50-54 years and >70 years at lumbar spine and for total hip at subgroup 55-59 years. No significant differences between treatment groups after 12 months on BMD change at lumbar spine and total hip. No fractures during the treatment.

Conclusion. The combined treatment Alendronate (generic) +Alfacalcidol+Calcium or other bisphosphonates+Alfacalcidol+Calcium increased BMD at lumbar spine and total hip. There are no significant difference between the treatment in the two groups after 12 months, but in some subgroups BMD was high significant improved. Alendronate (generic) was good like the other bisphosphonates. The combined therapy is an alternative solution.

Disclosures: **Corina Galesanu**, None.

MO0369

Effects of Denosumab on Bone Turnover Markers Compared to Zoledronic Acid in Severe Osteoporotic Women: A Randomized Head to Head Study. Marco Invernizzi^{*1}, Alessio Baricich², Maurizio Bevilacqua³, Stefano Carda⁴, Carlo Cisarì². ¹University of Eastern Piedmont, Novara, Italy, ²Department of Health Sciences, University of Eastern Piedmont "A. Avogadro", Italy, ³Department of Medicine, Luigi Sacco Hospital, University of Milan, Italy, ⁴Centre Hospitalier Universitaire Vaudois, Switzerland

Introduction: Denosumab is a fully human monoclonal antibody against RANKL that blocks its binding to RANK, inhibiting the development and activity of osteoclasts. Zoledronic Acid (ZOL) is an intravenous amino-bisphosphonate that binds to the skeleton and decrease osteoclast activity. Both drugs are able to decrease bone resorption, resulting in increased Bone Mineral Density (BMD). The efficacy of these two powerful antiresorptive agents in increasing BMD and reducing fracture risk in osteoporotic postmenopausal women has been demonstrated in numerous clinical trials; however at present time the effects of these two pharmacological agents on Bone Turnover Markers (BTM) have not been compared yet.

AIM: to determine the effects on BTM of Denosumab 60mg vs. 5mg intravenous ZOL in severe osteoporotic patients one month after administration .

Method: 77 severe osteoporotic post-menopausal woman were enrolled and randomly divided in two groups: 37 were treated with Denosumab 60mg subcutaneously and 40 with 5mg of intravenous ZOL. The inclusion criteria were: age > 70, presence of at least one vertebral or femoral osteoporotic fracture, a T-score at vertebral or hip site < -3. Previous treatment for osteoporosis were recorded. BMT (serum CTX, OC and BALP) were assessed at baseline and 1 month after treatment in both groups. Tolerability was evaluated by adverse experience (AE) reporting.

Results: One month after Denosumab treatment were found decreases of OC (-19.8%), serum CTX (-77.8%; p<0.01 vs. baseline) and B-ALP (-11%) compared to baseline values. Similarly 1 month after ZOL infusion we observed a decrease in OC (-10%), serum CTX (-42%; p<0.01 vs. baseline; p<0,05 vs. Denosumab group) and BALP (-7.2%) compared to baseline values. The percentage of treatment naive patient was 40,5% in Denosumab group and 48% in ZOL group respectively. Treatment-Naive patients in both groups showed no significant differences in BTM changes compared to previously treated patients. 2 patients (5,4%) experienced moderate self-limiting AE (myalgia and arthralgia) after Denosumab, while 18 patients (45%) experienced a self-limiting acute phase reaction after ZOL.

Conclusions: Denosumab treatment resulted in greater suppression of BTM compared with ZOL. Moreover it reported less AE than ZOL. The more rapid effect of Denosumab on BTM compared to ZOL may have clinical implications for therapeutic choices in severe osteoporotic patients.

Disclosures: Marco Invernizzi, None.

MO0370

Effects of Vitamin D Therapy on Bone Turnover Markers and PTH Levels in Postmenopausal Osteoporotic Women Treated with Alendronate. Jose Olmos¹, José L. Hernández², Javier Llorca³, Josefina Martínez², Daniel Nan², Carmen Valero⁴, Jesus Gonzalez-Macias⁵. ¹Hospital Universitario M. Valdecilla, Spain, ²Hospital Universitario Marqués de Valdecilla, Spain, ³Epidemiology Unit, Medical School, Universidad de Cantabria, Spain, ⁴Hospital Universitario Marqués De Valdecilla (HUMV), Spain, ⁵Universidad De Cantabria, Spain

It has often been stated that vitamin D supplementation is needed for an adequate response of osteoporotic bone to bisphosphonates (BPs). However, clear information about whether this is true, and if so, by how much, is still lacking. Therefore, the aim of the present study was to evaluate the extent to which bone turnover marker fall is influenced by serum 25OHD levels in patients on alendronate treatment. One hundred and forty postmenopausal osteoporotic women were randomized to receive either alendronate (ALN) or alendronate plus vitamin D (ALN+vitD) over a 3-month period. Serum 25OHD, PTH, CTX and PINP were measured at baseline and at the end of 3 months. As expected, patients allocated to ALN+vitD showed a significant increase in serum concentration of 25OHD ($p < 0.001$), while no significant changes were seen in patients treated with ALN alone. On the contrary, serum PTH remained at the baseline level in patients receiving ALN+vitD, but increased in the ALN group ($p < 0.001$). A significant decline in both serum CTX ($53 \pm 24\%$) and PINP ($46 \pm 19\%$) levels was seen after ALN alone administration. After ALN+vitD, the corresponding figures were $61 \pm 20\%$ for CTX ($p = 0.06$ compared to ALN) and $50 \pm 23\%$ for PINP ($p < 0.35$). When patients were divided into those below and above 20 ng/ml of serum 25OHD baseline, no differences were appreciated in CTX or PINP decreases between ALN+vitD and ALN groups in those above 20 ng/ml. However, in patients with basal 25OHD below 20 ng/ml, CTX decreases were $48 \pm 26\%$ in the ALN group and $61 \pm 17\%$ in the ALN+vitD group ($p = 0.015$); for PINP, the decreases amounted to $43 \pm 20\%$ and $50 \pm 23\%$ respectively ($p = 0.2$). We conclude that vitamin D administration is not an indispensable requirement for BPs to develop their bone antiresorptive effect, so that even in deficient patients bone marker decreases in the order of 50% are seen. However, in these patients vitamin D administration fostered the bone resorption marker CTX fall by about 25%. Further studies are needed to clarify whether this is due just to the inhibitory effect of vitamin D on bone resorption through PTH or other mechanisms are involved.

Supported by grants from the "Instituto de Salud Carlos III-FIS". Spain (PI08/0183; PI11/01092).

Disclosures: Jose Olmos, None.

MO0371

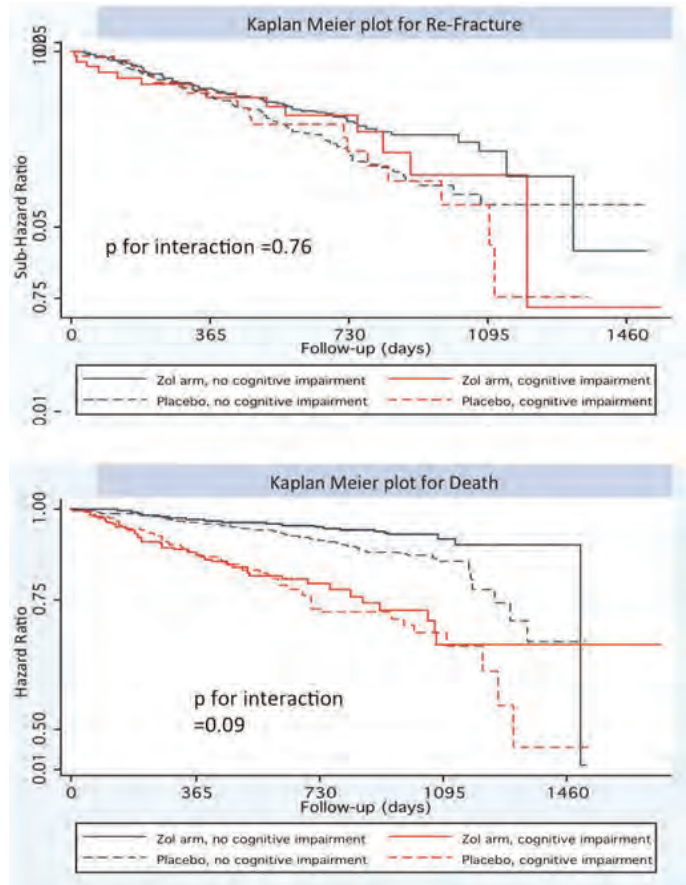
Fracture Prevention in Patients with Cognitive Impairment Presenting with a Hip Fracture: Secondary Analysis of Data from the HORIZON Recurrent Fracture Trial. Muhammad Javaid¹, Daniel Prieto-alhambra², Nigel Arden¹, Andrew Judge¹, Cyrus Cooper³. ¹University of Oxford, United Kingdom, ²Institut Municipal D'Investigació Mèdica, United Kingdom, ³University of Southampton, United Kingdom

Background: There is an established body of evidence for effective secondary fracture prevention using bisphosphonates. Patients with cognitive impairment presenting with a fracture are often denied therapy for a number of reasons. We therefore compared the effects of zoledronic acid on re-fracture and mortality in patients with normal vs. impaired cognitive status with a recent hip fracture within the HORIZON Recurrent Fracture Trial.

Method: We used data from the randomized, double blind, placebo-controlled trial of yearly intravenous 5mg zoledronic acid vs. placebo in patients with a recent hip fracture. The primary outcome was a new clinical fracture and secondary outcome was death. Short Portable Mental Status Questionnaire (SPMSQ) was measured at baseline; those > 2 were identified as moderate/severe cognitively impaired. Fine and Gray survival models for competing events were fitted to study the effect of zoledronic acid on time to re-fracture and standard Cox regression models for death. A multiplicative interaction term was introduced in the model to study a potential interaction between treatment and cognitive status on both outcomes.

Results: 350 (17.8%) participants had cognitive impairment and were balanced between treatment arms. In the placebo arm, those with cognitive impairment had a higher mortality at one year compared with those without cognitive impairment (12.5% vs. 3.2%, $p < 0.001$). The interaction term for the effect of cognitive status on zoledronic acid was non-significant for re-fracture rate ($p = 0.76$) and bordering significance for mortality ($p = 0.09$). The effect of zoledronic acid on survival was more pronounced in those with normal cognitive status (HR 0.56 (95%CI 0.40-0.80)) compared with those with impaired status (HR 0.90 (95%CI 0.59- 1.38)) (Figure).

Discussion: Given the sparse evidence base and rising prevalence of cognitive impairment in patients presenting with a hip fragility fracture, these exploratory findings require confirmation in future trials. In the interim, these results support the use of bisphosphonate therapy in those with cognitive impairment who are expected to live for more than 6 months.



Figure

Disclosures: Muhammad Javaid, Novartis, 2
This study received funding from: UO

MO0372

Withdrawn

MO0373

Prevalence of Renal Impairment among Osteoporotic Women in the US: Analysis of NHANES survey 2005-2008. Robert Lubwama¹, Allison Nguyen², Ankita Modi³, Paul Miller⁴. ¹Merck, USA, ²Merck & Co., Inc., USA, ³Merck & Company, USA, ⁴Colorado Center for Bone Research, USA

Background: Bisphosphonates have been recommended as first line treatment for patients with osteoporosis (OP) and at risk for fracture. Treatment options for OP patients with severe renal impairment are limited since bisphosphonates are not recommended in this population; however there are variations in the lower limit of Creatinine Clearance below which a therapy is not recommended: Alendronate < 35 ml/minute, Ibandronate and risedronate < 30 ml/minute, Zoledronic acid < 40 ml/minute.

Objective: To determine the proportion of women with OP aged 50 years or older who have renal impairment

Methods: Data from the 2005-2008 National Health and Nutrition examination survey (NHANES) were used to investigate the prevalence of renal impairment among OP women aged 50 years or older. OP was defined as prior hip or spine fracture, reported OP diagnosis or a lumbar spine or femoral neck BMD T-score < -2.5 . T-scores were calculated based BMD reference ranges at the lumbar spine and femoral neck among young adult white women in NHANES III. The 2005 Modification of Diet in Renal Disease (MDRD) formula was used to calculate the glomerular filtration rate (GFR). Moderate and severe renal impairment were defined as GFR < 60 and < 40 mL/min, respectively.

Results: The prevalence of OP among women aged 50+ (mean age 68.7) was 27% (12.7 million). 45.3%, 29.8% and 24.8% of the osteoporotic women were of normal body weight, overweight or obese, respectively. Nearly one quarter (23%; 10.3 million)

of the women with OP had moderate renal impairment and 637,504 (5.2%) had severe renal impairment.

Conclusion: Approximately 5.2% of US women age 50+ years with OP have severe renal impairment. These data reveal an unmet medical need in patients with both osteoporosis and severe renal impairment. The results warrant a need for better therapeutic alternatives or interventions which can be used in this patient population.

Disclosures: Allison Nguyen, Merck & Co Inc, 3
This study received funding from: Merck & Co Inc

MO0374

Prevention of Postmenopausal Osteoporosis With Two Intermittent Alendronate Regimens: Bone Mineral Density and Bone Markers Changes After 24 Months. Yves Boutsen¹, Jacques Jamart², Catherine Vynckier³, Thierry Vander Borgh³, Jean-Pierre Devogelaer⁴. ¹Cliniques Universitaires De Mont-Godinne, Belgium, ²Department of Biostatistics University Hospital in Mont-Godinne, Belgium, ³Department of Nuclear Medicine University Hospital in Mont-Godinne, Belgium, ⁴St. Luc University Hospital, Belgium

The aim of this prospective study was to compare the efficacy of two regimens of low-dose oral alendronate (ALN) for preventing postmenopausal osteoporosis in women who don't want or may not take hormone replacement therapy. Primary endpoint was lumbar spine (LS) bone mineral density (BMD) changes after two years. We present here changes in BMD and C-telopeptide crosslinks of type I collagen (S-CTX) levels after a two-year follow-up.

A total of 82 postmenopausal women (age range 45-60 years, at least 1 year since menopause) were randomly allocated to receive: ALN 70 mg (Fosamax®) every two weeks (group A); ALN 70 mg (Fosamax®) once-monthly (group B) or a placebo, similar to the ALN tablet, every two weeks (group C). Patients were recommended to take supplemental calcium 500 mg and vitamin D 400 IU daily. Randomisation was performed by a minimization procedure taking into account baseline BMD and S-CTX values. S-CTX levels were assessed using a one-step ELISA (β-CrossLaps*; Roche Diagnostics). Lumbar spine and hip BMD measurements were performed at baseline and repeated at 12 and 24 month. Treatment effects were compared among groups by analysis of variance (ANOVA), followed by 2 by 2 comparisons with the method of Least Significant Difference, and studied over time by ANOVA for repeated measurements.

Data were available at 24 months for 69 patients, drop-out rate being similar in groups A and C.

S-CTX levels decreased significantly at 3, 12 and 24 months in both ALN groups (p<0.001 for all comparisons, except p=0.029 for group B at 3 months). Significant difference in S-CTX level was observed between groups A and C after 3 months (p=0.008), 12 months (p=0.004) and 24 months (p=0.003) and between groups B and C after 12 months (p=0.028) and 24 months (p=0.004). Significant LS BMD increase was observed after 24 months in both ALN groups (group A 3.7%, p < 0.001; group B 2.6%, p=0.001) with a significant difference between groups A and C (p<0.001) and between groups B and C (p=0.001). At the femoral neck, BMD increase occurred in group A (0.9%, p=0.042) and BMD decrease in group C (-1.4%, p=0.025).

In conclusion, two years of intermittent ALN regimen, given 70 mg every two weeks or once-monthly, increased LS BMD with a significant difference as compared to placebo. Both ALN regimens were effective at decreasing rapidly osteoclastic activity in postmenopausal women, the response being slightly delayed with the monthly treatment.

| | Baseline | 3 months | 12 months | 24 months |
|------------------------------------|-------------------------|-------------------------|-------------------------|-------------------------|
| ALN every 2 weeks (Group A) | 522.3 ± 210.2 n = 28 | 300.7 ± 161.9 n = 27 | 285.9 ± 174.5 n = 26 | 250.1 ± 119.2 n = 22 |
| ALN once-monthly (Group B) | 539.1 ± 228.0 n = 28 | 394.5 ± 221.4 n = 28 | 327.6 ± 181.6 n = 28 | 257.7 ± 126.5 n = 27 |
| Placebo (Group C) | 526.6 ± 183.0 n = 27 | 440.2 ± 156.5 n = 25 | 444.4 ± 194.6 n = 22 | 393.2 ± 207.3 n = 20 |

*Normal values from the kit manufacturer <573 pg/ml for pre-menopausal women.

Table 1. S-CTX values expressed as mean ± SD (pg/ml).

Disclosures: Yves Boutsen, None.

MO0375

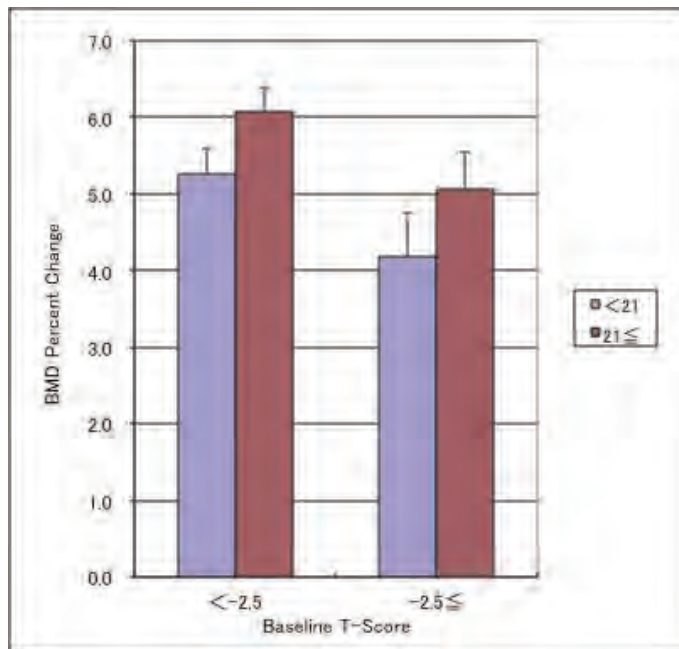
Relationship between Response to Treatment with Risedronate and Baseline Characteristics Including Age, BMD, and Vitamin D Level -Subanalyses of Japanese Risedronate Phase III Trials- Taro Mawatari¹, Ryoichi Muraoka², Yukihide Iwamoto¹. ¹Kyushu University, Japan, ²Ajinomoto Pharmaceuticals Co, Ltd., Japan

Purpose: Risedronate (RIS) increases bone mineral density (BMD) and reduces fracture risk. However, the response to the treatment may depend on the subjects' characteristics, such as baseline BMD, age, and vitamin D insufficiency. In this study, Japanese Phase III trials of RIS were subanalyzed to consider these issues.

Subjects and Methods: A total of 597 subjects whose baseline BMD, serum 25(OH)D level were measured prior to RIS treatment were included in this study. RIS was administered for 48 weeks without vitamin D supplementation in those trials. Relationship between baseline characteristics (BMD, serum 25(OH)D level, and age) and response to RIS treatment (BMD change and new fracture) were evaluated.

Results: Two-way analysis of variance showed that the percent change in BMD was higher when initial BMD (T-score) was < -2.5 than when it was ≥ -2.5 (least squares mean was 5.66% and 4.62%, respectively; P=0.032), and lower when baseline 25(OH)D level was < 21 ng/mL than when it was ≥ 21 ng/mL (least squares mean was 4.74% and 5.55%, respectively; P=0.043). (Figure) When subjects were divided into tertiles of age at start of RIS treatment, the percent change in BMD was higher in the subset of subjects aged between 63 and 70 years than other subsets (one-way ANOVA, P=0.004). Irrespective of baseline BMD, fracture rate was 2.28% in the population with a endpoint T-score < -2.5 and 1.22% in the population with a endpoint T-score ≥ -2.5.

Conclusions: These results suggest that bone density increases in response to RIS treatment even when the initial BMD is low, but early initiation of treatment would be more effective from the standpoint of preventing fracture. BMD response to RIS were smaller when 25(OH)D was less than 21 ng/mL than when it was not less than 21 ng/mL, suggesting the importance of vitamin D supplementation.



Figure

Disclosures: Taro Mawatari, None.

MO0376

Are There Differences in Those Sustaining Humeral Shaft Fragility Fractures with a Prior Osteoporosis Diagnosis? Debra Sietsema¹, Martin Hoffmann², Theresa Bacon-Baguley³, Clifford Jones¹. ¹Orthopaedic Associates of Michigan; Michigan State University, USA, ²Grand Rapids Medical Education Partners, USA, ³Grand Valley State University, USA

Background: Humeral shaft fractures occur in 3% of all fractures. Yet, humeral shaft fragility fractures are rarely screened for osteoporosis. The purpose of this study was to determine differences in those previously diagnosed with osteoporosis who have sustained a humeral shaft fragility fracture requiring surgical fixation as compared to those who were not previously diagnosed with osteoporosis. Methods: This study is a retrospective case control study of patients 50 years of age or older who were surgically treated for a humeral shaft fracture from a low-energy fall during the period of December 2008 through March 2011 at a Level I trauma center and treated at a large orthopaedic private practice. Patients were excluded who had known metastatic disease, periprosthetic fractures, and incomplete medical records. Results:

Sixty-eight patients met study criteria, of which 27 (40%) had a previous diagnosis of osteoporosis and/or a fragility fracture. More females were in the osteoporosis group (24, 89%) compared to the other group (23, 56%) ($\chi^2=0.004$). Those in the osteoporosis group had a smaller BMI (27.0, range 18.4-37.8) versus BMI 31.9 (range 19.9-50.1) in the nondiagnosed group ($t=2.544$, $\text{sig}=0.014$). Those diagnosed with osteoporosis had a lower rate of past smoking (7, 26%) compared those not diagnosed (23, 56%) ($\chi^2=0.013$). Fall prevention strategies were implemented more frequently in the previously diagnosed osteoporosis group (3 of 27, 11% vs. 0 of 41, 0%, $\chi^2=0.029$). Osteoporosis medication was prescribed at a higher rate in the previously diagnosed osteoporosis group (6, 22%) vs. the nondiagnosed group (2, 5%) ($\chi^2=0.030$). No other significant differences were found in the AO/OTA fracture classification, age, comorbidities, medication history, or osteoporotic lifestyle behavioral factors ($p>0.05$). Conclusions: As found overall in osteoporosis, more females and those with a smaller BMI with humeral shaft fragility fractures had a previous diagnosis of osteoporosis. Previous smoking occurred less frequently in the osteoporosis group. Treatment modalities were instituted more frequently after a humeral shaft fragility fracture when there was a previous diagnosis of osteoporosis. Surprisingly, no other differences were found. Astute screening, assessment, and treatment are needed to prevent initial and secondary fragility fractures.

Disclosures: Debra Sietsema, Eli Lilly, 2; Eli Lilly, 1

MO0377

Burden of Gastrointestinal Events on Osteoporosis Treatment Compliance: Administrative Claims Analysis of a Managed Care Population. Ethel Siris^{*1}, Shiva Sajjan², Jackson Tang³, Shuvayu Sen⁴, Ankita Modi². ¹Columbia University College of Physicians & Surgeons, USA, ²Merck & Company, USA, ³USA, ⁴Merck & Co., Inc., USA

Purpose: To describe the association of post-treatment gastrointestinal (GI) events and treatment compliance among a cohort of women taking osteoporosis (OP) therapy.

Method: A retrospective analysis using i3 Invision Datamart (Ingenix, Eden Prairie, MN); a large U.S. claims database with records from January 1, 2001 to December 31, 2010 (study period) was conducted. Women 50 years or older with a prescription of an oral bisphosphonate (BIS) (alendronate, ibandronate, risedronate) during study period with continuous enrollment one year prior to (baseline) and after (follow-up) the first BIS prescription date (index date) were included. Women with Paget's disease or malignant neoplasm in baseline or follow-up were excluded. Switching, discontinuing or augmenting from initial OP therapy to another therapy was assessed. Compliance was estimated using the medication possession ratio (MPR), calculated as the number of days supply of all OP medications received in the follow-up period divided by 365 days. Compliance was defined as $\text{MPR} \geq 0.80$. GI events were identified using ICD-9 diagnoses codes for GI symptoms in follow up. GI events could be new, recurrent or pre-existing (prior to the study period) during the follow up period. The study design does not ascribe causality of GI events. Multivariate logistic regression was used to examine the association of any post-treatment GI event (independent variable) and compliance (outcome variable) adjusting for covariates at baseline including age, osteoporosis fracture, GI events, Charlson comorbidity index, use of gastro-protective agents, nonsteroidal anti-inflammatory drugs, corticosteroids or estrogen.

Results: 99,788 women met study inclusion criteria of whom 27,445 (23.2 %) had developed at least one GI event in follow up. Among those with GI events, 67.4% discontinued BIS and 0.8% switched to a non-BIS. Patients with a GI event had a significantly lower MPR (Mean, [SD]: 0.5, [0.3] vs. 0.6, [0.3]) and significantly higher therapy discontinuation rates (67.1% vs. 57.2%) when compared with patients without GI events (p -value < 0.01). Patients with GI events were 29% less likely (Odds ratio (OR): 0.71, 95% CI [0.69-0.74]) to be compliant as compared to those without GI events.

Conclusion: Medication compliance was significantly lower among women with GI events as compared to those without GI events which may result in an incremental burden with respect to osteoporosis related healthcare resource use and costs.

Disclosures: Ethel Siris, Amgen, Lilly, 1
This study received funding from: Merck and Company

MO0378

Characterizing Gastrointestinal Events Among Patients Initiating Osteoporosis Therapy: A Retrospective Administrative Claims Database Analysis. Ethel Siris^{*1}, Tao Fan², Chun-Po Steve Fan³, Shiva Sajjan⁴, Shuvayu Sen⁵, Ankita Modi⁴. ¹Columbia University College of Physicians & Surgeons, USA, ²Merck, USA, ³AsclepiusJT LLC, USA, ⁴Merck & Company, USA, ⁵Merck & Co., Inc., USA

Purpose: To describe patient characteristics and rates of gastrointestinal (GI) events among patients on osteoporosis (OP) therapy.

Methods: A retrospective cohort study using i3 Invision Datamart; a large U.S. claims database records from January 1, 2001 to December 31, 2010 (study period) was conducted. Women 50 years or older, who had a prescription of an oral bisphosphonate (BIS) (alendronate, ibandronate, risedronate) from 2001–2010 and were continuously eligible in the 1 year prior to (baseline) and after (follow-up) the date of first BIS prescription (index date) during study period were included in the

study. Patients were excluded if they had any OP medications, Paget's disease or malignant neoplasm in baseline. Gastrointestinal events were defined as having a GI symptom related ICD-9 diagnosis and were assessed during the baseline (pre-treatment period) and at during 3, 6, and 12 months after OP treatment initiation in the follow-up. GI events were defined as having a diagnosis including esophagitis, esophageal reflux, ulcer, stricture, perforation, hemorrhage gastric, duodenal, peptic ulcer, acute gastritis, duodenitis, nausea, vomiting or dysphagia. GI events could be new, recurrent or pre-existing (i.e., present prior to the study period) during the follow up period. Rate of GI events were calculated based on percentage of individuals having at least one GI event divided by the sample denominator.

Results: The study population comprised 99,788 women who met study inclusion criteria with mean age of 61.5 years. In the baseline period, 26,045 (26.1%) individuals had GI events. Overall, 27,445 (27.5%) patients experienced GI events in the 12 month period post OP treatment initiation which comprised of either new, recurrent or pre-existing events. Among these, 14,207, 14.2 % developed a new GI event (not experienced by the subject in baseline) in the 12 month follow up period. Among the total sample, 10.5 % and 17.2% experienced GI events within first 3 months and 6 months of therapy respectively.

Conclusion: The background rate of GI events prior to initiating OP therapy was 26.1% close to the rate in follow up period (27.5%) in a managed care population. However, this study design does not ascribe causality of GI symptoms. Future research is needed to evaluate incremental burden of GI events related to quality of life and osteoporosis resource utilization among patients with osteoporosis.

Disclosures: Ethel Siris, Amgen, Lilly,; Amgen, Lilly, Merck, 2
This study received funding from: Merck and Company

MO0379

Reported Medication Initiation Rates are not Directly Comparable across Secondary Fracture Prevention Programs: Findings from a Systematic Review. Joanna Sale^{*1}, Dorcas Beaton², Josh Posen¹, Earl Bogoch¹. ¹St. Michael's Hospital, Canada, ²Keenan Research Centre, St Michael's Hospital, Canada

Purpose: To examine the methods used to calculate reported medication initiation rates in fracture secondary prevention programs.

Methods: A systematic review was conducted on post-fracture interventions that aimed to improve osteoporosis management in an orthopaedic environment. Two authors independently reviewed eligible articles to determine the numerator and denominator used to calculate rates of antiresorptive medication initiation based on author reports. In interventions with numerator and denominator combinations that appeared to be comparable, we examined the inclusion and exclusion criteria to confirm comparability.

Results: Fifty-seven articles reporting on 64 interventions from 11 countries were eligible for the systematic review. A total of 28 different combinations of numerators and denominators to calculate rates were reported for medication initiation across 49 of the 64 interventions. Of the remaining 15 interventions, one reported a rate for medication initiation but the numerator and denominator were unknown, four interventions reported no rate for medication initiation but reported a variety of numerators and denominators, two interventions reported pharmacotherapy data but not medication initiation, and eight interventions reported no pharmacotherapy data. After examining the inclusion and exclusion criteria for rates that appeared to be comparable, the highest number of interventions with a comparable rate was three.

Conclusions: Reporting processes for antiresorptive medication initiation outcomes in fracture secondary prevention programs used heterogeneous standards that obscured their results and prevented useful comparison of programs. Applying different numerator and denominator combinations meant that the same observed number of patients could have resulted in different reported rates. We propose standards for reporting in such programs.

Disclosures: Joanna Sale, None.

MO0380

Substantial Under-treatment among Women Diagnosed with Osteoporosis in a United States Managed Care Population. Ethel Siris^{*1}, Shiva Sajjan², Srinivasan Rajagopalan³, Shuvayu Sen⁴, Ankita Modi². ¹Columbia University College of Physicians & Surgeons, USA, ²Merck & Company, USA, ³Meddata Analytics, USA, ⁴Merck & Co., Inc., USA

Purpose: To describe characteristics and treatment initiation among women diagnosed with osteoporosis (OP) in a managed care population

Material and Methods: A retrospective cohort study using i3 Invision Datamart; a large U.S. claims database records from January 1, 2001 to December 31, 2010 (study period) was conducted. Inclusion criteria were women, ≥ 55 years, with a diagnosis of OP based on ICD-9 CM codes of 733.0x during the study period and enrolled for at least one year before and after the index diagnosis date. Index date was defined as the first date of OP diagnosis in the study period. Women who had a claim for Paget's disease, malignant neoplasm or a prescription for an OP medication prior to the index date were excluded. Users of estrogen therapy 12 months prior to index date were also excluded in the analysis. OP medications were identified based on NDC codes and included bisphosphonates (alendronate, etidronate, ibandronate, risedronate, zoledronic acid) and non-bisphosphonates (calcitonin, raloxifene, teriparatide). Subjects

were characterized as 'treated' if they received at least one pharmacological OP medication within the one year after OP diagnosis. Number and percent of individuals receiving pharmacological treatment were determined in this population. Patient characteristics such as age, Charlson comorbidity index, OP fracture history, gastrointestinal events, renal disease history, corticosteroid use, estrogen use and non-steroidal anti-inflammatory drug use in the pre-index period were assessed for all patients. Differences in baseline patient characteristics were assessed by Wilcoxon rank-sum tests for continuous variables and Chi-square tests for binary or categorical variables among the treated and untreated groups.

Results: Among 65,344 patients meeting study criteria with a mean age of 66 years, a majority, 64.3 % of the patients did not receive any pharmacological treatment within the one year of their diagnosis. Thirty-one percent of subjects initiated treatment with bisphosphonates and 4.9 % initiated non-bisphosphonates. Approximately 6.9 % of the patients had a history of OP fractures and about 27.3 % women had a history of gastrointestinal events during the baseline.

Conclusion: This analysis showed that a large proportion of women with osteoporosis did not receive any pharmacological treatment after their osteoporosis diagnosis warranting a need for further understanding the reasons for non-treatment despite diagnosis.

Disclosures: Ethel Siris, Amgen, Lilly and Merck, 2; Amgen, Lilly, 1
This study received funding from: Merck and Company

MO0381

The Effects of Bazedoxifene on Bone Structural Strength Evaluated by Hip Structure Analysis. Thomas Beck^{*1}, Thomas Fuerst², Kenneth Gaither³, Santosh Sutradhar⁴, Amy Levine⁵, Teresa Hines⁴, Robert Williams⁴, Arkadi Chines⁶. ¹Quantum Medical Metrics, LLC, USA, ²Synarc Inc, USA, ³Synarc, Inc., USA, ⁴Pfizer Inc., USA, ⁵Pfizer Primary Care Business Unit, USA, ⁶Amgen Inc., USA

Purpose: Bazedoxifene (BZA) is a selective estrogen receptor modulator that is effective for the treatment and prevention of postmenopausal osteoporosis. Hip structure analysis (HSA) is a method for extracting bone structural strength properties from hip bone mineral density (BMD) scans. This exploratory analysis evaluated changes in hip structure in postmenopausal women treated with BZA for 2 years.

Methods: Hip dual energy X-ray absorptiometry (DXA) scans were obtained from postmenopausal women enrolled in a phase 3 osteoporosis treatment study. The analysis was based on data for BZA 20 mg (approved dose) and placebo (PBO), primarily from women at increased fracture risk (1 moderate or severe or >1 mild vertebral fracture and/or femoral neck BMD T-score ≤ -3.0 at baseline) in addition to some women from the overall cohort. At baseline, mean (SD) age was 67.7 (6.3) years for BZA 20 mg and 67.4 (6.6) years for PBO; mean (SD) lumbar spine BMD T-score was -2.29 (1.13) for BZA 20 mg and -2.21 (1.22) for PBO. HSA was applied to hip DXA scans acquired in duplicate at screening and 24 months. Percent change from baseline in geometric parameters including section modulus (SM), cross-sectional area (CSA), outer diameter (OD), and buckling ratio (BR) as well as BMD were evaluated using an analysis of covariance, with baseline value, years since menopause category, fracture prevalence, study site, scanner type, and treatment in the model.

Results: In all regions, BMD increased and geometry trended toward improvement with increased CSA and SM and decreased BR with BZA. In the narrow neck, BZA 20 mg was associated with significant increases in SM ($P < 0.001$), CSA ($P < 0.001$), OD ($P < 0.05$), and BMD ($P < 0.01$) compared with PBO. In the intertrochanter region, BZA 20 mg significantly increased CSA and BMD and decreased BR versus PBO ($P < 0.05$ for all). Except for BMD ($P < 0.05$), effects at the shaft region with BZA 20 mg did not reach statistical significance.

Conclusion: Overall, BZA showed improvements in CSA, SM, BR, and BMD at all regions, suggesting geometry-related improvement in bone strength with regard to resistance to bending and compressive forces and local buckling. These improvements were more evident at common fracture locations in the femoral neck and intertrochanter regions of the hip. Findings are consistent with the significant treatment effect on nonvertebral fractures seen with BZA in higher-risk postmenopausal women with osteoporosis.

Disclosures: Thomas Beck, Quantum Medical Metrics, 8
This study received funding from: Pfizer Inc.

MO0382

A Cost Effectiveness Analysis of a Fracture Liaison Service. Daniel Solomon^{*1}, Amanda Patrick², John Schousboe³, Elena Losina². ¹Harvard Medical School, USA, ²Brigham & Women's Hospital, USA, ³Park Nicollet Clinic/University of Minnesota, USA

Background/Purpose: Post-fracture care is woefully inadequate in many settings. In the US, post-fracture care treatment occurs in less than 25% of older women. We examined the clinical and economic implications of a Fracture Liaison Service (FLS), in which an allied health provider (e.g., Nurse Practitioner) takes responsibility for post-fracture management, such as bone mineral density testing, laboratory investigation, osteoporosis (OP) treatment decision making, fall reduction education, and adherence counseling. Such an FLS would be supervised by a clinician.

Methods: We used a validated state transition Markov model of fracture care to estimate the effect of an FLS versus current usual care on subsequent fracture rates,

costs, and quality adjusted life expectancy (QALE). Estimates of fracture rates, costs, and quality of life post-fracture by fracture site were derived from the literature. We conservatively assumed: OP treatment rates with an oral bisphosphonate of 21% in usual care and 42% in FLS; FLS cost per patient US\$100 plus \$100 DXA and \$84 per year for treatment; and adherence to treatment declining to 55% and 40% of initial levels at 1 and 5 years. Re-fracture rates were drawn from a variety of high quality epidemiologic studies. We applied a 3% annual discount rate, a lifetime horizon and a modified societal perspective. We ran sensitivity analyses varying the FLS cost to US\$150 and the cost of treatment to US\$250, and increasing the FLS rates of treatment to 66% and 88%.

Results: In a simulated cohort of 10,000 65-year old women with prior hip fractures, over the ensuing 5 years, the cumulative incidence of new fractures was reduced from 2,635 to 2,483 (for a reduction of 152 fractures). Similar analyses in a cohort of 80-year old women find that the FLS would reduce the cumulative incidence of new fractures from 2,295 to 2,192 (for a reduction of 103 fractures). These reductions in fracture incidence lead to improved quality adjusted life expectancy (QALE) and reduced or minimally-increased costs (see Table).

Conclusions: An FLS is likely cost-neutral to cost-saving and improves quality adjusted life expectancy.

| Strategy | Cost, \$ | QALE | incremental costs | Incremental QALE | Incremental cost-effectiveness ratio |
|--------------------------|----------|-------|-------------------|------------------|--------------------------------------|
| 65 year old women | | | | | |
| usual care | 75,349 | 7.686 | --- | --- | reference |
| FLS 42% | 75,283 | 7.690 | -65 | 0.004 | cost-saving |
| FLS 66% | 74,981 | 7.697 | -368 | 0.011 | cost-saving |
| FLS 88% | 74,723 | 7.704 | -625 | 0.018 | cost-saving |
| 80 year old women | | | | | |
| usual care | 43,379 | 3.899 | --- | --- | reference |
| FLS 42% | 43,389 | 3.903 | 9 | 0.004 | 2,651 |
| FLS 66% | 43,150 | 3.908 | -229 | 0.009 | cost-saving |
| FLS 88% | 42,989 | 3.914 | -390 | 0.015 | cost-saving |

Table: Simulated costs, quality adjusted life expectancy and incremental cost-effectiveness ratios

Disclosures: Daniel Solomon, Lilly, 6; Amgen, 6

MO0383

Osteoporosis-Related Cost and Healthcare Utilization among Women Newly Initiated on Zoledronic Acid. Joice Huang^{*1}, Brad Stolshek², Emily Durden³, Elnara Eynullayeva³. ¹Amgen, USA, ²Amgen Inc, USA, ³Thomson Reuters, USA

Purpose: Oral bisphosphonates (BP) can be contraindicated or anticipated to be intolerant, so the BP of choice is sometimes zoledronic acid (ZA). We compared the OP-related utilization and direct healthcare costs for women who initiated ZA to a similar group of women treated with other OP therapies of interest.

Methods: Using MarketScan^a Commercial and Medicare claims databases, two cohorts of women aged ≥50 years with (1) a medical claim for ZA, or (2) a pharmacy or medical claim for a BP, teriparatide, or raloxifene between 8/1/2007 and 6/30/2009 were identified. Index dates were the date of the first claim for an OP therapy. Patients were observed for 12 months in the pre-index period to ensure new treatment initiation, and 18 months in the post-index period to account for ZA 2nd infusion. ZA patients without prior OP treatment were matched with a comparison cohort with no prior OP treatment who initiated a non-ZA OP drug using propensity scores. Outcome measures were costs and healthcare utilization (e.g. inpatient admissions, outpatient visits/services, and outpatient prescriptions) incurred in the 30-day and the 18-month post-periods, inclusive of the index date. Costs were adjusted to 2010 US dollars.

Results: Within the Commercial database, 64031 patients (1039 ZA, 62992 comparison) met all study criteria; likewise, 44663 Medicare patients (1412 ZA, 43251 comparison) were included. In the Commercial cohort, propensity score adjusted OP-related mean costs 30-day post-index were \$1766 vs. \$258 for ZA and the comparison groups, respectively ($p < 0.001$). OP-related mean costs in the 18-month post-period were \$3615 vs. \$1892 for ZA and the comparison groups, respectively ($p < 0.001$). In the Medicare cohort, 30-day post-index OP-related mean costs were \$1564 vs. \$286 for ZA and the comparison groups, respectively ($p < 0.001$). The 18-month post-period OP-related mean costs were \$3986 vs. \$2371 for ZA and the comparison groups, respectively ($p < 0.001$). Outpatient utilization including ZA prescription, laboratory, and day procedures, accounted for the majority of the increased expenditures during post-ZA infusion follow-up.

Conclusion: OP-related healthcare costs and utilization were significantly higher in the 30-day and 18-month post-periods for OP patients newly initiating ZA in contrast

with similar patients who initiated other OP drugs. When initiating OP treatment, this should be considered in determining the total cost of administering ZA.

Disclosures: Joice Huang, Amgen Inc, 3
This study received funding from: Amgen Inc

MO0384

The Correlations between Heel Quantitative Ultrasound and DXA Parameters - a Study in 336 Postmenopausal Women with Normal and Low BMD. Mara Carsote¹, Catalina Poiana^{*1}, Carmen Barbu², Crisitina Ene¹, Mihaela Popescu³, Valentin Radoi⁴, Gabriela Voicu⁵. ¹UMP DAVILA, Romania, ²Carol Davila University, Romania, ³Parhon, Romania, ⁴UMPh Davila, Romania, ⁵I.Parhon, Romania

Introduction: The use of Heel Quantitative Ultrasound (QUS) is important because of the low costs, portable, non ionizing devices compare to DXA. The direct correlations between the parameters from these 2 devices are still a matter of debate.

Aim: We correlated the results from DXA examination and those from QUS exam into 3 different groups of patients based on T-score values.

Patients and Method: 336 women between 45 and 81 yrs were included. They were in menopause for at least 1 year and not previously treated with specific anti-osteoporosis drugs. The patients were analyze by lumbar DXA (GE Lunar) and QUS (GE Lunar Achilles). We used for evaluation the parameter Stiffness Index (SI-QUS) at the left heel and Bone Mineral Density (BMD-DXA). The statistical analyze was performed with EPIINFO.

Results: The av. age was 58.4+/-12.3 yrs. The patients were included in 3 groups based on WHO 2004 criteria: normal (T-score less than -1)- 136 patients (p), osteopenia (T-score between -1 and -2.5) - 150 p, osteoporosis (T-score less than -2.5) - 50 p. The positive week correlation between SI and BMD was statistically significant for the patients with normal DXA ($r=0.245, p<0.005$), but in women with osteoporosis and osteopenia we found no correlation between the studied parameters.

Conclusion: We obtained good results in analyzing the BMD and SI in postmenopausal women with normal DXA, but not in patients with osteoporosis or osteopenia. Probably, more selective criteria (as decades of age or years after menopause) will enhance the accuracy of the results.

Disclosures: Catalina Poiana, None.

MO0385

Unmet Need for Osteoporosis Treatment in Real World Kyphoplasty/Vertebroplasty Patients. Yang Zhao^{*1}, Stephen Johnston², Donna McMorow², Kelly Krohn³, John Krege⁴. ¹Eli Lilly, USA, ²Thomson Reuters, USA, ³Lilly USA, LLC, USA, ⁴Eli Lilly & Company, USA

Purpose: Postmenopausal men and women aged 50+ presenting with vertebral fractures are recommended candidates for pharmacologic osteoporosis (OP) treatment according to National Osteoporosis Foundation (NOF) guidelines. This study examined real world patterns of OP treatment strategies among kyphoplasty/vertebroplasty (KV) patients.

Methods: A large US administrative claims database was used to identify patients aged 50+ with a KV between 1/1/2002-12/31/2010 (first observed KV = index). All patients included had 6+ months of pre-index continuous enrollment (baseline), no baseline evidence of teriparatide (TPTD), cancer, or Paget's disease. Patients were followed for up-to 36 months post-index to observe patterns in pharmacologic OP treatments. Five cohorts were constructed based on pre- and post-index use of OP treatment: patients with no observed evidence of OP treatment pre- or post-index (N/N); new bisphosphonate (BP) initiators with no baseline BP (N/BP); BP continuers with baseline BP (BP/BP); new TPTD initiators with no baseline BP treatment (N/TPTD); and TPTD initiators switching from prior BP (BP/TPTD). Demographics, clinical characteristics, and healthcare costs were compared across the 5 cohorts.

Results: Study included 23,241 patients. About 50% of the patients (11,667) had no OP treatment (N/N) over a median of 359 days of follow-up; 5,783 of whom had ≥ 1 year of follow-up. New BP initiators (N/BP; 4,742 patients) started BP treatment within a median of 68 days. BP continuers (BP/BP; 5,245 patients) resumed treatment within a median of 37 days. New TPTD initiators (N/TPTD; 680 patients) started TPTD treatment within a median of 70 days. TPTD initiators switching from prior BP (BP/TPTD; 907 patients) switched to TPTD treatment within a median of 38 days. Mean ages ranged from 74.2 (N/TPTD) to 77.6 (BP/BP) years. The N/N cohort had the highest proportion of males (44% vs. 14-26%), and the lowest baseline use rates of systemic glucocorticoids (33% vs. 36-47%) and dual energy X-ray absorptiometry scans (8% vs. 13-20%). Mean baseline healthcare costs were the lowest for the N/BP (\$13,536) and BP/BP (\$12,545) cohorts (vs. \$15,059-\$16,791).

Conclusions: Despite prominent recommendations for OP treatment in vertebral fracture patients within NOF guidelines, half of studied KV patients had no evidence of OP treatment over a median follow-up of 359 days. These data suggest substantial unmet need in the management of OP among high-risk patients.

Disclosures: Yang Zhao, Eli Lilly and Company, 7
This study received funding from: Eli Lilly and Company

MO0386

Denosumab - Identification of Patients and Tolerability in an Irish Bone Health Clinic Population. Rosaleen Lannon^{*}, Victoria Robinson, Conall Fitzgerald, Georgina Steen, Miriam Casey, JB Walsh. St James's Hospital, Ireland

Objective: Denosumab has been available for the treatment of severe osteoporosis in Ireland for 18 months. We reviewed the selection criteria applied by our physicians to prescribe denosumab, any reported side effects and initial biochemical response.

Method: We retrospectively reviewed the first 119 patients who received denosumab in our Bone Health Clinic. We looked at data from an existing database where patients demographics, bone density and biochemistry results are recorded. Prior medication and early side effects are also recorded here.

Results: We identified 110 females and 9 males. Table 1 documents demographic, biochemical and densitometric details of the 119 patients. The majority had severe established osteoporosis with 32% having vertebral fractures. Several had suboptimal vitamin D levels with PTH levels at the upper end of the normal reference range. Bone turnover was within the normal reference range. The majority of patients had normal renal function or mild dysfunction. However it should be noted that 54/119 patients had stage 3 chronic kidney disease (CKD) or worse.

Of those who commenced denosumab, 60/119 had been recently treated with at least one years course of a bisphosphonate, 15 of whom were treated with iv zoledronic acid. Other treatments were raloxifene (n=6), strontium ranelate (n=15) or rPTH (n=20). Due to the presence of CKD 18 patients received denosumab as first line treatment.

The main factors leading to commencement of denosumab were a lack of response to previous treatments, intolerance (specifically GI in 20%) of other treatments and non-compliance.

Follow up biochemical markers including serum PTH, serum calcium and bone turnover markers were carried out in 60 patients two weeks after administration of denosumab. There was a notable reduction in CTX at this stage (p=0.1) with trends towards a fall in serum calcium and rise in serum PTH also noted though this was not statistically significant. There were no clinically significant episodes of hypocalcaemia.

Clinically reported side effects were minimal: arthralgia (n=1), mild flu-like illness (n=2) and rash (n=1).

Conclusion: Denosumab is a very useful addition to the armamentarium of treatments for severe osteoporosis particularly in those with chronic kidney disease or gastrointestinal conditions. It is well tolerated with few side effects making it a safe as well as convenient treatment for our elderly population.

Table 1: Biochemical and densitometric characteristics of patients receiving denosumab.

| | Baseline mean \pm SD | 2 week mean \pm SD |
|-----------------------------------|------------------------|------------------------|
| Age | 74.9 yr \pm 10.8 | |
| 25(OH) Vit D (optimal > 75nmol/L) | 72.5nmol/L \pm 27 | |
| PTH (15-65pg/ml) | 44.9pg/ml \pm 14 | 67.6pg/ml \pm 13 |
| CTX (0.016-1.008ng/ml) | 0.315ng/ml \pm 0.092 | 0.053ng/ml \pm 0.001 |
| P1NP (16-74ng/ml) | 50.8ng/ml \pm 59 | 51.1ng/ml \pm 46 |
| Osteocalcin (13-48ng/ml) | 27.2ng/ml \pm 30 | 29.0ng/ml \pm 38 |
| Serum Calcium (2.2-2.7mmol/L) | 2.35mmol/L \pm 0.15 | 2.30mmol/L \pm 0.15 |
| T score spine | -2.79 \pm 1.19 | |
| T score total hip | -2.44 \pm 2.45 | |
| eGFR | 62ml/min \pm 21 | |

Biochemical and densitometric characteristics of patients receiving denosumab

Disclosures: Rosaleen Lannon, None.

MO0387

Effects of Denosumab on Bone Mineral Density (BMD) and Bone Resorption Marker in Men With Low BMD Compared With Men With Prostate Cancer Receiving Androgen Deprivation Therapy and Women with Postmenopausal Osteoporosis (PMO). Michael McClung*¹, Jean-Pierre Devogelaer², David Kendler³, Edward Czerwinski⁴, Osten Ljunggren⁵, Michael Bolognese⁶, Henry Bone⁷, E. Michael Lewiecki⁸, Paul Miller⁹, Ugis Gruntmanis¹⁰, Matthew Smith¹¹, Yuqing Yang¹², Andrea Wang¹², Carsten Goessl¹², Rachel Wagman¹³, Jesse Hall¹⁴, Steven Boonen¹⁵. ¹Oregon Osteoporosis Center, USA, ²St. Luc University Hospital, Belgium, ³Associate Professor University of British Columbia, Canada, ⁴Medical College Jagiellonian University, Poland, ⁵Uppsala University Hospital, Sweden, ⁶Bethesda Health Research, USA, ⁷Michigan Bone & Mineral Clinic, USA, ⁸University of New Mexico School of Medicine, USA, ⁹Colorado Center for Bone Research, USA, ¹⁰University of Texas Southwestern Medical Center, Dallas, USA, ¹¹Massachusetts General Hospital, USA, ¹²Amgen Inc, USA, ¹³Amgen, Incorporated, USA, ¹⁴Amgen, Inc., USA, ¹⁵Center for Metabolic Bone Disease & Division of Geriatric Medicine, Belgium

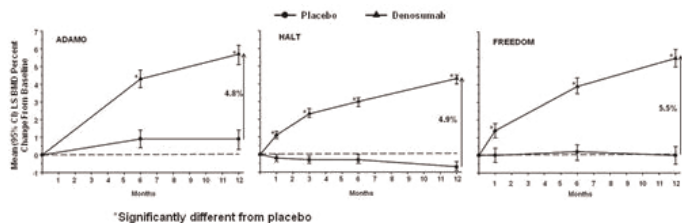
Purpose: Denosumab (DMAb) is a fully human monoclonal antibody against RANKL that decreases osteoclast formation, function, and survival. DMAB 60mg every 6 months (Q6M) has been shown to reduce bone turnover, increase BMD, and decrease risk for fractures in women with PMO (FREEDOM¹) and men with prostate cancer on hormone ablation therapy with low bone mass or a history of fragility fracture (HALT²). The efficacy and safety of DMAB in men with low BMD (ADAMO) has been shown through 12 months of treatment.³ The current analysis was conducted to evaluate the consistency of the effects of DMAB across these 3 populations with different etiologies for bone loss.

Methods: Efficacy result comparisons were based on data from the first 12 months of each study. For each BMD endpoint and serum CTX (sCTX), the analysis set included all randomized subjects who had both a baseline measurement and at least 1 post-baseline evaluation at or before 12 months.

Results: Baseline lumbar spine (LS) BMD T-scores and sCTX values are presented in the Table. While the mean baseline LS BMD T-scores for ADAMO were higher than that in FREEDOM but generally lower than that in HALT, the range of baseline LS BMD T-scores across all subjects showed considerable overlap among all 3 studies. Compared with baseline, men treated with DMAB in ADAMO showed gains in LS BMD of 5.7% compared to 4.3% and 5.5% to subjects in HALT and FREEDOM, respectively, and each were significantly greater than placebo (p<0.0001) (Figure). DMAB treatment reduced median sCTX levels by 81% from baseline at day 15 in ADAMO compared to 90% at month 1 in both HALT and FREEDOM, respectively. The safety profile observed in ADAMO at 12 months was consistent with that observed in the first 12 months of HALT and FREEDOM.

Conclusions: The magnitude of LS BMD increase at 12 months demonstrated the consistency of effects of DMAB across these 3 patient populations. HALT and FREEDOM demonstrated that increases in BMD with DMAB 60mg Q6M were associated with decreases in the risk of fracture, suggesting that the BMD increases observed in ADAMO are clinically meaningful. No new safety risks associated with DMAB treatment were identified in the ADAMO study compared with HALT and FREEDOM.

1. Cummings, et al. *NEJM* 2009;361:756
2. Smith, et al. *NEJM* 2009;361:745
3. Gruntmanis et al., *ENDO* 2012



Percent Change in Mean LS BMD at Month 12 for Subjects Enrolled in ADAMO, HALT and FREEDOM

| | ADAMO | | HALT | | FREEDOM | |
|-------------------------------------|----------------------------|----------------------------|---------------------------|---------------------------|----------------------------|----------------------------|
| | Placebo N = 121 | DMAB N = 121 | Placebo N = 734 | DMAB N = 734 | Placebo N = 3906 | DMAB N = 3902 |
| Gender | Men | | Men | | Women | |
| LS BMD T-score, mean (SD), (Q1, Q3) | -2.0 (1.0) (-2.8, -1.5) | -2.0 (1.1) (-2.8, -1.3) | -0.4 (1.8) (-1.6, 0.6) | -0.3 (1.8) (-1.5, 0.7) | -2.8 (0.7) (-3.3, -2.5) | -2.8 (0.7) (-3.2, -2.5) |
| sCTX ng/mL, median (Q1, Q3) | 0.37 (0.26, 0.51) | 0.36 (0.28, 0.48) | 0.81 (0.41, 0.83) | 0.82 (0.42, 0.87) | 0.54 (0.38, 0.72) | 0.54 (0.38, 0.71) |

Baseline Characteristics

Disclosures: Michael McClung, Merck, 6; Merck, 2
This study received funding from: Amgen Inc

MO0388

Evaluating the Effect of Yogurt Fortified With Calcium, Vitamin D and Milk Basic Protein on Bone Remodelling in Early Postmenopausal Women. Claudia Beaudoin*¹, Sonia Jean², Emilie Laurin³, Jonathan Adachi⁴, Susan I. Barr⁵, Jacques Brown⁶. ¹Crchuq Research Centre-chul, Canada, ²INSTITUT NATIONAL DE SANTÉ PUBLIQUE DU QUÉBEC, Canada, ³Les Aliments Ultima Foods inc., Canada, ⁴St. Joseph's Hospital, Canada, ⁵University of British Columbia, Canada, ⁶CHUQ Research CentreLaval University, Canada

Purpose: Previous studies have indicated that Milk Basic Protein (MBP) has beneficial effects on bone remodelling, but further studies are needed to assess if it can be provided as a supplement for bone health. The purpose of this 12-week open-label study was to evaluate the effect of daily intake of 200 g of yogurt fortified with 80 mg MBP, 660 mg calcium and 61.8 IU vitamin D (MBP-80 yogurt) on bone remodelling in early postmenopausal women with neither osteoporosis nor estrogen/progestin therapy.

Methods: Women who were vitamin D sufficient (≥40 nmol/L) were included and instructed to take MBP-80 yogurt daily from Day 0 to Day 84. Samples for the following bone turnover markers were collected on Day -28, 0, 28 and 84: serum C-terminal telopeptide of type I collagen (sCTX), serum osteocalcin (sOC), serum total N-terminal propeptide of type I procollagen (P1NP) and urinary collagen type I cross-linked N-telopeptide (uNTX). To assess the effect of MBP-80 yogurt on each marker's levels, percent changes from Day 0 to Day 28 and/or 84 were compared to those from Day -28 to Day 0. Analyses were performed on completers (defined as monthly adherence to yogurt intake ≥80%). One-sided Wilcoxon signed-rank tests were performed to determine whether differences in percent change (before vs. during the yogurt consumption period) distributions were significant (p<0.05).

Results: Eighty-six percent (43/50) of enrolled women were classified as completers and were included in analyses. For sCTX level, a median change of +4.09% was observed from Day -28 to 0 compared to median changes of -5.84% and -7.43% from Day 0 to 28 and from Day 0 to 84 respectively. According to the Wilcoxon signed-rank test, the percent change in the sCTX levels from Day -28 to 0 differed significantly from those from Day 0 to 28 (p=0.016) and from those from Day 0 to 84 (p=0.041). Thus, during the BMP-80 yogurt intake period, bone resorption decreased significantly. No significant change was observed for the other biochemical markers of bone turnover.

Conclusion: A daily consumption of BMP-80 yogurt during a period of 1 to 3 months resulted in a significant decrease in sCTX, a sensitive and specific biochemical marker of bone resorption. The magnitude of the effect is similar to calcium and vitamin D supplements (Bone H, J Clin Endocrinol Metab, 2008). Future studies could establish the effectiveness of dairy foods formulated with MBP on bone health in early postmenopausal women.

| Marker | K | Median % changes from... | | Difference in median % changes | One-sided signed-rank test [†] | |
|--------|----|--------------------------|------------|--------------------------------|---|-------|
| | | Day -28 to 0 | Day 0 to X | | N | p |
| sCTX | 84 | 4.09 | -7.43 | -11.52 | 43 | 0.041 |
| P1NP | 84 | 0.36 | -1.03 | -0.67 | 42 | 0.444 |
| sCTX | 28 | 4.09 | -5.84 | -9.93 | 43 | 0.016 |
| uNTX | 28 | -2.95 | -3.23 | -0.28 | 42 | 0.872 |
| uNTX | 84 | -2.95 | -6.33 | -3.38 | 42 | 0.354 |
| sOC | 84 | 0 | 0 | -0.55 | 43 | 0.429 |

[†]Yogurt consumption period: Day 0 to 84

[‡]Tests for equality of % change distributions were performed.

Median % change in the levels of bone turnover before and during the yogurt consumption period

Disclosures: Claudia Beaudoin, None.

This study received funding from: ULTIMA Foods inc.

MO0389

Lycopene Supplementation Improved Bone Resorption and Oxidative Stress Markers in Men \geq 50-65 Years: The CEOR Study. Mohammed-Salleh Ardawi*¹, Mohammed Qari², Abdulraheem Rouzi³. ¹Center of Excellence for Osteoporosis Research & Faculty of Medicine, Saudi Arabia, ²Center of Excellence for Osteoporosis Research & Department of Hematology, Faculty of Medicine & KAU Hospital, King Abdulaziz University, Saudi Arabia, ³Center of Excellence for Osteoporosis Research & Department of Obstetrics & Gynecology & KAU Hospital, Faculty of Medicine, King Abdulaziz University, Saudi Arabia

Background: No information is available on the role of lycopene, a known potent antioxidant found mainly in tomatoes and its products, in relation to bone loss and osteoporosis in men. We examined the effects of lycopene supplementation on biochemical bone turnover markers (BTMs), bone mineral density (BMD), and oxidative stress markers in men (age \geq 50-65 years) in a randomized controlled intervention study.

Methods: A total of 75 healthy men agreed to participate in the study and gave their informed consent. Inclusion criteria were: age of men \geq 50-65 years, independent mobility, and a femoral neck and/or lumbar spine (L₁-L₄) T-score values of \geq 1.0. Men were excluded if they had cancer or chronic diseases or treatment for metabolic bone disorders or with diseases known to be associated with increased oxidative stress. Men were randomized into 3 equal groups to follow a daily lycopene (Lyc-O-mato) supplementation protocol: (1) 30 mg/day (n=25); (2) 45 mg/day (n=25); and (3) placebo capsules containing 0 mg/day lycopene (n=25). Following a 4-week washout period with no lycopene-containing foods were consumed, and at 2, 4 and 6 months of lycopene supplementation, fasting blood and second-void early morning urine samples were collected. Men were medically examined and data were collected on lifestyle, level of physical activity and submitted a 4-day dietary records. Serum lycopene, total antioxidant status (TAS), total oxidant status (TOS), oxidative stress index (OSI), antioxidant enzymes, protein thiols, lipid peroxidation and BTMs (s-OC, s-PINP, s-CTX, and u-NTX) were measured at various time intervals. BMD was measured by X-ray absorptiometry at baseline and 6 months following supplementation.

Results: Lycopene supplementation for 6 months significantly increased serum lycopene compared to placebo (P<0.002) and decreased bone resorption (P<0.007) with increases in bone formation markers (P<0.05). Lycopene supplementation significantly increased TAS (P<0.001) and decreased TOS (P<0.001); OSI (P < 0.001); lipid peroxidation (P<0.001) and protein oxidation (P<0.001) variables as compared with placebo control, respectively.

Conclusions: Our findings demonstrate positive effects of 6-months lycopene supplementation on decreasing bone resorption markers and oxidative stress variables in men aged \geq 50-65 years: thus, lycopene may be beneficial in decreasing the risk of bone loss and/or osteoporosis.

Disclosures: Mohammed-Salleh Ardawi, None.

MO0390

Odanacatib, a Cathepsin-K Inhibitor, Has Similar Clinical Concentration-response Relationships for Urinary N-terminal Telopeptide (uNTx) and Deoxypyridinoline (uDPD). Stefan Zajic*¹, David Hreniuk², Rose Witter², Deborah Panebianco², Julie Stone², Aubrey Stoch³. ¹Merck Research Laboratories, USA, ²Merck Research Labs, USA, ³Merck & Co., Inc., USA

Purpose: Odanacatib is a cathepsin-K (cat-K) inhibitor under development for the treatment of osteoporosis. The N-terminal telopeptide collagen fragment (NTx) is a commonly used biomarker for bone resorption. Because NTx is a direct product of collagen cleavage by cat-K, it has been uncertain to what extent this biomarker can be viewed as a quantitative indicator of overall bone resorption in the presence of odanacatib, a cathepsin-K inhibitor. In this work, a PK/PD model was applied to clinical data on odanacatib and both urinary NTx (uNTx) and urinary deoxypyridinoline (uDPD), a non-cat-K-dependent biomarker of resorption that provides a direct measure of the mass of resorbed collagen, in order to compare the concentration-response relationships for these biomarkers.

Methods: Odanacatib concentrations and creatinine-adjusted urinary NTx and DPD concentrations were obtained from postmenopausal women and elderly men in eight Phase I studies for NTx and three Phase I studies for DPD. A population PK-PD inhibitory sigmoid Emax model previously developed to fit NTx and CTx data (Stoch et al., 2009) was fitted using NONMEM to concentration-biomarker datasets for uNTx and uDPD to determine Emax (maximum fractional inhibition from baseline) and EC50 values for each biomarker. DPD data were fitted as fractional change from baseline to account for study to study differences in absolute levels, while it was not necessary to baseline-adjust NTx data.

Results: Though uDPD data were more variable than uNTx, acceptable fits were obtained for both datasets. Population mean (%CV) EC50 values for NTx and uDPD were approximately 39 nM (38%) and 55 nM (102%), indicating a similar concentration-response relationship for the two biomarkers; these values are also consistent with the EC50 values observed for CTx in Stoch et al., 2009. The mean (%CV) percent of maximal reduction was approximately 66% (14%) for NTx and 39% (24%) for DPD, which is consistent with the known behavior of these biomarkers in the presence of anti-resorptive therapies.

Conclusions: These results demonstrate that in the presence of a cat-K inhibitor, uNTx and uDPD appear to have similar concentration-response relationships. Thus, uNTx appears to be an appropriate biomarker for assessing overall resorption inhibition for cat-K inhibitors, despite being a direct product of cat-K cleavage.

Disclosures: Stefan Zajic, Merck & Co., Inc., 3; Merck & Co., Inc., 7
This study received funding from: Merck Research Labs

MO0391

Osteoporosis-Related Trials in the ClinicalTrials.gov Dataset. Karen Barnard*¹, Wanda Lakey², Bryan Batch³, Karen Chiswell³, Asba Tasneem³, Jennifer Green³. ¹Duke University Medical Center, Durham VAMC, USA, ²Duke University Medical Center, USA, ³Duke University, USA

Background: More than 1.5 million fractures occur annually in the US and are associated with significant morbidity, mortality and healthcare costs. We examined the ClinicalTrials.gov database to determine if recently registered clinical trials will enhance osteoporosis care.

Methods: Investigators conducting interventional trials with at least one study site within the US are required to register trials of drugs, biologics, or devices into the ClinicalTrials.gov registry. A dataset of 96,346 studies registered was downloaded on September 27, 2010. The osteoporosis study subset of 240 interventional trials was created by selecting those trials with relevant disease condition terms. Trials evaluating orthopedic procedural interventions were excluded.

Results: At the time of the dataset download, 40,970 interventional trials had been registered since October 2007. Of these, 0.6% were osteoporosis-related. The primary purpose was treatment in 66.7%, prevention in 20%, supportive care in 5.8%, diagnostic in 3.1%, basic science in 3.1%, health service research in 0.9% and screening in 0.4%. The majority of studies included drug related interventions (60%). Other interventions were dietary/supplement (15%), behavioral (10%), procedural (7.1%), device (2.1%), and biological (1.3%). 91.8% of trials evaluated endpoints of safety, efficacy or both. Most of the trials (56.7%) enrolled only women, 39.2% of trials enrolled both men and women, and 4.2% enrolled only men. 88% of studies targeted those over the age of 18 years. 19.6% of trials excluded research participants older than 65 years and 33% of trials excluded those older than 75 years. The funding sources were industry (50.8%), NIH (6.3%), and other (42.9%). Most trials occurred in a single facility (65.8%) with the majority of trials registering at least one facility in North America (56.1%), Europe (33.5%), Eastern Asia (13.5%), or South America (7.0%).

Conclusion: The majority of osteoporosis-related trials registered between October 2007 and September 2010 examine the efficacy and safety of drug treatment and fewer trials examine prevention and non-drug interventions. Trials of interventions that are not required to be registered in ClinicalTrials.gov may be under represented in the dataset. Few trials are specifically studying osteoporosis in men and adults >75 years. Recently registered osteoporosis trials may not sufficiently address osteoporosis prevention and treatment in at risk populations.

Disclosures: Karen Barnard, None.

MO0392

Phase 3 Fracture Trial of Odanacatib for Osteoporosis – Baseline Characteristics and Study Design. Socrates Papapoulos*¹, Henry Bone², David Dempster³, John Eisman⁴, Susan Greenspan⁵, Michael McClung⁶, Toshitaka Nakamura⁷, Joseph Shih⁸, Albert Leung⁹, Arthur Santora⁹, Nadia Verbruggen¹⁰, Elizabeth Rosenberg¹¹, Antonio Lombardi¹¹. ¹Leiden University Medical Center, The Netherlands, ²Michigan Bone & Mineral Clinic, USA, ³Columbia University, USA, ⁴Garvan Institute of Medical Research, Australia, ⁵University of Pittsburgh, USA, ⁶Oregon Osteoporosis Center, USA, ⁷University of Occupational & Environmental Health, Japan, ⁸Robert Wood Johnson Medical School, USA, ⁹Merck Research Laboratories, USA, ¹⁰Merck Sharpe & Dohme, Belgium, ¹¹Merck & Co., Inc., USA

Odanacatib is a potent, selective and reversible inhibitor of cathepsin K, a collagenase secreted by osteoclasts, being evaluated for the treatment of osteoporosis. In a Phase 2 study of postmenopausal women with low BMD, oral odanacatib 50 mg once-weekly increased BMD progressively over 5 years by 11.9% at the lumbar spine and 9.8% at the femoral neck. A randomized, double-blind, Phase 3 trial designed to examine osteoporotic fracture reduction and safety has enrolled 16,231 postmenopausal osteoporotic women to receive odanacatib 50 mg or placebo once weekly (without regard to food). All participants also receive vitamin D₃ 5600 IU weekly, and calcium supplements as needed. This event-driven trial will be completed after 237 hip fractures have accrued. The trial has three primary endpoints: morphometric vertebral fracture, non-vertebral fracture, and hip fracture. Controls are employed for elevation of the false-positive error rate due to multiple primary endpoints. Clinical fractures are adjudicated centrally via clinical history, radiology reports, and/or x-rays. Secondary endpoints include clinical vertebral fractures, BMD, height, bone turnover markers, and safety and tolerability. Collection of extensive baseline clinical information, pharmacogenomic data, archived serum and urine samples for all

participants and trans-iliac bone biopsies from some participants will provide additional information. Postmenopausal women with (n=7,544) or without a prior radiographic vertebral fracture (n=8,687) were enrolled at 387 centers worldwide. At baseline they had a mean age of 73 years, were 57% Caucasian, and had mean BMD T-scores at lumbar spine -2.7, total hip -2.4, femoral neck -2.7, and trochanter -2.3. This trial will provide information on the efficacy and safety of once-weekly odanacatib 50 mg in reducing the risk of osteoporotic fractures in postmenopausal women with osteoporosis.

Disclosures: *Socrates Papapoulos, Merck Sharp & Dohme Corp., 2*
This study received funding from: *Merck Sharp & Dohme Corp.*

MO0393

Risk Factors for Developing Vertebral Fractures after Vertebroplasty (VP).

Angels Martinez-Ferrer^{*1}, Jordi Blasco², Jose Luis Carrasco³, Antonio López-Rueda², Ana Monegal⁴, Nuria Guanabens⁵, Pilar Peris⁶. ¹Hospital Clinic of Barcelona, Spain, ²Neurointerventional Department. Hospital Clinic Barcelona, Spain, ³Public Health Department. University of Barcelona, Spain, ⁴Rheumatology Department. Hospital Clinic Barcelona, Spain, ⁵Universitat De Barcelona, Spain, ⁶Hospital Clinic of Barcelona, Spain

We recently observed an increased risk (2.78-fold) for further vertebral fractures (VF) in a randomized controlled trial comparing the analgesic effect of VP versus conservative treatment (CT) in symptomatic VF (I). Therefore, the aim of the present study was to evaluate the risk factors related to the development of VF after VP in these patients.

Methods: Of the initial 125 patients randomized: 95 (47/64 in the VP arm and 48/61 in the CT arm) completed the 12-month follow-up. We evaluated the risk factors for developing VF in the 64 patients treated with VP analyzing: age, gender, baseline lumbar and femoral BMD, the number, type (wedge, biconcave or crush VF) and severity (grade I, II or III; based in Genant criteria) of vertebral deformities at baseline, the number of VP procedures, the presence and location of disk cement leakage during the procedure, bone remodeling (evaluated by determining serum PINP and urinary NTx) and vitamin D serum levels at baseline, associated glucocorticoid treatment and the type of antiosteoporotic treatment, among others.

Results: 29 radiologically new VF were observed in 17 of the 64 patients treated with VP. Increased risk of VF after VP was associated with age (>80 yr) (MR,5.6; 95% CI,1.35-18.8, p=0.019), vitamin D serum levels <20ng/ml (MR,4.3; 95% CI,1.36-13.8, p=0.005) and increased NTx values(>65nM/mM) (RR,3.11; 95% CI,1.1-8.8, p=0.01). Number, type and severity of vertebral deformities (> 2 wedge VF and/or grade II and III) were also associated with increased risk as was cement leakage into the inferior disk (RR,6.68; 95% CI,1.81-24.6, p=0.03). Procedure number > 1 also tended to be associated with a higher risk of fractures (MR,4; 95% CI,0.7-20.7, p=0.053).

Conclusions: Nearly 27% of patients with osteoporotic VF treated with VP had a new VF after the procedure. Age, especially over 80 years, low vitamin D serum levels and increased bone resorption were factors related to the development of new VF in these patients, as were the number, type and severity of VF at baseline and the presence of inferior disk cement leakage after the procedure.

(1) Blasco J et al. JBMR (in press).

Disclosures: *Angels Martinez-Ferrer, None.*

MO0394

The Impact of Different Health Dimensions on Overall Quality of Life Related to Kyphoplasty and Non-surgical Management.

Fredrik Borgström^{*1}, Oskar Ström², Steven Boonen³, Douglas Wardlaw⁴, Carolin Miltenburger⁵. ¹Karolinska Institutet, Sweden, ²Quantify Research, Sweden, ³Center for Metabolic Bone Disease & Division of Geriatric Medicine, Belgium, ⁴Orthopaedic Department, Woodend Hospital, NHS Grampian, United Kingdom, ⁵Medtronic International Trading SARL, Switzerland

Objective: The objective was to quantify the impact of different health dimensions on overall quality of life using the patient reported outcome measurements (PROMs) collected in the Fracture Reduction Evaluation (FREE) trial.

Materials and methods: The analysis was based on the patients included in the two year long randomised controlled Fracture Reduction Evaluation (FREE) trial that studied the efficacy and safety of balloon kyphoplasty (BKP) compared to non-surgical management (NSM). The PROMs included in the FREE trial was EQ-5D, SF-36, VAS-pain and the Roland-Morris Disability Questionnaire (RMDQ). The quality adjusted life year (QALY) improvement over two years was calculated by assuming that improvements over the baseline utility were solely due to treatment received. The dimensional contribution to the overall QALY was analysed by isolating the impact each dimension has on quality of life. A correlation analysis of the quality of life improvement was performed to investigate the relationships between the four instruments.

Results: The contributions (%) to the QALY gained of BKP vs. NSM from changes in each EQ-5D dimension are shown in figure 1. Changes in pain explained 60% of the QALY gained of BKP vs. NSM followed by mobility, self-care and usual

activities (EQ-5D dimensions). The results also indicate that health dimensions capturing the mental state do not seem to be an important factor for the QALY gained in this osteoporotic population. The SF-36 dimensional analysis showed similar results. The correlation analysis showed that the correlation of VAS-pain, RMDQ and QALY improvement were relatively weak.

Conclusions: Changes in the pain dimension of health are the most important driver for overall quality of life in patients treated with BKP or NSM. However, ignoring the impact of other dimensions would lead to an underestimation of the actual improvement in overall quality of life.

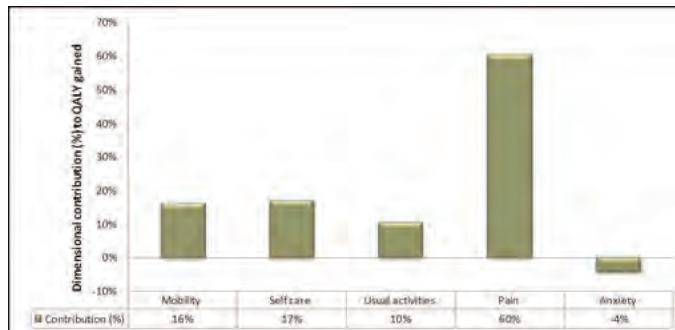


Figure 1 The contribution (%) to the QALY gained of BKP vs. NSM from changes in each EQ-5D dimension

Disclosures: *Fredrik Borgström, Medtronic, 2*
This study received funding from: *Medtronic*

MO0395

Different Bioavailability After a Single Oral or Intramuscular Administration of 600,000 IU of Cholecalciferol or Ergocalciferol in Elderly People: Implications for Treatment and Prophylaxis.

Cristiana Cipriani^{*1}, Stefania Russo², Luciano Carlucci³, Alessandro Ragno⁴, Donald MacMahon⁵, SARA PIEMONTE⁶, Antonella D'Angelo³, Claudia Castro³, Federica De Lucia⁷, Jessica Pepe³, Elisabetta Romagnoli⁸, Salvatore Minisola⁹. ¹University of Rome, Italy, ²Sapienza, University of Rome, Italy, ³"Sapienza" University of Rome, Italy, ⁴"Regina Apostolorum" Hospital, Italy, ⁵Columbia University, USA, ⁶POLICLINICO UMBERTO I-II CLINICA MEDICA, Italy, ⁷Universita Di Roma Sapienza, Italy, ⁸Dpt of Internal Medicine & Medical Specialties, University "Sapienza", Rome, Italy, ⁹"Sapienza", University of Rome, Italy

Purpose: We previously showed that a single high dose of oral cholecalciferol (D₃) sharply increases serum 25-hydroxyvitamin D [25(OH)D] while suppressing PTH serum levels in young people with vitamin D deficiency. The aim of the present study was to evaluate the bioavailability of a single oral or intramuscular high dose of ergocalciferol (D₂) and D₃ and the effect on serum calcitropic hormones in the elderly.

Methods: We studied 24 subjects (18 female and 6 male, mean age ± SD: 63.9 ± 7.1 years; age range 50-78 yrs) with vitamin D deficiency. Participants were randomized into four groups of six subjects each to receive a single dose of 600,000 IU of D₂ or D₃ by oral (po) or intramuscular (im) route. Serum 25(OH)D, parathyroid hormone (PTH) and 1,25-dihydroxyvitamin D [1,25(OH)₂D] were measured at baseline and at day (d) 30, 60, 90 and 120. We performed a data analysis by adjusting for the baseline serum levels for all the three assays.

Results: Figure 1 shows the effect of oral and im D₂ and D₃ preparations on the basal difference of serum 25(OH)D. With both oral forms there was a sharp increase at day 30 which is then followed by a slow decrease. On the contrary, both im preparations determined a slow increase during the observation period. Concerning serum levels of 1,25(OH)₂D, a significant increase after oral D₃ (10.2 ± 11.4 pg/mL), compared to both po and im D₂ at d 30 (p < 0.001 for both) and d 90 (p < 0.001 and p < 0.05, respectively), was observed. No significant change in PTH serum levels following the administration of each form was detected.

Conclusions: A single dose of 600,000 IU of oral D₂ and D₃ is initially more effective in increasing vitamin D serum levels than the equivalent im administration; oral D₃ has a greater effect in rapidly improving vitamin D status compared to the same oral dose of D₂. However, the im administration determined a sustained and gradual increase of serum 25(OH)D during all the observation period. These differences in pharmaceutical bioavailability should be taken into account when treating or preventing vitamin D deficiency states. Indeed, if fluctuations of 25(OH)D are considered harmful, then the im preparations should be preferred. The absence of long term changes of serum PTH following vitamin D administration in the elderly subjects is at variance with has been previously observed in young people, suggesting a perturbation of Vitamin D-PTH axis with ageing.

MO0397

The Effect of Different Doses of Vitamin D3 on Calcium Absorption in Older Women. Vinod Yalamanchili^{*1}, Lynette Smith², J. Christopher Gallagher¹.
¹Creighton University Medical Center, USA, ²University of Nebraska Medical Center, USA

Introduction: The major hormone that controls calcium absorption is 1,25 dihydroxyvitamin D (1,25 OH₂D₃). Previous studies show that serum 1,25 OH₂D₃ decreases when serum 25 hydroxyvitamin D (25OHD) falls below 10ng/ml but the level of serum 25OHD at which malabsorption of calcium occurs is not clear. Cross sectional data suggest that a threshold for normal calcium absorption occurred at a very low serum 25OHD level of 10 ng/ml. We performed a longitudinal placebo controlled trial of different doses of vitamin D to measure the effect on calcium absorption and looked for a threshold effect.

Methods: 163 Caucasian women, ages 57-94 years, were randomized to one of the doses of vitamin D₃ - 400, 800, 1600, 2400, 3200, 4000, 4800 IU/day or placebo for one year. Calcium intake was increased to 1200-1400 mg/day with calcium citrate. The main inclusion criteria was vitamin D insufficiency with serum 25OHD level less than 20ng/ml. Exclusion criteria were disease or medications known to affect calcium or vitamin D metabolism. Calcium absorption was measured at baseline and 12 months using a single isotope method with 100 mg elemental calcium and 5 microcuries ⁴⁵Ca. The single isotope correlates with a double isotope method. Serum 25OHD and 1,25 OH₂D₃ were measured by immunoassay (Diasorin). Multiple regression analysis was done with the variables age, dietary calcium intake, weight, serum 25OHD, dose and calcium absorption.

Results: Mean baseline serum 25OHD was 15.6 ng/ml (39nmol/L) and increased as a quadratic function reaching a plateau at around ~45ng/ml (110nmol/L). In the longitudinal analysis, there was a small but inconsistent effect of the vitamin D₃ dose on calcium absorption (p=0.046). However the increase in absorption was more highly correlated with final serum 25OHD (p=0.001). The increase in calcium absorption between serum 25 OHD levels of 20 to 60 ng/ml corresponded to an increase of 7% estimated from a double isotope method. In the baseline analysis serum 25OHD was divided into 3 groups (5-10,11-15,16-20 ng/ml) and as serum 25OHD decreased below 10ng/ml there was a non-significant decrease in calcium absorption.

Conclusions: The results show that vitamin D increases calcium absorption. The association with vitamin D dose was inconsistent and absorption was more clearly related to the serum 25OHD level. There was no clearly defined threshold for calcium absorption related to serum 25OHD level.

Disclosures: Vinod Yalamanchili, None.

This study received funding from: National Institute of Health-Aging

MO0398

Vitamin D Status and Effect of Food Supplementation in Rural White and American Indian Women. Irina Haller^{*1}, Diane Krueger², Jessie Libber², Ellen Fidler², Neil Binkley². ¹Essentia Institute of Rural Health, USA, ²university of Wisconsin, Madison, USA

This randomized, double-blind trial evaluated the effect of race (White and American Indian [AI]) on serum 25-hydroxyvitamin D [25(OH)D] and response to daily ingestion of D₃-fortified food for 4 months in healthy postmenopausal women from two rural communities. Women were randomly assigned within each race strata to receive a low calorie chocolate disk with ~2,500 IU of D₃ or an identical placebo disk daily. Measurements included serum chemistries, 25(OH)D, parathyroid hormone (PTH), markers of bone turnover and urinary calcium/creatinine ratio. Data were analyzed using t-test, chi-square test and general linear modeling.

The analysis sample included 59 women: 33 White and 26 AI. AI women were younger and had higher PTH concentrations, compared to White women (p<0.05). There were no baseline differences in clinical characteristics between D and placebo groups. Baseline prevalence of low D status (25(OH)D<30 ng/ml) was 34% among White women and 50% among AI women (NS). Compliance with the study preparation was >90% in all groups. After adjustment for baseline values, the mean 25(OH)D concentrations at follow-up were 48.1(2.0) ng/ml and 42.3(2.2) ng/ml among those who received a daily D-fortified disk in White and AI strata, respectively. Corresponding values in placebo groups were 29.6(2.1) ng/ml and 33.7(2.4) ng/ml. Adjusted for baseline and race difference in mean 25(OH)D concentrations between D and placebo groups was statistically significant (p<0.001). There was no statistically significant race effect on response to D-fortified food. Overall, after 4 months, low D status was observed in 7% of those who received a D-fortified disk compared to 50% among those who received placebo. There were no changes in serum calcium or urine calcium/creatinine ratio between baseline and follow-up. No statistically significant differences between D and placebo groups were observed at any of the study visits.

In conclusion, low D status is common among rural White and AI women. Food fortification with ~2,500 IU D₃ daily for 4 months is a safe and attractive option for improving D status in rural populations. Despite high compliance and use of a larger D dose than currently recommended, 7% remained low at the end-of-study. Further evaluation of the underlying mechanisms, including the importance of cytochrome P450 genotypes on response to D supplementation may shine light on the specific levels of vitamin D needed to maintain optimal status.

Disclosures: Irina Haller, None.

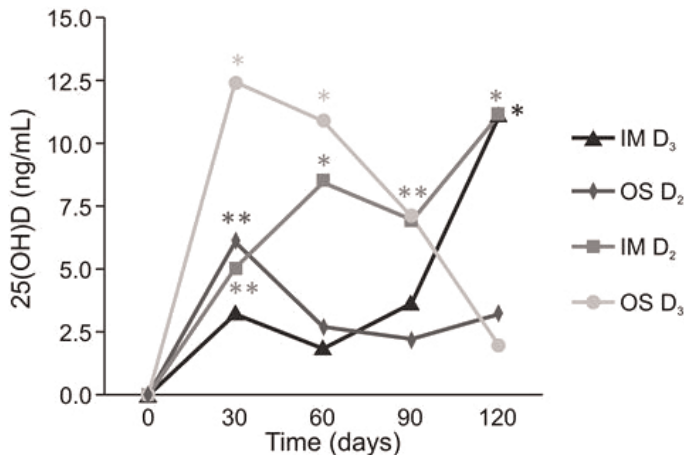


Figure 1: Effect of vitamin D supplementation on serum 25(OH)D basal difference:

OS D₃ vs IM D₃: p<0.01 at d 30 and 60

OS D₃ vs OS D₂: p<0.01 at d 30 and p<0.0001 at d 60

OS D₃ vs IM D₂: p<0.0001 at d 30 and p<0.05 at d 60

*p<0.0001 and **p<0.01 vs baseline

figure

Disclosures: Cristiana Cipriani, None.

MO0396

Skeletal & Non-Skeletal Beneficial Effects of Vitamin D. Sunil Wimalawansa*. Robert Wood Johnson Medical School, USA

Vitamin D deficiency is increasing worldwide. While, ultraviolet rays should provide more than 80% of vitamin D requirement, diet and supplements augment it. An additional 1,000 IU of vitamin D/day is generally sufficient for lighter-skinned individuals, whereas older people and dark-skinned individuals need an extra 2,000 IU/day to maintain normal serum 25(OH)D levels of over 30 ng/mL (50 nmol/L). Measurement of serum 25(OH)D is the most reliable way to evaluate vitamin D status. Rickets in childhood and osteomalacia in adults are manifestations of severe deficiency. Low vitamin D levels may aggravate a variety of non-skeletal disorders including cancer, diabetes, metabolic syndrome, infectious diseases, and autoimmune disorders. In addition to enhancing calcium absorption and mineralization of osteoid, vitamin D is important in neuro-modulation, muscle strength & coordination, release of insulin, and immune health. Whether vitamin D deficiency is related to the increasing incidences of cancer, type 2 diabetes, obesity and heart disease remains to be determined.

Several studies, Cochrane Reviews, and meta-analyses reported that doses of vitamin D over 800 IU lower fracture risks (Figure 1). Women's Health Initiative study suggested every 10 ng/mL decrease in serum vitamin D levels doubles the risk of hip fractures.

Low vitamin D status is endemic, and most common among the vulnerable groups and elderly. This is predominantly due to inadequate sun-exposure. Most patients who need vitamin D supplements are either not given or provide inadequate doses, and the long-term adherence to supplementation is poor; which can be improved with 50,000 IU doses administered once a month or twice a month. Such a regimen is efficacious and safe in replenishment of vitamin D and maintaining optimal serum 25(OH)D levels. Due to the high safety margin and the variability in measurements of serum 25(OH)D levels, to assure adequate serum vitamin D levels, a value around 40 ng/ml would be useful for maintenance.

Ref: Wimalawansa SJ. "Vitamin D: All you need to know." Karunaratne & sons, SL, 2012.

Ross, A.C., et al., *The 2011 report on dietary reference intakes for calcium and vitamin D from the Institute of Medicine: what clinicians need to know.* J Clin Endocrinol Metab,96: 53-8, 2011.

Holick, M.F., et al., *Evaluation, treatment, and prevention of vitamin d deficiency: an endocrine society clinical practice guideline.* J Clin Endocrinol Metab,96: 1911-30, 2011.

Disclosures: Sunil Wimalawansa, None.

MO0399

Vitamin D3 Dose Response on Serum 25 Hydroxyvitamin D: A Comparison of Caucasian and African American Women. J. Christopher Gallagher*¹, Vinod Yalamanchili¹, Munro Peacock², Lynette Smith³. ¹Creighton University Medical Center, USA, ²Indiana University Medical Center, USA, ³University of Nebraska Medical Center, USA

Introduction: There have been few controlled randomized trials that studied the effect of different doses of vitamin D3 on serum hydroxyvitamin D (25OHD) in human subjects.

Methods: We conducted a placebo controlled trial of the effect of vitamin D on serum 25OHD in 163 Caucasian and 110 African American older women, age range 57-94 years. They were randomized to vitamin D3 - 400, 800, 1600, 2400, 3200, 4000, 4800 IU/day or placebo for one year. Calcium intake was increased to 1200-1400mg/day with calcium citrate. The main inclusion criteria was vitamin D insufficiency with serum 25OHD level < 20ng/ml. Exclusion criteria were medical illness or medications known to affect calcium and vitamin D metabolism. Serum 25OHD was measured by immunoassay (Diasorin). The statistical analysis was a mixed effects model adjusted for covariates age, dietary calcium intake, body mass index (BMI) and baseline and serum 25OHD.

Results: The mean age for all subjects was 67 years. The mean baseline serum 25OHD was 14.5 ng/ml (36nmol/L). As the vitamin D dose increased the serum 25OHD changed as a quadratic function, on 800IU it was 30ng/ml (75 nmol/L), on 2400IU it was 39 ng/ml (97nmol/L) and plateaued at ~45ng/ml (110nmol/L) on the higher vitamin D doses. BMI had a significant effect on the dose response curves, however the curves were parallel suggesting that the variation in serum 25OHD is due to differences in volume distribution and not fat. In African Americans serum 25OHD reached similar levels to those of Caucasians on vitamin D. There was no significant difference in the dose response curves for serum 25OHD levels between Caucasian and African American women.

Summary: The results show that there is regulation of serum 25OHD level, that the serum 25OHD level is dependent on BMI and that the dose response to vitamin D is similar in African Americans to that of Caucasian women.

Disclosures: J. Christopher Gallagher, None.

This study received funding from: National Institute of Health-Aging

MO0400

What Organizational Factors Influence Vitamin D use in Nursing Homes?

Baseline Data from the ViDOS Cluster Randomized Controlled Trial. George Ioannidis*¹, Alexandra Papaioannou², Courtney Kennedy¹, Lora Giangregorio³, Lehana Thabane¹, Jacob Eappen¹, Sharon Marr¹, Robert Josse⁴, Lynne Lohfeld¹, Laura Pickard¹, Anna Sawka⁵, Lynn Nash¹, Jonathan Adachi⁶. ¹McMaster University, Canada, ²Hamilton Health Sciences, Canada, ³University of Waterloo, Canada, ⁴St. Michael's Hospital, University of Toronto, Canada, ⁵Toronto General Hospital, Canada, ⁶St. Joseph's Hospital, Canada

Background: The Vitamin D and Osteoporosis (ViDOS) study is a cluster randomized controlled trial of 40 long term care (LTC) homes (n=19 intervention, n=21 control) in Ontario, Canada. The overall purpose is to determine the feasibility and effectiveness of a multi-faceted knowledge translation intervention aimed at improving vitamin D supplementation and other evidence-based osteoporosis/fracture prevention strategies in LTC. In this analysis, we report the baseline vitamin D (≥ 800 IU/day) prescribing rates and examined whether facility-level characteristics influenced prescribing. **Methods:** De-identified clinical/prescribing data were downloaded from the database of a large pharmacy provider that services all study homes. Information on osteoporosis and fractures was gathered from Medication Administration Records. The following characteristics were collected from administrators/care directors or via publically available information on the health ministry web-site: size of home (small: < 100; medium: 100-199; large ≥ 200 beds); community size (small: <30,000; medium: 30,000-99,999, large: $\geq 100,000$ people); profit status (non-profit/profit); and chain affiliation (chain/non-chain). The generalized estimating equations technique, assuming an exchangeable correlation structure, was used to examine associations between facility-level characteristics and vitamin D (≥ 800 IU/day) use. The LTC home was used as the clustered variable in all analyses. **Results:** At baseline, there were 5454 residents [71% women, mean age=82.8 (standard deviation [SD] 10.8) years] and 108 physicians with 5 or more patients. Of the 40 study homes, the mean facility size was 142 residents (SD 79.5, range 43-378). Baseline prescribing rates for vitamin D (≥ 800 IU/day) were: 40% for all residents; 63% for residents with documented osteoporosis (n=769); and 58% for residents with a documented hip fracture (n=355). The table below presents the prescribing rates and odds ratios (95% confidence intervals) of individuals on vitamin D (≥ 800 IU/day) according to home characteristics. **Conclusion:** Vitamin D use was higher in residents with documented osteoporosis or hip fracture but was still sub-optimal. While further analyses are needed, there appears to be clinically relevant differences between vitamin D prescribing and home characteristics.

| | Percent (n/N) | Odds Ratio (95% Confidence Intervals) |
|-----------------------------|------------------|---------------------------------------|
| Size of home | | |
| Small (n=14) | 39.9 (348/872) | 1.20 (0.64, 2.27) |
| Medium (n=16) | 43.1 (949/2202) | 1.30 (0.72, 2.37) |
| Large (n=10) | 36.3 (865/2380) | Reference |
| Community size | | |
| Small (n=16) | 44.4 (597/1345) | 1.35 (0.81, 2.26) |
| Medium (n=4) | 52.4 (208/397) | 1.90 (0.55, 6.50) |
| Large (n=20) | 36.6 (1357/3712) | Reference |
| Not-for-profit (n=5) | 50.4 (576/1142) | 1.74 (0.92, 3.29) |
| For-profit (n=35) | 36.8 (1586/4312) | Reference |
| Chain affiliation | | |
| No (n=8) | 48.6 (697/1434) | 1.41 (0.84, 2.39) |
| Yes (n=32) | 36.4 (1465/4020) | Reference |

Residents Taking Vitamin D

Disclosures: George Ioannidis, None.

MO0401

BA058, a Novel Human PTHrP Analog, Restores Bone Mass in the Aged Osteopenic Ovariectomized Cynomolgus Monkey. Nancy Doyle¹, Aurore Varela*¹, Susan Y. Smith¹, Gary Hattersley². ¹Charles River Laboratories, Canada, ²Radius, USA

BA058 is a synthetic analog of hPTHrP (1-34) currently in Phase 3 of clinical development for the treatment of post-menopausal osteoporosis. The purpose of this study was to evaluate the effects of BA058 for a minimum of 4 months, on bone mineral density (BMD) measured by DXA and pQCT in the aged osteopenic, ovariectomized cynomolgus monkey. Female cynomolgus monkeys, ≥ 9 years of age, were randomly assigned to 5 groups based on whole body bone mineral content. Four groups of 16 or 17 animals were ovariectomized (OVX) and an additional group underwent Sham surgery (ovaries remained intact). Treatment commenced following a 9-month bone depletion period. Animals received daily subcutaneous injection of vehicle (Sham and OVX controls), or BA058 at 0.2, 1 or 5 $\mu\text{g}/\text{kg}$ for a minimum of 4 months. Blood and urine samples were analyzed for bone markers (NTx, CTx, BAP, PINP), and densitometry (DXA and pQCT) was measured for all animals once prior to OVX/sham operation, at the end of the bone depletion period, and after 4 months of treatment. DXA scans were obtained for the lumbar and thoracic spine, and proximal femur. Peripheral QCT scans were obtained at the proximal tibia metaphysis and diaphysis. At the end of the bone depletion period an increase in biochemical markers of bone turnover was observed for OVX animals compared to pre-OVX values or Sham controls, which was consistent with estrogen deprivation and subsequent decreases in bone density at all sites evaluated by DXA (up to -8%) and pQCT (up to -17% for trabecular BMD). Bone mass for Sham controls remained stable. The daily administration of BA058 for 4 months showed marked bone anabolic effects at all dose levels, with complete reversal of the OVX-induced osteopenia at 1 and 5 $\mu\text{g}/\text{kg}/\text{day}$. At Month 4, densitometry values were comparable to or above pre-surgery levels at the lumbar and thoracic spine and femoral neck as measured by DXA. Values increased up to 8% at the spine and 13% at the femoral neck compared to the end of bone depletion. Total slice BMD at the tibia metaphysis as measured by pQCT was significantly increased (up to 6% from the end of the bone depletion period) at all dose levels. Based on these results, BA058 potentially offers a number of important advantages as a new treatment for post-menopausal osteoporosis, including the ability to build new bone rapidly.

Disclosures: Aurore Varela, None.

This study received funding from: Radius Health

MO0402

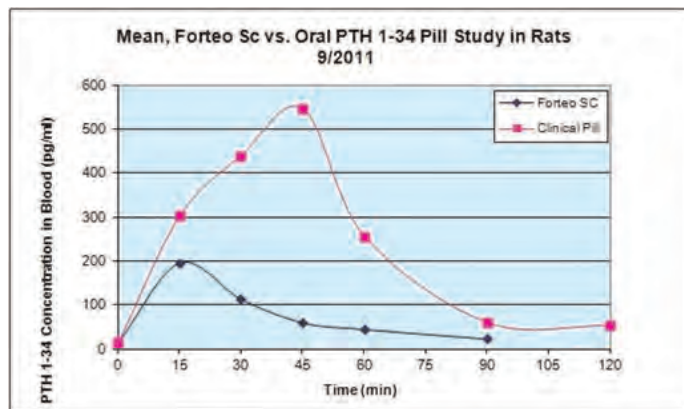
PTH Delivered Orally using a Novel Drug Delivery Technology -. Ed Arbrit¹, Phillip Schwartz², Hillel Galizer*³, Naifang Wang⁴. ¹NYU-Poly, USA, ²EnteraBio, Israel, ³New York Medical College, USA

A novel drug delivery technology that enables absorption of intact bioactive polypeptides and proteins through the gastrointestinal tract (GIT) has been used to deliver PTH in a rodent model, the first results are reported. The oral delivery technology is based on known pharmacopeia agents recognized as GRAS with no new chemical entities (NCEs). The Pk of the formulation is characterized by a rapid Tmax which is particularly suitable to simulate the anabolic profile of PTH.

Methods: Experiments were conducted in S.D. rats with an average weight of 250 mg. Animals were administered either Forteo by s.c injection (2.5 μg per rat) or by a solid dosage form (200 μg per rat) administered orally. Blood samples were withdrawn at regular intervals for Pk analysis.

Results: See attached graph

Discussion: GIT absorption of oral PTH was achieved in a consistent and reproducible manner in a rodent animal model using GRAS listed excipients. The PK of oral PTH was characterized by Tmax of 45 minutes and rapid elimination. This results are the first we have achieved with this novel technology with a suboptimal oral solid dosage form. The results are encouraging as they demonstrate the proof of concept that an oral absorption of PTH can be achieved. Further work is needed to optimize the dosage form to match that of the s.c. profile which should be readily achievable both in terms of Pk and with improved oral bioavailability. The oral drug delivery technology could be applied to other polypeptides and protein drugs that are currently only available as parenteral dosage forms. The Oral route of drug administration is the safest most convenient and most commonly used method, An oral PTH will fill an unmet medical need making this important drug accessible and convenient for use for a significant number of people with OP who are currently not able or willing to administer the drug parenterally.



Graph

Disclosures: Hillel Galizer, EnterBio, 3
This study received funding from: EnteraBio

MO0403

Rapid Transdermal Delivery of BA058 by sMTS Microneedle Arrays; Pharmacokinetics in Rats and Monkeys, and Reversal of Bone Loss in Osteopenic Rats. Gary Hattersley*¹, Amy Determan², Kris Hansen², C. Richard Lyttle³. ¹Radius, USA, ²3M Drug Delivery Systems, USA, ³Radius Health Inc, USA

BA058 is a novel analog of hPTHrP (1-34) developed as an anabolic therapy for osteoporosis treatment. Daily BA058 subcutaneous (SC) injection has produced promising safety and efficacy results thus far in Phase 1 and Phase 2 studies, and is currently enrolling in a Phase 3 fracture prevention study. There is a significant need for an alternate to injection for delivery of bone anabolic agents that improves patient convenience and compliance. To achieve this we investigated the use of 3M's solid microneedle array technology for transdermal BA058 delivery. sMTS (solid Microstructured Transdermal System) consists of a microneedle array containing ~320 microneedles that penetrate the skin to about 250 μ m, through the stratum corneum into the upper dermis. The pharmacokinetics of BA058 delivered by sMTS arrays were evaluated in rats and monkeys following application to the skin for 5 minutes. PK profiles from rats with BA058-sMTS (10, 25, 50 μ g) or BA058 SC injection (25 μ g) revealed an earlier Tmax with BA058-sMTS (5 min) compared to SC injection (15 min). The half-life (T1/2) was shorter with BA058-sMTS (25 min) than with SC injection (36 min). BA058-sMTS achieved a Cmax that exceeded SC injection, and as the dose increased, Cmax and AUC increased generally proportionally. A similar PK profile was observed in monkeys with BA058-sMTS (25, 50, 100 μ g). The Cmax for BA058-sMTS was again earlier than SC (5 min vs 1 hr) and T1/2 shorter with sMTS (30 min vs 80 min). Additional studies with longer skin contact times did not result in further BA058 release. The efficacy of BA058-sMTS was evaluated in ovariectomized osteopenic rats. Following an 8-week bone depletion period, rats were treated daily for 14 days with BA058-sMTS, placebo-sMTS, BA058 SC injection or placebo SC injection. After 14 days femur BMD increased 4.8% compared to placebo-sMTS, similar to the increase with BA058 SC (+4.2%). Lumbar spine BMD was also significantly increased with BA058-sMTS. Despite the short period of dosing, improvements in trabecular bone microstructure, assessed by μ CT, were seen in the distal femur metaphysis and lumbar spine. In summary, PK studies in rats and monkeys with BA058-sMTS demonstrate good delivery of BA058 with short wear times, and reversal of bone loss in osteopenic rats. Transdermal delivery of BA058 by sMTS potentially represents a convenient and compliance enabling new anabolic approach for the treatment of osteoporosis.

Disclosures: Gary Hattersley, Radius Health, 3

MO0404

Salvianolate Stimulates Bone Formation and Increases Bone Mass in SLE Mice. Liao Cui*¹, Yanzi Liu², Yang Cui³, Xiao Zhang³, Bilian Xu², Tie Wu². ¹Guangdong Medical College, Peoples Republic of China, ²Guangdong Medical College, China, ³Guangdong General Hospital, China

Recent studies have reported low bone mineral density and an increased risk of fracture among patients with systemic lupus erythematosus (SLE), combination treatment with glucocorticoid (GC) can accelerate bone loss in SLE patients. This study was to investigate the effects of salvianolate, an aqueous extract of *Radix Salviae Miltiorrhizae*, on bone tissue in a spontaneous SLE mice model by analysis of bone histomorphometry. Fifteen weeks old MRL/lpr mice were treated with vehicle, GC (prednisolone 6 mg/kg/d oral gavage)/salvianolate (60 mg/kg/d intraperitoneal injection) and GC plus salvianolate respectively for 12 weeks. MRL/lpr mice were very low bone mass with only 1.6% in trabecular area (Tb.Ar) comparing to wildtype mice which was with 10% in Tb.Ar. GC treated MRL/lpr mice remarkably decreased bone formation indices such as mineral apposition rate (MAR) and bone formation rate/bone volume (BFR/BV) but did not differ in bone mass when compared to MRL/lpr mice. Salvianolate treatment in GC treated MRL/lpr mice increased bone mass to 5.2% (increase of 123% in Tb.Ar, P<0.01) accompanied with increased in bone formation parameters (P<0.01) and femur bone biomechanics properties (P<0.01) when compared to GC treated MRL/lpr mice. Salvianolate treatment alone in MRL/lpr mice also increased bone mass to 3.1% (increase of 83% in Tb.Ar, P<0.05) accompanied with increased in bone formation rate/tissue volume (BFR/TV) (P<0.01) and femur bone biomechanics properties (P<0.01) when compared to MRL/lpr mice treated with vehicle. The data support further preclinical investigation of salvianolate stimulation of bone formation as a potential therapeutic strategy in treatment of SLE related bone loss.

Disclosures: Liao Cui, None.

This study received funding from: National Natural Science Foundation of China

MO0405

Single Dose Pharmacokinetics of PTH(1-34) and PTH-CBD, a Long-Acting Parathyroid Hormone Analog, in Sprague Dawley Rats. Robert Gensure*¹, Ranjitha Katikaneni², Joshua Sakon³, Robert Stratford⁴, Tulasi Ponnappakkam⁵. ¹Children's Hospital at Montefiore, Albert Einstein College of Medicine, USA, ²Childrens Hospital at Montefiore/Albert Einstein College of Medicine, USA, ³University of Arkansas, USA, ⁴Xavier University of Louisiana, USA, ⁵Childrens Hospital at Montefiore, New York/Albert Einstein College of Medicine, USA

PTH-CBD is a parathyroid hormone analog containing a collagen binding domain that targets its delivery to collagen rich areas such as bone and skin. PTH-CBD has been shown in mice and rats to have a sustained (6-9 month) anabolic action in bone after a single subcutaneous injection without causing hypercalcemia. Because of the absence of hypercalcemia, we hypothesized that PTH-CBD's effects are due to prolonged retention in the bone rather than a depot effect, leading to prolonged elevation of serum levels. To test this hypothesis, we determined the single dose serum pharmacokinetics of PTH-CBD in female Sprague-Dawley rats following subcutaneous administration and compared the results with those of human parathyroid hormone (hPTH (1-34)), using molar equivalent of 80 mg/kg of PTH(1-34). Serial blood samples were collected from the tail vein at times ranging from 0 to 360 minutes for measurement of human PTH and calcium. Pharmacokinetic analysis of hPTH serum concentrations was conducted with WinNonlin 6.2 (Pharsight, Inc) using a one-compartment model with first order absorption. PTH(1-34) and PTH-CBD showed similar area under the curve (AUC), indicating similar bioavailability. The terminal phase (declining concentration) half-life (K₁₀) was 3 times greater following PTH-CBD administration (56 minutes vs. 167 minutes). Estimation of the initial phase (increasing concentration) half-life (K₀₁) was similar for the two groups, and similar to the reported elimination half-life following intravenous bolus administration (5 – 8 minutes, Jones et al., 2006). The analysis suggest that the initial phase for both treatments actually represented elimination processes, while the terminal phase for PTH-CBD represented elimination plus ongoing absorption. Calcium concentration profiles were similar for the two groups. Results indicate that rate of absorption was reduced 3-fold when hPTH was administered as the CBD co-peptide. Thus, hPTH absorption was indeed slower when administered as PTH-CBD, but this prolonged absorption phase could only account for sustained serum levels of PTH-CBD for the first 12-24 hours after a single subcutaneous injection. Importantly, the systemic pharmacokinetic results obtained do not support long term (>6 months) presence of PTH-CBD in serum; thus, the prolonged anabolic bone effects of PTH-CBD are not due to substantially prolonged elevated serum levels.

Disclosures: Robert Gensure, BiologicsMD, 3

MO0406

Tailoring Drug - Loading Interactions to Rescue Periosteal Bone Formation at Senescence. Sundar Srinivasan¹, Dewayne Threet¹, Brandon Ausk¹, Leah Worton², Ronald Kwon¹, Edith Gardiner¹, Steven Bain¹, Ted Gross¹. ¹University of Washington, USA, ²The University of Washington, USA

Periosteal expansion, as induced by exercise, is a biomechanically optimal means to augment the structure of the fragile senescent skeleton. However, given that periosteal adaptation is muted with aging, we sought to identify therapeutic interventions that might rescue the adaptive response by focusing upon age-related alterations in mechano-sensitive Ca^{2+} /NFAT signaling. In this context, we recently found that when cyclical mechanical loading was augmented with Cyclosporin A (0.3, 3.0 mg/Kg; CsA), the induced periosteal bone formation in senescent mice (22 Mo) could be restored to levels observed in young animals (4 Mo). To examine this concept in the context of the numerous potential CsA dosage-loading combinations, we developed an *in-silico* model for how mechanical signals of varying potency would differentially modulate mechanotransduction. Based upon our analysis, we hypothesized that *bone formation in the senescent skeleton is substantially enhanced by factorial interactions between specific mechanical loading regimens and CsA dose.* We tested this hypothesis by exposing the right tibiae of senescent mice (n = 70, C57BL/6, 22 Mo) to 3-wks of either cyclical or 10-s rest-inserted loading supplemented with a range of CsA dosages (0 - 6 mg/Kg). The induced periosteal bone formation was contrasted with that observed in young animals (4 Mo, n = 17; without CsA). We found a significant interaction between CsA dose and loading regimen on induced bone formation ($p < 0.001$). The more potent mechanical signal (rest-inserted loading) required a 30-fold smaller CsA dosage to optimally enhance senescent bone formation (Fig 1). Supplementing either rest-inserted or cyclical loading with CsA, but at distinct optimal dosages (0.1, 3.0 mg/Kg, respectively), completely rescued periosteal bone formation in senescent mice to levels observed in young (Fig 1). These data suggest that attempts to augment mechanotransduction via adjuvants such as CsA will require consideration of drug - exercise interactions. While this increases the complexity of therapeutic applications, *in silico* models can serve to rapidly identify specific interactions with the most potent bone forming potential. Importantly, these mechano-pharmacologic interactions may be therapeutically exploited, as their occurrence suggests the possibility for optimizing interventions to account for individual patient differences (e.g., compliance, pre-existing conditions) when trialed in the elderly.

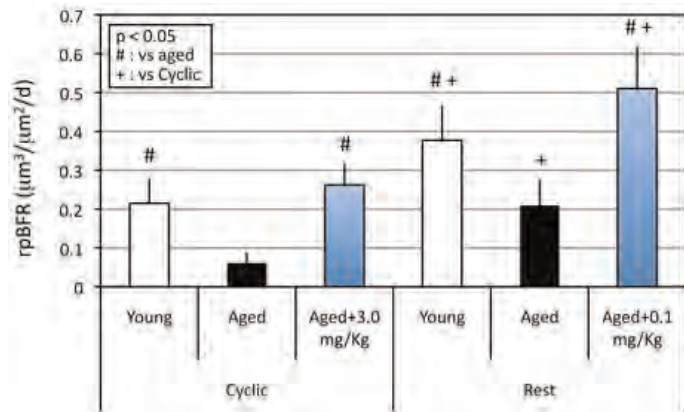


Fig 1: Periosteal adaptation at senescence can be rescued by optimal CsA dose-loading combinations.

Disclosures: Sundar Srinivasan, None.

MO0407

Effect of Sequential Treatment with Bisphosphonates after Teriparatide in Ovariectomized Rats: Comparison between Risedronate and Alendronate. Tetsuo Yano¹, Mei Yamada¹, Makoto Shiozaki¹, Daisuke Inoue². ¹Ajinomoto Pharmaceuticals Co., LTD, Japan, ²Teikyo University Chiba Medical Center, Japan

Background/Aim: Previous reports have demonstrated that patients previously treated with risedronate (RIS) exhibit a greater response to teriparatide (rhPTH1-34) than those previously treated with alendronate (ALN) in bone mineral density (BMD) gain. But effect of RIS and ALN after administration of PTH has not been directly compared. In the present study, we tested whether or not RIS has superior effect on bone quality to ALN, using ovariectomized rats, when administered after PTH.

Methods: Female Sprague Dawley rats at 12 weeks of age were divided into one sham-operated and eight ovariectomized groups (1: vehicle, 2: PTH, 3: PTH + vehicle, 4: PTH + RIS, 5: PTH + ALN, 6: PTH + vehicle, 7: PTH + RIS, and 8: PTH + ALN). PTH (0.1 mg/kg), RIS (0.01 mg/kg) and ALN (0.02 mg/kg) were given subcutaneously twice per week. RIS and ALN treated for 4 or 8 weeks after 4 weeks treatment of PTH. Four, eight or twelve weeks after PTH treatment, the rats were sacrificed and

BMD, bone strength and bone morphology of the lumbar vertebrae were evaluated using DEXA and biomechanical testing apparatus, respectively.

Result: PTH significantly increased BMD (+11.2%) in OVX rats after 4 weeks treatment. Eight weeks after PTH withdrawal, PTH + vehicle-treated group showed a BMD decline (-6.9%). In contrast, RIS and ALN significantly increased BMD by 11.5 and 14.6%, respectively, after 8 weeks of treatment with bisphosphonates. RIS and ALN decreased Tb.Sp by 17.2 and 4.2%, respectively. Additionally, RIS increased stiffness by 12.2% while ALN decreased it by 11.2%. Thus, RIS improved on Tb.Sp and stiffness to a greater extent than ALN.

Conclusion: The present study demonstrated that sequential therapy with bisphosphonates after teriparatide improved bone mass, structure and strength. Our results further suggest that RIS has a greater efficacy on bone structure and strength than ALN.

Disclosures: Tetsuo Yano, Ajinomoto Pharmaceuticals, 3

MO0408

High Doses of Zoledronic Acid Induce Persistent Osteonecrosis of the Jaw-Like Lesions in Rice Rats (*Oryzomys palustris*) with Periodontitis. Jose Aguirre¹, Donald Kimmel², Alicia Leeper³, Kathleen Neuville³, Marda Jorgensen⁴, Lakshmyya Kesavalu⁵, Thomas Wronski¹. ¹University of Florida, USA, ²Kimmel Consulting Services, USA, ³Department of Physiological Sciences, University of Florida, USA, ⁴Cell & Tissue Analysis Core, McKnight Brain Institute, University of Florida, USA, ⁵Department of Periodontology & Oral Biology, College of Dentistry, University of Florida, USA

We have already shown that oncologic doses of zoledronic acid (ZOL) induce osteonecrosis of the jaw (ONJ)-like lesions in rice rats (*Oryzomys palustris*) with periodontitis after 18 wks of treatment. Nitrogen (N)-containing bisphosphonate (BP)-associated ONJ has been defined as an area of exposed bone in the maxillofacial region that does not heal within 8 weeks after identification by a health care provider, in a patient who is receiving or had been exposed to an N-BP and had not had radiation therapy in the craniofacial region. Many investigators have shown overt, short-term ONJ-like lesions in different animal models. However, none of these studies assessed persistence of these lesions for a time period that complies with the ONJ definition. The purpose of this study was to determine whether the ONJ-like lesions observed in our model persist for at least a period of 6 wks. For this purpose, 28 day-old rice rats (10 males and 5 females/group) were fed a pelleted high sucrose and casein (H-SC) diet for periods of 24 wks. Simultaneously, animals were injected IV with vehicle or a high dose (HD) (80 $\mu g/kg$) of zoledronic acid (ZOL), which is equivalent to an oncologic dose in humans, until the end of the study. Rice rats treated with HD of ZOL developed gross/microscopic lesions that resemble ONJ. These ONJ-like lesions were similar to or with an even more destructive pattern compared to those observed after 18 wks of treatment. Lesions include: exposed necrotic alveolar bone, osteolysis, a honey comb-like appearance of the alveolar bone, and periodontal soft tissue destruction. Furthermore, bacterial biofilms morphologically resembling *Actinomyces sp.* were found attached to or within the necrotic alveolar bone, and also on the surface of the ulcerated gingival epithelium. As observed in rats treated with HD of ZOL for 18 wks, ZOL reduced mineralizing surface and BFR/BS, but not osteoclast number. Finally, blood vessel number was significantly decreased in rice rats treated with HD-ZOL compared to vehicle controls. Taken together, these data suggests that ONJ-like lesions in this model were not transient and persisted for at least 6 wks. Although this time period does not fully comply with the most recent definitions of N-BP-associated ONJ, it could represent a comparable persistence for a rodent animal model.

Disclosures: Jose Aguirre, None.

MO0409

Mucosal Irritative and Healing Impairment Effects of Risedronate, a Nitrogen-Containing Bisphosphonate, in Rats- Comparison with Alendronate and Minodronate -. Kikuko Amagase^{*}, Toshiko Murakami, Kaho Imanishi, Koji Matsumoto, Koji Takeuchi. Kyoto Pharmaceutical University, Japan

Background/Aim: Bisphosphonates (BPPs) are a class of compounds that have been developed as an anti-resorptive agent for treating the bone diseases. Clinical studies, however, showed that BPPs cause the untoward effects on the upper gastrointestinal tract. We recently found that alendronate produced ulcers in the antrum with severe edema and inflammation after refeeding. However, it remains unknown whether these unfavorable properties of alendronate are shared by other BPPs such as risedronate or minodronate. In the present study, we examined the mucosal irritative and healing impairment effects of risedronate on rat stomachs, in comparison with those of alendronate and minodronate. **Methods:** Male SD rats were used in the following 2 studies; 1) the ulcerogenic effects of alendronate, risedronate and minodronate in the antral mucosa, and 2) the healing impairment effect of these drugs on gastric ulcers induced by by thermocauterization. In the first study, each BPP was given PO once in 24 h-fasted rats, then the animals were fed normally and killed 3 days later. In the second study, each BPP was given once daily for 7 days starting from 3 days after induction of gastric ulcers. **Results:** A single administration

of BPPs to fasted rats produced ulcers in the antrum with severe edema and inflammation 3 days after refeeding, although the doses required for this action differed among these BPPs: alendronate > 100 mg/kg, risedronate > 300 mg/kg, minodronate > 10 mg/kg. The generation of antral ulcers induced by these BPPs was accompanied by an increase in MPO activity and lipid peroxidation as well as a decrease in SOD activity and GSH content in the mucosa; the extent order of these changes was minodronate > alendronate >> risedronate. On the other hand, the healing of gastric ulcers was significantly delayed by daily administration of alendronate (>30 mg/kg) and minodronate (>10 mg/kg), but not by risedronate, even at 60 mg/kg. Mucosal VEGF and bFGF protein expressions were up-regulated after ulceration, in parallel with angiogenesis. Alendronate and minodronate decreased these expressions and angiogenesis, while risedronate had no effect. Conclusion: The gastric adverse effect of risedronate is less potent than alendronate and minodronate. It is assumed that risedronate may be used more safely than other BPPs as an antiresorptive drug in patients.

Disclosures: Kikuko Amagase, None.

This study received funding from: Ajinomoto Pharma

MO0410

Rheumatologists Underestimate Daily Calcium Intake in Patients with Osteoporosis. Linda Rasch¹, Marian van Bokhorst - de van der Schueren², Lilian van Tuyl², Irene Bultink¹, Willem Lems^{*3}. ¹VU University Medical Center, The Netherlands, ²VU University Medical Center, Netherlands, ³Vrije Universiteit Medical Centre, The Netherlands

Background Calcium supplements are widely used for prevention and treatment of osteoporosis. However, literature shows a controversy whether or not excessive calcium supplementation may be associated with increased risk of cardiovascular events (1-2). In practice, rheumatologists at the VUmc use a short list to estimate dietary calcium intake. An accurate estimation is important to prescribe the adequate amount of calcium supplementation.

Objectives Validation of a short calcium list with a dietary history (DH), assessed by a dietician, as reference method.

Methods This cross-sectional study included patients attending the outpatient department of rheumatology at the VUmc. For participation, subjects had to be diagnosed with and treated for primary or secondary osteoporosis, based on a low T-score in hip and/or lumbar spine, with or without vertebral fracture. In addition, subjects with secondary osteoporosis were diagnosed with a rheumatic disorder. The short list calculated calcium intake by portions of milk, yoghurt (multiplied by 180mg calcium per portion), cheese (multiplied by 155mg calcium per portion), and 250mg calcium from other products. The short list was compared with a DH with specific focus on calcium and extra attention for portion sizes. On forehand, a difference of at least 250mg calcium between both methods was formulated as clinically relevant.

Results Sixty-six subjects (31 with primary and 35 with secondary osteoporosis) were included. Mean dietary calcium intake measured via the short list (825 ± 259 mg) was lower than via DH (1113 ± 424 mg) ($p < 0.001$). Furthermore, mean difference between both methods was 289 ± 346 mg calcium: in 37 of 66 patients (56.1%) the short list scored relevant lower than DH, in 4 of 66 patients (6.1%) the short list scored relevant higher than DH. In total, 55 patients (83.3%) reached an overall intake higher than the upper limit of the recommendation of 1200mg calcium per day.

Conclusion The short list gives a substantial and clinically relevant underestimation of dietary calcium intake in >55% of the patients. Therefore, the list is not an optimal method to measure calcium intake of patients with osteoporosis. This is a clinically relevant finding because of the rumour around an increased risk of cardiovascular events associated with a too high overall calcium intake.

References 1. Bolland MJ, et al. *BMJ* 2008 Feb 2;336(7638):262-6.

2. Lewis JR, et al. *J Bone Miner Res* 2011 Jan;26(1):35-41.

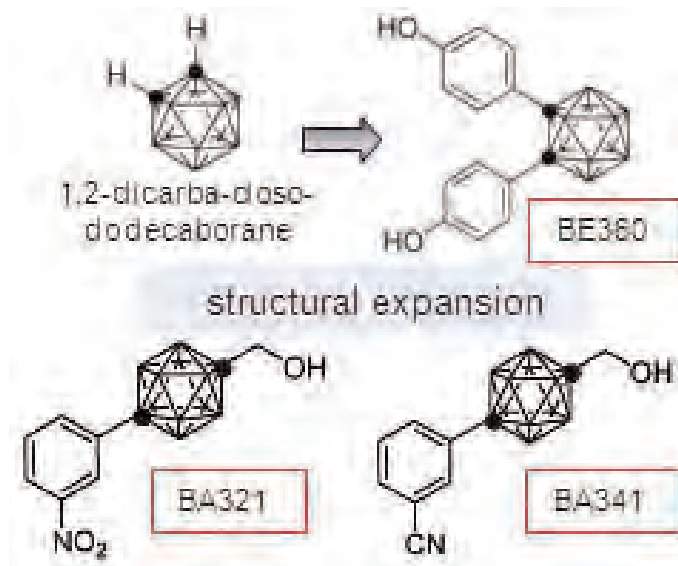
Disclosures: Willem Lems, None.

MO0411

Carborane BA321, One of The Carbon-containing Polyhedral Boron-cluster Compounds, is A New Type of Selective Androgen Receptor Modulator. Chiho Matsumoto¹, Masaki Inada¹, Michiko Hirata¹, Shinya Fujii², Tokuhito Goto³, Kiminori Ohta³, Yasuyuki Endo³, Chisato Miyaura^{*1}. ¹Tokyo University of Agriculture & Technology, Japan, ²Tokyo Medical & Dental University, Japan, ³Tohoku Pharmaceutical University, Japan

Carboranes (dicarba-closo-dodecaboranes) are a class of carbon-containing polyhedral boron-cluster compounds having exceptional hydrophobicity, and their features may allow a new medical application as a biologically active molecule that interact hydrophobically with steroid hormone receptors. We have reported carborane compound BE360 having carborane structure with two phenols, binds to estrogen receptor and exhibits estrogenic action in bone but not in uterus as selective estrogen receptor modulator (SERM). On the other hand, we have designed carborane compounds having affinity with androgen receptor (AR) and synthesized them to search effective compounds for osteoporosis in the male. Among several carborane compounds, we noticed two compounds, BA321 and BA341, as a putative AR antagonist, in which a benzene ring with electron-withdrawing group (-NO₂, -CN) and a hydroxyl group are placed at the opposite vertices of the hydrophobic carborane cage. In the competitive binding assay using human AR, both BA321 and

BA341 exhibited binding affinity to AR, and their affinities were 10-fold higher than that of the well-known anti-androgen hydroxyflutamide. In reporter gene assay using NIH3T3 cells transfected with a human AR, both BA321 and BA341 exhibited anti-androgenic activity 10-fold greater than that of hydroxyflutamide. To examine the effects of BA321 and BA341 in bone, male mice were orchidectomized (ORX) and some of the mice were treated with BA321 or BA341 (100 mg/head/day) subcutaneously for 4 weeks using a mini-osmotic pump. ORX mice showed severe bone loss due to androgen deficiency measured by femoral BMD, and the bone loss was completely recovered by the treatment with BA321 in ORX mice to sham level. BA341 significantly restored the bone loss in ORX mice, but the potency of BA341 was relatively less than that of BA321. Histological analysis by 3D-microCT showed that BA321 and BA341 significantly prevented the loss of trabecular bone in ORX mice. The weight of seminal vesicle was markedly reduced in ORX mice, and not influenced by the treatment of BA321 and BA341, indicating that these carborane compounds do not exhibit androgenic action in sex organ in the male. These results suggest the possible application of BA321 and BA341 to male osteoporosis as a new type of selective androgen receptor modulator (SARM).



Disclosures: Chisato Miyaura, None.

MO0412

(-)-epigallocatechin-3-gallate (EGCG) Alleviates Deterioration of Bone Microarchitecture in Ovariectomized Rats. Chung-Hwan Chen^{*1}, Lin Kang², Yin-Chih Fu³, Yi-Shan Lin¹, Mei-Ling Ho¹, Je-Ken Chang³. ¹Kaohsiung Medical University, Taiwan, ²National Cheng Kung University Medical College & Hospital, Taiwan, ³Kaohsiung Medical University & Hospital, Taiwan

Introduction: Green tea is one of the most popular beverages in the world. Among the catechins, (-)-epigallocatechin-3-gallate (EGCG) has received by far the most attention. Surveys have reported to reduce the risk of having a hip fracture with higher bone mineral density (BMD) by habitual tea drinkers. Our previous showed EGCG can enhance osteogenesis in a murine bone marrow cell line. Beside, we also found EGCG can inhibit osteoclastogenesis via NF- κ B. In this study, we evaluated the in vivo effect of EGCG.

Materials and Methods: Forty-eight rats aged 6 months were weight-matched and randomly allocated to 4 groups: (1) sham-operated control (SHAM) (n=8); (2) ovariectomized control (OVX) (n=14) (3) OVX with 0.34mg/kg/day EGCG treatment (OVX+1 EGCG) (n=12) (estimated peak serum concentration of 1 μ mol/L); (4) OVX with 3.4mg/kg/day EGCG treatment (OVX+10 EGCG) (n=14) (estimated peak serum concentration of 10 μ mol/L). EGCG was given intraperitoneally 3 months after ovariectomy for 12 weeks. After treatment, BMD, μ CT and histology over proximal tibia were examined. Besides, the biochemical profiles including liver function, renal function and electrolyte were also examined.

Results: BMD increased 1.66% in the SHAM group while BMD decreased 7.97% in the OVX group. Less decrease in BMD was noted in the OVX+10 EGCG group compared with the OVX group. There was significantly more trabecular number and volume in the SHAM and OVX+10 EGCG group than that in the OVX and OVX+1 EGCG group. Higher dose but not lower dose of EGCG supplement significantly increased BV/TV, Tb.Th, and Tb.N of the proximal tibiae. At the end of treatment, there was no obvious liver and renal toxicity.

Discussion: Our previous results indicated that EGCG (10 μ mol/L) significantly enhanced osteogenesis in murine bone marrow mesenchymal cells. We also found EGCG (10-100 μ mol/L) significantly suppressed the RANKL-induced differentiation of osteoclasts and the formation of pits in murine RAW 264.7 cells and bone marrow macrophages. In this study, we confirm the proximal tibia BMD and bone volume can be increased with intra-peritoneal injection of EGCG at the dose of 3.4 mg/kg/day

with the estimated peak serum concentration of 10 μmol/L. The effects in human need further studies. In conclusion, we first report the single molecule, EGCG, in GTP can mitigate the bone loss in OVX rats. Further studies are required to confirm the effects of EGCG on human.

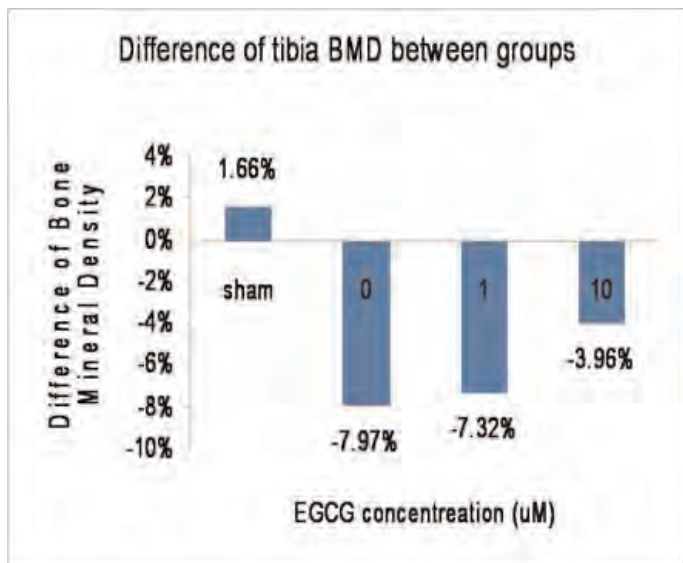


Figure . Less decrease in BMD was noted in the OVX+10 EGCG group compared with the OVX group.

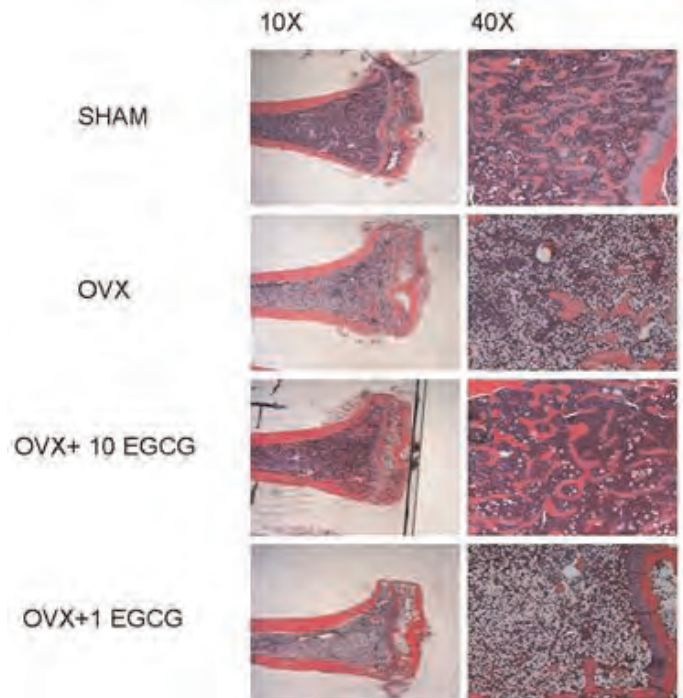


Figure 2. There was significantly more trabecular number and volume in the SHAM and OVX+ 10 EGCG gr

Thick :1.3mm
Length :4mm

Micro-CT (3D-image)

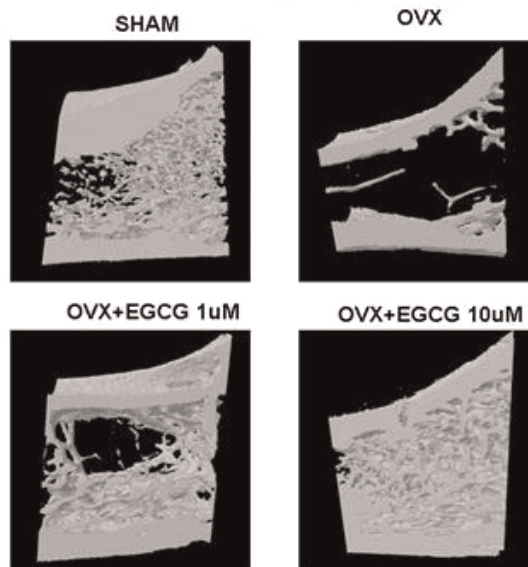


Figure 3. The structure of 3D reconstruction showed more trabecular volume in the SHAM and OVX+ 10

There was significantly more bone volume, trabecular thickness and less trabecular separation in the SHAM and OVX+ 10 EGCG group than that in the OVX and OVX+ 1 EGCG group.

| Trabecular bone | Sham | OVX | OVX+1 EGCG | OVX+10 EGCG |
|-----------------|---------------|---------------|---------------|----------------|
| BV/TV (%) | 42.34 ±5.32 | 18.80 ±3.22 | 15.81 ±0.54 | 27.38 ±4.63* |
| Tb.Th (mm) | 0.190 ±0.007 | 0.172 ±0.003 | 0.167 ±0.003 | 0.220 ±0.042* |
| Tb.Sp (mm) | 0.4631 ±0.107 | 0.9122 ±0.135 | 1.0968 ±1.097 | 0.6886 ±0.090* |

* P<0.05: compared with OVX group

Table 1

Disclosures: Chung-Hwan Chen, None.

This study received funding from: National Health Research Institute in Taiwan (NHRI-EX99-9935EI)

MO0413

A 6/12-month Toxicity Study of Denosumab in Cynomolgus Monkeys. Jeanine Bussiere*¹, Ian Pyrah². ¹Amgen Inc., USA, ²Amgen Inc, USA

A 6/12-month toxicity study with denosumab was conducted in adolescent cynomolgus monkey followed by a 3 month treatment-free period. The monkey is the only species in which denosumab is biologically active. Denosumab was administered once monthly by subcutaneous injections at 0 (control), 1, 10 or 50 mg/kg. No drug-related clinical signs were noted, nor were there treatment-related effects evident on body weight, food consumption, ophthalmic, cardiovascular, or clinical pathology parameters. Notably, there were no detrimental effects on the immune system, measured by circulating leukocyte counts, circulating immunoglobulin levels (IgG, IgM, and IgA) or lymphocyte subset numbers (T cells, B cells and NK cells). A male monkey in the 50 mg/kg group died on day 76 following prolonged diarrhea and body weight loss. Diarrhea was also seen in a majority of control animals and is a common background finding in monkeys occasionally leading to death. This death was therefore attributed to incidental disease and unrelated to denosumab. A second male monkey in the 50 mg/kg group was euthanized moribund on day 289 also following prolonged diarrhea. This animal had decreased serum levels of denosumab and lost pharmacodynamic effect (presumed due to anti-drug antibody formation) for at least 1 month prior to death. Thus, this death was also not attributed to denosumab. The only treatment-related histopathologic observations in the study were decreased chondroclasis characterized by retention of primary spongiosa and decreased numbers of osteoblasts and osteoclasts, reflecting decreased bone remodeling, in the tibia, sternum, and femur. Administration of denosumab increased vertebral bone mineral

density and femoral bone mineral content notably in males with bone mass significantly correlated with increased bone strength parameters. All treatment-related findings in this study were attributable to the expected pharmacology of denosumab, and restricted to bone. At the end of the 3-month treatment-free period, bone densitometry and strength parameters were similar among treated animals and controls, indicating normalization of bone following cessation of treatment. The NOAEL for this study was interpreted to be 50 mg/kg, the highest dose tested which represents an exposure margin of 150X the human dose for osteoporosis.

Disclosures: Jeanine Bussiere, Amgen Inc., 3
This study received funding from: Amgen Inc.

MO0414

Efficacy of ONO-5334, a Cathepsin K Inhibitor, on Bone Mineral Density, Geometry and Bone Strength in the Distal Radius in Ovariectomized Cynomolgus Monkeys. Hiroshi Mori^{*1}, Hiroyuki Yamada², Satoshi Nishikawa¹, Yasuaki Hashimoto¹, Yasutomo Nakanishi¹, Yasuo Ochi¹, Masafumi Sugitani¹, Yutaka Shichino¹, Kazuhito Kawabata¹. ¹Ono Pharmaceutical Co., Ltd., Japan, ²ONO PHARMA UK LTD., United Kingdom

We have previously reported that ONO-5334, an orally-active inhibitor of cathepsin K, increased areal BMD in the distal radius as well as lumbar vertebra in ovariectomized (OVX) monkeys (ASBMR2009, FR0420). In this study, we evaluated the efficacy of ONO-5334 on trabecular and cortical bone, and bone strength in the distal radius.

Female cynomolgus monkeys were assigned to one of the following 6 groups (20/group): sham-operated, OVX-control, ONO-5334 1.2, 6 or 30 mg/kg, or alendronate (ALN) 0.05 mg/kg. ONO-5334 was orally administered once daily from the day following OVX surgery for 16 months. ALN was administered intravenously once every 2 weeks. After necropsy, the distal radius (5% of total radius length from the distal end) were scanned using pQCT to measure volumetric BMD (vBMD) and geometric parameters. In addition, microarchitecture of trabecular bone was analysed by μ CT followed by a compression test at the distal radius (5-15% of total radius length from the distal end).

In the distal radius, OVX caused a significant decrease in trabecular vBMD and deterioration of trabecular architecture (decreases in trabecular bone volume, thickness, number, and connectivity density, and an increase in trabecular separation), but there were no changes in cortical vBMD and cortical geometry (cortical thickness, periosteal and endosteal perimeter) compared to the sham group. In trabecular bone, ONO-5334 at 30 mg/kg significantly increased trabecular vBMD (25%, $p < 0.01$ vs OVX), and prevented OVX-induced changes in trabecular microarchitecture ($p < 0.05$ vs OVX, except for trabecular thickness). In cortical bone, ONO-5334 at 6 and 30 mg/kg markedly increased cortical vBMD (23, 22% resp.) and thickness (51, 59% resp.), compared with the OVX-control group ($p < 0.01$). ONO-5334 at 6 and 30 mg/kg significantly decreased endosteal perimeter ($p < 0.01$ vs OVX), but did not affect periosteal perimeter. Bone strength (maximum load) at the distal radius decreased due to OVX ($p < 0.01$ vs sham), and markedly increased by treatment with ONO-5334 at 6 and 30 mg/kg (47, 52% resp., $p < 0.01$ vs OVX). ALN partially inhibited OVX-induced deterioration of trabecular microarchitecture, but did not affect trabecular and cortical vBMD, cortical geometry or bone strength.

These results suggest that increased cortical bone mass as well as improvement of trabecular microarchitecture by treatment with ONO-5334 induced prominent increase in bone strength in the distal radius.

Disclosures: Hiroshi Mori, None.

MO0415

Evaluation of MS-275 Skeletal Efficacy In Vitro and In Vivo. Ajit Regmi^{*1}, Masahiko Sato², Matthew Hamang¹, Lowell Gibson¹, Manuel Sanchez-Felix¹, Rachelle Galvin³, Timothy Richardson¹. ¹Eli Lilly & Company, USA, ²Lilly Research Labs, USA, ³Lilly Research Laboratories, USA

HDACs have been shown to interact with RUNX2 and other promoters to induce osteoblast maturation and matrix mineralization. MS-275, a class I specific HDAC inhibitor, was evaluated in BMP-induced adipose derive Stem Cells (ADSC) for its in vitro effects on osteogenesis. MS-275 in a concentration dependent manner induced alkaline phosphatase activity within 48 hours and increased matrix mineralization by day 8. It also induced DKK2 mRNA within 24 hrs. The compound decreased in vitro osteoclastogenesis in mouse marrow cells induced with soluble RANKL in a concentration dependent manner. We then set up to study if MS-275 promotes bone healing in a femoral cortical defect model (Komatsu et al. Endocrinology 2009). Female Sprague Dawley rats were ovariectomized at 6 months of age, allowed to lose bone for 2 months, and randomized into groups based on body weight. A 2 mm hole was drilled into the femoral diaphysis, and animals were treated with 10 μ L vehicle (58.3% wv PLG 50:50 (0.26-0.54) / 56.5% v v DMSO or collagen sponge 67% v v DMSO / 33% v v Water) or 10 μ L vehicle containing MS-275 (0.1, 0.2 and 0.4 mg). Treatments (10 μ L) were injected directly into the cortical defect at the time of surgery. Animals and the cortical defect site were evaluated longitudinally for 5 weeks by QCT. None of the treatments significantly increased mineralization (BMD or BMC) of the whole femur or of the cortical defect, relative to respective vehicle controls at study termination. The highest dose of 0.4 mg/kg decreased whole femur, anterior and

posterior cortex, and marrow BMD relative to vehicle controls in both formulations. These findings are in contrast to the recent findings by Kim et al (JBMR 2011) in which MS-275 enhanced healing of critical-sized calvarial defects in rats, when applied locally in a collagen sponge. The authors also reported that subcutaneous daily dosing with 7 mg/kg MS-275 increased femoral trabecular bone density within 10 days. In summary, MS-275 did not promote bone healing in a femoral cortical defect model despite in vitro pro-osteogenic activity. Discrepancies with previous efforts may be due to physiological differences in the calvaria and the femoral diaphysis bone healing models, and suggest that additional studies are required to clarify the skeletal effects of MS-275.

Disclosures: Ajit Regmi, Eli Lilly and Company, 3
This study received funding from: Eli Lilly and Company

MO0416

Nigella Sativa Shows Bone Protective Properties Against Postmenopausal Bone Loss in an Animal Model. Juan Guerra^{*1}, Erika Varela¹, Sara Reyna², Jameela Banu³. ¹Medical Research Division - Edinburg Regional Academic Health Center, University of Texas Health Science Center at San Antonio, USA, ²Department of Medicine, Medical Research Division - Edinburg Regional Academic Health Center, University of Texas Health Science Center at San Antonio, USA, ³University of Texas Health Science Center at San Antonio, USA

Over the past 20 years, the incidence of type 2 diabetes mellitus (T2DM) has increased significantly. One of the complications of T2DM, in elderly patients, is osteoporosis. Although both diseases are traditionally considered as separate diseases, there is increasing evidence that T2DM patients have decreased bone mass and are at high risk of undergoing fractures. Current treatments available for osteoporosis while efficacious in treating bone loss are not without severe side effects. Due to these effects, alternative treatments are now more actively sought out in treating bone loss. Previous studies have shown that *Nigella sativa* (NS) is a potent anti-diabetic drug with some bone strengthening properties. In the present study, we examined the effects elicited by NS and its major chemical constituent thymoquinone (T) on ovariectomy induced bone loss in Sprague Dawley rats.

Seven month old female Sprague Dawley rats were either sham operated or ovariectomized and divided into eight experimental groups: Baseline (B), age matched control (C), control ovarian (C S), control ovariectomy (C O), *Nigella sativa* sham (NS S), *Nigella sativa* ovariectomy (NS O), thymoquinone sham (T S) and thymoquinone ovariectomy (T O). After 3 months of treatment, animals were sacrificed. Femur, tibia and 4th lumbar vertebra were dissected for scanning using pQCT densitometer. Cancellous bone was analyzed at the proximal tibia metaphysis (PTM), distal femoral metaphysis (DFM) and vertebra.

In the PTM of C O group there was 87% and 89% decrease in cancellous bone mineral content (Cn BMC) and cancellous bone mineral density (Cn BMD), compared to the C S group. Cn BMC and BMD increased by 271% and 260% in the NS O group compared to C O group. Cn BMC and BMD decreased by 16% and 17% in the T O group compared to NS O group.

In the vertebra of the C O group there were 99% decreases in Cn BMC and BMD compared to C S group. Cn BMC and BMD increased by 14,168% and 5,746% in the NS O group from C O group. Cn BMC and BMD of T O group decreased by 78% and 66% from NS O group.

In the DFM, effect was not as pronounced as seen in the PTM and vertebra for the exception of 85% decreases in Cn BMC and Cn BMD from the C S to the C O groups.

We conclude that *Nigella sativa* and thymoquinone both display bone protective properties, NS having a more pronounced effect at the vertebra and PTM. This is possibly due to other naturally occurring compounds present in NS and could potentially be the focus of future research.

Disclosures: Juan Guerra, None.

MO0417

Osteocyte Apoptosis Induced by Glucocorticoids Is Prevented and Reversed by Anti-sclerostin Antibody in a Male Rat Model. Zahra Achiou^{*1}, Delphine Benaitreau², carine tournier², Eric Dolleans², Eric Lespessailles³, Michael Ominsky⁴, Stephane Pallu⁵, Claude Laurent Benhamou¹. ¹CHR ORLEANS, France, ²I3MTO, France, ³Centre Hospitalier Regional, France, ⁴Amgen Inc., USA, ⁵EA 4708 - I3MTO Orléans, France

Introduction: Long-term glucocorticoid therapy leads to osteoporosis and is associated with increased osteocyte and osteoblast apoptosis. Administration of antibodies anti-sclerostin, a product of the mature osteocyte, has been shown to increase bone formation and bone mass in various animal models, including in a mouse model of glucocorticoid mediated bone loss. In the current study, the effects of a sclerostin neutralizing monoclonal antibody (Scl-AbVI) on bone mass, bone strength, and osteocyte apoptosis were examined in a glucocorticoid-induced osteoporosis model in rats.

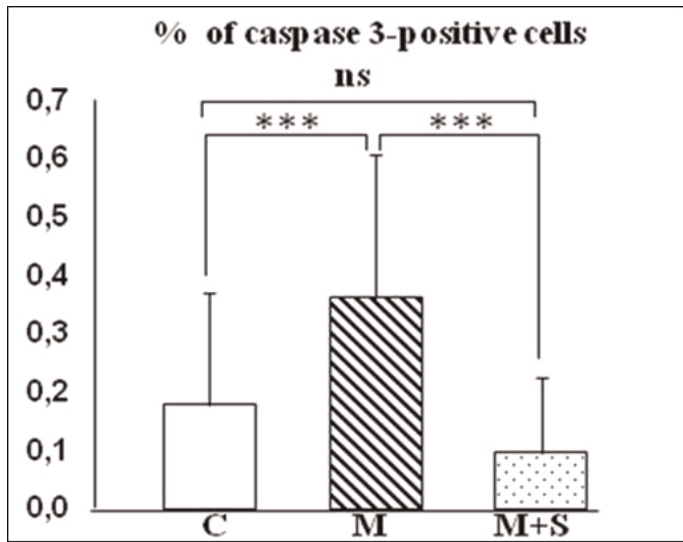
Methods: Forty five male Wistar rats, 4 month-old, were randomly assigned to 3 groups. Two groups were subcutaneously injected 5 days a week with vehicle (C) or 5 mg/kg methylprednisolone (M), with a third group injected with both methylprednisolone and Scl-Ab VI (25 mg/kg/day, 2 days a week) (M+S). After 9 weeks of

treatment, femoral BMD was analyzed by DXA, microarchitecture of the femoral trabecular and cortical bone was evaluated by micro-CT, and mechanical strength of the femur midshaft was determined by 3 point bending test. In addition, the percentage of apoptotic osteocytes in the cortical bone of the tibia was assessed by immunostaining of cleaved caspase-3.

Results: Methylprednisolone treatment induced a significant decrease in femoral BMD, Bone Volume/Tissue Volume, trabecular thickness, Trabecular number, and cortical thickness (all $p < 0.05$ vs C). Scl-Ab VI injections restored these parameters to levels higher than those observed in the control group (%BV/TV: +180% M+S vs C; +264% M+S vs M), with increased cortical thickness and decreased endocortical circumference.

Osteocyte apoptosis was increased by glucocorticoid treatment (+100% M vs C group) and was restored to a level statistically similar to controls, after Scl-Ab VI treatment (Figure). Moreover, the fractional number of apoptotic osteocytes was inversely correlated to femoral BMD ($r = -0.40$; $p < 0.04$) across all groups. Bone strength was significantly increased by Scl-Ab VI treatment at the femur midshaft versus glucocorticoid treatment (+16% in maximum load; $p < 0.05$).

Conclusion: These data have shown for the first time that Scl-Ab VI limits osteocyte apoptosis induced by glucocorticoids, the magnitude of which is negatively correlated with BMD. Moreover, Scl-Ab VI prevented glucocorticoid-induced changes in trabecular and cortical bone microarchitecture and bone strength.



Percentage of caspase-3 positive cells. Means \pm SD. ***: $p < 0.006$; ns: non significant

Disclosures: Zahra Achou, None.

This study received funding from: amgen

MO0418

Combination Treatment with Eldecalcitol (ED-71) and Raloxifene Improves Bone Mechanical Strength by Suppressing Bone Turnover and Increasing Bone Mineral Density in Ovariectomized Rats. Koichi Endo^{*1}, SATOSHI TAKEDA², Avako Shiraishi³, Nobuo Koike⁴, Masahiko Mihara⁴. ¹Chugai Pharmaceutical Co., Ltd., Japan, ²CHUGAI PHARMACEUTICAL CO.,LTD, Japan, ³Chugai Pharmaceutical Co.,Ltd., Japan, ⁴Chugai, Japan

Eldecalcitol (ED-71; ELD), a 2 β -hydroxypropyloxy derivative of 1 α ,25(OH)₂D₃, was approved for treatment of osteoporosis in Japan in 2011 and we have previously reported that ELD inhibits bone resorption more potently than alfacalcidol, a prodrug of 1 α ,25(OH)₂D₃, in ovariectomized rats. Raloxifene (RAL), a selective estrogen receptor modulator, is globally approved for the treatment and prevention of postmenopausal osteoporosis. In the present study, we compared the effects of the combination therapy of ELD and RAL with each monotherapy on bone turnover, bone mineral density (BMD) and bone mechanical strength using an estrogen-deficient osteoporosis rat model. Female 8-month-old Wistar-Imamichi rats were ovariectomized (OVX) and administered either ELD (7.5 ng/kg), RAL (0.3 mg/kg) or a combination of ELD and RAL daily by oral gavage for 12 weeks. Bone turnover markers were measured periodically at 4, 8 and 12 weeks. Lumbar and femoral BMD were measured by DXA, and the mechanical properties of the L5 vertebra and the femoral midshaft were tested by the compression test and the 3-point bending test, respectively. Bone histomorphometry was performed using the L3 vertebra. Urinary deoxyypyridinoline excretion was lower in all the treatment groups compared with the OVX control. The level in the combination group was lower than that of each monotherapy group after 4 weeks of treatment. The OVX-induced reduction of BMD at the lumbar and femur was prevented in all the treatment groups, but BMD of the combination group was higher than that of each monotherapy group. The mechanical strength of L5 was improved only by combination therapy. The femoral strength of the combination group was higher than that of the RAL-treated group. Bone histomorphometric analysis revealed that osteoblast surface (Ob.S/BS) and osteoclast

surface (Oc.S/BS) decreased in all the treatment groups and osteoid surface (OS/BS) and bone formation rate (BFR/BS) decreased in the ELD-treated and combination groups. The values of Ob.S/BS and OS/BS in the combination group were lower than those in each monotherapy group. The bone formation parameters in the combination group were not suppressed below the sham control level. These results indicated that the combination treatment of ELD and RAL suppresses bone turnover and increases BMD greater than the monotherapy, resulting in improved mechanical properties of lumbar vertebrae and femoral midshaft in OVX rats.

Disclosures: Koichi Endo, Chugai Pharmaceutical, 3

MO0419

Identification of Rare Genetic Variants on 1p13 and 8q22 Loci in Paget's Disease of Bone. Mariejka Beauregard^{*1}, Edith Gagnon¹, Jean Morissette¹, Jacques Brown², Laetitia Michou³. ¹CHUQ (CHUL) Research Centre, Canada, ²CHUQ Research CentreLaval University, Canada, ³Centre De Recherche Du CHUQ - CHUL, Canada

Background: Paget's disease of bone (PDB) has an autosomal dominant mode of inheritance in approximately 30 percent of cases. Mutations of the SQSTM1 gene account for only 37 percent of familial forms of PDB. Genome-wide association studies have identified significant associations between PDB and four single nucleotide polymorphisms (SNPs) located on 1p13 and 8q22 loci. Disease-causing rare genetic variants (RV) are often located near SNPs that are associated with a disease.

Purpose: To identify RV of candidate genes located on 1p13 and 8q22 loci and search for their genetic association with PDB in the French-Canadian population.

Methods: We selected genes on 1p13 and 8q22 loci involved in regulation of bone remodeling, in pathogenesis of bone diseases, in autophagy or apoptosis, and in detoxification of tobacco compounds. Exons, promoter and exon-intron junctions from 30 French-Canadian patients with familial PDB and 4 healthy individuals were amplified and sequenced. RV was defined by a minor allele frequency less than 0.05 or absent from dbSNP (NCBI). An association study of five RV is under way.

Results: We selected eight genes on 1p13 locus (ALX3, AMPD2, CSF1, EPS8L3, GSTM1, GSTM3, GSTM4, PSMA5) and three genes on 8q22 locus (CTHRC1, LRP12, DC-STAMP). We identified 66 RV in at least one individual with PDB; 56 RV were located on 1p13 locus and 10 RV were located on 8q22 locus. We located 36 of the 66 RV in an intron, 9 RV in an exon and 9 RV in an untranslated region. Among the five missense RV, two (EPS8L3; rs75744349, DC STAMP; rs62620995) are predicted to be damaging by two in silico analysis tools. rs62620995 alters a conserved amino acid (Leu397Phe). We also identified three PDB-specific RV (CTHRC1; rs35500845, EPS8L3; rs143958216, GSTM4; rs650985).

Conclusions: Nearly 30 percent of the 66 identified RV are located in very important gene regions. The study suggests a possible involvement of CTHRC1, a regulator of collagen matrix deposition, EPS8L3, currently of unknown function, GSTM4, involved in detoxification of oxidative stress products and DC-STAMP, involved in osteoclastogenesis through RANK signaling pathway, in the pathogenesis of PDB.

Disclosures: Mariejka Beauregard, None.

MO0420

Interaction Between OPTN And TNFRSF11A Gene Variants In Sporadic Paget's Disease of Bone. Daniela Merlotti^{*1}, Fernando Gianfrancesco², Luigi Gennari¹, Domenico Rendina³, Marco Di Stefano⁴, Salvatore Gallone⁵, Teresa Esposito⁶, Giovanna Morello⁶, Valentina D'Alessio⁶, Riccardo Muscarello³, Pasquale Strazzullo³, Giancarlo Isaia⁷, Ranuccio Nuti¹. ¹University of Siena, Italy, ²Institute of Genetics & Biophysics - National Research Council of Italy, Italy, ³Department of Clinical & Experimental Medicine, University of Naples Federico II, Naples, Italy, ⁴Surgical & Medical Disciplines, Section of Gerontology & Bone Metabolic Diseases, University of Turin, Italy, ⁵Department of Neuroscience, University of Turin, Italy, ⁶Institute of Genetics & Biophysics, CNR, Naples, Italy, ⁷University of Torino, Italy

Paget's disease of bone (PDB) is a skeletal disease with a consistent genetic component. Despite mutations in SQSTM1 gene have been detected in up to 50% of familial cases and associated with increased disease severity, their prevalence is low in sporadic PDB, likely due to the presence of additional predisposition genes. Recently, at least 7 genes were associated with PDB in genome-wide-association studies, including polymorphic variation in OPTN gene, encoding for optineurin. In particular, a single OPTN variant (rs1561570) was highly associated with PDB in our Italian replication cohort of 205 SQSTM1-negative patients. In this study we evaluated whether this OPTN variant is associated with PDB and the severity of phenotype in a larger population of 680 cases previously screened for SQSTM1 mutations. 200 age and sex-matched controls were also genotyped for comparison. Potential interactions with a TNFRSF11A polymorphism (rs1805034) previously associated with PDB severity were also explored. In the overall population we observed an increased prevalence of rs1561570 T allele in PDB patients than in controls (OR 1.6; $p < 0.01$). This association was higher in sporadic (OR 1.8) than in

familial cases (OR 1.5), while became non-significant in familial PDB cases without *SQSTM1* mutation. In contrast to the *TNFRSF11A* C variant, which was associated with increased disease severity in both *SQSTM1* negative or positive patients, the *OPTN* variant did not appear to interact with *SQSTM1*. In fact, the presence of the *OPTN* risk allele (T) was significantly associated with an early onset and an increased number of affected sites only in *SQSTM1* negative patients, and particularly in sporadic cases. Of interest, we observed a particularly higher prevalence of haplotype CC-TT (containing the homozygous risk alleles for both *TNFRSF11A* and *OPTN*, respectively) in sporadic than familial cases or controls (49% vs. 33% vs. 3% in sporadic, familial PDB and controls, respectively; $p < 0.01$). Moreover, sporadic *SQSTM1*-negative cases with CC-TT haplotype showed a higher number of affected sites and an earlier age at diagnosis than *SQSTM1*-negative cases with the other haplotypes. In summary, this study provides evidence that this *OPTN* variant affects the susceptibility to develop PDB and interacts with rs1805034 polymorphism in *TNFRSF11A* to cause the severity of the disorder in sporadic cases. A different susceptibility gene is probably involved in *SQSTM1* negative families.

Disclosures: Daniela Merlotti, None.

MO0421

Glucocorticoids Act Directly on Osteocytes to Reduce Bone Vascularity and Strength. Robert Weinstein^{*1}, Erin Hogan², Charles O'Brien¹, Stavros Manolagas¹. ¹Central Arkansas VA Healthcare System, Univ of Arkansas for Medical Sciences, USA, ²Central Arkansas VA Healthcare System, University of Arkansas for Medical Sciences, USA

Whether the negative impact of excess glucocorticoids on skeletal vascularity and strength is due to direct effects on bone cells, indirect effects on extracellular tissues, or both is unknown. Decrements in bone vascularity, blood flow, and water content contribute to the decrease in bone strength that occurs with glucocorticoid excess before and disproportionate to the decline in bone mass. To determine the contribution of osteoblasts and osteocytes to the adverse effects of glucocorticoids on bone vascularity, we blocked glucocorticoid action on these cells via transgenic expression of 11 β -hydroxysteroid dehydrogenase type 2 (11 β -HSD2), an enzyme that inactivates glucocorticoids in a pre-receptor fashion. Osteoblast/osteocyte-specific expression was obtained using the OG2 osteocalcin promoter. In a quantitative angiogenesis assay, 10 nM prednisone caused a 37% decrease in the vascular area of cultures of wild-type metatarsals, but this decrease was prevented in the metatarsals taken from the transgenic mice. Adult OG2-11 β -HSD2 transgenic mice have also been shown to be protected from glucocorticoid-induced osteoblast and osteocyte apoptosis, and reduced osteoid area, bone formation rate, and bone strength. These findings suggest that the adverse effects of glucocorticoid on bone vascularity and strength are not due to actions on extracellular tissues but rather from direct effects on osteoblasts, osteocytes, or both. To distinguish between these possibilities, we blocked glucocorticoid action on osteocytes via 11 β -HSD2 expression under control of the dentin matrix acidic phosphoprotein 1 (DMP-1) promoter. Osteocyte-specific activity of this promoter fragment has been demonstrated previously in DMP1-GFP mice, which express GFP in osteocytes but not in osteoblasts. At day 12 of the angiogenesis induction, DMP1-11 β -HSD2 mRNA was elevated in the transgenic metatarsal cultures but was absent from wild-type cultures. Prednisone caused a 60% decrease in vascular area and a 40% decrease in dendrite length in the metatarsals taken from the wild-type animals but these changes were prevented in the metatarsals obtained from the DMP-1-11 β -HSD2 transgenics. Taken together, these results strongly suggest that glucocorticoid excess adversely affects bone vascularity and strength via direct effects on osteocytes.

Disclosures: Robert Weinstein, None.

This study received funding from: NIH, VA Merit Award

MO0422

Selective Glucocorticoid Receptor Modulation Maintains Bone Mineral Density In Mice. Sylvia Thiele^{*1}, Elena Tsourdi², Karolien De Bosscher³, Jan Tuckermann⁴, Katrin Peschke⁵, Lorenz Hofbauer¹, Martina Rauner⁶. ¹Dresden University Medical Center, Germany, ²Division of Endocrinology & Metabolic Bone Diseases, Department of Medicine III, Technical University, Dresden, Germany, ³Department of Medical Protein Research, VIB, Ghent, Belgium; Department of Biochemistry, Faculty of Medicine & Health Sciences, Ghent University, Ghent, Belgium, ⁴Institute of Aging Research - Fritz-Lipmann Institute, Germany, ⁵Institute for Immunology, Technical University, Dresden, Germany, ⁶Medical Faculty of the TU Dresden, Germany

Glucocorticoids (GC) regulate various physiological processes, including bone remodeling. However, their long-term administration is associated with an increased fracture risk. Compound A (CpdA) is a novel GC receptor modulator with the potential of an improved benefit/risk profile. Here, we tested the effects of CpdA on bone as well as its anti-inflammatory potential in mice and compared it to a classical GC. Bone loss was induced in FVB/N mice by implanting slow-release pellets containing either placebo, prednisolone (PRED; 3.5 mg), or CpdA (3.5 mg). After a

total of 4 weeks, mice were killed to examine the effects on the skeleton. PRED reduced the total and trabecular bone density in the femur by 9% ($p < 0.05$) and 24% ($p < 0.05$) and in the vertebral body by 11% ($p < 0.01$) and 20% ($p < 0.01$), whereas CpdA did not impair these parameters. Histomorphometry confirmed these results and further showed that the mineral apposition rate was decreased by PRED whereas the number of osteoclasts was increased. These effects did not occur with CpdA. CpdA maintained osteoblast function while PRED decreased the mineralization rate, which was paralleled by a decline in serum P1NP, a reduced femoral expression of osteoblast markers, and increased mRNA levels of dickkopf-1 (DKK-1). In addition, serum CTX-1 and the femoral RANKL/OPG ratio were increased by PRED, but not by CpdA. In line with the in vivo data, CpdA did not affect the RANKL/OPG ratio in murine osteocytes, whereas dexamethasone (DEX) increased it 40-fold. Finally, while CpdA failed to transactivate DKK-1 expression in bone tissue and human bone marrow stromal cells (BMSC), its expression was 2-fold up-regulated ($p < 0.001$) in bone tissue and 2.5-fold ($p < 0.05$) increased in human BMSCs by the GC. To analyze the anti-inflammatory effects of CpdA arthritis was induced in DBA/1 mice using collagen type II. Once arthritis appeared, mice were treated with either PBS, DEX (2.5 mg/kg), or CpdA (7.5 mg/kg) for 10 days. Similar to DEX, CpdA significantly reduced paw swelling by 24% ($p < 0.05$) and the clinical score by 50% ($p < 0.01$). Also the paw temperature, which was assessed using an infrared camera, was decreased after DEX and CpdA treatment. At this concentration, CpdA also had no negative effect on bone mineral density. Thus, CpdA acts as an anti-inflammatory drug and does not impair bone. The underlying mechanisms remain to be elucidated.

Disclosures: Sylvia Thiele, None.

MO0423

Anabolic Effects of Icarin in Osteoblasts are Mediated through ERK and JNK Pathways that Interact with Estrogen Receptor Signaling. Lige Song^{*1}, Xiuzhen Zhang², Yun Zhou². ¹Tongji Hospital, Tongji University School of Medicine, Peoples Republic of China, ²Tongji Hospital, Tongji University School of Medicine, China

Icarin, the main active flavonoid glucoside isolated from *Herba epimedii* (HEF), largely accepted as a plant sex hormone, is an anabolic agent in bone that has been reported to prevent bone loss in ovariectomized rats and postmenopausal women. In vitro studies have shown that Icarin enhances osteoblast differentiation and mineralization; however, the detailed signaling mechanism for this anabolic action of Icarin has remained largely unknown. The present study shows that Icarin promotes osteoblast proliferation in a time and dose-dependent manner by increasing the gene expressions of Cyclin E and PCNA, positive regulators of cell cycle, and decreasing the levels of Cdkn2b, a negative regulator of cell proliferation, and the optimal concentration for the proliferation of osteoblasts is at 10-8mol/L ($p < 0.05$, N=5). Icarin also enhanced osteoblast mineralization and expression of early mineralization markers, ALP and Col I, and late mineralization markers, osteopontin, in a dose dependent manner ($p < 0.05$, N=5). To characterize the signaling pathway mechanisms for anabolic actions of Icarin, we examined the contribution of mitogen-activated protein kinase (MAPK) family. Icarin treatment rapidly induced ERK and JNK activation (in 5 min) but had no effect on activation of p38 kinase ($p < 0.05$, N=4). Furthermore, the proliferative effects of Icarin on were dramatically attenuated by treatment with specific inhibitors of MAPKs, U0126 (ERK pathway) and SP600125 (JNK pathway) ($p < 0.05$, N=5). Icarin has been largely presumed as a plant sex hormone, but whether its effects on the proliferation and differentiation of osteoblasts are mediated by the receptors of estrogen or androgen keeps undefined. Treatment of osteoblasts with estrogen receptor antagonist ICI182780 attenuated the proliferation and mineralization promoting effects of Icarin by more than 50% ($p < 0.05$, N=5), but no effect was observed about androgen receptor antagonist, Nilutamide. Furthermore, ICI182780 inhibited the activation of ERK and JNK pathways by Icarin to about 20% ($p < 0.05$, N=5). These observations provide a potential mechanism of anabolic actions of Icarin involving ERK and JNK pathway that interacts with estrogen receptor signaling.

Disclosures: Lige Song, None.

MO0424

Estrogen Signaling to Bone Is not Amplitude-Modulated in Adult Rats. Ingrid Kantner^{*1}, Hartmut Blode², Reinhold Erben³. ¹Vetmeduni Vienna, Austria, ²Bayer Pharma AG, China, ³University of Veterinary Medicine, Austria

There is evidence suggesting that use of low dose monophasic oral contraceptives may impair bone mass accrual in young women. One possible explanation could be that the response of bone to estrogen may be modulated by recurrent episodes of higher estrogen levels found in the preovulatory phase of the natural cycle, i.e., bone may respond to estrogenic amplitude modulation. Constant low doses of estrogen might not be the optimal stimulus for physiological accrual and maintenance of bone mass in women. It was the aim of this study to test this hypothesis by comparison of a continuous and a cyclical estradiol dosing regimen administered to adult ovariectomized (OVX) rats over 4 months. Six-month-old female Fischer 344 rats were either OVX or sham-operated. OVX rats allocated to the continuous regimen received 0.15, 0.5, 1.5, or 2.5 μ g 17 β -estradiol/kg per day subcutaneously (s.c.) throughout the experiment. Using the same mean doses averaged over a 5-day treatment period,

cyclical estradiol treatment was achieved by s.c. injection with half of the mean dose over 3 days, followed by 1 day with the 1.5-fold mean dose, and 1 day with the 2-fold mean dose, thus imitating the natural rat 4 - 5-day cycle. This cyclical 5-day administration regimen was repeated over the 4-month treatment period. Controls received vehicle (1% hydroxypropyl- β -cyclodextrin s.c.) alone. Treatment of OVX rats with estradiol in a continuous or cyclical fashion dose-dependently protected against loss of tibial and vertebral bone mineral density as measured by peripheral quantitative computed tomography (pQCT). In addition, bone formation and bone resorption was dose-dependently suppressed by continuous and cyclic estradiol as evidenced by bone histomorphometry in lumbar vertebrae and proximal tibiae, and by measurement of biochemical bone markers at the whole body level. However, regardless of the endpoint the main determinant of the skeletal response to estradiol was the mean dose administered, independent of a continuous or cyclical administration regimen. Thus, the current experiment suggests that the response of bone to estrogen is not amplitude-modulated in adult rats.

Disclosures: Ingrid Kantner, None.

This study received funding from: Bayer Pharma AG, Berlin, Germany

MO0425

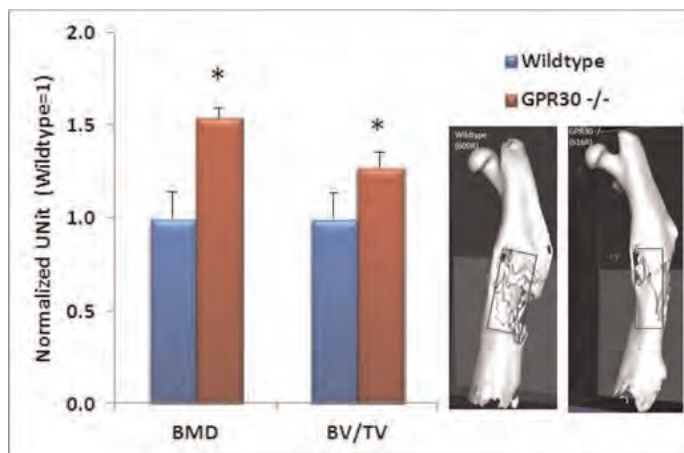
Genetic Inactivation of the G-Protein Coupled Estrogen Receptor 1 Enhances Fracture Healing in Mice. Orhan Oz*¹, Rahul Banerjee², Sagar Patel², Christopher Chen². ¹University of Texas Southwestern Medical Center, Dallas, USA, ²UT Southwestern Medical Center at Dallas, USA

Objectives: G Protein-coupled Estrogen Receptor 1 (GPER1), a novel receptor for estrogen, has been shown to play a role in bone mass and metabolism and chondrocyte proliferation in male mice and estrogen-promoted growth plate width suppression in female mice. The purpose of this study was to determine the role of GPER1 in fracture healing utilizing a closed mouse femur fracture model.

Methods: Wild-type (GPER1^{+/+}) mice (n=15) and knockout (GPER1^{-/-}) mice (n=19) underwent retrograde intramedullary nailing of the right femur followed by creation of a closed femur fracture utilizing a previously established model. Animals were sacrificed at 1 week and 6 weeks and the injured femur was analyzed using histology, microCT and biomechanical testing (three-point bending stiffness).

Results: At 1 week after fracture, histological analysis demonstrated increased Safranin-O staining in the GPER1-deficient mice (p=0.034), suggesting increased chondrogenesis. At 6 weeks after fracture, increased formation of hard tissue callus with mineralized tissue was found in both groups. Analysis of the fracture callus at 6 weeks using microCT demonstrated increased Bone Mineral Density and Bone Volume in the GPER1-deficient mice when compared to the wild-type mice (p<0.05), again suggesting an accelerated healing process. At 6 weeks after fracture, the three-point bending stiffness of the GPER1-deficient fractured femurs was also greater than those of the wild-type femurs (p =0.02) and approached 74% of the control (unfractured) femur.

Conclusions: Our findings showed that a deficiency of GPER1 in mice can accelerate the healing of a closed femur fracture as determined by histologic staining, microCT and biomechanical testing. This study demonstrates that GPER1 plays a significant role in the regulation of fracture healing. The GPER1 receptor may serve as a useful target for potential therapeutic modalities to enhance fracture healing.



GPER1 Fracture Healing by mCT

Disclosures: Orhan Oz, None.

MO0426

Transsexual Women have Low Bone Mass before Cross-sex Hormonal Treatment and Gonadectomy. Eva Van Caenegem*¹, Youri Taes², Stefan Goemaere³, Hans Zmierczak⁴, Katrien Wierckx⁵, Jean-Marc Kaufman⁶, Guy T'Sjoen⁵. ¹Ghent University, Belgium, ²Dept. Endocrinology Ghent University Hospital GhentDe Pintelaan 1859000 Gent, Belgium, ³University Hospital, Belgium, ⁴Ghent University Hospital, Belgium, ⁵Ghent University, Belgium, ⁶University Hospital of Ghent, Belgium

Context: Sex steroids have an important impact on gender differences in bone geometry acquired during puberty. Male-to-female transsexual persons (transsexual women) undergo extreme hormonal changes due to orchidectomy (sex reassignment surgery, SRS) and estrogen substitution, which leads to altered body composition and may change bone mass and size. **Objective:** To examine body composition, bone mass and geometry in transsexual women before cross-gender sex steroid exposure and SRS in comparison to age- and height-matched control men. **Design:** A prospective intervention study with 42 transsexual women (median age 31 years) with age- and height-matched control men. Grip strength, using a hand dynamometer, physical activity questionnaire, areal bone mineral density (aBMD), using DXA, bone geometry and volumetric bone mineral density (vBMD), using peripheral quantitative computed tomography, were measured, before the start of cross-sex hormonal therapy and SRS. **Results:** No differences were observed in weight, height, BMI, smoking and physical activity scores or fracture prevalence between transsexual women and controls. Body composition was also similar without significant differences in lean and fat mass, muscle mass and strength and waist and hip circumference. Prevalence of osteoporosis was higher in transsexual women (21%) compared to control men (3.4%) (p<0.05). They had a lower aBMD at the lumbar spine, hip and femoral neck (all p=0.01) and lower trabecular and cortical vBMD at the radius and tibia (all p<0.05) compared to control men. A significantly thinner radial and tibial cortex (both p=0.016), possibly due to a smaller periosteal and larger endosteal circumference (n.s.), was also found in transsexual women compared to control men. **Conclusions:** Transsexual women before the start of hormonal therapy appear to have a lower bone mineral density as well as a thinner bone cortex at the radius and the tibia compared to control men.

Disclosures: Eva Van Caenegem, None.

MO0427

A Liquid Chromatography Tandem Mass Spectrometric (LC-MS/MS) Method for the Quantification of 24,25-dihydroxyvitamin D₃ and 24,25-dihydroxyvitamin D₂ in Human Serum. Hemamalini Ketha*¹, Ravinder Singh¹, Rajiv Kumar². ¹Mayo Clinic, USA, ²Mayo Clinic College of Medicine, USA

Background: *Cyp24A1* activity can be assessed by measuring serum 24,25-dihydroxyvitamin D (24,25(OH)₂D). Indeed, inactivating mutations of the *CYP24A1* gene in humans are associated with elevated serum 1,25-dihydroxyvitamin D and calcium concentrations and reduced serum 24,25(OH)₂D (JCEM, 2012, 97(3):423-427). Current assays that measure 24,25(OH)₂D by competitive protein binding following lipid extraction and chromatography are time-intensive and not easily automated.

Objective: To develop and assess a LC-MS/MS method for the quantification of 24,25(OH)₂D₃ and 24,25(OH)₂D₂ in human serum.

Methods: Serum 24,25(OH)₂D concentrations were measured in 62 samples with a wide range of serum 25-hydroxyvitamin D (25(OH)D) concentrations (range 6-123 ng/mL; mean \pm SD 53.44 \pm 31.51 ng/ml). Of these, 31 samples (Group 1) had serum 25(OH)D concentrations <60 ng/mL (range 6-60, mean \pm SD 26.66 \pm 13), and 31 (Group 2) had serum 25(OH)D concentrations >60 ng/mL (range 60-123, mean \pm SD 80.22 \pm 15.56). Isotope-labeled internal standard was added to human serum samples. Samples were acidified and extracted on a C18 column. The eluants were dried and derivatized with 4-phenyl-1,2,4-triazoline-3,5-dione. Derivatized vitamin D metabolites were separated on an Agilent XDB-C8 column, and measured by positive ion electrospray ionization mass spectrometry using a multiple reaction monitoring mode.

Results: The Q1/Q3 ion pair used to quantify 24,25(OH)₂D₃ was 574.35 \rightarrow 298.20 and 586.35 \rightarrow 298.20 for 24,25(OH)₂D₂. The limit of detection for 24,25(OH)₂D₃ was 0.1 ng/ml whereas that for 24,25(OH)₂D₂ was 1 ng/ml. Serum 25(OH)D and 24,25(OH)₂D values were positively correlated (r² = 0.57) over the entire range of 25(OH)D concentrations. In Group 1, 25(OH)D < 60 ng/mL, 24,25(OH)₂D concentrations were 3.47 \pm 2.81 ng/ml, whereas for Group 2, 25(OH)D >60 ng/ml, 24,25(OH)₂D concentrations were 12.08 \pm 6.61 ng/ml. Serum 24,25(OH)₂D₃ and 24,25(OH)₂D₂ can be rapidly measured with high precision and accuracy using LC-MS/MS. Serum 24,25(OH)₂D concentrations are linearly correlated with serum 25(OH)D concentrations over a wide range.

Disclosures: Hemamalini Ketha, None.

MO0428

Ablation of CYP27B1 Accelerates Early Development of Mammary Hyperplasia and Triggers a Major Shift in Activation/deactivation of Growth Related Signaling Pathways Independent of CYP24A1. Jiarong Li*¹, Rene St-Arnaud², Timothy Reinhardt³, Anne Camirand⁴, William Muller¹, Richard Kremer⁵. ¹McGill University, Canada, ²Shriners Hospital for Children & McGill University, Canada, ³National Animal Disease Center, USDA, ARS, USA, ⁴McGill, Canada, ⁵McGill University, Royal Victoria Hospital, Canada

We hypothesize that the expression of 1 α -hydroxylase (CYP27B1) in the mammary epithelium could regulate 1, 25-dihydroxyvitamin D production locally and as a result influences critical steps in tumor progression. We disrupted CYP27B1 in the mammary epithelium of PyVMT mice using the Cre/LoxP recombination system. This transgenic mouse model reproduces the various phases of human breast cancer from hyperplasia at 4-5 weeks to adenocarcinoma with pulmonary metastasis at 12-13 weeks in 100% of animals. Ablation of CYP27B1 in PyVMT female animals, fed a normal vitamin D diet, resulted in accelerated transition from normal tissue architecture to hyperplasia followed by accelerated tumor growth. Same size tumors from control (PyVMT-CYP27B1^{lox/lox}Cre) (10 weeks old) and homozygous (PyVMT-CYP27B1^{lox/lox}Cre⁻) animals (8 weeks old) were analyzed for vitamin D metabolites content and gene expression arrays. Gene expression arrays were done using the Illumina Mouse Ref-6 v2.0 microarray platform with 45,200 probes interrogating 16,948 genes. Microarray data were analyzed using FlexArray (Genome Quebec, McGill University) at a p value of <0.05 and a two fold change in gene expression were considered significant. Signaling pathways influenced by CYP27B1 disruption were then analyzed using IPA, Ingenuity (Ingenuity Systems Inc). Circulating concentrations of 25-hydroxyvitamin D were not significantly different in controls (56.5 ± 14.30 ng/ml) and homozygous animals (63.4 ± 14.26 ng/ml). Tissue concentrations of 1,25(OH)₂D were significantly reduced in homozygous animals (265.9 ± 117 pg/ml) compared to control animals (762 ± 245 pg/ml). A total of 1971 probes were significantly unregulated or down regulated in the knockout tumors. Specifically, Rb-dependent repression of E2F-mediated transcription was down regulated, estrogen-dependent cell growth and proliferation mediators were up regulated, estrogen-dependent cell growth and proliferation mediators were up regulated and integrin / ERK, PI3K/AKT signaling was activated. Of particular interest was the absence of differential expression of CYP24A1 suggesting that this enzyme is not unregulated by 1, 25(OH)₂D in this setting and therefore does not accelerate 1, 25(OH)₂D degradation in vitamin D replete animals. In summary these studies demonstrate the critical role of CYP27B1 in breast cancer progression through its regulation of local 1, 25(OH)₂D productions independent of CYP24A1.

Disclosures: Jiarong Li, None.

MO0429

Influence of Seasonal Vitamin D Deficiency on Bone Metabolism Markers in Submariners Subjected to Prolonged Patrols. Xavier Holy*¹, Laurent Bégot¹, Frédéric Labarthe², Nicolas Granger-Veyron², Jean-Marc Collombet¹. ¹IRBA, France, ²Centre médical ESNLE, France

The aim of the study was to assess the influence of seasonal vitamin D status on bone, kidney and acid-base balance metabolisms in French submariners over 2-month patrols. To ensure a maximal discrepancy in vitamin D status between two patrols, submariners boarded either in September (summer patrol or SP) or in February (winter patrol or WP).

Urine and venous blood samples were collected before boarding (pre-patrol control values) and 20, 41 and 58 days after the beginning of submersion on both SP and WP crewmembers (n = 20 for each patrol). Vitamin D status was evaluated for WP and SP subjects. Extended parameters for acid-base balance (pCO₂, pH and bicarbonate), bone formation (bone alkaline phosphatase or BAP), bone resorption (C-terminal telopeptide of type I collagen or ICTP) and renal metabolism (creatinine) were scrutinized in blood serum. In addition, deoxypyridinoline (DPD) level, another bone resorption marker, was determined in submariner's urines.

As expected, SP vitamin D status was higher than WP vitamin D status regardless of the considered experimental time. A detrimental effect of submarine confinement was observed over the prolonged submersion. At patrol day 58, SP population was close to the vitamin D deficiency limit while WP subjects exhibited a severe vitamin D deprivation.

Based on serum pCO₂, pH and bicarbonate measurements, a mild chronic respiratory acidosis (CRA) was evidenced in both SP and WP submariners, up to patrol day 41. This CRA episode is mainly induced by a hypercapnia resulting from enriched CO₂ level encountered in submarines. Such a CRA occurrence paired up with an impaired bone remodeling coupling (reduced bone formation associated with a heightened bone resorption). This altered bone metabolism could constitute a physiological attempt to compensate respiratory acidosis via a bone buffering regulation. At the end of the patrol (day 58), a partial compensation of CRA episode combined with a recovered normal bone remodeling coupling was demonstrated in SP, however not in WP submariners. The discrepancy observed in terms of CRA-compensation between SP and WP populations may result from the seasonal influence on vitamin D status.

Disclosures: Xavier Holy, None.

MO0430

Ligand-dependent Actions of the VDR are Required for Activation of TGF- β Signaling During the Inflammatory Response to Cutaneous Injury. Hilary Luderer*¹, Rosalynn Nazarian², Eric Zhu³, Marie Demay⁴. ¹Massachusetts General Hospital, USA, ²Dermatopathology Unit, Pathology Service, Massachusetts General Hospital & Harvard Medical School, USA, ³Massachusetts General Hospital, Harvard Medical School, USA, ⁴Massachusetts General Hospital & Harvard Medical School, USA

The vitamin D receptor (VDR) has both 1,25-dihydroxyvitamin D (1,25(OH)₂D)-dependent and independent actions in the epidermis. While ligand-dependent actions of the VDR promote keratinocyte differentiation and regulate formation of the epidermal barrier, VDR actions on the hair cycle do not require 1,25(OH)₂D. Because ligand-dependent actions of the VDR play an important role in the immune system, and VDR-dependent anti-inflammatory actions of 1,25(OH)₂D influence the response to acute colonic and renal injury, studies were undertaken to determine if 1,25(OH)₂D-dependent or independent actions of the VDR regulate the inflammatory response to cutaneous injury.

Eight-week old control, VDR knock out (vdr^{-/-}), and vitamin D deficient mice were subjected to 3.5 mm full thickness cutaneous punch biopsy wounds. To evaluate the epidermal and dermal response, wounds were harvested two and five days post-injury. Although normal wound epithelialization was detected five days post injury, a dramatic defect in the dermal response was observed in vdr^{-/-} and vitamin D deficient mice compared to controls at both timepoints. While neutrophil recruitment was not affected, the absence of VDR signaling led to defects in macrophage recruitment and granulation tissue formation. Immunohistochemical and Western analyses were performed to identify the molecular basis for this phenotype. A significant reduction in expression of the macrophage-specific recruiting factor, Monocyte Chemoattractant protein-1 (MCP-1), was observed in the granulation tissue of both vdr^{-/-} mice and vitamin D deficient animals compared to controls, suggesting that ligand-dependent actions of the VDR are required for normal MCP-1 expression and, thus, macrophage recruitment during the inflammatory response to cutaneous injury. Impaired expression of Smad3, a downstream effector of the TGF- β signaling pathway, was detected in vdr^{-/-} and vitamin D deficient mice compared to controls, demonstrating that ligand-dependent actions of the VDR are required for activation of this pathway in response to cutaneous injury.

In sum, these investigations demonstrate that ligand-dependent actions of the VDR in the dermal component of cutaneous wound are essential for a normal inflammatory response to injury. Furthermore, they identify novel actions of the VDR that are required for induction of the TGF- β signaling pathway during this process.

Disclosures: Hilary Luderer, None.

MO0431

RNA-sequencing Analysis Defines 1,25-Dihydroxyvitamin D₃- and Calcium-modulated Gene Expression Patterns in the Duodenum of Cyp27b1 Null Mice on Normal and High Calcium/Phosphorus Rescue Diets. Seong Min Lee*¹, Erin Rilev¹, Mark Meyer¹, Nancy Benkusky¹, Lori Plum¹, Hector Deluca², J. Pike¹. ¹University of Wisconsin-Madison, USA, ²University of Wisconsin, Madison, USA

1,25-Dihydroxyvitamin D₃ (1,25(OH)₂D₃) plays an integral role in maintaining mineral homeostasis in higher organisms through its transcriptional actions in the intestine, kidney and skeleton. In the intestine, knockout studies suggest that many of the key genes involved in calcium absorption remain to be identified. To explore these networks in a more comprehensive fashion, Cyp27b1 null mice were placed on either a normal (16 mice) or a high calcium/phosphorus-containing rescue (16 mice) diet for 5 days without exogenous 1,25(OH)₂D₃. Mice from each of the two groups were then subjected to a single IP dose of either vehicle or 1,25(OH)₂D₃ (2 ng/g body weight) and sacrificed at 6 hr. Calcium, phosphorus, PTH and FGF23 determinations were made at termination of the experiment. Multiple tissues including duodenum were obtained at termination and used to isolate total RNA. Duodenal RNA samples were then subjected to deep sequencing analysis using an Illumina HiSeq instrument, at least 10⁸ reads mapped to the genome per sample and the data subjected to extensive bioinformatic analysis. All mice on the normal diet showed reduced whereas those on the rescue diet exhibited generally normal calcium and phosphorus levels; 1,25(OH)₂D₃ treatment did not raise blood calcium and phosphorus levels significantly above controls at 6 hr. 1,25(OH)₂D₃ strongly modulated large sets of genes under both the normal and rescue diet regimens. Surprisingly, the network of genes in the rescue diet-fed group was approximately 30% of that identified in the normal diet-fed group. Interestingly, while 80% of the genes were upregulated by 1,25(OH)₂D₃ under normal diet conditions (20% were suppressed), only 40% were upregulated under rescue diet conditions (60% were suppressed). Unexpectedly, the two sets of genes regulated by the hormone only modestly overlapped, although both sets contained genes reported to be involved in calcium uptake such as S100g, Trpv6 and Atp2b1, as well as others. We therefore suggest that high calcium conditions both restrict and alter response to 1,25(OH)₂D₃. A large network of genes uniquely modulated by the rescue diet alone was also observed; surprisingly, this set was similarly distinct from those induced by 1,25(OH)₂D₃. This study and further details confirm that dietary calcium and phosphorus strongly influence systemic mineral homeostasis but also reveal that global gene response patterns to 1,25(OH)₂D₃ are also significantly influenced as well.

Disclosures: Seong Min Lee, None.

MO0432

The Membrane-Mediated Effect of $1\alpha,25(\text{OH})_2\text{D}_3$ is Mediated by Ca^{2+} /CaM-Dependent Kinase II and Requires Caveolin-1 and PLAA. Maryam Doroudi*, Zvi Schwartz, Barbara Boyan, Georgia Institute of Technology, USA

$1\alpha,25$ -dihydroxyvitamin D₃ (1,25D₃) is known to regulate chondrocytes and osteoblasts via two different mechanisms: the classical pathway that is vitamin D receptor mediated, and rapid membrane-initiated signaling. In 1,25D₃-mediated membrane signaling, after 1,25D₃ binds its membrane-associated receptor Pdia3, phospholipase A2 (PLA2) activating protein (PLAA) is activated. PLA2 is stimulated, resulting in production of arachidonic acid, which can activate PKC. Caveolae and caveolin-1 (Cav-1) are required for rapid 1,25D₃-dependent PKC signaling. Pdia3 and PLAA are co-localized with Cav-1 in plasma membranes (PM). 1,25D₃ is a known regulator of Ca²⁺ homeostasis. Calmodulin (CaM) is a Ca²⁺ sensor and an effector protein that mediates many of the Ca²⁺-dependent signaling pathways. Ca²⁺ binding induces a conformational change in CaM resulting in activation of Ca²⁺/CaM-dependent kinase II (CaMKII). CaMKII is constitutively expressed in MC3T3-E1 cells. The aim of the present study was to determine the role CaMKII as a mediator of the membrane-mediated effects of 1,25D₃. To determine the time point at which 1,25D₃ activates CaMKII, MC3T3-E1 osteoblasts and confluent growth zone chondrocytes (GC) were treated for 3, 6, 9, 15, or 30 minutes with either vehicle or 1,25D₃. Whole cell lysates (WCL) were collected for the subsequent CaMKII activity, PM and caveolae isolation. MC3T3-E1 cells silenced for Cav-1 (shCav-1) and PLAA (shPLAA) were treated for 9 minutes with 1,25D₃ to determine Cav-1 and PLAA requirement in CaMKII activation. MC3T3-E1 and GC cells were pretreated with methyl- β -cyclodextrin (β -CD), which disrupts caveolar structure, and treated with 1,25D₃ for 9 minutes. WCL were collected for CaMKII activity and PM isolation. 1,25D₃ increased CaMKII activity in GC and MC3T3-E1 cells 9 minutes after treatment. CaM was detected in PM and caveolae of GC and MC3T3-E1 cells. 1,25D₃ treatment decreased the abundance of CaM in PM and caveolae of these cells. Unlike wild-type MC3T3-E1 osteoblasts, shCav-1 and shPLAA cells failed to activate CaMKII in response to 1,25D₃ treatment. β -CD pretreatment abolished 1,25D₃-mediated rapid activation of CaMKII and reduced the abundance of CaM in the PM. Taken together, the results suggest that 1,25D₃ rapidly activates CaMKII. PLAA, Cav-1 and caveolae are required for 1,25D₃-mediated CaMKII activation. 1,25D₃ stimulates CaM leaving PM, translocating to cytoplasm, leading to subsequent activation of CaMKII.

Disclosures: *Maryam Doroudi, None.*

MO0433

The Synergistic Effects of $1\alpha,25(\text{OH})_2\text{D}_3$ and BMP-2 on Osteoblast Mineralization Are Mediated through Both VDR and Pdia3. Jiaxuan Chen*¹, Christopher Dosier¹, Jung Hwa Park¹, Subhendu De¹, Asia Bailey¹, Robert Guldberg², Barbara Boyan¹, Zvi Schwartz¹. ¹Georgia Institute of Technology, USA, ²Parker H. Petit Institute for Bioengineering & Bioscience, USA

$1\alpha,25$ -Dihydroxyvitamin D₃ [$1\alpha,25(\text{OH})_2\text{D}_3$] and bone morphogenetic protein-2 (BMP-2) have been commonly used to stimulate osteoblastic differentiation of many cell types. $1\alpha,25(\text{OH})_2\text{D}_3$ regulates osteoblasts through both the classical vitamin D receptor (VDR) mediated genomic pathway and through protein disulfide isomerase family A, member 3 (Pdia3) mediated rapid responses. However, the role of VDR and Pdia3 in osteoblast differentiation by $1\alpha,25(\text{OH})_2\text{D}_3$ and interaction between $1\alpha,25(\text{OH})_2\text{D}_3$ and BMP-2 are not well known. In this study, we treated wild type, Pdia3-silenced and VDR-silenced pre-osteoblastic MC3T3-E1 cells with either BMP-2, $1\alpha,25(\text{OH})_2\text{D}_3$, or both and measured osteoblast marker expression in 2D culture and mineralization in a 3D poly ϵ -caprolactone scaffold model. Quantitative PCR was used to measure gene expression, while micro-CT, scanning electron microscopy (SEM) and X-ray photoelectron spectroscopy (XPS) were used to analyze mineralized volume, morphology and chemical composition, respectively. We found that $1\alpha,25(\text{OH})_2\text{D}_3$ and BMP-2 caused a synergistic increase in osteoblast marker expression including alkaline phosphatase, osteocalcin and osteopontin while silencing of both receptors attenuated this effect. Interestingly, $1\alpha,25(\text{OH})_2\text{D}_3$ and BMP-2 also synergistically increased VDR expression and $1\alpha,25(\text{OH})_2\text{D}_3$ treatment alone increased BMP-2 and its inhibitor- Noggin expression. This suggests there is a positive feedback between BMP-2 and $1\alpha,25(\text{OH})_2\text{D}_3$ pathways. A similar synergistic increase was found with mineralized volume in the 3D model. Silencing of Pdia3 resulted in no response to either or both factors, while silencing of VDR caused a significant decrease in mineralized volume after $1\alpha,25(\text{OH})_2\text{D}_3$ treatment. SEM also showed a unique morphology of mineralized matrix in the group treated with both factors. XPS data showed that combined treatment increased calcium and phosphate content and distribution in wild type cells. Silencing of Pdia3 also increased calcium and phosphate content and distribution compared to wild type. These data indicate a synergistic cross talk between $1\alpha,25(\text{OH})_2\text{D}_3$ and BMP-2 toward osteogenesis, as both VDR and Pdia3 regulated mineralization and also mediated the effect of $1\alpha,25(\text{OH})_2\text{D}_3$ and BMP-2.

Funding: W81XWH-11-1-03-06; Center for Advanced Bioengineering for Soldier Survivability (ARMY/MEDICAL RESEARCH)

Disclosures: *Jiaxuan Chen, None.*

MO0434

Vitamin D Supplementation as an Adjuvant Therapy for Saudi Patients with T2DM: an 18-month Interventional Study. Nasser Al-Daghri*, Khalid Alkharfy, Omar Al-Attas, Abdulaziz Al-Othman, King Saud University, Saudi Arabia

Background: Vitamin D deficiency has been shown to impair human insulin action, suggesting a role in the pathogenesis of Type 2 diabetes mellitus (T2DM). Despite the level of sunshine in Saudi the population has significant vitamin D deficiency based on our previous studies.

Objective: In this prospective interventional study we investigated the effect of vitamin D (Vit D) supplementation in the metabolic and glycemic profiles of the Saudi T2DM subjects pre and post supplementation to improve known Vit D deficiency compounded in metabolic states such as T2DM.

Method: T2DM Saudi subjects (men: age: 56.6 ± 8.7 yr, BMI, $n=34$; 29.1 ± 3.3 kg/m²; females: Age: 51.2 ± 10.6 yr, BMI 34.3 ± 4.9 kg/m²; $n=58$) were recruited and given 2000IU vitamin D₃ daily for 18 months. Anthropometrics and biochemical data was collected (0, 6, 12, 18 months) to monitor serum 25 hydroxyvitamin D [25(OH) D (nmol/L)] using a commercial ELISA, as well as glycemic and lipid profiles.

Results: In all T2DM subjects there was a significant increase in mean circulating 25(OH)D levels from baseline (32.2 ± 1.5 nmol/L) to 18 months (54.7 ± 1.5 nmol/L; $p < 0.001$) as well as with serum calcium [Baseline = 2.3 ± 0.23 mmol/L versus 18 months = 2.6 ± 0.1 mmol/L; $p = 0.003$]. A significant increase in HDL-cholesterol was noted only in females ($p < 0.001$), as well as a significant decrease in LDL- calcium [Baseline = 4.4 ± 0.8 mmol/L versus 18 months = 3.6 ± 0.8 mmol/L] and total cholesterol calcium [Baseline = 5.4 ± 0.2 mmol/L versus 18 months = 4.9 ± 0.3 mmol/L] ($p < 0.001$ and $p < 0.001$ respectively). In all subjects, glycemic parameters (glucose, insulin, HOMA-IR), blood pressure and BMI were comparable.

Conclusion: In summary, the results highlight that despite oral Vitamin D supplementation (2000IU/day) in Saudi subjects with T2DM; circulating 25(OH)D levels still remain deficient by 22% below normal 18 months post treatment. However, supplementation appeared to significantly improve lipid profile with a change in HDL/LDL ratio which was more pronounced in T2DM females, offering other benefits for health. This study suggests that T2DM Saudi subjects require a higher Vitamin D supplementation (3000IU/day) as a clinical recommendation to achieve normal vitamin D status.

Disclosures: *Nasser Al-Daghri, None.*

This study received funding from: King Abdulaziz City of Science and Technology (KACST Grant no: AT-29-38)

MO0435

Vitamin D₃ Supplementation Increases Intracellular Vitamin D Receptor Expression in Human Skeletal Muscle. Sathit Niramitmahapanya¹, Lisa Ceglia^{*1}, Susan Harris¹, Heike Bischoff-Ferrari², Roger Fielding³, Bess Dawson-Hughes¹. ¹Tufts University, USA, ²University of Zurich, Switzerland, ³Jean Mayer USDA HNRCA At Tufts University, USA

Background: The vitamin D receptor (VDR) has been identified in human skeletal muscle and is hypothesized to mediate effects of vitamin D on muscle cell differentiation and proliferation. Whether vitamin D supplementation alters VDR expression in skeletal muscle cells has not been reported.

Purpose: To determine whether a daily vitamin D₃ supplement alters intracellular VDR expression in skeletal muscle in older women with low vitamin D status. To assess if change in VDR expression is associated with change in 25-hydroxyvitamin D (25OHD) level.

Methods: In this randomized, double-blind, placebo-controlled pilot study, 14 healthy older women were given oral vitamin D₃ 4000 IU/d or placebo for 4 mos. Serum 25OHD level and a muscle biopsy of the vastus lateralis were performed at baseline and 4 mos. Muscle cross-sections were probed for VDR using an immunofluorescent technique. Intracellular VDR expression was calculated by counting the proportion of VDR-positive nuclei out of at least 300 nuclei per sample at baseline and 4 mos. We compared the percent (%) change (4 months-baseline) in intracellular VDR expression in the 2 groups.

Results: In the whole sample, mean (\pm SD) age was 78 ± 3 y and mean baseline 25OHD was 18.3 ± 4.1 ng/ml; these characteristics did not differ significantly in the 2 groups. Mean final 25OHD differed in the two groups (placebo [$n=8$]: 22.4 ± 7.5 ng/ml; vitamin D [$n=6$]: 32.3 ± 5.7 ng/ml; $p=0.006$). Mean baseline % intracellular VDR expression was similar in the 2 groups (placebo: $60.3 \pm 3.7\%$; vitamin D: $61.0 \pm 3.9\%$, $p=0.72$). Mean % change in intracellular VDR expression was $6.8 \pm 18.2\%$ in the placebo group vs. $29.8 \pm 11.7\%$ in the vitamin D group ($p=0.02$). Change in 25OHD was positively associated with % change in intracellular VDR expression independent of group ($r=0.86$, $p=0.005$; Figure).

Conclusion: Supplementation with vitamin D₃ for 4 mos significantly increased intracellular VDR expression in skeletal muscle of older women with low vitamin D status. Analyses to determine whether the increase in VDR-positive nuclei is fiber-type specific are ongoing. The rise in VDR expression is strongly associated with the rise in 25OHD level. This small study lends support to the concept that vitamin D acts on skeletal muscle by activation of the VDR.

MO0437

Characterization of the Alterations in Bone Composition Caused by Prostate Cancer Bone Metastasis Using Raman Spectroscopy. Xiaohong Bi¹, Julie Sterling², Alyssa Merkel³, Barbara Rowland³, Daniel Perrien⁴, Jeffrey Nyman⁴, Florent Elefteriou¹, Anita Mahadevan-Jansen⁵. ¹Vanderbilt University, USA, ²Department of Veterans Affairs (TVHS)/Vanderbilt University Medical Center, USA, ³Department of Medicine, Division of Clinical Pharmacology; Department of Veterans Affairs-Tennessee Valley Healthcare System (VISN9), USA, ⁴Vanderbilt University Medical Center, USA, ⁵Department of Biomedical Engineering, USA

Prostate cancer (PCa) is the most common primary tumor in men. PCa bone metastases result in pathologically active bone remodeling and generally cause a mix of osteoblastic and osteolytic bone lesions, leading to high risk of pathologic fractures. Detailed characterizations of cancer-induced changes in metastasis-bearing bone and the tumor-bone interaction are important for diagnosis and treatment. Raman Spectroscopy is an optical technique that probes molecular structure and constituents in tissues, and has been used to investigate changes in bone quality with age or disease. In this study, we used Raman spectroscopy to characterize cancer-induced alterations in the molecular structure and composition of bone in a mouse model of PCa with mixed lesions that mimic clinical PCa bone metastases. LNCap C4-2B PCa cells were injected into the right tibiae of 5- to 6-week-old male SCID mice, while the left tibiae were injected with phosphate buffered saline (PBS) as contralateral control (N = 10). Digital radiographs were acquired *in vivo* to assess the tumor burden at 8 weeks post-inoculation. Excised intact tibiae were analyzed *ex vivo* by Micro-CT to quantify cortical and trabecular architecture and mineralization, followed by Raman spectroscopy measurements to characterize the molecular composition of the tissue. The radiographs were used to calculate tumor burden and provide guidance for the selection of Raman spectra collection sites. The effect of tumor on the mineral and matrix composition of intact bone was determined by comparing Raman spectral parameters between tumor bearing and the contralateral control tibiae from each mouse. The degree of collagen mineralization as determined by phosphate v1/proline was 42.2% less (p<0.05) in the tumor-bearing bone than in the contralateral control bone. Hydroxyapatite crystallinity, a parameter indicative of mineral crystal size or stoichiometric perfection, also decreased significantly in the tumor-bearing tibiae relative to the control side. The carbonate substitution level determined by carbonate/phosphate v1 increased 10.6%, which could explain at least in part the decreased mineral crystallinity. Overall, these results suggest that the processes of prostate cancer growth in bone significantly change collagen mineralization and mineral crystal structure. Such alterations may be evidence of a previously undescribed mechanism by which cancer metastases increase fracture risk independent of bone loss.

Disclosures: Xiaohong Bi, None.

MO0438

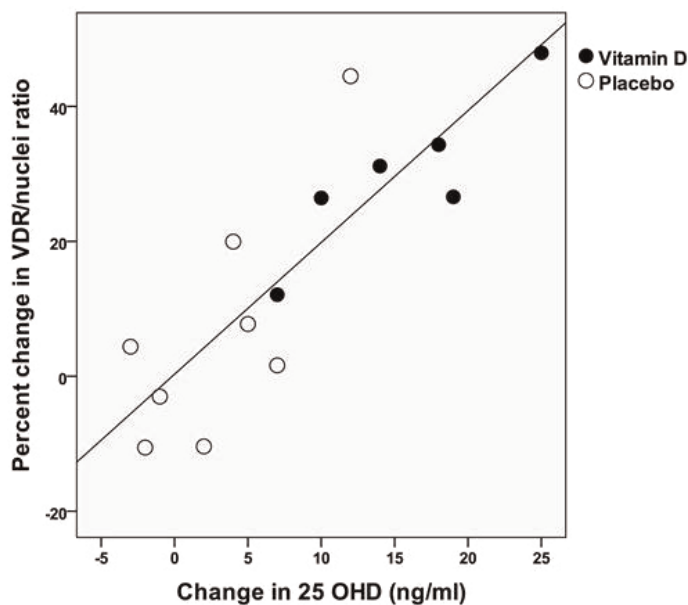
CXCL14 in Bone and Prostate Cancer Tumor Interaction. Alexander Dowell*, Gregory Clines. University of Alabama at Birmingham, USA

Discovery of novel factors implicated in the formation of prostate cancer bone metastasis is a vital first step in developing targeted therapies for this complication of malignancy. Tumor-secreted endothelin-1 (ET-1) is a critical factor that promotes prostate cancer osteoblastic bone metastasis by activating the osteoblast endothelin A receptor. The chemotactic factor C-X-C motif chemokine ligand 14 (CXCL14) is a target of ET-1 in the osteoblast. CXCL14 is also constitutively expressed by fibroblast epithelia in many normal tissues and is a known angiostatic factor and potent attractor of monocytes and dendritic cells. However, expression is lost in many tumor tissues and cell lines including the prostate cancer lines PC3 and DU145. The presence and function of CXCL14 in the bone microenvironment, until now, has remained unreported. Elucidation of the interaction between PCa secreted ET-1 and osteoblast secreted CXCL14 will provide insight into the mechanism of PCa tumor dissemination to the bone.

Utilizing gene expression array and qPCR validation, our laboratory has identified CXCL14 mRNA as highly up-regulated (2.13 fold increase; p = 0.049) in primary mouse calvarial osteoblast cultures when stimulated with ET-1. Further, we have shown this effect to be abrogated by hypoxia, supporting the established role of CXCL14 as an angiostatic agent. CXCL14 is moderately associated with late stage osteolytic prostate cancer bone metastasis in comparative gene expression array indicating a potential role of this chemokine in prostate cancer bone metastasis. Moreover, we have observed higher levels of staining in prostate cancer tumor cells in bone (H-score mean 172.5, n=113) vs. visceral metastasis (H-score mean 99.5, n=57) (p < 0.0001) in a prostate cancer bone metastasis tissue microarray.

CXCL14 is present in native bone cells of mice and prostate cancer bone metastases stromal cells. Endothelin-1 induces CXCL14 mRNA expression in mouse calvarial organ cultures and primary mouse osteoblasts. Immunostaining of a prostate cancer tissue micro-array provides strong visual evidence that the presence CXCL14 plays a role in human prostate cancer bone metastases. The presence and function of CXCL14 in the bone microenvironment, until now, has remained unreported.

Disclosures: Alexander Dowell, None.



Figure

Disclosures: Lisa Ceglia, None.

MO0436

Vitamin D Supplementation Prevents Hypocalcemia and Cortical Bone Loss Associated with Chronic Alcohol Feeding in Female Mice. Kelly Mercer*¹, Rebecca Wynne², Oxana Lazarenko², Charles Lumpkin¹, William Hogue¹, Larry Suva¹, Jin-Ran Chen³, Thomas Badger², Martin Ronis¹. ¹University of Arkansas for Medical Sciences, USA, ²Arkansas Children's Nutrition Center, USA, ³University of Arkansas for Medical Science, Arkansas Children's Nutrition Center, USA

Dietary cholecalciferol supplementation alone or combined with calcium has shown great promise in improving bone health, which has been attributed to endocrine actions involved in calcium regulation and/or paracrine/autocrine actions within bone. Indeed, we and others have suggested that dietary supplementation may also be an effective strategy to protect against EtOH-mediated bone loss in young females. Previously, we reported bone loss in cycling females receiving EtOH diets through intragastric infusion. EtOH-mediated bone loss was associated with excessive reactive oxygen species (ROS) production in osteoblastic populations resulting in the inhibition of bone formation and increased bone resorption. In addition, EtOH-generated ROS in the kidney increased CYP24A1 mRNA expression, which resulted in a reduction of circulating 1,25 hydroxyvitamin D₃ (1,25(OH)₂D₃) concentrations to below normal baseline levels, thus contributing to the disruption of normal vitamin D and calcium homeostasis. In the current study, 6 wk old, female C57BL/6J mice were pair-fed (PF) LieberDeCarli liquid diets containing 0% or 30% EtOH supplemented with 400 IU (EtOH/400) or 2000 IU (EtOH/2000) of cholecalciferol for 40 d. In the EtOH/400 group, chronic EtOH feeding resulted in decreased bone strength and stiffness (p<0.05), reductions in trabecular BV/TV and cortical volumetric BMD (p<0.05), and increased biochemical markers of bone resorption. The levels of circulating 1,25(OH)₂D₃ and ionized calcium were significantly decreased in the serum (p<0.05), and apoptosis was increased the bone marrow cells when compared to PF controls. In contrast, increasing daily cholecalciferol intake from 400 to 2000 IU/kg, completely prevented the cortical bone loss by reducing EtOH-mediated increases in bone resorption and protected against EtOH-mediated hypocalcaemia. In cultured cells, pre-treatment of 1,25(OH)₂D₃ in EtOH-treated ST2 cells protected against increased caspase-3 activity. In the EtOH/2000 mice, circulating 1,25(OH)₂D₃ was significantly lower compared to mice receiving EtOH alone, suggesting increased sensitivity to feedback control of vitamin D metabolism in the kidney. These data suggest that daily dietary intake of cholecalciferol of 2000 IU may protect against bone toxicity associated with chronic alcohol abuse in younger women, thus reducing the increased risk of osteoporosis and fracture that comes with age. Funded in part by R01 AA18282 (M.J.R.).

Disclosures: Kelly Mercer, None.

MO0439

Myeloid-Derived Suppressor Cells Promote Breast Cancer-Induced Bone Destruction. Sabrina Danilin¹, Alyssa Merkel², Rachelle Johnson³, Julie Sterling^{*4}. ¹VANDERBILT UNIVERSITY MEDICAL CENTER, USA, ²Vanderbilt Center for Bone Biology, USA, ³St. Vincent's Institute of Medical Research, Australia, ⁴Department of Veterans Affairs (TVHS)/Vanderbilt University Medical Center, USA

Myeloid-Derived Suppressor Cells (MDSC), identified as Gr-1+CD11b+ cells in mice, are well-established to expand in spleen and bone marrow (BM) of tumor-bearing mice and to be recruited to the primary cancer site where they promote tumor growth and metastasis. However, little is known about their role in bone metastases. We have previously demonstrated that MDSCs expand in the spleen and BM of athymic nude mice similar to the immune competent 4T1/Balbc model, and that MDSC expansion promotes tumor growth. In this study, we hypothesized that MDSCs create a favorable microenvironment for tumor cells and promote bone destruction. To address this question, we inoculated MDA-MB-231 cells into the left cardiac ventricle of nude mice and monitored disease progression weekly by X-ray and GFP fluorescence imaging. MDSCs were counted by fluorescence activated cell sorting (FACS) and isolated from normal and tumor-bearing mice before gene expression and *in vitro* function were assessed. Using FACS, we detected an increase in the Gr-1+CD11b+ population, but more importantly, the GR-1^{low}Ly6C+ subpopulation, which give rise to monocytic cells, also increased from 6 to 12%. Furthermore, *in vitro* experiments showed that MDSCs can differentiate into osteoclasts when cultured with RANKL and M-CSF and that they induce *PTHrP* mRNA expression in cancer cells, possibly via a 2 fold increase in TGF- β expression found in MDSCs isolated from tumor-bearing mice. We then reasoned that the increase in MDSCs in tumor bearing mice could increase the pool of osteoclast precursors, which could contribute to the osteolysis typical of breast tumor metastatic bone lesions. To address this, we inoculated tumor cells or PBS into the left cardiac ventricle of nude mice and co-injected MDSCs into their left tibia. MDSCs did not induce bone resorption in normal mice, but increased resorption and tumor burden significantly in tumor bearing mice. Importantly, using MDSCs purified from GFP mice, we found that MDSCs differentiate into osteoclasts in tumor bearing mice and that the number of TRAP+ and GFP+ cells was increased in tumor bearing animals. These results suggest that MDSCs have the ability of differentiating into osteoclasts, that this is stimulated in the presence of tumor, and that MDSCs expand in breast cancer bone metastases to contribute to bone destruction. Taken together this indicates an important role for MDSCs in the regulation of tumor growth and bone destruction.

Disclosures: Julie Sterling, None.

MO0440

PTHrP(12-48) Is A Novel and Predictive Biomarker of Breast Cancer Bone Metastasis. Charity Washam^{*1}, Archana Kamalakar², Nisreen Akel³, Stephanie Byrum³, Kim Leitzel⁴, Suhail Ali⁵, Alan Lipton⁴, Dana Gaddy³, Larry Suva³. ¹Department of Orthopaedic Surgery, Center for Orthopaedic Research, Winthrop P. Rockefeller Cancer Institute, University of Arkansas for Medical Sciences, USA, ²Department of Orthopaedic Surgery, Center for Orthopaedic Research, Winthrop P. Rockefeller Cancer Institute, University of Arkansas for Medical Sciences, USA, ³University of Arkansas for Medical Sciences, USA, ⁴Division of Oncology, Penn State Hershey Cancer Institute, Penn State Hershey Medical Center, USA, ⁵Division of Oncology, Penn State Hershey Cancer Institute, Penn State & Lebanon VA Medical Center, USA

Bone metastasis (BM) is a common complication of breast cancer (BC) that significantly compromises patient survival. Currently, no reliable methods exist that can consistently detect or predict patients at increased risk for developing BM. To address this issue we developed and utilized a validated plasma screening profile that identifies breast cancer patients with BM with high sensitivity (90.9%) and specificity (92.7%). The major discriminating protein in this profile (MW 4260.92Da) was identified by peptide mass fingerprinting, immunodepletion, and tryptic mapping as a novel PTHrP fragment, namely PTHrP(12-48). A *de novo* structural model of the PTHrP(12-48) peptide was derived and compared to all known PTHrP structures. The model predicts that PTHrP(12-48) is an alpha helix that unwinds into an unstructured region after residue 42. Structural alignment studies suggested that PTHrP(12-48) is unlikely to have any biological interactions with the PTH1 receptor. Peripheral blood mononuclear cells and human mesenchymal stem cell cultures were used to experimentally test the stimulatory or inhibitory effects of PTHrP(12-48) on osteoclastogenesis, osteoblastogenesis and adipogenesis. PTHrP(12-48) treatment had no stimulatory or inhibitory effects on osteoclast, osteoblast, or adipocyte differentiation at any dose tested. We next developed a mass spectrometry-based assay and specifically measured circulating PTHrP(12-48) concentrations in breast cancer patient plasma. Median plasma PTHrP(12-48) concentrations were significantly higher ($p < 0.0001$) in breast cancer patients with BM ($n = 21$) (7.6nM) compared with patients without BM ($n = 21$) (2.5nM). Logistic regression models were used to evaluate the diagnostic potential of PTHrP(12-48) as a single biomarker or in combination with the measurement of N-telopeptide of type I collagen (NTx). The PTHrP(12-48) logistic regression model, threshold 3.4nM, classified the two patient groups with high accuracy (Sn: 90.5%, Sp: 71.4%, AUC: 0.972). Interestingly, the

plasma concentration of PTHrP(12-48) in combination with the serum measurement of bone resorption (NTx) increased diagnostic specificity and accuracy (Sn: 85.7%, Sp: 95.2%, AUC: 0.986). These data demonstrate that PTHrP(12-48) circulates in breast cancer patient plasma and is a novel and predictive biomarker of breast cancer BM. The clinical measurement of PTHrP(12-48) in combination with NTx improves the detection of bone metastasis in breast cancer patients.

Disclosures: Charity Washam, None.

MO0441

β 2AR Stimulation of Host Osteoblasts Promotes Breast Cancer Bone Metastasis via RANKL. J. Campbell^{*1}, Matthew R Karolak², Sameena Masood², Daniel Perrien³, Julie Sterling⁴, Florent Elefteriou². ¹Vanderbilt Center for Bone Biology, USA, ²Vanderbilt University, USA, ³Vanderbilt University Medical Center, USA, ⁴Department of Veterans Affairs (TVHS)/Vanderbilt University Medical Center, USA

Bone and lung metastases are responsible for most deaths in patients with breast cancer. Emotional and psychosocial factors within this population precipitate time to recurrence and death, though the underlying mechanism(s) remain unclear. In this study, we addressed whether severe psychosocial stress, via activation of the sympathoadrenal axis, favored breast cancer metastasis. Two mouse models of bone metastasis were used: an orthotopic model using a bone selective 4T1 clone in the mammary fat pad of immunocompetent mice, and a model using MDA-231 intracardiac injections in nude mice. Chronic immobilization stress (CIS) and isoproterenol treatment (ISO) were used to examine the effect of sympathetic nervous system (SNS) activation on breast cancer bone metastasis. CIS or ISO treatment for 6 weeks significantly increased bone lesion number, area and tumor burden in both models, indicating that SNS activation increases metastatic cancer cells bone colonization or growth. ISO treatment for two weeks *before* cancer cell inoculation increased the number of MDA-231 cells in bones after 6 days and of bone lesions after 28 days, indicating a mechanism involving host cells, since cancer cells are not exposed to treatment in this model. Administration of propranolol to CIS mice decreased the number and area of bone lesions, indicating that SNS rather than hypothalamo-pituitary-adrenal activation contributes to this mechanism.

In vitro, induction of *Rankl* expression in osteoblasts following β 2AR stimulation increased the migration of MDA-231 cells, independently of SDF1-CXCR4 signaling. In addition, shRNA knockdown of RANK expression in MDA-231 cells decreased the incidence of bone metastasis *in vivo*. Lastly, using mouse 4T1 cells with low and high *Rank* expression, we observed a promotion of spontaneous bone metastasis upon ISO treatment specifically in the high RANK expressing 4T1 clone.

These results suggest that RANKL contributes to the effect of SNS activation in bone metastasis via promoting the invasion or retention of metastatic cancer cells within the bone environment, before the "vicious" cycle of bone destruction, and independently of bone turnover. The emerging clinical implication, supported by recent epidemiological data, is that β AR-blockers and drugs interfering with RANKL signaling could increase patient survival if used as adjuvant therapy to inhibit both the early colonization of bone and subsequent metastatic bone disease.

Disclosures: J. Campbell, None.

MO0442

The Role of RANK in Breast and Prostate Cancer Growth in a Murine Model of Bone Metastasis. Yu Zheng^{*1}, Shu-Oi Chow², Sarah Kim², Julian Kelly², Colin Dunstan³, Robert Sutherland⁴, Hong Zhou⁵, Markus Seibel¹.

¹Bone Research Program, ANZAC Research Institute, The University of Sydney, Australia, ²ANZAC Research institute, Australia, ³University of Sydney, Australia, ⁴Garvan Institute of Medical Research, Australia, ⁵Bone Research Program, ANZAC Research Institute, University of Sydney, Australia

Background: Most breast and prostate cancers express RANK with high expression concordance between primary tumors and their skeletal secondaries. We previously proposed that direct cross-talk between osteoblasts and cancer cells via RANKL and IL-6 enhances the growth of cancer metastases in the bone environment.¹ However, the role of tumor-expressed RANK within this pathway remained unknown. In the present study we determined whether knockdown of RANK in breast & prostate cancer cells affects tumor growth in bone and soft tissues.

Methods and Results: RANK expression was knocked down in breast (MDA-MB-231) and prostate (PC3) cancer cell lines. Non-target (NT) sequences served as controls. Knockdown (KD) efficacy was 80% (real-time RT-PCR & Western blot). *In-vitro*, RANK knockdown had no effect on cell growth of either cell line. *In-vivo*, however, and compared to the respective NT controls, intratibial injection of MDA_{RANK-KD} or PC3_{RANK-KD} cells resulted in significantly reduced radiographic osteolytic lesions at all time points ($p < 0.05$). Histologic analysis of bone sections at endpoint demonstrated significantly smaller total tumor areas ($p < 0.05$), reduced cortical bone destruction ($p < 0.01$) and fewer osteoclast-lined bone surfaces at the bone/tumor interface ($p < 0.05$) in mice injected with RANK knockdown cells compared to controls. In addition, tumors derived from RANK knock-down cells were characterised by lower mitotic activity ($p < 0.01$) and higher rates of apoptosis ($p < 0.01$), compared to controls.

Growth of MDA or PC3 cells implanted orthotopically into soft tissue was independent of whether animals were injected with RANK knockdown or NT cells. Interestingly, in the intratibial models, serum RANKL levels were significantly lower ($p < 0.05$) in animals injected with RANK knockdown cells compared to NT controls, while there was no difference between groups in the subcutaneous models.

Conclusions: Expression of RANK by breast and prostate cancer cells is an important determinant of tumor growth within the bone environment. Thus, RANK expression by tumor cells enables RANKL-expressing osteoblasts to directly communicate with the cancer cells in bone, inducing both increased IL-6 and RANK expression by the tumor.¹ Targeting the components of this novel feed-forward loop may offer potential new treatment strategies to control the growth of cancer bone metastases in humans.

Reference

1. Zheng *et al.*, *J Bone Miner Res* 26, Abstract, 2011.

Disclosures: Yu Zheng, None.

This study received funding from: ANZAC Research Institute

MO0443

Withdrawn

MO0444

DKK1 and Kremen Expression Predicts the Osteoblastic Response to Bone Metastasis. Katrina Clines, Gregory Clines*. University of Alabama at Birmingham, USA

The invasion of tumor cells into bone alters the bone microenvironment and initiates a skeletal response that is dependent on the type of tumor. Breast cancer typically results in massive osteolysis and prostate cancer classically forms osteoblastic lesions. Tumor-secreted Dickkopf homolog 1 (DKK1), an inhibitor of osteoblast canonical Wnt signaling, was hypothesized to dictate the osteoblast response to the invading cancer. The aims of this study were to determine if DKK1 expression predicts the bone response to metastasis and to discover mechanisms that regulate cancer DKK1 expression in bone. Real-time RT PCR was performed in a panel of breast and prostate cancer cell lines and a prostate cancer xenograft. DKK1 was highest in MDA-MB-231 and PC3 cells that yield osteolytic lesions in animal models of bone metastasis. LnCaP, C4-2, C4-2B, LuCaP23.1, T47D, ZR-75-1, MCF-7, ARCaP and ARCaPM cancer cells that generate osteoblastic, mixed or no bone lesions exhibited lower DKK1 expression. The DKK1 gene contains a CpG island surrounding the transcriptional start site and a portion of the first exon that serves as a focus for epigenetic regulation. Using methylation-specific sequencing, DKK1 promoter methylation was identified in the LnCaP, C4-2, C4-2B and T47D cancer cell lines. The C4-2B prostate cancer cell line was treated with the demethylating agent 5-aza-2'-deoxycytidine, which resulted in an approximately 500-fold increase in DKK1 mRNA concentration. In cells with absent DKK1 promoter methylation, Wnt signaling activity was analyzed since this signaling pathway itself regulates DKK1 expression. Wnt signaling was active in all cell lines examined, including MDA-MB-231 and PC3 cancer cells. In fact, these two cell lines secrete substantial DKK1 expected to suppress Wnt signaling. The combination of Wnt activation and high DKK1 secretion suggested a mechanism of DKK1 resistance. DKK1 binds to and is dependent on the high-affinity transmembrane Kremen receptors to downregulate Wnt signaling. A consistent pattern of low Kremen expression was found in MDA-MB-231 and PC3 cells. Kremen1 was overexpressed in MDA-MB-231 and PC3 cells, which partially restored DKK1-mediated Wnt signaling inhibition. Combined DKK1 and Kremen expression in cancer cells may predict the bone response of cancer in bone and may serve as therapeutic targets in bone metastasis.

Disclosures: Gregory Clines, None.

MO0445

Identification of Small Molecule Activators and Inhibitors of the Mutated G α responsible for Fibrous Dysplasia of Bone by High-Throughput Screening. Nisan Bhattacharyya*¹, Lesley A. Mathews², Catherine Z. Chen², Jeffrey TSAI¹, John K. Northrup³, Xin Hu², Noel T. Southall², Jaun J. Marugan², Wei Zheng², Marc Ferrer², Michael Collins⁴. ¹NIDCR, NIH, USA, ²Division of Pre-Clinical Innovation, NCATS, NIH, USA, ³Laboratory of Cell Biology, NIDCD, NIH, USA, ⁴National Institutes of Health, USA

Purpose: Fibrous dysplasia of bone/McCune-Albright syndrome (FD/MAS) is a disease defined by skeletal abnormalities sometimes associated with various forms of hyperfunctioning endocrinopathies. Missense mutations in the small subunit of the G-protein, G α (*gsp*), are directly correlated with this disease. The biochemical outcome of these mutations (R201H or R201C) is impaired GTPase activity and increased ligand-independent cAMP production. Clinically there is ligand-independent hypersecretion of hormones in endocrine cells and age-dependent apoptosis of bone cells. The aim of this study was to develop assay systems that can be used to discover small molecules that inhibit or activate *gsp*.

Methods: Several stable CHO cell lines that overexpress either the wild-type (WT) or *gsp* (R201C and R201H) were prepared. Using both ELISA and FRET-based

cAMP assays, several cell lines were optimized for use in a 1536-well plate high-throughput screening (HTS) format. Specific cell lines were identified and optimized to be able to identify either *gsp* stimulators or inhibitors. Stimulator- and inhibitor-optimized cell lines were used in screens of the MLSMR (Molecular Libraries Small Molecule Repository, NIH Chemical Genomics Center, NCGC) small molecule library ($\approx 350,000$ compounds) at multiple doses (0.6 μ M to 76.7 μ M).

Results: Approximately 1,408 and 1,460 compounds were identified by the initial screen that could either increase or decrease cAMP levels in the *gsp*-bearing cells, respectively. These compounds were counter-screened using cells expressing WT G α and cell toxicity assays. Clustering analyses of the selected inhibitory compounds indicated that there were 273 chemical clusters. Primary cultures of human bone marrow stromal cells (hBMSC) derived from an FD patient were also used for secondary screening to identify *gsp* inhibitors and 74 compounds were confirmed.

Conclusions: We have identified 74 compounds that may be specific inhibitors of *gsp*, and approximately 500 compounds with potential *gsp*-activating potential. These sets of compounds will undergo further screening to confirm specificity and activity, and eventually be tested further in preparation for the development of drugs for the treatment of FD/MAS and other *gsp*-mediated diseases.

Disclosures: Nisan Bhattacharyya, None.

MO0446

Increased Sclerostin Levels in Osteosarcoma. Avudaiappan Maran*¹, Scott Riester¹, Kristen Shogren¹, Glenda Evans², Michael Yaszemski¹. ¹Mayo Clinic College of Medicine, USA, ²Mayo Clinic, USA

Wnt signaling pathways are important for many physiological processes including cell proliferation, embryonic development and stem cell differentiation. Deregulation of the Wnt signaling pathway has been shown to correlate with cancer. Mutations in pathway components such as APC and β -catenin have been associated with a number of human neoplasms. Overexpression of Wnt proteins and/or silencing of Wnt antagonists such as DKK1, WISP, and sFRPs have led to the development of cancer in several in vitro and in vivo models. Wnt inhibitors are currently being investigated, in clinical trials, to treat a wide variety of cancers due to their demonstrated anti-tumor effects.

Osteosarcoma is the most common primary malignancy of bone and the sixth most common cancer in children. Upregulation of the Wnt signaling pathway has been demonstrated in osteosarcoma, and is believed to play a role in tumorigenesis. As expected, the expression levels of various Wnt ligands, receptors and coreceptors are highly induced in osteosarcoma, while the inhibitors of Wnt signaling are typically suppressed. To determine whether the Wnt inhibitor protein Sclerostin is modulated in osteosarcoma, pediatric and adult osteosarcoma tissues were utilized in this study. The expression of Sclerostin protein levels in normal control and osteosarcoma tissues were analyzed by western blot hybridization. Several histologic subtypes were analyzed including fibroblastic, chondroblastic, and osteoblastic osteosarcoma. Our results from osteosarcoma (n=17) and normal control (n=16) tissues indicate that Sclerostin protein levels increased in tumor tissues by 2- to 15-fold when compared to non-tumor tissues. Several published reports demonstrate that Wnt signaling is activated, and the expression of Wnt antagonists is suppressed with the progression of osteosarcoma. Hence, the observed increase in the Wnt inhibitor Sclerostin suggests that Sclerostin may be involved in other biological activities in the tumor microenvironment in osteosarcoma. Further investigation of the function of Sclerostin may lead to the development of novel therapeutic targets in the treatment of osteosarcoma.

Disclosures: Avudaiappan Maran, None.

MO0447

Myeloma Cells and Marrow Stromal Cells from Myeloma Patients Express Increased Levels of TAF12 which Increases their Sensitivity to 1,25-(OH)₂D₃. Noriyoshi Kurihara, Jumpei Teramachi*, G. David Roodman. Indiana University, USA

We reported osteoclast (OCL) precursors from patients with Paget's disease of bone (PD) were hypersensitive to 1,25-(OH)₂D₃ (1,25-D₃) and formed OCL at physiologic concentrations of 1,25-D₃ rather than the pharmacologic concentrations of 1,25-D₃ required for normal osteoclast formation in vitro. This enhanced sensitivity to 1,25-D₃ was due to increased expression of a novel VDR coactivator, TAF12, a member of the TFIID transcription complex. Further, we found TAF12 expression was increased in marrow stromal cells (BMSC) by the increased NF κ B signaling in pagetic OCL, and enhanced the capacity of BMSC to produce RANKL in response to low levels of 1,25-D₃. Because the marrow microenvironment in multiple myeloma (MM) and PD has many similarities in terms of increased OCL activity and enhanced NF κ B signaling in MM cells, we determined if MM cells induced TAF12 expression in BMSC of MM patients and enhanced RANKL production in BMSC of MM patients, even in patients with low levels of 1,25-D₃. We found both BMSC and CD138(+) primary myeloma cells from MM patients expressed increased TAF12 levels compared to normals. Further, coculture of myeloma cells with a normal human BMSC cell line, induced TAF12 expression and increased their sensitivity to 1,25-D₃. This increased TAF12 expression in BMSC didn't require cell to cell contact with MM cells. Consistent with these data, TNF α or IL-6 induced TAF12 expression in BMSC. Myeloma cells also produced increased amounts of RANKL in response to very low levels of 1,25-D₃. Further, low levels of 1,25-D₃ increased α 4 integrin expression on myeloma cells α 4 integrin mediates adhesive interactions between MM cells and

BMSC that increase MM growth, OCL formation and chemoresistance of MM cells. To confirm the role of TAF12 in the increased RANKL expression by MM cells treated with 1,25-D₃, we transfected MM1.S myeloma cells with a validated antisense construct to TAF12 or treated cells with a VDR antagonist and determined the effects on RANKL production in response to 1,25-D₃. Treatment of myeloma cells with either a VDR antagonist or antisense to TAF12 markedly decreased RANKL production in response to low levels of 1,25-D₃. These results suggest low levels of 1,25-D₃ can have profound effects on RANKL production by both MM cells and BMSC and enhance adhesive interactions between MM cells and stromal cells to increase MM cell growth and chemoresistance and OCL formation through TAF12 upregulation.

Disclosures: Junpei Teramachi, None.

MO0448

Pim-2 Suppresses BMP-2 Signaling as a Common Inhibitory Mediator of Osteoblastogenesis in Myeloma. Masahiro Hiasa^{*1}, Ryota Amachi¹, Keiichiro Watanabe², Takeshi Harada³, Shirou Fujii³, Shingen Nakamura³, Hirokazu Miki³, Kumiko Kagawa³, Kenzo Asaoka¹, Itsuro Endo³, Toshio Matsumoto³, Masahiro Abe⁴. ¹University of Tokushima Graduate School, Japan, ²Tokushima University Hospital, Japan, ³University of Tokushima Graduate School of Medical Sciences, Japan, ⁴University of Tokushima, Japan

In pursuing factors responsible for myeloma (MM) expansion and bone destruction, we have found that the serine/threonine kinase Pim-2 is over-expressed in MM cells as an anti-apoptotic mediator, and further up-regulated when MM cells are cocultured with bone marrow stromal cells (Leukemia, 2011). Interestingly, Pim-2 was found to be also up-regulated in bone marrow stromal cells, a precursor of osteoblasts, as a negative intracellular signaling mediator for osteoblastogenesis in the cocultures with MM cells. Various factors over-produced in MM bone lesions have been demonstrated to suppress osteoblastogenesis in MM. However, the association of Pim-2 with these factors remains unknown. In the present study, we further explored the regulation of Pim-2 expression in bone marrow stromal cells/osteoblasts in MM and the mechanisms of restoration of bone formation by Pim inhibition. Pim-2 protein expression was up-regulated in MC3T3-E1 preosteoblastic cells by addition of cytokines known as inhibitors of osteoblastogenesis in MM, including IL-3, IL-7, TNF-alpha, TGF-beta and activin A as well as MM cell conditioned media, suggesting Pim-2 as a common downstream mediator of these inhibitory factors. Enforced expression of Pim-2 abrogated BMP-2-induced smad1/5 phosphorylation and mineralized nodule formation in MC3T3-E1 cells. Conversely, Pim inhibition by the Pim inhibitor SMI-16a restored the mineralized nodule formation in MC3T3-E1 cells suppressed by MM cell conditioned media. The Pim inhibition also up-regulated smad1/5 phosphorylation by BMP-2 along with the expression of the BMP-2's downstream target Osterix, a critical transcription factor for osteoblastogenesis, while reducing Smad6, an inhibitory regulator for BMP signaling. However, the phosphorylation of beta-catenin and TCF/LEF reporter activity were not apparently affected by the Pim inhibition, suggesting marginal involvement of the canonical Wnt pathway. Collectively, these results demonstrate that Pim-2 is a common downstream mediator responsible for the suppression of osteoblastogenesis in MM, and that Pim-2 antagonizes BMP-2-mediated anabolic signaling. Therefore, Pim-2 is suggested to be an important therapeutic target to prevent both MM tumor progression and bone destruction.

Disclosures: Masahiro Hiasa, None.

MO0449

The ETS domain of FLI1 is Required for EWS-FLI-Mediated Repression of RUNX2 in Ewing's Sarcoma Family Tumors. Krista Bledsoe^{*1}, Jennifer Westendorf². ¹Mayo Graduate School, USA, ²Mayo Clinic, USA

Ewing's sarcoma family tumors (ESFTs) are aggressive pediatric tumors of bone and soft tissue. ESFTs affect 1 to 3 people per million every year and are the second most common pediatric bone malignancy after osteosarcoma. Approximately 85% of Ewing's sarcomas harbor the EWS-FLI fusion protein, which arises from a chromosomal translocation, t(11;22)(q24;q12), that fuses the N-terminal transcriptional regulatory portion of EWSR1 to the C-terminal DNA binding domain of FLI1 (Friend leukemia integration 1). We discovered that EWS-FLI binds RUNX2, inhibits its transcriptional activity, and blocks the differentiation of mesenchymal progenitor cells into osteoblasts. To understand the mechanism by which the oncogenic fusion protein EWS-FLI inhibits RUNX2 and prevents mesenchymal progenitor cell maturation a panel of FLI1 and EWS-FLI mutant proteins was constructed. In co-immunoprecipitation studies, only EWS-FLI and FLI1 proteins containing the ETS domain of FLI1 bound RUNX2. The ETS domain was also required for repression of RUNX2 transcription. Histone deacetylase inhibitors did not prevent FLI1 repression of RUNX2. Overexpression of FLI1 or EWS-FLI also did not alter binding of Runx2 to the DNA. Together our results indicate that the ETS domain of FLI1 and EWS-FLI is required for binding to Runx2 and inhibiting its transcriptional activity via Hdac-independent mechanisms.

Disclosures: Krista Bledsoe, None.

MO0450

The IRE1 α /XBPs Signaling in Bone Marrow Stromal Cells Is Critical for the Stromal Cell Support of Myeloma Cell Growth and Osteoclast Formation. Guoshuang Xu¹, Kai Liu², Judy Anderson³, Kenneth Patrene², Suzanne Lentzsch⁴, G. David Roodman⁵, Hong-Jiao Ouyang^{*2}. ¹The VA Pittsburgh Healthcare System, USA, ²University of Pittsburgh, USA, ³IUPUI, USA, ⁴Columbia University, USA, ⁵Indiana University, USA

Multiple myeloma (MM), a fatal neoplastic disease of B cell origin, is the most frequent cancer to involve the skeleton and induces osteolytic lesions that rarely heal. Multiple myeloma bone disease (MMBD) is featured by enhanced bone resorption and simultaneously repressed bone formation. Bone marrow stromal cells (BMSCs) are key players in the microenvironmental support of MM cell growth and bone destruction. The Inositol Requiring Enzyme-1 α (IRE1 α) is an ER transmembrane kinase/endoribonuclease, which upon ER stress, splices X box-binding protein 1 (*Xbp1*) mRNA to generate the spliced *Xbp1* (*Xbp1s*) via its endoribonuclease activity. XBPs, an active basic-region leucine zipper (bZIP) transcription factor of the CREB-ATF protein family, is highly expressed in MM cells and plays an indispensable role in MM pathogenesis. Our studies demonstrated that the IRE1 α endoribonuclease activity and consequently XBPs protein expression are strongly induced in MM patient BMSCs, compared with healthy donor BMSCs. XBPs overexpression in healthy donor BMSCs induced pathological behavior that are usually seen in MM patient BMSCs, such as heightened inflammatory cytokine secretion in response to MM cell/TNF α stimulation, and, thereby, enhanced BMSC support of MM cell growth and osteoclast formation in vitro. Moreover, overexpression of human XBPs in normal human bone marrow stromal cell line KM101 cells significantly enhanced the growth of the co-inoculated murine MM STGM1 cells and bone destruction in a myeloma bone disease mouse model. Importantly, knockdown of XBP1 in MM patient BMSCs greatly reversed their pathological behavior, such as their increased inflammatory cytokine secretion and their enhanced support of MM cell growth and osteoclast formation, to the levels that are comparable to healthy donor BMSCs. Our results, for the first time, demonstrate that the IRE1 α /XBPs is a pathogenic factor underlying BMSC support of MM cell growth and osteoclast formation, and represents a therapeutic target for MM bone disease. Since heightened stromal inflammatory cytokine secretion is a common pathological feature of many inflammatory bone diseases, such as rheumatoid osteoarthritis and other tumor bone metastases, our studies suggest that the IRE1 α /XBPs signaling in BMSC could also be a critical pathological factor in regulating the stromal cells support of the pathogenesis and/or progress of these inflammatory bone diseases.

Disclosures: Hong-Jiao Ouyang, None.

MO0451

Treatment of Chemotherapy Induced Alopecia in Mice with a Collagen Targeted Parathyroid Hormone Analog: Prophylaxis vs. Therapy. Ranjitha Katikaneni^{*1}, Tulasi Ponnappakkam², Joshua Sakon³, Robert Gensure⁴. ¹Childrens Hospital at Montefiore/Albert Einstein College of Medicine, USA, ²Childrens Hospital at Montefiore, New York/Albert Einstein College of Medicine, USA, ³University of Arkansas, USA, ⁴Children's Hospital at Montefiore, Albert Einstein College of Medicine, USA

Alopecia is a psychologically devastating complication of chemotherapy, for which there is currently no effective therapy, although parathyroid hormone analogs have shown promise in this disorder. While initial reports suggested that PTH antagonists promote hair growth, more recent data indicates that PTH agonists, through their effects on Wnt signaling in skin to increase production of beta-catenin, would be expected to have a greater effect by causing transition of hair follicles to the anagen, or growth, phase. PTH-CBD is a parathyroid hormone analog containing a collagen binding domain that targets drug delivery to the skin. We compared the effects of prophylactic vs. therapeutic administration of PTH-CBD in a mouse model of chemotherapy-induced alopecia which was designed to mimic the cycles of chemotherapy in clinical use. C57BL/6 mice were treated with a single subcutaneous injection of PTH-CBD (320 mcg/kg) or vehicle control, followed by 3 courses of cyclophosphamide chemotherapy (150mg/kg/week). After 1 year, mice pretreated with vehicle had evident hair changes (color change and hair loss), while those pretreated with PTH-CBD had a normal appearing coat. Vehicle mice were then divided into two groups, receiving either PTH-CBD (single subcutaneous injection, 320 mcg/kg) or vehicle control. After 4 months, mice receiving PTH-CBD showed partial recovery of the hair changes, while those receiving vehicle showed no recovery. After sacrifice, histological examination revealed dystrophic, mostly catagen hair follicles in mice receiving chemotherapy alone. Mice receiving PTH-CBD prophylaxis prior to chemotherapy showed normal-appearing anagen hair follicles. Mice receiving PTH-CBD therapy after chemotherapy showed intermediate histological features, with hair follicles mostly in the anagen phase. Overall, it appears that PTH-CBD is effective in both prevention and treatment of chemotherapy-induced alopecia in mice, but pre-treatment results in a better cosmetic outcome. PTH-CBD thus shows promise as an agent to prevent this complication of chemotherapy and improve the quality of life for cancer patients.

Disclosures: Ranjitha Katikaneni, None.

MO0452

α -CaMKII-induced VEGF Expression Is Critical for the Growth of Human Osteosarcoma. Paul Daft¹, Majd Zayzafoon². ¹The University of Alabama At Birmingham, USA, ²University of Alabama at Birmingham, USA

Osteosarcoma (OS) is a hyperproliferative malignant tumor that requires a high vascular density to maintain its large volume. Vascular Endothelial Growth Factor (VEGF) plays a crucial role in angiogenesis and acts as a paracrine and autocrine agent affecting both endothelial and tumor cells. Our lab previously demonstrated that the α -Ca²⁺/Calmodulin kinase two (α -CaMKII) protein is a critical regulator of OS growth. Others demonstrated that α -CaMKII regulates the expression of VEGF and its main transcription factor, hypoxia inducible factor-1 alpha (HIF-1 α). Therefore, we hypothesize that α -CaMKII-induced VEGF expression is critical for the growth of human OS. Here we show that the pharmacologic and genetic inhibition of α -CaMKII results in decreases in VEGF gene expression (50%) and protein secretion (45%) in the highly aggressive 143B OS cells, while α -CaMKII over-expression in nonaggressive cells (HOS) increases VEGF gene expression (100%) and protein secretion (500%). Endothelial cells treated with conditioned media from 143B cells lacking α -CaMKII failed to form vascular tube networks when compared to treatment with media from wild type cells, while cells treated with media from HOS α -CaMKII cells formed extensive networks. Using immunoblotting, we show that aggressive OS cells (143B, MG-63, M/HOS) express VEGF receptor-2 and respond to extracellular VEGF (100nm for 15 minutes) by increasing intracellular calcium, activation of α -CaMKII, and levels of HIF-1. This response was prevented by CBO-P11 (VEGFR-2 inhibitor) suggesting that secreted VEGF acts in an autocrine manner by further activating CaMKII and creating a positive feedback loop. Furthermore, using luciferase reporter assay and chromatin immunoprecipitation technique, we show that the inhibition of VEGF and α -CaMKII decreases the transactivation of the Hypoxia Response Element (HRE) and the binding of HIF-1 α to HRE on the VEGF promoter, suggesting that α -CaMKII regulates VEGF transcription by controlling HIF-1 α activation and DNA binding. Finally, using an intratibial nude mouse model, we injected 143B cells into 6-week old mice and allowed tumors to develop for 2 weeks. Mice were then treated with either vehicle or CBO-P11 (0.45mg/kg/day). After one week of treatment, a 4-fold decrease in tumor growth was observed in CBO-P11 treated mice when compared to controls. Taken together, our data suggest that VEGF expression in OS is controlled by CaMKII and is critical for tumor growth.

Disclosures: Paul Daft, None.

ADULT BONE AND MINERAL WORKING GROUP**WG1**

Seeking the Monitor: A Practical Approach to Tumor Localization and Post-operative Monitoring in Tumor-Induced Osteomalacia. William H. Chong¹, Diala El-Maouche², Panagiota Andreopoulou¹, Clara C. Chen³, James Reynolds³, Lori Guthrie¹, Marilyn Kelly¹, Richard Sherry⁴, Richard Chang³, Felasfa M. Wodajo⁵, Andrew Dwyer³, Michael T. Collins¹. ¹Skeletal Clinical Studies Unit, Craniofacial and Skeletal Disease Branch, National Institute of Dental and Craniofacial Research, National Institutes of Health, Bethesda, MD; ²Clinical Endocrinology Branch, National Institute of Diabetes, Digestive and Kidney Disease, National Institutes of Health, Bethesda, MD; ³Nuclear Medicine, Radiology and Imaging Sciences, Hatfield Clinical Research Center, National Institutes of Health, Bethesda, MD 20892; ⁴Surgery Branch, Center for Cancer Research, National Cancer Institute, National Institutes of Health, Bethesda, MD 20892; ⁵Musculoskeletal Oncology, Virginia Hospital Center, Arlington, VA 22204.

Purpose: Tumor-induced osteomalacia (TIO) is a rare disorder of acquired phosphate wasting due to excess fibroblast growth factor-23 (FGF23). While surgical resection is curative, tumor localization is difficult. We present a systematic approach to tumor localization and the post-operative biochemical changes from a large series of subjects with TIO.

Methods: 31 subjects with a history and biochemical findings consistent with TIO were seen at the National Institutes of Health between 1998 and 2012. Subjects had failed localization at outside institutions. Multiple imaging modalities were used in tumor localization. Functional imaging with 111-Indium-octreotide with single photon emission computed tomography (octreo-SPECT) and fluorodeoxyglucose positron emission tomography/CT (FDG-PET/CT) was performed first. Anatomic imaging with CT/MRI followed. Selective venous sampling (VS) was performed when multiple suspicious lesions were seen or high surgical risk was a concern. Subjects who underwent surgical resection were monitored post-operatively to investigate the biochemical response to tumor resection.

Results: Causative tumors were successfully localized in 20 (64.5%). 19/20 subjects underwent octreo-SPECT imaging, and 16/20 FDG-PET/CT imaging. 18/19 were positive on octreo-SPECT, and 14/16 on FDG-PET/CT. 12/20 subjects underwent VS; 12/12 were positive. Sensitivity, specificity, positive predictive value (PPV), and negative predictive value (NPV) calculations from this series yielded sensitivity=0.95,

specificity=0.64, PPV=0.82 and NPV=0.88 for octreo-SPECT; sensitivity=0.88, specificity=0.36, PPV=0.62 and NPV=0.50 for FDG-PET/CT. 16 subjects had their primary tumor resection performed at our institution; 15 showed no evidence of disease at last follow-up. Post-operatively, intact FGF23 (iFGF23) decreased to near undetectable levels within hours and in most cases returned to the normal range within 5 days. While C-terminal FGF23 (cFGF23) levels decreased immediately into the normal range, levels rebounded and were sustained within the high/high-normal range by 4 days and remained elevated for a sustained period. Serum phosphorus returned to normal in all patients, within 1 to 7 days. In most cases serum 1,25dihydroxyvitamin D (1,25D) levels rebounded to levels exceeding the normal range by 3 days. Alkaline phosphatase decreased early post-operatively in patients who had not been medically managed preoperatively. The first biochemical parameter to confirm successful resection was iFGF23 levels. Tubular reabsorption of phosphate (TRP) and 1,25D rose early as well.

Conclusions: These data define a multi-modal, systematic approach to TIO tumor localization. Octreo-SPECT was a more sensitive and specific modality for localizing tumors, but in most cases FDG-PET/CT was needed as a complementary modality. VS can discriminate between multiple suspicious lesions and increase certainty prior to surgery. Since iFGF23 is not commercially available, a rise in TRP and 1,25D within the first few days may be a practical parameter to monitor to prove successful resection. Interestingly, a sustained elevation in cFGF23 and 1,25D were observed, suggesting a mechanism by which low iFGF23 levels regulate FGF23 processing and 1,25D generation.

WG2

Case Report: Prolonged requirement for intravenous calcium supplementation following parathyroidectomy for tertiary hyperparathyroidism complicating X-linked hypophosphataemia (XLH). RK Crowley, M Kilbane, T King, S Gupta, M Morrin, MJ McKenna.

We describe a 32 year old woman with XLH secondary to a confirmed mutation in exon 22 of the PHEX gene. She presented at the age of nineteen months, with difficulty walking; was diagnosed with rickets secondary to XLH and managed with activated vitamin D and phosphate supplementation. When her care was transferred to adult services at age eighteen years, she was dependant on phosphate supplementation and became profoundly myopathic when phosphate was reduced or withdrawn. Ionised calcium (Cai) measured 1.39 mmol/L (1.19-1.35) and parathyroid hormone (PTH) 334 ng/L (12-64); over the next 7 years this rose to Cai 1.48 mmol/L and PTH 1107 ng/L. Bone turnover markers were elevated.

An attempt was made to stop phosphate supplementation for a trial of cinacalcet 30mg/day; Cai dropped to 1.22 mmol/L and PTH to 360 ng/L, but she became myopathic. On combined phosphate supplementation and cinacalcet therapy there was a paradoxical rise in PTH to 1345 ng/L with marked increase in bone turnover markers, and cinacalcet was discontinued. A trial of intravenous (IV) bisphosphonate therapy was complicated by an acute phase response, a hypersensitivity reaction and a transient drop in Cai attributed to hungry bone syndrome.

Sestamibiscintigraphy confirmed increased uptake in the parathyroids; she was referred for surgical resection of all glands. Post-operative hungry bone syndrome was anticipated and managed with IV calcium and oral vitamin D; in spite of early treatment she required Ca infusions for over 5 months at rates of up to 600ml of 10% calcium solution / day. In the 5 months after surgery, bone mineral density increased by 47% at hip and 58% at spine.

This was a complex case of XLH with tertiary hyperparathyroidism; dependence on phosphate supplements may explain the high PTH and may be related to this specific genetic mutation.

WG3

Long-term Teriparatide Therapy for Hypoparathyroidism Associated with Diffuse Painful Osteosclerosis. Nicole M. Gentile, M.D.¹, Robert A. Wermers, M.D.^{1,2}. ¹Department of Internal Medicine and ²Division of Endocrinology, Diabetes, Nutrition, and Metabolism, Mayo College of Medicine, Mayo Clinic, Rochester, Minnesota, USA.

Introduction: Acquired osteosclerosis, a rare disorder of bone formation, is an important consideration in adults with sclerotic bones or elevated bone density results. In this context, several diagnostic considerations include Paget's disease of bone, hepatitis C, fluorosis, hematologic malignancies, as well as both hyper- and hypoparathyroidism.

Case: A 28-year-old female status post total thyroidectomy in 2006 complicated by postoperative refractory hypoparathyroidism presents with a 3 to 4 year history of progressively worsening diffuse musculoskeletal pain. At the time of presentation she was on calcitriol 0.25 mcg twice daily, calcium carbonate (600 mg elemental calcium) 2400 mg four times daily, cholecalciferol 50,000 IU every 4 days, and teriparatide 20 mcg 2-3 times daily, which she has been on for the last 5 years due to the refractory nature of the hypoparathyroidism. Her ability to tolerate oral medication was limited by her daily migraines and nausea. Within the last year, she had approximately 30 emergency room visits for symptomatic hypocalcemia. At presentation, her laboratory evaluation was remarkable for: serum calcium 9.5 mg/dL, phosphorus 3.7 mg/dL, creatinine 0.8 mg/dL, 24 hour urine calcium 119 mg, bone alkaline phosphatase (BAP) 32 mcg/L (normal premenopausal < 14), beta-crossLaps (β CTX) 4155 pg/mL (normal premenopausal 25-573 pg/mL), 25-hydroxyvitamin D 32 ng/mL, PTH < 6.0 pg/mL, negative hepatitis C antibody screen, and normal TSH, protein

electrophoresis, and plasma fluoride. A skeletal survey demonstrated patchy areas of sclerosis throughout the majority of the visualized bones. MRI of the lower extremities was consistent with osteosclerosis involving the metadiaphysis of both femurs, tibiae, and fibulae. Bone scan revealed marked uptake through the calvarium, sternum, spine, and areas surrounding all major joints. With management of her migraine headaches, teriparatide was weaned off over 3 months with augmentation of calcitriol and the addition of hydrochlorothiazide. Her calcium stabilized and her bone pain improved. The BAP and β CTX dropped to 12 mcg/L and 91 pg/mL respectively at 4 months.

Conclusion: Improvement in symptoms and rapid decline in markers of bone turnover with reduction and discontinuation of teriparatide suggests there may be an association between chronic daily teriparatide treatment and the development of painful diffuse osteosclerosis.

WG4

SAPHO Syndrome. Marcio L Griebeler M.D., MatheniSathananthan M.D., Robert A. Wermers, M.D. Department of Internal Medicine and the Division of Endocrinology, Diabetes, Nutrition, and Metabolism, Mayo College of Medicine, Mayo Clinic, Rochester, Minnesota, USA.

Introduction: SAPHO Syndrome (synovitis, acne, pustulosis, hyperostosis and osteitis) is a rare disorder characterized by hyperostosis and palmoplantar pustulosis.

Case: A 52-year-old female presented with progressively worsening severe pain in the upper chest which began 8 months prior after an injury. She had minimal response to analgesics. Her medical history was significant for acne and dermatitis on her palms and feet. Physical exam revealed tenderness of the medial clavicular heads, with associated soft tissue swelling. She had residual scarring on her upper lip and chin and pustules on her hands and feet. Laboratory workup included a normal CBC, angiotensin converting enzyme, bone alkaline phosphatase, PTH, serum calcium and phosphorus, and plasma fluoride with an increased ESR and mild 25OH D deficiency. Radiographs showed sclerosis of the manubrium and clavicles with arthrosis of the sternomanubrial junction. CT chest showed marked symmetric sclerosis of the clavicles and upper sternum with associated soft tissue thickening consistent with hyperostosis and sclerosis of T9 and T10. A bone scan was remarkable for intense tracer uptake in the clavicles, manubrium and superior portion of the sternum. Subsequently, 16 patients meeting predefined inclusion criteria from 1/1/1996-11/26/2010 with clinical and radiographic features of SAPHO syndrome from our institution were identified.

Results: Eleven patients (68.8%) were female and patients ranged in age from 14-70 years at time of presentation (mean 43.4 years). The majority were Caucasian (n = 13, 81.3%). The duration of symptoms ranged from 2 days-23 years at time of presentation (mean 6 years). The majority of patients presented with either chest or sternoclavicular joint pain (n = 10, 62.5%). Eight patients (50%) had manifestations of severe acne, 12 (75%) palmoplantar pustulosis, 1 (6.3%) chronic recurrent multifocal osteomyelitis and 13 (81.3%) hyperostosis. Hyperostosis was present in sternocostoclavicular bones - 10 (76.9%) and spine - 3 (23.1%). Fourteen patients were smokers or had a history of smoking (87.5%). Erythrocyte sedimentation rate was elevated in 8/14 (57.1%) patients in whom it was measured. HLA-B27 antigen was positive in 2/7 patients (28.6%) where it was performed.

Conclusion: SAPHO syndrome often remains unrecognized based on the long duration of symptoms prior to diagnosis. Although not previously reported, smoking may be an important etiologic factor for this condition.

WG5

Sarcoidosis and Primary hyperparathyroidism coexisting in patients with hypercalcemia. Syed Hassan MD, Karthik Kannegolla MBBS, Sudhaker Rao MD. Division of Endocrinology, Henry Ford Hospital, Detroit-USA.

Sarcoidosis and Primary hyperparathyroidism are common causes of hypercalcemia, however the two have rarely been reported to coexist. We present here four cases with simultaneous occurrence of Primary hyperparathyroidism and Sarcoidosis, diagnosed at Henry Ford Hospital between (2005-2011). All the four patients are African American female with the average age at the time of diagnosis (63.5 \pm 10.5). Sarcoidosis was diagnosed at a much early age, by the presence of bilateral hilar lymphadenopathy and/or on biopsy showing non caseating granuloma. The diagnosis of Primary hyperparathyroidism was made in presence of elevated serum calcium levels with inappropriately high levels of intact parathyroid hormone (PTH) and normal levels of 1,25(OH)₂D. The initial presentation for hyperparathyroidism was presence of polyuria, vomiting and kidney stone with elevated serum calcium levels (10.9 \pm 0.2)mg/dl, ionized calcium (1.41 \pm 0.03)mmol/L and intact PTH levels (231.7 \pm 123)pg/ml. The serum levels of 1,25(OH)₂D concentration (48.25 \pm 18.5) were in the high normal range. Elevated levels of Serum Angiotensin converting enzyme (84 \pm 9.2) was noted due to presence of active Sarcoidosis. In the beginning, all the patients underwent steroid challenge test (prednisone 5-15mg once daily for 2-4weeks) with minimal response in three patients and no response in one. Finally due to persistence of symptoms, parathyroidectomy surgery was done in all, with removal of 1-2 glands. The average size of the largest gland removed was 240 \pm 123 mg. In one of the patients the parathyroid adenoma showed the presence of Sarcoid granuloma on biopsy. After the surgery, three patients showed excellent response within two weeks with resolution of symptoms and normalization of serum calcium and intact PTH levels. In one patient the surgery was a failure with persistence of hypercalcemia and elevated levels of intact PTH. The patients were

followed up for a period of 3-5 years with no recurrence of the disease. As very few cases exist, the pathophysiology is poorly understood, the best possible explanation could be the additive effect by the elevated plasma PTH in Primary hyperparathyroidism and vitamin D3 in Sarcoidosis. However in our patients it was the parathyroidectomy surgery and not the treatment for Sarcoidosis that treated them. Further studies are needed to understand the coexistence of these two entities.

WG6

Extremely High Bone Mineral Density Associated with Osteosclerosis. Vivien Lim and Bart Clarke. Mayo Clinic Division of Endocrinology, Diabetes, Metabolism, and Nutrition, Rochester, MN 55905 USA.

Many patients with high bone density and osteosclerosis have congenital skeletal dysplasias. Adults with high bone density may have a variety of disorders causing their osteosclerotic phenotype. We report a case of extremely high bone mineral density caused by metastatic oligodendroglioma.

A 60-year-old female was referred for evaluation of osteosclerosis incidentally discovered during evaluation for diffuse musculoskeletal pain. The patient was diagnosed 17 years earlier with an oligodendroglioma for which she underwent surgery and radiotherapy, without recurrence on follow-up. She developed diffuse moderate progressive musculoskeletal pain about 3 years before referral, which was attributed to polymyalgia rheumatica and treated with varying doses of prednisone between 5 to 7.5mg daily since mid-2009. She had no recognized disorders likely to cause osteosclerosis, and was on no medications or supplements that would cause this. Her family history was significant for 6 sisters without osteosclerosis. Initial workup showed no laboratory abnormalities except mildly increased serum bone alkaline phosphatase and beta-CTx. CT scan of her abdomen and pelvis was negative. Her skeletal survey showed patchy osteosclerosis sparing her distal extremities. She was advised against bone marrow biopsy due to lack of hematologic findings. She returned with progressive pain, more pronounced in her lower back and lower limbs, with difficulty walking. Her BMD showed her left femoral neck T-score -0.6, left total hip +3.1, right femoral neck +8.3, right total hip +11.0, and lumbar spine +6.7. Comparison to previous values a year earlier showed that her right total hip bone density had increased by 7.5%, and lumbar spine bone density increased by 6.8%. Her bone scan confirmed her previous skeletal survey findings. Her serum PTH was 37 pg/mL, beta-CTx 1,933 pg/ml, BSAP 25 mcg/L, 25-hydroxyvitamin D 44 ng/mL, hemoglobin 10.6 g/dL, and ESR 40 mm/hr. Her serum 1,25-dihydroxyvitamin D, PTH-rP, and ACE levels were normal. Her MRI of her lumbar spine showed significant epidural and paraspinal enhancing soft tissue masses and marrow infiltration at multiple levels. Her CT abdomen showed a 9.2-cm retroperitoneal mass. CT-guided needle biopsy of her right ilium and retroperitoneal mass yielded metastatic oligodendroglioma, without evidence of other pathology. This case of acquired osteosclerosis and extremely high bone density was attributed to metastatic oligodendroglioma. Oligodendrogliomas are only very rarely metastatic, and typically do not cause osteosclerosis or increased bone density. The differential diagnosis of high bone mineral density associated with osteosclerosis will be discussed.

WG7

Genotypic and Phenotypic Characteristics of X-linked Spondyloepiphyseal Dysplasia Tarda in Korean. Yumie Rhee¹, Tae Joon Cho², GyeYeon Lim³, HaeRyong Song⁴, Dong Kyu Jin⁵, Chul Ho Lee⁶, Woong-Yang Park⁷, Ok Hwa Kim⁸. ¹Department of Internal Medicine, Yonsei University College of Medicine, ²Orthopaedic Surgery, Seoul National University College of Medicine, ³Department of Radiology, Catholic University Hospital, ⁴Department of Orthopedic Surgery, Korea University Guro Hospital, ⁵Department of Pediatrics, Samsung Medical Center, Sungkyunkwan University, ⁶Department of Genetics, Yonsei University College of Medicine, ⁷Departments of Biomedical Sciences, Seoul National University College of Medicine, ⁸Department of Radiology, Ajou University College of Medicine.

Objectives. TRAPPC2 gene has been known to cause the X-linked spondyloepiphyseal dysplasia tarda (SEDT). This gene consists of six exons with open reading frame expanding 420bp encompassing exon 3 to 6 and until recently 47 different mutations have been reported. The purpose of this presentation is to document the radiological and genotypic findings of Korean SEDT. Materials and Methods. Clinical and radiological analysis of six patients (age range: 10-36 years) who had been misdiagnosed as other entities of short stature was reevaluated. DNA direct sequencing was done after PCR on TRAPPC2 gene. Results. All patients were male and showed disproportionate short trunk short stature. Progressive back pain and hip joint pain were noted. Characteristic hump-like elevation on the vertebral endplates with intervertebral disc spaces was noted in all patients. Humps of the vertebral endplates persistently noted in the adult patients. In addition, premature degenerative osteoarthritis of the hip and knee joints were evident in all patients. We have identified 2 novel mutations, 3 known ones and one case without any mutation. They were c.40del (p.Asp14IlesX27) in exon 3(novel), missense mutation of c.218C>T in exon 4, c.270_274 deletion in exon 5(novel), c364C>T mutation in exon 6, IVS2-2A>G in exon 2, and no mutation but duplication in exon 4, respectively. Conclusion. It should be noted that until all patients came to our notice in later ages and the exact diagnosis was under the labyrinth. This could be troublesome in clinical management as well as

the surgical option for the relief of symptoms. Therefore, awareness of skeletal manifestations of SEDT and exact molecular analysis can enhance the proper genetic counseling and clinical management.

WG8

A Problem Case: Managing Endocrine Disorders in the Adult OI Patient; Impact on Bone. Jay R. Shapiro, MD, Kennedy Krieger Institute and the Johns Hopkins School of Medicine, Baltimore; Thomas Trautman, MD, Southeast Radiation Oncology Group, Monroe, NC.

Osteogenesis Imperfecta (OI) is a systemic disorder due to gene mutations affecting the synthesis and tissue matrix deposition of type I collagen. Primary endocrine disorders are not a feature of OI. However, when endocrine disorders occur they may significantly impact skeletal function. A physician at a community hospital writes the following: I wonder if you could give me some advice on a nice gentleman who has osteogenesis imperfecta? He is 50 y.o. and very functional. He has pulmonary sarcoidosis, and has been on prednisone 10-15 mg daily for many months. Now he has high-risk prostate cancer and needs radiation, along with at least six months of androgen deprivation therapy (ADT). I am concerned that the chronic prednisone therapy and ADT will substantially weaken his already brittle bones. He does do regular exercise with small weights. The physician asks: (1) Is a bone density study useful? (2) I suspect that I should put him on calcium and vitamin D? How much? (3) Should a bisphosphonate be considered? Discussion points: (1) What is BMD in adult OI? How do these co-morbidities impact bone in OI? (2) Are Calcium and Vitamin D helpful in this situation? (3) What is the response to bisphosphonate treatment in adult OI and in this patient taking multiple drugs?

LATE-BREAKING ABSTRACTS

1217

Overexpression of PTHrP- related miRNA in Human Bone Marrow Derived Stem Cells Enhances Chondrogenesis and Inhibits Hypertrophy. *Gunil Im**¹, *Jong-Min Lee*², *Jung-Min Ahn*², *Jun-Ho Joe*². ¹Dongguk University Ilsan Hospital, Rok, ²Dongguk University Ilsan Hospital, South Korea

In this study, we tried microRNA microarray analysis with total RNAs from PTHrP-treated mesenchymal stem cells (MSCs). Four novel microRNAs were detected by microarray analysis, we confirmed that one of them can increase the chondrogenic potential of MSCs. In chondrogenic induction of PTHrP-treated hBMSCs, 9 novel miRNAs were up- and down-regulated. 4 miRNAs of them were up-regulated in PTHrP treatment (Fig 1A). miR-7, 8 and 9 expression patterns were gradually increased for 21 days. In case of miR-im6, expression pattern was increased by 7 days and then decreased at 21 days in spite of long-term treatment of PTHrP (Fig 1B and C). Each up-regulated miRNA was subcloned into lenti-viral expression vector and successfully overexpressed in hBMSCs by lentiviral infection at MOI=10 (Fig 1D and E). Amount of GAG/DNA measured in cultured lentiviral transduced pellets after 4 weeks of culture. GAG/DNA content of lenti-miR-im6 transduced hBMSCs was higher than other groups treated with TGF-β (Fig 2A). From safranin-O staining of each chondrogenic hMSC pellet, staining intensity of lenti-miR-im6 transduced hBMSCs was also stronger than TGF-β-treated positive control, similar to PTHrP-treated positive control (Fig 2B). Overexpression of miR-im6 in chondrogenic induction of hMSCs enhanced the expressions of chondrogenic markers (Type II collagen, SOX9) and suppressed the expression of hypertrophic markers (ALP, Type X collagen) (Fig 2C). Desert hedgehog (DHH), Wnt6, and Wnt9b were screened as target genes to miR-im6 in this pathway (Fig 2D). PTCH2, WNT6 and WNT9B of these proteins also were down-regulated in lenti-miR-im6- transduced and chondrogenesis-induced hMSCs pellets (Fig 2E). Luciferase activities were significantly decreased in Hela cells which were transformed with luciferase reporter vectors harboring PTCH1 or WNT6 3'UTR. This result demonstrates that PTCH1 and WNT6 are target genes of has-miR-im6. We are currently studying about another target gene (KLF10) of miR-im6, can be key regulator in novel PTHrP mediated chondrocyte hypertrophy blocking pathway (Fig 3C). Our results show that miR-im6 acts as a positive regulator of chondrogenic differentiation as well as a hypertrophy blocker in BMSCs by decreasing the ALP expression through unknown mechanism. To our knowledge, this is the first report showing that a specific microRNA, miR-im6, plays a crucial role in the course of chondrogenesis.

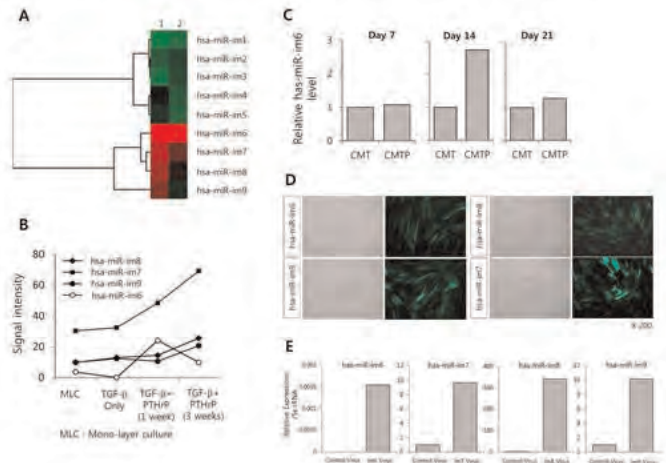


Figure 1

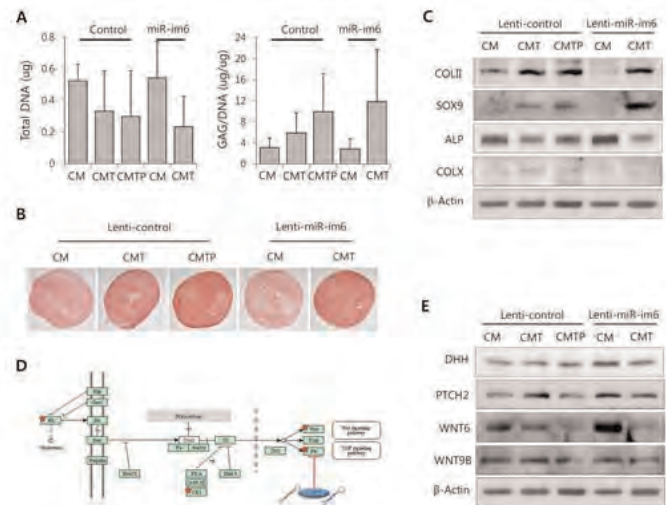


Figure 2

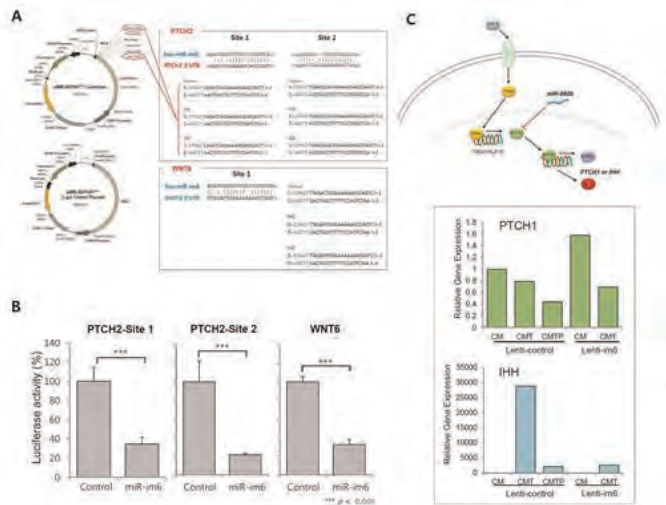


Figure 3

Disclosures: *Gunil Im, None.*
This study received funding from: National Research Foundation of Korea (2012-0006083)

XBP1S is Required for Chondrocyte Hypertrophy Through Associated with RUNX2. Fengjin Guo^{*1}, Yanna Liu², Jinghua Zhou², Wenjun Zhao², Xiaofeng Han², Peng Zhang². ¹Chongqing Medical University, Peoples republic of china, ²Department of Cell Biology & Genetics, China

Bone morphogenetic protein 2 (BMP2) is known to activate unfolded protein response (UPR) signaling molecules, including XBP1S and ATF6. However, the influence on XBP1S and ATF6 in BMP2-induced chondrocyte differentiation have not yet been elucidated. In this study we demonstrate that BMP2 mediates mild ER stress-activated ATF6 and directly regulates XBP1S splicing in the course of chondrogenesis. XBP1S is differentially expressed during BMP2-stimulated chondrocyte differentiation, and exhibits prominent expression in growth plate chondrocytes(Fig.1). This expression is probably due to the activation of XBP1 gene by ATF6 and spliced by IRE1a(Fig.2). Overexpression of XBP1S accelerates chondrocyte hypertrophy, as revealed by enhanced expression of type II Collagen, type X Collagen and Runx2; however, knockdown of XBP1S via RNA interference(RNAi) approach abolishes hypertrophic chondrocyte differentiation(Fig.3). In addition, XBP1S binds to Runx2 in micromass culture of ATDC5 cells treated with BMP2 for 7 days, however, this interaction can not be find in micromass culture of ATDC5 cells treated with BMP2 for 5 days. These results indicate that XBP1S and Runx2 can form a protein complex in hypertrophic chondrocyte differentiation. Besides, XBP1S obviously increased the Collagen X and MMP13 expression induced by Runx2. XBP1S associates with Runx2 and enhances Runx2-induced chondrocyte hypertrophy(Fig.4). Altered expression of XBP1S in chondrocyte hypertrophy was accompanied by altered levels of Indian hedgehog (IHH) and parathyroid hormone-related peptide (PTHrP). In conclusion, this study provides evidence showing that XBP1S acts as a novel mediator of chondrocyte hypertrophy is, at least partial, due to (1) the transactivation of XBP1 gene and increasing the expression of IRE1a-spliced XBP1S by ATF6 in chondrogenesis;(2)XBP1S enhances BMP2-induced chondrocyte differentiation; (3) the binding of XBP1S to Runx2 and acting as its cofactor for hypertrophic chondrocyte formation(Fig.5). Collectively, this study identifies XBP1S as a novel regulatory factor in the complex networks controlling growth plate chondrocyte prehypertrophy, hypertrophy and differentiation.

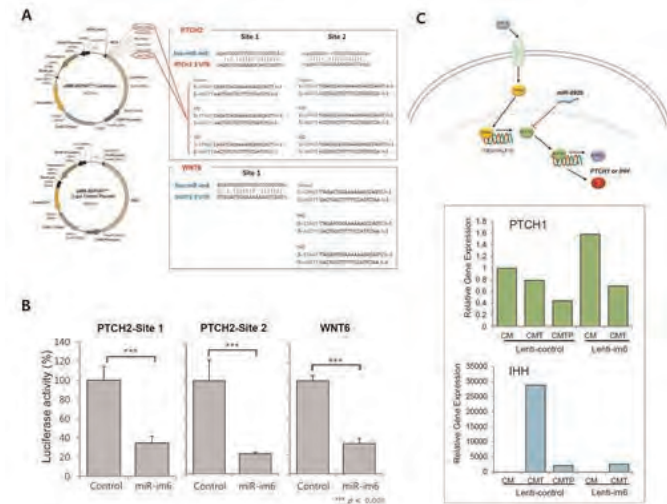


Fig.1 Expression of XBP1S during chondrogenesis both in vitro and in vivo.

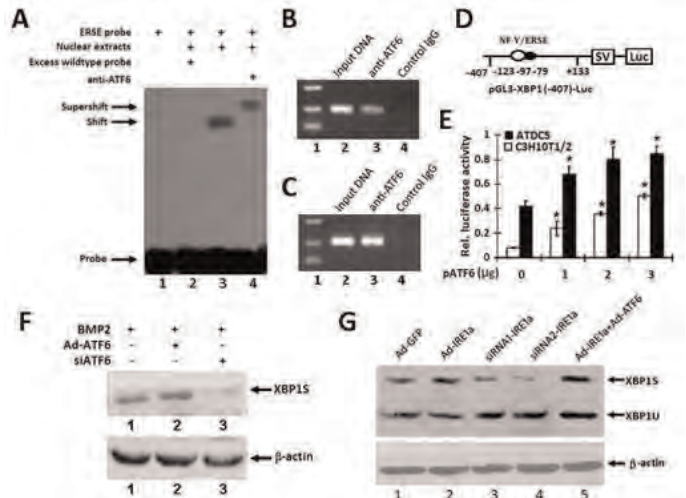


Fig.2 ATF6 increases the expression of XBP1S gene in chondrogenesis

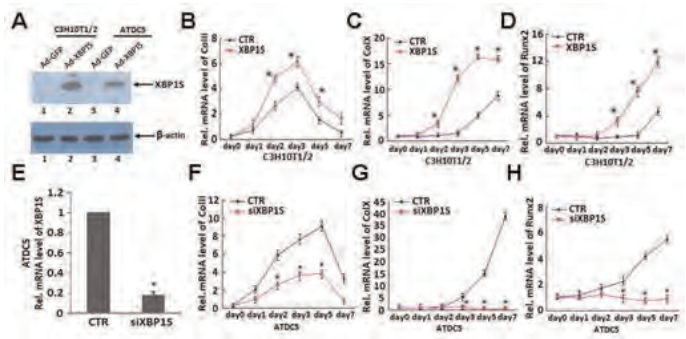


Fig.3 XBP1S enhances hypertrophic chondrocyte differentiation

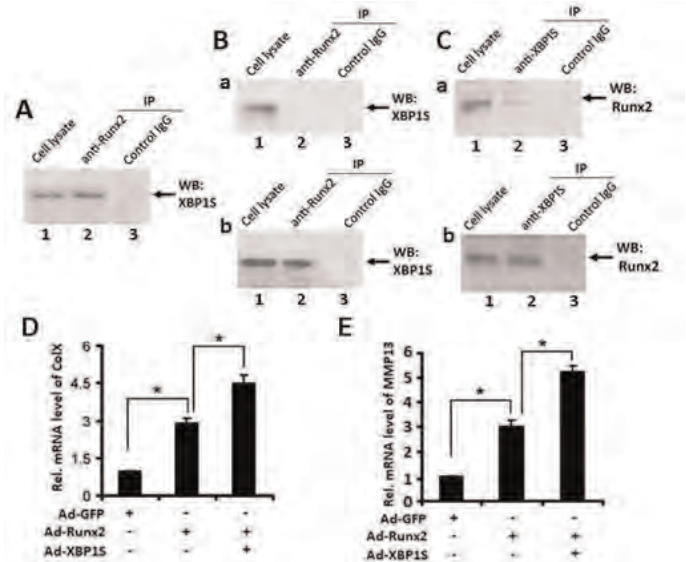


Fig.4 XBP1S associated with Runx2 and enhances Runx2-induced hypertrophic chondrocyte differentiation

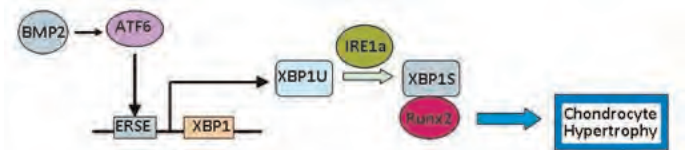


Fig.5 A proposed model for explaining the role and regulation of XBP1 in chondrocyte hypertrophy

Disclosures: Fengjin Guo, None. This study received funding from: NSFC

1219

“Phosphatase inhibition” - A Dual Drug Target Approach to Suppressing Calcification by Vascular Smooth Muscle Cells. Tina Moreira¹, Manisha Yadav², Dongxing Zhu³, Sonoko Narisawa⁴, Campbell Sheen⁴, Vicky E. MacRae⁵, Colin Farquharson⁶, Marc Hoylaerts⁷, Jose Luis Millan¹. ¹Sanford-Burnham Medical Research Institute, USA, ²Burnham Institute for Medical Research, USA, ³The Roslin Institute & R(D)SVSUUniversity of Edinburgh, United Kingdom, ⁴Sanford Burnham Medical Research Institute, USA, ⁵The University of Edinburgh, United Kingdom, ⁶Roslin Institute, University of Edinburgh, United Kingdom, ⁷Center for Molecular & Vascular Biology, University of Leuven, Belgium

Medial vascular calcification (MVC) is common in patients with chronic kidney disease, type II diabetes, obesity, and aging. MVC is an actively regulated process that resembles skeletal mineralization, resulting from chondro-osteogenic transformation of vascular smooth muscle cells (VSMCs), including the production of mineralization-competent matrix vesicles (MVs). We have previously shown that PHOSPHO1 and TNAP expression coincide during skeletal mineralization when MVs initiate deposition of hydroxyapatite through the intravesicular action of PHOSPHO1 while propagation of mineralization in the extravascular matrix is mediated by the action of tissue-nonspecific alkaline phosphatase (TNAP). The finding that TNAP upregulation is a common phenomenon at sites of medial calcification in several disease models has important translational implications and has motivated the development of potent inhibitors of the pyrophosphatase activity of TNAP. Here we present evidence that PHOSPHO1 is also a druggable target for MVC. Wild-type (WT) VSMCs cultured under calcifying conditions exhibited increased *Phospho1* gene expression and *Phospho1*^{-/-} VSMCs failed to mineralize *in vitro*. Using the natural PHOSPHO1 substrates phosphocholine and phosphoethanolamine, potent and specific inhibitors of PHOSPHO1 were identified via high-throughput screening and kinetic analyses. Then, the therapeutic potential of targeting PHOSPHO1 or TNAP alone and in combination to prevent VSMC calcification was assessed. The dual inhibition strategy inhibited VSMCs mineralization significantly better than inhibition of either target alone and the combination of inhibitors also affected expression of several mineralization-related enzymes, decreasing expression of *Colla1*, while increasing expression of the smooth muscle marker *Acta2*. In conclusion, we show that PHOSPHO1 plays a critical role in VSMC mineralization and that “phosphatase inhibition”, via the combined use of PHOSPHO1- and TNAP-specific inhibitors, offers a promising approach to prevent or attenuate MVC.

Kiffer-Moreira T., Yadav M.C., Zhu D., Narisawa S., Sheen C., Stec B., Cosford N.D., Dahl R., Farquharson C., Hoylaerts M.F., MacRae V.E., Millán J.L. Pharmacological inhibition of PHOSPHO1 suppresses vascular smooth muscle cell calcification. *J Bone Miner. Res.* 2012. In Press

Disclosures: Tina Moreira, None.

1220

A Dominant Mutation of *IFITM5* in Severe Osteogenesis Imperfecta Implicates an Interaction between Bril and PEDF in Bone. Charles Farber¹, ADI REICH², Aileen Barnes³, Wayne Cabral⁴, Ryan Riddle⁵, Douglas Digirolamo⁶, Thomas Clemens⁶, Joan Marini². ¹University of Virginia, USA, ²National Institute of Child Health & Human Development, USA, ³NICHD/NIH, USA, ⁴Bone & Extracellular Matrix Branch, NICHD, NIH, USA, ⁵Johns Hopkins University School of Medicine, USA, ⁶Johns Hopkins University, USA

Recessive mutations in the *SERPINF1* gene that encodes pigment epithelium-derived factor (PEDF) cause type VI osteogenesis imperfecta (OI). We identified a 25 year old proband with severe OI whose dermal fibroblasts have minimal secretion of PEDF in the absence of a *SERPINF1* mutation. The proband has relative macrocephaly, extreme short stature (50th centile for 28 month old girl), barrel chest and scoliosis. Long bones are severely bowed, with poor modeling and disorganized cystic appearance on radiographs. She has blue tinged sclerae. At age 6-8 years, multiple serum alkaline phosphatase values exceeded 900 mg/dl, but current value is 118 mg/dl. To identify the genetic basis of OI in this proband, we performed whole exome sequencing on the proband, both parents and an unaffected sibling. The exome sequence data were used to identify variants that were rare (allele frequency <1%) and fit a recessive or compound heterozygous mode of inheritance or were unique to the proband (*de novo* mutations). A total of 18 variants met these criteria. We next prioritized candidates based on their membership in a murine co-expression network module for cortical bone, which also contains all currently known OI genes. Of the 18 genes containing variants, interferon induced transmembrane protein 5 (*IFITM5*) was the only one that was a member of the module, suggesting it was the causal gene. *IFITM5* encodes the bone-restricted ifitm-like (Bril) protein that is specifically expressed in osteoblasts and has been shown to be involved in mineralized nodule formation *in vitro*. Sanger sequencing and restriction digestion confirmed the mutation was present in the proband and absent in family members. The nonsynonymous mutation in *IFITM5* leads to a S40L substitution and was predicted to impact Bril function. Interestingly, a single mutation in the 5'-UTR of *IFITM5*,

which creates a new start codon that adds 5 residues to the N-terminus of Bril, has recently been shown to cause dominant type V OI (Cho *et al.*, doi.org/10.1016/j.ajhg.2012.06.005; Semler *et al.*, doi.org/10.1016/j.ajhg.2012.06.011). We have shown that osteoblasts from type V OI probands have increased secretion of PEDF and decreased secretion of type I collagen. Conversely, we found that *Ifitm5* expression is increased in *Serpinf1* deficient murine calvarial osteoblasts. Together, these data suggest that *IFITM5* is a novel OI gene, whose product interacts with PEDF and plays an important role in bone mineralization.

Disclosures: Charles Farber, None.

1221

Dkk1 and Msx2-Wnt7 Signaling Reciprocally Regulate The Endothelial-Mesenchymal Transition In Aortic Endothelial Cells. Su-Li Cheng¹, Jian Su Shao¹, Abraham Behrmann², Karen Krchma², Dwight Towler². ¹Washington University in St. Louis School of Medicine, USA, ²Washington University in St. Louis, USA

Objective: Endothelial cells (ECs) can undergo an endothelial-mesenchymal transition (EnMT) during tissue fibrosis. Wnt- and Msx2-regulated signals participate in arteriosclerotic calcification and fibrosis. We therefore studied the impact of Wnt7, Msx2, and Dkk1 (Wnt7 antagonist) on EnMT in cultured primary aortic endothelial cells (AoECs). Methods and Results: Transduction of AoECs with vectors expressing Dkk1 suppressed EC differentiation and induced a mineralizing myofibroblastic phenotype. Dkk1 suppressed *claudin 5*, *PECAM*, *cadherin 5* (*Cdh5*), *Tiel* and *Tie2*. Dkk1 converted the cuboidal cell monolayer into a spindle-shaped multilayer and inhibited EC cord formation. Fibro-osteogenic markers such as *SM22*, *Osx*, *Runx2*, *type I collagen* and *alkaline phosphatase* were upregulated by Dkk1 via activin like kinase / Smad pathways. Dkk1 increased fibrosis and mineralization of AoECs cultured under osteogenic conditions – the inverse of mesenchymal cell responses. Msx2 or Wnt7 promoted the “cobblestone” morphology of differentiated ECs and EC marker expression. Targeting Wnt7b with the EC *Cdh5-Cre* transgene in *Wnt7b(f1/f1);LDLR-/-* mice upregulated aortic osteochondrogenic genes (*Osx*, *Sox9*, *Runx2*, *Msx2*) and increased collagen accumulation. Conclusions: Dkk1 enhances EnMT in AoECs, while Msx2-Wnt7 signals stabilize EC phenotype. EC responses to Dkk1, Wnt7, and Msx2 are the inverse of mesenchymal cell responses, coupling EC differentiation and fibro-osteogenic predilection during arteriosclerosis.

Disclosures: Su-Li Cheng, None.

1222

Exercise Strengthens Bone through Myokine Irisin. Jin Zhang¹, Yuwei Wu², Liming Yu¹, Shu Meng¹, Lan Zhang¹, Mengqi Huang¹, Qisheng Tu¹, Jake Jinkun Chen¹. ¹Tufts University School of Dental Medicine, USA, ²Tufts University, USA

Irisin, a newly discovered myokine induced in exercise, has potential effects in stimulating adipose tissue browning, fighting obesity and diabetes (NEJM, 366:1545, 2012; Nat 481:463, 2012). The present study aims, for the first time, to investigate the effects of irisin in bone metabolism.

Pre-osteogenic MC3T3-E1 and osteoclast precursor RAW264.7 cells were used. The cultured MC3T3-E1 cells were treated with ascorbic acid and irisin for 7, 10 and 14 days. RAW264.7 cells were exposed to irisin with or without RANKL for 1 and 3 days. The mRNA expression was detected by real-time PCR, and protein phosphorylation by Western blot.

For MC3T3-E1 cells, the mRNA expressions of osteogenic factors, *Runx2*, *Osterix* and *Satb2* were increased several folds after irisin treatment. The mature osteogenic genes, bone sialoprotein and osteocalcin were significantly upregulated in the late stage. Irisin increased protein phosphorylation of Smad 1/5/8 in 20nm, which was inhibited by BMP receptor inhibitor LDN193189. Thus irisin might increase osteoblast differentiation through BMP pathways.

It was also found that irisin inhibited RANKL-induced osteoclastogenesis of RAW264.7 cells through suppression of NFATc1 at 1d and 3d. Osteoclast differentiation marker, TRAP and cathepsin K, decreased to 30% at 3d. Irisin reduced the TRAP-positive osteoclast cells remarkably at 6d in a dose dependent manner. The signal genes of osteoclast differentiation, including *MITF* and *PU1*, were inhibited by irisin. *AKT1* gene expression and protein phosphorylation were reduced by irisin at 3d. NF-κB was not affected, while c-Fos and c-Myc were increased considerably. Therefore, irisin might specifically inhibit osteoclast differentiation through *AKT1*, *MITF* and *PU1-NFATc1* pathways.

Furthermore, irisin induced cytokine gene expression in RAW cells, including anti-inflammatory cytokines *IL-1ra* and *IL-10*, and pro-inflammatory cytokine *IL-1β*, *IL-6* and *TNF-α*. Irisin seems to exert complicated effects on osteoclast lineage through immune system as well.

In conclusion, we demonstrated that irisin promotes osteoblast differentiation partly through BMP pathway and inhibit osteoclast differentiation by suppressing the RANKL-AKT1/MITF/PU1-NFATc1 pathway. Hence the exercise-induced hormone irisin has initially proved to be a potent factor in strengthening bone by regulating bone metabolism, and a potential molecule for prevention and treatment of bone diseases such as osteoporosis.

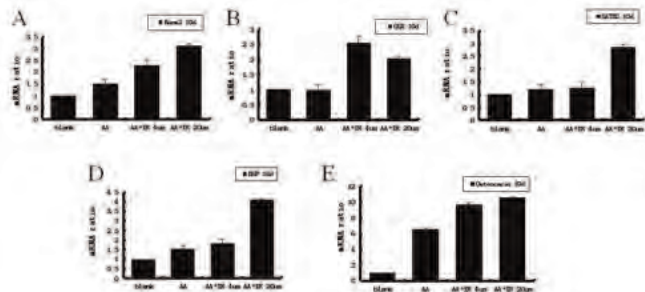


Figure 1: Irisin increased osteo-differentiation genes RUNX2(A), OSX(B) and SATB2(C) expression, and osteoblast marker gene BSP(D) and osteocalcin(E) after induced by Ascorbic acid for 10 days.

Figure 1

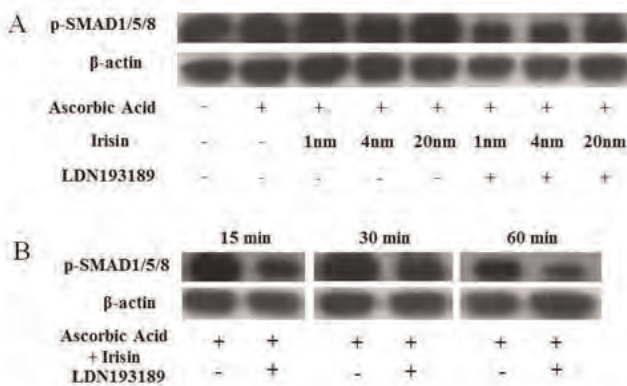


Figure 2: Irisin increased protein phosphorylation of Smad 1/5/8 in 20nm, which was inhibited by BMP receptor inhibitor LDN193189. A dose-dependent change, B time-dependent change.

Figure 2

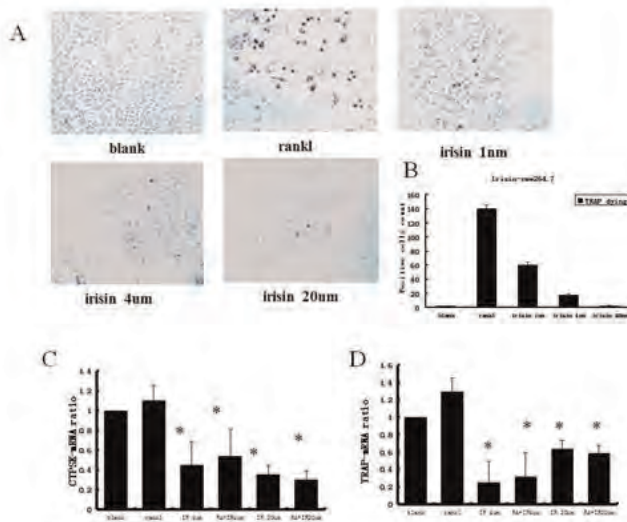


Figure 3: Irisin reduced osteoclastogenesis. A,B:the TRAP-positive osteoclast cells differentiated from raw 264.7 significantly at 6 days. A:TRAP staining, B:positive number,C,D:Osteoclast differentiation marker, TRAP(C) and cathepsin K(D), were decreased at 3d by irisin (*<0.05)

Figure 3

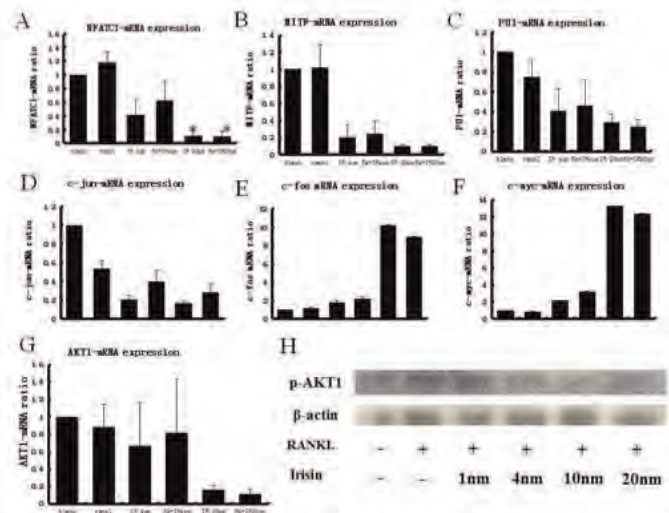


Figure 4: Some main signal gene expression of osteoclast differentiation were affected by irisin.A:The key transcription factors of osteoclast differentiation, NFATc1, were significantly inhibited (*<0.05).B,C,D:Several osteoclast signal gene were reduced by irisin,MIF(B) and PUF1(C) c-jun(D), E,F: c-fos(E) and c-myc(F) gene were increased significantly by irisin. G,H: AKT1 gene expression and protein phosphorylation were reduced by irisin at 3d. G, AKT1 mRNA expression, H, Dose-dependent reducing of AKT1 protein phosphorylation.

Figure 4

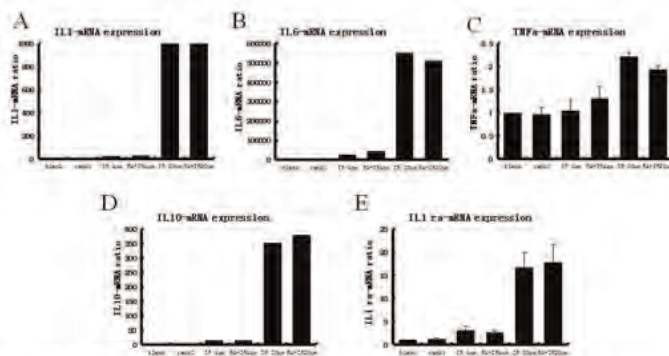


Figure 5: Irisin increased the mRNA expression of inflammation cytokine IL1β(A), IL6(B) and TNFα(C) and anti-inflammation cytokine IL10(D) and IL1-ra(E) significantly by real-time PCR.

Figure 5

Disclosures: Jin Zhang, None. This study received funding from: NIH Grants DE16710 and DE21464

1223

Micro-MRI Based Biomechanics Indicates Strength and Stiffness of the Tibia are Improved by Brief Daily Exposure to Low Magnitude Mechanical Signals in Patients with End-Stage Renal Disease. Chamith Rajapakse¹, Felix Werner Wehrli², Clinton Rubin³, Mary Leonard⁴. ¹University of Pennsylvania School of Medicine, USA, ²University of Pennsylvania Medical Center, USA, ³State University of New York at Stony Brook, USA, ⁴Children's Hospital of Philadelphia, USA

End stage renal disease (ESRD) is associated with markedly greater fracture rates compared with the general population. This study examines the potential of mechanical signals as a non-pharmacologic means of improving bone quality. Finite-element models developed from micro-MR images of the distal tibia were used to determine if low magnitude mechanical stimulation (LMMS) could enhance bone stiffness and strength in patients on dialysis.

This double-blind pilot study involved 28 patients with end-stage renal disease on maintenance hemodialysis. Participants were randomized to daily 20-min treatment standing on an LMMS active device (0.3g, 30 Hz) or a placebo control. Adherence was documented using internal monitor in the device. The three-dimensional microstructure of the distal tibial metaphysis was examined by high-resolution magnetic resonance imaging (μMRI) on a clinical 1.5 Tesla scanner at baseline and after 6 months of treatment. The distal lower extremity was chosen for imaging

because of the proximity to the site of the stimulus, and located on the direct transmission path of LMMS signals. Linear finite-element analysis was performed on the basis of μ MR images by simulating loading along the axial direction to obtain stiffness and failure strength, the latter by invoking thePistoi FAILURE criterion.

μ MR images of trabecular microstructure revealed noticeable bone accrual in LMMS patients (Fig.1). Intention to treat analyses indicated a 2.2% ($p=0.05$) and 4.4% ($p=0.1$) increase in stiffness and strength in the LMMS subjects, as compared to 1.6% ($p=0.2$) and 2.1% ($p=0.2$) increases in control (Table 1). In those subjects that were at least 70% compliant over the six month period, stiffness increased 4.7% ($p=0.05$) and strength increased 7.8% ($p=0.02$) from baseline, as compared to 1.9% ($p=0.4$) and 2.4% ($p=0.4$) in controls over the same time period. This work suggests that brief exposure to even low magnitude mechanical signals can enhance bone quantity and quality in patients with ESRD. The bone's response to mechanical signals achieved by this non-drug intervention may provide a means for mitigating fracture risk, without complicating the polypharmacy these patients inevitably must tolerate.

| Group and Parameter | Intention to treat analysis | | | | Subjects with >70% compliance | | | |
|---|-----------------------------|-------------|-------------|---------|-------------------------------|-------------|-------------|---------|
| | At Baseline | At 6 months | % Change | p Value | At Baseline | At 6 months | % Change | p Value |
| LMMS (8 males and 6 females) | | | | | | | | |
| Stiffness | 1167 ± 115 | 1190 ± 111 | 2.15 ± 5.21 | 0.1 | 1111 ± 93 | 1164 ± 113 | 4.69 ± 5.03 | 0.05 |
| Failure Strength | 4.50 ± 0.89 | 4.68 ± 0.88 | 4.18 ± 7.33 | 0.05 | 4.69 ± 0.43 | 5.05 ± 0.55 | 7.81 ± 6.30 | 0.02 |
| Placebo (8 males and 6 females) | | | | | | | | |
| Stiffness | 1193 ± 196 | 1211 ± 204 | 1.61 ± 6.90 | 0.2 | 1172 ± 160 | 1196 ± 191 | 1.84 ± 6.78 | 0.4 |
| Failure Strength | 4.78 ± 1.16 | 4.84 ± 1.06 | 2.14 ± 8.86 | 0.2 | 4.82 ± 0.91 | 4.90 ± 0.80 | 2.31 ± 7.67 | 0.4 |

Stiffness (MPa) and failure strength (kN) are means ± standard deviations.

Table 1

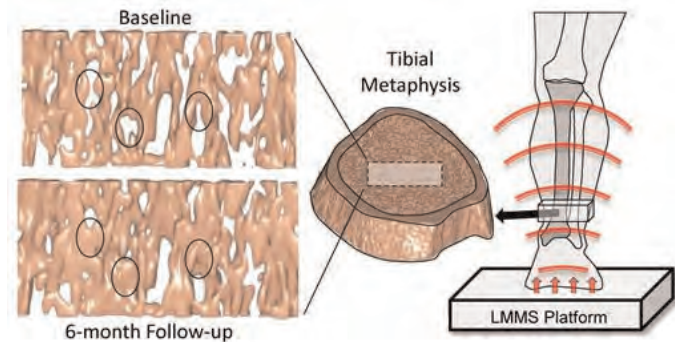


Figure 1:

Disclosures: Chamith Rajapakse, None.

1224

Differential Bone Loss Following Gastric Surgery: Comparison of Different Modalities at 12 Months. Malgorzata Brzozowska*, Nguyen Nguyen², John Jorgensen³, Jacqueline Center², Paul Baldock². ¹Garvan Institute of Medical Research, St Vincent's Hospital, Australia, ²Garvan Institute of Medical Research, Australia, ³St George Private Hospital, Australia

Obesity rates have increased markedly in recent decades. Gastric surgery is the most effective therapy. However, the skeletal consequences are not fully elucidated. We examined the skeletal response to 3 weight loss modalities: Medical Managed Dieting (MDD), Gastric Banding (GB) and Gastric Sleeve (GS).

We present preliminary 12 mth data from a 24 mth prospective trial. In addition to DXA at 0 and 12 mths, data were collected for calcium intake, 25-OH D, PTH, gut hormones and adipokines.

There were 10 MMD, 4 GB and 20 GS subjects. At baseline, average age was 51 ± 12 yrs (MMD 56 ± 10, GB 44 ± 14, GS 51 ± 13, ns). BMI was 40 ± 7 (MMD 38 ± 7, GB 37 ± 5, GS 43 ± 6, ns). Calcium intake, 25-OH D and PTH were normal. However, 25% of subjects had an osteopenic/osteoporotic DXA Z-score.

At 12 mths, differences in response were evident between groups. % weight change was small in MMD(-6; -7,-0.7), greater in GB(-15; -17,-13) and greatest in GS(-29; -33,-21), $P<0.0001$. (median: Q1,Q3), ANOVA. Despite weight loss among groups, % changes in total hip BMD were evident only in GS(-6; -8,-5) but minimal in MDD(-0.7; -1.9,0.3) and GB(-0.3; -0.6,0), $P<0.0005$.

We examined factors affecting bone loss:

1. In GS, all weight loss occurred in the first 6 mths post-surgery, however bone loss was ongoing: 3.5% by 6 mths, 6% by 12 mths. Moreover the 2 patients with 24 mth data had further bone loss to 11.6% suggesting that weight loss is not the sole determinant of bone loss.

2. Bone turnover markers increased in GS from baseline to 12 mths: osteocalcin ($8 \pm 3 \mu\text{g/L}$ to 14 ± 9 , $P<0.002$) and uNTX ($28 \pm 12 \text{nmol/mMcr}$ to 55 ± 24 , $P<0.02$) with no change in MDD and GB.

3. Calcium intake, vitamin D and PTH were normal throughout.

4. Gut-derived, pro-satiety hormone Peptide YY increases post-meal to reduce appetite and has a negative effect on bone. At baseline no PYY response was evident in any group. At 12 mths, %PYY increase at 90 minutes (median:Q1,Q3) was

MMD(23.7: 13.8,48.7), GB(34.4: 9.5,87.1), GS(121.6: 65.3,187.4), $P<0.01$. GLP-1 response was not significantly altered. Adiponectin increases matched weight loss MMD(6.6: -2.1,13.6), GB(27: 5.6,50.6), GS(51.9: 33.7,87.7), $P<0.0005$.

Different weight loss modalities produced varied skeletal responses. Bone loss was marked in GS but absent in GB despite weight loss. Bone loss post-GS may involve changes in PYY and adiponectin, in addition to weight loss.

Disclosures: Malgorzata Brzozowska, None.

1225

Too Fit To Fracture: A Consensus on Exercise Recommendations for Individuals with Osteoporosis and Osteoporotic Vertebral Fractures. Lora Giangregorio*, Alexandra Papaioannou², Norma MacIntyre³, Maureen Ashe⁴, Ari Heinonen⁵, Kathy Shipp⁶, John Wark⁷, Stuart McGill¹, Heather Keller¹, Ravi Jain⁸, Judi Laprade⁹, Micheal McLeod¹, Angela Cheung¹⁰. ¹University of Waterloo, Canada, ²Hamilton Health Sciences, Canada, ³McMaster University, Canada, ⁴University of British Columbia, Canada, ⁵Department of Health Sciences, University of Jyväskylä, Finland, ⁶Duke University Medical Center, USA, ⁷University of Melbourne Department of Medicine, Australia, ⁸Osteoporosis Canada, Canada, ⁹University of Toronto, Canada, ¹⁰University Health Network, Canada

Equipoise exists regarding whether exercise prevents fractures, in part due to the limitations of using bone mineral density (BMD) or falls as surrogate endpoints. Also, the potential for harm in high-risk individuals has not been well-studied.

Objective: To develop an international consensus on exercise recommendations for individuals: 1) with osteoporosis; and 2) with osteoporotic vertebral fracture(s).

Methods: The Grading of Recommendations Assessment, Development and Evaluation (GRADE) method was used to evaluate the quality of evidence and modifying factors (e.g., cost, preference, benefit vs. harm), and develop recommendations. Outcomes considered important for decision-making were nominated by an international panel of experts in physical therapy, geriatrics, endocrinology, internal medicine, dietetics and kinesiology, and 4 patient advocates. A majority vote by the panel and advocate feedback identified falls, fractures, BMD and adverse events for both target groups, as well as pain, quality of life and function for those with vertebral fractures. Meta-analyses published in 2011 or later evaluating the effects of exercise on the outcomes were reviewed by the panel. Observational studies or clinical trials were reviewed when meta-analyses were not sufficient to address the question. Quality ratings and preliminary recommendations were generated.

Results: The outcome for which evidence is strongest is falls (Table 1). We propose conditional recommendations for participating in exercise with the intent of reducing falls and fractures, or improving BMD in either target group, or for improving pain, quality of life and function in those with vertebral fracture. Multicomponent exercise programs or challenging balance exercises must be used if the intent is to reduce falls. Hyperkyphotic posture may affect fall or fracture risk. Point estimates of exercise effects on BMD are close to measurement error, and vary according to exercise type. There is very limited available evidence on the benefits or risks of exercise in those with vertebral fracture(s). Exercise has the potential to increase adverse events, but there is not enough evidence to quantify the risk or conclude if it is greater in those who exercise.

Conclusions: The preliminary consensus of our international panel is that exercise is recommended for individuals with osteoporosis or vertebral fracture, but our recommendations are conditional. Our next step is to seek broader input via a Delphi consensus process.

| Outcome | Individuals with diagnosis of osteoporosis | Individuals with osteoporotic vertebral fracture(s) |
|-----------------------|--|---|
| Falls | HIGH -Two meta-analyses provide evidence for effect -Evidence indirect but effect not suspected to be different -Effect similar in high and low risk individuals -Effect may be modified by hyperkyphotic posture -Balance exercises or multicomponent exercise programs | MODERATE -Two meta-analyses provide evidence for effect -Evidence indirect and effect may be different -Effect similar in high and low risk individuals -Effect may be modified by hyperkyphotic posture -Balance exercises or multicomponent exercise programs |
| Fractures | VERY LOW -Imprecise or sparse data -Inconsistency in direction and size of effect -Most data supporting an effect are observational -High risk of bias in available data | VERY LOW -Imprecise or sparse data -Inconsistency in direction and size of effect -Most data supporting an effect are observational -High risk of bias in available data |
| BMD | LOW -Indirect evidence, uncertain if effect is different -Imprecise or sparse data -Risk of bias | VERY LOW -Indirect evidence and effect may be different -Imprecise or sparse data -Risk of bias, participants on home drugs |
| Harm (adverse events) | VERY LOW -Inconsistency in direction and size of effect -High probability of reporting bias -Imprecise or sparse data | VERY LOW -Inconsistency in direction or size of effect -High probability of reporting bias -Imprecise or sparse data, indirect evidence |
| Pain | n/a | VERY LOW -Imprecision and risk of bias -Inconsistency in direction and size of effect |
| QOL | n/a | VERY LOW -Imprecise or sparse data, risk of bias |
| Mobility | n/a | LOW -Imprecise or sparse data, variable risk of bias -Inconsistency in size and direction of effect -Small positive effects in more than one trial |
| ADL | n/a | VERY LOW -Imprecise or sparse findings, variable risk of bias -Inconsistency in size and direction of effect |

Table 1

Disclosures: Lora Giangregorio, Merck Frosst, 6

1226

Diabetes Mellitus and Osteoporosis; Skeletal Effects of Diabetic Hyperglycemia and Glucose Lowering Anti-diabetic Therapies. Beata Lecka-Czernik*. University of Toledo College of Medicine, USA

Osteoporosis and diabetic disease have reached epidemic proportion and create significant public health concerns. The prevalence of these diseases is alarming, and indicates that in the US, 50% of elderly individuals are osteoporotic and almost 20% of population has either diabetic or prediabetic conditions (Centers for Disease Control and Prevention; <http://www.cdc.gov>). Diabetes mellitus and osteoporotic fractures are two of the most important causes of mortality and morbidity in older individuals. There is a close association between fragility fracture risk and diabetes mellitus, which not necessarily correlates with a reduced bone mineral density (BMD), however it correlates with a reduced biomechanical quality of the bone. Osteoporosis and diabetes share many features including genetic predispositions and molecular mechanisms. This concurs with recent findings indicating that bone status is closely linked to regulation of energy metabolism and insulin sensitivity. Indeed, bone and energy homeostasis are under the control of the same transcriptional and hormonal factors, including the peroxisome proliferator activated receptor gamma (PPAR γ), pancreatic hormone - insulin, hormones produced by adipose tissue - leptin and adiponectin, gastrointestinal hormones including ghrelin, glucose inhibitory protein (GIP) and glucagon inhibitory peptide (GLP), and bone derived hormone osteocalcin. These factors and related mechanisms control glucose homeostasis and fatty acids metabolism in peripheral tissues, which are pharmacological targets for anti-diabetic therapies. The same factors may contribute to the bone quality by their effect on bone cell differentiation and bone remodeling process creating a possibility that glucose lowering drugs may have adverse effects on bone. The review of skeletal effects of available anti-diabetic therapies indicate that they may either increase fracture risk (TZDs and insulin), or may not affect the risk (sulfonylurea), or may even decrease the risk (metformin and incretins). In conclusion, the linkage between osteoporosis and diabetes is multifactorial and includes common regulation of bone homeostasis and energy metabolism. This suggests vigilance for the skeletal effects of therapies which modulate energy metabolism.

Disclosures: Beata Lecka-Czernik, None.

1227

Associations of Long-term Dietary Calcium Intake with Fractures, Cardiovascular Events and Aortic Calcification in a Population-based, Prospective Cohort Study. Belal Khan*¹, Dallas English², Caryl Nowson³, Robin Daly⁴, Peter Ebeling⁵. ¹University of Melbourne, Australia, ²Melbourne School of Population Health, Australia, ³School of Exercise & Nutrition Sciences, Deakin University, Australia, ⁴Centre for Physical Activity & Nutrition Research, Deakin University, Australia, ⁵The University of Melbourne, Australia

Objective: To determine associations between dietary calcium intake and risk of fractures, cardiovascular events, mortality, vertebral deformities and aortic calcification.

Design: Prospective cohort study of 41,514 men and women aged 45-64 years followed 13-14 years for mortality, incident fractures and cardio-vascular events. 12,528 were eligible for fracture analysis, and 37,253 for cardiovascular and mortality analyses. A subset, having dietary calcium intakes of <500 mg/day (n=172) or \geq 1300 mg/day (n=174) at baseline, had lateral thoraco-lumbar spine x-rays.

Outcome measures (whole cohort): Cumulative self-reported incident fractures, non-fatal cardiovascular events (CVE), and mortality. Dietary calcium intake was assessed at baseline using a validated food frequency questionnaire and quartiles of energy-adjusted dietary calcium intake (CIQ) defined. Hazard ratios (HR) for mortality and odds ratios (OR) for self-reported events were calculated using Cox and logistic regression. In the subset, abdominal aortic calcification score (ACS, 24 point scale) and vertebral deformities (SQ method) were measured from x-rays. Linear, ordinal logistic and logistic regression measured coefficients for ACS; spinal deformity index (SDI) and OR for tertiles of AAC; and OR for ACS (\geq 6) and moderate to severe vertebral deformities.

Results: 824 (10.4%) reported incident fractures, 2,674 (12.9%) had incident non-fatal cardiovascular events; and 3,445 (9.3%) deaths occurred. After adjusting for potential confounders, the OR for incident fracture was 0.75 (CI 0.60-0.94) for the highest compared with lowest CIQ. The OR for incident CVE was 0.84 (CI 0.74-0.96); the OR for incident stroke was 0.87 (CI 0.62-0.97) and HR for all-cause mortality was 0.90 (CI 0.81-1.00) in the highest CIQ. In the subset, 103 (29.8%) had a vertebral deformity of which 36 (10.4%) were moderate to severe. AAC was present in 229 (66.2%) and 115 (33.2%) had ACS of \geq 6. The OR for vertebral deformity was 0.41 in the high dietary CI group (CI 0.25-0.68), including moderate to severe deformities (OR 0.33, CI 0.15-0.74). The SDI coefficient was also lower (-0.19, CI -0.33 to -0.05) and OR for severe aortic calcification (ACS \geq 6) was 0.41 (CI 0.17-0.99). Results were similar when dietary calcium unadjusted for energy was used. **Conclusion:** Higher dietary calcium intakes are beneficial to health and associated with decreased risks for all fractures, non-fatal cardiovascular events, stroke and vertebral deformity.

Disclosures: Belal Khan, None.

1228

Denosumab Compared With Risedronate in Postmenopausal Women Suboptimally Adherent With Alendronate Therapy: Efficacy and Safety Results From a Randomized Open-label Study. C Roux*¹, A Fahrleitner-Pammer², PR Ho³, F Hawkins⁴, LC Hofbauer⁵, M Micaelo⁶, S Minisola⁷, N Papaioannou⁸, M Stone⁹, J Wark¹⁰, MC Zillikens¹¹, I Ferreira³, S Siddhanti³, RB Wagman³, JP Brown¹². ¹Paris Descartes University, France, ²Medizinische Universitaet Graz, Austria, ³Amgen Inc., USA, ⁴Hospital Universitario, Spain, ⁵Dresden, University of Technology Medical Center, Germany, ⁶Instituto Portugues de Reumatologia, Portugal, ⁷Università di Roma, Italy, ⁸Laboratory for the Research of Musculoskeletal System University of Athens, Greece, ⁹University Hospital of Llandough, United Kingdom, ¹⁰The Royal Melbourne Hospital, The University of Melbourne, Australia, ¹¹University Hospital Rotterdam, Erasmus MC, Netherlands, ¹²CHUQ-CHUL Research Centre, Canada

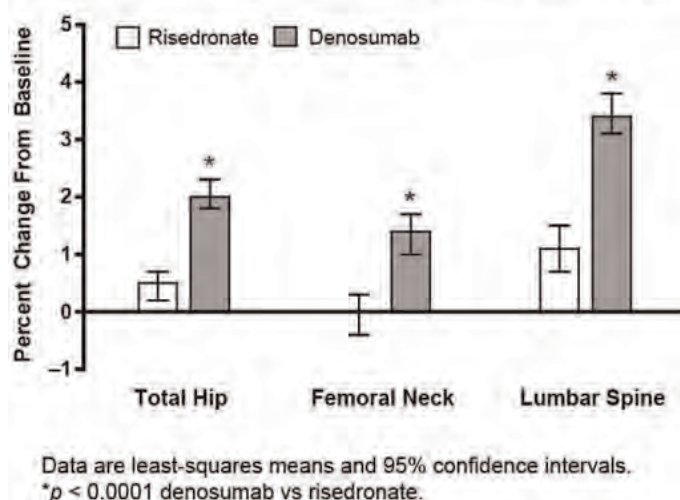
Denosumab (DMAB), a fully human monoclonal antibody that specifically targets RANKL to inhibit osteoclast formation, function, and survival, reduces the risk for new vertebral, nonvertebral, and hip fractures (Cummings NEJM 2009). In subjects who were treatment naïve or previously treated with alendronate, DMAB was associated with greater gains in bone mineral density (BMD) and decreases in bone turnover markers when compared with alendronate-treated subjects (Brown JBMR 2009; Kendler JBMR 2010). The purpose of this open-label trial was to compare the efficacy and safety of DMAB with risedronate over 12 months in postmenopausal women who transitioned from daily or weekly alendronate treatment and were considered to be suboptimally adherent with therapy.

This was a multicenter, international, randomized, open-label, parallel-group study in which postmenopausal women aged 55 and older were randomized 1:1 to receive open-label DMAB 60 mg subcutaneously every 6 months or risedronate 150 mg orally every month (one 75 mg tablet on each of two consecutive days) for 12 months. The primary endpoint was percent change from baseline in total hip BMD at month 12. Secondary endpoints included percent change from baseline in femoral neck and lumbar spine BMD at month 12, and percent change from baseline in serum CTX at months 1 and 6 (exploratory). Safety endpoints were also assessed.

A total of 870 subjects were randomized (435, DMAB; 435, risedronate) who had a mean (SD) age of 68 (7) years, mean (SD) BMD T-score of -1.6 (0.9), -1.9 (0.7), and -2.2 (1.2) at the total hip, femoral neck, and lumbar spine, respectively, and median CTX of 0.3 ng/mL. DMAB significantly increased BMD at the total hip compared with risedronate at month 12 (2.0% vs 0.5%, respectively; $p < 0.0001$; Figure). DMAB also significantly increased BMD at the femoral neck (1.4% vs 0%) and lumbar spine (3.4% vs 1.1%) compared with risedronate ($p < 0.0001$ at both sites). DMAB significantly decreased CTX compared with risedronate at month 1 (median change from baseline of -78% vs -17%; $p < 0.0001$) and month 6 (-61% vs -23%; $p < 0.0001$). In this open-label study, overall adverse events (AEs) and serious AEs were similar between groups.

In postmenopausal women who were suboptimally adherent with alendronate, switching to DMAB is more effective than risedronate based on significantly greater increases in BMD at all measured sites and greater reductions in CTX with DMAB.

Figure. Percent Change in BMD From Baseline at Month 12



Figure

Disclosures: C Roux, None.

1229

Femur Stress Fractures in Children with Osteogenesis Imperfecta and Intramedullary Rods on Long-term Intravenous Pamidronate Therapy.

Abdelsalam Hegazy^{*1}, Andrew Howard², Etienne Sochett³, LIANNE TILE⁴, Angela Cheung⁵. ¹Canada, ²The Hospital for Sick Children, Canada, ³Hospital for Sick Children, Canada, ⁴University of Toronto, Canada, ⁵University Health Network, Canada

Purpose: To describe femur stress fractures associated with long-term intravenous pamidronate therapy in children with Osteogenesis Imperfecta (OI) who have had femur osteotomies and intramedullary rod fixation. **Methods:** We reviewed the charts and x-rays of patients with OI who were followed at the Hospital for Sick Children in Toronto, Canada, between December 1999 and December 2011. All patients were receiving or had received intravenous pamidronate therapy, as well as vitamin D and calcium supplements. Blood biochemistry profile showed normal levels of alkaline phosphatase, phosphorous, 4 out of 6 patients had low 25-hydroxy vitamin D level at the time of these fractures, and none of the patients was on hormone or anabolic agent therapy during that period.

Results: Of the 72 patients (39 female, 33 male, age range 2-18) identified, six (3 female and 3 male) five patients had subtrochanteric and one had mid-diaphyseal femur stress fractures with minimal or no trauma. Prior to these stress fractures, all 6 had corrective osteotomies and intramedullary rod fixation for their femurs because of their deformities and/or multiple fractures, and have been on intravenous pamidronate therapy for more than five years. All 6 fractures happened after at least minimum period of eighteen months from the insertion of the rod, and were noncomminuted transverse or short oblique in configuration. None were related to previous osteotomies or due to delayed union. In addition, none were located at stress riser areas (such as tip of the implant) or at metaphysis (site of typical OI-related fractures), or at growth lines at the metaphysis because of cyclic pamidronate therapy. **Conclusion:** This is the first series describing femur stress fractures in children with OI and intramedullary rods on long-term intravenous pamidronate therapy. Subtrochanteric and mid-diaphyseal regions are the strongest sites in normal femurs and can usually withstand maximum tension and bending. These fractures resemble features described by the ASBMR Task Force for atypical femur fractures, and may provide clues to the etiology of atypical femur fractures.



Figure 1

Disclosures: Abdelsalam Hegazy, None.

1230

Predicting the Effects of Anti-Resorptive Drug Holiday on BMD and Tissue Age.

Christopher Hernandez^{*1}, Hellen Lopez¹, Joseph Lane². ¹Cornell University, USA, ²Hospital for Special Surgery, USA

Atypical femoral fractures have been implicated as an adverse side effect of long-term anti-resorptive treatment and are believed to be associated with increases in tissue age caused by reduced bone turnover. Drug holidays have been proposed as a way to limit increases in tissue age while maintaining most of the beneficial aspects of treatment (increased BMD, reduced fracture risk), although the effect of a drug holiday on tissue age is not known.

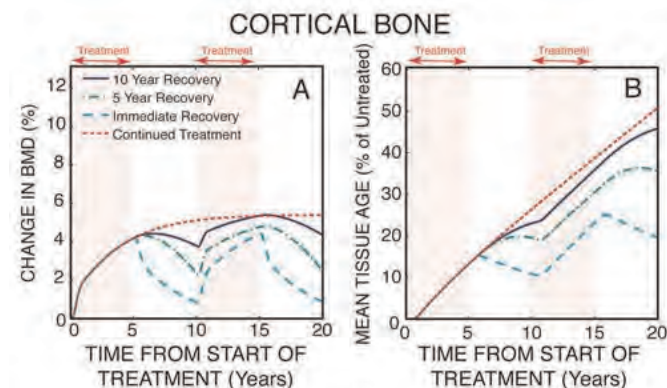
We used a computer model of the bone remodeling process to simulate drug treatment and drug holidays [1]. The simulation calculates the volume of bone tissue resorbed and formed during remodeling using histomorphometry data and determines the resulting changes in BMD and mean tissue age. Anti-resorptive therapy was simulated by reducing the activation frequency of bone remodeling by 85% (as seen in alendronate). The rate at which bone remodeling recovers after anti-resorptive treatment ends is not known and was simulated in three different ways to span the

range of possible responses: a) Immediate Recovery; b) 5 Year Recovery; and c) 10 Year Recovery. Drug holidays of 5 years, 3 years and 1 year in length were considered.

Simulations in which anti-resorptive treatment was ended after 5 years predicted that BMD would return to baseline within 5-10 years of cessation of treatment. However, mean tissue age recovered more slowly; ten years after ending treatment mean tissue age was predicted to be 8-55% greater than in a treatment naïve individual. Drug holidays caused oscillations in BMD and mean tissue age, but mean tissue age tended to increase over time (relative to an untreated individual) in most simulations, even with drug holidays (Figure).

Our findings suggest that after ending anti-resorptive treatment, BMD will recover much faster than mean tissue age. A drug holiday is therefore expected to cause loss of BMD long before mean tissue age returns to normal levels. While tissue age can be better controlled with anti-resorptive agents that are more rapidly removed from the body (simulated as Immediate Recovery), our simulations suggest that a drug holiday is unlikely to prevent accumulation of tissue age over long periods of care (more than 10 years) without loss of BMD. The risk of atypical femoral fractures is small compared to that of osteoporosis-related fractures (hip, wrist, spine) and drug holidays are not recommended for all patients.

1. Hernandez, CJ, et al. (2001). Bone 29(6): 511-16.



Figure

Disclosures: Christopher Hernandez, Musculoskeletal Transplant Foundation, 6

1231

A Comparison of Parathyroid Hormone-related Protein (1-36) and Parathyroid Hormone (1-34) on Markers of Bone Turnover and Bone Density in Postmenopausal Women: The PrOP Study.

Mara Horwitz^{*1}, Marilyn Augustine², Susan Sereika², Emily Martin², Raquel Carneiro³, Christine Oakley⁴, Angela Laslavic², Caren Gundberg⁵, Mary Beth Tedesco², Jane Cauley⁶, Andrew Stewart⁷. ¹University of PittsburghDiv of Endocrinology - EMRC, USA, ²University of Pittsburgh, USA, ³Universidade de Fortaleza, Brazil, ⁴Marshall University, USA, ⁵Yale University School of Medicine, USA, ⁶University of Pittsburgh Graduate School of Public Health, USA, ⁷University of Pittsburgh School of Medicine, USA

Background: PTHrP(1-36) increases lumbar spine (LS) bone mineral density (BMD), acting as a pure anabolic agent, but has not been directly compared to PTH(1-34).

Objective: A three month, randomized, prospective study in postmenopausal women with osteoporosis comparing PTHrP(1-36) to PTH(1-34) on markers of bone turnover, BMD, mineral metabolism and safety.

Design: 105 healthy postmenopausal osteoporotic women [LS, total hip (TH), or femoral neck (FN) T-score \leq -2.0] randomized to three groups: PTHrP 400 μ g/d; PTHrP 600 μ g/d; PTH 20 μ g/d, n=35/group. Exclusion criteria: any major medical disorder, fracture within 1 year, use of PTH for > 1 wk within 1 yr or >21 months ever, use of estrogen, SERMS, bisphosphonates, or any medication that could interfere with bone metabolism within 2 years. All had normal baseline 25(OH)D (> 20 ng/ml) and PTH.

Outcome measures: Primary outcome: change in PINP and CTX. Secondary outcomes: safety, vitamin D & mineral metabolism; changes in BMD.

Results: 90 subjects completed the study. Both PTH and PTHrP increased bone resorption (CTX): PTH = 53% day 60, 92% day 90 (p<0.005); PTHrP = 30% at day 90 (p<0.05). PTH also increased bone formation (PINP) (p<0.0005) to a greater extent (171%) than either dose of PTHrP (46-87%). The increase in PINP was earlier (day 15) and greater than the increase in CTX for all three groups. LS BMD increased equivalently by day 90 in all groups [PTH, PTHrP 400, PTHrP 600 = 1.8%, 1.5%, 2.1%, respectively (p<0.05 for all)]. TH increased (0.7%) significantly for both doses of PTHrP (p<0.05) and FN for PTHrP 400 (0.9%, p<0.05). There was no significant increase in TH or FN BMD for PTH. Forearm BMD declined non-significantly in all groups. PTH was not associated with hypercalcemia. PTHrP 400 induced mild (mean 9.95 mg/dl), transient (day 15), and largely self-limited hypercalcemia. PTHrP 600 required a dose reduction for hypercalcemia in 3 subjects. Each peptide induced a sustained increase in 1,25(OH)₂D, greatest for PTHrP 400. Adverse events (AE) were

similar among the three groups; AE-related terminations were 1 for PTH, 3 for PTHrP 400, and 4 for PTHrP 600.

Conclusion: PTHrP and PTH cause similar increases in LS BMD. PTHrP also increased TH and FN BMD. PTH induced greater changes in bone turnover than PTHrP. PTHrP was associated with mild transient hypercalcemia. Longer term studies using lower doses of PTHrP are needed to define the full clinical benefits of PTHrP.

Disclosures: *Mara Horwitz, None.*

1232

Transdermal Delivery of BA058, A Novel Analog of hPTHrP, with a Short Wear Time Microneedle Skin Patch in Post-Menopausal Women. Gary Hattersley¹, Kris Hansen², Amy Determan², Ken Brown², Kate McKay³, Jonathan Guerriero³, Dan McCarthy³, C. Richard Lyttle³, Louis O'Dea⁴. ¹Radius, USA, ²3M Drug Delivery Systems, USA, ³Radius Health Inc, USA, ⁴Radius Health Inc., USA

BA058 is a novel analog of hPTHrP (1-34) being developed as an anabolic therapy for the treatment of osteoporosis. Daily BA058 subcutaneous (SC) injection has produced promising safety and efficacy results thus far in Phase 1 and Phase 2 studies, and is currently enrolling in a Phase 3 fracture prevention study. There is, however, a significant need for an alternative to injection for delivery of bone anabolic agents that improves patient convenience and compliance. To achieve this we have investigated the use of a solid microneedle array technology (sMTS; 3M) for BA058 transdermal delivery. Three Phase 1 clinical studies were conducted to determine the pharmacokinetics, safety and tolerability of BA058 transdermal in healthy post-menopausal women after a single dose or repeat-daily administration up to 7 days. These studies were also designed to enable selection of wear time, wear site, and dose levels for further clinical studies. Periumbilical application of BA058 transdermal (100, 150 and 200 mcg) resulted in a desirable pharmacokinetic profile, with rapid delivery, early peak concentration and fast elimination of BA058. The Tmax of BA058 transdermal was ~ 8 minutes, compared to 15-25 minutes for BA058 SC injection, and the half-life (T1/2) was shorter, typically 15-30 minutes, again, compared to ~50-60 minutes for BA058 delivered via SC injection. BA058 transdermal also achieved a Cmax that matched or exceeded SC injection (80 mcg). BA058 microneedle array wear times of up to 24 hours were evaluated, with a 5-minute wear time found to be optimal to deliver BA058 and achieve desirable pharmacokinetics; skin contact times longer than 5-minutes did not result in further BA058 release. Seven consecutive days of repeat BA058 transdermal administration resulted in a marked increase in serum PINP, consistent with retention of pharmacological activity and bone anabolism. Overall, after more than 300 microneedle array applications to more than 100 subjects BA058 transdermal demonstrated a favorable safety profile, suitable for clinical development advancement. Transdermal delivery of BA058 using a short wear time microneedle skin patch potentially represents a convenient new anabolic approach for the treatment of osteoporosis that may increase patient compliance.

Disclosures: *Gary Hattersley, Radius Health, 3*

1233

Safety and Efficacy of Orally Administered Recombinant Salmon Calcitonin Tablets in the Prevention of Postmenopausal Osteoporosis in Women with Low Bone Mass: A Phase 2 Placebo-controlled Trial. Neil Binkley¹, Henry Bone², Michael Bolognese³, David Krause⁴. ¹University of Wisconsin, Madison, USA, ²Michigan Bone & Mineral Clinic, USA, ³Bethesda Health Research, USA, ⁴Tailsa Therapeutics Inc., USA

BACKGROUND: An oral preparation of recombinant salmon calcitonin (oral rsCT) has previously been shown to be safe and effective at increasing lumbar spine bone mineral density (LS BMD) in postmenopausal women with osteoporosis. METHODS: Eligible participants were women at least 5 years postmenopause with T-scores ≤ -1.5 and > -2.5 at the LS or total hip, femoral neck or trochanter but not ≤ -2.5 at any site, with a 10-year FRAX risk of at least 9.3% (major) or 1.2% (hip). After a 2 week placebo run-in period participants were randomized 2:1 to receive 200 µg/day of oral rsCT or identical appearing placebo for 1 year. Vitamin D and calcium citrate (1000IU/600mg daily) were provided. Replicate DXA scans were obtained at baseline, weeks 28 and 54, and read centrally. The 1^o efficacy variable was % change in LS-BMD over 52 weeks in the modified intent-to-treat (mITT) population. A serum bone resorption marker (CTX-1) was also assessed. Study medication was given h.s., until a protocol amendment changed the time of administration to dinner time. RESULTS: 144 subjects were enrolled at 7 US sites and entered the run-in period; 129 were randomized, 114 were in the mITT population. Their mean age was 67.2y and mean LS T-score -1.29. The mean change in LS BMD at the last visit was: (TABLE)

Oral rsCT was superior to placebo with respect to change in LS-BMD (delta 1.14% [95% CI: 0.14, 2.15], p=0.026). Time of administration (h.s. or dinner) did not affect the increase in LS BMD. The placebo-subtracted difference in fasting CTx-1 at the exit visit compared to baseline was -20.2 % (oral rsCT vs placebo, p =0.034). Tolerability was similar between groups; the most common adverse events (AEs) in each group were respiratory infections and gastrointestinal; few serious AEs and no deaths occurred. Most AEs were mild or moderate in severity. Few fractures occurred. CONCLUSIONS: In postmenopausal women, 1 year of oral rsCT treatment improved LS-BMD compared to placebo. The efficacy data (i.e., bone turnover and BMD) were robust, statistically significant and internally consistent. Administration

with a meal did not affect efficacy. The safety and tolerability profiles were similar to placebo. Oral rsCT has potential to provide an additional oral treatment option for postmenopausal women with low bone mass at risk of fracture.

| | % Increase LS BMD (SD) | Change From Baseline |
|-----------|------------------------|----------------------|
| Oral rsCT | 1.03 (2.50) | p < 0.001 |
| Placebo | -0.12 (2.39) | p = ns |

TABLE

Disclosures: *Neil Binkley, Tarsa, 6; Tarsa, 1*
This study received funding from: *Tarsa Therapeutics*

1234

Calcitonin Use and Risk of Malignancy: A Meta-Analysis of 17 RCTs in Patients with Osteoporosis. Markus Heep¹, Sylvia Lesperance¹, Juerg A. Gasser², Chien-Wei Chen³, R. Paul Aftring³. ¹Novartis Pharma AG, Switzerland, ²Novartis Institutes for Biomedical Research, Switzerland, ³Novartis Pharmaceuticals, USA

After a reported imbalance in prostate malignancies in clinical trials of an investigational formulation of salmon calcitonin,¹ we conducted a systematic meta-analysis of the occurrence of any malignancy in 17 randomized clinical trials (RCTs) in patients with osteoporosis treated with salmon calcitonin nasal spray (nSCT; Miacalcic®).

17 nSCT studies were analyzed for reported events of any malignancy. Clinical Study Reports were reviewed for type and onset of cases by 6 mo treatment time windows. Odds-ratios (ORs) for nSCT vs placebo (PBO) were obtained by Peto method. Effect of dose level on incidence of any malignancy was analyzed separately for each dose group. Time to malignancy event was evaluated based on number of malignant cases at each treatment period window. Only the randomized double-blind period was considered for each study. Four trials with zero events in both treatment groups were excluded in the meta-analysis, according to Peto method. Analysis included 2258 patients treated with nSCT and 976 PBO-treated patients.

In the meta-analysis of 13 RCTs, the OR of nSCT vs PBO for any malignancy was 1.61 (95% CI: 1.11–2.34), suggesting that the nSCT group had a higher risk compared with PBO. Comparisons of the events within individual studies were not significant. Analyses by dose level did not indicate a correlation of malignancy risk with dose (ORs were 1.52 (95% CI: 0.87–2.65) for 100 IU, 1.55 (95% CI: 0.94–2.55) for 200 IU, and 1.44 (95% CI: 0.87–2.37) for 400 IU). For patients with an event, the mean time of exposure was 21.8 months for nSCT compared with 22.4 for PBO (Table 1). The malignancy incidence rates at each 6-mo period over 5 years were similar between nSCT and PBO groups in the 0–6 mo period (0.9% vs 0.8%), whereas the calcitonin had a higher although variable incidence rate between 6–12 mos (1.2% vs 0.2%), 12–18 mos (0.7% vs 0.2%), 18–24 mos (0.6% vs 0.3%), 24–36 mos (3.2% vs 1.2%) and 36–48 mos (1.4% vs 0.6%) (Table 2).

Based on this meta-analysis of RCTs with nSCT, a small increase in the risk of any malignancy was observed for nSCT compared with PBO with long-term treatment (>6 months). This potential risk should be considered in the decision to treat with nSCT. No *in vivo* data have identified a mechanism for this observation.

References:

1. EMA. Meeting highlights from the CHMP, January 2011 http://www.ema.europa.eu/docs/en_GB/document_library/Press_release/2011/01/WCS00101076.pdf Meta-analysis conducted by Novartis Pharma AG

Table 1. Time to event is comparable in nasal calcitonin and placebo groups

| Time to event* (months) | Nasal calcitonin (n = 117) | Placebo (n = 25) |
|-------------------------|----------------------------|------------------|
| Mean | 21.8 | 22.4 |
| Median | 16.8 | 16.8 |
| Min | 0.03 | 0 |
| Max | 60.3 | 60.0 |

*For multiple malignancies within a patient, the first occurred malignancy is considered. †Eight missing time to event (5 for calcitonin group, 3 for placebo group) for nasal calcitonin trials.

Table 2. Patients in trials and first malignancy by time period

| | Nasal calcitonin* | | | | | | | |
|------------|-------------------|------|------|------|------|------|------|-----|
| | Months 0 | 6 | 12 | 18 | 24 | 36† | 48 | 60† |
| Patients | 2634 | 2377 | 2077 | 1885 | 1770 | 742 | 495 | 383 |
| Malignancy | 22 | 25 | 14 | 10 | 24 | 7 | 15 | |
| Percentage | 0.9% | 1.2% | 0.7% | 0.6% | 3.2% | 1.4% | 3.9% | |

| | Placebo | | | | | | | |
|------------|----------|------|------|------|------|------|------|-----|
| | Months 0 | 6 | 12 | 18 | 24 | 36† | 48 | 60† |
| Patients | 1234 | 1105 | 902 | 826 | 784 | 334 | 154 | 128 |
| Malignancy | 9 | 2 | 2 | 2 | 4 | 1 | 5 | |
| Percentage | 0.8% | 0.2% | 0.2% | 0.3% | 1.2% | 0.6% | 3.9% | |

*For multiple malignancies within a patient, only the first malignancy occurrence is considered. †Percentage is calculated based on the completers at each period. ‡The data by time period is not available for study MIA-16. †End of study follow-up may contribute to the higher incidence reported at 36 and 60 months

Nasal calcitonin trials meta-analysis

Disclosures: *Markus Heep, Novartis Pharma AG, 3*
This study received funding from: *Novartis Pharma AG*

LB-SA01

NBQX, a Glutamate Receptor (α -amino-3-hydroxy-5-methyl-4-isoxazolepropionic acid/kainate) Antagonist, Alleviates Inflammation, Pathology and Gait Abnormalities in Rat Antigen Induced Arthritis. Cleo Bonnet¹, Anwen Williams², Sophie Gilbert², Ann Harvey², Deborah Mason^{2*}. ¹Cardiff University, GBR, ²Cardiff University, United Kingdom

Introduction: Rheumatoid arthritis (RA) affects approximately 0.5-1% of the US and UK adult population and although treatment has been revolutionised by anti-cytokine therapies, around 30% of patients remain unresponsive. To tackle this treatment shortfall, we aim to identify potential new therapeutics. Glutamate concentrations are elevated in RA synovial fluids and activation of kainate (KA) glutamate receptors (GluRs) expressed by synoviocytes, increases interleukin-6 (IL-6) release [1]. Since IL-6 is an essential inflammatory arthritis mediator, we investigated whether the α -amino-3-hydroxy-5-methyl-4-isoxazolepropionic acid (AMPA)/KA GluR antagonist NBQX, attenuates disease progression in antigen induced arthritis (AIA) *in vivo*.

Methods: NBQX was injected intra-articularly into the affected knees of AIA rats at the time of arthritis induction. Knee swelling and gait patterns of AIA (n=15), AIA+NBQX (n=15) and naive rats (n=6) were measured over 21 days. On day 21, joint tissues were taken for QRT-PCR, x-ray, magnetic resonance imaging (MRI), histology (scored by two blinded observers using a modified Mankin score with a bone component from the OARSI score) and GluR/transporter immunohistochemistry.

Results: NBQX treatment significantly reduced knee swelling ($P < 0.001$, days 1-21), gait abnormalities (days 1-3), end-stage cartilage destruction ($P < 0.05$) and synovial inflammation ($P < 0.001$) scores, and meniscal IL-6 mRNA expression ($P < 0.05$). NBQX treatment reduced bone scores by 51% ($P < 0.001$), revealing smoother articular surface and fewer bone erosions by x-ray and MRI. Glutamate receptors (AMPA2, KA1) and transporters (GLAST, EAAC1) localised to areas of substantial bone and cartilage remodeling in AIA rats, but were less abundant in NBQX treated rats.

Discussion: Intra-articular NBQX treatment attenuates inflammation, pathology and pain related gait abnormalities in AIA *in vivo*. A substantial reduction in bone pathology indicates a significant osteo-protective effect of NBQX. Thus KA GluRs represent a potential disease modifying drug target for inflammatory arthritis. **Reference:** Flood, S. *et al.* (2007) Modulation of Interleukin-6 and Matrix Metalloproteinase 2 Expression in Human Fibroblast-like Synoviocytes by Functional Ionotropic Glutamate Receptors. *Arthritis and Rheumatism*, 56: 2523-2534.

Disclosures: Deborah Mason, None.

LB-SA02

Trabecular Bone Microarchitecture is Compromised in Obese Late Adolescent Females. Hannah Goff^{1*}, Christopher Modlesky², Emma Laing¹, Norman Pollock³, Harshvardhan Singh², Clifton Baile⁴, Richard Lewis¹. ¹The University of Georgia, USA, ²University of Delaware, USA, ³Georgia Health Sciences University Medical College of Georgia, USA, ⁴University of Georgia, USA

The influence of excess body fat on trabecular bone microarchitecture is unclear. The purpose of this cross-sectional study was to determine if tibia and radius trabecular bone microarchitecture are compromised in obese late adolescent white females. Participants 18 to 19 years of age were grouped into obese (OB; n = 12) and normal-weight (NW; n = 12) based on BMI/age percentile (OB > 95th and NW 20 - 85th) and %fat (OB > 32% and NW < 30%). Obese participants were carefully matched with NW participants for age and height. Tibia and radius trabecular bone microarchitecture indices [i.e., apparent trabecular bone volume to total volume (appBV/TV), apparent trabecular number (appTbN), apparent trabecular thickness (appTbTh), and apparent trabecular separation (appTbSp)] as well as mid-tibia and mid-radius cortical bone macroarchitecture indices [i.e., cortical volume, polar moment of inertia (J), section modulus (Z), cross-sectional moment of inertia (CSMI), medullary volume and total bone volume] were determined by MRI (GE 3.0 Tesla). Groups were compared using t-test and ANCOVA. OB compared to NW groups had higher body weight and fat and fat-free soft tissue masses ($P < 0.001$). OB participants also had lower appTbTh at the proximal tibia ($P < 0.03$), lower appBV/TV ($P < 0.002$) and appTbTh ($P < 0.03$) at the distal radius, and higher measures of appTbSp at the distal radius ($P < 0.02$). No differences were seen at the mid-tibia or mid-radius for cortical bone. Despite the fact that OB late adolescent females had higher body weights as well as higher fat and fat-free soft tissue masses compared to NW participants, trabecular bone microarchitecture was compromised in this group. Future studies should examine potential mechanisms and the clinical consequences.

Disclosures: Hannah Goff, None.

LB-SA03

TBS as a Predictor of Vertebral Fracture in Polish Men. Roman Lorenc¹, Wanda Horst-Sikorska^{2*}. ¹Specjalistyczny Ośrodek Wieków Dojrzałego Sp. Z O.o., Poland, ²ICP, Poland

Bone strength is determined by bone mass as well as trabecular bone microarchitecture, bone mineralization and turnover. BMD, measured by DXA, is of limited value for the osteoporotic fractures risk assessment. A new diagnostic tool TBSiNght provides information on bone microarchitecture and may improve the prediction of fracture risk. This is the first study that analyzes the cut off point for TBS in prediction of vertebral fracture (VF) in men.

The objective of the study was to assess whether TBS can predict vertebral fracture in men and to determine the cut-off point for male VF.

Methods

Male patients over 55 years with at least 1 clinical risk factor for osteoporosis or height loss >4 cm were recruited. Subjects with secondary osteoporosis were excluded. DXA scans and vertebral fracture assessment (VFA) were performed in every man. BMD was measured twice at the lumbar spine (L1-L4) with LUNAR Prodigy densitometer and TBS was calculated using the TBS Insight software (Medimaps). Statistical analysis was done with MedCalc software (MedCalc®, V 11.0.1). The groups were compared with Mann-Whitney U test and the correlation was calculated using Spearman's rank correlation coefficient. ROC analysis was performed to evaluate TBS and BMD as fracture discriminating factors. The accuracy of classification was tested by AUC (area under ROC curve). To obtain cut-off point OR (odds ratio) was calculated.

Results

A total of 94 male aged 71.6 ± 9.34 years were eligible for analysis. Fourty four patients had at least 1 vertebral fracture confirmed by VFA. Height loss >4cm was observed in 45 patients and was correlated with TBS ($r = -0.35$; $p = 0.0005$). Comparing fractured (VF) and non fractured men: mean BMD value was respectively: 0.94 ± 0.14 vs 1.01 ± 0.20 ($p = 0.0673$) while mean TBS: 0.96 ± 0.15 vs 1.06 ± 0.14 ($p = 0.0013$). ROC analysis showed that TBS can be a predictor of vertebral fracture (AUC = 0.69 95%CI [0.589 - 0.783]; $p = 0.0004$) and no prediction was found for spine BMD (AUC = 0.59; 95%CI [0.490 - 0.696]; $p = 0.1003$). The optimal cut-off point for TBS was determined ≤ 0.987 giving 60.47% of sensitivity and 80% specificity. For this value the risk for VF was over 5 times higher (OR = 5.7); 95%CI [2.271 - 14.28].

Conclusions:

Trabecular bone score in contrast to spine BMD can predict VF in men
TBS value ≤ 0.987 was cut off point related to over 5x higher risk of VF
TBS is significantly lower in fractured men and no significant difference was found for BMD

Horst-Sikorska W.¹, Ignaszak-Szczepaniak M.¹, Michalak M.² Sewerynek E.³, Lorenc R.⁴

¹Laboratory of Bone Metabolic Diseases, Department of Family Medicine, University of Medical Sciences, Poznan, Poland ²Department of Computer Science and Statistics, University of Medical Sciences, Poznan, Poland ³Medical University Łódź ⁴Biochemistry Department Children's Memorial Health Institute Warszawa

Disclosures: Wanda Horst-Sikorska, None.

LB-SA04

Osteo-chondrogenic Function of BMP is Directed Toward Osteogenesis by Hh-Gli1 in the Perichondrium. Hironori Hojo^{1*}, Shinsuke Ohba², Kiyomi Taniguchi³, Masataka Shirai³, Fumiko Yano⁴, Taku Saito⁵, Toshiyuki Ikeda⁶, Keiji Nakajima⁶, Yusuke Komiyama⁶, Naomi Nakagata⁷, Kentaro Suzuki⁷, Yuji Mishina⁸, Masahisa Yamada⁹, Tomohiro Konno⁶, Tsuyoshi Takato⁶, Hiroshi Kawaguchi¹⁰, Hideki Kambara³, Ung-Il Chung¹¹. ¹The Center for Disease Biology & Integrative Medicine, Japan, ²The University of Tokyo, Jpn, ³Hitachi Central Research Laboratory, Japan, ⁴University of Tokyo, Japan, ⁵University of Tokyo, Graduate School of Medicine, Japan, ⁶The University of Tokyo, Japan, ⁷Kumamoto University, Japan, ⁸University of Michigan, USA, ⁹The Okinawa Institute of Science & Technology, Japan, ¹⁰University of Tokyo, Faculty of Medicine, Japan, ¹¹University of Tokyo Schools of Engineering & Medicine, Japan

During endochondral ossification, osteo-chondroprogenitors (OCPs) are suggested to reside in the perichondrium. Hedgehog (Hh) and bone morphogenetic protein (BMP) are suggested to regulate the specification of OCPs into osteoblasts. However, the properties of OCPs and the regulatory mechanisms of the specification process are still poorly understood. We aimed to clarify these by combining a novel organ culture system and single-cell expression analysis with mouse genetics and biochemical analyses. In the metatarsal organ culture reproducing bone-collar formation, a Hh agonist SAG induced an ectopic bone collar, whereas a Hh inhibitor cyclopamine (Cyc) diminished bone-collar formation. The combination of BMP2 and SAG increased the thickness of the bone collar, while the combination of BMP2 and Cyc induced safranin O-positive chondrocyte-like cells in the perichondrium. In line with the results, the thickness of the bone collar was increased in *Ptch1^{+/+}; Prx1-cre; CAG-LoxP-caBmpr1a* mice, and *Ihh^{+/+}; Prx1-cre; CAG-LoxP-caBmpr1a* mice showed ectopic *Col2a1* expression in the perichondrium. Thus, BMP likely acts as an accelerator for both osteogenesis and chondrogenesis in the perichondrium, after

Hh-dependent specification has taken place. To further understand the specification process and characteristics of PCs, single-cell RT-qPCR analyses were performed on osteoblast and chondrocyte markers in PCs treated with or without SAG. Clustering analysis of the expression data showed that most PCs exhibited either of two features, a chondrocyte-like state or a non-osteochondrogenic (NOC) state. SAG-treated PCs showed more heterogeneity; some maintained the NOC state, but others expressed osteoblast markers or both osteogenic and chondrogenic ones. *In vitro* analysis revealed that SAG suppressed BMP2-induced expression of *Col2a1* in C3H10T1/2 cells, and the suppressive effect was reduced by *Gli1* knockdown. *Gli1* overexpression inhibited *Sox9* expression and *Sox9* recruitment onto its genomic enhancer. Indeed, ectopic expression of *Col2a1* was observed in the perichondrium of E17.5 *Gli1*^{-/-} metatarsals. Given that *Sox9* is shown to mediate the chondrogenic action of BMP, the inhibition of *Sox9* expression and function by *Gli1* may underlie the negative impact of Hh on BMP-mediated chondrogenesis. Taken together, Hh-*Gli1* alters the function of BMP to specify cells in the perichondrium into osteoblasts; the timing of Hh input and its target populations are critical for BMP function.

Disclosures: Hironori Hojo, None.

LB-SA05

Potential *Col10a1* Regulators Identified by Bioinformatics and Proteomic Methods. Junxia Gu^{*1}, Yaojuan Lu², Feifei Li³, Jeffrey Borgia², Qiping Zheng². ¹Jiangsu University, China, ²Rush University Medical Center, USA, ³Anhui Medical University, China

The type X collagen gene (*Col10a1*) is specifically expressed when chondrocytes undergo hypertrophy during endochondral bone formation. Abnormal *Col10a1* expression has been associated with multiple skeletal diseases. We have recently shown that Runx2 contributes to *Col10a1* expression through direct interaction with a 150 bp *Col10a1* cis-enhancer that contains a tandem-repeat Runx2 site. We have also shown that this interaction is required but not sufficient for *Col10a1* promoter activity, suggesting requirement of additional *Col10a1* regulators. To identify these factors, we have performed in silico sequence analysis of this cis-enhancer using web-based transcription factor analysis softwares. A variety of putative transcription factors were predicted to bind this *Col10a1* cis-enhancer. We have also performed yeast one-hybrid assay using the 150-bp fragment as a bait to screen a cDNA library generated from hypertrophic MCT cells. Multiple factors including Cox family members, Nedd4, and Psm1 were obtained. Interestingly, we detected upregulated Cox2 expression in hypertrophic MCT cells compared to proliferative MCT cells, suggesting its role in *Col10a1* regulation. Meanwhile, we have performed NanoLC-MS/MS experiment with the specific DNA/protein complexes formed by the short cis-enhancer and the MCT cell nuclear extract. We identified multiple factors, including EF1-alpha, Runx3, Nedd4, and some zinc finger proteins. These factors may interact with Runx2 and play a role in cell proliferation, apoptosis, and possibly, chondrocyte/osteoblast differentiation and skeletal development. Our results together suggest that multiple factors may interact with each other, or work with Runx2 to regulate *Col10a1* expression and chondrocyte maturation and thus, affect skeletal development and disease progression.

Disclosures: Junxia Gu, None.

LB-SA06

Receptor Activity Modifying Proteins alter the G-Protein activation response of PTH receptors to PTH and PTHrP. David Roberts¹, Gareth Richards¹, Aditya Desai¹, Timothy Skerry^{*2}. ¹University of Sheffield, United Kingdom, ²University of Sheffield Medical School, United Kingdom

The way that parathyroid hormone (PTH) exerts different effects in different cells, and functions differently in vivo by continuous or intermittent delivery have been long-standing questions in bone biology. Here we provide a novel mechanism that could explain these effects. Receptor activity modifying proteins (RAMPs) are accessory molecules discovered by their ability to influence ligand selectivity of Calcitonin (CT) and CT-like receptors. They have also been shown to be essential for trafficking of some receptors. Another role involves PTH receptors, that can translocate to the surface with or without an associated RAMP.

We used FRET to determine interactions and stoichiometry of PTH1&2 receptors with RAMPs and showed that RAMP2 and 3 could traffic with PTH1R but only RAMP2 trafficked with the PTH2R. Using a scintillation proximity assay to measure G-protein activation in membranes from COS cells transfected with different receptor/RAMP constructs, we determined effects of ligand activation of the receptors with and without RAMPs. Receptor numbers and affinity were determined by radioligand binding. Typical activation profiles are shown in A (n=6 at each point). Activation of Gq (PLC and *i/c* calcium activation: green line), begins at 10⁻¹²M. Gi activation (inhibition of adenylate cyclase activation: Blue line) exceeds Gs (adenylate cyclase: Red line) by c.50%. In membranes containing equal numbers of PTH1 receptors with RAMP2 (B), activation of Gq occurred at 10⁻⁸M[PTH] so that RAMP2 associated PTH receptors have a reduced Gq response to PTH than when expressed alone despite unchanged affinity. Both Gi and Gs had increased levels of activation with RAMP2 (c.75-100% respectively) compared with PTH1 receptors without RAMP2. PTHrP induced different patterns of PTH1 receptor activation that were changed differently again by the presence of RAMP2 in the membranes. Similar effects were recorded with PTH2 receptors and PTH(1-34) with and without RAMP3.

These data provide intriguing insights into the way that PTH receptors function. Expression of RAMPs by a cell confer the ability to alter effects of the same hormone acting on the same receptor, a novel layer of complexity and regulation in endocrinology. The differing sensitivity of activation of Gq by 100 fold different PTH dose with and without RAMP2 would impact on perception of transient intermittent doses in a way that could explain some of the current dilemmas regarding the hormone's action.

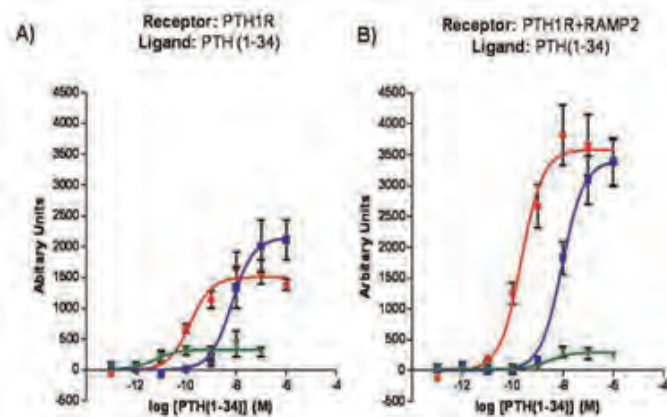


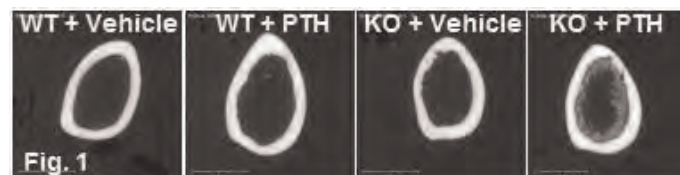
fig 1

Disclosures: Timothy Skerry, None.

LB-SA07

Continuous Infusion of PTH Stimulates New Bone Formation in Cyclooxygenase-2 (COX-2) Knockout Mice. Shilpa Choudhary^{*}, Adam Harris, Vilmaris Diaz-Doran, Douglas J. Adams, Carol Pilbeam. University of Connecticut Health Center, USA

In vivo intermittent PTH is anabolic and continuous infusion of PTH is catabolic. *In vitro* continuous PTH also inhibits osteogenesis in marrow stromal cells unless COX-2 expression/activity is absent, then it is osteogenic. We examined the impact of COX-2 knockout (KO) on continuous infusion of PTH *in vivo*. Male wild type (WT) and KO mice (n=7-9/group, 6 mo old) were infused with vehicle or 1-34 hPTH (40 µg/kg/d) via ALZET pump for 12 days. Measurements included serum at euthanasia; tibial mRNA (qPCR); % change in femur BMD (*in vivo* DXA); and trabecular (Tb) bone volume (BV/TV) and cortical parameters in femur (µCT). Histomorphometry is pending. Data were analyzed by 2-way ANOVA. PTH made both WT and KO mice hypercalcemic (11.4 and 11.0 mg/dl, respectively) compared to vehicle groups (9.76 and 9.77 mg/dl, respectively). (Two PTH-infused WT mice, euthanized on d 10 for weight loss and excluded from study, had serum Ca of 14.3 and 15.0 mg/dl.) PTH infusion decreased femur BMD in WT mice (-6.7%) but increased BMD in KO (+5.9%). On µCT, newly formed "fuzzy" bone was prominent along cortical endosteal surfaces of PTH-treated KO but not WT mice (Fig.1). Excluding this new bone, PTH decreased cortical thickness and increased % porosity similarly in WT and KO. Measurement of BV/TV in the distal femur included some new Tb bone along cortical endosteal surfaces, resulting in BV/TV being 90% greater in PTH-treated KO mice than in WT mice (p<0.02). PTH increased CTX, a serum marker of resorption, 3 times more in WT than KO mice (p<0.01). In contrast, PTH increased PINP, a serum marker of formation, 6 times more in KO than WT mice (p<0.01). PTH increased RANKL/OPG mRNA expression similarly in WT and KO (3.9-fold and 3.0-fold, respectively) but only increased osteocalcin mRNA (12-fold, p<0.01) in KO mice. In WT mice, PTH increased mRNA expression for inhibitors of bone formation, SOST (1.3-fold, not significant) and DKK1 (4.3-fold, p<0.01). In KO mice, PTH decreased SOST mRNA 56% (p<0.01) and had no effect on DKK1 mRNA. In summary, absence of COX-2 markedly increased the anabolic response to continuous PTH infusion, consistent with the inhibitory effects of COX-2/prostaglandins on PTH osteogenic effects seen *in vitro*. These data suggest a novel role for COX-2 in the anabolic effects of PTH and might lead to new protocols for enhancing the therapeutic potential of PTH.



Choudhary et al PTH infusion

Disclosures: Shilpa Choudhary, None.

LB-SA08

Fracture GWAS in the GEFOS Consortium Discovers New Loci Related to Hormonal and Neurological Pathways. Ling Oei¹, Hou-Feng Zheng², Evangelia Ntzani³, Carrie Nielson⁴, Karol Estrada¹, Unnur Styrkarsdottir⁵, Paul Ridker⁶, Yi-Hsiang Hsu⁷, Melissa Garcia⁸, Aaron Aragaki⁹, Emma Duncan¹⁰, Anke Enneman¹¹, Terho Lehtimäki¹², Tõnu Esko¹³, Stella Trompet¹⁴, Stephen Kaptege¹⁵, Joel Eriksson¹⁶, Najaf Amin¹¹, Annie Kung¹⁷, Carolina Medina-Gomez¹⁸, Evangelos Evangelou³, Konstantinos Tsilidis³, Gudmar Thorleifsson⁵, Lynda Rose⁶, Joseph Zmuda¹⁹, Ching-Ti Liu²⁰, Albert Vernon-Smith²¹, Priya Srikanth⁴, Scott Wilson²², Graeme Clark²³, Janda Viikari²⁴, Evelin Mihailov¹³, Alireza Moayyeri²⁵, Guo Li²⁶, Candace Kammerer¹⁹, Mattias Lorentzon²⁷, Natalia Rivera¹¹, Sumei Xiao²⁸, Jian Yang²⁹, David Karasik³⁰, Kristin Siggeirsdottir³¹, Edwin Oei³², Kari Stefansson⁵, Ville Aalto³³, Dana Willner²³, Nicholas Wareham³⁴, Ryan Minster³⁵, Joshua Bis²⁶, Cornelia van Duijn¹¹, Lizbeth Herrera¹¹, L. Adrienne Cupples²⁰, Thor Aspelund²⁶, Olli Raitakari³³, Paul Leo²³, Kay-Tee Khaw³⁷, John Robbins³⁸, Yongmei Liu³⁹, Stephan Breda¹¹, Robert Luben³⁷, Jane Cauley¹⁹, Alice Arnold²⁶, Lisette Stolk¹¹, Joyce Van Meurs¹, Pak Sham⁴⁰, Maria Zillikens³², Claes Ohlsson⁴¹, Bruce Psaty²⁶, Tamara Harris⁴², Jonathan Reeve³⁷, Wouter Jukema¹⁴, Andres Metspalu¹³, Mika Kahonen¹², Nathalie van der Velde¹¹, Matthew Brown⁴³, Vilmundur Gudnason³¹, John Ioannidis⁴⁴, Andre Uitterlinden⁴⁵, Steven Cummings⁴⁶, Tim Spector²⁵, Douglas Kiel³⁰, Rebecca Jackson⁴⁷, Unnur Thorsteinsdottir⁵, Daniel Chasman⁶, Eric Orwoll⁴, Brent Richards², Fernando Rivadeneira¹, for the GEFOS consortium.⁴⁸ ¹Erasmus University Medical Center, The Netherlands, ²McGill University, Canada, ³University of Ioannina Medical School, Greece, ⁴Oregon Health & Science University, USA, ⁵deCODE Genetics, Iceland, ⁶Brigham & Women's Hospital, USA, ⁷Hebrew SeniorLife Institute for Aging Research & Harvard Medical School, USA, ⁸NIA, NIH, USA, ⁹Division of Public Health Sciences, Fred Hutchinson Cancer Research Center, USA, ¹⁰Royal Brisbane & Women's Hospital, Australia, ¹¹Erasmus MC, Netherlands, ¹²University of Tampere & Tampere University Hospital, Finland, ¹³University of Tartu, Estonia, ¹⁴Leiden University Medical Center, Netherlands, ¹⁵University of Cambridge Bone Research Group, United Kingdom, ¹⁶University of Gothenburg, Center for Bone & Arthritis Research, Institute of Medicine, Sahlgrenska Academy, Sweden, ¹⁷Dr. Kung-Wai Chee Clinic, Hong Kong, ¹⁸Erasmus Medical Center, The Netherlands, ¹⁹University of Pittsburgh Graduate School of Public Health, USA, ²⁰Boston University School of Public Health, USA, ²¹Icelandic Heart Association & University of Iceland, Iceland, ²²University of Western Australia, Australia, ²³University of Queensland Diamantina Institute, Australia, ²⁴University of Turku & Turku University Hospital, Finland, ²⁵King's College London, United Kingdom, ²⁶University of Washington, USA, ²⁷Center for Bone Research at the Sahlgrenska Academy, Sweden, ²⁸The University of Hong Kong, ²⁹Queensland Institute of Medical Research, Australia, ³⁰Hebrew SeniorLife, USA, ³¹Icelandic Heart Association Research Institute, Iceland, ³²Erasmus MC, The Netherlands, ³³Research Centre of Applied & Preventive Cardiovascular Medicine, University of Turku, Finland, ³⁴Medical Research Council (MRC) Epidemiology Unit, United Kingdom, ³⁵University of Pittsburgh, USA, ³⁶Icelandic Heart Association, Iceland, ³⁷University of Cambridge, United Kingdom, ³⁸University of California, Davis Medical Center, USA, ³⁹Wake Forest University School of Medicine, USA, ⁴⁰The University of Hong Kong, China, ⁴¹Center for Bone & Arthritis Research at the Sahlgrenska Academy, Sweden, ⁴²Laboratory of Epidemiology, Demography, & Biometry, Intramural Research Program, National Institute of Aging, National Institutes of Health, USA, ⁴³Diamantina Institute of Cancer, Immunology & Metabolic Medicine, Australia, ⁴⁴Stanford University, USA, ⁴⁵Rm Ee 575, Genetic Laboratory, The Netherlands, ⁴⁶San Francisco Coordinating Center, USA, ⁴⁷The Ohio State University, USA, ⁴⁸Netherlands

Risk of osteoporotic fracture is heritable ($h^2 \sim 19\%$ Rotterdam Study). Over the last year, we have almost doubled sample size in our Genetic Factors of Osteoporosis (GEFOS) consortium GWAS meta-analysis to search for genetic risk factors associated with fracture risk. Cases were individuals (>18 years) with fractures confirmed by medical, radiological or questionnaire reports. When possible, high-trauma fractures and those of fingers, toes and skull were excluded. Results from 21 GWAS cohorts (n=93,364, 16,542 cases, mostly European ancestry) were meta-analyzed with inverse variance fixed-effects logistic regression models adjusted for age, height, weight (HapMap CEU release 22, build 36). Analyses were sex-combined

adjusted for sex, female-only and male-only. We used the Genome-wide Complex Trait Analysis (GCTA) conditional-joint-multiple SNP method to detect secondary signals. Signals associated at genome-wide significance (GWS, $P < 5 \times 10^{-8}$) mapped to 7q21.3 (closest gene *SHFMI*; $P = 2.3 \times 10^{-10}$, odds ratio = 1.10, 95% CI: 1.07-1.13) and 18p11.21 (*FAM210A*; $P = 1.4 \times 10^{-8}$, odds ratio = 1.09, 1.06-1.12). The *SHFMI* region is characterized by genomic re-arrangements leading to deletion of *DSSI*, *DLX5* and *DLX6*. The latter two code for members of the Wnt signaling pathway, and cause ectodactly when both are deleted or mutated. GCTA analysis identified additional GWS signals, including those in 13q21.33 (*KLHL1*; $P = 1.2 \times 10^{-9}$), 17q21.31 (*SOST*; $P = 1.2 \times 10^{-8}$), 6q24.3 (*SASH1*; $P = 1.3 \times 10^{-8}$), 15q26.1 (*RGMA*; $P = 2.8 \times 10^{-8}$), 3q24 (*ZIC4* and *ZIC1*; $P = 4.4 \times 10^{-8}$). *RGMA* and *KLHL1* are needed for neurite outgrowth, and the latter is overlapped by an antisense RNA implicated in spinocerebellar ataxia type 8. Heterozygous deletion of *ZIC1* and *ZIC4* is involved in Dandy-Walker cerebellar malformation, where affected individuals have motor deficits such as ataxia. In addition to the GWS loci we identified twenty suggestive ($P < 5 \times 10^{-6}$) signals, which are undergoing in-silico and de-novo replication in >80,000 individuals (~30,000 cases). One third of the GWS and suggestive loci are associated with BMD and mutations in some of the genes are known to cause skeletal abnormalities. Several of the loci have been found associated with height, malignancies (e.g., breast and prostate cancer), neurological or endocrine function. In conclusion, this large-scale GWAS meta-analysis discovered more than twenty new fracture loci involved in the regulation of bone mineral density, neurological or hormonal function.

Disclosures: Ling Oei, None.

LB-SA09

A Role for TGF- β RII Expressing Cells in the Regulation of MCP-5 during Post-traumatic Osteoarthritis. Lara Longobardi¹, Huseyin Ozkan², Alessandra Esposito³, Tieshi Li¹, Timothy Myers⁴, Joseph Temple⁵, Anna Spagnoli¹. ¹University of North Carolina at Chapel Hill, USA, ²University of North Carolina-Chapel Hill, USA, ³University of North Carolina, USA, ⁴UNC-Chapel Hill, USA

We have recently reported that low-expression levels of monocyte chemoattractant protein-5 (MCP-5) in developing joints are critical for proper joint formation and that the TGF- β Type II receptor (T β RII) signaling is needed to maintain such down-regulation. By generating a *Tgfb2- β -Gal-GFP-BAC* mouse, containing β -gal and GFP imaging reporters under the control of the *Tgfb2* promoter, our lab has described that T β RII expressing cells (T β RII⁺) localize in specific niches that are maintained through development and postnatal life (Li et al., ASBMR 2011). It has been reported that MCP-5, its human homologous MCP-1 and their sole common receptor CCR2, are increased in the inflamed joints of patients with different forms of arthritis and in rodent models for arthritis. We found that MCP-5 expression was up-regulated in arthritic joints of a murine model of osteoarthritis (OA) (destabilization of medial meniscus, DMM). Our *in-vivo* studies are aimed at determining whether: #1) the up-regulation of MCP-5 in arthritic joints correlates with OA progression and severity; #2) intra-articular implants of T β RII⁺ cells into DMM knees are able to prevent the up-regulation of MCP5. For purpose #1, knees of mice that underwent DMM or sham were harvested 4, 8 and 12 weeks after DMM and subjected to histological analyses using MCP-5 antibody. For purpose #2, by using GFP as positive marker for selection in FACS sorting, we isolated T β RII⁺ cells from E14.5 *Tgfb2- β -Gal-GFP-BAC* limb buds. Cells were injected in the intra-articular space of DMM and sham knees one week after DMM (25×10^5 cells/15 μ l PBS). Mice were euthanized 12-weeks after DMM and knees were subjected to immunofluorescence analyses. Sections were double-stained using conjugated fluorescent antibodies against GFP (to visualize exogenous T β RII⁺ cells) and MCP-5. We found that MCP-5 was highly expressed at the site of the OA lesions and its expression progressively increased from 4 to 12 weeks after DMM, while its expression was undetectable in sham controls. Implanted T β RII⁺ cells were detected in the articular cartilage of DMM knees and were able to abolish the MCP-5 up-regulation found in severe OA lesions (12 weeks after DMM). Our findings suggest a potential role for T β RII/MCP-5 axis in adult joint homeostasis and open novel perspective for the prevention and treatment of arthritis.

Disclosures: Lara Longobardi, None.

LB-SA10

Bone Resorption Inhibitory peptide Repairs Critical Size Defect on Calvariae in Mice. Neil Alles¹, Niroshani Surangika Sovsa², Masud Khan¹, Abudullah Al Mamun¹, YURIKO FURUYA³, Hisataka Yasuda⁴, Keiichi Ohya¹, Kazuhiro Aoki¹. ¹Tokyo Medical & Dental University, Japan, ²Faculty of Dental Sciences, Uni. of Peradeniya, Sri Lanka, ³ORIENTAL YEAST CO., LTD, Japan, ⁴Oriental Yeast Company, Limited, Japan

Our previous experiments have shown that TNF- α inhibits bone formation (Tomomatsu et al JBMR 24, 2009). But the role of RANKL in bone formation is not clarified well. W9 peptide (MW: 1226.2) was originally designed as a TNF- α antagonist-peptide, which has inhibitory effects on both TNF- α and RANKL. W9 is known to work as a bone resorption inhibitor *in-vitro* and *in-vivo* (Aoki et al. J Clin Invest, 2006). In this study we examined the direct effects of bone resorption

inhibitory peptide on bone formation *in-vitro* and *in-vivo*. *In-vitro* study, we used primary osteoblasts and ST-2 cells. The differentiation of these cells was significantly enhanced in W9 (140µm) treated cells, that was confirmed by increased ALP staining on day 7 and bone nodule formation on day 21 compared to vehicle-treated cells. We used two bone formation models *in vivo*. Five-week-old male C57BL/6J mice were used and received implantation of the type I bovine-collagen-carriers, containing BMP-2 (1µg), BMP-2+W9 (0.56mg) into the mice back muscle. Mice were sacrificed on day 12 after implantation. Micro-CT analysis revealed that the larger size of ectopic bone was observed in BMP-2 with W9 (0.56mg) group compared to the BMP-treated group. Quantitative analysis by DXA confirmed above observations. It is known that the size of the BMP-induced ectopic bone depends on the size of the carrier. In our experiment, the size of the ectopic bone in W9-treated group is much larger than the size of the carrier, suggesting the cartilage formation might be accelerated by W9. To further clarify the direct effect of W9 peptide on bone formation, calvarial defect model was used. Cholesterol-bearing pullulan (CHP)-hydrogels and gelatin hydrogels were used as a carrier of W9 peptide. Carriers containing W9 only (0.56mg/1.12mg) were placed on the mice calvarial defects and allowed to heal for 4 weeks. Soft-X-ray images showed that the defect was completely repaired in only one out of six mice in the 1.12 mg W9-containing CHP-hydrogel group. On the other hand, the bone defect of calvariae was partially repaired consistently in all mice, which had 0.56 mg W9-containing gelatin hydrogels. Both micro-CT and DXA analyses confirmed above observations of soft X-ray images. There data indicated W9-peptide itself could have bone formation ability to repair bone defect. Further studies are necessary to clarify the mechanism of anabolic effect of this peptide.

Disclosures: Neil Alles, None.

LB-SA11

Effect of Aroeira Extract in Mice Osteoblasts-like and in Human Osteoblasts. Adriana Matos*¹, Alessandra Cury Machado², Camila Peres Buzalaf³, Anne Bosqueiro Dokkedal⁴, Rodrigo Cardoso de Oliveira².

¹University of Sao Paulo, Brazil, ²Biochemistry, Department of Biological Sciences, Bauru Dental School, University of Sao Paulo, Brazil, ³Biochemistry, Department of Biological Sciences, Bauru Dental School, University of Sao Paulo, Brazil, ⁴ Department of Biological Sciences, UNESP, Brazil

Extracts of some plants have shown anti-inflammatory properties and bactericidal effect. One of Brazilian species used for these purposes, in folk medicine, is aroeira (*Myracrodruon urundeuva*). In addition, some studies have shown the effect of extract of the aroeira in controlling bone loss in periodontal disease, however, the exact mechanism of these effects have not yet been clarified. Thus, the aim of this study was to evaluate the action of the extract of aroeira on the viability of osteoblasts-like of mice (MC3T3) and human osteoblasts (HOAL), *in vitro*. The cells lines MC3T3 and HOAL were treated with different concentrations (1:10, 1: 100, 1: 1, 1,000 and 10,000) of extract of the aroeira hydroalcoholic in MEM (MC3T3) and DMEM (HOAL), in addition the control group (without the extract). After 24, 48, 72 and 96 hours were evaluated the viability of two cells lines through the reduction of MTT (3-(4,5-Dimethylthiazol-2-yl)-2,5-diphenyltetrazolium bromide), neutral Red uptake (VN) and Crystal Violet (CV). Comparing MC3T3 and HOAL, both exposed to the extract of the aroeira with different dilutions, it became apparent that the lineages behaved differently in the trials of the MTT and VN, but CV test cells had similar behavior. In MTT and VN tests there was a reduction of cell viability of MC3T3 with 1:10 compared to extract and control to other groups ($p < 0.05$). On the other hand, the HOAL, treated with the dilution of 1:10 had an increase of cell viability over the periods ($p < 0.05$). The MC3T3 treated with 1:10,000 demonstrated an increase in viability over the periods, however this same concentration resulted in reducing the viability of HOAL ($p < 0.05$). In CV testing, the standard maintained both by MC3T3 as HOAL was the reduction of cell proliferation with extract 1:10 and increased proliferation with 1:10,000 ($p < 0.05$). The aroeira extract modulates the viability of strains of MC3T3 and HOAL, however, the response to different concentrations of aroeira are distinct for each of these lineages.

Disclosures: Adriana Matos, None.
This study received funding from: FAPESP

LB-SA12

Resveratrol Partially Rescues Hematopoietic Defects through Improving Osteoblastic Niche in Bmi1 Deficient Mice. Jinbo Li*¹, Jianliang Jin¹, Dengshun Miao². ¹Nanjing Medical University, Peoples republic of china, ²Nanjing Medical University, Peoples republic of china

To determine whether osteoblastic niche defects contribute to hematopoietic defects occurred in Bmi1 knockout(KO) mice, Bmi1 KO and WT mice received lethal-dose irradiation and EGFP transgenic mouse-derived bone marrow(BM) transplantation subsequently. After 2 weeks, BM reconstruction was completed in WT mice, but was failed in Bmi1 KO mice. Total number of donor-derived EGFP⁺ BM cells and the percentage of EGFP⁺LSK cells both reduced dramatically, while percentage of EGFP⁺HPC cells increased obviously in Bmi1 KO mice. Decreased proliferation, increased senescence and apoptosis, down-regulated mRNA and protein expression levels of OPN, CXCL12, Ang-1 and Jagged1 and simultaneously reduced secreted

CXCL12 and Ang-1 were detected in Bmi1 KO osteoblast relative to WT osteoblast *in vitro*. Besides, percentage of LSK cells reduced while percentages of Ki67⁺LSK and HPC increased in both WT and Bmi1 KO BM cultures with conditioned medium(CM) from Bmi1 KO osteoblast cultures compared with CM from WT osteoblast cultures. Furthermore, Down-regulation of Sirt1 expression levels was confirmed in Bmi1 KO osteoblasts. To further elucidate whether the supplementation of resveratrol(RV), a Sirt1 activator, can rescue hematopoietic defects through improving osteoblastic niche, Bmi1 KO mice were fed on the normal diet without or with 250 mg RV/kg/day, their phenotypes were compared with each other and to WT mice fed on normal diet. The supplementation of RV in Bmi1 KO mice prolonged lifespan, enhanced osteoblastic bone formation, increased the number of BM cells and the percentage of LSK cells, enhanced the mean fluorescence intensity(MFI) of sca-1 of LSK cells. Reduced apoptosis, enhanced osteoblastic activity, up-regulated mRNA and protein expression levels of CXCL12, Ang-1 and Sirt1, and elevated secretion of CXCL12 and Ang-1 were observed in RV-treated Bmi1 KO osteoblasts. The percentage of LSK cells and sca-1 MFI increased significantly but percentages of Ki67⁺LSK and HPC decreased markedly in Bmi1 KO BM cultures with CM from RV-treated Bmi1 KO osteoblast cultures relative to CM from untreated Bmi1 KO osteoblast cultures. These changes were reversed by the addition of CXCL12 neutralized antibodies. Our results indicate that osteoblastic niche defects occur and contribute to the loss of HSC Pool and Stemness in Bmi1 deficient mice, and resveratrol can partially rescue these hematopoietic defects through promoting the synthesis and secretion of CXCL12 in osteoblastic niche.

Disclosures: Jinbo Li, None.

This study received funding from: National Natural Science Foundation of China

LB-SA13

The Crosstalk of Wnt5a and BMP2 during Dentin Repaired Process. Su Yingying, Wang Chenglin, Ye Ling*. State Key Laboratory of Oral Diseases, West China School of Stomatology, Sichuan University, China

Aims: In dental pulp repair process, the progenitor cells in human dental pulp will differentiate into odontoblasts or odontoblast-like cells and form dentin matrix. Regenerated pulp tissue should be functionally competent, e.g., capable of forming vascularized pulp tissue and producing hard tissue-dentin. The aim of the present study was to investigate the role of Wnt5a and BMP2 in mediating the differentiation of human dental pulp cells (HDPCs) into odontoblasts to regenerate dentin.

Methods: ALP and Alizarin red staining were applied to evaluate the differentiation capacity of HDPCs stimulated by Wnt5a condition medium or BMP2 or both. The activation of P38 and smad1/5 was determined by western blot using anti-P-p38 and P-smad1/5 antibody. Specific signaling inhibitor SB203580 and smad4 shRNA were utilized to block P38 pathway and the expression of smad4 protein respectively. RT-PCR was used to analyze the expression of related genes.

Results: ALPase and Alizarin red staining showed that Wnt5a and BMP2 could synergistically promote the differentiation of HDPCs. Both P38 pathway and smad4 were involved in the integration of Wnt5a and BMP2. BMP2 stimulated the phosphorylation of smad1/5 in a process requiring smad4/p38 and Wnt5a. Meanwhile, Wnt5a could increase the expression of BMP2 mRNA in a smad4- and P38-independent manner.

Conclusions: Wnt5a and BMP2 could synergistically promote the differentiation of HDPCs. P38 pathway and smad4 were involved in the integration of Wnt5a and BMP2 in the process of promoting cell differentiation.

Disclosures: Ye Ling, None.

LB-SA14

Dynamic Changes of Chromatin Accessibility During Early Osteoclastogenesis. KAZUKI INOUE*, Yuuki Imai. The University of Tokyo, Japan

Cell differentiation process is strictly controlled by a complex network of transcription factors and dynamic changes of chromatin structure in response to various environmental signals. Recent genome-wide studies revealed the dynamic changes of several histone modifications and binding patterns of specific transcription factors (TFs) during cellular differentiation by using ChIP-seq. However, genome-wide changes in chromatin accessibility and active *cis*-regulatory elements important for cellular differentiation are still unclear. Chromatin accessibility is changed at *cis*-regulatory regions by the *de novo* binding of sequence-specific DNA binding transcription factors and chromatin organizing proteins, resulting in increased hypersensitivity of local chromatin to DNase I attack. For this reason, genome-wide mapping DNase I hypersensitivity site (DHS) by using a deep sequence approach (DNase-seq) is a powerful tool to identify the genome-wide active *cis*-regulatory regions. Here, we used RANKL-stimulated osteoclastogenesis system as a model system of cellular differentiation, and performed *in vivo* DNase-seq to define the chromatin accessibility and *cis*-regulatory elements of early stage of osteoclastogenesis.

To investigate the temporal genome-wide changes in early stage of osteoclastogenesis, we used RANKL-stimulated Raw264 cells. After RANKL stimulation for 24 hrs, the nuclei were isolated, treated with DNase I, and collected small DNA fragments. DNase I-released fragments were subsequently subjected to deep sequencing using the Illumina HiSeq system. DHS regions were mapped by using MACS peak calling tool on Galaxy/Cistrome. Analysis of DNase-seq data from RANKL-stimulated Raw264 cells revealed 13545 DHS regions in the whole genome, and 5411 regions of the whole DHSs were unique in RANKL-stimulated Raw264 cells. Some of these

RANKL-stimulation specific DHSs were nearly located at the osteoclastogenic genes, such as *Jun*, *Nfatc1*, etc. Cis-regulatory element annotation system analysis revealed that 23.2% of these DHSs are mapped to promoter regions, and DNase footprints by binding transcription factors were detected within 0.5 kb from transcription start site. We searched the putative TFs bound to each footprint using SeqPos, and identified motifs of osteoclastogenic TFs, ATF2.3 and AP-1. These results provide a global view of the dynamic changes of chromatin structure during osteoclastogenesis, and we will find novel TFs regulating cell fate by DNase-seq.

Disclosures: KAZUKI INOUE, None.

LB-SA15

MiR-503 Regulates Osteoclastogenesis via Targeting RANK and Contributes to Osteoporosis. Chao Chen*, Peng Chen, Hui Xie, Li Yang, Gen-Qing Xie, Ru-Chun Dai, Zhi-Feng Sheng, Lin-Qin Yuan, Hou-De Zhou, Xian-Ping Wu, Er-Yuan Liao, Xiang-Hang Luo. The Second Xiangya Hospital of Central South University, China

The mechanism of postmenopausal osteoporosis remains unclear. Our study found circulating CD14⁺ peripheral blood mononuclear cells (PBMCs) in postmenopausal osteoporosis patients were more susceptible to macrophage colony stimulating factor (M-CSF) and receptor activator of nuclear factor- κ B ligand (RANKL)-induced osteoclastogenesis in vitro. Compared with control, receptor activator of NF- κ B (RANK) protein expression in CD14⁺ PBMCs of osteoporosis subjects increased, but mRNA levels had no change. It suggested that miRNAs played crucial roles in regulating RANK expression and osteoclast formation. We identified that in normal status, miR-503 in CD14⁺ PBMCs regulated osteoclastogenesis via target RANK. In postmenopausal osteoporosis subjects, miR-503 significantly decreased in CD14⁺ PBMCs, which making the progenitor cells more sensitive to M-CSF+RANKL-induced osteoclastogenesis through elevating RANK protein levels. In vivo, we simulated postmenopausal status using ovariectomy (OVX) mice. Our study showed that silencing of miR-503 using a specific antagomir in OVX mice increased RANK protein expression, promoted bone resorption and decreased bone mass. While, overexpression of miR-503 with agomir inhibited bone resorption for increasing bone mass and preventing bone loss in OVX mice. Furthermore, miR-503 promoter hypermethylation was identified in CD14⁺ PBMCs of osteoporosis subjects, which resulted in the down-regulated miR-503 expression and accelerated osteoclastogenesis. Thus, our study revealed that miR-503 play an important role in pathogenesis of postmenopausal osteoporosis via regulating osteoclast formation and contribute to a new therapeutic way for osteoporosis.

Disclosures: Chao Chen, None.

LB-SA16

Functional Status Relates to the Occurrence of Wrist or Proximal Humerus Fractures: The Study of Osteoporotic Fractures. Beatrice Edwards*¹, Dennis West², Alfred Rademaker², Bing Bing Weitner², Jaimee Holbrook², Teresa Hillier³, Jane Cauley⁴. ¹Northwestern University Medical School, USA, ²Northwestern University Feinberg School of Medicine, USA, ³Kaiser Center for Health Research, USA, ⁴University of Pittsburgh Graduate School of Public Health, USA

Background: Functional decline after hip fracture is well established but little is known about functional decline after wrist and proximal humerus fracture. The Study of Osteoporotic Fractures is an ongoing US multi-center prospective cohort study that evaluates risk factors for hip fracture in 9704 primarily white women aged 65 years and older.

Objective: The aims of this study included: 1) To determine whether functional status is a predictor of wrist and proximal humerus fractures; 2) To assess decline in functional status after wrist and proximal humerus fractures.

Methods: Women participated in standardized interviews and clinical examinations approximately every two years. The study group included women with an incident wrist, and/or humerus fracture. Functional status at each visit was measured using measures for gait speed, grip strength, chair stand, falls, and self-rated health. Decline in functional status was measured as the difference in these measures, the later visit minus the earlier visit. The change in functional status and other measures were analyzed using generalized linear model (GLM).

Results: Of the 9704 women, those with prior hip or wrist fracture, incomplete data or severe functional decline (>11/15) were excluded. The study group included 340 women with wrist fracture, 186 with proximal humerus fractures, 49 with both fractures, and 3130 women without fractures. Women with wrist fractures were younger ($p = 0.018$). Women with fractures had lower BMD ($p < 0.001$), and were less likely to have been estrogen users ($p < 0.001$). Women with both humerus and wrist fractures were more likely to have a prior stroke ($p = 0.043$), and have lower visual contrast sensitivity ($p = 0.007$). Hip abduction was lower in women with humerus fractures ($p = 0.037$) and they had a trend to lower gait speed ($p = 0.051$). Aim 1: Functional status, i.e., Grip strength, gait speed, chair stands and self-rated health did not decline prior to fractures. Aim 2: Grip strength declined after wrist ($p < 0.001$) and humerus ($p = 0.048$) fractures; gait speed declined after wrist ($p < 0.001$) and humerus ($p = 0.006$) fractures; chair stands declined post wrist fracture ($p < 0.001$) but not humerus fractures ($p = 0.206$). Falls and self-rated health were unchanged post fractures.

Conclusion: Women with both wrist and humerus fractures typically had a history of prior stroke and lower visual contrast sensitivity. Women with humerus fractures had lower hip abduction and gait speed. Pre-fracture functional changes were not significant prior to humerus or wrist fractures. However, decline in functional status for those with wrist and humerus fractures is evident.

Disclosures: Beatrice Edwards, Eli Lilly, 5; Warner, 5; Amgen, 5

LB-SA17

Decreased Circulating Sclerostin and Increased Immature Osteoprogenitor Cells in Postmenopausal Osteoporosis: The CEOR Study. Mohammed-Salleh Ardawi*¹, Mohammed Oari², Abdulrahim Rouzi¹, Sharifa Al-Sibiani³, Nawal Al-Senani³. ¹Center of Excellence for Osteoporosis Research & Faculty of Medicine, Saudi Arabia, ²Center of Excellence for Osteoporosis Research & Department of Hematology, Faculty of Medicine & KAU Hospital, King Abdulaziz University, Saudi Arabia, ³Center of Excellence for Osteoporosis Research & Department of Obstetrics & Gynecology & KAU Hospital, Faculty of Medicine, King Abdulaziz University, Saudi Arabia

Objective: Sclerostin is involved in the regulation of bone formation through the inhibition of the Wnt/ β -catenin signaling pathway. Circulating osteoprogenitor cells mineralize in vitro and in vivo and loss of osteogenic cells may contribute to bone loss and development of osteoporosis. We hypothesized that changes in circulating sclerostin are related to the number of circulating osteoprogenitor cells and bone mineral density (BMD) in postmenopausal women with and without osteoporosis.

Subjects and Methods: Circulating sclerostin (measured by ELISA); bone mineral density (BMD) [lumbar spine (L₁-L₄) and neck femur] (measured by DXA), together with the number of circulating alkaline phosphatase-positive (AP⁺), osteocalcin-positive (OCN⁺), AP⁺/CD34⁺, and OCN⁺/CD34⁺ cells (measured by flow cytometry) were determined in 275 postmenopausal women with osteoporosis and compared with 275 age-matched women without osteoporosis (controls).

Results: Serum sclerostin (pmol/L) was lower in women with osteoporosis (34.83 ± 7.06) as compared with controls [46.55 ± 8.94 ; ($P < 0.001$)]. The number of AP⁺ cells was lower in women with osteoporosis than in controls (138 ± 19 vs 246 ± 25 cells/ul; $P < 0.001$); higher numbers of AP⁺/CD34⁺ (2543 ± 630 vs 190 cells/ul; $P < 0.0001$), OCN⁺, and OCN⁺/CD34⁺ cells (7251 ± 1796 vs 2394 ± 569 cells/ul; $P < 0.0001$) were observed in women with osteoporosis than controls ($P < 0.001$ for all). Circulating sclerostin was inversely associated with AP⁺/CD34⁺ ($r = -0.586$, $P < 0.001$); and log OCN⁺/CD34⁺ cells ($r = -0.462$; $P < 0.001$). The number of AP⁺ cells showed positive correlations with BMD of both spine (L₁-L₄) ($r = 0.29$; $P = 0.008$) and neck femur ($r = 0.31$; $P < 0.005$) whereas inverse correlations were obtained between number of AP⁺/CD34⁺, OCN⁺, OCN⁺/CD34⁺ cells, and BMD values. Decreased AP⁺ cells and increased AP⁺/CD34⁺, OCN⁺, and OCN⁺/CD34⁺ cells together with changes in circulating sclerostin were predictors of low BMD, independent of traditional risk factors for osteoporosis.

Conclusions: Lower circulating sclerostin together with increased availability of circulating immature osteoprogenitor cells were found in postmenopausal women with osteoporosis as compared with age-matched controls. This interaction and cell imbalance may contribute to the pathogenesis of postmenopausal osteoporosis.

Disclosures: Mohammed-Salleh Ardawi, None.

LB-SA18

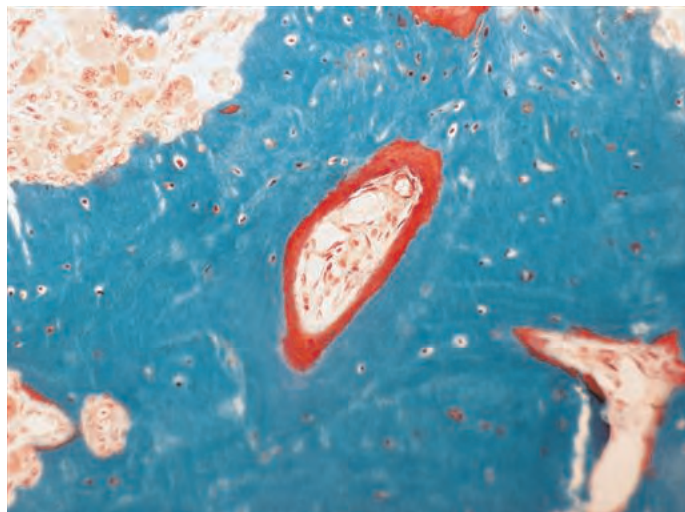
A Case of Atypical Femoral Fracture with Abnormal Cortical Bone Characterized by Impaired Mineralization and Pyrophosphate Accumulation. Maziar Shabestari*¹, Adolfo Diez-Perez², Erik Fink Eriksen³, Paul Roschger⁴, Sonia Gamsjaeger⁵, Eleftherios Paschalis⁶, Klaus Klaushofer⁷, Xavier Nogues⁸, Peter Ebeling⁹. ¹University of Oslo, Norway, ²Parc De Salut Mar, Spain, ³Oslo University Hospital, Norway, ⁴L. Boltzmann Institute of Osteology, Austria, ⁵Ludwig Boltzmann Institute of Osteologie, Austria, ⁶Ludwig Boltzmann Institute of Osteology, Austria, ⁷Hanusch Hospital, Austria, ⁸Institut Municipal D'Investigació Mèdica, Spain, ⁹The University of Melbourne, Australia

Long-term bisphosphonate use has been linked to atypical subtrochanteric and diaphyseal femoral fractures (AFF), the pathogenesis of which is still unknown. We therefore investigated bone remodeling, matrix properties and pyrophosphate distribution in a compact bone biopsy obtained at the fracture site from an 88 year old female with AFF, who had been treated with alendronate for 8 yrs. We used conventional histology, quantitative backscattered electron imaging (qBEI) and Raman spectroscopy (RS).

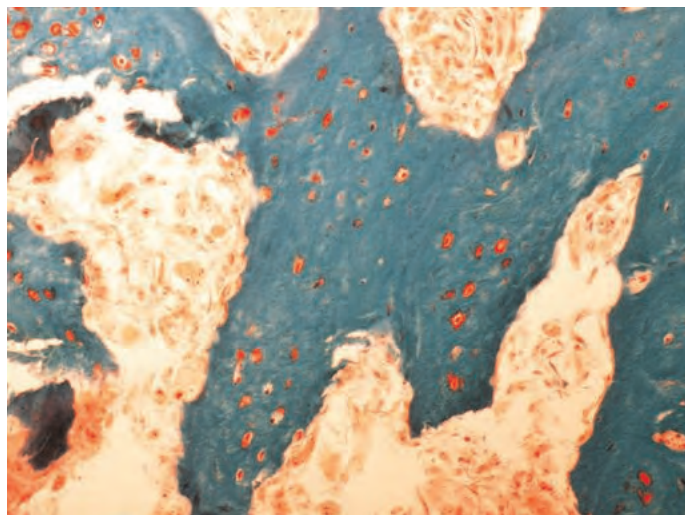
Histology revealed numerous osteoclasts on scalloped bone surfaces, widened osteoid seams and osteocytic osteolysis. On qBEI, AFF bone exhibited a scaffold of highly mineralized, porous bone matrix with numerous enlarged, randomly arranged osteocyte lacunae, on which osteonal bone was laid down. Bone mineralization density distribution (BMDD) was shifted towards lower and more heterogeneous mineralization compared to a normal reference database: Mean and mode calcium

content (CaMean -4.1% and CaPeak -1.8%), mineralization heterogeneity (CaWidth +29.3%), % bone with reduced mineralization (CaLow +111%) and % of bone with increased mineralization (CaHigh -2%). RS data obtained at similar anatomical locations (open osteons) were compared with iliac crest biopsies from 35 healthy premenopausal, 16 treatment-naïve osteoporotic women (PMC) and females with osteoporosis (OP) treated as follows: Alendronate (ALN) for 3-5 yrs. (N=33); ALN for > 5yrs (N=35), Risedronate (RIS) for 3-5 yrs (N=24); RIS for > 5 yrs (N=8) and zoledronic acid (ZOL) for 3 years (N=78). The mineral/matrix ratio of AFF bone was similar to the two ALN and the two RIS groups, lower than PMC, and higher than either OP or OP-ZOL groups. The proteoglycan content was higher in the AFF biopsy compared to all other groups. The mineral crystallinity of AFF bone was similar to both ALN groups, but higher compared to all other groups. Increased levels of pyrophosphate (rarely detectable in normal or bisphosphonate-treated bone) were demonstrable at the edge of the Haversian canals and highly mineralized matrix in the AFF biopsy.

In conclusion, bone from this case of AFF showed ongoing osteoclastic resorption, but also several abnormalities: 1) an altered arrangement of osteons; 2) impaired mineralization; 3) appreciable pyrophosphate accumulation, which might cause the impaired mineralization. Taken together, these changes may be responsible for the focally reduced bone strength at sites of AFF.



Osteoid



Scalloped surfaces

Disclosures: Maziar Shabestari, None.

LB-SA19

Efficacy and Safety of Zoledronic Acid in Chinese Women With Postmenopausal Osteoporosis. Xun Liu¹, Huiyong Shen², Lin Huang*². ¹The Sun Yat-Sen Memorial Hospital, Peoples republic of china, ²The Sun Yat-Sen Memorial Hospital, China

Aim: Zoledronic acid (ZOL) has been shown to significantly increase the spine and hip BMD in women with postmenopausal osteoporosis (PMO) (HORIZON study)¹. ZOL has been approved for treating PMO in China in 2009. This is the first study to

evaluate the efficacy and safety of ZOL in Chinese patients with PMO in a real-world setting.

Methods: This multicentre, non-interventional, post-marketing, observational, 12-month study enrolled patients with PMO with bone mineral density (BMD) T score of less than -2.5 or previous low-trauma fractures with BMD T score of -2.5 to -1.5. All eligible patients received one intravenous infusion of ZOL 5 mg. The primary efficacy endpoints were percentage changes from baseline in vertebral BMD and total hip BMD at 12 months. Secondary endpoints included changes in vertebral BMD and total hip BMD at 6 months, changes in alkaline phosphatase (ALP) at 12 months and safety. Subgroup efficacy analyses was performed across patients with age <65 and age ≥65.

Results: Of the 387 patients enrolled, 292 completed the study. There was an increase in vertebral BMD in 81.82% (216/264) of patients at 12 months. Vertebral BMD at 6 and 12 months increased by $5.31 \pm 0.77\%$ (95% CI 3.79%-6.83%, $P < 0.0001$) and $7.25 \pm 1.06\%$ (95% CI 5.16%-9.33%, $P < 0.0001$), respectively. An increase in total hip BMD was observed in 84.52% (202/239) of patients at 12 months. Total hip BMD increased by $7.54 \pm 1.24\%$ (95% CI 5.10%-9.98%, $P < 0.0001$) at 6 months and $9.96 \pm 1.24\%$ (95% CI 7.52%-12.40%, $P < 0.0001$) at 12 months, respectively. The percentage change in vertebral BMD and total hip BMD from baseline in the two age groups (<65 years and ≥65 years) at 12 months was not statistically significant. At 12 months, ALP decreased by an average of 8.29 ± 2.85 U/L ($P < 0.05$). Of the patients who completed the study, 91.44% (267) chose to continue ZOL treatment.

Adverse events were reported in 11.37% of patients, with the most common being systemic symptoms (7.49%), musculoskeletal symptoms (2.58%) and gastrointestinal symptoms (2.07%). Serious adverse events were reported in 4 cases (1.01%), including 3 deaths, which were not drug related. Hypocalcaemia was reported in 5 patients (1.80%).

Conclusion: The study demonstrated that ZOL was effective in the treatment of PMO in Chinese patients, which was independent of age, in a real-world setting. The drug was well tolerated with a general safety profile.

Disclosures: Lin Huang, Novartis Pharma, 1
This study received funding from: Novartis Pharma

LB-SA20

Evidence for a Vitamin D3 Like Endocrine System in an Ascomycete *Magnaporthe grisea*. Mihali Pandya*¹, Chandra Prakash², Mihir Sarang², Dr Bharat Chattop². ¹, India, ²Genome Research Center, India

Magnaporthe oryzae is the causal agent of the rice blast disease. This fungus destroys crop enough to feed over 10 million people. It produces a specialized structure called the appressorium which initiates infection on the leaf surface via a penetration peg. Several genes are known to be induced during the initial phase of infection, and among them, calcium pumps and calcium binding proteins may be involved in generating the cAMP surge. The latter signal is considered crucial in the downstream events leading to fungal infection. Fungi produce many secondary metabolites like the polyketides, antibiotics p450 end products and vitamins. The ascomycetes are known to harbor 67.82% of all known cytochrome P450 enzymes. We have used the GROMO and BroadMIT databases to identify a 25 hydroxyvitamin D 1 alpha hydroxylase based on sequence and motif similarity. Blast search showed a single hit with a high score for the catabolic enzyme 24 hydroxylase. Although no sequence identity was found for the vitamin D receptor (VDR) or its heterodimeric partner (RXR); there were significant similarities in the sequence of the ligand binding domain of the two receptors. Even in the absence of these receptors, the regulation of the fungal gene mimics its mammalian ortholog. It was shown to be induced > 30 fold in the presence of its precursor 25 hydroxy vitamin D, and inhibited nearly 10 fold in the presence of 1,25(OH)₂ D3. No VDRE like elements were identified in the upstream region suggesting that its regulation by vitamin D may be governed by a yet unknown protein. This is the first report of a P450 gene encoding a vitamin D3 synthesizing enzyme in a lower eukaryote.

Disclosures: Mihali Pandya, None.

LB-SU01

Lipoproteins are an Important Component of *Staphylococcus aureus* in the Induction of Bone Destruction. Ok-Jin Park*¹, Jiseon Kim², Jihyun Yang¹, Cheol-Heui Yun², Seung Hyun Han¹. ¹School of Dentistry, Seoul National University, South Korea, ²Seoul National University, South Korea

A Gram-positive bacterium, *Staphylococcus aureus*, has been recognized as one of the most important bacteria that causes bone diseases including bacterial arthritis and osteomyelitis. Although the cell wall components, such as lipoteichoic acid (LTA) and lipoproteins, of *S. aureus* are considered as major virulence factors, their roles in the bone-destructive diseases have been poorly understood. In this study, we investigated the effects of ethanol-killed *S. aureus* lacking LTA or lipoproteins on the differentiation of osteoblasts and osteoclasts *in vitro*, and bone resorption *in vivo*. While wild-type and LTA-deficient *S. aureus* enhanced the osteoclast differentiation of RANKL-primed macrophages, the lipoprotein-deficient mutant did not affect the osteoclast differentiation. In addition, wild-type and the LTA-deficient *S. aureus* attenuated osteoblast differentiation as determined by using bone marrow-derived osteoblasts and an osteoblast cell line, MC4. In contrast, the lipoprotein-deficient mutant slightly increased osteoblast differentiation. Intraperitoneal administration

with either wild or LTA-deficient *S. aureus* resulted in severe bone resorption in mice whereas no change was observed in mice given the lipoprotein-deficient mutant. Furthermore, we observed an increase of CD11b⁺B220⁻CD3⁻ osteoclast precursor cells from mice given *S. aureus* and the LTA-deficient mutant, but not in mice given the lipoprotein-deficient mutant. Taken together, we suggest that the lipoprotein might be a major component of *S. aureus* causing bone destructive diseases.

Disclosures: Ok-Jin Park, None.

LB-SU02

Bone Mineral Density in Nigerian Children after Discontinuation of Calcium Supplementation. Puja Umaretiya^{*1}, Tom Thacher¹, Philip Fischer¹, Stephen Cha¹, John Pettifor². ¹Mayo Clinic, USA, ²University of the Witwatersrand, South africa

Background: Young Nigerian children with low dietary calcium intakes showed an increase in forearm bone mineral density (BMD) after 18 months of calcium supplementation compared with placebo. However, it is not known whether this bone mineral accretion is sustained after calcium supplement withdrawal. We investigated whether calcium supplementation had a lasting effect on forearm BMD 12 months after supplement withdrawal.

Methods: Nigerian children aged 12-18 months from three urban communities were enrolled in a controlled trial of calcium supplementation. Two communities received daily calcium, one as calcium carbonate (400 mg), and the other as ground fish (529 ± 109 mg), for a duration of 18 months, and all three communities received vitamin A as placebo. Forearm BMD was measured 5 times during 18 months of calcium supplementation and 12 months after supplement withdrawal.

Results: Of 647 children enrolled, 390 completed the trial of calcium supplementation. During the 18 months of supplementation, there was a greater increase in both distal and proximal 1/3 radius and ulna BMD over time in the groups that received calcium relative to the placebo group (P<0.04). However, after calcium supplement withdrawal, the rate of increase in BMD did not significantly differ between the groups, and exhibited a nonsignificant relative decline of the distal radius and ulna BMD in the groups that received calcium compared with the placebo group. As a result, the positive effects of calcium supplementation on BMD were attenuated 12 months after withdrawal, and a significant difference did not remain between the calcium supplemented and placebo groups (P>0.12).

Conclusion: The benefit of calcium supplementation on forearm BMD in young children is not sustained after supplement withdrawal.

Disclosures: Puja Umaretiya, None.

LB-SU03

Effect of a Special Supplement in Preventing Loss of Bone Strength in Osteoporotic Sheep. Subrata Saha^{*1}, Westley Hayes², Racquel LeGeros³, Gavriel Feuer², Mrinal Musib², Dana Ruehlman⁴. ¹State University of New York Downstate Medical Center, USA, ²SUNY Downstate Medical Center, USA, ³New York University College of Dentistry, USA, ⁴Colorado State University, USA

Introduction: The long term objective of the study was to develop a calcium phosphate-based compound that will have a potential for osteoporosis therapy and prevention and be safe and affordable. This compound described as "synthetic bone mineral, SBM" consists of carbonate apatite incorporating magnesium (Mg), zinc (Zn) and with and without fluoride (F). Our studies on osteoporotic rats that SBM when administered by injection or as a diet supplement prevented bone loss. The present study aimed to test the efficacy of SBM in preventing bone loss in osteoporotic sheep.

Methods: Sheep were divided into four groups (7 sheep/group): A: sham-operated; B: ovariectomized (OVX); C: OVX given the diet supplemented with SBM (-F); D: OVX receiving diet supplemented with SBM (+F). All groups received low mineral diet and were given glucocorticoids. The animals were sacrificed after 8 months. Soft tissues were removed from the long bones (tibiae and femurs). The bones were scanned by CT and then tested mechanically in 4 point bending using an Instron mechanical testing machine (model 8874). The rate of deformation was 10 mm/mu. The bones were always kept in wet condition. From the automatically recorded load-deformation data, the maximum load, maximum deformation and the stiffness of the whole bones were calculated. Subsequently the maximum stress, maximum strain and the modulus of elasticity for the bone tissue were calculated for each group using the CT derived cross-sectional information. The mode of fracture for each bone was also examined and recorded.

Results: The maximum load (at 1 mm deformation) for the OVX sheep (Group B) was significantly lower than the sham operated group and groups with special diets (with and without fluoride). The sheep given the SBM (+F) showed the highest load carrying capacity. Similarly, the stiffness of the OVX sheep was also significantly lower than the sham operated and the groups given SBM (+F). The maximum stress and the Young's Modulus did not show any statistically significant difference among the four groups. The cortical cross-sectional areas of the femurs for the groups given SBM with and without F, was significantly higher than that of the OVX group.

Conclusion: Our results show that SBM (with and without F) added to the diet was able to prevent loss of bone strength induced by OVX and glucocorticoid treatments. [Supported by research grant AR056208 from NIAMS/NIH; PI, R.Z. LeGeros]

Disclosures: Subrata Saha, None.

LB-SU04

Small Leucine-Rich Proteoglycans Control Osteoclastogenesis. Vardit Kram^{*1}, Yanming Bi², Mildred Embree³, Tina Kilts², Azusa Maeda⁴, Marian Young¹. ¹National Institutes of Health, USA, ²NIDCR, USA, ³Columbia University, USA, ⁴Nih/nidcr, USA

Small leucine-rich proteoglycans (SLRP's) are macromolecules containing a protein core consisting of leucine-rich repeats (LRRs) flanked by conserved cysteine-rich regions and glycosaminoglycan (GAGs) side-chains. SLRP family members are abundantly expressed in the extracellular matrix (ECM) of mineralizing tissues and play a crucial role in collagen fibril formation and proper development of connective tissue. Biglycan (Bgn), a class I SLRP is highly expressed in bone and cartilage and has been shown to play an important role in proliferation, survival and differentiation of osteoblasts. Fibromodulin (Fmod), a class II SLRP, is highly expressed in cartilage, tendon and throughout the growth plate. In order to examine SLRP's role in mineralized tissue, double deficient mice, lacking both biglycan and fibromodulin (DKO) were generated. Our results show that these mice have low bone mass phenotype detectable as early as 5 weeks and becoming more pronounced with age. At 5 weeks of age DKO mice had 60-80% less BV/TV than the WT controls. The very low BV was the result of fewer and thinner trabeculae. These animals also displayed smaller diaphyseal diameters with thinner cortices. Morphological changes in the femoral bones of DKO mice were observed, including misalignment of the distal condyle and a distal bony protuberance, which may be the result of abnormal shear forces due to joint misarticulation. Additionally, these mice developed early onset osteoarthritis and ectopic ossification. BMSC derived from DKO mice had higher clonogenic potential compared to WT controls indicating that bone loss was not from defective osteoblastogenesis. Indeed, dynamic histomorphometry showed the low bone mass phenotype was not the result of decreased bone formation rate. Preliminary *in vivo* TRAP staining indicated that DKO mice have an increased number of osteoclasts, and when hematopoietic precursors were isolated from DKO mice and analyzed *in vitro*, the levels of TRAP positive cells and pit formation ability were both increased compared to WT controls. Since both bgn and fmod are expressed by cells of the osteoblastic lineage, we hypothesize a novel role for these SLRPs as coupling component that control osteoclast differentiation through their expression by osteoblast precursors. In summary our data indicate that bgn and fmod are novel extracellular elements that can control bone mass by negatively controlling osteoclastogenesis.

Disclosures: Vardit Kram, None.

LB-SU05

Modification of Mesenchymal Stem Cells with a Novel Cell-surface Reactive Polymer for Applications in Bone Disease. Sonia Dsouza^{*1}, Hironobu Murata¹, Moncy Jose¹, Jill Andersen¹, Richard R Koepsel¹, Alan J Russell². ¹University of Pittsburgh, USA, ²Carnegie Mellon University, USA

Bone destruction is one of the most prevalent problems due to injuries on the battlefield, accidents, or cancers affecting the bone. Our laboratory has explored how to influence the propensity of circulating cells to associate with bone by covalently attaching a custom designed polymer to the cell surface. The polymer has bisphosphonate groups attached at one end, which enables partitioning to bone and a terminal NHS group at the other end that enables binding to the surface of cells. We tested the ability of the polymer to bind cells and found that the polymer binds mesenchymal stem cells (MSC). Modification of the MSCs with the polymer did not affect cell viability or proliferation. In addition, the MSCs were able to differentiate into adipocytes and osteoblasts. Further, the MSCs that were modified with the polymer containing bisphosphonate bound bone in significantly higher numbers than MSCs that were modified with a control polymer lacking bisphosphonate. Thus, this polymer has the attributes necessary to change the partitioning of cells from the circulation to the bone *in vivo*, which is currently under investigation. Flexibility in the synthesis of the polymer allows for the attachment of different targeting molecules and/or binding moieties increasing its utility.

Disclosures: Sonia Dsouza, None.

LB-SU06

PTHrP Induces Lactation in the Absence of Pregnancy and Accelerates Breast Cancer. Kata Boras-Granic^{*1}, John Wysolmerski². ¹Yale School of Medicine, USA, ²Yale University School of Medicine, USA

Parathyroid hormone-related protein (PTHrP) contributes to normal mammary development and breast cancer. It is necessary for the development of embryonic breast tissue. During postnatal development, PTHrP is expressed in basal myoepithelial cells until late pregnancy, when its expression is also activated in

differentiating alveolar epithelial cells. During lactation, large amounts of PTHrP are secreted into milk and the circulation, where it regulates systemic calcium and bone metabolism. When PTHrP is secreted by breast cancers, it stimulates bone resorption, which promotes the growth of skeletal metastases and produces hypercalcemia. Less is known about the contribution of PTHrP to the development and/or progression of primary breast cancers. However, emerging studies have suggested that PTHrP accelerates breast cancer development and/or progression.

We generated a tetracycline-regulated, MMTV-driven transgenic model of PTHrP overexpression in the mammary gland (MMTV-rtTA;tetO-PTHrP mice). We find that overexpression of PTHrP causes alveolar hyperplasia in virgin mice that is associated with an increase in the numbers of alveolar progenitor cells upon FACS analysis of mammary stem/progenitor cell populations. Overexpression of PTHrP for 7 days in virgin mice activates a pattern of mammary gland gene expression characteristic of alveolar secretory differentiation. Remarkably, virgin transgenic mice produce milk and are able to feed fostered newborn pups for up to one week, despite never being pregnant themselves. These data suggest that PTHrP signaling operates downstream of systemic hormones to regulate the differentiation of luminal/alveolar progenitor cells during normal pregnancy. We also crossed MMTV-rtTA;tetO-PTHrP mice to MMTV-PyMT mice, a transgenic model of breast cancer. Overexpression of PTHrP in this model dramatically accelerated the formation of mammary tumors. All MMTV-rtTA;tetO-PTHrP;MMTV-PyMT mice develop palpable tumors in all mammary glands within 3-4 weeks of age, become hypercalcemic and die before 4.5 weeks of age. Mammary tumors display a papillary phenotype and secretory activity. Control MMTV-PyMT mice develop palpable tumors at 7 to 8 weeks of age and require sacrifice at 4 months. In summary, overexpression of PTHrP in luminal epithelial cells triggers premature secretory differentiation and greatly accelerates breast cancer formation.

Disclosures: *Kata Boras-Granic, None.*

LB-SU07

A Novel Function of an Old Hormone for Postmenopausal Health. Kim Henriksen*, Michael Feigh, Kim Andreassen, Sara Toftegaard Petersen, Claus Christiansen, Morten Karsdal. Nordic Bioscience A/S, Denmark

Salmon calcitonin is a pleiotropic molecule, with a well-established bone effect, while other functions are emerging. Early evidence indicating that oral administration of salmon calcitonin (sCT) has potent anti-diabetic effects in diet-induced obese (DIO) rats.

However, whether chronic oral sCT treatment influences energy balance and glucose homeostasis under estrogen deficient situations is unclear. Furthermore, the mechanism(s) of action for the glucoregulatory effects, i.e. the dependency on leptin signaling and the involvement of the incretin system are unclear.

To shed light on these aspects two studies of oral sCT were performed. 1) OVX and Sham rats fed a high fat diet, a model of postmenopausal obesity, high bone turnover and insulin resistance, were treated for 5 weeks, and 2) Zucker Diabetic Fatty rats, a leptin deficient overt diabetic model, were treated for 10 weeks. Effects on fasting blood glucose, post-prandial glucose and insulin, bodyweight and food intake were carefully monitored.

Oral administration of sCT for 5 wk reduced food intake, induced weight loss in HFD rats and prevented weight gain in HFD-OVX rats. Furthermore, oral sCT decreased fasting glycemia by 0.7 mM in both groups and decreased plasma insulin by 45% and 56% in HFD rats and HFD-OVX rats, respectively. Additionally, decreases in plasma leptin by 43% combined and HOMA-IR were observed. In the ZDF model, oral sCT treatment attenuated fasting and non-fasted hyperglycaemia during the intervention period, while showing no effect on bodyweight, with an overall reduction in glucose of ~9 mM and in HbA1c levels of 1.7%. Furthermore, a pronounced reduction in glucose excursions was observed during oral glucose tolerance test. Lastly, oral sCT treatment improved pancreatic beta-cell mass. In both models, oral sCT concomitantly improved glucose intolerance and ameliorated exaggerated secretion of pancreas and incretin glucoregulatory hormones during oral glucose tolerance test.

These novel findings demonstrate the beneficial effect of oral sCT treatment on energy balance and glucose metabolism in high-fat diet and ovariectomy-induced obese rats, and underscore the involvement of the leptin system in these effects. These data also indicate that glucose-lowering is obtained independent of weight loss and the leptin system, and hence clearly indicate clinical usefulness of oral sCT as anti-diabetic treatment in postmenopausal and obesity-associated insulin resistance and diabetes.

Disclosures: *Kim Henriksen, Nordic Bioscience, 3*
This study received funding from: Nordic Bioscience

LB-SU08

A Severe Case of Maffucci's Syndrome Complicated with Chondrosarcoma and Multigland Parathyroid Adenomas. Azar Khosravi*, Akshay Jain, Warren Chow. City of Hope, USA

Introduction: Maffucci's and Ollier's syndromes are characterized by enchondromas, with (Maffucci's) or without hemangiomas (Ollier's).

History of presentation: our patient is a 36-year-old woman. Hemangiomas first noted during infancy and progressively grew in size and number. She now has numerous subcutaneous and deep tissue hemangiomas, enchondromas and shortening of right lower extremity because of pathologic fracture of right femur.

Biopsy of a mass arising from the sacrum demonstrated transformation to a Grade 1 chondrosarcoma. Surgical options were declined by the patient. She was enrolled in

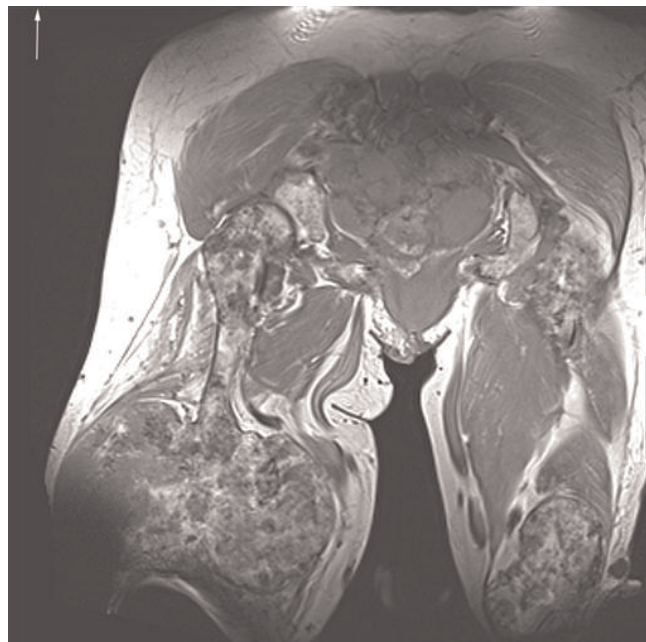
a trial with dasatinib for 4 years, with no interval growth of the lesion. However, she developed hypercalcemia and had to be taken off the trial. She was then started on pazopanib. Workup of hypercalcemia revealed primary hyperparathyroidism, with serum ionized calcium 1.96 mmol/L, phosphorus 3.3 mg/dL and PTH of 408 pg/mL. Serum calcium and parathyroid hormone levels normalized after surgical removal of 2 right adenomatous parathyroid glands. A biopsy of a right femoral lesion due to pain in the right groin and thigh was consistent with Grade 1 chondrosarcoma. Herlast CT identified a new 41 mm mass inferior to the right lobe of the liver, leading to discontinuation of the pazopanib.

Discussion: Isocitrate dehydrogenase 1 and 2 somatic mutations have been found in 92% of patients with Maffucci syndrome resulting from a postzygotic event. IDH mutation impairs histone demethylation and results in a block in cell differentiation and production of a potential oncometabolite, 2-hydroxyglutarate. Enchondromas have a 15-30% risk of transformation into chondrosarcomas, albeit often have an indolent rate of progression. Maffucci's syndrome is also associated with other tumors including endocrine tumors (parathyroid, thyroid, adrenal cortical and pituitary adenomas). Malignant tumors associated with this condition include chondrosarcoma, pancreatic cancer, ovarian tumors, lymphangiosarcoma, hemangiosarcoma and astrocytoma. Our patient has one of the most severe manifestations of Maffucci's syndrome documented in the medical literature, yet she is a highly functional individual.

Conclusion: Maffucci's syndrome is a rare disorder that is associated with profound psychosocial implications. The newly reported association of IDH 1 and 2 mutations opens new possibilities for future of therapies with targeted inhibitors of IDH-1 and 2.



CXR of numerous enchondromas



MRI of bilateral lower extremities enchondroma with malignant transformation in right femur



subcutaneous hemangiomas on bilateral hands

Disclosures: Azar Khosravi, None.

This study received funding from: City of Hope

LB-SU09

TRAIL Induces RANK Ligand Expression in Stromal/preosteoblast Cells.

Kumaran Sundaram¹, Christina Voelkel-Johnson², Sakamuri Reddy¹, Charles P. Darby Children's Research Institute, USA, ²Dept. of Microbiology & Immunology Medical University of South Carolina, USA

Receptor activator of nuclear factor kappa-B ligand (RANKL) is a critical osteoclastogenic factor expressed in bone marrow stromal/preosteoblast cells. RANKL-RANK receptor signaling is essential for osteoclast differentiation and bone resorption activity. TNF-related apoptosis-inducing ligand (TRAIL) is a member of TNF superfamily and has been shown to be elevated in pathologic conditions such as multiple myeloma and inflammatory arthritis. Osteoprotegerin (OPG) which inhibits osteoclastogenesis, is a decoy receptor for RANKL and also interacts with TRAIL. Previously, TRAIL has been shown to induce apoptosis in osteoclast cells. In contrast, recent evidence suggests that TRAIL induces osteoclast differentiation through TNF receptor associated factor-6 (TRAF-6) dependent signaling pathway. It has been demonstrated that osteoblast cells express TRAIL receptors (DR4 and 5), however, TRAIL do not induce apoptosis in these cells. Thus, the molecular mechanisms underlying TRAIL regulation of osteoclastogenesis is unclear. In this study, we show that TRAIL differentially regulates RANKL and OPG expression in human bone marrow derived stromal (SAKA-T) cells. Real-time PCR analysis demonstrated that TRAIL (0-100 ng/ml) treatment for 48 h induced RANKL mRNA expression in a dose-dependent manner in these cells. In contrast, TRAIL significantly decreased OPG mRNA expression. Further, TRAIL increased alkaline phosphatase (ALP) and decreased collagen 1A (Col1A) mRNA expression. However, there was no change in the levels of osteopontin, osteonin and osteocalcin mRNA expression. Western blot analysis identified that TRAIL increased (5.0 fold) c-Jun expression in SAKA-T cells. In addition, TRAIL treatment of SAKA-T cells transfected with the hRANKL promoter (-2 kb)-luciferase reporter plasmid showed increased levels of transactivation. These results suggest that TRAIL induce RANKL expression through specific transcriptional regulatory mechanisms and could be a potential therapeutic target to control enhanced osteoclast development/bone resorption activity associated with skeletal diseases.

Disclosures: Kumaran Sundaram, None.

LB-SU10

Osteoblast GSK-3 β Regulates Metabolism and Male Specific Diabetes.

Ryan Gillespie¹, Jason Bush², Gillian Bell², Laura Aubrey², Mathieu Ferron³, Barbara Kream⁴, James Woodgett², David Hess², Gerard Karsenty³, Frank Beier¹. ¹University of Western Ontario, Canada, ²Western University, Canada, ³Columbia University, USA, ⁴University of Connecticut Health Center, USA, ⁵Samuel Lunenfeld Research Institute/Mount Sinai, Canada

Glycogen synthase kinase 3 beta (GSK-3 β) is an essential negative regulator which acts as a "brake" on many anabolic-signalling pathways including Wnt and insulin. The global deletion of GSK-3 β results in perinatal lethality and in various skeletal defects. The goal of our research is to determine skeletal GSK-3 β cell autonomous effects and postnatal role. The role of Wnt and Insulin signalling on skeletal development has been studied individually before. However, since GSK-3 β is a node of regulation for both these pathways as well as for others, its role in skeletal development required further examination. We used Cre TG driven by the 3.6Kb *Col1a1* promoter to inactivate the *Gsk3b* gene (*Col1-Gsk3b* KO) in skeletal cells. Mutant mice exhibit decreased weight and postnatal bone growth as well as delayed

development of several skeletal elements. Surprisingly, the mutant mice display decreased circulating glucose and insulin levels, despite normal expression of GSK-3 β in metabolic tissues. We showed that these effects are due to an increase in global insulin sensitivity. Most of the male mutant mice died post weaning. Prior to death, blood glucose changed from low to high, suggesting a possible switch from insulin sensitivity to resistance. These male mice die with extremely large bladders that are preceded by damage to the urogenital tract, defects that are also seen type II diabetes. Our data suggests that skeletal-specific deletion of GSK-3 β affects global glucose metabolism and sensitizes male mice to developing type II diabetes.

Disclosures: Ryan Gillespie, None.

LB-SU11

Identification and Characterization of Human Menaquinone-4 Synthase

UBIAD1 Gene Promoter. YOSHIHISA HIROTA^{*}1, Kimie Nakagawa¹, Masato Watanabe¹, Nobuaki Funahashi¹, Kazuhiro Uenishi², Toshio Okano¹. ¹KOBE PHARMACEUTICAL UNIVERSITY, Japan, ²Kagawa Nutrition University, Japan

Vitamin K plays an important role in blood coagulation and bone formation. Vitamin K has two major homologues, the plant-derived phyloquinone(PK) and the bacterium-derived menaquinone-n(MK-n). We have previously identified a novel human enzyme, UBIAD1, responsible for the conversion of PK to MK-4 (*Nature* 2010). UBIAD1 is a key enzyme of MK-4 synthesis. However, mechanism of UBIAD1 gene regulation remains unclear. The aim of this study is to identify and characterize UBIAD1 promoter.

To identify the proximal promoter region of UBIAD1, seven promoter progressive 5'-deletion constructs spanning the positions from -3389 to +47 were generated and cloned in an upstream of the luciferase reporter gene in the pGL4.10-enhancer vector. Plasmids of pGL4.10[-3389/+47], pGL4.10[-1922/+47], pGL4.10[-896/+47], pGL4.10[-734/+47], pGL4.10[-517/+47], pGL4.10[-346/+47] and pGL4.10[-179/+47] were transiently transfected into human embryonic kidney cell line HEK293 cells. The constructs including pGL4.10[-1922/+47] to pGL4.10[-346/+47] showed similar or even higher luciferase activity compared to that of pGL4.10[-3389/+47]. However, pGL4.10[-179/+47] showed no luciferase activity. To further define the region involved in the differential regulation of UBIAD1, we then generated 3'-nasted deletion constructs of the -896 to +47 region. Deletion of the region from +47 to -266 resulted in no change of luciferase activity. However, further deletion from +47 to -306 substantially attenuated luciferase activity. Thus, UBIAD1 promoter may exist in the 40 bp region between -266 to -306. In order to define the enhancer region in UBIAD1 promoter, 100 bp interval deletion pGL4.10[-896/-266] constructs were generated. pGL4.10[-490/-440] displayed significantly decreased luciferase activity. Thus, this may be the enhancer region in UBIAD1 promoter. We then generated a biotin-labeled DNA probe corresponding to the enhancer region(-44 to -490) and searched factors capable of binding to this probe. A 110 kDa protein bound to this probe was identified as poly (ADP-ribose) polymerase 1(PARP-1) by MALDI-TOF/MS analysis. These results will help to better understand the mechanism underlying UBIAD1 gene expression and can provide useful information for the development of new drugs for therapeutic up-regulation of the UBIAD1 gene in osteoporosis.

Disclosures: YOSHIHISA HIROTA, None.

LB-SU12

Tet2 Plays an Important Role in Bone Remodeling by Regulating both

Osteoblasto- and Osteoclasto-genesis Through the Maintenance of 5-

Hydroxymethylcytosine in the Genome. Ling Li¹, Zhe Li¹, Craig Street²,

Jiapeng Wang¹, Steven Rhodes¹, Feng Pan¹, Yongzheng He¹, Khalid

Mohammad¹, Theresa Guise¹, Peng Jin², Mingjiang Xu³, Feng-Chun

Yang¹. ¹Indiana university, USA, ²Emory University, USA, ³Indiana

University School of Medicine, USA

Epigenetic mechanisms play an important role in the tissue-specific regulation of gene expression. DNA methylation is one of the most important epigenetic modifications. However, if DNA methylation underlies the physiology/pathophysiology of bone remodeling is not well established. Ten-eleven translocation proteins (TET1, 2, and 3), newly identified demethylating enzymes, catalyze the conversion of 5-methylcytosine (5-mC) to 5-hydroxymethylcytosine (5-hmC), therefore could alter methylation-driven gene silencing. Here, we challenged if the altered epigenetic modifications lead to dysregulation of critical genes controlling osteoblasto- and osteoclasto-genesis, and bone remodeling using Tet2-targeted mouse models. Using qPCR and Tet2:GFP reporter knock-in mice, we found that Tet2 is highly expressed in all osteoblast progenitors (mesenchymal stem cells, MSC) and preosteoclasts (preOCLs). Deletion of Tet2 dramatically reduced the 5-hmC levels and concomitantly increased the 5-mC levels in genomic DNA of MSCs and preOCLs. Tet2^{-/-} mice are slightly smaller and gradually develop osteopetrosis with significantly higher BMD and trabecular bone volume than WT littermates. Tet2^{-/-} mice had markedly increased number of marrow MSCs with skewed differentiation toward osteoblasts. Furthermore, Tet2^{-/-} preOCLs had impaired OCL differentiation capacity. To delineate the gene expression changes, RNA-Seq was performed with Tet2^{-/-} MSCs and preOCLs compared to their respective WT counterparts. A number of differentially expressed genes in Tet2^{-/-} MSCs (e.g. Sp7, Bmp2, Dlx3, Bglap2, Alpl)

and in Tet2^{-/-} preOCLs (*Stab2*, *Il6*, *Ccl3*, *Mitf*, *Gata2*) are implicated in the regulation of osteoblasto- and osteoclasto-genesis, respectively. Genome-wide 5-hmC profiling in WT and Tet2^{-/-} MSCs and preOCLs showed that the dysregulated gene expression correlated with specifically altered 5-hmC distribution patterns across selected gene loci. In addition, the genomic binding sites of Tet2 were mapped by ChIP-Seq in primary MSCs and preOCLs derived from Tet2:Flag/V5 knock-in mice with anti-Tag antibody. Our study identified potential Tet2 genetic targets and unveiled the regulatory network of Tet2 in MSCs and preOCLs. These results indicate that deletion of Tet2 dysregulates hydroxylation of 5-mC and gene expression in MSCs and preOCLs, which in turn alters their differentiation program, leading to osteopetrosis. These results demonstrate a pivotal role of DNA methylation in bone homeostasis.

Disclosures: Ling Li, None.

LB-SU13

Inorganic Polyphosphates Stimulate FGF23 Expression through FGFR Pathway. Ningyuan Sun^{*1}, Huawei Zou¹, Liang Yang¹, Ping Gong², Toshikazu Shiba³, Haiyang Yu¹, Quan Yuan¹. ¹State Key Laboratory of Oral diseases, West China School of Stomatology, Sichuan University, China, ²West China School of Stomatology, Sichuan University, China, ³Regenesis, Inc., Japan

Polyphosphate (polyP) is composed of linear polymers of orthophosphate residues linked by high energy phosphoanhydride bonds. It has been reported to improve osteoblastic differentiation, stimulate periodontal tissue regeneration, and accelerate bone repair. The aim of this study is to evaluate the effect of polyP on the expression of FGF23, a hormone mainly secreted from matured osteoblasts and osteocytes. In this study, different types of polyP were fabricated and co-cultured with osteoblast-like UMR-106 cells. The real-time PCR and western blot were employed to analyze the gene and protein expression of FGF23. We found that 1mM polyP was able to increase FGF23 expression after 4 hours and reach the peak after 12 to 24 hours, and go down at 48 hours. We also found that polyP could activate FGFR pathway, as evidenced by increased phosphorylation of FGFR, FRS2 and ERK1/2. When FGFR signaling was inhibited by a specific inhibitor SU5402, the effect of polyP on FGF23 was significantly blunted. Our results indicate that polyP is able to stimulate osteoblastic FGF23 expression, and this effect is associated with activation of FGFR pathway. These findings provide substantial mechanism and support for the clinical use of polyP for bone regeneration.

Disclosures: Ningyuan Sun, None.

LB-SU14

Osteoclast Resorptive Activity Utilizes Interactions of Plekhm1 and TRAFD1. Paul Odgren¹, Hanna Witwicka^{*2}, Hong Jia², Xiangdong Li³. ¹University of Massachusetts Medical School, USA, ²Univ. of Mass. Medical School Dept. of Cell Biology, USA, ³Chinese Academy of Sciences, China

Mutations in plekhm1 cause bone disease in humans and animals. Truncations cause deficient bone resorption by osteoclasts leading to osteopetrosis. A gain-of-function point mutation causes increased resorption leading to osteopenia. We and others have shown that plekhm1, a multi-modular protein, interacts with the small GTPase rab7 and is involved in vesicle trafficking, secretion, and membrane biogenesis. Investigating other interactions of plekhm1 by mass spectrophotometry, we found that TRAFD1 (FLN29) also interacts with plekhm1. Reciprocal pull-down assays confirmed the interaction and localized the regions of interaction. While TRAFD1 has been shown to suppress toxic shock by inhibiting innate immune responses in monocytes/macrophages via toll-like receptor signaling, a role in osteoclast biology has never been described. We found that, prior to stimulation of pre-osteoclasts with RANKL, there was no significant co-localization of TRAFD1 with plekhm1, whereas upon treatment with RANKL, co-localization increased to greater than 50%. Knockdown of TRAFD1 inhibited osteoclast resorbing activity and caused a marked decrease in acidification of the resorption lacuna. Cellular levels of acidification factors such as the ClC7 chloride channel, carbonic anhydrase II, and vATPase were unchanged, suggesting a defect in targeting these factors to their correct locations at the ruffled border. Together, these results imply a novel role for TRAFD1 in osteoclast vesicle transport and acidification.

Disclosures: Hanna Witwicka, None.

LB-SU15

Centrosome Fine Ultrastructure of the Osteocyte. Mechanosensitive Primary Cilium. Gael Y. Rochefort^{*1}, Delphine Maurel², Priscilla Aveline³, Stephane Pallu⁴, Claude Laurent Benhamou⁵, Rustem E. Uzbekov⁶. ¹EA4708 I3MTO, Orléans Hospital, France, France, ²Inserm Unit 658, Hôpital Porte Madeleine, France, ³Centre Hospitalier Régional D'Orléans, France, ⁴EA 4708 - I3MTO Orléans, France, ⁵CHR ORLEANS, France, ⁶Department of Microscopy, François Rabelais University, Tours, France, France

Introduction and Hypothesis: The centrosome is the principal microtubule organization center in cells, giving rise to microtubule-based organelles (e.g. cilia, flagella). The aim was to study the osteocyte centrosome morphology at an ultrastructural level in relation to its mechanosensitive function.

Methods: Osteocyte centrosomes and cilia in tibial cortical bone were explored by acetylated alpha-tubulin (A α Tub) immunostaining under confocal microscopy. For the first time, fine ultrastructure and spatial orientation of the osteocyte centrosome were explored by transmission electron microscopy on serial ultra-thin sections.

Results: A α Tub-positive staining was observed in 94% of the osteocytes examined (222/236). The mother centriole formed a short primary cilium and was longer than the daughter centriole due to an intermediated zone between centriole and cilium. The proximal end of the mother centriole was connected with the surface of daughter centriole by striated rootlets. The mother centriole exhibited distal appendages which interacted with the cell membrane and formed a particular structure called "cilium membrane prolongation". The primary cilium was mainly oriented perpendicular to the long axis of weight-bearing bones. This non-random orientation of the centriole can indicate that a "mechano-chemical" function may be related to the orientation of the bone growth, or to the loading axis.

Conclusions: Mother and daughter centrioles change their original mutual orientation during the osteocyte differentiation process. The short primary cilium is hypothesized as a novel type of fluid-sensing organelle in osteocytes.

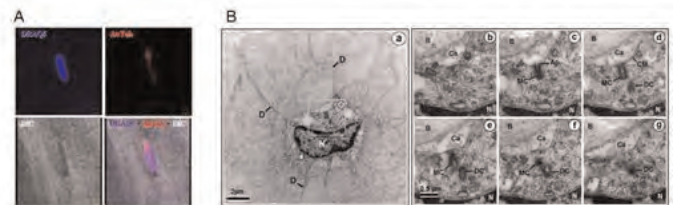


Figure 1: Primary cilium immunostaining (A) and ultrastructure (B) in osteocyte.

Disclosures: Gael Y. Rochefort, None.

This study received funding from: INSERM, Région Centre, Industry Department & the Loiret General Council, France

LB-SU16

The Assessment of Total Femur Bone Mineral Density in US Submariners. Heath Gasier^{*}, Linda Hughes, Colin Young, Annelly Richardson, David Fothergill. Naval Submarine Medical Research Laboratory, USA

The submarine environment (lack of sunlight and elevated carbon dioxide), coupled with insufficient vitamin D intake and weight-bearing exercise, may compromise bone strength and increase fracture risk. The purpose of this investigation was to determine if submarine duty is associated with bone mineral density (BMD) of the total femur. Male submariners (20-87 yrs), active duty (n=288) and those who left service (n=82), completed questionnaires to obtain information regarding past medical history, submarine service (underway time, type of submarine, duty status and rank), activity and dietary patterns. BMD (g/cm²) of dual total femur was determined by dual energy x-ray absorptiometry (DXA). Independent T-tests were used to determine differences in potential predictors of BMD between <50 yrs old (yo) and \geq 50 yo groups. Potential predictors of BMD including submarine service, anthropometric, and health related behaviors were identified using multiple regression with nonsignificant variables removed if p>0.05. Non-Hispanic white submariners (n=334) mean BMD and low BMD prevalence rates by age group (20-29, 30-39, 40-49, 50-59, and 60-69 yo) were compared to the National Health and Nutrition Examination Survey (NHANES) 2005-2008 data for Non-Hispanic white males. Age group differences were identified for 10 covariates, thus regression models were done for combined, <50 yo and \geq 50 yo groups. For the combined age model, age, body mass index, and gynoid body fat (%) predicted 23% of the variance in BMD. Similarly, for those <50 yo, age, height, weight, and gynoid body fat (%) predicted 22% of the variance in BMD. Interestingly, for the \geq 50 yo group, 24% of the variance in BMD was predicted by heart rate, calcium intake, and android body fat (%). In comparison to the NHANES data, submariners <60 yo had a significantly higher mean total femur BMD (p<0.05); however, no differences were determined for the 60-69 yo age group (p=0.97). All submariners <50 yo had normal BMD (Z-scores > -2.0). In contrast, 26% age-adjusted (27% crude) of submariners \geq 50 yo had low

BMD (T-score >-2.5 and <-1.0) compared to 14% age-adjusted prevalence of NHANES ($p=0.009$). These preliminary results revealed, 1) there was no association between submarine service predictors and BMD, 2) submariners <60 yo have higher total femur BMD than the general US population, and 3) the prevalence of low BMD in submariners ≥ 50 yo is nearly double the general US population.

Disclosures: Heath Gasier, None.

LB-SU17

Effect of Visceral Adiposity to One Year Change of Bone Mineral Density.

Kwang Joon Kim^{*1}, Yumie Rhee², Kyoung Min Kim³, Sung-Kil Lim³.
¹Severance Hospital, South Korea, ²Department of Internal Medicine, College of Medicine, Yonsei University, South Korea, ³Yonsei University College of Medicine, South Korea

Introduction: Several studies have documented relationships between adipose tissue and bone mineral density (BMD). However, there has been no longitudinal study that evaluated the effect of visceral adipose tissue on skeleton. Therefore, we investigated how the change of visceral adipose tissue effected on bone mass.

Method: A total of 87 healthy subjects have been enrolled in this study (45 male, 42 female) from Feb, 2011 to May, 2011. Visceral and subcutaneous adiposity was analyzed by computed tomography (CT), and bone mineral density (BMD) was measured by dual-energy X-ray absorptiometry for 2 years in a row. (2011 and 2012) Blood samples were collected to measure lipid profile, insulin resistance (HOMA-IR), hepatic enzymes, and hsCRP.

Result: In the cross sectional study, we found that baseline hsCRP, HOMA-IR, and visceral fat area but not subcutaneous fat area were inversely correlated with BMD and BMC. In the simple regression analysis, an increase in total visceral fat area which was measured by CT scan was negatively correlated with the change of BMD and BMC. ($r=-0.34$, $p < 0.01$) Furthermore, Δ insulin resistance (HOMA-IR) also negatively related with Δ BMC. ($r=-0.37$, $p < 0.01$) In the multiple regression analysis, the change of visceral fat area was an independent predictor of changes in BMD and BMC.

Conclusion: Visceral fat, but not subcutaneous fat, might be another risk factor of low BMD in Korean men and women.

Disclosures: Kwang Joon Kim, None.

LB-SU18

Atypical Femoral Shaft Fractures are a Separate Entity, Easily Diagnosed by its Radiographic Stress Fracture Characteristics. Analysis of 59 Atypical Fractures and 218 Controls..

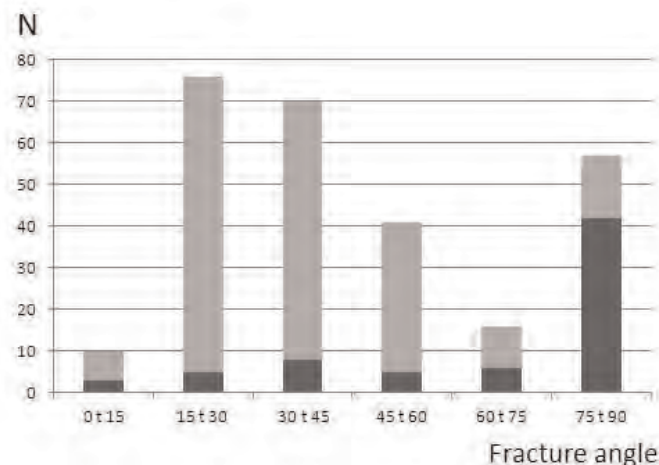
Per Aspenberg^{*}, Jörg Schilcher, Veronika Koepfen. Linköping University, Sweden

Background: The association between bisphosphonates and atypical femoral fractures is still debated. In a nation-wide study with radiographic adjudication, we found a relative risk of 47, suggesting a causative association. Others found a relative risk of only 2 in a large study with a similar design. A possible explanation for this discrepancy could be different radiographic definitions. We therefore re-analyzed the radiographs from our previous study, to estimate the relation between different radiographic features and bisphosphonate use.

Methods: In the previous nationwide study, 59 atypical and 218 ordinary subtrochanteric fractures were diagnosed. These fractures were identified by searching for a stress-type fracture pattern. All fractures were now re-assessed by an untrained physician, with no experience in radiology or orthopedics, after a briefing by the senior authors. All involved persons were blinded as regards bisphosphonate use. The fracture angle (0 – 90 degrees) was measured. Presence of a callus reaction (local lateral cortical thickening), more than 2 fragments, or a medial spike was noted. The reader then made a judgment whether the fracture appeared as a stress fracture, followed by a reassessment using the ASBMR criteria for atypical fracture.

Results: The new reader identified 56 of the previously diagnosed 59 stress fractures with no false positives. The fracture angle showed a significantly bimodal distribution (by frequency distribution analysis), with one peak between 75 and 90 degrees, and another, broader between 15 and 60 degrees. 42 of 57 patients in the 75 to 90 peak used bisphosphonates whereas only 27 of 213 others did. Presence of a callus reaction had a high specificity for bisphosphonate use (0.96; 95 % CI 0.92 to 0.98), but most other criteria had a good specificity too. The ASBMR criteria had a somewhat lower specificity, mainly due to problems defining the term "short oblique". Using the ASBMR criteria, the number of atypical fractures without bisphosphonate use increased from 13 to 31, leading to a corresponding decrease in relative risk associated with bisphosphonate use by more than half.

Interpretation: Stress fractures of the femoral shaft are a specific entity, which is easily diagnosed on radiographs and strongly related to bisphosphonate use. Differences in diagnostic criteria may partially explain the large differences in relative risk between different population-based studies.



Distribution of fracture angles. Dark part of bar signifies bisphosphonate users

Disclosures: Per Aspenberg, AddBio AB, 7; Eli Lilly corp., 2

LB-SU19

Estrogen Receptor Alpha Regulation of Bone Marrow Adipogenesis.

Susan Krum^{*}, Korinna Wend. UCLA, USA

A decrease in bone mineral density during menopause is accompanied by an increase in adipocytes in the bone marrow space. We show here that estrogen receptor alpha (ERα) knockout mice (ERαKO) also have an increase in lipid accumulation in the bone marrow compared to wildtype mice. Ovariectomy also leads to accumulation of fat in the bone marrow. Bone marrow cells from ERαKO mice that are differentiated to adipocytes *in vitro* also have increased lipid accumulation compared to cells from wildtype mice. Analysis of individual adipocytes show that wildtype mice have fewer, but larger, lipid droplets per cell than adipocytes from ERαKO mice. Furthermore, higher levels of Adipose Triglyceride Lipase (ATGL) protein in WT adipocytes correlate with increased lipolysis and fewer lipid droplets per cell. 17β-estradiol (E2) further increases ATGL mRNA and protein levels of ATGL. In contrast, ERαKO mice have higher levels of perilipin protein expression, which plays a role in lipogenesis. Together these results demonstrate that E2 signals via ERα to regulate lipid droplet size and total lipid accumulation in the bone marrow space.

Disclosures: Susan Krum, None.

LB-SU20

Expression of Measles Virus Nucleocapsid Protein (MVNP) Gene in Osteoclasts Induces Coupling Factors that Stimulate Bone Formation.

Jumpei Teramachi^{*1}, Norivoshi Kurihara¹, Jolene Windle², G. David Roodman¹. ¹Indiana University, USA, ²Virginia Commonwealth University, USA

We reported that 70% of Paget's disease (PD) patients express MVNP and that transgenic mice with expression of MVNP targeted to cells in the osteoclast (OCL) lineage express high levels of IL-6, form pagetic-like bone lesions and display both increased bone resorption and rapid new bone formation. In contrast, mice with knock-in of the p62^{P394L} mutation linked to PD have increased bone resorption but do not have increased bone formation *in vivo*. Loss of IL-6 in TRAP-MVNP mice prevents the development of pagetic OCLs and reduces bone resorption and formation in these animals. These results suggest that MVNP induction of IL-6 plays an important role in linking bone formation to bone resorption in PD. EphrinB2 and EphB4 were identified as key coupling factors for OCL and osteoblasts (OB). Since EphrinB2 is produced by OCL and dramatically enhances OB function and bone formation through specific interactions with EphB4 on OB, we determined if EphrinB2/EphB4 play a role in the effect of MVNP on bone formation. Protein lysates from wild type (WT), MVNP, MVNP/IL-6^{-/-} and p62^{P394L} knock-in (p62KI) mouse bones were tested for the expression of EphrinB2/EphB4. The levels of EphrinB2/EphB4 do not differ between WT and MVNP mice at 2 months of age. However, expression of EphrinB2 and EphB4 in MVNP mice was much higher than in WT, MVNP/IL-6^{-/-} and p62KI mice at 6 months of age. To examine if EphrinB2/EphB4 play a role in the effects of MVNP on bone formation *in vitro*, we cultured whole bone marrow cells from WT and MVNP mice and analyzed the effects of stimulating forward signaling by EphB4 on OBL differentiation with EphrinB2-Fc, and stimulating reverse signaling by EphrinB2 on OCL with EphB4-Fc. Addition of EphrinB2-Fc to osteoblastogenic cultures from MVNP mice significantly enhanced their differentiation as judged by increased ALP staining and Runx2 expression compared to WT and MVNP/IL-6^{-/-} cultures. Further, addition of EphB4-Fc to osteoclastogenic cultures suppressed OCL differentiation and bone resorption in WT, MVNP and MVNP/IL-6^{-/-} cultures. To determine if IL-6 was solely responsible for the

increased bone formation in MVNP mice, transgenic mice overexpressing IL-6 in OCL were examined but did not show increased coupling. These results suggest that MVNP induces EphrinB2/EphB4 to enhance bone formation in PD and that the increased levels of IL-6 induced by MVNP are necessary but not sufficient to mediate the effects of MVNP on bone formation *in vivo*.

Disclosures: *Junpei Teramachi, None.*
This study received funding from: NIAMS

LB-MO01

Alendronate Protects against Articular Cartilage Erosion by Inhibiting Subchondral Bone Loss in Ovariectomized Rats. Songsong Zhu^{*1}, Kan Chen¹, Yu Lan², Nan Zhang¹, Rulang Jiang², Jing Hu¹. ¹State Key Laboratory of Oral Diseases & Center of Orthognathic & Temporomandibular Joint Surgery, West China College of Stomatology, Sichuan University, China, ²Cincinnati Children's Hospital Medical Center, USA

Osteoporosis (OP) and osteoarthritis (OA) are major health problems in the increasing elderly population, particularly in postmenopausal women, but their relationship remains unclear. The present study was to investigate whether alendronate (ALN), a potent inhibitor of bone resorption, could protect articular cartilage from degeneration in a combined animal model of OP and OA induced by ovariectomy (OVX). Seventy-eight OVX rats were divided into five groups: OVX with either vehicle treatment, early ALN treatment at OVX, or late ALN treatment at 8 weeks after OVX and sham-operated with either vehicle or ALN treatment. Cartilage and subchondral bone changes were evaluated by histology and micro-CT. Osteoprotegerin (OPG) and receptor activator of nuclear factor- κ B ligand (RANKL) in the cartilage and subchondral bone were examined by RT-PCR and immunohistochemistry analysis. Matrix metalloproteinase 9 (MMP-9) and MMP-13 was also determined by immunohistochemistry. Early ALN treatment completely prevented both subchondral bone loss and cartilage surface erosion caused by OVX, as determined by histology, micro-CT and urine collagen degradation markers. Late ALN treatment inhibited subchondral bone loss and significantly reduced cartilage erosion, although they did not recover to normal levels. This protective effect of ALN was due to increased ratio of OPG/RANKL, possibly via inhibition of up-regulated MMP9 and MMP-13 expression. The subchondral bone plays a critical role during the interplay between menopause-related OP and OA. Treatment for OP with inhibitors of bone resorption reduces articular cartilage degeneration in postmenopausal women.

Disclosures: *Songsong Zhu, None.*

LB-MO02

Bone Health Determinants in Spinal Muscular Atrophy. Nataschia Di Iorgi^{*1}, Giorgia Brigati², Irene Olivieri¹, Marta Ferretti², Claudio Bruno², Mohamad Maghnie¹. ¹Department of Pediatrics, IRCCS Giannina Gaslini, University of Genoa, Italy, ²Unit of Muscular & Neurodegenerative Disease, IRCCS Giannina Gaslini, Genoa, Italy

Purpose. Severe osteopenia and fractures are reported in spinal muscular atrophy (SMA). Aim of our study was to evaluate determinants of bone status in SMA patients.

Methods. DXA measurements of total body less head bone mineral density (TB-BMD, g/cm² and Z-score), bone mineral content (TB-BMC, g), fat mass (FM%, kg) and fat free mass (FFM kg) were obtained in 17 SMA subjects (n=10 SMAII, 5 females, 5 males; n=7 SMAIII, 5 females, 2 males) at time T0 (12.0 \pm 6.4 yrs of age), T12 and T24 months. All patients underwent height (HT SDS), body mass index (BMI SDS), FMI (FM, kg/m²) measurements. Only 5 SMAIII patients were ambulant; 5 (n=3 males with SMAII, and 1 female and 1 male with SMAIII) reported fragility fractures.

Results. SMAII and SMAIII subjects did not differ at T0 for age, HT SDS, BMI, FM, FFM and FMI. SMAII were shorter and more muscularly atrophic (P= 0.07) than SMAIII subjects at all time points. In the former group BMI SDS decreased over time (P=0.03 at T12), with a significant loss of FFM (1,8 Kg, P=0,02) and no significant change of FM component (% Kg or FMI) between the first and the last evaluation.

TB-BMC, BMD and BMD-Z-score values were reduced in SMAII compared to SMAIII patients at all time points and significantly at T24 (P's=0,03). Both groups, however, showed a significant progressive reduction of BMD over 2 years (0,038 g/cm², P=0.03 and 0,100 g/cm², P=0.01, respectively), more pronounced in SMAII at T12 and in SMAIII at T24, with an absolute TB-BMC loss of 75.4 and 96,3 g during the observation period.

Age was inversely related to TB-BMD Z-score in SMAII; TB-BMD Z-score fell below normal values for age and sex in 70% of SMAII subjects by the age of 15 yrs; only 1 SMAIII showed low bone mass at the age of 22,5yrs. DXA parameters did not discriminate between fractured and not fractured SMA patients. In contrast BMI, FM and FMI were significantly higher and FFM significantly reduced in SMAII subjects with fractures compared to SMAII without bone events (P's<0,05).

Conclusions. Bone mass accrual is altered in both SMAII and SMAIII patients, although bone status is more compromised in SMAII. Body composition appears to be a major determinant of skeletal health in SMAII patients.

Disclosures: *Nataschia Di Iorgi, None.*

LB-MO03

Large-scale Population Imaging with Radiographic Assessment to Investigate the Genetic Epidemiology of Scheuermann's Disease: the Rotterdam Study. Ater Makurthou¹, Salih El Saddy^{*2}, Ling Oei³, Edwin Oei¹, Martha Castano-Betancourt³, Karol Estrada³, Albert Hofman⁴, Joyce Van Meurs³, Andre Uitterlinden⁵, Fernando Rivadeneira³. ¹Erasmus MC, The Netherlands, ²Erasmus University Medical Center, , ³Erasmus University Medical Center, The Netherlands, ⁴, Netherlands, ⁵Rm Ee 575, Genetic Laboratory, The Netherlands

PURPOSE

Scheuermann's disease is a form of osteochondrosis of the spine. It is characterized by increased posterior rounding of the thoracic spine in association with structural deformity of the vertebral elements. The exact prevalence of Scheuermann's disease is unclear; previous estimates vary between 0.4% and 10%. Although the etiology remains largely unknown, there is evidence that genetic factors play a role. A Danish twin study has found a heritability estimate of 74%. The aim of our study was to determine the prevalence of Scheuermann's disease and its radiographic criteria in the Dutch population and find susceptibility genes for Scheuermann's disease.

METHOD AND MATERIALS

Radiographs of the population-based Rotterdam Study Young cohort (RS-III; men and women aged 45 years and over) were scored for Scheuermann's disease. Cases were defined as those with a measured thoracic kyphosis angle of 45 $\text{\textcircled{3}}$ or more and endplate irregularities and wedging at a minimum of three vertebral levels. A genome-wide association study (GWAS) was conducted, testing both genotyped and imputed single nucleotide polymorphisms (SNPs) to identify genetic factors for Scheuermann's disease.

RESULTS

Out of 2753 lateral radiographs we distinguished 818 (29.7%) abnormal cases, of which 677 individuals (24.6%) had endplate irregularities and 140 (5.1%) had vertebral wedging. From this total, 127 radiographs fulfilled both criteria. These abnormalities were significantly more prevalent among men. In addition, 111 of these 127 combined cases had a kyphosis angle greater than 45 degrees. This resulted in a prevalence estimate of 4.0% (95% CI:3.3-4.7%) of Scheuermann's disease. We performed a GWAS and found a SNP on chromosome 4 associated at genome-wide significant level with Scheuermann's disease. The SNP maps to the Tolloid-like-1 gene (TLL1), which is involved in collagen and chordin synthesis.

CONCLUSION

Our results revealed a prevalence of 4.0% in the Dutch population. We found a SNP associated at genome-wide significant level with Scheuermann's disease mapping to TLL1. A replication study is necessary to confirm this finding.

CLINICAL RELEVANCE/APPLICATION

Scheuermann's disease is a relatively common, however, lesser known condition. Insights into its prevalence and pathophysiology have potential diagnostic (familial screening) and therapeutic benefits.

Disclosures: *Salih El Saddy, None.*

LB-MO04

Mir-34a Regulates Cytodifferentiation and Targets Multi-signaling Pathways in Human Dental Papilla Cells. Liwei Zheng^{*1}, Mian Wan², Bo Gao², Yin Tang², Feifei Sun², Yi Fan², Xin Zhou², Ling Ye², Xuedong Zhou¹. ¹West China School of Stomatology, Sichuan University, Peoples republic of china, ²State Key Laboratory of Oral Diseases, China

As well documented, odontogenesis relies on the reciprocal signaling interactions between dental epithelium and neural crest-derived mesenchyme which is sophisticatedly regulated by several signaling pathways. Subtle changes in the activity of these major signaling pathways can have dramatic effects on tooth growth. Machinery regulating such subtle pattern has been studied, one of which is the fine tuning function of microRNAs. However, the underlying mechanism remains elusive. Objective: This present study investigated the significant microRNAs during cytodifferentiation in human tooth germ, and studied microRNA-34a as a regulator of the dental papilla cells differentiation. Methods: Using microarrays, miRNA expression profiles have been established at selected times during development (early bell stage or late bell stage) of the human fetal tooth germ. Microarray data was validated using real-time PCR. MicroRNA-34a was selected and which mimics and inhibitors were transfected into human fetal dental papilla cells respectively. mRNA levels of predicted target genes were detected by quantitative real-time PCR. Coded protein levels were examined by western blotting and immunofluorescence. Odontogenic associated ALP and DSPP expression were also tested by qPCR, western

blotting and immunofluorescence. Results: Differentially expressed miRNAs during human tooth development were identified by microarray analysis. Among which mir-34a expression was significantly upregulated in late bell stage of human tooth germ. Odontogenic associated predicted targets of mir-34a: Lef1, Fgf2, Notch1, Bmp7 were down-regulated 72 hours after mimic oligonucleotide transfection, and up-regulated after inhibitor oligonucleotide transfection. However, Gli2 was not affected. Expression of ALP and DSPP were affected after oligonucleotide transfection as well. DSPP upregulated and ALP downregulated after mimic oligonucleotide transfection. Conclusion: Our analyses utilizing microarray technology, qPCR, western blotting, immunofluorescence, and target prediction tools have uncovered miRNA-34a that may play important roles in dental papilla cells differentiation during human tooth development by targeting multi-signaling pathway.

Disclosures: Liwei Zheng, None.

LB-MO05

Potential Roles for MAPK Signaling in Osteogenesis by Human Adipose-derived Stem Cells. Eric Tsang¹, Benjamin Wu¹, Patricia Zuk^{*2}. ¹UCLA, USA, ²University of California, Los Angeles, USA

The use of human adipose-derived stem cells (ASCs) as a potential source of osteoprogenitor cells for bone regenerative procedures is increasing in popularity. Most approaches choose to combine the ASC with upstream pro-osteogenic factors. However, such growth factors exert their effects through downstream signaling pathways, such as the MAPK cascade. Numerous studies on stem cells, including the ASC, suggest that the MAPK cascade plays a critical role in osteogenesis. To study this further, the roles of MAPK signaling was assessed upon the osteogenic differentiation of multiple human ASC populations. Microarray analysis of human ASCs identified several MAPK pathway genes whose expression changed with osteogenesis, suggesting a role for this pathway. Consistent with this, matrix mineralization and alkaline phosphatase activity could be inhibited through the administration of specific inhibitors to ERK, JNK or p38MAPK, with their effect on osteogenesis dependent upon the timing of their administration. Decreased mineralization was also observed upon transduction of osteo-induced ASCs with shRNA lentiviruses designed to knockdown ERK1/2 or JNK1/2. Using time-course western analysis, activation of either ERK1/2 or JNK1/2 was found to be directly associated with matrix mineralization, with activation of both kinases appearing to play a synergistic role in this event. A role for ERK and JNK in ASC osteogenesis was not limited to dexamethasone-driven differentiation as increased kinase activity and mineralization was also observed using vitamin D3 (VD3). However, ERK and JNK activity appeared to be essential for either dexamethasone or VD3-driven osteogenesis, as no link between kinase activity and matrix mineralization could be discerned in ASC populations induced in the absence of dexamethasone or in populations induced with hydrocortisone. In summary, it is apparent that MAPK signaling in ASC osteogenesis is a complex series of events that affects differentiation in kinase- and stage-specific manners and responds differentially to the presence of glucocorticoids, such as dexamethasone.

Disclosures: Patricia Zuk, None.

LB-MO06

Comparative Study of *Pth* null and WT Mice Reveal that FGF23 is Unresponsive to Substantial Changes in PTH, Calcitriol, Phosphorus, or Calcium that Occur Naturally During the Reproductive Cycle. Beth J. Kirby^{*1}, Yue Ma¹, Heather M. Martin¹, Andrew Karaplis², Christopher Kovacs¹. ¹Memorial University of Newfoundland, Canada, ²McGill University, Canada

FGF23 has been proposed to be a key regulator of serum phosphorus. It may be stimulated by hyperphosphatemia, calcitriol, and PTH, and inhibited by hypophosphatemia and hypocalcemia. But available evidence comes largely from study of non-physiological extremes: dietary phosphate loading and restriction, and genetic disorders of excess or absent FGF23 action.

Pregnancy and lactation cause marked changes in PTH, calcitriol, phosphorus, and calcium. For example, during pregnancy and lactation in mice, PTH decreases while calcitriol increases markedly. Therefore, unlike prior studies of FGF23 *in vivo* physiology, we kept diet and FGF23 genetics constant while using reproduction to invoke altered mineral metabolism. We hypothesized that studying WT and *Pth* null sister mice serially during reproductive cycles would reveal whether FGF23 responds to physiological changes in calcium, phosphorus, calcitriol, or PTH. The mice were maintained on a standard diet of 1% calcium and 0.75% phosphorus. FGF23 was measured using a 2-site intact assay (Kainos) validated and used extensively in mice.

Prior to pregnancy *Pth* null mice were hypocalcemic (1.86 vs. 2.20 mM in WT) and hyperphosphatemic (3.99 vs. 3.14 mM in WT). Serum calcitriol was 81.4 pM while serum FGF23 was 93.3 ± 21.3 pg/mL in *Pth* null; both values were no different than WT.

During pregnancy calcitriol increased 6-fold in *Pth* null to 449 pM, no different than the WT peak value. The hypocalcemia and hyperphosphatemia of *Pth* null mice were unchanged during pregnancy. FGF23 did not change significantly in either genotype.

During lactation, serum calcium (2.20 mM) and phosphorus (3.05 mM) normalized in *Pth* null and were no different than WT. FGF23 did not change significantly in either genotype.

At day 7 post-weaning, serum calcium remained normal (2.26 mM) while hyperphosphatemia recurred (3.50 mM) in *Pth* null. Calcitriol declined to 92.2 pM, no different than WT or pre-pregnancy. FGF23 continued to be unchanged in *Pth* null and WT vs. pre-pregnancy.

Urine P/Cr did not differ between genotypes at any time point.

In summary, intact FGF23 levels were not significantly altered by absence of PTH, 6-fold higher calcitriol during pregnancy, correction of hypocalcemia and hyperphosphatemia during lactation, or correction of hypocalcemia alone during recovery. In conclusion, FGF23 is unresponsive to loss of PTH or marked physiological changes in calcitriol, calcium, and phosphorus during the reproductive cycle.

Disclosures: Beth J. Kirby, None.

LB-MO07

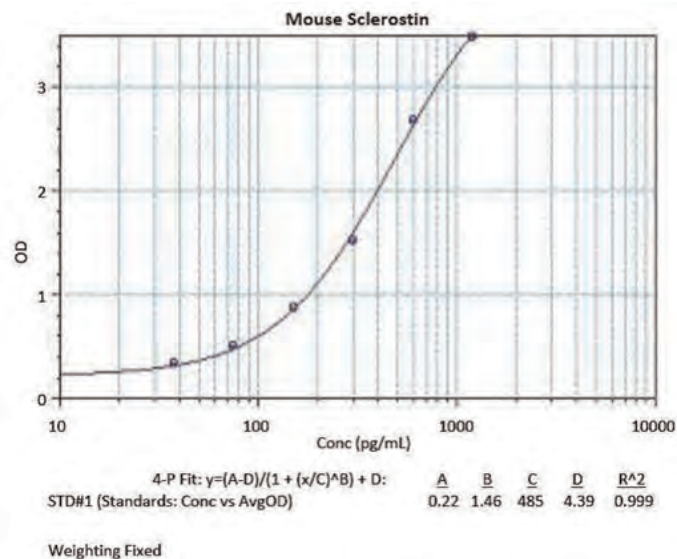
Measurement of Serum Sclerostin by an Enzyme-Linked Sandwich Assay in *Sost* Wild type and Knock-out Mice. Xiaobo Dai¹, Zachary Ryan^{*2}, Kelly Doering¹, Bethany Salerni¹, Chris Wisherd¹, Rajiv Kumar³. ¹ALPCO Diagnostics, USA, ²Mayo Clinic, USA, ³Mayo Clinic College of Medicine, USA

Sclerostin, a protein product of the SOST gene, inhibits osteoblast activity via antagonism of the wnt and BMP signaling pathways and plays a key role in the regulation of bone formation. Altered sclerostin expression and/or circulating levels could play a pathogenic role in demineralizing disorders such as immobilization-induced bone loss, osteoporosis, and rheumatoid arthritis.

The availability of an assay capable of measuring serum or plasma sclerostin concentrations in small volumes would be helpful in assessing the role of sclerostin in mouse models of bone disorders characterized by altered turnover. To this end, we developed a novel mouse sclerostin immunoassay and tested its specificity in a sclerostin knock out mouse. The assay utilizes a polyclonal antibody sandwich assay to detect mouse sclerostin and requires 25 µl of sample (serum or plasma) for duplicate measurements. Figure 1 shows a standard curve for sclerostin measurements. The lower level of detection of the assay is 17.4 pg/mL with a calibrated range of 37.5-1200 pg/mL. Spike/recovery studies using recombinant mouse sclerostin yielded recoveries ranging from 87 – 118%, dilution linearity ranged from 105 – 118% and intra- and inter-assay precision were <15%. For wild type mice, samples give OD determinations in the range of 0.32 to 0.57.

To ascertain the specificity of the assay, we generated a sclerostin knockout mouse and compared circulating sclerostin concentrations in wild-type (*sost*^{+/+}) and knockout (*sost*^{-/-}) mice. In sclerostin wild-type mice (n=7), sclerostin concentrations ranged from 432 – 810 pg/mL, while circulating sclerostin concentrations in sclerostin knockout mice (n = 8) were below the lower limit of quantitation of the assay (≤37 pg/mL). Of note, although the concentrations of sclerostin in *sost*^{-/-} mice were below the level of detection of the lowest standard, sera from knockout mice still showed OD determinations that were above background. This finding suggests that a blocking agent could be employed in order to normalize background in this assay. Alternatively, absorbance values obtained in sera from *sost*^{-/-} mice could be subtracted from those obtained in experimental samples.

These data demonstrate that the ELISA employed in this study is specific for mouse sclerostin and should therefore serve as a useful tool for exploring differences among mouse models of bone disease.



Mouse Sclerostin Standard Curve

Disclosures: Zachary Ryan, ALPCO Diagnostics, 9
This study received funding from: ALPCO Diagnostics

LB-MO08

Tissue-Specific Developmental Regulation of Allelic *Gαs* Silencing As a Plausible Explanation For Lack of Early Postnatal PTH-Resistance in Pseudohypoparathyroidism-Ia. Serap Turan¹, Eduardo Fernandez-Rebollo², Teuta Zoto³, Monica Reyes⁴, George Bounoutas⁴, Min Chen⁵, Lee Weinstein⁶, Reinhold Erben⁷, Vladimir Marshansky³, Murat Bastepe⁸. ¹Massachusetts General Hospital, Harvard Medical School, USA, ²Hospital Clinic de Barcelona, Spain, ³Massachusetts General Hospital & Harvard Medical School, USA, ⁴Massachusetts General Hospital, USA, ⁵NIH/NIDDK, USA, ⁶National Institute of Diabetes & Digestive & Kidney Diseases, USA, ⁷University of Veterinary Medicine, Austria, ⁸Massachusetts General Hospital, Harvard Medical School, USA

Pseudohypoparathyroidism (PHP) is characterized by hypocalcemia and hyperphosphatemia due to renal proximal tubular resistance to parathyroid hormone (PTH). PHP-Ia results from maternal mutations of *GNAS* that lead to loss of *Gαs* activity. *Gαs* expression is paternally silenced in the renal proximal tubule, and this genomic event is key to the development of PTH-resistance, as a patient displays impaired hormone action only if the mutation is located on the maternal allele. Mechanisms underlying this important process are unknown. PHP-Ia patients frequently lack hypocalcemia until after infancy, but it has remained uncertain whether PTH-resistance occurs in a delayed fashion. Analyzing reported cases of PHP-Ia with documented *GNAS* mutations and mice heterozygous for disruption of *Gnas*, we herein determined that PTH-resistance caused by the maternal loss of *Gαs* manifests itself gradually after early postnatal life, with elevation of serum PTH preceding hypocalcemia. To investigate whether this delay in PTH-resistance reflects gradual development of paternal *Gαs* silencing, we then analyzed *Gαs* mRNA expression in renal proximal tubules isolated by laser capture microdissection from mice with either maternal or paternal disruption of *Gnas*, thus measuring the paternal and maternal allele-specific expression, respectively. *Gαs* expression from the paternal allele in this tissue was significantly lower than that from the maternal allele at weaning ($42 \pm 5\%$ vs $61 \pm 5\%$ of total; $p < 0.05$) and in adulthood ($34 \pm 1\%$ vs $66 \pm 9\%$ of total; $p < 0.05$), whereas the contributions of the maternal and paternal *Gnas* alleles to *Gαs* expression were equal at postnatal day 3 (~50% of total each), indicating that the paternal *Gαs* allele is fully active in renal proximal tubules during early postnatal development. In contrast, paternal *Gαs* expression was already markedly repressed in brown adipose tissue at birth ($14 \pm 1\%$ of total). Our results show that the mechanisms underlying the paternal silencing of *Gαs* are developmentally regulated in a tissue-specific manner. Moreover, the absence of allelic *Gαs* silencing in early postnatal proximal tubules likely explains the latency of PTH-resistance in patients with PHP-Ia.

Disclosures: Murat Bastepe, None.

LB-MO09

Influenced Calvarial Bone Healing in the Absence of TLR2 and TLR4. Gregory Cooper, Dan Wang^{*}, James Gilbert, Melissa Shaw, Adam Kubala, Lauren Zammerilla, Sameer Shakir, Joseph Losee, Timothy Billiar. University of Pittsburgh, USA

OBJECTIVE: Toll-like receptor 2 (TLR2) and Toll-like receptor 4 (TLR4) are members of a highly conserved receptor family and are critical activators of the innate immune response after tissue injury. TLR2 and TLR4 signaling have been shown to regulate both the immune response and bone metabolism. Here we tested the hypothesis that bone healing would be enhanced in mice lacking the TLR2 and TLR4 genes.

METHODS: Circular bone defects were made in the parietal bones using a 1.8mm outer diameter trephine in WT (n=42), TLR2^{-/-} mice (n=28), and TLR4^{-/-} mice (n=36). Calvarial bone and surrounding soft tissues (e.g. skin and brain) were harvested and bone healing was assessed at different time points using radiographic, histologic analyses, and qRT-PCR was performed to assess the expression of 8 genes related to bone repair.

RESULTS: 1) Radiographic and histomorphometric analyses demonstrated accelerated calvarial healing in TLR4^{-/-} mice compared to WT mice on day 7 and day 14 ($p < 0.001$), while a similar amount of bone formation was observed by day 28 between WT and TLR4^{-/-} mice; significantly less bone healing was seen in TLR2^{-/-} mice compared to WT and TLR4^{-/-} mice by day 28. ($p = 0.070$). 2) differential expression of IL-1b, IL-6, BMP2 and TGF-β1 was observed between three groups of mice at early time points (3 hour, day 1 and day 4).

CONCLUSIONS: These data suggest that TLR2 signaling is needed for calvarial healing in our murine model and TLR4 signaling might delay the healing process. Further work is required to elucidate the role of inflammation in signaling through these pathways on calvarial repair.

Disclosures: Dan Wang, None.

LB-MO10

Dexamethasone-Induced Lipolysis Enhances the Lipotoxic Effect of Adipocytes on Osteoblasts. Dongqing Wang^{*1}, Azeb Haile², Lynne Jones³. ¹Johns Hopkins University, USA, ²Johns Hopkins University, USA, ³Johns Hopkins University School of Medicine, USA

The increased bone marrow lipid deposition in steroid-associated bone loss diseases indicates that abnormalities in fat metabolism are associated with disease development. Recent studies have suggested that bone marrow adipocytes are secretory cells and that they may have an inhibitory effect on the differentiation and function of osteoblasts. We hypothesized that bone-marrow-derived adipocytes exposed to corticosteroids secrete substances that exacerbate their deleterious effects on osteoblast metabolism and function. We focused on the direct effects of human bone marrow adipocytes on osteoblasts in the presence of dexamethasone. Adipocytes and osteoblasts derived from a human mesenchymal stem cell line (240 L) were co-cultured in the absence of direct cell contact with or without dexamethasone treatment. After 6 days of co-culture, osteoblasts demonstrated significantly lower levels of function based on lower mineralization, alkaline phosphatase activity and expression of osteogenic (Runx2, osteocalcin) mRNA markers. Dexamethasone treatment resulted in significantly lower levels of osteoblastic function as compared to co-cultured cells without dexamethasone. Furthermore, conditioned media from dexamethasone-treated adipocytes induced a similar toxic effect and increased apoptosis involving activation of caspases 3/7 as compared to conditioned media without dexamethasone treatment. The conditioned media exhibited a substantial increase in the levels of leptin and two saturated fatty acids (FAs; stearate and palmitate) with dexamethasone treatment. Although leptin supplementation failed to induce the inhibitory effect on osteoblasts, similar toxic results were produced with stearate and palmitate treatment, and an increase in intracellular reactive oxygen species was observed. Stearate- and palmitate-induced apoptosis was blocked by a reactive oxygen species scavenger pyrrolidine dithiocarbamate. These data show that saturated FAs secreted from adipocytes induce lipotoxic effects via mechanisms that may involve reactive oxygen species accumulation in osteoblasts. Our results support the hypothesis that inhibition of saturated FA secretion would protect osteoblasts against adipocytes in corticosteroid-associated bone loss diseases.

Fig.1

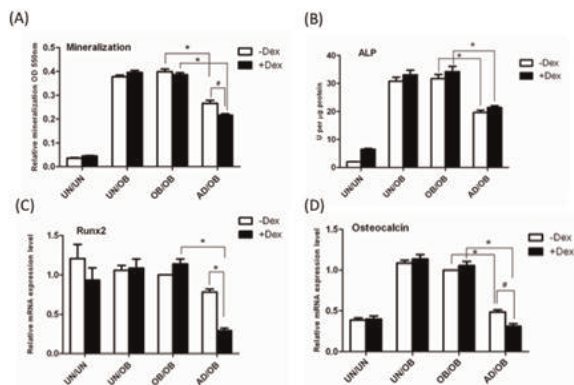


Figure 1

Fig.2

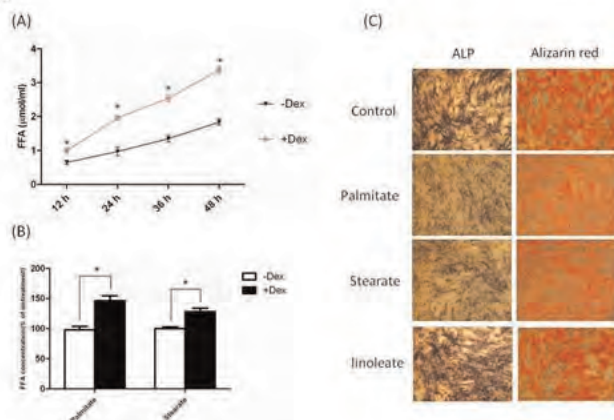


Figure 2

Fig.3

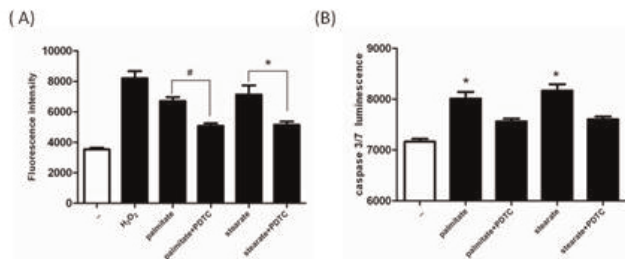


Figure 3

Disclosures: Dongqing Wang, None.

LB-MO11

PKC δ Is Required for Jagged-1 Induction of Osteoblast Differentiation.

Fengchang Zhu*¹, Mariya Sweetwyne¹, Hailu Shitaye², Kurt Hankenson¹.
¹University of Pennsylvania, USA, ²University of Pennsylvania, USA

Jagged-1 (Jag1) is a ligand in the Notch signaling pathway that is highly expressed by mesenchymal lineage cells. *JAG1* is variably mutated in Alagille Syndrome (ALGS), a disease condition which results in decreased bone mass and delayed bone regeneration. *JAG1* is also implicated as a determinant of bone mass through genome-wide association studies (GWAS). However, the role of Jag1 in human osteoblastogenesis is not fully understood. Plating primary human mesenchymal progenitor cells (hMSC) on Jag1 increases expression of osteoblastic genes in a dose-dependent manner. ALP and BSP were increased 1.5- and 1.2-fold respectively with 2 μ g/ml of Jag1 and 4.5- and 5.0-fold with 10 μ g/ml of Jag1. Jag1 also drives terminal osteoblastogenesis, as determined by increased alkaline phosphatase activity and mineralization. These results are in contrast to results observed with murine MSC where Jag-1 inhibits mineralization and osteoblast gene expression. ALP decreased 20% with 2 μ g/ml Jag1 and 50% with 10 μ g/ml Jag1 treatment. BSP decreased 50% with 2 μ g/ml Jag1 and 65% with 10 μ g/ml Jag1.

In hMSC, blocking Notch signaling with a gamma-secretase inhibitor prevents Jag1 induced mineralization; and overexpression of NICD is sufficient to induce osteoblast differentiation. hMSC overexpressing NICD increased ALP by over 34-fold and BSP by ~3.5-fold relative to control cells. Next a dominant negative construct of the mastermind-like protein (dnMAML), which blocks canonical Notch signaling, was used to determine whether hMSC Jag1 osteoblast induction requires canonical Notch signaling. dnMAML blocked Jag1-induced hMSC osteoblast gene expression and differentiation. Next we probed pathways that could interact with Jag1 to induce osteoblastogenesis. Treatment with 2 μ M of the PKC δ inhibitor Rottlerin blocks Jag1 induced hMSC osteoblast differentiation and decreases ALP expression up to 95%. Relatedly, Jag1 treatment results in PKC δ nuclear translocation and increases PKC δ kinase activity by 1.9-fold in 10 minutes and 2.6-fold in 4 hours. Moreover, Jag1 stimulates the physical interaction of PKC δ and NICD. Collectively, these results show that Jag1 is a potent inducer of hMSC osteoblast differentiation through the canonical Notch signaling pathway and that an intersection with the PKC δ pathway is required for this effect. Our study may define new therapeutic targets for the treatment of ALGS, and also demonstrates the deficiency in using a mouse model to study Jag1 effects on MSC.

Disclosures: Fengchang Zhu, None.

LB-MO12

Role of Zinc During Osteogenesis in Human Mesenchymal Stem Cells.

Kwang Hwan Park*, Dong Suk Yoon, Jin Woo Lee, Jae Myun Lee. Yonsei University College of Medicine, South Korea

Introduction : Many *in vivo* studies report that zinc deficiency is related with retardation of bone growth. Clinically, low serum zinc level is associated with osteopenia or osteoporosis in men and women. So, zinc might be very important trace element for osteogenesis in human mesenchymal stem cells (hMSC). But, there are very few studies that investigate role of zinc during osteogenesis in hMSC. In this study, we evaluated whether zinc is essential for osteogenesis and whether zinc enhance osteogenesis in hMSC.

Result : According to the proliferation assay, 100 μ M was maximal concentration of zinc for non-toxic to hMSC and human fetal osteoblast cell line (hFOB 1.19) and we used this concentration for osteogenesis with high dose zinc. During osteogenesis of hMSC, the activity and stain intensity of alkaline phosphatase (ALP) increased zinc dose-dependently. When hMSCs were induced osteogenic differentiation with zinc depleted osteogenic media (ZnD), the activity and stain intensity of ALP didn't increase significantly. At 7 days after initiating osteogenesis of hFOB, stain intensity of ALP and alizarin red S (ARS) significantly increased only in high dose zinc (ZnH) treated groups. Activity and stain intensity of ALP increased in ZnH treated group. Until 10 days, Activity and stain intensity of ARS increased earlier in ZnH treated group. But at 14 days, stain intensity of ARS in control group was higher than in ZnH

treated well. Normally, mRNA level of Runx2 was decreased in late stage of osteogenesis. But, in ZnH treated group, high mRNA level of Runx2 was maintained and mRNA level of Metallothionein 1 is markedly increased.

Conclusion : All of these results indicate that zinc has a role for the enhancement of osteogenesis in the human mesenchymal stem cells. Furthermore, depletion of zinc in the osteogenic media inhibits osteogenesis. In the future, we will investigate the molecular mechanisms for the enhancement of osteogenesis by zinc.

Disclosures: Kwang Hwan Park, None.

LB-MO13

Gene Array Analyses Reveal Distinct Expression Patterns in the Osteoclast and Chondroclast Populations within a Fracture Callus.

Kari Clifton¹, Do Soung², Jason Gibson³, Joseph Lorenzo², Marc Hansen², Hicham Drissi*².
¹University of Connecticut, USA, ²University of Connecticut Health Center, USA, ³UConn Health Center, USA

Chondroclasts form on calcified cartilage during endochondral ossification and fracture callus repair. Their principal function is to remove calcified cartilage. Chondroclasts appear similar to osteoclasts in that they are multinucleated, contain similar ultrastructural features and express tartrate resistant acid phosphatase (TRAP). However, there is ample evidence for phenotypic differences between osteoclasts, which resorb bone, and chondroclasts, which resorb mineralized cartilage matrices. We are currently limited in our understanding because they have not been studied to any great degree at a molecular level or *in vitro*. While the genes that are necessary for osteoclastogenesis and osteoclast function have been well characterized, the majority of our knowledge about chondroclasts comes from ultrastructural analysis. No information has been generated about the genomic signature of chondroclasts as compared to osteoclasts. To explore potential differences, we performed laser capture microdissection and isolated homogeneous populations of TRAP positive cells that interact with bone and TRAP positive cells that interact with mineralized cartilage on the same plane of murine femoral fracture callus sections (12 days post-fracture). RNAs were isolated from these harvested populations from several mice and gene expression analyses were performed using the Agilent Mouse GE 4X44K V2 microarray platform. Eight hundred and fifty one differentially expressed genes with greater than 2 fold difference in expression between chondroclasts and osteoclasts were identified. Custom TaqMan PCR arrays from Applied Biosystems were used to validate the microarray results. Condition and Gene Tree clustering of the expression data demonstrated a distinct pattern of differences in expression between chondroclasts and osteoclasts. Integrated gene ontology and pathways analyses revealed that the distinctions between these two cell types were in genes involved in migration, environmental sensing and interaction with the microenvironment as well as in transcriptional molecules that regulate these pathways. To our knowledge, this is the first demonstration of unique molecular signatures that differentiate osteoclasts from chondroclasts. Exploration of functional differences based on alteration of differentially regulated genes should yield targets that can be used to enhance skeletal development and repair.

Disclosures: Hicham Drissi, None.

LB-MO14

A Balance Between Osteoporosis and Osteopetrosis is Determined by the

Interaction of TRPC1 and I-mfa. E-Ching Ong*¹, Leonidas Tsiokas², Vasyly Nesin², Chang-Xi Bai², Jan Guz², Ivaylo Ivanov³, Joel Abramowitz⁴, Lutz Birnbaumer⁴, Mary Beth Humphrey⁵. ¹The University of Oklahoma Health Sciences Center, USA, ²OUHSC, USA, ³University of Utah, USA, ⁴NIEHS, USA, ⁵University of Oklahoma Health Sciences Center, USA

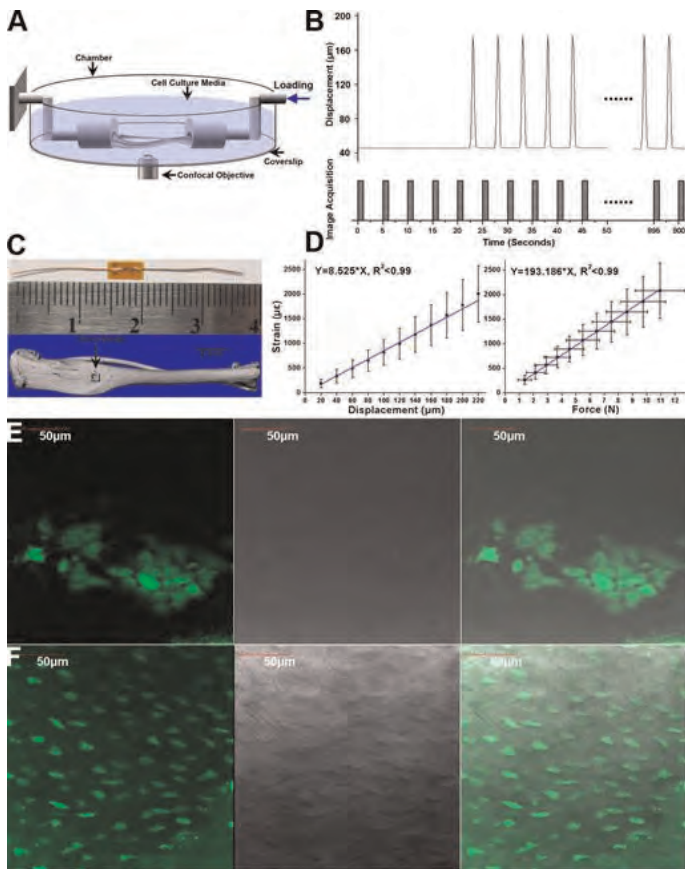
Ca²⁺ regulation is essential for bone homeostasis and skeletal development. Here we show that the Transient Receptor Potential canonical 1 (TRPC1) channel and the MyoD family inhibitor, I-mfa, function in the same pathway *in vivo* to regulate bone architecture through osteoclastogenesis. Specifically, deletion of *Trpc1* leads to decreased osteoclastogenesis and higher bone mass, whereas I-mfa null mice show the opposite effects, which are normalized in compound *Trpc1*^{-/-}; *I-mfa*^{-/-} mice. Mechanistically, TRPC1 enhances the activity of store-operated Ca²⁺ entry (SOCE) channels by forming a heteromultimeric complex with Ora1, a core component of a SOCE channel. I-mfa is recruited to this complex through TRPC1 and suppresses store-operated currents. The positive and negative modulation of SOCE channels by TRPC1 and I-mfa, respectively, increase the dynamic range of SOCE, implicating for the first time the I-mfa-mediated regulation of TRPC1 as a critical determinant of the balance between osteoporosis and osteopetrosis.

Disclosures: E-Ching Ong, None.

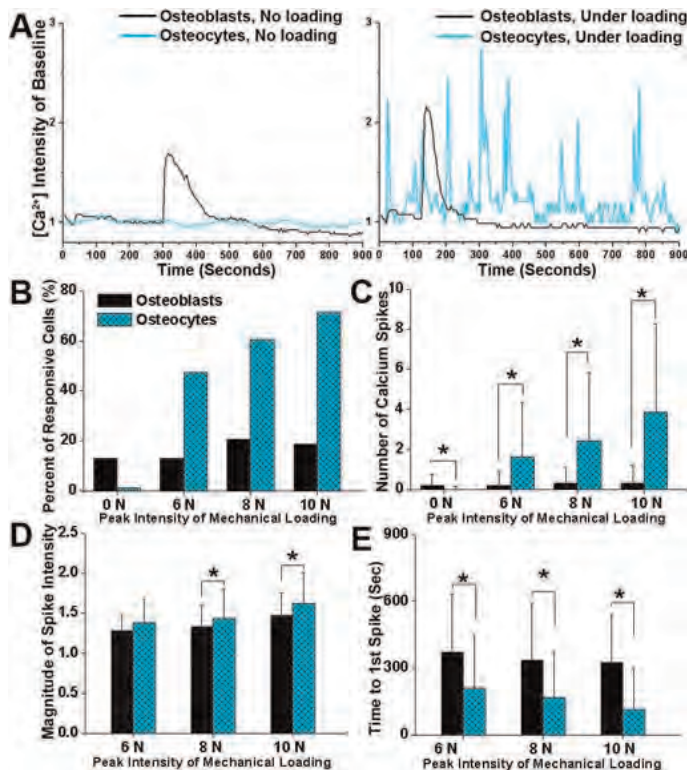
LB-MO15

Observing In Situ Intracellular Calcium Signaling of Osteocytes and Osteoblasts in Intact Mouse Tibiae under Cyclic Mechanical Loading. Da Jing*¹, Bin Zhou¹, Xin Lu¹, Liyun Wang², X Guo¹. ¹Columbia University, USA, ²University of Delaware, USA

Osteocytes are believed to act as the major mechanosensors in bone, and thus mediating osteoblastic and osteoclastic activities. Calcium signaling is one of the earliest mechanotransduction pathways, which is critical in osteocyte mechanobiology. However, this has never been studied with live osteocytes residing inside intact bone. In this study, *in situ* calcium responses of osteocytes or osteoblasts in intact mouse tibiae under cyclic mechanical loading were investigated. Tibiae from 3-month C57BL/6J female mice were dissected and dyed with Fluo-8 AM. Osteoblasts and osteocytes in the anterol-medial surface were imaged ~10 μm and 40 μm below the periosteal surface. 2-N preload with 6-N, 8-N or 10-N compressive peak load (0.5s ramp up, 0.5s ramp down and 4s dwell) were applied for 175 cycles. The peak tensile strain on the imaging region in the 3 loading groups was 773με, 1,159με and 1,546με measured with strain gauges. The loading system worked in the displacement control mode and confocal images were recorded after each loading cycle. This synchronization technique between mechanical loading and confocal imaging could effectively avoid the focus shift during mechanical loading. 4 tibiae (~500 cells) for osteocytes and 6 tibiae (~300 cells) for osteoblasts were used in each loading group. Our results showed that 13% osteoblasts spontaneously released one or two robust calcium spikes, but calcium curves of 98.7% osteocytes were flat. However, most osteocytes exhibited robust and repetitive calcium spikes under cyclic loading. The responsive cell percentage and calcium spike number in osteocytes were significantly higher than those in osteoblasts regardless of the loading magnitude ($P < 0.01$). As the loading intensity increased, the responsive cells and calcium spike number were dramatically increased in osteocytes, but not in osteoblasts. Osteocytes also released stronger spike intensities than osteoblasts under 8-N and 10-N peak loading groups ($P < 0.01$). Osteocytes also took shorter time to release the first spike than osteoblasts at all loading levels ($P < 0.01$). This study for the first time shows the unique *in situ* calcium oscillations in osteocytes under mechanical loading. Our findings highlight that osteocytes, possessing higher mechanical sensitivity than osteoblasts in detecting and processing mechanical loading signals, are qualified as a critical coordinator in bone modeling and remodeling.



Mechanical loading system, loading protocol, tension strain, and osteocytes and osteoblasts images



Comparison of autonomous or mechanical loading induced calcium response in osteocytes and osteoblast

Disclosures: Da Jing, None.

This study received funding from: NIH

LB-MO16

Utility of Testing for Monoclonal Bands in Serum of Patients referred to a Bone Health Clinic. Lorraine O’Keeffe¹, Niamh Murphy¹, Rosaleen Lannon*¹, Nessa Fallon¹, MC Casey¹, James Bernard Walsh². ¹St James’s Hospital, Ireland, ²Trinity College Dublin, The University of Dublin, Ireland

Introduction: In contrast to osteoporosis, multiple myeloma is a rare disease. However, vertebral fractures and pain are common to both and multiple myeloma would be expected to emerge more often in an osteoporosis clinic than another area of medicine. In addition monoclonal gammopathy of undetermined significance (MGUS) occurs in 5.3% of over 70’s. Risk of conversion to multiple myeloma has been quantified at 1% per year.

Methods: We conducted a retrospective observational study of patients attending our osteoporosis clinic who were newly referred for assessment of osteoporosis or fragility fractures. Our screen includes serum protein electrophoresis (SPEP) and urine for bence jones protein as well as bone density assessment and bone biochemistry.

Results: Results of 938 new patients were reviewed. Of these 64 (6.8%) patients were excluded as SPEP was not performed. A positive monoclonal band was seen in 33 (3.7%) patients with a further 12 (1.38%) patients having a minor abnormality. No positive monoclonal band was noted in patients <55 years (n = 165). Patients with a positive monoclonal band were significantly older (p < 0.01), had more renal impairment (p < 0.05) and tended to have a higher prevalence of osteoporosis. The prevalence of MGUS was most notable in patients between 75 and 85 years with a prevalence of 7.0% (13/186). Patients with hip fracture had a significant higher incidence of monoclonal bands (p = 0.03) compared to the rest of the population.

Conclusion: It is important that patients presenting with osteoporosis or fracture are tested for monoclonal bands in serum, as over 1 in 20 patients with newly diagnosed osteoporosis >50 years in our service had multiple myeloma or MGUS. Multiple myeloma is an important differential diagnosis in patients with suspected osteoporosis as it affects patients of the same age and can often be a cause of bone fragility. MGUS is a benign disorder but patients should be monitored for progression to malignancy.

Disclosures: Rosaleen Lannon, None.

LB-MO17

One Year Use of Oral Recombinant Salmon Calcitonin is Not Associated with Increased Risk of Cancer. David Krause^{*1}, Nigel A.S. Hernandez², Matthew Vitagliano², James Gilligan², Christine Buben². ¹Tailsa Therapeutics Inc., USA, ²Tarsa Therapeutics, USA

BACKGROUND: In July 2012 the European Medicines Agency recommended that calcitonin-containing medicines should be used only for short term treatment, due to a possible association with increased risk of (unspecified) cancer. It also recommended that intranasal calcitonin be withdrawn entirely. Although calcitonin has been in global use for at least 30 years, this association has not been previously reported, and historical carcinogenicity studies in rats and mice revealed an increased occurrence of pituitary adenomas (in rats) but no carcinogenicity signal. We recently completed two separate one-year trials of oral recombinant salmon calcitonin. **METHODS:** The ORACAL trial was a Phase 3 global (US, EU, Republic of South Africa) trial of oral rsCT compared to intranasal calcitonin and placebo (randomized 4:3:2) in postmenopausal women with frank osteoporosis. TAR01-201 was a Phase 2 US trial of oral rsCT compared to placebo (randomized 2:1) in postmenopausal women with low bone mass and increased risk of fracture, but without frank osteoporosis. In each trial the treatment duration was approximately 1 year and subjects randomized to oral rsCT received the same dose, 200 µg (1200 IU) per day, a dose of rsCT (200 µg) approximately 6 fold greater than present in nasal sCT formulations (33 µg). Neither trial specifically excluded individuals with cancer, but the presence of uncontrolled acute or chronic medical conditions was exclusionary. Subjects were seen at the clinical site 4 times after randomization in ORACAL and 5 times after randomization in 201. At each visit, as well as during regularly scheduled intervening phone calls, adverse events (AEs) were solicited and recorded. The safety databases from the two studies were integrated and AEs in the “Neoplasms benign, malignant and unspecified” system organ class were reviewed for AEs consistent with cancer. **RESULTS:** 678 women constitute the safety population. The mean age was approximately 67y, >95% of subjects were White. Adverse events consistent with cancer are displayed in the table. No deaths occurred.

TABLE
CONCLUSIONS: No carcinogenicity signal was noted in two trials of this preparation of oral recombinant salmon calcitonin.

| | Oral rsCT N=349 | Nasal ssCT N=182 | Placebo N=147 |
|---------------------------|--------------------|---------------------|------------------|
| Breast Cancer | 2 | 0 | 1 |
| Skin Cancer (unspecified) | 0 | 0 | 1 |
| Melanoma | 1 | 0 | 0 |
| Thyroid Cancer | 1 | 0 | 1 |
| Total (%) | 4 (1.1) | 0 (0.0) | 3 (2.0) |

Table
Disclosures: David Krause, Tarsa, 7; Tarsa, 3
This study received funding from: Tarsa Therapeutics

LB-MO18

Missing a Window of Opportunity: Surgical Management of Hip Fracture as a Sentinel Event to Identify and Treat Osteoporosis. Matthew Wolfson¹, Brian Kincaid², Sara Merwin³, Lewis Collins⁴, Ariel Goldman⁵, Stuart Weinerman^{*6}. ¹University of Central Florida, USA, ²North Shore-LIJ Health System, USA, ³North Shore-LIJ Health System, Hofstra North Shore LIJ School of Medicine, USA, ⁴University Orthopaedic Associates, USA, ⁵North Shore-LIJ Health System, Hofstra North Shore, LIJ School of Medicine, USA, ⁶Division of Endocrinology, USA

Purpose: Osteoporosis (OP) is a common condition characterized by decreased bone mass & increased fracture risk in postmenopausal women and elderly males. Many patients will not be evaluated/treated until recognized in conjunction with fragility fractures. Initiation of OP treatment following hip fractures (HF) occurs at rates of 5-30%. HF history is strongly predictive of subsequent fragility fractures. It is not standard practice among orthopaedic surgeons (OS) to manage OP after HF surgery; recent studies demonstrate that their participation improves treatment rates. Eisman proposed a Fracture Liaison Services (FLS) to prevent future fractures in OP patients by risk assessment & OS linkage with PCP for ongoing management. The objective of this study: determine OP diagnosis rates during hospital stay & frequency of OP treatment initiation in an OS practice. The investigators hypothesized: patients treated operatively for HF would not be routinely identified as osteoporotic at admission nor treated at discharge.

Methods: We performed chart reviews for patients with surgical HF treatment in a single surgeon's practice from 6/11 to 7/12. Inclusion criteria: age ≥ 55 years, femoral neck or intertrochanteric HF, hemiarthroplasty, intramedullary nail or cannulated screw fixation. Exclusions: high energy trauma, pathological fracture, nonoperative management. Measures/Outcomes: OP diagnosis/medication on admission, initiation of calcium & vitamin D during admission, OP documentation on discharge.

Results: Table 1
Conclusions: Although there were notable improvements in documentation of OP & a statistically significant increase in calcium and vitamin D orders after discharge for HF surgery, the study demonstrates a management gap in the identification &

treatment of OP in patients at high risk of fragility fractures for secondary prevention. Among patients with documentation of OP, females were more likely to be identified than males. Results are consistent with previous estimates of OP management in operative HF patients by OS. Based on these findings, management strategies are called for to optimize outcomes for HF patients presenting for surgical repair since there is substantial evidence of HF as a sentinel event presaging functional decline, future morbidity, and economic burden. Future studies should focus on systematic interventions to improve practices among OS & to create opportunities for more effective linkage with primary care providers for follow up.

Table 1: Patient characteristics, osteoporosis management after hip fracture surgery

| Parameter | Total N=109 | Males N=42 (38.53%) | Females N=67 (61.47%) |
|---|----------------|------------------------|--------------------------|
| Age (years) | | | |
| Mean | 83 | 83 | 83 |
| Median | 85 | 85 | 85 |
| Range | 55-105 | 55-96 | 57-105 |
| Procedure | | | |
| Intramedullary nail fixation | 59 (54.13%) | 19 (17.43%) | 40 (36.70%) |
| Arthroplasty | 28 (25.69%) | 17 (15.60%) | 11 (10.09%) |
| Cannulated screw fixation | 22 (20.18%) | 10 (9.17%) | 12 (11.92%) |
| 30-day all cause mortality | 5 (4.59%) | 3 (2.75%) | 2 (1.83%) |
| Number, percentage of males and females identified with osteoporosis on admission at discharge | | 2 (20%) 5 (21.74%) | 8 (30%) 18 (78.26%) |

Table 2 Osteoporosis documentation and management after hip fracture surgery, admission vs discharge

| | Osteoporosis documented on admission | Osteoporosis documented on discharge | P value |
|-------------|--------------------------------------|--------------------------------------|---------|
| Total N (%) | 10 (9.17%) | 23 (21.12%) | 0.02 |
| Male | 2 (1.83%) | 5 (4.59%) | |
| Female | 8 (7.34%) | 18 (16.51%) | |
| | Osteoporosis meds on admission | Osteoporosis meds on discharge | P value |
| Total N (%) | 4 (3.67%) | 16 (14.68%) | <0.005 |
| Male | 1 (0.92%) | 11 (10.09%) | |
| Female | 3 (2.75%) | 5 (4.59%) | |

Tables 1 and 2: Osteoporosis Management After Hip Fracture Surgery

Disclosures: Stuart Weinerman, None.

LB-MO20

Efficacy and Safety of Zoledronic Acid in Chinese Patients With Paget's Disease of Bone: A Phase IV Study. ou wang^{*1}, Hao Zhang², Yingying Hu¹, Zhenlin Zhang², Xiaoping Xing¹, XUNWU MENG³, Xun Liu⁴. ¹Department of Endocrinology, Peking Union Medical College Hospital, China, ²Shanghai Jiao Tong University Affiliated Sixth People's Hospital, China, ³PEKING UNION MEDICAL COLLEGE HOSPITAL, China, ⁴The Sun Yat-Sen Memorial Hospital, Peoples republic of china

Aim: A single infusion of zoledronic acid (ZOL) has been shown to produce rapid and sustained responses in Paget's disease of bone (PDB) in Whites and African Americans.¹ PDB is rare in China and there is no data available on ZOL use in this population. In this study, we aim to confirm the efficacy and safety of ZOL in the treatment of PDB in Chinese patients.

Methods: A total of 9 Chinese patients (M/F: 5/4) with PDB aged 59.3 ± 12.1 years were enrolled in this 6-month, open-label, single-arm, phase 4 study. All patients received a 5 mg infusion of ZOL over 30 minutes with elemental calcium 1000 mg/d and vitamin D3 800 IU/d supplementation. The primary efficacy endpoint was the rate of therapeutic response defined as a reduction of at least 75% in serum total alkaline phosphatase (ALP) or normalization of ALP at Month 6. The secondary efficacy variables included percent change in serum ALP, serum cross-linked C-telopeptides of type I collagen (CTX) and propeptide of N-terminal type I procollagen (PINP) at Months 3 and 6. Reductions in pain assessed by the visual analogue scale (VAS) were recorded. The safety endpoints included assessment of adverse events (AEs) and serious AEs.

Results: 100% therapeutic response rate was observed with 75.6% and 81.7% decrease in serum ALP levels at Months 3 and 6 compared with baseline, respectively. The percent changes of serum CTX and PINP were 54.08% and 82.60% at Month 3 and 64.73% and 86.30% at Month 6, respectively. The VAS decreased significantly from a median of 5.5 to 0.7 at 6 months. The median time to first therapeutic response and ALP normalization were 64 days (95% CI: 33, 66) and 65.5 days (95% CI: 60, 94), respectively, at the end of 6 months. All treatment-related AEs were of mild-to-moderate severity and occurred within 5 days post dose with a duration of ≤ 8 days. The most common AEs were general disorders and administration site conditions (6/9) and musculoskeletal and connective tissue disorders (4/9). There was one report of renal dysfunction due to increased serum creatinine levels, which reverted to normal levels in the out-of-study visits and two reports of decreased blood calcium. No serious AEs were reported.

Conclusions: This is the first study to prove the efficacy of a single infusion of 5 mg ZOL in Chinese patients with PDB. The drug was well tolerated with a low incidence of AEs.

Reference:
1. Reid IR et al. *N Engl J Med.* 2005;353(9):898-908.

Disclosures: ou wang, None.
This study received funding from: Novartis Pharma